

# The Toxicologist

Supplement to *Toxicological Sciences*

## 52<sup>nd</sup> Annual Meeting and ToxExpo™

March 10–14, 2013 • San Antonio, Texas



**OXFORD**  
UNIVERSITY PRESS

ISSN 1096-6080  
Volume 132, Issue 1  
March 2013

[www.toxsci.oxfordjournals.org](http://www.toxsci.oxfordjournals.org)

An Official Journal of  
the Society of Toxicology

**SOT** | Society of  
Toxicology

Creating a Safer and Healthier World  
by Advancing the Science of Toxicology

[www.toxicology.org](http://www.toxicology.org)



# 53<sup>rd</sup> Society of Toxicology Annual Meeting & ToxExpo Phoenix, Arizona

March 23–27, 2014  
Phoenix Convention Center

**Deadline for Proposals  
for SOT 2014  
Annual Meeting  
Sessions: April 30, 2013**

## Why Submit a Proposal?

1. To present new developments in toxicology.
2. To provide attendees an opportunity to learn about state-of-the-art technology and how it applies to toxicological research.
3. To provide attendees an opportunity to learn about the emerging fields and how they apply to toxicology.

## Session Types

**Continuing Education**—Emphasis on quality presentations of generally accepted, established knowledge in toxicology  
*Note: CE courses will be held on Sunday.*

**Symposia**—Cutting-edge science; new areas, concepts, or data

**Workshops**—State-of-the-art knowledge in toxicology

**Roundtables**—Controversial subjects

**Historical Highlights**—Review of an historical body of science that has impacted toxicology

**Informational Sessions**—Scientific planning or membership development

**Education-Career Development Sessions**—Sessions that provide the tools and resources to toxicologists that will enhance their professional and scientific development

**Regional Interest**—Central topics of relevance that describe public health and/or ecological problems of a particular region

Submit your proposal online at [www.toxicology.org](http://www.toxicology.org)

# The Toxicologist

Supplement to *Toxicological Sciences*

## 52<sup>nd</sup> Annual Meeting and ToxExpo™

March 10–14, 2013 • San Antonio, Texas



**OXFORD**  
UNIVERSITY PRESS

ISSN 1096-6080  
Volume 132, Issue 1  
March 2013

[www.toxsci.oxfordjournals.org](http://www.toxsci.oxfordjournals.org)

An Official Journal of  
the Society of Toxicology

**SOT** | Society of  
Toxicology

Creating a Safer and Healthier World  
by Advancing the Science of Toxicology

[www.toxicology.org](http://www.toxicology.org)

# Preface

**This issue is devoted to the abstracts of the presentations for the Continuing Education courses and scientific sessions of the 52nd Annual Meeting of the Society of Toxicology, held at the Henry B. Gonzalez Convention Center, March 10-14, 2013.**

**An alphabetical Author Index, cross referencing the corresponding abstract number(s), begins on page 536.**

**The issue also contains a Keyword Index (by subject or chemical) of all the presentations, beginning on page 561.**

**The abstracts are reproduced as accepted by the Scientific Program Committee of the Society of Toxicology and appear in numerical sequence.**



## **The New Mobile Event App**

Use these new planning and networking tools to access the latest meeting information, connect with fellow attendees, build your own schedule, view presentation details and abstracts, request meetings with attendees and exhibitors, and navigate ToxExpo with an interactive floor plan. In addition to these networking and meeting planning tools, use the app and website to access a complete San Antonio city guide including hotels, restaurants, attractions, nightlife, and shopping. One-on-one technology training and support is available during the meeting; visit the @SOT Center—Internet Access and Technology Training just across from Registration at the convention center or the SOT Pavilion in ToxExpo.

**Copies of *The Toxicologist* are available at \$50 each plus \$5 postage and handling (US funds) from:**

**Society of Toxicology  
1821 Michael Faraday Drive, Suite 300 • Reston, VA 20190**

**[www.toxicology.org](http://www.toxicology.org)**

**© 2013 Society of Toxicology**

*All text and graphics are © 2013 by the Society of Toxicology unless noted. Some San Antonio photos are courtesy of the San Antonio Convention & Visitors Bureau. For promotional use only. No advertising use is permitted. Some photos by Stephanie Colgan, Steve Moore, and Richard Nowitz.*

---

This abstract book has been produced electronically by ScholarOne, Inc. Every effort has been made to faithfully reproduce the abstracts as submitted. The author(s) of each abstract appearing in this publication is/are solely responsible for the content thereof; the publication of an article shall not constitute or be deemed to constitute any representation by the Society of Toxicology or its boards that the data presented therein are correct or are sufficient to support the conclusions reached or that the experiment design or methodology is adequate. Because of the rapid advances in the medical sciences, we recommend that independent verification of diagnoses and drug dosage be made.

## **CE 1 A Refresher of Immunoglobulin and Fc-Receptor Biology and Advances Related to Therapeutic Antibody Development.**

T. W. Salcedo. *Bristol-Myers Squibb Company, New Brunswick, NJ.*

The presentation will review the immunobiology of antibodies and Fc receptors and explore the field of therapeutic antibody development and advances in "antibody engineering" leading to the development of improved therapeutics. A basic overview will be provided on the structure and function of antibodies, as well as the various types and formats of antibody therapeutics and technological methods of production. In addition, the immunobiology of human leukocyte Fc receptors will be discussed. These receptors serve to link humoral immune responses to cellular activities within the immune system, and generally function as either antibody-binding receptors that trigger immune cell effector functions, or as transport receptors (FcRn). Highlights will include how immunoglobulin Fc sequences are now being tailored to trigger specific Fc receptors to improve therapeutic outcomes by introducing amino acid mutations, glycoengineering, or other approaches leading to next generation formats. Known species differences in immunoglobulins and Fc receptors that may be important for pharmacologic and toxicologic evaluations will be explored, as well as other challenges in assessing the nonclinical toxicities of new antibody formats. Building upon these basic themes, the presentation will explore the current landscape of approved therapeutics and forecasts for future developments in the field. The course will provide something for those seeking basic knowledge in the field of immunology and therapeutic antibody development, as well as those seeking to refresh and enhance their knowledge of recent advances.

## **CE 2 Basic Principles of Human Risk Assessment.**

Q. Zhao<sup>1</sup> and M. Meek<sup>2</sup>. <sup>1</sup>US EPA, Cincinnati, OH; <sup>2</sup>University of Ottawa, Ottawa, ON, Canada.

An overview of the fundamental, evolving guiding principles, and general methods used in chemical risk assessment will be provided. These principles and methods are addressed in presentations and discussions organized by the four components identified by the National Research Council in the Risk Assessment Paradigm: Hazard Identification and Characterization; Dose-Response Assessment; Exposure Assessment; and Risk Characterization. Guiding principles and key concepts in risk assessment will be illustrated by examples from the literature and sample calculations for dose-response assessment, exposure assessment, and risk characterization will be presented.

## **CE 3 Recent Developments in Cardiovascular Physiology-Based Toxicology.**

T. L. Knuckles<sup>1</sup> and W. McGuinn<sup>2</sup>. <sup>1</sup>West Virginia University, Morgantown, WV; <sup>2</sup>US FDA-CDER, Columbia, MD.

Contemporary drug development and toxicity assessments are focused on exploiting specific molecular targets that can improve disease outcomes with minimal untoward effects. Unfortunately, modern training in toxicology and pharmacology is directed primarily at specific ligand-receptor interactions at the expense of systems physiology. An overview of cardiovascular physiology, with a thematic focus on toxicology, will be provided. The presentations will include: overall physiological changes that manifest at the whole-animal level following toxicant exposure; in vivo, in vitro and ex vivo cardiac testing protocols in the regulatory environment, and how current testing strategies may potentially miss cardiac effects that manifest chronically; vascular and microvascular effects that result from toxicity initiated in other tissues; and microvascular physiology and toxicology in the context of model development, application, and underlying pathology. The course will be of interest to a broad scope of scientists that are increasingly being requested to consider the impact of novel compounds and toxicants on the physiology of the entire cardiovascular system.

## **CE 4 Approval of Biosimilar Monoclonal Antibodies: Scientific, Regulatory, and Legal Challenges.**

L. LeSauter<sup>2</sup> and J. D. Urban<sup>1</sup>. <sup>1</sup>ToxStrategies, Inc., Austin, TX; <sup>2</sup>Charles River Laboratories, Senneville, QC, Canada.

Technological advances have resulted in the development of a wide range of innovative monoclonal antibodies (mAb). As the patents for these monoclonal antibodies expire, there has been a growing interest in the market of "generic" follow-on

products, or biosimilars. These biosimilar drugs, however, are not generic in the same sense as small molecule drugs since they do not have identical active component(s) as the innovative drug product due to the differences in production. While established standard analytical methodologies enable manufacturers of generic small molecule drugs to demonstrate pharmaceutical equivalence, the complex and sensitive nature of even the most similar biological manufacturing systems (e.g., commercial cell lines) makes producing identical copies of the innovative monoclonal antibody products impossible. Therefore, the scientific and regulatory paradigm for demonstrating that the products are highly similar and that there are no clinically meaningful differences between a biosimilar product and an innovative therapeutic in order to obtain drug approval is necessarily much more complex. Adding to this complexity is the regulatory environment that impacts on the biosimilar approval process. Case studies will compare and contrast the scientific and regulatory approaches used for mAb biosimilar drug development. These examples will cover the GMP to clinical strategies in broad scope but focus on the preclinical breadth of studies conducted based on the extent of GMP and clinical similarity data available. Within these presentations the scientific rationale for similarity with the innovator drug will be highlighted. The basic concepts of the legal challenges and recent Biologics Price Competition and Innovation Act (BPCIA), which creates an abbreviated approval framework for biological products that are demonstrated to be "biosimilar" to or "interchangeable" with a US FDA-licensed biological product, along with the role the patent and data exclusivity provisions will play in biosimilar drug development, will also be discussed.

## **CE 5 The What, When, and How of Nonclinical Support for an IND Submission.**

P. Nugent<sup>1</sup> and D. Colagiovanni<sup>2</sup>. <sup>1</sup>Pfizer Worldwide Research and Development, Groton, CT; <sup>2</sup>N30 Pharmaceuticals, LLC, Boulder, CO.

The initiation of dosing of human subjects in a Phase 1 clinical trial represents the culmination of years of drug development, and immediately preceding the start of dosing, months of work to prepare and submit the Investigational New Drug (IND) application (or Clinical Trial Application (CTA)). A critical part of the submission dossier is the sections that describe the nonclinical data and interpretation that underwrite the clinical plan; specifically, the results of studies in pharmacology, pharmacokinetics, and toxicology, and their integration into a coherent argument that justifies the clinical starting dose, escalation of dose, and "stopping criteria" to be used in the clinical trial. The objective of the course is to elucidate the path to a successful IND/CTA submission by outlining what needs to be done (concentrating principally on the toxicology and safety pharmacology studies), the timeline and order of activities, and the presentation of the data and its integration into a coherent risk assessment to support introduction of the investigational compound into the clinic. The focus will be the content of the Nonclinical Overview (NCO), which represents an integrated detailed summary of the nonclinical studies conducted to support the clinical plan for first-in-human (FIH) dosing. The course will address the expectations of the two main "customers" for the NCO: the FDA pharmacology/toxicology reviewer evaluating the data to determine if it supports the safety considerations of the clinical plan, and the clinician designing the clinical protocol and conducting the FIH trial.

## **CE 6 The Practice and Implementation of Neural Stem Cell-Based Approaches to Neurotoxicology.**

T. J. Shafer<sup>1</sup> and A. B. Bowman<sup>2</sup>. <sup>1</sup>US EPA, Research Triangle Park, NC; <sup>2</sup>Vanderbilt University Medical Center, Nashville, TN.

The availability and use of human pluripotent stem cells (hPSC) and human neural stem cells (hNSC) for toxicology has dramatically increased in the past decade. hNSC are powerful tools for toxicologists and can provide tissue that would otherwise be unobtainable. This includes a renewable source of neural tissue from the same genetic stock that is not transformed or derived from a tumor, a source of normal human nervous system tissue, and sources of nervous system tissue from patients with clinical disease. However, culture and differentiation of hNSC are unique from culture of primary or transformed neural tissue. The course will bring together experts in the culture of various types of neural stem cells, including embryonic human derived neural stem cells, neurospheres, and neural cells derived from hPSC. Each expert will discuss the basic approaches to culturing different types of hNSC, including propagation of the cells in a progenitor status, as well as protocols for differentiation of the cells into different types of neurons. Pitfalls that are both common to the different models as well as unique ones will be described. The goal of the course is to provide the student with knowledge regarding different types of neural stem cell cultures, the techniques to successfully culture and differentiate these models, and application of these model systems to neurotoxicology. The course will conclude with an examination of appropriate outcome measures and discuss the possibility of personalized neurotoxicological assessment.

## CE 7 Toxic Effects of Metals.

M. F. Hughes<sup>2</sup> and M. P. Waalkes<sup>1</sup>. <sup>1</sup>NIEHS, Research Triangle Park, NC; <sup>2</sup>US EPA, Research Triangle Park, NC.

Human exposures to metals are a daily occurrence because of their natural presence in the environment—their uses in production of many commercial products—are byproducts of energy production and are found in many hazardous waste sites. The objective of the course is to highlight the fundamentals of metals toxicology. Metals have unique chemical and physical properties that distinguish them from organic-based chemicals. Even though some metals are essential to life, overexposure to these and other metals may result in a toxic effect in one or more organ systems. Upon exposure, metals may be absorbed, distributed throughout the systemic circulation, metabolized, and eliminated. The response of an organism following exposure to metals may be protective (e.g., induction of the metal-binding protein metallothionein), or toxicological by several mechanisms including oxidative stress. Key organ systems such as the central nervous system, the vascular system, as well as the skeleton system are affected by metals including manganese, lead, aluminum, and others. Accumulation of metals in bone has recently gained renewed interest as an eventual source of internal exposure. Noninvasive methods such as neutron activation are now being used to quantitate bone metal levels. Metals can influence gene expression, signal transduction, and epigenetics. Various toxic and carcinogenic metals such as arsenic and chromium alter the epigenetic program in cells; these effects on DNA methylation, histone tail modifications, and microRNA may be involved in metal-induced toxicity. Metals are known to cause cancer by several proposed mechanisms, including oxidative stress and the cancer stem cell hypothesis. Recent evidence suggests that developmental exposure to metals may affect stem cell population dynamics, which could result in adult onset of cancer. Overall, this is intended to be a basic course on metals toxicology, and is ideal to those who desire knowledge on the health effects of metals and useful tools used in metals toxicology research.

## CE 8 Advances in Nanotoxicology—Challenges.

S. M. Hussain<sup>1</sup> and S. F. Ali<sup>2</sup>. <sup>1</sup>US Air Force, Wright-Patterson AFB, OH; <sup>2</sup>US FDA-NCTR, Jefferson, AR.

Recent developments in nanotechnology have generated a degree of apprehension concerning the potential risk to human health and the environment from manufactured nanomaterials (MN). The unique chemical and physical properties of MN, coupled with their high surface area per unit mass, require an extensive suite of characterization tools to effectively assess the toxicity of MN. Not only must the size and surface area of the MN be characterized prior to cellular exposure, but also a number of other specific features must be additionally evaluated, such as the size distribution, chemical composition, crystallinity, surface structure, shape, and solubility. The ionic strength of biological fluids may produce MN instability, resulting in environmental-specific aggregation tendencies that may impact toxicological results. Since aggregation of MN can modify uptake rates, transport properties, and clearance by the cell model or organ system, it is critical to interpret the data from MN toxicity experiments with a detailed knowledge of the physicochemical properties of the MN at all experimental time points. Due to the lack of standardized methods to determine the physicochemical behavior of MN in biological systems, the mechanisms and nature of acute or chronic toxicity of engineered MN cannot be fully understood at this time. An understanding of a proper manner by which MN should be introduced to a biological environment has yet to be established, and consistency between cellular assay techniques has not been verified—both situations presenting clear challenges that must be addressed. This course raises issues to consider for the toxicity assessment of MN, and addresses recent advances and technical obstructions associated with conducting or interpreting *in vitro* or *in vivo* toxicity studies. The goal is to provide a comprehensive understanding of MN characterization, as well as facilitate valuable discussions of key challenges and advancements in the newly emerging field of nanotoxicology.

## CE 9 Gonadal Development, Function, and Toxicology.

B. McIntyre<sup>1</sup> and J. A. Flaws<sup>2</sup>. <sup>1</sup>NIEHS, Research Triangle Park, NC; <sup>2</sup>University of Illinois Urbana-Champaign, Urbana, IL.

The course objectives are to provide the basic tools for toxicologists who desire a better understanding of how to assess the effects of toxicants on the male and female gonads from development through adulthood. A focus on reproductive biology, study design considerations, reproductive endpoints, data interpretation, and

use of data in risk assessment will be highlighted. Reproductive toxicity studies are among the most complex and challenging studies in the field of toxicology. The studies assess multiple interrelated endpoints of male and female reproductive development and function. To properly design, conduct, and interpret these studies, a fundamental knowledge of male and female gonadal development, anatomy, physiology, and endocrinology are required. Individual lectures will discuss the anatomy and physiology of the male and female gonads, as well as endocrine regulation of these systems. Evaluation of toxicity endpoints to assess male and female reproductive function will also be discussed, including folliculogenesis, spermatogenesis, hormone analysis, cyclicity, fertility, histopathology, and proper use of statistical analysis. The regulatory expectations related to reproductive toxicity testing, interpretation of results, and how these results are ultimately used to assess potential risks to human reproduction, will be presented. The course will conclude with methodologies for *in vitro* reproductive toxicity assessments for screening and investigation of mode of action. In summary, key information required for the design of reproductive toxicity studies and interpretation of reproductive toxicity data, and provide guidance for use of the data for risk assessment of reproduction, will be presented.

## CE 10 The Reach Regulation and Safety Assessment Approaches for Chemicals That Come in Contact with the Skin.

J. Mortensen<sup>1</sup> and J. Heylings<sup>2</sup>. <sup>1</sup>CiToxLAB Scantox, Lille Skensved, Denmark; <sup>2</sup>Dermal Technology Laboratory Ltd., Keele University Science Park, United Kingdom.

REACH (Registration, Evaluation, Authorization, and Restriction of Chemical substances) is the European Union regulation on chemicals and their safe use, which came into force on June 1, 2007. The aim of REACH is to improve the protection of human health and the environment through better and earlier identification of the intrinsic properties of chemical substances. REACH places greater responsibility on the industry to manage the risks from chemicals, and to provide safety information on their substances. The regulation will come gradually into force in the period up to 2018. Under REACH, 30-40,000 new and existing chemicals will have to be (re)classified and registered. The regulation requires companies to conduct risk assessment and safety classification, with a minimal use of experimental animals, and to share information via databases managed by the European Chemicals Agency (ECHA). The skin (together with the respiratory system) is important as a route of chemical exposure, and as a target organ for toxicity induced by chemicals. Since under REACH so many chemicals need to be evaluated, it is important to use and develop testing methods that reliably predict human exposure and safety, while minimizing the use of experimental animals. An overview of the REACH regulation, and its practical implications for toxicological safety evaluation of chemicals marketed in Europe, will be given. Efforts to develop new methods and validation status of alternative methods that will limit the number of experimental animals to be used will be highlighted. Specifically, state-of-the-art investigational methods within dermal toxicology will be discussed since the skin is very important, both as a barrier to exposure and as a target organ. Practical examples of the use of the collected dermal safety data in the risk assessment of chemicals under REACH will be presented.

## CE 11 T4: Tools and Technologies in Translational Toxicology.

D. L. Mendrick<sup>2</sup> and V. S. Vaidya<sup>1</sup>. <sup>1</sup>Harvard Medical School, Boston, MA; <sup>2</sup>US FDA-NCTR, Jefferson, AR.

The last decade has seen revolutionary advances in the tools and technologies available for biomedical scientists such that researchers can now conduct transformative experiments to solve unmet medical needs moving from a single cell to whole organism, and vice versa. Novel tools and innovative technologies have facilitated the development of sophisticated molecular diagnostics, enabled the use of new approaches in safety evaluation and risk assessment, and led to the development of targeted therapeutics. The development and utilization of novel technologies and tools requires interaction between scientists of differing backgrounds and talents (e.g., biologists, chemists and programmers). Only with this shared effort can medicine transform itself to meet the needs of the 21st century. The panel of experts will decode and demystify the potential of these translational and transformative technologies over a wide variety of applications, including safety/efficacy screening of compounds, imaging, 'omics, and *in silico* modeling. The key goals are to enable you to understand how recent advances in "T4": 1) help in solving important problems that have been critical barriers to progress in the field and, 2) transform the field by generating foundational resources that will be widely used throughout biomedical science for safety evaluation and risk assessment.

## **CE** 12 Understanding Toxic Neuropathy in Drug Development: Both Clinical and Nonclinical Perspectives.

M. Kallman<sup>1</sup> and J. Benitez<sup>2</sup>. <sup>1</sup>Covance Research Laboratories, Greenfield, IN; <sup>2</sup>Vanderbilt University, Nashville, TN.

The topic of risk assessment of peripheral neuropathies is timely due to the increased clinical incidence of challenges related to multiple antecedents for the clinical presentation of neuropathies. The integration of both nonclinical and clinical dialogue on peripheral neuropathies will provide greater possibilities for successful drug development and improved patient outcomes. Peripheral nervous system toxicity is a common complication of exposure to industrial chemicals and drugs such as chemotherapeutics. Neuropathy can be caused by either limited or long-term exposure to drugs or chemicals, and toxic neuropathies can be classified by their presentation (e.g. motor vs. sensory), their electrodiagnostic features or their neuroanatomical location within the peripheral nerve. Identification of toxic neuropathology prior to human exposure in the drug development process requires a multidisciplinary approach. Presentations will include information on the preclinical and clinical syndromes that have been characterized and the specific techniques for assessment. The preclinical presenters will focus on the application of preclinical data to provide risk assessment and to direct clinical assessment possibilities. The clinical presenters will emphasize the clinical situation and current treatment approaches. The course will conclude with open discussion between the presenters and the audience about opportunities for future risk assessment and the application to clinical management.

## **CE** 13 Weighing in on Nutrition—Essential Concepts for Toxicologists.

D. M. Wilson<sup>1</sup> and A. L. Slitt<sup>2</sup>. <sup>1</sup>The Dow Chemical Company, Midland, MI; <sup>2</sup>University of Rhode Island, Kingston, RI.

There has been an exponential increase in the attention focused on the potential role of nutrition in reducing the risk for numerous health complications, ranging from birth defects to age-associated vascular disease. Underscoring the above is the increasing number of presentations and publications related to this subject, and hallmarks such as the recently revamped Food Pyramid into a Plate Icon. Chronic nutritional diseases are accepted to be a current crisis in our society; three nutrition-related diseases alone, obesity, Metabolic Syndrome, and Type 2 Diabetes, afflict over one-third of the American population. To better understand the components and etiology of nutritional diseases, it's essential for toxicologists to be well versed in the science of nutrition. A comprehensive understanding of nutrition has broad applications in toxicology, especially considering that many of us have roles in investigating the safety of nutrients, food additives or food ingredients, studying nutritional disease, or designing and interpreting preclinical or clinical studies wherein the need to consider and understand nutritional homeostasis is essential. The potential for intersection of normal nutritional metabolic pathways with adverse outcome pathways is becoming even more important to delineate. This course on general nutrition, the biochemistry of nutritional pathways, the essential role of vitamins, the channeling of nutrients such as carbohydrates, proteins and fats, cellular and molecular details of nutrition, and nutritional aspects of development and reproduction, will heighten awareness of their importance in human and animal health at multiple levels. The focus will be on relevant information, starting with an introduction to nutrition, followed by a review of biochemical and metabolic reactions in nutrition, with an emphasis on their relation to toxicology. How the nutritional status of a woman can modulate the developmental toxicity of a number of diverse toxicants, including alcohol, will be presented.

## **S** 14 Genetic and Epigenetic Determinants of Susceptibility to Environmental and Occupational Toxicants.

V. J. Johnson<sup>1</sup> and B. Yucesoy<sup>2</sup>. <sup>1</sup>BRT-Burleson Research Technologies, Morrisville, NC; <sup>2</sup>Toxicology and Molecular Biology Branch, NIOSH/CDC, Morgantown, WV.

The most common chronic disorders are multifactorial in nature, influenced by complex sequences of gene-gene and gene-environment interactions. While gene expression is a dynamic process that varies in response to a myriad of internal and external triggers and the surrounding microenvironment, the epigenetic mechanisms play a key role in mediating environmental influences on gene expression and epistatic interactions. In this respect, the expression of complex phenotypes should be assessed in a functional context that would look at the interplay between environmental, genetic, and epigenetic factors. Recent advances in genetic and epigenetic research offer new opportunities to integrate experimental approaches, including animal models and *in vitro/in vivo* translational research, with

computational strategies to predict such interactions at multiple levels of complexity. The focus of this session will be on current research investigating the role of genetic factors, epigenetic factors, and gene-environment interactions in the development and outcomes of complex diseases caused by environmental and occupational toxicants.

## **S** 15 Genetic Susceptibility to Occupational and Environmental Exposures.

D. C. Christiani. School of Public Health, Harvard Medical School, Boston, MA.

Due to their high prevalence in the general population, genetic polymorphisms in the susceptibility genes may predispose community members exposed to toxicants. Studies in genetic susceptibilities can eventually provide the following benefits: (1) to provide mechanistic insight of the etiology of disease; (2) to identify the more susceptible subpopulations with respect to exposure; (3) to provide valuable input in setting exposure limits by taking into account individual susceptibility. Research in this area has provided promising insights to occupational medicine, such as those illustrated by the NAT2 polymorphisms-aniline dyes and bladder cancer, and the HLA-DPB1Glu69 in chronic beryllium disease, a hypersensitivity-mediated inflammatory disorder. Nonetheless, even for the genetic susceptibility markers that have been shown scientifically to have a clear role in disease risk, the value of wide-scale genetic screening in occupational settings remains limited. In the general environmental setting, there are limited, but growing data on the role of common gene polymorphisms in predisposing children and adults to inflammation-related respiratory disorders induced by air pollution, and to heavy metal toxicity. The purpose of this presentation is to discuss state of knowledge with regard to gene variants interacting with environmental exposures in causing cancer and inflammatory disorders.

## **S** 16 Toxicogenomic and Systems Biology Approaches in the Understanding of Toxicity and Leukemogenesis Induced by Benzene.

C. McHale<sup>1</sup>, L. Zhang<sup>1</sup>, Q. Lan<sup>2</sup>, R. Thomas<sup>1</sup>, A. E. Hubbard<sup>1</sup>, R. Vermeulen<sup>3</sup>, G. Li<sup>4</sup>, S. M. Rappaport<sup>1</sup>, S. Yin<sup>4</sup>, M. T. Smith<sup>1</sup> and N. Rothman<sup>2</sup>. <sup>1</sup>School of Public Health, University of California Berkeley, Berkeley, CA; <sup>2</sup>Division of Cancer Epidemiology and Genetics, National Cancer Institute, Bethesda, MD; <sup>3</sup>Institute of Risk Assessment Sciences, Utrecht University, Utrecht, Netherlands; <sup>4</sup>Institute of Occupational Health and Poison Control, Chinese Center for Disease Control and Prevention, Beijing, China.

Benzene is an established cause of acute myeloid leukemia (AML) and may cause one or more lymphoid malignancies in humans. Occupational exposure to benzene, even at levels below the current U.S. occupational standard of 1 ppm, causes hematotoxicity. Toxicogenomics (e.g. genomics, transcriptomics and epigenomics) and systems biology (study of the interactions among toxicogenomic endpoints using bioinformatics) approaches in human populations, animals, and *in vitro* models, exposed to a range of benzene levels, are key to understanding gene-environment interactions in benzene toxicity and can identify biomarkers of exposure, early effect and susceptibility. Through analysis of the peripheral blood mononuclear cell (PBMC) transcriptomes of 125 workers exposed to a wide range of benzene levels, we recently reported highly significant widespread perturbation of gene expression at all exposure levels, as well as alterations in AML and immune response pathways. Sequencing of the PBMC transcriptomes from a subset of the study subjects revealed additional alterations in gene expression. From preliminary epigenomic data in the human subjects, we have identified benzene-induced alterations in the DNA methylome and miRNome. Using genomic screens in yeast, with subsequent confirmation in human cells, we have identified potential biomarkers of susceptibility. We are developing bioinformatic methods to integrate these and future toxicogenomic datasets, in a systems biology approach, to further understand pathways of benzene toxicity and to reveal potential biomarkers associated with a range of exposures.

Supported by NIH grant P42ES04705.

## **S** 17 Integrated Genetic and Genomic Approaches to Understand Susceptibility to Toxicant-Induced Lung Disease.

S. R. Kleeberger. Laboratory of Respiratory Biology, NIEHS, Research Triangle Park, NC. Sponsor: V. Johnson.

Genetic background has an important role in susceptibility to complex lung diseases, and the genetic contribution to disease phenotypes varies between populations. Understanding the mechanisms of interactions between genetic background

and exposures to environmental stimuli are critical to disease prevention. Animal models, particularly inbred mice, provide important insight to understand human disease etiologies because genetic background and environmental exposures can be controlled. Tools including *in silico* haplotyping, collaborative cross and diversity outcross mouse panels, bioinformatic applications, and -omics technologies have enhanced our ability to identify disease genes and pathways to guide translational investigations that apply these discoveries to human populations. Combined genetic and genomic approaches have yielded important insight to mechanisms of susceptibility to many complex traits and diseases. We have integrated inbred mouse and cell-based models with haplotype association mapping (genetic), global gene expression analyses (genomic), and expression quantitative trait locus mapping (eQTL or genetical genomics) to identify candidate susceptibility genes and associated gene networks important in toxicant-induced lung injury. The overarching goal of these investigations is to determine whether human homologues of these susceptibility genes associate with disease risk in human populations. Efforts to identify and validate susceptibility genes in mouse models of environmental disease with a goal towards translational application have enabled identification of individuals who are susceptible to disease. For example, epidemiological and clinical investigations have associated functional polymorphisms in human *NRF2* (NF-E2 related factor 2) and *TNF* (tumor necrosis factor alpha) with susceptibility to acute lung injury and ozone-induced changes in lung function, respectively. Importantly, these discoveries may also lead to novel intervention or therapeutic strategies to prevent disease.

## **S 18 Developmental Exposure to Bisphenol A and Lead: Effects on Metabolic Homeostasis and the Epigenome.**

D. Dolinoy. *University of Michigan, Ann Arbor, MI.*

Environmental exposures during early development and other critical life stages may induce changes to the epigenome resulting in potentially deleterious phenotypic effects including metabolic disease, cancer, and neurological disorders. The field of epigenetics is experiencing a rapid advancement in technology, methodology, and data acquisition that now allows for the identification of the constellation of genomic loci with altered epigenetic status following dose-dependent exposures. Thus, epigenomic profiling facilitates the identification of biomarkers of exposure, enabling clinicians to identify at-risk individuals prior to disease onset. Utilizing a multi-pronged approach with an *in vivo* mouse model, human clinical samples, and an ongoing 15-year longitudinal epidemiological study, the overall goal of this presentation is to elucidate the impact of perinatal bisphenol A (BPA) and lead (Pb) exposure on metabolic homeostasis and DNA methylation, and the interplay between the two. Developmental exposure to environmentally relevant levels of BPA has been shown to affect both global and gene-specific DNA methylation patterns in rodents. We now draw upon data from multiple whole-genome platforms to show that multiple dose levels of BPA affect DNA methylation in mice and humans and that these epigenetic effects are non-monotonic in dose response. Preliminary studies also indicate that Pb exhibits epigenetic effects that may contribute to its known neurotoxic and obesogenic activities.

## **S 19 Predictive Toxicology Paradigms for Understanding Carbon Nanotube Toxicity in the Lung.**

J. C. Bonner<sup>1</sup>, A. Nel<sup>2</sup>, D. W. Porter<sup>3</sup>, V. Castranova<sup>3</sup> and K. E. Pinkerton<sup>4</sup>.  
<sup>1</sup>NCSU, Raleigh, NC; <sup>2</sup>UCLA, Los Angeles, CA; <sup>3</sup>NIOSH, Morgantown, WV; <sup>4</sup>UC Davis, Davis, CA.

Nanotechnology is rapidly developing, resulting in the production of a variety of engineered nanoparticles. Carbon nanotubes (CNTs) represent an important family of nanoparticles because they have many potential uses in engineering, electronics, and medicine due to their ease of functionalization, unusual strength, and electrical conductivity. However, these novel nanostructures also represent a potential human health risk, due to the possibility of inhalation exposure and evidence that the lung and cardiovascular systems are targets for hazardous effects. Inhalation studies in rodents show that CNTs deposit within the distal regions in the lungs and migrate to the pleura to cause inflammatory and/or fibrotic effects. Presentations in this session are aimed at elucidating the pulmonary and cardiovascular effects of CNTs, and how an increasing variety of functionalized CNTs can be evaluated via high-content screening. Because functionalized CNTs vary in toxicological activity, we will address high-content screening for the development of structure-activity relationships relevant to inhalation toxicity and safer design of nanoparticles. This will include exploration of factors that mediate toxic effects such as high aspect ratio, durability, and residual metal content and discuss how removing metal catalysts or changing surface properties alters the pattern and timing of toxicity. While the lung is a major target organ, another goal is to determine the potential for inhaled CNTs to have toxic effects that reach beyond the lung to influence the cardiovascular system. Finally, we will discuss how susceptibility factors,

both genetic and environmental, determine pulmonary and cardiovascular toxicity to CNTs. The outcome of this session is to gain a better understanding of the structure-activity relationships, target organs, and susceptibility factors that will aid the development of predictive toxicology paradigms for understanding CNT toxicity.

## **S 20 Time Course of Pulmonary Responses to Inhaled Multiwalled Carbon Nanotubes.**

D. W. Porter<sup>1</sup>, A. F. Hubbs<sup>1</sup>, R. R. Mercer<sup>1</sup>, N. Wu<sup>2</sup>, W. McKinney<sup>1</sup>, B. T. Chen<sup>1</sup>, M. G. Wolfarth<sup>1</sup>, L. A. Battelli<sup>1</sup>, J. F. Scabilloni<sup>1</sup>, D. Schwegler-Berry<sup>1</sup>, S. Friend<sup>1</sup>, S. Tsuruoka<sup>3</sup>, M. Endo<sup>3</sup>, D. Frazer<sup>1</sup> and V. Castranova<sup>1</sup>.  
<sup>1</sup>NIOSH, Morgantown, WV; <sup>2</sup>Department of Mechanical & Aerospace Engineering, West Virginia University, Morgantown, WV; <sup>3</sup>Research Center for Exotic Nanocarbons, Shinshu University, Nagano, Japan.

In the present study, an aerosol of multi-walled carbon nanotubes (MWCNT) was produced with an acoustical generator, and airborne concentration and size distribution was determined. Mice were exposed by whole body inhalation to MWCNT (5 mg/m<sup>3</sup>, 5 hours/day, 12 days) and pulmonary responses were monitored at 1 day, 2, 4, 12, 24 and 48 weeks post-exposure. Pulmonary responses were investigated using whole lung lavage, histopathology, morphometry, and enhanced darkfield light microscopy studies. MWCNT lung burden was also measured to assess MWCNT clearance. Data indicate that the lung burdens of MWCNT in this study represent lung burdens relevant to estimated human occupational exposures and caused time-dependent pulmonary inflammation, damage and pulmonary fibrosis. Using enhanced darkfield microscopy, MWCNT fibers were found in lavage of the pleural space, parietal pleura, and respiratory muscles of the diaphragm and chest wall. The time course of pulmonary responses and their relationship to MWCNT lung burden and clearance will be discussed.

## **S 21 Establishment of Carbon Nanotube Structure-Activity Relationships (SARs) That Can Be Used to Understand Pulmonary Toxicity and Safer Design.**

A. Nel. *UCLA, Los Angeles, CA.*

There is a fundamental gap in understanding how the physicochemical properties of carbon nanotubes (CNTs) contribute to hazard generation in the lung. Without this knowledge, it is difficult to evaluate CNT safety in a predictive manner. Our goal is to develop a predictive toxicological paradigm for CNT safety assessment in which we define the structure-activity relationships (SARs) leading to hazard generation at the nano/bio interface, including ways to design safer materials that do not induce chronic inflammation and fibrosis. To achieve this goal, we are developing a series of single-wall and multi-wall CNT test materials that can be screened by robust cellular assays to perform hazard ranking and SAR analysis. We are looking at the role of CNT dimensions (including length, diameter and aspect ratio), dispersability, catalytic surface chemistry, electronic properties and purity in initiating cooperative cellular interactions in macrophages and cells of the epithelial-mesenchymal trophic (EMT), which are involved in the pathogenesis of pulmonary inflammation and fibrosis. The above physicochemical characteristics impact the lysosomal stability in macrophages in a hierarchical fashion, leading to cathepsin B release and assembly of the subunits of the NALP3 inflammasome. This leads to IL-1 beta release, which primes the EMT unit and initiates a march of events leading to TGF-beta and PDGF production and subsequent induction of chronic inflammation and fibrosis in the lung. Utilizing myeloid and epithelial cell lines, it is possible to study the induction of these biomarkers in relation to the property variations of the CNT materials, predicting the SARs that are associated with pulmonary inflammation and fibrosis. Moreover, we have also implemented surface coating and functionalization approaches that can change the hazardous characteristics, leading to the design of safer CNTs. The overall utility of this research exploration is to establish a predictive and quantitative toxicological paradigm for the safety assessment of CNTs and their safe implementation in the marketplace.

## **S 22 Surface and Chemical Modification of Single-Walled Carbon Nanotubes Does Not Necessarily Create a Safer Nanomaterial.**

K. E. Pinkerton. *University of California Davis, Davis, CA.*

We hypothesized iron (Fe) content and morphology of inhaled single-walled carbon nanotubes (SWCNTs) would influence the extent of cellular injury and alters homeostasis in the lung. Rats (SD) were exposed (1 mg/m<sup>3</sup>) to either aerosolized

SWCNTs (raw FeSWCNT or purified cSWCNT), carbon black (CB), crocidolite asbestos, or fresh air via nose-only inhalation for 6 hr/d for 10 d. SWCNTs containing varied amounts of iron. Depending on the endpoint of interest, pulmonary responses of SWCNTs sometimes followed that of CB while in other circumstances matched that of crocidolite. Notably, animals exposed to FeSWCNTs were unable to respond to an additional oxidant challenge and cSWCNTs exposed animals had a latent and persistent development of mucous cells in the distal airways. In summary, while some toxicity endpoints follow patterns comparable to CB or crocidolite, the respiratory effects of inhaled FeSWCNTs and cSWCNTs appear to be unique. These changes could be suggestive of precursor events to pathologic changes that could develop under more prolonged exposure conditions.

## **S 23 Cardiovascular Responses to Pulmonary Inhalation of Nanoparticles.**

*V. Castranova. Pathology & Physiology Research Branch, NIOSH, Morgantown, WV.*

Pulmonary exposure to various nanoparticles has been reported to cause lung inflammation and in some cases fibrosis. This presentation describes cardiovascular responses which occur following inhalation of titanium dioxide nanospheres or multi-walled carbon nanotubes in rats. Pulmonary exposure to nano titanium dioxide inhibits the ability of systemic and coronary arterioles to respond normally to dilators and affects heart rate and blood pressure in response to adrenergic agonists 24 hours post-exposure. This microvascular dysfunction is associated with adherence of polymorphonuclear leukocytes and generation of reactive species at the vessel walls, and resultant scavenging of nitric oxide secreted from dilator-stimulated endothelial cells. Neutrophil depletion or antioxidants partially reverse this vascular dysfunction. There also appears to be a neurogenic component to these cardiovascular changes, since inhibition of pulmonary sensory neurons or neuronal input to the arteriolar smooth muscle partially reverses these effects. Inhalation of multi-walled carbon nanotubes also inhibits coronary arterial responsiveness to dilators. This dysfunction occurs 24 hours after exposure and declines over several days thereafter. Human relevance of these rat data will be discussed.

## **S 24 Genetic and Environmental Factors That Determine Susceptibility to Inhaled Carbon Nanotubes.**

*J. C. Bonner. Toxicology, NC State University, Raleigh, NC.*

While studies with rodents suggest that inhaled carbon nanotubes could represent a human health risk for the development of pulmonary diseases, it is likely that individuals with pre-existing disease or those with specific genetic deficiency would be most susceptible to exposure and lung injury. The goal of this presentation is to emphasize genetic and environmental factors that determine susceptibility to inflammatory, immune, and fibroproliferative responses in the lungs of mice exposed to carbon nanotubes. Evidence will be presented showing that pre-existing non-allergic lung inflammation induced by bacterial lipopolysaccharide (LPS) or allergic airway disease induced by ovalbumin sensitization alters the immune response and fibroproliferative effects of carbon nanotubes as well as modulates other aspects of airway remodeling such as inflammatory cell infiltration and mucus hypersecretion. In addition, transgenic mouse studies show that susceptibility or resistance to carbon nanotubes is determined by the relative abundance or expression of specific genes that encode transcription factors involved in the innate immune response. Finally, the consequence of enhancing the physical or chemical properties of carbon nanotubes by atomic layer deposition will be addressed to better understand how post-synthesis engineering affects toxicity and disease pathogenesis.

## **S 25 Translatable Indicators of Testicular Toxicity: Inhibin B, microRNAs, and Sperm Signatures.**

*K. Boekelheide<sup>1</sup>, B. McIntyre<sup>3</sup>, M. Coulson<sup>4</sup> and R. E. Chapin<sup>2</sup>. <sup>1</sup>Brown University, Providence, RI; <sup>2</sup>Pfizer Drug Safety, DART Group, Groton, CT; <sup>3</sup>National Toxicology Program, NIEHS, NIH, Research Triangle Park, NC; <sup>4</sup>AstraZeneca R&D, Alderley Park, United Kingdom.*

The typical endpoints used in preclinical animal models for reproductive toxicity testing, such as histopathology, are not translatable for human clinical assessment, which typically focuses on the analyses of semen and serum hormones. Therefore, when testicular toxicity arises in preclinical toxicity testing, the methods currently

available to monitor this liability in clinical trials are limited. Because of these limitations, there is a need to develop sensitive and translatable indicators that reliably reflect testicular function. In this symposium, an introductory talk will set the stage by describing testicular physiology, preclinical tests of male reproductive toxicity, and current methods for assessing testicular function in men in clinical trials. The following three talks will discuss currently active efforts to develop improved translatable indicators of testicular toxicity in men. Serum inhibin B is a product of the testicular Sertoli cell and levels fall in response to testicular injury. Testis-specific miRNAs may be released upon testicular injury, and their measurement in serum may be a measure of effect. Sperm mRNA transcripts and DNA methylation may be indicators of testicular toxicity because they are easily measured and persistently altered after testicular injury. Developing reliable and predictive translatable indicators of testicular toxicity would be valuable for drug development in the pharmaceutical industry, and for monitoring men in occupational settings where exposure to potential testicular toxicants is a concern.

## **S 26 Biomarkers of Testicular Injury: Where Have We Been.**

*B. McIntyre. NIEHS/NIH, Research Triangle Park, NC.*

Toxicological findings in the male reproductive system are one of the most challenging events to put into perspective during nonclinical drug toxicity testing. These findings in animal models often consist of adverse changes in testicular histopathology and decreases in male fertility. Understanding the toxicological relevance of these findings to men enrolled in clinical trials is necessary for patient safety and is often paramount for continued development of the drug candidate. The mammalian testis is a complex tissue consisting specialized cell types that support spermatogenesis and reproduction. Although rodents, canines and non-human primates exhibit anatomical and physiological similarities, there are distinct differences that make extrapolation to human males challenging. Historically, alterations in non-invasive biomarkers such as hormone levels (e.g. testosterone and follicle stimulating hormone) and semen parameters (motility, morphology, count) have been used as indicators of altered testicular function. However, these changes are often insensitive and may require significant and potentially irreversible damage to the testes before biologically significant alterations in levels are evident in either animal models or humans. This has led to pragmatic nonclinical approaches where the pathogenesis of testicular toxicity is characterized with respect to both the potential for recovery/reversibility, and the margin of safety between the preclinical toxic exposure and the expected clinical exposure. Noninvasive (and often insensitive) biomarkers are often benchmarked against these exposures. This presentation with review the benefits of this sometimes challenging and inferential paradigm, but will also underscore that new tools and methodologies would be of value in understanding the human relevance of drug-induced testicular findings observed in animals.

## **S 27 Industry Efforts to Evaluate Inhibin B As Potential Biomarker for Testicular Toxicity.**

*M. Coulson. Safety Assessment, AstraZeneca, Macclesfield, United Kingdom. Sponsor: K. Boekelheide.*

Serum inhibin B is a hormone product of the seminiferous epithelium that has long been considered as The Next Great Biomarker. A HESI-sponsored effort in the early 2000's failed due to poor antibody behavior. A new antibody and a new assay kit have revived interest in this protein, and HESI has again sponsored a multi-company analysis of the analytic method and the protein's response to toxicity. This talk will introduce the biology, and the results of the consortium in evaluating the robustness of the analytic method, and the correlation between changes in inhibin B blood levels and the histologic state of the testis.

## **S 28 Circulating microRNAs As Biomarkers of Testicular Damage?**

*R. E. Chapin. DART, Drug Safety R&D, Pfizer, Inc, Groton, CT.*

MicroRNAs released into the blood following injury of specific tissues are emerging as promising biomarkers of toxicity, and the testis is no exception. A large multi-company effort under the auspices of the Predictive Safety Testing Consortium has

been working to define which miRNAs are testis-specific or -enriched, and to define their changes in the blood during testicular toxicant-induced injury. This presentation will briefly review the underlying biology and present an update of the work in this fast-moving area.

## **S** 29 **Sperm mRNA Transcripts and DNA Methylation Marks As Indicators of Testicular Injury.**

K. Boekelheide. *Brown University, Providence, RI.*

As a pure population of cells that have matured and differentiated within the seminiferous epithelium, sperm carry all of the information needed to fertilize an oocyte and initiate embryogenesis. Sperm deliver small and large RNAs and DNA to the oocyte. Using high throughput array technology, a panel of altered sperm mRNAs has been identified after exposure of rats to testicular toxicants. In men, the extent of sperm DNA methylation is related to sperm motility. The ultimate goal is to identify translatable sperm molecular signatures that will allow the rapid assessment of sperm effects in preclinical test species and exposed men.

## **W** 30 **Biology of Low-Dose Response for DNA-Reactive Chemicals.**

J. Klapacz<sup>1</sup> and B. P. Engelward<sup>2</sup>. <sup>1</sup>*TERC, The Dow Chemical Company, Midland, MI;* <sup>2</sup>*Department of Biological Engineering, Massachusetts Institute of Technology, Cambridge, MA.*

In the risk assessment process, DNA-reactive agents are generally considered to have no thresholds for their biological effects and this assumption formed the basis for linear low-dose extrapolation of any carcinogenic effects induced by these agents. On the other hand, cells have evolved to handle DNA lesions from endogenous and many exogenous DNA-reactive agents. In fact, DNA-repair processes are strictly conserved from bacteria to humans underlying their importance in protection against the effects of these agents, such as disease and aging. In recent years, low-dose response for DNA-reactive agents has been an active domain for research in toxicology, with publication of several datasets with large numbers of doses focused on the determination of no-observed-genotoxic-effect-level (NOGEL) values. This effort has included dose-response modelling to identify the best fit between linear and nonlinear models, such as bilinear (hockey-stick) and the benchmark dose (BMD) suite of models, and most datasets have supported a bilinear or nonlinear/threshold dose response as providing best fit based on statistical criteria. However, empirical demonstration of statistically-supported nonlinear/threshold dose response alone is not sufficient to achieve a paradigm shift in risk assessment. A clear understanding of the biological processes behind the shape of the low-dose response curve is similarly a critical piece of this journey, and one where less effort has been focused to date within toxicology. This workshop will explore some of the questions that need to be addressed to understand and bridge DNA-repair processes and cellular responses with the mode-of-action driving these nonlinear/threshold dose responses for genotoxic effects. The workshop will examine existing knowledge from the field of DNA repair and link it with response to low doses of DNA-reactive agents, in order to draw specific recommendations on a path forward.

## **W** 31 **Genotoxic Effects and Dose Response: What Do We Know So Far?**

L. H. Pottenger. *TERC, The Dow Chemical Company, Midland, MI.*

Low-dose genotoxic response for DNA-reactive alkylating agents has been actively investigated recently, with large datasets focused on low-dose response and determination of no-observed-genotoxic-effect-level (NOGEL) values. Most of these recent datasets include dose-response modelling analyses and have demonstrated a bilinear or non-linear/threshold dose-response as the statistically supported best fit, including datasets for directly DNA-reactive chemicals such as MMS, MNU, EMS, and ENU. Recent data have demonstrated the ubiquitous presence of endogenously-derived DNA adducts, some of which are identical to ones induced by exogenous exposure to DNA-reactive chemicals. Use of stable isotopes has permitted differentiation between the identical endogenously- and exogenously-induced DNA adducts, demonstrating that the exogenously-induced DNA adducts can have non-linear dose-responses at low doses; examples include formaldehyde and EO, both of which show that endogenous adduct levels can swamp the exogenously-induced ones at low exposures. Thus the available empirical evidence supporting the existence of non-linear/threshold dose-response for mutagenic effects from DNA-reactive agents is already compelling, while a growing body of evidence

is demonstrating similar non-linear/threshold dose-responses for exogenously-induced DNA adducts. However, statistically supported demonstration of non-linear/threshold dose-response alone is inadequate to achieve a paradigm shift in risk assessment. A clear understanding of the biology behind the shape of the dose-response is a critical piece for this journey, especially at low doses, although considerably less effort has transpired on this aspect to date. Addressing the biology and biologically plausible modes-of-action driving these non-linear/threshold dose-responses for genotoxic effects is the next task, one in which DNA repair mechanisms are likely to play a key role, both for adducts and for impact on dose-response for any resulting mutagenic effects.

## **W** 32 **CometChip and Recombomice Shed Light on Gene-Exposure Interactions That Impact Genomic Stability.**

B. P. Engelward. *Department of Biological Engineering, Massachusetts Institute of Technology, Cambridge, MA.*

We are interested in homologous recombination (HR) and base excision repair (BER) and the interaction between these DNA repair pathways. To explore HR in mammals, we created mice with recombination reporter systems (Recombomice) in which cells that have undergone an HR event fluoresce by combining tandem repeat of truncated copies of EYFP or EGFP gene. Here, we explore genetic and environmental factors that modulate susceptibility to HR in vivo. In particular, the impact of inflammation, producing endogenous oxidative and alkylating DNA damage, as both a modulator and an inducer of HR is presented. Exposure to low dose and high dose radiation causes many of the same changes to DNA as exposure to inflammation and can lead to severe inflammatory responses. Consequently, our inflammation studies have broad relevance. In addition, we have developed Comet assay called 'CometChip' for DNA damage analysis in single cells in an automated fashion. The approach increases throughput and improves reproducibility. Here, we show proof of principle of the technology as well as several applications of the CometChip for studies of gene-environment interactions. Together, this work and the technologies generated new biological insights.

HR has emerged as an important driver of carcinogenic sequence rearrangements. HR repairs double strand breaks in the S/G2 phases of the cell cycle resulting from endogenous and exogenous processes. While usually error free, errors in homologous recombination may result in sequence rearrangements and loss of heterozygosity, both of which are prominent features of cancer cells. BER is also a key DNA repair pathway. In this case, damaged bases are removed, the DNA backbone is cleaved, the ends are processed and the resulting gap is filled from the opposite strand. Both pathways are usually error-free, but there are still rare events where there are misalignments during HR, and misinsertions during BER. Also, both pathways are active in response to spontaneous DNA damage, and thus would be expected to be active in response to low dose radiation.

## **W** 33 **Role of Mismatch Repair in Mutagenesis, Cancer, and DNA-Damage Signaling.**

W. Edelmann. *Department of Cell Biology, Albert Einstein College of Medicine, Bronx, NY.* Sponsor: J. Klapacz.

The DNA mismatch repair (MMR) system is essential for maintaining the integrity of mammalian genomes by removing misincorporated nucleotides that result from erroneous replication. In addition, MMR participates in the early steps of checkpoint activation and apoptosis during the cellular response to alkylation induced O<sup>6</sup>MeG:T mismatches and many other DNA lesions, particularly relevant at low-dose, clinically-relevant exposures. Mutations in mammalian MMR genes result in increased spontaneous mutation rates and strong predisposition to colorectal cancers and other cancers. Eukaryotic MMR is a complex system that requires the interaction of several MutS and MutL proteins for the initiation of the repair reaction. Subsequent to mismatch recognition, downstream events are activated that lead to the excision of misincorporated or damaged nucleotides and the signaling of DNA damage-induced cell cycle arrest and apoptosis. The loss of the MMR-dependent DNA damage response is of significant clinical relevance as it results in increased resistance to many alkylating and chemotherapeutic agents. Our research program focuses on elucidating the functions of the individual MutS and MutL homologs in mammalian MMR and on assessing their importance for tumor suppression and the DNA damage response. Our results show that the DNA damage signaling by MMR is important for the suppression of tumorigenesis in the initial stages of the process. In addition, we found that MMR missense mutations can effectively separate the DNA repair and damage response functions and result in more heterogeneous cancer phenotypes than those caused by complete loss of function mutations.

## W 34 Computational Systems Biology Modeling of DNA-Damage Stress Pathways for Assessing Mutation Rates at Low Doses.

M. E. Andersen. *The Hamner Institutes for Health Sciences, Research Triangle Park, NC.*

Homeostasis with cellular stress response pathways involves negative feedback acting through a series of steps to reduce stressor concentrations. Many stress response pathways have rapid response, post-translational signaling and slower signaling through transcriptional upregulation of gene families. Our laboratory, in close collaboration with scientists from Unilever Safety and Environment Assurance Centre (SEAC), UK, has examined multiple biological read-outs in cells treated with several DNA-damaging compounds in order to create mechanistic computational models for micronuclei (MN) formation across wide dose ranges. The readouts in several cell types – AHH-1, HT-1080 and TK6 - included dose and time-dependent examination of whole genome gene expression, high content imaging of DNA-damage markers ( $\gamma$ H2AX and p53), semi-quantitative measures of key phosphoproteins (ATM, ATR, p38, Chk2, and p53), and MN as a measure of DNA-damage. Transcriptional upregulation only occurred in the regions of dose-response with clear increases in MN formation. Post-translational activation of rate constants for DNA-repair processes acting through activation of specific kinases appears to be the main contributor to regulation of DNA-damage at lower doses of these compounds. This talk describes stress pathway homeostatic feedback loops, shows our steps to populate high- and low-dose models for DNA-damage response pathways with etoposide, quercetin and methylmethanesulfonate, notes our progress in creating mechanistically-based low dose threshold models and discusses the value of these computational models in guiding new experimental approaches for assessing thresholds.

## W 35 Do Alkylating Agents Cause Genotoxic Thresholds through a DNA Repair Mode of Action?

G. E. Johnson, S. H. Doak, B. J. Rees, A. D. Thomas, J. R. Verma, Z. M. Zair and G. J. Jenkins. *College of Medicine, Swansea University, Swansea, United Kingdom.*

The long standing theory that linear dose responses exist for all DNA reactive genotoxic agents has recently been challenged. This paradigm shift towards accepting thresholds has been initiated by the scientific and regulatory community. High power non-linear dose responses are being produced in robust test systems. However, for the scientific community to accept a range of low doses as biologically irrelevant, a plausible mechanism of action must be shown experimentally. Many different research groups are tackling this issue for methyl- and ethyl-methane sulphonate (EMS and MMS) and methyl- and ethyl- nitrosourea (MNU and ENU) which have all been shown to exhibit non-linear dose responses for both mutagenicity and clastogenicity in vitro and in vivo. These alkylating agents induce specific DNA adducts (O6-alkylG, N7-alkyl-G and N3-alkyl-A), and recent work has been to investigate the roles of DNA repair in relation to their genotoxic thresholds. Specific DNA repair enzymes (N-methyl DNA purine glycosylase [MPG] and O6- alkyl guanine transferase [AGT]) have been shown to be up-regulated by low dose alkylating agents, and knocking down these specific DNA repair enzymes in vitro alters the shape of the dose response e.g. to EMS and MNU. Therefore, mono-functional alkylating agents have threshold dose responses through a DNA repair mode of action.

## W 36 Incorporation of Exposure Data and Chemical Properties into Early In Vitro Screening Studies: Putting Early Hazard Identification into Appropriate Context.

R. T. Dunn<sup>1</sup> and Y. Will<sup>2</sup>. <sup>1</sup>Discovery Toxicology, Amgen Inc, Thousand Oaks, CA; <sup>2</sup>Compound Safety Prediction, Pfizer R&D, Groton, CT.

Over the past several years, a multiplicity of innovative early-screening assays have been adopted to improve our ability to select drug candidates with the maximal opportunity to eventually succeed in later development. Examples of medium and high-throughput assays that can enable early hazard identification include ion channels related to cardiovascular safety (hERG, Nav1.5, and others), assays to understand CNS permeability and hepatobiliary transport (PgR, BSEP, etc.), and receptor and kinase screens, as well as screening ADME assays. These assays are typically employed early in the drug discovery process when little other data are available to help contextualize the early-screening result. Data output from these early screens is often produced, then utilized by project teams to select molecules for advancement, deprioritization, or to accumulate the knowledge base around a compound. In this model, the early-screening data may become a static entity, such as an IC50 value, which is then stored in a database often without further consideration or re-evaluation. There is a possibility that early-screening data in such a

model is underutilized or potentially misleading. An inherent problem with generating early-screening data is that it is often produced in the absence of accompanying data (e.g., *in vivo* exposure), which is information that can be leveraged to place these data into better context and enable more accurate predictions. In this workshop, several use case examples will be presented where *in vivo* exposure information and chemical compound properties have been weaved into early *in vitro* toxicity screening data enabling the discovery toxicologist to conduct a more robust assessment of the hazard identification assay data.

## W 37 Inclusion of Exposure Data to Early Toxicity Screening: Using the Bile Salt Export Pump (BSEP) Screen As an Illustrative Example.

R. T. Dunn, R. E. Morgan and H. K. Hamadeh. *Discovery Toxicology, Amgen Inc, Thousand Oaks, CA.*

Inhibition of the bile salt export pump (BSEP) is a recognized risk factor in the development of drug induced hepatic toxicity. To date there has not been an animal model that can be reliably used to predict toxicity arising from inhibition of bile salt transport. Thus, in order to provide project teams with an early hazard identification tool for BSEP inhibition, a vesicle-based BSEP assay was developed. Guidance for decision making or prioritization was initially based on a series of cutoff values, where potency on BSEP was used as a singular criterion for hazard flagging. As part of an effort to refine how early screening data are used, BSEP inhibition data was obtained from a compendium of approved and withdrawn drugs. The available human exposure data was then applied in a ratio calculation (BSEP IC50/Exposure) in order to provide an estimate of the safety multiple. Using the ratio-based data, a more robust evaluation of the IC50 data is now possible and the decision making power is enhanced. In addition, both false positive and false negative compounds were further analyzed and hypotheses generated to refine judgment around the hazard for individual molecules.

## W 38 High-Content Mechanistic Screening (HCMS) Technology to Impact Safety in the Context of Efficacy, Exposure, and Toxicity.

K. Tsaion. *Apredica, Watertown, MA.*

High content mechanism screening (HCMS) is a powerful platform that images numerous mechanistic toxicity endpoints in full dose response at various time points in cells of choice to generate IC50 based toxicity profiles presented as heatmaps. This allows to compare toxicity profiles of compounds across chemical series or within a series, with the goal to only take compounds forward that meet an acceptable safety profile and minimize the probability of attrition in later stages of development. We have successfully applied this approach to retrospective analysis for organ toxicity prediction as well as within our own portfolio. This work demonstrated that accurate prediction of clinical safety outcome depended on the availability of accurate information on clinical exposure levels. Rank ordering of compounds should be done in the context of exposure to most accurately define the safety window. When adjusted for clinical Cmax, retrospectively, the rank ordering of compounds fell in line with the FDA status and known clinical adverse events observations. This information was available to us for retrospective validation of the HCMS technology, but is not available for discovery compounds. To address this problem, as part of retrospective validation, we used industry-standard approach of using pharmacologically-based pharmacokinetic (PBPK) model and predicted human Cmax to normalize HCMS toxicity data. We demonstrated that when HCMS data were adjusted for predicted Cmax, that was calculated using PBPK model CloePK, rank order of the compounds fell in the same range as when we used clinical Cmax. In order to generate PBPK predictions a set of standard ADME data is used as an input.

## W 39 Lead Optimization Against Toxicological End Points in Drug Discovery: Recognition of Structural Determinants of Small Molecule Target Organ Exposure and Toxicity.

D. P. Hartley. *Array Biopharma, Boulder, CO.*

Target organ toxicity is a leading cause of attrition for novel small molecules in non-clinical drug discovery and early clinical development. Given the demands on drug discovery teams to produce molecules devoid of toxicity concerns, a paradigm shift has occurred such that toxicologists are now integral members of these teams with new responsibilities geared toward lead optimization. As such, it is no longer sufficient for the toxicologist to simply describe the observed organ toxicities of a new

compound, it is expected that we assess risk for toxicity in a predictive manner, or ascribe a mechanism to early toxicity findings, link the findings to an offending moiety within the structure, and assist in defining the chemical lead optimization path. In many instances, simple modifications to structural or physical chemical properties to molecules with insufficient safety profiles can quickly lead to new candidates with improved exposure and target organ toxicity profiles. Examples will be presented where recognition and subsequent modification of structural and physical chemical features were employed to reduce attrition of small molecules due to undesirable safety pharmacology or target-organ toxicity.

#### **W** 40 **The Challenges of Putting *In Vitro* Safety Assays into Context with *In Vivo* Data.**

N. Greene. *Compound Safety Prediction, Pfizer, Inc., Groton, CT.*

In the quest for higher-throughput, lower cost assays for safety assessment, many efforts have focused on cell based *in vitro* assays that generate a effect at a certain concentration level readout such as an LC50 etc. However, most of the efforts on correlating these *in vitro* concentration responses to *in vivo* effects have looked at the simple presence or absence of a phenotypic response in the *in vivo* study resulting in the potential misinterpretation of a result. In this presentation, we will describe efforts to more fully describe the *in vivo* responses in the context of compound exposure to enhance the interpretation and correlation of *in vitro* assays. We will highlight some of the issues in working with *in vivo* data such as the loosely controlled vocabularies used in describing the findings observed in a study and approaches we have taken to overcome these. Finally, we will show how this may then enhance the predictive value of an *in vitro* assay such as a simple ATP depletion assay.

#### **W** 41 **Relating Molecular Properties and *In Vitro* ADME/Tox Surrogate Assay Results to *In Vivo* Outcomes.**

D. E. Watson. *Lilly Research Laboratories, Indianapolis, IN.*

A primary goal of lead generation and lead optimization is to identify compounds with good pharmacological properties and optimal absorption, distribution, metabolism, excretion and toxicological (ADMET) characteristics. Chemists routinely consider molecular properties in designing compounds and utilize *in vitro* ADMET surrogate assays to select promising compounds for *in vivo* studies. A number of recent reports have investigated the relationship between computed molecular properties and *in vivo* ADMET outcomes. Although there is consensus that compound properties are important, one limitation of these analyses is a lack of controls for possible covariates (i.e. correlation vs. causation). We have examined the relationship between molecular properties and *in vitro* ADMET surrogate assays vs. *in vivo* properties within 175 chemical series identified from a database of 3792 compounds for which short term rodent pharmacokinetic and toxicology data are available. The role of confounding covariates was minimized by focusing on those variable associated with large differences in outcomes between compound pairs within chemically similar series of molecules. The analysis identified the following pairs of surrogates as most predictive among those examined: rat primary hepatocyte (RPH) cytolethality / volume of distribution (Vd) for *in vivo* toxicology outcomes, scaled microsome metabolism / calculated logP for *in vivo* unbound clearance, and calculated logD / kinetic aqueous solubility for thermodynamic solubility. An important practical outcome of the analysis is a set of guidelines defining the utility of specific surrogates for several *in vivo* ADMET endpoint and the magnitude of change required in a surrogate endpoint to achieve a desired *in vivo* result for novel drug candidates.

#### **W** 42 **Inhaled Mixtures: A Mode-of-Action Framework Applied to the Criteria Air Pollutants.**

E. O. Owens and C. C. Bowman. *National Center for Environmental Assessment, US EPA, Durham, NC.*

Although regulated individually, the criteria air pollutants, NO<sub>x</sub>, SO<sub>x</sub>, CO, PM, Pb, and O<sub>3</sub>, exist as a complex mixture in the atmosphere. Thus, the interactions and cumulative effects of multiple pollutants are important to consider when assessing the impact of ambient air exposures on health. The criteria air pollutants act through complex biological pathways to elicit health effects, but many share common modes of action, including oxidative stress and inflammation. Mode of action for a given toxic agent is defined as the set of key events involved in a given toxic effect. Key events are measurable endpoints along a continuum from exposure to effect, and are consistent with emerging concepts of how to use biomarkers, surrogate

endpoints, and toxicity pathways to characterize health risks. Recent discussions have proposed the use of mode of action to develop a unifying framework for the evaluation of mixtures containing multiple pollutants. This session convenes experts in the modes of action of criteria air pollutants to examine how this information can be organized, beginning with a description of an emerging framework for integrating mechanistic and biological plausibility information regarding the criteria air pollutants and a subset of ambient air toxics. Attendees will gain knowledge of how a mode-of-action framework can be used to consider mixtures, as well as emerging and established mechanisms of toxicity of air pollutants, focusing on potential interactions between pollutants encountered in a multipollutant context.

#### **W** 43 **Assessing Health Effects of Air Pollution Mixtures: Mode-of-Action Framework.**

B. Buckley. *National Center for Environmental Assessment, US EPA, Durham, NC.*  
Sponsor: C. Bowman.

To better understand the health effects resulting from exposures to mixtures of criteria pollutants (PM, particulate matter; sulfur oxides, SO<sub>x</sub>; nitrogen oxides, NO<sub>x</sub>; ozone, O<sub>3</sub>; lead, Pb and carbon monoxide, CO) that actually occur in ambient air, we are developing a framework for integrating information provided by toxicological, epidemiologic, and controlled human exposure studies based on mode of action. Mode of action for a given agent is defined as the set of key events which result in a toxic effect. Key events are measurable endpoints along the continuum from exposure to effect, and are consistent with emerging concepts of how to use biomarkers, surrogate endpoints, and toxicity pathways to characterize health risks. The approach elucidates commonalities in key events and pathways triggered by exposure to multiple pollutants. Available literature regarding the respiratory health effects of PM, SO<sub>x</sub>, NO<sub>x</sub> and O<sub>3</sub> indicates that all four pollutants activate neural reflexes, increase bronchial reactivity, initiate inflammation and modulate immune responses which may lead to the exacerbation of allergic responses, asthma and altered host defenses. Emerging evidence also demonstrates that exposure to either PM or O<sub>3</sub> may result in systemic inflammation, oxidative stress and impaired vasomotor function while exposure to NO<sub>x</sub> may result in pro-inflammatory circulating factors; all of which may lead to cardiovascular health effects. Exposure to CO may impair vasomotor function or lead to myocardial ischemia, while exposure to Pb may result in hypertension. Incorporation of important considerations for extrapolation in risk assessment such as adaptive responses, susceptibility factors, dose and duration of exposure, toxicokinetics, toxicodynamics and endogenous species into this framework is explored.

#### **W** 44 **The Effects of Criteria Pollutants in the Brain.**

M. L. Block. *Anatomy and Neurobiology, Medical College of Virginia, Richmond, VA.*

Increasing evidence links air pollution to central nervous system (CNS) disease, but the mechanisms remain poorly understood. Experimental studies and human case reports reveal that neuroinflammation and oxidative stress have emerged as a common deleterious pathway triggered by exposures to diverse criteria pollutants, including ozone and particulate matter. Thus, evidence indicates that not only does the brain's innate immune system respond to criteria pollutants, but that this has been linked to neurodegenerative-disease-like pathology in cell culture, rodent models, and humans. This presentation will focus on the cellular and peripheral mechanisms that may be driving the CNS effects of air pollution, as our work with diesel exhaust shows that both the peripheral immune system and microglia, the brain's resident innate immune cell, may be key to this process. In addition to providing new information on specific mechanisms of CNS disease development related to criteria air pollutant exposure, a mode of action framework will be used to describe the pathways leading to emerging health effects with uncertain mechanisms.

#### **W** 45 **Air Pollution and Pattern Recognition Receptors: Like a Wee LCMS in Every Mouse.**

M. J. Campen. *College of Pharmacy, University of New Mexico, Albuquerque, NC.*

Distinguishing among the toxicities of the numerous criteria pollutants and other unregulated air hazards that exist in the multipollutant environment challenges the most sophisticated human and animal studies. To adopt a more refined approach to assessing the effects of multipollutant exposures, it will be essential to better understand the shared mechanisms driving toxicity. One common pathway that several labs have recently elucidated relates to a class of receptors known as pattern recognition receptors (PRR). Research will be presented looking at the role of PRR in

driving allergic airway response, cardio-metabolic response, and the systemic vascular inflammatory response to combustion-source mixtures, such as gasoline and diesel emissions. These findings, combined with results from other laboratories, indicate a role for PRRs that may help refine our understanding of the link between the chemistry of pollutant interactions at the lung surface and the ultimate pathophysiological outcome.

**W 46 Differential Effects of PM Components: Toward a Better Understanding of Underlying Mechanisms.**

A. Rohr. *Air Quality, Electric Power Research Institute, Palo Alto, CA.*

Multiple epidemiological and toxicological studies have reported differential responses to fine particulate matter components, such as elemental carbon, organic carbon, sulfate, nitrate, and individual elements. While different PM components likely invoke unique pathophysiological pathways, it is also likely that there is overlap between mechanisms of action. For example, oxidative stress is a likely pathway for both organic PM components as well as trace elements. In a multipollutant setting, it is critical to understand the underlying mechanisms of adverse biological responses to these materials. This presentation will review what is currently known about pathophysiological pathways of response to PM components, with an emphasis on shared pathways.

**RI 47 Toxicological Challenges in Food Production in Texas and the Gulf Coast.**

L. M. Plunkett. *Integrative Biostrategies LLC, Houston, TX.*

With recent media attention on episodes of food contamination and the impact of chemicals in the environment on the food supply (i.e., bacterial contamination of food, as well as the 2010 BP oil spill), public awareness of food safety issues has grown. This symposium will explore the topic of food safety as it relates to unique features of food production in Texas and the Gulf Coast. Texas is a major source of fresh fruit and vegetable production for both regional and countrywide consumption, while the Gulf Coast is a major source of fresh fish and seafood for many parts of the United States. Topics covered in the symposium will include recent legislative initiatives such as the Food Safety and Modernization Act of 2010, current regulatory oversight of food safety in the Gulf Coast region, and key public and/or worker health issues associated with food production in the region. The goal of the symposium is to describe the strengths and weaknesses of current regulations and practices to ensure a safe food supply as well as worker safety, and provide dialog for ways to address unique concerns related to food production in Texas and the Gulf Coast. Symposium speakers work in academia, for the United States government (US FDA), and an organization representing the interests of the public (Center for Science in the Public Interest), which will allow for discussion of the topics from a variety of perspectives.

**RI 48 Multiagency Response to Seafood Safety Concerns following the 2010 Deepwater Horizon Oil Spill.**

R. W. Dickey. *US FDA, Dauphine Island, AL.* Sponsor: L. Plunkett.

The April 20, 2010 explosion and sinking of the Deepwater Horizon oil drilling platform (DWH) resulted in the largest oil spill in U.S. history. For a period of 87 days roughly 53 thousand barrels of oil per day flowed into the Gulf of Mexico (GOM). The U.S. Coast Guard estimated 4.9 million barrels of crude oil escaped before the damaged wellhead was sealed on July 15. The DWH spill threatened all States bordering the GOM, and crossed Federal and State jurisdictional boundaries. Agencies responded to the spill in a coordinated manner to execute a unified seafood safety risk assessment and protocol for testing and re-opening GOM fisheries.

Polycyclic aromatic hydrocarbons (PAH) are internationally recognized as the most appropriate indicators of potential human health risk from crude oil residues in seafood. A representative subset of 13 PAH and their alkylated homologues was selected for critical analysis of oil-impacted seafood. A standard set of calculations was used to determine seafood PAH tissue concentrations above which a 10-5 upper-bound risk for low dose, life-time cancer is exceeded. Levels of concern for non-cancer risks were also adopted from EPA IRIS reference dose values. Values for other event-specific variables were selected from the most recent and reliable information available.

FDA and NOAA tested more than 10,000 seafood specimens from state territorial and federal waters that were impacted by the oil spill. Waters were not reopened for fisheries harvest until oil had dissipated and testing showed that seafood was safe for consumption. The duration of fishery closures in the oil-impacted region ranged from 16 days for areas receiving little to no impact to greater than 24 months for areas more heavily oiled.

Most seafood samples that were tested after the oil spill had dissipated, and before waters were reopened for fishing, did not contain measurable levels of oil or dispersant residues. The samples that did contain measurable residues were consistently 100 to 1000-fold below levels of concern established in the unified seafood safety protocol.

**RI 49 Seafood Safety Challenges for the Texas Gulf Coast.**

D. W. Plunkett. *Center for Science in the Public Interest, Washington DC.* Sponsor: L. Plunkett.

Potentially toxic chemistry from the 2010 BP oil spill and clean-up efforts generated widespread public concern over the safety of seafood harvested from the Gulf of Mexico. Government agencies moved swiftly to contain the threat and reassure consumers. The effort, though, masked a larger truth. While contamination events caused by human activities draw public attention, naturally occurring toxins and deadly bacteria in Gulf waters sicken, maim and kill far more people than oil and chemical dispersants. Rare cases of neurotoxic shellfish poisoning occur in Texas. Much more common are illnesses and deaths from naturally occurring vibrios. Oysters harvested from Texas coastal waters have killed 53 people since 1995 and resulted in 45 serious illnesses from *Vibrio vulnificus* contamination. The presentation will cover the risks to human health from human and naturally occurring contaminants, focusing on shellfish. It will also cover responses, adequate and inadequate, by governmental food safety agencies and the fishing industry.

**RI 50 Occupational Hazards in Texas Food Production.**

E. Shipp. *Epidemiology and Biostatistics, Texas A&M School of Rural Public Health, College Station, TX.* Sponsor: E. Bruce.

A substantial number of hired farmworkers help Americans to put food on their tables. This largely foreign-born (>75%) workforce makes a huge contribution to the agricultural economy, yet the average family income ranges from \$15,000 to \$17,499 and less than a quarter are covered by health insurance. The agricultural industry also is among the most hazardous in the United States in terms of fatal and nonfatal injury. Common occupational hazards include: prolonged time in awkward postures, sun and heat stress, sharp implements, motorized farm equipment, inadequate safety training and field sanitation, and pesticides. Pesticides are especially a concern for farmworkers given the potential for long-term consequences such as skin problems, neurologic and motor problems, birth defects, and cancer. There are an estimated 10,000-20,000 cases of physician diagnosed pesticide poisoning among agricultural workers each year in the U.S. Many more cases likely go undiagnosed because symptoms can be flu-like and non-specific or the farmworkers lack access to healthcare. Worker training can reduce this exposure, but employers often do not provide training even when required to do so by law. In a study of adolescent farmworkers from Texas, only 21% had ever received any training in pesticide safety. This is troubling because adolescents are still developing both physically and mentally and may be especially vulnerable to chemical exposures. A recent pilot study showed that adolescent farmworkers who reported 5+ symptoms of neurotoxicity were nearly nine times as likely to report an acute injury compared to those reporting a lower number of symptoms (Whitworth et al., 2010). This presentation provides an overview of the occupational health and safety issues impacting farmworkers with a focus on pesticides and a current research study designed to examine this issue further in adolescents.

**RI 51 Occupational Heat Stress in Agricultural Settings.**

J. L. Levin. *Occupational Health Sciences, The University of Texas Health Science Center at Tyler, Tyler, TX.* Sponsor: E. Bruce.

Occupational heat stress and heat illness disproportionately affect agricultural workers compared with other occupations, including migrant and seasonal farmworkers. From 1992 to 2006, there were 423 occupational heat-related deaths in the United States. The mortality rate from occupational heat-related illness among crop workers was nearly twenty times as high as for all industries during that time frame. This presentation will review underlying causes and risk factors for occupational heat stress, recognition of the continuum of heat illness, and recommendations for monitoring and prevention. Presently, there is no federal occupational regulatory standard specifically regarding heat exposure. This presentation will also review fundamental differences between OSHA and NIOSH and emphasize the complexities of understanding recommended exposure limits. Case examples from outdoor work environments will be presented including one which culminated in adjudication before the Occupational Safety and Health Review Commission.

**PL 52**    **Developmental Toxicity and Neurobehavioral Effects of Dietary Flavonoids.**

S. M. Bugel and R. L. Tanguay. *Department of Environmental and Molecular Toxicology, Environmental Health Sciences Center, Oregon State University, Corvallis, OR.*

Flavonoids are a structurally diverse group of phytochemicals that are known hormone mimics (phytoestrogens), and are thought to have therapeutic properties. Humans are exposed to flavonoids through consumption of fruits, vegetables, and dietary supplements. These ubiquitous chemicals are found in baby formulas and foods, and are detected in human urine, plasma, and breast milk. Therefore, the potential for developmental effects should be explored. Using zebrafish (*Danio rerio*) as a model vertebrate, we tested the hypothesis that flavonoids exhibit structure-dependent effects on development. Embryos were treated with 5 representative flavonoids (apigenin, biochanin A, S-equol, galangin and kaempferol), 1-50  $\mu$ M, from 6 hours post fertilization (hpf) to 120 hpf. At 120 hpf, effects included yolk-sac and pericardial edemas, axis curvature, fin dysmorphogenesis and craniofacial abnormalities. For all 5 compounds, we also observed spastic pectoral fin and caudal tail movements at 72 hpf, suggestive of neurotoxicity. To test the hypothesis that flavonoids are stimulants, we assessed acute effects on neurobehavior in naïve 120 hpf larvae challenged with 16 flavonoids: apigenin, biochanin A, chrysin, daidzein, S-equol, fisetin, formononetin, galangin, genistein, kaempferol, luteolin, myricetin, naringenin, puerarin, quercetin and resveratrol. With the exception of puerarin, all induced hyperactive swimming behavior suggesting that flavonoids have psychoactive and stimulant properties. This zebrafish larval bioassay is amenable to rapid throughput screening for anxiogenic and anxiolytic properties, which we validate using neurotoxins chosen to represent diverse mechanisms (e.g. nicotine, chlorpyrifos, picROTOXIN, etc.). Using pharmacological intervention with receptor specific chemicals, this screen will be valuable for identifying interaction of dietary flavonoids and other chemicals of interest with neuro-receptors to identify the mechanism of toxicity in vivo. This research is supported by NIEHS grants P30 ES00210, RC4ES019764 and T32 ES07060.

**PL 53**    **Perinatal Toxicity and Carcinogenicity Studies of Styrene Acrylonitrile Trimer, a Ground Water Contaminant.**

M. Behl<sup>1,2</sup>, S. A. Elmore<sup>1</sup>, M. R. Hejtmančík<sup>3</sup>, D. K. Gerken<sup>3</sup> and R. S. Chhabra<sup>1</sup>. <sup>1</sup>Division of the National Toxicology Program, NIEHS, Research Triangle Park, NC; <sup>2</sup>Kelly Government Solutions, Research Triangle Park, NC; <sup>3</sup>Battelle Memorial Institute, Columbus, OH.

Styrene Acrylonitrile (SAN) Trimer is a by-product of the production of acrylonitrile styrene plastics. Following the report of a childhood cancer cluster in the Toms River section of Dover Township, New Jersey, SAN Trimer was identified as one of the groundwater contaminants at Reich Farm Superfund site in the township. The contaminants from the Reich Farm site's ground water plume impacted two wells at the Parkway well field. The National Toxicology Program (NTP) studied the toxicity and carcinogenicity of SAN Trimer in F344/N rats exposed during their perinatal developmental period and adulthood. The chronic toxicity and carcinogenicity studies in rats were preceded by 7 and 18-week perinatal toxicity studies to determine exposure concentrations for the 2 year studies. Pregnant dams were exposed to SAN-Trimer in the diet at 400, 800, or 1600 ppm during gestation, nursing and weaning periods of offspring followed by two years of adult exposure to both male and female pups. There was no statistically significant evidence of carcinogenic activity following SAN-Trimer exposure; however, rare neoplasms in the brain and spinal cord were noted in males and to lesser extent in female rats. These incidences were considered within the range of historical control background in the animal model used in the current studies. The major finding was a dose-related peripheral neuropathy associated with the sciatic nerves in females and spinal nerve roots in males and females, thereby suggesting that SAN-Trimer is a potential nervous system toxicant. Other non-neoplastic lesions included increased incidences of some lesions in the bone marrow and liver in males and females, and in the urinary bladder in females.

**PL 54**    **Does Developmental Hypothyroidism Produce Lasting Effects on Adult Neurogenesis?**

J. Nance<sup>1</sup>, R. C. Switzer<sup>2</sup>, A. Tennant<sup>1</sup>, A. F. Johnstone<sup>1</sup> and M. E. Gilbert<sup>1</sup>. <sup>1</sup>US EPA, Research Triangle Park, NC; <sup>2</sup>NeuroScience Associates, Knoxville, TN.

The subgranular zone of the dentate gyrus (DG) of the adult hippocampus generates new neurons throughout life. Thyroid hormones (TH) are essential for brain development, but impaired neurogenesis with adult hypothyroidism has also been reported. We investigated the role of milder degrees of TH disruption on adult neurogenesis following hypothyroidism induced during development, in adulthood, or

both. Pregnant dams were administered the TH synthesis inhibitor, propylthiouracil (PTU, 0 or 3ppm in drinking water) from gestational day 6 and pups were weaned to control water on postnatal day (PN)21. On PN60, offspring from control or PTU dams were either re-exposed to PTU (3ppm) for 1 month or maintained on control. Bromodeoxyuridine (BrdU 50 mg/kg, ip, twice daily) was administered to all animals on the last 5 days of the re-exposure period, and animals sacrificed 28 d later. Animals were perfused intracardially, the brains removed and embedded in a MultiBrain (NSA) array and freeze sectioned. Every 8th section throughout the hippocampus stained with an antibody against BrdU to mark actively dividing cells. The volume of the DG and the number of BrdU-positive cells were assessed from images captured on a Nikon microscope (400X) and Nikon Elements software. Preliminary findings indicate that developmental exposure to PTU produced a persistent reduction in the volume of the adult DG. BrdU cell counts were reduced similarly in all PTU-exposed groups. These data suggest that moderate levels of hypothyroidism decrease cell survival in the adult brain and that transient developmental hypothyroidism leads to persistent decreases in DG volume and cell survival. The degree to which these findings are determined by reductions in cell proliferation is currently under investigation. As neurogenesis in the adult recapitulates developmental processes of proliferation, differentiation, and migration, study of this neurogenic niche in the adult may provide a simpler means to assess the consequences of TH insufficiency on neurodevelopment. (Does not reflect EPA policy).

**PL 55**    **Dietary Administration of Paraquat for 13 Weeks Does Not Result in a Loss of Dopaminergic Neurons from the Substantia Nigra of Mice.**

N. Sturgess<sup>1</sup>, P. Botham<sup>1</sup>, M. Butt<sup>3</sup>, D. Minnema<sup>2</sup>, L. Smith<sup>1</sup> and J. Wolf<sup>4</sup>. <sup>1</sup>Syngenta, Bracknell, United Kingdom; <sup>2</sup>Syngenta, Greensboro, NC; <sup>3</sup>Tox Path Specialists, Frederick, MD; <sup>4</sup>EPL, Sterling, VA.

A number of publications have reported that i.p. administration of paraquat (PQ) to rodents (e.g. C57Bl6J mouse) at high doses results in a loss of dopaminergic neurons from the substantia nigra pars compacta (SNpc), the primary area of neuropathological damage in Parkinson's disease (PD). Such studies have been used to indicate mechanistic plausibility for epidemiological claims of a link between PQ exposure and PD. A major criticism of the i.p. mouse model is that it uses a route of administration and duration of exposure which is not relevant to human exposure. To better understand the relevance of the reported findings from the i.p. mouse model we have conducted a study where male C57Bl6J mice were exposed to PQ in the diet for 13 weeks, and the brains examined for evidence of dopaminergic neuronal cell loss using stereology, changes in striatal neurochemistry and pathological changes using stains to detect neuronal cell damage and inflammatory responses. Dietary concentrations of 10 & 50 ppm paraquat dichloride salt were used which resulted in achieved doses of 2.4 & 14.1 mg/kg/day. A low dose of N-1-methyl-4-phenyl-1,2,3,6-tetrahydropyridine (MPTP; 10 mg/kg administered i.p. to a separate group of male mice 4 times in a single day at 2 hr intervals, 7 days prior to the end of the dietary study) served as a positive control. PQ at either dose level did not induce a loss of tyrosine hydroxylase positive (TH+) dopaminergic neurons in the SNpc, alter the concentration of striatal dopamine and its metabolites or result in evidence of neuronal cell damage or astrocyte/microglial activation in the SNpc. In the MPTP group the number of TH+ neurons in the SNpc and striatal dopamine was reduced and there were significant pathological changes including neuronal necrosis and astrocyte/microglial activation. This study further brings into question the relevance of the findings from previous i.p. mouse studies as evidence for a link between PQ exposure and PD/parkinsonism.

**PL 56**    **Neurodevelopmental Effects of Inhaled Vapors of Gasoline and Ethanol in Rats.**

P. J. Bushnell<sup>1</sup>, T. E. Beasley<sup>1</sup>, W. M. Oshiro<sup>1</sup>, P. A. Evansky<sup>1</sup>, S. A. Martin<sup>1</sup>, V. C. Moser<sup>1</sup>, K. L. McDaniel<sup>1</sup>, P. M. Phillips<sup>1</sup>, J. Norwood<sup>1</sup>, M. E. Gilbert<sup>1</sup>, M. M. Taylor<sup>2</sup>, C. J. Gordon<sup>1</sup>, C. E. Grace<sup>1</sup> and J. M. Rogers<sup>1</sup>. <sup>1</sup>NHEERL/ORD, US EPA, Research Triangle Park, NC; <sup>2</sup>MMT Inc, Durham, NC.

Gasoline-ethanol blends comprise the major fraction of the fuel used in the US automotive fleet. To address uncertainties regarding the health risks associated with exposure to gasoline with more than 10% ethanol, we are assessing the effects of prenatal exposure to inhaled vapors of gasoline-ethanol blends. Pregnant Long-Evans rats are exposed to fuel vapors, 6.5 hr/day, on days 9–20 of gestation, and their offspring are assessed for a variety of neurodevelopmental effects. This report compares effects of inhaled gasoline vapor lacking ethanol (E0) at concentrations of 0, 3000, 6000, or 9000 ppm with previously-reported effects of inhaled ethanol (E100) at concentrations of 0, 5000, 10000 or 21000 ppm. Maximum concentrations were limited by the lower explosive limits of the vapors. As observed with

E100, E0 vapors caused no overt maternal toxicity, changes in litter size or weight, or weight gain of the pups. In contrast to E100, E0 did not alter locomotor activity of adults. Both E0 and E100 produced a few minor, unsystematic changes in the functional observational battery. In water maze tests, E100 altered search strategies (not dose-related) and impaired memory in females (no-platform probe trials, all doses); in contrast, E0 was essentially ineffective. No treatment affected working memory, as assessed in operant delayed-matching-to-position tests. In an operant reaction-time test, 21000 ppm E100 and 9000 ppm E0 increased hold failures, a measure of impulsivity, and increased decision times at the lower doses. Responses to a conditioned audiovisual cue were reduced in females at all doses of E100, but were not affected by E0; neither agent affected conditioning to context. Telemetered mean blood pressure (BP) was increased in male offspring by 9000 ppm E0 at PND 90 and 180; tail cuff tests corroborated these results at PND 180 only. E100 increased BP (tail cuff) in males at all doses on PND90 only. This abstract does not reflect EPA policy.

**PL 57 Postnatal Trichloroethylene Exposure Is Associated with Abnormal Behavior and Alterations Global DNA Methylation Patterns in Mouse Cerebellum.**

S. Blossom<sup>1</sup>, J. L. Rau<sup>1</sup>, S. B. Melnyk<sup>1</sup>, C. A. Cooney<sup>1</sup>, S. J. James<sup>1</sup> and W. D. Wessinger<sup>2</sup>. <sup>1</sup>*Pediatrics, Arkansas Children's Hospital Research Institute, Little Rock, AR;* <sup>2</sup>*Pharmacology and Toxicology, University of Arkansas for Medical Sciences, Little Rock, AR.*

Previous studies have shown that continuous exposure throughout gestation until the juvenile period to environmentally-relevant doses of trichloroethylene (TCE) in the drinking water of MRL+/+ mice promoted adverse behavior associated with glutathione (GSH) depletion in the cerebellum indicating increased sensitivity to oxidative stress. Here we extend these findings to further characterize the impact of TCE exposure on redox homeostasis, biomarkers of oxidative stress, transmethylation metabolites and global DNA methylation patterns in mice exposed to water only or two doses of TCE in the drinking water postnatally from birth until 6 weeks of age. The mice were subjected to a variety of open field behavioral tests in order to correlate behaviors with metabolic and methylation patterns observed in our model. Our results show that the cerebellum from male mice exposed to TCE have lower GSH and increased biomarkers of oxidative stress compared with controls. Methionine levels were also significantly reduced in the TCE-exposed mice which suggested compromised cellular methylation. Global DNA methylation, including hydroxymethylation patterns, were significantly lower in the cerebellum of TCE exposed mice, compared to controls. Mice exposed to TCE exhibited increased locomotor and exploratory activity compared to control mice suggesting increased novelty seeking behavior similar to that observed in humans with attention deficit disorder. Understanding the mechanisms of TCE neurotoxicity during sensitive windows of exposure is important in order to enhance mechanistic understanding of environmentally-related neurologic disorders in susceptible populations.

**PL 58 Perfluorohexane Sulfonate (PFHxS) Causes Adult Behavioral Disturbances in Male and Female Mice, after Neonatal Exposure.**

H. Viberg, I. Lee, A. Fredriksson and P. Eriksson. *Environmental Toxicology, Uppsala University, Uppsala, Sweden.*

Perfluorohexane sulfonate (PFHxS) is a perfluorinated compound (PFC) used as an industrial additive. PFC chemical properties make them suitable as surfactants and oil- and water repellents, which are frequently used in products for packaging and as protective coatings. However, the same properties also account for their extreme physico-chemical stability, making them practically non-biodegradable, accumulating in the global environment, causing concern, since little is known about the toxicity of the compound. We recently have seen that other PFCs, like perfluorooctane sulfonate (PFOS) and perfluorooctanoic acid (PFOA), can induce developmental neurotoxic effects and the purpose of the present study was to explore if neonatal exposure to PFHxS can affect behavior and cognitive function. In the present study we exposed male and female mouse pups to a single dose of PFHxS (0.61-9.2 mg/kg bw) during the defined critical period of brain development, on postnatal day 10. At two months of age male and female mice showed altered spontaneous behavior in a novel home environment, affecting cognitive function. Furthermore, these functional behavioral effects were long-lasting or irreversible since they were once again seen at four month of age. The nicotine-induced behavior test revealed that male and female mice neonatally exposed to PFHxS responded differently compared to control animals, when challenged with a dose of nicotine. The present findings show that PFHxS can cause developmental neurotoxicity, effects similar with effects earlier reported after neonatal exposure to PFOS and PFOA and other persistent pollutants, such as PBDEs and PCBs.

**PL 59 Acute Ozone-Induced Impairment of Glucose Regulation: Age-Related and Temporal Changes.**

V. L. Bass<sup>1</sup>, R. C. MacPhail<sup>1</sup>, D. L. Andrews<sup>1</sup>, B. Vallanat<sup>1</sup>, W. O. Ward<sup>1</sup>, M. C. Schladweiler<sup>1</sup>, A. D. Ledbetter<sup>1</sup>, D. B. Johnson<sup>2</sup>, K. A. Jarema<sup>1</sup>, C. J. Gordon<sup>1</sup> and U. P. Kodavanti<sup>1</sup>. <sup>1</sup>*EPHD/NHEERL/ORD, US EPA, Research Triangle Park, NC;* <sup>2</sup>*Curriculum in Toxicology, University of North Carolina at Chapel Hill, Chapel Hill, NC.*

Ozone (O<sub>3</sub>) is associated with adverse cardiopulmonary effects in humans and thought to produce metabolic effects, such as insulin resistance. We showed that episodic O<sub>3</sub> exposure increased insulin levels in aged rats. We hypothesized that O<sub>3</sub> could impair glucose homeostasis by altering insulin signaling and/or causing an unfolded protein response (UPR) in the liver. Brown Norway rats, 1, 4, 12, 21, and 24mo old, (a model of non-obese aging) were exposed to O<sub>3</sub> at 0, 0.25 or 1ppm, 6h/day for 2 consecutive days. As a follow-up study, 4mo old rats were exposed to 0 or 1ppm O<sub>3</sub> over 2 days to examine the time course of response. Glucose tolerance tests (GTT) directly followed exposure in all studies and additionally at 24h post-exposure in the time-course experiment. Liver gene expression was examined using Affymetrix RG-230PM Array strips. Liver and adipose tissues were also analyzed using RT-PCR for metabolic and UPR markers. Phospho-protein analysis to assess insulin signaling was done in the liver, adipose tissue, and muscle. GTT showed a marked impairment of glucose clearance among 1ppm O<sub>3</sub> exposed rats of all ages. The reduction in glucose regulation after O<sub>3</sub> exposure was most apparent in 1mo rats, who exhibited no baseline glucose intolerance. The 24mo rats exhibited glucose intolerance at baseline. Analyses of metabolic and acute phase response (APR) biomarkers show that the insulin signaling pathway is altered by O<sub>3</sub> in all three tissues and serum APR proteins were increased. Selected UPR genes were upregulated in the liver. Serum leptin increased acutely following 1 day (6h) O<sub>3</sub> exposure. Maximum effects of O<sub>3</sub> on insulin signaling and APR were seen directly following the second day of exposure. Our results suggest that glucose intolerance is a result of metabolic changes in response to O<sub>3</sub>. These findings raise concern about ambient O<sub>3</sub>'s potential to cause predisposition towards metabolic impairment. (Does not reflect US EPA policy).

**PL 60 Fine Particulate Matter (PM<sub>2.5</sub>) Exposure Impairs Vascular Insulin Signaling and Exacerbates Diet-Induced Systemic Insulin Resistance in Mice.**

P. Habertzell, J. McCracken, J. Lee, A. Bhatnagar and D. J. Conklin. *University of Louisville, Louisville, KY.*

Recent epidemiological studies suggest that increases in fine particulate matter (PM<sub>2.5</sub>) air pollution contribute to the rapidly evolving epidemics of obesity and diabetes. Because metabolic syndrome, diabetes and air pollution all induce endothelial dysfunction, and because we recently showed that short-term exposure to concentrated ambient PM<sub>2.5</sub> (CAP) impairs endothelial VEGF signaling and decreases circulating endothelial progenitor cells (EPCs), we examined the effects of CAP exposure (9-30 consecutive days, 6h/d) on endothelial and systemic insulin resistance and inflammation, adiposity and vascular function in mice fed normal chow or high fat-diet (HFD). Surprisingly, CAP exposure impaired vascular insulin signaling after only 9 or 30 days, and exacerbated HFD-induced systemic insulin resistance after 30 days without increasing adiposity. Insulin sensitivity and inflammation in adipose and liver were unaltered by CAP or HFD. In contrast, CAP exposure (30 days) impaired endothelial insulin signaling diet-independent in heart and aorta, but HFD-dependent skeletal muscle. Changes in insulin sensitivity were accompanied by organ-specific but not systemic inflammation and a decrease in circulating EPCs. Collectively, our results suggest that short-term CAP exposure provokes HFD-induced systemic insulin resistance by inducing inflammation and endothelial insulin resistance accompanied by decreased circulating EPC levels. Impaired vascular maintenance due to EPC suppression could contribute to vascular insulin resistance (or vice versa) thereby increasing systemic insulin resistance and the risk for the development of T2D and CVD by PM<sub>2.5</sub>.

**PL 61 Ozone (O<sub>3</sub>): A Potential Contributor to Metabolic Syndrome through Altered Insulin Signaling.**

D. B. Johnson<sup>3</sup>, D. L. Andrews<sup>2</sup>, V. L. Bass<sup>1</sup>, M. C. Schladweiler<sup>1</sup>, A. D. Ledbetter<sup>1</sup> and U. P. Kodavanti<sup>1</sup>. <sup>1</sup>*EPHD/NHEERL/ORD, US EPA, Research Triangle Park, NC;* <sup>2</sup>*RCU/NHEERL/ORD, US EPA, Research Triangle Park, NC;* <sup>3</sup>*Curriculum in Toxicology, University of North Carolina at Chapel Hill, Chapel Hill, NC.*

Air pollutants have been associated with diabetes and metabolic syndrome, but the mechanisms remain to be elucidated. We hypothesized that acute O<sub>3</sub> exposure will produce metabolic impairments through endoplasmic reticular stress (ER) stress

and altered insulin signaling in liver, muscle and adipose tissues in the Wistar Kyoto rats. Rats were exposed to air or 1ppm O<sub>3</sub>, 6hr/day for 1 or 2 days. Glucose tolerance tests were conducted immediately following each day or one day after 2-day exposure. Tissues were analyzed for insulin and ER stress signaling and serum for inflammation and metabolic biomarkers. O<sub>3</sub> produced severe hyperglycemia and glucose intolerance that was reversible following 1 day recovery. Phosphorylation of insulin receptor substrate (pIRS) decreased after 2nd day O<sub>3</sub> in all three organs. Downstream mediators, phospho-serine/threonine kinase and phospho-glycogen synthase kinase also decreased but only in adipose tissue. Serum insulin changes were correlated with tissue levels of pIRS. Serum IL-6, thought to link ozone-induced inflammation and metabolic alterations, did not increase at any time; however lipocalin and acute phase proteins increased after O<sub>3</sub>. Serum leptin was also increased sharply after 1-day O<sub>3</sub> exposure and it was correlated with O<sub>3</sub>-induced hyperglycemia, but not glucose intolerance. Genes downstream of unfolded protein response were changed in the liver indicating ER stress. To examine the role of liver ER stress in O<sub>3</sub> induced impairment of metabolism, we treated rats with ER-stress inhibitor, salubrinal prior to air or 1ppm O<sub>3</sub>. Salubrinal did not diminish O<sub>3</sub> induced hyperglycemia and glucose intolerance, suggesting that hyperglycemia likely did not result from ER stress. In conclusion, acute O<sub>3</sub> exposure alters insulin signaling in metabolic organs causing hyperglycemia and glucose intolerance, which might contribute to increased incidences of diabetes and metabolic syndrome. (Does not reflect USEPA policy).

## PL 62 Inhaled Ozone Induces Metabolic Abnormalities in Mice Fed a High-Fructose Diet.

K. M. Allen<sup>1,2</sup>, P. Brooks<sup>1</sup>, M. Dereski<sup>1</sup>, R. Lewandowski<sup>1,2</sup>, I. Hotchkiss<sup>1</sup>, D. Jackson-Humbles<sup>1</sup>, C. Brandenberger<sup>1</sup>, L. Bramble<sup>1,2</sup>, J. G. Wagner<sup>1,2</sup> and J. Harkema<sup>1,2</sup>. <sup>1</sup>Pathobiology, Michigan State University, East Lansing, MI; <sup>2</sup>Great Lakes Air Center for Integrated Environmental Research, Michigan State University, East Lansing, MI.

Results of recent inhalation toxicology studies have indicated that long-term exposure of mice to concentrated ambient particulate matter induces insulin resistance and potentiates other adverse metabolic effects brought on by consumption of a high fat diet. Similar adverse metabolic effects on insulin signaling and glucose homeostasis caused by gaseous air pollutants, such as ozone (O<sub>3</sub>), have not been investigated. In the present study, we tested the hypothesis that subacute inhalation exposure to O<sub>3</sub> enhances metabolic abnormalities, caused by a high fructose diet (HFrD), in mice. C57/Bl6 male mice were maintained on either a normal chow (NC) or a HFrD (from which 60% of the calories were derived from fructose) for the duration of the study. Mice were exposed to 0 (filtered air controls; FA) or 0.5 ppm O<sub>3</sub>, 4 h/day for 24 consecutive weekdays. No combination of exposure or diet caused changes in glucose metabolism, as measured by oral glucose tolerance testing. In contrast, mice fed the HFrD and exposed to O<sub>3</sub> had an increased fasting insulin (1519±128 pg/mL) as compared to all other groups (NC/FA: 646±62.73, HFrD/FA: 841±87.17, NC/O<sub>3</sub>: 535±48.32). Similarly, plasma leptin levels were markedly increased in the HF/O<sub>3</sub> group. HOMA-IR, an indicator of insulin resistance, was also increased in the HFr/O<sub>3</sub> (16.61±2.23) mice as compared to the NC/FA, HFr/FA or NC/O<sub>3</sub> mice (7.64±0.91, 7.98±0.7 and 5.23±0.44, respectively). In addition, O<sub>3</sub> exposure enhanced the severity of HFrD-induced hepatic steatosis. Overall these data in mice suggest that subacute inhalation exposure to O<sub>3</sub> may induce or enhance some adverse metabolic effects caused by a HFrD. The interaction of diet and air pollution exposure on human health requires further study. Funded by USEPA RD83479701

## PL 63 Suppressed Responses in Heart Rate Variability during Inhalation Exposure to Ozone and Ambient Fine Particles in Rats on a High-Fructose Diet.

J. G. Wagner<sup>1</sup>, H. Yang<sup>2</sup>, K. M. Allen<sup>1</sup>, M. Morishita<sup>2</sup>, B. Nan<sup>2</sup>, B. Mukherjee<sup>2</sup>, G. Fink<sup>1</sup> and J. Harkema<sup>1</sup>. <sup>1</sup>Michigan State University, East Lansing, MI; <sup>2</sup>University of Michigan, Ann Arbor, MI.

People with diet-induced cardiometabolic disorders (diabetes, hypertension) may be more susceptible to the adverse cardiovascular effects of air pollution. The present study was designed to determine if a high-fructose diet affects cardiovascular responses to inhaled air pollutants. We used a mobile air research laboratory located in an industrial area of Dearborn, MI, to expose male Sprague Dawley rats, to filtered air (FA), ozone (O<sub>3</sub>; 0.5 ppm), concentrated ambient fine particles (CAPs; 400 µg/m<sup>3</sup>) or the combination of O<sub>3</sub> & CAPs. Rats were fed a normal (ND) or high-fructose diet (HFD) for 8 weeks prior to exposure and during exposure. Inhalation exposures were 8h/day for 9 days (4-5 days/week). Heart rate (HR) and ECG waveforms were collected by radiotelemetry every 5 minutes during exposures, and measures of heart rate variability (HRV, indicated as SDNN and

rMSSD) were calculated and analyzed by a linear mixed model. Compared to FA-exposed rats fed ND, rats fed HFD had significantly greater HR (328 ± 27.5 vs 299 ± 35 bpm, respectively) and lower SDNN (44.6 ± 78.8 vs 64.4 ± 86 ms). All exposures caused decreases in HR that were greater in HFD rats (25-40 bpm) than in ND rats (6-15 bpm). However responses in HRV were dependent on the specific exposure and diet. Exposure to O<sub>3</sub>&CAPs induced significant decreases in HRV in ND- but not HFD-fed rats, with a 55% decrease in SDNN over the nine days of exposure. By comparison exposure to O<sub>3</sub> alone had the opposite effect on HRV, with a 48% increase in SDNN, but with no effect in HFD rats. Lastly, ND-fed rats exposed to CAPs alone had a modest decrease in SDNN (23%), while similarly exposed HFD-fed rats again had no change. In summary, while HR was decreased in all experimental groups, the degree and direction in change of HRV depends on the specific exposure and diet. The mechanism(s) underlying altered autonomic responses in HFD rats to single- or multi-pollutant exposures requires further study. US EPA RD83479701

## PL 64 Oxidative Stress and the Acceleration of Atherosclerosis in Susceptible Mice after Exposure to Semivolatile Components of Ultrafine Particulate Matter.

A. J. Keebaugh<sup>1</sup>, P. Pakbin<sup>2</sup>, L. B. Mendez<sup>1</sup>, Z. Ning<sup>2</sup>, G. Gookin<sup>1</sup>, C. Sioutas<sup>2</sup> and M. T. Kleinman<sup>1</sup>. <sup>1</sup>Community and Environmental Medicine, University of California Irvine, Irvine, CA; <sup>2</sup>Environmental Engineering, University of Southern California, Los Angeles, CA.

Exposure to ultrafine particulate matter (UF-PM) has been associated with adverse cardiovascular health effects. UF-PM contains semi-volatile organics (SVOCs) that are bound to particles but can partition to the vapor phase after emission. SVOCs contain species such as polycyclic aromatic hydrocarbons and quinones that can induce oxidative stress and may be responsible for the exacerbation of cardiovascular disease by UF-PM. Therefore, we hypothesized that the removal of SVOCs from an aerosol should decrease the ability of the particle to cause oxidative damage and consequently the acceleration of atherosclerotic plaque formation. ApoE <sup>-/-</sup> mice, which are prone to developing atherosclerosis, were exposed to UF concentrated ambient particles (CAPs), CAPs with the SVOC components removed, or SVOC components without the particle core. A control group was exposed to purified, filtered air. Particles were concentrated using a VACES, and SVOCs were separated from the particle core using a thermal denuder. The exposures took place 5 hours/day, 4 days/week for 8 weeks in downtown Los Angeles, 100m downwind of a major freeway. Plaque formation in the aortic arch and total and LDL cholesterol in the serum were measured to evaluate the progression of atherosclerosis. Serum concentrations of lipid peroxidation, protein carbonyl content, and glutathione were assessed to determine systemic oxidative stress. Aortic plaque formation in mice exposed to unmodified CAPs was higher than in those exposed to CAPs with no SVOCs. Similarly, higher levels of lipid peroxidation were measured in mice exposed to unmodified CAPs and SVOC components of CAPs compared to those exposed to CAPs without SVOCs. The corresponding trends in plaque formation and lipid peroxidation support the notion that exposure to SVOCs may contribute to the acceleration of atherosclerosis via an oxidative stress pathway.

## PL 65 Acrolein-Induced Increases in Blood Pressure and Heart Rate Are Coupled with Decreased Blood Oxygen Levels during Exposure in Hypertensive Rats.

C. M. Perez<sup>1</sup>, A. D. Ledbetter<sup>2</sup>, M. S. Hazari<sup>2</sup>, N. Haykal-Coates<sup>2</sup>, A. P. Carll<sup>1</sup>, D. W. Winsett<sup>2</sup>, D. L. Costa<sup>3</sup> and A. K. Farraj<sup>2</sup>. <sup>1</sup>University of North Carolina at Chapel Hill, Chapel Hill, NC; <sup>2</sup>Environmental Public Health Division, US EPA, Research Triangle Park, NC; <sup>3</sup>ORD, US EPA, Research Triangle Park, NC.

Exposure to air pollution increases the risk of cardiovascular morbidity and mortality, especially in individuals with pre-existing cardiovascular disease. Recent studies link exposure to air pollution with reduced blood oxygen saturation suggesting that hypoxia is a potential mechanism that mediates the adverse cardiovascular effects of air pollution. The purpose of this study was to characterize the cardiovascular effects of exposure to acrolein, a potent irritant and component of cigarette smoke and diesel exhaust and determine if acrolein exposure causes decreased blood oxygen levels. We hypothesized that hypertensive rats would be more sensitive to the adverse cardiovascular effects of acrolein and that the cardiovascular effects of acrolein would be coupled with decreased arterial blood oxygen levels during exposure. Spontaneously hypertensive (SH) and Wistar Kyoto (WKY; rats with normal blood pressure) rats implanted with biopotential radiotelemetry transmitters were exposed once for 3 hours to 3 parts per million acrolein gas or filtered air (control) in whole body plethysmograph chambers while cardiovascular and ventilatory parameters were monitored. In a separate cohort of rats, arterial blood samples were drawn before, during, and after exposure to acrolein to monitor blood oxygen saturation. We found that hypertensive, but not normal rats, had significant increases

in heart rate, blood pressure, breathing frequency, and minute volume during acrolein exposure. These effects were coupled with significant decreases in arterial blood pO<sub>2</sub> and K<sup>+</sup> levels and significant increases in pCO<sub>2</sub>. The data suggest that hypertension predisposes to the adverse health effects of air pollution exposure and that hypoxia may have an important role in mediating these physiologic responses (This abstract does not reflect EPA policy).

## PL 66 PM<sub>2.5</sub> Exposure and RAGE: Insight into an Emerging Risk for Diabetes.

J. M. Vaughan, J. T. Zelikoff, B. Narayanan, A. Schmidt and L. Chen. *Environmental Health Science, New York University, Tuxedo, NY.*

Diabetics are a particularly vulnerable population to the adverse cardiopulmonary effects of particulate air pollution (PM)—often attributed to enhanced inflammation and endothelial dysfunction. Recent reports have implicated activated receptors for advanced glycation end-products (RAGE) as an integral factor in the inflammatory processes of cardiovascular dysfunction and diabetes; nonetheless, it is unclear whether ambient PM alone/or in combination w/ other endogenous factors may contribute to RAGE activation. Levels of soluble RAGE (sRAGE) were measured in human serum samples (n=60) from two cities in Gansu, China (Jinchang (JC) and Zhangye (ZH)—albeit similar ambient levels of PM; Ni, Cu, As, and Se in JC were 76, 25, 17, and 7 fold higher than ZH, respectively). In addition, human pulmonary endothelial cells were exposed to PM (collected from the same region) to investigate RAGE-mediated vascular dysfunction. Lastly, to examine the link between PM and overt diabetic endpoints, B6C3F<sub>2</sub> mice were exposed to concentrated ambient PM (CAPS). Results: sRAGE was significantly higher (p=0.04) in residents of JC (538.7±37.5ng/ml) than that measured in ZH (452.6±29.1ng/ml). Multiple regression analyses revealed PM<sub>2.5</sub> concentration as a significant (p=0.03) predictor of RAGE outcome. In the in vitro work, after 48h of PM<sub>2.5</sub> exposure, a dose dependent increase in cell proliferation and small increases in sRAGE activity at higher doses of PM was evident. Immunofluorescence detection showed an elevation in cells positive for membranous RAGE expression; accompanied w/ a 2-fold increase in mRNA for RAGE & NF-κB and >2 fold increase of ATF4 & NF-κB in cells treated w/ PM+BSA. These findings suggest plausible interaction between PM & RAGE resulting in enhanced expression of NF-κB, ATF4 and RAGE. Finally, preliminary mouse exposures have yielded supportive findings: progeny of CAPs exposed pregnant mice have shown significantly decreased glucose tolerance compared to controls (p=0.03). Collectively, these data offer valuable insight into PM-mediated RAGE activation / its influence on diabetes.

## PS 67 Integration of Jacketed Telemetric Hemodynamics in a Toxicology Study Design: Assessment of Sensitivity and Distribution and Impact of Erroneous Values.

H. Holzgrefe, S. Tichenor, R. Kaiser and D. Meyer. *Toxicology, Charles River Laboratories, Reno, NV.*

Integration of telemetered hemodynamics in toxicology studies is an emerging trend which offers detailed information on potential cardiovascular safety issues that are only identified with repeat dosing. Jacketed external telemetry (JET) is an enabling technology for which the intrinsic variability of the associated minimally invasive blood pressure (BP) device (PA-C10, DSI, St. Paul, Minn.) has not been extensively characterized. Accordingly, we evaluated the intrinsic and extrinsic beat-to-beat pressure measurement errors of JET BP in 10 male cynomolgus monkeys (2.7-3.7 yrs, 3.0±0.2 kg). BP catheters were advanced to the descending aorta via the femoral artery. BP (24 h) was continuously digitized (500 Hz) in a quiet radio frequency environment and retrospectively analyzed in beat-to-beat increments (Life Sciences Suite, ver. 5.0, DSI). Data are presented as mean±std. Sham dosing occurred at 2.5 h post acquisition start to mimic a typical toxicology study design. Erroneous values were categorized as beats where either systolic pressure, pulse height, and/or +dP/dt were 60<>240, 20<>80, or 600<>4000 native units, respectively. Transducer stability was assessed as the beat-to-beat change (Δ) in systolic pressure. Over 24 h, systolic pressure was 130.6±8.5 mmHg and Δ was 0.0±2.67 mmHg. During a quiescent nocturnal period (10 h) systolic pressure was 131.9±8.5 mmHg and Δ was 0.0±2.42 mmHg. Erroneous values (8874/2428462 beats, 0.36%) were infrequent and temporally random. These data confirm that the JET BP device conformed to, or exceeded, design sensitivity (± 3 mmHg) at all times. Systolic pressures exhibited stable diurnal variances of ± 8.5 mmHg yielding ~ 80% power to detect a 10 mmHg change (p<0.05) with n=6. The sparse, sporadic incidence of non-physiologic hemodynamic values was insufficient to influence mean BP values aggregated over times ≥ 5 min. Consequently, resources devoted to the beat-to-beat filtering of JET BP values will not improve the accuracy, precision, or power of these data.

## PS 68 Evaluation of an in Line Filter for Reducing Noise in Subcutaneous Telemetered ECGs.

C. M. Kelly<sup>1</sup>, M. Miyamoto<sup>1</sup>, M. Brockway<sup>2</sup> and B. Brockway<sup>2</sup>. <sup>1</sup>Huntingdon Life Sciences, East Millstone, NJ; <sup>2</sup>VivaQuant, St. Paul, MN.

EMG noise and movement artifact are barriers to obtaining accurate interval measurements in ambulatory subjects in preclinical studies. Herein we report the results of testing of a new device, an In Line Filter (ILF) that employs Multi-Domain Signal Processing™ (MDSP) technology, for real-time noise and artifact suppression in telemetered subcutaneous ECG recordings. Prior evaluations of MDSP technology using ECGs already acquired by the Dataquest™ system showed that it reduces the amplitude of in-band noise by > 95% without distorting ECG morphology and provides a corresponding increase in the number of analyzable beats. In this work, studies of ILF performance were conducted using freely moving subjects instrumented with DSI™ D70-PCT telemetry transmitters. An ILF was inserted between the telemetry receiver and the Dataquest system to filter out noise. Raw and filtered ECG signals were collected from multiple species commonly used in safety studies and were analyzed with emka ECGauto using standard methods. Results obtained from filtered and unfiltered recordings were evaluated to assess the impact of filtering on parameter measurement accuracy, the increase in beats available for analysis, and the amount of labor required to perform interval analysis. Results show that, on average in all species tested, filtering the ECGs using the ILF prior to analysis increased the analyzable portion of the data to roughly that reported in the literature for telemetered epicardial and intravenous ECG sensors and significantly reduced the amount of labor required to perform interval analysis. There was no degradation in the accuracy of parameter measurements as a result of filtering the signal. Use of the ILF could make routine beat-to-beat analysis of 24-hour subcutaneous ECG recordings practical and cost-effective without the complications and complexities associated with epicardial, endocardial, and intravenous ECG sensing leads.

## PS 69 The Application of Telemetry EEG and EMG in Conscious Dogs and Monkeys for Safety Assessment and Translational Science.

X. Cheng, C. Cao, N. N. Niu, K. H. Chen, S. L. Sun and A. Hu. *Toxicology and Safety Pharmacology, Pharmaron, Beijing, China.*

The species differences are the common and major concerns in safety assessment and translational science, particular in situations where results from CV and CNS safety studies in the same species are required or the receptor subunits expression are significantly difference cross species etc. In this study, we have used the radio-telemetry technique to record EEG and EMG from conscious, non-sedated dogs and monkeys and validated the model with a proconvulsant, pentylenetetrazole (PTZ).

Beagle dogs and cynomolgus monkeys were implanted with four electrodes epidural over the motor cortex and connected to the radio-transmitter (DSI) placed subcutaneously in the lateral neck region. Two additional electrodes were inserted into the ridge cervical muscle for EMG recording simultaneously. The signals captured by the receiver were routed via a data matrix board to a PC and sampled at a rate of 500Hz.

Subcutaneous (s.c) administration of PTZ dose-dependently (10, 20 and 50 mg/kg s.c) induced paroxysmal activity, clonic convulsion and tonic convulsion in both dogs and monkeys, indicating a remarkable CNS safety issue of PTZ as positive control article. When PTZ administrated i.v at 1.5mg/kg/min and 1.5mL/min, both dogs and monkey showed similar level of paroxysmal spike-and-wave activity associated with clonic convulsions occurred between 17 and 36 min after the start of infusion at 4-5Hz.

The data indicate that the electroencephalogram (EEG) and electromyogram (EMG) are the most sensitive and valuable biomarkers in identifying pathologic CNS activity, in particular for safety pharmacology evaluation and translational application.

## PS 70 Established Method to Assess Cardiorespiratory Parameters in Inhalation Safety Pharmacology Studies in Conscious Beagle Dogs.

T. Ziegelhofer, J. Sheehan, J. Sentz, M. Miyamoto and A. Curran. *Safety Pharmacology, Huntingdon Life Sciences, East Millstone, NJ.*

A critical aspect of cardiorespiratory safety pharmacology studies is the collection of good quality cardiovascular and respiratory data immediately prior to dose, during dose and immediately after dose to be able to recognize any acute effects of the test

article. This is especially challenging when the test article is administered via inhalation. This poster describes the method for achieving a successful outcome in these types of studies, including the factors that must be considered in the design and execution. Effects of proper habituation to equipment and carefully scheduled study activities were assessed based on the overall character of cardiorespiratory response from 3 different studies.

Prior to the first data collection, all animals were surgically implanted with DSI telemetry transmitters and habituated to the exposure/data collection system. Respiratory parameters were collected using respiratory inductance plethysmography (RIP). Telemetry data were collected continuously while animals were in their home cage, after transfer to the exposure suite but prior to either air or the vehicle, during the exposure period, and for 24 hours post dose in 3 different studies. Each study used a different vehicle and an air (sham) control was administered to assess the vehicle effect.

Administration of the vehicle produced no effects on blood pressure, heart rate, body temperature, respiratory rate, tidal volume and minute volume during pre-dose, exposure period and for the 24 hour post dose recording period when compared to air (sham) control in all 3 studies. Very similar patterns in blood pressure and heart rate were noted in all 3 studies; however, each study has a specific pattern for body temperature and respiratory parameters, which was attributed to individual variation in these parameters. This poster presents a consistent and reliable method of collecting cardiorespiratory data from conscious beagle dogs prior to, during and after inhalation exposure in our Testing Facility.

**PS 71 Assessment of QT-Interval Prolongation in Nonclinical Safety Study Using External Telemetric Device in Conscious Beagle Dogs: Application of QT Shift and Probabilistic Methods.**

L. Renaud<sup>1</sup>, P. Champeroux<sup>2</sup>, S. Ruillon<sup>1</sup>, N. Velasquez<sup>1</sup>, P. Desbois<sup>1</sup>, O. Wattrelos<sup>1</sup> and N. Claude<sup>1</sup>. <sup>1</sup>*Drug Safety, Servier, Gidy, France;* <sup>2</sup>*Centre de Recherches Biologiques, CERB, Baugy, France.*

The detection of delayed ventricular repolarization, characterized by a QT interval prolongation, is one of the main issues for the preclinical evaluation of potential risk of pro-arrhythmia for a new drug candidate. This study was designed to compare different methods of QT interval prolongation assessment in conscious beagle dogs using external telemetric device. The same 6 dogs (3/sex) were given vehicle or reference compounds known to induce QT interval prolongation using a sequential design (single oral dosing of Sotalol at 30 mg/kg and Moxifloxacin at 30 then 90 mg/kg or repeated oral dosing for 6 days of Thioridazine at 20 mg/kg/d and Terfenadine at 30 mg/kg/d). Electrocardiograms were recorded during a treatment-free period and on day 1 and/or day 6 for approximately 20 h post dosing. QT intervals were measured from a beat to beat analysis over 10-min periods centred on selected timeslots and corrected according to the Van de Waters formula (QTvdw). QT shift calculations and an analysis based on the principles of the Holzgrefe's probabilistic method (QTh, using a minimum 250 beats/timeslot) were also performed. All methods allowed an accurate evidence of QT effect for Sotalol and Moxifloxacin. The QT shift and QTh methods gave more evidences for Terfenadine effect than QTvdw. As expected, the marked increase in heart rate (HR) induced by Thioridazine resulted in no apparent effect on QT and a statistically significant overcorrection for QTvdw whereas QT shift and QTh gave more accurate and reliable results. The statistical sensitivity threshold detection of QT prolongation was low, i.e. 10 to 15 ms for QT shift and QTh methods. Thus, external telemetry in non-clinical safety dog studies allows new perspectives for a better assessment of QT prolongation when associated to QT shift and Holzgrefe's probabilistic methods, especially in case of slight drug-induced QT effect or marked changes in HR.

**PS 72 Integration of Automated Patch Clamp Systems and Logistic Models in the Cardiochannelgramtm (CCGTM) for Better Prediction of Cardiac Risk.**

J. W. Kramer<sup>1</sup>, G. J. Myatt<sup>2</sup>, C. A. Obejero-Paz<sup>1</sup>, A. Bruening-Wright<sup>1</sup>, Y. A. Kuryshev<sup>1</sup> and A. M. Brown<sup>1</sup>. <sup>1</sup>*ChanTest Corporation, Cleveland, OH;* <sup>2</sup>*Leadscope Inc., Columbus, OH.*

Drug-induced inhibition of the cardiac hERG potassium channel is recommended by ICH and FDA to predict delayed cardiac repolarization (DR) and cardiac risk. The consequent QTc prolongation is a surrogate marker of Torsade de Pointes (TdP), a rare but potentially lethal iatrogenic outcome. Drugs with effective therapeutic plasma concentrations (ETPC) within 30-fold of their hERG IC50s are thought to be dangerous despite the fact that multiple ion channel effects (MICE)

can mitigate DR. Here we demonstrate that logistic regression models, which integrate MICE, predict TdP with much greater certainty than the hERG safety ratio (hERG IC50/ETPC or safety margin (SM)) alone. To this end we measured hERG, Nav1.5, Cav1.2, Kir2.1 and KvLQT1/minK IC50 values of 56 drugs (33 +TdP and 23 -TdP) from multiple classes using automated patch clamp systems including Qpatch and PatchXpress. The sensitivity of the automated patch clamp platforms was evaluated in a comparison to manual patch clamp. ETPC values and the torsadogenic liability of drugs was obtained from the literature, package inserts and Arizona CERT. Eleven logistic regression models were constructed; one using the hERG SM alone, the others integrating hERG SM, Nav1.5 SM and/or Cav1.2 SM data. The predictive power of each model was evaluated using the likelihood ratio test. Leave-one-out cross validations were performed and each model's accuracy was determined by comparing receiver-operating characteristics (ROC, sensitivity vs. 1-specificity). Models that include Nav1.5, Cav1.2 or both variables are statistically significant better predictors of TdP liability than the model that contains only hERG (Model 1). Model 1 had a ROC area under the curve (AUC) of 0.80 and Model 11, that includes hERG, Nav and Cav1.2 SMs, significantly improved accuracy showing a ROC AUC of 0.94. Thus, Model 11 that incorporates the concept of MICE in the CardioChannelGramTM (CCGTM) is a robust nonclinical predictor of cardiac risk.

**PS 73 Characterization of Jacketed External Telemetry with Blood Pressure in Conscious Nonhuman Primates in Pen-Style Housing Administered Etilefrine, Sotalol, or Hydralazine.**

L. Kreckler, J. Kopshinsky, J. Schneider, G. Hanson, D. Morris and C. Foley. *Covance Laboratories, Inc., Madison, WI.*

An important component of nonclinical safety assessment is the evaluation of electrocardiography (ECG) and hemodynamic parameters. Jacketed external telemetry with an implanted telemetry blood pressure transmitter (JET-BP) is a minimally invasive technology being utilized in general toxicology studies to assess ECG and blood pressure measurements in conscious, unrestrained animals. We characterized JET-BP in nonhuman primates (NHPs) housed in pen-style caging with three reference compounds with known effects on blood pressure or ECG parameters. Thirty-six male NHPs were implanted with a telemetry blood pressure device and group-housed in pen-style caging (3 animals/pen). Four animals per group were given reference material or a concurrent control article. Etilefrine, a sympathomimetic, was given at 1 or 10 mg/kg; hydralazine, a vasodilator, at 1 or 10 mg/kg; and sotalol, a non-specific  $\beta$ -blocker, at 3 or 30 mg/kg. JET-BP measurements were recorded for at least 90 minutes prior to dosing and continuously for at least 20 hours postdose. The following ECG and hemodynamic parameters were determined as one (light phase) or two-hour (dark phase) averages: PR, QT and rate-corrected QT; systolic, diastolic, and mean arterial pressures; heart rate; and arterial pulse pressure. In addition, blood was collected at seven postdose timepoints for each test article for pharmacokinetic analysis. Etilefrine significantly increased mean arterial pressure, systolic blood pressure and pulse height, while diastolic blood pressure remained unchanged. Sotalol significantly prolonged QT with no significant change in blood pressure. Administration of hydralazine did not significantly change blood pressure at the dose levels administered. In summary, ECG and blood pressure changes caused by three different reference compounds were detectable using JET-BP technology in group-housed NHPs.

**PS 74 Differential Cardiovascular Physiology and Pathology in Selected Lineages of Miniature Swine.**

A. Stricker-Krongrad<sup>1</sup>, T. J. Madsen<sup>1</sup>, B. C. Hanks<sup>1,2</sup>, D. Brocksmitz<sup>2</sup>, J. Liu<sup>1</sup>, L. D. Brown<sup>1,2</sup> and G. F. Boucard<sup>1,2</sup>. <sup>1</sup>*Sinclair Research Center, LLC, Columbia, MO;* <sup>2</sup>*Sinclair BioResources LLC, Auxvasse, MO.*

The miniature swine has been increasingly recognized as a valid alternative to canine and non-human primates in regulatory toxicity. This poster presents the results of cardiovascular assessments in the Yucatan, Hanford, and Sinclair miniature swine conducted during clinical investigations and control toxicity testing. Anatomic parameters were obtained at necropsy. Blood vessels diameter, velocity, and flow were obtained by Doppler ultrasonography. Cardiac electrophysiology was obtained using clinical ECG and surgical monitor units. Macroscopic lesions and histopathology assessments were conducted on heart and kidneys. Data were compared to published measurements of adult human illustrating similarities or differences (for practicality, male data are reported here). Across the three lineages, heart-to-body weights ratio ranged from 0.41 to 0.50 and were higher than human (0.42). The geometric corrections for heart rate adjustment to body size ranged from 215 to 297 and were comparable to human (241), indicating that heart volume and function were well adjusted to the reduction in body size. The miniswine

hearts showed a coronary artery distribution comparable to human. The right coronary internal diameters ranged from 1.44 to 1.79 mm and were comparable to human (3.9 mm) when adjusted to body surface area (weight range: 10-30 kg). External femoral blood flows at rest averaged 93 mL/min and were slightly lower than human (260 mL/min) when adjusted to body size. Electrophysiological heart segments duration (e.g. RR ranged from 360 to 662 msec) and their ratio (QT/RR) were proportional to human and well-adjusted to body size. Macroscopic lesions were nonexistent. Histopathology findings were rare and limited to sub-level myocardial inflammation with low incidence in the Hanford lineage. In conclusion, the similarities between the cardiovascular systems make these three lineages of miniature swine suitable animals to model the human counterpart.

## PS 75 Whole Heart Energetics and Stress Test As an Indicator of Drug-Induced Cardiac Toxicity.

K. A. Henderson<sup>1</sup>, R. Borders<sup>1</sup>, J. Ross<sup>1</sup>, A. Jalil<sup>2</sup>, W. Brandon<sup>1</sup>, J. Ma<sup>1</sup> and R. M. Brian<sup>1</sup>. <sup>1</sup>Battelle Memorial Institute, Columbus, OH; <sup>2</sup>Ohio State University, Columbus, OH.

Cardiac toxicity, manifested as compromised contractility or ischemic heart disease, comprises 26.9% of post-approval drug failures. The heart has a high demand for a constant energy supply which can be affected by many sources of stress and thus may be a good indicator of potential toxicity. The purpose of this research was to utilize the ex vivo heart model to assess contractility and whole heart energetics in response to drugs with known/unknown mechanisms of toxicity. We used FCCP and verapamil as positive and negative controls and doxorubicin (dox), doxorubicin-ol, sunitinib, and sorafenib as the chemotherapies associated with latent toxicity. Rat hearts were removed, perfused with Modified Henselet Krebs, and LVP was monitored via insertion of a fluid-filled balloon. The perfused heart was inserted into an 11.7 NMR magnet. Whole heart phosphogen content was assessed before and during 60 min of drug exposure and then during 20 min of 0.1 μM isoproterenol (iso) with drug to assess energy reserve. Control heart contractility and energetics were stable throughout the experiment until the iso challenge, where contractility increased as expected and PCr and ATP decreased and Pi increased. FCCP treated hearts showed a decline in contractility and PCr and reduced reserve during the iso challenge. Verapamil treated hearts did not change in energetics during treatment or during the iso challenge. Dox increased contractility, while the other chemotherapies showed very little change in contractility during drug treatment. Dox treated hearts demonstrated a drop in Pi, PCr, and ATP. In addition, during the iso challenge contractility increased compared to control and PCr decreased. Dox and sorafenib may be enhancing part of the beta-agonist pathway, causing a more pronounced response to iso and thus resulting in an increased work load for the heart. This may be a possible pathway to investigate as a mechanism for latent toxicity, as well as an early indicator of potential drug induced cardiac issues after treatment.

## PS 76 Simultaneous Recording of Action Potentials and Calcium Transients from Stem-Cell Derived Cardiomyocytes: Applications for Cardiotoxicity Testing.

R. Whittaker<sup>1</sup>, F. Cerignoli<sup>1</sup>, R. Vega<sup>1</sup>, R. Ingermans<sup>1</sup>, R. Towart<sup>2</sup>, D. Gallacher<sup>2</sup>, M. Mercola<sup>3</sup> and J. Price<sup>1,3</sup>. <sup>1</sup>Vala Sciences Inc, San Diego, CA; <sup>2</sup>Center of Excellence for Cardiovascular Safety Research, Janssen Pharmaceuticals, Beerse, Belgium; <sup>3</sup>Sanford-Burnham Medical Research Institute, La Jolla, CA.

Current methods for preclinical cardiotoxicity testing generally examine the effects of candidate compounds on the activity of single ion channels using manual or planar patch clamp methods. Limitations in these assays require that the tests be performed with cell lines which stably express the ion channel of interest. This reductionist approach grossly underestimates the complexity of cardiomyocyte excitability and physiology. We have developed a new automated image cytometer and associated software which facilitates a more physiologically relevant test of compound effects on cardiomyocyte excitation-contraction coupling. This new approach utilizes a dual channel automated Image cytometer that allows for simultaneous measurement of the cardiomyocyte action potential and calcium transient using voltage and calcium sensitive dyes. By using these advanced imaging techniques this system frees the need for the assay apparatus to interact physically with the cells, allowing the use of a wide array of cell types including more clinically relevant models such as cardiomyocytes derived from human induced pluripotent stem cells (hiPSC). Here we demonstrate the application of this system to a small scale screen of known cardioactive compounds in hiPSC derived cardiomyocytes. Our results suggest that the ability to identify perturbations in the cardiomyocyte action potential and/or calcium transient due to exposure to cardioactive compounds is on par with existing technologies. However, this system demonstrates a

much higher throughput than existing systems and provides a more complete analysis of compound effects on excitation-contraction coupling in the cardiomyocyte.

## PS 77 Effect of Cell Culture Media on the Growth and Viability of Neonatal Rat Cardiomyocytes.

L. Baeva, D. Chan, H. Dinesdurge, M. W. Betz and R. P. Brown. *CDRH, US FDA, Silver Spring, MD.*

We studied the suitability of serum-free medium, reduced serum medium, and chemically defined medium with serum replacement for growing rat neonatal cardiomyocytes. The cardiac cells were grown for up to 48 hours under six different culture conditions: the base make up (Dulbecco's Modified Eagle Medium (DMEM) containing 100 μM BrdU, 10 mM HEPES, 50 U/mL penicillin and 50 μg/mL streptomycin) with 10% Fetal Bovine Serum (FBS)-(A), or 10% Goat Serum-(C), or 10% Knockout Serum Replacement (KRS)-(D) or no serum -(B); Knockout DMEM(Gibco) (E) and Advanced DMEM(Gibco) (F) were supplemented by 15% KSR and 2% FBS, respectively. The beating rates and viabilities of the cells were evaluated by counting the beats of cells under a phase contrast microscope and Neutral Red Assay method, respectively. The cell damage and cytotoxicity were determined by measuring lactate dehydrogenase (LDH) activity and the troponin I release from the cardiomyocytes were examined by rat cardiac Troponin ELISA. The results indicate poor cell beating and viability for medium C without serum. The media D, E, and F had relatively low background troponin level, provided good viability and morphology and low cytotoxicity, and may be used for the cardiotoxicity study.

## PS 78 Understanding the Relationship of PI3K Inhibition to HERG Liabilities and QT Prolongation.

D. Puppala<sup>1</sup>, H. Cheng<sup>3</sup>, A. Rosado<sup>2</sup>, K. McKiernan<sup>2</sup>, S. Sun<sup>2</sup>, B. Fermini<sup>2</sup> and K. Leach<sup>1</sup>. <sup>1</sup>Compound Safety Prediction, Pfizer Inc, Groton, CT; <sup>2</sup>Global Safety Pharmacology, Pfizer Inc, Groton, CT; <sup>3</sup>Oncology Medicinal Chemistry, Pfizer Inc, Groton, CT.

Off target promiscuity is one of the biggest issues that kinase targeting drug discovery teams have to overcome in order to achieve efficacy with limited toxicity. In a recent paper, Zhongju Lu et al (Science Translational Medicine 25 April 2012 Vol 4 Issue 131) showed that suppression of Phosphoinositide 3-Kinase(PI3K) signaling directly or indirectly via tyrosine kinase inhibition prolongs the QT interval by affecting multiple ion channels, including HERG. In an effort to understand the role of PI3K inhibitors and HERG channels, we investigated the effects of Pfizer PI3Ka inhibitors both in a Dofetilide binding assay that determines their affinity for HERG channels as well as in a patch clamp assay that assesses their functional activity on these channels. Out of 48 PI3K inhibitors selected from four structurally distinct series and with PI3Ka Ki less than 1 nM, 47 exhibited Dofetilide Ki values > 10 uM, and one demonstrated a Ki value of ≈ 2.0 uM, a concentration > 2000-fold above its kinase activity. 8 compounds, including the one with a Dofetilide Ki of 2.0 uM, were tested in the HERG functional assay and all showed IC50 values > 30 uM.

In addition, 16 marketed drugs, which are known HERG blockers and that have been shown to induce QTc prolongation (14/16) and/or cause Torsades de Pointes in the clinic (8/14), were tested in a PI3Ka enzyme assay. Only Verapamil, a calcium channel blocker that inhibits HERG current (IC50: 0.2 uM) but does not prolong the QTc interval or cause TdP in the clinic exhibited activity on PI3Ka (IC50: 33 uM), while the rest showed IC50 > 100 uM.

In summary, the data obtained from both Pfizer potent PI3Ka inhibitors and marketed drugs demonstrate the absence of the correlation between PI3Ka inhibition and HERG activity.

Furthermore, our results support the notion that HERG inhibition, in the absence of PI3K inhibition, is sufficient to prolong the QT interval.

## PS 79 Characterization of Cell Signaling Events in Human Cardiomyocytes.

S. Eldridge<sup>1</sup>, M. Davis<sup>1</sup>, J. Mussio<sup>2</sup> and R. Parchment<sup>2</sup>. <sup>1</sup>DCTD, NCI, Bethesda, MD; <sup>2</sup>SAIC-Frederick, Frederick National Laboratory for Cancer Research, Frederick, MD.

Cardiotoxicity is a significant concern for anticancer therapeutics. "On-target" toxicity may result when a drug target that regulates cancer growth also serves an important role in normal cardiac function. To explore mechanisms of cardiac toxicity

associated with anti-cancer agents, in vitro approaches are key investigative tools. iCell® cardiomyocytes (Cellular Dynamics International, Madison, WI) are highly purified human cardiomyocytes derived from induced pluripotent stem cells through reprogramming adult cells, and are becoming widely used for the assessment of cardiac toxicity. To begin to inform the utility of these cells to monitor cellular events involved in critical cardiac myocyte signaling, we measured expression and activity of ErbB receptors, Erk1, Erk2, AKT, troponins, and endothelin-1 (ET-1) receptors A and B. Untreated iCell® cardiomyocytes expressed ErbB2 and ErbB4 receptors, Erk1, Erk2, AKT, cardiac troponin I, cardiac troponin T and ET-1 receptors A and B, but not ErbB1 or ErbB3 receptors. Furthermore, treatment with neuregulin-1 (a natural ligand for ErbB4) activated ERK1/2 and AKT as demonstrated by increased levels of phosphorylated proteins measured by western blotting with phospho-specific antibodies. Ligand-activated ErbB2/ErbB4 signaling was both dose and time dependent. We also examined the effect of tyrosine kinase inhibitors (lapatinib, sorafenib and staurosporine) and anthracyclines (doxorubicin) on cell death and mitochondrial membrane potential (MMP) using a high content multiplexed imaging system, and on troponin release into the cell culture media using the Meso Scale Discovery® platform. All of these anticancer agents induced a dose-dependent release of cardiac troponins I and T and caused a reduction in MMP. Based on these results, this model may present an opportunity to explore and “back-translate” mechanisms of cardiotoxicity using human cardiomyocytes in vitro. Funded by NCI Contract No HHSN261200800001E.

## PS 80 Mitochondria and Intrinsic Apoptotic Pathway Mediate Cardiac Toxicity of Environmentally Persistent Free Radicals (EPFR).

G. C. Chuang<sup>1</sup>, B. Dellinger<sup>2</sup> and K. J. Varner<sup>1</sup>. <sup>1</sup>Pharmacology, Louisiana State University Health Sciences Center, New Orleans, LA; <sup>2</sup>Chemistry, Louisiana State University and A&M College, Baton Rouge, LA.

Epidemiology studies have linked combustion-derived particulate matter to increased cardiac morbidity and mortality. To conduct prospective controlled-exposure studies, we synthesized the model EPFR, DCB230, by chemisorption of 1,2-dichlorobenzene to 0.2 µm silica particles containing 5% Cu(II)O at 230°C. Electron paramagnetic resonance showed that DCB230 generates radicals in solution similar to those produced by EPFRs found in environmental samples. We have shown that DCB230 inhalation produces inflammation and oxidative stress in both lung and heart. Since oxidative stress and apoptosis are mechanisms implicated in cardiac injury, we hypothesized that DCB230 exposure exerts cardiotoxicity by activating apoptotic pathways. HL-1 cardiomyocytes were dosed with 0-200 µg/mL DCB230 for 8 h and assessed for cytotoxicity and apoptotic markers. DCB230 dose-dependently increased lactate dehydrogenase (LDH) release, a marker of late cell death. Caspase 3, caspase 9, and poly (ADP-ribose) polymerase 1 cleavage also increased concomitant with DCB230 concentration, indicating apoptotic signaling activation. Next, HL-1 cardiomyocytes were treated with 0-200 µg/mL DCB230 for 2 h to examine early signaling events. While neither LDH release nor caspase 3 cleavage were detected after 2 h, increased caspase 9 cleavage suggests that mitochondrial dysfunction initiated early intrinsic apoptotic signaling. Confocal microscopy showed that mitochondrial membrane potential decreased after 2 h treatment with DCB230. Lastly, fluorescence data was validated as mitochondrial via FRET and co-localization with MitoTracker Green. Taken together, DCB230 exposure depolarized mitochondria in cardiomyocytes, leading to the activation of canonical intrinsic apoptotic signaling and resulting in cell death. Future studies will assess mitochondrial permeability transition and autophagy as contributing mechanisms. Supported by NIH P42-ES013648, sub-award 61365.

## PS 81 Evaluation of Cellular Impedance Assays for Drug Screening in Cardiomyocytes.

M. Peters, C. W. Scott, S. D. Lamore and Y. P. Dragan. *Safety Assessment, AstraZeneca, Waltham, MA.*

Cardiovascular (CV) toxicity is a leading contributor to drug withdrawal and late-stage attrition. Earlier screening is a validated approach to build-in CV safety, as demonstrated for hERG screening to reduce arrhythmia. There is an urgent need for novel in vitro assays to extend this success to contractility, heart rate, hypertrophy, structural damage, and non-HERG arrhythmia. Advances in cellular impedance technology enables label-free tracking of spontaneous synchronized beating of cultured cardiomyocytes (CM). To validate and translate CM impedance assays, we tested a set of drugs with established CV effects in humans- 22 neg. inotropes, 8 pos. inotropes, and 21 inactives (previously tested in canine CM Tox Appl Pharm 260(2):162). The data clearly indicate that beat rate and amplitude are independent variables, capable of providing robust potency data. Consistent with the balance of negative inotropes, the most frequent response was a dose-dependent decrease in

amplitude until beating stopped. The cessation of beating was not linked to cytotoxicity (judged by ATP and cell index) indicating specific changes in CM function. Since rat neonatal (and stem cell-derived) CMs have a negative frequency-force relationship, it is not surprising that the decrease in amplitude was linked to a concomitant increase in rate. However, for another subset of validation compounds, rate initially decreased, whereas amplitude showed no associated change until higher drug concentrations. Moreover, for a test compound not in the validation set (that was selected for inducing myocarditis in 2 days), beat rate increased with no change in amplitude or cytotoxicity. Together this data demonstrates that impedance assays can detect and differentiated functional changes in CMs. The changes are sensitive to electrical and mechanical aspects of contraction, yield robust data, and offer a versatile format with moderate throughput making this platform a candidate for addressing gaps in early phase screening for CV toxicity.

## PS 82 Cellular Impedance Assays for Predictive Preclinical Drug Screening of Kinase Inhibitors in Cardiovascular Toxicity.

S. D. Lamore, C. W. Scott, Y. P. Dragan and M. Peters. *Safety Assessment, AstraZeneca, Waltham, MA.*

Cardiotoxicity is the leading cause for late stage drug attrition and withdrawals from the market. Serious adverse cardiac events have emerged as a prevalent risk for kinase inhibitors (KI). Although current in vivo screens can reduce known risks due to arrhythmia, there is urgent need for novel in vitro assays with sufficient throughput to identify risks and support the development of SAR against other prevalent cardiovascular (CV) toxicities. Recently, cellular impedance technology has been adapted for detecting spontaneous, synchronized beating of cultures of cardiomyocytes (CM) in a real-time, label-free format. Impedance technology is a good candidate for detecting the pleiotropic cellular effects of kinases since it detects morphological changes thereby giving a readout that is downstream of key toxicity targets in the contraction cascade (i.e. cardiac action potential, calcium flux, mechanical elements of contraction). We evaluated the application of impedance-based assays for screening KI effects on rat neonatal CM. We selected compounds from a MAP-microtubule affinity-regulating kinase (MARK) inhibitor program that failed in late-stage preclinical development with dramatically decreased blood pressure in anesthetized dogs as an example for the earlier detection of CV toxicity. Two MARK inhibitors were tested and both dose-dependently influenced CM beat rate and amplitude without causing cell death as judged by cell index, cellular ATP levels, or cardiac troponin release assays. The relative potency of the two compounds on reducing beat amplitude in impedance assays (EC<sub>50</sub>= 4.31 µM and 0.55 µM; 20 min exposure) aligned with the ~10-fold difference in affinity for MARK isoforms 1-4. Knockdown of pan-MARK expression reduced beat amplitude by 40%. These MARK data indicate that impedance assays can specifically detect non-cytotoxic functional effects of KIs on CM. Our data support the validation of cellular impedance-based assays for an early preclinical CV toxicity screening of KIs.

## PS 83 Activation of Human Monocytic NADPH Oxidase by Chlorinated Cyclodiene Insecticides.

L. C. Mangum, J. E. Chambers and M. K. Ross. *CVM Basic Sciences, Mississippi State University, Mississippi State, MS.*

Although the mechanistic relationship between bioaccumulative organochlorine (OC) insecticide exposure and increased atherosclerosis risk is poorly defined, elevated systemic oxidative stress stemming from OC-mediated induction of NADPH oxidase activity may play a significant role in disease development. Activation of phagocytic Nox2-containing NADPH oxidase can result in a rapid intracellular accumulation of superoxide-derived reactive oxygen species (ROS) that may be directly linked to the progression of atherosclerosis. This study measured the ability of two legacy OC compounds to induce Nox2-containing NADPH oxidase activity in vitro, in addition to providing evidence for a possible mechanism of action. Human THP-1 monocytes exposed to micromolar amounts (1-20 µM) of the cyclodiene OC insecticides trans-nonachlor and dieldrin exhibited increased levels of serine phosphorylation of the p47phox regulatory subunit of NADPH oxidase, a necessary process for enzyme assembly and translocation, with trans-nonachlor demonstrating several fold greater potency than dieldrin. OC treatment also induced elevated levels of intracellular ROS, as shown by 2',7'-dichlorofluorescein-diacetate fluorescence assay, suggesting increased superoxide anion production. Pretreatment of monocytes with arachidonyl trifluoromethyl ketone, a specific inhibitor of cytosolic phospholipase A2, prior to cyclodiene treatment abrogated p47phox serine phosphorylation and blocked the induction of arachidonic acid and prostanoid liberation, as determined by UPLC-ESI MS/MS, suggesting that this enzyme may play a crucial role in the induction of NADPH oxidase activity by cyclodienes via the modulation of intracellular arachidonic acid levels. The results suggest that trans-nonachlor and dieldrin are capable of altering intracellular ROS levels via an

inducible NADPH oxidase dependent mechanism that may be significant in the etiology of atherosclerosis associated with exposure to bioaccumulative cyclodiene insecticides. (NIH R15ES015348)

#### PS 84 Mechanistic Studies of Drug-Induced Cardiac Hypertrophy in H9c2 Cell.

Z. Lin and Y. Will. *Compound Safety Prediction, Pfizer Global Research & Development, Groton, CT.*

Drug induced cardiotoxicity can manifest itself through a variety of mechanisms including mitochondrial toxicity, apoptosis, oxidative stress and ion channel disturbance. However, cardiac hypertrophy is the most common safety finding. Here, we aimed at established an in vitro platform which could reliably characterize hypertrophic responses. Fifty drugs reported to cause hypertrophy in vivo were utilized in this study and consistent of a variety of drug classes such as anthracyclines, statins, kinase inhibitors and catecholamines. Compounds were characterized in H9c2 cell assessing the following endpoints: cell size, protein synthesis, fetal gene expression (ANP, BNP, MYH7), cell viability and reactive oxygen species (ROS).

Our results indicate that unlike the traditional cardiac hypertrophy which is driven by ventricular wall stress and hormonal factors including angiotensin II, endothelin-1, and catecholamine, compound-induced cardiac hypertrophy (increase in protein and cell size) may be initiated by the same mechanisms that drive cytotoxicity. In contrast, fetal gene expression is different from the mechanisms that drive cell size and protein increase.

Specifically, our results demonstrate that: 1) all protein synthesis-inducing compounds (23) caused significant cytotoxicity; 2) all compounds causing increase in cell size also induced protein synthesis; 3) both protein and cell size increase were compound-concentration dependent with protein increase occurring always ahead of cell size increase; 4) of the total of 50 drugs known to cause hypertrophy in vivo, 28 compounds induced fetal gene expression; 5) Oxidative stress was associated with the hypertrophic response (25%).

In summary, our data suggest the initial trigger(s) of compound-induced hypertrophic response are multi-factorial; one of which shares the same mechanism that induces cytotoxicity. Not all compounds known to cause hypertrophy in vivo were accurately characterized by our in vitro approach. Whether stem cells and additional mechanistic parameters can improve our assay is subject to future studies.

#### PS 85 Optical Measurements of Electrical Activity from hiPSC-Derived Cardiomyocytes Is a Robust and High-Throughput Method for Measuring NCE-Effects on the Cardiac Action Potential.

G. Smith<sup>2</sup>, B. D. Anson<sup>1</sup>, M. A. Craig<sup>3</sup> and I. Ghouri<sup>2</sup>. <sup>1</sup>*Cellular Dynamics International, Madison, WI*; <sup>2</sup>*University of Glasgow, Glasgow, United Kingdom*; <sup>3</sup>*Clyde Biosciences, Glasgow, United Kingdom*. Sponsor: K. Kolaja.

Pro-arrhythmic assessment of new chemical entities (NCEs) is a vital component of toxicological and safety profiling. Manual patch clamp interrogation of the cardiac action potential (AP) is a gold standard for proarrhythmia assessment; however this technique is laborious, requires highly skilled scientists, and neither the technique nor traditional tissue cells have been readily amenable to higher throughput techniques. Optical measurements of electrical activity with human cardiomyocytes may offer a solution. We present data here characterizing and demonstrating the suitability of a novel optical platform used in conjunction with hiPSC-derived cardiomyocytes to assess NCE-mediated pro-arrhythmogenicity.

Cardiac electrical activity was monitored from spontaneously beating hiPSC-cardiomyocyte syncytia with di-4-ANEPPS at a 10kHz over 60 second time windows from 2-3 areas per well over 3 wells for both experimental and control values. Small molecule effects on Na<sup>+</sup>, hERG, and Ca<sup>2+</sup> channels were assessed and compared with time matched controls. Ion channel block by all agents produced dose-dependent changes in the expected AP parameters relative to controls. Na<sup>+</sup> channel block by 3μM mexiletine produced a 244±86% (n=3) increase in AP rise time, hERG channel block by 30nM E4031 produced a 39±14% (n=3) increase in APD90, and Ca<sup>2+</sup> channel block by 300nM nifedipine produced an approximate 50% shortening in APD90. Experimental measurements for a single compound were completed in less than 3 hours. Similar data was obtained across cellular manufacturing batches and experimental days. This dataset demonstrate that optical measurements of electrical activity on hiPSC-derived cardiomyocytes is a suitable methodology for assessing NCE arrhythmogenic potential with a robustness that approaches that of manual patch clamp and throughput that is an order of magnitude greater.

#### PS 86 Multiparameter In Vitro Assessment of Drug Effects on Cardiomyocyte Physiology Using iPSCs.

O. Sirenko<sup>1</sup>, C. Crittenden<sup>1</sup>, A. Blake<sup>2</sup>, I. Rusyn<sup>3</sup> and E. F. Cromwell<sup>1</sup>.

<sup>1</sup>*Molecular Devices LLC, Sunnyvale, CA*; <sup>2</sup>*Cellular Dynamics International, Madison, WI*; <sup>3</sup>*University of North Carolina at Chapel Hill, Chapel Hill, NC.*

Highly predictive in vitro assays suitable for high throughput screening (HTS) for potential cardiotoxicity are critical to drug safety testing. Adult human stem cell derived cardiomyocytes show promise for screening compounds during early drug development. We developed methods for measuring the impact of drug candidates on the beating rate of human iPSC derived cardiomyocytes using fast kinetic fluorescence imaging. Cardiomyocyte contraction rate and pattern are characterized by monitoring changes in intracellular Ca<sup>2+</sup> measured using calcium sensitive dyes. The assay was optimized for HTS and allows characterization of beating profiles by using multi-parameter analysis outputs such as beating rate, peak frequency and width, or waveform irregularities. The assay is suitable for assessment of short-term (minutes) and delayed (days) effects. Next, we tested known cardiotoxic compounds including alpha and beta blockers, hERG inhibitors, ion channel blockers, etc., as well as control drugs. IC50 values showed a significant rank correlation with published values determined by other cardiotoxicity models as well as good concordance with reported human plasma Cmax values. The assay was further tested using commercially available cardiotoxicity library representing different classes of compounds including receptor antagonists, ion channel blockers, anti-cancer and anti-inflammatory drugs, and kinase inhibitors. The estimated balanced prediction accuracy of the assay was greater than 80%, and multi-parameter characterization of beating profiles allowed identification of specific patterns defining hERG or Na channel blockers. We conclude that this assay shows utility for screening compounds for potential to cause arrhythmic and non-arrhythmic cardiotoxicity.

#### PS 87 Nucleoside Reverse Transcriptase Inhibitors Induced Premature Senescence in Aortic Endothelial Cells.

V. Y. Hebert, K. Slaybaugh, C. N. Robinson, S. Xue, D. Hayes, M. C. Glover and T. R. Dugas. *Pharmacology, LSU Health Sciences Center, Shreveport, LA.*

HIV patients undergoing antiretroviral therapy exhibit an increased incidence of cardiovascular events and their associated diseases. Though HIV therapy generally involves a combination drug approach, nucleoside reverse transcriptase inhibitors (NRTI) are considered a backbone of this therapy. Prior studies in rodents suggested that NRTI promote HIV-associated endothelial dysfunction, an initiating factor in atherosclerosis. Further, this cellular dysfunction was associated with mitochondrial injury. In cultured endothelial cells, NRTI treatment increased mitochondrial ROS production, while decreasing ATP production and the activities of mitochondrial electron transport chain (ETC) complexes I-IV. While these effects were observed for acute treatment, in other studies, we noted that when the mitochondria were exposed to low doses of NRTI, damaged mitochondria were removed through a process known as mitophagy. Thus, our hypothesis was that with chronic treatment, this repair mechanism may be overwhelmed, so as to promote premature endothelial senescence. In these studies, human aortic endothelial cells (HAEC) were exposed to chronic NRTI treatment. ROS production, cell proliferation rate and levels of senescence were determined. Our findings were that NRTI treatment increased ROS production, at least initially. Also, the rate of cell proliferation decreased from passage 1 to passage 8, and the level of NRTI-induced senescence increased. In addition, co-treatment with the mitochondrial antioxidant coenzyme (Q10) resulted in a delayed onset of senescence. In conclusion, long term NRTI treatment resulted in ROS production, reduced cell proliferation rate and premature endothelial senescence. Moreover, our findings may suggest approaches for reducing the cardiovascular side effects of NRTI therapy.

#### PS 88 Fluoride Prevents Ectopic Calcification of Vascular Cells through Inhibition of Crystal Nucleation.

A. Martin-Pardillos<sup>1</sup>, A. Millan<sup>2</sup> and V. Sorribas<sup>1</sup>. <sup>1</sup>*Laboratory of Molecular Toxicology, University of Zaragoza, Zaragoza, Spain*; <sup>2</sup>*Institute of Materials Science, CSIC, Zaragoza, Spain*. Sponsor: A. Anadon.

Fluoridation of public water to improve dental and bone health can involve a risk during degenerative processes such as ectopic calcification.

We have analysed the effect of fluoride (F) on the calcification of rat aortic vascular smooth muscle cells. Cytotoxicity in vitro was determined by a lactate dehydrogenase (LDH) assay. F did not affect cell viability at the normal plasma concentrations of fluoridation (2.5-10 μM), but surprisingly, it reduced the cell death generated during calcification conditions. 5 and 10 μM fluoride also decreased the

calcification caused by 2 mM Pi by 25 and 59% in VSCMs, respectively. A dose-response relationship of calcification inhibition with increasing concentrations of pyrophosphate (PPi) revealed that the IC50 shifted from 4.26  $\mu$ M to 2.14 in the presence of 5  $\mu$ M NaF, therefore indicating that less PPi is necessary to prevent calcification when F is present in the calcification medium. Similar effect was obtained with phosphonoformic acid.

Electron microscopy (TEM, SEM, ED and EDS) observations have revealed that the calcification deposits consist of spherulites of intergrowth particles that had an amorphous character, a low density, and a laminar particle shape, in the absence of F-. With increasing F- concentration, the deposits turn more dense and compacted, while the particle shape becomes clearly fibrillar. F is not incorporated in the deposits, therefore suggesting a modification of crystallization process and inhibition of nucleation, which could explain the prevention of calcification. This effect was similar both in living and dead (fixed) cells, which indicates an intrinsic effect of F-ions on the calcification process independent of cellular activity. Furthermore, F- decreases the Pi-induced expression of osteogenes, most likely as the consequence of the reduced calcium phosphate deposits.

In conclusion, F addition to drinking water can have a beneficial effect in preventing vascular calcification originated during hyperphosphatemic conditions.

## PS 89 Development of an *In Vitro* Multiwell Cardiovascular Microelectrode Array (MEA) Toxicity Assay with Human IPS-Derived Cardiomyocytes.

S. Qin<sup>1</sup>, J. Ross<sup>2</sup>, M. Brock<sup>2</sup>, J. Bradley<sup>1</sup>, H. Luthardt<sup>1</sup>, J. Gilbert<sup>1</sup> and C. Strock<sup>1</sup>. <sup>1</sup>Cyprotex, Watertown, MA; <sup>2</sup>Axion Biosystems, Atlanta, GA.

Cardiotoxicity represents the most common reason for attrition of compounds due to toxicity. Current *in vitro* assays fail to predict the many causes of cardiac toxicity. Cytotoxicity assays only identify the most overtly toxic compounds, while assays to measure more specific liabilities such as hERG or other ion channels measure only a specific risk target, potentially missing the overall physiological response a compound elicits in cardiac cells. Additionally, *in vivo* animal studies rely on determination of compound activity in a different species, which does not always model human responses. Therefore, an ideal assay would screen compounds in human cardiomyocytes and provide a comprehensive assessment of their effects on electrophysiology. Here we demonstrate the successful use of multiwell MEAs to screen for cardiotoxic liabilities in human IPS derived cardiomyocytes (hsCM). MEAs measure the electrical activity in cells and therefore can be used to capture the field potential of the cardiomyocytes, producing a virtual EKG. This data can then be extracted to report effects of test compounds on the different phases of the heart-beat. Response endpoints that can be reported include: field potential duration ("QT"), conduction velocity, beat rate, as well as field potential metrics (Amplitude, Slope, etc.). The recent development of the multiwell MEA has allowed for an increased throughput for cardiotoxicity screening as well as the ability to generate dose curve responses for each compound. Here we demonstrate the different electrophysiological responses observed when we test compounds with different targets and liabilities (hERG, other ion channels, etc.). The compounds tested are E4031, Nifedipine, Sotalol, isoproterenol, Ouabain, Mexiletine, ZD7288, Amitriptyline, Cisapride, Terfenadine, and Verapamil. In summary, we show that use of multiwell MEAs with hsCM is highly effective for screening test compounds for toxic liabilities.

## PS 90 Development of Improved hESC-Based High-Throughput Screening Assays for Cardiotoxicity Assessment.

H. Xian, C. Blanco, J. Lam and R. Snodgrass. VistaGen Therapeutics Inc., South San Francisco, CA.

The limitations of current pre-clinical drug testing systems contribute to the high failure rate of drugs. Unexpected human cardiotoxicity is one of the two major reasons for failure of drugs and drug candidates due to safety concerns. Incorporating human embryonic stem cell-derived cardiomyocytes (hESC-CMs) assays into the pre-clinical drug development offers the potential to improve the predictability of toxicity and efficacy testing and to decrease drug development costs. Our goal is to utilize hESC-CMs to develop reproducible and predictive assays for cardiac function and toxicity prediction. We have developed protocols that, without selection, reproducibly yield >80% hESC-CMs that function reliably in various established, and newly developed, assays relevant to cardiac drug effects. In addition, the CD172a cell surface marker enables the production of substantially pure (>95%) hESC-CMs. Here we expand our previous electrophysiological assessments, and describe the development of a series of fluorescence or luminescence based high-throughput assays that were used to assess drug-induced necrosis, apoptosis, mitochondrial toxicity and oxidative stress of hESC-CMs. These assays were validated using well-known cardiotoxic compounds. These compounds include inhibitors of

various kinases, DNA intercalating agents, hERG trafficking blockers and K<sup>+</sup> channel blockers. These assays were able to measure drug effects, with high sensitivity, consistent with known biology of the compounds. In addition, a medium throughput multi-electrode array (MEA) system was used to evaluate electrophysiological functions of the hESC-CMs. The effects of selective ion channel blockers and compounds associated with QT prolongation on field potentials and beat rates were assessed. The observed cardiac electrophysiology was reproducible and consistent with the known effects of the compounds. Our data suggest that these hESC-CM based screening systems are valuable tools for preclinical cardiac safety screening, which we believe will contribute to the efficient and rapid identification of safer drugs.

## PS 91 Vascular Effects Induced by 15nm Gold Nanoparticles in Isolated Rat Aortic Rings.

M. Gonzalez Castillo<sup>1,2</sup>, S. Salazar-García<sup>1</sup>, D. Maldonado Ortega<sup>1</sup>, G. Palestino Escobedo<sup>1</sup>, M. Ramirez Lee<sup>1</sup>, A. Mendez Mancilla<sup>1</sup> and S. F. Ali<sup>2</sup>. <sup>1</sup>Universidad Autonoma de San Luis Potosí, San Luis Potosí, Mexico; <sup>2</sup>National Center for Toxicological Research, US FDA, Jefferson, AR.

Gold nanoparticles (AuNPs) have been used in biomedicine as therapeutic tool. However, their role on the vascular physiology, have not been fully studied. The purpose of the present work was to evaluate the effects of 15 nm AuNPs on the vasculature, using a rat aortic rings model, pre-contracted with phenylephrine, a well known contractile agent. Adult male Sprague Dawley rats were sacrificed; aorta was excised, and maintained in an organic bath chamber with physiological solution. Each individual aorta rings were treated under isometric conditions, in presence and absence of endothelium (E), along with increasing concentrations (0.1-100  $\mu$ g/mL) of AuNPs. AuNPs exerted a vasodilator effect independent on E, the relaxation was exerted in the same magnitude that was found in presence of E. Relaxation induced by the Au-NPs were not dependent on nitric oxide (NO), since, L-Nitro-arginine methyl ester (L-NAME), an inhibitor of the NO production and a potent vasodilator mediator, did not block this effect. However, a pretreatment with indomethacin, an inhibitor of prostanooids synthesis, blocked partially the vasodilation induced by AuNPs, suggesting that prostanooids could be, at least in part, mediators of these actions. Further studies are underway to evaluate the mechanisms of action which are underlying the relaxation induced by AuNPs, and the implications that they could confer in the cardiovascular physiology.

## PS 92 Nano-Cerium Dioxide Exposure and Arteriolar Dysfunction: Exposure Route Dependency.

T. R. Nurkiewicz<sup>1</sup>, P. A. Stapleton<sup>1</sup>, E. M. Sabolsky<sup>2</sup> and V. C. Minarchick<sup>1</sup>.

<sup>1</sup>Center for Cardiovascular and Respiratory Sciences, West Virginia University, Morgantown, WV; <sup>2</sup>Mechanical Engineering, West Virginia University, Morgantown, WV.

Nano-cerium dioxide (CeO<sub>2</sub>) is being used or developed as a fuel catalyst (diesel), a protective drug (radiation and ischemia) and as a contrast agent (medical imaging). These diverse uses possess the potential for human exposures that are beyond the well studied pulmonary route. Our laboratory has assessed the arteriolar effect of nano-CeO<sub>2</sub> 24hrs post-pulmonary exposure; however, other routes of exposure such as systemic and gastrointestinal have not been investigated. Therefore, our aim was to analyze the microvascular effects of nano-CeO<sub>2</sub> via instillation, injection, and gavage. Sprague-Dawley rats were intratracheally instilled (100  $\mu$ g), intravenously injected (100 or 900 $\mu$ g), or gavaged (100 or 600 $\mu$ g) with nano-CeO<sub>2</sub> suspended in Normosol (5% serum). 24hrs later the mesentery was harvested, and 4<sup>th</sup> or 5<sup>th</sup> order arterioles were dissected and prepared for isolated vessel experiments. Arteriolar reactivity was evaluated by determining endothelium-dependent (acetylcholine, 10<sup>-9</sup>-10<sup>-4</sup>M), and -independent dilation (spermine NONOate, 10<sup>-9</sup>-10<sup>-4</sup>M), vasoconstriction [phenylephrine (PE), 10<sup>-9</sup>-10<sup>-4</sup>M], and mechanotransduction [myogenic responsiveness (0-105 mmHg) and shear stress (0-30 $\mu$ l/min)]. Endothelium-dependent and -independent dilation for all three exposure routes (instillation: 30% and 50%, injection: 45% and 55% and gavage: 36% and 64% vs sham arterioles, respectively) was significantly impaired. Arteriolar responsiveness to PE or pressure was unaltered for the exposure routes. There was an impaired dilation in response to flow for the rats injected or gavaged (53% and 35% vs sham, respectively). This arteriolar dysfunction was exposure route dependent because little to no arteriolar dysfunction was observed in rats injected or gavaged with 100 $\mu$ g of nano-CeO<sub>2</sub> as compared in instilled rats. These results provide evidence that microvascular dysfunction is present 24hrs after nano-CeO<sub>2</sub> exposure and is dependent on the exposure route.

NIH-RO1-ES015022, RC1-ES018274(TRN) and NSF-1003907(VCM)

**PS 93 Simulated Metabolism in the Langendorff Isolated Rat Heart: A Comparison of Novel and Traditional Dosing Techniques for 5-Fluorouracil and Doxorubicin.**

J. B. Ross, K. A. Henderson, R. Borders, P. S. Hong, W. M. Black and B. M. Roche. *Battelle, Columbus, OH.*

There is a clear need for more predictive and translatable assays in early drug discovery. It is important to take a multi-scale approach to translate data to pre-clinical and clinical trials. The Langendorff isolated heart model provides a tool to assess cardiotoxicity in the whole organ in the absence of in-vivo variables. We used the Langendorff to assess both acute and latent cardiotoxicity of 5-fluorouracil (5-FU) and doxorubicin. Physiologically Based Pharmacokinetic (PBPK) models were developed to determine clinically relevant doses. A reverse extrapolation from human physiological and physiochemical parameters to rat was performed. The resulting pharmacokinetic (PK) curves led to some challenging dose considerations; both 5-FU and doxorubicin are rapidly cleared in humans and rats, never reaching a steady state. Other PK parameters such as Area Under the Curve (AUC) and the maximum concentration (Cmax) pose problems as well. AUC will accurately represent the total amount of drug over a given period of time; however, a single concentration derived from the AUC could potentially underestimate a biological response. In contrast, Cmax would greatly overestimate the total amount of drug, potentially leading to false toxicity. Computer generated dosing schemes were developed and characterized in an effort to fit the modeled PBPK curves. Initial concentrations (Cmax) were diluted with deionized water and perfused through the Langendorff system in the absence of a heart. Perfusate was collected at various time points, analyzed with HPLC, and concentration curves were generated for proof of concept. An acceptable fit was observed between the computer generated and the tested curves. This dosing technique was applied to an isolated rat heart; multiple endpoints were collected and compared to previous data collected at constant perfusion concentrations. The novel dose schemes proved to be a better representation of in-vivo concentrations in our ex-vivo model.

**PS 94 Oxidative Stress Uncovers  $\beta$ 2-Adrenergic Mediated Dilation to Curcumin Mimicked by Preventing Clathrin Endosome Formation.**

M. Frame<sup>1,2</sup>, B. Calizo<sup>2</sup>, A. M. Dewar<sup>1</sup> and S. Scarlata<sup>2</sup>. <sup>1</sup>*Biomedical Engineering, Stony Brook University, Stony Brook, NY;* <sup>2</sup>*Physiology/Biophysics, Stony Brook University, Stony Brook, NY.* Sponsor: T. Nurkiewicz.

The nutraceutical, curcumin, has anti-oxidative properties, but also is a potent adrenergic receptor (AR) agonist, with an EC50 for dilation in the nM range (beta, bAR). Our goal was to determine how oxidative stress impacted vasoactive responses to curcumin. Intravital microscopy of small arterioles in the hamster cheek pouch was performed (N=10; pentobarbital 70mg/kg i.p.). Oxidative stress (OX) was induced by applying exogenous nitric oxide for 2 minutes in the tissue bath. Before OX, dilation to micropipette applied curcumin was dose dependent, with a maximum from 10-9 to 10-6M. After OX, dilation was eliminated in the nM and higher range, and significantly left shifted to a narrow peak from 10-15 to 10-10M, which was inhibited by the  $\beta$ 2-adrenergic receptor inverse agonist, carazolol (1nM). We next tested whether preventing clathrin endosome formation with dynasore altered dilation to curcumin. Dynasore (80uM) alone eliminated dilation to curcumin in the uM range, and uncovered a dilation in the pM range. Dynasore with OX further increased the potency, and increased the efficacy of dilation to curcumin over the range 10-15 to 10-10M. To understand the mechanism of this OX induced narrow potency range, we tested whether curcumin and the bAR were internalized and co-localized using FRET in HEK cells. Before OX, curcumin was rapidly internalized (seconds), and co-localized with bAR. After OX (1mM CoCl<sub>2</sub>), curcumin was internalized, but bAR remained at the plasma membrane. Thus, in cells, OX prevented internalization of curcumin with bAR. In situ, inhibition of clathrin endosome formation mimicked and enhanced the vasoactive responses after OX. (AHA 0655908T)

**PS 95 Diminished Oxygen Supply in Microvessels following Inflammatory Oxidative Stress.**

A. M. Dewar, M. Frame, N. Zhou and C. Du. *Biomedical Engineering, Stony Brook University, Stony Brook, NY.* Sponsor: T. Nurkiewicz.

Increased heterogeneity of flow accompanies many inflammatory states, including oxidative stress (OX) with toxicant exposure or thermal injury. Red blood cell (RBC) flux along nutrient flow paths is an indicator of oxygen delivery; many inflammatory mediators result in a specifically located arteriole-venule RBC shunt pathway. Our goal was to directly measure oxy- vs deoxy-hemoglobin (HbO v

HbR) to determine whether OX induced shunt paths resulted in heterogeneity of oxygen supply. A controlled thermal burn model in the hamster cheek pouch tissue localized OX so that unequivocal control vs OX spatial locations could be observed. Adult male hamsters (N=10, isoflurane) were prepared for intravital microscopy of the cheek pouch tissue. Fluorescently labeled RBC flow markers confirmed shunt pathways after a thermocouple controlled 50 degree C 300um spot burn (same location before vs 15m-1hr after, within 500um of burn rim). Multi-wavelength laser speckle contrast imaging was used (1-2h after burn) to determine HbO and HbR at 630 and 570nm at locations within 500um of the burn rim (near) vs. locations >1mm from the burn rim (far); values of changes in HbO and HbR were obtained in [Hb] mM. Total Hb in the large vessels was consistent with a local tube hematocrit of 5-40%, as is typically found using fluorescent RBC. HbO was 30% less in perfused large arterioles near vs far from the burn, and 24% less in perfused large venules near vs far from the burn. Within the terminal arteriolar networks far from the burn, HbO is 7% higher along the shunt pathway vs the non-shunt pathway, consistent with RBC flux values. Near the burn, HbO is 71% greater along the shunt pathway vs the non-shunt pathway, also consistent with RBC flux values. Comparing HbO along shunt pathways, HbO is decreased 52% near vs far from the burn rim. Thus, in this model of inflammation, RBC flux and HbO values together suggest that a diminished oxygen shunt pathway is initiated by inflammation and maintained for several hours after the inflammatory event. (NIH HL55492; AHA 0655908T)

**PS 96 Validation of the Amphibian Metamorphosis Assay for Potential Endocrine Disrupting Chemicals with Xenopus Laevis.**

J. J. Burlingham, C. A. Jenkins, J. Pawsey, I. Taylor and L. Haynes. *Aquatic Ecotoxicology and Biodegradation, HLS, Eye, United Kingdom.* Sponsor: C. Auletta.

The new European Union Plant Protection Products Regulation (PPPR 1107/2009) identifies the need to consider whether a substance is a potential endocrine disrupter in aquatic non-target organisms and the current draft of the PPP data requirements refers to three screening assays for ecotoxicological endocrine-disrupting potential. Of these, we describe in detail our experience in the establishment and validation of the amphibian metamorphosis assay (OECD 231; OPPTS 890.1100) with the African Clawed Frog.

In this method, in order to satisfy validity criteria in the rearing phase, conditions necessary to allow tadpoles to develop from fertilisation to development stage 51 as defined by Nieuwkoop and Faber (1994) were established, and individuals selected for the exposure phase and transferred to test vessels. To establish the assay, 400 tadpoles were exposed to a range of levels of the three reference substances, thyroxine (T<sub>4</sub>) which produces stimulatory effects on the normal function of the hypothalamic-pituitary-thyroid (HPT) axis, sodium perchlorate (which retards development) and iopanoic acid (which affects hind limb development) and levels of each were verified using an appropriate analytical method. At Day 7, 80 randomly selected individuals at each exposure level were removed and assessed (body weight, developmental stage, hind limb and snout to vent length). Exposure continued for a further two weeks and the study terminated on Day 21 when all the remaining individuals were assessed as on Day 7. Following developmental stage matching, 80 individuals were selected for thyroid removal and histopathological analysis.

We found that our results were similar to the ring test results published by the OECD (Series on Testing and Assessment Document Number 77) and make a number of observations on methodology that may improve the reproducibility of these assays.

**PS 97 Mammary Gland Morphology and Gene Expression Signature of Prepubertal Male and Female Rats following Exposure to Exogenous Estradiol.**

M. Ronis<sup>1,2</sup>, I. R. Miousse<sup>1,2</sup>, N. Sharma<sup>2</sup>, J. Vantrease<sup>2</sup>, L. Hennings<sup>1</sup>, K. Shankar<sup>1,2</sup>, H. Gomez-Acevedo<sup>1,2</sup>, M. Cleves<sup>1,2</sup> and T. M. Badger<sup>1,2</sup>. <sup>1</sup>*UAMS, Little Rock, AR;* <sup>2</sup>*Arkansas Children's Nutrition Center, Little Rock, AR.*

In order to properly understand whether xenoestrogens act as true estrogen agonists, it is essential to possess a solid portrait of the physiological effects of exogenous 17 $\beta$ -estradiol (E2). Because the estrogen-dependent gene expression is one of the primary indicators of estrogenic action, we have assessed effects of three doses of exogenous E2 (0.1, 1.0 and 10  $\mu$ g/kg of body weight/day) on the mammary gland morphology and gene expression profiles of prepubertal male and female rats of both sexes compared to untreated controls. The mammary gland was more responsive to E2 treatment in males than in females with 1392 genes modulated >1.5-fold up or down relative to controls at the highest E2 dose compared to 463 genes. There

was an increase in the number of terminal end buds in males ( $P < 0.05$ ), and a corresponding increase in the expression of the gene encoding amphiregulin ( $P < 0.05$ ), a protein known to drive the differentiation of terminal end buds. In intact females, the highest dose of E2 tested induced an increase in the expression of genes encoding milk components, as well as muscle proteins. Lower doses had limited effects on gene expression. Therefore, the prepubertal rat male mammary gland is a very sensitive tissue to evaluate estrogenicity using morphological changes coupled to microarray-analysis of gene expression. Intact prepubertal females were comparatively poorly responsive to exogenous E2, although many modulated genes were common to both sexes. Supported by USDA CRIS-6251-51999-007-04S.

## PS 98 Potential Endocrine Disruption of a Drinking Water Sample from the State of São Paulo, Brazil.

M. M. Solano<sup>1</sup>, C. M. Raimundo<sup>2</sup>, I. C. Pescara<sup>2</sup>, W. F. Jardim<sup>2</sup>, D. D. França<sup>3</sup>, G. A. Quinaglia<sup>3</sup>, J. A. Anselmo-Franci<sup>4</sup>, R. G. Carolino<sup>4</sup>, J. L. Luvizutto<sup>1</sup>, G. A. Umbuzeiro<sup>5</sup> and J. V. de Camargo<sup>1</sup>. <sup>1</sup>Botucatu Medical School, Department of Pathology, São Paulo State University- UNESP, Botucatu, Brazil; <sup>2</sup>Institute of Chemistry, University of Campinas- UNICAMP, Campinas, Brazil; <sup>3</sup>Environmental Toxicology, Genotoxicity and Microbiology Division - CETESB, São Paulo, Brazil; <sup>4</sup>School of Dentistry, Department of Morphology, Stomatology and Physiology, University of São Paulo- USP, Ribeirão Preto, Brazil; <sup>5</sup>Faculty of Technology, University of Campinas- UNICAMP, Limeira, Brazil.

Many xenoestrogens, natural and synthetic estrogens may end up in the water bodies through sewage discharges. Contaminated rivers are conventionally treated by Water Treatment Plants (WTP) to produce drinking water, but emerging contaminants may remain. This study investigated the potential for endocrine disruption of a drinking water sample from a São Paulo State WTP, using two harmonized bioassays. Female rats 21 days old were exposed by gavage to drinking water extracts during 03 days (uterotrophic assay; OECD 440) or 20 days (pubertal development female rat assay, EPA 890.1450) at 33.3, 166.5, and 333.0 mL equivalent of water/kg body weight, modeling a daily ingestion of 2 L, 5 L and 10 L of drinking water by a 60 kg human being. Traces of caffeine (5.8 ug/L), estrone (1 ng/L) and atrazine (11.2 ng/L) were detected in the extracts by LC-MS/MS. Androgen or estrogen agonistic activity of the water extract resulted negative by the bioluminescent yeast assay (BLYES, BLYAS). Accordingly, both in vivo assays were negative: there was no significant increase of the uterus wet weight in the uterotrophic assay and no alteration of the moment for vaginal opening in the pubertal assay. However, the serum levels of LH, FHS, PRL and 17 $\beta$ -estradiol were altered, with a significant dose-response increase. Therefore, it has to be assumed that the tested drinking water sample induced steroidogenic dysregulation in vivo.

## PS 99 Development of Medium-Throughput Thyroperoxidase Inhibition Assays for Screening.

K. B. Paul<sup>1,2</sup>, J. M. Hedge<sup>2</sup>, K. M. Crofton<sup>2</sup>, M. W. Hornung<sup>3</sup> and S. O. Simmons<sup>2</sup>. <sup>1</sup>ORISE, US EPA, Research Triangle Park, NC; <sup>2</sup>Integrated Systems Toxicology Division, NHEERL, ORD, US EPA, Research Triangle Park, NC; <sup>3</sup>Mid-Continent Ecology Division, NHEERL, ORD, US EPA, Duluth, MN.

Thyroperoxidase (TPO), the catalyst for thyroid hormone (TH) synthesis, is a target for thyroid-disruptors, including methimazole (MMI), isoflavones, benzophenone-2, and malachite green; however, no medium- to high-throughput screening methods for TPO inhibition are available. To adapt the low-throughput guaiacol oxidation assay for TPO inhibition to chemical screening, we replaced guaiacol with a fluorescent peroxidase substrate in a rat thyroid-based assay and developed an in vitro human TPO model. We tested the hypothesis that use of a peroxidase substrate (Amplex UltraRed, AUR, LifeTech) in 96- or 384-well plate formats with automated reagent delivery could increase the TPO assay throughput with thyroid microsomes. The IC<sub>50</sub> of MMI-induced TPO inhibition was reduced with AUR compared to the guaiacol assay, with average IC<sub>50</sub>s of 0.15  $\mu$ M and 5  $\mu$ M, respectively. AUR signal was stable from 30-120 min after initiation. The dynamic range of the assay with MMI was 6- to 10-fold using 96- or 384-well formats, with Z' scores of 0.75 to 0.9. A 21 chemical training set is being used to validate the assay for screening. One limitation of this model is the availability of human thyroid microsomes. Preliminary work demonstrated that lentiviral-transduction of a human cell line (HEK293T) with recombinant TPO could also be used to test for human TPO inhibition. TPO activity measured by the AUR assay in cell fractions was maximally inhibited by MMI at 100  $\mu$ M. This approach to improving and developing medium-throughput assays for thyroid-disruptor screening demonstrates the feasibility of screening 100s to 1000s of chemicals for TPO inhibition, and drastically reduces the need for animal tissue. This abstract does not necessarily reflect the policy of the US EPA.

## PS 100 High-Throughput Detection of Estrogenic Compounds Using Autonomously Bioluminescent Human Breast Cancer Cells.

T. Xu<sup>1</sup>, D. Close<sup>2</sup>, S. L. Price<sup>1</sup> and G. S. Saylor<sup>1,2</sup>. <sup>1</sup>The University of Tennessee, Knoxville, TN; <sup>2</sup>490 BioTech Inc., Knoxville, TN. Sponsor: S. Ripp.

Substantial public health concerns exist over the potential endocrine disrupting capabilities of a wide variety of untested or under-tested natural and industrial chemicals. It is clear that the development of accurate, high-throughput, and inexpensive testing regimens will be key to mitigating public concern. Here we report on the development of a novel screening assay for estrogenic activity that utilizes an autonomously bioluminescent human cell line to provide direct bioavailability data. To construct this cell line, estrogen-responsive human breast carcinoma cells (T-47D) were genetically engineered to express the full bacterial bioluminescence gene cassette (*luxCDABEfp*), generating an autonomously bioluminescent cell line (T-47D/Lux) capable of maintaining bioluminescent output independent of substrate addition. Bioluminescence emitted from T-47D/Lux cells was correlated tightly ( $R^2 > 0.99$ ) to the number of cells present in a population, permitting the use of light production dynamics as an indicator of cell proliferation. Additionally, the substrate-free nature of the lux system allowed for continuous, near real-time monitoring of the same cell population throughout exposure to the tested compounds. A significant change in bioluminescent production ( $p < 0.05$ ) compared with unexposed control was observed 3 days after exposure to concentrations of 17 $\beta$ -estradiol (E2) as low as 1 pM. The EC<sub>50</sub> for E2 in this assay was determined to be approximately 10 pM. These results are similar to those obtained using a traditional cell proliferation assay, but offer the advantage that data acquisition can be performed in a fully automated fashion since the need for sample destruction or substrate addition is removed, making it an ideal candidate for high-throughput analysis.

## PS 101 Cryopreserved Rainbow Trout Hepatocytes Model Endocrine Disruption As Detected by Protein and Gene Expression of Vitellogenin.

L. K. Markell, R. T. Mingoia, H. M. Peterson, J. P. Finn, D. L. Nabb and X. Han. DuPont Haskell Global Centers for Health and Environmental Sciences, Newark, DE.

The toxicity of environmental pollutants may occur through modes of action that alter normal endocrine functions, resulting in altered development, growth and reproduction of aquatic species. Consequently, there is a need to develop assay endpoints capable of identifying endocrine disruption in fish. Our lab has previously shown the utility of cryopreserved trout hepatocytes. Here we use this cell culture method to identify the potential estrogenicity of chemicals through vitellogenin (VTG) expression. This biomarker indicates an estrogenic effect when the protein is expressed by male trout hepatocytes, both in vivo in plasma and in vitro in cell culture media. To test the performance of cryopreserved trout hepatocytes, reference chemicals estradiol (E2), estrone (E1) and diethylstilbestrol (DES) were used and culture media was collected for ELISA 96-hrs post-treatment. Our results show that the levels of protein detected with cryopreserved trout hepatocytes are similar to results previously published using fresh trout hepatocytes, ranking the compounds E2  $\geq$  DES  $>$  E1. To determine whether transcriptional regulation of VTG correlated with protein expression, quantitative real-time PCR was performed. mRNA was collected from cryopreserved hepatocytes treated for 24 hours with the same doses of reference chemicals. VTG gene expression correlated well with protein expression, ranking the compounds similarly. In addition, the negative control corticosterone showed no increase in gene expression at any dose, indicating that this is a sensitive, yet specific endpoint. These studies demonstrate both ELISA and transcription-based methods can be used with cryopreserved trout hepatocytes for screening chemicals for potential estrogenic effects, enabling greater access to this model system and potentially improving the turn-around time for generating results through detection of VTG mRNA levels.

## PS 102 Permethrin Does Not Have Endocrine Disrupting Properties As Evaluated by the US EPA's Endocrine Disruptor Screening Program (EDSP) In Vivo Assays.

L. Zorrilla<sup>1</sup>, S. J. Borghoff<sup>1</sup> and T. G. Osimitz<sup>2</sup>. <sup>1</sup>Integrated Laboratory Systems, Inc, Durham, NC; <sup>2</sup>Science Strategies, Charlottesville, VA.

Permethrin, a pyrethroid insecticide, was evaluated for potential endocrine activity in 3 of 4 in vivo US EPA EDSP assays. The maximum tolerated dose (MTD) of permethrin used in these assays was selected based on the results of dose range finding studies. Sprague Dawley rats were administered permethrin in corn oil by oral gavage for 10 (Hershberger Bioassay, OPPTS 890.1400, castrated model), 21/22

(female pubertal assay, OPPTS 890.1450), or 31/32 (male pubertal assay, OPPTS 890.1500) days based on daily body weights. The Hershberger Bioassay, which evaluated agonist and antagonist androgenic activity, was negative; no significant changes in any androgen-dependent tissue weights up to the MTD of 120 mg/kg/day were observed. The male pubertal assay, administered a MTD of 120 mg/kg/day, showed no effects on male pubertal development with no differences observed in reproductive organ weights, the day of preputial separation, or serum testosterone levels compared to controls. Liver weight was significantly increased, with a decrease in thyroxine ( $T_4$ ) and a corresponding increase in thyroid stimulating hormone (TSH) compared to controls. No changes were observed in thyroid gland weights or histopathology. The female pubertal assay, administered a MTD of 150 mg/kg/day, showed no effects on female pubertal development with no differences observed in the day of vaginal opening, estrus onset, cyclicity, or reproductive organ weights. The liver and thyroid gland weights were significantly increased, and serum TSH concentrations were increased with a corresponding decrease in serum  $T_4$  following administration permethrin, however, the thyroid gland showed no histopathological changes. In summary, permethrin did not show androgen or estrogen activity in these assays, and the effects observed in the thyroid likely are secondary to liver enzyme induction, a phenomenon known to occur following repeated dosing with permethrin, and not a reflection of a direct effect on the thyroid.

### PS 103 Linking *In Vitro* Enzyme Activity To *In Vivo* Effects: Thyropoxidase Inhibition in Methimazole-Exposed Rats.

J. M. Hedge<sup>1</sup>, K. M. Crofton<sup>1</sup>, S. O. Simmons<sup>1</sup>, M. W. Hornung<sup>2</sup> and K. B. Paul<sup>1,3</sup>. <sup>1</sup>Integrated Systems Toxicology Division, NHEERL, ORD, US EPA, Research Triangle Park, NC; <sup>2</sup>Mid-Continent Ecology Division, NHEERL, ORD, US EPA, Duluth, MN; <sup>3</sup>Oak Ridge Institute for Science Education, US EPA, Research Triangle Park, NC.

The anti-thyroid drug methimazole (MMI) inhibits thyropoxidase (TPO), the enzymatic catalyst for thyroid hormone (TH) production and a target for thyroid-disrupting chemicals. Our development of a medium-throughput screening assay for TPO inhibitors using a fluorescent peroxidase substrate (Amplex UltraRed) has instigated characterization of the relationship between *in vitro* TPO inhibition using thyroid microsomes and *in vivo* TH status. This work tested the hypothesis that TPO activity would be decreased in thyroids from rats exposed *in vivo* to MMI doses that decreased serum THs. Weanling female Long-Evans rats received MMI in corn oil (0, 0.1, 0.3, 1, 10, 20, 30 mg/kg/day po) for 4 days and were sacrificed 24 hr later. Pooled thyroid microsomes (n=8/pooled treatment) were used in the TPO inhibition assay. As a positive control, the vehicle control microsomes were exposed *in vitro* to MMI (0.015 – 200  $\mu$ M), which yielded an assay dynamic range of 6-fold, an IC<sub>50</sub> = 0.14  $\mu$ M, and Z' = 0.9. TPO was inhibited in a dose-dependent manner, up to 53% of vehicle control at 30 mg/kg/day, which corresponded to significant serum thyroxine ( $T_4$ ) decreases of 60% and thyroid gland weight increases of 64% (p<0.05). TPO inhibition in the 10-30 mg/kg/day MMI corresponded to *in vitro* MMI concentrations of 0.14-0.44  $\mu$ M. These results suggest that MMI-induced serum  $T_4$  decreases *in vivo* correspond to significant TPO activity decreases *in vitro*. Continued work will aim to strengthen understanding of the association between the degree of TH perturbation *in vivo* and the magnitude of TPO inhibition in the AUR screening assay. This abstract does not necessarily reflect the policy of the US EPA.

### PS 104 Endocrine Disruption Potential of Benfenin: Weight of Evidence Evaluation.

S. Papineni<sup>1</sup>, K. K. Coady<sup>2</sup>, S. Marty<sup>2</sup>, V. J. Kramer<sup>1</sup> and S. C. Gehen<sup>1</sup>. <sup>1</sup>Dow AgroSciences, Indianapolis, IN; <sup>2</sup>The Dow Chemical Company, Midland, MI.

Benfenin, a pre-emergent herbicide, was included on List 1 of chemicals to be screened under US EPA's Endocrine Disruptor Screening Program (EDSP). Following completion of 11 Tier 1 EDSP assays, a Weight of Evidence (WoE) evaluation was conducted using all available data to determine if benfenin has potential to interact with the estrogen, androgen or thyroid (EAT) systems following the five (5) – tiered OECD conceptual framework. For the *in vitro* assays, benfenin was negative for androgen and estrogen receptor binding, and negative in the aromatase and steroidogenesis assays but induced a weak positive response in the estrogen receptor transactivation assay (ERTA). However, this slight positive response in the ERTA assay was not corroborated in other estrogen sensitive assays estrogen receptor (ER) binding, uterotrophic, estrogen-sensitive endpoints in the female pubertal, and vitellogenin levels in the fish short-term reproduction assay (FSTRA) that were negative. Anti-androgenic and anti-estrogenic effects were observed in the pubertal assays and in the Hershberger assay only at the high dose levels. However, the WoE evaluation of the data does not support a direct interaction; rather, an indirect mode-of-action (MoA) due to enhanced liver enzyme induction and hormone

clearance appears evident. Similarly, results for thyroid effects in the pubertal assays were consistent with previously demonstrated MoA data which support an indirect MOA due to enhanced thyroxine clearance not relevant to humans. Furthermore, benfenin was negative in the amphibian metamorphosis assay designed to detect thyroid agonists and antagonists. A high-degree of coherence and consistency is observed in results from the higher-tiered data and previous toxicity studies showing no direct interaction with the endocrine system. In conclusion, the vast majority of Tier 1 studies/endpoints were clearly negative and those few positive responses were seen only at high-dose levels and were either isolated (e.g., ERTA) in nature or secondary to other effects.

### PS 105 Endocrine Exposure at Environmentally-Relevant Concentrations.

K. C. Fussell<sup>1</sup>, S. Schneider<sup>1</sup>, S. Melching-Kolmuss<sup>2</sup>, S. Gröters<sup>1</sup>, V. Strauss<sup>1</sup>, B. Siddeek<sup>3</sup>, M. Benahmed<sup>3</sup>, M. Frericks<sup>2</sup> and B. van Ravenzwaay<sup>1</sup>. <sup>1</sup>Experimental Toxicology and Ecology, BASF SE, Ludwigshafen am Rhein, Germany; <sup>2</sup>Product Safety, BASF SE, Ludwigshafen am Rhein, Germany; <sup>3</sup>U895, équipe 5, Centre Hospitalier l'Archet 2, Inserm, Nice, France.

Endocrine disruption has become an important topic of public concern. Despite an increasing amount of attention, little is understood about how doses of endocrine disrupting chemicals (EDCs) at environmental concentrations affect homeostasis. To address these concerns, we performed a pre-/post-natal reproductive toxicity study to measure the developmental toxicity of low doses of three anti-androgenic compounds: vinclozolin, flutamide, and prochloraz. The tested doses were selected to mimic low-effect levels, the no observed adverse effect levels (NOAEL) for endocrine effects, and the acceptable daily intake (ADI). Despite mild maternal toxicity in parental females treated with the top dose of prochloraz, sufficient offspring were produced to evaluate the developmental effects of the three EDCs. While female offspring developed normally, the male offspring showed effects known for anti-androgens. One sensitive clinical parameter was the retention of nipples and/or areolas by male animals on PND 12. This effect was largely transient, as all had regressed by PND 21, with the exception of the offspring exposed to the flutamide top dose. The young adult male offspring displayed additional anti-androgen effects including, delayed sexual maturation and reduced male sex organ weights. These alterations were observed at the effect doses of all three anti-androgens, and at the putative flutamide NOAEL. Offspring from the flutamide top dose group had an increased incidence of developmental sexual defects including hypospadias, short penis, and cryptorchidism. No effects at all were noted at the low doses, as expected for the ADI. Assessment of sexual steroid hormones and their precursors revealed no effects at any of the dose levels. Taken together, the weight of evidence of the clinical and pathological findings suggests a lack of a non-monotonic dose-response curve.

### PS 106 Assessment of Estrogenic and Androgenic Impairment of Iowa Surface Water by Chemical Analysis and Bioassays.

S. Flor<sup>1</sup>, J. Vargo<sup>2</sup> and G. Ludwig<sup>1</sup>. <sup>1</sup>University of Iowa, Iowa City, IA; <sup>2</sup>Iowa State Hygienic Lab, Coralville, IA.

Limited data are available regarding the presence of hormones and steroids in Iowa surface water. To obtain more information about the hormonal impairment, river water samples were collected in October 2011 up- and downstream of Iowa City and Des Moines. Chemical analysis of water extracts was performed by LCMSMS using drinking water method EPA 539 that assesses equilin, estriol, 17 $\alpha$ - and 17 $\beta$ -estradiol, estrone, 17 $\alpha$ -ethynylestradiol, androstenedione, testosterone, progesterone, and 17 $\beta$ -trenbolone concentrations. For endocrine disrupting activity of the water extracts the E- and A-screen with human MCF-7 breast cancer cells (estrogenic and androgenic activity) and the H295R assay with adrenal cancer cells (interference with steroid hormone synthesis) were used. A goal of this study was to determine how well chemical testing for targeted hormones and steroids reflects the total androgenic and estrogenic activity determined by bioassay tests. Preliminary evaluation revealed that the added preservative 2-mercaptopyridine-1-oxide or a derivative that was formed during the extraction procedure was highly cytotoxic to the cells. However, extracts preserved with sulfuric acid could be used in the bioassays. The chemical analysis detected only a few hormones and those that were detected were found at low- or sub-ng/L concentrations in the Iowa surface waters. The Iowa River up- and downstream extracts showed an estrogenic activity in the E- and A-screen and the Des Moines River extracts had a small androgenic and antiestrogenic activity. The H295R hormone concentration tests revealed no obvious changes in testosterone and cortisol levels in the medium but the extracts tended to increase the estradiol levels. Additional tests with synthetic samples prepared according to the analytical test results are needed to examine whether the detected hormones alone caused these biological effects or whether other, still undetermined endocrine disrupting chemicals were involved. (Funded by ES05605 from NIEHS)

**PS 107 Endocrine Disruption: Weight of the Evidence for Low-Dose Effects of TCDD on Sperm Counts.**

K. L. Hentz, A. L. Williams and J. C. Lamb. *Exponent, Alexandria, VA.*

Considerable debate is ongoing regarding the potential for endocrine-mediated low-dose effects. One of the examples that has been presented as evidence for low dose effects is exposure to 2,3,7,8-tetrachlorodibenzo-dioxin (TCDD) and the impact on sperm counts in the male offspring. Although one epidemiological study has reported reduced sperm counts in males exposed to TCDD, the results of this study are limited by the small number of subjects, evaluation of a single sperm sample, potential differences in sexual activity, and lack of control in the collection/transport of the sperm sample. We have conducted a weight-of-the-evidence review of the toxicological studies investigating the impact of maternal TCDD exposure on sperm counts in their offspring and the results have been highly variable. Epididymal sperm counts have been reported to be reduced at doses as low as 64 ng TCDD/kg, but other studies have failed to show effects at doses of 800 ng TCDD/kg or higher. Several other animal studies have not reported effects on sperm counts at doses between 10 and 50 ng TCDD/kg, suggesting a potential threshold. While sperm effects have been reported in experimental animal studies at 64 ng TCDD/kg, this dose should not be considered a low dose because human exposures are much lower. This dose is not relevant to current human exposures to TCDD based on estimated intakes that are 100-fold lower for all dioxins and furans combined based on TEQ (toxic equivalents). Thus, discussions regarding the potential endocrine disruptive effects of TCDD on sperm counts are misleading and do not occur at the low doses experienced by general American public.

**PS 108 Effects of Pesticides on Cytochrome P450 17 (CYP17) and Androgen Receptor (AR) Function in Human H295R Adrenocortical and LNCaP Prostate Cancer Cells.**

C. Robitaille, P. Rivest and T. Sanderson. *INRS-Institut Armand-Frappier, Laval, QC, Canada.*

Exposures to endocrine disrupting chemicals, including pesticides, are thought to be contributing to the increased incidence of certain endocrine-related cancers in the human population, such as prostate cancer. Prostate cancer growth is initially androgen-dependent and under control of the nuclear androgen receptor (AR), which increases the gene transcription of proteins involved in cell proliferation, such as prostate specific antigen (PSA). CYP17 is a key enzyme in the biosynthesis of androgens and increased expression is associated with increased prostate cancer risk. We evaluated the effects of several pesticides suspected or known to modulate hormonal function in androgen-dependent LNCaP human prostate cancer cells and in an *in vitro* steroidogenesis model, the H295R human adrenocortical carcinoma cell line. Benomyl, vinclozolin and prochloraz reduced dihydrotestosterone (DHT)-stimulated LNCaP cell proliferation and nuclear AR protein accumulation concentration-dependently (0.1-30  $\mu$ M). Levels of an active phosphorylated form of AR, pAR-Ser81, were increased by 10 nM DHT, whereas benomyl, vinclozolin and prochloraz decreased these stimulated levels (after a 1 or 6 h exposure). All three pesticides reduced DHT-stimulated PSA secretion by LNCaP cells. We found AR to be expressed in H295R cells but levels of AR and pAR-Ser81 were not affected by DHT, although they were increased by 30  $\mu$ M atrazine. Benomyl and vinclozolin (10 and 30  $\mu$ M) and prochloraz (1 and 3  $\mu$ M) decreased CYP17 mRNA expression in H295R cells at sub-cytotoxic concentrations and prochloraz strongly inhibited CYP17-catalyzed conversion of pregnenolone to DHEA (24h exposure). In H295R and LNCaP cells, CYP17 protein expression was increased by atrazine (30  $\mu$ M). In conclusion, certain pesticides exert combined antiandrogenic effects in androgen-dependent prostate cancer cells at the level of CYP17 and AR, the latter by reducing AR phosphorylation at serine 81.

**PS 109 Metabolomics Characterization of the Effects of Estradiol in Human Breast Cancer Cell Lines.**

L. Zhao<sup>1</sup>, S. Odwin-DaCosta<sup>1</sup>, M. M. Vantagoli<sup>2</sup>, H. T. Hogberg<sup>1</sup>, M. Bouhifd<sup>1</sup>, A. Kleensang<sup>1</sup>, L. Smirnova<sup>1</sup>, K. Boekelheide<sup>2</sup>, J. D. Yager<sup>1</sup> and T. Hartung<sup>1</sup>. <sup>1</sup>Department of Environmental Health Sciences, Johns Hopkins University, Bloomberg School of Public Health, Baltimore, MD; <sup>2</sup>Department of Pathology and Laboratory Medicine, Brown University, Providence, RI.

Estradiol (E2 or 17 $\beta$ -estradiol) is the most potent naturally occurring estrogen. Its effects on cell function during development and in adults in a variety of tissues are mediated through estrogen receptors located in the nucleus, cytoplasm, mitochondria and at the cell membrane. Our objective is to employ high-throughput liquid chromatography mass spectrometry based metabolomics analysis to map pathways affected by estradiol in MCF-7 and T47D cells and then compare them with pathways affected by endocrine disrupting compounds (e.g. BPA and others).

Concurrent cell growth and gene expression studies are also being carried out. Cells were exposed to estradiol at different concentrations and times. Stimulation of cell growth was observed at 0.1nM in association with changes in the metabolome at 6 and 24hrs. A time course study at 100nM estradiol revealed that some metabolites were significantly altered at various time points. The metabolites and pathways most affected included metabolites from cellular energy-related pathways (e.g. Malate, Fumarate, Pyruvate) and amino acid synthesis pathways (e.g. Arginine, Valine, Ornithine, Leucine/Isoleucine, 2-Methylmalate). Further investigation is underway and should give more insight into the identification of metabolism pathways affected by estradiol and endocrine disruptors.

**PS 110 Creating *In Vitro* Test Methods for Endocrine Disruptor Risk Assessment: Assay Development.**

C. Le Sommer, S. M. Ross, P. D. McMullen, M. E. Andersen and R. A. Clewell. *The Hamner Institutes, Research Triangle Park, NC.*

Endocrine disruptor test programs in the US are moving forward to identify active compounds and prioritize them for subsequent in-life toxicity studies. Our focus is on developing *in vitro* tests for cellular responses to endocrine active substances that will be sufficient for health risk assessment without moving on to in-life toxicity tests. We have begun a research effort for the estrogen receptor (ER) pathway to: 1) map signaling pathways for estrogen mediated proliferation, 2) define the dose-response for perturbation of estrogen signaling by xenobiotics and 3) develop computational models to predict chemical effect on uterine epithelium. The first phase develops a cell-based assay in human Ishikawa endometrial cell line expressing the three major ERs: ESR1, ESR2 and G-protein coupled receptor GPER. The dose-response for 17 $\beta$ -estradiol (E2) and 17 $\alpha$ -ethynyl estradiol (EE) (0.001 – 10 nM) were examined at 1, 2, 3, 4, 5, and 6 days of exposure for proliferation and induction of protein and gene targets of ESR1, including alkaline phosphatase (ALP), proliferation associated gene GREB1 and progesterone receptor (PGR). E2 and EE increased proliferation and ALP activity by day 3 at 0.01 nM, while gene induction (GREB1, ALP, PGR) occurred earlier (day 1). Cells were also treated with selective receptor agonists PPT, DPN, and G1 targeting ESR1, ESR2 and GPER. PPT increased proliferation, ALP activity and gene expression similar to EE. DPN induced proliferation and ALP only at higher doses associated with cross-reactivity with ESR1. GPER plays a role in regulating uterine proliferative response; however, we saw no change in proliferation upon treatment with G1 alone. This may result from low GPER expression in our cells. We also conducted expression analysis of studies with Ishikawa cells from our laboratory and published sources to evaluate dose-response of GO-categories by these receptor specific ligands. *In vitro* responses have been analyzed in light of *in vivo* rodent uterotrophic assay transcriptomic data to show consistency between *in vitro* and *in vivo* assays.

**PS 111 Leaching of Chemicals with Estrogenic Activity from Packaging into Popular Lab Animal Feeds.**

D. Klein<sup>1</sup>, C. Z. Yang<sup>2</sup>, G. J. Kollessery<sup>2</sup> and G. D. Bittner<sup>1,2,3</sup>. <sup>1</sup>PlastiPure, Inc., Austin, TX; <sup>2</sup>CertiChem, Austin, TX; <sup>3</sup>University of Texas, Austin, TX. Sponsor: M. Stoner.

A robotized MCF-7 cell proliferation assay currently undergoing validation by IC-CVAM/NICEATM was used to quantify the total estrogenic activity (EA) of chemical mixtures leaching from lab animal feed bags into feed over time. A standard open-formula (low phytoestrogen AIN-93G) feed was purchased from Harlan®, Research Diets™, and TestDiet®. The TestDiet® feed was packaged in EA-Free bags recently developed by PlastiPure for PMI® LabDiet® and other customers. All diets were analyzed 0, 2, and 4 weeks after purchase. All leachates were quantified relative to the percentage of the maximum DNA produced per well induced by a test chemical with respect to the maximum DNA produced per well induced by the 17 $\beta$ -estradiol positive control (%RME2) and corrected by the cell response to the vehicle (negative) control. The significance level ( $p < 0.01$ ) to detect EA was a %RME2 value 3 standard deviations more than the VC. According to this conservative criterion, EA levels in 72 hour ethanol extracts of commercial bags for TestDiet®, Harlan®, and Research Diets™ were non-detectable (ND), significantly positive, and significantly positive, respectively. In the feed study, there was no detectable EA activity in TestDiet® feed at any time point. Feed samples from Harlan® and Research Diets™ were ND at week 0 but significantly positive following storage for 2 and 4 weeks after purchase. EA readings for Harlan® and Research Diets™ increased from week 0 to week 2 and again from week 2 to week 4. These data suggest that leaching of chemicals having EA from the non-EA free plastic packaging can alter the hormonal activity of semi-purified animal feeds. Such leaching of chemicals having EA from plastic packaging into animal feeds may impact research protocols that examine hormonally-responsive end-points.

## PS 112 Endocrine Disruption Potential of Trifluralin: Weight of Evidence Evaluation.

S. Marty<sup>1</sup>, S. Papineni<sup>2</sup>, V. J. Kramer<sup>2</sup>, S. C. Gehen<sup>2</sup> and K. K. Coady<sup>1</sup>. <sup>1</sup>The Dow Chemical Company, Midland, MI; <sup>2</sup>Dow AgroSciences LLC, Indianapolis, IN.

Trifluralin was included on List 1 for the EPA's Endocrine Disruptor Screening Program (EDSP). EDSP screens chemicals for their potential to interact with the estrogen, androgen, or thyroid pathways. A battery of 11 Tier 1 EDSP assays was completed for trifluralin and a Weight of Evidence (WoE) evaluation was conducted. **Estrogen pathway:** Trifluralin was weakly positive in the estrogen receptor (ER) transactivation assay, but it did not affect other estrogen-sensitive assays (i.e., ER binding, uterotrophic, estrogen-sensitive endpoints in the female pubertal, and vitellogenin levels in the fish short-term reproduction assay (FSTRA)). **Androgen pathway:** Trifluralin was negative for androgen receptor binding and while positive in the Hershberger assay, this result was due to enhanced testosterone metabolism. The male pubertal assay showed some indications of antiandrogenicity; however, we believe these effects were indirect. In a previous two-generation study, mating/reproductive indices, litter size/survival and reproductive organ histopathology were unaffected. The FSTRA was potentially positive; however, interpretation was complicated by overt toxicity and the absence of a cohesive link between study observations and known endocrine modes-of-action (MoA). **Thyroid pathway:** The female pubertal assay was positive for thyroid changes due to liver enzyme induction and enhanced thyroxine clearance. Thyroxine levels were decreased in the male pubertal assay, but other thyroid-related endpoints were not altered. Trifluralin increased thyroid tumors in a previous carcinogenicity study via a mode-of-action that is understood to be not relevant to humans. The amphibian metamorphosis assay was negative. Thus, there was no consistent evidence of effects on the estrogen pathway and effects on the androgen pathway did not fit a mode-of-action fingerprint for antiandrogenicity. Trifluralin alters the rodent thyroid system via an indirect effect on the liver; these effects are not expected in humans, who are quantitatively less sensitive than rats.

## PS 113 Cosmetics Products Have Detectable Estrogenic and Antiestrogenic Activity.

C. Z. Yang<sup>1</sup>, G. J. Kollessery<sup>1</sup>, M. Stoner<sup>1</sup>, A. W. Wong<sup>1</sup> and G. D. Bittner<sup>1,2</sup>. <sup>1</sup>CertiChem, Inc., Austin, TX; <sup>2</sup>The University of Texas, Austin, TX.

We have used a roboticized MCF-7 cell proliferation assay and a BG1-Luc assay undergoing validation by ICCVAM/NICEATM to quantify estrogenic activity (EA) and anti-estrogenic activity (AEA) in saline (hydrophilic), ethanol (hydrophobic), and DMSO extracts of over 50 commercially available cosmetic products. These included lipsticks, colognes, shampoos, hair conditioners and skin lotions sent to CertiChem for testing by the National Toxicology Program and the Breast Cancer Fund or purchased for testing by CertiChem from local stores. The total EA in extracts was quantified relative to the maximum response of 17 $\beta$ -estradiol (%RME2) and defined as the percentage of the maximum DNA/well produced by an extract with respect to the maximum DNA/well produced by E2 at any dilution and corrected by the cell response to the vehicle (negative) control (VC). The total AEA in extracts was quantified relative to the AEA of ICI 162,780 (%RMICI). As previously reported (see Yang et al, 2011, EHP 119:989-998), %RME2 and %RMICI values >15% are significantly (P<0.01) greater than the VC, i.e. are detectable for EA or AEA. In both MCF-7 and BG1-Luc assays, over 60% of the cosmetics products tested had easily detectable EA in either saline, ethanol or DMSO extracts. Some products exhibited AEA. When multiple extracts and tests were done on eight cosmetic samples, 7 out of 8 had detectable EA or AEA in at least one extract. Our results indicate that many cosmetics products contain components that exhibit easily detectable EA when tested on two human cell lines in vitro. EA or AEA in widely used cosmetics may account for some epidemiological data suggesting hormonal perturbations in the early onset of puberty in girls, development of uterine fibroids in adult females, and other adverse health effects (e.g., breast cancer). The study was supported by NTP and Breast Cancer Fund.

## PS 114 Use of Novel Assays to Screen Large Chemical Inventories for Functional Estrogen Receptor (ER) Activity.

K. Houck<sup>1</sup>, M. Martin<sup>1</sup>, R. Judson<sup>1</sup>, D. Rotroff<sup>1</sup>, J. Melnick<sup>2</sup>, J. Lamedin<sup>2</sup> and J. Weswick<sup>2</sup>. <sup>1</sup>NCCT, US EPA, Research Triangle Park, NC; <sup>2</sup>Odyssey Thera, San Ramon, CA.

Rapid, efficient screening assays are important for providing the means to prioritize large inventories of environmental chemicals for potential endocrine disrupting effects. Past efforts focused on transcriptional activation (TA) assays for estrogen, androgen and thyroid receptors. The complexities of nuclear receptor (NR) biology,

however, limit this approach as a comprehensive strategy to identify all NR modulators. For example, selective ER modulators can have cell type-specific activity dependent on the particular coregulator proteins expressed. We thus examined alternative, complimentary assay methodologies that provide unique functional information for chemical modulation of the ER pathway. We measured the ability of 1848 chemicals to induce ER dimerization and nuclear translocation, initial and required steps in ligand-induced activation of the ER pathway, using fluorescent imaging in intact cells at multiple time points. We also determined receptor selectivity using distinctly tagged ER $\alpha$  and ER $\beta$  receptors and found the great majority of compounds to have similar potency for both receptors. Secondly, we determined the activity of these 1848 chemicals in an ER/chromatin assay that visualizes active ER transcriptional loci and provides functional information as to the level of agonist versus antagonist activity of the ligand. Overall assay results showed chemicals could be categorized into several groups. First, there were unequivocal ER agonists active under virtually all testing conditions. Second, antagonists and partial agonists with weak or no activity in TA assays run in agonist mode were readily detected by these assays. Finally, there are spurious or artifactual results for each assay that must be taken into account when performing large scale assays such as this and are apparent by looking at data across multiple assays and formats. These results demonstrate the value of multiple, complimentary assay approaches in understanding complex biological responses with in vitro systems.

## PS 115 Effect of Technical Variation and Bioinformatics on the Biological Discovery in a Mechanistic Toxicogenomics Study.

B. Gong<sup>1</sup>, J. Xu<sup>1</sup>, Z. Su<sup>1</sup>, H. Hong<sup>1</sup>, J. Meehan<sup>1</sup>, H. Fang<sup>1</sup>, W. Ge<sup>1</sup>, S. S. Auerbach<sup>2</sup>, C. Wang<sup>3</sup>, L. Shi<sup>1</sup> and W. Tong<sup>1</sup>. <sup>1</sup>Division for Bioinformatics and Biostatistics, National Center for Toxicological Research, US FDA, Jefferson, AR; <sup>2</sup>National Toxicology Program, NIEHS, Durham, NC; <sup>3</sup>Department of Molecular Medicine, City of Hope National Medical Center and Beckman Research Institute, Duarte, CA.

Whole-transcriptome sequencing using next-generation sequencing technologies, i.e., RNA-Seq, has drawn a significant attention as a ground-breaking tool for clinical application and safety assessment. However, critical assessment of RNA-seq to toxicology needs to be carefully conducted to understand whether the technology is robust and reproducible and how the choice of the bioinformatics approaches impacts study of the toxicity mechanisms and predictive toxicology. In this study, we conducted a specific study design to evaluate the impact of sequencing platforms and library preparation to the differentially expressed genes (DEGs) obtained, as well as the impact of different methods for DEG identification. Specifically, RNA samples from six rats' livers were collected, three of them were treated with aflatoxin (AFL) and the other three were matched controls. Two libraries were separately prepared for the samples and two sequencing platforms (Illumina HiSeq2500 and HiSeq2000 systems) were used. The investigation was based on the results derived from 6 different bioinformatics pipelines; each pipeline consists of a workflow including a specific genome template, mapping algorithm, quantification and normalization. Several methods for DEG identification were compared. The preliminary results show that library preparation introduces more variance than sequencing platform on gene expression quantification. Additionally, more variance has been observed for the low-expressed genes and thus increases the false positive rate in DEG identification among those genes. We proposed two filters for data reliability control prior to DEG analysis, one on the low expression level and another on high variance. Comparison was also carried out at functional module and pathway levels.

## PS 116 Structural Classification of 1848 Chemicals Evaluated for Estrogenic Activity in 13 HTS Assays.

R. Judson<sup>1</sup>, D. Rotroff<sup>1</sup>, M. Martin<sup>1</sup>, D. Reif<sup>1</sup>, K. Houck<sup>1</sup>, P. Kothia<sup>1</sup>, N. S. Sipes<sup>1</sup>, T. B. Knudsen<sup>1</sup>, M. Xia<sup>2</sup> and R. Huang<sup>2</sup>. <sup>1</sup>US EPA, Research Triangle Park, NC; <sup>2</sup>NCGC, Rockville, MD.

High-throughput screening (HTS) assays are seeing increasing use for identifying chemicals that can cause toxicity via key biological pathways. However, biological complexities often mean that a single assay will fail to correctly classify all compounds for pathway activity. Here we use multiple orthogonal HTS assays to classify chemicals for their ability to interact with the estrogen receptor (ER) pathway among a structurally diverse library of 1848 chemicals, including pesticidal actives and inerts, industrial chemicals, food additives, cosmetics and drugs. The assays are: reporter gene assays in HepG2 cells selected to maximize metabolic activity, HEK293 cells, BG1 cells, CHO-K1 cells; cell-free binding assays (human, mouse, bovine); assays for ER dimerization (ER $\alpha$ -ER $\alpha$ , ER $\alpha$ -ER $\beta$ , ER $\beta$ -ER $\beta$ ) in HEK293 cells; a transcription-factor/DNA binding assay in HeLa cells; and an ER-sensitive cell proliferation assay in T47D cells. Multiple assay readouts used (fluorescence,

luminescence, sequencing, electronic impedance) allowed determination of possible assay interference. Non-ER related assays (cytotoxicity, cell stress, chemical fluorescence, unrelated endpoints) in the same engineered cells were also included. Assay data were compared with chemical structure clusters. A total of 237/1848 chemicals were active in at least 4 assays. (Note: the library was enriched in chemical classes expected to be estrogenic). This survey identified well known structural classes of estrogenic compounds including steroids, phenols, chlorobenzenes, anilines and perfluorinated alkanes. In metabolically competent assays, we also observed bioactivation in classes of compounds including permethrins and anthracene derivatives. In addition, we confirmed classes of compounds that consistently cause false activity in certain assays, including surfactants. Finally, there were novel compounds active in many assays that will require more analysis and follow-up studies to confirm their activity. This abstract does not necessarily reflect Agency policy.

## PS 117 Categorizing Tobacco Related Documents by Salient Topics for Regulatory Examination with Topic Modeling.

K. Yu<sup>1</sup>, Y. Ding<sup>1</sup>, R. Perkins<sup>1</sup>, W. Aaronson<sup>2</sup>, D. Sholtes<sup>2</sup>, Y. Tian<sup>2</sup>, G. Rochester<sup>2</sup>, X. Xu<sup>1,3</sup> and W. Tong<sup>1</sup>. <sup>1</sup>Division of Bioinformatics and Biostatistics, National Center for Toxicological Research, US FDA, Jefferson, AR; <sup>2</sup>Center for Tobacco Products, US FDA, Rockville, MD; <sup>3</sup>Department of Information Science, University of Arkansas at Little Rock, Little Rock, AR.

The FDA's Center for Tobacco Products (CTP) has received a large volume of documents from its regulated industries, and even more documents are forthcoming. The documents are unstructured and in various formats, including email, PowerPoint slides, memoranda and others. These documents contain diverse information related to such areas as marketing, safety and risk. The language is free text often containing ambiguous semantic descriptions, posing difficulty in retrieving useful information in a consistent and accurate fashion that is needed for regulatory review. Moreover, the sheer volume makes manual reading of the entire corpus impractical. To increase the review efficiency, the FDA requires submitters to include key word tags corresponding to FDA supplied question areas. The goal of this study is to identify the hidden topics or concepts from the submitted documents using topic modeling, and to assess whether the extracted topics reflect the FDA defined questions and thus facilitate review. As a pilot study, more than three thousand menthol-related tobacco documents were used to develop a topic model with latent Dirichlet allocation (LDA). The number of topics was optimized based on an information-loss approach. After generating the topics, a cosine similarity based approach was used to map FDA questions to the extracted topics. The results demonstrated that the extracted topics reflect the concepts of regulatory questions. The majority of documents clustered by topic modeling coincided with those grouped by FDA defined requests. This study demonstrates the potential utility of topic modeling as an unsupervised machine learning technique to classify the submitted documents based on the hidden topics, and thus provides an alternative means to support the review process.

## PS 118 Gene Expression Analysis to Predict the Dermal Carcinogenic Potential of Petroleum Streams.

K. Mathijs<sup>1</sup>, J. van Delft<sup>1</sup>, M. van Steensel<sup>2</sup>, K. Goyak<sup>3</sup>, H. Ketelslegers<sup>3</sup>, J. Freeman<sup>3</sup> and R. Phillips<sup>3</sup>. <sup>1</sup>Department of Toxicogenomics, Maastricht University, Maastricht, Netherlands; <sup>2</sup>Department of Dermatology, Maastricht University, Maastricht, Netherlands; <sup>3</sup>ExxonMobil Biomedical Sciences Inc., Annandale, NJ.

Certain poorly refined petroleum streams that contain high levels of polycyclic aromatic compounds have been shown to cause skin cancer in mice, as determined by the appearance of skin tumors after chronic dermal administration, which has cost and time constraints. We wish to identify biomarkers for petroleum-induced skin tumorigenesis, based on toxicogenomic responses in treated mouse skin from which predictive short-term tests can be developed. C3H/HeNcrI mice were treated dermally three times for one week with carcinogenic (C) or non-carcinogenic (NC) petroleum streams or with the solvent control. 24 h after the last treatment, sections of dorsal skin from sacrificed mice were used for immunohistochemistry (IHC), RNA and DNA isolation. Gene expression profiling using Agilent microarrays was done to select altered genes and molecular pathways related to individual test substances and substance classes for use in class prediction analyses to discriminate C from NC. No clear differences in IHC markers for hyper-proliferation, differentiation, or apoptosis were found between control, C and NC. Increased  $\gamma$ H2AX, a DNA damage marker, was found in C vs control and NC. Clear differences in gene expression profiles occurred between C and NC. Based on the gene expression profiles, correct prediction occurred; the top 10 classifier genes (which included *Cyp1a1*, *Cyp1b1*, *Nqo1*, *Ahr*, *Arnt*) are mainly involved in xenobiotic metabolism and oxidoreductase reactions. Classification based on pathway expression changes correctly predicted only NC and the highest concentrations of C; the top classifier

in the pathway analysis was the KEGG pathway "xenobiotic metabolism by cytochrome P450". Our results indicate that gene expression responses from a short-term dermal mouse study can predict C and NC petroleum streams, and that the AhR receptor pathway warrants further evaluation as a biomarker of exposure for petroleum-induced skin tumorigenesis.

## PS 119 Structure-Based Virtual Screening: Identification of New Targets for Triclosan.

D. Montes-Grajales and J. Olivero-Verbel. Environmental and Computational Chemistry Group Pharmaceutical Sciences, University of Cartagena, Cartagena, Colombia.

Triclosan (TCS; 2,4,4'-trichloro-2'-hydroxy-diphenylether) is a broad-spectrum antimicrobial agent used in personal care products. It has cytotoxic and endocrine-disrupting properties, and may be bioaccumulated from daily use. However, its impact on human health is largely unexplored with little evidence for deleterious effects in humans. A total of 248 proteins involved in different pathological processes were evaluated by *in silico* virtual screening to find new possible human protein targets for TCS. The 3D-structures of the proteins were downloaded from PDB, prepared and optimized by Sybyl X-2.0. The TCS structure was optimized by DFT at the B3LYP/6-31G level in Gaussian 0.9. Docking studies were performed in AutoDockVina 2.0 using a blind docking strategy, exhaustiveness of 25 and 10 runs. Calculated binding affinities were then employed for ranking proteins. A redocking step of 100 runs and exhaustiveness of 100, as well as the interaction analysis with Ligand Scout, LigPlot and MMV were carried out on the complexes presenting the best docking results. The greatest affinity scores were found for CDC2-like kinase 4 (CLK4,  $-8.4 \pm 0.0$  kcal/mol), oligomeric death domain complex (CRADD/PIDD,  $-8.3 \pm 0.1$  kcal/mol); progesterone receptor (PGR,  $-8.1 \pm 0.0$  kcal/mol); and estradiol 17-beta-dehydrogenase 1 (17-beta-HSD 1,  $-8.1 \pm 0.1$  kcal/mol), proteins involved in endocrine disruption and breast cancer-related processes. Validation showed our protocol predicted the binding site for the 17-beta-HSD and PGR native ligands, in agreement with crystallographic data. Moreover, TCS interacts in the same binding site occupied by the 17-beta-HSD 1 native ligand, but in a different one from that used by progesterone in PGR. Protein-ligand binding included hydrophobic and hydrogen bonding interactions. These results suggest TCS may target different proteins, probably altering pathways involved in pathophysiological disorders. Vice-Rector for Research. UniCartagena. 2011-2012. Colciencias-UniCartagena: Grants 110745921616 (2009) and 110751929058 (2010).

## PS 120 Generation of *In Vitro* Margin of Exposure (MOE) Values to Support the Postulated Mode of Action (MOA) for Selected Tobacco Smoke Toxicants.

S. A. Fiebelkorn, E. H. Cunningham, E. L. Bishop, D. M. Dillon and C. Meredith. Group R&D, British American Tobacco, Southampton, United Kingdom.

Over the last ten years there has been increasing interest in the identification and characterisation of tobacco smoke toxicants. We propose the use of a biologically relevant risk assessment framework incorporating both *in vivo* and *in vitro* data for the prioritisation of such toxicants. We have previously described the use of *in vivo* data in the generation of Margin of Exposure (MOE) values alongside Mode of Action (MOA) reviews. We have also proposed that individual toxicants are tested for activity in a battery of *in vitro* assays including *in vitro* micronucleus, Ames and mouse lymphoma assays.

MOE assessments are used as an initial tool to segregate tobacco smoke toxicants into high or low priority for risk reduction research. As recommended by EFSA, MOE values above 10,000 can be considered a low priority for risk management actions. We have generated *in vitro* MOEs for a number of tobacco smoke toxicants in conjunction with MOA reviews and *in vivo* MOEs (where suitable data is available). Where the *in vivo* MOEs generated for individual toxicants do not provide a conclusive evaluation and are split across the critical value of 10,000 (e.g. NNK and arsenic) or where the available *in vivo* data is unsuitable for MOE generation (e.g. hydroquinone and catechol), the use of *in vitro* data can provide an alternative source of information. We present here MOE data for five different tobacco smoke toxicants:

Benzo[a]pyrene: *in vitro*:  $42,469 - 3.0 \times 10^7$ ; *in vivo*:  $16,805 - 2.4 \times 10^6$ .

NNK: *in vitro*:  $1.0 \times 10^6 - 3.7 \times 10^8$ ; *in vivo*:  $338 - 3.7 \times 10^5$ .

Arsenic: *in vitro*:  $2.95 \times 10^7$ ; *in vivo*:  $13 - 4.9 \times 10^5$ .

Catechol: *in vitro* 938-12,094; *in vivo*: No data.

Hydroquinone: *in vitro*: 1651-10,304; *in vivo*: No data.

The incorporation of *in vitro* data into our suite of assessment methods allows us to generate additional MOEs to support the MOAs and provide further mechanistic understanding of individual toxicants. There is also the potential to incorporate such *in vitro* data into the future development of PBPK models for individual toxicants.

**PS 121** **Developing a Gene-Gene Interaction Network for Nonsyndromic Orofacial Clefts Using Computational Analysis.**

J. McKone, A. N. Van, E. Lachenauer and D. Johnson. *University of California Berkeley, Berkeley, CA.*

Orofacial clefts (OFCs) are caused by malformations in the closing of the lip or the soft palate. Although OFCs are considered to be one of the most common congenital birth defects, the underlying mechanisms of its etiology have yet to be clearly elucidated. This study sought to systematically determine how candidate genes previously identified in the literature interact, potentially implicating specific pathways for nonsyndromic OFC formation. OFC gene candidates were derived from genome-wide association studies (GWAS), the Comparative Toxicology Database, and Thomson Reuter's GeneGo. The compiled OFC genes were analyzed in conjunction with genes associated with the metabolic pathways of vitamin A and folic acid, factors shown to be implicated in OFC formation. Utilizing GeneGo and the candidate gene list, a gene-gene interaction network was constructed. Analysis of the network led to the identification of the TCF/LEF gene family, members of which regulate several downstream targets identified in the GWAS and/or are associated with vitamin A or folic acid metabolism. The TCF/LEF genes were shown in the network to be regulated by genes involved with the WNT signaling pathway, suggesting a mechanistic relationship between WNT signaling and orofacial cleft formation. Through computational analysis, this study proposes a potential gene-gene interaction mechanism for OFC formation via the WNT signaling pathway and ultimately identifies the TCF/LEF family as possible target gene candidates for further studies.

**PS 122** **Role of Beta-Methylamino-L-Alanine in GRIK1-Mediated Amyotrophic Lateral Sclerosis Disease Pathway.**

S. Firouzbakht, Y. Iizuka and D. Johnson. *University of California Berkeley, Berkeley, CA.*

Amyotrophic Lateral Sclerosis (ALS) is a debilitating neurodegenerative disease that affects about 30,000 people in the United States alone. Only a small fraction of cases are linked to genetics, making it likely that the overwhelming majority are induced by environmental factors. Therefore, the elucidation of a toxicity pathway is critical to the understanding of the vast majority of the ALS disease population. Amongst potential environmental exposures, neurotoxin beta-N-Methylamino-L-alanine (BMAA) has shown strong association with ALS in a small disease cluster in Guam. However, the several proposed mechanisms are insufficient in explaining the entire disease pathway. In this study, we utilized computational predictions with GeneGo, STITCH, BLAST, PubChem, and KEGG to generate the most feasible pathway for BMAA toxicity. The results from PubChem structure clustering between a highly kainate-specific ligand and BMAA- $\beta$ -carbamate revealed a statistically significant 3D Tanimoto score, implicating a comparable receptor repertoire. BLAST sequencing comparisons between GRIK1-5 and GLUL, an ALS associated gene, showed significant overlap between the two nucleotide sequences, further suggesting that kainate receptors are crucial to the ALS disease pathway. Incorporating these computational studies with current knowledge, there is compelling evidence suggesting a primary disease pathway in which BMAA- $\beta$ -carbamate binds to the kainate receptor GRIK1 at the presynaptic motor neuron, leading to increased glutamate release and subsequent neurodegeneration.

**PS 123** **Computational Analysis of a Potential Mechanistic Relationship between Depleted Uranium (DU) Exposure and Risk of Spina Bifida Cystica.**

S. Aghaee, H. Ngo and D. Johnson. *University of California Berkeley, Berkeley, CA.*

Prolonged weapon use in war zones increases the environmental levels of potentially teratogenic metals which may have a direct relationship to increased incidences of birth defects. In Fallujah, Iraq since 2003, high levels of depleted uranium (DU) in the environment and in hair samples of residents suggests that constant exposure to

DU may play a role in the alarming rates of congenital defects found in Iraqi children. One particular birth defect, Spina bifida, is a congenital defect of the spinal column with two major subclasses: spina bifida occulta and spina bifida cystica. Cystica is the most severe form of the disease but also the least prevalent. However, this has not been the case in Fallujah, Iraq where from 2003 cystica has been found to be the most prevalent form of spina bifida. The purpose of this study was to search for any commonalities between the genes and biological pathways associated with exposure to uranium and development of spina bifida cystica. Computational methods and tools utilized included the Comparative Toxicogenomics Database (CTD), PubChem, ToxNet, Pathway Commons, and unpublished exposure/defect data from Iraq. Out of the 292 genes reportedly affected by uranium exposure, 155 were also associated with spina bifida cystica. Biological pathway analysis revealed three genes, NT5E, PED, and TALDO1, associated with uranium are also involved in upstream pathways of folic acid synthesis. Research has shown that a lack of folate is known to be related to spina bifida. This study provides a broad look at the genetic and molecular similarities between response to uranium exposure and spina bifida cystica, and may offer options for preventive therapeutic interventions. Further studies examining gene ontologies of populations exposed and not exposed to depleted uranium would offer a clearer picture of the relationship between uranium and spina bifida.

**PS 124** **Computational Analysis of Catechins in Teas and Potential Relationship to Cardiovascular Health.**

C. Lei, M. Nhan, C. Ha and D. Johnson. *University of California Berkeley, Berkeley, CA.*

Consumption of green tea has been reported to have beneficial effects on a variety of health-related issues. Of interest is the beneficial differences between green, oolong, and black teas, all produced from the leaves of *Camellia sinensis*. Of the five main groups of bioactive compounds in the *Camellia sinensis* plant, catechins were found to be the most bioactive. Of the six main catechins in tea, epigallocatechin-3-gallate (EGCG), the most abundant and bioactive of the catechins was found to be in the highest concentration in green tea as compared to oolong and black teas and subsequently was considered to be the most health-relevant component. The potential health benefits of tea depend on their level of fermentation, which is correlated to the amount of oxidation the catechins undergo during processing. EGCG is most abundant in green tea, which is not fermented, and highest in fresh unprocessed leaves from *Camellia sinensis*. Green tea extract has also been reported to have increased biological activities. EGCG and pro-drugs have also been shown to be potential epigenetic modulators. DNA methylation is catalyzed by DNA methyltransferase (DNMT) with S-adenosyl-methionine (SAM) as the methyl donor. EGCG has been shown to reduce DNMT indirectly by reducing SAM and increasing S-adenosyl homocysteine (SAH) and homocysteine levels in the MCF-7 breast cancer cell line. In this study, primarily utilizing GeneGo Metadrag and MetaCore we report a proposed overlap between EGCG affected pathways and the atherosclerosis disease pathway. EGCG was found to competitively block hydroxy-3-methyl-glutaryl-CoA, and non-competitively inhibit squalene epoxidase, two rate limiting enzymes in the cholesterol biosynthesis pathway. In addition, previous animal studies have reported a decrease in LDL levels in rats given the three teas with the highest response coming from green tea treatment. This study provides an analysis of antioxidant compound levels found in tea and their relation to its effect on cardiovascular health, providing a possible explanation to the differences in beneficial effects found in different types of teas.

**PS 125** **Computational Analysis of Environmental Factors Potentially Associated with Multiple Sclerosis Susceptibility.**

F. Su, M. Gooding, G. Anderson and D. Johnson. *University of California Berkeley, Berkeley, CA.*

Multiple Sclerosis (MS), an autoimmune disease of the CNS, may have associated environmental risk factors. A relationship between distance from the equator and MS risk reinforces the belief that UVB radiation and subsequent Vitamin D synthesis act protectively. The Human Leukocyte Antigen b chain, HLA-DRB1 is activated by Vitamin D and its receptor, and a polymorphism, HLA-DRB1\*15.01, has been associated with MS susceptibility. Computational methods utilized to explore environmental factors beyond UVB radiation that might influence MS disease pathways included the Comparative Toxicogenomics Database (CTD), STITCH, GWAS data, GeneGo, and the EPA Toxic Release Inventory (TRI). Historical MS clusters in the US were identified and toxic release data obtained through TRI. Lead (Pb 2+), was found as a top contaminant among the MS clusters. Although lead has been proposed as a risk factor for MS, no previous published studies have clearly linked lead and MS. To identify and investigate genes,

cellular pathways and disease interactions, CTD was utilized with STITCH to generate association networks between genes and proteins and to identify another intermediate protein, ALAD. Binding assays show that a polymorphism of ALAD, ALAD2, causes red blood cells to bind lead more tightly and previous research has implicated ALAD as an important factor in lead susceptibility. VDR polymorphisms are also associated with lead susceptibility. Although a correlation between VDR B and higher blood, urine, and plasma lead levels has been reported, the mechanism and systemic effect of the allele are not well understood. Maps of the frequency of haplotypes in different populations for VDR B, ALAD2 and HLA-DRB1 were obtained from GWAS and correlating biological pathways involving MHCII, ALAD, and VDR were constructed with GeneGo. In combination, the relationships identified suggest that ALAD2 and VDR B haplotypes confer an individual with heightened lead susceptibility. Furthermore, the results suggest that elevated levels of lead are associated with decreased expression of HLA-DRB1 and greater risk of MS.

**PS 126 Profiling the Activity of Environmental Chemicals in Causing Testicular Dysgenesis Syndrome Using the US EPA Toxicity Reference Database (ToxRefDB).**

M. C. Leung<sup>1</sup>, K. W. McLaurin<sup>1</sup>, J. Phuong<sup>1</sup>, N. S. Sipes<sup>1</sup>, N. C. Baker<sup>1</sup>, N. Kleinstreuer<sup>1</sup>, A. M. Frame<sup>1</sup>, R. Judson<sup>1</sup>, G. R. Klinefelter<sup>2</sup>, M. T. Martin<sup>1</sup> and T. B. Knudsen<sup>1</sup>. <sup>1</sup>National Center of Computational Toxicology, US EPA, Research Triangle Park, NC; <sup>2</sup>Reproductive Toxicology Division, US EPA, Research Triangle Park, NC.

Hypogonadism, cryptorchidism, hypospadias, and testicular cancer are increasingly common male reproductive defects. Clinical and experimental evidence suggest that these defects are associated with testicular dysgenesis syndrome (TDS). We hypothesize an Adverse Outcome Pathway (AOP) framework for TDS starting with disruption of cell signaling and structural targets of the fetal testis during embryogenesis, followed by a series of key events that lead to male reproductive defects. Since understanding chemical-endpoint associations is an approach in building the AOP conceptual models, we mined 4209 guideline animal studies in EPA's ToxRefDB, which included 963 compounds tested in rats, mice, and rabbits. Testicular neoplasia was an outcome for 60 (6.2 %) chemicals. Sperm abnormalities were an outcome for 72 (9.8 %) chemicals tested in chronic and subchronic toxicity studies and 44 (5.7 %) chemicals tested in prenatal developmental and/or multigenerational fertility studies. Reductions in anogenital distance were recorded for 15 (3.5 %) chemicals tested in multigenerational studies, and 11 (1.5 %) chemicals tested caused hypospadias or cryptorchidism in developmental or multigenerational studies. The chemical classes showing the broadest activity across different TDS endpoints were pesticides (amdro, benomyl, primisulfuron-methyl, tetrachlorobenzene, and vinclozolin) and phthalates (butyl benzyl phthalate, dibutyl phthalate, and diethylhexyl phthalate) with a lowest effect level on the order of ~300 mg/kg/day. The most potent TDS-actives (17 $\beta$ -estradiol, flutazepam, and tebutimfos) produced testicular effects below 0.1 mg/kg/day. These results suggest a hierarchical pattern of male reproductive defects in ToxRefDB which can be used as an AOP anchor for TDS. [This work does not reflect EPA policy].

**PS 127 Compound Toxicity Profiling and Prioritization Using Tox21 Phase I Quantitative High-Throughput Screening (qHTS) Cytotoxicity Data.**

J. Hsieh<sup>1</sup>, A. Sedykh<sup>2</sup>, R. Huang<sup>3</sup>, M. Xia<sup>3</sup> and R. R. Tice<sup>1</sup>. <sup>1</sup>Division of the National Toxicology Program, NIEHS, NIH, Research Triangle Park, NC; <sup>2</sup>University of North Carolina at Chapel Hill, Chapel Hill, NC; <sup>3</sup>National Center for Advancing Translational Sciences, Bethesda, MD.

Using in vitro data to prioritize compounds for in vivo toxicity testing is a goal of Tox21. Phase I profiled 1408 NTP compounds against 126 cell-based qHTS assays; those that measured cytotoxicity record the ability of a chemical to adversely perturb multiple cellular pathways in a concentration-response fashion. The curves from 39 cytotoxicity assays (9 human cell types, 4 rodent cell types, 13 sets of identical twin lymphoblastoid cell lines) were curated to filter noise and remove artifacts. To quantify the activity of each compound in these assays, we calculated a weighted version of Area Under the Curve (wAUC) intended to capture potency and efficacy simultaneously, as well as the conventional half-maximal activity concentration (AC50) value. The average wAUC or AC50 values across the 39 cytotoxicity assays were used to rank compounds and the rankings were compared, for 880 compounds, with available rat acute oral toxicity data. The compounds were categorized as toxic or non-toxic based on various "Globally Harmonized System of Classification and Labelling of Chemicals" (GHS) acute toxicity thresholds (50,

300, 500, 2000 mg/kg). The wAUC approach consistently prioritized more toxic compounds at the early stage (up 1% non-toxic compounds of dataset) at all thresholds. The best receiver operating characteristic (ROC) enrichment value at 1% and AUC value are 14.3 [95% CI=1.8-26.8] and 0.73 [95% CI=0.65-0.80], respectively, at a threshold of 50 mg/kg. Also, some toxic compounds (e.g., actinomycin D, colchicine, daunomycin) had higher ranks based on wAUC due to their ill-fitted curves in some of the cell lines, resulting in missing AC50 values. We conclude that the wAUC provides an additional and useful metric to estimate the toxicity potential of compounds for Tox21 qHTS assays. Based on this metric, compounds screened in Tox21 can be prioritized for more extensive testing.

**PS 128 Predicting Cellular Dynamics and Key Events in Developmental Toxicity with a Multicellular Systems Model.**

T. B. Knudsen<sup>1</sup>, M. R. Rountree<sup>1</sup>, S. Hunter<sup>2</sup>, N. C. Baker<sup>3</sup>, R. Spencer<sup>3</sup>, R. S. DeWoskin<sup>4</sup> and W. Setzer<sup>1</sup>. <sup>1</sup>NCCT, US EPA, Research Triangle Park, NC; <sup>2</sup>NHEERL, US EPA, Research Triangle Park, NC; <sup>3</sup>Lockheed Martin, Research Triangle Park, NC; <sup>4</sup>NCEA, US EPA, Research Triangle Park, NC.

Computer simulation of cellular networks is one possible solution for modeling key events in developmental toxicology. We constructed a multicellular agent-based model (ABM) of early limb-bud development in CompuCell3D ([www.compu-cell3d.org/](http://www.compu-cell3d.org/)). The model simulates key cellular behaviors (mitosis, apoptosis, adhesion, migration, chemotaxis, shape, secretion), organizing centers (AER, ZPA) and signals (FGFs, SHH, BMPs, RA). It effectively emulates hindlimb-bud development during a 42h period in mouse (Theiler stages 16-19) and 160h in human (Carnegie stages 13-16). The ABM reflects biological variability across parallel simulations for spatio-temporal expression of biochemical gradients and cell behaviors, ultimately manifesting in trajectories of outgrowth. To evaluate the model as a tool for predictive toxicology, we selected 5-Fluorouracil (5FU) as a prototype. 5FU perturbed 13 of 650 ToxCast assays based on AC50s (or LECs) at or below 15  $\mu$ M. 5FU effects observed in the assays were disruption of stem cell (mES) growth and differentiation, suppression of TGF $\beta$ 1 signaling and mitochondrial density, p53-induction, mitotic arrest, reduced cell proliferation and increased cell death. Challenging the ABM with concentration-response data derived from mES cell number produced a dose-dependent wave of mitotic arrest and apoptosis, disrupting outgrowth. Varying the dose and time of exposure localized the primary key event to arrest of SHH-expressing cells and their geometric relationships to cells expressing GREM1, a BMP antagonist maintained by SHH signals. Different outcomes emerged when perturbation of the SHH/GREM1/BMP loop was switched between mitotic arrest and excessive apoptosis, indicating the importance of considering both cellular consequences together. These findings support the application of multi-cellular ABMs as tools to translate cellular dynamics into simulation of emergent (higher order) tissue effects for predictive toxicology. [This abstract does not necessarily reflect EPA policy.]

**PS 129 Chemical Structure-Based *In Silico* Phototoxicity Prediction: An Approach from a Combination of Photochemical Properties.**

Y. Haranosono, S. Nemoto, M. Kurata and H. Sakaki. Senju Pharmaceutical Co., Ltd., Kobe, Japan.

Some photochemical properties are essential factor for prediction of phototoxicity, since phototoxicity is caused by photo-activation of the compounds. Highest Occupied Molecular Orbital – Lowest Unoccupied Molecular Orbital Gap (HLG) is a photochemical property of needful energy for photo-activation, and HLG was reported to be related with phototoxicity based on *in vitro* 3T3 Neutral Red Uptake assay (3T3 NRU assay). However there are few reports to predict of phototoxicity using photochemical property including HLG. In this research, we established the stepwise approach using Maximum-Conjugated- $\pi$ -Electron- Number ( $PEN_{MC}$ ) of the compounds in addition to HLG for *in vitro* phototoxicity prediction. HLG and  $PEN_{MC}$  were calculated by ChemDraw<sup>®</sup> and Chem3D<sup>®</sup> for total 64 compounds which were known the results of 3T3 NRU assay (32 positive and 32 negative). As step 1, we set the cut lines of HLG as follows; the compounds that have over 8.0 of HLG were determined as negative, and the compounds that have less than 5.2 of HLG were determined as positive. On the other side, the compounds that have HLG from 5.2 to 8.0 showed no predicting performance to phototoxicity, and then we defined this range of HLG as gray zone. As step 2, we employed  $PEN_{MC}$  for the gray zone compounds. We found that  $PEN_{MC}$  also indicated correlation to *in vitro* phototoxicity, and therefore set the cut lines as follows; the compounds that have 12 and more than of  $PEN_{MC}$  were determined as positive, and 11 or less of  $PEN_{MC}$  were determined as negative. This stepwise approach for phototoxicity prediction

was validated by the following results; sensitivity (84.4%), specificity (81.3%), positive rate (81.8%), negative rate (83.9%) and concordance (82.8%). We concluded that the stepwise approach with combination of HLG and PEN<sub>MC</sub> for prediction of phototoxicity is adaptable and useful for drug development as *in silico* screening, because it showed high sensitivity and negative rate from only chemical structure.

**PS 130 High-Content Screening of ToxCast Compounds for Developmental Endpoints Related to Adipogenesis and Angiogenesis.**

D. L. Filer, N. Kleinstreuer, M. Martin, K. Houck and D. Reif. *National Center for Computational Toxicology, US EPA, Research Triangle Park, NC.*

The US EPA's ToxCast research program gathers toxicity information for over 1000 chemicals utilizing high-throughput toxicity screening (HTS) assays with human gene and protein targets to inform prioritization of chemicals with little or no toxicity information for further testing. Vala Sciences provides high content multiplexed assays utilizing quantitative digital imaging of cultured cells, tissues and small model organisms. We measured the ToxCast Phase I\_v2 chemical library, (293 unique compounds, primarily food-use pesticides with associated *in vivo* toxicity data), with 12 Vala Sciences assays in six-point concentration response from 0.013  $\mu$ M to 100  $\mu$ M. Assays examined chemical effects on embryonic stem cell differentiation, neuronal function, pancreatic  $\beta$  cell differentiation, germ layer proliferation, adipogenesis, adipocyte lipolysis, hepatic steatosis, and junctional proteins critical to developmental angiogenic processes and tumor progression. We subjected concentration response data to automated curve-fitting using modified Hill functions, outlier detection algorithms, and uncertainty analysis to determine the half-maximal activity concentration (AC50) and Lowest Effective Concentration (LEC) for each chemical/assay combination. Assays showed high reproducibility, both within triplicate replicate sets and in blinded compound replicate sets. Across the entire Phase I chemical set, 5% of chemical/assay combinations demonstrated significant (> 50% change over control baseline) activity. Early response targets in this data set provide toxicological and mechanistic insight to complement other ToxCast assays and lead to stronger predictive toxicity models. Collectively, these results add important data to ToxCastDB that will help identify and prioritize possible developmental toxicants, endocrine disruptors, liver toxicants, and carcinogens to inform targeted testing strategies. *This abstract does not necessarily reflect U.S. EPA policy.*

**PS 131 In Silico Models for Dermal Absorption from Complex Formulations.**

K. Guth<sup>1</sup>, J. E. Riviere<sup>2,3</sup>, J. Brooks<sup>2</sup>, M. Schäfer-Korting<sup>4</sup>, M. Dammann<sup>1</sup>, E. Fabian<sup>1</sup>, B. van Ravenzwaay<sup>1</sup> and R. Landsiedel<sup>1</sup>. <sup>1</sup>Experimental Toxicology and Ecology, BASF SE, Ludwigshafen am Rhein, Germany; <sup>2</sup>Toxicology Research and Pharmacokinetics, North Carolina State University, Center for Chemical, Raleigh, NC; <sup>3</sup>Institute of Computational Comparative Medicine, Kansas State University, Manhattan, KS; <sup>4</sup>Institut für Pharmazie, Freie Universität, Berlin, Germany.

Dermal exposure is a relevant parameter for risk assessment of chemicals, cosmetics and pesticides. Here, we present potential *in silico* models for prediction of dermal absorption based on realistic exposure scenarios in complex mixtures. The calculations were based on 342 individual dermal absorption *in vitro* experiments using human or rat skin samples for 56 chemicals (mainly pesticides) in more than 150 different mixtures containing up to 20 ingredients like water, organic solvents, surfactants or thickeners. The first approach was based on the Abraham solute descriptors, mixture factors (MFs) as suggested by Riviere and Brooks and the logarithmic maximal permeability coefficient (logmaxKp) as response<sup>1,2</sup>. Additionally, an indicator variable for the species (SpI) was introduced. In a second approach class variables – which bundled substance-specific information – were used in combination with mixture factors. Validation was performed in accordance with the OECD Guidance document for QSAR models. The final validated Abraham-based model comprised the solute excess molar refractivity of the penetrant, SpI and topological polar surface area of the mixture (R<sup>2</sup>:0.38, Q<sup>2</sup>Ext: 0.41). Despite the low correlation, the model was suitable to estimate Marzulli classes of penetration for unknown penetrants in specific mixtures<sup>3</sup>. Furthermore, precise prediction of mixture effects on well-known substances was possible with the substance-based approach (R<sup>2</sup>:0.75, Q<sup>2</sup>Ext: 0.73). Taken together, both applications are suitable screening tools in early stages of product development.

1 Abraham et al. 1999. *Pesticide Science* 55, 78-88

2 Riviere and Brooks 2005. *Toxicology and Applied Pharmacology* 208, 99-110

3 Marzulli and Brown 1969. *Toxicology and Applied Pharmacology* 3, 76-83

**PS 132 Development of Improved Salmonella Mutagenicity QSAR Models Using Structural Fingerprints of Known Toxicophores.**

L. Stavitskaya<sup>1</sup>, B. L. Minnier<sup>2</sup>, R. Benz<sup>1</sup> and N. L. Kruhlik<sup>1</sup>. <sup>1</sup>US FDA, Silver Spring, MD; <sup>2</sup>GlobalNet Services, Inc., Rockville, MD.

The current draft of the International Conference on Harmonisation (ICH) M7 guidance describes the use of *in silico* models to qualify genotoxic impurities during the drug safety evaluation and approval process. In order to attain the highest accuracy and improve the domain of applicability of the current Salmonella mutagenicity quantitative structure-activity prediction models, continuous updates to the training set must be made to accommodate new genotoxic findings. In this study, we first assessed our current Salmonella mutagenicity training set using fingerprints of known genotoxic structural alerts to determine the domain of applicability and performance characteristics of several commercial (Q)SAR models. We then enhanced the previous version of our non-proprietary training database for Salmonella mutagenicity with data for 431 new compounds harvested from FDA approval packages and the published literature, to give a total of 3965 compounds. Of the 431 chemicals, 247 are drug molecules marketed between 1970 and 2011. Data gaps within the training set were identified and, using structural features derived from known toxicophores, 141 examples containing functional groups such as azides, amine oxides, hindered epoxides, propiolactones, quinones, amine halides, diazines, azo compounds, diazoniums, sulfates, aziridine chlorides, nitrites, hydrazines, nitriles, isocyanates, and sulfur mustards were added. Moreover, the new training set was expanded to include over 40 compounds containing previously unmodeled atoms such as boron, silicon, selenium, and tin. A hierarchical clustering analysis of the final training set showed representation of an additional 44 structural clusters over which the model can make a prediction.

**PS 133 Evaluation of QSPR Models to Predict Evaporation Rates of Hazardous Chemicals from the Skin Surface.**

T. Liu, M. Rauma and G. Johanson. *Institute of Environmental Medicine, Karolinska Institutet, Stockholm, Sweden.*

The skin serves as a barrier against hazardous agents in the environment. However, the barrier is incomplete in that chemicals may penetrate the skin and cause toxicity. The absorbed dose depends not only on the absorption rate but also the evaporation rate (assuming a fixed dose and skin area). The limited data available suggest that rates vary by several orders of magnitude between chemicals. However, there is a huge lack of data and new approaches are needed. One attractive possibility is to use quantitative structure-permeability relationship (QSPR) models. The aim of the present study was to examine different QSPR models addressing evaporation rate. We calculated evaporation rates for nine volatiles (methanol, n-propanol, acetone, methyl ethyl ketone, hexane, n-heptane, octane, benzene and toluene) at three air velocities and three air temperatures, using four semi-empirical models; McCready & Saghir, EPA, Mackay & Matsugu, and BAU. The predictions were compared with experimental data published by the EPA<sup>1</sup>. None of the four models were able to predict the evaporation rate at all wind speeds. For comparison, we also developed linear solvation energy relationships (LSER) and partial least squares projections to latent structures (PLS) models. Seven solvents were used for calibration and two to test predictive performance. The LSER and PLS models showed good correlation (R<sup>2</sup> 0.95 and 0.92) and predictive performance (Q<sup>2</sup> 0.86 and 0.95) and seem more suitable than the semi-empirical models to predict evaporation rate. The semi-empirical models, EPA and Mackay & Matsugu at higher air velocity (5.08 m/s) and lower temperature (280.35 K), showed a fair agreement between predictive and experimental values. As a result, evaporation rates can be adequately predicted from available physicochemical properties of the volatile organic compounds (VOCs).

Reference

1. Braun, K.O. and Caplan, K.J. (1989) *Evaporation rate of volatile liquids*, final report, 2nd edition. EPA/744-R-92-001, NTIS PB92-232305, Springfield.

**PS 134 Regulatory Targets of CDKN2A in Lung Epithelial Cells.**

J. Mehta and G. Acquah-Mensah. *Massachusetts College of Pharmacy and Health Sciences, Worcester, MA.*

Cyclin Dependent Kinase Inhibitor 2A (CDKN2A) is a tumor suppressor protein in humans. It is capable of inducing cell cycle arrest in the G1 and G2 phases. p16INK4a is a major component of the RB pathway. p14ARF is part of an ARF-MDM2-TP53 system that exercises a negative control on hyper-proliferative signals originating from oncogenic stimuli. ARF binds to MDM2 and blocks its cytoplasmic transfer and thereby sequesters it in the nucleus. This hinders the MDM2 action, thereby blocking degradation of p53 and thus enhancing transactivation

and apoptosis. The purpose of this study was to identify additional regulatory targets of CDKN2A in lung epithelial cells, using Bayesian networks. Using the Robust Multi-Array Average procedure, a compendium of lung epithelial cell microarray data was generated based on Gene Expression Omnibus datasets GSE 19027 and GSE 994. The best-scoring regulatory networks, given the gene expression data, were then learned using the Bayesian Network Inference with Java Objects toolkit (BANJO) for static Bayesian Network inference. A set of known regulatory relationships involving CDKN2A was used as the initial network to focus the search space. Two proposers concurred in predicting IL1RN, IL6ST, IL1RAPL1, IGFALS, and WNT10B as regulatory targets for CDKN2A. These genes are known to interact with a range of chemicals, including certain environmental toxicants. Furthermore, CDKN2A was predicted to be a direct regulator of RB1. These hypotheses warrant additional study as they lend valuable insights into the functions of CDKN2A in Chronic Obstructive Pulmonary Disease (COPD) and cancer. E2F3 was predicted, and validated in the literature, to be a regulator of MDM2 and TP53. Thus, Bayesian networks are a valuable tool for drawing signaling insights from gene expression data.

### PS 135 Irreversible Inhibition of Acetylcholinesterase by Soman.

G. S. Sirin<sup>1,2</sup> and Y. Zhang<sup>2</sup>. <sup>1</sup>ATSDR, Atlanta, GA; <sup>2</sup>New York University, New York, NY. Sponsor: P. Ruiz.

Acetylcholinesterase (AChE) is a key enzyme in the cholinergic nervous system that hydrolyses acetylcholine and terminates synaptic signals. Organophosphate compounds, such as nerve agents, can covalently inhibit AChE by phosphorylating the enzyme's catalytic serine residue. The phosphorylated adducts can either be reactivated to some limited extent by nucleophilic compounds with oxime functional unit or undergo an aging reaction. Phosphorylation and subsequent aging leads to irreversible AChE inhibition, resulting in overstimulation of the nervous system. By employing *ab initio* QM/MM molecular dynamics simulations with umbrella sampling, we characterized the phosphorylation reaction mechanism between AChE and the nerve agent soman (GD), as well as the aging mechanism of GD phosphorylated AChE. The phosphorylation reaction between AChE and GD follows an associative nucleophilic substitution mechanism that is initiated when the nucleophilic Ser200 attacks GD's phosphorus atom, with His440 acting as a general base. In the elimination step, Tyr121 of the catalytic gorge forms hydrogen bonds with the leaving fluorine atom prior to its dissociation from the active site. Once a stable covalent adduct is formed, the aging reaction begins with excision of the alkoxyl covalent bond connecting the bound GD's alkyl group to the phosphonate moiety. This cleavage is swiftly followed with a methyl group rearrangement of the alkyl group resulting in a stable tertiary carbenium, which is hydrated to an alcohol by a reactive water molecule facilitated by Tyr121. The characterized mechanisms and simulation results provide new detailed insights into this important process. Such mechanistic details are of significant interest for the development of novel strategies to reduce the toxic effects of GD poisoning by facilitating the search and design of novel compounds capable of slowing the aging of nerve-agent-inhibited AChEs as well as effective reactivators for the aged conjugates. Lastly, this work may also facilitate the design of aging-resistant pseudo-catalytic scavengers capable of sequestering nerve agents.

### PS 136 Computational Elucidation of Energetic Trends for DNA Intercalation.

H. W. German and M. J. Novak. *Chemistry, Florida Institute of Technology, W. Melbourne, FL.* Sponsor: L. Valerio.

The prediction of general energetic trends from intercalation of polycyclic aromatic compounds with DNA can provide insight into these pertinent interactions from a pharmacological and toxicological perspective. Compounds chosen for this study are nucleotide base pairs (AT, GC, AA) and two novel intercalating agents (4-azatryptanthrin and coralyne). Unfortunately, neither of these compounds have an established crystal structure when intercalated into DNA. The absence of this computational starting place gives rise to the need for a strong alternative computational method.

Since dispersion forces have been shown to drive optimal orientation based on  $\pi$ -stacking, this method utilizes the electrostatic potential (ESP) maps of both interacting species. Presented herein is our improved method that uses more pertinent variables, overcomes the weakness of a center of mass method, and improves the efficiency with which computational studies can provide insight to experimental design by relying primarily on visual intuition of the ESP alignments. The simplicity of this study leads to the decrease in the time cost and the consideration of dispersion forces increases confidence in our results.

Our computational methods utilize SPARTAN and GAUSSIAN software, a Ground State Density Functional Theory (DFT), Local Spin-Density Approximation (LSDA) method, and a 6-311++G(d,p) basis set. Initial results in-

dicate a preferential intercalation of 4-azatryptanthrin with the GC base pair over an AT base pair based on energetic stabilization due to  $\pi$ -stacking. Identification of trends such as this can be valuable in designing future experimental studies targeting GC or AT rich regions associated with genetic disorders such as Myotonic Dystrophies, Fragile X, and Friedreich's Ataxia.

### PS 137 Efficient *In Vivo* Developmental and Neurotoxicity Screen of ToxCast Phase I and II Compounds in Zebrafish.

L. Truong<sup>1,2,3</sup>, C. Miller<sup>1,2,3</sup>, D. Haggard<sup>1,2,3</sup>, G. Gonnerman<sup>1,2,3</sup>, L. Chalker<sup>1,2,3</sup>, K. Nhan<sup>1,2,3</sup> and R. L. Tanguay<sup>1,2,3</sup>. <sup>1</sup>Environmental and Molecular Toxicology, Oregon State University, Corvallis, OR; <sup>2</sup>Environmental Health Sciences Center, Corvallis, OR; <sup>3</sup>Sinnhuber Aquatic Research Laboratory, Corvallis, OR.

The United States Environmental Protection Agency launched the ToxCast program to begin to predict the potential chemical toxicity of 1,078 compounds made up of pesticides, pharmaceuticals, "green" chemicals, chemicals in cosmetics and other consumer products. Early life stages are often sensitive to chemical insult, which make embryonic zebrafish an ideal platform to investigate the developmental and neurotoxicity of these compounds. We developed an efficient *in vivo* phenotypic screen using embryonic zebrafish to assess all 1,078 compounds. Using a wide range of concentrations (0.0064 to 64  $\mu$ M, 10 fold serial dilution); all compounds were assessed for developmental toxicity beginning at 6 hours post fertilization (hpf). We kept exposed embryos completely in the dark until 24 hpf, and assessed photo-motor responses using the Photo-motor Response Assessment Tool (PRAT) that we developed. PRAT quantifies individual embryonic photo-motor response following two pulses of bright light. The initial pulse normally results in pronounced movement, and the second light pulse usually produces no activity. At 120 hpf, using Viewpoint Zebrafish, we assessed photo-induced larval locomotor activity. The locomotor activity is tracked for 25 minutes (10 in the light, 10 in the dark, and 5 in the light). Afterwards, each larva was assessed for changes in a suite of 20 morphological endpoints. We have successfully conducted the phenotypic screen on all 1,078 compounds, and a summary of the results will be discussed. Collectively, we have demonstrated the efficiency of the zebrafish model as a phenotypic screening platform to identify hazardous chemicals. This research is supported by NIEHS grants P30 ES00210 and RC4ES019764.

### PS 138 *In Silico* and *In Vitro* Analyses of the Hormonal Activity of Hydroxylated Polychlorinated Biphenyl on Human Thyroid Receptor.

C. Dassuncao, O. Faroon, J. Wheeler and P. Ruiz. *DTHHS, ATSDR/CDC, Chamblee, GA.*

Hydroxylated polychlorinated biphenyl (OH-PCBs) may disrupt thyroid hormone status because of their structural similarity to thyroid hormone. However, the molecular mechanisms of interactions with thyroid hormone receptors (TRs) are not fully understood. The integrated application of omics studies, bioinformatics, and computational modeling can provide to biological systems an enhanced understanding of the mechanisms underlying the toxicity of endocrine disruptor chemicals and support the study of disease etiology and prevention. In the present study, we examined the interactions between OH-PCBs and TRs to identify critical structural features and molecular properties of OH-PCBs related to their hormonal activity and to develop quantitative structure-activity relationship (QSAR) models for the thyroid hormone activity of OH-PCBs. Molecular descriptors were computed, selected, and used to characterize the ligand-receptor binding, and subsequently develop an *in silico* model. The *in silico* model had good robustness, predictive ability, and mechanism interpretability. Lipophilic distribution, hydrophobic and electrostatic interactions between OH-PCBs and TRs are important factors governing thyroid hormone activities. The OH-PCBs with higher ability to accept electrons, ortho position of the hydroxyl group, low dipole-dipole interactions tend to have weak binding with TRs and subsequently lower thyroid hormone activities. Hence, this *in silico* model can be used as a screening tool for further targeted toxicity testing and risk assessment, generate hypotheses about potential mechanistic pathways leading to adverse outcomes, and reduce time and cost of OH-PCBs testing.

**PS 139 A Systematic Analysis of ToxCast *In Vitro* Assays Associated with *In Vivo* Hepatic Outcomes.**

J. Liu<sup>1,2</sup>, M. T. Martin<sup>1</sup>, C. Corton<sup>3</sup>, C. Wood<sup>3</sup> and I. Shah<sup>1</sup>. <sup>1</sup>NCCT/EPA, Durham, NC; <sup>2</sup>University of Arkansas, Little Rock, AR; <sup>3</sup>NHEERL/EPA, Durham, NC.

The U.S. EPA's ToxCast™ program uses hundreds of high-throughput, *in vitro* assays to screen chemicals for bioactivity. The EPA Virtual Liver project combines ToxCastDB data with guideline rodent toxicology data to map hepatic adverse outcome pathways (AOPs). Here our objective is to reveal meaningful relationships between *in vitro* assays and *in vivo* liver outcomes. 289 ToxCast phase I chemicals were organized into 15 categories based on 272 histopathological lesions reported in guideline testing studies from ToxRefDB. Based on lesions reported at the study end, 242(83.7%) chemicals produced hypertrophy, 39(13.5%) chemicals resulted in hyperplasia, and neoplastic lesions were found for 79(24.9%). We compared the AC50 concentrations of chemicals for each of the 973 ToxCast assays and identified assays with at least 10 chemicals per category and the mean potency was significantly different ( $p < 0.05$ ). Out of the 973 assays, 28/147(19%) of the high-content imaging assays (APR) had associations with 7 liver injury categories. 6/83(7.2%) multiplexed transcription reporter assays (ATG) and 15/112(13.4%) protein complementation (OT) assays were also significant for liver injury. A number of the assays such as, cell loss, enzyme induction and enzyme inhibition, were generally significant across most categories. On the other hand, some assays were quite specific to certain categories. For instance, APR\_StressKinase\_72hr\_pos (stress kinase pathway activation) and ATG\_CRE\_CIS (transcription factor DNA binding activity) were significant for chemicals that showed regeneration vs ATG\_VDRE\_CIS (nuclear receptor transcription activity) for hypertrophy. The results suggest the utility of HTS assays for screening hepatotoxicity, and for linking biological events in the pathways to specific adverse outcomes. Such assays are not only mechanistically relevant but also aid in defining cell-based toxicity signatures for rapidly screening thousands of environmental chemicals. Abstract does not represent EPA policy.

**PS 140 Interpreting QSAR Toxicity Predictions in Hazard Assessments: An Acrylamide Case Study.**

R. S. DeWoskin, L. D. Burgoon and G. M. Woodall. US EPA, Research Triangle Park, NC.

Toxicity predictions based on QSAR are used to screen large numbers of chemicals with little to no toxicity data into prioritized categories for further toxicity testing, development as "green" chemicals, or candidates for efficacious drug therapy. As databases incorporate more information on adverse pathways and potential targets, QSAR results may also contribute to hazard assessment for chemicals considered "data rich" (based on the availability of a full suite of traditional animal bioassays), but which are often "data poor" when it comes to characterizing the mode of action (MOA), severity progression, or potential adverse human clinical effects not monitored in animal bioassays. Presented here is an exercise to evaluate QSAR results within the context of extant hazard assessments on a data rich chemical, in this case, acrylamide (AA), and its less well studied active metabolite, glycidamide (GA). Results from four QSAR programs – two freeware programs (VEGA and OECD's QSAR) and two proprietary programs (MetaCore™ and Discovery Studio/TopKat™) provided considerable new information in the areas mentioned above. Potential AA and GA induced adverse effects of clinical relevance to humans were identified as well as likely biological targets for AA, GA, and analogous chemicals. The results further supported the qualitative characterization of the MOAs, potential endpoints to consider in dose-response arrays, and identification of potentially important early biomarkers to aid future bioassay or human study design. Conversely, extant AA and GA ADME data and PBPK models helped assess the likelihood of AA or GA reaching biological targets predicted by the QSAR programs. This exercise demonstrated the value of integrating QSAR results into traditional hazard assessment for improved qualitative information. The next step is to integrate high throughput screening /content (HTS/HTC) assay results into the assessment to further quantitate dose-response for a wider array of effects. [The views expressed are those of the authors and do not necessarily reflect the views or policies of the U.S. EPA]

**PS 141 Health-Related Effects Reported by Electronic Cigarette Users in Online Forums.**

M. Hua, M. Alfi and P. Talbot. Cell Biology and Neuroscience, University of California, Riverside, Riverside, CA.

Electronic cigarettes (e-cigarettes) are battery-operated devices that deliver aerosolized nicotine to users without burning tobacco. Because little data exists on their health effects, we explored the symptoms that e-cigarette use has on humans

by analyzing online user posts from three e-cigarette forums with "health and safety" sections. Basic information (location, age, and gender) and health (symptoms and doctor diagnosed signs) information were collected. A total of 405 symptoms (78 positive, 326 negative and 1 neutral) were reported in three forums. Most data analysis was performed on Electronic Cigarette Forum (ECF) posts. A total of 12 systems/anatomical regions were affected in e-cigarette users. Systems most often affected include: mouth and throat, respiratory, neurological, sensory, and digestive. The majority of negative health effects occurred in the respiratory system. We further consolidated reported symptoms into categories to determine which anatomical regions/physiological processes were most affected for each system. For consolidated data, symptoms were most frequently reported for: bronchi/lungs (e.g., wheezing, shortness of breath, difficulty breathing), throat; neurological (headaches), intestine/digestion, and sight. To analyze interactions between systems, interactomes were created with Cytoscape software. Interactions were most frequently seen between circulatory/neurological; respiratory/mouth and throat; respiratory/chest, and digestive/neurological systems. Increased blood pressure was the most frequently reported sign diagnosed by physicians treating e-cigarette users. While some positive health effects were reported, a significant proportion of the data showed a correlation with e-cigarette use and onset of adverse health effects. This study is the first to compile and quantitatively assess health data associated with e-cigarette use from online forums.

**PS 142 The Relationship Between T-Box Transcription Factors CAMK2B and PITX2 in the Expression of Collagen Protein COL4A3 in COPD.**

B. Nguyen, G. Acquah-Mensah and C. Ngo. Pharmaceutical Sciences, MCPHS, Worcester, MA.

The T-Box transcription factors are known have recently been highlighted for their expression role in epithelial cells in Chronic Obstructive Pulmonary Disease (COPD), which genes, including COL4A3, TBX2, TBX3, TBX5, PML, CFLAR, GULP1, CASP10, PAX3, BOK, and PITX2 are connected in transcriptional regulatory networks of lung epithelial cells. The type IV, alpha 3, collagen gene (COL4A3) involves into extracellular matrix construction as the major structural component of basement membrane. COL4A3 is known to have suppressed expression in COPD3. The A polymorphism of the COL4A3 is also indicated of associated with the risk of developing COPD. COL4A3's C terminus binds to autoantibodies at basement membranes in Goodpasture syndrome and is phosphorylated by calcium/calmodulin-dependent protein kinase II beta (CAMK2B), which is activated by the promyelocytic leukemia protein (PML). The paired-like homeodomain 2 (PITX2) regulates the expression of N-cadherin. N-cadherin changes the adhesion of extracellular matrix (ECM) by interacting with collagen proteins. PITX2 gene is regulated by different kinase pathways, such as MAPK and Akt. However, the relationship between these factors is still not well studied. Thus, we have come up with the question that if is PITX2 gene also regulated by CAMK2B. We conducted the study in focus on exploring the relationship between PITX2 and CAMK2B genes by applying Bayesian Network Structural Learning (BNSL). Version 2.2 of Bayesian Network Inference with Java Objects (Banjo) was employed in the study. The result was used to compare to the known interactions between COL4A3, CAMK2B, PITX2 and PML. The study has shown the possible novel phosphorylation of PITX2 by CAMK2B.

**PS 143 Validation of a Systems Toxicology Based Adverse Outcome Pathway Prediction with Functional Outcome: Effect of Exposure to 2, 4-Dinitrotoluene on Energy Metabolism and Exercise Endurance.**

M. S. Wilbanks<sup>1</sup>, K. Gust<sup>1</sup>, S. Atwa<sup>2</sup>, I. Sunesara<sup>3</sup>, S. A. Meyer<sup>2</sup> and E. J. Perkins<sup>1</sup>. <sup>1</sup>Engineer R & D Center, US Army Corps of Engineers, Vicksburg, MS; <sup>2</sup>Department of Toxicology, University of LA-Monroe, Monroe, LA; <sup>3</sup>Center of Biostatistics and Bioinformatics, University of MS Medical Center, Jackson, MS.

2,4-dinitrotoluene (2,4DNT), commonly used in industrial and explosive manufacturing processes, is known to contaminate artillery ranges, demilitarization areas and munitions manufacturing facilities leading to its listing on US EPA's Contaminant Candidate List. Previous transcriptomic and lipidomic studies identified energy metabolism as a potential target of DNT toxicity. The impact of such perturbations of energy metabolism on exercise endurance is largely unknown. We hypothesized that organism-level impacts of 2,4DNT dosing were the result of energy metabolism deficits, especially lipid metabolism, from involving interference with PPAR $\alpha$  signaling and its downstream pathways. To validate this adverse outcome pathway, we linked molecular changes caused by 2,4DNT exposure to effects

on whole animals. PPAR $\alpha$  (-/-) and wild-type (WT) mice exposed to a sublethal 2,4DNT dose (134 mg/kg/day for 14 days) or vehicle were given an exercise challenge (a forced swim) 1 day after the last dose to determine how 2,4DNT and/or PPAR $\alpha$  impairment affected overall performance. Observations were collected at multiple levels of biological organization including genes involved in fatty acid and glucose metabolism, PPAR activation and response, biochemistry (serum triglycerides and glucose), and swimming endurance. Decreased swim times were observed with DNT in WT and PPAR $\alpha$  (-/-) mice, but DNT effect was significantly less in knock-down mice indicating that knock down of PPAR $\alpha$  expression partially rescued mice from DNT-induced energy metabolism deficits. Our results support the proposed hypothesis by demonstrating that 2,4DNT's impact on energy metabolism, especially lipid metabolism, occurs via perturbation of PPAR $\alpha$  signaling resulting in reduced exercise endurance at the individual level. (Support: US Army Corps of Engineers)

## PS 144 Modelability of ToxCast Phase I Datasets.

A. Golbraikh<sup>1,2</sup>, A. Sedykh<sup>1</sup>, E. Muratov<sup>1</sup>, R. Shah<sup>2,3</sup>, W. A. Boyd<sup>4</sup>, M. Smith<sup>4</sup>, G. Zhao<sup>5</sup>, H. Zhu<sup>6</sup>, J. H. Freedman<sup>4</sup> and A. Tropsha<sup>1,2</sup>. <sup>1</sup>University of North Carolina at Chapel Hill, Chapel Hill, NC; <sup>2</sup>Sciome LLC, Research Triangle Park, NC; <sup>3</sup>SRA International, Durham, NC; <sup>4</sup>NIEHS, Research Triangle Park, NC; <sup>5</sup>AstraZeneca, Shanghai, China; <sup>6</sup>Rutgers University, Camden, NJ.

One of the problems in Quantitative Structure-Activity Relationships (QSAR) analysis is to establish, whether it is possible to build a predictive model for a given dataset. For some datasets, all attempts to build a predictive model using different sets of descriptors and QSAR/QSTR methodologies fail raising a question, whether it is possible to evaluate the dataset modelability prior to modeling. We have devised several modelability criteria such as dataset diversity, new activity cliff indices, correct classification rate (CCR) for similarity search models (ssCCR), CCR=0.5\*(sensitivity+specificity), etc. These criteria were applied to 40 binary datasets, for which QSAR models were built using Dragon 5.5 descriptors and/or ToxCast in vitro assays treated as biological descriptors, and kNN, Random Forest and SVM methods. The best modelability criterion was found to be the ssCCR, which had the correlation coefficient of 0.73 with the QSAR/QSTR model CCR. We consider a model predictive, if its CCR as well as both sensitivity and specificity are at least 0.70. We found that to satisfy this condition, ssCCR should be at least 0.68. ssCCR values were obtained for ToxCast datasets with 24 ToxRefDB in vivo assays as end points, which had at least 30 toxic compounds among 212 compounds of the curated ToxCast dataset. None of the ssCCR for these datasets was as high as 0.60 except for the rat cholinesterase inhibition assay, for which it was 0.85, and sensitivity and specificity were 0.83 and 0.88, respectively. We conclude that with the latter exception, ToxCast Phase I datasets with ToxRefDB in vivo assays as end points do not appear to be modelable using QSAR approaches. This conclusion agrees with the recent empirical observations of Thomas et al (Toxicol Sci. 2012, 128:398-417).

## PS 145 Celastrol Decreases Specificity Proteins (Sp) and Fibroblast Growth Factor Receptor-3 (FGFR3) in Bladder Cancer Cells.

G. Chadalapaka<sup>1</sup>, I. D. Jutooru<sup>1</sup> and S. H. Safe<sup>1,2</sup>. <sup>1</sup>Department of Veterinary Physiology and Pharmacology, Texas A&M University, College Station, TX; <sup>2</sup>CEGM, Institute of Biosciences & Technology, Houston, TX.

Bladder cancer is the ninth most common cancer worldwide and ranks 13th as a cause of cancer deaths. MVAC (methotrexate, vinblastine, adriamycin and cisplatin) chemotherapy has been extensively used for treatment of advanced bladder cancer and is accompanied by toxic side effects and, thus, it is important to develop less toxic alternate chemotherapeutic therapies and dietary management strategies for prevention of this disease. Celastrol (CSL) is a naturally occurring triterpenoid acid that exhibits anticancer activity, and in KU7 and 253JB-V bladder cells, 0.5 to 2.5  $\mu$ M CSL induced apoptosis, inhibited growth, colony formation and migration and CSL decreased bladder tumor growth in vivo. CSL also decreased expression of specificity protein (Sp) transcription factors Sp1, Sp3 and Sp4 and several Sp-regulated genes/proteins including vascular endothelial growth factor, survivin and cyclin D1. CSL also decreased fibroblast growth factor receptor-3 (FGFR3), a potential drug target for bladder cancer therapy. Results of RNA interference and knockdown of Sp proteins show that FGFR3 is a Sp-regulated gene downregulated by CSL. The mechanism of Sp downregulation by CSL was cell context-dependent due to activation of proteasome-dependent (KU7) and -independent (253JB-V) pathways. In 253JB-V cells, CSL induced reactive oxygen species (ROS) and inhibitors of ROS such as glutathione blocked CSL-induced growth inhibition and

repression of Sp1, Sp3 and Sp4. This response was due to induction of the Sp repressors ZBTB10 and ZBTB4 and downregulation of miR-27a and miR-20a/17-5p, respectively, which regulate expression of these transcriptional repressors. Thus, the anticancer activity of CSL in 253JB-V cells is due to induction of ROS and ROS-mediated induction of Sp repressors (ZBTB4/ZBTB10) through downregulation of miR-27a and miR-20a/17-5p and this is emerging as a characteristic pathway observed for many ROS inducers in cancer cells.

## PS 146 Raloxifene Potentiates the Cytotoxicity-Induced by RL91, a Second Generation Curcumin Analog, in PC3 Prostate Cancer Cells.

A. Mazumder<sup>1</sup>, M. Gould<sup>2</sup>, S. Taurin<sup>1</sup>, H. D. Nicholson<sup>2</sup> and R. J. Rosengren<sup>1</sup>. <sup>1</sup>Pharmacology & Toxicology, University of Otago, Dunedin, New Zealand; <sup>2</sup>Anatomy, University of Otago, Dunedin, New Zealand.

The survival rate for men with hormone refractory prostate cancer has not changed significantly in the last 30 years. Thus there is a need for new drug treatments for this aggressive cancer. Our lab has had success with second generation curcumin derivatives as novel therapies for aggressive breast cancer. In this study we examined the combination of raloxifene and 2,6-bis(pyridin-4-ylmethylene)-cyclohexanone (RL91), a potent 2nd generation curcumin derivative as a novel treatment for hormone refractory prostate cancer (HRPC). The combination treatment showed highly potent cytotoxicity toward PC3 prostate cancer cells compared to individual treatments. Specifically, EC50 values of 2  $\mu$ M and 10  $\mu$ M were produced by RL91 and raloxifene, respectively. Moreover, this combination decreased cell number by 85% compared to control after 96 h of treatment, as determined by the sulforhodamine B assay. Raloxifene is known to modulate the activity of estrogen receptor alpha (ER $\alpha$ ) and beta (ER $\beta$ ). The activation of these receptors as well as the epidermal growth factor receptor (EGFR), is crucial for the proliferation of HRPC. To determine how raloxifene potentiates the cytotoxic effect of RL91, the localization of these receptors was examined by fluorescent microscopy. The results showed that ER $\alpha$ , ER $\beta$ , the androgen receptor (AR) and EGFR were expressed in PC3 cells. However, raloxifene treatment (10  $\mu$ M for 48 h) promoted EGFR internalization in the cytoplasm. A similar effect was also seen for ER $\beta$  where raloxifene promoted a translocation from the nucleus to the cytoplasm. However, no change was observed for either ER $\alpha$  or the AR. These results suggest that raloxifene-mediated changes in the localization of ER $\beta$  and the EGFR provide a mechanism by which raloxifene enhances the cytotoxicity of RL91 toward PC3 cells. This novel mechanism should be explored further in order to develop new therapies for HRPC.

## PS 147 Evaluation of Wild Yam (*Dioscorea Villosa*) Root Extract As a Potential Epigenetic Agent in Breast Cancer Cells.

P. Aumsuwan<sup>1,2</sup>, S. I. Khan<sup>1,3</sup>, I. A. Khan<sup>1,3</sup>, L. A. Walker<sup>1,2</sup> and A. K. Dasmahapatra<sup>1,2</sup>. <sup>1</sup>National Center for Natural Product Research, University of Mississippi, University, MS; <sup>2</sup>Department of Pharmacology, University of Mississippi, University, MS; <sup>3</sup>Department of Pharmacognosy, University of Mississippi, University, MS.

Aberrant epigenetic alterations in the genome, is believed to be a potential cause of some forms of cancer. Due to their reversibility, epigenetic modifications are considered potentially useful in drug development approaches (epi-drugs). The current available synthetic epi-drugs are non-specific and induce adverse effects. Natural products might offer advantages and find utility for cancer treatment. The present study was designed to evaluate the efficacy of wild yam root extract as a potential demethylating agent using two breast cancer cell lines, MCF-7 (Estrogen receptor positive, ER+) and MDA-MB-231 (ER negative, ER-), and a gene, *GATA-3*, a potential marker of breast cancer development. Moreover, *GATA-3* expression is methylation-specific, being higher in ER+ cells with promoter hypomethylation and insignificant in ER- with promoter hypermethylation. In this study, cells, approximately at 70 % confluency, were treated with wild yam root extract (0-50  $\mu$ g/ml) for 72h and then used for viability, mRNA, and methylation analyses. It was observed that wild yam significantly reduced viability of both cell lines and enhanced the mRNA contents of DNMTs (*DNMT1*, *3A*, and *3B*) and *GATA-3* in a dose-dependent manner. Global DNA methylation, analyzed as 5'-methyl-2'-deoxycytidine (mC) and 5-hydroxymethylcytosine (hmC), showed that mC was increased only in MCF-7 cells, whereas hmC level was reduced in both cell lines. Since hmC is generated from mC by ten-eleven-translocation (TET) enzymes, the present data suggest that enhanced expression of *GATA-3* and *DNMT* enzyme mRNAs followed by a reduction in hmC in MCF-7 and MDA-MB-231 cells are the result of interruption of TET enzyme functions in the epigenome by wild yam root extract. This plant with a long history of traditional use should be further explored with regard to its potential as an epigenetic agent in breast cancer therapy.

**PS 148 Mucosa-Associated Enteropathogenic Escherichia coli As an Internal Exposome Triggers Tumor Cell Dissemination via Macrophage Inhibitory Cytokine 1.**

H. Choi, J. Kim, S. Park, K. Do, C. Oh and Y. Moon. *Laboratory of Mucosal Exposome and Biomodulation, Department Microbiology and Immunology, Pusan National University School of Medicine and Medical Research Institute, Yangsan, Republic of Korea.*

Commensal bacterial community shifts in the pathogenic colonic environment and chronic colonization of mucosa-associated Escherichia coli (MAEC) has been linked to colonic tumorigenesis. Enteropathogenic Escherichia coli (EPEC) is one of commonly identified MAEC in colorectal cancer patients. The aim of this study is to address the contribution of MAEC colonization to human carcinogenesis. EPEC infection of cancer cell caused alterations in affect locomotion-related behaviors of cancer cell including detachment, migration, cytoskeleton rearrangement, dissemination and survival via induction of macrophage inhibitory cytokine 1 (MIC-1). Mechanistically, MIC-1 induced RhoA GTPase which mediated survival of the detached cancer cells. In terms of signaling pathway, MIC-1 triggered TGF-beta-activated kinase 1 (TAK-1), which enhanced expression of RhoA GTPase. In conclusion, mucosal EPEC enhanced MIC-1 gene expression in the human intestinal cancer cells, which was associated with enhanced tumor cell resistance to anoikis and subsequent survival via enhanced TAK-1 and RhoA GTPase (This work was supported by the Basic Science Research Program through the National Research Foundation of Korea, funded by Ministry of Education, Science, and Technology Grant 2012R1A1A2005837).

**PS 149 Ring-Substituted Analogs of 3, 3'-Diindolylmethane (DLM) Induce Apoptosis and Necrosis in Androgen-Dependent and -Independent Prostate Cancer Cells.**

A. Goldberg<sup>1</sup>, V. I. Titorenko<sup>2</sup>, A. Beach<sup>2</sup>, S. H. Safe<sup>3,4</sup> and T. Sanderson<sup>1</sup>. <sup>1</sup>Toxicology, INRS, Laval, QC, Canada; <sup>2</sup>Biology, Concordia University, Montréal, QC, Canada; <sup>3</sup>Veterinary Physiology and Pharmacology, Texas A&M University, College Station, TX; <sup>4</sup>Institute for Bioscience and Technology, Houston, TX.

We have recently reported that novel ring-substituted analogs of 3,3'-diindolylmethane (ring-DIMs), exhibit anti-androgenic and anti-proliferative activities in androgen-dependent prostate cancer cells. We hypothesized that the anti-proliferative effects of ring-DIMs may be due to their ability to induce cell death. Ring-DIMs inhibited androgen-stimulated LNCaP cell proliferation and induced apoptosis and necrosis in LNCaP and PC-3 prostate cancer cells with 2-4 fold greater potencies than DIM. DIM and the ring-DIMs increased caspases-3, -8 and -9 activity and induced PARP cleavage in both cell lines. The cytotoxicity of the most potent ring-DIM, 4,4'-dibromoDIM, but not the other ring-DIMs, was decreased by caspase-3 inhibition. The 4,4'-dibromoDIM was primarily found in the extracellular media, whereas the ring-DIMs were located intracellularly in both cell lines. Ring-DIMs were more potent inhibitors of cell growth and survival in LNCaP and PC-3 cells than DIM and the differential structure-dependent cell death mechanisms indicates ring-DIMs have clinical potential as chemopreventive and chemotherapeutic agents in prostate cancer, regardless of hormone-dependency.

**PS 150 Ellagitannins and Anthocyanins Constituents of Pomegranate Suppress Colorectal Aberrant Crypt Foci (ACF) and Inflammation: Possible Role of miR126.**

N. Banerjee<sup>1,2</sup>, H. Kim<sup>2</sup> and S. U. Mertens-Talcott<sup>1,2,3</sup>. <sup>1</sup>Toxicology, Texas A&M University, College Station, TX; <sup>2</sup>Nutrition and Food Science, Texas A&M University, College Station, TX; <sup>3</sup>Veterinary Physiology & Pharmacology, Texas A&M University, College Station, TX.

The antitumorigenic efficacy of polyphenols ellagitannins and anthocyanins extracted from pomegranate (*Punica granatum* L.) has been extensively studied where cytotoxic, anti-inflammatory and antioxidant effects were demonstrated in various cancer models. The objective of this study was to investigate the role of post-transcriptional regulation of apoptotic and inflammatory biomarkers by specific microRNAs in cells treated with pomegranate polyphenols (PP).

mRNA, microRNA expression were measured by RT-PCR, protein by western blotting and multiplex bead assay. In vivo studies were performed with Sprague Dawley rats (10rats/group) that received PP (2504.74mg/L GAE) for 10 weeks and were injected with azoxymethane (AOM) subcutaneously (15 mg/kg) at weeks 3 and 4.

PP juice suppressed the number of high multiplicity aberrant crypts foci (HMAF) >4 ACF) by 42% (P<0.05) and lowered Ki67 (proliferation marker) antigen. Correspondingly, cell proliferation was also inhibited by PP (5 -25 µg/mL) in colon

cancer cells HT-29. In vitro and in vivo results were accompanied by a downregulation of expression including NF-κB, inducible nitric oxide synthase (iNOS), cyclooxygenase-2 (COX-2), vascular adhesion molecule-1 (VCAM-1) and insulin growth factor (IGF). PP also inhibited phosphorylation of PI3K/Akt, and mTOR signaling pathways. miRNA 126 is frequently lost in colon cancer and targets VCAM-1 and PI3K that are involved in inflammation and cell survival. PP increased miR126 expression in both in vitro and in vivo, corresponding to the observed decrease in VCAM-1 and PI3K. In vitro, the involvement of miR-126 was confirmed using the antagomir for miR-126, where PP reversed the effects of the antagomir.

In summary PP inhibited HT29 cell proliferation, suppressed number of HMAF formation and colon tumorigenesis through the involvement of microRNA 126-regulated pathways.

**PS 151 Dichloroacetate (DCA) Increases Radiation Sensitivity of A549 and H1299 Lung Cancer Cells.**

J. B. Watkins<sup>1</sup>, K. T. Allen<sup>1</sup>, H. Chin-Sinex<sup>2</sup>, J. D. Sherer<sup>2</sup>, J. M. Jesseph<sup>1</sup>, J. G. Foley<sup>1</sup> and M. S. Mendoca<sup>2</sup>. <sup>1</sup>Medical Sciences Program, Indiana University School of Medicine, Bloomington, IN; <sup>2</sup>Department of Medical and Molecular Genetics, Indiana University School of Medicine, Indianapolis, IN.

Dichloroacetate (DCA) is a synthetic small molecule inhibitor of pyruvate dehydrogenase kinase used to treat metabolic diseases with low toxicity in human patients for decades. Recent reports suggest that DCA is cytotoxic to several cancer cell types including non-small-cell lung cancers (NSCLC). The cytotoxicity to cancer cells appears to be a result of a reversal of the Warburg effect through partial restoration of mitochondrial glucose oxidation away from cytoplasmic aerobic glycolysis. With the increase in glucose oxidation, ROS production is augmented leading to the opening of the mitochondrial transition pore to release cytochrome c and apoptosis inducing-factor (AIF) into the cytoplasm. The consequence is mitochondria membrane depolarization and induction of cell death in a caspase-dependent or -independent manner. Given the potential therapeutic translation of DCA to human cancer treatment, we investigated the efficacy of DCA to sensitize NSCLC to X-ray induced killing *in vitro* after both single and fractionated X-ray exposure. Treatment with DCA decreased plating efficiency (PE) and enhanced radiation-induced cell killing by dose modification factors of 1.5 in A549 and 1.4 in H1299. The decrease in PE was not due to induction of apoptosis or necrosis. X-ray fractionation showed that DCA inhibited split-dose recovery/repair by 3.5 fold in A549 and 1.5 fold in H1299. Flow cytometry analysis with propidium iodide indicated significant cell cycle arrest at G1/S in A549 and at G2/M in H1299. The data suggest that DCA enhances X-ray-induced NSCLC cell killing through inhibition of DSB repair and/or alteration of cell cycle distribution.

**PS 152 Mango Polyphenolics Reduce Inflammation in Intestinal Colitis—Potential Involvement of the miR-126/PI3K/AKT/mTOR Pathway *In Vitro* and *In Vivo*.**

H. Kim<sup>1</sup>, N. Banerjee<sup>1,2</sup>, S. Talcott<sup>1</sup> and S. U. Mertens-Talcott<sup>1,2</sup>. <sup>1</sup>Department of Nutrition and Food Science, Texas A&M University, College Station, TX; <sup>2</sup>Interdisciplinary Program of Toxicology, Texas A&M University, College Station, TX.

Mango polyphenolics including gallic acid, mangiferin and gallotannins, have shown antioxidant, anti-inflammatory and anticarcinogenic properties in several studies. However, anti-inflammatory mechanisms relevant to the prevention of colon cancer have not been well investigated.

This study investigates the potential role of the miRNA-126/PI3K/AKT/mTOR signaling pathway in the anti-inflammatory effects of mango polyphenolics in human CCD-18Co colon-myofibroblastic cells and on DSS-induced colitis in rats. Animals were administered control juice (15.7g sugar and 0.05g citric acid/100ml) or mango juice (total phenolic content of 475.80mg/L GAE), and exposed three cycles of 3% DSS. The mRNA and protein levels were measured by RT-PCR, western blot analysis and multiplex bead assay.

In vitro mango extract and gallic acid suppressed the expressions of inflammatory mediators such as NF-κB (p65) and IL-1β and reduced the expressions of AKT and HIF1α involved in AKT/mTOR pathway at mRNA and protein level in a dose dependent manner. Correspondingly, miRNA-126, which negatively regulates the Akt/mTOR pathway, was induced by mango extract and gallic acid. In the rat colitis model, mango juice intake suppressed cell proliferation as measured by Ki-67 staining, and resulted in protection against DSS-induced colon inflammation during chronic colitis compared to control juice. The juice significantly attenuated the expressions of pro-inflammatory cytokines such as TNF-α, IL-1β, IL-6, and IL-10 at protein and mRNA level. Moreover, the phosphorylation of AKT and mTOR were suppressed, and the expression of PI3K was reduced while miRNA-126 that has a target site in the mRNA of PI3K was upregulated by the juice.

These results suggest that mango polyphenols attenuated inflammatory response by modulating the miR-126/PI3K/AKT/mTOR pathway both in vitro and in vivo, and is a potential therapeutic for colitis and colon cancer.

## **PS 153** Loss of the Tumor Suppressor Protein PTEN Contributes to Increased Nrf2 Signaling.

P. M. Shelton<sup>1</sup>, M. I. Vitolo<sup>2</sup>, S. S. Martin<sup>2</sup> and A. K. Jaiswal<sup>1</sup>. <sup>1</sup>Pharmacology, University of Maryland, Baltimore, Baltimore, MD; <sup>2</sup>Marlene and Stewart Greenebaum Cancer Center, University of Maryland, Baltimore, Baltimore, MD.

Nrf2 is a master regulator of cyto-protective genes involved in the maintenance of cellular redox balance. In recent studies, the PI3K/Akt pathway is reported to positively regulate the Nrf2 pathway. The protein phosphatase PTEN counteracts the action of PI3K by removing the phosphate from PIP3. This led us to hypothesize that loss or mutation of PTEN, an event that occurs frequently in cancers, might increase Nrf2 activity that promotes the survival and proliferation of cancer cells. In our study we investigated the role of PTEN in prostate and breast cancer, commonly reported to have either loss of heterozygosity or mutations in PTEN. Using the PTEN-null human prostate cancer cell line PC3, we found that expression of wild-type but not mutant PTEN decreased the basal and anti-oxidant induced expression of Nrf2 target genes. More common clinically, patients have loss of a single allele of PTEN. Therefore, we also investigated the Nrf2 pathway in cells heterozygosity for the PTEN gene. Using a murine prostate tumor cell line with a spontaneous loss of a single allele in PTEN (PTEN-P8, +/-) and an isogenic cell line that had deletion of the second allele (PTEN-CaP8, -/-) we found that complete loss of PTEN resulted in higher expression of the Nrf2 target genes. In order to fully address the role of PTEN haploinsufficiency that could mimic the cellular progression from benign to malignant we also looked at Nrf2 activity in the immortalized breast epithelial cell line MCF-10a that had both alleles intact (+/+), deletion of a single allele (+/-), or deletion of both alleles (-/-) of PTEN. As expected, we found that both the basal and inducible expression of the prototypical Nrf2 target gene NQO1 inversely correlated with PTEN status. Together this suggests that the loss of PTEN contributes to increased Nrf2 transcriptional activity, which likely provides cells with an altered proteome that favors oncogenesis.

## **PS 154** Formaldehyde-Induced Replication Stress Causes Activation of ATR Kinase Leading to p53-Mediated Apoptosis and Senescence in Human Lung Cells.

J. Morse, V. Wong and A. Zhitikovich. Brown University, Providence, RI.

Formaldehyde (FA) is a recognized human carcinogen with documented inhalation exposures in many occupational groups. Here we examined stress signaling pathways and cell fate decisions triggered by FA in human lung cells (normal lung fibroblasts, H460 lung epithelial cells and primary bronchial epithelial cells). We found that FA induced a rapid activation of the DNA damage-responsive ATR kinase that preferentially targeted the p53 transcription factor at low and moderate damage levels. Activation of p53 was evidenced by its strong Ser-15 phosphorylation, protein stabilization and upregulation of its target genes, such as MDM2 and CDKN1A (p21). Knockdown experiments with shRNA confirmed the p53 dependence of the gene expression responses. FA also caused a depletion of the p53 inhibitor MDM4 via its enhanced proteolysis. The use of biochemical markers of individual cell cycle phases and replication status manipulations showed that activation of ATR-p53 signaling by FA occurred exclusively in the S phase. The p53 played a major role in FA-induced apoptosis in lung epithelial cells, which was associated with upregulation of the proapoptotic gene BBC3 (PUMA). The presence of p53 was also required for permanent growth arrest (senescence) in FA-treated lung fibroblasts. Overall, our results indicate that replication stress and ATR-activated p53 are responsible for cytotoxic responses in FA-exposed human lung cells. Acknowledgements. This work was supported by grant ES020689 from NIEHS.

## **PS 155** Down-Regulation of Telomerase Activity and Shortening of Telomere Length by Polychlorinated Biphenyls (PCBs) in HL-60 Cells.

X. Xin<sup>1</sup>, S. Pl<sup>1</sup>, J. L. Schnoor<sup>1,2</sup> and G. Ludewig<sup>1</sup>. <sup>1</sup>Interdisciplinary Graduate Program in Human Toxicology, The University of Iowa, Iowa City, IA; <sup>2</sup>Department of Civil and Environmental Engineering, The University of Iowa, Iowa City, IA.

We reported that PCBs, environmental persistent organic pollutants and probable human carcinogens, can down-regulate telomerase activity in vitro in immortal human keratinocytes (HaCaT). The most efficacious congener was the dioxin-like

PCB126, a potent arylhydrocarbon receptor (AhR) agonist. To analyze whether this effect of PCB126 is tissue specific and to gain insight into the mode of action (MOA) we exposed another cell type, human promyelocytic leukemia (HL-60) cells, to PCB126 and also to PCB153, not an AhR activating congener. Both compounds reduced telomerase activity, visible after 6 days of exposure, and telomere length, to about 50% within 30 days of exposure, PCB126 more so than PCB153. This reduction in telomerase activity and telomere length was seen in both cell lines, but only HaCaT also showed a strong increase in cytochrome P450 1A1 mRNA and activity, the hallmark of AhR activation. This suggests that AhR activation may be one, but not the only mechanism for this effect of PCBs. HL-60 can differentiate which is accompanied by a reduction in telomerase activity. However, the continuous proliferation of the PCB-exposed cells makes this mechanism less likely. Telomeric repeat binding factors (TRF1, TRF2) are involved in the stabilization of telomeres. Up-regulation of TRF1/2 was seen in PCB126-exposed HaCaT, pointing to a possible mechanism. Experiments with both cell lines, representing different target tissues of PCB toxicity, are under way to elucidate the MOA of PCBs on telomeres and the possible significance of this effect on precursor cells of the hematopoietic pathway. (Supported by NIEHS P42 ES013661)

## **PS 156** Chronic Exposure to Particulate Hexavalent Chromium Disrupts Shugoshin1 Localization in Human Lung Cells.

C. Falank<sup>1</sup> and J. Wise<sup>1,2,3</sup>. <sup>1</sup>Wise Laboratory of Environmental and Genetic Toxicology, University of Southern Maine, Portland, ME; <sup>2</sup>Maine Center for Toxicology and Environmental Health, University of Southern Maine, Portland, ME; <sup>3</sup>Department of Applied Medical Science, University of Southern Maine, Portland, ME.

Chromosomal instability (CIN) is a hallmark of cancer and can be caused by spindle assembly checkpoint disruption or chromosome missegregation during mitosis. Hexavalent chromium (Cr(VI)) is a well-known human lung carcinogen, and has shown to induce numerical CIN, however its mechanisms for inducing aneuploidy remain unknown. In this study we are investigating whether Cr(VI) affects a key centromeric cohesion protein, Shugoshin 1 (Sgo1). Sgo1 maintains and protects centromeric cohesion in G2 and continues to maintain proper sister-chromatid cohesion during mitosis. This protection mechanism prevents sister-chromatids from prematurely separating during mitosis. Disruption of Sgo1 localization has been shown to lead to chromosome missegregation. We have found that chronic exposure to particulate Cr(VI) disrupts the localization of Sgo1 in G2 cells. Specifically, after a 24 h exposure to 0.1, 0.2, or 0.3 µg/cm<sup>2</sup> lead chromate we did not observe any changes in the percent of G2 cells with Sgo1 localization at the kinetochores. However, a 120 h exposure to the same concentrations showed a concentration-dependent decrease in the percent of G2 cells with Sgo1 localization at the kinetochores. Specifically 0.1, 0.2 or 0.3 µg/cm<sup>2</sup> disrupted localization in 36, 88, and 90% of G2 cells, respectively. Our findings suggest that particulate Cr(VI)-induced CIN is mediated through disrupting Sgo1 localization to the kinetochores during G2 cells, thus leading to chromosome missegregation and ultimately aneuploidy. This work was supported by NIEHS grant ES016893 (J.P.W.).

## **PS 157** Ultraviolet B-Irradiated L-Tryptophan Induces Human UDP-Glucuronosyltransferase 1A1 and 1A8 Expressed in the Human Skin.

R. Fujiwara, M. Kawana, E. Kouno, S. Takano, T. Narawa and T. Itoh. School of Pharmacy, Kitasato University, Tokyo, Japan.

Benzo[a]pyrene is a widespread environmental contaminant and its active metabolite, benzo[a]pyrene-7,8-dihydrodiol-9,10-epoxide, is associated with the development of ultraviolet (UV) B-induced skin cancer. While UDP-glucuronosyltransferase (UGT) is involved in the detoxification of benzo[a]pyrene, the protective role of UGT in the defensive mechanism against UVB-induced skin cancer has not been elucidated yet. Here, we investigated the effects of UVB irradiation on the expression of human UGT1A enzymes as well as on cytochrome P450 (CYP) 1A1 in HaCaT cells. Multiple UGT1A isoforms such as UGT1A1, UGT1A3, UGT1A4, and UGT1A8 were expressed in human skin and HaCaT cells. When HaCaT cells were treated with 6-formylindolo[3,2-b]carbazole (FICZ), which is one of the tryptophan derivatives formed by UVB, UGT1A1 and UGT1A8 along with CYP1A1 were significantly induced. While UVB-irradiated tryptophan also induced those enzymes, the formation of FICZ was not detected in the irradiated tryptophan solution, indicating that tryptophan derivatives other than FICZ formed by UVB might have the potential to activate the aryl hydrocarbon receptor. While UVB induces CYP1A1, increasing the bioformation of benzo[a]pyrene-7,8-dihydrodiol-9,10-epoxide from benzo[a]pyrene, it also induces UGTs, accelerating the detoxification of benzo[a]pyrene. Specific induction of skin UGT1A1 and UGT1A8 without inducing CYP1A1 might protect individuals from developing skin cancer.

**PS 158 The Cannabinoid WIN 55, 212-2 Decreases Specificity Protein (Sp) Transcription Factor and the CaP Protein eIF4E in Colon Cancer Cells.**

S. Sreevalsan<sup>1</sup> and S. H. Safe<sup>1,2</sup>. <sup>1</sup>VTPP, Texas A&M University, College Station, TX; <sup>2</sup>Institute of Biosciences and Technology, Texas A&M Health Science Center, Houston, TX.

The eukaryotic translational initiation factor (eIF4E) is an essential component of the cellular translational machinery and is responsible for binding ribosomes to the cap structure of mRNAs. The phosphorylated form (serine-209) of eIF4E plays a critical role in cancer cell growth and transformation. Treatment of colon cancer cells with a synthetic cannabinoid WIN 55,212-2 (WIN) inhibited cancer cell growth, induced apoptosis and downregulated specificity protein (Sp) transcription factors and Sp-regulated gene products associated with cancer cell growth (EGFR and Cyclin D1), angiogenesis (VEGF and VEGFR) and survival (survivin and bcl-2). The anticancer activity of WIN is accompanied by induction of multiple phosphatases and some of the effects of WIN are blocked by the phosphatase inhibitor sodium orthovanadate (SOV). Treatment of SW480 cells with 7.5  $\mu$ M WIN alone also decreased levels of eIF4E and co-treatment with 0.35 mM SOV blocked WIN-induced downregulation of eIF4E and knockdown of Sp proteins confirmed that eIF4E was an Sp-regulated gene. Protein phosphatase 2A (PP2A) catalyzes dephosphorylation of both eIF4E and Mnk-1, an upstream kinase that phosphorylates eIF4E. Treatment of SW480 cells with 7.5  $\mu$ M WIN and knockdown of PP2A by RNA interference blocked downregulation of eIF4E, Sp proteins and some Sp-dependent genes. Several anticancer agents inhibit Sp transcription factors by inducing zinc finger binding protein ZBTB10 and by suppressing microRNA-27a (miR27a). Treatment of SW480 cells with 7.5  $\mu$ M WIN induced ZBTB10 protein and decreased miR27a expression and knockdown of PP2A reversed these responses demonstrating that WIN-induced downregulation of Sp and eIF4E was due to PP2A-mediated disruption of miR27a:ZBTB10 axis.

**PS 159 HOTTIP, a lncRNA, Exhibits Pro-Oncogenic Activity in Pancreatic Cancer.**

I. D. Jutooru<sup>1</sup>, G. Chadalapaka<sup>1</sup>, K. Kim<sup>2</sup> and S. H. Safe<sup>1,2</sup>. <sup>1</sup>TAMU, College Station, TX; <sup>2</sup>IBT, Texas A&M Health Science Center, Houston, TX.

Recent studies have demonstrated that non-coding RNAs (ncRNAs) are differentially expressed and play an important role in gene regulation and influence normal and cancer cell phenotypes. About 3000 lncRNAs have been identified and some of these act as scaffolds regulating molecular (protein, RNA and DNA) interactions required for various signaling networks and this is accomplished, in part, by association with chromatin-modifying complexes. HOXA transcript at the distal tip (HOTTIP) is a 3,764-bp lncRNA transcribed from 5' tip of HOXA gene cluster and is expressed in anatomically distal cells such as hand and foot fibroblasts. Previous studies in our laboratory showed that HOTAIR is a negative prognostic marker in pancreatic cancer and this is due, in part, to interaction of HOTAIR with Polycomb Repressive Complex 2. In contrast, HOTTIP was reported to interact with MLL complexes by specifically binding to WDR5 adapter protein leading to broad loss of H3K4me3 across HOXA locus. In this study, we investigated the functional role of HOTTIP in Panc1 and L3.6pL pancreatic cancer cell lines. Knockdown of HOTTIP by RNA interference studies (iHOTTIP) resulted in ~50% reduction in cell survival within 72 hr after transfection and iHOTTIP also decreased pancreatic cancer cell migration which was determined in a Boyden chamber assay. iHOTTIP enhanced Annexin V staining and PARP cleavage associated with induction of apoptosis in both Panc1 and L3.6pL cells. Knockdown of HOTTIP also decreased expression of cyclin D1, VEGF and survivin which play an important role in cell proliferation, angiogenesis and survival. An in vivo study was performed using L3.6pL cells transfected with iHOTTIP in a mouse xenograft model and after 15 days of knockdown there was a significant reduction in tumor volumes and weights ( $\geq 70\%$ ). RNASeq analysis of HOTTIP knockdown in Panc1 cells resulted in significant (>1.5 fold) changes in expression of ~1467 genes and analysis of data suggest that HOTTIP mediated gene regulation has a critical role in pancreatic cancer progression.

**PS 160 Metformin Causes Degradation of Fatty Acid Synthase and PI3 Kinase Signaling Proteins in Pancreatic Cancer Cells through Downregulation of Specificity Protein (Sp) Transcription Factors.**

V. Vasanthakumari<sup>1</sup> and S. H. Safe<sup>1,2</sup>. <sup>1</sup>VTPP, Texas A&M University, College Station, TX; <sup>2</sup>IBT, TAMHSC, Houston, TX.

Metformin or N,N'-dimethyl biguanide is an oral hypoglycemic drug with a remarkable record of safety that has been prescribed worldwide for treatment of Type II diabetes. In addition to its antidiabetic property it also exhibits antineoplastic ef-

fects which include inhibition of angiogenesis through decreased levels of vascular endothelial growth factor (VEGF) and blocks cell cycle progression through decreased expression of cyclin D1. Fatty Acid Synthase (FAS) a key enzyme in lipid metabolism is overexpressed in cancer cells, which is one of the phenotypic alterations in cancer progression. Here we show that expression of FAS was significantly decreased when pancreatic cancer cells were treated with metformin. FAS expression is stimulated by growth factors and their receptors, like EGFR and IGFR. Effects of these receptors on FAS complex involve cross talk between various signal transduction pathways. One such signaling pathway include PI3kinase/ mTOR pathway. Specificity protein (Sp) transcription factors - Sp1, Sp3 and Sp4 play a complex role in malignant transformation of pancreatic cancer cells. We report for the first time that metformin downregulates specificity protein (Sp) transcription factors (Sp1, Sp3, Sp4) in cancer cells. Furthermore metformin downregulates the expression of growth factor receptors like EGFR, IGFR and phosphorylation/expression of major PI3K effectors like AKT and mTOR. Knockdown of Sp1, Sp3, and Sp4 proteins by RNA interference decreased the expression of FAS, pmTOR and pAKT indicating that FAS and these signaling proteins are regulated by Sp proteins. However when cells were pretreated with SOV (Sodium Ortho Vanadate), a phosphatase inhibitor, there was a reversal of Sp downregulation and phosphorylation of mTOR by metformin. The effects of metformin on downstream targets of PI3 kinase pathway and the specific phosphatases which play a major role in the antineoplastic effects of metformin are currently being investigated.

**PS 161 Overexpression of STAT-3 Induces Anoikis Resistance, Promotes Cell Migration, and Metastatic Potential in Cancer Cells.**

N. M. Fofaria and S. K. Srivastava. Biomedical Sciences and Cancer Biology Center, Texas Tech University Health Sciences Center, Amarillo, TX.

Anoikis is an anchorage independent cell death. Resistance to anoikis is one of the key features of the metastatic cells. In the current study, we have shown the role of STAT-3 in anoikis resistance in various melanoma and pancreatic cancer cells. Marked anoikis was induced as such in the cells that were grown in anchorage-independent conditions. The melanoma and pancreatic cancer cells that resisted anoikis were observed to have higher rate of migration as compared to the cells that were exposed to anchorage dependent growth, as observed in cell migration and invasion assays. These anoikis resistant cells also had significantly higher expression and phosphorylation of STAT-3 at Tyr 705, than the cells that were attached to the basement membrane. Treatment of these cells with IL-6, a cytokine which phosphorylates STAT-3, prevented the induction of anoikis. STAT-3 inhibitors AG490 and piplartine induced anoikis in a concentration-dependent manner, whereas IL-6 blocked anoikis. Over-expression of STAT-3 by transfection, not only increased the anoikis resistance but also protected cancer cells from piplartine-induced anoikis, confirming the role of STAT-3 in anoikis resistance. On the other hand, silencing STAT-3 decreased the potential of cancer cells to resist anoikis. Furthermore, STAT-3 (-/-) cancer cells were more sensitive to anoikis as well as to the effect of piplartine as compared to STAT-3 (+/+) cells. The STAT-3 (+/+) cells also had enhanced migration potential as compared to STAT-3 (-/-) cells. In summary, our results establish STAT-3 as a critical player that renders anoikis resistance to the cancer cells and enhance their metastasis potential. The role of STAT-3 in anoikis in breast and ovarian cancer is currently under investigation. The outcome of this study has great clinical implications as it will serve as a platform to devise rational therapeutic approaches to treat metastatic cancers. [Supported in part by R01 grants CA106953 and CA129038 (to S.K.S) awarded by the National Cancer Institute].

**PS 162 Indole and Related Compounds Exhibit AhR Antagonist/Agonist Activities.**

S. H. Safe<sup>1</sup>, A. Jayaraman<sup>2</sup>, R. Alaniz<sup>2</sup> and U. Jin<sup>2</sup>. <sup>1</sup>Texas A&M University, College Station, TX; <sup>2</sup>IBT, Texas A&M University System, Houston, TX.

Indole-derived compounds including diindolylmethane (DIM), indole-3-carbinol, tryptophan photoproducts and metabolites have been identified as agonists of the aryl hydrocarbon receptor (AHR). Indole and tryptophan metabolites tryptamine (TA) and indole 3-acetate (IAA) are produced by gut microflora and there is evidence that AHR ligands modulate gut inflammatory pathways. We therefore investigated the AHR agonist/antagonist activities of indole, TA and IAA using Ah-responsive breast and colon cancer cells as in vitro models. In MDA-MB-468 breast cancer cells TA (0-500  $\mu$ M) induced CYP1A1 mRNA and protein with an EC50 < 500  $\mu$ M; IAA and indole also induced CYP1A1 mRNA (only IAA induced CYP1A1 protein) however < 30 and < 10% of the maximal induction responses were observed at 1000  $\mu$ M concentrations of IAA and indole respectively. The effects of these compounds as inhibitors of 2,3,7,8-tetrachlorodibenzo-p-dioxin

(TCDD) induced responses were also investigated in cells treated with the indole compound alone or in combination with TCDD. Indole (500 and 1000  $\mu$ M) significantly inhibited TCDD-induced CYP1A1 mRNA and protein levels and similar results were observed for 500  $\mu$ M TA however the former compound was a significantly more potent AHR antagonist. In contrast IAA did not exhibit AHR antagonist activity. These results were somewhat variable among different cell lines however, it was evident that the major gut microbiome product, indole, was an AHR antagonist and this may impact AHR-dependent gut inflammatory pathways.

**PS 163 Tolfenamic Acid Inhibits Colon Cancer Cell and Tumor Growth and Downregulates Specificity Protein (Sp) Transcription Factors.**

S. Pathi<sup>1</sup> and S. H. Safe<sup>1,2</sup>. <sup>1</sup>Veterinary Physiology and Pharmacology, Texas A&M University, College Station, TX; <sup>2</sup>Institute of Bioscience and Technology, Houston, TX.

**Introduction:** Tolfenamic acid (TA) is a nonsteroidal anti-inflammatory drug (NSAID) and is a potential chemotherapeutic agent for treatment of colon cancer; however, the mechanism of action of TA is unknown and was investigated in this study.

**Methods:** Inhibition of colon cancer cell growth and induction of apoptosis by TA was investigated using cell counting and Annexin V staining, and modulation of specificity protein (Sp) transcription factors Sp1, Sp3, Sp4 and Sp-regulated gene products was determined by western blot analysis of whole cell lysates. Mechanisms of TA-induced Sp downregulation were investigated using specific pathway inhibitors and the in vivo anticancer activity of TA was determined in athymic nude xenograft studies using RKO cells as xenografts.

**Results:** TA induced apoptosis and decreased colon cancer cell growth and this was accompanied by caspase-dependent proteolysis of Sp1, Sp3 and Sp4 and decreased expression of Sp-regulated gene products including bcl-2, survivin, VEGF, VEGFR1, cyclin D1 and c-MET. TA also inhibited colon tumor growth and decreased Sp1, Sp3, Sp4 and Sp-dependent gene product expression in tumors.

**Conclusion:** TA-induced repression of Sp transcription factors and Sp-regulated genes play a role in the cancer chemotherapeutic effects of TA. Since TA acts as anticancer agent in several tumor types, results of this study suggest for the first time that TA is a potential chemotherapeutic agent for treatment of colon cancer. Clinical applications of TA alone or in combined treatment of colon cancer are enhanced since this agent is relatively non-toxic and has previously been used as a non-steroidal anti-inflammatory drug. The prior use of TA, as an NSAID will also facilitate approval of the drug for application as a cancer therapeutic agent.

**PS 164 Ni<sup>2+</sup>-Induced Chromosome Aberrations/Gene Amplification/Gene Silencing Alter Cytoskeleton, Ca<sup>2+</sup> Distribution, and Global Gene Expression, Causing Morphol./Neoplast. Transformation of 10T1/2 Mouse Embryo Cells.**

J. R. Landolph<sup>1,3,2</sup>, A. DaSilva Pehl<sup>2,3</sup>, P. Samala<sup>1,3</sup>, S. Keliipaakaua<sup>2,3</sup> and K. Akinwumi<sup>1,3</sup>. <sup>1</sup>Department of Molecular Microbiology and Immunology, University of Southern California, Los Angeles, CA; <sup>2</sup>Department of Pathology, University of Southern California, Los Angeles, CA; <sup>3</sup>USC Cancer Center, University of Southern California, Los Angeles, CA.

Ni refinery workers inhaling Ni sulfidic ore dusts/smoking cigarettes contracted lung/nasal cancers. Inhaled Ni3S2/green NiO induced lung cancer in rats. Ni3S2/green-black NiOs induced chromosome aberrations/morph-neoplas transformation (Tx) in 10T1/2 mouse cells. Ni/MCA-Tx cell lines showed a) ect-2 gene amplification/higher ect-2 mRNA/protein, b) no DRIP80 c) no  $\beta$ -centaurin-2 mRNA. We hypothesized Ni+2 1) amplified ect-2 gene, causing higher levels of microtubules (MTs); 2) silenced  $\beta$ -centaurin-2 gene, causing higher levels of microfilaments (MFs); and 3) silenced DRIP gene, altering Ca+2 distribution/Tx 10T1/2 cells. We tested these hypotheses by staining cells with fluor. phalloidin to decorate MFs; fluor. Ab to  $\alpha$ -tubulin to decorate MTs; Fluor 3AM to stain Ca+2; DAPI to decorate nuclei; then examined cells by confocal microscopy. In non-Tx 10T1/2 cells, MFs/MTs were arranged in long fibers. In NiS/green NiO-Tx cell lines, MFs/MTs were over-expressed, aggregated in areas, absent/other areas, changing cell shapes. Low density non-Tx cells had high nuclear/low cytoplasmic Ca+2 concentrations (State I); high density near-confluent cells had low nucl./high cyto. Ca+2 (State II). Ni/MCA-Tx cell lines were largely in State II. We conclude Ni+2 ions 1) amplified ect-2/silenced  $\beta$ -centaurin-2 genes, causing over-expression of MTs/MFs, altering cell shapes, changing global gene expression; 2) silenced DRIP80 gene, altering Ca+2 distributions in Tx cells; and 3) induced mutations/methylations in 15 genes, causing differential expression of 130 genes, contributing to induction/maintenance of Tx phenotypes in Ni+2/MCA-Tx cell lines. Support: R01 ES03341/NIEHS (PI JRL); Cancer Center Core Grant 5 P30 CA09320/NCI; MS Program/Discret. Funding (JRL).

**PS 165 Benzoquinone-Induced Topoisomerase Modifications: Linking Benzene Myelotoxicity and Leukemia.**

C. L. Kuhlman, G. Tsapralis, T. J. Monks and S. S. Lau. *Southwest Environmental Health Sciences Center, Department of Pharmacology and Toxicology, University of Arizona, Tucson, AZ.*

Protein adduction by reactive electrophiles can induce structural and functional changes that contribute to toxicity and disease progression. Such electrophiles are often products of xenobiotic metabolism or generated endogenously via oxidative stress and lipid peroxidation. Relevant to this phenomenon are the redox-active and electrophilic metabolites of benzene, which are believed to contribute to its myelotoxic effects. When the benzene metabolites hydroquinone (HQ) and phenol (PHE) are administered to rats, HQ oxidizes to 1,4-benzoquinone (BQ) and in the presence of GSH gives rise to multi-GSH conjugates detectable in bone marrow. These HQ-GSH conjugates retain the ability to adduct proteins and to redox cycle. Here we report that bone marrow malondialdehyde levels in PHE/HQ treated rats are significantly elevated, indicative of lipid peroxidation and the consequent generation of other reactive electrophilic aldehydes, such as 4-hydroxy-2-nonenal (4HNE). Indeed, proteomics profiling revealed bone marrow proteins targeted by benzene metabolites and 4HNE, including 14-3-3 protein zeta/delta, protein disulfide isomerase A3, peroxiredoxin 2, and calreticulin. Adduction of topoisomerase II  $\alpha$  (topo II $\alpha$ ) has been implicated in benzene-induced leukemia, and cancer chemotherapeutic topo II $\alpha$  inhibitors are a leading cause of therapy-induced leukemia. We next reacted purified topo II $\alpha$  (6 units) with BQ (0.5  $\mu$ M) or 4HNE (1.3  $\mu$ M). A marked reduction in the ability of topo II $\alpha$  to decatenate the kDNA substrate was observed. Proteomic analysis of 4HNE-reacted topo II $\alpha$  revealed multiple amino acid sites of adduction, including K893 and K1480 adducts. Adduction of these lysine residues could impair topo II $\alpha$ -DNA binding, or inhibit topo II $\alpha$ 's ATP-dependent formation and annealing of DNA strand breaks. The consequences of BQ- and 4HNE-induced functional alterations in topo II $\alpha$  are currently under investigation.

**PS 166 Overexpression of CRM1 in Normal Human Lung Epithelial Cells Changes Cellular Morphology and Cytotoxic Responses to Tobacco-Specific Carcinogen NNK.**

C. Lu, W. Zhu and W. Gao. *The Institute of Environmental and Human Health, Texas Tech University, Lubbock, TX.*

Chromosome region maintenance 1 (CRM1), the major nuclear export receptor with a broad substrate range, is not only required for transport of many RNAs and proteins but also involved in various modulations within the cell such as mitosis, cell arrest, and apoptosis. Our recently published study showed that CRM1 played critical roles in response to tobacco-specific carcinogen, 4-(methylnitrosamino)-1-(3-pyridyl)-1-butanone (NNK), in BEAS-2B cells (a normal human lung epithelial cell line). The objective of the present study was to further examine the significance of CRM1 in lung cancer development using BEAS-2B cells stably overexpressing CRM1 (BEAS-2BCRM1+ cells). The overexpression of CRM1 in BEAS-2BCRM1+ cells was confirmed by real-time PCR and western blot. As compared to BEAS-2B cells, BEAS-2BCRM1+ cells were prone to form colonies. Soft-agar assay further demonstrated increased colony formation and larger colony size in BEAS-2BCRM1+ cells in comparison with BEAS-2B cells. In addition, the cytotoxic effects in response to NNK was measured by 3-(4,5-dimethylthiazol-2-yl)-5-(3-carboxymethoxyphenyl)-2-(4-sulfophenyl)-2H-tetrazolium (MTS) assay in both cells. Cells were treated with 0-500  $\mu$ M NNK for 24, 48, and 72 h. The inhibitory effects were dose and time dependent in both cells ( $p < 0.05$ ). However, BEAS-2BCRM1+ cells showed different sensitivity to NNK as compared to BEAS-2B cells. Taken together, our results indicate that CRM1 overexpression changes cellular morphology and cytotoxic response to tobacco carcinogen in human lung epithelial cells. The potential molecular mechanisms involving these changes are being evaluated to better understand the critical role of CRM1 in chemical carcinogenesis after NNK exposure.

**PS 167 ARNT Isoforms Mediate Opposing Effects on NF- $\kappa$ B Signaling.**

K. Gardella<sup>1,2</sup>, I. Muro<sup>1,2</sup> and C. Wright<sup>1,2</sup>. <sup>1</sup>Division of Pharmacology and Toxicology, The University of Texas at Austin, Austin, TX; <sup>2</sup>The Center for Molecular and Cellular Toxicology, The University of Texas at Austin, Austin, TX.

We have previously shown that the arylhydrocarbon receptor nuclear translocator (ARNT) regulates the chromatin binding activity of the RelB NF- $\kappa$ B subunit. ARNT is a transcription factor that is integral in the regulation of xenobiotic and hypoxic responses but our studies suggest that ARNT also participates in NF- $\kappa$ B

signaling. ARNT is expressed as two isoforms, isoform 1 and 3, but whether these isoforms differentially regulate NF- $\kappa$ B activity is unclear. Isoform 1 is identical to isoform 3 except for an additional 15 amino acids near the N-terminus. The extra amino acids in isoform 1 provide a phosphorylation site, which has been shown to inhibit its DNA binding. Interestingly, we have observed in lymphoid malignancies that ARNT isoform 1 is expressed at much higher levels than isoform 3 as compared to normal lymphocytes where the ARNT isoforms are expressed at equal levels. We find that ARNT isoform 1 potentiates while ARNT isoform 3 abrogates NF- $\kappa$ B activity. In light of our previous ARNT-RelB model, these opposing effects of the ARNT isoforms in NF- $\kappa$ B signaling appear to hinge on their ability to associate with RelB as ARNT isoform 3 binds much more strongly than isoform 1. Lastly, we found that the co-expression of a GFP-tagged p100 in combination with the ARNT isoforms promoted p100 nuclear translocation, possibly through a RelB bridge, resulting in diminished transactivation of NF- $\kappa$ B responsive genes. Thus, our current working model is one in which lymphoid malignancies shift toward the production of ARNT isoform 1, which in turn enhances NF- $\kappa$ B activity, as a contributing factor to their growth and survival.

## PS 168 Co-Exposure to Arsenic and Estrogen Leads to Enhanced Transformation of Normal Human Prostate Epithelial Cells.

J. Treas, T. Tyagi and K. P. Singh. *The Institute of Environmental and Human Health, Texas Tech, Lubbock, TX.*

Exposure to both arsenic and estrogen are known risk factors for prostate cancer, however the carcinogenic effect of their co-exposure is not known. Therefore, the objective of this study was to evaluate the transformation potential and its mechanism in human prostate epithelial cells by co-exposure to these two chemicals. To achieve this objective, the human prostate epithelial cells, RWPE-1 were treated for 6 months with sodium-meta arsenite and 17 $\beta$ -estradiol, both alone and in combination, at concentrations of 100 pg/mL and 100 ng/mL. Cell counts and MTT assay was performed to determine the effects on growth, and soft agar assay was performed to evaluate the cell transformation by exposure to arsenic and estrogen. Potential role of estrogen receptors and aromatase in mediating the cellular response to these chemicals was evaluated by measuring their expression at transcript level. The result of this study revealed that the growth and transformation of RWPE-1 cells were significantly greater in arsenic and estrogen co-exposed cells as compared to cells individually exposed to these two chemicals. The data of quantitative real time PCR revealed that expression of estrogen receptor beta was significantly increased whereas aromatase was significantly decreased in arsenic and estrogen co-exposed cells. These findings together with our recently published data on aberrant expression of epigenetic regulatory genes, such as, DNMTs, HDACs and MBDs in arsenic and estrogen co-exposed cells suggest that co-exposure to these two chemicals enhances carcinogenicity through epigenetic mechanisms.

## PS 169 Effects of Polycyclic Aromatic Hydrocarbons with Estrogen Receptors $\alpha$ and $\beta$ in Breast Cancer Cells.

T. T. James<sup>1,2</sup>, C. K. Sievers<sup>2</sup>, E. Shanle<sup>1,2</sup>, S. S. Hecht<sup>3</sup>, C. A. Bradfield<sup>1,2</sup> and W. Xu<sup>1,2</sup>. <sup>1</sup>Molecular and Environmental Toxicology Center, University of Wisconsin-Madison, Madison, WI; <sup>2</sup>Oncology, University of Wisconsin-Madison, Madison, WI; <sup>3</sup>Masonic Cancer Center, University of Minnesota, Minneapolis, MN.

Polycyclic aromatic hydrocarbons (PAHs) are widespread environmental pollutants found in cigarette smoke, contaminated soil, vehicle exhaust, among others, known to cause adverse health effects including carcinogenesis and endocrine disruption. The metabolites of PAHs have been implicated in endocrine disruption. Some PAHs are known to have estrogenic effects by interacting with estrogen receptors (ERs). Estrogens have diverse roles including regulation of mammary gland development and morphogenesis, and maturation of uterus and ovaries. These functions are mediated by two subtypes of estrogen receptors, ER $\alpha$  and ER $\beta$ , which function in dimer forms (i.e. ER  $\alpha$ , $\beta$  homodimers and ER $\alpha$ / $\beta$  heterodimers). ER $\alpha$  is known to be proliferative while ER $\beta$  is known to be antiproliferative in the mammary gland. The estrogenic effects of PAHs have been mostly focused on their effects on ER $\alpha$ . Recently our lab reported that the monohydroxylated metabolites of naphthalene, phenanthrene and pyrene showed differential effects with ER $\alpha$  and ER $\beta$ . These PAHs were selected because they are found at high levels in contaminated environments. The ability of the PAH compounds to promote estrogenic effects were revealed by luciferase assays in isogenic reporter cell lines, competitive binding assays and bioluminescent resonance transfer (BRET) assays. The PAHs metabolites were more selective for ER $\beta$  and were able to activate ER $\beta$  target genes suggesting that these compounds can interfere with ER $\beta$  signaling in human breast cancer cells. In this study we screened additional PAHs and their monohydroxylated metabolites to determine their estrogenic effects. These studies demonstrate the impact of monohydroxylated PAHs on ER signaling and provide basis for the determination of the effects of other environmental compounds on ER. Supported by NIEHS Predoctoral Training Grant T32 ES007015

## PS 170 Alternative Splicing of ATG5 in DU145 Human Prostate Cancer Cells Inactivates Autophagy and Promotes Xenograft Tumor Growth.

D. J. Wible<sup>1,2</sup>, T. M. Calhoun-Davis<sup>2</sup>, D. G. Tang<sup>2</sup> and S. B. Bratton<sup>2</sup>. <sup>1</sup>Institute for Cellular and Molecular Biology, The University of Texas at Austin, Austin, TX; <sup>2</sup>Molecular Carcinogenesis, Virginia Harris Cockrell Cancer Research Center at The University of Texas MD Anderson Cancer Center Science Park, Smithville, TX.

Autophagy is a highly conserved pathway that targets cytoplasmic cargo to the lysosome for degradation. Excess or aberrant organelles, large protein aggregates and non-selective portions of the cytosol can be targeted by the autophagosome and delivered to the lysosome in order to maintain cellular homeostasis or survival in response to stress. In this study, we show that DU145 human prostate cancer cells alternatively splice Autophagy-related protein 5 (ATG5), an essential protein for autophagosome formation. These novel ATG5 splice forms are unable to conjugate normally to ATG12 and instead are rapidly ubiquitinated and turned over by the proteasome. The absence of ATG5-ATG12 conjugate in DU145 cells prevents autophagosome formation and autophagic degradation. Stable expression of full-length ATG5 using lentiviral infection rescued both ATG5-ATG12 conjugation and autophagy. Autophagy is currently thought to be tumor suppressive by eliminating potentially genotoxic protein aggregates and damaged organelles. However, the role it plays in tumor progression and metastasis remains unclear. To address this question, we performed subcutaneous injections of autophagy-deficient and autophagy-proficient DU145 cells into immunodeficient mice and monitored tumor formation and growth. In initial experiments, autophagy deficient tumors had a significantly longer latency period, yet grew at a faster rate than autophagy competent tumors. This suggests that autophagy can promote initial tumor establishment, while suppressing later tumor growth. Currently there are numerous clinical trials investigating the therapeutic potential of drugs that inhibit autophagy. Since it's not yet clear how these opposing aspects affect cancer metastasis, further study is essential to ensure effective therapy.

## PS 171 The Aryl Hydrocarbon Receptor Regulation during Epithelial-to-Mesenchymal Transition.

S. S. Kishinhi and S. E. Eltom. *Biochemistry & Cancer Biology, Meharry Medical College, Nashville, TN.*

The aryl hydrocarbon receptor (AhR) is a ligand-activated transcription factor that plays a role as a mediator of the xenobiotic signaling pathways. Recently, the AhR emerged as a major player in breast carcinogenesis. We have shown previously that ectopic overexpression of AhR in immortalized normal human mammary epithelial cells (HMEC) resulted in the development of malignant phenotypes, most notably the epithelial-to-mesenchymal transition (EMT). This EMT phenotype however, is not rigid but is in a dynamic state; with cells moving back and forth between epithelial and mesenchymal states. We asked the question whether this flux of phenotypes is due to changes in AhR levels or activity. A clone of HMEC overexpressing AhR, with either epithelial (E) or fibroblastic (F) phenotypes was compared to an empty vector (EV) control cells. We employed Western blotting, immunocytofluorescence (ICF) staining and RT-PCR techniques to assess the AhR expression as well as the epithelial and mesenchymal markers, E-Cadherin and vimentin, respectively. Our results showed that although at the mRNA levels AhR expression was similar, the AhR protein was higher in E- than in F-type cells. The AhR protein levels were always higher when cells were grown at higher density. Nuclear localization as assessed by ICF and CYP1A1 expression as assessed by RT-real time PCR, were used as surrogates for AhR activation. Our analysis showed that AhR activation was much higher in F-type cells and is more pronounced at higher cell density. In contrast, a 3h treatment with TCDD, a potent AhR agonist resulted in a steeper induction of CYP1A1 in E-type than the F-type cells, which is further enhanced at higher density. The observed difference in AhR protein levels and activity may be due to a differential stability of the protein associated with the two morphological forms, which is under investigation.

## PS 172 Expression and Role of ALDH1B1 in Pancreatic Cancer.

S. Singh<sup>1</sup>, K. Quackenbush<sup>2</sup>, A. Purkey<sup>2</sup>, J. Arcaroli<sup>2</sup>, Y. Chen<sup>1</sup>, D. J. Orlicky<sup>3</sup>, W. Messersmith<sup>2</sup> and V. Vasilou<sup>1</sup>. <sup>1</sup>Department of Pharmaceutical Sciences, University of Colorado, Aurora, CO; <sup>2</sup>Division of Medical Oncology, University of Colorado, Aurora, CO; <sup>3</sup>Department of Pathology, University of Colorado, Aurora, CO.

Recent studies show that ALDH activity selectively defines an enhanced tumor-initiating cell population in human pancreatic adenocarcinoma. The specific ALDH isozyme(s) contributing to the high ALDH activity in these cells are unknown. We have recently shown that the mitochondrial aldehyde dehydrogenase 1B1

(ALDH1B1) is a potential biomarker for colon cancer. The aim of the current study was to examine expression and the role, if any, of ALDH1B1 in pancreatic adenocarcinoma. In normal pancreas, ALDH1B1 is abundantly expressed in glandular cells, but sparsely in the ducts (ALDH1B1 immunopositivity =  $16.7 \pm 1.7$ ). In pancreatic ductal carcinoma, we found a rather high ALDH1B1 expression in ductal cancerous tissues (ALDH1B1 immunopositivity =  $197.2 \pm 29.4$ ). Our data were also confirmed by analyzing human pancreatic adenocarcinoma tissue microarrays. Furthermore, ALDH1B1 appears to be contributing to ALDH activity in some, but not all, human pancreatic cancer explants examined. The variation of ALDH1B1 expression was also observed in 16 human pancreatic cancer cell lines. Two high and two low ALDH1B1 expressing cell lines were subjected to siRNA ALDH1B1 knockdown and cell proliferation was evaluated. High ALDH1B1 cell lines showed a 35% reduction in cell growth whereas proliferation was not affected in low ALDH1B1 cell lines. Treatment of high ALDH1B1 cells with gemcitabine resulted in greater ALDH1B1 mRNA levels and enzyme activity. In contrast low ALDH1B1 cells showed no such effect. Collectively our data show for the first time that ALDH1B1 is expressed at very high levels in pancreatic cancer and it contributes to proliferation of these tumor cells. These data suggest a potential role of ALDH1B1 in pancreatic cancer.

**PS 173 Gene Expression Changes in Human Endometrial and Mammary Cells Exposed to Tamoxifen.**

E. Hernandez Ramon<sup>1</sup>, E. Asaki<sup>2</sup>, O. Olivero<sup>1</sup> and M. C. Poirier<sup>1</sup>. <sup>1</sup>LCBG, NCI, NIH, Bethesda, MD; <sup>2</sup>Division of Computational Bioscience, CIT, NIH, Bethesda, MD.

Tamoxifen (TAM), a selective estrogen receptor modulator used for adjuvant therapy and chemoprevention of breast cancer, also increases the risk of endometrial and myometrial cancer. We hypothesized that comparison of gene expression patterns in cultured normal breast and endometrial cells may elucidate TAM-induced mechanisms. Gene expression studies in normal human mammary epithelial cells (NHMECs) exposed to 10  $\mu$ M TAM for 48 hr, using NIH DNA-oligonucleotide microarrays (Schild et al., 2003), demonstrated up-regulation of genes active in the interferon and immune-response pathways. Here we used the same NHMECs and TAM exposure conditions, and evaluated gene expression by Human Gene 1.0 ST Affymetrix expression array. Results using the Affymetrix array confirmed TAM-induced up-regulation of interferon signaling and complement pathways. Genes significantly overexpressed include some reported before (IFI27, IFIT1, IFIT3, IFI44L, IFITM1 and OAS3), and new genes involved in the same pathway (IFI44, IFI35, and IFIH1), as well as genes in the complement system (C1S, C1R and SERPING1). To contrast breast with endometrium, we used human endometrial stromal cells (HESC cells), also exposed to 10  $\mu$ M TAM for 48 hr. The primary genes up-regulated included some involved with biosynthesis of steroids (DHCR7, FDPS and MVD), and SREBF2, a sterol transcription factor. In addition, there was up-regulation of PPARG, a gene involved in cell proliferation and cancer, and down-regulation of CC1, a gene with anti-tumor activity. Expression changes of the most highly altered genes have been confirmed by qRT-PCR, and the microarray data are being subjected to extensive pathway analysis. However, these preliminary data show induction of different gene expression patterns in normal human mammary and endometrial cells exposed to TAM, confirming that immune-response pathways are induced in the breast, and showing that steroidal and proliferative pathways are induced in the endometrium.

**PS 174 Revealing the Role of Cancer Testes Antigens in Hif Signaling.**

C. Okechukwu<sup>1</sup>, A. Whitehurst<sup>2</sup>, J. Wooten<sup>2</sup> and K. Corcoran<sup>2</sup>. <sup>1</sup>Chemistry and Pharmaceutical Sciences, North Carolina Central University, Durham, NC; <sup>2</sup>Pharmacology, University of North Carolina Chapel Hill, Chapel Hill, NC. Sponsor: A. Baines.

The hypoxia-inducible factor-1 (HIF-1), is a transcription factor that responds to changes in oxygen homeostasis. Furthermore, the HIF pathway has been observed to contribute to tumor aggressiveness. The overexpression of HIF proteins has been observed to increase malignancy in tumor cells. Identifying the mechanisms that regulate HIF is essential to developing therapeutic strategies to inhibit its function. Here, we asked whether any members of the cancer-testes (CT)-antigen (CTA) family support HIF signaling. We combined an siRNA mediated loss of function approach with a luciferase reporter fused to a HIF Response Element (HRE) to determine consequences on HIF signaling following individual depletion of 120 CTAs. This screen revealed a subset of CT-antigens that positively support HIF induced transcription. This regulation appears to be at the level of the HIF1 $\alpha$  protein as depletion of a subset of these CTAs, MAGEA3/6 and IGF2BP3 reduced induc-

tion of HIF1 $\alpha$  protein. These findings suggest that CTAs may support stress signaling, particularly under hypoxic conditions and further demonstrate that CTAs may be playing functional roles in supporting tumor cell survival.

**PS 175 Aryl Hydrocarbon Receptor (Ahr)-Active Pharmaceuticals Are Selective Ahr Modulators in Triple Negative Breast Cancer Cell Lines.**

U. Jin<sup>1</sup>, S. Lee<sup>1</sup> and S. H. Safe<sup>1,2</sup>. <sup>1</sup>CEGM, Institute of Biosciences & Technology, Houston, TX; <sup>2</sup>VTPP, Texas A&M University, College Station, TX.

The aryl hydrocarbon receptor (AHR) plays an important role in multiple biological processes including regulation of drug-metabolizing enzymes, inflammatory pathways, immune responses and modulation of tumor cell formation and growth. Activation of the AHR by 2,3,7,8-tetrachlorodibenzo-p-dioxin (TCDD) or the selective AHR modulator 6-methyl-1,3,8-trichlorodibenzofuran (MCDF) inhibited metastasis/invasion of triple negative MDA-MB-231 breast cancer cells in vitro and in vivo and identification of other antimetastatic AHR ligands was further investigated among a group of previously identified AHR-active pharmaceuticals. Treatment of BT474, MDA-MB-468 and MDA-MB-231 breast cancer cells with 4-hydroxytamoxifen, flutamide, leflunomide, mexiletine-HCl, nimodipine, omeprazole, sulindac, or tranilast gave highly variable results for their AHR agonist activity which was structure and cell context-dependent. The most striking data were observed in MDA-MB-468 cells where tranilast exhibited partial AHR agonist/antagonist activities and mexiletine inhibited TCDD-induced CYP1A1 gene expression and was a full AHR antagonist in this cell line. We also investigated the potential AHR-mediated inhibition of MDA-MB-231 cancer cell migration and invasion by this panel of pharmaceuticals using scratch and Boyden Chamber invasion assays. Only omeprazole blocked cell migration and invasion in this cell line and these responses were inhibited by knockdown of the AHR by RNA interference or co-treatment with the AHR antagonists, 3'-methoxy-4'-nitroflavone or 3,4-methoxy- $\alpha$ -naphthoflavone. These in vitro antimetastatic responses were accompanied down-regulation of the prometastatic gene CXCR4, previously been reported as an AHR ligand-inducible gene. Omeprazole and related benzimidazole analogs also exhibited anti-invasion activities in vitro suggesting that this AHR-pharmaceutical class may have clinical importance for treating advanced basal-type breast cancer that metastasizes to other tissues. (Supported by NIH-R01-CA-136571).

**PS 176 A Retrospective Analysis of Vehicle-Related Effects on Body Weight Gain and Survival from Two-Year Sprague-Dawley Rat Carcinogenicity Studies.**

R. Yeager<sup>1</sup>, C. Papagiannis<sup>2</sup>, D. Poage<sup>2</sup>, R. Pimentel<sup>2</sup>, T. Henriques<sup>1</sup>, C. Lin<sup>3</sup> and L. Shu<sup>3</sup>. <sup>1</sup>Preclinical Safety Toxicology, Abbott Laboratories, Abbott Park, IL; <sup>2</sup>MPI Research, Inc., Mattawan, MI; <sup>3</sup>Non-Clinical Statistics, Abbott Laboratories, Abbott Park, IL.

Depending on the proposed clinical indication, two-year rat carcinogenicity (CA) studies are conducted in support of the marketing application for new chemical entities (NCEs). The vehicle(s) used to formulate NCEs for the preclinical GLP rat toxicology studies are often utilized in the CA studies. Therefore, the objective of this study was to conduct a retrospective analysis of vehicle-related effects on body weight gain and survival from rat CA studies. The data set consisted of 30 individual vehicle groups, which included the following vehicles: water, methylcellulose, ad libitum diet/feed, and a lipid mixture. Survival was analyzed by the proportional hazard model and body weight gain was analyzed by the Gompertz non-linear mixed model. For males and females, there was higher variability in survival with diet compared to other vehicles. In males, there was a marginally significant ( $p = 0.069$ ) increase in survival with diet compared to water. In addition, there was a significant decrease in survival with the lipid mixture vehicle compared to all other vehicles. This significant decrease in survival with the lipid mixture vehicle corresponded with a decrease in body weight gain in this group compared to all other vehicles. In females, there was a significant increase in survival with methylcellulose compared to diet; however, there were no other significant differences in survival among other vehicle groups in females. Moreover, there was not as profound of an effect on body weight gain in females administered the lipid mixture vehicle, compared to other vehicles, as was observed in males. In conclusion, this analysis demonstrates that complex vehicle formulations, such as lipid mixtures, may affect body weight gain and survival on two-year rat carcinogenicity studies.

**PS 177** **Modifying Effect of Glycidol Fatty Acid Esters on *N*-Methyl-*N*-Nitrosourea Induced Mammary Carcinogenesis in Rats.**

Y. Cho<sup>1</sup>, T. Toyoda<sup>1</sup>, S. Onami<sup>1</sup>, Y. Mizuta<sup>1</sup>, A. Nishikawa<sup>2</sup> and K. Ogawa<sup>1</sup>.  
<sup>1</sup>Division of Pathology, NIHS, Tokyo, Japan; <sup>2</sup>Biological Safety Research Center, NIHS, Tokyo, Japan.

Glycidol fatty acid esters (GEs), trace contaminants in edible oils which are possibly formed during refining processes, have recently been detected in vegetable fat-containing products, including infant formulas. The level of GEs was ten times higher in enzymatically processed diacylglycerol-rich oil than that in the regular cooking oil containing triacylglycerols as major components. Although there is no toxicological data available yet on the GEs, the primary toxicological concern is based on the potential release of genotoxic carcinogen, glycidol from the parent esters. In the present study, to detect the modifying effects of GEs on the mammary gland, one of the carcinogenic target organs of glycidol, we pretreated 7-week-old SD rats with *N*-methyl-*N*-nitrosourea (50 mg/kg i.p.) and then administered glycidol (800 ppm) or GEs (3600 ppm, glycidol oleate (GO) or glycidol linoleate (GL)) in the drinking water for 26 weeks. The dose levels being selected on the basis of carcinogenic dose levels in rat carcinogenicity study of glycidol (37.5 and 75 mg/kg/day) and on the equal moles of the esters. In body weights, significant decrease was noted in the glycidol group compared to control group from week 2 through experimental period due to obvious decrease of water consumption. The calculated glycidol intake was 43 mg/kg per day and on the assumption that all treated GEs would be completely metabolized to glycidol, intake of glycidol in GO and GL groups was 93 and 74 mg/kg per day, respectively. The multiplicity and volume of histopathologically diagnosed mammary tumors, in particular poorly differentiated mammary carcinomas were significantly increased in the glycidol group as compared with the control. In the GO group, the multiplicity and volume of mammary tumors showed a slight tendency to increase, but no change was noted in the GL group. These results provide evidence of a mammary tumor promoting activity of glycidol, but not GEs in the present model.

**PS 178** **Spontaneous Thymoma Observed in Carcinogenicity Study of Wistar Han Rats.**

C. Maraschiello<sup>1</sup>, W. Henderson<sup>1</sup>, H. Iwata<sup>1,2</sup>, K. Weber<sup>1,2</sup>, S. Gachle<sup>1</sup> and T. Anzai<sup>1</sup>. <sup>1</sup>Harlan Laboratories, Inc., Indianapolis, IN; <sup>2</sup>AnaPath GmbH, Oberbuchsen, Switzerland.

Wistar Han rats are an appropriate model for toxicity and carcinogenicity studies in rodents and spontaneous thymoma is sometimes recorded in carcinogenicity studies of this strain of rats. The incidence of thymoma in historical control data of Harlan Laboratories is as follows: benign thymoma 0.64% for males, 2.39% for females; malignant thymoma 0.50% for males, 0.63% for females. The incidence of benign thymoma is higher in females with a range of 0% to 17.02% in these data. Histologically, these tumors commonly appear as solitary lesions with expansive growth, consisting of a mixture of thymic epithelial cells and lymphocytes with medullary differentiation. It was not always clear and requires careful consideration to distinguish between hyperplastic lesions and benign thymoma, and also between benign and malignant thymoma for many cases. In this report, we introduce typical hyperplastic lesions, thymoma and also the rarer epithelial cell type thymoma observed in Wistar Han rats.

**PS 179** **Mechanisms of Acetylugenol Nanocapsules on Melanoma Development: *In Vitro* and *In Vivo* Assays.**

C. C. Drewes<sup>1</sup>, C. G. Bexiga<sup>1</sup>, L. A. Fiel<sup>2</sup>, V. F. de Paula<sup>1</sup>, A. R. Pohlmann<sup>2,3</sup>, S. S. Guterres<sup>2</sup> and S. P. Farsky<sup>1</sup>. <sup>1</sup>Department of Clinical and Toxicological Analyses, Universidade de São Paulo, São Paulo, Brazil; <sup>2</sup>Department of Pharmacy, UFRGS, Porto Alegre, Brazil; <sup>3</sup>Department of Organic Chemistry, UFRGS, Porto Alegre, Brazil. Sponsor: S. Barros.

Eugenol displays antiproliferative and pro-apoptotic activities in different types of cancer cells, although effects of Acetylugenol (AC) and Acetylugenol Nanocapsules (NCAC) have not been elucidated. Here the role of NCAC on *in vivo* melanoma model and their actions on *in vitro* melanoma and endothelial cell cultures were investigated. Murine melanoma cells (B16F10, 8X105/100μL) were s.c. injected in the dorsal region of C57BL6 mice. Animals were i.p. or p.o. treated with Saline, AC, NCAC (50 mg/kg/day) or with their respective controls during 7 days. *In vitro* human endothelial cells (HUVEC) and melanoma cells (SK-Mel-28) were incubated with RPMI, DMSO, NC, AC or NCAC. Cell viability, nitric oxide (NO), clonogenic survival and cell adherence were monitored. Only NCAC

(100μM and 300μM), treatment reduced the endothelial and melanoma cell viability. NC and NCAC (60μM) treatments reduced the clonogenic survival only in melanoma cells and AC (30 and 60μM) treatment reduced clonogenic survival in both endothelial and melanoma cells. AC and NCAC (60μM) treatments inhibited endothelial and melanoma cells adherence. Both NC and NCAC (10, 30 and 60μM), but not AC, treatments increases the NO production by endothelial and melanoma cells. I.p. injection of NC or NCAC reduced melanoma growth, nevertheless they caused loss of weight, due to lower food intake and reduced the number of platelets. These *in vivo* toxic effects may be caused by accumulation of NC or NCAC in the peritoneum. P.o. administration of NC or NCAC reduced melanoma growth more than AC, and NC, AC or NCAC treatments decreased the number of circulating leukocytes. Together, data obtained show that i.p. route is not feasible to NC treatments, and the efficiency of NCs on tumor cell growth detected by p.o. may be due to their higher activity on clonogenic survival and adherence of melanoma cells.

**PS 180** **Natural Compounds As Chemopreventive Agents for the Inhibition of Protein Targets Involved in Cancer Induced by UV Radiation.**

W. Maldonado-Rojas, M. Ojeda-Cuello and J. Olivero-Verbel. *Environmental and Computational Chemistry Group Pharmaceutical Sciences, University of Cartagena, Cartagena, Colombia.*

Skin cancer is one of the most common worldwide, with an increasing incidence in recent years. This disease is mainly caused by excessive exposure to solar ultraviolet (UV) radiation. Currently, there is a high demand for natural chemopreventive compounds that may work on the biochemical mechanisms involved in the development of the disease. In this study, *in silico* molecular protein-ligand docking was performed with Autodock Vina to assess the interaction of 44 natural bioactive compounds with protein kinases (ERK1/TVO, p38/2YIX, JNK/2ZDT) and cyclooxygenase-2 (3LN1), widely recognized protein targets in the signaling cascades of skin tumor formation induced by UV radiation. The results showed these compounds presented theoretical binding affinity scores of similar magnitude to those recorded for known inhibitors of these proteins. The best binding affinity values were registered for cyaniding-3-rutinoside docked to ERK and JNK (-10.3±0.1 kcal/mol), and to cyclooxygenase-2 (9.7±0.1 kcal/mol). In the case of p38, the greatest affinity was found for epigallocatechin-3-gallate (-9.2±0.0 kcal/mol). The affinities obtained for the inhibitors of 1TVO, 2YIX, 2ZDT and 3LN1 were -9.4±0.0 (FR-180204), -7.0±0.0 (CE-159167), -7.3±0.0 (C46), and -10.3±0.0 kcal/mol (celecoxib), respectively. These theoretical results are good indicators that natural bioactive compounds may work as potential chemopreventive agents against skin cancer induced by UV exposure, probably by a mechanism involving their direct binding on key protein targets associated with the disease. Vice-Rectoría for Research. UniCartagena. 2011-2012. Colciencias-UniCartagena, Colombia: Grants 110745921616 (2009) and 110751929058 (2010).

**PS 181** **Genetic Polymorphism of Human Microsomal Epoxide Hydrolase As a Determinant of Polyaromatic Hydrocarbon Metabolism and Toxicity.**

X. Cai<sup>1</sup>, W. D. Hedrich<sup>1</sup>, E. M. Laurenzana<sup>1</sup>, B. E. Sell<sup>1</sup>, K. John<sup>1</sup>, A. K. Sharma<sup>2</sup>, S. G. Amin<sup>2</sup> and C. J. Omiecinski<sup>1</sup>. <sup>1</sup>Center for Molecular Toxicology and Carcinogenesis, The Pennsylvania State University, University Park, PA; <sup>2</sup>Department of Pharmacology, Hershey College of Medicine, Hershey, PA.

Microsomal epoxide hydrolase (mEH, EPHX1) is a key catalytic determinant in the formation of diol-epoxide metabolites of certain polyaromatic hydrocarbons (PAHs), noted as potent and ultimate mutagenic moieties. Epidemiological associations between EPHX1 genetic status and the incidence of certain diseases, including lung cancer, have been reported, yet the mechanistic bases for these associations remain unclear. Further, PAH diol-epoxides have never been evaluated as substrates for human EPHX1. Using enzymatic analyses, we evaluated substrate selectivity of the most common mEH genetic variants in the hydrolysis of planar vs. the highly tumorigenic non-planar fjord region PAH epoxides, together with their respective abilities to metabolize bay region and fjord region PAH diol-epoxide intermediates. Among the mEH variants, Y113/H139 wild type allele displayed highest capacity for hydrolysis of the bay region benzo[a]pyrene (BaP)-4,5-epoxide. The H113/H139 variant exhibited lowest affinity for the bioactivation of the fjord region dibenzo[a]pyrene-8,9-epoxide (-11-fold higher *K<sub>m</sub>* vs. wild type). Surprisingly, all of the human mEH variant enzymes were capable of hydrolyzing the bay region BaP-7,8-diol-9,10-epoxide, although displaying differential activity toward the fjord region dibenzo[a,l]pyrene-11,12-diol-13,14-epoxides. Results

from Comet assays and in situ DNA damage assays conducted in COS1 cells transfected with the mEH variants and treated with the corresponding epoxides generally corroborated the enzymatic activity data. Overall, these findings demonstrate marked substrate selectivity among the mEH variants with respect to PAH epoxide metabolism and provide mechanistic support for published epidemiology data suggesting that the H113 mEH allele is associated with a reduced risk of lung cancer.

## PS 182 Cotinine Levels and Gene Polymorphisms in Asthmatic Children Exposed to Tobacco Smoke in Northern Mexico.

A. Albores<sup>1</sup>, B. S. Barron-Vivanco<sup>1,2</sup>, V. M. Davila-Borja<sup>3</sup>, E. Juárez-Pérez<sup>4</sup>, A. E. Rojas-García<sup>2</sup>, C. López-Campos<sup>4</sup>, B. Muñoz<sup>5</sup> and I. Poblete-Naredo<sup>1</sup>. <sup>1</sup>Toxicology, Cinvestav, Mexico City, Mexico; <sup>2</sup>Laboratorio de Contaminación y Toxicología Ambiental, UAN, Tépica, Mexico; <sup>3</sup>Laboratorio de Toxicología Genética, Instituto Nacional de Pediatría, Mexico City, Mexico; <sup>4</sup>Departamento de Pediatría, UMAE 71, IMSS, Torreón, Mexico; <sup>5</sup>Escuela de Ciencias de la Vida, ITESM-Ciudad de México, Mexico City, Mexico.

Tobacco smoke (TS) represents a serious health threat to consumers and passively exposed individuals. However, passive exposure receives much less attention than smokers. In addition, more than 700 million children worldwide are passively exposed to TS, meaning an increased risk to develop tobacco related diseases later in life; among them children with respiratory impairments, like asthmatics, are a particularly vulnerable group since the lung is the main route of TS entrance. Asthma is a multifactorial disease and the environment quality is a relevant etiology factor. We investigated children exposure to tobacco smoke in an asthmatic population (n=100 individuals; 6.98 ± 0.85 years), and non-asthmatic children (n=100, 7.1 ± 0.82 years) living in Región Lagunera, Northern Mexico. There was a statistically significant difference in urinary cotinine between the exposed and non-exposed groups. Urinary cotinine levels showed a small positive correlation between children and smoking adults (r= 0.1205 and p= 0.244). Although, cotinine levels were higher in asthmatic children compared to non-asthmatic, such difference was not statistically significant. In addition, no association between cotinine levels and asthma severity was observed in this study. As for the allelic frequencies of GSTT1 null and CYP2A6\*2 (1799 T-A) polymorphisms, were significantly different comparing TS exposed asthmatic and non-asthmatic children. This study suggests children response to passive TS exposure may be affected by asthma and GSTT1 or CYP2A6 polymorphisms (Supported by the grant SEP-Conacyt (60463) and a BBV scholarship (Conacyt-6544).

## PS 183 Identification of Genomic Regions Linked to Epigallocatechin Gallate Induced Liver Toxicity Using the Diversity Outbred Stock.

R. J. Church<sup>1</sup>, D. M. Gatti<sup>2</sup>, J. Eaddy<sup>1</sup>, P. B. Watkins<sup>1</sup>, D. Threadgill<sup>3</sup> and A. H. Harrill<sup>1</sup>. <sup>1</sup>The Hamner-UNC Institute for Drug Safety Sciences, The Hamner Institutes, Research Triangle Park, NC; <sup>2</sup>The Jackson Laboratories, Bar Harbor, ME; <sup>3</sup>North Carolina State University, Raleigh, NC.

Epigallocatechin gallate (EGCG), an abundant polyphenol in green tea, has caused idiosyncratic liver toxicity when taken as an herbal supplement. The identification of genetic risk factors utilizing mouse population-based approaches, and validated in patient cohorts, could improve clinical management of EGCG-induced liver injury. In order to map genomic loci related to EGCG induced hepatotoxicity, we utilized the Diversity Outbred (DO) stock. DO mice are derived from eight inbred founder strains and have high genetic diversity, enabling high resolution mapping in this population. We hypothesized that Quantitative Trait Locus (QTL) mapping in DO mice exposed to EGCG would allow us to identify candidate genomic regions influencing the hepatotoxicity of EGCG. Male DO mice were treated once daily, for 3 days, with EGCG (50 mg/kg i.g.) or vehicle. Twenty four hours after the final dose, animals were sacrificed and serum and liver tissue were collected. Similar to humans, EGCG treatment in DO mice precipitates wide variation in hepatotoxic response. In treated animals, serum alanine aminotransferase (ALT) fold changes (terminal compared to pre-dose) ranged from 0.46-495.5 (mean: 24.8 ± 65.4) and percent liver necrosis ranged from 0-86.8% (mean: 6.3 ± 14.1). QTL mapping in treated animals identified two suggestive loci— one on chromosome 12 and one on chromosome X. In a follow-up study, we will genotype suspected risk alleles in DNA collected by the Drug Induced Liver Injury Network (DILIN) from patients with suspected EGCG-induced liver toxicity. We have demonstrated the first application of the DO mice to the detection of xenobiotic risk alleles of toxicity responses. While further validation is needed, our data suggest that QTL mapping in DO mice may aid in identification of pharmacogenetic risk alleles for compounds causing liver injury.

## PS 184 Pharmaco-Genomics and -Genetics of 5-Fluorouracil in Koreans.

M. Yang and M. Bae. Sookmyung Women's University, Seoul, Republic of Korea.

Genetic polymorphisms of several enzymes such as dehydropyrimidine dehydrogenase (DPYD), methyltetrahydrofolate reductase (MTHFR) and thymidylate synthase (TS) have been emphasized for pharmacogenomics and -genetics of 5-FU, which has been used for half century as a representative therapy for various cancers, however, shown individual variations in its various toxicities including life-threatening toxicity. Focusing on the three genes, we performed a pharmacogenomic and -genetic study of 5-FU in a Korean population. Most of genotypes and gene expression were analyzed with 7500 Realtime PCR System (ABI). As results, we found genetic polymorphisms in DPYD-85, -1627, and -1896 sites, 5'-ER, and 3'-UTR at TS, and MTHFR-222, and -429 sites among the Korean subjects (N=133; normal, N=105; head and neck patients, N=28). There was a significant association between 3'-UTR genetic polymorphism at TS and its genetic expression (p<0.05). From 5-FU pharmacokinetic (PK) analyses, each genotype did not show any effect on PK parameters. However, the combination of genetic polymorphisms in MTHFR -222T/C, DPYD- 1896T/C and 3'-UTR at TS showed significant differences in AUC of 5-FU and 5-FU/5-FUH2 ratios (p<0.01). Therefore, this study provides association between TS expression and its 3'-UTR polymorphism. Moreover, combination of the three genetic polymorphisms of the three genes can affect PK of 5-FU in Koreans.

## PS 185 PON1 Genotypes of Black Females from the Mississippi Delta Are Different from Those in the Rest of the State and Country.

M. Dail, P. Eden, C. McDaniel, E. C. Meek and J. E. Chambers. Center for Environmental Health Sciences, Mississippi State University, Mississippi State, MS.

Paraoxonase (PON1) is named for its ability to hydrolyze paraoxon, the active metabolite of the insecticide parathion. It is implicated in cardiovascular and metabolic diseases, such as Type 2 diabetes as well as tolerance of organophosphate insecticides. The human PON1 gene has several single nucleotide polymorphisms (SNPs). The SNP of an arginine (R) to glutamine (Q) substitution at codon 192 is associated with catalytic efficiency while the SNP of a methionine (M) to leucine (L) substitution at codon 55 is linked with serum levels. Since the Mississippi Delta has the highest rate of metabolic disease in the country, and a historically high use of pesticides, we compared the PON1 genotypes of black female Mississippi Delta clinic patients to those of black females from northeastern Mississippi and military populations. Genomic DNA was isolated from whole blood and the SNP codon areas were amplified by PCR. Since there is a native Alw I restriction site at codon 192, the QQ, RR, and QR SNPs yield different digest patterns. A native NlaIII restriction site at codon 55 generates different digest patterns for the LL, MM, and LM allozymes. Genotypic frequencies were different for the Q192R SNP. QR was most frequent in the military (45%) and northeastern Mississippians (50%), but RR was most frequent in the Delta group (54%). Similarly, the most common combination of polymorphisms was QRLL in the military (24%) and northeastern Mississippi groups (36%), but in the Delta group it was RRLL (48%). Using Fisher's exact test to analyze genotypic frequencies, the largest differences were between the Delta and military groups with Q192R P=0.0024 and L55M P=0.000176. When all three groups were compared, Q192R ratios were significantly different at P=0.00007 and L55M ratios at P= 0.00001. The significant differences seen in the Delta population may be associated with the region's health disparities.

## PS 186 In Vitro Toxicogenomic Screen Developed Using Genetically Diverse Mouse Inbred Cell Lines: Developing In Vivo Validations.

T. Wiltshire<sup>1</sup>, O. Suzuki<sup>1</sup>, B. B. Parks<sup>2</sup>, O. Trask<sup>2</sup>, C. Benton<sup>1</sup>, A. Frick<sup>1</sup>, N. Butz<sup>1</sup>, E. Chan<sup>1</sup>, E. Healy<sup>2</sup> and R. S. Thomas<sup>1</sup>. <sup>1</sup>Eshelman School of Pharmacy, University of North Carolina at Chapel Hill, Chapel Hill, NC; <sup>2</sup>The Hamner Institute for Health Sciences, Durham, NC.

Cell-based assays provide unprecedented means to globally and systematically screen for drugs and chemicals likely to display high inter subject toxicity variability. Genetic determinants of toxicity identified in these screens can guide clinical trial design or identify susceptible subpopulations. Here, we developed an innovative in vitro genetic screen using mouse embryonic fibroblast (MEFs) cells isolated from 32 inbred strains and screened them against 69 different drugs and chemicals. Using high-content imaging, we measured multiplexed cell health parameters, including cell loss, mitochondrial membrane potential, and cytochrome c release at

24 and 72 hours post treatment. We looked for genetic loci significantly linked to inter-strain cellular responses to treatment and found a 1.2 Mb locus on Chr X that was significantly linked to variable cytotoxic responses to a known mitochondrial toxicant, rotenone ( $-\log P > 4.0$ ). Within this putative locus is cytochrome b-245, beta polypeptide (Cybb) gene, which encodes for a voltage-gated H(+) channel that mediates pH in the mitochondria. We conducted a series of experiments to examine the role of Cybb in mediating toxic responses to rotenone in vivo, given that mitochondrial dysfunction has been shown to underlie idiosyncratic adverse drug reactions. We found that strains belonging to different Cybb haplotypes scored differently in the treadmill exercise stress test for aerobic endurance after chronic treatment with rotenone. Our study demonstrates that cell-based genetic assays using MEFs are an effective tool for identifying genes underlying drug and chemical toxicity. Importantly, mouse strains that exhibit differential in vitro sensitivity, from a cell-based screen, also display a differential in vivo phenotype. This in vitro-to-in vivo validation is difficult, but a fundamental step toward recognition of cell-based toxicity screens.

## PS 187 P-Glycoprotein Transport in the Disposition of Neurotoxicants.

S. Lacher, K. Skagen, R. Dalton, F. Cardozo-Pelaez and E. Woodahl.  
CEHS/BMED, The University of Montana, Missoula, MT.

Background: P-glycoprotein (P-gp), encoded by the *ABCB1* (or *MDR1*) gene, is an efflux xenobiotic transporter expressed in many tissues important in xenobiotic disposition. P-gp is highly expressed at the blood-brain-barrier and protects the brain from substances circulating in the blood. Although the importance of P-gp in drug disposition is clear, its role in disposition of environmental neurotoxicants is not well understood. Our goal is to investigate the role of P-glycoprotein in neurotoxicant accumulation in the brain, particularly pesticides that have been associated with Parkinson's disease such as rotenone, maneb, paraquat, and MPP+. Methods: We used polarized kidney epithelial control cells, LLC-PK1, and *ABCB1*-transfected cells, LLC-MDR1, to characterize pesticides as substrates or inhibitors of P-gp using flow cytometry, cytotoxicity, and transepithelial permeability assays. P-gp-stimulated ATPase activity was also measured to evaluate compounds as P-gp substrates in a membrane-based system. Results: We observed weak inhibition of rhodamine-123 (R123) efflux in *ABCB1*-expressing cells by flow cytometry in the presence of 100  $\mu$ M rotenone or maneb,  $16.2 \pm 1.53$  and  $11.6 \pm 4.53\%$ , respectively. Paraquat and MPP+ showed no R123 inhibition. ATPase assays showed that rotenone is a P-gp substrate with a  $K_m = 26.7 \pm 12.9 \mu$ M and  $V_{max} = 35.8 \pm 6.5$  nmol Pi/mg protein/min. This compares to the known P-gp substrate verapamil with kinetic constants of  $K_m = 8.22 \pm 3.79 \mu$ M and  $V_{max} = 42.9 \pm 5.5$  nmol Pi/mg protein/min. Paraquat, maneb, and MPP+ showed no ATPase stimulation. Conclusions: In combination these data suggest that rotenone acts both as a substrate and a weak inhibitor of P-gp, whereas maneb acts only as a weak inhibitor. MPP+ and paraquat are neither substrates nor inhibitors of P-gp. We will further confirm these results using cytotoxicity and transepithelial permeability studies. Our studies will provide data to show the role of P-gp in the disposition of pesticides associated with Parkinson's disease.

## PS 188 Polymorphic Enzymes, Urinary Bladder Cancer Risk, and Structural Change in the Local Industry.

K. Golka<sup>1</sup>, D. Ovsiannikov<sup>2</sup>, S. Selinski<sup>1</sup>, M. Lehmann<sup>1</sup>, M. Blaszkewicz<sup>1</sup>, O. Moormann<sup>2</sup>, M. W. Haenel<sup>3</sup> and J. G. Hengstler<sup>1</sup>. <sup>1</sup>Leibniz Research Centre for Working Environment and Human Factors, Dortmund, Germany; <sup>2</sup>Department of Urology, St.-Josefs-Hospital Dortmund-Hörde, Dortmund, Germany; <sup>3</sup>Max-Planck-Institut für Kohlenforschung, Mülheim an der Ruhr, Germany.

In the 1990s, the highest percentage of glutathione S-transferase M1 (GSTM1) negative urinary bladder cancer cases (70%) ever reported was observed in the greater Dortmund area. The question arose whether this uncommonly high percentage of GSTM1 negative urinary bladder cancer cases was due to environmental and/or occupational exposure decades ago. Thus, 15 years later, another study on urinary bladder cancer was performed in the same area after the coal, iron and steel industries had finally closed in the 1990s. In total 196 bladder cancer patients from a local department of urology and 235 controls with benign urological diseases were investigated by a questionnaire and genotyped for GSTM1, GSTT1 and the N-acetyltransferase 2 (NAT2) tag SNP rs1495741. The frequency of the GSTM1 negative genotype was 52% in bladder cancer cases and in the controls as well and thus much lower, compared to a previous study performed from 1992-95 in the same area (70%). NAT2 genotypes were distributed equally among cases and controls (63% slow acetylators). Less GSTT1 negative genotypes were present in cases

(17%) than in controls (20%). The normal frequency of the GSTM1 negative genotype in bladder cancer cases in the present study supports the assumption that the highly increased percentage of GSTM1 negative bladder cancer patients observed in the preceding study may be related to past occupational and environmental exposures decades ago.

## PS 189 CTNNA3 ( $\alpha$ -Catenin) Gene Variants Are Associated with Diisocyanate Asthma in Occupationally-Exposed Workers.

B. Yucesoy<sup>1</sup>, M. L. Kashon<sup>1</sup>, Z. L. Lummus<sup>2</sup>, V. J. Johnson<sup>3</sup>, K. L. Fluharty<sup>1</sup>, D. Gautrin<sup>4</sup>, J. Malo<sup>4</sup>, A. Cartier<sup>4</sup>, D. R. Germolec<sup>5</sup>, M. I. Luster<sup>1</sup> and D. I. Bernstein<sup>2</sup>. <sup>1</sup>Health Effects Laboratory Division, CDC/NIOSH, Morgantown, WV; <sup>2</sup>Division of Immunology, Allergy and Rheumatology, University of Cincinnati, Cincinnati, OH; <sup>3</sup>BRT-Burleson Research Technologies, Morrisville, NC; <sup>4</sup>Hôpital du Sacré-Cœur de Montréal, Université de Montréal, Montréal, QC, Canada; <sup>5</sup>Toxicology Branch, DNT/NIHES, Research Triangle Park, NC.

A genome-wide association study conducted recently in Korean subjects identified three CTNNA3 ( $\alpha$ -T catenin) single nucleotide polymorphisms (SNPs) (rs10762058, rs7088181, and rs4378283) associated with diisocyanate induced occupational asthma (DA). We conducted a candidate gene association study to replicate these findings in Caucasian workers. Genotyping was performed on genomic DNA, using a 5' nuclease PCR assay. Genotyping of these SNPs was performed in 410 diisocyanate-exposed and predominantly Canadian workers including: 132 workers with DA confirmed by a specific inhalation challenge (DA+); 131 symptomatic workers in whom DA was excluded by a negative challenge (DA-); and 147 HDI-exposed asymptomatic workers (AWs). CTNNA3 rs7088181 and rs10762058 SNPs were significantly associated with DA+ when compared to AWs ( $p \leq 0.05$ ) but not in comparison to DA- workers. After adjusting for potentially confounding variables of age, smoking status and duration of exposure, minor allele homozygotes of rs7088181 and rs10762058 SNPs were at increased risk for DA compared with AWs [OR = 9.05 (95% CI: 1.69, 48.54) and OR = 6.82 (95% CI: 1.65, 28.24), respectively]. In conclusion, we replicated association between two closely linked CTNNA3 gene SNPs and DA in Caucasian workers. These findings suggest that genetically altered expression of CTNNA3 might influence cellular adherence and epithelial barrier function in the airways and play a role in the pathogenesis of DA.

This work was supported in part by an NIEHS IAG (Y1-ES-0001) and NIOSH/CDC R01 OH 008795.

## PS 190 Prevalence and Functional Characterization of the NADH Cytochrome *b<sub>5</sub>* Reductase I1M\*6C>T Intronic Variant.

K. L. Blanke<sup>1,2</sup>, J. Sacco<sup>1</sup> and L. Trepanier<sup>1,2</sup>. <sup>1</sup>Department of Medical Sciences, School of Veterinary Medicine, University of Wisconsin - Madison, Madison, WI; <sup>2</sup>Molecular & Environmental Toxicology Center, University of Wisconsin - Madison, Madison, WI.

Women exposed to cigarette smoke may have an increased risk of breast cancer, although this is controversial. In addition, African American, but not Caucasian, women showed an association with smoking and breast cancer in the Carolina Breast Cancer Study (CBCS) population. We hypothesized that this could be due to race-associated genetic variability in the pathways that detoxify tobacco carcinogens such as 4-aminobiphenyl (4-ABP) and 2-amino-1-methyl-6-phenylimidazo [4,5-*b*] pyridine (PhIP). Both are mammary procarcinogens that are bioactivated to hydroxylamine metabolites, which form DNA adducts and are thought to initiate cancer. Cytochrome *b<sub>5</sub>* (CYB5A) and NADH cytochrome *b<sub>5</sub>* reductase (CYB5R3) comprise a detoxification pathway that reduces 4-ABP and PhIP hydroxylamine metabolites back to their parent compounds. The purpose of this study was to determine whether CYB5A and CYB5R3 polymorphisms were over-represented in African American women in the CBCS, and to evaluate their role in the association with smoking and breast cancer risk. Several CYB5A and CYB5R3 single nucleotide polymorphisms (SNPs) were more prevalent in African Americans than in non-African Americans in the CBCS population. One intronic SNP in CYB5R3, I1M\*6C>T, previously found in tissue samples with low *b<sub>5</sub>* reductase protein expression, was found with a minor allele frequency that was 100-fold higher in African American subjects (MAF = 0.0428,  $P < 0.0001$ ). Among smokers, this variant was significantly over-represented in African American women with breast cancer compared to same-race controls (OR 2.10, 95% CI, 1.08-4.06). The I1M\*6C>T CYB5R3 variant is being functionally characterized for promoter and repressor function using a dual-luciferase reporter assay. These studies suggest that the I1M\*6C>T intronic variant in CYB5R3 may increase the risk of breast cancer among African American women that smoke.

**PS 191 Influence of Genetics on Paraoxonase 1 Activity in Monozygotic and Dizygotic Twins.**

L. Podolefsky<sup>1</sup>, K. M. Kelly<sup>2</sup>, J. C. Murray<sup>3</sup>, T. J. Raife<sup>4</sup> and G. Ludewig<sup>1, 2</sup>.

<sup>1</sup>Grad Program in Human Toxicology, University of Iowa, Iowa City, IA;

<sup>2</sup>Occupational and Environmental Health, University of Iowa, Iowa City, IA;

<sup>3</sup>Pediatrics, University of Iowa, Iowa City, IA; <sup>4</sup>Pathology, University of Iowa, Iowa City, IA.

Paraoxonase 1 (PON1) is an important HDL-associated endogenous antioxidant found to play a major role in susceptibility to health effects from pesticides and oxidative stress. A number of gene polymorphisms influence both protein concentration and substrate specificity, as do certain lifestyle factors. However, reports about the influence of PON1 genetics have varied widely in the literature. The goal of this study was to examine the influence of genes and health data in a group of monozygotic and dizygotic twins to better understand the effect of genetics on PON1 activity levels. DNA, serum, and standard blood donation information was obtained from 6 sets of dizygotic twins and 13 sets of monozygotic twins. DNA was genotyped for polymorphisms within PON1, PON2, C-reactive protein (CRP), and tumor necrosis factor (TNF). PON1 activity was determined using phenyl acetate (PA) and CMPA [4-(Chloromethyl)phenyl acetate] as substrates, and genotyping was performed using the TaqMan-Applied Biosystems 7900 HT System. Using a general linear model, PON1 Q192R, L55M and C-108T were significantly associated with both PA and CMPA activity, with CMPA activity showing a stronger association with genetic variants. PON2 S311C was significantly associated with PA activity, but not CMPA. Activity for either substrate was not found to be associated with CRP or TNF polymorphisms. BMI was found to significantly correlate with CMPA activity, but not PA activity (correlation = -.34), while gender did not correlate with either substrate. Pair-wise analysis of all twins with identical PON genotypes showed no difference in PON activity variance between siblings, regardless of zygosity. Though other shared or variant genetic and lifestyle factors may influence PON1 activity, the findings in this twin population suggest a strong link between PON activity and specific PON polymorphisms.

**PS 192 Contribution of Environmental and Genetic Factors to Pancreatic Cancer.**

S. Chittiboyina, A. A. Bond, L. M. Kamendulis and B. A. Hocevar.

*Environmental Health, Indiana University School of Public Health, Bloomington, IN.*

Pancreatic cancer is the fourth leading cause of cancer deaths in the United States with a five year survival rate of less than 6%. Several environmental risk factors have been identified for pancreatic cancer, including dietary factors. In particular, high dietary intake of folate has been associated with a decreased incidence of pancreatic cancer, while low plasma folate levels are associated with an increased cancer risk. In conjunction with diet and lifestyle determinants, an individual's folate pathway status is determined by their genetic makeup. In the present study, we determined the expression of selected SNPs in the folate metabolic pathway in a cohort of pancreatic cancer patients and healthy related and unrelated control groups. In agreement with other cancer studies, we show that cancer cases were more likely to express the TT allele of the methylene tetrahydrofolate reductase (MTHFR) C677T polymorphism compared to controls. Expression of this allele has been associated with low folate levels and elevated homocysteine (Hcy) levels. In support of this, we found that pancreatic cancer patients display elevated serum Hcy levels in comparison to both control groups. In addition, 48% of the pancreatic cancer patients exhibited hyperhomocysteinemia, as defined by a value >15 µM/L, (range 11.15 - 26.17 µM/L), while no subjects in either control group exhibited hyperhomocysteinemia. In addition, we found that SNPs in betaine hydroxymethyltransferase (BHMT; rs 3733890) and serine hydroxymethyl transferase (SHMT; rs 1979277) exhibited significantly different distributions between the case and control groups (p < 0.05). While a clear association was not seen between cancer risk and alcohol or smoking use in our population, self reported environmental exposure data suggested an association between pancreatic cancer and exposure to welding fumes. These findings underlie the necessity to investigate further the interaction between environmental exposures and genetic factors which could provide further insight into the etiology of pancreatic cancer.

**PS 193 The Impact of CYP2S1 Single Nucleotide Polymorphisms on the Metabolic Activation of the Anticancer Prodrug, AQ4N.**

N. Bajaj, N. M. Singh and A. M. Rowland. *Chemistry and Biochemistry, NMSU, Las Cruces, NM.*

Cytochrome P450 2S1 (CYP2S1) is one of the most recent additions to the P450 superfamily of enzymes. Although its physiological role has not yet been defined, it has been shown to influence metabolism of bioactive lipids, including

prostaglandins and retinoids. CYP2S1 is predominantly expressed in extra-hepatic epithelial cells. Its expression is elevated in cancer and catalyzes the metabolic activation of the anticancer prodrug, AQ4N, under hypoxic conditions. Interestingly our lab has also demonstrated that increased CYP2S1 expression may protect against AQ4 cytotoxicity under normoxic (21% O<sub>2</sub>) conditions. The main objective of this study is to determine whether individual variability in the CYP2S1 enzyme alters sensitivity of human lung cells to AQ4N and AQ4-mediated cytotoxicity. Five published CYP2S1 allelic variants have been published: CYP2S1\*2 (R380C), CYP2S1\*3 (P466L), CYP2S1\*4 (S61N), CYP2S1\*5 (L230R). According to the NCBI database, two additional non-synonymous variants have been identified in cancer (A205T and L189F) and L189F is restricted to African American populations. We generate each of the polymorphisms in a CYP2S1-Flag mammalian expression vector, using site directed mutagenesis. Thus far, two stable lines (S61N and L189F) in bronchial epithelial cells (BEAS-2B) and four stable (S61N, R166H, A205T, and P466L) alveolar carcinoma cell lines (A549) have been made. Examination of AQ4N and AQ4 cytotoxicity in BEAS-2B cells revealed that both mutants (S61N and L189F) exhibit significantly increased cytotoxicity in response to AQ4N compared with wild type CYP2S1-Flag and pcDNA3.1 controls. Interestingly, the S61N polymorphism was significantly more sensitive to AQ4 than any of the other cell lines. This effect appears to be selective because cytotoxicity is not altered in response to a similar topoisomerase II inhibitor, mitoxantrone. We are currently testing the effects of these polymorphisms on AQ4N and AQ4 levels, using HPLC. Research funded by NIH NIGMS Grant # R25GM061222.

**PS 194 The Remarkable Genotoxic Effect of Exposure to Ethyl Tertiary Butyl Ether in ALDH2 Knockout Mice.**

R. Wang, Z. Weng, K. Ohtani, M. Suda, Y. Yanagiba and T. Suzuki. *Japan National Institute of Occupational Safety and Health, Kawasaki, Japan.*

Ethyl Tertiary Butyl Ether (ETBE) is used in gasoline for vehicles as a biofuel. ETBE exposure induced liver damage and other health effects only at high concentrations in our previous studies, and its No Observed Adverse Effect Level (NOAEL) was calculated to be 500 ppm. However, in mice without ALDH2 enzyme activity, ETBE could induce DNA damage even at the NOAEL. To find out how low concentration at which ETBE shows its genotoxic effect, we did the exposure experiment with mice at low range of ETBE concentrations. METHODS: Male Aldh2<sup>-/-</sup> (KO), Aldh2<sup>+/-</sup> (HT) as well as C57BL/6 strain (WT), at 8 weeks old were exposed to ETBE at 0, 50, 200 and 500 ppm, 6 hr/day and 5 days/week, for 9 weeks. Blood, liver, epididymides were sampled 20 hr after the last exposure, and DNA damages were analyzed with comet assay in these tissues. RESULTS: The tail intensity (TI) was used to evaluate the degree of DNA damage. In the leukocytes of WT mice, the TI value was not affected in any exposure group as compared to the control. However, the TI was significantly increased in 200 and 500 ppm groups of KO mice. Similar results were also obtained in HT mice, but there was no difference between the two types of mice. In liver cells and sperm, ETBE also induced DNA damage, but this effect was only observed in KO and HT mice as in the leukocytes. The NOAEL was 50 ppm in these types of mice. These results suggest that ALDH2 deficiency may increase the susceptibility to the health effect of ETBE exposure. We thank Ms. S. Watanabe for her assistance in the manipulation of the animals.

**PS 195 MGMT Haplotypes Alter MGMT Expression and Can Thus Affect Response to Alkylating Agents.**

M. Xu, I. Nekhayeva, C. E. Cross, C. M. Rondelli and S. Z. Abdel-Rahman. *OB/Gyn, UTMB, Galveston, TX.*

Glioblastoma (GB) is rapidly fatal. However, treatment with temozolomide (TMZ) and radiation is beneficial, but only for some patients. TMZ alkylates tumor DNA to form O6-alkylguanine (O6-AG) DNA adducts, inducing apoptosis. Because O6-AG is repaired by O6-methylguanine-DNA methyltransferase (MGMT), levels of MGMT are critical in determining tumor response to TMZ. Single nucleotide polymorphisms (SNPs) in the promoter/enhancer (P/E) region of the MGMT gene can alter its transcription and thus alter MGMT protein levels. Genetic variants are not arrayed as individual SNPs but as combinations forming specific "haplotypes". To date, no studies have determined the haplotypes structure of the P/E region of MGMT or their effect on its transcription. We sequenced 104 DNA samples from healthy individuals and identified 8 SNPs in this region (7/Y, 135/K, 290/R, 485/M, 575/M, 666/R, 777/M and 1099/Y). Using bioinformatics, we inferred the haplotypes encompassing these SNPs. We identified 21 potential haplotypes ranging in frequency from 0.39 to 0.00005, of which 10 were identified in our sample population as 20 paired haplotype combinations. We hypothesized that these haplotypes alter the regulation of MGMT transcription. Luciferase-reporter constructs containing different MGMT haplotypes were transfected into a GB cell

line and the effects of the haplotypes on *MGMT* transcription were determined using a Dual-Luciferase Reporter Assay. Compared with the most common (reference) haplotype, haplotypes 7 and 18 induced a significant 60% and 65% reduction in expression, respectively ( $P < 0.001$ ). However, haplotype 11 significantly increased expression by 70% ( $P < 0.001$ ). These data indicate that *MGMT* haplotypes regulate *MGMT* transcription and thus could play a major role in tumor response to TMZ treatment. Work is in progress to define the underlying mechanisms and to develop sensitive and specific markers that can distinguish those patients who would most be likely responsive to chemotherapy from those who would not (supported by P30 ES006676; T32-07454; 1 R03 NS065392-01 grants).

## PS 196 Associations between Genetic Polymorphisms of the Genes Mediating Inflammatory Response and Acute Pancreatitis Risk.

B. Alpertunga and G. Ozhan. *Pharmaceutical Toxicology, Istanbul University, Faculty of Pharmacy, Istanbul, Turkey.*

Acute pancreatitis is a common inflammatory disease. The reported incidence is approximately 30 to 40 per 100,000 population per year and 25% will develop severe or life-threatening complications. Inflammation is typified by the activation of immunocytes such as monocytes and macrophages, and the secretion of inflammatory mediators such as nitric oxide, prostaglandin E2, and tumour necrosis factor- $\alpha$  (TNF- $\alpha$ ). Nitric oxide is especially controlled by the inducible nitric oxide synthases (iNOS). Prostaglandin E2 is produced from arachidonic acid metabolites by the catalysis of cyclooxygenase-2 (COX-2). TNF- $\alpha$ , thought to be the first cytokine released, is a principal mediator of immune responses. Genetic factors may play important roles in susceptibility to pancreatic injury, as well as in the severity and evolution of the inflammatory process. The aim of our study was to determine if polymorphisms in iNOS, COX-2, TNF- $\alpha$  genes were associated with acute pancreatitis. For that, three iNOS (Ser608Leu, 1173C/T, 954G/C), seven COX-2 (rs5275, rs2206593, rs4648262, rs4648261, rs2066826, rs5277, rs2745557) and two TNF- $\alpha$  (308G/A, 238 G/A) variants were determined using polymerase chain reaction-restriction fragment length polymorphism analysis in patients with acute pancreatitis and healthy controls. Odds ratios (ORs) and 95% confidence intervals (CI) were estimated. In conclusion; the association was seen with COX-2 rs5275 ( $P = 0.03$ ); specifically, patients carrying the TT genotype in comparison to patients carrying the CC genotype had a significantly lower risk of disease (OR=1.88; 95%CI:1.06-3.34). Both SNPs of TNF- $\alpha$  were not genetic risk factor for acute pancreatitis susceptibility. It was also found that iNOS Ser608Leu polymorphism was more frequent among cases with acute pancreatitis compared to controls (OR=2.88; 95%CI:1.49-5.57;  $P = 0.002$ ). We believe that the findings may be beneficial to the development of efficacious preventive strategies and therapies for inflammation-associated diseases.

## PS 197 In Vitro Toxicity of Antibacterial Silver Ions Released by Low Intensity Direct Electric Current (LIDC) Stimulation.

R. A. Shirwaiker<sup>1,2</sup>, M. E. Samberg<sup>2</sup>, Z. Tan<sup>1</sup> and N. A. Monteiro-Riviere<sup>2,3</sup>. <sup>1</sup>E. P. Fitts Department of Industrial and Systems Engineering, North Carolina State University, Raleigh, NC; <sup>2</sup>Joint Department of Biomedical Engineering, University of North Carolina at Chapel Hill and North Carolina State University, North Carolina State University, Raleigh, NC; <sup>3</sup>Nanotechnology Innovation Center of Kansas State, Kansas State University, Manhattan, KS.

Medical devices related surgical site infections and their treatment are a major cause of concern in the global healthcare system. The problem is compounded by the presence of antibiotic-resistant bacteria such as methicillin-resistant *Staphylococcus aureus* (MRSA) in healthcare environments, because infections caused by these bacteria are difficult to treat with conventional antibiotics. To prevent transmission of such infections, a prophylactic surface system that provides protracted release of antibacterial silver ions from interdigitated silver electrodes using low intensity direct electric current (LIDC) stimulation was developed and successfully validated against four pathogenic bacterial strains including *S. aureus*, *Escherichia coli*, *Enterococcus faecalis* and *Pseudomonas aeruginosa*. The objective of this study was to evaluate the toxicity of the LIDC system to human epidermal keratinocytes (HEK) and human dermal fibroblasts (HDF) with alamarBlue, using parameters proven to be antibacterial (28 $\mu$ A at 6V). It was found that 1.5h exposure to the silver ion-releasing surface system was not toxic to HEK or HDF, which suggests that the applications of the antibacterial system for surfaces that come into contact with skin epithelial cells or connective tissue for less than 1.5h are not expected to cause toxicity in vivo. The application of this technology is particularly relevant for high contact surface areas in medical devices such as stethoscopes, scalpel handles, endoscopes, and forceps that are prone to microbial contamination. In conclusion, the lack of toxicity in vitro provides support for future in vivo or clinical studies. (Supported by ArgentumCidalElectrics, Inc.)

## PS 198 Safety Assessment of Colorants Used in a Short Term Blood Contacting Medical Device—Challenges in Color Extraction Testing.

F. K. Hsia<sup>1</sup>, H. J. Beckord<sup>1</sup>, M. P. Beauchane<sup>1</sup>, C. J. Anderson<sup>2</sup>, D. R. Kent<sup>3</sup> and E. E. Reverdy<sup>1</sup>. <sup>1</sup>Corporate Toxicology and Biocompatibility Services, Boston Scientific Corporation, Maple Grove, MN; <sup>2</sup>Materials, Testing, Analysis, and Characterization, Boston Scientific Corporation, Maple Grove, MN; <sup>3</sup>Product Safety and Validation, NAMS, Northwood, OH.

Use of colorants in medical devices continues to be scrutinized by the FDA. In response to the FDA questions on a recent PMA submission and to be compliant with ISO 10993 *Biological Evaluation of Medical Devices - Part 1: Evaluation and Testing within a Risk Management Process*, Boston Scientific completed extraction studies on colorants as part of the safety assessment. The challenges and successes in demonstrating the safety of the colorants used in a short-term blood-contacting catheter are presented here. A color elution study was conducted to demonstrate the potential bioavailability of four colorants. Devices were extracted at 37°C for 24 hours in acetone. These aggressive extraction conditions maximized the potential to extract colorant and were not intended to represent clinical use. Non-volatile residue (NVR) portions of the extracts were microwave digested and then analyzed using ICP-OES against control colorant samples of known concentration. The estimated maximum amounts of extracted colorant ranged from <LOQ - 2.4 mg/device. These values together with the NVR value (0.1 mg/device) from the USP Physicochemical test were used as "worst case" estimates in the safety assessment. Variable process spike recovery results and device degradation during extraction contributed to uncertainty in the reported results. The safety assessment was conducted following ISO 10993-17: *Establishment of Allowable Limits for Leachable Substances*. The existing toxicological and biological safety data were included in the risk assessment. The threshold of toxicological concern (TTC) approach was applied for colorants with insufficient toxicological data. We concluded that the colorants used in this short-term catheter are eluted from the device at toxicologically insignificant amounts when extrapolated to the clinical exposure.

## PS 199 Comparison of Results from 2 In Vitro Cytotoxicity Tests Used in the Evaluation of Medical Devices.

D. E. Malek<sup>1</sup> and R. T. Przygoda<sup>2</sup>. <sup>1</sup>Malek Toxicology Delaware LLC, Greenville, DE; <sup>2</sup>Life Cycle Materials, Johnson & Johnson, Cincinnati, OH.

ISO 10993-1 includes an *in vitro* cytotoxicity test as part of a biological evaluation of medical devices. Two cytotoxicity tests commonly used in this evaluation are the MEM elution (ME) and Colony Formation (CF). The results from 43 samples used in medical devices were analyzed to evaluate the utility of both tests. Twenty-eight test samples also were evaluated for *in vivo* irritation, sensitization and systemic toxicity. The ME test was performed according to ISO 10993-5, section 8.2 including serial dilution of the extract, and CF test was performed according to ISO 10993-5, Annex B. The *in vivo* tests were performed according to the appropriate ISO 10993 standard. The ME and CF test results from 36 test samples showed agreement (84% agreement). Seven test samples were non-toxic in ME but toxic in the CF test (16% disagreement). Toxicity was not observed in any of the *in vivo* tests on the 12 samples that were toxic in either the ME, CF, or both cytotoxicity tests. When compared to the results of the 28 sets of *in vivo* tests, the ME test was 71 % in agreement and the CF test was 46% in agreement. Cytotoxicity was not observed in ME or CF tests for the 3 samples that failed for irritation. The results from this comparison demonstrate that *in vitro* cytotoxicity is not predictive of *in vivo* irritation, sensitization or systemic toxicity; and the lack of cytotoxicity does not guarantee acceptable *in vivo* test results. The ME test with serial dilutions is more in agreement with results from *in vivo* tests, and when toxicity is observed provides comparable results to CF test.

## PS 200 Evaluation of Sample Preparation Methods in the ISO 10993-12 Standard: Implications for the Biocompatibility Assessment of Medical Devices.

R. P. Brown, H. Dinesdurge, J. Goode and M. Ghosh. *US FDA, Silver Spring, MD.*

The ISO 10993-12 standard outlines suitable extraction conditions for the preparation of test samples for the biological evaluation of medical devices. The standard provides a list of temperature, time, and solvent conditions recommended for the preparation of extracts for toxicity testing, but no guidance is offered on which specific extraction conditions are optimal for various types of materials. The goal of this study is to identify extraction conditions that can be used to differentiate toxic from nontoxic polymeric materials in an indirect hemolysis assay without resulting

in the degradation of the material. A "toxic" material is defined in this study as one that produces a positive response in a modified MEM Elution cytotoxicity test. A wide range of polymeric materials (e.g., BUNA, nitrile, butyl, neoprene, latex, silicone rubbers; polyurethane, polyethylene, PVC) was extracted in a closed glass vial in phosphate buffered saline (PBS) using the default conditions outlined in the ISO 10993-12 standard (37°C x 24 hrs, 37°C x 72 hr, 50°C x 72 hr, 70°C x 24 hr, 121°C x 1 hr). In addition, the polymers were extracted in 5% or 50% ethanol (EtOH) or acetone at 37°C for 24 hours. The 50% EtOH extracts were diluted to 5% with PBS for the hemolysis assay. The acetone extracts were evaporated under a nitrogen stream, then reconstituted with PBS. Our results show that rigorous extraction conditions (acetone, 50% EtOH) are necessary to correctly differentiate toxic from nontoxic materials. For example, latex and BUNA were positive in the cytotoxicity assay, positive when 50% EtOH extracts were used in the hemolysis assay, but negative when extracted in PBS using the standard extraction conditions in the ISO 10993-12 standard (e.g., 50°C x 72 hrs). Since the use of acetone as an extraction vehicle resulted in the degradation of some materials, such as PVC, the use of EtOH:PBS solvent mixture represents a promising approach for preparing samples for the biological evaluation of medical device materials.

**PS 201 Can There Be a Universal Extraction Solvent for Medical Device Biocompatibility Testing? Comparison of Extraction Efficiencies among Five Solvents Used to Extract Polymeric Dental Devices.**

L. H. Moilanen<sup>1</sup>, J. K. Dahms<sup>2</sup>, B. D. Bagley<sup>1</sup> and E. F. Hope<sup>1</sup>. <sup>1</sup>Medical Department, 3M, St. Paul, MN; <sup>2</sup>3M ESPE, 3M, St. Paul, MN.

The biocompatibility of medical devices is often evaluated using extracts prepared from the final product. The selection of the most appropriate extraction solvent(s) for product chemical characterization and biocompatibility assessment remains a subject of active discussion within the medical device standards community. For this study, we examined extraction data obtained for nine experimental dental product prototypes extracted using five solvents of varying polarity to address both clinical use and exaggerated extraction scenarios. The extracted prototypes included four composite restoratives, a resin-modified glass ionomer, a polymeric polishing brush, a temporary cement, a self-etch adhesive, and a dental sealant. ISO 10993-12 compliant samples of each product were extracted in aqueous 5% ethanol solution, acetone, methanol, heptane, and 50:50 cyclohexane:isopropanol at 37°C with a target sample:solvent extraction ratio of 0.2 g/mL. Extraction time intervals ranged from 24 hours to 28 days. Gravimetric and HPLC analyses of the extracts show that in most cases use of methanol either resulted in the highest concentration of extractables or gave results similar to acetone. In the remaining cases, either acetone or water extracted the largest amount of residue. These results confirm the utility of methanol as an exaggerated solvent for many polymeric dental products, but also highlight the importance of proper solvent selection based on detailed knowledge of product chemistry.

**PS 202 Determination of Total Leachable Bisphenol A from Polysulfone Membranes in Hemodialyzers and Hemoconcentrators.**

S. M. Cho, Y. Choi, H. Luu and J. Guo. US FDA, Silver Spring, MD.

Bisphenol A (BPA) is a high-production-volume chemical widely used to manufacture polysulfone (PS), polycarbonate, epoxy resin, etc. Over the past ten years, BPA has been the subject of numerous risk assessment reviews and research worldwide because of its potential to produce adverse health effects through endocrine disruption. Although there is a significant body of literature focused on the adverse effects of BPA at low doses, there are discrepancies in the relevance and reliability of the published results. These make it difficult to properly evaluate the hazards of BPA. To reduce discrepancies and variation in research results, it is essential to establish reproducible/accurate analytical methods. In this study, we evaluated the BPA levels eluted from porous PS membranes used in hemodialyzers and hemoconcentrators using single and multiple consecutive extractions under clinically relevant extraction condition. The levels of BPA release were determined using solid phase extraction (SPE) coupled with high performance liquid chromatography-mass spectrometry (HPLC-MS). We demonstrated that it was difficult to determine the total amount of BPA released from the PS membranes using a single extraction method with finite solvent volume because of the chemical equilibrium between the extraction solution and the polymer phase. A general equation was derived to fit the BPA elution data and deepen our understanding on the equilibrium phenomenon during the extraction. The results revealed that repeated consecutive extractions of the PS membranes are needed to accurately determine the total leachable BPA in porous membranes.

**PS 203 Bisphenol A Content in Polycarbonate from Medical, Automotive and Consumer Suppliers.**

R. T. Przygoda<sup>1</sup>, J. A. Anim<sup>1</sup>, D. E. Malek<sup>2</sup> and D. J. Caldwell<sup>3</sup>. <sup>1</sup>Life Cycle Materials, Johnson & Johnson, Cincinnati, OH; <sup>2</sup>Malek Toxicology Delaware, LLC, Greenville, DE; <sup>3</sup>Worldwide Environment, Health, and Safety, Johnson & Johnson, New Brunswick, NJ.

Bisphenol A (BPA) is an organic compound used to make polycarbonate (PC) polymers and epoxy resins. The presence of BPA has the potential to produce human reproductive and developmental effects. Three sources of PC's were utilized in this study: from medical, automotive, and consumer suppliers (cups). Sterilized and unsterilized samples were extracted using ethanol (EtOH) or isopropanol (IPA) and incubated at 37 degrees C for 24 hours. Extracts were analyzed by high performance liquid chromatography (HPLC). In addition, exhaustive extraction by Soxhlet with IPA was performed on a medical grade PC. BPA was below the level of detection (0.5µg/g) in EtOH and IPA extracts with the exception of the cups. In extracts from cups, between 4 to 5.8µg BPA/g of test sample was detected, however BPA was not detected in the non-sterilized sample extracted with EtOH (limit of detection was 0.51µg). Assuming a 10g cup and the worst-case of 5.8µg BPA/g, an adult male (70kg) would be exposed to 0.829µg BPA/kg/day. Using exhaustive Soxhlet extraction with IPA, BPA was below the limit of detection (0.51µg/g) for automotive PC. Assuming a 10g sample and the worst-case of 0.5µg/g, an adult male would be exposed to 0.071µg/kg/day. The average BPA amount found in medical grade PC by exhaustive Soxhlet extraction with IPA was 0.25µg/g. For a 10g medical device, the calculated exposure for an adult male is 0.036µg/kg/day. The US FDA acceptable Daily Intake (ADI) and/or EU Tolerable Daily Intake (TDI) for BPA is 50µg/kg/day. The adult male exposures to BPA from consumer, automotive, and medical grade PC are 58, 704, and 1300 times less than US FDA ADI or EU TDI. The extractable BPA from automotive and medical grade PC was significantly less than that observed from the consumer PC.

**PS 204 Local Effects of Microelectrode Implantation in Rabbit Muscles.**

J. Yoon<sup>1</sup>, E. Cho<sup>1</sup>, S. Kim<sup>1</sup>, J. You<sup>1</sup>, Y. Kim<sup>1</sup>, E. Kwon<sup>1</sup>, B. Kang<sup>1,2</sup> and J. Che<sup>1</sup>. <sup>1</sup>Biomedical Research Institute, Seoul National University Hospital, Seoul, Republic of Korea; <sup>2</sup>Graduate School of Immunology, Seoul National University, Seoul, Republic of Korea. Sponsor: K. Lim.

The purpose of this study was to evaluate the biocompatibility of various polymer-based microelectrodes (PBMs) after implantation in rabbit muscle tissues following a standardized method. Three types of PBMs were examined: silicone-based platinum, polyimide-based gold, and liquid crystal polymer-based gold microelectrodes. All experimental procedures followed the International Organization for Standardization (ISO) 10993-6:2007(E). Six female rabbits were used for this study. The PBMs were implanted into the left paravertebral muscle of the dorsal region of the rabbits for 12 weeks, each type being implanted into two rabbits. Control article (high density polyethylene, HDPE) was implanted in the equivalent site on the right side of each rabbit. No changes in the clinical signs, mortality, body weight, and gross findings related to the PBMs were noted. The results of histopathological evaluation suggest that the PBMs did not induce any cellular changes. Thus it could be concluded that the three types of PBMs are all non-toxic, non-irritating, and biocompatible.

**PS 205 Subchronic Systemic Toxicity of Subcutaneous Implantation of Microelectrodes in Rats.**

E. Cho<sup>1</sup>, S. Kim<sup>1</sup>, J. You<sup>1</sup>, Y. Kim<sup>1</sup>, E. Kwon<sup>1</sup>, B. Kang<sup>1</sup>, J. Che<sup>1,2</sup> and J. Yoon<sup>1</sup>. <sup>1</sup>Biomedical Research Institute, Seoul National University Hospital, Seoul, Republic of Korea; <sup>2</sup>Graduate School of Immunology, Seoul National University, Seoul, Republic of Korea. Sponsor: K. Lim.

The purpose of this study was to evaluate the biocompatibility of various polymer-based microelectrodes (PBMs) through the subchronic systemic toxicity of subcutaneous microelectrode implantation in rats following a standardized method. Three types of PBMs were examined: silicone-based platinum, polyimide-based gold, and liquid crystal polymer-based gold microelectrodes. All experimental procedures followed the International Organization for Standardization (ISO) 10993-6:2007(E) and ISO 10993-11:2006(E). Ten female rats were used for four each groups. Control article (high density polyethylene, HDPE) and three types of PBMs were implanted subcutaneously in the same site in each group and were left in place for 13 weeks. No effects related to the microelectrodes were observed in any tested criteria, included mortality, clinical signs, body weight, food and water consumption, hematology and serum biochemistry parameters, urinalysis and ophthalmoscopy,

organ weight, gross findings, or histopathological findings. These results suggest that no subchronic systemic toxicity is induced by subcutaneous implantation of these three types of PBMs under the conditions used in this study.

**PS 206 Comprehensive Health-Based Risk Assessment of Material from an Ingestible Medical Device.**

M. A. Nascarella<sup>1</sup>, G. M. Savage<sup>2</sup>, G. Moon<sup>2</sup> and B. D. Beck<sup>1</sup>. <sup>1</sup>Gradient, Cambridge, MA; <sup>2</sup>Proteus Biomedical, Inc., Redwood City, CA.

We present an analysis of the potential toxicity of an ingestible medical device. The primary toxicological concern is an 8  $\mu\text{M}$  layer of copper (Cu), with an area of approximately 1.0  $\text{mm}^2$ , that is a component of the device's battery. The Cu content is approximately 20-33.1  $\mu\text{g}/\text{device}$ . We calculated the potential toxicological risks of Cu leached from the device, assuming a maximum use of 30 devices/event. Depending upon fluid in the stomach, an individual could have a stomach dose of approximately 219  $\mu\text{g}$  Cu, resulting in a stomach concentration ranging from 0.25-2.73  $\mu\text{g}$  Cu/mL. These concentrations may be compared to a threshold Cu concentration for gastrointestinal (GI) toxicity of 1.4  $\mu\text{g}/\text{mL}$ . In the most plausible scenario, the predicted concentration of Cu in the stomach is below the concentration associated with GI symptoms in humans, consisting of mild, reversible effects and no associated systemic toxicity. The higher potential stomach concentrations somewhat exceed the threshold concentration, but potential GI symptoms could be mitigated by ingesting the devices with food. We also estimated the potential total intake of Cu from all sources, including the device. Ingestion of the device, combined with the ingestion of median levels of Cu in food, water, and multivitamins, is estimated to be well below the 10  $\text{mg}/\text{day}$  IOM determined level of safe daily intake for the general population. We also evaluated the cytotoxicity of the extractable material from this device, based on ISO-compliant tests of device extractions using simulated gastric fluid. Using open-source software, we calculated the number of devices that would be associated with a cytotoxic effect according to ISO standards. This analysis indicated that plausible use of the devices would not lead to cytotoxic effects. Overall, we conclude that ingestion of the medical device under plausible use conditions is unlikely to present a toxicological concern for Cu.

**PS 207 Comparative Pulmonary Response to Aerosolized Humidifier Disinfectants by Intratracheal Instillation and Inhalation Exposure.**

Y. Kim<sup>1</sup>, S. Choi<sup>2</sup>, Y. Yang<sup>2</sup>, Y. Kim<sup>1</sup>, C. Song<sup>1</sup>, J. Cho<sup>1</sup>, C. Ha<sup>2</sup> and K. Lee<sup>2</sup>. <sup>1</sup>Korea Institute of Toxicology, Daejeon, Republic of Korea; <sup>2</sup>Jeonbuk Department of Non-Human Primate, Korea Institute of Toxicology, Jeongup, Republic of Korea. Sponsor: S. Park.

Mice intratracheal instillation (IT) and rat inhalation exposure (IH) were conducted to identify the toxicity of 3 representative humidifier disinfectants (products A, B, and C containing polyhexamethylene guanidine (PHMG), 5-chloro-2-methylisothiazol-3-(2H)-one/2-methylisothiazol-3(2H)-one (CMIT/MIT), and oligo(2-(2-ethoxy)ethoxyl guanidinium chloride (PGH), respectively). In mice administered by multiple 7-9 IT at 0.05 ml for 2 wk, severe necrotic obliterative bronchiolitis (OB) was found in product A and C. But no adverse treatment effect was observed in product B. In rat inhalation study (IH), necrotizing inflammation was observed in nasal cavity, larynx, trachea, and lung airways at repeated IH with product A at 0.4  $\text{mg}/\text{m}^3$  and product C at 1.75  $\text{mg}/\text{m}^3$ . However, necrotizing inflammatory lesions in the upper airways were not present in the IT due to direct administration of test substance to the lung via trachea. Granulomatous OB, bronchitis, collagenized fibrosis, alveolar bronchiolarization, and extensive squamous metaplasia were observed in product A at 10 wk IH, and product C at 7 wk IH. No treatment-related adverse effects were observed in 13 wk IH with product B at 1.80  $\text{mg}/\text{m}^3$ . Lung lesions induced by IT and IH with product A and C were comparable and no treatment-related lesions were present with product B in both IT and IH exposure. It was difficult to evaluate dose-related toxicity by IT dosing. However, IT with low dose was a useful methodology to screen and identify toxicity of test substances in this study.

**PS 208 Effect of Fuel Composition on Chemistry and Pulmonary Toxicity in Mice Exposed to Biomass Pyrolysis Vapor.**

I. Gilmour<sup>1</sup>, E. Mutlu<sup>3</sup>, B. Elizabeth<sup>1</sup>, D. Mary<sup>1</sup>, L. Copeland<sup>1</sup>, C. King<sup>1</sup>, T. Krantz<sup>1</sup>, I. George<sup>2</sup>, M. Hays<sup>2</sup>, J. Dye<sup>1</sup>, M. Higuchi<sup>1</sup> and C. Lee<sup>2</sup>. <sup>1</sup>NHEERL, US EPA, Durham, NC; <sup>2</sup>NRMRL, US EPA, Durham, NC; <sup>3</sup>CEMALB, University of North Carolina at Chapel Hill, Chapel Hill, NC.

Biomass pyrolysis is a method to form oil through the thermal degradation of organic material in the absence of oxygen. The process results in a mix of gaseous oxides, organic vapors and particulate matter that could pose an inhalation hazard. In

this study, we characterized aerosol emissions from three different fuels (corn, pine, maple) pyrolyzed under similar conditions, and compared pulmonary and systemic toxicity endpoints in CD-1 mice after a 4h inhalation exposure. Particle number counts/cc were 37000, 48000 and 34000 for corn cob, pine and maple respectively, with median count diameters of 221, 254 and 225 nm. Particle mass was 409, 689 and 362  $\mu\text{g}/\text{m}^3$  for the three fuels, and CO measurements were 37, 39 and 45 ppm. Volatile organic analysis by GC-MS showed acrolein being 1.3, 1.7 and 2.3 ppm, with lower levels of propylene, acetone and vinyl acetate. Pulmonary responses were assessed in a plethysmograph immediately before and after exposure, as well as 4 and 24h post-exposure, when mice were euthanized. All fuels altered breathing parameters immediately following exposure, and this effect persisted at the 4h time-point for the corn cob and maple atmospheres before returning to control levels at 24h. Total protein was increased in the BALF of animals exposed to corn cob (4h and 24h post), pine (24h post), and maple (4h post), with corn having the highest effect. No other indices were affected except BALF LDH for pine, and increased hematocrits for corn cob at 24h. Because these atmospheres were considered to have high irritant characteristics, nasal lavage was also performed and although some increases in inflammatory cells were seen for the corn cob and maple atmospheres, the effects were variable. We conclude that corn cob and maple pyrolysis products seemed to have a more potent effect on pulmonary function and toxicity parameters than pine emissions. (This abstract does not reflect EPA policy).

**PS 209 Gene Expression in Bronchiolitis Obliterans-Like Lesions in Rats Exposed to 2, 3-Pentanedione.**

D. L. Morgan<sup>1</sup>, B. A. Merrick<sup>1</sup>, K. E. Gerrish<sup>2</sup>, P. S. Stockton<sup>1</sup>, J. F. Foley<sup>1</sup>, W. M. Gwinn<sup>1</sup> and G. P. Flake<sup>1</sup>. <sup>1</sup>Division of the National Toxicology Program, NIEHS, Research Triangle Park, NC; <sup>2</sup>Division of Intramural Research, NIEHS, Research Triangle Park, NC.

Obliterative bronchiolitis (OB) is an irreversible lung disease characterized by progressive fibrosis in the small airways with eventual obliteration of the airway lumens. OB is most commonly associated with lung transplant rejection; however, OB has also been diagnosed in workers exposed to artificial butter flavoring (ABF) vapors. Research has been limited by the lack of an adequate animal model of OB, and as a result the mechanism is unclear and there are no effective treatments for this condition. A rat model of chemical-induced OB using the ABF component, 2,3-pentanedione (PD), was found to cause airway lesions histopathologically similar to OB lesions in humans. We used this model to evaluate changes in gene expression in the distal bronchi of rats with OB. Male Wistar Han rats were exposed to 200 ppm PD or air (controls) 6hr/d, 5d/wk for 2-wks. Distal bronchial tissues were laser microdissected from serial sections of frozen lung. In exposed lungs, both fibrotic and nonfibrotic airways were collected. Following RNA extraction and microarray analysis, differential gene expression was evaluated. In exposed nonfibrotic bronchi, 1548 genes were significantly altered relative to air-exposed controls with notable downregulation of many inflammatory cytokines and chemokines. In contrast, in PD-exposed fibrotic bronchi, 2504 genes were significantly altered with a majority of genes being upregulated in affected pathways. TGF-beta2 and downstream genes implicated in fibrosis were significantly upregulated in fibrotic lesions. Genes for collagens and extracellular matrix proteins were highly upregulated. In addition, expression of genes for peptidases and for peptidase inhibitors were significantly altered suggesting tissue remodeling that may contribute to fibrosis. These data will be used to gain a better understanding of the molecular mechanisms of OB and to identify potential therapeutic targets.

**PS 210 Polyhexamethyleneguanidine Phosphate Induces Severe Lung Inflammation, Fibrosis, and Thymic Atrophy.**

J. Song<sup>1</sup>, H. Park<sup>1</sup>, H. Yang<sup>1</sup>, M. Yang<sup>1</sup>, C. Song<sup>2</sup> and K. Lee<sup>1</sup>. <sup>1</sup>Inhalation Toxicology Center, Jeonbuk Department of Nonhuman Primate, Koeran Institute of Toxicology, Jeongup, Republic of Korea; <sup>2</sup>Korean Institute of Toxicology, Daejeon, Republic of Korea. Sponsor: S. Park.

Polyhexamethyleneguanidine phosphate (PHMG-ph) has been widely used as a disinfectant due to its strong bactericidal activity. But The Korea Centers for Disease Control and Prevention (KCDC) and Ministry of Health and Welfare reported that humidifier disinfectants might cause of the unknown pulmonary disease in 2011. The purpose of this study was to assess the potential adverse effect of PHMG-Ph, a ingredient of humidifier disinfectant, exposed to lung directly. 0.0125%, 0.0375%, and 0.0625% PHMG-Ph was instilled intratracheally into mice. Seven and fourteen days after instillation, lungs were collected and proinflammatory cytokines, chemokines and fibrotic markers were measured from lung lysates. We also performed flow cytometry to evaluate the cell distribution of thymus and RT-PCR to measure the mRNA expression associated with T cell development.

As a result, single exposure of 0.0125%, 0.0375%, and 0.0625% PHMG-Ph induced inflammatory response with increased proinflammatory cytokines and immune cell infiltration to the lungs, and interestingly, this inflammation did not resolved till the end of the experiments (14 days after instillation). The histopathology showed the both inflammation and pulmonary fibrosis exacerbated at day 14 after exposure in dose-dependent manner. Also PHMG-Ph decreased the total cell number and the CD4+/CD8+ cell proportion in thymus and induced severe medulla reduction based on histopathology data. These observations demonstrated that PHMG-Ph exposed to lung lead to pulmonary inflammation and fibrosis as well as to thymic atrophy.

## PS 211 Inhalation of a Spot Welding Aerosol Using an Adhesive Increased Airway Resistance but Not Lung Inflammation.

J. M. Antonini, A. Afshari, J. A. Thompson, J. S. Fedan, W. McKinney, T. G. Meighan, M. C. Jackson, B. T. Chen, D. Schwegler-Berry, A. Erdely, D. Frazer and P. C. Zeidler-Erdely. *NIOSH, Morgantown, WV.*

Spot welding (SW) is used in the automotive and aircraft industries where high speed repetitive welding is needed and relatively thin metal sections are welded. Epoxy adhesives are applied as sealers to the seams of the metals that are joined. SW produces complex aerosols composed of both metal and volatile compounds which may cause bronchitis and asthma in workers. The goal was to assess the effect of SW fumes on lung function and toxicity. Male Sprague-Dawley rats were exposed by inhalation to 20 mg/m<sup>3</sup> of SW aerosol in the presence of an adhesive for 4 hr/d x 8 d. Controls were exposed to air. Size distribution of the aerosol as determined by a MOUDI particle impactor was tri-modal with a MMAD of 1.66 µm in the large-fine mode, 0.30 µm in the small-fine mode, and 0.01-0.05 µm in the ultrafine mode. Two distinct particle morphologies were observed- a brownish metal particle that predominated in the small-fine particle fraction and a black, glue-like particle that was in the large-fine fraction. The metal fraction was found to be >90% Fe. Significant amounts of volatiles (e.g., benzene, toluene, others) were present, likely produced from the vaporization of the adhesive. At different times after exposure, bronchoalveolar lavage (BAL) was performed to assess lung toxicity. Lung resistance (R<sub>L</sub>) was evaluated in a separate set of animals before and after challenge with inhaled methacholine (MCh). Immediately after exposure, baseline R<sub>L</sub> was significantly elevated in the group exposed to the SW fumes. Basal R<sub>L</sub> returned to control level by 1 d after exposure. Reactivity to MCh was not affected at any time point after fume exposure. No significant increase in lung inflammation (neutrophil influx) or injury (cytotoxicity and lung epithelial permeability) was observed in BAL fluid at 1 and 5 d after exposure to SW fume. Acute inhalation of SW fumes at occupationally-relevant concentrations may act as an irritant as evidenced by the increased R<sub>L</sub> but had little effect on toxicity.

## PS 212 Cardiopulmonary Health Effects of Traffic-Related Air Pollutants in a Healthy Population.

J. E. Mirowsky<sup>1</sup>, R. Peltier<sup>2</sup>, M. Lippmann<sup>1</sup>, L. Griffith<sup>1</sup>, J. Carter<sup>3</sup>, D. Diaz-Sanchez<sup>3</sup>, W. Cascio<sup>3</sup> and T. Gordon<sup>1</sup>. <sup>1</sup>Environmental Medicine, New York University, Tuxedo, NY; <sup>2</sup>Environmental Health Science, University of Massachusetts, Amherst, MA; <sup>3</sup>US EPA, Research Triangle Park, NC.

There is emerging evidence that inhaling certain components of ambient particulate matter, specifically traffic pollutants, is associated with adverse health effects. We hypothesized that exposure to air pollution components of diesel exhaust-rich traffic, compared to cars-only traffic, produces greater adverse cardiopulmonary effects. In this case-crossover study, 23 participants were recruited to measure pulmonary function, exhaled NO, blood cytokines, heart rate variability, and blood pressure prior to, immediately after, and 24 hours after intermittent walking along 3 diverse roadways. Exposures lasted for 1.5 hours between June and September in 2011 and 2012, and personal exposures to pollutants were collected. The 3 locations differed by traffic type: the George Washington Bridge (GWB) carries truck and car traffic, the Garden State Parkway (GSP) carries only car traffic, and Sterling Forest, NY (SF) acted as a control location. Levels of PM<sub>2.5</sub>, PM<sub>10</sub>, black carbon, elemental carbon, and organic carbon were found to be highest at GWB and lowest at SF for all pollutants measured. The traffic count was similar between GSP and GWB. Using a repeated measures 2-way ANOVA, p-values were generated for time, location, and interactions between time and location. Location was a significant factor for FVC (p = 0.04) and FEV<sub>1</sub> (p = 0.05); a significant interaction term for pulse pressure was also observed (p < 0.01). Upon further analysis, systolic and pulse pressures varied significantly amongst locations when comparing the baseline and 24 hr-post measurement, while IL-1β varied amongst locations between the baseline and immediately after exposure. A trend of increasing eNO at the GWB was seen immediately after exposure, but did not reach significance (p = 0.06). These results suggest that acute effects of traffic-related pollution are observed in a small, healthy population; these effects differed by traffic type.

## PS 213 Ventricular Transcriptional Data Provide Mechanistic Insights into Diesel Exhaust-Induced Attenuation of Cardiac Contractile Response and Blood Pressure.

U. P. Kodavanti, V. L. Bass, J. Crooks, B. Vallanat, H. Ren, M. C. Schladweiler, R. F. Thomas, T. Krantz, C. King, C. J. Gordon and A. D. Ledbetter. *EPHD/NHEERL/ORD, US EPA, Research Triangle Park, NC.*

Human exposure to diesel exhaust (DE) has been associated with cardiovascular impairments however the mechanisms and the role of hypertension are not well understood. We have shown that DE reduces blood pressure (BP) and cardiac contractility in healthy normotensive Wistar Kyoto (WKY) rats. We hypothesized that DE would induce differential myocardial gene expression changes that modulate contractility in WKY and spontaneously hypertensive (SH) rats, and that lowering BP in WKY and SH with hydralazine (HYD) would increase this effect of DE. Male WKY and SH rats were treated with HYD (150 mg/L) in drinking water for 10 days prior to exposure and until necropsy. All rats were exposed to clean air or freshly-generated whole DE (1500 µg/m<sup>3</sup>), 5-hrs/day for 2-days. Systolic BP was monitored using the tail-cuff method on days -10, 0, and 2. Left ventricular genome-wide expression was analyzed using Illumina RatRef-12 BeadChips. As expected, WKY and SH rat's ventricular gene expression patterns differed markedly. Surprisingly, DE exposure caused differential expression of 256 genes in WKY but none in SH rats. In WKY rats, the effect of HYD on expression patterns were nearly identical to changes induced by DE (same genes with same directional change); while HYD was without effect on expression changes in SH rats despite lowering BP. Genes inhibited by DE or HYD in WKY were induced at baseline in SH and vice versa. These genes inhibited by DE and HYD were related to sequestration of oxidants, inhibition of proteases, and membrane stability. The genes up-regulated by DE and HYD in WKY included those involved in decreasing BP and muscle contraction as well as calcium homeostasis and apoptosis. In conclusion, acute DE exposure caused gene expression changes only in normotensive WKY rats; these changes mimicked those induced by HYD and are associated with decreased cardiac contractility and BP in healthy rats. (Abstract does not reflect USEPA policy)

## PS 214 Comparative Cardiopulmonary Toxicity of Soy Biofuel and Diesel Exhausts in Healthy and Hypertensive Rats.

M. C. Schladweiler<sup>1</sup>, V. L. Bass<sup>1</sup>, R. F. Thomas<sup>1</sup>, J. E. Richards<sup>1</sup>, D. Johnson<sup>2</sup>, D. L. Andrews<sup>4</sup>, A. Nyska<sup>3</sup>, T. Krantz<sup>1</sup>, C. King<sup>1</sup> and U. P. Kodavanti<sup>1</sup>. <sup>1</sup>EPHD/NHEERL/ORD, US EPA, Research Triangle Park, NC; <sup>2</sup>Curriculum in Toxicology, University of North Carolina at Chapel Hill, Chapel Hill, NC; <sup>3</sup>Tel Aviv University, Tel Aviv, Israel; <sup>4</sup>RCU/NHEERL/ORD, US EPA, Research Triangle Park, NC.

Increased use of renewable energy sources raise concerns about health effects of emissions from such sources. We conducted a comprehensive analysis of relative cardiopulmonary health effects of exhausts from 1) 100% soy biofuel (B100), 2) 20% soy biofuel + 80% low sulfur petroleum diesel (B20), and 3) 100% petroleum diesel (B0) in rats. Normotensive Wistar Kyoto and spontaneously hypertensive rats were exposed to these 3 exhausts at 0, 50, 150 and 500 µg/m<sup>3</sup>, 4 h/day for either 2d or 4 wk (5 d/wk) to mimic near environmental concentrations. Additionally, WKY rats were exposed for 1d and responses were analyzed 0 hr, 1d or 4d later for time course analysis. Hematological parameters, in vitro platelet aggregation, bronchoalveolar lavage fluid (BALF) markers of pulmonary injury and inflammation, ex-vivo aortic ring constriction, heart and aorta mRNA markers of atherogenesis, and serum biomarkers of acute cardiac injury as well as cytokines were analyzed. The presence of pigmented macrophages in the lung alveoli was clearly evident with all 3 exhaust exposures. Overall, exposure to all 3 exhausts produced only modest effects in most endpoints analyzed in both rat strains. BALF γ-glutamyl transferase (GGT) activity was the most consistent marker shown to be increased in both strains with all 3 fuels (B0>B100>B20) without increases in BALF neutrophils. Small inconsistent changes in aorta mRNA markers of inflammation, vasoconstriction and thrombosis, and those of serum biomarkers need to be interpreted cautiously. Our comparative evaluations show modest cardiovascular and pulmonary effects at low concentrations of all exhausts. Additionally, our study highlights the value of BALF levels of GGT activity as the most sensitive biomarker in low level inhalation studies. (This abstract does not represent USEPA policy).

**PS 215 Acute and Delayed Effects of Intermittent Ozone on Cardiovascular and Thermoregulatory Responses of Young and Aged Rats.**

A. F. Johnstone<sup>1</sup>, R. C. MacPhail<sup>1</sup>, C. Aydin<sup>2</sup> and C. J. Gordon<sup>1</sup>. <sup>1</sup>TAD, NHEERL, US EPA, Research Triangle Park, NC; <sup>2</sup>Physiology, University of Uludag, Bursa, Turkey.

Ozone (O<sub>3</sub>) is associated with cardiovascular and respiratory diseases. The aged population is considered to be more sensitive to air pollutants but relatively few studies have demonstrated increased susceptibility in animal models of aging. To study the acute and delayed physiological responses to O<sub>3</sub>, core temperature (T<sub>c</sub>) and heart rate (HR) monitored by telemetry in adult (12 m) and senescent (24 m) Brown Norway rats exposed to intermittent O<sub>3</sub> (1.0 ppm, 6 hr/d for 2 consecutive d for 12 wk). T<sub>c</sub> and HR dropped precipitously in both age groups during the 1st bout of O<sub>3</sub> exposure; T<sub>c</sub> decreased from ~38 to ~35 °C while HR decreased from ~300 to ~175 b/min. These acute responses were attenuated during the 2nd day of O<sub>3</sub>. As O<sub>3</sub> exposures continued, the acute T<sub>c</sub> and HR responses abated but the aged animals were consistently less affected than the young adults throughout the 12 wk exposure period. During 5 d of recovery in home cages, both young and senescent rats displayed a fever-like ~0.5 °C elevation in daytime T<sub>c</sub>. HR was also elevated in the young adults during recovery. The rise in T<sub>c</sub> persisted for 2-3 d after O<sub>3</sub>. The O<sub>3</sub>-induced fever was marked following the 1st exposure, abated by the 3rd exposure week but then gained in magnitude throughout the remainder of the study. We postulate that inflammatory responses of the respiratory system to O<sub>3</sub> are exacerbated in younger animals, leading to accentuated acute physiological responses compared to that of senescent rats. This is an abstract of a proposed presentation and does not reflect US EPA policy.

**PS 216 Dose and Effect of Inhaled Ozone in Resting versus Exercising Human Subjects: Comparison with Resting Rats.**

G. E. Hatch, J. McKee, J. S. Brown, B. McDonnell, E. Seal, J. Soukup, R. Slade, K. Crissman and R. B. Devlin. Environmental Public Health Division, US EPA, Research Triangle Park, NC.

**Rationale:** Human controlled exposure studies have generally focused on subjects exposed to ozone (O<sub>3</sub>) while exercising. We exposed resting subjects to labeled O<sub>3</sub> (<sup>18</sup>O<sub>3</sub>, 0.4 ppm, for 2 hr) and compared O<sub>3</sub> dose and effects with our previously published study of exercising subjects.

**Methods:** We measured O<sub>3</sub> dose as the concentration of <sup>18</sup>O in cells and extracellular material of nasal, bronchial and bronchoalveolar lavage fluid (BALF) immediately post exposure and related these measurements to O<sub>3</sub> effects on inflammation, epithelial permeability and phagocytosis in the same fluids and to breathing parameters measured during the <sup>18</sup>O<sub>3</sub> exposure. A parallel study of resting subjects examined FEV<sub>1</sub> changes during and immediately following a 2 hr exposure to 0.18, 0.25, 0.3 and 0.4 ppm O<sub>3</sub>.

**Results:** Subjects exposed while resting had <sup>18</sup>O concentrations in BALF and nasal lavage that were proportional to the amount of air breathed during exposure. Significant but small changes were observed in BALF total cells and neutrophils and in BALF cell phagocytosis following resting O<sub>3</sub>, however, most indicators of O<sub>3</sub> effects that were observable in exercising subjects (including increased BALF supernatant protein, lactate dehydrogenase, interleukin-6 and low molecular weight antioxidants) were not observed in resting subjects. The <sup>18</sup>O incorporation into BALF of resting humans was similar to that of similarly exposed resting F344 rats. FEV<sub>1</sub> changes in resting human subjects showed a much attenuated response compared to exercising subjects.

**Conclusions:** Quantitative measures of alveolar O<sub>3</sub> dose and toxicity that were observed previously in exercising subjects were greatly reduced or non-observable in O<sub>3</sub> exposed resting subjects. Resting rats and resting humans have similar alveolar O<sub>3</sub> dose. **Disclaimer:** This abstract does not represent E.P.A. policy.

**PS 217 Biological Responses in Rats Exposed to Mainstream Smoke from a Heated Cigarette Compared to a Conventional Reference Cigarette.**

H. Fujimoto<sup>1</sup>, H. Tsuji<sup>1</sup>, I. Fukuda<sup>1</sup>, T. Nishino<sup>1</sup>, M. K. Lee<sup>2</sup>, R. Renne<sup>3</sup> and H. Yoshimura<sup>1</sup>. <sup>1</sup>R&D Group, Japan Tobacco Inc., Yokohama, Japan; <sup>2</sup>Scientific and Regulatory Affairs, Japan Tobacco International S.A., Geneva, Switzerland; <sup>3</sup>Roger Renne ToxPath Consulting, Sumner, WA.

The heated cigarette (HC) generates mainstream smoke (MS) primarily by vaporizing the components of the tobacco rod using a carbon heat source at the cigarette tip. Consequently, MS of HC contains markedly less chemical constituents compared to conventional (combusted) cigarettes. In this study, MS from a non-ventilated HC (nvHC) was generated under a modified Canadian Intense Regimen

(CIR) and its biological activities were compared to those of Reference (3R4F) cigarettes, using nose-only inhalation studies. In a 5-week inhalation study, female SD rats were exposed to MS of either cigarette at 600 or 1000 µg wet total particulate matter (WTPM) /L for 1 hr, 2 times/day, 7 days/week for 5 weeks. Pulmonary inflammation was significantly weaker in nvHC groups compared to 3R4F groups, based on the neutrophil counts and deviation enzyme levels in bronchoalveolar lavage fluid (BALF). After a 4-week recovery, BALF parameters of nvHC groups were similar to the air-exposed Sham group, while those of 3R4F groups remained elevated. In a 13-week inhalation study, male and female SD rats were exposed to MS from each cigarette at 200, 600, or 1000 WTPM µg/L for 1 hr/day, 7 days/week for 13 weeks. Histopathological changes in the respiratory tract were significantly lower in incidence/severity for nvHC groups, especially in respiratory epithelial hyperplasia and accumulation of pigmented macrophages in alveoli. After a 13-week recovery, the lesions were completely or partially regressed, except for accumulation of pigmented macrophages in alveoli, in both nvHC and 3R4F groups. In conclusion, nvHC demonstrated clearly and significantly lower biological activities compared to 3R4F, based on the BALF parameters and histopathology.

**PS 218 A Cross-Regulatory T Cell Response in Pulmonary Hypertension.**

G. Grunig, W. Chen, C. Hoffman, T. Gordon and S. Park. NYU Medical Center, Tuxedo, NY.

Exposure to urban air pollution (fuel emissions, particulate matter) has been associated with the exacerbation of autoimmune diseases. Our studies are focused on the mechanism of immune response induced pulmonary hypertension. We have shown that co-exposure of mice to inhaled antigen and urban particulate matter (PM) exacerbates pulmonary arterial remodeling and induces pulmonary hypertension. The current studies were performed with neutralizing anti-cytokine antibodies to identify the critical mediators for pulmonary hypertension and the interactions in the mediator-network.

Sensitized mice were intranasally challenged with either antigen (Ovalbumin) combined with urban PM2.5 (collected in New York City), or given saline. Groups of mice were injected with neutralizing anti-Interleukin (IL)-13, or anti-IL-17A/F antibodies alone or in combination, or control antibody. Right ventricular systolic pressures and immune response markers in the lungs were measured.

Intranasal challenge with antigen and urban PM significantly increased right ventricular systolic pressures. Only combined, but not single, injections with IL-13 and IL-17A/F-blockers significantly reduced this outcome. Surprisingly, injections with single neutralizing antibodies not only significantly reduced the inflammatory markers known to be regulated by IL-13 or IL-17A/F, but also revealed cross-inhibition of these markers. For example, the increased expression of the antigen presentation molecule, major histocompatibility class II (MHCII), by airway dendritic cells was inhibited by the IL-13 blocker given alone or in combination, while the IL-17A/F blocker lead to an increase in MHCII expression. Conversely, infiltration of the airways with neutrophils was inhibited by the administration of the IL-17A/F blocker given alone or in combination, while injections with the IL-13 blocker increased neutrophil influx.

In conclusion, exposure to antigen and urban PM induced pulmonary hypertension by elaborating a mixed immune response that has at least two, cross-regulatory arms that are controlled by IL-13 and IL-17A/F, respectively.

**PS 219 Capsule-Based Aerosol Generator (CBAG)—Validation in a Rat Model of LPS-Induced Nonallergic Pulmonary Inflammation.**

S. Jordan, S. Moore and R. Armstrong. Huntingdon Life Sciences, Huntingdon, United Kingdom. Sponsor: E. Moore.

Intratracheal (IT) insufflation is the principal method of delivery of inhaled drug substances to conscious non-clinical species in early drug development; however, this achieves particulate deposition dissimilar to conscious inhaled delivery and can produce artefactual toxicological and pharmacological results. The CBAG was developed(1) as an alternative to IT insufflation whilst providing representative inhalation exposure by demonstrating the effectiveness of the CBAG in the rat model of LPS-induced non-allergic airway inflammation. Rats were exposed to 0.01, 0.1 or 1.0 mg/kg of inhaled fluticasone propionate (FP) over a 20-minute period using nominally 1 mg filled hydroxypropyl methyl cellulose size 2 capsules at blend strengths of 1, 10 and 100% w/w of FP respectively. Two concurrent control groups were exposed to lactose only using the same regime. Twenty minutes after the end of the inhalation exposure the animals were challenged with either aerosolised LPS (0.1 mg/mL) for the FP groups and one control group or 0.9% w/v saline (second control group) for 30 minutes. Rats were euthanized 4hrs following the challenge

and a bronchoalveolar lavage (BAL) investigation performed. A BAL total and differential cell count was used to evaluate the efficacy of FP. Delivered doses of 0.0103, 0.117 and 0.863 mg/kg were achieved, which were within 14% of target. This resulted in a dose dependent inhibition of BAL neutrophils of 40%, 79% and 98% respectively compared with the lactose/LPS control group. In conclusion, the results give confidence that the CBAG is a viable alternative to IT methodology for studies in early drug development and has the added advantage of producing results representative of inhaled exposures.

(1) Paul G, Somers G, Moore S and Goodway R, Respiratory Drug Delivery 2012, Vol. 2, 525-530.

## PS 220 Distinct Inflammatory Macrophage Subpopulations and Myeloid-Derived Suppressor Cells Accumulate in the Lung and Spleen following Exposure of Mice to Inhaled Ozone.

D. L. Laskin<sup>1</sup>, H. M. Choi<sup>1</sup>, J. D. Laskin<sup>2</sup> and M. Mandal<sup>1</sup>. *Pharmacology and Toxicology, University of Arizona, Tucson, AZ.*

Ozone is an ubiquitous urban air pollutant known to damage the lung. Activated macrophages (MP) and inflammatory mediators they produce have been implicated in ozone toxicity. However, the phenotype and origin of these cells have not been established. In these studies, techniques in flow cytometry were used to assess macrophage subpopulations in the lung, spleen and bone marrow following ozone inhalation. Exposure of C57Bl/6 male mice to ozone (0.8 ppm, 3 h) resulted in increased bronchoalveolar lavage (BAL) protein levels after 24-72 h, indicative of alveolar epithelial injury. This was correlated with a rapid and persistent increase in the percentage of CD11b+F4/80+ inflammatory macrophages in BAL. An increase in F4/80 negative CD11b+Ly6C+Ly6G+ myeloid-derived suppressor cells (MDSCs) was also observed in BAL, a response most prominent 24 h post ozone exposure. Conversely, F4/80 positive CD11b+Ly6C+Ly6G+ MDSCs decreased in BAL after ozone exposure. We also found that ozone exposure resulted in a persistent decrease in CD11b+F4/80+ inflammatory macrophages, and a transient increase in CD11b-F4/80+Ly6C+Ly6G+ MDSCs in the spleen. In contrast, there were no changes in bone marrow cell subpopulations after ozone inhalation. Taken together, these results suggest that the spleen is a source of inflammatory MP in the lung following ozone exposure; moreover, subpopulations of MDSCs originating in the lung and the spleen may contribute to early inflammatory responses in the lung and to processes of injury and repair. Supported by NIH grants GM034310, ES004738, CA132624, AR055073, ES007148, ES005022.

## PS 221 Compare *In Vitro* Endothelial Cell Release of Endothelium Derived Vasodilators in Response to Diesel, Biodiesel Blend and Biodiesel Neat Combustion Extract.

L. Bhavaraju<sup>1</sup>, A. Williams<sup>2</sup>, T. Kormos<sup>3</sup> and M. Madden<sup>4</sup>. <sup>1</sup>Toxicology, University of North Carolina at Chapel Hill, Chapel Hill, NC; <sup>2</sup>National Renewable Energy Laboratory, Golden, CO; <sup>3</sup>NERL, ORD, US EPA, Research Triangle Park, NC; <sup>4</sup>EPHD, NHEERL, US EPA, Chapel Hill, NC.

Diesel exhaust exposure in controlled human chamber studies found exposure induced inhibition of vasodilation. Particles emitted in exhaust can translocate into the vascular system however when particles are dissolved in solvents of various polarity the insoluble fraction separates from the soluble fraction. We collected the soluble fraction of combusted particles dissolved in DMSO for evaluation of the extract to interfere with the release of endothelium derived vasodilators. Endothelium dependent vasodilation is dependent on 6-keto PGF1alpha (6keto) a vaso-active metabolite of arachidonic acid. We have investigated the effects of diesel, biodiesel blend and biodiesel neat for a change in 6 keto release from three cell lines: endothelial hybrid cell line (EA hy 926 cells), primary human umbilical vein endothelial cells (HUVEC) and primary human coronary artery endothelial cells (HCAEC). ELISA results of EA hy 926 cells with extract exposure for 24hrs indicate a statistically significant (p<0.009) increase in 6keto from control and 100µg/mL of biodiesel neat (B100). However ELISA results from HUVEC and HCAEC exposed to extract for 6, 8 and 24hrs indicate no statistically significant change in 6keto release. QPCR data from extract exposure indicates there is no increase in markers of inflammation. However there is a measureable increase in heme oxygenase-1(HO-1) gene expression. HUVEC and HCAEC with 8hr extract exposure to B100 at 100µg/mL have over two fold increase in HO-1. The B100 particle composition analysis indicates high levels of Zn and Fe compared to biodiesel blend and diesel. In our work we address a possible mechanism for attenuation of vaso-active arachidonic acid metabolites in endothelial cells exposed to diesel, biodiesel blend and biodiesel neat particle extracts. [This is an abstract of a proposed presentation and may not necessarily reflect official US EPA Policy.]

## PS 222 Role of CD36 in Ozone (O<sub>3</sub>)-Induced Lung Injury, Inflammation, and Vascular Dysfunction.

S. Robertson, S. N. Lucas, P. Hall, M. Paffett and M. J. Campen. *University of New Mexico, Albuquerque, NM.*

Ground level O<sub>3</sub> can damage the cardiovascular system. A lack of a clear mechanism explaining O<sub>3</sub>-induced vascular health effects hinders the effectiveness of policies for achieving better health. Evidence suggests that inhaled pollutants evoke a systemic inflammatory response that causes endothelial injury and dysfunction. Using serum from O<sub>3</sub>-exposed mice, we found that circulating components impaired acetylcholine (ACh) vasorelaxation in aortas from naïve wild type (WT) mice. However, the mechanistic interaction(s) between circulating factors and endothelial cells is unknown. To address this issue we turned our attention to pattern recognition receptors (PRRs), such as CD36 (cluster of differentiation 36), as mediators of vascular abnormalities following O<sub>3</sub> exposure. PRRs are capable of detecting danger signals released by stressed or injured cells. We hypothesized that activation of endothelial CD36 following acute O<sub>3</sub> exposure mediates cross-talk between lung-derived circulating factors and vascular endothelium, culminating in endothelial dysfunction.

Female C57 wild type (WT) and CD36 knockout (KO) mice were exposed to filtered air (FA) or 1 ppm O<sub>3</sub> for 4 h. Indices of pulmonary (quantified by lavage inflammatory cells) inflammation was assessed 24 h later. The effects of exposure on ACh-induced vasorelaxation were studied using the aortic ring preparation. Parallel experiments were performed in aortas from naïve WT mice incubated with serum from exposed mice.

O<sub>3</sub>-induced infiltration of macrophages and neutrophils into the airspace in WT mice were absent in CD36 KO mice. ACh-evoked vasorelaxation of thoracic aorta of WT mice, but not CD36 KO mice, was significantly reduced after inhalation of O<sub>3</sub>. *Ex vivo* assays utilizing homologous serum demonstrated that the vascular damage caused by O<sub>3</sub>-induced circulating factors was dependent on vascular CD36 receptor expression.

Collectively, our data demonstrate that an as yet unidentified circulating factor, or factors, induced by O<sub>3</sub> exposure leads to vascular dysfunction mediated, in part, by CD36 binding in the vascular tissue.

## PS 223 *In Vitro* Endothelial Cell Model to Assess the Impact of Systemic Inflammation on Vascular Health.

M. Aragon, E. S. Colombo, M. J. Campen and S. Lucas. *Department of Pharmaceutical Sciences, University of New Mexico, Albuquerque, NM.*

Assessing the adverse vascular health effects of systemic inflammation caused by inhaled toxins has presented a substantial research challenge. Current models rely on anatomically disputable direct application of xenobiotics, especially airborne particulate matter, on cultured endothelial cells. Such assay systems fail to account for the complex interactions and toxicokinetics that occur *in vivo*. We have developed a model that takes these factors into account to better elucidate the mechanisms involved in a living system. This approach utilizes plasma or serum from exposed animals as the endothelial stimulus, as this is the component in direct contact with endothelial cells. Briefly, the serum/plasma isolated from exposed animals is incubated on endothelial cells and canonical activation pathways are assessed. In this way the endothelial cells act as a "biosensor", expressing markers of inflammation, especially cell surface adhesion molecules. In addition, nitric oxide (NO) bioavailability via electron paramagnetic resonance can be directly measured in the supernatant. We have characterized this model paradigm using primary endothelial cells from rats and mice, using known mediators (IL-6, TNF-α) to assess the range of response in order to compare endothelial cell responses to serum obtained from ozone-exposed rodents. Serum obtained 24h following exposure to 1ppm ozone for 4h caused a 2-fold increase in vascular cell adhesion molecule-1 cell surface expression on rat aortic endothelial cells, as compared to serum from filtered air-exposed rats. Similarly, we observe reductions in NO generation and elevated mRNA expression of specific markers of endothelial cell activation. The potential for this assay extends beyond the toxic effects of air pollution, with potential applications to drug safety and efficacy, as well as having prognostic value for vascular disease.

**PS 224 Interaction of Human Bronchial Epithelial Cells and Alveolar Macrophages Modifies the Innate Immune Response to Ozone.**

R. N. Bauer<sup>1</sup>, L. Mueller<sup>2</sup>, L. Brighton<sup>2</sup> and I. Jaspers<sup>1,2</sup>. <sup>1</sup>Curriculum in Toxicology, University of North Carolina at Chapel Hill, Chapel Hill, NC; <sup>2</sup>Center for Environmental Medicine, Asthma, and Lung Biology, University of North Carolina at Chapel Hill, Chapel Hill, NC.

The lining of the airway consists of airway epithelial cells and resident immune cells, which together coordinate the innate immune response to oxidant pollutants. Oxidant pollutants can damage airway epithelial cells and induce the production of soluble mediators that attract nearby immune cells, such as alveolar macrophages, and activate innate immune pathways. Using ozone (O<sub>3</sub>) as a model oxidant pollutant, we developed a human bronchial epithelial cell (HBE) and alveolar macrophage (AM) co-culture model to assess how the interaction between HBE and AM modifies the innate immune response to oxidant air pollutants. AM derived from the bronchoalveolar lavage of healthy volunteers were co-cultured with the HBE cell line 16HBEo- on transwell cell culture inserts or on transwells alone. Co-cultures, AM alone, and HBE alone were exposed to 0.4 ppm O<sub>3</sub> or clean air for 4 hours and analyzed 1 and 24 hours after O<sub>3</sub> exposure. O<sub>3</sub>-induced secretion of interleukin (IL)-1 $\beta$  and IL-8 was compared between the cultures to determine the specific cellular sources and whether the interaction between AM and HBE modifies the inflammatory response. Using flow cytometry, co-cultures or AM alone were examined for AM surface receptor expression, particularly CD44, Toll-like Receptor 4 (TLR4) and its co-receptor CD14, which recognize soluble mediators produced in response to oxidative damage. Our results suggest that co-culture of AM and HBE modifies O<sub>3</sub>-induced secretion of IL-1 $\beta$ , but not IL-8. Whereas the co-cultures had robust O<sub>3</sub>-induced IL-1 $\beta$  production, this response was blunted in both AM and HBE cultured alone. Both O<sub>3</sub>-exposed AM had altered CD14, TLR4, and CD44 expression, and co-culture further modified surface marker expression. These results suggest that HBE and AM coordinate the inflammatory response to O<sub>3</sub>, and that the interaction between HBE and AM is an important determinant of the innate immune response to inhaled oxidant pollutants.

**PS 225 Behaviour of Lactose Blends in Nonclinical Respiratory Safety Assessment Studies.**

S. Moore<sup>1</sup> and S. Cracknell<sup>2</sup>. <sup>1</sup>Huntingdon Life Sciences, Huntingdon, United Kingdom; <sup>2</sup>Huntingdon Life Sciences, East Millstone, NJ. Sponsor: D. Mitchell.

Drug/lactose powder blend range and complexity has also grown proportionally as the potency of drug molecules has increased. This review, therefore, addresses the relationship between the active drug moieties and total particulate over a range of lactose powder blend formulations before and after aerosolisation to ensure enhanced study control. Test atmosphere concentration data from studies were chemical or gravimetric analysed for drug:total particulate (TP) ratios and compared with the original blend strength (BS). Results for unmiconised blends indicated up to a 13-fold increase in drug:TP ratio for lower drug blend strengths (0.25% w/w) for non-rodent exposure systems and 9-fold for rodent systems. The fold change (FC) decreased exponentially with increasing drug BS for unmiconised blends and by 40% w/w; the FC was only 2-fold. Greater variation between different drug actives was also evident at lower blend strengths. Using stabilisers or additives resulted in a slight increase (between 0.25 and 0.50 w/w) in the drug:TP ratio over the same BS range. Comparison of 3 different lactose types indicated varying proportions of FC depending on the particle size of the lactose. Miconised Lactohale LH301 gave marginal increase in FC between BS of 0.25 and 40% w/w (1.02 to 1.11) but the FC exhibited for unmiconised Respirose SV008 gave a much greatest change over the same BS range. The FC using the same BS with different size inhalation chambers showed no difference with chamber level implying that the animals receive the same drug:lactose ratio irrespective of their position within the chamber. Comparison between the Flow-Through and Flow past chambers with different blend strengths gave a greater FC for the latter chamber type (up to 67%) due to increased lactose sedimentation related to internal geometry of the chamber. In conclusion, this approach will allow greater prediction and confidence that the gravimetric aerosol concentrations will be an accurate representation of the active drug moiety when the frequency of chemical analysis is reduced.

**PS 226 An In Vitro Cell-Based Assay to Measure the Solubilization of Indium-Containing Particles by Macrophages.**

W. M. Gwinn<sup>1</sup>, W. Qu<sup>1</sup>, R. W. Bousquet<sup>2</sup>, M. P. Waalkes<sup>1</sup> and D. L. Morgan<sup>1</sup>. <sup>1</sup>NTP Laboratory, NIEHS, Research Triangle Park, NC; <sup>2</sup>Alion Science and Technology, Research Triangle Park, NC.

Inhaled or airway-delivered indium-containing particles (ICPs) such as indium phosphide (InP) and indium tin oxide (ITO) exhibit pulmonary toxicity and are carcinogenic. Many ICPs are highly insoluble compounds which are engulfed by alveolar macrophages; however, the mechanism(s) of ICP-induced pathogenesis within the lung is unclear. We have previously shown that ICPs are cytotoxic to macrophages in vitro which is dependent upon phagolysosome acidification. In the current study, we hypothesized that macrophages phagocytose and solubilize ICPs which generates free indium ions- likely the cytotoxic constituent of ICPs. Adherent RAW 264.7 macrophages were treated with 200  $\mu$ g/ml InP particles for 24 hrs. In some groups, macrophages were pre-treated for 30 min with 5  $\mu$ g/ml cytochalasin D (cytoD), an inhibitor of phagocytosis, and then co-treated with InP + cytoD for 24 hrs. CytoD treatment blocked both the phagocytic uptake and cytotoxicity of InP particles. Cell culture supernatants were collected after 24 hrs of treatment and centrifuged to pellet any residual cells and InP particles. Cell and particle-free supernatants were then acid digested overnight and the concentration of total indium was measured using atomic absorption spectroscopy. The concentration of extracellular indium in cell culture supernatants from macrophages treated with InP particles in the absence of cytoD (91.2  $\mu$ g/L) was significantly increased and approximately 3-fold greater compared to macrophages treated with InP in the presence of cytoD (29.8  $\mu$ g/L). These data indicate that macrophages phagocytose and solubilize InP particles within lysosomes resulting in cell death and the extracellular release of free indium metal species. This cell-based assay can potentially be applied to other ICPs to determine if the in vitro macrophage solubility of different ICPs correlates with in vivo pulmonary toxicity.

**PS 227 Acute Pulmonary Heme Oxygenase-1 Protein Response to Particulate Matter in Naïve Animals As an Indicator of Allergic Adjuvant Potential.**

C. Carosino, A. Castaneda, L. E. Plummer, K. Green, Y. Zhao, K. J. Bein, A. S. Wexler and K. E. Pinkerton. Center for Health and the Environment, University of California Davis, Davis, CA.

The San Joaquin Valley (SJV) of California is home to high PM pollution and asthma symptom prevalence. Recently, source oriented sampling (SOS) approaches have been employed in the SJV to collect commonly occurring particle source combinations in the normal milieu of PM typical to the region to allow for the evaluation of their differential toxicities. Acute toxicity studies to assess differential pulmonary inflammation were performed. Additional studies were performed in an acute model of allergic airway inflammation. Studies utilized BALB/c mice, 8-10 weeks old and re-suspended particles collected and extracted by SOS methods. Naïve studies utilized dosing via oropharyngeal aspiration of 50 $\mu$ g SOS PM with tissues examined for pulmonary inflammation 24-hours post dosing. Allergic studies utilized intranasal aspiration dosing on day 1, 3, and 5 of a) vehicle control, b) 25 $\mu$ g endotoxin purified D. Farinae house dust mite allergen, HDM (allergic control), or c) HDM and 15 $\mu$ g SOS PM (45 $\mu$ g total dose). Animals were challenged on day 11, 12, and 13 with allergen alone and tissues collected on day 14. All allergen-treated animals exhibited cellular profiles indicative of an allergic response with elevations in leukocytes characterized by neutrophils, lymphocytes and eosinophils. Heme oxygenase-1 (HO-1) protein levels in homogenized pulmonary tissue of acutely exposed naïve mice were quantified as a biomarker of oxidative stress. Analysis of correlations revealed large associations between total cell, lymphocytic, eosinophilic and neutrophilic pulmonary inflammation in allergic animals in contrast to HO-1 protein levels in the tissue of acutely exposed naïve animals. Cellular inflammation in naïve acute studies did not correlate with HO-1 protein and did not accurately predict adjuvant potential. These studies suggest that pulmonary HO-1 levels in naïve acute studies and existing archived tissue may be a valuable indicator of particle adjuvant potential. Support: CARB/EPRI

**PS 228 Toxic and Mutagenic Effects of World Trade Center Dust on Cultured Human Lung Cells.**

A. M. DiLorenzo, C. Lambrousis, S. Choi and P. Rivera. Montclair State University, Montclair, NJ.

The terrible events of the September 11, 2001 World Trade Center (WTC) tragedy left many dead, injured, devastated and emotionally scarred. The effect of this tragic event was noticed even a decade later in many upper-respiratory complica-

tions resulting from the exposure to the toxic dust. The purpose of these experiments was to investigate the extent of cellular damage resulting from WTC dust exposure. This research project was conducted with cultured human lung fibroblast cells exposed to WTC dust. To determine if cell proliferation levels were affected, cultured cells were exposed to WTC dust at various concentrations ranging from 2.5 to 250 parts per million (ppm) in simulated physiological stress environments. LD 50 had previously been determined in choosing sample concentrations. Decreased serum levels were also utilized to mimic stress conditions which were to be correlated to the stress levels experienced in the exposed human population. The cultures under the various conditions were studied using both Cell Titer 96 Aqueous Non-radioactive Assay and Caspase Glo 3/7 Assay (Promega). Results indicated that cell proliferation levels decreased as WTC dust concentrations increased reaching a peak at 250ppm. This pattern persisted regardless of stress induced serum level. The serum concentrations used were 10% Fetal Bovine Serum (FBS), which represented a non-stressed system, with 2.5 and 1% FBS concentrations used to simulate stressed environments. Assessment for apoptosis, programmed cell death, resulted in higher than baseline levels in cells exposed to WTC dust in both MRC-5 (male) and WI-38 (female) human lung fibroblasts. In summary, results determined that exposure to WTC dust led to decreased cell proliferation and increased apoptosis levels. These findings evidence need for future research regarding possible mutagenic properties of World Trade Center dust. Further clarification of the small differences seen relative to gender of the exposed sample lung cells is also needed.

## PS 229 Dose Response to Sacramento Particulate Matter.

L. S. Van Winkle, D. Anderson, K. E. Pinkerton, F. Tablin, D. Wilson, K. J. Bein and A. S. Wexler. *University of California Davis, Davis, CA.*

Particulate matter (PM) exposure contributes to respiratory diseases and cardiopulmonary mortality. The toxicity of PM could be related to sources, such as vehicle exhausts, and composition, such as abundance of polycyclic aromatic hydrocarbons (PAHs). We exposed adult male balb/c mice, via oropharyngeal aspiration, to a range of doses of PM<sub>2.5</sub> collected during the winter in downtown Sacramento near a major freeway interchange (SacPM). Because the relative contribution of PAHs in SacPM might be important, and since filter extraction may alter PM biological effects, we tested two PM preparation methods (sonication/spin-down and sonication/lyophilization) at 10, 50 and 100 µg doses and analyzed the lung tissue response at 24 hrs after dosing. We analyzed 1) leukocytes and total protein in BALF, 2) airway-specific and whole lobe expression of PAH sensitive genes (CYP1B1 and CYP1A1) and IL-1b and 3) lung histology. We found both PM extraction methods stimulated similar biological responses, but the spin-down method was more robust at producing IL-1b and CYP1B1 gene responses and the lyophilization method induced whole lung CYP1A1. Neutrophils in the BALF were increased 5-fold at 50 µg and 10-fold at 100 µg. Total protein in the BALF was significantly increased at both the 50 and 100 µg doses. Histopathology scores were dose responsive and more robust in mice treated with spin-down derived PM. CYP1B1 gene expression in whole lung increased 3-fold at the 50 and 100 µg dose for this method as well, but was increased less than 1.5-fold for the lyophilization method. In microdissected airways all doses of the spin-down PM increased CYP1B1 gene expression significantly, but the lyophilized PM did not change CYP1B1. We conclude 1) the method of filter extraction can influence the degree of biological response at a given dose, 2) for SacPM the minimal effective dose for this strain of mouse and route of exposure is 50µg and 3) P450s in airways and the lung parenchyma have differential ability to be upregulated in response to PAH-containing PM. (Supported by California Air Resources Board)

## PS 230 Subchronic Inhalation Exposure of Rats to Libby Amphibole and Amosite Asbestos: Effects at 1 and 3 Months Postexposure.

G. A. Willson<sup>1</sup>, D. E. Dodd<sup>2</sup>, K. Roberts<sup>2</sup>, H. G. Wall<sup>1</sup>, J. M. Cyphert<sup>3</sup>, A. M. Jarabek<sup>4</sup> and S. H. Gavett<sup>4</sup>. <sup>1</sup>Experimental Pathology Laboratories, Inc., Research Triangle Park, NC; <sup>2</sup>The Hamner Institutes for Health Sciences, Research Triangle Park, NC; <sup>3</sup>Curriculum in Toxicology, University of North Carolina School of Medicine Chapel Hill, Chapel Hill, NC; <sup>4</sup>US EPA, Research Triangle Park, NC.

Increased asbestosis, lung cancer, and mesothelioma rates are evident after exposures to Libby amphibole (LA). To support dosimetry model development and compare potency, a subchronic nose-only inhalation study (6 hr/d, 5 d/wk, 13 wk) was conducted in male F344 rats. Rats were exposed to air (control), LA (LO, MED, HI; 1.01, 3.33, 10.08 mg/m<sup>3</sup>; 300, 701, 4050 fibers/cc), or amosite (AM; 3.35 mg/m<sup>3</sup>; 1035 f/cc). Toxicity endpoints, pathology, and fiber burden evaluation

were determined 1 d and 1, 3, and 18 mo post-exposure. Previously reported results (Dodd, SOT 2012) showed comparable inflammatory and fibrogenic responses 1 d after exposure to MED LA and AM. Here we report BAL neutrophils were increased in HI LA and AM groups at 1 mo, but only in HI and MED LA groups at 3 mo. Macrophages were decreased in the HI and MED LA groups at 3 mo. AM and MED LA groups had comparable increases in BAL LDH and protein at 1 and 3 mo. Lung tissue cytokine production and activation of pro-fibrotic and cellular growth signaling pathways were also comparable between AM and MED LA. Histopathological examination of the lung found a minimal increase in alveolus inflammation, interstitial fibrosis, bronchiolization, and foreign body presence in both AM and LA groups compared to controls. Alveolus inflammation was most severe in HI LA rats at 1 and 3 mo compared to all other exposure groups. Only HI LA rats had bronchiole epithelial hyperplasia, but only 1 mo after exposure. These results show comparable fibrogenic responses 1 and 3 mo after subchronic exposure of rats to LA and AM asbestos. Tissue fiber burdens are being measured to support dosimetry model development of deposition and clearance (Asgharian, SOT 2012; Jarabek, SOT 2013); comparison of responses between fibers may change based on dosimetry modeling. (This abstract does not represent US EPA policy)

## PS 231 Exposure to Sumas Mountain Chrysotile Induces Similar Gene Expression Changes As Libby Amphibole but Has Greater Effect on Long-Term Pathology and Lung Function.

J. M. Cyphert<sup>1,2</sup>, A. Nyska<sup>3</sup>, R. K. Mahoney<sup>4</sup>, M. C. Schladweiler<sup>2</sup>, U. P. Kodavanti<sup>2</sup> and S. H. Gavett<sup>2</sup>. <sup>1</sup>Curriculum in Toxicology, UNC School of Medicine, Chapel Hill, NC; <sup>2</sup>EPHD, NHEERL, US EPA, Research Triangle Park, NC; <sup>3</sup>Sackler School of Medicine, Tel Aviv University, Timrat, Israel; <sup>4</sup>EMSL Analytical, Inc., Libby, MT.

This study was designed to provide understanding of the toxicity of naturally occurring asbestos (NOA) including Libby amphibole (LA), Sumas Mountain chrysotile (SM), El Dorado Hills tremolite (ED) and Ontario ferroactinolite cleavage fragments (ON). Rat-respirable fractions (aerodynamic diameter ≤ 2.5 µm) were prepared by water elutriation and a dose of 1.5 mg/rat delivered via a single intratracheal (IT) instillation. Bronchoalveolar lavage (BAL), gene expression, histopathology, and lung function were analyzed 1 d, 3 mo, or 15 mo post-instillation.

One day after exposure, although inducing less acute inflammation than other samples, LA and SM induced a greater degree of lung injury. A similar trend was also observed in gene expression profiles, as both LA- and SM-exposed rats differed significantly from dispersion media (DM) controls. Changes were suggestive of dysregulation of both extracellular matrix and fibrosis pathways. By three months, most BAL parameters had returned to DM control levels. However, significant time-dependent fibrosis was evident in rats exposed to LA or SM. By 15 months, the greatest fibrotic changes were observed in SM-exposed rats; while no fibrosis was noted in the cleavage-fragment or DM control group (SM>LA>ED>ON=DM). Consistent with the greatest degree of fibrosis, only SM-exposed rats exhibited persistent, long-term changes in lung function parameters. These data demonstrate that, in the rat, SM resulted in more significant long-term effects after a single IT exposure than LA. This study suggests that there may be cause for concern for people at risk of being exposed to NOA from the Sumas Mountain landslide, and highlights the need for further study of sites where NOA is present. (This abstract does not represent U.S. EPA policy).

## PS 232 Lack of Sex Difference in Nasal Glutathione Response to Naphthalene.

J. A. Cichocki<sup>1</sup>, L. S. Van Winkle<sup>2</sup>, G. J. Smith<sup>1</sup> and J. B. Morris<sup>1</sup>. <sup>1</sup>Toxicology, University of Connecticut, Storrs, CT; <sup>2</sup>Veterinary Medicine, University of California Davis, Davis, CA.

At concentrations of 10 ppm or greater, naphthalene (NA) is a nasal carcinogen inducing respiratory adenomas in male and olfactory neuroblastomas in female rats, respectively. The proposed carcinogenic mode of action includes metabolic activation via CYP450 to an electrophile with subsequent glutathione depletion, escape of electrophile, and covalent binding. Respiratory and olfactory mucosa are tumor target sites and both contain NA CYP450 activating capacity; the activity in olfactory exceeds that in respiratory mucosa by 3-fold. To fully define the effect of NA on nasal glutathione, male and female F344 rats were exposed to 0, 10, or 30 ppm NA for 1, 4, or 6 hours. Following exposure, nasal olfactory and respiratory tissues were analyzed for reduced/oxidized glutathione levels (GSH/GSSG). Female control rats had twice the levels of GSH compared to male controls, but NA exerted similar effects on GSH in both genders. GSH was depleted at all times; in females,

respiratory and olfactory mucosal levels were ~45 and 70% of control levels (respectively) after 10 or 30 ppm, an effect that did not correlate with local CYP450 activation rates. Similar trends were seen for male rats. To fully define the concentration response, rats were exposed to 0, 0.5, 1, 3, 10, or 30 ppm NA for 4 hours. Significant GSH depletion occurred at all exposure levels in respiratory and olfactory mucosa with maximal depletion (about 30 and 60% of control levels, respectively) occurring at or above 1 ppm. Similar trends were seen in both males and females. NA, at concentrations well below those shown to be carcinogenic, causes significant depletion of GSH in the nose. The degree of GSH depletion in different nasal regions does not correlate with activation rates, suggesting that other factors contribute to the GSH response. No sex difference was observed in GSH response, suggesting that the sex difference in tumor response cannot be attributed to this step in the carcinogenic mode of action. (Supported by the Naphthalene Research Council)

**PS 233 Acetaminophen at Low Doses Depletes Airway Glutathione and Alters Respiratory Reflex Responses.**

G. J. Smith, J. A. Cichocki, J. E. Manautou and J. B. Morris. *Toxicology Program, University of Connecticut, Storrs, CT.*

In the past three decades the prevalence of asthma has more than doubled. The reasons for this increase are unknown. Several hypothetical mechanisms have been proposed, but none have been proven. The "acetaminophen (APAP) hypothesis", first derived from epidemiological data, postulates that pediatric use of acetaminophen, by decreasing lung antioxidant defenses, increases asthma risk. APAP (N-acetyl-para-aminophenol, is an analgesic thought to be safe at therapeutic doses. APAP is activated by CYP450 to a reactive intermediate that conjugates with, and depletes, the important antioxidant, glutathione (GSH). To determine if this occurs in the airways, female C57Bl/6J mice were administered APAP (ip) at non-hepatotoxic doses (30, 60, or 100 mg/kg) followed by measurement of tissue non-protein sulfhydryl (NPSH) (~90% of which is GSH). A dose and time dependent reduction in NPSH levels occurred with maximal depletion to ~60% of control at 1 hr in the liver, and at 2 hrs in the lung, trachea, and nose. Inhalation exposure to reactive electrophilic vapors, such as acrolein, stimulates the trigeminal nerve Transient Receptor Potential A1 (TRPA1) receptor and elicits the sensory irritation response. (The role of TRPA1 has been confirmed in our model via use of TRPA1 knockout mice.) Acrolein acts at intracellular N-terminal cysteines of the TRPA1 receptor; we reasoned that APAP, by decreasing GSH would increase the amount of acrolein available to interact with TRPA1. APAP (100 mg/kg 1 hr prior to acrolein exposure) increased the irritation response by 75% over that of acrolein alone. Nasal NPSH levels in acrolein/APAP exposed mice were reduced to 88, 69, and 59% of control at 30, 60, and 100 mg/kg, respectively. These results suggest that APAP, at near therapeutic doses, causes depletion of airway GSH to levels sufficient to modulate acute respiratory responses. These findings lend support to the APAP hypothesis. (Supported by the UConn Presidents Research Award)

**PS 234 Upper Respiratory Lesions in Rats Administered Amiodarone Hydrochloride Solution Orally for 4 Days by Intraesophageal Dosing: Absence of the Lesion by Intragastric Dosing.**

S. Ogata, Y. Nezu, T. Watanabe, S. Takada, Y. Tani and W. Takasaki. *Medicinal Safety Research Laboratories, Daiichi-Sankyo, Tokyo, Japan.*

Upper respiratory (UR) tract can be damaged by compounds administered orally. Retrograde exposure of nasal passage to dose formulation from the esophagus has been suggested as one of the toxicological mechanisms (Damsch et al. *Toxicol Pathol*, 2011). However, literatures are limited with this toxicity of orally administered drugs in clinical use and the toxicological significance remains unclear. Amiodarone hydrochloride (AM) is an antiarrhythmic agent administered orally and intravenously in clinical use. We demonstrated AM induces UR lesions in rats by gavage dosing for 4 days with a metallic tube. Retrograde exposure of the nasal passage to dose formulation was suggested because incidence of the lesion was higher in the posterior nasal passage than the anterior one (Ogata et al., *JSTP Annual Meeting*, 2011). Furthermore, irritability of the dose formulation to nasal epithelium was confirmed based on induction of UR lesions after single intranasal dosing (Ogata et al., *JSOT Annual Meeting*, 2012). To examine the effect of the dosing procedure on the lesions, rats were administered 150 mg/kg AM by a catheter instead of a metallic tube and the UR lesions were compared histopathologically with those obtained in the former study with a metallic tube. In this study, no UR lesions were observed in rats given AM with a catheter. Cmax and AUC was

equivalent between dosing procedures with the catheter and metallic tube after a single dose. The results suggest that the UR lesions in rats given AM by a metallic tube is not attributable to systemic exposure alone. Dependence on metallic tube dosing may suggest low toxicological relevance of the UR lesions. Furthermore, catheter dosing would be an option to evaluate toxicological significance of gavage-related UR lesion, with equivalent Cmax and AUC obtained by metallic tube dosing, and without possible concern specific to dosing from parenteral or feeding routes.

**PS 235 A High-Fructose Diet Attenuates Adaptation of Nasal Epithelium to Subacute Ozone Exposure in Mice.**

J. Harkema<sup>1,2</sup>, P. Brooks<sup>1</sup>, K. M. Allen<sup>1,2</sup>, M. Dereski<sup>1</sup>, R. Lewandowski<sup>1,2</sup>, D. Jackson<sup>1</sup>, L. Bramble<sup>1,2</sup> and J. G. Wagner<sup>1,2</sup>. <sup>1</sup>Michigan State University, East Lansing, MI; <sup>2</sup>US EPA Great Lakes Air Center for Integrated Environmental Research, East Lansing, MI.

**INTRODUCTION:** Ozone (O<sub>3</sub>) is a common oxidant air pollutant and inhaled respiratory toxicant. Repeated inhalation exposures to high ambient concentrations of O<sub>3</sub> cause an adaptive epithelial change, mucous cell metaplasia (MCM), in the nasal airways of laboratory rodents and nonhuman primates. Since airway mucus is a known anti-oxidant, MCM with increases in mucus-secreting cells, is a defensive response of airway epithelium to minimize further oxidant injury caused by inhaled irritants. Unhealthy diets associated with the metabolic syndrome may adversely affect the host's normal response to inhaled pollutants. The present study was designed to determine the effect of a high fructose diet (HFD) on the adaptive MCM response of nasal epithelium to O<sub>3</sub>. **METHODS:** C57/Bl6 male mice were exposed to 0 (controls) or 0.5 ppm O<sub>3</sub>, 4h/day, for 24 consecutive week days. Half of the mice were fed a normal diet (ND) and the other half were fed a HFD. Mice were sacrificed 24h after the last day of O<sub>3</sub> exposure. Nasal tissues were processed for light microscopy and morphometric analysis. **RESULTS:** No exposure-related nasal lesions were found in filtered air-exposed control mice fed either diet. ND-fed mice exposed to O<sub>3</sub> developed marked MCM in nasal transitional epithelium that was accompanied by a mucosal influx of eosinophils. In contrast, HFD-fed mice had minimal nasal MCM and few mucosal eosinophils (85 and 60% less, respectively, compared to ND mice) after O<sub>3</sub> exposure. **CONCLUSIONS:** In mice, a HFD significantly altered the MCM adaptation of nasal epithelium to O<sub>3</sub> exposure. Underlying mechanism(s) responsible for this diet-induced alteration in host response and its possible human health implications are yet to be determined. Funded by USEPA RD83479701.

**PS 236 Morphometric Assessment of Concentration- and Time-Dependent Injury in the Nasal Airways of Rats Exposed to Chlorine Gas.**

A. M. Jarabek<sup>2</sup>, A. Watkins<sup>1</sup> and J. Harkema<sup>1</sup>. <sup>1</sup>Michigan State University, East Lansing, MI; <sup>2</sup>US EPA, Research Triangle Park, NC.

Chlorine (Cl<sub>2</sub>) is an oxidizing chemical used in industrial processes and as a household disinfectant. It is also an inhaled toxicant that causes airway injury, ranging from minor irritation to death, depending on exposure conditions. Due to its toxicity and availability, Cl<sub>2</sub> is considered a chemical threat agent. Understanding the airway pathology of inhaled Cl<sub>2</sub> is critical to both preventing and treating its toxicity. In rodents, the nose is a primary target organ for inhaled Cl<sub>2</sub>. Risk assessment approaches rely on the daily concentration times time (C x t) product for extrapolation of effect levels across studies of different duration (Haber's Rule). This Cl<sub>2</sub> inhalation study in rats was designed to determine the contribution of daily C x t product and exposure duration to the severity of nasal injury. Cl<sub>2</sub> was one of the gases on which Haber's Rule was based, but emerging understanding of its pathobiology suggests that the relationship does not hold. We hypothesized that the daily C x t product does not capture the occurrence and magnitude of Cl<sub>2</sub>-induced toxicity. Rats were exposed to equivalent combinations of daily C x t inhaled Cl<sub>2</sub> for acute (6 ppm for 1 h; 1 ppm for 6 h; 0.25 ppm for 24 h) or subacute and subchronic (1 ppm, 6h/d for 5d, 10d or 90d) durations. The amount of histochemically stained mucosubstances in nasal transitional epithelium was morphometrically determined as a quantitative measure of the severity of Cl<sub>2</sub>-induced mucous cell metaplasia (MCM). Only rats subacutely or subchronically exposed to Cl<sub>2</sub> developed this lesion and the magnitude of MCM markedly increased with duration. Our results indicate that daily C x t product alone is not a good estimator of Cl<sub>2</sub>-induced MCM and exposure duration is an important determinant of the risk to Cl<sub>2</sub>-induced nasal toxicity. Funded by EP-12-C-000052. (The views expressed in this abstract are those of the authors and do not necessarily represent the views or policies of the U.S. Environmental Protection Agency.)

**PS 237 Diacetyl-Induced Respiratory and Olfactory Toxicity in Mice: Influence of Ubiquitination, Gender, and Dicarboxyl/L-Xylulose Reductase Gene Knockout.**

A. F. Hubbs<sup>1</sup>, K. L. Fluharty<sup>1</sup>, M. P. Goravanahally<sup>2,1</sup>, R. J. Edwards<sup>2,1</sup>, M. L. Kashon<sup>1</sup>, L. Sargent<sup>1</sup>, R. R. Mercer<sup>1</sup>, M. C. Jackson<sup>1</sup>, A. M. Cumpston<sup>1</sup>, W. T. Goldsmith<sup>1</sup>, J. S. Fedan<sup>1</sup>, R. D. Dey<sup>2</sup>, L. A. Battelli<sup>1</sup>, T. Munro<sup>1</sup>, W. B. Moyers<sup>1</sup>, P. A. Willard<sup>1</sup>, K. McKinstry<sup>1</sup>, S. Friend<sup>1</sup> and K. Sriram<sup>1</sup>.  
<sup>1</sup>HELD, NIOSH, Morgantown, WV; <sup>2</sup>West Virginia University, Morgantown, WV.

The  $\alpha$ -dicarbonyl butter flavoring, diacetyl (2,3-butanedione), is associated with flavorings-related constrictive bronchiolitis in workers who make or use flavorings. Diacetyl causes protein damage in a process believed to be dependent upon the  $\alpha$ -dicarbonyl structure. A protective response to damaged protein is ubiquitination with subsequent proteasomal processing. Diacetyl is also metabolized to the less reactive  $\alpha$ -hydroxyketone, acetoin, by dicarbonyl/L-xylulose reductase (Dcxr). We examined the role of Dcxr and gender on acute toxicity of inhaled diacetyl by exposing Dcxr knockout and wildtype mice of both sexes to diacetyl at target concentrations of 0, 100, 200 or 300 ppm for 6 hr. At 1 day post-exposure, endpoints were semi-quantitative histopathology and morphometric measurement of ubiquitin immunofluorescence in nose and lung sections. Ubiquitin was principally localized to nasal and intrapulmonary airways, increased in large bronchioles at concentrations  $\geq 100$  ppm, and in the nose at 300 ppm. Diacetyl-induced ubiquitin in the nose and lung was modified by both gender and Dcxr. In lung histopathology, diacetyl caused vacuolation of airway epithelium of large bronchioles at concentrations  $\geq 100$  ppm. In olfactory bulb (OB) of male mice inhaling 300 ppm diacetyl, mRNA expression of inflammatory mediators and olfactory marker protein (Omp), a marker of olfactory neuron axons, were assayed by real-time PCR. Diacetyl elevated Il6, Cxcl2, and Tnfa and decreased Omp in OB. The data suggest that ubiquitin expression is a sensitive biomarker of diacetyl-induced protein damage in airway epithelium. Further, diacetyl causes neuroinflammation and potential loss of axons of olfactory neurons in OB, suggestive of neurotoxicity.

**PS 238 Subchronic Exposure to Ambient Particulate Matter Induces Oxidative Stress Responses in Brain Tissue of ApoE-/- Mice.**

L. B. Mendez<sup>1</sup>, A. J. Keebaugh<sup>1</sup>, L. Chen<sup>2</sup>, M. Lippmann<sup>2</sup> and M. T. Kleinman<sup>1</sup>. <sup>1</sup>University of California Irvine Irvine, CA; <sup>2</sup>New York University, New York, NY.

Exposure to particulate matter (PM), present in urban environments, has been shown to induce pro-inflammatory and oxidative stress responses in the central nervous system (CNS) of apolipoprotein E knockout (ApoE-/-) and Balb/c mice. In this study oxidative stress responses in different subcellular fractions of the ApoE-/- mouse brains were evaluated after a subchronic exposure to fine ( $\leq 2.5$   $\mu$ m) concentrated ambient particles (CAPs). Apo E-/- mice were exposed to either CAPs or particle-free air for 5 hours a day, 5 days per week, for a period of 6 months. The whole-body inhalation exposures were conducted in two urban cities (Seattle, WA and Detroit, MI) with distinct sources and chemical composition of PM. Brain tissue was collected after the exposures were completed and analyzed for biomarkers of oxidative stress. The antioxidant glutathione was reduced in the brains of mice exposed to CAPs in Michigan but not in Washington. In contrast the lipid peroxidation product 4-hydroxyalkenal (HNE) was significantly increased in the membrane fraction of brain tissue of mice exposed to CAPs in Washington but not in Michigan. No significant differences were observed in protein carbonyl levels, a biomarker of protein oxidation, although the levels were slightly higher in the cytoplasmic fraction of brain tissue from animals exposed to CAPs when compared to controls regardless of exposure site. The results suggest that PM from different sources can modulate oxidative stress responses in a distinct fashion and that different subcellular fractions in the brain can be more susceptible to the effects of PM.

**PS 239 Co-Exposure to Ultrafine Particulate Matter and Ozone Causes Electrocardiogram Changes Indicative of Increased Arrhythmia Risk in Mice.**

N. Kurhanewicz<sup>1</sup>, R. McIntosh-Kastrinsky<sup>1</sup>, L. Walsh<sup>2</sup>, A. K. Farraj<sup>2</sup> and M. S. Hazari<sup>2</sup>. <sup>1</sup>University of North Carolina at Chapel Hill, Chapel Hill, NC; <sup>2</sup>Environmental Public Health Division, US EPA, Research Triangle Park, NC.

Numerous studies have shown a relationship between acute air pollution exposure and increased risk for cardiovascular morbidity and mortality. Due to the inherent complexity of air pollution, recent studies have focused on co-exposures to better understand potential interactions. This study was designed to evaluate the cardiac effects of concentrated ambient fine (PM<sub>2.5</sub>) and ultrafine (UFP) particles with and without ozone (O<sub>3</sub>) co-exposure. We hypothesized that ozone co-exposure

would enhance the acute effects of particles, particularly UFP. Conscious unrestrained C57BL/6 mice implanted with radiotelemeters were exposed by whole-body inhalation to either 250  $\mu$ g/m<sup>3</sup> PM<sub>2.5</sub> or 100  $\mu$ g/m<sup>3</sup> UFP with or without 0.3 ppm O<sub>3</sub> (4hrs); separate groups were exposed to either filtered air or O<sub>3</sub> only. Heart rate (HR) and electrocardiogram (ECG) were recorded continuously before, during and after exposure. Control animals experienced a decrease in HR during exposure. Neither PM<sub>2.5</sub> nor UFP alone caused any HR change; however with O<sub>3</sub> co-exposure, HR remained transiently elevated above control levels. Exposure to UFP+O<sub>3</sub> caused decreased PR-interval, a transient increase in QRS, and increased QTc. PM<sub>2.5</sub> alone caused QRS to decrease and O<sub>3</sub> alone caused a decrease in QRS interval and QTc. There were no other significant differences in the ECG parameters measured of any groups. Lastly, only animals exposed to UFP+O<sub>3</sub> had an increase in the number of non-conductive P-waves; there were no differences in other arrhythmia counts. These data suggest that O<sub>3</sub> co-exposure might worsen the stress response to PM, especially UFP, and cause repolarization heterogeneity in the heart, which increases the risk for arrhythmogenesis. As such, this indicates that the cardiovascular effects of particle and gas co-exposures are not easily characterized, potentially increasing the complexity of risk assessment. (This abstract does not reflect EPA policy)

**PS 240 An Air-Liquid Interface *In Vitro* Approach for Studying Toxic Effects of Exhaust Emissions Using a Heavy Duty Truck.**

I. M. Kooter<sup>1</sup>, M. Alblas<sup>1</sup>, J. van Triel<sup>2</sup>, A. Jedynska<sup>1</sup>, M. Steenhof<sup>1</sup>, M. Houtzager<sup>1</sup> and M. van Ras<sup>1</sup>. <sup>1</sup>EELS, TNO, Utrecht, Netherlands; <sup>2</sup>TAP, TNO Triskelion, Zeist, Netherlands. Sponsor: R. Woutersen.

Classically *in vitro* diesel exhaust (DE) studies have been performed with submerged cell cultures which are exposed to collected DE particles. Major drawback of this exposure method is that cells are not exposed to the whole complex and dynamic mixture of compounds DE is composed of. In recent years, air-liquid interface exposures have become more widely used, enabling *in vitro* exposures to mixtures of gases and particles. The main objective of this study was to investigate the feasibility of exposing human lung epithelial cells at the air-liquid interface to complete DE generated by a heavy-duty truck in the state-of-the-art TNO power train facilities.

Human epithelial lung cells (A549) were directly exposed at the air liquid interface to DE generated by a heavy-duty Euro III truck (turbo diesel model 2002). The truck was tested at a steady-state cycle at a speed of ~70 kmh<sup>-1</sup> to simulate free-flowing traffic at a motorway on a transient engine dynamometer. Cells were exposed to DE for 1.5 hours. After a 24 hours post-incubation period, cells were analysed for markers of oxidative stress (glutathione levels, GSH; heme oxygenase 1 protein levels, HO-1), cytotoxicity (lactate dehydrogenase release, LDH; Alamar Blue assay) and inflammation (interleukine-8 protein levels, IL-8).

DE exposure resulted in a decreased cell viability (significantly decreased Alamar Blue levels in the incubation medium and slightly increased LDH levels), and an increased oxidative stress response (significantly increased HO-1 levels and reduced GSH/GSSH ratio). However, the pro-inflammatory response seemed to decrease (non-significant decrease in IL-8).

The results presented here demonstrate that our *in vitro* exposure approach is indeed well suited for testing complex particulate and gaseous pollutant mixtures from diesel trucks. Our results confirm previous *in vitro* studies showing cytotoxicity and oxidative stress responses due to DE exposure.

**PS 241 Comparative Toxicity of Soy Biodiesel and Diesel Emissions in Healthy and Allergic Mice.**

S. H. Gavett<sup>1</sup>, M. A. Williams<sup>1</sup>, J. M. Cyphert<sup>2,1</sup>, E. H. Boykin<sup>1</sup>, M. E. Daniels<sup>1</sup>, L. B. Copeland<sup>1</sup>, D. L. Andrews<sup>3</sup>, J. H. Richards<sup>1</sup> and I. Gilmour<sup>1</sup>. <sup>1</sup>EPHD, NHEERL, US EPA, Research Triangle Park, NC; <sup>2</sup>Curriculum in Toxicology, UNC School of Medicine, Chapel Hill, NC; <sup>3</sup>Research Cores Unit, Proteomic Research Core, US EPA, Research Triangle Park, NC.

Toxicity from combustion of 100% soy-based biodiesel (B100) was compared to that of petrodiesel (B0) or a 20% biodiesel / 80% petrodiesel mix (B20) in healthy and house dust mite (HDM)-allergic Balb/c mice. Exhaust from combustion of B0, B20, or B100 was diluted to target concentrations of 50, 150, or 500  $\mu$ g/m<sup>3</sup> as determined by real-time Tapered Element Oscillating Microbalance. Studies in healthy mice showed greater levels of MIP-2 and neutrophils in bronchoalveolar lavage (BAL) fluid 2 hr after a single 4 hr exposure to B0 compared with exposure to biodiesel emissions (air control neutrophils = 1x, B0 = 11.9x, B20 = 4.4x, B100 = 2.1x). However these differences were attenuated 24 hr after exposure and no consistent differences were observed 2 or 24 hr after 5 d (4 hr/d) or 4 wk (5 d/wk) exposures. Mice sensitized and challenged intranasally with HDM and exposed to B0, B20, or B100 for 4 wk (5 d/wk) had no emissions-related differences in airway

hyperresponsiveness to MCh aerosol (determined by total lung resistance in anesthetized, paralyzed and ventilated mice). Non-significant trends of decreased eosinophils and IL-5 in BAL fluid were found after exposure to the 500 µg/m<sup>3</sup> concentration of all 3 fuels. Proliferative responses of peribronchiolar lymph node cells in response to HDM antigens in vitro were not significantly affected by exposure to fuel emissions. We conclude that alternative soy biofuel emissions have comparable or reduced adverse effects relative to diesel emissions in healthy mice or a mouse model of allergic asthma. (This abstract does not represent U.S. EPA policy.)

**PS 242 Mechanisms Underlying Anti-Inflammatory Effects of Selective Diindolylmethane Compounds Using RAW264.7 Cells.**

M. F. Afzali<sup>1</sup>, G. P. Dooley<sup>1</sup>, S. H. Safe<sup>2</sup>, W. H. Hanneman<sup>1</sup> and M. E. Legare<sup>1</sup>.  
<sup>1</sup>Center for Environmental Medicine, Environmental and Radiological Health Sciences, Colorado State University, Fort Collins, CO; <sup>2</sup>Center for Environmental and Genetic Medicine, Institute of Biosciences and Technology, Texas A&M Health Sciences, Houston, TX.

Chronic inflammation has been associated as the root cause of many serious illnesses including heart disease, Alzheimer's disease and many cancers. Tolfenamic Acid (TA) a non-steroidal anti-inflammatory (NSAID) drug has been shown to have multiple anti-inflammatory effects in RAW264.7 murine macrophages. This study compares the anti-inflammatory effects of selected diindolylmethane (DIM) compounds in activated RAW264.7 cells. Results indicate a significant decrease in production of prostaglandin E (2), D (2) and F (2). In addition, there was a decrease expression of mediators of inflammation including cyclooxygenase-2 (COX-2) in LPS-induced RAW 264.7 cells. These results underscore the potential use for these DIM compounds in ameliorating inflammation in disease processes and therapeutic regimens.

**PS 243 Fyn Kinase Inhibitors Attenuate Manganese Nanoparticles Induced Neuroinflammatory Signaling in BV2 Microglial Cells and Primary Microglia.**

K. Kanthasamy, N. Panicker, A. Ngwa, C. Jeffery, M. Neal, A. Kanthasamy and V. Anantharam. Iowa State University, Ames, IA.

Manganese (Mn) nanoparticles are currently used in a multitude of industrial and biomedical applications, including magnetic resonance imaging, high capacity batteries, industrial coatings, biosensors, plastics, ultrahigh density storage devices, nanofibers, and catalysts. Yet, the potential impacts of these particles on human health and the environment are not well understood. Notably, the cellular mechanisms underlying Mn nanoparticle induced neurotoxicity are yet to be identified. Because nanoparticles are similar in size to microbes, we hypothesize that Mn nanoparticles exposure may activate phagocytic microglial cells to induce a neurotoxic response. We exposed BV2 microglia and primary microglial cultures to various doses of Mn nanoparticles and then measured inflammatory markers. Exposure of 0-50 µg/mL Mn nanoparticles to BV2 microglia over 24 hr period resulted in a dose-dependent increase in iNOS, ROS, TNFα, IL-6, IL-12, and RANTES levels. Additionally, Mn nanoparticles induced over a threefold increase in ROS generation in primary microglial cells. Interestingly, Mn nanoparticles also activated the non-receptor tyrosine kinase Fyn in BV2 microglia. In order to determine whether Fyn kinase plays a role in the Mn induced inflammatory response, we tested a series of Fyn kinase inhibitors, including rosmarinic acid, dinitro-rosmarinic acid and caffeic acids. Rosmarinic and caffeic acids showed EC50s of 33 and 32 µM, respectively, against Mn induced iNOS activation. In addition, Fyn kinase inhibitors significantly blocked Mn-nanoparticle induced TNFα, IL-6, IL-12 release and ROS generation, indicating that Fyn kinase may play a central role in the Mn nanoparticle neuroinflammation and oxidative stress. Taken together, our results demonstrate that Mn nanoparticles activate microglial cells via a Fyn kinase dependent mechanism and that Fyn kinase inhibitors may serve as efficacious therapeutic agents against the metal nanoparticle induced neuroinflammatory insult (supported by NIH grants ES10586 and NS65167).

**PS 244 Proinflammatory Cytokines Present in the Tumour Microenvironment Induce Phenotypic Change in Colorectal Cancer Cell Lines.**

S. Patel and N. J. Gooderham. Surgery and Cancer, Imperial College London, London, United Kingdom.

Colorectal cancer (CRC) is the third most common cancer worldwide with metastatic disease responsible for high mortality rates. The cellular microenvironment is modified during malignancy to support tumor development and metastasis, however mechanisms by which this occurs remain unclear. Previous data from

our laboratory has shown an overexpression of cytochrome P450 (CYP) drug metabolizing enzymes 1B1 and 2E1 and pro-inflammatory cytokines interleukin (IL) 1β and IL6 in neoplastic tissue resected from colorectal cancer patients compared to matched non-neoplastic controls. In the current study, the presence of these cytokines in the tumour microenvironment was investigated in vitro using two CRC cell lines HCT116 and SW480, differing in metastatic potential. Treatment with conditioned media from activated THP1 monocytes, known to secrete an array of cytokines (including IL6, IL1β and TNFα), was able to induce the invasive properties of the metastatic cell line HCT116 as measured using wound and migration chamber assays. Treatment with IL6 alone (0-1000 pg/ml) was also shown to promote cell motility and invasion in a bell-shaped dose response, characteristic of cytokine function. The non-metastatic cell line SW480 did not respond to the conditioned media and was more resistant to IL6, generating a response only at the higher doses. Additionally, CYP 1B1 and 2E1 expression were increased following treatment with the conditioned media as well as with IL6 on its own. Taken together, these data indicate that pro-inflammatory cytokines, in particular IL6, are able to cause phenotypic change in CRC cells by inducing CYP expression and promoting ability for the cells to migrate and invade surrounding tissue, thus demonstrating the important role of tumor microenvironment in disease progression.

**PS 245 A Novel Anti-Inflammatory Peptide: Potential Therapy of Sepsis Induced by Bacterial Endotoxin.**

U. Wormser<sup>1</sup>, M. Aschner<sup>2</sup>, Y. Finkelstein<sup>3</sup>, E. Proscura<sup>1</sup>, B. Brodsky<sup>1</sup> and E. Shapira<sup>1</sup>. <sup>1</sup>Institute of Drug Research, The Hebrew University, Jerusalem, Israel; <sup>2</sup>Department of Pharmacology, Center for Molecular Toxicology, and the Kennedy Center for Research on Human Development, Vanderbilt University School of Medicine, Nashville, TN; <sup>3</sup>Neurology and Toxicology Service and Unit, Shaare Zedek Medical Center, Jerusalem, Israel.

Sepsis is a syndrome of infection complicated by vital organ dysfunction and considered one of the leading causes of mortality in intensive care units. It is characterized by a generalized inflammatory response caused by systemic activation of macrophages and other immune and microvascular endothelial cells. The present study demonstrates the efficacy of a novel anti-inflammatory peptide termed IIMM1 in ameliorating sepsis induced by the bacterial endotoxin lipopolysaccharide (LPS). A single injection of the peptide 3 days prior to lethal dose of LPS increased animal survival by 60%. Shorter or longer intervals between IIMM1 and LPS administration reduced peptide efficacy. LPS-induced increase in liver, kidney and spleen mass was reverted by peptide treatment. Thioglycolate-induced peritonitis, expressed by increased number of macrophages in the peritoneal cavity, was reduced by 38% in IIMM1-treated mice. A bell-shape dose-response effect was observed in both peritonitis and sepsis models reaching maximal effect at 1mg/kg. Chemical modifications such as omission of the C- or N-terminal residues weakened the anti-inflammatory activities of the peptide. Serum levels of interleukin 6 and tumor necrosis factor alpha were reduced by 32% and 53%, respectively, in IIMM1-treated mice intoxicated by LPS. Similar cytokine profile was observed in LPS-activated peritoneal macrophages treated in vitro with the peptide. In view of these data IIMM1 is a promising drug candidate for treatment of sepsis induced by bacterial endotoxin.

**PS 246 S-Adenosylhomocysteine Inhibits NF-κB Activity in the Nucleus of Hepatocytes and Confers Sensitivity to TNF Cytotoxicity.**

W. Watson<sup>1</sup>, T. Burke<sup>1</sup> and C. McClain<sup>1,2</sup>. <sup>1</sup>Department of Medicine/GI, University of Louisville, Louisville, KY; <sup>2</sup>Louisville VAMC, Louisville, KY.

Chronic alcohol exposure results in liver injury that is largely driven by inflammatory cytokines such as tumor necrosis factor-α (TNF). Hepatocytes are normally resistant to the cytotoxic effects of TNF, but they become sensitized to TNF by chronic alcohol exposure. Recently we reported that the decrease in the ratio of S-adenosylmethionine (SAM) to S-adenosylhomocysteine (SAH) that occurs with alcoholic liver injury renders hepatocytes sensitive to TNF cytotoxicity. The purpose of the present study was to determine whether inhibition of the transcription factor NF-κB contributed to TNF-induced cell death in hepatocytes with high levels of SAH. HepG2 cells were pre-incubated with a combination of adenosine plus homocysteine to increase SAH levels. Following stimulation with TNF, viability was determined by the MTT assay, and activation of the NF-κB pathway was assessed by measuring degradation of cytosolic IκB, translocation of NF-κB to the nucleus, and expression of an NF-κB -dependent reporter gene as well as endogenous targets of NF-κB related to cell death. The results showed that NF-κB was indeed inhibited in cells with high SAH, and that this inhibition occurred at the level of the nucleus; the cytoplasmic inhibitor IκB-α was degraded and NF-κB translocated to the nucleus in response to TNF stimulation of HepG2 cells in both control cells and in

cells with high SAH levels. Nuclear NF- $\kappa$ B was not transcriptionally active, however, when SAH levels were high. As a result, I $\kappa$ B- $\alpha$  was not re-synthesized and NF- $\kappa$ B remained in the nucleus. It is likely that cross-talk with other transcription factors is perturbed under these conditions, resulting in still other changes in gene expression.

**PS 247** **Cyanobacterium *Anabaena* sp. Lipopolysaccharide (LPS) Elicits Release of MIP- $\alpha$ , Interleukin-6, and Matrix Metalloproteinase-9 from Rat Brain Microglia *In Vitro*.**

D. Macadam<sup>1</sup>, M. L. Hall<sup>1</sup>, D. Feher<sup>2</sup>, P. Williams<sup>2</sup> and A. M. Mayer<sup>1</sup>.  
<sup>1</sup>Pharmacology, Midwestern University, Downers Grove, IL; <sup>2</sup>Chemistry and Biochemistry, University of Hawaii at Manoa, Honolulu, HI.

We recently reported that freshwater cyanobacterium *Anabaena*LPS (AnaLPS) elicited release of superoxide anion (O<sub>2</sub><sup>-</sup>), thromboxane B<sub>2</sub> (TXB<sub>2</sub>), and tumor necrosis alpha (TNF- $\alpha$ ) by rat microglia (BMG) *in vitro* (The Toxicologist CD 126 (S-1), 2012). We hypothesized that AnaLPS-activated BMG might additionally release the cytokine interleukin-6 (IL-6), the chemokine MIP-1 $\alpha$  (MIP-1 $\alpha$ ), and the matrix metalloproteinase-9 (MMP-9) *in vitro*. **Methods:** AnaLPS was prepared by hot phenol/water extraction. BMG were isolated from neonatal rats, and treated *in vitro* with 0.1-10<sup>5</sup> ng/mL AnaLPS at 35.9 °C for 17 hours. TNF- $\alpha$ , MIP-1 $\alpha$  and IL-6 were determined by Milliplex® MAP rat cytokine/chemokine immunoassays, and MMP-9 by zymography. **Results:** MIP-1 $\alpha$ , TNF- $\alpha$ , and IL-6 generation were observed at AnaLPS >10 ng/mL (MIP-1 $\alpha$ ), and > 1,000 ng/mL, respectively. In contrast, MMP-9 release was significant at AnaLPS 10,000 ng/mL. **Conclusions:** Treatment of BMG with AnaLPS confirmed previously reported TNF- $\alpha$  release, and furthermore demonstrated for the first time the release of MIP-1 $\alpha$ , IL-6 and MMP-9. Taken together, our results suggest that *in vitro* proinflammatory mediator release by cyanobacterial AnaLPS-treated BMG is complex, including lipids (TXB<sub>2</sub>), free radicals (O<sub>2</sub><sup>-</sup>), cytokines (TNF- $\alpha$  & IL-6), chemokines (MIP-1 $\alpha$ ) and enzymes (MMP-9), all of which might play a yet unknown role in the putative immunotoxicity of AnaLPS *in vivo*. Continued investigation of AnaLPS chemistry and immunotoxicology are currently ongoing in our laboratories. Supported by Midwestern University and the University of Hawaii at Manoa.

**PS 248** **Spleen As a Source of Inflammatory Macrophages: Role in Acetaminophen-Induced Hepatotoxicity.**

M. Mandal<sup>1</sup>, A. Dragomir<sup>1</sup>, H. M. Choi<sup>1</sup>, J. D. Laskin<sup>2</sup> and D. L. Laskin<sup>1</sup>.  
<sup>1</sup>Pharmacology & Toxicology, Rutgers University, Piscataway, NJ; <sup>2</sup>Environmental & Occupational Medicine, UMDNJ-RWJMS, Piscataway, NJ.

Activated macrophages (MP) have been implicated in the hepatotoxicity of acetaminophen (APAP). However, the origin of these cells has not been established. Splenic monocytes (mono)/MP have been shown to accumulate at inflammatory sites following tissue injury. In the present studies, we analyzed the contribution of splenic mono/MP to liver inflammation and injury induced by APAP. Mice were fasted overnight prior to administration of APAP (300 mg/kg, i.p.) or PBS. Spleen, bone marrow (BM) and liver were collected 24-96 h later and analyzed by flow cytometry and immunofluorescence for the presence of activated mono/MP. APAP intoxication was associated with a time-dependent increase in CD11b+Ly6C+ proinflammatory MP, and a decrease in F4/80+ resident MP in the liver; this was correlated with a significant decrease in CD11b+F4/80+Ly6C-Ly6G- resident mono/MP in the spleen at 24 and 48 h post APAP, with no effect on BM mono/MP. Conversely, CD11b+F4/80+Ly6C+ inflammatory mono/MP increased in the spleen after 48-96 h, but decreased in the BM. To assess the role of splenic mono/MP in APAP hepatotoxicity, we used splenectomized (spx) mice. APAP-induced hepatotoxicity was significantly decreased in spx mice, as measured by decreases in serum transaminases. Histologic evidence of hepatic necrosis was also reduced. This was associated with a significant decrease in inflammatory mono/MP subsets (CD11b+F4/80-Ly6C+ and CD11b+F4/80+Ly6C+) in the BM at 24 h post APAP when compared to sham control mice. In addition, in spx mice, a decrease in CD11b+F4/80+Ly6C+Ly6G+ myeloid derived suppressor cells (MDSCs) was observed in BM at 96 h post-APAP. Taken together, these results indicate that splenic mono/MP contribute to early inflammation and hepatotoxicity induced by APAP. Moreover, removal of the splenic reservoir of mono/MP results in emigration of MDSCs out of the BM following APAP administration and this may contribute to tissue repair. Supported by NIH GM034310, ES004738, CA132624, AR055073, ES007148, ES005022.

**PS 249** **Exaggerated Hepatotoxicity of Acetaminophen (APAP) following Administration of Clodronate Liposomes Is Associated with the Persistence of Classically-Activated Macrophages in the Liver.**

A. Dragomir<sup>1</sup>, R. Sun<sup>1</sup>, M. Mili<sup>1</sup>, J. D. Laskin<sup>2</sup> and D. L. Laskin<sup>1</sup>. Joint Graduate Program in Toxicology, Rutgers University/UMDNJ-Robert Wood Johnson Medical School, Piscataway, NJ.

Toxic doses of APAP are known to cause centrilobular hepatic necrosis. Evidence suggests that classically and alternatively activated macrophages play distinct roles in APAP-induced hepatotoxicity. In the present studies, we investigated the effects of macrophage depletion using clodronate liposomes (CL) on activated macrophage subpopulations accumulating in the liver in response to APAP intoxication. Mice were administered empty liposomes (EL) or CL (100  $\mu$ L, i.v.) 48 h before APAP (300 mg/kg, i.p.) or PBS control. In mice pretreated with EL, increases in serum transaminases and hepatic necrosis were observed within 24 h; this was correlated with hepatic accumulation of CD11b+Ly6C+ classically activated macrophages in the liver and increased expression of galectin-3, a marker for these cells. These effects were significantly increased in mice pretreated with CL at 72 and 96 h post APAP, and were associated with increases in CD11b+Ly6C+F4/80-/inflammatory monocytes in the bone marrow, suggesting a potential origin of these cells. In contrast, APAP-induced expression of the alternative macrophage activation markers Fizz-1 and Ym1, and the anti-inflammatory cytokine IL-10, were significantly reduced in livers of mice treated with CL when compared to EL. Expression of TNF- $\alpha$ , the chemokine CCL2, and its receptor CCR2, cytokines critical for repair of APAP-induced injury, were also decreased in CL-pretreated mice relative to EL-treated mice. Taken together, these results suggest that increased APAP-induced hepatotoxicity following macrophage depletion using CL is due, in part, to persistent accumulation of classically activated macrophages in the liver. Supported by NIH GM034310, ES004738, CA132624, AR055073 and ES005022.

**PS 250** **Bone Marrow Inflammation Precedes Delayed Myelosuppression from Hexahydro-1-Nitroso-3, 5-Dinitro-1, 3, 5-Triazine (MNX) Induced in Rats.**

S. Jalgama<sup>1</sup>, V. M. Kale<sup>2</sup>, M. S. Wilbanks<sup>3</sup>, E. J. Perkins<sup>3</sup> and S. A. Meyer<sup>1</sup>.  
<sup>1</sup>Toxicology, University of Los Angeles Monroe, Monroe, LA; <sup>2</sup>College Pharmacy, Roseman University Health Science South Jordan, UT; <sup>3</sup>US Army Engineer Research & Development Center, Vicksburg, MS.

MNX (hexahydro-1-nitroso-3, 5-dinitro-1, 3, 5-triazine), an environmental nitroreduced product of munitions RDX, contaminates military sites. Our previous studies identified bone marrow (BM) and spleen as hematological targets of acute oral exposure to MNX in rats in the form of splenic hemosiderosis and loss of BM Granulocyte Macrophage Colony Forming Cells (GM-CFCs). To address whether delayed loss of GM-CFCs and blood granulocytes (NOAELs 24, 47 mg/kg resp) at 14 days after exposure to MNX is due to persistence of early hematological effects or is late-onset due to required expression period, female Sprague-Dawley rats were orally gavaged with MNX from 0 to 94 mg/kg and different toxicological endpoints were evaluated over a time course at 2, 7, 10, 12, and 14d. Significant decrease in relative spleen weight and increased macrophage activity in splenic red pulp at 2d ( $\geq$  47 mg/kg); and persistent splenic hemosiderosis at 2d ( $\geq$  47 mg/kg), 7d (NOAEL 24 mg/kg) and 14d were observed. A significant increase in blood granulocytes and circulating levels of RANTES, a leukocyte chemokine, indicate that an acute inflammatory response occurs at 2d after exposure to MNX. Also, persistent BM macrophage infiltration was observed in MNX (94 mg/kg) treated rat iliums (24h, 2d and 10d) and activation of NF $\kappa$ B signaling pathway in BM cells was evident at 10d. Further, significant increase in adherent BM mesenchymal stromal cell colonies constituting macrophages, endothelial cells and fibroblasts was observed in MNX (94 mg/kg) treated rats. Collectively, these data suggest that while splenic effects are early onset and persist for at least 14d, myelosuppression is delayed until 10d presumably due to development of inhibitory effects of preceding BM inflammation on myelopoiesis. (Support: DoD/CDMRP, US Army Corps of Engineers)

**PS 251** **Reversibility of Prostate Fibrosis in Response to Bacterial-Induced Chronic Inflammation.**

L. Wong<sup>1</sup>, P. Hutson and W. A. Bushman. University of Wisconsin-Madison, Madison, WI.

Introduction: Benign prostatic hyperplasia (BPH) and its associated lower urinary tract symptoms (LUTS) are common in aging men. Chronic inflammation and increased stromal collagen are common features observed in BPH. Recent study has

shown that the collagen content is correlated with the degree of LUTS and tissues stiffness, suggesting a role of prostate fibrosis in BPH/LUTS. Using the bacterial-prostatic inflammation mouse model, we have shown that prostatic inflammation induces collagen content. The goal of this study is to investigate the reversibility of prostate fibrosis during bacterial-induced chronic inflammation.

**Methods:** We transurethrally instilled uropathogenic E-coli into adult C3H/HeOuJ male mice to induce chronic inflammation in the prostate. Naïve, saline and E-coli instilled animals were sacrificed after 1 month. Other animals were treated with Baytril in drinking water to resolve the infection and underwent an additional 2-month resolution. The prostate tissues were used for bacterial culture and measurement of hydroxyproline level as collagen content using high-pressure liquid chromatography.

**Results:** The uropathogenic E-coli was present in the prostates of all E-coli infected animals after 1-month post-instillation and treatment of Baytril completely resolved the bacterial infection. We further found that hydroxyproline content in the prostates was significantly increased in the E-coli infected mice compared to the saline. Infected mice treated with Baytril with an additional 2-month resolution had a significant increase in hydroxyproline level in the prostates compared to the saline, but the level was significantly lowered to the E-coli infected prostates.

**Conclusion:** This study suggests that prostate fibrosis in response to bacterial-induced chronic inflammation is only partially reversed. Given that prostate fibrosis is suggested to strongly associate with the loss of prostate compliance and the development and progression of BPH/LUTS, an understanding on the mechanisms of the irreversible collagen deposition is required for improvement of therapeutic treatment.

## PS 252 Topical Application of TRPV1 Antagonist Effectively Inhibits PTD-Induced Sensitization in Murine Skin.

K. Lim, K. Jung, W. Jang and Y. Park. *AMOREPACIFIC Co. R&D Center, Gyeonggi-do, Republic of Korea.*

Transient receptor potential vanilloid type 1 (TRPV1) is expressed in the skin and plays a role in migration of dendritic cells to lymph nodes in allergic diseases. However, it has been unaddressed if TRPV1 blockade can suppress chemical-induced contact dermatitis. 1,4-toluenediamine (PTD) and 1,4-phenylenediamine (PPD) are widely used as permanent hair dye but repeated use of PTD can induce contact hypersensitivity by the induction of regulatory T cells in the draining lymph node and of inflammation in the exposed skin. In this study, the inhibitory effect TRPV1 antagonist, PAC-14028 on PTD-induced dermatitis and dendritic cell (DC) function was explored. This study was performed according to the method of nonradioactive local lymph node assay using flow cytometry. Groups of mice (N=4-5) were treated with 25 µl of the PTD alone, PAC-14028 alone, PTD and PAC-14028 or vehicle alone on the dorsal area of both ears daily for 3 consecutive days (Day 1, 2 and 3) and were sacrificed at Day 6. The local response was measured by ear swelling and by histological examinations (H&E staining). We also used immunohistochemistry staining and western blot assays to evaluate the activation of specific inflammation makers and key mediators of signaling pathway in the mouse skin. The DCs migration markers in the draining lymph nodes were analysed by flow cytometry. TRPV1 antagonist suppressed PTD-induced edema in skin and proliferation of lymphocyte and inhibits the migration of CD11c+ DC and CD207+ Langerhans cells (LC) to the draining lymph nodes (LNs).

## PS 253 Comparative Inflammatory Effects of Differential Particulate Matter Species in an OVA-Sensitization and Challenge Model.

M. A. Williams<sup>1</sup>, M. J. Daniels<sup>1</sup>, E. H. Boykin<sup>1</sup>, T. Smith<sup>1</sup>, N. Hykal-Coates<sup>2</sup>, L. B. Copeland<sup>1</sup>, D. L. Andrews<sup>2</sup>, J. H. Richards<sup>1</sup> and L. Gilmour<sup>1</sup>.

<sup>1</sup>Environmental Public Health Division, US EPA, Research Triangle Park, NC;

<sup>2</sup>Research Core Unit, US EPA, Research Triangle Park, NC.

Exposure to respirable ambient particulate matter (APM) provokes allergic immunity that may also occur on exposure to environmental diesel exhaust particles (eDEP) or emission source DEP (cDEP). Our hypothesis tested whether APM, eDEP or cDEP provide immune adjuvancy in an antigen (OVA) sensitization and challenge model. We assayed for oxidative stress, inflammatory and cytokine analytes in BALF, assay of lung infiltrating cells, assay of serological analytes (total IgE, IgG1, IgG2a), and antigen-specific recall responses of primary lymph node cells (pLNC). All PM species increased markers of airway or allergic inflammation. However, eDEP or cDEP sensitized mice had lower levels of superoxide dismutase as compared APM, without affecting other oxidative stress markers (p<0.005). By contrast, all PM species enhanced eosinophil and neutrophil infiltration to the lung as compared saline or OVA alone (p<0.001). These effects for APM (p<0.005) and cDEP (p<0.05) were concordant with enhanced levels of pro-Th2 cytokines like

IL-5 in BALF. Assay of isotype class-switching was less informative. All PM species partially augmented total IgE as compared saline, but not when compared to LPS control or each other, and dampened secretion of IgG2a (p=0.07) and IgG1 (p=0.059) as compared low-dose LPS/OVA. In OVA-specific recall responses, pLNC proliferation was enhanced in mice sensitized with eDEP and particularly cDEP, which provoked robust IL-5 and IL-13 secretion (p<0.01). We conclude that all PM species provoked airway and allergic inflammation. However diesel PM, and particularly cDEP were most effective in sensitizing mice and driving Th2-type cytokine and OVA-specific responses ex vivo. This study supports the realization that respirable PM differentially provoke allergic inflammation, and provides new insights on signaling changes contributing to these effects. This abstract does not reflect US EPA policy.

## PS 254 Role of Ortho-Phthalaldehyde in IgE-Induced Airway Hyperresponsiveness As a Hapten and an IgE-Selective Adjuvant-Like Activity in Mice Treated with Ovalbumin.

Y. Ishihara<sup>1</sup>, M. Nakao<sup>1</sup>, T. Morinaga<sup>1</sup>, G. Hasegawa<sup>1</sup>, M. Yamaguchi<sup>1</sup>, T. Nishikawa<sup>2</sup> and H. Kawashima<sup>3</sup>. <sup>1</sup>Public Health, Kurume University, Kurume, Japan; <sup>2</sup>Surgical Pathology, Tokyo Women's Medical University, Tokyo, Japan; <sup>3</sup>Microbiology & Immunology, University of Shizuoka, Shizuoka, Japan.

**[Purpose]** We previously reported that ortho-phthalaldehyde (OPA) disinfectant induces acute inflammation and enhances allergen-specific IgE production without allergen-specific IgG in ovalbumin (OVA)-sensitized mice. However, etiology of this disorder is not fully understood. The purpose of this study is to explore relationship between airway hyperresponsiveness and host immunity in OPA-treated OVA sensitized mice. **[Methods]** Female ICR mice were divided into five groups; OPA + OVA group, aluminum hydroxide (Alum) +OVA group, OPA group, OVA group, and Control group. The mice were sensitized twice with OVA and challenged with OVA inhalation one day prior to testing airway responsiveness to acetylcholine (Ach) under anesthesia. **[Results]** Airway hyperresponsiveness to Ach was observed in the OPA + OVA and Alum +OVA groups compared with the responses observed in the OPA, OVA and control groups. OPA-specific IgE and IgG antibodies and OVA-specific IgE antibody increased markedly, whereas OVA-specific IgG antibody did not increase in the OPA + OVA group due to the masking of OVA's antigenicity for IgG production by the aldehyde group of OPA. **[Conclusion]** These results strongly suggest that OPA functions as both a hapten and an allergen-specific, IgE-selective adjuvant, leading to significant airway inflammation and hyperresponsiveness to Ach.

## PS 255 Dual Oxidase Modulates Airway Neutrophil Recruitment in Allergic Airways.

S. Chang<sup>1,2</sup>, A. L. Linderholm<sup>2</sup>, H. Grasberger<sup>3</sup> and R. W. Harper<sup>2</sup>. <sup>1</sup>Pharmacology Toxicology, University of California Davis, Davis, CA; <sup>2</sup>Internal Medicine, University of California Davis, Davis, CA; <sup>3</sup>Internal Medicine, University of Michigan, Ann Arbor, MI.

**Introduction/Rationale:** Reactive oxygen species (ROS) plays an important role in maintaining lung homeostasis. However dysregulation of ROS, specifically hydrogen peroxide, has been linked to respiratory diseases such as chronic obstructive pulmonary disease, cystic fibrosis and asthma. Dual Oxidase (DUOX) is an NADPH oxidase, whose function is regulated production of hydrogen peroxide, localized to the lung epithelium. DUOX activity and expression are upregulated by IL-4 and IL-13 which are key cytokines in allergic airways. Interestingly, the role of DUOX in asthma has never been evaluated in vivo. The objective of this study was to determine the role of DUOX derived hydrogen peroxide in asthmatic airways, using a DUOX system knock out mouse. **Methods:** Wild-type and dual DUOX A1/DUOX A2 knockout mice were sensitized with ovalbumin (day 0 and 14) and subsequently exposed to aerosolized ovalbumin for a period of 2 weeks to evaluate the role of DUOX in allergic asthma. Measurement of forced expiratory nitric oxide concentrations, airway compliance, live cell counts, bronchoalveolar lavage fluid (BALF) cell differentials and histology were performed and compared between the two groups. **Results:** Wild-type mice with functional DUOX had a greater influx of neutrophils than knockout mice when subjected to ovalbumin as observed in BALF as well as semi quantitative counts in lung tissue. **Conclusion:** These findings suggest that DUOX derived hydrogen peroxide has an important role in signaling neutrophils into allergic airways.

This research was supported by NIH(R01 HL085311& R01 HL085311-S1).

**PS 256 Epithelial-Derived Hypoxia Inducible Factor-1 $\alpha$  Plays a Role in Programming the Innate Immune Response of the Lung.**

K. Greenwood, S. P. Proper, Y. Saini, D. Jackson-Humbles, J. G. Wagner, J. Harkema and J. J. LaPres. *Michigan State University, East Lansing, MI.*

Allergic airway disease (AAD) involves a complex interaction between various cell types within the lung, including inflammatory and epithelial cells. The inherent inflammation of AAD also leads to localized hypoxia. Communication between inflammatory cells, such as macrophages and T cells, and the epithelia in these hypoxic conditions is hypothesized to be critical to the progression of AAD. To characterize the role of epithelial-mediated hypoxia-induced signaling in AAD, epithelial and lung-specific conditional hypoxia inducible factor-1 $\alpha$  (HIF1 $\alpha$ ), HIF2 $\alpha$ , and HIF1 $\alpha$  and HIF2 $\alpha$  (HIF1/2 $\alpha$ ) knockout mouse models were created. Previous research in our lab has shown that the HIF1 $\alpha$ -deficient (HIF1 $\alpha$  $\Delta/\Delta$ ) mice exhibit an exacerbated response to the ovalbumin (OVA) model of AAD. To determine the role of HIF2 $\alpha$  in AAD and characterize possible compensation between the two HIFs following OVA challenge, recombination was induced early in post-natal development and control and HIF-deficient mice were then sensitized/challenged with OVA via a standard paradigm. In contrast to the HIF1 $\alpha$  $\Delta/\Delta$  model, the HIF2 $\alpha$  $\Delta/\Delta$  mice displayed no increase in eosinophil infiltration, T helper 2 cytokines, or airway resistance following OVA treatment. The HIF2 $\alpha$  $\Delta/\Delta$  mice appear phenotypically identical to OVA-treated littermate controls. Interestingly, when HIF1/2 $\alpha$  $\Delta/\Delta$  mice were sensitized/challenged with OVA, these animals appeared similar to HIF2 $\alpha$  $\Delta/\Delta$  and littermate controls, suggesting that HIF2 $\alpha$  plays a role in the exacerbated inflammation observed in the HIF1 $\alpha$  $\Delta/\Delta$  model. These data suggests that epithelial-derived HIF signaling plays an important role in establishing the immunity of the lung and that a proper balance between the two HIFs is required for a normal inflammatory response. The observed changes in the inflammatory response of the various models also suggest that early life exposures that alter the expression or function of HIF1 $\alpha$  and/or HIF2 $\alpha$  might have profound effects on the lung's response to toxicant challenge upon reaching adulthood.

**PS 257 ODSH Improves Survival in PA Pneumonia by Increased Bacterial Clearance and Reduced Lung Injury.**

L. Sharma<sup>1</sup>, J. Wu<sup>1</sup>, V. Patel<sup>1</sup>, R. Sitapara<sup>1</sup>, N. Rao<sup>3</sup>, T. P. Kennedy<sup>4</sup> and L. L. Mantell<sup>1,2</sup>. <sup>1</sup>*St. John's University, New York, NY;* <sup>2</sup>*The Feinstein Institute for Medical Research, Manhasset, New York, NY;* <sup>3</sup>*University of Utah, Salt Lake City, UT;* <sup>4</sup>*Pulmonary and Critical Care Medicine, Georgia Health Sciences University, Augusta, GA.*

Nosocomial Pneumonia (NP) or Hospital Acquired Pneumonia (HAP) is associated with infections originated from the hospital borne pathogens. Resistance against antimicrobial agents is the most common feature of these infections which results in persistent infection leading to high mortality rates and therapeutic costs. Due to the involvement of multidrug resistant bacteria, alternative or supportive therapies are required. *Pseudomonas aeruginosa* (PA), gram negative pathogen, is one of the prominent pathogens associated with NP. PA pneumonia increases the secretion of inflammatory cytokines, neutrophil infiltration and subsequent lung damage. HMGB1, one of the inflammatory cytokines, has been shown to play important roles in PA lung infections. HMGB1 can compromise innate immunity by impairing phagocyte function mediated by its receptors TLR2 and TLR4. Heparin, a well-known anticoagulant, exhibits anti-inflammatory properties that are independent of anticoagulant property. 2-O, 3-O -desulfated heparin (ODSH), heparin, has been proven to have anti-inflammatory properties with minimal anticoagulation effect. ODSH has been shown to reduce lung injury in sterile inflammation and reducing inflammatory lung damage. In this study, we examined the effect of ODSH on PA pneumonia. Here we demonstrate that ODSH not only reduces PA-induced lung injury, illustrated by reduced total protein content in lung lavage fluids, it also significantly increases bacterial clearance. This improved lung injury and bacterial clearance resulted in marked improvement in overall survival of the mice with PA infection. The attenuation in lung injury and improved bacterial clearance was associated with reduced airway HMGB1. In addition, ODSH inhibits binding of HMGB1 with receptors TLR2 and TLR4. These data indicate a novel role of ODSH in the treatment of PA pneumonia.

**PS 258 Role of Mannose-Binding Lectin in the Pulmonary Response to Ozone.**

J. Ciencewicki, K. E. Gerrish, P. Bushel and S. R. Kleeberger. *NIEHS, Research Triangle Park, NC.* Sponsor: *D. Harbourt.*

Ozone is a common pollutant and a potent oxidant in many areas of the country. Inhalation causes airway hyperactivity, lung hyperpermeability, inflammation and cell damage in humans and laboratory animals, and exposure to ozone has been as-

sociated with exacerbation of asthma, altered lung function, and mortality. Currently the mechanisms of ozone-induced lung injury and differential susceptibility are not fully understood. Ozone exposure induces a number of pro-inflammatory events in the lung, some of which are mediated by the innate immune system. We hypothesized that mannose binding lectin (MBL), which plays a central role in the activation of the complement pathway of innate immunity, is needed to elicit some of the pro-inflammatory events caused by ozone-mediated activation of the innate immune system. Wild-type (Mbl<sup>+/+</sup>) and MBL deficient (Mbl<sup>-/-</sup>) mice were exposed to ozone (0.3 ppm) for 24, 48, and 72 hours. Compared to Mbl<sup>+/+</sup> mice, significantly less neutrophilic infiltration and the neutrophil attractants CXCL2 (MIP-2) and CXCL5 (LIX) were found in the lungs of Mbl<sup>-/-</sup> mice exposed to ozone. We then used mRNA microarray analyses to gain additional mechanistic insight to the role of MBL in this model. We identified significant differences in expression response profiles and networks at baseline and after exposure between Mbl<sup>+/+</sup> (WT) and Mbl<sup>-/-</sup> (KO) mice, providing potential roles for MBL at steady-state and in the innate immune pulmonary response to ozone inhalation. For example, we found gene enrichment for lipid metabolism and hematological disease at baseline, and innate immunity and cell morphology after ozone exposure. These novel findings demonstrate that MBL function contributes to ozone-induced pulmonary inflammation and may be mediated through the activation of the complement cascade.

Research supported by intramural research program at NIEHS.

**PS 259 Anti-Inflammatory Effect of Imipramine in Silica-Induced Inflammation.**

R. Biswas, R. Hamilton and A. Holian. *Center for Environmental Health Sciences, University of Montana, Missoula, MT.*

Environmental or occupational exposure to silica particles over an extended period of time is associated with the development of progressive inflammation and silicosis. Silicosis remains a prevalent health problem throughout the world. Currently, treatment choices for silicosis are limited and at present there is no cure for the disease. Therefore, it is essential to investigate potential therapeutic agents in silicosis treatment. Imipramine (IMP) is an approved tricyclic antidepressant, and a lysosomotropic agent. The aim of this study was to determine the protective effect of IMP on silica-induced inflammation and determine the mechanism by which IMP inhibits inflammation. C57BL/6 wild-type (WT) mice were used throughout the study. The protective effect of IMP was evaluated in vitro and 24 hours and 42 days following silica exposure in vivo. Silica was administered once a week for 4 weeks and IMP was delivered for 42 days via osmotic pumps implanted subcutaneously. Collagen levels were determined by hydroxyproline content. IMP treatment decreased collagen levels compared to the silica-exposed group. Lung histopathology improved on IMP treatment. WT mice were pretreated with IMP 25 mg/kg, and subsequently exposed to silica 1mg/kg during the in vivo acute study. IMP inhibited silica-exposed neutrophil infiltration, IL-1 $\beta$  and IL-6 in the lavage fluid. For in vitro experiments, WT alveolar macrophages (AM) were pretreated with 25  $\mu$ M IMP and subsequently exposed to LPS (20 ng/ml) and silica (100  $\mu$ g/ml). IMP was highly effective in blocking silica-induced inflammasome activation without any toxic effects on AM. The effect of IMP on acid sphingomyelinase (A-SMase) was determined since A-SMase has been associated with acute lung injury. A-SMase was significantly inhibited by IMP treatment. The results demonstrate that IMP inhibits silica-induced inflammation and IMP may be exhibiting anti-inflammatory properties through its effect on lysosomes. The work was supported by NIH grants P20 RR017670 and R01 ES 15294

**PS 260 Higher Susceptibility of Male Mice to Diesel Exhaust Neurotoxicity.**

L. G. Costa<sup>1,2</sup>, G. Giordano<sup>1</sup>, A. Engstrom<sup>1</sup>, C. S. Weldy<sup>3</sup>, F. Farin<sup>1</sup> and T. J. Kavanagh<sup>1</sup>. <sup>1</sup>*Department Environmental Occupational Health Sciences, University of Washington, Seattle, WA;* <sup>2</sup>*Department of Neuroscience, University of Parma, Parma, Italy;* <sup>3</sup>*Division of Cardiology, University of Washington, Seattle, WA.*

In addition to increased morbidity and mortality caused by respiratory and cardiovascular diseases, air pollution may also contribute to CNS diseases. Traffic-related air pollution is a major contributor to global air pollution, and diesel exhaust (DE) is its most important component. DE contains more than 40 toxic air pollutants and is a major constituent of ambient particulate matter (PM), particularly of ultrafine-PM. Limited information suggest that exposure to DE may cause oxidative stress and neuroinflammation in the CNS. We hypothesized that males may be more susceptible than females to DE neurotoxicity, because a lower level of expression of paraoxonase 2 (PON2), an anti-oxidant mitochondrial enzyme. Acute exposure to DE (250  $\mu$ g/m<sup>3</sup> for 6h) causes significant oxidative stress (lipid peroxidation as determined by the malonyldialdehyde assay) in several brain regions (particularly the olfactory bulb, the hippocampus and the cerebellum) and the ef-

fect is consistently higher in male mice than in females. A number of pro-inflammatory cytokines (IL-1 alpha, IL-1 beta, IL-3, IL-6, TNF-alpha) were also measured in olfactory bulb and hippocampus by the Luminex xMAP® technology. Levels of all cytokines increased significantly in both brain regions upon acute DE exposure, and in most cases gender differences were present. For example, in the hippocampus, levels of IL-6 increased by 18-fold and 8-fold in male and female mice, respectively. Such differences may also be due to a gender-dependent, differential expression of PON2, which has been shown to have anti-inflammatory actions in the periphery, and may have similar effects in the CNS. These findings indicate that acute exposure to DE causes oxidative stress and neuroinflammation in several brain regions, and suggests that gender plays an important role in modulating susceptibility to DE neurotoxicity, with male mice being more sensitive (Supp. in part by DEOHS).

**PS 261 Pilot Study Using an Alzheimer's Disease Animal Model to Assess the Role of Particulate Matter Exposure in Neuroinflammation and Amyloid Production.**

S. Lung<sup>1</sup>, L. B. Mendez<sup>2</sup> and A. Campbell<sup>1</sup>. <sup>1</sup>Pharmaceutical Science, Western University of Health Science, Pomona, CA; <sup>2</sup>Medicine, University of California Irvine, Irvine, CA.

Alzheimer's Disease (AD) is a neurodegenerative disease that is associated with severe memory loss and dementia. One of the major pathological markers for AD is formation of senile plaques, which are composed of amyloid beta peptides derived from amyloid precursor protein (APP). In this pilot study, we examined the effect of exposure to fine particulate matter (PM2.5) on proinflammatory markers and potential association with enhanced amyloid levels. Mice with the human Swedish mutation (Tg2576) in the APP gene and wild-type control animals were exposed to filtered air or PM2.5. Brain APP levels, NF-κB activation, and IL-1β levels were determined. Microglia and TLR2 activation in hippocampus were demonstrated. Brain levels of Aβ40 and Aβ42 were also assessed. Results showed APP levels were expressed only in brains of Tg2576 mice and not in wild type animals. The Aβ40 and Aβ42 brain level after PM2.5 exposure showed upregulation. NF-κB activation was also increased in the brain of both wild type and transgenic animals after PM2.5 exposure. IL-1β increased only in transgenic mice exposed to PM2.5. In transgenic animals, the hippocampus region showed enhanced staining for both TLR-2 and microglia after PM2.5 exposure compared to filtered air. The results of our pilot study suggest PM2.5 exposure may lead to the activation of innate immune response mediated by NF-κB pathway. The upregulation of Aβ levels in the brain of PM2.5 exposed animals suggest that there could be a link between PM2.5 exposure and enhancement of amyloid production. The results of this pilot project justify the need for a more extensive study assessing the effect of particulate matter on potentiating amyloid pathology in AD.

**PS 262 Subchronic Exposure to Deltamethrin Causes Hippocampal Neuroinflammation and Deficits in Learning and Memory.**

M. M. Hossain and J. Richardson. *Environmental and Occupational Medicine, Robert Wood Johnson Medical School, Piscataway, NJ.*

Previously, we have reported that in vitro exposure of neuroblastoma cells to deltamethrin causes apoptosis through the ER stress pathway, leading to calpain and caspase-3 activation (Hossain and Richardson, 2011). Others have found that acute high-dose deltamethrin (12.5 mg/kg) exposure causes hippocampal apoptosis in adult rats (Wu and Liu, 2000). However, little is known about the effects of longer-term lower level exposure that does not result in acute poisoning. Here, we investigated the effects of deltamethrin at a dose of 3mg/kg every 3 days for 2 months on hippocampal ER stress, neuroinflammation, and learning and memory in adult mice. Deltamethrin treatment did not result in over toxicity. However, we observed increased spectrin cleavage in the hippocampus of deltamethrin-treated mice, indicating activation of calpain. Deltamethrin also significantly increased the hippocampal mRNA expression of glial fibrillary acidic protein (GFAP; 23%) and the pro-inflammatory cytokines tumor necrosis factor-alpha (121%) and Interleukin-1 alpha (96%), indicating an ongoing neuroinflammatory process. Finally, we found that subchronic deltamethrin exposure causes profound deficits in hippocampal-dependent learning and memory in the Morris water maze, which was accompanied by a decreased mRNA expression (30%) and protein level (39%) of nerve growth factor (NGF), respectively. Together, these data suggest activation of the ER stress pathway and neuroinflammation by repeated exposure to deltamethrin may contribute to the down-regulation of NGF in the hippocampus, which may result in subsequent impairment in learning and memory in mice. Supported by NIH ES015991 and ES005022.

**PS 263 Ambient Endotoxins Possible Links to Toll-Like Receptors Gene Polymorphisms in Puerto Rican Asthmatics.**

M. G. Ortiz-Martínez<sup>1,2</sup> and B. D. Jiménez-Vélez<sup>1,2</sup>. <sup>1</sup>Biochemistry, University of Puerto Rico-Medical Sciences Campus, San Juan, Puerto Rico; <sup>2</sup>Center for Environmental and Toxicological Research, University of Puerto Rico-Medical Sciences Campus, San Juan, Puerto Rico.

African Dust Storms also referred as Events (ADE) are believed to be associated to high prevalence of respiratory diseases such as asthma in Puerto Rico (PR). Endotoxins (ENX) have been previously reported as constituents associated with ADE particulate matter (PM). These ENX and related compounds are known to promote pro-inflammatory responses in lung cells and in susceptible individuals. Since ENX have been shown to work through the following receptors, we have evaluated a number of Toll-like receptors (TLR2/4) as well as the co-receptor, Cluster of Differentiation 14 (CD14) single nucleotide polymorphisms (SNPs) in the Puerto Rican population. Contradictory results exist, which link SNPs to increased asthma prevalence and/or risk in some populations. A total of 6 SNPs have been evaluated in the Puerto Rican asthmatic population. TLR2 (+596C/T, +6686T/A, +399A/G), TLR4 (+896A/G, +1196C/T) and CD14 (+1188C/G) SNPs were measured in 62 asthmatics and 59 non-asthmatic controls using Taqman® probes through a genotyping assay (Real Time PCR). Minor allele frequencies (n=121) were determined for those variants as 0.35, 0.37, 0.32, 0.07, 0.06 and 0.09, respectively. Two (+596C/T and +399A/G) TLR2 SNPs showed to be more represented in the asthmatic group (89% and 65%), combining C/T plus T/T and A/G plus G/G genotypes, respectively. TLR4 SNP +896A/G analysis revealed only 1 G/G genotype (2%) on the asthmatic group. The CD14 SNP was similarly represented in both groups. The identification of specific TLR SNPs will be valuable to understand action mechanisms of environmental ENX, which have been associated with the triggering of asthma in PR. Moreover, it will help to reveal the relevance of TLR pathway genes as potential candidates for gene-environment interactions in Puerto Ricans. Study approved by the UPR-MS-IRB (#A8570111) and supported by MBRS-RISE Grant R25GMO61838.

**PS 264 Cytotoxicity Effect and Utilization of *Mytilus edulis* Shell in the Diet of *Clarias gariepinus*.**

A. A. Idowu<sup>1</sup> and S. O. Ayoola<sup>2</sup>. <sup>1</sup>Aquaculture and Fisheries Management, Federal University of Agriculture, Abeokuta, Abeokuta, Nigeria; <sup>2</sup>Marine Sciences, University of Lagos Akoka, Lagos, Lagos, Nigeria.

Five isonitrogenous diets (100% DCP compounded feed, 75% DCP Compounded feed and 25% *Mytilus edulis* shell, 50% DCP Compounded feed and 50% *Mytilus edulis* shell, 25% DCP compounded feed and 75% *Mytilus edulis* shell, 100% *Mytilus edulis* shell) were formulated. The *Mytilus edulis* shell was washed, sun dried for 5 days and later grinded and added to the feed and were fed to 150 juveniles of *Clarias gariepinus* which were distributed into 15 different plastic bowls. Ten specimens were stocked in each of the plastic bowls and they were fed twice daily for an experimental period of 12 weeks. In the cytotoxicity, five fishes were picked randomly from each triplicate and their blood collected carefully with syringe from the anal region and kept in sample bottles. The blood was smeared on slides and were air-dried for 24 hours, fixed in ethanol for 20 minutes and followed by 10% Giemsa staining. Each fish had 2000 erythrocytes examined and to detect micronuclei in erythrocytes, the slides were analysed using a 1000X oil-immersion lens. This implies that *Mytilus edulis* shell can be utilized best with compounded feed at a ratio of 50 to 100%. Therefore, this ratio should be adopted by fish farmers whose intention is to increase the calcium mineral level of their fishes. The obtained results for micronucleus reveals that T1 (25% MES) had the highest number of micronucleated cells while the rest (T2, T3, and T4) including the control had no significant differences. Results for BN reveal that T1 having the highest number of BN and T0 (control) having the least number of BN. While in LB, BL, and NT there were no significant differences in all the treatments. From the results it showed that *Mytilus edulis* shell (MES) has no toxins since there are less micronucleus and other aberrations in the haematopoietic cells. Hence, *Mytilus edulis* shell can be included from 50 – 100%.

**PS 265 Using a Sequence Homology-Based Predictive Strategy to Address Current Demands for Focused Toxicity Testing in Ecological Risk Assessment.**

C. LaLone<sup>1</sup>, D. L. Villeneuve<sup>1</sup>, L. D. Burgoon<sup>2</sup>, C. Russom<sup>1</sup>, H. Helgen<sup>4</sup>, J. Berninger<sup>3</sup>, J. Tietge<sup>1</sup>, M. Severson<sup>1</sup>, J. Cavallin<sup>5</sup> and G. T. Ankley<sup>1</sup>. <sup>1</sup>US EPA, Duluth, MN; <sup>2</sup>US EPA, Research Triangle Park, NC; <sup>3</sup>National Research Council, Duluth, MN; <sup>4</sup>Computer Sciences Corporation, Duluth, MN; <sup>5</sup>ORISE Research Participation Program, Duluth, MN.

The lack of resources available for comprehensive toxicity testing, international interest in limiting the quantity of animals used in testing, and a mounting list of anthropogenic chemicals produced world-wide have led to the exploration of innovative means for identifying chemicals that are potentially hazardous to the environment and its inhabitants. Predictive toxicological approaches, which utilize publically available, a priori, knowledge of a chemical and its known molecular, cellular, or whole organism interactions, show promise for focusing current toxicity testing strategies. Using modern bioinformatic techniques, we have created a computational tool, which mines the extensive genomic and proteomic sequence repositories available through the National Center for Biotechnology Information and strategically compares homology metrics associated with primary and secondary protein sequences/structural domains across taxa. These comparisons are used to identify and rank species most likely to be susceptible to a chemical acting through a known molecular initiating event and can therefore aid in designing toxicity studies for species of concern. This presentation will identify the domains of applicability for this tool and describe examples related to predicting species sensitivities to pharmaceuticals and pesticides. An assessment of honey bee sensitivity to various pesticides will demonstrate the applicability of this tool for existing questions in risk assessment. The contents of this abstract neither constitute nor reflect official US EPA policy.

**PS 266 Alteration in Behaviour, Histoarchitecture of Liver, Lung, and Kidney of Male Wistar Rats Exposed to Open Refuse Dump.**

P. U. Nwoha<sup>1,2,3</sup>, G. E. Waritimi<sup>2</sup>, A. D. Atoni<sup>2</sup>, F. Onyije<sup>2</sup> and O. M. Ijomone<sup>1</sup>. <sup>1</sup>Anatomy and Cell Biology, Obafemi Awolowo University, Ile-Ife, Nigeria; <sup>2</sup>Human Anatomy, Niger Delta University, Wilberforce Island, Nigeria; <sup>3</sup>Environmental Neurobiology and Toxicology, Centre for Scientific Investigations and Training, Owerri, Nigeria.

Household wastes are disposed in the open in Nigeria, and most third world countries. These could have serious consequences on the health of humans and animals in the vicinity. Yet not much is known on the effects of such exposure on behaviour, and organs of the body. The present work exposed weaned male Wistar rats to open refuse dump continuously for five months. During this period the rats were housed in a building on the dump, kept in clean plastic cages, fed normal rat chow, and provided clean drinking water. Control rats were housed in Niger Delta University Animal Holding. At the end of the period, behaviour of the rats was tested on Open, and Elevated plus maze, for exploratory activity and for anxiety respectively. The animals were sacrificed, liver, lung, kidney dissected, examined macroscopically, and prepared for histological examination with H & E staining. Data obtained and analysed with student t-test showed that rats exposed to refuse dump spent significantly less time in open arms of the elevated plus maze than their unexposed controls ( $p < 0.05$ ). Organs showed massive infiltration with fat, while the histology showed destruction of the radial liver architecture, thinning and collapse of alveolar wall of lung, and tubular wall of the kidney. Thus indicating that such exposure could induce anxiety, and massive destruction of organs of the body, leading to serious health consequences.

Key words: refuse exposure, anxiety, destruction, liver, lung, kidney

**PS 267 In Vitro Fish Metabolism Using Rainbow Trout Liver S9 Fractions to Evaluate the Bioaccumulation Potential of Fragrance Ingredients.**

G. Adamson<sup>1</sup>, H. Laue<sup>2</sup>, K. J. Jenner<sup>3</sup>, H. Gfeller<sup>2</sup>, S. Kern<sup>2</sup>, J. W. Nichols<sup>4</sup> and A. Natsch<sup>2</sup>. <sup>1</sup>Givaudan US, East Hanover, NJ; <sup>2</sup>Givaudan Schweiz AG, Duebendorf, Switzerland; <sup>3</sup>Givaudan UK Ltd., Ashford, United Kingdom; <sup>4</sup>US EPA, Duluth, MN.

Bioaccumulation in aquatic species is a critical endpoint in the evaluation of novel chemicals as part of PBT assessment (persistent, bioaccumulative, and toxic) by the U.S. EPA. In vivo determination of the bioconcentration factor (BCF) requires the use of large numbers of animals. Predictive models are commonly used if no in vivo

BCF data are available. These models generally acknowledge the possibility that biotransformation can reduce the extent of accumulation. Lacking measured data, however, modeled biotransformation rates are commonly set equal to zero. In vitro systems have been proposed as alternative methods that can be used to provide metabolic data needed to refine BCF computer model estimates.

The goal of our study was to determine the in vitro metabolic stability of common chemical classes of fragrance ingredients (esters, alcohols and ketones) using rainbow trout liver S9 fractions and to use in vitro clearance rate to model the bioaccumulation potential. Metabolic stability was determined by monitoring the disappearance of the parent molecule by GC MS and metabolite formation by GC-MS and LC-MS.

Slow enzymatic turnover was found with isolongifolanone (CAS 23787-90-8). The ester serenolide (477218-42-1) was transformed rapidly. Alcohols like Ambermax (929625-08-1) and ketones like spirogalbanone (224031-70-3) were transformed moderately to rapidly. Metabolic routes, identified by selective use of cofactors and metabolite identification, involve ester cleavage, hydroxylations, reductions and conjugation with glucuronic acid and glutathione. When clearance rates measured in vitro were used as inputs to the BCF model a good correlation was observed between predicted BCFs and measured in vivo values. In vitro S9 metabolism data in combination with new refined BCF models are a valuable tool to assess bioaccumulation potential as part of a weight-of-evidence approach for chemical registrations.

**PS 268 The Role of Aquaporin 3 in the Uptake of Arsenite through the Intestine of the Atlantic Killifish (*Fundulus heteroclitus*).**

D. Jung<sup>1,2</sup>, M. A. Adamo<sup>2</sup>, R. M. Lehman<sup>2</sup>, R. Barnaby<sup>1</sup>, B. P. Jackson<sup>3</sup>, J. R. Shaw<sup>4,2</sup> and B. A. Stanton<sup>1,2</sup>. <sup>1</sup>Microbiology and Immunology, Geisel School of Medicine at Dartmouth, Hanover, NH; <sup>2</sup>Mount Desert Island Biological Laboratory, Salisbury Cove, ME; <sup>3</sup>Earth Sciences and Chemistry, Dartmouth College, Hanover, NH; <sup>4</sup>School of Public and Environmental Affairs, Indiana University, Bloomington, IN.

Aquaglyceroporins (AQPs) are proteins that mediate movement of water and small solutes across cellular membrane. Previously, we cloned kAQP3a from the gill of the killifish (*Fundulus heteroclitus*), an environmental sentinel species. kAQP3a, the only AQP expressed in gill, is the first AQP3 described that does not transport arsenite. This finding accounts for the low levels of cellular arsenite in gill of killifish exposed to environmental arsenite. Another homolog of AQP3 (kAQP3b), which transports arsenic, was identified as the consensus from a transcriptome database. In this study, we sought to identify the AQPs in the intestine, a major route of arsenite uptake. First, we examined AQP mRNA expression by qRT-PCR in the killifish intestine. Among the AQPs examined, only AQP3 was significantly expressed above background levels. Western blot studies with a polyclonal antibody that did not discriminate among kAQP3 variants, revealed that kAQP3 abundance was higher in killifish acclimated to FW compared to SW. Intriguingly, whereas only kAQP3a was expressed in the intestine of FW killifish, both kAQP3a and a new variant, kAQP3c, were expressed in the intestine of SW fish. When kAQP3c was transfected into HEK293T cells, cells took up arsenic as effectively as cells transfected with kAQP3b. When we examined arsenic levels in the intestine of FW fish and SW fish exposed to 1000 µg/L arsenite for 72h, the amount of arsenic detected in the intestine of SW fish was higher than the amount detected in FW fish. Results indicate that arsenite uptake in the killifish mostly likely occurs via ingestion, and that killifish acclimated to SW take up more arsenite than FW acclimated fish, because kAQP3c expression is up-regulated in SW fish and because SW fish drink more water than FW fish.

**PS 269 Characterization of DCOIT Bioaccumulation Mechanism via In Vitro Incubation with Rainbow Trout Liver S9.**

F. Zhang, D. L. Rick, M. Bartels and G. A. Hazelton. <sup>1</sup>Global Environmental Health Sciences, Tulane University, New Orleans, LA; <sup>2</sup>Tulane Cancer Center, Tulane University, New Orleans, LA; <sup>3</sup>Department of Biomedical Sciences, Tulane University, New Orleans, LA; <sup>4</sup>Department of Sociology, Washington State University, Pullman, WA; <sup>5</sup>Mary Queen of Vietnam Community Development Corporation, New Orleans, LA.

4, 5-Dichloro-2-(n-Octyl)-4-Isothiazolin-3-one (DCOIT) is an important biocide widely used in a variety of industrial processes. In supporting DCOIT regulatory registration, a bioaccumulation study in bluegill sunfish was conducted with 14C-DCOIT and indicated the bioconcentration factor (BCF) was 750 ml/g with less than 1 % of radioactivity in tissues attributed to DCOIT. To understand the findings in the in vivo fish bioaccumulation study, the in vitro metabolism of DCOIT was examined by using rainbow trout liver S9 (Fish S9) and glutathione (as protein

surrogate) in the presence or absence of NADPH. The potential metabolites including glutathione conjugates were identified and quantified via LC/MS-MS methodologies and radioactivity counting, and the protein binding activity of DCOIT was also quantified. Overall, more than nineteen metabolites (all chlorine-free) were identified with a majority of these metabolites conjugated to glutathione or cysteine. Incubations containing Fish S9 and DCOIT in the absence of glutathione resulted in much higher protein binding than those incubations containing glutathione. This demonstrated that glutathione present in the incubation medium acts as a useful surrogate of endogenous Fish S9 proteins to competitively react with DCOIT (or DCOIT active metabolites). The results from the present study provide evidence that the BCF value measured in vivo can be attributed to ring-opened metabolites binding high molecular weight tissue fractions- likely the sulphhydryl moieties in proteins. These data confirm that parent DCOIT does not bioaccumulate in fish, but the parent molecule is extensively metabolized to metabolites which were bound to high molecular weight components of the fish tissue (i.e., proteins).

## PS 270 Zinc Content Determines the Toxicity of Tire Leachate in *Girardia tigrina*.

R. Sneed, E. Coleman and E. Rice. *Biology, Chemistry, and Physics, University of the District of Columbia, Washington DC.* Sponsor: P. Ganey.

The practice of recycling old tires into various outdoor structures such as playground surfaces and landfill liners poses the risk of tire components moving into local watersheds and possibly affecting aquatic organisms. In this study we tested the hypothesis that the zinc content of tire leachate is a significant factor in its toxicity to *Girardia tigrina* (Girard, 1850), a freshwater planarian common to North American waterways. Planarians were cultured in tire leachate containing either 49.5 mg/L of zinc (BALT) or 0.13 mg/L (FRESH) of zinc or a control of extraction medium (EM) over a time period of 24 hours. All planarians in the BALT group died within 24 hours while no planarians died in either the FRESH or EM groups. To verify that zinc was the causative agent in the observed toxicity, planarians were maintained in a solution containing an equivalent amount of zinc (from zinc sulfate) for 24 hours. The survival rate of planarians in this group was not significantly different from the survival rate observed in the BALT group. These data strongly indicate zinc as the toxic agent. In addition to the lethality demonstrated by both high-zinc solutions, planarians displayed signs of distress indicated by increased activity, writhing, and loss of motor coordination prior to death when compared to controls, suggesting that neurotoxicity may be the mechanism of action. Future studies will examine the dose-response relationship of zinc toxicity in *G. tigrina* as well as evidence of neurotoxicity. (Support: NSF Award 0928444.)

## PS 271 Harmonizing Use of the 3Rs in Fish Toxicity Testing.

C. Willett<sup>1</sup>, S. Belanger<sup>2</sup>, M. Embry<sup>3</sup>, T. Iguchi<sup>4</sup>, M. Halder<sup>5</sup>, A. Lillicrap<sup>6</sup>, H. Rufli<sup>7</sup>, L. Touart<sup>8</sup> and S. Zok<sup>9</sup>. <sup>1</sup>The Humane Society of the United States, Gaithersburg, MD; <sup>2</sup>Procter & Gamble, Cincinnati, OH; <sup>3</sup>Health and Environmental Sciences Institute, Washington DC; <sup>4</sup>National Institute for Basic Biology, Okazaki, Japan; <sup>5</sup>ECVAM, Joint Research Centre, Ispra, Italy; <sup>6</sup>Norwegian Institute for Water Research, Ecotoxicology and Risk Assessment, Oslo, Norway; <sup>7</sup>Ecotoxolutions, Basel, Switzerland; <sup>8</sup>Office of Science Coordination and Policy, US EPA, Washington DC; <sup>9</sup>BASF, Ludwigshafen, Germany.

Pursuit of methods that refine, reduce or replace animals is often discussed in the context of human health hazard and risk assessment; however, several approaches that are in common use for human health are more frequently being applied in ecological hazard and risk assessment as well. Organized testing frameworks such as tiered frameworks or integrated strategies can be used to prioritize information needs and focus testing on tests that would be the most informative for a given regulatory need. Specific application of integrated strategies has been used to minimize fish used for acute toxicity testing, for example the limit and threshold approaches. There are principles that can be applied to specific test protocols that minimize animal use, for example the use of historical controls where appropriate or using statistical analyses to define the minimum individuals needed to obtain statistically significant results. Computer modeling can assist in extrapolating information from one species to another or in predicting acute toxicity, bioaccumulation and other biological activity in fish. While limited embryo, ex-vivo, and in vitro approaches are currently used in fish toxicity testing, opportunities exist for expanding the repertoire, particularly in the area of 'omics technologies. This presentation will describe these approaches as currently applied and present recommendations for improving the application and harmonization of 3Rs approaches to fish toxicity

testing, as presented in Chapter 5 of the Fish Toxicity Testing Framework Guidance Document prepared by the Organization of Economic Cooperation and Development (August 2012).

## PS 272 Concentrations of Metals Associated with Crude Oil from the BP Macondo Well in Sediments and Fish from the Northeastern Gulf of Mexico.

A. C. Nichols, D. A. Steffy and L. J. Morgan. *Physical and Earth Sciences, Jacksonville State University, Jacksonville, AL.*

To investigate if metals associated with crude oil from the BP Macondo Well were entering the marine food chain, sediment and scad mackerel (*TRACHURUS LATHAMI*) samples were analyzed by ICP for five of these metals: chromium, nickel, lead, thallium and vanadium. Samples were collected from the carbonate shelf along the west coast of Florida in fall, 2010. A subset of these samples was collected from the western Florida Panhandle. This area was south of the Florida beaches where tar balls washed ashore during the summer of 2010. Nickel levels in samples from this subset ranged from 2.85 to 11.18 micrograms/g in dry sediments, and 0.00 to 0.86 micrograms/g in dry fish tissues. Chromium levels in samples from this area ranged from 7.08 to 12.43 micrograms/g in sediments, and from 0.00 to 0.76 micrograms/g in scad. Vanadium levels ranged from 3.32 to 10.07 micrograms/g in sediments. Vanadium was the only one of these metals not detected in any of the fish. Lead levels ranged from 1.13 to 5.89 micrograms/g in sediments, and 0.00 to 0.36 micrograms/g in scad. Thallium appears to be biomagnified in scad, as concentrations in fish ranged from 0.72 to 1.42 micrograms/g, while sediment levels ranged from 0.00 to 0.30 micrograms/g.

## PS 273 The Effect of Tributyltin (TBT) on Zebrafish Sexual Differentiation.

C. L. McGinnis. *Quinnipiac University, Hamden, CT.*

Tributyltin (TBT), an antifouling agent, has been implicated in the masculinization of fish species worldwide, however the molecular mechanism is not fully understood. Our lab has previously examined the actions of TBT as an endocrine disruptor in zebrafish (*Danio rerio*) and determined, in vitro, that TBT inhibits zER specific activity in a dose dependent manner and may potentially act through the RXR portion of the PPAR-RXR (peroxisome proliferator-activated receptor gamma - retinoid X receptor alpha) heterodimer. Additionally, zebrafish were exposed to increasing concentrations of TBT and sexual differentiation genes were analyzed via qPCR. Results from qPCR focused our experimental efforts on the candidate gene, SRY-box containing gene 9a (Sox9a). Sox9a is a key regulator in mammalian testis differentiation, where it is shuttled to the nucleus upon differentiation; this appears to be a conserved mechanism across fish, marsupials and placental mammals. Developing zebrafish embryos were exposed to 1pM and 2.5pM TBT from 10 days post hatch (dph) to 90 dph and sampling was done at 25, 35, 40, 45, 60 and 90 dph. Fish were treated three times per week with either TBT, estrogen or vehicle. Following treatments, immunohistochemical (IHC) analysis was performed to assess Sox9a nuclear or cytoplasmic localization.

## PS 274 Heavy Metal Response in *Daphnia magna*: An Ecologically-Relevant Nonmodel Organism.

S. Roy and M. E. Pfrender. *Biology, University of Notre Dame, Notre Dame, IN.*

Environmental health issues have become a major focus of ecotoxicology research over the last decade. Due to rapid industrialization and urbanization, ecosystems are currently, and into the foreseeable future, under the threat of potential damage. In order to mitigate these risks, environmental scientists build predictive models to gauge the impact of pollutants, perform risk assessment studies to measure water quality, and protect organisms from potential damage due to the effects of pollutants.

One major pollutant is heavy metal. Since aquatic systems are the major sinks of industrial effluents they are often more highly impacted by heavy metals than area terrestrial ecosystems. Numerous studies on individual organisms and populations have demonstrated the effects of acute exposure to metal pollutants, but few studies are available that show the consequences of long-term low dose metal exposure to aquatic organisms.

In regular risk assessment practice, acute and high dose/concentration exposure is a common approach to predict which metal/chemical has potentially harmful effects on a particular organism. This approach is informative, but not predictive of the long-term low dose/concentration scenario that is more likely happening in our

day-to-day life. Further, aquatic toxicity tests have historically been largely limited to model organisms. However, not all organisms show the same physiological response to a particular metal/chemical making these assessments species specific. Our approach is to use quantitative genetics/genomics tools applied in an ecological relevant non-model organism to determine the genetic basis and mechanisms of response to a common, toxic metal pollutant. We use *Daphnia magna*, a widespread freshwater invertebrate, as a model organism to understand and interpret the genetic mechanisms of response to cadmium.

**PS 275 Characterization of the Hepatic Metabolome of Migrating Sockeye Salmon in British Columbia, Canada.**

J. P. Benskin<sup>1,2</sup>, M. G. Ikonomou<sup>2</sup>, N. Veldhoen<sup>3</sup>, C. Dubetz<sup>2</sup>, C. C. Helbing<sup>3</sup> and J. R. Cosgrove<sup>1</sup>. <sup>1</sup>Product Development, AXYS Analytical Services Ltd., Sidney, BC, Canada; <sup>2</sup>Fisheries and Oceans Canada, Institute of Ocean Sciences, Sidney, BC, Canada; <sup>3</sup>Biochemistry and Microbiology, University of Victoria, Victoria, BC, Canada.

The health of British Columbia wild sockeye salmon (*Onchorhynchus nerka*) is of increasing concern due to recent extreme variation in the number of fish returning to spawn annually. Causes of this variability are unclear but may be related to contaminant or viral exposures, climate change, or food shortages. Two key migratory routes for Pacific sockeye are the Fraser and Skeena River watersheds. These watersheds represent highly contrasting environments for spawning salmon; the former flows through populous and industrialized regions of Vancouver, while the latter flows through fairly remote regions with little industrial input. A recent comparison of hepatic mRNA profiles between Fraser and Skeena sockeye revealed stark differences in estrogen-associated signaling in Skeena fish, despite these fish spawn in a relatively pristine environment. In contrast, the status of hepatic gene transcripts for Fraser River sockeye showed normal reproduction-related changes in estrogen-associated signaling. To expand upon available toxicological endpoints and further define potential sources of exposure resulting in the observed hepatic mRNA profiles in Skeena River salmon, we compared aspects of the hepatic metabolome of fish from both populations. A total of 186 metabolites from 6 different metabolite classes were measured using a recently developed assay. Molecular targets included acylcarnitines (n=40), amino acids (n=21), glycerophospholipids (n=90),  $\Sigma$ hexose, sphingolipids (n=15), and biogenic amines (n=19). Major metabolites quantified in Sockeye salmon liver included glycine, carnitine, phosphatidylcholine acyl-alkyl C38:6, and sphingomyeline C24:1. The combined transcriptomic and metabolomic data provides a comprehensive molecular profile of fish health, and sheds light on the biochemical changes arising from alteration of estrogen-associated signaling.

**PS 276 Elevated Metals and Organic Concentrations Linked to Biomarkers' Alterations in Organisms Exposed to Mining Effluent.**

O. T. Olubambi and V. Wepener. Centre for Aquatic Research, Department of Zoology, University of Joburg, Johannesburg, South Africa.

The Blesbokspuit wetland, South Africa, continuously receives diffuse and point source releases of mining effluent till date. Results are presented from a first time study conducted in the system on metals and organic bio-accumulation in sediments, residents and transplanted organisms. A suite of biomarkers assay was also carried out in bio-indicators. During the 2008 low and high flow periods, resident catfish, *Clarias gariepinus* and tilapia, *Tilapia sparrmanii* species were collected from 5 sites in a field survey. During the 2009 high flow, a transplantation study (active bio-monitoring - ABM) was conducted using laboratory reared *Tilapia* spp. at four of the five sites in cages for four weeks. Biomarkers of exposure: cytochrome P-450 (CYT-P450) and acetylcholine esterase (AChE) and biomarkers of effect: catalase (CAT) and superoxide dismutase (SOD) responses were determined in all samples. Metal and organic concentrations measured varied among sites and were elevated ( $p < 0.05$ ) during the field survey high flow than the low flow in most cases. This was always high for both periods in Site 1 which is upstream and close to mine dumps. Biomarkers were found altered both in resident and transplanted organisms at all sites. For example, triggered CAT activity and inhibition of SOD both indicative of oxidative stress was observed. CYT-P450 and AChE activities inhibition, which indicates organometallic and pesticides exposure was also observed. Biomarker responses were similar for both resident and transplanted fishes for the high flow periods ( $p < 0.05$ ). Site 5 (reference site) generally showed the least altered responses during the field survey low flow but not during the high flow and ABM. Biomarkers were able to successfully demonstrate biological effects from toxicants in the system. It was possible to link these effects to observed elevated metal and organic concentrations found in bio-indicators. This approach can be applied within the proposed integrated management plan for the Blesbokspuit as well as other catchments.

**PS 277 Effects of Two Progestins, Norethindrone and Levonorgestrel, on Reproduction in a Marine Fish, *Tautoglabrus adspersus*.**

L. Mills<sup>1</sup>, D. Borsay Horowitz<sup>1</sup>, G. Zarogian<sup>1</sup>, B. Rashleigh<sup>1</sup>, B. W. Riffle<sup>2</sup> and S. C. Laws<sup>2</sup>. <sup>1</sup>Atlantic Ecology Division, US EPA, ORD, NHEERL, Narragansett, RI; <sup>2</sup>Toxicology Assessment Division, US EPA, ORD, NHEERL, Research Triangle Park, NC.

Endocrine-active pharmaceuticals that enter the aquatic environment through sewage effluent may have unintended impacts on reproduction in fish, which in turn may affect the sustainability of exposed populations. Laboratory experiments were conducted with the marine fish cunner (*Tautoglabrus adspersus*) to evaluate whether norethindrone (NOR) and levonorgestrel (LNG) affected reproduction in spawning adults. Both progestins are used in human contraceptive formulations and have been detected in low (ng/L) concentrations in aquatic environments. Synthetic progestins in aquatic environments are of special concern because some fish use natural progesterones as pheromones to coordinate reproduction, and evidence suggests progestins may be selectively taken up through the gills in some species. Reproductive endpoints of egg production, viability and fertility were assessed daily in spawning cunner treated with NOR or LNG (nominal concentrations of 0, 0.075 or 0.75 mg/kg) by oral gavage on days 0, 4, 8, 12 and 16 of the experiment. All fish were sacrificed on day 17 and gonadosomatic index (GSI) was determined. In NOR-treated fish, egg production per gram female was significantly reduced relative to controls at both concentrations, while egg fertility and viability was notably decreased, although not significantly, only in the 0.75 mg/kg treatment. GSI was significantly reduced in both males and females from the 0.75 mg/kg treatment. Female mortality in this treatment group was more than twice that in controls, indicating an increase in male aggression. In LNG-treated cunner, no significant effect was seen on egg production, fertility, viability, or GSI compared to control fish. Results indicate some progestins can impact fish reproduction, even in short-term exposures. Research is planned to determine if these fish selectively take up progestins from the aquatic environment. This abstract does not reflect U.S. EPA policy.

**PS 278 Effects of Fungicides on Honey Bee Development and Behavior.**

L. A. Hoooven. Oregon State University, Corvallis, OR.

Pesticides may contribute to the health challenges facing honey bees. Bees experience chronic exposures through contaminated beeswax and stored pollen and honey. There is a need to study possible sublethal or delayed effects from such exposures, which may ultimately result in the collapse of the colony. Fungicides are thought to have little effect on insects, and are routinely sprayed while bees are pollinating crops. Multiple fungicides are transported with pollen into the colony, and some are known to persist in beeswax. Beekeepers suspect that fungicides may have an effect on honey bee development, and some laboratory tests have demonstrated adverse effects of fungicides on bee larvae. We have developed laboratory methods to chronically expose young adult bees to pesticide-contaminated beeswax, in concentrations similar to those found in hives. By using Noldus Ethovision to track the behavior of bees on video, we have found that the major contaminants of beeswax, including the fungicide chlorothalonil, delay behavioral development as measured by the initiation of circadian activity rhythms. Young adult bees consume pollen and secrete proteinaceous brood food and royal jelly to feed developing larva and the queen. In semi-field experiments, we fed pollen spiked with fungicides to colonies of bees, similar to field concentrations. By evaluating colonies weekly, we found that chlorothalonil and iprodione affect larval development, and ziram affects queen health several weeks after initial exposure. These results suggest that chronic contact exposure through wax and ingestion of fungicides through pollen may target the development and social function of young worker bees, and may have detrimental effects on the colony.

**PS 279 The Mediterranean Gecko, *Hemidactylus turcicus* (Gekkonidae : Squamata)—An Alternative Model for the Study of Redox Potential.**

M. Y. Farooqui and R. Bloom. Biology, University of Texas Pan American, Edinburg, TX.

Glutathione and similar sulfhydryl groups play an important role in redox cycling in mammals. In this study we have investigated the role of sulfhydryls in the Mediterranean Gecko, *Hemidactylus turcicus* (Gekkonidae : Squamata). Concentrations of hepatic sulfhydryls were determined in the field controls and the geckos maintained at various temperatures. Concentrations of sulfhydryls in livers

of field controls were  $46.3 \pm 5$   $\mu\text{moles/g}$  and were significantly elevated (141 and 151 % of controls) in geckos maintained at 15 and 100°C, respectively. Female geckos had significantly higher (139 %) concentrations of sulfhydryls than did the males. This study indicates that this oxidative biochemical pathway is operative in geckos. Geckos may provide a very inexpensive alternative animal model for redox studies.

## PS 280 Recent Emergence of Perfluorohexanoate in Tap, River, and Sea Water in Japan.

N. Saito, K. Sasaki and S. Tsuda. *Iwate Institute of Environmental Health Sciences, Morioka, Japan.*

Environmental waters such as river water (RW) and sea water (SW) are expected to be the major exposure sources of Perfluoroalkyl acids (PFAA) to humans via tap water (TW) and food fish. At the 2012 Annual Meeting of SOT, we reported the trend in PFAA contaminations in Japanese RW and TW from 2003 to 2010, based on the results of measurement of Perfluorocarboxylates (from C5 to C12 carbon backbone) and perfluorosulfonates (CS4, CS6, CS8 and CS10). The major PFAA (C6, C8, C9 and CS8) concentrations in both RW and TW were always highest in Kinki area. In 2010 extremely high RW C6 concentrations (46 and 24  $\mu\text{g/L}$ ) were detected in the lower reaches at the foot of a fluorochemical plant, where extremely high concentrations of C8 (67 and 24  $\mu\text{g/L}$ ) had been detected in 2003. From 2003 to 2010, Kinki showed drastic reduction of RW C8 concentration to one tenth. C6 concentration in TW in 2007 showed as low as 2.3 % of RW in 2010 compared to 42.3% for that of C8. The conclusion there was that the release of C6 to the environment had begun recently from the source in Kinki. In the present study, we measured PFAA (from C4 to C16; and CS4, CS6, CS8 and CS10) in RW (12 locations) and TW (6 locations) in the Kinki area and costal SW around Japan (31 locations) collected in 2011 using LC-MS/MS. The highest RW Perfluorocarboxylates (from C4 to C10) were detected in the lower reaches at the foot of the fluorochemical plant (for C6: 49 and 43  $\mu\text{g/L}$ ). The highest TW C6 concentration in the 2011 samples was 2.85 ng/L, which was greater than the highest C6 concentration (1.51 ng/L) in the 2007 samples. The highest SW C6 concentration in Kinki was far greater than the samples from the other areas and was 129 ng/L. From these results it was concluded that C6 release from the source to the river of recent onset is rapidly contaminating surrounding SW and gradually contaminating TW in the nearby areas.

## PS 281 Distributions of Metals (Cadmium, Lead, Iron, Manganese, Zinc, and Copper) in Water, Aquatic Plant, and Fish.

K. A. Abdou<sup>1</sup>, A. S. Mahmoud<sup>2</sup>, M. S. Housen<sup>1</sup> and K. I. Ahmed<sup>1</sup>. <sup>1</sup>Department of Toxicology and Forensic Medicine, Faculty of Veterinary Medicine, Beni Suef University, Beni Suef, Egypt; <sup>2</sup>Department of Toxicology and Forensic Medicine, Faculty of Veterinary Medicine, Assiut University, Assiut, Egypt. Sponsor: A. Kadry.

Concentrations of cadmium (Cd), lead (Pb), iron (Fe), manganese (Mn), zinc (Zn) and copper (Cu) were measured in water, Ceratophyllum demersum (C. demersum) aquatic plant, Clarias lazera fish (C. lazera) collected from nine sampling stations along El Ebrahimia canal and two districts located at the east bank of the Nile in the province of Beni Suef, Egypt during 2009-2010.

Atomic Absorption analysis revealed that the studied metals were higher than the limit of detection (LOD) in all the examined samples. In water, Pb had the highest concentration among the metals detected in seven of the nine tested locations (0.3 - 0.9 ppm). The concentrations of Pb, Fe, and Mn were above the maximum Egyptian permitted limits in all tested sites, while Zn and Cu concentrations were below the permitted limits (4 mg/l and 2 mg/l) in the nine districts. Comparisons were made of the metal concentrations in water and aquatic plants with those in the catfish tissues obtained from water. The metal concentrations found in the C. demersum aquatic plant samples taken in the nine studied districts were distributed in this order;  $\text{Mn} > \text{Zn} > \text{Cu} > \text{Pb} > \text{Fe} > \text{Cd}$ , and were higher than the water. In fish, metals accumulated in the various examined tissues at several levels, but the metal concentrations in muscles (edible part) were below the metal levels in the other organs (nonedible) in the fish samples. The concentrations of Cd, Pb and Fe in fish tissues were above the international standard, while the concentrations of Mn, Zn and Cu were below this standard. The high concentrations of these metals in water, aquatic plants and fish in El Ebrahimia canal may be the result of both anthropogenic activities producing industrial, agricultural and domestic waste and accidental pollution incidents.

## PS 282 Cytochrome P450 Monooxygenases Expression in Human Epithelial Lung Cell Lines.

M. Niehof and T. Hansen. *Fraunhofer ITEM, Hannover, Germany.* Sponsor: C. Dasenbrock.

The pulmonary epithelium is the first barrier for airborne xenobiotics and inhaled drugs. Cytochrome P450 monooxygenases (CYP) participate in metabolic inactivation of xenobiotics. Beyond that some compounds require enzymatic activation to exert their toxic effects or their desirable functions. The bronchial epithelial cell line Calu-3 and the type II-like pulmonary epithelial cell line A549 serve as cell culture models for the human respiratory epithelium. So far, there is little information regarding their metabolic properties especially for Calu-3 cells. The goal of this study was to further characterize both cell lines regarding their basal and inducible CYP isoform expression.

CYP expression was determined using real-time reverse transcription quantitative polymerase chain reaction (RT-qPCR). Basal expression of CYP1B1, CYP1A1, CYP2D6, CYP2B6/7, CYP3A5, and CYP2J2, and slight amounts of further CYPs were detected in both cell lines, which is consistent with expression in the human lung.

Furthermore, potential CYP inducers were analyzed. Omeprazole acts on aryl hydrocarbon receptor (AhR) activation and induced CYP1A1 and CYP1B1 in both cell lines. Rifampicin acts on pregnane x receptor (PXR) and phenobarbital acts predominantly on constitutive androstane receptor (CAR), however, both receptors are not expressed in the lung. Accordingly, both agents did not induce any CYP in these cells. Besides PXR, dexamethasone acts on glucocorticoid receptors and we found induction of members of the CYP3A family, mainly CYP3A7 in Calu-3 cells, and CYP3A5 and CYP3A7 in A549 cells. CITCO is known to act as a CAR agonist and is normally used to induce CYP2B6/7. However, it is a potent inducer of CYP1B1 in Calu-3 cells, and of CYP1A1 and CYP1B1 in A549 cells.

Thus, Calu-3 cells and A549 cells express a broad range of CYPs with preserved inducibility and are valuable models of the airway epithelial barrier for metabolic in vitro experiments.

## PS 283 Role of Renal Proximal Tubule P450 Enzymes in Chloroform-Induced Nephrotoxicity.

S. Liu<sup>1,2</sup>, Y. Yao<sup>1</sup>, S. Lu<sup>1</sup>, X. Ding<sup>1</sup>, C. Mei<sup>1</sup> and J. Gu<sup>1</sup>. <sup>1</sup>Wadsworth Center, Albany, NY; <sup>2</sup>Changzheng Hospital, Shanghai, China.

The kidney is a primary target for numerous toxicants. Cytochrome P450 enzymes (P450s), responsible for the metabolic activation of various chemical compounds, are predominantly expressed in proximal tubules in the kidney. However, the specific role of proximal tubule P450s in chemical-induced nephrotoxicity is unclear. The aim of this study was to test the hypothesis that renal proximal tubule P450s are critical for the metabolic activation and nephrotoxicity of chloroform. To test this hypothesis, we have developed two new mouse models, one having proximal tubule-specific deletion of the cytochrome P450 reductase (Cpr) gene (the enzyme required for all microsomal P450 activities), named kidney-Cpr-null, and the other with proximal tubule-specific rescue of CPR activity in a model with global suppression of CPR activity in all extra-renal tissues, named extra-renal Cpr-low. The kidney-Cpr-null, extra-renal-Cpr-low, Cpr-low, and wild-type (WT) control mice were treated with a single oral dose of chloroform at 200 mg/kg. Blood, liver and kidney samples were obtained at 24 h after the treatment. Kidney toxicity was assessed by measuring serum levels of BUN and creatinine, and by pathological examination. The blood and tissue levels of chloroform were also determined. Chloroform-induced proximal tubular lesions and increases in BUN and creatinine levels were observed in all four genotypes, but the severity of toxicity was less in kidney-Cpr-null and Cpr-low mice, compared to WT and extra-renal-Cpr low mice, respectively. There was no significant difference in chloroform levels in the blood, liver, or kidney, between kidney-Cpr-null and WT mice, or between extra-renal-Cpr-low and Cpr-low mice. These findings indicate that local P450 dependent metabolic activation plays an important role in renal toxicity induced by chloroform. Our results also demonstrate the utility of these novel mouse models for studies on the renal toxicity of other chemicals.

## PS 284 Green Tea Epigallocatechin Gallate Inhibits Drug Metabolizing Enzymes by Covalent-Binding to the Proteins and Formation of Protein Aggregates.

Z. Weng and Q. Shi. *Division of Systems Biology, US FDA, NCTR, Jefferson, AR.* Sponsor: X. Yang.

Green tea supplements have been reported to cause hepatotoxicity but the mechanisms of the toxic metabolite, epigallocatechin gallate (EGCG), are unknown. In this study, the rat liver microsomes were treated with 1 - 100  $\mu\text{M}$  EGCG for 30

min, and the EGCG-binding proteins were affinity purified and probed with antibodies against glyceraldehyde-3-phosphate dehydrogenase (GAPDH), actin, cytochrome P450 (CYP) 1A1, CYP1A2, CYP2B1/2, CYP2E1, CYP3A, catechol-O-methyltransferase (COMT) and microsomal glutathione transferase 1 (MGST1). All but actin and soluble COMT were positively detected at  $\geq 1 \mu\text{M}$  EGCG, indicating EGCG selectively bound to a subset of proteins including membrane-bound COMT. The binding correlated well with inhibition of CYP activities, except for CYP2E1 whose activity was unaffected despite evident binding. When microsomes were probed on Western Blots, all but the actin and CYP2E1 antibodies showed a significant reduction in binding at  $\geq 1 \mu\text{M}$  EGCG, suggesting that a fraction of the indicated proteins formed aggregates that were not recognizable by antibodies against the intact proteins. Protein aggregate formation was also observed in Coomassie Blue-stained SDS-PAGE gels. EGCG effects were partially abolished in the presence of 1 mM glutathione. We conclude that EGCG inhibits drug metabolizing enzymes by covalent-binding to the target proteins and formation of protein aggregates.

## PS 285 Metabolism of Rutaecarpine in Freshly Isolated Hepatocytes from Rats and Mice.

T. Jeong, D. Lee, D. Oh, J. Kim, Y. Jahng and M. Kang. *Pharmacy, Yeungnam University, Gyeongsan, Republic of Korea.*

Rutaecarpine is an alkaloid originally isolated from *Evodia rutaecarpa* that has been used for the treatment of gastrointestinal disorders in Asia. In the present study, Phase I and Phase II metabolisms of rutaecarpine were investigated in freshly isolated hepatocytes from rats and mice. The results indicated that the metabolism of rutaecarpine in rats and mice was different. When rutaecarpine was incubated with fresh hepatocytes isolated from either rats or mice for 2 hr, 5 major Phase I metabolites were observed in both hepatocytes with different extents. Likewise, the production of sulfate conjugates also showed difference. In rat hepatocytes, 4 sulfate conjugates were observed, whereas only two conjugates were observed in murine hepatocytes. The results indicated that the species selection would be concerned in the process of preclinical investigation. Supported by a grant from National Research Foundation of Korea (2010-00266220).

## PS 286 Effects of Intestinal Microflora on Oral Pharmacokinetics of Baicalin in Normal and Antibiotic-Treated Mice.

D. Oh, M. Kong, J. Kim, M. Kang, W. Kang and T. Jeong. *Pharmacy, Yeungnam University, Gyeongsan, Republic of Korea.*

Baicalin (baicalein-7-glucuronide) is an ingredient of *Scutellaria baicalensis* Georgi that has been used as one of the most popular herbs in Korea for treatment of inflammation, cardiovascular diseases, hypertension, and microbial infections. In the present study, effects of intestinal microflora on oral pharmacokinetics of baicalin were investigated in normal SPF and antibiotic-treated mice. To control the number of intestinal bacteria, mice were pre-treated orally with erythromycin, oxytetracycline and cefadroxil for 3 consecutive days, followed by an oral administration with 100 mg/kg baicalin. Then baicalin and its possible metabolites in serum were determined by using liquid chromatography/electrospray ionization mass spectrometry. By the pre-treatment with antibiotics, the number of intestinal microflora was significantly reduced. In addition, serum concentrations of baicalin and its metabolite, baicalein-6-glucuronide, were remarkably changed by treatment with antibiotics when compared with control mice. These results indicated that the intestinal microflora might have a critical role in modulating oral pharmacokinetics of baicalin. Supported by the grant from KFDA (09172KFDA996) and from National Research Foundation of Korea (2010-00266220).

## PS 287 Role of Intestinal Microflora in Oral Pharmacokinetics of Baicalin in a Germ-Free Mouse Model.

J. Kim<sup>1</sup>, D. Oh<sup>1</sup>, M. Kang<sup>1</sup>, W. Yun<sup>2</sup>, H. Kim<sup>2</sup> and T. Jeong<sup>1</sup>. <sup>1</sup>Pharmacy, Yeungnam University, Gyeongsan, Republic of Korea; <sup>2</sup>Biomedical Mouse Resource Center, KRIBB, Ochang, Republic of Korea.

Baicalin and its aglycone baicalein are bioactive flavonoids originally isolated from the root of *Scutellaria baicalensis* Georgi, a medicinal plant that has been used for the treatment of inflammation, hypertension, cardiovascular and allergic diseases. In the present study, role of intestinal microflora in baicalin metabolism was investigated following a single oral administration with 100 mg/kg baicalin in germ-free and control mice. Baicalin and its metabolites were determined by HPLC coupled with a tandem mass spectrometry. Serum concentrations of baicalin and its

metabolite in germ-free animals were significantly lower than those in control mice having normal intestinal microflora. Likewise, transient hepatotoxicity induced by baicalin in germ-free mice was significantly different from that in control mice. These results indicated that the intestinal microflora might play a key role in metabolism of baicalin orally ingested. Supported by the grant from KFDA (09172KFDA996) and from National Research Foundation of Korea (2010-00266220).

## PS 288 Importance of Chirality Considerations in Risk Assessments: Enantiomer-Specific Pharmacological Metabolism with Rainbow Trout (*Oncorhynchus mykiss*) S9.

K. Connors<sup>1</sup>, B. Du<sup>1</sup>, P. N. Fitzsimmons<sup>2</sup>, C. K. Chambliss<sup>1</sup>, J. W. Nichols<sup>2</sup> and B. W. Brooks<sup>1</sup>. <sup>1</sup>Baylor University, Waco, TX; <sup>2</sup>US EPA, Duluth, MN.

Enantiomers are capable of having significantly different biological effects, selectivity for receptors/transporters/enzymes, potency, and biodegradation rates. Differences in environmental fate, bioavailability and toxicity have also been reported. Despite this knowledge, enantiomers are often treated as a single chemical entity in environmental monitoring and risk assessment. Enantiomer-specific differences in pharmaceuticals are especially well documented within mammalian literature. Finding a way to leverage existing pharmaceutical safety data and pharmacology information through biological "read-across" may aid our ability to perform more accurate environmental assessments. In this study, we examined the comparative metabolism of R, S and the racemate of three pharmaceuticals (propranolol, ibuprofen and fluoxetine) in rainbow trout liver S9 using a substrate depletion approach. An isotope dilution liquid chromatography tandem mass spectrometry (LC-MS/MS) method was employed for quantitation of parent chemical concentrations. Differential substrate depletion rates were observed for propranolol enantiomers. The fastest clearances rates were observed with rac-propranolol, followed by S and R-propranolol, respectively. Ibuprofen appeared to undergo limited metabolism; however, the resulting depletion curves did not differ statistically from those obtained for denatured controls. No substrate depletion was observed for rac, R or S fluoxetine. Mammalian clearance rates will be compared and risk assessment implications discussed.

## PS 289 The Role of Interstrain Differences in Trichloroethylene Metabolism in Kidney Effects in Mice.

H. Yoo, B. U. Bradford, L. B. Collins, O. Kosyk, S. Shymonyak, W. M. Bodnar, L. M. Ball, A. Gold and L. Rusyn. *Department of Environmental Sciences and Engineering, University of North Carolina at Chapel Hill, Chapel Hill, NC.*

Trichloroethylene (TCE) is a well-known environmental and occupational toxicant contaminating air, water, and soil. The U.S. EPA recently issued the final IRIS assessment of TCE and classified TCE as carcinogenic to humans. Still, several issues critical for assessing human health risks from TCE remain unresolved, such as (1) the amount of glutathione (GSH)-conjugated metabolites formed in various tissues, and possible inter-individual and inter-species differences; and (2) the mode of action involved in kidney toxicity/carcinogenesis. The aim of this study was to use a panel of inbred mouse strains to investigate the relationship between inter-strain differences in TCE metabolism and kidney toxicity. TCE (600 mg/kg/day, in 5% Alkamuls EL-620 in saline) was administered by gavage to male mice (6-8 weeks old) from 7 inbred strains (129S1/SvImJ, A/J, BTBR T+tf/J, C57BL/6J, CAST/EiJ, NOD/ShiLtJ, NZW/LacJ) for 5 days. Liver, kidney, and serum were collected at 2 and 8 hrs after the last dose. Quantification of S-(1,2-dichlorovinyl)glutathione (DCVG), S-(1,2-dichlorovinyl)-L-cysteine (DCVC), and trichloroethanol (TCOH) was performed. In addition, blood urea nitrogen, kidney-to-body weight ratio, proximal tubular cell proliferation, expression of peroxisome proliferator marker genes (*Ppara*, *Acox1*, and *Cyp4a10*), kidney injury molecule-1 in kidney were evaluated. Inter-strain variability in the levels of DCVG, DCVC, and TCOH in liver, serum, and kidney were observed. Overall, the level of TCOH was 10,000-fold greater than that of DCVG and DCVC in both liver and kidney. In conclusion, the inter-strain differences in TCE metabolism provide a mechanistic basis for examining the inter-strain differences in TCE organ-specific toxicity. This work was supported by the Superfund Basic Research Program grant P42 ES005948.

**PS 290 Interpretation of Multiroute Data for Chloroform-Induced Renal Toxicity in Rats and Mice Using an Updated Physiologically-Based Pharmacokinetic Model.**

A. F. Sasso<sup>1</sup>, P. M. Schlosser<sup>2</sup>, G. L. Kedderis<sup>6</sup>, M. Genter<sup>3</sup>, J. E. Snawder<sup>4</sup>, Z. Li<sup>1</sup>, S. Rieth<sup>1</sup> and J. C. Lipscomb<sup>5</sup>. <sup>1</sup>National Center for Environmental Assessment, US EPA, Washington DC; <sup>2</sup>National Center for Environmental Assessment, US EPA, Research Triangle Park, NC; <sup>3</sup>Department of Environmental Health and Center for Environmental Genetics, University of Cincinnati, Cincinnati, OH; <sup>4</sup>NIOBH, CDC, Cincinnati, OH; <sup>5</sup>National Center for Environmental Assessment, US EPA, Cincinnati, OH; <sup>6</sup>Independent Consultant, Chapel Hill, NC.

Chloroform (CF) is a trihalomethane present in drinking water as a byproduct of disinfection, and the kidney is one of the targets of toxicity in experimental animals. Since CF induces toxic effects via production of reactive metabolites, proper characterization of metabolism is essential for risk assessment. A revised physiologically-based pharmacokinetic (PBPK) model, in conjunction with benchmark dose (BMD) modeling, was used to interpret rat and mouse renal toxicity markers in three oral and inhalation studies. Large species differences in potency as a function of external dose became minimal when expressed in terms of a renal dose metric (daily mg CF metabolized per L cortex), indicating that species differences in susceptibility may be primarily mediated by toxicokinetics, rather than differences in toxicodynamics. The external BMD result for nuclear enlargement was 6 ppm for the mouse, but 40 ppm for the rat—a 7-fold difference. When the measure of dose was changed from inhaled concentration to the renal dose metric, the BMD result becomes 62 mg/L in the mouse, and 47 mg/L in the rat—a difference of 30%. Since results derived from drinking water data were also consistent with inhalation data, the work presented here increases confidence in the PBPK model, and the use of site-specific chloroform metabolism as the internal dose-metric. The views expressed in this publication are those of the authors and do not represent the views and policies of their respective Agencies

**PS 291 The Use of Cytochrome P450-Embedded Nanodisks to Enhance Metabolism and Elimination of Chemical Toxicants.**

M. Malfatti<sup>1</sup>, E. Kuhn<sup>1</sup>, A. Kohlgruber<sup>1</sup>, Y. Li<sup>2</sup>, K. Lam<sup>2</sup> and M. Coleman<sup>1</sup>. <sup>1</sup>Lawrence Livermore National Laboratory, Livermore, CA; <sup>2</sup>University of California Davis, Davis, CA.

Exposure to toxic chemicals and how to eliminate them from the body is a topic of great concern. Developing safe and effective methods that can mitigate exposures is critical for responding to many different exposure scenarios. In this study we are capitalizing on the body's endogenous detoxification capabilities by supplementing existing metabolic enzymes to increase the natural capacity for transforming toxic agents into less harmful constituents. We are developing a novel system that packages cytochrome P450 proteins, liposomes, and telodendrimer into nanodisks, in an effort to enhance the metabolism of toxic chemicals into inactive compounds. Microsomes expressing human cytochrome P4503A4 (CYP3A4) were combined with POPC lipid and 1% telodendrimer, comprised of an octamer of cholic acid linked to the terminal end of a linear 5kDa PEG molecule. Assembly of CYP3A4 telodendrimer nanodisks (TND) was achieved after overnight incubation at 4° C. Activity of CYP3A4 in the TND was assessed by fluorescent intensity, using the P450-Glo assay (Promega), and determined to be 57.0 FU. This was comparable to the CYP3A4 positive control of 64.8 FU, indicating successful incorporation of functional CYP3A4 into the TND. Functional stability was assessed by monitoring TND-CYP3A4 activity over time at 4° C. TND-CYP3A4 activity was stable for 7 days post assembly. After 7 days, activity decreased by 42% and remained at that level for the 24-day study duration. In vitro metabolism tests demonstrated that the TND was able to metabolize the model substrate testosterone to 6 $\beta$ -OH-testosterone at rates comparable to the CYP3A4 microsomal control incubations. These results indicate that this system has the potential to improve one's ability to detoxify chemicals. Further studies are needed to determine the capability of the TNDs to metabolize chemicals in vivo.

This work was performed under the auspices of the U.S. DOE by LLNL under Contract DE-AC52-07NA27344 and supported by LLNL LDRD 11-ERD-012.

**PS 292 Sulfonation of 1-Methyl-Phenanthrene and 9-Ethyl-Phenanthrene in Human Hepatoma (HepG2) Cells.**

M. Huang, I. A. Blair and T. M. Penning. Centers of Excellence in Environmental Toxicology and Cancer Pharmacology, Department of Pharmacology, University of Pennsylvania, Philadelphia, PA.

Exposure to petrogenic polycyclic aromatic hydrocarbons (PAHs) in the food-chain is the major human health hazard associated with the Deepwater Horizon gulf-oil spill. Risk assessment is based on the assumption that petrogenic and pyrogenic

PAHs have similar toxicological profiles yet information on the metabolism of petrogenic PAHs is lacking. We report the metabolic fate of 1-methyl-phenanthrene and 9-ethyl-phenanthrene as representative alkylated petrogenic PAHs in human hepatoma (HepG2) cells. The structures of the metabolites were identified by HPLC-UV-fluorescence detection and LC-MS/MS. Both 1-methyl-phenanthrene and 9-ethyl-phenanthrene showed the formation of O-sulfated mono-phenols, O-sulfated bis-phenols, O-sulfated dihydrodiols, and O-sulfated catechols. The identification of these sulfate conjugates supports metabolic activation of 1-methyl-phenanthrene and 9-ethyl-phenanthrene by P450 and AKR isozymes followed by metabolic detoxification by SULT isozymes. (Supported by U19ES020676-01 to TMP)

**PS 293 N-Acetyltransferase 1 (NAT1) Expression and Activity during Keratinocyte Differentiation and Cell Cycle Progression.**

J. Bonifas and B. Blömeke. Environmental Toxicology, University of Trier, Trier, Germany.

N-acetyltransferase 1 (NAT1) dependent N-acetylation is an important detoxification pathway for arylamines including certain dyes. Proliferating keratinocytes have high N-acetylation capacities, but the influence of differentiation on NAT1 is not clear.

Keratinocyte differentiation is associated with an arrest of cells in the G0/G1 phase of the cell cycle. In order to analyze NAT1 regulation in the different cell cycle phases we synchronized HaCaT keratinocytes by serum starvation (83 $\pm$ 4% G0/G1) and re-addition for 20hrs (66 $\pm$ 1.7% S-phase) as well as by double thymidine block (68 $\pm$ 2% G0/G1, 72 $\pm$ 6% S-Phase) and analyzed NAT1 activity, protein and mRNA expression. In line with the high N-acetylation capacity of the skin, NAT1 activity was, compared to S-phase, elevated (about 40 $\pm$ 2%) in the G0/G1 phase, which is the predominant state of keratinocytes in the epidermis. NAT1 protein levels were also higher in G0/G1 phase, while NAT1 promoter P1 dependent steady state mRNA levels were not enhanced.

In the next step, we differentiated the keratinocyte cell line HaCaT and primary keratinocytes in vitro and analyzed NAT1 mRNA expression and NAT1 activity. With increasing differentiation we found no NAT1 variation after in vitro differentiation and detected NAT1 protein staining throughout the entire epidermis using human skin slices.

These results indicate that in vitro differentiated keratinocytes do not lose N-acetylation capacity, although cell proliferation is terminated, possibly due to high NAT1 activities in G0/G1 phase arrested cells. However, variations of the keratinocyte cell cycle phase distribution may influence NAT1 activity and thereby detoxification capacities.

**PS 294 Characterization of Peroxidase Activity in SkinEthic™ Reconstructed Skin Models Compared with Ex Vivo Human Skin Samples.**

J. Eilstein, G. Lereaux, A. Garrigues-Mazert, J. Meunier and D. Duché. L'Oréal Research & Innovation - Advanced Research, Aulnay-sous-Bois, France. Sponsor: E. Dufour.

Skin metabolism is becoming a major consideration in the development of new cosmetic ingredients, skin being the first organ exposed to them. Consequently, the use of ex vivo samples of normal human skin (NHS) or reconstructed human skin models (skin models) as alternative tools to animal testing requires to characterize and compare their abilities to metabolize xenobiotics. In this work, we determined if they possessed a functional peroxidase activity. Previous studies showed that NHS and skin models from SkinEthic™ Laboratories such as Episkin™, SkinEthic-RHE™ and the full thickness model of Episkin™ expressed the mRNAs of several peroxidase isoforms (mainly in GPx and COX families). The catalytic activity of these enzymes was measured from dose-response studies using cumene hydroperoxide as substrate. Apparent Vmax, Km and ratio Vmax/Km (assessing metabolic clearance) were calculated for each biological model from 2-phenyl-2-propanol quantification. Results showed that in NHS and skin models, a peroxidase activity was demonstrated to be functional and that the obtained enzymatic parameters could be influenced by the lack of the glutathione co-factor. To conclude, a peroxidase activity is present and functional in NHS and skin models which can be easily used for studying the biotransformation process of peroxides and assessing their impact on cellular biomarkers.

**PS 295 Covalent Thiol Adducts Arising from Cocaine and Morphine Biotransformation.**

K. J. Schneider and A. P. DeCaprio. *Department of Chemistry & Biochemistry and International Forensic Research Institute, Florida International University, Miami, FL.*

Covalent protein adduction, which can underlie drug toxicity and/or reflect exposure, is largely unstudied in the case of illicit drugs of abuse. This research investigates the formation of protein adducts resulting from cocaine and morphine biotransformation using *in vitro* assay systems. Human liver microsomal preparations were incubated for 1.5 or 6 h with cocaine or morphine in the presence of thiol-containing trapping agents at 37°C, pH 7.4. Thiols included N-acetylcysteine (NAC), glutathione (GSH), and a synthetic hexapeptide (AcPAACAA). Microsomes were removed by centrifugation and supernatants were subjected to LC-MS/MS analysis for characterization of metabolites and adducts. Isomeric hydroxycocaine adducts from thiol adduction on the arene ring were the major products with all three model thiols. Eight isomers of cocaine-adducted NAC were separated and characterized. While the structural complexity of adducted GSH and model peptide diminished the ability to separate isomers, MS/MS data supported adduct structures analogous to those with NAC. With morphine, two distinct metabolites were identified as the likely species responsible for thiol adduction, the known reactive metabolite morphinone and a novel metabolite, morphine quinone methide. Reaction between morphinone and NAC formed two isomeric products which underwent secondary reduction to form three additional stereoisomeric products. Likewise, morphine quinone methide formed two structural isomers, although no secondary reduction was noted. Individual structural isomers of morphine adducts with GSH and AcPAACAA could not be isolated; however, morphine-derived adduction products were nevertheless present. Analysis using recombinant cytochrome P450s determined that formation of cocaine adduction products was mediated by CYPs 1A2, 2C19, and 2D6, while those from morphine were produced by CYP3A4. Results obtained from this study enhance the existing knowledge of illicit drug metabolism and demonstrate novel mechanisms for covalent protein modification by these compounds.

**PS 296 The Enantioselective Oxidation of 2, 2', 3, 3', 6, 6'-Hexachlorobiphenyl (PCB136) by Liver Microsomes Is Species Dependent.**

H. Lehmler, X. Wu and A. Kammerer. *Department of Occupational and Environmental Health, College of Public Health, The University of Iowa, Iowa City, IA.*

The adverse neurodevelopmental effects of chiral PCBs, such as PCB 136, are mediated by the enantiospecific sensitization of Ryanodine receptors and may be influenced by enantioselective PCB metabolism. Since the enantioselective disposition of PCBs is only poorly investigated, we tested the hypothesis that the enantioselective oxidation of PCB 136 to hydroxylated metabolites by liver microsomes is species dependent. Racemic PCB 136 was incubated with liver microsomes obtained from different species (i.e., male guinea pig, hamster, monkey, mouse, and rabbit; female dog) or pooled human liver microsomes. According to gas chromatographic analysis, 2,2',3,3',6,6'-hexachlorobiphenyl-4-ol (4-136) was the major metabolite in incubations with monkey, rabbit and human microsomes. 2,2',3,3',6,6'-Hexachlorobiphenyl-5-ol (5-136) was the major metabolite in incubations using dog, guinea pig, hamster and mouse microsomes. 4-136 to 5-136 ratios were 0.1, 0.1, 0.1, 13, 0.6, 1.7 and 1.8 for dog, guinea pig, hamster, monkey, mouse, rabbit and human microsomes, respectively. Furthermore, enantioselective analyses showed species-dependent difference in the enrichment pattern of atropisomers of 4-136 and 5-136. Taken together, these observations suggest that species-dependent enantioselective metabolism needs to be considered in studies investigating the developmental neurotoxicity of PCBs and other chiral pollutants.

**PS 297 CYP2F1 Expression and Activity Toward Naphthalene in a CYP2A13/2F1-Humanized Mouse Model.**

L. Li<sup>1</sup>, K. Jia<sup>1</sup>, Y. Wei<sup>1</sup>, L. V. Winkle<sup>2</sup> and X. Ding<sup>1</sup>. <sup>1</sup>Health Research Inc., Albany, NY; <sup>2</sup>Center for Health and the Environment, University of California Davis, Davis, CA.

The aim of this study is to characterize the expression and activity of CYP2F1, a human P450 expressed preferentially in the respiratory tract, using a recently generated CYP2A13/2B6/2F1-transgenic (TG) mouse model. CYP2F1 has been proposed to metabolize several lung toxicants, including naphthalene. However, conclusive data on how efficient CYP2F1 is in the bioactivation of these compounds are still unavailable, as it has been difficult to obtain functional CYP2F1 protein

through heterologous expression. Both CYP2F1 and CYP2A13, but not CYP2B6, are expressed in the lung and nasal mucosa (NM) of the TG mice. The level of CYP2A13 protein was 100 and 0.2 pmol/mg protein in nasal and lung microsomes, respectively, of the TG mice. The level of CYP2F1 protein was not determined previously, for lack of a suitable CYP2F1 standard. Here, using a newly developed LC-MS/MS method, we have determined that the level of CYP2F1 was 8 and 2 pmol/mg protein in nasal and lung microsomes, respectively, of the TG mice. To determine the activity of CYP2F1, we further crossed the TG mouse to a newly generated Cyp2abfgs-null (null) mouse, in which all mouse Cyp2abfgs genes are deleted, and the naphthalene bioactivating activities of nasal and lung microsomes were substantially decreased. In the resultant CYP2A13/2B6/2F1-humanized mice (TG/null), nasal and lung microsomal activity toward naphthalene was significant higher than in the null mice (2-fold for lung and 8-fold for NM). Thus, CYP2A13 and/or CYP2F1 are active toward naphthalene in the humanized mouse. Further analysis of the activities in the humanized mice provided evidence that, while the activity in the NM was primarily contributed by CYP2A13, the activity in the lung was mainly contributed by CYP2F1.

**PS 298 Effect of Vinclozolin Exposure during Pregnancy on *In Vitro* Testosterone Metabolism.**

F. G. García-Montes de Oca, M. L. Lopez-Gonzalez, D. C. Escobar-Wilches and A. Sierra-Santoyo. *Toxicology, CINVESTAV-IPN, Mexico City, Mexico.*

Vinclozolin (V) is a fungicide used for agricultural settings. V is classified as an endocrine disruptor by inhibiting competitively the androgen receptor. V exposure during pregnancy alters morphogenesis of the masculine reproductive system. V regulates liver cytochrome P450 (CYP) expression and may affect the biotransformation of endogenous substances, such as testosterone (T) which is an important hormone during pregnancy. There is no information about the effect of V exposure during pregnancy on testosterone metabolism. The objective of this study was to evaluate the effect of V exposure during the pregnancy on *in vitro* testosterone metabolism. Pregnant Wistar rats were orally administered with V at the dose of 150 mg/kg/d from gestational days 14 to 21 suspended in corn oil. Two control groups were included, pregnant and non-pregnant rats in oestrus phase and received only vehicle. Animals were sacrificed at 2 h after last dose by asphyxia with CO<sub>2</sub>. Liver was removed and processed to obtain microsomes to carry out *in vitro* enzyme assays using T as substrate. T and its metabolites were analyzed by HPLC. The pregnancy decreased 50% the liver total CYP content as well as the formation of metabolites 7 $\alpha$ -hydroxytestosterone (-OHT), 16 $\beta$ -OHT, androstenedione (AD) and 6 $\beta$ -OHT, 78, 40, 97 and 28%, respect to non-pregnant rats. V exposure significantly decreased the weight gain during pregnancy and increased 27% the content of total CYP, respect to the non-treated pregnant group. Moreover, V increased the formation of 7 $\alpha$ -OHT, 2 $\beta$ -OHT, 16 $\beta$ -OHT, AD, 6 $\beta$ -OHT and 16 $\alpha$ -OHT, 1.7-, 1.7-, 3.0-, 1.5-, 4.3- and 1.7-fold, respectively. These results suggest that V affects the pregnancy by reducing weight gain and modulates liver CYP expression. In addition, they also suggest that V exposure during pregnancy may alter the biotransformation of testosterone and affecting physiological processes regulated by this hormone. These effects may represent another mechanism of action associated to V exposure during the pregnancy.

**PS 299 *In Vitro* Metabolism of Benzo[a]pyrene and Dibenzo[Def, P]Chrysene in Rodents and Humans.**

S. Hanson-Drury<sup>1</sup>, S. R. Crowell<sup>1</sup>, J. Soelberg<sup>1</sup>, R. A. Corley<sup>1</sup> and D. E. Williams<sup>2</sup>. <sup>1</sup>Systems Toxicology, Pacific Northwest National Laboratory, Richland, WA; <sup>2</sup>Oregon State University, Corvallis, OR.

Polycyclic aromatic hydrocarbons (PAHs) are ubiquitous and often carcinogenic contaminants released into the environment during natural and anthropogenic combustion processes. Benzo[a]pyrene (BaP) is the prototypical carcinogenic PAH, and dibenzo[def,p]chrysene (DBC) is a less prevalent, but highly potent transplacental carcinogenic PAH. Both are metabolically activated by isoforms of the cytochrome P450 (CYP450) enzyme superfamily to form reactive carcinogenic and cytotoxic metabolites. Metabolism of BaP and DBC was studied in hepatic microsomes of male Sprague Dawley rats, naïve and pregnant female B6129SF1/J mice, and female humans, corresponding to available pharmacokinetic data. Michaelis Menten saturation kinetic parameters were calculated from substrate depletion data. Maximum rates of metabolism (V<sub>MAX</sub>, nmol/min/mg microsomal protein) and rates of intrinsic clearance (CL<sub>INT</sub>, ml/min/kg body weight) were higher for BaP than DBC, regardless of species. Clearance for both BaP and DBC was highest in naïve female mice (1705 and 182 ml/min/kg) and lowest in female humans (27.2 and 7.5 ml/min/kg). Clearance rates of BaP and DBC in male rat (52.2 and

18.8 ml/min/kg) were more similar to female human than to female mice. Clearance of DBC in pregnant mice (136 ml/min/kg) was reduced compared to naïve mice, possibly contributing to elevated tissue concentrations and residence times observed in pharmacokinetic data. These parameters have been used in the development of physiologically based pharmacokinetic (PBPK) models of PAH exposure and dosimetry for rodents and humans, which accurately describe available pharmacokinetic data. Supported by Award Number P42 ES016465 from the National Institute of Environmental Health Sciences.

**PS 300 Hyperoxia Attenuates Cytochrome CYP1B1 Expression in Human Bronchial Epithelial Cell BEAS-2B: Implications for Oxygen-Mediated Lung Injury.**

D. Dinu, C. Chu, W. Jiang, B. Shivanna, X. Courouci and B. Moorthy.  
*Pediatrics, Baylor College of Medicine, Houston, TX.*

Supplemental oxygen, used to treat premature infants with pulmonary insufficiency, contributes to the development of bronchopulmonary dysplasia (BPD) in animal models and infants by mechanisms that are not entirely known. We recently observed that cyp1b1-null mice are less susceptible to hyperoxic lung injury, suggesting a pro-oxidant role for CYP1B1. Hyperoxia inhibits the growth of the cells, and  $\beta$ -naphthoflavone (BNF) was reported to protect cells from hyperoxic injury. This study tested the hypotheses: 1. hyperoxia attenuates endogenous and BNF inducible CYP1B1 expression in human lung cell line, BEAS-2B; 2. downregulation of CYP1B1 protects cells from hyperoxic injury while overexpression augments the damage.

BEAS-2B cells treated with DMSO (control) or BNF were maintained in room air or hyperoxia for 24, 48, and 72 h. CYP1B1 promoter activity, mRNA and protein expression were evaluated. Cell proliferation, cell viability, apoptotic markers and reactive oxygen species were assessed.

BEAS-2B cells expressed endogenous CYP1B1 protein, which was diminished by about 50% by 24 or 48 h of hyperoxia. BNF induced CYP1B1 mRNA and protein expression. Hyperoxia attenuated endogenous and BNF inducible CYP1B1 protein expression and mRNA expression. Also, hyperoxia attenuated luciferase driven CYP1B1 promoter activity. BNF had minimal improvement in cell viability. Downregulation of CYP1B1 using siRNA improved cell viability in hyperoxia, and overexpression of CYP1B1 was associated with a significant decrease in viability.

Our finding that hyperoxia decreases CYP1B1 protein, mRNA and promoter expression suggests transcriptional or post-transcriptional mechanisms. The finding that downregulation of CYP1B1 improves cell viability, while the overexpression decreases the cell viability supports the role of CYP1B1 as pro-oxidant in hyperoxic injury. As CYP1B1 appears to contribute to lung injury mediated by hyperoxia, understanding the mechanisms of regulation of CYP1B1 may lead to new strategies to prevent or treat BPD.

**PS 301 Metabolism of Deltamethrin (DLM) and Trans-Permethrin (TPM) by Human Hepatic and Intestinal Preparations.**

B. G. Lake<sup>1</sup>, R. J. Price<sup>1</sup>, B. Ing<sup>1</sup>, M. Scott<sup>1</sup>, R. N. Hines<sup>2</sup>, H. J. Clewell<sup>4</sup>, D. W. Gammon<sup>5</sup>, N. Assaf<sup>3</sup>, M. Yoon<sup>4</sup>, S. S. Anand<sup>6</sup> and T. G. Osimitz<sup>7</sup>. <sup>1</sup>LFR Molecular Sciences, Leatherhead, United Kingdom; <sup>2</sup>Medical College of Wisconsin, Milwaukee, WI; <sup>3</sup>Valent Biosciences, Libertyville, IL; <sup>4</sup>The Hamner Institutes for Health Sciences, Research Triangle Park, NC; <sup>5</sup>FMC, Ewing, NJ; <sup>6</sup>DuPont Haskell, Newark, DE; <sup>7</sup>Science Strategies LLC, Charlottesville, VA.

Pyrethroids can be metabolised by both cytochrome P450 (CYP) and carboxylesterase (CES) enzymes. DLM and TPM metabolism was studied using the substrate depletion approach in pooled human hepatic S9, microsomes and cytosol and intestinal S9 fractions. Studies with liver S9 in the presence and absence of NADPH indicated that DLM was metabolised mainly by CES enzymes, whereas TPM was metabolised by both CES and CYP enzymes. Rates of DLM and TPM clearance in liver microsomes were 22.3 and 11.9 ml/min/mg protein, respectively, and in liver cytosol were 2.6 and 5.3 ml/min/mg protein, respectively. The hepatic clearance of both pyrethroids is thus due to both microsomal and cytosolic enzymes. Addition of cofactors for glucuronidation and sulfation did not enhance the metabolism of DLM and TPM by hepatic S9, suggesting that the rate limiting step for hepatic clearance of both pyrethroids is predominantly due to phase I enzymes and not to phase II enzymes. Rates of DLM and TPM clearance by intestinal S9 were 0.6 and 0.8 ml/min/mg protein, respectively. Rates of pyrethroid metabolism were not reduced in the absence of NADPH, suggesting that both compounds are largely metabolised by only intestinal CES enzymes. The metabolic data obtained with human tissue fractions will be used to develop PBPK models for DLM and TPM (Supported by CAPHRA).

**PS 302 Biological Impact of a Dysfunctional CYP1/AhR Auto-Regulatory Feedback Loop.**

E. Wincent<sup>1,2</sup>, A. Kubota<sup>2</sup>, A. R. Timme-Laragy<sup>2</sup>, M. E. Hahn<sup>2</sup>, A. Rannug<sup>1</sup> and J. Stegeman<sup>2</sup>. <sup>1</sup>Institute of Environmental Medicine, Karolinska Institutet, Stockholm, Sweden; <sup>2</sup>Biology Department, Woods Hole Oceanographic Institution, Woods Hole, MA.

The toxicity of slowly metabolized AHR agonists (e.g., dioxins) can be explained by their persistent activation of the receptor, whereas transient AHR activation by readily metabolized chemicals leads to toxicity through cytochrome P4501 (CYP1)-dependent bioactivation of PAHs to toxic products. Still, CYP1A inhibition has been shown to amplify carcinogenic and teratogenic effects of PAHs, emphasizing the complex relationship between CYP1 induction and toxicity. The endogenous and proposed physiological ligand 6-formylindolo[3,2-b]carbazole (FICZ) has the highest AHR affinity found to date and is an almost perfect substrate for CYP1A, resulting in an efficient auto-regulatory feedback of its actions. The importance of CYP1/AHR feedback regulation to in vivo responses to FICZ are unknown.

We tested the hypothesis that blocking CYP1A expression would result in FICZ becoming toxic in vivo. Studies were performed using zebrafish (zf; Danio rerio) embryos with morpholino knockdown of CYP1A (CYP1A-KD) or AHR2 (AHR2-KD). Zf embryos were exposed to vehicle (DMSO) or FICZ (10 or 100nM) starting at 24 hr post fertilization (hpf), and morphology was monitored from 54 to 96 hpf. In the CYP1A-KD embryos FICZ caused a dose-dependent increase in the incidence and severity of pericardial edema and circulation failure, and increased lethality. Hatching frequency was reduced and swimbladder inflation abolished. In control-KD and AHR2-KD embryos, FICZ (100nM) had no significant morphological effects.

The results show that a functioning CYP1/AHR feedback loop is crucial for regulation of AHR signaling by a potential physiological ligand. Considering the large number of chemicals and drugs known to inhibit CYP1s, we suggest a novel mechanism of toxicity whereby chemicals inhibit the metabolism of FICZ, resulting in prolonged activation of the AHR. [FORMAS grant 2011-963; NIH grants R01ES015912, F32ES017585, and R01ES006272; JSPS Postdoctoral Fellowship for Research Abroad 820]

**PS 303 Metabolism and Disposition of 2-Ethylhexyl-P-Methoxycinnamate in Male and Female Harlan Sprague-Dawley Rats and B6C3F<sub>1</sub>/N Mice After Gavage and Intravenous Administration.**

S. Waidyanatha<sup>1</sup>, R. Snyder<sup>2</sup>, Y. Hong<sup>2</sup>, S. Watson<sup>2</sup>, S. Black<sup>2</sup>, B. McIntyre<sup>1</sup> and J. Mathews<sup>2</sup>. <sup>1</sup>Division of National Toxicology Program, NIEHS, Research Triangle Park, NC; <sup>2</sup>RTI International, Research Triangle Park, NC.

2-Ethylhexyl-*p*-methoxycinnamate (EHMC) was nominated to the National Toxicology Program for toxicological evaluation based on its presence as one of the most common active ingredients in sunscreens. Therefore, the current study was undertaken to investigate the metabolism and disposition of [<sup>14</sup>C]EHMC in male and female Harlan Sprague Dawley rats and B6C3F<sub>1</sub>/N mice 24 h or 72 h following gavage and intravenous administration. Intravenous doses to male rats and mice were 8 mg/kg. Gavage doses of 8, 80 or 800 mg/kg to rats were mostly excreted in urine (73-80% in 72 h), with 3-8% of the radioactivity recovered in feces and 1-4% as CO<sub>2</sub>; volatiles accounted for less than 0.25% of the radioactivity for the 800 mg/kg dose. Radioactive residues in tissues were <1% of the dose. There were no sex or route differences in disposition in rats. In male and female mice administered 8 mg/kg gavage and intravenous doses of EHMC, radioactivity was excreted mostly in urine (57-73% in 72 h), recovery in CO<sub>2</sub> and volatiles traps was only 2-4% and 1%, respectively, and tissues contained <0.3% of the radioactivity 72 h post dosing without any apparent sex- or route-related differences in disposition. Urinary metabolites following gavage administration of 800 mg/kg EHMC were associated with hydrolysis of the ester and hydroxylation of the ring; no parent EHMC was detected in urine. The metabolites 2-ethylhexanol and 2-ethylhexanoic acid, which are developmental toxicants, were identified by GC-MS in plasma from rats 1 and 2 h following a gavage dose of 800 mg/kg EHMC. These data indicate that oral doses of EHMC are well absorbed, completely metabolized and excreted chiefly in urine with no species or sex difference. [Supported by NIH, N01ES75563]

**PS 304 Immunochemical Characterization of Xenobiotic-Metabolizing Enzyme Expression in Adult Rat Testis.**

R. R. Gilibili<sup>1</sup>, W. A. Vogl<sup>2</sup>, T. K. Chang<sup>1</sup> and S. M. Bandiera<sup>1</sup>. <sup>1</sup>Faculty of Pharmaceutical Sciences, University of British Columbia, Vancouver, BC, Canada; <sup>2</sup>Faculty of Medicine, University of British Columbia, Vancouver, BC, Canada.

Relatively little is known about the protein expression of xenobiotic-metabolizing enzymes, such as cytochrome P450 (CYP) and epoxide hydrolase (EH) in rat testis. These enzymes are expressed in liver and many other organs, and are known to play an important role in the oxidative biotransformation of various endogenous and exogenous compounds. Some xenobiotics such as benzo[a]pyrene are bioactivated to form genotoxic and/or carcinogenic metabolites. Formation of reactive metabolites in the testis could cause severe adverse effects on steroidogenesis and germ cell development. In the present study, we characterized the expression of various xenobiotic-metabolizing enzymes in adult rat testis using immunoblot and immunohistochemical analyses. Testicular microsomes prepared from adult male Sprague-Dawley rats were separated using SDS-PAGE and electrophoretically transferred onto membranes and probed with different antibodies. Immunoblot results indicated that CYP1B1, CYP2A1, NADPH-cytochrome P450 reductase, and EH were expressed in testicular microsomes isolated from adult rats. By comparison, CYP1A1, CYP1A2, CYP2B1, CYP2E1, CYP2D1, CYP2D2, CYP2C6, CYP2C7, CYP2C11, CYP2C12, CYP2C13, CYP3A1, CYP3A2, CYP4A1, CYP4A2 and CYP4A3 were not detected in the testicular microsomal samples. In addition, tissue sections were prepared from frozen adult rat testis and probed with antibodies to CYP1B1, CYP2A1, NADPH-cytochrome P450 reductase, and EH. Fluorescent staining indicated that CYP1B1 and CYP2A1 were expressed in interstitial cells, which are comprised mainly of Leydig cells, but not in seminiferous tubules. In contrast, EH and NADPH-cytochrome P450 reductase were expressed in both interstitial cells and in seminiferous tubules. In summary, among the CYP enzymes studied, only CYP1B1 and CYP2A1 were detected in testicular microsomes and appeared to be confined to interstitial cells.

**PS 305 Demographic Differences by Age, BMI, Gender, and Disease States of Phase I and Phase II Enzyme Activities in Cryopreserved Human Hepatocytes.**

T. Moeller, C. Six, S. Dennell, T. Rose and C. Watt. *Celsis In Vitro Technologies, Halethorpe, MD.* Sponsor: M. Xia.

Human hepatocytes are a key in vitro reagent for making predictions of in vivo drug metabolism, interactions and intrinsic clearance in drug discovery and development. However, inter-individual differences in drug metabolizing enzyme activities complicate pharmacokinetics, leading to varying efficacy and drug-drug interactions. To delineate the potential influences, we have reviewed phase I (CYP1A2, 2A6, 2C9, 2C19, 2E1 and 3A4) and phase II (UGT and SULT) enzymatic activities as they relate to age, BMI, gender and ethnicity. The data was generated using cryosuspension hepatocytes with specific substrates (CYP1A2: phenacetin, 2A6: coumarin, 2C9: tolbutamide, 2C19: mephenytoin, 2E1: chlorzoxazone, 3A4: testosterone, UGT: 7-hydroxycoumarin and SULT: 7-hydroxycoumarin) near Km concentrations, as well as with multiple enzyme substrate 7-ethoxycoumarin (ECOD). From a minimum of 180 donors, several statistically significant trends were observed. For age-dependent differences, a loss of activity was observed for ECOD and CYP2C19, and an increase in CYP1A2 activity as the age increased from 1 to 89 years old. As BMI increased, ECOD, CYP1A2 and CYP2C19 decreased between the range of 14 and 53. As for gender-related differences, men showed higher activities in ECOD and CYP2E1. Diabetic donors had lower CYP2C9, CYP2C19 and CYP3A4 activities compared to non-diabetics. Overall, choosing appropriate hepatocyte preparations for metabolism studies as a reflection of "average" are dependent upon gender, age, BMI and disease states in many drug metabolizing enzymes.

**PS 306 Metabolism of Benzo(a)pyrene (BaP) and Fluoranthene (FLA) in Gastrointestinal Tract Subcellular Fractions of the APC<sup>Min</sup> Mouse.**

K. L. Harris, P. V. Rekha Devi, D. L. Digges, A. C. Huderson, J. A. Mantey, L. D. Banks, M. S. Niaz and A. Ramesh. *Biochemistry & Cancer Biology, Meharry Medical College, Nashville, TN.*

The objective of the present study was to investigate whether subcellular fractions (nuclear, cytosolic, mitochondrial, and microsomal) from the gastrointestinal (GI) tract of a colon cancer mouse model were capable of metabolizing BaP, a combustion byproduct, which is released into the environment from automobile exhausts, cigarette smoke, and industrial emissions. A significant intake of BaP is also expected in people who consume barbecued foods, and diet rich in saturated fat. In

this study, subcellular fractions (SCF) were isolated by differential centrifugation from a tumor-bearing APC<sup>Min</sup> mouse induced by subchronic doses of 50µg/kg BaP and incubated with either BaP or FLA (3µM each) alone or in combination and appropriate control groups. Subsequent to incubation, samples were extracted with ethyl acetate and analyzed for BaP and FLA metabolites by reverse-phase HPLC with fluorescence detection. The SCF from tumor tissues metabolized BaP to a greater extent than those from the non-tumor tissues. The rate of BaP metabolism (pmol of metabolite/min/mg protein) was found to be more when fractions from BaP-pretreated mice were exposed to BaP alone. The SCF from BaP-pre-exposed mice generated greater proportion of BaP 7,8-diol, BaP 3,6- and 6,12-diones compared to other experimental groups. Furthermore, SCF from BaP-pretreated mice produced greater proportion of FLA 2, 3-diol, and 2, 3 D FLA when fractions were incubated with FLA alone or a combination of BaP and FLA. Our studies revealed that the tumor SCF were competent to metabolize BaP and FLA either individually or as a binary mixture. The metabolism of BaP and FLA as a consequence of prior or simultaneous exposure to BaP may influence the growth of tumors. Our findings are of relevance to long-term dietary intake of these toxicants and the consequent acceleration of the GI tract carcinogenesis process in humans (supported by 5R01CA142845-02, 1F31ES017391-01, 1F31ES019432-01A1, 5R25GM059994-11 and SREB grants).

**PS 307 Studies of Styrene, Styrene Oxide and 4-Hydroxystyrene Toxicity in CYP2F2 Knockout and CYP2F1 Humanized Mice Support Lack of Human Relevance for Mouse Lung Tumors.**

G. Cruzan<sup>1</sup>, J. Bus<sup>2</sup>, J. A. Hotchkiss<sup>2</sup>, R. Sura<sup>2</sup>, M. Banton<sup>3</sup> and S. Sarang<sup>4</sup>. <sup>1</sup>ToxWorks, Bridgeton, NJ; <sup>2</sup>Dow Chemical Company, Midland, MI; <sup>3</sup>LyondellBasell Company, Houston, TX; <sup>4</sup>Shell International, Houston, TX.

Styrene (S) is lung tumorigenic in mice but not in rats. In previous mode of action (MOA) studies, S and its alkene-oxidized metabolite styrene oxide (SO) were not lung toxic in CYP2F2(-/-) [knockout] mice, indicating S-induced mouse lung tumors are mediated through mouse-specific CYP2F2-generated cytotoxic ring-oxidized metabolite(s) producing repeated localized cytotoxicity in Clara cells and associated cumulative cell proliferation in lung bronchioles. This conclusion is consistent with the observation that 4-hydroxystyrene (4HS) is toxic to Clara cells in mice at doses lower than S or SO. The human relevance of the CYP2F MOA was assessed by insertion of a human CYP2F1, 2A13, 2B6 transgene into CYP2F2(-/-) mice; CYP2F1 expression and activity were confirmed in the transgenic (TG) mice. No evidence of cytotoxicity or increased cell proliferation (BrdU labeling) was seen in TG mice treated with either S or SO (200 mg/kg/day ip for 5 days), while cytotoxicity was apparent and BrdU labeling was increased ~10-fold in wild-type (WT) mice. Consistent with the hypothesis, 4HS (60 or 105 mg/kg ip for 5 days) increased BrdU labeling 5-10 fold in WT mice, and was attenuated to less than a 3 fold increase in KO mice and a 2-4 fold increase in TG mice. The limited response of 4HS in both KO and TG mice suggests that direct administration of high doses of 4HS are either intrinsically lung toxic or are capable of limited metabolism by either CYP2F1 and/or other lung CYPs in KO and TG mice to lung toxic metabolite(s). Regardless of the MOA of the limited 4HS toxicity in KO or TG mice, these findings indicate that the CYP2F-mediated tumorigenic MOA in WT mice is not operative for S, SO, or for 4HS putatively derived from metabolism of S by CYP2F1 in humans, and thus S-induced mouse lung tumors are unlikely to be relevant to human risk.

Sponsor: Styrene Information and Research Center

**PS 308 Metabolism and Disposition of Bisphenol AF in Male and Female Harlan Sprague-Dawley Rats following Gavage and Intravenous Administration.**

T. Fennell<sup>1</sup>, R. Snyder<sup>1</sup>, P. Patel<sup>1</sup>, S. Black<sup>1</sup>, J. Mathews<sup>1</sup>, M. Mercado-Feliciano<sup>2</sup> and S. Waidyanatha<sup>2</sup>. <sup>1</sup>Pharmacology and Toxicology, RTI International, Research Triangle Park, NC; <sup>2</sup>Division of National Toxicology Program, NIEHS, Research Triangle Park, NC.

Bisphenol AF (BPAF) is used as a cross linking agent in polymers. BPAF was nominated to the National Toxicology Program for toxicological evaluation based on its moderate production levels, structural similarity to bisphenol A, and lack of adequate toxicity data. The current study was undertaken to investigate the metabolism and disposition of [<sup>14</sup>C]BPAF in male and female Harlan Sprague Dawley (HSD) rats. Following gavage administration of 3.4, 34 or 340 mg/kg to male rats, the administered dose was mostly excreted in feces (73-80%) with < 6% of the dose recovered in urine and cage rinse at 72 h. Radioactivity in tissues was 0.2-1.5% of the dose 72 h post dosing compared to 7% at 24 h following a dose of 34 mg/kg.

Urinary excretion at 72 h post administration was higher in females (~15%) compared to males (~4%) following a 34 mg/kg dose. Distribution of an intravenous dose of 34 mg/kg was similar to that following gavage, but with less excreted in urine in both males (0.62% for intravenous vs. 4.32% for gavage) and in females (7% for intravenous vs. 15% for gavage). About 52% of a 340 mg/kg gavage dose was excreted in bile by 24 h, indicating that high excretion in feces is not due mostly to unabsorbed BPAF. BPAF glucuronide (major metabolite), diglucuronide, glucuronide-sulfate, and sulfate were identified in bile using LC/MS/MS. This study demonstrated that BPAF is well absorbed following gavage administration in rats, metabolized by glucuronidation and sulfation, and excreted mainly in feces. [Supported by NIH, N01ES75563].

**PS 309 Absorption, Distribution, Metabolism, and Excretion Studies of *n*-Butylbenzenesulfonamide in Harlan Sprague-Dawley Rats following Gavage Administration.**

S. Black<sup>1</sup>, S. Watson<sup>1</sup>, J. Mathews<sup>1</sup>, C. Rider<sup>2</sup> and S. Waidyanatha<sup>2</sup>.  
<sup>1</sup>Pharmacology and Toxicology, RTI International, Research Triangle Park, NC;  
<sup>2</sup>Division of National Toxicology Program, NIEHS, Research Triangle Park, NC.

*n*-Butylbenzenesulfonamide (NBBS) is used as a plasticizer and an antifungal agent. There is high potential for human exposure to NBBS due to its likely occurrence in drinking water and leaching from NBBS-containing products. The limited toxicity data in rodents suggests that NBBS can cause toxicity to the hematopoietic, nervous, and male reproductive systems. The present studies were conducted to investigate the clearance of NBBS in male Harlan Sprague Dawley (HSD) rat and B6C3F1/N mouse hepatocytes in vitro and metabolism and disposition of NBBS following gavage administration in HSD rats in vivo. The half-lives of disappearance of NBBS (1  $\mu$ M) in rat and mouse hepatocytes were  $136 \pm 24$  and  $320 \pm 41$  min, respectively. Following gavage administration of ring-labeled [<sup>14</sup>C]NBBS to male HSD rats at 2 and 200 mg/kg and sacrificed at 72h, NBBS was excreted primarily in urine (70-76%) with feces accounting for about 12% of the administered dose. Retention in tissues was 5-7% at 72 h, with no tissue exhibiting high concentrations of radioactivity relative to blood. Profiling of urine showed presence of numerous metabolites; however, the parent NBBS was not observed. Some of the polar metabolites were diminished upon treatment with  $\beta$ -glucuronidase or acylase, indicative of glucuronides and mercapturates, but minimal changes were observed after sulfatase treatment. In conclusion, NBBS is well absorbed following gavage administration and metabolized to products including glucuronides and mercapturates. [Supported by NIH, N01ES75563].

**PS 310 Biotransformation of BDE-47 to Potentially Toxic Metabolites Is Predominantly Mediated by Human CYP2B6: Implications for Interindividual Variability in Metabolism and Retention of BDEs.**

J. R. Olson<sup>1</sup>, M. S. Gross<sup>2</sup>, M. L. Feo<sup>3</sup>, S. T. Singleton<sup>1</sup>, A. L. Crane<sup>1</sup>, B. P. McGarrigle<sup>1</sup>, E. Eljarrat<sup>3</sup>, D. Barcelo<sup>3</sup> and D. S. Aga<sup>2</sup>.  
<sup>1</sup>Pharmacology and Toxicology, University at Buffalo, Buffalo, NY; <sup>2</sup>Chemistry, University at Buffalo, Buffalo, NY; <sup>3</sup>Environmental Chemistry, IDAEA CSIC, Barcelona, Spain.

Recent studies suggest that bioactivation by oxidative metabolism may add considerably to the neurotoxic potential of polybrominated diphenyl ethers (PBDEs), but critical data are lacking on PBDE metabolism in humans. The purpose of this study was to characterize the in vitro metabolism of 2,2',4,4'-BDE (BDE-47), the most abundant PBDE detected in human serum, by human liver microsomes (HLMs) and recombinant human cytochrome P450s (CYPs), and to identify the CYP(s) that are active in the oxidative metabolism of BDE-47. Human CYPs (CYP1A1, 1A2, 1B1, 2A6, 2B6, 2C8, 2C9, 2C19, 2D6, 2E1, 3A4) were incubated with BDE-47 (20  $\mu$ M) and metabolites were measured and characterized using GC/MS/MS. For kinetic studies, CYP2B6 and pooled HLMs were incubated with BDE-47 (0-60  $\mu$ M). CYP2B6 was the predominant CYP capable of forming six different OH-BDEs, including 3-OH-BDE-47, 5-OH-BDE-47, 6-OH-BDE-47, 2'-OH-BDE-66, 4-OH-BDE-42, and 4'-OH-BDE-49. GC/MS analysis also revealed formation of novel metabolites, di-OH-BDE-47 and di-OH-dioxin. Kinetic studies of BDE-47 metabolism by CYP2B6 and pooled HLMs found  $K_m$  values ranging from 4.1-6.9  $\mu$ M and 7.8-13  $\mu$ M, respectively, indicating the high affinity towards the formation of OH-BDEs. Interindividual variability in the in vitro metabolism of BDE-47 will be assessed utilizing CYP2B6 genotyped HLMs, with up to a 100-fold range in the level of CYP2B6 activity, and recombinant polymorphic variants of human CYP2B6 (\*4, \*5, \*6, \*7, \*18). Our findings support the predominant role of CYP2B6 in the metabolism of BDE-47 and suggest that in addition to variable exposures to PBDEs, genetic variability in CYP2B6-specific metabolism may contribute to interindividual variability in the body burden of PBDEs and the formation of potentially toxic metabolites. (NIEHS, grant # ES021554)

**PS 311 Coculture of Antigen-Presenting Cells and Keratinocytes Increases Responsiveness to Prohaptens.**

J. Hennen<sup>1</sup>, C. Cohrs<sup>1</sup>, A. John<sup>2</sup>, A. Seidel<sup>2</sup> and B. Blömeke<sup>1</sup>.  
<sup>1</sup>Department of Environmental Toxicology, University Trier, Trier, Germany; <sup>2</sup>Biochemical Institute for Environmental Carcinogens, Prof. Dr. Gernot Grimmer Foundation, Grosshansdorf, Germany.

Small chemical compounds can induce sensitization to humans that results in tolerance or allergic contact dermatitis after repeated skin exposure. A subgroup of chemicals (prohaptens) can induce an immune response only following metabolic activation, e.g. by cytochrome P450 (CYP). Related in vitro assays currently consist of either skin cells or dendritic cells (DC) but importance of cross talk between these two cell types including xenobiotic metabolism is becoming even more evident (Modi et al., 2012). To study this cross talk in more detail we established a coculture model consisting of THP-1 cells as DC-like cells and HaCaT keratinocytes (Hennen et al., 2011). Upregulated expression of costimulatory molecule CD86 was clearly increased in coculture after incubation with prohaptens and depended on phase I/II enzyme activity. It is not known whether proximate or ultimate metabolites are transported between these two cell types or whether coculture enhances THP-1 responsiveness towards prohaptens. As relevant metabolites have not been identified for most prohaptens, we used the strong sensitizer benzo[a]pyrene (B[a]P) as model prohapten. In single cultured THP-1 cells, B[a]P neither induces CYP1 enzymes nor CD86 expression, whereas in coculture with HaCaTs CYP1A1 (>100-fold) and CYP1B1 (13-fold) as well as CD86 are clearly induced. In preliminary experiments, we could detect several B[a]P metabolites in both HaCaT and THP-1 supernatants, but the suspected ultimate metabolite was only formed in HaCaT cells and in coculture as indicated by the presence of B[a]P tetrol in the supernatants. Whether and how metabolites are transported needs further investigation, but results indicate that both cell types are needed for the activation of antigen-presenting cells and likely sensitization.

**PS 312 Early Vertebrate Origin of ALDH1B1 from ALDH2 Gene and Inactivation of ALDH1B1 by Heteromerization with ALDH2\*2.**

B. C. Jackson<sup>1</sup>, R. S. Holmes<sup>3</sup>, D. S. Backos<sup>1</sup>, P. Reigan<sup>1</sup>, D. C. Thompson<sup>2</sup> and V. Vasilou<sup>1</sup>.  
<sup>1</sup>Department of Pharmaceutical Sciences, University of Colorado Anschutz Medical Campus, Aurora, CO; <sup>2</sup>Department of Clinical Pharmacy, University of Colorado Anschutz Medical Campus, Aurora, CO; <sup>3</sup>School of Biomolecular and Physical Sciences, Griffith University, Nathan, QLD, Australia.

Vertebrate ALDH2 genes encode mitochondrial enzymes capable of metabolizing acetaldehyde and other biological aldehydes in the body. Mammalian ALDH1B1, another mitochondrial enzyme sharing 72% identity with ALDH2, is also capable of metabolizing acetaldehyde but has a tissue distribution and pattern of activity distinct from that of ALDH2. Bioinformatic analyses of several vertebrate genomes were undertaken using known ALDH2 and ALDH1B1 amino acid sequences. Phylogenetic analysis of many representative vertebrate species (including fish, amphibians, birds and mammals) indicated the presence of ALDH1B1 in many mammalian species and in frogs (*Xenopus tropicalis*); no evidence was found for ALDH1B1 in the genomes of birds, reptiles or fish. Predicted vertebrate ALDH2 and ALDH1B1 subunit sequences and structures were highly conserved, including residues previously shown to be involved in catalysis and coenzyme binding for human ALDH2. Studies of ALDH1B1 sequences supported the hypothesis that the ALDH1B1 gene originated in early vertebrates from a retrotransposition of the vertebrate ALDH2 gene. Given the high degree of similarity between ALDH2 and ALDH1B1, it is surprising that individuals with an inactivating mutation in ALDH2 (ALDH2\*2) do not exhibit a compensatory increase in ALDH1B1 activity. We hypothesized that the similarity between the two ALDHs would allow for dominant negative heterotetramerization between the inactive ALDH2 mutants and ALDH1B1. Computational-based molecular modeling studies examining predicted protein-protein interactions indicated that heterotetramerization between ALDH2 and ALDH1B1 subunits was highly probable and may partially explain a lack of compensation by ALDH1B1 in ALDH2\*2 individuals.

**PS 313 Epigallocatechin-3-Gallate Abrogates Cytotoxicity and DNA Damage Induced by Benzo[a]pyrene in Lung Epithelial Cells.**

W. Zhu, W. Gao and Q. Cai. The Institute of Environmental and Human Health, Lubbock, TX.

Epigallocatechin-3-gallate (EGCG) is an active component isolated from green tea which has chemopreventive and anticancer properties. However, the molecular mechanisms of EGCG in these processes are still not very clear. The objective of the

present study is to evaluate the potential protective effects of EGCG on benzo[a]pyrene (BaP)-induced cytotoxicity and DNA damage in BEAS-2B, a human normal lung epithelial cell. BEAS-2B cells were treated with vehicle control (0.1% DMSO), BaP or BaP+EGCG for 24 hours. The cytotoxicity, cell cycle, benzo[a]pyrene diol epoxidation (BPDE)-DNA adducts, and mRNA expression levels of cytochrome P450 (CYPs) were determined by MTT assay, flow cytometry, high performance liquid chromatography (HPLC), and quantitative real-time PCR (qRT-PCR), respectively. BaP induced cell growth inhibition in a dose-dependent manner; while EGCG dose-dependently reversed this inhibition ( $P < 0.05$ ). The flow cytometry analysis showed that BaP caused significant G2/M phase arrest compared to controls, however, increased S phase and decreased G2/M phase were observed in cells co-treated with BaP and EGCG compared to BaP group ( $P < 0.05$ ). BEAS-2B cells exposed to BaP had a significant induction of BPDE-DNA adducts when compared with controls ( $P < 0.01$ ). Moreover, these adducts were diminished significantly by EGCG treatment with an 80% reduction. CYP1A1 and CYP1B1 expression levels analyzed by qRT-PCR dramatically increased after BaP exposure compared to controls (CYP1A1: 130.2-folds; CYP1B1: 6.0-folds;  $P < 0.001$ ). EGCG significantly reduced BaP-induced CYP1A1 and CYP1B1 expression (CYP1A1: 1.6-folds; CYP1B1: 1.2-folds; BaP vs. BaP+EGCG,  $P < 0.05$ ). On the other hand, CYP1A2 and CYP3A4 did not show any changes among the control, BaP-treated, and BaP and EGCG co-treated groups. In summary, BaP-induced adverse effects could be prevented by EGCG, suggesting a possible chemopreventive role for this natural polyphenol against the development of lung cancer.

### PS 314 17 $\beta$ -Estradiol Benzoate and Bisphenol A Suppress Xenobiotic-Metabolizing Enzyme Expression in Adult Rat Testis.

S. M. Bandiera, R. R. Gilibili and T. K. Chang. *Faculty of Pharmaceutical Sciences, University of British Columbia, Vancouver, BC, Canada.*

Previous studies showed that 17 $\beta$ -estradiol benzoate (EB) (at 4  $\mu$ mol/kg) decreased testicular expression of cytochrome P450 1B1 (CYP1B1) in adult male rats. Bisphenol A (BPA) is an endocrine disrupting chemical that has been reported to exert estrogenic activity in vitro and in vivo. In the present study, we investigated the effect of treatment with EB and BPA at varying dosages on the expression of CYP and other xenobiotic-metabolizing enzymes in rat testis. In Experiment 1, five groups of adult male Sprague-Dawley rats ( $n = 4$  per group, except for control,  $n = 5$ ) were injected sc with EB (0.004, 0.04, 0.4 or 4  $\mu$ mol/kg) or vehicle (propylene glycol, 1ml/kg), once daily for 14 days. Immunoblot analysis indicated that treatment with EB at 0.004, 0.04, 0.4 or 4  $\mu$ mol/kg decreased testicular CYP1B1 (by 15, 56, 70 and 80 %), CYP2A1 (by 48, 79, 97 and 95%) and CYP17A1 (by 15, 44, 94 and 98 %) protein levels, respectively, when compared with vehicle-treated rats. The constitutive expression of EH and NADPH-cytochrome P450 reductase was not affected by EB at 0.004  $\mu$ mol/kg, but EH (by 56, 70 and 80 %) and NADPH-cytochrome P450 reductase (by 53, 58 and 48 %) protein levels were decreased following EB treatment at 0.04, 0.4 and 4  $\mu$ mol/kg, respectively. In Experiment 2, adult male rats ( $n = 4$  per group) were injected sc with saline, vehicle (propylene glycol, 1ml/kg) or BPA at 400, 800 or 1600  $\mu$ mol/kg, once daily for 14 days. Treatment with BPA at 400, 800 or 1600  $\mu$ mol/kg decreased CYP1B1 (by 51, 87 and 89%), CYP2A1 (by 79, 92 and 92%), EH (by 50, 67 and 67%) and NADPH-cytochrome P450 reductase (by 43, 67 and 67%) protein levels, respectively, when compared with saline- or vehicle-treated rats. CYP17A1 protein levels were decreased by 49% by BPA at 400  $\mu$ mol/kg dose and were not detectable at other BPA doses. In conclusion, testicular expression of CYP1B1, CYP2A1, CYP17A1, EH and NADPH-cytochrome P450 reductase was down-regulated by exogenous estradiol and BPA, at higher dosages, produced a similar effect.

### PS 315 Acute Lead Exposure Induces Cardiotoxicity In Vivo and In Vitro Rat Model through the Cytochrome P450 1A1 Signaling Pathway.

H. M. Korashy, M. A. Ansari and Z. H. Maayah. *Pharmacology & Toxicology, King Saud University, Riyadh, Saudi Arabia.* Sponsor: S. Al-Bakheet.

Lead (Pb2+) is a naturally occurring systemic toxicant heavy metal that has been reported to affects several organs in the body including the kidneys, liver, central nervous system, and the cardiovascular system. However, Pb2+-induced cardiotoxicity has never been investigated yet and the exact mechanism of Pb2+ associated cardiotoxicity has not been studied. Therefore, the current study was designed to investigate the potential effect of Pb2+ to induce cardiotoxicity in vivo and in vitro rat model and explore the molecular mechanisms and the role of cytochrome P4501A1 (CYP1A1) in Pb2+-mediated cardiotoxicity. For these purposes, Wistar albino rats were treated with Pb2+ (25, 50 and 100 mg/kg, i.p.) for three days to study its effect on physiological and histopathological parameters of cardiotoxicity. On the other hand, rat cardiomyocyte H9c2 cell line, which was utilized as an in vitro model, were incubated with increasing concentration of Pb2+ (25, 50, and

100  $\mu$ M) and the expression of hypertrophic genes,  $\alpha$ - and  $\beta$ -myocin ( $\alpha$ -MHC and  $\beta$ -MHC) and CYP1A1 were determined at the mRNA and protein levels using real-time PCR and Western blot analysis, respectively. Our results showed that Pb2+ significantly induced cardiotoxicity and heart failure as evidence by increase cardiac enzymes, lactate dehydrogenase and creatine kinase-MB) and changes in histopathology *in vivo*. In addition, Pb2+ treatment induced  $\beta$ -MHC whereas inhibited  $\alpha$ -MHC mRNA levels in a time- and dose-dependent manner *in vivo* and *in vitro*. Importantly, these changes were accompanied with a proportional increase in the expression of CYP1A1 mRNA and protein expression levels, suggesting a role for the CYP1A1. The direct evidence for the involvement of CYP1A1 in the induction of cardiotoxicity by Pb2+ was evidenced by the ability of CYP1A1 blocker, resveratrol, to significantly inhibit the Pb2+-modulated  $\beta$ -MHC and  $\alpha$ -MHC mRNAs. It was concluded that acute lead exposure induced cardiotoxicity through CYP1A1 mediated mechanism.

### PS 316 Reciprocal Roles of Cytochromes P4501a1 and 1A2 in Lung Carcinogenesis Mediated by Polycyclic Aromatic Hydrocarbons (PAHs) in Mice.

W. Jiang<sup>1</sup>, L. Wang<sup>1</sup>, G. Zhou<sup>2</sup>, X. Couroucl<sup>1</sup> and B. Moorthy<sup>1</sup>. <sup>1</sup>*Pediatrics, Baylor College of Medicine, Houston, TX;* <sup>2</sup>*Institute of Biosciences and Technology, Texas A&M University Health Science Center, Houston, TX.*

Humans are constantly exposed to polycyclic aromatic hydrocarbons (PAHs). Cytochrome P4501A (CYP1A) enzymes play important roles in the activation of PAHs such as 3-methylcholanthrene (MC) to DNA-binding metabolites, which in turn mediate carcinogenesis in target organs such as lung. In this study, we tested the hypothesis that CYP1A1 and 1A2 have reciprocal roles in PAH-mediated tumorigenesis. Eight week-old female wild type (WT) (A/J) mice or mice lacking the gene for CYP1A1 or CYP1A2 on the A/J background were treated with a single dose of MC (40  $\mu$ mol/kg), or vehicle (corn oil), and liver and lung tumors were studied after 28 weeks. While 100% of WT or Cyp1a2-null mice exposed to MC showed lung tumors after 28 weeks, about 80% of the Cyp1a1-null mice showed lung tumors. However, there were striking differences in the Cyp1a1-null and Cyp1a2-null mice in regard to lung tumor multiplicities. The WT mice treated with MC had about 15 lung tumors/animal. On the other hand, the Cyp1a2-null mice displayed about 40 lung tumors/animal, while the Cyp1a1-null mice showed about 2-3 tumors/mouse. DNA adduct studies at early time points (8 days) showed increased MC-DNA adducts in lungs of Cyp1a2-null mice compared to WT mice, and decreased adduct formation in the Cyp1a1-null mice, supporting the hypothesis that DNA adducts are early biomarkers of PAH-mediated carcinogenesis. Overall, our results suggest that CYP1A1 contributes to the formation of tumorigenesis by PAHs, while CYP1A2 protects against carcinogenesis mediated by PAHs, presumably through its role in PAH detoxification. In conclusion, our results strongly suggest that CYP1A1 and 1A2 could be novel candidates for cancer prevention and therapy through either inhibition of CYP1A1 or induction of CYP1A2. (Supported by NIH grant ES009132.)

### PS 317 Activity-Based Protein Profiling of Metabolizing Enzyme Ontogeny and Response to PAH Exposure in Rodents and Humans.

N. Sadler<sup>1</sup>, S. R. Crowell<sup>1</sup>, A. Wright<sup>1</sup>, D. E. Williams<sup>2</sup> and R. A. Corley<sup>1</sup>. <sup>1</sup>*Systems Toxicology, Pacific Northwest National Laboratory, Richland, WA;* <sup>2</sup>*Oregon State University, Corvallis, OR.*

Activity-based protein profiling (ABPP) has recently emerged as a post-genomic technology for characterizing functional proteins in complex biological systems. This approach applies chemical activity-based probes that monitor the functional activity of enzymes under physiological conditions, thereby providing high-content proteomic information beyond the reach of standard gene- and protein-expression profiling. We have previously developed a suite of activity based probes that display broad coverage across mouse and human phase I and II metabolizing enzymes. Each probe contains three moieties: (1) a reactive group that forms a covalent bond to a functional P450 through a mechanism-based reaction, (2) a binding group that targets a probe towards P450s, and (3) an alkyne (C2) handle to exploit the bio-compatible click chemistry reaction for attachment of an enrichment moiety or fluorescent reporter. In this study, we measured enzyme activity at key life stages in mouse, including fetal development, normal adulthood, and pregnancy, as well as in human fetal tissues. Additionally, we compared the effects of exposure to the transplacental carcinogenic polycyclic aromatic hydrocarbon (PAH) dibenzo[def,p]chrysene (DBC) on enzyme activity in the mouse. We have determined that the activity of most hepatic phase I enzymes associated with PAH metabolism (e.g., CYP 1A1, CYP2E1, epoxide hydrolase) was reduced by 2-10 fold during pregnancy in mice. By incorporating these reductions in enzyme activity

into a physiologically based pharmacokinetic (PBPK) model, along with normal changes in anatomy and physiology, we were able to describe the significantly elevated concentrations of DBC in blood and tissues of pregnant mice versus naïve mice, following equivalent exposures. We additionally report, for the first time, developmentally driven changes in enzyme activity in both mice and humans. Supported by Award Number P42 ES016465 from the NIEHS, and DOE Laboratory Directed R&D Project 90001.

### PS 318 Elucidating the Catalytic Mechanisms of the Novel Styrene Detoxification System in *Pseudomonas* Bacteria.

N. Okonkwo and G. T. Gassner. *Chemistry and Biochemistry, San Francisco State University, San Francisco, CA.* Sponsor: E. Bayliss.

As the world becomes more polluted with styrene-based polymers, it is essential to consider how the 28 million tons of Styrofoam and commercial plastics produced in the United States impact human health. Styrene and its metabolites act as biological membrane disrupters and intracellularly where they are transformed by cytochrome p450 isoforms to styrene oxide and vinylphenol, which have biological activity as pulmonary and hepatic poisons. This toxic vinyl benzene is a danger to living systems and for this reason we focused our research on the styrene detoxification pathway in *Pseudomonas* bacteria. The first enzyme, styrene monooxygenase (SMO), a two component flavoenzyme with an NADH specific reductase, SMOB, and a FAD specific epoxidase, SMOA, catalyzes the epoxidation of styrene to yield styrene oxide. Here, SMOB binds NADH and oxidized FAD as substrates and catalyzes the reduction of FAD by a hydride-transfer mechanism. Many details of the SMOB catalyzed flavin reduction and transfer still need to be explained. This research evaluates the catalytic mechanism of N-terminally histidine-tagged styrene monooxygenase reductase (N-SMOB) from *Pseudomonas putida* S12 bacteria. Over expression of N-SMOB in *E. coli* BL21(DE3) cells produces high amounts of the enzyme, which we purified using nickel affinity chromatography. A Spectromax190 microplate reader was used to measure the rate at which the hydride ion is transferred from NADH to FAD at 340nm. Previous data showed the native SMOB enzyme follows a sequential mechanism under identical conditions. However, preliminary data of N-SMOB at 10 °C suggests that a double displacement reaction with NADH as the leading substrate could be prevalent mechanism. These studies of N-SMOB at 10°C provided estimates of the Km of NADH, Km of FAD and Vmax of N-SMOB at 5.0 uM, 3.7 uM, and 38.0 uMs<sup>-1</sup>, respectively. Through the use of high resolution kinetic analysis at 30°C, we confirm that the double displacement mechanism is the preferred reaction for N-SMOB and these findings will be used to elucidate the flavin-transfer reaction.

### PS 319 Impact of Liver-Specific Loss of Cytochrome P450 Reductase on the Expression and Function of Intestinal P450 Enzymes.

Y. Zhu<sup>1</sup>, X. Ding<sup>1</sup>, C. Fang<sup>2</sup> and Q. Zhang<sup>1</sup>. <sup>1</sup>Wadsworth Center, Albany, NY; <sup>2</sup>American Clinical Solutions, Tampa, FL.

Tissue-specific deletion of the cytochrome P450 reductase (CPR) gene in either liver or intestine leads to upregulation of many P450 genes in the tissue with the Cpr deletion. The aim of this study was to test whether a loss of hepatic CPR would also lead to upregulation of P450 expression in the small intestine (SI). We found that in the liver-specific Cpr-null (LCN) mouse, SI expression of CYP2B, 2C and 3A proteins was increased, by 2- to 3-fold, relative to that in wild-type (WT) mice. This increase was accompanied by increases in rates of SI microsomal metabolism of lovastatin (LVS), a CYP3A substrate (by 2.1-fold). The overall impact of the loss of hepatic P450 function and the increase in SI P450 expression on systemic clearance of orally administered LVS was dependent on LVS dose: the rates of clearance were increased at an LVS dose of 5 mg/kg, unchanged at 25 mg/kg, but decreased at 50 mg/kg, in the LCN mice, compared to WT mice. Thus, we show for the first time that hepatic CPR/P450 deficiency leads to compensatory increases in SI P450 expression and capacity of first-pass metabolism of oral drugs; this finding may aid in the prediction of drug exposure in patients with compromised hepatic P450 function. We also found that SI FGF15 and IBABP mRNA levels were significantly lower (by 15- and 5-fold, respectively) in LCN than in WT mice, while the levels of PXR and FXR mRNAs were unchanged. Furthermore, treatment of mice with FGF19 (the human counterpart of mouse FGF15) abolished the difference between WT and LCN mice in SI CYP3A levels. Thus, SI FGF15 may play a previously unrecognized, direct role in the regulation of SI P450 expression. Overall, our results not only provide the basis for further mechanistic studies of physiological regulation of SI P450 expression, but will also help with data interpretation for numerous studies utilizing the LCN mouse model to determine roles of hepatic P450s in the disposition of orally administered drugs.

### PS 320 Organ-Specific *Ugt1* Locus Profiling in Defining the Toxic Response Towards Irinotecan Anticancer Drug Therapy.

S. Chen, V. Devaraj, M. Fagan and R. H. Tukey. *Laboratory of Environmental Toxicology, Departments of Chemistry & Biochemistry and Pharmacology, University of California San Diego, La Jolla, CA.*

Irinotecan (CPT-11) has been used as a first line drug in the treatment of colorectal cancer. However, its efficacy and safety is compromised because of severe late onset diarrhea, a result of enterocyte toxicity from the active metabolite SN-38. SN-38 is inactivated primarily by hepatic UGT1A1 catalyzed glucuronidation to form SN-38 glucuronide, which is excreted via the biliary ducts into the gastrointestinal (GI) tract, where it serves as a substrate for bacterial  $\beta$ -glucuronidase. Free SN-38 is then re-absorbed by entry through the GI tract. Since an abundance of the UGT1 proteins are rich in the GI tract, it was important to examine the association between SN-38 glucuronidation and the pending intestinal tissue damage resulting from CPT-11 therapy. To carry out these experiments, we have generated mouse models targeting deletion of the *Ugt1* locus specifically in liver (*Ugt1<sup>ΔHep</sup>*) and the intestines (*Ugt1<sup>ΔGI</sup>*). Wild type (*Ugt1<sup>WT</sup>*), *Ugt1<sup>ΔHep</sup>*, and *Ugt1<sup>ΔGI</sup>* adult male mice were treated by the intraperitoneal route with CPT-11 daily for four constitutive days. At a daily dose of 75 mg/kg, survival curves of the *Ugt1<sup>ΔHep</sup>* mice showed a 50% lethality rate, comparable to the LD50 values of CPT-11 treated *Ugt1<sup>WT</sup>* mice. Deletion of the *Ugt1* locus in hepatic tissue had no impact on liver or GI toxicity when compared to wild type mice. Alternatively, *Ugt1<sup>ΔGI</sup>* mice were highly susceptible to CPT-11-induced diarrhea, developing severe ileocolitis. At a CPT-11 dose of 25 mg/kg, bloody diarrhea was observed in all *Ugt1<sup>ΔGI</sup>* mice and was associated with 100% lethality, while no diarrhea or lethality was observed in *Ugt1<sup>ΔHep</sup>* or *Ugt1<sup>WT</sup>* mice at that dose. Thus, intestinal expression of the UGT1A proteins is critical towards the detoxification of SN-38. Regulation of the intestinal UGT1A1 gene may serve as a target for improving the therapeutic index and efficacy associated with CPT-11 treatment. (Supported by USPHS grants ES010337 and CA171008)

### PS 321 Selective Criteria for Determining Catalytic Competency in CYP3A4: A Combined Docking and Pharmacophore Study on Triazole Fungicide Metabolism.

D. T. Chang<sup>1</sup>, C. M. Grulke<sup>1</sup>, M. Goldsmith<sup>1</sup>, J. F. Kenneke<sup>2</sup>, S. Rawat<sup>3</sup>, S. A. Marchitti<sup>2</sup>, C. S. Mazur<sup>2</sup>, K. Holm<sup>1</sup>, M. B. Phillips<sup>1</sup>, Y. Tan<sup>1</sup>, R. Tornero-Velez<sup>1</sup> and C. C. Dary<sup>4</sup>. <sup>1</sup>National Exposure Research Laboratory, US EPA, Research Triangle Park, NC; <sup>2</sup>National Exposure Research Laboratory, US EPA, Athens, GA; <sup>3</sup>Student Services Authority, Athens, GA; <sup>4</sup>National Exposure Research Laboratory, US EPA, Las Vegas, NV.

Cytochrome P450 (CYP) 3A4 is one of the major isoforms of enzymes that catalyzes via Phase I oxidation a wide variety of endogenous and exogenous compounds (i.e., broad substrate specificity) including environmental xenobiotics like chiral pesticides. In particular, several chiral pesticides are well-known to undergo differential kinetics within the homochiral environment of biological systems. The current ability to model such metabolic processes within physiologically-based pharmacokinetic model from an exposure-dose perspective is limited by specific chiral information coupled together with accurate kinetic data. With available in-house stereospecific (i.e., individual stereoisomer) *in vitro* data, we have utilized a ligand-based approach to develop a prototype CYP3A4 pharmacophore model for triazole fungicides based on the observed stereoselective CYP3A4 clearance. The developed model was further used to discriminate between single isomeric configurations thereby enriching the dataset and providing further criteria on putative ligand-receptor interactions. We also utilized a combined pharmacophore and docking approach within the CYP3A4 binding cavity (2V0M PDBID) to provide estimates on putative ligand stereoselective rate constants for a test set of triazole compounds. Observations and comparisons between high and low binding affinity poses as well as homolytic dissociation bond energy estimates at purported sites of metabolism indicate that this method may be helpful for selecting catalytically competent ligand substrates for CYP3A4 and thereby reducing the uncertainty within exposure-based pharmacokinetic models of chiral substrates. Although this work was reviewed by EPA and approved for publication, it may not necessarily reflect official Agency policy.

### PS 322 Chlorpyrifos Affects Specific Types of Zebrafish Larval Behavior If Administered during Distinct Developmental Time Periods.

H. Richendrer and R. Creton. *MCB, Brown University, Providence, RI.*

Pesticides are widely used in agriculture and are found ubiquitously in the environment. While adults have enzymes that are able to break down pesticides, developing embryos lack the necessary enzymes for toxicant removal. Low doses of organophosphate pesticides during early embryonic development in animal models

and in humans have been documented to affect brain development and behavior. It is important to determine at which stages of development embryos are most affected by the exposure to organophosphate pesticides. Using zebrafish as a model system for pesticide exposure is advantageous because embryos can be exposed to organophosphates immediately after fertilization and large numbers of larvae can be used for high-throughput behavioral analysis. Behaviors such as swim speed, preference for edge of a well, and avoidance of a moving stimulus can be quickly obtained. In the present study, employing a high-throughput assay unique to our lab, we show that exposure to low doses of a widely used organophosphate, chlorpyrifos, affect discrete behaviors if administered during specific developmental time periods. The results indicate that even low levels of chlorpyrifos have the potential to impact behavior when administered during critical periods of development and these behavioral abnormalities are emerge from pesticide exposure during different critical points. The results of the present study have the potential to affect food consumption guidelines, especially in pregnant women. Future studies will include larval zebrafish confocal brain imaging to detect neural patterning changes after chlorpyrifos exposure.

### PS 323 The Ahr Pathway and Aromatic Hydrocarbon-Mediated Teratogenicity in the Atlantic Killifish.

R. T. Di Giulio<sup>1</sup>, C. W. Matson<sup>2</sup> and B. W. Clark<sup>1</sup>. <sup>1</sup>Duke University, Durham, NC; <sup>2</sup>Baylor University, Waco, TX.

Exposure of developing fish to polycyclic aromatic hydrocarbons (PAHs) and halogenated aromatic hydrocarbons (HAHs) results in a suite of defects including cardiac malformation, pericardial and yolk sac edema, craniofacial defects and hemorrhaging. Several populations of Atlantic killifish (*Fundulus heteroclitus*) on the Atlantic coast of the United States are resistant to the developmental toxicity caused by PAHs and HAHs; this resistant phenotype displays strong down-regulation of the aryl hydrocarbon receptor (AHR) pathway. The AHR is known to mediate many toxic responses to PAHs and HAHs in vertebrates. A single AHR has been identified in mammals, but killifish and other fish species have multiple AHRs and their roles in contaminant response and development are not clear. In this study, translation-blocking and splice-junction morpholino gene knockdown was used to determine the roles of AHR1 and AHR2, as well as CYP1A, in mediating cardiac teratogenesis induced by  $\beta$ -naphthoflavone (BNF), benzo[k]fluoranthene (BkF), and 3, 3', 4, 4', 5-pentachlorobiphenyl (PCB-126). Here we report that AHR2 and not AHR1 knockdown resulted in rescue of cardiac teratogenicity induced by BNF, BkF, and PCB-126 in laboratory-reared offspring of non-adapted of parents from unpolluted sites. Knockdown of CYP1A enhanced the toxicity of PAHs but not PCB126. Furthermore, knockdown of AHR2 partially rescued the severe cardiac teratogenicity caused by extracts of sediments from the Atlantic Wood (AW) Superfund site (Elizabeth River, VA, USA), a site heavily contaminated with a complex mixture of creosote-derived PAHs (and home to a resistant population of killifish). These data demonstrate that AHR2 is an important mediator of cardiac teratogenesis caused by multiple aryl hydrocarbons in killifish and suggest that suppression of the AHR pathway through modulation of AHR2 is a plausible mechanism for PAH resistance in adapted fish. CYP1A, which is recalcitrant to induction in the AHR down-regulated AW population, appears to play a protective role against PAH developmental toxicity.

### PS 324 Characterization of glo1 Gene Expression during Development and Alterations Induced by Atrazine Exposure in Zebrafish.

G. Ryan<sup>1</sup>, G. J. Weber<sup>1</sup>, S. M. Peterson<sup>1</sup>, M. S. Sepulveda<sup>2</sup> and J. L. Freeman<sup>1</sup>. <sup>1</sup>Health Sciences, Purdue University, West Lafayette, IN; <sup>2</sup>Forestry and Natural Resources, Purdue University, West Lafayette, IN.

Atrazine is a commonly used herbicide that is an endocrine disruptor and a suspected carcinogen. Although atrazine was recently banned by the European Union for widespread contamination risks in potable water supplies, this herbicide is still commonly used in the United States with a current maximum contaminant level (MCL) of 3 ppb. The health risks associated with this MCL are currently being reviewed by the Environmental Protection Agency, but the mechanisms of atrazine toxicity are not well defined. In this study, we are using [1] global gene expression analysis to identify altered genes, [2] in situ hybridization to qualitatively analyze spatial gene expression throughout development, and [3] quantitative PCR (qPCR) to assess gene expression levels of specific targets throughout development in the zebrafish model system. In a previous study completed in our laboratory, zebrafish were exposed to 0.3, 3, or 30 ppb atrazine or a control treatment throughout development (1-72 hours post fertilization [hpf]). This analysis showed that expression alterations were enriched with genes associated with neuroendocrine development and function, cell cycle regulation, and carcinogenesis. From this list of genes, glyoxylase 1 (GLO1) was targeted for further study. GLO1 is part of the glyoxylase system which converts methylglyoxal to S-D-lactoylglylutathione. Upregulation of

GLO1 is linked to cell proliferation and is associated with various cancers in humans. To further our understanding of this genetic target, expression was analyzed at five developmental time points: 24, 36, 48, 60, and 72 hpf. In situ hybridization and qPCR were coupled to determine spatial and quantitative gene expression of glo1 throughout development under normal conditions and after atrazine treatment. This data is furthering our understanding of glo1 expression during development and alterations induced by atrazine exposure.

### PS 325 Developmental Effects of 6-Formylindolo[3, 2-B]Carbazole in Birds.

M. E. Jönsson<sup>1</sup>, S. Shaik<sup>1,2</sup>, A. Rannug<sup>2</sup> and B. Brunström<sup>1</sup>. <sup>1</sup>Environmental Toxicology, Uppsala University, Uppsala, Sweden; <sup>2</sup>Institute of Environmental Medicine, Karolinska Institutet, Stockholm, Sweden.

Birds show a strikingly large species variation in susceptibility to developmental toxicity of dioxins and coplanar polychlorinated biphenyls (PCBs). The chicken is the most sensitive to these compounds among avian species, while e.g. the Japanese quail is much more resistant. Such differences are proposed to depend on binding affinity of dioxin to the aryl hydrocarbon receptor (AHR), i.e., the degree of sensitivity is linked to variation in a few amino acids in the ligand binding domain of avian AHRs. The proposed endogenous AHR ligand 6-formylindolo[3,2-b]carbazole (FICZ) has high AHR binding affinity and causes strong transient induction of CYP1 mRNA in human cells and zebrafish embryos. In *Xenopus tropicalis* tadpoles FICZ is almost as potent an inducer of CYP1A as in zebrafish embryos. However, *Xenopus* tadpoles are much less sensitive to PCB126-induced toxicity than zebrafish embryos. The goal of the present study was to determine mRNA expression responses and other effects of FICZ in developing birds. Peanut oil-lecithin emulsions with or without FICZ were injected into the yolks of day-4 chicken embryos (0, 2, 20, or 200  $\mu$ g FICZ/kg egg) and day-3 quail embryos (0, 2, or 200  $\mu$ g FICZ/kg egg). Twenty four hours post-injection CYP1A4 and CYP1A5 showed dose-dependent induction by FICZ in both chicken and quail, and the degree of induction was similar in the two species. The CYP1B1 level in both species and the CYP1C1 level in chicken were unaffected by FICZ exposure. In chicken embryos exposed to 200  $\mu$ g FICZ/kg the CYP1A levels remained induced in liver and thymus 13 days post-injection (day 17). Furthermore, liver lesions were observed in 48% of these animals, suggesting that FICZ is toxic at high doses. Our results suggest that while there is a large species variation in sensitivity to dioxin-like compounds the strong AHR activation by FICZ is evolutionary conserved, indicating an important physiological function. Funding: The Swedish Research Council Formas and Carl Tryggers Stiftelse.

### PS 326 Aryl Phosphate Esters within a Major PentaBDE Replacement Induce Cardiotoxicity in Developing Zebrafish Embryos: Potential Role of the Aryl Hydrocarbon Receptor.

D. Volz<sup>1</sup>, S. McGee<sup>1</sup>, A. Konstantinov<sup>2</sup> and H. Stapleton<sup>3</sup>. <sup>1</sup>University of South Carolina, Columbia, SC; <sup>2</sup>Wellington Laboratories, Guelph, ON, Canada; <sup>3</sup>Duke University, Durham, NC.

Firemaster 550 (FM550) is an additive flame retardant formulation of brominated and aryl phosphate ester (APE) components introduced in 2004 as a major replacement for the commercial polybrominated diphenyl ether mixture (known as PentaBDE) used primarily in polyurethane foam. Due to rapid adoption, certain FM550 components have been detected at elevated concentrations within indoor environments. However, little is known about the potential effects of FM550-based ingredients during early vertebrate development. Therefore, we first screened the developmental toxicity of each FM550 component using zebrafish as an animal model. Based on these initial screening assays, we found that exposure to triphenyl phosphate (TPP) or mono-substituted isopropylated triaryl phosphate (Mono-ITP) – two APEs comprising almost 50% of FM550 – resulted in targeted effects on cardiac looping and function during embryogenesis. As these cardiac abnormalities resembled aryl hydrocarbon receptor (AHR) agonist-induced phenotypes, we then exposed developing embryos to TPP or Mono-ITP in the presence or absence of a selective AHR antagonist (CH223191) or AHR2-specific morpholino. Based on these studies, we found that CH223191 blocked the cardiotoxic effects of Mono-ITP but not TPP, while AHR2 knockdown failed to block the cardiotoxic effects of both components. Moreover, using a cell-based human AHR reporter assay, we found that Mono-ITP (but not TPP) exposure resulted in a significant increase in human AHR-driven luciferase activity at similar nominal concentrations as a potent reference AHR agonist ( $\beta$ -Naphthoflavone). Overall, our findings suggest that two major APE components of FM550 induce severe cardiac abnormalities during early vertebrate development, raising questions about the potential health risks of these APEs resulting from indoor exposure.

**PS 327 Cytochrome P450 Gene Transcripts in Early Development of Zebrafish *Danio rerio*.**

J. Stegeman, A. Kubota, B. Woodin, E. Hawley, Z. Janes, B. Lemaire and J. Goldstone. *Biology, WHOI, Woods Hole, MA.*

Understanding the roles of cytochromes P450 (CYPs) in zebrafish is important to the use of this non-mammalian model in toxicological, pharmacological and carcinogenesis research. In this study, we determined whether maternally derived transcripts for many CYP genes are present in zebrafish oocytes, and how levels change up to the mid-blastula transition (MBT) (3 hours post fertilization, hpf), focusing on genes involved in xenobiotic and endobiotic metabolism. The maternal contribution to transcript abundance in the eggs varied greatly among CYP genes examined. CYP2V1 showed the highest levels in the oocytes, followed by CYP20 and CYP1A. The transcript levels of all CYPs examined were similar between unfertilized eggs and fertilized eggs at < 2 cell stage (prior to the first division). Many of CYPs including CYP1B1, 1C1, 1C2, 2P6, 2R1, 2AA4, 11C1, 17A2, and 26A1 showed significant increases in their transcript levels at 3 hpf (1,000 cells). In contrast, CYP1A and the steroidogenic CYPs 11A1, 17A1, and 19A1, showed constant levels of transcript from egg to 3 hpf. Other CYPs, including CYP2V1, 2AA3, 3C1, and CYP51 showed an increasing trend at 2 hpf (64 cells), well before the MBT. We also examined the effect of exposure to an aryl hydrocarbon receptor agonist, 3,3',4,4',5-pentachlorobiphenyl (PCB126) on transcript levels of CYP1 and selected other genes in oocytes. Exposure of females to waterborne PCB126 caused increases in the transcript levels of CYP1A, 2AA3, 3C1, 11A1, and CYP51 genes in eggs as compared to those from vehicle-exposed females. The results reveal maternal transcript deposition of a suite of CYP genes in the egg, and also show that temporal patterns of CYP transcript levels during early development from egg to the MBT differ substantially among different CYP genes. Maternal exposure to chemical was shown to cause change in the transcript deposition of some CYPs in the eggs. [Support: JSPS Postdoctoral Fellowships for Research Abroad no. 820 (A.K.), and NIH Superfund Research Program grant P42ES00738 (J.S.)]

**PS 328 Benzo[a]pyrene Exposure Effects on Reproductive Success, Development, and Transcriptome in Zebrafish.**

K. L. Willett<sup>1</sup>, C. Thornton<sup>1</sup>, J. Corrales<sup>1</sup>, X. Fang<sup>1</sup>, M. White<sup>1</sup>, K. Mislan<sup>1</sup>, L. Ballard<sup>2</sup> and B. E. Scheffler<sup>2</sup>. <sup>1</sup>Pharmacology and Environmental Toxicology, University of Mississippi, University, MS; <sup>2</sup>Genomics and Bioinformatics, USDA ARS, Stoneville, MS.

Benzo[a]pyrene (BaP) is an environmentally relevant carcinogenic and endocrine disrupting compound that causes multigenerational effects in mammals. We hypothesized that, like in humans, BaP exposure would adversely affect zebrafish gene expression, reproduction and cause quantifiable pathologies across generations. Adult zebrafish (2 females x 2 males, N=10 replicate tanks per treatment) were fed 2% body weight/day flake food treated with 0, 11.6, 110, 1086 µg BaP/g flake (equivalent to 0, 0.23, 2.2, and 22 µg BaP/g fish/day) for 22 days. Parental gonad pathology and reproductive success, and F1 and F2 survival and morphological abnormalities were measured. The total number of eggs produced and fertilization success was non-significantly reduced in a dose-dependent manner, and parental ovarian atresia was significantly decreased. Mortality was significantly increased in F1 larvae whose parents were exposed to 2.2 and 22 µg BaP/g fish by 48 and 56 hours post-fertilization (hpf), respectively. High dose BaP F1 fish hatched sooner (48 hpf) compared to control (56 hpf). Body and tail shape and swim bladder were negatively impacted after parental exposure to 2.2 and 22 µg BaP/g fish. Moreover, differential gene expression by RNA-Seq of embryos and larvae was documented after a seven day parental embryonic water-borne BaP exposure. As expected, CYP1 genes in 96 hpf BaP-exposed embryos were induced as was vtg7. Based on these results, BaP negatively impacted zebrafish reproduction and development. Supported by NIEHS R21ES019940.

**PS 329 Molecular Pathway of Neurotoxicity Caused by Developmental Exposure to Bisphenol A in Embryonic Zebrafish.**

S. R. Das<sup>1</sup>, K. S. Saili<sup>1</sup>, S. M. Bugel<sup>1</sup>, M. M. Corvi<sup>1</sup>, S. C. Tilton<sup>2</sup>, K. M. Waters<sup>2</sup> and R. L. Tanguay<sup>1</sup>. <sup>1</sup>Environmental and Molecular Toxicology, Oregon State University, Corvallis, OR; <sup>2</sup>Computational Biology and Bioinformatics, Pacific Northwest National Laboratory, Richland, WA.

Bisphenol A (BPA) is an endocrine disrupting compound widely used in consumer product manufacturing. Developmental exposure to 0.1 µM BPA results in a hyperactive phenotype in zebrafish larvae and impairment of learning in adults. The

mode of action underlying these effects presumably involves impacts on nervous system development through activation of classical estrogen receptors (ERs) or other receptors such as estrogen related receptor gamma (ERR3) and G-protein coupled estrogen receptor (GPER). Transient knockdown of ERR3 using an antisense morpholino rescued the hyperactive phenotype in the zebrafish larvae suggesting a role of ERR3 in the developmental toxicity induced by BPA. We further used global mRNA and miRNA expression analysis to investigate the transcriptional effects of BPA exposure and to identify candidate genes and signaling pathways that mediate the observed behavioral response. Zebrafish embryos were exposed to either of 0.1% DMSO, 0.1 µM BPA, 0.1 µM 17β-estradiol, 0.1 µM GSK4716 (an ERR3 agonist) from 8 hours post fertilization (hpf) to 24 hpf. At 24 hpf RNA was isolated to identify transcriptional changes that precede behavioral response using a 135K NimbleGen microarray platform. Functional analysis of differentially expressed genes revealed CREB and prothrombin activation as top canonical pathways impacted by both BPA and E2 exposure, and suppressed expression of key genes involved in nervous system development and function. For miRNA expression analysis, total RNAs isolated at 24 hpf after exposure to either 0.1% DMSO or 0.1 µM BPA were labeled and hybridized onto a Exiqon miRCURY LNA miRNA array (v. 11). The expression of a number of miRNAs was altered by BPA exposure. These results provide insight into potential modes of action underlying BPA's neurodevelopmental toxicity in zebrafish. Supported by NIEHS T32 ES7060, R21 ES018970, P30 ES000210, P42 ES016465.

**PS 330 Methylmercury-Induced Notch Signaling Points to a Role for Muscle Targets in Motor Nerve Development in *Drosophila*.**

C. T. Mahapatra<sup>2</sup>, M. D. Rand<sup>1</sup>, G. Engel<sup>1</sup> and A. Delwig<sup>1</sup>. <sup>1</sup>Environmental Medicine, University of Rochester, Rochester, NY; <sup>2</sup>College of Agriculture, Purdue University, West Lafayette, IN.

Methylmercury (MeHg) is a ubiquitous environmental toxicant that targets the developing fetal nervous system. Despite a wide variety of toxic mechanisms ascribed to MeHg, its specificity for neural targets is not completely understood. Previous work in mammalian and insect cells has shown that MeHg induces expression of Notch pathway target genes, notably the Enhancer of split m-delta (E(spl)mδ) gene. We have shown earlier that MeHg induction of E(spl)mδ can occur independent of the Notch receptor and thus may directly influence neural development. In this study we examine the effects on MeHg on E(spl) gene expression in parallel with neural development events in the *Drosophila* embryo. We now show that E(spl)mδ is specifically upregulated in MeHg-exposed embryos. We exclude the possibility that MeHg-induced E(spl)mδ expression is a by-product of a general stress response or a shift in developmental timing. MeHg phenotypes are apparent in the outgrowth of the embryonic intersegmental and segmental motor nerves. Genetic manipulations causing overactivity of the Notch pathway in neurons can mimic these phenotypes. Unexpectedly, induced expression of E(spl)mδ in neurons does not cause a failure of motor nerve outgrowth. We now demonstrate that endogenous E(spl)mδ expression localizes to developing muscle and that E(spl)mδ overexpression in embryonic muscle causes a segmental nerve phenotype similar to MeHg treatment. Closer examination shows altered patterning in muscle fields stemming from either MeHg treatment or E(spl)mδ overexpression. In contrast, targeting expression of the closely related E(spl)mγ to developing muscle shows no embryonic phenotype, whereas E(spl)mγ targeted to neurons is embryonic lethal. In summary these data highlight a novel mechanism whereby MeHg can engage the activity of a Notch pathway target gene to alter coordinated development of muscles and motor neurons.

**PS 331 Effects of Benzo[a]pyrene on Early Zebrafish Development.**

K. M. Alharthy, F. T. Booc, J. Corrales, C. Thornton and K. L. Willett. Department of Pharmacology and ETRP, University of Mississippi, Oxford, MS.

Benzo[a]pyrene (BaP) is a ubiquitous environmental contaminant that is an endocrine disrupting and carcinogenic high molecular weight polycyclic aromatic hydrocarbon. Our previous work found that BaP significantly decreased fish brain aromatase (CYP19b) expression, a key enzyme in steroidogenesis. We hypothesized that BaP deregulates the steroid hormone hypothalamus-pituitary-gonad feedback loop adversely affecting reproductive development and physiology. Zebrafish embryos were exposed to waterborne concentrations of BaP (0, 10, and 50 µg/L) for 96 hours postfertilization (hpf). Fifty µg/L BaP significantly increased mortality compared with the control and 10 µg/L groups at 24, 48, 72, and 96 hpf, whereas mortality was not significantly increased until 96 hpf in the 10 µg/L BaP group. In order to quantitate effects on larval estrogen and testosterone concentrations, larvae were collected at 48, 72, 96, 168 and 504 hpf. Histopathological assessment of gonad maturation was done on paraffin embedded and sectioned fish at 28, 32, 35, and 52 days post fertilization. In a treatment-blinded morphological assessment of larvae at 96 hpf, the high BaP dose significantly decreased the body length, optic vesicle, and swim bladder size while increasing pericardial and abdominal edema

compared to control and 10 µg/L treatments. Body and tail shape and fin malformation scoring also indicated a dose-dependent adverse impact of BaP-treatment on development. Results extend previous studies highlighting the adverse impacts on early development of BaP-exposure. (Supported by NIEHS R03 ES018962)

**PS 332 Drosophila CYP6g1 and Its Human Homolog CYP3A4 Confer Tolerance to Methylmercury during Development.**

M. D. Rand<sup>1</sup>, J. A. Lowe<sup>1</sup> and C. T. Mahapatra<sup>2</sup>. <sup>1</sup>*Environmental Medicine, University of Rochester, Rochester, NY;* <sup>2</sup>*College of Agriculture, Purdue University, West Lafayette, IN.*

The fetal nervous system is a well-known primary target for methylmercury (MeHg) toxicity. Despite knowledge of numerous cellular processes that are affected by MeHg, the mechanisms that ultimately influence tolerance or susceptibility to MeHg in the developing fetus are not well understood. Using transcriptomic analyses of developing brains of MeHg tolerant and susceptible strains of *Drosophila*, we previously identified members of the cytochrome p450 (CYP) family of monooxygenases/oxidoreductases as candidate MeHg tolerance genes. CYP genes encode Phase I enzymes best known for xenobiotic metabolism in the liver as well as synthesis and degradation of essential endobiotics, such as hormones and fatty acids, that are critical to normal development. We now demonstrate that natural and induced variation in expression CYP genes can strongly influence MeHg tolerance in the developing fly. We show that modulating expression of a single CYP, CYP6g1, specifically in neurons or the fat body (liver equivalent) is sufficient to rescue *Drosophila* development in the presence of MeHg in the diet. Furthermore, we identify CYP3A4 as a human homolog of CYP6g1 and show that it similarly confers MeHg tolerance when ectopically expressed in flies. Finally, pharmacological induction of endogenous CYPs with caffeine also results in elevated tolerance to MeHg in developing flies. These findings establish a previously unidentified role for CYPs in modulating MeHg toxicity and point to a potentially conserved role of CYP genes to influence susceptibility to MeHg toxicity across species.

**PS 333 Systems Approaches to Define the Developmental Toxicity of Polybrominated Diphenyl Ethers.**

M. T. Simonich, L. Truong, S. M. Bugel, B. C. Goodale, W. Bisson, D. C. Koch, S. K. Kolluri and R. L. Tanguay. *Environmental & Molecular Toxicology, Oregon State University, Corvallis, OR.*

Polybrominated diphenyl ethers (PBDEs) are high production volume flame retardants used in a number of consumer products. PBDEs are ubiquitous environmental pollutants due to their widespread usage, persistence and lipophilicity. Developmental exposure to PBDEs is associated with a number of neurological and developmental effects in humans and wildlife. A major complexity in assessing the hazard and risk posed by PBDEs is the diversity of chemical congeners; chemical structure-toxicity relationships are not established for these compounds. Our hypothesis was that developmental toxicity of PBDEs is highly structure dependent and that the molecular targets of these compounds are distinct. We performed rapid throughput assessment of PBDE developmental and neurotoxicity in zebrafish with PBDE congeners 47, 77, 99, 100, 153, 154, and 183. All exposures were from 6 until 120 hours post fertilization (hpf) at which time larvae were assessed for photo-induced locomotor activity and changes in a suite of 20 morphological endpoints. Preliminary global gene expression data suggested that some PBDE congeners may activate the aryl hydrocarbon receptor (AHR). We used our AHR PAS domain homology model for molecular docking analysis, which predicted that PBDE 47, 77, and 99 would bind to the human and zebrafish AHR. Immunohistochemistry confirmed CYP1A induction for PBDE 77 and PBDE 99. Mammalian AHR dependent *in vitro* reporter assays supported these results. Finally, PBDE exposures in AHR2 null fish confirmed that AHR2 is necessary for PBDE 77, and 99 neuro and developmental toxicity. Collectively these data indicate that some PBDEs induce toxicity primarily via activation of the AHR, while others act through uncharacterized AHR-independent pathways, and we are now positioned to identify these distinct mechanisms of PBDE action. This research is supported by NIEHS grants P30 ES00210, T32 ES07060 and RC4ES019764.

**PS 334 Evaluating Morphological, Neurological, and Gene Expression Changes in Response to Developmental PAH Exposures.**

A. Knecht and R. L. Tanguay. *Oregon State University, Corvallis, OR.*

Polycyclic aromatic hydrocarbons (PAHs) are ubiquitous environmental contaminants present in urban air, dust, and soil resulting from incomplete combustion of organic materials or fossil fuels. It is widely recognized that PAHs pose risks to

human health, especially for the developing fetus and infant where PAH exposures have been linked to low birth weight and in-utero mortality and lower intelligence. Using the embryonic zebrafish model, we evaluated the developmental and neurotoxicity after exposure to two PAHs: benzo[a]pyrene (B[a]P) and dibenzo[a,l]pyrene (DB[a,l]P). Dechorionated embryos were exposed from 6 to 120 hours post fertilization (hpf) to a broad concentration range of PAHs and assessed for mortality and 20 unique endpoints at 120 hpf. Using the Viewpoint Zebrafish, we identified that larvae exposed to B[a]P exhibited a hyperactive phenotype. To determine if this behavioral defect persists throughout development, a subset of exposed animals were raised to adulthood and assessed for learning and memory deficiencies using shuttleboxes. Previously, we have demonstrated that exposure to PAHs resulted in an induction of the oxidative stress genes set. Using the Seahorse Extracellular Flux Analyzer, we measured oxidative stress *in vivo* in 24hpf embryos exposed to PAHs from 6 – 24 hpf. The Seahorse results confirm the presence of oxidative stress and that exposure to PAHs cause decreased oxygen consumption rates and acidification rates suggesting the presence of mitochondrial damage. To explore what transcriptional events are occurring prior to the onset of developmental and neurotoxicity, a global gene expression analysis using RNA-seq was performed on 48 hpf embryos exposed to 1 and 10ppm B[a]P and 10ppm DB[a,l]P. Analysis of our collective data will be discussed and provide insight into potential mechanism of action for some PAHs. This research was supported by the NIEHS grants P42 ES016465 and P30 ES000210.

**PS 335 Defining Pathways of Polycyclic Aromatic Hydrocarbon Developmental Toxicity in Zebrafish Using Systems-Based Transcriptional Profiling.**

B. C. Goodale<sup>1</sup>, S. C. Tilton<sup>2</sup>, A. Knecht<sup>1</sup>, A. Swanson<sup>1</sup>, K. Anderson<sup>1</sup>, K. M. Waters<sup>2</sup> and R. L. Tanguay<sup>1</sup>. <sup>1</sup>*Environmental and Molecular Toxicology, Oregon State University, Corvallis, OR;* <sup>2</sup>*Computational Biology and Bioinformatics, Pacific Northwest National Laboratory, Richland, WA.*

Polycyclic aromatic hydrocarbons (PAHs) are ubiquitous in the environment as components of fossil fuels and by-products of combustion. Defining toxicity mechanisms for this large family of multi-ring structures and substituted derivatives is a substantial challenge. In addition to the well-studied carcinogenic properties of several PAHs such as benzo(a)pyrene, reports of cardiac and developmental effects have increased concern about health risks of exposure to PAHs. Some PAHs induce toxicity via activation of the aryl hydrocarbon receptor (AHR), while others act through uncharacterized AHR-independent pathways. We employed the zebrafish model to rapidly assess developmental toxicity, global transcriptional responses and AHR activation in embryos exposed to parent, oxygenated PAHs (OPAHs) and environmental mixture samples during development. Using comparative analysis of mRNA expression profiles from microarrays with embryos exposed to benz(a)anthracene (BAA), dibenzothiophene (DBT) and pyrene (PYR), we identified expression biomarkers and disrupted biological processes that precede developmental abnormalities. These transcriptional responses were associated with PAH body burdens in the embryos detected by GC-MS. We found that uptake data was essential for discerning molecular pathways from dose-related differences, and identified two primary toxicity profiles. While BAA disrupted transcripts involved AHR signaling and vasculogenesis, DBT and PYR misregulated ion homeostasis and muscle-related genes. Biomarkers of these toxicity pathways are under investigation with a diverse group of OPAHs, and comparative analysis of embryos exposed to OPAHs with different proposed molecular mechanisms using RNA-seq will expand and refine pathways of PAH-induced developmental toxicity. This research is supported by NIEHS grants P30ES00210, P42ES016465 and T32ES07060.

**PS 336 Ebselen As a Countermeasure for Nitrogen Mustard Vesicant-Induced Toxicity.**

J. D. Laskin<sup>1</sup>, Y. Jan<sup>1</sup>, D. E. Heck<sup>2</sup>, R. P. Casillas<sup>3</sup> and D. L. Laskin<sup>4</sup>. <sup>1</sup>*Environmental & Occupational Medicine, UMDNJ-RWJMS, Piscataway, NJ;* <sup>2</sup>*Environmental Health Science, New York Medical College, Valhalla, NY;* <sup>3</sup>*MRI Global, Kansas City, MO;* <sup>4</sup>*Pharmacology & Toxicology, Rutgers University, Piscataway, NJ.*

Mechlorethamine (HN2), a nitrogen mustard vesicant, is a bifunctional alkylating agent commonly used as a model to study sulfur mustard-induced lung injury. Previously, we reported that HN2 selectively targeted antioxidants in lung A549 epithelial cells including the selenoprotein thioredoxin reductase (TrxR) forming intra- and inter-molecular cross links. This resulted in dimer and oligomer formation, and enzyme inactivation, a process contributing to oxidative stress and toxicity. In this study, we examined the effects of ebselen, a selenium-containing antioxidant, on HN2-induced toxicity. In A549 cells, HN2 was found to be cytotoxic

(LD50 = 25  $\mu$ M). Both pre- and post-treatment with ebselen (50  $\mu$ M) significantly attenuated HN2-induced toxicity. This was correlated with reduced inhibition of TrxR enzyme activity and decreased formation of TrxR dimers and oligomers. Ebselen treatment was found to induce TrxR protein expression in A549 cells, suggesting that inhibition of toxicity was due to both reduced TrxR damage and increased TrxR enzyme activity. Using purified rat liver TrxR, ebselen also protected against enzyme inactivation by HN2. This was due to a decrease in HN2 binding to the catalytic residues on TrxR, thus preventing enzyme inactivation. Taken together, our data suggest that ebselen has the potential to be an effective countermeasure for HN2-induced lung injury. Support: NIH grants AR055073, ES004738, CA132624, ES05022 and GM034310.

### PS 337 Identification of Thioredoxin As a Molecular Target for Sulfur Mustard Analog Vesicants.

Y. Jan<sup>1</sup>, I. Wohlman<sup>2</sup>, D. E. Heck<sup>3</sup>, R. P. Casillas<sup>4</sup>, D. L. Laskin<sup>2</sup> and J. D. Laskin<sup>1</sup>. <sup>1</sup>Environmental & Occupational Medicine, UMDNJ-RWJMS, Piscataway, NJ; <sup>2</sup>Pharmacology & Toxicology, Rutgers University, Piscataway, NJ; <sup>3</sup>Environmental Health Science, New York Medical College, Valhalla, NY; <sup>4</sup>MRIGlobal, Kansas City, MO.

The thioredoxin system, composed of thioredoxin reductase, thioredoxin and NADPH, is a cellular disulfide reduction system important in antioxidant defense and cell growth control. We reported previously that thioredoxin reductase is a target of both monofunctional [2-chloroethyl ethyl sulfide (CEES)] and bifunctional (HN2, nitrogen mustard) vesicating agents. These vesicants were found to covalently bind to selenocysteine/cysteine residues in the redox centers of the enzyme, leading to its inactivation and toxicity. Thioredoxin contains two catalytic cysteine and three structural cysteine residues. In these studies, we determined if vesicants also target thioredoxin. Both CEES and HN2 treatment were found to cause time- and concentration-dependent inhibition of thioredoxin in A549 cells. Western blot analysis revealed that a band corresponding to tetramers of thioredoxin was present in HN2-, but not CEES-treated cells, suggesting that HN2 caused inter-molecular thioredoxin cross-links. Using recombinant enzyme and mass spectrometry, we found that both CEES and HN2 alkylated cysteine and lysine residues on thioredoxin, including cysteine-32 and cysteine-35 in the redox center of the enzyme. In addition, several inter-peptide cross links were identified in HN2-treated thioredoxin, providing a mechanism for the formation of thioredoxin tetramers in A549 cells. These data demonstrate that thioredoxin is a molecular target of sulfur mustard vesicants. Agents that can reactivate the thioredoxin system may be effective countermeasures for sulfur mustard-induced tissue injury. Support: NIH grants AR055073, ES004738, CA132624, ES05022 and GM034310.

### PS 338 Novel Therapeutic Compounds YEL001 and YEL002 Mitigate Radiation-Induced Toxicity Authors.

Y. Rivina and R. H. Schiestl. Pathology; Environmental Health Sciences, Radiation Oncology, University of California Los Angeles, Los Angeles, CA.

The possibility of a radiation disaster from a nuclear detonation or accident has existed for over 50 years and spawned much of the basic research in radiobiology in the 1950-60s. The recent Fukushima accident was yet another reminder that there remains a dire need to develop novel therapies against radiation-induced toxicities. Here we report on the development of two novel radiation countermeasure therapies: Yel001 and Yel002. These small, biologically active, drug-like molecules were uncovered in the DEL high throughput assay reducing radiation-induced cyto- and geno-toxicity in yeast. Radiation-modulating activity was further confirmed in yeast plate-based DEL Assay: addition of either Yel001 or Yel002 to irradiated cultures reduced cell death and genomic instability. Further, Yel compounds increases survival to 75% in vivo following an LD100/30 dose of ionizing radiation (IR) with the first therapeutic injection administered 24 hours post exposure followed by injections at 48, 72, 96, and 120 hours. Additionally, treatment with Yel001 and Yel002 compounds reduces radiation-induced leukemia from 90% to 50% and 40% respectively. Of note, treatment with either Yel001 or Yel002 reduced spontaneous leukemia rate from 10% to 0%. Treatment with Yel002 following IR accelerates the recovery of the hematopoietic cells after sub-lethal exposures. In addition, treatment with Yel002 reduces EMS, MMS, UV, cigarette smoke extract as well as nitrogen mustard induced toxicity as well as genotoxicity showing a broad application spectrum. Toxicity has not been observed in neither in vitro or in vivo administrations. Overall, Yel compounds have much potential as stockpile therapies for radiation-induced lethality and cancer: they are highly effective when administered up to 24 hours post exposure, they reduce radiation-induced sequelae such as leukemia, and appear to have an acceptable toxicity profile.

### PS 339 Show Bispyridinium Nonoximes Direct Interactions with Muscle-Type Nicotinic Acetylcholine Receptors?

H. Thiermann, T. Seeger, F. Worek and K. V. Niessen. Bundeswehr Institute of Pharmacology and Toxicology, Munich, Germany.

Objective: In poisoning with some organophosphorus nerve agents, e.g. soman, therapeutic efficacy of oximes is limited. For such cases, a direct intervention at nicotinic acetylcholine receptors (nAChR) might be an alternative. Studies with the bispyridinium non-oxime MB327 (1,1'-(propane-1,3-diyl)bis(4-tert-butylpyridinium) di(iodide)) demonstrated a therapeutic effect against soman in vitro and in vivo. As MB327 was found to interact most probably with muscle-type nAChRs, improved therapeutic efficacy could possibly be achieved with compounds that show enhanced activity. To identify potential candidates, homologous series of substituted and non substituted analogues (linker C1-C10) of MB327 were investigated in binding and functional assays. In addition, their inhibitory activity was assessed with human acetylcholinesterase (AChE).

Experimental procedures: In competition radioligand binding assays, the influence on [3H]epibatidine binding sites of Torpedo californica nAChR was investigated. Functional assessments were performed with cell-free electrophysiology based on solid supported membranes (SSM). AChE inhibitory properties of the compounds were assayed with a modified Ellmann assay using haemoglobin-free human erythrocyte ghosts.

Results: MB327 and several bispyridinium structure analogues exhibit no regular displacement curves at [3H]epibatidine binding sites. Compounds with unsubstituted pyridinium ring and long linkers (> C7) show regular competition but no intrinsic effect. Inhibition of human AChE (IC50 < 1  $\mu$ M) for both bispyridinium compound series (unsubstituted and with p-tert-butyl in both pyridine rings) was observed with increasing distance between the pyridinium N (> C9 and > C6 respectively).

Conclusion: The interaction with [3H]epibatidine binding sites and functional improvement of Torpedo californica nAChRs depend on the substitution and C-linker between the pyridine N. Further research is necessary for better understanding how these compounds interact with the nAChR.

### PS 340 Novel Pyridinium Oximes Offer Neural Protection in the Central Nervous System against Nerve Agent Surrogates.

R. B. Pringle<sup>1</sup>, E. C. Meek<sup>1</sup>, H. W. Chambers<sup>2</sup>, J. M. Gearhart<sup>3</sup> and J. E. Chambers<sup>1</sup>. <sup>1</sup>College Veterinary Medicine, Mississippi State University, Mississippi State, MS; <sup>2</sup>Biochemistry, Molecular Biology, Entomology and Plant Pathology, Mississippi State University, Mississippi State, MS; <sup>3</sup>AFRL, Wright-Patterson AFB, Dayton, OH.

Organophosphates (OPs), including nerve agents, target the cholinergic system via inhibition of acetylcholinesterase (AChE), with subsequent overstimulation resulting in neural damage and potential detrimental long-term effects. The efficacy of novel pyridinium oxime reactivators, created with moieties to increase blood-brain barrier penetration, was tested using highly relevant sarin and VX surrogates. Glial fibrillary acidic protein (GFAP; an indicator of neural damage) and monoamines (dopamine, serotonin (5-HT) and their metabolites) were measured in select brain regions via immunohistochemistry and HPLC, respectively. Adult male rats were treated ip with high, sub-lethal doses of surrogates for sarin or VX, nitrophenyl isopropyl methylphosphonate (NIMP; 0.325mg/kg) or nitrophenyl ethyl methylphosphonate (NEMP; 0.4mg/kg), respectively. Surrogate treatment was followed after 1 hr by im administration of novel oxime (0.1mmol/kg). Seizure activity was monitored, and kainic acid (KA; 10mg/kg) served as a positive control. Administration of KA or surrogate (NIMP or NEMP) significantly (p<0.05) increased GFAP expression compared to control animals. Two different formulations of oxime (bromide vs. mesylate salt) attenuated seizures and reduced GFAP levels over NIMP or NEMP treatments alone to levels near those of controls (p<0.05) in both the piriform cortex and dentate gyrus region of the hippocampus, while 2-PAM did not provide protection. Serotonergic activity was also altered in several brain regions, including the piriform cortex (significant increase in both 5-HT and 5-HIAA; p<0.05), one hr after NIMP treatment, with early markers of oxidative stress (isoprostanates) also being tested. These results indicate the potential therapeutic efficacy of these oximes and suggest this innovative chemistry may protect against neural damage induced by OPs. Supported by Defense Threat Reduction Agency: 1.E0056\_08\_AHB\_C

**PS 341** **Sulforaphane Induces Antioxidants and Glutathione-S-Transferase A1 and Protects against Vesicant-Induced Toxicity in Mouse Keratinocytes.**

R. G. Udasin<sup>1,4</sup>, M. Shakarjian<sup>2,3</sup>, V. Mishin<sup>4</sup>, D. E. Heck<sup>3</sup>, R. P. Casillas<sup>5</sup>, D. L. Laskin<sup>1,4</sup> and J. D. Laskin<sup>1,6</sup>. <sup>1</sup>Joint Graduate Program in Toxicology, Rutgers University/UMDNJ, Piscataway, NJ; <sup>2</sup>Department of Medicine, UMDNJ-RWJMS, Piscataway, NJ; <sup>3</sup>Department of Environmental Health Science, New York Medical College, Valhalla, NY; <sup>4</sup>Pharmacology & Toxicology, Rutgers University, Piscataway, NJ; <sup>5</sup>MRI Global, Kansas City, MO; <sup>6</sup>Environmental & Occupational Medicine, UMDNJ-RWJMS, Piscataway, NJ.

Sulfur mustard and the related skin vesicant nitrogen mustard (mechlorethamine hydrochloride, HN2) are bifunctional alkylating agents known to cause oxidative stress and persistent tissue damage including blistering. In the present studies we determined whether HN2-induced oxidative stress and cytotoxicity in mouse keratinocytes could be mitigated by upregulating antioxidant enzymes. Sulforaphane (SFN), an isothiocyanate found in cruciferous vegetables including broccoli, is a well characterized inducer of antioxidants and phase II metabolizing enzymes through a pathway mediated by the transcription factor nuclear factor-erythroid 2-related factor 2 (Nrf2). Treatment of PAM212 mouse keratinocytes with HN2 inhibited keratinocyte growth (IC<sub>50</sub> = 1.0  $\mu$ M). Pretreatment of the cells with 3  $\mu$ M SFN for 3 hours protected against growth inhibition (IC<sub>50</sub> = 6.0  $\mu$ M). SFN also protected primary mouse epidermal keratinocytes from HN2 (IC<sub>50</sub> = 2.0  $\mu$ M and 30  $\mu$ M with and without SFN, respectively). SFN also decreased HN2-induced phosphorylation of histone H2A.X, a marker of DNA damage, in PAM212 cells. SFN was functionally active causing Nrf2 to translocate from the cytosol to the nucleus. This was associated with a marked increase in expression of the antioxidants heme oxygenase-1, thioredoxin reductase 1, and NADPH quinone oxidoreductase-1, as well as the phase II metabolizing enzyme glutathione-S-transferase A1. Taken together, these data indicate that oxidative stress is important in HN2-induced toxicity in mouse keratinocytes and that SFN may be an effective countermeasure against vesicant-induced toxicity. Supported by NIH grants AR055073, ES004738, CA132624, GM034310 and ES005022.

**PS 342** **Effects of Delayed Treatment with a Centrally Active Oxime on Acetylcholinesterase and Survival following Sarin Intoxication.**

T. Shih, R. K. Kan, T. M. Myers and I. Koplovitz. *Research Division, US Army Medical Research Institute of Chemical Defense, Aberdeen Proving Ground, MD.*

Organophosphorus (OP) nerve agents (NA), such as sarin, irreversibly inhibit the enzyme acetylcholinesterase (AChE), which leads to an excess of acetylcholine in the synapses, causing numerous toxic effects, such as convulsions, respiratory distress, and death. The current NA treatment regimen includes 2-pralidoxime (2-PAM) to reactivate NA-inhibited AChE. The quaternary structure of 2-PAM, however, does not allow it to cross the blood brain barrier to reactivate brain AChE and to mitigate CNS toxicity. We have shown earlier that the tertiary oxime monoisonitrosacetone (MINA), when given soon after NA exposure, provided some AChE reactivation in the brain, enhanced survival and mitigated the seizure activity following NA exposure. In this study, we evaluated the efficacy of delayed MINA therapy in reactivating brain AChE and enhancing survival following lethal sarin intoxication. For the reactivation study, guinea pigs were treated with MINA (30, 60, or 120 mg/kg, im) 30 min after one LD<sub>90</sub> of sarin, and AChE was assessed 60 min later. MINA was capable of producing a dose-related reactivation of brain (from 5.8 to 27.4% recovery) and peripheral tissue (from 4.1 to 21.0% recovery) AChE activity that was inhibited by sarin. In a 24-hour survival study, animals were challenged with 3 x LD<sub>50</sub> of sarin and treated 1 min later with intramuscular atropine (0.5 mg/kg) and 2-PAM (25 mg/kg), and MINA (56 mg/kg, im) was given as an adjunct at 1, 3, 5, 15, or 30 min after sarin. Treatment with atropine and 2-PAM at 1 min resulted in 67% mortality, while additional therapy with MINA ensured 100% survival anytime from 3 to 30 min. These findings suggested that delayed therapy with a centrally active AChE reactivator for up to 30 min following lethal exposure to sarin is still capable of reactivating NA-inhibited AChE and saving lives. Thus, inclusion of a CNS penetrating oxime in the therapeutic regimen for OP NA intoxication is beneficial even when the therapy would be delayed.

**PS 343** **Novel Oximes That Penetrate the Blood-Brain-Barrier (BBB) and Reactivate Organophosphate (OP) Inhibited Acetylcholinesterase (AChE).**

E. C. Meek<sup>1</sup>, H. W. Chambers<sup>2</sup>, R. B. Pringle<sup>1</sup>, J. E. Chambers<sup>1</sup> and J. M. Gearhart<sup>3</sup>. <sup>1</sup>College of Veterinary Medicine, Mississippi State University, Mississippi State, MS; <sup>2</sup>Department of Biochemistry, Molecular Biology, Entomology and Plant Pathology, Mississippi State University, Mississippi State, MS; <sup>3</sup>AFRL, Wright-Patterson AFB, Dayton, OH.

Inhibition of AChE following exposure to toxic OPs (nerve agents and pesticides), results in the overstimulation of the nervous system. The approved therapies include an oxime, e.g. 2-PAM, to reactivate OP inhibited AChE; however these oximes have little, if any ability to cross the BBB. A series of novel pyridinium oximes has been synthesized that incorporate moieties that increase BBB penetration and AChE reactivation. Oximes were screened *in vitro* for their ability to reactivate AChE inhibited by a sarin surrogate, phthalimidyl isopropyl methylphosphonate (PIMP), or a VX surrogate, nitrophenyl ethyl methylphosphonate (NEMP), which phosphorylate AChE with the same moiety as sarin or VX, as well as with paraoxon, the active metabolite of the insecticide parathion. Rat brain homogenate was incubated with a concentration of OP that yielded about 80% AChE inhibition, followed by an oxime (0.1mM) and AChE activity measured. *In vitro* AChE reactivation varied among oximes but was similar for each of the nerve agent surrogates; PIMP 14-79%, and NEMP 23-76%, but differed for paraoxon 16-93%. Oxime lipophilicities ranged from 0.009 to 2.244 ( $K_{ow}$ ) and were greater than for 2-PAM (0.006). A subset of oximes that demonstrated AChE reactivation  $\geq 40\%$  *in vitro* were selected for testing *in vivo* in rats with the nerve agent surrogates. A high sublethal dose of a stable sarin surrogate, nitrophenyl isopropyl methylphosphonate (NIMP) (0.325mg/kg) or NEMP (0.4mg/kg) was administered ip, yielding about 80% brain AChE inhibition, followed by an im injection (0.1mmol/kg) of an oxime at the time of peak brain AChE inhibition (1hr). Twelve of 25 novel oximes tested yielded 10-35% brain AChE reactivation and attenuated OP induced seizures, indicating their ability to cross the BBB, reactivate brain AChE and thus demonstrating their therapeutic potential. Supported by DTRA: 1.E0056\_08\_AHB\_C

**PS 344** **Toxicokinetics of ST-246, an Antiviral Product Developed for the Treatment of Human Pathogenic Orthopoxvirus Infection, in Cynomolgus Monkeys.**

M. Trinh<sup>1</sup>, A. Amantana<sup>2</sup>, J. M. Leeds<sup>2</sup>, Y. Chen<sup>2</sup>, K. Honeychurch<sup>2</sup>, D. E. Hruby<sup>2</sup>, B. M. Saville<sup>3</sup>, C. Chang<sup>1</sup>, J. F. Marier<sup>1</sup> and M. Beliveau<sup>1</sup>. <sup>1</sup>Pharsight Consulting Services, Pharsight Corporation, Montréal, QC, Canada; <sup>2</sup>SIGA Technologies, Inc., Corvallis, OR; <sup>3</sup>Charles River Laboratories Preclinical Services, Reno, NV.

Smallpox is still considered a serious bioterror threat even though worldwide surveillance and vaccination eradicated the virus from the natural environment. ST-246 is an antiviral drug developed for the treatment of pathogenic orthopoxvirus infections (includes smallpox and monkeypox). Efficacy trials previously demonstrated that treatment of monkeypox virus-infected monkeys with ST-246 provided significant survival benefit at doses  $\geq 3$  mg/kg. Once daily, 6-h IV infusions of 3, 10 and 30 mg/kg ST-246 were administered for 14 days in a total of 19 male and female cynomolgus monkeys. Toxicokinetic (TK) parameters of ST-246 were evaluated with non-compartmental analysis methods on Day 1 and 14. Mean AUC<sub>0-24</sub> and C<sub>max</sub> increased in a dose-proportional manner on Day 14, with values ranging from 6839 to 76908 ng.h/mL and 904 to 12827 ng/mL, respectively. The accumulation ratio (AUC<sub>0-24</sub> Day 14 vs. Day 1) ranged from 1.00 to 1.54, suggesting minimal accumulation after repeated dosing. Mean CL (415 to 766 mL/h/kg) were consistent with liver blood flow in a typical 5-kg monkey (612 mL/h/kg). Mean V<sub>ss</sub> (1200 – 2503 mL/kg) were markedly higher than the total body water in a typical 5-kg monkey (693 mL/kg), suggesting extensive distribution in peripheral tissues. Steady state concentrations (range: 285 to 3205 ng/mL) were markedly higher than *in vitro* inhibitory concentrations associated to 50% of the maximum effect (IC<sub>50</sub>) against monkeypox virus and different variola strains (10.8 and 12.3 ng/mL, respectively). Overall, ST-246 displayed favorable TK parameters, such as dose-proportional increase in exposure, limited accumulation following repeated dosing, and extensive distribution in peripheral tissues.

**PS 345 Prediction of Human Equivalent Dose (HED) of Levofloxacin (LEVO) in New Zealand White Rabbits (NZW) to Support Efficacy of Combination Treatment with Novel Therapeutics against Inhalation Anthrax (IA).**

M. Beliveau<sup>1</sup>, A. L. Menard<sup>1</sup>, J. F. Marier<sup>1</sup>, J. T. Troyer<sup>2</sup> and E. K. Leffel<sup>2</sup>.  
<sup>1</sup>Pharsight Consulting Services, Pharsight Corporation, Montréal, QC, Canada;  
<sup>2</sup>PharmAthene, Inc., Annapolis, MD.

Regulatory agencies have suggested that novel therapeutics for treatment of IA do not diminish the efficacy of the standard-of-care (SOC) antibiotics in combination therapy, which would be the likely treatment. The NZW is an accepted animal model for IA where the SOC LEVO is both well tolerated, efficacious and where benefits of combination therapy would therefore need to be demonstrated. However, for proper demonstration of the added benefit of the new drug, the administered dose of LEVO must not be supra-therapeutic. Therefore, a HED of LEVO in NZW must be used. The objective of the current analysis was to determine pharmacokinetic (PK) parameters of LEVO in NZW and to determine the NZW dose equivalent to the HED of 7.14 mg/kg (500 mg QD) for IA. LEVO was administered to NZW by either PO or IV bolus administration and blood for PK analysis was collected at various times up to 48h post dose. Plasma samples were assayed for concentrations of LEVO using a validated LC/MS/MS method. Following calculation of PK parameters such as clearance (CL) and volume (Vss) by standard non-compartmental methods, the NZW HED was extrapolated from the clinical dose using the following equation:  $\text{Dose}_{\text{rabbit(HED)}} = (\text{HED}/\text{CL}_{\text{human}}) \times \text{CL}_{\text{rabbit}}$  where the HED = 500 mg and the  $\text{CL}_{\text{human}}$  was taken from the literature (175 mL/min). Following IV dosing, mean  $\text{CL}_{\text{rabbit}}$  and Vss of LEVO were 17.7 mL/min/kg and 1619 mL/kg, respectively. Bioavailability in NZW was dose dependent and ranged from 37.9% to 79.7%. Using  $\text{CL}_{\text{rabbit}}$ ,  $\text{CL}_{\text{human}}$  and the HED, the dose of LEVO in NZW corresponding to the HED was 50.5 mg/kg IV. If administered PO, the NZW HED would range from 53.8 mg/kg to 63.1 mg/kg. In conclusion, the above results suggest that LEVO IV dosing of 50.5 mg/kg or PO dosing of 53.8 to 63.1 mg/kg in NZW in combination with novel anthrax therapeutics are expected to allow sufficient demonstration of any added benefit of the novel drug.

**PS 346 The Beneficial Effect of a Treatment with Macrophages on Sulfur Mustard Cutaneous Burns.**

S. Dachir<sup>1</sup>, D. Kamus-Elimeleh<sup>1</sup>, R. Sahar<sup>1</sup>, E. Fishbine<sup>1</sup>, R. Gez<sup>1</sup>, J. S. Graham<sup>2</sup>, A. Eisenkraft<sup>3</sup>, V. Horwitz<sup>1</sup> and T. Kadar<sup>1</sup>. <sup>1</sup>Pharmacology, Israel Institute for Biological Research, Ness Ziona, Israel; <sup>2</sup>Office of the Commander, USAMRICD, Aberdeen Proving Ground, MD; <sup>3</sup>NBC Protection Division, Ministry of Defense, Tel Aviv, Israel.

Sulfur mustard (HD) is a potent vesicant that its toxicology has been for many years a subject for research, yet, the exact mechanism of its toxicity is still elusive and treatment is only partially effective. Macrophages are known to play an essential role in almost every stage of wound healing and there is evidence for their beneficial effects in treating decubital ulcers and deep sterna wound infections in human. This study was aimed to investigate the efficacy of a treatment with activated macrophages in ameliorating acute and long-term HD induced skin injuries in the hairless guinea pig (HGP) model. HGP were exposed to HD vapor creating superficial dermal skin lesions. They were treated with either a single or multiple intra-dermal injections of human activated macrophages (hAMS) into the wound bed. Clinical and histological evaluations were conducted up to four weeks post-exposure. A single intra-dermal injection into the wound bed administered early (15min or 6hr) after exposure inflicted an initial positive effect on the extent of the damage, demonstrating a temporal decrease in clinical symptoms, reduced number of acidophilic epithelial cells and less micro-vesications compared to untreated control. Repeated injections with hAMS (15min, 48hr and 7d post-exposure), decreased significantly the wounds' area and improved the integrity of the barrier function as expressed by trans-epidermal water loss measurements up to 10 days. Still, at 21 days there were no differences between the experimental groups. The results demonstrated a beneficial effect of macrophages on HD induced lesions. Further investigation is required to determine whether macrophages are required during the early phase of wound development or during the late phase of scar formation and remodeling. This work was supported by the US Army Medical Research and Material Command under award #: W81XWH-08-2-0128.

**PS 347 Comparative Anticonvulsant Effects of Diazepam in Rats Exposed to DFP, Paraoxon and the Chemical Warfare Nerve Agent Soman.**

R. K. Kan, J. A. Leuschner, T. T. Dao, S. W. Kaski, J. F. Irwin, C. Acon-Chen, C. R. Braue, E. A. Johnson, H. Hoard-Fruchey and T. Shih. *Pharmacology, USAMRICD, Aberdeen Proving Ground, MD.*

Diazepam is routinely used to control organophosphate-induced seizures. The present study was designed to evaluate the effectiveness of diazepam to control seizures induced by soman (GD), diisopropylfluorophosphate (DFP) and paraoxon. Prior to experimentation, animals were instrumented with cortical electrodes for monitoring brain activity. Animals exposed to GD (180 ug/kg, sc) were pretreated with HI-6 (125 mg/kg, ip) 30 min prior to GD challenge and treated with atropine methylnitrate (2.0 mg/kg, im). Animals exposed to DFP (4.0 mg/kg, sc) were pretreated with pyridostigmine (0.026 mg/kg, ip) 30 min prior to DFP challenge and treated with atropine sulfate (AS; 0.2 mg/kg, im) and 2-PAM (25 mg/kg, im). Animals exposed to paraoxon (1.05 mg/kg, sc) were treated with AS (2.0 mg/kg, im) and 2-PAM (25 mg/kg, im). In all cases, diazepam (10 mg/kg, im) was given at 40 min after the onset of seizures. Diazepam was effective in terminating DFP- and paraoxon-induced seizures, but it was ineffective in terminating GD-induced seizures. In addition, neuropathology in animals treated with diazepam at 40 min after DFP or paraoxon-induced seizures was markedly reduced at 24 hr after seizure onset. In contrast, diazepam treatment at 40 min after the onset of seizures-induced by GD did not prevent or attenuate brain injury. DFP and paraoxon models were developed as surrogate animal models for nerve agent (NA) biomedical research for evaluation of putative therapeutics. The difference in the effectiveness of diazepam in controlling seizures and reducing neuropathology induced by GD, DFP or paraoxon indicates that DFP and paraoxon are not suitable simulants for NA biomedical research, at least not for screening of potential anticonvulsants to control on-going seizures. Novel anticonvulsants that are effective in terminating seizures induced by DFP or paraoxon may not be efficacious against NA-induced seizures.

**PS 348 Determination of Cholinesterase Levels in the Blood and Brain following Galantamine Administration in the Guinea Pig Model.**

C. Wilhelm<sup>1</sup>, A. Moulder<sup>1</sup>, G. Platoff<sup>2</sup>, D. Jett<sup>2</sup>, D. Yeung<sup>2</sup> and M. C. Babin<sup>1</sup>. <sup>1</sup>Battelle, Columbus, OH; <sup>2</sup>CounterACT Program, NIH OD, Bethesda, MD.

The CounterACT Program at the National Institutes of Health is investigating galantamine hydrobromide (GAL) as a treatment for organophosphorus nerve agent (NA) intoxication and is establishing a dose response representation to determine optimal doses for future efficacy studies. GAL is a reversible acetylcholinesterase (AChE) inhibitor that crosses the blood-brain barrier and is presently approved for the treatment of mild to moderate Alzheimer's disease. It has shown some efficacy against NA toxicity in animal studies. Ongoing studies are investigating the efficacy of GAL when administered either as a pre-treatment or post-treatment and when used in conjunction with standard NA treatments atropine and 2-PAM (pralidoxime). The objective of this study was to correlate clinical biomarkers and pharmacodynamics with clinical observations after treatment with GAL. Blood and brain levels of GAL and ChE inhibition were determined at various time-points along with standardized clinical observations. Cohort A used 36 animals with six dose levels of 0, 2, 4, 8, 12 and 16 mg/kg and serial blood collections from 5 minutes to 24 hours post treatment. These samples were assayed to determine the percent AChE activity at seven time-points. Cohort B used 144 male Hartley guinea pigs with six dose levels of 0, 2, 4, 8, 12 and 16 mg/kg with designated sacrifice time-points on 4 animals for each dose level at 5, 30, 60 min, 2, 4 and 24 hours post treatment. Clinical observations showed a trend of increasing severity of clinical observations as the dose level increased. All clinical signs started at 5 minutes post treatment and all animals were normal by the 24 hour post treatment time-point. Significant observations of toxicity were present at and above the 12 mg/kg dose level, combined with the greatest inhibition of AChE. Inhibition of AChE was seen at the 5 minute time-point (post treatment) with results showing a dose dependent inhibition from low to high dose levels.

**PS 349 Characterization of Protein Adducts of Nitrogen Mustards As Potential Exposure Biomarkers.**

V. R. Thompson and A. P. DeCaprio. *Department of Chemistry & Biochemistry and International Forensic Research Institute, Florida International University, Miami, FL.*

Protein adducts are useful as longer-term biomarkers of exposure to electrophilic xenobiotics, including chemical warfare agents (CWA) and their metabolites. The purpose of this study was to characterize protein adducts of the nitrogen mustards

HN-2 and HN-3 as potential exposure biomarkers. Limited data exist on HN adducts to protein thiols but not other nucleophilic sites such as lysine and histidine. Initial *in vitro* experiments used three model peptides (AcPAAXAA; X = C, K, or H) incubated with HN-2 and -3 (100-fold molar excess) at pH 7.4, 37°C to mimic physiological conditions. Adduct formation was monitored by LC-QQQ-MS/MS analysis at various incubation times. Rapid adduction by both agents occurred at all three nucleophilic sites. Major reaction products included S- and N-(2-chloroethylaminoethyl) adducts (determined by MS isotopic ratios) and S- and N-(2-hydroxyethylaminoethyl) hydrolysis products. Adduct stability was assessed by extended incubation of modified peptides after removal of unreacted agent via C<sub>18</sub> SPE. LC-MS/MS analysis demonstrated that adducts were stable for up to three weeks. In addition, hemoglobin (Hb) as a model protein was incubated with HN-2 at a mustard:protein molar ratio of 100:1. LC-QTOF MS demonstrated a mass shift on each Hb subunit corresponding to up to two modifications. Trypsin digestion of modified protein followed by LC-MS/MS confirmed adduction at C, K, and H. Finally, *in vitro* results were compared to *in silico* calculations (Gaussian 03W software) to predict relative electrophilic reactivity of HN-2 and -3 with protein nucleophiles. Calculated parameters showed good concordance to the experimental data with regard to kinetics and comparative adduct formation. Results of this study confirm that nitrogen mustards can stably adduct nucleophilic protein sites including lysine and histidine. Current work involves assessing the specificity of binding in both Hb and serum albumin, with the ultimate goal of developing adduct-based biomarkers for these important potential CWA.

### PS 350 Glucocorticoid Exposure Primes the Neuroinflammatory Response to the Nerve Agent DFP in a Model of Gulf War Illness.

K. A. Kelly<sup>1</sup>, D. B. Miller<sup>1</sup>, S. M. Lasley<sup>2</sup> and J. P. O'Callaghan<sup>1</sup>. <sup>1</sup>CDC-NIOSH, Morgantown, WV; <sup>2</sup>University of Illinois College of Medicine, Peoria, IL.

We have shown previously that chronic exposure to the glucocorticoid corticosterone, (CORT), at levels associated with high physiological stress, can prime the CNS proinflammatory response to neurotoxic insults. Persistent sickness behavior, a prominent component of Gulf War (GW) Illness, is associated with neuroinflammation. Veterans of the 1991 GW were exposed to the stresses of war, prophylactic treatment with the reversible acetylcholinesterase (AChE) inhibitor, pyridostigmine bromide (PB), the insect repellent, DEET, and, potentially, acutely to the nerve agent sarin. Previously, we showed that subchronic CORT pretreatment primed the CNS to mount a neuroinflammatory response to these GW exposures when provoked 24 h after the termination of CORT treatment. Here, we investigated the persistence of this priming effect on neuroinflammation and the minimal amount of CORT required to produce the priming response. Male C57BL/6 mice were pretreated with chronic (14 days) PB (2mg/kg/day, s.c.) and DEET (30 mg/kg/day, s.c.), as well as subchronic CORT (200 µg/ml in drinking water on days 7-14) or acute CORT (20 mg/kg, s.c., 2 injections, 7 h interval on day 14) exposures. Acute doses (days 15 or 45) of the sarin surrogate and irreversible AChE inhibitor diisopropyl phosphorofluoridate (DFP, 4 mg/kg, i.p.) or known inflammogen lipopolysaccharide (LPS, 2 mg/kg, s.c.) were used to provoke neuroinflammation. We found that both acute and chronic CORT exposure greatly augmented neuroinflammation in response to LPS and DFP. Marked neuroinflammation in response to DFP was found even when the exposure was 30 days after the cessation of the subchronic CORT treatment (a time point equivalent to 6 years in humans). Our findings are suggestive of a possible critical and yet unrecognized link between the stressful environs of the 1991 GW theater and agent exposure(s) unique to this war, exposures in which the CNS is primed to amplify future exposure to pathogens, injury or toxicity. (Supported by CDMRP W81XWH-09-2-0098)

### PS 351 Evaluation of Selected Organoselenium Analogs of Ebselen As Protective Agents against HN2 Toxicity in A-431 Skin Cells.

M. A. Pino<sup>1,2</sup>, B. Billack<sup>2</sup> and M. Pietka-Ottlik<sup>3</sup>. <sup>1</sup>Basic Sciences, TouroCOM, New York, NY; <sup>2</sup>Pharmaceutical Sciences, St. John's University, New York, NY; <sup>3</sup>Division of Organic and Pharmaceutical Technology, Faculty of Chemistry, Wrocław University of Technology, Wrocław, Poland.

Our lab has previously demonstrated that the organoselenium compound ebselen (EB-1) possesses the ability to reduce the cytotoxicity of mechlorethamine (HN2), a sulfur mustard surrogate, *in vitro*. The main objective of the present study was to determine the extent to which three structurally related compounds, namely EB-2, EB-3 and EB-4, could mimic this effect in human epidermoid carcinoma cells (A-431). Using MTT cell viability analysis, we found that in the absence of any test analog, a reproducible and robust cell death was observed in the cells following incubation with HN2 (25 µM, 24 h), while cells treated with test analog alone (15,

30 or 60 µM) for a similar period of time were generally unaffected. When incubated in the presence of both HN2 and test analog for 24 h, we observed that all analogs reduced HN2 toxicity to varying degrees, with the EB-4 analog being the most effective. An examination of cellular morphology using light microscopy analysis confirmed cytoprotection among cells treated with organoselenium analogs. It is noteworthy that all analogs of EB-1, at a test concentration of 60 µM, were capable of reducing the levels of HN2-induced thiobarbituric acid reactive substances (TBARS), suggesting an antioxidant activity. Among the EB-1 analogs tested, EB-4 was found to be the most potent at reducing TBARS while EB-2 was the least potent in this regard. Taken together, these data identify a cadre of organoselenium analogs which are active against a mustard gas surrogate *in vitro*. Future studies are warranted to determine whether or not said compounds will be effective at reducing mustard-related injury *in vivo*.

### PS 352 Hydroxamate Inhibition of EMMPRIN, an MMP Inducer, after Mustard Exposure.

A. S. Rodrigues<sup>1</sup>, A. Miller<sup>1</sup>, R. A. Hahn<sup>1</sup>, M. Patel<sup>1</sup>, C. Lacey<sup>2</sup>, A. N. Pillai<sup>2</sup>, S. Young<sup>2</sup>, R. A. Flowers<sup>2</sup>, N. Dennisova<sup>1</sup>, M. A. Gallo<sup>3</sup>, D. R. Gerecke<sup>1</sup>, K. K. Svoboda<sup>4</sup>, N. D. Heindel<sup>2</sup> and M. K. Gordon<sup>1</sup>. <sup>1</sup>Pharmacology and Toxicology, EMSOP, Rutgers University, Piscataway, NJ; <sup>2</sup>Department of Chemistry, Lehigh University, Bethlehem, PA; <sup>3</sup>Environmental and Occupational Health, UMDNJ, Robert Wood Johnson Medical School, Piscataway, NJ; <sup>4</sup>Biomedical Sciences, Baylor College of Dentistry, Texas A&M University, Dallas, TX.

Mustards are blistering agents injuring the eye, skin and lungs. Corneal mustard injury causes separation at the epithelial-stromal border, resulting in epithelial sloughing. ADAM17 is a transmembranous enzyme that cleaves collagen XVII, a transmembranous hemidesmosomal component that is part of the anchoring complex riveting the epithelium to the stroma. ADAM17 is activated in rabbit corneal organ cultures immediately after nitrogen mustard (NM) exposure, and persists 24 hr post exposure, correlating with the degree of epithelial-stromal separation. To promote epithelial-stromal integrity after mustard exposure, two hydroxamates were tested for their inhibition of ADAM17 to reduce collagen XVII cleavage. The hydroxamates olvanil OH (NDH4409) or retro olvanil 8 (NDH4417) were applied 4 times to organ cultures over the course of 22 hrs, beginning 2 hours post NM exposure. Epithelial sloughing at 24 hr was reduced. Surprisingly, only NDH4417 significantly inhibited ADAM17 activity. However, both drugs reduced matrix metalloproteinase-9 (MMP-9). To further evaluate why corneal epithelial-stromal integrity was preserved after NM exposure, the effects of each drug on expression of EMMPRIN was tested. EMMPRIN is an MMP inducer. EMMPRIN was greatly upregulated after mustard exposure. Both NDH4409 and NDH4417 significantly reduced EMMPRIN expression. Our data indicate that hydroxamates inactivate ADAM17 and MMPs, and may also preserve corneal epithelial-stromal integrity by attenuating the vesicant-induced upregulation of the MMP-inducer EMMPRIN. Supported by UMDNJ-Rutgers Counteract Center of Excellence NIAMS U54AR055073; NIH NEI EY009056; and NIEHS P30ES005022

### PS 353 Sulfur Mustard Induces Cytotoxicity and Apoptosis in Mouse Skin Hair Follicles.

L. Joseph<sup>1</sup>, J. A. Cervelli<sup>1</sup>, G. M. Composto<sup>1</sup>, M. C. Babin<sup>2</sup>, R. P. Casillas<sup>3</sup>, P. J. Sinko<sup>1</sup>, D. R. Gerecke<sup>1</sup>, D. L. Laskin<sup>1</sup>, J. D. Laskin<sup>4</sup> and D. E. Heck<sup>5</sup>. <sup>1</sup>Rutgers University, Piscataway, NJ; <sup>2</sup>Battelle, Columbus, OH; <sup>3</sup>MRI Global, Kansas City, MO; <sup>4</sup>UMDNJ-Robert Wood Johnson Medical School, Piscataway, NJ; <sup>5</sup>New York Medical College, Valhalla, NY.

Sulfur mustard (SM), a potent vesicant, damages follicular and interfollicular epidermis. We examined the effects of SM vapor on pilosebaceous units in dorsal skin of 5 wk old male SKH1-Hr mice. Control skin contains prominent sebaceous glands, atypical hair shafts, isolated utriculi, and small follicular cysts. Fatty acid synthase and proliferating cell nuclear antigen (PCNA) were expressed in sebocytes. PCNA was also expressed in hair root sheaths and dermal papillae. Three to seven days following SM exposure, alterations in the pilosebaceous unit were evident including epithelial cell karyolysis within hair root sheath, infundibulum and isthmus, as well as loss of sebocytes. Utriculi, some with connections to the skin surface, and engorged dermal cysts were observed. One day post SM exposure phosphoroylated H2A.X (γH2A.X), a DNA damage marker, and cleaved caspase-3, a marker of apoptosis, were expressed in the pilosebaceous unit and epidermis. Although evident in the pilosebaceous unit, PCNA was not expressed in the interfollicular epidermis. Decreased numbers of pilosebaceous units and increased numbers of inflammatory cells were observed surrounding utriculi and cysts 3 days post SM. Decreased expression of γH2A.X, PCNA, and fatty acid synthase was noted, whereas cleaved caspase-3 was upregulated in the hyperplastic hair root sheath. By 7 days post SM, there were no hair follicles or sebaceous glands within the wound;

only remnants, including utriculi and large follicular cysts. By 14 days, follicular cysts within the hyperplastic epidermis were greatly enlarged. Significant amounts of PCNA and cleaved caspase-3 were expressed in cells surrounding the follicular cysts. Taken together, these data indicate that the hair follicle is an important target contributing to SM-induced skin injury. Support: NIH AR055073, ES004738, CA132624, GM034310, and ES005022.

### PS 354 Acute Respiratory and Neurological Toxicity in Rats following Inhalational Exposure to Lethal Doses of Soman.

B. Wong, M. Perkins, G. Murphy, D. A. Alves, A. M. Rodriguez, J. Devorak, R. K. Kan, J. A. Leuschner, T. Dao and A. M. Sciuto. *USAMRICD, Aberdeen Proving Ground, MD.*

Soman (GD) is a potent chemical warfare nerve agent (CWNA). GD irreversibly inhibits acetylcholinesterase (AChE), resulting in accumulation of the neurotransmitter acetylcholine (ACh). High ACh at synapses results in prolonged stimulation of muscarinic and nicotinic receptors leading to cholinergic crises. This study developed a novel head-out inhalation exposure system to serve as a realistic and applicable model for a mass casualty-type scenario to study the development of acute respiratory and neurological toxicity. GD vapor (520, 560, 600 and 825 mg×min/m<sup>3</sup>) was generated in a saturator cell and carried by filtered N<sub>2</sub> into a customized glass exposure chamber. Male rats (250-300 g) were restrained in head-out exposure tubes and exposed to GD for 4-10 minutes. The probit analyzed LC<sub>50</sub> of vaporized GD was 593.1 mg×min/m<sup>3</sup>. A majority of the animals developed severe cholinergic responses followed by convulsions and died within 4-8 min post-exposure (PE). Mild to severe convulsions and muscular fasciculations were observed up to 24 h in animals exposed to 560 and 600 mg×min/m<sup>3</sup>. GD exposures produced significant, concentration-dependent inhibition in cardiac blood AChE activity. AChE activity was inhibited in bronchoalveolar lavage (BAL) fluid, lung and whole brain tissues. Rats exposed to a 600 mg×min/m<sup>3</sup> exhibited severe brain damage in the piriform cortex, neocortex, dentate hilus, amygdala and thalamus. Analyses of lung tissue showed morphologic changes in alveolar histiocytosis, hemorrhage and inflammation consisting of neutrophilic exudate. Respiratory and neurological toxicity induced by GD vapor was determined by clinical observations, histopathology and biochemical analyses of tissues 24 h PE. We integrated novel technologies in inhalation toxicology and physiology to evaluate CWNA toxicity to develop an improved model suitable for testing medical countermeasures in a mass casualty scenario.

This research was supported by the Defense Threat Reduction Agency project #3.F0014.

### PS 355 Inflammatory Profile and Macrophages Population in Sulfur Mustard (SM)-Exposed Skin Wound Repair.

Y. Chang<sup>1</sup>, M. Soriano<sup>1</sup>, J. D. Laskin<sup>2</sup>, R. P. Casillas<sup>3</sup>, M. K. Gordon<sup>1</sup> and D. R. Gerecke<sup>1</sup>. <sup>1</sup>Pharmacology and Toxicology, EOHHS, Rutgers University, Piscataway, NJ; <sup>2</sup>UMDNJ-RWJMS, Piscataway, NJ; <sup>3</sup>MRI Global, Kansas City, MO.

Cutaneous SM induced injury is characterized by a severe inflammatory response and delayed wound repair. Development of quantifiable inflammatory biomarkers is needed for screening anti-inflammatory drugs against SM injury. Since most inflammatory marker studies with SM exposed skin are only available for early time points (less than 24h), we extended this study to 7 days to better understand the inflammatory profile induced by SM. We examined the macrophage population and inflammatory profile using the mouse ear vesicant model (MEVM). RT-PCR data showed neutrophil collagenase/MMP8 was significantly unregulated 6h, 12h, and 168h post-SM exposure and macrophage elastase/MMP12 was significantly unregulated at 24h post SM exposure, increasing as time progressed. Immunohistochemical studies using a macrophage specific marker, F4/80 identified increased numbers of macrophages at 72h and 168h post-SM exposure. RT-PCR data showed early upregulation of IL6, IL1b, CCL3, CCL4, CXCL2, CXCL5, CXCL7 and CXCR4. Upregulation at 72 h post-SM exposure included: IL1r1, IL2rg, IL4ra, IL10ra, CSF2rb2, Tnfrsf1b, and Tnfsf11. Using a mouse cytokine/chemokine multiplex protein assay, we showed upregulation and persistent expression of IL6 and KC/CXCL1, and downregulation of IL10. CCL2 significantly increased over time beginning at 24h post-SM exposure. CCL3, GCSF, and IP10/CXCL10 were significantly increased at 72h and 168h post-SM exposures. These findings suggest that the cytokine/chemokines pattern we observed may be related to the persistent macrophage population that is generally seen in SM-exposed skin wounds. In addition, this inflammatory profile may be useful as in vivo biomarkers for evaluating anti-inflammatory drugs against SM-induced skin injury. This work is supported by ES005022, EY09056, and AR05507

### PS 356 Activation of the Endoplasmic Reticulum Stress and Unfolded Protein Responses for Protection against Sulfur Mustard-Induced Skin Injury.

D. R. Gerecke<sup>1</sup>, J. D. Wang<sup>1</sup>, J. D. Laskin<sup>2</sup>, M. K. Gordon<sup>1</sup> and Y. Chang<sup>1</sup>. <sup>1</sup>Pharmacology and Tox, EOHHS, Rutgers University, Piscataway, NJ; <sup>2</sup>UMDNJ-RWJMS, Piscataway, NJ.

The endoplasmic reticulum (ER) stress response, a cell survival pathway upregulated when cells are under severe stress, contributes to the pathogenesis of various diseases. It triggers the unfolded protein response (UPR) which initiates ER-to nucleus signaling pathways to protect against cell death via several types of UPR sensor proteins. One of these, ATF6, is proteolytically cleaved and translocated into the nucleus to regulate gene expression. Skin exposed to the vesicant sulfur mustard (SM) results in increased expression of specific chaperone proteins. We performed time course studies with SM using the mouse ear vesicant model (MEVM) and showed progressive histopathologic changes including edema, separation of the epidermis from the dermis, prolonged inflammation, and delayed wound repair from 24h to 168h post exposure. This study explored the contribution of UPR and increased ER chaperones in ER stress induced by SM injury. RT-PCR analysis of the ER stress survival gene GRP78; UPR gene ATF6; and ER stress apoptotic gene CHOP, demonstrated at least a 2 fold increase as time progressed. Western blot analysis confirmed upregulation of GRP78 and CHOP as time progressed. Both the full length cytoplasmic ATF6 and the 50 kDa cleaved nuclear fragment of ATF6 were increased after 24h post SM. Immunofluorescent data showed cytoplasmic staining at 24h post exposure and significant nuclear staining in the proliferating keratinocytes at 168h post exposure. Double-labeled immunofluorescent studies of GRP78 and CHOP indicated GRP78 staining in the basal, proliferating keratinocytes. In contrast, expression of CHOP was greater in the outermost migrating cells. These data suggest the ER stress response and UPR are activated in the proliferating keratinocytes to protect cells against SM induced skin injury. This work is supported by ES005022, EY09056, and AR055073.

### PS 357 Detection of Sulfur Mustard or Half Mustard-Induced DNA Adducts in Human Skin Cells.

K. Kehe, V. Schrettl, D. Steinritz and H. Thiermann. *Bundeswehr Institute of Pharmacology and Toxicology, München, Germany.* Sponsor: A. Bürkle.

Introduction: Sulfur mustard (SM) and 2-chloroethyl ethylsulfide (CEES) are bi- and monofunctional DNA alkylating agents, respectively. SM is an old chemical warfare agent causing blisters (vesicant). Both chemicals react with N7 guanine. SM will form 7-Hydroxyethylthioethylguanine for SM and CEES 7-ethyl thioethylguanine for CEES. A specific monoclonal antibody (2F8) exists which detects SM and CEES adducts at N7 position.

Aim: The 2F8 antibody was used to develop a slot blot technique for detection of SM and CEES exposure in human keratinocytes (HaCaT cells).

Methods: HaCaT cells were exposed with different concentrations of SM or CEES (30 min). After exposure, cells were scraped and DNA was isolated, normalized and transferred to a Nylon membrane using slot blot technique. After incubation with 2F8 antibody, the DNA adducts were visualized with DAB staining.

Results: DNA adducts were detected after CEES and SM exposure below 30 µM which is the vesicant threshold.

Conclusion: The presented technique is potentially able to confirm SM or CEES exposure in blister roofs of exposed patients.

### PS 358 Differential Inhibition of Cytoplasmic and Mitochondrial Thioredoxin and Thioredoxin Reductase by Nitrogen Mustard in A549 Lung Epithelial Cells.

I. Wohlman<sup>1</sup>, Y. Jan<sup>2</sup>, D. E. Heck<sup>3</sup>, R. P. Casillas<sup>4</sup>, D. L. Laskin<sup>1</sup> and J. D. Laskin<sup>2</sup>. <sup>1</sup>Pharmacology & Toxicology, Rutgers University, Piscataway, NJ; <sup>2</sup>Environmental & Occupational Medicine, UMDNJ-Robert Wood Johnson Medical School, Piscataway, NJ; <sup>3</sup>Environmental Health Science, New York Medical College, Valhalla, NY; <sup>4</sup>MRI Global, Kansas City, MO.

The thioredoxin system, consisting of thioredoxin reductase (TrxR) and thioredoxin (Trx), plays an important role in cellular antioxidant defense. Both cytosolic (TrxR1, Trx1) and mitochondrial (TrxR2, Trx2) forms of the enzymes have been identified in mammalian cells. Previously, we reported that the bifunctional nitrogen mustard vesicant, mechlorethamine (HN2), targeted cytosolic TrxR1 by alkylating catalytic residues in the enzyme's redox centers. In the present studies, we compared the effects of HN2 on the cytoplasmic and mitochondrial forms of TrxR and Trx in A549 lung epithelial cells. HN2 treatment was found to cause a concentration- and time-dependent inhibition of the activities of both cytoplasmic and

mitochondrial forms of TrxR and Trx. HN2 was significantly more efficient in inhibiting cytosolic, when compared to mitochondrial forms of the enzymes. For TrxR1 and TrxR2, the IC50's for inhibition of enzyme activity were 2.7  $\mu$ M and 14.3  $\mu$ M, respectively. Immunoblot analysis of subcellular fractions from control cells on denaturing SDS-PAGE showed TrxR (57 kDa) and Trx (14 kDa) monomers. HN2 treatment cross-linked Trx1 and Trx2 forming tetramers, and TrxR1 and TrxR2 forming dimers and oligomers. These data demonstrate that HN2 can target the thioredoxin system in cytosolic and mitochondrial fractions of A549 cells by cross-linking proteins. Disruption of this system in lung cells provides a mechanism for nitrogen mustard-induced oxidative stress and toxicity. Support: NIH grants AR055073, ES004738, CA132624, ES005022 and GM034310.

**PS 359 Nitrogen Mustard (NM)-Induced Pulmonary Injury and Inflammation Are Associated with Alterations in Histone Methylation and Acetylation.**

A. Venosa<sup>1</sup>, R. Malaviya<sup>1</sup>, J. D. Laskin<sup>2</sup> and D. L. Laskin<sup>1</sup>. <sup>1</sup>Pharmacology and Toxicology, Rutgers University, Piscataway, NJ; <sup>2</sup>Environmental & Occupational Medicine, UMDNJ-Robert Wood Johnson Medical School, Piscataway, NJ.

NM (mechlorethamine hydrochloride) is a highly toxic vesicant which acts by alkylating DNA and proteins and generating oxidative stress. The lung is known to be a major target for NM. Exposure to NM results in rapid structural changes including perivascular edema and thickening of the alveolar wall followed by bronchiolization of the epithelium which progresses to lung fibrosis. We have previously shown that inflammatory mediators including reactive nitrogen species and tumor necrosis factor- $\alpha$  contribute to NM-induced lung injury. Expressions of genes for these mediators, as well as antioxidants, are known to be regulated by methylation and acetylation of histones. In these studies we determine if NM-induced injury and inflammatory/antioxidant protein expression is associated with histone modification. Lung samples were collected 1 d – 28 d after exposure of male Wistar rats to NM (0.125 mg/kg, intratracheal) or PBS control. NM intoxication resulted in increased expression of inducible nitric oxide synthase, cyclooxygenase-2 and heme oxygenase-1 in the lung within 1 d, a response which persisted for 28 d; Mn-superoxide dismutase was also up regulated beginning at 7 d. Analysis of lung homogenates by western blotting using specific antibodies revealed that this was correlated with a time-dependent increase in acetylation on histone 3 lysine 9 (H3K9Ac) which returned to baseline by 28 d. In contrast H3K4 methylation decreased 1 d – 7 d post-NM; this was followed by an increase at 28 d. Additionally, whereas H3K36 methylation increased beginning 3 d post-NM and persisted up to 28 d, increases in H3K27 methylation were only evident 28 d after NM exposure. These data suggest that NM-induced lung injury leads to specific alterations in chromatin structure which may contribute to pro-inflammatory and antioxidant gene expression. Supported by NIH Grants AR055073, ES004738, CA132624, GM034310, and ES005022.

**PS 360 Dose Modulation of a Potential Therapeutic for Neovascularization from Ocular Exposure to Sulfur Mustard.**

M. L. Meade<sup>1</sup>, J. J. Schlager<sup>2</sup> and M. C. Babin<sup>3</sup>. <sup>1</sup>Henry M Jackson Foundation, Wright-Patterson AFB, OH; <sup>2</sup>711th Human Performance Wing, Wright-Patterson AFB, OH; <sup>3</sup>Battelle Biomedical Research Center, Jeffersonville, OH.

Sulfur mustard is a potent alkylating agent affecting the skin, respiratory tract and eyes. Ocular exposure to HD can result in long term injuries including corneal neovascularization (NV) and blindness. The immunosuppressant, cyclosporine A, has shown promise for protecting epithelial cells against apoptosis in *in vitro* experiments. To investigate the effects of cyclosporine A *in vivo*, two studies were conducted, an initial long term study for 112 days, and a 28 day study using the white rabbit ocular model to evaluate the effects of different concentrations of cyclosporine A. The right cornea was insulted with 0.4  $\mu$ l (0.51 mg) of neat HD while using the left as a control. Cyclosporine was administered beginning at five days post exposure for three weeks decreasing the frequency throughout the regimen. Clinical assessments, including stromal damage and corneal thickness were performed throughout the study. Following the study, corneas were harvested and shipped to Wright Patterson AFB for quantitative proteomic analysis. In the initial 16 week study, cyclosporine performed significantly better than did no treatment or other potential therapeutics thought to aid in NV prevention. H&E staining shows continued inflammation in the stroma in the untreated eyes at 15 weeks post exposure, while the cyclosporine treated eyes appear normal. A follow up study using differing concentrations of cyclosporine A was also performed. The clinical assessment data acquired during this study showed that all concentrations of cyclosporine performed well in eliminating stromal opacity at 28 post exposure compared to no treatment. The 2% cyclosporine group performed better than other concentrations

in preventing NV with only one animal in the group experiencing NV at the conclusion of the study. Quantitative proteomics of the epithelium and endothelium of the corneas also showed protein expression levels consistent with the unexposed eyes in the 2% cyclosporine group.

**PS 361 Development and Optimization of *In Vitro* Models of Chemical Ocular Injury for High-Throughput siRNA Screening.**

J. G. Lehman, S. L. Beach, R. D. Causey and A. L. Ruff. US Army Medical Research Institute of Chemical Defense, Aberdeen Proving Ground, MD.

Chemically induced ocular injuries are considered one of the few true ocular emergencies based on their high potential to inflict rapid and significant tissue damage. Currently there are no specific therapeutics to treat chemically induced corneal injury, and there is a pressing need to rapidly screen therapeutics to discover a treatment. Understanding of the molecular mechanisms of this injury is necessary to aid in rational therapeutic development. We intend to utilize high throughput small inhibitory RNA (siRNA) screening to elucidate the mechanisms of chemical cornea injury and to identify therapeutic targets. Herein we present the development of the *in vitro* models for this screening effort. Two immortalized human corneal epithelial cell lines will be used for screening: SV40 large T antigen immortalized corneal epithelial cells (SHECs) and telomerase immortalized corneal epithelial cells (TCECs). Hydrofluoric acid (HFA) is used for the induction of chemical injury. The major conditions optimized included cell line plating density, exposure dose, and transfection conditions. Matrices of these conditions were evaluated to ensure optimal target knockdown without sacrificing cell viability. Transfection conditions were optimized using siRNA targeting cyclophilin b, and knockdown was assessed using the QuantiGene Plex assay, a bead based assay using hybridization to amplify specific mRNAs allowing for quantification. A dose-response study of HFA injury was performed, and the HFA-induced production of the cytokines was evaluated by multiplex bead-based assay for a panel of 30 cytokines. Once optimized, these models will be used to screen subgenomic siRNA libraries targeting HF-induced ocular inflammation.

Disclaimer: The views expressed in this article are those of the author(s) and do not reflect the official policy of the Department of Army, Department of Defense, or the U.S. Government. This research was supported by the Defense Threat Reduction Agency – Joint Science and Technology Office, Medical S&T Division.

**PS 362 Multirray Gene Expression Approach Analyzing Cultured Primary Human Astrocytes and Neurons following Chemical Warfare Nerve Agent Exposure.**

C. Rothwell, S. Swayze, J. E. Dillman and H. Hoard-Fruchey. USAMRICD, Gunpowder, MD.

Chemical warfare nerve agents (CWNAs) are irreversible organophosphorus cholinesterase inhibitors that cause seizure. Within 24 h of CWNA exposure, neuronal degeneration, astrocytic activation and cellular death can be observed in various brain regions. In this study, we investigated the effects of CWNA exposure on primary cultures of neurons and astrocytes to determine direct molecular alterations in the absence of CWNA-induced seizure activity. Cultured primary human astrocytes were exposed to 100  $\mu$ M of the CWNAs sarin, soman, VX, or VR and harvested at 24 h. Similarly, cultured primary human neurons were exposed to 100  $\mu$ M soman or VX and harvested at 24 h. Total RNA was isolated from exposed cells, processed for microarray analysis, and hybridized to Affymetrix Human Genome U133 Plus 2.0 arrays. Principal component analysis (PCA) of the astrocyte data did not show distinct profile differences based on agent type, indicating few if any significant differences in transcript expression in response to agent exposure. However, PCA of the neuronal data showed a distinct profile difference based on agent type. For both cell types, the dataset was filtered by agent type, and an analysis of variance (ANOVA) was performed using agent as the factor. Using these combined data, the pathways significantly affected by agent type in cultured human primary neurons were identified. The genes differentially expressed in response to soman exposure mapped to canonical pathways containing inflammatory molecules. Using the same samples, real-time PCR was utilized to provide quantitative measurements of gene transcription across genes associated with the human immune response. These data suggest a non-cholinergic effect of soman that induces transcriptional expression of inflammatory molecules as well as components of the GABA pathway. In addition, these data suggest that an in-depth analysis of *in vivo* transcriptomic data focusing on the GABA pathway may reveal new targets within that pathway for improved medical countermeasures to these toxic agents.

**PS 363 MicroRNA Microarray Analysis of Human-Induced Pluripotent Stem Cell-Derived Neurons and Cardiomyocytes following Exposure to the Organophosphate Nerve Agents Soman and VX.**

E. K. Yego, J. F. Dillman and H. Hoard-Fruchey. *Research Division, US Army Medical Research Institute of Chemical Defense, Aberdeen Proving Ground, MD.*

Chemical warfare nerve agents (CWNA) are potent cholinesterase inhibitors that may also have non-cholinesterase effects. Several in vivo studies have demonstrated CWNA-induced damage in the brain and heart following CWNA exposure. The mechanisms of this damage have been a critical area of research for the development of medical countermeasures. This study utilized microRNA (miRNA) analysis to evaluate potential direct cellular effects of the nerve agents soman (O-Pinacolyl methylphosphonofluoridate) or VX (o-ethyl-s-[2 (diisopropylamino) ethyl]) on human-induced pluripotent stem cell (iPSC)-derived neurons and cardiomyocytes. This approach was taken since miRNA expression changes are stimulus specific and no previous studies of miRNA profiles have been conducted for CWNA exposure. Cells were treated with soman or VX at concentrations of 0  $\mu$ M, 0.1  $\mu$ M or 100  $\mu$ M for either 1 hr or 6 hr. Following treatment, isolated total RNA was processed for miRNA microarray analysis and analyzed for significant changes. Soman- and VX-treated samples were analyzed separately. Principal component analysis (PCA) was used to identify major sources of variability in the dataset. PCA analysis of neurons identified differences in miRNA expression only for cells exposed for 6 hr to soman. Targets that were significantly altered under these conditions were miR-2277, miR-1910 and miR-1972. miR-2277 was significantly altered in soman- and VX-exposed neuron data sets that were analyzed by both time and dose. Minimal sample variability was observed with cardiomyocytes as determined by PCA analysis. One-way ANOVA with time as the factor identified miR-3178 as the only target that was altered significantly by both soman and VX in cardiomyocytes. This miRNA modulates several targets including complexin-1 and splicing factor-1. This study demonstrates the feasibility of using miRNA microarray analysis for the study of CWNA cellular effects.

**PS 364 Toxidromes—A Decision-Making Tool for Early Response to Chemical Mass Exposure Incidents.**

M. Kirk<sup>1</sup>, P. J. Hakkinen<sup>2</sup>, J. S. Ignacio<sup>3</sup>, O. Kroner<sup>4</sup>, A. Maier<sup>4</sup> and J. Patterson<sup>4</sup>. <sup>1</sup>University of Virginia, Charlottesville, VA; <sup>2</sup>National Library of Medicine, Bethesda, MD; <sup>3</sup>Department of Homeland Security, Washington DC; <sup>4</sup>TERA, Cincinnati, OH.

A common language to describe and recognize clinical manifestations of toxic chemical exposures is essential for emergency responders and hospital first receivers to be prepared to provide rapid and appropriate medical care for victims of industrial chemical mass exposures and terrorist attacks. In these situations, when the identity of the chemical is not known, first responders need a tool to rapidly evaluate victims and identify the best course of treatment. Military and civilian emergency response communities use a "toxic syndrome" (toxidrome) approach to quickly assess victims and determine the best immediate treatment when information on chemical exposures is limited. Toxidromes can be defined by a unique group of clinical observations, such as vital signs, mental status, pupil size, mucous membrane irritation, and lung and skin examinations. Data on over 20 toxidrome systems were evaluated to identify salient features and develop a consistent lexicon for use by state, local, tribal, territorial, and federal first responders and first receivers. A workshop of over 40 practitioners and experts in emergency response, emergency medicine, and medical toxicology developed names and definitions for 12 unique toxidromes that describe and differentiate the clinical signs and symptoms from exposures to chemicals. These toxidromes focus on acute signs and symptoms caused by inhalation and dermal exposures. Each toxidrome is characterized by exposure routes and sources, organs/systems affected, initial signs and symptoms, underlying mode of action, and treatment/antidotes. Toxidrome names and definitions are designed to be readily understood and remembered by users. Communication in a crisis requires accurate and succinct terms that can quickly convey the health conditions of patients. These toxidromes lay the foundation for a consistent lexicon, that if adopted widely, will improve response to chemical mass exposure incidents.

**PS 365 Activation of DNA Damage Repair Pathways in Response to Nitrogen Mustard-Induced DNA Damage and Toxicity in Skin Keratinocytes.**

S. Inturi<sup>1</sup>, N. Tewari-Singh<sup>1</sup>, C. Agarwal<sup>1</sup>, C. W. White<sup>2</sup> and R. Agarwal<sup>1</sup>. <sup>1</sup>Pharmaceutical Sciences, University of Colorado Denver, Aurora, CO; <sup>2</sup>Pediatrics, University of Colorado Denver, Aurora, CO.

Alkylating agent nitrogen mustard (NM), a structural analog of chemical warfare agent sulfur mustard (SM), upon exposure to tissues, forms adducts and crosslinks with DNA, RNA and proteins. The major mechanism of NM-induced toxicity involves DNA interstrand crosslinks (ICL) formation resulting in either induction of cell cycle arrest to facilitate DNA damage repair or cell death, in the case of inadequate repair. Consistently, NM (0.75  $\mu$ M) exposure in mouse epidermal JB6 cells decreased cell growth and caused S-phase arrest by 16 h after exposure. Cells were then released to G2-M phase by 24 h and resumed normal cell cycle progression by 48 h after exposure. Repair of NM-induced DNA ICLs involves formation of DNA double strand breaks (DSB). Our studies showed an increase in comet tail extent moment starting between 4 and 8 h of NM exposure, as well as an increase in levels of DNA DSB repair molecules (phospho H2A.X and p53, rad50 and XRCC1). The repair of DNA double strand breaks occurs via homologous recombination repair (HRR) or through the non homologous end joining pathway (NHEJ). The activation of the HRR pathway was evidenced by formation of Rad51 foci at 4 h after NM exposure, and activation of NHEJ pathway was indicated by increases in phospho and total DNA-PK levels. To confirm this, NHEJ and HRR pathways were inhibited by using DNA-PK inhibitor NU7026 and Rad51 siRNA, respectively. Inhibition of NHEJ did not result in a significant decrease in total cell number after 48 h of NM exposure and also did not affect the NM-induced S-phase arrest at 16 h. However, inhibition of the HRR pathway caused a 28% decrease in cell number, and a lack of NM-induced S-phase arrest, probably leading to an increase in the observed cell death. These studies indicate that HRR may be a key pathway involved in repair of NM-induced DNA DSBs. These findings may be useful in developing new therapeutic strategies against NM-induced skin toxicity.

**PS 366 Progression of Injury and Toxic Effects following Nitrogen Mustard Exposure in SKH-1 Hairless and C57BL/6J Mice Skin: Clinical and Pathological Significance.**

N. Tewari-Singh<sup>1</sup>, A. K. Jain<sup>1</sup>, S. Inturi<sup>1</sup>, D. J. Orlicky<sup>2</sup>, C. W. White<sup>3</sup> and R. Agarwal<sup>1</sup>. <sup>1</sup>Pharmaceutical Sciences, University of Colorado Denver, Aurora, CO; <sup>2</sup>Pathology, University of Colorado Denver, Aurora, CO; <sup>3</sup>Pediatrics, University of Colorado Denver, Aurora, CO.

Lack of availability of relevant skin injury models and clinically applicable biomarkers are major limitations in developing therapies to rescue skin injury and vesication by chemical warfare agent sulfur mustard (SM). Consequently, we conducted studies to establish useful clinical and histopathological endpoints with primary vesicating agent nitrogen mustard (NM). NM possesses strong vesicating and alkylating properties and causes damage to cellular macromolecules, exerting severe skin toxicity comparable to SM. Our comprehensive studies employing NM (3.2 mg) exposure for 12, 24, 72 and 120 h in both SKH-1 and C57BL/6J mice showed clinical sequelae of toxicity, including visible microblistering (12-24 h), edema (12-120 h), erythema (12-24 h), and hyper- and hypopigmentation, wounding, xerosis and scaly dry skin (72-120 h) that were comparable in both the mouse strains, and similar to those reported with SM in humans. In addition, 40% mortality was observed by 120 h after NM exposure in C57BL/6J mice. H&E stained skin sections of both mice showed that NM (12-120 h recovery) caused increased skin bi-fold thickness; histopathological effects such as hyperproliferation, microvesication, epidermal and dermal necrosis, denuding and scab formation, and parakeratosis (24-120 h), hypercornification (12-120 h), acanthosis and re-epithelialization (72-120 h); increase in inflammatory cells; and red blood cell extravasation into the dermis. These histopathological effects with NM were comparable to those reported in humans and other animal species with SM, and were quantified as percent of skin sections showing these effects, fold increases in histopathologic abnormalities, and prevalence among mice (% that showed these effects). These NM-induced effects are novel clinically relevant biomarkers to be used in screening and optimization of rescue therapies for skin injuries due to NM and SM in humans.

**PS 367 Long-Range Assessment and Treatment of Lung and Systemic Injury in Rats Exposed to Inhaled Sulfur Mustard.**

D. S. Olivera, T. R. Varney, D. A. Alves, K. Whitten, V. I. Morthole, R. K. Kan, J. L. Collins, J. B. Simons, J. L. Devorak, A. M. Rodriguez, C. M. Bowens, A. M. Witriol, E. A. Lyman, R. R. Deckert, S. L. Russell and A. M. Sciuto. *Analytical Toxicology, USAMRICD, Gunpowder, MD.*

Sulfur mustard (HD) causes severe chemical burns to the skin, eyes, and airways. HD was used as a chemical warfare agent (CWA) in the Iran/Iraq conflict, and more than half of surviving HD-exposed casualties suffer from permanent lung injuries. The mechanisms and timing of the development of these pathologies are poorly defined, and there is no effective antidote. Rats were intubated and ventilated for 10 min with nebulized HD or vehicle to achieve doses of 0, 0.5, 1.75, 2.25, and 3 mg/kg. Pulmonary function was analyzed by whole-body plethysmography. Rats were euthanized at various time-points  $\leq$  6 months post-exposure, blood chemistry was analyzed, broncho-alveolar lavage fluid was analyzed for cytokines/ redox state, and lungs were subjected to pathologic analysis. The data show high correlation between blood gas perturbations, upper airway necrosis and pulmonary function in the 24 h to 48 h after the 3 mg/kg HD exposure. In longer-ranging animals, the 3 to 7 wks period was a significant challenge because 15% of the 3 mg/kg group and 10% of the 2.25 mg/kg group died suddenly or required withdrawal from the study during this time. Alveolar exudates, edema, oxidative stress, and inflammation peaked at 3 wks and correlated with changes in pulmonary function and respiratory distress. Therefore, the first day and the second to third wks post-exposure may be crucial windows in the progression of HD inhalation injury, and treatment at these times may be the best approach. Based on this, we have evaluated single and multiple infusions of mesenchymal stem cells as a treatment and have found success in reducing HD-induced edema, necrosis, inflammation, and death at 5 wks post-exposure. This study provides the first long-term examination of HD-induced lung injury and systemic effects, and demonstrates the feasibility of stem cell therapies for treatment of HD inhalation injury.

**PS 368 Therapeutic Efficacy of Serum-Derived Human Butyrylcholinesterase against Topical Challenges of VX in the Hartley Guinea Pig.**

T. Snider<sup>1</sup>, J. D. Johnson<sup>1</sup>, K. G. McGarry<sup>1</sup>, G. H. Van der Zwaag<sup>1</sup>, R. L. Malek<sup>2</sup>, B. Peterson<sup>2</sup> and A. N. Nunley<sup>2</sup>. <sup>1</sup>Battelle, Columbus, OH; <sup>2</sup>Chemical Biological Medical Systems/Medical Identification and Treatment Systems, Frederick, MD.

The protective efficacy of human serum butyrylcholinesterase (HuBChE) was assessed in the guinea pig against topical challenges of VX. Male Hartley guinea pigs with jugular catheters were clipped on the left flank and challenged with neat VX at multiples of the 24-hr median lethal dose (LD<sub>50</sub>). Two hours after challenge, animals received either 1.04 mL/kg saline or HuBChE at 26 mg/1.04 mL/kg by intravenous (IV) infusion. Blood samples were collected at 5 min before challenge, 5 min before therapy, and 48 and 96 hr after challenge, and assayed for acetylcholinesterase (AChE) and butyrylcholinesterase (BChE) activity. Clinical signs, recorded for up to 96 hr after challenge, indicated that VX rapidly penetrated skin. The protective ratio of HuBChE, 2.8, was calculated as the LD<sub>50</sub> determined by probit analysis among IV therapy-receiving guinea pigs (0.39 mg/kg) divided by the LD<sub>50</sub> for unprotected guinea pigs (0.14 mg/kg). VX was lethal to all guinea pigs challenged at 4x and 8x LD<sub>50</sub>. AChE activity among survivors, likely through VX dissociation, rebounded to more than 80% of the baseline value by 96 hr. BChE activity among survivors increased after therapy and remained at more than 30 times endogenous levels over the 4-day study. In a follow-on study, the therapeutic window was characterized by fixing the topical VX challenge dose at the LD<sub>15</sub> (0.34 mg/kg) and changing the time interval to IV therapy. Probit modeling indicated that 50% lethality would be expected after a 4.3 hr delay post-challenge of HuBChE therapy. Blood AChE activity profiles declined with delay in therapy followed by a rebound among survivors. BChE activity increased after therapy and remained at 30 to 54 times endogenous levels over the 4-day study. This work was conducted under the CBRNIAC Contract No. SF0 700-00-D-3180, Delivery Order 0599, Task 789.

**PS 369 A Comparative Study of Biomarkers of Nitrogen Mustard-Induced Skin Injury in Male SKH-1 Hairless and C57BL/6J Mice.**

A. K. Jain<sup>1</sup>, N. Tewari-Singh<sup>1</sup>, S. Inturi<sup>1</sup>, D. J. Orlicky<sup>2</sup>, C. W. White<sup>3</sup> and R. Agarwal<sup>1</sup>. <sup>1</sup>Pharmaceutical Sciences, University of Colorado Denver, Aurora, CO; <sup>2</sup>Pathology, University of Colorado Denver, Aurora, CO; <sup>3</sup>Pediatrics, University of Colorado Denver, Aurora, CO.

Sulfur mustard (SM) is a primary vesicating warfare agent that upon exposure causes severe skin injuries. Currently, we lack effective antidote against SM-induced skin injuries, in part due to lack of appropriate animal model(s) that can be used for mechanistic and efficacy studies in laboratory settings. Our earlier studies have established biomarkers related to inflammation and vesication in SKH-1 hairless mice using 2-chloroethyl ethyl sulfide (CEES), an SM analog. However, CEES is a monofunctional alkylating agent that is less toxic than SM. Therefore, to develop a more relevant skin injury model, we have now used nitrogen mustard (NM); a primary vesicant and a bifunctional alkylating agent that induces toxic effects comparable to SM. We compared the effect of NM (3.2 mg) exposure for 12, 24, 72 and 120 h in SKH-1 hairless and C57BL/6J mice. NM caused significant increases in skin microvesication, cell proliferation, apoptotic cell death, inflammatory cells (neutrophils, macrophages, and mast cells) and MPO activity in both mouse strains. However, in SKH-1 mice there was a more prominent increase in epidermal thickness, macrophages and mast cell infiltration, relative to that seen in C57BL/6J mice. NM also caused collagen degradation at early time points (12-24 h) with a decrease in collagen trichrome staining and an increase in dermal thickening, due, at least in part, to edema. However, at later time points (72 and 120 h), dense collagen staining with reduced dermal edema was observed, indicating a healing process. This study indicates that both mouse strains have comparable susceptibility to NM injury, as shown by inflammation and vesication. However, some inflammatory responses were more pronounced in NM-induced skin injury in SKH-1 mice. These newly established biomarkers in a more accessible and relevant NM skin injury model should aid in identifying effective therapies for treatment of skin injuries due to NM and SM.

**PS 370 24 h LD<sub>50</sub> for Subcutaneous Exposure to Chemical Warfare Nerve Agents in Rats: Comparison across Multiple Age Groups.**

L. K. Wright, R. B. Lee, S. H. Robertson, K. M. Licht, M. F. Stone, M. C. Moffett and L. A. Lumley. *US Army Medical Research Institute of Chemical Defense, Aberdeen Proving Ground, MD.*

In a mass casualty situation involving the release of chemical warfare nerve agents (CWNA), infants, children and adolescents are likely to be exposed. These subgroups of the population may be more susceptible than adults to the toxicological effects of CWNA exposure because of their closer proximities to a ground source, smaller body masses, higher respiratory rates, greater skin permeabilities and immature brains and metabolic systems. Unfortunately, there have only been a handful of studies on the effects of CWNA in younger animals, and more research is needed to confirm this hypothesis. Using a stagewise, adaptive dose design, we determined the 24 h LD<sub>50</sub> for subcutaneous (sc) exposure to sarin (GB), as well as VX, in both male and female Sprague-Dawley rats at five different time points during their development (postnatal day [PND] 7, 14, 21, 42 and 70). For males, the 24 h LD<sub>50</sub> for both GB and VX increased from PND 7 thru PND 42 and then slightly decreased at PND 70. Similar results were observed for females; however, fewer significant differences between age groups were observed. Regardless of CWNA, no significant differences were observed between males and females for any age group. Thus, younger rats are more susceptible to the lethal effects of subcutaneously administered CWNA than older rats. The views expressed in this abstract are those of the authors and do not reflect the official policy of the Department of Army, Department of Defense, or the U.S. Government. The experimental protocol was approved by the Animal Care and Use Committee at the United States Army Medical Research Institute of Chemical Defense (USAMRICD), and all procedures were conducted in accordance with the principles stated in the Guide for the Care and Use of Laboratory Animals and the Animal Welfare Act of 1966 (P.L. 89-544), as amended. This research was supported by interagency agreement between the Biomedical Advanced Research and Development Authority and USAMRICD.

**PS 371 Mechanisms of Vesicating Agent Nitrogen Mustard-Induced Skin Injury in SKH-1 Hairless Mice.**

D. Kumar<sup>1</sup>, N. Tewari-Singh<sup>1</sup>, S. Inturi<sup>1</sup>, C. Agarwal<sup>1</sup>, A. K. Jain<sup>1</sup>, D. Dhar<sup>1</sup>, C. W. White<sup>2</sup> and R. Agarwal<sup>1</sup>. <sup>1</sup>Pharmaceutical Sciences, University of Colorado Denver, Aurora, CO; <sup>2</sup>Pediatrics, University of Colorado Denver, Aurora, CO.

Lack of a comprehensive understanding of molecular mechanisms and signaling pathways involved in skin injuries due to chemical warfare agent sulfur mustard (SM)- is a major limitation in developing mechanism-based therapies for rescue of skin injuries by vesicating agents. Our recent studies in SKH-1 hairless mice show that exposure to nitrogen mustard (NM; 3.2 mg) for 12, 24, 72, 120 or 168 h triggers an inflammatory response, vesication, apoptotic cell death, and either initiation of healing or 40% mortality by 168 h of exposure. Both SM and NM vesicant-induced tissue injury is mainly due to alkylating properties, with DNA damage resulting from direct toxicity and/or oxidative stress. In this study we extended our efforts to identify the mechanism/s involved in NM-induced toxic response at 12-120 h after exposure. In skin tissue of SKH-1 mice, NM exposure caused p53 ser15 phosphorylation and increased p53 accumulation, both indicating DNA damage. Our results also showed that NM exposure, with recovery for 12-168 h, induced expression of inflammatory mediators COX-2 and iNOS in mouse skin, and >2-fold increase in expression of protease MMP-9, that may contribute to NM-induced vesication. NM exposure, with recovery for 12-168 h, also was associated with phosphorylation of mitogen-activated protein kinases (MAPKs; ERK1/2, JNK, and p38) and increased oxidative stress, as indicated by enhanced 4-HNE (lipid peroxidation) and DMPO protein adduct formation. Our results thus far indicate that NM induces activation of upstream signaling pathways including MAPKs and oxidative stress that could, in part, be responsible for DNA damage, cell death, and expression of inflammatory and proteolytic mediators contributing to the inflammatory response and vesication. These molecular targets could be useful in developing therapeutic interventions against NM- and SM-related skin injuries.

**PS 372 Ovarian Hormones Affect the Physiological Response to VX in Female Rats.**

C. Smith, L. K. Wright, J. E. Schwartz, S. H. Robertson, K. M. Licht and L. A. Lumley. *US Army Medical Research Institute of Chemical Defense, Aberdeen Proving Ground, MD.* Sponsor: J. McDonough.

Chemical warfare nerve agents (CWNAs), such as VX, irreversibly bind to acetylcholinesterase, which induces a "cholinergic crisis" that causes numerous physiological events including seizures and death. Females are historically an understudied subset of the population, largely because of conflicting data related to the effects of CWNAs both within groups of females and in comparison to males. The profound impact of circulating ovarian hormones on biological processes is well known, and parsimony suggests that these hormones contribute to these observed differences. To date, few studies have investigated the impact of naturally circulating ovarian hormones in animals exposed to CWNAs. In the current study, we examined the effects of VX (1.0 x LD<sub>50</sub>) in female rats that had their ovaries removed (OVEX) or left intact. The estrous cycles of females left intact were monitored, and they were further divided by stage of the cycle (estrus or diestrus). Results show that females in estrus survived for a significantly longer period of time than OVEX rats. Seizure activity was also significantly different, with 5/8 OVEX, 2/8 diestrous, and 0/8 estrous female rats exhibiting seizures. These data suggest that ovarian hormones, including estrogen, progesterone, and their metabolites, which rise the evening before estrus, offer protection against the seizure-inducing and lethal effects of VX. The views expressed in this abstract are those of the authors and do not reflect the official policy of the Department of Army, Department of Defense, or the U.S. Government. The experimental protocol was approved by the Animal Care and Use Committee at the United States Army Medical Research Institute of Chemical Defense and all procedures were conducted in accordance with the principles stated in the Guide for the Care and Use of Laboratory Animals and the Animal Welfare Act of 1966 (P.L. 89-544), as amended. This research was supported by the U.S. Army's In-house Laboratory Independent Research (ILIR) program.

**PS 373 Inflammatory Response following Neurogenic Cardiotoxicity Induced by Exposure to the Chemical Warfare Agent Soman.**

H. Hoard-Fruchey, C. J. Smith, M. A. Guignet, J. F. Irwin, T. L. Dao, J. A. Leuschner, E. A. Johnson, J. F. Dillman and R. K. Kan. *US Army Medical Research Institute of Chemical Defense, Aberdeen Proving Ground, MD.*

Chemical warfare nerve agents (CWNAs) are potent inhibitors of cholinesterase activity, causing inhibition of acetylcholinesterase and accumulation of acetylcholine (ACh) at synaptic junctions. Excess ACh causes hyperstimulation of the central and

peripheral cholinergic systems, and seizure activity ensues in susceptible brain regions. Because of the extensive neuronal damage and death caused by the resulting seizure activity, studies of CWNA-induced injury have focused primarily on the effects to the central nervous system with few studies focused on other organ systems. Previous studies have demonstrated cardiac damage following exposure to seizurogenic doses of the CWNAs soman and sarin. Following acute exposure to soman, up to 88% of rats display cardiac lesions in the interventricular septum and left ventricular wall. To initiate molecular characterization of soman-induced cardiotoxicity, we used multiplex immunoassays to determine concentrations of inflammatory and cardiac markers altered in left ventricle samples from rats exposed to a seizurogenic dose of soman. Increased concentrations of cytokines such as IL-1 beta, IL-4, IL-5, IL-13, and IFN gamma were observed within 24 hours of soman-induced seizure. Cytokine IL-6 concentrations peaked 3 hr after soman-induced seizure, indicating early involvement of inflammatory response in cardiac tissue. Chemokines MCP-1 and CXCL1 also increased, indicating that signals for neutrophil and monocyte recruitment to cardiac tissue are present following soman exposure. In addition, increases in TIMP-1 and VEGF concentrations within 6 hr of soman exposure suggest that cardiac injury occurs within hours of seizure initiation and that in response, repair mechanisms are activated. These results support development of anti-inflammatory medical countermeasures to treat the peripheral as well as the central effects of chemical warfare nerve agents.

**PS 374 Development of an Inhalation Exposure System to Control Concentration and Time Profile of a Test Gas to Evaluate the Predictivity of "Toxic Load" Models.**

B. A. Wong, R. James, B. C. Sharits and L. M. Sweeney. *Naval Medical Research Unit - Dayton, Wright Patterson Air Force Base, OH.*

For dose calculations of an inhaled toxic material, a time-varying concentration scenario is generally modeled as a constant concentration times a specified duration (step profile) that yields the same cumulative exposure, such as in the toxic load model ( $C_n \times T$ ). The adequacy of the toxic load model to predict mortality from a realistic exposure scenario based on step profile laboratory experiments is under review. An inhalation exposure system was set up to provide separate pulses of a test atmosphere at different concentrations and time durations as a first approximation of a time varying exposure.

A test atmosphere was generated by mixing a test gas from a cylinder (hydrogen cyanide in oxygen and nitrogen) with clean air to a target concentration. A combination of two generation systems, one at a high target concentration and one at a low target concentration was used to produce a specified change in concentration. The two generation systems could be switched on and off to insert a time gap between the two exposure concentrations, if desired. Precision mass flow controllers were used to control the flow of test gas and dilution air to achieve the target concentrations. Electric solenoid valves were used to change the different gas flows for precise timing. A Fourier Transform Infrared Spectrometer was used to measure the test material concentration in the exposure air entering the breathing zone of the test subject. A 12-port nose-only exposure unit was used to expose animals to the test atmosphere. Three basic patterns were generated, a single constant concentration for a defined time duration, a high concentration and low concentration pulse with no separation, and a high concentration and low concentration with a clean air gap between pulses. Test generation results showed excellent control of time and concentration of the exposure atmospheres.

**R 375 A Decade of Nanotoxicology: Where Do We Stand Now?**

S. M. Hussain and J. J. Schlager. *Air Force Research Laboratory, US Air Force, Wright-Patterson, Dayton, OH.*

The last ten years have seen an explosion in the development and evolution of nanotoxicology. This milestone of a decade of research provides a great opportunity to look back and evaluate both the progress made, as well as identify challenges that can potentially plague future research. Early studies had few materials to work with. However, advances in material science have resulted in a large array of nanomaterials (NM) with controlled size, shape, and surface functionalities. From early on, it became apparent that the unique properties associated with NMs, (i.e., primary size, agglomeration patterns, crystal structure, shape, etc.) can dictate the observed effects. Systematic evaluation of toxicity mechanisms necessitated development of novel tools to assess NM physicochemical properties that include: enhanced microscopy techniques, dynamic and static light scattering, and quantitation of cellular uptake. However, adaptation of such characterization tools within the nanotoxicity community has been slow, due to convoluted literature reports of the same NM property measured with different techniques. Recently, the question of dosimetry has become a focus of inquiry due to such conflicting reports. Experiments are being performed to evaluate and compare the effect of dosage by

mass, surface area, and number of particles. However, the evaluation of aggregation state has largely ignored the structure of aggregation, which can substantially influence NM mass exposure and uptake. In addition, another challenge in nanotoxicity is the lack of strategies to accurately extrapolate *in vitro* results to predict *in vivo* responses. This generates the need for enhanced cell model development and implementation in nanotoxicity research. The emerging field of nanotoxicology has made remarkable progress over the past decade and holds immense promise for the next. The focus of this discussion will be to highlight the current state of nanotoxicity and determine key gaps in dosimetry, interpretation of characterization to decipher mechanistic toxicity, and translating data to reliable assessment of human exposure and risk.

### **R** 376 **Predicting Human Thorough QT (TQT) Study Outcomes with Nonclinical Data—How Good Are We and How Good Do We Need to Be?**

J. Valentin<sup>1</sup>, O. Della Pasqua<sup>2</sup>, J. Koerner<sup>3</sup>, D. Leishman<sup>4</sup>, L. Ewart<sup>1</sup> and M. Krucoff<sup>5</sup>. <sup>1</sup>AstraZeneca, Macclesfield, United Kingdom; <sup>2</sup>Leiden University, Leiden, Netherlands; <sup>3</sup>US FDA, Silver Spring, MD; <sup>4</sup>Lilly, Greenfield, IN; <sup>5</sup>Duke University Medical Center, Durham, NC.

The ability to predict and thus prevent drug-induced ventricular arrhythmia and Torsades de Pointes (TdP) is a significant public health issue and a primary focus of regulatory safety pharmacology studies. Data are generated both nonclinically (via hERG, ECG, APD studies) and clinically primarily via a thorough QT study (TQT). The speakers in this roundtable session will consider the predictive value of each of these studies individually and their utility as a panel overall. Specifically, speakers will discuss concordance between nonclinical and clinical data for safety pharmacology endpoints; discuss optimization of nonclinical study design and data collection; identify opportunities for data from additional metrics; and discuss perspectives on the collection and use of nonclinical data to inform clinical trials. The panelists will also be challenged to identify strengths and weaknesses in current testing approaches and propose recommendations to improve or modify these approaches in the future. Participants will be engaged in these discussions and provide input in the debate of the predictive value of nonclinical QT studies as well as the potential for alternative assays or extrapolations to improve our ability to anticipate clinical outcome.

### **HH** 377 **Diesel and Gasoline Exhaust and Cancer.**

A. M. van Erp<sup>1</sup>, J. D. McDonald<sup>3</sup>, R. O. McClellan<sup>2</sup> and E. Garshick<sup>4</sup>. <sup>1</sup>Health Effects Institute, Boston, MA; <sup>2</sup>Toxicology and Human Health Risk Analysis, Albuquerque, NM; <sup>3</sup>Lovelace Respiratory Research Institute, Albuquerque, NM; <sup>4</sup>Veterans Administration Boston Health Care System, Boston, MA.

In 1989, the International Agency for Research on Cancer (IARC) classified whole diesel exhaust as a "probable human carcinogen" and whole gasoline engine exhaust as a "possible human carcinogen." Since then, stringent regulations on diesel engine emissions have been introduced, and there have been significant developments in engine technology and introduction of ultra-low sulfur fuel resulting in marked reductions in the hazardous components in diesel exhaust. These changes are expected to provide substantial benefits to air quality and human health. The time course for realizing the benefits will be related to the rate at which old engines are replaced with new technology. In June 2012, IARC re-evaluated the carcinogenic hazard of diesel and gasoline exhaust based on new information that has become available from studies in humans and animals, which has led to the current designation of diesel exhaust as a "known human carcinogen." This session provides a historical overview of diesel engine technology and emissions, and the significant changes that have occurred over the past decades. We also take a look at what is known about the health effects of diesel and gasoline exhaust and its public perception over the years. We provide a detailed characterization of the June 2012 IARC Working Group re-evaluation of the carcinogenic hazard classification of diesel exhaust and gasoline emissions, both regarding the toxicologic and epidemiologic evidence, and discuss potential implications of the new hazard classification for public policy. Although the Working Group discussed whether to distinguish between "traditional diesel exhaust" and "new technology diesel exhaust" in the cancer hazard assessment, they concluded that this was not possible due to a lack of data on health effects associated with exposure to new technology diesel exhaust.

### **EC** 378 **From New Submissions to Competitive Renewals: Different Phases of Grant Writing.**

C. E. Sulentic<sup>1</sup> and B. L. Kaplan<sup>2</sup>. <sup>1</sup>Wright State University, Dayton, OH; <sup>2</sup>Michigan State University, East Lansing, MI.

Grant writing is a challenging endeavor. One must effectively communicate the significance, innovation, and approach of their research project in a clear, but concise manner with appropriate grammar. While there are some aspects of grant writing that apply regardless of the grant application phase, such as a clearly stated hypothesis and specific aims, the style, and required elements of the various phases of the grant writing process can differ significantly. Thus, the goals of this session are to discuss the various phases of the grant writing process, including preparing a new application versus a competitive renewal, composing the rebuttal and revised grant application, how best to create a "new" grant if a grant has not been funded after two review cycles, and an overview of the review process, and choosing the best scientific review group. Three speakers from NIEHS and a well-funded fourth speaker, who is also an experienced grant reviewer, will expertly cover these topics and participate in a panel discussion at the end of the session.

### **PS** 379 **Erionite Induces Th-17 Pathway Cytokines *In Vitro* and *In Vivo*.**

N. Zebedeo and J. Pfau. Idaho State University, Pocatello, ID.

Erionite is a fibrous zeolite with similar morphological and physical properties to amphibole asbestos. Erionite can also cause malignant mesothelioma and other diseases similar to what is seen in individuals who have been exposed to asbestos. There is little known about how erionite affects the immune system or whether it is associated with systemic autoimmune diseases.

Given these similarities to amphibole asbestos, the hypothesis of this study is that erionite will evoke autoimmune reactions similar to what has been seen upon asbestos exposure. Certain cytokine profiles from macrophages and lymphocytes that may indicate autoimmunity were examined after exposure to asbestos. The cytokines belonging to the Th17 pathway have been implicated in the development of pathologies in some autoimmune diseases.

*In vitro* exposures were done using bone marrow derived macrophages from a cell line and macrophages and lymphocytes from spleens of C57BL/6 mice. Mice were also exposed *in vivo* through peritoneal injections for 1, 3 and 7 days. Cytokines from peritoneal fluid and splenocyte cultures were examined using ELISAs.

Data has shown that erionite causes an increased production of cytokines belonging to the Th17 profile including IL-17, IL-6 and TNF- $\alpha$ . This may be a marker that indicates autoimmune reactions associated with erionite. There are populations in the United States that may be at risk to developing diseases due to erionite exposure. Understanding the mechanism of disease caused by erionite can provide targets for therapies and help implement regulations on its use.

### **PS** 380 **Resistance to Asbestos-Induced Apoptosis with Continuous Exposure to Crocidolite on a Human T Cell.**

T. Otsuki<sup>1</sup>, M. Maeda<sup>2</sup>, S. Yamamoto<sup>1</sup>, N. Kumagai-Takei<sup>1</sup>, S. Lee<sup>1</sup>, H. Mastuzaki<sup>1</sup> and Y. Nishimura<sup>1</sup>. <sup>1</sup>Hygiene, Kawasaki Medical School, Kurashiki, Japan; <sup>2</sup>Biofunctional Chemistry, Graduate School of Natural Science and Technology, Okayama University, Okayama, Japan.

We have been investigating the immunological effects of asbestos. The establishment of a low-dose and continuously exposed human T cell line, HTLV-1 immortalized MT-2, to chrysotile (CB) revealed reduction of CXCR3 chemokine receptor and production of IFN- $\gamma$  that caused a decline of tumor immunity. These effects were coupled with upregulation of IL-10, TGF- $\beta$ , and BCL-2 in asbestos-exposed patients. To observe the immunological effects of crocidolite (CR) on human T cells, a trial to establish a low-dose and continuously exposed model was conducted and compared with a previously reported CB-exposed model (MT-2CB). Transient exposure of MT-2 original cells to CB or CR induced a similar level of apoptosis and growth inhibition. The establishment of a continuously exposed subline to CR (MT-2CR) revealed resistance against CR-induced apoptosis and upregulation of the BCL-2/BAX ratio similar to that recorded for MT-2CB. Both sublines showed reduced production of IFN- $\gamma$ , TNF- $\alpha$ , and IL-6 with increased IL-10. cDNA microarray with network/pathway analyses focusing on transcription factors revealed that many similar factors related to cell proliferation were involved following continuous exposure to asbestos in both MT-2CB and MT-2CR. These results indicate that both CB and CR fibers affect human T cells with similar degrees even though the carcinogenic activity of these substances differs due to their chemical and physical forms. Trials to identify early detection markers for asbestos exposure or the occurrence of asbestos-inducing malignancies using these findings may lead to the development of clinical tools for asbestos-related diseases and chemoprevention that modifies the reduced tumor immunity.

**PS 381 Effect of Asbestos Exposure on Regulatory Role of NK Cells for Expanded Autologous CD4<sup>+</sup> T Cells.**

Y. Nishimura, N. Kumagai-Takei, H. Matsuzaki, S. Lee and T. Otsuki. *Hygiene, Kawasaki Medical School, Kurashiki, Japan.*

We have studied about effect of asbestos exposure on anti-tumor immunity to date, which demonstrated altered function of natural killer (NK) cells exposed to asbestos, showing decreased cytotoxicity against cancer cells with altered expression of NK cells receptors. Recently, it has been become known that NK cells show cytotoxicity for not only abnormal cells but also healthy autologous cells, by which NK cells play a regulatory role in immune response. Therefore, the present study examined effect of asbestos exposure on regulatory role of NK cells for CD4<sup>+</sup> or CD8<sup>+</sup> T cells. Human peripheral blood mononuclear cells (PBMCs) were cultured in IL-2-supplemented media with or without chrysotile B asbestos or silica, while CD4<sup>+</sup> or CD8<sup>+</sup> T cells were freshly sorted from PBMCs magnetically, and cultured upon stimulation by antibodies to CD3 and CD28. After 7 days, expanded CD4<sup>+</sup> or CD8<sup>+</sup> T cells were cultured with CD3-CD56<sup>+</sup> NK cells isolated from harvested PBMCs by flow cytometry for a day. The culture with NK cells caused a decrease in the percentage of viable CD4<sup>+</sup> T cells. However, CD4<sup>+</sup> T cells cultured with NK cells exposed to asbestos, but not with silica-exposed those, showed more decrease in viable cells, compared with control culture. In addition, the expression levels of cell surface CD25 and CXCR3, activation and effector markers respectively, decreased in those CD4<sup>+</sup> cells. In contrast, CD8<sup>+</sup> T cells did not show alteration in percentage of viable cells and expression of FasL and CXCR3 by culture with NK cells. These results indicate that asbestos-exposed NK cells show enhanced function to regulate expanded CD4<sup>+</sup> T cells, in which effector cells are reduced more. The enhanced regulatory function might lead to insufficient anti-tumor response.

**PS 382 Long-Term Exposure of Asbestos on MT-2 Cell Affects Cell Cycle Progression and Cell Death.**

S. Lee<sup>1</sup>, H. Matsuzaki<sup>1</sup>, M. Maeda<sup>2</sup>, N. Kumagai-Takei<sup>1</sup>, Y. Nishimura<sup>1</sup> and T. Otsuki<sup>1</sup>. <sup>1</sup>*Hygiene, Kawasaki Medical School, Kurashiki, Japan;* <sup>2</sup>*Laboratory of Functional Glycobiology, Department of Biofunctional Chemistry, Division of Agricultural and Life Science, Graduate School of Environmental and Life Science, Okayama University, Okayama, Japan.*

Asbestos is a silicate mineral that causes serious illness such as malignant mesothelioma and lung cancer. Regulatory T cells (Treg), are known as a suppressor of immune activity and cause a less anti tumor immunity. We have hypothesized that asbestos causes less immune reaction including tumor immunity through the enhancement of Treg function. Here we used MT-2 cell line, an HTLV-transformed human FoxP3 positive Treg model cell line, and established 7 sub-cell lines from original MT-2. They were exposed to 3 kinds of asbestos (Chrysotile A, Chrysotile B and Crocidolite) at low concentration (10 µg/ml or 25 µg/ml) for long term (more than 8 months). Microarray analysis revealed that transcriptional factor FoxO1 was remarkably decreased in these all of sub-cell lines. Since FoxO1 regulates expression of several cell cycle regulatory molecules, in this study we focused on the cell cycle regulation in these sub-cell lines. Real time PCR analysis showed cyclin dependent kinase (CDK) inhibitors, p21Cip1, p57Kip2, p18Ink4c, p19Ink4d were decreased and CyclinD1 was remarkably increased in these sub-cell lines. Western blot analysis also showed us p21Cip1 was decreased and CyclinD1 was increased in these sub-cell lines. Annexin V/PI staining showed some sub-line cells contained more living cells than original MT-2. We detected significantly less Fas-ligand mRNA expression in all sub-cell lines. These results suggested that long-term exposure of asbestos might accelerate cell cycle progression, and decrease cell death, and conduct them increase. Abnormal proliferation of Treg may down regulate tumor immunity. Further study is required to elucidate whether the down regulation of FoxO1 is implicated cell cycle progression in these sub-cell lines.

**PS 383 Difference in Functional Property of CD8<sup>+</sup> Lymphocytes between Patients with Pleural Plaque and Malignant Mesothelioma.**

N. Kumagai-Takei<sup>1</sup>, Y. Nishimura<sup>1</sup>, M. Maeda<sup>2</sup>, H. Matsuzaki<sup>1</sup>, S. Lee<sup>1</sup>, T. Kishimoto<sup>3</sup>, K. Fukuoka<sup>4</sup>, T. Nakano<sup>4</sup> and T. Otsuki<sup>1</sup>. <sup>1</sup>*Department of Hygiene, Kawasaki Medical School, Kurashiki, Japan;* <sup>2</sup>*Department of Biofunctional Chemistry, Graduate School of Natural Science and Technology, Okayama University, Okayama, Japan;* <sup>3</sup>*Okayama Rosai Hospital, Okayama, Japan;* <sup>4</sup>*Division of Respiratory Medicine, Department of Internal Medicine, Hyogo College of Medicine, Nishinomiya, Japan.*

[Background and Purpose] We have demonstrated effect of asbestos on in vitro development of cytotoxicity in CD8<sup>+</sup> lymphocytes, and reported the property of CD8<sup>+</sup> cells in people positive for pleural plaque (PL), a mark of asbestos exposure, last year. In the present study, CD8<sup>+</sup> lymphocytes of malignant mesothelioma

(MM) patients as well as PL-positive people were examined by flow cytometry. [Materials and Methods] Freshly prepared PBMCs were assayed for cell number of CD3<sup>+</sup>CD8<sup>+</sup> cells and percentages of granzyme B<sup>+</sup>, perforin<sup>+</sup>, and CD45RA<sup>+</sup> cells in CD8<sup>+</sup> lymphocytes by flow cytometry. PBMCs were stimulated with PMA/ionomycin for 4h and assayed for percentages of IFN-γ<sup>+</sup>, CD107a<sup>+</sup>, granzyme B<sup>+</sup> and perforin<sup>+</sup> cells in CD8<sup>+</sup> lymphocytes. [Results] CD3<sup>+</sup>CD8<sup>+</sup> cells in PL and MM showed lower cell number than those of healthy volunteers (HV). There was no difference in % CD107a<sup>+</sup>, showing degranulation, and % IFN-γ<sup>+</sup> cells in stimulated CD8<sup>+</sup> lymphocytes among three groups. Although % granzyme B<sup>+</sup> cells in fresh CD8<sup>+</sup> lymphocytes of PL and MM were similar to that of HV, % perforin<sup>+</sup> cells of PL and MM was higher than that of HV. However, the stimulated CD8<sup>+</sup> lymphocytes of MM showed more decrease in % perforin<sup>+</sup> cells than those of the other groups. The CD8<sup>+</sup> lymphocytes of PL and MM groups showed higher percentages of CD45RA<sup>+</sup> cells than that of HV. [Discussion] These results indicate that PL and MM groups share increase in CD45RA<sup>+</sup> and perforin<sup>+</sup> CD8<sup>+</sup> cells, suggesting effect of asbestos on tumor immunity. In addition, the results indicate the enhanced decrease in perforin<sup>+</sup> CD8<sup>+</sup> cells of MM after stimulation, implying impairment in stimulation-induced cytotoxicity.

**PS 384 Cadmium Exposure Effects on the Class- Switch Recombination in Burkett's Lymphoma Cell Lines.**

V. Poltoratsky. *Pharmaceutical, St. John's University, Queens, NY.* Sponsor: L. Trombetta.

Cadmium is an environmental and industrial pollutant, which enhances susceptibility to pathogens and autoimmune disease. It has been demonstrated that exposure to cadmium modulates the human humoral and cell-mediated immunity. Exposure to cadmium in high doses causes a decrease in B and T cell concentrations and exposure to low doses causes selective inhibitory effect on immunoglobulin isotypes. While the effect of the high concentrations of cadmium in induction of the oxidative stress and apoptosis is well documented, the effect of lower cadmium concentrations on modulating humoral immune response has not been fully understood.

It has been previously demonstrated that low concentrations of cadmium specifically inhibit the miss matched repair pathway, by inhibiting the ATPase activity of MSH2 and MSH6 proteins (Clark and Kunkel, 2004). On other hand, Msh2 and Msh6 deficient mice are defective in class switch recombination (Wiesendanger et al, 2000). In this study, we suggested that exposure to the low concentrations of the cadmium is affecting mismatch repair and the class switched recombination in B lymphocytes, due to its effects on the MSH2 and MSH6 proteins.

Here we tested the effect of low concentrations of cadmium on the miss matched repair and class switched recombination in human B cells. Cadmium at micromolar concentrations inhibited CSR in Burkett's lymphoma cells but did not significantly affect the mRNA level of the activation induced cytosine deaminase and MSH2 and MSH6 genes. The study also covered relations between cadmium concentrations and mismatch repair activity.

**PS 385 Arsenic Species Have Differential Impacts on *Pseudomonas aeruginosa* Induced Immune Response in Human Bronchial Epithelial Cells.**

E. Notch, R. Barnaby, B. Coutermarsh, V. Taylor, B. Jackson, T. Hampton and B. Stanton. *Geisel School of Medicine at Dartmouth, Hanover, NH.*

Arsenic is the number one environmental contaminant of concern with regard to human health. In animal and epidemiological studies arsenic exposure has been associated with a variety of deleterious health outcomes. *In utero* and early life stage arsenic exposure has been linked to lung disease, including acute and chronic bacterial infections, and chronic obstructive pulmonary disease, all of which are associated with *Pseudomonas aeruginosa* (Pa) infection. Animal models have also shown that chronic arsenic exposure decreased immune response to viral challenge. However, little is known about the mechanisms by which these alterations occur or the relative contributions of different arsenic species. This study examined the impacts of inorganic sodium arsenite (iAs<sup>III</sup>) and two major metabolites, monomethylarsonous acid (MMA<sup>III</sup>) and dimethylarsenic acid (DMA<sup>V</sup>), on Pa induced cytokine secretion by primary human bronchial epithelial cells (HBEC, n=4 donors). HBEC cells did not metabolize iAs<sup>III</sup>, MMA<sup>III</sup> or DMA<sup>V</sup>. Exposure of HBEC to 10ppb iAs<sup>III</sup> for 6 days did not alter Pa induced cytokine secretion. In contrast, 10ppb DMA<sup>V</sup> for 6 days significantly decreased IL-8, IL-6, CXCL1 and CXCL2 secretion after Pa stimulation compared to cells exposed to Pa alone. Exposure to 10ppb MMA<sup>III</sup> increased Pa induced IL-8, and Gro-b secretion. HBEC exposed to DMA<sup>V</sup> also had significantly decreased mRNA levels of IL-8, IL-6, CXCL1 and CXCL2 after Pa stimulation. These data provide the first evidence of arsenic species dependent alterations of the immune response of HBEC to infection by Pa. IL-8, IL-6, CXCL1 and CXCL2 are key proinflammatory cytokines that recruit monocytes, macrophages and neutrophils to clear Pa. Thus, MMA<sup>III</sup> and DMA<sup>V</sup>-induced

changes in cytokine secretion by HBEC in response to *Pa* are likely to contribute to the observation that exposure to arsenic dramatically increases the incidence of acute and chronic bacterial infections. Supported by Dartmouth Superfund Program P42 E507373.

**PS 386 Evidence for Low-Dose Suppression of T Cell Proliferation by Arsenite in Certain Normal HPBMC Donors *In Vitro*.**

F. T. Lauer, K. Liu, L. G. Hudson and S. W. Burchiel. *College of Pharmacy, University of New Mexico, Albuquerque, NM.*

Arsenic exposures in the United States and elsewhere in the world have been associated with numerous chronic diseases. People are exposed to arsenic via drinking water, diet, and air vectors. Arsenic exposure is now considered a top environmental public health concern worldwide. Several epidemiologic studies have shown that T cell proliferation is suppressed in individuals exposed to arsenic via drinking water. Previous studies in our laboratories have shown that sodium arsenite suppresses T cell proliferation in HPBMC obtained from normal donors. We have previously reported that some individuals respond to extremely low concentrations (<1 nm) of sodium arsenite when exposed to T cell mitogens (phytohemagglutinin, PHA) and arsenite *in vitro* for 72 hrs. We have now extended these studies to additional individuals and have examined additional assays for assessing T cell proliferation, including PHA-induced 3H-thymidine incorporation and a flow cytometry-based CFSE assay. Using the CFSE assay, we are examining differentially affected T cell subsets. In addition, the work has been extended to the activation of human T cells using anti-CD3/anti-CD28 beads. We find excellent agreement between the results obtained using 3H-thymidine incorporation and CFSE. In this poster we will demonstrate examples of the inter-individual variations in responses to arsenic and polycyclic aromatic hydrocarbons (PAHs) as well as potential synergistic interactions between these chemical classes of agents.

This work was supported by NIH 1R01ES019968-01A1.

**PS 387 The Aryl Hydrocarbon Receptor and Th17 Polarization: Relevance of Receptor Affinity.**

M. D. Hayes<sup>1</sup>, A. Smith<sup>2</sup>, I. Kimber<sup>1</sup> and R. J. Dearman<sup>1</sup>. <sup>1</sup>*Faculty of Life Sciences, Manchester University, Manchester, United Kingdom;* <sup>2</sup>*MRC Toxicology Unit, Leicester, United Kingdom.*

There are in mice well-characterized strain differences in responsiveness of the aryl hydrocarbon receptor (AhR) to its archetypal ligand 2,3,7,8-tetrachlorodibenzo-p-dioxin that result from genetic variants of AhR displaying variable affinities. Thus, C57BL/6 are categorized as being very responsive, with DBA strain mice being the least responsive. Importantly, the human AhR is defined as being of low affinity comparable with the DBA strain receptor. The AhR is expressed relatively ubiquitously but in T cells it is restricted to the T helper (Th) 17 and T regulatory cell subsets. Furthermore, it has been reported that AhR activation is required for optimal Th17 cell polarization. However, such studies have used exclusively the high affinity C57BL/6 strain. We have investigated whether the class of AhR affects optimal *in vitro* polarization of Th17 cells using various mouse strains including an AhR null mouse. Th (CD4<sup>+</sup>) cells were isolated by negative selection from the peripheral lymph nodes of naive mice and polarized into Th17 cells with anti-CD3 and anti-CD28 antibodies and cytokines interleukin (IL)-6, IL-1 $\beta$  and TGF- $\beta$ . Th17 cell differentiation was assessed as a function of mRNA and protein expression for key IL-17 cytokines and the frequency of IL-17<sup>+</sup> cells by intracellular cytokine staining. Using an AhR antagonist (CH-223191), the majority of Th17 cell activity was shown to be dependent upon AhR ligation in all wild type mouse strains (C57BL/6, DBA and BALB/c), regardless of AhR affinity phenotype. Residual Th17 responses (IL-17A<sup>+</sup> cells and IL-17A and IL-17F mRNA and protein) were detected in all strains and in AhR null mice. These data demonstrate that natural ligands can stimulate Th17 development through the AhR and that also relative AhR affinity appears not to influence the impact of natural agonists on Th17 polarization. These data suggest that despite their low affinity receptor, endogenous AhR ligands could play a major role in driving human Th17 cell differentiation.

**PS 388 2, 3, 7, 8-Tetrachlorodibenzo-p-dioxin (TCDD) Reduces *Leishmania major* Burdens in Mice but Not in Macrophages *In Vitro*.**

R. E. Teagarden, J. L. Lenberg, A. R. Dunn and G. K. DeKrey. *Biological Sciences, University Northern Colorado, Greeley, CO.*

A previous study by Bowers et al. (*Am. J. Trop. Med. Hyg.*, 75: 749, 2006) reported significantly lower parasite burdens in *L. major*-infected C57BL/6 mice when pre-treated with TCDD at a dose of 40  $\mu$ g/Kg or higher. This result was unexpected

given that 1) TCDD suppresses T helper cell responses in mice, and 2) resistance to *L. major* infection in mice normally depends upon appropriate T helper cell function. To explain this, we hypothesized that TCDD reduces *L. major* burdens in mice by a mechanism that does not involve T cells. Severe combined immunodeficient (SCID) mice were treated with peanut oil or TCDD (50 or 200  $\mu$ g/Kg) one day prior to infection with 10<sup>4</sup> stationary phase *L. major* promastigotes. A dose- and time-dependent reduction of lesion size and lesion parasite numbers was observed with the greatest effect on day 45 in the highest dose group: 12% of control ( $p < 0.05$ ) and 2% of control, respectively. These results suggested that T cells are not required for reduced *L. major* burdens in TCDD-treated mice. Because macrophages are the primary host cell for *L. major* *in vivo*, we hypothesized that TCDD reduces *L. major* burdens in mice by inhibiting macrophage infection. Using a WST-1 cell viability assay and mouse RAW 264.7 cells, we found that TCDD exposure (0 or 10<sup>-10</sup> to 10<sup>-7</sup> M for up to 48 hours) did not significantly change macrophage viability. Using light microscopy and starch-elicited C57BL/6 mouse peritoneal macrophages, we found that TCDD exposure (0 or 10<sup>-10</sup> to 10<sup>-7</sup> M for 48 hours) did not significantly change the number of intracellular parasites (4.2 *L. major*/infected macrophage, overall) at 24 hours after infection with stationary phase promastigotes. These results suggest a mechanism other than altered parasite uptake by macrophages or macrophage cytotoxicity to explain reduced parasite burdens in TCDD-treated mice.

**PS 389 Carbamate Pesticides Induce Apoptosis in Human NK-92CI Cells.**

Q. Li, M. Kobayashi and T. Kawada. *Department of Hygiene and Public Health, Nippon Medical School, Tokyo, Japan.*

Purpose:

Carbamate pesticides are widely used throughout the world in agriculture as fungicides and insecticides. We previously found that ziram, a dithiocarbamate fungicide, significantly inhibited natural killer (NK) activity in a dose-dependent manner (1). To explore the mechanism of carbamate pesticide-induced inhibition of NK activity, we investigated carbamate pesticide-induced apoptosis and its underlying mechanism in human NK cells.

Methods:

NK-92CI cells, a human NK cell line, were treated with carbaryl (insecticide), maneb (fungicide), thiram (fungicide), and ziram (fungicide) at different concentrations for 2-24 h at 37°C. Apoptosis was determined by FITC-Annexin-V/PI staining. To explore the mechanism of apoptosis, intracellular levels of active caspases 3 and mitochondrial cytochrome-c release were determined by flow cytometry (2-3).

Results and Conclusions:

Ziram and thiram significantly induced apoptosis in NK-92CI cells in a dose- and time-dependent manner. Maneb also significantly induced apoptosis in NK-92CI cells at higher concentrations (more than 20  $\mu$ M). On the other hand, carbaryl, a carbamate insecticide, showed a very weak effect on apoptosis in NK-92CI cells even at 40  $\mu$ M. Moreover, ziram and thiram significantly increased the intracellular level of active caspase 3 and Z-VAD-FMK, a caspase inhibitor, partially but significantly inhibited the apoptosis, respectively. Ziram and thiram also significantly caused mitochondrial cytochrome-c release. These findings indicate that carbamate pesticides can induce apoptosis in NK-92CI cells, and the apoptosis is mediated by both the caspase-cascade and mitochondrial cytochrome-c pathways. The strength of the apoptosis-inducing ability differed among these pesticides, and the order was as follows: thiram, ziram > maneb > carbaryl.

References:

1. Li et al. *Arch Toxicol.* 2012;86(3):475-81.
2. Li et al. *Arch Toxicol.* 2011;85:355-61.
3. Li et al. *Arch Toxicol.* 2012;86(4):615-23.

Acknowledgements:

This work was supported by a Grant-in-Aid for Scientific Research in Japan.

**PS 390 PCB126 Inhalation Reduces the Number and Function of Lymphocytes in Rats.**

A. B. Shimada, W. S. Cruz, A. Nakasato and S. H. Farsky. *Clinical and Toxicological Analysis, University of São Paulo, São Paulo, Brazil.* Sponsor: S. Moraes Barros.

Polychlorinated biphenyls (PCBs) are persistent organic pollutants and ubiquitous environmental contaminants that resist to degradation and accumulate in the food-chain. PCB126 was widely used in industrial processes and is the most potent aryl hydrocarbon receptor agonist. Once respiratory tract is an important pathway of PCB 126 absorption, this work aimed to investigate the effects caused in the immune system by PCB126 inhalation in rats. Male Wistar rats were exposed to

PCB126 at doses of 0.1; 1 or 10 µg/kg of body weight, for 15 days, by nasal instillation. Control animals were exposed to vehicle (saline + 0.5% DMSO). Five hours following the last exposure, animals were killed and bone marrow and blood leukocytes were evaluated as following: a) total number cells by hemocytometer; b) differential bone marrow cells were evaluated by anti-granulocyte, CD3 and CD45R expression analyzed by flow cytometer and differential leukocyte blood cells were quantified in stain smear; c) the expression adhesion molecules on circulating lymphocytes membranes were evaluated by flow cytometer at basal or *in vitro* fMLP stimulation conditions (N-formyl-methionine-leucine-phenylalanine; 10-8M; 1 hour). All the experiments were conducted according to Ethics Committee in Animal Experiments approved by protocol number CEUA/FCF/315. Exposure to 10 µg/kg of PCB126 reduced the number of total circulating leukocytes and bone marrow cells, which reflected reduced CD45 labeled lymphocytes in the bone marrow cells and lymphocytes in the blood. Exposure to 1 or 10 µg/kg of PCB126 reduced the expression of CD62L on circulating lymphocytes at basal conditions and *in vitro* fMLP stimulation impaired CD18 and CD31 expression in these cells. Our data indicates that PCB126 exposure modify the pattern of adhesion molecules expression by blood lymphocyte and it may affects the lymphocytes production, maturation or traffic between the body compartments. These effects may affect the host defense, as lymphocytes are pivotal cells in the immune response. Financial support: FAPESP and CNPq.

### PS 391 Alternariol Induces Differentiation of Macrophages.

A. Solhaug<sup>1</sup>, C. Wisbech<sup>1</sup>, T. E. Christoffersen<sup>2,3</sup>, L. Olsen<sup>2</sup>, T. Lea<sup>2</sup>, L. L. Vines<sup>4</sup>, J. Pestka<sup>4</sup>, J. A. Holme<sup>5</sup> and G. S. Eriksen<sup>1</sup>. <sup>1</sup>Norwegian Veterinary Institute, Oslo, Norway; <sup>2</sup>Norwegian University of Life Sciences, Ås, Norway; <sup>3</sup>Ostfold University College, Halden, Norway; <sup>4</sup>Michigan State University, East Lansing, MI; <sup>5</sup>Norwegian Institute of Public Health, Oslo, Norway.

Mycotoxins are often found, as contaminants of food and feed, and may pose a risk for disease in humans and animals. Mycotoxins sometimes aberrantly affect the immune system and cause immune stimulation as well as immune suppression. The fungi *Fusarium* and *Alternaria* often co-occur in grain, and mixtures of mycotoxins are often more potent than the level of the pure well known toxins (eg. the trichothecenes from *Fusarium*) would indicate. The objective of this study was therefore to examine the potential immune effects of a frequently co-occurring mycotoxin, alternariol (AOH; *Alternaria* toxin). RAW 264.7 mouse macrophages as well as primary peritoneal mouse macrophages and human primary macrophages were therefore used as a model system. AOH was found to induce DNA damage, abnormal nuclei and cell cycle arrest in RAW 264.7 cultures. However, only low levels of cell death were observed. Instead the cells were found to change morphology into star-shaped cells, with increased expression of several cell surface receptors (CD80, CD11b, MHCII) increased TNF-alpha secretion as well as increased endolytic activity. Interestingly, the cells entered a senescent state after prolonged AOH exposure, possibly as a response to the different stresses induced by this mycotoxin. In contrast to RAW 264.7, peritoneal mouse macrophages and human primary macrophages do not proliferate in culture and as a likely consequence, did not exhibit abnormal nuclei upon AOH exposure. Interestingly, AOH was found to change the morphology and most of the cells got a dramatically elongated or a star-like shape, with no increase in cell death which is possibly associated with phenotypic changes. AOH-induced differentiation of macrophages might contribute in part to the observed effects of mycotoxins mixtures on the immune system.

### PS 392 Analysis of Epigenetic Reprogramming of CD8<sup>+</sup> T Cell Responses by Developmental Aryl Hydrocarbon Receptor Activation.

B. Winans<sup>1</sup>, A. Nagari<sup>2</sup>, M. Chae<sup>2</sup>, W. Kraus<sup>2</sup> and B. Lawrence<sup>1</sup>. <sup>1</sup>University of Rochester Medical Center, Rochester, NY; <sup>2</sup>University of Texas Southwestern Medical Center, Dallas, TX.

The developing immune system is susceptible to environmental insults, leading to altered immune function later in life. The aryl hydrocarbon receptor (AhR) is a ligand-activated transcription factor that acts as an environmental sensor and binds many dioxins and polychlorinated biphenyls (PCBs), pollutants to which humans are constantly exposed. AhR also plays a role in the development and function of the immune system. Human and animal data demonstrate that early life exposure to AhR-binding ligands leads to persistent alterations in immune function, supporting the idea that inappropriate AhR activation influences the developing immune system. In order to study the susceptibility of the immune system to perturbation by AhR signaling, our laboratory uses 2,3,7,8-tetrachlorodibenzo-*p*-dioxin (TCDD) as a model developmental immunotoxicant and influenza A virus as a prototypical human pathogen. Mice exposed to TCDD during development have persistently reduced clonal expansion and differentiation of CD8<sup>+</sup> T cells. This

functional alteration is due to direct AhR signaling in the offspring, and results from a direct effect on hematopoietic cells. Furthermore, this altered function occurs without detectable changes in lymphoid organ cellularity or the distribution of immune cell subpopulations in naïve animals. These findings suggest the novel idea that inappropriate activation of AhR influences the epigenetic regulation of the developing immune system, leading to persistent changes in immune function. To test this idea directly we have examined genome-wide DNA methylation patterns in naïve and activated CD8<sup>+</sup> T cells isolated from developmentally exposed mice, and correlated these with changes in gene expression. These novel data provide an important framework for understanding how changes in epigenetic marks, cued by developmental exposure, may affect gene expression and T cell function.

### PS 393 DES and Methoxychlor Metabolite, HPTE, Induction of Cell Death and Alteration of Thymocyte Development: Timing of Induction of Apoptosis.

C. Broussard, L. Leung Liu, C. Zambrano, F. Mourad, Z. Muscato and P. Escalante. *Biology, University of La Verne, La Verne, CA.*

Estrogen and putative endocrine-disrupting chemicals, such as diethylstilbestrol (DES) and methoxychlor, induce death of thymocytes and alter T cell development. Such alterations have the potential to profoundly affect the functioning of the immune system in the long term, particularly when they occur during gestation. We have previously shown that exposure of embryonic thymocytes to two EDCs, DES and hydroxyphenyl-trichloroethane (HPTE; the primary physiological metabolite of methoxychlor), results in death of the thymocytes and alteration of the development of T cells. We undertook the current study to elucidate the mechanism of action of DES and HPTE. C57BL/6 embryonic thymocytes were cultured in the presence of DES or HPTE in an assay that mimics the *in vivo* process of positive selection. Using Annexin V and propidium iodide staining we identified the time course for induction of cell death in the treated thymocytes. By six hours of treatment with DES or HPTE, thymocytes began to express markers of apoptosis, Annexin V+ and PI-. In addition, we assessed the induction of caspase activity, a later event in the apoptotic pathway. The induction of caspase activity distinguished the cell death we observed from other forms of cell death including necrosis and necroptosis. Our results suggest that death induced by DES and HPTE is rapid (beginning by 6 hours of exposure) and caspase-dependent, hallmarks of signal-mediated death induction.

<sup>^</sup>This research is supported by NIEHS ES017345-01. The opinions expressed in this work are solely the authors'.

<sup>\*</sup>At the time the work was completed, these individuals were undergraduate researchers at the University of La Verne.

### PS 394 Genetic Alterations by Prenatal Exposure to Mercury.

K. L. Kracke, D. L. Shirley and J. F. Nyland. *Pathology, Microbiology & Immunology, University of South Carolina School of Medicine, Columbia, SC.*

**Background:** Mercury (Hg) is an ubiquitous environmental toxicant which bioaccumulates and can produce many biological effects, including on the nervous and immune systems. Because Hg can cross the placenta and concentrates in the fetal compartment, the developing fetus is particularly vulnerable. We hypothesize that developmental exposure to Hg will cause immunological changes, leading to an increased susceptibility to, or exacerbation of, immune disorders later in life. Therefore, we exposed pregnant female mice to low doses of Hg for a short duration and examined the genetic effects related to immune function in the offspring. **Methods:** Pregnant BALB/c mice were exposed to Hg (200 µg/kg HgCl<sub>2</sub> in PBS by subcutaneous injection) or vehicle control every other day from gestation day (GD) 5 to GD15. Female offspring remained with the dam until weaning and were euthanized at 8 weeks of age with no further exposures to Hg. Splenic RNA was isolated using RNeasy (Qiagen), then gene expression changes quantitated by microarray (Affymetrix). Gene expression data were analyzed with GeneSpring and differences in expression levels interrogated through Ingenuity Pathway Analysis software.

**Results:** We found that a number of genes were differentially expressed when mice were prenatally exposed to Hg. Focusing on cytokines, macrophage activation, and regulatory T cells, we found that expression of IL-1, CTLA4, CX3CL1 and IGHM was upregulated at least two fold with prenatal Hg exposure.

**Discussion:** In this project, we demonstrate that prenatal Hg exposure can produce lasting programming changes in the immune system. Increased expression of pro-inflammatory cytokine IL-1 has been associated with autoimmune disorders, while pro-inflammatory chemokine CX3CL1 has been associated with microglial (macrophage-lineage cells of the brain) activation. These changes may increase the

risk of developing autoimmune disorders or the possibility of exacerbating existing immune disorders later in life. Future studies will include examining sex differences in the effects of prenatal Hg exposure effects.

### PS 395 Cannabinoid Receptors and PPAR-Gamma Interactions in Endocannabinoid-Modulated Differential CD8<sup>+</sup> T Cell Responses.

S. T. Pike<sup>1</sup>, R. B. Crawford<sup>1</sup>, B. L. Kaplan<sup>1,2</sup> and N. E. Kaminski<sup>1,2</sup>. <sup>1</sup>Center for Integrative Toxicology, Michigan State University, East Lansing, MI; <sup>2</sup>Department of Pharmacology and Toxicology, Michigan State University, East Lansing, MI.

Endogenous cannabinoids (endocannabinoids), eg, anandamide (AEA), bind cannabinoid receptors, CB1 and CB2, and modulate immune responses. In addition, PPAR $\gamma$ -dependent but cannabinoid receptor-independent suppression of immune responses has been reported by endocannabinoids; however, the relationship between cannabinoid receptor-dependent and independent events is poorly characterized. In addition, phytocannabinoids, but not endocannabinoids, have been shown to both enhance and suppress immune function. Using AEA and an in vitro model mimicking the CD8<sup>+</sup> T cell response to early HIV infection, we are seeking answers to two questions: 1) Do endocannabinoids differentially modulate CD8<sup>+</sup> T cell responses? and 2) What roles do cannabinoid receptor-dependent and independent signaling play in these effects? In this model, the percentage of interferon-gamma (IFN $\gamma$ ) producing CD8<sup>+</sup> T cells activated by a HIVgp120-expressing antigen presenting cell line is measured. These studies showed that in the presence of sub-optimal activation (Vh groups <28% CD8<sup>+</sup>IFN $\gamma$ <sup>+</sup> cells), AEA significantly (~10%) enhanced IFN $\gamma$  production. Under supra-optimal activation conditions (>68%), the CD8<sup>+</sup> T cell response decreased by ~5%. If activation was optimal (between 28% and 68%), little AEA-effect was observed. In addition, enhanced responses were AEA concentration-dependent. Using CB1-/-/CB2-/- mice, an increased baseline CD8<sup>+</sup> T cell response (~8%) was observed compared to wild type mice, but an AEA-induced increase above this response was not evident. Surprisingly, addition of a PPAR $\gamma$  antagonist over a range of activation levels was additive (~5%) to AEA-induced T cell effects. Overall, our results show endocannabinoids differentially modulate immune responses with cannabinoid receptors involved in the initial activation of CD8<sup>+</sup> T cells. In addition, the AEA effects were PPAR $\gamma$ -dependent. (Supported in part by R01DA020402 & F32DA030167)

### PS 396 Perinatal Exposure to Bisphenol A through Maternal Diet Alters Allergen-Induced Lung Inflammation in Adult Offspring.

E. O'Brien<sup>1</sup>, D. Dolinoy<sup>1</sup>, M. Peters-Golden<sup>2</sup>, Z. Zaslona<sup>2</sup> and P. Mancuso<sup>1</sup>. <sup>1</sup>Environmental Health Sciences, School of Public Health, University of Michigan, Ann Arbor, MI; <sup>2</sup>Internal Medicine, School of Medicine, University of Michigan, Ann Arbor, MI.

Bisphenol A (BPA), a monomer of polycarbonate plastics and epoxide resin, is a high production volume chemical that has been implicated in asthma pathogenesis when exposure occurs to the developing fetus. However, few studies have examined the effect of in utero and early-life BPA exposure on the pathogenesis of asthma in adulthood. Using an allergen-induced model of asthma, we examined whether perinatal BPA exposure through maternal diet alters lung inflammation in adult offspring by measuring cellular recruitment, cytokine production, lipid mediator production, and serum IgE levels. Two weeks before mating, BALB/c dams were randomly assigned to a diet containing low (50 ng BPA/kg diet), medium (50  $\mu$ g), or high (50 mg) levels of BPA or a BPA-free control diet. Dams remained on the assigned diet throughout gestation and lactation until postnatal day 21 when offspring were weaned onto the BPA-free diet. Twelve-week-old offspring were sensitized to ovalbumin with alum by intraperitoneal injection and subsequently challenged with aerosolized ovalbumin to induce an allergic inflammatory response. Offspring exposed to medium or high levels of BPA exhibited increased serum anti-ovalbumin IgE levels compared to controls, while animals exposed to the low dose displayed increased lymphocyte recruitment, RANTES production, and TNF- $\alpha$  and IFN- $\gamma$  production from splenocytes. Offspring exposed to low or high doses of BPA exhibited decreased macrophage, neutrophil, and eosinophil recruitment and decreased production of TNF- $\alpha$ , IFN- $\gamma$ , IL-4, IL-13, cysteinyl leukotrienes, and prostaglandin D2. Our data show that perinatal BPA exposure has quantitatively different effects on various measures of allergen-induced inflammation. These data indicate that perinatal BPA exposure does not worsen allergen-mediated inflammation in the adult lung, but suggests that exposure may increase inflammation on a systemic level.

### PS 397 Direct Evidence of Altered Conformation and Evidence for a Binding Site on TLR3 for Ethanol at Relevant Concentrations.

S. B. Pruett<sup>2</sup>, V. Le<sup>1</sup>, E. Lewis<sup>1</sup>, S. Gwaltney<sup>1</sup>, B. Manikantan<sup>1</sup> and A. Shack<sup>2</sup>. <sup>1</sup>Chemistry, Mississippi State University, Mississippi State, MS; <sup>2</sup>Basic Sciences, Mississippi State University, Mississippi State, MS.

The mechanism by which ethanol causes a complex array of changes in animal models and humans has been vigorously debated and investigated for more than 50 years. Some progress has been made on the direct effects of ethanol on conformation and function of receptors for neurotransmitters, which apparently cause many of the neurological effects of ethanol. However, there has been no similar investigation of any component of the immune system. We selected TLR3 for this purpose because its 3-dimensional structure has been published, it forms dimers in solution in the presence of ligand which is also the initial event in signaling in vivo, the cytokines and other inflammatory mediators induced by this receptor are inhibited substantially by ethanol, and TLR3 plays an important role in innate immunity to viruses. We used molecular docking software (Autodock 4.2) to determine that there is a highly probable binding site for ethanol in both human and mouse TLR3, and they are at different locations. They are not within the ligand binding region of the molecule, so they should not directly affect ligand binding (though indirect effects are possible). We used circular dichroism to evaluate the dose-response effects of ethanol on the conformation of human or mouse TLR3 with ligand (poly I:C). The difference in rotation of light (millidegrees) in control and ethanol treated samples at 220 nm exhibits a biphasic concentration-response pattern with a peak at ~40 mM (a concentration which is not uncommon in human binge drinkers) and the lowest value at ~80-100 mM (a near lethal concentration of ethanol). The concentration at the peak of the response curve is near the binding constant calculated by the docking software, suggesting that conformational change may be related to the ethanol binding site on TLR3. This is the first report that ethanol at relevant concentrations alters the conformation of an immunological receptor.

### PS 398 Developmental Aryl Hydrocarbon Receptor (AhR) Activation Attenuates Hematopoietic Stem Cell (HSC) Capacity to Undergo Lymphocyte Differentiation.

L. Ahrenhoerster, P. A. Lakatos and M. D. Laiosa. Zilber School of Public Health, University of Wisconsin—Milwaukee, Milwaukee, WI.

HSCs are the foundational cells of the blood system, responsible for balancing self-renewal and differentiation into mature effector cells. Environmental exposures to the HSCs in utero can profoundly affect future development of immune diseases. Indeed, transplacental exposure to 2,3,7,8 Tetrachlorodibenzo-p-dioxin (TCDD) leads to numerous later-life immunological deficits. TCDD mediates this developmental immunotoxicity by binding to and activating the AHR, which is an important regulator of immunological development and function. Given the centrality of hematopoiesis in immune development throughout the life-course, we investigated the effect AHR activation by TCDD has on murine HSCs. Since it is known that the AHR maintains HSCs in a state of non-proliferative quiescence, we hypothesized that persistent developmental AHR activation modulates HSC differentiation capacity and self-renewal ability. To test this hypothesis, pregnant dams were exposed to 3  $\mu$ g/kg TCDD or vehicle control. On gestational day 14.5, lineage negative, cKit<sup>+</sup>, Sca-1<sup>+</sup> (LSK) cells were harvested, quantified, and placed into T-lymphocyte differentiation cultures using a limiting dilution approach. We found approximately 2.5 fold more LSKs present in fetuses exposed to TCDD in utero. Measuring potential, we found approximately 1 in 17 vehicle-exposed LSKs had the capacity to undergo T-cell differentiation while only 1 in 39 did if developmentally exposed to TCDD. These effects are mediated by the AHR in the individual fetuses as supported by studies conducted in offspring from AHR<sup>+/+</sup> crosses. Specifically, the T-cell differentiation potential of LSKs from TCDD-exposed AHR<sup>-/-</sup> fetuses approximates that of vehicle-exposed wild type LSKs. Conversely, the TCDD-exposed AHR<sup>+/+</sup> and AHR<sup>+/+</sup> siblings produce LSKs with a diminished T-cell precursor potential. These data suggest that developmental AHR activation in HSCs reprograms the balance between self-renewal and differentiation, potentially affecting future immune system development and function.

**PS 399 Immunotoxicity of the Nasal Associated Lymphoid Tissue Induced by the Black Mold Toxin Satratoxin-G in Rhesus Monkeys.**

S. A. Carey<sup>1</sup>, V. M. Takala<sup>1</sup>, D. M. Hyde<sup>2</sup>, J. Pestka<sup>1</sup> and J. Harkema<sup>1</sup>.  
<sup>1</sup>Michigan State University, East Lansing, MI; <sup>2</sup>University of California Davis, Davis, CA.

Damp Building-Related Illnesses (DBRI) include many respiratory and immunological symptoms etiologically linked to exposure to *Stachybotrys chartarum*, a black mold that grows in water-damaged indoor environments. The mechanisms by which airborne exposure to *S. chartarum* causes immune dysfunction remain poorly understood. Epidemiological evidence suggests that children may be particularly vulnerable to the harmful effects of airborne toxicants. To assess the potential risk of nasal injury and immunotoxicity in children, we developed an *in vivo* model of intranasal mycotoxin exposure in juvenile monkeys, whose nasal airways are morphologically and functionally similar to those of children. We recently reported that intranasal exposure to Satratoxin-G (SG), a trichothecene mycotoxin produced by *S. chartarum*, causes apoptosis of olfactory sensory neurons. The present study tests the hypothesis that intranasal exposure to SG causes apoptosis of the nasal associated lymphoid tissue (NALT). Juvenile male rhesus macaques received either a single intranasal instillation of 20 µg SG (n=3), or daily instillations of 5 µg SG (n=3) for four consecutive days in the right nasal passage. Saline vehicle was administered to the left nasal passage. Left and right nasal passages were sectioned and preserved for light microscopic, immunohistochemical, and morphometric analyses of the NALT. Both single dose and repeated dose exposure to SG caused atrophy of the NALT, resulting in a 19% (single) and 70% (repeated) reduction in the area of NALT along the nasal septum in the SG-exposed nasal passages, compared to the respective saline-exposed nasal passages. NALT apoptosis was identified morphologically and using immunohistochemistry for caspase-3. SG exposure caused a 2.75-fold increase in caspase-3 immunoreactivity in septal NALT compared to saline exposure. The results in this model provide new insight into a potential mechanism of immune dysregulation associated with exposure to damp indoor environments.

**PS 400 Prenatal Exposure to Benzo(a)pyrene Confers an Enhanced Susceptibility of Macrophage Membranes to Microbial Infection.**

R. S. Clark<sup>1</sup>, A. Ramesh<sup>2</sup>, M. Maguire<sup>1</sup> and D. B. Hood<sup>1</sup>. <sup>1</sup>Neuroscience and Pharmacology, Environmental Health Disparities and Medicine, Center for Molecular and Behavioral Neuroscience, Meharry Medical College, Nashville, TN; <sup>2</sup>Biochemistry and Cancer Biology, Meharry Medical College, Nashville, TN.

The purpose of this study was to elucidate the mechanism of benzo(a)pyrene, [B(a)P]-induced immune suppression by determining whether exposure suppresses macrophage function and alters membrane components to increase susceptibility to infection. C57BL and SCID times pregnant dams were exposed to varying concentrations of B(a)P by oral gavage on embryonic days 14-17. An *ex vivo* macrophage experimental model system was generated from offspring spleen where monocyte differentiation, phagocytic activity, ROS production and modulation of lipid raft cholesterol homeostasis were quantified. Exposure-induced modulatory effects on differentiation was quantified by adhesion assays in the presence or absence of GM-CSF then verified using CD11, F4/80 antibodies and a WST-1 assay. Macrophage respiratory burst activity detection was performed by incubating PMA-stimulated macrophages with dihydrorhodamine, an ROS intermediate sensitive probe. ROS intermediate production was measured by flow cytometry. To determine whether B(a)P modulates lipid raft homeostatic cholesterol levels, lipid rafts from cultured macrophages were isolated by discontinuous sucrose gradient centrifugation and the lipid fractions were verified by CD59 and CD55, two lipid raft proteins. In parallel the fractions were analyzed by HPLC for B(a)P metabolites. The preliminary results demonstrate that *in utero* B(a)P exposure suppresses macrophage functional indices and alters macrophage lipid raft cholesterol levels in offspring. Future studies are directed at establishing whether B(a)P increases macrophage susceptibility to microbial infection.

**PS 401 The CpG Adjuvant Increases Immune Responses to Ovalbumin (OVA) following Sublingual Immunization in C57/BL6 Mice.**

L. A. Coney<sup>3</sup>, A. Parlapiano<sup>2</sup>, A. Curran<sup>5</sup>, G. Bannish<sup>4,1</sup>, M. Perpetua<sup>1</sup>, J. Doughty<sup>1</sup>, A. Beavis<sup>1</sup> and E. Dadey<sup>2</sup>. <sup>1</sup>Biologics and Biomarker Analysis, Huntingdon Life Sciences, East Millstone, NJ; <sup>2</sup>MonoSol Rx, LLC, Warren, NJ; <sup>3</sup>Group Strategic Marketing, Huntingdon Life Sciences, Huntingdon, United Kingdom; <sup>4</sup>Group Strategic Marketing, Huntingdon Life Sciences, East Millstone, NJ; <sup>5</sup>Safety Assessment, Huntingdon Life Sciences, East Millstone, NJ.

The sublingual route of administration has been demonstrated to modulate humoral responses. A protease resistant, phosphorothioate CpG oligonucleotide induces TH1 immune responses through a TLR9-mediated activation of B lymphocytes and dendritic cells and was used as an adjuvant to evaluate its utility in sublingual immunizations. Mice were immunized sublingually with either 4.0ug or 175ug ovalbumin in the presence of 0.5ug or 8.8ug CpG adjuvant on up to 4 occasions (Days 1, 8, 22, 29) and terminated on Day 36. As a control, additional cohorts of animals were treated with vehicle or dosed intraperitoneally (i.p.) with ovalbumin in incomplete Freund's adjuvant (IFA), or ovalbumin in CpG adjuvant. Robust immune responses were observed in the control animals with either IFA or CpG adjuvant on Days 22 and 36. No antibody responses specific to OVA were observed with sublingual dosing on Day 22 in both groups and on Day 36 with 4.0ug OVA and 0.5ug CpG. In contrast, detectable specific antibody responses to OVA were observed on Day 36 with sublingual dosing of 175ug OVA and 8.8ug CpG in 3 of 4 animals. The response was clearly positive but notably lower in magnitude compared to i.p. immunization. Flow cytometry evaluation of B lymphocyte subsets, NK lymphocytes, and T lymphocyte subsets in the spleen revealed no detectable systemic changes. Finally, ELISpot evaluation of splenic cells stimulated with an OVA peptide generated detectable responses in 2 of 4 animals in both the control group using CpG adjuvant and high dose sublingual group. In conclusion, these results are consistent with the known TH1 effects of the CpG adjuvant in C57/bl6 mice and demonstrate the ability to generate a humoral response via sublingual immunization under these conditions.

**PS 402 Effects of Early Life Farm Exposure on Phenotype and Functional Properties of Dendritic Cells and Contribution to the Risk of Disease.**

H. Kääriö<sup>1</sup>, J. Nieminen<sup>2</sup>, K. Huttunen<sup>1</sup>, M. Hirvonen<sup>1,3</sup>, J. Pekkanen<sup>3</sup>, O. Vaarala<sup>2</sup> and M. Roponen<sup>1</sup>. <sup>1</sup>Environmental Science, University of Eastern Finland, Kuopio, Finland; <sup>2</sup>Viral Diseases and Immunology, National Institute for Health and Welfare, Helsinki, Finland; <sup>3</sup>Environmental Health, National Institute for Health and Welfare, Kuopio, Finland. Sponsor: M. Viluksela.

Dendritic cells (DCs) are the major antigen presenting cells that play a central role in the induction of the cellular immune response. Exposure to farm-associated microbes might alter DC numbers or accelerate their maturation, thereby enhancing the development of healthy immune tolerance that would protect against allergic sensitization and disease. In early childhood still immature DCs are very susceptible to environmental exposure. Therefore, the objective of this study was to investigate if numbers or functional properties of DCs in 4.5 year old Finnish children (a selected part of a European birth cohort study, EFRAIM) are associated with the farm exposure and/or atopic outcome. Myeloid DC1 (mDC1, CD11c<sup>+</sup>CD11c<sup>+</sup>), mDC2 (CD141<sup>+</sup>), plasmacytoid DC (pDC, CD123<sup>+</sup>CD303<sup>+</sup>), monocytes (CD14<sup>+</sup>), functional markers (CD80, CD86, TLR4) and intracellular cytokines (IL-6, TNF-α) were analyzed by flow cytometry per se and following 6 hour stimulation with lipopolysaccharide. The frequency of subpopulation mDC1 was lower in non-asthmatic children who had lived in farm environment, as compared to non-farmer children. Also, lower frequency of pDC subpopulation was associated clearly with food atopy. Consequently, the ratio of pDC/mDC1 was lower in children with food atopy. Other associations between DC phenotype/function and atopy were more complicated and dependent on the type of the atopy/sensitisation and the selected IgE cut-off concentration. The main conclusions are that 1) the farm exposure seems to reduce the frequency of circulating mDC1 cells, possibly affecting the antigen-presenting function of the exposed children, 2) the reduced number of pDC cells predisposes children to the development of food atopy and 3) the definition of atopy is crucial when associations between DCs and atopy are studied.

**PS 403 Role of PKC Beta in Allergen-Induced CD86 Expression and IL-8 Release in THP-1 Cells.**

V. Galbiati, M. Marinovich, E. Corsini and C. L. Galli. *DiSFeB, Università degli Studi di Milano, Milan, Italy.*

Protein kinase C (PKC) is a family of twelve serine-threonine kinases, involved in signal transduction of hormones, neurotransmitters, and cytokines. We have found an age-related alteration in PKC signaling and TNF- $\alpha$  release in epidermal cells exposed to different stimuli, including contact allergen DNCB. We demonstrated an age-related decrease in the receptor for activated C kinase (RACK-1) expression, which underlies defective PKC  $\beta$  activation and age-related functional deficit in Langerhans cells (LC) responsiveness (1). It has been indeed demonstrated that LC cannot migrate from the epidermis when PKC  $\beta$  is inhibited, indicating that PKC  $\beta$  transduces the signal for migration of LC from the epidermis (2).

The purpose of this study was to investigate the role of RACK-1 and PKC  $\beta$  in contact allergen-induced CD86 expression and IL-8 release. The human promyelocytic cell line THP-1 was used as surrogate of dendritic cells, while dinitrochlorobenzene (DNCB), p-phenylenediamine (PPD) and diethylmaleate (DEM) were used as reference allergens. CD86 expression was evaluated by FACS analysis and IL-8 release by commercially available ELISA. The selective cell-permeable inhibitor of PKC  $\beta$ , the specific kinase isoform interacting with RACK-1, and the broad PKC inhibitor GF109203X, completely prevented allergen-induced CD86 expression and significantly modulated the release of IL-8 (50% reduction). The use of a RACK-1 pseudosubstrate, which directly activates PKC, resulted in a dose-related increase in CD86 expression and IL-8 release. These effects were not due to cytotoxicity, as assessed by lactate dehydrogenase leakage, or to endotoxin contamination of RACK-1 pseudosubstrate, as assessed using polymyxin B. Overall, we demonstrate a role of PKC  $\beta$  and RACK-1 in allergen-induced CD86 expression and IL-8 production, confirming the pivotal role of PKC in immune cell activation.

Acknowledgement. This project was supported by Ministero dell'Istruzione, dell'Università e della Ricerca (PRIN2009).

**References**

- (1) Br J Dermatol 160:16-25, 2009
- (2) Immunology 79:621-6, 1993

**PS 404 Perfluorooctanoic Acid Exposure Suppresses T-Independent Antibody Responses.**

J. DeWitt<sup>1</sup>, N. Creech<sup>1</sup>, Q. Hu<sup>1</sup>, W. Williams<sup>2</sup> and R. Luebke<sup>1</sup>. <sup>1</sup>Pharmacology and Toxicology, East Carolina University, Greenville, NC; <sup>2</sup>Cardiopulmonary & Immunotoxicology Branch, Research Triangle Park, NC.

Exposure to  $\geq 3.75$  mg/kg of perfluorooctanoic acid (PFOA) for 15d suppresses T-dependent antibody responses (TDAR), suggesting that T helper cells and/or B cells/plasma cells may be impacted. This study evaluated effects of PFOA exposure on the T cell-independent antibody response (TIAR) to dinitrophenyl-ficoll (DNP). Adult female C57BL/6 mice were given 0, 0.94, 1.88, 3.75, or 7.5 mg/kg of PFOA in drinking water for 15d and immunized with 1  $\mu$ g of DNP in 0.2 ml of sterile saline on d11 of dosing. Seven days after immunizations and 3d after dosing ended, animals were euthanized and bled; sera were evaluated for IgM anti-DNP titers by ELISA. PFOA exposure did not alter body or lymphoid organ weights. Mean (log2) IgM serum titers of animals dosed with  $\geq 1.88$  mg/kg PFOA were statistically suppressed, on average, by 10% relative to control responses. Splenic B and T cell subset phenotypes were evaluated in separate groups of animals dosed with 0, 3.75 or 7.5 mg/kg of PFOA for 10, 13, or 15d. Animals exposed for 13 or 15d were immunized with sheep erythrocytes on d11 of dosing. In animals exposed for 15d, the mean percentage of B cells was increased by all doses. Within the CD3+ T cell population, the following changes were observed in the mean percentage of cells: CD4+CD8- T cells were increased at doses of 3.75 and 7.5 mg/kg after 10, 13, and 15d of exposure; CD4+CD8+ T cells were increased after 13d of exposure across all doses relative to 10 and 15d of exposure; CD4-CD8+ and CD4-CD8- T cells had dose and duration interactions, with no clear effect of dose or duration of exposure. Overall, PFOA exposure did not reduce splenic B or T cell populations. Suppression of TDAR and TIAR, in the absence of obvious lymphocyte subpopulation loss, suggests that effects on humoral immunity are likely mediated, at least in part, by disruption of normal B cell/plasma cell function. This abstract does not represent EPA policy.

**PS 405 African Dust Fine PM Induce the Expression of GSTp, HO-1, IL-6 and IL-8 in BEAS-2B.**

R. I. Rodríguez<sup>1,2</sup> and B. D. Jiménez-Vélez<sup>1,2</sup>. <sup>1</sup>Biochemistry, University of Puerto Rico-Medical Sciences Campus, San Juan, Puerto Rico; <sup>2</sup>Center for Environmental and Toxicological Research, University of Puerto Rico-Medical Sciences Campus, San Juan, Puerto Rico.

African dust travels seasonally across the Atlantic Ocean and impacts Puerto Rico increasing the airborne particulate matter (PM) load and the probability of developing an oxidant atmosphere over the Island. The impact of this global event on the general health of Puerto Ricans is still uncertain. We evaluated the generation of reactive oxygen species (ROS) by African dust (ADE) atmospheric load on bronchial epithelial cells (BEAS-2B). In addition, we also measured antioxidant [Glutathione-S-Transferase (GSTp); Heme Oxygenase 1, (HO-1)] and pro-inflammatory (Interleukins, IL-6 and IL-8) gene expressions in cells exposed to PM organic extracts. Cells were treated with extracts (50 $\mu$ g/ml) from ADE and Non-ADE and the contribution of metals determined using 50  $\mu$ M deferoxamine mesylate (DF). Cells were co-treated with N-acetyl-L-cysteine (NAC) to evaluate the extract oxidant capacity. The rate of ROS formation was monitored with 2'7 dichlorofluorescein diacetate for 2 hrs reading fluorescence every 15 min. Quantitative fluorogenic amplification of cDNA was performed using the TaqMan Gene Expression Assays. ADE and Non-ADE induce the generation of ROS, which was significantly reduced with DF. GSTp and HO-1 mRNA expression increased 6 and 8-folds respectively after 4 hrs with ADE extract treatment. The use of DF or NAC significantly reduced both GSTp and HO-1 expression. ADE extracts also induced IL-8 mRNA (7 folds) and IL-6 (5 folds) after 8 hrs. DF or NAC co-treatments similarly reduced cytokine expression confirming the importance of metals in the extracts. African dust arriving Puerto Rico increases local concentrations of trace elements and other constituents in ambient PM<sub>2.5</sub>, which generate ROS and induce the expression of antioxidant and inflammatory gene responses as demonstrated in vitro by the use of BEAS-2B. Supported by MBRS-RISE Grant R25GMO61838 and by NCRR 2G12-RR00305 and NCMHD 8G12-MD007600.

**PS 406 Aminogluthethimide-Induced Immune Changes and Idiosyncratic Drug Reactions.**

W. Ng and J. Uetrecht. Faculty of Pharmacy, University of Toronto, Toronto, ON, Canada.

Aminogluthethimide (AMG) is an aromatic amine aromatase inhibitor associated with a high incidence of idiosyncratic blood dyscrasias, especially agranulocytosis. Despite evidence for immune involvement, the mechanisms of idiosyncratic drug reactions (IDRs) are poorly understood. Animal models of IDRs represent an essential tool to study these reactions; however, like humans, treating animals with drug alone does not usually induce an IDR. Conversely, studying the lack of response may be crucial to understanding why only certain people develop an IDR to a specific drug. Therefore, the objective of this study was to characterize the immune response of Brown Norway rats treated with 125 mg AMG/kg/day and to determine whether immune suppression may prevent the induction of IDRs. An early increase in peripheral blood neutrophils in AMG-treated rats corresponded to changes in the bone marrow that were consistent with an increase in the myeloid cell population. Expression of CD62L on neutrophils decreased at both 24 and 48 hours after AMG treatment, which suggests neutrophil activation, and this was followed by elevated serum levels of Gro/KC and MCP-1. In the spleen, increased proliferation was observed in the white pulp after 14 days of AMG treatment, which was attributed to CD4+ T-cells; however, this may be a local response because it did not extend to the auricular lymph nodes. Furthermore, an early increase in IL-17-expressing CD4+ T-cells in the spleen of the AMG-treated was followed by increased expression of IL-10 after 48 hours, which could modulate the immune response. These results suggest that the major immune response to AMG involves the innate immune system. Although there is some evidence to suggest activation of an adaptive immune response, further investigation of how the innate and adaptive immune interact may provide a better understanding of the mechanisms of IDRs. This research was funded by grants from the Canadian Institutes of Health Research.

**PS 407 The Dermal Exposure to Silica Nanoparticles Induces IgE-Mediated Hypersensitivity.**

T. Hirai<sup>1</sup>, Y. Yoshioka<sup>1</sup>, H. Takahashi<sup>1</sup>, K. Ichihashi<sup>1</sup>, N. Nishijima<sup>1</sup>, T. Yoshida<sup>1</sup>, H. Nabeshi<sup>2</sup>, T. Yoshikawa<sup>1</sup>, S. Tsunoda<sup>3,4</sup>, K. Higashisaka<sup>1</sup> and Y. Tsutsumi<sup>1,3,4</sup>. <sup>1</sup>Laboratory of Toxicology and Safety Science, Graduate School of Pharmaceutical Sciences, Osaka University, Osaka, Japan; <sup>2</sup>National Institute of Health Science, Tokyo, Japan; <sup>3</sup>Laboratory of Biopharmaceutical Research, National Institute of Biomedical Innovation, Osaka, Japan; <sup>4</sup>MEI Center, Osaka University, Osaka, Japan.

To fully utilize the potential benefits of nanomaterials (NMs), it is crucial to evaluate the hazard associated with NMs on human health. Previously, we reported that amorphous silica nanoparticles (nSPs), one of the most frequently used NMs in cosmetics, could penetrate the skin barrier and might have potential risk to enhance allergic responses (Hirai T et al. Part. Fibre Toxicol. 2012). Thus, to ensure the safety of nSPs, it is needed to investigate the effect of dermal exposure to nSPs on allergic diseases. Here, we identified hazard of dermal exposure to nSPs using atopic dermatitis (AD) model mice. The mixture of mite extract antigen (Dp) and nSPs with diameter of 30 nm (nSP30) were swabbed on upper back and both ears for 4 weeks. To evaluate whether nSP30 affects severity of Dp-induced AD, ear thickness and Dp-specific immune responses were measured. Dermal exposure to nSP30 did not affect Dp-induced ear swelling, indicating that nSP30 did not aggravate AD-like skin lesion. The levels of Dp-specific IgE were also not affected by dermal exposure to nSP30. In contrast, the level of Dp-specific IgG in nSP30 (Dp+) groups were significantly lower than those in Dp alone. Furthermore, we showed that the decrease of IgG levels in nSP30 (Dp+) groups induced IgE-mediated hypersensitivity in Dp-mediated anaphylaxis model. Recent epidemiologic study revealed that allergen exposure through the epidermis is important factor to initiate not only AD but also other allergic diseases such as asthma and food allergy. Considering our results together, it is important to examine the relationship between the dermal exposure to NMs and initiation of allergic diseases more precisely.

**PS 408 Effects of Clozapine on the Bone Marrow and Immune Cells in Rodents and Humans: Implications for Drug-Induced Agranulocytosis.**

A. R. Lobach and J. Uetrecht. *Leslie Dan Faculty of Pharmacy, University of Toronto, Toronto, ON, Canada.*

Clozapine is a very effective antipsychotic agent, but its use is limited by the risk of drug-induced agranulocytosis. At the start of treatment, the majority of clozapine patients display evidence of an inflammatory response paired with elevated neutrophil counts. These immune changes appear to be accompanied by changes in the bone marrow, specifically a faster release of neutrophils to the blood. To further investigate these immunomodulatory effects, studies were carried out in rats focused on the peripheral blood and bone marrow responses.

Methods: Rats were treated with clozapine for up to 10 days and bone marrow was collected at study endpoint. Flow cytometry was employed to measure changes in the balance of myeloid, lymphoid, and erythroid compartments in the bone marrow. Progenitor cell changes in vivo were assessed by the methylcellulose assay. Patient studies have been initiated in which the T cell response (ie. Th1/2, Th17, Treg) at the start of clozapine therapy will be monitored in the blood using flow cytometry.

Results: Clozapine treatment in rats was found to significantly elevate the number of mature myeloid cells in the bone marrow. This increase was found to be due to an upstream increase in the number of myeloid progenitor cells. Furthermore, these progenitor cells were observed to favor the formation of granulocyte (G) colonies over macrophage (M), or mixed GM colonies.

Conclusions: Clozapine alters the normal production of hematopoietic cells in the rat bone marrow by promoting the formation of granulocyte colonies. This is reflected in the blood as an increase in neutrophil counts, which is also observed in patients at the start of therapy. The mechanism of clozapine-induced agranulocytosis remains unclear; however, other studies suggest that it may be the result of clozapine-induced neutrophil apoptosis. Clozapine-induced agranulocytosis may occur in cases where this damage leads to an immune response, which doesn't resolve with tolerance. This research was supported by grants from the Canadian Institutes of Health Research.

**PS 409 A Mechanistic Analysis of Silica Nanoparticle-Induced Immune-Modulating Effect in Murine Dendritic Cells.**

H. Takahashi<sup>1</sup>, Y. Yoshioka<sup>1</sup>, T. Hirai<sup>1</sup>, K. Ichihashi<sup>1</sup>, N. Nishijima<sup>1</sup>, T. Yoshida<sup>1</sup>, H. Nabeshi<sup>2</sup>, T. Yoshikawa<sup>1</sup>, S. Tsunoda<sup>3,4</sup>, K. Higashisaka<sup>1</sup> and Y. Tsutsumi<sup>1,3,4</sup>. <sup>1</sup>Graduate School of Pharmaceutical Sciences, Osaka University, Laboratory of Toxicology and Safety Science, Suita, Japan; <sup>2</sup>National Institute of Health Science, Setagaya, Japan; <sup>3</sup>National Institute of Biomedical Innovation, Laboratory of Biopharmaceutical Research, Ibaraki, Japan; <sup>4</sup>Osaka University, MEI center, Suita, Japan.

Nanomaterials (NMs) exhibit unique physicochemical properties and innovative functions, and they are increasingly being used in a wide variety of fields. Ensuring the safety of NMs is now an urgent task. Recently, we reported that amorphous silica nanoparticles (nSPs), one of the most widely used NMs, induced immune modulating effect via the cross-presentation (CP) in murine dendritic cells (DCs). Here we investigated the mechanism of nSP-induced CP in DCs for the development of safer nSPs. It is known that CP is induced by internalized antigens entered the cytosol via endosomes, and these antigens are then degraded by proteasomes. To examine whether this pathway is necessary for nSP-induced CP, we investigated the effect of the potent proteasome inhibitor lactacystin on nSP-induced CP. Lactacystin treatment strongly inhibited nSP-induced CP. In addition, we analyzed the effect of cellular uptake of nSPs on the induction of CP. Because some reports have shown that scavenger receptor (SR) was related to the uptake of nSPs, we examined nSP-induced CP after treatment with Poly I, which is a SR inhibitor. nSP-induced CP was inhibited with Poly I treatment. These results suggest nSPs enhanced CP in proteasomes- and SR-dependent manner. We believe a detailed analysis of the mechanisms of nSP-induced CP will be invaluable for the design of safe nSPs.

**PS 410 Programmed Death-1 Receptor Interactions with Its Ligands May Play a Role in Inhibiting Drug-Induced Liver Injury Mediated by the Adaptive Immune System.**

K. Semple, P. Ryan, M. Chakraborty, W. R. Proctor and L. Pohl. *Molecular and Cellular Toxicology Section, Laboratory of Molecular Immunology, National Heart, Lung and Blood Institute, Bethesda, MD.*

Although clinical evidence suggests that many cases of serious idiosyncratic drug-induced liver injury (SIDILI) are mediated by hepatic protein adducts of drugs and the adaptive immune system, detailed experimental proof for this mechanism of toxicity has remained elusive due to the lack of animal models. We have hypothesized that SIDILI is as rare in animals as it is in humans due at least in part to the tolerogenic nature of the liver, which consists of multiple negative regulators of the adaptive immune system. One negative regulatory pathway that may play a role in modulating the incidence of SIDILI involves the interaction of programmed death-1 receptor (PD-1) on the surface of activated T and B cells with its ligands (PD-L1 and PD-L2) found on a variety of other cells. This possibility has now been tested in an established murine model of halothane-induced liver injury. Twenty-four hours after female Balb/cJ mice were treated with halothane, analysis of the liver revealed perivenous necrosis and an infiltration of CD4+ and CD8+ T cells as well as neutrophils and eosinophils determined by flow cytometry. Further study revealed that T cells expressed PD-1 on their surface, while neutrophils and eosinophils too a lesser extent expressed PD-L1, but not PD-L2 on their surface. These findings suggest that neutrophils may play a role in directly regulating the adaptive immune system. This possibility can be tested in vitro and in vivo by modulating the activities PD-L1 and PD-1 and may have a role in determining susceptibility to SIDILI that is mediated by cells of the adaptive immune system.

**PS 411 In Vitro Characterization of Immunostimulation by siRNA-Lipid Nanoparticles.**

P. Kasperkovitz, R. Duncan, B. Bettencourt, J. Harrop, G. Warner and S. Barros. *Amylam, Cambridge, MA.*

The treatment of human diseases using RNA interference (RNAi) therapeutics requires efficacious and safe delivery of short interfering RNA (siRNA) to target tissues. A well-established strategy for systemic delivery is formulation of siRNA in lipid nanoparticles (LNP). Our current multi-component lipid formulation has been shown to be highly efficient for liver delivery and silencing of therapeutically relevant gene targets. Similar to liposomal drug products, siRNA-LNP delivery can also cause minor transient increases in serum cytokines or complement activation in a small subset of patients. The aim of this study was to systematically assess factors influencing cytokine responses to siRNA-LNP *in vitro* to obtain insight into the mechanistic basis of immunostimulation. We established a consistent healthy

blood donor pool that gave us the unique opportunity to analyze both population heterogeneity and response consistency by repeat-characterization of single donors (41 donors, mean 3.7 visits per donor). Whole blood was incubated *in vitro* with siRNA-LNP and plasma levels of 13 cytokines were determined using multiplex analysis. As anticipated, we observed considerable variability in cytokine responses between donors. For large-scale analysis of 13-dimensional cytokine data, we applied Principal Component Analysis (PCA) to reduce redundancy among variables and to identify data patterns. We found that Principal Components 1 and 2 captured ~85% of variance in our dataset. Moreover, individual donors could be sub-classified into three categories (High, Intermediate, Low) based on responsiveness to siRNA-LNP. Using an algorithm to analyze the reliability of our subclassification, we demonstrated that donor sensitivity to *in vitro* siRNA-LNP immunostimulation was consistent over time. Our data suggest that the observed heterogeneity in sensitivity to siRNA-LNP immunostimulation is due to stable, intrinsic immune differences.

#### **PS 412 Characterization of Suppression of the Innate Immune System by Sodium Methylthiocarbamate.**

W. Tan, B. Jan, X. Deng, M. Gadson and S. B. Pruett. *Basic Sciences, Mississippi State University, Mississippi State, MS.*

Sodium methylthiocarbamate (SMD) is the most widely used soil fumigant in the US. The parent compound and its major breakdown product – methylisothiocyanate (MITC) have been reported to suppress innate immunity in animal models. Our studies indicated that both SMD and MITC altered pro- and anti-inflammatory cytokine and chemokine production in a mouse sepsis model, and increased mortality in a similar manner at 72 hr. Experiments described here were conducted to understand the mechanisms by which SMD alters innate immunity. In NF- $\kappa$ B reporter mice, both SMD and MITC decreased the signal strength of NF- $\kappa$ B, which clearly suggested that the NF- $\kappa$ B pathway was inhibited by both compounds. Therefore, it is important to determine how SMD alters NF- $\kappa$ B signaling. Early studies showed that *in vivo* administration of SMD decreased the concentration of reduced glutathione in mouse peritoneal macrophages, which indicated that SMD administration induced oxidative stress. NF- $\kappa$ B signaling is known to be sensitive to oxidative stress. However, our studies showed that neither BSO nor NAC altered the signal inhibition of NF- $\kappa$ B induced by SMD, which indicated that other mechanisms are more important. Interestingly, NF- $\kappa$ B p65 was not altered by SMD. In contrast, NF- $\kappa$ B p50 was downregulated at the level of mRNA expression in microarray analysis. Meanwhile, microarray analysis indicated that other pathways could be potentially involved in the suppression of innate immune responses induced by SMD, such as hormone pathways, recognition receptors of bacteria and viruses, and others. Therefore, further studies are necessary to determine the interaction of these impaired pathways after methylthiocarbamate treatment. This work was supported by grant R01ES013708 from the National Institute of Environmental Health Sciences.

#### **PS 413 Submicrometer-Sized Iron Oxide Particles and Inflammation.**

A. M. Nilsen and D. Mihaylova. *Norwegian University of Science and Technology, Trondheim, Norway.*

Iron-containing nano- and sub-micrometer particles are increasingly used in daily life products such as clothes and paint as well as in nanomedicine. Thus, it is of importance to find if such particles might cause harmful inflammatory responses. The aim of the study was to determine if two types of iron oxide particles activate isolated immune cells and initiate inflammatory responses in blood, and if they differ in their potential for doing so.

We compared two super paramagnetic iron oxide particle types (100 nm and 1  $\mu$ m diameter) functionalized with carboxyl or glucuronic acid carboxyl and determined if they activate human monocytes in culture or activate cells and initiate inflammatory responses in human whole blood. Activation of the immune cells were determined by quantification of secreted cytokines by ELISA and multi-plex, by induced expression of surface proteins (CD11b) on monocytes and granulocytes in whole blood using flow cytometry and by determining activation of the complement system (TCC) by ELISA.

The results suggest that the 100 nm beads caused a dose dependent activation of isolated monocytes as seen by elevated levels of secreted IL-1 $\beta$  and TNF- $\alpha$  6h after adding the beads. Multi-plex confirmed the increase in IL-1 $\beta$  and demonstrated in addition an elevation in IL-2, IL-6, GM-CSF and IFN- $\gamma$ . The 1  $\mu$ m beads were found much less potent in inducing the secretion of these pro-inflammatory cytokines. Priming of the cells using LPS (100 pg/ml for 2h) gave very minor effects

on the cytokine responses to the particles. From the whole blood analysis it was found that the 100 nm beads at the highest concentration (100  $\mu$ g/ml) caused an elevated level of CD11b on both monocytes and granulocytes, activated complement, and increased the secreted levels of IL-1 $\beta$ , IL-2, IL-6 and TNF- $\alpha$ . The 1  $\mu$ m beads gave no cytokine changes compared to the negative control except for an activation of the complement system that was similar to the smaller beads. The functionalized 100 nm iron oxide particles seem to induce a higher inflammatory response in human monocytes and whole blood than the 1  $\mu$ m beads.

#### **PS 414 A 28-Day Inhalation Immunotoxicity Study of Methyl Isothiocyanate in Female B6C3F1 Mice.**

J. Weinberg<sup>1</sup>, D. Kirkpatrick<sup>1</sup>, V. Peachee<sup>2</sup>, V. Piccirillo<sup>3</sup>, A. Jonynas<sup>3</sup> and J. Hauswirth<sup>3</sup>. <sup>1</sup>WIL Research, Ashland, OH; <sup>2</sup>ImmunoTox, Inc., Richmond, VA; <sup>3</sup>MITC Task Force, Washington DC.

The objective of this study was to evaluate potential immunotoxic effects of methyl isothiocyanate (MITC) when administered via whole-body inhalation to female B6C3F1 mice for 28 consecutive days. MITC is the active metabolite of metam sodium, an organosulfur compound used as a soil fumigant for protection against soil fungi and nematodes. Groups of 10 female mice were exposed to target vapor concentrations of 0, 1, 3 and 10 ppm. All animals were immunized with an intravenous injection of sheep red blood cells (sRBC) on study day 24. A concurrent positive control group received once daily intraperitoneal injections of cyclophosphamide monohydrate (CPS) at a dosage level of 50 mg/kg/day on study days 24-27. All animals were observed at the midpoint of exposures for signs of toxicity. Body weights were recorded twice weekly and food consumption was recorded weekly. A gross necropsy was conducted on all animals on study day 28. Spleen and thymus weights were recorded at necropsy. Immunotoxicity assessment was based on the results of a splenic antibody-forming cell (AFC) assay to assess the T-cell dependent antibody response. There were no MITC-related effects on survival, body weights, food consumption, macroscopic findings or spleen and thymus weights. An increase in eye closure was observed in mice at the 3 and 10 ppm exposure levels. Spleen cellularity, specific activity (AFC/106 spleen cells) and total activity (AFC/spleen) of splenic IgM antibody-forming cells to the T cell-dependent antigen sRBC were unaffected. CPS administration resulted in an expected suppression of the humoral component of the immune system. There was no suppression of the humoral component of the immune system when female B6C3F1 mice were exposed to concentrations of 1, 3 and 10 ppm MITC vapor by whole-body inhalation for 28 consecutive days. In the absence of MITC-related effects on the AFC response, the No-Observed-Effect-Concentration (NOEC) on the immune system was greater than 10 ppm.

#### **PS 415 Activation of the Aryl Hydrocarbon Receptor during Development Leads to an Altered Cd4<sup>+</sup> T Cell Response to Influenza Virus.**

L. Boule<sup>1</sup> and B. Lawrence<sup>2,1</sup>. <sup>1</sup>Immunology, Microbiology, and Virology, University of Rochester Medical Center, Rochester, NY; <sup>2</sup>Environmental Medicine, University of Rochester Medical Center, Rochester, NY.

Recent reports suggest developmental exposures to certain pollutants lead to lower antibody responses to childhood immunizations, but the mechanism by which this occurs is unknown. An intracellular receptor activated by a variety of chemicals is the transcription factor aryl hydrocarbon receptor (AhR). It is expressed by many cell types, including immune cells, and can alter their function upon activation. Previously, we have shown that developmental triggering of the AhR by one of its most potent ligands, the pollutant 2,3,7,8-tetrachlorodibenzo-p-dioxin (TCDD), results in a decrease in the class-switched antibody response to influenza virus infection. CD4<sup>+</sup> T cells differentiate into various effector subsets dependent on the environment in which they are activated. CD4<sup>+</sup> T cells that secrete IFN $\gamma$  and express the transcription factor TBet are defined as Th1 cells, and these Th1 cells are critical effectors in the class-switched antibody response to influenza virus. We examined the CD4<sup>+</sup> T cell response to influenza virus in developmentally exposed mice and found that there are fewer activated and virus-specific CD4<sup>+</sup> T cells in the draining lymph nodes of infected adult mice that were developmentally exposed to TCDD. In addition, there are fewer Th1 cells in the MLN of these mice. Conversely, the percentage of CD4<sup>+</sup>CD25<sup>+</sup>Foxp3<sup>+</sup> regulatory T cells (Tregs), responsible for suppressing immune responses, is increased the MLNs of developmentally exposed mice. This is the first report in the context of an influenza virus infection that AhR activation during development disrupts the normal function and differentiation of CD4<sup>+</sup> T cells, an effect of which may lead to decreased antibody responses to both infections and immunizations.

**PS 416 Exposure to Triclosan Augments the Allergic Response to Ovalbumin in a Mouse Model of Asthma.**

C. M. Long<sup>1,2</sup>, J. Franko<sup>3</sup>, M. L. Kashon<sup>1</sup>, K. L. Anderson<sup>1</sup>, A. E. Hubbs<sup>1</sup>, E. Lukomska<sup>1</sup>, B. J. Meade<sup>1</sup> and S. Anderson<sup>1</sup>. <sup>1</sup>HELD/ACIB, CDC-NIOSH, Morgantown, WV; <sup>2</sup>West Virginia University, Morgantown, WV; <sup>3</sup>Bethany College, Bethany, WV.

During the last decade there has been a remarkable and unexplained increase in the prevalence of asthma. These studies were conducted to investigate the role of dermal exposure to triclosan, an endocrine-disrupting compound, on the hypersensitivity response to ovalbumin (OVA) in a murine model of asthma. Triclosan has had widespread use in the general population as an antibacterial and antifungal agent and is commonly found in consumer products such as soaps, deodorants, toothpastes, shaving creams, mouth washes, and cleaning supplies. For these studies, BALB/c mice were exposed dermally to concentrations of triclosan ranging from 0.75-3% (0.375-1.5 mg/mouse/day) for 28 consecutive days. Concordantly, mice were intraperitoneally injected with OVA (0.9 ug) and aluminum hydroxide (0.5 mg) on days 1 and 10 and challenged with OVA (125 ug) by pharyngeal aspiration on days 19 and 27. Compared to the animals exposed to OVA alone, increased spleen weights, OVA-specific IgE, Interleukin (IL)-13 cytokine levels, and lung eosinophils were demonstrated when mice were co-exposed to OVA and triclosan. Statistically significant increases in OVA-specific and non-specific airway hyperreactivity (AHR) were observed for all triclosan co-exposed groups when compared to the vehicle and OVA controls. In these studies exposure to triclosan alone was not demonstrated to be allergenic, however co-exposure with a known allergen resulted in enhancement of the hypersensitivity response to that allergen, suggesting that triclosan exposure may augment the allergic responses to other environmental allergens.

**PS 417 Oral Exposure to Genistin but Not Daidzein Increased Natural Killer (NK) Cell Activity in Female B6C3F1 Mice.**

T. Guo<sup>1</sup>, R. D. Brown<sup>2</sup> and J. F. Zheng<sup>2</sup>. <sup>1</sup>University of Georgia, Athens, GA; <sup>2</sup>Virginia Commonwealth University, Richmond, VA.

Genistin (GIN), the glycoside form of phytoestrogen genistein (GEN), is the predominant isoflavone found in soy products. The objective of this study was to determine if exposure to GIN (2, 6 or 20 mg/kg) by daily gavage for 28 days modulated immune responses in female B6C3F1 mice in comparison with daidzein (DAZ), another soy isoflavone. There were no significant changes in the body weight and absolute weights of thymus, spleen, lungs, kidneys, or liver in either GIN or DAZ-treated mice. However, exposure to GIN increased relative kidney weight (20 mg/kg; 11%). In contrast, exposure to DAZ decreased relative spleen weight (2 mg/kg; 21%; 6 mg/kg; 24%; 20 mg/kg; 24%), relative kidney weight (6 mg/kg; 15%), relative liver weight (6 mg/kg; 14%; 20 mg/kg; 14%), and relative lung weight (20 mg/kg; 24%). In the thymus, GIN exposure increased the percentages of CD4+CD8+ cells (2 mg/kg; 22%; 20 mg/kg; 26%) and CD44-CD25- cells (20 mg/kg; 5%) but decreased the percentages of CD4+CD8- cells (20 mg/kg; 28%), CD4-CD8- cells (2 mg/kg; 41%; 20 mg/kg; 41%), and CD44-CD25+ cells (20 mg/kg; 53%). Exposure to DAZ increased the percentages of CD44-CD25- cells (2 mg/kg; 5%) while decreased that of CD4+CD8- cells (2 mg/kg; 30%), CD44-CD25+ cells (2 mg/kg; 51%), and CD44-CD25+ cells (2 mg/kg; 71%; 6 mg/kg; 45%; 20 mg/kg; 43%). In the spleen, GIN exposure increased the percentages of NK cells (20 mg/kg; 86%), T cells (20 mg/kg; 74%), and neutrophils (2 mg/kg; 148%) while DAZ exposure increased the percentages of T cells (20 mg/kg; 112%), CD4+ T cells (20 mg/kg; 58%), CD8+ T cells (6 mg/kg; 69%; 20 mg/kg; 133%) but decreased the percentage of neutrophils (20 mg/kg; 48%). In correlation with observed increased %NK cells, exposure to GIN but not DAZ increased NK cell activity. Taken together, the differential effects of GIN and DAZ suggest that both the estrogenic and non-estrogenic properties of these compounds contribute to their immunomodulatory roles (Supported in part by NIEHS contract NO1-ES05454).

**PS 418 Neural Autoimmunity and Low-Level Mercury Exposure.**

C. Wright, D. L. Shirley and J. F. Nyland. Pathology, Microbiology & Immunology, University of South Carolina School of Medicine, Columbia, SC.

Multiple Sclerosis (MS) is an autoimmune disease of the central nervous system (CNS) involving demyelination; the mechanism of disease pathology involves stimulated auto-reactive T cells that are elicited against myelin proteins and primarily strikes more women than men. Mercury (Hg), a heavy metal found in many consumer products and as an environmental contaminant, affects the immune system,

although there is little data linking low-level Hg exposure to the development of autoimmunity. Contrarily, high-level Hg exposure has proven to be toxic to the human CNS, specifically on neurons and glial cells. Since glial cells are CNS-resident immune lineage cells, we hypothesized that low-level Hg pre-exposure will increase neural autoimmunity in the animal model of MS, experimental autoimmune encephalomyelitis (EAE), induced with myelin oligodendrocyte glycoprotein (MOG). Adult C57BL/6 male mice were first pre-treated with HgCl<sub>2</sub> or PBS every other day by subcutaneous injection for 2 weeks pre-disease induction, then divided into 3 groups: (1) Hg only, (2) disease (MOG<sub>35-55</sub> peptide) only, and (3) Hg+ disease. Clinical scores were recorded daily until day 25 when mice were euthanized. Brain, spinal cord, and spleen tissues were collected and analyzed for 9 cytokines (pro- & anti-inflammatory) using a multiplex assay. Hg alone raised levels of both pro-inflammatory and anti-inflammatory cytokines in the spinal cord; however, in diseased animals, Hg did not have the same effects and only increased IFN- $\gamma$  in the brain. Low-level Hg alone is insufficient to prompt disease in males but exposure does upregulate cytokine levels in the CNS (IFN- $\gamma$ ) when disease is present. These data indicate that low-dose Hg interacts with components of the CNS milieu, specifically cytokine-producing cells of the immune system. Future studies will focus on exploring sex-specific effects of disease severity with Hg pre-treatment in female mice of the same animal model.

**PS 419 Modulation of HIV<sub>GP120</sub>-Specific T Cell Responses by  $\Delta^9$ -Tetrahydrocannabinol *In Vitro* and *In Vivo*.**

W. Chen<sup>1,3</sup>, B. L. Kaplan<sup>2,3</sup>, S. T. Pike<sup>3</sup> and N. E. Kaminski<sup>2,3</sup>. <sup>1</sup>Microbiology and Molecular Genetics, Michigan State University, East Lansing, MI; <sup>2</sup>Pharmacology and Toxicology, Michigan State University, East Lansing, MI; <sup>3</sup>Center for Integrative Toxicology, Michigan State University, East Lansing, MI.

Approximately 25% of HIV patients use marijuana for its putative therapeutic benefit; however, it is unknown how cannabinoids affect the immune status of immunocompromised HIV patients. A surrogate *in vitro* mouse model was established to investigate the effects of cannabinoids on the early stages of the anti-HIV response. Specifically, T cell responses to HIV<sub>gp120</sub> were induced using gp120-expressing antigen presenting cells and target cells. CD8<sup>+</sup> T cell proliferation and gp120-specific IFN $\gamma$  production were observed, which was suppressed or enhanced by  $\Delta^9$ -tetrahydrocannabinol (THC), the predominant psychoactive compound in marijuana, depending on the magnitude of cellular activation. To further determine the molecular mechanisms by which THC differentially modulates T cell responses, PMA/ionomycin (Io) or anti-CD3/CD28 were used as stimuli. THC suppressed or enhanced IFN $\gamma$  or IL-2 production under optimal or suboptimal activation, respectively, but increased intracellular Ca<sup>2+</sup>, regardless of the activation levels, suggesting that appropriate or excessive Ca<sup>2+</sup> affected T cell activation differentially. To determine whether THC has similar effects *in vivo*, a mouse model to stimulate HIV<sub>gp120</sub>-specific response has also been established. Vector plasmid VRC2000 or gp120-expressing plasmid VRC<sub>gp120</sub> was injected intramuscularly into mice. The gp120-specific IFN $\gamma$  response was detected by ELISPOT, when splenocytes were restimulated with the pool of gp120-derived peptides 81-84, which were identified as the putative immunodominant ones among 211 tested peptides. The THC effect on the gp120-specific response *in vivo* will be characterized. Overall, our data will provide in-depth understanding of cannabinoid effects on HIV antigen-specific T cell responses *in vitro* and *in vivo*. (Supported by NIH DA07908)

**PS 420 Cannabinoid Enhancement of Humoral Immunity in CB<sub>1</sub>/CB<sub>2</sub> Null Mice Is Correlated with Enhanced Splenic Norepinephrine (NE) Concentration.**

T. J. Simkins<sup>1,2,3</sup>, K. J. Lookingland<sup>2,3</sup> and B. L. Kaplan<sup>1,2,3</sup>. <sup>1</sup>Center for Integrative Toxicology, Michigan State University, East Lansing, MI; <sup>2</sup>Pharmacology and Toxicology, Michigan State University, East Lansing, MI; <sup>3</sup>Neuroscience Program, Michigan State University, East Lansing, MI.

Cannabinoid compounds, such as  $\Delta^9$ -tetrahydrocannabinol (THC), are immune suppressive as evidenced, in part, by their ability to inhibit T cell-dependent B cell responses. In response to sheep erythrocytes, THC suppresses immunoglobulin M (IgM) antibody production in a cannabinoid receptor (CB) 1 and/or CB2-dependent manner. Moreover, previous studies demonstrated that the magnitude of IgM production in response to sheep erythrocytes was higher in CB1/CB2 null mice as compared to wild type mice, suggesting endogenous cannabinoid control of humoral immunity. Thus, the focus of the present studies was to determine the mechanisms by which cannabinoids regulate humoral immunity. A direct comparison of female and male wild type and CB1/CB2 null mice demonstrated that CB1/CB2 null mice produce more circulating IgM and IgG, even in the absence of immune

sensitization. In response to various antigens, including influenza and lipopolysaccharide (LPS), CB1/CB2 null mice also produced more IgM. It has been demonstrated that NE engagement of  $\beta 2$  adrenergic receptor ( $\beta 2$ AR) on B cells is part of the normal physiological mechanism that contributes to antibody production, and in fact, splenic NE concentration and  $\beta 2$ AR expression on B cells were higher in CB1/CB2 null mice as compared to wild type mice. These results provide a correlation between splenic NE concentration and antibody production, suggesting the possibility that cannabinoid-mediated suppression of NE release from splenic sympathetic neurons contributes to cannabinoid-induced inhibition of antibody responses. (Supported in part by NIH DA007908).

**PS 421 Differential Effects of Delta(9)-Tetrahydrocannabinol on NF $\kappa$ B Activation in T Cell-Dependent Humoral Immune Response in Humans.**

T. Ngaotepprutaram<sup>1,2</sup>, B. L. Kaplan<sup>1,2</sup> and N. E. Kaminski<sup>1,2</sup>. <sup>1</sup>Pharmacology and Toxicology, Michigan State University, East Lansing, MI; <sup>2</sup>Center of Integrative Toxicology, Michigan State University, East Lansing, MI.

Delta(9)-Tetrahydrocannabinol (THC), a major psychoactive constituent found in marijuana, modulates immune function. Previously, our laboratory demonstrated that THC inhibits humoral immune responses to T cell-dependent antigens in mice by suppressing sheep erythrocyte or CD40 ligand (CD40L)-induced immunoglobulin M (IgM) secretion and antibody forming cell (AFC) response. CD40 is constitutively expressed on B cells, whereas CD40L is induced in activated T cells. Thus, the objective of this study was to investigate the role of the CD40-CD40L interaction in THC-mediated suppression of the T cell-dependent humoral immune response in humans. These studies show that THC suppressed the anti-CD3/CD28-induced DNA binding activity of NFAT and NF $\kappa$ B, two transcription factors critical in the upregulation of CD40L in activated human CD4<sup>+</sup> T cells. An assessment of the effect of THC on proximal T cell-receptor signaling induced by anti-CD3/CD28 revealed modest impairment of sustained elevation in intracellular calcium, but no significant effect on the phosphorylation of Zap70, PLC $\gamma$ , Akt, and Gsk3 $\beta$ . Additional findings, using an in vitro T cell-dependent antibody response model, which employs cell surface-expressed CD40L and recombinant cytokines [interleukin (IL)-2, IL-6, and IL-10], to induce B cell responses demonstrated that THC suppressed STAT3, but not NF $\kappa$ B activation in B cells. Moreover, THC impaired B cell activation and proliferation, ultimately resulting in suppression of IgM AFC response. Collectively, these findings suggest that THC exhibits stimulation- and/or cell type-specific selectivity in NF $\kappa$ B inhibition, and identifies many aspects of the multi-faceted mechanism by which THC suppresses T cell-dependent humoral immunity in humans. Supported in part by DA07908 and Royal Thai Government Scholarships.

**PS 422 Phenotypic Comparison of Leukocyte Populations between Wild Type and Aryl Hydrocarbon Receptor (AhR) Null Rat in the Developing and Mature Spleen and Thymus.**

R. B. Crawford<sup>1</sup>, N. Joshi<sup>1</sup>, R. S. Thomas<sup>2</sup> and N. E. Kaminski<sup>1</sup>. <sup>1</sup>Department of Pharmacology & Toxicology and Center for Integrative Toxicology, Michigan State University, East Lansing, MI; <sup>2</sup>Institute for Chemical Safety Sciences, The Hamner Institutes for Health Sciences, Research Triangle Park, NC.

The immunotoxic effects produced by dioxin and dioxin-like polycyclic aromatic hydrocarbons are mediated through the AhR; however, little is known concerning the role of the AhR in the development or functionality of the immune system. The objective of the present study was to investigate whether targeted deletion of the AhR in the Sprague-Dawley rat altered the leukocyte composition within the developing (3 weeks) and/or mature (8 weeks) thymus or spleen of male and female rats. No significant differences were observed between AhR null and wild type rats in the spleen or thymus body to organ weight ratios or cellularity of the thymus or spleen at 3 or 8 weeks of age. Similarly, leukocyte populations as characterized by comprehensive phenotyping using multiple panels of antibodies directed against specific cell surface proteins (i.e., B cells, T cell subtypes, monocyte-derived lineages, neutrophils and NK cells) using flow cytometry showed no significant differences in the cellular composition of the thymus between the wild type and AhR null rat. Similar analysis of the spleen showed an increase in the CD8<sup>+</sup>NK<sup>+</sup> (NKT) population at week 3 in the AhR null rat. A trend toward an increase in NKT cells was also present at week 8 but this difference was not statistically significant. These studies show that targeted deletion of the AhR in the Sprague-Dawley rat has minimal effects on the leukocyte composition of the developing and mature rat thymus and spleen. (Supported in part by the Dow Chemical Company)

**PS 423 Differential Expression Kinetics of miRNA Involved in Allergic Chemical Sensitization following Dermal Exposure in a Murine Model.**

S. Anderson<sup>1</sup>, K. Beezhold<sup>2</sup>, E. Lukomska<sup>1</sup>, J. Richardson<sup>1</sup>, C. M. Long<sup>1</sup>, K. Anderson<sup>1</sup>, J. Franko<sup>3</sup>, B. J. Meade<sup>1</sup> and D. H. Beezhold<sup>1</sup>. <sup>1</sup>NIOSH, Morgantown, WV; <sup>2</sup>University of Pittsburgh, Pittsburgh, PA; <sup>3</sup>Bethany College, Bethany, WV.

Allergic disease is an important occupational health concern with work related asthma and allergic contact dermatitis among the most frequently diagnosed occupational illnesses. The development of rapid and sensitive methods for hazard identification of the responsible agents is critical. MicroRNAs (miRNAs) are small non-coding RNAs 20-22 nucleotides long whose primary function is to regulate gene expression by functioning as endogenous inhibitors of protein translation. Allergic disease is characterized by an imbalance between Th1 and Th2 cytokines; however the role of posttranscriptional mechanisms like the ones regulated by miRNAs is just starting to be explored. These studies describe the kinetics of miRNA expression during the sensitization phase of an allergic response following dermal exposure to prototypical chemical sensitizers in a mouse model. Using microarray and other data, six miRNAs were identified for further analysis with RT-PCR including mi-21, 22, 210, 155, 133a, and 27b. These data demonstrate that miRNAs may have a central role early in the allergic response focused on establishing the fine balance of Th1 versus Th2 responses to chemical sensitizers. Identification of unique miRNA expression profiles may help to elicit the mechanisms by which exposure to sensitizing chemicals induce immune cell activation and can potentially help to identify biomarkers for new treatments and preventions.

**PS 424 Potential for Immune Sensitization following Dermal Exposure to Indium Tin Oxide.**

B. J. Meade<sup>1</sup>, E. Lukomska<sup>1</sup>, K. Brock<sup>2</sup>, C. M. Long<sup>1</sup>, K. Anderson<sup>1</sup> and S. Anderson<sup>1</sup>. <sup>1</sup>NIOSH, Morgantown, WV; <sup>2</sup>West Virginia University, Morgantown, WV.

Pulmonary disease including pulmonary fibrosis, emphysema and pulmonary alveolar proteinosis has been observed in workers in the indium industry. The mechanisms underlying this disease and its natural history have not been fully elucidated. Among other findings, following inhalation exposure to Indium-tin Oxide (ITO) animal studies have revealed hyperplasia of mediastinal lymph nodes and granulomas of mediastinal nodes and bronchus-associated lymphoid tissue. These studies were undertaken to investigate the potential for ITO to induce immune sensitization using the mouse Local Lymph Node Assay. Furthermore studies were conducted following exposure to both intact and abraded skin to begin to evaluate the potential for dermal penetration of the nanoparticles. BALB/c mice (5 animals/per group for both intact and abraded skin groups) were exposed to either vehicle (dimethyl sulfoxide), increasing concentrations 2.5%-10% ITO (90:10 indium oxide/tin oxide, particle size <50 nm) or positive control (30% alpha-hexylcinnamaldehyde). A dose response was observed in both groups reaching statistical significance and a SI of 4 in the 5% intact dose group (EC3 value of 2.6). Students t-test showed no statistical differences when responses were compared between intact and breach skin exposures at the same dose levels. These studies demonstrate the potential for ITO to induce sensitization following dermal exposure and suggest that the particles may have similar bioavailability through intact and abraded skin.

**PS 425 Rat Bioassay of Diisocyanate Asthma: Comparison of Thresholds of the Asthmagenic Response and Pulmonary Irritation.**

J. Pauluhn. Toxicology, Bayer Pharma AG, Wuppertal, Germany.

Occupational exposure to polymeric diphenylmethane-diisocyanate (MDI) and the more volatile toluene-diisocyanate (TDI), known human asthmagens, can be attributed to two potential routes: the skin and the respiratory tract. Both routes were systematically compared in the Brown Norway (BN) rat MDI asthma model. Induction utilized either 2 topical exposure sessions or inhalation exposures on 5 consecutive days at concentration x exposure time (C x t) relationships of 1000, 5000, and 10000 mg MDI/m<sup>3</sup> x min using exposure durations of either 10- or 360-min. This was followed by four 30-min inhalation challenges to 40 mg MDI/m<sup>3</sup> on every alternate follow-up week. This comparison revealed that a 'high dose' dermal exposure is markedly more efficacious to produce 'asthmatic rats' than a repeated high-dose/high-concentration inhalation protocol. Therefore, further testing was focusing solely on the topical route for induction. Under otherwise similar conditions, rats were challenged to 80 mg TDI/m<sup>3</sup>. This overcomes the loss of dose due to the vapor retention in the upper airways of rats and associated drop in

ventilation. Two independent methods were used to characterize the asthma-like response at the last challenge, the analysis of pulmonary inflammatory by bronchoalveolar lavage (BAL) and physiologic endpoints showing changes in respiration delayed in onset. The most distinct outcomes characterizing the asthmatic response in this bioassay were increased neutrophils in BAL and the delayed respiratory response. These data demonstrated further that the vigor of asthma-like response after challenge is clearly dependent on the inhalation elicitation dose ( $C \times t$ ) of pre-challenged rats to attain the asthmatic state. This relationship of the elicitation response served as basis for the dose-response analysis and estimation of the benchmark NOAEL. After adjustments accounting for differences exposure durations, in the rat-to-human pulmonary doses, and the intra-human variability, the resultant threshold  $C \times t$  of asthmatic rats and humans converged into the same threshold limit value.

**PS 426 Identification of Novel Exposure and Lung Cancer Gene Markers in Carbon Nanotube-Exposed Human Lung Epithelial Cells.**

T. A. Stueckle<sup>1</sup>, A. Mishra<sup>1</sup>, R. Derk<sup>1</sup>, T. Meighan<sup>1</sup>, V. Castranova<sup>1</sup>, Y. Rojanasakul<sup>2</sup> and L. Wang<sup>1</sup>. <sup>1</sup>NIOSH, Morgantown, WV; <sup>2</sup>West Virginia University, Morgantown, WV.

Concern for increased risk of CNT-induced lung cancer has arisen due to asbestos-like high aspect ratio, pulmonary persistence and fibrosis. Our previous study found that chronic in vitro exposure to dispersed single (D-SWCNT) and multi wall CNT (D-MWCNT) resulted in neoplastic transformation in human small airway epithelial cells (SAEC). Genome profiling identified oncogene signaling mechanisms in CNT SAECs that were quite different from asbestos-exposed (ASB) SAEC. Few in vivo studies identified whole lung gene markers associated with MWCNT exposure, but did not compare CNT vs. asbestos genetic response. Here, toxicogenomic profiling with correlation feature selection strategies identified particle-specific, key gene markers from our previous study. D-SWCNT, D-MWCNT, ASB, ultrafine carbon black (UFCB) and control SAEC genome profiles were subjected to comparative marker and class neighbor analyses followed by multistep cross validation to identify genes with highly correlated expression for each treatment. Specific treatment markers and genome profiles were subjected to Ingenuity Pathway and Biomarker Analysis to determine both specific markers performance and identify disease markers. Gene marker subsets and disease markers were validated using rtPCR and protein expression. Here, we present robust SWCNT, MWCNT, ASB and UFCB specific gene marker sets for in vitro chronically exposed SAEC. Matching our original analysis, both D-MWCNT and D-SWCNT markers were associated with lipid metabolism and cancer while ASB and UFCB centered on inflammatory response and senescence, respectively. Biomarker Analysis identified known lung and other cancer markers (MYC, PPARG) in CNT SAECs which differed from inflammation-associated cancer markers (IL-1B) in ASB SAECs. In conclusion, toxicogenomic profiling in a chronic in vitro exposure model identified particle-specific gene markers and known lung cancer markers which can potentially aid in assessing CNT exposure and detection of early disease markers.

**PS 427 ROS Evaluation for Series of CNTs Using ESR Method and Its CNT Concentration Effects.**

S. Tsuruoka<sup>1</sup>, K. Takeuchi<sup>2</sup>, K. Koyama<sup>2</sup>, F. Tristan-Lopez<sup>1</sup>, H. Matsumoto<sup>3</sup>, N. Saito<sup>4</sup>, Y. Usui<sup>4</sup>, M. Endo<sup>1</sup>, M. Terrones<sup>1</sup>, D. W. Porter<sup>5</sup> and V. Castranova<sup>5</sup>. <sup>1</sup>ENCs, Shinshu University, Nagano, Japan; <sup>2</sup>Faculty of England, Shinshu University, Nagano, Japan; <sup>3</sup>Department of Organic and Polymeric Materials, Tokyo Institute of Technology, Meguro, Japan; <sup>4</sup>Department of Applied Physical Therapy, Shinshu University, Nagano, Japan; <sup>5</sup>NIOSH, Morgantown, WV.

Carbon nanotubes (CNTs) are becoming important materials in industries. It is a concern that CNTs may induce carcinogenic responses through pulmonary exposure. It has been recently reported that CNTs scavenge ROS, which is utilized for toxicological evaluations. Although the electron charge transfer seems the noticeable phenomena of toxicological chemical reactions, any comprehensive evaluation of ROS scavenging capabilities using a variety of CNTs has not been demonstrated well. The present work specifically investigates ROS scavenging capabilities using the series of CNTs and their derivatives: more than 15 kinds of CNTs. Those ROS scavenging properties were measured by ESR with DMPO. Highly crystallized, mechanically chopped, mechanically de-bulked, and metal doped CNTs were evaluated (Group A). Furthermore, several of commercially available CNTs (Group B) were compared with Group A. Interestingly the ROS scavenging rate was not significantly influenced by mechanical treatments, but depended on crystallization at high temperature. Very thin DWCNTs showed elimination of OH radical almost, implying existence of diameter threshold. The ratio of CNTs to DMPO influenced

the scavenging rate of CNTs but not titanium dioxide, as a higher concentration of CNTs showed the lower scavenging rate, this suggests that DMPO is partly adsorbed on the CNT surface and decreases the activity. The results suggest that the electron transfer on the CNT surface is the fundamental mechanism of ROS scavenging. Dangling bonds are not a key factor for scavenging, though. ROS is affected by CNT/DMPO ratio.

**PS 428 The Biological Response to Carbon Nanotubes in the BEAS-2B Cell Line Is Affected by Medium Conditions.**

H. Haniui<sup>1</sup>, N. Saito<sup>2</sup>, Y. Matsuda<sup>3</sup>, Y. Usui<sup>4</sup>, K. Aoki<sup>1</sup>, S. Takanashi<sup>1</sup>, S. Kobayashi<sup>1</sup>, H. Nomura<sup>1</sup>, M. Okamoto<sup>1</sup> and H. Kato<sup>1</sup>. <sup>1</sup>Department of Orthopaedic Surgery, Shinshu University School of Medicine, Matsumoto, Japan; <sup>2</sup>Department of Applied Physical Therapy, Shinshu University School of Health Sciences, Matsumoto, Japan; <sup>3</sup>Clinical Pharmacology Educational Center, Nihon Pharmaceutical University, Ina-machi, Japan; <sup>4</sup>Research Center for Exotic Nanocarbons, Shinshu University, Matsumoto, Japan. Sponsor: T. Kadota.

There are many reports on the use of an SV-40/adenovirus-transformed normal human bronchial epithelial cell line (BEAS-2B) to evaluate nanomaterials, especially multi-walled carbon nanotubes (MWCNT). However, the results have been controversial; one explanation is that while some experimental culture media contained serum, others did not. Here, we clarified the influence of serum on the BEAS-2B response to MWCNT compared with that on normal human bronchial epithelial cells (NHBE; Cell application) and studied its effect on MWCNT endocytosis. Cytotoxicity and cytokine secretion profiles of MWCNT on BEAS-2B cells or NHBE were examined in media with or without serum (Ham's F12 containing 10% fetal bovine serum [Ham's F12] and serum free growth medium [SFGM]). Cellular uptake of MWCNT was observed by fluorescence microscopy and analyzed by flow cytometry. We also examined if MWCNT uptake was suppressed by two kinds of endocytosis inhibitors. BEAS-2B cells cultured in Ham's F12 and NHBE cultured in SFGM exhibited similar biological responses to internalized MWCNT in terms of cell growth inhibition and cytokine secretion. BEAS-2B cells cultured in SFGM did not internalize MWCNT, and the IC<sub>50</sub> value of this cell line was 10 times higher than that in Ham's F12. MWCNT uptake was suppressed both by clathrin- and caveolae-mediated endocytosis inhibitors for BEAS-2B cells cultured in Ham's F12 and NHBE in SFGM. We conclude that the BEAS-2B cell line in serum-containing medium exhibits clathrin- and caveolae-mediated endocytosis of MWCNT, and displays the biological responses suitable for safety assessment of nanomaterials as a model of NHBE.

**PS 429 Evaluation of the Effect of Carbon Nanotubes on the Expressions of Endothelial Genes Implicated in Different Pathways of Cellular Death.**

O. Janouskova<sup>1</sup>, M. Orecna<sup>2</sup>, T. Tegegn<sup>2</sup>, S. Lacerda<sup>2</sup>, K. Holada<sup>1</sup> and J. Simak<sup>2</sup>. <sup>1</sup>First Faculty of Medicine, Charles University, Prague, Czech Republic; <sup>2</sup>Division of Hematology, CBER, US FDA, Rockville, MD.

Carbon nanotubes (CNTs) are attractive for various nanomedicine applications including their intravascular use. Therefore, the vascular biocompatibility of CNTs is a critical safety issue. Here we investigate the effect of carboxylated multi-walled CNTs (M60COOH) and their pristine counterparts (M60) on cultured human umbilical vein endothelial cells (HUVECs) by evaluating the changes in the expression of selected genes with known involvement in autophagy, apoptosis or necrosis. We have utilized Death PathwayFinder RT<sup>2</sup> Profiler PCR Array (Qiagen), to monitor expression of 84 selected genes. HUVECs were treated for 24 h with 100 µg/ml of M60 or M60COOH. Controls included HUVECs with serum starvation, or treatment with 1 µM camptothecin for 24h, or incubation with 1 mM H<sub>2</sub>O<sub>2</sub> for 2h. The cDNA was constructed from isolated RNA and the level of gene expression was analyzed by real time PCR using the PCR Array Data Analysis software (Qiagen).

Out of 84 monitored genes just 40 genes changed the expression significantly ( $P < 0.05$ ) often only after one or two treatments. The Bonferroni correction reduced the number of significantly changed genes to 14. Expression profiles after treatment with M60 and M60COOH differed ( $P < 0.05$ ). Both nanomaterials up-regulated different proapoptotic genes. In contrast to M60, only M60COOH up-regulated autophagy related genes for NFKB1, SQSTM1, and INS. Comparably, these gene array results complement our previous finding of a significant accumulation of the autophagosome protein marker LC3B in M60COOH but not in M60 treated HUVECs.

Our study suggests that the screening of mRNA levels of cell death pathway genes may be a valuable complementary tool in the testing of cellular toxicity of nanomaterials. However, further gene selection, standardization and validation of assays are required.

**PS 430 Carboxylated Multiwalled Carbon Nanotubes Induce mTOR Independent Autophagosome Accumulation in Endothelial Cells by Blockade of Autophagic Flux.**

M. Orecna<sup>1</sup>, S. Lacerda<sup>1</sup>, O. Janouskova<sup>2</sup>, T. Tegegn<sup>1</sup>, K. Holada<sup>2</sup> and J. Simak<sup>1</sup>. <sup>1</sup>Division of Hematology, CBER, US FDA, Rockville, MD; <sup>2</sup>First Faculty of Medicine, Charles University, Prague, Czech Republic.

Carbon nanotubes (CNTs) are attractive for various nanomedicine applications including their intravascular use. Therefore, the vascular biocompatibility of CNTs is a critical safety issue.

We have previously shown that in contrast to their pristine counterparts M60, carboxylated multiwalled carbon nanotubes M60COOH at 100µg/ml induced increase in the LC3B autophagosome protein marker in cultured human umbilical vein endothelial cells (HUVECs). Here we investigate a mechanism of this process. The autophagosome accumulation in M60COOH treated HUVECs was visualized by Laser Scanning Confocal Microscopy (LSCM) using immunodetection of the LC3B as well as in HUVECs transfected with Promo<sup>TM</sup> Autophagy Sensor LC3B-Green Fluorescent Protein using the baculovirus BacMam 2.0 technology. Moreover, western blotting (WB) analysis confirmed accumulation of LC3B in M60COOH treated HUVECs. The autophagosome accumulation can be caused either by induction of autophagy or by blockade of autophagic flux. The WB analysis of p62 (SQSTM1), a protein which is preferentially degraded by autophagy, showed that the induction of autophagy by serum starvation caused a significant decrease in p62 protein levels, while no change in p62 was observed in M60COOH treated HUVECs. The classical pathway of induction of autophagy involves inhibition of the mTOR kinase. The WB analysis of the mTOR substrate p-p70S6K showed no changes in levels of phosphorylation of this protein after M60COOH treatment. In addition, the LSCM kinetic study of HUVECs treated with Alexa555-conjugated M60COOH indicated the autophagic flux blockade. Our results showed that the accumulation of autophagosomes in HUVECs induced by M60COOH likely resulted from the blockade of autophagic flux, rather than induction of autophagy. This presentation reflects the views of the author and should not be construed to represent FDA's views or policies. (2CR grant LH12014)

**PS 431 Effects of the Protein Corona on the Interaction of Carbon Nanotubes with Blood Platelets.**

S. Lacerda<sup>1</sup>, L. L. Diduch<sup>2</sup>, M. Orecna<sup>1</sup>, T. Tegegn<sup>1</sup>, E. Karnaukhova<sup>1</sup> and J. Simak<sup>1</sup>. <sup>1</sup>US FDA, Bethesda, MD; <sup>2</sup>NIST, Gaithersburg, MD.

With the potential uses of carbon nanotubes (CNTs) in medicine and related CNT toxicity concerns, the importance of CNT-protein interaction studies cannot be stressed enough. We have shown that CNTs activate store operated calcium entry in blood platelets (De Paoli Lacerda SH et al, ACS Nano 2011). Here, we investigate how the PLT-activating effect of multiwalled carboxylated-CNTs (M60COOH) is influenced by interaction of M60COOH with different human proteins: albumin (HSA), fibrinogen (FBG), Gamma-globulins (HGG) and histone H1 (H1). Pymol molecular visualization was used to determine protein dimensions, electrostatic potential surfaces, and the number of aromatic residues available for binding to the M60COOH. Dissociation constants  $K_D = 0.049, 0.053, 0.079$  and  $0.165$  mg/mL for H1, FBG, HSA and HGG, respectively, were calculated for binding of these proteins to M60COOH. Circular dichroism revealed that the secondary structure of the studied proteins changed upon binding to M60COOH surface. Platelet (PLT) aggregometry showed that pre-incubation of M60COOH with HSA, HGG, and FBG reduced PTL-aggregating effect compared to bare M60COOH. In contrast, pre-incubation of M60COOH with H1 markedly increased their PLT-aggregating activity which was comparable to the effect of 20µM TRAP. In addition, the flow cytometry analysis of PTL membrane microparticles (CD41+CD62P+MP) showed that H1-M60COOH induced marked increase in CD41+CD62P+MP release compared to bare M60COOH. It is likely that positively charged H1 strongly interacts with the negatively charged plasma membrane of PTLs enhancing the nanopenetration of CNTs through the platelet plasma membrane. FBG leads M60COOH to self-assembly resulting in loss of the CNT surface area for interaction with PTLs which possibly explains the decrease in PLT-aggregating activity of FBG-treated M60COOH. In conclusion, binding of different proteins to CNTs greatly modulate their interactions with blood platelets. This presentation reflects the views of the author and should not be construed to represent FDA's views or policies.

**PS 432 Genotoxicity of Multiwalled Carbon Nanotubes.**

S. H. Reynolds<sup>1</sup>, C. Dinu<sup>2</sup>, D. T. Lowry<sup>1</sup>, M. L. Kashon<sup>1</sup>, A. F. Hubbs<sup>1</sup>, B. Stanley<sup>3</sup>, J. L. Salisbury<sup>4</sup>, J. Mastovich<sup>5</sup>, B. Kristin<sup>3</sup>, J. Sturgeon<sup>5</sup>, M. Keane<sup>1</sup>, C. Lorenzo<sup>1</sup> and L. Sargent<sup>1</sup>. <sup>1</sup>CDC/NIOSH, Morgantown, WV; <sup>2</sup>West Virginia University, Morgantown, WV; <sup>3</sup>NSA, Knoxville, TN; <sup>4</sup>Mayo Clinic, Rochester, MN; <sup>5</sup>RJ Lee, Monroeville, PA.

Carbon nanotubes have many unique applications in industry and medicine. Although the low density and small size of carbon nanotubes makes respiratory exposures to workers likely during the production or use of commercial products, the genotoxicity is not fully investigated. We have previously shown mitotic spindle aberrations in cultured primary and immortalized human airway epithelial cells exposed to single-walled carbon nanotubes (SWCNT). In order to investigate whether mitotic spindle damage was unique to SWCNT, we examined mitotic spindle aberrations following dosing of cells to multi-walled carbon nanotubes (MWCNT) at concentrations anticipated in the workplace. MWCNT induced a dose responsive increase in disrupted centrosomes, abnormal mitotic spindles and aneuploid chromosome number. The data further showed that monopolar mitotic spindles comprised 95% of the disrupted mitoses. Cell cycle analysis demonstrated a greater number of cells in G1 and S-phase in MWCNT-treated compared to diluent control, indicating a G1/S block in the cell cycle. The monopolar phenotype of the disrupted mitotic spindles and the G1/S block in the cell cycle is in sharp contrast to the multi-polar spindle and the G2 block in the cell cycle observed in SWCNT-induced disruption. Three dimensional reconstructions showed carbon nanotubes integrated with the microtubules, the DNA and within the centrosome structure. The lower doses did not cause cytotoxicity or apoptosis 24 hours after exposure; however, after 72 hours, significant cytotoxicity was observed in the MWCNT-exposed cells. One month following exposure, MWCNT-treated cells had a dramatic increase in both size and number of colonies. Our results demonstrate significant disruption of the mitotic spindle by MWCNT at occupationally relevant doses.

**PS 433 Loss of Epithelial Monolayer Integrity following Exposure of Primary Human Airway Cells to Multiwalled Carbon Nanotubes.**

R. J. Snyder<sup>1</sup>, S. Hussain<sup>1</sup>, R. Wine<sup>2</sup>, J. Roberts<sup>2</sup>, J. M. Brown<sup>3</sup>, N. J. Walker<sup>4</sup> and S. Garantzotis<sup>1</sup>. <sup>1</sup>Division of Bioinformatics and Biostatistics, National Center for Toxicological Research, US FDA, Jefferson, AR.

Pulmonary health effects due to inhaled multi-walled carbon nanotubes (MWCNT) have been a growing concern, as MWCNT become more widely used due to their unique physical and chemical properties. Studies have implicated MWCNTs in the pathogenesis of pulmonary fibrosis and inflammation. Airway epithelia are crucial for the maintenance of airway homeostasis and epithelial injury leads to airway remodeling and inflammation. We therefore tested the effect of MWCNT on airway epithelial integrity. In vivo mouse exposure to MWCNTs induced loss of airway columnar and ciliated epithelium within 7 days, and changes consistent with airway epithelial metaplasia. We then explored the mechanism for these changes in vitro. Bronchial epithelial cells (BECs) were obtained from healthy human volunteers via bronchoscopy, grown on E10+ electrode arrays until confluent, and electrical resistance across monolayers was measured continuously for 7 days after treatment with either dispersion medium, nanographene shape control (12ug/ml), or MWCNT (3 or 12 ug/ml). MWCNT treatment induced a significant reduction in epithelial resistance over time, suggesting breakdown of monolayer integrity, as well as alterations in cell morphology, but cytotoxicity was observed only in the higher MWCNT dose. Epithelial-mesenchymal transition was ruled out by western blotting, RT-PCR and staining for relevant markers. Microarray analysis revealed that MWCNT induced significant downregulation of cornulin, cadherins, and keratins, as well as upregulation of genes involved in retinoid signaling. These results suggest that MWCNT disrupt airway epithelial integrity through cytotoxicity and metaplasia linked to by retinoid-related dedifferentiation.

**PS 434 Human Pleural Mesothelial MeT-5A Cells Are a Limited In Vitro Model for Detection of Potential Asbestos-Like Genotoxic Effects of Multiwall Carbon Nanotubes.**

C. Ziemann, S. Reamon-Büttner, A. Hackbarth, H. Brockmeyer, H. Rahmer and B. Bellmann. *Fraunhofer Institute for Toxicology and Experimental Medicine, Hannover, Germany.* Sponsor: C. Dasenbrock.

Multiwall carbon nanotubes (MWCNT) are nanomaterials with important technological impact. But, depending on diameter and length some MWCNT may induce fiber-like toxicity/genotoxicity, similar to asbestos. Thus, a project funded by

the German Federal Ministry of Education and Research (contract No. 03X0109A) focuses on potential adverse biological effects and toxicity determining characteristics of divers MWCNT, both *in vivo* and *in vitro*, using long fiber amosite asbestos (LFA) as positive control. Since mesothelial cells are targets for adverse effects of asbestos, notably mesothelioma development, human SV40-transformed, non-malignant pleural mesothelial MeT-5A cells were initially chosen as *in vitro* model. In this study part, their usefulness for investigation of potential asbestos-like adverse effects of MWCNT *in vitro* was characterized. Proliferation parameters and a MWCNT-optimized lactate dehydrogenase assay indicated concentration-dependent cytotoxicity of LFA (2, 10 and 20  $\mu\text{g}/\text{cm}^2$ ) in MeT-5A cells. LFA also induced DNA-strand breaks and oxidative DNA-damage in the hOGG1-modified comet assay. For determination of MWCNT-related aneugenic effects/spindle fiber damage, basal frequency of micronuclei, chromosome aberrations, and altered meta-, ana- and telophase morphology was firstly determined. MeT-5A cells exhibited highly variable chromosome numbers (6.5% cells with normal 46 chromosomes), a markedly higher spontaneous micronucleus frequency, compared to rodent bone marrow erythrocytes (~15-fold) and V79 cells ~5-fold), and a high frequency of aberrant mitosis stages (bridges, lagging chromosomes, multipolar divisions). In conclusion, MeT-5A cells are a limited *in vitro* model to study potential asbestos-like effects of MWCNT. Cells are responsive to asbestos, but demonstrate marked genomic instability and thus limited significance concerning genotoxic effects. LP9 and LP9/TERT-1 cells are thus currently characterized as alternative models.

#### PS 435 Multidisciplinary Approach to Determination of C<sub>60</sub> Fullerene Presence in Lipid Membranes.

K. A. Russ<sup>1</sup>, P. T. Williamson<sup>3</sup>, P. Elvati<sup>2</sup>, A. Dews<sup>1</sup>, T. Adzemovic<sup>1</sup>, M. Ray<sup>1</sup>, A. Violi<sup>2</sup>, P. Smith<sup>4</sup> and M. A. Philbert<sup>1</sup>. <sup>1</sup>Environmental Health Sciences, University of Michigan, Ann Arbor, MI; <sup>2</sup>Mechanical Engineering, University of Michigan, Ann Arbor, MI; <sup>3</sup>Centre for Biological Sciences, University of Southampton, Southampton, United Kingdom; <sup>4</sup>Institute for Life Sciences, University of Southampton, Southampton, United Kingdom.

The incorporation of C<sub>60</sub> fullerenes into cell membranes was confirmed by computational modeling, <sup>31</sup>P and <sup>2</sup>H solid-state NMR, and transmission electron microscopy. Computational modeling shows that the free energy required for C<sub>60</sub>s to exist in or near the lipid bilayer is lowest when the C<sub>60</sub> is positioned between the lipid tails of the membrane. Static <sup>31</sup>P and <sup>2</sup>H solid-state NMR were used to study the interaction of the C<sub>60</sub> with model lipid bilayers composed of deuterated 1-palmitoyl-2-oleoylphosphatidylcholine. Temperature-dependent <sup>31</sup>P NMR spectra show that C<sub>60</sub>s are able to enter the membrane. Reduced magnetic deformation in the <sup>31</sup>P spectra suggests that C<sub>60</sub>s increase the rigidity of the membrane. Increased motional averaging in the phosphate groups and reduction in quadrupolar splitting (resulting in a higher density of motions occurring on the microsecond timescale in the glycerol backbone) were also seen with increasing concentrations of C<sub>60</sub>s. Transmission electron microscopy (TEM) shows C<sub>60</sub>s are able to enter the cell via three mechanisms: endocytosis (well-known), diffusion through the membrane, and an unknown mechanism allowing entry into the nucleus. Freeze fracture TEM images of RAW 264.7 immortalized cells show decreasing C<sub>60</sub> aggregate size with increasing proximity to the membrane as well as structures within the membrane space. This multidisciplinary approach clarifies some of the complex questions of nanomaterial-membrane interaction. Alteration of membrane composition via the addition of C<sub>60</sub>s may alter the structure/function of the cell. Further research will elucidate interactions between C<sub>60</sub> and receptors in the membrane that may in turn alter the normal functions of the cell. Supported by ES 08846, U01 ES020128-01, NIEHS Training Grant T32-ES007062-26 and NSF-CAREER Award CBET 0644639.

#### PS 436 Single-Walled Carbon Nanotubes Increase Influenza Virus Infectivity in Lung Cells.

P. Sanpui<sup>1</sup>, J. Loeb<sup>1</sup>, J. Lednický<sup>1</sup>, N. B. Saleh<sup>2</sup> and T. Sabo-Attwood<sup>1</sup>. <sup>1</sup>Department of Environmental & Global Health, University of Florida, Gainesville, FL; <sup>2</sup>Department of Environmental Engineering, University of South Carolina, Columbia, SC.

Possibility of engineered nanoparticles to influence the behavior of infectious agents, such as influenza A viruses (IAV) can have critical consequences. We are mainly interested in single-walled carbon nanotubes (SWNTs) because of their ever-increasing use in consumer products and structural resemblance with asbestos that may be relevant to their long-term health effects. Here, we aim to identify mechanisms controlling the immune response of lung epithelial cells (LEC) exposed to SWNTs and determine their influence on IAV infection. We concentrate on the role of toll-like receptors (TLRs) which are activated by pathogens to stimulate production of immune proteins. To examine the impact of SWNTs on TLRs and immune genes, LEC were exposed to SWNTs for 24 hours and expression of

84 genes were quantified using a TLR-selective array. Results revealed an immunosuppressive profile with 3 genes (CLEC4E, CD14, CSF3) being significantly downregulated. Since exposure to IAV results in a robust immune response we investigated whether SWNTs could enhance IAV infectability. LEC were exposed to SWNTs for 24 hours followed by co-incubation with H1N1 IAV. After immunofluorescence staining with an H1N1-specific antibody, we observed that LEC pre-exposed to SWNTs had significantly higher levels of IAV infection (~10%). These results were consistent with the quantified number of virus particles released into the cell culture media as determined by a titer assay showing an increase of 5.6 times over cells exposed to IAV only. To investigate the impact of SWNT on immune response, we measured secretion of a panel of cytokines (TNF $\alpha$ , IFN $\gamma$ , G-CSF, GM-CSF, IL1 $\alpha$ , IL8, IP10, Rantes) in media of exposed cells. The overall profiles showed that cytokines induced by IAV were repressed or enhanced in presence of SWNT. Overall results from these studies indicate that SWNTs have the potential to increase the susceptibility of lung cells to IAV infection and modulate IAV-associated classical immune response.

#### PS 437 Accumulation of Lipids and Oxidatively Damaged DNA in Hepatocytes Exposed to Particles.

P. Moller, L. K. Vesterdal, P. H. Danielsen, J. K. Folkmann, L. F. Jespersen, M. Roursgaard and S. Loft. Department of Public Health, University of Copenhagen, Copenhagen K, Denmark. Sponsor: M. Campen.

Exposure to particles has been suggested to generate hepatosteatosis by oxidative stress. We investigated lipid accumulation in cultured human hepatocytes (HepG2) and rat liver after exposure to Printex 90 carbon black (CB) particles. HepG2 cells were exposed to particles for 3 h and subsequently incubated for another 18 h to manifest lipid accumulation. There was a concentration-dependent increase after exposure to CB (50 and 100  $\mu\text{g}/\text{ml}$ ), which was only observed after co-exposure to oleic/palmitic acid. Similar results were observed in HepG2 cells that were exposed to diesel exhaust particles (SRM2975), fullerenes C60 or single-walled carbon nanotubes. All four types of particles at a concentration of 25  $\mu\text{g}/\text{ml}$  generated oxidatively damaged DNA, assessed as formamidopyrimidine (FPG) sensitive sites by the comet assay, in HepG2 cells after 3 h exposure. We have previously shown that a single oral exposure to 0.64 mg/kg of CB increased the level of 8-oxo-7,8-dihydro-2'-deoxyguanosine in the liver of rats (Danielsen et al., Toxicol Sci 118: 574-585, 2012). Recently we have assessed the level of hepatosteatosis by Oil Red staining in lean and obese Zucker rats that had been exposed to 0.064, 0.64 or 6.4 mg/kg of CB by a single oral administration (Folkmann et al., Toxicol Sci 129:98-107, 2012). There was slightly increased lipid load in the liver after exposure to 0.64 mg/kg (P=0.077) and statistically significant increased lipid load in lean Zucker rats that had received 6.4 mg/kg of CB (P<0.05). This was not associated with increased iNOS staining in the liver, indicating that the oral CB exposure was associated with hepatic steatosis rather than steatohepatitis. The obese Zucker rats had higher level of lipid load compared to the lean counterparts, whereas the oral CB exposure did not affect the lipid load level. In conclusion, our results indicate that exposure to particles is associated with accumulation of lipids in hepatocytes, concomitantly with signs of oxidatively damaged DNA.

#### PS 438 IL-4 and IL-13 Suppress IL-1 $\beta$ Production by Human THP-1 Macrophages after Exposure to Multiwalled Carbon Nanotubes.

K. A. Shipkowski, A. J. Taylor and J. C. Bonner. Toxicology, North Carolina State University, Raleigh, NC.

Introduction: Multi-walled carbon nanotubes (MWCNT) are prominent in the field of nanotechnology due to their novel properties, but represent a potential health hazard for human lung disease as mice exposed to MWCNT develop pulmonary inflammation and fibrosis. It has also been shown that mice with allergen-induced lung inflammation, driven largely by the Th2 cytokines interleukin (IL)-4 and IL-13, are susceptible to MWCNT-induced fibrosis. IL-1 $\beta$  is a pro-inflammatory cytokine secreted by MWCNT-activated macrophages via multi-protein scaffolds known as inflammasomes. In this study, MWCNT were evaluated as a stimulator of IL-1 $\beta$  expression by human THP-1 macrophages in the presence of IL-4 or IL-13 to model the microenvironment in allergic asthma. Methods: THP-1 cells, a human monocytic cell line, were activated with vitamin D3, differentiated with 12-O-tetradecanoylphorbol 13-acetate (TPA), primed with lipopolysaccharide (LPS), and dosed with either MWCNT alone (1-100  $\mu\text{g}/\text{mL}$ ) or MWCNT with IL-4 or IL-13 (10 ng/mL). IL-1 $\beta$  mRNA and protein levels were measured via TaqMan quantitative real-time RT-PCR and ELISA, respectively. Protein levels of phosphorylated and total STAT-6, an intracellular transducer of IL-4 and IL-13, were measured by Western blotting. Results: THP-1 cells treated with MWCNT showed a dose-dependent increase in IL-1 $\beta$  mRNA and protein levels. IL-1 $\beta$  induction was

significantly greater in differentiated cells, showing that activation of THP-1 cells increases their response to MWCNT stimulation. Cells co-exposed to IL-4 or IL-13 showed a significant decrease in MWCNT-induced IL-1 $\beta$  levels. Western blotting showed that IL-13, but not MWCNT, activated STAT-6 in THP-1 cells. Conclusions: IL-4 and IL-13 suppress MWCNT-induced expression of IL-1 $\beta$  in macrophages via STAT-6 phosphorylation. Our data suggest that Th2 cytokines up-regulated in asthma inhibit the innate immune response of macrophages to carbon nanotubes. (Funded by NIEHS RC2 ES018772 and R01 ES020897)

**PS 439 Zinc Oxide Surface Modification of Multiwalled Carbon Nanotubes Enhances Chemokine and Growth Factor Production in Human Monocytes and Lung Fibroblasts *In Vitro*.**

A. J. Taylor<sup>1</sup>, C. K. Devine<sup>2</sup>, G. N. Parsons<sup>2</sup> and J. C. Bonner<sup>1</sup>. <sup>1</sup>*Department of Environmental and Molecular Toxicology, North Carolina State University, Raleigh, NC;* <sup>2</sup>*Department of Chemical and Biomolecular Engineering, North Carolina State University, Raleigh, NC.*

Carbon nanotubes, a product of emerging nanotechnologies, are gaining increasing attention due to possible health risks from occupational and environmental exposures. Previous studies with rodents have shown that MWCNTs stimulate the production of pro-fibrogenic growth factors such as transforming growth factor- $\beta$ 1 (TGF- $\beta$ 1) & platelet-derived growth factor (PDGF) *in vivo*. Thin-film coating of MWCNT with metal oxides by a process called atomic layer deposition (ALD) modifies and enhances the functionality of MWCNTs in electronics and engineering. We hypothesize that metal oxide surface coating of MWCNT with zinc oxide (ZnO) alters the production of pro-inflammatory cytokines & chemokines as well as pro-fibrogenic growth factors by human monocytes (THP-1) and human lung fibroblasts (HLF-16Lu). To test our hypothesis MWCNTs were coated with ZnO via ALD. THP-1 and HLF-16Lu were exposed to coated or uncoated MWCNT for 24 hr and then we measured mRNAs levels (via RT-PCR) of the growth factors PDGF and TGF- $\beta$ 1, the pro-inflammatory cytokine IL-1 $\beta$ , and the mononuclear cell chemokine CXCL10. THP-1 cells exposed to ZnO-coated MWCNTs showed a 6-fold increase in IL-1 $\beta$  mRNA expression, and ~2-fold increase in TGF- $\beta$ 1 mRNA and PDGF mRNA levels. In the HLF-16Lu fibroblasts, ZnO-coated MWCNTs increased the mRNA expression of TGF- $\beta$ 1 3-fold and CXCL10 6-fold but proved to be cytotoxic at higher doses. Uncoated MWCNTs had no effect on any of the target mediators in either cell line. Our findings indicate that surface modification of MWCNTs with ZnO enhances the production of pro-fibrogenic proteins by macrophages and fibroblasts *in vitro*. These findings suggest that MWCNT modified by ALD coating with ZnO could increase the toxicity and pathogenicity of MWCNT in the lung.

(Funded by: NIEHS Grants R01ES020897 & RC2-ES018772)

**PS 440 Metabolomic Analysis of Liver Cells Exposed to Carbon Nanotubes and Graphene Oxide.**

W. M. Henderson<sup>1</sup>, D. Bouchard<sup>1</sup>, X. Chang<sup>2</sup>, I. Chowdhury<sup>3</sup>, B. Foster<sup>2</sup>, S. Aronson<sup>2</sup> and Q. Teng<sup>1</sup>. <sup>1</sup>*National Exposure Research Laboratory, Office of Research and Development, US EPA, Athens, GA;* <sup>2</sup>*Student Service Authority Contractor to US EPA, Athens, GA;* <sup>3</sup>*Grantee to US EPA via National Research Council Cooperative Agreement, Athens, GA.*

Carbon nanotubes (CNTs) and other graphenic nanomaterials are being used extensively in industrial, consumer, and mechanical applications based in part on their unique structural, optical and electronic properties. Due to the widespread use of these nanoparticles (NPs), human and ecological exposure is probable and inevitable. To determine the effects CNTs and graphene oxide (GO) have on biochemical processes, metabolomics-based profiling of human (C3A) and zebrafish (ZFL) liver cells was utilized. Cell cultures were exposed to 0, 10, or 100 ng/mL of covalently or non-covalently modified nanomaterial for 24 and 48 hrs while particle size distribution, charge, and aggregation kinetics were monitored concurrent with exposure studies. Following NP exposure, metabolites were extracted and derivatized prior to GC/MS analysis or lyophilized and buffered for 1H NMR analysis. Acquired spectra and chromatograms were subjected to multivariate analysis to determine the consequence of NP exposure on the metabolite profile of C3A and ZFL cells. The resulting scores plots illustrated temporal and dose dependent responses to all classes of NPs tested. Loadings plots coupled with univariate analysis were then used to identify metabolites of interest. Preliminary data suggest that CNT and GO exposure causes perturbations in processes involved in cellular oxidation as well as fluxes in lipid metabolism and fatty acid synthesis. Dose-response

trajectories are apparent for each nanomaterial tested and spectral components related to both dose and NP modifications were determined. Correlations of the significant changes in metabolites will aid in identifying potential biomarkers associated with carbonaceous nanoparticle exposure in both humans and ecologically relevant species.

**PS 441 Physical Characterization of Multiwalled Carbon Nanotubes for Inhalation Studies.**

B. T. Chen, D. Schwegler-Berry, W. McKinney, S. Stone, J. L. Cumpston, S. Friend, D. W. Porter, V. Castranova and D. Frazer. *PPRB, NIOSH, Morgantown, WV.*

Animal inhalation studies have reported that adverse pulmonary, cardiovascular, and immune reactions may result from exposure to multi-walled carbon nanotubes (MWCNTs). At the present time, however, there is little guidance for adequate sampling and characterization of MWCNT aerosols for evaluating exposures and obtaining an applicable dose metric for risk assessment. This is mainly because MWCNTs tend to agglomerate and form complex structures making them difficult to characterize. To address this problem, we conducted detailed sampling and characterization studies of MWCNTs that had similar particle morphologies to those found in the workplace. Representative samples were collected using filters, a cascade impactor, and direct reading instruments, and they were used for microscopic observation, gravimetric analysis, and real-time monitoring. Particle number distributions on a filter (0.008–0.10 particles/ $\mu$ m<sup>2</sup>), and mass distributions using an impactor (0.1–0.3 mg on peak stages) were determined. Microscopic analyses indicated that MWCNTs can be classified into three shape categories: irregular, isometric, and fibrous particle structures. Each particle structure contained a mean of 18 nanotubes, and 1  $\mu$ g of MWCNTs contained 2.7 x 10<sup>6</sup> particle structures composed of 4.9 x 10<sup>7</sup> individual nanotubes. Impactor measurements showed that the mass median aerodynamic diameter of the aerosol was 1.5  $\mu$ m with a geometric standard deviation of 1.67. The shape factor of individual fibers was 1.94–2.71, and the isometric particles had an effective density of 0.71–0.88 g/cm<sup>3</sup>. Results also indicated that real-time particle number counts were realistic, but without an index of agglomeration, they were insufficient for adequate risk assessment. Information from this study can be used to estimate initial lung burden and to design an improved lung deposition model that considers three individual MWCNT particle shapes. The described methods can be used as guidance for sampling and characterizing other engineered nanoparticles.

**PS 442 Cellular Responses Induced by Single-Wall Carbon Nanotubes with Varying Physical Properties in Alveolar Epithelial Cells.**

K. Fujita<sup>1,2</sup>, M. Fukuda<sup>2</sup>, S. Endoh<sup>2</sup>, H. Kato<sup>1,2</sup>, N. Shinohara<sup>1,2</sup>, R. Nagano<sup>2</sup>, M. Horie<sup>3</sup>, S. Kinugasa<sup>1,2</sup>, H. Hashimoto<sup>1</sup> and A. Kishimoto<sup>1,2</sup>. <sup>1</sup>*AIST, Tsukuba, Japan;* <sup>2</sup>*TASC, Tsukuba, Japan;* <sup>3</sup>*University Occupational Environmental Health, Kitakyushu, Japan.*

Concern over the influence of carbon nanotubes (CNTs) on human health has risen due to advances in the development of nanotechnology. Some studies have shown that unpurified CNTs induced high levels of cellular responses than those of purified CNTs. They suggest that the residual metals involved in CNTs attribute to induction of oxidative stress. Here, we examine our hypothesis that the physicochemical properties of single-wall carbon nanotubes (SWCNTs) may have important implications for biological responses. We have developed novel dispersion procedure of CNTs with their different physical properties in culture medium. *In vitro* cytotoxicity assays were performed on human alveolar epithelial cell lines (A549) using impurity-free SWCNTs with varying physical properties and commercial SWCNTs with residual metals as a reference. Cell viability, apoptosis, intracellular reactive oxygen species (ROS) generation, cell cycle distribution, and cellular uptake of SWCNTs were investigated. Impurity-free SWCNTs with their different physical properties (CNT-1, CNT-2) and SWCNTs containing trace amounts of metals (CNT-3) did not cause significant inhibition of cell proliferation, induction of apoptosis and arresting cell cycle progression. On the other hand, all samples significantly increased level of the intracellular ROS production after 24h incubation. These results show that residual metals involved in SWCNTs may not be a definitive parameter for induction of oxidative stress. The relatively short line shape of SWCNTs small bundles were observed in the vacuoles of cells exposed to CNT-1. The relatively long line shape of SWCNTs large bundles were observed in the cytoplasm and vacuoles of cells exposed to CNT-2. A large number of aggregated SWCNTs with punctate structures were observed in the cytoplasm and vacuoles of cells exposed to CNT-3. We suggest that the physical properties of SWCNTs are closely related to the cellular uptake and induction of oxidative stress.

**PS 443 Sonolytic Degradation of Pluronic® Surfactants to Toxic Byproducts: Implications for Nanotoxicity Testing.**

R. K. Draper<sup>1,2</sup>, R. Wang<sup>1,2</sup>, H. Tyler<sup>1</sup>, S. Beck<sup>1</sup>, S. Vakili<sup>1</sup>, S. Li<sup>1</sup> and P. Pantano<sup>2</sup>. <sup>1</sup>Molecular & Cell Biology, University of Texas at Dallas, Richardson, TX; <sup>2</sup>Chemistry, University of Texas at Dallas, Richardson, TX.

Poloxamers (known by the trade name Pluronic®) are triblock copolymer surfactants that contain two polyethylene glycol blocks and one polypropylene glycol block of various sizes. Poloxamers are widely used as nanoparticle dispersants for nanotoxicity studies wherein nanoparticles are sonicated with a dispersant to prepare suspensions. It is known that poloxamers can be degraded during sonication and that reactive oxygen species contribute to the degradation process. However, the possibility that poloxamer degradation products are toxic to mammalian cells has not been well studied. We report here that aqueous solutions of poloxamer 188 (Pluronic® F-68) and poloxamer 407 (Pluronic® F-127) sonicated in the presence or absence of multi-walled carbon nanotubes (MWCNTs) can become highly toxic to cultured cells. Moreover, toxicity correlated with the sonolytic degradation of the polymers. These findings suggest that caution should be used in interpreting the results of nanotoxicity studies where the potential sonolytic degradation of dispersants was not controlled.

**PS 444 Effects of Carbon Black Nanoparticles on Human Pulmonary Cell Lines and Precision Cut Lung Slices.**

T. Hansen<sup>1</sup>, J. Kopf<sup>1</sup>, O. Danov<sup>1</sup>, M. Ströbele<sup>3</sup>, A. Braun<sup>1</sup>, K. Sewald<sup>1</sup>, P. Steinberg<sup>4</sup> and H. Fehrenbach<sup>2</sup>. <sup>1</sup>Fraunhofer Institute for Toxicology and Experimental Medicine, Hannover, Germany; <sup>2</sup>Research Center Borstel, Borstel, Germany; <sup>3</sup>Karlsruhe Institute of Technology (KIT), Karlsruhe, Germany; <sup>4</sup>University of Veterinary Medicine Hannover, Hannover, Germany. Sponsor: C. Dasenbrock.

Carbon black nanoparticles (CBNPs) are among the most abundantly used nanomaterials and have been reported to cause adverse health effects after inhalation exposure. The aim of this study was to compare the effects of Printex® 90 and acetylene soot particles in human pulmonary cell lines (16HBE14o-, Calu-3, A549) and precision cut lung slices (PCLS) of mice, rats and humans using a wide concentration range. Particle size distribution in the cell culture medium was determined by dynamic light scattering. Viability assays were LIVE/DEAD® staining and WST-1 assay for PCLS and WST-8 and neutral red assay for cell lines. CBNP-induced formation of reactive oxygen species (ROS) was assessed in A549 and 16HBE14o-cells by flow cytometry using the DCFH-DA assay. Furthermore, the effect of CBNP exposure on the transepithelial electrical resistance (TEER) was investigated in Calu-3 cells after 24, 48 and 120h treatment with 10 and 50 µg/ml CBNPs. With PCLS, the inflammatory response was assessed by measuring pro-inflammatory cytokines (i.e. IL-1α, TNF-α, IL-8). Both CBNPs tested were not toxic in physiologically relevant concentrations. Significant cytotoxicity was observed in the WST-8 assay for both CBNPs at 50 µg/ml after 48h, whereas no effects were found in the neutral red assay. Increased ROS formation was observed with both CBNPs after 24 and 48 h. Interestingly, acetylene soot particles cause significant TEER reduction at both dose levels and all time points tested whereas Printex® 90 reduced the TEER only after 120h at the high dose. Neither Printex® 90 nor acetylene soot particles induced the secretion of proinflammatory cytokines in mouse and rat PCLS. In conclusion, the combination of in vitro and ex vivo models provides a valuable tool to assess the acute irritation and inflammation effects of CBNPs on lung tissue.

**PS 445 Rho-Kinases Are Involved in Caspase-1-Mediated IL-1β Secretion following In Vitro Exposure to Multiwalled Carbon Nanotubes and Asbestos in Human Monocyte.**

S. Kanno<sup>1</sup>, S. Hirano<sup>2</sup>, S. Chiba<sup>1</sup>, H. Takeshita<sup>1</sup>, T. Nagai<sup>1</sup>, M. Takada<sup>1</sup> and T. Mukai<sup>1</sup>. <sup>1</sup>Department of Legal Medicine, St. Marianna University School of Medicine, Kawasaki, Japan; <sup>2</sup>Research Center for Environmental Risk, National Institute for Environmental Studies, Tsukuba, Japan.

It has been reported that fibrous particles such as asbestos and carbon nanotubes (CNT) trigger interleukin (IL)-1β release through NLRP3 inflammasome in phagocytotic cells. GTPase effector Rho-kinases (ROCK1, and 2), are known to be associated with the organization of the actin cytoskeleton during phagocytosis. In this study we examined whether ROCKs are involved in asbestos- or multi-walled CNT (MWCNT)-induced IL-1β release in human monocytic THP-1 cells. THP-1 were differentiated to macrophages by PMA and were exposed to crocidolite, MWCNT or lipopolysaccharide (LPS) in the presence or absence of Y27632 (ROCKs inhibitor) or Z-YVAD (caspase-1 inhibitor). Concentrations of IL-1β in

the culture medium were measured using ELISA. Cell-associated MWCNT or asbestos were assayed by turbidimetry. Protein levels of ROCK1 and ROCK2 were analyzed by western blotting. Treatment with PMA increased expression of ROCK1, whereas that of ROCK2 was not changed in THP-1 cells. Exposure of the cells to asbestos or MWCNT provoked IL-1β secretion the secretion was suppressed by either Y27632 or Z-YVAD, whereas LPS-induced IL-1β secretion was inhibited only by Z-YVAD, but not by Y27632. These results indicate that IL-1β secretion was increased by caspase-1 activation and ROCKs are involved in both asbestos- and MWCNT-induced IL-1β secretion. On the contrary, treatment with Y27632 did not change the amount of those fibrous particles associated with the cells. To further examine the effect of ROCK1 and ROCK2 on asbestos and CNT-induced IL-1β secretion, differentiated THP-1 were transfected with siRNA to knockdown ROCKs. siRNA designed for both ROCK1 and ROCK2 decreased asbestos- or MWCNT-induced IL-1β secretion and did not change LPS-induced IL-1β secretion, indicating that ROCKs are implicated in fiber-induced inflammatory responses.

**PS 446 Multiwalled Carbon Nanotubes Damage the Mitochondria to Increase Reactive Oxygen Radical Production, Activate NF-κB Signaling to Induce Inflammatory Cytokines, and Stimulate Transforming Growth Factor β1 and Platelet-Derived Growth Factor Expression to Promote Fibroblast-to-Myofibroblast Transformation.**

X. He<sup>1</sup>, S. Young<sup>2</sup>, D. Schwegler-Berry<sup>2</sup>, W. P. Chishom<sup>3</sup>, J. E. Fernback<sup>4</sup> and Q. Ma<sup>1</sup>. <sup>1</sup>Toxicology and Molecular Biology Branch, NIOSH, Centers for Disease Control and Prevention, Morgantown, WV; <sup>2</sup>Pathology and Physiology Research Branch, NIOSH, Centers for Disease Control and Prevention, Morgantown, WV; <sup>3</sup>Exposure Assessment Branch, NIOSH, Centers for Disease Control and Prevention, Morgantown, WV; <sup>4</sup>Chemical Exposure & Measuring Branch, NIOSH, Centers for Disease Control and Prevention, Cincinnati, OH.

Carbon nanotubes (CNTs) are novel material with unique electronic and mechanical properties. Here, we report that multi-walled carbon nanotubes (MWCNT) have potent, dose-dependent toxicity on cultured human cells. Molecular characterization revealed that MWCNT induced substantial ROS production and mitochondrial inner membrane depolarization at sub-toxic doses. MWCNT stimulated the secretion of a panel of inflammatory cytokines and chemokines (TNFα, IL-1β, IL-6, IL-10 and MCP1) from macrophages (Raw264.7) by activating the canonical NF-κB signaling pathway. Activation of NF-κB signaling involves rapid degradation of IκBα, nuclear accumulation of NF-κBp65, binding of NF-κB to specific DNA-binding sequences, and transactivation of target gene promoters. Finally, MWCNTs induced the production of fibrogenic growth factors TGFβ1 and PDGF that function as paracrine signals to promote the transformation of lung fibroblasts into myofibroblasts, a key molecular step in the development of lung fibrosis. These results demonstrated that MWCNT elicit multiple and intertwining molecular signaling events involving oxidative damage, inflammatory cytokine production, and myofibroblast transformation, which potentially underlie the toxicity and fibrosis in human lungs by MWCNTs.

**PS 447 Functionalization-Associated Effects of Carboxylated Fullerenes on Cellular Aging.**

J. Gao and I. Rashi. Bioscience Division, Los Alamos National Laboratory, Los Alamos, NM.

The systematic evaluation of critical cellular responses such as apoptosis, cellular proliferation, reproductive clonogenicity and cell cycle responses in lung cells by distinctly functionalized fullerenes demonstrated that fullerene-mediated responses are dependent on their ability to perturb cell division that ultimately impact cellular fate. Moreover, we postulate that the observed cellular responses were charge and functionalization specific, in that the positively charged fullerenes were cytotoxic as opposed to the negatively charged fullerene. Interestingly, the negatively charged fullerenes inhibited cellular apoptosis and necrosis. On further investigation we discovered that, depending on the functionalization, the negatively charged fullerenes could induce senescence in bronchial epithelial cells, a cellular response that we have previously reported as a potential toxicological endpoint of fullerenes in dermal cells. We demonstrate that the observed non-cytotoxic or cyto-protective effect of fullerenes may in fact be due to a more novel function of fullerenes to induce premature senescence in cells. In the present study we utilized immortalized but not tumorigenic human bronchial epithelial cells (Beas-2b) and normal human-derived bronchial epithelial cells (NHBE) to perform a systematic evaluation of the effect of a suite of positively and negatively charged engineered fullerenes on key biological

responses. We found that the biological response(s) elicited by fullerenes on interaction with lung cells may depend upon their ability to perturb cell cycle checkpoints potentially inducing senescence. Further elucidation of the underlying molecular mechanisms involved in this senescence response indicated the involvement of GADD45a, p16, p21 and p53a, a response characteristic of cells undergoing senescence. Finally, we correlated the physicochemical properties of engineered fullerenes with the observed biological responses to obtain a better understanding of property-dependent bioactivity of fullerenes.

#### PS 448 An In Vitro Assay Detects Enhancement of Mouse T Cell Sensitization to Ovalbumin by Carbon Nanoparticles.

D. E. Lefebvre<sup>1</sup>, B. Pearce<sup>1</sup>, E. Chomyshyn<sup>1</sup>, N. Ross<sup>1</sup>, S. Halappanavar<sup>2</sup>, A. F. Tayabali<sup>2</sup>, I. Curran<sup>1</sup> and G. S. Bondy<sup>1</sup>. <sup>1</sup>Bureau of Chemical Safety, Food Directorate, Health Products and Food Branch, Health Canada, Ottawa, ON, Canada; <sup>2</sup>Environmental Health Science and Research Bureau, Environmental and Radiation Health Sciences Directorate, Healthy Environments and Consumer Safety Branch, Health Canada, Ottawa, ON, Canada.

**RATIONALE AND SCOPE:** Previous studies suggested that some nanomaterials can promote allergic sensitization. At present there are no in vitro tools to study this risk. The hypothesis was that an in vitro screening assay could be developed to assess the adjuvant activity of agglomerated carbon black nanoparticles (CBNP). **EXPERIMENTAL PROCEDURES:** DO11.10 transgenic mice have a T cell receptor which recognizes the ovalbumin (OVA) protein from chicken egg. Splenic leukocytes from these mice were cultured with 0, 0.012, 0.12, 1.2 or 12 µg/mL CBNP, OVA, or OVA with CBNP. T cell mitosis rate was quantified by flow cytometry on day 3 post-exposure. T helper (Th1/Th2) cytokine production was measured by qPCR and ELISA. **RESULTS:** Printex 90 and Aldrich carbon CBNP products were characterized. These powders consisted of micron-sized agglomerates made up of 22 nm and 39 nm diameter CBNP base particles, respectively. Following sonication in saline RP-10 solution, the fraction of agglomerates smaller than 220 nm was purified by filtration for cell exposure. These particles did not induce T cell mitosis, and they did not modify this parameter during the response to OVA. These CBNP alone did not induce Th1/Th2 cytokine expression. However, OVA in combination with 12 µg/mL of either Printex 90 or Aldrich carbon significantly increased the allergy-related Th2 cytokines IL-4, IL-10 and IL-13 compared with OVA alone ( $p \leq 0.05$ ;  $n = 3-5$ /group). This was concurrent with a decrease in the Th1 transcription factor Stat4. Lower CBNP doses had no effect. **CONCLUSIONS:** An in vitro immunotoxicology tool was developed. At the highest dose, carbon nanoparticles enhanced allergy pathways in mouse immune cells responding to ovalbumin. This assay will be used to further characterize nanomaterials for risk assessment purposes.

#### PS 449 Role of Transforming Growth Factor-β1 Pathway in Carbon Nanotube Stimulated Collagen Production in Human Lung Cells.

A. Mishra<sup>1,2</sup>, T. A. Stueckle<sup>1</sup>, R. Derk<sup>1</sup>, V. Castranova<sup>1,2</sup>, Y. Rojanasakul<sup>2</sup>, J. Yuan<sup>3</sup> and L. Wang<sup>1,2</sup>. <sup>1</sup>Pathology and Physiology Research Branch, Health Effects Laboratory Division, NIOSH, Morgantown, WV; <sup>2</sup>School of Pharmacy, West Virginia University, Morgantown, WV; <sup>3</sup>School of Public Health, Hebei United University, Tangshan, China.

Accumulated studies have shown that carbon nanotubes (CNT) induce rapid and progressive lung fibrosis in animal models but the mechanisms are not clear. Following CNT exposure transforming growth factor β (TGF-β), a pro-fibrogenic mediator, was induced both in vivo and in vitro models and was correlated with in vivo fibrosis and in vitro collagen induction. To understand the signaling mechanism of this fibrogenic response, we investigated the contribution of TGF-β signaling in CNT-induced collagen production, a hall mark of fibrosis, using cultured human lung cells and determined the role of TGF-β receptor-Smad (TGF-βR1-Smad) signaling as a potential mechanism for CNT-induced fibrosis. Human lung epithelial (BEAS2B) cells and fibroblast (CRL1490) cells were exposed to doses relevant to in vivo exposure (0.02-0.6 µg/cm<sup>2</sup> in vitro ~ 10-80 µg/mouse lung) of well characterized and dispersed multi-walled CNT (MWCNT), single walled CNT (SWCNT) and ultrafine carbon black (UFCB). Protein expression was measured by immunofluorescence, western blotting and ELISA. Present results indicate: 1) CNT exposure caused induction of TGF-β1 production in lung epithelial cells; 2) TGF-β, TGF-βR1, p-Smad-2, and collagen type I were overexpressed in CNT-exposed fibroblast cells; 3) collagen I stimulating effects of MWCNT were partially blocked in TGF-βR1 and Smad-2 knockdown fibroblast cells. In conclusion, CNT stimulate lung fibroblasts to induce collagen I in vitro through activation of the TGF-β R1-Smad Signaling pathway.

#### PS 450 Factors Associated with the Releasability of Carbon Nanotubes (CNTs) from Nanocomposites in Potential Consumer or Industrial Applications.

M. Kovochich, R. Avnani and A. K. Madl. *ChemRisk, Aliso Viejo, CA.*

Engineered nanomaterials offer innovative advancements for a wide range of industrial and consumer product technologies which promise to have global economic impact. Engineered nanomaterials in composites (nanocomposites) are currently being used in applications ranging from basic consumer goods to critical national defense technologies, with carbon nanotubes (CNTs) being popular for nanocomposites due to their enhanced mechanical, thermal, and electrical properties. With comparisons of CNTs to other high aspect ratio fibers, some concerns have been raised regarding the potential implications for exposure and health risk of nanocomposites containing CNTs. We hypothesized that the physical and chemical interactions between CNTs and the composite matrix, as well as settings in which nanocomposites are handled will influence the release of these nanomaterials. We analyzed available data on the release of CNTs from different composites as a result of various stressors. Although no release was detected under UV weathering conditions, CNT surface aggregation was detected in thermoplastic and epoxy composites compared with cementitious material. Matrix type, nanomaterial dispersion within the matrix, and chemical bonding were critical determinants for releasability. Mechanical stress tests such as cutting, grinding, sanding, and abrasion showed both positive and negative releasability results. Taken together, data indicate that physical, chemical, and environmental factors can affect the release of CNTs from nanocomposites including the location of the CNTs within the matrix, the chemical and physical bonding between the CNTs and the matrix, as well as the physical stress applied to the matrix. Analytical methods distinguishing release of CNTs versus matrix nanoparticles are critical to characterizing nanomaterial exposure. Understanding the factors that play a role in the release of CNTs will aid in technological development and safe handling of nanocomposites while minimizing any potential health risks.

#### PS 451 In Vitro Endothelial Exposure to Carbon Nanotubes Produce Reactive Oxygen Species.

Y. Rodriguez Yanez<sup>1</sup>, I. Poblete-Naredo<sup>1</sup>, B. Chavez-Munguia<sup>2</sup>, B. Cisneros<sup>3</sup> and A. Albores<sup>1</sup>. <sup>1</sup>Toxicology, Cinvestav, Mexico City, Mexico; <sup>2</sup>Infectomics and Molecular Pathology, Cinvestav, Mexico City, Mexico; <sup>3</sup>Genetic and Molecular Biology, Cinvestav, Mexico City, Mexico.

Recent studies are focused to carbon nanotubes (CNT) effects on blood coagulation, and have demonstrated that CNT are able to induce platelet aggregation and vascular thrombosis. However, there is little information on CNT effects on fibrinolysis. Therefore, we investigated the role of CNT on fibrinolysis and their contribution to elicit a prothrombotic process in vascular endothelium and the reactive oxygen species (ROS) participation. In the present study we examined the CNT oxidative potential by ROS production and the induction of fibrinolysis-related gene expression in human umbilical vein endothelial cells (HUVEC) isolated from the vein of the umbilical cord. Primary HUVEC cultures were exposed to single-walled carbon nanotubes (SWCNT) at 5, 25 and 50 µg/ml during 24 h, and oxidation potential (free-cell dithiotreitol oxidation assay), cytotoxicity (propidium iodide stain) and cell morphology (transmission electron microscopy, TEM) were assessed. SWCNT exposure resulted in concentration-dependent changes: a) oxidation potential increases that suggest a ROS increase and, b) viability decreases. Additionally, morphological changes in mitochondria, chromatin and nucleus were observed by TEM. It is expected that the oxidative stress caused by ROS may affect the transcription of the fibrinolysis related genes, activators: tissue- and urokinase-activator, tissue kallikrein, [tPA, uPA, KLK1]); and inhibitors: plasminogen activator inhibitor type 1 and kallistatin [serpine1, serpin4]), altering the physiological fibrinolysis pathway in the vascular endothelium (Supported by grants SSA/IMSS/ISSSTE/CONACYT grant 162391 and ICyTDF51/2012, YRY received a Conacyt scholarship 203482).

#### PS 452 Transport of Inhaled MWCNT to the Pleura, Respiratory Muscles and Systemic Organs.

R. R. Mercer, A. F. Hubbs, J. F. Scabilloni, L. Wang, L. A. Battelli, V. Castranova and D. W. Porter. *PPRB, NIOSH, Morgantown, WV.*

Inhalation exposure studies of mice were conducted to determine if multi-walled carbon nanotubes (MWCNT) distribute to the parietal pleura, respiratory musculature and systemic organs. Male C57BL/6J mice were exposed in a whole-body inhalation system to a 5 mg/m<sup>3</sup> MWCNT aerosol for 5 hours/day for 12 days (4 times/week for 3 weeks). At 1 day and 48 weeks after the 12 day exposure period,

mice were anesthetized and lungs and systemic tissues were preserved by whole body vascular perfusion of paraformaldehyde while inflated with air. A separate, clean-air control group was studied. Sirius Red stained sections from lung, diaphragm, chest wall, heart, kidney and liver were analyzed. Enhanced darkfield microscopy and morphometric methods were used to detect and count MWCNT in tissue sections. Counts in tissue sections were expressed as number of MWCNT per cm<sup>2</sup> of tissue (mean±SE, N=8 mice per group). Although agglomerates account for approximately 60% of lung burden, only singlet MWCNT were observed in diaphragm, chest wall and systemic tissues. At one day post exposure, the average length of singlet MWCNT in diaphragm was comparable to that of singlet MWCNT in the lungs 5.6 ± 0.6 versus 5.1 ± 0.6 μm, respectively. There were 26 ± 13 and 134 ± 25 per cm<sup>2</sup> in tissue sections of diaphragm at 1 day and 48 weeks post exposure, respectively. On average, there were 18 ± 5 and 50 ± 20 per cm<sup>2</sup> singlet MWCNT observed in systemic organ tissue sections at 1 day and 48 weeks, respectively. The burden of singlet MWCNT in parietal pleura, respiratory musculature and systemic organs at 48 weeks post exposure was significantly higher than at 1 day post exposure. Results demonstrate that inhaled MWCNT, which deposit in the lungs, are transported to the parietal pleura, the respiratory musculature and the systemic organs in a singlet form and accumulate with time following exposure.

#### PS 453 Genotoxicity of Long, Tangled Carbon Nanotubes in Mice.

J. Catalán<sup>1,2</sup>, H. Järventaus<sup>1</sup>, S. Suhonen<sup>1</sup>, K. Siivola<sup>1</sup>, C. Moreno<sup>2</sup>, E. Rossi<sup>1</sup>, J. Koivisto<sup>1</sup>, E. Vanhala<sup>1</sup>, H. Wolff<sup>1</sup>, H. Alenius<sup>1</sup>, K. Savolainen<sup>1</sup> and H. Norppa<sup>1</sup>. <sup>1</sup>Nanosafety Research Centre, Finnish Institute of Occupational Health, Helsinki, Finland; <sup>2</sup>University of Zaragoza, Zaragoza, Spain.

Long, needle-like multiwalled carbon nanotubes (MWCNTs) have been described to induce inflammation, genotoxic effects and mesothelioma in the respiratory system of mice, but the mechanisms behind these adverse effects are not well understood. The stiffness of the CNTs has been suggested to play a crucial role in their clearance from the lungs, affecting their toxicity. We have earlier observed that long, needle-like MWCNTs increase DNA damage in murine lungs. To find out whether the shape of the CNTs could affect their genotoxic properties, we examined here whether also long, but tangled MWCNTs (outer diameter 8-15 nm; Cheaptubes Inc), administered either by pharyngeal aspiration or inhalation, could be genotoxic in C57BL/6J mice locally in the lungs or systematically in peripheral leukocytes and bone marrow erythrocytes. Cell samples were collected 24-h after a single pharyngeal aspiration (0.02-4 mg/ml) or a 4-day inhalation exposure (4 h/day; 17.5 mg/m<sup>3</sup>) to the MWCNTs. DNA damage was assessed by the comet assay in bronchoalveolar lavage (BAL) cells and lung cells. DNA double strand breaks were assessed by the γ-H2AX assay in peripheral leukocytes and (after pharyngeal aspiration) in lung cells. Micronuclei, a biomarker of chromosome damage, were analyzed in bone marrow polychromatic erythrocytes sampled 24 h after the end of the inhalation exposure. No significant dose-dependent increase in DNA damage (comet assay) was seen in the BAL or lung cells of mice treated by pharyngeal aspiration or by inhalation exposure. The long, tangled MWCNTs neither induced systemic genotoxic effects in peripheral leukocytes or bone marrow. Our findings suggest that the stiffness of long MWCNTs is a central characteristic with respect to their genotoxicity in vivo, with thinner and flexible tangled MWCNTs, which tend to form agglomerates, showing no genotoxic effects. (Funded by the Finnish Work Environment Fund)

#### PS 454 High-Fat Diet Leads to Increased Lung Inflammation and Airway Resistance following Multiwalled Carbon Nanotubes Exposure.

T. A. Brown. Center for Environmental Health Sciences, University of Montana, Missoula, MT.

Obesity has become a worldwide epidemic responsible in large part for the rising costs of health care. Obesity leads to systemic low-grade inflammation increasing risk for the development of diseases such as diabetes, but the link for respiratory disease is less clear. We investigated the effect of a high fat diet on lung inflammation and lung physiology when exposed to multi-walled carbon nanotubes (MWCNT). Nanomaterials, including MWCNT, are used in an increasing number of consumer products. Given their small dimensions with large surface area and often very unique properties with high deposition efficiency they can induce significant immune responses in the lung. In this study, C57BL/6 mice were kept on a high fat diet for 6 weeks and then exposed to MWCNT, via oropharyngeal instillation. Measurements were taken 24 hr later to determine changes in inflammation and respiratory physiology, specifically lung resistance. Mice given particle on the high fat diet had significantly increased levels of IL-1β, a pro-inflammatory cytokine produced by the inflammatory complex the inflammasome, as well as increased lung resistance compared to mice on the control diet given particle. In order

to further investigate inflammatory changes due to the high fat diet additional studies examined the influx of inflammatory cells in response to MWCNT exposure. Mice on the high fat diet exposed to MWCNT had a greater influx of neutrophils and eosinophils compared to control diet mice exposed to particle. These results indicate that a high fat diet leads to an increase inflammatory response with measurable physiological alterations in the lungs when exposed to MWCNT. This work was supported by NIH grants RC2 ES018742 and P20 RR017670.

#### PS 455 Multiwalled Carbon Nanotubes Cause Mild Inflammation in the Aorta without Pulmonary Toxicity in a Rapidly Aging Mouse Model.

K. Luyts, S. Smulders and P. Hoet. *Environment and Health, Kuleuven, Leuven, Belgium.*

Exposure to ambient particulates has been shown to cause co-morbidity in elderly. Brain and muscle ARNT-like protein-1 (Bmal1) clock gene-deficient mice, with an accelerated aging and prothrombotic phenotype, were used to study the pulmonary and cardiovascular toxicity of multiwalled carbon nanotubes (CNTs). At the age of 8 weeks, wildtype and knockout Bmal1 mice were oropharyngeally aspirated once weekly during 5 consecutive weeks with 6.4 μg (32 μg in total), 25.6 μg (128 μg in total) of CNTs or the vehicle as control.

Cell counts in the bronchoalveolar lavage fluid indicated no inflammatory response 24 hours or 2 months after the last aspiration despite the presence of particle-laden macrophages. Cytokine measurements in lung homogenates showed trends for IL-1β, IL-6 and KC increases only in the wildtype mice aspirated with 128 μg CNTs but this response disappeared after 2 months.

In wildtype mice, aspiration of 128 μg CNTs caused a non-significant decrease in platelet and red blood cell counts, no significant differences for the aPTT and PT clotting tests were found and clotting factor FVIII was (non-significantly) decreased 24 hours after the last aspiration and increased 2 months later. In the Bmal1 knockout mice, FVIII was increased after 24 hours but decreased after 2 months.

A macrophage staining (MAC-3) on sections of the aorta showed endothelial activation and vascular inflammation in 60% of the 128 μg dosed knockout animals. There were no changes observed in the aortas of the wildtype mice.

In this study we showed that multiple dosing (5 weekly doses) of CNTs induced a mild vascular inflammation in the high dosed Bmal1 knockout mice in the absence of pulmonary toxicity.

ENPRA Project NMP4-SL-2009-228789

IWT 101061

#### PS 456 Investigation of the Pulmonary Bioactivity of Double-Walled Carbon Nanotubes.

T. M. Sager<sup>1</sup>, M. Wolfarth<sup>1</sup>, D. W. Porter<sup>1</sup> and T. Steinbach<sup>2</sup>. <sup>1</sup>NIOSH, Morgantown, WV; <sup>2</sup>Experimental Pathology Laboratories, Sterling, VA.

Nanotechnology is one of the world's most promising new technologies. In turn, carbon nanotube production is estimated to reach into the millions of tons within the decade. Our laboratory has previously established that exposure to multi-walled carbon nanotubes (MWCNT) causes lung inflammation and fibrosis in mice after pharyngeal exposure. However, the bioactivity of double-walled carbon nanotubes (DWCNT) has not been determined. In this study we explored the hypothesis that DWCNT would promote pulmonary toxicity by analyzing the pulmonary bioactivity of the DWCNT. To test this hypothesis, male mice (C57BL/6J) were given a single dose of one of the following by pharyngeal aspiration: 1) 0.9% saline with 0.3% (w/v) carboxymethyl cellulose (CMC; vehicle control), or 2) DWCNT (0-40 μg/mouse) suspended in vehicle [0.9% saline with 0.3% (w/v) CMC]. Whole lung lavage (WLL) was conducted at 1 and 7 days post-exposure. Lungs of non-lavaged animals were also collected and processed for histopathologic analysis at 7 and 56 days post-exposure. The results show the DWCNT exposure caused a dose-dependent increase in WLL polymorphonuclear leukocytes, indicating that DWCNT exposure initiates pulmonary inflammation. DWCNT exposure also caused a dose-dependent increase in LDH activity as well as albumin levels in WLL fluid, indicating that DWCNT exposure promotes cytotoxicity as well as decreases in the integrity of the blood-gas barrier in the lung. Also, at 56 days post-exposure, the presence of fibrosis was noted in the highest dose exposure group (40 μg/mouse). In conclusion, this study provides insight into the previously uninvestigated pulmonary bioactivity of DWCNT exposure. The results confirm that DWCNT exposure does promote inflammation and fibrosis in the lung. The results also indicate that DWCNT have a similar pulmonary bioactivity as the previously studied MWCNT.

## PS 457 Multiwalled Carbon Nanotube-Induced Lung Tumors.

L. Sargent<sup>1</sup>, D. W. Porter<sup>1</sup>, D. T. Lowry<sup>1</sup>, L. A. Battelli<sup>1</sup>, K. Siegrist<sup>1</sup>, M. L. Kashon<sup>1</sup>, B. T. Chen<sup>1</sup>, D. Frazer<sup>1</sup>, L. Staska<sup>2</sup>, A. E. Hubbs<sup>1</sup>, W. McKinney<sup>1</sup>, M. Andrew<sup>1</sup>, S. Tsuruoka<sup>3</sup>, M. Endo<sup>3</sup>, V. Castranova<sup>1</sup> and S. H. Reynolds<sup>1</sup>. <sup>1</sup>CDC/NIOSH, Morgantown, WV; <sup>2</sup>Integrated Laboratory Systems, Durham, NC; <sup>3</sup>Shinshu University, Nagano, Japan.

Carbon nanotubes have many promising applications. Although the low density and small size of carbon nanotubes makes respiratory exposures to workers likely during the production or use of commercial products, there is limited data on carcinogenicity of inhaled multi-walled carbon nanotubes (MWCNTs). We have therefore utilized a two stage initiation/promotion protocol to determine whether inhaled MWCNTs act as a complete carcinogen and/or promote the growth of cells with existing DNA damage. Six week old, male, B6C3F1 mice received a single dose of either methylcholanthrene (MC, 10 µg/g BW, i.p.) or vehicle (corn oil). One week after i.p. injections, mice were exposed by inhalation to MWCNTs (5 mg/m<sup>3</sup>, 5 hours/day, 5 days/week) or filtered air (controls) for a total of 15 days. The B6C3F1 mouse used in this study has intermediate susceptibility to lung carcinogenesis, and data obtained will have relevancy to existing human lung tumor data because lung tumors in this mouse strain exhibit many molecular and morphological similarities to human pulmonary tumors. At 17 months post-exposure, mice were euthanized and examined for lung tumor formation. Twenty percent of the filtered air controls, 33% of the MWCNT-exposed, and 50% of the MC followed by air-exposure, had a mean of one tumor per mouse. By contrast, 100% of the mice which received MC followed by MWCNTs had tumors with an average of 3.6 tumors per mouse. Additionally, mice exposed to MWCNTs or MC followed by MWCNTs had larger tumor volumes than their corresponding air-exposed control groups. Our preliminary data suggests that MWCNT exposure promotes the growth of spontaneously and chemically initiated lung cells, resulting in the development of lung tumors. In this study, mouse MWCNT lung burden approximates feasible human occupational exposures. Therefore, the results of this ongoing study indicate that caution should be used to limit human exposures to MWCNTs.

## PS 458 Toxicological Evaluation of Pulmonary Exposure to Graphenes of Different Sizes.

J. R. Roberts<sup>1,2</sup>, A. Kenyon<sup>1</sup>, S. S. Leonard<sup>1,2</sup>, N. R. Fix<sup>1</sup>, D. W. Porter<sup>1,2</sup>, T. M. Sager<sup>1,2</sup>, M. Wolfarth<sup>1</sup>, B. M. Yingling<sup>2,1</sup>, I. S. Chaudhuri<sup>3</sup>, A. Kyrilidis<sup>3</sup>, S. A. Bilgesu<sup>1</sup>, R. R. Mercer<sup>1,2</sup>, D. Schwegler-Berry<sup>1</sup>, V. Castranova<sup>1</sup> and A. Erdelyi<sup>1,2</sup>. <sup>1</sup>NIOSH, Morgantown, WV; <sup>2</sup>WVU, Morgantown, WV; <sup>3</sup>Cabot Corporation, Billerica, MA.

Research on the uses and manufacturing of nano graphene has increased dramatically in the past decade. Thus, worker inhalation of graphene nanopowders is likely. The goal of this study was to evaluate the lung toxicity of three non-oxidized graphene (Gr) samples of different sizes [20 µm lateral x 7-10 nm thick (Gr20), 5 µm lateral x 7-10 nm thick (Gr5), and <2 µm lateral x 1-2 nm thick (Gr1)]. Gr samples were diluted in physiological dispersion medium (DM) and characterized for size, surface reactivity, and free radical generation *in vitro*. Male C57BL/6J mice received 4 or 40 µg of Gr1, Gr5, or Gr20, or 40 µg of carbon black (CB; particle control), or DM (vehicle control) by aspiration. Mice were sacrificed at 4 hr (day 0), 1, 7, and 28 days post-exposure. Lung lavage was performed, the fluid and cells were retained, and indices of lung injury and inflammation were examined. Particle/aggregate size ranged from ~ 5-300 µm, 0.5-60 µm, and 0.2-5µm for Gr20, Gr5, and Gr1, respectively, with CB being similar to Gr1. Electron spin resonance (ESR) indicated that all Gr samples and CB had low to no surface reactivity as compared to a positive control (α-quartz). *In vitro*, ESR showed all Gr samples induced free radical production by mouse monocytes with significantly greater response in Gr20- and Gr5-treated cells compared to Gr1- and CB-treated cells. Indices of lung injury in lavage fluid were increased for the 40 µg doses of Gr20 and Gr5 on days 0, 1, and 7 when compared to control. Gr1 (40 µg) produced an increase only at day 7. Increased lung injury in the CB group was comparable to Gr20 and Gr5 on days 1 and 7. Injury decreased in all groups by day 28. Inflammation was elevated in the 40 µg Gr20, Gr5, Gr1 and CB groups on day 1, but only in the 40 µg Gr20 and Gr5 groups on days 0 and 7. In summary, the larger Gr particles appeared to produce more toxicity at the early time points post-exposure when compared to controls.

## PS 459 A 28-Days Repeated Dose of Multiwalled Carbon Nanotubes (MWCNTs) in Sprague-Dawley Rats.

J. Sung<sup>2</sup>, B. Choi<sup>2</sup>, K. Song<sup>2</sup>, J. Kim<sup>2</sup>, K. Ahn<sup>3</sup>, G. Lee<sup>3</sup>, J. Lee<sup>5</sup>, J. Shin<sup>5</sup>, J. Lee<sup>1</sup>, K. Jeon<sup>4,3</sup> and I. Yu<sup>1</sup>. <sup>1</sup>Institute of Nanoparticle Safety Research, Hoseo University, Asan, Republic of Korea; <sup>2</sup>Bioconvergence Department, KCL, Incheon, Republic of Korea; <sup>3</sup>Mechanical Engineering, Hanyang University, Ansan, Republic of Korea; <sup>4</sup>HCT, Icheon, Republic of Korea; <sup>5</sup>Occupational Lung Diseases Institute, Korea Workers' Compensation Welfare Service, Icheon, Republic of Korea.

There is a lack of available information on the human health and environmental hazards of MWCNTs. For this reason, the current study investigated the inhalation toxicity potential of MWCNTs. Eight-week-old rats were divided into 4 groups (10 rats in each group), including the fresh air control (0 mg/m<sup>3</sup>), low-concentration group (0.2 mg/m<sup>3</sup>), middle concentration group (0.5 mg/m<sup>3</sup>), and high-concentration group (1.0 mg/m<sup>3</sup>), and exposed to MWCNTs for 5 days (6 hrs/day) in nose-only inhalation exposure system. Then the rats were allowed to recover for 1 and 3 months by ceasing the exposure. At the end of the study, the rats were subjected to a full necropsy. Cellular differential counts and inflammatory measurements, such as albumin, lactate dehydrogenase (LDH), total protein, and cytokines were also monitored in the a cellular bronchoalveolar lavage (BAL) fluid of the rats exposed to the MWCNTs for 28 days. Histopathological, hematological and clinical chemistry examinations indicated that there were no significant findings related to MWCNT exposure after 28 days of MWCNT inhalation exposure.

## PS 460 Toxic Effects of MWCNT *In Vivo* and *In Vitro*.

A. Schlichting<sup>1</sup>, C. Ziemann<sup>1</sup>, A. Leonhardt<sup>2</sup>, R. Susanne<sup>1</sup>, S. Dirk<sup>1</sup> and B. Bernd<sup>1</sup>. <sup>1</sup>Fraunhofer ITEM, Hannover, Germany; <sup>2</sup>Leibniz Institute for Solid State and Materials Research, Dresden, Germany. Sponsor: C. Dasenbrock.

Multiwall carbon nanotubes (MWCNT) are discussed to exhibit a toxic potential depending on their length and fiber-like shape. For this reason, potential adverse biological effects *in vivo* (rat) and *in vitro* (human peritoneal mesothelial LP9/TERT-1 cells) of MWCNT are investigated in a project funded by the German BMF (contract No. 03X0109A). In this project MWCNT data are compared with long amosite asbestos as a positive control and more particle-like MWCNT (Baytubes®, milled MWCNT, and Printex 90) as negative controls. For this study custom made MWCNT with different length and diameter were produced. To investigate the carcinogenic potential of these MWCNT, they were suspended in artificial lung-like medium using a sonotrode. The separated MWCNT were applied to the rats by intraperitoneal injection. In addition to the carcinogenicity study, the proliferation of cells in the diaphragm was investigated as a short time screening test after 3 month, using a BrdU method. To determine cytotoxicity *in vitro* LP9/TERT-1 cells were incubated for 24h with the same MWCNT, suspended in culture medium, and the toxic potential was estimated by cell counting and subsequent calculation of the relative increase in cell count (RICC). Suspension, size, and distribution of MWCNT were always monitored by SEM. CNT3 (length: 8.57 µm; diameter: 0.085 µm) and long amosite (length: 13.95 µm; diameter: 0.39 µm) led to significant thickening of the diaphragm, as compared to the negative control. With CNT2 (length: 10.24 µm; diameter: 0.04) a high amount of BrdU positive cells were noted. In the *in vitro* study part both CNT1 (length: 7.91 µm; diameter: 0.037 µm), CNT2, CNT3 and long amosite asbestos mediated strong reduction in cell number, compared to the particle controls, indicating a marked cytotoxic potential. In conclusion, some MWCNT mediate enhanced proliferation in rat diaphragm which may result in mesothelioma development and certain MWCNT exhibit a cytotoxic potential in mesothelial cells *in vitro*.

## PS 461 Carbon Nanotubes Enhance Metastatic Growth of Lung Carcinoma via Up-Regulation of Myeloid-Derived Suppressor Cells.

M. Shurin<sup>1</sup>, A. V. Tkach<sup>2</sup>, E. Kisin<sup>2</sup>, T. Khaliullin<sup>2</sup>, S. Stanley<sup>2</sup>, D. Gutkin<sup>1</sup>, A. Star<sup>4</sup>, Y. Chen<sup>4</sup>, G. Shurin<sup>1</sup>, V. Kagan<sup>3</sup> and A. A. Shvedova<sup>2</sup>. <sup>1</sup>Department of Pathology, University of Pittsburgh, Pittsburgh, PA; <sup>2</sup>PPRB, HELD, NIOSH, Morgantown, WV; <sup>3</sup>Department of Environmental and Occupational Health, University of Pittsburgh, Pittsburgh, PA; <sup>4</sup>Department of Chemistry, University of Pittsburgh, Pittsburgh, PA.

Expanding applications of nanomaterials, particularly carbonaceous nanoparticles (CNP), in new technologies, consumer products and biomedicine, imply their increasing levels of manufacturing. There are numerous attempts to utilize nanoparticles for better delivery of drugs and nucleic acid-based therapeutics to disease sites in the lung, particularly to the lung epithelium. The inhalation of drug nano-for-

mulations propelled the development of new strategies in therapy of several human lung diseases such as asthma, cystic fibrosis, chronic obstructive pulmonary disease, lung cancer, tuberculosis, etc. Safety and lack of adverse health effects remain the major pre-requisites for broader applications of these novel technologies. Toxicological assessments of nano-particles typically are performed on normal animals. Thus possible effects of CNP on tumor growth have not yet been considered. The immune system safeguards the host from infections and malignancies. Recognition and undesirable interactions of CNP with cells of the immune system may lead to immunomodulation, hence increasing the host's susceptibility to infections and cancer. Here, we show that single wall carbon nanotubes (SWCNT) promote metastatic establishment and growth of Lewis lung carcinoma in C57BL/6J mice. The effect was mediated by increased local and systemic accumulation of myeloid-derived suppressor cells (MDSC), as their depletion abrogated pro-tumor activity in vivo. These data are important for the design of novel theranostics platforms with modules capable of depleting or functionally suppressing MDSC to ensure effective immunosurveillance in the tumor microenvironment.

**PS 462 IL-33 Modulates Chronic Airway Resistance Changes Induced by Multiwalled Carbon Nanotubes.**

X. Wang, J. Shannahan and J. M. Brown. *Pharmacology & Toxicology, East Carolina University, Greenville, NC.*

As the field of nanotechnology rapidly grows, the potential health hazards for human exposure rise. We have previously demonstrated that oropharyngeal instillation of multi-walled carbon nanotubes (MWCNTs) in C57BL/6 mice leads to increases in total respiratory system resistance (R) and Newtonian resistance (Rn), which is a measure of central airway resistance. In this study, we hypothesized that IL-33, a critical immune system alarmin, modulates mechanisms of pulmonary toxicity following exposure to MWCNTs. We assessed lung histology and pulmonary function in C57BL/6 and IL-33<sup>-/-</sup> mice 30 days following oropharyngeal aspiration of MWCNTs. The total number of bronchoalveolar lavage cells and the recruitment of neutrophils was increased in C57BL/6 mice following MWCNT exposure. In contrast, IL-33<sup>-/-</sup> mice exposed to MWCNTs did not demonstrate alterations in bronchoalveolar lavage cell content. Furthermore, C57BL/6 mice displayed increased inflammation around the airways demonstrated by histopathology which was unseen in IL-33<sup>-/-</sup> mice. To determine if these histopathological changes impact airway resistance, MWCNT exposed C57BL/6 were challenged with cumulative doses of methacholine (Mch) between 1.5 mg/ml and 24 mg/ml. Aerosolized Mch increased R and Rn in a dose-dependent manner in all groups with MWCNT instilled C57BL/6 mice responding with significantly higher R and Rn compared to control C57BL/6 mice. Importantly, increases in R and Rn induced by MWCNT were dependent on IL-33, as there was no significant difference between MWCNT treated and control IL-33<sup>-/-</sup> mice. In conclusion, these results indicate IL-33 plays an important role in pulmonary toxicity induced by MWCNT by influencing airway resistance via an inducible inflammatory response. This work supported by NIH RO1 ES019311.

**PS 463 Pulmonary Toxicity Assessment of Multiwalled Carbon Nanotubes after Single Intratracheal Instillation in a One-Year Bioassay of Rats.**

M. Naya, N. Kobayashi, K. Honda, M. Ema and J. Nakanishi. *National Institute of Advanced Industrial Science and Technology (AIST), Tsukuba, Japan.*

Well-dispersed multi-wall carbon nanotubes (MWCNTs) were instilled intratracheally at dosage of 1.0 or 2.6 mg/kg body weight to male Wistar rats. A negative (vehicle) control, 0.5 mg/mL Triton X-100 was administered in a similar manner. After instillation, the bronchoalveolar lavage fluid (BALF) was assessed for the inflammatory biomarkers, and the lung, liver, kidney, spleen, and cerebrum were examined histopathologically at 1-day, 3-day, 1-week, 4-week, 3-month, 6-month, and 12-month post-exposure. Transient pulmonary inflammatory responses were observed up to 3-month post-exposure. In the histopathological examination, 1.0 and 2.6 mg/kg of MWCNTs deposited in the lungs were phagocytosed by the alveolar macrophages and these macrophages were accumulated in the alveoli up to 12-month post-exposure. There was no evidence of chronic inflammation, such as angiogenesis or fibrosis which induced by MWCNT instillation. These results suggest that MWCNTs were being processed and cleared by alveolar macrophages.

**PS 464 Thirteen-Week Inhalation Toxicity Study with a Multiwall Carbon Nanotube Test Material in Wistar Rats.**

D. Schuler<sup>1</sup>, K. L. Reed<sup>2</sup>, M. P. DeLorme<sup>2</sup>, Y. Okazaki<sup>1</sup>, Y. Muro<sup>4</sup>, H. J. Chevalier<sup>3</sup> and D. B. Warheit<sup>2</sup>. <sup>1</sup>Harlan Laboratories Ltd., Fuellinsdorf, Switzerland; <sup>2</sup>DuPont Haskell Lab, Wilmington, DE; <sup>3</sup>Anapath GmbH, Oberbuchsitzen, Switzerland; <sup>4</sup>Showa Denko K.K., Tokyo, Japan.

A subchronic inhalation toxicity study of an inhaled vapor-grown multiwall carbon nanotube (MWCNT) test substance was conducted in male and female Wistar rats. The test sample was composed of > 99.5% carbon, containing limited (Fe) catalyst metals; BET surface area measurements of ~25 m<sup>2</sup>/g; and average lengths/diameters of 9 µm and 100 nm, respectively. Four groups of rats per sex were exposed nose-only, 6 h/day, for 5 days/week to aerosol concs. of 0, 0.013 (low), 0.055 (mid) or 0.53 (high) mg/m<sup>3</sup> MWCNT (MMAD ranging from 0.85 – 1.64 µm) over a 91-day period and evaluated 1 day later. Toxicity evaluations included clinical and histopathology methods, and bronchoalveolar lavage fluid (BALF) analyses. Additional control and high exposure groups were evaluated at 3 months PE. Results demonstrated that MWCNT exposures produced no significant adverse extrapulmonary effects. Absolute and relative lung weights were increased in high exposure conc. vs. controls and to a lesser extent after the recovery period. The results of BALF studies demonstrated increased GGT, LDH and ALK PHOS levels vs. controls in mid/high exposure groups. In addition, increased numbers of BALF cells were recovered at 0.53 mg/m<sup>3</sup> MWCNT. Principal histopathological findings consisted of granulomatous lesions in centriacinar regions of male/female rats exposed to 0.53 mg/m<sup>3</sup>, and in some females at 0.055 mg/m<sup>3</sup>. The lesion was characterized by aggregation of pulmonary macrophages and focal pulmonary hypertrophy/hyperplasia of lung epithelial cells. In the nasal cavities, an increase of eosinophilic inclusions in the respiratory/olfactory epithelium was noted at 0.53 mg/m<sup>3</sup> which was followed by the olfactory epithelial injury in the recovery animals. Based on the findings in respiratory tract tissues (lungs and nasal cavities), the overall LOAEL was considered to be 0.055 mg/m<sup>3</sup>, and the corresponding NOAEL was determined to be 0.013 mg/m<sup>3</sup> under the conditions of this study.

**PS 465 Carbon Nanotube Dosimetry: From Workplace Exposure Assessment to Inhalation Toxicology.**

M. Dahm<sup>1</sup>, B. T. Chen<sup>2</sup>, M. E. Birch<sup>1</sup>, D. E. Evans<sup>1</sup>, M. K. Schubauer-Berigan<sup>1</sup>, T. Hulderman<sup>2</sup>, S. A. Bilgesu<sup>2</sup>, H. D. Leonard<sup>2</sup>, W. McKinney<sup>2</sup>, D. Frazer<sup>2</sup>, J. M. Antonini<sup>2</sup>, D. W. Porter<sup>2</sup>, V. Castranova<sup>2</sup>, P. C. Zeidler-Erdely<sup>2</sup> and A. Erdely<sup>2</sup>. <sup>1</sup>NIOSH, Cincinnati, OH; <sup>2</sup>NIOSH, Morgantown, WV.

Relevant dosimetry for toxicology studies involving multi-walled carbon nanotubes (MWCNT) has not been well described due to a lack of detailed occupational exposure assessments. In response, exposure assessment findings from U.S.-based MWCNT manufacturers and users were extrapolated to results of an inhalation study in mice. Inhalable and respirable personal breathing zone (PBZ) samples from 9 facilities were collected for the mass concentration of elemental carbon. Upon analysis, 95% of the PBZ samples found exposure concentrations to be <10 µg/m<sup>3</sup> with an average inhalable concentration of 8.5 µg/m<sup>3</sup>. At facilities where respirable and inhalable PBZ samples were collected, respirable samples were approximately 25% of the inhalable size fraction. Using 10 µg/m<sup>3</sup>, standard worker ventilatory parameters, and assuming 11% alveolar deposition, alveolar deposition was calculated to be 10.56 µg/d. Extrapolation to mouse equivalence by surface area equals 5.2 ng/d. In complement, a 19 d inhalation exposure to MWCNT with daily alveolar depositions of 1250 ng (=240 d of human exposure at 10 µg/m<sup>3</sup>), 125 ng (=24 d), and 12.5 ng (=2.4 d) was conducted. Mice were sacrificed at day 0, 3, 28, and 84 post-exposure. Pulmonary cytotoxicity (LDH activity) and polymorphonuclear cell (PMN) influx were evident at the high dose through day 84. For the middle dose, no PMN influx was evident and cytotoxicity was significant only at day 0. Lung inflammatory gene expression was increased at the high and middle dose. Alveolar macrophages harvested after exposure and stimulated with LPS showed enhanced cytokine release at the high dose and day 0 for the middle dose. No exposure effects were observed at the lowest dose. These results show a no effect dose lies somewhere in between the middle (=456 d at 10 µg/m<sup>3</sup>) and low dose (=45.6 d). The findings stress the importance of exposure assessment when extrapolating results of animal MWCNT exposures to potential human outcomes.

**PS 466 Pharmacokinetics and Pharmacodynamics of C60 and Nanosilver in Nonpregnant, Pregnant, and Lactating Rats.**

R. Snyder<sup>1</sup>, S. Sumner<sup>1</sup>, S. Black<sup>1</sup>, A. Lewin<sup>1</sup>, R. Tyl<sup>1</sup>, M. Levine<sup>1</sup>, C. J. Wingard<sup>2</sup> and T. Fennell<sup>1</sup>. <sup>1</sup>Discovery Sciences, RTI International, Research Triangle Park, NC; <sup>2</sup>Department of Physiology, East Carolina University, Greenville, NC.

Pregnancy and lactation represent periods in which the female and her offspring may be more sensitive to adverse effects from exposure to nanoparticles. The distribution of nanoparticles during pregnancy and lactation has not been comprehensively investigated. We therefore examined the absorption, distribution, and excretion of C60 and two sizes of nanosilver (NS) in nonpregnant, pregnant, and lactating rats. Rats were dosed via tail vein injection with [<sup>14</sup>C]C60 solubilized with polyvinylpyrrolidone (PVP) in saline. [<sup>14</sup>C]C60 was administered to pregnant rats on gestational day (gd) 11, 15, or 18 and lactating rats on postnatal day (pnd) 8. Nonpregnant and pregnant rats (gd 18) were dosed via tail vein injection (1 mg/kg) or oral gavage (10 mg/kg) with 20 nm or 110 nm NS stabilized with PVP in water, equivalent doses of silver acetate, or vehicle. Urine, feces, blood, and tissues were collected following dosing, and quantitative whole body autoradiography of [<sup>14</sup>C]C60 was conducted. The largest portion of the [<sup>14</sup>C]C60 derived radioactivity was detected in the liver (~29%), lung (~31%), and spleen (~5%) after a single iv dose in the pregnant rat, and detected in the liver (~54%), lung (~8%), and spleen (~4%) in the lactating rat. Radioactivity was above background for many additional tissues. Less than 1% of the radioactivity recovered was found in urine and feces at all time points for the pregnant rats. The majority (55%) of the recovered oral 110 nm NS dose was found in feces after 48 hr. Following iv dosing, 11% of the dose was recovered in feces for the 110 nm NS and 27% for the 20 nm NS. The highest concentration of nanosilver was found in the spleen for both sizes of NS. Plasma cytokine and urinary 8-hydroxydeoxyguanosine levels were determined. This study demonstrated substantial differences in the retention of C60 compared with nanosilver. (Supported by NIEHS U19ES019525)

**PS 467 Signal Transducer and Activator of Transcription 1 (STAT-1) Suppresses Pulmonary Inflammation following Allergen Sensitization & Exposure to Multiwalled Carbon Nanotubes.**

E. E. Anderson Thompson, A. J. Taylor, E. E. Glista-Baker, B. C. Sayers and J. C. Bonner. *Environmental and Molecular Toxicology, North Carolina State University, Raleigh, NC.*

Multi-walled carbon nanotubes (MWCNT) pose a potential risk to human health, especially in individuals with pre-existing lung diseases such as asthma. A key factor in asthma is an imbalance of T-helper type 1 (Th1) and type 2 (Th2) cells. STAT-1 is a transcription factor that maintains Th1 development. We postulated that mice deficient in STAT-1 would be susceptible to ovalbumin (OVA) allergen challenge and display increased airway disease to MWCNT. STAT-1<sup>-/-</sup> and wildtype (WT) mice were sensitized to OVA by i.p. injection on days 0 & 12, followed by OVA intranasal challenge on days 26, 28, & 32. On day 34, mice were exposed to 4 mg/kg MWCNT or saline/0.1% pluronic surfactant by oropharyngeal aspiration. Necropsy was performed 1 & 21d post-MWCNT exposure. Lungs were lavaged to collect inflammatory cells and bronchoalveolar lavage fluid (BALF), right lung was collected for RNA & protein, and left lung for histopathology. Ashcroft scoring of H&E-stained lung sections revealed that OVA-sensitized STAT-1<sup>-/-</sup> mice displayed significantly greater inflammation compared to vehicle control treated STAT-1<sup>-/-</sup> mice at 21 d, and this was not exacerbated by MWCNT. However, BALF differential cell counts revealed that OVA-sensitized STAT-1<sup>-/-</sup> mice treated with MWCNT had significantly increased numbers of neutrophils & eosinophils compared to similarly treated WT mice at 21 d. Quantitative morphometry of Alcian blue PAS & trichrome stained lung sections revealed that the OVA-sensitized STAT-1<sup>-/-</sup> mice also produced significantly more airway mucus and collagen after exposure to MWCNT. ELISA performed on BALF showed significant increases in the pro-fibrogenic mediators IL-1 $\beta$ , TGF- $\beta$ 1, and osteopontin in the OVA sensitized STAT-1<sup>-/-</sup> mice treated with MWCNT at 21d. Taken together, these results suggest that STAT-1 suppresses the exacerbation of lung disease by MWCNT in individuals with asthma. (Funded by NIEHS RC2 ES018772 and R01 ES020897)

**PS 468 Resolution of Inflammatory and Surfactant Alterations Mediated by Carbon Black and Silver Nanospheres.**

D. Botelho<sup>1</sup>, S. Sarker<sup>2</sup>, F. Chung<sup>3</sup>, A. Porter<sup>3</sup>, S. Schwander<sup>2</sup> and A. Gow<sup>1</sup>. <sup>1</sup>Toxicology, Rutgers The State University of New Jersey, Piscataway, NJ; <sup>2</sup>UMDNJ, Piscataway, NJ; <sup>3</sup>Imperial College London, London, United Kingdom.

Environmental exposure to engineered nanomaterials (ENMs) is on the rise, in particular inhalation exposure. The consequences of ENM interaction with the lung are not well understood, including the effects on function and inflammation. We

have examined how carbon and silver nanospheres interact with the lung lining and alter pulmonary function and inflammation. C57Bl6/J male mice were intratracheally instilled with saline (control), low (0.05  $\mu$ g/g) or high (0.5  $\mu$ g/g) doses of either silver or carbon black 15nm nanospheres. Lung histology, cytology, surfactant composition and function, inflammatory gene expression, and pulmonary function were measured at 1, 3, and 7 days post exposure. One-day post exposure, high dose carbon black resulted in a classic inflammatory response: increased neutrophilia ( $19 \pm 0.002$  v.  $2.5 \pm 0.0004 \times 10^3$  cells), increased cytokine production (IL-1 $\beta$  2.6 and IL-6 1.7 mRNA fold induction vs control), peribronchial infiltration, and increased low-pressure lung elastance. Low dose carbon black did not differ significantly from control. Examination of these markers 3 days post exposure shows a classic injury response with neutrophilia ( $28.7 \pm 6.1$  vs  $2.7 \pm 0.2 \times 10^3$  cells) and increased macrophage numbers ( $139 \pm 0.006$  v.  $147 \pm 2.6 \times 10^3$  cells at day 1 v. 3). At day 7, neutrophilia has resolved, while macrophage numbers remain high ( $198 \pm 5.6 \times 10^3$  cells). Carbon nanospheres persist within recruited macrophages. Neither low nor high dose silver particles resulted in inflammation 1 day post exposure. There was significantly increased tissue stiffness compared to control, which was paralleled by reduced surfactant function and disrupted surfactant protein expression. Lung function begins to resolve 3 days post exposure to silver particles; however, there is a delayed inflammatory response which is resolving by day 7. These data suggest that silver nanoparticles may have a unique toxicological profile that is dependent upon disruption of lung function.

**PS 469 Biocompatibility of Graphene Nanoplatelets in Terminal Arterioles.**

S. Chowdhury<sup>1</sup>, M. Frame<sup>1</sup>, A. M. Dewar<sup>1</sup>, S. Kanakia<sup>1</sup>, J. Touissant<sup>1</sup>, W. Moore<sup>2</sup> and B. Sitharaman<sup>1</sup>. <sup>1</sup>Biomedical Engineering, Stony Brook University, Stony Brook, NY; <sup>2</sup>Radiology, Stony Brook University, Stony Brook, NY. Sponsor: T. Nurkiewicz.

Carbon-based nanomaterials are currently being tested for a range of medical uses from drug delivery vehicles to contrast enhancing agents for magnetic resonance imaging (MRI). Ensuring biocompatibility is essential for each compound and formulation. Our goal was to evaluate the microvascular effect of graphene nanoparticles known as graphene oxide nanoplatelets (GNPs). The hydrophobic GNPs (20-60nm by 15-35nm, 3-4nm thick) were water-solubilized via non-covalent functionalization with 3.5 mg/ml of the biocompatible natural polymer dextran (GNP-Dex). Adult male hamsters (N=11) were anesthetized (isoflurane) and prepared for intravital microscopy observation of the cheek pouch tissue terminal arterioles; these arterioles control nutrient flow. GNP-Dex (0-50mg/ml) were micropipette applied to small terminal arterioles (~10um dia., 30s), where 0 mg/ml was dextran alone, 2.5mg/ml was the projected therapeutic circulation dose, and 50mg/ml was the highest expected i.v. injection dose when used as a drug delivery or MRI contrast agent. Based on the pipette delivery conditions, the dose of 50mg/ml would expose that arteriole to 127 pg of GNP-Dex. GNP-Dex induced a dose dependent dilation (EC50  $6.9 \pm 0.6$ mg/ml, maximal dilation  $70 \pm 2\%$  increase from baseline). Dextran alone was not vasoactive. We next tested whether acute exposure to 50mg/ml induced endothelial dysfunction, a hallmark sign of cardiovascular inflammation. Comparing before vs. after GNP-Dex exposure, dilator (acetylcholine, 10-4M) and constrictor (phenylephrine, 10-4M) responses were unchanged, unlike our prior work with single-walled carbon nanotubes, which induced a profound endothelial dysfunction. Thus, the direct effect of GNP-Dex is dilation, but there is no residual adverse effect of this formulation on terminal arteriole control of tone. (NIH HL55492; AHA 0655908T; Wallace H. Coulter Foundation)

**PS 470 In Vitro Penetration of Amine Terminated Dendrimer Nanoparticles into Pig and Human Skin.**

M. E. Kraeling<sup>1</sup>, V. D. Topping<sup>1</sup>, X. Gao<sup>1</sup>, O. A. Ogunsola<sup>1</sup>, K. Schlick<sup>2</sup>, E. Simanek<sup>2</sup>, S. Man<sup>3</sup>, A. K. Patri<sup>3</sup>, R. L. Sprando<sup>1</sup> and J. J. Yourick<sup>1</sup>. <sup>1</sup>Office of Applied Research and Safety Assessment, US FDA, Laurel, MD; <sup>2</sup>Department of Chemistry, Texas Christian University, Fort Worth, TX; <sup>3</sup>Nanotechnology Characterization Laboratory, SAIC-Frederick, Frederick National Laboratory for Cancer Research, Frederick, MD.

Dendrimers are highly branched stable polymeric nanoparticles with terminal functional groups capable of binding other molecules. There is concern about the potential for dendrimers to increase skin absorption of ingredients currently considered safe in cosmetics. We evaluated the skin penetration of amine-terminated generation 3 (G3), generation 4 (G4), generation 5 (G5) and generation 6 (G6) polyamidoamine (PAMAM) dendrimer nanoparticles (positive surface charge). Alexa Fluor 568 (~1 equivalent per dendrimer) was conjugated to terminal amines on PAMAM dendrimers via amide bonds for confocal imaging. Free unconjugated

fluorophore was removed by ultrafiltration followed by gel filtration, and characterized. Dendrimers were applied (0.2% concentration) in aqueous solutions or cosmetic emulsion formulation onto viable pig or human cadaver skin assembled in diffusion cells. After a 24 hour exposure, the skin surface was washed to remove unabsorbed dendrimer. The extent of skin penetration was determined by laser scanning confocal microscopy. Most fluorescence from the applied dendrimers appeared on or in the stratum corneum, in hair follicles, or in folds of both pig and human skin. Fluorescence appeared in the upper regions of the epidermis of pig skin with the small generation dendrimers using both the solution and emulsion application. Fluorescence also appeared deeper in the dermal layers of pig skin when smaller generation dendrimers were applied at a higher dose. In human skin, small generation dendrimers penetrated skin at the low and high dose application. Dendrimers applied in emulsions did not penetrate beyond the stratum corneum of human skin. Further studies will examine dendrimer surface functionalization on skin penetration.

**PS 471 Identifying Data Gaps and Prioritizing Research Areas Necessary for Risk Assessment of Multiwalled Carbon Nanotubes.**

K. Fedak, A. Turner, A. Harris and D. Burch. *ICF International, Durham, NC.*

The pace of chemical hazard assessment has not maintained pace with the introduction of new chemicals into the market place, with much of the growth in consumer products applications. As a result, scientists must prioritize resources towards research that fills key data gaps and enables better risk assessment and management. The application of the first step of an iterative comprehensive environmental assessment (CEA) process is used to describe hazard and identify research priorities as well as inform risk management decisions for a range of different chemicals, products, and technologies. The CEA framework allows risk assessors to evaluate the state-of-the-science regarding a new chemical for application in hazard assessment. A case study on an emerging nano-enabled consumer product—multiwalled carbon nanotube flame retardant coatings on upholstery textiles—was conducted using the CEA framework to identify what is known and not yet known about the substance. Side-by-side information on decabromodiphenyl ether (decaBDE), a non-nanoenabled flame retardant that is currently in the process of being phased out, was presented as a comparison to illustrate the suitability of available MWCNT data for informed risk assessment and risk management decisions. For each material, the case study synthesized the available data on primary and secondary contaminants, analytical techniques, fate and transport processes, cumulative and aggregate exposure, and ecological and human health impacts throughout the life cycle of the product. The case study was subsequently used as an informative tool in a stakeholder-involved collective judgment process to identify data gaps and prioritize research areas critical to future risk assessment of MWCNTs and carbon nanomaterials in general.

Disclaimer: The views expressed in this abstract are those of the authors and do not necessarily represent the views or policies of the U.S. Environmental Protection Agency.

**PS 472 Association of Rice and Grain Consumption with Urinary Concentrations of Total Arsenic and Dimethylarsinic Acid in US Adults.**

Y. Wei<sup>1</sup>, J. Zhu<sup>2</sup> and A. Nguyen<sup>1</sup>. <sup>1</sup>Department of Community Medicine, Mercer University School of Medicine, Macon, GA; <sup>2</sup>Department of Mathematics and Computer Science, Fort Valley State University, Fort Valley, GA.

Exposure to inorganic arsenic in the general population occurs mainly from drinking water and food sources. In the United States, levels of exposure are relatively low and the drinking water might not be the main source of exposure, compared to those endemic regions where the pump well water has been used as drinking water supply. To this end, we examined the association between dietary intake and urinary concentrations of arsenic in the U.S. adult population, aged 20-85 years, in the 2003-2006 National Health and Nutrition Examination Survey. Total arsenic (tAs) and dimethylarsinic acid (DMA) were detected in urine of 99% and 87% of the study participants, respectively, and were analyzed in the study. Statistical analyses were performed using SAS 9.3. To control for urine dilution in spot urine samples, creatinine-adjusted urinary concentrations of tAs and DMA were determined. Urinary concentrations of tAs and DMA were categorized into low and high exposure groups by a cutoff value of 50th percentiles. A significantly higher percentage of high exposure to both arsenic species was found in participants who consumed rice and grain  $\geq$  once per week, compared to the reference group with consumption

< once per week (55.67% vs. 45.33% for tAs;  $p < 0.0001$  and 59.61% vs. 43.48% for DMA;  $p < 0.0001$ ). Logistic regression analysis revealed a statistically significant association between rice and grain consumption and urinary concentrations of tAs [adjusted OR=1.39 (1.03, 1.87)] and DMA [adjusted OR=1.97 (1.41, 2.74)] after adjustment for age, gender, race, family income, education, seafood intake (the main source of organic arsenic), and source of drinking water. This study demonstrated that rice and grain consumption contributed to inorganic arsenic exposure in U.S. adults. Racial groups consuming high amounts of rice and grain showed significantly higher exposure to arsenic, especially to DMA.

**PS 473 Prenatal Exposure to Inorganic Arsenic in Gómez Palacio, Mexico, Links to Contaminated Drinking Water.**

J. E. Laine<sup>2</sup>, M. Rubio-Andrade<sup>4</sup>, A. F. Olshan<sup>2</sup>, M. Styblo<sup>3</sup>, G. G. Garcia-Vargas<sup>4</sup> and R. C. Fry<sup>1</sup>. <sup>1</sup>Environmental Sciences and Engineering, University of North Carolina at Chapel Hill, Chapel Hill, NC; <sup>2</sup>Epidemiology, University of North Carolina at Chapel Hill, Chapel Hill, NC; <sup>3</sup>Nutrition, University of North Carolina at Chapel Hill, Chapel Hill, NC; <sup>4</sup>Facultad de Medicina, Universidad Juárez del Estado de Durango, Gómez Palacio, Mexico.

Exposure to inorganic arsenic (iAs) from drinking water is a global public health problem, however much is still unknown about the amount of exposure in susceptible populations, such as pregnant women. The aim of this study is to examine arsenic (As) exposure levels in a new prospective cohort in Gómez Palacio, Mexico. IAs and its methylated metabolites (e.g. methylarsonic acid (MMA) and dimethylarsinic acid (DMA)) were measured in a cohort of pregnant women in Gómez Palacio, Mexico. Levels of As in drinking water and urine were measured using hydride generation atomic absorption spectrometry (AAS). In the case of urine analysis, As species were separated by cryotrapping in liquid nitrogen prior to AAS detection. All women had detectable levels of As in their drinking water ( $n=202$ ). The mean iAs concentration in drinking water was 24.5  $\mu\text{g/L}$ , with a range of 0.46  $\mu\text{g/L}$  to 236  $\mu\text{g/L}$ . Over half ( $n=107$ ) of women's household samples had values that were above the WHO's safe drinking water guidelines of 10  $\mu\text{g/L}$ , and 21 percent were above the MCL (50  $\mu\text{g/L}$ ) for Mexico. There was an association with iAs in drinking water and urine ( $p < 0.01$ ). Most women ( $n=188$ ) had detectable levels of As in their urine. Mean concentrations were 46.7  $\mu\text{g/L}$ , 6.8  $\mu\text{g/L}$ , and 35.3  $\mu\text{g/L}$  for total iAs, total MMA and total DMA, respectively. These data show that pregnant women are exposed to iAs in their drinking water in Mexico. Findings from this study support the need for further investigation into the association of health effects from prenatal exposure to arsenic contaminated drinking water.

**PS 474 Is the Relationship Between Prenatal Exposure to Polychlorinated Biphenyls (PCB) and Birthweight Attributable to Pharmacokinetics?**

M. Verner<sup>1,2</sup>, R. McDougall<sup>3</sup>, A. Glynn<sup>4</sup>, M. E. Andersen<sup>5</sup>, H. J. Clewell<sup>5</sup> and M. P. Longnecker<sup>6</sup>. <sup>1</sup>Channing Laboratory, Brigham and Women's Hospital, Harvard Medical School, Boston, MA; <sup>2</sup>Institute of Environmental Medicine, Karolinska Institutet, Stockholm, Sweden; <sup>3</sup>Faculty of Engineering and Applied Science, University of Ontario Institute of Technology, Oshawa, ON, Canada; <sup>4</sup>Swedish National Food Administration, Uppsala, Sweden; <sup>5</sup>The Hamner Institutes for Health Sciences, Research Triangle Park, NC; <sup>6</sup>Epidemiology Branch, National Institutes of Environmental Health Sciences, Research Triangle Park, NC.

Epidemiologic studies have reported an association between exposure to PCBs and reduced birthweight. However, gestational weight gain is associated negatively with PCB levels during pregnancy and positively with birthweight, so whether the reported association is mainly driven by noncausal, pharmacokinetic effects is unclear. We evaluated the influence of gestational weight gain on the association between PCB exposure and birthweight using a previously developed physiologically based pharmacokinetic (PBPK) model that was modified to account for the relations between maternal weight and fat gain and birthweight. We ran Monte Carlo simulations to generate realistic profiles of blood PCB-153 levels throughout pregnancy. The association between PCB-153 levels and birthweight was evaluated in the simulated population using linear regression analyses. We observed a small negative association between maternal blood levels and birthweight. In models that did not adjust for maternal weight gain, at delivery, a 69 g decrease in birthweight was observed for each 10-fold increase in blood PCB-153. However, the effect size was reduced to 8 g when we adjusted for gestational weight gain. Results from this study suggest that the association between prenatal exposure to PCBs and birthweight is strongly confounded by gestational weight gain. Epidemiologic studies on lipophilic persistent organic pollutants that do not control for gestational weight gain may strongly overestimate the size of the association.

**PS 475 Association of Serum Levels of PCBs with IL-8 mRNA Expression in Blood Samples from Asthmatic and Nonasthmatic Japanese Children.**

M. Tsuji<sup>1,2</sup>, T. Kawamoto<sup>2</sup>, C. Koriyama<sup>3</sup>, S. Akiba<sup>3</sup>, C. Vogel<sup>1</sup>, Y. Hsu-Sheng<sup>2</sup> and F. Matsumura<sup>1</sup>. <sup>1</sup>Department of Environmental Toxicology and the Center for Health and the Environment, University of California Davis, Davis, CA; <sup>2</sup>Department of Environmental Health, University of Occupational and Environmental Health, Kitakyusyu, Japan; <sup>3</sup>Department of Epidemiology and Preventive Medicine, Kagoshima University Graduate School of Medical and Dental Sciences, Kagoshima, Japan.

Polychlorinated biphenyls (PCBs) are one of the most commonly found toxins in the environment. One suggested outcome of PCB exposure during early developmental periods in humans is childhood asthma. The primary objective of the current study was to clarify the causal relationship between PCB exposure and development of childhood asthma through the development of reliable biomarkers. Blood samples from fifteen asthmatic children and an equal number of non-asthmatic children (averaging 2 years of age) were collected and analyzed for select marker expression using qRT-PCR. At the time of collection, an interview included questions about the number of siblings, duration of breast feeding, smoking habits of parents, the parental history of allergic diseases and history of allergies of the study subjects.

Among biomarkers examined IL-8 expression was significantly correlated to serum levels of PCB #163+#164 (P=0.022), #170 (P=0.046), #177 (P=0.022), #178 (P=0.022) and #180+#193 (P=0.046) in a dose-dependent manner, which was found only among asthmatic children. In contrast to IL-8, significant correlations between COX-2 mRNA levels and individual congener levels were recognized only among control subjects, and not among asthmatic subjects.

In conclusion, the most important finding from the current study is that there exist significant correlations between children's exposure to PCBs and the occurrence of childhood asthma, which could be recognized by the use of a reliable biomarker such as IL-8 and selecting certain individual PCB congeners.

**PS 476 Pulmonary Function Testing in Emergency Responders.**

S. Harbison, G. Johnson, J. McCluskey, P. Xu, S. Morris, J. Wolfson and R. D. Harbison. *Environmental and Occupational Health, University of South Florida, Tampa, FL.*

Emergency responders may be exposed to a variety of fumes, gases, and particulates during the course of their job that may affect pulmonary function (PF) and may require the use of respiratory protection. This investigation used occupational health monitoring examination data to characterize PF in a population currently employed as emergency responders in the state of Florida. PF tests for workers (n=127) who required health examinations to ensure fitness for continued respirator use were compared to NHANES III Raw Spirometry subjects (n=9,792) to determine if decreased PF was associated with employment as an emergency responder. Mean FVC and FEV1 values were determined and multivariate regression was used to evaluate the impact of emergency responder status on PF after adjusting for confounders. Emergency responders produced a higher mean FVC of 5.11L (95%CI 4.95-5.26) compared to a mean NHANES III subject value of 4.01L (95%CI 3.99-4.03) (p<0.0001). Emergency responders also produced a higher mean FEV1 of 4.06L (95%CI 3.92-4.19) compared to a mean NHANES III subject value of 3.21L (95%CI 3.19-3.23) (p<0.0001). Stratification by age, sex, height, and smoking history yielded similar results. Multivariate regression analysis demonstrated significant predictors of FEV1 included age, height, sex, smoking history, and emergency responder status (p<0.0001). Significant predictors of FVC included age, height, sex, and emergency responder status (p<0.0001). The direction of effect for emergency responder status was beneficial for lung function (parameter estimates 0.45L FEV1 and 0.54L FVC). Logistic regression was used to determine the effect of PF predictors on generating and FEV1/FVC ratio less than 0.8. Emergency worker status was not associated with the production of a FEV1/FVC ratio less than 0.8. The modest increase in PF observed in emergency responders in multivariate analysis is likely due to a combination of effective exposure controls in the workplace and the healthy worker effect among aging workers.

**PS 477 Association between Copper, Iron, and Zinc Levels in Private Wells and Birth Defects Prevalence in North Carolina.**

A. P. Sanders<sup>1</sup>, T. A. Desrosiers<sup>1,2</sup>, A. H. Herring<sup>1</sup>, D. Enright<sup>2</sup>, A. F. Olshan<sup>1</sup>, R. E. Meyer<sup>2</sup> and R. C. Fry<sup>1</sup>. <sup>1</sup>University of North Carolina Chapel Hill, Chapel Hill, NC; <sup>2</sup>State Center for Health Statistics, Division of Public Health, Raleigh, NC.

Environmental metals including copper, iron and zinc are typically considered essential metals that are able to cross the placental barrier from mother to fetus. In excess, however, many essential metals are developmental toxicants. In this population-based study, we assessed the association between essential metal concentrations in private well water and birth defect prevalence in North Carolina. We conducted an ecologic study including 3,923 infants born between 2003 and 2005 with selected birth defects (cases) identified by the North Carolina Birth Defects Monitoring Program, and 347,587 non-malformed infants (controls). Residence at birth as well as over 20,000 measurements of metal concentrations in residential wells were geocoded. Analyses were conducted at the Census Tract level. Prevalence ratios (PR) with 95% confidence intervals (CI) were calculated to estimate the association between average concentration of each metal within Census Tracts and the prevalence of birth defects, adjusted for maternal age and race. The highest quartile of iron exposure was associated with a higher prevalence of conotruncal heart defects (PR: 2.2; 95%CI: 1.1-4.1) and a decreased prevalence of chromosomal defects (PR: 0.5; 95%CI: 0.3-0.9). In addition, the highest quartile of zinc exposure was associated with a higher prevalence of heart defects (PR: 2.3; 95%CI: 0.7-7.1) and reduction defects of the limbs (PR: 1.7; 95%CI: 0.8-3.5). Sensitivity analyses revealed similar associations. Our findings suggest evidence of a possible relationship between levels of environmental metals in drinking water and specific birth defects. Further research is needed to evaluate the potential associations. Given the known health effects of in utero metal exposure, these data suggest that it would be prudent for pregnant women relying on private wells for drinking water to have their wells tested.

**PS 478 Lack of an Association between Cumulative Exposure to Diacetyl and Changes in Pulmonary Health among Workers at a Food Flavorings Manufacturer.**

C. J. Ronk, D. M. Hollins, M. J. Jacobsen, A. M. Foda, D. A. Galbraith and D. J. Paustenbach. *ChemRisk, San Francisco, CA.*

Declines in metrics of pulmonary health have recently become a topic of interest for researchers studying the health effects of inhalation exposures to food flavorings such as diacetyl. To study the effects that occupational exposures to food flavorings may have on declines in the metrics, forced expiratory volume in one second (FEV1) and forced vital capacity (FVC), we examined data on a cohort of workers at a food flavorings manufacturer. Data were extracted from medical records, pulmonary health records, employment records, and industrial hygiene records to assess and estimate changes in FEV1 and FVC over time in relation to cumulative exposure to diacetyl and time worked in job positions that involve the handling and use of diacetyl and other food flavorings. Through the use of these data, tenure in various job tasks was calculated and linked with industrial hygiene data on diacetyl to form a job-exposure matrix and estimates of cumulative exposure (e.g., dose). For this analysis, total cumulative exposure for each worker was estimated by summing area-specific cumulative exposures (i.e., time spent in each work area multiplied by the median 8-hour time weighted average of diacetyl measured in those areas). Generalized estimating equation (GEE) models were used to evaluate the associations between cumulative dose to diacetyl and declines in FEV1 and FVC. GEE models were adjusted for obesity status, change in weight, hypertension status, age, race/ethnicity, gender, and smoking status. It was found that cumulative dose did not significantly affect changes in FEV1 (p=0.42) or FVC (p=0.34). The associations between tenure at the facility and changes in FEV1 and FVC were not statistically significant (p=0.79 and p=0.40, respectively). Tenure in positions that handled food flavorings was not associated with changes in FEV1 (p=0.49) or FVC (p=0.56). In this cohort of food flavoring manufacturing workers, changes in FEV1 and FVC over time were not affected by exposure to diacetyl.

**PS 479 DDT/DDE and Breast Cancer: NHANES 1999-2004 Analyses and a Meta-Analysis.**

S. Z. Ingber, F. Scinicariello, H. R. Pohl, H. G. Abadin and H. Murray. *DTHHS, ATSDR/CDC, Chamblee, GA.* Sponsor: P. Ruiz.

The biological basis for an investigation of dichlorodiphenyltrichloroethane (DDT) exposure and breast cancer risk stems from research indicating that DDT has estrogenic effects in both in vitro and animal systems. A meta-analysis report published in 2004 by Lopez Cervantes et al. found no relationship between DDE and breast cancer.

The objective of this study was: (1) to update the Lopez Cervantes meta-analyses and, (2) to analyze NHANES 1999–2004 data for any relationship between DDE exposure and breast cancer prevalence.

**Methods** Meta-Analyses: PubMed and Web of Science databases were searched for studies published through June 2012 assessing DDT exposure and breast cancer. From the 500 studies screened, 40 studies were used for the meta-analyses to quantify the summary Odds Ratios (OR) for breast cancer to DDT exposure in the highest versus the corresponding lowest exposed group. Both random and fixed effect models were used. Heterogeneity across studies was calculated using the I<sup>2</sup> measure of inconsistency. Heterogeneity was resolved through stratification analyses by study design, tissue sample type, and control population. Publication bias was assessed by the Begg and Egger tests.

**Survey Analyses:** Data from NHANES 1999–2004 female participants aged 20 years and older for levels of DDE were analyzed in relation to self-reported breast cancer (n=51). Logistic regression models were adjusted for age, race/ethnicity, education, alcohol intake, smoking status, body mass index and c-reactive protein.

**Results:** Slightly elevated, but not statistically significant summary ORs were found for the selected studies for DDE (1.05; 95%CI: 0.93 – 1.18) and DDT (1.02; 95%CI: 0.92 – 1.13). Logistic regression of NHANES data showed that women in the higher serum DDE tertile had a not-statistically significant OR (0.89; 95% CI: 0.27 – 2.94; p= 0.75) to have breast cancer compared to those in the lowest serum DDE tertile.

**Conclusion:** The existing information does not support the hypothesis that exposure to DDT/DDE increases the risk of breast cancer in humans.

#### PS 480 Assessing Model Prediction Quality for a Dynamic Population Simulation Model (DPSM).

J. P. Monteleone<sup>1</sup>, R. Gunawan<sup>1</sup> and K. Lee<sup>2</sup>. <sup>1</sup>Pharsight Corporation, Cary, NC; <sup>2</sup>JT International SA, Geneva, Switzerland.

An increasing amount of tobacco-control literature use DPSMs to predict changes in tobacco-related excess mortality (EM) and smoking prevalence (SP), typically using point estimates as model inputs. Point estimate information is often criticized because estimates are based on limited data and difficult to defend resulting in potentially questionable model predictions. One method for testing prediction quality is sensitivity analysis (SA), which tests predictions using specific values for point estimates. Unfortunately, for complex models, only limited subsets of values are typically tested. An alternative method uses a prediction interval (PI), which provides information on the expected distribution of the predictions from numerous randomly generated sets of point estimates. In this study, these methods for assessing prediction quality were evaluated using a tobacco-related DPSM from the literature. After reproducing the DPSM, a SA was performed using the author's simulation scenarios (consisting of a limited selection of point estimate model inputs). A PI was also constructed by applying a uniform distribution to the minimum and maximum values for each of the model inputs and randomly drawing samples (using Monte Carlo simulation) to create 1,000 unique sets of model inputs. Predictions for EM or SP were simulated annually for the years 2010 to 2050. A 90% PI plot was created by removing the highest and lowest 5% of the predicted values for each of the 40 years. When the two approaches were compared, most of predictions from the author's SA fell within the PI, while the SA results were constrained to only a small region of the PI, most likely because only a limited number of scenarios were tested. Furthermore, the PI demonstrated how variability among multiple model inputs can interact with each other by illustrating expected variability in the EM or SP predictions. A PI approach may therefore prove robust and efficient, compared to SA, in assessing how well point estimate model inputs predict outcomes from complex simulation models.

#### PS 481 Multiple Myeloma Risk and Benzene Exposure among Pliofilm Workers—A Reanalysis Using an Internal Reference Group.

S. Lamm<sup>1</sup>, J. Britt<sup>2</sup> and R. James<sup>2</sup>. <sup>1</sup>Consultants in Epidemiology and Occupational Health, Washington DC; <sup>2</sup>ToxStrategies, Tallahassee, FL.

The Pliofilm worker cohort (Rinsky et al., 2002) is comprised of 1,291 benzene-exposed and 554 unexposed workers with follow-up for leukemia and multiple myeloma (MM) mortality through 1996. Five of the exposed workers and three of the unexposed workers died from MM. Prior risk analyses of this benzene cohort were limited to the exposed cohort using U.S. death rates as the external reference population. We propose, for this cohort whose unexposed group is 43% the size of the exposed population (545/1,291 = 43%), that the risk analysis be done by using the unexposed population as an internal reference group. The crude mortality ratio (CMR) for MM for the exposed population (5/1,291 = 0.004) is 0.4 % (95% CI, 0.1-0.9), and CMR for the unexposed population (3/554=0.005) is 0.5% (95% CI, 0.1-1.6). The relative risk is 0.72 (95% CI, 0.17-2.98; Fisher two-tailed p-value, 0.70). When the analysis is limited to males as all the MM deaths were male,

the relative risk is 0.62 (95% CI, 0.15-2.59, Fisher two-tail p-value = 0.45). The CMR analysis indicates that the MM risk in benzene-exposed workers is actually not greater than that of the unexposed. The marginally lower difference seen here is not significant. These results, like others reported in the literature, reinforce the importance of examining an internal reference group analysis when evaluating the potential risks associated with occupational chemical exposures. Analytic use of an internal reference population reduces bias from the healthy worker effect or other risk factors associated with employment.

#### PS 482 Expression of DNA Repair Genes in Breast Cancer Tumors from Puerto Rican Women.

J. L. Matta<sup>1</sup>, L. Morales<sup>1</sup>, A. Cruz<sup>2</sup>, M. Bayona<sup>3</sup>, J. Dutil<sup>4</sup>, A. Gjyshi<sup>5</sup>, A. Monteiro<sup>5</sup> and E. Suarez<sup>6</sup>. <sup>1</sup>Pharmacology Physiology and Toxicology, Ponce School of Medicine and Health Sciences, Ponce, Puerto Rico; <sup>2</sup>Hematology-Oncology Fellowship Program, SJCH with VACHS, San Juan, Puerto Rico; <sup>3</sup>US FDA, Division of Epidemiology/OSB/CDRH, Silver Spring, MD; <sup>4</sup>Biochemistry, Ponce School of Medicine and Health Sciences, Ponce, Puerto Rico; <sup>5</sup>H. Lee Moffitt Cancer Center, Tampa, FL; <sup>6</sup>Cancer Epidemiology Program, University of Puerto Rico, Ponce, Puerto Rico.

DNA repair is a critical defense system in the human body aimed at protecting the integrity and stability of the genome from the harmful effects of cancer-causing agents. Specific genetic alterations in DNA repair genes have been clinically associated with risk, survival, aggressiveness, and treatment outcome of breast cancer (BC). Even though diminished DNA repair capacity is recognized as a risk factor for BC, no studies to date have identified gene expression profiles in tumors from Puerto Rican women. Study participants were women with histopathologically confirmed primary BC (n =35) and normal breast tissue obtained during cosmetic surgery (n=2). Tumors were snap frozen in liquid nitrogen and RNA was extracted. Microarrays data were obtained from Affymetrix Plus 2.0 chip to assess whole genome gene expression. The assessment of differentially expressed genes was performed using Permutation method with 5% false discovery rate. Genome-wide gene expression levels were initially measured using the Affymetrix Plus 2.0 array, and DNA repair genes showing significant changes in expression levels were validated by RT-PCR. Most of the DNA repair genes were over expressed. Twenty-three candidate DNA repair genes were found to be differentially expressed (including PARP-1, therapeutic target). Of these 21 were overexpressed and 2 were underexpressed (p<0.001). This is the first report of DNA repair candidate genes in Puerto Rican women with BC, a population with mixed ancestry. Supported by grants S06 GM008239-20, 1SCA157250-2 and 5U56CA126379 from the NCI Center to Reduce Health Disparities and NIH-MBRS Program (NIGMS).

#### PS 483 Investigation of Route-Dependent Exposure and Metabolism of Bisphenol A (BPA) in Neonatal Mice following Oral and Subcutaneous Administration of <sup>3</sup>H-BPA.

D. Draganov<sup>1</sup>, D. Markam<sup>2</sup>, D. Beyer<sup>3</sup>, J. Moore<sup>1</sup>, T. Riehl<sup>1</sup>, J. Waechter<sup>2</sup>, S. Dimond<sup>4</sup>, R. Shiotsuka<sup>5</sup>, K. Ehman<sup>6</sup> and S. Hentges<sup>7</sup>. <sup>1</sup>Metabolism, WIL Research, Ashland, OH; <sup>2</sup>The Dow Chemical Co., Midland, MI; <sup>3</sup>Bayer Healthcare AG, Wuppertal, Germany; <sup>4</sup>SABIC, Pittsfield, MA; <sup>5</sup>Bayer Material Science, Pittsburgh, PA; <sup>6</sup>TRS, Inc., Charlottesville, VA; <sup>7</sup>ACC, Washington DC.

Orally administered bisphenol A (BPA) undergoes efficient first-pass metabolism in the liver to produce inactive metabolites, including BPA-glucuronide (BPA-G) and BPA-sulfate (BPA-S). The current study was conducted to evaluate the pharmacokinetics of BPA and its conjugated metabolites, specifically BPA-G and BPA-S, in juvenile mice following a single oral or subcutaneous (SC) administration. This study had 3 phases: 1) Mass-balance phase in which effective dose delivery procedures for oral or SC administration of <sup>3</sup>H-BPA to post natal day (PND) 3 mouse pups were developed; 2) Pharmacokinetic phase during which systemic exposure to total <sup>3</sup>H-BPA-derived radioactivity in female PND 3 mice was established; and 3) Metabolite profiling phase in which two groups of 50 female PND 3 mice received either a single oral or SC dose of <sup>3</sup>H-BPA at 400 µg/kg bw with ≈ 4.4 mCi/kg bw of radioactivity. Blood was collected from 5 pups/route/time point at 5, 10, 20, and 30 minutes, and 1, 2, 3, 4, 6, and 24 hours post-dosing and processed to plasma. The plasma samples were pooled by group and time point and profiled by HPLC with fraction collection. Fractions were analyzed for total radioactivity and data used to generate radiochromatograms and integrate individual peaks. The identity of the BPA, BPA-G and BPA-S peaks was confirmed using authenticated standards and LC-MS/MS analysis. Metabolic profiles and key parameter as AUC<sub>0-24hr</sub> and C<sub>max</sub> were derived for free-BPA, BPA-G and BPA-S. The result of this study revealed that female PND 3 mice have metabolic capacity to metabolize BPA to BPA-G, BPA-S and other metabolites after both routes of administration and that systemic exposure to free-BPA is route-dependent as the plasma concentrations were lower following oral administration compared to SC injection.

**PS 484 Disposition and Kinetics of Tetrabromobisphenol A (TBBPA) in Female Wistar-Han Rats.**

G. A. Knudsen, J. M. Sanders, A. M. Sadik and L. S. Birnbaum. *Toxicology and Toxicokinetics, NCI at NIEHS, Research Triangle Park, NC.*

Tetrabromobisphenol A (TBBPA) is the brominated flame retardant with the largest production volume (~150,000 tons/year), representing nearly 60% of all worldwide demand for brominated flame retardants. TBBPA is used in printed circuit boards, ABS plastic casings, and laminates. Studies were conducted to characterize the disposition and toxicokinetic profile of TBBPA in female Wistar-Han rats following single oral bolus (25, 250 or 1,000 mg/kg) or intravenous (25 mg/kg) administration. All dosing solutions provided 50  $\mu\text{Ci/kg}$  of [ $^{14}\text{C}$ ]-labeled TBBPA. Following oral administration of [ $^{14}\text{C}$ ]-TBBPA the primary route of elimination of radioactivity was in feces; dose recoveries in 72h were  $95.7 \pm 3.5\%$ ,  $94.3 \pm 3.6\%$  and  $98.8 \pm 2.2\%$ , respectively. After a single IV administration of 25 mg/kg of [ $^{14}\text{C}$ ]-TBBPA, ~10% of the administered radioactivity was eliminated in the feces within 6h. Recoveries in urine ranged from 0.2-2% of dose. Less than 0.1% of the administered [ $^{14}\text{C}$ ]-radioactivity was detected in tissues collected at 72h following oral doses. Preliminary toxicokinetic profiles were estimated based on total [ $^{14}\text{C}$ ]-radioactivity detected in whole blood. Oral dosing (250 mg/kg) resulted in a rapid absorption of compound, with an apparent  $\text{C}_{\text{max}}$  occurring at 3h post-dose and the subsequent distribution phase was consistent with a one-compartment model. Following IV administration (25 mg/kg), [ $^{14}\text{C}$ ]-radioactivity concentrations in whole blood decreased rapidly with less than 2% of the administered radioactivity remaining at 6h post dose. The time-concentration profile for total [ $^{14}\text{C}$ ]-radioactivity following IV administration of [ $^{14}\text{C}$ ]-TBBPA was consistent with a two compartment model. These early results suggest low systematic bioavailability. These data indicate that TBBPA has a similar ADME/TK profile in female Wistar-Han rats as that reported for male Fischer-344 rats. This research was supported in part by the Intramural Research Program of NIH/NCI; this abstract may not reflect official NIH policy.

**PS 485 Investigation of BPA-Glucuronide As a Substrate for Human BCRP, MDR1, MRP2, and MRP3 Transporters.**

M. V. Driscoll and A. L. Slitt. *Biomedical and Pharmaceutical Sciences, University of Rhode Island, Kingston, RI.*

Bisphenol A (BPA) is a chemical used in plastic manufacturing that is present in polycarbonate bottles, food containers, and resins that line metal cans. Exposure to BPA occurs mainly through consumption of food products that are in direct contact with plastics and polycarbonates. Recently, BPA exposure in humans has been linked to the development of obesity and diabetes, as well as having effects on reproductive health and cancer. BPA is metabolized to BPA-glucuronide (BPA-gluc) and BPA-sulfate by Phase II enzymes and is eliminated by ATP-binding cassette (ABC) transporters. In humans, BPA-gluc is predominantly excreted through urine, whereas in rodents, it is excreted through bile into feces. One class of ABC transporters, multidrug resistance-associated proteins (MRPs) is thought to be involved in BPA clearance. There are nine known human MRPs (MRP1-9), and mouse orthologs exist for all human MRP genes except MRP8. Multidrug resistance protein (MDR1) and breast cancer-resistant protein (BCRP) are also possible transporters for BPA metabolites. However, despite numerous studies, the mechanism of BPA metabolite clearance remains unclear. In this study we examined whether BPA-gluc is a substrate for human xenobiotic transporters BCRP, MDR1, MRP2, or MRP3. Membranes expressing human BCRP, MDR1, MRP2, or MRP3 were used in a colorimetric ATPase assay. The amount of inorganic phosphate ( $\text{P}_i$ ) released from BPA-gluc-stimulated ATP hydrolysis was measured. Preliminary data suggest that BPA-gluc is a substrate for MRP3 ( $\text{K}_m$ : 48.2  $\mu\text{M}$ ). Furthermore, BPA-glucuronide is a potential activator of MRP2 at low concentrations, with an ATPase transporter activation >30% at 0.046  $\mu\text{M}$ , but inhibits transport at higher concentrations. Low to negative percent ATPase activation values for MDR1 strongly suggests that MDR1 is inhibited by BPA-glucuronide. As differences exist between rodents and humans, identification of the ABC transporters involved in BPA clearance will be an important tool in the pharmacokinetic assessment of BPA.

**PS 486 A Physiologically-Based Pharmacokinetic Model for Bisphenol A in Rats at Different Developmental Ages.**

X. Yang, D. R. Doerge and J. W. Fisher. *National Center for Toxicological Research, US FDA, Jefferson, AR.*

Bisphenol A (BPA) is an industrial chemical that has been used in the manufacture of a wide variety of consumer products such as hard plastic products and the lining of metal food and beverage cans. Widespread exposure to BPA has raised public health concerns about BPA in food and the environment. A physiologically based

pharmacokinetic model (PBPk) was developed to describe the pharmacokinetic behavior of BPA and its metabolites (Phase II conjugates) in adult and neonatal rats. The model was calibrated using published BPA studies on in vitro hepatic and intestinal metabolism, in vivo biliary excretion of BPA metabolites, and in vivo serum time course data after oral and intravenous administration of BPA. Metabolism of BPA in the small intestine was predicted to substantially reduce the oral bioavailability of BPA and enterohepatic recirculation of BPA metabolites was predicted to prolong the systemic levels of BPA and its metabolites. The dosimetry of the aglycone BPA was age-dependent, in part, because of immature phase II metabolism in neonatal rats.

**PS 487 Dose-Response Relationship of an Environmental Mixture of Pyrethroids following an Acute Oral Administration in the Rat.**

M. F. Hughes<sup>1</sup>, D. G. Ross<sup>1</sup>, J. M. Starr<sup>2</sup>, E. J. Scollon<sup>1,3</sup>, M. J. Wolansky<sup>4</sup>, K. M. Crofton<sup>1</sup> and M. DeVito<sup>1,5</sup>. <sup>1</sup>ORD/NHEERL, US EPA, Research Triangle Park, NC; <sup>2</sup>ORD/NERL, US EPA, Research Triangle Park, NC; <sup>3</sup>OPP/HED, US EPA, Arlington, VA; <sup>4</sup>University of Buenos Aires, Buenos Aires, Argentina; <sup>5</sup>NIEHS/INTP, Research Triangle Park, NC.

Human exposure to multiple pyrethroid insecticides may occur because of their wide use on crops and for residential pest control. To address the potential risk from exposure to pyrethroids, it is important to understand their toxicity and disposition in target organs such as the brain and surrogates such as the blood. The objective of this study was to compare motor activity with pyrethroid concentrations in blood and brain of rats after oral administration of a pyrethroid mixture. Male Long-Evans rats were dosed with a mixture of  $\beta$ -cyfluthrin (12.9% of dose), cypermethrin (28.8%), deltamethrin (3.4%), esfenvalerate (2.7%) and *cis*- (20.9%) and *trans*-permethrin (31.3%) in corn oil at one of seven doses (maximum total pyrethroid dose = 27.4 mg/kg). From 2 to 3 h post-administration, gross motor activity was assessed. At 3.5 h, blood and brain were collected and analyzed for parent pyrethroid using HPLC-tandem mass spectrometry. There was a linear dose-related increase in concentrations of the pyrethroids in blood and brain. Cypermethrin (56-62%) and *cis*-permethrin (57-70%) were the predominant pyrethroids detected in blood and brain, respectively, at all dose levels. The pyrethroids with the lowest percentage in tissue were *trans*-permethrin (0.6-2.7%) and  $\beta$ -cyfluthrin (0.4-1.2%) in blood and deltamethrin (1.1-3.5%) and esfenvalerate (2.4-4.7%) in brain. The approximate ED<sub>30</sub> for decrease in motor activity was 300 ng/ml and 200 ng/g of total pyrethroid in blood and brain, respectively. More research is needed to understand the dosimetry of pyrethroids in blood and brain of rat and how this relates to neurotoxic effect. (This abstract does not represent U.S. EPA or NIEHS/INTP policy).

**PS 488 Partition Coefficients of Deltamethrin (DLM) and Cis-Permethrin (CIS) in Male Sprague-Dawley Rats.**

M. Amarani<sup>1</sup>, D. Gullick<sup>1</sup>, P. Sethi<sup>1</sup>, T. Mortuza<sup>1</sup>, T. Osmitz<sup>2</sup>, S. S. Anand<sup>3</sup>, D. W. Gammon<sup>4</sup>, C. A. White<sup>1</sup>, J. V. Bruckner<sup>1</sup> and B. S. Cummings<sup>1</sup>. <sup>1</sup>University of Georgia, Athens, GA; <sup>2</sup>Science Strategies, LLC, Charlottesville, VA; <sup>3</sup>DuPont Haskell, Newark, DE; <sup>4</sup>FMC, Ewing, NJ.

Pyrethroid insecticides are widely used to control a wide variety of pests in and around homes, food handling establishments, in mosquito control, and in agriculture. Partition coefficients are essential to the construction of PBPk models, because of their role in determining systemic distribution. The main aim of this study was to determine tissue:blood partition coefficients ( $\text{K}_t:\text{p}$ ) of two commonly used pyrethroids, DLM and CIS. In vitro plasma to RBC partition coefficients, as determined by HPLC analysis, ranged from 0.7 to 1.0 for DLM, and 1.1 to 1.7 for CIS. The steady state levels of both DLM and CIS were obtained in vivo by constant infusion (0.36 mg/hr) using subcutaneous implantation of Alzet<sup>TM</sup> pumps, combined with oral loading doses of 34 mg/kg for DLM, or 150 mg/kg for CIS given 4 hr after the implantation of the pump in male rats. The time to reach steady-state was determined by analyzing blood samples collected by tail vein puncture 24, 48 and 72 hr post loading. Rats were sacrificed at 72 hr and blood and tissues collected and analyzed for DLM and CIS using a modified GC-MS method. DLM levels in plasma after 72 hr of constant infusion were 960 ng/mL, compared to 222 ng/mL in brain, 272 ng/mL in liver, 132 ng/mL in muscle and 1,384 ng/mL in fat. This corresponded to  $\text{K}_t:\text{p}$  values of 0.23 for brain, 1.45 for fat, 0.28 for liver and 0.14 for muscle. In contrast, the CIS level in plasma was 78 ng/mL, compared to 43 ng/mL in brain, 27 ng/mL in liver, 107 ng/mL in muscle and 1,625 ng/mL in fat. These corresponded to  $\text{K}_t:\text{p}$  of 0.55 for brain, 20.78 for fat, 0.34 for liver and 1.37 for muscle. These data show that both pyrethroids are sequestered in fat, and that differences exist in  $\text{K}_t:\text{p}$  for DLM and CIS, as  $\text{K}_t:\text{p}$  values were generally higher for CIS. Supported by the Council For Advancement of Pyrethroid Human Risk Assessment.

**PS 489 Preliminary Toxicokinetics of N-Butylbenzenesulfonamide after a Single Intravenous or Gavage Administration to Harlan Sprague-Dawley Rats and B6C3F1/NMice.**

S. Hong<sup>1</sup>, S. Gibbs<sup>1</sup>, S. Graves<sup>1</sup>, D. Kobs<sup>1</sup>, C. Rider<sup>2</sup>, A. Martone<sup>2</sup> and S. Waidyanatha<sup>2</sup>. <sup>1</sup>Battelle Memorial, Columbus, OH; <sup>2</sup>Division of National Toxicology Program, NIEHS, Research Triangle Park, NC.

N-butylbenzenesulfonamide (NBBS) is a common plasticizer with limited toxicity data that has been detected in environmental samples. A preliminary toxicokinetic study was conducted in Harlan Sprague Dawley rats and B6C3F1/N mice following a single intravenous (2 mg/kg) and gavage (2 or 200 mg/kg) administration of NBBS, and plasma and brain toxicokinetics were evaluated. Intravenous and gavage TK profiles of NBBS were characterized by a one-compartment kinetic model in both rats and mice. Following intravenous administration, male and female elimination ( $k_{10}$ ) half-life values were 0.300 and 0.387 hours, respectively, in rats, and 0.383 and 0.268 hours, respectively, in mice. Following gavage administration, male and female elimination half-life values were 0.657 and 1.11 hours (2 mg/kg) and 4.88 and 3.86 hours (200 mg/kg), respectively, in rats, and 1.21 and 0.494 hours, respectively, in mice. Male and female AUC<sub>∞</sub> values following gavage administration were 43.0 and 166 hr\*ng/mL (2 mg/kg) and 17,800 and 46,800 hr\*ng/mL (200 mg/kg), respectively, in rats indicating saturation of elimination kinetics around 200 mg/kg. The absolute bioavailability of NBBS after gavage administration at 2 mg/kg was 13% and 39% for male and female rats, respectively. AUC<sub>∞</sub> values for male and female mice after gavage administration were 20,000 and 15,500 hr\*ng/mL, respectively. The absolute bioavailability of NBBS after gavage administration to mice at 200 mg/kg was 25% for both sexes. NBBS was extensively distributed into the brain with concentrations similar to plasma in mice but greater than plasma in rats. [Supported by NIH, HHSN273201000016C]

**PS 490 Gestational and Lactational Physiologically-Based Pharmacokinetic (PBPK) Models for the Herbicide Atrazine in Rats: Development and Optimization.**

Z. Lin<sup>1,2</sup>, J. W. Fisher<sup>3</sup> and N. M. Filipov<sup>1,2</sup>. <sup>1</sup>Physiology and Pharmacology, University of Georgia, Athens, GA; <sup>2</sup>Interdisciplinary Toxicology Program, University of Georgia, Athens, GA; <sup>3</sup>National Center for Toxicological Research, US FDA, Jefferson, AR.

Atrazine (ATR) is a widely used chlorotriazine herbicide that is commonly detected in the environment and in human specimens, including pregnant women's urine, umbilical cord blood and breast milk. To help address concerns about reported adverse effects of ATR exposure during development, gestational and lactational PBPK models for ATR in the rat were developed. The models accounted for potential differences in the metabolism of ATR in dams, fetuses, and neonates and between single and repeated daily oral exposures and incorporated binding of ATR and its major metabolite didealkylatrazine (DACT) with target tissue (maternal/neonatal brain and fetus), plasma proteins, and red blood cells. Model predictions correlate well with recently reported measured data on the concentrations of ATR and its metabolites in maternal/neonatal plasma, tissue, fetus, and milk following repeated daily oral exposure to the dam during gestation, lactation, or both, including with data from a study (lactational exposure) not used for model calibration. The model simulations indicate that: (1) the fetus is exposed to ATR and DACT at levels that are similar to maternal plasma levels, (2) the neonate is exposed mostly to DACT at levels about two-thirds of the maternal plasma DACT levels and (3) gestational carryover of DACT greatly affects neonatal dosimetry up until mid-lactation. Hence, excessive exposure to ATR and/or its metabolites during pregnancy or early lactation may be of particular concern. These models provide insights into designing and interpreting early life toxicity and pharmacokinetic studies with this herbicide and could be used in fetal and neonatal tissue dosimetry prediction and for improvement of ATR's exposure assessment.

**PS 491 Characterization of the Fate of  $\beta$ -Hexabromocyclododecane (HBCD) in Mice.**

J. M. Sanders, G. A. Knudsen, A. M. Sadik and L. S. Birnbaum. *NIH/NCI, Research Triangle Park, NC.*

1,2,5,6,9,10-Hexabromocyclododecane (HBCD) is a high production volume cycloaliphatic used primarily as an additive flame retardant in polystyrene foam building materials. Commercial HBCD mixtures contain three major stereoisomers, alpha ( $\alpha$ ), beta ( $\beta$ ) and gamma ( $\gamma$ ), at a typical ratio of 1.2:0.6:8.2. Toxicity (e.g. developmental neurotoxicity, immune effects, liver hypertrophy, and endocrine disruption) in rodents exposed to HBCD mixtures may be affected by differential kinetics of the isomers. Previous work from our laboratory demonstrated

that  $\alpha$ -HBCD has greater bioavailability and potential for accumulation in mice than  $\gamma$ -HBCD. The present investigation provides comparative disposition data for  $\beta$ -HBCD to support toxicological evaluations of HBCD mixtures. In these studies, a single dose of [<sup>14</sup>C]-labeled  $\beta$ -HBCD (3 mg/kg), administered orally, was absorbed rapidly in the female C57BL/6 mouse. The C<sub>max</sub> for  $\beta$ -HBCD-derived radioactivity in blood and other assayed tissues, except adipose, was observed 3 hours following gavage. Approximately 90% of the total dose was eliminated in urine and feces by 24 h postdosing. The extent of dose absorption was  $\geq 85\%$  based on HPLC analysis of feces extracts and comparison of oral and iv excretion data.  $\beta$ -HBCD-derived metabolites were excreted in urine and feces. Approximately 8% of the total dose was excreted in feces as  $\gamma$ -HBCD. Oral administration of either 30 or 100 mg/kg of  $\beta$ -HBCD resulted in initial slower rates of [<sup>14</sup>C] elimination; however, cumulative excretion data were similar across the dosing range 4 days following gavage. Residual concentrations of [<sup>14</sup>C] in tissues of these mice were highest in adipose and liver.  $\beta$ -HBCD-derived radioactivity accumulated in these tissues following four consecutive daily doses of 3 mg/kg by gavage. In conclusion,  $\beta$ -HBCD, like  $\gamma$ -HBCD, was extensively metabolized, rapidly excreted, and had less potential for accumulation in tissues over time in female C57BL/6 mice than  $\alpha$ -HBCD. (Research supported in part by Intramural Research Program of NIH/NCI; abstract may not reflect official NIH policy).

**PS 492 OATs and OATPs Are Involved in the Disposition of Perfluoroalkyl Sulfonates in Rats.**

W. Zhao<sup>1</sup>, J. Zitzow<sup>2</sup>, D. J. Ehresman<sup>2</sup>, S. Chang<sup>2</sup>, J. L. Butenhoff<sup>2</sup> and B. Hagenbuch<sup>1</sup>. <sup>1</sup>Pharmacology, Toxicology and Therapeutics, Kansas University Medical Center, Kansas City, KS; <sup>2</sup>Medical Department, 3M Center, St. Paul, MN.

Perfluoroalkyl sulfonates (PFSA) are a group of persistent environmental contaminants that have been detected in wildlife and human serum. Based on estimations from retired fluorocarbon production workers, the elimination half-lives of certain PFSA, such as perfluorohexanesulfonate (PFHxS) and perfluorooctanesulfonate (PFOS), are very long (several years). Pharmacokinetic studies in animal models indicate that the long half-lives of these compounds are due to slow renal clearance and strong hepatic accumulation. In previous studies we have demonstrated certain organic anion transporters expressed in the kidney and the liver are involved in the disposition of another family of perfluoroalkyl substances, perfluoroalkyl carboxylates (PFCAs), in rats. However, so far it is unknown whether PFSA are also substrates for the same drug transporters. Therefore, we wanted to test whether the organic anion transporters involved in the disposition of PFCAs are also responsible for the disposition of PFSA. We used HEK293 cells overexpressing rat OAT1, OAT3 and OATP1A1 and measured the uptake of model substrates in the absence and presence of PFSA with different carbon chain-lengths, namely perfluorobutanesulfonate (PFBS), PFHxS and PFOS. PFHxS showed the strongest inhibition for both rat OAT1 and OAT3, while rat OATP1A1 was only inhibited by PFOS. Direct uptake determination of these PFSA demonstrated that rat OAT1 and OAT3 can transport PFBS and PFHxS while rat OAT3 and OATP1A1 might transport PFOS. In conclusion, these results suggest that the same families of transporters in the rat that are involved in the disposition of PFCAs are also involved in the disposition of PFBS, PFHxS and PFOS.

**PS 493 Toxicokinetics of Inhalation, Metabolism and Elimination of 6:2 FTOH and 8:2 FTOH in Rats.**

M. W. Himmelstein, T. L. Serex, R. C. Buck and M. H. Russell. *E.I. DuPont de Nemours & Co Inc., Wilmington, DE.*

This study compares the in vivo metabolism of two fluorotelomer alcohols (6:2 FTOH and 8:2 FTOH). Single 6-h inhalation exposures were conducted in Crl:CD(SD) rats followed by analysis of per- and poly-fluorinated acid metabolites in plasma. Both substances were readily absorbed and rapidly eliminated via conjugation and oxidative metabolism. Following exposure to either 0.5 or 5.0 ppm 6:2 FTOH, the terminal metabolites included perfluorobutanoic acid (PFBA), perfluorohexanoic acid (PFHxA), perfluoroheptanoic acid (PFHpA) and 5:3 Acid (C<sub>5</sub>F<sub>11</sub>CH<sub>2</sub>CH<sub>2</sub>COOH). 5:3 Acid was the dominant acid metabolite in plasma which, based on toxicokinetic modeling, represented 0.2-3.8 mol% and 1.2-2.8 mol% of the inhaled dose of 6:2 FTOH in male and female rats, respectively. Corresponding yields of PFHxA were 0.1-2.8 mol% and 0.5-1.7 mol% in male and female rats, respectively. The sum of all modeled acid analytes ranged between 0.5 and 7.1 mol% with higher yields of all analytes observed at lower inhaled 6:2 FTOH doses. After 6:2 FTOH exposure cessation, the fluorinated acids observed in plasma were rapidly eliminated with typical elimination half-lives of a few hours. A single 8:2 FTOH 6-h exposure of rats to 0.16 or 1.6 ppm resulted in dose proportional formation of perfluorooctanoic acid (PFOA) and 7:3 Acid (C<sub>7</sub>F<sub>15</sub>CH<sub>2</sub>CH<sub>2</sub>COOH) as the major fluorinated acid metabolites. In male and female rats, toxicokinetic calculations of 7:3 Acid in plasma resulted in yields of 0.9-2.1 mol% in male and female rats while PFOA yields ranged between 0.3 and 1.1

mol%. 7:3 Acid was eliminated with calculated half-lives of 1-7 hrs in male and female rats while the elimination of PFOA showed distinct gender differences with half-lives of 6-8 hrs in female rats and no measurable decline in male rats over the 18-h period of depuration. For both fluorotelomer alcohols, the major terminal acids formed metabolically in rats were 5:3 Acid and PFHxA from 6:2 FTOH and 7:3 Acid and PFOA from 8:2 FTOH. This study demonstrates rapid bioelimination of inhaled fluorotelomer alcohols from plasma.

#### PS 494 Absorption, Distribution, Metabolism, and Elimination of [<sup>14</sup>C] 6:2 Fluorotelomer Alcohol in the Rat.

R. T. Mingoia<sup>1</sup>, S. C. Carpenter<sup>1</sup>, T. L. Whyte<sup>1</sup>, M. W. Himmelstein<sup>1</sup>, T. A. Snow<sup>1</sup>, L. Cox<sup>1</sup>, S. A. Gannon<sup>1</sup> and R. C. Buck<sup>2</sup>. <sup>1</sup>DuPont Haskell Global Centers for Health and Environmental Sciences, Newark, DE; <sup>2</sup>E. I. duPont de Nemours and Company, Inc., Chemicals and Fluoroproducts, Wilmington, DE.

Fluorotelomer alcohols (FTOHs; F(CF<sub>2</sub>)<sub>x</sub>C<sub>2</sub>H<sub>4</sub>OH, x=6, 8, or 10) are used in the manufacture of specialty fluorinated surfactants and polymers. Fluorotelomer manufacturers are moving away from raw materials that are potential precursors to perfluorooctanoic acid (PFOA), such as the higher fluorotelomer alcohol homologues, to products based on 6:2 FTOH as a raw material. To better understand 6:2 FTOH biological fate, the absorption, distribution, metabolism, and elimination of [1,2-<sup>14</sup>C] 6:2 FTOH was investigated following a single oral dose administration of 5 and 125 mg/kg to male and female rats. The maximum concentration of total radioactivity in plasma following oral dosing at 5 and 125 mg/kg occurred by 2 h post dose in both male and female rats. The plasma terminal elimination half-life values for total radioactivity were approximately 79 h in male rats at both dose levels and 78 and 63 h in female rats following a 5 and 125 mg/kg dose, respectively. Terminal elimination half-life values in red blood cells were approximately twice that in plasma, ranging from 121 h to 160 h. The internal dose as measured by area under the concentration-time curve to infinity (AUC<sub>inf</sub>) was similar for both male and female rats. The increase in AUC<sub>inf</sub> was slightly less than dose proportional from 5 mg/kg to 125 mg/kg. Preliminary material balance and tissue distribution data following an oral 5 mg/kg dose suggests that at 7 days postdose, less than 5% of the administered radioactivity was present in tissues with the highest concentrations occurring in fat, adrenals, and thyroid. The majority of the [1,2-<sup>14</sup>C] 6:2 FTOH dose was excreted in feces with 65% and 50% excreted in male and female rats, respectively. Renal excretion was also a significant elimination pathway with 10% and 18% excreted in urine in male and female rats, respectively.

#### PS 495 Analysis of tris(2-Chloroisopropyl)phosphate Metabolites in Rat Plasma for Toxicology Studies.

B. Collins<sup>2</sup>, S. Waidyanatha<sup>2</sup>, M. Stout<sup>2</sup>, A. Gutierrez<sup>1</sup>, R. Mathias<sup>1</sup>, C. Dillon<sup>1</sup>, D. Slade<sup>1</sup>, C. Crouch<sup>1</sup>, K. Aillon<sup>1</sup>, J. Algaier<sup>1</sup> and R. Harris<sup>1</sup>. <sup>1</sup>MRI Global, Kansas City, MO; <sup>2</sup>National Toxicology Program, NIEHS, Research Triangle Park, NC.

Tris(2-Chloroisopropyl)phosphate, TCP, is an organophosphate compound used as a flame retardant and plasticizer especially in polyurethane foam in furniture and in home insulation. Due to its environmental prevalence and resulting human exposure, TCP is under study by the NTP. In support of NTP toxicological studies, MRI Global developed methods to analyze TCP and two major metabolites, Mono (MCPP, 2 isomers) and Bis 2-chloroisopropyl phosphate (BCPP, 3 isomers) in rodent plasma and blood. Because of its similarity to Tris(2-chloroethyl)phosphate, BCPP was expected to be the major TCP metabolite. During the analytical method development, multiple isomers of MCPP were observed and hence were included in the method. The 5 isomers of the two metabolites were characterized using synthetic standards following derivatization with BSTFA/pyridine prior to analysis by GC/MS without using an internal standard. The ions monitored in the selected ion monitoring mode were for MCPP, m/z 211, 227, 283 and for BCPP, m/z 155, 171, 197.

The quantitation of MCPP and BCPP was achieved without derivatization using LC/MS/MS following extraction of 100 µL of plasma with 200 µL acetonitrile, removing acetonitrile by evaporation, and reconstituting the residue in 100 µL of 2% MeOH in water containing 50 mM tributylamine, TrBA (pH 5 with formic acid) with internal standard dibenzylphosphate. The LC/MS analysis used a phenylhexyl column, which resulted in good linearity with a preliminary limit of detection value of 5 to 10 ng/mL of plasma ranging to over 500 ng/mL. Multiple MCPP and BCPP isomers were quantified as one MCPP and one BCPP peak.

Plasma samples from rats and mice from single and multiple exposures to TCP were analyzed to show the applicability of this method. The data show the presence of MCPP and BCPP at levels significantly higher than the parent TCP.

#### PS 496 In Vitro-In Vivo Extrapolation of 7-Ethoxycoumarin Metabolism Using 3D-Organotypic Liver Bioreactor.

K. Choi<sup>1</sup>, J. Campbell<sup>1</sup>, W. P. Pfund<sup>2</sup>, J. McKim<sup>3</sup>, E. L. LeCluyse<sup>1</sup> and H. J. Clewell<sup>1</sup>. <sup>1</sup>The Hamner Institutes for Health Sciences, Research Triangle Park, NC; <sup>2</sup>RealBio Technology, Inc., Kalamazoo, MI; <sup>3</sup>CeeTox Corp., Kalamazoo, MI.

A liver bioreactor system was developed to simulate the metabolism and clearance of compounds similar to the liver in vivo to provide better prediction of in vivo clearance and metabolite profiles of compounds from in vitro data. Primary rat and cryopreserved human hepatocytes were maintained in a RealBio D4™ Culture System for approximately a month. General metabolic and liver-specific functions and cellular damage of rat/human hepatocytes inside liver bioreactor were monitored. Stable levels of biomarkers and related functional endpoints were achieved after a 7-10 day period for both rat and human liver bioreactors, respectively (glucose 64.6 – 86.6/152 – 182 mg/dL; lactate 0.6 – 1.9/0.1 – 3.7 mmol/L; pH 7.4 – 8.0/7.4 – 7.5; albumin 0.8 – 1.0/1.0 – 1.1 mg/mL; total protein 7.5 – 8.8/1.8 – 20 mg/mL; ALT 4.9 – 13.6/6.0 – 9.9 U/L; AST 6.8 – 25.4/18.9 – 53.1 U/L). The activities of rat CYP2B, CYP2C11 and CYP3A were monitored by the production of 16β-OH testosterone, 16α-OH testosterone and 6β-OH testosterone, respectively. Rat hepatocytes at 28 days in a liver bioreactor and treated with 5 µM dexamethasone for 24hr showed 3-fold increase in CYP3A activity. Metabolism of 7-ethoxycoumarin (7-EC) was characterized in the rat liver bioreactor. 7-Hydroxycoumarin was the predominant metabolite produced, which was further metabolized to the glucuronide and sulfate conjugates. The depletion of 7-EC showed mono-exponential decay with an estimated intrinsic clearance of 113.3 µL/min/106 cells. Scaling of the in vitro CL<sub>int</sub> to in vivo CL<sub>int</sub> yielded in vivo prediction of 135.98 mL/min/rat body weight (250g). In conclusion, hepatocytes maintained in a 3D organotypic liver bioreactor showed stable liver functional capacity and intrinsic clearance over an extended period. This system may help resolve current limitations in assessing the clearance mechanisms and long-term effects of compounds and their major metabolites on chemical-induced liver toxicity.

#### PS 497 Enhanced Intranasal Delivery of Gemcitabine to the Central Nervous System.

M. Krishan<sup>1</sup>, G. Gudelsky<sup>2</sup>, P. Desai<sup>2</sup> and M. Genter<sup>1</sup>. <sup>1</sup>Environmental Health, University of Cincinnati, Cincinnati, OH; <sup>2</sup>College of Pharmacy, University of Cincinnati, Cincinnati, OH.

Delivery of therapeutics to the brain to treat neurological diseases is a challenge due to impenetrable nature of the blood brain barrier (BBB). Intranasal (IN) drug administration is a non-invasive approach for rapid direct drug delivery from the nose to the central nervous system (CNS), thereby minimizing systemic exposure. The current study focuses on a strategy to enhance the delivery of the nucleoside drug gemcitabine (GEM) to the CNS via IN administration. Our approach takes advantage of the fact that the BBB and olfactory epithelial (OE) tight junctions (TJs) share many proteins in common. We hypothesized that by transiently increasing the permeability of nasal epithelial tight junctions using the BBB permeabilizer piperazine (PV), we will increase the concentration of GEM reaching the brain extracellular fluid (BECF) following IN delivery, with the goal of delivering therapeutic concentrations of nucleoside drugs to the CNS. Experimental methods included IN administration of fluorescein isothiocyanate-dextran beads (FD4), in-vitro GEM recovery, in vivo brain microdialysis for BECF collection, HPLC analysis to measure GEM in BECF, histopathology, and western blot analysis. Distribution studies with FD4 showed significant deposition in the ethmoid turbinates, suggesting drug uptake through OE. Clinically-relevant doses of PV (up to 1.4% IN) did not cause histological evidence of cytotoxicity or inflammation in nasal epithelia, lung, liver, spleen, or kidney. Pharmacokinetics of GEM in BECF showed area under the curve (AUC) = 5.55±0.84 µg.h/mL for PV (1.4%) + GEM (50mg/kg) treated animals, compared to 1.5±0.29 µg.h/mL for GEM without PV treatment. Western blot analysis suggested that IN PV treatment increased permeability through OE TJs by transiently decreasing the levels of TJ protein occludin. Thus, it appears that transient permeabilization of nasal epithelial TJs provides a non-invasive means to enhance delivery of nucleoside drugs to the CNS.

#### PS 498 Altered Irinotecan Pharmacokinetics in Diet-Induced Obesity.

P. Shah, A. Gandhi and R. Ghose. *Pharmaceutical and Pharmacological Sciences, University of Houston, Houston, TX*. Sponsor: R. Ghose.

Purpose: Irinotecan (CPT-11) is a topoisomerase I inhibitor that has been shown to be highly effective in treatment of variety of cancers. It has recently been shown that CPT-11 administration is associated with liver toxicity and this effect is compounded by baseline obesity. It was found that patients with a BMI index of >25

were twice as much susceptible to developing liver toxicity than patients with BMI index of <25. CPT-11 metabolizes to SN-38, which then undergoes glucuronidation by uridine glucuronosyl transferase (UGT) 1A1 to form SN-38 glucuronide (SN-38G). Excess accumulation of the toxic metabolite SN-38 is known to cause fatal diarrhea in cancer patients. We hypothesize that accumulation of SN-38 is associated with increased liver toxicity of CPT-11 in obesity.

Methods: For metabolism studies, liver S9 fractions were prepared from diet-induced obese (DIO, 60% fat) and lean mice (10% fat). UGT1A-mediated metabolism of SN-38 was determined in liver S9 fractions. For pharmacokinetic studies, mice were injected with a single oral dose of 10 mg/kg CPT-11 and blood and feces samples were collected from 0-8hr. Samples were analyzed for CPT-11 and SN-38 concentrations using LC-MS/MS. Liver tissues were harvested for real-time PCR studies. The mRNA and serum TNF $\alpha$  levels were measured in liver and plasma samples, respectively.

Results: We found that the rate of formation of SN-38G was 2 fold lower in the DIO mice compared to the lean controls. This corresponded with reduced expression of UGT1A1 in DIO mice livers. We did not observe significant changes in the area under the curve (AUC) or clearance of CPT-11 between the DIO and lean mice. However, plasma and fecal exposure of SN-38 was increased by 2 folds in the DIO mice compared to the lean controls. We also observed significantly higher mRNA and serum levels of TNF $\alpha$  in the DIO mice as compared to the lean mice. Higher TNF $\alpha$  levels are known to be associated with liver toxicity.

Conclusion: CPT-11 dosage should be closely monitored for effective and safe chemotherapy in obese patients who are at a higher risk of developing liver toxicity.

#### PS 499 Interaction of Immunosuppressants with Human Organic Anion Transporters 1 and 3 and Multidrug Resistance Proteins 2 and 4.

R. Greupink<sup>1</sup>, A. A. El-Sheikh<sup>2</sup>, H. Wortelboer<sup>3</sup>, J. J. Van den Heuvel<sup>1</sup>, M. Schreurs<sup>1</sup>, J. B. Koenderink<sup>1</sup>, R. Masereeuw<sup>1</sup> and F. G. Russel<sup>1</sup>. <sup>1</sup>Department of Pharmacology and Toxicology, Radboud University Nijmegen Medical Centre, Nijmegen, Netherlands; <sup>2</sup>Department of Pharmacology, Faculty of Medicine, Minia University, Minya, Egypt; <sup>3</sup>TNO, Zeist, Netherlands.

Renal proximal tubule transporters can play a key role in excretion, pharmacokinetic interactions and toxicity of immunosuppressant drugs. Basolateral organic anion transporters (OATs) and apical multidrug resistance proteins (MRPs) contribute to active tubular uptake and urinary efflux, respectively. Combining immunosuppressants during therapy may lead to drug-drug interactions occurring at the transporter level, resulting in toxicity. We studied the effect of different immunosuppressants on OAT1- and OAT3-mediated uptake of [3H]-methotrexate ([3H]MTX) in cells, and on ATP-dependent [3H]MTX transport in membrane vesicles isolated from HEK293 cells over-expressing human MRP2 and MRP4. For the uptake transporters, we found that cyclosporine, dexamethasone, azathioprine and 6-mercaptopurine did not affect either transporter. Cytarabine, vinblastine, vincristine, hydrocortisone and mitoxantrone significantly inhibited OAT1 ( $p < 0.05$  at 10  $\mu$ M), whereas these compounds did not inhibit OAT3. In contrast to other compounds, mycophenolic acid (10  $\mu$ M) inhibited OAT3 more effectively than OAT1, reducing [3H]MTX uptake by  $86 \pm 4\%$  and  $52 \pm 5\%$  of control, for OAT3 and OAT1 respectively. Subsequent studies showed that the IC<sub>50</sub> of mycophenolic acid for OAT3 was 4.3  $\mu$ M (95% CI: 2.7-6.9  $\mu$ M), which is close to its reported C<sub>max</sub>, unbound ( $\sim 1$   $\mu$ M). With regard to the apical transporters, cyclophosphamide, hydrocortisone, tacrolimus and mycophenolic acid inhibited both MRP2 and 4. Cyclosporine, vincristine and vinblastine only inhibited MRP2, while 6-mercaptopurine only inhibited MRP4. In conclusion, immunosuppressants may alter renal transport activity. From a drug safety perspective, the observed differences in transporter inhibition profiles may provide a selection criterion when combining immunosuppressive drugs.

#### PS 500 Accumulation of $\beta$ -N-methylamino-L-Alanine in Tissues following Repeat Oral Administration to Harlan Sprague-Dawley Rats.

C. Garner<sup>1</sup>, C. J. Wegerski<sup>1</sup>, M. Doyle-Eisele<sup>1</sup>, J. Lucak<sup>1</sup>, S. Waidyanatha<sup>2</sup>, J. D. McDonald<sup>1</sup> and J. M. Sanders<sup>2</sup>. <sup>1</sup>Lovelace Respiratory Research Institute, Albuquerque, NM; <sup>2</sup>National Toxicology Program, NIEHS, Research Triangle Park, NC.

$\beta$ -N-methylamino-L-alanine (L-BMAA) was nominated to the National Toxicology Program for toxicological assessment based on widespread environmental distribution and evidence that the potentially neurotoxic compound may accumulate in CNS tissue. Data describing metabolism and disposition of L-BMAA are needed to support planned NTP toxicity studies. Male Harlan Sprague-Dawley rats were dosed by gavage with [1,2-<sup>14</sup>C]-L-BMAA (1 mg/kg/d) for 1, 5, and 10 consecutive days. Excreta and tissues were collected for up to 72 hours after the final

dose. The majority of <sup>14</sup>C was recovered as <sup>14</sup>CO<sub>2</sub> (50-60%) across 10 days of dosing and <10% of dose was excreted in urine. HPLC profiles of urine showed multiple polar metabolites and L-BMAA was not detected. Over 10 days of dosing <sup>14</sup>C continued to accumulate in tissues including the brain. After single and up to 10 day repeat doses the majority of the <sup>14</sup>C recovered in tissues was found in liver, adipose, muscle, and skin; < 0.01% dose was recovered in the brain. Accumulation rate of brain <sup>14</sup>C over 10 days exceeded elimination by >3 fold. On days 1, 5, and 10 a majority of <sup>14</sup>C in brain tissue 24 h following the final dose was recovered in the protein after exhaustive extraction. The nature of BMAA associated with brain protein was investigated in vitro. Incubation of [1,2-<sup>14</sup>C]-L-BMAA in vitro with rat brain homogenates released <sup>14</sup>CO<sub>2</sub> and <sup>14</sup>C was incorporated into protein. HPLC analysis of in vitro protein hydrolysates showed that [<sup>14</sup>C]-L-BMAA itself and other <sup>14</sup>C-equivalents made up the radioactive components. Thus accumulation of L-BMAA and its equivalents in brain tissue may be due in part to incorporation into protein. Brain tissue from repeat dose administration in rats is currently being analyzed to investigate the nature of the radiolabel associated with the protein. This work was conducted for the NTP under NIEHS Contract N01-ES-75562.

#### PS 501 Comparative Nonclinical Ocular Tissue Distribution of the Visual Cycle Modulator (VCM) Emixustat in Rats, Beagle Dogs, and Cynomolgus Monkeys.

T. Podoll<sup>1</sup>, R. J. Eyre<sup>1</sup>, S. Al-Fayoumi<sup>1</sup>, E. Austin<sup>1</sup>, E. Prescott<sup>2</sup>, G. Sun<sup>2</sup>, M. Orme<sup>1</sup> and R. Kubota<sup>1</sup>. <sup>1</sup>Acucela Inc., Seattle, WA; <sup>2</sup>Covance, Madison, WI.

Emixustat HCl is a novel, non-retinoid VCM that inhibits a key step in regeneration of 11-cis-retinal by retinyl ester isomerase RPE65. Emixustat is currently in late Phase 2 clinical development as an orally administered treatment for geographic atrophy associated with dry age-related macular degeneration (AMD). In ADME studies, very low plasma concentrations of emixustat are seen as it is extensively metabolized, producing pharmacologically inactive metabolites. Interestingly, the pharmacological activity of emixustat has been shown to be prolonged beyond the time at which its plasma concentrations are no longer measurable. Ocular distribution studies using <sup>14</sup>C emixustat were undertaken in rat, dog, and monkey to better understand the time course of emixustat ocular tissue exposure in relation to observed pharmacology activity in animal models.

Pigmented and albino rats received single oral doses of 1 mg/kg, and were prepared for QWBA, or a repeated oral dose (QD for 7 days) and were prepared for ocular dissection. Dogs received 0.3 mg/kg as a single or a repeated oral dose (QD for 7 days). Monkeys received 0.9 mg/kg/day as a single or a repeated oral dose (TID for 7 days). Eye levels were observed for up to six weeks postdose.

The mean recovery of radioactivity was >95% in rat and dog, and >90% in monkey. The half life of removal of radioactivity from eye tissues was longer in all species than that observed in plasma. Consistent among the three species, emixustat parent molecule was the major component found in eye tissues. In all three species, the retina C<sub>max</sub> of emixustat were >50 fold higher than respective plasma C<sub>max</sub> on a ng $\cdot$ equiv/g basis. Although high levels of the major metabolites were observed in plasma, they were not observed in eye tissues. Preclinical ocular distribution results indicated emixustat parent is the predominant molecule in the eye responsible for pharmacological activity.

#### PS 502 Development of Sustained Release Buprenorphine for Use As an Improved Analgesic in Toxicology Studies: Assessment of Formulation Pharmacokinetics.

L. Koetznar<sup>1</sup>, W. Stokes<sup>2</sup>, W. Lance<sup>3</sup>, G. Wnorowski<sup>1</sup>, N. South<sup>4</sup> and J. Boulet<sup>1</sup>. <sup>1</sup>Product Safety Labs, Dayton, NJ; <sup>2</sup>NICEATM, NIEHS, Research Triangle Park, NC; <sup>3</sup>Wildlife Pharmaceuticals, Fort Collins, CO; <sup>4</sup>Battelle, Columbus, OH.

Acute toxicology safety testing procedures can involve animal pain and distress. U.S. regulatory agencies and the OECD recently adopted and updated procedures that incorporate the routine use of systemic analgesics to avoid or reduce pain and distress for eye irritation testing procedures. Buprenorphine is recommended as a useful analgesic for such toxicology studies. However, buprenorphine requires a minimum of twice-daily dosing at 12 hour intervals to maintain effective analgesia. A study was therefore conducted to evaluate sustained release formulations to determine their usefulness for once-per-day or less frequent dosing. The pharmacokinetics of two sustained release formulations of buprenorphine were compared to buprenorphine in saline using male 2-2.5 kg New Zealand White rabbits. Sustained release formulations were prepared using N-methyl-pyrrolidone (NMP) or Triacetin as the vehicle. Following subcutaneous dosing, blood samples were collected at intervals to four days; plasma buprenorphine was determined using liquid chromatography with mass spectrometry. Both the NMP and Triacetin formulations produced higher plasma buprenorphine concentrations than the saline formulation at time points from 12 hours on. The Triacetin formulation also resulted in higher concentrations at earlier time points, as well as concentrations near or

above 0.1 ng/mL—a concentration previously associated with analgesic activity in other species—to 96 hours post-dosing. Body weight and food consumption were recorded, and did not show adverse effects of treatment with sustained release formulations. No abnormal clinical signs or local lesions were observed. These results suggest that the Triacetin sustained release formulation of buprenorphine can significantly reduce the dosing interval required and can be a useful replacement for twice-daily treatments.

## **PS 503 Acute Rat Inhalation Pharmacokinetic Study of 10.9 kD Protein with or without Pegylation.**

J. Gould<sup>1</sup>, I. Carvajal<sup>1</sup>, T. Davidson<sup>1</sup>, A. Kozhich<sup>1</sup>, J. Laporte<sup>2</sup>, J. Li<sup>1</sup>, N. Mathias<sup>1</sup>, L. Schneeweis<sup>1</sup>, S. Thompson-Iritani<sup>1</sup>, J. Valentine<sup>1</sup>, B. Wang<sup>1</sup> and H. H. Haggerty<sup>1</sup>. <sup>1</sup>Bristol-Myers Squibb, New Brunswick, NJ; <sup>2</sup>Charles River Laboratories Preclinical Services Montréal Inc, Senneville, QC, Canada.

Biologics are an evolving protein-based therapeutic approach in the pharmaceutical industry. As part of assessing hazards, an Occupational Exposure Limit (OEL) is developed internally for proprietary biologics to support worker safety. Biologics are considered to be less hazardous than small molecules due to suspected lower systemic bioavailability (BA) from the lung and degradation in the GI tract. To investigate fate after inhalation (Inh), SD rats were exposed to RGE (10.9 kD protein), RGE-PEG (40 kD PEG+10.9 kD protein) or saline by nose-only Inh for 1 hr. The pharmacokinetic (PK) profile was investigated in blood and bronchial alveolar lavage fluid (BAL). The measured experimental exposures were 42 and 48 mg/m<sup>3</sup>, corresponding to a calculated dose of 1.8 and 2.1 mg/kg, and a mean mass aerodynamic diameter of 1.8 and 1.9  $\mu$ m for RGE and RGE-PEG, respectively. The systemic PK profile for RGE and RGE-PEG included AUC(INF) of 169 and 357 ng.h/mL; C<sub>max</sub> of 19.8 and 10.1 ng/mL; T<sub>max</sub> of 2 and 9 hrs; and t<sub>1/2</sub> of 5.5 and 21 hrs; respectively. When compared to an IV study, systemic BA was 1.4 and 0.05%, respectively. From BAL levels, the left lung lobe contained 4.2 and 3.2% of the calculated dose at end of exposure and the lung t<sub>1/2</sub> was 4.5 and 7.2 hrs, respectively. These results indicate that after Inh exposure, systemic BA was low, with the PEG-RGE being markedly less than the unmodified RGE. However, the overall AUC(INF) for both proteins was similar. Compared to systemic results, the lung PK for the two proteins were similar with respect to t<sub>1/2</sub> and reduced percent of dose delivered to the lung. These PK results suggest that compared to small molecule drugs, there may be a decreased hazard for proteins, which would be demonstrated by applying these data-derived PK factors to the OEL calculation. Further studies on additional biologics would be needed to generalize across proteins.

## **PS 504 Simulation of Perfluoroacid Accumulation in Humans Exposed to Perfluorotelomer Alcohol Products.**

W. Roth and P. Rice. *Office of Food Additive Safety, US FDA, College Park, MD.*

Perfluorochemical grease-proofing agents derived from perfluorotelomer alcohols are commonly used in fast-food packaging, and have been of concern because of the toxicity and potential for biopersistence of components of these products, such as the surfactant perfluorooctanoic acid (PFOA) and related perfluoroalkyl carboxylic acids (PFCAs). Although the predominant products of perfluoroalkyl-ethanol (PFAE) metabolism are usually conjugates such as PFAE-O-glucuronide or PFAE-S-glutathiones, studies in the rat indicated that small amounts of PFCAs are also formed, and might lead to accumulation in other species (especially humans) under the appropriate kinetic conditions. We have previously conducted pharmacokinetic modeling of the metabolism of PFOE based on the rat experiments of Fasano et al. (2006), and were able to explain the metabolic appearance of PFOA with fitted kinetic coefficients. Since that time, additional in vitro data from human, rat, and mouse hepatocyte incubations has become available (Naab et al., 2007; Fasano et al., 2009), allowing us to extend our PK model to predict accumulation of PFCAs derived from PFAE products in the mouse and humans. Although neither the PK model prediction nor the in vitro data are definitive, this combination of alternative methods provides insight into PFAE exposures and consequent levels of PFCAs.

## **PS 505 Uptake and Disposition in Humans of Hydrofluorocarbons (HFCs) Used As Refrigerants.**

L. Ernstgård, B. Sjögren and G. Johanson. *Work Environmental Toxicology, Institute of Environmental Medicine, Karolinska Institutet, Stockholm, Sweden.*

A variety of hydrofluorocarbons (HFCs) have replaced the ozone-depleting chlorofluorocarbons (CFC) and hydrochlorofluorocarbons (HCFC) during the last decades. There are few data on uptake and disposition of HFCs in humans. In a se-

ries of experiments, we therefore exposed healthy volunteers to vapors of four commonly used HFCs, namely difluoroethane (HFC152a; 0, 200 and 1000 ppm), trifluoroethane (HFC143a; 500 ppm), tetrafluoroethane (HFC134a; 500 ppm) and pentafluoropropane (HFC245fa; 0, 100 and 300 ppm). In parallel, blood:air, saline:air and olive oil:air partition coefficients (PCs) were determined in vitro. The inhalation exposures were performed for 2 h during light physical exercise (50 W) in an exposure chamber. Capillary blood, urine and exhaled air were sampled until next day and analyzed for the parent substance by head-space gas chromatography. Fluoride and other potential metabolites were analyzed in urine using an ion selective electrode and 19F-NMR analysis, respectively. All HFCs had similar toxicokinetic profiles in blood with a rapid initial increase of HFC and an apparent steady-state reached within a few minutes. The area under the concentration-time curves (AUC) of HFC152a and HFC245fa in blood was proportional to the exposure level, suggesting first-order kinetics. For all four HFCs, the inhalation uptake was low (less than 4%) and only minor amounts were excreted unchanged in breath and urine after exposure. No signs of metabolism were detected except a slightly increased urinary excretion of fluoride after exposure to 1000 ppm HFC152a. No other urinary metabolites were detected. The observed time courses in blood and breath could be well described with a physiologically-based pharmacokinetic (PBPK) model. In conclusion, the uptake and disposition of the four HFCs are consistent with the PCs determined in vitro and with zero or insignificant biotransformation.

## **PS 506 Ethanol Toxicokinetics Resulting from Inhalation Exposure in Human Volunteers and Toxicokinetic Modeling.**

J. Dumas-Campagna, G. Charest-Tardif, R. Tardif and S. Haddad. *Environmental and Occupational Health, IRSPUM, Université de Montréal, Montréal, QC, Canada.*

There is a lack of information and increased interest on the risks associated with chronic inhalation exposures to low levels of ethanol (< 1000 ppm). A physiologically based pharmacokinetic model (PBPK) for inhaled ethanol was previously developed based on exposed volunteers but only for levels above 5000 ppm. Uncertainty still remains about the validity of this model to predict the blood levels of ethanol (BE) for lower level exposures. This project aims to determine the BE resulting from exposure to low concentrations (<1000 ppm) in order to adjust/validate the PBPK model. Ten volunteers (5 men and 5 women) were exposed for 4 h to vapors of ethanol (125, 250, 500, 750 and 1000 ppm) in resting conditions in an inhalation chamber. An additional exposure to 750 ppm that included 4 periods of 12 minutes of exercise at 50W was performed. Blood samples and alveolar air were collected during and after the exposure. Results show that there is a linear relationship between the ethanol inhaled air concentrations and (i) BE (women: r<sup>2</sup> = 0.98/men: r<sup>2</sup> = 0.99), as well as (ii) ethanol concentrations in the alveolar air at end of exposure period (men: r<sup>2</sup> = 0.99/women: r<sup>2</sup> = 0.99). Furthermore, exercise resulted in a significant increase (2 to 3 times) in BE after each period of 12 min of exercise. Overall, the model predictions were overestimated at exposure levels < 2616 ppm for men and < 2300 ppm for women. At lower exposure concentrations, limiting the clearance to the liver compartment was insufficient to account for total ethanol clearance. Adjusting the model by adding extra-hepatic biotransformation of high affinity and low capacity associated with the richly perfused tissues allowed the model to fit adequately the low and high exposure level toxicokinetic data. These new toxicokinetic data and improved PBPK model for ethanol will facilitate the refinement of risk assessment for chronic inhalation exposure to low levels of ethanol. (Project funded by ANSES, France).

## **PS 507 Physiologically-Based Pharmacokinetic (PBPK) Modeling: Extrapolation from In Vitro to In Vivo, a Case Study Using a Novel Dermal Compartment.**

M. V. Evans<sup>1</sup>, C. A. Wilson<sup>2</sup>, L. J. Beesley<sup>2</sup>, L. S. Leon<sup>2</sup>, R. A. Pegram<sup>1</sup>, E. L. Croom<sup>1</sup>, C. R. Eklund<sup>1</sup> and M. E. Sawyer<sup>2</sup>. <sup>1</sup>PB, US EPA, Research Triangle Park, NC; <sup>2</sup>REU 2012, North Carolina State University, Raleigh, NC.

PBPK models are useful extrapolation tools requiring time course data for calibration. A unique data set for rodents and humans was used with an existing PBPK model for species extrapolation. This same data set also enabled an in vitro to in vivo extrapolation, an emerging application tool for PBPK modeling. By adding a dermal compartment, a refined rodent PBPK model for orally administered lindane was developed and optimized using time-course tissue concentration data for Wistar rats. This refined PBPK model also provided blood and skin partition coefficients (P<sub>blood</sub> = 1.72 and P<sub>skin</sub> = 26.2); other partition coefficients were obtained from the literature. Next, a human in vivo model was extrapolated from the rodent model using physiological values from the literature. In addition, a novel in vitro model of human skin containing a follicular compartment was developed to

improve the fit to the available in vitro absorption data. In vitro dermal permeability coefficients were estimated using two different methods: 1) a permeability coefficient of 0.013 cm/hr was derived with the Potts-Guy equation; simulations generated with this coefficient matched the upper error results from the in vivo data; and 2) a permeability coefficient of 0.0043 cm/hr resulted from the dermal in vitro model; simulations generated with this coefficient matched the lower error results from the same in vivo data. The permeability value obtained using the in vivo PBPK model was 0.0060 cm/hr, which provided the best fit to the data. This result is between the in vitro and the Potts-Guy estimates, and PBPK simulations generated with this in vivo permeability fit through the averaged data points. In summary, PBPK modeling was found to be a powerful in vitro to in vivo extrapolation tool, particularly when time course datasets are available. (This abstract does not reflect EPA policy).

**PS 508 Evaluation of Toxicity Adjustment Factors Used for the Risk Assessment of Chlorpyrifos Oxon in Drinking Water.**

M. Bartels<sup>1</sup>, S. Marty<sup>2</sup>, J. E. Chambers<sup>3</sup>, J. J. Galligan<sup>4</sup>, D. W. Lickfeldt<sup>5</sup> and D. R. Juberg<sup>5</sup>. <sup>1</sup>Toxicology, Dow Chemical, Midland, MI; <sup>2</sup>Toxicology, Dow Chemical, Midland, MI; <sup>3</sup>College of Veterinary Medicine, Mississippi State University, Mississippi State, MS; <sup>4</sup>Neuroscience Program, Michigan State University, East Lansing, MI; <sup>5</sup>Regulatory Laboratory, Dow AgroSciences LLC, Indianapolis, IN.

In the Preliminary Human Health Risk Assessment for chlorpyrifos (CPF), EPA has derived toxicity adjustment factors (TAF) for chlorpyrifos oxon (Oxon), for both acute and chronic dietary scenarios, of 12 and 18, respectively, based on relative inhibition of RBC acetylcholinesterase (AChE) by Oxon, relative to CPF. However, a comprehensive evaluation of the biological effects of Oxon, following oral exposure, has shown that this test material undergoes complete first-pass metabolism, via chemical and/or enzymatic processes in the GI tract, GI tissue, portal vein blood and liver. As a result, no test material is systemically available at  $\leq 10$  mg/kg, as shown by non-detectable levels of Oxon in blood and no inhibition of brain ChE activity at doses up to 10 mg/kg in adult rats. Numerous datasets on tissue sensitivity to Oxon show that effects in brain are predictive and conservative for ChE inhibition, relative to other target tissues. Minor effects seen in the GI tract, at dose levels  $\geq 5$  mg/kg, are limited to the portal of entry (i.e., do not directly affect other tissues), are not considered to have long-term clinical consequences, and would not be expected given the predicted, low level exposures to Oxon in drinking water. As a result of these analyses, it is proposed that the potency of Oxon be based on a relevant toxicity endpoint (e.g., brain effects seen at  $> 10$  mg/kg) and not on RBC ChE inhibition, which is an indicator of low levels of Oxon that are not systemically available.

**PS 509 Effects of Leucine Administration on Plasma and Brain Levels of Other Amino Acids.**

K. Yu, L. Narayanan, J. Gearhart, J. J. Schlager, F. Lobo-Menendez, D. A. Mahle and P. Robinson. *AFRL, Wright-Patterson AFB, Dayton, OH.*

Leucine (leu), one of the essential branch-chained amino acids (AAs), has been shown to activate mTOR to increase protein synthesis, and for the brain, may provide enhanced cognitive memory deposition. However, little is known regarding leu kinetics. Investigations into the leu kinetics revealed that it was eliminated very fast from the blood after dosing, and leu levels in brain were higher than blood, indicating active transport of leu across the blood brain barrier (BBB). The objective of this work was to investigate the effects of leu administration on blood and brain levels of 20 AAs, and the BBB role (if any) to leu kinetics. A rodent model was dosed leu via iv (5 & 12.9 mg/kg) for dose-response and time-course studies, and orally (319 mg/kg) for time-course analysis. Tissue leu levels were measured at various time points (5m–6h, iv and 30m–4h, orally). Interestingly, more than 65% of all AAs were increased in brain. At the 5 mg/kg dose, valine, lysine and proline in brain were increased, while aspartic acid and isoleucine levels decreased. At the 12.9 mg/kg dose, serine, tryptophan, lysine and proline in brain were increased, while threonine and methionine decreased (all relative to control,  $p < 0.05$ ). With oral dosing, 16 AAs in brain were increased at the 1h time point. Isoleucine (time point 1 & 4h), lysine (0.5 & 1h), histidine (0.5 & 1h) and proline (all time points: 0.5, 1, 2, and 4h) in brain were increased significantly from control at  $p < 0.05$  or less. Brains to plasma AA ratios were increased following dosing for lysine, methionine and valine at 5 mg/kg, proline at 12.9 mg/kg and isoleucine and proline for oral dosing groups. Our results indicate that leucine administration initiate complex time- and dose- dependent responses in both plasma and brain levels of the other AAs. These preliminary data show that neither the specific BBB transport system for AAs (most AAs use the L1 large neutral AA transporter for crossing the BBB), nor obvious general chemical or biological AA properties determine the brain levels and uptake behavior observed in these studies.

**PS 510 Screening for Substrates of the P-Glycoprotein Transporter.**

R. A. Pegram<sup>1</sup>, E. L. Croom<sup>1</sup> and J. A. Campbell<sup>2</sup>. <sup>1</sup>NHEERL/ORD, US EPA, Research Triangle Park, NC; <sup>2</sup>NCBA/SEE Program, Washington DC.

P-glycoprotein (Pgp) is an ATP-dependent efflux transporter of xenobiotic compounds with broad substrate specificity. Pgp is an important component of the blood-brain barrier and frequently mediates resistance of tumors to chemotherapeutic agents. Attempts to predict the in vivo toxicity of environmental chemicals based upon in vitro screening test results can be erroneous if transporter effects are not considered. In this study, a multi-tiered in silico/in vitro testing approach was used to predict Pgp substrates within a set of ToxCast chemicals. An in silico analysis using a support vector machine predicted 45 of the 280 chemicals to be Pgp substrates; these predictions matched the results of a separate in silico docking analysis. Only 5% of the chemicals with MW  $< 400$  (and none with MW  $< 300$ ) were predicted as substrates, while 87% with MW  $> 400$  were predicted substrates. In vitro cell-based assays were used to further screen for Pgp substrates among chemicals with MW  $> 300$ . Dye efflux experiments were conducted with NIH 3T3 MDR1 cells that stably express human Pgp. A number of potential substrates were identified by this assay (including ivermectin and abamectin), as shown by their capability to interfere with efflux of Hoechst 33342 dye from the cells. A more definitive assay was used to test chemicals with known cytotoxicity by comparing toxicity in the MDR1 cells and wild type 3T3 cells. Pgp substrates (i.e., chemicals that were less toxic to MDR1 cells) included captan, naled, pyriproxyfen, thiophanate, thiodicarb, abamectin, niclosamide, and rotenone. These results demonstrate that a systematic approach involving a combination of in silico and cell-based in vitro assays can successfully predict Pgp substrates within large chemical test sets. In vitro toxicants that are identified as Pgp substrates will require additional toxicokinetic assessment to correctly predict their potential in vivo toxicity. (This abstract does not reflect EPA policy.)

**PS 511 Transport Mediated Mechanism for Nucleoside Penetration of the Blood-Testis Barrier.**

D. M. Klein<sup>1</sup>, R. N. Hardwick<sup>1</sup>, K. K. Evans<sup>2</sup>, W. H. Dantzler<sup>2</sup>, S. H. Wright<sup>2</sup> and N. J. Cherrington<sup>1</sup>. <sup>1</sup>Pharmacology/Toxicology, University of Arizona, Tucson, AZ; <sup>2</sup>Physiology, University of Arizona, Tucson, AZ.

The blood-testis barrier (BTB) is formed by tight junctions between Sertoli cells and prevents the entry of many therapeutics into the lumen of the seminiferous tubules (STs) shielding developing germ cells from chemical exposure. One drug class of HIV therapeutics, nucleoside reverse transcriptase inhibitors (NRTIs), can penetrate the BTB and be detected in human seminal plasma at concentrations higher than that of blood plasma. The purpose of this study is to determine the mechanisms by which NRTI drugs are transported across the BTB. Transport studies in isolated rodent seminiferous tubules using H3uridine (Kt 89.72uM) as a model nucleoside substrate indicate that seminiferous tubules take up nucleosides almost exclusively via equilibrative nucleoside transporter 1 (ENT1). The IC50 for NBMPR, an ENT inhibitor, is 12.9 nM. Trans-epithelial transport of uridine by primary rat Sertoli cells can also be blocked by ENT1 inhibition. Blocking ENT1 function on the basolateral membrane also prevents uridine uptake into cells. These data correspond with immunohistochemical staining of rat testes showing ENT1 on the basolateral membrane, whereas ENT2 is on the apical membrane of Sertoli cells. This localization suggests that ENT1 acts as an uptake transporter and ENT2 may facilitate the efflux of nucleosides and NRTI drugs into the lumen of STs. Uridine transport can also be inhibited by NRTI drugs. We also demonstrate transepithelial transport of radiolabeled NRTIs zidovudine (AZT) and didanosine (ddI) through primary Sertoli cells is partially blocked by ENT1 inhibition (88% and 67% for AZT and ddI respectively). These data indicate a novel ENT dominant mechanism for the transepithelial transport of nucleosides and NRTI drugs across the BTB.

**PS 512 Pharmacokinetics and Bioavailability Testing of Levofloxacin in Rats.**

K. K. Kabirov, A. Banerjee, E. Onua, M. Hautmann and A. Lyubimov. *Toxicology Research Laboratory/UIC, Chicago, IL.*

Drug exposure of the antibiotic levofloxacin was examined in male and female Sprague Dawley rats following oral and intravenous administration. Pharmacokinetic modeling and determination of bioavailability were conducted following single dose treatment and subsequent measurements of levofloxacin levels in plasma. Dose levels studied were 50 mg/kg oral (PO) and 25 mg/kg intravenous

(IV). There were no abnormal clinical signs observed following dosing, which might have otherwise affected the pharmacokinetic modeling. The systemic bioavailability of levofloxacin in rats after PO administration ranges between 33.7–42.7%, and appears to be lower in males. The volume of distribution ( $V_z$ ) appeared to be higher in female than in male rats following IV administration. Other pharmacokinetic parameters appeared to be similar in both male and female rats for both routes of administration. Levofloxacin appears to distribute widely in rat tissues and possibly exhibits a large affinity for tissue proteins. The half-life of the drug is short (4.33 hr and 4.96 hr in males and females, respectively, following PO administration; 1.38 hr and 1.55 hr in males and females, respectively, following IV administration), probably due to a high systemic clearance. Levofloxacin single IV (25 mg/kg) and PO (50 mg/kg) doses were well tolerated by male and female rats. Mean ( $\pm$ SD) AUC<sub>0-inf</sub> values following IV administration were  $11339.0 \pm 572.3$  hr\*ng/mL and  $9422.7 \pm 1169.4$  hr\*ng/mL, in males and females, respectively, and following PO administration were  $8051.4$  hr\*ng/mL and  $10211.6$  hr\*ng/mL in males and females, respectively. Based on mean  $T_{max}$  and terminal elimination half-life values, levofloxacin is rapidly absorbed and eliminated.

**PS 513 Comparative Disposition and Metabolism of 2, 2'-Dithiobisbenzanilide following Dermal, Oral, and Intravenous Administration to Harlan Sprague-Dawley Rats and B6C3F1/N Mice.**

J. Lucak<sup>1</sup>, C. Garner<sup>1</sup>, C. J. Wegerski<sup>1</sup>, J. M. Sanders<sup>2</sup>, M. Doyle-Eisele<sup>1</sup>, J. D. McDonald<sup>1</sup> and S. Waidyanatha<sup>2</sup>. <sup>1</sup>Lovelace Respiratory Research Institute, Albuquerque, NM; <sup>2</sup>National Toxicology Program, NIEHS, Research Triangle Park, NC.

2, 2'-Dithiobisbenzanilide (DTBBA) is used as a peptizing agent in tires and rubber products and occupational exposure to DTBBA may occur mainly through dermal contact. Potential systemic exposure via the dermal route was investigated in rodents and compared to intravenous and oral routes. A single dermal dose of [<sup>14</sup>C]DTBBA (4 mg/kg, in acetone) were applied (protected from oral grooming) to male Harlan Sprague-Dawley rats and B6C3F1/N mice and its disposition and metabolism 72 h after was compared to 4 mg/kg intravenous and gavage doses. Following a dermal dose of [<sup>14</sup>C]-DTBBA in rats and mice,  $10.9 \pm 2.9\%$  and  $10.6 \pm 2.9\%$  of the dose was absorbed, respectively. Excretion of absorbed dose was via urine ( $18.4 \pm 3.3\%$ ;  $34.7 \pm 7.7\%$ ) and feces ( $32.6 \pm 10.7\%$ ;  $49.5 \pm 10.8\%$ ) for rats and mice, respectively. Following gavage administration in both species, the absorption was complete. Excretion of [<sup>14</sup>C] after rat intravenous doses was mostly via urine ( $73.1 \pm 7\%$ ). After mouse intravenous, mouse or rat dermal or gavage doses ~30% to ~40% was recovered in urine and feces. The percent dose in tissues after dermal dosing was  $4.58 \pm 1.92\%$  for the rat and  $0.98 \pm 1.13\%$  for mouse and in both species non dose site skin had the highest [<sup>14</sup>C] levels. Radioactivity remaining in tissues followed the trend of dermal  $\geq$  intravenous > gavage in rat and intravenous > gavage  $\approx$  dermal in mouse. DTBBA was not detected in urine. Urine metabolite profiles were qualitatively similar between species but the levels of some metabolites varied between dose routes. The structure of the predominant urinary metabolite was identified as thiobisbenzanilide-S-glucuronide by LC/MS/MS and <sup>1</sup>H and <sup>13</sup>C-NMR. This work was conducted for the NTP under NIEHS Contract N01-ES-75562.

**PS 514 Effect of Vehicle on the Dermal Absorption of 2-Hydroxy-4-Methoxybenzophenone Harlan Sprague-Dawley Rats and B6C3F1/N Mice.**

C. J. Wegerski<sup>1</sup>, C. Garner<sup>1</sup>, M. Doyle-Eisele<sup>1</sup>, J. M. Sanders<sup>2</sup>, J. D. McDonald<sup>1</sup>, S. S. Auerbach<sup>2</sup> and S. Waidyanatha<sup>2</sup>. <sup>1</sup>Lovelace Respiratory Research Institute, Albuquerque, NM; <sup>2</sup>National Toxicology Program, NIEHS, Research Triangle Park, NC.

2-Hydroxy-4-methoxybenzophenone (HMB) is used as sunscreen agent with significant human exposure. To support a vehicle selection for potential dermal studies in rodents, the effect of different dermal vehicles on absorption and disposition of 0.1 or 10 mg/kg [<sup>14</sup>C]HMB was investigated in male and female Harlan Sprague Dawley Rats and B6C3F1/N Mice 72 h following application. The vehicles investigated were ethanol, ethanol:coconut oil (1:1), coconut oil, light paraffin oil, or a lotion (olive oil:emulsifying wax:water, 15:15:70). In rats, the greatest absorption was observed with paraffin oil ( $79.8 \pm 6.9\%$ ). Absorption across all vehicles followed the trend of paraffin oil > ethanol:coconut oil > ethanol > coconut oil > lotion. Dose did not have an impact on absorption in rats at 10 and 0.1 mg/kg when paraffin oil was used as the vehicle ( $79.8 \pm 6.9$  and  $72.5 \pm 8.5\%$  dose, respectively

( $p > 0.05$ ). Ethanol gave a large difference in absorbed dose between rats ( $67.8 \pm 3.2\%$  dose) and mice ( $43.7 \pm 3.7\%$  dose) ( $p < 0.001$ ). The absorbed dose was similar between rats ( $34.6 \pm 8.5\%$  dose) and mice ( $36.8 \pm 8.2\%$  dose) when using the lotion vehicle. There was also no significant difference in the absorbed dose between male and female mice using the lotion ( $36.8 \pm 8.2\%$  and  $46.2 \pm 7.3\%$  dose, respectively) ( $p > 0.05$ ). In rats, the percent dose recovered in tissues ranged from 2.8–8.3 for all dosing vehicles, which was higher than the percent recovered in tissues for mice (0.6–1.2). Non-dose site skin was the site of greatest tissue burden in both species. In conclusion, these studies indicate use of paraffin oil as the vehicle provides the highest systemic absorption of HMB and there is a difference in absorption between rats and mice. This work was conducted for the NTP under NIEHS Contract N01-ES-75562.

**PS 515 Lipophilicity and Membrane Affinity of Munitions Constituents Using Biolipid Beads.**

A. B. Goins<sup>1</sup>, D. R. Johnson<sup>2</sup>, C. Y. Ang<sup>1</sup>, A. M. Scott<sup>2</sup>, A. J. Bednar<sup>2</sup>, T. M. Reese<sup>3</sup> and F. C. Hill<sup>2</sup>. <sup>1</sup>Environmental Laboratory, US Army Engineer Research & Development Center, Vicksburg, MS; <sup>2</sup>Badger Technical Services, Vicksburg, MS; <sup>3</sup>Jackson State University, Jackson, MS.

Bioaccumulation of organic molecules into fat can be predicted by chemical lipophilicity which is measured by the octanol:water partition coefficient (Kow). Newly developed methods use the liposome:water partition coefficient (Klipw) with phosphatidylcholine (PC) instead of octanol to more accurately represent the capacity of membrane lipids to accumulate neutral organic chemicals. In this study, a new technique for measuring Klipw using solid-supported PC liposomes attached to silica beads (TRANSIL® Sovicell, Leipzig, Germany) was used to assess the membrane affinity (i.e., Klipw) of 10 munitions compounds (MCs) and 5 environmental breakdown products (BPs). Nitroaromatic compounds studied were 2,4,6-trinitrotoluene [TNT], 2,4-dinitrotoluene [2,4-DNT], 2,6-dinitrotoluene [2,6-DNT], 1,3,5-trinitrobenzene [TNB], 2,4-dinitroanisole [DNAN]; cyclic nitramine compounds studied were hexahydro-1,3,5-trinitro-1,3,5-triazine [RDX], octahydro-1,3,5,7-tetranitro-1,3,5,7-tetrazocine [HMX], hexanitrohexaazaisowurtzitan [CL-20]; and other nitrogenous compounds studied were 5-nitro-2,4-dihydro-3H-1,2,4-triazol-3-one [NTO] and 2,2-dinitro-1,1-ethenediamine [FOX-7]. Results indicate that nitroaromatic and cyclic nitramine compounds have lipophilicities with log Klipw ranging from 1.55–3.22, with TNT and RDX log Klipw 2.18 and 2.26, respectively. RDX-like compounds and the TNT BP 4-aminodinitrotoluene (4-ADNT) have Klipw >1 log units higher than computational and literature-based log Kow. NTO and FOX-7 were found to have very low lipophilicity (log Klipw < 1, below biolipid assay detection limit). In conclusion, use of Klipw from biolipid beads rather than Kow from literature or computational sources may allow scientists and risk assessors to avoid underestimating chemical bioconcentration.

**PS 516 Less Is More: Better Toxicity Data from Fewer Rodents Using Plasma Microsampling.**

G. Schmitt, A. Eichinger-Chapelon, D. Zaugg and T. Singer. *Toxicology, F. Hoffmann-La Roche, Basel, Switzerland.*

The standard design of drug development rodent toxicity studies today involves numerous large volume blood samplings to characterize the toxicokinetics of a drug candidate. Due to the large volume and generally required anesthesia, standard practice is to use additional satellite animals. Using the plasma microsampling technique developed by Ove Jonsson et al. (Bioanalysis (2012), 4(6), 661–674) would change this. With this technique, satellite animals for kinetic bleedings are no longer required (3R-Reduce), anesthesia is no longer required for small (i.e.,  $\mu$ L) blood volume sampling from the tail vein (3R-Refine), and lastly less animals means less test compound is needed. Ultimately, plasma microsampling would be used for toxicokinetic blood collection in all types of rodent toxicology studies performed at or under sponsorship of F. Hoffmann-La Roche. To reach this goal, a method validation study has been initiated using acetaminophen and an anti-CD20 monoclonal antibody as model compounds. These compounds were selected to investigate the different analytical methods needed for small versus large molecule, i.e., liquid chromatography coupled to mass spectrometry versus an enzyme-linked immunosorbent assay, respectively. For each compound, one low and one high dose were selected to check for dose exposure dependence. The validation study design would use both the microsampling and conventional large volume sampling in the same animals in an authentic 14-day rat toxicity study and compare the exposure data obtained from each technique. If successful (i.e., comparable exposure data), the use of the microsampling technique in rodent toxicity studies will

lead to i) a significant reduction in animal use (e.g., 32 instead of 48 rats in a 14-day dose-range finding study), ii) the abandonment of anesthesia for toxicokinetic blood sampling, and iii) better data as effect and exposure are gathered in the same animal leading to better assessments of drug-related effects.

**PS 517 Using PBPK Modeling to Address Diurnal Variation and Age Differences in Hexavalent Chromium Toxicokinetics in Humans.**

C. R. Kirman<sup>1</sup>, C. M. Thompson<sup>2</sup>, D. M. Proctor<sup>3</sup>, M. Suh<sup>3</sup>, L. C. Haws<sup>4</sup>, M. A. Harris<sup>2</sup> and S. M. Hays<sup>5</sup>. <sup>1</sup>Summit Toxicology LLP, Orange, OH; <sup>2</sup>ToxStrategies, Katy, TX; <sup>3</sup>ToxStrategies, Rancho Santa Margarita, CA; <sup>4</sup>ToxStrategies, Austin, TX; <sup>5</sup>Summit Toxicology LLP, Allenspark, CO.

A physiologically based pharmacokinetic (PBPK) model has been developed to describe the toxicokinetics of hexavalent chromium [Cr(VI)] in mice, rats, and humans. The PBPK model was used to support a human health risk assessment (HHRA) based upon mouse small intestinal (SI) tumors. Key factors contributing to the delivery of Cr(VI) to the SI were identified by sensitivity analyses, and include gastric pH, gastric transit time, and gastric reducing equivalents. These factors affect the rate of Cr(VI) reduction in gastric contents, with a higher delivery of Cr(VI) resulting from higher pH values (which causes slower rates of Cr(VI) reduction), shorter stomach transit times, and lower reducing equivalent concentrations. The PBPK model was used to address 4 important sources of variation. First, the model was used to account for normal diurnal variation in gastric lumen factors (e.g., in normal individuals, baseline gastric pH is typically between 1-3 between meals, but rises rapidly to levels of 5-7 at the start of a meal, then returning to baseline levels within a 2-3 hours). Second, the model was used to simulate exposures to different age groups, including infants, children, youths, adults, and elderly, since some age groups (e.g., infants) normally exhibit higher pH values than adults. Age-specific differences in the key factors were incorporated in the modeling to estimate human equivalent lifetime average daily dose corresponding to point of departures determined for mouse SI lesions. Third, the model was used to assess risk to specific populations (proton-pump inhibitor users) that may be sensitive to Cr(VI) due to alterations in gastric pH. Lastly, the model was used to assess the impact of the timing of Cr(VI) exposure events on delivery of Cr(VI) to the SI with respect to their occurrence during or between meals. The implications to HHRA are quantified and discussed.

**PS 518 Advantages of Using Quadrupole Time-of-Flight (QTOF) in the Bioanalysis of Large Therapeutic Peptides.**

F. Garofolo. *Bioanalytical Services, Algorithme Pharma, Laval, QC, Canada.*  
Sponsor: K. Draper.

**Purpose.**

MUC5AC13, hepcidin, and calcitonin were selected as model compounds to demonstrate the advantages of QTOF in large therapeutic peptides bioanalysis for toxicokinetic (TK) and pharmacokinetic (PK) studies.

**Methods.**

Samples were prepared by spiking MUC5AC13, hepcidin or calcitonin in plasma. They were extracted using protein precipitation followed by solid phase extraction. UPLC was used for chromatography. MUC5AC13 and Calcitonin were analyzed on TripleTOF5600 with DuoSpray. A KinetexC18 column and 0.6mL/min flow rate in gradient conditions were used. For hepcidin, electrospray Chip emitters TriVersaNanoMate on TripleTOF5600 with AtlantisT3 column at 0.5mL/min flow rate in gradient conditions were used.

**Results.**

MUC5AC13 showed multiple charge states +2 and +3 as the most abundant ions in QTOF full scan. Summing +2 and +3 charge states with a 10mDa extraction window was used for quantification, over 3.5 orders of linear range (0.4-2000ng/mL), a precision of <9.3% and an accuracy between 86-113% were obtained. In hepcidin quantification, full scan and parent ion quantification showed interferences even with narrow extraction window (2-5mDa). The interference peaks might be in source fragments and thus eliminated by the first quadrupole (Q1). Hence, quantification of hepcidin was performed in QTOF tandem mass spectrometry and summing +4 charge state isotopomers of parent ion at a 10mDa extraction window and it showed 3 orders of linear dynamic range (2-2048ng/mL) a precision of <9% and an accuracy between 80-112%. Calcitonin quantification showed +3, +4 and +5 charge states as the most abundant ions. QTOF full scan and summing +3, +4 and +5 charge states of parent ion at a 10mDa extraction window were used for quantification. The observed LLOQ was 50pg/mL with 4 orders of linear dynamic range. The precision was better than 15% and the accuracy between 83-118%.

**Conclusion.**

The benefits of QTOF bioanalytical quantification for large therapeutic peptides (minimum drug optimization; generic method and non-targeted quantification) were confirmed and it can be used for TK & PK studies.

**PS 519 A New Strategy to Effectively Reduce Matrix Effect Caused by Phospholipids in Plasma Samples under Hydrophilic Interaction Liquid Chromatography (HILIC).**

M. Raigneau and F. Garofolo. *Bioanalytical Services, Algorithme Pharma Inc., Laval, QC, Canada.* Sponsor: K. Draper.

**Purpose.**

Significant reduction of matrix effect due to phospholipids (PL) in plasma sample by using aprotic solvent to improve the performance of bioanalytical methods used for drug quantification in toxicokinetic and pharmacokinetic studies.

**Methods.**

Rivastigmine was extracted using liquid-liquid extraction and injected using HILIC column with ammonium acetate / Acetonitrile (ACN) with a flow rate=0.8mL/min. Analysis was performed on ABSciexAPI3000 with electrospray(+). Lower limit of quantification=10pg/mL. PL were monitored at m/z 184. The PL extractability was evaluated by samples evaporated in polypropylene (PP) instead of glass tubes and reconstituted with ACN.

**Results.**

Extracted plasma samples were reconstituted in mobile phase (MP blank) or in ACN blank and injected with post-column infusion of rivastigmine. The post-column infusion of MP and ACN blanks showed no suppression at the drug retention time. However, the baseline from the post-column infusion of MP blank dropped by 35% after seven injections. However, ion-suppression was not observed for the ACN blank. These results suggest that the late eluting suppressors are not reconstituted in ACN. PL peak was observed after seven MP blank injections suggesting that the late eluting suppressors in the MP blank are phospholipids. This peak was not observed in ACN blank. These results suggest that PL are reconstituted in mobile phase and elute as late eluting suppressors under the chromatographic conditions. However, PL are not reconstituted using ACN. The extracted blank plasma samples were reconstituted in PP tubes with ACN and compared to MP and ACN blanks reconstituted in glass tubes to determine if the PL are insoluble in ACN or if adsorption occurred on the glass tube surface. The PP ACN & MP blanks chromatograms were identical thus demonstrating that PL are soluble in ACN but were adsorbed on silica surface.

**Conclusion.**

The reconstitution of extracted samples in glass test tube using 100% ACN successfully eliminates the matrix effect caused by phospholipids.

**PS 520 Impact of Organic Solvent Additive on the Integrity of Plasma Samples over Time in Bioanalysis by LC-MS/MS.**

C. Dicaire and F. Garofolo. *Bioanalytical Services, Algorithme Pharma Inc., Laval, QC, Canada.* Sponsor: K. Draper.

**Purpose.**

Evaluation of plasma integrity over time due to addition of organic solvent in quality control samples (QCs) for morphine-6-glucuronide (M6G) bioanalytical method that was validated to be used in pharmacokinetic studies.

**Methods.**

The samples were extracted using solid phase cartridges. The injection of the samples was performed on XBridge Phenyl column (2.1x50mm, 5µ) in gradient conditions on Agilent1100 coupled with ABSciex API5000 in electrospray(+). The QCs were prepared with M6G alone and M6G + naltrexone (Co-Administered Drug - CAD) at 1.0% organic content vs. 1.5% respectively. M6G and M6G-D3 (IS) were monitored at m/z 462/201 and 465/289 respectively. Full scans and post-columns infusion were performed to evaluate the presence and determine the impact of interfering compounds.

**Results.**

A significant decrease in signal (~35%) was observed for M6G/IS over time for the QC containing naltrexone. A post-column infusion profile of these QCs showed the presence of suppressors which co-eluted with M6G/IS. Chromatographic separation was achieved between naltrexone and M6G/IS thus eliminating any possible suppression from naltrexone. Full scan experiments enabled the detection of two specific masses co-eluting with M6G/IS only in the QCs stored over time and containing naltrexone. QCs containing only the analyte and others containing the analyte with naltrexone were prepared in different plasma matrices. Some blank matrices were tested alongside with blank matrix containing different organic solvent percentage. The freshly prepared QCs did not show ion suppression; either in the presence of naltrexone or of the extra organic solvent. The long-term evaluation of the matrices in the presence of organic solvent (1.5%), showed two unknown compounds to appear over time and elute at the retention time of M6G thus creating a suppression zone.

## Conclusion.

The amount of organic solvent added impacted the integrity of the plasma samples over time. The ion suppression observed in plasma was not due to the addition of the CAD (naltrexone) but due to the amount of organic.

## PS 521 Dried Blood Spots (DBS) On-Card Derivatization: An Easy & Alternative Form for Sample Handling to Overcome the Biological Matrix Instability of Thiorphan.

R. Sabelli and F. Garofolo. *Bioanalytical Services, Algorithm Pharma Inc., Laval, QC, Canada.* Sponsor: K. Draper.

**Purpose:** Use of in-house pre-treatment of DBS cards to overcome stability challenges of thiorphan in toxicokinetic and pharmacokinetic studies.

### Methods.

Thiorphan was spiked in whole blood (range of 5-600ng/mL) and 40uL of whole blood were applied on untreated or in-house pretreated cards with 2-bromo-3'-methoxyacetophenone FTA DMPK-A, B and C cards. Disks (6mm) were punched from the blood spots, transferred into tubes and 200uL of internal standard (thiorphan-D5) in methanol was added. Samples were vortexed and left on bench for one hour. 100uL of the supernatant was transferred into 96wellplate already containing 100uL of water prior to injection on a Zorbax BonusRP column eluted using a gradient. Analysis was performed on an ABSciex API3000 in electrospray(+).

### Results.

The instability of thiorphan in biological matrix was demonstrated and minimized by derivatization to thiorphan-MP with 2-bromo-3'-methoxyacetophenone (BMP). In order to simplify sample handling process, on-card derivatization using DBS was investigated. The instability of thiorphan on-card, without derivatization, was demonstrated on all DBS cards used. Therefore, on-card derivatization technique was investigated. BMP could be added directly to the card for at least 2 days prior to blood spotting without compromising thiorphan derivatization. Although the on-card derivatization of thiorphan was successful on the A and C cards, the derivatization reaction seemed to be inhibited on the B card. Linearity of a calibration curve for a range of 5-600ng/mL was demonstrated using A and C cards pretreated with 0.5M BMP. Precision was 2-8% and the accuracy was 97-104%. Results showed on-card stability of thiorphan-MP for at least 2 days.

### Conclusion.

It was clearly demonstrated that DBS on-card derivatization offers a practical alternative for the bioanalysis of thiorphan in TK & PK studies since it requires less manipulation than the regular sample handling process.

## PS 522 Superparamagnetic Iron Oxide Loaded Cross-Linked Nanoassemblies Improve Tumor Accumulation and Magnetic Resonance Imaging *In Vivo*.

M. Dan<sup>1,2</sup>, M. T. Dickerson<sup>1</sup>, P. A. Hardy<sup>3</sup>, Y. Bae<sup>1</sup> and R. A. Yokel<sup>1,2</sup>.  
<sup>1</sup>Pharmaceutical Sciences, University of Kentucky, Lexington, KY; <sup>2</sup>Toxicology, University of Kentucky, Lexington, KY; <sup>3</sup>Anatomy and Neurobiology, University of Kentucky, Lexington, KY.

**Purpose:** To improve accumulation and contrast-enhanced magnetic resonance imaging of glioma using cross-linked nanoassemblies loaded with superparamagnetic iron oxide nanoparticles (CNA-IONPs) for potential glioma theranostic applications.

**Methods:** CNA-IONPs were synthesized and characterized. Gd-DTPA was used to monitor glioma tumor growth as a T1 contrast agent. CNA-IONPs were injected via the tail vein of a glioma xenograft rat model. T2 weighted MR images were taken 10 min and 2 h after the injection. T2\* was used to predict CNA-IONPs concentration increases. Glioma tumor, contralateral brain tissue, blood, and peripheral organs were collected at 2 or 6 h and iron concentrations analyzed by inductively coupled plasma mass spectrometry (ICP-MS).

**Results:** CNA-IONPs had a neutral zeta potential, hydrodynamic size ~ 30 nm, and were highly stable in medium containing serum at 37 °C over 30 h. CNA-IONPs showed significant T2 and T2\* contrast enhancement 2 h after injection. Gd-DTPA (0.3 mmol/kg) enhanced the tumor on T1 images acquired immediately after injection. T1 images acquired 2 h after injection showed Gd-DTPA was almost entirely cleared. In certain regions of the tumor, R2\* (1/T2\*), which is proportional to iron concentration, increased 48% from 10 min to 2 h after CNA-IONP injection. ICP-MS iron concentration in glioma tissue was 3 to 9 times higher than in contralateral brain tissue at 2 h. The iron concentrations in blood and peripheral organs did not significantly change from 2 to 6 h.

**Conclusions:** CNA-IONPs had desirable physicochemical properties for in vivo application. They preferentially accumulated in glioma and the concentration increased with time consistent with their long blood circulation time. CNA-IONPs have the potential to improve MRI diagnosis and provide a platform for incorporating glioma therapeutics.

Support: NCI Cancer Nanotechnology Training Center grant R25CA153954.

## PS 523 Age-Dependent Capability of Drug Metabolism in Commercially Available Human Hepatocytes.

M. Sunouchi<sup>1</sup>, K. Nakazawa<sup>1</sup>, R. Kikura-Hanajiri<sup>2</sup>, K. Kobayashi<sup>3</sup>, H. Kojima<sup>1</sup> and M. Usami<sup>1</sup>. <sup>1</sup>Pharmacology, National Institute of Health Sciences, Tokyo, Japan; <sup>2</sup>Pharmacognosy and Phytochemistry, National Institute of Health Sciences, Tokyo, Japan; <sup>3</sup>Shizuoka Prefectural Agriculture and Forestry College, Iwata, Japan. Sponsor: H. Kojima.

Primary human hepatocytes have been worldwide used as a good tool to evaluate the safety of chemicals containing environmental pollutants, pesticides and drugs. On the other hand, it is known that the drug-metabolizing enzyme activities of hepatocytes are changing with aging. There, however, are large interindividual variations in the levels of CYP enzyme activities and the response to inducers among hepatocyte donors. Therefore, in this study we analyze the relation between the enzyme activities and the induction levels of the enzymes.

We analyzed the enzyme activities of CYP1A1, CYP2B6, CYP3A4, CYP2C8, CYP2C9, CYP2C19, CYP2D6 and UGT and their responses to CYP inducers by comparing the data of cryopreserved human hepatic cell suspension and plateable hepatocytes regarding the enzyme activities and the levels of mRNA's encoding the enzymes presented from multiple suppliers. Total samples used in this study were obtained from more than 100 donors (3 months - 82 years old).

CYP1A2 activities in hepatocytes from young donors (< 4 years old) tended to be reduced in cell suspension and were largely induced both in the activity and the mRNA levels in plateable hepatocytes by beta-naphthoflavone. The enzyme activities and the mRNA levels of CYP3A4 and CYP2B6 in the young donors were positively induced by rifampicin. There was large variability in CYP activities and the abilities of the inducers. The utility of these cryopreserved human hepatocytes as an evaluation system for the safety of chemicals will be discussed.

## PS 524 AHR-Mediated Epigenetic Modulation of CYP19 and BCRP in Human Breast Adipose Fibroblasts and MCF-7 Cells.

M. B. van Duursen, S. M. Nijmeijer, M. de Dreu and M. van den Berg. *Institute for Risk Assessment Sciences, Utrecht University, Utrecht, Netherlands.*

The epithelial-stromal microenvironment in breast cancer largely determines chances of therapeutic success, due to modulation of tumor cell gene expression and drug resistance. In breast adipose fibroblasts (BAFs) surrounding a tumor, expression of aromatase (CYP19), the enzyme responsible for local estrogen production, is elevated. In breast cancer cells, over-expression of breast cancer resistance protein (BCRP) is one of the major causes of multi-drug resistance and chemotherapy failure. Both BCRP and CYP19 over-expression have been related to hypomethylation of the promoter regions by DNA methyltransferases (DNMTs). Earlier studies have suggested that the aryl hydrocarbon receptor (AHR) can function as an epigenetic regulator. Here, the effect of the non-toxic AHR agonist tranilast on CYP19 and BCRP expression was investigated in BAFs and MCF-7 cells. In BAFs, tranilast caused a significant 70% reduction of CYP19 expression, which concurred with a 1.3/pI to 1.4-promoter switch. In MCF-7 cells, tranilast induced expression of the AHR-responsive gene CYP1A1 (15-fold) and breast cancer resistance protein (BCRP, 2-fold), but had no effect on the expression of DNMT1, 3a and 3b. CYP19 expression in MCF-7 cells was too low to be detected. Inhibition of DNA methylation by 5-aza-2'-deoxycytidine (5-aza-dC, 10 µM) significantly up-regulated expression of CYP19, BCRP (28-fold) and DNMTs (2 to 5-fold) in vehicle control-treated MCF-7 cells. In combination with tranilast, the induction of gene expression by 5-aza-dC was attenuated, except for CYP1A1 expression. Changes in EROD (CYP1A1) and aromatase activity in MCF-7 cells concurred with the gene expression profiles. These data show that AHR activation by tranilast leads to epigenetic modulation. This results in downregulation of CYP19 possibly through alternate promoter use and potential abrogation of multidrug resistance as result of BCRP overexpression. Our results indicate that the AHR might provide a multimodal target in the emerging field of epigenetic therapeutics.

## PS 525 The Ah Receptor Recruits Protein Kinases to Phosphorylate Ser10 in Histone H3 of the CYP1A1 Promoter Chromatin.

H. Kurita and A. Puga. *Department of Environmental Health, University of Cincinnati, Cincinnati, OH.*

Halogenated aromatic hydrocarbons such as 2,3,7,8-tetrachlorodibenzo-*p*-dioxin (TCDD) cause many types of toxicity via the aryl hydrocarbon receptor (AHR). One of the best known proteins induced by TCDD is the cytochrome P450 1A1

(CYP1A1). Induction of this enzyme requires AHR ligand-dependent activation followed by the activated AHR binding to xenobiotic responsive elements (XRE) in the promoter region of the *Cyp1a1* gene. Histone modifications are well-known epigenetic markers modulating the activity of transcription factors by alteration of chromatin states. Among histone modifications, phosphorylation of serine-10 in histone H3 (H3S10ph) by various kinases has been reported to play a role in mitosis. Prior work from this lab had shown that the level of H3S10ph in the XRE enhancer region of the *Cyp1a1* promoter was elevated by AHR activation, which led us to search for responsible kinases that would be recruited by the ligand-activated AHR. To search for candidate kinases that phosphorylate H3S10 in an AHR dependent manner, we performed chromatin immunoprecipitation (ChIP) assays for the enhancer region of *Cyp1a1* in TCDD-treated Hepa-1 cells by using antibodies for AHR, H3S10ph and various kinases previously reported to phosphorylate this site. We found that binding of a subset of these kinase, including IKK $\alpha$ , MSK1, MSK2 and SRK, to the *Cyp1a1* enhancer region was absent in control cells and significantly increased by TCDD treatment. Given the known role of the AHR in cell cycle and differentiation, these data suggest that H3S10ph might be an activated AHR-dependent marker that signals cellular proliferation and mitosis. *Supported by NIH grant R01 ES 06273*

## PS 526 Epigenetics of Arsenic Carcinogenesis and Location of Methylated DNA Sites Underlying Gene Expression Changes.

B. A. Merrick<sup>1</sup>, E. J. Tokar<sup>1</sup>, D. P. Phadke<sup>2</sup>, R. R. Shah<sup>2</sup>, M. Wang<sup>3</sup>, O. Gordon<sup>3</sup>, G. M. Wright<sup>3</sup>, M. Burke<sup>3</sup>, S. A. Baxter<sup>3</sup>, K. E. Pelch<sup>1</sup>, R. R. Tice<sup>1</sup> and M. P. Waalkes<sup>1</sup>. <sup>1</sup>DNTP, NIEHS, Research Triangle Park, NC; <sup>2</sup>Bioinformatics, SRA, Durham, NC; <sup>3</sup>Genomics, DHMRI, Kannapolis, NC.

Inorganic arsenic (As) is an environmental human carcinogen and the prostate gland is among its many target organs. CAsE-PE transformed cells, developed after prolonged As exposure of normal human RWPE-1 prostate cells, have aberrant methylated DNA (MeDNA) patterns. We hypothesized that MeDNA changes might influence gene expression in As transformation. MeDNA changes were studied on a genome-wide level after affinity enrichment followed by bisulfite reduction and Illumina deep sequencing. Gene expression was determined by RNA-Seq. Analysis of RNA-Seq data showed 1,068 genes increased and 1,046 decreased at >2X fold change,  $p < 0.05$ . Key upregulated genes included vesicular trafficking protein, Syn3 (594X), the gluconeogenic enzyme FBP1 (321X), the peptidase, GGT5 (414X), and the oncogene, K-Ras (146X); downregulated genes at <100X fold control included high mobility group HMGA1, fibronectin-1, filamin B and the glycolytic enzyme, PKM2. Alignment of bisulfite sequencing data showed 1000's of cytosine methylations throughout the genomes of these cells. However, the number of methylation sites either nearby or within gene coding regions that might influence expression was a much smaller proportion of total. Several genes had notable decreases in expression and increased methylation. For example, nestin is an intermediate filament protein and progenitor marker, which was reduced 14X fold in CAsE-PE transformed cells vs RWPE-1 controls and that had a concurrent average increase in methylation of cytosines at 27X fold above control within a CpG island in the 5' region. Similarly, neurotrimin is an adhesion molecule whose expression in CAsE-PE cells was reduced by >100 fold vs controls and had a 25X fold increase in methylation of the promoter region. These data suggest deep sequencing of MeDNA enrichments can provide new insight into effects of environmental carcinogens on the epigenetic landscape leading to a malignant phenotype.

## PS 527 Age- and Sex-Related Alterations in Renal Global DNA Methylation during the Life Cycle of Rats.

T. Han, C. L. Moland, J. C. Kwekel, V. Desai and J. C. Fuscoe. *Division of Systems Biology, National Center for Toxicological Research, US FDA, Jefferson, AR.*

Epigenetic modifications of DNA, such as methylation of cytosine, are critical to regulating gene and miRNA expression, cellular differentiation, and X-chromosome inactivation, and have been shown to be involved in human diseases including cancer. The role of epigenetic changes in renal development and diseases has been noted. However, comprehensive study is needed to understand the epigenetic effects on renal disease susceptibility and progression at different life stages and between the sexes. Recent advances in high throughput technologies such as high density methylation array and next generation sequencing make it possible to monitor the methylation status at the whole genome level. In this study, kidney tissues from Fischer 344 rats at 2, 5, 6, 8, 15, 21, 78, and 104wk of age for both sexes were examined for sex- and age-specific alterations in DNA methylation using Roche 385k rat promoter methylation microarrays, which cover 15,398 CpG island regions. The raw image data were analyzed by DEVA (v1.2.1) to compute the methylation changes in these samples. Biweight mean centering normalization was applied before downstream analysis. Hierarchical clustering analysis indicated that the

overall methylation patterns are similar between the age groups, but there are distinct methylation patterns between male and female rats. The results indicate that there are slightly more methylated sites at 2wk of age compared to later ages. A higher number of methylated sites were found on the X chromosome in females than males, suggesting involvement in repression of X-inactivated genes. These results provide a comprehensive global view of the DNA methylation status in the kidney over the entire rat life cycle. These age- and sex-related differences in DNA methylation may provide insights in susceptibility to kidney disease and its progression.

## PS 528 Phylogenetic Identification of Variably Methylated Transposons As Biomarkers for Early Environmental Exposures.

C. Faulk, A. K. Barks and D. Dolinoy. *Environmental Health Sciences, University of Michigan, Ann Arbor, MI.*

A small number of retrotransposons in the long terminal repeat (LTR) class are known to exhibit environmental sensitivity in DNA methylation status, and are termed "metastable epialleles". Two of the sequenced examples, the agouti viable yellow (Avy) and the CDK5 activator-binding protein (CabpIAP) result from a recently inserted LTR, an intracisternal A particle (IAP) element. These insertions are from the same family, and show high sequence identity (98.5%). Additionally, both act as biomarkers of early exposure. Until now, neither the full extent of variability at these metastable epialleles, nor the phylogenetic relationship underlying variable elements was well understood. Using a computational approach, we identified 10,802 IAP LTRs in mice, and filtered by subtype to yield 1,388 IAP LTRs in the family that includes Avy and CabpIAP. Phylogenetic analysis revealed duplication and divergence events subdividing this family into three clades. To characterize variation across clades, DNA from isogenic mice was subjected to combined bisulfite and restriction analysis (CoBRA) at 21 LTR transposons (7 per clade). To validate our candidate IAP LTRs for interindividual variation, we assayed 17 isogenic mice for shifts in liver DNA methylation patterns. Methylation levels at individual LTRs varied widely with mean methylation ranging from a low of 59% to a high of 89%. Among mice, average methylation across all LTRs was not significantly different (71%-74%,  $p > 0.99$ ). Finally we determined that the clade with the most conserved elements had significantly higher average methylation across LTRs than either diverged clade. Thus, we increase the number of known epigenetically modifiable loci and provide evidence that sequence identity is predictive of methylation level. Since repetitive elements comprise nearly half of mammalian genomes, they are likely targets for toxicological disruption, especially during early development. The characterization of murine metastable epialleles is crucial for the development of treatments for environmentally-induced disease.

## PS 529 Chromatin Context Modulates Genome-Wide p53 Sequence-Specific Occupancy and Exposure-Induced Gene Expression.

D. A. Bell, D. Su, M. R. Campbell and X. Wang. *NIEHS, Research Triangle Park, NC. Sponsor: B. McIntyre.*

DNA damaging agents activate p53 to bind to DNA response elements leading to transactivation of p53 pathway genes and directing cells toward arrest or apoptosis. To understand the determinants of treatment-specific and tissue-specific responses to DNA damage we have carried out treatments using ENCODE cells in an exposure model and generated genome-wide data (p53 ChIPseq, H3K4me3 ChIPseq, sequence specificity, evolutionary conservation and gene expression). Effects of doxorubicin and nutlin-3 treatments in lymphoid cells have been compared with other cell types and analyzed in relation to chromatin context based on the ENCODE chromatin hidden Markov model (ChromHMM). We identified novel chromatin interactions that modulate the transcriptional response to p53 activation following DNA damage. Highly induced p53 genes typically display both low H3K4me3 marks and low baseline expression. Among the 2568 high confidence p53-occupied genes detected by p53 ChIP-seq, 45% have active promoter marks (H3K4me2, H3K4me3, H3k27ac, H3K9ac) prior to treatment. Surprisingly, based on ChromHMM categorization, ~22% of p53 genes displayed repressive chromatin states; including many highly-induced p53 response genes. Many p53 peaks were located in genomic regions with preexisting states classified as promoters (16%) or enhancers. However, notably a large percentage (31%) of all p53 binding peaks were found in repressed or heterochromatin regions far distant from a transcription start site. Thus p53 binding occurs in regions of both accessible and inaccessible chromatin although induced expression was most commonly associated with inaccessible chromatin. We identified p53 DNA binding motifs in 95% of p53 ChIPseq peaks and used a position weight matrix model (PWM) to score similarity to the consensus p53 motif. PWM strength and spacer length have distinctive distribution patterns between different chromatin states. Thus both epigenetic and sequence-based factors modulate the DNA damage response regulated by p53.

**PS 530 Mercury Exposure and DNA Methylation among Dental Professionals.**

J. Goodrich, N. Basu, A. Franzblau and D. Dolinoy. *Environmental Health Sciences, University of Michigan, Ann Arbor, MI.*

Epigenetic alteration may be a key mechanism linking chemical exposures to toxicity and disease. Recent, yet limited, animal and human data suggest that mercury (Hg) modifies the epigenome, specifically DNA methylation. This study hypothesizes that methylmercury and inorganic Hg exposures from fish consumption and dental amalgams, respectively, alter DNA methylation patterns at multi-copy repeats and candidate genes. Dental professionals were recruited at meetings of both the Michigan and American Dental Associations (MDA, ADA). Subjects provided survey data (e.g. exposure sources, demographics) and samples for Hg measurement and epigenetic analysis. Total Hg was quantified via atomic absorption spectrophotometry in hair and urine, indicative of methylmercury and inorganic Hg exposures, respectively. Methylation was assayed globally by pyrosequencing of long interspersed elements (LINE-1) and site-specifically at *DNMT1*, *SEPW1*, and *SEPP1* in bisulfite converted DNA (isolated from buccal mucosa or saliva in the MDA; blood leukocytes and saliva in the ADA). In the MDA cohort (n=158), hair Hg (mean  $\pm$ SD:  $0.55 \pm 0.54$   $\mu$ g/g) and urine Hg ( $1.05 \pm 1.08$   $\mu$ g/L) overlapped with levels of the general US population. Multivariate linear regression displayed a trend of hypomethylation at LINE-1 and three candidate genes with increasing hair Hg levels. Only in males, this trend was significant ( $p < 0.05$ ) in models of mean *SEPP1* methylation, methylation of each *SEPP1* CpG site, and of one LINE-1 site. Relationships between urine Hg and DNA methylation were not significant. Associations between Hg biomarker levels and DNA methylation will be further explored using samples from the ADA cohort (n>500). This work suggests that methylmercury modifies DNA methylation at labile regions in males. Epigenetic modification by Hg should be further investigated to elucidate this pathway as a mechanism of toxicity.

**PS 531 Alteration of Gene Methylation in the Testis of Rats and Mice Chronically Exposed to Low-Dose Cadmium.**

B. Wang<sup>1,2,3</sup>, L. Yang<sup>2</sup>, Y. Tan<sup>3</sup> and C. Lu<sup>3</sup>. <sup>1</sup>Department of Pathology, Inner Mongolia Forestry General Hospital, Hulunbuir, China; <sup>2</sup>Department of Pathophysiology, Jilin University, Changchun, China; <sup>3</sup>Department of Pediatrics, University of Louisville School of Medicine, Louisville, KY.

Testicular cancer has a unique epigenetic phenotype and Cadmium is known to be human carcinogens. To further evaluate gene methylation alterations of testis by Cadmium (Cd) treatment, this study was designed to aim at genome-wide screening of the altered methylation genes in the testis of rats chronically exposed to low-dose Cd. First, rats were exposed to Cd at 20 nmol/kg every other day for 4 weeks and gene methylation was analyzed at the 52nd week with methylated DNA immunoprecipitation-CpG island (CGI) microarray. Among the 490 altered genes, there were 134 genes whose promoter CGIs were all hypermethylated, 346 genes whose promoter CGIs were hypomethylated, and 10 genes whose promoter CGIs were some hypermethylated and some hypomethylated. Furthermore, *Rassf1* gene promoter CGI hypermethylation was detected and confirmed in Cd treated mice at the 60th week by mouse tumor suppressor gene array. In mice model, mice were given chronic exposure of Cd with and without methylation inhibitor (5-aza-2'-deoxycytidine, 5-aza) for 6 weeks and at the 60th week *Rassf1* promoter CGI hypermethylation was prevented. Results showed that testis of mice previously exposed to chronic Cd displayed an increased *Rassf1* CGI methylation, which was prevented by 5-aza treatment. These results suggest that DNA methylation of *Rassf1* gene promoter down-regulated its activity, leading to a reduction of testicular apoptosis, and may be a potential cause of Cd-induced testis cancer.

**PS 532 Epigenetic Modifications from Lead Exposure: Influences of Sex, Exposure Level, and Developmental Timing of Exposure on DNA Methyltransferases and Methyl Cytosine-Binding Proteins.**

S. Kidd, D. Anderson and J. Schneider. *Thomas Jefferson University, Philadelphia, PA.*

Maintaining normal DNA methylation levels is critical during development and in adults, DNA methylation may maintain a subtle balance of global gene expression pattern, crucial for normal neuronal function. DNA methylation is catalyzed by a family of DNA methyltransferases (Dnmts) that include the maintenance enzyme *Dnmt1* and the de novo methyltransferase *Dnmt3a*. DNA methyltransferase (*Dnmt*) expression is subject to active regulation under both physiologic or pathologic conditions and is critical to the regulation of synaptic plasticity in the mature brain. Dysregulation of *Dnmts* has been associated with a variety of cognitive disorders. Likewise, methyl cytosine-binding proteins such as MeCP2 and MBD1

play important roles in transcriptional regulation. The present study investigated the extent to which these enzymes are affected by developmental Pb exposure. Long Evans dams were fed Pb-containing food (RMH 1000 with or without added Pb acetate: 0, 150, 375, 750 ppm) prior to breeding and stayed on the same diet through weaning at postnatal day 25 (perinatal exposure group (Peri)). Other animals were exposed to the same doses of lead but exposure started on postnatal day 1 and continued through postnatal day 25 (early postnatal exposure group (EPN)). A third group had Pb exposure from postnatal day 1 through day 45 (long postnatal exposure (LPE)). All animals were euthanized on day 45 and hippocampi were removed, frozen and stored until processed. Analyses showed significant effects on *Dnmt1* and MeCP2 in particular, lesser effects on *Dnmt3a* and MBD1, with effects modified by sex, developmental window of exposure and level of Pb exposure. Interestingly, the degree of modulation appeared to be more related to when the exposure occurred developmentally than to the absolute duration of the exposure. These data suggest epigenetic effects of developmental Pb exposure on DNA methylation that depend on sex, level of exposure and developmental period of exposure. Supported by NIH RO1-ES015295.

**PS 533 A Clinical Study to Clarify Effect of Blueberry (*Vaccinium spp.*) on Oxidative Stress and Global Methylation.**

M. Kim and M. Yang. *Sookmyung Women's University, Seoul, Republic of Korea.*

Blueberry (*Vaccinium spp.*) has shown a broad spectrum of biomedical functions including anti-oxidative and anti-inflammatory effects through in vitro or animal studies. However, its human studies are relatively few. In addition, food-born epigenetic modulators, e.g. folate, genistein, etc., can recover environmental exposure-related epigenetic alterations. Therefore, epigenetics can be a useful screening method to find a new functional food. We performed a two weeks- intervention study to evaluate anti-oxidative and epigenetic effects of blueberry in young women (N=8, age= 22.6 $\pm$ 0.7 yrs, BMI=20.2 $\pm$ 1.97 kg/m<sup>2</sup>). Among the subjects, two persons took vt C (1 g/day) as positive controls and the others took blueberry juice [240 ml (total polyphenol 300mg, anthocyanin 76mg)/day]. From genomic DNA of their peripheral blood, we analyzed global methylation-status with MethylationFlashTM methylated DNA quantification kit (Epigentek). We also analyzed urinary malondialdehyde (MDA), a biomarker of oxidative stress with HPLC/UVD. As a result, we found that blueberry did not reduce urinary MDA levels as much as vt C did. In addition, both blueberry and vt C treatment somewhat increased global DNA methylation. There were no significant differences in the global DNA methylation between the two treatments ( $p=0.89$ ). Therefore, anti-oxidative activity of blueberry was not found in this trial, compared to vt C. However, its epigenetic effects can be similar to vt C's. In conclusion, the present study provides that a medicinal function of blueberry can be induced by global hypermethylation rather than anti-oxidative effects.

**PS 534 The Role of microRNAs in the Pathogenesis of MMPi-Induced Skin Fibrodysplasia.**

D. P. Tonge<sup>1</sup>, J. D. Tugwood<sup>2</sup> and T. W. Gant<sup>1</sup>. <sup>1</sup>CRCE, Health Protection Agency, Oxford, United Kingdom; <sup>2</sup>Global Safety Assessment, AstraZeneca, Cheshire, United Kingdom.

This study sought to investigate the role of microRNAs (miRNAs) in the pathogenesis of matrix metalloproteinase inhibitor (MMPi) induced skin fibrodysplasia (FD) in the dog.

MicroRNAs are short non-protein-coding RNAs that modulate protein translation from specific mRNAs. Certain miRNAs exhibit tissue specificity, and are dysregulated in response to specific pathologies. MicroRNAs are detectable in biological fluids, paving the way for their use as biomarkers. Matrix metalloproteinases (MMPs) are a family of proteolytic enzymes and have been an attractive pharmacological target for a number of indications. However, development has been hampered by the propensity of these compounds to cause connective tissue pathologies. The broad-spectrum MMPi AZM551248 has been shown to induce such effects in the dog, characterised by fibroblast proliferation and collagen deposition in subcutaneous tissues.

Thirty 12-month old female beagle dogs were assigned to six groups. Animals were dosed orally once daily with vehicle, or with vehicle plus 20mg/kg/day AZM551248 for between 4 and 17 days. miRNA expression profiles in subcutaneous skin were determined by high-throughput sequencing (SOLiD 4.0).

Following 4 days MMPi administration, 13 miRNAs were differentially expressed in the skin compared with vehicle treated animals. Several of these were members of the miR-200 family and were attenuated in response to MMPi. As the severity of FD increased at the later time-points, miRNAs associated with TGF $\beta$  synthesis were modulated. Evidence of epithelial to mesenchymal transition was present at all study time points. Receiver operator curve analysis revealed that miR-21 expression in the cervical subcutaneous tissue was a sensitive and specific biomarker of FD incidence.

We have described a role for miRNAs in processes relevant to the key histopathological events associated with MMPi-induced FD. Furthermore, we have identified key miRNAs with the potential to be used as informative biomarkers of FD.

### PS 535 Exposure of Pregnant Mice to Chlorpyrifos-Methyl Alters Embryonic H19 Gene Methylation Patterns.

H. Kang<sup>1</sup>, H. Shin<sup>1</sup>, J. Seo<sup>1</sup>, S. Park<sup>1</sup>, Y. Park<sup>1</sup>, S. Son<sup>1</sup>, S. Jeong<sup>3</sup> and J. Kim<sup>2</sup>.  
<sup>1</sup>Veterinary Toxicology and Chemistry, National Veterinary Research and Quarantine Service, Anyang, Republic of Korea; <sup>2</sup>Toxicology Laboratory, College of Veterinary Medicine, Konkuk University, Seoul, Republic of Korea; <sup>3</sup>GLP Research Center, College of Natural Science, Hoseo University, Asan, Republic of Korea.

The aim of this study was to identify whether chlorpyrifos methyl (CPM) exposure during pregnancy leads to changes in the methylation patterns of H19 gene. CPM 4, 20, 100mg/kg bw/day was administered to 4 pregnant mice per group between 7 and 12 days post coitum (d.p.c.). Pregnant mice were killed at 13 d.p.c. and genomic methylation in primordial germ cells (PGCs) and fetal organs (the liver, intestine, and placenta) was examined. Four polymorphism sites in the H19 alleles of maternal (C57BL/6) and paternal (CAST/Ei) alleles were identified at nucleotide position 1407, 1485, 1566 and 1654 and the methylation patterns of 17 CpG sites were analyzed. The methylation level in male and female PGCs was not altered by CPM treatment in the maternal allele H19. The methylation level of the paternal H19 allele was altered in only male PGCs in response to the CPM treatment. The methylation level at a binding site for the transcriptional regulator CTCF2 was higher than that at the CTCF1 binding site in all CPM-treated groups. In the placenta, the aggregate methylation level of H19 was 56.89% (control) and ranged from 47.7% to 49.89% after treatment with increasing doses of CPM. H19 gene from theliver and intestine of 13 d.p.c. fetuses treated with CPM was hypomethylated compared with controls, although H19 mRNA expression was unaltered. In the placenta, H19 expression was slightly increased in the CPM-treated group, although not significantly. IGF2 expression levels were not significantly changed in the placenta. In conclusion, CPM exposure during pregnancy alters the methylation status of the H19 gene in PGCs and embryonic tissues. We infer that these alterations are likely related to changes in DNA demethylase activity.

### PS 536 Autoimmune Disease Triggered by Trichloroethylene Is Associated with Epigenetic Alterations in Cd4<sup>+</sup> T Cells.

K. Gilbert<sup>1</sup>, S. Blossom<sup>1</sup> and C. Cooney<sup>2</sup>. <sup>1</sup>University of Arkansas for Medical Sciences/Arkansas Children's Hospital Research Institute, Little Rock, AR; <sup>2</sup>Central Arkansas Veterans Healthcare System, Little Rock, AR.

Previous studies have shown that chronic (32-week) exposure to occupationally-relevant concentrations of trichloroethylene (TCE) in the drinking water of female MRL+/+ mice promoted autoimmune hepatitis. This was accompanied by the expansion of CD4<sup>+</sup> T cells that secreted increased levels of IFN- $\gamma$  and expressed an activated (CD44<sup>hi</sup>CD62L<sup>lo</sup>) phenotype. The current study was initiated to determine the mechanism by which TCE altered CD4<sup>+</sup> T cell function. The study constituted a longitudinal evaluation of mouse TCE exposure over 40 weeks. Alterations in IFN- $\gamma$  production corresponded to changes in the expression of markers used to assess DNA methylation, namely retrotransposons Iap (Intracisternal A Particle) and Muerv (murine endogenous retrovirus). In addition, global DNA methylation was significantly altered in CD4<sup>+</sup> T cells from TCE-treated mice. Most recently, bisulfite sequencing revealed that DNA methylation of CpG sites associated with the Ifng promoter was significantly, and time-dependently altered by TCE exposure. Thus, for the first time, a toxicant known to promote autoimmune disease has been shown to alter epigenetic processes (DNA methylation) in the cell type that mediates pathology, namely CD4<sup>+</sup> T cells.

### PS 537 Is the Current Product Safety Assessment Paradigm Protective for Transgenerational Epigenetic Effects?

R. A. Alyea<sup>1</sup>, M. J. LeBaron<sup>1</sup>, R. Sura<sup>1</sup>, J. A. Murray<sup>1</sup>, I. P. Pogribny<sup>2</sup>, J. K. Passage<sup>1</sup>, R. G. Ellis-Hutchings<sup>1</sup>, N. P. Moore<sup>3</sup>, E. W. Carney<sup>1</sup>, B. Gollapudi<sup>1</sup> and R. J. Rasoulpour<sup>1</sup>. <sup>1</sup>The Dow Chemical Company, Midland, MI; <sup>2</sup>Division of Biochemical Toxicology, National Center for Toxicological Research, US FDA, Jefferson, AR; <sup>3</sup>Dow Europe GmbH, Horgen, Switzerland.

Placement of epigenetic effects appropriately into the product safety paradigm is challenging due to an incomplete understanding of causal associations between epigenetics and apical adverse effects. To begin to understand this relationship, groups of 25 pregnant F0 CD-1 mice were administered ~10  $\mu$ g/kg/day diethylstilbestrol (DES) or ~30  $\mu$ g/kg/day 17 $\beta$ -estradiol (E2) via the diet or by subcutaneous injection (SC) from gestation day 9 – lactation day 20. F1 offspring were mated for two

additional generations, with F1-F3 offspring evaluated for uterotrophic effects on postnatal day (PND) 21 and 18 months. F1 generation weanlings in the DES and E2 diet groups had a 3-4-fold increase in relative uterine weights, which corresponded to hyperplasia and hypertrophy of the endometrial epithelium and hypertrophy of the myometrium. Gene array analysis of these groups showed an increase in cancer and reproductive associated biofunctional and canonical pathways. The F1 18 month DES SC and diet group had an increase in squamous metaplasia of the endometrium and squamous cell carcinoma in the DES diet group, but no histopathological effects in either E2 group at 18 months. When comparing gene lists in the PND 21 E2 and DES diet groups, ~1500 known genes were unique for DES, of which 24 remained significantly altered up to 18 months. These gene sets provided candidates for further epigenetic analysis. The F2 generation DES diet group had a marginal increase in mean PND 21 uterine weights and a treatment-related increase in leiomyoma/leiomyosarcoma at 18 months. In the F3 generation, there was no effect on uterine weight or histopathology at PND 21 or 18 months. Under the conditions of this study, there were no transgenerational effects associated with DES or E2, which would suggest that a typical margin of exposure risk assessment would be protective.

### PS 538 Genome-Wide Methylation Profiling in Rat Tissues for Nongenotoxic Carcinogens Using Medip-Chip.

S. Ozden<sup>1</sup>, N. Turgut Kara<sup>2</sup>, T. Chen<sup>3</sup>, B. Alpertunga<sup>1</sup>, K. Chipman<sup>4</sup> and A. Mally<sup>2</sup>. <sup>1</sup>Department of Pharmaceutical Toxicology, Faculty of Pharmacy, Istanbul University, Istanbul, Turkey; <sup>2</sup>Division of Molecular Biology and Genetics, Faculty of Science, Istanbul University, Istanbul, Turkey; <sup>3</sup>School of Public Health, Soochow University, Suzhou, China; <sup>4</sup>School of Biosciences, University of Birmingham, Birmingham, United Kingdom; <sup>5</sup>Department of Toxicology, University of Würzburg, Würzburg, Germany.

DNA methylation is an epigenetic mark that has a crucial role in chemical carcinogenesis. The aim of the study was to perform a genome-wide analysis of DNA methylation profile of non-genotoxic hepatocarcinogens including tetrachlorodibenzo-p-dioxin (TCDD), hexachlorobenzene (HCB), methapyrilene (MPY) and the male rat kidney carcinogens, d-limonene, p-dichlorobenzene (DCB), chloroform and ochratoxin A (OTA) in their respective target tissues in rats dosed under bioassay conditions. Methylated DNA immunoprecipitation (MeDIP) was used in conjunction with a NimbleGen promoter plus CpG island array to identify differentially methylated DNA regions (DMRs) on a genome-wide basis. We first identified a total of 76 candidate DMRs for OTA, 1 DMR for MPY and 4 DMRs for chloroform by the MeDIP-Chip method. No change was observed in rats treated by TCDD, HCB, DCB and d-limonene. It is expected that results from this study will contribute to a better understanding of the key molecular events which occur during early stages of chemical carcinogenesis and aid in identification of mechanism-based biomarkers for early detection of non-genotoxic carcinogens.

### PS 539 Modulation of DNA (Cytosine-5)- Methylation in the Mouse Embryonic Stem Es-D3 Cell- and in the Human Intestinal CaCo2-Cells by Okadaic Acid.

E. E. Creppy, S. Moukha, E. Renault and B. Sangare-Tigori. *Toxicology, University Bordeaux Segalen, Bordeaux, France.*

Okadaic acid (OA) a polyether fatty acid produced by marine plankton (dinoflagellates) accumulates in the black sponge and in mussels and oysters and causes shellfish diarrhetic syndrome in consumers. It is also suspected of causing gut tumours in humans. It is a tumour promoter in mouse skin, inhibitor of protein phosphatase 1 and 2A (IC50=x109M<sup>-1</sup>) and a potent and specific inhibitor of protein synthesis in cell-free system (IC50=33.7x1011M<sup>-1</sup>). The cell death induced by OA occurs by both apoptosis and necrosis. OA induces hypermethylation and/or hypomethylation of deoxycytidine residues in the DNA concentration-dependently. We have investigated the effects of okadaic acid on the methylation of [poly(dIdC-dIdC)] by DNAMtase of ES-D3 cells in the presence of [3Hmethyl]-SAM, and 3H-labelled OA. The methylation rate was evaluated by the determination of the total [3H]-label in the trichloroacetate precipitated material after incubation (37°C for 60 min. in initial velocity conditions) and then by the radioactive counts of the peak corresponding to the [3H]m5dC by HPLC and Flo-one Packard coupled to UV detection. m5dC was also quantified by ELISA. In parallel, parameters such as lipoperoxidation, DNA-oxidized bases related to oxidative stress, ILs production, NF-kB, 8OH-dG, caspase-3, bax and bcl2 activation were determined. The results of three independent experiments showed hypermethylation for low concentrations of OA (maximum + 90% at 15nM) and hypomethylation for cytotoxic concentrations. Altogether these data point at an epigenetic mechanism of action of OA in the pathway for its tumour promotion. Since the epigenetic effects are already induced by low concentration of OA (hypermethylation-mitogenic activity) it should be taken into account when assessing the risk for human.

**PS 540 Methylation Profiles of CpG Islands Localized in the Upstream Regions of the Human Microsomal Epoxide Hydrolase Gene Promoters.**

C. J. Omiecinski, X. Cai, S. Su and W. D. Hedrich. *Center for Molecular Toxicology and Carcinogenesis, Pennsylvania State University, University Park, PA.*

Previous studies from our laboratory demonstrated that expression of the human epoxide hydrolase gene (EPHX1) is driven by a far upstream E1-b promoter in most human tissues, whereas the proximal E1 promoter selectively drives hepatic EPHX1 expression. The molecular mechanisms underlying the differential promoter usage are not well elucidated. CpG islands are short stretches of DNA harboring relatively higher frequencies of the cytosine/guanine repeat sequence, potentially reflective of higher gene methylation modifications. In-silico analysis of the human EPHX1 gene indicated that the upstream regions of E1 and E1b promoters of human EPHX1 gene are both rich in CpG islands. As methylation status of CpG islands around gene promoter regions is often associated with transcriptional repression of genes, we investigated the methylation status of CpG islands proximal to the upstream regions of the E1b and E1 promoters in several human cell lines and in primary human hepatocytes. Our data demonstrate that the methylation status of all the CpG islands in upstream regions of the E1b promoter from different cell lines is essentially the same and only sparsely methylated (<10%). In contrast, the CpG islands located at regions close to the E1 promoter are highly methylated (>60%) in cell lines originating from lung and kidney. In contrast, in hepatocellular carcinoma HepG2/C3A cells, the CpG islands localized at -128bp, -89bp, -48bp and +8bp of the E1 promoter are 0%, 0%, 0%, 0% and 25% methylated, respectively. Similarly, the CpG islands located at -724bp, -602bp, -128bp, -89bp, -48bp and +8bp of the E1 promoter in human primary hepatocytes are all unmethylated. The methylation status of these promoters from human hepatic and non-hepatic tissues are also consistent with our results from different cell lines and primary hepatocytes. These findings suggest that differential methylation status determines tissue selective promoter usage for EPHX1 expression in humans.

**PS 541 Identification of Arsenic-Responsive microRNAs in Rats by Genome-Wide High-Throughput Sequencing.**

Y. Ge<sup>1</sup>, J. R. Olson<sup>1</sup>, H. Wu<sup>2</sup> and X. Ren<sup>1</sup>. <sup>1</sup>*Social and Preventive Medicine & Pharmacology and Toxicology, The State University of New York at Buffalo, Buffalo, NY;* <sup>2</sup>*School of Environment and Public Health, Wenzhou Medical College, Wenzhou, China.*

Consumption of drinking water contaminated with arsenic, a naturally occurring carcinogenic metalloid, constitutes a major public health problem. Although the relationship between exposure and carcinogenesis is well documented, the mechanisms by which arsenic participates in tumorigenesis are not fully elucidated. Epigenetic modifications are often dysregulated in cancer and occur following exposure to a number of carcinogenic chemicals and are suggested to play a key role in arsenic-induced carcinogenesis. Beyond DNA methylation, other epigenetic mechanisms, in particular miRNA expression, that play a critical role in regulation of gene expression, have yet to be adequately investigated for arsenic. In the current study, male rats were exposed to sodium arsenite (As(3+)) up to 150ppm in drinking water for 60 days. miRNAs was extracted from rat liver, the primary tissue for arsenic metabolism and potential target of arsenic carcinogenesis, following As(3+) treatment. Genome-wide profiling of miRNA in rat livers was generated to identify As(3+)-responsive miRNAs by next generation high-throughput sequencing technology. The preliminary results indicate that exposure to environmentally-relevant levels of As(3+) lead to aberrant expression of multiple miRNAs in rat liver. Additional analysis will identify miRNAs whose levels are most differentially expressed in rats due to arsenic treatment, and potentially identify early pre-disease epigenetic biomarkers of arsenic exposure. The results may also provide insights into the role of miRNAs in arsenic carcinogenesis (This work was supported by Zhejiang Natural Science Foundation, China (H.W.); and Startup fund (to X.R.) provide by SUNY at Buffalo).

**PS 542 Benzo(a)pyrene Enhances Line-1 Reactivation in the Absence of Retinoblastoma Proteins: Implications for Global Epigenetic Silencing and Heterochromatin Regulation.**

D. E. Montoya-Durango and K. S. Ramos. *Biochemistry and Molecular Biology, University of Louisville, Louisville, KY.*

Benzo(a)pyrene (BaP) is a ubiquitous environmental pollutant that induces DNA mutations and disease. At the molecular level, BaP induces the reactivation of LINE-1 (or L1), a parasitic DNA element that normally remains silent in differentiated cells. L1 epigenetic silencing involves promoter DNA hypermethylation, recruitment of transcriptional repressors such as retinoblastoma (RB), and small

RNAs. Since RB proteins control the cell cycle and help recruit transcriptional corepressors to chromatin, we hypothesized that i) L1 expression may follow cell cycle progression, and ii) absence of RB is associated with derepression of L1. In the present studies, ES-D3 mouse embryonic stem cells were stained live and sorted for different phases of the cell cycle, followed by measurements of L1 message by quantitative PCR. L1 message was most abundant in the G1 phase of the cell cycle, coinciding with the stage where RB becomes inactivated by hyperphosphorylation. In separate experiments, isolates of mouse embryo fibroblast (MEFs) deficient for the RB family of proteins (TKO MEFs) were exposed to BaP for 12 hours and real time PCR used to quantify changes in the abundance of L1 transcripts. Compared to wild type counterparts, RB null cells dramatically overexpressed L1 in the presence of BaP. Cytochrome P450 genes involved in BaP metabolism also showed an enhanced inducibility in mutant cells, suggesting increased chromatin accessibility to transcription factors. Collectively, these data indicate that L1 is regulated in a cell-cycle dependent manner and that mutation or loss of RB proteins in humans in the face of environmental stress may contribute to the deregulation of L1 in somatic cells. Such deregulation may compromise differentiation programs and induce acquisition of neoplastic phenotypes.

**PS 543 DNA Methylation Patterns Represent "Environmental Footprints" of Transcription Factor Occupancy.**

D. Rojas<sup>1,2</sup>, K. Bailey<sup>2</sup>, A. Sanders<sup>2</sup>, L. Smeester<sup>2</sup>, B. Ahir<sup>2</sup>, J. E. Rager<sup>2</sup>, Z. Drobná<sup>3</sup> and R. C. Fry<sup>1,2</sup>. <sup>1</sup>*Curriculum in Toxicology, UNC School of Medicine, University of North Carolina at Chapel Hill, Chapel Hill, NC;* <sup>2</sup>*Department of Environmental Sciences and Engineering, UNC Gillings School of Global Public Health, University of North Carolina at Chapel Hill, Chapel Hill, NC;* <sup>3</sup>*Department of Nutrition, UNC Gillings School of Global Public Health, University of North Carolina at Chapel Hill, Chapel Hill, NC.*

Previous research has demonstrated that binding of transcription factors (TFs) to promoters can alter the DNA methylation patterns within these regions. While previous research was conducted in the context of stem cell differentiation, the impact of environmental toxicants on TF binding and subsequent effects on DNA methylation has not been examined. Our group recently identified genes in human leukocyte DNA and mouse livers that exhibit differential CpG island methylation following exposure to metals/metalloids including cadmium and arsenic. Among these genes, we have identified enrichment for transcription factor binding sites that we postulate represent "environmental footprints" of transcription factor occupancy. For example, we identified enrichment of the Metal-Responsive Transcription Factor-1 (MTF-1) binding site in the promoter regions of genes in which DNA methylation status of white blood cells was associated with cadmium or arsenic exposure in two different human populations. Based on these results, we hypothesize that in response to environmental stimuli, selective occupancy of DNA regions by transcription factors can alter the access of epigenetic modifiers to DNA, resulting in gene-specific DNA methylation patterns. To support our hypothesis, we utilized in vitro culture of human cells to study changes in genome-wide promoter DNA methylation patterns associated with specific changes in transcription factor binding induced by cadmium and arsenic. These results provide crucial information relating to the mechanism by which specific genes display toxicant induced patterns of DNA methylation.

**PS 544 Increased Growth Inhibition of Human Breast Cancer Cells by Co-Treatment with EGCG and 5-aza-2'-deoxycytidine Is Modulated through Epigenetic Mechanisms.**

T. Tyagi, J. Treas and K. P. Singh. *Environmental Toxicology, Texas Tech University, Lubbock, TX.*

Breast cancer is the leading cause of cancer deaths in women. Both genetic and epigenetic processes are implicated in breast carcinogenesis. Aberrations in DNA methylation pattern contribute to cancer development. Studies show that half of all the tumor suppressor genes are inactivated more often by epigenetic, rather than genetic mechanisms in all types of cancer. As epigenetic changes like DNA methylation are reversible, demethylating drugs, such as, 5-aza-2'-deoxycytidine (5-aza) are being clinically used as cancer chemotherapeutics. However, there are cytotoxic effects associated with high doses of these drugs. Alternative dietary compounds like EGCG, a green tea polyphenol are known to possess anticancer properties with minimal or no toxic effects on normal cells. EGCG is also reported to have DNA demethylation and histone modification activity. Therefore, the purpose of this study was to investigate the efficacy of co-treatment of EGCG and 5-aza, at low doses in inhibiting growth of MCF-7 breast cancer cells. MCF-7 cells were treated with either 5-aza, (5µM), EGCG (50µM, 100µM) or their combination. MTT assay showed that co-treatment significantly decreased cell viability as compared to

individual treatment. Both compounds arrest separate phases of cell cycle, but co-treatment eventually increased the percentage of growth arrested and apoptotic cells. Increased hypomethylation due to co-treatment was also observed in global genomic methylation analysis. Downregulation of DNMT1 expression was significantly greater in co-treatment than individually treated cells. These data suggest that co-treatment with EGCG and 5-aza, at low doses can synergistically reverse hypermethylation induced gene silencing and hence can be used for inhibition of breast cancer growth while minimizing cytotoxicity on normal cells.

**PS 545 Differential Expression of Long Intervening Noncoding RNAs in the Livers of Female B6C3F1 Mice Exposed to the Carcinogen Furan.**

L. Recio<sup>1</sup>, S. Phillips<sup>1</sup>, T. Maynor<sup>1</sup>, M. D. Waters<sup>1</sup>, F. Jackson<sup>2,3</sup> and C. Yauk<sup>2</sup>. <sup>1</sup>ILS, Research Triangle Park, NC; <sup>2</sup>Environmental Health Science and Research Bureau, Healthy Environments and Consumer Safety Branch, Health Canada, Ottawa, ON, Canada; <sup>3</sup>Department of Biology, Carleton University, Ottawa, ON, Canada.

The mammalian genome is transcribed into mRNAs that code for protein as well as a broad spectrum of other noncoding (nc) RNA products. Long ncRNAs (lncRNA), defined as noncoding RNA species > 200 nucleotides long, are emerging as important epigenetic regulators of gene expression and are involved in a spectrum of biological processes of relevance to toxicology. We have conducted a gene expression profiling study in liver using female B6C3F1 mice exposed to the carcinogen furan at 0.0, 1.0, 2.0, 4.0, and 8.0 mg/kg for 3 weeks. LncRNAs showed a non-linear dose response with no lncRNAs differentially expressed at 1.0 or 2.0 mg/kg and two lncRNAs differentially expressed at 4.0 mg/kg furan. At 8.0 mg/kg furan, 13.3% (83/632) of the differentially expressed transcriptome was comprised of lncRNAs. Among the lncRNAs observed, a number showed transcriptional clustering with nearby protein coding genes. For example, in furan-exposed mouse liver there was increased expression of lncRNA-p21. LncRNA-p21 is an anti-sense transcript that is 15 kb downstream from Cdkn1a locus and is known to be induced by p53 in human cells. LncRNA-p21 appeared to be co-transcribed with the protein coding gene Cdkn1a in response to 8.0 mg/kg furan. These data suggest that lncRNAs are transcriptional targets of furan-induced cytotoxicity and cell proliferation. We hypothesize that lncRNAs have potential as epigenomic biomarkers of carcinogenic exposures and we are currently examining lncRNA expression in the liver of mice exposed to a number of other carcinogens.

**PS 546 ROS-Generation Leads to 5-Hydroxymethylcytosine Formation and DNA Demethylation.**

J. B. Coulter<sup>1,2</sup>, C. M. O'Driscoll<sup>1,2</sup> and J. P. Bressler<sup>1,2</sup>. <sup>1</sup>Environmental Health Sciences, Johns Hopkins University Bloomberg School of Public Health, Baltimore, MD; <sup>2</sup>Neurology, Hugo Moser Research Institute at Kennedy Krieger, Baltimore, MD.

DNA methylation is a chemical modification at the 5' position on cytosine residues involved in gene repression. Notably, DNA methylation plays a vital role in stem cell differentiation. A better understanding of the dynamic processes controlling methylation and demethylation is critical to identifying chemicals with potential to disrupt programming of the methylome and may uncover targets in diseases such as neurodegenerative disease and cancer. While enzymes which methylate cytosines neighboring guanines (CpG's) have been identified, no demethylase has been discovered in mammalian cells. Inhibition of DNA methyltransferases leads to demethylation, though these mechanisms depend on cell division and may not explain active demethylation in post-mitotic cells such as neurons. Recent work has uncovered the role of Tet proteins in converting 5-methylcytosine to 5-hydroxymethylcytosine (5-hmC). Subsequent deamination by cytidine deaminases followed by base excision repair results in unmethylated cytosine. Here, we show that sub-lethal exposures of the benzene metabolite hydroquinone (HQ) led to formation of 5-hmC in HEK293 cells and a human neural progenitor cell line. In HEK293 cells, HQ exposure led to increases in reactive oxygen species (ROS), reactivation of a methylation-silenced reporter plasmid, and demethylation of CpG's within its promoter. Both 5-hmC formation and plasmid reactivation were inhibited by the antioxidants  $\alpha$ -tocopherol and N-acetyl-L-cysteine, indicating ROS formation was involved. Moreover, reactivation of the silenced plasmid by HQ was enhanced in cells overexpressing cytidine deaminase APOBEC2. These effects were observed with no detectable changes in Tet gene expression, though activity may have changed. Our data indicate toxicant-induced ROS leads to CpG demethylation in a manner consistent with oxidation-deamination mechanisms catalyzed by Tet proteins and suggest a link between cellular redox status and maintenance of the epigenome.

**PS 547 A Critical Review of Epigenetic Transgenerational Inheritance following Environmental Exposures.**

J. Heilman, E. Freeman and B. Polakoff. *Exponent, Inc, Washington DC.*

Epigenetic transgenerational effects are phenotypic traits passed down from generation to generation via heritable modifications in the epigenetic landscape. There are several accounts in the literature investigating the effects of environmental factors on the transgenerational inheritance of purportedly epigenetic traits. Epigenetic transgenerational effects have been suggested through animal models to lead to such conditions as polycystic ovarian disease, prostate disease phenotype, abnormal sperm parameters, altered discrete brain nuclei, fetal abnormalities, increased tumor frequency, altered immune function, and indications of kidney disease. Certain compounds have received particular attention with respect to transgenerational epigenetic changes, with some publications claiming to demonstrate transgenerational epigenetic effects and others refuting the existence of these effects. Recently, increasingly more diverse compounds have been tested for the ability to induce transgenerational epigenetic changes either alone or in mixtures, including pesticides, plastics components, and hydrocarbons. Although many publications claim to demonstrate clear evidence of transgenerational epigenetic effects, an equally clear mechanism explaining how the effect is conveyed is often lacking. Additionally, it remains to be explained how any particular chemical, that is not, for example, a methyl donor, could impact such a diverse collection of phenotypic outcomes. While the possibility of epigenetic transgenerational inheritance is not questioned, it is suggested that a clear or strong mechanistic link has not been established between many of the compounds purported to effect epigenetic transgenerational inheritance, and the subsequently observed phenotypes. A critical analysis of a selection of the evidence assessing epigenetic transgenerational inheritance following exposure to environmental agents and chemicals will be presented with particular focus on mechanisms of epigenetic inheritance, discrepancies in the literature, study quality, reproducibility and transparency.

**PS 548 Effect of Increased Reactive Oxygen Species on microRNA Expression in First Trimester Placental Trophoblasts.**

C. E. Cross, C. M. Rondelli, M. Xu and S. Z. Abdel-Rahman. *Obstetrics & Gynecology, UTMB, Galveston, TX.*

In early pregnancy, the conceptus is highly sensitive to reactive oxygen species (ROS). Expression of superoxide dismutase, catalase, glutathione peroxidase and high levels of glutathione, taurine, and vitamins A and D protect the conceptus by 5 weeks. During implantation, maternal spiral artery remodeling and trophoblast invasion serves as the beginning of placental development and would result in increased protection of the fetus to normal ROS signaling. However, improper invasion and remodeling can result in disease development. Although debated, the current proposed model for preeclampsia, which manifest as abnormally high blood pressure (>140/80) after 20 weeks gestation in a previously normotensive woman, is aberrant maternal spiral artery remodeling, subsequent altered angiogenesis and localized ischemia/reperfusion due to continued muscularization of the spiral arteries. Preeclampsia is associated with low birth weight, preterm labor, small gestational age, and intrauterine growth restriction as well as altered gene expression in the placenta as a result of increased ROS production. Epidemiological screening studies for preeclampsia indicate alterations in placental microRNA (miRNA) expression as a result of increased trophoblast apoptosis. The goal of this project is to determine the effect of increased ROS during early placental development on miRNA expression to better understand the time frame of gene expression alteration. The villous 3A first trimester cell line was exposed to varying concentrations of H<sub>2</sub>O<sub>2</sub> over 24 hours to determine the amount of intracellular ROS generated from this model. Using an optimal exposure of 50  $\mu$ M, we then determined the effect of increased ROS exposure on the expression of 1008 miRNAs using the human miRNome PCR array (Qiagen). The miRNAs shown to be altered from increased ROS production are being selected for pathway analysis and further study using miRNA mimics and inhibitors (Supported by T32-07454; P30-006676).

**PS 549 Identification of Mode-of-Action Specific Toxicity Transcript Profiles In Vitro Using a Connectivity Mapping Approach.**

J. M. Naciff<sup>1</sup>, N. DeAbrew<sup>1</sup>, G. Overmann<sup>1</sup>, R. Adams<sup>1</sup>, G. Carr<sup>1</sup>, R. Settivari<sup>2</sup>, J. Tiesman<sup>1</sup>, C. Edward<sup>2</sup> and G. Daston<sup>1</sup>. <sup>1</sup>Procter & Gamble, Cincinnati, OH; <sup>2</sup>Dow Chemical Company, Midland, MI.

We hypothesize that it is possible to predict toxicity by assessing changes in gene expression in a small number of cell types enriched in toxicologically relevant pathways. We have evaluated the transcriptional profile elicited by 34 chemicals in HepG2, Ishikawa and MCF7 cells, using microarrays (U219, Affymetrix). These chemicals act via a number of modes of toxicity and do not involve direct chemical

reactivity, as this can be adequately detected by a number of simple in vitro methods. Each of the 34 chemicals was tested at 3 doses and at 3 different time points; however, data presented here are for only one dose and one time point (6h). The relatedness of each transcript profile to each other was analyzed using the cMAP platform (Broad Institute). The results indicate that not all cell lines responded to all chemicals. For example the response of the Ishikawa cells to methotrexate is minimal (16 genes significantly affected), while the MCF7 and HepG2 cells have a robust response to this chemical (>3000 genes significantly affected). A comparison of responses to chemicals that share similar modes of action (MOA) exhibited very high correlation, even among different cell lines. These correlations held true for both agonists (cMAP score  $\leq 1$ ) and antagonists (score  $\leq -1$ ) and extended to MOAs mediated through receptors (AR, ER, FX, PR, etc.) and enzyme inhibition (histone deacetylase, DHFR, etc.). For example, using the signature from valproic acid (VA) treated cells to query the cMAP database yield high positive connectivity scores for VA in all three cell lines tested, as well as with other HDAC inhibitors (vorinostat, trichostatin, bufexama, depudecin and HC toxin), regardless of cell lines or concentrations. The transcript profile elicited by chemicals with various MOAs in selected cell types, coupled with a cMAP approach for the analysis of the response, offers relevant biological data to predict biological activity and MOA, and thus toxicity, in a defined in vitro system.

## PS 550 Analysis of Longitudinal Metabolomic Data from Endocrine Disruption Studies: The A-SCA Method.

C. Canler<sup>1,2</sup>, M. Tremblay-Franco<sup>1,2</sup>, N. J. Cabaton<sup>1,2</sup>, R. Gautier<sup>1,2</sup>, L. Debrauwer<sup>1,2</sup>, A. M. Soto<sup>3</sup> and D. Zalko<sup>1,2</sup>. <sup>1</sup>INRA, UMR 1331 TOXALIM Research Center in Food Toxicology, Toulouse, France; <sup>2</sup>Université de Toulouse, INP, UMR1331, TOXALIM, F-31000, Toulouse, France; <sup>3</sup>Department of Anatomy and Cellular Biology, Tufts University School of Medicine, Boston, MA.

Metabolomics are increasingly being used in the field of toxicology. Experimental designs involving the study of dynamic changes in the metabolome raise new methodological challenges in the field of data analysis, regarding long term and perinatal in vivo studies. Multivariate analysis of variance (MANOVA), often used to analyze experimental data, is not always appropriate for metabolomics, especially when sample size is much smaller than the total number of variables, which prevents the testing of underlying hypotheses (normality, homoscedasticity). Multivariate methods, such as Principal Component Analysis (PCA) or Partial Least Squares-Discriminant Analysis (PLS-DA), often used to analyze metabolomic data, do not take into account data's temporal structure, resulting in a loss of information when used alone. In this study, we applied a method combining ANOVA and PCA: A-SCA (Anova-Simultaneous Component Analysis; SCA is a generalization of PCA) taking into account the experimental design, as well as the relationship between variables, to allow data modelisation. Data were first separated into blocks corresponding to the different sources of variation (experimental design factors). Then SCA was independently applied on each block, and permutations test was used to evaluate the significance of model parameters. This method was applied to the study of the effects of low doses of bisphenol A (BPA) on global metabolism in SD rats exposed in the perinatal period, (NIEHS project #5RC2ES018822). Pregnant rats were exposed to DMSO (vehicle-control), 0.25, 2.5, 25 or 250 ng BPA/kg BW/day. Serum samples of the F1 generation were collected on days 21, 50, 90, 140 and 200 of the experiment, and submitted to 1H NMR spectroscopy. Using the A-SCA method, time effects were demonstrated.

## PS 551 A Systems Chemical Biology Approach to Predict Effects from Chemical Cocktail Exposure.

K. Kongsbak<sup>1,2</sup>, N. Hadrup<sup>1</sup>, A. Vinggaard<sup>1</sup> and K. Audouze<sup>2</sup>. <sup>1</sup>National Food Institute, Technical University of Denmark, Søborg, Denmark; <sup>2</sup>Center for Biological Sequence Analysis, Department of Systems Biology, Technical University of Denmark, Kgs. Lyngby, Denmark.

Purpose: In its report, Toxicity Testing in the 21st Century, the National Research Council called for the development of new approaches to human health risk assessment that would rely, in part, on computer-based models rather than animal testing and epidemiology (National Research Council 2007).

Using a systems chemical biology approach, we have studied the five commonly used pesticides epoxiconazole, mancozeb, prochloraz, procymidone, and tebuconazole that are all known to have effects on male reproductive development. The purpose of this study was to apply a method previously described by Audouze and Grandjean (Audouze & Grandjean, 2011) to generate hypotheses on the mechanisms linking relevant human outcomes to specific compounds.

Methods: An integrative systems biology approach was adapted to investigate similar or shared modes of action for the chemicals in the mixture of the five pesticides. Human chemical-protein/gene associations were collected from the databases ChemProt, STITCH, and CTD. These associations were then enriched using

known protein-protein interactions (PPIs) to yield associations between the chemicals and PPI networks. Subsequently, data integration was performed using in-house tools to extrapolate data to human diseases and pathways affected by the selected chemicals.

Results: The applied method on these chemicals is capable of identifying known effects on male reproductivity and of predicting novel effects on human health.

With the successful identification of known effects, a thorough data analysis is likely to help the linkage between the investigated compounds and their potential effects on other aspects of human health.

Perspectives: As the systems chemical biology approach relies on existing data it serves as an important tool in the efforts to apply alternative methods to animal testing. Furthermore, the method integrates data from many sources, which allows for unraveling of previously unidentified pathways of toxicity.

## PS 552 Modeling Species-Specific Metabolic Responses to TCDD in Mice and Rats Using a Reconstructed Metabolic Network.

R. Nault<sup>1,4</sup>, M. Wu<sup>3</sup>, C. Chan<sup>2,3,4</sup> and T. R. Zacharewski<sup>1,4</sup>. <sup>1</sup>Center for Integrative Toxicology, MSU, East Lansing, MI; <sup>2</sup>Chemical Engineering & Material Science, MSU, East Lansing, MI; <sup>3</sup>Computer Science & Engineering, MSU, East Lansing, MI; <sup>4</sup>Biochemistry & Molecular Biology, Michigan State University, East Lansing, MI.

2,3,7,8-tetrachlorodibenzo-*p*-dioxin (TCDD) elicits species-specific transcriptomic and metabolomics responses. Using a reconstructed metabolic network and published microarray datasets, we examined the ability of the network to predict hepatic metabolomic responses based on TCDD-elicited differential gene expression profiles. Previously published temporal whole-genome microarray datasets (2-168h) for TCDD-treated female C57BL/6 mice (30 µg/kg) and female Sprague-Dawley rats (10 µg/kg) were used. Context-specific metabolic networks were generated using the Gene Inactivity Moderated by Metabolism and Expression (GIMME) method by including induced genes (fold change  $\geq 1.5$ , P1(t)  $\geq 0.99$ ) and reactions necessary to maintain a steady-state flux. The mouse context-specific metabolic network revealed more reactions involved in fatty acid (FA) activation and triglyceride synthesis suggesting an increased flux towards lipid synthesis relative to the rat. Meanwhile, mice had fewer reactions involved in FA oxidation, carnitine shuttling, and glycerophospholipid metabolism suggesting FA catabolism is induced in rats exposed to TCDD. Moreover, the predicted induction of glycerophospholipid metabolism is consistent with reported changes in phosphoethanolamine in mice, and phosphocholine and phosphatidylserine in rats. In summary, we show that context-specific metabolic networks based on transcriptomic data are consistent with observed species-specific metabolomic changes elicited by TCDD including hepatic lipid accumulation observed in mice and species-specific glycerophospholipid metabolism effects. Moreover, the reconstructed metabolic network facilitated differential gene expression interpretation by providing valuable insights into the species-specific disruption of metabolic responses. Funded by SRP P42ES04911.

## PS 553 Multiscale Modeling for Individualized Spatiotemporal Prediction of Drug Effects.

J. G. Diaz Ochoa, J. Bucher, J. Niklas and K. Mauch. *InSilico Biotechnology AG, Stuttgart, Germany*. Sponsor: C. Yang.

Recently, in silico models for biokinetics have become a relevant way to test the distribution and metabolism of substances in single cells and in organisms. Its relevance is accentuated by the fact that in the next future an animal free toxicity assessment must be implemented in the European Union. Inside the COSMOS project (HEALTH-F5-2010-266835), which is funded by the European Union and a consortium of cosmetic industries (Cosmetics Europe), the central aim is to develop computational methods and in silico models for the prediction of long term toxicity upon repeated exposure to compounds. The power of such methods is (i) to derive quantitative predictions and (ii) to extrapolate results from in vitro measurements into in vivo predictions.

In this contribution, we present a case study that addresses acetaminophen induced hepatotoxicity. Based on a metabolic network model assigned to individual cells, which includes transport, drug metabolism, and intracellular mechanisms leading to toxicity, we were able to predict the metabolism of acetaminophen and production of toxic substances in the liver lobules in different time periods. Depending on the accumulation of these substances, the cell integrity in the liver was estimated. Such estimation is relevant not only for the prediction of physical changes in the organ but also for the prediction of changes in the clearance of the liver under high or repeated drug dosage. Our model also predicted variations of drug toxicity depending on alterations in metabolic enzyme activities. Variations in enzyme activities reflect genetic characteristics or diseases of individuals, thus allowing stratified or even personalized predictions of drug toxicity as well as drug efficacy.

**PS 554 Toxicogenomic Analysis of Environmental PAH Mixtures in a Model of Transplacental Carcinogenesis.**

S. C. Tilton<sup>1</sup>, L. K. Siddens<sup>2</sup>, A. J. Larkin<sup>2</sup>, B. N. Do<sup>2</sup>, K. C. Dunn<sup>2</sup>, E. P. Maden<sup>2</sup>, S. K. Krueger<sup>2</sup>, K. M. Waters<sup>1</sup>, W. M. Baird<sup>2</sup> and D. E. Williams<sup>2</sup>. <sup>1</sup>Pacific Northwest National Laboratory, Richland, WA; <sup>2</sup>Oregon State University, Corvallis, OR.

Several polycyclic aromatic hydrocarbons (PAHs) are bioavailable to the fetus *in utero*, can generate DNA damage after transplacental exposure and result in increased incidence of carcinogenesis in offspring in an arylhydrocarbon (Ahr)-dependent manner. However, little is known about the effects of environmental PAH mixtures or mechanisms of carcinogenesis. Therefore, we utilized a mouse model of transplacental carcinogenesis to investigate the effect of PAH mixtures collected from environmental samples compared to the known carcinogen, dibenzo[def,p]chrysene (DBC). *Ahr*<sup>b-1/d</sup> (responsive) females were bred with *Ahr*<sup>d/d</sup> (non-responsive) male mice at eight weeks of age. Females were gavaged on gestation day 17 with DBC, an artificial atmospheric PAH mixture or PAH extract collected from Portland Harbor Superfund Site. Subsamples from each treatment (n=4) were euthanized 24 hrs post-treatment to collect fetal thymus, lung and liver for microarrays. At 3-6 months of age, 79% of the offspring from DBC-treated dams were euthanized due to severe T-cell lymphoma, as expected, which was not detected in the other treatment groups. Exposure of mice to both DBC and the artificial atmospheric mixture resulted in significant (p<0.05) increase in the overall incidence of lung nodules, 100% and 46%, respectively, in offspring at 10 months of age compared to controls. Global transcriptional analysis of fetal tissues 24 hrs post-treatment results in treatment-dependent, tissue-dependent and genotype-dependent gene signatures. A pathway-based approach was utilized to identify mechanisms of exposure and link gene signatures to tumor outcome. Network and transcription factor analysis of the gene clusters further resulted in identification of upstream regulators associated with PAH-induced carcinogenesis. These data describe potential mechanisms for DBC and PAH mixtures *in utero* that may be linked to downstream carcinogenesis in offspring. Supported by P42\_ES016465.

**PS 555 Functional Profiling to Reveal Toxicity Pathways.**

C. Vulpe<sup>1</sup>, W. Varsally<sup>3</sup>, R. Thomas<sup>2</sup>, I. Gerlovina<sup>2</sup>, B. Gaytan<sup>1</sup>, Y. De La Rosa<sup>1</sup>, M. North<sup>1</sup>, A. E. Hubbard<sup>2</sup>, P. Antczak<sup>3</sup> and F. Falciani<sup>3</sup>. <sup>1</sup>Nutritional Science and Toxicology, University of California Berkeley, Berkeley, CA; <sup>2</sup>Biostatistics, School of Public Health, University of California Berkeley, Berkeley, CA; <sup>3</sup>University of Liverpool, Liverpool, United Kingdom.

We contend that functionally conserved toxicity pathways underlie adverse cellular responses to toxicants. Therefore, we are using functional profiling in *Saccharomyces cerevisiae*, to identify the pathways involved in cellular toxicity. In this approach, the ~4500 viable deletion strains are pooled, grown for multiple generations in the presence of a toxicant, and sensitivity of each strain is individually quantified. If a deletion strain is significantly sensitive/resistant, then it provides evidence that the gene product absent in that strain plays a functional role in toxicity. We utilized this approach to identify key susceptibility genes to a wide variety of toxicants. We then applied reverse engineering to infer functional relationships between gene products and assemble functional networks. We used the network inference ARACNE algorithm (using a mutual information threshold of 0.35 (equating to a p-value of 10E-16) to infer a network containing 2604 nodes and 33593 edges representing functional linkage between non-essential genes. We identified key network modules enriched in different functional properties (e.g. mitochondrial function) that may represent common toxicity "hubs" and/or endpoints. We evaluated the relationship between these functional hubs and individual toxicants. We found enrichment of strains affected by individual toxicants in different hubs, perhaps indicative of the functional components associated with toxicity for each toxicant. We suggest that this functional approach in yeast and development of functional networks provides a unique insight into both the shared and unique molecular responses to toxicant exposure.

**PS 556 Prenatal Exposure to Transition Metals in Ambient PM2.5 Up-Regulates Nitrotyrosine in Human Cord Blood.**

C. Barros Veguilla<sup>1</sup>, J. Niu<sup>2</sup>, B. Yan<sup>2</sup>, N. Li<sup>2</sup>, Q. Qu<sup>1</sup> and L. Chen<sup>1</sup>. <sup>1</sup>Nelson Institute of Environmental Medicine, New York University School of Medicine, Tuxedo, NY; <sup>2</sup>School of Public Health, Lanzhou University, Lanzhou, China.

Objective: Our previous study indicated that the ambient levels of nickel (Ni), copper (Cu), arsenic (As), and selenium (Se) in Jinchang were 76, 25, 17, and 7 fold higher than Zhangye, respectively. This pilot study was conducted in both cities to

assess potential adverse effects of prenatal exposures to these high levels of pollutants on the fetus. Methods: A total of 60 healthy nonsmoking pregnant women were recruited in Jinchang and Zhangye for collection of paired maternal and cord blood samples. ICP-MS was used to measure the concentrations of Ni, Cu, As, Se, and Co in blood samples. ELISA kits were used to measure human C-reactive protein (CRP), interleukin 6 (IL-6), nitrotyrosine, and cotinine. Results: All metals measured were elevated in both maternal and cord blood collected from Jinchang as compared to those from Zhangye, while significant differences were only detected for As, Co, and Se. In addition, Ni and As in cord blood were significantly higher than those in maternal blood with cord/maternal ratios of 1.56 ± 0.13 and 1.41 ± 0.25, respectively. Surprisingly, the levels of Cu in cord blood were significantly lower than paired maternal blood (cord/maternal ratios of 0.41 ± 0.04). The cord blood level of nitrotyrosine in Jinchang was significantly higher than that in Zhangye (p<0.0001). The other inflammatory biomarkers were not significantly different between these two groups. In contrast, CRP in maternal blood was 9 fold higher than cord blood (p<0.0001). The levels of IL-6 and nitrotyrosine were higher in cord blood compared with maternal blood although the differences were not statistically significant. Conclusion: The results suggest that the blood-placenta barrier may effectively prevent transportation of Cu from mother to fetus. On the other hand, Ni and As may easily penetrate placenta barrier and accumulated in cord blood, which may be responsible for the up-regulation of nitrotyrosine.

**PS 557 A Global Genomic Screening Strategy Reveals Genetic and Chemical Activators of Peroxisome Proliferator-Activated Receptor Alpha (PPARalpha).**

C. Corton<sup>1</sup>, N. Vasani<sup>1</sup>, M. B. Rosen<sup>1</sup>, B. D. Abbott<sup>1</sup>, C. Lau<sup>1</sup>, W. Ward<sup>1</sup>, R. S. Thomas<sup>2</sup>, D. Applegate<sup>3</sup> and K. Oshida<sup>1</sup>. <sup>1</sup>US EPA, Research Triangle Park, NC; <sup>2</sup>The Hammer Institutes for Health Sciences, Research Triangle Park, NC; <sup>3</sup>Regenomed, San Diego, CA.

A comprehensive survey of chemical, diet and genetic perturbations that activate PPARalpha in the mouse liver has not been carried out but would be useful to identify factors that may contribute to PPARalpha-dependent liver tumors. A gene signature dependent on PPARalpha activation was identified by comparing the transcript profiles after exposure to three PPARalpha activators (Wy-14,643, fenofibrate, perfluorooctanoic acid) in wild-type and PPARalpha-null mice. In independent experiments using transcript profiles from the livers of chemically-exposed male or female mice, the signature correctly predicted activation by 2 known PPARalpha activators but not 10 activators of other pathways. Individual genes in the signature (i.e., Cyp4a10, Pdk4) were used in RT-PCR experiments to show the specificity of the response to PPARalpha activators compared to chemical-induced activation of other xenobiotic-activated transcription factors. The signature was used with standard classification methods to identify perturbations in which PPARalpha was activated in an Affymetrix compendium of ~750 mouse liver transcript comparisons encompassing a broad range of chemical, dietary and genetic perturbations. We found that PPARalpha is activated by a number of novel chemicals, dietary regimens and genetic mutations. Specific findings include activation by 1) chemicals that cause steatosis (e.g., TCDD, BaP), 2) dietary regimens of triglycerides, "fast food" and "cafeteria" diets, and fish oil, and 3) nullizygous mutations in a number of genes (Mfp2, Erc1, Por, Hnf1a, Fah/p21, Udf2, Hif1a, Hif2a) that could be secondary to steatosis. The findings increase our understanding of the factors that impact PPARalpha activation and that could contribute to increases in PPARalpha-dependent liver tumors. (This abstract does not represent EPA policy.)

**PS 558 Proteomic Analysis of Biological Responses from Exposures to Chemical Mixtures.**

M. E. Bruno<sup>1</sup>, W. Winnik<sup>2</sup>, A. Swank<sup>2</sup>, K. Wallace<sup>1</sup>, S. Leavitt<sup>1</sup> and Y. Ge<sup>1</sup>. <sup>1</sup>ISTD, US EPA, Research Triangle Park, NC, NC; <sup>2</sup>US EPA, Research Triangle Park, NC. Sponsor: K. Kitchin.

Nickel (Ni), cadmium (Cd) and chromium (Cr) are human lung carcinogens but the key events leading to their toxic effects are not fully elucidated. In addition, little is known about the molecular basis and the underlying toxic mechanisms of co-exposure of these carcinogenic metals which are frequently observed in environmental exposures. In this study, we investigated the biological responses and effects of the exposures of three metals, individually and in combinations, in BEAS-2B human lung epithelial cells. Utilizing two dimensional gel electrophoresis and mass spectrometry, we identified 455 differentially expressed proteins in BEAS-2B cells exposed to the metals and their mixtures at different doses. The identified protein changes were validated using Western blot and protein functional assays. These altered proteins were mapped to protein interaction networks, toxicity lists, and

canonical pathways using Ingenuity Pathway Analysis. The number of pathways affected in cells exposed to single metals or metal mixtures were: Ni (4 up and 5 down), Cd (1 up and 7 down), Cr (6 up and 0 down), Cd-Cr binary (12 up and 9 down) and Cd-Cr-Ni ternary (11 up and 5 down). The proteins and pathways that were unique or common to the specific metals and their mixtures were also identified. For instance, ubiquitin conjugated enzyme E2 protein was present only in mixtures. At the pathway level, Rho A signaling was changed only in mixtures. Specific effects of a metal in a binary mixture was also ascertained. Exposure to Cr (1.8  $\mu\text{m}$ ) resulted in upregulation of the protein ubiquitination pathway. In contrast, coexposure to a Cd (7.5  $\mu\text{M}$ ) and Cr (1.8 $\mu\text{m}$ ) binary mixture had the opposite effect on this pathway. In summary, this study enabled us to (1) distinguish single metals from metal mixtures at both the protein and pathway level and (2) determine the contribution of a metal in a metal mixture.

This abstract does not necessarily reflect EPA policy

**PS 559 Environmentally Relevant Concentrations of the Flame Retardant BDE-209 in Sediment Linked to Potential Developmental and Neurotoxic Effects on Zebrafish Embryos.**

N. G. Reyero Vinas<sup>1</sup>, L. Escalon<sup>2</sup>, E. Prats<sup>3</sup>, J. Stanley<sup>2</sup>, B. Thienpot<sup>3</sup>, N. Melby<sup>2</sup>, P. Babin<sup>4</sup>, E. J. Perkins<sup>2</sup> and D. Raldua<sup>3</sup>. <sup>1</sup>Mississippi State University, Vicksburg, MS; <sup>2</sup>US Army, Vicksburg, MS; <sup>3</sup>CSIC, Barcelona, Spain; <sup>4</sup>University of Bordeaux, Bordeaux, France.

Decabromodiphenyl ether (BDE-209) is a fully brominated diphenyl ether compound used as a flame retardant in polystyrene applications such as casings for computers, upholstery textile and televisions. It is highly lipophilic and persistent and as such it is prone to bioaccumulation and biomagnifications in the food chain. Increasing concentrations of polybrominated diphenyl ethers in wildlife have been documented since the mid 1990s. BDE-209 is a very large molecule, and the general thought was that due to its size it was not bioavailable, and therefore could not bioaccumulate in wildlife. Several studies now have proven this concept wrong, as BDE-209 has been found in many aquatic and terrestrial organisms. Exposure to BDE-209 has been linked to decreased learning and memory in mice, behavioral changes in mice and inhibition of neural stem cells into neurons in culture. As many of the toxic effects of BDE-209 have been found on laboratory exposures, here we analyze the potential effects of an environmentally relevant dose of BDE-209 on zebrafish (*Danio rerio*) embryo. Zebrafish embryos were exposed to sediments that contained 12,500  $\mu\text{g/kg}$  BDE-209 for eight days. We analyzed gene expression changes, thyroid function, and morphometric parameters. Gene expression analysis highlighted the potential effects of BDE-209 on development, neurotoxicity, and liver toxicity. We then analyzed the effects of BDE-209 on zebrafish behavior. BDE-209 affected zebrafish response to light as well as movement. Our results show that environmentally relevant doses of BDE-209 are not only bioavailable but can have adverse effects on organisms.

**PS 560 The Induction of Oxidative Stress by Mixtures of Dichloroacetate and Trichloroacetate in the Livers of Mice after Subchronic Exposure.**

E. Hassoun and J. Cearfoss. *Pharmacology, University of Toledo, Toledo, OH.*

Dichloroacetate (DCA) and trichloroacetate (TCA) are drinking water chlorination byproducts and were previously found to induce oxidative stress (OS) in the hepatic tissues of B6C3F1 male mice after subacute and subchronic exposures. In order to determine the effects of mixtures of DCA and TCA on OS induction in the hepatic tissues, groups of male B6C3F1 mice were treated daily, by gavage, with 3 different mixtures (Mix I, Mix II and Mix III) of the compounds for 13 weeks. The concentrations of the compounds in Mix I, II and III, respectively corresponded to those producing approximately 15%, 25% and 35% of maximal induction of OS by the individual compounds in the subchronic studies. The mice were euthanized at the end of the treatment period and livers were assayed for the biomarkers of OS that included production of superoxide anion, lipid peroxidation and DNA single strand breaks. While the effects on all of the biomarkers in response to Mix. I and II were additive, they were greater than additive in response to Mix III. The induction of OS in the livers of B6C3F1 mice after long term exposure to DCA and TCA was previously suggested as an important mechanism in the long term hepatotoxicity/hepatocarcinogenicity of the compounds, hence exposure to mixtures of the two compounds are expected to significantly increase the risk of exposure to the individual compounds. (Supported by NIH/NIEHS grant # R15ES013706-01A2)

**PS 561 Ultrafine Particles Are Not Major Carriers of Carcinogenic PAHs and Their Genotoxicity in Size-Segregated Aerosols.**

J. Topinka<sup>1</sup>, A. Milcova<sup>1</sup>, J. Schmuczerova<sup>1</sup>, J. Krouzek<sup>2</sup> and J. Hovorka<sup>2</sup>. <sup>1</sup>Genetic Ecotoxicology, Institute of Experimental Medicine AS CR, Prague, Czech Republic; <sup>2</sup>Institute for Environmental Studies, Faculty of Science, Charles University in Prague, Prague, Czech Republic.

Some studies suggest that genotoxic effects of the combustion related aerosol are induced by carcinogenic polycyclic aromatic hydrocarbons (c-PAHs) and their derivatives forming organic fraction of the ambient air particulate matter (PM). The proportion of the organic fraction in PM is known to vary with particle size. The ultrafine fraction is hypothesized to be the most important carrier of c-PAHs, since it possesses the highest specific surface area of PM. To test this hypothesis, the distribution of c-PAHs in the organic extracts (EOMs) was compared from 4 size fractions of ambient-air aerosols: coarse ( $1 < d_{ae} < 10 \mu\text{m}$ ), upper ( $0.5 < d_{ae} < 1 \mu\text{m}$ ), and lower ( $0.17 < d_{ae} < 0.5 \mu\text{m}$ ) accumulation, and ultrafine ( $d_{ae} < 0.17 \mu\text{m}$ ). High-volume aerosol samples were collected consecutively in 4 localities differing in the extent of environmental pollution. The genotoxicity of EOMs was measured by the analysis of DNA adducts induced in the acellular assay consisting of calf thymus DNA with/without rat liver microsomal S9 fraction coupled with <sup>32</sup>P-postlabelling. The upper accumulation fraction was the major size fraction in all 4 localities forming 37-46 % of the total PM mass. As per  $\text{m}^3$  of sampled air, this fraction also binds the highest amount of c-PAHs. Correspondingly, the upper accumulation fraction induced highest DNA adduct levels. As per PM mass itself, the lower accumulation fraction is seen to be the most efficient at binding DNA-reactive organic compounds. Interestingly, the results suggest that the fraction of ultrafine particles of various ambient air samples is neither a major carrier of c-PAHs nor a major inducer of their genotoxicity, which is an important finding for the extensively discussed toxicity and health effects of ultrafine particles. Support: Grant Agency of the Czech Republic (CZ: P503/12/G147).

**PS 562 Acute, Five- and Ten-Day Inhalation Study of Hydroprocessed Esters and Fatty Acids-Mixed Fats (HEFA-F) Jet Fuel.**

D. R. Mattie<sup>1</sup>, A. L. Carter<sup>1</sup>, P. Eden<sup>1</sup>, J. Z. Hezel<sup>1</sup>, T. R. Sterner<sup>2</sup>, D. A. Dodd<sup>3</sup>, G. A. Wilson<sup>4</sup>, K. L. Mumy<sup>5</sup> and B. A. Wong<sup>5</sup>. <sup>1</sup>711 HPW/RHDJ, Wright-Patterson AFB, OH; <sup>2</sup>HJF, Wright-Patterson AFB, OH; <sup>3</sup>The Hammer Institutes for Health Sciences, Research Triangle Park, NC; <sup>4</sup>EPL, Research Triangle Park, NC; <sup>5</sup>NAMRU-D, Wright-Patterson AFB, OH.

The U.S. Air Force is pursuing development of alternative fuels to augment or replace JP-8 jet fuel. Hydroprocessed Esters and Fatty Acids from Mixed Fats (HEFA-F) jet fuel was administered as an aerosol and vapor mixture to 5 male and 5 female Fischer-344 rats per group. Inhalation exposures lasted 6 hours per day for 1 day (with and without an 11-day recovery period), 5 days or 10 days (5 days per week for 2 weeks). Concentrations for each exposure were 0, 200, 700 and 2000  $\text{mg/m}^3$ ; mean aerosol percents were 0, 7, 22 and 28%, respectively. There were no significant changes in male or female body weights due to HEFA-F exposure at any time point. Food and water consumption, urinalysis, clinical pathology, lung cytokine/chemokine and blood cytokines were measured at 10 days. Decreased mean food consumption in male rats was significant at 2000  $\text{mg/m}^3$ . A 10% decrease in mean water consumption was observed in all HEFA-F exposed female rats. Urinalysis changes included a slight decrease in pH in all exposed rats, as well as a small elevation in ketones and the presence of leukocytes and hemoglobin in the 2000  $\text{mg/m}^3$  males. There were no changes in standard clinical chemistry or hematology parameters. Caudal lung tissue was analyzed for cytokines, chemokines and receptors using a PCR array for rat inflammatory cytokines and receptors kit; no significant changes were seen. Proinflammatory blood cytokines showed no significant differences, although a trend for increasing MCP-1 with increasing dose was seen. Male kidney weight increases were likely related to hyaline droplet formation, relevant only to male rats. Nasal cavity changes included olfactory epithelial degeneration at 2000  $\text{mg/m}^3$ . Alveolus inflammation was seen in the 2 higher doses at 10 days. To examine sensory irritation, male Swiss-Webster mice were exposed nose-only to 2000  $\text{mg/m}^3$  HEFA-F for 30 minutes, resulting in 23% respiratory depression.

**PS 563 Global Gene Expression Changes Induced by Organic Extracts of Air Pollutants in Human Lung Cells.**

H. Libalova<sup>1</sup>, K. Uhlirova<sup>1</sup>, J. Klema<sup>2</sup>, M. Machala<sup>3</sup>, M. Ciganek<sup>3</sup>, J. Topinka<sup>1</sup> and R. J. Sram<sup>1</sup>. <sup>1</sup>*Institute of Experimental Medicine AS CR, Prague, Czech Republic*; <sup>2</sup>*Czech Technical University, Prague, Czech Republic*; <sup>3</sup>*Veterinary Research Institute, Brno, Czech Republic*.

Many adverse effects of the ambient air pollution have been linked to polycyclic aromatic hydrocarbons (PAHs) occurring in the complex mixture adsorbed onto airborne particles. Besides their genotoxic effect, some of them are known to act via aryl hydrocarbon receptor (AhR)-mediated nongenotoxic and tumor promoting mechanism. This study employed human lung adenocarcinoma cells (A549) to investigate the effect of complex mixture of the air pollutants on the global gene expression changes. We determined whole-genome gene expression profiles (Illumina platform) of cells treated with organic extracts (EOMs) from particulate matter (<2.5 µm) collected in four localities in the Czech Republic differing in the level of the air pollution. Simultaneously, detailed chemical analysis of EOMs from each locality was performed. Despite various sources, EOMs exhibited equal qualitative composition although the absolute level of PAHs and other pollutants in the most polluted locality was much higher comparing to other localities. Gene expression profiles of cells treated with equal amounts of EOM from each locality showed similar patterns. No significant diversity among localities was found. Goeman's global test and KEGG pathway database were applied to identify the most deregulated pathways and contributing genes. We observed significantly deregulated processes and genes common for all localities including metabolism of amino acids such as glycine, serine and threonine (SHMT2, PSAT1), xenobiotic metabolism (CYP1B1, ALDH3A1), vitamin B6 metabolism (PDXK), TGF-beta signaling (SMAD3), immune system and infectious diseases (IL8, PTGS2) or cell cycle (E2F2, CCND3). It has been proposed that most of them are modulated by activated Ah-receptor. Our results suggest the prominent role of activated Ah-receptor and other events possibly leading to the metabolic reprogramming and tumor promotion in A549 cells. Support: Grant Agency of the Czech Republic (CZ:P503/11/0142).

**PS 564 Evaluation of Additivity of Binary Mixtures of Perfluoroalkyl Acids (PFAAs) on Peroxisome Proliferator-Activated Receptor-Alpha (PPARα) Activation *In Vitro*.**

C. J. Wolf<sup>1</sup>, C. Rider<sup>2</sup>, C. Lau<sup>1</sup> and B. D. Abbott<sup>1</sup>. <sup>1</sup>*Toxicity Assessment Division, US EPA, ORD, NHEERL, Research Triangle Park, NC*; <sup>2</sup>*National Toxicology Program, NIEHS, Research Triangle Park, NC*.

Perfluoroalkyl acids (PFAAs) are found globally in the environment and in animal tissues, and are present as mixtures of PFAA congeners. Mechanistic studies have found that *in vivo* effects of PFAAs are mediated by PPARα. Our previous studies showed that individual PFAAs activate PPARα transfected into COS-1 cells. Here we evaluated whether binary combinations of perfluorooctanoic acid (PFOA, C8) and other PFAAs interact in an additive fashion to activate PPARα. COS-1 cells in 96 well plates were transiently transfected with mouse PPARα luciferase reporter plasmid. After 24 hours, cells were exposed to either vehicle control (0.1 % DMSO or water), PPARα agonist (WY14643, 10 µM), C8 or perfluorononanoic acid (C9) at 1 - 128 µM, perfluorohexanoic acid (C6) at 8 - 1024 µM, or perfluorooctane sulfonate (C8S) at 4 - 384 µM to generate sigmoidal dose-response curves. In addition, cells in the same plate were exposed to binary combinations of C8 + either C6, C9, or C8S, in an 8x8 factorial design. After 24 hours of exposure, cells were lysed and luciferase activity was measured. Data were transformed on a fold-induction and % maximal response basis. The dose-response data for individual chemicals were fit to sigmoidal curves and analyzed with nonlinear regression to generate EC50s and Hill slopes, which were used in response-addition and dose-addition models to calculate predicted responses for mixtures. All PFOA+PFAA combinations produced dose-response curves that were closely aligned with the predicted curves for both response addition and dose addition. However, at higher concentrations of all chemicals, the observed response curves deviated upward from the predicted models of additivity, although with more variability. We conclude that at the lower concentration ranges, binary combinations of PFAAs behave additively in activating PPARα in the COS-1 cell system. This abstract does not necessarily reflect USEPA policy.

**PS 565 Reference Dose (RfD)-Based Chronic Human Health Hazard Ranking System for Complex Mixtures—Assessment of Polar Nonhydrocarbons in Groundwater at Biodegrading Petroleum Sites.**

A. K. Tiwary<sup>1</sup>, R. I. Magaw<sup>1</sup>, D. A. Zemo<sup>2</sup>, K. T. O'Reilly<sup>3</sup>, R. E. Mohler<sup>1</sup> and K. A. Synowicz<sup>1</sup>. <sup>1</sup>*CETC, San Ramon, CA*; <sup>2</sup>*Zemo & Associates LLC, Incline Village, NV*; <sup>3</sup>*Exponent, Inc., Bellevue, WA*.

Chronic human health hazard evaluations of chemical mixtures are challenging and generally rely on similarities in toxicity mechanisms and dose-additivity of chemicals in the mixture. However, such assessments are inadequate for highly complex mixtures such as those present in groundwater at biodegrading petroleum sites where thousands of compounds representing many distinct structural classes of chemicals may be present. A hazard ranking system based on USEPA Reference Doses (RfDs) was developed to evaluate the potential chronic human health hazards presented by complex mixtures of polar petroleum biodegradation products in water. Equivalent risk-based drinking water concentrations for the range of identified RfDs were derived using the USEPA Regional Screening Level (RSL) equation for Tap Water Screening Levels (SLwater-nc-ing).

Based on the RfDs of representative chemicals for each structural class of potential biodegradation products, overall summary hazard rankings of "Low", "Low to Moderate", and "Moderate", were assigned. Classes constituting chemicals with RfDs ≥ 0.1 mg/kg/day were defined as being of "Low" hazard; "Low to Moderate" if 0.1 > RfD ≥ 0.01 mg/kg/day, and "Moderate" if 0.01 > RfD ≥ 0.001 mg/kg/day. These three groups included essentially all of the potential polar biodegradation products for which RfDs were available. This RfD based system is consistent with similar systems developed by USEPA OPPTS and UN GHS programs and was validated by review of USEPA summary documents.

The ranking system was applied to groundwater samples collected from biodegrading petroleum sites and the results show that the vast majority of the polar biodegradation products are in structural classes that may present "Low" hazard to humans. Overall, the polar mixtures are unlikely to present a significant risk to human health if consumed as drinking water.

**PS 566 Repeat-Dose and Developmental Toxicity Assessment of Crude Oil.**

R. H. McKee<sup>1</sup>, M. J. Nicolich<sup>2</sup>, T. Roy<sup>3,4</sup>, R. White<sup>5</sup> and W. Daughtrey<sup>1</sup>. <sup>1</sup>*Toxicology and Environmental Sciences, ExxonMobil Biomedical Sciences, Inc., Annandale, NJ*; <sup>2</sup>*COGIMET, Lambertville, NJ*; <sup>3</sup>*Port Royal Research, Hilton Head, SC*; <sup>4</sup>*University of South Carolina, Beaufort, SC*; <sup>5</sup>*American Petroleum Institute, Washington DC*.

**Abstract**

Petroleum (commonly called crude oil), CAS number 8002-05-9, is a complex substance of variable composition, primarily composed of hydrocarbon constituents. The principal acute toxicological hazards are those associated with exposure to volatile hydrocarbon constituents and hydrogen sulfide, and chronic hazards are associated with exposure to benzene and polycyclic aromatic compounds (PAC). To further characterize the potential for repeated dose and/or developmental effects from dermal contact, the PAC content of 46 crude oils was measured using a method based on DMSO extraction followed by GC separation and quantitation of the aromatic ring classes (ARC). Statistical models were then used to predict the potential for target organ and developmental toxicity of the 46 crude oils based on their ARC profiles. We compared model predictions to empirical data from previously tested crude oils, showing that one of the previously tested oils approximated a "worst case" situation. Thus, this modeling exercise demonstrated that data from previously tested crude oils could be used to form a reasonable basis for characterizing the repeated dose and developmental toxicological hazards of crude oils in general.

**PS 567 Insights from Initial Analysis for Harmful and Potentially Harmful Constituents (HPHC) in Tobacco Products.**

M. Oldham, D. DeSoi, K. A. Wagner and M. J. Morton. *Altria Client Services, Richmond, VA*.

A total of 20 commercial cigarette and 16 commercial smokeless tobacco products were initially assayed for 96 HPHC (Draft HPHC list, Federal Register, August 12, 2011) prior to draft guidance by FDA (March 30, 2012). The FDA Draft Guidance specified a reduced list of HPHC with more replicates than initially tested. Three contract laboratories were used to complete all testing. The same lots of commercial product were used for all testing. Cigarettes were tested using both the ISO and Canadian intense smoking regimens. In general, the levels of HPHC

constituents in the commercial products tested were consistent with levels previously reported in the literature. Approximately 12% of HPHC measured for cigarettes and smokeless tobacco products were not found or were below the limit of quantification. Comparison of initial HPHC results with results from additional replicates demonstrated statistically significant differences for most HPHC (i.e. temporal variability). Therefore, simple conventional comparisons, such as two-sample t-tests are inappropriate for comparing products tested at different points in time from the same laboratory or from different laboratories. Additionally, all of the HPHC in mainstream cigarette smoke were correlated to tar yield as previously reported in the literature.

Although each analytical assay was validated within a laboratory, some HPHC results were quite different between laboratories. These differences demonstrate the need for standardized methods between laboratories with defined repeatability and reproducibility determined by inter-laboratory collaborative testing for each HPHC using certified reference standards. Since no one-to-one relationship of tobacco constituent to human disease exists, the biological relevance of these HPHC results to human disease is unknown.

## PS 568 Different Toxicity Outcomes in Rats Correlated with EPR and NMR Spectra of Crude Oil from Various Sources.

S. A. Meyer<sup>1</sup>, S. Jaligama<sup>1</sup>, K. A. El Sayed<sup>2</sup> and T. R. Dugas<sup>3</sup>. <sup>1</sup>Toxicology, University LA-Monroe, Monroe, LA; <sup>2</sup>Basic Pharmaceutical Sciences, University LA-Monroe, Monroe, LA; <sup>3</sup>Pharmacology, Toxicology & Neurosciences, LSU Health Sciences Center, Shreveport, LA.

Crude oil varies with source in its relative composition of alkanes, simple and polycyclic aromatics, nitrogen, sulfur, asphaltene and porphyrin nickel and vanadium. Here, we identify several toxicological effects upon acute exposure of rats to crude oil from several sources and correlate these with peaks of select constituents from spectra of the crude oils obtained with EPR and <sup>1</sup>H- and <sup>13</sup>C-NMR. Sources of oil were Louisiana sweet crude, Nigerian (Qua Iboe) sweet crude and Iraqi high sulfur (ONTA, Inc., Toronto, Canada). Female Sprague-Dawley rats were given 2 daily doses of 2.5 and 5 ml/kg of oil or vehicle (0.5% DMSO in corn oil) by oral gavage. Rats were euthanized after 48 h and blood was taken for hematology, clinical chemistry and immunoassay for cytokines and vasoactive agents. Femur bone marrow cells were assayed for CFU-GM myeloid progenitors. All oils elevated serum alkaline phosphatase (ALP) with LA oil being least active, in agreement with liver pathology. Liver weight increased 25-75% and CYP1A1 protein was elevated with all, Iraqi oil being most effective. Granulocytes increased ~2-fold by high dose of LA and Iraqi oil. Spleen weights decreased 30% with high dose of Iraqi and Nigerian oil. CFU-GMs decreased only with high dose of LA oil (40%). Vasoconstrictor endothelin-1 increased 2-fold in serum from rats treated with Iraqi and Nigerian oils. <sup>1</sup>H- and <sup>13</sup>C-NMR spectra gave qualitatively similar alkane peaks for all oils, but differing aromatic peaks, e.g., benzene (<sup>1</sup>H-NMR 7.38 ppm) of Iraqi oil was least intense. EPR spectra of all oils exhibited asphaltene free radical peak with intensity greatest for Iraqi oil. Vanadium porphyrin was detected in Iraqi oil only. Summarizing, LA sweet crude oil was uniquely myelosuppressive and with lesser effect on spleen and liver weights and ALP. Iraqi oil, richest in asphaltene free radical and vanadium porphyrin and lowest in benzene, most affected liver weight and CYP1A1 (LA Board of Regents)

## PS 569 Complex Mixtures of PAHs Are More Potent Than Benzo[a]pyrene at Inducing Cellular Inflammatory and DNA-Damage Response.

K. Dreijl<sup>1</sup>, I. W. Jarvis<sup>1</sup>, C. Bergvall<sup>2</sup>, M. Bottai<sup>1</sup>, G. A. Umbuzeiro<sup>3</sup>, R. Westerholm<sup>2</sup> and U. Stenius<sup>1</sup>. <sup>1</sup>Institute Environmental Medicine, Karolinska Institutet, Stockholm, Sweden; <sup>2</sup>Department Analytical Chemistry, Stockholm University, Stockholm, Sweden; <sup>3</sup>Faculty of Technology, State University of Campinas, Limeira, Brazil. Sponsor: G. Johanson.

Complex mixtures of polycyclic aromatic hydrocarbons (PAHs) are present in air particulate matter (PM) and have been associated with many adverse health effects including cancer and cardiovascular disease. We hypothesize that interactions between different PAHs stand for a major biological effect. We have previously showed that soil PAH extracts induce persistent DNA damage including prolonged activation of DNA damage markers H2AX and Chk1. To further study the effects of mixtures of PAHs biological testing of air PM extracts were performed using human HepG2 and H1395 cells and sensitive cellular endpoints relevant for carcinogenesis (DNA damage response) and cardiovascular pathogenesis (inflammatory signaling). The cellular response was compared to benzo[a]pyrene (BP) and dibenzo[a,l]pyrene (DBP). The results showed a more than additive response for binary mixtures of BP and DBP on activation of Chk1. Persistent activation of DNA damage signaling was observed at significantly lower concentrations of air PM extracts than BP alone. Activation of DNA damage signaling was more persistent in

air PM fractions containing PAHs with more than four aromatic rings suggesting larger PAHs contribute more to the genotoxicity of PAHs in air PM. Furthermore, we observed significant up-regulation of pro-inflammatory stress responsive genes including several cytokines in response to air PM extracts corresponding to 1 nM BP. Employing specific inhibitors showed that the activation of inflammatory signaling was mediated through the Ah-receptor and MAPK signaling. Taken together, our data indicate synergistic effects on important cellular signaling events due to PAH interactions. This suggests that human health risk assessment based on additivity such as toxicity equivalency factor scales may significantly underestimate the risk of exposure to complex mixtures of PAHs.

## PS 570 Individual and Cumulative Health Risk Assessment of 17 PFASs in the Swedish Population.

D. Borg<sup>1</sup>, B. Lund<sup>2</sup>, N. Lindquist<sup>2</sup> and H. Håkansson<sup>1</sup>. <sup>1</sup>Institute of Environmental Medicine (IMM), Karolinska Institutet, Stockholm, Sweden; <sup>2</sup>Swedish Chemicals Agency (KemI), Stockholm, Sweden.

Perfluoroalkylated and polyfluoroalkylated substances (PFASs) are a large class of chemicals that have emerged as global environmental contaminants. This study, carried out in accordance with the European chemicals legislation (REACH) guidelines for risk assessment, evaluated possible health risks of 17 PFAS congeners in the Swedish population. The exposure assessment was based on blood and serum levels from biomonitoring studies in the Swedish population. Population groups considered were the general population and occupationally exposed professional ski waxers. The hazard assessment primarily considered hepatotoxicity and reproductive toxicity which were endpoints shared by the selected congeners. Read-across was performed to the closest most potent congener for 12/17 congeners lacking toxicological data and/or internal dose levels. The result of the risk characterization showed no cause for concern for hepatotoxicity or reproductive toxicity in the general population, except for hepatotoxicity in a subpopulation eating PFOS-contaminated fish. However, a cause for concern was identified for the non-conventional endpoints disrupted mammary gland development and immunotoxicity. For the occupationally exposed professional ski waxers safe use could not be shown based on concern for liver toxicity by PFOA and by all congeners in combination, for reproductive toxicity by all congeners in combination as well as for disrupted mammary gland development and immunotoxicity. This is the first attempt to assess the health risks to a combination of a large number of PFASs.

## PS 571 Mixtures of Benzo(A)Pyrene with Direct or Indirect Acting Mutagens Have a Nonmonotonic Mutation Profile.

R. David and N. J. Gooderham. Imperial College, London, United Kingdom.

Genotoxic carcinogens are present in the human diet, and Benzo(a)pyrene (BaP), 2-Amino-1-methyl-6-phenylimidazo[4,5-b]pyridine (PhIP) and acrylamide (AC) represent three important examples. BaP is a polycyclic aromatic hydrocarbon generated by incomplete combustion of organic substances such as lipids, thus contaminating numerous foodstuffs, PhIP is a heterocyclic amine formed when meat is cooked, and AC forms when foods, such as potatoes and cereals, are cooked at temperatures exceeding 100°C. Individually these have been shown to be genotoxic but the biological consequences of exposure to mixtures of these chemicals have not been systematically examined.

The aim of the current study was to examine the biological response of MCL-5 cells (metabolically competent human lymphoblastoid cell line) to mixtures of these genotoxins at concentrations relevant to human exposure (µM to sub-nM). Cells were exposed to the chemicals individually or in mixtures for 24h and mutagenicity was assessed through resistance to trifluorothymidine at the thymidine kinase (TK) locus and 6-thioguanine at the hypoxanthine-guanine phosphoribosyltransferase (HPRT) locus.

At the TK locus the mixtures produced non-monotonic mutation responses; 100nM BaP combined with some low, non-mutagenic concentrations of other mutagens showed synergism, while antagonism was observed for 10µM BaP in mixtures with higher concentrations of other genotoxins. Responses differed between the two loci, with a higher than anticipated mutation frequency (MF) observed for high concentration combinations at HPRT compared to TK. Combining 10µM BaP with 100µM PhIP reduced the number of cells in S phase with a corresponding increase in sub-G1 and G1. Moreover, ethoxoresorufin-O-deethylase (EROD; CYP1A) activity and CYP1A1 mRNA levels significantly correlated with each other and with the MF at TK emphasising the involvement of the CYP1A family in this mutation response. This non-monotonic MF is of significance when considering risk assessment, especially at low concentration combinations where the individual chemicals are not measurably mutagenic.

**PS 572 Preliminary Steps in a Whole Mixture Strategy for Risk Evaluation.**

K. Joshi and C. Gennings. *Virginia Commonwealth University, Richmond, VA.*

When assessing risks posed by environmental chemical mixtures, whole mixture approaches are preferred to component approaches. When toxicological data on whole mixtures as they occur in the environment are not available, EPA guidance states that toxicity data from one or more mixtures considered "sufficiently similar" to the environmental mixture(s) can serve as surrogates. However, the selection process of which mixtures to experimentally evaluate is an open line of inquiry. The objective of our study was to demonstrate a proof-of-concept strategy for the selection process using a mixture of 17 polychlorinated dibenzo-p-dioxins (PCDDs), polychlorinated dibenzofurans (PCDFs) and polychlorinated biphenyls (PCBs) based on (i) human biomonitoring data from the National Health and Nutrition Examination Survey (NHANES); and (ii) single chemical dose response models from the literature. Principal component (PC) analysis was conducted to identify patterns of chemicals present in humans as measured in serum concentrations in the US population using NHANES data. Five different concentration patterns were found to represent 82% of the variation in the mixture concentrations for these 17 chemicals. Population-based median concentration estimates for the chemicals identified by large absolute values in the PCs were used to define mixing proportions for the five mixtures. Robust optimal designs, using a maximin optimization criterion which is robust to model misspecification, were determined for the mixtures using published dose-response models in Crofton et al (2005, EHP). The approach provides design information for conducting mixtures studies in support of a whole mixtures risk assessment. Next steps include estimating the dose values required to approximate the blood concentrations in the mixtures. Determining how representative these mixtures are to the population concentrations while testing for sufficient similarity is a long-range research goal. (The authors gratefully acknowledge the support from #R01ES015276, #T32 ES007334, and #UL1TR000058.)

**PS 573 Coexposure to Low-Dose Model Testicular Toxicants Induces Gene Alterations.**

N. Catlin, S. M. Huse and K. Boekelheide. *Brown University, Providence, RI.*

Testicular effects of chemical mixtures may differ from those of the individual chemical constituents. This study assesses the co-exposure effects of the model germ cell- and Sertoli cell-specific toxicants, X-radiation (x-ray) and 2,5-hexanedione (HD), respectively. X-ray induces germ cell apoptosis and HD has been shown to attenuate the x-ray effect on germ cells. Adult rats were exposed to different levels of x-ray (0.5Gy, 1Gy, 2Gy), HD in the drinking water for 18 days (0.33%, 1%), alone or in combination. Custom PCR arrays were generated based on a panel of genes identified through microarray studies; hierarchical clustering of these PCR arrays identified dose-dependent treatment effects on the apoptosis-related genes Fas, Aen, and Casp3. The 5Gy + 1% HD co-exposure induced Aen and Casp3 expression, with a maximum fold induction of 3.1 and 2.6, respectively. Also, Fas was significantly induced 2.6-fold at this co-exposure dose, despite no induction of Casp3, Fas, or Aen expression by x-ray or HD alone. In order to assess cell type-specific attenuation of HD effects with x-ray co-exposure, we used laser capture microdissection (LCM) to examine a panel of apoptosis-related transcripts using PCR arrays. Several pro-apoptotic genes were identified, which increase with a fold change greater than 1.4 after 2Gy x-ray exposure, including Traf3, Tnfrsf10 and Fas. We also identified an anti-apoptotic gene, Bcl2a1d, which increases in fold change across the different exposures (0.33% HD, 1.3 fold; 2Gy x-ray, 1.6 fold; 0.33% HD + 2Gy, 3.1 fold). Ingenuity Pathway Analysis of the gene expression data produced two over-represented pathways across all treatment groups examined with LCM: Induction of Apoptosis by HIV1 and Death Receptor Signaling. We amplified LCM RNA and examined the same apoptosis transcripts. When compared to our unamplified RNA, we found a Pearson correlation coefficient of 0.64, indicating that use of amplified LCM RNA may introduce significant bias. These results provide insight into environmentally relevant low-dose co-exposures of model testicular toxicants.

**PS 574 Development of a Portable In Vitro System for Lab. and Field Aerosol Exposure Studies.**

J. Zavala, K. Lichtveld, S. Ebersviller, G. W. Walters, H. E. Jeffries, K. G. Sexton, W. Vizuete, I. Rusyn and I. Jaspers. *Environmental Sciences and Engineering, University of North Carolina at Chapel Hill, Chapel Hill, NC.*

There is a growing interest in studying the toxicity of multi-pollutant mixtures found in ambient air, and the U.S. Environmental Protection Agency (EPA) is moving towards setting standards for these types of mixtures. Conventional in vitro

exposure methods do not properly emulate human exposures and are not adequate to meet the EPA's strategic plan to demonstrate a direct link between air quality and health effects. Exposure of cells at the air-liquid interface (ALI) is the most realistic approach to emulate in vivo exposures. A new portable in vitro system that uses electrostatics to deposit particles onto the cells has been developed and this study demonstrates the efficacy of this device. The portable system provides a viable environment within its electric field for cultured human lung cells grown on permeable membrane supports. This method provides an efficient and effective way to expose cells to particles without prior collection and subsequent resuspension in a liquid medium. Cell viability testing included maintaining normal cell culture conditions for exposures across the ALI for periods of up to 4 hours outside of a tissue culture incubator. Results from all cell viability testing with A549 human lung cells show that no parts, components, materials or operating characteristics of the portable sampler induce any cytotoxicity, as measured by lactate dehydrogenase (LDH), or inflammatory response, as measured by interleukin-8 (IL-8). A549 cells were then exposed to photochemically-aged diesel exhaust (DE) using the UNC rooftop smog chamber. An exposure dose of 3.6 µg of DE particles in air was delivered to the cells and a 3-fold increase in LDH and IL-8 was observed when compared to controls. This new device can serve as a stepping-stone for researchers and engineers to develop new and improved in vitro exposure technology suitable for field use.

**PS 575 Chemical Dispersants Used in the Gulf of Mexico Are Cytotoxic to Human Lung and Skin Fibroblasts.**

J. Wise<sup>1,2</sup>, S. Wise<sup>1,2,3</sup>, H. Xie<sup>1,2,3</sup>, J. Griffith<sup>4</sup> and J. Wise<sup>1,2,3</sup>. <sup>1</sup>Wise Laboratory of Environmental and Genetic Toxicology, University of Southern Maine, Portland, ME; <sup>2</sup>Maine Center for Toxicology and Environmental Health, University of Southern Maine, Portland, ME; <sup>3</sup>Department of Applied Medical Science, University of Southern Maine, Portland, ME; <sup>4</sup>Department of Coastal Sciences, University of Southern Mississippi, Ocean Springs, MS.

Chemical dispersants are chemicals compounds that can be used to aid in the cleanup of crude oil spills. In 2010, they became a significant public health concern due to the BP Deepwater Horizon Oil Crisis; when millions of gallons of chemical dispersants specifically Corexit® 9527 and 9500 were applied via aerial spray and deepwater injection to break up the crude oil. Toxicity of Corexit® to humans is unknown, and the primary routes of exposure to these chemical dispersants are inhalation, direct dermal contact and ingestion. The objective of this study is to determine the cytotoxicity and genotoxicity of these two dispersants in human lung (WTHBF-6) and skin (BJhTERT) fibroblasts. Cells were treated with and without S9 fractions with cofactors, because fibroblast cells may not readily express cytochrome P450 enzymes necessary to metabolize chemicals. Corexit® 9500 was cytotoxic to lung and skin cells. Specifically in skin, 50, 250, 350 and 500 ppm, it induced 95, 89, 52, and 3 percent relative survival, respectively. S9-mediated metabolism increased toxicity inducing 78, 84, 39 and 2 percent relative survival, respectively. Corexit® 9527 was cytotoxic to lung and skin cells. Specifically in skin, 500, 650, 850 and 1000 ppm, it induced 89, 56, 73, and 24 percent relative survival, respectively. S9-mediated metabolism increased toxicity inducing 65, 60, 22 and 0 percent relative survival, respectively. Our genotoxicity data is less clear. Corexit® 9527 induced 8 aberrations per 100 metaphases at 850 ppm, but caused cell cycle arrest at 875 ppm. Similarly Corexit® 9500 induced 14 aberrations per 100 metaphases at 350 ppm, but caused cell cycle arrest at 425 ppm. Ongoing and future work will consider the effects of dispersed oil.

**PS 576 Micronanoparticle Suspension Formulation Development for Medical Chemical Countermeasures.**

L. Cabell<sup>1</sup>, J. McDonough<sup>1</sup>, A. Clark<sup>1</sup>, T. Belski<sup>2</sup> and L. Mobley<sup>2</sup>. <sup>1</sup>SWRI, San Antonio, TX; <sup>2</sup>CBMS/IMTS, Frederick, MD. Sponsor: J. Johnson.

Current U.S. medical chemical countermeasures require battlefield stability and an effective shelf life. One example is bis-pyridinium oximes that are used for the treatment of Organophosphate (OP) intoxication to counter the effects of AChE inhibition. This class of oximes possesses poor thermal stability in an aqueous formulation due to hydrolytic cleavage. CBMS and SwRI have developed non-Newtonian suspension formulations of oximes in cottonseed oil (CSO) vehicles that impart oxime solid stability characteristics to oxime/CSO liquid suspension formulations. MMB4 DMS and HI-6 DMS have shown superior thermal stability in these liquid suspension formulations compared to aqueous formulations and equal thermal stability compared to solid formulations. These types of formulations have shown bioavailability comparable to parent active pharmaceutical ingredients (API) in aqueous formulations. C<sub>max</sub> and T<sub>max</sub> for these APIs are relatively the same with absorption and elimination not substantially affected. In principle, these types of

suspension formulations can be used to stabilize any drug that is prone to hydrolytic cleavage. In addition, the nature of these suspensions inhibits drug-drug interaction in the formulations as well as promotes differential drug controlled release if designed appropriately. We have designed these suspensions with high zero-shear viscosity, which allows it to resist sedimentation and non-Newtonian behavior that causes shear thinning, such that the viscosity decreases and the product flows easily under a shear force, such as injection through a needle. Furthermore, the viscosity and sedimentation behavior are controlled by formulation parameters such as particle size and concentration. DISTRIBUTION STATEMENT A. Approved for public release; distribution is unlimited.

**PS 577 Application of Generalized Concentration Addition to Receptors That Dimerize.**

T. Webster, *Department Environmental Health, Boston University School of Public Health, Boston, MA.*

Concentration addition is a standard toxicological method for analyzing mixtures of similarly acting compounds. A significant limitation of concentration addition is that it cannot be used to describe the effect of mixtures containing partial agonists at response levels above that for the compound with lowest efficacy. Unfortunately, partial agonism is a common phenomenon, limiting the application of concentration addition. We previously proposed generalized concentration addition (GCA) as a solution to this issue and successfully used this method to describe data from experiments involving mixtures of full and partial agonists of the AhR receptor. GCA requires the use of dose-response functions that are invertible over the relevant range. This posed no problem for the AhR-ligand systems described by a Hill function with a Hill coefficient of one. Receptors that dimerize (or receptors that bind two ligands) are often modeled using Hill functions with Hill coefficients of two, but these functions are not appropriately invertible. We used mathematical models based on equilibrium kinetics and mass balance to describe a simple pharmacodynamic model of binding of ligands to receptors followed by dimerization: e.g.,  $A + R_{AR, AR+AR} \rightleftharpoons ARRA$ , where A is a ligand, R is a receptor, AR is a ligand-receptor complex, and ARRA is the dimerized complex. This leads to theoretical dose-response functions that are invertible and different from Hill functions but approximated by them at low doses. Such models may be applicable to examining mixtures of full and partial agonists of several systems of receptors that dimerize including the androgen and estrogen receptors.

**PS 578 Generalized Concentration Addition Models Some but Not All Interactions of Mixtures of Androgen- and Estrogen-Receptor Active Compounds in High-Throughput Screening Assays.**

F. Parham<sup>1</sup>, M. DeVito<sup>1</sup>, R. Huang<sup>2</sup>, M. Xia<sup>2</sup>, B. Collins<sup>1</sup>, C. Rider<sup>1</sup> and R. R. Tice<sup>1</sup>. <sup>1</sup>NTP, NIEHS, Research Triangle Park, NC; <sup>2</sup>NCATS, NIH, Bethesda, MD.

As part of the U.S. Tox21 collaboration, 69 mixtures of compounds previously found to be active in estrogen or androgen receptor (ER or AR) reporter assays were tested in ER and AR high throughput screening assays in agonist and antagonist mode. ER-active compounds used were acetochlor, alachlor, bisphenol A, butyl benzyl phthalate, chlordecone, DDT, dicumyl peroxide, ethylenediamine, p-n-nonylphenol, and zearalenone. AR-active compounds were androstenedione, dexamethazone, flouxymestron, hydroxyflutamide, medroxyprogesterone acetate, o-methoxyphenol, oxymetholone, and progesterone. Of the 69 mixtures, 32 were AR-active compounds only, 23 were ER-active compounds only, and 14 were both groups of compounds. Mixtures contained between 2 and 18 chemicals and were equipotent mixtures, mixtures of equal concentration and mixtures that varied potency of the individual chemicals. The 18 compounds were also tested individually. A generalized concentration addition model for partial agonism and antagonism was used to model the concentration-response of the mixtures as a function of the parameters of the response for the mixture components. The parameters were derived using two optimization methods. In the first method, the parameters for the mixtures components were derived by fitting the model to the single-component data, and then the model was used to predict the mixture effects. In the second method, the parameters were obtained by fitting the model to all the data (both single-component and mixture) simultaneously. The second method generally accurately models both the single-component and mixture data, although there were several mixtures that were not accurately represented by the model. The first method was inaccurate for many more mixtures. The experiment demonstrates that high-throughput assays can be used to evaluate dose addition theory for large numbers of individual chemicals and mixing ratios.

**PS 579 Cumulative Risk Assessment of Radon and Confounder Mixtures.**

M. Mumtaz<sup>1</sup>, L. Keith<sup>1</sup>, D. Wohlers<sup>2</sup> and E. Murray<sup>1</sup>. <sup>1</sup>Division of Toxicology and Human Health Sciences, CDC ATSDR, Atlanta, GA; <sup>2</sup>SRG, Inc., North Syracuse, NY.

Cumulative risk assessment is a challenging proposition because it involves integration and collective distillation of all available data capturing the essence of the potential risks of multiple stressors, chemical and nonchemical. The conclusions of such assessments must also integrate the inherent disparities, the constraints of the data gaps, and address data uncertainties. More recently communities and stakeholders have also voiced concerns about health effects beyond the single stressor-specific critical effects and the role of interactions in the overall toxicity of real life exposures. Most often the focus has been on chemical toxicity; here we present a case of chemical plus radiological effects. The Agency for Toxic Substances and Disease Registry (ATSDR) has updated the Toxicological Profile for Radon to comprehensively evaluate its systemic toxicity and carcinogenicity. It features information from individual and pooled epidemiological studies of miner and residential cohorts to assess radon carcinogenicity. These studies largely accounted for smoking and arsenic as confounders. Crystalline silica and diesel exhaust carcinogenicity was not integrated into the miner assessments. Thus, radon carcinogenicity may have been overestimated in miners. Residential epidemiological studies of radon have assessed cancer risk addressing smoking as a confounder and suggested that lung cancer mortality in radon-exposed populations may be 25 times higher among smokers than never-smokers. It is not possible to avoid exposure to radon and its progeny since they are ubiquitous. For this reason, to limit potential health effects, EPA recommends keeping radon air level <4 pCi/L in residential settings. Diesel exhaust and other indoor chemicals/non-chemical stressors, including biologics, might enhance the health effects of residential radon and should be considered as part of any risk assessment. (The views expressed in this abstract are those of the authors and do not necessarily represent the views or policies of ATSDR.)

**PS 580 90-Day Inhalation Toxicity Study with Hydroprocessed Esters and Fatty Acids Jet Fuel from Camelina (HEFA-C) in Rats.**

K. L. Mumy<sup>1</sup>, W. R. Howard<sup>1</sup>, B. A. Wong<sup>1</sup> and D. R. Mattie<sup>2</sup>. <sup>1</sup>Naval Medical Research Unit - Dayton, Wright Patterson Air Force Base, OH; <sup>2</sup>711 HPWIRHDJ, Wright Patterson Air Force Base, OH.

The Department of Defense is actively pursuing the development of alternative fuels to augment or replace petroleum-based jet fuels. Towards these efforts, numerous synthetic and biologically-based fuels are currently under consideration for military use. Given the widespread use of fuels within the military, the health effects associated with occupational exposure to fuels remains a concern. Toxicity studies are being performed with the fuels in order to assess any possible health effects related to fuel exposure. Hydroprocessed Esters and Fatty Acids jet fuel (HEFA) is a type of hydrotreated renewable jet fuel currently under consideration. One specific type of HEFA is generated from oils extracted from the camelina plant (*Camelina sativa*; HEFA-C). In order to evaluate potential toxicity of HEFA-C, an *in vivo* 90-day whole body inhalation study was performed with the fuel (concentrations of 0, 200, 700 and 2000 mg/m<sup>3</sup> for 6h/day, 5 days/wk) using male and female Fischer 344 rats. Following exposure, a series of toxicity endpoints was evaluated, including food consumption and body weight, genotoxicity by micronucleus (MN) test, neurotoxicity and histopathology. There was no change in food consumption attributed to fuel exposure and the average body weight was found to slightly decrease (not statistically significant) in animals exposed to the high concentration. MN test was negative for evidence of genotoxicity. No significant effects were observed on clinical chemistry or hematology evaluations and no significant neurobehavioral effects were observed based on functional observational battery and motor activity tests. Minimal effects attributable to exposure to HEFA-C were observed with histopathology. These effects included goblet cell hyperplasia and olfactory epithelium degeneration at the highest concentration of exposure. These data will help guide the establishment of an occupational exposure limit for this alternative jet fuel.

**PS 581 Chemical Characterization of Complex Aromatic Flame Retardants for Toxicological Studies.**

R. Harris<sup>1</sup>, M. Kroenke<sup>1</sup>, J. Van Scoy<sup>1</sup>, Q. Lawrence<sup>1</sup>, B. O'Brien<sup>1</sup>, A. Ammenhauser<sup>1</sup>, L. Siemann<sup>1</sup>, K. Aillon<sup>1</sup>, J. Algaier<sup>1</sup>, B. Collins<sup>2</sup> and S. Waidyanatha<sup>2</sup>. <sup>1</sup>MRIGlobal, Kansas City, MO; <sup>2</sup>National Toxicology Program NIEHS, Research Triangle Park, NC.

Aromatic phosphates (APs), which are replacing polybrominated diphenyl ethers as flame retardants, contain multiple isomeric forms and are formulated with other flame retardants in commercial products. Manufacturer and lot-to-lot variation add to the complex nature of AP products, making toxicity data interpretation difficult with respect to individual product components.

Six APs [triphenyl phosphate (TPP), tert-butylphenyl diphenyl phosphate (BPDP), tricresyl phosphate (TCP), 2-ethylhexyl diphenyl phosphate (EHDP), isodecyl diphenyl phosphate (IDDP), and phenol, isopropylated phenol phosphate (3:1) (IPP)] were nominated to the National Toxicology Program (NTP) for toxicity testing. MRIGlobal supported the NTP by performing chemical identity and purity studies on the selected chemicals.

GC/FID was used to separate components of each AP and GC/MS or NMR was used to identify components. TPP and EHDP were of low complexity. TPP contained a single component with chromatographic purity of 99.8% and no variation between 2 lots of a supplier. EHDP from 2 suppliers contained 3 components and had chromatographic purities of 98.5 and 97.4%. Both lots contained TPP at similar concentrations (1.5 vs. 2.5%). BPDP and TCP were considered to be moderately complex. A lot of BPDP contained 6 major components, identified as BPDP isomers and TPP. A lot of TCP contained 10 major components identified as TCP isomers and TPP. IDDP and IPP were considered highly complex with over 20 major components. Seven lots of IPP, from 5 vendors, contained TPP and 14 other major components identified as IPP isomers. Three IDDP lots from 3 vendors contained TPP and more than 30 components, identified as IDDP isomers or structurally similar analogs. Both IPP and IDDP demonstrated a high degree of lot-to-lot variability and large supplier differences.

**PS 582 Preparation of Toxicological Studies: Principal Component Analysis of Isopropylated Phenol Phosphate.**

J. Algaier<sup>1</sup>, M. Kroenke<sup>1</sup>, L. Lucas<sup>1</sup>, K. Bauer<sup>1</sup>, K. Aillon<sup>1</sup>, L. Siemann<sup>1</sup>, R. Harris<sup>1</sup>, B. Collins<sup>2</sup> and S. Waidyanatha<sup>2</sup>. <sup>1</sup>MRIGlobal, Kansas City, MO; <sup>2</sup>National Toxicology Program, NIEHS, Research Triangle Park, NC.

Phenol, isopropylated Phosphate (3:1), IPP, is one of many multi-component aryl phosphate flame retardants also used as plasticizers in products such as polyurethanes, textile coatings, and paints. Due to potential consumer exposure and the lack of adequate toxicity data, IPP has been selected for evaluation by the National Toxicology Program (NTP). MRIGlobal supported the NTP by procuring seven different IPP lots from five suppliers and chemically characterizing the material. IPP characterization will not only inform the NTP of the material's complexity, but may allow for source identification of IPP used in product mixtures.

Each IPP lot was analyzed and chromatographically fingerprinted following the development of a gas chromatographic/flame ionization detection method. Each lot contained 25 to 30 components pointing towards the existence of mono- bis- or tris-isopropylated phenyl groups and multiple positional isomers. With this many component peaks, simple chromatographic overlays do not allow for complex data evaluation and understanding of the dynamic nature of these lots.

To achieve a better understanding of IPP component complexity Principal Component Analysis (PCA) was performed. PCA, a common multivariate statistical technique for finding patterns in data of high dimension, was used to find potential groupings with respect to suppliers in the dataset generated for 11 key IPP chromatographic components in 48 sample runs of 7 lots from 5 suppliers. Of the 11 possible principal components, the first 2 explained 56% and the first 3 explained 75% of the total variance in the data. A 3-D plot of the data clearly demonstrated supplier grouping, enabling identification of specific suppliers. Commercial products may now be compared to these fingerprints for possible source identification.

**PS 583 The Effects of Atrazine Exposure on Genome Wide Expression Levels in Male *Drosophila melanogaster*.**

M. Xie<sup>1</sup>, J. Walters<sup>2</sup> and A. C. Fiumera<sup>1</sup>. <sup>1</sup>Biological Sciences, Binghamton University, Binghamton, NY; <sup>2</sup>Ecology and Evolutionary Biology, University of Kansas, Lawrence, KS. Sponsor: A. Fiumera.

Atrazine (2-chloro-4-ethylamino-6-isopropylamino-1,3,5-triazine) is one of the most commonly applied herbicides in the United States to control broad leaf and grassy weeds. Although beneficial in agriculture, atrazine can also be a potential environmental toxicant. It has been detected at low concentrations in surface water,

ground water and precipitation. In addition, many studies demonstrate that atrazine is a potent endocrine disruptor and affects a variety of reproductive traits in vertebrates, such as sperm number and motility, as well as, sperm capacitation. We are studying the effects of atrazine exposure on genome wide expression levels (RNA-seq) in the model genetic system, *Drosophila melanogaster*. Male flies were reared throughout their entire life cycle on either control food or food containing 20 ppm atrazine and flash frozen at 4 to 6 days old. Two biological replicates, each consisting of a pool of 40 flies, were prepared for each condition and were multiplexed in a single lane of an Illumina HiSeq2000, yielding at least 10 million reads per replicate. We used different combinations of read-counting procedures (HTseq, RSEM) and testing statistics (DEseq, baySeq) in all 4 possible combinations to determine differentially expressed genes. Twenty six genes that showed consistent expression differences (i.e. ranked in the top 50 significant genes of the different analyses) were analyzed using qRT-PCR (20 control and exposed replicates). Eleven of these 26 genes were significantly changed after 20 ppm atrazine exposure. Most of these genes are currently uncharacterized and have not been previously shown to be affected by environmental stressors. Future work will investigate how polymorphisms in these genes impact susceptibility.

**PS 584 Effects of Atrazine Exposure on Male Reproductive Performance in *Drosophila melanogaster*.**

A. R. Vogel and A. C. Fiumera. *Biological Sciences, Binghamton University, Vestal, NY.* Sponsor: A. Fiumera.

Atrazine is the one of the most commonly applied herbicides in the United States. In a variety of vertebrate classes, atrazine can feminize males and reduce their reproductive performance, likely through its effects on aromatase. Much less is known, however, about the effects of atrazine on invertebrates. In this study, we investigate the effects of larval atrazine exposure (4 ecologically relevant concentrations and unexposed controls) on reproductive performance of adult male *Drosophila melanogaster*. We scored male mating rate when mating to virgins (mating rate) and previously mated females (remating rate), as well as, a male's ability to prevent the female from remating (refractoriness). We also scored measures of male induced female fertility, including egg laying rate and total progeny production. Atrazine exposure significantly negatively affected male mating rate ( $p = 0.010$ ), male induced egg laying rate ( $p = 0.001$ ) and total progeny production ( $p = 0.012$ ). It had no effect on refractoriness. In general, we observed non-monotonic responses such that the intermediate exposure levels showed the largest reduction in male reproductive performance. For example, male remating rate was reduced between the unexposed controls and individuals reared on food with 2 ppM atrazine ( $p < 0.05$ ) but not for flies reared on 20 ppM food. Ongoing work is investigating sperm sperm transfer, storage and utilization rates.

**PS 585 Effects of the Herbicide Trifluralin in HepG2 Cell Culture.**

M. F. Franco<sup>1</sup> and D. J. Dorta<sup>2</sup>. <sup>1</sup>Universidade de São Paulo (USP). Faculdade de Ciências Farmacêuticas de Ribeirão Preto (FCFRP), Ribeirão Preto, Brazil; <sup>2</sup>Departamento de Química, Universidade de São Paulo (USP). Faculdade de Filosofia, Ciências e Letras de Ribeirão Preto (FFCLR), Ribeirão Preto, Brazil.

The emerging contaminants are a new category of xenobiotics widely distributed in the environment. These contaminants include pesticides, within them are the herbicides, a heterogeneous category of chemical products, designed to control weeds. Trifluralin ( $\alpha, \alpha, \alpha$  - trifluoro - 2,6 - dinitro - N,N - dipropyl - p - toluidine) is a herbicide used on many agronomic crops. The present study aimed to evaluate the cytotoxic effects of the Trifluralin in HepG2 cell culture through the assays of cell proliferation, cell viability and mitochondrial membrane potential. It was used concentrations of 1, 5, 10, 20, 50 and 100  $\mu$ M of trifluralin dissolved in dimethyl-sulfoxide. The time of exposure was 24, 48 and 72 hours. The assessment of cell proliferation was performed with the dye sulforhodamine B (SRB Assay), the test of cell viability was done using the dye bromide 3 - (4,5-dimethylthiazol-2-yl) -2,5 diphenyl tetrazolium (MTT Assay), and for the analysis of the mitochondrial membrane potential, cells were incubated with a solution tetramethylrhodamine methyl ester. All experiments were performed in triplicate. The ANOVA test was applied followed by Dunnett. The results of SRB assay at 24, 48 and 72 hours of exposure showed a significant difference from the control at concentrations of 50 and 100  $\mu$ M of trifluralin. Effects on the MTT assay and mitochondrial membrane potential showed a similar pattern, being significant from the control at the concentrations of 50 and 100  $\mu$ M of trifluralin. We can conclude that trifluralin affects the HepG2 cells by inhibiting cell proliferation and/or inducing cell death and disrupting mitochondrial membrane potential at concentrations of 50  $\mu$ M and higher. Further studies will be performed to better understand the effects of trifluralin on HepG2 cells.

**PS 586 Effect of p, p'-DDE on Adipogenesis and Macrophage Activation.**

L. Mangum<sup>1</sup>, G. E. Howell<sup>1,2</sup>, S. B. Pruett<sup>1</sup>, M. K. Ross<sup>1</sup> and J. E. Chambers<sup>1</sup>.  
<sup>1</sup>Center for Environmental Health Sciences, Mississippi State University, Mississippi State, MS; <sup>2</sup>Biological Sciences, Mississippi College, Clinton, MS.

There is evidence that exposure to organochlorine compounds, such as DDE, may contribute to dyslipidemia, obesity, and insulin resistance, a cluster of signs that comprise the metabolic syndrome. Obesity results from adipocyte hyperplasia and hypertrophy which leads to recruitment of immune cells to adipose tissue and eventually contributes to localized chronic low-grade inflammation and adipocyte dysfunction. This study investigated a potential COX-2 dependent mechanism by which DDE could modulate normal physiological function and facilitate an increased risk of developing metabolic syndrome following exposure. Murine (J774a.1) and human (THP-1) macrophage cell lines and murine preadipocytes (3T3-L1) were used to investigate the effects of DDE on inflammation and adipogenesis. Macrophage cell lines were exposed to DDE or a known COX inhibitor for 18 hr before treatment with an inflammatory challenge of lipopolysaccharide (LPS) or palmitic acid (PA). Cell culture supernatants were analyzed for the presence of prostaglandins PGE<sub>2</sub>, PGD<sub>2</sub>, PGF<sub>2α</sub>, arachidonic acid (AA), and thromboxane (TBX) and for proinflammatory cytokines, including tumor necrosis factor (TNFα). 3T3 preadipocytes were induced to differentiate to adipocytes using a sub-optimal differentiation cocktail in the presence of DDE or a COX-2 inhibitor, with or without TNFα, a known COX inducer and suppressor of adipogenesis. Mature adipocytes were analyzed for intracellular lipid accumulation by Oil Red O staining. Both DDE and COX inhibitors increased adipogenesis in a dose-dependent manner in all treatments. In macrophages, DDE exposure followed by LPS or PA challenge reduced secretion PGE<sub>2</sub>, PGF<sub>2α</sub>, and PGD<sub>2</sub> and caused a slight increase in secretion of TNFα over vehicle. COX enzymes have a complex role in both inflammation and adipogenesis, and these results suggest that DDE exposure may contribute to altered adipogenesis and increased inflammation, potentially through a COX-2 dependent mechanism.

**PS 587 Organophosphorus Pesticides Activate Mast Cells Ex Vivo and In Vivo.**

A. C. Grodzki and P. J. Lein. *Molecular Biosciences, University of California Davis, Davis, CA.*

Mast cells are immune cells involved in diverse inflammatory diseases and are best known for their critical role in allergic reactions and asthma. In asthma, mast cells are activated by the cross-linking of FcεRI (the high affinity IgE receptor) with antigen-specific IgE, but these cells can be activated via several additional mechanisms. We hypothesized that organophosphorus pesticides (OPs) can activate mast cells in an IgE-independent manner. OPs are known to modulate immune function at levels that do not cause significant inhibition of cholinesterases, and previous studies of total peritoneal cells exposed to the OP malathion *in vivo* suggested that at least this OP modulates primary macrophage functions as an indirect consequence of mast cell degranulation. To determine whether OPs can target mast cells directly, we evaluated cellular degranulation using morphologic criteria, and release of β-hexosaminidase, a marker for mast cell degranulation, in percoll gradient-purified and non-purified rat peritoneal and mesentery mast cells following exposure to OPs. Preliminary experiments indicated that *ex vivo* exposure to paraoxon induced significant mast cell degranulation within 1 h and increased release of β-hexosaminidase in a concentration dependent manner. *In vivo* treatment with parathion caused mast cell degranulation with increased β-hexosaminidase release in the peritoneal cavity. Therefore, the data suggests that parathion and paraoxon affect mast cell stability, provoking degranulation and consequent release of inflammatory mediators. Ongoing studies are exploring the action of other OPs, carbamates and pyrethrins on mast cells and evaluating the mechanism by which these pesticides affect mast cell integrity. This work was supported by funding from the National Institutes of Health (grant R01 ES017592 to P.JL) and a postdoctoral fellowship to ACGG (T32 HL007013).

**PS 588 Detection of Dichlorvos Targets in Hepatocytes.**

T. Bui-Nguyen<sup>1</sup>, W. Dennis<sup>2</sup>, J. A. Lewis<sup>2</sup> and D. A. Jackson<sup>2</sup>. <sup>1</sup>Oak Ridge Institute for Science and Education (ORISE), Frederick, MD; <sup>2</sup>US Army Center for Environmental Health Research, Frederick, MD.

Toxicity of dichlorvos (DDVP), an organophosphate (OP) pesticide, classically results from modification of the serine in the active sites of cholinesterases. However, DDVP also forms adducts on unrelated targets such as transferrin and albumin,

suggesting that DDVP causes cellular perturbation by modifying non-cholinesterase targets. Here, we identify novel DDVP-modified targets in lysates of a human hepatocyte-like cell line (HepaRG) in competitive pull-down experiments using DDVP and a biotin-linked organophosphorus compound (10-fluoroethoxyphosphinyl-N-biotinamidopentyldecanamide; FP-biotin), which competes with DDVP for similar binding sites. Using the competition assay and mass spectrometry, we show that DDVP forms adducts to six new target proteins, including Glyceraldehyde-3-Phosphate Dehydrogenase (GAPDH). We validated the results using purified GAPDH incubated with DDVP and found that GAPDH Tyr-314, a residue in the known active site, is modified by DDVP. GAPDH activity is inhibited in a concentration dependent manner in DDVP-treated HepaRG cells, suggesting that the modification directly inhibits the enzyme. These results may help explain the chronic metabolic effects of DDVP exposure.

Opinions, interpretations, conclusions, and recommendations are those of the authors and are not necessarily endorsed by the U.S. Army. Citations of commercial organizations or trade names in this report do not constitute an official Department of the Army endorsement or approval of the products or services of these organizations. The research described herein was sponsored by the USAMRMC and Military Operational Medicine Research Program. This research was supported in part by an appointment to the Postgraduate Research Participation Program at the U.S. Army Center for Environmental Health Research (USACEHR) administered by the Oak Ridge Institute for Science and Education through an interagency agreement between the U.S. Department of Energy and USACEHR.

**PS 589 Neonicotinoid Insecticides: Formaldehyde Generation As a Proposed Mechanism of Mouse-Specific Hepatotoxicity and Hepatocarcinogenicity of Thiamethoxam.**

T. Swenson and J. Casida. *Graduate Group in Molecular Toxicology, University of California Berkeley, Berkeley, CA.*

Thiamethoxam (TMX), one of the most important insecticides, is carcinogenic and hepatotoxic in mice but not in rats. Green *et al.* (*Toxicol. Sci.* **86**, 36-47, 2005) established that TMX is a much better substrate for mouse liver cytochrome P450s than the corresponding rat or human enzymes in forming desmethyl-TMX (dm-TMX), which is also hepatotoxic, and clothianidin (CLO), which is not hepatotoxic or carcinogenic. The present investigation examines the hypothesis that liberation of formaldehyde (HCHO) or an N-methylol intermediate during TMX and dm-TMX metabolism to CLO and dm-CLO, respectively, provides a molecular explanation for the mouse-specific toxicity. Mouse liver microsomes were compared to rat and human liver microsomes in the metabolism of the seven commercial neonicotinoids and dm-TMX in the presence or absence of the cofactor, NADPH. HCHO production was determined by derivatization with 2,4-dinitrophenylhydrazine and monitoring by HPLC while other TMX metabolites (dm-TMX, CLO and dm-CLO) were quantitated by LC/MS. TMX and dm-TMX yielded more HCHO than any of the six other commercial neonicotinoids and mouse microsomes gave much higher conversion than rat or human microsomes. HCHO or an N-methylol intermediate in TMX and dm-TMX metabolism is therefore the candidate reactive hepatotoxicant. The N-methylol intermediates are difficult to analyze because of their chemical instability. These results provide HCHO liberation as an alternative to the earlier explanation of TMX hepatotoxicity in which dm-TMX is the proposed reactive metabolite and its toxicity is exacerbated by dm-CLO inhibition of inducible nitric oxide synthase (iNOS) (Green *et al.*, 2005). Although the HCHO generation proposal versus the dm-TMX/iNOS inhibition hypothesis for TMX toxicity is not fully resolved, the mouse vs. rat vs. human comparison of TMX metabolism reconfirms that the rat (showing no carcinogenic effects) is the best risk assessment model for humans.

**PS 590 Chiral Pesticide Pharmacokinetics: A Range of Values.**

J. F. Kenneke<sup>1</sup>, S. A. Marchitti<sup>1</sup>, S. Rawat<sup>2</sup>, D. T. Chang<sup>3</sup>, C. M. Grulke<sup>3</sup>, C. S. Mazur<sup>1</sup> and M. R. Goldsmith<sup>3</sup>. <sup>1</sup>US EPA, Athens, GA; <sup>2</sup>Student Services Authority, Athens, GA; <sup>3</sup>US EPA, Research Triangle Park, NC.

Approximately 30% of pesticides are chiral and used as mixtures of two or more stereoisomers. In biological systems, these stereoisomers can exhibit significantly different pharmacokinetics (absorption, distribution, metabolism, and elimination). In spite of these differences, these "mixtures" are often treated as a single compound in exposure and hazard assessment. To evaluate the impact of pharmacokinetic differences on internal exposure (dose) estimates, we studied the stereoisomer-specific metabolism of twenty chiral 1,2,4-triazole fungicides in hepatic microsomes, hepatocytes, and purified cytochrome P450s (P450). Additionally, we measured the metabolism of the pure stereoisomers for three of the

fungicides. Studies indicated that CYP3A4 was a major metabolizing enzyme for a majority of the fungicides. In general, the stereoisomers of each fungicide (pure and in the fungicide mixture) exhibited significantly different clearance rates. With some compounds, one or more stereoisomers inhibited the clearance of the other stereoisomers. Results were consistent across genders. In an effort to explain the observed stereoisomer clearance rates, we utilized a directed ligand-based pharmacophore analysis to identify key ligand features. Triadimefon was the only fungicide that preferentially underwent stereoselective carbonyl reduction rather than P450-mediated oxidation. Reduction of the prochiral carbonyl produced four stereoisomers of triadimenol. Relative formation of the triadimenol stereoisomers varied among 16 vertebrate species; the individual triadimenol stereoisomers differentially inhibited CYP3A4 metabolism. These results suggest that treating a chiral pesticide as a single chemical rather than a mixture could introduce errors in risk assessment. Although this work was reviewed by EPA and approved for publication, it may not necessarily reflect official Agency policy.

**PS 591 Alpha-Cypermethrin Metabolism and Exposure Assessment in Egyptian Agricultural Workers.**

S. T. Singleton<sup>1</sup>, J. B. Knaak<sup>1</sup>, L. Chi<sup>1</sup>, B. P. McGarrigle<sup>1</sup>, F. M. Farahat<sup>2</sup> and J. R. Olson<sup>1</sup>. <sup>1</sup>Pharmacology and Toxicology, University at Buffalo, Buffalo, NY; <sup>2</sup>Menoufia University, Shibin el Kom, Egypt.

Pyrethroids are neurotoxic insecticides that exert their effects by prolonging the opening time of sodium channels and increase the duration of neuronal excitation. Alpha-cypermethrin (aCM) is derived from the 8-stereoisomer containing pyrethroid cypermethrin, and is one of the most common pyrethroids being used in agriculture throughout the world. Pyrethroids are extensively metabolized in the liver by both esterases and oxidative enzymes. In vitro metabolism assays with human liver microsomes and cytosol demonstrate that aCM undergoes metabolism to the detoxified metabolites, 3-phenoxybenzoic acid (3-PBA) and cis-3-(2,2-dichlorovinyl)-2,2-dimethylcyclopropane carboxylic acid (cis-DCCA) in both liver fractions. Previous studies suggest that 3-PBA may be a general biomarker of human exposure to pyrethroids, while cis-DCCA is a specific biomarker of aCM. A sensitive GC-MS NCI method was developed and daily urinary cis-DCCA and 3-PBA concentrations were quantitated for Egyptian agriculture workers who were applying alpha-cypermethrin to cotton fields for up to 10 consecutive days. Both cis-DCCA and 3-PBA were detected in the urine of all workers and ranged from 0.07-17.7 µg/g creatinine and 0.5-19.7 µg/g creatinine, respectively. This study is the first to use these biomarkers to quantify occupational exposures to alpha-cypermethrin. The in vivo biomarker data and in vitro metabolism kinetic data will be useful in future efforts to model human exposures to alpha-cypermethrin. (This research was supported in part by U.S.EPA STAR grant R833454 and NIEHS R01 ES016308)

**PS 592 4'-OH-Deltamethrin Metabolite-Induced Changes in Oxidative Stress Biomarkers in SH-SY5Y Cells and Alleviation Effect of Melatonin.**

M. R. Martinez-Larrañaga, A. Romero, E. Ramos, V. Castellano, M. A. Martinez, I. Ares, M. Martinez and A. Anadon. *Toxicology & Pharmacology, Complutense University, Madrid, Spain.*

Oxidative damage has been recognized as one of the primary causes of subcellular toxicity pesticides. Studies on pyrethroid insecticides have also suggested a putative role for free radicals in the lipid peroxidation and other oxidative stress-mediated injuries. Although initially it was thought that metabolites of deltamethrin, a  $\alpha$ -cyano pyrethroid insecticide, should be less toxic than the parent compound, we studied the oxidative stress-inducing effect of both the oxidative metabolite 4'-OH-deltamethrin and the parent compound in SH-SY5Y neuroblastoma cells. Cell line SH-SY5Y was used by their vulnerability to the oxidative damage. Lipid peroxidation induced by deltamethrin and 4'-OH-deltamethrin with or without melatonin was evaluated. Intracellular malondialdehyde (MDA) production was quantified using a thiobarbituric acid reactive substance assay. Changes in nitric oxide (NO) production were measured indirectly as the accumulation of nitrites (the end-product of NO metabolism) in the medium using Griess assay. In the present study, the levels of both NO and lipid peroxides measured as MDA, which can lead to a loss of membrane structure and function, were found to be significantly increased in deltamethrin and 4'-OH-deltamethrin treated cells. Both deltamethrin (10 µM) and 4'-OH-deltamethrin (10 µM) induced a significant increase in MDA levels (3- and 3.5-fold above basal,  $p < 0.001$  respectively) as well as increased by 3.5- and 5-fold,  $p < 0.001$ , NO production. Our results also demonstrated that melatonin (1 µM) significantly reversed the effects of deltamethrin and 4'-OH-deltamethrin.

In the present in vitro study, it is demonstrated that the metabolite 4'-OH-deltamethrin, is more cytotoxic than the parent compound deltamethrin. This work was supported by projects Refs. GR35/10-A UCM-BSCH, S2009/AGR-1469 and Consolider-Ingenio CSD/2007/00063 (FUN-C-FOOD), Madrid, Spain.

**PS 593 Effect of Age on Plasma Protein Binding of Deltamethrin, Cis-Permethrin, and Trans-Permethrin in Rats.**

P. Sethi<sup>1</sup>, S. Muralidhara<sup>1</sup>, M. Amaraneni<sup>1</sup>, T. Mortuza<sup>1</sup>, C. Chen<sup>1</sup>, B. S. Cummings<sup>1</sup>, J. V. Bruckner<sup>1</sup>, N. Assaf<sup>2</sup>, D. Minnema<sup>3</sup> and C. A. White<sup>1</sup>. <sup>1</sup>Department of Pharmaceutical and Biomedical Sciences, University of Georgia, Athens, GA; <sup>2</sup>Valent BioSciences, Libertyville, IL; <sup>3</sup>Syngenta Crop Protection, Greensboro, NC.

Plasma protein binding (PPB) can influence the toxicokinetics of highly-bound chemicals, by limiting the amount of compound free to reach target organs and sites of elimination. Because the influence of age on PPB of common pyrethroids is unclear, this study was undertaken to determine if binding of deltamethrin (DLM), cis-permethrin (CIS) or trans-permethrin (TRANS) changes during maturation. The PPB of DLM, CIS and TRANS was studied in plasma of 10-, 15-, 21- and 90-day-old (adult) rats. A solvent extraction method was developed to quantify the binding of these highly hydrophobic compounds to rat plasma (RP) proteins and lipoproteins. A 10-µl aliquot of 14C-DLM, -CIS or TRANS was mixed with 90 µl of plasma and cold compound yielding concentrations of 250-100,000 nM. Samples were incubated and shaken at 37°C for 3 hr. The unbound fraction was extracted with 200 µl of isooctane, the lipoprotein-bound fraction with 200 µl of octanol, and the albumin-bound fraction with 200 µl of acetonitrile. Samples were treated with 10 µl of a 0.64 M solution of sodium fluoride to inhibit carboxylesterases. The free fractions of DLM, CIS and TRANS were higher in 10-day-old RP ( $27.1 \pm 6.1$  to  $29.9 \pm 6.4$  %) than adult RP ( $19.2 \pm 1.5$  to  $21.3 \pm 2.1$  %). The fractions of DLM, CIS and TRANS bound to lipoproteins were slightly higher in the pre-weanlings, however the fractions bound to protein were substantially lower. In 15-day-old rats the free fraction and lipoprotein-bound fraction of DLM, CIS and TRANS decreased somewhat. At day 21, PPB reached adult levels. The lower PPB in pre-weanlings is consistent with lower total plasma protein levels. Their lower albumin levels appear to account for the relatively low protein binding of DLM, CIS and TRANS. (Supported by the Council for Advancement of Pyrethroid Human Risk Assessment)

**PS 594 Assessment of an In Vitro Human Dermal Absorption Database for Pesticide Formulations to Establish Scientifically-Based Default Dermal Absorption Values.**

M. Aggarwal<sup>1</sup>, A. Hueser<sup>2</sup>, C. Strupp<sup>3</sup>, C. Wiemann<sup>4</sup>, P. Fisher<sup>5</sup>, B. Parr-Dobrzanski<sup>6</sup>, M. Soufi<sup>7</sup> and R. Billington<sup>1</sup>. <sup>1</sup>Dow AgroSciences, Abingdon, United Kingdom; <sup>2</sup>Dr Knoll Consult GmbH, Leverkusen, Germany; <sup>3</sup>Feinchemie Schwebda GmbH, Kleines Wiesental, Germany; <sup>4</sup>BASF Oesterreich GmbH, Vienna, Austria; <sup>5</sup>Bayer CropScience, Sophia-Antipolis, France; <sup>6</sup>Syngenta, Bracknell, United Kingdom; <sup>7</sup>DuPont de Nemours (Deutschland) GmbH, New-Isenburg, Germany.

Dermal absorption (DA) values for plant protection products (PPP) are required as inputs to risk assessment models used in the EU for assessing non-dietary risk for sprayers, workers, residents and bystanders. DA values are generated using undiluted PPP and representative field spray dilutions. The European Food Safety Authority (EFSA) published guidance on dermal absorption for PPP that includes highly conservative default DA values of 25% and 75% for undiluted PPP and field spray dilutions, respectively. Moreover, a default DA value of 75% applies to the undiluted PPP if it contains  $\leq 5\%$  active substance. To determine the validity of these default values, data from over 300 in vitro DA studies using human skin have been collected, collated and evaluated to establish the scientific validity of the default values and other endpoints. All studies that complied with the principles of OECD test guideline #428 were chosen for this analysis. These studies were performed on a wide range of formulation types and concentrations. The analysis was carried out considering two definitions of DA: (i) radioactivity present in receptor fluid and receptor chamber wash, plus skin minus the first two tape strips (i.e., worse-case definition) and (ii) radioactivity present in receptor fluid and receptor chamber wash plus skin minus stratum corneum (best-case definition). The analysis suggests that the default DA values for concentrate and spray dilution should not be more than 5% and 40%, respectively, considering the worse-case DA definition. Preliminary ranking for influence of formulation type on DA for undiluted PPP is EC = EW > SL = SE = SC > CS = solid formulations = FS. Data will also be presented on the influence of formulation types on DA for field spray dilutions.

**PS 595** **Determination of Pyrethroids in Rat Blood and Tissues Using Gas Chromatography (GC) Negative Chemical Ionization Mass Spectrometry.**

D. Gullick<sup>1</sup>, X. Wang<sup>1</sup>, J. V. Bruckner<sup>1</sup>, B. S. Cummings<sup>1</sup>, D. Minema<sup>2</sup>, M. Krolski<sup>3</sup> and M. G. Bartlett<sup>1</sup>. <sup>1</sup>PBS, University of Georgia, Athens, GA; <sup>2</sup>Syngenta Crop Protection, Greensboro, NC; <sup>3</sup>Bayer Crop Science, Research Triangle Park, NC.

Pyrethroids are the more stable synthetic structural analogues of naturally occurring pyrethrins, which are potent insecticides that exhibit low mammalian toxicity. A reproducible and sensitive bioanalytical method was developed to monitor the uptake and elimination of pyrethroids in plasma and tissues following oral dosing of rats as part of an approach to assess their risk to human health by physiologically based pharmacokinetic (PBPK) models. Blood and tissue homogenates (100 µL) were spiked with Deltamethrin, cis- or trans-permethrin. 1% phosphoric acid (100 µL) was added (to reduce binding of pyrethroids to proteins) and mixed. Internal standard (another pyrethroid) and 400 µL acetonitrile were added and mixed (to precipitate the proteins and extract the pyrethroids) and centrifuged. Supernatant (500 µL) was evaporated to dryness, reconstituted with toluene (300 µL), filtered (0.2 µm PTFE syringe filter), evaporated, and reconstituted with toluene (50 µL) for analysis. Samples were injected into an Agilent 6890 gas chromatograph using pulsed splitless injection onto a Zebtron® ZB5-MS capillary column eluting into a 5973 quadrupole mass analyzer in negative chemical ionization mode. Fragment ions were monitored using selected-ion monitoring for quantitation and verification of the analyte. The method was linear from 1 ng/mL to 1 µg/mL from tissues and blood. The limit of detection was 0.5 ng/mL, the limit of quantitation was 1 ng/mL, and the intraday precision and accuracy of the method were better than 15% across the linear range. Absolute recovery from blood and tissues was greater than 50%. The method was successfully used to monitor the uptake and elimination of pyrethroids in blood and tissues following oral dosing of rats. (Supported by the Council for the Advancement of Pyrethroid Human Risk Assessment).

**PS 596** **Toxicokinetics of Low Doses of the Pyrethroid, Deltamethrin (DLM), in Rats.**

C. Chen<sup>1</sup>, S. Muralidhara<sup>1</sup>, D. Gullick<sup>1</sup>, T. Mortuza<sup>1</sup>, M. Amaraneni<sup>1</sup>, P. Sethi<sup>1</sup>, D. W. Gammon<sup>2</sup>, S. S. Anand<sup>3</sup>, T. G. Osimitz<sup>4</sup>, C. A. White<sup>1</sup>, B. S. Cummings<sup>1</sup> and J. V. Bruckner<sup>1</sup>. <sup>1</sup>PBS, University of Georgia, Athens, GA; <sup>2</sup>FMC, Ewing, NJ; <sup>3</sup>DuPont Haskell, Newark, DE; <sup>4</sup>Science Strategies LLC, Charlottesville, VA.

Pyrethroid insecticides are the widely used to control a wide variety of pests in and around homes, in food handling establishments, in mosquito control, and in agriculture. Pre-weanling and weanling rats are much more sensitive to lethality from a single high dose of the Type II pyrethroids deltamethrin (DLM) and cypermethrin than are adult rats. The hypothesis is that this is due to the incomplete development of the detoxification enzymes in the young rats. No age-related sensitivity to lethality or acoustic startle response has been noted at low doses of DLM. Our hypothesis is that, despite immature detoxification enzymes, sufficient metabolic capability is present to readily eliminate low doses. The current work was conducted to generate low-dose DLM blood and tissue time-course data to test this hypothesis and to provide input to a physiologically based pharmacokinetic model. Time-courses for 0.1, 1 and 5 mg DLM/kg have been delineated in adult rats dosed orally with DLM in 1 or 5 ml corn oil/kg or in 1 ml glycerol formal/kg. Serial sacrifices of groups of 3–5 rats have been conducted at intervals from 15 min to 96 hr post-dosing to obtain blood, brain, and other tissue samples for GC-MS analysis. Dose-dependent increases in peak DLM blood and non-adipose tissue levels were manifest from 2 to 6 hr. The larger volume of corn oil resulted in a relatively broad peak or plateau in blood levels and a more gradual decrease over the monitoring period than with the low volume. Brain levels at comparable times were significantly lower with the larger dosing volume. A significant portion of each dose of DLM was sequestered in fat, with slow release resulting in prolonged elevation of blood levels and thus availability to other tissues. (Supported by the Council for the Advancement of Pyrethroid Human Risk Assessment)

**PS 597** **Dislodgeable Foliar Metabolites of Malathion and Fenpropathrin May Contribute to Aggregate Harvester Exposure Estimates Using Urine Biomonitoring.**

Y. Liu<sup>2</sup>, G. Sankaran<sup>1,2</sup>, L. T. Tang<sup>2</sup>, L. Chen<sup>2</sup>, A. Krieger<sup>2</sup>, J. H. Ross<sup>3</sup>, H. Vega<sup>2</sup> and R. Krieger<sup>1,2</sup>. <sup>1</sup>University of California Riverside, Riverside, CA; <sup>2</sup>University of California Riverside, Riverside, CA; <sup>3</sup>Gem Quality Risk, Inc., Carmichael, CA.

Parent insecticide residues dissipate on sprayed leaf surfaces and may yield derivatives used as biomarkers of exposure to the pesticide on foliar surfaces. It is imperative to determine if surface derivatives actually contribute to the apparent aggregate exposure of harvesters based upon urine biomonitoring. If pesticide derivatives that are potential urine biomarkers persist longer than the parent insecticide on treated plants and they are bioavailable, their absorption and excretion may confound harvester exposure reconstruction for risk assessment. Strawberry harvester exposures to malathion and fenpropathrin use were studied during July 2012 at Santa Maria, CA. Quantitative measurements of parent residues and corresponding biomarker residues on leaf surfaces determined using nitrile gloves worn by workers and 24 hr urine samples from harvesters (and matched controls with no occupational exposure) were conducted at specified intervals post malathion and fenpropathrin application on strawberry fields. Urine biomonitoring allows reconstruction of absorbed dose/day from all possible routes of pesticide and biomarker exposure using rapidly excreted urine biomarkers. Preliminary data show that when foliar malathion residue transferred to cotton cloths (µg/cm<sup>2</sup>; 0.238 to 0.027) and harvester gloves (µg/pair; 13944 to 3435) declined by 90% and 75% respectively in the 3d between the first picking and the second picking; corresponding malathion transferred foliar biomarkers dropped only by 16% and 11%, respectively. These data suggest surface derivatives last longer than parent residues on foliar surfaces. Structurally similar derivatives are dermally absorbed and this may explain why biomonitoring historically has indicated exposure to parent long after the parent has dissipated.

**PS 598** **Soil Concentrations and Human Exposures to Contaminated Soil in the Remote First Nation Community of Fort Albany, Ontario, Canada.**

E. N. Liberda<sup>1</sup>, E. S. Reyes<sup>1</sup> and L. J. Tsuji<sup>2</sup>. <sup>1</sup>School of Occupational and Public Health, Ryerson University, Toronto, ON, Canada; <sup>2</sup>Department of Environment and Resource Studies, University of Waterloo, Waterloo, ON, Canada.

A study was conducted in the James Bay Region of Ontario, Canada to examine the concentration of dichlorodiphenyltrichloroethane and metabolites (o,p'-DDE, p,p'-DDE, o,p'-DDD, p,p'-DDD, o,p'-DDT, p,p'-DDT, and ΣDDT) in potentially contaminated soil sites, and to assess the exposure pathways to ΣDDT by comparing the estimated daily intake (EDI) to acceptable daily intake (ADI) values. The contaminated soil plots were analyzed by a gas chromatograph equipped with a 63Ni electron capture detector (GC/ECD) or by gas chromatography with a mass spectrometer as a detector (GC/MS). The samples were first extracted using a Soxhlet apparatus with dichloromethane as the solvent and sample cleanup was applied using a Florisil extraction column. The mean ΣDDT found in the soil plots were distributed irregularly with values ranging from not detected to 4.19 mg/kg. From the soil plots analyzed, Plot A had the highest ΣDDT concentration of 1.12 mg/kg, followed by Plot B and Plot C which were 0.09 mg/kg and 0.01 mg/kg, respectively. The exposure analysis showed that the risks to humans was below governmental guidelines, even though the DDT concentration in the soil was above Canada's soil guidelines of 0.7 mg/kg as set by the Canadian Council of Ministers of the Environment. The DDT concentration in Plot A breached maximum levels, therefore this land cannot not be used for agricultural as planned nor for recreational purposes. However, both Plots B and C were below maximum threshold limits, and this land may be used to grow safe food resources.

**PS 599** **Effect of Soil Fumigation with Methyl Bromide against Earthworm, *Aporrectodea caliginosa*.**

N. S. Ahmed, S. S. Desouky, A. H. Elsebae and S. S. Soliman. *Pesticide Chemistry, Alexandria University, Alexandria, Egypt.*

Methyl bromide, MBr, is a soil and food commodity fumigant that is used to control most kind of pests that born from or affect them, respectively. Earthworms, *Aporrectodea caliginosa*, are very important for healthy and productive soil. Although, MBr has been added to the list of chemicals that deplete the ozone layer (Montreal Protocol), its use still allowed under several condition worldwide. Effect of MBr against earthworm was investigated in this study. Worms were exposed to one fumigation level of 30 gm/m<sup>2</sup> where worms were distributed in several depths

of the used soil. Mortality and some biochemical effects in the exposed worms compared to control were measured at 24, 48, and 72 hours after exposure. MBr at the tested level caused 100% mortality in worms crawling at 10 and 30 cm depth in all tested intervals. At the 50 cm depth, mortality rates were 80, 90, and 90 percent at the 24, 48, and 72 hours after exposure, respectively. The effect of MBr against protein content of earthworm crawling at the 50 cm depth was measured. Results showed that, after 24, 48 hours, the protein content increased significantly. There was no significant difference after 72 h of exposure in protein content between exposed worms and the control. Effect of MBr at the tested level on the activities of earthworms glutathione-S-transferases, GS-T; acetylcholinesterase, AChE; and cellulase were also determined in worms crawling at the 50 cm depth. Results showed only slight significant increase in AChE activity at 24 and 48 hours after exposure relative to control. MBr at the tested level caused significant increase in GS-T activity of the exposed earthworm at all tested exposure intervals. On the other hand, there was a significant increase in cellulase activity after 24 h as compared to control. However, this difference disappeared at 48 and 72 hours following exposure. These results indicate that MBr is a very potent soil fumigants that also kill the beneficiary earthworms in soil and protection of earthworms must be taken into consideration while searching for alternative to MBr.

## PS 600 Mechanism of Paraquat-Induced Pulmonary Fibrosis and Intervention of Pyrrolidine Dithiocarbamate.

M. Huang<sup>1,2</sup>, P. Zhang<sup>3</sup>, X. Chang<sup>2</sup>, Q. Wu<sup>2</sup> and Z. Zhou<sup>2</sup>. <sup>1</sup>Occupational Health Science, Ningxia Medical University, Yinchuan, China; <sup>2</sup>Occupational Health Science and Toxicology, Fudan University, Shanghai, China; <sup>3</sup>Occupational Health, Centers for Disease Control and Prevention of Jiading, Shanghai, China.

The mechanism of Paraquat-induced pulmonary fibrosis and potential therapeutic effect of pyrrolidine dithiocarbamate (PDTC) were studied. Male SD rats were divided into control group (0.9% NaCl, gavage), PDTC group (100mg/kg, ip), PQ (80mg/kg, gavage) group and PQ+PDTC (100mg/kg, ip) group. On the 1st, 3rd, 7th, 14th, 28th and 56th day after treatment, The expressions of connective tissue growth factor (CTGF) and  $\alpha$  smooth muscle actin ( $\alpha$ -SMA) in lung tissues were measured. The mRNA levels of CTGF, Fn, Col I, Col III and integrin  $\alpha 5$  were analyzed with quantitative RT-PCR. Meanwhile, the lung pathological changes were observed and the content of Hydroxyproline (Hyp) was measured. The expression of CTGF in PQ group increased gradually compared with control group ( $P < 0.05$ ). CTGF mRNA level significantly increased from the 1 st to the 14 th day compared with control group ( $P < 0.05$ ). PQ significantly increased Fn mRNA level on all time points and integrin  $\alpha 5$  mRNA level from the 3 rd to 56 th day compared with control group ( $P < 0.05$ ). Col I mRNA level significantly increased from the 7 th to the 56 th day and Col III mRNA level appears to be decreased from the 14 th to the 56 th day. PDTC treatment significantly decreased the levels of those factors compared with PQ group in corresponding time points ( $P < 0.05$ ). Noteworthy, PDTC strongly attenuated histopathological changes and decreased the content of Hyp. These results suggested that CTGF plays a key role in paraquat-induced pulmonary fibrosis, which is characterized by increased Fn, integrin  $\alpha 5$ , Col I and Col III mRNA levels. PDTC may inhibit NF- $\kappa$ B activity and further significantly decrease expressions of CTGF leading to drastically attenuated pulmonary fibrosis. However, the mechanisms of PDTC intervention still remain to be explored.

## PS 601 Testicular Toxicity of Fluorochloridone in Adult Sprague-Dawley Rats.

L. Xu<sup>2,1</sup>, Z. Zhou<sup>2</sup>, Q. Zhao<sup>2</sup>, D. Lou<sup>2</sup>, X. Chang<sup>2</sup>, P. Xiao<sup>3</sup>, X. Hong<sup>3</sup> and X. Yu<sup>1</sup>. <sup>1</sup>Department of Environmental Health Science, University of Georgia, Athens, GA; <sup>2</sup>School of Public Health, Fudan University, Shanghai, China; <sup>3</sup>Shanghai Municipal Center for Disease Control & Prevention, Shanghai, China.

Fluorochloridone (FC) a widely used herbicide in Europe and the US, has been recognized as a potential reproductive and developmental toxicant. However, there is little data available concerning its male reproductive toxicity. In this study, we examined the testicular toxicity of FC in SD male rats. Adult rats were treated by gavage with FC at doses of 0, 30, 150, 750 mg/kg/d for four weeks. FC exposure resulted in a decrease in the absolute and relative weight of testes and a decrease in the absolute weight of epididymides as compared with the control. Cauda epididymal sperm count decreased dramatically in a dose-dependent manner. In addition, histological lesions were also found in the testes of the treated animals. A dose-effect (response) relationship analysis suggested that changes in cauda epididymal sperm count and testicular histological structure could be the most sensitive indicators for FC induced testicular toxicity.

## PS 602 Carbofuran Is Not an Endocrine Disruptor—Weight-of-Evidence of US EPA's Tier 1 Endocrine Disruptor Screening Program Assays and Higher Tier Studies.

D. W. Gammon, B. Sharma, S. Longacre, G. Mitchell, S. Mukhi, M. Oh and Z. Liu. APG, FMC Corp, Ewing, NJ.

Carbofuran, the active ingredient in FMC Corporation's FURADAN® Insecticide/ Nematicide products, underwent testing in EPA's Tier I endocrine disruption screening program (EDSP), as required for all US registered pesticide active ingredients, to assess whether carbofuran had the potential to interact with endocrine systems. Nine of the eleven carbofuran Tier 1 EDSP assays showed no potential to interact with endocrine systems. The slight increase in estradiol in the in vitro steroidogenesis assay, and the mild to moderate thyroid hypertrophy and mild thyroid hyperplasia in the amphibian metamorphosis assay observed with relatively high carbofuran concentrations were not corroborated by any of the other assays. Only the highest concentration (100  $\mu$ M) was positive in the steroidogenesis assay, several orders higher than the concentration required for AChE inhibition. Previously conducted higher tier in vivo carbofuran developmental, reproductive and chronic toxicity studies showed no endocrine-mediated effects. The overall lack of effects in the carbofuran Tier 1 EDSP assays is consistent with the lack of endocrine-mediated effects in the previously conducted carbofuran higher tier in vivo studies. The collective results of the carbofuran Tier 1 EDSP assays and previously conducted higher tier in vivo studies indicate carbofuran is not an endocrine disruptor, and that there is no concern for endocrine effects resulting from the use of FURADAN® products according to label instructions.

## PS 603 Reproductive Outcomes in Women Para-Occupationally Exposed to Pesticides in an Agricultural Community in Southern Mexico.

G. López-Manzanero<sup>1</sup>, N. Pérez-Herrera<sup>1</sup>, L. Dzib-Cocom<sup>1,2</sup>, P. García-Molina<sup>1,2</sup>, M. Vera-Avilés<sup>1</sup>, T. Castillo-Burguete<sup>3</sup>, L. González-Navarrete<sup>1</sup>, J. Alvarado-Mejía<sup>1</sup>, B. Jiménez-Delgadillo<sup>1</sup>, J. Arias-León<sup>1</sup>, V. Suárez-Solis<sup>1</sup>, M. Cárdenas-Marrufo<sup>1</sup>, I. Vado-Solis<sup>1</sup>, C. Pérez-Osorio<sup>1</sup>, I. Hernández-Ochoa<sup>4</sup> and B. Quintanilla-Vega<sup>4</sup>. <sup>1</sup>Faculty of Medicine, Autonomous University of Yucatán, Mérida, Mexico; <sup>2</sup>Faculty of Chemistry, Autonomous University of Yucatán, Mérida, Mexico; <sup>3</sup>Human Ecology Department, CINVESTAV, Mérida, Mexico; <sup>4</sup>Toxicology Department, CINVESTAV, Mexico City, Mexico.

Epidemiological studies have shown that farmers are at high risk of developing adverse effects including reproductive problems. However, reproductive outcomes by para-occupational exposure to pesticides in wives of farmers are poorly documented. We reported reproductive alterations such as poor semen quality in farmers and spontaneous abortions and preterm birth in wives of agricultural workers mostly exposed to organophosphate pesticides (OP). Thus we evaluated the scenery of para-occupational pesticide exposure and its associated reproductive outcomes in wives of farmers. A transversal study was conducted in Yucatán, Mexico in wives of farmers exposed to pesticides (n=28) and wives of workers without pesticide exposure (n=45). Women donated a blood sample and responded a questionnaire. The TORCH profile was determined as potential confounders. General characteristic and TORCH profile were similar between two groups. Age at menarche was marginally lower in wives of farmers (11.5 $\pm$ 1.06 vs. 12.13 $\pm$ 1.56 years, p=0.07). Difficulty getting pregnant was more prevalent in wives of farmers (63 vs 13%, p=0.0003), preterm births were marginally more frequent in these women (7 vs 0%, p=0.07), and the birth weight of the first child was slightly lower in couples of farmers (2.94 $\pm$ 0.55 vs 3.16 $\pm$ 0.48 Kg, p=0.09). A complex scenery of pesticides exposure was observed, paraquat, glyphosate, 2,4-D amine, methamidophos and chlorpyrifos were among the most used pesticides. Results show that pesticide para-occupational exposure in wives of farmers may be involved with reproductive outcomes. Supported by PROMEP-SEP-México.

## PS 604 Extension of a Nasal Dosimetry Model for Acetaldehyde to Account for Vasodilation.

P. M. Schlosser<sup>1</sup>, M. H. Lumpkin<sup>2</sup> and J. B. Morris<sup>3</sup>. <sup>1</sup>NCEA, US EPA, Research Triangle Park, NC; <sup>2</sup>ENVIRON International Corporation, Atlanta, GA; <sup>3</sup>School of Pharmacy, University of Connecticut, Storrs, CT.

Acetaldehyde (AAld) is an important industrial chemical, used in manufacturing a wide range of products, but sources also include volcanoes, forest fires, biological waste degradation, and respiration by plants. Subchronic inhalation causes olfactory and nasal respiratory tissue degeneration in rats at  $\geq$  150 ppm and nasal tumors in both regions at  $\geq$  750 ppm. The toxicity of AAld is likely due to its metabolism to acetic acid in nasal tissues. A series of physiologically-based

pharmacokinetic (PBPK) models have been published which use results from computational fluid dynamics to specify regional airflow and air-phase transport resistance in the nose. Most recently, Teeguarden et al. (Inhal. Toxicol., 20:375-390, 2008) developed a version which included polymorphisms in human high-affinity acetaldehyde dehydrogenase (ALDH2). However, Stanek et al. (Inhal. Toxicol., 13:807-822, 2001) showed that AALD causes vasodilation, increasing uptake of acetone with co-exposure of the two. Vasodilation will also increase uptake of AALD. If this is not included in the model, the extent of metabolism estimated by fitting a PBPK model to nasal AALD uptake data could be over-predicted at concentrations where dilation is significant. Therefore we revised the PBPK model of Teeguarden et al. to include vasodilation (increases in nasal blood flow), with the amount of dilation estimated from the data of Stanek et al. using a parallel acetone PBPK model. An error in model code calculation of tissue phase mass transfer resistance was also corrected. The net result is an increase in the estimated  $V_{max}$  for ALDH2 and a dose-dependent change in total metabolism in rats: increased at lower concentrations where ALDH2 is not saturated, but decreased at 1500 ppm where vasodilation is significant. Quantifying the impact of this revision requires integration of model results with dose-response (i.e., benchmark dose) modeling. (Views expressed here are those of the authors and do not necessarily reflect the views or policies of the U.S. EPA.)

## PS 605 An In Silico Model of Spermatogenesis for Use in Predictive Toxicology.

A. M. Frame, M. C. Leung, T. B. Knudsen and R. Judson. *US EPA, Research Triangle Park, NC.*

EPA's toxicity reference database (ToxRefDB), covering 963 compounds tested in 4209 animal studies, indicated testicular atrophy as an adverse outcome for 278 (28.9 %) chemicals and reduced sperm quality or quantity for 72 (9.8 %) chemicals tested in chronic and subchronic rodent toxicity studies. The sensitivity of the male reproductive system, coupled with the biological complexity of testicular function and the large number of untested chemicals, motivates the need for predictive computational models of male reproductive function based on high-throughput screening (HTS) and in vitro data. Toward this end, we are building a virtual tissue model of the hypothalamic-pituitary-gonadal system (vHPG) that integrates computational approaches for kinetic modeling and dynamic simulation. As a proof of concept, we have constructed a multicellular agent-based model of the rat seminiferous tubule using CompuCell3D. The model integrates cell signaling networks for hormonal effects (FSH, testosterone), growth factor and cytokine stimulation (GDNF, TNF $\alpha$ , TGF $\beta$ , IL1 $\alpha$ ) and transcription factors (e.g. ERM, RhoX5, SOX8, WT1) responsible for regulating key events in the spermatogenic cycle. It also enables Sertoli cell interactions including cytoskeletal restructuring and protein secretion. To test our model, over 1900 chemicals associated with toxic effects on sperm were characterized for effects on spermatogenesis and mechanisms of action. We then identified chemicals targeting specific key aspects of spermatogenesis: cellular division (bleomycin, cisplatin, doxorubicin), cell/cell adhesion (adjudin, indenopyridines, indazole-3-carboxylic acid), and Sertoli cell death ( $\beta$ -benzene hexachloride), as well as putative endocrine disruptors (e.g. atrazine, bisphenol A, ketoconazole). Preliminary results indicate that the model responds appropriately, in terms of sperm production, to the disruption of key signaling events. This abstract does not necessarily reflect Agency policy.

## PS 606 Development of PBPK Models for Gasoline in Adult and Pregnant Rats and Their Fetuses.

S. A. Martin<sup>1</sup>, W. M. Oshiro<sup>1</sup>, P. A. Evansky<sup>1</sup>, J. Ford<sup>1</sup>, L. L. Degen<sup>1</sup>, H. A. El-Masri<sup>1</sup>, W. R. LeFevre<sup>1</sup>, E. D. McLanahan<sup>2</sup>, D. MacMillan<sup>1</sup>, W. K. Boyes<sup>1</sup> and P. J. Bushnell<sup>1</sup>. <sup>1</sup>National Health and Environmental Effects Research Laboratory, US EPA, Durham, NC; <sup>2</sup>National Center for Environmental Assessment, US EPA, Durham, NC.

Concern for potential developmental effects of exposure to gasoline-ethanol blends has grown along with their increased use in the US fuel supply. Physiologically-based pharmacokinetic (PBPK) models for these complex mixtures were developed to address dosimetric issues related to selection of exposure concentrations for in vivo toxicity studies. Sub-models for individual hydrocarbon (HC) constituents were first developed and calibrated with published literature or QSAR-derived data where available. Successfully calibrated sub-models for individual HCs were combined, assuming competitive metabolic inhibition in the liver, and a priori simulations of mixture interactions were performed. Blood HC concentration data were collected from exposed adult non-pregnant (NP) rats (9K ppm total HC vapor, 6h/day) to evaluate performance of the NP mixture model. This model was then converted to a pregnant (PG) rat mixture model using gestational growth equations that enabled a priori estimation of life-stage specific kinetic differences. To address the impact of changing relevant physiological parameters from NP to PG, the PG

mixture model was first calibrated using the NP data. The PG mixture model was then evaluated against data from PG rats that were subsequently exposed (9K ppm/6.33h gestation days (GD) 9-20). Overall, the mixture models adequately simulated concentrations of HCs in blood from single (NP) or repeated (PG) exposures (within ~2-3 fold of measured values of most HCs), indicating that the blood data from PG rats were not highly sensitive to PG-specific physiological parameters. This PG model will be used to estimate internal HC concentrations in the total fetus during in utero exposure to HC vapors. This is an abstract of a proposed presentation and does not necessarily reflect EPA policy.

## PS 607 Strategy to Support Clearance Model of Inhaled Libby Amphibole Asbestos Fibers in Rat and Human Respiratory Tract.

B. Asgharian<sup>2</sup>, O. T. Price<sup>2</sup>, S. H. Gavett<sup>1</sup> and A. M. Jarabek<sup>1</sup>. <sup>1</sup>US EPA, Research Triangle Park, NC; <sup>2</sup>ARA, Inc., Raleigh, NC.

To characterize inhaled Libby amphibole (LA) asbestos fibers as retained dose (RD), we developed a strategy to integrate experimental data with compartmental modeling. Compartments extend our model structure for inhalability and deposition (Asgharian, 2012) to estimate RD in major respiratory tract (RT) regions (upper respiratory tract, URT; tracheobronchial, TB; and pulmonary, PU), pleural lining (PL), and lymph nodes (LN). The strategy provides data to derive 3 clearance mechanisms in the respiratory tract (RT): mucociliary (MC), translocation (TR), and dissolution (DS). Initial mass in each region is calculated using the deposition model verified with fiber burden data in the URT, trachea/larynx, 5 lung lobes and pleural casts in F344 rats from a 6-hr exposure of LA at 0, 3.5, or 25 mg/m<sup>3</sup>. MC rates of the URT and TB regions are estimated by refining published rate constants with fitting mass burdens measured in URT, TB, LN and PL compartments of a 5-d study in rats at those 3 concentrations with post-exposure time course (0-, 6-, 12-, and 24-hr). Burden data in rats from a 13-wk study at 0, 3.3, 1, and 10 mg/m<sup>3</sup> with post-exposure time course (1-d and 1-, 3- and 18-mo) refine TR rates from PU to TB, PL and LN compartments and evaluate overload. The initial DS rate is based on burden data from the URT coupled with in vitro data on DS of LA incubated with synthetic lung lining fluid. Data from in vitro incubation of LA with acid refine DS rate for TB and PU regions. This integrated strategy is the first to derive characterization of MC, TR and DS rates in the rat RT. For humans, DS rates were not scaled, published human MC rates are adjusted based on mass conservation (Asgharian et al., 2001), TR rates to PL and LN compartments are scaled on MC, and PU TR is scaled from the rat by an approach described for particles (Jarabek et al., 2005) based on regional surface area. (The views expressed in this abstract are those of the authors and do not necessarily represent the views or policies of the U.S. Environmental Protection Agency.)

## PS 608 A Modified PBPK Model for RDX (hexahydro-1, 3, 5-trinitro-1, 3, 5-triazine) to Improve Rat to Human Toxicokinetic Extrapolation.

A. E. Loccisano<sup>1,3</sup>, R. S. DeWoskin<sup>2</sup>, P. M. Schlosser<sup>2</sup>, A. F. Sasso<sup>3</sup> and L. J. D'Amico<sup>3</sup>. <sup>1</sup>Oak Ridge Institute for Science & Education, Oak Ridge, TN; <sup>2</sup>ORD/NCEA, US EPA, Research Triangle Park, NC; <sup>3</sup>ORD/NCEA-IRIS, US EPA, Washington DC.

RDX is a military explosive that has been detected in air, soil, and ground water at or near military bases and munitions plants and storage facilities. Studies in rats provide evidence of mortality, reproductive toxicity, and neurotoxicity associated with RDX exposure. Physiologically-based pharmacokinetic (PBPK) models can aid in interpreting toxicological data and extrapolations across dose, species and exposure routes. Presented here is the further development and application of an RDX PBPK model for rats and humans originally published by Sweeney et al. (Regul. Toxicol. Pharmacol., 2012 v. 72, p. 107-114). The differences in the GI tract submodel and absorption parameters for different formulations of RDX in the Sweeney model are problematic for risk assessment because there is no rationale or predictability to the changes. Modifications to the model include a consistent submodel for the GI tract, a consistent set of absorption parameters to simulate oral exposures to RDX, and oral absorption rate constants keyed to different formulations of administered RDX per the kinetic data in the literature. Model code was also added to simulate drinking water and inhalation exposures relevant to human chronic exposures. The resulting model simulations are consistent with observed differences in the time course blood level data from a variety of PK studies, RDX formulations, and dosing regimens. Blood concentrations of RDX did not differ considerably when simulating inhalation exposure as compared to oral exposure. Model fits to rat data resulting from a subchronic drinking water exposure demonstrated achievement of steady state levels, lack of metabolic induction over time

from repeated doses, and the utility of the modified RDX model for use in estimating and extrapolating blood levels following repeated exposure. [The views expressed are those of the authors and do not necessarily reflect the views or policies of the U.S. EPA.]

**PS 609** **Developing New Methods to Measure Reactive Oxygen Species Related to Aerosol Components.**

W. Huynh<sup>1</sup>, E. Browne<sup>2</sup> and R. E. Peltier<sup>1</sup>. <sup>1</sup>Public Health - Environmental Health Sciences, University of Massachusetts Amherst, Amherst, MA; <sup>2</sup>Veterinary & Animal Sciences, University of Massachusetts Amherst, Amherst, MA.

Reactive oxygen species (ROS) have been shown to be an important indicator of adverse toxicological effects and has been widely studied in the context of ambient air pollution exposure research. ROS is formed *in vivo* as a result of exposure to ambient air pollutants and is thought to be a convenient approach to understanding responses arising from air pollution exposures. Current methods of measurement for ROS typically follow a labor-intensive and time-consuming method of collection and extraction of particles from the field, which are then introduced (often at very high concentrations) *in vitro*. The objectives of this research are to streamline these approaches by developing and characterizing a new instrument capable of automated, semi continuous quantification of ROS. The work presented here attempts to fill this gap by repeatedly inducing reactive oxygen on plated immortalized pulmonary epithelial cells (BEAS-2B) which have been loaded with 2',7'-dichlorofluorescein diacetate (DCFH-DA). The data presented here are based on a method using 96-well plates and standard fluorescent spectrometry methods. These results are compared with similar approaches using a system of horseradish peroxidase and DCFH-DA. Tested elements include micromolar concentrations of hydrogen peroxide, solutions of ammonium sulfate and nitric acid, and quinones. We show that, with notable limitations, plated cells can respond to repeated dosing of simulated air pollution, suggesting that this method is suitable for further instrument method development.

**PS 610** **Designing Quantitative Structure Activity Relationships (QSAR) to Predict Specific Toxic Endpoints for Polybrominated Diphenyl Ethers (PBDE) in Mammalian Cell Culture Systems.**

S. Rawat<sup>1,2</sup> and E. D. Bruce<sup>2,3</sup>. <sup>1</sup>US EPA, Athens, GA; <sup>2</sup>Department of Environmental Science, Baylor University, WACO, TX; <sup>3</sup>Department of Civil Engineering, Texas A&M University, College Station, TX.

Polybrominated diphenyl ethers (PBDEs) are flame retardants that have had vast industrial application in consumer products, such as plastics, building materials, electronics and textiles. They are structurally similar to thyroid hormones that are responsible for regulating metabolism in the body. Therefore, PBDEs compete for the thyroid hormone binding receptors and this can adversely affect thyroid hormone transport and metabolism. Due to their potential threat to human health, this study aimed to design Quantitative Structure Activity Relationship (QSAR) models for predicting specific toxic endpoints, namely, cell viability and apoptosis. Human hepatocarcinoma (Hep G2) cells were exposed to PBDEs and were used as a model system to evaluate cell viability using Janus Green dye and apoptosis using a caspase assay. Data collected from the experiments were used to create QSAR models using the Genetic Function Approximation (GFA) method of generating predictive models. Cell viability and apoptosis responses elicited by the PBDEs were successfully modeled with an  $r^2$  of 0.97 and 0.94 respectively. Van der Waal's surface area and Gasteiger charges were found to be the important properties that characterize cell viability. Molar refractivity, Kappa-3, and VSA\_PartialCharge figured as the most appropriate descriptors to characterize apoptosis.

**PS 611** **A Preliminary Physiologically-Based Pharmacokinetic (PBPK) Model of Squalene in Vaccines.**

M. A. Tegenge and R. J. Mirkus. CBER, US FDA, Rockville, MD.

Adjuvants are often added to vaccine formulations to potentiate the immune response to antigen. Aluminum salts are the oldest and most widely used adjuvants; however, in recent years, oil-in-water emulsion adjuvants have emerged as alternative adjuvant systems. Two emulsion adjuvants, MF59® and ASO3®, for example, have been developed commercially using the triterpene oil, squalene. Although

squalene is a natural component of the diet and an endogenous precursor of cholesterol, its fate following intramuscular (IM) injection as a vaccine adjuvant constituent is not fully understood. In the absence of experimental pharmacokinetic data in humans, we constructed a whole body physiologically based pharmacokinetic (PBPK) model for intramuscularly injected squalene-in-water emulsion in adults. Based on published information, we assumed a mean diameter of 160 nm for the emulsion and stabilization by nonionic surfactants. Hence, preferential uptake into the lymphatics, rather than the blood, would be expected following IM injection. Tissue-blood partition coefficients for squalene were estimated by an algorithm approach that considered its binding potential to neutral lipids and lipoproteins. Physiological and biochemical parameters were obtained from standard sources in the published literature. The results of our modeling indicate that intramuscular squalene emulsion will transfer from the site of injection into the lymphatics rapidly and will be essentially cleared from the deltoid muscle in two days. The major proportion of the injected squalene was predicted to distribute to the draining lymph nodes and accumulate in distal adipose tissues. Our model indicated slow clearance from the latter compartment most likely because of partitioning into neutral lipids and a low rate of squalene biotransformation there. However, the predicted contribution of administered squalene was still only ~0.1% of the endogenous pool of squalene in adipose tissue. In conclusion, our results provide important pharmacokinetic information that may help to explain the pharmacodynamic activity of a new class of vaccine adjuvants that contain squalene.

**PS 612** **A Model for Elucidating the Role of the Aryl Hydrocarbon Receptor in TCDD-Mediated IgM Suppression in Human B Cells.**

N. Kovalova<sup>1,2</sup>, M. Manzan<sup>2</sup>, R. B. Crawford<sup>2</sup> and N. E. Kaminski<sup>1,2</sup>. <sup>1</sup>Pharmacology/Toxicology, Michigan State University, East Lansing, MI; <sup>2</sup>Center for Integrative Toxicology, Michigan State University, East Lansing, MI.

The aryl hydrocarbon receptor (AHR) is a transcription factor mediating toxic effects of 2,3,7,8 tetrachlorodibenzo-p-dioxin (TCDD). The objective of the present study was to establish a human B cell model for elucidating the role of the AHR in TCDD-induced suppression of the IgM production by B cells. The SKW6.4 cell line used here is an Epstein-Barr virus-transformed, IgM-secreting human B cell line. Wild-type SKW 6.4 cells are AHR null. We have used a lentiviral transduction system to establish a SKW 6.4 cell line that stably expresses the human AHR cloned from hepatoma HepG2 (SKW E8). An expression vector was designed to produce an AHR-GFP fusion protein under the control of a doxycycline-inducible promoter. SKW E8 and HepG2 cells express similar levels of AHR mRNA, as determined by qRT-PCR. TCDD treatment significantly induced Cyp1B1 mRNA expression in SKW E8 but not in SKW 6.4 cells, indicating that the transduced AHR retained its transactivational activity. To assess the effects of TCDD on IgM secretion, increasing concentrations of TCDD were added to pokeweed mitogen (PWM) or lipopolysaccharide (LPS) activated SKW cell lines, induced IgM was measured by ELISA. IgM secretion by PWM- or LPS-stimulated SKW E8 but not SKW6.4 cells was suppressed by TCDD in a concentration-dependent manner. Further analysis of the TCDD-induced suppression of the IgM response in SKW E8 cells revealed that to suppress IgM production, TCDD must be added within the first 12 h post-LPS activation. A similar window of sensitivity for the TCDD-induced suppression of the IgM response was previously described in primary mouse B lymphocytes. We demonstrate that the introduced AHR is functional and induction of IgM production is suppressed by TCDD-treatment as shown in primary B cells. These results suggest that human SKW6.4 E8 cells represent a model for elucidation of the molecular mechanisms involving AHR signaling in IgM suppression.

**PS 613** **The Impact of Variation in Scaling Factors on the Estimation of Internal Dose Metrics: A Case Study Using Bromodichloromethane.**

E. M. Kenyon<sup>1</sup>, R. A. Pegram<sup>1</sup>, C. R. Eklund<sup>1</sup> and J. C. Lipscomb<sup>2</sup>. <sup>1</sup>ORD/NHEERL, US EPA, Durham, NC; <sup>2</sup>ORD/NCEA, US EPA, Cincinnati, OH.

Physiologically based pharmacokinetic (PBPK) models can include values for metabolic parameters extrapolated from *in vitro* metabolism studies using scaling factors such as mg of microsomal protein per gram of liver (MMPGL) and liver weight (LW). Variation in scaling factor values impacts metabolic rate parameter estimates ( $V_{max}$ ) and hence estimates of internal dose used in dose response analysis. The impact of variation in MMPGL and LW on estimates of internal dose was assessed using a human PBPK model for bromodichloromethane (BDCM). Internal dose metrics evaluated were area under the curve for blood BDCM (AUC), maximum concentration of BDCM in blood ( $C_{max}$ ) and amount metabolized in liver per

hour (AML) - for two exposure scenarios (single 0.25 liter drink of water or 10 minute shower) under typical (10 ppb) and plausible high level (50 ppb) water concentrations. MMPGL and LW (as a fraction of body weight) values used in the analysis reflect the range of values reported for adult humans. For each concentration, each dose metric was changed less than 5% for the showering scenario (inhalation and dermal exposure) because  $V_{max}$  for hepatic metabolism is not a very influential parameter for dose metrics related to blood concentration following low level exposures. In contrast, an 8-fold difference in  $C_{max}$  and AUC was observed for each oral exposure concentration, but AML was relatively unchanged. Sensitivity analysis for AUC for the oral exposure scenario revealed that MMPGL was the most influential parameter, followed closely by LW, with blood flow to the liver being moderately influential. This analysis demonstrates that variability in the scaling factors used for in vitro to in vivo extrapolation (IVIVE) of metabolic rate parameters can have a significant impact on estimates of internal dose metrics under environmentally relevant exposure scenarios. This indicates the need to evaluate both uncertainty and variability for scaling factors used for IVIVE. (This abstract does not necessarily reflect USEPA policy).

**PS 614 Kinetic Modeling Reveals the Roles of ROS Scavenging and DNA-Repair Processes in Shaping the Dose-Response Curve of  $KBrO_3$ -Induced-DNA Damage.**

D. J. Miller and M. A. Spassova. *National Center for Environmental Assessment, US EPA, Washington DC.* Sponsor: S. Vulimiri.

We have used kinetic modeling to investigate how DNA repair processes and scavengers of reactive oxygen species (ROS) can affect the dose-response shape of pro-oxidant induced DNA damage. We used as an example chemical  $KBrO_3$ , a water ozonation by-product and environmentally present pro-oxidant with genotoxic and carcinogenic effects. In our model,  $KBrO_3$  is activated via interaction with glutathione and forms reactive intermediates that directly interact with DNA to form 8-hydroxy-2-deoxyguanosine DNA adducts (8-OH-dG) – an effect convincingly established in literature. The single strand breaks (SSB) that can result from failed base-excision repair of these adducts were considered in the model as an effect downstream from 8-OH-dG. We previously demonstrated that in the presence of effective base-excision repair, 8-OH-dG can exhibit threshold-like dose-response dependence, while the downstream SSB can still exhibit a linear dose-response. We now further demonstrate that this result holds for a variety of model variants. In particular, we investigated how the presence of a scavenger of the bromate reactive intermediates affects the dose-response shape of 8-OH-dG and SSB. It has been shown that melatonin, a terminal antioxidant, inhibits  $KBrO_3$ -caused oxidative damage. Our modeling revealed that a single pulse exposure to  $KBrO_3$  in the presence of such a terminal scavenger can lead to a sublinear/threshold-like dependence of the response for both 8-OH-dG and SSB. However, sustained exposure to  $KBrO_3$  can lead to fast scavenger exhaustion, in which case the dose-response shapes for both endpoints are not substantially affected. The results are important to consider when forming conclusions on a chemical's toxicity based on the dose-response of early genotoxic events.

**PS 615 A Compartmental Pharmacokinetic (PK) Model for Bromate in F344 Rats.**

N. Kolisetty<sup>1</sup>, C. A. White<sup>1</sup>, R. J. Bull<sup>2</sup>, J. A. Cotruvo<sup>3</sup>, J. W. Fisher<sup>4</sup> and B. S. Cummings<sup>1</sup>. <sup>1</sup>Pharmaceutical and Biomedical Sciences, University of Georgia, Athens, GA; <sup>2</sup>Mo Bull Consulting, Richland, WA; <sup>3</sup>Joseph Cotruvo & Assoc. LLC, Washington DC; <sup>4</sup>National Center for Toxicological Research, US FDA, Jefferson, AR.

Bromate ( $BrO_3^-$ ) is a toxic water disinfection by-product formed during ozonation of source water containing bromide ( $Br^-$ ). It is a proven animal and probable human carcinogen (group 2B). However,  $BrO_3^-$  pharmacokinetics (ADME) at low doses is not fully understood. To better understand  $BrO_3^-$  ADME, we developed a pharmacokinetic (PK) model based on the raw data from our recent publication (Bull et al. 2012). Based on goodness of fit, and the model diagnostics, a pharmacokinetic model fitted with individual animal data and weight-2 (1/Y<sup>2</sup>) weight scheme was chosen as a model of choice to describe  $BrO_3^-$  disposition in female F344 rats.  $BrO_3^-$  disposition after IV bolus was best described using a 1-compartmental pharmacokinetic model for doses up to 0.5 mg/kg; and by using a 2-compartmental pharmacokinetic model for doses of 1-2.5 mg/kg potassium bromate ( $KBrO_3$ ).  $BrO_3^-$  disposition was best described using a 1-compartmental model following its oral administration (0.5 to 20 mg/kg  $KBrO_3$ ) in female F344 rats. Analysis of  $BrO_3^-$  PK parameters following oral administration, suggested that  $BrO_3^-$  absorption occurs in a first order manner with a rate constant ( $K_a$ ) of ~0.16 min<sup>-1</sup>.  $BrO_3^-$  appears to undergo extensive first pass reduction, resulting in

bioavailability of ~19-25%. Approximately 90% of orally administered  $BrO_3^-$  is reduced to  $Br^-$  in the body, and the remaining  $BrO_3^-$  appears to be excreted from the body as  $BrO_3^-$  in the urine at 0.002 L/min/kg. In conclusion,  $BrO_3^-$  undergoes extensive reduction to  $Br^-$  in liver and blood following its oral administration in female F344 rats, which limits  $BrO_3^-$  distribution to the peripheral tissues to exert its toxic effects.

**PS 616 A Strategy for Developing a PBPK Model to Describe the Kinetics of Silver Nanoparticles.**

M. Yoon<sup>1</sup>, S. Sumner<sup>2</sup>, R. Snyder<sup>2</sup>, T. Fennell<sup>2</sup> and H. J. Clewell<sup>1</sup>. <sup>1</sup>The Hammer Institutes for Health Sciences, Research Triangle Park, NC; <sup>2</sup>RTI International, Research Triangle Park, NC.

Our previous model for C60 was proposed as a general platform for PBPK modeling of engineered nanoparticles (NPs). Since the structure was based on biological mechanisms that govern NP disposition, the platform can be applied to other NPs by changing parameters to account for particle-to-particle variance in biological processes. In this study, the model was parameterized for silver (Ag) NPs using tissue concentration data collected in adult female SD rats after a single intravenous (IV) dose (1 mg/kg) of Ag NPs (20 or 110 nm) in water stabilized with polyvinyl pyrrolidone (PVP) or Ag acetate in PVP. Parameterization was based on size-dependent dissolution potential of Ag NPs under physiological conditions as well as generally applicable size-dependent endocytosis efficiency for particles. Due to the dissolution potential, a combination of two kinetic models, one for Ag NPs and the other for ionic forms of Ag was used. The model successfully simulated observed concentrations of total Ag in various tissues as well as in urine and feces after a single IV dose of Ag NPs. The model was then extrapolated to Ag NPs with other coating agents. The published data for tissue concentrations of total Ag in adult male Wistar rats after single or multiple (~0.1 mg/kg/day) IV administration of Ag NPs in phosphate buffer (20 or 110 nm) was simulated. For this evaluation, the impact of different coatings on Ag NPs stability in size, shape and surface properties was also considered in the parameterization. The current model captured the time courses of total Ag concentration in blood, liver, lung, spleen, and heart both for single and multiple exposures from this study. The overall success in extending the C60 model to Ag NPs demonstrated the applicability of our model structure, as a general platform, to other NPs when combined with nanoparticle-specific properties for the given material (This work was supported by NIEHS Award #U19ES019525, but solely expresses the view of the authors).

**PS 617 A Physiologically-Based Pharmacokinetic Model to Describe the Pharmacokinetic Disposition for Hexamethyldisiloxane, a Linear Volatile Methyl Siloxane, following Inhalation Exposures in the Rat.**

T. McMullin, J. Y. Domoradzki, D. A. McNett, J. Durham and K. P. Plorazke. *Health and Environmental Sciences, Dow Corning Corporation, Midland, MI.*

The purpose of this work was to expand a previously developed physiologically based pharmacokinetic (PBPK) model for hexamethyldisiloxane (HMDS) (Dobrev et al., 2003) with additional kinetic data to further examine the processes regulating the pharmacokinetic disposition of HMDS. Time-course concentrations of parent HMDS and total metabolites in multiple tissues, blood and exhaled breath in male and female F344 rats during and following nose only vapor inhalation exposure to 5000ppm 14C-HMDS were used to extend the model. A 15 day inhalation study was also conducted to understand impacts, if any, following repeated exposures. Based on similarities in physicochemical properties, the HMDS model structure was adapted from another volatile methylsiloxane (VMS) octamethylcyclotetrasiloxane (D4) model structure (Andersen et al., 2001). This updated model now includes saturable metabolism in the liver, a diffusion-limited uptake of HMDS in the fat compartment and a blood lipid pool where a fraction of HMDS is sequestered and unavailable for exchange into blood and exhalation from the lung. HMDS and its metabolites in blood, liver, lung, fat and exhaled breath following both single and multiple exposures are well described with this model using a single set of parameters. Consistent with D4 kinetic behavior, low blood:air partitioning and extensive metabolism lead to rapid clearance of free HMDS from the body following both single and repeated exposures. Despite retention of bound HMDS in tissues at the extended time points following exposure, the extensive and rapid clearance mechanisms of HMDS lead to tissue and exhaled breath concentrations of HMDS that are similar following both multiple day exposures and single exposures. This PBPK model is a starting point from which the pharmacokinetic disposition of HMDS and, upon extension, other linear VMSs, can be evaluated for risk assessment.

**PS 618 Use of a Physiologically-Based Pharmacokinetic Model to Simulate the Time Course of 3-Hydroxybenzo(a)Pyrene Metabolite in Workers Exposed to Polycyclic Aromatic Hydrocarbons and Predict Most Plausible Exposure Scenarios.**

R. Heredia-Ortiz<sup>1</sup>, A. Maitre<sup>2</sup> and M. Bouchard<sup>1</sup>. <sup>1</sup>Department Environmental and Occupational Health, University of Montréal, Montréal, QC, Canada; <sup>2</sup>CHU de Grenoble, Université Joseph Fourier, Grenoble, France.

Mathematical modeling has become an important tool to assess xenobiotic exposure in humans. In the present study, we have used a human physiologically-based pharmacokinetic (PBPK) model to reproduce the time-course of 3-hydroxybenzo(a)pyrene (3-OHBP) in the urine of industrially exposed workers and in turn predict most plausible exposure scenarios. Urinary voids from a dozen workers highly exposed to polycyclic aromatic hydrocarbons (PAHs) in the Rhone-Alpes region in France have been collected during a typical workweek (beginning and end-of-shift) and subsequent days off; urinary concentrations of 3-OHBP were then determined. Based on the information obtained for each worker (airborne BP concentration, daily shift hours, tasks, protective equipment), the time courses of 3-OHBP in the urine of the different workers have been simulated using the PBPK model, considering the various possible exposure routes, oral, dermal and inhalation, as well as combined exposure. The model was constructed from *in vivo* experimental data in rats and then extrapolated from animals to humans after assessing and adjusting most sensitive model parameters as well as species specific physiological parameters. The model was able to closely reproduce the observed time course of 3-OHBP and establish most plausible exposure route depending on the worker. It appears as a useful tool to better interpret biomonitoring data of PAH exposure on the basis of 3-OHBP biomarker levels.

**PS 619 Computational Modeling of the Pathway Linking Oxidant Exposure with a Fluorescent Reporter Protein in Human Airway Epithelial Cells.**

W. Cheng<sup>1</sup>, J. M. Samet<sup>2</sup> and R. B. Conolly<sup>3</sup>. <sup>1</sup>Environmental Science and Engineering, University of North Carolina at Chapel Hill, Chapel Hill, NC; <sup>2</sup>EPHD, US EPA, Chapel Hill, NC; <sup>3</sup>ISTD, US EPA, Chapel Hill, NC.

Air pollution is one of the most common environmental exposures imposed on humans in urban areas on a daily basis. Mixtures of gaseous and particle pollutants contain hundreds of thousands of compounds with the potential for numerous interactions. Many pollutants operate through modes of action involving oxidative stress. We use the genetically engineered fluorescent reporter roGFP to assess oxidative stress in transformed human airway epithelial cells. The specific goal of current study was to develop a computational model of the biochemical pathway linking oxidant exposure with oxidation of roGFP. Models of this type can provide insights into the structure and kinetics of these pathways that complement the information obtained directly from the laboratory studies. As our initial effort at model development, we used live cell imaging to monitor roGFP oxidation by micromolar H<sub>2</sub>O<sub>2</sub>. roGFP was fully oxidized within 20 min and recovery to its reduced state took several hours. These kinetics were well described by the model. Furthermore, the model-based quantitative analysis has shown that the observed response for oxidation of roGFP is nonlinear with dose and consistent with Michaelis-Menten kinetics. These latter results reflect the underlying sequence of enzymatic reactions, e.g., glutathione peroxidase, glutaredoxin and glutathione reductase, through which the oxidizing effect of H<sub>2</sub>O<sub>2</sub> is transmitted to roGFP. These results illustrate how computational modeling of modes of action of oxidants can provide insights that complement laboratory observations and that will be needed as we seek to understand the health risks associated with air pollution exposures. This presentation reflects the views of the authors and does not necessarily reflect EPA policy.

**PS 620 Comparative Toxicokinetic and Toxicodynamic Study of Trichloroethylene and Tetrachloroethylene in the Mouse.**

V. Soldatow<sup>1</sup>, H. Yoo<sup>1</sup>, B. Wanda<sup>1</sup>, L. B. Collins<sup>1</sup>, S. Kim<sup>2</sup>, K. Xia<sup>1</sup>, W. Sun<sup>1</sup>, E. Wright<sup>1</sup>, W. A. Chiu<sup>1</sup>, K. Guyton<sup>3</sup> and I. Rusyn<sup>3</sup>. <sup>1</sup>University of North Carolina at Chapel Hill, Chapel Hill, NC; <sup>2</sup>Seoul National University, Seoul, Republic of Korea; <sup>3</sup>NCEA, US EPA, Washington DC.

Trichloroethylene (TCE) and tetrachloroethylene (PCE) are ubiquitous environmental and occupational agents hazardous to human health. Several important gaps in our understanding of their potential toxicity have been identified: 1) extent of inter-individual variability in toxicity, 2) complexities associated with linking metabolites to specific organ toxicity, and 3) comparative analysis of toxicokinetics (TK) and toxicodynamics (TD) of these closely related agents. This project aimed

to fill these gaps by providing TK and TD data using a panel of mouse strains as a model for inter-individual variability. We focus on key metabolites of TCE and PCE: trichloroacetic acid (TCA), dichloroacetic acid (DCA), trichloroethanol (TCOH), S-(1,2,2-trichlorovinyl)-L-cysteine (TCVC), S-(1,2-dichlorovinyl)-L-cysteine (DCVC), and S-(1,2,2-trichlorovinyl)glutathione (TCVG), and S-(1,2-dichlorovinyl)glutathione (DCVG). In the TK and TD studies, a single oral dose of TCE or PCE (24-800 mg/kg or 30-1,000 mg/kg, respectively, in 5% Alkamuls EL-620 in saline) was administered to male mice from three strains (C57BL/6J, NZW/LacJ and B6C3F1/J). Quantification of metabolites (up to 36 hours post dosing) was performed in serum, liver, kidney, spleen, brain, lung, and bone marrow. In addition, RNA Sequencing was used to identify dose-response changes in gene expression in liver. These data are relevant for human health assessments of TCE and PCE as they provide data for kinetic modeling, dose-response analysis of the toxicity mechanisms, and evaluation of inter-individual differences in susceptibility to these chemicals. Funded by P42 ES005948. Disclaimer: The views expressed here are the authors' and not necessarily those of the US EPA.

**PS 621 A Mechanistic Model of GABAA-Receptor Trafficking during Status Epilepticus.**

E. Merrill<sup>1</sup>, J. Gearhart<sup>1</sup>, C. Ruark<sup>1</sup>, D. A. Mahle<sup>2</sup> and P. Robinson<sup>1</sup>. <sup>1</sup>AFRL/RHDJ, Henry M. Jackson Foundation, Wright Patterson Air Force Base, OH; <sup>2</sup>Human Performance, AFRL/RHDJ, Wright Patterson Air Force Base, OH.

The efficacy of benzodiazepines (BZ) to abolish seizures diminishes rapidly with time after onset of status epilepticus (SE). This progressive loss of efficacy is associated with the rapid internalization of BZ-sensitive GABAA receptors, together with a slight increase in localization of BZ-insensitive GABAA receptors to the synaptic membrane. We developed a compartmental model of receptor localization and movement in the dendritic spine that includes surface receptors within the post-synaptic density (PSD), including those bound to gephyrin scaffold proteins, and the extrasynaptic membrane (ESM), as well as internalized receptors. The model includes movement of receptors between these compartments as well as receptor synthesis and degradation. The model was used to simulate receptor trafficking under normal (non-seizure) and status epilepticus conditions. Data from *in vitro* studies using various neuronal cell cultures as well as HEK cells modified to express GABAA receptors were used to parameterize and validate the model. Increases in receptor endocytosis rate and lateral movement from PSD to ESM (or a decrease in gephyrin binding) were found to be sufficient to simulate SE conditions. By integrating the current GABAA receptor trafficking model with a physiologically-based pharmacokinetic (PBPK) model for diazepam, a time-dependant therapeutic dose can be predicted. The model suggests that approximately 55% occupancy of the original receptor number is required to reverse ongoing seizures. This is up from a reported 37% occupancy required to prevent the initiation of seizures in the rat, when diazepam is administered as a prophylaxis.

**PS 622 Multichemical Bayesian Calibration of a Generic Physiologically-Based Pharmacokinetic (PBPK) Model to Calculate Biological Limit Values for Lipophilic Volatile Organic Compounds.**

R. McDougall<sup>1</sup>, M. Verner<sup>2,3</sup>, G. Charest-Tardif<sup>4</sup>, R. Tardif<sup>4</sup> and G. Johanson<sup>2</sup>. <sup>1</sup>Faculty of Engineering and Applied Science, University of Ontario Institute of Technology, Oshawa, ON, Canada; <sup>2</sup>Institute of Environmental Medicine, Karolinska Institutet, Stockholm, Sweden; <sup>3</sup>Channing Laboratory, Brigham and Women's Hospital, Harvard Medical School, Boston, MA; <sup>4</sup>Département de santé environnementale et santé au travail, Université de Montréal, Montréal, QC, Canada.

Biomonitoring provides an integrative measure of internal exposures in workers exposed to contaminants in the occupational setting. PBPK models validated against empirical data can be used to estimate the variability in biological levels following specific exposure conditions. Given the large array of contaminants in the workplace, the calibration of a generic PBPK model could be useful to generate biological limit values for chemical with little or no available human data. We aimed to develop a generic PBPK model for lipophilic volatile organic compounds (VOCs) in end-exhaled air, which can be obtained non-invasively, and to calibrate it using Markov Chain Monte Carlo (MCMC) techniques and human data from controlled exposures. We built a simple 3-compartment PBPK model (liver, adipose tissue and rest of the body) that runs on three chemical-specific parameters: intrinsic clearance and octanol:water and blood:air partition coefficients. Global sensitivity analysis was used to identify the most influential parameters on end-exhaled air

levels. MCMC analysis was employed to infer population and individual distributions for these significant parameters based on levels measured in 12 individuals exposed to styrene, n-hexane or toluene. The generic VOC PBPK model calibrated by MCMC analysis was able to predict end-exhaled air levels for the 12 individuals and 3 compounds. The chains from the converged MCMC runs will be used to derive distributions of end-exhaled air for given exposure scenarios. Our next steps will be to include more individuals, compounds and exposures scenarios with variable workloads to better describe variability in the population.

## PS 623 Development of a New 3D Human Small Intestinal Tissue Model.

S. Aychunie, Z. Stevens, T. Landry, P. Hayden and M. Klausner. *MatTek Corporation, Ashland, MA.*

The epithelial lining of the gastrointestinal (GI) tract is a gatekeeper for entry of orally ingested nutrients and xenobiotics including medications. The intestinal lining has a well organized structure containing proliferative cells which migrate along the crypt-villi axis and differentiate into functional mature epithelial cells. Currently, the most common in vitro model utilized for study of drug absorption at the intestinal mucosa is based on a 2-D cell culture model of the colon carcinoma cell line, Caco-2. These cells differentiate into monolayers of polarized enterocytes that are connected by tight junctions, but lack mucus-secreting goblet cells and show inter-passage inconsistency. Others have developed small intestinal organoids which are not suitable for apical application of test articles. Here, we report the reconstruction of a human organotypic small intestinal tissue (SI) generated from primary human SI epithelial cells that grow in tissue culture inserts using serum free medium. Human SI epithelial cells and myofibroblasts were expanded in monolayer culture and seeded on a microporous membrane containing a fibroblast-collagen-gel substrate to reconstruct three dimensional organotypic SI tissues. Tissue morphology and biomarker expression of the SI model were characterized by H&E staining and immunohistochemistry, respectively. Basal cell proliferation markers, cytokeratins (CK) and mucin were monitored over an 11-day culture period. Analysis of the SI tissue model revealed: 1) wall-to-wall growth of the epithelial layer, 2) columnar epithelial cell morphology similar to that of native SI tissue, 3) expression of muc-2, CK19, and villin at the surface of the epithelium, and 4) Lgr5+ (crypt stem cell marker) positive cells. In conclusion, the new human cell based 3D SI tissue model will likely serve as a valuable tool to evaluate pre-clinical therapeutic drug candidates intended for oral administration and study microbiomes and microbial infection of the GI tract.

## PS 624 Evaluating Dose-Response Parameters of an *In Vitro* DNA-Chemical Interaction Using a Mechanistic Biological Model.

A. Nong, K. Lyon, J. M. Gavina and Y. Feng. *Environmental Health Science and Research Bureau, Health Canada, Ottawa, ON, Canada.*

Benchmark dose modeling of genomic data is a trending approach in toxicity testing, and system biology modeling attempts to understand quantitative data in light of what we expect from more complex biological systems. Biological modeling approaches can incorporate different forms of kinetic and dynamic data of a chemical interaction in vitro. The objective of this effort was to interpret a biological model mechanism and parameters describing a chemical doubled stranded oligonucleotide interaction assay for a series of chemicals (tetrachlorohydroquinone, styrene-7,8-oxide, methyl methane sulfonate, phenyl glycidyl ether, and benzo(a)pyrene diol epoxide), with both time series and dose-ranged measurements. The chemicals have been analyzed with time series, dose-response and inhibition mixture response analysis. A model using mixed Michaelis-Menten kinetic and multiple binding was determined to be best suited with the data coherency between the biological and mathematical expectations. This was based on the results of the model, as well as the poorer results of other considered models (e.g. constant rate constants, linear rate constants, multi-step reactions, Hill functions). Correlations between coefficients and various chemicals, as well as sensitivity analysis, gave evidence of a deeper mechanism underlying nucleotide perturbations (e.g. relations amongst the half-life, dose and the curvature of the reactions). Two model parameters, molecular binding coefficient (range from 0.1 to 2.6) and nonlinear affinity rate constant (ranging from 30 to 5300  $\mu\text{M}$ ), were dose dependant and specific to each chemical. These kinetic parameters are suitable candidates for a quantitative structure-activity analysis with chemical descriptors for nucleotide binding sites and interaction efficacy as indicators of adduct formation. These biological models fit the biological expectations for the governing mechanisms, giving further evidence of the effectiveness of statistical and benchmark dose modeling in toxicity testing.

## PS 625 Developing Predictive Approaches to Characterize Adaptive Responses of the Reproductive Endocrine Axis to Aromatase Inhibition: Computational Modeling.

M. Breen<sup>1,2</sup>, D. L. Villeneuve<sup>3</sup>, G. T. Ankley<sup>3</sup>, D. Bencic<sup>4</sup>, M. S. Breen<sup>5</sup>, K. H. Watanabe<sup>6</sup>, A. L. Lloyd<sup>2</sup> and R. B. Conolly<sup>1</sup>. <sup>1</sup>ISTD, NHEERL, ORD, US EPA, Research Triangle Park, NC; <sup>2</sup>Biomathematics Program, Department of Mathematics, NCSU, Raleigh, NC; <sup>3</sup>Mid-Continent Ecology Division, US EPA, Duluth, MN; <sup>4</sup>Ecological Exposure Research Division, US EPA, Cincinnati, OH; <sup>5</sup>NERL, US EPA, Research Triangle Park, NC; <sup>6</sup>Environmental and Biomolecular Systems, Oregon Health & Science University, Beaverton, OR.

Exposure to endocrine disrupting chemicals can affect reproduction and development in both humans and wildlife. We developed a mechanistic mathematical model of the hypothalamic-pituitary-gonadal (HPG) axis in female fathead minnows to predict dose-response and time-course (DRTC) behaviors for endocrine effects of a well-defined aromatase inhibitor, fadrozole (FAD). The model includes a regulatory feedback that mediates adaptive responses to endocrine stress by controlling the secretion of a generic gonadotropin (LH/FSH) from the hypothalamic-pituitary complex. Plasma 17 $\beta$ -estradiol (E2) and ovarian cytochrome P450 (CYP) 19A aromatase mRNA data from two time-course experiments, each of which included both an exposure and a depuration phase, and plasma E2 data from 4 days exposure experiment were used to develop and evaluate the model. Model parameters were estimated using E2 concentrations for 0, 0.5, and 3  $\mu\text{g/L}$  FAD concentrations, and good fits to these data were obtained. The model accurately predicted CYP19A mRNA fold changes for controls and three FAD doses (0, 0.5, or 3  $\mu\text{g/L}$ ), and venous E2 dose-response during FAD exposure on day 4. Comparing the model-predicted DRTC with experimental data provided insight into how the feedback control mechanisms embedded in the HPG axis mediate these changes: adaptive changes in plasma E2 levels occurring during exposure and "overshoot" occurring post-exposure. This study demonstrates the value of mechanistic computational modeling to examine and predict the possible dynamic behaviors. This abstract does not necessarily reflect US Environmental Protection Agency policy.

## PS 626 Mitochondrial Dysfunction-Induced by Sertraline, an Antidepressant Agent.

L. Couch<sup>1</sup>, Y. Li<sup>1</sup>, J. Fang<sup>1</sup>, M. Higuchi<sup>2</sup> and L. Guo<sup>1</sup>. <sup>1</sup>NCTR, US FDA, Jefferson, AR; <sup>2</sup>Department of Biochemistry and Molecular Biology, University of Arkansas for Medical Sciences, Little Rock, AR.

Sertraline, a selective serotonin reuptake inhibitor (SSRI), has been used for the treatment of depression. Although it is generally considered safe, cases of sertraline-associated liver injury have been documented; however, the possible mechanism of sertraline-associated hepatotoxicity is entirely unknown. Here we report that mitochondrial impairment may play an important role in liver injury induced by sertraline. In mitochondria isolated from rat liver, sertraline uncoupled mitochondrial oxidative phosphorylation and inhibited the activities of oxidative phosphorylation Complexes I and V. Additionally, sertraline induced Ca<sup>2+</sup>-mediated mitochondrial permeability transition (MPT), and the induction was prevented by bongkrekic acid, a specific MPT inhibitor targeting adenine nucleotide translocator (ANT), implying that the MPT induction is mediated by ANT. In freshly isolated rat primary hepatocytes, sertraline rapidly depleted cellular ATP and subsequently induced lactate dehydrogenase (LDH) leakage; both were attenuated by bongkrekic acid. Our results, including ATP depletion, induction of MPT, inhibition of mitochondrial respiration complexes, and uncoupling oxidative phosphorylation, indicate that sertraline-associated liver toxicity is possibly via mitochondrial dysfunction.

## PS 627 Mouse Liver Protein Sulfhydryl Depletion Induced by Acetaminophen Exposure.

X. Yang<sup>1</sup>, J. Greenhaw<sup>1</sup>, Q. Shi<sup>1</sup> and W. F. Salminen<sup>2</sup>. <sup>1</sup>Division of Systems Biology, US FDA, National Center for Toxicological Research, Jefferson, AR; <sup>2</sup>PAREXEL, Benton, AR.

Since Acetaminophen (APAP) remains the leading cause of acute liver failure in the western world, a large body of research has been conducted to understand the mechanisms behind the pathogenesis. The role of protein sulfhydryl depletion in APAP-induced liver injury was investigated in this study and compared to protein adducts and classical measures of toxicity. A single oral gavage dose of 150 or 300 mg/kg APAP in B6C3F1 mice produced increased serum alanine aminotransferase levels, liver necrosis, and glutathione depletion in a dose-dependent manner. The levels of global free protein sulfhydryls were significantly decreased at 1 hour and

remained as such through 24 hours postdose. Histochemical detection of free protein sulfhydryls showed a zonal pattern of sulfhydryl depletion within the liver lobule. The centrilobular areas exhibited dramatic decreases in protein free sulfhydryls while the periportal regions were essentially spared. Oxidation of the free protein sulfhydryls occurred in the same regions of cells that contained APAP-protein adducts and developed necrotic changes. Interestingly, the majority of free protein sulfhydryl depletion was due to reversible oxidation since the global and lobule-specific effects were essentially reversed with TCEP, a sulfhydryl reducing agent, prior to maleimide labeling. The changes in protein sulfhydryl oxidation may act as the sensor for oxidants, such as ROS and RNS. Therefore, investigating the protein sulfhydryl depletion may have important clinical ramifications in understanding the pathogenesis of APAP-induced hepatocellular injury.

**PS 628 Purinergic Receptor Antagonist A438079 Protects against Acetaminophen-Induced Liver Injury by Inhibiting P450 Isoenzymes Not Inflammasome Activation.**

Y. Xie, C. Williams, M. R. McGill, M. Leborfsky, A. Ramachandran and H. Jaeschke. *Pharmacology, Toxicology & Therapeutics, University of Kansas Medical Center, Kansas City, KS.*

Acetaminophen (APAP) overdose is the most frequent cause of acute liver failure in the western world. Controversy exists regarding the hypothesis that the hepatocyte injury is amplified by a sterile inflammatory response, rather than being the result of intracellular mechanisms alone. A recent study suggested that the purinergic receptor antagonist A438079 protects against APAP-induced liver injury by preventing the activation of the Nalp3 inflammasome in Kupffer cells and thereby preventing inflammatory injury. To test the hypothesis that A438079 actually affects the intracellular signaling events in hepatocytes, C57BL/6 mice were treated with APAP (300 mg/kg) and A438079 (80 mg/kg) or saline and GSH depletion, protein adduct formation, c-Jun-N-terminal kinase (JNK) activation, oxidant stress and liver cell necrosis was determined between 0-6h after APAP administration. APAP caused rapid GSH depletion, extensive protein adduct formation in liver homogenates and in mitochondria, JNK phosphorylation and mitochondrial translocation of phosphor-JNK within 2h, oxidant stress, and extensive centrilobular necrosis at 6h. A438079 significantly attenuated GSH depletion, which resulted in a 50% reduction of total liver and mitochondrial protein adducts and substantial reduction of JNK activation, mitochondrial P-JNK translocation, oxidant stress and liver injury. The same results were obtained using primary mouse hepatocytes. A438079 did not directly affect JNK activation induced by tert-butyl hydroperoxide and GSH depletion. However, A438079 dose-dependently inhibited hepatic P450 enzyme activity. Thus, the protective effect of A438079 against APAP hepatotoxicity in vivo can be explained by its effect on metabolic activation and cell death pathways in hepatocytes without involvement of the Nalp3 inflammasome.

**PS 629 The Role of Choline Depletion in Perfluorooctanesulfonate-Induced Hepatic Steatosis.**

P. Krishnan<sup>1</sup>, A. D. Patterson<sup>1</sup>, D. J. Ehresman<sup>2</sup>, P. B. Smith<sup>1</sup>, M. K. Scavell<sup>1</sup>, S. Chang<sup>2</sup>, J. L. Burenhoff<sup>2</sup> and J. M. Peters<sup>1</sup>. <sup>1</sup> Pennsylvania State University, University Park, PA; <sup>2</sup>3M Company, St. Paul, MN.

In toxicological studies, perfluorooctanesulfonate (PFOS) exposure has resulted in hepatic steatosis and hypolipidemia, believed to be the result of decreased production and secretion of VLDL and HDL and increased uptake of VLDL-triglyceride. The hypothesis that PFOS produces hepatic steatosis via ionic sequestration of available choline necessary for the production of VLDL was examined. Plausibility was supported by identification of an ion-triad between two molecules of choline and one molecule of PFOS in vitro. We fed male C57BL/6 mice either a control diet or a marginal methionine/choline-deficient (mMCD) diet, both with and without PFOS. After a two-week run-in period on diets without PFOS, control or mMCD diets containing 0, 30, 60, or 120 mg K+PFOS/kg diet were fed for three weeks. There was a dose-dependent increase in the relative liver weight in both control and mMCD fed mice. Dietary PFOS was also associated with dose-dependent decreases in body weight, increases in hepatic triglyceride concentration, and increases in serum ALT, ALP, and bile acids, all with larger effects observed in mice fed mMCD compared to those fed the control diet. Serum and liver concentrations of PFOS were increased in a dose-dependent manner on both diets; however, serum PFOS concentrations were higher and liver concentrations lower in mMCD-fed mice compared to corresponding control-fed mice. This is surprising because the evidence suggested that PFOS-induced hepatotoxicity was exacerbated in the mMCD diet fed mice. Metabolomic analysis demonstrated that PFOS caused a significant decrease in the hepatic concentration of many phosphatidylcholines in the PFOS-fed mice compared to controls. Further, the average serum concentration of choline was reduced by dietary PFOS. These studies are the first to provide evidence that PFOS may cause hepatic steatosis through depletion of choline required for hepatic VLDL production and export.

**PS 630 Platelet Depletion Reduces Acetaminophen Hepatotoxicity in Mice.**

K. Miyakawa<sup>1,2</sup>, R. Albee<sup>3</sup>, M. Scott<sup>1</sup>, P. E. Ganey<sup>2,3</sup>, J. Luyendyk<sup>1,2</sup> and R. Roth<sup>2,3</sup>. <sup>1</sup>Department of Pathobiology and Diagnostic Investigation, Michigan State University, East Lansing, MI; <sup>2</sup>Center for Integrative Toxicology, Michigan State University, East Lansing, MI; <sup>3</sup>Department of Pharmacology and Toxicology, Michigan State University, East Lansing, MI.

Acetaminophen (APAP) overdose is the major cause of acute liver failure in the U.S. Previous studies identified decreases in blood platelet concentration in patients with APAP toxicity, but the role of platelets in APAP-induced liver injury is unclear. We tested the hypothesis that platelets contribute to liver injury in a mouse model of APAP hepatotoxicity. Blood platelet concentration was reduced 6-36 h after administration of APAP (300 mg/kg, ip) to mice, and immunofluorescent labeling showed increased platelets within livers at 2-6 h. Pretreatment of mice with anti-CD41 IgG to reduce circulating platelet concentrations to 1/10th of control reduced liver injury at 6, 12 and 24 hr after APAP administration, as evaluated by plasma alanine aminotransferase activity and the area of hepatic necrosis. The erythrocyte-to-hepatocyte volume ratio in the livers of APAP-treated mice was also reduced by anti-CD41 IgG pretreatment, suggesting a reduction in congestion or hemorrhage. The early (30 min) APAP-mediated consumption of reduced glutathione (GSH) was unaffected by platelet depletion, suggesting that the reduction in injury was not a consequence of diminished APAP bioactivation. Activated platelets provide a thrombogenic surface for amplification of thrombin generation; indeed, platelet depletion significantly reduced the increase in plasma concentration of thrombin-antithrombin complexes, a biomarker of thrombin generation, at 3h. Addition of thrombin to cultures of primary hepatocytes in vitro did not affect APAP-induced cytotoxicity, suggesting that thrombin does not contribute to toxicity through a direct action on hepatocytes. Taken together, the results suggest that platelets support thrombin generation and contribute to congestion or hemorrhage and hepatocellular injury after APAP overdose. (Supported by NIH grant R01 DK087886.)

**PS 631 Acute Biliary Hyperplasia in F344 Rats Administered the Indole-3-Carbinol Analog, NSC 743380.**

M. Davis<sup>1</sup>, S. Eldridge<sup>1</sup>, K. Elsass<sup>2</sup>, T. Horn<sup>3</sup> and J. Morris<sup>1</sup>. <sup>1</sup>DCTD, NCI, Bethesda, MD; <sup>2</sup>Battelle, Columbus, OH; <sup>3</sup>IITRI, Chicago, IL.

Biliary hyperplasia discovered in preclinical safety assessment represents a severe finding due to being unmanageable and non-monitorable in the clinical setting. NSC-743380 (1-[(3-chlorophenyl) methyl]-1H-indole-3-methanol) is in early stages of development as an anticancer agent at the NCI. In an exploratory toxicity study in rats, acute hepatotoxicity, characterized by biliary hyperplasia and inflammatory hepatic necrosis, was observed 5 days after dosing orally at 100 mg/kg/day. The hepatotoxicity noted was also apparent from the clinical chemistry results that showed marked increases in alkaline phosphatase, alanine aminotransferase and aspartate aminotransferase levels by day 2 dosing relative to controls. In contrast, IV dosing with NSC-743380 (6.25 – 25 mg/kg/day), produced no microscopic lesions or clinical chemistry changes relative to controls either on day 2 or after day 5 of dosing. Plasma levels of NSC-743380 and its aldehyde and acid metabolites obtained for IV administration were higher than that achieved from oral administration; however, liver toxicity, as determined by clinical chemistry and histopathology, was observed only after administration of the parent compound and not the aldehyde or acid metabolite. In addition, the toxicity profiles of a structurally similar inactive molecule and a structurally diverse molecule (with the same efficacy profile) were compared to NSC-743380 to explore scaffold versus target-mediated toxicity. Following 2 days of oral dosing at 100 mg/kg/day, the structurally different compound produced a similar toxicity profile, although less severe, than NSC-743380. Taken together, the hepatotoxicity associated with NSC-743380 appears to be related to the parent molecule rather than its major metabolites and related to target-modulation representing on-target toxicity. Furthermore, this molecule offers a unique opportunity to explore biomarkers for biliary hyperplasia using a short-duration toxicology study design. N01CM201100019/N01CM201100027

**PS 632 Identifying Proregenerative Signaling after Acetaminophen-Induced Acute Liver Failure in Mice Using Incremental Dose Model.**

B. Bhushan, C. Walesky, P. Borude, G. Edwards and U. Apte. *Department of Pharmacology, Toxicology, and Therapeutics, University of Kansas Medical Center, Kansas City, KS.*

Overdose of acetaminophen (APAP) is the major cause of acute liver failure (ALF) in the US with very limited treatment options. Recent studies suggest that liver regeneration is a critical determinant of overall survival following APAP overdose and

has highlighted the potential of regenerative therapies for ALF. However, the mechanisms of liver regeneration following APAP-induced ALF are not completely clear. In the present study, we studied the major signaling pathways involved in liver regeneration following APAP-induced ALF using an incremental APAP dose model. Two-month-old male C57BL/6 mice were treated with either 300 mg/kg (APAP300) or 600 mg/kg (APAP600) APAP and liver injury and regeneration was studied over a time course of 0 to 48 hr. Mice treated with APAP300 developed extensive liver injury followed by significant liver regeneration resulting in resolution of APAP-induced injury by 48 hr. In contrast, mice treated with APAP600 exhibited significant injury but substantial decrease in liver regeneration. The inhibition of liver regeneration in APAP600 group was associated with decreased Cyclin D1 mRNA and protein expression, decreased phosphorylation of Rb protein and sustained expression of p21. Further analysis of several signaling pathways revealed differences in pro-mitogenic signaling between APAP300 and APAP600. EGFR, c-Met, and downstream activation of MAPK pathways were highly activated in APAP600, where regeneration was inhibited. However, canonical Wnt/ $\beta$ -catenin pathway and NF- $\kappa$ B signaling were activated in APAP300 where liver regeneration was stimulated and inhibited in APAP600 group where regeneration was decreased. Finally, a TaqMan-based PCR array of 15 growth factor genes revealed rapid induction of several growth factors including HGF, VEGF, Kit-L, and PDGF $\alpha$  specifically in APAP300 group. Taken together, our study has identified Wnt and NF- $\kappa$ B signaling as potential pathways that regulate liver regeneration after APAP overdose.

**PS 633 Potential Hepatoprotective Effects of Licorice Root (*Radix glycyrrhizae*) Extract against Carbon Tetrachloride-Induced Hepatotoxicity in Isolated Rat Hepatocytes.**

O. S. El-Tawil<sup>1</sup>, A. A. Shalaby<sup>2</sup> and E. A. Mohamed<sup>3</sup>. <sup>1</sup>Department of Toxicology and Forensic Medicine, Faculty of Veterinary Medicine, Cairo University, Cairo, Egypt; <sup>2</sup>Department of Biochemistry, Faculty of Veterinary Medicine, Suez Canal University, Ismailia, Egypt; <sup>3</sup>Department of Pharmacology and Toxicology, Faculty of Pharmacy, Al-Azhar University, Cairo, Egypt. Sponsor: A. Kadry.

*Radix glycyrrhizae* is one of the native Mediterranean plants. Licorice root is a popular soft drink in Egypt. Literatures cited therapeutic effects of licorice. The present work is to evaluate the potential hepatoprotective effects of aqueous licorice root extract against the cytotoxic effects and the oxidative stress induced by carbon tetrachloride (CCl<sub>4</sub>) in isolated primary rat hepatocytes. Hepatocytes were isolated by collagenase perfusion technique. Cytotoxicity was determined by assessing cell viability and leakage of cytosolic enzymes, such as lactate dehydrogenase (LDH), alanine aminotransferase (ALT) and aspartate aminotransferase (AST). Oxidative stress was assessed by determining reduced glutathione (GSH) level and lipid peroxidation as indicated by thiobarbituric acid reactive substances (TBARS) production. Exposure of isolated rat hepatocytes to CCl<sub>4</sub> (5mM) caused cytotoxicity and oxidative injury, manifested by loss of cell viability and significant increase in LDH, ALT and AST leakages. As well as, CCl<sub>4</sub> caused progressive depletion of intracellular GSH content and significant enhancement of TBARS accumulation. Preincubation of hepatocytes with either licorice (25  $\mu$ M/ml) or silymarin (0.5mM) which is a known hepatoprotective agent, ameliorated the hepatotoxicity and oxidative stress induced by CCl<sub>4</sub>, as indicated by significant improvement in cell viability, significant decrease in LDH, ALT and AST leakages, significant prevention of GSH depletion and significant decrease in TBARS formation as compared to CCl<sub>4</sub> alone-treated cells. The present results indicate that CCl<sub>4</sub> has a potential cytotoxic effect in isolated rat hepatocytes; and licorice extract possess a highly promising hepatoprotective effects against CCl<sub>4</sub> - induced hepatotoxicity.

**PS 634 Lack of Human Health Relevance of Increased Hepatocellular Adenoma in Male Cd1 Mouse Treated with Cyproconazole or Propiconazole.**

D. Cowie<sup>1</sup>, R. Green<sup>1</sup>, E. Barnes<sup>1</sup>, R. Currie<sup>1</sup> and R. Peffer<sup>2</sup>. <sup>1</sup>Syngenta, Bracknell, United Kingdom; <sup>2</sup>Syngenta, Greensboro, NC.

In 18- to 24-month carcinogenicity studies, treatment with cyproconazole (CCZ) or propiconazole (PPZ) with high levels (100 to 200ppm and 2500ppm, respectively) in the diet resulted in increased incidences of hepatocellular adenoma in male CD1 mice. The proposed non-genotoxic mode of action (MOA) for induction of these tumours involves a number of common key events that define a common toxicity pathway. The first key event is activation of the constitutive androstane receptor (CAR). This stimulates increased DNA replication and hepatocellular proliferation along with differential expression of genes that result in

a suppression of apoptosis. Following prolonged exposure, this pro-proliferative milieu along with suppression of apoptosis promotes the growth and progression of spontaneously transformed cells eventually producing hepatocellular adenoma. The ability of CCZ and PPZ to elicit these key events *in vivo* was confirmed by measuring Cyp2b and Cyp3a induction as a surrogate for CAR activation and replicative DNA synthesis to assess hepatocellular proliferation. In addition, the requirement for CAR activation for increased hepatocellular proliferation was demonstrated for CCZ using CAR knock-out mice. Furthermore, reporter gene assays demonstrated that PPZ is a direct activator of both mouse (potent) and human (weak) CAR. Following experimental demonstration of the proposed MOA for mice, the lack of human relevance was assessed by comparing the effects of PPZ or CCZ on primary cultures of mouse and human hepatocytes. Consistent with the *in vivo* observations, treatment of mouse hepatocytes with CCZ or PPZ resulted in increases in Cyp2b, Cyp3a and replicative DNA synthesis. In contrast, treatment of human hepatocytes with these compounds resulted in increased Cyp2b and Cyp3a, but not replicative DNA synthesis. These data demonstrate a qualitative species difference in response to CAR activation. The lack of proliferative response in human hepatocytes means it is reasonable to conclude that neither CCZ nor PPZ are hepatotumorigenic in humans.

**PS 635 In Vivo Lead Hepatotoxicity in Mice Is Reversed by a Molluscan C-Reactive Protein Purified from *Achatina fulica* (Bowdich).**

S. Mukherjee, S. Sarkar, S. Chatterjee and S. Bhattacharya. Zoology, Visva Bharati University, Santiniketan, India.

Vertebrate liver is affected by several heavy metals among which lead (Pb) occupies a significant position. Lead induced prooxidant/ anti-oxidant balance contributes to tissue injury via oxidative damage to critical biomolecules (lipids, proteins, and DNA). We have earlier reported amelioration of lead induced toxicity by the application of C-reactive protein (CRP) isolated from a mollusc *Achatina fulica* in rat hepatocytes *in vitro* (SOT, 51st Annual Meeting, 2012), however, the mechanism of anti-stress property of ACRP has not been clarified. We evaluated *in vivo* hepatoprotective role of ACRP against Pb(NO<sub>3</sub>)<sub>2</sub> induced toxicity in mice, where CRP is not an acute phase protein (Du Clos, 2003). Adult male albino mice weighing 20 $\pm$ 2 g were segregated in 3 groups of 5 animals each. Group I served as control and received intraperitoneal (ip) normal saline. Group II received ip 14.8 mg/kg body weight Pb(NO<sub>3</sub>)<sub>2</sub> (1/10 LD<sub>50</sub>) for 7 consecutive days. Group III received ip Pb(NO<sub>3</sub>)<sub>2</sub> once daily for 7 days and from day 5 onwards ACRP (100  $\mu$ g/mouse) was co-administered ip with Pb(NO<sub>3</sub>)<sub>2</sub> until day 7. Generation of superoxides in liver was routinely assessed by TBARS assay (Buege and Aust, 1978) and the level of endogenous anti-oxidant GSH was determined (Sedlak and Lindsay, 1968). Administration of Pb(NO<sub>3</sub>)<sub>2</sub> significantly depleted liver glutathione and enhanced lipid peroxidation by 2 fold against control. Interestingly, ACRP co-treatment significantly reversed glutathione level and lipid peroxidation towards control while enhanced expression of Nrf2 and MAPKs (ERK, JNK and p38) indicated expression of several antioxidant genes. Protective role of ACRP against lead toxicity is further evidenced by profound induction of HSP70. It is concluded that ACRP reduces metal toxicity by triggering the survival pathway and inducing several anti oxidant genes in lead treated mice.

**PS 636 Eosinophils Not Neutrophils Mediate Halothane-Induced Liver Injury in Mice.**

W. R. Proctor, M. Chakraborty, J. C. Morrison, L. S. Chea, J. D. Berkson, K. Semple, M. Bourdi and L. R. Pohl. Molecular and Cellular Toxicology Section, Laboratory of Molecular Immunology, National Heart, Lung and Blood Institute, Bethesda, MD.

Liver eosinophilia has often been associated with drug induced liver injury, though its role in the etiology of this disease remains unclear. We decided to investigate this problem in a murine model of halothane-induced liver injury, where neutrophils have been reported to play a pathogenic role. When female Balb/c mice were administered halothane, eosinophils were detected by flow cytometry in the liver within 12 hours and increased thereafter proportionally to liver damage. Infiltrating neutrophils did not increase significantly until 18 hours after halothane administration. Chemokines CCL11 and CCL24, which are known to attract eosinophils, increased in response to halothane-treatment. Immunohistochemical staining for the cytotoxic eosinophil granule protein, major basic protein, revealed that eosinophils accumulated exclusively around areas of hepatocellular necrosis. The severity of HILI was decreased significantly when the study was repeated in wild-type mice partially depleted of eosinophils by pretreatment with Siglec-F antibody, while the

number of hepatic neutrophils remained unchanged. Conversely, selective depletion of neutrophils by pretreatment with low concentrations of Gr-1 antibody failed to reduce the extent of HILI when levels of eosinophils remained unchanged. The pathologic role of eosinophils was confirmed when halothane induced hepatotoxicity was significantly reduced in the eosinophil lineage ablated  $\Delta\text{dblGata}^{-/-}$  mice, which are neutrophil competent. Our findings indicate that eosinophils, not neutrophils, have a pathologic role in HILI in mice and suggest that they may contribute similarly in many clinical cases of DILI.

### PS 637 Effect of Ligand Activation of PPAR $\beta/\delta$ in Kupffer Cells.

G. Balandaram<sup>1</sup>, J. M. Peters<sup>1</sup> and E. J. Gonzalez<sup>2</sup>. <sup>1</sup>Veterinary and Biomedical Sciences, Pennsylvania State University, University Park, PA; <sup>2</sup>Laboratory of Metabolism, NCI, Bethesda, MD.

Peroxisome proliferator-activated receptor  $\beta/\delta$  (PPAR $\beta/\delta$ ) can inhibit pro-inflammatory activities in the liver. Since activated Kupffer cells can modulate hepatic inflammation, the role of PPAR $\beta/\delta$  in modulating Kupffer cell activities was examined. Kupffer cells were isolated from wild-type, Ppar $\beta/\delta$ -null or Ppar $\beta/\delta$ -null mice expressing a DNA binding mutant form of PPAR $\beta/\delta$  in the Kupffer cells (PPAR $\beta/\delta$  DBM). Cultured Kupffer cells from the three genotypes phagocytized latex beads demonstrating relative purity. Ligand activation of PPAR $\beta/\delta$  in Kupffer cells increased expression of the PPAR $\beta/\delta$  target gene, adipocyte differentiation-related protein (Adip) in wild-type but not in Ppar $\beta/\delta$ -null or PPAR $\beta/\delta$  DBM Kupffer cells. Ligand activation of PPAR $\beta/\delta$  attenuated lipopolysaccharide (LPS)-induced expression of the pro-inflammatory gene, tumor necrosis factor- $\alpha$  (Tnf $\alpha$ ) mRNA in Kupffer cell cultures from wild-type and PPAR $\beta/\delta$  DBM mice but not from Ppar $\beta/\delta$ -null mice. Wild-type Kupffer cells treated with LPS to induce an M1 phenotype exhibited increased expression of the pro-inflammatory macrophage markers Tnf $\alpha$ , interleukin-6 (IL-6), interleukin-1 $\beta$  (IL-1 $\beta$ ) and chemokine ligand-4 (Ccl4) and ligand activation of PPAR $\beta/\delta$  attenuated these responses. Wild-type Kupffer cells treated with IL-4 to induce an M2 phenotype exhibited increased expression of the anti-inflammatory markers arginase type-1 (Arg-1), macrophage galactose N-acetyl-galactosamine specific lectin-1 (Mgl-1), c-type lectin domain family 7, member A (Clec7A) and interleukin-10 (IL-10), but ligand activation of PPAR $\beta/\delta$  did not influence these responses. Combined, results from these studies suggest that PPAR $\beta/\delta$  inhibits hepatic inflammation, at least in part, via transrepression of pro-inflammatory signaling in Kupffer cells. Since this effect can be found with a DNA binding mutant form of PPAR $\beta/\delta$ , this suggests that the attenuation of pro-inflammatory signaling could be due to direct protein-protein interaction of PPAR $\beta/\delta$  with other inflammatory signaling molecules such as NF- $\kappa$ B.

### PS 638 Hepatocyte Tissue Factor Triggers the Procoagulant Response Associated with Acetaminophen-Induced Liver Injury and Hepatocyte Transplantation.

J. Luyendyk<sup>1</sup>, A. K. Kopec<sup>1</sup>, N. Joshi<sup>1</sup>, H. Cline<sup>1</sup>, S. Bishop<sup>1</sup>, K. M. Kassel<sup>1</sup>, C. E. Rockwell<sup>2</sup>, N. Mackman<sup>3</sup> and B. P. Sullivan<sup>1</sup>. <sup>1</sup>Pathobiology and Diagnostic Investigation, Michigan State University, East Lansing, MI; <sup>2</sup>Pharmacology and Toxicology, Michigan State University, East Lansing, MI; <sup>3</sup>Department of Medicine, University of North Carolina at Chapel Hill, Chapel Hill, NC.

The localization and regulation of tissue factor (TF) activity in hepatocytes (HPCs) is poorly understood and a role for HPC TF in vivo has not been established. We characterized the expression of TF by mouse HPCs and evaluated the role of HPC TF in mouse models of HPC transplantation and acetaminophen (APAP) overdose. TF mRNA, protein, and total procoagulant activity (PCA) were significantly reduced in isolated HPCs and in liver homogenates from TF<sup>flox/flox</sup>/albumin-Cre mice (HPC<sup>ΔTF</sup> mice) compared to TF<sup>flox/flox</sup> mice (control mice). TF protein on the surface of intact HPCs had PCA that was reduced by cell-impermeable lysine conjugating reagents, but was unaffected by an inhibitory TF antibody that competes for factor VII binding. Intact mouse HPCs clotted factor VII-deficient human plasma and TF-dependent factor Xa generation by HPCs occurred without exogenous factor VIIa. Thrombin generation in a model of HPC transplantation was dependent on donor HPC TF expression. Thrombin generation was also dramatically reduced in APAP-treated HPC<sup>ΔTF</sup> mice compared to APAP-treated control mice. The results indicate that TF expressed on the surface of mouse HPCs is preloaded with VII/VIIa, and that HPC TF is essential for coagulation induced by hepatocellular injury in vivo. Moreover, the expression of TF by HPCs implies that most hepatotoxic responses are likely accompanied by activation of the extrinsic pathway of blood coagulation.

### PS 639 Hepatoprotective Effects of Fibrin(ogen) in Chronic Xenobiotic-Induced Cholestatic Liver Injury: Potential Involvement of Platelets.

N. Joshi<sup>2</sup>, K. M. O'Brien<sup>2</sup>, B. L. Copple<sup>2</sup>, K. J. Williams<sup>1</sup> and J. Luyendyk<sup>1</sup>. <sup>1</sup>Pathobiology and Diagnostic Investigation, Michigan State University, East Lansing, MI; <sup>2</sup>Pharmacology & Toxicology, Michigan State University, East Lansing, MI.

Coagulation cascade activation and hepatic fibrin(ogen) deposition are evident in a model of chronic alpha-naphthylisothiocyanate (ANIT)-induced cholestatic liver injury. We have shown previously that complete fibrin(ogen) deficiency increases liver necrosis in mice fed a diet containing ANIT. The mechanism whereby fibrin(ogen) deficiency worsens injury in this model is not known, nor is it clear whether stabilizing hepatic fibrin would be hepatoprotective. One possibility is that fibrin(ogen)-dependent platelet activation protects the liver from chronic ANIT diet-induced injury. We tested the hypothesis that stabilizing hepatic fibrin(ogen) inhibits ANIT-induced chronic cholestatic liver injury by supporting hepatic platelet accumulation/activation. Mice fed a diet containing 0.025% ANIT for 2 weeks developed liver injury consisting of multifocal acute hepatocellular necrosis and inflammation, peribiliary fibrosis, lymphocytic inflammation and bile duct epithelial hyperplasia. Immunofluorescent CD41 (alpha<sub>IIb</sub> integrin) staining revealed a marked increase in platelets in livers of mice fed the ANIT diet compared to mice fed control diet. Administration of the anti-fibrinolytic drug tranexamic acid (1200 mg/kg, ip, bid) significantly reduced liver injury in mice fed the ANIT diet, but did not affect platelet accumulation. Administration of the platelet inhibitor clopidogrel significantly increased serum alanine aminotransferase (ALT) levels and liver necrosis in mice fed the ANIT diet. Moreover, serum ALT activity was increased in mice deficient in protease activated receptor-4 (PAR-4), a primary thrombin receptor on mouse platelets. The results indicate that stabilization of hepatic fibrin with antifibrinolytic therapy significantly reduces liver injury in mice fed ANIT diet. Moreover, the results suggest that platelets are also hepatoprotective in mice fed the ANIT diet.

### PS 640 Effects of Acetaminophen and Oxidative Stress on Primary Human Hepatocytes Derived from a Steatotic Liver.

M. J. Liguori, D. J. Cugier, R. Ciurlionis, A. C. Ditewig, J. Lai-Zhang, G. D. Gagne and E. A. Blomme. Department of Cellular and Molecular Toxicology, AbbVie, Abbott Park, IL.

Primary human hepatocytes are a favored in vitro system for characterization of some types of hepatotoxicity. Donor demographics, disease states, and lifestyles result in significant donor to donor variability and can have a strong influence on the sensitivity of primary hepatocytes to hepatotoxins. Here, we describe a unique primary human hepatocyte system originating from the liver of a female donor (SMK) with severe metabolic syndrome and pre-conditioned steatosis. The cells had a lipid-rich phenotype that was clearly visible both using standard light microscopy and lipid fluorescent stain, which showed a 400% increase in signal intensity compared to a standard lot of hepatocytes. In general, steatotic cells have enhanced sensitivity to the presence of reactive oxidative stress (ROS). To test whether SMK cells were more susceptible to ROS, SMK and cells from a normal donor were exposed to acetaminophen, a drug with a well characterized ROS-mediated mechanism of toxicity, at a dose range of 0.5 to 20 mM for 72h using standard culture conditions. SMK hepatocytes were 2.7-fold more susceptible to APAP induced cytotoxicity compared to their normal counterparts. The lipid signal was slightly reduced upon high levels of APAP. Total RNA was isolated from SMK both from naïve and APAP treated cells and subjected to whole genome transcriptomic profiling. When compared to a pool of non-diseased hepatocyte donors, naïve SMK cells showed extensive gene expression changes that were largely associated with bioenergetic pathways with marked downregulation of lipid processing control and synthesis genes (e.g. SREBP). Agglomerative hierarchical cluster analysis revealed a clear distinction between SMK and its normal counterparts of the global expression profiles induced after treatment with APAP. In summary, this study demonstrates that hepatocytes with marked steatosis can serve as interesting molecular models for ROS-mediated hepatotoxic injury.

**PS 641 Meso-Dihydroguaiaretic Acid Inhibits Alcoholic and Nonalcoholic Fatty Liver by Antagonizing LXR $\alpha$  Activity.**

W. Sim<sup>1</sup>, S. Park<sup>1</sup>, K. Lee<sup>1</sup>, Y. Jye<sup>1</sup>, H. Yin<sup>1,4</sup>, Y. Choi<sup>1</sup>, S. Sung<sup>1</sup>, S. Park<sup>2</sup>, H. Park<sup>2</sup>, K. Shin<sup>3</sup> and B. Lee<sup>1</sup>. <sup>1</sup>College of Pharmacy, Seoul National University, Seoul, Republic of Korea; <sup>2</sup>School of Pharmacy, Sungkyunkwan University, Suwon, Republic of Korea; <sup>3</sup>College of Pharmacy, The Catholic University, Bucheon, Republic of Korea; <sup>4</sup>Molecular Pharmacology and Physiology, University of South Florida Health Sciences Center, Tampa, FL.

Collaborative regulation of liver X receptor (LXR) and sterol regulatory element binding protein (SREBP)-1 are main determinants in hepatic steatosis. Recent studies indicate that selective intervention of overly functional LXR $\alpha$  in the liver shows promise in treatment of fatty liver. In the present study, we evaluated the effects of meso-dihydroguaiaretic acid (MDGA) on LXR $\alpha$  activation and its ability to reverse fatty liver in mice. An LXR $\alpha$  co-activator recruitment assay and molecular docking analysis were performed to evaluate the binding of MDGA to the ligand-binding domain (LBD) of LXR $\alpha$ . The ability of MDGA to inhibit LXR $\alpha$ -dependent steatosis was investigated in an ethanol- or high-fat-diet (HFD)-induced steatosis model. MDGA inhibited activation of the LXR $\alpha$ -LBD by competitively binding to the pocket for agonist T0901317 and decreased the luciferase activity in LXRE-tk-Luc-transfected cells. MDGA attenuated the expression of LXR $\alpha$  and hepatic neutral lipid accumulation in ethanol- and HFD-induced fatty liver. MDGA reduced the expression of LXR $\alpha$  co-activator protein RIP140 in HFD-fed mice. While MDGA decreased the expression of LXR $\alpha$ , SREBP-1, SCD-1, and FAS proteins, genes associated with reverse cholesterol transport such as ABCA1 and ABCG1 were not affected. These results demonstrate that MDGA has the potential to reverse alcoholic and nonalcoholic steatosis mediated by selective inhibition of LXR $\alpha$  in the liver.

**PS 642 Toxicity of Diethylnitrosamine (DEN) in the Liver of Constitutive Androstane Receptor (CAR)-Knockout (KO) Mice.**

K. Inoue<sup>1</sup>, M. Takahashi<sup>1</sup>, Y. Sakamoto<sup>1</sup>, K. Tamura<sup>1</sup>, S. Matsuo<sup>1</sup>, Y. Kodama<sup>2</sup> and M. Yoshida<sup>1</sup>. <sup>1</sup>Division of Pathology, National Institute of Health Sciences, Tokyo, Japan; <sup>2</sup>Division of Toxicology, National Institute of Health Sciences, Tokyo, Japan.

CARKO mice showed high mortality after injection of DEN. To clarify the cause of high susceptibility in CARKO mice to the toxicity of DEN, 6-week old male CARKO and C3H mice were intraperitoneally injected 90 mg/kg body weight of DEN, and their livers were collected at days 1, 3, 7 and 14 after DEN treatment. Relative weight, pathological changes, mRNA expression and enzyme activity levels of CYP2B10 and CYP2E1 in the liver of CARKO mice were compared with controls injected saline or with wild mice. DEN significantly reduced relative liver weights in both genotypes and the decreased liver weights in CARKO mice were significantly lower than wild mice at days 7 and 14. Microscopically, pale cytoplasm of the hepatocytes in the centrilobular area was observed by DEN treatment at day 1, and the area of this change was larger in CARKO than in wild mice. DEN treatment also increased slight to mild single necrosis of hepatocytes and mononuclear cell infiltration in the centrilobular area from day 1 and from day 3, respectively. The intensities of single necrosis and mononuclear cell infiltration in CARKO mice were comparable to wild mice. While the expression level of Cyp2b10 in the liver of wild mice increased by DEN with or without significance, compared with their controls, the level in CARKO mice remarkably diminished in both control and DEN groups at all time points. As for testosterone hydroxylase activity (CYP2B10), there were no difference between controls and DEN groups or both genotypes at days 1 and 7. DEN treatment significantly decreased Cyp2e1 and aniline hydroxylase activity (CYP2E1) level in both genotypes at day 1, compared with each control, and the decreased level of aniline hydroxylase activity was significantly lower in CARKO than in wild mice. Judging from these results, high susceptibility in CARKO mice to the toxicity of DEN might be caused by immediate decrease of CYP2E1 activity after DEN treatment.

**PS 643 Leptin Modulates Toxicity Associated Steatohepatitis through Peroxynitrite in Kupffer Cells.**

S. Das<sup>1</sup>, A. Kumar<sup>2</sup>, D. Ganini<sup>2</sup>, E. J. Tokar<sup>3</sup>, J. Corbett<sup>2</sup>, M. Kadiiska<sup>2</sup>, M. P. Waalkes<sup>3</sup>, A. Diehl<sup>4</sup>, R. P. Mason<sup>2</sup> and S. Chatterjee<sup>1,2</sup>. <sup>1</sup>Environmental Health Sciences, University of South Carolina, Columbia, SC; <sup>2</sup>Laboratory of Toxicology and Pharmacology, NIEHS, Research Triangle Park, NC; <sup>3</sup>Inorganic Toxicology, NIEHS, Research Triangle Park, NC; <sup>4</sup>Gastroenterology, Duke University, Durham, NC.

Progression from steatosis to toxin-mediated steatohepatitis (TASH) lesions is hypothesized to require a second hit. These lesions have been associated with increased oxidative stress, often ascribed to high levels of leptin and other proinflam-

matory mediators. Here we have examined the role of leptin in inducing oxidative stress and Kupffer cell activation in toxin-mediated steatohepatic lesions of obese mice. Male C57BL/6 mice fed with a high fat diet (60%kcal) at 16 weeks were administered CCl<sub>4</sub> to induce steatohepatic lesions. Approaches included use of immuno-spin trapping for measuring free radical stress, gene-deficient mice for leptin, p47 phox, iNOS and adoptive transfer of leptin primed macrophages in vivo. Diet-induced obese (DIO) mice, treated with CCl<sub>4</sub> increased serum leptin levels and leptin receptor expression. Oxidative stress was significantly elevated in DIO mice liver but not in OB/OB mice, or in DIO mice treated with leptin antibody. In OB/OB mice, leptin supplementation restored markers of free radical generation. Markers of free radical formation were significantly decreased by the peroxynitrite decomposition catalyst FeTPPS, the iNOS inhibitor 1400W, the NADPH oxidase inhibitor apocynin, or in iNOS or p47 phox-deficient mice. These results correlated with the decreased expression of TNF-alpha and MCP-1 and decreased leptin receptor expression. Kupffer cell depletion eliminated oxidative stress and inflammation, whereas in macrophage-depleted mice, the adoptive transfer of leptin-primed macrophages significantly restored inflammation. These results, for the first time, suggest that leptin action in macrophages of steatotic liver through induction of iNOS and NADPH oxidase caused peroxynitrite-mediated oxidative stress thus activating Kupffer cells and modulating leptin receptor expression in the liver. (NIH-4-R00-ES19875)

**PS 644 Occupational Vinyl Chloride Exposures Are Associated with Significant Changes to the Plasma Metabolome: Implications for Toxicant Associated Steatohepatitis.**

B. Wheeler<sup>1</sup>, M. Cave<sup>1,2</sup>, K. Falkner<sup>1</sup> and C. McClain<sup>1,2</sup>. <sup>1</sup>Department of Medicine/GI, University of Louisville, Louisville, KY; <sup>2</sup>Louisville VAMC, Louisville, KY.

Occupational vinyl chloride (VC) exposure has been associated with steatohepatitis (TASH) and liver cancer, although the modes of action are unknown. Metabolomics has recently been utilized for the evaluation of drug-induced liver injury, but has not previously been performed for occupational VC exposures. Plasma samples from 17 highly-exposed VC workers without liver cancer and 27 unexposed healthy volunteers were obtained from a specimen bank. GC/MS (Thermo-Finnigan Trace DSQ fast-scanning single-quadrupole mass spectrometer) and LC/MS2 (Waters ACQUITY UPLC, Thermo-Finnigan LTQ mass spectrometer) were performed. Software was used to match ions to a library of standards for metabolite identification and quantitation by peak area integration. Statistical significance was determined using Welch's t-tests. 613 unique named metabolites were identified. Of these, 189 metabolites were significantly increased in the VC exposure group while 94 metabolites were significantly decreased. The most striking differences occurred in lipid metabolites. Essential (7 of 7) and long chain free fatty acids (19 of 19, including arachidonic acid, 6 fold) were significantly increased with VC exposure. Lipid peroxidation products were likewise increased by VC exposure: monohydroxy fatty acids (8 of 9, including 13-HODE, 211 fold); fatty acid dicarboxylates (8 of 13); oxidized arachidonic acid products (7 of 7, including 5-HETE, 9-HETE, and 15-HETE, up to 616 fold). Other arachidonic acid products including leukotriene B<sub>4</sub> (52 fold) were also up-regulated with VC exposure. Abnormalities were also noted in amino acid metabolism, and particularly the transmethylation and transsulfuration pathways. VC exposure was associated with increased plasma free fatty acids and lipid peroxidation products. Lipotoxicity, pro-inflammatory lipid peroxidation products, and impaired transmethylation/transsulfuration pathways represent novel modes of action for VC hepatotoxicity.

**PS 645 Pregnancy-Related Lactogenic Hormones Alter the Expression of Uptake and Efflux Transporters in Primary Human Hepatocytes.**

J. E. Moscovitz<sup>1</sup>, C. J. Gibson<sup>1</sup>, H. J. Chung<sup>2</sup>, H. Y. Jeong<sup>3</sup> and L. M. Aleksunes<sup>1,4</sup>. <sup>1</sup>Department of Pharmacology and Toxicology, Rutgers University, Piscataway, NJ; <sup>2</sup>College of Pharmacy, Gyeongsang National University, Jinju, Republic of Korea; <sup>3</sup>Department of Pharmacy Practice, University of Illinois, Chicago, IL; <sup>4</sup>Environmental and Occupational Health Sciences Institute, Rutgers University, Piscataway, NJ.

The secretion of lactogenic hormones prolactin (PRL) and placental lactogen (PL) increases steadily throughout pregnancy and reaches the highest levels just prior to parturition. The effects of lactogenic hormones on the expression of hepatic transporters critical for the excretion of endogenous chemicals, drugs, and toxicants have not been characterized. To investigate the regulation of transporters by lactogenic hormones, sandwich-cultured, freshly isolated human hepatocytes from three adult female donors were treated for 72 hours with vehicle (carbonate-buffered saline),

human PRL (150 ng/ml) or human PL (6 µg/ml), and total RNA was isolated. Gene expression was quantified by microarray analysis and validated with quantitative real-time PCR (qPCR). qPCR analysis shows PRL and PL have differential effects on the gene expression of hepatic transporters. PRL caused the up-regulation of mRNA for the uptake transporter OAT2 by 60%, and down-regulation of the efflux transporters MRP3, MRP6, and BCRP between 15 and 20%. PL decreased mRNA expression for all uptake transporters tested, significantly for NTCB, OCT1, OATP1B1, and OATP1B3. In addition, PL increased efflux transporter gene expression for ABCA1 and BSEP by 100%, but reduced MDR1, MRP2, MRP3, MRP5, MRP6, and BCRP mRNAs. Taken together, these data suggest hormones secreted during pregnancy may globally suppress the maternal gene expression of many uptake and efflux transporters crucial for chemical excretion by the liver. Supported by ES020522, DK080774, ES007148, ES005022, HD065532.

**PS 646 Acrolein Cytotoxicity in Hepatocytes Involves Endoplasmic Reticulum Stress, Mitochondrial Dysfunction, and Oxidative Stress.**

M. Mohammad<sup>1</sup>, D. Avila<sup>1</sup>, J. Zhang<sup>1</sup>, S. Barve<sup>1</sup>, G. Arteel<sup>3</sup>, C. McClain<sup>1,2</sup> and S. Joshi-Barve<sup>1</sup>. <sup>1</sup>Department of Medicine/GI, University of Louisville, Louisville, KY; <sup>2</sup>Louisville VAMC, Louisville, KY; <sup>3</sup>Pharmacology and Toxicology, University of Louisville, Louisville, KY.

Acrolein is a common environmental, food and water pollutant and a major component of cigarette smoke. Also, it is produced endogenously via lipid peroxidation and cellular metabolism of certain amino acids and drugs. Acrolein is cytotoxic to many cell types including hepatocytes; however the mechanisms are not fully understood. We examined the molecular mechanisms underlying acrolein hepatotoxicity in primary human hepatocytes and hepatoma cells. Acrolein, at pathophysiological concentrations, caused a dose-dependent loss of viability of hepatocytes. The death was apoptotic at moderate and necrotic at high concentrations of acrolein. Acrolein exposure rapidly and dramatically decreased intracellular glutathione and overall antioxidant capacity, and activated the stress-signaling MAP-kinases JNK, p42/44 and p38. Our data demonstrate for the first time in human hepatocytes, that acrolein triggered endoplasmic reticulum (ER) stress and activated eIF2 $\alpha$ , ATF-3 and -4, and Gadd153/CHOP, resulting in cell death. Notably, the protective/adaptive component of ER stress was not activated, and acrolein failed to up-regulate the protective ER-chaperones, GRP78 and GRP94. Additionally, exposure to acrolein disrupted mitochondrial integrity/function, and led to the release of pro-apoptotic proteins and ATP depletion. Acrolein-induced cell death was attenuated by N-acetyl cysteine, phenyl-butyric acid, and caspase and JNK inhibitors. Our data demonstrate that exposure to acrolein induces a variety of stress responses in hepatocytes, including GSH depletion, oxidative stress, mitochondrial dysfunction and ER stress (without ER- protective responses) which together contribute to acrolein toxicity. Our study defines basic mechanisms underlying liver injury caused by reactive aldehyde pollutants such as acrolein.

**PS 647 Interstrain Differences in Progression from Simple Liver Steatosis to Fibrosis Are Associated with Altered Hepatic Iron Metabolism in Mice.**

S. Shpileva<sup>1</sup>, L. Muskhelishvili<sup>2</sup>, M. Pogribna<sup>1</sup>, C. Cozart<sup>1</sup>, M. Bryant<sup>1</sup>, F. A. Beland<sup>1</sup> and I. P. Pogribny<sup>1</sup>. <sup>1</sup>Division of Biochemical Toxicology, NCTR, US FDA, Jefferson, AR; <sup>2</sup>Toxicologic Pathology Associates, NCTR, US FDA, Jefferson, AR.

Nonalcoholic fatty liver disease (NAFLD) is a major health problem and a leading cause of chronic liver disease in the United States and other developed countries. The pathogenesis of NAFLD is often conceptualized as a two-step process that consists of hepatic triglyceride accumulation leading to steatosis as a first step, followed by a second step that includes oxidative stress, inflammation, and fibrogenesis. However, there is a lack of consensus on the significance of these events and the underlying mechanisms responsible for the disease progression and, more importantly, for differences in inter-individual disease severity and sensitivity. In a previous study we demonstrated that the inter-strain variability in severity of NAFLD was associated with dysregulation of lipid metabolism (first step). Emerging evidence indicates the importance of altered iron metabolism in the mechanism of the second step leading to progression from simple hepatic steatosis to fibrosis. The goal of this study was to investigate whether or not inter-individual differences in the intracellular iron metabolism are associated with development and severity of fibrosis induced by methyl-donor-deficiency among individual inbred strains of mice. Feeding male A/J, 129S1/SvImJ, and WSB/Eij mice a choline- and folate-deficient (CFD) diet for 12 weeks caused liver injury similar to NAFLD, with the magnitude being A/J < 129S1/SvImJ < WSB/Eij. The inter-strain variability in severity of

NAFLD and its further progression to fibrosis, which was characterized by hepatic stellate cell activation and up-regulation of fibrosis markers, was associated with the extent of hepatic iron metabolism deregulation. This was evidenced by strain-dependent alterations in the expression of iron-regulatory genes (Tfr, Fth1, Slc40a1, and Hfe2), which was correlated tightly with the degree of hepatic fibrotic changes in the livers of the mice fed the CFD diet.

**PS 648 Dose-Dependent Hepatic Physiological, Histopathological, and Gene Expression Responses in C57BL/6 Mice following Repeated TCDD Exposure.**

T. R. Zacharewski<sup>1,3</sup>, K. A. Fader<sup>1,3</sup>, J. Harkema<sup>2,3</sup> and R. Nault<sup>1,3</sup>. <sup>1</sup>Biochemistry & Molecular Biology, Michigan State University, East Lansing, MI; <sup>2</sup>Pathobiology and Diagnostic Investigations, Michigan State University, East Lansing, MI; <sup>3</sup>Center for Integrative Toxicology, Michigan State University, East Lansing, MI.

2,3,7,8-Tetrachlorodibenzo-p-dioxin (TCDD) is a potent aryl hydrocarbon receptor (AhR) agonist. We have previously reported that exposure to a single oral dose of 1 µg/kg TCDD induces hepatic steatosis in mice. A complementary 28 day repeated-dose dose-response study was performed to further investigate the effects of TCDD on steatosis and its progression to steatohepatitis and cirrhosis. C57BL/6 mice were gavaged every 4 days with sesame oil vehicle control or 0.001 - 30 µg/kg TCDD. Although repeated dosing did not significantly affect body weight gain, gonadal white adipose tissue (gWAT) weight was 50% lower at 30 µg/kg while relative liver weight was increased at 3, 10, and 30 µg/kg TCDD. Histopathology revealed dose dependent alterations with minimal centrilobular microvesicular lipid accumulation (hepatic steatosis) at 3 µg/kg, mild to moderate hepatic lipid accumulation with mild inflammation at 10 µg/kg (steatohepatitis), and widespread micro- and macro-vesicular lipid accumulation in the centrilobular, mid-zonal, and periportal regions of the liver, inflammation, and perivascular fibrosis suggesting early cirrhosis at 30 µg/kg. QRT-PCR revealed dose-dependent induction of *Cyp1a1*, *Cyp1a2*, *Cyp1b1*, *Dysf*, *Gstp2*, *Notch1*, *Nqo1*, *Pla2g12a*, *Serpina6a*, *Srxn1*, *Tiparp*, and *Tnfrsf2*, as well as down-regulation of *Got1* and *Pck1*. Dose-response modeling (ToxResponse modeler) revealed similar ED50's to 24h single dose TCDD studies. These results suggest that simple steatosis can progress to steatohepatitis with fibrosis following repeated TCDD exposure, due to persistent AhR-mediated differential gene expression associated with lipid transport, processing, and metabolism. Funded by SRP P42ES04911.

**PS 649 Impaired Glycosylation and Membrane Localization of Uptake and Efflux Transporters in Human Nonalcoholic Fatty Liver Disease.**

J. Clarke<sup>1</sup>, P. Novak<sup>2</sup>, A. D. Lake<sup>1</sup>, R. N. Hardwick<sup>1</sup> and N. J. Cherrington<sup>1</sup>. <sup>1</sup>Pharmacology and Toxicology, University of Arizona, Tucson, AZ; <sup>2</sup>Biology Centre ASCR, Institute of Plant Molecular Biology, Ceske Budejovice, Czech Republic.

The prevalence of non-alcoholic fatty liver disease (NAFLD) and the more severe non-alcoholic steatohepatitis (NASH) is estimated to be 30-40% and 5-17%, respectively. We have previously demonstrated a loss of N-linked glycosylation and decreased membrane localization of the efflux transporter ABCG2 in rodent and human NASH resulting in the altered disposition of drugs. N-linked glycosylation of proteins has been shown to be critical for proper protein folding and trafficking to the plasma membrane. The purpose of this study was to assess the transcriptomic expression of genes involved in protein glycosylation and processing through the endoplasmic reticulum (ER), and to determine the effect of altered glycosylation on key drug transporters during the progression of human NAFLD. For this study, human liver samples diagnosed as healthy, steatosis, NASH with fat, and NASH without fat were analyzed. Using bioinformatics methods we discovered that genes involved in protein processing in the ER and biosynthesis of N-glycans were significantly enriched for downregulation in NAFLD progression. Included in the N-glycan biosynthesis category were genes involved in the oligosaccharyltransferase complex, N-glycan quality control, N-glycan precursor biosynthesis, N-glycan trimming to the core, and N-glycan extension from the core. In contrast to down-regulation of these genes, N-glycan degradation genes were unaltered in the progression to NASH. Immunoblot analysis of the uptake transporters OATP1B1 and OATP1B3 and the efflux transporters ABCG2 and BCRP demonstrated a significant loss of glycosylation, while immunohistochemical analysis revealed impaired membrane localization of ABCG2. We propose that the loss of glycosylation and impaired membrane localization of key uptake and efflux transporters in human NASH is a potential mechanism for the occurrence of altered drug disposition in NASH.

**PS 650 High Dietary Fructose Induced Copper Deficiency Contributes to Alcoholic Liver Disease Progression.**

M. Song<sup>1</sup>, T. Chen<sup>3</sup> and C. McClain<sup>1,2,3</sup>. <sup>1</sup>Department of Medicine/GI, University of Louisville, Louisville, KY; <sup>2</sup>Louisville VAMC, Louisville, KY; <sup>3</sup>Pharmacology and Toxicology, University of Louisville, Louisville, KY.

**Background/Aims:** The increased consumption of fructose parallels the increased prevalence of obesity and the metabolic syndrome in the United States and worldwide. Noteworthy is that obesity potentiates the severity of alcohol-induced liver injury. High fructose feeding impairs intestinal copper absorption and leads to copper deficiency in rodents. Moreover, Copper deficiency is associated with the decreased antioxidant defenses and mitochondrial dysfunction. In this study, we investigated whether high fructose diet induced obesity potentiates chronic alcohol drinking induced liver injury.

**Methods:** Six-week-old male C57BL/6J mice were fed either control diet or high fructose diet (60%, w/w) for 18 weeks. 20% (w/v) ethanol was given ad libitum after 8-weeks high fructose feeding until the end of the experiment. Copper status, hepatic injury and steatosis were assessed.

**Results:** High fructose diet feeding led to copper deficiency as indicated by decreased plasma ceruloplasmin, Cu, Zinc superoxide dismutase (SOD1) and increased copper chaperone for SOD1 (CCS). Liver injury was significantly induced in mice fed with high fructose diet followed by chronic alcohol drinking as evidenced by robust increased plasma ALT, AST, chemokine (mouse KC) and liver histology. Both liver triglyceride and plasma triglyceride were significantly increased with chronic alcohol drinking, however, neither additive nor synergistic effects was observed in mice fed with high fructose diet followed by chronic alcohol.

**Conclusion:** Our data suggest that high fructose diet-induced obesity may potentiate chronic alcohol drinking induced liver injury. High fructose feeding induced copper deficiency might be a priming factor to chronic alcohol drinking induced liver injury. The potential mechanism might relate to the decreased antioxidant defense caused by copper deficiency.

**PS 651 Steroid Sulfatase Enhances Hepatic Estrogen Activity and Protects Mice from Obesity and Type 2 Diabetes.**

W. Xie and M. Jiang. University of Pittsburgh, Pittsburgh, PA.

The enzyme steroid sulfatase (STS) is responsible for the formation of biologically active estrogens by the hydrolysis of estrogen sulfates and regulates estrogen homeostasis. In this report, we showed that hepatic over-expression of STS in female STS transgenic mice elicited metabolic benefits that protected mice from high fat diet (HFD) induced obesity and type 2 diabetes. STS transgenic mice subjected to HFD challenge displayed significant decrease in fat mass and body weight, and increased energy expenditure without alterations in food intake compared with their wild-type counterparts. Moreover, STS transgenic mice had improved glucose tolerance. The metabolic benefit was associated with inhibition of hepatic gluconeogenic genes and inflammation related genes. Silencing the transgene expression through tet-off regulatory system abolished the metabolic benefit, indicating that the protection is caused by transgene itself rather than non-specific effects from random transgene insertion sites. The hepatic estrogen signaling was enhanced in STS transgenic mice, whereas elimination of the primary source of estrogens by ovariectomy abolished the protective metabolic phenotype, suggesting the metabolic action is mediated by increased estrogenic activity in STS transgenic mice liver. In summary, our results have revealed an important metabolic function of STS and may establish it as a novel therapeutic target for the prevention and treatment of obesity and type 2 diabetes.

**PS 652 Effect of Diallyl Disulfide on the Cytokines Expression in Cadmium Chloride-Treated Liver Cells.**

S. Smith, C. Odewumi, V. Badisa, A. Abdulla and L. M. Latinwo. *Biology, Florida A&M University, Tallahassee, FL.* Sponsor: A. Becker.

Cadmium is one of the most hazardous metals in the environment. Studies have shown that exposure to cadmium causes damage to many organs that may alter biological activities of the cells and may lead to cancer in mammalian systems. In the presence of toxicants, cells produce various cytokines in the body to reduce the toxic effect of the toxicants. Diallyl disulfide (DADS), an organosulfur compound in the garlic extract has been used in many countries as a preventive compound for various diseases. DADS can act as chelator and/or as an antioxidant. This project was designed to study the preventive effect of DADS on the cytokines expression in cadmium chloride (CdCl<sub>2</sub>) treated normal rat liver CRL1439 cells. For the viability assay, the cells were treated with CdCl<sub>2</sub> alone (0, 50 and 150  $\mu$ M), DADS alone (150 and 300  $\mu$ M) or co-treated with 2 h pre-treatment of DADS (150 and 300  $\mu$ M) prior to CdCl<sub>2</sub> (150  $\mu$ M) for 24 h and the cells viability was measured by the

crystal violet assay. For the cytokine array analysis, the cells were treated with CdCl<sub>2</sub> alone (0, and 150  $\mu$ M), DADS alone (150  $\mu$ M) or co-treated with 2 h pre-treatment of DADS (150  $\mu$ M) prior to CdCl<sub>2</sub> (150  $\mu$ M) for 6 h and the cytokines expression was measured using the Ray Biotech human cytokine array 7 kit. Viability results revealed that 150  $\mu$ M of DADS showed the greatest protection against CdCl<sub>2</sub> toxicity. In the cells treated with CdCl<sub>2</sub> alone, 22 cytokines were up-regulated and 2 cytokines were down-regulated. However, in the co-treated cells, the pattern of cytokines expression observed was reversed, indicating the protective effect of DADS against CdCl<sub>2</sub> toxicity. Cytokines that were up-regulated in CdCl<sub>2</sub> alone are involved in the alterations of cell cycle control system and cell mediated immunity. The present study clearly shows the preventive effect of DADS on the cytokines expression in the CdCl<sub>2</sub> treated liver cells and suggests that DADS can be used as preventative agent for cadmium toxicity.

**PS 653 The Effect of Fenugreek Leaf Extract on Gene Expression Profile of Cadmium Chloride Treated Normal Rat Liver Cells.**

R. L. Lyles, C. Odewumi, V. Badisa and L. M. Latinwo. *Biology, Florida A&M University, Tallahassee, FL.* Sponsor: A. Becker.

**Rationale and Scope of the Study:** Cadmium is a toxic and carcinogenic metal pollutant that has been known to cause DNA damage. It targets many human organs, mainly lungs, liver, and kidneys. Many chemo-preventive agents have been used against the toxic effect of many heavy metals. Fenugreek belongs to the family Leguminosae and well known for its medicinal value. In our study, the effect of Fenugreek Leaf Extract (FLE) on the viability and total gene expression profile in cadmium treated rat liver cells was evaluated. **Experimental Procedure:** The cells were treated with CdCl<sub>2</sub> (0, 25  $\mu$ M) alone or pretreated with FLE (0.005  $\mu$ g/ml) for 4 h followed by CdCl<sub>2</sub> (25  $\mu$ M) for 36 h or 48 h at 37°C in a 5% CO<sub>2</sub> incubator. The viability was measured by crystal violet dye staining method. The total gene profiles were determined using RG230 PM whole genome microarray which was processed by Affymetrix Gene Atlas system. The Partek Express software analyzes the genes up or down regulated in the treated samples. The Partek pathway software identifies the pathways affected by the treatment. **Results:** In CdCl<sub>2</sub> alone treated cells, the viability was reduced to 37.1%, while in the cells pretreated (4 h) with FLE followed by CdCl<sub>2</sub>, the viability was increased to 102% respectively, in comparison to the control cells (100%). In CdCl<sub>2</sub> alone treated cells, out of 31,139 genes on the array 61 were up regulated (>2 fold) and 124 were down regulated ( $\leq$  2 fold) respectively in comparison to control cells. In the cells pretreated with FLE followed by CdCl<sub>2</sub>, 181 genes were up regulated (>2 fold) and 161 genes were down regulated ( $\leq$  2 fold). The main pathways affected in above treatment groups were ribosome, TCA cycle and DNA replication. **Conclusion:** Our results indicate that pretreatment with FLE for 4 h affects gene expression profile in the cadmium treated cells. The alteration in the genes expression in the FLE pretreated cells may be responsible for the protective effect against cadmium toxicity. Therefore, our study suggests that fenugreek leaves can be used to reduce cadmium toxicity.

**PS 654 Evidence for a Functional Keap1-Nrf2 Cell Defence Pathway in Human Liver.**

I. M. Copple<sup>1</sup>, C. Rowe<sup>1</sup>, R. P. Jones<sup>2,1</sup>, S. W. Fenwick<sup>2</sup>, H. Z. Malik<sup>2</sup>, C. Goldring<sup>1</sup>, N. R. Kitteringham<sup>1</sup> and B. Park<sup>1</sup>. <sup>1</sup>MRC Centre for Drug Safety Science, University of Liverpool, Liverpool, United Kingdom; <sup>2</sup>Department of Hepatobiliary Surgery, Aintree University Hospital NHS Foundation Trust, Liverpool, United Kingdom. Sponsor: D. Mendrick.

The transcription factor Nrf2 regulates a battery of cell defence processes that protect against drug-induced liver injury in rodents, yet very little is known regarding the role of Nrf2 in regulating resistance to drug-induced stress in man. Utilising hepatocytes isolated from surgically resected healthy liver tissue (n=6), we provide the first comprehensive delineation of the Nrf2 pathway in human liver. Hepatocytes were isolated using a standard collagenase perfusion protocol, seeded onto Type I collagen-coated culture plates and reverse-transfected with 20 nM of an siRNA duplex targeted against Nrf2, Keap1 or a scrambled non-targeting control siRNA duplex. siRNA depletion of Nrf2 was associated with a decrease in the mRNA and protein levels of the established Nrf2 target genes GCLC, NQO1 and SRXN1. Furthermore, following siRNA depletion of Keap1, the cytosolic repressor of Nrf2, the total cellular abundance of Nrf2 protein was increased, as was the mRNA and protein levels of GCLC, NQO1 and SRXN1. The potent Nrf2 activator CDDO-Me induced a robust stabilisation of Nrf2 in human hepatocytes, and this was associated with a time and Nrf2-dependent increase in the mRNA and protein levels of GCLC, NQO1 and SRXN1. Under the same conditions, CDDO-Me provoked a

time and Nrf2 -dependent increase in total glutathione levels. Therefore, the Keap1-Nrf2 pathway regulates the basal and inducible activity of key cell defence processes in human hepatocytes, and may therefore be a novel marker of chemical stress and/or a promising therapeutic target in man. Notably, there was marked (up to 5-fold) inter-individual variation in the basal and inducible level of Nrf2 protein across hepatocytes isolated from patients. Such inter-individual variation in the activity of Nrf2 may have important consequences for susceptibility to disease and drug-induced toxicity in man.

## PS 655 Dibenzofuran and Mitochondrial Function: Interaction with Adenine Nucleotide Translocator.

C. M. Palmeira<sup>1,2</sup>, F. V. Duarte<sup>1,2</sup>, A. P. Gomes<sup>1,2</sup>, J. S. Teodoro<sup>1,2</sup>, A. T. Varela<sup>1,2</sup>, A. J. Moreno<sup>1</sup> and A. P. Rolo<sup>2,3</sup>. <sup>1</sup>Department of Life Sciences, University of Coimbra, Coimbra, Portugal; <sup>2</sup>Center for Neurosciences and Cell Biology, University of Coimbra, Coimbra, Portugal; <sup>3</sup>Department of Biology, University of Aveiro, Aveiro, Portugal.

Dioxins and furans are very toxic and exposure to these environmental pollutants, such as fuel constituents, is linked to several diseases. Dibenzofuran is listed as a pollutant of concern due to its persistence in the environment, bioaccumulation and toxicity to humans and the environment.

Mitochondrial function is very important in cellular homeostasis and keeping a proper energy supply for eukaryotic cells is essential in the fulfillment of the tissues energy-demand. The main objectives of this work concerned Dibenzofuran effects on mitochondrial function. We isolated mitochondria from rat liver and incubated them with Dibenzofuran to analyze the effects of this pollutant at the level of mitochondrial function.

The effects of Dibenzofuran exposure include a markedly increase in the lag phase that follows depolarization induced by ADP, indicating an effect in the phosphorylative system. Experiments performed using carboxyatractyloside (CAT) suggested an interaction of Dibenzofuran with the ANT carrier. Dibenzofuran exposure also produces an inhibition of mitochondrial permeability transition and an increase in calcium retention capacity, which may also be explained by a putative interaction of Dibenzofuran with ANT.

Clarifying the role of pollutants in some mechanisms of toxicity, such as unbalance of bioenergetics status and mitochondrial function, may help to explain the progressive and chronic evolution of diseases derived from exposure to environmental pollutants.

Duarte FV (SFRH/BD/38372/2007), Teodoro JS (SFRH/BD/38467/2007), Gomes AP (SFRH/BD/44674/2008) and Varela AT (SFRH/BD/44796/2008) are recipients of a Fundação para a Ciência e a Tecnologia (Portugal) scholarship.

## PS 656 Trovafloxacin-Induced TNF Expression in Raw Cells Is ATR-Dependent.

K. L. Poulsen<sup>1,2</sup>, P. E. Gancay<sup>1,2</sup> and R. A. Roth<sup>1,2</sup>. <sup>1</sup>Pharmacology and Toxicology, Michigan State University, East Lansing, MI; <sup>2</sup>Center for Integrative Toxicology, Michigan State University, East Lansing, MI.

Trovafloxacin (TVX) is a fluoroquinolone antibiotic associated with idiosyncratic drug-induced liver injury (IDILI) in humans. The mechanism underlying this toxicity remains unknown. An animal model of IDILI in mice revealed that TVX synergizes with a concurrent inflammatory stress from bacterial lipopolysaccharide (LPS) to result in liver injury. This hepatotoxic interaction depended upon prolongation of the LPS-induced appearance of tumor necrosis factor- $\alpha$  (TNF) in the plasma of animals coexposed to TVX. We established a model in vitro in RAW 264.7 murine macrophages (RAW cells) in which exposure to TVX alone or in combination with LPS increases both cellular TNF mRNA and TNF protein released into the culture medium. TVX is a bacterial topoisomerase inhibitor, and in a cell-free assay it inhibited mammalian topoisomerase II- $\alpha$  as well. Interestingly, TVX also caused a concentration-dependent increase in DNA double-strand breaks (DSBs) in RAW cells. Inasmuch as DSBs can activate kinases such as ataxia telangiectasia mutated (ATM) and Rad3-related (ATR), kinase inhibitors were tested for their ability to diminish TVX-induced synthesis and release of TNF from RAW cells. A selective ATM inhibitor (KU55933) had no effect on TNF mRNA or TNF release from TVX-exposed RAW cells. In contrast, a novel ATR inhibitor (NU6027) significantly attenuated the TVX-induced increase in TNF mRNA. NU6027 also eliminated the interaction between TVX and LPS, significantly decreasing TNF release in cells treated with TVX-LPS to the level induced by LPS alone. These findings suggest that ATR plays an important role in TNF expression in response to TVX exposure. (Supported by NIH grant R01 DK061315 and T32 ES007255)

## PS 657 3, 3'-Diindolylmethane Attenuates Lipopolysaccharide/D-Galactosamine-Induced Fulminant Hepatic Failure by Inducing Changes in microRNA Expression in the Liver-Infiltrating Mononuclear Cells.

S. Tomar, P. Nagarkatti and M. Nagarkatti. Pathology, Microbiology and Immunology, School of Medicine, University of South Carolina, Columbia, SC.

Lipopolysaccharide/D-Galactosamine (LPS/D-GalN) induced acute liver injury is a widely used animal model of human fulminant hepatic failure. Our studies demonstrate that pretreatment with 3,3'-Diindolylmethane (DIM), a plant derived compound and a ligand for Aryl hydrocarbon receptor (AhR) reduces LPS/D-GalN induced acute liver injury in BALB/c mice. This was demonstrated by decreased mortality, serum levels of pro-inflammatory cytokines such as TNF $\alpha$  and IL-6, serum Alanine Transaminase (ALT) enzyme, liver damage by histology, liver infiltration of mononuclear cells and the myeloperoxidase (MPO) activity in the liver tissues of mice treated with DIM prior to induction of liver injury. DIM treatment also suppressed Caspase 3 activity, nuclear NF- $\kappa$ B translocation and activation of ERK MAP kinase in the liver tissues. DIM treatment also causes a reduction in absolute numbers of activated macrophages that infiltrate the liver. In vitro studies showed that DIM causes suppression in the expression of activation markers, CD69, CD86 and MHCII, and increased apoptosis of B cells after LPS treatment. Interestingly, AhR antagonist CH223191 was able to cause a reversal of these DIM-mediated in vitro effects, indicating that the effects of DIM were mediated through the AhR. miRNA expression microarray revealed that DIM causes a differential change in the expression of several miRNAs that regulate multiple pathways of immune cell responses including MAP kinases, STAT proteins, TNF $\alpha$ , IL-6 and NF- $\kappa$ B signaling within the liver infiltrating mononuclear cells. Our results indicate that DIM suppresses acute liver injury by regulating miRNA expression within the liver infiltrating mononuclear cells and that DIM could be a potential therapeutic strategy for acute liver injury. (Supported in part by NIH grants P01AT003961, R01AT006888, R01ES019313, R01MH094755, P20RR032684 and VA Merit Award BX001357).

## PS 658 Multiple Mechanisms for the Appearance of Acetaminophen-Protein Adducts in Plasma: Basic Science and Clinical Implications.

M. R. McGill, Y. Xie, M. Bajt, M. Yang, C. Williams and H. Jaeschke. Pharmacology, Toxicology, and Therapeutics, University of Kansas Medical Center, Kansas City, KS.

Acetaminophen (APAP) overdose is a major cause of acute liver failure. The drug is metabolized to an intermediate (NAPQI) which binds to proteins. Protein binding in the liver initiates a cascade of intracellular signaling events leading to necrosis. Interestingly, APAP-protein adducts can also be detected in plasma. Initially, this was thought to be due to release of hepatocyte contents during cell death. However, it has been shown that plasma adducts can appear without injury. Here, we have confirmed this by showing that plasma adducts increase before ALT at toxic doses, are detectable after non-toxic doses, and are detectable in APAP-resistant rats. How this occurs is not yet known. To explore this further, primary mouse hepatocytes were treated with APAP in medium with or without serum. In serum-free medium we could measure extracellular proteins within 3 h (Coomassie), demonstrating active protein secretion. Adducts were detected in both regular and serum-free medium at this time point ( $0.77 \pm 0.08$  and  $0.31 \pm 0.01$  nmol/mL, respectively), suggesting that secretion is one mechanism by which extracellular adducts appear. The difference may be due to diffusion of NAPQI and direct serum-protein binding. Cell adducts were higher in cultures without serum ( $0.42 \pm 0.02$  vs.  $0.24 \pm 0.02$  nmol/mg protein), indicating that serum absence did not reduce metabolism. To test if necrosis can increase serum adducts, we treated mice with doses of APAP that did not cause injury and induced necrosis with ischemia-reperfusion. A significant increase in serum APAP-protein was observed. This could have implications for the clinical use of this parameter in patients with non-APAP liver injury and incidental APAP ingestion. Conclusions: Multiple mechanisms are involved in appearance of serum APAP-protein adducts, including secretion and passive release during necrosis. Caution should be used in the clinical interpretation of APAP-protein adducts.

## PS 659 Insulin-Mimetic Effects of Arsenic: Modulation of FoxO Signaling to Affect Selenoprotein P Expression.

I. Hamann and L. Klotz. Faculty of Pharmacy and Pharmaceutical Sciences, University of Alberta, Edmonton, AB, Canada.

Epidemiological studies have indicated a dose-response relationship between the prevalence of diabetes mellitus and arsenic exposure from drinking water. Mechanisms by which arsenic may cause this diabetogenic effect are largely unknown. Recent studies indicate that arsenic may impair insulin-stimulated glucose

uptake. The phosphoinositide 3'-kinase (PI3K)/Akt signaling pathway plays an important role in glucose metabolism, in part by regulating the activity of forkhead box/class O (FoxO) transcription factors. The present study aimed at investigating the effect of As<sup>3+</sup> (arsenite) on FoxO activity in human hepatoma cells, the role of PI3K/Akt signaling therein and the modulation of the expression of FoxO target genes, such as that of selenoprotein P (SeP), a hepatokine causing insulin resistance. We analyzed changes in phosphorylation of Akt and FoxO1a/3a in HepG2 human hepatoma cells in response to As<sup>3+</sup> by Western blotting and found a concentration-dependent increase in phosphorylation of Akt at S473, with arsenite being effective already at low micromolar concentrations. Arsenite exposure caused phosphorylation of FoxO1a and FoxO3a at sites known to be phosphorylated by Akt, T32 and T24, respectively. Phosphorylation of FoxOs was prevented by wortmannin, pointing to the involvement of PI3K. The functional inactivation of FoxOs by As<sup>3+</sup> was observed in an ELISA-based DNA binding assay and at the level of FoxO target gene expression: SeP and glucose-6-phosphatase mRNA levels were clearly downregulated after 24h exposure to nanomolar As<sup>3+</sup> concentrations, as demonstrated by real-time RT-PCR. Curiously, As<sup>3+</sup> showed a biphasic effect on SeP protein levels, inducing a small increase in the nanomolar and a distinct decrease in the micromolar concentration range. In conclusion, As<sup>3+</sup> may perturb cellular signaling pathways involved in fuel metabolism: it stimulates insulin-like signaling in HepG2 cells and affects the expression of FoxO target genes and the release of the hepatokine SeP, which is known to modulate insulin sensitivity.

## PS 660 The Role of Multidrug Resistance Protein 4 (Mrp4, Abcc4) in Protecting against Acetaminophen (APAP)-Induced Hepatotoxicity.

A. M. Bataille and J. E. Manautou. *Pharmaceutical Sciences, University of Connecticut, Storrs, CT.*

Mrp4 is a member of the ABC family of membrane transport proteins that functions as an efflux transporter for a wide variety of substrates. Previous studies in our laboratory have shown that Mrp4 is the most significantly induced hepatic transporter by toxic acetaminophen (APAP) treatment. The basal expression of Mrp4 in normal human and naïve C57BL/6J mouse liver is very low. However, Mrp4 expression is greatly induced by exposure to hepatotoxins that cause oxidative stress, suggesting that this transporter is up-regulated to assist in defending against cellular stress. Additional studies in our laboratory demonstrated that a low hepatotoxic dose of APAP protects against subsequent administration of a higher dose of APAP. This phenomenon is referred to as APAP autoprotection and liver Mrp4 induction is even more pronounced in this mouse model. Despite these findings, the precise role that enhanced Mrp4 expression plays in protecting against APAP hepatotoxicity remains unclear. To study this, we analyzed the responsiveness of Mrp4 heterozygous mice (Mrp4<sup>+/-</sup>) to APAP hepatotoxicity and the ability of these mice to exhibit resistance to APAP upon toxicant re-exposure. The results showed that APAP hepatotoxicity in Mrp4<sup>+/-</sup> mice is significantly higher than in wild-type mice. However, the ability of these mice to develop tolerance to APAP liver injury is unchanged. Analysis of potential differences in gene expression of other hepatic membrane transporters, oxidative stress-related genes and drug detoxification enzymes revealed that there are no significant changes that could account for the differential susceptibility of Mrp4<sup>+/-</sup> mice to APAP toxicity. Based on these results, we conclude that Mrp4 plays a critical role in preventing APAP-induced hepatotoxicity but that its role in APAP autoprotection may be less substantial.

## PS 661 Dual Role of Macrophages in Injury and Repair in Acetaminophen-Induced Hepatotoxicity.

C. R. Gardner<sup>1</sup>, H. M. Choi<sup>1</sup>, J. D. Laskin<sup>2</sup> and D. L. Laskin<sup>1</sup>. <sup>1</sup>Rutgers University, Piscataway, NJ; <sup>2</sup>UMDNJ-RWJ Medical School, Piscataway, NJ.

Activated macrophages and the mediators that they release play a key role in acetaminophen (APAP)-induced hepatotoxicity; however, their role is dependent on their phenotype and timing of appearance in the liver. Whereas classically activated M1 macrophages contribute to tissue injury, alternatively activated M2 macrophages are involved in tissue repair. To assess the role of these macrophage subpopulations in APAP hepatotoxicity, we used gadolinium chloride (GdCl<sub>3</sub>) and clodronate liposomes (CL), which block M1 and M2 macrophages, respectively. Male Long Evans hooded rats were treated with GdCl<sub>3</sub> (7 mg/kg, iv) or CL (0.4 ml/100 g body weight), 24 and 48 h prior to APAP (600 mg/kg, ip). Cells were isolated 24 h later. Treatment of rats with APAP resulted in a decrease in CD163<sup>+</sup> resident repair macrophages in the liver after 24 h, with no significant effect on infiltrating CD11b/CD68<sup>+</sup> M2 repair macrophages. Pretreatment of rats with GdCl<sub>3</sub>, which protects against APAP hepatotoxicity, resulted in a decrease in macrophage expression of inducible nitric oxide synthase, a prototypical marker of classical activation. This was associated with an increase in CD163<sup>+</sup> resident and

CD11b/CD68<sup>+</sup> infiltrating repair macrophages in the liver. Conversely, CL pretreatment, which exacerbates APAP hepatotoxicity, markedly decreased both of these repair macrophage populations. Expression of markers of alternative M2 macrophage activation including STK, macrophage stimulating protein, and arginase-1, as well as the anti-inflammatory cytokine IL-10 were also reduced in CL treated rats. Taken together these data support the concept that macrophages play distinct role in APAP hepatotoxicity depending on their functional capacity. Supported by NIH GM034310, ES004738, CA132624, AR055073 and ES005022.

## PS 662 Induction of Hepatic Bcrp Transporter Expression in Mice Treated with Perfluorooctanoic Acid.

M. Little<sup>1,2</sup>, L. Eldasher<sup>2</sup>, X. Wen<sup>2</sup>, K. M. Bircsak<sup>2</sup>, L. L. Yacovino<sup>2</sup> and L. M. Aleksunes<sup>2,3</sup>. <sup>1</sup>Department of Chemistry and Biochemistry, Montclair University, Montclair, NJ; <sup>2</sup>Department of Pharmacology and Toxicology, Rutgers University, Piscataway, NJ; <sup>3</sup>Toxicology Division, Environmental and Occupational Health Sciences Institute, Rutgers University, Piscataway, NJ.

Perfluorooctanoic acid (PFOA) is an industrial chemical that has been associated with negative health outcomes. The purpose of this study was to determine whether PFOA alters the expression of the breast cancer resistance protein (BCRP/ABCG2), an efflux transporter found in hepatocytes and renal proximal tubule cells, in mice and to determine whether PFOA interferes with BCRP transport in vitro. To test this, Bcrp mRNA and protein expression were measured in the kidneys and livers of male C57BL/6 mice treated with PFOA (1 or 3 mg/kg/d po) for 7 days. In addition, ATPase and membrane vesicle experiments were used to assess whether PFOA alters human BCRP activity. As expected, PFOA treatment increased liver weights as well as the mRNA and protein expression of the known target, cytochrome P450 4a14, in the liver and kidneys of mice. Compared to vehicle-treated control mice, PFOA treatment increased hepatic, but not kidney, Bcrp mRNA and protein between 2- and 3-fold. Immunofluorescent staining revealed enhanced canalicular Bcrp staining in liver sections from PFOA-treated mice. In the ATPase assay, PFOA decreased transporter activity in sulfasalazine-activated BCRP membranes. In addition, PFOA inhibited BCRP-mediated transport in membrane vesicles between 47 and 69% at high concentrations (>25 µM). In conclusion, PFOA induces hepatic Bcrp expression in mice and may inhibit human BCRP function at high concentrations. Supported by DK080774, ES020522, ES020721, ES005022 and ASPET SURF.

## PS 663 Xenosensors Mediated Regulation of ATP Binding Cassette Transporter B6 (ABCB6).

H. D. Chavan and P. Krishnamurthy. *Pharmacology, Toxicology & Therapeutics, Kansas University Medical Center, Kansas City, KS.*

Cytochromes P450 (P450s) are induced in response to therapeutic drugs and environmental contaminants, leading to increased detoxification and elimination of the xenobiotics. Xenosensors like PXR, CAR and AhR play a major role in drug and environmental contaminant induced expression of P450s. Each P450 is composed of an apoprotein moiety and a heme prosthetic group, which is required for P450 activity. Thus, under conditions of P450 induction, there is a coordinate increase in heme biosynthesis to compensate for the increased expression of P450s. ABCB6, a mitochondrial ABC transporter, is shown to regulate heme biosynthesis by modulating coproporphyrinogen transport from the cytoplasm into the mitochondria. However, it is not known if exposure to xenobiotics induces ABCB6 expression, to assure an adequate and apparently coordinated supply of heme for the functional P450. In the present study, we evaluated the role of xenosensors PXR, CAR and AhR in the regulation of Abcb6. Our results demonstrate that AhR and CAR but not PXR regulate ABCB6 expression. AhR mediated regulation of Abcb6 expression was observed both in mice and in human cell lines, while CAR mediated regulation of Abcb6 expression was seen only in mice and not in human cell lines. Further, promoter activation studies demonstrate that both AhR and CAR induce Abcb6 expression by interacting with their respective response elements in the 5' flanking region of the Abcb6. These studies are the first to describe direct transcriptional activation of both mouse and human ABCB6 by xenobiotics similar to those found in inducible P450s. The results presented in this work have both pharmacological and toxicological significance. AhR ligands have the ability to precipitate porphyria and both AhR and CAR ligands have been shown to promote cell growth and proliferation. We have previously shown that ABCB6 expression promotes cell growth and proliferation during carcinogenesis. Thus, ABCB6 induction by xenosensors AhR and CAR could be a potential contributing factor in drug induced porphyria and carcinogenesis.

**PS 664** **Hepatic Flavin-Containing Monooxygenase-3 (FMO3) Protein Is Inducible by Acetaminophen Treatment.**

S. Rudraiah and J. E. Manautou. *University of Connecticut, Storrs, CT.*

Flavin-containing monooxygenase 3 (FMO3) is a drug-metabolizing enzyme with functions similar to CYP450. Hepatic expression of human FMO3 gene is highly variable and is important in the detoxification of xenobiotics. Fmo3 was thought to be non-inducible but recent data showed that activation of the Ah receptor induces Fmo3 mRNA in mice. Recent microarray work by our group also showed a drastic induction of liver Fmo3 mRNA expression in a mouse model of resistance to acetaminophen (APAP) hepatotoxicity (autoprotection). In addition to APAP, alpha-naphthyl isothiocyanate treatment and bile duct ligation in mice markedly increase Fmo3 gene expression. The purpose of this study was to evaluate the Fmo3 gene regulation and protein expression during APAP hepatotoxicity. Among all Fmo isoforms analyzed for mRNA expression, Fmo3 was most significantly induced following a single dose of APAP (400mg/kg). Although Fmo3 mRNA levels increased significantly by APAP, its protein expression was marginally changed. Consistent with this, the catalytic activity of Fmo3 measured by oxygenation of methimazole did not change significantly either. By contrast, both Fmo3 mRNA and protein expression are significantly higher in mice pretreated and re-exposed to APAP (autoprotection model). In agreement with greater Fmo3 protein expression in livers of autoprotected mice, its catalytic activity was also significantly higher. In summary, the dramatic changes in Fmo3 gene expression produced by a single dose APAP are not accompanied by concomitant changes in protein and enzyme function, whereas livers from mice pretreated and re-exposed to APAP exhibit induction of both Fmo3 protein expression and catalytic function. Additional work is currently underway to determine the functional significance of enhanced Fmo3 protein function and which factors and signaling pathways mediate Fmo3 gene and protein expression during APAP toxicity. Taken together, these findings establish for the first time induction of not only Fmo3 gene expression, but also significant protein levels and function. Supported by NIH DK069557.

**PS 665** **Vanin-1 Knockout Mice Exhibit Alterations in Compensatory Immune Infiltration and Hepatocyte Proliferation following Acetaminophen Toxicity.**

D. Ferreira<sup>1</sup>, F. Galland<sup>2</sup>, P. Naquet<sup>2</sup> and J. E. Manautou<sup>1</sup>. <sup>1</sup>Department of Pharmaceutical Sciences, University of Connecticut, Storrs, CT; <sup>2</sup>Centre d'Immunologie de Marseille-Luminy CNRS-INSERM, Université de la Méditerranée, Marseille, France.

Previously we have shown that Vanin-1 (Vnn1) knockout mice are more susceptible to APAP hepatotoxicity (400mg/kg, i.p.) despite no differences in hepatic glutathione (GSH) content or gene expression of APAP metabolizing enzymes or transporters. Here we show that in vitro, livers from both genotypes showed similar capacities to bioactivate APAP to its reactive metabolite (~1.8 nmol APAP-NAC/min/mg protein) and to detoxify the parent compound by glucuronidation (~1.7 nmol APAP-Gluc/min/mg protein) and sulfation (~15.6 pmol APAP-Sulf/min/mg protein). Together, these data strongly suggest that the enhanced susceptibility of Vnn1 knockout mice to APAP toxicity is not due to differences in APAP metabolism. Immunohistochemistry of formalin-fixed liver sections following APAP treatment revealed a lack of PCNA positive hepatocytes and F4/80 positive macrophages in and around areas of centrilobular necrosis in Vnn1 knockouts at 48 hours after APAP. qRT-PCR from total RNA isolated from whole livers indicated that inducible nitric oxide synthase (iNos) and interleukin-4 were reduced by 2.9 and 4.3 fold, respectively, in control treated Vnn1 knockout mice relative to wild-types. Additionally, interferon  $\gamma$  was 2.7 fold lower in Vnn1 knockout mice at 48 hours after APAP treatment in comparison to wild-types. Myeloperoxidase and iNos exhibited a trend of decreased expression in Vnn1 knockouts at 48 hours, but these differences were not statistically significant. Together, these results indicate that a lack of Vnn1 expression may alter the normal compensatory repair and immune responses following toxic APAP exposure although it is unknown to what extent these mechanisms contribute to the enhanced susceptibility of Vnn1 knockout mice to APAP hepatotoxicity.

**PS 666** **Transcription Regulation by Novel Interaction of Kruppel-Like Factor 6 with Aryl Hydrocarbon Receptor at the NC-XRE.**

A. D. Joshi, D. P. Jackson, S. R. Wilson and C. Elferink. *Pharmacology and Toxicology, University of Texas Medical Branch, Galveston, TX.*

The Aryl Hydrocarbon Receptor (AhR) is a ubiquitous, ligand mediated basic helix-loop-helix transcription factor of Per/ARNT/Sim family that regulates adaptive and toxic responses to variety of chemical pollutants such as polycyclic aromatic hydrocarbons (PAH) and halogenated aromatic hydrocarbons, most notably

2,3,7,8-tetrachlorodibenzo-p-dioxin (TCDD). Upon ligand activation, the AhR translocates into the nucleus and binds to DNA at the XRE along with aryl receptor nuclear translocator (ARNT) and facilitates transcription of cytochrome P450 family members. In addition, AhR-regulated gene expression is known to regulate G1 phase cell cycle progression. Recent DNA microarray experiments by our group showed that plasminogen activator inhibitor 1 (PAI-1) is a TCDD responsive gene lacking the XRE. Subsequent characterization identified a novel non-consensus XRE (NC-XRE) located within the PAI-1 promoter that supports direct binding of AhR independent of ARNT. While the XRE and NC-XRE are distinct entities, the NC-XRE shares marked homology with the DNA binding sequence of the Kruppel-like Factor (KLF) family of transcription factors. The KLF superfamily of proteins are related to Sp1 and characterized by three zinc finger domains in their C-termini that confer binding to a GC-box linked to diverse target genes. Our results indicate that AhR interacts directly with KLF6 at the NC-XRE in a dioxin-dependent manner. Furthermore, sequential deletion studies demonstrate the importance of the AhR C-terminal and KLF6 N-terminal domains in this interaction. Since KLF6 is a liver specific tumor suppressor that has been shown to induce transcription of the G1 cyclin-dependent kinase inhibitor p21Cip1, the potential exists for overlapping or common roles involving both proteins in cell cycle regulation. Our further studies will focus on mapping the AhR complex at NC-XRE and understanding the role of this complex in transcription regulation. This work was supported by R01ES007800 and P30ES006676.

**PS 667** **Mild Endoplasmic Reticulum Stress Preconditioning Attenuates Methylmercury-Induced Cellular Damage by Inducing Favorable Stress Responses.**

F. Usuki<sup>1</sup>, M. Fujimura<sup>2</sup> and A. Yamashita<sup>3</sup>. <sup>1</sup>Clinical Medicine, National Institute for Minamata Disease, Minamata, Japan; <sup>2</sup>Basic Medical Sciences, National Institute for Minamata Disease, Minamata, Japan; <sup>3</sup>Molecular Biology, Yokohama City University School of Medicine, Yokohama, Japan. Sponsor: A. Naganuma.

Methylmercury (MeHg) toxicity is a continuous environmental problem to human health. Failure to protect cells against MeHg-induced early oxidative stress triggers subsequent endoplasmic reticulum (ER) stress and apoptosis. Here, we demonstrate the protective effects of mild ER stress preconditioning against MeHg toxicity on a MeHg-susceptible cell line. Cells preconditioned with low concentrations (0.1-0.3  $\mu$ g/ml) of an inhibitor of ER  $\text{Ca}^{2+}$ -ATPase, thapsigargin (TPG), showed resistance to MeHg cytotoxicity through several favorable stress responses, which included phosphorylation of eukaryotic initiation factor 2 alpha (Eif2 $\alpha$ ), accumulation of activating transcription factor 4 (Atf4), and upregulation of stress-related proteins (glucose regulated protein of 78 kDa (Grp78) and metallothionein 1 (Mt1)). Atf4 accumulation was mediated by translation inhibition of its upstream open reading frame (uORF) and translation facilitation of its protein-coding ORF by the phospho-Eif2 $\alpha$ . Nonsense-mediated mRNA decay (NMD) activity was suppressed by the combined effects of decreased expression of several NMD components besides the phospho-Eif2 $\alpha$ -mediated general suppression of translation initiation, resulting in accumulated Atf4 mRNA but not protein. Integrated stress responses led to a delay of MeHg-induced oxidative stress and the activation of extracellular signal-regulated kinase pathways to promote cell survival in preconditioned cells exposed to MeHg. Finally knockdown experiments demonstrated that Grp78 plays a crucial role in protecting preconditioned cells against MeHg cytotoxicity. These results suggested that mild ER stress preconditioning is a useful therapeutic intervention against MeHg toxicity, the underlying mechanism being the induction of integrated stress responses.

**PS 668** **Differences in Regulation of Gene Expression Profiles of the Bone Marrow between C57BL/6 and C3H/He Mice after Benzene Treatment.**

Y. Hirabayashi<sup>1</sup>, B. Yoon<sup>2</sup>, K. Igarashi<sup>1</sup>, J. Kanno<sup>1</sup> and T. Inoue<sup>3,4</sup>. <sup>1</sup>Cell & Molecular Toxicology Division, Biology Safety & Research Center, National Institute of Health Sciences, Tokyo, Japan; <sup>2</sup>Histology & Molecular Pathogenesis Laboratory, School of Veterinary Medicine, Kangwon National University, Chuncheon, Republic of Korea; <sup>3</sup>Function & Structural Medicine Department, Nihon University School of Medicine, Tokyo, Japan; <sup>4</sup>National Institute of Health Sciences, Tokyo, Japan.

We focused on the differences in the regulation in gene expression profiles of the bone marrow, which predict benzene-specific early responses related to plausible leukemogenic changes, between C57BL/6 (B6), a lymphoid-neoplastic-prone mouse strain, and C3H/He (C3H), a myelogenous-leukemia-prone mouse strain. Previously, we showed a latent potential of induction of myelogenous leukemias by benzene in both strains, but with different mechanistic propensities. Consequently, reciprocal differences between B6 and C3H mice in gene expression profiles related

to leukemogenesis were found by gene chip analyses 28 days after benzene treatment. Because leukemia did not develop in all mice even under the optimal condition, we further analyzed the data, focusing on not only strain differences but also individual differences. Two types of gene expression profile were recognized: one, corresponding to common gene profiles obtained by one-way analysis of variance or Welch's t-test, which were commonly shared by all mice in the same group each; and the other, corresponding to stochastic gene-expression profiles obtained by principal component analysis, which were unique genes in each individual mouse. The results clearly elucidated that the predicted gene expression profiles in the regulation of transcription factors (TFs) for proliferation were essentially different in each strain. The selected TFs, i.e., 20 for B6 and 11 for C3H, were less overlapped among each mouse in the same strain, and their regulation showed the coexistence of both suppression and activation signals in B6, whereas suppressive signals were generally predominant in C3H. These differences in regulatory gene-expression profiles may be essentially related to the strain differences in the incidence and spectrum of the leukemogenesis after benzene treatment.

## PS 669 Biphase Influence of Arsenic, Cadmium, Mercury, and Nickel on Aryl Hydrocarbon Receptor (AhR) Signaling.

A. Rannug<sup>1</sup>, A. Mohammadi-Bardbori<sup>1</sup>, L. Vikström Bergander<sup>1</sup> and U. Rannug<sup>2</sup>. <sup>1</sup>Institute of Environmental Medicine, Karolinska Institutet, Stockholm, Sweden; <sup>2</sup>Department of Genetics, Microbiology and Toxicology, Stockholm University, Stockholm, Sweden.

Interaction of oxidants with the metabolic turnover of the endogenous AHR ligand 6-formylindolo[3,2-b]carbazole (FICZ) seems to play critical roles in downstream AHR-mediated signaling. Production of superoxide leading to increased proliferation was observed after exposure of immortalized human keratinocytes (HaCaT) to low levels of As<sup>3+</sup>, Cd<sup>2+</sup>, Hg<sup>2+</sup> and Ni<sup>2+</sup>. Higher concentrations lowered the intracellular GSH levels and led to temporal inhibition of FICZ-stimulated cytochrome P4501A1 (CYP1A1) activity and increased adaptive antioxidant responses as measured by expression of antioxidant genes. After addition of FICZ (150 pM) together with the metals a temporal inhibition of the metabolic degradation of FICZ occurred, as determined by HPLC analyses. At these inhibitory concentrations, the metals themselves activated CYP1A1 at late time points. Transcriptional activation of CYP1A1 was estimated with a luciferase reporter assay in human hepatoma HepG2-XRE-Luc cells and the ability of the metals to activate the AHR only in the presence of the natural ligand FICZ was established by comparing AHR activation in commercial DMEM medium and in DMEM medium free from background levels of FICZ. NADPH oxidase (NOX) activity was critical for the stimulation of proliferation by the metals as determined by lack of proliferative responses in human X-CGD myeloid cells carrying a mutated gp91phox gene. In addition, influence of NOX on CYP1A1 gene expression was indicated by lower metal-stimulated luciferase activity in HepG2 cells treated with the NOX inhibitor diphenyliodonium. Pretreatment with the metals led 24 h later to elevated GSH levels and increased sensitivity of the AHR to low levels of FICZ (superinduction). We propose that the AHR/CYP1-dependent auto-regulatory feed-back mechanism, which ensures low steady-state levels of FICZ, works in close concert with the NADPH oxidase system.

## PS 670 Differential Gene Expression Responses by Hepatic Lobe in Fischer Rats Treated with Carcinogens Phenobarbital and Diethylnitrosamine.

B. Li<sup>1</sup>, M. W. Trimble<sup>2</sup>, D. Henderson<sup>1</sup>, S. Stepanians<sup>1</sup>, M. L. Parrish<sup>1</sup>, B. Kevin<sup>2</sup>, A. Sharma<sup>2</sup>, G. A. Boorman<sup>3</sup> and S. Williams<sup>2</sup>. <sup>1</sup>Covance Genomics Laboratories, Inc., Seattle, WA; <sup>2</sup>Covance Laboratories, Inc., Madison, WI; <sup>3</sup>Covance Laboratories, Inc., Chantilly, VA.

Rodent liver is a primary organ for assessing compound toxicity. Non-genotoxic carcinogens such as phenobarbital (PB) and genotoxic carcinogens such as diethylnitrosamine (DEN) induce morphological and physiological changes in the liver that may vary by lobe. For example, DEN induces more tumors in the right liver lobe than in the left and median lobes. To elucidate the molecular mechanisms underlying the differential compound responses, as well as the differences among the three liver lobes, groups of male Fischer rats were treated with 0 or 7.5 mg/kg/day of DEN, or 0 or 65 mg/kg/day of PB, by daily oral gavage for two and four weeks. Samples of the right lateral (RL), right median (RM), and left lateral (LL) hepatic lobes were obtained for gene expression analysis and pathological assessment. DEN induced slight apoptosis/necrosis of individual hepatocytes in all lobes, while administration of PB was associated with centrilobular hypertrophy that was much less prominent in the left lateral lobe compared with the other lobes. Gene expression profiles were assessed for three animals/group/interval using whole genome

microarrays. The data showed that PB and DEN both induced robust, yet quite distinct, transcriptional changes in the animals, which could partially explain the differential morphological/physiological outcomes. In both groups of vehicle-treated rats, the transcriptional profile of the LL lobe was much different from those of the RL and RM lobes, whereas the latter two were quite similar to each other. In animals given DEN or PB, such lobe difference was much reduced, slightly more so in the rats given DEN than in those given PB. Overall, the gene expression profile may provide clues to the mechanism of PB- and DEN-induced liver tumors, and possible molecular biomarkers for predicting liver toxicity.

## PS 671 In Vitro Effects of Aldehydes Present in Tobacco Smoke on Gene Expression in Human Lung Alveolar Epithelial Cells.

N. Cheah<sup>1,2,4</sup>, J. Pennings<sup>2</sup>, J. Vermeulen<sup>2</sup>, F. J. van Schooten<sup>1</sup> and A. Opperhuizen<sup>1,3</sup>. <sup>1</sup>Toxicology, Maastricht University, Maastricht, Netherlands; <sup>2</sup>Laboratory for Health Protection Research, National Institute for Public Health and the Environment, Bilthoven, Netherlands; <sup>3</sup>Risk Assessment, Netherlands Food and Consumer Product Safety Authority, Utrecht, Netherlands; <sup>4</sup>Cigarette Testing Laboratory, Health Sciences Authority, Singapore, Singapore. Sponsor: H. van Loveren.

Tobacco smoke consists of thousands of harmful components. A major class of chemicals found in tobacco smoke is formed by aldehydes, in particular formaldehyde, acetaldehyde and acrolein. The present study investigates the gene expression changes in human lung alveolar epithelial cells upon exposure to formaldehyde, acrolein and acetaldehyde at sub-cytotoxic levels. We exposed A549 cells in vitro to aldehydes and non-aldehyde chemicals (nicotine, hydroquinone and 2,5-dimethylfuran) present in tobacco smoke and used microarrays to obtain a global view of the transcriptomic responses. We compared responses of aldehydes with that of the non-aldehydes. Formaldehyde gave the strongest response; a total of 66 genes was greater than 1.5-fold differentially expressed mostly involved in apoptosis and DNA damage related processes, followed by acetaldehyde (57 genes), hydroquinone (55 genes) and nicotine (8 genes). Acrolein and mixture gave effects to oxidative stress genes, no gene expression effect found on the exposure to 2,5-dimethylfuran. Overall, aldehyde responses are primarily indicative for genotoxicity and oxidative stress. These two toxicity mechanisms are linked to respiratory diseases such as cancer and COPD, respectively. The present findings could be important in providing further understanding of the role of aldehydes emitted from cigarette smoke in the onset of pulmonary diseases.

## PS 672 Regulation of the Metabolic Switch between Ductal Carcinoma In Situ (DCIS) and Invasive Breast Cancer (IBC).

K. C. Scribner<sup>1</sup>, Y. Fan<sup>2</sup>, M. Ragavan<sup>3</sup>, R. Chapkin<sup>2</sup>, C. Hilty<sup>3</sup>, H. Payne<sup>4</sup>, R. Mounieime<sup>4</sup>, F. Behbod<sup>5</sup> and W. Porter<sup>1</sup>. <sup>1</sup>Integrative Biosciences, Texas A&M University, College Station, TX; <sup>2</sup>Integrative Nutrition and Complex Diseases, Texas A&M University, College Station, TX; <sup>3</sup>Chemistry, Texas A&M University, College Station, TX; <sup>4</sup>Image Analysis Laboratory, Texas A&M University, College Station, TX; <sup>5</sup>Pathology and Laboratory Medicine, University of Kansas Medical Center, Kansas City, KS.

Ductal carcinoma in situ (DCIS) accounts for 15-25% of breast cancers. However, there is a gap in our understanding of the factors that regulate the progression of DCIS to invasive breast cancer (IBC). Deregulation of cell metabolism is a defining feature of tumor cells, which utilize glycolysis instead of oxidative phosphorylation. Since altered metabolism promotes invasion and metastasis, the mechanisms regulating this switch could be critical in mediating the transition from DCIS to IBC.

Single-minded-2s (Sim2s) is present in early stage DCIS lesions and lost in IBC. Re-establishment of SIM2s in the MCF10DCIS.com model inhibits tumor growth, invasion, and metastasis. We hypothesize that SIM2s plays a key role in mediating the switch between DCIS and IBC.

To determine the effect of SIM2s on metabolism in DCIS progression, we analyzed SIM2s over and under-expressing MCF10DCIS.com cells for energy dependent differences in growth, autophagy, and metabolism. Live cell imaging and TEM were used to determine SIM2s' effect on mitochondria and autophagy. Nuclear Magnetic Resonance and Seahorse analysis was employed to compare differences in metabolic signatures and measure oxidative phosphorylation and glycolytic capacity.

Re-establishment of SIM2s induced oxidative phosphorylation and adaptation to metabolic stress through increased oxygen consumption, whereas loss of SIM2s promoted glycolysis by elevating glucose uptake and lactate production.

These results suggest that SIM2s plays a critical role in DCIS progression and loss of SIM2s is required for the switch from oxidative phosphorylation to glycolysis.

**PS 673 Hypoxia Perturbs PCB-Induced Aryl Hydrocarbon Receptor Signaling and CYP1A1 Induction in Human Cells.**

S. U. Vorrink and F. E. Domann. *Human Toxicology, The University of Iowa, Iowa City, IA.*

The aryl hydrocarbon receptor (AhR) pathway controls cellular responses to exposure of foreign substances by activating genes that aid in xenobiotic metabolism. The ligand-activated AhR forms a heterodimer with its binding partner aryl hydrocarbon receptor nuclear translocator (ARNT) and subsequently induces the transcription of genes such as CYP1A1, a member of the cytochrome P450 family and a phase I detoxifying enzyme. Notably, ARNT proteins also dimerize with hypoxia-inducible factors (HIF $\alpha$ ) which mediate the cellular response to low oxygen (hypoxia). During hypoxia, HIF $\alpha$ :ARNT heterodimers form and activate the transcription of genes that promote cell survival in low oxygen environments. Since HIF $\alpha$  and AhR share a common subunit, ARNT, the possibility for signaling crosstalk exists at this axis. We hypothesized that hypoxic conditions cause HIF $\alpha$  to sequester ARNT and thus inhibit the activation of a robust AhR transcriptional response in response to a polychlorinated biphenyl (PCB) AhR ligand. To test this hypothesis we queried several human cell lines for their responses to PCBs. Our results indicate that CYP1A1 mRNA expression was induced by 3,3',4,4',5-pentachlorobiphenyl (PCB 126) in an AhR-specific manner. Exposure of the cells to hypoxia (1% oxygen for 8 hours) significantly inhibited the induction of CYP1A1 mRNA by up to 74%. EMSA and CYP1A1 promoter:Luciferase reporter assays to measure DNA binding and transcriptional activities of AhR complexes further showed an inhibitory effect of hypoxia treatment on PCB-induced AhR signaling. Growth curve and MTT assays demonstrated significant growth inhibition following PCB 126 treatment. Taken together, these findings indicate that hypoxia significantly interferes with AhR-mediated responses to PCBs. Our future studies will investigate whether the observed effects also occur at the protein level and whether hypoxia can prevent the growth inhibitory effect of PCB treatment. (Supported by grant NIEHS P42 ES 013661.)

**PS 674 Characterizing Chronic Nicotine Exposure-Induced Behaviors and Gene Regulations in *Caenorhabditis elegans*.**

J. R. Polli, F. A. Taki, M. A. Smith and X. Pan. *Biology, East Carolina University, Greenville, NC.* Sponsor: J. DeWitt.

Nicotine is one of the most abused substances. Nicotine binds nicotinic acetylcholine receptors (nAChRs), stimulates the mesolimbic dopamine system, and leads to addiction. With chronic exposures to low concentrations of nicotine are a common scenario, this study aims to characterize chronic nicotine exposure-induced behaviors and explore affected gene pathways in the model organism, *Caenorhabditis elegans* (*C. elegans*). *C. elegans* were treated with control, 6.17  $\mu$ M, and 61.7  $\mu$ M of nicotine for 24-hour and locomotion behaviors were characterized using a worm tracking system. Our preliminary data has determined several additive behavioral patterns following chronic low range micromolar nicotine exposures, including stimulation, withdrawal, and tolerance. Locomotive behaviors were stimulated in control worms that were exposed to nicotine. Withdrawal behaviors were observed as increased locomotion speeds when nicotine dosages were disrupted in nicotine-dependent worms. We also detected the expressions of 39 functional genes implicated in cholinergic signaling, locomotion, egg-laying, and stress-response. Findings showed that gene expressions are most active in low but not in high concentration dosages. The expression profiles of all the tested protein-coding genes were affected with a range from 12.5 fold down-regulation (old-1) to 138.1 fold up regulation (hlh-14). Nicotine exposure also affected the expression of microRNAs, an extensive class of a small regulatory RNAs.

**PS 675 TNIP1 Regulates the Cell Stress Response through Repression of Heat Shock Proteins A6 and A1A.**

V. P. Ramirez<sup>1</sup>, M. Stamatis<sup>2</sup>, A. Shmukler<sup>2</sup>, C. Zhang<sup>3</sup> and B. J. Aneskievich<sup>3</sup>.

<sup>1</sup>Pharmacology & Toxicology Program, University of Connecticut, Storrs, CT;

<sup>2</sup>PharmD Program, University of Connecticut, Storrs, CT; <sup>3</sup>Department of Pharmaceutical Sciences, University of Connecticut, Storrs, CT.

TNIP1 protein represses gene expression otherwise activated by NF- $\kappa$ B, RAR, and PPAR. Additionally, TNIP1 expression is increased in several cutaneous inflammatory diseases and wound healing. Thus, while some transcription factor targets and pathologies have been recognized, the spectrum of genes possibly affected by TNIP1 is unknown. To identify additional gene expression changes due to increased TNIP1 levels, we conducted a microarray analysis from keratinocytes transiently overexpressing TNIP1.

In addition to repression of genes known to be activated by NF- $\kappa$ B, RAR, and PPAR, a surprising result of decreased HSP gene family expression was observed (ex. 20x and 3.2x for HSPA6 and A1A, resp.). This reduction was confirmed by

qPCR and western blot. Both HSPA6 and A1A have similar functions in cell protection where knockdown of either HSP reduced cell viability post-cell stress. Since HSPA6 basal and induced expression was decreased by TNIP1, it was chosen for further studies.

To guide analysis of how HSPA6 may be regulated by TNIP1, we isolated and performed in silico analyses on the HSPA6 3-kb promoter. Putative PPAR, RAR and NF- $\kappa$ B sites were found. PPAR $\alpha$  and RAR ligands had no effect, but PPAR  $\beta/\delta$  and  $\gamma$  ligands increased HSPA6 expression ~4x. To search for TNIP1-responsive region(s), we cloned 5'-HSPA6 promoter deletions into a reporter construct. Intriguingly, the most repressed region lacks PPREs, RAREs, and NF- $\kappa$ B sites. These results suggest that although PPAR can regulate HSPA6 and TNIP1 may be repressing HSPA6 through this transcription factor, there is an additional TNIP1-sensitive region independent of its previously identified PPAR, RAR and NF- $\kappa$ B targets. Moreover, our data suggests TNIP1-mediated HSPA6 repression is independent of PPAR, RAR or NF- $\kappa$ B, suggesting there may be additional, as yet unrecognized, targets where interaction with TNIP1 results in reduced transcriptional activity.

**PS 676 Erk1/2 Pathway Inhibition Attenuates BoNT/A-Induced Neurite Outgrowth in Motor Neurons.**

L. Liu and J. A. Coffield. *University of Georgia, Athens, GA.*

Botulinum neurotoxin A (BoNT/A) is known to be neurotoxic due to its paralytic effect at cholinergic synapses with extremely high potency. Independent of that, BoNT/A has been found to stimulate neurite outgrowth of motor neurons both in vivo and in vitro, which may account at least in part for the initiation of recovery from botulism. The signaling pathways regulating the BoNT/A-induced neurite outgrowth process have not been identified. In the current study, we used pharmacologic kinase inhibition to investigate the more relevant outgrowth pathways. GFP positive motor neurons were directly differentiated from HBG3 mouse embryonic stem cells, and treated with a MEK1/2 inhibitor in the presence of 1nM BoNT/A. Following 6 and 24h post BoNT/A exposures, single motor neurons were image-captured. The total neurite length and number of branches of primary and secondary neurites were measured and counted. Significant differences were determined using one-way or two-way ANOVA with post hoc tests. Preliminary results showed that 10  $\mu$ M of the MEK1/2 inhibitor specifically blocked BoNT/A's stimulatory effect on secondary branching at 6h compared to toxin only treated controls, suggesting an early, transient role in BoNT/A-induced signal transduction. In addition, there was no effect of MEK1/2 inhibition on the toxin's enzymatic action to cleave SNAP-25. Collectively, these data suggest that ERK1/2 pathway may play an important role in the early phases of BoNT/A-induced neurite outgrowth.

**PS 677 Inhibition of TGF $\beta$ -Induced Integrin- Growth Receptor Cooperative Signaling by Cucurbitacin B, Causes Breast Cancer Growth Suppression.**

P. Gupta and S. K. Srivastava. *TTUHSC, Amarillo, TX.*

Integrins have recently been shown to play an important role in promotion of cell motility and survival in various cancers through cooperative signaling with EGFRs. Integrins transmit cell survival signals through ILK-Paxillin complex and further play role in activating AKT signaling. Cucurbitacin B (CuB) is a steroidal class of chemical present in the plants belonging to cucurbitaceae family. CuB has shown cytotoxic potential in several cancers by causing G2/M cell cycle arrest and inhibition of JAK/STAT3 pathway. However, the exact mechanism of CuB and its role in metastasis and cell survival is not known. Our results show that CuB significantly suppressed the growth of MDA-MB-231, SKBR3, MCF-7, MDA-MB-231 (HER2) and MCF-7 (HER2), five different breast cancer cells in a concentration and time-dependent manner. CuB also induced apoptosis and down-regulated ILK1 expression. In addition, CuB down-regulated ITGB4 and ITGA6 protein expression and suppressed the phosphorylation of AKT at Ser473, paxillin at Tyr118. Previous studies have shown that TGF $\beta$  mediates physical association of ITGB4 and HER2, through Src kinase to enhance cell survival and motility. Interestingly we observed significant downregulation of Src, EGFR and HER2 in different breast cancer cells, suggesting that CuB suppresses cooperative signaling of Integrins and HER2. We also observed that TGF $\beta$  pretreatment imparted protection from CuB's cytotoxic effects, indicating that CuB modulates TGF $\beta$  mediated Integrin signaling. Taken together our results indicate the anti-cancer effects of CuB in breast cancer cells by targeting ITGB4/ITGA6, Src, ILK and TGF $\beta$ . Further detailed mechanistic work is in progress. [Supported in part by R01 grants CA106953 and CA129038 (to S.K.S.) awarded by the National Cancer Institute].

Key: ITGB4 – Integrin  $\beta$ 4, ITGA6 – Integrin  $\alpha$ 6, TGF $\beta$  – Transforming growth factor  $\beta$ , ILK- Integrin linked kinase, EGFR – Epidermal growth factor receptor, CuB – Cucurbitacin B

**PS 678 High Content Live-Cell Imaging of Nrf2 and NF- $\kappa$ B Signaling Reporters As Predictive Tools to Classify Drug-Induced Liver Injury Responses.**

B. Herpers, L. Fredriksson, Z. Di, H. de Bont and B. van de Water. *Toxicology, Leiden University, Leiden, Netherlands.*

Drug-induced liver injury (DILI) is an important clinical problem and predicting human DILI for novel candidate drugs is difficult. Current models indicate that in many cases DILI is linked to reactive metabolite formation and involves activation of innate immune systems. Here we systematically evaluated the combined application of high content live cell imaging-based analysis of 1) NRF2 activation as a measure for reactive metabolite stress, 2) perturbations of the normal NF- $\kappa$ B activation mediated by TNF $\alpha$ ; and 3) synergistic induction of apoptosis by DILI compounds and TNF $\alpha$ . Fifteen drugs associated with DILI were evaluated. Most DILI compounds induced NRF2 stabilization-dependent activation of the downstream target SRXN1 (11 out of 15). Various DILI compounds affected the TNF $\alpha$ -induced activation of NF- $\kappa$ B (6 out of 15), which strongly correlated to the strength of NRF2 activation. In particular for those compounds that show strong NRF2 activation and perturbation of NF- $\kappa$ B signaling, a significant drug-cytokine synergy for apoptosis was observed, which included carbamazepine, diclofenac, ketoconazole, clozapine, nefazodone and amiodarone. Together, our data support that mechanism-based high content imaging strategies involving combined analyses of cellular stress responses contribute to DILI hazard identification.

**PS 679 Translation Initiation Factor EIF4A1 Determines TNF $\alpha$ -Mediated Apoptosis in Drug-Induced Liver Injury through the Stress Protein Chop.**

L. Fredriksson, B. Herpers, S. Wink, J. Meerman and B. van de Water. *Toxicology, Leiden University, Leiden, Netherlands.*

Drug-induced liver injury (DILI) is an important clinical problem and to minimize it a more detailed knowledge about the mechanism is essential. Here we used a functional genomics approach to establish the critical drug-induced toxicity pathways that act in synergy with the pro-inflammatory cytokine tumor necrosis factor  $\alpha$  (TNF $\alpha$ ) to cause apoptosis of liver HepG2 cells. Transcriptomics-based analysis of the toxicity response pathways activated by hepatotoxicants diclofenac (DCF) and carbamazepine (CBZ) revealed significant activation of the nuclear factor-erythroid 2 (NF-E2)-related factor 2 (Nrf2) oxidative stress response, and endoplasmic reticulum (ER) stress/translational initiation signaling. Importantly, significant activation of these pathways after drug exposure could be confirmed by transcriptomics of primary hepatocyte cultures as well as *in vivo*. Systematic siRNA-mediated knockdown of the individual toxicity pathway determinants established the critical roles of these pathways for the drug/TNF $\alpha$ -induced apoptosis in the HepG2 cell system. Pre-induction of the cytoprotective Nrf2 pathway by knockdown of its negative regulator Kelch-like ECH-associated protein 1 (Keap1) suppressed the drug/TNF $\alpha$  synergy. Furthermore, ER stress signaling by selective protein kinase R-like ER kinase (PERK) activation and subsequent expression of C/EBP-homologous protein (CHOP) was crucial in the onset of drug/TNF $\alpha$ -induced apoptosis independent of drug-induced oxidative stress. Interestingly, CBZ and DCF caused an enhanced expression of the translational initiation factor EIF4A1. Importantly, depletion of EIF4A1 almost completely inhibited CHOP expression in association with protection against the drug/TNF $\alpha$ -mediated cell killing. We propose a model in which enhanced drug-induced translation initiates PERK-mediated CHOP signaling thereby sensitizing towards caspase-8-dependent TNF $\alpha$ -induced apoptosis.

**PS 680 The Effect of Thermal Stress on *Drosophila melanogaster* Gene Expression.**

K. Silkaitis<sup>1,2</sup>, A. Branco<sup>1</sup> and B. Lemos<sup>1</sup>. <sup>1</sup>Molecular and Integrative Physiological Sciences, Department of Environmental Health, Harvard School of Public Health, Boston, MA; <sup>2</sup>Temple University, Philadelphia, PA. Sponsor: V. Vaidya.

Genetic tools can be used to dissect the biological pathways mediating stress response. Studying *Drosophila melanogaster* responses to environmental stress is informative because prior studies have shown that resistance to one type of environmental stress often confers resistance to additional stresses. In particular, temperature stress can alter thermal homeostasis, which can affect the biological dosage of an environmental toxicant. In *D. melanogaster*, thermal stress has been shown to affect males differently than females, demonstrated not only by male sterility but also in autosomal and X-linked gene expression. Gene expression is further controlled by the geographic origin of the Y chromosome. We investigated the effect of cold stress on two genotypes of *D. melanogaster* that contained a Y chro-

mosome from a natural population in either Massachusetts (Ymass) or Democratic Republic of the Congo (Ycongo), temperate and tropical climates, respectively. Newly emerged male flies were collected and reared at 25°C or 16°C. The flies were then flash frozen, total RNA was extracted and hybridized to a microarray, and differential expression (DE) of genes was assessed with Bioconductor/Limma. We identified more than 1,000 DE genes ( $p < 0.001$ ) in common between the comparisons of Ymass 16°C to 25°C and Ycongo 16°C to 25°C. Gene expression in the testes was most affected by temperature among the 27 tissues examined, while genes relating to calcium binding, metabolism, and cell proliferation showed high levels of DE. In tandem, we examined the effects of parental growth temperature on gene expression in male F1 progeny. We found that maternal exposure to cold stress differentially affected the expression of genes in progeny involved in cell death, metabolism, and responses to sodium. Together, these results suggest that responses to environmental stressors, including toxicants, may depend on both temperature and Y chromosome genotype.

**PS 681 Dual Mechanisms for Controlling Chk1 Protein Levels.**

F. Zhang, S. S. Lau and T. J. Monks. *Department of Pharmacology and Toxicology, College of Pharmacy, University of Arizona Health Sciences Center, Tucson, AZ.*

2,3,5-tris(glutathion-S-yl)hydroquinone (TGHQ), a metabolite of benzene, catalyzes the generation of reactive oxygen species (ROS), and caspase-dependent apoptosis in HL-60 cells. We now report that TGHQ induced severe DNA damage, as evidenced by DNA ladder formation and histone H2AX phosphorylation, and the subsequent engagement of checkpoint response pathways. Thus, TGHQ induced the activation of both ATR and ATM, which initiate the mammalian DNA damage response via the phosphorylation of the effector proteins Chk1 and Chk2. Perturbation of Chk1 signaling abrogates the TGHQ-induced S-phase arrest, indicating an important role for Chk1 in the S-phase checkpoint following TGHQ-induced DNA damage. Moreover, Cdc25A, which is required for the intra-S phase checkpoint, was degraded in HL-60 cells treated with TGHQ. TGHQ also substantially decreased Chk1 levels, primarily by decreasing the Chk1 gene transcription. Consistent with these findings, MG-132, a proteasome inhibitor, failed to restore Chk1 protein levels. Interestingly, MG-132 itself ( $> 0.1 \mu\text{M}$ ) decreased Chk1 expression, whilst simultaneously inducing Ser-345 Chk1 phosphorylation. RT-PCR data revealed that MG-132 down-regulates Chk1 gene expression. Finally, following S-phase cell synchronization with aphidicolin, TGHQ strikingly attenuated the S-phase arrest, which may drive HL-60 cells into premature mitosis in the presence of un-repaired DNA damage. In summary, TGHQ-induced DNA damage triggers the ATM/ATR-Chk1/Chk2-Cdc25 pathway and induces Chk1-dependent S-phase arrest in the p53-deficient HL-60 cells. The results are consistent with the view that targeting of Chk1 is an effective chemotherapeutic strategy. However, the data also reveal that in addition to the established mechanism of Chk1 protein degradation engaged by the majority of anti-cancer agents, a novel mechanism to modulate Chk1 protein expression can be engaged at the transcriptional level.

**PS 682 Atrazine-Elicited Differential Gene Expression in BLTK1 Leydig Cells.**

A. L. Forgacs<sup>1,2</sup> and T. R. Zacharewski<sup>1,2</sup>. <sup>1</sup>Biochemistry & Molecular Biology, Michigan State University, East Lansing, MI; <sup>2</sup>Center for Integrative Toxicology, Michigan State University, East Lansing, MI.

Atrazine (ATR) is a widely used triazine herbicide associated with impaired reproductive development and function. We have previously demonstrated that ATR affects basal and recombinant human chorionic gonadotropin (rhCG)-induced steroidogenic activity in BLTK1 murine Leydig cells as early as 2 hrs. ATR elicited dose-dependent induction of Star, Hsd3b6 and Hsd17b3 mRNA levels while repressing Hsd3b1, Cyp17a1 and Srd5a1 expression at 24 hrs. The current study evaluates the temporal gene expression effects (1-48 hrs) of 300  $\mu\text{M}$  ATR on Agilent 4 X 44K oligonucleotide microarrays using a dye-swap independent reference design. ATR differentially regulated the expression of 797 unique genes (fold change  $> 1.5$ ,  $P(t) > 0.999$ ), with 389 up-regulated and 416 down-regulated at a minimum of one time point. Most changes were observed at later time points (12-48 hrs) suggesting early ATR induction of testosterone (T) levels in media are independent of gene expression. However, sustained T levels coincide with the induction of Star mRNA. Database for Annotation, Visualization and Integrated Discovery (DAVID) and Ingenuity Pathway Analysis (IPA) identified over-represented gene functions associated with reproductive system development and function, tissue morphology, and regulation of hormone metabolism, consistent with ATR effects on BLTK1 cell morphology and steroidogenesis. The IPA transcription

factor tool predicted the activation of SREBF1 and SREBF2 comprising the induction of cholesterol uptake (Ldlr), cholesterol biosynthesis (Hmgcr, Hmgcs1, Lss, Sqle, Cyp51) and cholesterol transporter (Star) gene expression. Additionally, the predicted activation of CREB1, CREB2, CEBPA and CEBPB suggest increased cAMP-mediated gene expression such as the induction of Vegfa, Gadd45a, and Bcat1 involved in cell morphology and growth. Collectively, these results suggest the later effects of ATR on BLTK1 murine Leydig cell steroidogenesis are mediated by SREBF- and CREB-mediated changes in gene expression.

## PS 683 Hepatic Gene Expression Analysis of 2-Aminoanthracene-Exposed Fisher-344 Rats Reveal Patterns Indicative of Liver Carcinoma and Type 2 Diabetes.

W. E. Gato<sup>1</sup>, B. D. Hales<sup>2</sup> and J. C. Means<sup>3</sup>. <sup>1</sup>Chemistry, Augustana College, Rock Island, IL; <sup>2</sup>Physiology, Southern Illinois University Carbondale, Carbondale, IL; <sup>3</sup>Environmental Science & Management, University of California Santa Barbara, Santa Barbara, CA.

The goal of the present study was to examine hepatic differential gene expression patterns in Fisher-344 rats in response to dietary 2-aminoanthracene (2AA) ingestion for 14 and 28 days. Twenty four post-weaning 3-4 week old F-344 male rats were exposed to 0 mg/kg-1-diet (control), 50 mg/kg-1-diet (low dose), 75 mg/kg-1-diet (medium dose) and 100 mg/kg-1-diet (high dose) 2AA for 14 and 28 days. This was followed by analysis of the liver for global gene expression changes. In both time points, the numbers of genes affected seem to correlate with the dose of 2AA. Sixteen mRNAs were differentially expressed in all treatment groups for the short-term exposure group. Similarly, 51 genes were commonly expressed in all 28-day exposure group. Almost all the genes seem to have higher expression relative to the controls. In contrast, cytochrome P450 family 4, subfamily a, polypeptide 8 (Cyp4a8), and monocyte to macrophage differentiation-associated (Mmd2) were down-regulated relative to controls. Differentially expressed mRNAs were further analyzed for associations via DAVID. GO categories show the effect of 2AA to be linked with genes responsible for carbohydrate utilization and transport, lipid metabolic processes, stress responses such as inflammation and apoptosis processes, immune system response, DNA damage response, cancer processes and circadian rhythm. The data from the current study identified altered hepatic gene expression profiles that may be associated with carcinoma, autoimmune response, and/or type 2 diabetes. Possible biomarkers due to 2AA toxicity in the liver for future study include Abcb1a, Nhej1, Adam8, Cdkn1a, Mgmt, and Nrcam

## PS 684 Utilizing RNA Sequencing and the DNA-Damage Response to Model Chemical Toxicity: How PKC-Activating Tumor Promoters Create a Path of Their Own.

K. P. Glover<sup>1</sup>, L. K. Markell<sup>1</sup>, E. Donner<sup>1</sup>, Z. Chen<sup>2</sup> and X. Han<sup>1</sup>. <sup>1</sup>DuPont Haskell, Newark, DE; <sup>2</sup>DuPont Information & Computing Technologies, Wilmington, DE.

The DNA damage response (DDR) is an essential cellular pathway for maintaining genomic integrity and preventing neoplastic transformation. Although tumor promoting compounds do not directly cause fixed mutations, they have been previously shown to alter many different cellular processes that also impact normal DDR signaling. Therefore, the purpose of this study was to profile PKC activating tumor promoting chemicals by their respective alterations to normal DDR signaling induced by short-wavelength ultraviolet light (UVC). Human lymphoblastoid TK6 cells were exposed to 1 nM 12-O-tetradecanoyl-phorbol-13-acetate (TPA) for 72 hours which caused a reduction in cell growth and changes in cellular morphology. Following UVC exposure (10 J/m<sup>2</sup>), TPA treated cells displayed a synergistic increase in apoptosis and a significant delay in  $\gamma$ H2AX clearance. Other PKC activating tumor promoters including other phorbol esters, mezerein, sapintoxin D, (-)-indolactam V, and resiniferonol 9,13,14-ortho-phenylacetate caused similar changes in cell morphology and a synergistic increase in apoptosis following UVC exposure. RNA sequencing was used to capture the global transcriptomic profile 8 hours after UVC-induced DNA damage following TPA pretreatment. Principle component analysis of UVC treated cells revealed a relationship between gene expression patterns and the concentration of TPA (0.2, 0.5 and 1 nM). These findings indicate a deviation from the normal DDR response. TPA pretreatment at 1 nM caused greater than 300 of the UVC-regulated genes to be downregulated and greater than 80 UVC-regulated genes to be upregulated compared to the normal UVC expression profile. These results show that the tumor promoter TPA has a unique gene expression profile following DNA damage that can be potentially used to profile this class of chemical.

## PS 685 Reactive Nitrogen Species Regulate Autophagy through ATM-AMPK-TSC2-Mediated Suppression of mTORC1.

D. N. Tripathi<sup>1</sup>, R. Chowdhury<sup>2</sup>, L. J. Trudel<sup>2</sup>, G. N. Wogan<sup>2</sup> and C. L. Walker<sup>1</sup>. <sup>1</sup>Center for Translational Cancer Research, IBI, Texas A&M HSC, Houston, TX; <sup>2</sup>Department of Biological Engineering, Massachusetts Institute of Technology, Cambridge, MA.

Reactive intermediates such as reactive oxygen species (ROS) and reactive nitrogen species (RNS) play essential roles in the cell as signaling molecules, but in excess, constitute a major source of cellular damage in both physiological (i.e. mitochondrial respiration) and pathophysiological (i.e. inflammation) settings. Recently, ROS were shown to induce autophagy via a novel ATM signaling pathway in the cytoplasm. Activation of cytoplasmic ATM by ROS engages LKB1 and AMPK kinases to activate the TSC2 tumor suppressor, which represses mTORC1 (a negative regulator of autophagy) to induce autophagy. However, whether RNS engage this or similar signaling pathway(s) to regulate mTORC1 and induce autophagy is unclear. We found under conditions of steady-state nitric oxide (NO) exposure, rapid activation of ATM and downstream signaling by this stress kinase to LKB1-AMPK and the TSC2 tumor suppressor. As a result, mTORC1 was repressed as evidenced by decreased phosphorylation of the direct mTORC1 targets S6K, 4EBP1, and ULK-1, the target for mTORC1 repression of autophagy. Induction of autophagy concordant with decreased ULK-1 phosphorylation by mTORC1 at S757 and increased phosphorylation at S317 by AMPK was demonstrated by increased ratio of LC3-II/LC3-I, formation of GFP-LC3 puncta, increase in acidic vesicles and decreased p62 levels, indicative of increased autophagic flux. While autophagy has been shown to have pro-death and pro-survival functions, induction of autophagy by NO caused loss of cell viability, suggesting it functions primarily as a cytotoxic response to excess nitrosative stress. These data indicate that nitrosative stress, like oxidative stress, regulates autophagy. As cancer cells are particularly sensitive to nitrosative stress, these data open new therapeutic avenues capitalizing on the ability of NO and RNS to induce autophagic cell death.

## PS 686 CYP2S1 Expression Influences Cytotoxicity of the Anticancer Prodrug, AQ4N, in Human Bronchial Epithelial Cells.

N. M. Singh and A. M. Rowland. Chemistry and Biochemistry, NMSU, Las Cruces, NM.

Cytochrome P450 2S1 (CYP2S1) is one of the most upregulated P450s identified in human cancers and correlates with poor prognosis. The underlying cause of elevated CYP2S1 expression and the consequence of elevated expression is not known. The only recognized substrate for CYP2S1 is AQ4N (Baxanthrone). AQ4N is a bioreductive prodrug under clinical investigations for hypoxic tumors. AQ4N is metabolically reduced in hypoxic environments to the topoisomerase II inhibitor, AQ4. CYP2S1 is recognized as one of the most efficient enzymes to catalyze this reduction. The objective of this study was to determine: i) whether human CYP2S1, like the mouse CYP2s1, is elevated in response to hypoxia and ii) whether changes in CYP2S1 expression influence CYP2S1-mediated metabolism of AQ4N. To determine whether CYP2S1 was induced in response to hypoxia we evaluated mRNA expression in the presence of 1% oxygen as well as the hypoxia mimetics cobalt chloride and o-phenanthroline. CYP2S1 mRNA was significantly increased by approximately 8-, 3-, and 50-fold in response to 1% oxygen, cobalt chloride, and o-phenanthroline. These results suggest that human CYP2S1 mRNA is elevated in response to hypoxia. To determine whether changes in CYP2S1 expression influence AQ4N metabolism we examined the effects of AQ4N and AQ4 on cell viability in bronchial epithelial cells (BEAS-2B) cells differentially expressing CYP2S1. Cytotoxicity was estimated using alamar blue reduction in cells expressing high (CYP2S1-flag), medium (control plasmids: pcDNA3.1 and scrambled shRNA), and low CYP2S1 expression (CYP2S1 shRNA). Preliminary results demonstrate that elevated CYP2S1 expression does enhance cytotoxicity under hypoxic conditions (0.2%-1% O<sub>2</sub>). Interestingly, our results also suggest a protective role for CYP2S1 in normoxic conditions (21% O<sub>2</sub>). These data suggest that elevated CYP2S1 expression may have a dual role in protecting normal cells while promoting AQ4N-mediated cytotoxicity in hypoxic cells.

**PS 687 Transcriptome Analysis Reveals Novel Pathway Regulation in Response to Differential Expression of CYP2S1 in Human Lung Cells.**

T. W. Madanayake<sup>1</sup>, A. M. Rowland<sup>1</sup>, N. Devitt<sup>2</sup> and I. Lindquist<sup>2</sup>. <sup>1</sup>Chemistry and Biochemistry, NMSU, Las Cruces, NM; <sup>2</sup>National Center for Genomics Research, Santa Fe, NM.

Cytochrome P450 2S1 (CYP2S1) is considered an orphan P450s with an unknown biological function. Data from our laboratory and others suggests that CYP2S1 may have an important physiological role in modulating the synthesis and metabolism of bioactive lipids, including prostaglandins and retinoids, respectively. CYP2S1 expression is elevated in epithelial-derived cancers. Whether increased CYP2S1 expression in proliferative disease is protective, detrimental, or fails to impact disease progression remains to be determined. To elucidate its role, we need to understand the physiological significance of CYP2S1. We reasoned that transcriptome analysis of human bronchial epithelial cells (BEAS-2B) differentially expressing CYP2S1 would reveal metabolic shifts in key regulatory pathways linked to CYP2S1-mediated metabolism. To test this idea, we established four stable BEAS-2B cell lines expressing high (CYP2S1-Flag), medium (pcDNA3.1 and scrambled shRNA), and low (CYP2S1 shRNA) CYP2S1 expression. Expression levels confirmed using qRT-PCR and western analysis. Alterations in the transcriptome were determined using RNA-sequencing (RNA-seq) analysis. RNA was isolated from three biological replicates from each of the four experimental conditions (CYP2S1-Flag vs pcDNA3.1 and CYP2S1 shRNA vs SCRAM shRNA). Eight to fourteen million sequencing reads were generated from each of the 12 samples. Four distinct population clusters were identified using principal component analysis, representing each of the transformed cell lines. Approximately 1000 genes were differentially expressed in response to CYP2S1. Among these were key regulatory enzymes involved in prostaglandin synthesis. RNA-seq also identified novel changes in the mTOR pathway, which regulates cell size. Significant differences in cell size was in lung cells differentially expressing CYP2S1, revealing a potentially novel role for CYP2S1 in cell size regulation.

**PS 688 In-Depth Examination of How Exposure to Long-Term Low-Dose Chromium Alters the Transcriptional Response to BaP.**

J. Ovesen, Y. Fan and A. Puga. University of Cincinnati, Cincinnati, OH.

Complex mixtures and their toxicity are a significant and growing problem that must be addressed by applied toxicology. Techniques for the assessment of similar compounds in a mixture based on relative toxicity are inadequate for the assessment of complex mixtures with different types of components. In complex mixtures, multiple exposures generate specific changes in gene expression that cannot be attributed to any single mechanism. Data on the responses to these kinds of mixtures are rare and often contradictory. Our previous work demonstrated that epigenetic regulation of gene transcription plays an important role in chromium's toxic response, and that Cr is capable of altering the transcriptional regulation of known BaP responsive genes, like Cyp1a1. Here we use RNA-seq after long-term low-concentration exposure to chromium to examine the extent to which chromium exposure can alter BaP induced transcriptional responses throughout the transcriptome. We find that mouse hepatoma cells exposed to long-term low concentrations of sodium chromate, in the range of 0.1 – 0.5  $\mu$ M, accumulate double-strand DNA breaks, and that the percentage of cells undergoing apoptosis increases concurrently with either increased concentration or longer period of exposure to Cr. Using RNA-seq we determined that the transcription of genes critical to several important processes are regulated differently by BaP if the cells were previously chronically exposed to a low concentration of Cr. In cells grown normally genes related to critical functions like cell cycle and tissue development are down-regulated but cells treated with low concentration Cr for a long period of time do not down-regulate these functions in response to acute BaP treatment. These findings can serve as a guide for studies to determine what biological functions normally regulated by BaP may be abnormally regulated when there are previous exposures to chromium. Supported by NIH grant ES010807.

**PS 689 Expression of the Nuclear Receptor Corepressor Tnfr1 in Mouse Tissues.**

N. Francis, C. Zhang and B. J. Aneskievich. University of Connecticut, Willimantic, CT.

Tnfr1 regulates multiple signaling pathways (NF- $\kappa$ B, ERK2, PPAR and RAR) involved in either executing or responding to toxic insults. Altered Tnfr1 expression levels are associated with certain human inflammatory diseases. These cell signaling and pathology studies revealed some molecular targets and potential organ end-

points. Additionally, body-wide data on expression of Tnfr1 is incomplete. To gain a better understanding of Tnfr1's expression pattern and functional role, we developed a Tnfr1 gene trap knock out (KO) mouse to identify possible new signaling and organ targets.

The Tnfr1 gene trap KO mouse was created via a  $\beta$ -Geo cassette ( $\beta$ -galactosidase and neomycin resistance genes) insertion into the Tnfr1 first intron. Expression from the cassette allowed for evaluation of Tnfr1 promoter activity in different tissues qualitatively via X-gal staining, immunofluorescent (IF) staining for  $\beta$ -Galactosidase ( $\beta$ -Gal), and quantitatively via Q-PCR. With WT tissues as a control, all heterozygote (Tnfr1 +/-) tissues turned blue with X-gal staining. Results of IF  $\beta$ -Gal staining in Tnfr1 +/- mouse tissues were similar to that of X-gal whole organ staining and paralleled the Tnfr1 antibody staining. For most organs, both  $\beta$ -Gal and Tnfr1 were homogeneously expressed across the tissue. However, for kidney, both  $\beta$ -Gal and Tnfr1 glomerular staining was significantly reduced compared to convoluted tubules suggesting distinct expression levels and fidelity of the  $\beta$ -Gal marker for the endogenous Tnfr1 expression. Q-PCR results revealed that the Tnfr1 promoter activity, determined by steady state levels of  $\beta$ -Gal mRNA, varied among different tissues and mirrored the Tnfr1 mRNA levels. These results suggest Tnfr1 is expressed at varying levels in different mouse tissues. Recent studies report a high rate of lethality in Tnfr1 KO mouse embryos due to fetal liver apoptosis (Oshima et al, 2009, Zhou et al, 2011). By contrast, we demonstrate there are tissues other than liver expressing Tnfr1 and that biological function of these organs may be impacted by changes in levels of Tnfr1 protein.

**PS 690 Evaluating the Role of Kinase Activation Involved in Chemical-Dependent p53 Response to DNA Damage.**

B. Reidel<sup>1</sup>, B. Sun<sup>1</sup>, A. Scott<sup>2</sup>, Y. Adeleye<sup>2</sup>, M. E. Andersen<sup>1</sup> and R. A. Clewell<sup>1</sup>. <sup>1</sup>The Hammer Institutes, Durham, NC; <sup>2</sup>Unilever, PLC, London, United Kingdom.

Post-translational modifications (PTMs) of p53, individually and in combination, help determine the function of p53 in DNA damage response, e.g. cell cycle arrest, apoptosis and DNA repair. The dose-response for p53 activation, cell cycle, apoptosis and mutation (micronuclei) were studied for etoposide (ETP), methylmethane sulfonate (MMS) and quercetin (QUE). Cellular response was chemical specific, despite similar induction of DNA damage (double strand breaks) and p53. Here, we investigated activation of mitogen-activated protein kinases (MAPKs) and phosphoinositide 3-kinases (PI3Ks) in response to MMS, ETP, and QUE across doses and time (1 – 24 hrs) in human fibrosarcoma cells (HT1080). The MAPKs were studied by measuring p-p38, p-ERK1/2, p-JNK1/2, and p-MEK1 using immunoblot and Luminex assays, and the PI3Ks: p-ATM, p-ATR, p-DNA-PK and p-Chk 2 by immunoblot and flow cytometry. MAPKs and ATM were activated by all three chemicals. Although p-ATM, p-p38, p-ERK and p-JNK increased at 1, 3 and 24 hrs, they showed different patterns of activation that may lead to observed differences in cell fate. While ETP and MMS showed maximal p-ERK1/2 and p-ATM at 24 hr, QUE displayed a much stronger p-ERK and p-ATM response at 1 hr, which may indicate more efficient repair, and is in agreement with less micronuclei observed with QUE vs. ETP or MMS. p-p38 - associated with p-p53 (ser46) leading to apoptosis - was induced quickly with ETP (1 hr), but more slowly with QUE, an observation consistent with observed apoptosis by ETP, but not QUE in HT1080 cells. ETP showed a much stronger induction of p-ATR than either MMS or QUE, and only QUE inhibited p-ATR. Our results indicate that, types and timings of the activated kinases are chemical specific and likely to determine the downstream actions of p53. Currently, we are evaluating treatment dependent PTMs of p53 by proteomics, as well as kinase specific inhibitors to further confirm the relationship between kinase modification of p53 and cell fate.

**PS 691 Global Transcriptional Analysis of Zebrafish Embryos following Acute Exposure to Cadmium.**

M. J. Jenny<sup>1</sup>, E. E. Linney<sup>2</sup>, B. O'Shields<sup>1</sup>, A. Holowiecki<sup>1</sup> and A. McArthur<sup>1</sup>.

<sup>1</sup>Department of Biological Sciences, University of Alabama, Tuscaloosa, AL;

<sup>2</sup>Department of Molecular Genetics and Microbiology, Duke University Medical Center, Durham, NC.

Although cadmium (Cd) exerts its toxic effects through the generation of oxidative stress, many of the cellular mechanisms involved in Cd toxicity are not fully established. Utilizing zebrafish embryos as a model, we undertook a transcriptomic-based approach to investigate the role of Cd as a developmental toxicant and assist in the identification of novel mechanisms of cellular dysfunction. Zebrafish embryos (24, 48, 72 and 96 hpf) were continuously exposed to Cd (25, 50, 100, 150  $\mu$ M) for 24 hours prior to mortality assessment. No significant mortality was observed prior to 72 hpf. However, at 96 and 120 hpf the 50  $\mu$ M Cd dose resulted in 20% and 40% mortality, respectively, while the 100 and 150  $\mu$ M Cd doses resulted in an average of 75% and >95% mortality, respectively. To investigate global changes in gene expression, zebrafish embryos (72, 96 and 120 hpf) were exposed

to 50  $\mu\text{M}$  Cd for 4 or 8 hours. Global gene expression profiling was performed using the Agilent 4x44K Zebrafish Oligo Microarray. Overall, 788 probes were significantly upregulated, while 679 probes were downregulated in one or more treatments. Principle component analysis was employed to find trends among the various treatments. The first principle component separated out the 96 and 120 hpf Cd-treated embryos, consistent with the mortality curves suggesting that zebrafish embryos become most sensitive to Cd toxicity around 96 hpf. The majority of genes altered by Cd exposure resulted in the upregulation of a large subset of genes responsive to oxidative stress, genes involved in glutathione synthesis and heme/iron homeostasis, mitochondrial uncoupling proteins, and various solute carriers with roles in zinc transport/homeostasis or mitochondrial oxidative phosphorylation. The majority of genes downregulated by Cd were involved in cell cycle control and DNA replication. A thorough analysis of genes differentially regulated by Cd during zebrafish development will be presented. [R00ES017044]

## PS 692 Role of Chromatin Structural Changes in Regulating Human CYP3A Ontogeny.

N. L. Giebel<sup>1</sup>, J. D. Shadley<sup>1</sup>, K. Dorko<sup>2</sup>, S. C. Strom<sup>3</sup>, P. M. Simpson<sup>1</sup>, K. Yan<sup>1</sup> and R. N. Hines<sup>1</sup>. <sup>1</sup>Pediatrics, Medical College of Wisconsin, Milwaukee, WI; <sup>2</sup>Pharmacology, Toxicology and Therapeutics, University of Kansas Medical Center, Kansas City, KS; <sup>3</sup>Laboratory Medicine, Karolinska University Hospital, Stockholm, Sweden.

Variability in drug metabolizing enzyme (DME) developmental trajectories contributes to differential susceptibility to chemical toxicity and adverse drug reactions, particularly in the first years of life. Factors linked to variability are largely unknown and molecular mechanisms regulating ontogeny are likely involved. To evaluate chromatin structure dynamics as a contributing mechanism, age-dependent changes in histone marks were evaluated within known *CYP3A4*, *CYP3A7*, *FMO1*, and *FMO3* regulatory domains. Chromatin immunoprecipitation with fetal and adult primary human hepatocyte chromatin pools followed by qPCR was used to determine relative histone mark occupancy. Histone mark occupancy is consistent with many regions of bivalent chromatin (i.e., exhibiting histone marks associated with active and repressive transcription) in adult and fetal hepatocytes with the exception of the *CYP3A7* XREM and C/EBP $\beta$  domains in adult hepatocytes. For *CYP3A4*, the bivalent regulatory domains are consistent with a low level of fetal liver expression. Differential histone mark occupancy indicates adult histone mark and transcription factor occupancy have a developmental trajectory towards an active transcriptional state. In contrast, the bivalent *CYP3A7* regions in fetal hepatocytes do not correspond with high expression and surprisingly, adult hepatocytes had less histone mark occupancy, particularly the repressive mark H3K27me3. These findings for *CYP3A7* suggest mechanisms other than chromatin structural changes involved in regulating ontogeny. Chromatin structural change is an important mechanism controlling DME ontogeny, particularly for those whose specific activity increases substantially after birth. Supported in part by NIH grant GM081344

## PS 693 6-Formylindolo(3, 2-b)carbazole (FICZ) Positively Regulates the Signosome Responsible for Retinoic Acid (RA)-Induced Differentiation of Leukemic Blast Model HL-60.

R. Bunaciu and A. Yen. Cornell University, Ithaca, NY.

Tryptophan is an essential amino acid that absorbs strongly in UV (extinction coefficient: 5,050 M<sup>-1</sup>cm<sup>-1</sup> for 280 nm). Both in cell free conditions (such as cell culture media exposed to light) and in the cells (such as skin keratinocytes exposed to sunlight), tryptophan yields a multitude of photoproducts. One such photoproduct is 6-Formylindolo(3,2-b)carbazole (FICZ). FICZ has a high affinity for AhR (K<sub>d</sub>=7x10<sup>-11</sup> M). It is proposed to be an endogenous AhR agonist and also a cytochrome P450 family 1 substrate. FICZ and a multitude of its metabolites have been shown to be present in human fluids. Currently all the complete parenteral nutrition formulations contain tryptophan. The bags for total parenteral nutrition are made of clear plastic. Since many cancer patients receive both parenteral nutrition and chemotherapy (generally enhancing AhR expression and activity), it is of significant interest to assess potential effects of FICZ on cell differentiation and in particular on RA-induced leukemic cell differentiation. HL-60 leukemic cells were untreated or treated with RA alone or RA in combination with FICZ for 48 h. To assess the involvement of AhR, other cells were treated either with  $\alpha$ -naphthoflavone and RA or  $\beta$ -naphthoflavone and RA. Expression of cell surface differentiation markers, cell cycle distribution and respiratory burst response were quantified by flow cytometry. Western blots were performed to assess the proteins known to be part of the signosome driving the RA-induced differentiation. FICZ augments the RA-induced differentiation as evidenced by CD38 and CD11b receptors, inducible respiratory burst, G0 cell cycle arrest and growth curves.

Signaling molecules previously shown to be upregulated by RA and to drive RA induced differentiation were enhanced by FICZ: MAPK signaling axis, Src family kinases, Cbl, VAV, SLP-76, PI3K, and IRF-1. Moreover, AhR is associated with the c-CBL adaptor in the signosome, as shown by IP. In conclusion, FICZ modulates RA induced differentiation.

## PS 694 Nrf2 Gene Regulation during Oxidative Stress in Embryonic Development.

A. R. Timme-Laragy<sup>1,2</sup>, S. I. Karchner<sup>1</sup>, R. C. Harbeitner<sup>1</sup>, A. G. MacArthur<sup>3</sup> and M. E. Hahn<sup>1</sup>. <sup>1</sup>Biology, Woods Hole Oceanographic Institution, Woods Hole, MA; <sup>2</sup>Public Health, University of Massachusetts, Amherst, MA; <sup>3</sup>AGM Consulting, Hamilton, ON, Canada.

Nrf2 is a transcription factor that regulates antioxidant defenses in response to oxidative stress. Embryonic development is highly susceptible to disruption by exposure to chemicals, including those that alter redox balance. The role of Nrf2 in the oxidative stress response (OSR) during embryonic development remains unclear. Our previous work identified a novel Nrf2 paralog, *nrf2b*, in zebrafish (*Danio rerio*). This study builds upon that work to elucidate the roles of *nrf2a* and *nrf2b* in regulating the OSR during vertebrate embryonic development. Zebrafish embryos were micro-injected with antisense morpholino oligonucleotides (MO) to knock down translation of either *nrf2a* or *nrf2b*, or a standard morpholino control (co-MO). At 48 hours post fertilization, embryos were exposed to the pro-oxidant and Nrf2 activator, *tert*-butylhydroquinone (tBHQ) or vehicle (DMSO) for 4 hours, and preserved for RNA isolation. Microarrays were conducted using Agilent's V3 44k array, and selected genes validated by QPCR. In response to tBHQ, 71 probes were up-regulated in the co-MO group, including *gstp1*, *gclc*, *ferritin*, *peroxiredoxin1*, *hsp70*, *sod1*, and other genes typically found as part of the OSR. Interestingly, we found that an important and often overlooked part of the OSR is the down-regulation of genes, including *cathepsin*, various complement components, and *apolipoprotein Ea*. Knockdown of Nrf2a or Nrf2b blocked some but not all of the tBHQ-induced changes in OSR gene expression and the effects of Nrf2a-MO and Nrf2b-MO were distinct. The results show that Nrf2 paralogs primarily regulate distinct gene sets, with some overlapping targets, in response to oxidative stress in embryos. This study also highlights the importance of gene down-regulation as a component of the OSR during embryonic development. [F32ES017585, R01ES016366].

## PS 695 On Breast Cancer Treatment, Synergistic Effects of Akt1 shRNA and Paclitaxel-Incorporated Conjugated Linoleic Acid-Coupled Poloxamer Thermosensitive Hydrogel.

S. Hong<sup>1</sup>, C. Cho<sup>2</sup> and M. Cho<sup>1</sup>. <sup>1</sup>Laboratory of Toxicology, Seoul National University, Seoul, Republic of Korea; <sup>2</sup>Agricultural Biotechnology, Seoul National University, Seoul, Republic of Korea.

The phosphoinositide 3-kinase (PI3K)/Akt1 signaling pathway has emerged as a target for treatment of cancer therapy. In this study, we develop a strategy to enhance Akt-targeted therapy. We thought that combination of Akt1-targeted therapy with conventional chemotherapy using paclitaxel-incorporated conjugated linoleic acid-coupled poloxamer (CLA-CP) thermosensitive hydrogel may have synergistic effects in cancer therapeutic efficiency compared with chemotherapy alone. MDA-MB-231 cell, the human breast cancer cell line, was inoculated into 6-week-old female BALB/C nu/nu athymic mice. After 2 weeks of inoculation, shAkt1 and CLA-CP treatments were subcutaneously injected into the tumor. We found that the combination of shAkt1 with paclitaxel showed synergistic anti-cancer effects, thus, inhibiting the growth of human breast cancer cells, and breast cancer xenografts in mice as well. The combination therapy showed enhanced anti-cancer effects through inhibiting Akt1 signaling, inducing apoptosis. In addition, it suppressed angiogenesis and proliferation, also. It suggests that the presented strategy of combination of shAkt1 with paclitaxel may have a potential for the treatment of breast cancer.

Acknowledgements

This work was partly supported by the National Research Foundation (NRF-2011-0000380), Ministry of Education, Science and Technology (MEST) in Korea.

## PS 696 TBX5 As Targets for Treatment of Chronic Obstructive Pulmonary Disease.

J. Lee and G. Acquah-Mensah. Massachusetts College of Pharmacy Health and Sciences, Worcester, MA.

Chronic Obstructive Pulmonary Disease (COPD) is a progressive disease of the respiratory system which is characterized by destruction of the epithelium cells of lungs. Current therapies alleviate symptoms of COPD but do not treat the under-

lying causes. It has been recognized in the literature that the T-box transcriptional factor TBX5 is suppressed in patients with COPD. The purpose of the study was to identify regulatory target genes of TBX5 and their significance in future treatment of COPD. A compendium of lung epithelium microarray datasets was created using GSE 19027 and GSE 994 from the Gene Expression Omnibus database. Probe IDs for TBX5 and genes that have known interactions with the TBX5 transcription factor were used to generate an initial network. Bayesian Network Inference with Java Objects was then used to generate a new regulatory network, given the gene expression data. Cytoscape was used to visualize the difference between the initial and predicted networks. In addition, analysis of GSE 1650, which compared lung tissue from smokers with severe emphysema and smokers with mild or no emphysema, was done. The resulting network indicates that STAT3 regulates TBX5, NKX2-5, GATA4, ID2 and TAZ. The regulatory relationships between STAT3 and TBX5, NKX2-5, GATA4, ID2 have been validated in the published literature. However, a relationship between STAT3 and TAZ has not been established. It is known that TAZ regulates TBX5. This presents with a possible feed-forward relationship among TBX5, STAT3 and TAZ. STAT3 is known to be involved in cell growth, apoptosis, and regulation of anti-inflammatory response by controlling genes involved in the inflammatory response. This result suggests a potential inhibitory relationship between STAT3 and TBX5 since STAT3 was up-regulated in smokers with severe emphysema and TBX5 was suppressed in patients with COPD. The result suggests that future therapies targeting STAT3 or TBX5 can regulate inflammatory response involved in COPD. Further research is warranted to investigate how TBX5, STAT3 and TAZ play a role in the inflammatory response of COPD.

**PS 697** **Suppressive Effect of HES1 (*Drosophila* Hair and Enhancer of Split-1) on Human Hepatic Multidrug Resistance-Associated Protein 4 (MRP4) Gene Expression and Induction of HES1 by Oxidative Stress.**

X. Gu and J. E. Manautou. *Department of Pharmaceutical Sciences, University of Connecticut, Storrs, CT.*

Previous in silico studies in our laboratory identified a total of 107 canonical HES1-binding N-boxes (CANNAG) in a 10kb DNA fragment upstream to the translation start site of the multidrug resistance-associated protein 4 (MRP4/ABCC4). In this study, we investigated the role of HES1 in regulating MRP4 gene expression. We have identified a 16-bp DNA fragment in the MRP4 promoter-proximal region containing a non-canonical N-box (GGCGTG) for HES1 that accounts for a profound suppression of MRP4 promoter transcription activity in HepG2 cells. A point mutation in this cis-element (GGCGTC) resulted in the loss of this suppressive effect of HES1. Furthermore, suppression of MRP4 reporter genes containing 230 bp, 5 kb or 7 kb of 5' flanking regulatory sequences was observed by over-expression of HES1 but not by a dominant negative mutant form of HES1 which is unable to bind to DNA. From these findings we hypothesized that the MRP4 induction we have previously reported under conditions of oxidative stress might be due in part to down-regulation of HES-1 expression. To our surprise, HES1 mRNA levels are significantly increased in the human liver cell line HC04 treated with the pro-oxidant chemicals tert-butylhydroperoxide or tert-butylhydroquinone (100-300µM). We also detected HES1 protein accumulation in nuclei of HC04 treated with these chemicals in a dose- and time- dependent manner. Similarly, treatment of mice with toxic doses of APAP increases liver HES1 mRNA levels. These increases in expression and function of the repressive factor HES1 by oxidative stress seem inconsistent with the induction of MRP4 that also occurs under oxidative stress conditions. Studies are currently underway to investigate whether HES1 directly regulates MRP4 gene expression in vivo by oxidative stress and to determine the interplay of HES1 with other activating and repressive transcription factors known to regulate MRP4. Supported by NIH Grant DK069557.

**PS 698** **Exposure to Metals Mixtures: Genomic Alterations of Infectious Disease Response Pathways in Children Exposed to Environmental Metals.**

J. Gruber<sup>1,2</sup>, R. D. Patel<sup>1</sup>, J. E. Rager<sup>1</sup>, A. P. Sanders<sup>1</sup>, S. Edwards<sup>3</sup>, J. E. Gallagher<sup>3</sup> and R. C. Fry<sup>1</sup>. <sup>1</sup>*Environmental Sciences and Engineering, University of North Carolina at Chapel Hill, Chapel Hill, NC;* <sup>2</sup>*Department of Epidemiology, University of North Carolina at Chapel Hill, Chapel Hill, NC;* <sup>3</sup>*National Health and Environmental Effects Research Laboratory, US EPA, Research Triangle Park, NC.*

Exposure to toxic metals can have harmful health effects, particularly in children. Although studies have investigated the individual effects toxic metals have on gene expression and health outcomes, there are no studies assessing the effect of metal mixtures on gene expression profiles. Here, we assessed the mixture effect of six

toxic metals (arsenic, beryllium, cadmium, chromium, mercury, and lead) on gene expression profiles in children in Detroit, Michigan. As part of the Mechanistic Indicators of Childhood Asthma (MICA) cross sectional study, we assessed metal exposure in 131 children in Detroit using fingernail metals levels. A metals mixture score was calculated and compared to gene expression profiles across the population adjusting for age and race. There were 145 unique genes that were significantly differentially expressed when comparing children exposed to low and high levels of the metals mixture. Of the genes differentially expressed, 107 (74%) had increased expression while 38 (26%) had decreased expression. The main biological function associated with multiple metals was infectious disease. Within that group, genes were associated with infection of respiratory tract ( $P < 10^{-6}$ ) severe acute respiratory syndrome ( $P < 10^{-5}$ ), and sepsis ( $P < 10^{-3}$ ). Taken together, these data demonstrate that exposure to metals mixtures may activate gene networks related to infectious disease response. This abstract does not necessarily reflect the views or policies of the EPA.

**PS 699** **Transcriptomics Analysis of Lung Tissues of Brown Norway Rats Exposed to the Sensitizers Trimellitic Anhydride (TMA), Oxazolone (OXA) or Dinitrochlorobenzene (DNCB).**

F. Kuper<sup>2</sup>, M. Radonjic<sup>2</sup>, J. van Triel<sup>1</sup>, Y. Staal<sup>1</sup>, R. Woutersen<sup>2</sup> and R. Stierum<sup>2</sup>. <sup>1</sup>*TNO Triskelion, Zeist, Netherlands;* <sup>2</sup>*The Netherlands Organisation for Applied Scientific Research, TNO, Zeist, Netherlands.*

TMA is a respiratory allergen, OXA is a potent contact allergen in man, but elevates serum IgE levels and Thelper2 cytokines in test animals, suggesting that it has also respiratory allergenic potential. DNCB is a contact allergen. Brown Norway rats (BN) were sensitized by two dermal applications of TMA, OXA or DNCB. The animals were provoked by inhalation on day 21. TMA and OXA both induced elevation of serum IgE, breathing pattern changes and the same type of allergic laryngeal inflammation. However, microarray analysis of the lung (sampled 24 hrs after provocation) indicated that OXA may act through different mechanisms than TMA, despite a certain overlap in activated genes. TMA upregulated strongly Th2-associated genes and genes associated with lung remodeling, whereas OXA activated predominantly Th1-associated genes. The variability in balance between Th1- and Th2-associated genes may reflect different subtypes of respiratory allergies. DNCB induced a very mild inflammation in the larynx, which resembled DNCB-induced inflammation in the skin; only a few Th1-associated genes were differentially expressed in the lung. The transcriptomics analysis supports the idea that classification of allergens based on single genes is unreliable. Omics data contribute to our understanding of respiratory allergy and may help in the design of a predictive toxicity test for sensitization.

**PS 700** **In Vivo Expression of p16INK4a in Response to Toxicological Exposures.**

J. Sorrentino<sup>1,3</sup>, N. Sharpless<sup>1,2,3</sup> and C. Burd<sup>4</sup>. <sup>1</sup>*Toxicology, University of North Carolina at Chapel Hill, Chapel Hill, NC;* <sup>2</sup>*Departments of Medicine and Genetics, University of North Carolina at Chapel Hill, Chapel Hill, NC;* <sup>3</sup>*Lineberger Comprehensive Cancer Center, University of North Carolina at Chapel Hill, Chapel Hill, NC;* <sup>4</sup>*Molecular Genetics, Ohio State University, Columbus, OH.*

In mammals, expression of p16INK4a is highly regulated. Excess expression can lead to cellular senescence and aging, while impaired activation is associated with cancer. The precise mechanism of p16INK4a regulation in vivo is poorly understood. In vitro systems have limited utility since proliferation in culture induces p16INK4a. Both extrinsic (chemotherapy and ionizing radiation) and intrinsic (telomere shortening and improper DNA damage repair) stimuli can induce p16INK4a, but the kinetics of and cellular responses to these genomic insults have not been examined in vivo. To address this question, we developed a murine strain with firefly luciferase 'knocked-in' to the endogenous p16INK4a locus and under control of the p16INK4a promoter (p16-LUC). We exposed p16-LUC mice to 50ppm arsenic, 42% fat diet, 350 J/m<sup>2</sup> UVB light, or cigarette smoke for a minimum of 6 months. Every other month, p16-LUC mice were imaged to measure luciferase induction. At 30 weeks of exposure, mice exposed to cigarette smoke displayed 2 times higher levels of whole body luciferase activity than no-smoke controls. Additionally, mice exposed to UVB exhibited 1.5 times higher levels of luciferase activity by 6 weeks of exposure that reached 8 times over control mice by 24 weeks. In arsenic exposed mice, there was only a slight induction of p16INK4a by 24 weeks (not statistically significant). We observed no differences in p16INK4a expression in mice on high fat diet (42% fat) compared to normal fat diet (4%) after 78 weeks. Currently, we are correlating luciferase expression in different organs with tissue damage and mRNA expression of p16INK4a. The data generated from these experiments will demonstrate how environmental exposures are associated with expression of p16INK4a, a mediator of tumor suppression and aging. (Supported by T32 ES07126, HHMI Translational Medicine Program, and UO1-CA141576)

**PS 701 Reprogramming of the HepG2 Genome by Long Interspersed Nuclear Element-1: Regulatory Control of Epithelial to Mesenchymal Transition Is Independent of Reverse Transcriptase.**

P. Bojang<sup>1</sup>, M. Anderton<sup>2</sup>, R. Roberts<sup>2</sup> and K. S. Ramos<sup>1,3</sup>. <sup>1</sup>Biochemistry and Molecular Biology, University of Louisville, Louisville, KY; <sup>2</sup>General Toxicology Sciences, AstraZeneca, Manchester, United Kingdom; <sup>3</sup>Center for Environmental Genomics and Integrative Biology, University of Louisville, Louisville, KY.

Long Interspersed Nuclear Element-1 (LINE-1 or L1) is an autonomous, mobile element within the human genome that transposes via a "copy and paste" mechanism and relies upon L1-encoded endonuclease and reverse transcriptase (RT) activities to compromise genome integrity. Because the complexity of L1 biology is not understood, studies were conducted to evaluate the impact of L1 on epithelial to mesenchymal transition (EMT) in HepG2 cells. Forced expression of synthetic wild type or mutant (D702Y) L1 deficient in RT activity was associated with formation of cytoplasmic foci and minor association with the nuclear compartment. Random de novo L1 retrotransposition was identified in cells expressing wild type L1, but not the D702Y mutant. Both synthetic wild type and mutant L1 induced marked reductions in the expression of epithelial markers and overexpression of mesenchymal markers. These data establish L1 as a key regulator of genome plasticity in HepG2 cells via RT-dependent and RT-independent mechanisms which do not couple to intrinsic retrotransposition activity.

**PS 702 Interoperability Case Study: Connecting Models across Exposure and Dose-Response Arenas for Characterization of Vinyl Chloride Hepatotoxicity.**

D. S. Womack<sup>1</sup>, S. M. Beaulieu<sup>1</sup>, A. B. Parks<sup>1</sup>, M. Mumtaz<sup>2</sup>, P. Ruiz<sup>2</sup>, J. Babendreier<sup>3</sup> and A. M. Jarabek<sup>4</sup>. <sup>1</sup>RTI, Research Triangle Park, NC; <sup>2</sup>ATSDR, Atlanta, GA; <sup>3</sup>US EPA, Athens, GA; <sup>4</sup>US EPA, Research Triangle Park, NC.

The 2012 SOT workshop "Building for Better Decisions: Multi-scale Integration of Human Health and Environmental Data" advanced seamless data and model integration for support of sustainability and improved risk characterizations. It highlighted the need for interoperability of models across the source/exposure/dose-response/cost/benefit continuum. We conducted a case study to illustrate interoperability issues for characterizing aggregate risk of liver cancer or hepatotoxicity for inhaled and ingested vinyl chloride (VC). Exposure models used were the EPA's Assessment System for Population Exposure Nationwide (ASPEN) using data of the National-scale Air Toxics Assessment (NATA) for inhalation, and the Human and Ecological Exposure and Risk in Multimedia Environmental System (HE<sup>2</sup>RMES) domain within the Framework for Risk Analysis in Multimedia Environmental Systems (FRAMES) with Data for Environmental Modeling (D4EM) of the Agency's integrated exposure modeling (iem) technologies. The dose-response was characterized by data on the Integrated Risk Information System (IRIS) and the physiologically-based pharmacokinetic (PBPK) model for VC available in the ATSDR PBPK toolkit. Output from ASPEN and HE<sup>2</sup>RMES for inhaled VC exposure illustrates the value to efficient model comparison if plug-and-play capability is provided by interoperability. Conflicting assumptions regarding key parameters between exposure and dose-response arenas were highlighted when computing aggregate risk from oral and inhalation routes; these conflicts must be rectified prior to proper model integration. This exercise readily shows how the ability to transparently integrate such models impacts current approaches and enhances understanding of each discipline. (The views expressed in this abstract are those of the authors and do not necessarily represent the views or policies of the U.S. Environmental Protection Agency or the Agency for Toxic Substances and Disease Registry.)

**PS 703 Modeling Acute Exposure Guideline Levels (AEGs).**

M. T. Chu, C. M. Nordberg, R. Manimaran, Y. Tie and E. Demchuk. ATSDR, Atlanta, GA.

Acute Exposure Guideline Levels (AEGs) are comprehensively peer-reviewed health guidance values for assessing the risk of acute once-in-a-lifetime or rare exposures to hazardous inhalation chemicals. Each AEG is a concentration designed to prevent health effects of a certain type (AEG-1: reversible, AEG-2: disabling, AEG-3: life-threatening) at one of the five exposure durations (1/6, 1/2, 1, 4, 8h). Currently only 272 compounds have published AEGs and among them 114 have unassigned AEGs-1. The objective of present work was to develop a novel *in silico* approach for rapid estimation of provisional AEG-1 thresholds, specifically at 8h (AEG-1<sub>8h</sub>). Correlation and multivariate linear regression analyses were employed

to assess significant predictors for AEG-1. AEGs-2 and -3 were identified as perspective explanatory variables, controlled for physiochemical properties and chemical-specific qualitative data used to extrapolate AEGs (e.g. species, target health endpoint, uncertainty factors).  $\chi^2$ - and *t*-tests were used to assess the homogeneity of covariates in the training and test sets. Variable selection involved multicollinearity, interaction, and confounding assessments. An exhaustive all-possible-subset selection was employed to determine the best information-entropy model. Available toxicological LOAEL or NOAEL data were used to validate the model. The final model was developed for AEG-1<sub>8h</sub>. It relied on AEG-2<sub>8h</sub> values as the main explanatory variable, controlled for chemical volatility, testing species, and uncertainty factors. For the chemicals without the AEG-1<sub>8h</sub> assigned, approximately 70% of model-predicted concentration thresholds were within a 10-factor of their extrapolated LOAEL or NOAEL values. The proposed 1D-QSAR model provides a meaningful and statistically-valid method to derive provisional AEG-1 thresholds that is consistent with available toxicological data. Such *in silico* methods offer a complementary approach when biological or toxicological evidence is insufficient, budget is limited, and/or rapid assessment is necessary, as in an emergency response.

**PS 704 Concentration-Time Relationships for Short-Term Inhalation Exposures to Hazardous Substances.**

R. Manimaran and E. Demchuk. Agency for Toxic Substances and Disease Registry, Atlanta, GA. Sponsor: P. Ruiz.

Acute Exposure Guideline Levels (AEGs) are developed by the USEPA AEG committee for controlling acute exposures to airborne chemical hazards. AEGs are the threshold exposure limits for once-in-a-lifetime or rare chemical exposures at five exposure durations (1/6, 1/2, 1, 4, 8h). AEGs are derived from various published and unpublished experimental studies described in Technical Support Documents prepared by the committee. An AEG concentration (C) for a specific duration (t) is extrapolated from available experimental data. Extrapolations are carried out using the exponential function,  $Cn \cdot t = k$ , where n, the temporal scaling factor (TSF), is chemical-specific. Preferably, it is derived experimentally, but thus far experimental TSFs for few chemicals have been derived. For most of 272 chemicals on the AEG list, TSFs are unknown. For these chemicals, the AEG committee has adopted a rule by which n = 1 when extrapolating from short- to long-term durations, and n = 3, when extrapolating from long- to short-term durations. However, for many chemicals with unknown TSFs, this rule has been abandoned in favor of chemical-specific information deemed appropriate by the committee. Thus, the AEG database contains rich expert-validated chemical-specific information about temporal extrapolation. The objective of the present study was to extract this information. Using regression analysis for each chemical in the database, a surrogate TSF was derived. In addition to being chemical-specific, TSFs were found to be health-effects-specific. The relationship between median TSFs for mild/reversible ( $n_1=2.9$ , AEG-1 tier), disabling/irreversible ( $n_2=2.0$ , AEG-2), and life-threatening effects ( $n_3=1.8$ , AEG-3) was  $n_1 > n_2 > n_3$ . A geometric mean TSF for the AEG-3 tier,  $n_3 = 1.88$  [95% CI: 1.77, 1.99], was closest to n = 1 in Haber's rule, which applies to combat exposures to chemical warfare agents. This observed agreement indicates that model-derived TSFs may be appropriate for temporal extrapolation of AEG concentrations to durations of exposure for which experimental durations are not available.

**PS 705 Refined Animal Toxicity Testing Using Unequally Sized Dose Groups and Benchmark Dose Analysis.**

M. Öberg, J. Ringblom, F. Kalantari and G. Johanson. Institute of Environmental Medicine, Karolinska Institutet, Stockholm, Sweden.

Benchmark dose (BMD) analysis has been recommended as a more robust alternative to the No Observed Adverse Effect Level (NOAEL) as it makes use of all the data from the study to derive the point of departure. In this study, we used simulations to examine the possibility to optimize the study design for BMD analysis by introducing unequally sized dose groups. In addition, this BMD-aligned design of experiment was evaluated regarding animal distress. Experimental data were generated by Monte Carlo simulations for fixed doses and equally sized groups. We started with the OECD standard of 4 dose groups (logarithmic dose spacing: 0-1-3-10 mg/animal) with 20 animals per group and assumed a sigmoidal dose-effect curve. The distribution of animals between dose groups was then altered before performing the next set of simulations. The quality of the simulated BMD was evaluated against the "true" dose-effect curve and the standard 4x20 design. The procedure was repeated for scenarios with different effect variability and dose placements on the dose-effect curve. The designs with more animals in the low dose groups generally showed significantly better quality than the standard design with equally sized dose groups. With these designs it was also possible to reduce animal distress with 45%, under the assumption that the distress is proportional to dose. To reduce

the number of animals in the high dose group would be an important refinement of animal testing since the primary parameter for setting the high dose is the tolerability determined by clinical signs of moderate severity, e.g. weight loss of up to 20%, hunched intermittently, intermittent convulsions or transient prostration. In conclusion, our simulations suggest that toxicological studies can be improved by unequally sized dose groups, which also results in substantially reduced distress. The study illustrates how regulatory testing may be refined (one of the R's in 3R – Reduce, Refine, Replace) by use of BMD-aligned experimental design.

## PS 706 A Novel Screening System for Classifying Potential Health and Environmental Impacts Associated with Hydraulic Fracturing Fluids.

C. N. McFarland and D. B. Davies. *Intrinsic Environmental Inc., Calgary, AB, Canada.*

Public opposition to hydraulic fracturing or “fracking” is being witnessed across many communities in the U.S.A., Canada and elsewhere. Concerns over this practice include the potential impacts of fracking on groundwater and surface water quality, air quality, human health, and terrestrial and aquatic ecosystems. These concerns have prompted some jurisdictions to place temporary moratoriums on the practice until a better understanding of these potential impacts is gained. Numerous initiatives are now underway to heighten this understanding, including measures aimed at increasing awareness of the chemical additives that are used during the process. Many jurisdictions are now mandating public disclosure of these additives, and chemical registries that list the additives delivered down-hole on a well-by-well basis have emerged. Although these registries identify the chemicals used, they provide no indication of the potential health and environmental risks that the additives could present. To help fill this void, a novel risk-based screening system was developed to improve the understanding of the potential health and environmental impacts of the chemical additives used in hydraulic fracturing. The system relies on the results of toxicity and environmental fate studies for a number of key endpoints to assess the potential risks involved. The endpoints include acute and chronic oral toxicity, reproductive and developmental toxicity, mutagenicity, carcinogenicity, aquatic toxicity, environmental persistence and bioaccumulation potential. The outcomes of the screening process are used to assign the chemical additive products to one of several categories depending upon the potential risks involved. This categorization process allows the product users to take appropriate steps to manage the potential hazards. The screening system has been used to classify more than 1,500 products to date, has proven to be reliable and effective, and is currently being adopted on an industry-wide basis in Canada.

## PS 707 Analysis of the Validated Epiderm Skin Corrosion Test (EpiDerm SCT) and a Prediction Model for Sub-Categorization According to the UN GHS and EU CLP.

S. Letasiova<sup>2</sup>, H. Kandarova<sup>2</sup>, T. Milasova<sup>2</sup> and M. Klausner<sup>1</sup>. <sup>1</sup>MatTek Corp, Ashland, MA; <sup>2</sup>MatTek IVLSL, Bratislava, Slovakia. Sponsor: P. Hayden.

Skin corrosion refers to the production of irreversible damage to the skin manifested as visible necrosis through the epidermis and into the dermis. In 2004, OECD adopted two ECVAM-validated reconstructed human skin model assays (EpiDerm and EPIKIN) for testing skin corrosion (OECD TG 431). However, OECD TG 431 does not satisfy international labeling guidelines for transport of dangerous goods since none of the methods were validated for sub-categorization. The UN-GHS utilizes 3 corrosion sub-categories (1A-very dangerous, 1B-medium danger and 1C-minor danger). Labeling a chemical as 1A has important consequences for transport, including very small volume package limits for air transport, prohibition from passenger aircraft, protective storage conditions, costly containers, and low market acceptance. Animal tests are still utilized for assessing the packaging subclasses. An in vitro method that discriminates between the 1A and 1B/1C classes will therefore have a substantial impact on reducing animal tests for this purpose.

The current study evaluates whether the EpiDerm SCT can discriminate between UN-GHS classes 1A, 1B/1C and non-corrosives (NC) based on the MTT viability assay. Data obtained during the ECVAM validation study (Liebsch et al, 2000) indicated sensitivity of 100% for class 1A. In the current study (> 80 chemicals), sensitivity for class 1A was obtained in a range of 77 – 87% depending on cutoff chosen following a 3 min exposure. None of 1A chemicals was under-predicted as NC. Specificity for NC chemicals was 80%.

As demonstrated by results of this study, EpiDerm SCT allows a partial sub-classification of corrosives into sub-category 1A, 1B/1C, and NC. Adoption of the new prediction model based on a 3 min endpoint into the validated EpiDerm SCT design would allow identification of severely corrosive substances and would lead to significant reduction in animal use for corrosion sub-group package labeling.

## PS 708 Physiologically-Based Pharmacokinetic (PBPK) Modeling for the Development of Provisional Advisory Levels (PALs): A Case Study with Fentanyl.

H. Shankaran<sup>1</sup>, F. Adeshina<sup>3</sup> and J. G. Teeguarden<sup>2</sup>. <sup>1</sup>Computational Biology and Bioinformatics, Pacific Northwest National Laboratory, Richland, WA; <sup>2</sup>Systems Toxicology, Pacific Northwest National Laboratory, Richland, WA; <sup>3</sup>National Homeland Security Research Center, US EPA, Washington DC.

Provisional advisory levels (PALs) are tiered exposure limits for toxic chemicals in air and drinking water that are developed to assist in emergency responses. Physiologically-based pharmacokinetic (PBPK) modeling can support this process by enabling extrapolations across doses, and exposure routes, thereby addressing gaps in the available toxicity data. Here, we describe the development of a PBPK model for Fentanyl – a synthetic opioid used clinically for pain management – to support the establishment of PALs. Starting from an existing model for intravenous Fentanyl, we first optimized distribution and clearance parameters using several additional IV datasets. We then calibrated the model for oral and inhalation exposures using pharmacokinetic datasets for various Fentanyl formulations. Predictions of the calibrated model were in good agreement with the >50 datasets considered here. For aerosolized pulmonary Fentanyl,  $F=1$  and  $t_{90}<1$ min indicating complete and rapid absorption. The  $F$  value ranged from 0.35 to 0.74 for oral and various trans-mucosal routes. Oral Fentanyl was absorbed the slowest ( $t_{90} \sim 300$ mins); the absorption of intranasal Fentanyl was relatively rapid ( $t_{90} \sim 20$ -40mins); and the various oral trans-mucosal routes had intermediate absorption rates ( $t_{90} \sim 160$ -300mins). Based on these results, for inhalation exposures, we assumed that all of the Fentanyl inhaled from the air during each breath directly, and instantaneously enters the arterial circulation. We present model predictions of Fentanyl blood concentrations in oral and inhalation scenarios relevant for PAL development, and provide an analytical expression that can be used to extrapolate between oral and inhalation routes for the derivation of PALs.

## PS 709 Pooled Analysis for Chronic Dietary Studies of Di-Isononyl Phthalate.

C. M. North<sup>1</sup>, M. J. Nicolich<sup>2</sup>, K. M. Kransler<sup>3</sup> and R. A. Barter<sup>1</sup>. <sup>1</sup>ExxonMobil Biomedical Sciences, Amundale, NJ; <sup>2</sup>Cogimet, Lambertville, NJ; <sup>3</sup>ExxonMobil Chemical Company, Houston, TX.

Point of departure selection for risk assessment can be complicated when more than one study is available for evaluation. Differences in dose spacing and post-mortem evaluation can result in differing conclusions, leading to uncertainty and additional conservatism in the overall assessment. Here, several analysis methods were utilized to estimate the point of departure using the pooled data from two rat chronic toxicity studies on di-isononyl phthalate (DINP), a general purpose plasticizer used in flexible vinyl applications. Two chronic dietary administration studies (two year) were conducted in DINP-exposed F344 rats. Dietary administration in the two studies were different, with doses of approximately 0, 15, 152, and 307 (Study I) or 0, 29, 88, 359, and 733 (Study II) mg/kg/day. In addition, the number of liver sections evaluated between the two studies differed, impacting the overall incidence of observed liver effects. In both studies, a dose-related increase in the incidence of spongiosis hepatitis was observed in male rats. Separate NOAELs of 15 (Study I) or 88 (Study II) mg/kg/day were determined from the two studies; separate Benchmark Doses (BMDs) were estimated at 38 and 203 mg/kg/day, respectively. A pooled data approach, rather than a combining of the NOAEL or BMDs from the individual studies was utilized to derive a rational, data-based NOAEL or BMD. A generalized linear model with a logistic link function was used to determine a NOAEL for the pooled analysis. The NOAEL was the lowest dose group whose model coefficient was not statistically significantly different from the control group coefficient at the 5% significance level. The calculated NOAEL using the pooled data was 152 mg/kg/day. A BMD10 of 72.4 mg/kg/day with a 95% BMDL10 of 61.0 mg/kg/day were calculated with the pooled data. Pooled analysis, combined with robust statistical analysis, is a useful and rigorous method for deriving a point of departure that considers data from multiple, compatible studies.

## PS 710 A Systematic Approach for Identifying, Evaluating, and Presenting Mode-of-Action Evidence in IRIS Toxicological Reviews.

M. E. Kushman<sup>1,3</sup>, A. D. Kraft<sup>2</sup>, K. Guyton<sup>2</sup>, B. Sonawane<sup>2</sup>, W. A. Chiu<sup>2</sup>, S. Makris<sup>2</sup> and I. Rusyn<sup>3</sup>. <sup>1</sup>ORISE/US EPA, Washington DC; <sup>2</sup>NCEA, US EPA, Washington DC; <sup>3</sup>University of North Carolina at Chapel Hill, Chapel Hill, NC.

Recent National Research Council recommendations on the process of hazard assessment include improving transparency and standardization of evidence collection, selection, presentation, and evaluation. Per this recommendation, we designed

a process that was tested using di(2-ethylhexyl)phthalate (DEHP) liver tumorigenesis as a case study. We identified relevant modes of action (MOAs) from published reviews and devised an overall search strategy. Literature search strings containing relevant synonyms and wildcards for DEHP and its metabolites, MOAs, and species of interest were tested in PubMed. Specific tiered assessment criteria for exclusion/inclusion into the search were also defined and literature was searched and screened according to these tiered criteria. For MOAs with large databases, additional screening criteria were applied through manual curation of the articles. The evidence gathering process was documented as a literature tree, clearly describing each step of the search, inclusion/exclusion, and curation. Studies satisfying the assessment criteria were summarized into evidence tables. Narratives for each liver cancer related MOA were composed. Literature was organized in the EPA's Health and Environmental Research Online (HERO) database using tags in accordance with assessment criteria. This approach streamlines and exemplifies transparent mechanistic evidence capture and reporting for DEHP liver carcinogenicity. Large amounts of information are effectively managed and appraised, and enabled for analysis of concordance across studies and species in MOA determinations for hazard assessment. This research was supported in part by an appointment to the Research Participation Program for the U.S. EPA, Office of Research and Development, administered by ORISE through an interagency agreement between the U.S. Department of Energy and EPA. Disclaimer: The views expressed in this abstract are those of the authors and do not necessarily represent the views or policies of the US EPA.

**PS 711 A Nonparametric Bayesian Approach for Benchmark Dose Estimation from Continuous Data.**

K. Shao<sup>1</sup>, J. S. Gift<sup>2</sup>, L. Kopylov<sup>3</sup> and W. A. Chiu<sup>3</sup>. <sup>1</sup>NCEA-ORISE, US EPA, Research Triangle Park, NC; <sup>2</sup>NCEA, US EPA, Research Triangle Park, NC; <sup>3</sup>NCEA, US EPA, Washington DC.

The current approach for benchmark dose (BMD) estimation from continuous data (e.g., body weight, relative liver weight), proposed by Crump (1984) and used in EPA's BMD software (BMDs), models the responses at each dose level as a population described by mean and variance. Then, various dose-response models (e.g. Hill, Exponential, Power and Polynomial) and variance models are fit to the means, and the model parameters, as well as the variance, are estimated using the maximum likelihood estimation (MLE) approach for BMD calculation. Due to limited data, a common situation in risk assessment, the selection of a particular model and modeling assumptions such as the distribution of the responses (i.e., normal or log-normal distribution) is usually based on limited biological and toxicological information and empirical fit. Consequently, the selection of appropriate BMD and BMDL estimates from the results of a set of acceptable dose-response models is often criticized as being somewhat arbitrary. The non-parametric Bayesian (NPB) approach proposed in the present study models endpoints as a single-point mean response at each dose level without assuming the format of dose-response models or the distribution of responses. The NPB is a data-driven approach and the only assumption employed is that the curve is monotonically increasing or decreasing. The methodology is illustrated through both existing and simulated dose-response datasets, and compared with prevailing parametric methods available in the standard BMDs. The results of these analyses suggest that the NPB method can adequately fit the data and provide comparable BMD estimates (to the standardized models in BMDs). The NPB can provide flexibility in model fitting, and with further research, could be refined into a promising supplemental tool for BMD estimation.

**PS 712 Material Threat Assessment Chemical and Scenario Selection Process.**

J. Moser<sup>1,2</sup>, D. Howell<sup>1,2</sup> and R. Jablonski<sup>1,3</sup>. <sup>1</sup>Chemical Security Analysis Center, Department of Homeland Security, Gunpowder, MD; <sup>2</sup>Battelle Memorial Institute, Columbus, OH; <sup>3</sup>Edgewood Chemical Biological Center, Aberdeen Proving Ground, MD.

The Department of Homeland Security (DHS) Chemical Security Analysis Center (CSAC) and the Department of Health and Human Services (DHHS) Biomedical Advanced Research and Development Authority Division of Analytic Decision Support (BARDA ADS) jointly assess public health hazards and consequences related to potential chemical agent attacks on the U.S. homeland. To provide a realistic appraisal of the type of threats chemical agents pose to the U.S. populace, the CSAC and BARDA ADS evaluate a broad range of chemicals to assess an adversary's potential to cause significant adverse consequences. This is accomplished through the development of Material Threat Assessments (MTAs), which examine the potential acquisition of a chemical and whether effective dissemination on a target can cause significant severe or lethal effects. Each MTA consists of an analysis of a single chemical or group of chemicals that have a similar mechanism of action,

while modeling these chemicals across a standard set of scenarios to enable comparison among chemicals and scenarios. MTAs include a comparison of public health consequences of a chemical attack with and without the use of consequence mitigating countermeasures. This presentation describes how the Chemical Terrorism Risk Assessment (CTRA) is used to inform the MTA process and describes the tools and assumptions employed to select high risk and high consequence chemicals and scenarios.

**PS 713 Use of REACH Registration Data for Improving Thresholds of Toxicological Concern (TTC).**

V. Mostert<sup>1</sup>, N. Wieneke<sup>1</sup>, C. Wiegand<sup>1</sup>, C. Jakupoglu<sup>1</sup>, M. Sica<sup>1</sup>, G. Werle-Schneider<sup>2</sup> and N. Jägemann<sup>2</sup>. <sup>1</sup>ICB EHS TOX-L, Dr. Knoell Consult GmbH, Leverkusen, Germany; <sup>2</sup>ICB TOX-C, Dr. Knoell Consult GmbH, Mannheim, Germany.

The Threshold of Toxicological Concern (TTC) concept is utilised to identify human exposures that are so low that in-depth toxicological investigations are expendable. This is called "exposure-based waiving".

Exposure-based waiving serves to focus available resources on substances with relevant human exposure potential.

Important work into establishing TTC values has been published by Munro et al. (1996). The initial report used a database of 613 organic substances compiled from publicly available sources. In total, 2941 NOELs were collected in this fashion. The Munro concept used the Cramer classification to categorise substances according to their hazard potential.

We broadened the TTC database by including NOAELs published on the EChA website as per 19 July 2012, containing data for more than 7600 substances. Only non-gaseous mono-constituent substances with oral NOAELs were included in the TTC database. Organophosphates and genotoxic substances were excluded from the database as well as NOAELs obtained for surrogate substances. NOAELs for all systemic endpoints (general toxicity, developmental toxicity, fertility, neoplasia) were taken into account. Where appropriate, default assessment factors of up to 6 were used to establish chronic NOAELs for each substance.

For every eligible substance, we collected the published CLP category for acute oral toxicity as a potential predictor of overall hazard potential. This gives rise to five categories of acute oral toxicity.

A TTC is calculated from the 5th percentile of NOAELs in each of these categories using the REACH rules for establishing DNELs for workers and the general population.

This poster presents the preliminary results for more than 1500 substances. The results indicate that the TTC concept becomes more robust when using the very broad EChA database. It also suggests that acute oral toxicity categories can be used as a predictor for the overall hazard potential of a substance.

**PS 714 Evaluation of the Toxrttool for Assessing Quality of Toxicological Studies for Risk Assessments.**

D. Segal<sup>1</sup>, S. Makris<sup>1</sup>, D. Bergfelt<sup>1</sup>, A. D. Kraft<sup>1</sup>, A. Bale<sup>1</sup>, K. Raffaele<sup>1</sup>, K. Crofton<sup>3</sup>, M. E. Gilbert<sup>3</sup>, M. Selgrade<sup>2</sup>, R. Blain<sup>2</sup> and K. Fedak<sup>2</sup>. <sup>1</sup>US EPA, Washington DC; <sup>2</sup>ICF International, Durham, NC; <sup>3</sup>US EPA, Research Triangle Park, NC.

In order to improve transparency and consistency, both the European Union and National Academy of Sciences have recommended the standardization and documentation of criteria used to evaluate the quality of studies considered in health risk assessments of xenobiotics. Although peer reviewed publication is an important criterion for judging scientific data, the quality of studies and reporting of results vary tremendously. To find a means to efficiently assess the quality of these studies, we evaluated a publicly available algorithm (Toxicological data Reliability assessment Tool, ToxRTTool) recently developed by the European Commission. The ToxRTTool builds on the Klimisch score, a method for categorizing the reliability of toxicological studies, but adds important criteria that should be present in a high-quality journal article used to support health risk assessments. To evaluate the ToxRTTool, 20 peer-reviewed studies on thyroid disrupting chemicals were selected, ranging in quality from excellent to poor as determined a priori by a thyroid expert on the team. Eight scientists with various levels of expertise then used the ToxRTTool to evaluate the papers, and the consistency and reliability of scores were compared across evaluators. Scores were most consistent for previously judged 'high-quality' papers with greater variability among scores as the quality of papers diminished. The basis for inconsistencies appeared to be related to the subjective nature and lack of clarity for responding to many criteria. In conclusion, by providing more objective criteria and better instructions for responding, the ToxRTTool would likely be extremely useful for systematic evaluations of peer reviewed studies being considered for health risk assessments.

(Disclaimer: The views in this abstract are those of the authors and do not necessarily reflect the views or policies of the EPA.)

**PS 715 GO-Quant Systems-Based Quantitative Analysis of Dynamic Signaling Pathways during Neurodevelopment and Implication for Risk Assessment.**

X. Yu and L. Xu. *Environmental Health Science, University of Georgia, Athens, GA.*

The most critical biological process during neurodevelopment is the timely controlled signaling pathways. Many reports provided qualitative data demonstrating the critical role of neuro-developmentally related pathways. However, only few have provided quantitative evaluation of the dynamic pathways during these processes. These differences in dynamic signaling pathways are believed to be tightly associated with the sensitivity of window of exposure to toxicants, but still have not been clearly examined. Genome-wide scale evaluation of gene expression has proven to be a powerful tool in understanding molecular mechanism during neurodevelopment. Thorough analysis of these genomic data during development will inevitably lead to a greater understanding of how changes in transcriptome relate to functional and structural changes in the neurodevelopment. However, the integration of these gene expression data into a description of dynamic signaling pathways within specific events of development has proven to be a difficult task. We constructed and established meta-database for neurodevelopment and applied systems-based GO-Quant program to quantitatively map the developmental stage-specific landmark of signaling pathways. Our GO-Quant analysis with rat gene expression array data demonstrated the dynamic changes of multiple signaling pathways during different stages of development. The mapping of the dynamic pathways greatly improves our understanding of time-dependent role of each signaling pathway during neurodevelopment. The systems-based identification of developmental stage-specific landmark signaling pathways helps to create sensitive, breakthrough early biomarkers for neurodevelopmental toxicity.

**PS 716 Safety Assessment of a Novel Antibiotic Using a Mouse Population-Based Approach Predicts Risk of DILI in Humans Where Classical Models Fail.**

M. Mosedale<sup>1</sup>, C. Kurtz<sup>1</sup>, J. Eaddy<sup>1</sup>, K. Adkins<sup>2</sup>, H. Wu<sup>2</sup>, P. B. Watkins<sup>1,3</sup> and A. H. Harrill<sup>1,3</sup>. <sup>1</sup>The Hammer Institutes for Health Sciences, Research Triangle Park, NC; <sup>2</sup>Pfizer, Inc., Groton, CT; <sup>3</sup>The University of North Carolina at Chapel Hill, Chapel Hill, NC.

Development of the macrolide antibiotic PF-04287881 was suspended following elevations in liver function tests observed in a Phase I clinical trial. The potential for drug-induced liver injury (DILI) due to this compound was not predicted by standard nonclinical toxicology studies. We hypothesized that a mouse diversity panel (MDP), comprised of genetically diverse inbred strains, could predict the DILI potential of PF-04287881. Additionally, using the MDP offers the ability to identify genetic loci that underlie PF-04287881 DILI susceptibility. In this study, we collected serum and liver tissue from 34 mouse strains treated with PF-04287881 (600 mg/kg, i.g.) or vehicle once daily for 7 days. Significant elevations in serum alanine aminotransferase (ALT) levels in PF-04287881-treated animals relative to vehicle-treated controls were observed in 31 of the 34 strains ( $p < 0.05$ ). The average fold change in ALT varied greatly across strains (from 1.6 - 14.2). Microscopic findings of single cell necrosis, hepatocellular hypertrophy and Kupffer cell vacuolation were observed together or individually depending on strain. Genome wide association analysis conducted using ALT fold change identified 51 significantly associated single nucleotide polymorphisms, 12 of which occurred in known genes. These genes are involved in pathways important for transcriptional regulation, mitochondrial function, and cell structure and signaling. Taken together, these data support our hypothesis that the MDP can predict DILI liability for compounds without a clear hepatotoxicity signal in standard preclinical species. These findings also demonstrate the potential for this population-based approach to improve human risk assessment in drug-safety testing as well as yield mechanistic insights into the toxicity mechanisms via pharmacogenetic investigation.

**PS 717 An Investigation of Factors Associated with Mortality Patterns across the Midwestern United States.**

M. P. Chan. *Environmental Sciences Program, Southern Illinois University Edwardsville, Edwardsville, IL.*

Various studies have indicated that mortality rates are positively correlated with social inequalities, air pollution, elevated ambient temperature, age, availability of medical care and other factors. This study develops a model that uses indicators for multiple factors to predict the mortality rates for selected diseases by county across

the Midwestern United States. A total of 1,055 counties from 12 states in the Midwestern region were studied. Systematic random sampling was used to select a subset of counties from the 1,055 counties to validate the model. Appropriate statistical analyses were used to predict the relationship between environmental pollutants, socio-economic factors, risk factors, social capital, weather, crime, social and other factors to explain variations in county-specific mortality rates for the leading causes of death and lifespan in the US. It is anticipated that this study would suggest the complex inter-relationships of multiple factors that influence mortality and lifespan, and suggests the need for a better understanding of the pathways through which these factors, mortality, and lifespan are related at the community level, particularly in urban versus rural settings. The resulting findings might assist policy makers at local, state, and federal levels in developing effective prevention strategies in this region.

**PS 718 Establishment of the Cumulative Margin of Exposure for a Group of Polychlorinated Biphenyl (PCB) Congeners.**

F. Kalantari<sup>1</sup>, C. Bergkvist<sup>1</sup>, M. Berglund<sup>1</sup>, E. Fattore<sup>3</sup>, A. Glynn<sup>2</sup>, H. Håkansson<sup>1</sup> and S. Sand<sup>2</sup>. <sup>1</sup>Karolinska Institutet, Stockholm, Sweden; <sup>2</sup>National Food Agency, Uppsala, Sweden; <sup>3</sup>Institute for Pharmacological Research, Milano, Italy.

Due to the fact that humans are exposed to mixtures of chemicals, the development of methods that can assess the combined risk resulting from cumulative exposure to a several chemicals is of high interest. The aims of this study were: (1) to estimate a cumulative margin of exposure (MOE) for a group of polychlorinated biphenyls (PCBs) using reduction of hepatic vitamin A as an example endpoint; (2) To compare a relative potency factor (RPF) based approach with a RPF-free approach for estimating the cumulative MOE.

The MOE was defined as the ratio between a reference dose, derived using the benchmark dose (BMD) approach (based on experimental dose-response data), and the estimated human dietary PCB exposure. A distribution for the cumulative MOE was established, taking into account inter- and intra-individual variability as well as uncertainty in data measurements. The cumulative MOE reflected mainly the MOE for PCB 126; other PCB congeners had little contribution to the cumulative exposure and MOE. The median of the 0.1st percentile for the cumulative MOE was about 20 for women; depending on the percentile, the cumulative MOE was 2 - 4 times higher for men compared to women. Furthermore, a relative potency factor (RPF) based approach was compared to an RPF-free approach for estimating the cumulative MOE. The RPF-free approach more completely accounts for variability and uncertainty on the other hand, the RPF-based approach is less data intensive and can be more easily implemented in practice, allowing for a use of existing data on RPFs. Consideration of the discussed approaches may contribute to improving cumulative health risk assessments.

**PS 719 A Prototype for Integrating Toxicokinetics into the Human Health Risk Assessment Process for Agrochemicals: Sulfoxaflor.**

C. Terry<sup>1</sup>, M. Aggarwal<sup>1</sup>, A. T. McCoy<sup>2</sup>, L. G. McFadden<sup>2</sup>, R. J. Rasoulpour<sup>2</sup>, M. Bartels<sup>2</sup> and R. Billington<sup>1</sup>. <sup>1</sup>Human Health, Dow AgroSciences, Oxfordshire, United Kingdom; <sup>2</sup>The Dow Chemical Company, Midland, MI.

Toxicokinetics (TK) has played a central role in the pharmaceutical industry for decades and this data can provide valuable information for human health risk assessment. However, historically, limited internal dose data have been routinely generated for agrochemicals. In recent years this trend has begun to change; the main drivers for this being: ILSI/HESI-ACSA principles, new EU Regulation (1107/2009 EC) and OECD guidelines.

Integrated TK in toxicity studies is now routine at Dow AgroSciences for all new active substances. This approach involves no additional animal usage.

This abstract describes the advantages of integrated TK to each stage of the risk assessment process and specific examples are provided from the toxicology programme of the new insecticide, sulfoxaflor, to show that integrated TK allows:

1. Hazard identification:
  - a. More relevant routes of administration for toxicity studies – comparison of systemic dose across different routes of exposure, for example in rat and rabbit developmental toxicity studies.
  - b. Kinetically-derived maximum dose approach – allowing more appropriate dose levels to be selected for the mouse carcinogenicity study, for example.
2. Dose-Response Assessment:
  - a. All life-stages of test species to be addressed – application of TK data in developmental and reproduction studies, for example.
3. Exposure Assessment:
  - a. Refinement of default 'external' (mg/kg bw/day) exposure assessments – for example, use of TK data from animals in 'TK Modeler', to predict systemic human exposure.
4. Risk Characterisation:

- a. Integrated Mode-of-Action (MoA) and human relevance investigations – for example, anchoring *in vitro* MoA test concentrations to the *in vivo* effect levels in animals.
- b. Setting of ‘internal’ Reference Doses (RfDs) – for example, proposing the corresponding blood concentration from critical *in vivo* studies used to set RfDs (such as the acceptable daily intake (ADI) or acute reference dose (ARfD), as an ‘internal’ RfD.

**PS 720 Refinement of the Exposure Component of the Human Health Risk Assessment Process for Agrochemicals: Development of a Simple Tool.**

A. T. McCoy<sup>1</sup>, C. Terry<sup>2</sup> and G. Drummond<sup>2</sup>. <sup>1</sup>The Dow Chemical Company, Midland, MI; <sup>2</sup>Dow AgroSciences, Milton Park, United Kingdom.

Traditional human health risk assessments include Uncertainty Factors (UFs) to account for toxicokinetic (TK) and toxicodynamic differences between animals and humans. Predictions of systemic exposure in humans, based on animal TK data or measured human biomarker levels, could allow for science-based refinements in the UFs related to interspecies differences in TK. These refinements could provide more realistic reference dose values, while predictions of human blood levels could help to inform calculations of biomonitoring equivalents.

The aims of this project were two-fold. The first was to develop a user-friendly modeling method that could accurately predict systemic bioavailability via parenteral exposure routes (i.e. dermal) in humans. Ideally, this model could predict exposure levels in both urine and blood. The second was to utilize animal TK data (measured or modeled from alternate exposure routes) to predict systemic exposure in humans from either occupational, bystander or residential exposures, using a simple TK modeling approach.

TK Modeler is an Excel-based program developed for prediction of blood levels of a test material and optimal sampling time selection for TK analysis. This program was successfully used to predict human blood levels, both, after exposure by parenteral routes (dermal), and using data derived only from animals. Three data-rich Dow AgroSciences molecules were used as case studies: haloxyfop, triclopyr and picloram. Attempts were made to achieve both of the above aims with each molecule, though this was not always possible due to limited available data. Overall, accurate predictions of human blood levels were achieved in most cases where adequate data were available. The only exceptions were due to large species differences between animal and human kinetics. A greater understanding of these animal/human systemic exposure comparisons will help to reduce interspecies uncertainty related to TK that are used in regulatory risk assessments.

**PS 721 An Approach for Characterizing Uncertainty in Relative Potency Factors.**

H. Carlson-Lynch<sup>1</sup>, J. Stickney<sup>1</sup>, A. Bacom<sup>1</sup>, G. Diamond<sup>1</sup>, B. Thayer<sup>1</sup>, P. McClure<sup>1</sup>, L. Flowers<sup>2</sup>, C. Chen<sup>2</sup>, M. Gehlhaus<sup>2</sup> and M. Pratt<sup>2</sup>. <sup>1</sup>SRC, Inc., East Syracuse, NY; <sup>2</sup>US EPA, Washington DC.

Relative potency factors (RPFs) for cancer may be calculated as the ratio of the slopes of two dose-response curves, each estimated by linear extrapolation from a benchmark dose (BMD) value. BMD values are subject to uncertainties stemming from study design features such as dosing interval and numbers of animals tested, as well as uncertainties pertaining to modeling, such as model choice, goodness-of-fit, and choice of benchmark response (BMR) relative to the observable data range. Quantitative characterization of the uncertainty in a RPF estimate is desirable both for comparing different estimates and for use in characterizing uncertainty in risk estimates obtained with a RPF. Because it is estimated as a ratio, a RPF poses certain challenges with respect to statistical approaches to characterizing uncertainty. Analytic approaches to calculating a confidence interval for a ratio (e.g., Hinkley 1969) were explored as a means of characterizing the uncertainty in a number of RPF estimates for benzo[b]fluoranthene (relative to benzo[a]pyrene). In addition, a Monte Carlo simulation method was investigated. For both approaches, the RPF estimate was simplified as a ratio of BMDs estimated at the same BMR (10% extra risk), and the standard error of the BMD was approximated using the upper and lower 90% confidence limits reported by the BMD software. For the Monte Carlo method, the benchmark dose was simulated as a lognormal distribution. Each iteration of the Monte Carlo simulation consisted of random samples from the probability distributions of BMDs for benzo[b]fluoranthene and benzo[a]pyrene, and calculation of an RPF for each random draw. The Monte Carlo simulation approach, unlike the analytic approach, provided plausible confidence limits and therefore, useful quantitative estimates of the uncertainty in the RPFs. (The views expressed are those of the authors and do not necessarily reflect the views or policies of the U.S. EPA).

**PS 722 The Chemical Terrorism Risk Assessment Medical Mitigation Model: Approach, Toxicology, and Medical Endpoints.**

D. Winkler<sup>1</sup>, M. T. Whitmire<sup>2</sup>, K. Good<sup>1</sup> and J. A. Cox<sup>2</sup>. <sup>1</sup>Battelle Memorial Institute, Columbus, OH; <sup>2</sup>DHS Chemical Security Analysis Center, Gunpowder, MD. Sponsor: H. Salem.

The Chemical Terrorism Risk Assessment (CTRA) is a probabilistic risk assessment that considers threat, vulnerability, consequences, and mitigation to yield a comprehensive estimate of chemical terrorist risk to the Nation. The Medical Mitigation (MedMit) model is a key component of the CTRA; it is a stock and flow model with parameters defined by toxicology and emergency medicine subject matter experts. The MedMit model estimates the number and type of injured victims according to dose, and determines the number of victims that may be saved or benefitted by the public health response. This presentation will discuss the approach to parameter quantification. It includes the definition of chemical-specific toxicity values for life-threatening, severe, and mild to moderate injury types, the desire and benefits of including these different victim types in the Medical Mitigation model, the segregation of more than 100 chemicals into toxidromes, and the data collection process. The application of toxicology to the CTRA enables a more realistic representation of event consequences and the public health response. Consequently, the model makes it possible to assess the effectiveness of the existing public health response system and examine improvement strategies. Such a capability permits policy makers to make informed decisions regarding resource allocation, and assists responders' understanding of chemical terrorist events and areas of potential improvement.

**PS 723 A Decision Tool for Assessing Polymers and Polymeric Substances with Potential Hazards to Human Health.**

B. K. Gadagbui<sup>1</sup>, A. Maier<sup>1</sup>, P. Nance<sup>1</sup>, M. Jayjock<sup>2</sup> and C. Franklin<sup>2</sup>. <sup>1</sup>Toxicology Excellence for Risk Assessment, Cincinnati, OH; <sup>2</sup>The LifeLine Group, Annandale, VA.

Polymers display a wide variety of characteristics – e.g., presence of non-bound residual monomers, polymerization chemicals, degradation products, and additives – that may pose a potential health hazard. There is a paucity of direct testing data on many polymers to adequately evaluate their toxicity, but several regulatory agencies have provided guidance for assessing polymer safety. We evaluated each of these approaches and identified the strengths and weaknesses of each. No single published model appears to cover all characteristics of interest. This suggests the need to develop a comprehensive decision tool to identify polymeric substances that may pose potential toxicological hazards to human health. We developed a decision tool that incorporates a weight of evidence approach integrating information for many individual hazard flags. Hazard flags were placed into four broad categories: (1) empirical hazard information on the polymer or residual monomer; (2) evidence of toxicity based on structural properties (i.e., based on polymer class, monomer components, or reactive functional groups); (3) potential for significant tissue dose (i.e., based on molecular weight distribution or systemic bioavailability); and (4) hazard based on foreseeable special use considerations. Some of these hazard flags have not been considered previously by the regulatory agencies. We tested this approach for a number of polymers to demonstrate how the new tool (integrates) incorporates all available regulatory approaches as well as the new features and provides a comprehensive decision framework for evaluating polymer safety.

**PS 724 The h-NAG-1 Transgenic Mouse Serves As an Animal Model for Obesity.**

G. J. Moser<sup>1</sup>, K. Chrysovergis<sup>2</sup>, J. Kosak<sup>2</sup>, J. Kim<sup>2</sup>, M. Nixon<sup>1</sup>, E. Gilas<sup>1</sup>, M. Streicker<sup>1</sup> and T. Eling<sup>2</sup>. <sup>1</sup>Investigative Toxicology, Integrated Laboratory Systems, Inc., Durham, NC; <sup>2</sup>NIEHS, Research Triangle Park, NC.

NSAIDS-activated gene-1 (h-NAG-1) transgenic mice (C57BL/6-Tg(CAG-GDF15)) over express human NAG-1/ Growth/differentiation factor-15 (GDF15). Hemizygous h-NAG-1 mice are significantly leaner than their wild-type littermates and have less abdominal white fat despite comparable food intake. To improve our understanding of the mechanisms of obesity development, h-NAG-1 mice and WT were put on a 10 or 60% diet for 12 weeks and blood was collected. Final body and abdominal white fat weights were increased in WT relative to h-NAG-1 mice. The h-NAG-1 mice on the high and low fat diet had lower circulating levels of the inflammatory adipokine leptin, although the difference on the high fat diet was much greater (3.5 +/- 1.1; h-NAG-1 and 55.4 +/- 8.7 ng/ml; WT) than on the low fat diet (2.3 +/- 0.7; h-NAG-1 and 15.8 +/- 6.8 ng/ml; WT). Similarly, serum insulin levels were significantly decreased in h-NAG-1 mice on both diets. Because obesity, via

higher leptin levels, can increase inflammatory responses, hNAG-1 mice and WT were injected with the inflammatory agent lipopolysaccharide (LPS) and serum inflammatory cytokine measured. The levels of KC, IL-6, MCP-1 and TNF $\alpha$  were lower in the leaner h-NAG-1 transgenic mouse. The data indicate the h-NAG-1 mouse may serve as a model for investigating obesity and how environmental exposures may be altered by obesity.

## PS 725 Extended Exenatide Treatment Causes Pancreatic Stress and Injury in a Rodent Model of Insulin Resistance.

R. L. Rouse, S. R. Stewart, B. A. Rosenzweig, K. L. Thompson, K. I. Shea, D. G. Goodwin and J. Zhang. *CDER, US FDA, Silver Spring, MD.*

A possible association between use of the anti-diabetic drug exenatide and acute pancreatitis has been suggested by the analysis of post-approval adverse event data but remains controversial. Studies were undertaken to determine whether an animal model could be developed to reveal potential safety signals consistent with pancreatitis following exposure to drug. Subcutaneous exenatide injection (3, 10, or 30  $\mu$ g/kg for 6 weeks) of Sprague-Dawley rats, caerulein-treated rats, and Zucker fatty diabetic rats demonstrated no consistent histopathologic pancreatic injury signal on standard chow or a high fat, high carbohydrate diet (HFD). However, C57BL/6 mice placed on HFD for 6 weeks exhibited a dose and time dependent pancreatic responses to single daily subcutaneous exenatide injections (3, 10, or 30  $\mu$ g/kg, for up to 12 weeks) that were exacerbated by the HFD. Focal areas of acinar cell necrosis progressing to edema, inflammation, and general tissue fibrosis and atrophy were identified in control mice but were much more prevalent in exenatide treated mice. Other findings included acinar cell hypertrophy and hyperplasia with increased incidence of autophagy and apoptosis in proportion to necrosis and inflammation. Regardless of exenatide exposure, mice on HFD had increased body weight and significantly elevated blood glucose and serum pro-inflammatory cytokines compared to mice on standard chow. The type of stress and injury produced in this study do not approximate the acute necrotizing pancreatitis described in adverse event reports but represent a reproducible pancreatic signal that might be useful for the preclinical safety evaluation of pancreatic injury induced by anti-diabetic drugs.

## PS 726 Adipose Deficiency of Nrf2 in Ob/Ob Mice Results in Severe Metabolic Syndrome.

P. Xue, Y. Hou, Y. Chen, B. Yang, J. Fu, H. Zheng, K. M. Yarbrough, C. G. Woods, Q. Zhang, M. E. Andersen and J. Pi. *The Hamner Institutes for Health Sciences, Durham, NC.*

Nuclear factor E2-related factor 2 (Nrf2) is a transcription factor that functions as a master regulator of the cellular adaptive response to oxidative stress. Our previous studies showed that Nrf2 plays a critical role in adipogenesis by regulating expression of CCAAT/enhancer-binding protein  $\beta$  and peroxisome proliferator-activated receptor  $\gamma$ . To determine the role of Nrf2 in the development of obesity and associated metabolic disorders, the incidence of metabolic syndrome was assessed in whole body or adipocyte-specific Nrf2-knockout mice on a leptin-deficient ob/ob background, a model with an extremely positive energy balance. On the ob/ob background, ablation of Nrf2, globally or specifically in adipocytes, led to reduced white adipose tissue (WAT) mass, but resulted in an even more severe metabolic syndrome with aggravated insulin resistance, hyperglycemia and hypertriglyceridemia. Compared to wild-type, WAT of ob/ob mice expressed substantially higher levels of many genes related to antioxidant response, inflammation, adipogenesis, lipogenesis, glucose uptake and lipid transport. Absence of Nrf2 in WAT resulted in reduced expression of most of these factors at mRNA and/or protein levels. Our findings support a novel role for Nrf2 in regulating adipose development and function, by which Nrf2 controls the capacity of WAT expansion and insulin sensitivity and maintains glucose and lipid homeostasis.

## PS 727 Effect of a Purified Openstandard Diet (OSD) on Body Weight (BW), Adiposity, and Glucose Tolerance (GT) in Male C57BL/6 Mice.

M. A. Pellizzon, M. R. Ricci and E. A. Ulman. *Research Diets, Inc., New Brunswick, NJ.* Sponsor: *P. Marone.*

Purified diets (PDs) offer biologists the ability to have fine control over diet composition compared to grain-based chows which often contain phytoestrogens and toxic heavy metals. However, common PDs such as the AIN-76A (76A) and AIN-93G (93G) may predispose rodents to moderate elevations in BW, blood and liver lipids, and reduced GT, vs. chows. The relatively higher levels of sucrose, lower total

fiber (~5% in PDs vs. ~20% in chow) and lack of soluble fiber in PDs (0 vs. ~2% in chows) may be responsible for these effects. Therefore, we tested two new PDs for their metabolic effects vs. chow (Purina 5002), 76A and 93G: 1) a PD with no sucrose and 9% fiber (7% insoluble, 2% soluble fiber; OSD) and 2) OSD with a fiber level and type similar to chow (18% insoluble, 2% soluble fiber; OSD+F). 75 weanling male C57BL/6N mice (n=15/grp) were fed ad-lib for 88 days. Other than BW (weekly) and an oral GT test (OGTT; day 83), all other measures (adiposity index [AI=adipose depot wt\*100/carcass wt]), liver triglycerides [TG], 6 hr fasted serum glucose, insulin and leptin were terminal. Baseline (17 $\pm$ 0.4 g) and terminal BW (31 $\pm$ 1 to 37 $\pm$ 1) were similar for all groups, but BW gain over time in OSD and 93G was higher (-2.3 g, p<0.05) vs. other groups. AI was similar in all groups but higher in OSD vs. 93G (13 $\pm$ 0.004% vs. 11 $\pm$ 0.01%, p<0.05). Serum leptin was higher in OSD (34 $\pm$ 1 ng/ml) and 93G (36 $\pm$ 2) vs. chow (22 $\pm$ 3) and OSD+F (23 $\pm$ 2, p<0.05). All groups had similar fasting glucose and insulin. Glucose area under the curve during OGTT was higher (p<0.05) for 76A (38,400 $\pm$ 2,500 mg/dl/120 min) and 93G (36,500 $\pm$ 3,000) vs. both chow (27,300 $\pm$ 1,400) and OSD (26,400 $\pm$ 1,600), while OSD+F (32,400 $\pm$ 1,800) was intermediate and not different from 76A and 93G or chow and OSD. Liver TG levels were no different between chow (4.5 $\pm$ 0.2 mg/g), OSD+F (8 $\pm$ 1) and 76A (6.5 $\pm$ 1) but were higher (p<0.001) for OSD (10 $\pm$ 1) and 93G (10 $\pm$ 1). These data suggest that PDs with no sucrose and higher fiber can improve GT over established PDs.

## PS 728 Development of an Oral Exposure Model to Predict Drug Hypersensitivity Using Brown Norway Rat.

A. Tamura, I. Miyawaki, T. Yamada, J. Kimura and H. Funabashi. *Safety Research Laboratories, Dainippon Sumitomo Pharma Co., Ltd., Osaka, Japan.*

**Background:** It is important in new drug development to evaluate the potential of drug hypersensitivity as well as the other adverse effects in non-clinical study, but validated methods are not available yet. Brown Norway (BN) rat is a strain that seems susceptible to substances that induce immune-mediated adverse reaction, and thus this particular strain has been used in studies on chemical-induced autoimmunity and food allergy. In the present study we examined whether it would be possible to develop a new predictive model of drug hypersensitivity using BN rat.

**Methods:** As representative drugs with the potential of drug hypersensitivity in humans, phenytoin (PHT), carbamazepine (CBZ), amoxicillin (AMX), and sulfamethoxazole (SMX) were orally administered to BN rats for 28 days to investigate their effects on these animals. The examinations included observation of clinical signs, hematology, determination of serum IgE levels, histology, and flow cytometric analysis of lymphocyte subsets.

**Results:** Skin rashes similar to what are often seen in humans were not observed in any animals treated with these drugs. Circulating inflammatory cells and serum IgE levels increased only in the animals treated with CBZ and SMX. Only germinal center hyperplasia was commonly noted in spleen and/or mesenteric lymph nodes in the animals treated with all the drugs. The changes of proportions of lymphocyte subsets were only noted in spleen of the animals treated with PHT and CBZ for 7 days and not for 28 days.

**Conclusion:** The potential of drug hypersensitivity was detected in BN rats by performing histological examination of secondary lymphoid organs/tissues. The present data suggested that BN rat could provide a useful animal model to evaluate the potential of drug hypersensitivity. Compared to existing models, the advantages of using this model are capable to evaluate 1) by oral administration, 2) not using reporter antigen, and 3) in easy method (general histological examination).

## PS 729 Behavioral, Neurochemical and Histological Characterization of a Novel MitoPark Mouse Model for Neurotoxicity and Neuroprotection Studies.

M. R. Langley, A. Ghosh, M. Ay, A. Kanthasamy, H. Jin, V. Anantharam and A. G. Kanthasamy. *Biomedical Sciences, Iowa Center for Advanced Neurotoxicology, Iowa State University, Ames, IA.*

Parkinson's disease is now recognized as a neurodegenerative condition caused by a complex interplay of genetic and environmental factors. The animal models presently available, created by neurotoxic insults or genetic defects, do not fully recapitulate the chronic and progressive nature of the nigrostriatal dopaminergic neurodegenerative process. Recently, the MitoPark mouse model was created by inactivation of mitochondrial transcription factor Tfam in the nigrostriatal pathway through the control of a DAT promoter. In this study, we tested the utility of MitoPark mice for neurotoxicological and neuroprotective studies using behavioral, neurochemical and histological analyses. Measurement of locomotor activity in MitoPark mice over 8-25 weeks revealed that motor function started to decline at 12 weeks of age and progressed over time, leading to severe deficits at 17-25 weeks.

MitoPark mice also showed a dramatic loss of striatal dopamine and its metabolites compared to wild type C57 mice. In order to determine the gene-environmental interaction, we exposed MitoPark mice to Mn (10 mg/kg, p.o) daily for 30 days. Motor deficits were significantly exacerbated in Mn-treated Mitopark mice beginning at week 10 compared to vehicle treated MitoPark mice. The depletion of striatal dopamine, DOPAC and HVA content in MitoPark mice was exacerbated in Mn-treated MitoPark mice. We also evaluated the neuroprotective efficacy of a novel mitochondrial-targeted antioxidant, mitoapocynin. Oral administration of mitoapocynin (10 mg/kg, p.o) three times a week to MitoPark mice through 13-24 weeks of age restored behavioral deficits, striatal dopamine depletion and TH neuronal cell loss in MitoPark mice. Our results demonstrate that the MitoPark mouse is an excellent model to study the gene-environmental interactions associated with mitochondrial defects in the nigral dopaminergic system as well as to evaluate the neuroprotective efficacy of novel neuroprotective agents.

### PS 730 Continuous Infusion in Genetically-Altered Down Syndrome Mice.

H. van Wijk. *Covance Laboratories Ltd., Harrogate, United Kingdom.* Sponsor: S. Kirk.

Performing femoral vein catheterisation surgery with tail cuff exteriorisation directly at the performing laboratory offers various advantages. Implanted mice avoid transport from a third party supplier post-surgery. This reduces the risks associated with post operative transport (expression of disease), requires a shorter total recovery time, and allows utilisation of unusual strains not surgically available.

In this study we investigated the feasibility of performing femoral vein catheterisation with tail cuff exteriorisation surgery in-house on B6EiC3Sn a/A-Ts(1716)65Dn (Ts65Dn) Euploid Ts65Dn mice (Jackson Laboratories, Bar Harbour, Maine, USA) to avoid tube restraint necessary for iv bolus administration and allow behavioural monitoring.

Ts65Dn is a widely accepted mutant strain model of Down's syndrome allowing assessment of medicines for potential unwanted side effects in disease patients. The chromosomal complement of the Ts65Dn mouse is incomplete relative to conventional mice; however the animals do not require special husbandry conditions, housing or maintenance and are considered to show normal behaviour in most respects. They are not affected by heart abnormalities common in humans affected by Down's Syndrome.

The mean bodyweight of the control euploid mice is greater than the Ts65Dn mice (~ 40g and 30g respectively). The mean body length for Ts65Dn mice is shorter (~ 1 cm nose - base of tail; 1.5 cm nose - tip of tail) presenting challenges in surgery and tail cuff attachment. To ensure tail size was not likely to impede exteriorisation of the catheter, a range of tail cuff sizes were used.

Of the 16 Ts65Dn and 16 wild type mice that were surgically prepared, only one Ts65Dn mouse failed to recover and was humanely killed three days post surgery. No unexpected clinical signs were seen after surgery and infusion and body weights started to regain six days post surgery, which is quicker than previously described by Arts et al 2012.

In conclusion, in-house catheterisation of Ts65Dn mice was shown to be more humane than obtaining and transporting surgically prepared mice from a third party, reducing the chance of disease expression.

### PS 731 Generation and Characterization of a Humanized *C. elegans* Transgenic Animal That Results in Early Onset, Age-Dependent Complete Loss of DA Neurons.

S. Jamadar, N. VanDuyn and R. M. Nass. *Pharmacology and Toxicology, Indiana University School of Medicine, Indianapolis, IN.*

Background: Parkinson's disease (PD) is a slowly progressive neurodegenerative disease characterized by the selective loss of dopamine (DA) neurons. Despite over 50 years of intensive research into the disorder, the origin of the pathogenesis and the molecular determinants involved in PD have not been elucidated. A significant hindrance in dissecting these molecular components is the lack of facile *in vivo* genetic models to explore the mechanisms involved in age-dependent cell death. Aims/Objectives: Our goal in this study was to develop and characterize a viable *C. elegans* animal that has early onset, age-dependent complete loss of DA neurons. Methods: We utilized transgenic *C. elegans*, reverse genetics, biochemical assays, immunofluorescence, mRNA and miRNA arrays, RT-PCR, Western analysis, and neuronal morphology analysis to characterize expression, localization and the role of human alpha-synuclein, parkin and mutant genes in DA neuron pathology. Results: We generated genetic crosses with *C. elegans* containing human A53T alpha-synuclein, an endogenous parkin mutation and other genetic modifications. One product of this study is the generation of a *C. elegans* transgenic animal that results in a robust DA neurodegeneration phenotype. Immediately after hatching, the animals have their full complement of DA neurons as determined by confocal analysis and DA levels by HPLC, yet animals approximately 8 days old exhibit a

complete loss of DA neurons. Our data suggests that post-translational modifications play significant roles in DA neuron vulnerability to PD-associated genes and toxicants. Conclusions: We have generated a novel transgenic, the first animal (vertebrate or invertebrate) that has a complete loss of DA neurons as a function of age. This animal is proving to be invaluable in determining molecular basis of gene- and toxicant-associated DA neuron vulnerability. Support: NIEHS ES014459 and ES003299 to RN, and EPA STAR Graduate Fellowship to NVD.

### PS 732 Development of Animal Models of Idiosyncratic Drug-Induced Liver Injury.

I. G. Metushi and J. Uetrecht. *Pharmacology and Toxicology, University of Toronto, Toronto, ON, Canada.*

Background: Idiosyncratic drug-induced liver injury (IDILI) remains a serious health problem and it also significantly increases the risk of drug development. Unfortunately, not much is known about the mechanism of IDILI and a main reason is because there are no good animal models. We set out to develop animal models of IDILI by focusing on two drugs: Isoniazid (INH) and Amodiaquine (AQ), both of which cause IDILI in humans. Results: INH was found to covalently bind to mouse and to a lesser extent rat liver macromolecules. Treatment of Balb C, C57BL/6 mice, Wistar or Brown Norway rats with INH did not result in significant liver injury. Treatment of Cbl-b<sup>-/-</sup>, PD1<sup>-/-</sup> and NAT 1/2<sup>-/-</sup> mice resulted in mild liver injury. One possible reason that these animals did not develop more extensive liver damage is immune tolerance. Immunization of C57BL/6 mice with S100 hepatic protein modified with INH produced a greater degree of autoimmune hepatitis than S100 alone, but when INH was subsequently given orally this prevented the autoimmune hepatitis. Treatment of female C57BL/6 mice with AQ resulted in a mild transaminase (ALT) increase at week 3 and this resolved by week 5. Immunohistochemical staining and flow cytometry showed that AQ-induced liver injury in C57BL/6 mice was associated with infiltration of immune cells such as F4/80, CD11b, CD4, CD8 and CD45R in the liver and spleen. Treatment of Cbl-b<sup>-/-</sup> and PD1<sup>-/-</sup> mice with AQ resulted in more severe liver injury, but ALT still resolved despite continued treatment. Treatment of Cbl-b<sup>-/-</sup> mice with FICZ and Anti-CD25 Ab to break immune tolerance was not effective. Treatment of RAG1<sup>-/-</sup> mice also resulted in a mild increase in ALT but the ALT did not appear to resolve as it did in the C57BL/6 mice. Conclusion: These data suggest that the dominant response to these drugs is immune tolerance. Treatment of female C57BL/6 mice with AQ results in delayed onset of mild liver injury which resolved despite continued treatment; this is similar to what happens in humans and this model is being further characterised. Supported by grants from CIHR.

### PS 733 Role of Myeloid-Derived Suppressor Cells in a Murine Model of Drug-Induced Liver Injury Mediated by the Adaptive Immune System.

M. Chakraborty, L. S. Chea, J. D. Berkson, W. R. Proctor, J. C. Morrison, K. Semple and L. R. Pohl. *Molecular and Cellular Toxicology Section, Laboratory of Molecular Immunology, National Heart, Lung and Blood Institute, Bethesda, MD.*

Although clinical evidence suggests that many cases of serious idiosyncratic drug-induced liver injury (SIDILI) are mediated by hepatic protein adducts of drugs and the adaptive immune system, detailed experimental proof for this mechanism of toxicity has remained elusive due to the lack of animal models. We have hypothesized that SIDILI is as rare in animals as it is in humans due at least in part to the tolerogenic nature of the liver, which consists of multiple negative regulators of the adaptive immune system. This idea has now been tested in an established murine model of halothane-induced liver injury where the toxicity is initiated by the metabolism of halothane to form trifluoroacetylated liver proteins and enhanced by the innate immune system, which are prerequisites for activating the adaptive immune system. Twenty-four hours after female Balb/cj mice were treated with halothane, analysis of the liver revealed perivenous necrosis and an infiltration of CD11b<sup>+</sup> Gr-1<sup>High</sup> neutrophils, as reported by other researchers. Further study revealed that the neutrophils contained a subpopulation of myeloid-derived suppressor cells (MDSC) that inhibited the proliferation of both CD4<sup>+</sup> and CD8<sup>+</sup> T cells isolated from naïve mice. When MDSC were depleted from the liver with Gr-1 antibodies prior to two treatments with halothane, enhanced liver injury was observed nine days after the second exposure of halothane as compared to mice that were pretreated with isotype control antibodies before halothane treatments. Moreover, the liver injury was associated with elevated levels of hepatic T cells and serum antibodies that both reacted with trifluoroacetylated liver proteins isolated from halothane treated mice. Collectively, our data provides a rational approach for developing animal models of SIDILI mediated by the adaptive immune system and suggests that deficiencies in liver tolerance may predispose patients to SIDILI.

**PS 734 Defective Platelet Function in a Mouse Model of Progressive Cholestasis.**

Y. Zhang<sup>1</sup>, F. Li<sup>2</sup>, S. Cheepala<sup>1</sup>, Y. Wang<sup>1</sup>, E. J. Gonzalez<sup>2</sup> and J. D. Schuetz<sup>1</sup>.

<sup>1</sup>Pharmaceutical Sciences, St. Jude Children's Research Hospital, Memphis, TN;

<sup>2</sup>Laboratory of Metabolism, Center for Cancer Research, NCI, National Institutes of Health, Bethesda, MD.

We have recently demonstrated that Abcb11-deficient mice recapitulate the human genetic disease PFIC2 (progressive familial intrahepatic cholestasis type 2) attributed to loss of function of the ABC transporter, ABCB11 (1). Cholestatic liver diseases lead to coagulopathies, however it is unclear if these are due to defects in the liver's production of fibrinogen and procoagulant factors or defects in platelet function. By metabolomic analysis we demonstrated that lysophosphatidylcholine (lysoPC) (16:1 and 18:1) concentrations were elevated 2 to 5 times (vs. WT) in the liver and sera of Abcb11-null mice before evidence of frank liver damage. Because lysoPC inhibits platelet aggregation (2) we hypothesized that platelets of Abcb11-null mice might have aggregation defects due to elevated serum lysoPC. Platelet counts were comparable between the Abcb11-null mice and WT mice and platelet-rich plasma was used to test platelet aggregation. Agonist-induced aggregation of Abcb11-null platelets was impaired for agonists: ADP, collagen and thrombin. This ubiquitous defect is consistent with reduced expression of dense granule marker P-selectin and platelet receptor protein GPVI. As there are no changes in the downstream signaling genes *Plcγ1*, *Syk*, and *FcRγ1*, in platelets of Abcb11-null mice; our results suggest that defective aggregation of Abcb11-null platelets is the result of down-regulation of GPVI and P-selectin which may be secondary to lysoPC exposure.

1. Zhang Y, Li F, Patterson AD, Wang Y, Krausz KW, Neale G, Thomas S, Nachagari D, Vogel M, Gonzalez FJ, and Schuetz JD. (2012) Abcb11 Deficiency Induces Cholestasis Coupled to Impaired beta-Fatty Acid Oxidation in Mice. *J Biol Chem* 287, 24784-94.

2. Yuan Y, Jackson SP, Newnham HH, Mitchell CA, Salem HH. (1995) An essential role for lysophosphatidylcholine in the inhibition of platelet aggregation by secretory phospholipase A2. *Blood* 86, 4166-74.

**PS 735 Validation of ROS As a Toxicity Marker in Zebrafish.**

W. Seng, C. Li and P. McGrath. *Phylonix, Cambridge, MA.*

Oxidative stress, associated with an increased level of reactive oxygen species (ROS), is a key factor in both drug-induced toxicity and disease pathogenesis. However, conventional methods for assessing ROS damage are labor intensive and slow hampering widespread use as a toxicity marker. Because of their genetic and physiological similarity to humans, zebrafish have shown promise as an efficient and predictive animal model for assessing drug toxicity, safety and efficacy. Similar to effects in mammals, ROS levels have been shown to increase in zebrafish after drug treatment and irradiation. In this study, we developed a quantitative whole zebrafish microplate-based ROS assay format that relies on a commercially available fluorogenic dye (5-[and-6]-chloromethyl-2,7-dichlorodihydrofluorescein diacetate, acetyl ester, CM-H2DCFDA). We validated the assay using 7 characterized mammalian ROS inducers: TSA [Trichostatin A], PMA [4β-phorbol 12-myristate 13-acetate], Cisplatin, DCA [Dichloroacetate], Menadione, TBHP [tert-Butyl hydroperoxide] and Ethanol and 1 negative control compound, NAC [N-Acetyl-L-cysteine]. In order to optimize the assay, we assessed: ROS level by zebrafish developmental stage, linear relationship between number of animals per microwell and fluorescence intensity, signal to noise (S/N) ratio, effect of carrier DMSO, assay specificity, and assay reproducibility and robustness.

To confirm results using the whole animal microplate format, we also visually assessed site of ROS induction in transparent animals using fluorescent based morphometric image analysis. Using both the microplate format and whole mount morphometric image analysis, compared to mammals, the overall correct prediction rate in zebrafish was 100%, which according to the European Centre for the Validation of Alternative Methods (ECVAM), is considered "excellent". These results underscore the high conservation of toxicity pathways among species and support use of the whole zebrafish ROS assay as a rapid, predictive in vivo assay for compound screening.

**PS 736 The Effect of Fluoride on the Bones and Teeth of ICR-Derived Glomerulonephritis (ICGN) Mice by Subacute Exposure.**

M. Hosokawa<sup>1</sup>, C. Sugaya<sup>2</sup>, M. Tsunoda<sup>2</sup>, K. Itai<sup>3</sup>, Y. Kodama<sup>4</sup>, Y. Sugita-Konishi<sup>4</sup>, H. Ohta<sup>5</sup>, Y. Ito<sup>6</sup>, M. Shimahara<sup>6</sup>, K. Yokoyama<sup>1</sup> and Y. Aizawa<sup>7</sup>.

<sup>1</sup>Epidemiology and Environmental Health, Juntendo University, Tokyo, Japan;

<sup>2</sup>Preventive Medicine, Kitasato University, Sagami, Japan; <sup>3</sup>Iwate Medical University, Morioka, Japan; <sup>4</sup>National Institute of Health Sciences, Tokyo, Japan;

<sup>5</sup>Environmental, Occupational Health and Toxicology, School of Allied Health Science, Kitasato University, Tokyo, Japan; <sup>6</sup>Oral surgery, Osaka Medical College, Takatsuki, Japan; <sup>7</sup>Kitasato University, Tokyo, Japan.

Dental fluorosis and osteofluorosis by drinking water contaminated with fluoride (F) have been reported in China and India. Because fluoride is excreted from the kidney, the toxic effects of F may be affected more significantly by F in ICR-derived glomerulonephritis (ICGN) mice that have commonly been used as a model of renal failure. In this study, we administered F to ICGN and ICR mice to compare the effects of F on the teeth and bones between mice with and without renal failure. Both male and female ICGN and ICR mice were administered F at the concentrations of 0, 25, 50, 100, and 150 ppm in the drinking water for 4 weeks. The mice's femurs were sampled and photographed with a standard aluminum scale. The photographs were analyzed by microdensitometry, and the indexes calculated were: bone mineral content and bone density. The teeth were decalcified in EDTA solution and stained with HE. All the ICGN mice exposed to 150 ppm died. However, no ICR mice died. The mean bone density was significantly lower in the female ICGN mice exposed to 150 ppm compared to the control. The mean mineral content and bone density of the female 100 ppm ICGN group were significantly lower than those of the control. There were no significant differences in the bone indexes among the male ICGN groups. In ICR mice, the mean bone mineral content and bone density were higher in the 150-ppm group for both male and female. The heterogeneity of calcification in the tooth enamel was observed in the ICGN mice exposed to 150 ppm. The decrease in bone density in the mice exposed to F may be due to systemic effects of F. ICR mice exposed to F may be used as a model of osteofluorosis.

**PS 737 A Population-Level Mouse Model to Investigate the Genetic Determinants of Susceptibility to Environmental Toxicants.**

M. C. DeSimone<sup>1</sup>, S. H. Jennings<sup>2</sup>, A. B. Rogers<sup>3</sup> and D. Threadgill<sup>1</sup>. <sup>1</sup>Genetics, North Carolina State University, Raleigh, NC; <sup>2</sup>Veterinary Medicine, North Carolina State University, Raleigh, NC; <sup>3</sup>Pathology, University of North Carolina at Chapel Hill, Chapel Hill, NC.

Carcinogenesis bioassays have lacked the genetic component critical for the evaluation of underlying disease susceptibility genes. Here we used a systems biology approach to model the genetic heterogeneity of exposed human populations, including the inter-individual variation in drug metabolism and transport. We developed a novel intercross population derived from FVB/N<sup>Abcb1a/1b/-/-</sup>, a multi-drug resistant p-glycoprotein knockout mouse model, and CAST/EiJ a wild-derived strain that is genetically distinct from the FVB/N background. Using this intercross to model human biology, including using a western diet, environmentally-relevant doses of trichloroethylene (TCE) and inorganic arsenic (iAs), were evaluated for their effects on toxicity susceptibility. A study cohort of 900 FVB/N<sup>Abcb1a/1b/-/-</sup> x CAST/EiJ F3 mice was divided into nine dose groups, each containing 50 female and 50 males, and was administered TCE and sodium arsenite via the drinking water and chow, respectively, at environmentally-relevant concentrations for 56 weeks using a dose-ratio approach. At harvest, biofluids and tissues were either formalin fixed for pathology, or flash frozen for molecular analysis. Mice co-exposed to TCE and iAs developed hepatocellular carcinoma, as well as renal cysts, clear cell foci and dilated renal tubules consistent with human renal disease pathogenesis. Whole genome expression analysis of kidney tissues revealed a distinct response signature for the combinatorial exposures, including overexpression of oncogenes implicated in the development of human renal cell carcinoma. Genome-wide allelotyping of each mouse using a 7,851 SNP genotyping array will reveal the genetic variants underlying toxicity response. This experimental paradigm has successfully modeled the population-level variability in disease response and has the potential to identify individuals sensitive to toxicity.

**PS 738 Human Antibodies Can Cross Guinea Pig Placenta and Bind Its Neonatal Fc Receptor: Implications for Evaluating Immune Therapy during Pregnancy.**

L. Ma<sup>1</sup>, L. Zhong<sup>1</sup>, D. M. Toibero<sup>3</sup>, A. Hoglund<sup>2</sup>, J. Beren<sup>4</sup>, M. G. Norton<sup>1</sup>, P. Zhang<sup>1</sup> and E. B. Struble<sup>1</sup>. <sup>1</sup>Laboratory of Plasma Derivatives, Division of Hematology, OBRR, CBER, US FDA, Bethesda, MD; <sup>2</sup>Division of Veterinary Services, CBER, US FDA, Bethesda, MD; <sup>3</sup>University of Maryland, College Park, MD; <sup>4</sup>OC TEC, CDER, US FDA, Silver Spring, MD.

Disclaimer: The findings and conclusions in this presentation have not been formally disseminated by the Food and Drug Administration and should not be construed to represent any Agency determination or policy.

Despite increased use of monoclonal and polyclonal antibody therapies, including during pregnancy, there is little data on appropriate animal models that could humanely be used to understand determinants of protection, and to evaluate safety of these biologics in the mother and the developing fetus. We have demonstrated that pregnant guinea pigs can transport human IgG transplacentally at the end of pregnancy. Using an intravenous anti-hepatitis B specific immune globulin preparation as an example, we show that IgG subclasses one, two and three are measurable in both the sows and their piglets. Given that IgG4 can be transferred transplacentally in the guinea pig, our observations indicate that all human IgG subclasses can pass guinea pig placenta during the last third of pregnancy. In addition, we found that all human IgG subclasses are capable of binding to a soluble form of the guinea pig neonatal Fc receptor *in vitro* in a manner similar to that demonstrated for the human variant. This result suggests that transplacental transport of human IgG subclasses in guinea pig mirrors the receptor-based mechanism seen in humans. Together, our studies lay the groundwork in introducing pregnant guinea pigs as an appropriate model for the evaluation of antibody therapies during pregnancy and advancing the health of women and neonates.

**PS 739 Gender and Perinatal Exposure to Bisphenol A Affect Markers of Inflammation in the Brain and Spleen of Young Rats.**

J. Rodriguez-Santiago<sup>1</sup>, Z. Varguaz-Villarrubia<sup>1</sup>, D. R. Mierke<sup>3</sup>, R. N. Sadowski<sup>2</sup>, L. M. Wise<sup>2</sup> and S. N. Laverne<sup>3</sup>. <sup>1</sup>Aguadilla, University of Puerto Rico, Aguadilla, Puerto Rico; <sup>2</sup>Psychology, University of Illinois, Urbana, IL; <sup>3</sup>Comparative Biosciences, University of Illinois, Urbana, IL.

Bisphenol A (BPA) is an environmental estrogen disruptor that has been extensively studied for its repro- and neurotoxicity. It has also been shown to activate the immune system and to induce inflammation. This study therefore evaluated markers of inflammation in the brain and spleen of young rats exposed perinatally to BPA. Pregnant rats were dosed with 400 ug/kg/day of BPA during pregnancy, and rat pups continued to be dosed during PND1-PND9; they were then weaned, and eventually humanely euthanized at PND23. The spleens and brains were collected and snap frozen straight away, and stored at -80°C. MHCII levels in the spleens were estimated semi-quantitatively using immunohistochemistry. Cytokine levels were measured in both the spleens and the brains, using a multibead kit. Female rats had higher MHCII levels in their spleen in the vehicle group; this gender effect was absent in the BPA exposed animals where both genders showed similarly high levels. Spleens showed higher levels of IL-1b than brains, but IL-6 and TNFa levels were similar in both organs. In the spleen, IL-1b and IL-6 were higher in females in the vehicle group, but they were higher in males in BPA exposed animals; TNFa levels were higher in females in the control group, but they were similar between genders in the BPA group. BPA decreased IL-1b, increased TNFa, but did not affect IL-6 in male brains. Work is underway to investigate the effect of BPA on inflammation status depending on the exposure timing during development.

**PS 740 Comparing Minimal Supportive Care Models of Hematopoietic Acute Radiation Syndrome in Nonhuman Primates.**

R. Guilmette, M. Doyle-Eisele, W. Weber and D. Melo. *LRRI, Albuquerque, NM.*

Currently male Rhesus Macaques are the standard non-human primate model for hematopoietic acute radiation syndrome however the availability of these animals may limit the drug development studies conducted with treatment candidates. As an alternative, LRRI recently performed a comparison study using male and female cynomolgus macaques. Animals were irradiated with a 6-MV Varian 600c linear accelerator using a two-dimensional irradiation scheme (bilateral) at a dose of 3.5 Gy. Blood was collected prior to irradiation (baseline) and at the following time points post irradiation: 1, 2, 3, 6, 8, 13, 15, and 20 days. Antibiotics, supplemental fluids,

and nutritional support were administered throughout the study. In accordance with the rhesus macaque published data, an initial spike in neutrophils was followed by neutropenia 24 hours following irradiation. By 7 days post irradiation, the platelet levels dropped. At Day 22, an LD100 for females was established. Males began recovering and survived to their scheduled necropsy at Day 30. Baseline measurements for c-reactive protein were consistent with literature values. A biphasic increase occurred between days 1-3 and days 20-27 post irradiation. In addition to CRP, Flt-2L (a hematopoietic growth factor) was also consistent with the literature which showed an increase around day 5 and 20-23 post irradiation. Based on the results, male cynomolgus macaques react similarly to rhesus macaque following external irradiation exposure at this dose level and may be a useful substitute based on their availability. In addition, these data suggest a sex sensitivity in this species.

**PS 741 Development of a Phosgene-Induced Acute Lung Injury in the Conscious Pig.**

S. Graham<sup>1</sup>, A. J. Smith<sup>1</sup>, R. L. Perrott<sup>1</sup>, S. J. Rutter<sup>1</sup>, P. Marshall<sup>1</sup>, T. Mann<sup>1</sup>, B. J. Jugg<sup>1</sup> and A. M. Sciuto<sup>2</sup>. <sup>1</sup>Biomedical Sciences, DSTL, Salisbury, United Kingdom; <sup>2</sup>Medical Toxicology, USAMRICD, Aberdeen Proving Ground, MD.

The toxic industrial chemical (TIC) phosgene (CG) is a reactive intermediate used in a range of industrial processes. Exposure to high concentrations of CG results in an asymptomatic period (2-6 h) before pulmonary oedema develops. There are no specific medical countermeasures for such poisoning, treatment being supportive in an intensive care setting. Evidence based treatment guidelines are needed for health care practitioners to guide treatment. Small animal models have been used to screen candidate therapies, extrapolation of therapeutic benefit to man requires verification in a larger animal model e.g. the pig. There is, therefore, a requirement to develop a conscious large animal model of CG-induced lung injury in which to verify efficacious treatments. If successful, this model will allow assessment of therapeutic interventions to CG-induced lung injury in a species closer to man.

After a period of socialisation, animals were surgically prepared to allow physiological measurements (arterial blood pressures, ECG, temperature and activity via telemetric implant) and blood samples (via exteriorised catheters) to be taken. After a 1 week recovery from surgery and baseline measurements (1 week) animals were exposed to either air or phosgene under anaesthesia, then recovered and monitored for 24 h.

Air-exposed and phosgene-exposed animals were successfully recovered and monitored to 24 h post exposure. The phosgene-exposed animals had a severe but non-lethal phosgene-induced lung injury at 24 h compared to air-exposed controls, demonstrated by changes in arterial blood gas measures, gross pathology and histopathology.

The feasibility of this unique model has been demonstrated. Further refinement of the telemetry technology may be required to add robustness and improve confidence in extrapolation to man. We intend to use the model to test therapeutic candidates proven efficacious in a small animal model.

**PS 742 Sex Differences in Inflammatory Response in a DAPM-Induced Rat Model of Pulmonary Hypertension.**

M. A. Carroll Turpin, V. Y. Hebert, H. Wensler, T. Chotibut, C. Robinson and T. R. Dugas. *Pharmacology, Toxicology and Neuroscience, LSUHSC-Shreveport, Shreveport, LA.*

Pulmonary Arterial Hypertension (PAH) is a cardiovascular disorder characterized by elevated pulmonary artery pressure as a result of arterial wall thickening. Patients survive, on average, 2.8 yr after diagnosis and are 3-4 times more likely to be women than men. There is no cure - the few therapies available can only slow progression. Our purpose was to develop a relevant animal model of PAH in order to identify sex differences that contribute to disease progression, and in doing so, identify potential new treatment strategies. 4,4'-Methylenedianiline (DAPM) is an aromatic amine used industrially in the synthesis of polyurethanes. Chronic, intermittent treatment of rats with DAPM results in medial hyperplasia of pulmonary arterioles, exclusively in females, coupled to increases in pulmonary arterial pressures. After 12 wk, significant increases in plasma levels of endothelin-1 (ET-1) and serotonin (5-HT), but decreases in nitrite (NO<sub>2</sub><sup>-</sup>), were observed in females (not males) treated with DAPM. A decrease was observed in the serum ratio of the estrogen metabolites 2-hydroxyestradiol (2-OHE)/16α-hydroxyestrogen (16α-OHE; p = .07). In females, ET-1, NO<sub>2</sub><sup>-</sup> and 2-OHE/16α-OHE were significantly correlated with peak pressure gradient, an indirect measure of pulmonary arterial pressure. In DAPM-treated females, serum IL-10 decreased 37% (p = .0129). INF-γ increased by 48% and IL-6 increased 3-fold (as determined by Bio-Plex cytokine assay). These changes were not significant. However, there were significant interactions between sex and treatment. Future studies will address the contributions of these inflammatory cytokines in PAH initiation and progression in females.

**PS 743 Cynomolgus Macaque (*Macaca fascicularis*) As a Potential Animal Model for Studying Bleomycin-Induced Pulmonary Fibrosis.**

M. Doyle-Eisele<sup>1</sup>, J. Villalba<sup>1</sup>, Y. Shi<sup>1</sup>, J. D. McDonald<sup>1</sup> and I. O. Rosas<sup>1,2</sup>.  
<sup>1</sup>LRRI, Albuquerque, NM; <sup>2</sup>Harvard Brigham and Women's Hospital, Boston, MA.

Bleomycin Sulfate-Induced Pulmonary Fibrosis has been extensively described in mice. However, to our knowledge few non-murine animal models have been implemented before. Here we investigated the pathogenic/inflammatory potential of Bleomycin administration in Cynomolgus Macaques (*Macaca fascicularis*), a surrogate model for human pulmonary fibrosis. Fifteen Cynomolgus Macaques (6 insulin resistant on high fat diet and 9 on standard primate chow) were challenged via a bolus insufflator with varying doses of Bleomycin Sulfate (0.1-1.9 mg/kg). Animals were followed during 10 weeks of study by twice daily cage-side clinical observations. Bronchoalveolar lavage (BAL) and pulmonary function tests (PFTs) were performed biweekly until necropsy. PFTs were completed for each animal (previously anesthetized) using a whole body plethysmograph. A subset of inflammatory potential markers was further analyzed in BAL cell mRNA. Macroscopic lung abnormalities were examined at necropsy. Increases in PYCARD and TXNIP were noted in all animals that received high fat diet compared to those on normal primate chow irrespective of the bleomycin dose. Interestingly, NLRP3, PYCARD, PR2X7, TXNIP, and IL-18 mRNA expression showed an inverse relationship with the bleomycin dose for both feed types. The development of fibrosis in monkeys mimics more of a chronic process as seen in humans. Though our animals presented structural/molecular changes, all of them were asymptomatic. Animals fed a high fat diet have increased inflammasome activation than those fed the standard diet however there is no significant association with the bleomycin dose and the inflammasome activation. These findings suggest that Cynomolgus Macaques may be a potential animal model for studies of Bleomycin-induced pulmonary fibrosis, and this might prove to be a prerequisite for translational research.

**PS 744 Cue-Induced vs Cocaine+Cue-Induced Reinstatement: Two Different Animal Models of Relapse.**

D. Pushett, G. Froget, D. Virley, V. Castagné and C. Froger-Colleaux. *Porsolt SAS, Le Genest-St-isle, France.*

Both environmental factors and abused drugs play a role in drug-seeking. The aim of this work was to compare two models of cocaine-induced reinstatement (i.e. cue- and cocaine+cue). Rats were subjected to daily sessions in operant chambers during which they could receive i.v. infusions of cocaine (0.35 mg/kg/infusion): when rats pressed the active lever, a cue light and a tone signal were turned on together with activation of the infusion pump. When cocaine self-administration was acquired, rats were moved to extinction sessions where active lever-presses no longer produced cocaine infusion, cue light/tone presentation or noise from the pump. Once rats had met extinction criteria, they were subjected to a single reinstatement session. Rats were pretreated with vehicle or raclopride (0.08 or 0.15 mg/kg s.c., -30 min). The cue-induced reinstatement session began with a tone and cue light. The remainder of the session was identical to the self-administration session except that no cocaine was delivered. For the cocaine+cue-induced reinstatement session, rats were administered with a non-contingent administration of cocaine (10 mg/kg i.p.) prior to being placed in the chamber. In rats treated with vehicle, a greater number of active lever presses were observed during the cocaine+cue-induced reinstatement session as compared with the cue-induced reinstatement session. A consistent inhibitory profile on cocaine-seeking behavior was demonstrated for raclopride at the higher dose (0.15 mg/kg s.c.) in both models. However the suppressing effect of raclopride at the lower dose (0.08 mg/kg s.c.) was only observed in the cue-induced reinstatement model. These data demonstrate that the cocaine+cue-induced reinstatement model induces a higher level of drug-seeking which is more difficult to reverse than the drug-seeking produced in the cue-induced reinstatement model. Conversely, the cue-reinstatement model may be more sensitive to detect relapse-facilitating effects of test substances.

**PS 745 Early Juvenile Exposure to High-Dose Acetaminophen Impacts Adult Murine Social Behavior in a Strain-Dependent Manner.**

G. G. Gould<sup>1</sup>, C. Smolik<sup>1,2</sup>, T. Gu<sup>1</sup>, M. Vitela<sup>1</sup>, M. F. Valdez<sup>2</sup>, J. Hensler<sup>2</sup>, A. Seillier<sup>2</sup>, A. Giuffrida<sup>2</sup> and S. T. Schultz<sup>3</sup>. <sup>1</sup>Physiology, UTHSCSA, San Antonio, TX; <sup>2</sup>Pharmacology, UTHSCSA, San Antonio, TX; <sup>3</sup>Family and Community Medicine, UTHSCSA, San Antonio, TX.

Pediatric acetaminophen use has increased since 1980, while baby aspirin use declined after its association with Reye Syndrome. It has been hypothesized that increased exposure of children under 5 years old to acetaminophen may be contributing to the rise in autism incidence. Cumulative acetaminophen doses < 75

mg/kg/day for 2 days are within recommended guidelines, but may be problematic for children in whom conjugative disposition pathways are impaired. Alternative metabolic pathways, either via deacetylation to promote endogenous cannabinoid neurotransmission or via oxidative pathways, may be harmful at vulnerable stages of brain development. We sought to model this scenario to clarify possible mechanisms using juvenile mice. We hypothesized that high-dose (>100 mg/kg/day) acetaminophen exposure in weanling (PD18-21) mice would produce impairments in the social behavior of C57BL/6J mice and would worsen them in BTBR mice. Male pups of each strain were exposed for 4 days to 4x daily injections of acetaminophen (100 mg/kg), WIN 55,212 (0.1 mg/kg) or vehicle (saline + 10% DMSO), and matured to adulthood (PD 80). Three chamber sociability tests of C57BL/6 mice revealed a significant (p<0.05) reduction in social interaction relative to vehicle controls that was comparable to prenatal treatment with valproic acid. However, the social behavior of BTBR mice was unaffected. Levels of 2-arachidonoylglycerol and serotonin transporter binding site density were also reduced in both strains. In contrast C57BL/6 mice exposed for 4 days to 1.5 mg/ml of acetaminophen were unaffected. Thus, exposure to supratherapeutic doses of acetaminophen or cannabinoid full agonists indicates a possible role for cannabinoid receptors in modulating social behavior, at least in juvenile mice. This research was supported by US Navy contracts and a sub-award from UTHSCSA Institute for Integration of Medicine and Science CTSA grant #UL1RR025767.

**PS 746 Interlaboratory Comparison of Clearance Rates of Xenobiotics by Cryopreserved Trout Hepatocytes for the Prediction of Bioaccumulation Potential.**

K. Fay<sup>1</sup>, R. T. Mingoia<sup>2</sup>, I. Goeritz<sup>3</sup>, D. L. Nabb<sup>2</sup>, A. D. Hoffman<sup>1</sup>, B. D. Ferrell<sup>2</sup>, H. M. Peterson<sup>2</sup>, J. W. Nichols<sup>1</sup>, H. Segner<sup>3</sup> and X. Han<sup>2</sup>. <sup>1</sup>US EPA, Duluth, MN; <sup>2</sup>DuPont Haskell Global Centers for Health & Environmental Sciences, Newark, DE; <sup>3</sup>University of Bern, Bern, Switzerland.

Hepatic biotransformation is an important determinant of chemical bioaccumulation in fish. Consequently, improvements to bioaccumulation models can be made using estimates of chemical biotransformation rates. Cryopreserved trout hepatocytes have previously been used to measure the clearance rates of some compounds. The use of this information within a regulatory context requires, however, that such results be reproducible across laboratories. In this study, three independent laboratories performed a round-robin study using cryopreserved rainbow trout (*Oncorhynchus mykiss*) hepatocytes. Six compounds were selected for testing: benzo[a]pyrene, 4-nonylphenol, di-tert butyl phenol, fenthion, methoxychlor and o-terphenyl. Pre-trial studies were performed to streamline the assay protocol, standardize hepatocyte counting procedures, and characterize potential sources of variability. The results confirmed first-order depletion kinetics for the selected compounds and highlighted the effects of assay temperature as well as lot variability. Each laboratory then conducted clearance assays for the six compounds using a substrate depletion approach. The analyses for each substrate were conducted at one institute to focus the comparison on the assay itself. Compounds determined to be poorly (o-terphenyl; <0.05 ml/h/106 cells) or rapidly metabolized (benzo[a]pyrene; >0.3 ml/h/106 cells) were similarly determined across laboratories. Coefficients of variation across the three laboratories were generally 30% or better, suggesting this method of determining intrinsic clearance is transferable and reproducible. This inter-laboratory comparison strongly supports the use of cryopreserved trout hepatocytes as a tool for estimating hepatic clearance for bioconcentration factor predictions.

**PS 747 Pharmacokinetics of Dichloroacetate in a Canine Model.**

H. W. Maisenbacher<sup>1</sup>, A. L. Shroads<sup>2</sup>, G. Zhong<sup>3</sup>, A. D. Daigle<sup>1</sup>, M. M. Abdelmalak<sup>2</sup>, I. Sosa Samper<sup>1</sup>, B. D. Mincey<sup>1</sup>, M. O. James<sup>3</sup> and P. W. Stacpoole<sup>2</sup>. <sup>1</sup>Small Animal Clinical Sciences, University of Florida, Gainesville, FL; <sup>2</sup>Medicine, University of Florida, Gainesville, FL; <sup>3</sup>Medicinal Chemistry, University of Florida, Gainesville, FL.

Dichloroacetate (DCA) is an investigational drug for mitochondrial diseases, pulmonary arterial hypertension (PAH), and cancer in humans. It is metabolized to glyoxylate by glutathione transferase zeta 1/maleylacetoacetate isomerase (GSTZ1/MAAI), which also catalyzes the penultimate step in tyrosine catabolism. DCA is a mechanism-based inhibitor of GSTZ1/MAAI, thereby inhibiting its metabolism and causing accumulation of reactive tyrosine intermediates, such as maleylacetone (MA). Human haplotype variation in GSTZ1 also confers variable rates of DCA biotransformation that may impact chronic safety. Dogs express GSTZ1/MAAI and develop PAH and cancer; thus, they may be a valuable model of human diseases in which DCA is used. Accordingly, we characterized the pharmacokinetics and dynamics of DCA in a canine model.

Based on an initial 2 day dose-response study, 3 dogs were orally administered 6.25mg/kg q12h DCA for 4 weeks. Between day 1 and 14, Cmax was significantly different ( $p < 0.01$ ) and clearance approached significance ( $p = 0.067$ ). The differences between day 1 and 28 approached significance for  $t_{1/2}$  ( $p = 0.058$ ) and clearance ( $p = 0.065$ ). Urinary levels of DCA ( $p = 0.074$ ) and MA ( $p = 0.056$ ) tended to increase during DCA exposure. There were no differences in packed cell volume, blood alanine aminotransferase, aspartate aminotransferase or glucose levels, or nerve conduction velocities between day 0 and 28. Liver biopsies on day 0 and 27 demonstrated complete inhibition of GSTZ1 protein expression and activity ( $0.305 \pm 0.030$  vs.  $0.012 \pm 0.009$  nmol glyoxylate formed/min/mg protein,  $p < 0.01$ ). Dogs demonstrate slower clearance and greater inhibition of DCA metabolism than rodents and most humans. The plasma kinetics of DCA in dogs is similar to humans with GSTZ1/MAAI polymorphisms that confer exceptionally slow plasma clearance. Thus, dogs may be a useful model to further investigate the toxicokinetics of DCA.

#### PS 748 Determination of Onset of Sexual Maturity in Female Göttingen Minipigs.

B. Peter<sup>1</sup>, H. Lorentsen<sup>2</sup>, E. van Duijnhoven<sup>1</sup>, M. van Tuyll<sup>1</sup>, B. van Rozendaal<sup>1</sup> and H. Emmen<sup>1</sup>. <sup>1</sup>Toxicology, WIL Research Europe B.V., 's-Hertogenbosch, Netherlands; <sup>2</sup>Ellegaard Göttingen Minipigs A/S, Dalmose, Denmark.

Minipigs are often used in safety assessment studies with pharmaceuticals. Based on breeding experience, female minipigs are considered to reach sexual maturity at 4-5 months of age. However, more exact scientific data on sexual maturity is lacking. This information is pivotal for the design and interpretation of toxicity studies during drug development.

First, a pilot study was initiated to find useful parameters for the detection of estrous cycle in adult female Göttingen minipigs. Three sows at 10-11 months of age housed adjacent to adult boars were monitored daily for signs of heat (specific behavior, changes of the vulva) for 29 days. In addition, rectal body temperature was recorded, vaginal smears were taken for estrous cycle determination and the reproductive hormones progesterone and  $17\beta$ -oestradiol were measured in serum. Progesterone analysis was the most valuable method, showing a cyclic pattern of release. The outcome of the examination of vulva and vaginal smears was less clear. Other external signs of heat did not reveal a cyclic pattern.

Subsequently, the approximate age at which female minipigs reach onset of sexual maturity was determined. For this, two gilts at 2 months of age, housed in the same room as adult boars, were used. Investigations included progesterone analysis, observations of the vulva, estrous cycle determination and recording of body weights. Progesterone levels increased first at approximately 5.5 and 6.5 months of age (body weight: 12.7 and 17.3 kg), respectively. The hormone release was indicative for a functional corpus luteum. For one female progesterone analysis was continued for nearly 3 months. The cycle duration was approximately 3 weeks which is in line with published data (18-21 days). However, the different stages of the cycle could not easily be distinguished by evaluation of vaginal smears. This information will be used in a following study to further investigate onset of sexual maturity in a female minipig population.

#### PS 749 Recording of the Full-Field Electroretinogram in the Göttingen Minipig.

R. Forster<sup>1</sup>, A. Augsburger<sup>2</sup>, V. Haag<sup>1</sup> and J. Legrand<sup>1</sup>. <sup>1</sup>CiToxLAB France, Evreux, France; <sup>2</sup>DMV Clinique Vétérinaire, Bois-Guillaume, France.

The purpose of this work was to evaluate a simple electroretinographic protocol on a representative sample of Göttingen minipigs. Electroretinogram recordings were conducted on 162 healthy minipigs (81 males and 81 females) aged 4-6 months. After a 1.5-h light adaptation period, the animals were placed under general anesthesia. First, binocular full-field photopic electroretinogram recordings were conducted under photopic conditions. Subsequently, scotopic electroretinogram recordings were conducted during dark adaptation every 4 min over a 20-min period. At the end of this period, the maximal combined rod-cone response was recorded by measuring the retinal response to a single high-intensity flash. We used sclerocorneal clips as active electrodes and needle electrodes for the reference and ground. The a-wave and b-wave peak times and amplitudes were measured and statistically analyzed. For each of the statistical comparisons, normality and homogeneity of variances were evaluated. No significant gender differences were observed, with the exception of a higher b-wave amplitude for the photopic ERG recordings in females ( $48.14 \pm 12.91$  IV vs.  $42.88 \pm 10.67$  IV;  $p < 0.005$ ). The process of dark adaptation was evaluated, and the maximal combined rod-cone response was measured (a- and b-wave amplitudes and peak time). In conclusion, photopic and scotopic electroretinogram recordings were performed in the minipig using a protocol based on light adaptation followed by dark adaptation. Sclerocorneal clip electrodes allowed a quick assembly and examination.

#### PS 750 Normal Physiological Ranges for Hanford Miniature Swine.

J. Liu<sup>1</sup>, L. D. Brown<sup>1,2</sup>, T. J. Madsen<sup>1</sup>, S. Schlink<sup>1</sup>, M. Freeman<sup>1</sup>, B. C. Hanks<sup>1,2</sup>, A. Stricker-Krongrad<sup>1</sup> and G. F. Bouchard<sup>1,2</sup>. <sup>1</sup>Sinclair Research Center, LLC, Columbia, MO; <sup>2</sup>Sinclair BioResources LLC, Auxvasse, MO.

The miniature swine have been increasingly recognized as a non-rodent model in regulatory toxicity. Members of the FDA have even published on the use of miniature swine as an alternative to canine and non-human primates in regulatory toxicity. The similarities between the cardiovascular, renal, and digestive systems make the miniature swine a suitable animal to model the human counterpart. The miniature swine are also the most recognized species for dermal toxicology. The Hanford miniature swine (HMS) has other attractive traits that make them a good substitute to model humans. They are omnivorous, easy to handle, prone to obesity, and will develop atherosclerosis and dyslipidemia if fed a high fat diet. With the advent of new techniques, all routes of compound administration can be used with miniature swine. The HMS should be considered as one of the non-rodent species in toxicity testing. In an effort to generate a database on baseline information about the normal physiological status of the Hanford miniature swine, we report expanded and updated physiological data from normal intact and naïve juvenile and young adult miniature swine of both genders. The normal physiological data gathered includes growth parameters, hematology, serum chemistry, coagulation profile, urinalysis, ECG rhythm and segment intervals, and organ weights.

#### PS 751 A Six-Month Feeding Study for WistarHannover gpt Delta Transgenic Rat.

H. Takagi<sup>1</sup>, Y. Nozaki<sup>1</sup>, A. Kawada<sup>1</sup>, M. Yamada<sup>2</sup>, K. Masumura<sup>2</sup> and T. Nohmi<sup>3</sup>. <sup>1</sup>Biotechnical Center, Japan SLC, Inc., Hamamatsu, Japan; <sup>2</sup>Division of Genetics and Mutagenesis, National Institute of Health Sciences, Tokyo, Japan; <sup>3</sup>Biological Safety Research Center, National Institute of Health Sciences, Tokyo, Japan. Sponsor: A. Nishikawa.

Transgenic rodent gene mutation assays, recently adopted as OECD test guideline TG488, are useful methods to evaluate *in vivo* mutagenicity of chemicals in a target organ. The multiple copies of genetically neutral transgenes that contain reporter genes for mutation analysis are integrated in the chromosome of the transgenic rodents. However, biological identities between the transgenic and non-transgenic animals are not well demonstrated. To evaluate the characteristics of WistarHannover gpt delta transgenic (Tg) rat in general toxicity study, we investigated the clinical and pathological features of the gpt delta transgenic and non-transgenic WistarHannover rats in six months feeding study. The six week-old Slc:WistarHannover/Rcc (gpt delta) and Slc:WistarHannover/Rcc (40 animals/sex/strain) were employed for this assessment. Twenty animals in each sex were subjected to necropsy at 13 and 26 weeks after starting, then, clinical and pathological assessments were conducted. In Slc:WistarHannover/Rcc(gpt delta), the values of several parameters in hematology, clinical biochemistry and organ weights were different from those in Slc:WistarHannover/Rcc with statistical significance. These alterations, however, were within the range of historical control data of in housed Slc:WistarHannover/Rcc, and thus were considered to be incidental. In histopathology, spontaneous lesions in WistarHannover such as fibrosis in the heart, microgranuloma in the liver and so on were observed in both strains. These results suggested that there were no remarkable differences which indicate phenotypic modulation in Tg rats, and supported the conclusion that Slc:WistarHannover/Rcc(gpt delta) has similar characteristics to WistarHannover.

#### PS 752 A Medium-Term Animal Model Using gpt Delta Rats for Predicting Chemical Carcinogenicity and Related Mechanisms of Action.

K. Matsushita<sup>1</sup>, Y. Ishii<sup>1</sup>, S. Takasu<sup>1</sup>, K. Kuroda<sup>1</sup>, A. Kijima<sup>1</sup>, T. Nohmi<sup>2</sup>, K. Ogawa<sup>1</sup>, A. Nishikawa<sup>2</sup> and T. Umemura<sup>1</sup>. <sup>1</sup>Division Path., National Institute Health Science, Tokyo, Japan; <sup>2</sup>BSRC, National Institute Health Science, Tokyo, Japan.

In this study, an animal model (GPG46) capable of rapidly detecting chemical carcinogenicity with the underlying mechanisms of action was developed in gpt delta rats using a reporter gene assay to detect mutations and a medium-term rat liver bioassay to detect tumor promotion. The standard protocol for the GPG46 model was developed based on the results of dose-response exposure to diethylnitrosamine (DEN) and treatment with phenobarbital over time following DEN administration. Briefly, gpt delta rats were exposed to various chemicals for 4 weeks, followed by a partial hepatectomy (PH) to collect samples for the *in vivo* mutation assay. The mutant frequencies (MFs) of the reporter genes were examined as an indication of tumor initiation. A single i.p. injection of 10 mg/kg DEN was administered in rats 18 h after the PH to initiate hepatocytes. Tumor promoting activity was evaluated

based on the development of glutathione S-transferase placental form (GST-P) positive foci at week 10. The genotoxic carcinogens 2-acetylaminofluorene (2-AAF), 2-amino-3-methylimidazo[4,5-f]quinoline (IQ) and safrole (SF), the non-genotoxic carcinogens piperonyl butoxide (PBO) and phenytoin (PHE), the non-carcinogen acetaminophen (APAP) and the genotoxic non-hepatocarcinogen aristolochic acid (AA) were tested to validate the GPG46 model. The MFs of the gpt genes were significantly increased in rats treated with 2-AAF, IQ, SF and AA. The number and area of GST-P positive foci were increased in the livers of rats treated with 2-AAF, IQ, SF, PBO and PHE. APAP treatment did not elevate the MFs of the gpt genes and inhibited the development of GST-P positive foci. The validation results indicate that the GPG46 model could be a powerful tool in understanding chemical carcinogenesis and provide valuable information regarding human risk hazards.

**PS 753 Age-Related Changes in Body Composition in Laboratory Rats: Strain and Gender Comparisons.**

R. C. MacPhail, P. M. Phillips, C. J. Gordon and K. A. Jarema. *NHEERL, US EPA, Research Triangle Park, NC.*

Long Evans (LE), Sprague Dawley (SD), Fischer 344 (F344), and Brown Norway (BN) rats are all commonly used as laboratory research subjects. These strains have been studied under many conditions, but few studies have measured changes in body composition as the animals age. Understanding strain differences with regard to body composition, age and growth are essential for understanding toxicity mechanisms, specifying deprivation regimens for studies on food-rewarded learning and performance, and developing accurate pharmacokinetic models of toxicity. This study used a Bruker body composition analyzer to compare the changes in body fat, lean tissue, and fluid for male (n=12/strain) and female (n=12/strain) LE, SD, F344 and BN rats. We found dramatic differences in body composition between the four rat strains. In both male and female rats, body weights were similar for the LE and SD strains, and much lower for the F344 and BN strains. In all cases, body weights for females were less than males. Lean mass for both genders followed a similar pattern as body weight, with the LE and SD rats differing from the BN and F344 rats, and males differing from females. Total fat content differed substantially between strains. The LE rats had the highest fat content, followed by SD, then F344, and finally BN, which had the lowest fat content. These strain differences were seen with both males and females. When body fat was calculated as a percentage of total body weight, the LE rats still had the highest values and the BN rats had the lowest values. However, the male SD and F344 rats appeared to be nearly identical in percent fat. Moreover, the female SD and F344 had similar percent fat values early in development, but these values diverged as they continued to age. These results show marked differences in body composition between four rat strains commonly used in toxicology research.

(This is an abstract of a proposed presentation and does not reflect US EPA policy.)

**PS 754 Assessment of Cardio-Respiratory Function in Conscious Rats: Use of Combined Telemetry and Plethysmography.**

E. Hayes, S. Rompion, E. Gascoin, M. Maujeul, M. Lepage and G. Froget. *Porsolt SAS, Le Genest-St-isle, France.*

In vivo safety pharmacology assessment of cardiovascular (CV) and respiratory function is a regulatory requirement during pre-clinical drug development. Combination of both assessments in a single model could be useful with respect to reducing animal use. We established a model of combined telemetry and plethysmography to evaluate the time-dependent effects of various reference compounds on CV and respiratory function in conscious rats. Male Sprague Dawley rats (n=5-6) were implanted with DSI telemetric devices and placed into plethysmographic chambers (EMKA) with receivers (DSI). Clonidine, verapamil and theophylline were examined for their effects on heart rate, HR; mean arterial blood pressure, MAP, minute volume, MV; tidal volume, TV; respiratory rate, ReR and enhanced pause, Penh before and for 360 min after drug administration. Data were compared by two-way ANOVA (group, time). In controls, a transient decrease in TV (-22%) and Penh (-21%) and a transient increase in ReR (+121%) and MV (+69%) were observed but returned to baseline values within 90 min and remained stable thereafter. No change in MAP or HR occurred in controls. Clonidine (1 mg/kg, i.p.) reduced HR (-55%), MV (-39%) and TV (-39%) but increased ReR (+95%) and Penh (+96%). Verapamil (30 mg/kg, p.o.) reduced MAP (-39%) but had no effect on ventilation. Theophylline (100 mg/kg, p.o.) exhibited respiratory stimulant and bronchodilatory properties (MV, +125%; ReR, +313%; TV, +40%; Penh, +28%) with concomitant tachycardia (HR, +63%). Overall the expected pharmacological actions of the reference compounds on cardio-respiratory function were adequately determined using a combined telemetry and plethysmography system in conscious rats. Combined use of telemetry-plethysmography in the same study may be useful for the development of new compounds that can be compared to established drugs. This model also allows for a reduction in animal use requirements for CV and respiratory safety pharmacology and fulfills the ethical rule of 3R.

**PS 755 Comparison of Ophthalmologic Findings in Young Adult CrI: CD SD and Wister Han Rats.**

H. Kuno<sup>1</sup>, S. McPherson<sup>2</sup>, Q. Kong<sup>2</sup>, S. Mason<sup>2</sup> and Q. He<sup>2</sup>. <sup>1</sup>NTOLLC, Abiko-shi, Japan; <sup>2</sup>WuXi AppTec Co. Ltd., Suzhou, China.

With more than one strain of rat now being used in toxicology studies, a study was instigated to see if there were differences in the incidence and nature of background lesions between the CrI: CD SD and the Wister Han rat.

The results of pretest ophthalmologic examinations of Wister Han (Charles River USA) and CrI:CD rats purchased from Charles River USA and BioLASCO Taiwan Co., Ltd respectively were analyzed. The percentage incidences (total number of lesion(finding)/total number of rats) of the findings were compared for evidence of any significant differences between the two strains and sexes to see if any particular finding was unique or predominately expressed in one of the two strains/sexes.

Corneal opacity along with the palpebral fissure is commonly observed in rats. Wister Han rats showed both a dense and higher incidence of this lesion when compared with CrI: CD rats. In addition, for Wister Han rats a higher incidence was observed for females as compared with males. This gender difference was not apparent for CrI: CD rats. Based on the differences of corneal opacity, the number eyes of CrI: CD rats that were considered normal was higher than that recorded for Wister Han rats. In addition, unilateral or bilateral posterior cortical multifocal pinpoint opacity was observed for Wister Han rats but not CrI: CD rats. In conclusion, there is a clear difference in the incidence of spontaneous ocular findings observed for both Wister Han and CrI:CD rats; with CrI:CD rats showing a lower incidence of corneal opacity along with interpalpebral fissure and no posterior cortical lens opacity.

**PS 756 Feasibility of 3-Month Intravenous Bolus Injections via the Femoral Vein and an External Access Port in Sprague-Dawley Rats.**

J. Perron<sup>1</sup>, R. Tavcar<sup>1</sup>, L. Armer<sup>1</sup> and R. Forster<sup>2</sup>. <sup>1</sup>CiToxLAB North America, Laval, QC, Canada; <sup>2</sup>CiToxLAB France, Evreux, France.

Long term intravenous (IV) dosing continues to be critical in non-clinical development of many drugs (e.g., anti-cancer agents, large molecules), or pharmaceuticals that cannot achieve high systemic exposure by other routes. The IV route is commonly used in Sprague-dawley rats and the most common injection site is the tail vein. Although daily tail vein injection is normally feasible in acute and sub-acute studies (1, 7 or 14-day duration), sub-chronic and chronic studies (28-days, ≥ 3-months duration), once, twice and even multiple daily administration may be technically challenging and require additional animals at each dose level to assure an adequate number of animals to complete the study. Vehicle selection can also influence the success of long term daily or multiple daily tail vein injections and the use of the vena cava allows for a greater pool of blood to minimize secondary effects caused by non-ideal formulations. In alignment with the 3Rs (Reduction, replacement, refinement), our laboratory has demonstrated that daily intravenous injection via the femoral vein in the rat and external access port was feasible over a period of up to 3 months, which helped minimizing the number of animals per dose level to the minimum required by regulations. A medical grade polyurethane-based catheter was surgically implanted in the vena cava via the femoral vein and connected to a Quick-connect harness with a Luer Valve. A heparin-based locking solution was used to fill the catheter and the injection cap. Sodium chloride for injection (0.9% Saline) was injected daily for up to 3 months via the injection cap, at a dose volume of 5 mL/kg. The experimental procedures were well-tolerated and no adverse effects were observed in clinical signs, body weight, and clinical pathology. Histopathological tissue changes were comparable to findings in catheterized animals. The IV bolus injection via the femoral vein and an external access port was shown to be a suitable alternative to tail vein injection for rat sub-chronic and chronic studies.

**PS 757 Noninvasive Airway Resistance Measurements in Large Animals by High-Frequency Airwave Oscillometry.**

T. F. Schuessler<sup>1</sup>, A. Robichaud<sup>1</sup>, R. Forster<sup>2</sup>, M. Pouliot<sup>2</sup>, A. Asch<sup>2</sup>, E. Troncy<sup>3</sup> and S. Authier<sup>2,3</sup>. <sup>1</sup>SCIREQ Scientific Respiratory Equipments, Montréal, QC, Canada; <sup>2</sup>CiToxLAB North America, Laval, QC, Canada; <sup>3</sup>Faculty of Veterinary Medicine, University of Montréal, St-Hyacinthe, QC, Canada.

Large animals are generally more sensitive than rodents to drug induced respiratory changes. Methodologies to measure airway resistance in large animals normally require an esophageal pressure probe placed under anesthesia or a surgically implanted pleural pressure catheter. Both approaches could alter experimental endpoints in toxicology studies, which limit their use in drug development. A

non-invasive methodology to measure airway resistance by high frequency airway oscillometry was evaluated in conscious Beagle dogs and cynomolgus monkeys. A forced oscillation system was used to assess airway resistance and obtain conventional respiratory parameters (tidal volume, respiratory rate) before and after an intravenous treatment with a bronchoactive agent. Respiratory mechanics measurements were performed using 16 second long single (19 Hz) or composite (6, 10, 14, 19, 26 and 31 Hz) high frequency waveforms, which were applied at each time point at the subject's airway opening via a face mask. During measurements, pressure and flow signals were recorded. After collection of baseline measurements, methacholine was administered to Beagle dogs (n=4) and cynomolgus monkeys (n=4) at 8 and 68 mcg/kg, respectively. A peak increase in airway resistance (+64% in Beagle dogs and +30% in cynomolgus monkeys) was observed after intravenous methacholine administration in both species with return to baseline comparable levels within 10 min. Airway resistance data analysis for individual animals revealed mean percent variations from baseline ranging from 9.5 to 18.6% for dogs and from 4.4% to 6.9% for cynomolgus monkeys, suggesting stable and reproducible assessment of lung function. Airway oscillometry appears to be suitable for non-invasive respiratory mechanics measurements in large animal toxicology studies.

**PS 758 Seizure Liability Models: Seizure Characterization and Automated Detection in Telemetered Nonhuman Primates.**

S. Authier<sup>1,2</sup>, S. Maghezzi<sup>1</sup>, M. Pouliot<sup>1</sup>, S. Bernasconi<sup>3</sup>, T. de Geyer d'Orth<sup>3</sup>, P. Zitoun<sup>3</sup> and R. Forster<sup>1</sup>. <sup>1</sup>CiToxLAB North America, Laval, QC, Canada; <sup>2</sup>Faculty of Veterinary Medicine, University of Montréal, St-Hyacinthe, QC, Canada; <sup>3</sup>NOTOCORD, Croissy-sur-Seine, France.

Seizure liability studies in non human primates generally aim to: 1) confirm drug-induced seizures are self-limiting, 2) determine plasma level at seizure onset 3) identify prodromal clinical signs which can be monitored in clinical trials 4) confirm that conventional drugs (e.g. diazepam) can treat drug-induced seizure and 5) confirm the no observed adverse effect level (NOAEL) by absence of paroxysmal activity. To achieve these goals, typical study designs include video-EEG monitoring. Continuous telemetry monitoring generates a considerable amount of data which translates into lengthy analysis when solely relying on manual EEG review. A new application for seizure detection was developed in non-human primates (NHP). The prototype evaluates temporal and spectral features and compares them to features extracted from a sliding reference window. Detected seizures are validated based on a decision tree and artifact rejection algorithms. The automated prototype was used to evaluate periods of up to 68h of continuous EEG data and all detections were subject to a visual review. All animals presented at least one epileptic event. A detection sensitivity of 86.4% with 2.3 false positives per hour of signal was achieved using the default parameters of the prototype. Detection sensitivity increases to 100% when selecting optimal settings for each individual. The processing time was approximately 5 minutes for a 24h EEG telemetry signal. These promising results reflect progress in an era computerized data analysis. Further improvements are investigated to maintain a detection sensitivity of 100% essential with the model, while keeping the number of false detections low to increase data analysis efficiency.

**PS 759 Comparing Data Obtained by Refined Restraint Methods to Traditional Methods in Nonhuman Primate Studies.**

N. Lalayeva<sup>1</sup>, N. Bailey<sup>1</sup>, J. Kenfield<sup>1</sup>, N. Makori<sup>1</sup>, P. Franklin<sup>1</sup>, T. Beck<sup>1</sup> and R. Nagata<sup>2</sup>. <sup>1</sup>Safety Assessment, SNBL USA, Ltd., Everett, WA; <sup>2</sup>Corporate, Shin Nippon Biomedical Laboratories, Ltd., Kagoshima, Japan.

As nonhuman primates continue to be an important model in nonclinical toxicology/pharmacology studies, improving methods of animal handling during procedures is essential. The aim of this study is to present historical background data collected using a refinement in the restraint technique, the Procedure Cage (PC). Use of the PC has the potential to contribute to minimizing inter- and intra-animal data variability when compared to data collected using other restraint methods (e.g. Restraint Chair [RC]). Historical control pregnancy loss ratio of 16.3% (range 0–31.3%) obtained using the PC is relatively low when compared to published data (17.8%, Hendrie et al. 1996, Am J Primat 40:41; and 29.6%, Wehner et al. 2009, BDR [B] 86:144). Restraint-associated stress can also influence values of hemodynamic and cardiovascular measurements. In a telemetry study comparing cardiovascular parameters for restraint in the Restraint Chair (RC) vs. Procedure Cage (PC), six telemetry implanted animals were monitored and data analyzed for heart rate (HR) and mean arterial blood pressure (BP) using a validated Notocord Telemetry System. In a series of procedures performed, HR for RC animals was on average 1.2 times (range 147–198 bpm) that of PC animals (range 139–167 bpm). BP for RC animals was on average 1.1 times (range 102–109) that of PC animals (range 90–96). The RC animals returned to baseline HR and BP levels only 22 and 33% of the time, beginning at 15 and 30 min post procedure, respectively. In contrast, the

PC animals returned to baseline HR and BP levels 50 and 91% of the time beginning at 5 and 10 min post procedure, respectively. In summary, it is evident that use of the PC method has potential to contribute to obtaining more robust data and, thus, could eventually lead to use of fewer animals on study.

**PS 760 Comparative Analysis of Noninvasive Blood Pressure Data by High-Definition Oscillometry (HDO) in Cynomolgus Monkeys of Mauritian and Asian Origin.**

B. Niggemann and U. Zuehlke. Covance Laboratories GmbH, Muenster, Germany. Sponsor: G. Weinbauer.

Cardiovascular investigations - among other diagnostic parameters - are essential for the detection and interpretation of untoward findings in preclinical studies. As cardiovascular toxicity in general and blood pressure determination in particular is concerned with adverse effects of xenobiotics on the circulatory system, a representative analysis of non-invasive blood pressure data is mandatory for the right interpretation of apparent circulatory findings.

Cynomolgus monkeys are frequently used in toxicity studies and animals from various sources such as Mauritius and Asia are available from acknowledged breeders. The aim of the present work was to compare non-invasive blood pressure data from group housed, untreated and unsedated cynomolgus monkeys of Mauritian and Asian origin.

Individual data from 150 Mauritian and 92/128 Asian male and female animals, each were analysed for systolic, diastolic and mean arterial blood pressure.

Blood pressure data of male and female animals of either origin showed slight but significant differences ( $P \leq 0.05$  to  $P \leq 0.001$ ) and values for males were higher than for female animals. Comparison of blood pressure data from monkeys of Mauritian and Asian origin revealed that systolic pressure (+9.0 % M; +10.4 % F), diastolic pressure (+12.0 % M; +14.1 % F) and mean arterial pressure (+10.1 % M; +11.7 % F) were significantly ( $P \leq 0.01$  and  $P \leq 0.001$ ) elevated in monkeys from Mauritius when compared to monkeys from Asia.

**PS 761 Procedure Refinement and Reduced Restraint Enables Extended 6-Hour-Daily Inhalation Dosing in Beagle Dogs.**

A. Dumais<sup>1</sup>, M. Stoute<sup>1</sup>, R. Tavcar<sup>1</sup> and R. Forster<sup>2</sup>. <sup>1</sup>CiToxLAB North America, Laval, QC, Canada; <sup>2</sup>CiToxLAB France, Evreux, France.

Extended duration of dosing for preclinical assessment of inhaled pharmaceuticals is considered advantageous when testing products of expected low toxicity. Technical limitations have often determined the maximum time of exposure in non-rodents such as Beagle dogs. Increased exposure time can improve the chances and accuracy of determining the maximum tolerated dose rather than being limited to a maximum feasible dose. A study was undertaken to confirm whether reduced restraint (platform) combined with procedural refinements would enable routine 4 hr daily dosing (5 days) and even 6 hr daily dosing (3 days). Prior to delivery from the supplier, a number of dogs were presented to platform restraint and inhalation facemask for up to 15 min and those demonstrating acceptance were selected. Following receipt, the four dogs were gradually acclimated for increasing periods of time (up to 4 hrs) to the inhalation equipment over 13 consecutive days. During the acclimation period, the dogs were monitored for behavior changes (excessive salivation, trembling, vocalization, struggling and increases in respiratory rate). Reinforcement through positive behavior by voice and minimal animal contact during the sham dosing where emphasized. Verbal rewards, petting and treats were provided after completion of each session. All animals underwent the 4 hr daily sham dosing except one female for which the sham dosing had to be interrupted on Days 2 to 4. The 6 hr sham dosing was initiated and successfully conducted using the remaining 3 dogs. There were no changes in clinical signs, body weights or food consumption throughout the study. In conclusion, extended daily inhalation dosing in Beagle dogs is made possible by combining animal screening at the supplier, extensive acclimation, positive behavior re-enforcement and reduced restraint. This enables to more accurately determine the NOEL and improve the determination of a MTD while improving animal welfare by reducing the level of restraint and stress.

**PS 762 Reducing Blood Volume for Hematology and Clinical Chemistry Analysis in Mice.**

A. Prefontaine, C. Copeman, L. Huard, D. Lourdel, K. Petitclerc and F. Poirout. Charles River, Montréal, QC, Canada. Sponsor: M. Vézina.

Blood volume limitations are a challenge with mice when used as a preclinical model. Cohorts of mice are often needed, sampled terminally to meet requirements. This is a sub-optimal use of animals and implies more animals, test materials, technical personnel and costs. To permit interim sampling and reduce blood

volume for hematology and clinical chemistry, we investigated dilution of small blood volumes collected by jugular venipuncture. Whole blood (300 uL instead of 1.2 mL) collected from 46 mice was split; 150uL for hematology and 150 uL for clinical chemistry. For hematology, 2 blood and 2 reticulocyte smears were prepared prior to diluting 100 uL of blood with 200 uL of ADVIA sheath rinse solution®. The 1:3 dilution was analyzed on the ADVIA 120 hematology analyzer (Siemens). All flagged values were verified by microscopic blood smear evaluation. Serial blood dilutions yielded adequate precision up to 1:5 dilution. For clinical chemistry, 40 to 50 uL of serum was diluted 1:3 in saline. Samples were analyzed on the Modular Analytics biochemistry analyzer (Roche) with exception of electrolytes. Serial dilutions of all chemistry parameters evaluated had previously demonstrated acceptable precision up to 1:5 dilution in saline. Jugular vein versus abdominal aorta sample results, were compared using historical ranges. Twelve of 46 (hematology) and 8 of 46 (clinical chemistry) samples were inadequate for analysis, similar incidence to abdominal aorta sampling. Jugular vein samples had slightly higher RBC and platelet counts, while clinical chemistry parameters were comparable except for slight elevations in aspartate aminotransferase. These dilutions necessitated more technical sample processing, but allowed clinical pathology analysis with only 300 uL of blood (ie. 4X reduction), presenting clear advantages, including interim study sampling, reduction in animals, combination of endpoints for in a given mouse, improving correlations and interpretation.

**S 763 Human Health and Environmental Concerns around Natural Gas Production Using Hydraulic Fracturing.**

*Z. Naufal. Chevron Energy Technology Company, Houston, TX.*

Natural gas production from shale rock formations using hydraulic fracturing has expanded greatly over the last decade across the United States and other parts of the world. The expansion came as a result of advances in horizontal drilling technology which helped unlock large natural gas supplies in shale and other tight rock formations across the country. Calls to reduce greenhouse gas emissions, the high cost of energy, and other economic pressures also contributed to the rapid growth of shale gas drilling using hydraulic fracturing. As a result, natural gas production is the highest it has been in the United States in decades. However, with the expansion of hydraulic fracturing into rural communities and areas traditionally not familiar with oil and gas explorations, questions about public health and environmental impacts have been raised by some residents living in proximity to fracturing operations. Data gaps may exist since the growth of fracturing operations has outpaced the research efforts conducted by the broad scientific community around this issue. In general, recent research activities have focused on understanding the potential impacts of the chemical components of the fluids used to fracture rock formations. Other issues raised by the public include the increase in noise, air, and light pollution in hydraulic fracturing areas and the potential for accidental contamination of air or groundwater. This session will provide an overview of the current and projected extent of the use of hydraulic fracturing to meet energy needs, and a discussion of the questions surrounding the public health and environmental impacts of this technology.

**S 764 Current Status of Tight Oil and Gas Development Using Hydraulic Fracturing.**

*J. Imse. ENVIRON International Corporation, Denver, CO. Sponsor: Z. Naufal.*

The industry is rapidly evolving - as a result of the variations in world pricing, and greater public and regulatory scrutiny. The practices of only a few years ago have been replaced in this changing industry. As a result, there has been increasing scrutiny into the process of hydraulic fracturing and how current practices may result in potential exposure pathways that may pose risks to human health. Chemical additives used in this process - the disclosure of those chemicals is now required in states representing approximately 90% of the US production - have evolved at a rapid pace and have evolved from hazardous constituents to food grade substances. Furthermore, additives once viewed as benign (sand) are now receiving greater scrutiny when evaluated in a safety context - e.g. silica (sand). Monitoring and exposure evaluations implemented at sites where hydraulic fracturing occurs will need to evolve rapidly to match the evolving additives in use. Similarly, studies with an objective of evaluating historical exposures will require a major study component focused on determining the actual additives used and the concentrations used at each site.

**S 765 An Assessment of Exposure Pathways and Potential Impacts to Human Health Associated with Shale Gas Drilling and Production Operations.**

*A. Harris. ENVIRON International Corporation, Little Rock, AR.*

Shale gas drilling operations continue to expand in the US, leading to increasing focus on identifying and understanding potential impacts to human health. The primary concern is the potential contamination of air and groundwater in communities located near shale gas drilling sites. Air quality may be affected from drilling and fracturing activities as well as emissions from vehicles and equipment. Air quality studies have been conducted both at drilling sites and near community receptors. VOCs, when detected, have been at concentrations below health-based benchmarks. Multiple studies have also been conducted to evaluate potential impacts to groundwater by additives of fracturing fluid, petroleum constituents and methane. Migration of fracture fluids to groundwater aquifers have been proposed although there is currently little data indicating that groundwater has been impacted by fracture fluids. Other exposure pathways of concern include leaks or spills of undiluted additives to surface water and inadequate containment of flowback and produced wastewater.

**S 766 The Potential Toxicological Impacts of Shale Gas Drilling: An Overview.**

*B. Goldstein and J. Kriesky. University of Pittsburgh, Graduate School of Public Health, Pittsburgh, PA.*

The pace of development of hydraulic fracturing technology to extract natural gas from shale formations has outstripped that of the research necessary to ensure that we maximize the benefits and minimize the risk of this important activity. Issues of particular toxicological concern include the potential impact of the evolving list of chemical and physical agents which are used in hydrofracturing. Concerns also extend to upstream processes, such as the mining of silica and the delivery of chemical and physical agents to the site; the on-site drilling, hydrofracturing and long term extraction processes, including contamination of groundwater, and emissions and noise from diesel compressors; and downstream activities such as the distribution of the hydrocarbon products and the safe disposal of the literally millions of gallons of fluid that comes up from underground containing such agents as brine components, arsenic and radioactive agents. Of particular toxicological importance is the potential adverse consequences of the mixtures of hydrofracturing agents, hydrocarbons and natural agents brought to the surface. Air pollution also has been documented and there is concern about the nearby impacts of the release of hydrofracturing agents and volatile hydrocarbons, as well as regional ozone issues. The longer term legacy of site specific pollution is also an issue.

**S 767 Community Exposure and Risk Near Natural Gas Production Sites: Impacts and Research Needs.**

*J. Adgate. Colorado School of Public Health, University of Colorado, Aurora, CO. Sponsor: A. Harris.*

The current boom in domestic natural gas production has focused national attention on the environmental and health impacts of this process. Increased development of unconventional natural gas resources (i.e., from shales, coal beds and tight sands) using hydraulic fracturing ("fracking") has raised concerns about impacts on environmental quality and human health, especially as development has moved into populated areas. While public concerns tend to focus on potential water contamination, the well development process also results in emissions of multiple air toxics when injected water "flows back" to the surface with the natural gas, accompanying petroleum condensate and fracking chemicals. Studies in Colorado and elsewhere indicate that multiple air toxics and chemicals used in well production activities are emitted from gas development and production sites. Research on non-occupational exposure indicates that air pollution is a major concern because health-based risk estimates for nearby residents are greater than for individuals living further from well development sites. Human exposures and risks vary with proximity to wells, specific activities at well pads, topography/meteorology, and individual operator practices and controls. This talk explores our current understanding of exposure and health risks around well development sites, identifies major information gaps and uncertainties, and outlines research that will improve our understanding of the health risks associated with natural gas development.

## **S** 768 **Air Quality Impacts of Natural Gas Operations in Texas.**

M. Honeycutt, S. Ethridge and T. Bredfeldt. *Texas Commission on Environmental Quality, Toxicology Division, Austin, TX.*

Texas is home to the Barnett Shale, a shale-containing geological formation in a highly-populated area which is currently being actively drilled using hydraulic fracturing. The Texas Commission on Environmental Quality (TCEQ) is charged with regulating sources of air emissions from natural gas operations and has spent considerable resources examining emissions from these sources. The TCEQ has utilized flyovers of helicopters outfitted with infra-red (IR) cameras capable of visualizing volatile organic compound (VOC) emissions, conducted numerous mobile monitoring trips, and has installed an extensive ambient air fixed-site monitoring system in areas with intensive drilling. Between August 1, 2009, and June 30, 2012, the TCEQ has surveyed 2,307 sites in the Barnett Shale area using hand-held IR cameras, and at 2,263 of these sites, hand-held survey instruments were also used. These surveys included citizen complaint investigations, compliance investigations, mobile monitoring trips, and follow-up investigations based on helicopter flyovers. As a result of observations with the hand-held IR camera and measurements collected using the survey instruments, 1,167 short-term field canister samples have been collected and analyzed for VOCs. Less than 5% of VOC canister samples measured short-term levels of concern. Short-term samples have also been collected and analyzed for carbonyls, NO<sub>x</sub>, and sulfur compounds and none of the analyses have measured chemicals at short-term levels of concern. Six stationary VOC monitors were operational in the Barnett Shale area in 2009, thirteen are operational now. No VOCs have been detected to date at levels of long-term health concern.

## **S** 769 **Role of Metabolic Syndrome and Perivascular Adipose in Exposure-Induced Vascular Dysfunction.**

D. J. Conklin<sup>1</sup> and M. J. Campen<sup>2</sup>. <sup>1</sup>*Cardiovascular Medicine, University of Louisville, Louisville, KY;* <sup>2</sup>*Department of Pharmaceutical Sciences, University of New Mexico, Albuquerque, NM.*

Recent epidemiological studies indicate that ambient air pollution enhances the progression from metabolic syndrome to diabetes but not by increasing obesity. Because vascular dysfunction and vascular insulin resistance are two early events associated with metabolic syndrome and air pollution exposure, the mechanisms by which these alterations occur in the vasculature could be informative of changes in overall cardiovascular disease risk. Similarly and increasingly, there is a growing recognition that the perivascular adipose tissue (PVAT) is an important regulator of vascular tone under normal homeostatic conditions and PVAT is altered during disease states, including metabolic syndrome and diabetes. The perivascular adipose tissue structure and function are changed to a proinflammatory state both by disease, angiotensin II, and by exposure to environmental pollutants, implicating these alterations in subsequent endothelial and vascular dysfunction. This symposium will provide both an introduction to the role of perivascular adipose tissue in health and metabolic disease states and draw on evidence from environmental and experimental model studies to emphasize specific alterations in perivascular adipose tissue and how these changes contribute to subsequent vascular dysfunction and potentially increase the risk of cardiovascular disease.

## **S** 770 **Turning Vascular Disease Inside Out: Role of Perivascular Adipose Tissue in Coronary Artery Disease.**

N. Weintraub. *Division of Cardiovascular Diseases, University of Cincinnati, Cincinnati, OH.* Sponsor: D. Conklin.

Adipose tissue surrounding the great vessels [perivascular (PV) adipose tissue, or PVAT] expands during obesity and correlates with the extent of visceral fat and insulin resistance in humans. Moreover, both the amount of PVAT and the degree of PVAT inflammation correlate with the presence of atherosclerotic coronary artery disease. Studies in isolated perivascular adipocytes indicate that the cells display a reduced state of adipogenic differentiation, and enhanced pro-inflammatory cytokine expression, as compared with subcutaneous and visceral adipocytes. In response to just two weeks of high fat feeding in mice, adipogenic gene expression is markedly reduced, while pro-inflammatory cytokine expression is up-regulated, in PVAT. Using a novel model of PVAT transplantation to the mouse carotid artery in the setting of high fat feeding, we demonstrate that PVAT enhances atherosclerosis and wire injury-induced neointimal hyperplasia, triggering inflammatory cell infiltration and proliferation of vasa vasorum. Our data suggest that PVAT plays a pathogenic role in vascular disease, linking metabolic signals to inflammation and angiogenesis of the blood vessel wall.

## **S** 771 **Perivascular Adipose and Vascular Dysfunction in Mice after Combined High-Fat Diet and Concentrated Ambient Particulate Matter Exposure.**

D. J. Conklin and P. Haberzettl. *Cardiovascular Medicine, University of Louisville, Louisville, KY.*

Exposure to inhaled fine particulate matter induces endothelial dysfunction and increases the risk of cardiometabolic disease, insulin resistance and the risk of diabetes, however, the mechanisms by which PM<sub>2.5</sub> enhances this risk are unclear. Because diabetes and air pollution are worldwide health problems, we examined whether high fat diet (HFD) enhanced concentrated ambient particulate matter (CAP)-induced EPC suppression and insulin resistance to ascertain the relationship between these important changes. Mice (male; C57BL/6) maintained on low fat (LFD, 10% kcal fat) or high fat (HFD, 60% kcal fat) were exposed to HEPA-filtered air or urban Louisville CAP (80-100 µg/m<sup>3</sup>) for 9 or 30 consecutive days (6h/d). CAP exposure or HFD prevented insulin-induced Akt and eNOS phosphorylation in isolated aorta, and aortic contractility was progressively dysfunctional under CAP, HFD and combined HFD+CAP treatments. Moreover, only combined HFD+CAP treatment increased glucose intolerance without increasing obesity, and thus, worsened the metabolic syndrome and progression toward diabetes. These data implicate alterations in vascular structure such as increased perivascular adipose in the combined effects of HFD+CAP on vascular dysfunction and insulin resistance.

## **S** 772 **NADPH Oxidase and Perivascular Superoxide Production with Particulate Matter Exposure.**

Q. Sun. *Environmental Health Sciences, The Ohio State University, Columbus, OH.*

Reactive oxygen species from oxidant-releasing enzymes such as NAD(P)H oxidase are known to play a causal role in certain disease development, and air pollutants, such as PM<sub>2.5</sub>, are known to cause vascular dysfunction in major cardiovascular diseases. To evaluate the role of exposure to airborne fine particulate matter (diameter, <2.5 µm, PM<sub>2.5</sub>) pollution on metabolic parameters, inflammation, and adiposity, PM<sub>2.5</sub> inhalation exposure was performed in C57BL/6 mice and mice deficient in the cytosolic subunit of the nicotinamide adenine dinucleotide phosphate (NADPH) oxidase p47phox (p47phox<sup>-/-</sup>) with normal or high fat diet. We found that PM<sub>2.5</sub>-exposed C57BL/6 mice exhibited metabolic abnormalities consistent with insulin resistance. Ex vivo-labeled and infused monocytes demonstrated increased adherence in the microcirculation of normal diet- or high-fat diet-fed PM<sub>2.5</sub>-exposed mice. p47phox<sup>-/-</sup> mice exhibited an improvement in parameters of insulin resistance, vascular function, and visceral inflammation in response to PM<sub>2.5</sub>. We concluded that exposure to high levels of PM<sub>2.5</sub> is a risk factor for subsequent development of insulin resistance, adiposity, and inflammation, and reactive oxygen species generation by NADPH oxidase appears to mediate this risk. Other NAD(P)H oxidase subunits and their roles in PM<sub>2.5</sub> exposure-induced cardiovascular diseases will also be summarized.

## **S** 773 **Role of Perivascular Adipose in Regulation of Vascular Function by the Aryl Hydrocarbon Receptor.**

M. K. Walker. *Department of Pharmaceutical Sciences, University of New Mexico, Albuquerque, NM.*

The aryl hydrocarbon receptor (AHR) has been demonstrated to be required for normal blood pressure regulation as demonstrated by the hypotensive phenotype in the global AHR knockout mouse. Notably, conditional deletion of the AHR solely from endothelial cells results in a nearly identical blood pressure phenotype as observed in the global knockout. Thus, we hypothesized that AHR plays a critical role in the vascular regulation of blood pressure. We generated ECahr<sup>-/-</sup> mice by crossing AHR floxed mice (ahr<sup>flx/flx</sup>) to mice expressing Cre recombinase driven by an EC-specific promoter. BP was assessed by radiotelemetry prior to and following an acute injection of the potent vasoconstrictor, angiotensin (Ang) II, or chronic treatment with an inhibitor of Ang II formation, Ang converting enzyme inhibitor (ACEi). ECahr<sup>-/-</sup> mice exhibited significantly different responses to Ang II and ACEi. While Ang II increased BP in both genotypes, the increase was sustained in ECahr<sup>+/+</sup>, whereas the increase in ECahr<sup>-/-</sup> mice steadily declined. Area under the curve (AUC) analysis showed that Ang II-induced increase in diastolic BP (DBP) over 30 min was significantly lower in ECahr<sup>-/-</sup> mice (AUC: ECahr<sup>+/+</sup> 1297±223 mmHg/30 min; ECahr<sup>-/-</sup> 504±138 mmHg/30 min, p<0.05). In contrast, while ACEi decreased BP in both genotypes, the subsequent rise in DBP after treatment was significantly delayed in the ECahr<sup>-/-</sup> mice. ECahr<sup>-/-</sup> mice also exhibited reduced vascular and adipose Ang II type 1 receptor (AT1R) expression, and reduced aortic Ang II-dependent vasoconstriction in the presence of vascular

adipose. Taken together these data suggest that hypotension in ECahr-/- mice results from reduced vascular responsiveness to Ang II that is influenced by AT1R expression and perivascular adipose.

## **S** 774 **Role of Perivascular Adipose Tissue in Angiotensin II-Induced Vascular Diseases.**

L. A. Cassis. *Graduate Center for Nutritional Sciences, University of Kentucky, Lexington, KY.* Sponsor: D. Conklin.

Adipocytes express all components of the renin-angiotensin system necessary to synthesize and respond to angiotensin II (AngII). We have previously demonstrated that infusion of AngII to hyperlipidemic male mice augments atherosclerosis and causes the formation of abdominal aortic aneurysms (AAAs). Mechanisms for AngII-induced AAAs include inflammation that extends to perivascular adipose tissue surrounding the abdominal aorta. Inflammation in perivascular adipose tissue was augmented by genetic or diet-induced obesity, and resulted in marked increases in susceptibility to AngII-induced AAAs. Moreover, weight loss in previously obese mice resulted in remodeling of AAAs. Vascular changes in mice experiencing weight loss included reduced adventitial neovascularization, with alterations in stem cell populations in perivascular adipose tissue. Current studies are examining effects of deficiency of components of the renin-angiotensin system in adipocytes on AngII-induced vascular diseases.

## **W** 775 **Environmental Factors in Neurodegenerative Diseases.**

E. Tiffany-Castiglioni<sup>1</sup> and A. G. Kanthasamy<sup>2</sup>. <sup>1</sup>*Veterinary Integrative Biosciences, Texas A&M University, College Station, TX;* <sup>2</sup>*Biomedical Sciences, Iowa State University, Ames, IA.*

Exposures to environmental pollutants are implicated in the development of neurodegenerative diseases and protein conformational diseases, including Parkinson's Disease (PD) and Alzheimer's Disease (AD). The purpose of this workshop is to bring together experts to discuss etiologic factors associated with PD and AD, particularly environmental pesticides, heavy metals, and other pollutants, and to discuss new directions for identifying suitable targets for therapeutic strategies. Two very promising lines of investigation into the mechanisms of dopaminergic cell death in PD will be discussed, as well as the interaction of senescence-related, genetic, and environmental factors likely contributes to the etiology of late-onset neurodegenerative diseases such as PD and AD. The interactions of heavy metals with chaperone proteins that regulate protein folding and cell death as related to protein conformational diseases will also be discussed. The workshop will address six questions: 1) Despite equivocal results, why are genetic factors still considered the primary etiologic factor in late-onset neurodegenerative disease?; 2) How can existing models of neuronal cell death in neurodegenerative diseases be integrated?; 3) How can cell culture models be integrated into a better understanding neurodegenerative disease processes?; 4) Are there common pathways or mechanisms that are relevant to environmental exposures in protein folding diseases, including PD and AD?; 5) How do chemicals in a similar class of compounds elicit very different effects on the neurodegenerative processes?; 6) What is the evidence that early exposures to environmental factors predispose to neurodegenerative diseases?

## **W** 776 **ER Chaperone-Metal Interactions: Links to Protein Folding Disorders.**

E. Tiffany-Castiglioni and Y. Qian. *Veterinary Integrative Biosciences, Texas A&M University, College Station, TX.*

Chaperones in the endoplasmic reticulum play vital roles in the folding, assembly, and post-translational modification of secretory proteins and also recycle, refold, or initiate degradation of misfolded proteins. Chaperone deficiencies are implicated in protein folding disorders of the CNS. We present evidence that the master chaperone 78 kD glucose regulated protein (GRP78) becomes pathologic through deleterious interactions with Pb and Cu. The key points of this presentation are that metals, including Cu and Pb, are implicated in the etiology of protein folding disorders, Cu and Pb induce the expression GRP78, Cu and Pb bind to GRP78, and metals impair GRP78 function when they bind to GRP78. Recent data from our lab demonstrate that GRP78 is involved in Cu homeostasis in primary astrocyte and C6 rat glioma cultures. Astrocytes cultured in medium containing 0.3 micromolar Cu accumulated Cu and expressed increased levels of GRP78 but not metallothionein (MT1/2). Cu isotope radiography and Cu affinity column analysis with cytosolic fractions of C6 cells showed that GRP78 bound to Cu. However, the level of GRP78 expression was not proportional to Cu accumulation in astrocytes and C6

cells: astrocytes expressed low protein levels of GRP78 compared to C6 cells but accumulated significantly more Cu. Furthermore, GRP78 depletion by RNA interference increased Cu accumulation by C6 cells. Whereas our findings implicated GRP78 in Cu homeostasis but not storage, we examined the possibility that GRP78 affected Cu accumulation through its role as a protein chaperone. We found that antibody to the Cu-extrusion pump Atp7a precipitated GRP78, but antibody to GRP78 did not precipitate Atp7a. We postulate that GRP78 may chaperone Atp7a as a client protein in cytosolic trafficking for the removal of Cu from the cell. Specific questions to be addressed include: Are there common pathways or mechanisms that are relevant to environmental exposures in protein folding disorders? How can cell culture models be integrated into a better understanding of neurodegenerative disease processes?

## **W** 777 **Novel Oxidative Cell-Death Signaling in Neurotoxicity Models of Parkinson's Disease.**

A. G. Kanthasamy. *Department of Biomedical Sciences, Iowa State University, Ames, IA.*

Although oxidative stress and apoptosis are known to be important in the degenerative process in dopaminergic neurons in PD, the apoptotic signaling mechanisms downstream of caspase-3 that contribute to the degeneration of dopaminergic neurons are poorly understood. We have identified that protein kinase C-delta (PKCδ), a member of the novel PKC isoform family, is highly expressed in nigral dopaminergic neurons, and that the kinase is persistently activated via a novel mechanism by which caspase-3 proteolytically cleaves to permanently dissociate the catalytic subunit from the regulatory subunit of PKCδ. We demonstrated that PKCδ proteolytic activation contributes to apoptotic cell death of dopaminergic neurons during oxidative damage induced by Parkinsonian toxicants such as 6-OHDA, MPTP and other dopaminergic neurotoxins. We also unexpectedly identified that protein kinase D1 (PKD1) is activated by a PKCδ dependent mechanism to protect dopaminergic neurons from the early stages of neurotoxic insult. The current status of our systematic characterization of PKCδ-PKD1 oxidative signaling in nigral degenerative processes using cell culture and animal models of PD as well as human postmortem PD brains will be presented. Potential therapeutic strategies targeting the signaling pathway will be discussed. The proposed PKCδ-PKD1 signaling will provide comprehensive information about signaling pathways associated with protective responses at the early stages of neurotoxicant-induced oxidative stress, as well as the cell signaling mechanisms that override them during prolonged oxidative insult in nigral dopaminergic neurons. Specific questions to be addressed will include: How can existing models of dopaminergic cell death in PD be integrated in relation to PKCδ-PKD1 signaling? Are there common pathways or mechanisms that are relevant to environmental exposures in PD and other neurodegenerative diseases? What are major interplay/interactions between genetic and environmental risk factors associated with neurodegenerative diseases? (supported by NIH grants ES10586, NS 074443, ES19267).

## **W** 778 **Industrial Toxicants and Parkinson's Disease.**

G. W. Miller. *Environmental Health, Emory University, Atlanta, GA.*

The exposure of the human population to environmental contaminants is recognized as a significant contributing factor for the development of Parkinson's disease (PD) and other forms of parkinsonism. While pesticides have repeatedly been identified as risk factors for PD, these compounds represent only a subset of environmental toxicants that we are exposed to on a regular basis. Non-pesticide contaminants, such as metals, solvents, and other organohalogen compounds (polychlorinated biphenyls (PCBs), polybrominated diphenyl ethers, trichloroethylene), have also been implicated in the clinical and pathological manifestations of these movement disorders. Here we report a relationship between PCBs and PD pathology. Post-mortem brain samples from control and PD patients were obtained from the Emory University Brain Bank and from the Nun Study. Concentrations of eight prevalent PCB congeners were extracted from post-mortem brain tissue and analyzed using gas chromatography-mass spectrometry. PCB congeners 153 and 180 were significantly elevated in the brains of Parkinson's disease patients. When stratified by sex, the female Parkinson's disease group demonstrated significantly elevated concentrations of total PCBs and specifically congeners 138, 153, and 180 compared to controls, whereas PCB concentrations in males were not significantly different between control and Parkinson's disease groups. In a separate population of women (Nun Study) who had no clinical signs or symptoms of PD, elevated concentrations total PCB and congeners 138, 153 and 180 were also observed in post-mortem brain tissue exhibiting moderate nigral depigmentation compared to subjects with mild or no depigmentation. These quantitative data demonstrate an association between brain PCB levels and Parkinson's disease-related pathology. Recent evidence from cellular and animal studies suggests that PCBs may induce

pathology by disrupting the normal storage and release of dopamine and related neurotransmitters. Dr. Miller will also present novel high throughput approaches that will be used to further study this association. Supported by NIEHS P01ES016731.

## **W 779 Integrating Epidemiological and Basic Research to Assess the Role of Pesticide Exposure in Neurodegenerative Disease.**

**J. Richardson.** *Robert Wood Johnson Medical School, Piscataway, NJ.*

Although a significant amount of research effort and resources have been focused on determining genetic contributors to Parkinson's disease (PD) and Alzheimer's disease (AD), purely genetic contributions account for only a fraction of the cases. Our laboratory has been specifically interested in the potential role of pesticides in the etiology and pathogenesis of both PD and AD. Recently, we have found that serum levels of a long-lasting residue of the organochlorine pesticide hexachlorocyclohexane ( $\beta$ -HCH) was significantly higher in the serum of PD patients, while the DDT metabolite, p,p'DDE, was significantly higher in patients with AD. DDE levels were 3.8-fold higher in serum of AD patients ( $2.61 \pm 0.35$  ng/mg cholesterol;  $n = 86$ ) when compared to controls ( $0.69 \pm 0.10$  ng/mg cholesterol;  $n = 79$ ;  $p < 0.001$ ). After controlling for age, sex, education, race, and sample collection site, the OR for increased risk of AD in the highest tertile of DDE levels was 4.26 (95% CI: 3.41-5.32;  $p < 0.001$ ). To determine whether DDT exposure alters the expression of AD-related genes in vivo, male C57BL6 mice were dosed with 3 mg/kg DDT every 3 days for 30 days. DDT significantly increased the mRNA levels of APP (25%), NEP (77%), and ApoE (150%) in the hippocampus. These data suggest that DDT selectively alters the expression of AD-related genes in a brain-region specific manner with the hippocampus being more sensitive than the frontal cortex. Specific Questions to be addressed will include: Despite equivocal results, why are genetic factors still considered the primary etiological factor in late-onset neurodegenerative disease? Are there common pathways or mechanisms that are relevant to environmental exposures in both PD and AD? How do chemicals in a similar class of compounds elicit very different effects on the neurodegenerative processes?

## **W 780 Life-Course Models for Ensuring Children's Health Protection.**

**S. P. Darney<sup>1</sup> and E. M. Faustman<sup>2</sup>.** <sup>1</sup>ORD, US EPA, Research Triangle Park, NC; <sup>2</sup>Environmental & Occupational Health Sciences, University of Washington, Seattle, WA.

New knowledge about environmental risks to human reproduction and development directly relevant to children's health protection derives from the fields of developmental and reproductive toxicology, exposure science, epidemiology, risk assessment, and public health. Together, this information highlights the importance of the intrauterine environment in setting the stage for lifelong health, along with the complexities of the physical, chemical, and social factors that operate during critical windows of development to impact health and wellbeing. For example, breakthroughs in genetic polymorphisms and epigenetics are extending our understanding of inherent and acquired susceptibility to effects of environmental contaminants and showing how various intrauterine stressors such as nutrition, toxicants, and social stress may alter developmental programming at the start and throughout life. These scientific advances point to the need for innovative cumulative risk assessment methods and public health intervention approaches in order to account for risks that accrue across the developmental continuum from cradle to cradle. This workshop brings together the interdisciplinary expertise needed to begin integrating new knowledge into life-course models for children's health and wellbeing. Topics include research findings from toxicity testing and epidemiology studies specific to critical windows of exposure during pre-conception, pregnancy, and early childhood life stages to stimulate discussion on the broad challenge of optimizing testing and risk assessment models and enabling analyses across the whole life course. The workshop also features an innovative approach for evaluating and communicating complex scientific information about reproductive risks and interventions to diverse audiences including health care providers, parents (present and future), and regulators.

## **W 781 Today's Challenge for Protecting Children's Environmental Health for a Lifetime.**

**E. M. Faustman.** *University of Washington, Seattle, WA.*

Evidence continues to build for the increasing importance of early life experiences in defining not only childhood development and normal health trajectories but also the potential for chronic disease risk throughout later life. Thus, a critical need for

protecting children's health is recognition that our models require a dynamic context, a lifecourse framework in order to address the key differences in developmental landmarks, functionality and the windows of susceptibility to environmental impact. Such a framework is also needed to provide the context for incorporation of the multitude of research findings across lifespan and discipline and to develop effective public health interventions. To set the stage for the workshop this talk will identify the emerging issues and most pressing questions for reproductive and developmental toxicologists, epidemiologists, and risk and health assessors in lifecourse study. Research from contemporary science, including community-based cohort studies, coupled with research to elucidate molecular toxicity pathways and genetic polymorphisms will be presented to illustrate these important lifestages. Critical questions and research will be discussed within the framework and will include: What does this research tell us about critical windows of exposure, susceptibility and impact across lifecourse? What sorts of statistical models are needed to account for multiple stressors over time? How can this new science be used to build a case for developing a lifecourse approach to risk assessment and children's health protection? How can research in this arena be informed by the parents who live in communities which are highly impacted by environmental stressors? Research by developmental and reproductive biologists, toxicologists, epidemiologists and exposure and risk scientists are required and hence determination of how this multidisciplinary science can be integrated within the lifecourse models is essential. Presentation of both evidence and modeling approaches will be the basis for describing the lifecourse framework for risk assessment.

## **W 782 Periconception Parental Metal Exposures, Couple Fecundity, and Child Health: Delineating the Chicken and Egg Question.**

**G. M. Buck Louis, R. Sundaram and J. Maisog.** *Division of Epidemiology, NICHD, Bethesda, MD.* Sponsor: **S. Darney.**

Growing evidence suggests that human fecundity and fertility may be informative about the subsequent health and well-being of couples' offspring. This avenue of study is in keeping with the early origin for health and disease hypothesis (DOHAD), and the need for a life course approach for assessing health across the lifespan. Early evidence suggests that gynecologic and urologic disorders may be associated with adverse pregnancy outcomes such as genital-urinary malformations or diabetes in affected children. Similarly, couples experiencing conception delays are reported to be at higher risk of delivering infants of diminished gestation and birth size, outcomes associated with developmental disabilities and other childhood morbidities. This evolving body of evidence underscores the importance of exposure assessments in both partners in keeping with the couple-dependent nature of human reproduction and development. For illustrative purposes, this talk utilizes data from the recently completed Longitudinal Investigation of Fertility and the Environment (LIFE) Study to demonstrate the relation between couples' exposures to persistent environmental chemicals (i.e., cadmium, lead and mercury) and fecundity as measured by time-to-pregnancy (in menstrual cycles), and infant health outcomes such as gestation and birth weight. Blood cadmium concentrations in female partners (range 0.02-2.87  $\mu\text{g/L}$ ) and blood lead in male partners (range 0.34, 6.91  $\mu\text{g/dL}$ ) were significantly associated with a longer time to pregnancy as measured by fecundity odds ratio (FORs) below one (FOR=0.78; 95% CI 0.63, 0.97 and FOR=0.85, 95% CI 0.73, 0.98, respectively). When jointly modeling both partners' metal exposures as a continuous exposure, female lead and male cadmium exposures were associated with reductions in gestation and birth weight. Further analysis is underway to determine if the reduction in gestation and birth weight is mediated indirectly through reduced couple fecundity or directly on fetal growth and development.

## **W 783 Prenatal Pesticide Exposures and Children's Neurodevelopment across the Life-Course Continuum—Lessons from the Fields.**

**B. Eskenazi, A. Bradman, K. Harley and N. Holland.** *Center for Environmental Research and Children's Health, University of California Berkeley, Berkeley, CA.* Sponsor: **S. Darney.**

A growing body of evidence suggests that prenatal pesticide exposure may be related to adverse effects on neurodevelopment of children. In 2000-2001, we initiated CHAMACOS (Center for the Health Assessment of Mothers and Children of Salinas), a longitudinal birth cohort study, with the primary aim to investigate the association of prenatal and postnatal exposure to agricultural chemicals and health and development of children. We enrolled 601 pregnant women into this community-based participatory research project. The participants were primarily low-income Latinas from the agricultural community in the Salinas Valley, Monterey,

California. We conducted detailed neurodevelopmental assessment of the CHAMACOS children at multiple time points and currently the children are reaching their 12th birthday. During these years, we have monitored their exposures to a number of chemicals including pesticides such as organophosphates, organochlorines and fungicides. We have also examined potential genetic susceptibility to exposure with analyses of the PON1 polymorphisms and enzyme activity and we are now beginning analyses of epigenetic endpoints. These studies highlight the advantages of longitudinal cohort studies for evaluating the long-term impact of prenatal and early life exposures on children's health and development. Results of the CHAMACOS study to date, coupled with those of other longitudinal studies demonstrate how in utero exposure to certain pesticides can impact neurodevelopment. Furthermore, our results suggest that certain children by virtue of their genetic make-up may be more susceptible. Lastly, we have identified limitations in assessing exposures to pesticides that challenge our ability to determine "causal" relationships. Primary funders: Children's Center grant from NIEHS, NIH and US EPA

## **W 784** New Strategies for Addressing Toxicity Testing across the Lifespan.

P. M. Foster. *National Toxicology Program (NTP), NIEHS, Research Triangle Park, NC.*

A previous NTP workshop evaluating the utility of the cancer bioassay for detecting hormonally-related cancers (particularly breast, prostate, ovary and testis), concluded that the standard approach, commencing exposure as young adults (~ 6 weeks of age) is likely missing important windows during early development that could be critical for cancer outcomes and therefore assessment of lifetime risk. NTP used the workshop results to adopt a new default for rat cancer bioassays to incorporate early life exposures into the assay. NTP had previously conducted perinatal bioassays, but required specific justification; now, such studies are conducted routinely, unless there is a scientific rationale not to do so. This study begins exposure at implantation and continues until the offspring reach 2 years of age. Embarking on a cancer study requires preliminary dose setting information. For a cancer bioassay, this is normally a 90 d study, but would now require exposure from implantation thru weaning prior to the 90d component to evaluate target organ toxicity. Such an approach, would also lend itself easily to evaluations of multiple other end points from the same exposure paradigm, including developmental neurotoxicity and immunotoxicity and, if one bred the F1 offspring at adulthood, both fertility/fecundity and pre-natal developmental toxicity (teratology) - the NTP modified one-generation study. Each of these end points could be considered interchangeable "cassettes" depending on the type of toxicity that NTP was required to assess. Compared to the individual, stand alone studies, this would have considerable savings in time, cost and animal usage, yet generate high quality developmental and reproductive toxicity information for risk assessment. This is a similar approach to the OECD extended one-generation study, but has several major advantages, most importantly is a significantly improved ability to detect potential effects on fertility and fecundity in the same animals on which structural changes are evaluated, together with a pre-breed exposure that is consistent with the length of rat spermatogenesis.

## **W 785** Advancing Risk Communication and Decision Tools for Children's Health Protection.

T. J. Woodruff and P. Sutton. *Program on Reproductive Health and the Environment, UCSF, San Francisco, CA.* Sponsor: S. Darney.

Parents and physicians who take care of them and their children read and hear a plethora of information, some contradictory, about environmental and chemical risks to children's health. Better tools are needed to evaluate and synthesize this information and translate it into meaningful prevention strategies for health professionals, the public and policy-makers. Methods to synthesize the science into evidence-based decisions have been developed and validated in clinical arenas. But because of differences in approaches, the evidence-base and decision-context of clinical health sciences methods are not seamlessly applicable to environmental exposures. To meet this need, UCSF's Program on Reproductive Health and the Environment undertook an interdisciplinary collaboration to craft a systematic and transparent methodology to evaluate environmental contaminants and their potential effects on reproductive and developmental health. The result is the Navigation Guide, the product of a yearlong collaboration of 22 clinical and environmental health scientists and/or practitioners, from governmental and non-governmental organizations in the U.S. and Europe. Government agencies can use the Navigation Guide methodology to craft evidence-based statements regarding the relationship

between an environmental exposure and health. Government agencies called on to make risk management decisions can also apply the Navigation Guide to grade the strength of recommendations for prevention. Professional societies, healthcare organizations, and other potential guideline developers working with toxicologists can use the Navigation Guide to craft consistent and timely recommendations to improve patient, and ultimately population, health outcomes. Development of the first case studies applying the Navigation Guide methodology is extremely timely as it coincides with growing recognition of the need for updated methods in risk assessment, and related calls for government agencies such as the U.S. Environmental Protection Agency to incorporate systematic approaches into decision-making.

## **W 786** Nanoinformatics: Computational Challenges for Nanomaterial Hazard Assessment.

K. M. Waters<sup>1</sup> and S. Harper<sup>2</sup>. <sup>1</sup>*Systems Toxicology, Pacific Northwest National Lab, Richland, WA;* <sup>2</sup>*Environmental & Molecular Toxicology, Oregon State University, Corvallis, OR.*

Hazard evaluation of the growing number of nanomaterials can be expedited and enhanced through the identification of underlying quantitative relationships between their structural, chemical, and physical properties and responses in key biological systems. The Toxicity in the 21st century testing paradigm holds particular promise for nanoparticles because whole animal testing is not economically practical or feasible for every new material introduced to the marketplace. Important advancements have been made in this emerging but critical field, yet many challenges remain. Distillation of the large amount of phenotypic data regarding *in vitro* cytotoxicity and inflammation down to *in vivo*-relevant adverse events is a daunting task, given the vast differences in microenvironment, temporal dynamics, and exposure. The use of systems biology approaches will enable the identification of relevant target organs/cell types, the development of mechanism-based assays for hazard assessment and computational modeling for predicting potential toxicity from human relevant exposures. This session will address computational challenges in data standards, data integration, and modeling of dose response and structure-activity relationships, including talks by experts in the areas of informatics, *in vitro* screening, *in vivo* exposures and PB/PK modeling. Included is an opening by the co-chair of the US-EU Nanoinformatics Community of Research, which seeks to facilitate intercommunication between researchers, regulators, and granting agencies on environmental health and safety issues for manufactured nanomaterials. Speakers will include current experimental and computational approaches as well as future research needs to identify relevant *in vitro* assays that are predictive for nanomaterial hazard assessment based on *in vivo* mode of action and realistic human exposures.

## **W 787** US-EU Nanotechnology Databases and Ontology Community of Research.

N. A. Baker<sup>1</sup> and H. Rauscher<sup>2</sup>. <sup>1</sup>*Pacific Northwest National Laboratory, Richland, WA;* <sup>2</sup>*DG Joint Research Centre Unit Nanobiosciences/TP 202, European Commission, Ispra, Italy.* Sponsor: K. Waters.

This talk will provide an overview on the work of a new US-EU Nanotechnology Safety Community of Research (CoR) focused on nanotechnology databases and ontology with specific examples and highlights from our own research. CoRs are groups of people who share a significant interest in nano safety, work together to develop a shared repertoire of resources, and have regular contact to address key global research challenges. Interconnected information systems are urgently needed for collating nanoscale material descriptions; their intrinsic and context-dependent properties and their interactions; and their interactions with biological entities. One goal of the CoR is to enable the sharing, searching, and analysis of nanoscale material characterization data across a wide range of experimental sources and guide the structuring of these data to enable their widest possible use. Achievement of this goal will deliver important new capabilities to allow integration of risk assessment data among labs throughout the world, to provide situational awareness of data coverage across nanomaterial categories, and to enable predictive computational models for bridging physical properties and biological outcomes with exposure, dispersal and fate. In order to realize this goal, the CoR will initially focus on the following three areas of investigation: Identification of the data elements necessary to establish common data-sharing models for this domain; specification of requirements for sharing data between research groups and repositories in human- and machine-interpretable forms; definition of concepts necessary to support the above activities and representation of those concepts in an ontological framework. This will include descriptors for the material itself as well as for its interaction with the environment and elements to characterize intermediate effects in adverse outcome

pathways. Through these activities the CoR will provide tools for improving the overall quality of experimental data being generated in EU and US research communities.

**W 788 High-Throughput Screening of Nanomaterial Bioactivity/Toxicity: The Computational Side Is Just As Important As the Testing Assays and Characterization.**

A. Wang. *US EPA, Research Triangle Park, NC.*

High-throughput screening (HTS) of bioactivity/toxicity is currently the only cost-efficient and rapid tool to screen the numerous nanomaterials (NMs) in use and under development. In the EPA ToxCast program, diverse classes of NMs and their micro-particle and ionic salt counterparts are tested in HTS assays to help prioritize NMs for further targeted testing. While the measured HTS endpoints are the same as those tested for traditional soluble chemicals, specific challenges arise for NMs for both experimental procedures and computational analysis. Challenges include no standard nomenclature, comparison of potency between different classes of NMs each tested at a different concentration range, linking NM physicochemical (pchem) characterization data into the analysis, and assay interference by NMs. With no standard nomenclature, we identified NMs by combining information on group (nano, micro, ion), chemical composition of the core and coating, primary particle size, and source. CAS numbers were purposely not used for NMs to avoid data being aggregated with bulk counterparts. We accounted NM exposure potential and tested NM at various concentrations, while all soluble chemicals were tested at the same concentrations in ToxCast and their sigmoidal AC50s were compared. NM bioactivity data is being analyzed using various dose metrics (e.g., either NM mass or surface area per medium volume or cell surface area) and potency estimates (LEC, sigmoidal AC50, etc.) for NM toxicity ranking. To link NM pchem properties into the bioactivity data, we choose to build a distinct database of NM pchem characterization results, instead of modifying the existing ToxCast database of bioactivity results. While HTS assays we used have successfully screened hundreds of soluble chemicals, inspecting the NM bioactivity results carefully resulted in discontinuing the use of one of the testing platforms because NMs interfere with the assay. Future research needs include developing computational models using NM pchem properties and/or in vitro data to predict in vivo effects.

**W 789 Computational Dosimetry for Nanomaterial Risk Assessment from Transcriptomic and HTP Data.**

J. G. Teeguarden<sup>1</sup>, V. Mikheev<sup>2</sup>, J. G. Pounds<sup>1</sup> and B. D. Thrall<sup>1</sup>. <sup>1</sup>*Systems Toxicology, Pacific Northwest National Lab, Richland, WA;* <sup>2</sup>*Battelle Memorial Institute, Columbus, OH.*

The convergence of evolutionary changes to the field of toxicology and the rapid emergence of an immense new class of toxicologically untested nanoscale materials has led to development of new genomic and high-throughput in vitro screening tools for toxicological assessment of nanomaterials. These advancements and refinements in the measurement and analysis of response have not however, been followed by equally important advancements nanoparticle kinetics and in the measurement of cellular or tissue exposure to test materials. The absence of adequate dosimetry data for nanomaterial toxicity studies is one of the largest sources of uncertainty in current testing paradigms. We present an integrated computational dosimetry framework for placing the results of in vitro genomics and high throughput (HTP) toxicity data in the context of in vivo animal and human exposures and improving the basis for hazard rankings. The framework is applied in three case studies to demonstrate the impact of an evolution from "exposure" to target cell dose based nanotoxicity assessments: 1) the disruption of macrophage pathogen clearance by macrophages in vitro; 2) in vitro cytotoxicity screening and hazard ranking of 25 metal oxides; and 3) in vitro screening and hazard ranking of nanomaterials from the U.S. EPA's ToxCast program.

**W 790 Integrative Nanotoxicology: Linking Rapid Assays and Informatics to Predict Nanomaterial-Biological Interactions.**

S. Harper<sup>1,2</sup>. <sup>1</sup>*Environmental and Molecular Toxicology, Oregon State University, Corvallis, OR;* <sup>2</sup>*Chemical, Biological and Environmental Engineering, Oregon State University, Corvallis, OR.*

While numerous nanotechnology and nanomaterial-based applications promise benefit to human health or the environment, the potential health and environmental risks associated with the unique properties of nanoscale materials are unknown and may lead to unintended health and safety consequences. The current gap in

nanoparticle toxicological data dictates the need to develop rapid, relevant and efficient testing strategies to assess these emerging materials of concern prior to large-scale exposures. Among these are informatics approaches to speed the rate at which we can gain information on the fundamental relationships between specific nanomaterial features and their behavior in the environment as well as their interactions with living systems. Data compiled using a dynamic whole animal (in vivo) assay to reveal whether a nanomaterial produces adverse responses have been made available through the Nanomaterial-Biological Interactions (NBI) knowledgebase (nbi.oregonstate.edu). Endpoints such as mortality, development, malformations and behavior were assessed in the embryonic zebrafish model. Data compression of the 23 individual endpoints provided the numerical representation of overall mortality and morbidity elicited by a particular nanomaterial at a given concentration. Computational analysis performed on 82 nanomaterial datasets has revealed the importance of surface chemistry as a driver for nanomaterial toxicity across material classes. Furthermore, data mining techniques to model the biological effects of nanomaterials were applied to this case study. Results illustrate that individual endpoints have different predictability given the same set of algorithms and cumulatively the combined values can provide significant insight into the potential toxicity associated with nanomaterials for use in hazard ranking.

**W 791 Usefulness of In Vivo Genomics for In Vitro Screening in Nanotoxicity.**

A. Erdely and P. C. Zeidler-Erdely. *NIOSH, Morgantown, WV.*

Literature-based network analysis of in vivo microarray data, which yields biologically relevant molecular networks from the dataset, is becoming an increasingly useful tool to identify nanoparticle-induced signaling. This approach can be used to discover molecules that contribute to endpoint health effects and otherwise unknown mechanisms of action. While animal inhalation exposures may be the most relevant for predicting human health effects of nanomaterials, it is not always feasible because of the vast number of particles being manufactured. Therefore, in vitro high-throughput screening (HTS) is being used to predict their potential toxicity. While HTS may be necessary, in vivo genomic studies still provide useful information for screening broad classes of nanomaterials. Similar to physiological experiments in which three results are expected—increased, decreased, and no change—the question of whether network-based genomics from in vivo studies is useful for in vitro screening can be answered yes, no, and maybe. The output from these studies provides significant molecular detail of an exposure. Advanced analysis can indicate specific transcription factors involved in the response, upstream, and downstream signaling, and also which cell type may be the most affected by a particular nanomaterial. However, there are challenges to converting genomic data from in vivo exposures to in vitro screening. These include responsiveness of the cell type in vitro vs observed in vivo changes, distinguishing temporal effects, and an isolated single cell response in vitro that lacks regulatory effects occurring in vivo. The in vivo genomic findings also have limitations including whether altered molecular networks from studies in rodents are applicable to the human, and therefore applicable to studies utilizing human cell lines. In addition, experimental design (e.g., dosing relevant to human exposure levels) should be evaluated when interpreting genomic analysis from in vivo studies. In summary, genomic analysis from in vivo studies, although not without limitations, can offer insight for HTS.

**W 792 Scientific and Regulatory Advances in Genetic Toxicology Safety Assessment.**

M. Aardema<sup>1</sup> and B. Mahadevan<sup>2</sup>. <sup>1</sup>*Toxicology, BioReliance, Rockville, MD;* <sup>2</sup>*Medical Safety & Surveillance, Abbott Laboratories, Columbus, OH.*

Recent reviews of genotoxicity assay performance, the use of these data in the safety evaluation process, and the development of new assays have led to important advancements in regulatory and scientific recommendations in the area of genetic toxicology. For instance, the International Conference on Harmonization (ICH) has recently finalized guidelines on genetic toxicology testing for drugs. The OECD is updating 15 year-old guidelines for genetic toxicology assays. International validation of new assays like the Comet assay have been completed. Workshops held by international expert groups on new approaches for genetic toxicology assessments highlight the importance of incorporating new approaches in drug safety evaluations. In recent years, significant progress has been made in incorporating quantitative approaches to genotoxicity dose response in order to identify a point of departure for application in risk assessment process. These important initiatives impact the science and practice of genetic toxicology safety assessments globally and across all sectors including drugs, chemicals, and consumer products. This workshop brings together international experts representing key geographies involved in leading these efforts. In an effort to discuss scientific and regulatory advances in genetic toxicology safety assessment, the following key aspects will be addressed in this workshop: (1) US FDA implementation of ICHS2 (R1) guidelines, (2) Latest updates and new approaches in international guidelines for genetic toxicology assays,

(3) Outcomes on the JACVAM Comet validation and OECD guideline development, and (4) New approaches for genotoxicity assessments and guidance on dealing with positive results. In addition, this workshop will provide a forum to discuss the scientific advances that have led to the latest regulatory guideline changes, and their implementation.

### **W 793 US FDA Implementation of the ICH S2(R1) Guideline.**

M. W. Powley. *CDER, US FDA, Silver Spring, MD.*

The genetic toxicology testing paradigm to support drug development was recently updated in ICH S2(R1) "Guidance on Genotoxicity Testing and Data Interpretation for Pharmaceuticals Intended for Human Use". Although the guideline contained a variety of revisions, the most substantial impact was on the selection and conduct of genetic toxicology assays. Historically, *in vitro* and *in vivo* assays were performed to detect gene mutations as well as structural and numerical chromosome damage. While the revised ICH testing battery addresses these same endpoints, the guideline provides options weighted toward *in vitro* or *in vivo* assessments. Another update was the inclusion of the *in vitro* micronucleus assay and *in vivo* comet assay as potential components of the primary evaluation. Additional changes included a reduced limit dose for *in vitro* mammalian cell assays (i.e., the lower of 1 mM or 0.5 mg/mL) and an emphasis on designing studies to evaluate multiple endpoints. Ultimately, the revisions were intended to improve performance characteristics of the genetic toxicology testing battery, provide options to Sponsors of drug development, and maintain patient safety while preventing unnecessary delays in developing drugs.

As ICH S2(R1) was adopted in November 2011, regulatory agencies and Sponsors are just beginning to gain experience with the guideline. This presentation will briefly review the guideline and discuss implementation by the U.S. Food and Drug Administration's Center for Drug Evaluation and Research. Emphasis will be placed on key factors considered in regulatory decision making and highlighted by a discussion of case studies where appropriate.

### **W 794 New Approaches in International Guidelines for Genetic Toxicology Assays: Latest Updates on OECD Guidelines.**

V. Thybaud<sup>1</sup>, J. van Benthem<sup>2</sup>, N. Delrue<sup>3</sup>, G. Douglas<sup>4</sup>, E. Lorge<sup>5</sup>, M. M. Moore<sup>6</sup>, R. Schoeny<sup>7</sup> and T. Singer<sup>4</sup>. <sup>1</sup>*Drug Disposition, Preclinical Safety and Animal Research, Sanofi, Vitry-sur-Seine, France;* <sup>2</sup>*National Institute for Public Health and the Environment (RIVM), Bilthoven, Netherlands;* <sup>3</sup>*Organization for Economic Co-operation and Development (OECD), Paris, France;* <sup>4</sup>*Health Canada, Ottawa, ON, Canada;* <sup>5</sup>*Servier Group, Orleans-Gidy, France;* <sup>6</sup>*National Center for Toxicological Research, US FDA, Jefferson, AZ;* <sup>7</sup>*Office of Research and Development, US EPA, Washington DC.*

In March 2010, the 22nd meeting of the Working Group of National Coordinators of the OECD Test Guidelines Programme (WNT) approved a project for updating the Test Guidelines on genotoxicity, with Canada, the Netherlands, France and the USA identified as lead countries for this work. An Expert Working Group (EWG) comprised of international experts was established and has since met twice. The EWG has recommended the deletion of several Test Guidelines, including the assays conducted in yeast and *Drosophila*. The EWG is currently working on revisions to the *in vitro* Test Guidelines for the micronucleus test (TG487), chromosomal aberration test (TG473) and gene mutation test (TG476), as well as the *in vivo* assays for the mammalian erythrocyte micronucleus test (TG474), the mammalian bone marrow chromosomal aberration test (TG475), the dominant lethal test (TG478) and the spermatogonial chromosomal aberration assay (TG483). A new guideline dedicated to the thymidine kinase locus is also under development. In addition, an update has been initiated of the Introduction Document to the genetic toxicology test guidelines, which is intended to provide succinct and useful guidance to guideline users. The purpose of the presentation at the SOT meeting will be to provide information on the status of the revision process and its main accomplishments to date. The opinions in this abstract are those of the authors and do not represent the policies of the U.S. EPA and FDA.

### **W 795 JACVAM Comet Validation and OECD Guideline.**

M. Hayashi. *Public Interest Incorporated Foundation, BioSafety Research Center, Shiobinden, Iwata, Japan.*

The *in vivo* rodent alkaline comet assay is used world-wide to detect genotoxicity of chemicals. The assay, however, has not been formally evaluated for its reliability and relevance. Thus, the Japanese Center for the Validation of Alternative Methods

(JACVAM) has organized with ECVAM, ICCVAM and NICEATM. This validation study has been also supported by JEMS/MMS and the consultation team including statisticians and specialists for the comet assay. We had the kick-off meeting for this trial in 2006. We have studied on the protocol optimization, intra- and inter-laboratory reproducibility before starting the predictive capability as the 4th phase. In the 4th phase- 1st step validation study, the purpose was to examine the extent of reproducibility and variability of assay results among labs using coded test chemicals and the positive control EMS, when experiments were conducted in accordance with the Comet assay protocol-version 14. In review of the data, Validation Management Team (VMT) confirmed the reproducibility and variability of assay results among laboratories. Thus the VMT decided to move on to the 4th phase- 2nd step validation study with an expanded set of test chemicals in accordance with the Comet assay protocol-version 14.2. The purpose of the 2nd step is to investigate the predictive capability of the assay against carcinogenicity of test chemicals. In the 2nd step, we selected 40 test chemicals, which include different characteristics in chemical classes including: Genotoxic carcinogen, Genotoxic non-carcinogen, Non-genotoxic carcinogen, and Non-carcinogen. Each test chemical was examined in one lab, because reproducibility was robustly confirmed in the 1st step validation study. We will disclose all data shortly but up to now VMT satisfied the outcomes. We are finalizing the validation report of our whole trial and we are also preparing the Comet Assay Atlas to guide how to select nuclei to be analyzed. Now, we are on the line of OECD TG through the peer review of our validation report and we have started to draft test guideline on *in vivo* comet assay.

### **W 796 New Approaches for Genotoxicity Assessment and Guidance on Dealing with Positive Results.**

B. Gollapudi, V. Thybaud and J. Kim. *ILSI-HESI IVGT Project Committee, Washington DC.*

Exposure to mutagens can lead to adverse health consequences such as cancer and genetic diseases. A battery of short-term tests has been in use for decades to identify potential mutagenic agents. However, the relevance of findings from these assays in predicting human risk continues to be a subject of discussion, centering around three major topics on how to 1) improve the existing assays, 2) integrate emerging technologies, and 3) deal with positive findings. An international initiative consisting of experts from academia, industry and the government has been addressing these issues to enable more accurate assessment of human risk from exposure to mutagenic agents. In the area of improving the existing *in vitro* assays, the experts have been examining the choice of cell lines (e.g., human vs. rodents; p53 deficient vs. competent) and the metabolic activation systems (human vs. rodent) in order to make recommendations for future testing protocols. New technologies being considered as potential replacements and/or complements of the standard testing battery include the application of stem cells, 3-D skin/ liver tissues, humanized animal models, high throughput assays (Tox21), incorporation of biomarkers of epigenetic changes with potential transgenerational significance, and the utilization of non-invasive imaging technologies to probe into time/age-related changes in the same animal with parallel anatomical and functional assessments. Results from the genotoxicity assays have traditionally been interpreted in a qualitative manner without analysis of the dose-response relationships. An expert group examined several quantitative approaches to the analysis of the dose-response data to identify a point of departure (POD) that could be combined with mode of action analysis to determine whether exposure(s) below a particular level (i.e., POD corrected by safety and uncertainty factors) constitute a significant risk for humans. These, along with other ongoing national and international initiatives are paving the way for a paradigm shift in the field of genetic toxicology.

### **PL 797 Early Markers for Screening Workers Exposed to Nephrotoxic Chemicals.**

F. M. Merwally and A. ElSafty. *Environmental & Occupational Medicine Department, National Research Center, Giza, Egypt.*

Routine renal function tests are insensitive for detection of subclinical renal impairment. A marker of early renal affection is needed to be used for screening of workers at risk. In this study the activity of the urinary N—acetyl-B-D-glucosaminidase (NAG) was measured to detect early renal changes in workers exposed to nephrotoxic chemicals. The efficacy of NAG was also compared with that of urinary B2-microglobulin. The studied groups included 50 chemical laboratory workers exposed to aliphatic hydrocarbon solvents, 40 car painters exposed to aromatic hydrocarbon solvents, 36 plumbers exposed mostly to lead fumes and a control group of 36 clerks, matched the exposed groups in age, sex, smoking habits and socioeconomic status.

Approval of the Medical Research Ethics Committee at the National Research Center and Consent of all participants in the study were obtained. Exposure indices included lifetime hydrocarbon exposure score (HES), Lead in blood (Ug/dL), and lifetime exposure score for lead (LES-Pb).

Levels of urinary NAG differed significantly in all groups compared to controls. Unlike B2-microglobulin, NAG levels also expressed a strong and consistent correlation with cumulative exposure indices (HES&LES-Pb). Furthermore, an exposure-effect relationship existed between NAG and HES in solvent-exposed normotensive subjects. Values of NAG were higher in solvent-exposed hypertensives than normotensives. These results support the use of urinary NAG in the periodic screening of workers at risk, especially hypertensives and those with renal disease.

## PL 798 Is Indoor Exposure to DEHP a Health Risk?

A. Gotti<sup>1</sup>, D. A. Sarigiannis<sup>1,2</sup> and S. P. Karakitsios<sup>1,2</sup>. <sup>1</sup>Chemical Engineering, Aristotle University of Thessaloniki, Thessaloniki, Greece; <sup>2</sup>Chemical Process and Energy Resources Institute, Centre for Research and Technology Hellas, Thessaloniki, Greece.

The study describes a mechanistic approach for assessing the timecourse of the source-to-dose exposure to DEHP. The overall modelling framework was built on asclxtreme and consists of:

- Multiphase indoor air quality model, for estimating DEHP concentrations in the gas, particle and dust phase starting from gaseous emissions of products containing DEHP.

- Exposure assessment model that incorporates all possible exposure pathways and routes (inhalation of DEHP, skin exposure through dust rubbing off, non-dietary oral exposure through dust ingestion).

- Internal dose model, for the assessment of DEHP and its 3 major metabolites (MEHP, 5-OH MEHP and 5oxo-MEHP) in human tissues and urine through a multi-compartmental PBPK model.

- Uncertainty/variability analysis tool across all stages of the assessment.

Under a typical scenario in a common residential dwelling (surface area of 270 m<sup>2</sup> and air exchange rate of 0.5hr<sup>-1</sup>) characterized by DEHP gaseous emissions of 200 µg/h (vinyl flooring and other plastic materials), the concentrations of DEHP in the gaseous, particles and dust phase are equal to 1.5 µg/m<sup>3</sup>, 21 µg/m<sup>3</sup> and 4400 µg/g settled dust. Overall daily intake varies between 0.2 to 10 µg/kg-bw, depending on the exposure scenarios considered. The latter are age-dependent: adults are exposed mostly through inhalation and infants through non-dietary ingestion. For a common repeated aggregate exposure scenario of 2 µg/kg-bw, the DEHP internal dose in venous blood and in adipose tissue (where bioaccumulation is clearly observed) reach a quasi-state equilibrium of 0.07 and 0.4 µg/L respectively. The expected urinary concentrations of MEHP, 5-OH MEHP and 5oxo-MEHP are 3.1, 16 and 8 µg/gCr respectively. These findings are in good accordance to existing biomonitoring data from NHANES. They are also one order of magnitude below the Biomonitoring Equivalent value of 660 µg/gCr for the sum of all DEHP metabolites measured in urine showing that DEHP concentrations in dwellings does not pose any significant risk.

## PL 799 Identifying the Sources of Uncertainty in the Process of Reconstructing Exposures to Carbaryl Using Exposure-to-Dose Modeling.

K. Holm<sup>1</sup>, R. McDougall<sup>2</sup>, M. Yoon<sup>3</sup>, B. Young<sup>4</sup>, H. J. Clewell<sup>3</sup>, R. Tornero-Velez<sup>1</sup>, R. Goldsmith<sup>1</sup>, D. T. Chang<sup>1</sup>, C. M. Grulke<sup>1</sup>, M. B. Phillips<sup>1</sup>, C. C. Dary<sup>5</sup> and C. Tan<sup>1</sup>. <sup>1</sup>US EPA ORD NERL, Research Triangle Park, NC; <sup>2</sup>The AEgis Technologies Group, Oshawa, ON, Canada; <sup>3</sup>The Hamner Institute, Research Triangle Park, NC; <sup>4</sup>Bayer CropScience, Research Triangle Park, NC; <sup>5</sup>US EPA ORD NERL, Las Vegas, NV.

"Exposure reconstruction" is a process for estimating distributions of exposures that are consistent with observed biomarker levels, and comparable to risk-based guidance values. The research identified uncertainties in reconstructed carbaryl exposure estimates stemming from data gaps. Sources of uncertainty were identified by evaluating exposure reconstruction results in a simulated population for which we know the exposure level. The "Cumulative and Aggregate Risk Evaluation System" (CARES) exposure model was used to generate time-concentration profiles for 500 virtual individuals exposed to carbaryl in food and drinking water for 365 days. Time-concentrations profiles were the inputs for a human physiologically based pharmacokinetic (PBPK) model for carbaryl, and biomarker (metabolite 1-naphthol) concentrations in spot urine sample were simulated. Three mathematical techniques (namely, Exposure Conversion Factor, Discretized Bayesian, and Markov Chain Monte Carlo (MCMC)) were used to reconstruct mean daily carbaryl intake for the virtual population given the distribution of spot biomarker levels. We found that MCMC was the most precise method. Using MCMC for exposure reconstruction, we found that MCMC iterations did not converge to an

exposure distribution if either the PBPK parameters or the urine flow rate were varied. Variation in the time between exposure events and spot sampling also contributed to the uncertainty in the reconstructed exposure. We recommend measuring urine flow rate, obtaining accurate estimates of PBPK model parameters, and monitoring time between exposure events and sample collection for improving reconstructed exposure estimates for rapidly metabolized compounds such as carbaryl.

[This abstract has been cleared by the US-EPA but solely expresses the view of the authors]

## PL 800 A Novel Design of Experiments Approach to Assess Biomarker Usage with Experiments Involving PBPK Models.

J. Ivy, M. A. Lyons, A. N. Mayeno and B. Reisfeld. Department of Chemical and Biological Engineering, Colorado State University, Fort Collins, CO.

In exposure assessment, samples from the environment and population are collected and analyzed to estimate the magnitude, frequency, and duration of exposure to an agent. In this and other applications, an appropriate design of experiments is critical to assure the optimal usage of resources and the efficient gathering of data necessary to answer important public health questions. To aid in such designs, physiologically based pharmacokinetic (PBPK) models are increasingly used to help elucidate chemical disposition, identify key biomarkers, and characterize the effects of uncertainty and variability. Although a number of approaches have been used to help optimize the design of experiments based on PBPK models, significant gaps remain in the efficiency and utility of these methods.

Here we describe a new approach in experimental design that can be used to identify quantities useful in exposure assessment experiments, such as maximally-informative biomarkers, types of biospecimen, and sampling times. This method involves the integration of an efficient sampling algorithm and metrics to assess information loss within a Bayesian inference framework containing a PBPK model. These features expand upon the capabilities of existing tools to include hierarchical statistical models and design comparison without random error.

To test the methodology, several models relevant to toxicology were evaluated, including those for styrene, methylmercury, dichloromethane, and chlorpyrifos. Results from these studies showed that the use of information loss as a design metric lead to precise and accurate reconstructions of simulated exposure data. These results also included a characterization and ranking of various biomarker- and exposure-related quantities in terms of their utility in conducting both forward and reverse dosimetry.

We expect that the proposed methodology will be useful in the design of exposure assessment experiments and related studies and will expand the field of Bayesian inference in environmental and human toxicology.

## PL 801 Antioxidants and Oxidative Modification of Biomolecules: Can They Identify a Biomarker of Ozone Oxidative Stress?

M. Kadiiska. NIEHS/NIH, Research Triangle Park, NC.

The effect of ozone exposure on antioxidants and oxidation products of lipids, proteins and DNA in the plasma and urine of rats was studied by the international biomarker of oxidative stress study sponsored by NIEHS/NIH. The goal of this multi-laboratory study was to identify a biomarker of ozone oxidative stress and to assess whether inconsistent results often found in the field of ozone oxidative stress might be due to a lack of comparability of the available methods where various oxidative products are measured as biomarkers. The time and dose-dependent effects of ozone exposure of rats on plasma and urine lipid hydroperoxides, TBARS, malondialdehyde, isoprostanes, protein carbonyls, methionine sulfoxidation, various tyrosine oxidation products, and DNA changes were investigated with different techniques. Effects of ozone on ascorbic acid, tocopherols, coenzyme Q, glutathione and uric acid were measured to determine if the oxidative effects of ozone would result in decreases of antioxidants in blood plasma and bronchoalveolar lavage fluid as expected. Generally, antioxidants were not changed or showed only high-dose and/or single time point. Ozone exposure did not cause statistically significant differences in plasma concentration products of lipid peroxidation or protein and DNA oxidation in a time- and dose-dependent pattern. However, urinary concentrations of isoprostanes measured with an immunoassay were increased by two different doses of ozone 8 h, 56 h and 70 h post-exposure. Since elevation of isoprostanes in urine was consistent at three time points studied, it is concluded that it fulfilled the oxidative stress biomarker criterion of significant effects measured in biological fluid and seen at both doses at more than one time point. Measurements of low molecular weight antioxidants in plasma are not sensitive biomarkers for oxidative damage induced by the ozone and may not be the tool of choice for the assessment of oxidative damage by ozone in vivo.

**PL 802 Enhancing PM Epidemiological Concentration-Response Functions by Incorporating Lung Deposition and Oxidative Potential.**

S. P. Karakitsios<sup>1</sup>, D. A. Sarigiannis<sup>1,2</sup>, V. Kalaitzis<sup>1</sup> and M. Kermenidou<sup>1</sup>.

<sup>1</sup>Chemical Engineering, Aristotle University of Thessaloniki, Thessaloniki, Greece;

<sup>2</sup>Chemical Process and Energy Resources Institute, Centre for Research and Technology Hellas, Thessaloniki, Greece.

Despite the fact that well documented associations have been established between urban air PM and mortality/morbidity, incorporating internal exposure and toxicity metrics would be expected to significantly improve risk assessment and management.

Thus, existing concentration response functions were modified taking into account the fraction of particles deposited across the respiratory tract (using the MPPD lung deposition model) and the relevance to the corresponding health endpoint. The latter also depends on the actual size distribution for a given PM mass concentration, which is better described by the particle number count (PNC). Finally, the oxidative potential of particles of different size was also taken into account to derive revised exposure-response functions.

To investigate the feasibility of using this approach an extensive measurement campaign was carried out in a large Metropolitan area. PM size and number distributions were recorded in four sites. PM<sub>10</sub>, PM<sub>2.5</sub> and PM<sub>1</sub> samples were analyzed for oxidative potential by measuring Reactive Oxygen Species (ROS) using the DTT protocol. The results showed that the fraction of ultra-fine and fine particles is higher in the city center than in the suburbs. The same is true for oxidative potential especially for the smaller particles. Thus, the actual exposure for endpoints related to lower respiratory tract deposition and possibly translocation within the systemic circulation (e.g. cardiovascular disease, adverse pregnancy outcomes) might rise to up to 4 times higher to the one estimated by the respective differences in mass concentration. Besides their implications for spatial epidemiology, our results show that future epidemiological studies would be greatly improved by incorporating evidence based on toxicity metrics, resulting in more robust associations between ambient air PM exposure and ill-health.

**PL 803 Continuous, Near Real-Time Toxicological Screening Using an Autonomously Bioluminescent Human Cell Line: A Transitory Preclinical Imaging Approach.**

D. Close<sup>1</sup>, T. Xu<sup>2</sup>, J. Webb<sup>2</sup>, S. Ripp<sup>1</sup> and G. Saylor<sup>1</sup>. <sup>1</sup>490 BioTech Inc., Knoxville, TN; <sup>2</sup>The University of Tennessee, Knoxville, TN.

Continuous toxicity monitoring using human cell-based bioreporters can report on the bioavailability and efficacy of toxic substances but is logistically challenging because of the cells' relatively high autofluorescent background or the expense and/or sample destruction required to perform bioluminescent substrate (i.e., luciferin) addition. To facilitate this process, we have synthetically optimized the bacterial luciferase gene cassette to function autonomously in human cells without the need for external substrate addition. A proof-in-principle demonstration using human kidney cells (HEK293) revealed that bioluminescent output declined in response to challenge with the DNA damaging antibiotic Zeocin in a dose response fashion. This response was similar to that displayed using commercially available firefly luciferase reporter assays, but allowed for repeated monitoring of the same samples, leading to a lower overall cost and increased data acquisition potential. Similarly, autobioluminescent reporter cells were designed using a tetracycline activated promoter and were demonstrated to be capable of autonomously initiating a bioluminescent response in reaction to treatment with the antibiotic doxycycline within 2.5 hours at a concentration of 100 ng/ml. The resultant bioluminescent signal was comparable to existing firefly luciferase-based reporter systems at  $1.33 (\pm 0.1) \times 10^7$  photons/second and was significantly greater than uninduced background ( $p < 0.01$ ). Additionally, we have validated the imaging capabilities of these autobioluminescent cells in a mouse model, demonstrating that the same system can be utilized for both high throughput culture based testing and low throughput animal studies. This approach therefore provides a route for the direct comparison of results as toxicological investigations transition across multiple levels of complexity.

**PL 804 Provisional Biomonitoring Equivalents for a Screening Level Evaluation of Urinary 3-Phenoxybenzoic Acid Concentrations in a Risk Assessment Context.**

L. Aylward<sup>1</sup>, S. M. Hays<sup>2</sup>, K. Irwin<sup>3</sup>, A. St-Amand<sup>3</sup> and A. Nong<sup>3</sup>. <sup>1</sup>Summit Toxicology, LLP, Falls Church, VA; <sup>2</sup>Summit Toxicology, LLP, Allenspark, CO; <sup>3</sup>Health Canada, Ottawa, ON, Canada.

3-phenoxybenzoic acid (3-PBA) is a common metabolite of a number of commonly-used pyrethroid pesticides of differing structures and relative potency and also exists as a residue in foods resulting from environmental degradation of parent

pyrethroid compounds. Thus, 3-PBA in urine cannot be used as a specific biomarker of exposure to specific pyrethroid compounds. However, an approach derived from the use of Biomonitoring Equivalents (BE), which are estimates of steady-state biomarker concentrations consistent with exposure guidance values, can be used in an assessment of nine pyrethroid compounds in order to estimate a conservative initial screening value for a tiered assessment of population data on 3-PBA in urine. The most recent USEPA reference doses (RfDs) for these pyrethroids were identified. An average urinary excretion fraction (FUE) for 3-PBA was estimated from four pyrethroid compounds with human excretion fraction data and then applied to all nine parent compounds. Estimated steady-state urinary 3-PBA concentrations associated with the RfD for each of the nine compounds ranged from 6 ug/L for cyhalothrin to 1,875 ug/L for permethrin. The lower end of this range can be used as a highly conservative screening value for assessment of population urinary 3-PBA data through an implicit assumption that all exposures leading to the observed 3-PBA were to the most potent parent compound and no direct exposure to 3-PBA has occurred. If population data do not exceed this level, it is unlikely that cumulative exposures to multiple pyrethroids are exceeding the RfD equivalent for the mixture. If population data do exceed this level, more detailed assessment and weighting of individual pyrethroid provisional BE values can be considered.

**PL 805 Beyond Biological Equivalents to Biologically Effective Dose.**

D. A. Sarigiannis<sup>1,2</sup>, S. P. Karakitsios<sup>1,2</sup> and A. Gotti<sup>1</sup>. <sup>1</sup>Chemical Engineering, Aristotle University of Thessaloniki, Thessaloniki, Greece; <sup>2</sup>Chemical Process and Energy Resources Institute, Centre for Research and Technology Hellas, Thessaloniki, Greece.

This paper deals with the refinement of the Risk Characterization Ratio (RCR) calculation by employing the enhanced Biomonitoring Equivalences (BEs) – Biologically Effective Dose (BED) concept, using a generic PBTK model. The overall methodology was demonstrated for Bisphenol-A and DEHP.

A generic multi-compartmental two generations (mother-fetus) PBTK model was developed so that it could be adaptable for humans, mice and rat. The model incorporates route and intra-species extrapolations, allowing the direct translation of animal NOAELs into human BEDs and BEs. The model was parameterized for BPA and DEHP based on existing human and rodents toxicokinetic data.

To estimate the BEs values, we estimated the BED for rodents corresponding to the steady-state concentration of orally administered doses as described in the respective guideline studies (5 mg/kg\_bw/day in mice for BPA and 592 mg/kg\_bw/day in Sprague-Dawley Rat for DEHP) from where the respective NOAELs were derived. The corresponding BED derived for mice (BPA) and rat (DEHP) respectively, were then translated by reverse modeling into human external exposure doses. Lastly, the corresponding BEs were derived by running the human parameterized PBTK models.

The direct extrapolation of observed NOAELs into human urine BEs through BEDs, resulted in higher values than the ones derived based on using human equivalent NOAELs and simple pharmacokinetic considerations. This comes as result of physiology-dependent differences in clearance and entero-hepatic recirculation between rodents and humans. In addition inter-individual variability is explicitly addressed via this approach. Thus, translating in vivo testing results into equivalent human exposure regimes and expected biomonitoring values is facilitated; uncertainties are minimized and unnecessary conservatism in population exposure/risk characterization is avoided.

**PL 806 Liver Effects in CD1 Mice Prenatally-Exposed to Low Doses of Perfluorooctanoic Acid (PFOA): Novel Modes of Action.**

S. E. Fenton<sup>1</sup>, A. J. Filgo<sup>1,4</sup>, C. A. Cummings<sup>5</sup>, M. Hoenerhoff<sup>2</sup>, D. Malarkey<sup>2</sup> and E. M. Quist<sup>1,2,3</sup>. <sup>1</sup>NTP Labs, DNTP, NIEHS, Research Triangle Park, NC; <sup>2</sup>Cellular and Molecular Pathology Branch, NIEHS, Research Triangle Park, NC; <sup>3</sup>Comparative Biomedical Sciences, College of Veterinary Medicine, North Carolina State University Raleigh, NC; <sup>4</sup>Curriculum in Toxicology, University of North Carolina at Chapel Hill, Chapel Hill, NC; <sup>5</sup>Experimental Pathology Labs, Inc, Research Triangle Park, NC.

Perfluorooctanoic acid (PFOA) is a perfluoroalkyl acid primarily used as an industrial surfactant. It persists in the environment and has been linked to potentially toxic and/or carcinogenic effects in animals and people. As a known activator of peroxisome proliferator-activated receptors (PPAR), PFOA can cause alterations that lead to defects in fatty acid oxidation, lipid transport, and inflammation. Here, CD1 mice were orally gavaged with 0, 0.01, 0.1, 0.3 and 1 mg PFOA/kg body weight from gestation days (GD) 0 through 17. On postnatal day (PND) 21, histopathologic changes in the liver of offspring included hepatocellular hypertrophy and periportal inflammation that increased in severity by PND91 in an apparent dose-dependant response. In an earlier study, similarly exposed wildtype and PPARα KO SV129 and CD1 mice also developed significant hepatocellular hypertrophy by 72 weeks (high-dose groups). A significant dose dependent increase in

bile duct hyperplasia and hepatocellular hypertrophy in the PPAR $\alpha$  KO mice suggest a mechanism of hypertrophy independent of that previously reported for PPAR $\alpha$ -induced peroxisome proliferation in the current literature. Transmission electron microscopy (TEM) of selected liver sections from PND91 mice revealed PFOA-induced cellular damage and mitochondrial abnormalities with no evidence of peroxisome proliferation. These mitochondrial changes may represent PFOA-induced alterations in the beta-oxidation pathway regulated by PPAR $\alpha$  and/or may represent an earlier change that proceeds, or is independent of, PPAR $\alpha$ -induced peroxisome proliferation. This abstract does not necessarily reflect NIEHS policy.

## PL 807 Dose-Dependent Incidence of Murine Hepatic Tumors following Perinatal Bisphenol A Exposure.

C. Weinhouse<sup>1</sup>, O. S. Anderson<sup>1</sup>, I. L. Bergin<sup>2</sup> and D. Dolinoy<sup>1</sup>. <sup>1</sup>*Environmental Health Sciences, University of Michigan, Ann Arbor, MI*; <sup>2</sup>*Unit for Laboratory Animal Medicine, University of Michigan, Ann Arbor, MI*.

Epidemiological and animal studies have now critically established that environmental exposures during early embryonic development have the ability to influence adverse health outcomes in adulthood. This study evaluated adult health outcomes of perinatal exposure to the endocrine disruptor bisphenol A (BPA) in a mouse model. Prior studies have linked BPA exposure with precancerous lesions in mammary and prostate glands, and uterus, as well as with hepatic dysfunction. We exposed isogenic mice (n=69) perinatally through the maternal diet to 3 physiologically relevant doses of BPA (50 ng, 50  $\mu$ g, or 50 mg of BPA per kg diet) or a control diet. 23% (16/69) of 10-month offspring presented with hepatic tumors (hepatocellular carcinoma or hepatic adenoma), with a risk ratio of 7.15 for the 50 mg group (p=0.0280) and significant dose-response on Cochran-Armitage test of trend (p=0.0295). Importantly, observed early disease onset and lack of characteristic sexual dimorphism in tumor incidence support a non-classical etiology. Notably, the 1982 National Toxicology Program chronic feed study finding of multinucleated hepatocytes (MH) was replicated here. MH were present in 7 animals, exclusively in low-dose groups (n=4 in 50 ng group, n=3 in 50  $\mu$ g group); these abnormal cells may be associated with increased hepatocyte proliferation. The significance of this study includes: (1) these data represent the first report of frank tumors, in addition to precancerous lesions, in any organ following perinatal or adult BPA exposure; (2) these data represent the first report of neoplasms in a non-reproductive estrogen-target organ; (3) this study underscores the critical importance of exposure timing; and (4) this study implicates an environmentally ubiquitous chemical in development of hepatocellular carcinoma in mice, with potential implications for human disease. Funding: ES017524 and DK089503.

## PL 808 Liver Hypertrophy Is Not a Key Event in Constitutive Androstane Receptor (CAR)-Mediated Liver Tumor Development in Mice Treated with Triazoles.

K. Tamura<sup>1</sup>, K. Inoue<sup>1</sup>, M. Takahashi<sup>1</sup>, S. Matsuo<sup>1</sup>, K. Irie<sup>1</sup>, Y. Kodama<sup>2</sup>, S. Ozawa<sup>3</sup> and M. Yoshida<sup>1</sup>. <sup>1</sup>*Division Pathology, National Institute Health Sciences, Setagaya-ku, Tokyo, Japan*; <sup>2</sup>*Division Toxicology National Institute Health Sciences, Setagaya-ku, Tokyo, Japan*; <sup>3</sup>*School Pharmacology, Iwate Medicine University, Morioka, Iwate, Japan*.

Liver hypertrophy is accepted to be a key event in CAR-mediated liver tumor development in rodents. Many triazoles (TRIs) have been reported to induce hypertrophy and tumors in the livers of rodents. In this study, we clarified the involvement of CAR in TRI-induced liver hypertrophy and tumor development using CAR knockout mice (CARKO). Seven-week-old male CARKO and wild-type mice (WT) were treated with cyproconazole (Cypro), tebuconazole (Teb), or fluconazole (Flu) for 27 weeks at 200, 1500, or 200 ppm, respectively, in the diet. Tumors were initiated by a single i.p. injection of diethylnitrosamine (DEN) before the treatment. At interim kills at 4 (without DEN) and 13 weeks (with DEN), increases in liver weight and severe centrilobular/diffuse hepatocellular hypertrophy were detected in WT treated with TRIs. In CARKO, Teb induced severe liver hypertrophy, whereas Cypro and Flu induced very mild hypertrophy compared to that in corresponding WT. After 27 weeks of treatment, Cypro significantly increased eosinophilic altered foci/adenomas in WT. In CARKO, both types of lesions were clearly reduced compared to WT, but the multiplicity of foci was marginally higher than in the control. Teb increased eosinophilic foci in WT, but significantly depressed formation of these foci in CARKO. Flu and Teb had similar profiles in both genotypes. Basophilic foci/adenomas were also reduced in CARKO compared to WT for all TRI groups, but the effects were weak compared to changes in eosinophilic ones. Our present study indicated that CAR was the major mediator involved in liver hypertrophy for Cypro and Flu, but another pathway also existed. In particular, CAR was not involved in Teb-induced hypertrophy. Meanwhile, the involvement of CAR was crucial for TRI-induced tumors. These results suggested that liver hypertrophy was not a key event in CAR-mediated liver tumor development in mice.

## PL 809 Fluopyram: Mechanistic Investigations to Elucidate the MoA for Liver Tumor Formation in the Rat.

H. Tinwell<sup>1</sup>, D. Rouquié<sup>1</sup>, O. Blanck<sup>1</sup>, P. Maliver<sup>1</sup>, F. Schorsch<sup>1</sup>, S. Wason<sup>1</sup>, D. Geter<sup>2</sup> and R. Bars<sup>1</sup>. <sup>1</sup>*Bayer CropScience, Sophia Antipolis, France*; <sup>2</sup>*Bayer CropScience, Research Triangle Park, NC*.

Fluopyram, a broad spectrum fungicide, caused hepatomegaly, liver hypertrophy and resulted in an increased incidence of hepatocellular carcinomas and adenomas in female Wistar rats following chronic exposure (24 months) at the highest dose evaluated (1500 ppm equating to 89 mg/kg/d) in the guideline carcinogenicity study. Mechanistic studies were subsequently conducted in the female rat to identify the initial key events responsible for the tumor formation and to establish thresholds for each of the early hepatic changes. Studies showed increased expression of constitutive androstane receptor (CAR) and pregnane X receptor (PXR) inducible genes from as early as 3 days of treatment. Further confirmation of CAR/PXR activation was provided by increased activity of specific Phase I enzymes (PROD and BROD respectively). Increased hepatocellular proliferation (measured by Ki67) was observed, particularly in the centrilobular region, starting from 3 days of treatment. Cell proliferation was also increased after 7 and 28 days of treatment but to a lesser extent than that following a 3 day exposure. In these studies, dose responses and clear thresholds were established for gene expression, enzyme activity and cell proliferation. Furthermore, these early hepatic changes were shown to be reversible following compound withdrawal. Other modes of action (MoAs) for liver tumor formation such as genotoxicity or peroxisome proliferation were not observed. In conclusion, fluopyram is a threshold carcinogen and the resultant hepatocellular carcinomas in the female rat are due to hepatocellular proliferation mediated by CAR/PXR activation. It is unlikely that fluopyram would induce liver tumors in humans as the CAR/PXR induced hyperplastic response has been shown to be absent in human hepatocytes exposed to other known rodent hepatocarcinogens with the same MoA.

## PL 810 Mechanistic Investigation of Technical Toxaphene (TT)-Induced Mouse Liver Tumors.

Z. Wang<sup>1</sup>, B. H. Neal<sup>2</sup>, J. C. Lamb<sup>2</sup> and J. E. Klaunig<sup>1</sup>. <sup>1</sup>*Indiana University, Bloomington, IN*; <sup>2</sup>*Exponent Inc, Alexandria, VA*.

Chronic exposure to technical toxaphene (TT) resulted in an increase in liver tumors in B6C3F1 mice, with male mice showing higher response. TT appears to act on the tumor promotion process. The current study was performed to further investigate the mode of action (MOA) of TT inducing mouse liver tumors. In a preliminary dose range-finding study, mice were given TT (0, 10, 40, 80, 160 and 320 ppm) in diet continuously for two weeks. A decrease in body weight gain compared to control was observed in mice treated with 320 ppm TT in diet (3.27 g vs. -1.22 g). Body weight gains were also significantly decreased in the 80 ppm and 160 ppm treatment groups. A significant dose dependent increase in relative liver weight was observed in mice treated with 0, 40, 80, 160 and 320 ppm TT diet (4.81, 5.32, 6.05, 6.55 and 7.43 g respectively). A similar trend was observed in the liver weight. A dose dependent increase in liver centrilobular hypertrophy was seen in mice treated with 80, 160 and 320 ppm TT; this was not observed at the 10 and 40 ppm doses. Similarly, a significant dose dependent increase in hepatocyte DNA synthesis (BrdU incorporation) was seen in mice treated with 40 ppm, 80 ppm, 160 ppm and 320 ppm, compared with the untreated controls with labeling indices of 3.28, 6.34, 11.10, and 15.61 respectively, compared with 1.06 in the control group). The increase in labeling index showed agreement with the absolute and relative liver weight results. Based on findings of the range-finding study, a second study using 0, 3, 32 and 320 ppm TT diet was initiated to define the MOA for the TT mouse liver tumorigenic effects. Using phenobarbital as a positive control, the well-established hepatic tumor modes of action are being investigated including: cytotoxicity; receptor activation (PPAR $\alpha$ , CAR, estrogen, and AhR) and oxidative stress in TT treated B6C3F1 mice.

## PL 811 In Vitro Cross-Species Comparative Analysis of Pharmacokinetic and Molecular Responses Mediated by a Labile AhR Activator.

L. A. Murphy<sup>1</sup>, D. L. Rick<sup>1</sup>, L. McClymont<sup>1</sup>, J. McFadden<sup>1</sup>, M. Bartels<sup>1</sup>, N. J. Stagg<sup>2</sup>, R. Billington<sup>2</sup>, R. J. Rasoulpour<sup>1</sup> and D. L. Eisenbrandt<sup>2</sup>. <sup>1</sup>*The Dow Chemical Company, Midland, MI*; <sup>2</sup>*Dow AgroSciences, LLC, Indianapolis, IN*.

A novel herbicide in development, XDE-729 methyl, induces rodent liver effects through an aryl hydrocarbon receptor (AhR)-mediated mode-of-action (MoA). To further characterize species differences in these effects, mouse, rat, and human *in vitro* assays were used to elucidate differences in 1) AhR activation, 2) hydrolysis

rates to non-AhR activator metabolites, and 3) systemic exposure as predicted by a physiologically based pharmacokinetic (PBPK) model. AhR transactivation and binding assays indicated that XDE-729 methyl exhibits weak AhR agonism in mouse cells, no AhR agonism in human cells, and binds weakly to the rat AhR ligand and binding domain. Fresh hepatocytes from CD-1 mouse, Sprague Dawley rat, and human (6 donor livers) were used to compare XDE-729 methyl mediated CYP1A1 induction, a sensitive biomarker for AhR activation. Gene expression analysis indicated that rats are the most sensitive species with regards to XDE-729 methyl mediated CYP1A1 induction with maximal induction at 100  $\mu$ M of 147.7-fold in rat, versus 37.8-fold in mouse, and 2.9, 4.5, 6.2, 8.7, 10.3, and 34-fold in the six human livers. An *in vitro* study to determine hydrolysis rates of XDE-729 methyl to the major metabolite, XDE-729 acid, which does not activate AhR, indicated that: 1) the hydrolysis rate in human liver S9 is faster than rodents; 2) hydrolysis in human synthetic gastric fluid is faster than rodents 3) hydrolysis of XDE-729 methyl is slowest in human whole blood versus rat or mouse. A PBPK model using the *in vitro* hydrolysis rates predicted similar blood and liver levels of XDE-729 methyl in rat and human after XDE-729 methyl dietary exposure. However, the *in vitro* mechanistic data indicate that humans are less sensitive than rats based on faster liver hydrolysis rates of XDE-729 methyl and limited AhR activation; therefore, a margin of exposure risk assessment using the *in vivo* rat toxicity studies is protective of human health.

**PL 812 Developmental Exposure to 2, 3, 7, 8 Tetrachlorodibenzo-*p*-dioxin (TCDD) Affects Leukemogenesis in Adult Tumor Prone Mice by Interacting with the Thymus Expressed Notch1.**

M. D. Laiosa, L. Ahrenhoerster, D. Almagro and P. A. Lakatos. *Zilber School of Public Health, UW-Milwaukee, Milwaukee, WI.*

Reprogramming of progenitor cells during development can have profound impacts on later life disease susceptibility and is dependent on the interaction between genetic susceptibility of the child, the maternal intrauterine environment, and the timing of exposure to potential insults. In particular, developmental exposure to the persistent contaminant TCDD, acting through the aryl hydrocarbon receptor (AHR), is known to cause immunosuppression and is associated with hematological malignancies later in life. For example, at least 50% of all T-cell leukemias are associated with activating mutations in Notch1. Notch1 is a transmembrane receptor required for T-cell lineage commitment in the thymus. Moreover, preliminary data suggest a potential interaction between AHR and Notch1 signal transduction. To test for a possible gene-environment interaction between the AHR and Notch1, we hypothesized that leukemia prone Notch1 transgenic mice would have a more severe disease if exposed to TCDD during development. To test this hypothesis, timed pregnant dams were exposed to 0 to 3  $\mu$ g/Kg TCDD throughout pregnancy. We found that while there was no difference in disease onset, severity or incidence, there was a significant difference in the cell-type of T-cell thymomas that developed in these mice and this difference was observed only in males. Specifically, whereas Notch-TG control mice developed CD4<sup>+</sup> tumors, Notch-TG mice exposed to TCDD in utero developed CD8<sup>+</sup> tumors. This lineage switch in disease phenotype suggests a reprogramming of a hematopoietic precursor or tumor stem cell during development leading to a reversal in the T-lineage choice in the adult life. These data suggest that early life AHR activation has a long-term effect on Notch1-mediated thymocyte lineage choice throughout the life-course. These data have implications for disease susceptibility in vulnerable populations that may possess genetic instability in the Notch locus and/or have been exposed to AHR agonists developmentally.

**PL 813 Critical Evaluation of the Mode of Action of Carcinogenicity for Acrylonitrile.**

J. M. Fritz and A. M. Luke. *ORD/NCEA/IRIS, US EPA, Washington DC.*

Acrylonitrile (AN) is an aliphatic nitrile used as a reagent in industrial processes, and is polymerized into injection-molded plastics used to create pipes, automobile dashboards and children's building blocks. Annually, over 1.5 million tons are produced in the U.S. alone, where AN is regulated by EPA as a hazardous air pollutant. Industrial cohort studies suggest a potential association between AN exposure and increased risk of cancer mortality and experimental evidence demonstrates that acrylonitrile induces tumor formation at multiple sites in rodent species following oral and inhalation exposure. A comprehensive cancer mode of action (MOA) analysis has been conducted and may inform the correspondence between the human and animal datasets. The AN literature was reviewed for evidence pertaining to genotoxicity and other potential MOAs; data were sorted by species, endpoint, and study design, and effects were critically evaluated for consistency, magnitude, specificity, plausibility and coherence. Early effects in relevant adverse

outcome pathways were further assessed for causality, to determine if effects could indicate key events in AN-induced carcinogenesis. Critical analysis of the AN dataset supports potential contributions from multiple MOAs, including genotoxicity. Brain region-specific increases in lipid peroxidation and dose-dependent accumulation of 8-oxodG could support genotoxicity concurrent with oxidative stress *in vivo*, while covalent-binding to proteins and nucleic acids, liver DNA alkylation, leukocyte cell micronuclei formation and dose-dependent induction of forward mutations all support genotoxicity occurring prior to other cellular effects. While data-rich in some areas, other endpoints evaluated in the course of this analysis were data-poor. Some of these data gaps include a comprehensive evaluation of DNA repair and adducts, fixed mutations, and source of AN-induced oxidative species in rodent cancer target tissues. The views expressed are those of the authors and do not necessarily reflect the views or policies of the U.S. EPA.

**PL 814 Long-Term Inhalation Study with Nanomaterials: Pulmonary Effects of Nanoscale CeO<sub>2</sub> and BaSO<sub>4</sub> in a Rat 28-Day Range Finding Study.**

J. Keller<sup>1</sup>, S. Gröters<sup>1</sup>, L. Ma-Hock<sup>1</sup>, V. Strauss<sup>1</sup>, K. Wiench<sup>2</sup>, B. van Ravenzwaay<sup>1</sup> and R. Landsiedel<sup>1</sup>. <sup>1</sup>*Experimental Toxicology and Ecology, BASF SE, Ludwigshafen am Rhein, Germany;* <sup>2</sup>*Product Safety, BASF SE, Ludwigshafen am Rhein, Germany.*

Inhalation exposure has been considered as the major route of concern for nanomaterials. Recent published literature reveals a distinct gap of long-term inhalation studies, especially on industrial relevant poorly soluble bio-persistent particles (PSP), including their carcinogenic potential. Nanoscale CeO<sub>2</sub> and BaSO<sub>4</sub> will be accurately examined in a combined chronic and carcinogenicity inhalation study. Emphasis is placed on the relationship of inflammatory reactions, particle overload and lung tumor formation.

For this purpose, a 28 day range finding study according to the OECD Guideline 412 was performed. Groups of female Wistar rats (5 rats/ group) were whole body exposed to 0.5, 5, 25 mg/m<sup>3</sup> CeO<sub>2</sub> and 50 mg/m<sup>3</sup> BaSO<sub>4</sub> for 28 days. A concurrent control group was exposed to clean air. The exposure concentrations for CeO<sub>2</sub> were selected to achieve lung burden below and above particle overload.

Biological effects were examined immediately after last exposure and in a post-exposure period. Examined endpoints considered bronchoalveolar lavage, hematology and clinical chemistry, gross necropsy, histological examination of the respiratory tract and cell proliferation of the lung as well as systemic genotoxicity in peripheral blood cells.

Increased lung weights in the high dose test group of CeO<sub>2</sub> (25 mg/m<sup>3</sup>) and significant changes in lung lavage parameters (cell cytology, protein and enzyme levels) in the mid (5 mg/m<sup>3</sup>) and high dose test group of CeO<sub>2</sub> are indicative for early treatment-related findings. Subsequent results of particle related biological effects associated with an appropriate particle lung burden of the range finding study will be presented here. The outcome of the 28 day study will serve as basis for concentration selection for the upcoming long-term inhalation study.

**PL 815 Pulmonary Responses in Rats after Inhalation Exposure to Cerium Oxide Nanoparticles Generated by the Harvard Versatile Engineered Nanomaterial Generating System (Venges).**

V. Castranova<sup>1</sup>, M. Barger<sup>1</sup>, W. Goldsmith<sup>1</sup>, D. Frazer<sup>1</sup>, B. Hines<sup>1</sup>, W. McKinney<sup>1</sup>, G. Pyrgiotakis<sup>2</sup>, S. Gass<sup>2</sup>, P. Demokritou<sup>2</sup> and J. Ma<sup>1</sup>. <sup>1</sup>*HELD, NIOSH, Morgantown, WV;* <sup>2</sup>*Harvard University, Boston, MA.*

Recently cerium compounds have been used in a variety of consumer products including semiconductors, UV shields and diesel fuel additives to increase fuel combustion efficiency and decrease diesel soot emissions. Our previous studies have shown that exposure of rats to CeO<sub>2</sub> by intratracheal instillation not only induces sustained pulmonary inflammation, but also lung fibrosis. In the present study, the aerosols of CeO<sub>2</sub> or CeO<sub>2</sub> coated with a nanothin layer of amorphous SiO<sub>2</sub> (aSiO<sub>2</sub>-CeO<sub>2</sub>) were generated by the Harvard VENGES. The aerosols were diluted with air and delivered to a whole body exposure chamber. Male Sprague Dawley rats were exposed to CeO<sub>2</sub> or aSiO<sub>2</sub>-CeO<sub>2</sub> at 2.7 mg/m<sup>3</sup>, 2h/day for 4 days along with air controls. Animals were sacrificed at 1 or 84 days post exposure. Morphometric analysis of the CeO<sub>2</sub> and aSiO<sub>2</sub>-CeO<sub>2</sub> particle cores showed diameters of 12.8 and 19.2 nm, respectively. Mobility diameter modes of 82 and 96 nm were measured for the CeO<sub>2</sub> and aSiO<sub>2</sub>-CeO<sub>2</sub> aerosols aggregates in the breathing zone of the animals. Alveolar macrophages (AM) were obtained by bronchoalveolar lavage (BAL), and alveolar BAL fluids (BALF) were saved for further analysis. At 1 day after CeO<sub>2</sub> exposure, but not aSiO<sub>2</sub>-CeO<sub>2</sub>, significantly induced PMN infiltration and lactate dehydrogenase activity in the BALF. CeO<sub>2</sub> significantly increased collagen

degradation enzymes, matrix metalloproteinases (MMPs)-2 and tissue inhibitor of MMP-1 in the BALF, which may be involved in the modification of extracellular matrix. At 84 days post exposure, none of the particle treatment groups induced lung inflammation, cellular injury or alteration of hydroxyproline content in lung tissues. These results demonstrated that a thin coating of aSiO<sub>2</sub> on CeO<sub>2</sub> protected lungs from CeO<sub>2</sub>-induced acute lung toxicity, suggesting that a thin coating of aSiO<sub>2</sub> may potentially be used to modify other nanoparticle-induced lung toxicity.

## PL 816 Gene Expression Profiling of Human Lung Epithelial Cell Lines Exposed to Manufactured CoO and CeO<sub>2</sub> Nanoparticles.

I. Nelissen<sup>1</sup>, S. Verstraelen<sup>1</sup>, E. Casals<sup>2</sup>, S. Remy<sup>1</sup>, P. De Boever<sup>1</sup>, H. Witters<sup>1</sup> and V. Punters<sup>2</sup>. <sup>1</sup>Flemish Institute for Technological Research (VITO NV), Mol, Belgium; <sup>2</sup>Institut Català de Nanotecnologia (ICN), Barcelona, Spain. Sponsor: P. Hoet.

Exposure to manufactured nanoparticles (NPs) via inhalation can cause adverse human health effects. A transcriptomics study was performed to identify molecules and cellular pathways that are specifically triggered by in vitro exposure of the human bronchial BEAS-2B and alveolar A549 epithelial cell lines to 7-nm CoO and 4-nm CeO<sub>2</sub> NPs. We aimed to investigate whether 1) the same lung cell type responds similarly to the NPs, 2) alveolar vs. bronchial epithelial cells respond differently to the same NP, and 3) immunological processes are influenced. Non-cytotoxic exposure concentrations of monodispersed NPs were used. Statistically significant changes in gene expression as compared to solvent-treated cells (median |fold-change| > 1.5, p < 0.05) were evaluated after 3, 6, 10, and 24 hours.

The kinetics of the cell responses induced by the 2 NPs were similar within, but different between the 2 cell models. BEAS-2B cells were found to be more sensitive for NP toxicity, as they showed a higher total number of differentially expressed transcripts (DET) at a 10-fold lower NP-concentration than A549 cells. Hierarchical biclustering of all DET indicated that the transcriptional responses were quite heterogeneous among the 2 cell types and 2 NPs. Between 1% and 14% DET encoding markers involved in immune system processes were observed in the BEAS-2B and A549 cell lines, resp., with the highest fractions observed in BEAS-2B cells. Most of these genes, i.e. ITGB2, TLR6, PAG1, HLA-DRB3, TIRAP, and HLA-A, are involved in immune signalling or yet unassigned pathways. Nanoparticle exposure mainly induced suppression of immune gene transcription, rather than immune stimulation. The AKT1 gene was identified as a possible generic marker of lung epithelial cell-NP interaction.

Our data suggest that CoO- and CeO<sub>2</sub>-NP give rise to a distinct immunological response in bronchial and alveolar epithelial cells.

## PL 817 Mechanistic Insights into the Toxicity of Multiwalled Carbon Nanotubes and Cerium Dioxide Nanoparticles in Primary Human Bronchial Epithelial Cells.

S. Hussain<sup>1</sup>, R. Snyder<sup>1</sup>, S. M. Anderson<sup>1</sup>, J. D. Marshburn<sup>1</sup>, A. B. Rice<sup>1</sup>, N. J. Walker<sup>2</sup> and S. Garantziotis<sup>1</sup>. <sup>1</sup>Clinical Research Program, NIEHS (NIEHS)/National Institute of Health (NIH), Durham, NC; <sup>2</sup>DNTP, NIEHS, Research Triangle Park, NC.

Cerium dioxide nanoparticles (CeO<sub>2</sub> NPs) and multi-walled carbon nanotubes (MWCNT) are priority materials for urgent risk assessment due to wide spread industrial, consumer product and environmental utilizations. We aimed at deciphering the impact of CeO<sub>2</sub> NPs and MWCNTs on primary human bronchial epithelial cells (BEC) following an ex-vivo exposure. CeO<sub>2</sub> NPs and MWCNT suspensions were thoroughly characterized, including using transmission electron microscopy (TEM), dynamic light scattering (DLS), and zeta potential analysis. Cells were then exposed to nanomaterials for 18 - 24 hours and mechanisms of cell injury were studied. TEM revealed that both CeO<sub>2</sub> NPs and MWCNTs are internalized by bronchial epithelial cells and are found either in vesicles or free in the cytoplasm. CeO<sub>2</sub> NPs fail to elicit a toxic response in BECs at environmentally relevant doses. However, diesel exhaust particles and CeO<sub>2</sub> NPs co-exposure leads to significant increase in cytotoxicity. MWCNT exposure in bronchial epithelial cells leads to a time-dependent decrease in viability, increased reactive oxygen species production, NF-κB (p65)/Rel A phosphorylation and nuclear translocation. Moreover, we observed caspase-1 activation and increased numbers of autophagic vesicles in MWCNT-treated cells as compared to control cells. An increase in p62 levels indicated a blockage of autophagic turnover rather than autophagy induction in these cells which was associated with cytoskeletal alterations induced by MWCNT. In conclusion we demonstrate that nanomaterials exposure leads to

toxic events in primary human bronchial cells. Moreover, we show that doses of CeO<sub>2</sub> NPs and diesel exhaust particles that are innocuous in themselves can result in toxicity when given as a co-exposure.

## PL 818 Inflammatory and Free Radical Generation Characteristics of Nano-Cerium Dioxide.

V. C. Minarchick<sup>1</sup>, D. W. Porter<sup>2</sup>, N. R. Fix<sup>2</sup>, S. S. Leonard<sup>2</sup>, E. M. Sabolsky<sup>3</sup> and T. R. Nurkiewicz<sup>1</sup>. <sup>1</sup>Center for Cardiovascular and Respiratory Sciences, West Virginia University, Morgantown, WV; <sup>2</sup>National Institute for Occupational Safety and Health, Morgantown, WV; <sup>3</sup>Mechanical Engineering, West Virginia University, Morgantown, WV.

Nano-cerium dioxide (CeO<sub>2</sub>) possesses the potential for use in human health by protecting against the deleterious effects of ischemia and radiation. However, the literature is polarized about the effects this compound has *in vivo*. Our laboratory has shown that pulmonary nano-CeO<sub>2</sub> impairs arteriolar reactivity 24 hrs post-exposure. The mechanisms of this impairment are currently unknown but may be linked to the free radical scavenging or inflammatory properties of this nanoparticle. The aims of this study were to: 1) thoroughly assess the physical and chemical characteristics of the nano-CeO<sub>2</sub>, 2) examine the antioxidant potential of nano-CeO<sub>2</sub> via electron spin resonance (ESR), and 3) assess the pulmonary inflammation in Sprague-Dawley rats 24 hrs post-intratracheal nano-CeO<sub>2</sub> instillation. The primary particle size of the nano-CeO<sub>2</sub> was calculated to ~3 nm (via transmission electron microscopy and surface area measurements). Dynamic light scattering determined the agglomerate size (~80 nm) and x-ray photoelectron spectroscopy determined the valence state of the nano-CeO<sub>2</sub>. The ESR measurements indicated that nano-CeO<sub>2</sub> alone did not generate free radicals and in the presence of cells (Raw264.7), nano-CeO<sub>2</sub> quenched the free radicals generated by these cells. Finally, bronchial alveolar lavage from rats instilled with 0, 10, 100 or 400 µg of nano-CeO<sub>2</sub> revealed an increase in polymorphonuclear leukocytes (0.6±0.2, 0.8±0.3, 7.1±0.9, and 10.3±0.9 per 106 cells), and lactate dehydrogenase (90±12, 100±9, 453±33, and 602±32 units/L) but there was no change in albumin. These findings provide evidence that pulmonary inflammation is present after exposure but does not damage to the epithelial/endothelial cellular barrier. Additionally, these nanoparticles are capable of quenching free radicals there by exerting a systemic effect.

NIH-RO1-ES015022 and RC1-ES018274 (TRN), and NSF-1003907 (VCM)

## PL 819 Nanoceria Distribution and Biopersistence in Rats Is Not Consistently Affected by Particle Size, Shape, Dose, or Dosing Schedule.

R. A. Yokel<sup>1,2</sup>, R. C. MacPhail<sup>5</sup>, J. M. Unrine<sup>3</sup>, P. Wu<sup>4</sup> and E. A. Grulke<sup>4</sup>. <sup>1</sup>Pharmaceutical Sciences, University of Kentucky, Lexington, KY; <sup>2</sup>Graduate Center for Toxicology, University of Kentucky, Lexington, KY; <sup>3</sup>Plant and Soil Sciences, University of Kentucky, Lexington, KY; <sup>4</sup>Chemical and Materials Engineering, University of Kentucky, Lexington, KY; <sup>5</sup>Toxicology Assessment Division, US EPA, Research Triangle Park, NC.

Background: Nanoceria is a diesel fuel additive, an abrasive in integrated circuit fabrication, and is being developed as an antioxidant therapeutic. Objectives: Determine the influence of nanoceria size, shape, dose, and dosing schedule on its distribution and biopersistence. Methods: Aqueous dispersions of citrate-stabilized cubic or polyhedral ceria and a ceria nanorod (10 x 40 to 600 nm), synthesized and characterized in-house, were iv infused into rats (single infusion of 5 nm @ 11, 56 or 85 mg/kg, 15 nm @ 70 mg/kg, 30 nm @ 6 or 85 mg/kg, 55 nm @ 50 mg/kg, nanorod @ 20 or 50 mg/kg; and 5 nm @ 11 mg/kg for 5 consecutive days). They were terminated 1 h to 90 days later. Controls received vehicle. Multiple organs were weighed and samples collected from multiple sites and blood for cerium determination. Results: The greatest % of the dose was in the liver, spleen and bone marrow; these levels decreased over time only in liver for the 30 nm ceria @ 6 mg/kg, and increased in spleen and bone marrow over time in several cases. There were no consistently significant differences in the % of the dose in the liver or spleen for the different sizes, shapes, doses, or dosing schedules other than tendencies for more nanorod accumulation in the spleen than the 5 nm polyhedral ceria and more nanorod accumulation in the bone marrow than the 5 or 30 nm ceria. Brain nanoceria was low; little to none was in brain parenchyma. Conclusions: Nanoceria, an insoluble metal oxide, was cleared into mononuclear phagocyte system organs in which it persisted for 90 days. Size, shape, dose, and dosing schedule had little effect on its distribution or persistence, suggesting repeated exposure will likely produce accumulation, perhaps reaching a level shown to be toxic after single high-dose administration. Support: US EPA STAR Grant RD-833772.

**PL 820 Metal Oxide Nanoparticles Alter Spontaneous Activity and Pharmacological Responses in Neuronal Networks Grown on Microelectrode Arrays.**

J. D. Strickland<sup>3,2</sup>, W. R. LeFev<sup>1</sup>, K. Dreher<sup>2</sup> and T. J. Shafer<sup>1</sup>. <sup>1</sup>IISTD, ORD, US EPA, Research Triangle Park, NC; <sup>2</sup>EPHD, ORD, US EPA, Research Triangle Park, NC; <sup>3</sup>North Carolina State University, Raleigh, NC.

The widespread use of engineered nanoparticles (NP) has increased their exposure potential and made it necessary to assess potential impacts on human health. Previous studies indicate that NPs can enter the brain via the olfactory nerve or by crossing the blood-brain barrier; thus, it is essential that their effects on neuronal function be examined. In the present study, 5 CeO<sub>2</sub> (7 to 1288 nm), and 4 TiO<sub>2</sub> (6 to 200 nm) NPs were examined to determine their ability to alter network function in primary cultures of cortical neurons grown on 12 well microelectrode array (MEAs) plates. NPs were dispersed in Neurobasal A medium containing 20% FBS (dispersant). Between days 14 to 21 in vitro, 1 hr of baseline activity was recorded prior to exposure to NPs. Changes in spontaneous mean firing rate (MFR) relative to the dispersant control were assessed 1, 24, and 48 hrs after exposure to NPs (3–50 µg/ml). Following the 48 hr recording, the response to a pharmacological challenge with the GABA<sub>A</sub> antagonist bicuculline (BIC; 25 µM) was assessed. In all, 3 of 5 CeO<sub>2</sub>, and 2 of 4 TiO<sub>2</sub> NPs decreased MFR below threshold following 1 hr exposure. All 4 TiO<sub>2</sub> NPs altered MFR beyond threshold at 24 hrs. At 48 hr, the MFR for all 9 NPs deviated from minimum threshold. BIC increased MFR in dispersant treated networks; of the 9 NPs tested, 3 TiO<sub>2</sub> particles and 1288 nm CeO<sub>2</sub> increased the BIC response in MFR, while <7 nm CeO<sub>2</sub> suppressed the BIC-induced change in MFR relative to control. Most notably, the results show that changes in network function occur in the absence of cytotoxicity and were observed at all time points regardless of particle type. The results indicate that metal oxide NPs can disrupt both spontaneous and GABA<sub>A</sub> receptor-mediated neuronal activity in vitro. Additional studies are necessary to investigate the mechanisms underlying these observations and understand the implications of NP exposure to neuronal function in vivo. (This abstract does not reflect Agency Policy.)

**S 821 Systems and Computational Biology As Foundations for Toxicology Research.**

L. D. Lehman-McKeeman. Bristol-Myers Squibb Company, Princeton, NJ.

Systems and computational approaches are holistic methods to elucidate and understand the complex interactions among components of a biologic response network and are central to the comprehensive understanding of all biological processes. The field requires the integration of concepts from biology and physiology, computer science and applied mathematics, as well as physics and engineering. Toxicology is also a multidisciplinary science and application of systems and computational approaches can aid in unraveling the dynamic and complex nature of toxic responses. In light of the broad utility of systems biology approaches to toxicology and risk assessment, the goal of this session is to feature eminent scientists who have made seminal contributions and advances in systems and computational biology. The broad areas to be addressed include:

- general concepts of systems biology tools including network mapping and statistical challenges in assuring the validity of network analyses along with the newest tools and approaches for gaining insight into the regulation and function of complex systems;
- applications of systems biology approaches to studying fundamental biological responses such as cell signaling and kinase networks;
- perspectives on the application of systems networks to biomedical research and particularly for studying disease etiology and prevention;
- computational strategies that inform the prediction of pharmacologic and toxicologic responses including the prediction of adverse drug reactions; and,
- novel applications of machine learning and cell imaging to evaluate subcellular organization and function that inform hypothesis testing and translational details that may be useful in drug development.

**S 822 Turning Protein Networks into Gene Ontologies.**

T. Ideker. Department of Medicine, University of California San Diego, La Jolla, CA. Sponsor: L. Lehman-McKeeman.

Ontologies have been very useful for capturing knowledge as a hierarchy of concepts and their interrelationships. In biology, a prime challenge has been to develop ontologies of gene function given only partial biological knowledge and inconsistency in how this knowledge is curated by experts. I will present a method by which large networks of gene and protein interaction, as are being mapped systematically for many species, can be transformed to assemble an ontology with equivalent cov-

erage and power to the manually-curated Gene Ontology (GO). The network-extracted ontology contains 4,123 biological concepts and 5,766 relations, capturing the majority of known cellular components as well as many additional concepts, triggering subsequent updates to GO. Using genetic interaction profiling we provide further support for novel concepts related to protein trafficking, including a link between Nnf2 and YEL043W. This work enables a shift from using ontologies to evaluate data to using data to construct and evaluate ontologies.

**S 823 Network2Canvas: Network Visualization on a Canvas with Enrichment Analysis.**

A. Ma'ayan. Department of Pharmacology and Systems Therapeutics, Mount Sinai School of Medicine, New York, NY. Sponsor: L. Lehman-McKeeman.

Networks are vital to computational systems biology research, but visualizing them can be a challenge. For networks larger than ~100 nodes and ~200 links, ball-and-stick diagrams fail to convey much information. To address this, we developed Network2Canvas (N2C), a web application that provides an alternative way to view networks. N2C visualizes network nodes by placing them on a square toroidal grid. These nodes are then clustered together on the grid using simulated annealing to maximize local connections. For visualizing the canvas, a node's brightness is made proportional to its local fitness; the brighter a node is, the stronger its connections to its neighbors. The grid is interactive, implemented in HTML5 and the Java Script library D3. We applied N2C to create canvases for 25 gene-gene functional association networks connecting human and mouse genes, and six drug-drug networks connecting FDA approved drugs based on their shared properties. N2C also has functions to perform enrichment analysis. Given lists of genes or drugs, N2C highlights enriched terms on the grid as well as computes the degree of clustering for these enriched nodes. We applied N2C to analyze nine cancer cell lines by comparing their enrichment signatures to enrichment signatures of matched normal tissues. Such analysis provides a global visualization of critical differences between normal tissues and cancer cell lines. In particular, we observed a common pattern of up regulation of the polycomb group and enrichment for the histone mark H3K27me3 in many of cancer cell lines. In summary, N2C provides a new flexible method to visualize large networks and to perform and visualize enrichment analysis on functional drug and gene networks. N2C is freely available at <http://www.maayanlab.net/N2C>

**S 824 Computational Approaches to Predicting Adverse Drug Reactions and Mitigating Off-Target Liabilities in Early-Stage Drug Discovery.**

L. Urban<sup>1</sup>, S. Whitebread<sup>1</sup>, E. Lounkine<sup>1</sup> and P. Müller<sup>2</sup>. <sup>1</sup>Center for Proteomic Chemistry, Novartis Institutes for Biomedical Research, Cambridge, MA; <sup>2</sup>Preclinical Safety, Novartis Institutes for Biomedical Research, Cambridge, MA.

Identifying unintended off-targets associated with adverse drug reactions (ADRs) is daunting by empirical methods alone. Many of these are unrelated to the therapeutic target and it would need hundreds of assays to reveal their involvement in clinical side effects. However, latest development in *in vitro* assay technologies, tools for pharmacovigilance, and establishment of clinical data warehouses laid the foundation for the development of computational strategies to predict side-effect targets and even their associations with pathways and complex biological systems. However, many of the early methods focused on cheminformatic aspects of lead optimization with little attention for translational value, not to mention the safety aspects of the chemical structures and individual molecules. Introduction of several theoretical methods to explore drug-target-adverse reactions changed the landscape of safety assessment and the translational value of these new methods has been increasing significantly. The methods could be characterized as statistical models, expert or rule-based systems, quantum mechanics calculations, and structure based approaches. Data used by these models are largely generated in *in vitro* assays and obtained from clinical observations. Novartis, in collaboration with UCSF and SeaChange has conducted a large-scale experimental test of the SEA method to predict drug activities on targets linked to ADRs, and a guilt-by-association method to associate that activity with side-effects and provided evidence that a drug-target-ADR network approach could have wide application to de-risking toxicological liabilities in drug discovery. In this presentation, we will highlight the various methods and applications developed for early risk assessment, and provide insight of their practical applications.

## **S** 825 **Image-Derived Models of Subcellular Organization and Perturbation.**

R. F. Murphy. *Biological Sciences, Carnegie Mellon University, Pittsburgh, PA.*  
Sponsor: L. Lehman-McKeeman.

Because of their complexity, cutting-edge machine-learning methods will be critical for building systems models of cell and tissue behavior and for future drug development. Such models require accurate information about the subcellular distributions of proteins, RNAs and other macromolecules in order to be able to capture and simulate their spatiotemporal dynamics. Unfortunately, information with sufficient resolution and for different cell and tissue types is currently very limited. Microscope images provide the best source of this information, and new tools are being developed to build models of cell organization directly from such images. The number of possible experiments needed is prohibitive, but active machine learning methods can be used to help choose which experiments are needed in order to construct sufficient models of how cell organization changes with cell type and with disease. In order to use these models for drug development, information on how thousands of cell components respond to millions of potential therapeutics is also needed in order to minimize toxicity. Active-learning methods can also guide experimentation to overcome the dimensionality of this problem.

## **S** 826 **From Inhaled Particles to Cardiovascular Disease and Toxicity: Evidence from Studies in Volunteers, Experimental Animals, and Cell-Based Systems.**

F. R. Cassee<sup>1</sup> and H. Kipen<sup>2</sup>. <sup>1</sup>*Centre for Environmental Health Research (MGO), National Institute for Public Health and the Environment (RIVM), Bilthoven, Netherlands;* <sup>2</sup>*Environmental & Occupational Medicine, UMDNJ-Robert Wood Johnson Medical School, Piscataway, NJ.*

The adverse effects of air pollution on cardiovascular health have been established in a series of major observational studies. Even brief exposures to air pollution have been associated with marked increases in cardiovascular morbidity and deaths from myocardial ischemia, arrhythmia, and heart failure. The breadth, strength, and consistency of the evidence provide a compelling argument that air pollution, especially traffic-derived pollution, causes cardiovascular disease. However, these observational data are limited by imprecision in the measurement of pollution exposure, and the potential for environmental and social factors to confound these apparent associations. For a causal association to have scientific credence, a clear mechanism must be defined. What are the potential pathways through which air pollution mediates these adverse cardiovascular effects and diseases? And are the effects caused by the nano-sized particles? This session will focus on the underlying biological mechanisms of complex particle mixtures.

## **S** 827 **Acute Increases in Exhaled Breath Condensate No Metabolites Suggests Oxidative Stress As a Mechanism for the Health Effects of Traffic-Related Pollutants.**

H. Kipen<sup>1</sup>, R. J. Laumbach<sup>1</sup> and A. J. Gow<sup>2</sup>. <sup>1</sup>*Environmental & Occupational Medicine, UMDNJ-Robert Wood Johnson Medical School, Piscataway, NJ;* <sup>2</sup>*School of Pharmacy, Rutgers University, Newark, NJ.*

Explication of a mechanism lends substantial scientific credence to epidemiologic associations. For example, there are strong epidemiologic associations between increases in air pollution, specifically traffic-related air pollution, and adverse cardiopulmonary outcomes, but our understanding of explanatory mechanistic pathways is incomplete. What are the potential pathways through which air pollution mediates these adverse cardiopulmonary effects? This presentation will focus on some of the underlying biological mechanisms. One specifically hypothesized mechanism is acutely increased oxidative stress/inflammation in the airways, as reflected in exhaled breath condensate (EBC) nitrite and nitrate in human subjects. Nitric oxide (NO) is formed in the lung epithelium from activities of all three NO synthases, and may then diffuse into the airway lining fluid where it is subject to oxidation to nitrite and nitrate by multiple pathways. Data showing an increase in exhaled breath condensate nitrite and nitrate following either controlled diesel exhaust inhalation or acute highway traffic exposure will be reviewed. Multiple oxidative pathways for the acute increases in EBC nitrite will be discussed, along with implications for generation of cardiopulmonary effects.

## **S** 828 **Health Effects from Traffic Particles and Noise in Road Workers.**

M. Riediker<sup>1</sup>, R. Meier<sup>1</sup>, A. Ghio<sup>4</sup>, F. R. Cassee<sup>2</sup> and W. Cascio<sup>3</sup>. <sup>1</sup>*Department Workers' Health, Institute for Occupational Health Sciences, Lausanne, Switzerland;* <sup>2</sup>*Centre for Environmental Health Research (MGO), National Institute for Public Health and the Environment (RIVM), Bilthoven, Netherlands;* <sup>3</sup>*Environmental Public Health Division, US EPA, Research Triangle Park, NC;* <sup>4</sup>*Human Studies Division, US EPA, Research Triangle Park, NC.*

Fine particulate matter (PM<sub>2.5</sub>), gaseous co-pollutant, and noise exposure were assessed in panels of workers that spend most of their professional activities on or near roads. To quantify workers' exposure and related short term health effects, up until now, we observed 13 road maintenance workers, each over 5 non-consecutive work days. We used a methodology based on personal and work site measurements to assess the workers' exposure to particles, noise and co-pollutants. For examination of personal exposures during and after work, the workers were equipped with a personal particulate monitor (PM<sub>2.5</sub>) and a noise dosimeter. Additional exposure parameters measured at the work site provided a detailed evaluation of exposure during work. These included ultrafine particle counts, measurement of carbon monoxide, nitrogen dioxide and ozone as well as PM sampling for compositional analysis. Cardiovascular health endpoints were assessed before, during and 15 hours post work shift. These included a continuous ECG from before until 15 hours post work, measurement of blood pressure and lung function before and 15 hours post work as well as measurement of exhaled nitric oxide and blood markers 15 hours post work shift. Noise levels are generally high with extreme levels during certain activities. Mean work shift PM<sub>2.5</sub> Mass concentrations ranged from 17.0 µg/m<sup>3</sup> to 321.0 µg/m<sup>3</sup> (mean 56.8 µg/m<sup>3</sup>) and UFP counts were between 15,538 particles/cm<sup>3</sup> and 408,518 particles/cm<sup>3</sup> (70,721 particles/cm<sup>3</sup>). Results suggest that PM<sub>2.5</sub> induces cardiovascular effects and inflammation. PM<sub>2.5</sub> and noise were only weakly correlated, allowing further assessment of these associations.

## **S** 829 **Air Pollution Is Associated with Chronic Progression of Cardiovascular Disease.**

A. K. Lund. *Lovelace Respiratory Research Institute, Albuquerque, NM.*

Traffic-generated pollutant-exposures appear to have a strong correlation to these adverse vascular outcomes, as shown through roadway proximity studies. Controlled toxicological studies highlight potential interactions between vehicle-source emissions and upregulation of signaling molecules associated with progression of atherosclerosis. Mechanistically, a role for both innate and adaptive immune responses is emerging, with important recent findings demonstrating that receptors such as the lectin-like oxidized LDL receptor (LOX)-1 may play a role in communicating airway exposures to cardiovascular outcomes. Using a mixed vehicle emission (MVE: gasoline and diesel engine, 100 PM µg/m<sup>3</sup>) model we show that atherosclerotic Apolipoprotein E null (ApoE<sup>-/-</sup>) exhibit increased oxidized LDL, associated with proinflammatory responses and lipid accumulation, as well increased vascular LOX-1 expression, when exposed by inhalation 6 h/d for 7 days, compared to filtered air-exposed controls. Furthermore, we observe a significant upregulation of vascular factors downstream of the LOX-1 receptor that are associated with atherogenic plaque growth and rupture, including reactive oxygen species, endothelin (ET)-1 and matrix metalloproteinase (MMP)-9 in MVE-exposed Apo E<sup>-/-</sup> mice, expression of which are attenuated with anti-LOX-1 antibody treatment. These data indicate that vascular effects of inhalation exposure to traffic-generated pollutants, resulting in progression of atherosclerosis and onset of clinical cardiovascular events, may be mediated through scavenger receptor ligand binding, internalization, and downstream signaling pathways.

## **S** 830 **Effects on the Vascular System of Source-Specific Particles.**

M. E. Gerlofs-Nijland<sup>1</sup>, F. R. Cassee<sup>1,2</sup>, M. Steenhof<sup>1,2</sup>, M. Strak<sup>1,2</sup> and N. A. Janssen<sup>1</sup>. <sup>1</sup>*Centre for Environmental Health Research (MGO), National Institute for Public Health and the Environment (RIVM), Bilthoven, Netherlands;* <sup>2</sup>*Institute for Risk Assessment Sciences (IRAS), Utrecht University, Utrecht, Netherlands.*

Oxidative potential as a metric to predict source specific cardiovascular toxicity? Presentation Description: Much attention has been paid to the role of tail pipe emissions on pulmonary and cardiovascular toxicity. Although the focus in the past few years has been on diesel engine exhaust, PM is emitted from other non-exhaust sources like brakes as well. Some sources have shown to have a much higher oxidative potential compared to diesel soot. Oxidative stress has been suggested as a key aspect leading to cardiovascular toxicity and worsening of diseases. It is therefore very important to measure oxidative stress to check on the health status. A simple

metric for oxidative stress in vivo could be the oxidative potential of particles indicating the possibility of PM to produce oxygen radicals and cause damage in vivo. The focus of this presentation will be on the oxidative potential of PM from different sources as a measure to predict source specific cardiovascular toxicity in vivo. Systemic effects in rats exposed for 4-weeks to diesel engine exhaust occurred including decreased numbers of white blood cells and reduced von Willebrand factor protein in the circulation. In addition, lung tissue factor activity is reduced in conjunction with reduced lung tissue thrombin generation. We have also shown in studies in which volunteers were exposed to air pollution at various locations dominated by different sources of emission that organic carbon, nitrate and sulfate to be most consistently linked with different biomarkers (e.g. high-sensitivity C-reactive protein, fibrinogen, von Willebrand factor and plasminogen activator inhibitor-1) of acute cardiovascular risk. Associations for PM mass concentrations and OP were less consistent, while other measured components of the air pollution

### **S 831 Diesel Exhaust: The Many Ways That Nanoparticles Can Impair Cardiovascular Health.**

M. Miller, J. P. Langrish, N. L. Mills, K. Donaldson, P. W. Hadoke and D. E. Newby. *Centre for Cardiovascular Sciences, University of Edinburgh, Edinburgh, United Kingdom.* Sponsor: F. Cassee.

The detrimental effects of air pollution on the cardiovascular system are now well established, however, the mechanisms underlying these effects remain to be determined. Using diesel exhaust as an example of a common air pollutant, rich in combustion-derived nanoparticles, this presentation will give an overview of the multiple ways urban air pollution can alter cardiovascular function. Studies in both animals and man have demonstrated that this pollutant impairs vascular function, promotes thrombosis, exacerbates cardiac ischemia and accelerates the development of atherosclerosis. The presentation will focus on preclinical experiments with diesel exhaust particulate (DEP) that provide insight into potential mechanisms for these effects, including oxidative stress, endothelial dysfunction, inflammation, particle translocation, as well as considering with constituents of DEP may be responsible for these harmful effects.

### **S 832 The Dynamics of Neuroinflammation and Inflammatory Cell Responses in Neurologic Disease.**

G. J. Harry<sup>1</sup> and C. P. Curran<sup>2</sup>. <sup>1</sup>*NTP Laboratory, NIEHS, Research Triangle Park, NC;* <sup>2</sup>*Northern Kentucky University, Highland Heights, KY.*

An increasing body of evidence indicates that neuroinflammation and activation of immune cells within the nervous system are associated with neurodegenerative disease, neurodevelopmental disorders, and potentially in reaction to environmental exposures. However, it is also increasingly obvious that these responses may be beneficial or detrimental, and discriminating between these has only recently been addressed. Understanding the process by which these responses are triggered and the spatiotemporal dynamics of the response is critical to developing a strategy for translating neuroinflammatory and immune response to effective prevention or treatment of neurologic disease/injury. Three well-known neurotoxins: trimethyltin, manganese, and mercury will be used as chemical probes to explore differences in the timing of inflammatory effects and consequences in the brain. We will conclude by discussing approaches to manipulate the lesion microenvironment and/or brain macrophage such that inflammation favors tissue repair in the spinal cord.

### **S 833 Microglia Heterogeneity in Neuroinflammation and Neurotoxicity.**

G. J. Harry. *NTP Laboratory, NIEHS, Research Triangle Park, NC.* Sponsor: C. Curran.

Microglia cells are the resident immune cells of the brain; however, they are also critical neural specific cells with multiple roles. The response of microglia has been associated with environmental exposures and is present in diagnosed neurodegenerative disease. In many cases, what is considered a microglia response is often a brain macrophage response that can be derived from both resident microglia and infiltrating blood-borne monocytes. In order to better understand the resident microglia response, data will be presented from a delayed neuronal death model following trimethyltin intoxication. This compound induces death of the dentate granule neurons across multiple species and is accompanied by a robust microglia response and elevation in pro-inflammatory cytokines. The process is tightly regulated and with the phagocytic clearance of the neuronal debris, the system actively

undertakes repair. Using this model of resident microglia activation, the dynamic sequence of events will be described that characterize the microglia response within areas of neuronal death, synaptic loss, and neuronal activity. Using this model we are able to identify the various functions of microglia and potentially identify a profile of molecular and morphological responses that will identify the different functions of the microglia. This will serve to identify those processes of microglia that need to be fostered and those that need to be mitigated by therapeutic intervention.

### **S 834 Neuroinflammation and Developmental Vulnerability to Manganese.**

R. B. Tjalkens<sup>1,2</sup>. <sup>1</sup>*Center for Environmental Medicine, Colorado State University, Fort Collins, CO;* <sup>2</sup>*Toxicology Section, Department of Environmental and Radiological Health Sciences, Colorado State University, Fort Collins, CO.*

There is increasing evidence that activation of microglia and astrocytes during development can influence susceptibility to neurodegeneration later in life. Environmental insults such as infectious agents, pesticides, and heavy metals have all been implicated in neuronal injury leading to increased activation of glial cells and development of chronic neuroinflammation. Exposure to elevated levels of the essential element manganese (Mn) causes a spectrum of neurochemical and neuropathologic changes that can culminate in irreversible neuronal injury in subcortical and cortical structures. Children are more vulnerable to Mn than adults and recent epidemiological evidence links high Mn in drinking water to cognitive and behavioral impairment. Mn neurotoxicity is associated with astrogliosis in the basal ganglia and studies conducted in our laboratory and others suggests that glial-derived inflammatory cytokines and nitric oxide (NO) influence the progression of neuronal injury. Increased expression of iNOS/NOS2 by activated glial cells in response to Mn results in nitrosative stress throughout the basal ganglia and enhanced apoptosis within selected populations of neurons in the globus pallidus and striatum. NOS2 is exclusively expressed in glia and produces high levels of NO, which forms highly reactive peroxynitrite anion (ONOO-) upon combining with superoxide, resulting in electrophilic nitration of cellular proteins that damages neurons. Peroxynitrite-mediated nitrosative stress is also implicated in a number of neurological disorders, including Alzheimer's and Parkinson's diseases. Inflammatory changes in glial cells may therefore be an important link between neurotoxic injury and persistent neurological dysfunction during aging.

### **S 835 Spontaneous and Mercury-Induced Antibodies to Brain Antigens Affect Fetal Brain Development.**

D. A. Lawrence<sup>1</sup>, Y. Zhang<sup>1</sup>, Y. Heo<sup>2</sup> and D. Gao<sup>1</sup>. <sup>1</sup>*Immunology, Wadsworth Center, Albany, NY;* <sup>2</sup>*Occupational Health, Catholic University of Daegu, Daegu, Republic of Korea.*

BTBR mice spontaneously develop a high level of serum IgG of which a proportion are antibodies (Abs) to brain antigens. These Abs enter the brain and are associated with expression of inflammatory cytokines, which are suggested to be related to presence of activated microglia and mast cells. The neurodevelopmental effects of BTBR mice are posited to be autoimmune due to elevated presence of activated CD4+ T cells driving Ab production, and the offspring have behaviors that resemble autism. IgG from BTBR mice intravenously injected into B6 pregnant dams caused offspring to have lowered social interactions; likewise, B6 embryos that are born from BTBR dams have lowered sociability. Changes in mitochondrial functions can alter these behavioral outcomes of BTBR mice, but the mechanisms remain unknown. Abs causing behavioral deficits is not a new finding, in that Abs induce neuropsychiatric syndromes in lupus-prone mice. Additionally, certain strains such as A.SW, which are sensitive to Hg-induced autoimmune responses, generate autoantibodies to brain antigens upon developmental exposure to HgCl<sub>2</sub> and have behavioral deficits as adults, and inflammatory cytokines in multiple brain regions are associated with the behavior changes; however, the HgCl<sub>2</sub>-induced effects are dependent on the genetics of the strain and sex of the developmentally exposed mice.

### **S 836 Manipulating Microglia and Macrophages to Promote Repair of Injured Spinal Cord.**

P. G. Popovich. *Department of Neuroscience, The Ohio State University, Columbus, OH.* Sponsor: C. Curran.

Following traumatic or ischemic/reperfusion injury to spinal cord or brain, macrophages derived from resident microglia and infiltrating blood monocytes accumulate in the affected area. Collectively, these cells exert diverse and conflicting effects on neurons and glia. Indeed, microglia/macrophages can cause neuronal cell death, axonal injury and demyelination but can also promote neuron survival, axon regeneration, remyelination and revascularization. Over the past few years, we have

used a number of strategies to manipulate resident and recruited macrophages in an effort to understand their seemingly paradoxical functions, specifically in the context of rodent models of traumatic spinal cord injury (SCI). Data will be presented showing that SCLelicits CNS macrophages with a distinct molecular phenotype, one that simultaneously favors cell killing and axon growth/regeneration. Newer data also will be presented to show that it is possible to manipulate the lesion microenvironment and/or the CNS macrophages such that the natural course of inflammation progresses to favor tissue repair without concomitant cell killing. In this context, preliminary applications of therapeutic gene transfer and bioengineering will be discussed. Supported by NIH-NINDS and The Craig H. Neilsen Foundation.

### **W 837 Advances in Carcinogenic Risk Assessment of Low-Level Genotoxic Impurities in Pharmaceuticals.**

W. W. Ku<sup>1</sup> and D. Jacobson Kram<sup>2</sup>. <sup>1</sup>*Nonclinical Drug Safety US, Boehringer Ingelheim Inc., Ridgefield, CT*; <sup>2</sup>*Center for Drug Evaluation and Research, US FDA, Silver Spring, MD.*

Pharmaceutical syntheses involve the use of reactive starting materials, intermediates, and reagents, some of which are known or potential genotoxicants and carcinogens. Therefore, genotoxic and potentially carcinogenic impurities may appear in the final drug product. Risk assessment approaches have focused on defining impurity limits which pose acceptable risk over a patient's duration of drug treatment. Over the past decade, regulatory guidances (EMA, US FDA draft) have been introduced. Drug-associated genotoxic impurities became an ICH guideline topic (M7) in 2009, and an Expert Working Group is currently developing a harmonized guideline. The ICH M7 effort presents an opportunity to review existing guidelines, evaluate new information and experiences since their introduction, and improve the integration of safety and quality aspects for detection, risk management and control. This workshop will provide a historical overview and introduce newer concepts to SOT members for discussion on several approaches being considered in M7. The workshop will cover the following topics along with case studies: (1) a brief overview of regulatory risk assessment approaches developed over the past decade and introduce current M7 concepts being considered; (2) review current *in silico* Q(SAR) and genotoxicity testing approaches to predict or identify hazards and qualify impurity risk; (3) introduce advances in the framework and rationale for applying less-than-lifetime acceptable risk limits during clinical development and marketing; (4) highlight differences in chemical space between pharmaceutical synthetic intermediates or impurities and that used to derive the original lifetime threshold of toxicological concern (TTC) limit, and its potential implications for risk characterization; and (5) review approaches for addressing risk of multiple genotoxic impurities in a drug product.

### **W 838 Genotoxic Impurities—Regulatory Advances in Risk Assessment Approaches.**

P. Kasper. *Federal Institute for Drugs and Medical Devices, Bonn, Germany.* Sponsor: W. Ku.

The control of impurities in drug substances/products is regulated by internationally harmonized guidelines (ICH Q3A/B). However, these documents lack any specific instructions on how to treat impurities with a genotoxic potential. This has led to considerable differences between regulatory authorities on what levels of daily intake of genotoxic impurities are acceptable and prompted the European Medicines Agency (EMA) to release a "Guideline on the Limits of Genotoxic Impurities" in 2007 followed by publication of a draft guidance by CDER/FDA in 2009. Several basic principles are common to both documents and are currently under discussion for further development in the ICH process.

Genotoxic impurities are defined as compounds that are DNA-reactive and have the potential to directly cause DNA damage when present at low levels leading to mutations and therefore, potentially causing cancer. Consequently, *in silico* prediction of DNA reactivity/mutagenicity and Ames mutagenicity testing are basically the recommended approaches for hazard identification. Since risk assessment based on such limited set of data is not feasible a generic "Threshold of Toxicological Concern" (TTC)-value of 1.5 µg/day corresponding to a 10<sup>-5</sup> lifetime risk of cancer is used as a pragmatic approach for control of impurities that are Ames-positive. Derived from linear extrapolation of rodent potency data from over 700 carcinogens and based on an accumulation of worst-case assumptions the TTC value is a very conservative and therefore sufficiently safe limit. Possible deviations from the default TTC approach are currently under discussion and include cases when more extensive and appropriate data for a proper assessment of potential risks are available, e.g., data from carcinogenicity studies with the impurity or mechanistic data providing evidence for a threshold. Also specific clinical aspects may justify an adjustment of accepted daily intake levels of mutagenic impurities, such as for instance treatment of life-threatening condition, short life expectancy of patients, or indications with less-than-lifetime exposure.

### **W 839 Advances in Mutagenic Impurity Hazard Assessment: Best Practices and Current Developments.**

K. Dobo. *Drug Safety Research and Development, Pfizer Global Research and Development, Groton, CT.* Sponsor: W. Ku.

For many years, pharmaceutical companies have been using *in silico* methods as a primary tool for the identification of mutagenic impurities or degradants in drug substances or products as recommended in the European Medicines Agency (EMA) guidance, as well as the CDER/FDA draft guidance. Although neither guideline provides specific recommendations on the conduct of *in silico* assessments, a recently published survey of industry practice showed that the *in silico* methods employed by 8 companies are highly similar. More importantly, the survey showed that *in silico* analysis alone or in conjunction with an expert evaluation provides a high degree of confidence that an impurity that is predicted non-mutagenic will produce a negative result in the Ames assay. Despite the encouraging survey results, there remain many specific points of concern which are currently being addressed by a European pharmaceutical industry (EFPIA) working group in collaboration with regulators. The working group intends to provide recommendations on the conduct of (Q)SAR assessments, which, if followed, would be considered sufficiently rigorous methodology. Although many pharmaceutical impurities can be confidently categorized as mutagenic or non-mutagenic based on *in silico* methodology alone, there are instances in which biological testing is necessary. The Ames assay is considered to be the most practical and appropriate test for the identification of directly DNA reactive substances that warrant TTC control. In most cases the outcome of this assay is sufficient to define and implement appropriate impurity control measures. However, on occasion (e.g. Ames positive degradant that can't be controlled to TTC limits) additional testing is necessary to further address the biological relevance and risk of Ames positive results. Case studies will be used to illustrate potential scenarios warranting additional testing and factors to take into consideration when deciding what studies to conduct.

### **W 840 Less Than Lifetime (LTL) Carcinogenic Risk Limits for Mutagenic Impurities during Clinical Development and in Marketed Products.**

L. Mueller. *Non-Clinical Drug Safety, F. Hoffmann-La Roche Ltd., Basel, Switzerland.*

Mueller et al have provided in 2006 a framework for the application of the threshold of toxicological concern concept to pharmaceuticals with introduction of a "staged TTC". In this staged approach, acceptable daily intake levels were defined for the clinical development phase of pharmaceuticals, i.e. for up to 1 year intake. In the meantime, this "staged concept" was also introduced into regulatory framework in the existing EU regulatory process on genotoxic impurities. In the ICH M7 group, the principle has been expanded based on the application of Haber's Rule relating concentration (or dose) and duration of exposure. According to a recent review by Felter et al. (2011), the majority of carcinogens are more potent in rodents if the same cumulative dose is given over a shorter period (e.g. three months) than a longer one (e.g. two years). Although the number of compounds tested in such scenarios is low and it is unclear if these data can be extrapolated to very low exposure scenarios, it was proposed to adjust the acceptable daily exposure to mutagenic carcinogens for shorter durations with an extra uncertainty factor in comparison to longer durations of intake. On the other hand, it was recognized that medication treatment durations are often less than lifetime and depend on many factors (indication, nature of disease being treated and late onset of disease in life). Hence, it appeared unreasonable to propose the lifetime TTC or 1.5 µg/day for mutagenic carcinogens in most marketed pharmaceuticals. In adopting this consideration, it is currently proposed to place clinical trials of longer duration (>1 year) and medical intervention schemes of shorter than 10 years into one category of "up to 10 years" with the assignment of an adjusted TTC of 10 µg/day. The presentation will include examples for such clinical trials and pharmaceuticals in use.

### **W 841 Many Potential Mutagens Used in Pharmaceutical Syntheses Are in Less Potent Classes Than the Carcinogens Used to Derive the TTC, Justifying Higher Levels without Increasing Risk.**

S. Galloway. *Merck Research Laboratories, West Point, PA.* Sponsor: W. Ku.

The TTC for mutagenic impurities was derived using several worst-case assumptions, and was based on the more potent carcinogens in the public databases. The TTC is needed only when insufficient information exists to estimate safe levels of a mutagen. Most reactive chemicals used in pharmaceutical syntheses are not in the categories of potent carcinogens on which the TTC was based (Delaney, Reg.Tox.

Pharm 49, 107-24, 2007), confirmed here by data from 12 companies and 602 "alerting" structures. Thus, for many synthetic intermediates with structural alerts for mutagenicity, higher daily intakes are appropriate without increased risk. Especially in early stages of pharmaceutical development the risks from exposure to potentially mutagenic impurities are negligible without imposing the default TTC for each. The most common classes are alkylating agents and aromatic amines. For alkyl halides, the relation between the complexity of the structure and carcinogenic potency is well established, (Brigo and Muller, in Teasdale, "Genotoxic Impurities", Wiley 2010) and justifies an acceptable daily intake for mono-functional alkyl halides 10 times the default TTC. Aromatic amines have a wide range of carcinogenic potencies, and we lack sufficient knowledge to define the likely potency of each new one. However the structural characteristics of the most potent carcinogens are well defined, so one can rule out that a new aromatic amine is a highly potent one. The "cohort of concern" (COC) was highlighted as so potent that even the default TTC did not provide sufficient control of exposure. The COC comprises aflatoxins and N-nitroso compounds, not usually relevant to pharmaceuticals, but also azoxy structures. The known alkyl azoxy compounds are thought to be mutagenic by forming carbocations and alkylating DNA. In pharmaceutical syntheses, aromatic azoxy groups are used, which cannot form the alkyl carbocation, so are not in the highly potent class and need not be excluded from the TTC/ADI approach.

#### **W 842 Addressing Risks of the Potential Presence of Multiple Genotoxic/Carcinogenic Impurities in Pharmaceuticals.**

J. Bercu. *Amgen Inc., Thousand Oaks, CA.*

There has been an evolution of risk assessment and regulatory guidance for multiple genotoxic/carcinogenic impurities in pharmaceuticals. While experiences from other relevant industries have been adapted to pharmaceutical impurities (e.g. food, environmental), there are also unique aspects applied to pharmaceutical process development. Scientific discussions have included application of a probabilistic risk assessment to low level genotoxic substances, impacts of structurally/mechanistic similar impurities versus non-similar impurities, and the risk of synergism/potentiation. The science has shaped regulatory guidance to ensure product quality and patient safety throughout development and in registered use. The European Medicines Agency (EMA) and US Food and Drug Administration (FDA) have developed guidances (USFDA is in draft) which include control of multiple genotoxic/carcinogenic impurities. The International Conference on Harmonization (ICH) is developing guidance (i.e., ICH M7) on DNA reactive (mutagenic) impurities. According to the ICH M7 concept paper, one of the issues to resolve is multiple impurities. Industry is developing strategies to implement these regulatory guidances. In conclusion, there are many challenges and issues to resolve, but the advancement of risk assessment for multiple genotoxic/carcinogenic impurities will best occur through science and regulatory guidance.

#### **W 843 Health Risks of Sodium (Salt) Intake: Too Much or Too Little?**

M. G. Soni<sup>1</sup> and P. M. Bolger<sup>2</sup>. <sup>1</sup>Soni & Associates Inc, Vero Beach, FL; <sup>2</sup>Charles Street, Annapolis, MD.

Public health advocates have been concerned for decades that Americans consume unhealthy amounts of dietary sodium. Recently, the Institute of Medicine (IOM) recommended a Tolerable Upper Intake Level of 2,300 mg sodium/day and an Adequate Intake of just 1,500 mg/day, based on risks of adverse health effects, particularly hypertension. However, the average sodium intake is estimated to be 3,500 mg/day. The risk for morbidity and mortality due to excessive or insufficient salt intake varies because of biochemical individuality. The available evidence from a wide variety of clinical trials shows a direct relation between salt intake and blood pressure. A recent meta-analysis suggests that salt reduction tended to increase levels of hormones (renin, aldosterone), cholesterol, and triglycerides, which are all thought to be risk factors for heart disease. It has been asserted that while the risks of consuming too much salt are real, the risks have been exaggerated for the general population, or that the studies done on the consumption of salt can be interpreted in many different ways. There have also been recent scientific debates upon whether "excess" sodium in our diet has any adverse effect at all on healthy individuals and whether the last 50 years of scientific research that strongly correlates salt intake and hypertension might just be a well intentioned misinterpretation of the scientific data. In an effort to broaden the understanding of the aforementioned issues pertaining to salt intake and risk, the following key aspects will be addressed in this session: (1) Health risks associated with sodium intake; (2) Should salts' GRAS status be modified? (3) Any unintended consequences of salt reduction. (4) Is there a sufficient evidence for salt reduction?

#### **W 844 Sodium Homeostasis and Cardiovascular Health.**

P. M. Bolger. *Charles Street, Annapolis, MD.*

Under normal circumstances the mammalian physiological system is a highly complex and exceedingly efficient homeostatic system for monitoring and regulating electrolyte levels throughout the human body. These essential mechanisms include neurological (e.g., pituitary function) and endocrinological (e.g., adrenal) components as well as various organs (e.g., kidneys) and are vital in maintaining a healthy cardiovascular system. In this regard, it is important to understand various homeostatic control systems for key electrolytes, with particular attention to the critical role of sodium in the maintenance of cellular function and cardiovascular health. The key sodium dependent mechanisms with particular emphasis on those that involve renal function also need attention. An integrative approach will be needed to demonstrate the multi-factorial and organ system functions that are involved in the overall systemic homeostatic system to regulate sodium status.

#### **W 845 Strategies to Reduce Sodium Intake in the United States.**

J. Henney. *College of Medicine, University of Cincinnati, Cincinnati, OH.* Sponsor: M. Soni.

Reducing sodium intake is a critical public health need for all Americans. In spite of nearly 40 years of voluntary effort to reduce sodium intake, Americans average daily intake of more than 3,400 mg. of sodium (approx. 1.5 teaspoons) exceeds the existing maximum intake level 2,300 mg/d (1 teaspoon of salt) established by the 2005 Dietary Guidelines for Americans. High sodium intake puts the population-young and old, male and female, and all ethnic groups at risk for hypertension, and subsequent cardiovascular and/or renal events. The study committee convened by the Institute of Medicine consulted many sources and was provided additional information and insight at its public meeting and through the committee's website. The committees recommendations were in three categories: Primary; Supporting and Interim. Primary Recommended Strategy: A coordinated approach to set mandatory standards for safe levels of sodium in food using existing FDA authorities to modify the Generally Recognized as Safe (GRAS) status of salt and other sodium containing compounds. Supporting strategies: A nationally organized campaign to educate the public about risks, healthy food choices and support for government, industry and consumer effort; Update nutrition labeling; Training for restaurant /food service operations; Purchasing specifications by large food purchasers; Enhanced monitoring; Research. Interim strategies: Food manufacturers and restaurant/food service operations voluntarily accelerate and broaden efforts; The food industry, government, professional and public health partners should work together to promote voluntary collaborations to reduce sodium in foods. The specific recommendations and rationale for each strategy will be discussed along with the actions taken since the release of the report.

#### **W 846 The Effects of Sodium Reduction on Blood Pressure, Hormones, Lipids, and Mortality.**

N. Graudal. *Department of Internal Medicine/Infectious Medicine/Rheumatology, Copenhagen University Hospital, Copenhagen, Denmark.* Sponsor: M. Soni.

The average normal salt (NaCl) intake in the world is about 9 g per day. The result of a meta-analysis of 167 intervention studies randomly allocating participants to a low salt diet or a normal salt diet indicates that the effect of a reduced salt intake of about 6 g on blood pressure is less than 1 mmHg in people with normal blood pressure and about 3 mmHg in people with hypertension. These effects were contrasted by significant increases in variables associated with a poor survival prognosis, such as renin, aldosterone, cholesterol and triglyceride. It is therefore not obvious that sodium reduction leads to health benefits. In agreement with this, population studies generally cannot confirm that people on low sodium diets have less morbidity or mortality than people on normal sodium diets, on the contrary these studies show a trend towards increased all cause mortality among individuals on low sodium diet.

#### **W 847 Unintended Consequences of Salt Reduction.**

M. Satin. *Science and Research, Salt Institute, Alexandria, VA.* Sponsor: M. Soni.

While there is considerable clinical evidence to indicate that substantial reductions in dietary sodium intake may result in single digit reductions in systolic blood pressure for salt-sensitive individuals, further evidence reveals that these same reductions may cause a significant increase in morbidity and mortality across a broad

range of the population. It is generally agreed that most of these negative health outcomes are a consequence of the increase in renin-angiotensin-aldosterone system activity that accompanies reductions in salt consumption. Other negative health outcomes may result from the changes in nutrient consumption patterns that accompany recommended salt reductions. The ideal level of sodium consumption for individuals will result from a rational balance of positive and negative health outcomes. As new research findings continue to emerge and concern over potential unintended consequences of restricting sodium intake grows, it is imperative to ensure that nutrition policies reflect the most current, robust and scientifically sound research.

#### **W 848 The Importance of Population-Wide Sodium Reduction As a Means to Prevent Cardiovascular Disease and Stroke.**

D. Arnett. *Department of Epidemiology, University of Alabama at Birmingham, Birmingham, AL.* Sponsor: M. Soni.

High blood pressure is one of the leading causes of preventable mortality and morbidity, worldwide. National health agencies and professional societies around the world recommend reduction in dietary sodium as a means to lower blood pressure and preventing CVD. The American Heart Association (AHA) recommends limiting daily sodium intake to less than 1,500 mg/d for all Americans. For the estimated one in three who will develop high blood pressure in their lifetime, a high-sodium diet may be to blame. Many consumers do not realize that sodium is ubiquitous in the environment and found in many unsuspecting foods at levels that are often unnecessary. Consequently, consumers continue to purchase foods that are relatively high in sodium and increase their risk of hypertension and related health risks. There is overwhelming scientific evidence that lowering sodium intake improves cardiovascular outcomes. Even a modest reduction in sodium intake is likely to result in substantial health benefits, especially when it is achieved in the general population. The AHA has undertaken an organizational approach to sodium reduction in the United States. The health risks associated with consuming too much sodium in the diet are clear and cannot be ignored.

#### **W 849 Unique Challenges in Biologic Drug Development: Separating Mechanism of Action from Mechanism of Toxicity.**

L. Andrews<sup>1</sup> and M. Todd<sup>2</sup>. <sup>1</sup>Genzyme, Framingham, MA; <sup>2</sup>Pfizer, La Jolla, CA.

A common safety concern of biotherapeutic agents is toxicity associated with mechanism of action (MoA). The term MoA refers to the specific biochemical interaction through which a drug substance produces its pharmacological effect. This workshop will address areas of significant impact to biotherapeutic drug development where there is a known disassociation of MoA and MoT in toxicity studies and/or in translation to the clinic. Most nonclinical toxicity studies are conducted in healthy animals which may not predict the effects of a biotherapeutic when used in the patients with specific diseases. The latest paradigms for using animal disease models, including study conduct and interpretation, will be explored. For many years, the likelihood of off-target toxicity was considered to be very low for most biotherapeutics. Data will be presented highlighting that off-target toxicity, particularly hematotoxicity, can occur and may be more prevalent than previously thought. Effort has also been put into better understanding the development and impact of antidrug antibodies (ADA) in nonclinical toxicity studies and their relevance to clinical ADA. In addition to impacting biotherapeutic drug exposure, ADA may also cause a variety of non-MoA associated toxicities including acute hypersensitivity, immune complex disease, and neutralization of the endogenous target. The incidence of ADA-associated toxicities has been increasing and the current understanding of these toxicities and their clinical relevance will be discussed.

#### **W 850 Introduction to the Mechanism of Action/Mechanism of Toxicity Challenges of Biotherapeutics.**

C. Grimaldi. *Boehringer Ingelheim, Ridgefield, CT.* Sponsor: L. Andrews.

Toxicities associated with biologics are often attributed to the mode of action (MoA). Mechanisms of toxicity (MoT) can be caused by "exaggerated pharmacology" which can occur as a direct effect of the biotherapeutic on the intended cell type or biochemical pathway, or as an indirect effect on unintended cell types or pathways. The extent of the pharmacologic response can be influenced by numerous factors including, but not limited to, biophysical properties of the biotherapeutic agent such as binding potency, effector function and immune stimulatory properties, drug dose and/or duration, tissue distribution of the target, perturbation of

signaling networks and disease state. Since the expected pharmacologic mode of action of biotherapeutics is usually understood, the mechanisms of toxicities may be predicted using relevant test systems. To this end, specialized pharmacologic endpoints are needed in addition to the conventional nonclinical safety assays for toxicity testing in animals. Important considerations to evaluate MoA/MoT include the use of alternative animal models, safety biomarkers, drug exposure and immunogenicity, impact of drug delivery routes and modalities, novel drug formats and the impact of process changes and engineering on drug safety. Challenges for nonclinical toxicity testing of biotherapeutics include how and when to incorporate "fit-for-purpose" investigational approaches, and importantly how to extrapolate in vitro and in vivo data to the clinical setting.

#### **W 851 Use of Animal Models of Disease in Safety Assessments of Biotherapeutics—Is This the Future?**

J. Cavanaugh. *Access Bio, Boyce, VA.*

A guiding principle in the design of preclinical safety studies is to parallel as closely as possible the clinical conditions of use and exposure. In accordance with this principle, much attention is paid to the dosing regimen with respect to route of administration, duration of treatment and dosing interval. With respect to mirroring the characteristics of the patient population to be exposed normal animals appropriately parallel the typical Phase I population in normal subjects (healthy volunteers). Where toxicologists deviate from the principle of correlation of clinical conditions of exposure is in the evaluation of potential toxicity in patients in the later safety and activity/efficacy clinical trials. The deviation from this principle relates primarily to the physiological state of the clinical populations involved as they are no longer healthy volunteers but rather individuals who either have a specific disease and/or are very ill. Therefore a relevant question for the toxicologist to ask is whether toxicology studies in "normal animals" adequately assess the risks in "sick people". The answer to this question has even greater significance for biopharmaceuticals when first in human (FIH) Phase I trials are conducted in subjects with disease for ethical and practical reasons. Thus animal models of disease are being used not only to establish preclinical POC but also to assess exaggerated pharmacology and toxicity in an attempt to improve relevance and extrapolation of results to the intended disease population.

#### **W 852 Antidrug Antibodies: Interpreting Toxicology Studies and Translating Nonclinical Findings to the Clinic.**

C. Horvath. *Genzyme, Framingham, MA.*

Animals frequently mount an anti-drug antibody (ADA) response to biological drugs during toxicology studies. In some cases ADAs have no effect on the product's behavior; while in others they may produce a variety of undesirable effects. ADAs may affect the pharmacodynamics, pharmacokinetic, bioavailability and efficacy of a test article. For example, enhanced clearance of a test article from the circulation by ADAs will affect exposure in a toxicology study. The production of ADAs can also result in potentially life-threatening adverse effects. A histamine mediated Type I hypersensitivity response can be experienced when dosing large foreign proteins into rodents. This response can often be mitigated by co-medicating with antihistamines, such as diphenhydramine, but can significantly affect the ability to conduct repeat dosing in rodent models. A Type III hypersensitivity reaction can lead to tissue injury, such as vasculitis, as a result of the formation of immune complexes. Additionally, the neutralization of an endogenous protein may occur when the ADA directed against the drug cross-reacts with an endogenous protein. The level and resulting toxic effects of an ADA response to a particular product can be different in various animal species and are not predictive from one species to another. In general, immunogenicity in animals does not predict immunogenicity in humans, however, caution must be taken when translating the relevancy of any ADA-mediated toxicity observed in an animal to human safety. It is important to consider the implications of ADAs when interpreting the results of a toxicity study and include a comprehensive investigation of potential ADA-mediated lesions to determine if they are solely related to the presence of ADAs or to the pharmacology of the target. The ramifications of nonclinical ADA-mediated toxicity on the clinic can range from additional clinical monitoring to product development termination.

#### **W 853 Unexpected Toxicities of Biotherapeutics on Peripheral Blood Cells.**

N. Evers. *Amgen, Seattle, WA.* Sponsor: L. Andrews.

Monoclonal antibodies and other biotherapeutics are an increasing proportion of drugs being developed by pharmaceutical companies. Unintended effects of biotherapeutics on peripheral blood cells may occur in nonclinical testing or only after

clinical trials or product launch. Nonclinical studies generally predict clinical hematotoxicity for recombinant cytokines and growth factors, but have not been predictive for the majority of biotherapeutics with clinical hematologic liabilities, especially those that are immune mediated and/or of low incidence. Hematotoxicities may be species-specific and affect one or multiple blood cell lineages. Mechanistically, hematotoxicity caused by monoclonal antibodies or other biotherapeutics can be directly related to the activity of the test article, or can be indirect generally due to immune-related events. Direct effects can be due to binding to the intended target or to an off-target molecule. Recently, several publications have demonstrated species-specific hematotoxicity due to off-target binding; these effects have been observed in both rats and NHPs. Indirect hematotoxicity is often due to autoimmunity, biological cascades, antidrug antibodies, or other immune system responses. Hematotoxicities due to biological cascades generally involve mediators of systemic inflammation, such as cytokines, complement, and immune complexes, and often are observed as acute post-dosing events. Platelets are particularly susceptible to effects of biotherapeutics, perhaps due to the high expression of activating FcRs. In vitro assays can be utilized to further investigate and understand the pathogenesis of unexpected effects of large molecules on blood cells. Characterizing the hematotoxicity (e.g. primary or secondary, relevance to humans, underlying mechanism, monitorability, etc) is important for risk assessment. Despite the potential for unexpected hematologic toxicity, the risk-benefit profile of most biotherapeutics is favorable; hematologic effects are readily monitorable and managed by dose modification, drug withdrawal and/or therapeutic intervention.

**PS 854 Effectopedia: The Online Encyclopedia and Graphical Editor for AOPs.**

A. Clippinger<sup>1</sup>, H. Aladjov<sup>2</sup> and G. Veith<sup>3</sup>. <sup>1</sup>*People for the Ethical Treatment of Animals, Norfolk, VA*; <sup>2</sup>*Institute of Biophysics and Biomedical Engineering, Bulgarian Academy of Sciences, Sofia, Bulgaria*; <sup>3</sup>*International QSAR Foundation, Two Harbors, MN*. Sponsor: K. Sullivan.

The 21st-Century shift to more prospective hazard identification and hypothesis generation requires greater strategic application of systems biology, QSAR and archived toxicological data in the form of adverse outcome pathways (AOPs). AOPs describe the causal linkages among biological responses to chemicals over time. The complexity of integrating science can be a barrier to progress in terms of the toxicity pathways and networks involved as well as the need to organize knowledge from many disciplines.

Effectopedia is an open-knowledge aggregation and collaboration tool for delineating AOPs in an encyclopedic and predictive manner. It includes discrete cause-effect studies and critical reviews that are relevant to toxicology. To achieve human and machine interpretability, Effectopedia uses an ontology-enhanced, natural language interface that offers clarifying questions and special tags to define the semantic knowledge while preserving the natural language description of the AOP's elements. The use of ontologies also allows Effectopedia contributors to publish their contributions as nanopublications.

Effectopedia serves as a graphical editor to delineate causal linkages at any level of biological organization and test species. It creates a common organizational space that (1) helps experts identify gaps in knowledge of causal linkages of biological responses and (2) acts as a web-based conference room for dialogue and synthesis by experts with interest in specific AOPs. Effectopedia's live documents are instantly open for focused discussions and feedback, whilst giving credit to original authors and reviewers. New contributions are immediately distributed to interested parties, keeping all information current and documented. Uncoupling the contribution and review processes also permits organizations to define their own seals of approval and associate them with special interest pathways without slowing down the Wiki-inspired stream of contributions.

**PS 855 Exposure Data Curation for Integration into the Comparative Toxicogenomics Database (CTD).**

C. G. Murphy, C. Mattingly and A. P. Davis. *Biology, North Carolina State University, Raleigh, NC.*

Toxicology research is rapidly transitioning from the observational study of adverse effects of chemical exposures on living organisms to a predictive science based on mechanistic understanding of chemical actions. Integration of exposure information into the network of interactions among chemicals, genes, diseases, and molecular pathways is essential to this transition. Therefore, we initiated a project to curate exposure data for inclusion into the publicly available Comparative Toxicogenomics Database (CTD; <http://ctdbase.org>). CTD is a manually curated database containing over 16 million toxicogenomic relationships of chemical-gene-disease interactions and Gene Ontology and pathway annotations that are integrated with analysis tools to promote understanding of the molecular mechanisms

underlying environmental diseases. Building on the community-based development of the ExO exposure ontology, (<http://ctdbase.org/downloads/#exposures>), biocurators manually curate four types of inter-related exposure data from the scientific literature: Exposure Stressor, Exposure Receptor, Exposure Event, and Exposure Outcome. Both controlled vocabulary and free text data fields are used to allow searches among variables, while retaining details specific to the exposure study. Inclusion of exposure information into CTD will create a centralized exposure data resource that will facilitate the identification of connections between real-world exposures, chemicals, genes, proteins, diseases, and molecular pathways. Here we describe our exposure curation paradigm, initial content, and vision for integration into CTD.

**PS 856 Expansion of Toxicity Reference Database (ToxRefDB) Study Data for In Vivo Phenotypic Modeling.**

K. W. McLaurin, S. Sneed, I. Thillainadarajah and M. T. Martin. *NCCT/ORD, US EPA, Durham, NC.*

The US EPA's Toxicity Reference Database (ToxRefDB) was originally populated with pesticide registration toxicity. ToxRefDB now incorporates guideline-like studies from the pharmaceutical industry, National Toxicology Program (NTP), and publicly available research literature. ToxRefDB now captures 5000 animal studies on 1000 chemicals and study data was captured using a standardized, multilayered effect vocabulary across varied study types and species. Seven predominant, data rich study type and species combinations were examined in this analysis: subchronic rat (590), chronic rat (590), chronic mouse (518), chronic dog (325), developmental rat (663), developmental rabbit (512), and multigenerational reproduction rat studies (504). While the majority of chemicals did not have complete toxicity study coverage, there was substantial overlap with study type and species combinations. Of 590 chemicals tested in chronic rat studies: 488 have been tested in chronic mouse studies, 416 in subchronic rat studies, 415 in developmental rat studies, 372 in developmental rabbit studies, and 373 multigenerational rat studies. Differences in key study parameters such as dosing duration, species, strain, and life-stage provided a heterogeneous view of chemical toxicity profiles while helping to gain evidence as common phenotypic outcomes arise. Across 382 chemicals with a subchronic and chronic rat study, 42% observed liver pathology in both (correlation = 0.486). The hierarchical effect vocabulary was mapped from study type and species combination to endpoint supercategory, category, subcategory, class, and subclass, down to effect type, target and description covering over 27000 effect possibilities. This multilayered vocabulary allows for comparison of effects occurring within a biological continuum creating a more effective comparison of hundreds of chemicals now captured by ToxRefDB.

This abstract does not necessarily reflect US EPA policy.

**PS 857 Application of US FDA, Center for Food Safety and Applied Nutrition's Knowledge-Base to Two Use Cases for Food Contact Substances: FCS Inventory Assessment by Read-Across and Prediction Models.**

K. Arvidson<sup>1</sup>, J. Aungst<sup>1</sup>, S. Boyer<sup>2</sup>, C. Hasselgren<sup>2</sup>, E. Matthews<sup>1</sup>, K. Muldoon-Jacobs<sup>1</sup>, A. McCarthy<sup>1</sup>, J. Rathman<sup>3</sup> and C. Yang<sup>3</sup>. <sup>1</sup>*US FDA, College Park, MD*; <sup>2</sup>*AstraZeneca R&D, Mölndal, Sweden*; <sup>3</sup>*Altamira LLC, Columbus, OH.*

The Chemical Evaluation and Risk Estimation System (CERES) project at FDA Center for Food Safety and Applied Nutrition delivers a foundation providing workflows for decision support activities for both pre-market and post-market safety assessments of food additives, food contact substances, and potential contaminants. CERES v1.0 is a data repository and platform for database searching and computational tools. The content includes chemical structures and properties, regulatory records, toxicity studies, and other biological screening assays. CERES is also an institutional knowledgebase where historical regulatory decisions on a given substance are found. The system also assists new decision-making processes in a systematic and consistent manner. In cases where no information is available for a particular substance, CERES provides tools to estimate the toxicity and to assist with other aspects of safety assessment. Two use cases of the CERES system are described in this presentation. One is the read-across process within the CERES system to estimate a carcinogenicity potential of a compound. The analog searching capability along with the supporting experimental data as well as genetic toxicity and carcinogenicity models based on mode-of-actions are employed. Various information types are combined using a weight-of-evidence (WOE) decision theory method. The second use case is a post-market analysis of all historical food-contact substances in the database of the Office of Food Additives Safety using the MOA (mode-of-action) QSAR models within CERES, e.g., genetic toxicity endpoints, carcinogenicity, and reproductive-developmental endpoints. In addition, a plan to connect CERES to other predictive methods to enhance the system will be discussed.

**PS 858 Flexible and Transparent Computational Workflows for the Prediction of Target Organ Toxicity.**

A. N. Richarz<sup>1</sup>, S. J. Enoch<sup>1</sup>, M. Hewitt<sup>1</sup>, J. C. Madden<sup>1</sup>, K. Przybylak<sup>1</sup>, C. Yang<sup>2</sup>, M. R. Berthold<sup>3</sup>, T. Meinl<sup>3</sup>, P. Ohl<sup>3</sup> and M. T. Cronin<sup>1</sup>. <sup>1</sup>*School of Pharmacy and Chemistry, Liverpool John Moores University, Liverpool, United Kingdom*; <sup>2</sup>*Altamira LLC, Columbus, OH*; <sup>3</sup>*KNIME.com AG, Zurich, Switzerland*.

In silico modeling of target organ toxicity has been held back in part by an inability to capture all relevant information into a meaningful reductionist approach. It has also been considered at times too simplistic, using data of often variable quality and seldom allowing the user to assess the relevance to the intended use. The purpose of this study was to develop a novel computational toxicology workflow system, to allow the users greater control and understanding of the target organ toxicity prediction. The workflows were built on the KNIME open-access platform which allows pipelining via a graphical user interface. Various building blocks, known as nodes, were incorporated, to access chemical inventories and/or databases, to profile structures and calculate properties and to report prediction results. The “basic” user sees a web-interface, whilst a “trained” user can go behind this to interrogate the nodes and, if required, link to additional data sources or investigate and update the models. The workflow was developed to address in particular the prediction of target organ toxicity of cosmetic ingredients. It comprises an inventory of over 4,400 unique chemical structures (cosmetic ingredients and related substances). The database contains repeat dose toxicity data for over 1,100 compounds including NOEL values. Thus, a user is able to search for similar compounds in the inventory file or database. The compound is then profiled using relevant structural alerts and chemotypes, currently comprising 108 alerts for protein reactivity, 85 for DNA binding, 32 for phospholipidosis and 16 for other liver toxicity endpoints. The workflows are flexible and transparent, they are successful in guiding a user through the process of making a prediction of target organ toxicity. Supported by the EU FP7 COSMOS Project.

**PS 859 Chemotypes: A New Structure Representation Standard for Incorporating Atom/Bond Properties into Structural Alerts for Toxicity Effects and Mechanisms.**

C. Yang<sup>1</sup>, K. Arvidson<sup>2</sup>, A. Detroyer<sup>3</sup>, J. Gasteiger<sup>4</sup>, J. Maruszczyk<sup>4</sup>, J. Rathman<sup>1</sup>, A. M. Richard<sup>5</sup>, S. Ringeissen<sup>3</sup>, C. Schwab<sup>4</sup>, A. Tarkhov<sup>4</sup> and A. Worth<sup>6</sup>. <sup>1</sup>*Altamira, LLC, Columbus, OH*; <sup>2</sup>*US FDA, College Park, MD*; <sup>3</sup>*L'Oréal, Aulnay S/S, France*; <sup>4</sup>*Molecular Networks, Erlangen, Germany*; <sup>5</sup>*US EPA, RPT, NC*; <sup>6</sup>*JRC, Ispra, Italy*.

The representation of structural moieties that carry biological activity information, historically referred to as structural alerts, has a long association with Structure Activity Relationships (SAR). Typically, structural knowledge development is performed only by experts and implemented using SMARTS or proprietary formats. With few exceptions, scientists have generally not been able to query structures with customized substructure rules. Furthermore, there are needs for standardized representations and the ability to encode attributes such as atomic and/or bond properties within structural constructs. Recent efforts to apply cheminformatics to systems-biology have called for innovation in this SAR area by integrating properties with structure connectivity. To this end, an XML-based representation of chemotypes has been developed to define substructures in which each atom and bond can be annotated with atomic, bond, and/or electronic properties, adhering to a controlled vocabulary, that go beyond the confines of conventional structural classes. These chemotypes have been implemented in a publicly free software application to enable search and data filtering. This chemotyper has been developed as part of a project from FDA's Center for Food Safety and Applied Nutrition to aid in updating FDA structure categories used by toxicology reviewers and to support the mode-of-action modeling (MOA) approach adopted in the Chemical Evaluation and Risk Estimation System. A series of chemotypes have been developed to incorporate SAR-informed annotations associated with phenotypic effects in hepatotoxicity and developmental morphology, as well as skin irritation and sensitization. These chemotypes enhanced accuracy of categorizations and MOA model predictions. This abstract does not necessarily reflect EPA policies.

**PS 860 In Silico Models of Sequence-Specific Mutagenicity: Exploring Chemical-Mutation Site Associations.**

A. Sedykh<sup>1</sup>, Y. Low<sup>1</sup>, S. Chakravarti<sup>2</sup>, R. Saiakhov<sup>2</sup> and A. Tropsha<sup>1</sup>. <sup>1</sup>*Eshelman School of Pharmacy, University of North Carolina at Chapel Hill, Chapel Hill, NC*; <sup>2</sup>*MultiCASE, Beachwood, OH*.

The Ames Salmonella test for genotoxicity has undergone several transformations since its introduction in 1971. The initial strains, histidine-deficient mutants involving different mutation-prone DNA sequences, were designed to detect specific

frameshifts and base substitutions. Later, many strains with the same target sequence but improved antibiotic resistance, cellular permeability or impaired repair mechanisms were introduced as more sensitive alternatives. However, most existing Quantitative Structure-Activity Relationship (QSAR) models predict either mutagenicities in major strains or overall mutagenicity. We hypothesized that using additional sensitive strains can provide more refined models predicting sequence-specific mutations. Hence, we curated the Chemical Carcinogenesis Research Information System (CCRIS) database (n=6,545) and the CASE Ultra data set (n=5,438) to create a larger database of 6,967 molecules with fewer missing entries (42% vs 33-39% in original sources). Using mutagenicities reported either in the presence or absence of metabolizing enzymes, we built QSAR models for five sequence-specific mutation sites (hisD3052, hisD3018, hisD6610-hisO1242, hisG46 and hisC3076). These 10 models were compared with the previous strain-specific models in CASE Ultra. Sequence-specific models generally exhibited greater sensitivity (68-88%) and dataset coverage (88-98%) but lower specificity (51-72%). Conversely, previous strain-specific models, built on unbalanced data sets, exhibited high specificity (82-99%) but low sensitivity (17-82%). We have further analyzed the models in terms of statistically significant chemical fragments that were interpreted as structural alerts, highlighting the susceptibility of targeted DNA sequences to certain chemical features. For example, fluorenes, due to their planar structures, are good intercalators often associated with frameshifts in hisD3052. The curated data, models, and new structural alerts will be included in future releases of CASE Ultra.

**PS 861 ToxML: A Structured and Serialisable Exchange Standard for Toxicology.**

M. A. Ali<sup>1</sup>, M. L. Patel<sup>1</sup>, P. N. Judson<sup>2</sup> and D. R. Benz<sup>3</sup>. <sup>1</sup>*Lhasa Limited, Leeds, United Kingdom*; <sup>2</sup>*Judson Consulting Service, Harrogate, United Kingdom*; <sup>3</sup>*US FDA Center for Drug Evaluation and Research, Silver Spring, MD*.

The amount of toxicity data available for those wishing to share and communicate knowledge, or to use for data mining and modelling, is continually growing within the biomedical disciplines. The challenge with this expanding amount of data is that it exists in a multitude of different formats. ToxML is an open standard based on Extensible Markup Language (XML) that consists of an XML Schema (XSD) defining the toxicology schema and lists of controlled vocabulary that ensure consistency of usage. The use of XML means that the data can be created, stored and transported in a structured format that is not bound to a specific software application or programming language. The data file model resulting from this approach is very versatile and allows for the aggregation of experimental data up to the compound level in the detail needed to support areas such as quantitative structure-activity relationship (QSAR) development. ToxML formats have been developed, so far, for 27 toxicity study types. These cover both in vivo and in vitro, and currently include the following super toxicity endpoints: genetic toxicity, carcinogenicity, skin sensitisation, skin penetration, in vivo repeat dose toxicity, in vivo single dose toxicity and ecotoxicity.

Informatics groups at the FDA CDER-CFSAN use ToxML to populate repositories with the results of FDA toxicological and clinical data harvesting efforts, and employ the resulting information to model QSARs. We describe an example of how ToxML could be used as a practical data exchange standard for genetic toxicology information. The standard is maintained by a curation team overseen by the ToxML organisation. The standard is published on a web site ([www.toxml.org](http://www.toxml.org)) together with tools to view, edit and download it. Contributions from the user community to the ongoing evolution of the standard are facilitated in an open forum via a wiki on the web site.

**PS 862 ToxCast™ Workflow: High-Throughput Screening Assay Data Processing, Analysis and Management.**

P. G. Kothiyal<sup>1,2</sup>, M. T. Martin<sup>1</sup>, A. M. Frame<sup>1</sup>, A. M. Richard<sup>1</sup>, R. Judson<sup>1</sup> and D. Reif<sup>1</sup>. <sup>1</sup>*National Center for Computational Toxicology, Office of Research and Development, US EPA, Research Triangle Park, NC*; <sup>2</sup>*Bioinformatics Program, North Carolina State University, Raleigh, NC*.

USEPA's National Center for Computational Toxicology (NCCT) is developing the ToxCast program with the aim of providing high-quality screening data on thousands of chemicals. The huge library of compounds and wide diversity of high-throughput assays in ToxCast present daunting practical challenges with respect to data processing, analysis, and management with the goal of providing transparent and sustainable data outputs across these massive data sets. To successfully address these goals, the data analysis workflow was designed with 8 levels of processing from raw data to finalized hit calls and is distributed within two major portions of the workflow: “Pipeline” (levels 1-4) and “Curve fit” (levels 5-8). The pipeline portion takes incoming raw data files, performs automated chemical and assay mapping, provides plate/batch effect correction, and assay specific data normalization to supply highly consistent data formats for the curve fitting process. The curve-fitting

and hit-calling process consists of cytotoxicity-point and outlier detection/masking, concentration activity estimates using dose response modeling, systematic data confounder detection (e.g., fluorescence or non-specific activity). The finalized results are subsequently uploaded into ToxCastDB for data integration and analysis as well as to serve as the primary portal for publication and data release. In addition, the ToxCast workflow has data quality and error identification features quantifying assay performance and quality. The ToxCast data workflow has been systematically developed to efficiently address data management challenges, increase curve-fitting and hit-calling accuracy, and to allow for technology specific customization resulting in repeatable and transparent analyses. This work does not necessarily reflect Agency policy.

**PS 863 High-Throughput Electronic Literature Libraries (E-Libraries) to Support Development of Toxicity Prediction Models and Adverse Outcome Pathways (AOPs).**

N. C. Baker<sup>1</sup>, T. B. Knudsen<sup>2</sup> and K. M. Crofton<sup>2</sup>. <sup>1</sup>Lockheed Martin/US EPA, Research Triangle Park, NC; <sup>2</sup>NCCT, US EPA, Research Triangle Park, NC.

The elucidation of adverse outcome pathways (AOPs) and mechanistic models of toxicity depends on a thorough understanding of the relationships among protein targets, molecular pathways, cellular processes, adverse outcomes, and exogenous chemicals in a given biological system. Scientists rely on the biomedical literature for a significant portion of this information; however, common tools and resources such as PubMed are designed primarily for article retrieval and may fall short in synthesis of important relationships from the large amounts of available literature. We developed a series of electronic libraries (e-libraries) to provide investigators a way to streamline information retrieval from the biomedical literature and focus the retrieval on key relationships. The foundation for the e-libraries is a broad literature database in the form of a compilation of the MeSH annotations extracted from each MEDLINE record. These annotations are processed and organized so that the relationships among target proteins, biological effects, and chemicals are more easily extracted. For a particular area of interest (e.g., cleft palate, limb development, endocrine disruption) or for a particular set of chemicals (e.g., ToxCast) the literature database is batch-searched for articles containing the corresponding MeSH terms and the co-annotated terms. To produce the e-library, the terms are organized and written to Excel spreadsheets. Finding relevant articles is facilitated by allowing users to use built-in filtering capabilities. A filtering flag for species for instance, will allow the user to see only the rows about a desired species. The e-libraries have been constructed around subject areas as diverse as cleft palate, zebrafish, retinal development, flame retardants, and endocrine disruption. Access to e-libraries has been used to assist all kinds of research from basic exploratory research to development of AOPs and computer simulations. [This abstract does not necessarily reflect EPA policy.]

**PS 864 Interactive Web Application (Dashboards) to Integrate Data on Chemical Hazard and Exposure.**

S. Watford, M. Martin, A. M. Frame, R. Judson, N. C. Baker, I. Shah, J. F. Wambaugh and D. Reif. National Center for Computational Toxicology, Office of Research and Development, US EPA, Research Triangle Park, NC.

The USEPA has developed web-based interfaces (Dashboards) to synthesize multiple sources of data from Aggregated Computational Toxicology Resource (ACToR) into customized information displays. Users may select subsets of chemicals and data types to focus on for the assessment process. The data are organized into custom classes to present all relevant information for a given task. While not all chemicals will have complete information across all classes, each class reports available data including relevant high-throughput assay results, regulatory information, relevant articles from the biomedical literature, exposure data, and in vivo toxicity data. Custom widgets display each type of data according to its nature (e.g. dose-response plots or tables for assay data and summary tables for exposure data). Chemical-specific summary scores that consider all information in each class are presented in a dynamic summary table that highlights areas deserving additional attention. Transparency in decision-making is preserved since Dashboards record and save all user selections and decisions. Expert judgment can be used to override score criteria if necessary, again with such events recorded for transparency purposes. The scores are carried over into a prioritization process where the chemicals are ranked in a weight-of-evidence scheme to identify candidates for focused assessment. For example, the Dashboard created to support analysis of potential endocrine disruptors contains over 8000 chemicals with the classes Estrogen, Androgen, Thyroid, Steroidogenesis, Exposure, Occurrence, and Health Effects. The aggregation of relevant data and use of Dashboards to generate custom displays streamlines the toxicity assessment process and allows users to zoom from larger chemical subsets down to very focused chemical-wise views. While the initial Dashboards have been created to support EPA programmatic needs, future versions will include a public-facing web interface. This abstract does not necessarily reflect US EPA policy.

**PS 865 Literature Visualization and Navigation to Facilitate Development and Application of Computational Biological Models.**

N. Pena, S. R. Crowell, S. Dowson, D. McQuerry and J. G. Teeguarden. Systems Toxicology, Pacific Northwest National Laboratory, Richland, WA.

Physiologically based pharmacokinetic (PBPK) and quantitative structure activity relationship (QSAR) modeling rely heavily on mining of published literature for model development and parameterization, a time and resource intensive process. Because PBPK and QSAR modeling are relatively new disciplines, there is a need for readily accessible and high quality resources to support the increasing model use. Resource needs are broad, ranging from parameter values to model archives and publication archives. A common thread is the need to organize the available model related literature in a fashion that supports rapid access and organization according to data needs and more detailed analysis. We have developed a tree map application, a powerful, visually intuitive literature navigation interface, which exploits the naturally hierarchical nature of information used in biological modeling. Tree maps organize data thematically, and can be navigated by the user choosing a theme of interest, and then drilling down through sub-themes to the level of individual documents (existing models or relevant publications). Subject matter experts developed a taxonomy of themes in biological modeling, and relevant documents were identified in the literature by means of specific search strings. IN-SPIRE Visual Document Analysis was used to identify linguistically significant themes within the data, and to develop and test search strings used by the tree map to identify relevant documents from within the database of biological modeling publications. Documents were then labeled with their relationships within the class structure, loaded into a database, and a tree map user interface generated. With continuing refinement of search strings and development of the tree map application, this work has the potential to yield a powerful, evergreen (automatically updating) search tool specifically designed to aid in biological model development and utilization. An external demo of the tree map can be found at <https://nvacdemo.pnl.gov/srs/dashboard/epa/>

**PS 866 Database of Chemicals Assayed for Estrogenic Activity in the US FDA's Endocrine Disrupting Knowledge Base (EDKB).**

J. Shen, L. Xu, W. Tong and H. Hong. <sup>1</sup>University of Georgia, Athens, GA; <sup>2</sup>Jiangnan University, Wuxi, China.

Endocrine disruptors (EDs) are chemicals with ability to disrupt endocrine system. EDs have sparked intense international scientific discussion and debate and provoked regulatory action. The FDA's National Center for Toxicological Research (NCTR) developed a publicly available Endocrine Disrupting Knowledge Base (EDKB) (<http://goo.gl/Qn0nv>) 13 years ago. It has been a widely used resource in the scientific community. Currently, we are expanding the data collection in the EDKB by including the most up-to-date literatures. Since many EDs display estrogenic activities and affect the normal estrogen signaling pathway, we first updated the estrogenic data and developed a database of chemicals assayed for estrogenic activity as a component in EDKB. The database contains over 16,500 activity data of about 7,000 compounds from many public resources. The activity data are categorized based on assay types into binding assay, reporter gene assay and cell proliferation assay. The database also contains protein subtypes and domains used in the assays. Original data were converted into the same units such as logRBA for binding data (RBA=Relative Binding Affinity). Quality control was performed to ensure the data quality. The database was implemented using Instant JChem. A user-friendly interface was designed and developed for rapid navigating and searching the database. Searching multiple fields such as chemical structure, substructure, chemical name, CAS, assay type, assay species, activity range, and references can be conducted using logical operations. To the best of our knowledge, this database is the most comprehensive collection of chemicals assayed for estrogenic activity. It provides the scientific and regulatory communities a free source to search estrogenic activity data for chemicals of interest and to develop predictive models for predicting chemicals for which no assay data are available.

**PS 867 The Comparative Toxicogenomics Database.**

C. Mattingly<sup>1</sup>, C. G. Murphy<sup>1</sup>, R. Johnson<sup>2</sup>, J. M. Lay<sup>2</sup>, K. Lennon-Hopkins<sup>2</sup>, C. Saraceni-Richards<sup>1</sup>, D. Sciaky<sup>2</sup>, B. L. King<sup>2</sup>, M. C. Rosenstein<sup>2</sup>, T. C. Wieggers<sup>1</sup> and A. P. Davis<sup>1</sup>. <sup>1</sup>North Carolina State University, Raleigh, NC; <sup>2</sup>MDIBL, Salisbury Cove, ME.

The goal of the Comparative Toxicogenomics Database (CTD; <http://ctdbase.org>) initiative is to inform hypothesis development about mechanisms of chemical actions and the impact of environmental exposures on human health. CTD is a freely

available tool that provides a foundation of manually curated data describing chemical-gene interactions and chemical-disease and gene-disease relationships. Curated data are integrated with external data sets (e.g., Gene Ontology and pathway data) and tools that allow users to navigate and analyze over 16 million biological relationships relevant to environmental health sciences (EHS). Here we describe CTD functionality and highlight several new analysis and data visualization features, including: a Gene Set Enricher tool that provides deeper insight into the functional themes and pathways associated with user-defined genes or genes forming the basis of inferred chemical-disease relationships; filtering options that allow users to better customize queries and analyses; and a 'slim' list for our disease vocabulary that was implemented with graphical views to provide visual summaries of disease categories associated with chemicals in CTD. We also present information about emerging projects, including the use of curated data for developing chemotypes (a chemical substructure that carries information about biological activity), text-mining workflows for identifying chemical-gene-disease data, novel pathway development tools, and exposure data curation. We continue to expand the depth and functionality of CTD to meet the evolving needs of the EHS research community.

## PS 868 Mode-of-Action Ontology: An Application Ontology for Risk Assessment Data Mining.

K. L. Painter<sup>1</sup> and L. D. Burgoon<sup>2</sup>. <sup>1</sup>Oak Ridge Institute for Science and Education, Research Triangle Park, NC; <sup>2</sup>National Center for Environmental Assessment, US EPA, Research Triangle Park, NC.

Automated natural language processing (NLP) will make the practice of risk assessment more efficient. In the future, computer algorithms will use NLP to screen the literature for appropriate studies, identify relevant data, and help synthesize mode of action (MOA) evidence across several studies. However, before we can utilize the data from NLP searches, ontologies must be built to facilitate efficient data storage and sharing using existing standards. We developed the Mode of Action Ontology (MOAO) to support automated NLP discovery, integration, and management of mode of action knowledge. MOAO is a semantic model that 1) describes MOA knowledge, 2) easily combines data from multiple sources, 3) makes MOA knowledge more transparent and easily available to the public via semantic web interfaces, and 4) will allow computers to discover latent information and relationships via logical inference. MOAO is the first ontology we are aware of that describes mode of action information for toxicological purposes. MOAO was conceptualized as an application ontology, borrowing terms from existing high-quality ontologies produced for various biological sub-specialties. This allows us to maximize integration with outside data sources. In this way, MOAO can be a model for how other sub-domains in toxicology can reap the benefits of ontologies without the overhead of constructing one completely from scratch. We leverage the work by the Open Biological and Biomedical Ontologies (OBO) Foundry and the Basic Formal Ontology (BFO) to facilitate the integration of our ontology with others. The reference ontologies which MOAO uses include the Gene Ontology (GO), ChEBI (Chemical Entities of Biological Interest), the Uber Anatomy Ontology (UBERON), the NCBI Taxonomy, and the NCI Thesaurus. The views expressed in this abstract are those of the authors and do not necessarily represent the views or policies of the U.S. Environmental Protection Agency.

## PS 869 Development of a COSMOS Database to Support *In Silico* Modelling for Cosmetics Ingredients and Related Chemicals.

J. Rathman<sup>1,2</sup>, C. Yang<sup>1</sup>, K. Arvidson<sup>3</sup>, M. T. Cronin<sup>5</sup>, S. Enoch<sup>5</sup>, D. Hristozov<sup>3</sup>, Y. Lan<sup>6</sup>, J. C. Madden<sup>5</sup>, D. Neagu<sup>6</sup>, A. N. Richarz<sup>5</sup>, M. Ridley<sup>6</sup>, O. Sacher<sup>4</sup>, C. Schwab<sup>4</sup> and L. Yang<sup>6</sup>. <sup>1</sup>Altamira, LLC, Columbus, OH; <sup>2</sup>The Ohio State University, Columbus, OH; <sup>3</sup>Office of Food Additive Safety, CFSAN US FDA, College Park, MD; <sup>4</sup>Molecular Networks, Erlangen, Germany; <sup>5</sup>Liverpool John Moores University, Liverpool, United Kingdom; <sup>6</sup>University of Bradford, Bradford, United Kingdom.

The Seventh Amendment of the EC's Cosmetics Directive foresees a deadline in 2013 for the replacement of animal testing of cosmetic products for repeated dose/reproductive toxicity and toxicokinetics. To this end, the COSMOS project has been initiated to fill the gap in knowledge and technology via *in silico* toxicology. The management and sharing of chemical, biological and toxicity data play a central role. The COSMOS database activities cover three main directions: an overview of toxicity data sources and studies; the design of the data model and the data entry tool for the database; and the definition of a data curation strategy. The new COSMOSDB provides a publicly available web-based searching/retrieval system and also serves for sharing resources, models and supporting workflow developments. The database is "compound-centred" and represents both EU COSING and US PCPC inventories for cosmetics ingredients. For biological data, the database supports repeated dose toxicity, metabolism information and dermal absorption data. The data have been collected, curated, quality-controlled, stored and

managed in a flexible and sustainable manner to support predictive modelling tasks. An effective curation strategy for toxicity data has also been reflected in building the data entry system. Based on the review of existing approaches on good practice to assess quality entries, the reliability of the toxicity data is supported by all available data from multiple sources. Additional functionalities for data aggregation within a data governance framework are described. The COSMOS project is funded by European Community's 7th Framework Program (FP7/2007-2013) and by Cosmetics Europe.

## PS 870 The Toxbank Infrastructure Project to Support the Replacement for Repeated Dose Toxicity.

G. J. Myatt<sup>1</sup>, E. Benfenati<sup>3</sup>, D. Bower<sup>1</sup>, R. Ceder<sup>2</sup>, K. P. Cross<sup>1</sup>, R. C. Grafström<sup>2</sup>, L. Healey<sup>4</sup>, C. Helma<sup>5</sup>, N. Jeliakova<sup>6</sup>, V. Jeliakova<sup>6</sup>, L. Kidane<sup>4</sup>, P. Kohonen<sup>2</sup>, S. Maggioni<sup>3</sup>, S. Miller<sup>1</sup>, M. Rautenberg<sup>6</sup>, G. Stacey<sup>4</sup>, J. Wiseman<sup>8</sup> and B. Hardy<sup>7</sup>. <sup>1</sup>ReD, Leadscope, Columbus, OH; <sup>2</sup>Karolinska Institutet, Stockholm, Sweden; <sup>3</sup>Istituto di Ricerche Farmacologiche Mario Negri, Milan, Italy; <sup>4</sup>National Institute for Biological Standards and Control, Potters Bar, United Kingdom; <sup>5</sup>In silico toxicology, Basel, Switzerland; <sup>6</sup>Ideaconsult, Sofia, Bulgaria; <sup>7</sup>Douglas Connect, Zeiningen, Switzerland; <sup>8</sup>Pharmatope, Wayne, PA. Sponsor: R. Benz.

The aim of the €50 million SEURAT-1 (Safety Evaluation Ultimately Replacing Animal Testing-1) research cluster, sponsored by the European Union and Cosmetics Europe, is to generate a proof-of-concept replacement for repeated dose systemic toxicity testing on animals. The SEURAT-1 strategy is to adopt a mode-of-action framework to describe repeated dose toxicity, combining *in vitro* and *in silico* methods in an intelligent manner to derive predictions of *in vivo* toxicity responses. ToxBank is the cross-cluster infrastructure project whose activities include the development of a data warehouse, the selection of reference compounds for use across the cluster to support the mode-of-action framework, a physical compounds repository, and a reference resource for biomaterials. The ToxBank data warehouse provides a web-accessible shared repository for protocols and experimental results supporting SEURAT-1 research objectives such as toxicity pathway elucidation and biomarker discovery. Information in ToxBank is uploaded from the research activities of the cluster partners and relevant information on the reference compounds from public databases. In this poster we describe the data warehouse and implementation based on open standards, the selection of reference compounds, and an analysis linking the reference compounds to public omics data.

## PS 871 Software for Integration of Experimental, Chemical, and Environmental Data.

E. Peterson<sup>1</sup>, K. Hobbie<sup>2</sup>, S. C. Tilton<sup>1</sup>, R. L. Tanguay<sup>2</sup>, K. Anderson<sup>2</sup> and K. M. Waters<sup>1</sup>. <sup>1</sup>PNNL, Richland, WA; <sup>2</sup>OSU, Corvallis, OR.

The Oregon State University Superfund Research Program evaluates the potential health effects of polycyclic aromatic hydrocarbons (PAHs). More than 100 parent PAH compounds, and an unknown number of PAH derivatives and metabolites have been identified. PAHs raise concern at over 800 Superfund Sites and serve as the risk driver for remediation at 20% of all Superfund sediment sites. Assessing the health effects of PAHs is a major challenge because environmental exposures to these chemicals are from complex mixtures of PAHs and other toxicants. Integration of exposure data with biological activity and pharmacokinetics is essential to evaluate the effects presented by these mixtures on human health. Increasingly researchers are generating data streams of high content data from analytical, high-throughput, and 'omic' studies, which make direct applications from these technologies out of reach for clinicians and regulators. However, more accurate and precise thresholds for risk assessments and prediction will ultimately arise from leveraging the integration of data from across disciplines. Therefore, the principle challenge for mixture assessments, epitomized by PAHs, is the efficient integration of large and diverse data sets. To this end we've extended PNNL's Experimental Data Management System (EDMS) to create a seamless data workflow among researchers and analysts. EDMS has been extended to track and manage relationships among any and all data points across a project. This allows us to integrate chemical and biological data for environmental extracts (LIMS and EDMS) with analogous data on pure chemical compounds. EDMS provides a query mechanism that will reach through all the relationships of data from chemical compounds to the analytics and statistics run on the experimental data. Query results, visualizations, and data processing results are all also stored together with and related to the experimental information. This reduces data replication and supports a streamlining of analysis, collaboration and experimental design allowing researchers to take advantage of all the data generated.

**PS 872 Computational Methods to Reveal Cross-Species, Dose-Response Patterns in Nonclinical Studies.**

S. Nath, J. Kimball, S. Madhavan, V. Krishnan and L. Prabhakar. *PointCross Life Sciences, Foster City, CA*. Sponsor: *R. Guy*.

Drug development scientists and regulatory reviewers alike have a need to understand toxicity patterns of a drug candidate across animal species prior to human trials. Effective exploitation of collected study data has previously been impeded by differences in mnemonics, terminologies and units across sponsor and CRO data. Moreover, computational techniques to analyze large volumes of disparate quantitative and qualitative study data, and their respective endpoints, have not been routinely available for use by practicing toxicologists and reviewers.

To address these common challenges for the FDA and the Industry, we have developed new repository techniques to prepare and hold in vivo harmonized datasets (including standardized formats like SEND, the Standard for Exchange of Nonclinical Data), and extracted metadata, as a first step towards advanced analytics and study reviews. Predictive, comparative and cluster analysis techniques have been performed on large study repository datasets to reveal similarities and differences in dose-response patterns across species in terms of their magnitude, shape and trends. Finally, signal processing techniques such as Z-transform box plots have been adapted to present trends in ways that scientists and regulatory reviewers can easily use to interpret potential toxicity patterns and their inter-relationships. Collectively, new computational tools are available to better exploit legacy and ongoing data that are already being collected, provide better decision support for species selection and protocol design, and advance our understanding of how dose-response patterns translate across species for the same compound and to detect other compounds that share similar responses. Implications of applying such computational methods to improve safety prediction across species, and eventually into humans, will be discussed particularly in light of the FDA's mandate to require standardized e-Data submissions, including SEND datasets, as a way to further regulatory science.

**PS 873 ToxCast High-Throughput Screening Assay Annotation Using Bioassay Ontology and Expanded Assay Target Information.**

J. Phuong<sup>1,2</sup>, K. Houck<sup>1</sup> and M. T. Martin<sup>1</sup>. <sup>1</sup>NCCT, US EPA, Research Triangle Park, NC; <sup>2</sup>Environmental Science & Engineering, University of North Carolina at Chapel Hill, Chapel Hill, NC.

The ToxCast assay library includes 427 high- to Low-throughput screening assays with a total of 700 assay components. Assessing a battery of cellular, pathway, protein and gene perturbations, the total number of assay endpoints (assay\_component\_endpoints) generated is 1106. Selecting the appropriate data sets to use for modeling purposes encounters questions such as suitable cell type, assay design specifics, protein form, measured target and detection method. To simplify these concepts, the BioAssay Ontology was applied to annotate 36 descriptors for assay design and target information and to create a scheme for identifying assay\_component\_endpoints. Assay design information is distinguished by assay design types (n=23), detection technology types (n=11), and cell types (n=36), which consists of 14 species and 18 tissues. Assay target information is separated by technological target mapped to gene(s) (n=381), technological target types (n=15), intended target genes (n=362), intended target families (n=145), intended target types (n=14), and biological process targets (n=11). An example of applying the assay target information to identify all applicable assay\_component\_endpoints is given for the Aryl Hydrocarbon Receptor (AhR). AhR is assessed by four assay\_components (ATG\_AhR\_CIS, Tox21\_AhR\_BLA\_Agonist, CLZD\_CYP1A1, and CLZD\_CYP1A2) in eight assay\_component\_endpoints. The ATG\_AhR\_CIS assay uses an mRNA induction design to target transcription factor activity. The Tox21\_AhR\_BLA\_Agonist assay uses a beta lactamase reporter gene induction design to measure receptor activity. Lastly, the CLZD assays measure the mRNA induction of two AhR target genes, CYP1A1 and CYP1A2, at multiple time-points to measure AhR receptor gene regulation activity. With this approach, the intended assay targets and the means used to measure their activities can be clearly communicated in explicit ways to allow for integration into larger systems-models. This abstract does not necessarily reflect U.S. EPA policy.

**PS 874 A Novel Hybrid Approach in Combining a QSAR-Based Expert System and a Quantitative Read Across Methodology to Achieve Better In Silico Genotoxicity Assessment of Drugs, Impurities and Metabolites.**

S. Chakravarti<sup>1</sup>, R. Saiakhov<sup>1</sup> and G. Klopman<sup>1,2</sup>. <sup>1</sup>Multicase Inc., Beachwood, OH; <sup>2</sup>Chemistry, Case Western Reserve University, Cleveland, OH.

**Purpose:** Purpose of this study is to develop and apply a novel technique of combining the predictions of the CASE Ultra expert system models and a new quantitative read across modeling methodology to obtain better genotoxicity predictions as opposed to using just one technique. The hybrid methodology successfully provides the interpretability of toxicity alerts and reduces false positives, false negatives while increasing the test coverage. This in silico tool can be successfully used for assessment of potential toxicity or beneficial therapeutic effects of new drug candidates, impurities and metabolites.

**Method and Data:** CASE Ultra is a computer program that automatically extracts structure-activity knowledge from chemical databases and applies the knowledge for predicting activity in test chemicals. It also gives a very clear explanation of its predictions so that they are easily interpretable by chemists and toxicologists. Recently we have developed a novel read across modeling technique for quantitative prediction of toxicity that uses the full neighborhood profiles of chemicals. In case of Salmonella mutagenicity predictions, the read across prediction was applied in a systematic way on top of the predictions from the CASE Ultra mutagenicity models, and significant improvements in the sensitivity, specificity and coverage were achieved. The details of the methodology and results of prediction for a large external test set are presented.

**Results of the Study:** The improvements in the predictive performance as a result of the hybrid technique is demonstrated for Salmonella mutagenicity prediction in an external test set. Improvements in the prediction sensitivity, specificity and coverage were in the order of 3-5%, 2-5% and 5% respectively.

**PS 875 Systematic 'Omics Analysis Review Tool to Support Risk Assessment.**

E. McConnell<sup>1</sup>, S. Bell<sup>1</sup>, I. Cote<sup>2</sup>, R. Wang<sup>3</sup>, E. J. Perkins<sup>4</sup>, N. Garcia-Reyero<sup>5</sup>, P. Gong<sup>4</sup> and L. D. Burgoon<sup>6</sup>. <sup>1</sup>Oak Ridge Institute for Science and Education, Research Triangle Park, NC; <sup>2</sup>NCEA, US EPA, Washington DC; <sup>3</sup>NERL, US EPA, Cincinnati, OH; <sup>4</sup>USACE, Vicksburg, MS; <sup>5</sup>Mississippi State University, Starkville, MS; <sup>6</sup>NCEA, US EPA, Research Triangle Park, NC.

Incorporating data from molecular and systems biology studies, especially omics data, presents a major challenge for risk assessors. Omics studies of varying quality and relevance are currently reported in the literature. Risk assessors need a standardized, transparent way of screening literature based on study quality prior to performing in-depth analyses of the data and including the results in human health risk assessments (HHRA). The Systematic Omics Analysis Review (SOAR) tool is a spreadsheet of 35 objective questions, currently focused on transcriptomic microarray studies, developed by domain experts. The tool will identify if a study meets basic published quality criteria, such as those defined by the Minimum Information About a Microarray Experiment (MIAME) guideline and the Toxicological data Reliability assessment (ToxR) Tool. Although the tool is currently constructed for human use in reviewing microarray literature, future work will automate the literature screening process using natural language processing as a first pass filter, with fewer subjective questions left for human determination afterward. The questions cover four sections (Test System, Test Substance, Experimental Design, and Microarray Data). Seven scientists were recruited to validate the tool by using it to rate 16 published manuscripts that study chemical exposure with microarrays. Using their feedback, questions were weighted based on importance of the information and a suitability cutoff was set for each of the four question sections. The SOAR tool was found to be simple, systematic way of performing a first-pass screening of microarray literature, which will introduce modern research methodologies into traditional HHRA procedures.

The views expressed in this abstract are those of the authors and do not necessarily represent the views or policies of the U.S. Environmental Protection Agency.

**PS 876 Web-Based Benchmark Dose Modeling Module As a Prototype Component of an Informatics-Based System for Human Health Assessments of Chemicals.**

A. J. Shapiro<sup>1,4</sup>, N. Cook<sup>1</sup>, P. Ross<sup>4</sup>, J. Fox<sup>2</sup>, V. Coglianò<sup>2</sup>, W. A. Chiu<sup>2</sup>, N. Wang<sup>2</sup>, L. Zeise<sup>3</sup>, K. Guyton<sup>2</sup> and L. Rusyn<sup>1</sup>. <sup>1</sup>University of North Carolina at Chapel Hill, Chapel Hill, NC; <sup>2</sup>NCEA, US EPA, Washington DC; <sup>3</sup>Scientific Affairs Division, Cal/EPA, San Francisco, CA; <sup>4</sup>ICF International, Fairfax, VA.

We propose developing a modular, cloud-ready, informatics-based system to synthesize multiple data sources into overall human health assessments of chemicals. This system would seamlessly integrate and document the overall workflow from literature search and review, data extraction, and evidence synthesis, to dose-response analysis and uncertainty characterization. Crucial benefits of such a system include improved data integrity, greater transparency, standardization of data presentation, and increased consistency. By including both a web-based workspace for assessment teams, and complementary web-based portal for reviewers and stakeholders, all interested parties would have dynamic access to completed and ongoing assessments. The modular approach will also facilitate rapid prototyping, testing, review, and incorporation of methodological improvements. Here we present a prototype module for benchmark dose (BMD) modeling used to develop points-of-departure, from which toxicity values are derived. Previously-developed BMDS Wizard and DRAGON Excel-based programs were used to develop a web-based tool where assessment teams can view/upload/enter dose-response data sets into the module, perform BMD modeling, and export results. Example summary views and plots are available online, or can be converted to report format. In addition, multiple nested views of the data and analyses enable interested users to rapidly "dive into the details." We conclude that given new data streams, diverse user needs, and multiple stakeholder interests, assuring the utility, integrity, and objectivity of human health assessments will be greatly facilitated by a modular, upgradeable, informatics-based system for their development, review, and dissemination. Disclaimer: The views expressed in this abstract are those of the authors and do not necessarily represent the views or policies of the US or California EPA.

**PS 877 An Optimized Cheminformatics Method for Determining Hazard Communication Information for Research Samples.**

N. M. Berdasco, D. M. Wilson, P. S. Price, J. A. Hammond and C. M. Thornton. *TERC, The Dow Chemical Company, Midland, MI.*

A Research Sample Safety Data Sheet (RSSDS) is a hazard communication document, which describes health and safety properties and characteristics of a chemical substance, typically for one-time-use only. This document enables research samples to be safely packaged and shipped worldwide using commercial carriers in compliance with all regulatory requirements. It is the critical vehicle for communicating relevant toxicity information to workers, shippers and first responders in case of unplanned release. It can be a time critical service where the client expectation is that cycle time (CT) will be short, typically 24-48 hrs. Implementation of the Global Harmonized System (GHS) around the world necessitates the inclusion of GHS classifications for substances and mixtures. This requirement has greatly increased the complexity of RSSDS hazard assessment, especially in situations where hazard profiles must be estimated for novel chemicals where only the structure is known. This poster describes an optimized method for the delivery of hazard information as developed by The Dow Chemical Company. The method utilizes cheminformatics tools such as QSAR modeling, read-across and identification of analogs to enhance the ability to predict hazards for novel chemicals, enabling clients to comply with complex international regulations and product stewardship while still meeting competitive timelines for product development and sampling.

**PS 878 California Communities Environmental Health Screening Tool (CalEnviroScreen).**

G. V. Alexeeff<sup>1</sup>, J. Faust<sup>1</sup>, L. August<sup>1</sup>, R. Cendak<sup>1</sup>, W. Wieland<sup>1</sup>, T. Kadir<sup>1</sup>, L. Cushing<sup>2</sup>, K. Randles<sup>1</sup>, C. Milanese<sup>1</sup> and L. Zeise<sup>1</sup>. <sup>1</sup>OEHH, Cal/EPA, Oakland and Sacramento, CA; <sup>2</sup>Energy and Resources Group, University of California Berkeley, Berkeley, CA.

Many Californians are burdened by multiple sources of pollution and some people are more vulnerable to the exposures. We developed a method, called CalEnviroScreen, which uses existing environmental, health and socioeconomic data to create a cumulative impacts score for different geographic area across California. We conducted a preliminary statewide screen at the ZIP code level to identify communities most burdened by multiple sources of pollution with populations that may be especially vulnerable to its effects. The method uses a concept of

total pollution burden based on measures of exposure, public health effects and environmental effects. This is modified by measures of sensitive populations and relevant socio-economic factors. The screen considered data for ambient ozone and PM<sub>2.5</sub> concentrations, traffic density, toxic releases from facilities, pesticide use, cleanup sites, impaired water bodies, leaking underground storage tanks, solid and hazardous waste facilities, low birth weight infants, asthma, prevalence of children and elderly, educational attainment, income, poverty and race/ethnicity. The analysis consisted of a relative comparison of approximately 1800 ZIP codes in California using a relative risk model structure. The comparisons can be viewed by individual indicators, measures of burden or measures of vulnerability. The results are presented graphically using Geographic Information System tools for each indicator and are summarized by categories of exposures, environmental effects, public health effects, sensitive individuals and socioeconomic factors. Sensitivity analyses are used to test the model structure and the usefulness of each indicator selected.

**PS 879 Cellesis: A Novel System Biology Toxicology Tool.**

C. F. Biscarrat, P. Picamal and N. A. Compagnone. *Department of Toxicology, ICDD, Meyreuil, France.* Sponsor: Y. Will.

Understanding and predicting adverse drug reactions (ADRs) are crucial goals in toxicology, since unrecognized toxicity is the most frequent reason for drug withdrawal. We have developed a novel technology based on dynamical image analysis of intracellular organelles in live cells. Mitostream®, the dynamic measure of the mitochondrial behavior, is a system biology experimental technology predictive of the severity and incidence of ADRs. It is a powerful HCA to help identify drug-induced toxicity, differentiate risk between compounds and evaluate the potential for rare but severe adverse events. Mitostream® decodes the mitochondrial behavior, quantifying motility, morphology, permeability and network organization with multiple endpoints associated to qualitative descriptors to model their interrelationship. We developed the Cellesis algorithm to identify classifiers and predictors able to fuse the matrix of recorded multi-modal markers into a unique statistical toxicity index.

An original set of 27 molecules was studied to classify drugs on a toxicity scale. The algorithm classified properly 83% of the drugs with 94% specificity and 75% sensitivity. We extended the set to include more non-toxic compounds and compounds with rare but severe toxicity as well as compounds that did not target the mitochondria. The second training set included 47 compounds and yielded 85% proper classification, a specificity of 91% and a sensitivity of 92%. Independent industrial validation was performed through the Consortium for Technology Evaluation at the DSEC, testing 10 new compounds. Chosen by our industrial partners these compounds classified properly with similar performances, showing a good association between Cellesis-predicted ADRs and the lowest tolerable dose seen in the clinic. A set of NSAID was further studied. Results showed 86 % proper classification through Cellesis-predicted ADRs. Specificity was 92%, sensitivity was reduced to 85%, some apparent false positive had a below threshold reported clinical ADRs despite having been withdrawn post-marketing due to idiosyncratic hepatotoxicity.

**PS 880 Development of a Systems Computational Model to Investigate Early Biological Events in Hepatic Activation of Constitutive Androstane Receptor (CAR) by Phenobarbital.**

H. A. El-Masri<sup>1</sup>, S. Hester<sup>1</sup>, C. E. Wood<sup>1</sup>, I. Shah<sup>2</sup>, D. C. Wolf<sup>1</sup> and C. Corton<sup>1</sup>. <sup>1</sup>NHEERL, US EPA, Research Triangle Park, NC; <sup>2</sup>NCCT, US EPA, Research Triangle Park, NC.

Activation of the nuclear receptor CAR (constitutive active/androstane receptor) is implicated in the control several key biological events such as metabolic pathways. Here, we combined data from literature with information obtained from *in vitro* assays in the US EPA ToxCast database, and *in vivo* outcomes in the US EPA ToxRef database to link CAR activation to a proposed adverse outcome pathway (AOP) of hepatic tumors. Key *in vivo* pathological events for this proposed hepatic tumor AOP are similar to those of other non-genotoxic receptor-mediated chemicals (i.e., hypertrophy, cellular proliferation, preneoplastic foci, and neoplasia), highlighting the importance of upstream biological mechanisms mediating the early proliferative signals of CAR activation. Using phenobarbital (PB), a known rodent tumor promoter and CAR activator, we developed a computational model for the early initiating events of CAR activation leading to its nuclear translocation. Based on literature evidence, the computational model describes the cascade of biological events leading to CAR nuclear translocation. These events are initiated by PB activation of Adenylyl Cyclase (AC) leading to an increase in the rate of ATP transformation to cyclic AMP. In turn, cyclic AMP increases intercellular calcium levels which inhibit the activity of AC via a negative feedback loop mechanism. However, the resulting transient increase in cyclic AMP levels activates protein

phosphatase 2A (PP2A) which inhibits ERK. This inhibition is required for the nuclear translocation of CAR and the subsequent binding to a PB-enhancer module (PBREM) indicated by CYP2B6 gene induction. Future work will bridge these events with key targets mediating proliferative responses in the proposed AOP for hepatic nuclear receptor mediated carcinogenesis. Our computational systems model illustrates the impact of early events for dose-response modeling of receptor-mediated AOPs. This abstract does not reflect EPA policy.

## PS 881 Mechanistic Modeling Illuminates the Most Important Unknowns in Bile Acid Mediated DILI.

J. L. Woodhead<sup>1</sup>, K. Yang<sup>2</sup>, K. L. Brouwer<sup>2</sup>, P. B. Watkins<sup>1</sup>, S. Q. Siler<sup>1</sup> and B. A. Howell<sup>1</sup>. <sup>1</sup>The Hamner-UNC Institute for Drug Safety Sciences, Research Triangle Park, NC; <sup>2</sup>UNC-Eshelman School of Pharmacy, Chapel Hill, NC.

BSEP inhibition and consequent bile acid (BA) buildup has been proposed to be an important mechanism in drug-induced liver injury (DILI). There are many gaps in the knowledge of BA homeostasis and its disruption by transporter inhibitors. Modeling can help us understand which of these knowledge gaps should be filled first in order to provide maximum understanding. We have constructed a model of BA homeostasis and toxicity within DILIsym<sup>TM</sup>, a mechanistic model of DILI that includes bile acid flux into and out of hepatocytes, the role of the farnesoid X receptor (FXR) in the regulation of BA transport and synthesis, and gallbladder BA release and recirculation. We first analyzed our system's behavior in the presence of a simulated BSEP inhibitor similar to glibenclamide. We predict a 41% increase in total hepatocyte content of amide conjugated chenodeoxycholic acid (CDCA). However, the simulated BSEP inhibition resulted in no change in either unconjugated CDCA or the amide-conjugated lithocholic acid (LCA), and the hepatocyte content of unconjugated LCA decreased by 15%. We next performed a sensitivity analysis on our system's response to BSEP inhibition in order to determine which parameter has the greatest effect on hepatocyte content of BAs and hence BSEP inhibitor-induced hepatotoxicity. We found that the most important unknown in the system is the intrahepatic BA concentration that triggers FXR-mediated regulation of BA transporters, while other parameters such as the affinity constants for transport of CDCA and LCA and ileal LCA transport efficiency were less important. We conclude that the highest priorities for wet lab research to inform our model and enhance our understanding of BSEP inhibitor mediated DILI are: 1) quantifying the relationship between intrahepatic concentrations of individual bile acids and FXR activation, and 2) quantifying the link between intracellular CDCA amide conjugates and toxicity.

## PS 882 Quantitative Dose-Response in a Virtual Hepatic Lobule.

J. F. Wambaugh<sup>1</sup>, J. Jack<sup>1</sup>, J. Liu<sup>1</sup>, H. A. El-Masri<sup>2</sup>, J. Davis<sup>1</sup>, W. Setzer<sup>1</sup> and I. Shah<sup>1</sup>. <sup>1</sup>National Center for Computational Toxicology, US EPA, Research Triangle Park, NC; <sup>2</sup>National Health and Environmental Effects Research Laboratory, US EPA, Research Triangle Park, NC.

The U.S. EPA Virtual Liver (vLiver) is a cellular systems model of hepatic tissue that provides simulated *in vivo* context for liver-relevant ToxCast and other *in vitro* data. To protect public health it is necessary to quantitatively estimate the risk of long-term low dose exposure to environmental pollutants. The vLiver model currently allows testing of early key events in adverse outcome pathways (AOP) by integrating multiple types of *in vitro* data in order to predict *in vivo* (animal) data. The model was used to simulate hepatocyte proliferation in 28 day repeat dose studies as an early event in non-genotoxic liver cancer AOPs. *In vitro* hepatocyte assays are often limited in assessing proliferation, in part due to the cells being removed from a tissue context – this context is created via simulation. A hepatic lobule microdosimetry model, developed in conjunction with a high throughput physiologically-based pharmacokinetic model, links whole-body exposure to cell-scale concentrations. For seven chemicals (fenarimol, imazalil, azoxystrobin, bifenazate, fenamidone, fluoxastrobin, and paclobutrazol) free chemical concentrations in the liver were predicted as a function of dose and time. A ToxCast assay for up-regulation of activator protein 1 (AP-1) in HepG2 cells – a transcription factor for cell-cycle initiation and progression – was used as a surrogate for hepatocyte proliferation. Model simulations predicted the administered dose (mg/kg/day) needed for excess proliferation *in vivo*. Five of the seven chemicals displayed non-proliferative liver lesions in rats (ToxRefDB) at similar doses, while the two without lesions were among the three chemicals predicted to require the highest dose. This demonstrates the potential for *in silico* models to predict the *in vivo* administered doses that, based on *in vitro* data, may lead to *in vivo* adverse effects. This abstract does not necessarily reflect EPA policy.

## PS 883 Quantitative Extrapolation of *In Vitro* Data to Risk Management Decisions: Using Hepatic Ah Receptor and Its Agonists As an Example.

X. Chang<sup>1</sup>, M. DeVito<sup>1</sup> and M. Easterling<sup>2</sup>. <sup>1</sup>DNTP, NIEHS, Research Triangle Park, NC; <sup>2</sup>SRA International, Research Triangle Park, NC.

A critical question in human risk assessment is how best to incorporate *in vitro* data. In a quantitative *in vitro* to *in vivo* extrapolation, one assumption is that media concentration equals blood concentration. Here, we evaluate this assumption by applying physiologically based pharmacokinetic (PBPK) models to predict cellular responses in primary rat hepatocytes exposed to an aryl hydrocarbon receptor (AhR) agonist. PBPK models for AhR agonists (e.g., TCDD, PeCDF, PCB126) were developed based on NTP two-year rat carcinogenicity bioassay data. The model predicts tissue concentrations and CYP1A1 induction well and demonstrates that ligand binding affinity is an important parameter for AhR-mediated enzyme induction and distribution of these chemicals. Using this model, we predicted the dose response for Cyp1a1 induction in whole rat liver at 48 h after an oral dose of TCDD. The predicted results were compared to literature data on rat primary hepatocyte treated with TCDD for 48 hours. The EC50 obtained for Cyp1a1 induction *in vitro* is about 100 fold less than that predicted *in vivo* (i.e., the primary cell culture system is about 100 times more sensitive). To identify which factors might contribute to this difference, we built a primary hepatocyte culture model, based on rat primary hepatocyte data from the literature and incorporated the same parameters used in the *in vivo* PBPK model of AhR agonists. Based on differences in parameter values between the two models, we identified critical factors determining the difference in sensitivity between *in vivo* and *in vitro* (e.g., TCDD availability). The hepatocyte culture model built for TCDD can predict the toxicities or downstream events for other AhR agonist by changing the parameter associated to AhR binding affinity only. This evaluation provides a model example of a quantitative *in vitro* to *in vivo* extrapolation for nuclear receptors and informs on how to better use *in vitro* data for risk assessment. This abstract does not necessarily reflect the policies or views of NIH.

## PS 884 Predicting Plasma Profiles following Oral Dosing for Drug Liver Transporter Substrates Using Physiologically-Based Pharmacokinetic Modeling.

H. A. Barton<sup>1</sup>, Y. Lai<sup>1</sup>, J. R. Gosset<sup>2</sup> and H. M. Jones<sup>2</sup>. <sup>1</sup>Pharmacokinetics, Pharmacodynamics, and Metabolism, Pfizer, Inc., Groton, CT; <sup>2</sup>PDM, Pfizer, Inc., Cambridge, MA.

A novel prediction approach for OATP substrates was developed using *in vitro* sandwich cultured hepatocyte (SCHH) data as input into a physiologically based pharmacokinetic (PBPK) model and was validated for intravenous (iv) dosing (Jones et al., 2012). The aim of our work was to extend this to the prediction of oral profiles. Data for plasma concentrations following oral doses were obtained from literature. Simple descriptors of oral absorption (fa, ka) were predicted using a physiologically based gastrointestinal (GI) tract model, which were then used in the published transporter PBPK model with a single compartment for oral absorption. The seven literature compounds were bosentan, cerivastatin, fluvastatin, pravastatin, repaglinide, rosuvastatin, and valsartan. *In vitro* passive permeability and solubility under fed and fasted conditions were measured as inputs to the GI model. We tested whether the oral absorption parameters were reasonable by combining them with the transporter parameters obtained from fitting the iv plasma data. Characterizing plasma pharmacokinetics using area under the curve to infinity (AUC(0-inf)), maximum concentrations (Cmax), and time to maximum concentration (Tmax), the fold error for the seven compounds was 1.6, 2.3, and 1.9 respectively, indicating the oral absorption parameters were reasonable. Forward predictions for the seven compounds based on SCHH data and the oral absorption parameters provided a test of both aspects of predicting oral plasma time course. The average fold errors for the seven compounds increased somewhat to 2.5, 3.3, and 2.4, respectively. This method was then applied to oral plasma data for four in-house compounds resulting in reasonable predictions for three of the four. An initial prediction method has been developed using *in vitro* and *in silico* inputs to estimate plasma profiles and pharmacokinetic parameters for iv and oral dosing of anionic drugs that are substrates for liver transporters.

**PS 885 A Mechanistic Approach to Understand Idiosyncratic Toxicity of Perhexiline and Sulindac.**

S. Das, R. Kumar, N. Rajeswara, S. Raghavan, Y. Chandrasekaran, N. Mandyam, S. Louha, A. Khanna, D. Srivastava, K. Ra and K. Subramanian. *Strand Life Sciences, Bangalore, India.*

Idiosyncratic DILI is one of the most common causes of safety-related post-marketing drug withdrawals. We have developed a dynamic systems based integrative approach that aids in its understanding by combining a mathematical model along with a panel of in vitro enzyme and transporter assays.

We tested perhexiline and sulindac in this assay system and fed the assay results into a mathematical model of liver biology. Our simulations identified the key mechanism behind the steatohepatitis caused by perhexiline. They predict perhexiline induced alterations in mitochondrial function, i.e. inhibition of oxidative phosphorylation, generation of oxidative stress along with inhibition of mitochondrial beta-oxidation leads to steatosis. An interesting insight gained in this process was the fact that whole cell measurements such as ATP or GSH alone can provide an erroneous understanding of the impact of a compound in vivo. On the other hand measuring various enzymatic functions enabled us to quantify the impact of ROS in vivo.

In the case of Sulindac, intracellular accumulation of GSH in HepG2 cell line indicated impairment of transport system. Applying this impairment in the model, our simulations predict bile and bilirubin accumulation indicating the potential for idiosyncratic cholestasis.

Thus our system enables us to understand mechanistic insights into the effect of leads and make predictions on their effects in vivo without necessitating the use of whole animal studies.

**PS 886 An Integrated Structure-Based Systems Approach to Predict Hepatotoxicity.**

A. Das, N. Mandyam, N. Tiwari and K. Subramanian. *Strand Life Sciences, Bangalore, India.*

We have developed a systems biology model for hepatotoxicity prediction. The input for the model is a set of in vitro assays that capture the effects of a chemical compound on selected proteins. The model takes these assay results as input, simulates their likely effects on selected pathways in a liver cell and outputs the toxicity effects in vivo. Though this approach has good predictive value and provides mechanistic insights into the toxicity response, the time consuming and expensive assays are a bottleneck for using the model in a high-throughput manner.

Using structure based approaches, we have virtualised the assays to use this model to rapidly evaluate hepatotoxicity of molecules. The binding affinity of a molecule to each of the proteins is estimated using structure prediction, flexible and induced docking and pharmacophore approaches and classified as low, intermediate or high. This forms the input to the systems model which then estimates the integrated impact of these perturbations on various pathways in the liver. We expected that the model output, though not as precise as with in vitro inputs, can flag likely hepatotoxicity of a molecule.

As an initial proof of concept, we tested this approach in a set of molecules, pioglitazone, tolcapone, rofecoxib, quiniacrine, propantheline bromide, benoxinate, bumetanide, AZ177 and acetaminophen. We found that this method is able to flag the key toxic mechanisms of each of these molecules and is able to predict synergistic toxic effects. We believe that this approach can be used as screening tool to rapidly and accurately assess mechanistic toxic effects and has utility during lead discovery and optimization.

**PS 887 Application of an In Silico Approach to Predict Intrinsic In Vitro Cytotoxicity for Compounds in Primary Human Hepatocytes during Preclinical Development.**

R. Pai, B. Wei, P. Chang, J. Crawford, W. Young, D. Ortwine, D. Misner and D. Dambach. *Genentech Inc., S. San Francisco, CA.*

Drug-induced liver injury is a major cause of compound attrition in preclinical and clinical development and, often, intrinsic hepatotoxicity can be related to chemical structure. Screening in primary human hepatocytes has been routinely used to assess toxicity in the preclinical setting to allow for assessment of metabolic contribution. However, the knowledge gained from this screening has not been fully utilized to drive medicinal chemistry design before compound synthesis. Herein, we present work in progress in the development of a computational model that is used to predict the outcome of hepatocyte screening for a set of preclinical compounds with significant accuracy. Cytotoxicity was determined by treating cryoplateable human hepatocytes with individual compounds and evaluating cellular ATP levels. In vitro

cytotoxicity was classified based on IC50 values into three buckets: high (<50  $\mu$ M), medium (50-100  $\mu$ M) and low toxicity (>100  $\mu$ M) groups. Using a machine learning approach, a large set of structural and non-structural descriptors were evaluated for their usefulness to classify cytotoxicity on a training set of 72 compounds. Three calculated physicochemical properties emerged as the most predictive descriptors (most-basic-pKa, plasma protein binding % and logP), and were used to construct a decision tree model. Subsequently, predictions were made for 102 compounds prospectively. The positive predictive values were 77% & 65%, and negative predictive values were 72% & 85% for high (H) and low (L) toxicity groups, respectively. Interestingly, addition of structural descriptors did not improve the accuracy of prediction, suggesting that the intrinsic toxicity of those compounds were not specific to their structures. We show that this model proved useful in reducing compound attrition for an ongoing project. Furthermore, the physicochemical property space that this work has implicated as being associated with toxicity may also provide clues toward understanding the underlying mechanism(s).

**PS 888 In Vitro In Vivo Correlation: Apparent or Ambiguous? Analysis of Pfizer Compounds in US EPA's ToxCast Chemicals-Assay Space.**

F. Shah and N. Greene. *Compound Safety Prediction, Worldwide Medicinal Chemistry, Pfizer Worldwide Research and Development, Groton, CT.*

In 2009, Pfizer collaborated with EPA in their ToxCast initiative to identify predictive bioactivity signatures for toxic compounds using 'dead' pharmaceuticals. A total of 52 Pfizer compounds with preclinical data were profiled in multiple assay platforms measuring bioactivity against diverse assay end-points. The first part of this work was focused on the analysis of Pfizer compounds in ToxCast chemicals and pharmacological space. These include a) comparison of bioactivity profile of Pfizer compounds with other pharma and EPA compounds; b) analysis of compounds sharing similar chemical and pharmacological space as of Pfizer compounds; and c) ability of assay platforms to reproduce the primary mode of action of Pfizer compounds. Analysis revealed that compound from EPA set seemed to have different pharmacological and chemistry space than pharma compounds. It also highlighted assay platforms and sensitive endpoints that are more relevant to understand the off-target activities of compounds. The second part involves correlation of in vitro ToxCast assay signals with in vivo findings related to liver injury, observed either in preclinical or clinical studies. The analysis pinpointed diverse cytotoxicity endpoints within ToxCast as markers of compound potential to cause preclinical or clinical liver injury.

**PS 889 Improved In Silico Methods to Group Liver Toxicants Related to Adverse Outcome Pathways.**

M. T. Cronin, S. J. Enoch, M. Hewitt, J. C. Madden, M. Nelms, K. Przybylak and A. N. Richarz. *School of Pharmacy and Chemistry, Liverpool John Moores University, Liverpool, United Kingdom. Sponsor: C. Yang.*

Prediction of repeat dose toxicity by in silico methods remains an elusive goal. Current quantitative structure-activity relationship (QSAR) approaches have acknowledged limitations. A more pragmatic approach is to identify relevant molecular initiating events associated with an adverse effect – integrated into the Adverse Outcome Pathway (AOP) concept – and attempt to group chemicals accordingly. Such an approach will have a greater probability of success if targeted at organ level toxicity. The purpose of this study was to develop novel structural alerts to enable to the grouping of potential liver toxicants. Specifically, the utility of current approaches for grouping according to protein reactivity (relating to reactive hepatotoxicity) was investigated along with novel methods to group chemicals and extract usable information from the grouping, placing in the context of relevant AOPs. The objective, therefore, was not to necessarily provide a better predictive model for liver toxicity, but to improve structural alerts to group compounds to perform read-across for liver toxicity. Data for over 900 compounds classified as either being toxic or non-toxic to the liver were assessed in this study. Attempts to group compounds on the basis of protein reactivity (the OECD Profiler in the OECD QSAR Toolbox) had poor predictivity, only identifying approximately 34% of liver toxicants, whilst nearly 25% of non-toxicants were found to contain a reactive structural alert. Therefore, the liver toxicants were grouped according to structural similarity using the ToxMatch software. Over 80 categories were found by this automated method from which 16 robust categories were manually curated, many of which were associated to mitochondrial toxicity AOPs. The suite of reactive and non-reactive MIEs, defined by structural alerts and chemotypes, provides a basis for grouping potential liver toxicants. Supported by the EU FP7 COSMOS and eTox Projects.

**PS 890 Construction of a Human Hepatotoxicity Database for QSAR Modeling.**

N. L. Kruhlak and X. Zhu. *CDER/OPS/OTR/DDSR, US FDA, Silver Spring, MD.*  
Sponsor: R. Benz.

Drug-induced liver injury (DILI) represents the second most common reason for pre-market attrition of drug candidates and post-market withdrawal of approved products, prompting the need for better tools to predict these serious effects. Quantitative structure-activity relationship (QSAR) modeling uses computational algorithms in conjunction with large chemical data sets to identify correlations between molecular structural features and biological activity, and lends itself well to the task of improving the prediction of drug safety by exploiting FDA's vast institutional knowledge of DILI and other adverse event (AE) data. This report describes the development of a new method for creating a DILI QSAR training set based on FDA's Adverse Event Reporting System data. The method utilizes the Multi-item Gamma Poisson Shrinker (MGPS) algorithm, the gold standard used by FDA CDER's Office of Surveillance and Epidemiology for AE signal identification, to generate Empirical Bayesian Geometric Mean (EGBM) scores for all drugs in the database binned by MedDRA preferred term. A set of 38 preferred terms (PTs) describing serious hepatic events, such as hepatic failure, hepatocellular injury, and hepatic cirrhosis, was selected based on related physiology and their adverse event counts were pooled to provide a more robust dataset for scoring purposes. An independently obtained verification set of 107 known hepatotoxins with evidence ranging from clinical manifestations (n=93) to market withdrawals (n=14), was used as a calibration set to determine whether the standard EGBM cutoff of 2.0 was appropriate for partitioning the training set. While 92% of the withdrawn drugs were correctly classified, only 50% of the positives with clinical manifestations were correctly classified, emphasizing the need for additional parameters and/or PTs to supplement the AE data used in the training set. This method created a set of over 2000 unique molecular entities that were structurally suitable for QSAR modeling.

**PS 891 Virtual Liver: Mapping Pathways to Liver Injury by Linking In Vitro Assays to In Vivo Outcomes.**

I. Shah<sup>1</sup>, J. Liu<sup>1</sup>, C. Corton<sup>2</sup>, S. Hester<sup>2</sup>, K. Houck<sup>1</sup>, T. B. Knudsen<sup>1</sup>, H. A. El-Masri<sup>2</sup>, J. Simmons<sup>2</sup>, J. F. Wambaugh<sup>1</sup> and C. Wood<sup>2</sup>. <sup>1</sup>NCCT, US EPA, Durham, NC; <sup>2</sup>NHEERL, US EPA, Durham, NC.

The EPA ToxCast project uses high-throughput screening (HTS) to evaluate in vitro bioactivity of chemicals. Here we are attempting to bridge HTS data with histopathological effects in ToxRefDB using a data-driven computational approach. Starting with 2,200 guideline studies for 763 chemicals stored in ToxRefDB, we defined 8 broad categories of hepatic histological effects consisting of hypertrophy, cytotoxicity, inflammation, regeneration, steatosis, fibrosis, preneoplasia, and neoplasia. A subset of 560/763 chemicals were screened in 500 ToxCast assays. Univariate statistical analysis found 91 assays in which chemicals had a significantly ( $p < 0.05$ ) greater potency for hepatic effects. We identify mechanistic relationships between the molecular and cellular targets of these assays from literature and use an information-theoretic criterion to calculate the most plausible sequence of key events for each outcome. The results are summarized as a dependency network including molecular initiating events (e.g. AhR, PXR, and PPAR), signal transduction (PI3K/AKT, p53, NFkB, JNK), cellular alterations (oxidative stress, mitochondrial dysfunction, cytoskeletal changes, cell cycle arrest and apoptosis), and histological effects. The analysis also suggests markers of hepatic lesion severity: chemicals that cause hypertrophy without injury have a 3-fold potency ( $p < 0.05$ ) for stress kinase activation; for hypertrophy and injury a 2-fold greater potency for G2/M arrest and p53 activation; and for steatosis a 2-fold greater potency for mitochondrial dysfunction. This work should inform current efforts to translate HTS data from a molecular scale to clinically-relevant health effects.

This work was reviewed by EPA and approved for publication but does not necessarily reflect official agency policy.

**PS 892 A Multiscale Dose-Response Model of AhR Toxicity Pathway Activation in the Human Liver.**

S. Bhattacharya, P. D. McMullen and M. E. Andersen. *Institute for Chemical Safety Sciences, The Hamner Institutes for Health Sciences, Research Triangle Park, NC.*

We have developed a spatial, multicellular agent-based computational model of the human liver lobule to study the contribution to hepatotoxic injury from multiple levels of biological organization. This multi-scale "virtual tissue" model combines

molecular circuits in individual hepatocytes with cell-cell interactions and blood-mediated transport of toxicants through hepatic sinusoids, and dosimetry estimated by whole-body PBPK models, to enable quantitative, mechanistic prediction of dose-response. We use the activation of the aryl hydrocarbon receptor (AhR) toxicity pathway in hepatocytes exposed to 2,3,7,8-tetrachlorodibenzo-p-dioxin (TCDD) and other dioxin-like compounds (DLCs) as a case study for data integration and multi-scale model development for mechanistic dose-response prediction. By explicitly accounting for basal gradients in AhR expression across the lobule and stochastic uptake of TCDD molecules by individual hepatocytes, we were able to reproduce experimentally observed zonal heterogeneity in TCDD accumulation and cytochrome P450 1A1 expression. A detailed implementation of the AhR signaling and transcriptional cascade in each hepatocyte in this multicellular model enabled us to characterize differential dose response for various AhR-mediated endpoints at the tissue level, including cytotoxicity and cell proliferation.

**PS 893 Evaluation of Perchlorate Intake on Maternal and Fetal Serum T4 Levels Using a BBDR Model.**

A. Lumen<sup>1,3</sup>, D. R. Mattie<sup>2</sup> and J. W. Fisher<sup>3</sup>. <sup>1</sup>HJF, Rockville, MD; <sup>2</sup>711 HPW/RHDJ, Wright-Patterson AFB, OH; <sup>3</sup>US FDA/NCTR, Jefferson, AR.

Perchlorate (ClO<sub>4</sub><sup>-</sup>) is both a naturally occurring and man-made chemical widely distributed in the environment with low levels detected in food and drinking water. Disturbances in the maternal hypothalamic-pituitary-thyroid (HPT) axis leading to hypothyroxinemia and hypothyroidism have been shown to cause negative effects on the neurodevelopment of the fetus. Downstream perturbations of maternal and fetal HPT axes following ClO<sub>4</sub><sup>-</sup> competitive inhibition of sodium iodide symporter-mediated thyroidal iodide (I<sup>-</sup>) uptake have not been evaluated quantitatively. In order to quantitate effects of dietary I<sup>-</sup> intake, ClO<sub>4</sub><sup>-</sup> exposure and their interactions on maternal and fetal HPT axis, a biologically based dose response (BBDR) model for HPT axes in the pregnant woman and fetus was developed. The BBDR model includes sub-models for I<sup>-</sup>, ClO<sub>4</sub><sup>-</sup>, thyroxine (T<sub>4</sub>) and triiodothyronine (T<sub>3</sub>). The model was successfully calibrated for euthyroid, marginal iodide deficiency and ClO<sub>4</sub><sup>-</sup> exposure. Serum thyroid hormone changes were predicted for dietary I<sup>-</sup> intake ranging from 75 to 250 µg/day and for ClO<sub>4</sub><sup>-</sup> exposures of 0.01 to 1000 µg/kg/day. Model simulations suggest that ClO<sub>4</sub><sup>-</sup> at environmentally relevant ranges of exposure (~0.1 µg/kg/day) does not result in significant decreases in maternal and fetal free serum T<sub>4</sub> concentrations for maternal I<sup>-</sup> intake of 75 to 250 µg/day. For a daily I<sup>-</sup> intake of 200 µg/day, the daily dose of ClO<sub>4</sub><sup>-</sup> required to reduce serum free T<sub>4</sub> (fT<sub>4</sub>) levels from representative euthyroid region to a hypothyroxinemic state was estimated to be about 50-fold greater (32 µg/kg/day) than the current reference dose (RfD, 0.7 µg/kg/day). As I<sup>-</sup> intakes were lowered (150, 100 and 75 µg/day), ClO<sub>4</sub><sup>-</sup> doses required for similar reductions in fT<sub>4</sub> levels were reduced to 28, 16, and 4 µg/kg/day, respectively. This BBDR-HPT axis model for pregnancy provides a novel tool for public health assessments for endocrine active chemicals found in food and the environment. Funded by the Air Force Center for Engineering & the Environment through 711 HPW/RHDJ, WPAFB, OH.

**PS 894 Cross-Species and Life Stage PBPK Modeling of Dibenzo[def,p]chrysene.**

S. R. Crowell<sup>1</sup>, S. Hanson-Drury<sup>1</sup>, J. Soelberg<sup>1</sup>, N. Sadler<sup>1</sup>, A. Wright<sup>1</sup>, A. Sharma<sup>2</sup>, E. P. Madsen<sup>3</sup>, D. E. Williams<sup>3</sup> and R. A. Corley<sup>1</sup>. <sup>1</sup>Pacific Northwest National Laboratory, Richland, WA; <sup>2</sup>Penn State University, Hershey, PA; <sup>3</sup>Oregon State University, Corvallis, OR.

Polycyclic aromatic hydrocarbons (PAHs) are ubiquitous, often carcinogenic environmental contaminants generated as by-products of combustion processes. PAHs are found at almost half of Superfund sites, and are drivers for remediation in a significant percentage of those sites. Dibenzo[def,p]chrysene (DBC) is a high molecular weight and highly potent transplacental carcinogenic PAH. We developed the first species- and life stage-specific physiologically based pharmacokinetic (PBPK) models for high molecular weight PAHs that can be used to predict target tissue doses of PAH metabolites important to their carcinogenic mode of action. In rodents, we measured metabolic enzyme activity, rates of metabolism, and pharmacokinetics during vulnerable life stages such as pregnancy and fetal development. Pregnant animals had elevated tissue concentrations of DBC and its metabolites (2 – 4 fold increase in C<sub>MAX</sub>), and suppressed rates of clearance compared to naïve mice. Using activity-based protein profiling (ABPP), a unique proteomic approach for characterizing functional proteins in complex biological systems, to measure and compare enzyme activity, we found that multiple enzymes important for PAH metabolism have significantly altered activity during pregnancy and development in rodents and humans. Incorporating changes in anatomy and physiology during pregnancy as well as measured reductions in P450 enzyme activity accounted for

observed pharmacokinetic differences in mice. We have extrapolated our PBPK models to describe human dosimetry on the basis of human anatomy and physiology, and chemical specific human *in vitro* metabolic rates. In order to evaluate the extrapolated human model, a controlled human pharmacokinetic study of DBC at environmentally relevant exposure levels (30 ng bolus exposure) has been performed by our collaborators. Initial simulations of DBC concentrations in blood are remarkably similar to those observed in preliminary data from human volunteers.

**PS 895 Evaluating Early-Life Sensitivity to Pyrethroids by Physiologically-Based Pharmacokinetic (PBPK) Modeling Using *In Vitro* to *In Vivo* Extrapolation.**

H. Wu<sup>1</sup>, M. Yoon<sup>1</sup>, S. Anand<sup>2</sup>, B. G. Lake<sup>3</sup>, T. Osimitz<sup>4</sup>, N. Assaf<sup>5</sup>, A. Efremenko<sup>1</sup> and H. J. Clewell<sup>1</sup>. <sup>1</sup>The Hammer Institute for Health Sciences, Research Triangle Park, NC; <sup>2</sup>DuPont Haskell, Newark, DE; <sup>3</sup>LFR Molecular Sciences, Leatherhead, United Kingdom; <sup>4</sup>Science Strategies, LLC, Charlottesville, VA; <sup>5</sup>Valent BioSciences, Libertyville, IL.

The increased sensitivity of post-natal day (PND) 21 (weanling) rats to acute high-dose neurotoxicity of deltamethrin (DLM) poses the question of whether children will be more sensitive than adults both of whom are exposed to a much lower dose than rats. Age-related pharmacokinetic (PK) differences are hypothesized to be responsible for the observed differences in rats. We developed a PBPK model for human children based on rat PK and rat and human *in vitro* data. Our model incorporated species and age-dependent differences in metabolism of DLM as well as physiological changes during growth. The predicted age-dependent changes in brain C<sub>max</sub> correlated well with the maturation of metabolic capacity suggesting the lower metabolic clearance as a mechanism for the increased sensitivity in neonatal rats. The predicted C<sub>max</sub> in brain of PND 21 pups after a single oral dose of 4 mg/kg was 50% higher compared to PND 70 rats. The human model was developed similarly by incorporating maturation physiology and developmental changes in DLM metabolizing enzymes. Unlike the rat, the predicted brain C<sub>max</sub> of DLM was comparable between children and adults. After a single oral dose of DLM (0.1 mg/kg), the predicted C<sub>max</sub> was 1.4, 1.7, 2.4, and 2.0 pg/g, respectively, for children ages 1, 5, and 10 years old, and adults. The observed species differences in age-dependent PK seems to be largely attributable to the species differences in enzyme ontogeny and resulting metabolic clearance rates for DLM as well as differences in doses. In conjunction with age-specific exposure data, the current model will enable us to evaluate early life sensitivity in humans under environmentally relevant exposure conditions for this chemical and can be readily applicable to other pyrethroids with proper parameterization (supported by CAPHRA).

**PS 896 Evaluating Age-Related Sensitivity to Carbaryl-Induced Behavioral Changes by PBPK/PD Modeling.**

D. Billings<sup>1</sup>, M. Yoon<sup>1</sup>, V. C. Moser<sup>2</sup>, R. C. MacPhail<sup>2</sup> and H. J. Clewell<sup>1</sup>. <sup>1</sup>The Hammer Institutes for Health Sciences, Research Triangle Park, NC; <sup>2</sup>TAD/NHEERL/ORD, US EPA, Research Triangle Park, NC.

Due to its reversible inhibition of cholinesterases (ChEs), acute neurotoxicity is the primary effect of concern for carbaryl. Sensitivity to acute behavioral neurotoxicity of carbaryl was observed to be greater in aged rats, which was not fully attributable to differences in ChE inhibition. We used a PBPK/PD model to evaluate appropriate dose metrics to describe the observed age-related sensitivity to carbaryl in Brown Norway rats, using the change in horizontal motor activity as a marker of biological effect. The current model extends our previous PBPK/PD model in adult Sprague-Dawley rats that describes carbaryl disposition and inhibition of ChE in brain and blood. Age-appropriate physiological parameters were incorporated in the model in conjunction with age-specific metabolism parameters determined in primary hepatocytes isolated from young adult and aged rats (4, 12 and 24 month old). The model-simulated values compared well with the data both for peak and time-dependent changes in carbaryl concentration in the brain, liver and plasma as well as inhibition of ChE in brain and erythrocytes after a single oral exposure of carbaryl (3, 7.5, 15, or 22.5 mg/kg). While changes in motor activity were correlated with the degree of ChE inhibition at the time of peak effect (40 min), the model did not reproduce the recovery of activity in the older rats up to 240 min. The age-related difference was not explained by kinetics of reaction with ChE by carbaryl, but suggested differences in recovery dynamics in aged rats. The current study demonstrated the use of a PBPK/PD model to describe age-dependent acute effects and recovery from carbaryl, and provided a novel explanation for prolonged recovery in old animals. This is an abstract of a proposed presentation and does not reflect EPA policy (supported by EPA STAR grant R833452 and ACC-LRI).

**PS 897 Interpreting Biomonitoring Data for Di-n-Butyl and Di-(2-Ethylhexyl) Phthalate Metabolites in Urine Using a Physiologically-Based Pharmacokinetic Model and Reverse Dosimetry: Estimation of Cumulative *In Utero* Exposure.**

J. Campbell, R. A. Clewell, M. E. Andersen and H. J. Clewell. The Hammer Institutes for Health Sciences, Research Triangle Park, NC.

At high doses, several phthalate esters, including d-n-butyl and di-2-ethylhexyl phthalate (DBP and DEHP respectively), disrupt normal male reproductive development in rats. Human biomonitoring data have demonstrated phthalate exposure in humans of all ages based on serum, urine, cord blood and breast milk measurements. We used PBPK modeling and reverse dosimetry to infer likely environmental exposures from human biomonitoring data on phthalates in urine. Human PBPK models for DBP and DEHP and their primary metabolites – mono-n-butyl and mono-2-ethylhexyl phthalate (MBP and MEHP) – during pregnancy were developed from published rodent PBPK models and human data. To estimate daily intake of DBP and DEHP consistent with population measures of urinary metabolite levels, Monte Carlo analyses were performed to generate an inverted distribution between urine concentration and steady state exposure. Based on the NHANES III biomonitoring data, the predicted distribution of daily intake for DBP in the U.S. had a median of 0.65 µg/kg/day with a 95th percentile of 5.0 µg/kg/day. For DEHP the estimated daily intakes were higher, with a median of 1.86 µg/kg/day and a 95th percentile of 20.4 µg/kg/day. Applying forward dosimetry with the pregnancy PBPK model, the 95th percentile exposure concentration resulted in an average fetal plasma concentration of 6.77 µg/L for MBP and 1.4 µg/L for MEHP. These values can be compared to an average concentration of 1680 µg/L for MBP and 71.2 µg/L for MEHP in rat fetal plasma, simulated with the rat PBPK models at the NOAELs of 30 and 5 mg/kg, respectively, for developmental effects.

**PS 898 Species Extrapolation of Life-Stage PBPK Models to Investigate Ethanol Developmental Toxicity Using *In Vitro* to *In Vivo* Methods.**

E. D. McLanahan<sup>1</sup>, S. A. Martin<sup>2</sup>, S. Hunter<sup>2</sup> and H. A. El-Masri<sup>2</sup>. <sup>1</sup>ORD/NCEA, US EPA, Research Triangle Park, NC; <sup>2</sup>ORD/NHEERL, US EPA, Research Triangle Park, NC.

Ethanol (EtOH), which induces fetal alcohol spectrum disorder-related effects, was selected to investigate the use of PBPK models in a quantitative *in vitro* to *in vivo* extrapolation (IVIVE) paradigm. Mouse whole embryo culture data on EtOH time-concentration dependent induction of neural tube defects (NTDs) was used to assess embryotoxicity. Initially, published rat life-stage PBPK models were extrapolated to adult non-pregnant and pregnant mice and humans using species specific (SS) growth equations and parameters. Each model was able to predict blood EtOH concentrations (BEC) following multiple routes of exposure. Once calibrated with published data, the mouse and human models produced adequate simulations (within factor of 2) of time-course BEC data. An IVIVE was performed by estimating SS BECs in rat and mouse dams using *in silico* simulations for induction of NTDs *in vitro*. Then, a human model IVIVE was performed using rodent *in vitro* and pregnant human toxicity and epidemiological reports of EtOH exposure during windows of gestational susceptibility. As reported in the human literature, 150 mg/dl BEC is associated with developmental neurotoxicity. In human embryonic stem cells (hESCs), 145 mg/dl EtOH is associated with apoptosis and altered neuroprogenitor differentiation and proliferation. The similarity in effective concentration illustrates the utility of using BEC in pregnant women as a predictor of adverse developmental effects. However, since hESCs are more sensitive to EtOH-induced effects than mouse conceptuses *in vitro*, a human IVIVE based on mouse *in vitro* data exceeds the reported 150 mg/dl BEC. The human model predicted exposure scenarios within a factor of 2 of the observed toxic BECs. This research demonstrates both the capability of models to extrapolate between *in vitro* animal and *in vivo* human studies and the first pregnancy models for EtOH in mice and humans. The views expressed in this abstract are those of the authors and do not necessarily represent the views or policies of the U.S. EPA.

**PS 899 A Simple *In Vitro* Approach for the Rapid Detection of Neurotoxicity.**

Q. Gu, S. Lantz, M. G. Paule and L. Schmued. Division of Neurotoxicology, US FDA National Center for Toxicological Research, Jefferson, AR.

Neurodegeneration is the underlying cause of a vast majority of neurological disorders and often a result of brain trauma, stroke, or neurotoxic insult. A widely used and reliable method for labeling degenerative neurons in *ex vivo* brain tissue involves the use of the Fluoro-Jade stains. Recently we described a novel method for

the labeling of degenerating neurons in unfixed brain tissue samples using Fluoro-Jade-C (FJC) (Gu et al. *Journal of Neuroscience Methods* 2012, 28:40-43). This method is simple, fast, and applicable to unfixed brain tissue sections and works at neutral pH. Based on these features, we extended our experimentation by examining the utility of FJC in vitro using cell cultures. Using neural stem cells, for example, we report here specific FJC labeling following treatment with neurotoxicants such as cadmium. The FJC labeling appears to be specific to neural cells, since other cell types such as cultured kidney epithelial cells did not show similar labeling even when cells were dying or dead. Further characterization and validation of this in vitro approach is underway. By employing FJC labeling in multi-well culture plates and using high-content time-lapsed recordings and additional techniques, a primary goal will be to achieve high-throughput monitoring and analysis of morphological, biochemical and molecular changes associated with the entire neurodegenerative process in cell culture models after neurotoxicant exposures. This in vitro approach has the potential to not only reduce animal use and suffering in toxicity tests but also to facilitate high-throughput screens for potentially neurotoxic compounds.

Supported by NCTR Protocols E07460 and E07477.

## PS 900 Evaluation of the Neuroactivity of ToxCast Compounds Using Multiwell Microelectrode Array Recordings of Primary Cortical Neurons.

P. Valdivia<sup>1,2</sup>, M. Martin<sup>3</sup>, W. LaFew<sup>4</sup>, J. Ross<sup>2</sup>, K. Houck<sup>3</sup> and T. J. Shafer<sup>4</sup>.

<sup>1</sup>Duke University, Durham, NC; <sup>2</sup>Axion Biosystems, Atlanta, GA; <sup>3</sup>NCCT, ORD, US EPA, Research Triangle Park, NC; <sup>4</sup>ISTD, ORD, US EPA, Research Triangle Park, NC.

Assessment of spontaneous activity in neuronal cultures on microelectrode arrays (MEA) is a sensitive method to detect responses to drugs, chemicals, and particles. While single-well MEA systems lack the efficiency to screen large numbers of compounds, recently developed multi-well MEA systems have increased throughput of MEAs. The present experiments examined the ability of a subset of EPA's ToxCast library of compounds to alter neuronal activity using 48 well MEA plates. Sixty-eight compounds were selected from the ToxCast Phase I and II chemical libraries based on known neuroactivity or data from 14 ToxCast in vitro assays indicating that they interacted with ion channels. Two compounds expected not to alter neuronal function, acetaminophen and saccharin, were included as negative controls. One hr of baseline activity was recorded prior to exposing the cortical networks to 40  $\mu$ M of each compound for 1 hr and the weighted mean firing rate (wMFR) was determined in the absence and presence of each chemical. All experiments were conducted on day in vitro 14 or 15. Based on DMSO-treated wells, chemicals that increased or decreased activity by  $>23.6\%$  were considered hits. Of the 68 compounds, 47 altered wMFR by more than the threshold. Saccharin and acetaminophen did not change wMFR beyond the threshold. Four of six pyrethroids, and 3/3 conazoles were detected as hits. Interestingly only 1/7 nicotinic agonists (nicotine&neonicotinoids) were hits, but were close to the threshold. These data demonstrate that multiwell MEAs can be used efficiently to screen chemicals for potential neurotoxicity and that the results are concordant with predictions from 14 ToxCast ion channel assays. Further, changes in wMFR may not be a sensitive measure to detect nicotinic effects in this culture model (This abstract was supported by CRADA #644-11 with Axion Biosystems. This abstract does not reflect Agency Policy).

## PS 901 Development of an In Vitro Multiwell Microelectrode Array (MEA) Neurotoxicity Assay with Human IPS-Derived Neurons.

J. Bradley<sup>1</sup>, J. Ross<sup>2</sup>, M. Brock<sup>2</sup>, H. Luithardt<sup>1</sup>, J. Gilbert<sup>1</sup> and C. Strock<sup>1</sup>.

<sup>1</sup>Cyprotex, Watertown, MA; <sup>2</sup>Axion Biosystems, Atlanta, GA.

Seizurogenic neurotoxicity produces significant drug attrition during drug discovery. Current available in vitro assays fail to predict this toxicity due to the failure of general cytotoxicity assays to predict sublethal target specific electrophysiological liabilities. Ion channel and receptor activity assays can be used to predict some seizure potential, but this only focuses on specifically measured targets for prediction and may miss a response which relies on a combination of endpoints. Most evaluation of seizure inducing compounds occurs later in preclinical development in in vivo studies which have higher costs and could result in species specific results. Therefore, the development of an in vitro assay to screen compounds for seizurogenic potential in a human neural model would give the potential to screen compounds earlier at lower cost and greater reliability. Here we demonstrate the use of

multiwell MEAs to screen for seizurogenic compounds in human IPS derived neurons (hsN). HsNs were seeded in 48 well MEAs and spontaneous activity began at 3 days post plating with greater activity at 7 days when the assay is performed. Neural action potentials were detected and the results were reported as mean firing rate (MFR). The seizurogenic compounds tested show dose dependent increase in MFR with changes in spike train organization, while all of the negative controls were unaffected. The seizurogenic compounds tested were Picrotoxin, Gabazine, L-Glutamate, and pentylenetetrazole (PTZ). Negative compounds tested were acetaminophen, naproxen, and DMSO. To further demonstrate the responsiveness of the cells in the assay, we tested Domoic Acid, a neurotoxin known to cause amnesia, and found that it completely blocked network activity while not causing cell death. These results illustrate the power of the human Neural MEA assay for predicting compound induced neural toxicity, especially the seizurogenic response.

## PS 902 In Vitro Neurotoxicity of Tetrabromobisphenol-A (TBBPA).

R. H. Westerink, R. G. van Kleef, M. van den Berg and H. S. Hendriks. *Neurotoxicology Research Group, Institute for Risk Assessment Sciences (IRAS) - Utrecht University, Utrecht, Netherlands.*

Tetrabromobisphenol-A (TBBPA) is a widely used brominated flame retardant. Studies on the in vitro neurotoxic potential of TBBPA focused on cytotoxicity and presynaptic effects of neurotransmission, while recent studies indicate that persistent organic pollutants can also affect postsynaptic inhibitory human GABAA and excitatory  $\alpha 4\beta 2$  nicotinic acetylcholine (nACh) receptors. Possible effects of TBBPA on these neurotransmitter receptors are of considerable interest as these receptors are critically involved in neurotransmission, synaptic plasticity and brain development. We therefore investigated the effects of TBBPA on these receptors, expressed in *Xenopus* oocytes, using the two-electrode voltage-clamp technique. Our results demonstrate that TBBPA acts as full ( $\geq 10 \mu$ M) and partial ( $\geq 0.1 \mu$ M) agonist on human GABAA receptors, while it acts as antagonist ( $\geq 10 \mu$ M) on human  $\alpha 4\beta 2$  nACh receptors. To further study the effects of TBBPA on calcium-permeable nACh receptors, effects in B35 cell were examined using single cell fluorescent calcium imaging. TBBPA ( $\geq 1 \mu$ M) inhibits ACh receptors in B35 cells as evidenced by a reduction in the ACh-evoked increases in the intracellular calcium concentration ( $[Ca^{2+}]_i$ ). Additionally, TBBPA ( $>1 \mu$ M) induces a strong and concentration-dependent increase in basal  $[Ca^{2+}]_i$  in B35 cells. In dopaminergic PC12 cells, TBBPA ( $>1 \mu$ M) also increases basal  $[Ca^{2+}]_i$ . The increase in basal  $[Ca^{2+}]_i$  is also evident under calcium-free conditions, indicating it originates from intracellular calcium stores. Moreover, depolarization-evoked increases in  $[Ca^{2+}]_i$  are strongly reduced by TBBPA ( $\geq 1 \mu$ M), indicating TBBPA-induced inhibition of voltage-gated calcium channels. Our in vitro studies thus demonstrate that TBBPA exerts multiple adverse effects on functional endpoints for neurotransmission, justifying the quest for flame retardants with reduced neurotoxic potential. Funding: EU-FP7 (ENFIRO; grant agreement FP7-ENV-2008-1-226563).

## PS 903 Modulation of Nicotinic Acetylcholine Receptor by Brominated and Alternative Halogen-Free Flame Retardants.

H. S. Hendriks, R. G. van Kleef and R. H. Westerink. *Institute for Risk Assessment Sciences, Utrecht University, Utrecht, Netherlands.*

The large scale use of brominated flame retardants (BFRs) is associated with ecological and toxicological concerns. Previous *in vitro* research demonstrated that nicotinic acetylcholine (nACh) receptors are a direct target for e.g., PBDEs and TBBPA. These (neuro)toxic effects of BFRs argue for replacement by safe(r) and less persistent alternatives. Since it is essential to assess the (neuro)toxic potential of proposed halogen-free flame retardants (HFFRs) before they are used on large scale and in high volume, we measured the effects of three frequently used BFRs and 13 possible halogen-free substitutes on the function of human  $\alpha 4\beta 2$  nACh receptors, expressed in *Xenopus* oocytes, using the two-electrode voltage-clamp technique. Our initial rank-order potency based on the *in vitro* inhibition of nACh receptors indicates the neurotoxic potential of the HFFR triphenylphosphate (TPP), aluminium diethylphosphinate (Alpi), ammonium polyphosphate (APP), and the nanoclay cloisite 30B (MMT). However, additional studies focusing on expected concentrations in humans and the environment are required before these compounds can be excluded as viable alternatives. Importantly, five out of the sixteen tested compounds (brominated polystyrene (BPS), bisphenol-A bis(diphenylphosphate) (BDP), resorcinol bis(diphenylphosphate) (RDP), 9,10-dihydro-9-oxa-10-phosphaphenanthrene-10-oxide (DOPO), and zinc stannate (ZS)) are classified as not potent. Based on this specific neurotoxic endpoint, these five compounds could therefore be selected for additional testing to further assess the viability of these HFFRs as alternatives to replace current BFRs.

**PS 904 Neurotoxic Effects of Bisphenol AF by the Calcium-Induced ROS and MAPKs.**

S. Kim and S. Lee. *Pharmacology, Kyungpook National University Medical School, Daegu, Republic of Korea.*

Bisphenol AF (BPAF), a newly introduced chemical structurally related to bisphenol A (BPA), is used extensively in fluoroelastomers and polyesters, and has been known to induce estrogen-dependent responses. However, the toxicity of BPAF is largely unknown except for its endocrine-related effects. In this study, we investigated the neurotoxicity of BPAF and underlying mechanisms of action using hippocampal cell line (HT-22) and mouse primary neuronal cells. We found that BPAF induced apoptosis in both HT-22 and primary neuronal cells. To clarify the underlying mechanisms of BPAF-induced apoptosis, various signaling molecules were evaluated. BPAF increased the level of intracellular calcium, followed by the generation of reactive oxygen species (ROS). BPAF upregulated the phosphorylation of mitogen-activated protein kinase (MAPK): extracellular signal-regulated kinase (ERK), p38 and c-Jun N-terminal kinase (JNK), and nuclear translocation of nuclear factor (NF)- $\kappa$ B. Using specific inhibitors, we confirmed that calcium, ROS, p38, and JNK mediated the BPAF-induced apoptosis. In addition, BPAF inhibited microglial activation in a microglia/neuroblastoma coculture model by the reduction of nitric oxide production. We found that BPAF interrupted the normal physiological functions of microglia at non-toxic levels. Taken together, our results suggest that BPAF, the substitute of BPA, also have neurotoxic properties.

**PS 905 Potent Induction of a Series of Endogenous Antioxidative Enzymes by Triterpenoid CDDO-IM Leads to Neuprotection Against Oxidative and Electrophilic Injury.**

A. Speen, C. Jones, R. Patel and Z. Jia. *Department of Biology, University of North Carolina Greensboro, Greensboro, NC.*

Evidence suggests oxidative and electrophilic stress as a major factor contributing to the neuronal cell death in neurodegenerative disorders, especially Parkinson's disease (PD). Early depletion in the levels of thiol antioxidant glutathione (GSH), which may lead to generation of reactive oxygen species, is an important biochemical feature of PD. However, whether induction of endogenous antioxidative enzymes by a novel triterpenoid CDDO-IM (2-cyano-3,12 dioxoooleana-1,9 dien-28-oyl imidazoline) affords protection against oxidative and electrophilic neurocytotoxicity has not been carefully investigated. Retinoic acid-induced differentiation of human neuroblastoma SH-SY5Y cells are known to possess properties of mature neurons and thus have been widely used in vitro model for the study of neurotoxicity and neuprotection. In this study, we showed that incubation of retinoic acid-induced differentiation of human neuroblastoma SH-SY5Y cells with nanomolar concentrations of CDDO-IM (1-400 nM) for 24 h resulted in significant increase in the levels of reduced glutathione (GSH) and NAD(P)H:quinone oxidoreductase 1 (NQO1), two critical cellular defenses in detoxification of reactive oxygen species and electrophilic quinone molecules. Pretreatment of the cells with CDDO-IM was found to afford remarkable protection against the neurocytotoxicity elicited by acrolein, 4-hydroxynonenal, 3-morpholininosynonimine hydrochloride, xanthine oxidase/xanthine, and hydrogen peroxide. Taken together, this study demonstrates for the first time that CDDO-IM potentially induces the cellular GSH system and NQO1 in retinoic acid-induced differentiation of human neuroblastoma SH-SY5Y cells, which is accompanied by dramatically increased resistance of these cells to the damage induced by various neurotoxicants. The results of this study may have important implications for the development of novel neuroprotective strategies.

**PS 906 1, 3-Dinitrobenzene Induces Age-Specific Responses in Primary Neurons.**

L. Maurer<sup>1</sup>, N. D. Hein<sup>2</sup>, J. D. Latham<sup>1</sup>, R. Landis<sup>3</sup>, I. Speirs<sup>1</sup> and M. A. Philbert<sup>1</sup>. <sup>1</sup>Toxicology Program, University of Michigan, Ann Arbor, MI; <sup>2</sup>Neurology, University of Michigan, Ann Arbor, MI; <sup>3</sup>Kalamazoo College, Kalamazoo, MI.

During the normal aging process, the brain successively loses the ability to cope with pathophysiological stressors. The accumulation of iron in the aging brain potentially contributes to this by increasing redox activity. Astrocytes participate in the preservation of neurons during chemically induced stress by releasing adenosine, thereby silencing the electrical (hence energetic and metabolic) requirements

of neurons. 1,3-dinitrobenzene (DNB) stimulates adenosine release from astrocytes, and is used as a neural stressor probe in this study. Primary neurons and astrocytes were exposed to DNB (0, 100nM, or 100  $\mu$ M) and 10  $\mu$ M adenosine with 100nM or 100 $\mu$ M DNB. Neurons were isolated from male F344 rats (1 mo, 3 mo, & 18 mo), maintained for two weeks and exposed to DNB. Astrocytes were isolated and maintained for five weeks and cocultured with neurons. Adenosine triphosphate (ATP) was measured in both cell types. Neurons from 3 mo brains exhibited higher ATP than neurons from other age groups. Cocultured astrocytes had higher ATP levels than neurons at all age groups. Neurons were assayed at a later timepoint for lactate dehydrogenase (LDH). Neurons from brains of 1 mo and 18 mo rats, but not 3 mo rats, exposed to DNB exhibit statistically significantly higher LDH than neurons treated with both DNB and adenosine. Immunocytochemistry for the presence of transferrin (Tf) and mitochondrial frataxin (mtFr) was performed on neurons. Increases in Tf were observed in older neurons. Colocalization of Tf and mtFr was observed in the oldest age group. These results suggest that neurons from older animals sequester more mitochondrial iron than younger cohorts, increasing potential for higher redox activity, rendering them more vulnerable to chemical insults such as DNB. Future work will elucidate the significance of mitochondrial iron in the aging process.

This work was supported by NIH 2R01 ES00846 (LM, JDL, ICS, MAP), NIH 2T32 ES007062 (LM), HHMI Award (RL), NIH R01 NS069700 and SPF N014262 (NDH).

**PS 907 Magnetic Resonance Imaging and Spectroscopic Markers of Kainic Acid-Induced Excitotoxicity in the Rat Brain.**

S. Liachenko<sup>1</sup>, J. Ramu<sup>1</sup>, M. G. Paule<sup>1</sup>, L. Schmued<sup>1</sup> and J. P. Hanig<sup>2</sup>. <sup>1</sup>Neurotoxicology, NCTR/US FDA, Jefferson, AR; <sup>2</sup>Office of Testing & Research, CDER/US FDA, White Oak, DC.

Neurotoxicity assessment in drug development is typically accomplished using microscopic analysis, which may be time consuming and not always comprehensive. In this study we describe changes in brain after acute administration of kainic acid (KA) using non-invasive magnetic resonance imaging (MRI) and spectroscopy (MRS) in comparison to histopathology. Adult male Sprague-Dawley rats (N = 24, 361  $\pm$  36 g) were anesthetized with isoflurane and positioned inside a 7 tesla MRI scanner. T2 relaxation mapping of the whole brain and proton MRS in the left hippocampus were performed. KA (10 mg/kg, ip) was then administered to all animals after baseline scans and imaging was continued for another 2 hours. One group of animals (N = 6) was euthanized at this time. The MRI procedure was repeated one day (N = 6) and 2 days later (N = 12) and these animals were then euthanized. All rats were perfusion-fixed and their brains underwent histopathological assessment. KA led to an increase in T2 in the hippocampus as early as 1 hour after administration. These changes were more pronounced at 2 hours and drastically so at 1 and 2 days after the treatment at which point the findings spread to wider areas of the brain, including the amygdala, thalamus, and cortex. MRS revealed immediate increases in glutamate and glutamine concentrations right after KA administration followed by decreases at 1 and 2 days, at which point N-acetyl-aspartate signal was also decreased. Lactate was not detectable in the normal brain but appeared at 15 min and increased to a maximum at 2 hours after treatment. At 1 and 2 days lactate was still detectable. The T2 water relaxation correlated with histopathological changes in the brain at all time points. These data provide the basis for the development of imaging biomarkers for the early detection of neurotoxicity, which would benefit public health by increasing the number of tools available for safety evaluation of new drugs. (Supported by NCTR and CDER, FDA, #E0741801).

**PS 908 Effect of Acute Administration of Beta-N-Methylaminoalanine (L-BMAA) on Rat Hippocampus Neurochemical Profile Determined with 1H Magnetic Resonance Spectroscopy (MRS).**

J. Ramu<sup>1</sup>, J. P. Hanig<sup>2</sup>, E. C. Garner<sup>3</sup>, M. G. Paule<sup>1</sup> and S. Liachenko<sup>1</sup>. <sup>1</sup>Neurotoxicology, NCTR/US FDA, Jefferson, AR; <sup>2</sup>Office of Testing & Research, CDER/US FDA, White Oak, MD; <sup>3</sup>Lovelace Respiratory Research Institute, Albuquerque, NM.

L-BMAA is a non-proteogenic amino acid present in cyanobacteria and in cycad seed, exposure to which is implicated in western Pacific amyotrophic lateral sclerosis and parkinsonism-dementia complex (ALS-PDC). After absorption, L-BMAA is transported into the brain, metabolized, and L-BMAA and/or its metabolites may accumulate in brain protein. This bound form may serve as a sink from which L-BMAA or its metabolites are released, contributing to its neurotoxic effect. L-BMAA has been shown to be excitotoxic, acting as a glutamate receptor agonist. In

this study we used non-invasive <sup>1</sup>H-MRS to investigate the changes in the hippocampal neurometabolic profile after single dose of L-BMAA. Nine adult male Sprague-Dawley rats (390 ± 8 g) were anesthetized with isoflurane and positioned in 7 tesla MRI scanner. MRS in the left hippocampus (voxel size 4 x 4 x 2 mm) was performed before and for 1.5 hrs after BMAA administration (100 mg/kg, ip). Signal intensity of N-acetyl-aspartate, gamma-aminobutyric acid (GABA), creatine, choline, glutamate, glutamine, myo-inositol, and taurine were measured relative to water peak in water-unsuppressed reference spectrum. At the end of observation period the GABA signal was elevated relative to the baseline (+23%, P = 0.051) and taurine was decreased (-10%, P = 0.014). Signal intensity of other neurotransmitters did not change. These data may be consistent with L-BMAA mediated glutamate agonist activity. Both GABA and taurine are released into extracellular space after stimulation of NMDA receptors. Increase in GABA may be due to a combination of uptake and increased synthesis. The lowering of hippocampal taurine may reflect a reduction in re-uptake after release. These data suggest that L-BMAA has measurable effect on glutaminergic pathways in undisturbed, intact tissues in rats.

## PS 909 Pattern of Pathologic Changes Observed in the CNS of Chronic Toluene Abusers.

D. Pyatt<sup>1,2</sup> and P. Kerzic<sup>3</sup>. <sup>1</sup>Summit Toxicology, Superior, CO; <sup>2</sup>Schools of Pharmacy and Public Health, University of Colorado, Denver, CO; <sup>3</sup>Cinpathogen, Los Angeles, CA.

Toluene is a common volatile organic chemical (VOC) found in petroleum-based products and has wide-spread industrial use as a solvent in paints, lacquers, inks, adhesives and cleaning agents (degreasing). The toxicity of toluene has been well described in experimental animals, occupationally exposed humans and healthy volunteers. Considerable toxicological data has also been obtained from individuals who purposely expose themselves to high levels of toluene and/or toluene containing solvents to achieve the narcotic effect common to most organic solvents. Collectively, this data has demonstrated that high-dose prolonged exposure to toluene can cause neurological toxicity, ranging from non-specific, reversible symptoms to permanent pathological changes in the 'white matter' of the brain. Evaluation of chronic toluene abusers by magnetic resonance imaging (MRI) have revealed a series of pathologic alterations that appear to be common to most, if not all, toluene abusers that suffer from permanent neurological alterations. These individuals almost always provide evidence of direct toxic insult, including diffuse atrophy in the brain and/or areas of de-myelination and axonal dying. Other frequently reported pathological changes include hypo-intensity of the thalamus region and basal ganglia, high T2 signal intensity in the periventricular white matter and a loss of grey-white demarcation or differentiation. Most authors report a clear dose-response relationship, describing exposures (durations as well as intensities) necessary to cause these lesions observed in the white matter. While none of the reported alterations are dispositive of toluene exposure, the consistent pathological pattern observed in the MRIs of chronic toluene abusers (or those with severe occupational exposures) has not been previously appreciated or reported. The existing scientific evidence relevant to this issue, including exposure-response data (where available), has been comprehensively evaluated and is presented herein.

## PS 910 Effects of Short- and Long-Term Exposure to 1-Bromopropane on Neurogenesis in Adult Rats.

L. Zhang<sup>1</sup>, T. Nagai<sup>2</sup>, K. Yamada<sup>2</sup>, D. Ibi<sup>2</sup>, S. Ichihara<sup>3</sup>, K. Subramanian<sup>1</sup>, Z. Huang<sup>1</sup>, S. Sheik Mohideen<sup>1</sup>, H. Naito<sup>1</sup> and G. Ichihara<sup>1</sup>. <sup>1</sup>Department of Occupational & Environmental Health, Nagoya University Graduate School of Medicine, Nagoya, Japan; <sup>2</sup>Neuropsychopharmacology, Nagoya University Graduate School of Medicine, Nagoya, Japan; <sup>3</sup>Mie University Graduate School of Regional Innovation Studies, Tsu, Japan.

**Purpose:** People with 1-bromopropane (1-BP) intoxication show depression and reduction of cognitive function and memory. The present study tested the hypothesis that 1-BP suppresses neurogenesis in the dentate gyrus which is involved in higher cerebral function in adult rats.

**Methods:** Four groups of twelve male Wistar rats were exposed to 1-BP at 0, 400, 800 and 1000 ppm, 8 hrs/day for 7 days. Other four groups of six rats were exposed to 1-BP at 0, 400, 800 and 1000 ppm for two weeks and 0, 200, 400 and 800 ppm for another 2 weeks. The other four groups of six rats were exposed to 1-BP at 0, 200, 400 and 800ppm for 4 weeks. Rats were injected with 5-bromo-2'-deoxy-uridine (BrdU) after four-week exposure at 1000/800 ppm to examine neurogenesis in the dentate gyrus using immunostaining. Factors known to affect neurogenesis, including monoamine level in different brain regions, hippocampal brain-derived neurotrophic factor (BDNF) and glucocorticoid receptor (GR) mRNA expression levels were measured.

**Results:** BrdU positive cells decreased significantly at 800/1000 ppm after 4-week exposure to 1-BP. 1-week exposure to 1-BP at 800 and 1000 ppm significantly reduced noradrenalin level in the striatum. 4-week exposure to 1-BP decreased significantly noradrenalin level in the hippocampus, prefrontal cortex and striatum at 800 ppm. 1-BP also reduced hippocampal BDNF and GR mRNA levels.

**Conclusion:** Long-term exposure to 1-BP decreased neurogenesis in the dentate gyrus. Downregulation of mRNA expression of BDNF and GR and low hippocampal norepinephrine levels might partly contribute to the reduced neurogenesis.

## PS 911 Nitrosative Stress in Chemoconvulsant-Induced Epileptogenesis.

K. Ryan<sup>1,2</sup>, L. Liang<sup>1</sup> and M. Patel<sup>1</sup>. <sup>1</sup>Toxicology, Skaggs School of Pharmacy and Pharmaceutical Sciences; University of Colorado Anschutz Medical Campus, Aurora, CO; <sup>2</sup>NTP, NIEHS, Morrisville, NC.

Reactive oxygen and nitrogen species (ROS/RNS) are mediators of oxidative stress and are increased in the brain as a result of seizure activity and reactive gliosis; yet their contributing role in the process by which injury leads to epilepsy (i.e. epileptogenesis) is largely unknown. Our previous work in the kainate model of chemoconvulsant-induced epilepsy has confirmed significant oxidative macromolecular damage to hippocampal mitochondria (Ryan et al 2012). The primary goals of this study were to assess the consequences of nitrosative stress in cellular compartments to gain greater mechanistic insight into mitochondrial dysfunction during epileptogenesis. Rats were exposed to a single high dose of kainate (11mg/kg) or vehicle and monitored by video and/or EEG for seizure activity 6 wks. Nitrosative stress was measured in the susceptible hippocampal brain region acutely after kainate administration (8hr, 24hr, and 48hr), 1wk after kainate prior to development of epilepsy (latent period) and during the chronic stages of epilepsy (3wk and 6wk). Analysis from frozen hippocampal sections indicated global astrogliosis (GFAP) and microgliosis (Iba-1) after kainate. Hippocampal nitric oxide spiked 2-fold 8hr after kainate and remained elevated throughout epileptogenesis. Preliminary results suggest this could be associated with increased iNOS detected by immunohistochemical staining. Furthermore, cellular and mitochondrial 3-nitrotyrosine (3NT) progressively and significantly increased during epileptogenesis indicating protein nitration and subsequent immunofluorescent co-labeling showed that 3NT is localized to hippocampal neurons (NeuN). This study demonstrates a probable mechanism for gliosis-mediated nitric oxide production and downstream protein damage to hippocampal neurons in epileptogenesis. These studies propose a role for targeting oxidative and nitrosative species to delay or prevent disease progression by inhibiting detrimental protein nitration. NS039587 (M.P.) and NS R21 NS072099 (M.P.)

## PS 912 Ozone-Induced Changes in Oxidative Stress Parameters in Brains of Adult, Middle-Age, and Senescent Brown Norway Rats.

P. S. Kodavanti, J. E. Royland, J. E. Richards, D. I. Agina-Obu and R. C. MacPhail. NHEERL, US EPA, Research Triangle Park, NC.

Understanding life-stage susceptibility is a critical part of community based human health risk assessment following chemical exposure. Recently there is growing concern over a common air pollutant, ozone (O<sub>3</sub>), and adverse health effects including dysfunction of the pulmonary, cardiac, and nervous systems. Oxidative stress (OS) is a known contributor in multiple organ toxicities and plays an important role in age-related diseases. Growing evidence implicates OS in O<sub>3</sub> toxicity. The current study explored OS as a potential toxicity pathway for O<sub>3</sub> exposure and addressed whether these effects are life stage-dependent. OS-related measures included reactive oxygen species (ROS) production [NADPH Quinone oxidoreductase 1 (NQO1), NADH Ubiquinone reductase (UBIQ)], antioxidant homeostasis [total antioxidant substances (TA), superoxide dismutase (SOD), γ-glutamylcysteine synthetase (γ-GCS)], and oxidative damage (total aconitase). Male Brown Norway rats (4, 12, and 24 months) were exposed to O<sub>3</sub> (0, 0.25 or 1 ppm) via inhalation for 6 h/day, 2 days per week for 13 weeks. Frontal cortex (FC), cerebellum (CB), striatum (ST), and hippocampus (HP) were dissected 24 hours after last exposure, quick frozen, and stored at 80°C until analysis. Results indicated life stage-related increases in ROS production (~ 2x in UBIQ and > 1.5x in NQO1 in striatum), slight decreases in antioxidant homeostatic mechanisms (TAS, γ-GCS, and SOD), and a decrease in aconitase activity. The effects of O<sub>3</sub> exposure were brain area-specific, with the striatum being more sensitive than other brain regions. With regard to life stage, the effects of O<sub>3</sub> appeared to be greater in 4 month old than 12 or 24 month old rats. These results indicate OS could be a potential toxicity pathway for O<sub>3</sub>, but the complex interactions between age, exposure and brain region require further investigation. (This abstract does not necessarily reflect USEPA policy).

**PS 913 Protective Role of Carnosine Against Ischemic Brain Damage through Modulation of Mitochondrial Function and Autophagy.**

O. Bae<sup>1</sup>, S. Baek<sup>2</sup> and A. Majid<sup>3</sup>. <sup>1</sup>College of Pharmacy, Hanyang University, Ansan, Republic of Korea; <sup>2</sup>College of Pharmacy, Ajou University, Suwon, Republic of Korea; <sup>3</sup>Department of Neurology and Manchester Academic Health Sciences Centre, Salford Royal Hospital, Salford, United Kingdom.

We recently found that carnosine, an endogenous pleiotropic dipeptide, has a neuroprotective activity against ischemic stroke. To investigate the mechanism of carnosine neuroprotection, we examined the effect of carnosine on mitochondrial dysfunction and autophagic process in ischemic brain. In rat permanent middle cerebral artery occlusion models, intravenous treatment with carnosine exhibited robust neuroprotection. Carnosine treatment improved brain mitochondrial function as found in mitochondrial respiration, and fusion/fission signaling. Interestingly, autophagic pathways were activated in brain following ischemic insults, such as reduction of phosphorylated mTOR/p70S6K and the conversion of LC3 I to LC3 II, as found in western blot analysis of isolated brain homogenates. Treatment of carnosine attenuated the autophagic signaling in ischemic brain, while the change of ERK phosphorylation was not detected. Taken together, our data suggest that carnosine neuroprotection is mediated by mitochondrial protection, inhibiting excessive autophagic processes. We believe that our finding contributes to the development of carnosine as a strong candidate for stroke treatment, providing a new insight into the role of mitochondrial damage and autophagic pathways in ischemic brain damage.

**PS 914 The Neurotoxic Effects of Tributyltin on Tokai High Avoicer (THA) Rats Evaluated by the Sidman Electric Shock Avoidance Test.**

M. Tsunoda<sup>1</sup>, T. Kido<sup>2</sup>, M. Hosokawa<sup>3</sup>, C. Sugaya<sup>1</sup>, H. Endo<sup>4</sup>, T. Watanabe<sup>4</sup> and Y. Aizawa<sup>5</sup>. <sup>1</sup>Preventive Medicine, Kitasato University School of Medicine, Sagami-hara, Japan; <sup>2</sup>Public Health and Environmental Medicine, Jikei University School of Medicine, Tokyo, Japan; <sup>3</sup>Epidemiology and Environmental Health, Faculty of Medicine, Juntendo University, Tokyo, Japan; <sup>4</sup>Basic Clinical Science and Public Health, Tokai University School of Medicine, Isehara, Japan; <sup>5</sup>Kitasato University, Tokyo, Japan.

Tributyltin (TBT) compounds have been known as environmental pollutants. Although neurotoxicity is one of the major toxicities of TBT, the effects of TBT on learning ability have not yet been clearly demonstrated. Wistar-derived Tokai High Avoicer (THA) rats, which were developed at Tokai University, can achieve stable learning ability in the Sidman electric shock avoidance test because of their innate high-level avoidance ability and small individual differences. We evaluated the neurotoxicity of TBT in THA rats by Sidman electric shock avoidance test. The male and female THA rats were administered TBT in their food at 0 and 125 ppm after weaning (males, n = 5/group; females n = 4/group). From 6 weeks of age, the Sidman test sessions were performed for 60 min/day for 10 consecutive days. Rats can avoid electric shocks by pressing a lever. Avoidance rates for shock exposures were calculated for the first and second halves (30 minutes each) of each session. The mean values of the avoidance rates were compared between the control and TBT groups for each sex, and those of the TBT-exposed group were lower than those of the control for both sexes for all the sessions. Significantly lower mean values of the avoidance rates compared to the control were observed in the first 30 minutes of the sessions in male rats on days 2 and 5. It is suggested that learning ability was impaired in the THA rats exposed to TBT at 125 ppm. To detect the statistically significant differences in future studies, more THA rats should be used.

**PS 915 Protein Biomarker Panel of Cisplatin-Induced Neurotoxicity in a Preclinical Model.**

O. Y. Glushakova<sup>1</sup>, S. Mondello<sup>1</sup>, D. Johnson<sup>1</sup>, C. Heldermon<sup>2</sup>, J. Streeter<sup>1</sup> and R. L. Hayes<sup>1</sup>. <sup>1</sup>Banyan Biomarkers, Inc., Alachua, FL; <sup>2</sup>University of Florida, Gainesville, FL. Sponsor: C. Markgraf.

Background: Neurotoxic brain damage is a widely recognized adverse effect of chemotherapy affecting overall outcome and quality of life cancer survivors. Effective clinical monitoring of neurotoxicity using simple and reliable assays could provide timely information to clinicians allowing them to adjust treatment and reduce neurologic and cognitive side effects of chemotherapy. The goal of this study was to investigate spatiotemporal distributions in the brain, CSF and serum of glial, of neuronal and inflammatory biomarkers: ubiquitin C-terminal hydrolase-1 (UCH-L1), glial fibrillary acidic protein (GFAP),  $\alpha$ -spectrin break down products (SBDPs), microtubule-associated protein 2 (MAP2), myelin basic protein (MBP), MBP break down products (MBP-BDP), intercellular adhesion molecule (ICAM) and their relationships to cisplatin-induced neuropathology in rats.

Methods: Neurotoxicity in adult rats was induced by cisplatin (10 mg/kg, i.p.). The levels and localization of biomarkers in the brain were examined by immunohistochemistry (IHC) and their levels in CSF and serum were evaluated by ELISA. Results: IHC revealed that cisplatin caused abnormal changes in the brain starting at 6 h and increasing at 24 and 48 h including gliosis, determined by increased GFAP level, dendritic damage determined by decreased MAP2 level, neuronal demyelination determined by increased level of MBP-BDP, and inflammation determined by increased level of ICAM. Serum levels of UCHL-1, GFAP and SBDP150 were significantly increased at 24 h after cisplatin administration as compared to controls. The levels of these biomarkers were correlated with IHC brain pathologies and survival.

Conclusion: This study demonstrated the potential of using levels of glial and neuronal proteins in blood for assessment of cisplatin induced neurotoxicity. In addition, assessment of serum levels of biomarkers can provide information on underlying mechanisms of neurotoxicity and facilitate a personalized treatment to minimize side effects during and after chemotherapy.

**PS 916 Effects of a Smokeless Tobacco, Gutkha on Neurotransmitter Levels and Associated Parameters in the Mouse Brain.**

D. E. Lauterstein<sup>1</sup>, C. Hoffman<sup>1</sup>, M. M. Hossain<sup>3</sup>, J. Richardson<sup>3</sup>, F. Ganey<sup>2</sup> and J. T. Zelikoff<sup>1</sup>. <sup>1</sup>Environmental Medicine, New York University, Tuxedo, NY; <sup>2</sup>Memorial Sloan-Kettering Cancer Center, NY, NY; <sup>3</sup>Rutgers University, New Brunswick, NJ.

Many studies have been performed on the relationship between smoked tobacco and adverse effects on health. However, fewer data are available on the toxicity of smokeless tobacco. Gutkha, a smokeless tobacco (ST) product manufactured in India and readily available in the U.S. (used extensively by South Asian communities), is composed of powdered tobaccos, slake lime, and spices. To assess the effects of Gutkha usage on the brain, adult male mice (B6C3F1) were exposed daily via the oral mucosa to water (control), 50  $\mu$ L of a 21 mg water-soluble Gutkha solution or of a 8 mg/kg nicotine solution for 3 days and changes in brain levels of dopamine (DA), serotonin (5-HT), and norepinephrine (NE) were assessed in the striatum. Monoamine oxidase and tyrosine hydroxylase (enzymes important for neurotransmitter (NT) breakdown and synthesis, respectively) levels were assessed in the striatum, frontal cortex, and locus coeruleus. Serum cotinine levels for all the groups were analyzed upon sacrifice within 1 hr post-exposure; Gutkha- and nicotine-exposed mice had comparable cotinine levels ranging between 18-50 ng/mL and 20-60 ng/mL, respectively. HPLC studies measuring NT levels in the brain demonstrated that Gutkha-exposed mice had a significant increase in NE compared to those exposed to either nicotine or water. In contrast, Gutkha-exposed mice had a significant decrease in DA and 5-HT compared to the control and nicotine-exposed groups. The results here suggest that: effects of Gutkha on certain brain parameters may be due to Gutkha-associated toxicants other than nicotine; Gutkha may provide an additional biological stressor for the brain compared to nicotine alone; and, Gutkha may be more addictive than nicotine alone based on the rapid depletion rate of catecholamines in the brain. Studies supported by funds from the NYU Cancer Center and NYU NIEHS Center.

**PS 917 3, 4-Methylenedioxymethamphetamine (Ecstasy)-Mediated Acute and Long-Term Effects Are Reduced in SERT-Knockout Rats.**

L. E. Lizarraga, A. B. Cholanians, J. M. Herndon, S. S. Lau and T. J. Monks. Pharmacology and Toxicology, University of Arizona, Tucson, AZ.

3,4-Methylenedioxymethamphetamine (MDMA, Ecstasy) is a ring-substituted amphetamine derivative structurally related to the psychomotor stimulant amphetamines and the hallucinogen mescaline. The neuropharmacological effects of MDMA are biphasic in nature. MDMA initially causes synaptic monoamine release, primarily of serotonin (5-HT), producing hyperthermia and hyperactivity (5-HT syndrome). The long-term effects of MDMA manifest as a prolonged depletion in 5-HT, and structural damage to 5-HT nerve terminals. The effects of MDMA are in part mediated by an ability to inhibit the presynaptic 5-HT reuptake transporter (SERT). Using a SERT-knockout (SERT-KO) rat model, we determined the effects of SERT deficiency on MDMA (10mg/kg, sc, X 4 at 12h intervals)-mediated hyperthermia, locomotor activity, and neurotoxicity in SERT-KO or Wistar-based wild-type (WT) rats. Open-field activity cages equipped with photo-beam sensor rings revealed that WT rats were 2.4-fold more active (displaying higher horizontal movement distance and mean velocity) than their SERT deficient counterparts. Exposure to MDMA stimulated total movement by 4.2-fold in both WT and SERT-KO rats. Although the peak hyperthermic response in SERT-KO (38.9C & 38.4C) and WT animals (39.1C & 38.8C) were similar after the first and third doses of MDMA, the response was delayed and prolonged in WT animals. Thus the cumulative (temp X time) elevation in temperature was significantly

( $p < 0.01$ ) higher in the WT rats. Finally, SERT KO animals were insensitive to MDMA-mediated long-term (7 days) depletions in 5-HT and its metabolite, 5-hydroxyindoleacetic acid (5-HIAA), in both cortex and striatum. In conclusion, SERT deficiency in KO animals attenuated MDMA-induced hyperthermia and neurotoxicity but not locomotor activity. The data confirm that SERT is essential for the manifestation of the acute and long-term effects of MDMA (NIH R01 DA023525, P30ES006694, and T32ES007091).

**PS 918 Structurally-Distinct Dopaminergic Neurotoxins Acutely Decrease ATP-Dependent Calcium Signaling in Astrocytes by Inhibiting TRPC3.**

K. Streifel, A. Gonzales, B. Trout, B. Mohl, S. Earley and R. B. Tjalkens. *Environmental and Radiological Health Science, Colorado State University, Fort Collins, CO.*

Dopaminergic nuclei within the basal ganglia are important for control of motor function but are highly sensitive to damage from oxidative stress, inflammation, and environmental neurotoxins. Here we propose that inhibition of transmitter-evoked calcium ( $Ca^{2+}$ ) signaling in astrocytes may contribute to this sensitivity because ATP-dependent  $Ca^{2+}$  waves in these cells modulate diverse trophic functions in the CNS, including metabolism, synaptic activity, and regional cerebral blood flow. To examine mechanisms underlying alterations in  $Ca^{2+}$  signaling in astrocytes, we postulated that cationic neurotoxins of the basal midbrain would acutely inhibit ATP-induced  $Ca^{2+}$  signals in astrocytes through a common channel. To test this hypothesis, we examined the capacity of MPP<sup>+</sup> and 6-Hydroxydopamine (6-OHDA) to block ATP-dependent  $Ca^{2+}$  waves and transients in primary striatal astrocytes. Calcium imaging studies revealed a dose-dependent decrease in ATP-induced intracellular  $Ca^{2+}$  transients and mechanically stimulated  $Ca^{2+}$  waves following acute application of both MPP<sup>+</sup> and 6-OHDA. These compounds also acutely inhibited OAG-induced  $Ca^{2+}$  influx, suggesting the transient receptor potential channel, TRPC3, as a probable target. MPP<sup>+</sup> inhibited OAG-induced intracellular  $Ca^{2+}$  transients similarly to the TRPC3 channel antagonist, pyrazole-3, whereas 6-OHDA only partly suppressed OAG-induced  $Ca^{2+}$  transients. In whole cell patch clamp experiments conducted in TRPC3-overexpressing cells, acute application of MPP<sup>+</sup> completely blocked TRPC3-like currents, whereas only partial inhibition was detected in the presence of 6-OHDA. These findings indicate that dopaminergic neurotoxins that have cationic properties differentially inhibit TRPC3 in astrocytes, thereby diminishing the amplitude of ATP-induced  $Ca^{2+}$  transients. These compounds may therefore share a common mechanism of neurotoxicity in their capacity to acutely disrupt astrocytic trophic functions reliant on this signaling mechanism.

**PS 919 Comparative Toxicity of Amphotericin B and Amphotericin B Methyl Ester in Oligodendrocytes *In Vitro* and *In Vivo*.**

O. U. Nnodi<sup>1</sup>, C. P. Schaffner<sup>2</sup> and K. R. Reuhl<sup>1</sup>. <sup>1</sup>*Pharmacology & Toxicology, Rutgers University, Piscataway, NJ;* <sup>2</sup>*Waksman Institute, Rutgers University, Piscataway, NJ.*

Amphotericin B methyl ester (AME) is a polyene macrolide antibiotic highly effective against systemic fungal infections. Introduced more than 40 years ago, AME is less toxic than the commonly used Amphotericin B (AMB), which has serious dose-limiting nephrotoxicity. Nevertheless, reports of neurotoxicity led to cessation of its clinical use. Research in our lab using pure AME suggest that the reported myelin toxicity was due to contamination by AMB which injures myelin-producing oligodendrocytes in the CNS. To test this hypothesis, adult female Balb/c mice were administered to AMB or AME (5 mg/kg, ip) or vehicle for 28 days and 54 days. Histopathologic analysis of mice using Fluoromyelin dyes demonstrated white matter vacuolation and demyelination, with accumulation of myelin debris within macrophages. AMB also induced apoptosis of glial cells. AME-treated mice were normal. Quantitative dose-response assessment using an immortalized human oligodendroglial cell line (MO3.13) exposed to 0.5-30  $\mu$ g/ml AMB or AME demonstrated that AME was at least 10-fold less toxic than AMB as measured by dye exclusion. The lowest concentration of AMB to induce cell membrane injury in MO3.13 cells was 1  $\mu$ g/ml. AMB induced an apoptotic phenotype at concentrations ten times lower than AME as determined by nuclear area factor assessment. AMB induces the mitochondrial intrinsic apoptotic pathway in the MO3.13 cells. A direct effect of AMB on the mitochondrial membrane was confirmed by labeling with JC-1, a fluorescent marker of mitochondrial membrane potential ( $\Delta\Psi_m$ ), which revealed diminished intensity following AMB treatment at 1  $\mu$ g/ml. Changes in  $\Delta\Psi_m$  were not rescued by Trolox, a mitochondrial membrane pore inhibitor. AME concentrations below 10  $\mu$ g/ml did not alter  $\Delta\Psi_m$ . These data suggest that AMB, but not pure AME, causes potentially lethal injury to oligodendrocytes by inducing plasma membrane permeability and mitochondrial perturbation, with consequent apoptosis. (Supported by ES005022 and ES07148).

**PS 920 Effects of "Uptake 2" Blockade and/or Risperidone on Murine 5-HT Uptake, Social and Repetitive Behavior.**

C. Smolik<sup>1,2</sup>, M. Javors<sup>1</sup>, J. Hensler<sup>1</sup>, W. Koek<sup>1</sup>, L. C. Daws<sup>1</sup> and G. G. Gould<sup>1</sup>. <sup>1</sup>*CBN, UTHSCSA, San Antonio, TX;* <sup>2</sup>*Biology, UTSA, San Antonio, TX*

Uptake 2 mechanisms in the brain such as organic cation transporters (OCTs) may play a major role in the modulation of monoamine neurotransmission. OCTs have affinity for and/or transport many endogenous and xenobiotic compounds. Their blockade produces similar effects to selective serotonin (5-HT) reuptake inhibitors. The pseudoisocyanine 1,1'-diethyl-2,2'-cyanine iodide (decynium-22 or D-22) blocks 5-HT uptake in vivo and produces antidepressant-like effects in mice. Administration of D-22 (0.01-0.1 mg/kg) or diazepam (1 mg/kg) increased social approach in BTBR mice 50 min afterward ( $p < 0.05$ ,  $N=6$ ), in contrast to risperidone (0.1 mg/kg). Unlike diazepam or risperidone, D-22 failed to reduce BTBR marble burying. D-22 (0.01 mg/kg) increased social sniffing of stranger mice by SERT -/- mice ( $p < 0.05$ ,  $N=12$ ), with a similar lack of effect on marble burying. We hypothesized that D-22 produces its effects on social behavior by blocking OCTs or other uptake-2 sites in the mouse brain. Saturation binding of [<sup>3</sup>H] D-22 in mouse hippocampal homogenates revealed a  $K_D$  of  $\approx 3-4$  nM, and a  $B_{max}$  of  $700 \pm 167$  fmol/mg protein ( $N=3$ ). Binding of [<sup>3</sup>H] D-22 is partially blocked by the neurotoxin 1-methyl-4-phenylpyridinium (MPP<sup>+</sup>), a substrate of OCTs. We confirmed that [<sup>3</sup>H] MPP<sup>+</sup> uptake by hOCT expressing HEK cells was blocked by D-22 with IC50 values ranging from 3-8  $\mu$ M ( $N=5$ ). We also found that D-22 blocks hippocampal 5-HT uptake (IC50=197 nM), albeit more weakly than striatal DA uptake (IC50=35 nM), in synaptosomes from mice ( $N=4-7$ ). Through HPLC measurements D-22 was detectable in the brain when administered by intraperitoneal (i.p.) injection at 10 mg/kg, but not at lower doses. D-22 has a serum clearance half-life of 30 min in BTBR mice. OCT3 blockade appears to be a promising therapeutic strategy for social interaction deficiencies. Research was supported by NIH-NINDS #R25NS080684 START-UP Program, NIH-NIMH #R03MH086708 and DOD AR110109.

**PS 921 Social Behaviors, Monoamine Transporter Function, and Brain Mitochondrial Efficiency in Insulin-Resistant Mice.**

R. Lozano<sup>1,2</sup>, W. Q. Zhang<sup>1</sup>, C. Smolik<sup>1</sup>, P. A. Barba-Escobedo<sup>1</sup>, M. Gamez<sup>1</sup>, H. Van Remmen<sup>3</sup>, L. C. Daws<sup>1</sup> and G. G. Gould<sup>1</sup>. <sup>1</sup>*Physiology, UTHSCSA, San Antonio, TX;* <sup>2</sup>*Psychology, Texas A&M University, College Station, TX;* <sup>3</sup>*Barshop Center, UTHSCSA, San Antonio, TX.*

Insulin resistance and elevated blood glucocorticoids are key components of the metabolic syndrome that often comes before type 2 diabetes. Use of atypical antipsychotics can increase the risk for developing metabolic syndrome, yet the impact of elevated insulin on drug response, monoamine systems and behavior is poorly understood. In streptozotocin-treated rats and in type 1 diabetes, insulin production is suppressed and dopamine transporter function is impaired. Conversely, we hypothesized that high circulating insulin and corticosteroid levels, as seen in type 2 diabetes, may instead enhance monoamine transporter function and impair sociability. We tested this hypothesis using BTBR x C57BL/6 (BL6) F1 male mice, which exhibit insulin resistance as adults, and their parent strains. BTBRxBL6 F1 mice had increased abdominal adiposity, but their serum levels of corticosterone were intermediate ( $89 \pm 8$  ng/ml) to higher BTBR and low BL6 levels ( $N=5-8$ ). Their social behavior in three chambered tests and marble burying was similar to that of socially-deficient BTBR mice. Yet BTBRxBL6 F1 were more impulsive than either parent strain in the tube test for social dominance. Brain tissue from BTBR and BTBRxBL6 F1 mice had lower  $H_2O_2$  production from mitochondrial electron transport than BL6 mice ( $P < 0.05$ ,  $N=5$ ). Binding of [<sup>3</sup>H] citalopram to serotonin transporters in hippocampal synaptosomes was reduced in BTBR and BTBRxBL6 mice, but [<sup>3</sup>H] 5-HT uptake was similar to BL6 mice ( $N=4-6$ ). In contrast, [<sup>3</sup>H] WIN 35,428 binding to dopamine transporters in striatal synaptosomes was similar among strains, but [<sup>3</sup>H] dopamine uptake was significantly increased in BTBR mice ( $N=4-6$ ). Based on [<sup>3</sup>H] domperidone binding in cortical synaptosomes, dopamine receptor density may be increased in BTBR and BTBRxBL6 F1 mice. Hence dopamine transmission could be suppressed in these insulin-resistant mice, which may alter their responsiveness to antipsychotics.

**PS 922 Impact of Pair Housing and Selection of Photobeam-Based Motor Activity Parameters for Neurobehavioral Evaluation.**

P. Mukerji, S. S. Anand, L. A. Malley, N. P. Betts and S. E. Loveless. *DuPont Haskell Global Centers for Health & Environmental Sciences, Newark, DE.*

Social housing is widely considered to be beneficial to the welfare of laboratory animals, compared with single housing, and is recommended by the Guide for the Care and Use of Laboratory Animals. Therefore, the impact of social housing on

measurable neurobehavioral endpoints was evaluated. Socially defeated or submissive rats exhibit body weight loss and decreased exploratory behavior relative to socially dominant rats. It was hypothesized that any impact of social dominance on a neurobehavioral endpoint (e.g., motor activity) would correlate with a difference in bodyweight gain between the two pair-housed rats. However, the control data from five 90-day studies (N=114) indicated no significant correlation between the difference in bodyweight gain within each cage and the difference in motor activity, grip strength, hindlimb splay, or body temperature values within the same cages. Our second objective was to optimize the use of a photobeam-based system which computes multiple parameters for motor activity assessment and is widely used in the industry. We evaluated baseline data from eight studies (N=816), to select two representative motor activity parameters from a list of multiple options. Duration of movement and number of ambulatory movements offered the greatest unique value (lowest correlation coefficients) and were the best predictors (highest R-squared values) of the remaining motor activity parameters. A positive control study conducted with carbaryl and amphetamine using pair housing conditions demonstrated neurobehavioral effects that were consistent with previously published literature. Based on the analysis of data from multiple studies including a positive control, we concluded that pair housing does not interfere with neurobehavioral evaluations and that motor activity can be characterized effectively using duration of movement and number of ambulatory movements in a photobeam-based system.

## PS 923 Feasibility Study of EEG Measurements in Chair Restrained Cynomolgus Monkeys.

C. B. Rose, S. H. Korte and B. Niggemann. *Covance Laboratories GmbH, Muenster, Germany*. Sponsor: G. Weinbauer.

Quantitative EEG is one of the most sensitive non-invasive approaches for the detection of drug effects on the brain. Therefore, a validation study was performed using 4 male and 4 female cynomolgus monkeys. Two electrodes each were placed on the frontal, central and occipital cortex, with the reference electrode either placed at CZ (central region) or the mastoid. The electrode positions were calculated and marked with a tattoo on the head of the sedated animal 1-3 weeks before start of EEG measurements to guarantee exact electrode placement over the course of the study. The animals were habituated to the primate chair before start of the study. At the day of EEG recordings, the animals were habituated to the room approximately 5-10 minutes prior to EEG recordings. Subcutaneous steel needle electrodes as well as a reference electrode were fixed on the primate head and connected to the EEG system (EEG Kit for Neuropack S1, MEB-9400, Nihon Kohden). For determination of artefacts, ECG recordings were simultaneously performed. Sedating effects were shown using the drug lorazepam. An intermittent slowing of Delta- and/or Theta- waves was observed for all animals dosed intravenously with 0.2 mg/kg lorazepam, however the expected increase in frontal beta-activity was only recorded after a lorazepam dose of 0.4 mg/kg. For the 0.4 mg/kg dose level, an antidote was applied after sedating effects were observed in the EEG. To demonstrate seizure-inducing effects, female animals of an inhouse project were treated with pentylenetetrazole (PTZ) under anesthesia until seizures were visible. Anesthesia was induced with ketamine, the animals were ventilated and anesthesia was maintained with a mixture of oxygen and nitrous oxide. To avoid muscle artefacts in the EEG recordings, rocuronium was used as peripheral muscle relaxant. Seizures were observed at a single intravenous dose of 20 mg/kg PTZ at a dose volume of 0.2 mL/kg. In conclusion, this validation study demonstrated the feasibility of EEG recordings in chair-restrained cynomolgus monkeys since sedating as well as seizure-inducing effects could be demonstrated.

## PS 924 Characterization of Urinary microRNA in Cisplatin-Induced Nephrotoxicity in Rats.

M. Kanki<sup>1</sup>, A. Moriguchi<sup>1</sup>, D. Sasaki<sup>1</sup>, H. Mitori<sup>1</sup>, A. Yamada<sup>2</sup>, R. Hirota<sup>1</sup> and Y. Miyamae<sup>1</sup>. <sup>1</sup>Astellas Pharma Inc., Osaka, Japan; <sup>2</sup>Astellas Research Technologies Co., Ltd., Osaka, Japan.

Recent studies with urinary microRNA (miRNA) report that some urinary miRNAs detect renal dysfunction and histopathological damages. The purpose of this study is to find urinary miRNAs that can detect the drug-induced nephrotoxicity in rat as one of novel biomarkers.

Male Sprague-Dawley rats were given a single intraperitoneal injection of saline (10 animals) or cisplatin (6 mg/kg, 20 animals) and the urine was collected from 4 to 5 days (17hr) after administration. To examine the effects of feeding condition, half of animals in each group were fed and the others were fasted during urine collection. The kidney and serum were collected at 5 days after administration. Eighteen

protein biomarkers of nephrotoxicity in the urine were also measured. Urinary miRNAs were individually isolated from 5 animals in each group and miRNA expression data was obtained by TaqMan® rodent microRNA array cards.

In cisplatin-treated groups, moderate or marked proximal tubular necrosis was observed in the kidney and blood urea nitrogen and creatinine were significantly increased in the serum. Furthermore, most of protein biomarkers were significantly increased in the urine. There were no noteworthy differences in these items due to the feeding conditions. Regarding miRNAs, approximately 80 miRNAs showed statistically significant difference in the expression levels between fed and fasted condition. These miRNAs might be affected by feeding condition and were excluded when we explore changed miRNAs in cisplatin-treated groups. Approximately 30 miRNAs were found to be up- or down-regulated in cisplatin-treated group regardless of feeding condition during urine collection. Some of up-regulated urinary miRNAs, such as miR-192, were reported their expression in the rat kidney, so that these miRNAs might be derived from the injured kidney tissue. In conclusion, the feeding condition during urine collection affects the urinary miRNA profiles and we could identify some of urinary miRNAs that can detect the cisplatin-induced nephrotoxicity in rats.

## PS 925 Circulating miR-208a As Potential Cardiac Toxicity Biomarker.

J. Wang, L. Ling, S. Aquirre, W. W. Collette, M. Ko, F. Sace, Q. Peng, R. L. Yafawi, Q. Zong and A. John-Baptiste. *Drug Safety Research and Development, Pfizer, La Jolla, San Diego, CA*.

Literature is rife with information about several potential miRNAs that are involved in acute cardiac injury. In this dose finding study, we evaluated miR-1, -133a, -208a and -499-5p as potential biomarkers for cardiac injury in an oxidative stress mouse model and compared them alongside Troponin I.

Isoproterenol Hydrochloride (80, 160 or 320 mg/kg) was administered to female SOD2 +/- mice intraperitoneally once daily for one day to induce cardiac injury. EDTA plasma samples were collected at 6 and 24 hours for assessing miR-1, -133a, -208a, and -499-5p by Taqman real time PCR and Troponin I, the current golden standard for detecting early cardiac injury via MSD® ELISA kit. Cardiac damage was confirmed microscopically in heart tissues collected at day 10 and by measuring conventional serum biomarkers ALT, AST, ALP and GLDH at day 10.

Treatment related findings at doses  $\geq 80$  mg/kg at 6 and 24 h consisted of increased of cTn I in a dose-response fashion. Levels of cTn I declined after 6 hours. Concordant with cTn I results, miR-208a was elevated significantly. A similar, yet smaller, magnitude of response was noted for miR-499-5p while miR-1 and miR-133a appeared to be the least sensitive. Microscopically, mild myocardial inflammation and fibrosis at the heart base was observed in some mice given 160 mg/kg while ALT, AST, ALP and GLDH were not changed.

In conclusion, the release profile of miR-208a is comparable to cTn I suggests its utility as a putative cardiac injury biomarker. A dose level of 160 mg/kg caused significant elevations in cTn I and miR-208a which correlated with histopathologic findings in the heart.

## PS 926 Evaluation of the Pancreas-Specific microRNAs, miR-216a, and miR-217 As Biomarkers of Acute Pancreatitis.

D. G. Goodwin, J. Zhang, S. R. Stewart, L. Xu, B. A. Rosenzweig, K. L. Thompson and R. L. Rouse. *CDER, US FDA, Silver Spring, MD*.

Pancreatitis is a serious side effect associated with nearly half of the 100 most prescribed medications that is often under- or misdiagnosed because of its non-specific symptoms and the relative insensitivity of the clinical biomarkers, serum amylase and lipase. MicroRNAs (miRs) are short, non-coding RNA sequences involved in the regulation of gene expression. Serum miR-216a has been reported as a potential biomarker of acute pancreatitis, and our results suggest that miR-217 may also serve that purpose. miR-216a and miR-217 are selectively expressed in pancreatic acinar cells and are present at very low or undetectable levels in serum under normal conditions. To further evaluate the possible utility of miR-216a and miR-217 as serum biomarkers of pancreatitis, we investigated their performance in models of acute pancreatitis induced by caerulein, L-arginine, and ductile ligation in both rats and mice. Liver and acute kidney injury models were used to demonstrate the specificity of miR-216a and miR-217 for pancreatic injury. Both miR-216a and miR-217 showed a time and dose dependent correlation with the severity of pancreatitis in each of the pancreatic injury models and with amylase and lipase levels. The preliminary data suggest that miR-216a and miR-217 may be more sensitive and specific indicators of pancreatic injury than amylase and lipase in mice and rats and useful in pre-clinical drug development. Given the highly conserved nature of these microRNAs, a translation to clinical use would be also anticipated.

**PS 927 Multilaboratory Assessment of Best Practices for Quantification of microRNAs Associated with Isoproterenol-Induced Myocardial Injury in the Urine and Plasma of Rats.**

K. Thompson<sup>1</sup>, S. J. Nielsen<sup>2</sup>, T. Chen<sup>3</sup>, P. Coutter<sup>4</sup>, H. Ellinger-Ziegelbauer<sup>5</sup>, M. Kanki<sup>6</sup>, J. Kelsall<sup>7</sup>, E. Boitier<sup>8</sup>, R. Nassirpour<sup>9</sup>, G. Searfoss<sup>10</sup>, C. Spire<sup>11</sup>, P. Yuen<sup>12</sup> and R. O'Lone<sup>13</sup>. <sup>1</sup>CDER, Silver Spring, MD; <sup>2</sup>Exiqon, Vedbæk, Denmark; <sup>3</sup>NCTR, Jefferson, AR; <sup>4</sup>Novartis Pharma AG, Basel, Switzerland; <sup>5</sup>Bayer Pharma AG, Wuppertal, Germany; <sup>6</sup>Astellas Pharma Inc, Osaka, Japan; <sup>7</sup>AstraZeneca, Macclesfield, United Kingdom; <sup>8</sup>Sanofi, Vitry-sur-Seine, France; <sup>9</sup>Pfizer, Andover, MA; <sup>10</sup>Lilly, Indianapolis, IN; <sup>11</sup>Servier, Gidy, France; <sup>12</sup>NIDDK, NIH, Bethesda, MD; <sup>13</sup>ILSI Health and Environmental Sciences Institute, Washington DC.

MicroRNAs are promising noninvasive biomarkers of drug-induced toxicities due to their tissue-selective expression, rapid release post-injury, and stability in biofluids, but their low levels in biofluids present challenges to their reliable quantification. The HESI Genomics committee initiated a collaborative study to assess best practices for measuring injury-related microRNAs in biofluids. Samples were derived from a model of acute cardiotoxicity in male Wistar rats induced by a single s.c. injection of 0.5 mg/kg isoproterenol. The heart-enriched microRNAs miR-208, miR-499, and miR-1 increased by approximately 10-fold in serum and plasma 4 hr after treatment. In a follow-up study using the same model system, urine was collected overnight and plasma at 24 hr post-injection. Biofluids were pooled from 5 rats per group and aliquots were sent to 10 laboratories for analysis of levels of the 3 heart-enriched microRNAs. At each site, samples were assayed using a standard protocol and the data normalized to levels of a spiked-in ath-miR159a control. The results from this interlaboratory analysis of multiple preanalytical and technical issues provide guidelines for the accurate measurement and reporting of injury-related microRNAs in biofluids.

**PS 928 Circulating miR-9\* and miR-384-5p As Potential Indicators for Trimethyltin-Induced Neurotoxicity.**

K. Ogata<sup>1,2</sup>, K. Sumida<sup>1</sup>, K. Miyata<sup>1</sup>, M. Kushida<sup>1</sup>, M. Kuwamura<sup>2</sup> and J. Yamate<sup>2</sup>. <sup>1</sup>Environmental Health Science Laboratory, Sumitomo Chemical Co., Ltd., Osaka, Japan; <sup>2</sup>Laboratory of Veterinary Pathology, Division of Veterinary Sciences, Graduate School of Life and Environmental Sciences, Osaka Prefecture University, Izumisano, Japan. Sponsor: T. Yamada.

MicroRNAs (miRNAs) are believed to be promising biomarkers due to their tissue-specific expression and high stability in blood. Our study was conducted to determine nervous system-specific miRNAs in blood as potential indicators for neurotoxicity. Using trimethyltin (TMT)-induced neurotoxicity model, we analyzed serum miR-9\* and miR-384-5p which were reported to be highly or specifically expressed in the nervous system, and compared the sensitivity as neurotoxicity parameters with nervous symptoms and histopathology.

Seven-week-old SD rats were orally given a single dose of 6, 9 and 12 mg/kg of TMT. Nervous tissues (brain, spinal cord and sciatic nerve) and blood were collected 1, 4 and 7 days after administration (D1, 4 and 7). Daily observation of symptoms and histopathology were conducted. Immunohistochemistry (PCNA, GFAP, Iba1) and TUNEL method were performed on brain. Expressions of miR-9\* and miR-384-5p in serum and hippocampus were analyzed by RT-PCR.

TMT induced tremor, hypersensitivity and decreased auditory response after D2 at 12 mg/kg and after D4 at 9 mg/kg. Neural cell death including apoptosis and glial reaction in cerebrum (mainly hippocampus) and cerebellum was observed after D1 at 12 mg/kg and after D4 at 6 and 9 mg/kg, and the severities increased in a dose- and time-dependent manner.

Expression levels of miR-9\* (D4 and 7 at 12 mg/kg and D7 at 6, 9 mg/kg) and miR-384-5p (D4 at 9 mg/kg, D7 at 12mg/kg) in serum were significantly higher than the vehicle control, but not changed in hippocampus. Increased serum level of these miRNAs might be due to leakage from damaged nervous tissue.

The detection sensitivity of neurotoxicity of serum miR-9\* miR-384-5p was similar to observation of nervous symptoms, therefore they were considered possible novel indicators of neurotoxicity.

**PS 929 Assessment of microRNA 122 As a Preclinical and Clinical Biomarker of Hepatotoxicity Utilizing Affymetrix QuantiGene Technology.**

S. J. Schomaker<sup>1</sup>, D. Burt<sup>1</sup>, R. Warner<sup>2</sup>, K. Johnson<sup>2</sup> and J. Aubrecht<sup>1</sup>. <sup>1</sup>Safety Sciences, Pfizer Inc, Groton, CT; <sup>2</sup>Department of Pathology, University of Michigan Medical School, Ann Arbor, MI.

Hepatotoxicity is major challenge in drug development. While alanine aminotransferase (ALT) remains the gold standard biomarker of liver injury, the availability of alternative biomarkers to better predict the potential for drug induced liver injury is essential. In this study we evaluated the utility of miRNA122 as a biomarker of liver

injury in both preclinical and clinical serum samples utilizing Affymetrix QuantiGene Technology. The Affymetrix system is a 96-well plate based assay that uses a sandwich nucleic acid hybridization platform to detect miRNA directly without a reverse transcription step followed by signal amplification via a branched DNA amplifier and chemiluminescence signal generation. In this study, male Sprague-Dawley rats were treated with a single dose of 1400mg/kg acetaminophen (APAP), 100mg/kg naphthylisothiocyanate (ANIT), or 0.2mg/kg microcystin-LR (MC) to induce hepatocellular necrosis which was confirmed by histopathological examination. Statistically significant increases ( $p < 0.01$ ) in miRNA122 were observed after treatment with all three of the model hepatotoxins. miRNA122 was also assessed in cohorts of human subjects including 27 healthy subjects, 31 patients with a variety of liver impairments, and 7 cases of APAP poisoning collected from the University of Michigan health care system under an approved IRB. In the absence of histopathologic evaluation that was not feasible due to ethical and practical reasons, miRNA122 values were correlated with ALT levels as an indicator of liver injury. A Spearman's rank correlation analysis between miRNA122 and ALT of the 65 human samples yielded a correlation coefficient of  $r_s = 0.88$ . Analysis of miRNA122 in the APAP poisoned subjects resulted in increases of 13-95 fold when compared to miRNA122 levels from healthy subjects. This study demonstrates the utility of miRNA122 as a preclinical and clinical biomarker of liver injury utilizing Affymetrix QuantiGene Technology.

**PS 930 Urinary microRNA Profiles After Glomerular vs Proximal Tubular Injury.**

B. Riefke<sup>2</sup>, M. Pavkovic<sup>1</sup>, I. Groetcke<sup>1</sup>, A. Frisk<sup>2</sup>, F. McDonald<sup>2</sup> and H. Ellinger-Ziegelbauer<sup>2</sup>. <sup>1</sup>Bayer Pharma AG, Wuppertal, Germany; <sup>2</sup>Bayer Pharma AG, Berlin, Germany.

MicroRNAs (miRNAs) are small, conserved, non-coding RNAs that modulate gene expression post-transcriptionally. They are remarkably stable in various body fluids like urine and thus suggested as new non-invasive biomarkers (BM) of tissue injury, especially since some miRNAs are produced in cell- or tissue specific manners offering the possibility to identify the site of injury. Furthermore, their tissue expression profiles may be used for investigation of the mechanistic details of compound-induced toxicities.

We investigated miRNAs in urine of male Crl:WI (Han) rats treated with nephrotoxics: Cisplatin (Cp), to specifically elicit proximal tubular injury; and male Wistar Kyoto rats treated with a nephrotoxic serum (NTS) containing antibodies against the glomerular basement membrane to induce glomerular damage. The expected tissue injury was confirmed by histopathology. Total RNA including small RNAs was isolated from urine on day 3, 5, 8, 15 and 26 after a single dose of Cp (0, 1 and 3 mg/kg) and on day 8 and 14 after NTS injection (0.1, 0.25 and 0.5 mL/100g bw). Urinary miRNA profiles were measured with TaqMan® MicroRNA Cards (TLDA). MiRNA levels were normalized to a non-endogenous spiked-in control miRNA and to urinary creatinine. Comparing Cp-high dose vs. control samples and NTS-high dose vs. control samples we identified 131 and 68 miRNA, respectively, with significantly increased urinary levels. About 65 miRNAs were affected by both treatments, whereas app. 10 and 35 urinary miRNAs were exclusively affected by NTS and Cp treatment, respectively. Furthermore, TLDA analysis of kidneys from NTS-treated rats showed deregulation of many miRNAs upon glomerular injury.

Our results suggest that urinary miRNAs may be used as promising new and site-specific BMs for nephrotoxicity and encourage further investigations of their role in different types of kidney injury.

**PS 931 Proposed Workflow for microRNA Analysis in Urine.**

H. Ellinger-Ziegelbauer<sup>1</sup>, M. Pavkovic<sup>1</sup>, B. Riefke<sup>2</sup> and R. Khan-Malek<sup>3</sup>. <sup>1</sup>Bayer Pharma AG, Wuppertal, Germany; <sup>2</sup>Bayer Pharma AG, Berlin, Germany; <sup>3</sup>Sanofi-Aventis, Bridgewater, NJ.

MicroRNAs (miRNAs) have emerged as new non-invasive biomarkers (BM) for various diseases and tissue injuries due to their release into body fluids upon tissue damage. At least some of these miRNAs are produced in a cell- or tissue specific manner.

For evaluation of miRNAs, urine was collected from male Wistar rats treated with the nephrotoxicant Cisplatin (Cp). Tissue injury was confirmed by histopathology. Total RNA was isolated from urine on days 3, 5, 8, 15 and 26 after a single dose of Cp (0, 1 and 3 mg/kg). Using TaqMan® MicroRNA Cards (TLDA) urinary miRNA profiles were measured. Since currently a commonly accepted endogenous control miRNA is not available, and since we could not identify invariant miRNAs in our study, we describe here a normalization procedure based on the spiked-in control miRNA (ath-miR159a) and urinary creatinine (uCreat). For other urinary BMs uCreat is commonly used to account for different urine volumes.

For the TLDA- derived PCR data, a modified  $\Delta\Delta C_t$  method was applied: delta-Ct values obtained by subtracting ath-miR-159a Cts from target miRNA Cts were de-logarithmized and divided by the corresponding uCrea value. This normalization reduced the variation of the delta-Ct values for miRNAs across samples. Then ratios were calculated between treated and time-matched control groups. With this method we identified 131 miRNAs with significantly increased urinary levels on days 3 and 5. Twenty miRNAs with distinct time-dependent profiles were then measured using TaqMan® MicroRNA Assays. The data were analysed either with the modified  $\Delta\Delta C_t$  method, or absolutely quantified using synthetic miRNA standard curves run in parallel. With both methods we obtained comparable results with respect to observed direction of changes and time course of affected urinary miRNAs.

Our results indicate that urinary miRNAs may be used as BMs for nephrotoxicity in rats.

Furthermore, normalization to uCrea, which is recommended for urinary BMs, appears feasible for analysis based either on the PCR-generated Ct values only, or including absolute quantification.

### PS 932 **MiR-122 Is a Sensitive Indicator of Stem Cell-Derived Hepatocyte-Like Cell Maturity with Utility in Hepatotoxicity Screening.**

C. Rowe, C. Goldring, L. Kelly, N. Hanley, H. Z. Malik, R. Jones, D. Tosh, R. Kia, N. R. Kitteringham and B. Park. *MRC Centre for Drug Safety Science, University of Liverpool, Liverpool, United Kingdom.* Sponsor: *D. Mendrick.*

Consistent differentiation of embryonic, or induced pluripotent, stem cells into functional hepatocyte-like cells available on demand for hepatotoxicity screening would be a valuable resource for drug development programs. Assessments of stem cell-derived hepatocyte-like cell maturity often lack quantitative comparisons with primary human hepatocytes and the presumed fetal-like phenotype currently achieved is concluded from observations of cell morphology and the detection of a small number of proteins such as albumin, alpha fetoprotein and alpha 1 antitrypsin. The identification of a hepatocyte-specific marker that can be quantified absolutely would aid the assessment of cells and be useful for inter-laboratory comparisons. miRNA-122 is a micro-RNA species that is very highly enriched in hepatocytes. We hypothesised that this molecule would be a useful biomarker of differentiation and could also serve as a more sensitive indicator of hepatocyte-specific injury. Our study demonstrates that miR-122 is a specific and sensitive marker of hepatocyte phenotype, present at high levels in primary human hepatocytes and in fetal liver samples but of low abundance or absent in hepatoma and non-hepatic human cell lines. Expression of miR-122 was greatly elevated in stem cell-derived hepatocyte-like cells compared to the undifferentiated stem cell lines. Furthermore we demonstrate miR-122's utility as a sensitive marker of hepatotoxicity in primary hepatocytes and a potential adjunct to screens such as lactate dehydrogenase release and ATP depletion. We conclude that quantitative measurement of miR-122 may be used as sensitive and specific marker during the hepatocyte differentiation process or to confirm the hepatocyte-like status of stem cell-derived material following hepatotoxicity screening assays.

### PS 933 **Potential Utilization of microRNA As Circulating Biomarkers in Th2-Mediated Disorders Such As Asthma and Ulcerative Colitis.**

H. Lin<sup>1</sup>, M. Kasaian<sup>2</sup>, A. Brennan<sup>2</sup> and S. Ramaiah<sup>1</sup>. <sup>1</sup>DSRD, Pfizer Inc., Andover, MA; <sup>2</sup>Immunology & Autoimmunity, Pfizer Inc., Cambridge, MA.

MicroRNAs (miRNAs) are single-stranded RNAs which constitute a class of non-coding RNAs which have emerged as key regulators of gene expression. They are generally thought to inhibit translational activities or promote degradation of mRNA targets. miRNA profiles have been proposed as a diagnostic tool to predict survival and relapse in lung and colon cancer patients. Moreover, circulating miRNAs have been proposed as a new class of biomarker of human diseases and toxicities. IL-4 and IL-13 are central Th2 cytokines in the immune system and potent activators of inflammatory responses during Th2-mediated inflammation. In particular, an essential role for Th2-mediated immune response has been demonstrated in animal models of allergic asthma and experimental colitis. We hypothesized that miRNAs may be involved in the homeostatic regulation of IL-4/-13 expression in disease, or may be modulated during the course of therapeutic antagonism of IL-4/-13 in order to maintain homeostasis of IL-4/-13 expression. Using web based databases that provide literature information on the predicted mRNA targets of miRNAs related to the Th2 immune response, distinct subsets of miRNAs were selected and used to construct a Taqman miRNA assay panel for miRNA screening of sera from asthmatic and ulcerative colitis patients. We found that the profile of circulating miRNAs is capable of distinguishing healthy volunteers from patients with asthma or ulcerative colitis. The results described here have

implications for the use of serum or plasma miRNA profiles as biomarkers for Th2-associated diseases. The overlap with tissue miRNA expression as described in the literature suggests that circulating miRNA expression may be a sensitive indicator of disease activity in the target organ.

### PS 934 **Circulating Nucleic Acids As Lead Exposure Biomarkers in a Mammalian Model System.**

S. Lee and M. E. Gillespie. *Pharmaceutical Sciences, St. John's University, Queens, NY.*

Exposure to lead (Pb) causes numerous deleterious health effects including developmental and cognitive abnormalities in children. Early detection of lead exposure is critical to reduce serious health problems arising from chronic lead toxicity. Circulating nucleic acid based biomarkers are present in various bodily fluids such as blood, serum, and urine. A number of studies have reported the use of circulating nucleic acids as biomarkers for pathological conditions and developmental stages. In this study, a Long Evans rat model system is used to identify lead exposure-induced circulating nucleic acid biological markers in peripheral blood. Two different groups of animals are used, females and time-pregnant Long Evans rats. Females are exposed to 112 parts per million (ppm) Pb (lead acetate) via drinking water ad libitum for 5 days then switched to 19 ppm Pb treatment for an additional 15 days. Dams are exposed to 112 ppm Pb (lead acetate) via drinking water ad libitum from gestation day 16 through 21 then switched to 19 ppm Pb treatment on postnatal day 1 through 15. Animals are euthanized at the conclusion of treatment and blood and brain tissue are collected for analysis. Inductively coupled plasma optical emission spectrometry (ICP-OES) is used to determine blood lead levels of all samples. A microarray approach was initially used to identify differentially expressed circulating nucleic acid sequences only present in animals exposed to Pb. This data highlighted 3 genes of interest: Nt5c3, Skap1, and Coq7. Circulating nucleic acid expression levels in blood samples will be quantified using real-time RT-PCR analysis. Comparison between lead exposed females and pregnant females will identify unique genes as biomarkers of lead exposure and confirm the origin of the circulating nucleic acids.

### PS 935 **Examination of Oxidative Stress As a Possible Risk Factor for Colorectal Cancer Susceptibility.**

R. Sellamuth, S. Dickinson, Z. Wang, S. Zhou and J. E. Klaunig. *Indiana University, Bloomington, IN.*

The present study investigated the role of oxidative stress as a possible risk factor for colorectal cancer in humans. Blood samples were collected from 232 subjects including 102 healthy controls, 90 patients with polyps, 39 patients diagnosed with colorectal cancer. We measured both direct and oxidative DNA damage in peripheral white blood cells (WBCs) using alkaline (direct DNA damage) and formamidopyrimidine DNA glycosylase modified (oxidative DNA damage) Comet assay. Trolox equivalent total antioxidant capacity (TEAC) in plasma was also determined spectrophotometrically. Results showed that Oxidative Stress induced DNA damage was associated with a significantly higher probability of colorectal cancer in males ( $p = 0.008$ ) but not in females ( $p = 0.675$ ) compared to healthy controls. Direct DNA damage also showed a marginally significant effect on colorectal cancer ( $p = 0.071$ ). Results from the TEAC assay showed a positive trend on colorectal cancer, but was not statistically significant ( $p = 0.230$ ). Oxidative stress induced DNA damage, TEAC, and direct DNA damage did not show significant relationships with probability of polyps. Females showed significantly higher probability of developing polyps ( $p < 0.01$ ); and older patients showed significantly lower probability of polyps in this study ( $p < 0.001$ ). Further, these results were not affected by life-style related oxidative stress such as smoking and alcohol. Selected SNPs for oxidative damage, detoxification and DNA repair were examined. Initial results suggested a correlation between SNPs in hOGG and GSTM and colorectal cancer. The results of this study suggest that high level of oxidative stress induced DNA damage is associated with increased risk of colorectal cancer in males, not in females.

### PS 936 **Circulating mRNA Changes in Rat Serum Associated with Drug-Induced Vascular Injury.**

M. Scicchitano, D. Dalmás, K. Roland and H. Thomas. *GlaxoSmithKline, King of Prussia, PA.*

Drug-induced vascular injury (DIVI) continues to be an obstacle to early drug-development due to the lack of biomarkers and by a limited understanding of the pathologic mechanism/s. Recently, a novel gene panel has been developed, for use in rat mesenteric arteries, which can potentially be used to identify and/or predict

the occurrence of drug-induced medial arterial necrosis (MAN) in rats; however, a non-invasive method for detecting this type of injury is currently lacking. To determine whether these genes regulated in mesenteric arteries have the potential to be utilized as circulating serum genomic biomarkers, the gene panel was assessed in mRNA isolated from the serum of rats given a vasotoxic dose of Fenoldopam or Dopamine and compared to mRNA data obtained from serum of rats given Yohimbine, a vasoactive compound which does not cause histologic evidence of vascular injury. Out of the 69 potential circulating biomarkers, 10 genes, including *Lrrc59*, *Tubb6*, *Kpna2*, *Abca8a*, *Prosl*, *S100a11*, *IL-8R*, *CTGF*, *Nfkbiz*, and *Daf1*, were observed to be upregulated (5 fold or greater) and correlated with histologic evidence of MAN following treatment with a vasotoxic dose of Fenoldopam. Six of the 10 genes including *Lrrc59*, *Abca8a*, *S100a11*, *IL-8R*, *Nfkbiz* and *Daf1*, were also upregulated (4 fold or greater), in the serum of rats given Dopamine. With exception of *S100a11*, these genes were not regulated in the serum of rats given Yohimbine thereby, providing further evidence of their association with vascular injury, namely mesenteric MAN. Although further studies are required to fully assess the utility of these serum-derived mRNAs as biomarkers of DIVI, they have the potential to help improve the characterization of DIVI in rats for early safety assessment in drug development.

**PS 937 Identification and Quantitative Evaluation of Novel Circulating Liver-Specific mRNAs in Rats Treated with Various Hepatotoxic Compounds: Validation for Biomarkers of Drug-Induced Liver Injury.**

S. Okubo<sup>1,2</sup>, M. Miyamoto<sup>1,2</sup>, K. Takami<sup>1,2</sup>, M. Kanki<sup>2,3</sup>, A. Ono<sup>2,4</sup>, N. Nakatsu<sup>2</sup>, H. Yamada<sup>2</sup>, Y. Ohno<sup>4</sup> and T. Urushidani<sup>2,5</sup>. <sup>1</sup>Drug Safety Research Laboratories, Takeda Pharmaceutical Company Limited, Kanagawa, Japan; <sup>2</sup>Toxicogenomics Informatics Project, National Institute of Biomedical Innovation, Osaka, Japan; <sup>3</sup>Astellas Pharmaceutical Incorporated, Osaka, Japan; <sup>4</sup>National Institute of Health Sciences, Tokyo, Japan; <sup>5</sup>Doshisha Women's College of Liberal Arts, Kyoto, Japan.

In our previous report, circulating liver-specific albumin (Alb) and  $\alpha$ -1 microglobulin/bikunin precursor (Ambp) mRNAs have been shown to be potential biomarkers for drug-induced liver injury (DILI). We identified apolipoprotein h (ApoH) and group specific component (Gc) mRNAs as additional biomarkers, and quantified total of four mRNAs in plasma from rats treated with wide variety of hepatotoxicants to validate circulating liver-specific mRNAs as biomarkers for DILI. Bioinformatic and molecular biological analyses revealed the high liver-specificity of ApoH and Gc mRNAs, and increased plasma levels of these mRNAs were confirmed by real-time quantitative RT-PCR in rats treated with thioacetamide (TAA). To examine the characters of the four circulating liver-specific mRNAs, seven hepatotoxicants were administered to rats. The severities of liver injury were variable among individuals and compounds. At 24 hr after single dosing, parallel increases of the four circulating liver-specific mRNAs were noted and the levels correlated with changes in the ALT values and hepatocellular necrosis scores. In addition, all the four mRNAs increased with greater magnitude than the ALT values. Time course analysis within 24 hr after single dosing of TAA showed that the plasma levels of Alb and Gc mRNAs increased remarkably before the ALT elevations and the timing of the increase was different among mRNA species, indicating that circulating liver-specific mRNAs may predict the beginning of liver damage and enable us to know the stages of injury. This validation study clearly demonstrated that the four circulating liver-specific mRNAs would be reliable and useful biomarkers for DILI.

**PS 938 Metabolomics and Transcriptomics Evaluation of Preclinical Biomarkers of Hepatotoxicity: An Update.**

R. D. Beger<sup>1</sup>, L. K. Schnackenberg<sup>1</sup>, S. Jinchun<sup>1</sup>, L. Pence<sup>1</sup>, T. Schmitt<sup>1</sup>, Y. Ando<sup>2</sup>, X. Yang<sup>1</sup>, J. Greenhaw<sup>1</sup>, S. Slavov<sup>1</sup>, S. Bhattacharyya<sup>1,3</sup>, W. E. Salminen<sup>1</sup> and D. L. Mendrick<sup>1</sup>. <sup>1</sup>NCTR, US FDA, Jefferson, AR; <sup>2</sup>Daiichi Sankyo Co. Ltd., Tokyo, Japan; <sup>3</sup>Arkansas Children's Hospital Research Institute, Little Rock, AR.

Drug-induced hepatotoxicity represents a major reason that drugs are recalled post market. Furthermore, it has been estimated that 10% of acute liver failure is due to idiosyncratic events. While there is no standard definition for "idiosyncratic," the term is generally applied to compounds that induce a relatively low incidence of hepatotoxicity in humans and fail to exert liver damage using classical toxicity endpoints in commonly used preclinical testing species such as rats and dogs. The inability to identify such compounds with classical preclinical markers of

hepatotoxicity has necessitated the need to discover new biomarkers. In order to identify biomarkers of idiosyncratic toxicity, a systems biology study was initiated to evaluate omics endpoints in urine, blood and liver tissue from rats dosed with compounds that have been shown to be overt hepatotoxicants, idiosyncratic hepatotoxicants, and negative hepatotoxicants. The two overt hepatotoxicants were acetaminophen (APAP) and carbon tetrachloride (CCl<sub>4</sub>). Three additional compounds have been studied; one is generally classified as idiosyncratic in nature, felbatol (FEL), while the other two are considered to not cause liver injury, meloxicam (MEX) and penicillin (PEN). Since idiosyncratic and non-hepatotoxicant drugs do not cause overt hepatotoxicity, doses were used to induce some adverse effect (e.g., a decrease in body weight) to provide a phenotypic anchor. Early results show that increases in blood levels of multiple acyl carnitines could be an indication of hepatic mitochondrial injury and altered levels of bile acids may be related to drug-induced hepatotoxicity, activation of liver transporters or due to effects on gut microflora. Blood levels of lysoPCs were decreased in the rats treated with a high dose of APAP, CCl<sub>4</sub> and FEB at 6 and/or 24 hr.

**PS 939 Whole Transcriptome RNA-Seq of FFPE Liver.**

S. S. Auerbach<sup>1</sup>, B. A. Merrick<sup>1</sup>, R. R. Shah<sup>2</sup>, D. Phadk<sup>2</sup>, B. Xie<sup>3</sup>, J. Shin<sup>3</sup>, Y. Gao<sup>3</sup> and R. R. Tice<sup>1</sup>. <sup>1</sup>Division of the National Toxicology Program, NIEHS, Research Triangle Park, NC; <sup>2</sup>SRA International, Durham, NC; <sup>3</sup>Lieber Institute for Brain Development, Johns Hopkins University, Baltimore, MD.

Formalin fixed, paraffin embedded (FFPE) pathology specimens represent a potentially rich resource for transcriptomic-based biomarker discovery. While a number of approaches have been developed that employed targeted, amplification dependent microarray analysis, no one has employed the agnostic approach of whole transcriptome RNA-seq to the analysis of RNA extracted from FFPE samples. Here, we compare whole transcriptome using RNA-seq performed on fresh frozen (FF) and FFPE RNA samples obtained from Fischer F344 rats exposed to Aflatoxin B1 (AFB1) at 1 ppm in feed for 90d and paired control animals. ~70% of reads generated from each FFPE sample aligned to Rn4and mapping corresponded well with defined transcription boundaries for most RefSeq genes. Whole transcriptome PCA indicated clear distinction between FFPE and FF however robust, parallel differentiation between AFB1 and control samples was obvious in both data sets. A rank based comparison of global transcript abundance was strongly correlated between FF and FFPE, suggesting the global liver biology at the transcript level remained intact in the FFPE samples. Differential expression analysis indicated that of the 405 RefSeq genes altered by AFB1 in FF samples, 288 (of 487 showing differential expression) were also differentially expressed in FFPE samples. Expression of selected genotoxic carcinogenicity biomarker genes (e.g., Adam8, Mybl2, Cdh13, Cngl1, Ddit4l, Cdkn1c) were concordantly up-regulated in FF and FFPE by AFB1 treatment. Comparison of the genomic response to AFB1 in FF and FFPE at a pathway level using GSEA found concordant regulation of cell cycle, autophagy, xenobiotic metabolism, and p53 signaling and discordant regulation of proteasome and NOD-like signaling pathways. We have demonstrated that accurate whole transcriptome profiling is possible with RNA extracted from FFPE samples. The success of this approach opens up new avenues for performing signature-based biomarker discovery.

**PS 940 Hepatic Hemangiosarcoma Due to Occupational Vinyl Chloride Exposure Generates a Distinct Plasma Metabolite Profile.**

M. Cave<sup>1,2</sup>, B. Wheeler<sup>1</sup>, K. Falkner<sup>1</sup> and C. McClain<sup>1,2</sup>. <sup>1</sup>Department of Medicine/GI, University of Louisville, Louisville, KY; <sup>2</sup>Louisville VAMC, Louisville, KY.

Occupational vinyl chloride (VC) exposure has been associated with the development of hepatic hemangiosarcoma (HS), an extremely aggressive and otherwise unusual form of liver cancer. Routine liver biochemistries are typically normal even in advanced hemangiosarcoma. The purpose of this study is to determine if VC-related hemangiosarcoma alters the plasma metabolome. Plasma samples from 16 highly-exposed VC workers with hemangiosarcoma (VC+/HS+), 17 highly-exposed VC workers without hemangiosarcoma (VC+/HS-), and 27 unexposed healthy volunteers (VC-/HS-) were obtained from a specimen bank. GC/MS and LC/MS2 were performed following metabolite extraction. Software was used to match ions to a library of standards for metabolite identification and quantitation by peak area integration. Random Forest analysis was performed. Welch's Two Sample t-test comparisons were made between the means of each biochemical. Results of Random Forest analyses of all 613 named and 518 unnamed biochemicals observed in plasma yielded an overall predictive accuracy of 82% for classifying

samples within each group, strongly indicating that hemangiosarcoma generates a distinct global metabolic profile in plasma from those that were exposed but failed to develop the disease. When comparing VC+/HS+ vs. VC+/HS-, 65 named biochemicals were up-regulated while 50 were down-regulated. Likewise, 43 unnamed biochemicals were up-regulated and 27 were down-regulated. Four key metabolite subclasses containing named biochemical were identified. Hemangiosarcoma increased metabolite levels in these classes accordingly: Class A (8/10 metabolites, up to 6 fold increase); Class B (5/7 metabolites, up to 121 fold increase); Class C (3/3 metabolites, up to 84 fold increase); Class D (9/15 metabolites, up to 92 fold increase). In chemical workers with high-level vinyl chloride exposures, hemangiosarcoma generates a distinct plasma global metabolic profile from those that were exposed but failed to develop the disease.

#### PS 941 **Metabolomic Biomarkers in Long-Term Smokers and Moist Snuff Consumers.**

G. L. Prasad<sup>1</sup>, B. A. Jones<sup>1</sup>, P. Chen<sup>1</sup> and A. D. Kennedy<sup>2</sup>. <sup>1</sup>R & D, RJ Reynolds Tobacco Co., Winston-Salem, NC; <sup>2</sup>Metabolon Inc, Durham, NC. Sponsor: G. Krautter.

The long-term health effects associated with cigarette smoking have been shown to be more harmful compared to those associated with the use of non-combustible tobacco products, such as moist snuff. To investigate the long-term effects of tobacco exposure, we evaluated the biochemical profiles of 40 smokers, 40 moist snuff consumers (MSC), and 40 non-tobacco consumers (NTC) using UHPLC-mass-spectrometry based global metabolomics. Matching twenty-four-hour urine and plasma samples were collected from study subjects to generate metabolomic profiles. In this global profiling study, a total of 511 biochemicals (290 known and 221 unknown metabolites) were detected in the plasma, whereas 972 biochemicals (396 known and 596 unknown) were found in urine. The "named" metabolites could be grouped into diverse physiological pathways such as glucose, lipid, bile acid and amino acid metabolism.

Based on the differential levels of metabolites, random forest analyses separated non-tobacco consumers (NTC), smokers, and MSC with high accuracy (96%) when all metabolites were included. On the other hand, MSC showed more subtle changes in metabolomic profiles, and were more difficult to separate from NTC when nicotine metabolites were excluded from the analyses. The metabolomic changes suggest that smokers exhibited exacerbated oxidative stress and inflammatory pathways relative to MSC and NTC cohorts. Biochemical changes in glucose, lipid amino acid and xenobiotic metabolism were also noted in the study cohorts. These metabolites could be used as potential biomarkers of effect, pending further validation. In summary, global metabolomic profiles and panels of selected biomarkers could potentially be used to assess the effects of tobacco use.

#### PS 942 **Effect of Benzo(a)pyrene Exposure Dose on Levels of Exposure Biomarkers, DNA Adducts, and Gene Expression in Rats.**

M. Moreau<sup>1</sup>, P. Ayotte<sup>2</sup> and M. Bouchard<sup>1</sup>. <sup>1</sup>Department Environmental and Occupational Health, University of Montréal, Montréal, QC, Canada; <sup>2</sup>Institut national de santé publique du Québec, Québec, QC, Canada.

The effect of benzo(a)pyrene (BaP) doses on levels of several biomarkers of exposure and early effects was studied in rats intravenously injected with 0.4, 4, 10 and 40 µmol/kg of BaP. Blood, tissues and excreta were collected 8 h and 24 h post-treatment. BaP and several of its metabolites, 3- and 7-OHBP, 4,5- and 7,8-BaPdiols, tetrol, 1,6-, 3,6- and 7,8-BaP-diones, were simultaneously measured in blood, tissues and excreta by UHPLC/fluorescence. BaPDE-DNA adducts in lungs were quantified in parallel using an ultrasensitive immunoassay with chemiluminescence detection. Expression of various genes in lungs of treated rats (lung RNA) compared to control rats was also assessed by qRT-PCR. There was a dose-dependent increase in blood and tissue levels as well as excretion of BaP metabolites. At 8 h and 24 h postinjection, BaP and 3-OHBP were found in higher concentrations in blood and tissues compared to the other analytes. However, BaPdiols were excreted in greater amounts in urine and apparently more quickly than hydroxyBaP. Mean percentages (± SD) of injected dose excreted in urine as 4,5-diol-BaP during the 0-8 and 0-24-h period post-treatment were 0.16 ± 0.03% and 0.14 ± 0.08%, respectively. Corresponding values for 3-OHBP were 0.004 ± 0.001% and 0.026 ± 0.014%. Diones were not detectable in blood, tissues and excreta using the developed method and BaP-7,8-diol and 7-OHBP were found to be more minor metabolites. There was also a dose-dependent increase in DNA adduct formation. Analysis of gene expression further showed a modulation of cyp1a1, cyp1b1, nqo1, nrf2, fos and Ahr expression at the 10 and 40 µmol/kg doses, but not at the lower

doses. This study confirms the interest of measuring multiple metabolites in combination with DNA adducts and alteration of gene expression for a more comprehensive assessment of links between biomarkers of BaP exposure and early effects.

#### PS 943 **Biomarker Discovery for Early Detection of Hepatocellular Carcinoma (HCC) in Hepatitis C (HCV) Infected Patients.**

G. M. Mustafa<sup>1</sup>, J. R. Petersen<sup>1</sup>, J. Hyunsu<sup>1</sup>, L. Cicalese<sup>1</sup>, N. Snyder<sup>2</sup>, S. J. Haidacher<sup>1</sup>, L. Denner<sup>1</sup> and C. Elferink<sup>1</sup>. <sup>1</sup>University of Texas Medical Branch, Galveston, Galveston, TX; <sup>2</sup>Kelsey Seybold Clinic, Galveston, TX.

The projected rise in HCC (the most common primary liver cancer) cases in the US is mainly due to HCV infections with onset of HCC coming several decades after initial infection. However, additional environmental risk factors including alcohol, tobacco and other dietary insults that induce liver injury also increase the incidence of HCC. The poor prognosis for HCC is largely due to late stage diagnosis making successful intervention difficult. Existing biomarkers for early HCC detection lack the specificity and sensitivity to be very effective. Our aim is to develop serum-based biomarkers suitable for early HCC detection that will provide a sensitive yet specific screen. Serum was obtained from individuals positive for HCV who were clinically diagnosed with liver disease (pre-HCC) or HCC. Serum was pre-fractionated using an aptamer-based technology and further fractionated using 2D-Difference In Gel Electrophoresis. Pre-HCC and HCC profiles were compared and the peptides located in 24 different 2D-DIGE spots exhibiting a statistically significant ≥1.5-fold change between pre-HCC and HCC samples were identified by mass spectrometry (MS). Stable isotope O18/O16 labeling was used to verify the identity of proteins identified by 2D-DIGE and to aid in development of Selected Reaction Monitoring (SRM) assays. ApoA1 was selected to develop an SRM as proof of concept in this biomarker discovery protocol. Using a Triple Quadrupole MS (Agilent), Optimizer (Agilent) and skyline (MacCoss) to assist in the design we developed an SRM assay to quantify this candidate biomarker using labeled internal standards (AQUA peptides). The SRM is capable of reliably detecting a >30% reduction in ApoA1 in HCC serum samples relative to the pre-HCC samples. Future multiplexing of SRM assays for other candidate biomarkers is envisioned to develop a biomarker panel for subsequent verification and validation studies.

#### PS 944 **Effects of Acrylamide Exposure on Gene Expression in the Thyroid of Male and Female RccHan Wistar Rats.**

R. C. Colli-Dula<sup>1</sup>, M. A. Friedman<sup>2</sup> and N. Denslow<sup>1</sup>. <sup>1</sup>CEHT, University of Florida, Gainesville, FL; <sup>2</sup>TR Services, Oviedo, FL.

Acrylamide is a chemical commonly utilized to make polymers used in industry including waste water treatment, mining, among other uses. It became a public health concern when it was detected in food products. Daily exposure to acrylamide has been associated with neurological toxicity in different animal species and with tumors in the mammary gland, testicular tunica vaginalis, and thyroid. In relation to its potential for forming tumors, it is important to distinguish its ability to act as genotoxin from a hormone mimic. The goal of this study was to use microarray analysis to determine changes in gene expression in the thyroid gland of male and female RccHan Wistar rats treated at 3 mg/kg in drinking water from gestational day 6 to pnd (post natal day) 30. Thyroid glands were collected from rats at 10 PM to reflect non-quietest thyroid activity. The transcriptome analysis showed that acrylamide caused a significant alteration in the expression of genes related to phase II detoxifying enzymes and oxidative stress, neurotoxicity, apoptosis, and tumorigenesis. Results from enrichment and pathway analysis showed that in both genders, acrylamide caused differential regulation of genes associated with cell processes of protein folding, microtubule cytoskeleton assembly, DNA replication, DNA repair and ROS generation. These data suggest a potential involvement of this chemical in cell processes other than mutagenicity which may be associated with tumorigenesis. Furthermore, our study, by identifying affected gene ontologies and pathways, provides insight into a potential mechanism of action and may have substantial impact on risk assessment.

#### PS 945 **Development of a Quantitative Proteomics Multiplexed Assay for the Predictive Assessment of Drug-Induced Organ Toxicity in the Preclinical Setting.**

M. Gharib<sup>1,2</sup>, P. Thibault<sup>2</sup>, A. Nelson<sup>3</sup>, D. Chelsky<sup>1</sup>, L. Di Donato<sup>1</sup> and L. McIntosh<sup>1</sup>. <sup>1</sup>Caprion Proteome Inc, Montréal, QC, Canada; <sup>2</sup>Université de Montréal, Montréal, QC, Canada; <sup>3</sup>ITR Canada, Baie d'Urfé, QC, Canada. Sponsor: W. Lee.

Drug-induced organ toxicity is the primary reason for the withdrawal of drugs from the market and the failure of lead compounds during drug development. Detection of organ toxicity early in the development pipeline would not only reduce the cost

of drug development but also prevent injuries to patients in the clinic. Limitations of traditional approaches highlight the need for more sensitive and specific tools to predict drug toxicity. With the recent regulatory qualification of seven renal safety biomarker for use during drug development, biomarkers are increasingly viewed as potential means for providing toxicity assessments. Here, we have employed a targeted mass spectrometry (MS) approach, known as multiple reaction monitoring (MRM) to quantitatively measure changes in organ-specific toxicity biomarkers in rats. A highly multiplexed MRM assay, targeting 192 candidate protein biomarkers of hepatotoxicity, nephrotoxicity, cardiotoxicity as well as muscle, vascular and neurotoxicity, was developed. Results show that markers for all organs covered in our toxicity biomarker panel are detectable in serum and urine under normal conditions. Significantly, GGT5 and MDH-1, important liver injury biomarkers currently under investigation as well as qualified kidney injury biomarkers cystatin-C, clusterin and  $\beta$ -2-microglobulin and albumin were successfully detected in serum and urine, respectively. We tested the predictive value of our panel on cyclophosphamide treated rat blood samples. In agreement with the literature, we found that serum biomarkers for the kidney, the vascular system and the liver were markedly increased following toxicity. The present MRM assay has the potential to become standard practice for pre-clinical drug safety assessments. Further studies will be centered on applying this assay to monitor urinary kidney injury biomarkers following cisplatin-induced nephrotoxicity of rats.

**PS 946 Development of a LC/MS Serum Bile Acid Profiling Method for Sensitive Detection of Biliary Injury in Dogs.**

J. M. Maher, T. Sharapova, R. Yeager, E. Blomme and S. Cepa. *R45M, Abbott Laboratories, Abbott Park, IL.*

Currently there are many non-invasive methods for assessing hepatic toxicity in large animal species, but biliary injury is often difficult to detect in lieu of histopathology. Notably hepatobiliary biomarkers such as liver transaminases, alkaline phosphatase, gamma glutamyl transferase, and total bilirubin suffer from poor specificity or sensitivity in detection of biliary injury. Quantification of serum bile acids has been utilized in veterinary medicine in the diagnosis of biliary disease with success, but the current methods of quantification suffer from technical hurdles and lack robustness. Thus the purpose of the current study was to develop a method for detection of serum bile acids in dogs using liquid chromatography-mass spectrometry (LC/MS) for sensitive and rapid detection of hepatobiliary injury by quantifying the individual bile acid species in tandem. Twenty bile acids species were assessed with the current LC/MS method, including primary cholic and chenodeoxycholic bile acids and secondary bile deoxycholic and lithocholic bile acids, including the glycine- and taurine-conjugated forms. A diagnostic reference range was established from more than 50 untreated, fasted beagles of both genders to assess normal variability with benchmarked clinical pathology. These individual serum bile acid levels ranged from approximately 900 pmol/ml to levels below the limits of detection, with all taurine-conjugated species notably detected in serum. The applications of this method in assessing the sensitivity and specificity of serum bile acids versus existing methods will be discussed in the early detection of drug-induced hepatobiliary injury.

**PS 947 Lack of Concordance in Microarray Gene Expression Responses to Phenobarbital in Companion-Aged FFPE and Frozen Liver Samples.**

S. Hester, G. Carswell, B. Vallanat, A. B. DeAngelo and C. E. Wood. *US EPA, Durham, NC.*

Despite the immense potential value of public and private biorepositories, direct utilization of archival tissues for molecular profiling has been limited. A major reason for this limited use is the difficulty in obtaining reliable transcriptomic profiles from formalin-fixed paraffin-embedded (FFPE) tissue samples with highly fragmented nucleic acid. The goal of this study was to evaluate transcriptional responses in 16 year-old FFPE and companion frozen (FROZ) liver samples from F344 rats treated for 2 yrs with control water or water with 0.06% Phenobarbital (PB), a known CAR/PXR inducer and rodent liver mitogen. RNA isolation and gene expression was performed using the Rat Illumina Bead Array® for 16 samples, paired FFPE and FROZ. The RNA integrity numbers (RINs) ranged from 2-3 for FFPE and 3-5 for FROZ, and RNA yield for both FFPE (2 10 $\mu$ m sections) and FROZ (20 mg) samples was 2-4 micrograms. Nugen Ovation® and Encore® reagents optimized for FFPE tissues were used to amplify and label the RNA followed by hybridization to arrays. We selected 12 of 16 samples based on successful hybridization performance for analysis. Differential gene expression was assessed using Rank Products followed by pathway mapping. Results showed only 10 significantly altered PB-responsive genes in common between paired FFPE (n=1373) and FROZ (n=721) samples whereas pathway analysis identified only a 10% overlap in pathways significantly altered by PB between FFPE and FROZ samples. Pathway profiles for both FFPE and FROZ samples were unique to their respective

sample type. The lack of concordance in genomic responses to PB suggests that traditional microarray platforms are inadequate for genomic profiling of aged FFPE samples, despite improved RNA isolation and labeling methods. Further work will evaluate more recent next-generation sequencing (NGS) technologies for transcriptomic analysis of archival specimens. This abstract does not reflect EPA policy.

**PS 948 Formaldehyde-Induced Changes in microRNA Signaling.**

J. E. Rager<sup>1</sup>, B. C. Moeller<sup>2</sup>, M. Doyle-Eisele<sup>3</sup>, J. A. Swenberg<sup>1,2</sup> and R. C. Fry<sup>1,2</sup>. <sup>1</sup>Environmental Sciences and Engineering, The University of North Carolina at Chapel Hill, Chapel Hill, NC; <sup>2</sup>Curriculum in Toxicology, The University of North Carolina at Chapel Hill, Chapel Hill, NC; <sup>3</sup>Lovelace Respiratory Research Institute, Albuquerque, NM.

MicroRNAs (miRNAs) are critical regulators of gene expression, yet much remains unknown regarding miRNA changes resulting from environmental exposures and whether they influence pathway signaling across various cell types and time. To gain knowledge on these novel topics, we set out to investigate in vivo miRNA responses to inhaled formaldehyde, an important air pollutant known to disrupt miRNA expression profiles. Rats were exposed by inhalation to either 0 or 2 ppm formaldehyde (6 hours/day) for 7 days, 28 days, or 28 days followed by a 7 day recovery. Genome-wide miRNA expression profiles and associated signaling pathways were assessed within the nasal respiratory mucosa, circulating mononuclear white blood cells (WBC), and bone marrow (BM). We found that miRNAs were responsive to formaldehyde exposure in the nose and WBC, but not the BM. A transcriptomics-based analysis was performed in the nose and WBC of the rats exposed for 28 days. In the nose, formaldehyde altered the expression of 42 transcripts; of these, 15 (36%) were computationally predicted to be regulated by formaldehyde-responsive miRNAs. Conversely, in the WBC, formaldehyde altered the expression of 130 transcripts; of these, 18 (14%) were predicted to be regulated by miRNAs. Systems-level analyses revealed that the transcripts regulated by miRNAs play diverse roles in cell signaling. Key players include dosage suppressor of mck1 homolog, meiosis-specific homologous recombination (Dmcl1) and secreted frizzled-related protein 4 (Sfrp4) within the nose, involved in cell death signaling. In WBC, key players were v-akt murine thymoma viral oncogene homolog 3 (protein kinase B, gamma) (Akt3) and integrin, alpha 2 (Itga2), involved in inflammation signaling. Our study informs critical knowledge towards the biological consequences of inhaled formaldehyde exposure.

**PS 949 Dermal Sensitization to Toluene Diisocyanate in Mice Is Manifested by Early Changes in the Proteome of Auricular Lymph Nodes and Serum.**

S. Haenen<sup>1,3</sup>, E. Clynen<sup>2</sup>, V. De Vooght<sup>1</sup>, L. Schoofs<sup>3</sup>, B. Nemery<sup>1</sup>, P. Hoet<sup>1</sup> and J. Vanoirbeek<sup>1</sup>. <sup>1</sup>Occupational, Environmental and Insurance medicine, KU Leuven, Leuven, Belgium; <sup>2</sup>Biomedical Research Institute, Hasselt University, Diepenbeek, Belgium; <sup>3</sup>Research Group of Functional Genomics and Proteomics, KU Leuven, Leuven, Belgium.

**Introduction.**

Diisocyanates are capable of initiating an allergic response, which can lead to occupational asthma after a latency period. Clinical symptoms such as cough, wheezing and dyspnea occur only late, making it difficult to intervene at an early stage.

We explored proteome changes, before asthma is apparent, in the local draining lymph nodes and serum of mice dermally sensitized once or twice with toluene diisocyanate (TDI) to explore biomarkers of sensitization.

**Methods.**

The proteomes of male BALB/c mice (6 weeks old, 20g), sensitized once (n=12) or twice (n=12) with 0.3% TDI, were individually compared with control mice (n=12) using two-dimensional difference gel electrophoresis (2D-DIGE). A level of p<0.01 (Student's t-test) was considered significant.

Western blot or ELISA was used to verify a subset of the differential proteins. A level of p<0.05 (unpaired t-test) was considered significant.

**Results.**

In the lymph nodes, we found between TDI-treated and control mice 38 and 58 differential proteins after one and two treatments, respectively. In serum, 7 and 16 differential proteins were detected after one and two treatments, respectively. We identified 80-85% of these proteins by mass spectrometry. Among them, lymphocyte specific protein-1, coronin 1a and hemopexin were verified in an independent group of mice by Western blot or ELISA.

**Conclusion.**

Our study revealed, in a mouse model, alterations in the proteome during sensitization. If validated in humans, these changes could lead to earlier diagnosis of exposed workers.

All animal experiments were approved by the Local Ethical Committee for animal experiments of the KU Leuven.

## PS 950 Smoking-Induced microRNA Changes in Human Sperm.

E. L. Marczylo<sup>1</sup>, J. Janus<sup>3</sup>, A. A. Amoako<sup>2</sup>, J. C. Konje<sup>2</sup>, T. H. Marczylo<sup>1</sup> and T. W. Gant<sup>1</sup>. <sup>1</sup>CRCE, Health Protection Agency, Didcot, United Kingdom; <sup>2</sup>Reproductive Sciences, Leicester Royal Infirmary, Leicester, United Kingdom; <sup>3</sup>Cardiovascular Sciences, University of Leicester, Leicester, United Kingdom.

Recent work has suggested that some of the constituents of cigarette smoke, along with other environmental chemicals, can have adverse effects not just on the exposed individuals, but also on their progeny. Although the mechanisms underlying multigenerational toxicity are not well understood, a number of studies have implicated heritable microRNA-mediated epigenetic modifications. Using microarray profiling and pathway analysis, we have shown that cigarette smoke induces specific differences in the spermatozoa microRNA content of human smokers compared with non-smokers, and that these altered microRNAs appear to predominantly mediate pathways vital for healthy sperm and normal embryo development, particularly cell death and apoptosis. MicroRNA-mediated perturbation of such pathways may explain how harmful phenotypes can be induced in the progeny of smokers. Consequently, we have also been developing an *in vitro* system for investigating the potential roles of microRNAs in toxicology. By differentiating embryonic stem cells into embryoid bodies we have been able to generate and subsequently isolate sets of clonal primordial germ cell lines. These cell lines can be produced in the presence and absence of environmental chemicals (for example 17 $\beta$ -estradiol and di-butyl-phthalate), and exhibit chemically-induced differential microRNA expression. This model (including both the embryoid bodies and the resulting primordial germ cell lines) shows promise for further investigating the mechanisms of microRNA-mediated toxicity induced by environmental chemicals, including cigarette smoke. All work was approved by the Leicestershire, Rutland and Northamptonshire Ethics (Institutional Ethics) Committee and written informed consent to partake in the study was obtained from all volunteers.

## PS 951 New Data from Old Studies: Development of qRT-PCR Signature Assays for Assessment of Mode-of-Action from Formalin Fixed Paraffin Embedded Archival Tissues.

S. Phillips<sup>2,1</sup>, L. Recio<sup>1,2</sup>, T. Maynor<sup>1</sup> and M. D. Waters<sup>1</sup>. <sup>1</sup>ILS, Research Triangle Park, NC; <sup>2</sup>ILS Genomics, Morrisville, NC.

Archival formalin fixed paraffin embedded (FFPE) tissue samples collected over decades from toxicological studies represent a rich source of biological materials with detailed pathological evaluations from the testing of numerous substances. Until recently, the application of 'omics technologies to toxicology studies has been primarily limited to fresh frozen tissue samples collected at necropsy. Archival FFPE tissues represent a rich and largely untapped resource of invaluable information. There is a clear need to develop methods to apply 'omics based technologies to FFPE tissue banks. ILS and ILS Genomics have developed a systematic approach using bioinformatics and laboratory testing for the de novo design of gene specific qRT-PCR assays for use on FFPE archival tissue samples. For these studies, mouse liver carcinogen furan was administered by oral gavage at 0.0, 2.0, 4.0 and 8.0 mg/kg with 5 animals per group for three weeks. Animals were necropsied at 4 hrs after the final administration, liver sections were flash frozen in liquid nitrogen and stored at -80°C. Other liver sections were fixed in formalin for 18-24 hrs, transferred to ethanol for 2 days and then processed into FFPE tissue blocks. Total RNA was extracted from paired frozen and FFPE tissues (10  $\mu$ m sections) for subsequent qRT-PCR analysis. Custom designed qRT-PCR assays using TaqMan technology with amplicons of approximately 70 bp were tested to demonstrate equal primer efficiencies between frozen and FFPE tissue RNA isolations. Using this strategy we have validated a set of 8 genes and 2 lncRNAs (Chek1, Cyp4a14, Egr1, Ephx2, Cdkn1a, Xrcc1, Dppa5a, Gsta1 lncRNA-p21 and lncRNA-Chr9: 78107225-78118850) and normalization gene Actb to quantify mRNA levels in liver RNA isolated from FFPE compared to frozen tissues. These studies demonstrate that quantitative analysis of mRNA levels from FFPE tissue samples can be done using highly specific mRNA qRT-PCR assays.

## PS 952 Identification of Novel Biomarkers for Drug-Induced Renal Papillary Necrosis in Rats by Toxicoproteomic Techniques.

D. Sasaki<sup>1,2</sup>, M. Kanki<sup>1</sup>, K. Nishihara<sup>1</sup>, M. Hiramoto<sup>1</sup>, M. Yuri<sup>1</sup>, H. Umeno<sup>1</sup>, A. Moriguchi<sup>1</sup>, H. Mitori<sup>1</sup>, R. Hirota<sup>1</sup>, J. Seki<sup>1</sup>, Y. Miyamae<sup>1</sup>, G. Hwang<sup>2</sup> and A. Naganuma<sup>2</sup>. <sup>1</sup>Astellas Pharma Inc., Osaka and Tsukuba, Japan; <sup>2</sup>Graduate School of Pharmaceutical Sciences, Tohoku University, Sendai, Japan.

Renal papillary necrosis (RPN) is a type of kidney injury that is often observed in diabetics and patients taking nonsteroidal anti-inflammatory or anticancer drugs. However, no prognostic biomarkers (BMs) for RPN in humans have been identified. Here, we searched for novel BMs suitable for early RPN detection using toxicoproteomic techniques.

Urine from rats with RPN induced by a single injection of 2-bromoethylamine hydrobromide (BEA; 0, 3, 10, 30, and 100 mg/kg) was pooled into 4 groups. Urinary proteins in each group were analyzed by 2-dimensional LC-MS/MS coupled with isobaric tags (iTRAQ) to identify BM candidates. The urinary levels of BM candidates were quantified in individual rats after BEA treatment to assess the ability of these markers to detect RPN in comparison with FDA- and/or EMA-approved BMs for assessing preclinical kidney injury. The identified BM candidates were also measured in the urine of rats with glomerular- or proximal tubular (PT)-injury induced by puromycin, cisplatin, or gentamicin to verify the site specificity of the kidney lesions. In BEA-treated rats, 75 proteins with >2-fold increases in urinary concentrations compared with those in control rats were identified. Among these proteins, the selectivity and sensitivity of Es2, fetuin-A, and fibrinogen for RPN were evaluated. Es2 levels in urine were elevated rapidly after BEA treatment compared to those of serum BUN, creatinine, urinary clusterin, KIM-1, and RPA-1, and were also increased in glomerular- or PT-injury rats, suggesting that Es2 is a highly sensitive, but nonselective for RPN. In contrast, fetuin-A and fibrinogen were selective for RPN, as no marked changes in their urinary concentrations were observed in glomerular or PT-injury rats, but had low sensitivity for RPN detection. In conclusion, we identified three BM candidates for RPN with kidney lesion-site specificity and different sensitivities.

## PS 953 Determination of Formaldehyde Specific DNA-Protein-Crosslinks.

B. C. Moeller<sup>1</sup>, W. M. Bodnar<sup>2</sup> and J. A. Swenberg<sup>1,2</sup>. <sup>1</sup>Curriculum in Toxicology, University of North Carolina at Chapel Hill, Chapel Hill, NC; <sup>2</sup>Environmental Sciences and Engineering, University of North Carolina at Chapel Hill, Chapel Hill, NC.

Formaldehyde (FA) is classified as a known human and animal carcinogen. It is a ubiquitous environmental pollutant and is used in a number of consumer products or industrial applications. FA is also endogenously produced as part of normal cellular metabolism. FA is a genotoxic agent, causing a number of effects on cells including DNA monoadducts, DNA-DNA crosslinks and DNA-protein-crosslinks (DPC). DPCs are believed to be one of the critical lesions involved in FA induced carcinogenesis and is thought to provide a key initiating step in the Mode-of-Action. Currently, there are no available methods to distinguish between endogenous and exogenous FA induced DPCs. To investigate the possible link between inhaled FA and the formation of both endogenous and exogenous DPCs, several analytical techniques are being developed. *O*-Alkylguanine-DNA alkyltransferase (AGT) is a DNA repair enzyme that is known to form DPCs with FA and other crosslinking agents at the active Cys145 residue. Using AGT as a model protein, a series of experiments were undertaken to understand the formation, stability and degradation of the DNA-protein-crosslink at the reactive cysteine and the *N*<sup>2</sup> position of deoxyguanosine. Digestion conditions for both DNA and protein cleavage were investigated to determine approaches that would allow for the isolation and identification of either cysteine-CH<sub>2</sub>-dG or AGT peptide-CH<sub>2</sub>-dG crosslinks using sensitive and selective Liquid Chromatography – Mass Spectrometry. Further experiments investigating the ability to distinguish between crosslinks formed by both [<sup>13</sup>CD<sub>2</sub>]-FA and unlabeled FA were accomplished. Further validation and development of these approaches may allow for accurate and quantitative determination of endogenous and exogenous FA specific DPCs in cell culture and animal models. This information will be critical in advancing the understanding of the risks associated with inhaled FA and its role as a human carcinogen.

## PS 954 Pulmonary Toxicity and Global Gene Expression Profile in Response to Crystalline Silica Exposure in Rats.

R. Sellamuthu, C. Umbright, J. R. Roberts, S. Young, D. Richardson, W. McKinney, B. T. Chen, D. Frazer, S. Li, M. L. Kashon and P. Joseph. National Institute for Occupational Safety and Health (NIOSH), Morgantown, WV.

The ability to detect target organ toxicity as well as to determine the molecular mechanisms underlying such toxicity by employing surrogate biospecimens that can be obtained either by a non-invasive or minimally invasive procedure has significant advantage in toxicology. Pulmonary toxicity and global gene expression profiles in the lungs, blood and bronchoalveolar lavage (BAL) cells were determined in rats 44-weeks following inhalation exposure to crystalline silica (15 mg/m<sup>3</sup>, 6-hours/day, 5 days). A significant elevation in lactate dehydrogenase activity and albumin content in the BAL fluid as well as histological alterations, mainly type II pneumocyte hyperplasia and fibrosis, observed in the lungs suggested silica-induced pulmonary toxicity in the rats. A significant increase in the number of neutrophils and elevated monocyte chemotactic protein 1 in the BAL fluid indicated silica-induced pulmonary inflammation in the rats. Determination of global gene expression profiles in the lungs, BAL cells, and blood of the silica exposed rats identified 175, 273, and 59 significantly differentially expressed genes (SDEGs) (FDR <0.05 and >1.5 fold change in expression), respectively, compared with the corre-

sponding control samples. Bioinformatics analysis of the SDEGs demonstrated a remarkable similarity in the biological functions, molecular networks and canonical pathways that were significantly affected by silica exposure in the lungs, BAL cells and blood of the rats. Induction of inflammation was identified as the major molecular mechanism underlying the silica-induced pulmonary toxicity. These findings demonstrated the potential application of global gene expression profiling of blood and BAL cells as a valuable minimally invasive approach to study silica-induced pulmonary toxicity.

**PS 955 Comparison of a New Skin Penetration System Containing an Automated Toxicokinetic Modul with Franz Diffusion Cells.**

A. G. Schepky, I. Herberz, M. Akhiani, S. Müller, H. Wenck and D. Gerstel.  
4218-Research Toxicology, Beiersdorf AG, Hamburg, Germany.

Critical endpoints in in vitro testing of cosmetic ingredients are the determination of the bioavailability of test substances in different skin layers and the examination of the toxicokinetic profile. Skin penetration studies are so far performed in Franz diffusion cells using pig skin. Unfortunately with these cells an automated toxicokinetic determination of percutaneously penetrated substance is not receivable.

To perform toxicokinetic studies, we developed a new Vitrocell systems skin penetration system (SPS) with eight parallel running diffusion cells, which is able to take samples from the receptor fluid automatically. To substitute the Franz diffusion cells with the SPS it is important to compare both systems in terms of performance and reproducibility. Therefore we compared the penetration of caffeine through full thickness pig skin in Franz diffusion cells with manual sampling from the receptor fluid with the prototype of the SPS that provides automated sampling from the receptor fluid.

We could show toxicokinetic profiles for manual and automated samples with comparable lag times and recovery rates. Furthermore we could even show lower standard deviations using the SPS.

In conclusion, the new SPS is highly comparable to the Franz diffusion cell with the additional advantage to allow the automated detection of toxicokinetic profiles from the receptor fluid.

**PS 956 Risk Assessment for Cosmetic Ingredients Using Alternative Methods—Skin Sensitization.**

T. Atobe<sup>1</sup>, K. Tsujita<sup>1</sup>, S. Oeda<sup>1</sup>, M. Hirota<sup>1</sup>, T. Ashikaga<sup>1</sup>, H. Kouzuki<sup>1</sup>, T. Yoshida<sup>2</sup> and S. Aiba<sup>3</sup>. <sup>1</sup>Safety Technology Development Group, Shiseido Research Center, Yokohama, Japan; <sup>2</sup>Department of Biochemical Toxicology, Showa University School of Pharmacy, Tokyo, Japan; <sup>3</sup>Department of Dermatology, Tohoku University Graduate School of Medicine, Sendai, Japan.

Development of non-animal safety evaluation methods for chemicals is necessary from the viewpoint of animal welfare and to meet the 7th amendment of the European cosmetics directive. As an in vitro skin sensitization test, we have established two methods. One was the human cell line activation test (h-CLAT) detecting augmentation of CD86 and CD54 expression in THP-1 cells exposed by skin sensitizers. The other was the SH test taking advantage of changing cell-surface thiols on THP-1 cells induced by skin sensitizers. Recently the Antioxidant Response Element (ARE) assay measuring oxidative stress caused by skin sensitizers have been attracted attention. However, hazard assessment of skin sensitization has been unable to predict by only one test in vitro yet. Furthermore, non-animal methodologies in risk assessment how much a chemical has skin sensitization potency has just started in earnest. This study attempted to verify how to combine tests in vitro or in silico to assess chemical skin sensitizers. EC3 values from LLNA were accumulated by non-linear analysis using each endpoint from in vitro skin sensitization test and then some descriptors suggesting correlation to LLNA threshold values were selected. Correlation between the descriptors and EC3 values were analyzed by Artificial Neural Network (QwikNet Ver. 2.23). Molecular orbital of the three-dimensional chemical structures was also used in silico. As a result, the model obtained from tests in vitro or in silico reveals good correlation to in vivo data, thus the combination of in vitro and in silico method could be a sophisticated non-animal testing for risk assessment in skin sensitization.

**PS 957 Application of a Modified Keratinsens Assay to Predict Sensitization Hazard for Botanical Extracts.**

D. Gan<sup>1</sup>, K. Norman<sup>2</sup>, N. Barnes<sup>2</sup>, H. Raabe<sup>2</sup>, C. Gomez<sup>1</sup> and J. W. Harbell<sup>1</sup>.  
<sup>1</sup>Mary Kay Inc., Addison, TX; <sup>2</sup>IIVS, Gaitersburg, MD.

An essential step in the safety review of cosmetic/personal care ingredients is hazard assessment, including dermal sensitization potential. In vitro methods to identify allergic (haptenic) potential are based on electrophilic interaction with marker pep-

tides or cellular target systems. These assays use a specific molar ratio of the test chemical to the test system. Botanical extract ingredients, as mixtures, preclude specific molar ratio determination. Often, the botanical extract portion is a small fraction of the complete ingredient. To assess these mixtures, the KeratinoSens assay was selected because it operates over a wide dose range and sets cytotoxicity limits on doses used to measure marker gene expression (Emter et al, 2010). Induction of a luciferase gene, under the control of the antioxidant response element (ARE), was measured. Cytotoxicity was assessed by both NRU and MTT assays. Concentrations up to 1 mg/mL (of complete ingredient) were tested and a test dose was considered positive if the fold induction of luciferase was 1.5x (EC1.5) and viability  $\geq 70\%$  relative to the solvent controls. The goal of the study was to measure the activity of 3 known sensitizers (gluteraldehyde (GA) [strong], dimethyl maleate (DM) [moderate] and cinnamic aldehyde (CA) [moderate] spiked into four different botanical ingredients (with different excipient solvent systems). Activity was measured, relative to the EC1.5 of the neat sensitizer, as a function of sensitizer concentration and ingredient composition. Three independent trials were performed. No appreciable cytotoxicity was observed. The recovery of the GA spike required at least a 3-fold increase in concentration relative to the chemical alone and one extract reduced the activity below detection. The DM and CA showed activity at about the same effective concentrations as the neat chemicals although the DM showed reduced activity in one extract as well. These data suggest that the KeratinoSens assay has the potential to identify electrophile allergens within a botanical extract ingredient matrix.

**PS 958 Development of a Highly Reproducible Three-Dimensional Chinese Skin Reconstructed Model for Evaluating Drug and Cosmetic Skin Irritation.**

J. Wang<sup>1</sup>, Z. Du<sup>1</sup>, Z. Wang<sup>2</sup> and X. Zhang<sup>1</sup>. <sup>1</sup>Foreland Biopharma Co. Ltd., Beijing, China; <sup>2</sup>Boston University, Boston, MA. Sponsor: J. Wang.

In vitro models to study irritation, corrosivity and phototoxicity are important tools for research and development in the pharmaceuticals and cosmetic industries. Human skin is the best possible model for such in vitro studies. The commercially reconstructed human epidermis models are similar to the morphology, lipid composition and biomarkers of native human tissue and have been approved by European Centre for the Validation of Alternative Methods (ECVAM) for the validation of cosmetics. The models are available in many countries but not in China. Here, we describe the development of a constructed three-dimensional (3D) model using Chinese human skin, which consists of a "dermis" with fibroblasts embedded in rat collagen matrix and an "epidermis" comprised of differentiated keratinocytes. The fibroblasts and keratinocytes were first separated from foreskins of Chinese adults after incubating in dispase and collagenase solutions. Then, rat type I collagen was constructed onto the polycarbonate membrane of a culture insert. After gels solidified at room temperature, a collagen matrix with Chinese dermal fibroblasts was constructed above the acellular collagen layer. Keratinocytes were added to the surface of the contracted collagen gels and allowed to attach to the matrix to generate a confluent cellular monolayer. The reconstructed tissues were raised to an air-liquid interface to enable complete stratification and differentiation. After exposure and incubation, MTT assay was performed for cell viability. Nine well-known irritants or corrosive chemicals caused cell viability rates less than 50%. Cosmetics both from Western nations and China were also tested in the model. We found the Western cosmetics did not influence the cell viability compared to some of Chinese cosmetics which dramatically decreased cell viability 1 hour after exposure. Our data indicate that the reconstructed 3D Chinese skin model is highly reproducible and sensitive to assess skin irritation to chemicals and cosmetics.

**PS 959 Incorporation of Reconstructed Human Epidermal Tissues into a Corporate Toxicology Laboratory: Use of In Vitro Test Data for Diverse Safety and Risk Assessment Applications.**

L. M. Milchak, D. H. Brandwein and J. Zappia. Corporate Medical Department, 3M, St. Paul, MN.

The 3M Strategic Toxicology Laboratory (STL) is an internal corporate resource providing toxicology support to 3M businesses. An objective in the STL is to routinely incorporate *in vitro* test methods, with a recent focus on the use of reconstructed human epidermis tissues. The first model utilized has been EpiDerm™, which is currently validated for classification of chemicals for dermal irritation in OECD 439, and also dermal corrosion in OECD 431. Following the process outlined in the standard protocols for demonstration of technical proficiency, both test methods have been validated and used to assist with classification of chemistries for consumer and industrial use, utilizing the standardized MTT based cell viability assay. In addition, custom protocols have been performed using the tissues in time course irritation studies to evaluate the release of the inflammatory marker cytokine

IL-1 $\alpha$ . This approach has been advantageous for the simultaneous screening of multiple formulations for irritation potential during research and development for new products. Other customized studies have evaluated the efficacy of various skin washing agents at removal of a viscous coating from the skin tissues, in a simulated washing study to help formulate occupational health recommendations for workers. These studies evaluated irritation potential using MTT, IL-1 $\alpha$  and LDH release, and also analyzed the dermal penetration of an amine component in the coating. In summary, incorporation of these test methods has been very useful for the evaluation of a multitude of dermal exposure scenarios. The tissues have been used in standardized irritation and corrosion assays, as well as custom protocols utilizing additional markers of cell damage, and also specialized skin washing and dermal penetration studies. The results of these studies have provided valuable information for safety and risk assessment purposes, particularly during the product development phases, and have permitted these evaluations without animal use.

**PS 960 Intralaboratory Reproducibility of the Direct Peptide Reactivity Assay (DPRA) to Assess the Robustness of the Current Prediction Model.**

L. Foertsch and F. Gerberick. *Central Product Safety, Procter & Gamble Company, Cincinnati, OH.*

One characteristic of a chemical allergen is its ability to react with proteins prior to the induction of skin sensitization. The majority of chemical allergens is electrophilic and reacts with nucleophilic amino acids such as cysteine or lysine. In the DPRA, test chemicals are incubated for 24 hours with two synthetic peptides containing a cysteine or lysine residue, and the reactions are analyzed by HPLC to measure peptide depletion. We have previously demonstrated that reactivity correlates with sensitization potential and have developed a prediction model to assign a reactivity category for each material tested in the assay (Gerberick et al. *Tox Sci* 2007; 97:417-427). In order to assess the robustness of this prediction model and its ability to distinguish reactive skin sensitizers from minimally reactive non-sensitizers, a historical DPRA dataset of 133 chemicals was analyzed retrospectively with a modified prediction in which the cut-off between minimal and low reactivity was changed from 6.38% to 8% depletion. Regardless of cut-off, the accuracy of the prediction model remained at 86% with little to no change in sensitivity, specificity, and positive and negative productivity. To further investigate the robustness and reproducibility of the prediction model, a small intra-laboratory study was conducted. In this study, 9 chemicals were tested blindly in three independent runs. The depletion data was analyzed using the current prediction model as well as the described modified prediction model. In both cases, 7 out of 9 chemicals showed the same reactivity prediction in all 3 runs. Neither the retrospective analysis nor the intra-laboratory study provided any compelling evidence to adjust this cut-off value from the current model. Taken together, these studies further display the reproducibility and robustness of the DPRA and its prediction model.

**PS 961 A Novel Animal-Free Approach to Dermal Sensitization Hazard Identification and Potency Assessment.**

J. McCauley. *Toxicology Assessment & Compliance Assurance, 3M, St. Paul, MN.*  
Sponsor: D. Luebker.

International regulatory efforts have played a major role in advocating for the Three R's of animals used in safety evaluations for toxicological endpoints. These efforts support a movement away from the current in vivo-dependent toxicity testing state, to an animal-free toxicity testing state that includes in vitro human biology and a computational systems approach. To accomplish this goal, key stakeholders have proposed an ITS methodology to assess the skin-sensitizing potential of test chemicals to facilitate safety evaluation decision-making. The use of this ITS model integrated both novel and literature-reported data on 116 chemicals of known skin-sensitizing potential. Two in vitro assays and one in silico prediction model were used to cover four key sources of toxicological information: peptide reactivity; induction of ARE dependent luciferase activity; calculated octanol-water partition coefficient; and TIMES-SS model in silico prediction. The results from the in vitro assays were scaled into five classes from 0 to 4 and then compared with the LLNA data, which were also scaled from 0 to 4. Using an optimized model, an 87.9% overall accuracy was obtained for predicting sensitizers with a linear relationship between the LLNA scores and the in vitro scores. The use of clogP to account for potential differences in the bioavailability of the test chemicals did not reduce the correlation. With the increasing number of large-scale toxicology risk assessment programs for chemicals and emerging or expanding areas of chemical use, the development and acceptance of an ITS model appears to be the solution needed to strike a balance between safety, speed, cost and animal welfare. Along with ITS data refinements and the inclusion of other in vitro assays and in silico models accompanied by larger data sets, consideration should be given to defining a validation strategy focused on regulatory acceptance of an ITS model for skin sensitization.

**PS 962 Development of a Compromised Skin Model In Vitro Using a Tape Stripping Method.**

J. Heylings<sup>2</sup>, D. Davies<sup>2</sup>, M. C. Correa<sup>1</sup> and T. J. McCarthy<sup>1</sup>. <sup>1</sup>Johnson & Johnson, Skillman, NJ; <sup>2</sup>Dermal Technology Laboratory Ltd., Keele, United Kingdom.

Dermal absorption of chemicals from topically applied products is studied in a variety of *in vitro* and *in vivo* models. Skin barrier function may be impaired due to intrinsic or extrinsic factors. To our knowledge there is not a standardized model for evaluation of dermal absorption in compromised skin barrier conditions. Our objective was to validate an *in vitro* model of altered barrier function generalizable across compromised skin states. To investigate the permeability properties of compromised skin compared to normal skin, we explored the relationship between non-invasive (Trans Epidermal Water Loss, TEWL) and invasive (Electrical Resistance, ER; Tritiated Water Flux, TWF) markers of barrier function in slaughterhouse pig skin before and after tape stripping. Skin samples were randomly divided into groups and subjected to a standardized tape stripping procedure. The pre-and post-values for the 3 measures of skin integrity were recorded for 0, 5, 10, 15 and 20 tape strips. A full analysis of the distribution of TEWL, ER and TWF for 70 separate skin samples revealed that only ER was robust enough to discriminate between the barrier property changes effected by sequential tape stripping. The measurement of water flux through the skin (TEWL, TWF) required a long period of stabilization and proved to be unsuitable as a short term test. However, a significant difference could be observed with ER between control and each group of 5-20 tape strips ( $p < 0.01$ ,  $n = 53$ ). Further analysis of the data revealed that removal of 10 tape strips provided a loss of barrier function approximately equivalent to a 3-4 fold increase in TEWL, which approximates the altered barrier function clinically observed in atopic dermatitis, psoriasis, and diaper dermatitis. In conclusion, we have developed an *in vitro* model of compromised skin barrier function that is simple and robust and can be used to study the dermal absorption of chemicals that may come in contact with skin with impaired barrier properties.

**PS 963 A Predictive High-Content Imaging Cell-Based Assay As an Alternative to the Local Lymph Node Assay for Skin Sensitization.**

R. N. Ghosh, M. J. Tomaszewski, M. L. Pietila and J. R. Haskins. *ThermoFisher Scientific, Pittsburgh, PA.*

Allergic contact dermatitis (ACD) is a health effect that can develop in those exposed to skin sensitizing chemicals. To decrease the occurrence of this adverse reaction, regulations require that testing be performed to identify which chemicals are responsible for this effect, and be labeled accordingly. The current standard for ACD measurement is the Local Lymph Node Assay (LLNA), which is both animal and labor intensive. The LLNA testing procedure is based upon enumerating the responding cells in the draining lymph nodes of the mouse after treatment. Alternatives for this assay have depended on the measurement of phenotypic changes of a defined cell line, which would be analogous to a prior step in the pathway of induction of sensitization than that of the LLNA endpoint. To the end of developing an assay that more comprehensively mimics the role of the immune system during ACD *in vitro*, we describe a phenotypic and functional cell based assay that can be used to predict the sensitizing potential of compounds. The prediction method of this assay is based upon the up-regulation of cell surface molecules and proliferation indicative of the induced maturation of the cell line after compound treatment, and also a functional response whereby the treated cells are exposed to chemotaxis inducing reagents and migration measured. These features can easily be captured and measured via an automated fluorescent imaging and analysis platform. The measurement of these features when combined allow for prediction of sensitizing potential, but also provide toxicity data which allows for compounds to be easily re-screened at lower concentrations. Tested compounds ( $n=24$ ) yielded a high sensitivity rate (100%) and a high concordance (82%) to the LLNA. In summary, this assay shows promise in its ability to predict in vivo responses and may offer a viable alternative to traditional animal studies. In addition, it could provide a valuable first level triage for chemicals entering the consumer and industrial products pipeline.

**PS 964 Performance Standards and Alternative Assays: Practical Insights from Skin Sensitization.**

D. Basketter<sup>2</sup>, S. N. Kolle<sup>1</sup>, S. Casati<sup>3</sup>, W. S. Stokes<sup>4</sup>, J. Strickland<sup>6</sup>, H. Vohr<sup>5</sup>, B. van Ravenzwaay<sup>1</sup> and R. Landsiedel<sup>1</sup>. <sup>1</sup>Experimental Toxicology and Ecology, BASF SE, Ludwigshafen am Rhein, Germany; <sup>2</sup>DABMEB Consultancy Ltd., Sharnbrook, United Kingdom; <sup>3</sup>ECVAM, European Commission, Ispra, Italy; <sup>4</sup>Interagency Center for the Evaluation of Alternative Toxicological Methods, National Toxicology Program, NIEHS, Research Triangle Park, NC; <sup>5</sup>Bayer Health Care, Wuppertal, Germany; <sup>6</sup>Integrated Laboratory Systems, Inc, Research Triangle Park, NC.

To encourage the development and validation of alternative toxicity test methods, the effort required for validation of test methods proposed for regulatory purposes should be minimised. Performance standards (PS) facilitate efficient validation by requiring limited testing. Based on the validated method, PS define accuracy and reliability values that must be met by the new similar test method. The OECD adopted internationally harmonized PS for evaluating new endpoint versions of the local lymph node assay (LLNA). However, in the process of evaluating a lymph node cell count alternative, the LNCC, simultaneous conduct of the regulatory LLNA showed that this standard test may not always perform in perfect accord with its own PS. The LNCC results were similar to the concurrent LLNA; discrepancies between PS, LLNA and LNCC were largely associated with "borderline" substances and the variability of both endpoints. Two key lessons were learned: firstly, the understandable focus on substances close to the hazard classification borderline are more likely to emphasise issues of biological variability, which should be taken into account during the evaluation of results; secondly, variability in the results for the standard assay should be considered when selecting reference chemicals for PS.

**PS 965 Alternative Method in Practice: Postvalidation Experience of the Skin Sensitization *In Vitro* Test Strategy.**

S. N. Kolle, B. van Ravenzwaay and R. Landsiedel. *Experimental Toxicology and Ecology, BASF SE, Ludwigshafen am Rhein, Germany.*

Several *in vitro* methods including dendritic cell line activation (e.g. MUSST and h-CLAT), keratinocyte activation (e.g. LuSens and KeratinoSens) and *in chemico* (e.g. DPRA) assays have been described as promising animal-free tools to qualitatively predict skin sensitizing potential. While these methods are currently undergoing evaluations in the different stages of formal validation, testing strategies have been proposed based on the combination of these assays. Yet to use suggested methods and prediction models for the diverse industrial sectors, such as the cosmetic, industrial chemical, pharmaceutical and maybe even the agrochemical sector, the scope of the substance classes tested as part of the initial validation exercise needs to be extended. Typically in a first validation phase novel alternative methods are evaluated against their gold standard *in vivo* assays using model substances selected from literature for their well described toxicological endpoint effects. The substances tested in the first validation phase, do, however, usually not reflect the typical test substance portfolio of the different industrial sectors. Therefore in this study we present the post-validation evaluation of 40 additional substances with available *in vivo* skin sensitization data from various substance classes including acrylates, surfactants, isocyanates, plant extracts, and agrochemical formulations in state of the art *in vitro* methods to assess skin sensitization. This additional data provides valuable information to understand the predictive capacity in terms of the applicability domains and may also help to manage expectations what can be achieved with those assays.

**PS 966 Alternative Methods in Practice: Testing of Acrylate and Methacrylate Esters with the Skin Sensitization *In Vitro* Test Strategy.**

K. Wiench<sup>2</sup>, S. N. Kolle<sup>1</sup>, H. Müllerschön<sup>3</sup>, M. Pemberton<sup>5</sup>, L. Andrews<sup>4</sup> and R. Landsiedel<sup>1</sup>. <sup>1</sup>Experimental Toxicology and Ecology, BASF SE, Ludwigshafen am Rhein, Germany; <sup>2</sup>Product Safety, BASF SE, Ludwigshafen am Rhein, Germany; <sup>3</sup>Chemicals Management, Evonik Industries, Darmstadt, Germany; <sup>4</sup>The Dow Chemical Company, Midland, MI; <sup>5</sup>Systox Ltd., Wilmslow, United Kingdom.

Allergic contact dermatitis is a common skin disease and is elicited by repeated skin contact with an allergen. In the regulatory context, up to now only data from animal experiments have been accepted to assess the skin sensitizing potential of substances. Animal welfare concerns and the EU Cosmetic Directive/Regulation call for the implementation of animal-free alternatives for safety assessments. The mechanisms that trigger skin sensitization are complex and various steps are involved. Therefore, a single *in vitro* method may not be able to accurately assess this

endpoint. An *in vitro* testing battery that addresses different stages of the sensitization process was developed based on protein reactivity (direct peptide reactivity assay, DPRA), activation of the Keap-1/Nrf2 signaling pathway (LuSens and KeratinoSensTM) and dendritic cell activation assays (MUSST and h-CLAT). Based on an in-house validation this *in vitro* test strategy for the identification of skin sensitizers showed an accuracy comparable to that of the LLNA assay (94% compared to 89% for the LLNA). In this in-house validation, model substances selected from literature for their well characterized sensitizing potential were selected but did not necessarily reflect to typical testing portfolio. Therefore in this study, the in-house validation was extended by acrylates and methacrylate esters with available *in vivo* skin sensitization data. Further, the *in vitro* test battery has been used as a replacement for more than a dozen acrylates and methacrylate esters.

**PS 967 IVSA: *In Vitro* Sensitization Assay.**

M. Troese, L. F. Pratt, D. R. Cerven and G. L. DeGeorge. *MB Research Laboratories, Spinnerstown, PA.*

Regulatory agencies worldwide are seeking non-animal or *in vitro* testing methods that embrace the 3Rs philosophy. Strong support now exists in the consumer products, pharmaceutical and cosmetics industries to develop and validate alternative assays for use in preclinical safety testing programs. Our group has adapted the Sensitization *in vitro* sensitization NCTC2594 IL-18 response assay of Corsini, et al. (Toxicol In Vitro 23 (5):789-796, 2009) for use in the MatTek EpiDerm™ model, measuring IL-18 secretion into the media to identify dermal sensitizers. In intra-lab validation tests, IL-18 release was measured after a 24-hour topical exposure using twelve sensitizers and five irritants/non-sensitizers. Either distilled water or EtOH was used as solvent vehicles. A Stimulation Index (SI) was calculated relative to the solvent vehicle for each test material. An SI > 1.6 result was considered biologically significant and best fit the data for identification of a positive sensitizer using a 2x2 contingency table and Cooper statistics. The overall Accuracy of the assay was 94%, with no false positives. The Sensitivity, Specificity, Positive and Negative Predictivity were 92%, 100%, 100% and 83%, respectively. The *In Vitro* Sensitization Assay (IVSA) produced a dose-dependent release of IL-18 upon treatment with increasing concentrations of 4-nitrobenzyl bromide. In addition, IVSA correctly identified two photosensitizers (+UVA): chlorpromazine and olaquinoxid. Thus, in this initial evaluation, IVSA has proven to be a useful and highly predictive tool for identifying dermal sensitizers without the use of animals.

**PS 968 Evaluation of Skin Irritation for Household Products Using a Reconstructed Human Epidermis Model.**

F. Yamaguchi, N. Takebuchi and J. Sato. *Lion Corporation, Odawara-shi, Japan.*  
Sponsor: H. Kojima.

Classification for irritation using reconstructed epidermis test methods have been developed. These test methods have been validated with the ability of dividing chemicals into skin irritants or non-irritants, in accordance with the UN Globally Harmonized System of Classification and Labeling (GHS). Application of these models to dermal safety evaluation of household products, which are consisted of several chemical substances, is of highly importance from the point of view to ensure product safety.

The aim of this research is to estimate skin irritation potential of household products comparing cell viability patterns on reconstructed epidermis when household products are applied.

We select LabCyte EPI-MODEL24 (Japan Tissue Engineering Co., Ltd) model with JACVAM validated protocol for GHS classification of chemical substances. Twenty five commercial household detergents in Japan including laundry detergents, dishwashing detergents, fabric softeners and household cleaners were tested. It appeared that the cell viability becomes comparable in some product categories. The products which contains highly anionic surfactants tends to show low cell viability. Fabric softeners which were based on cationic surfactants showed no cytotoxicity in this model. Powder laundry detergents tend to show low cytotoxicity. Liquid laundry detergents, dishwashing detergents and household cleaners shows various cell viability. It seemed that category and/or its concentrations of contained surfactants might be affected the results.

These results suggested that reconstructed epidermis test methods useful for the products safety assessment by performing comparative assessment in each product category.

**PS 969 Collaborative Project in JCIA for Testing Strategy of Skin Sensitization Using h-CLAT, DPRA and DEREK.**

O. Takenouchi<sup>1,11</sup>, K. Okamoto<sup>2,11</sup>, N. Imai<sup>3,11</sup>, D. Kyotani<sup>4,11</sup>, Y. Kato<sup>5,11</sup>, T. Kasahara<sup>6,11</sup>, A. Toyoda<sup>7,11</sup>, S. Watanabe<sup>8,11</sup>, Y. Seto<sup>9,11</sup>, T. Ashikaga<sup>10,11</sup> and M. Miyazawa<sup>1,11</sup>. <sup>1</sup>Kao Co., Tochigi, Japan; <sup>2</sup>Kanebo Cosmetics Inc., Kanagawa, Japan; <sup>3</sup>Kose Co., Tokyo, Japan; <sup>4</sup>Cosmos Technical Co., Ltd., Tokyo, Japan; <sup>5</sup>Nippon Menard Cosmetic Co., LTD., Aichi, Japan; <sup>6</sup>Fujifilm Co., Kanagawa, Japan; <sup>7</sup>Pola Chemical Industries, Inc., Kanagawa, Japan; <sup>8</sup>Lion Co., Kanagawa, Japan; <sup>9</sup>P&G Japan K.K., Hyogo, Japan; <sup>10</sup>Shiseido Co., LTD., Kanagawa, Japan; <sup>11</sup>Working Group for *In Vitro* Skin Sensitization Evaluation in Japan Cosmetic Industry Association (JCIA), Tokyo, Japan. Sponsor: J. Avalos.

For the replacement of the LLNA, the combination of several alternative methods is necessary. JCIA organized a working group to investigate testing strategies. In this study, considering the applicable domain, we demonstrated the utility of a testing strategy using the human Cell Line Activation Test (h-CLAT), Direct Peptide Reactivity Assay (DPRA) and the in silico system, DEREK. A total of 133 chemicals, some of which exhibit poor water-solubilities, were evaluated. For h-CLAT, THP-1 cells were exposed to each test chemical for 24 hours. The CD86 and CD54 expressions were analyzed by flow cytometry. For DPRA, model peptides were mixed with test chemical for 24 hours. The depletion of peptides was analyzed by HPLC. For DEREK, the alert of chemical structure was examined. For 133 chemicals, the accuracy of h-CLAT, DPRA and DEREK to predict LLNA results was 78, 74 and 74%, respectively. Next, we investigated 3 testing strategies: the Integrated Testing Strategy (A), a tiered approach (B), and a multiple regression analysis model (C). Each strategy had a high potential prediction (A:84%, B:81%, C:84%). Regarding false negative chemicals, some chemicals induced no cytotoxicity and other chemicals crystallized or separated in the medium and the buffer. The logP values of these chemicals were mostly above 3.5. If hydrophobic chemicals (logP>3.5) were removed from analysis, the accuracy was improved to A:88%, B:86%, C:87%. The sensitivity was improved to A:96%, B:97%, C:100%. All strategies provided an accuracy of 73% for the potency prediction. These results suggested that every strategy has high predictivity for the potential and potency.

**PS 970 Refinement of the Prediction Model of the Myeloid U937 Skin Sensitization Test (MUSST).**

C. Piroird, F. Ibanez, J. Faugere, C. Gomes, N. Alépée and S. Martinozzi-Teissier. *L'Oréal Research & Innovation, Aulnay sous Bois, France*. Sponsor: E. Dufour.

**Background:** In line with the 3Rs concept, in vitro alternatives methods are being developed based on the early events of the skin sensitization process. One of these is the capacity of skin dendritic cells to recognize a chemical as a danger. Since the late nineties, L'Oréal has actively worked on the Myeloid U937 Skin Sensitization Test (MUSST) which models this early event by measuring the up-regulation of CD86 expression, a co-stimulatory receptor. Year's in house use of this assay allowed us to demonstrate its value in combination with other assays (DPRA, Nrf-2 activation) for the prediction of sensitization hazard (Sensitizer S /NonSensitizer NS) of cosmetic ingredients. A third class was defined as "Inconclusive (INC)" where the MUSST is not able to conclude S or NS. The aim of this study was to refine the predictive model in order to reduce the number of INC, by maintaining the predictive capacities of the MUSST.

**Methods:** 208 substances with LLNA data were analyzed. MUSST results on this set gave 92 S, 56 NS predictions and 60 INC. Statistical methods based on a stacking scoring method were applied on raw data of these 60 INC in order to find additional rules to classify these substances into S or NS.

**Results:** a combination of 6 rules was identified, that allows to classify 44/60 INC into 23 S and 21 NS with a sensitivity of 95% and a specificity of 91%. The predictive performances of the MUSST on the 208 substances with the optimized prediction model composed of the original prediction model and the additional 6 rules-based model show 84% concordance, 87% sensitivity and 79% specificity against LLNA data. No false negative are observed among the extreme and strong sensitizers.

**Conclusion:** The optimized MUSST is an efficient assay for the skin sensitization hazard characterization, promising as a tool to be integrated within a battery of assays to perform a skin sensitization risk assessment.

**PS 971 *In Vitro* Phototoxicity Screening Assay for Systemically-Administered Pharmaceuticals Using a Reconstructed Skin Model EpiDerm.**

P. Hayden, Y. Kaluzhny, M. W. Kinuthia, L. d'Argembeau-Thornton, H. Kandarova and M. Klausner. *MatTek Corporation, Ashland, MA*.

According to current regulatory guidelines, photosafety testing is required for new compounds if they absorb light in the range of 290–700 nm or partition into the skin or eyes. The only approved non-animal in vitro phototoxicity assay, the 3T3 Neutral Red Uptake (3T3 NRU-PT), is overly-sensitive in predicting the in vivo photosafety hazard to humans and thereby eliminates valuable, new active pharmaceutical ingredients (API) from further development, even though they are safe to humans.

EpiDerm™, a normal human 3-dimensional (NHu-3D) skin model, is highly reproducible, contains an in vivo-like barrier, possesses in vivo-like biotransformation capabilities, and has been pre-validated for determining phototoxicity of topically applied materials. Here, we utilized EpiDerm to develop an in vitro assay for screening the phototoxicity of pharmaceuticals following systemic administration (sPHO). Test articles (n=42) were added into the culture medium and allowed to partition into the epidermal tissue. Tissues were exposed to solar radiation and phototoxic effects were determined by the comparing the tissue viability of UV irradiated vs. non-irradiated tissue models, using the MTT assay. A prediction model (PM) was established: a material is phototoxic after systemic administration if one or more test concentrations in the presence of irradiation (+UVR) decreases tissue viability by ≥30% when compared to identical concentrations in the absence of irradiation (-UVR); a material is non-phototoxic if the decrease in tissue viability is < 30%. The PM resulted in high sensitivity (91.7%) and specificity (100.0%) for 42 test materials (24 phototoxic/18 non-phototoxic). Results of sPHO assay were compared to in-house 3T3-NRU-PT assay.

The current protocol extends phototoxicity testing using EpiDerm for risk assessment to systemically administered chemicals and medications and will provide the pharmaceutical industry with an in vitro screening method to assess the phototoxic risk of new API.

**PS 972 Validation of *In Vitro* and Clinical Safety Assessment of Behentrimonium Chloride-Containing Leave-on Body Lotions Using Postmarketing Adverse Event Data.**

D. Cameron<sup>1</sup>, G. Costin<sup>2</sup>, L. Kaufman<sup>3</sup>, J. Avalos<sup>1</sup>, M. Downey<sup>1</sup>, W. Billhimer<sup>1</sup>, S. Gilpin<sup>1</sup>, N. Wilt<sup>2</sup> and A. F. Simion<sup>1</sup>. <sup>1</sup>Kao USA, Inc., Cincinnati, OH; <sup>2</sup>Institute for In Vitro Sciences, Inc. (IIVS), Gaithersburg, MD; <sup>3</sup>Scripterra Scientific, Cincinnati, OH.

Behentrimonium chloride (BTC) is a straight-chain alkyltrimonium chloride compound commonly used as an antistatic, hair conditioning, emulsifying-surfactant or preservative agent in personal care products. Although the European Union restricted the use of alkyltrimonium chlorides and bromides as preservative to ≤0.1%, these compounds have been safely used at ≤10% in hundreds of cosmetic products for other uses than as a preservative. *In vitro*, clinical, and controlled consumer usage tests in barrier-impaired individuals were conducted to determine if whole body, leave-on skin care products containing 1-3% BTC cause dermal irritation or any other skin reaction with use. BTC-containing formulations were predicted to be non-irritants by the EpiDerm™ skin irritation test and the bovine corneal opacity and permeability (BCOP)/chorioallantoic membrane vascular assay (CAMVA) ocular irritation test battery. No evidence of allergic contact dermatitis or cumulative dermal irritation was noted under the exaggerated conditions of confirmatory human occlusive patch tests. No clinically assessed or self-reported adverse reactions were noted in adults or children with atopic, eczematous, and/or xerotic skin during two-week and four-week monitored home usage studies. These results were validated by post-marketing data for five body lotions, which showed only 0.69 undesirable effects (skin irritation) reported per million shipped consumer units during 2006-2011. No serious undesirable effects were reported during in-market use of the products. Therefore, if formulated in appropriate conditions at 1-3%, BTC will not likely cause dermal irritation or delayed contact sensitization when used in a whole-body, leave-on product.

**PS 973 Collaboration Study on Eye Irritation Alternative Method with Human Corneal Model; LabCyte Cornea-Model24.**

H. Kojima<sup>1,2</sup>, N. Annaka<sup>2</sup>, S. Tsuchiya<sup>2</sup>, Y. Yoshitake<sup>2</sup>, R. Xu<sup>2</sup>, M. Suzuki<sup>2</sup>, W. Shimatani<sup>2</sup>, A. Kajita<sup>2</sup>, M. Nakamura<sup>2</sup>, M. Watanabe<sup>2</sup>, M. Nakajima<sup>2</sup>, K. Sakamoto<sup>2</sup>, R. Takeda<sup>2</sup>, M. Hisama<sup>2</sup>, H. Ikeda<sup>2</sup>, A. Inagaki<sup>2</sup>, Y. Munekihika<sup>2</sup>, Y. Yamamoto<sup>2</sup>, T. Kasahara<sup>2</sup>, T. Fukuda<sup>2</sup>, S. Nakahara<sup>2</sup>, S. Watanabe<sup>2</sup>, H. Kurata<sup>2</sup>, S. Shinoda<sup>2</sup> and M. Katoh<sup>3,2</sup>. <sup>1</sup>Division of Pharmacology, National Institute of Health Sciences, Tokyo, Japan; <sup>2</sup>Japanese Society for Alternative to Animal Experiments, Tokyo, Japan; <sup>3</sup>Japan Tissue Engineering Co., Ltd., Aichi, Japan.

LabCyte CORNEA-MODEL24 is a human corneal model that was developed by Japan Tissue Engineering Co., Ltd. (J-TEC) as an alternative to animal tests for ocular irritation. It has been reported to provide highly-accurate predictions. A first step toward the future inclusion of this method in test guidelines is to verify transferability of the protocol. In collaboration with the Planning Committee of the Japan Society for Alternative to Animal Testing, a call for collaborating partners was issued, with respondents participating in a technical training session and a collaboration study to identify potential problems with the protocol. A total of twenty-four laboratories responded to the call for collaborating partners. These laboratories were divided into four groups, and four chemicals as well as a positive control were distributed to each group without coding. These sixteen chemicals and their control groups were tested using a WST-8 assay to determine cytotoxicity and thereby verify transferability of the protocol. As a result, we had a good inter- and intra-laboratory reproducibility in this study. On the other hand, a number of problematic points have already been noted, including several difficult-to-understand parts of the protocol and an inability to clear standard values for negative controls. The future inclusion of this method in established guidelines requires smooth implementation of a validation process, and a first step in that process is to verify the transferability of a suitable protocol.

**PS 974 Assessing Eye Irritation Potential of Cosmetic Products Using the STE Test.**

T. Abo<sup>1</sup>, Y. Nukada<sup>1</sup>, K. Ooshima<sup>2</sup>, T. Hayashi<sup>2</sup>, D. Araki<sup>2</sup>, D. Cameron<sup>3</sup>, J. Avalos<sup>3</sup>, A. F. Simion<sup>3</sup>, A. Kirst<sup>4</sup>, A. Fuchs<sup>4</sup>, R. Fautz<sup>4</sup>, H. Sakaguchi<sup>1</sup> and N. Nishiyama<sup>1</sup>. <sup>1</sup>Kao Corporation, Tochigi, Japan; <sup>2</sup>Kanebo Cosmetics Inc., Kanagawa, Japan; <sup>3</sup>Kao USA, Cincinnati, OH; <sup>4</sup>Kao Germany, Darmstadt, Germany.

Various in vitro assays that have been developed as an alternative for the Draize test are currently used to evaluate the eye irritation potential of cosmetic products and ingredients. A Short Time Exposure (STE) test, which we developed as a potential alternative test for eye irritation using rabbit cornea cells (SIRC), is planned for peer review and expected to be accepted as an OECD test guideline for classifying materials as Non-irritant/Irritant (NI/I). The test is expected to be able to evaluate cosmetic products as well as chemicals and cosmetic ingredients. Firstly, we evaluated the accuracy of the STE test against GHS classification for 20 cosmetic products (14 rinse-off and 6 leave-on products). Secondly, the results of STE test (including various rinse-off and leave-on products) were compared with the results of 43 cosmetic products tested in BCOP (bovine cornea opacity and permeability) test, 20 cosmetic products tested in HET-CAM, and 40 cosmetic products tested in CAMVA (two hen egg chorioallantoic membrane tests) in order to confirm the homology of in vitro assays used for evaluating eye irritation of the cosmetic products. In the first step, the accuracy for STE classifying a product as NI/I, compared to GHS, was 90% (18/20). Furthermore, STE test is able to provide a rank order (minimal irritant, moderate irritant and severe irritant) for materials based on the cell viability. The accuracy which compared GHS classification to a rank order of STE test was 75% (15/20). In the second step, comparison between STE test and three in vitro assays demonstrated that the accuracy of STE classifying a product as NI/I compared to BCOP, HET-CAM, and CAMVA was 79% (34/43), 80% (16/20), and 90% (36/40), respectively. Our findings show that STE test can be an alternative for the Draize test as well as for the three in vitro assays used to evaluate a cosmetic product.

**PS 975 The Interlaboratory Reproducibility of the STE Test for Assessing Eye Irritation of Cosmetic Products.**

Y. Nukada<sup>1</sup>, T. Abo<sup>1</sup>, A. Hilberer<sup>2</sup>, A. Heppenheimer<sup>3</sup>, M. Watanabe<sup>4</sup>, K. Ooshima<sup>5</sup>, D. Cameron<sup>6</sup>, A. Kirst<sup>7</sup>, H. Sakaguchi<sup>1</sup> and N. Nishiyama<sup>1</sup>. <sup>1</sup>Kao Corporation, Tochigi, Japan; <sup>2</sup>Institute for In Vitro Sciences, Inc., Gaithersburg, MD; <sup>3</sup>Harlan Cytotest Cell Research GmbH, Rosdorf, Germany; <sup>4</sup>Food and Drug Safety Center, Kanagawa, Japan; <sup>5</sup>Kanebo Cosmetics, Inc., Kanagawa, Japan; <sup>6</sup>Kao USA, Cincinnati, OH; <sup>7</sup>Kao Germany, Darmstadt, Germany.

The Short Time Exposure (STE) test, a potential alternative test for eye irritation using rabbit cornea cells (SIRC), is planned for peer review and expected to be accepted as an OECD test guideline for classifying materials as Non-irritant/Irritant (NI/I). Currently, we evaluated the technical transfer and inter-laboratory reproducibility of the STE test at 3 contract research laboratories and lead laboratory (Kao Corp). We first assessed the technical transfer at the 3 contract labs by using 5 chemicals (sodium lauryl sulfate, calcium thioglycolate, Tween 80, 1-octanol, and dodecane). Cell viability, following exposure to a 5% concentration, was used as an indicator of eye irritation potential, where a material is considered a NI if the viability was more than 70% and an I if the viability was less than 70%. Furthermore, a rank order (minimal irritant, moderate irritant and severe irritant) was given to materials based on scores obtained from exposures to 5% and 0.05% concentration. All 3 contract labs had reproducible and similar results for the 5 chemicals confirming the technical transfer among the contract labs. The inter-laboratory reproducibility was confirmed by using 21 cosmetic products (13 rinse-off and 8 leave-on products) and assessed by comparing the accuracy (i.e., ability to classify same materials as either NI or I, and same rank order) of the results among the 3 contract labs and Kao Corp. The respective accuracy for classifying as either NI/I for Lab A, B and C were 100, 81 and 95%. The respective accuracy for obtaining the same rank order for Lab A, B and C were 95, 67 and 76%. Overall, our findings show that a good inter-laboratory reproducibility was obtained for STE test using the finished cosmetic products.

**PS 976 Choosing the Appropriate Solvent for Solid Materials Tested in the Bovine Corneal Opacity and Permeability (BCOP) In Vitro Assay.**

G. Costin<sup>1</sup>, Y. Jeong<sup>2</sup>, D. Anderson<sup>2</sup>, J. E. Bader<sup>1</sup>, L. Krawiec<sup>1</sup>, J. R. Nash<sup>1</sup> and H. Raabe<sup>1</sup>. <sup>1</sup>Institute for In Vitro Sciences, Inc. (IIVS), Gaithersburg, MD; <sup>2</sup>The Dow Chemical Company, Midland, MI.

In compliance with OECD Test Guideline 437 for eye irritation (BCOP assay), non-surfactant solid materials are typically tested as 20% dilutions prepared in 0.9% sodium chloride solution, distilled water, or other solvent that has been demonstrated to have no adverse effects on the test system. However, the limited solubility of some chemicals adds technical challenges in finding a vehicle that would ensure the material's availability to the excised corneas and that itself would not affect the test system. In this study, we evaluated five solvents frequently used in the BCOP assay: distilled water, mineral oil, corn oil, polyethylene glycol (PEG)-400, and methocel solution (0.5%). Based on the available classification systems, our preliminary data showed that water, methocel, mineral oil and corn oil were predicted as non-irritants, while PEG-400 was predicted as a mild irritant. To demonstrate the influence of the type of solvent on the outcome/prediction of the BCOP assay for solid materials, we tested a 20% suspension of benzoic acid (BA) prepared in these solvents. BA has a non-polar benzoic ring that would preferably dissolve in non-polar solvents and a polar acidic group with affinity for polar solvents, thus making it a good model for testing its effect on corneas when dissolved in various solvents. Previous animal tests reported moderate to severe eye irritation induced by BA. Our results demonstrated that when mixed in water, mineral oil, corn oil, or methocel, BA was predicted to be a corrosive/severe irritant, while it was predicted to be a moderate irritant when mixed in PEG-400. These results support the need for further investigation of the solvent's influence in the BCOP assay to allow the correct prediction of the irritation potential of solid materials.

**PS 977 Predicting Eye Irritation of Agrochemical Formulations According to Different Classification Schemes by *In Vitro* Methods.**

S. N. Kolle<sup>1</sup>, A. Büchse<sup>2</sup>, T. Knieriemens<sup>3</sup>, M. Rey-Moreno<sup>1</sup>, W. Meyer<sup>3</sup>, A. van Cott<sup>4</sup>, S. Gröters<sup>1</sup>, B. van Ravenzwaay<sup>1</sup> and R. Landsiedel<sup>1</sup>. <sup>1</sup>*Experimental Toxicology and Ecology, BASF SE, Ludwigshafen am Rhein, Germany*; <sup>2</sup>*Scientific Computing, BASF SE, Ludwigshafen am Rhein, Germany*; <sup>3</sup>*Agricultural Products Formulation Development, BASF SE, Ludwigshafen am Rhein, Germany*; <sup>4</sup>*Agricultural Products - Global Product Safety & Registration, BASF Corporation, Research Triangle Park, NC.*

The bovine corneal opacity and permeability (BCOP) test has been adopted by OECD for the identification of ocular corrosive and severe irritants (GHS category 1) for single component substances and multi-component formulations. Further, human reconstructed tissue models have been suggested for incorporation into a tiered test strategy to ultimately replace the Draize rabbit eye irritation test (OECD TG 405) and the value of the EpiOcular Eye Irritation Test (EIT) for the prediction of ocular non irritants (GHS no category) has been shown previously. The purpose of this study was to evaluate whether the BCOP including corneal histology and the EIT could be used to predict eye irritancy of agrochemical formulations according to different classification schemes including UN GHS, EPA and ANVISA systems. We have assessed opacity, permeability and histology in the BCOP assay and relative tissue viability in the EIT for 50 agrochemical formulations with available *in vivo* eye irritation data. Using the OECD TG guideline evaluation scheme for opacity and permeability in the BCOP did not prove predictive with respect to severe eye irritation potential for the 50 agrochemical formulations assessed here, while corneal histology grades and the EpiOcular tissue viabilities were useful predictors of eye irritancy potencies. Further we describe here statistical evaluation based on the experimental *in vitro* data to predict eye irritancy for the different classification schemes.

**PS 978 A Preliminary Investigation in the Use of Porcine Corneas As a Substitute for Bovine Corneas in the BCOP Assay.**

D. Wolfinger and D. R. Cerven. *MB Research Laboratories, Spinnerstown, PA.*  
Sponsor: G. DeGeorge.

The Bovine Cornea Opacity and Permeability Assay (BCOP) has been used since 1992 to provide estimates of ocular irritation. It has been accepted as an alternative to the use of rabbit in acute ocular safety testing. However in some areas of the world, access to bovine eyes is limited, and the Draize eye-scoring test, performed in rabbits, is still being utilized. In response to this, we have been investigating the replacement of excised bovine corneas with porcine corneas for evaluation of acute ocular irritation (PCOP). This preliminary investigation involved the evaluation of 100% ethanol, 0.1% Benzalkonium Chloride (BAK), and four cosmetic products, all of which had previously been tested in the BCOP as well as the Chorioallantoic Membrane Vascular Assay (CAMVA). Initially the results from the ethanol and BAK testing in the porcine corneas showed no correlation to the results from bovine corneas. These suggested the need for certain modifications to the trimming and mounting procedures for the porcine corneas, which are smaller than the bovine corneas. Thus, the trimming process to excise the cornea was modified, and the same chambers supplied with the opacitometer for use with bovine eyes was also used for the porcine eyes. After modifying the pre-testing procedures, we proceeded to test four cosmetic compounds successfully in the BCOP and PCOP. These investigations indicate that the *In Vitro* Scores obtained with porcine eyes are similar to those in bovine eyes. Additional evaluation with a wider range of chemical entities is underway.

**PS 979 *In Vitro* Ocular Irritation Testing Strategy for Prototype Cleaning Products.**

M. Bauman<sup>1</sup>, K. Norman<sup>2</sup>, G. Mun<sup>2</sup> and H. Raabe<sup>2</sup>. <sup>1</sup>*S.C. Johnson & Son, Inc., Racine, WI*; <sup>2</sup>*Institute for In Vitro Sciences, Gaithersburg, MD.*

The Bovine Corneal Opacity and Permeability (BCOP) assay can be used for predicting mild, moderate, and severe ocular irritation through quantitative assessment of the changes in opacity and permeability of bovine corneas. In addition, histological evaluation of the corneas may be performed to assess the depth of damage. The BCOP assay with histology was used to determine the ocular irritation potential of prototype cleaning products with antimicrobial claims according to the guideline provided by the EPA-Office of Pesticide Programs (OPP). Several prototype cleaners of similar formulation were evaluated along with a reference material. The results of the BCOP assay showed noticeable differences among the products. The *in vitro* score, determined by changes in opacity and permeability of the

corneas, ranged from ~15 to 80. These scores indicate mild, moderate, and severe irritation according to the guideline provided by the EPA-OPP. In addition, the histological evaluation of the corneas showed differences in the depth of damage to the stroma between moderate and severe category products, confirming the classification of the products by the *in vitro* score. These results demonstrate the utility of the BCOP assay with histology as a stand-alone assay for eye irritancy evaluation in the EPA-OPP program. Furthermore, this testing strategy distinguished the ocular irritation potential among similar prototypes demonstrating its effectiveness in the product development process.

**PS 980 Development of a Human Corneal Full Thickness Tissue for Eye Irritation Testing.**

L. d'Argembeau-Thornton, Y. Kaluzhny, H. Kandarova, P. Hayden and M. Klausner. *MatTek Corporation, Ashland, MA.*

The FDA and other regulatory agencies require ocular irritation testing of ophthalmologic pharmaceuticals and consumer products. Human reconstructed tissue models have been suggested for incorporation into a tiered testing strategy to replace the Draize eye irritation test (OECD TG 405) and for use as highly reproducible and cost effective *in vitro* alternatives.

A newly developed Ocular-Corneal Full Thickness (OCFT) tissue model includes epithelial, stromal, and endothelial layers. This model has been characterized in terms of tissue morphology, expression of specific markers for human corneal epithelium (Cytokeratins 12, 14, and 19, stratifin, tight junction proteins ZO-1, occluding, and claudin), and NaFl leakage and transepithelial electrical resistance (TEER) in response to chemical insults. Histological evaluation of the tissues was used to provide information on the type and depth of the chemical insult. Also, the OCFT model was used to assess tissue recovery following exposure to increasing concentrations of surfactants and TA spanning the range of irritancy. Significant recovery at 24 and 48 hours was observed for non-irritants (NI) chemicals. The OCFT tissue was also evaluated in a response to a battery of test articles (TA, n=65) spanning the range from ocular corrosives and severe irritants (I) to non-irritants (NI). *In vivo* irritancy levels were obtained from a published database and *in vitro* effects were determined using the MTT tissue viability assay and TEER. Using a tissue viability cutoff of 50%, the OCFT model was able to detect "I" with 100.0/75.0 and 87.7% specificity/sensitivity/accuracy.

The OCFT model will address the needs of ophthalmic and other formulators who need to screen their products for irritancy and efficacy. Similar to other *in vitro* assays, high levels of reproducibility at a low cost are anticipated. The OCFT model will facilitate the development and testing of ophthalmologic pharmaceuticals and allow for basic studies related to corneal physiology, wound repair, and pathologies.

**PS 981 Validation of *In Vitro* Eye and Skin Irritation Assays for Structurally Complex Pharmaceutical Chemicals.**

N. Foglio<sup>2</sup>, C. Villano<sup>1</sup>, C. Risatti<sup>1</sup>, H. Raabe<sup>3</sup> and J. Gould<sup>1</sup>. <sup>1</sup>*Bristol-Myers Squibb, New Brunswick, NJ*; <sup>2</sup>*Rutgers University School of Pharmacy, Piscataway, NJ*; <sup>3</sup>*Institute for In Vitro Sciences, Gaithersburg, MD.*

Identification of local ocular and dermal irritation effects is important for occupational health and hazard communication. OECD has published Test Guidelines (TG) 439 for *In Vitro* Skin Irritation (EpiDerm™ System, MatTek) and TG 437 for the Bovine Corneal Opacity and Permeability Test Method (BCOP) to replace or supplement *in vivo* tests, but their applicability to complex molecules found in the pharmaceutical industry has not been fully investigated. A validation study was conducted to compare *in vivo* eye (OECD TG 405) and skin irritation (OECD TG 404) to *in vitro* study data for Bristol-Myers Squibb (BMS) proprietary compounds. The validation set consisted of 15 compounds, which were selected to represent the BMS chemical space within six chemical classes:  $\alpha\beta$  unsaturated carbonyls,  $\alpha$ -halo ketones, aminoalcohols, boronic acids/esters, halogenated heterocycles, and nitroaromatics. The assay results were interpreted using OECD and GHS classification schemes and *in vitro* and *in vivo* results were compared using basic statistics. The BCOP assay accurately predicted 12 of 15 compounds when non- and mildly irritating classifications were grouped together. Both boronic compounds were under-predicted by BCOP, suggesting the assay may not be appropriate for this chemical class. The *in vitro* skin assay demonstrated high specificity by correctly identifying 12 of 13 negative *in vivo* skin irritants, but, the sensitivity could not be interpreted from the limited number of positive skin irritants in this study. Additional data are needed to assess the predictivity of positive skin irritants with greater confidence. Overall, the replacement of *in vivo* studies with these alternative *in vitro* irritation methods reduces and refines the tiered testing strategy for ocular and dermal hazard identification of pharmaceutical chemicals.

**PS 982 Surfactant Responses in the Bovine Corneal Opacity and Permeability Assay: Points to Consider for *In Vitro* Eye Irritation Testing.**

J. E. Bader, G. Costin, A. Hilberer, G. Mun, J. R. Nash, K. Norman, N. Wilt and H. Raabe. *Institute for In Vitro Sciences, Gaithersburg, MD.*

The Bovine Corneal Opacity and Permeability (BCOP) assay is an *ex vivo* test used to evaluate the ocular irritation of a broad range of chemicals. In the regulatory classification and labeling arena, BCOP can be used to identify severe and corrosive eye irritants according to the OECD Test Guideline (TG) 437. However, BCOP has historically under-predicted certain anionic surfactants, when tested according to the standard liquid protocol. TG 437 specifies that liquid surfactants may be tested as 10% aqueous dilutions for 10 minutes (although alternate dilutions and exposure times may be conducted with scientific rationale), and the relevant guidance document (GD) No. 160 suggests that solid and concentrated liquid surfactants may be diluted to 10% for testing. However, GD No. 160 further directs that surfactant-based formulations are usually tested neat, but could be diluted with justification, imparting some confusion in identifying the most appropriate test methods. Since neither the basis for selecting the appropriate surfactant test methods, nor the justification for modifications are clearly presented in TG 437 or GD No. 160, we present on the testing of sodium lauryl sulfate (SLS) in the BCOP assay, using standard and modified dilutions and exposures, to elucidate the impact of these variables on eye irritation prediction. For example, *in vitro* scores of 20.7, 28.4, and 28.3 were obtained when testing SLS at concentrations of 50, 20, and 10% for 10 minutes, showing that irritation responses were not fully concentration-dependent, but demonstrated optimally at intermediate doses. When tested using modified exposure times, SLS showed time-related responses, with improvements in irritation predictions at the 20 and 30 minute exposures. Histopathology was performed to assess the surfactant-induced corneal changes. Based upon these results, a framework for testing surfactants, and surfactant-based formulations is proposed.

**PS 983 New Detecting Method for Estimating the Eye Irritation Potential of Chemicals: An Alternative to the Draize Test.**

S. Cho, G. Nam, J. Kim, J. Cho and K. Shin. *AMOREPACIFIC Corporation R&D Center, Yongin-si, Republic of Korea.*

Determination of eye irritation potential is an essential part of the safety assessment of chemicals, pharmaceuticals, and cosmetics. For many years, the ocular irritation potential of chemicals has been mainly evaluated by the Draize rabbit eye irritation test (OECD Test Guideline 405). Because Draize rabbit eye irritation test is based on subjective visual scoring evaluation, significant variability has been observed. In addition, the test causes considerable discomfort and pain to the animal, and it has also been identified that the eye irritation response of rabbits does not always correspond to those of humans. For scientific reasons, animal welfare issues and the ban of cosmetics in animal eye irritation tests in the European Union (EU), there are many efforts to develop alternative methods replacing animal study. Using a human corneal cell line (HCE-T cells), we developed a new alternative method to assess the eye irritation potential of chemicals. We exposed HCE-T cells to 3 fixed concentrations of the 38 chemicals (5%, 0.5%, and 0.05%) for 1 h and measured the relative cell viability (RCV) at each concentration. Using the RCV values at 5%, 0.5%, and 0.05%, we developed a new criterion for eye irritation potential (total eye irritation score, TEIS) and estimated the ocular irritancy. We then assessed the correlation of the results of TEIS with those of the Draize rabbit eye irritation. TEIS results exhibited good correlations (sensitivity: 80.77%, specificity: 83.33%, and accuracy: 81.58% for TEIS). We conclude that the new *in vitro* model using HCE-T cells is a good alternative evaluation model for the prediction of the eye irritation potential of chemicals.

**PS 984 Neonatal Hyperoxia Promotes Lung Fibrosis Independent of Excessive Leukocyte Recruitment to the Lung following Influenza A Virus Infection.**

B. W. Buczynski<sup>1</sup>, M. Yee<sup>2</sup>, P. Lawrence<sup>1</sup> and M. A. O'Reilly<sup>2</sup>. <sup>1</sup>*Environmental Medicine, The University of Rochester, Rochester, NY;* <sup>2</sup>*Pediatrics, The University of Rochester, Rochester, NY.*

There is a growing appreciation that environmental exposures during critically important periods of development can influence the onset of many childhood and adult diseases. For example, preterm infants prematurely exposed to excess levels of oxygen (hyperoxia) at birth are at increased risk for impaired lung development and are often more sensitive to respiratory viral infections later in life. Similarly, adult

mice exposed to 100% oxygen during PND 0-4 exhibit persistent lung simplification, as well as an increase in inflammation and fibrosis following infection with influenza virus. Levels of the inflammatory chemokine MCP-1 are selectively increased following infection in these mice. Since increased levels of MCP-1 are often associated with pulmonary inflammation and fibrosis, we hypothesized that *Mcp-1*<sup>-/-</sup> mice exposed to hyperoxia at birth would have an attenuated inflammatory response and reduced fibrotic repair following infection with influenza virus. Prior to infection, lung simplification was evident and indistinguishable amongst *Mcp-1*<sup>+/-</sup> and *Mcp-1*<sup>-/-</sup> mice exposed to hyperoxia at birth. When infected, *Mcp-1*<sup>-/-</sup> mice exposed to hyperoxia had reduced mean body weight loss and leukocyte recruitment to the lung in comparison to *Mcp-1*<sup>+/-</sup> mice exposed to hyperoxia. Although leukocyte recruitment was not excessive following infection in *Mcp-1*<sup>-/-</sup> mice exposed to hyperoxia, they still developed pulmonary fibrosis, which was not observed in infected *Mcp-1*<sup>-/-</sup> mice exposed to room air. Thus, the aberrant fibrotic repair observed following infection in mice exposed to hyperoxia at birth occurs independently of excessive leukocyte recruitment to the lung. Our findings identify novel neonatal hyperoxia-mediated pathways disrupted in response to influenza virus infection, which may provide insight into how early-life exposure to high levels of oxygen leads to childhood and adult diseases later in life.

**PS 985 Integrating Genome and Transcriptome Data to Understand Susceptibility to Postnatal Lung Injury.**

J. Nichols<sup>1</sup>, A. Burkholder<sup>1</sup>, J. Lu<sup>1</sup>, Z. McCaw<sup>1</sup>, O. Suzuki<sup>2</sup>, D. Fargo<sup>1</sup>, P. Bushel<sup>1</sup>, T. Wiltshire<sup>2</sup> and S. R. Kleeberger<sup>1</sup>. <sup>1</sup>*NIEHS, Durham, NC;* <sup>2</sup>*Eshelman School of Pharmacy, University of North Carolina at Chapel Hill, Chapel Hill, NC.*

Late lung development is a critical window of susceptibility as perturbations impair alveolarization and vascular development. Currently, genetic control of differential gene expression during lung development and injury is incompletely understood. We hypothesized that integration of genetics and genomics in expression quantitative trait loci (eQTL) analysis will identify genetic factors contributing to variability in the neonatal lung and characterize genetic susceptibility. Full term neonates from 30 inbred strains of mice were maintained in room air or exposed to 95% oxygen for 72hrs beginning on postnatal day 1 (P1). Lungs were collected from 3 neonates/group for each strain on P4. RNA was isolated for transcriptomic analysis using Illumina WG6v2.0 BeadChips. Transcript intensities were analyzed for differential expression, and associations between genetic polymorphisms and transcript intensity (eQTLs) were identified by haplotype association mapping with FastMap. 4513 differentially expressed transcripts were identified on P4, and cis-eQTL analysis, or associations between a transcript and polymorphism in the same gene, yielded 29 genes. Biologically interesting candidate genes included Adam17, Prdx1, Tnfip2, and Eif2ak2. After hyperoxia exposure, 5386 transcripts were differentially expressed. 1230 were specifically hyperoxia-induced and related to developmental and inflammatory pathways. 23 cis-eQTLs were identified and biologically interesting candidates included Vcp, Casp9, and Trim30. These analyses identified significant interstrain variation in transcript levels in the developing lung that is, in part, due to genetic background. Furthermore, network and pathway analysis of these candidate genes pointed to a novel role for the integrated stress response and proteostasis in neonatal lung development and injury.

**PS 986 Analysis of the Developmental Origins of Health and Disease (DOHaD) Grant Portfolio at the NIEHS.**

A. Haugen, T. T. Schug and J. J. Heindel. *Division of Extramural Research and Training, NIEHS, Research Triangle Park, NC.* Sponsor: M. Humble.

Environmental exposures combined with genetics can have a persistent influence on common chronic health conditions of children and adults. A growing body of research at the National Institute of Environmental Health Sciences (NIEHS) is focusing on environmental effects during early-life development and disease occurrence over the lifespan—a branch of scientific study referred to as Developmental Origins of Health and Disease or the “DOHaD paradigm.” This paper describes the evolution of DOHaD research at NIEHS and how extramural events, including Requests for Applications (RFA) in the areas of Fetal Basis of Adult Disease (FeBAD), children's health, and epigenetics, have stimulated the field of environmental health science as it relates to DOHaD. In order to build and analyze a portfolio of active NIEHS-funded grants in the area of DOHaD, the electronic Scientific Portfolio Assistant (eSPA) software application was used. DOHaD portfolios for the years 1991, 2001, and 2011 were analyzed for exposures, disease/organ endpoints, windows of exposure, study design, and impact on the field based on publication data. Priority exposures in the 1991 and 2001 portfolios comprise of metals (e.g. lead and mercury), PCBs, and air pollutants; but by 2011, the portfolio has evolved to include or expand the variety of endocrine disruptors (e.g. BPA, phthalates), pesticides/Persistent Organic Pollutants (POPs) (e.g.

organophosphates, organochlorines, PBDE, PAH), and metals (e.g. arsenic, manganese). Several disease endpoints related to brain/CNS are apparent across all three portfolios, whereas reproduction and cancer increase steadily over the same time period, and new endpoints like obesity are introduced by 2011. The analysis of NIEHS-funded DOHaD research provides insight into the institute's impact on the field, and will help determine how to improve the quality and health impact of future, funded DOHaD projects.

**PS 987 Effects of Gutkha Use during Pregnancy on Hepatic Parameters Later in Life.**

S. P. Doherty-Lyons<sup>1</sup>, C. Hoffman<sup>1</sup>, J. Odin<sup>3</sup>, I. Fiel<sup>3</sup>, F. Ganey<sup>2</sup>, D. J. Conklin<sup>4</sup> and J. T. Zelikoff<sup>1</sup>. <sup>1</sup>Environmental Medicine, New York University School of Medicine, Tuxedo, NY; <sup>2</sup>Memorial Sloan-Kettering Cancer Center, New York, NY; <sup>3</sup>Mount Sinai School of Medicine, New York, NY; <sup>4</sup>University of Louisville, Louisville, KY.

Gutkha, a popular smokeless tobacco (ST) herbal concoction made in India and sold throughout India and the U.S., is a combination of tobacco, lime, betel and areca nut, spices, and catechu. Recent evidence demonstrates that consuming gutkha during pregnancy may be linked to adverse obstetric consequences. However, whether gutkha exposure during pregnancy increases offspring risk of chronic disease later on in adulthood, as with combustible tobacco products, remains unknown. For this study, pregnant B6C3F1 mice were exposed daily to 21 mg of a water-soluble gutkha solution beginning on gestational day (GD) 2-4 until parturition. The main objectives of this study were to evaluate whether prenatal exposure to gutkha altered offspring susceptibility for hepatic disease later in life. After male pairing, female mice were exposed to a gutkha solution via the oral mucosa. Serum cotinine levels in pregnant mice were measured weekly and ranged from 24-44 ng/ml. Cotinine levels, also measured in the amniotic fluid and fetal liver on -GD 15, averaged 21-22 ng/ml. Beginning at 12-wk-of-age, a sub-group of male and female offspring were fed a high fat (HF) diet for 14 days. Male offspring prenatally exposed to gutkha and fed subsequently a HF diet had increased hepatic fat mass, fibrosis, and inflammation compared to the other groups. Additionally, female offspring exposed to gutkha alone had significantly higher serum levels of the hepatic injury markers, alanine transaminase and aminotransferase. In conclusion, findings from these studies demonstrate that gutkha usage during pregnancy may have persistent later life effects that increase the risk of adult liver disease. As gutkha use by pregnant women in the South Asian communities are increasing exponentially, such a menacing public health behavior requires immediate attention. Supported by Memorial Sloan Kettering Cancer Institute.

**PS 988 Transcriptomic Profiling of Embryos and Adult Female Brain Tissue Links a Developmental Origin of Atrazine-Induced Reproductive Alterations in Zebrafish.**

G. J. Weber<sup>1</sup>, S. M. Peterson<sup>1</sup>, S. S. Lewis<sup>2</sup>, M. S. Sepulveda<sup>2</sup> and J. L. Freeman<sup>1</sup>. <sup>1</sup>Health Sciences, Purdue University, West Lafayette, IN; <sup>2</sup>Forestry and Natural Resources, Purdue University, West Lafayette, IN.

Atrazine, an herbicide commonly applied to agricultural areas throughout the Midwest and a common contaminant of potable water supplies, is implicated as an endocrine disruptor and potential carcinogen. The specific adverse health effects associated with atrazine exposure and the underlying molecular mechanisms of these effects are not well defined. In an effort to delineate the mechanisms of atrazine toxicity, we exposed zebrafish embryos to environmentally relevant concentrations of atrazine shortly after fertilization through 72 hours post fertilization (hpf). Transcriptomic profiles immediately following the embryonic atrazine exposure were obtained and subsequent analyses identified an enrichment of genes with altered expression patterns that are involved in neuroendocrine development and function, cell cycle regulation and carcinogenesis. From these exposures a subset of individuals was permitted to mature under normal conditions to evaluate later life effects of the developmental exposure and in unexposed subsequent generations. A significant difference in the number of pairs that successfully bred in one of the atrazine treatment groups coupled with distinct altered reproductive histological and morphological alterations in female adult zebrafish was observed indicating a later life effect of the developmental atrazine exposure. Furthermore, gene ontology analysis from microarrays performed on adult female zebrafish brains showed enrichment for genes involved in neuroendocrine system function and disease. The reproductive alterations observed in the adult females along with decreased mating success and altered transcriptomic profiles provide support to the endocrine disrupting effects of this herbicide and warrant further mechanistic investigation. Current efforts are aimed at assessing transgenerational effects of this developmental atrazine exposure in subsequent unexposed generations.

**PS 989 Bisphenol A and Diethylstilbestrol Treated Mice Respond Differently to a Very High Fat Diet.**

L. Chalifour<sup>1,2</sup>, B. Patel<sup>1,2</sup> and I. A. Sebag<sup>1,2</sup>. <sup>1</sup>Lady Davis Institute, Montréal, QC, Canada; <sup>2</sup>McGill University, Montréal, QC, Canada.

**Rationale:** Bisphenol A (BPA) is an estrogenizing endocrine disruptor, and diethylstilbestrol (DES) is a non-steroidal estrogen. Some data suggest that BPA is an obesogen. We hypothesized that BPA and/or DES would increase the metabolic impact of a very high fat diet and that this obesity would reduce heart structure/function. **Methods:** C57bl/6n mice were exposed to Vehicle, oral BPA (5.0µg/kg/da) from gestation day 11 to weaning and then (0.5µg/kg/da) to 4 months, or diethylstilbestrol (DES, 1µg/kg/da) from GD 11-14. Mice were fed control (CD, 10% calories from fat) or very high fat (HFD, 60% calories from fat) diets from weaning. Body weight (BW) and body length (BL) were measured monthly. Body mass index (BMI) and body surface area (BSA) were calculated. Glucose tolerance was tested at 15 weeks. Echocardiography, organ weights and serum for cholesterol, triglycerides and leptin were collected at 16 weeks.

**Results:** All HFD mice had increased BW, BL, BMI and BSA. HFD VEH and BPA males had similar increases in total fat and total fat indexed to BW or BSA, but HFD BPA males were smaller in BW, BMI and BSA. HFD VEH and BPA females had similar total fat and total fat indexed to BW or BSA, BW, BMI and BSA. In contrast, HFD DES treated males and females had the least fat gain, BW, BMI and BSA. Cholesterol and triglycerides were increased with HFD in all males and leptin was increased in BPA and DES males. Cholesterol, triglycerides and leptin were increased with HFD identically in VEH, BPA and DES females. Glucose tolerance was reduced with HFD equally in all mice. Fractional shortening was unaffected, but HFD induced eccentric cardiac hypertrophy in VEH and BPA with DES mice showing the greatest increase.

**Conclusions:** Neither BPA nor DES worsened the response to a very HFD. VEH and BPA mice responded similarly to a very HFD. DES mice had a blunted metabolic response to a very HFD. Cardiac function was unaffected, but cardiac structure was affected by HFD.

**PS 990 Analysis of Transcriptional Profiles and Functional Clustering of Global Cardiovascular Gene Expression in Response to In Utero B(a)P Exposure.**

G. E. Jules<sup>1</sup>, S. Pratap<sup>2</sup>, A. Ramesh<sup>3</sup> and D. B. Hood<sup>1</sup>. <sup>1</sup>Neuroscience and Pharmacology, Meharry Medical College, Nashville, TN; <sup>2</sup>Microbiology & Immunology, Microarray/Bioinformatics Core, Meharry Medical College, Nashville, TN; <sup>3</sup>Biochemistry and Cancer Biology, Meharry Medical College, Nashville, TN.

Interest in the correlation between environmental toxicants and cardiovascular diseases has increased considerably over the past few decades. However, little is known of B(a)P's effect on the developing heart or the specific biological pathways altered by B(a)P. Functional comparative genomic analysis of the cellular and developmental effects of different polycyclic aromatic hydrocarbon (PAH) compounds is considered a helpful approach to distinguish the complex and specific effects of B(a)P exposure in utero. Using timed-pregnant Long Evans Hooded rat offspring, we characterize the genetic modulation in cardiovascular related genes for three concentrations of B(a)P (0, 600, and 1,200 µg/kg/BW) at postnatal days 0 and 53 (P-0 and P-53). In utero exposure to B(a)P at both 600 and 1,200 µg/kg/BW significantly modulated the expression of 89 out of 45,000 genes in offspring. The focused microarray approach identified important subgenomic differences in the pattern of cardiovascular disease cell-related gene expression in response to in utero B(a)P exposure. These molecular targets and deduced networks may be employed as a guide for classifying, monitoring and manipulating the molecular and pathological specificities of different PAHs in key cardiovascular related cell systems and for potential pharmacological application.

**PS 991 Maternal DDT Exposure Increases Risk of Metabolic Syndrome in Adult Offspring.**

M. La Merrill<sup>1,2</sup> and C. Buettner<sup>3,2</sup>. <sup>1</sup>Environmental Toxicology, University of California Davis, Davis, CA; <sup>2</sup>Metabolism Institute, Mount Sinai School of Medicine, New York, NY; <sup>3</sup>Endocrinology, Diabetes, Bone Disease, Mount Sinai School of Medicine, New York, NY; <sup>4</sup>Preventive Medicine, Mount Sinai School of Medicine, New York, NY.

DDT is associated with altered carbohydrate and lipid homeostasis in animals that have been exposed to relatively high doses, and with increased risk of type 2 diabetes and hypertension in human studies. We hypothesized that maternal exposure

to DDT would increase the risk of metabolic syndrome in the adult offspring of mice. We administered DDT to C57BL/6J mice from gestational day 11.5 to postnatal day 5, when litters were culled to six pups. We performed comprehensive metabolic phenotyping in offspring. Maternal DDT exposure increased diastolic and systolic blood pressure in adult offspring. Maternal DDT exposure also caused a mild obese phenotype in female offspring that was due to impaired thermoregulation (increased cold intolerance) and decreased energy expenditure while food intake was not different. When these female offspring were fed a diet high in fat, they developed elevated fasting insulin and lipids. Thus, the results from the current study suggest that maternal DDT exposure leads to metabolic syndrome in adult offspring.

**PS 992 Mechanisms Underlying Neurodevelopmental Defects in Weanling and Adult Rats Associated with Prenatal Exposure to Methylmercury.**

D. De Groot<sup>1</sup>, C. De Esch<sup>1</sup>, M. de Groot<sup>1</sup>, C. Kuper<sup>1</sup>, R. Stierum<sup>1</sup>, A. Wolterbeek<sup>1</sup>, E. De Vries<sup>2</sup>, N. Cappaert<sup>3</sup>, M. Radonjic<sup>1</sup> and R. Woutersen<sup>1</sup>.  
<sup>1</sup>TNO the Netherlands, Zeist, Netherlands; <sup>2</sup>Groningen University Medical Center, Groningen, Netherlands; <sup>3</sup>University of Amsterdam, Amsterdam, Netherlands.

A Developmental Neurotoxicity (DNT) study with MeHg was carried out in Wistar rats [Guidelines US-EPA OPPTS 870.6300/8600]. To map neurodevelopmental defects of MeHg and uncover underlying mechanisms, cerebellum and cerebrum of female F1-rats, prenatally exposed to MeHg via maternal diet (GD6 - PD10), were sampled at weaning (PD18-21) and adulthood (PD61-70). Brain tissues were analysed by [18F]FDG PET functional imaging, synaptic excitation analysis and microarray gene expression profiling. Brain activity and functionality of neurotransmission assessed by [18F]FDG PET imaging and synaptic excitation analysis revealed a delay in brain activity and impaired neural function. The findings were substantiated by genome-wide transcriptome analysis. The discovered transcriptional patterns revealed that exposure to MeHg causes (1) a delay in onset of neural development and/or function and (2) alterations in pathways related to structural and functional aspects of nervous system development. The latter includes changes in gene expression of developmental regulators, developmental-phase associated genes, small GTPase signaling molecules and representatives of all processes required for synaptic transmission. Marked repression of genes regulating brain development and neural function were observed particularly at PD70, showing that prenatal exposure to MeHg has long-lasting effects in adult brain. No effects of MeHg were found in tests proposed in DNT guidelines.

Summarizing, structural and functional defects associated with MeHg were demonstrated with [18F]FDG PET functional imaging, synaptic excitation analysis and microarray gene expression profiling, and molecular mechanisms underlying these developmental defects identified. The findings are relevant from a health perspective, but also show that the approaches used are sensitive and superior to conventional tests proposed in current DNT guidelines.

**PS 993 Vulnerability Windows of the Developing Rat Brain to TBTO Demonstrated by Animal-Friendly MRI.**

M. Berk<sup>1,2</sup>, S. Folkertsma<sup>1</sup>, M. de Groot<sup>1,3</sup>, A. Knaapen<sup>1</sup>, I. Waalkens<sup>1</sup>, A. Wolterbeek<sup>1</sup>, R. Woutersen<sup>1</sup>, A. Veltien<sup>2</sup>, A. Heerschap<sup>2</sup> and D. De Groot<sup>1</sup>.  
<sup>1</sup>TNO, the Netherlands, Zeist, Netherlands; <sup>2</sup>Radboud University Medical Center Nijmegen, Nijmegen, Netherlands; <sup>3</sup>IRAS, Utrecht University, Utrecht, Netherlands.

To design a proper strategy for safety evaluation of drugs for children and adolescents information on the vulnerability of the brain during critical phases of development is essential. In this study developmental and juvenile exposure windows proposed in current guidelines for toxicity testing were studied in a rat model with tributyltin oxide (TBTO).

Rats were exposed to 8mg TBTO/kg BW/day during development (TBTOdev: gestation day (GD)8 to postnatal day (PD)10) or adolescence (TBTOjuv: PD22-PD62). Brain weight (cerebrum and cerebellum separately) was determined at weaning (PD22) and young adult age (PD62). Brain (region) volume was estimated from magnetic resonance (MR) images. Brain specific gravity (SG) was calculated from the ratio [weight / volume]. Relative growth for these brain measures was calculated over time (from PD22 to PD 62) for control and TBTO-exposed brains.

Effect of TBTOdev included reduced cerebral weight but increased volume at PD22, whereas at PD62 both weight and volume appeared reduced. Effects of TBTOjuv implied reduced weight and increased volume at PD62. Effect of TBTOdev on brain SG was most pronounced on cerebrum at PD22, which was no

more observed at PD62. Effect of TBTOjuv (PD62) was most pronounced on SG of cerebellum/brainstem. MRI scans demonstrated that effects within cerebrum were located in particular in anterior regions.

Together, the results demonstrate the relevance of exposure windows relative to the vulnerability of the developing brain; under the circumstances of this study the brain appeared more vulnerable when exposed during development with largest effects on cerebrum at adolescent age (PD22). Effects of juvenile exposure appeared mild, and seemed to affect both cerebrum and cerebellum/brainstem (PD62). The results are discussed in light of TBTO-induced delayed development, persistent effects at adult age and a speculative role of TBTO as obesogen.

**PS 994 The Effects of Endocrine Disruption on the Maturation of the Developing Human Fetal Prostate.**

C. Saffarini<sup>1</sup>, E. V. McDonnell<sup>1</sup>, A. Amin<sup>2</sup>, S. J. Hall<sup>1</sup> and K. Boekelheide<sup>1</sup>.  
<sup>1</sup>Pathology and Laboratory Medicine, Brown University, Providence, RI; <sup>2</sup>Pathology and Laboratory Medicine, Rhode Island Hospital, Providence, RI.

The etiology of prostate cancer is unknown, although it has been suggested that early life exposures to various toxicants, such as estrogenic chemicals, may play an important role. Previous studies in rat models have demonstrated that early life exposures to estrogens is responsible for causing epithelial and stromal hyperplasia, inflammation, and prostatic intraepithelial neoplasia (PIN) lesions. We have developed a xenograft rodent model to characterize the growth and differentiation of human fetal prostate implants (gestational age 12-24 weeks). This model encompasses the effects of both early and later-life exposures to either corn-oil (control) or 250 ug/kg/body weight of 17 $\beta$ -estradiol 3-benzoate post-transplant. To ensure proper growth of implants, the renal subcapsular space was chosen as the site of implantation to allow for appropriate growth and vascularization of prostate tissue. This model was characterized based on the expression of key immunohistochemical markers responsible for epithelial and stromal maturation including p63, cytokeratins 18, alpha smooth muscle actin, vimentin, caldesmon, ki-67, prostate specific antigen, estrogen receptor- $\alpha$ , and androgen receptor. As expected, the human fetal implants grew and matured as demonstrated by the histopathology seen in 7, 14, 30, 90, 200 and 400 day xenografts. Interestingly, the human prostate xenografts exhibited marked differences in response to estrogen exposure compared to their endogenous rodent prostate counterparts. The endogenous rodent prostates exhibited atypical hyperplasia along with the presence of massive cellular debris after estrogen exposure, while the human prostates demonstrated basal cell hyperplasia as indicated by p63 staining. This study of human fetal prostate tissue will allow for future mechanistic studies investigating the origins of prostate disease.

**PS 995 Characterizing Later-Life Spatial Discrimination Deficit Phenotypes following *In Utero* Exposure to Benzopyrene.**

M. M. McCallister<sup>1</sup>, M. Maguire<sup>1</sup>, R. Rhoades<sup>1</sup>, B. Hudson<sup>2</sup>, A. Ramesh<sup>3</sup>, M. Newland<sup>2</sup> and D. B. Hood<sup>1</sup>. <sup>1</sup>Neuroscience and Pharmacology, Center for Molecular and Behavioral Neuroscience, Meharry Medical College, Nashville, TN; <sup>2</sup>Department of Psychology, Auburn University, Auburn, AL; <sup>3</sup>Department of Biochemistry and Cancer Biology, Meharry Medical College, Nashville, TN.

To characterize observed behavioral learning deficit phenotypes in offspring adult rodents arising from *in utero* exposure to benzo(a)pyrene [B(a)P], timed-pregnant Long Evans Hooded rats or Cytochrome p450- reductase (Cprlox/lox) mice were exposed to either B(a)P (0, 150, 300, 600 and 1200 $\mu$ g/kg BW or aerosol 100ug/m<sup>3</sup> on embryonic days 14 to 17. In the pre-weaning period, B(a)P metabolites were examined in cerebral cortex. No detectable levels of metabolites were found in the control offspring during the pre-weaning period but dose-related increases in B(a)P metabolites were seen in cerebral cortex and revealed a time-dependence for elimination during this period. Reversal learning was evaluated using a spatial discrimination-reversal procedure in adult offspring. Offspring that were exposed *in utero* to 600 and 1200  $\mu$ g/kg BW or 100ug/m<sup>3</sup> required a significantly higher number of sessions to complete the first reversal than control offspring. However, with original discrimination and subsequent reversals, exposed offspring behavioral profiles resembled their respective controls. This effect was seen in errors of commission, indicative of perseveration or resistance to extinction. Offspring that were exposed *in utero* also had shorter choice latencies than controls during the first session of a reversal. Activity related-cytoskeletal associated protein (Arc), an experience-dependent cortical protein marker known to be up-regulated in response to acquisition of novel behaviors, was also upregulated in B(a)P exposed animals that were trained in the behavioral paradigm. Collectively, the findings support the hypothesis that *in utero* exposure to B(a)P during the critical window for peak neurogenesis produces later-life learning deficit phenotypes in offspring.

**PS 996 Does the Barker Hypothesis Apply to Maternal Nanomaterial Exposure and Fetal Microvascular Function?**

P. G. Stapleton<sup>1</sup>, V. C. Minarchick<sup>1</sup>, J. Yi<sup>1</sup>, C. R. McBride<sup>1</sup>, K. Engles and T. R. Nurkiewicz<sup>2</sup>. *Physiology and Pharmacology, West Virginia University, Morgantown, WV.*

The continued development of engineered nanomaterials (ENM) has given rise to concerns over the potential for human health effects. While the lung is the primary site of exposure, the cardiovascular system is a principal site of impact. One of the most complex and acutely demanding circulations is the enhanced maternal system to support fetal development. The "Barker Hypothesis" proposes that metabolic impairments during gestation predispose future sensitivity. Herein we initiated testing at the microvascular level.

Pregnant (gestation day 10) Sprague-Dawley rats were exposed to nano-titanium dioxide aerosols (count mode aerodynamic diameter of 137 nm, 10 mg/m<sup>3</sup>, 4 hrs/day) for 10 days to evaluate the maternal and fetal consequences of maternal exposure. The calculated daily maternal deposition was 20 µg.

These exposures lead to fetal irregularities and maternal microvascular dysfunction. Isolated maternal uterine arteriolar (< 150 µm) reactivity was significantly impaired overall, consistent with a metabolically impaired profile. This dysfunction presented as blunted endothelium-dependent reactivity (acetylcholine, Ach, 10-9-10-4 M), reduced adrenergic responsiveness (phenylephrine, 10-9-10-4 M), and impaired myogenic responsiveness (transmural pressure, 15-120 mm Hg).

With respect to the fetal group, maternal exposures lead to a significant decrease in total fetal weight. Fetal tail arteries (< 150 µm) were isolated to assess microvascular alterations after maternal exposure. Interestingly, the vessels from the exposed group also demonstrate significant impairment to increasing concentrations of ACh (10-9-10-4 M), spermine-NONOate (10-9-10-4 M), and increases in transmural pressure.

Collectively, impaired uterine microvascular reactivity after ENM exposure during pregnancy can reduce nutrient exchange, drastically impacting fetal weight and number. This prenatal exposure may also lead to cardiovascular consequences for the developing fetus.

NIH-RO1-ES015022 and RC1-ES018274 (TRN)  
NSF-1003907 (VCM)

**PS 997 The AhR Contributions to Cardiovascular Development, Developmental Toxicity, and Adult Disease.**

V. S. Carreira<sup>1</sup>, Y. Fan<sup>1</sup>, J. Rubinstein<sup>2</sup>, M. Jiang<sup>2</sup> and A. Puga<sup>1</sup>. *<sup>1</sup>Environmental Health, University of Cincinnati, Cincinnati, OH; <sup>2</sup>Internal Medicine, University of Cincinnati, Cincinnati, OH.*

Developmental disruption has been increasingly recognized as a key contributor to adult disease. Exposures to ubiquitous environmental persistent organic pollutants (POPs), which includes the pervasive organic pollutant 2,3,7,8-Tetrachlorodibenzo-p-dioxin (TCDD), can result in abnormalities of the cardiovascular system at the structural and functional levels. TCDD is a prototypical aryl-hydrocarbon receptor (AHR) ligand but the precise pathogenesis and phenotype of TCDD developmental toxicity remains poorly characterized. Our work aims at understanding how developmental perturbations (TCDD-exposure) or absence (knockout) of the AHR pathway affects the cardiovascular system in the embryo and adult. To characterize the toxicity phenotype, C57BL/6J pregnant dams were oral-gavaged with different doses of TCDD (0.1, 0.5, 1, 2.5, 5, and 50 µg/Kg) or vehicle control at key murine cardiogenesis time points (E7.5, 9.5, and 11.5). Embryos were harvested at E13.5, 15.5, and 18.5 or carried to term and adulthood. Additionally, C57BL/6J Ahr<sup>-/-</sup> mice were included in postnatal functional studies. At all studied doses, embryos could be carried to term; however, pups died within 24 hours post-partum at the three highest doses. Embryo cardiac toxicity was characterized by dynamic changes in morphometric parameters (right and left ventricular free wall thickness, cellular density, nuclear size, and extracellular matrix) as well as the changes in the expression of the Ahr and cellular proliferation proteins. The postnatal functional studies highlighted LV cavity dilatation in the Ahr<sup>-/-</sup> mice at PND60 and 90. These results corroborate the heart as a target of developmental disruption by in-utero exposure to a POP. Moreover, since all biological effects of TCDD exposure are believed to be mediated through AHR signaling, these results underscore the critical role for the AHR pathway in normal cardiovascular development. Supported by NIH Grant R01ES06273.

**PS 998 Exposure to 2, 3, 7, 8-Tetrachlorodibenzo-p-dioxin (TCDD) Changes Morphology of Dendritic Spines in the Developing Anteroventral Periventricular Nucleus (AVPV).**

J. Del Pino Sans<sup>1,2</sup> and S. Petersen<sup>2</sup>. *<sup>1</sup>Toxicologia y Farmacologia, University Complutense of Madrid, Madrid, Spain; <sup>2</sup>Veterinary and Animal Sciences, University of Massachusetts, Amherst, MA.*

Developmental exposure to TCDD interferes with masculinization of luteinizing hormone release patterns and sexual behaviors. Consequently, female-typical luteinizing hormone LH surge release and mating postures can be elicited by ovarian hormones in exposed males. Thus, it is likely that TCDD interferes with processes important for masculinization of the brain. Dendritic spine plasticity plays a role in sexual differentiation of preoptic areas important for sexual behavior, but no work has examined whether similar processes regulate differentiation of the anteroventral periventricular nucleus (AVPV), the brain region that controls LH surge release. Likewise, no work has previously investigated the effects of TCDD on modulation of dendritic spines morphology. In these studies, we used Golgi staining to examine sex differences and lasting effects of TCDD exposure on spine density and shape in the AVPV of rats. We found that compared with female counterparts, Postnatal Day 30 (PD30) control males had significantly more dendritic spines overall. In addition, the shapes of the spines differed between the sexes with males having more mushroom and stubby spines, but fewer thin dendritic spines than females. Lactational exposure to TCDD (600 ng p.o. to dams on PND1) did not change the overall density of dendritic spines in the AVPV. However, exposed males had more thin dendritic spines and stubby spines, but fewer mushroom spines than controls. These findings suggest that TCDD interferes with AVPV development by both replacing the high surface area mushroom dendritic spines with thin and stubby spines. Dendritic spines play a major role in neuronal plasticity and integration of signals, so by altering the number and shape, TCDD exposure during development may permanently alter gonadotropin release mechanisms.

**PS 999 Breast Cancer 1 (BRCA1)-Deficient Mice Develop Normally but Are More Susceptible to Ethanol- and Methamphetamine-Initiated Embryopathies.**

A. M. Shapiro<sup>1</sup>, L. Miller<sup>2</sup> and P. G. Wells<sup>1,2</sup>. *<sup>1</sup>Pharmaceutical Science, University of Toronto, Toronto, ON, Canada; <sup>2</sup>Pharmacology and Toxicology, University of Toronto, Toronto, ON, Canada.*

Brcal1 is a DNA repair gene associated with certain familial breast and ovarian cancers, and heterozygous (+/-) Brcal1-deficient mice develop normally but are more susceptible to cancer later in life. Little information is available on the developmental consequences of Brcal1 deficiencies, but homozygous (-/-) Brcal1 knockout mice are embryolethal and no confirmed cases of human -/- knockouts exist, even in families where both parents are carriers. To further investigate the role of Brcal1 deficiencies during embryonic development, a conditional Brcal1 knockout, driven by a Sox2 promoter, was implemented in an embryo culture system. Sox2-promoted Cre-expressing hemizygous males were mated overnight with floxed Brcal1 females (plug designated gestational day (GD) 1). On GD 9, embryos were explanted and grown in culture for 24 hours. Western blot analysis indicated a 35% reduction of Brcal1 expression in +/- conditional knockout progeny. As previously reported, untreated +/- Brcal1-deficient embryos developed normally relative to their wild-type littermates. However, following exposure to the reactive oxygen species (ROS)-initiating teratogens methamphetamine and ethanol, +/- Brcal1-deficient progeny exhibited increased embryopathies at concentrations that were not toxic in their wild-type Brcal1-normal littermates. Preliminary studies suggested an increase in oxidatively damaged DNA, measured as 8-oxoguanine (8-oxoG), in drug-exposed embryos, which was further enhanced with Brcal1 deficiencies. Ongoing studies are underway to localize the 8-oxoG lesions and investigate other forms of DNA damage. The protection by Brcal1 against embryonic ROS suggests a novel role for Brcal1, and has implications for drug exposure during pregnancy. [Support: Canadian Institutes of Health Research]

**PS 1000 Validation of a ToxCast Predictive Signature for Vascular Disruption in a Complex Angiogenesis Assay.**

N. Kleinstreuer<sup>1</sup>, R. Sarkanen<sup>2</sup>, T. Heinonen<sup>2</sup> and T. B. Knudsen<sup>1</sup>. *<sup>1</sup>NCCT, US EPA, Research Triangle Park, NC; <sup>2</sup>FICAM, Tampere, Finland.*

Analysis of the ToxCastDB Phase-I dataset revealed a strong in vitro signature for vascular disruption and developmental toxicity (>90% correlation) based on multiple angiogenic growth factors, chemokines, and receptors. Computer simulation with a multicellular agent-based model (ABM) predicted phenotypic effects on the structural integrity and complexity of a developing endothelial network.

Embryonic vascular development can be disrupted by diverse compounds (thalidomide, estrogens, endothelins, dioxin, retinoids, cigarette smoke, metals). Collaborative studies are underway to test these predictions across an array of assays (whole embryo culture, aortic explants, endothelial tubulogenesis, transgenic zebrafish, etc.). Here, we describe initial results with a complex human-cell based in vitro angiogenesis assay, on the first 7 of 20 ToxCast Phase I chemicals selected by a range of predicted activity as vascular disruptors (pVDCs). Degree of endothelial tubule formation in vitro was scored by AC50 values relative to cytotoxicity. Both chemicals predicted as non-pVDCs, imazamox and pymetrozine, showed no inhibitory activity. The predicted inhibitory potential of 5 pVDCs was confirmed for 4 out of 5 chemicals. Pyridaben, predicted as a strong pVDC, inhibited tubule formation in a concentration-dependent manner in the FICAM assay, first evident at 0.001  $\mu$ M and complete at 0.01  $\mu$ M. Other predicted pVDCs with different ToxCast activity profiles (BPA, oxytetracycline, fluazinam) inhibited endothelial tubulogenesis at concentrations ranging from 5- to 500  $\mu$ M. PFOS was the one inactive pVDC tested; however, the ToxCast prediction was based on inhibition of Ang1/Tie2 signaling that controls later stages of vessel stabilization – a subtle outcome in the ABM simulation. Overall, concordance between the tubulogenesis assay and computer ABM simulation demonstrates the utility of these in vitro and in silico models for predictive modeling and mechanistic understanding of vascular disruption in higher-order biological tissues. [This work does not reflect EPA policy].

### PS 1001 A Metabolite-Based Biomarker Approach to Predict Developmental Toxicity Using Human Embryonic Stem Cells.

A. M. Smith, J. A. Palmer, P. R. West, K. R. Conard, L. A. Egnash, M. E. Ross, B. R. Fontaine, P. Bais, E. L. Donley and R. E. Burrier. *Stemina Biomarker Discovery, Inc., Madison, WI*. Sponsor: L. Recio.

Birth defects are the largest cause of infant morbidity and mortality in the United States. Teratogens, defined as substances that cause fetal abnormalities during development, are responsible for 5-10% of all birth defects. The application of more predictive developmental toxicity screens would reduce the prevalence of birth defects and increase pharmaceutical and chemical safety. Human embryonic stem cell (hESC) technology provides an innovative and robust alternative in vitro model system to predict developmental toxicity of chemicals. We have developed a targeted, rapid and highly predictive assay based on specific biomarker metabolites identified after analysis of metabolomics data obtained from hESCs exposed to 23 known human teratogens and non-teratogens. The new model predicts the concentration at which hESCs respond to treatment indicating the potential teratogenicity based on treatment dose. We have tested this approach in over 60 compounds with varying degrees of toxicity in animal tests. hESCs were exposed to a 9-point dose curve of each compound. Spent media was collected and analyzed by high resolution LC/MS using a targeted metabolomics approach to determine the relative abundance of the biomarkers present in the model. We have built a database of the expected teratogenicity of the tested compounds in in vivo and in vitro tests. The results show excellent concordance with both human and animal teratogenicity data and compare well to other commonly used in vitro assays for developmental toxicity. This new targeted biomarker approach continues to utilize LC/MS analysis while allowing for an 8-fold increase in instrument throughput and simplified analysis. This biomarker based assay is an attractive new quantitative model providing faster turn around and lower cost, while retaining high predictivity for early assessment of the developmental toxicity potential across a broad range of chemicals at multiple treatment levels in an all human derived system.

### PS 1002 Metformin-Induced Folate Deficiency-Like Malformations in Cultured Rat Embryos: Potential for Novel Species Sensitivity.

C. Zhang<sup>1</sup>, J. Panzica-Kelly<sup>1</sup>, G. L. Gong<sup>2</sup> and K. Augustine<sup>1</sup>. <sup>1</sup>Bristol-Myers Squibb, Pennington, NJ; <sup>2</sup>Bristol-Myers Squibb Co., Princeton, NJ. Sponsor: L. Lehman-McKeeman.

Metformin has been used alone or in combination with other drugs, including those recently approved, for patients with Type II diabetes. Even though there has not been metformin associated teratogenic outcomes, about 7% of patients treated with metformin present subnormal vitamin B12 levels, suggesting the drug may attenuate folate metabolism. Some reports in rats indicated that metformin may have weak teratogenic properties resulting in a low incidence (~0.5-1%) of rare neural tube abnormalities, similar to those caused by folate deficiency. Mouse embryos cultured with metformin also presented delayed neural tube closure. Our objectives were to evaluate whether metformin causes adverse effects on neural tube development in rats (a standard test species for GLP teratology studies) using whole em-

bryo culture, and metabolomics to determine whether the compound disrupts folate processing. Neurulating rat embryos were exposed to metformin at concentrations observed in rats and humans. Embryos were evaluated for viability, growth, morphology, and metabolite profiles. Methotrexate was used as a positive control for adverse morphology and metabolomic profiles induced by disrupted folate signaling. Metformin caused concentration-related neural tube malformations and embryo lethality occurring at human clinical concentrations. Co-administered folic acid with metformin completely rescued the malformations as well as altered metabolites at rat concentrations and partially rescued the adverse effect at the sub-lethal human exposure concentration. Together, the studies suggested that rat neurulation may be sensitive to metformin, and the effects were related in part to folate signaling. Given the severity of neural tube findings at clinical concentrations that only caused recoverable anomalies in cultured mouse embryos and no reported effects in human pregnancy, the study suggests that the rat embryo may present novel species-sensitivity to metformin.

### PS 1003 Placental Transfer of <sup>125</sup>Iodinated Humanized Immunoglobulin G2Aa in the Sprague-Dawley Rat.

P. S. Coder<sup>1</sup>, J. A. Thomas<sup>1</sup>, D. B. Stedman<sup>2</sup> and C. J. Bowman<sup>2</sup>. <sup>1</sup>WIL Research, Ashland, OH; <sup>2</sup>Pfizer Inc, Groton, CT.

Biopharmaceuticals are a growing segment of the health care therapeutic arsenal and indications for these agents are rapidly expanding into patient populations that include women of child bearing potential. The fetus is typically not a target of these drug therapies, and thus effects on the developing conceptus are generally undesirable. While small molecules generally cross the placenta via passive diffusion throughout gestation, transfer of large molecules is limited and may be species dependent. Antibody-like biopharmaceuticals (Abs), that contain an Fc region, are unique and cross the placenta using active transport pathways normally reserved for maternal immunoglobulin G (IgG). Embryo/fetal, placental and maternal tissue concentrations of an Ab in Sprague Dawley rats were evaluated by 2 different biodistribution techniques following maternal injection of <sup>125</sup>Iodinated hIgG2Aa on different gestation days. Blood and tissue samples were collected for gamma counting or whole maternal carcasses were processed for quantitative whole body autoradiography. The results indicate the presence of maternally injected IgG in the conceptus as early as Gestation Day (GD) 11 and a >1000 fold increase in that amount by GD 21, with the overall tissue concentration generally remaining unchanged during gestation (within the same order of magnitude). In addition, fetal-maternal tissue concentration ratios remain stable during organogenesis with only a slight increase at the end of gestation. These data indicate that Abs with a target present in the developing conceptus have the potential to elicit an unintended biological response depending on the Ab affinity and potency. These data also demonstrate that maternally-administered Abs may be present during organogenesis and have the potential for adverse developmental outcomes in the rat based on direct embryo/fetal exposure.

### PS 1004 Evidence That Perfluorooctanoic Acid (PFOA) Does Not Activate Estrogen Receptor (ER) Activities In Vivo or In Vitro.

P. Yao<sup>1</sup>, D. J. Ehresman<sup>2</sup>, J. M. Caverly-Rae<sup>3</sup>, S. Chang<sup>2</sup>, S. R. Frame<sup>3</sup>, J. L. Butenhoff<sup>2</sup>, G. L. Kennedy<sup>3</sup> and J. M. Peters<sup>1</sup>. <sup>1</sup>The Pennsylvania State University, University Park, PA; <sup>2</sup>3M Company, St. Paul, MN; <sup>3</sup>Haskell Global Centers for Health and Environmental Sciences, Newark, DE.

We evaluated the potential of perfluorooctanoate to produce estrogenic activity in both an in vivo uterotrophic assay and an in vitro estrogen receptor (ER) activation assay. In the in vivo study, pre-pubertal female CD-1 mice born to dams fed an estrogen-free diet from PND 14 through weaning on postnatal day (PND 18) were given daily oral doses of 0, 0.005, 0.01, 0.02, 0.05, 0.1 or 1 mg/kg PFOA on PND 18-20. In addition, a positive control received daily 17 $\beta$ -estradiol (E2, 0.5 mg/kg). On PND 21, the uterus and vagina were weighed and prepared for histology. Transcripts concentrations for the ER responsive genes pS2, progesterone receptor (PR), and trefoil factor (TFF) were quantitated in the uterus (quantitative RT-PCR). Serum PFOA concentrations were determined by LC-MS/MS. PFOA caused no changes in body weights, uterine weights, transcripts for ER target genes, or in squamous hyperplasia and cornification of the vaginal epithelium. E2 administration produced increased relative uterine weight, increases in transcript concentrations for ER-responsive genes, and squamous hyperplasia and cornification of the vaginal epithelium. Mean serum PFOA ranged from 5 to 1200 ng/mL. In the in vitro study, PFOA at 0, 0.0005, 0.001, 0.005, 0.01, 0.05, 0.1, 0.5, 1, 5 or 10  $\mu$ g/ml in media failed to affect estrogen response element activity in a human ovarian carcinoma cell line (BG1-Luc4E2) that carried an estrogen response element (ERE)-luciferase reporter construct; whereas, E2 exhibited a marked increase. Collectively, these data do not support an estrogenic effect of PFOA either in vivo or in vitro.

**PS 1005 Effects of Di(2-Ethylhexyl)-Phthalate Exposure during the Peripubertal Period: An Analysis of the Evidence.**

A. D. Kraft, D. Segal and S. Makris. *National Center for Environmental Assessment, US EPA, Washington DC.*

Di(2-ethylhexyl)phthalate (DEHP) is a widely-used plasticizer and ubiquitous environmental contaminant. DEHP exposure during late gestation in rodents has been shown to cause a spectrum of adverse effects related to altered androgen function, collectively termed the "phthalate syndrome". Thus, many studies on DEHP have focused on exposures during this critical period of organ development and outcome measures in male offspring. A more limited database exists for other endpoints or following exposures that do not encompass fetal development. One such exposure paradigm involves DEHP treatment in young adult animals during the period of sexual maturation. Several of these peripubertal exposure studies suggest that the observed responses differ from those manifested following gestational DEHP exposure. In an effort to evaluate the consistency of these observations, data were collected from studies analyzing the effects of DEHP on adolescent humans or animals exposed during the peripubertal period. This evidence was cumulated by endpoint, the specific timing of DEHP exposure, and the age that the outcome was assessed. The observations were then compared to evidence from exposures during fetal development. The human evidence was difficult to interpret, as exposure timing could not be ascertained. Based on the animal data, several outcomes, including male reproductive system toxicity, showed evidence of differential effects following peripubertal exposure. Mechanisms that may explain these differences, such as proposed effects on postnatal androgen biosynthesis, were considered in light of biological plausibility to inform the interpretation of these data. Overall, our analysis suggests that the peripubertal period may be a stage of development sensitive to DEHP exposure; however, more comprehensive studies are needed to determine the impact of DEHP exposure on sexually immature adolescents. Disclaimer: The views expressed are those of the author and they do not represent U.S. EPA policy or guidance.

**PS 1006 Diet Acclimation of NZW Rabbits for Use in Embryo-Fetal Development Studies.**

K. Robinson<sup>1</sup>, A. I. Martin<sup>1</sup>, M. Freke<sup>1</sup>, I. Primakova<sup>1</sup>, R. Perras<sup>2</sup>, E. Lewis<sup>3</sup> and A. M. Hoberman<sup>3</sup>. <sup>1</sup>*Reproductive & Juvenile Toxicology, Charles River, Montréal, QC, Canada;* <sup>2</sup>*Charles River, St. Constant, QC, Canada;* <sup>3</sup>*Charles River, Horsham, PA.*

Poor food intake in pregnant rabbits can lead to adverse outcomes including abortion. Initial validation studies with a line of New Zealand White (NZW) rabbits, showed a high incidence of inappetence and adverse pregnancy outcomes. Several studies were conducted to optimize diet acclimation procedures at the breeding facility to match the certified diet used at the Testing Facility. Once the diet acclimation procedure was optimized, a study was conducted that met the ICH guideline for evaluation of embryo-fetal development (EFD). Naturally bred adult female NZW (CrI:KBL[NZW]) rabbits were received from Charles River, Canada on Day 0 or 1 postcoitum (pc). For the premating diet acclimation the does were fed increasing percentages of an irradiated version of PMI 5322 for 10 days before being given this diet alone at 150 or 180g/day for a further 10 days. The animals were fed 180g/day of PMI 5322 during the study. The does (22/group) were dosed with standard vehicles from Days 7 to 19 pc by oral gavage, intravenous injection, or inhalation; in addition there was a room control. Food consumption was measured daily and body weights were collected twice weekly. Clinical observations and any signs of abortion or premature delivery were recorded twice daily. Terminal examinations on Day 29 pc included a necropsy, corpora lutea counts and evaluation of the uterine contents. Live fetuses were weighed and examined for external, visceral and skeletal abnormalities. The does showed a high pregnancy rate and a low abortion rate. The occurrence of periods of inappetence during gestation was negligible. Ovarian, uterine and fetal parameters were comparable to other lines of NZW rabbits, but with slightly higher litter sizes and consequently slightly lower fetal weights noted. In conclusion, the diet acclimation procedure decreased the inappetence that was seen in previous rabbit reproductive toxicology studies and this line of NZW rabbit is considered suitable for use on EFD studies.

**PS 1007 Epigenetic and Physiologic Effects of Perinatal Lead Exposure.**

A. K. Barks, C. Faulk, J. Goodrich, O. S. Anderson, K. E. Peterson and D. Dolinoy. *Environmental Health Sciences, University of Michigan School of Public Health, Ann Arbor, MI.*

Epidemiological and animal data suggest that development of chronic conditions such as obesity in adulthood is influenced by early life exposures. A proposed mechanism for this link is epigenetic modification. This study investigates effects of perinatal

lead (Pb) exposure on DNA methylation and alterations in physiologic parameters, including body composition and spontaneous activity. Using the viable yellow agouti (Avy) mouse, perinatal Pb exposure was modeled by a/a maternal exposure via drinking water supplemented with 0 ppm (control), 3.7 ppm (low), 27 ppm (medium), and 55 ppm (high) Pb two weeks prior to mating with an Avy/a male. Pb exposure continued through gestation and lactation. Epigenetic effects were evaluated by scoring coat color of Avy/a offspring (N=172), and physiologic parameters were evaluated in 3 month old wildtype a/a offspring (N=72) at the University of Michigan Nutrition and Obesity Research Center (MNORC). A statistically significant shift towards yellow coat color, indicative of DNA hypomethylation at the Avy allele, was observed in high dose Avy/a offspring, compared to controls (p=0.01). In a/a offspring, body weight was increased in high dose females, compared to controls (p=0.04). Females had increased % body fat and decreased % lean body mass across all exposure groups, compared to controls (p<0.05). Males showed significant differences in medium (decreased % lean mass) and high (increased % fat mass) Pb doses, compared to controls (p<0.05). Spontaneous activity was significantly decreased in females, but not males, in medium and high doses, compared to controls (p<0.05). There were no significant differences in food intake. Thus, perinatal Pb exposure resulted in both epigenetic and physiologic responses. Activity and body weight effects were more pronounced in females. Future work includes quantitation of methylation at specific target genes and life-course analysis of physiologic parameters of a/a offspring at 6 and 9 months of age. Funding: P20 ES018171/RD83480001 and P30 DK08950.

**PS 1008 Embryotoxic Potential of Epoxiconazole In Vitro and In Vivo.**

B. Flick<sup>1</sup>, F. DiRenzo<sup>2</sup>, S. Schneider<sup>1</sup>, S. Stinchcombe<sup>1</sup>, E. Menegola<sup>2</sup> and B. van Ravenzwaay<sup>1</sup>. <sup>1</sup>*Experimental Toxicology and Ecology, BASF SE, Ludwigshafen am Rhein, Germany;* <sup>2</sup>*Department of Biology, University of Milan, Milan, Italy.*

Some triazoles cause CYP26 inhibition of all-trans retinoic acid (RA) metabolism during organogenesis known to cause cleft palate (CP), via a mode of action (MoA) where altered tissue RA concentrations disrupt neural crest cell (NCC) migration, impairing development of the branchial arches (BA). Since very high-dose epoxiconazole (EPX) treatment induces clear maternal toxicity, causing CPs, we examined whether these are also caused by this MoA.

Both whole embryo culture tests (WEC) and in vivo studies were performed where the development of the embryos was examined morphologically, NCCs were visualized using whole immunostaining (WIS) for cellular retinoic acid binding protein, and embryonic tissue levels of EPX were analyzed with UPLC.

In WEC, embryos were exposed to 0, 1, 3, 10, 20, 30 mg/l for 48 hours starting at gestation day (GD) 9.5. EPX caused alterations in BA in 30% of the embryos at the LOAEC (3 mg/l) and dysmorphogenesis in 92% of embryos at 30 mg/l (embryonic tissue conc. = 8 mg/l). Embryos exposed to at least 10 mg/l exhibited an abnormal NCC distribution in the craniofacial region.

In the in vivo study, embryos were harvested on GD 11 from dams gavaged since GD6 with 0, 50, 100, and 180 mg/kg bw/d (the maximal tolerated dose which also causes CP). EPX caused maternal toxicity at 100 and 180 mg/kg; however, these embryos (embryonic tissue conc. = 6.4 mg/l) developed similarly to controls. No treatment-related increase in dysmorphogenesis, no alterations of BA, and no disturbance of NCC distribution were found.

The observed dysmorphogenesis of BAs and the impaired migration of the NCCs in the in vitro study supports the thesis that EPX alters CYP26-mediated RA metabolism, causing CP. But, despite comparable embryonic tissue levels in the in vivo study, neither the morphology nor the NCCs distribution was affected by EPX. These data do not support the theory that EPX-induced cleft palate in vivo is caused by alterations in RA metabolism.

**PS 1009 Perfluorooctanoic Acid-Induced Cytotoxicity in Primary Cardiomyocyte Culture.**

Q. Jiang and J. DeWitt. *Department of Pharmacology and Toxicology, East Carolina University, Greenville, NC.*

Perfluorooctanoic acid (PFOA) is a perfluorinated compound (PFC) that is widely used as a polymerization aid in the production of fluoropolymers. PFOA is environmentally persistent and is now detected ubiquitously in biota. Numerous studies have shown that PFOA can induce developmental toxicity in laboratory animal models. Epidemiological studies have demonstrated that PFOA exposure is associated with increased cholesterol levels and cardiovascular disease risk. We have previously reported that PFOA induces developmental cardiotoxicity in chicken embryos and hatchlings. To investigate the mechanism, we developed primary

cardiomyocyte cultures from D10 chicken embryo hearts and evaluated cell viability and reactive oxygen species (ROS) generation after in vitro PFOA exposure. Primary cardiomyocytes were treated with vehicle (0.1% DMSO in medium) or 0.1, 1, 10, 50, 75 or 100 µg/ml of PFOA for 1h or 36h. No statistical differences were detected between untreated and vehicle-treated groups. Viability was decreased by 74.5% in cells treated with 100 µg/ml of PFOA relative to the vehicle group ( $n=4-6$ ,  $P<0.05$ ) at the 1h time point. At the 36h time point, viability was statistically decreased at 10, 50, 75 and 100µg/ml concentrations, relative to the vehicle group (18.1%, 18.7%, 34.6% and 70.0%, respectively;  $n=4-6$ ,  $P<0.05$ ). At the 1h time point, an increase in ROS generation was observed at all doses; however, only 50 µg/ml of PFOA statistically increased ROS generation relative to the vehicle group (316.8%;  $n=3$ ,  $P<0.05$ ). Our results indicate that direct PFOA exposure to primary cardiomyocytes can induce cytotoxicity and ROS generation. Although additional studies are necessary to verify this effect in vivo, induction of cell death and generation of ROS may partially contribute to developmental cardiotoxicity associated with in ovo PFOA exposure in an avian model.

## PS 1010 Estradiol Modulates Paraoxonase-2 Expression in Mouse Brain.

G. Giordano<sup>1</sup>, C. E. Furlong<sup>2</sup>, T. B. Cole<sup>2</sup> and L. G. Costa<sup>1,3</sup>. <sup>1</sup>Department Environmental Occupational Health Sciences, University of Washington, Seattle, WA; <sup>2</sup>Division of Medical Genetics and Department of Genome Sciences, University of Washington, Seattle, WA; <sup>3</sup>Department of Neuroscience, University of Parma, Parma, Italy.

Paraoxonase 2 (PON2), a member of the PON gene family, is expressed in mouse brain; levels are highest in dopaminergic areas (e.g. striatum), and are higher in astrocytes than in neurons or microglia. As in other tissues, PON2 exerts a potent antioxidant effect in the CNS, and protects mouse neurons and astrocytes against oxidative stress. In all mouse tissues, including the brain, PON2 levels are higher in female than in male mice. In primary striatal astrocytes and neurons PON2 protein level in females is 2-3-fold higher than in males. Levels of PON2 mRNA and lactonase activity show similar gender differences. Male astrocytes and neurons are more sensitive (by 3-4-fold) than female cells to oxidative stress-induced toxicity, though GSH levels do not differ between cells isolated from the two genders. In contrast, no significant gender difference in susceptibility is seen in cells from PON2<sup>-/-</sup> mice, suggesting that PON2 is a major determinant of gender differences in susceptibility to oxidative stress-mediated neurotoxicity. Estradiol induces a time- and concentration-dependent increase in the levels of PON2 protein and mRNA in male (4.5-fold), and also in female (1.8-fold), astrocytes. Such effect is due to activation of estrogen receptors alpha. In ovariectomized mice serum estradiol levels are decreased to male levels; PON2 protein and mRNA are also decreased to male levels in brain areas and in liver. Neuroprotection by estradiol against oxidative stress-induced neurotoxicity is seen only in astrocytes from wild type mice, but not in cells from PON2<sup>-/-</sup> mice, suggesting again that PON2 represent a major, gender-dependent, factor in protective CNS cells against neurotoxins. The lower expression of PON2 in males may have broad ramifications with regard to susceptibility to diseases involving oxidative stress, including neurodegenerative diseases (Supp. in part by ES04696).

## PS 1011 Suppression of H19 Methylation in Mouse Exposed to Chlorpyrifos Methyl during Organogenesis Period.

H. Shin<sup>1</sup>, J. Seo<sup>1</sup>, S. Jeong<sup>2</sup>, S. Park<sup>1</sup>, Y. Park<sup>1</sup>, S. Son<sup>1</sup> and H. Kang<sup>1</sup>. <sup>1</sup>Toxicology & Residue Chemistry Division, QIA, Anyang, Republic of Korea; <sup>2</sup>GLP Research Center, Hoseo University, Asan, Republic of Korea.

Chlorpyrifos-methyl (CPM) is widely used organophosphorus insecticide. In Korea, more than sixty-five tons per year are used in agriculture. In our previous study, CPM showed anti-androgenic endocrine disruption activity. Lots of EDC shows the alteration of methylation in imprinting gene, which inherit to next generation. This study was performed to examine the effect of CPM on the H19 methylation in mouse.

After mating CAST/Ei (♂) and B6 (♀), CPM was administered at dose of 4 (CPM4), 20 (CPM20) and 100 (CPM100) mg/kg bw/day from embryonic day (ED) 7 to ED 17. Anogenital distance (AGD) was measured at post natal day (PND) 21. Clinical signs, body weights, feed and water consumption, organs weights, serum hormone values and H19 methylation level of organ and sperm were measured at PND63.

Body weights were significantly ( $p$  value  $<0.0.1$ ) lower than control until PND 6. AGD was significantly ( $p$  value  $<0.0.1$ ) decreased at CPM100 group in male and increased at CPM20 group in female. The weight of thymus and epididymis were

significantly ( $p$  value  $<0.0.1$ ) increased at all of CPM treatment in male. In CPM20 group, liver, kidney, heart, lung, spleen, prostate gland and testes were significantly increased. Testosterone level in serum was significantly ( $p$  value  $<0.0.1$ ) increased by CPM treatment in both male and female. H19 methylation level of liver and thymus showed decreased pattern by dose-dependent manner in male. The levels of H19 methylation in sperm were  $73.76\pm7.16\%$ (CTL),  $57.84\pm12.94\%$ (CPM4),  $64.24\pm3.79\%$ (CPM20) and  $64.24\pm3.79\%$ (CPM100).

CPM can disturb the early development of offspring development and disrupt H19 methylation in organ and sperm. Those altered methylation pattern may pass down to next generation through sperm.

## PS 1012 In Utero Growth Restriction and Dibutyl Phthalate Exposure May Cooperatively Disrupt Steroidogenesis.

J. Pike<sup>1</sup>, E. McDowell<sup>2</sup>, A. Kisilewski<sup>2</sup> and K. Johnson<sup>2</sup>. <sup>1</sup>Biological Sciences, University of Delaware, Wilmington, DE; <sup>2</sup>AI Dupont Hospital for Children, Wilmington, DE.

Masculinization of the male reproductive tract occurs in human gestational weeks 10-22, and rat gestational days 16-21. Fetal testes produce a surge of testosterone causing reproductive masculinization. Disruption leads to reproductive abnormalities including cryptorchidism and hypospadias. In humans, in utero growth restriction (IUGR) is a risk factor for cryptorchidism and hypospadias. Rat work shows that fetal steroidogenesis is disrupted by exposure to the anti-androgen dibutyl phthalate (DBP). While these fetal circumstances increase the prevalence of the same birth defects individually, we examined a possible cooperative effect of these treatments on steroidogenesis. A maternal under-nutrition model was examined in the rat. Pregnant Wistar rats were restricted to 50% ( $n=9$ ) of the food eaten by ad libitum controls ( $n=8$ ) beginning on gestational day (GD) 3. Restriction through GD17 caused a significant decrease in pup weight with no decrease in litter size. Fetal testes showed decreased testosterone production (40%) by radioimmunoassay. mRNA levels of steroidogenic genes including Scarb1 and Star were significantly decreased in the fetal testis after growth restriction. Food restriction ( $n=11$ ) from GD3-18 caused no malformations at postnatal days 1, 14, or 28 as compared to controls ( $n=10$ ). A coexposure study of IUGR and maternal dosing with the anti-androgen DBP was performed examining a cooperative effect on steroidogenesis. Analysis of fetal testes (GD17) following 50% food restriction from GD3-17 ( $n=11$ ) or exposure to DBP (250mg/kg/day) from GD15-17 ( $n=7$ ) showed a significant decrease in the expression of the steroidogenic genes Cyp11a1, Cyp17a1, Scarb1, and Star as compared to controls ( $n=7$ ). When 50% restriction was coupled with DBP exposure ( $n=10$ ), further decreased steroidogenic gene expression. While IUGR and DBP lead to a decrease in steroidogenesis separately, they also appear to work cooperatively to cause further disruption.

## PS 1013 A Comparison of Social Housing Opportunities during Developmental Toxicity Evaluation in Cynomolgus Monkeys.

S. M. Henwood<sup>1</sup>, C. Luetjens<sup>2</sup>, A. Fuchs<sup>2</sup> and G. F. Weinbauer<sup>2</sup>. <sup>1</sup>Nonclinical Safety Assessment, Covance Laboratories Inc., Madison, WI; <sup>2</sup>Nonclinical Safety Assessment, Covance Laboratories GmbH, Munster, Germany.

The demand for developmental toxicity studies in nonhuman primates (NHPs) has increased, mainly driven by biopharmaceutical drug development. Social housing of NHPs has become mandatory in many countries and this poses a specific challenge since NHPs with timed pregnancies cannot be obtained commercially. The cynomolgus fertility rate in a mating programme is typically 35-45% per mating cycle and 60% per female animal upon repeated mating trials. Hence, social housing of pregnant cynomolgus monkeys requires special approaches until a cage is populated by animals with confirmed pregnancy. Formation of new groups of sexually mature female cynomolgus monkeys has pronounced effects on ovarian cyclicity to the extent that some animals exhibit transient amenorrhea. Concern has been raised that social housing of pregnant animals might interfere with maintenance of gestation due to rank order fights, incompatibility, and other group-related adverse effects. On the other hand, in a social setting, animals experience birth events and handling of neonates by watching cage mates, and infants have cage mates of comparable ages to interact with. In the present work, qualitative assessment in more than 200 hundred pregnant control animals under social housing indicated good compatibility with little aggression toward each other. Interestingly, a reduction of pre- and postnatal loss by 25-30% was encountered under social housing when compared to single housing. Conceivably, the delivery process and managing the newborn was facilitated by social maternal housing. Moreover, maternal and infant body weight gains were significantly increased under social housing

compared to single housing. In conclusion, social housing is feasible for developmental toxicity studies in NHPs and provides distinct advantages over single housing and is, therefore, recommended for the conduct of NHP developmental toxicity studies and is now the default at Covance Laboratories.

#### **PS 1014 Feasibility of Mouse Continuous Intravenous Infusion for Fertility and Embryo-Fetal Development Studies.**

R. S. Bartlett and H. van Wijk. *Covance Laboratories Ltd., Harrogate, United Kingdom.* Sponsor: S. Kirk.

The rat and rabbit are routinely used in pre-clinical reproductive and developmental toxicity (DART) studies. However, where the rat and/or rabbit are not suitable, the mouse is an alternative model.

A model of continuous intravenous infusion using a surgically-implanted femoral vein catheter with tail cuff exteriorisation has been previously developed in the mouse. The reliability of this method decreased over time, with a success rate of only 74% after 28 days because of tail cuff constraints due to animal growth.

This study aimed to (1) determine whether a larger diameter tail cuff (6 mm) could extend the continuous infusion duration, and (2) determine the feasibility of evaluating DART parameters in mice using this surgical model in a combined fertility and embryo-foetal development study.

33 CD-1 female mice (approximately 7-9 weeks old) were surgically implanted with a femoral vein catheter exteriorised with a 6 mm tail cuff. After 6 days of recovery, they were intravenously administered 0.9% sodium chloride, by continuous infusion (4 mL/kg/hr) for 2 weeks prior to pairing, during pairing (with uncatheterised males) and through Gestation Day (GD) 18 (42 days). On GD18, females were killed and uterine contents examined.

Technical failure occurred in 9 females; this was attributed to the larger diameter of the tail cuff, which slipped down and allowed the catheter to be chewed. Of the 24 female mice remaining on study at the end of pairing, 23 (96%) were successfully mated and 22 (96%) were confirmed pregnant. Catheter failures or poor tail conditions resulted in early removal of 5 additional mice. However, those surviving to necropsy, uterine and foetal data were within background ranges, indicating no effects on reproductive or developmental parameters.

It is concluded that continuous intravenous infusion via this surgical model is a viable method of dosing mice in DART studies. The larger tail cuff did not increase reliability of the infusion technique for a period greater than 28 days, therefore separate fertility and embryo foetal development studies are recommended for mice.

#### **PS 1015 Addressing the Mode of Action for Developmental PFOA-Induced Mammary Gland Delays.**

M. B. Macon<sup>1,2</sup> and S. E. Fenton<sup>2</sup>. <sup>1</sup>*Curriculum in Toxicology, University of North Carolina, Durham, NC;* <sup>2</sup>*NTP Labs, NIEHS, NIH, Research Triangle Park, NC.*

Perfluorooctanoic acid (PFOA) exposure alters mammary gland (MG) development and function in mice. The mode of action (MOA) for these effects has not been elucidated, although activation of peroxisome proliferator activated receptor alpha (PPAR $\alpha$ ) has been implicated. To begin elucidation of a MOA, time pregnant CD-1 mice were gavaged with 0.0, 0.01, 0.1, or 1.0 mg PFOA/kg body weight on gestation days (GD) 10-17. Female offspring MGs were removed and prepared for RNA on multiple postnatal days (PND). A comparison of MG RNA from control and 1.0 mg/kg groups with Affymetrix 420.2 microarrays found differential regulation of 710 and 41 genes at PND 7 and 14, respectively. Adiponectin, estrogen receptor alpha, and WNT expression were reduced in PFOA-treated glands. PPAR $\alpha$  expression was not changed. These data were validated by PCR of MG RNA, using TBP as a reference gene. At PND 7, PFOA induced differential regulation of several genes compared to controls, even at 0.01 mg/kg. When considering developmental scores, glands with higher scores or more normal growth had increased RNA expression of WIF1, ESR1 and PGR at PND 21 and FABP3 and UCP1 at PND 56. PND 56 MG sections stained for PPAR $\alpha$  protein displayed robust expression in all glands regardless of treatment, yet there was higher expression in stromal tissues surrounding ducts in PFOA exposed mice compared to controls. Collectively, these findings suggest that PPAR pathway genes are altered in conjunction with PFOA-induced MG changes along with other pathways. Observed altered genes are involved in signaling of all PPAR isoforms including  $\alpha$ ,  $\beta/\delta$ , and  $\gamma$ . Both up and down regulation of these genes were found which suggests that multiple PPAR isoforms may work together to regulate PFOA-induced MG aberrations. In addition, prenatal PFOA exposure at 0.01 mg/kg leads to mammary gene changes at human-relevant levels. Future investigations will examine related gene pathways and protein levels compared to observed morphological and hormone outcomes. This abstract does not necessarily reflect NIEHS policy.

#### **PS 1016 Evaluation of Reproductive and Developmental Toxicity of Multiwall Carbon Nanotubes in Pregnant Mice After Intratracheal Instillation.**

N. Kobayashi<sup>1</sup>, M. Kawabe<sup>2</sup>, H. Nakashima<sup>2</sup>, T. Numano<sup>2,3</sup>, R. Kubota<sup>1</sup>, N. Sugimoto<sup>1</sup> and A. Hirose<sup>1</sup>. <sup>1</sup>*National Institute of Health Sciences, Setagaya, Japan;* <sup>2</sup>*DIMS Institute of Medical Science Inc., Ichinomiya, Japan;* <sup>3</sup>*Department of Molecular Toxicology, Nagoya City University Graduate School of Medical Sciences, Nagoya, Japan.*

Some studies have reported that maternal exposure to nanoparticles may induce teratogenicity or transfer to their fetuses and affect the development and function of the central nervous systems. In order to evaluate the reproductive and developmental toxicity of multi-wall carbon nanotubes (MWCNTs) via inhalation exposure, we conducted intratracheal instillation study of MWCNTs dispersed in two different media (blood serum obtained from female mice and 2% of sodium carboxymethyl cellulose (CMC-Na) solution) in pregnant mice. MWCNTs (MWNT-7) dispersions were prepared by ultrasonication using an ultrasonic bath for 30 min. The above MWCNT dispersions were administered to pregnant Crlj:CD1(ICR) mice with gestation day 9 at dosage of 0, 3.0, and 5.0 mg/kg bw. Five mice per group were evaluated. The mice were dissected at 18 days of gestation period. MWCNT depositions in the tissues and the effect to embryos and fetuses were evaluated. The MWCNTs were deposited in the lungs as the black spots. No statistically significant difference between the control group and MWCNT-exposed groups in the number of corpora lutea, implantations, dead fetuses (early or late resorption site), live fetuses, and sex ratio. However, body weight of fetuses and placental weights were dose-dependently decreased in the both MWCNT-exposed groups. Furthermore, external malformations (i.e., oligodactyly, extensive contracture, cleft lip) were observed in the 3 mg/kg of CMC-Na treated MWCNT-exposed group and 5 mg/kg of blood serum treated MWCNT-exposed groups. Further information is needed to clarify the potential for the reproductive and developmental toxicity of MWCNTs.

#### **PS 1017 Histology of Selected Organs from the Göttingen Minipig Fetus from Days 60 (Midterm) and 110 (Term) of Gestation.**

M. Perron Lepage, J. Briffaux, C. Thuilliez, E. Marsden and M. Leroy. *Ricerca Biosciences SAS, St. Germain sur l'Arbresle, France.*

In a previous study, we demonstrated that chemically induced fetal abnormalities could be detected in the Göttingen Minipig shortly after mid term. At this time, it is possible to sex the minipig fetus by observation of the external genital area, although at gross soft tissue examination, the location, size and shape of the male and female gonads are similar at this stage. The aims of the present study were to compare the histological features of selected organs in the Göttingen Minipig fetus at GD 60 and GD 110 and to validate histologically the method of sexing the fetuses by macroscopic observation of the external genital area.

Four 7- to 13-month-old virgin Göttingen Minipig females were mated. Caesarean sections were performed on two females at mid term (GD 60) and on two others at term (GD110). The fetuses were weighed, sexed and submitted to standard gross external and visceral examinations. Selected organs (adrenal glands, heart, kidneys, liver, lungs, ovaries, thymus, thyroid gland, urinary bladder, uterus, vagina, epididymides and testes) were sampled and fixed in 10% formalin or modified Davidson's fluid. Five male and 5 female fetuses obtained at GD 60, and 2 male and 6 female fetuses obtained at GD110 were available for histological examination. The microscopic appearances and the differences between the two timepoints were described for each organ.

The histological appearance of the organs at GD110 was similar to that of juvenile minipigs. At GD 60, however, although all organs were identifiable, maturation and growth were obviously still incomplete.

This study reported the histology of selected organs in minipig fetuses at GD 60 and GD 110. At GD 60, there was complete concordance in establishing the sex of each fetus by microscopic examination and evaluation of the external genitalia.

#### **PS 1018 Mono-Ethylhexyl Phthalate (MEHP) Exposure Reduces Embryonic Nutrition and Induces Structural Defects in Mouse Whole Embryo Culture.**

K. E. Sant and C. Harris. *Environmental Health Sciences, University of Michigan, Ann Arbor, MI.*

Di-2-ethylhexyl phthalate (DEHP) is a highly lipophilic endocrine disruptor and is the most abundant phthalate plasticizer in the environment. Exposure to DEHP and its primary active metabolite, mono-ethylhexyl phthalate (MEHP), have been associated with several adverse health effects, ranging from obesity to reproductive

dysfunction. The objective of this study was to determine whether MEHP can induce structural defects during embryonic development in vitro in whole embryo culture (WEC) and to assess whether decreased embryonic nutrition contributes to these defects. Gestational day (GD) 8 CD-1 mouse conceptuses were explanted into WEC. MEHP or DEHP at concentrations ranging from 100-1000 µg/ml were added directly to the culture media and conceptuses were exposed for 26 hours before complete morphological scoring and collection of visceral yolk sac (VYS) and embryo (EMB) tissues on GD 9. MEHP treatment significantly reduced total morphological scores at all doses, reaching a maximal decrease of 67% ( $p < 0.03$ ), while DEHP failed to produce any significant decreases in total morphology score. Morphological comparison of neural tube-specific endpoints revealed that MEHP produced a significant increase in incomplete neural tube closure ( $p < 0.001$ ). Clearance of FITC-albumin by the VYS was assessed after 3 h exposure to 100 or 250 µg/ml MEHP on GD 9 as a measure of histiotrophic nutritional activity. Treatment significantly reduced total clearance in a dose-dependent manner ( $p < 0.008$ ) by 29% and 43% for 100 and 250 µg/ml treatment, respectively. This work demonstrates that MEHP treatment reduces embryonic nutrition, limiting the substrates essential for normal metabolic activities, and induces structural defects, especially preventing closure of the neural tube.

**PS 1019 Development and Validation of an Analytical Method for Monobutylphthalate, a Metabolite of Di-n-Butylphthalate, in Harlan Sprague-Dawley Rat Plasma and Amniotic Fluid by UPLC-MS/MS.**

V. G. Robinson<sup>2</sup>, M. A. Silinski<sup>1</sup>, T. A. Freed<sup>1</sup>, R. A. Fernando<sup>1</sup>, C. S. Smith<sup>2</sup> and S. Waidyanatha<sup>2</sup>. <sup>1</sup>RTI International, Research Triangle Park, NC; <sup>2</sup>Division of National Toxicology Program, NIEHS, Research Triangle Park, NC. Sponsor: K. Levine.

Di-n-butyl phthalate (DBP) is a common plasticizer used in a variety of consumer products. Its major metabolite is its monoester. Exposure to DBP is widespread, and its potential toxicity has been, and continues to be, investigated. The objective of this work was to develop, validate, and apply a method to quantitate mono-n-butyl phthalate (MBP), the major metabolite of DBP, in rat plasma and amniotic fluid. Samples were extracted by spiking 25 µL of plasma or amniotic fluid with 25 µL of water, 25 µL of internal standard solution (MBP-d4 in water), and 425 µL of 0.1% formic acid in acetonitrile. After centrifugation, 5 µL of supernatant was injected onto an Acquity UPLC HSS T3 column, and separation was performed using gradient elution. MS/MS analysis was conducted using electrospray ionization in negative ion mode and multiple reaction monitoring. The method was successfully validated over the range 25-5000 ng/mL in plasma, with cross-validation for amniotic fluid. Validation parameters included linearity ( $r > 0.99$ ), recovery, selectivity, sensitivity (LOD = 6.9 ng/mL), precision (%RSD < 15%), accuracy (%RE < 15%), and stability (% of Day = 100 +/- < 20%). It was also demonstrated that samples as high as 516,000 ng/mL could be accurately and precisely diluted into the calibration range.

The method is being applied for the analysis of MBP in plasma and amniotic fluid samples from rats administered 0, 300, 1000, 3000, or 10,000 ppm DBP in feed.

**PS 1020 Developmental and Reproductive Studies in Sprague-Dawley Rats with Gevokizumab, a Novel Monoclonal Antibody Targeting IL-1 Beta.**

C. A. Gasper<sup>1</sup>, B. Thorsrud<sup>2</sup>, L. Cao<sup>1</sup>, J. Chen<sup>1</sup>, L. Wong<sup>1</sup>, K. Der<sup>1</sup>, J. Ma<sup>1</sup>, A. Ahene<sup>1</sup> and K. Meyer<sup>1</sup>. <sup>1</sup>Nonclinical Safety Evaluation, XOMA (US) LLC, Berkeley, CA; <sup>2</sup>Developmental & Reproductive Toxicology, MPI Research, Mattawan, MI.

Gevokizumab, also coded XOMA 052 or S78989, is a humanized IgG2 monoclonal antibody that binds with high affinity to human interleukin-1 (IL-1) beta. Gevokizumab inhibits the activation of the IL-1 receptor, thereby modulating the cellular signaling events producing inflammation. Currently, gevokizumab is in Phase 3 clinical trials for non-infectious uveitis and Behçet's uveitis and in Phase 2 proof-of-concept studies for moderate to severe acne and erosive osteoarthritis of the hand. Developmental and reproductive studies (embryo fetal, fertility, and pre/postnatal development) in Sprague Dawley rats evaluated the effects of gevokizumab when administered subcutaneously once weekly at 3, 30, and 90 mg/kg/dose. The rat (usual rodent model for evaluating developmental and reproductive toxicity) was selected due to similar binding affinity and in vitro functional activity between human and rat IL-1 beta. Standard ICH S5(R2) study designs were followed. Observations included clinical signs, body weight, food consumption, drug levels in serum and milk, anti-drug antibodies (ADA), maternal uterine and ovarian examinations, fetal evaluations, macroscopic pathology, reproductive

performance, parturition, lactation to weaning, and F1 physical growth and development. Gevokizumab did not produce any mortality or significant adverse effects. Measurement of gevokizumab in serum (maternal, fetal, neonate) and maternal milk confirmed adequate exposure during the dosing periods. ADAs were detected in a few dams, without neutralizing activities. The NOAEL for maternal and developmental toxicity including teratogenicity, general reproductive toxicity in male and female rats, and general toxicity in the dam, including developmental and reproductive toxicity in the F1 offspring was considered to be at least 90 mg/kg/dose, the highest dose level tested. No gevokizumab-related findings were observed in any of the reproductive and developmental studies.

**PS 1021 Weight of Evidence Considerations for Developmental Toxicity Classification of Boric Acid.**

W. Ball and M. Harrass. Rio Tinto Minerals, Greenwood Village, CO.

Although reproductive and developmental effects have been demonstrated in laboratory animals exposed to high doses of boric acid (BA), similar effects have not been observed in highly exposed human populations or workers. Workers in boron (B) mining/processing industries represent the maximum possible human exposure. A weight of evidence approach was used in evaluating numerous independent studies on the determination of the hazard of BA to humans. Information that was considered together included results of in vitro tests, animal data, worker exposure data, epidemiological studies and mechanistic data. Extensive evaluations of sperm parameters in highly exposed workers in Turkey and China demonstrated no effects on male fertility. No evidence of developmental effects in humans attributable to B has been observed in studies of populations with high exposures to B. Collectively the epidemiological studies consistently show an absence of effects in highly exposed populations. A comparison of blood, semen and target organ B levels in studies of lab animals and B workers shows B industry worker exposures are lower than untreated control rats. Recent studies provide evidence that BA may act by similar mechanisms in causing developmental effects in mice as sodium salicylate (natural deacetylated form of aspirin) including effects on Hox gene expression and inhibition of embryonic histone deacetylases. Although aspirin is known to cause developmental effects in laboratory animals, similar effects have not been seen in controlled human studies. Similar mechanisms of action of BA and aspirin and the absence of effects in humans ingesting aspirin suggest that BA related developmental effects in humans are unlikely. Also, there is evidence that Zinc (Zn) interacts with B in the body reducing the toxicity of B. Zn levels in soft tissue in humans are over 2 x greater than in lab animals explaining in part the absence of fertility and developmental effects in humans. Based on the total weight of evidence, the data show that it is improbable that BA will cause reproductive or developmental effects in humans.

**PS 1022 Embryonic DNA Repair and Ethanol-Initiated Behavioural Deficits in Oxoguanine Glycosylase 1 (OGG1) Knockout Mice: A Role for Oxidatively-Damaged DNA and Protection by a Free Radical Spin Trapping Agent.**

L. Miller<sup>1</sup>, D. J. Pinto<sup>1</sup> and P. G. Wells<sup>1,2</sup>. <sup>1</sup>Pharmacology and Toxicology, University of Toronto, Toronto, ON, Canada; <sup>2</sup>Pharmaceutical Sciences, University of Toronto, Toronto, ON, Canada.

A mother's consumption of alcohol (ethanol, EtOH) during pregnancy can cause a spectrum of structural, cognitive and behavioural problems in the developing child termed Fetal Alcohol Spectrum Disorders (FASD). Reactive oxygen species (ROS) have been implicated in the mechanism of behavioural teratogenicity, although the role of embryonic DNA damage and repair are unclear. To determine the latter, DNA repair-deficient heterozygous (+/-) oxoguanine glycosylase 1 (OGG1) knockout mice were mated, and pregnant dams were treated once on gestational day 17 with EtOH (2 g/kg i.p.) or its saline vehicle, with or without pretreatment with the free radical spin trapping agent alpha-phenyl-N-tert-butyl nitro (PBN) (40 mg/kg i.p.). Saline-exposed progeny exhibited an ogg1 gene dose-dependent learning deficit in the passive avoidance test compared to wild-type (WT) littermates, demonstrating for the first time a phenotype in OGG1-deficient mice. EtOH-exposed progeny exhibited an enhanced learning deficit compared to saline controls at 6 and 9 weeks of age, also in an ogg1 gene dose-dependent fashion. PBN pretreatment significantly protected both WT and KO progeny, although this protection for EtOH was slightly less effective in +/- and -/- KO progeny. These results provide the first evidence to date that ROS-initiated embryonic DNA oxidation is involved in EtOH-initiated behavioural deficits, and embryonic DNA repair status may be a determinant of teratological risk. (Support: Canadian Institutes of Health Research)

**PS 1023 Hyperactivity of Rat and Mouse Induced by Lactational Exposure to Hydroxylated PCB (OH-PCB106).**

N. Koibuchi, A. Haijima, R. Lesmana, I. Amano, Y. Takatsuru, T. Iwasaki and N. Shimokawa. *Department of Integrative Physiology, Gunma University Graduate School of Medicine, Maebashi, Japan.*

Polychlorinated biphenyls (PCBs) are persistent environmental pollutants that may cause adverse health effects. Previous in vitro studies including ours have shown that various PCB congeners affect neurodevelopment through different mechanisms. However, behavioral alterations induced by lactational exposure to PCB and its neurochemical mechanisms have not yet been fully studied. In the present study, hydroxylated-PCB 106 (OH-PCB 106; 4-hydroxy-2',3,3',4',5'-pentachlorobiphenyl) was administered to lactating rat and mouse dams via gavage every second day from day 3 to 13 after delivery. The exposure did not affect the body weight of the dams or the physical development of the newborn pups in both sexes. Male rats and mice exposed to OH-PCB 106 showed hyperactivity that was characterized by increased locomotor activity in open field and circadian period. OH-PCB 106-exposed rats displayed abnormally high levels of dopamine and D2 dopamine receptor (D2DR), but not D1DR and D5DR, in the striatum, an important center for the coordination of behavior. These findings indicate that OH-PCB 106 has a significant neurotoxic effect on rodent behavior, which may be associated with increased D2DR mediated signals.

**PS 1024 Di-isobutyl Phthalate (DIBP) Hazard Identification.**

S. Y. Euling<sup>1</sup>, K. Hogan<sup>1</sup>, G. Cooper<sup>1</sup>, C. Cai<sup>1</sup>, K. Y. Christensen<sup>1</sup>, M. Lorber<sup>1</sup>, X. Arzuaga<sup>1</sup>, C. Sheth<sup>1</sup>, A. F. Sasso<sup>1</sup>, M. Pratt<sup>1</sup>, A. K. Hotchkiss<sup>2</sup> and J. C. Lambert<sup>3</sup>. <sup>1</sup>NCEA, US EPA, Washington DC; <sup>2</sup>NCEA, US EPA, Research Triangle Park, NC; <sup>3</sup>NCEA, US EPA, Cincinnati, OH.

The hazard potential for DIBP is being evaluated as part of EPA's Integrated Risk Information System (IRIS) Toxicological Review. DIBP is a plasticizer that confers flexibility and durability in industrial and consumer products. The epidemiology and animal toxicology databases are both relatively small. The small DIBP epidemiological database includes studies that assessed the relationship between urinary concentrations of the DIBP metabolite mono-isobutyl phthalate (MIBP) and developmental, neurodevelopmental, immunological or breast cancer outcomes. There is limited support for associations between MIBP and inflammatory biomarker levels, and decreased masculine play behavior. The animal toxicological database includes studies that assessed male reproductive developmental endpoints that constitute the phthalate syndrome after in utero DIBP exposure. The largest developmental study, Saillenfait et al. (2008), reported changes in anogenital distance, male reproductive organ weights, and litter incidence of phthalate syndrome endpoints in the lower dose range after early gestational exposure. Other studies observed increased fetal mortality, male postnatal and adult growth decrements, decreased fetal testicular testosterone and changes in expression of genes involved in androgen production pathways. The developmental reproductive effects observed in animal studies are consistent with the reduced testicular testosterone mode of action that is well-characterized for developmentally toxic phthalates. Effects on liver and kidney weight and function in both male and female adults were also reported. Research needs include epidemiologic studies that examine DIBP exposure, testosterone and related outcomes throughout development as well as multigenerational reproductive toxicity studies and cancer bioassays. The views expressed are those of the authors and do not necessarily reflect the views or policies of the US EPA.

**PS 1025 Establishment of a Molecular Embryonic Stem Cell Developmental Toxicity Assay.**

J. Panzica-Kelly<sup>1</sup>, K. Brannen<sup>2</sup>, Y. Ma<sup>1</sup>, C. Zhang<sup>1</sup>, O. Flint<sup>1</sup>, L. D. Lehman-McKeeman<sup>1</sup> and K. Augustine<sup>1</sup>. <sup>1</sup>Discovery Toxicology, Bristol-Myers Squibb, Princeton, NJ; <sup>2</sup>Charles River, Horsham, PA.

Efforts to reduce animal use for embryotoxicity testing of chemicals lead to the development of the embryonic stem cell test (EST), a 10-day low-throughput assay. The objective of this study was to shorten the assay's duration and increase throughput by incorporating molecular endpoints to detect aberrant changes in embryonic stem cell differentiation. Monolayers of mouse D3 embryonic stem (ES) cells were used to identify IC50 values in a 3-day cytotoxicity assessment. ES D3 cells were grown for 4 days as embryoid bodies for transcriptional profiling of 12 developmentally regulated genes (nanog, fgf5, gsc, cd34, axin2, apln, chst7, lhx1, fgf8, sox17, foxa2, and cxcr4). Embryoid bodies were exposed to a single compound concentration selected from the cytotoxicity assessment (0.1x IC20). A decision-tree model to classify compounds for teratogenicity potential was built with IC50 and relative expression values of the target genes after exposure to 65 compounds

(33 teratogens, 32 non-teratogens) of known in vivo teratogenicity. Compounds with IC50 values <22 µM were classified as teratogens without the use of transcriptional profiling. Compounds with IC50 values between 22 and 200 µM were categorized as teratogenic if ≥8 genes were deregulated by 10%. Compounds with IC50 values greater than 200 µM were categorized as positive for teratogenic potential if all 12 genes were deregulated by 10%. For teratogenic predictions of unknowns, the concordance for teratogens is 76% (22 out of 29), and for non-teratogens is 69% (25 out of 36) with a total concordance of 72% (47 out of 65) with a false positive error rate of 24%. The model was further tested with 12 additional compounds (5 positive, 7 negative) in which 10 were identified correctly (83% concordance) with a 0% false positive error rate. Increased throughput in combination with its low false positive error rate makes this assay ideal for first tier hazard identification screening of pharmaceutical compounds.

**PS 1026 A Tiered Screening Platform for Optimizing Predictivity, Throughput and Cost Effectiveness of In Vitro Developmental Toxicity Assays.**

K. Augustine, C. X. Zhang and P. Julie. *Discovery Toxicology, Bristol-Myers Squibb, Pennington, NJ.* Sponsor: L. Lehman-McKeeman.

In recent years, various laboratories have focused on generation and/or refinement of in vitro developmental toxicology assays for classification of teratogenic liability of small molecules. The impetus for this effort is multifaceted including increasing animal rights pressure, REACH legislation of chemicals and need for proactive safety optimization of pharmaceutical compounds. In response to these needs, our laboratory has developed three in vitro developmental toxicology assays: a molecular embryonic stem cell assay (MESCA), a dechorinated zebrafish embryo culture (ZEC) assay and a streamlined rat whole embryo culture (rWEC) assay. Individually, all three assays have demonstrated good utility for screening compounds for teratogenic liability, achieving ~80% overall concordance and relatively balanced error rates. This study describes the results of evaluating a test set of ~60 compounds across the 3 assays and generation of a tiered testing strategy. The cross-assay assessment identified the assays' attributes and deficiencies. For instance, the MESCA and ZEC assays were found to have 2 limitations: compound solubility and high misclassification rates of compounds with H1 receptor or GABAergic activity. In contrast, solubility limitations were rarely encountered in the streamlined rWEC assay and it also presented <20% misclassification error rates of compounds with H1 and GABAergic activity. As such, rWEC assay was found to be a cost effective stand alone assay for supporting poorly soluble compounds and/or ones with H1 or GABAergic activity. For all other compounds, using MESCA as a first tier and the dechorinated ZEC assay as a 2nd tier assay minimizes animal use and optimizes error rates, throughput and cost. To this end, compounds receive a final classification if found positive in the MESCA assay, and those that are negative are followed up in the ZEC assay resulting in overall error rates below 15%.

**PS 1027 The Devtox Project: A Comprehensive Source of Information on Developmental Abnormalities.**

J. Buschmann<sup>1</sup>, I. Chahoud<sup>2</sup>, R. Kellner<sup>1</sup> and R. Solecki<sup>2</sup>. <sup>1</sup>Fraunhofer ITEM, Hannover, Germany; <sup>2</sup>Federal Institute for Risk Assessment, Berlin, Germany; <sup>3</sup>Institute of Clinical Pharmacology and Toxicology, Berlin, Germany. Sponsor: C. Dasenbrock.

The potential of a compound to cause adverse effects in the developing embryo or fetus is an important consideration in human health risk assessment. The terms and diagnostic criteria used to describe fetal anomalies in animal experiments need to be consistent from one laboratory to another and must be harmonized between regulatory agencies.

Consequently, the DevTox Project ([www.devtox.org](http://www.devtox.org)) has the main objectives to harmonize the nomenclature used to describe developmental anomalies in laboratory animals and to assist in the visual recognition of developmental anomalies with the aid of photographs.

The use of a harmonized and internationally accepted nomenclature is a basic requirement for the operation of DevTox. A first approach of establishing such a harmonized terminology was made in 1997 by a publication of the International Federation of Teratology Societies IFTS (Teratology 55, 249-292, 1997). This terminology has recently been updated (Reproductive Toxicology 28, 371-434, 2009). In addition, in a series of Berlin Workshops working definitions for the two classification categories "malformation" and "variation" were agreed.

The results of all these activities were used to establish the DevTox data base. The easy-to-use Web interface allows different views of the nomenclature, images and data and a quick navigation throughout the complete site. DevTox currently contains more than 2,500 images, showing examples of external, skeletal, soft tissue and maternal-fetal anomalies in rats, mice, rabbits, hamsters, primates, Guinea

pigs, minipigs, dogs and birds. It provides short descriptions of each finding and in some cases synonyms and further diagnostic notes as well as a hierarchical structure for the localizations. The system is publicly accessible and allows the electronic download of the current version of the harmonized terminology.

**PS 1028 Reference Images for the Skeletal Examination of Cynomolgus Monkey Fetuses and Thalidomide-Induced Malformations.**

O. Foulon, F. Spezia, C. Dauzat, M. Da Silva, P. Barrow, B. Palate and R. Forster. *CiToxLAB, Evreux, France.*

In this poster selected images are presented to illustrate the normal and (drug-induced) abnormal skeletal morphology of the cynomolgus monkey at 100 days post-coitum. Very little is available in the literature in terms of reference images for the skeletal examination of cynomolgus monkey (*Macaca fascicularis*) fetuses in teratology studies. This poster will present photographs of the fetal skeleton on day 100 post-coitum. Normal (control) fetuses will be presented and compared with fetuses showing thalidomide-induced malformations. A total of 20 control and 3 thalidomide-treated fetal specimens were photographed. Dams were 3 to 8 years old at mating and weighed 2.0 to 4.5 kg. Mating was confirmed by the presence of sperm in a vaginal smear during cohabitation with a male. Pregnancy was confirmed 18 or 19 days later by ultrasound examination. The treated dams were given 20 mg/kg/day of thalidomide by oral gavage from days 25 to 30 of gestation. The control dams received a similar volume of water (10 mL/kg). The fetuses were removed by caesarean section on day 100 of gestation. Fetal and placental weights were recorded. Morphometric measurements (head circumference and crown rump-length) were taken. Each fetus was then given a detailed necropsy examination prior to processing for skeletal examination by the Dawson method: the ossified skeletal structures were visualised following clearing of the soft tissues in potassium hydroxide and staining with Alizarin Red S. The normal variation in the degree of skeletal maturity and the corresponding patterns of ossification can be assessed using the control images.

**PS 1029 Regulatory Embryofetal Development Studies in Minipigs: Optimisation of Techniques.**

A. Makin, T. K. Andreassen and J. Løgstød. *CiToxLAB, Lille Skensved, Denmark.*

Rats and rabbits are traditionally the species of choice for developmental toxicity (embryofetal development) studies. If for any reason these species are found unsuitable (e.g. due to issues of metabolism) a non-rodent alternative choice of species is the minipig. In our facility we have several years of experience with EFD studies in the Gottingen minipig. When working with non-standard species for studies of this nature, a reliable study design producing robust data is imperative. Control data are presented from 9 preliminary studies and 4 main studies performed over the last 5 years and intended for regulatory submission. On the basis of this experience, study designs have been reviewed and refined to ensure reliable and consistent results. Consideration was given to factors such as efficient synchronisation of estrus with the use of Regumate® (altrenogest) to maximise mating success. Using this approach a success rate of close to 100% is attained. In this way the required number of pregnant sows for the study can be accurately provided, allowing precise scheduling of the number of sows mated per day according to the facility capacity to perform the caesarean sections on the required day of gestation. The data presented show that our methods give a mating success and an average litter size that are superior to the published literature, thus ensuring that there are sufficient fetuses for interpretation of findings. Estrus synchronisation is also useful for the provision of neonatal piglets for juvenile toxicology studies. The present poster presents background data for all of the fundamental litter-based parameters and demonstrates the robustness of the methods. Data for Pregnancy rate, Uterus Weight, Litter Size, Resorptions, Implantations, Corpora Lutea and Pre and Post-implantation Loss are also presented.

**PS 1030 Exploring the Role of the Mediator Gene 'Med31' in Proliferation and Limb Development during Mouse Embryogenesis.**

K. Wolton<sup>2</sup>, J. Wright<sup>1</sup>, R. Doran<sup>1</sup> and K. Henges<sup>2</sup>. <sup>1</sup>*Faculty of Life Sciences, Manchester University, Manchester, United Kingdom;* <sup>2</sup>*Product Safety, Syngenta, Bracknell, United Kingdom.* Sponsor: *P. Botham.*

Birth defects are recognised as a common global human health concern and they may arise as a result of a multitude of factors. In terms of ameliorating such anomalies, it is important to gain a better understanding of the fundamental mechanisms

controlling embryonic development. A role for the Mediator complex gene Med31 in the developing embryo has been recognised using a random mutagenesis screen in mice. Developing embryos which lack the Med31 protein are substantially smaller than their wild type littermates, and show a delay in development. This is particularly noticeable in the developing limbs, which fail to grow to the same length as wild type, and demonstrate delays in normal ossification patterns. Analysis of embryonic fibroblast cultures has revealed a significant defect in cell proliferation in Med31 mutants, which is recapitulated in the Med31 mutant limb bud, at embryonic day (E)10.5.

Med31 forms part of the mediator complex, which acts as a bridge between transcription factors and the RNA Polymerase II to initiate transcription. Mutant embryos lacking Med31 have a reduction in the expression of the cell cycle genes mTOR and Cyclin B. In situ hybridisation has demonstrated that the mutants do not express Sox9, a master regulator of chondrogenesis, and this is particularly evident in the limb bud at E10.5, while genes such as Fgf8, a marker of limb patterning, retain a normal expression pattern.

These findings are being further investigated by exploring the genes which are under the transcriptional regulation of Med31 in limb development. These experiments will provide new insights into the mechanisms by which Mediator complex proteins regulate developmental processes.

1) Risley, M.D. Clowes, C. Yu, M. Mitchell, K. Hentges, K.E. (2010) *Developmental Biology*. 342. 146-156.

**PS 1031 Investigation of Methods for Anesthetization and Euthanization of Rat and Rabbit Fetuses in Developmental Toxicity Studies.**

H. Kato, R. Katagiri, A. Arima, Y. Ooshima and R. Nagata. *Shin Nippon Biomedical Laboratories, Ltd., Drug Safety Research Laboratories, Kagoshima, Japan.*

Japan Association for Laboratory Animal Medicine recommends humane handling of laboratory animal fetuses. However, it is a challenge to accept proposed euthanizing methods such as cervical dislocation, decapitation and/or intracardiac injection of potassium chloride, because these methods would damage fetal specimens for skeletal and visceral examinations in developmental toxicity studies. The present study aimed at finding better methodologies for rat and rabbit fetal euthanasia and anesthesia. We focused on, and evaluated, two parameters: fetal heart rate and response to touch stimulus. We were unable to accomplish fetal euthanasia directly in either species; however, we were able to euthanize fetuses under pain-controlled anesthesia.

Rat fetuses immersed in physiological saline at 10°C showed complete loss of reaction to touch stimulus within 10 minutes, and a mean heart rate of less than 20 bpm, suggesting that deep anesthesia had been achieved very rapidly. Therefore, it is recommended that hypothermia by immersion in cold physiological saline is an appropriate method for anesthetization of rat fetuses.

Rabbit fetuses intraperitoneally injected with pentobarbital sodium at 3.24 mg/body and retained in filter paper impregnated with physiological saline at 18°C showed complete loss of reaction to touch stimulus within 30 minutes. Therefore, it is recommended that intraperitoneal injection of pentobarbital sodium and hypothermia induced by cold physiological saline form an appropriate method for anesthetization of rabbit fetuses.

We further recommend that the fetuses should be euthanized promptly upon reaching anesthesia by exsanguination, removal of vital organs, or immersion in appropriate fixatives.

**PS 1032 Acute Intravenous Exposure to Silver Nanoparticles during Pregnancy Induces Particle Size and Vehicle-Dependent Changes in Vascular Reactivity.**

A. K. Vidanapathirana<sup>1</sup>, L. C. Thompson<sup>1</sup>, M. Herco<sup>1</sup>, J. O. Dawkins<sup>1</sup>, S. C. Sumner<sup>3</sup>, T. Fennell<sup>3</sup>, J. M. Brown<sup>2</sup> and C. J. Wingard<sup>1</sup>. <sup>1</sup>*Physiology, East Carolina University, Greenville, NC;* <sup>2</sup>*Pharmacology & Toxicology, East Carolina University, Greenville, NC;* <sup>3</sup>*RTI International, Research Triangle Park, NC.*

With increasing use of engineered silver nanoparticles (NP) in different settings there are concerns regarding their safety particularly in vulnerable life stages such as pregnancy. Effects of silver NP on maternal vascular reactivity have not been extensively investigated despite potential occupational, therapeutic and environmental exposure. Our hypothesis was: the acute intravenous (IV) exposure to silver NP during late stages of pregnancy increases the vasoconstrictor response in the uterine artery. Pregnant (17-19 days) Sprague Dawley rats were exposed to a single dose of 20 or 110 nm silver NP (200 µg) suspended in polyvinylpyrrolidone (PVP) or citrate solutions. 24 h post-exposure vasomotor responses of segments of the main uterine artery and thoracic aorta were assessed using wire myography. Cumulative dose-response curves were constructed for acetylcholine, angiotensin II, endothelin

1 and Rho kinase inhibitor (HA1077). The response to phenylephrine was studied in the presence and absence of COX inhibitor, indomethacin. Dose-response curves, maximum stress and EC50 values were different for silver NP exposed animals when compared with vehicle controls. Reciprocal changes were seen between the aortic and uterine vessels: greater vasoconstriction in uterine artery and greater vasodilation in aorta following 110 nm silver exposure. Exposure to 20 nm silver NP increased the HA1077 mediated vasodilation in aortic segments suggesting a possible mechanism underlying the changes of agonist mediated vasoconstrictor response following NP exposure. NP suspensions in citrate lead to higher stress generation in both vessels. IV exposure to silver NP during pregnancy induces particle size and vehicle dependent changes in vascular reactivity which can potentially influence blood supply to the fetus. This work is supported by NIEHS U19 ES019525.

### PS 1033 Gamma Secretase Inhibition: Effects on Fertility and Embryo-Fetal Development in Rats.

L. Sivaraman<sup>1</sup>, K. Thompson<sup>1</sup>, G. Pilcher<sup>2</sup>, T. Sanderson<sup>2</sup> and M. E. McNeerney<sup>1</sup>. <sup>1</sup>Bristol-Myers Squibb Co., New Brunswick, NJ; <sup>2</sup>Bristol-Myers Squibb Co., Mt. Vernon, IN.

BMS-708163 (avagacestat) inhibits  $\gamma$ -secretase (GS), a protease that cleaves amyloid precursor protein to produce amyloid  $\beta$  (A $\beta$ ) and amyloid plaques that are prominent lesions in Alzheimer's disease (AD). As part of the nonclinical reproductive safety evaluation, studies of embryo-fetal development as well as fertility and early embryonic development were conducted in female Sprague-Dawley rats. In the embryo-fetal development study, BMS-708163 was administered (oral gavage) to pregnant rats at 3, 10 and 30 mg/kg/day from Gestation Day (GD) 6 through GD 15. Cesarean sections were conducted on GD 21. Assessments of maternal well-being included clinical observations, body weight, and food consumption; evaluation of fetal viability, morphology and body weights comprised the assessment of developmental toxicity. BMS-708163 was a selective developmental toxicant at all doses tested, with dose-related increases in the incidence and severity of fetal malformations and variations in the absence of maternal toxicity. Malformations and variations included axial and appendicular skeletal anomalies. In the study of fertility and early embryonic development in female rats, BMS-708163 was administered for 14 days prior to cohabitation; then throughout cohabitation and early gestation, until presumed GD 7 at 1, 5, and 15 mg/kg/day. Mid-gestation cesarean sections were conducted (GD 13-15). Reproductive end points included estrus cycle length, mating and fertility rates, implantation and conceptus viability. Dose-dependent reductions in female fecundity at doses  $\geq$  5 mg/kg/day were attributed to impaired ovarian follicular development; this was reflected in dose-dependent reductions in implantation sites, litter size, and gravid uterine weights. These results occurred at exposures above those which lower brain A $\beta$  in rats; are consistent with inhibition of GS-mediated Notch processing, a key signaling pathway in cell-fate determination and embryonic development; and are considered no risk to the intended AD (> 65 yr) patient population.

### PS 1034 Flubendazole Embryotoxicity in Rat Embryos and Fetuses.

P. A. Colombo<sup>1</sup>, M. Longo<sup>1</sup>, S. Zanoncelli<sup>1</sup>, M. Messina<sup>1</sup>, R. Schnurbus<sup>1</sup>, I. Scandale<sup>2</sup> and G. Mazué<sup>3</sup>. <sup>1</sup>Accelera, Nerviano MI, Italy; <sup>2</sup>DNDi, Geneva, Switzerland; <sup>3</sup>Consultant, Mantry, France.

Filarial diseases affect millions in poverty-stricken areas. DNDi investigated Flubendazole Amorphous Solid Dispersion (ASD) as a possible drug candidate. Within its preclinical characteristics in particular potential embryotoxicity was evaluated. With this aim flubendazole ASD was administered orally to Sprague Dawley rats at 0, 2, 3.46, 6.32 and 13 mg/kg/day as flubendazole, during the recognized susceptible organogenetic period on GD (gestation day) 9.5 and 10.5 as identified in a previous whole embryo culture study. Fetuses were evaluated on GD 20. Flubendazole was embryolethal from 6.32 mg/kg/day (Cmax after single administration 0.801 ug/mL). In addition Flubendazole was teratogenic at 3.46 mg/kg/day (Cmax after single administration 0.539 ug/mL). No increase in resorptions was seen however 80% of fetuses showed malformations namely exencephaly, micro-/anophthalmia, small/absent kidneys, markedly enlarged renal pelvis/ureters, absent tail, anal atresia and disruption of skeletal ossification of head, spine and thoracic cage. Flubendazole did not interfere with rat embryonic development, apart from a minimal reduction in fetal and placental weights, at 2 mg/kg/day (Cmax after single administration 0.389 ug/mL) with treatment restricted to two days during pregnancy and with a limited number of animals. In order to evaluate the embryotoxic nature of Flubendazole, embryos of dams treated as above, were evaluated on GD 11.5 and 12.5, as a window for observing the origin of alterations detected at term.

Flubendazole confirmed to be embryolethal and teratogenic through its cytostatic properties.

At 6.32 mg/kg/day it initially induced a block of embryonic development through its cytostatic action, followed by cytotoxicity which led to 100% embryolethality within 48h while at 3.46 mg/kg/day, it markedly reduced embryonic development through its cytostatic action but did not show cytotoxic effects. Therefore, embryos still alive markedly retarded with consequent morphological alterations in specific areas namely brain vesicles, eye, maxillary structures and body axis.

### PS 1035 Double-Staining Technique for Minipig Fetal Skeletons at Gestation Day 60.

S. Baudet, J. Briffaux, C. Pique, P. Quesada and A. Jocteur-Monrozier. *Ricerca Biosciences SAS, St. Germain sur l'Arbresle, France.*

In a previous study, we have demonstrated that fetal abnormalities associated with a known human and swine teratogen (Pyrimethamine) could be detected in the minipig with fetal examinations performed close to mid-term instead of at term. The principal objective of the present study was to validate a double staining method for bone and cartilage of minipig fetuses obtained by caesarean section close to gestation day (GD) 60 in order to support skeletal examinations.

Two virgin Göttingen Minipig females were mated at the testing facility and subsequently submitted to caesarean section close to GD 60. Ten fetuses (5 in each litter) were available for the trials and the sexes were evenly split.

The fetuses were used in a number of staining trials based on our own established methods for other species, including the rat and rabbit. In the first step, the fetuses were stained, without prior fixing, following evisceration and skinning. Varying concentrations of ethanol, mixed together with Alizarin red S, Alcian blue and acetic acid, were tested to obtain the desired results. In order to establish the best conditions to fix the staining, the fetuses were then transferred to baths containing different concentrations of ethanol for varying durations. Following fixation, the specimens were transferred into potassium hydroxide solutions for maceration of the soft tissue. Finally, the soft tissues were cleared, firstly using Malls solution followed by glycerol at increasing concentrations. The fetuses from the successful trial were then ready for skeletal examination.

The technique is slightly more labour intensive than the single staining technique using Alizarin red S only. However, the time required to process the specimens for examination is approximately the same for both methods. Moreover, this new technique enhances the examination process for mid-term minipig fetal skeletons, at a time when ossification of the skeleton is obviously less advanced than at term. Our next step is to generate an atlas of the mid-term minipig fetal skeleton.

### PS 1036 Retrospective Review of Skin Irritation and Corrosion Hazards on the Basis of Existing Human Data.

D. Basketter<sup>1</sup>, D. Jirova<sup>2</sup> and H. Kandarova<sup>3</sup>. <sup>1</sup>DABMEB Consultancy Ltd., Sharnbrook, United Kingdom; <sup>2</sup>National Institute of Public Health, Prague, Czech Republic; <sup>3</sup>MarTek IVLSL, Bratislava, Slovakia.

Regulatory classification of skin irritation has historically been based on rabbit data, however current toxicology processes are transitioning to in vitro alternatives. The in vitro assays have to provide sufficient level of sensitivity as well as specificity to be accepted as replacement methods for the existing in vivo assays. This is usually achieved by comparing the in vitro results to classifications obtained in animals. Significant drawback of this approach is that neither in vivo nor in vitro methods are calibrated against human hazard data and results obtained in these assays may not correspond to situation in human.

The main objective of this review was to establish an extended database of substances classified according to their human hazard to serve for further development of alternative methods relevant to human health as well as resource for improved regulatory classification.

The literature has been reviewed to assemble all the available information on the testing of substances in the human 4 h human patch test, which is the only standardized protocol in humans matching the exposure conditions of the regulatory accepted in vivo rabbit skin irritation test.

A total of 81 substances tested according to the defined 4 h human patch test protocol were found and collated into a dataset together with their existing in vivo classifications published in the literature. While about 50% of the substances in the database are classified as irritating based on the rabbit skin test, on using the 4 h HPT test, less than 20% were identified as acutely irritant to human skin.

Based on the presented data, it can be concluded that the rabbit skin irritation test largely over-predicts human responses for the evaluated chemicals. Correct classification of the acute skin irritation hazard will only be possible if newly developed in vitro toxicology methods will be calibrated to produce results relevant to man.

**PS 1037 Influence of Acidic Extraction Conditions on Formazan Assay: Assessment of Test Substances Using *In Vitro* EpiSkin Skin Irritation Test Method by HPLC and Colorimetry.**

M. H. Grandidier, N. Alépée, B. Micheau, S. Grégoire and J. Cotovio. *L'Oréal Research & Innovation, Aulnay sous Bois, France.* Sponsor: E. Dufour.

The skin irritation potential of a test substance is typically determined by measuring cell viability in treated tissues by means of the colorimetric MTT reduction assay after topical application of a test substance. In the EpiSkin validated skin irritation test method, tetrazolium salt-based formazan assay is performed by using acidified isopropanol extraction conditions (ESAC 2007, OECD TG439 2010). The current work evaluated the data obtained with the EpiSkin model for the 20 reference chemicals (listed in the OECD TG439) following formazan extraction with acidified (IPA) or non acidified (IP) isopropanol solutions to evaluate the influence of acidic extraction conditions. Therefore the objectives of this work was to establish the use of HPLC measurements as a complementary assay to standard photometry assay for detection of reduced MTT, a known limitation for test substances that are highly coloured.

The cell viability in EpiSkin quantitatively measured after acidified (IPA) or non acidified (IP) isopropanol extractions from tissues were equivalent ranging from 6.4 to 104% by colorimetry (reference method). Following HPLC measurement, formazan quantitative analyses were comprised between 7.9 to 99.2%. The standard deviation between those 2 conditions was +/- 18%. Therefore, within-laboratory variability assessed in 3 runs showed similar concordance of classification for each condition. The sensitivity (based on 10 GHS Cat.2 substances) was 90% and the specificity (based on 10 No-category substances) was 70%. The HPLC provides data comparable to those using standard photometry assays for 20 test substances indicative of the use of HPLC as a complementary assay to photometry in EpiSkin skin irritation test method. Therefore, those results suggest that acidified isopropanol extraction conditions did not affect the EpiSkin skin irritation outcomes.

**PS 1038 Cytotoxic Effects of Dicyclohexylamine and Three Metalworking Fluids on Human Epidermal Keratinocytes.**

A. D. Linthicum<sup>1</sup>, A. O. Inman<sup>2</sup>, N. A. Monteiro-Riviere<sup>2</sup> and R. E. Baynes<sup>1</sup>.

<sup>1</sup>Center for Chemical Toxicology Research and Pharmacokinetics, North Carolina State University, Raleigh, NC; <sup>2</sup>Nanotechnology Innovation Center of Kansas State, Kansas State University, Manhattan, KS.

Many of the 1.2 million workers in the metal machining industry within the United States will be exposed to metalworking fluids via the dermal route, making it a major occupational health and safety concern. Dicyclohexylamine (DCHA), an anticorrosive agent used in the metalworking industry to prevent corrosion of fabricated materials, is known to permeate the skin and could potentially elicit a toxic response on human epidermal keratinocytes (HEK). HEK were exposed only to DCHA or one of the following three generic metalworking fluids: soluble oil, synthetic oil and semi-synthetic oil for 24h. Cells were dosed with solutions ranging from concentrations of 200-5000µg/ml. The highest concentration of 5000µg/ml is the relevant occupational exposure dose in the metal machining industry. Cells exposed to 200-5000µg/ml of DCHA resulted in a 24-91% decrease in cell viability in comparison to the media control. The soluble oil and semi-synthetic oil dosed from 200-5000µg/ml resulted in an 80-83% and 81-85% decrease in cell viability, respectively, in comparison to the media control. For synthetic oil, there was a 52-85% decrease in cell viability in comparison to the media control. DCHA and all metalworking fluid treatments caused a significant (p<0.05) decrease in HEK viability. In conclusion, metalworking fluids and DCHA had a cytotoxic effect to HEK. This data suggests that the concentration of DCHA in metalworking fluid formulations should be reduced while safer metalworking fluid formulations are developed. (Supported by NIOSH R01-01-03669)

**PS 1039 Aryl Hydrocarbon Receptor Repressor (AhRR) Function Revisited: Repression of Cyp1 Activity in Human Skin Fibroblasts Is Not Related to AhR Expression.**

J. Tigges<sup>1</sup>, H. Weithardt<sup>1</sup>, G. Christine<sup>1</sup>, I. Foerster<sup>1</sup>, H. F. Merk<sup>2</sup>, T. Haarmann-Stemmann<sup>1</sup>, J. Krutmann<sup>1</sup> and E. Fritsche<sup>1</sup>. <sup>1</sup>Leibniz Institute for Environmental Medicine, Duesseldorf, Germany; <sup>2</sup>Dermatology and Allergology, University Clinic RWTH, Aachen, Germany.

The skin reacts to environmental noxae by inducing cytochrome P450 (CYP)-catalyzed reactions via activation of the aryl hydrocarbon receptor (AhR). A drawback of this response is the generation of oxidative stress, which is especially dangerous for postreplicative cells such as dermal fibroblasts, in which damage may accumulate over time. Accordingly, in dermal fibroblasts, CYP1 expression is repressed and

it has been proposed that this is due to the AhRR, which is supposedly overexpressed in fibroblasts as compared with other skin cells. Here, we revisited this "AhRR hypothesis", which has been mainly based on ectopic overexpression studies and correlation analyses of high AhRR gene expression with CYP1A1 repression in certain cell types. In primary human skin fibroblasts (NHDFs) of 25 individuals, we found that (i) the AhRR was expressed only at moderate RNA copy numbers and that, against the common view, (ii) in some fibroblast strains, CYP1A1 mRNA expression could be induced by AhR activators. However, even the highest induction did not translate into measurable CYP1 enzyme activity, and neither basal expression nor mRNA inducibility correlated with AhRR expression. In addition, enhancement of CYP1A1 mRNA expression by trichostatin A, which inhibits AhRR recruited histone deacetylases at the CYP1A1 promoter, failed to induce measurable CYP1 activity. Finally, AhRR deficient mouse embryonic fibroblasts were not induced to biologically relevant CYP1 enzyme activity despite impressive mRNA induction. These data clearly indicate that repressed CYP1 activity in NHDFs is not causally related to AhRR expression, which may serve a different, yet unknown, biological function.

**PS 1040 Citotoxic Effect of the Temporary Hair Dye Basic Red 51 on Human Keratinocytes(HaCaT): Development and Application on a Reconstructed (3D) Artificial Skin.**

T. B. Zannoni<sup>1</sup>, M. T. dos Santos<sup>2</sup>, S. Barro<sup>2</sup>, S. Maria-Engler<sup>2</sup> and D. de Oliveira<sup>1</sup>. <sup>1</sup>Environmental Toxicology, University of São Paulo, Ribeirão Preto, Brazil; <sup>2</sup>Laboratory of Pathology and Clinical Cytology, University of São Paulo, São Paulo, Brazil.

Nowadays, hair dyes are being commonly used for cosmetics purposes. However in 2001, the Scientific Committee on Cosmetic products and Non-Food Products intended for consumers (SCCNFP) of the European Union recommended that hair dye ingredients should be re-analyzed. Since 2006, 22 hair dyes have been banned for not being considered safe. On the present work, we evaluated the cytotoxicity of a temporary hair dye "Basic Red 51" (CAS: 77061-58-6), an azo dye (-N=N-) that is currently being revised by the EU. We tested the toxicity of the "Basic Red 51" in immortalized keratinocytes (HaCaT) that are the primary route of exposure. Moreover, we reconstructed a human (3D) epidermis using HaCaT cells and dermal fibroblasts in order to create a new approach that would better represent the real exposure. For HaCaT cells in monolayer, the Basic Red 51 IC50 was 12.9 µg/mL, determined by Tripan Blue assay. Besides, this concentration of the dye induced cell cycle arrest at G2 phase. Using the clonogenic assay, we observed that 2.5 µg/mL of the dye was sufficient to inhibit completely cell growth after 48 hours of exposure. In the artificial skin model, we demonstrated that the exposure to Basic Red 51 at IC50 reduces the skin thickness, decreasing the number of cell layers. We also observed that the cells appear to be injured and undergoing apoptosis. It is important to point out that the IC50 used for these experiments (12.9 µg/mL) is much lower than the commercial concentration (2000µg/mL). We suggest that similar effects could be induced in humans after the exposure to Basic Red 51, mainly considering the effects in artificial skin. So, we concluded that the use of Basic Red 51 for cosmetic proposes should be carefully evaluated.

**PS 1041 Skin and Eye Lesions in the Long Evans Rat Produced by Oral 8-Methoxy-Psoralen (8-MOP) Application and Subsequent UV-A Irradiation.**

M. Sieber<sup>1</sup>, C. Simon<sup>1</sup>, K. Broich<sup>1</sup>, C. Maraschiello<sup>1</sup> and K. Weber<sup>2</sup>. <sup>1</sup>Harlan Laboratories Ltd., Itingen, Switzerland; <sup>2</sup>AnaPath GmbH, Oberbuchsiten, Switzerland. Sponsor: T. Ansai.

For assessment of the dermal and ocular response to the model phototoxicant 8-MOP, 6 female HsdBLu:LE (SPF) Long Evans rats received a single dose of 5.0 mg/kg body weight 8-MOP by oral gavage. 6 control rats were treated with the vehicle only. One pigmented and one unpigmented skin site were clipped free of hair and irradiated with 15 J/cm<sup>2</sup> UV-A (Bio-Spectra irradiation chamber, Vilber Lourmat Deutschland GmbH). Irradiation was performed 30 min after 8-MOP application under pentobarbitone anaesthesia. Visual assessment of the skin 4 h after irradiation showed erythema on the irradiated pigmented and non-pigmented skin of 8-MOP-treated rats and in control rats which increased in severity in 8-MOP-treated rats after 20 h and receded in control rats. Injection of Evans Blue showed moderate vascular leakage 24 h and 48 h after irradiation in all 8-MOP-treated rats, while only few of the control rats were affected at a lower severity. Histopathologically, corneal single cell necrosis was recorded in the irradiated eye of 2 of the 8-MOP-treated rats, but not in control rats. Dermal lesions in pigmented and unpigmented skin of 8-MOP-treated rats consisted of focal/multifocal epidermal hyperplasia, focal erosions/scab formation, ulceration, subcutaneous and/or dermal infiltration, follicular inflammation, focal/multifocal epidermal necrosis

and subcutaneous and/or dermal inflammation, showing a slightly higher incidence and severity in non-pigmented than in pigmented skin. An identical experiment with a higher irradiation dose of 35 J/cm<sup>2</sup> UV-A led to erythema and correlating histopathological findings in the skin of both 8-MOP-treated and control rats; however, corneal affections consisting of focal or single cell corneal necrosis, corneal epithelial vacuolation and/or focal corneal keratosis were recorded in 8-MOP-treated rats only. The results of the experiment confirmed that the test system is appropriate for the assessment of systemic phototoxicity.

### PS 1042 13-Week Dermal Toxicity of Triclosan in B6C3F1 Mice.

M. M. Vanlandingham<sup>1</sup>, J. Fang<sup>1</sup>, F. A. Beland<sup>1</sup>, B. E. Juliar<sup>1</sup>, G. R. Olson<sup>1</sup>, W. A. Harrouk<sup>2</sup> and R. E. Patton<sup>1</sup>. <sup>1</sup>National Center for Toxicological Research, US FDA, Jefferson, AR; <sup>2</sup>Center for Drug Evaluation and Research, US FDA, Silver Spring, MD.

Triclosan [5-chloro-2-(2, 4-dichlorophenoxy)phenol] is widely used as an antimicrobial agent, and humans in all age groups have the potential to receive lifelong exposures. We recently demonstrated that the dermal application of triclosan to mice results in systemic distribution of the compound. The goal of the present study was to evaluate the toxicities of triclosan administered dermally to B6C3F1 mice for 13 weeks and provide a scientific basis for dose selection for a subsequent chronic dermal carcinogenicity study. Groups of 10 male and 10 female mice received dermal application of 0, 5.8, 12.5, 27, 58, or 125 mg triclosan in ethanol per kg bw daily seven days per week for a period of 13 weeks. All mice survived the 13-week treatment. Body weights of female mice were not affected, while male mice administered 58 and 125 mg/kg weighed 91% and 83% of the control male mice. The mean weight of livers from females receiving 58 and 125 mg/kg was 11% and 40% greater than the controls; in males, the highest dose led to a higher mean liver weight (38% greater than the controls). Skin lesions (epidermal hyperplasia, inflammation, necrosis, ulceration, and parakeratosis; dermal fibrosis and inflammation) were observed in both sexes. The severity of the lesions was minimal at the 12.5 mg/kg dose, and both the severity and incidence of the lesions increased as the dose was increased. The highest dose of triclosan increased the percentage of reticulocytes in both sexes and the percentage of micronucleated normochromatic erythrocytes in females; in addition, the 58 mg/kg dose increased the percentage of reticulocytes in females. A significant dose-dependent decrease in the levels of T4 and cholesterol was observed in both sexes. There were no differences between treated and control mice in sperm or vaginal cytology measurements. The NOAEL, under the conditions of this subchronic assay, was 5.8 mg/kg. (Supported by Interagency Agreement between NCTR/FDA IAG #224-12-0003 and NIH AES12013.)

### PS 1043 Dermal Toxicokinetic Studies of Triclosan in B6C3F1 Mice.

J. Fang<sup>1</sup>, M. M. Vanlandingham<sup>1</sup>, F. A. Beland<sup>1</sup> and W. A. Harrouk<sup>2</sup>. <sup>1</sup>Division of Biochemical Toxicology, National Center for Toxicological Research, FDA, Jefferson, AR; <sup>2</sup>Center for Drug Evaluation and Research, FDA, Silver Spring, MD.

Triclosan [5-chloro-2-(2, 4-dichlorophenoxy)phenol] is widely used as an antimicrobial agent in personal care products, household items, and clinical settings. Due to its extensive use, there is potential for humans in all age groups to receive lifelong exposures to triclosan; however, data on the chronic dermal toxicity/carcinogenicity of triclosan are still lacking. The goal of the present study was to determine the absorption, distribution, metabolism, and excretion of triclosan following dermal administration to B6C3F1 mice. A single dose of [<sup>14</sup>C(U)]triclosan (10 or 100 mg per kg bw, 10 µCi per mouse) was administered to mice in two separate experiments: a vehicle selection experiment to compare the bioavailability of triclosan in male mice using propylene glycol, ethanol, and a generic lotion as vehicles; and a toxicokinetic experiment to evaluate sex differences in the absorption and deposition of triclosan and its metabolites. Three mice per sex in each group were killed at 0.5, 1, 2, 4, 6, 8, 12, 24, 48, and 72 h after administration, and excreta and tissues were collected and analyzed for radioactivity. Ethanol has the best properties of the vehicles evaluated. Maximum absorption of triclosan (80 ~ 86%) was obtained at 12 h after dermal application. There was some saturation of absorption at the 100 mg/kg. Radioactivity appeared in the excreta and in all tissues examined, with the highest level in gall bladder and the lowest level in brain. Triclosan was readily metabolized to triclosan sulfate and glucuronide conjugates, 2,4-dichlorophenol, and hydroxytriclosan. The metabolite profile was tissue-dependent and the predominant route of excretion was the feces (65 ~ 78%). There were no differences in bioavailability between males and females. Slightly lower absorption was observed with Elizabethan collar, suggesting some oral ingestion due to the normal behavior grooming. (Supported by Interagency Agreement between NCTR/FDA IAG #224-12-0003 and NIH AES12013.)

### PS 1044 Confocal Raman Microscopy—The Future for Dermal Absorption Studies.

T. Patel<sup>1</sup>, A. Ghaemmaghami<sup>1</sup>, P. Williams<sup>1</sup>, J. Wright<sup>2</sup>, C. Roberts<sup>1</sup> and F. Rose<sup>1</sup>. <sup>1</sup>School of Pharmacy, University of Nottingham, Nottingham, United Kingdom; <sup>2</sup>Syngenta Ltd., Bracknell, United Kingdom. Sponsor: P. Botham.

The activity and absorption of pesticides into the skin of the user is increasingly becoming a major problem within the Agrochemical industry. Fewer formulations are passing the regulatory process of pesticide approval as a result of unknown compound dermal accumulation and toxicity. Currently, 2 gold-standard methods are used to monitor dermal absorption and determine compound flux (µg/cm<sup>2</sup>/h) across the skin but limitations in measuring dermal accumulation most often results in compound failure. Confocal Raman Microscopy (CRM) is novel label free, rapid, optical method which allows compounds to be identified within dermal tissue at depths of ~300 µm. The aims of the investigations were to develop and establish CRM methods for in vitro dermal absorption investigations across ex vivo pig skin. A Lab Ra HR CRM was employed for the analysis of a range of concentrations (0.0 - 50.0 mg/mL) of benzoic acid, caffeine (both in 50% (v/v) ethanol (EtOH)) set at the following: IR laser at 785 nm a filter intensity of 100%, a hole 300 µm with a x50 objective. Depth profiling was also preformed on fresh pig skin samples from the surface to a maximum depth of ~300 µm (~50 µm increments). CRM spectra for the pig skin investigations demonstrated good reproducibility with some spectral differences noticed. Intensity of the spectra decreased with increased depth as expected. It was observed that a concentration of 50% (v/v) EtOH appeared to mask the signal of prominent identifiable peaks for benzoic acid and caffeine solutions at and below a concentration of 6.25 mg/mL. Compound concentrations equal to or higher than 20.0 mg/mL within a 50% (v/v) EtOH solution could be detected. This data suggests that this masking effect by EtOH requires further exploration to better understand the limitations of the technique. The CRM method has the potential to qualitatively determine dermal compound accumulation within mixed media and solutions ultimately, providing a powerful tool in identifying toxic compounds early on.

### PS 1045 Development of an Alternative Model for Assessing Barrier Function and Permeability for Infant Skin.

T. J. McCarthy<sup>1</sup>, N. K. Tierney<sup>1</sup>, S. G. Raney<sup>2</sup> and P. A. Lehman<sup>2</sup>. <sup>1</sup>Johnson & Johnson, Skillman, NJ; <sup>2</sup>PRACS Institute, Fargo, ND.

Recent published literature of non-invasive measures of skin barrier function of full-term human infants indicates a dynamic maturation process over the first year of life indicative of adaptation from in utero to the external environment. During this period, infant skin may be more vulnerable to penetration of topically applied ingredients, however, the magnitude of differences in non-invasive measures may not correlate to the magnitude of the difference in penetration of topical agents. While thriving demonstrates that a functional skin barrier exists at birth, differences in dermal permeability compared to adult skin could have an impact on the exposure assessment and safety of topically applied ingredients. The purpose of this study was to compare various indicators of skin barrier function (electrical impedance, TEWL), and permeability (tritiated water, <sup>14</sup>C-octanol, and 24-hr aqueous caffeine) across skin from donors of different ages. Fresh neonatal and pubescent porcine skins (animals culled for other purposes) were collected from a breeding colony. Cryopreserved ex vivo adult human skins were purchased from a skin bank. All measures of skin barrier function and permeability were equally applied to all skin samples. The barrier functions in the porcine skin varied, depending upon the measure. Average impedance indicated parity across age. TEWL and tritiated water flux was lower through neonatal skin versus either mature species. Neonatal skin octanol flux showed parity versus pubescent porcine skin while immaturity versus human cadaver skin. Caffeine absorption ranged from 1.5x to 4.5x higher through neonate skin than seen in either mature species. These data demonstrate that non-invasive measures of barrier function may be indicative, but not definitive, for determining the absorption of topical compounds. The current 10x intra-species safety factor used in risk assessment adequately captures the difference in neonatal barrier function.

### PS 1046 Modelling Diffusion of Therapeutic Drugs through the Skin In Vitro Does the Model Need to Be Complicated?

J. Jenner<sup>1</sup>, O. Payne<sup>1</sup>, C. Dalton<sup>1</sup>, S. Graham<sup>1</sup>, J. Azeke<sup>2</sup>, E. Braue<sup>2</sup> and J. S. Graham<sup>2</sup>. <sup>1</sup>Biomedical Sciences, DSTL, Salisbury, United Kingdom; <sup>2</sup>USAMRICD, Edgewood, MD.

A mathematical model accurately simulating diffusion of chemicals through the skin would be useful for predicting percutaneous absorption and aid understanding penetration mechanisms. Models of varying complexity have been validated using

in vivo and in vitro data. In the present study data from the penetration of four drugs was used to test the output of a simple one compartment model based on Fick's 1st law of diffusion.

Methods: Drugs, as off the shelf formulations, were applied to pig skin (500  $\mu$ m dermatomed slice) in Franz type diffusion static cells using stirred ethanol:water (1:1) as a receptor; surface temperature 32°C. Penetration of hydrocortisone, capsaicin, clobetasol and diclofenac were measured in the receptor fluid using Ultra Performance Liquid Chromatography. The experimental permeability constant (Kp) was estimated from the maximum flux rate (assumed to be steady state; Jss) and the applied concentration of drug (C0) using the equation:

$$Kp = Jss / C0$$

A penetration profile was predicted using a model with the skin as a single compartment of a thickness approximating the stratum corneum and using the experimental Kp to calculate flux of drug from vehicle into the barrier layer and from barrier layer into receptor fluid. A best fit (determined by least squares) was then obtained by adjusting the experimental Kp by a factor which gave an estimate of the accuracy of the model in predicting the experimental data.

Results: Model predictions needed to be adjusted by factor of between 1.1 and 1.35 to fit the experimental data as judged by a least squares method and assuming a membrane thickness of between 0.025 and 0.04 mm.

Discussion: this work has demonstrated that a very simple model is able to predict quite closely the penetration of some non-volatile compounds applied to the skin in a vehicle.

This work is supported by the US Army Medical Research and Materiel Command under contract W81XWH-08-C-0070.

© Dstl Crown Copyright 2012

#### **PS 1047 Prediction of Skin Disposition After Topical Application of Drugs—Simcyp Platform As a Tool for Capturing System Information and Safety Assessment.**

S. Polak<sup>1,2</sup>, N. Patel<sup>1</sup>, M. Jamei<sup>1</sup> and A. Rostami Hodjegan<sup>1,3</sup>. <sup>1</sup>Simcyp (a Certara Company), Sheffield, United Kingdom; <sup>2</sup>Faculty of Pharmacy, Jagiellonian University Medical College, Krakow, Poland; <sup>3</sup>School of Pharmacy and Pharmaceutical Sciences, University of Manchester, Manchester, United Kingdom. Sponsor: B. Wetmore.

There are reports where topical application of drugs, which is generally considered safe, results in health threatening side effects or drug-drug interactions. Simcyp platform separates the system information from those of drug and uses in vitro in vivo extrapolation approach to predict disposition of the topically administered drugs (Polak 2012). Administration of a single 0.4 mg of erythromycin (topical - 2cm<sup>2</sup> area of the forearm) with 40 mg simvastatin (oral) is used as a model scenario to assess anticipated interactions mimicking corresponding clinical study (van Hoogdalem 1996). Lotion formulation was simulated by modification of permeability/partition parameters (factor of 50 for stratum corneum and viable epidermis). Simulated residual amounts of erythromycin collected from the skin surface at various time and fraction of the dose recovered from stratum corneum after 6 hours were compared with the observed values. The results were consistent with observations and indicate significant systemic absorption. Subsequently oral simvastatin (40 mg SID) and topical ketoconazole (0.4 mg BID for two weeks, applied on upper arm) were simulated in 100 healthy individuals and by modification permeability/partition parameters (factor of 5 for stratum corneum) to account for occlusion. The average AUC<sub>inf</sub>/AUC and Cmax<sub>inf</sub>/Cmax ratios were 1.17 and 1.11 respectively, suggesting safe concomitant use. The maximum simulated ratios were 1.51 (AUC) and 1.32 (Cmax) indicating potential risk of significant interaction in some individuals. This is in agreement with the clinical observations suggesting general safety with rare occurrence of major side effects (e.g. Lareb Q 2009 report; myalgia).

References: (1) Polak et al. JPharmSci 2012; 101(7):2584-95. (2) van Hoogdalem et al. SkinPharmacol 1996;9:104-110.

#### **PS 1048 In Vitro Human Epidermal Penetration of IMX-101 Munitions Chemicals.**

W. C. McCain, L. R. Williams and G. Reddy. Toxicology Portfolio, US Army Public Health Command, Army Institute of Public Health, Aberdeen Proving Ground, MD.

Dermal exposure to ammunition chemicals is a major concern of the Army in assessing risk during manufacturing and field operations. The US Army Environmental Quality Technology (EQT) program is creating new, insensitive ordnance formulations to replace highly energetic compounds such as RDX and TNT. There are limited data on dermal absorption of munitions chemicals to support health risk assessment. We studied in vitro dermal penetration of a newly-developed munition, IMX-101 (Insensitive Munitions explosive) (as a mixture) and

its individual chemicals, 2,4-dinitroanisole (DNAN), 3-nitro-1,2,4-triazol-5-one (NTO), and nitroguanidine (NQ). Human epidermal membranes were prepared from frozen cadaver skin according to OECD guidelines and were mounted in Franz static diffusion receptor cells so that the visceral side was in contact with the receptor fluid. Neat test chemicals at infinite dose (100 mg powder) were carefully placed on the mounted skin in the donor chamber and at different times (1, 2, 4, 6 and 8 hrs) 0.1 mL of receptor fluid (buffer) was collected and quantified by HPLC. The rate of diffusion per cm<sup>2</sup> was calculated for each chemical. The analysis of absorbed chemical in the receptor fluid showed that steady state fluxes of neat NTO, DNAN and NQ were 332, 1.10 and 31.25  $\mu$ g/cm<sup>2</sup>/hr respectively. When complete IMX-101 was tested as 100 mg of mixture, the fluxes for NTO, DNAN and NQ independently were 135.9, 1.80, and 236  $\mu$ g/cm<sup>2</sup>/hr, respectively. NTO and NQ showed about 0.4 and 7 times greater rate of penetration in the combination mix than as individual compounds. These estimated values will be used to determine occupational exposure levels with dermal exposure.

#### **PS 1049 In Vitro Human Skin Penetration of Acetyl Hexapeptide-8 from a Cosmetic Formulation.**

O. A. Ogunsola<sup>1</sup>, W. Zhou<sup>2</sup>, P. G. Wang<sup>2</sup> and M. E. Kraeling<sup>1</sup>. <sup>1</sup>Office of Applied Research and Safety Assessment, US FDA, Laurel, MD; <sup>2</sup>Office of Regulatory Science, US FDA, College Park, MD.

Peptides are being incorporated into cosmetic creams marketed as anti-aging/anti-wrinkle products. Acetyl hexapeptide-8 may penetrate into the deep layers of the skin and potentially stimulate biological activity by interfering with neuromuscular signaling as its anti-wrinkle effect. The skin penetration of commercially available acetyl hexapeptide-8 (Ac-EEMQRR-amide) from a cosmetic formulation was determined in human cadaver skin assembled into in vitro diffusion cells. An oil-in-water emulsion containing 10% Ac-EEMQRR-amide was applied to skin at a dose of 2 mg/cm<sup>2</sup>. After a 24 hour exposure, the skin surface was washed to remove unabsorbed peptide. Skin discs were taped stripped to determine the amount of peptide in the stratum corneum. Removal of the stratum corneum layers was verified by confocal microscopy. The epidermis was heat separated from the dermis and each skin fraction was homogenized. Skin penetration of Ac-EEMQRR- was measured in skin layers by hydrophilic interaction liquid chromatography with tandem mass spectrometry (HILIC-MS/MS) using electrospray ionization (ESI) in the positive mode. Stable isotopically labeled hexapeptides were used as internal standards for the quantitation of native hexapeptides to correct for matrix effects associated with ESI. Results (% of applied dose) found the majority of the Ac-EEMQRR-amide was not absorbed and removed by washing (87%). Stratum corneum peptide levels decreased as each layer was removed by tape stripping. Total Ac-EEMQRR-amide found in the stratum corneum was 0.22 % and 0.01% in the epidermis. No peptide was detected in the dermis or receptor fluid. Hairless guinea pig skin penetration of Ac-EEMQRR-amide showed similar results where 0.51% remained in the stratum corneum and 0.01% penetrated into the viable epidermis. This skin penetration data will be useful for evaluating the safety of cosmetic products containing short-chain peptides.

#### **PS 1050 Nevirapine-Induced Skin Rash Is Caused by a Reactive Sulfate Metabolite Formed in the Skin.**

A. M. Sharma and J. Uetrecht. Pharmacy, University of Toronto, Toronto, ON, Canada.

Rationale: Nevirapine (NVP) treatment is associated with significant idiosyncratic immune-mediated skin rash and hepatotoxicity in humans. NVP causes a very similar rash in female Brown Norway rats, and we had previously shown that 12-hydroxylation of NVP is required to induce the rash. In this study we studied the further metabolism and covalent binding of NVP in the rat model and in human skin. Immune activation via IL-1 $\beta$  in the skin was also examined. Methods: An anti-NVP antibody was produced and used in immunoblotting studies to detect covalent binding of NVP, 12-OH-NVP, or NVP-sulfate to skin and liver proteins from rodents and humans. In vitro incubations of NVP or metabolites with hepatic microsomes or skin cytosolic fractions from humans, mice, or rats were also performed. The ability of SULT 1A1\*1 to metabolize NVP was studied and cutaneous IL-1 $\beta$  levels were examined by ELISA. Results: Covalent binding was observed in the epidermis of NVP or 12-OH-NVP-treated rats. Major modified bands appeared between 40K-60K. Depletion of PAPs decreased blood levels of NVP-sulfate but did not prevent rash or covalent binding in skin. Topical administration of 1-phenyl-1-hexanol (sulfotransferase inhibitor) prevented rash and covalent binding where applied, and also prevented covalent binding of 12-OH to cytosolic skin fractions and SULT 1A1\*1 in vitro. IL-1 $\beta$  levels were significantly upregulated in skin of rats with a rash as well as skin isolates. No skin rash or covalent binding was observed in the skin of NVP treated mice. Conclusions: In contrast to covalent

binding in the liver, which involves direct oxidation to a quinone methide, the reactive metabolite that covalently binds in the skin is a sulfate. The sulfate responsible for the rash is formed in the skin of rats and in human skin incubations but not in mice which develop no rash. Further work is being done to confirm the role of IL-1 $\beta$  in NVP-induced skin rash. Funding: Canadian Institutes of Health Research.

**PS 1051 In Vitro Discrimination of Skin Sensitizing Haptens and Prohaptens in a Modified Keratinsens Assay with an Added Metabolic Activation Step.**

A. Natsch<sup>1</sup>, T. Haupt<sup>1</sup> and G. Adamson<sup>2</sup>. <sup>1</sup>Givaudan Schweiz AG, Duebendorf, Switzerland; <sup>2</sup>Givaudan US, East Hanover, NJ.

Prohaptens are chemicals which may cause skin sensitization after being converted into electrophilic molecules by skin enzymes. In vitro sensitization assays ideally should detect the potential of molecules to act as prohaptens. The metabolic activation system most commonly used in in vitro toxicology is Aroclor-induced rat liver S9 fraction. Even if this system contains higher enzyme activities as compared to those reported in skin, it may serve as a surrogate system to study the potential of chemicals to form reactive, skin sensitizing metabolites. To test this concept, the luciferase induction in KeratinoSens reporter cells treated with chemicals in presence and absence of S9 fractions was measured. Suspected prohaptens such as methylisoeugenol, eugenol, trans-anethol or benzo(a)pyrene gave no, or weak, gene induction in absence of S9 fractions, and a strongly enhanced luciferase induction in presence of S9 proving their prohapten status. Haptens like DNCB or cinnamic aldehyde gave a reduced response in presence of S9. We then evaluated whether this metabolic activation assay might be implemented in a tiered screening strategy to screen negatives in the classical KeratinoSens<sup>TM</sup> assay to enhance sensitivity. To this aim all chemicals classified negative in the classical KeratinoSens<sup>TM</sup> assay were retested with this activation step. Among the 77 chemicals found as correct-negatives, 74 were also negative in presence of metabolic activation, thus this counter-screen does only slightly reduce specificity. However, based on this comprehensive screening, we found that only a small fraction of the known skin sensitizers need activation by the S9/P450 system, and thus the KeratinoSens<sup>TM</sup> -S9 assay may be useful for the in vitro evaluation of specific classes of potential prohaptens, rather than as a general screening approach. These results will be presented along with results on the predictivity and reproducibility of the KeratinoSens<sup>TM</sup> assay as accumulated during the prevalidation studies conducted for ECVAM.

**PS 1052 Toxicogenomic Characterization of Sensitizer and False-Positive Responses in the Local Lymph Node Assay (LLNA).**

D. Adenuga<sup>1</sup>, I. Kimber<sup>2</sup>, R. Dearman<sup>2</sup>, M. Woolhiser<sup>1</sup>, M. Black<sup>3</sup>, R. S. Thomas<sup>3</sup> and D. R. Boverhof<sup>1</sup>. <sup>1</sup>The Dow Chemical Company, Midland, MI; <sup>2</sup>University of Manchester, Manchester, United Kingdom; <sup>3</sup>The Hammer Institutes for Health Sciences, Research Triangle Park, NC.

Recent publications have highlighted chemistries which yield false positive responses in the LLNA when compared with guinea pig and human data. A toxicogenomic approach was applied to provide insight into the molecular and cellular mechanisms that may explain these differential responses. Auricular lymph node gene expression responses were evaluated in female CBA mice exposed to equipotent doses of 9 chemical sensitizers and 7 false positives per the standard LLNA dosing regimen. Lymph nodes were analyzed for 3HTdR incorporation on day 6 and gene expression responses on study days 4 and 6. Statistical analyses identified 779 and 473 differentially expressed genes (DEGs) between sensitizers and false positives on days 4 and 6. Class-based comparison of DEGs showed that the most enriched functional categories in the sensitizer-specific subsets were consistent with mechanisms involved in the acquisition of antigen-mediated skin sensitization. Key immune responses at the 4 day time point were restricted to genes involved in early T-cell development including pathways involved in IL2 regulation (IL2 and Egr4), Tbeta and the pre T-cell receptor alpha (Ptcra). Day 6 responses were more consistent with a mature T-cell response and included genes involved in the DC/T-cell maturation process such as IL21, Lag3 and Fxyd4. In contrast, false positives exhibited a strong pro-inflammatory expression profile including markers for activated macrophages and neutrophils such as Cd51, IL12b, Mpo, Defa4 and class I steffins. Expression of these genes in the absence of dermal irritation suggested these responses were not solely driven by skin irritation. These gene expression profiles suggest a differential cellular recruitment to the lymph nodes following skin exposure to true sensitizers and false positives and provide a potential new endpoint that could be applied to address false positives and enhance the predictive value of the LLNA.

**PS 1053 Inductive Effects on Reactivity of the Contact Allergen Benzoquinone and Its Derivatives to Proteins.**

W. Mbiya<sup>1</sup>, I. Chipinda<sup>2</sup>, P. Seigel<sup>2</sup> and R. Simoyi<sup>1</sup>. <sup>1</sup>Chemistry, Portland State University, Portland, OR; <sup>2</sup>Health Effects Laboratory Division, NIOSH, Morgantown, WV.

Benzoquinone (BQ) and substituted benzoquinones (SB) are used for dye and cosmetics production. BQ is an electrophile known to covalently modify proteins via Michael Addition (MA) but the reactivity, reaction mechanistic domains and allergenicity of SB are unknown. Electron withdrawing and electron donating substituents on BQ were assessed for effects on BQ reactivity and allergenicity. Alternative potential protein binding mechanisms were explored. BQ binding to Cys34 on human serum albumin (HSA) was studied and for BQ and SB reactivity studies, nitrobenzenethiol (NBT) was used as a model nucleophile. Hammett and Taft (HT) constants were used to evaluate the influence of these substituents on chemical reactivity. Both NBT binding studies and HT values demonstrated chlorine SB to be more reactive than methyl and t-butyl SB. Production of semiquinone radicals from SB and characterization of SB-NBT adducts demonstrated that haptenation may also occur via free radical mechanism which is pH dependent, and vinylic substitution mechanisms, in addition to the predominant MA. BQ and SB dermal allergenicity as evaluated in the murine local lymph node assay (LLNA) was consistent with that predicted by reactivity and HT data. These results demonstrate the effect of substituents on BQ reactivity and allergenicity while suggesting potential utility of chemical reactivity data and HT values for electrophilic allergen identification and potency ranking.

**PS 1054 Interaction of Para-Phenylenediamine with Human N-Acetyltransferases.**

S. Scheitza, D. Dierolf, J. Bonifas and B. Blömeke. Department of Environmental Toxicology, University Trier, Trier, Germany.

The contact allergen para-phenylenediamine (PPD) is known as a good substrate for N-acetyltransferase 1 (NAT1) but we also found that concentrations above 50  $\mu$ M are accompanied by inhibition of NAT1 activity in human keratinocytes. Here, we investigated the substrate and inhibition characteristics of PPD on NAT enzymes. First we measured whether next to PPD and mono-acetylated PPD (MAPPD) the PPD oxidation product Bandrowskis Base (BB) can also be acetylated. We therefore incubated PPD, MAPPD and BB with human recombinant NAT1 and NAT2 and found them to be good substrates for both enzymes. NAT1 inhibition characteristic of PPD was further studied using the THP-1 cell line which served as model for antigen-presenting cells. Both PPD and MAPPD are N-acetylated by THP-1 and the acetylation is accompanied by NAT1 inhibition. Concentrations above 1  $\mu$ M PPD clearly reduced enzyme activity already after 8h while 47% reduction was measured after 24h (200  $\mu$ M). Independent of the substrate-based enzyme inhibitions, certain compounds are known to oxidize the catalytic cysteine or form adducts with NAT protein. Therefore we studied whether PPD, MAPPD and/or oxidized PPD including BB also interact with recombinant NAT protein itself in the absence of acetyl coenzyme A. All but MAPPD interact with the protein after 2h and the greatest inhibition was found for oxidized PPD (up to 50%). From these results we can conclude that the observed NAT inhibition may be caused by both substrate dependent and independent effects. NAT1 activity in PPD-treated THP-1 cells was completely restored after incubation in fresh culture medium for 24h, whereas inhibition caused by 24h treatment with MAPPD could be restored for only 10%. In sum our data indicate that PPD and its oxidation products can inhibit NAT in two different ways. In addition we demonstrated that PPD and BB are acetylated by NAT1 and 2, suggesting that certain amounts of PPD and eventually formed BB inside the body may be detoxified by NAT1 in skin and additionally by NAT2 expressing organs.

**PS 1055 Pharmacodynamic Profiling of EGFR Inhibitors in HaCaT Cells.**

K. Balavenkatraman, P. Couttet, A. Vicart, B. Bertschi, M. Marcellin, N. Rathfelder, U. Hopfer, O. Grenet, R. Funhoff, S. Chibout, A. Lambert, J. Moggs, E. Pognan and A. Wolf. Discovery and Investigative Safety, Novartis Institutes for Biomedical Research Basel, Basel, Switzerland.

Skin Rash is a serious adverse effect of EGFR inhibitors observed during anticancer therapy in the clinic and appears to be linked to inhibition of the target pathway. The EGFR inhibitors erlotinib and afatinib were investigated at increasing concentrations (0, 0.001, 0.01, 0.1, 1 and 10  $\mu$ M) in the human keratinocyte cell line

HaCaT at different time points (0, 4, 8, 24 hours). Apoptosis, cytokine gene expression and protein release, and the EGFR-downstream signaling events Akt and Erk phosphorylation, were investigated as EGFR pathway pharmacodynamic read-outs.

The tested EGFR inhibitors induced dose-dependent pharmacodynamic responses in HaCaT cells that reflected their differential potencies in recombinant EGFR protein IC50 assays. Analysis of cytokine modulation (CCL-2, CCL-5 CXCL-10, IL-8, TGF- $\alpha$ ) also revealed a very good correlation between the mRNA and protein levels upon treatment with EGFR inhibitors.

These results suggest that HaCaT cells might be a useful model for the profiling of new compounds for potential EGFR pathway inhibitory activities.

## PS 1056 Cytokine-Induced Liver Hepatotoxicity of Trovafloxacin in Co-Culture of Hepatocytes and Kupffer Cells.

E. L. LeCluyse<sup>1</sup>, K. Rose<sup>1</sup>, K. Freeman<sup>2</sup>, S. S. Ferguson<sup>2</sup> and R. P. Witek<sup>2</sup>. <sup>1</sup>The Hammer Institutes for Health Sciences, Research Triangle Park, NC; <sup>2</sup>Life Technologies, Durham, NC.

Immune-mediated chemical-induced hepatotoxicity, i.e. indirect hepatocellular toxicity resulting from immune cells activating liver inflammatory responses, is often overlooked as a potential mode of action due to unavailability of appropriate in vitro models. Kupffer cells are the largest population of resident macrophages in the liver and thus play a critical role in immune-mediated hepatotoxicity and liver injury. For this reason, we have established a co-culture system of rat primary hepatocytes and Kupffer cells that can be used to model chemical-induced immune reactions resulting in acute hepatotoxicity. Hepatocytes and Kupffer cells were cultured for 24-72 hours with various amounts of lipopolysaccharide (LPS) and trovafloxacin (TVX), a compound associated with immune-response-mediated hepatotoxicity in vivo. IL-6 and TNF $\alpha$  levels were assessed by ELISA or Luminex<sup>®</sup> bead assays and CYP3A was measured using Luciferin-IPA as a probe substrate to monitor endotoxin-induced functional changes in metabolic capacity. LPS-treated co-cultures showed marked down-regulation of CYP3A activity, which correlated with up-regulation of IL-6 production. This response was blunted in co-cultures treated with LPS and TVX, showing no changes to CYP3A activity and significantly lower production of IL-6. However, TNF $\alpha$  production was unaffected in TVX/LPS-treated co-cultures and markedly up-regulated in Kupffer cell monocultures. LPS/TVX-treated co-cultures also exhibited increased hepatocellular injury, represented by decreased ATP content and increased LDH leakage. This data suggests that shifts in cytokine profiles, especially IL6/TNF $\alpha$  ratios may play a role in immune-mediated chemical-induced hepatotoxicity. Co-culture of hepatocytes and Kupffer cells may represent a powerful in vitro tool to predict adverse liver effects resulting from indirect adaptive immune reactions during chemical exposure.

This project was supported by funding from the Long-Range Research Initiative (LRI) of the American Chemistry Council (ACC).

## PS 1057 Drugs Associated with Idiosyncratic Drug-Induced Liver Injury Synergize with Inflammatory Mediators to Produce Cytotoxicity in a Human Hepatoma Cell Line.

A. Maiuri<sup>1,2</sup>, R. Parkins<sup>3</sup>, P. E. Ganey<sup>1,2</sup> and R. Roth<sup>1,2</sup>. <sup>1</sup>Pharmacology and Toxicology, Michigan State University, East Lansing, MI; <sup>2</sup>Center for Integrative Toxicology, Michigan State University, East Lansing, MI; <sup>3</sup>College of Veterinary Medicine, Michigan State University, East Lansing, MI.

Idiosyncratic drug-induced liver injury (IDILI) typically occurs in a small fraction of patients and often results in removal of otherwise efficacious drugs from the pharmaceutical market. The mechanisms of IDILI are unknown, and animal models of IDILI are few. Several animal models have been developed that suggest that inflammation plays an important role in IDILI. Moreover, the inflammatory mediators tumor necrosis factor alpha (TNF $\alpha$ ), interferon gamma (IFN $\gamma$ ), and neutrophil-derived elastase (EL) are essential to the pathogenesis of liver injury in these models. The goal of the present study was to determine if two non-steroidal anti-inflammatory drugs associated with IDILI in humans synergize with TNF $\alpha$ , IFN $\gamma$  +/- TNF $\alpha$ , or EL +/- TNF $\alpha$  in producing hepatocellular toxicity in vitro. HEPG2 cells were treated with either diclofenac or sulindac sulfide (the active metabolite of sulindac) and with TNF $\alpha$ , IFN $\gamma$  +/- TNF $\alpha$ , or EL +/- TNF $\alpha$ . Cytotoxicity was significantly increased when cells were treated with diclofenac or sulindac in the presence of TNF $\alpha$  compared to cells treated with drug or TNF $\alpha$  alone. IFN $\gamma$  potentiated the cytotoxicity caused by either drug in the presence of TNF $\alpha$ . EL increased the cytotoxicity caused by diclofenac in the presence of TNF $\alpha$ . These results indicate that some of the events that occur in drug-inflammatory stress models in vivo can be reproduced in cultured cells and suggest the possibility of developing in vitro systems that can predict IDILI liability of drug candidates. (Supported by NIH grant RO1DK061315 and T32 GM092715-01A1).

## PS 1058 Serial Survival Liver Biopsies in Dogs and Monkeys.

V. Dinkel, M. Taschwer, J. Nelson, R. Haas, A. Wathen, A. Kamholz, J. Stuhler, J. Lindsay and F. Thalacker. Covance Laboratories Inc., Madison, WI.

The liver plays a key role in metabolism and excretion of endogenous compounds and xenobiotics and is an area of strong experimental focus. The liver may also be a target for efficacy (e.g. antiviral therapeutics) or toxicity. Animal models are critical for studying xenobiotic metabolism, biomarkers, and pharmacological/toxicological effects on the liver; however the ability to obtain adequate liver tissue samples for analyses in a survival model has been lacking. A surrogate matrix (e.g. blood, plasma, bile) is often used as an indirect measure for liver as its location within the body cavity makes it generally inaccessible for non-terminal sampling. In general, terminal sampling procedures have been needed when larger samples are required and survival procedures have typically been limited to a single collection per animal; the prospect of additional collections being dependent on whether minor (laparoscopic) or major techniques were used. The limitation of a single collection per animal increases the number of animals required to obtain the same data. We have developed laparoscopic surgical techniques for serial survival liver biopsies of ~100 mg, 18 hours apart in dogs and monkeys. We have also developed techniques, at least one laparoscopic, for serial survival biopsies of 1+ g in monkeys with samples taken over a period of weeks. All techniques allow for multiple phases and animal use has been decreased from 50-88%. In all cases, animals recovered completely following each procedure. They have been BAR (bright, alert, responsive), eating and mobile on the same day of surgery and display no signs of pain or distress, indicating exceptional pain management. Also, there have been no significant changes in body weight or clinical pathology and no surgical complications. Overall this work has resulted in the ability to obtain serial liver biopsies in multiple species, providing a significant advantage over current techniques and supporting the 3R philosophy through substantial reductions in animal use without compromising animal welfare.

## PS 1059 Quantitative Relationship Between Intracellular Lithocholic Acid (LCA) and Toxicity in Rat Sandwich-Cultured Hepatocytes (SCH): Incorporation into a Mechanistic Model of Drug-Induced Liver Injury (DILI).

K. Yang<sup>1</sup>, J. L. Woodhead<sup>2</sup>, R. St. Claire<sup>3</sup>, P. B. Watkins<sup>2</sup>, S. Q. Siler<sup>2</sup>, B. A. Howell<sup>2</sup> and K. L. Brouwer<sup>1</sup>. <sup>1</sup>University of North Carolina at Chapel Hill, Chapel Hill, NC; <sup>2</sup>The Hammer-UNC Institute for Drug Safety Sciences, Research Triangle Park, NC; <sup>3</sup>Qualyst Transporter Solutions, Research Triangle Park, NC.

One proposed mechanism of DILI is inhibition of the bile salt export pump resulting in cellular accumulation of toxic bile acids (BAs). The purpose of this study was to establish the quantitative relationship between intracellular LCA concentrations and toxicity. This information is essential to link BA kinetics to toxicity in a BA transport inhibition model constructed within DILIsym<sup>™</sup>, a mechanistic model of DILI. Day3 rat SCH in 24-well plate were incubated with LCA (25–200 $\mu$ M) for 6, 12, and 24hr. Cytotoxicity was assessed by LDH release from damaged cells and intracellular ATP levels. Intracellular LCA/metabolites were measured by LC-MS/MS analysis of lysate after hepatocytes were incubated for 5min with Ca<sup>2+</sup>-free HBSS buffer to open tight junctions using B-CLEAR<sup>®</sup> technology. LCA, and its taurine (TLCA) and glycine (GLCA) conjugates, accumulated extensively in rat SCH. Cellular LCA concentrations increased with increasing LCA medium concentrations; cellular TLCA and GLCA decreased at LCA doses above 100 $\mu$ M, potentially due to saturation of amidation. LC<sub>50</sub> values estimated based on medium and intracellular LCA concentrations at 12hr were 143 and 1098 $\mu$ M, respectively. An E<sub>max</sub>-type relationship was observed between cellular LCA exposure (AUC<sub>LCA</sub>) and toxicity; half maximal toxicity was observed at AUC<sub>LCA</sub> of 10.4 and 16.3mM\*hr for the 12 and 24hr incubations, respectively. Decreased intracellular ATP concentrations preceded the toxicity measured by LDH. AUC<sub>ATP,0-24hr</sub> was correlated with toxicity at 24 hr (r<sup>2</sup>=0.97) and AUC<sub>LCA,0-24hr</sub> (r<sup>2</sup>=0.95). These results provide mechanistic insight that increased cellular exposure of unconjugated LCA leads to ATP depletion and subsequent toxicity.

Supported by NIH R01 GM41935 and DILI-sim initiative.

## PS 1060 Transformation of CO<sub>2</sub> Evolution Assays into Multiwell Plate Format Assays to Assess Effects of Compounds on Substrate Oxidation in Rat Hepatoma H4IIE Cells.

P. A. Cosgrove and J. W. Lawrence. Comparative Biology and Safety Sciences, Amgen Inc., Thousand Oaks, CA. Sponsor: S. Sawant.

Perturbations of metabolic processes are involved in several pathologies including cardiac hypertrophy, hepatic vacuolation, and steatosis. Different substrates can be used to distinguish between electron transport chain, the citric acid cycle,  $\beta$ -oxida-

tion, glycolysis, and amino acid metabolism pathway inhibition. The conventional assay for assessing substrate oxidation is through the use of  $^{14}\text{C}$ -labeled substrates and measuring the formation of  $^{14}\text{CO}_2$ . Historically, these assays are run with septum sealed flasks that are awkward to use, prone to sample loss, and have low throughput. We have adapted the  $\text{CO}_2$  capture method to a 96-well format by using a standard 96-well plate for cell incubation with substrate. A neoprene gasket is used to seal the environment to ensure  $\text{CO}_2$  is collected on a 96-well capture filter plate aligned on top.  $^{14}\text{C}$ -labeled glucose, pyruvate, glutamine, butyrate, octanoate, or palmitate were used as substrates and their oxidation was assessed in H4IIE cells. Etomoxir, an inhibitor of carnitine palmitoyl transferase-1, demonstrated a concentration dependent decrease in palmitate oxidation, however, glucose oxidation increased after treatment suggesting a fuel switching to compensate for the defect in fatty acid oxidation. Methylene cyclopropyl acetic acid (MCPA), a reported inhibitor of medium-chain acyl-CoA dehydrogenase, inhibited both butyrate and octanoate oxidation and had minimal effects on palmitate oxidation. An increase in glucose oxidation was observed after MCPA treatment, similar to that observed with etomoxir suggesting a similar fuel switching. Antimycin A, an electron transport chain inhibitor, decreased the oxidation of multiple substrates with similar potencies, suggesting inhibition at a point in the metabolic pathway common to all substrates. In conclusion, by transforming the classical  $\text{CO}_2$  evolution assay into a 96-well format, the effect of various compounds on various substrates can be assessed in an easier, higher throughput manner.

**PS 1061 Effect of Trichloroethylene Exposure on Autoimmune-Mediated Cholangitis in NOD.c3c4 Mice.**

A. K. Kopec, B. P. Sullivan and J. Luyendyk. *Pathobiology and Diagnostic Investigation, Michigan State University, East Lansing, MI.*

Epidemiological studies support the hypothesis that exposure to environmental chemicals increases the risk of developing autoimmune liver diseases. Despite this association, the identity of specific chemical perpetrators and the mechanism whereby environmental chemicals modify liver disease is unclear. Previous studies have shown that trichloroethylene (TCE) can trigger autoimmunity in susceptible mice. We investigated whether modulation of hepatic gene expression by TCE exposure modified the pathogenesis of autoimmune cholangitis in mice. NOD.c3c4 mice spontaneously develop autoimmune-mediated liver disease with features including biliary cyst formation, portal lymphocytic inflammation, and fibrosis. Nine-week-old NOD.c3c4 mice were exposed to TCE (0.5 mg/ml) or its vehicle (1% Cremaphor-EL) via the drinking water for 4 weeks. TCE exposure had little effect on changes in clinical chemistry, biliary cyst formation, or CD3 T cell accumulation. Rather, global microarray profiling and Ingenuity Pathways (IPA) analysis revealed marked differential expression of PPAR $\alpha$  target genes, in agreement with a computational IPA prediction of PPAR $\alpha$  activation. TCE exposure significantly down-regulated cholesterol metabolism genes, and resulted in a ~3-fold suppression of early growth response 1 (Egr1). Consistent with a link between Egr1 suppression and liver fibrosis, we found that TCE exposure increased Type 1 collagen mRNA and protein levels in livers of NOD.c3c4 mice. In contrast, TCE exposure did not increase type 1 collagen expression in Nod.ShilT mice, which do not develop liver disease. These results suggest that in the context of concurrent autoimmune liver disease with a genetic basis, modification of hepatic gene expression by TCE may increase profibrogenic signaling in liver. Moreover, these studies further highlight the potential use of NOD.c3c4 mice as a model to study gene-environment interactions critical for development of autoimmune-mediated liver disease.

**PS 1062 Identification and Categorization of Transcriptional Profiles and Potential Biomarkers of Liver Injuries Related to a Drug Pair.**

Y. Wang, W. Ge, Z. Liu, M. Lee and W. Tong. *Bioinformatics and Biostatistics, National Center for Toxicological Research, US FDA, Jefferson, AR.*

Amiodarone and benziodarone share similar chemical structure and pharmacological effects, but induce different types of liver injuries in humans. This aspect of the difference can not be seen with the current conventional preclinical toxicity assessments. We hypothesize that the difference in liver gene expression profiles between two drugs correlate with the difference in their injury types. Thus, the aims of this study are to differentiate the drug-induced liver injury mechanisms between amiodarone and benziodarone by analyzing liver gene expression profiles in rats exposed to both drugs. Gene expression profiles of rat liver treated with amiodarone or benziodarone for consecutively 28-days were analyzed and compared to their concurrently control rats to identify the transcriptional changes. Three doses were used, where maximum tolerated dose (MTD) determined from dose range finding studies were considered as the high dose for each molecule while low and middle

doses were calculated from the ratios of the MTD. Several common upstream regulators such as PPAR- $\alpha$ , pirinixic acid, clofibrate were identified spontaneously in rat livers treated with two drugs. Sets of genes were detected to show a dose-response pattern from liver tissues treated with amiodarone and benziodarone, respectively. We suspected that this alteration of genes may be important in the biological progress relating to the different liver injuries caused by the drug pair. Using these differentially expressed genes, biological pathways and networks were developed to categorize the correlation and interaction of each factor in relating to liver injuries and in differentiating hepatotoxicity induced by amiodarone and benziodarone. The results of this study suggested that genomic profiles can be a good starting point in developing mechanism-based biomarkers for prediction and differentiation of liver injuries related to amiodarone benziodarone in early stage of drug discovery and development.

**PS 1063 In Vitro Assessment of Drug Induced Liver Injury (DILI) Using a High Content Cellular Imaging System.**

M. L. Wolfe<sup>1</sup>, S. Einhorn<sup>2</sup>, V. Ott<sup>2</sup> and H. Ma<sup>1</sup>. <sup>1</sup>*Cellular and Molecular Biology, MPI Research, Maitland, MI;* <sup>2</sup>*Cellular Dynamics International, Madison, WI.*  
Sponsor: T. Rogers.

Drug-induced liver injury (DILI) is a leading cause of drugs failing during clinical trials and being withdrawn from the market. In vivo safety testing in pre-clinical species ensures that drugs which enter clinical trials do not cause reproducible and dose-dependent liver injury in man, but is of limited value for exploration of underlying mechanisms and does not assess potential to cause rare idiosyncratic DILI. Implementation of an in vitro cell-based predictive assay early in the drug discovery process would help improve early compound attrition and develop safer drug candidates. We tested compound-treated human hepatocellular carcinoma Hep G2 cells, human induced pluripotent stem cell (iPSC)-derived hepatocytes (iCell® Hepatocytes) and primary human hepatocytes using the Thermo Scientific ToxInsight® IVT platform and DILI Assay Cartridge to determine the hepatotoxicity risk of a compound through the measurement of multiple toxicity biomarkers in individual cells. The compounds we investigated include a number of known hepatotoxic compounds (Ticlopidine, Troglitazone, Naladixic acid, Mefenamic acid, Phenylbutazone and Aflatoxin B1) and non-hepatotoxic compounds (Aspirin, Fluoxetine and Melatonin). Each compound was tested at eight concentrations in triplicate. The DILI Assay Cartridge allows for the high sensitivity and specificity for predicting hepatotoxicity by simultaneously detecting five multiplexed cellular targets and properties associated with cell loss, cellular redox stress, and mitochondrial stress. The hepatotoxicity prediction using the multiparametric data generated for the test compounds demonstrates high specificity across the three hepatocyte models but varying sensitivity for each hepatocyte model system.

**PS 1064 Altered-Hepatic Catabolism of Branched Chain Amino Acids in Progressive Human Nonalcoholic Fatty Liver Disease.**

A. D. Lake<sup>1</sup>, P. Novak<sup>3</sup>, P. Shipkova<sup>2</sup>, N. Aranibar<sup>2</sup>, D. Robertson<sup>2</sup>, M. D. Reily<sup>2</sup>, L. D. Lehman-McKeeman<sup>2</sup>, R. R. Vaillancourt<sup>1</sup> and N. J. Cherrington<sup>1</sup>. <sup>1</sup>*Pharmacology & Toxicology, University of Arizona, Tucson, AZ;* <sup>2</sup>*Bristol-Myers Squibb Co., Princeton, NJ;* <sup>3</sup>*Institute of Plant Molecular Biology, Ceske Budejovice, Czech Republic.*

Branched chain amino acids (BCAAs) and their catabolism have essential roles in metabolic homeostasis. BCAAs are capable of activating the mammalian target of rapamycin (mTOR) during states of over-nutrition resulting in an increased risk of insulin resistance and altered lipid homeostasis. Nonalcoholic fatty liver disease (NAFLD) is closely associated with features of the metabolic syndrome and over-nutrition. Approximately 30-40% of the United States population is afflicted with NAFLD while 5.7-17% is estimated to have severe nonalcoholic steatohepatitis (NASH). A 'two-hit' model has been used to describe the pathological progression of NAFLD to steatosis and then NASH, although the exact mechanisms for disease progression are not known. The hypothesis of this study is that these two 'hits' drive alterations in hepatic branched chain amino acid (BCAA) composition and catabolism while enhancing disease progression. Hepatic transcriptomic and metabolomic data sets representing the entire spectrum of human NAFLD (healthy, steatosis, NASH Fatty, and NASH Not Fatty livers) were utilized to investigate the role of BCAAs in the mechanisms of NAFLD pathophysiology. An increase of the BCAAs leucine (127% of normal), isoleucine (139%) and valine (147%) were observed in NASH samples. Increased BCAA catabolism through upregulated branched chain aminotransferase enzyme appears to drive increases of acylcarnitine products that include butyryl carnitine (353% of normal) and lauryl carnitine (403% of normal). The hepatic overload of BCAAs also potentiates mTOR signaling thereby increasing metabolic dysregulation. Overall, these findings demonstrate altered catabolism of BCAAs in NASH with important downstream signaling implications for lipotoxicity and insulin resistance in the progression of NAFLD.

**PS 1065 Altered Hepatic and Renal Drug Transporter Expression in Multiple Rodent Models of Nonalcoholic Steatohepatitis.**

M. Canet, R. N. Hardwick, A. D. Lake and N. J. Cherrington. *Pharmacology and Toxicology, University of Arizona, Tucson, AZ.*

Nonalcoholic fatty liver disease (NAFLD) is the most common form of chronic liver disease in Western society representing a spectrum of liver damage ranging from simple steatosis to the more advanced nonalcoholic steatohepatitis (NASH). Experimental models of NASH include diet-induced models such as the methionine and choline deficient (MCD) diet and genetically obese models such as the leptin-deficient, ob/ob mice. Previous studies have demonstrated alterations in the expression and activity of multiple drug transporters in human NASH, but little information is known regarding the most appropriate animal models for predictive toxicology to extrapolate in vivo hepatic and renal drug disposition data to human NASH populations. The purpose of the current study was to determine which experimental NASH model best recapitulates human disease pathology as well as alterations in drug transporter expression. Both rat and mouse NASH models were utilized in this investigation and include; MCD diet, atherogenic diet, ob/ob and db/db mice, and fa/fa rats. Histologic and pathological evaluations confirmed that the MCD and atherogenic rats and MCD, ob/ob and db/db mice all developed NASH. In contrast, the fa/fa rats did not develop pathological NASH. Hepatic mRNA levels of drug transporters showed that the rat and mouse MCD diet model and the ob/ob and db/db mice best recapitulate the expression profile seen in human NASH. In general, the majority of efflux transporters are induced whereas uptake transporters are decreased. Similar to the liver, efflux transporter expression in the kidney is also induced at both the mRNA and protein level. However, renal uptake transporter expression across these models is differentially altered and is transporter and model-specific. These results suggest that the MCD rat, and the ob/ob and db/db mouse models may be more useful preclinical models to determine the effect of NASH on drug disposition as well as determining extra-hepatic alterations in drug transporter expression.

**PS 1066 Regulation of ABCC2 Internalization in Nonalcoholic Steatohepatitis.**

A. L. Dzierlenga, R. N. Hardwick, J. Clarke and N. J. Cherrington. *Pharmacology & Toxicology, University of Arizona, Tucson, AZ.*

Non-alcoholic fatty liver disease affects 30-40% of the United States population and can progress to non-alcoholic steatohepatitis (NASH) which is characterized by an accumulation of fat, oxidative stress, fibrosis and inflammation. It has been previously shown that NASH can have a significant effect on the disposition of many drugs and potentially contribute to the occurrence of adverse drug reactions. NASH-associated altered drug disposition has, in part, been linked to stress-induced alterations of the expression and function of hepatic transporters such as ABCC2. ABCC2 is located on the canalicular membrane and transports xenobiotic substrates into the bile for elimination from the body. By mechanisms that are not entirely understood, ABCC2 has been shown to be internalized in rodent and human NASH livers, as well as the in vitro conditions of acute oxidative stress and lipopolysaccharide exposure. Previous reports have suggested that the activation and cellular localization of radixin, protein phosphatase 1, phosphoinositide 3-kinase, protein kinase A, and protein kinase C (PKC) may be involved in the internalization of ABCC2. The purpose of this study is to identify potential mechanisms responsible for ABCC2 internalization in NASH. Sprague-Dawley rats were fed a control methionine and choline supplemented diet or a methionine choline deficient diet (MCD) to model NASH. It was found that in NASH livers there was an increase in the membrane association of the PKC $\epsilon$  isoform compared to control livers, but not PKC $\delta$  or PKC $\alpha$ , implicating PKC $\epsilon$  as a potential regulator of ABCC2 internalization. Additionally, the cellular localization of radixin was not found to change in NASH livers. Further insight into the mechanisms behind functional perturbations of hepatic drug transporters such as ABCC2 has implications for improved understanding and identification of targets for alleviating adverse drug reactions in clinical NASH.

**PS 1067 A RNA-Interference Screen Identifies Novel Regulators of the Ubiquitinase A20/TNFAIP3 As Critical Determinants of Drug-Induced Liver Injury Responses.**

B. van de Water, B. Herpers, L. Fredriksson, G. Benedetti and M. de Graauw. *Division of Toxicology, Leiden University, Leiden, Netherlands.*

The cytokine tumor necrosis factor alpha (TNFalpha) acts in synergy with different drugs, including diclofenac, to initiate drug-induced liver injury (DILI). This is directly related to the inhibition by these drugs of TNFalpha-induced NFkB activation as demonstrated by an inhibition of the NFkB nuclear oscillatory translocation

response. Here we investigated the underlying mechanism of the drug/TNF synergy. We used a live-cell imaging-based siRNA screen to identify individual kinases, (de)ubiquitinases and sumoylases that control the NF-kB oscillatory response. We applied high content confocal laser scan microscopy in combination with multiparametric image analysis to follow the NF-kB oscillation in ~300 individual cells per condition simultaneously. Out of the ~1500 genes screened, we identified 115 that significantly affected the NF-kB oscillatory response. Using 4 individual siRNAs, we confirmed the action for 46 genes, which affected: i. the amplitude or duration of nuclear oscillations; ii. the time between oscillations, leading to an increase or decrease of the number of nuclear translocations; or iii. an inhibition of the response altogether. In this last category we identified six genes, four novel, whose reduced expression protected against the diclofenac/TNFalpha-induced apoptosis. Interestingly, the knockdown of these six genes led to a basic up-regulation of A20 expression. In accordance, A20 knockdown promoted the NF-kB oscillation and enhanced apoptosis. Double knockdown experiments indicated a direct relationship between these four genes and A20 in the control of the NF-kB activation. These findings indicate that the (de)ubiquitinase A20 is a master regulator in the life-death decision upon TNFalpha stimulation in drug-induced hepatotoxic responses, which, in turn, is kept under control by a network of genes that control its expression level.

**PS 1068 Hepatic Transporters in HepaRG Cells and Sandwich-Cultured Human Hepatocytes.**

C. Guugen-Guillouzo<sup>1,2</sup>, P. Bachour-El Azzi<sup>1,3</sup>, R. Li<sup>2</sup>, A. Charanek<sup>1</sup>, Z. Abdel-Razzak<sup>3</sup>, A. Guillouzo<sup>1</sup> and C. Chesne<sup>2</sup>. <sup>1</sup>INSERM 991, Rennes University, Rennes, France; <sup>2</sup>BIOPREDIC, Rennes, France; <sup>3</sup>Lebanese University, Hadath, Lebanon. Sponsor: M. Robin.

Reestablishment of polarized excretory function and maintenance of expression and activity of transporters in liver cell models are critical for in vitro analysis of drug and bile acid excretion as well as toxicity testing. Previous studies have shown that conventional primary hepatocytes and HepG2 cells do not correctly mimic the in vivo situation whereas sandwich-cultured hepatocyte conditions do restore cell polarity for a few days. In the present work we have analyzed expression, activity and distribution of several canalicular and basolateral transporters in hepatocytes from human HepaRG cells compared to sandwich-cultured primary human hepatocytes. Differentiated HepaRG hepatocytes exhibited high polarity with typical bile canalicular structures characterized by F-actin accumulation and restricted by connexin 32-positive tight junctions. In previous reports, most influx and efflux transporters were found to be expressed in HepaRG cells and adult hepatocytes, at the transcriptional level. Using the immunofluorescence technique and imaging analysis their specific distribution was investigated. MRP2 was localized in both models, at the canalicular membrane domain while both MRP3 and MRP4 and the influx transporter NTCP, were demonstrated at the basolateral plasma membrane domains. Trafficking polarization toward canalicular structures through MRP2 and MDR1 was evidenced by using specific substrates coupled with fluorescein and/or mitotracker and Ca<sup>2+</sup> regulation of canalicular excretion was clearly documented. In addition, uptake and release of bile acid taurocholate was investigated in HepaRG cells using H3-taurocholate; both active influx via NTCP activity and canalicular efflux were evidenced. Moreover, addition of chlorpromazine, a compound known to induce cholestasis in vivo, resulted in bile salt efflux inhibition mainly at the canalicular pole. Together, these data support the view that HepaRG hepatocytes represent a suitable in vitro model to investigate human drug and bile acid excretion.

**PS 1069 Deep Sequencing of miRNA in Livers of Rats Exposed to Hepatotoxics.**

M. Flores Torres<sup>1</sup>, J. Wright<sup>1</sup>, R. Currie<sup>2</sup>, C. Koufaris<sup>1</sup> and N. J. Gooderham<sup>1</sup>. <sup>1</sup>Biomolecular Medicine, Imperial College London, London, United Kingdom; <sup>2</sup>Safety Assessment, Syngenta, Jealotts Hill, United Kingdom.

MicroRNAs (miRNAs) are small non-protein coding RNAs. They act as regulators of gene expression, by inhibiting mRNA translation or promoting mRNA degradation, and are involved in diverse physiological and pathological events. Recently we have shown (Koufaris et al. Toxicol Sci: 128, 532, 2012) that the CAR activator phenobarbital (PB) induces deregulation of the hepatic miRNAome in the livers of rats. Next Generation Sequencing (NGS) analysis of small RNAs is a powerful tool that can be used for miRNA expression profiling, and offers a deeper understanding of molecular toxicology. Here we explore the liver miRNAome associated with CAR activation, and to compare this with the effects of the hepatotoxicant dimethylarsinic acid (DMA), which is known to induce mitochondrial perturbation. Male rats were dosed with PB (50 or 1000 ppm) or DMA (4 or 40 ppm) in the diet for 28 days, and sacrificed after 2, 4, 15, and 28. Histopathological evaluation revealed centrilobular hypertrophy at 15 and 28 days after PB treatment and multifocal inflammatory foci with necrosis at 28 days after DMA treatment. Total RNA

was isolated from frozen samples, and library constructs for NGS were generated (TrueSeq Small RNA kit, Illumina). Bioinformatics was used to prioritise potential gene targets of deregulated miRNAs, and qPCR to validate expression of miRNA families and potential gene targets. Consistent with our previous report, miR200 family was induced by 28 days of treatment with PB at 1000ppm, but not by 50ppm. There was a dose-dependent reduction in the zeb1 and zeb2 transcription factors, which are known and validated targets of the miR200 family. The zeb1 and zeb2 transcription factors regulate the epithelial to mesenchymal transition, thus PB-mediated miR200 family induction appears to be a homeostatic response to protect the epithelial nature of hepatocytes. NGS permits a more detailed exploration of the response of the miRNAome to hepatotoxicants such as PB, thereby aiding an understanding of the underlying pathways.

#### PS 1070 High-Content Imaging of Rat Hepatocytes Long-Term Cultures to Predict Specific Drug-Induced Liver Toxicity.

D. Germano, M. Uteng, P. Couttet, O. Grenet, S. Chibout, F. Pognan and A. Wolf. *Discovery and Investigative Safety, Novartis Institutes for Biomedical Research Basel, Basel, Switzerland.*

Primary rat hepatocytes were investigated for liver-specific functional changes after repetitive treatments with model liver toxicants at low concentrations for two weeks. Cells were cultured in the Collagen I/Matrigel™ sandwich configuration. High content imaging (HCI) was performed by using the Cellomics™ Arrayscan®. The liver-specific pathologies cholestasis/hyper-bilirubinemia, steatosis and phospholipidosis were investigated by means of fluorescence dyes. Mrp2-mediated canalicular transport, intra-cellular accumulation of neutral lipids and phospholipids were assessed by carboxy-DCFDA, BODIPY or LipidTOX™ Red, respectively. Unspecific cytotoxicity was measured by ATP contents and LDH releases. Cyclosporin A (CsA), Amiodarone (AMD), Rosiglitazone (RGZ), Chlorpromazine (CPZ), Troglitazone (TGZ), Metformin (MET), Fenofibrate (FFB), Ibuprofen (IBU), Acetaminophen (ACT), Valproic Acid (VPA) and EMD335823 (EMD) were evaluated at four different concentrations and at five time points (day 1, 3, 7, 10, 14). The results showed that inhibition of canalicular transport, induction of phospholipidosis and steatosis occurred after multiple treatments at clinical relevant doses in absence of cytotoxicity in the hepatocytes. CsA, CPZ and TGZ treatment caused time- and concentration-dependent inhibition of Mrp2-mediated transport, while AMD and CPZ induced dose-dependent accumulation of phospholipids. CsA was also associated with intracellular accumulation of lipids, whereas VPA did not induce steatosis. Taken together, the current data suggest that the current testing strategy has a high predictive value for compounds inducing hyperbilirubinemia/cholestasis and phospholipidosis, but not for drug-induced steatosis. In addition, the present work illustrates that HCI is a sensitive and reproducible tool for the evaluations of specific cellular functions and that HCI can be applied in safety profiling of drug candidates. Study is part of the European FP7 PREDICT-IV consortium (grand no 202222).

#### PS 1071 Gene Expression Profiling Identifies Molecular Mechanisms of Tamoxifen-Induced Hepatotoxicity in Mice.

V. Tryndyak, T. Han, M. Churchwell, B. Montgomery, J. C. Fuscoe, J. R. Latendresse, F. A. Beland and I. P. Pogribny. *US FDA-NCTR, Jefferson, AR.*

Tamoxifen is an anti-estrogenic drug widely used for the treatment and prevention of estrogen-receptor-positive breast cancer. However, despite the indisputable benefits of tamoxifen, its use has been associated with the induction of hepatic steatosis. The goal of this study was to investigate the underlying molecular mechanisms associated with tamoxifen-induced hepatotoxicity. Female and male WSB/Eij mice were fed a diet containing 420 ppm tamoxifen for 12 weeks. The livers of tamoxifen-fed mice exhibited moderate pathomorphological changes, as evidenced by glycogen depletion, despite having profound genotoxic and non-genotoxic alterations. Specifically, the livers of tamoxifen-fed mice were characterized by extensive sex-independent accumulation of tamoxifen-DNA adducts and marked changes in the gene expression. To identify tamoxifen-responsive genes that were differentially expressed between the control and tamoxifen-exposed mice, a t-test,  $p < 0.01$ , coupled with a fold-change cut-off  $> 1.5$  was applied. A total of 1245 and 2100 genes were found to be differentially expressed in the livers of tamoxifen-exposed female and male mice, respectively. Interestingly, 361 of the genes were differentially expressed in both female and male mice treated with tamoxifen. Most of these genes were associated with altered lipid metabolism, inflammation, cell death and proliferation, and development of liver fibrosis. These results demonstrate the importance of gene-expression profiling in identify early hepatic molecular events associated with the chronic administration of tamoxifen.

#### PS 1072 A 3D Co-Culture Model-Based Assay to Assess Liver Kupffer-Cell Activation and Functionality.

S. Shetty<sup>2</sup>, K. Adkins<sup>2</sup>, M. Roy<sup>2</sup>, I. Agarkova<sup>1</sup>, J. M. Kelm<sup>1</sup> and S. Messner<sup>1</sup>. <sup>1</sup>InSphero AG, Zurich, Switzerland; <sup>2</sup>Drug-Safety R&D, Investigative Toxicology, Pfizer, Groton, MA. Sponsor: A. Wolf.

Adverse drug reactions in the liver are one of the major causes of attrition in drug development with both small and large molecules. Novel therapeutic modalities such as antibodies and other biologicals can be taken up by non-parenchymal cells, such as phagocytic cells in the liver (mainly Kupffer cells) and can limit drug exposure and cause liver toxicity. Therefore, evaluating Kupffer-cell uptake can serve as an indirect screen for liver toxicity. However, due to lack of suitable organotypic in vitro models, Kupffer cell uptake has been difficult to study. Here, the use of primary heterotypic 3D rat liver microtissues for assessment of drug-induced Kupffer-cell activation is demonstrated. Morphological characterization of rat liver microtissues demonstrated the presence of ED1 and ED2-positive Kupffer cells within the hepatospheres. Electron-microscopy confirmed layering of Kupffer cells between hepatocytes in the rat liver microtissues. Lipopolysaccharide (LPS) treatment of the rat liver microtissues resulted in increased uptake of acetylated LDL (ac-LDL), whereas incorporation of ac-LDL was reduced when the phagocytosis inhibitor gadolinium chloride was applied, indicating ac-LDL uptake by Kupffer cells is dependent on phagocytosis. An increase in IL-6 secretion was also observed at 48 and 120 hrs post-treatment with LPS, indicating Kupffer cell activation. Together these data demonstrate the suitability of heterotypic rat liver microtissues for assessing Kupffer cell activation and functionality by external stimuli, and highlight the potential of 3D rat liver models for evaluating liver toxicity.

#### PS 1073 Organic Solute Transporter Ostα-Ostβ As a Potential Therapeutic Target for the Metabolic Syndrome.

S. Gorman, C. Hammond, P. Hinkle and N. Ballatori. *Environmental Medicine, University of Rochester, Rochester, NY.*

The metabolic syndrome has increased in occurrence in recent decades, and as a result has become a major health concern. Environmental contaminants have been linked to this, as common toxicants have been found to increase susceptibility to weight gain and/or insulin resistance, key features of the metabolic syndrome. This has resulted in a need for pharmaceuticals that lower fat accumulation and improve insulin sensitivity, and this study identifies a novel potential therapeutic target, the bile acid transporter Ostα-Ostβ. Our laboratory has generated an Ostα<sup>-/-</sup> mouse in the C57Bl6 background, a strain susceptible to age-related weight gain. Interestingly, Ostα<sup>-/-</sup> mice have a significant reduction in bile acid pool size. The major purpose of bile acids is to emulsify dietary lipids in the small intestine and facilitate their absorption, but they have also recently been shown to function as signaling molecules that affect lipid and glucose homeostasis. This study aimed to explore differences in lipid and glucose homeostasis in Ostα<sup>-/-</sup> mice. A comparison of whole body and fat pad weights of Ostα<sup>-/-</sup> and wild type mice at 5 and 12 months of age revealed no differences in these parameters at 5 months, but at 12 months, Ostα<sup>-/-</sup> mice had accumulated less fat and had lower total body weights. Similarly, extraction of liver lipids indicated less accumulation of total lipid and cholesterol in hepatic tissue with age. At both ages, increased fecal lipid excretion and altered expression of genes involved in bile acid and lipid homeostasis were noted, and glucose and insulin tolerance tests also revealed significant improvement in glucose tolerance and insulin sensitivity at both ages. These studies indicate that Ostα<sup>-/-</sup> mice excrete more lipids in feces, are resistant to age related weight gain and have improved insulin sensitivity and glucose tolerance, suggesting an inhibitor of Ostα-Ostβ may be useful in treating the metabolic syndrome. (NIH Grant DK067214, NIEHS Training Grant ES07026 and Center Grant ES01247)

#### PS 1074 Predictivity of Drug-Induced Liver Toxicity Using High-Content Screening in 384-Well Cultures of HepG2 Cells and Primary Human Hepatocytes.

K. F. Marcoe<sup>1</sup>, H. J. Garside<sup>2</sup>, J. Chesnut-Speelman<sup>1</sup>, A. J. Foster<sup>2</sup>, U. Warrior<sup>1</sup>, J. Baumgartner<sup>1</sup>, D. Muthas<sup>3</sup>, J. G. Kenna<sup>2</sup> and J. Bowes<sup>2</sup>. <sup>1</sup>Eurofins Panlabs, Bothell, WA; <sup>2</sup>Global Safety Pharmacology, AstraZeneca, Macclesfield, United Kingdom; <sup>3</sup>Global Safety Assessment, AstraZeneca, Molndal, Sweden. Sponsor: J. Valentin.

Drug-induced liver injury (DILI) is a major cause of failed drug development and drug withdrawal. Predictive toxicology screening assays are therefore required for early de-selection of compounds that may cause DILI. Although previous investigators have reported several potentially promising in vitro approaches, it is unclear which cell systems and endpoints can provide the greatest predictive power. In this

study we used multiplexed high content screening, with automated fluorescence microscopy and image analysis, to assess the *in vitro* toxicity of 122 drugs associated with DILI in man and 22 drugs not reported to cause DILI. Studies were undertaken in HepG2 cells with and without rat S9 fraction and in cryopreserved primary human hepatocytes. Toxicity was determined at 4, 24 or 48 h. The parameters assessed were: cell proliferation (nuclear dyes); apoptosis (anti-activated caspase 3); cell cycle (anti-pHistone H3); stress (anti-HSP70/72); reactive oxygen species generation (H2DFFDA dye); mitochondrial damage (TMRE dye); phospholipid and neutral lipid accumulation. All cell systems provided highly specific discrimination (>90%) between those that caused DILI and non-hepatotoxic drugs. The highest sensitivity was observed in HepG2 cells without S9, using the apoptosis (29%) and phospholipidosis (22%) endpoints. Addition of S9 did not increase the sensitivity of any of the parameters studied. In human hepatocytes, the 24 h H2DFFDA assay had a sensitivity of 20%, whereas the other endpoints had sensitivities of <11%. We conclude that toxicity studies in HepG2 cells enabled detection of compounds which may cause DILI in humans with high specificity but low sensitivity and that neither the addition of S9 nor the use of human primary hepatocytes provided improved predictivity.

## PS 1075 Studying Drug-Induced Cholestasis with a Novel Cellular Model Coexpressing Major Bile Salt Transporters in the Liver.

M. S. Warren, J. X. Zhang, J. Huang, P. Druzgala and Y. Huang. *Optivia Biotechnology Inc., Menlo Park, CA.*

Drug induced cholestasis and hepatocellular injury are two major manifestations of drug induced liver disease (DILI). Research has shown such injuries are often attributed to inhibition of bile salt transporters in the liver. NTCP, OATP1B1, BSEP and MRP2 have been identified as the major transporters modulating hepatic clearance of bile salts and their conjugates.

We recently demonstrated that canalicular excretion and intracellular retention of bile salts can be studied with a polarized MDCK cell model concomitantly expressing three major bile salt transporters in the liver, i.e., OATP1B1, NTCP and BSEP. To evaluate the utility of this model in studying drug-induced cholestasis, we tested 20 drugs and their major metabolites that have been reported to cause cholestasis in the human. More than half of the drugs or their metabolites, including traglitzone, benzbromarone and bosentan, significantly inhibited B>A transcellular transport (canalicular excretion) of [3H]Taurocholate at clinically relevant concentrations, suggesting that blocking transporter mediated canalicular excretion of bile salts is a major mechanism of drug induced-cholestasis *in vivo*. Furthermore, a few drugs, such as Rifampicin, remarkably elevated intracellular concentration of Taurocholate (which has been suggested to lead to hepatocellular damage), suggesting that at high concentrations, these drugs are more likely to cause cholestatic hepatitis than the others. Other agents, such as estradiol-17-beta-glucuronide, tamoxifen and pyrazinamide, did not exhibit significant inhibitory effect on Taurocholate transport under the test conditions, which suggests there may be other mechanism(s) involved.

In summary, our study demonstrates that the novel OATP1B1/NTCP/BSEP triple transporter expression model can be a useful economical tool for early-stage screening and for mechanistic study of compounds with cholestasis liability.

## PS 1076 Use of a Multiplexed Endpoint Assay Strategy to Assess Model Bioactivated Compounds in Sandwich-Cultured Hepatocytes.

K. Wille<sup>1</sup>, A. L. Niles<sup>2</sup>, J. J. Cali<sup>2</sup> and E. L. LeCluyse<sup>1</sup>. <sup>1</sup>The Hammer Institutes for Health Sciences, Research Triangle Park, NC; <sup>2</sup>Promega Corporation, Madison, WI.

Sandwich-cultured rat hepatocytes (SCRH) represent a metabolically competent *in vitro* model for screening and identifying potentially hepatotoxic compounds that correlates well with *in vivo* results. In this study, we employ a novel strategy for multiplexing a broad complement of metabolic plater reader assays using SCRH to measure hepatotoxicity of model bioactivated compounds, such as acetaminophen (APAP). This approach yields a profile of early toxicity indicators that provides greater mechanistic insight from fewer experimental replicates. SCRH in 24- or 48-well plates were exposed to 8 concentrations of APAP in the presence or absence of the CYP inducer, dexamethasone (DEX); CYP inhibitor, 1-aminobenzotriazole (ABT); and the glutathione synthesis inhibitor, L-buthionine sulfoximine (BSO). Toxicity was assessed at 24 and 48 hours for Cyp3A activity (Promega P450-Glo<sup>TM</sup>), ATP content (Promega CellTiter-Glo<sup>®</sup> Assay), lactate dehydrogenase leakage (Promega CytoTox ONE<sup>TM</sup> Homogenous Membrane Assay), and glutathione content (Promega Glutathione-Glo<sup>TM</sup> Assay). Resulting ATP, glutathione, and LDH data showed dose- and time-dependent APAP toxicity which was moderated, especially at the 24 hour time point, by ABT and exacerbated by DEX. CYP3A ac-

tivity was induced up to 4-fold by DEX and significantly inhibited by ABT (5% of DMSO controls). BSO nearly eliminated intracellular glutathione levels by 48 hours and increased hepatocyte APAP sensitivity. Collectively, these data demonstrate the utility of SCRH as a model to assess bioactivated compounds for hepatotoxicity. The multiparameter assay approach offers greater mechanistic insight into the nature and timing of the toxicity.

This project was supported by the Long-Range Research Initiative (LRI) of the American Chemistry Council (ACC) and Promega Corporation, Madison, WI.

## PS 1077 Cytotoxic Interaction of Inflammagens with Trovafloxacin in Spheroid Cultures of Rat Liver Cells.

R. A. Roth<sup>1</sup>, P. C. Wilga<sup>2,1</sup>, K. L. Poulsen<sup>1</sup>, K. M. Beggs<sup>1</sup>, J. Prezenger<sup>2</sup>, A. Maiuri<sup>1</sup>, P. E. Ganey<sup>1</sup> and J. McKim<sup>2</sup>. <sup>1</sup>Pharmacology and Toxicology, Michigan State University, East Lansing, MI; <sup>2</sup>CeeTox, Inc., Kalamazoo, MI.

Idiosyncratic, drug-induced liver injury (IDILI) typically escapes detection in pre-clinical safety evaluation of drug candidates due to paucity of predictive models. Recently, models have arisen in which liver injury occurs in rodents treated with trovafloxacin (TVX) or other IDILI-associated drugs and coexposed to an inflammagen such as bacterial lipopolysaccharide (LPS). The hepatocellular injury depends on tumor necrosis factor- $\alpha$  (TNF) and possibly other cytokines released by nonparenchymal cells (NPCs) and therefore cannot be reproduced in monocultures of hepatic parenchymal cells (HPCs). Accordingly, the cytotoxicity of TVX in the presence and absence of LPS was evaluated in 3-dimensional (3D) spheroid cultures (InSphero) containing equal numbers of HPCs and NPCs and compared to data obtained from HPCs in standard sandwich culture. Spheroids or standard HPC cultures were exposed to various concentrations of TVX (10 -100  $\mu$ M) alone or with LPS (10  $\mu$ g/ml) or TNF (10 ng/ml) for 24 hr. TNF was detected in the culture medium of spheroids cotreated with LPS and TVX, but not with either agent alone, and no TNF was detected in HPC cultures treated similarly. Cytotoxicity, as assessed by decreases in intracellular ATP content, was evident only in spheroids cotreated with LPS and TVX. In contrast, treatment of either spheroids or HPC cultures with TNF in the absence or presence of TVX did not result in consistent cytotoxicity. Levofloxacin (LVX) is in the same pharmacological class as TVX, but has far less IDILI liability; interestingly, there was no cytotoxic interaction with LVX and LPS or TNF. These results show that LPS-stimulated inflammatory mediator production and cytotoxicity occurred in 3D spheroid cultures containing NPCs cotreated with TVX. 2D-sandwich HPC cultures were less sensitive to cytotoxicity from the TVX-inflammation interaction, suggesting that spheroids may afford advantages in evaluating interactions between drugs and inflammatory mediators.

## PS 1078 Trovafloxacin Induces Cell Cycle Arrest and Sensitizes HepG2 Cells to TNF-Induced Cytotoxicity by an ATR-Dependent Mechanism.

K. M. Beggs<sup>1,3</sup>, K. Miyakawa<sup>2,3</sup>, M. A. Scott<sup>2</sup>, P. E. Ganey<sup>1,3</sup> and R. A. Roth<sup>1,3</sup>. <sup>1</sup>Pharmacology and Toxicology, Michigan State University, East Lansing, MI; <sup>2</sup>Pathobiology and Diagnostic Investigation, Michigan State University, East Lansing, MI; <sup>3</sup>Center for Integrative Toxicology, Michigan State University, East Lansing, MI.

Trovafloxacin (TVX) is an antibiotic associated with idiosyncratic hepatotoxicity in humans, though the mechanism for this toxicity is unknown. In mice, TVX is not hepatotoxic by itself but synergizes with tumor necrosis factor- $\alpha$  (TNF) to produce liver injury. Moreover, treatment with combinations of TVX and TNF were cytotoxic to HepG2 human hepatoma cells, whereas neither TVX nor TNF alone caused cytotoxicity. It was demonstrated previously that TVX is a weak inhibitor of eukaryotic topoisomerase-II  $\alpha$  activity and inhibits HepG2 cell proliferation. These results led to the hypothesis that signaling mechanisms important in cell cycle regulation contribute to cytotoxicity from TVX/TNF interaction. In HepG2 cells treated with both TVX and TNF, activities of caspases 9 and 3 were increased starting 8 hr after treatment, which is a time before the onset of cell death. Cytologic evaluation revealed that cells treated with TVX or with TVX/TNF were arrested in the prophase of mitosis compared to vehicle or TNF-treated cells, which appeared in all stages of the cell cycle. The PI3K-like kinases, ataxia telangiectasia mutated (ATM), ataxia telangiectasia and Rad3-related (ATR), and DNA protein kinase (DNAPK), as well as the tumor suppressor protein p53, all play a role in regulating cell cycle. Pharmacologic inhibitors of ATM, DNAPK, and p53 had no significant effect on the cytotoxicity caused by TVX/TNF treatment, whereas an inhibitor of ATR attenuated cytotoxicity. Taken together, these data suggest that increased activity of caspases 9 and 3 is associated with TVX/TNF-induced cytotoxicity of HepG2 cells and that ATR plays a role in this cell death response. (Supported by NIH grant R01DK061315.)

**PS 1079 MicroRNA Regulation of Alcoholic and Nonalcoholic Fatty Liver Disease.**

S. Kondraganti<sup>1</sup>, T. K. Varma<sup>2</sup>, B. S. Kaphalia<sup>1</sup> and G. Ansari<sup>1</sup>. <sup>1</sup>Pathology, The University of Texas Medical Branch, Galveston, TX; <sup>2</sup>Anesthesiology, The University of Texas Medical Branch, Galveston, TX.

Alcoholic liver disease (ALD) and non-alcoholic fatty liver disease (NAFLD) are histologically similar diseases as both induce fatty liver (hepatic steatosis) through mechanisms not yet fully understood. MicroRNAs (miRNAs), small non-coding RNAs are involved in regulation of various biological process and dysregulated microRNA expression is observed in various diseases including fatty liver. To understand the role of miRNAs in inducing hepatic steatosis, miRNAs were analysed in the livers of both ALD and NAFLD models. Male Fischer-344 rats were fed with or without 5% alcohol via Lieber-DeCarli diet for one, two or three months or L- aminoacid rodent diet with or without methionine-choline for one week. We observed differential expression of eleven miRNAs in both treatment models. Increased expression of miR-122 and miR-34a was observed in ethanol treated rat livers as time progressed while miR-122 expression decreased and no change in miR-34a expression was observed in rat livers fed with methionine-choline deficient (MCD) diet. Contrary, expression of miR-451 was increased in both ethanol fed rats with time as well as MCD diet fed rats. However, the increase in miR-451 expression was more pronounced in MCD diet fed rat livers. miR-122 is known to be involved in hepatic lipid metabolism and sterol synthesis, miR-34a is involved in lipid metabolism, cell cycle and apoptosis while miR-451 is involved in regulation of insulin dependent (gluconeogenesis) pathway. Our miRNA expression data also supported the differential regulation of genes involved in lipid metabolism such as sterol regulatory element-binding protein (SREBP), AMP-activated protein kinase (AMPK), peroxisome proliferator-activated receptor alpha (PPAR- $\alpha$ ), sirtuin-1 and acyl-CoA synthetase long-chain family member 1 (ACSL-1). In conclusion, our studies show that differential expression of miRNAs results in steatosis in both models but could be via different mechanisms.

**PS 1080 Characterization of HepaRG-EP Cells As a Surrogate for Primary Human Hepatocytes.**

J. J. Cali<sup>1</sup>, M. Sobol<sup>1</sup>, D. Ma<sup>1</sup> and D. Steen<sup>2</sup>. <sup>1</sup>Research, Promega Corporation, Madison, WI; <sup>2</sup>Biopredic International, Overland Park, KS. Sponsor: T. Riss.

HepaRG-EP (EP) cells are a next generation version of HepaRG (HRG), a human hepatoma cell line with substantial similarity to primary human hepatocytes (HH). We characterized cryopreserved EP from Biopredic International to evaluate their suitability as a HH surrogate for in vitro toxicity and ADME studies, and for comparison to HRG (Biopredic). The DMSO content of the EP cryopreservation medium was low enough for compatibility with a no spin thaw/recovery protocol that yielded about 90% viable cells (HRG required DMSO removal). One cryopreserved vial of EP provided for two full confluent 96 well plates of cells, which exceed the yield from typical commercially sourced vials of HH. EP cell viability was relatively constant over a period of 7 days in culture. Like HRG, EP established an adherent co-culture of hepatocytes and cholangiocytes but EP had a higher hepatocyte/cholangiocyte ratio. Consistent with this hepatocyte enrichment, EP also had higher activity for CYP1A2, -2D6, -2B6 but similar CYP3A4 activity, and these activities were within the range typically observed in HH. The initial EP CYP3A4 activity remained elevated for the first 24 hours, but then declined to a lower yet still robust level that averaged about 25% of the initial activity over the next 6 days. As a marker of metabolic capacity, the sustained CYP3A4 activity suggests EP will provide a good model for acute or extended drug metabolism studies. Omeprazole, phenobarbital and rifampicin respectively caused substantial inductions of CYP1A2, -2B6 and -3A4 activities with a more pronounced CYP1A2 response in EP compared to HRG. In common with HH, dose-dependent aflatoxin-B1 toxicity was observed with HRG and EP, indicating their competence for detecting metabolism-based toxicities. In summary, EP provides a convenient model for hepatotoxicity, metabolism and CYP induction studies with the reproducibility inherent to a cell line. For the properties tested EP is a reasonable HH surrogate with enhanced metabolic capacity and convenience over HRG.

**PS 1081 Use of a Multiparametric Assay on Isolated Mouse Liver Mitochondria to Predict Drug-Induced Liver Injury in Human.**

A. Borgne-Sanchez<sup>1</sup>, M. Porceddu<sup>1</sup>, N. Buron<sup>1</sup>, C. Roussel<sup>1</sup> and B. Fromenty<sup>2</sup>. <sup>1</sup>Mitologies Research Laboratory, Mitologies SAS, Paris, France; <sup>2</sup>INSERM U991, Faculté de Pharmacie, Rennes, France. Sponsor: N. Claude.

Drug-induced liver injury (DILI) is difficult to predict using classical in vitro assays and regulatory animal studies leading to interruption of clinical trials or even to market withdrawal after commercialisation. Consequently, drug-induced mito-

chondrial dysfunction should be detected early, ideally during pre-clinical screening of potential drug candidates. This could be done by investigation of drug-induced mitochondrial dysfunction which appears as a major mechanism of DILI. To achieve this detection, we have developed a dedicated high-throughput screening platform using isolated mouse liver mitochondria to measure several parameters related to mitochondrial function and integrity. Indeed, this multiparametric assay measures in isolated mouse liver mitochondria: 1) global mitochondrial membrane permeabilization (swelling), 2) transmembrane potential, 3) outer membrane permeabilization (cytochrome c release) and 4) oxygen consumption through respiratory chain complex I and complex II. A pool of 124 drugs was tested revealing a highly significant relationship between drug-induced mitochondrial toxicity and DILI occurrence in patients ( $P < 0.001$ ) with an excellent sensitivity (94 or 92% depending on cut-off) and a high positive predictive value (89 or 82%) [1]. Moreover, our study disclosed for the first time the identification of several drugs triggering mitochondrial toxicity. Investigation of drug-induced loss of mitochondrial integrity and function with this assay should be considered for integration into basic screening processes at early stage to select drug candidates with lower risk of DILI in human. This multiparametric assay is also a valuable tool for assessing the mitochondrial toxicity profile and investigating the mechanism of action of new compounds and marketed drugs.

[1] Porceddu M, Buron N, Roussel C, Labbe G, Fromenty B, Borgne-Sanchez A. (2012). *Toxicol Sci.* 129: 332-45.

**PS 1082 CAR Activation Increases Bile Flow, Excretion of Major Bile Acids, and Bile Acid Synthesis, As Well As Transport Genes in Mice.**

A. J. Lickteig, I. L. Csanaky, M. Pratt-Hyatt and C. D. Klaassen. *Internal Medicine (Division Gastroenterology), University of Kansas Medical Center, Kansas City, KS.*

Activation of Constitutive Androstane Receptor (CAR) has been shown to protect against bile acid (BA)-induced liver injury. However, the effect of CAR activation on bile flow, BA profile, and BA synthesis and transport genes in liver is not well understood. Therefore, the purpose of the present study was to determine the effect of CAR activation on BA homeostasis. The CAR ligand 1,4-Bis-[2-(3,5-dichloropyridyloxy)]benzene (TCPOBOP) was administered intraperitoneally (3 mg/kg) daily to male C57BL6/N wild-type mice for 4 days, followed by collection of serum, liver, and bile. BAs of serum and bile were quantified by UPLC-MS/MS. TCPOBOP induced a CAR-dependent increase in bile flow by 67%. TCPOBOP increased biliary excretion of two of the three quantitatively major bile acids in mice, T $\alpha$ MCA (3.5-fold) and T $\beta$ MCA (80%), as well as the quantitatively minor bile acids TUDCA (38%) and TCDCA (224%). Additionally, TCPOBOP increased biliary excretion of unconjugated bile acids by 74%. These increases in biliary excretion correlated with increased liver mRNA of the two major canalicular efflux transporters Mrp2 (3.2-fold) and Bsep (2.4-fold). Interestingly, TCPOBOP induced BA synthesis genes Cyp7a1 (4.3-fold) and Cyp27a1 (110%). Also in livers of TCPOBOP-treated mice, the sinusoidal efflux transporters Mrp3 (17-fold) and Mrp4 (14-fold) were markedly increased. Surprisingly, there were no changes in serum concentrations of total BAs, taurine-conjugated BAs, unconjugated BAs, or primary BAs, but the serum secondary BAs were decreased 61%. In summary, while CAR activation has relatively minor effects on serum BA profile, CAR activation increases bile flow and biliary excretion of T $\alpha$ MCA, T $\beta$ MCA and total unconjugated BAs. (R01ES009649, R01DK081461, F32DK092069)

**PS 1083 Role of Aryl Hydrocarbon Receptor (AhR) in Maintaining Plasma Concentrations and Biliary Excretion of Bile Acids.**

I. L. Csanaky, A. J. Lickteig, M. Pratt-Hyatt and C. D. Klaassen. *Department of Internal Medicine, University of Kansas Medical Center, Kansas City, KS.*

Failure in regulation of bile acid (BA) homeostasis contributes to several liver diseases. It is generally accepted that hepatic FXR-SHP and intestinal Fgf15/19 regulate BA homeostasis. However, the contribution of other hepatic transcription factors to BA homeostasis is not clear. The adaptive role of the aryl hydrocarbon receptor (AhR) in protecting against BA related liver damage is unknown. The AhR may be critical for mediating an adaptive response that involves induction of genes responsible for the metabolism or transport of BAs. To study the role of the AhR in BA homeostasis, sera, livers, and bile of 12-week-old male wild-type and AhR-null mice were collected, and BA concentrations in serum and bile, as well as the mRNA expression of hepatic BA synthesis and transport genes were quantified. Surprisingly the lack of AhR increased serum total BAs (62-fold), taurine conjugated-BAs (52-fold), and unconjugated-BAs (113-fold). Similarly the biliary excretion of total BAs (2.3-fold), taurine conjugated-BAs (2.3-fold), and unconjugated-BAs (3.8-fold) increased in AhR-null mice compared with controls. In livers of

AhR-null mice the mRNA expression of Fgfr4 (111%), SHP (83%), Cyp7a1 (170%), Cyp8b1 (70%), BAL (60%), Bsep (50%), and Mrp3 (80%) were increased, whereas Cyp7b1 (-64%) was decreased in comparison to wild-type mice. In conclusion, lack of the AhR receptor results in an increase in (1) mRNA of the majority of BA synthesis and transport genes, (2) conjugated and unconjugated BAs in serum, as well as (3) the biliary excretion of conjugated and unconjugated BAs. These findings suggest that AhR has a fundamental role in suppressing synthesis, transport, plasma concentrations, and biliary excretion of BAs. (Supported by NIH grants ES009649, ES013714, DK092069)

#### PS 1084 Screening of AMPK Activator from Herbal Extract.

S. Lee and M. Dong. *School Lifesciences and Biotechnology, Korea University, Seoul, Republic of Korea.* Sponsor: B. Lee.

AMP-activated protein kinase (AMPK) is a key sensor and regulator of glucose, lipid, and energy metabolism throughout the body. Activation of AMPK improves metabolic abnormalities associated with metabolic diseases including obesity and type-2 diabetes. AMPK phosphorylation inhibits sterol regulatory element-binding protein-1 (SREBP-1) activity which plays an important role in lipid metabolism. In this study, we established in vitro screening methods for potential activators of AMPK from herbal extracts to develop the inhibitor of hepatic steatosis. First, the phosphorylation of AMPK and its substrate ACC-1 were screened by In-cell-western assay which is an immunocytochemical assay performed in 48 well-microplate format and then confirmed them using Western blot in HepG2 cells. Oil Red O staining is performed to observe the accumulation of lipid droplets in cell and then tested the expression of genes related lipid synthesis and metabolism. When we screened over 50 herbal extracts, we found three extracts which were significantly increased the phosphorylation of AMPK and its substrate ACC-1 in a dose-dependent manner. They also reduced the palmitic acid induced lipid droplets accumulation determined by Oil Red O staining. Among them, one extract was selected and observed SREBP-1 transcriptional activity using a SRE-luc reporter gene assay and SREBP-1 target genes expression using RT-PCR. In this study, we could identify the natural extracts for the development of AMPK activator for diabetes and the metabolic syndrome.

#### PS 1085 Gender Differences in mRNA and Protein Expression of Nuclear Factor Erythroid 2-Related Factor 2 (Nrf2) and Nrf2-Dependent Genes.

P. Rohrer and J. E. Manautou. *Department of Pharmaceutical Sciences, University of Connecticut, Storrs, CT.*

Nuclear factor erythroid 2-related factor 2 (Nrf2) is a transcription factor that positively regulates the expression and activity of cytoprotective genes during periods of oxidative stress. It has previously been shown that some of these cytoprotective genes are more highly expressed in livers of female than male mice. This could explain previously reported gender-related differences in susceptibility to acetaminophen (APAP) hepatotoxicity in mice. In this study, we examined the presence of differences in basal mRNA and protein expression for Nrf2 and Nrf2-dependent genes between naïve fed male and female mice. Hepatic mRNA and protein levels were measured by quantitative PCR and western blotting, respectively. Basal Nrf2 mRNA expression was significantly lower in livers of female than male mice. Furthermore, mRNA expression of the Nrf2-regulated genes NAD(P)H quinone oxidoreductase 1 (Nqo1), heme oxygenase 1 (Ho-1) and multidrug resistance-associated protein transporter 4 (Mrp4) was less pronounced in livers of male than female mice, although these differences were not statistically significant. Conversely, mRNA levels of glutamate cysteine ligase catalytic subunit (Gclc), glutamate cysteine ligase modifier subunit (Gclm), and multidrug resistance-associated protein transporter 3 (Mrp3) appeared more pronounced in male mice than female mice, but these difference were not significant either. Protein levels of Nqo1 and Mrp4 were similar between genders, while protein levels of Mrp3 and Gclm were significantly lower in livers of female than male mice. In agreement with mRNA levels of Nrf2, lower protein expression of Nrf2 was seen in female mice, although this difference was not significant. Collectively, these results indicate that female mice do not have higher global expression of Nrf2-related genes and that other factors might be responsible for the lower susceptibility of female mice to APAP hepatotoxicity. Supported by NIH DK069557.

#### PS 1086 Metabolomics Evaluating Protective Effects of Green Tea Extract on Acetaminophen-Induced Hepatotoxicity in Mice.

J. Sun<sup>1</sup>, Y. Lu<sup>1,2</sup>, X. Yang<sup>1</sup>, J. Greenhaw<sup>1</sup>, W. F. Salminen<sup>1,3</sup>, D. L. Mendrick<sup>1</sup> and R. D. Beger<sup>1</sup>. <sup>1</sup>NCTR/US FDA, Jefferson, AR; <sup>2</sup>Jiangsu Institute for Food and Drug Control, Jiangsu, China; <sup>3</sup>PAREXEL International, Boston, MA.

Green tea has a considerable amount of polyphenolic catechins (potent antioxidants) and it has shown to have protective effects on oxidative stress-related diseases. Acetaminophen (APAP) is a widely used analgesic drug that can cause liver injury if overdose. The aim of this study was to explore the effects of green tea extract (GTE) on APAP-induced hepatotoxicity using an LC/MS-based metabolomic approach. Male B6C3F1 mice were orally administered GTE (500 or 1000 mg/kg) either 3 h prior to 200 mg APAP/kg oral treatment, or for three consecutive days (once daily) followed by 300 mg APAP/kg on the fourth day. Blood and liver tissue samples were collected 24 h after APAP administration for clinical chemistry, histopathological and metabolomic analysis. LC/MS-based metabolomics profiling was utilized to examine metabolic changes in liver extracts. The partial least squares discriminant analysis of the LC/MS data showed that groups dosed with APAP alone were the most distinct from controls, while animals dosed with 500 mg GTE/kg followed by APAP treatment were located between these two and those pre-treated with 1000 mg GTE/kg groups were nearest to control group. These results were consistent with histopathological data showing that 3h single or 3d consecutive dosing with 1000 mg GTE/kg prior to APAP exposure significantly alleviated some of the hepatocyte necrosis. Similar results were observed for ALT and AST. Dose dependent changes were observed in the energy pathway-related metabolites, including acylcarnitines (mitochondrial injury biomarker) and lysophosphatidylcholines, which returned to controls levels after 3h or 3d consecutive dosing GTE prior to APAP treatment compared to APAP treatment alone. These results indicate that GTE treatments prior to APAP dosing could relieve liver injury.

#### PS 1087 Oleoic Acid Produces Cholestatic Liver Injury in Mice.

J. Liu, Y. Lu, Y. Zhang, K. C. Wu and C. D. Klaassen. *Internal Medicine, University of Kansas Medical Center, Kansas City, KS.*

Oleoic acid (OA) is a triterpenoid that exists widely in fruits and medicinal herbs. OA is effective in protecting against hepatotoxins. However, we recently found that whereas a low dose of OA is hepatoprotective, higher doses and long-term use of OA produce cholestasis. This study characterized OA-induced cholestatic liver injury. Adult C57BL/6 mice were given OA at doses of 0, 50, 100, 200, and 300 µmol/kg, sc (suspended in 2% Tween-80 saline) for 5 days, and cholestatic liver injury was observed at doses of 200 µmol/kg and above, as evidenced by increases in serum total bilirubin, serum activities of alanine aminotransferase and alkaline phosphatase, as well as by histopathology with feathering-like degeneration indicative of cholestasis. Serum bile acid (BA) concentrations were dramatically increased not only for unconjugated bile acids (CA, CDCA, DCA, αMCA and βMCA), but also for taurine conjugated bile acids (TCA, TCDCA, TDCA, TUDCA, and TaβMCA), as determined by UPLC-MS/MS. The mRNAs of hepatic bile acid uptake transporter for unconjugated BAs Oatp1b2 and conjugated BAs Ntcp, as well as canalicular efflux transporter Bsep were decreased in a dose-dependent manner. OA decreased OSTα but increased OSTβ. Hepatic uptake transporter Oatp1a1, 1a4, and 2b1 were suppressed, while the efflux transporters Abca1, Abst, and Bcrp were increased. OA decreased the mRNA of the nuclear receptors CAR, FXR, PPARα, but had no effects on AhR and PXR. The mRNA of the BA biosynthesis limiting enzyme Cyp7a1 was decreased. Taken together, higher doses of OA produces cholestatic liver injury in mice and this effect appears to be associated with the alteration of liver transporters resulting in disruption of BA homeostasis.

#### PS 1088 Apoptogenic, Necrogenic, and Unique Patho-Morphological Changes Induced by Bio-Activation-Dependent Hepatotoxins.

P. Patel, M. E. Kiersma and S. D. Ray. *Pharmaceutical Sciences, Manchester University College of Pharmacology, Fort Wayne, IN.*

The diagnosis of drug-induced liver disease is an intriguing question often accompanied by insufficient clinical data and the difficulty of interpreting histopathology after exposure to toxins. This study investigated the histopathological changes induced by several different bioactivation-dependent hepatotoxins, such as, acetaminophen (an analgesic; 500mg/Kg, ip), carbon tetrachloride (CCl4; a hepatotoxin), dimethylnitrosamine (DMN; a potent carcinogen), doxorubicin (DOX; an antineoplastic agent), furosemide (FUR; a loop diuretic) and streptozotocin (STZ;

an inducer of hyperglycemia) to characterize most common and most uncommon pathological traits in order to hypothesize whether a subset of lesions can be used to diagnose toxicity profile of a particular toxin. Mice were administered CCl<sub>4</sub> (1ml/Kg, po), DMN (50 mg/Kg, ip), DOX (60 mg/Kg, ip), Fur (500 mg/Kg, ip) and STZ (100 mg/Kg, ip 2 consecutive doses) and sacrificed 24-72 hours later. Blood was collected for serum chemistry and liver sections for histopathology. PAS or H&E stained liver sections were examined under a brightfield microscope to determine similarities concerning: sinusoidal dilatation, centrilobular necrosis, excessive vacuolization, cells with apoptotic morphology, microvesicular steatosis, ballooning degeneration, pericentral or periportal or indiscriminate necrosis, glycogen depletion trend, inflammation, and formation of ground glass hepatocytes. Results indicated that all the toxins caused massive liver injury with limited overlapping profiles. The most common features were indiscriminate glycogen depletion and ballooning of hepatocytes. Results also indicated various other characteristic morphological changes such as macrovesicular steatosis, bridging necrosis, portal tract fibrosis and some unique but yet to be reported feature induced by DOX, i.e., prominent sinusoidal dilation. Thus, our study made a serious effort in differentiating and profiling the varied patho-morphological changes induced by diverse hepatotoxins. [Suppo. by Dept. of PSCs, AMS Coll of Pharm & HSCs]

### PS 1089 Cholestyramine Liver Effects in Healthy Human Subjects.

R. Singhal<sup>1</sup>, A. H. Harrill<sup>3</sup>, F. Menguy-Vacheron<sup>2</sup>, Z. Jayyosi<sup>1</sup>, H. Benzerdjeb<sup>2</sup> and P. Watkins<sup>3</sup>. <sup>1</sup>Sanofi, Inc., Framingham, MA; <sup>2</sup>Sanofi, Chilly-Mazarin, France; <sup>3</sup>The Hammer Institute, Research Triangle Park, NC.

Cholestyramine is an orally administered, an ion exchange non-absorbable resin with a high affinity for biliary acids used as a cholesterol lowering agent as well as to accelerate clearance from the body of xenobiotics and to treat itching in patients with advanced cholestatic liver disease. This treatment has been associated with elevations in serum alanine aminotransferase (ALT), a sensitive biomarker of liver injury, but has never been associated with clinically important liver injury. A recent clinical trial in healthy adults receiving cholestyramine provided an opportunity to use current serum biomarkers to investigate mechanisms underlying this phenomenon. After a double blind, placebo controlled study cholestyramine (8 gm/tid X 11 days) was administered to healthy adult subjects to accelerate clearance of the new drug candidate given in the active arm. During cholestyramine therapy, eleven subjects previously treated with placebo experienced elevations in serum ALT levels exceeding three-fold the upper limit of normal (>3x ULN; mean 6.9 fold; range 3-28 fold). Serum samples from those subjects were assayed for additional mechanistic biomarkers. Compared to predose baseline values, there was a significant (<0.05) 13-fold mean increase in miR-122 confirming a liver source for the serum ALT. Mean serum levels of GLDH (8-fold), cytokeratin 18, and HMGB1 (1.7 fold) were elevated supporting ongoing necrosis. Caspase-cleaved cytokeratin 18 was also increased (1.7 fold) supporting apoptosis. Serum ALT elevations observed during cholestyramine treatment reflect both hepatocellular necrosis and apoptosis. The wealth of clinical data available with cholestyramine indicate that this effect on the liver is self-limited and not a significant safety concern.

### PS 1090 Sterile Inflammation and Neutrophil Activation during Injury Resolution following Acetaminophen Overdose in Mice and Humans.

C. D. Williams, M. R. Sharpe, M. R. McGill, M. Bajt and H. Jaeschke. <sup>1</sup>UAMS, Little Rock, AR; <sup>2</sup>Arkansas Children's Nutrition Center, Little Rock, AR.

Following acetaminophen (APAP)-overdose, there is a robust inflammatory response triggered by the release of cellular contents from necrotic hepatocytes into systemic circulation which recruits neutrophils (PMNs) into the liver. PMNs do not contribute to APAP-induced injury in mice, but their role, and the role of NADPH oxidase, in injury resolution is unclear. C57BL/6 mice were treated with APAP and were euthanized (6h - 72h) for assessment of liver injury and regeneration. Informed and consented human APAP-overdose patients (ALT >800U/L) had serial blood draws during injury and recovery phases for determination of liver function tests (LFTs) and flow cytometric analysis. Blood PMNs (mouse, human) and liver PMNs (mouse) were evaluated by flow cytometry (CD11b, reactive oxygen priming, phagocytosis). To test the importance of phagocyte ROS production, gp91phox-/- (NADPH oxidase defective) mice were compared to C57BL/6 mice for hepatocyte proliferation and injury resolution. PMNs in the peripheral blood of mice showed increasing activation status during and after the peak of injury but returned to baseline levels prior to injury resolution. Hepatic sequestered PMNs showed an increased and sustained CD11b expression, but no ROS priming was

observed. Confirming that NADPH oxidase is not essential for recovery, gp91phox-/- mice following APAP-overdose displayed no difference in injury resolution. APAP-overdose patients also showed increased PMN activation status after the peak of injury, and PMNs remained in an activated state even as LFTs began to normalize. The time course of PMN activation status in the peripheral blood was similar in mice and humans, and markers of activation were increased and sustained well after active liver injury had subsided. The similar findings between surviving patients and mice indicate PMN activation may be a critical event for injury resolution following APAP-overdose in man, but not a contributing factor to APAP-induced injury.

### PS 1091 Ethyl Tertiary-Butyl Ether Induces Oxidative Stress and 8-OHdG Formation in the Liver of F344 Rats via Activation of CAR, PXR and PPAR Nuclear Receptors.

A. Kakehashi<sup>1</sup>, A. Hagiwara<sup>2</sup>, N. Imai<sup>2</sup>, Y. Doi<sup>2</sup>, K. Nagano<sup>3</sup>, M. Banton<sup>4</sup>, F. Nishimaki<sup>5</sup>, H. Wanibuchi<sup>1</sup> and S. Fukushima<sup>6</sup>. <sup>1</sup>Department Pathology, Osaka City University Graduate School of Medicine, Osaka, Japan; <sup>2</sup>DIMS Institute of Medical Science, Ichinomiya, Japan; <sup>3</sup>Nagano Toxicologic-Pathology Consulting, Kanagawa, Japan; <sup>4</sup>Toxicology and Risk Assessment, LyondellBasell Corporate HSE, Houston, TX; <sup>5</sup>Japan Petroleum Energy Center, Tokyo, Japan; <sup>6</sup>Japan Bioassay Research Center, JISHA, Kanagawa, Japan.

To elucidate the mode of action (MOA) of hepatotumorigenicity in rats for non-genotoxic chemical ethyl tertiary-butyl ether (ETBE), male F344 rats were treated with ETBE at doses of 300 and 2000 mg/kg/day by gavage and 500 ppm phenobarbital (PB) in diet for the comparison analysis for 1 and 2 weeks. Significant increases of hydroxyl radicals and P450 total content levels at weeks 1 and 2 in 300, 2000 mg/kg/day ETBE and PB groups accompanied the accumulation of P450 isoenzymes CYP2B1/2, CYP3A1/2 and CYP2C6 in the cytoplasm of hepatocytes. Specific up-regulation of CYP2E1 and CYP1A1 was obvious in the high dose ETBE group. Conspicuous elevation of 8-hydroxydeoxyguanosine (8-OHdG) and apoptosis in the liver tissue observed in 2000 mg/kg/day ETBE and PB groups was associated with suppression of Ki-67 positive-cell index, cyclin D1 mRNA expression and down-regulation of 8-OHdG repair enzyme, DNA glycosylase 1 (Ogg1) after 2 weeks of application. Results of QSTAR LC/MS/MS and IPA analyses indicated that upstream regulators of gene expression altered by ETBE included CAR, PXR and PPAR. High dose ETBE induced peroxisome proliferation in hepatocytes at week 2 detected by TEM. These results indicated that MOA of ETBE hepatotumorigenicity in rats is due to induction of oxidative stress and 8-OHdG formation, subsequent cell cycle arrest and apoptosis, suggesting regenerative cell proliferation, predominantly induced by activation of CAR and PXR nuclear receptors by a mechanism similar to that of PB, and furthermore peroxisome proliferation by specific activation of PPAR. The MOA of ETBE hepatotumorigenicity in rats is indicated to be not relevant to human.

### PS 1092 Expression Profiles of Hematopoietic Stem Cell, Endothelial Cell, and Myeloid Cell Antigens in Spontaneous and Chemically Induced Hemangiomas and Hemangiosarcomas in Mice.

S. Kakiuchi-Kiyota<sup>1,2</sup>, C. A. Torrie<sup>3</sup>, L. L. Arnold<sup>1</sup>, K. L. Pennington<sup>1</sup>, J. C. Cook<sup>2</sup>, D. Malarkey<sup>4</sup> and S. M. Cohen<sup>1</sup>. <sup>1</sup>Pathology and Microbiology, University of Nebraska Medical Center, Omaha, NE; <sup>2</sup>Drug Safety Research & Development, Pfizer Inc., Groton, CT; <sup>3</sup>Experimental Pathology Laboratories, Research Triangle Park, NC; <sup>4</sup>National Toxicology Program, NIEHS, Research Triangle Park, NC.

It is unclear whether the process of spontaneous and chemically induced hemangioma (HA) and hemangiosarcoma (HS) formation in mice involves the transformation of differentiated endothelial cells (ECs) or recruitment of multipotential bone marrow-derived hematopoietic stem cells or endothelial progenitor cells (EPCs) which show some degree of endothelial differentiation. In the present study, immunohistochemical staining for hematopoietic stem cell markers (CD45 and CD34), EC markers (VEGFR2, CD31, and Factor VIII-related antigen (FVIII RAg)), and a myeloid lineage marker (CD14) was used to assess the origin of HA and HS in mice and compare with results of canine and human EC tumors reported in previous literature. We showed that the staining for CD45, FVIII RAg, and CD14 was negative in spontaneous and chemically induced HA and HS, whereas cells stained positive for CD34, VEGFR2, and CD31 in these tumors. These results indicate that mouse HA and HS are composed of cells derived from EPCs expressing CD34, VEGFR2, and CD31, but not FVIII RAg. The lack of

CD45 expression suggests that mouse vascular tumors may arise from EPCs that are at a stage later than hematopoietic stem cells. Since FVIII RAg expression is known to occur later than CD31 expression in EPCs, our observations may indicate that these tumor cells are arrested at a stage prior to complete differentiation, in contrast to vascular tumor cells in humans and canines, which express both CD31 and FVIII RAg. In addition, unlike human infantile HA or canine HS, myeloid lineage cells do not appear to contribute to HA and HS formation in mice. Our results may indicate that mouse HA and HS may arise by a different mechanism than canine or human EC tumors.

### PS 1093 Role of the Circadian Clock in the Differential Susceptibility of Rat Strains to Mammary Carcinogenesis.

M. Fang and H. Zarbl. *Environmental Occupational Medicine, University of Medicine and Dentistry of New Jersey, Piscataway, NJ.*

Disruption of circadian rhythm is associated with increased risk of breast cancer incidence and malignancy. DNA damage responsive and repair pathways are controlled by and also modulate the molecular circadian oscillators. In order to investigate the role of the circadian clock on the susceptibility to mammary tumor, we compared circadian expression patterns of genes involved in circadian rhythm and DNA damage responsive and repair pathways in mammary glands of susceptible Fisher 344 (F344) and resistant Copenhagen (COP) rats. The mammary tissue of susceptible F344 rats showed a 4-hr delay in the rhythmic expression of clock genes (e.g., *Per2* and *Bmal1*) and much higher amplitude on *Rev-ErbA $\alpha$*  expression compared to resistant COP rats. In mammary glands of COP rats, 45.1% of DNA responsive and repair genes (total 82 genes) were up-regulated in a circadian pattern with peak expression levels over 2 folds at Zeitgeber Time (ZT)12 (lights off) compared to ZT0 (lights on). By contrast, in the susceptible F344 rats, 30.5% of these genes showed a circadian pattern of down-regulation, with only one gene being up-regulated in the active phase. Exposure to a single carcinogenic dose of N-nitroso-N-methylurea (NMU) disrupted the rhythmic expression of *Per2* in mammary gland of F344 rats after two days and further abolished after 30 days. In contrast, NMU induced a significant increase in the rhythmic expression of *Per2* gene in the COP rats in 2 days, and the increase was sustained for at least 30 days post exposure. Moreover, the ratio of NAD<sup>+</sup>/NADH and NAD<sup>+</sup>-dependent Sirt1 activity, were also significantly increased in NMU-treated COP, but were dramatically decreased in treated F344 rats. Taken together, we speculate that the genetic block to tumor progression in COP is, at least in part, due to the ability to maintain or enhance circadian rhythm, and hence DNA repair upon exposure to carcinogens. (Supported by NIEHS grants, U19ES011387, P30ES007033, and P30ES005022).

### PS 1094 Transcriptomic Profiling of Hepatoblastomas and Associated Hepatocellular Carcinomas in B6C3F1 Mice.

S. Bhusari<sup>1</sup>, A. Pandiri<sup>1,4</sup>, Y. Wang<sup>1</sup>, J. Foley<sup>1</sup>, H. Hong<sup>1</sup>, T. Ton<sup>1</sup>, K. R. Shockley<sup>2</sup>, S. Peddada<sup>2</sup>, K. E. Gerrish<sup>3</sup>, D. Malarkey<sup>1</sup>, R. Sills<sup>1</sup> and M. Hoenerhoff<sup>1</sup>. <sup>1</sup>Cellular and Molecular Pathology, National Toxicology Program, NIEHS, Research Triangle Park, NC; <sup>2</sup>Biostatistics Branch, NIEHS, Research Triangle Park, NC; <sup>3</sup>Microarray Core, NIEHS, Research Triangle Park, NC; <sup>4</sup>Experimental Pathology Laboratories, Research Triangle Park, NC.

The cell of origin of hepatoblastoma (HB) is unknown; it is thought to be a transformed hepatocyte, an oval cell, or a multipotent hepatic progenitor cell. Many investigators believe that HBs arise solely within hepatocellular carcinoma (HCC), and therefore are a more malignant form of HCC. Comparison of differential gene expression changes in HB to HCC in which they arise may identify alterations specific to each tumor type, as well as alterations shared by both tumor types. Such studies may provide information on the possible cell of origin and pathogenesis of these tumors. In the current study, frozen samples from chemically-induced HB, associated HCC, tumor-associated normal (AN) liver, and vehicle control normal (VN) liver from a 2-year National Toxicology Program (NTP) bioassay were laser capture microdissected from B6C3F1 mouse liver tumor samples. RNA was isolated, amplified, and global gene expression profiling was performed to identify differential transcriptomic changes between sample groups. Principal component analysis of the normalized transcriptomic data showed that the HB samples clustered distinctly from HCC. When compared to AN, there were increased numbers of differentially expressed genes in HB (10,386 genes) compared to HCC (1,073 genes). Genes involved in Wnt/ $\beta$ -catenin signaling, hepatic embryonic stem cell-like phenotype and genomic imprinting were significantly altered in HB compared to HCC, pathways prominent in human HB pathogenesis. Meta-analysis of HB tumors revealed high concordance with murine embryonic liver E10.5 to 12.5d gene expression. Understanding the molecular differences between HB and HCC

will provide a more accurate assessment of the pathogenesis of chemically-induced HB and HCC, and may have an impact on hazard identification of compounds important in human health risk.

### PS 1095 Methionine Sulfoxide Stimulates Hepatocarcinogenesis in Mouse; Possible Role of Free Radical-Mediated DNA Methylation.

K. Kawai<sup>1</sup>, H. Kasai<sup>1,4</sup>, Y. Li<sup>1</sup>, M. Song<sup>1</sup>, A. Kakehashi<sup>2</sup>, H. Wanibuchi<sup>2</sup> and A. Ootsuyama<sup>3</sup>. <sup>1</sup>Department of Environmental Oncology, University of Occupational and Environmental Health, Kitakyushu, Japan; <sup>2</sup>Department of Pathology, Osaka City University Medical School, Osaka, Japan; <sup>3</sup>Department of Radiation Biology, University of Occupational and Environmental Health, Kitakyushu, Japan; <sup>4</sup>OHG Institute, Kitakyushu, Japan.

Methylation of the cytosine C-5 position in the promoter region of tumor suppressor genes is an important mechanism of carcinogenesis in addition to gene mutation. However, the actual mechanisms of de novo methylation are not clear. We have reported the formation of 5-methylcytosine from cytosine in vitro, with methyl radicals generated from methionine sulfoxide (MetO). To confirm this reaction in vivo, MetO was added to the drinking water and administered to non-alcoholic steatohepatitis (NASH) mice, which develop hepatitis caused by endogenous oxidative stress. All of the animal experimental procedures were performed in accordance with the guidelines for the care and use of laboratory animals at Univ. Occup. Environ. Health. Histopathological examinations revealed incidences of hepatocellular carcinoma of 16.7% and 90% in the 0% and 3% MetO groups, respectively. Higher DNA methylation was detected in the promoter region of the *p16* gene isolated from the livers of MetO-treated mice. The higher incidence of liver tumors may be due to the methyl radical-mediated formation of 5-methylcytosine in DNA, which triggers epigenetic changes.

References: 1) Kawai K, et al. DNA methylation by dimethyl sulfoxide and methionine sulfoxide triggered by hydroxyl radical and implications for epigenetic modifications. *Bioorg Med Chem Lett.* 2010; 20: 260-5. 2) Kasai H, et al. DNA methylation at the C-5 position of cytosine by a methyl radical: a link between environmental agents and epigenetic change. *Genes and Environment.* 2011; 33: 61-5. 3) Kawai K, et al. Methionine sulfoxide stimulates hepatocarcinogenesis in non-alcoholic steatohepatitis (NASH) mouse: possible role of free radical-mediated DNA methylation. *Genes and Environment.* 2012; 34: 123-8.

### PS 1096 Differential Activation of Mitogenic Signaling through the Insulin Receptor or the Insulin-Like Growth Factor 1 Receptor of Various Clinical Relevant Insulin Analogues.

B. ter Braak<sup>1</sup>, K. Siezen<sup>3</sup>, B. van de Water<sup>1</sup> and J. van der Laan<sup>2,3</sup>. <sup>1</sup>Toxicology, LACDR, Leiden University, Leiden, Netherlands; <sup>2</sup>National Institute of Public Health and the Environment (RIVM), Bilthoven, Netherlands; <sup>3</sup>Medicines Evaluation Board (MEB), Utrecht, Netherlands.

Several epidemiological studies suggest an association between the use of some insulin analogues and cancer incidence in diabetic patients. Different insulin analogues might affect the affinity and activation of these analogues towards the insulin receptor (INSR) and the insulin-like growth factor 1 receptor (IGF1R). A switch towards higher IGF1R affinity is likely to emphasize cellular signalling pathways that promote mitogenesis rather than glucose metabolism.

To investigate this hypothesis we have performed in vitro exposure experiments with several insulin analogues including glargine, AspB10, aspart, glulisine, lispro and detemir. To separate INSR versus IGF1R activation motifs of these analogues, we used human breast cancer cell lines (MCF7) that either ectopically express the INSR (A or B isoform) in conjunction with a stable knockdown of the IGF1R, or the IGF1R in conjunction with a stable knockdown of the INSR. Using Western blots we measured the activation of INSR and IGF1R as well as downstream mitogenic signalling cascades including ERK and Akt. We revealed differences in activation patterns between the different insulin analogues tested. While insulin primarily acted through the INSR, the mitogenic signalling activation pattern of the long-acting insulin glargine was highly similar to that of known mitogenic compounds like insulin AspB10 or insulin like growth factor 1 (IGF1) and acted mainly via the IGF1R. These findings correlated with the proliferative effect of insulin glargine: at low insulin glargine concentrations a clear increase in cell proliferation was observed. This occurred despite the fact that the EC50 for the proliferative effect was not much different from regular insulin. Therefore, these data suggest that insulin glargine is similar in mitogenic potency to AspB10 and IGF1, at least at low and presumably physiological concentrations.

**PS 1097 Deletion of Hepatocyte Nuclear Factor 4 Alpha Promotes Diethylnitrosamine-Induced Hepatocellular Carcinoma.**

C. Walesky<sup>1</sup>, S. Gunewardena<sup>2</sup>, G. Edwards<sup>1</sup>, P. Borude<sup>1</sup> and U. Apte<sup>1</sup>.  
<sup>1</sup>Pharmacology, Toxicology, and Therapeutics, University of Kansas Medical Center, Kansas City, KS; <sup>2</sup>Kansas Intellectual and Developmental Disabilities Research Center, University of Kansas Medical Center, Kansas City, KS.

HNF4 $\alpha$  is known as the master regulator of hepatocyte differentiation. However, role of HNF4 $\alpha$  in regulation of hepatocyte proliferation is not known. We investigated role of HNF4 $\alpha$  in regulation of hepatocyte proliferation using a novel tamoxifen-inducible hepatocyte specific HNF4 $\alpha$  knockdown mouse model. Hepatocyte specific deletion of HNF4 $\alpha$  in adult mice resulted in increased hepatocyte proliferation with a significant increase in liver/body weight ratio. RNA sequencing-mediated global gene expression analysis revealed that a significant number of the 500+ up-regulated genes are associated with cell proliferation and cancer. Further, a combined bioinformatics analysis of ChIP-sequencing and RNA-sequencing data indicated that a substantial number of up regulated genes are putative HNF4 $\alpha$  targets. IPA-mediated functional analysis revealed the most significantly activated gene network after HNF4 $\alpha$  deletion is regulated by c-Myc. To determine role of HNF4 $\alpha$  in pathogenesis of HCC, we performed the classic initiation-promotion experiment using diethylnitrosamine (DEN). Deletion of HNF4 $\alpha$  resulted extensive promotion of DEN-induced hepatic tumors. HNF4 $\alpha$  deletion resulted in 4-fold higher hepatic tumors, which were highly proliferative and less differentiated. Further, the HCC observed in HNF4 $\alpha$  deleted mice exhibited significant up regulation of c-Myc and its target genes. These data indicate that HNF4 $\alpha$  inhibits hepatocyte proliferation, is a potential tumor suppressor in the liver and plays a critical role in chemical carcinogenesis.

**PS 1098 EGCG Elicits Stage-Specific Sensitivity in a Novel Prostate Cancer Progression Model.**

M. A. Moses<sup>1</sup>, W. A. Ricke<sup>2</sup> and T. A. Gasiewicz<sup>3</sup>. <sup>1</sup>Department of Pathology, University of Rochester, Rochester, NY; <sup>2</sup>Department of Urology, University of Wisconsin-Madison, Madison, WI; <sup>3</sup>Department of Environmental Medicine, University of Rochester, Rochester, NY.

Epigallocatechin gallate (EGCG), a major tea catechin, has been shown to have protective effects in a mouse model of PRCA, however, the relevance to human PRCA and the mechanism of action are less understood. We made the novel discovery that EGCG is a heat shock protein 90 (hsp90) inhibitor. Therefore, we utilized non-tumorigenic, tumorigenic, and metastatic PRCA cells from a human PRCA progression model to test the hypothesis that malignant cells are more sensitive to EGCG in a stage-specific manner and that sensitivity is related to the ability of EGCG to act as a hsp90 inhibitor. Treatment of cells with EGCG (25-50 $\mu$ M) *in vitro* decreased the viability and proliferation, and induced apoptosis selectively in PRCA cells compared to non-tumorigenic cells. EGCG also led to a decrease in the motility of tumorigenic PRCA cells, as analyzed by scratch assay, at the same concentrations tested. Moreover, when tumorigenic or metastatic cells were grown *in vivo*, mice supplemented with 0.06% EGCG in drinking water had significantly smaller tumors than those of the untreated group. To elucidate the mechanism of EGCG sensitivity, we performed affinity chromatography with EGCG-sepharose. Binding assays revealed that hsp90 from metastatic cells had a higher affinity for EGCG than non-tumorigenic cells. Furthermore, EGCG disrupted hsp90 complex formation, as analyzed by Native PAGE, leading to an accumulation of dimeric hsp90, and promoted the degradation of hsp90-client proteins such as HER2, p-Akt, and Raf1 in metastatic cells at concentrations that affected viability. These data suggest that EGCG may be an efficacious small molecule for the treatment of PRCA because it selectively targets PRCA cells and inhibits a molecular chaperone involved in many pro-cancer signaling cascades. Future studies will test if analogs of EGCG are more stable/bioavailable, and therefore more potent hsp90 inhibitors, for the treatment of PRCA. Funded by NIH Grant AT006366.

**PS 1099 Fluopyram: Mechanistic Investigations to Elucidate the Moa for Thyroid Tumor Formation in the Mouse.**

D. Rouquié<sup>1</sup>, O. Blanck<sup>1</sup>, H. Tinwell<sup>1</sup>, P. Maliver<sup>1</sup>, F. Schorsch<sup>1</sup>, S. Wason<sup>1</sup>, D. Geter<sup>2</sup> and R. Bars<sup>1</sup>. <sup>1</sup>Bayer CropScience, Sophia Antipolis, France; <sup>2</sup>Bayer CropScience, Research Triangle Park, NC.

Fluopyram, a broad spectrum fungicide, caused an increased incidence of thyroid follicular cell (TFC) adenomas in males at the highest dose evaluated (750 ppm equating to 105 mg/kg/d) in the mouse oncogenicity study. Mechanistic studies were conducted in the male mouse to characterize the mode of action (MoA) for the thyroid tumor formation and to determine if thresholds exist for each key event. The proposed MoA consists of an initial effect on the liver by activating the

constitutive androstane (CAR) and pregnane X (PXR) nuclear receptors causing increased elimination of thyroid hormones followed by an increased secretion of in thyroid stimulating hormone (TSH). This change in TSH secretion results in an increase of TFC proliferation which leads to hyperplasia and eventually adenomas after chronic exposure. CAR/PXR nuclear receptors were shown to be activated from as early as 3 days of treatment as indicated by increased activity of specific Phase I enzymes (PROD and BROD respectively). Furthermore, evidence of increased T4 metabolism was provided by the induction of phase II enzymes known to preferentially use T4 as a substrate. Additional support for the proposed MoA was given by an increase of Tsh transcripts in the pituitary gland. Finally, increased TFC proliferation (BrdU incorporation) was observed after 28 days of treatment. In these dose response studies, clear thresholds were established for liver enzyme activities, T4 and TSH changes and TFC proliferation. Furthermore, each early change was shown to be reversible following fluopyram withdrawal. In conclusion, these studies indicate that fluopyram is a threshold carcinogen and the resultant increased incidence of TFC adenoma in the male mouse is mediated by CAR/PXR activation, with subsequent TFC proliferation. Since liver mediated thyroid toxicity has been reported to be rodent specific, it is unlikely that fluopyram would induce thyroid changes and tumours in humans.

**PS 1100 Oncogene PKC Epsilon Inhibits Transcription Factor Nrf2 through Phosphorylation of Its Regulatory Molecule INrf2 (Keap1).**

S. K. Niture and A. K. Jaiswal. *Pharmacology, University of Maryland, Baltimore, MD.*

Nrf2:INrf2 (Keap1) serve as sensors of chemical and radiation stress and are critical in protection against oxidative stress and cellular transformation. INrf2 functions as an adaptor protein for Cul3-Rbx1-mediated ubiquitination and degradation of Nrf2. Exposure to stressors leads to dissociation of Nrf2 from INrf2, stabilization and nuclear translocation of Nrf2 and activation of Nrf2 downstream cytoprotective proteins leading to cellular protection and survival. The molecular signal(s) that control INrf2 control of Nrf2 remains elusive. In this report, we demonstrate that oncoprotein protein kinase C epsilon (PKC $\epsilon$ ) phosphorylates INrf2 at amino acid positions Ser599 and Ser602 that is essential for INrf2:Nrf2 interaction and ubiquitination/degradation of Nrf2. Therefore, PKC $\epsilon$  by regulating INrf2 controls Nrf2 and expression of downstream cytoprotective proteins and cell survival. PKC $\epsilon$  phosphorylation of INrf2 appears specific for recognizing Nrf2 since it does not affect INrf2 interaction with other proteins including ubiquitin factors Cul3/Rbx1. Inhibition of PKC $\epsilon$  or MEFs lacking PKC $\epsilon$  or INrf2S602A mutant all failed to phosphorylate INrf2 and led to reduced degradation of Nrf2 and enhanced Nrf2 downstream signaling resulting in increased cell survival, proliferation and drug resistance. An analysis of protein microarray data from human lung and liver tumors showed lower PKC $\epsilon$  and higher Nrf2. This inverse relationship between PKC $\epsilon$  and Nrf2 in tumors presumably contributed to cancer cell survival and drug resistance. In conclusion, this is the first report that demonstrates a role of PKC $\epsilon$  in phosphorylation of INrf2 and control of Nrf2 with significant implications in survival of cancer cells that often express lower levels of PKC $\epsilon$ .

**PS 1101 A Weight-of-Evidence Approach to Determine the Leydig Cell Tumor Mode-of-Action (MoA) for Pronamide.**

R. J. Rasoulpour<sup>1</sup>, A. K. Andrus<sup>1</sup>, M. J. LeBaron<sup>1</sup>, S. Marty<sup>1</sup>, L. H. Pottenger<sup>1</sup>, S. Papineni<sup>2</sup> and D. L. Eisenbrandt<sup>2</sup>. <sup>1</sup>The Dow Chemical Company, Midland, MI; <sup>2</sup>Dow AgroSciences, Indianapolis, IN.

Pronamide, a herbicide, caused an increased incidence of Leydig cell tumors (LCT) in CD rats at 1000 ppm (27% vs. 9% in controls) and liver hypertrophy after two years of dietary exposure. There was no Leydig cell hyperplasia or tumors at the 12-month interim necropsy. Dose levels of 40 or 200 ppm had LCT incidences similar to controls, identifying a clear effect threshold. A series of studies was performed to elucidate the MoA for rat LCT and its relevance to humans. Pronamide was negative for mutagenicity/clastogenicity, which is the only known LCT MoA with clear human relevance. Other LCT MoAs have little to no relevance to humans and all commonly affect the endocrine system. Pronamide was negative for androgen and estrogen receptor binding, aromatase inhibition, steroidogenesis alterations, and estrogen receptor transactivation. Despite no evidence of direct action upon the endocrine system, *in vivo* MoA studies revealed a slight, but consistent, increase in circulating levels of luteinizing hormone (LH), estradiol, and estrone in rats at  $\geq$  1000 ppm. It is proposed that the high-dose hormonal alterations are secondary to induction of liver-based testosterone metabolism/inactivation, coincident with liver hypertrophy and increased cytochrome P450s. Secondary increases in LH are proposed to result in mitogenic stimulation of rat Leydig cells, which are quantitatively more sensitive than human Leydig cells to LH-driven proliferative response, based

primarily upon >10-fold more LH receptors per cell in rats vs. humans. This difference in sensitivity is supported by the >1,000-fold difference between background incidence of human LCT vs. the rat. Overall, the weight-of-evidence for pronamide-induced rat LCT supports a threshold-response (i.e., nonlinear) approach for risk assessment due to the lack of genotoxicity, absence of direct endocrine effects, clear NOAEL for the LCT response (200 ppm), and an adequate margin of exposure for an effect in a uniquely sensitive animal model.

## PS 1102 Hepatic Nongenotoxic Carcinogen-Induced Temporal Changes in the Hepatic miRNAome.

K. Chen<sup>1</sup>, W. Jayne<sup>2</sup>, R. Currie<sup>2</sup>, C. Koufaris<sup>1</sup> and N. J. Gooderham<sup>1</sup>.

<sup>1</sup>Biomolecular Medicine, Imperial College London, London, United Kingdom; <sup>2</sup>Safety Assessment, Syngenta, Jealotts Hill, United Kingdom.

Non-genotoxic carcinogens are capable of inducing carcinogenesis via means other than direct modification of DNA structure. While there are many tests readily available for detecting genotoxic substances, methods for detecting and screening non-genotoxic chemical carcinogens are limited. Here we explore the potential of miRNA dysregulation as an indicator of non-genotoxic carcinogens by assessing the temporal-dependent changes in the miRNAome of Fisher rats. Ten chemical compounds, including: Phenobarbital (PB, 1000ppm), Chlorendic Acid (Chl Ac, 1250ppm), Diethylhexylphthalate (DEHP, 1200ppm), Monuron (Mon, 1500ppm), Methapyrilene Hydrochloride (MP HCl, 250ppm), 2-Aminoacetylfluorene (genotoxic, 2-AAF, 40ppm), cinnamon anthranilate (CA, 30,000ppm), Diethylhexyldipate (DEHA, 25,000ppm), Benzophenone (BP, 1250ppm) and Diethylthiourea (DETU, 250ppm), were fed in the diet to Fisher rats for a period of up to three months and liver samples were harvested at 7, 28 and 90 days. The total RNA was purified and analysed with Agilent Rat miRNA Microarrays Kit (Release 16.0). The expression of multiple hepatic miRNAs was found to be altered in response to chemical treatment in a temporally-dependent manner. Chemicals with a similar mode of action (eg: DEHP and DEHA) induced similar responses on the hepatic miRNAome, confirmed by hierarchical clustering analysis qPCR. In the case of DEHA and DEHP, miR-101 family and miR-212 were transiently elevated (at least 3 fold) at 7 days of treatment. In contrast MiR-200 family expression was unaffected at 7 days but was significantly induced at 90 days of treatment. MiR-101 family and miR-212 family are predicted to regulate MAPK3 pathway and target myc gene in the p53 feedback pathway, whereas the miR-200 family are involved in regulating the epithelial-mesenchymal transition and metastasis. These data suggest that miRNAs are potential biomarkers of nongenotoxic hepatocarcinogens and understanding the consequences of miRNA dysregulation aids the understanding of the mechanisms of carcinogens.

## PS 1103 Dietary Carcinogen PhIP Induces Early DNA Damage and p53 Pathway Activation in CYP1A-Humanized Transgenic Mice.

J. Chen<sup>1,2</sup>, G. Li<sup>2</sup>, H. Wang<sup>2</sup>, A. Liu<sup>2</sup> and C. S. Yang<sup>2</sup>. <sup>1</sup>Joint Graduate Program in Toxicology, UMDNJ-Rutgers University, Piscataway, NJ; <sup>2</sup>Department of Chemical Biology, Rutgers, The State University of New Jersey, Piscataway, NJ.

2-Amino-1-methyl-6-phenylimidazo[4,5-b]pyridine (PhIP) is a dietary carcinogen and the most abundant heterocyclic amine generated from high temperature cooking of meat and fish. PhIP is activated via N2-hydroxylation to a proximate carcinogen primarily by cytochrome 1A2. CYP1A-humanized (hCYP1A) mice, which replaced the murine Cyp1a1 and Cyp1a2 with human CYP1A1 and CYP1A2, mimic human metabolism of PhIP. Previous study in our lab demonstrated that in hCYP1A mice, a single oral administration of PhIP induces high-grade prostatic intraepithelial neoplasia, mainly in the dorso-lateral glands (DLGs). Because murine DLGs correspond to the human prostate peripheral zone, the most common site of prostate cancer, PhIP-induced carcinogenesis in hCYP1A mice is a relevant mouse model for studying early stage prostate carcinogenesis. Herein, we investigated the early cellular and molecular events induced by PhIP in the dorso-lateral prostate of hCYP1A mice. Using immunohistochemistry, we detected strong positive staining of 8-Oxo-2'-deoxyguanosine as well as  $\gamma$ -H2AX in the DLGs on Days 1 and 3 after PhIP treatment, suggesting DNA damage and DNA strand breaks. Through gene expression profiling analysis and RT-qPCR, we found changes in expression of numerous p53-associated genes, including p21 and cyclin D1, indicating p53 activation and likely cell cycle arrest in PhIP-treated hCYP1A mice. Similar gene alterations were not observed in the PhIP-treated wild-type C57BL/6J mice. Altogether, these results suggest PhIP-induced DNA damage causing activation of the p53 pathways that may be involved in the early stage of carcinogenesis in the prostate. (Supported by NIEHS training grant 5T32ES007148-25 and NIH grant RO1CA133021 as well as shared facilities funded by CA72720 and ES05022).

## PS 1104 Reexamination of Initiator Dose in Ultra-Short-Term Carcinogenicity Study in RASH2 Mice.

H. Tsutsumi<sup>1</sup>, K. Urano<sup>1</sup>, M. Suguro<sup>2</sup>, M. Kawabe<sup>2</sup>, T. Numano<sup>2,3</sup> and F. Furukawa<sup>2</sup>. <sup>1</sup>Testing department, Central Institute for Experimental Animals, Kawasaki, Japan; <sup>2</sup>DIMS Institute of Medical Science, Inc., Ichinomiya, Japan; <sup>3</sup>Nagoya City University Graduate School of Medical Sciences, Nagoya, Japan.

We have established an ultra-short-term carcinogenicity study in which the target organ was the skin, one of the common targets in rasH2 mice. Although we previously reported that the suitable dose of 7,12-dimethylbenz[a]anthracene (DMBA) as an initiator was 50 mg at SOT 2010, several tumors were induced in DMBA treated groups without promotion, suggesting the dose of DMBA as an initiator was too high. In this study, we reexamined the suitable dose of DMBA as an initiator. Several compounds were applied to shaved dorsal skin of female rasH2 mice one week after 12.5 or 25  $\mu$ g DMBA application: oleic acid diethanolamine condensate (OADC, 30 mg/kg, 7 times/week) or benzethonium chloride (BC, 1.5 mg/kg, 5 times/week), known to have no promoting effect, 99.5 % ethanol (7 times/week) or anhydrous ethanol (5 times/week) as vehicles, or benzoyl peroxide (BPO, 20 mg/head, 5 times/week) as a positive tumor promoter. Applied skin was studied histopathologically at eight weeks after DMBA application. Although no tumors were induced in OADC, BC or vehicle treated groups, skin tumors were induced at five weeks after DMBA application in BPO treated groups, and the incidence of skin tumors reached 100 % by seven weeks after DMBA application. The number of skin tumors, which were diagnosed as hyperplasia and/or papilloma, at necropsy were 29.2 and 35.6 in 12.5  $\mu$ g and 25  $\mu$ g DMBA treated groups, respectively. Therefore, we concluded that 12.5  $\mu$ g DMBA was suitable to initiate the skin of rasH2 mice in an ultra-short-term skin carcinogenicity study.

## PS 1105 Modulation of Cocarcinogenic Effect of Aflatoxin B1 and Fumonisin B1 in a Short-Term Bioassay by Uniform Particle Size NovaSil Clay.

L. Tang<sup>1</sup>, G. Qian<sup>1</sup>, S. Lin<sup>1</sup>, Z. Yang<sup>1</sup>, M. Kang<sup>1</sup>, N. J. Mitchell<sup>2</sup>, J. Su<sup>1</sup>, W. Gelderblom<sup>3</sup>, R. Riley<sup>4</sup>, T. Phillips<sup>2</sup> and J. Wang<sup>1</sup>. <sup>1</sup>University of Georgia, Athens, GA; <sup>2</sup>Texas A&M University, College Station, TX; <sup>3</sup>Medical Research Council, Tygerberg, South Africa; <sup>4</sup>USDA ARS, Athens, GA.

Co-contamination of AFB1 and FB1 in corn-based food and feed is a health concern for their combinative toxic effects as well as potential co-carcinogenic effect. Uniform particle size NovaSil (UPSN) clay has been used as an enterosorbent to reduce AFB1 and FB1 exposure in animals and humans. In this study male F344 rats (150g) were randomly divided into five groups: negative control group, AFB1+FB1 group, AFB1+ FB1+low UPSN (0.25%) group, AFB1+FB1+high UPSN (0.5%) group, and positive control group treated with diethylnitrosamine and 2-acetylaminofluorene. All treated animals were sacrificed after their last exposure. Liver were dissected and processed with regular H&E staining for examination of histological alterations. Liver tissue slides were also immunohistochemically stained for examination of formation of placental form glutathione S transferase positive (GST-P+) foci. No detectable lesions were found in the negative control group, while the positive control group showed significant high rates of dysplasia (262  $\pm$  29), prolific foci (53  $\pm$  16), and nodules (15  $\pm$  10), as well as high rate of GST-P positive liver foci (58  $\pm$  11), which demonstrates the success of the experiments. Co-exposure to AFB1 and FB1 induced comparable rate of dysplasia (258  $\pm$  40) to the positive control group and a higher rate of apoptosis (26  $\pm$  8) than the positive control group (4  $\pm$  4). UPSN in both low and high groups significantly inhibited formation of preneoplasia in liver: For dysplasia, reduction of 46% (140  $\pm$  29) and 56.6% (113  $\pm$  20); for apoptosis, reduction of 42% (15  $\pm$  4) and 57% (11  $\pm$  4); for prolific foci, reduction of 74% and 94%; for GST-P positive foci numbers, areas, and mean areas, the reduction of 77% and 88%; 83% and 94%; and 31% and 53% were found, respectively. These results demonstrate significant modulation of UPSN on reducing potential co-carcinogenic effect in this short-term bioassay.

## PS 1106 Validation of Cocarcinogenic Effects of Aflatoxin B1 and Fumonisin B1 in a Short-Term Bioassay.

J. Wang<sup>1</sup>, G. Qian<sup>1</sup>, S. Lin<sup>1</sup>, L. Tang<sup>1</sup>, Z. Yang<sup>1</sup>, M. Kang<sup>1</sup>, N. J. Mitchell<sup>2</sup>, J. Su<sup>1</sup>, W. Gelderblom<sup>3</sup>, R. Riley<sup>4</sup> and T. Phillips<sup>2</sup>. <sup>1</sup>University of Georgia, Athens, GA; <sup>2</sup>Texas A&M University, College Station, TX; <sup>3</sup>Medical Research Council, Tygerberg, South Africa; <sup>4</sup>USDA ARS, Athens, GA.

A short-term animal assay using Aflatoxin B1 (AFB1) as the initiator and fumonisin B1 (FB1) as the promoter demonstrated dramatic increase in formation of placental form glutathione S transferase positive (GST-P+) foci in rat liver. In this

study, we validated this short-term bioassay and studied potential interactions between AFB1 and FB1 on the biochemical and histological changes and the formation of liver GST-P+ foci through a modified treatment protocol. AFB1 (150 ppb) containing diet caused dramatic dysplastic hepatocytes, mild bile duct proliferation and necrosis, and proliferation foci formation. In contrast, FB1 (250 ppm) containing diet induced less dysplastic hepatocytes and more apoptotic bodies while no proliferation foci were found. Additive effects on increasing serum ALP, ALT and AST activities were found in co-exposed animals as compared to single AFB1 or FB1 treated. Sequential co-exposure to AFB1 and FB1 lead to significantly increased numbers of dysplastic hepatocytes, apoptosis and proliferation foci. Co-exposure of AFB1 and FB1 also significantly increased the numbers of liver GTP-P+ foci by approximately 7.2 and 12.2 folds ( $p < 0.01$ ), and increased the mean sizes of GST-P+ foci by 6.0 and 7.5 folds ( $p < 0.01$ ), as compared to single AFB1 or FB1 treated, suggesting strong synergistic effects in enhancing the preneoplastic lesion in liver. This study validates co-carcinogenic effects of AFB1 and FB1 in the short-term bioassay in rat liver and provides evidence for the use of this model in future intervention studies and mechanistic investigations.

## PS 1107 Tumor Promoter Action of Chromium-Containing Stainless Steel Welding Particulate Matter in the Lungs of A/J Mice.

P. C. Zeidler-Erdely, T. G. Meighan, A. Erdely, L. A. Battelli, M. L. Kashon, M. Keane and J. M. Antonini. *HELD, NIOSH, Morgantown, WV.*

Epidemiology studies show that occupational exposure to metal-rich welding particulate matter (PM) increases lung cancer risk. However, animal studies are lacking to conclusively link welding with an increased cancer risk. PM derived from stainless steel (SS) welding practices, in particular, contains carcinogenic metals such as hexavalent chromium and nickel. Previously, we found that PM derived from gas metal arc (GMA) welding of SS caused a borderline increase in lung tumor incidence and a significant, chronic immune response in the lungs of mice. Thus, we hypothesized that welding PM may act as a tumor promoter and increase lung tumor multiplicity. In this study, the capacity of GMA-SS welding PM to promote lung tumors was evaluated using a 2-stage (initiation-promotion) model in lung tumor susceptible A/J mice. Age and weight-matched male mice ( $n=26-29/\text{group}$ ) were treated either with the initiator 3-methylcholanthrene (MCA; 10  $\mu\text{g/g.i.p.}$ ) or vehicle (corn oil; CO) followed by 5 weekly pharyngeal aspirations of GMA-SS (340 or 680  $\mu\text{g}$ ) or PBS. Lung tumors were enumerated at 30 weeks following initiation with MCA. Body weights were recorded at 2 week intervals and no effect of treatment was found. MCA initiation followed by GMA-SS exposure promoted lung tumor multiplicity in both the lower dose ( $12.0 \pm 1.5$  tumors/mouse;  $p=0.0001$ ) and high dose ( $14.0 \pm 1.8$  tumors/mouse;  $p=0.0001$ ) groups significantly above that of MCA/PBS ( $4.77 \pm 0.7$  tumors/mouse). Not only was this highly significant for the average total number per mouse, multiplicity was also increased ( $p < 0.004$ ) across all five individual lung regions of GMA-SS-exposed mice. No treatment effects were found in the corn oil groups at 30 weeks and also, as expected, tumor incidence was greater than 93% in the MCA treated groups which verified its carcinogenic potency. In conclusion, GMA-SS welding PM acts as a lung tumor promoter in vivo. These novel findings implicate that susceptible individuals may be at greater risk for lung cancer development after exposure to welding PM.

## PS 1108 Induction of 1, 3-Dichloropropene Rat Liver Tumors through a Nongenotoxic Mode of Action.

S. C. Gehen<sup>1</sup>, R. Billington<sup>2</sup>, Z. Wang<sup>3</sup>, P. J. Klein<sup>3</sup> and J. E. Klaunig<sup>3</sup>. <sup>1</sup>Dow AgroSciences LLC, Indianapolis, IN; <sup>2</sup>Dow AgroSciences LLC, Abingdon, United Kingdom; <sup>3</sup>Indiana University, Bloomington, IN.

1,3-Dichloropropene (1,3-D) is a soil fumigant used for control of parasitic nematodes. It was previously shown that dietary exposure to 1,3-D was associated with an increased incidence of benign hepatocellular adenomas in male rats in one of two rat cancer studies. In in vivo genotoxicity studies, 1,3-D was shown consistently to be non-mutagenic in studies where physiologic levels of glutathione and glutathione S-transferases were present and genotoxic stabilizers were not present, thus supporting liver tumorigenesis through a non-genotoxic mode-of-action (MoA). The present study was undertaken to investigate the hypothesis that 1,3-D induces rat liver tumors by acting as a tumor promoter in the liver carcinogenesis process. To assess potential 1,3-D tumor promotion, diethylnitrosamine-initiated Fischer 344 rats were treated by gavage with 25 mg/kg/day 1,3-D or 80 mg/kg/day phenobarbital (PB) for either 30 or 60 days, or for 30 days followed by 30 days recovery. Staining for the placental form of glutathione S-transferase (GSTP) was conducted post-exposure as a phenotypic marker of preneoplastic foci. While having no effect on GSTP positive foci, 1,3-D significantly enhanced the number and size of GSTP negative lesions at 30 and 60 days. Importantly, after 30 days recovery, the number and size of GSTP negative lesions in 1,3-D treated animals returned to control levels thus demonstrating 1,3-D promotion of foci and not

tumor initiation. Also supportive of tumor promotion, the hepatocyte labeling index in GSTP-negative preneoplastic foci was significantly increased in 1,3-D treated rats at 30 and 60 days and returned to control levels after 30 days recovery. PB, a well recognized non-genotoxic rodent liver carcinogen, produced an expected reversible increase in number and size of the GSTP positive lesions. The results presented are consistent with 1,3-D inducing liver carcinogenesis through a non-genotoxic MoA by induction of reversible proliferation of non-GSTP staining focal populations of hepatocytes.

## PS 1109 Effects of Long-Term Administration of the Tissue-Selective Estrogen Receptor Modulator Bazedoxifene on Survival and Tumor Formation in Rats.

D. J. Wright<sup>1</sup>, R. Perry<sup>1</sup>, C. A. Thompson<sup>2</sup>, N. J. Earnhardt<sup>3</sup>, S. Bailey<sup>1</sup>, B. Komm<sup>4</sup>, D. R. Minck<sup>5</sup> and M. A. Cukierski<sup>1</sup>. <sup>1</sup>Drug Safety, Pfizer, Groton, CT; <sup>2</sup>Abbott Laboratories, Abbott Park, IL; <sup>3</sup>Pharmacokinetics, Dynamics, and Metabolism, Pfizer, La Jolla, CA; <sup>4</sup>Medical Affairs, Pfizer, Collegeville, PA; <sup>5</sup>Division of Metabolism and Endocrinology, US FDA, Silver Spring, MD.

Bazedoxifene acetate (BZA) is a selective estrogen receptor modulator that is approved in a number of countries for the prevention and/or treatment of osteoporosis in postmenopausal women. To assess for carcinogenic potential, BZA was administered ad libitum in the diet to male and female rats for 2 years. BZA resulted in a reduction and a delayed onset in total tumor burden in both male and female rats. Survival rates were enhanced due to decreased pituitary (males and females) and mammary tumors (females) and decreased body weight gain in BZA-treated animals compared to controls. BZA caused an increased incidence of benign ovarian tumors and renal tubular tumors (males). Results from separate studies suggested that BZA caused an increase in LH, which stimulated formation and persistence of ovarian cysts, which eventually progressed into benign ovarian granulosa cell tumors. The reductions in pituitary and mammary gland tumors were attributed to BZA-related antagonism of endogenous estrogens at the estrogen receptors. The greater increase in renal tumor incidence in male rats given BZA was associated with the increased survival and increased time for development of late onset tumors. These findings are consistent with a non-genotoxic mechanism, unique to male rats, that involves test article-induced corticomedullary mineralization, renal tubular injury, and exacerbation of naturally occurring chronic progressive nephropathy in aged male rats that leads to proliferative changes and tumor formation. In conclusion, BZA elicited agonistic or antagonistic effects in a tissue-selective manner which was generally consistent with expression and/or activity of estrogen receptors in those tissues.

## PS 1110 Resveratrol Exposure Reduces Benzo(a)pyrene-DNA Adduct Concentrations in Apc<sup>Min</sup> Mouse Model of Colon Cancer.

A. C. Huderson, P. V. Rekhadevi, M. S. Niaz, S. E. Adunyah and A. Ramesh. *Biochemistry & Cancer Biology, Meharry Medical College, Nashville, TN.*

Colon cancer is the third leading cause of cancer cases and related deaths as per the statistics provided by the American Cancer society. Exposure to toxicants such as benzo(a)pyrene (BaP) is one of the contributing factors to the development of sporadic colon cancer. Our studies have shown a decrease in the size, and number of adenomas in the colon of mice exposed to BaP and resveratrol (RVT), compared to BaP exposure alone. We have also shown that RVT exposure caused a decrease in the expression and activity of CYP1A1/1B1 enzymes and BaP metabolite concentrations both in liver and colon. Since DNA damage is one of the key events in carcinogenesis, the objective of this study was to investigate whether RVT exposure simultaneously or prior to BaP treatment alters BaP-DNA adduct concentrations in Apc<sup>Min</sup> mouse. The treatment consisted of BaP only administration (in peanut oil) at a dose of 100  $\mu\text{g/kg}$  bw via oral gavage over a 60 day period (group I); BaP (100  $\mu\text{g/kg}$  bw) co-administered with RVT (in 10% ethanol + 90% deionized water) at a dose of 45  $\mu\text{g/kg}$  bw (group II); RVT administered for 1 week prior to BaP dosing (group III). Post exposure, DNA was isolated from colon and liver samples, and analyzed for BaP-DNA adducts by the <sup>32</sup>P-postlabeling method using a four-directional TLC system. The adduct concentrations showed a trend that mirrored the concentrations of BaP metabolites in the organs studied with low concentrations in RVT-treated mice compared to BaP-treated mice. Between the two RVT-treatment strategies, concurrent administration of RVT appeared to affect the BaP bioactivation compared to RVT treatment prior to BaP exposure as reflected by the low adduct concentrations in the former group III compared to groups I & II. Overall, our results suggest that RVT provides a preventive effect against BaP-induced colon cancer progression in Apc<sup>Min</sup> mouse (funded by NIH grants 1F31ES019432-01A1, 5R01CA142845-02, 5T32HL007735-12, and 5R25GM059994-11).

**PS 1111 Triclosan Promotes the Development of Hepatocellular Carcinoma in Mice.**

M. Yueh, V. Jiang and R. H. Tukey. *Laboratory of Environmental Toxicology, Departments of Chemistry & Biochemistry and Pharmacology, University of California San Diego, La Jolla, CA.*

Triclosan (TCS), a chlorophenol, is used in a large number of personal care products as an antibacterial agent. TCS has endocrine disruption properties, has been detected in microgram per liter levels in various water ways in the US, and is considered to be a major environmental contaminant in aquatic ecosystems. Daily exposure to TCS has resulted in its detection in humans with studies showing its presence in plasma, breast milk, and urine. Studies have increasingly linked TCS to a range of health and environmental effects; however, there are no mechanism-based studies that directly address TCS exposure to negative health effects in humans. Using wild type and Car-/- mice, TCS has been shown to effectively induce hepatic Cyp2b10 in a CAR-dependent manner. However, transient transfection experiments revealed that TCS is not a direct CAR agonist but behaves as a phenobarbital-like inducer that indirectly activates CAR and facilitates its translocation to the nucleus. Using the chemical procarcinogen diethylnitrosamine (DEN) to initiate tumorigenic episodes in mice, TCS exposure through drinking water promotes the development of hepatocellular carcinoma (HCC). The development and promotion of HCC by TCC compared to DEN-only treated mice proceeds in a CAR-independent fashion. This finding stands in contrast to CAR-dependent tumor induction with the liver tumor promoter phenobarbital. HCC tumors produced by DEN-TCS exposure lead to a number of changes in the liver including histological alteration in hepatocytes, increases in liver-to-body weights, elevated levels of  $\alpha$ -fetoprotein, and enhanced levels of tumor-promoting cytokines IL-6 and TNF $\alpha$ . In addition, tumor-bearing livers significantly alter the expression profile for genes associated with drug metabolism. The identification of TCS as a liver tumor promoter may be significant because of its abundance and long term use in consumer products and its propensity for rapid absorption into the systemic circulation. (Supported by USPHS grant ES010337)

**PS 1112 Kupffer Cells Modulate Wyeth-14, 643 and Phenobarbital-Induced Hepatocyte Proliferation in Naïve and Diethylnitrosamine (DEN)-Initiated Mice.**

T. Peat, Z. Wang, S. Zhou and J. E. Klaunig. *Indiana University, Bloomington, IN.*

Kupffer cells (KC) play an important role in liver homeostasis. Upon activation, KC release inflammatory and growth regulatory mediators that have been linked to acute and chronic liver responses including hepatic cancer. Wyeth 14,643 (WY) and Phenobarbital (PB) are non DNA reactive hepatic carcinogens in rodents. The present study was conducted to investigate the role of KC in liver cell proliferation in naïve and focal lesion containing mice. In our initial study, KCs in male C3H mice were depleted using liposome encapsulated clodronate (Lip-clod, 0.1 ml/10 g, iv). LPS, a known KC activator, was used as a positive control (1 mg/kg, ip, 2X/wk). Lip-clod treatment resulted in depletion of 99% of KC as confirmed by F4/80 positive staining cells. WY treatment increased the relative liver weight and DNA synthesis in naïve mice after 7 and 21 d treatment. LPS and PB increased hepatic DNA synthesis (7 and 21 d). Following KC depletion, the induction of DNA synthesis by LPS and PB were significantly decreased, while WY-induced DNA synthesis was not altered. In the second study, mice were injected with DEN (50 mg/kg, ip, 1X/wk for 4 wk). Following development of focal lesions, mice were treated with WY or PB for 28 d. Treatment with PB or WY increased the relative focal volume and depletion of the KC decreased the relative focal volume. WY and PB increased DNA synthesis in both basophilic and eosinophilic lesions, similar to LPS. Upon KC depletion, a decrease in DNA synthesis was seen in PB treated mice. In the surrounding non-lesion tissue, PB produced a marginal increase in DNA synthesis (2-fold) and that was decreased following KC depletion compared to control. In comparison, DNA synthesis increased greatly (10-fold) when treated with WY. These results show that the KC modulated hepatocyte proliferation both in naïve mice and in the preneoplastic focal lesions in PB and WY treated mice.

**PS 1113 Bioassay-Directed Fractionation of Diesel and Biodiesel Emissions.**

E. Mudu<sup>1,2</sup>, S. H. Warren<sup>1</sup>, C. King<sup>1</sup>, W. P. Linak<sup>1</sup>, D. G. Nash<sup>1,3</sup>, I. Gilmour<sup>1</sup> and D. M. DeMarini<sup>1</sup>. <sup>1</sup>US EPA, Research Triangle Park, Durham, NC; <sup>2</sup>University of North Carolina at Chapel Hill, Chapel Hill, NC; <sup>3</sup>ORISE, Oak Ridge, TN.

Biofuels are being developed as alternatives to petroleum-derived products, but published research is contradictory regarding the mutagenic activity of such emissions relative to those from petroleum diesel. We performed bioassay-directed frac-

tionation and analyzed the polycyclic aromatic hydrocarbon (PAH) levels of particles generated using petroleum diesel (B0) and those from soy-based biodiesel where the soy accounted for 20, 50 or 100% of the fuel (B20, B50, B100) from a Yanmar L70 diesel engine. We also evaluated a composite sample of diesel-exhaust particles (C-DEP) generated from petroleum diesel with a 30-kW 4-cylinder Deutz BF4M1008 diesel engine connected to an air compressor. The biodiesel and C-DEP particles were extracted with dichloromethane (DCM), and the percentage of extractable organic material of these complex environmental mixtures were determined. The extracts were then solvent exchanged into dimethyl sulfoxide and evaluated for mutagenicity in various *Salmonella* strains +/-S9. We calculated the mutagenic emission factors (revertants/megajoule, rev/MJ) from data from strain TA100 +S9, which responds to PAH-type mutagenicity. These mutagenic emission factors for the biodiesels were 3X less (B20), 6X less (B50), and 8X less (B100) than that of petroleum diesel (B0). The whole extract of C-DEP (petroleum diesel) was sequentially fractionated with solvents of increasing polarity, and >50% of the mass eluted in fraction 1; this fraction was not mutagenic. The 2nd fraction had 60% of the TA100+S9 activity, indicative of PAHs; the 3rd fraction contained 60% of the TA98-S9 activity, indicative of nitroarenes. We conclude that under these experimental conditions, emissions from biodiesel were less mutagenic than those from petroleum diesel, and based on the fractionation of the C-DEP, most of the activity is associated with PAHs. [Abstract does not necessarily reflect the views or policies of the U.S. EPA.]

**PS 1114 Phenotypic Characterization of CarG-box Binding Factor-A (CBF-A) Knock-out Mice.**

J. T. Barrett<sup>1</sup>, X. Zhang<sup>3</sup>, J. Richardson<sup>1,2</sup>, M. Fang<sup>1,2</sup> and H. Zarbl<sup>1,2,3</sup>. <sup>1</sup>Environmental and Occupational Medicine, Robert Wood Johnson Medical School, UMDNJ, Piscataway, NJ; <sup>2</sup>Environmental and Occupational Health Sciences Institute, Robert Wood Johnson Medical School, Piscataway, NJ; <sup>3</sup>Environmental and Occupational Health Sciences, Robert Wood Johnson Medical School, Seattle, WA.

CarG-box binding factor-A is a member of the heterogeneous nuclear ribonucleoprotein (hnRNPs) family of RNA-binding proteins involved in a variety of cellular functions, including transcriptional regulation. We showed that CBF-A (hnRNP A/B) regulates the expression of the Ha-ras oncogene by binding to enhancer elements (ets-like) in the promoter region. Deregulated expression of CBF-A isoforms is associated with mammary carcinogenesis in NMU-treated rats. CBF-A is a regulator of epithelial-mesenchymal transition (EMT), an important process in the cancer progression. To evaluate the role of CBF-A, we generated knock-out mice. Behavioral evaluation in the elevated plus maze showed that CBF-A null mice spent ~300% more time in the open arms of the maze compared to the wild-type, suggesting that loss of CBF-A results in a low-anxiety behavioral phenotype. This behavioral abnormality may be related to the role of CBF-A in regulating the expression of vasopressin in the brain. To further study the role of CBF-A in tumorigenesis, we exposed wild-type mice, as well as CBF-A null and heterozygous mice to a single dose of the mutagenic, DNA-alkylating agent ENU (10 mg/mL at 9-10 weeks of age). While administration of ENU decreased the survival rate in all genotypes compared to vehicle control mice, CBF-A null mice had a decreased survival rate and tumor-free survival rate compared to the wild-type. Taken in concert, these data suggest that CBF-A plays an important role in maintaining both normal growth control and behavior.

Supported by Grants from the DOD(BC971045), the NIEHS funded Toxicogenomics Research Consortium (ES011387), NIEHS Center Grants (ES005022 and ES007033) and CINJ (CA072720).

**PS 1115 Inhibition of Hepatocyte Nuclear Factor 1 and 4 Alpha (HNF1 $\alpha$  and HNF4 $\alpha$ ) As a Mechanism of Arsenic Carcinogenesis.**

A. Hernandez<sup>1,2</sup>, A. Pastor<sup>1</sup> and R. Marcos<sup>1,2</sup>. <sup>1</sup>Genetics and Microbiology, Autonomous University of Barcelona, Bellaterra, Spain; <sup>2</sup>CIBER-ESP, ISCIII, Madrid, Spain. Sponsor: A. Sampayo-Reyes.

Inorganic arsenic (i-As) is a naturally occurring toxic metalloid affecting millions of people worldwide. It is known to be carcinogen, liver being a potential target, and related to the prevalence of diabetes in arseniasis-endemic areas. Hepatocyte nuclear factor 1 and 4 alpha (HNF1 $\alpha$  and HNF4 $\alpha$ ) are key members of a transcriptional network essential for normal liver architecture. Changes in HNF1 $\alpha$  and HNF4 $\alpha$  expression are clearly associated with the development of liver malignancies and diabetes in humans. In this work, hepatic HepG2 cells and Golden Syrian hamsters were exposed to sub-toxic, environmentally relevant doses of sodium arsenite (SA; up to 10  $\mu$ M in vitro, 15 mg/L in vivo) in order to evaluate whether arsenic is able to compromise the expression of hepatocyte nuclear factors (HNFs). Also, liver hisopathological examination was carried out and several markers of hepatocyte dif-

ferentiation and glucose metabolism status were determined as a measure of i-As-induced effects. Results show a consistent down-regulation of HNF1 $\alpha$  and HNF4 $\alpha$  under an scenario of exposure where HepG2 cells (i) gained resistance to arsenic-induced toxicity/apoptosis, (ii) attained loss of tissue specific features (as shown by the observed downregulation of ALDOB, PEPCK and CYP1A2, the triggering of the epithelial-to-mesenchymal transition program (EMT) and the hypersecretion of matrix metalloproteinase-2 and 9), (iii) failed to maintain balanced the expression of the "stemness" genes C-MYC, OCT3/4, LIN28 and NOTCH2 and (iv) showed glucose metabolism impairment. We conclude that the i-As-induced down-regulation of HNF1 $\alpha$  and HNF4 $\alpha$  under chronic settings may play a central role in the features of disease and cancer observed both in vivo and in vitro.

## PS 1116 Carcinogenicity of Diesel (DEE) and Gasoline Engine Exhausts (GEE).

L. Benbrahim-Tallaa, R. Baan, Y. Grosse, B. Secretan-Lauby, F. El Ghissassi, V. Bouvard, N. Guha, D. Loomis and K. Straif. *IARC Monographs, IARC, Lyon, France.*

Recently, an IARC Monographs Working Group (WG) reevaluated the carcinogenic hazards to humans of DEE and GEE. DEE was classified as "carcinogenic to humans" (Group 1) and GEE as "possibly carcinogenic to humans" (Group 2B). A US study in non-metal miners included a cohort analysis and a nested case-control analysis adjusted for tobacco smoking. Both showed positive trends in lung cancer risk with increasing exposure, with a 2-3-fold increased risk in the highest categories of cumulative or average exposure. A 40% increased risk for lung cancer was observed in U.S. railroad workers exposed to DEE. Indirect adjustment for smoking and a more accurate exposure assessment strengthened the validity of the results. A large cohort study reported a 15-40% increased lung cancer risk in US truck drivers and dockworkers with exposure to DEE, with a significant trend of increasing risks with longer duration of employment, adjusted for tobacco smoking. Findings in other occupational groups and case-control studies including various occupations with similar exposures supported the WG's conclusion of "sufficient evidence" in humans for the carcinogenicity of DEE. The WG concluded that there was "sufficient evidence" in experimental animals for the carcinogenicity of whole DEE, DEE particles, and extracts of the particles, which also induced, in vitro and in vivo, various forms of DNA damage. Positive genotoxicity biomarkers of exposure and effect were also observed in humans exposed to DEE. The WG concluded that there is "strong evidence" for the ability of whole DEE to induce cancer in humans through genotoxicity. GEE and cancer risk was investigated in only a few epidemiological studies and, because of the difficulty to separate the effect of DEE and GEE, evidence for carcinogenicity was evaluated as "inadequate". Organic extracts of GEE condensate induced a cancer in mice, and in rats, GEE condensate also induced cancer in rats. The WG concluded that there was "sufficient evidence" in experimental animals for the carcinogenicity of condensates of GEE.

## PS 1117 Suicide Inhibition Is Responsible for the Paradoxical Absence of CYP2B10 Enzyme Activity in Mouse Liver following Nitrapyrin- or Pronamide-Induced CAR Activation.

M. J. LeBaron<sup>1</sup>, H. L. Kan<sup>1</sup>, M. R. Schisler<sup>1</sup>, S. Papineni<sup>2</sup>, D. L. Eisenbrandt<sup>2</sup> and B. Gollapudi<sup>1</sup>. <sup>1</sup>The Dow Chemical Company, Midland, MI; <sup>2</sup>Dow AgroSciences, Indianapolis, IN.

Establishing a mode of action (MoA) for a toxicological finding requires the identification of key events (both causal and associative) that progress to the apical end point of interest. In the case of constitutive androstane receptor (CAR)-mediated rodent hepatocarcinogenesis, the first key event is activation of the CAR signaling pathway, which is often measured via the empirically observable biomarker of Cyp2b10 induction (transcript, protein, and/or enzyme activity). The agrochemicals pronamide (herbicide) and nitrapyrin (nitrification inhibitor) induced hepatocellular tumors in mice as a result of high-dose, long-term dietary administration. Subsequent MoA studies for each chemical were consistent with a role for CAR-activation in the mouse liver tumorigenesis. With both chemicals significant increases in Cyp2b10 transcript as well as protein were observed; however, there was no associated change in the activity of the enzyme as measured by PROD. To investigate the role for suicide inhibition in this paradoxical finding, *in vitro* experiments were conducted with phenobarbital (PB)-induced microsomes. These microsomes were treated with PB (negative control), curcumin (positive control), nitrapyrin, or pronamide. In this system, nitrapyrin and pronamide inhibited PROD activity in a dose-related manner and up to 97% and 56% at 500  $\mu$ M, respectively. While PB had no effect on PROD activity, curcumin had a dose-related inhibition of Cyp2b-mediated PROD activity of up to 63% at 40  $\mu$ M. These results indicate that the two agrochemicals and/or their metabolites irreversibly inhibit Cyp2b10-mediated PROD activity and elucidate the apparent inconsistency between protein levels and enzyme activity of treated livers while supporting the CAR-mediated MoA for liver

tumorigenesis. Further, these data indicate that measurement of transcript levels as biomarkers for CAR activation is more appropriate than traditional enzyme activity (e.g., PROD) measurements.

## PS 1118 Structure-Dependent Effect of Diindolylmethane Derivatives on Inactivation of the Oncogenic NR4A1/NR4A2 Receptor in Colon Cancer Cells.

X. Li<sup>1</sup>, S. Lee<sup>2</sup> and S. H. Safe<sup>1, 2, 3</sup>. <sup>1</sup>College of Medicine, Texas A&M Health Science Center, College Station, TX; <sup>2</sup>Institute of Biosciences & Technology, Texas A&M Health Science Center, College Station, TX; <sup>3</sup>Veterinary Physiology and Pharmacology, Texas A&M University, College Station, TX.

The nuclear receptor 4A (NR4A) subfamily members TR3 (NR4A1) and Nurrl (NR4A2) have been investigated in this laboratory as novel drug targets for clinical treatment of pancreatic cancer. Inactivating of these oncogenic transcription factors by analogs derived from the chemopreventive phytochemical diindolylmethane (DIM) exhibit promising in vitro and in vivo chemotherapeutic effects. Knockdown of NR4A1 and NR4A2 by RNA interference in colon cancer cells decreased cell proliferation, induced apoptosis and inhibited colon cancer cell invasion. Using NR4A-responsive promoter elements (monomer-binding NBRE and dimer-binding NurRE) linked to a luciferase reporter gene, we investigated the structure-dependent activity of over forty 1,1-bis(3'-indolyl)-1-(substituted phenyl)methane (DIM-C-Ph) and 1,1-bis(3'-indolyl)-1-(heteroaromatic)methane (DIM-C-heteroaromatic) analogs as inactivators of NR4A1, NR4A2 or both receptors. In colon cancer cells we identified DIM-C-Ph analogs containing para-hydroxy, chloro, methyl, or trifluoromethoxy groups that inactivated NR4A1 and the 3-pyridine analog (DIM-C-Pyr-3) inactivated NR4A2-mediated transactivation. In contrast, several other p-substituted phenyl analogs containing fluoro, iodo or cyano groups were potent inactivators of both receptors. The mechanisms of NR4A inactivation by C-DIMs were investigated and the possible role of site-specific phosphorylation was determined using several protein kinase inhibitors including LY294002, PD98059 and SP600125. The results show that in RKO colon cancer cells transfected with NBRE-luciferase construct and treated with DIM-C-pPhCN, NR4A inactivation was inhibited by PD98059. These results indicate that the chemotherapeutic properties of C-DIMs are outcomes of NR4A inactivation and the NR4A1/NR4A2-dependent pathways and role of kinases are currently being investigated.

## PS 1119 Evaluation of microRNAs in Blood for Detection of Chemical-Induced Carcinogenesis.

T. Chen<sup>1</sup>, F. Meng<sup>1</sup>, J. Yan<sup>1</sup> and K. L. Thompson<sup>2</sup>. <sup>1</sup>National Center for Toxicological Research, US FDA, Jefferson, AR; <sup>2</sup>Center for Drug Evaluation and Research, US FDA, Silver Spring, MD.

MicroRNAs (miRNA) are emerging as a valuable tool in toxicological applications due to their role in regulation of gene expression in different biological pathways. Multiple studies have revealed that miRNAs are present and relatively stable in clinically accessible biofluids such as blood. miRNAs in biofluids may provide a non-invasive way of detecting chemical carcinogenicity. In this study, we evaluated whether microRNA profiling and individual miRNAs in mouse blood can predict carcinogenesis induced by N-ethyl-N-nitrosourea (ENU). Male B6C3F1 mice were treated with either a single dose of 140 mg/kg ENU or vehicle alone. Blood was collected on post-treatment days (PTDs) 1, 2, 3, 7, 14, 28, and 42. Profiling of total miRNAs in the blood showed that a number of miRNAs associated with carcinogenesis were altered by the ENU treatment. The temporal alteration of one of these miRNAs, miR-34a, a tumor suppressor, by ENU was characterized further. The level of miR-34a expression was significantly increased by ENU as early as PTD 1, reached a maximum level of about 10-fold over controls at PTD 7, and then decreased to control levels at PTD 42. Serum levels of miR-34a were also examined to assess the contribution of blood cells to miR-34a levels in whole blood. The results suggest that miRNAs have potential use as early sensitive circulating biomarkers of carcinogen exposure.

## PS 1120 Hemodynamic Changes, Arrhythmias, and Sudden Death in Dogs following Repeated Dosing of AKT/pp70S6K Inhibitor.

E. Blasi<sup>1</sup>, P. Harris<sup>1</sup>, M. Engwall<sup>2</sup>, S. Ralston<sup>3</sup> and L. Burns Naas<sup>4</sup>. <sup>1</sup>Drug Safety, Pfizer, San Diego, CA; <sup>2</sup>Drug Safety, Amgen, Thousand Oaks, CA; <sup>3</sup>Drug Safety, Abbott, Abbott Park, IL; <sup>4</sup>Drug Safety, Gilead, San Francisco, CA.

PF-04176340 (PF) is an inhibitor of AKT & pp70S6K. Target organs in GLP repeat dose studies in dogs included eye, GI, liver, testes. In addition, unexplained deaths were observed. In a 10d dose range-finding study (3, 10, 30 mpk/d), mor-

tality occurred in 1/4 male dogs at 30 mpk/d on d4 with no preceding signs. Similar observations were noted on d2 & d4 in a 1mo IND-enabling study in 2/5 male dogs at 20 mpk/d. In a SP study in telemetered male dogs (n=4), 10 & 15 mpk caused a significant increase in BP & dP/dT. Peak effect & duration were not related to expected exposure profile. An early study was conducted to investigate if the unexplained deaths were related to CV events as there was no evidence of direct cardiac toxicity in those animals. Conscious, unrestrained telemetered male dogs (n=4) were treated with VH or 20 mpk/d PF-04176340 continuously for 5d. Serum drug concentrations, glucose, insulin, troponin, clin chem, & electrolytes were measured predose & 5h postdose daily. Clinical signs were assessed by visual monitoring. PF produced transient cardiac arrhythmias (isolated PVC, polymorphic tachyarrhythmias) on d2 (Dog 3) & d3 (Dog 2) approx 6h postdose, and were associated with significant changes in LVP & dramatic drops in BP, and spontaneously resolved. Arrhythmias repeated multiple times on the day they were observed but were not on any other day. Arrhythmias were prolonged in Dog 3. Arrhythmic events did not appear to be correlated with plasma drug levels. During arrhythmic events, dogs were observed to be sleeping. Remaining telemetry data were consistent with the prior SP study. Treatment with PF also produced marked increases in glucose & insulin. No changes were noted in troponin, clinical chemistry, or electrolytes. It was concluded that the cardiovascular events observed in Dog 3 may explain the mortality in the repeat dose studies since without spontaneous resolution, prolonged arrhythmias may instigate a fatal decrease in cardiac output.

### PS 1121 The Role of Endothelial Cell-Specific Nitric Oxide Synthase in Causing Drug-Induced Vascular Injury.

G. A. Tobin<sup>1</sup>, D. G. Goodwin<sup>1</sup>, C. González<sup>1</sup>, J. Zhang<sup>1</sup>, L. Xu<sup>1</sup>, S. Stewart<sup>1</sup>, A. Knapton<sup>1</sup>, M. P. Lawton<sup>2</sup>, B. E. Enerson<sup>2</sup> and J. L. Weaver<sup>1</sup>. <sup>1</sup>Division of Drug Safety Research, US FDA, Silver Spring, MD; <sup>2</sup>Drug Safety Research and Development, Pfizer, Inc., Groton, CT.

The finding of drug-induced vascular injury (DIVI) in preclinical toxicology studies is a major cause of attrition in the development of many classes of drugs. In previous studies with the phosphodiesterase-4 inhibitor, CI-1044, we found that elevation of serum Nitric Oxide (NO) levels through endothelial cell-specific Nitric Oxide Synthase (eNOS) was critical for producing mesenteric vascular lesions in a rat model of DIVI. Furthermore, phosphorylation of key regulatory amino acids in eNOS such as S615, S1177, and S633 was significantly altered in response to CI-1044. The aim of the current study was to examine if other classes of drugs would produce similar lesions and whether these effects are mediated through eNOS activity. We examined the effect of a phosphodiesterase-3 inhibitor (SK&F 95654), a vasopressor (midodrine), and a vasodilator (nicorandil), in causing mesenteric vascular lesions in the rat. We also used SIN-1 or L-NAME to determine if levels of NO production, as measured by serum nitrate levels, correlated with vascular lesions. The combination of SK&F 95654 and SIN-1 led to a ~2-fold increase in serum nitrate and vascular injury over controls, while SK&F 95654 in combination with L-NAME caused a complete inhibition of vascular injury, with a three-fold inhibition of serum nitrate production, suggesting that this drug acts in a similar way to CI-1044. Interestingly, phosphorylation at S1177 was increased in response to SK&F 95654, in contrast to CI-1044. Although SIN-1 caused a ~2-fold increase in serum nitrate by midodrine, this led to a 4-fold inhibition of DIVI. Nicorandil, an NO donor, caused a ~300-fold increase in serum nitrate, either alone or in combination with SIN-1 or L-NAME. Our results illustrate that among the wide variety of drugs that can cause DIVI, modulation of eNOS activity may be a common feature of the mechanism leading to vascular injury.

### PS 1122 Soluble Components of Ultrafine Particles Induce Cellular Procoagulant Activity through Oxidant Signaling.

S. J. Snow<sup>1</sup>, A. Wolberg<sup>2</sup> and M. Carraway<sup>3</sup>. <sup>1</sup>Toxicology, University of North Carolina at Chapel Hill, Chapel Hill, NC; <sup>2</sup>Pathology and Laboratory Medicine, University of North Carolina at Chapel Hill, Chapel Hill, NC; <sup>3</sup>NHEERL, US EPA, Chapel Hill, NC.

Mechanisms that underlie the strong association between air pollution exposure and adverse cardiovascular health remain unknown. We hypothesize that soluble components of ultrafine particles (soluble UF) initiate procoagulant activities in endothelial cells through tissue factor (TF) induction via reactive oxygen species (ROS) production. Human coronary artery endothelial cells (HCAEC) were exposed to soluble UF and assessed for their ability to trigger procoagulant activity in platelet free plasma. HCAEC triggered faster thrombin generation and fibrin clot formation following exposure, which was abolished by an anti-TF antibody, indicating that the effects are TF-dependent. We found that TF mRNA expression was increased following soluble UF exposure without significant compensatory changes in mRNA levels of key anti-coagulant proteins, confirming that TF upregulation

plays an important role in this imbalance in the coagulation system. To study early events that might regulate TF expression, we measured H<sub>2</sub>O<sub>2</sub> production in HCAEC following exposure to soluble UF. There was an immediate induction of extra- and intracellular H<sub>2</sub>O<sub>2</sub> production following soluble UF exposure, and pretreatment with antioxidants attenuated the UF-induced upregulation of TF, linking the procoagulant response to ROS formation. Multiple chemical inhibitors indicated NOX as the source of increased TF mRNA, which was confirmed by the finding that NOX-4 siRNA prevented UF-induced upregulation of TF mRNA. These data show that exposure to soluble UF induces endothelial procoagulant activity, which requires new TF synthesis through ROS production and by NOX-4. These novel findings provide mechanistic insight into the enhanced thrombosis and endothelial dysfunction associated with air pollution exposure and increased risk for CV morbidity and mortality.

### PS 1123 Evaluation of Age and Sex Effects on Mitochondria-Related Gene Expression in Rat Heart.

V. Vijay, T. Han, C. Moland, J. C. Kwekel, J. C. Fuscoe and V. Desai. *Systems Biology, National Center for Toxicological Research, US FDA, Jefferson, AR.*

Age-related susceptibilities and sex-based differences in cardiovascular diseases are known and the underlying mechanisms need further investigation. Mitochondria are critical for normal cardiac function so alterations in such at different ages and sexes may affect the way the heart responds to drugs. To understand the role of mitochondria in age- and sex-related differences in the heart, we investigated the expression levels of mitochondria-related genes. Gene expression in the heart of male and female Fischer 344 rats at 8 (young), 21 (adult) and 78 (old) weeks of age was measured using Agilent whole genome rat arrays. Out of 18,435 unique genes on the Agilent rat microarray, 869 unique genes were determined to be mitochondria-related. Age effect was evaluated by using ANOVA coupled with pair-wise t-test (p<0.05) between each age group, and sex difference was evaluated at each age using t-test (p<0.05). The expression levels of genes involved in oxidative phosphorylation (Ox Phos), membrane transporters, and fatty acid (FA) metabolism were the highest at 21 wks compared to 8 or 78 wks in both males and females. A significant age related effect was observed in 21% and 7% of Ox Phos genes and 15% and 7% of membrane transporter genes in males and females, respectively, at all age groups. Only male rats showed significant age-related effects on the expression levels of genes (21%) involved in FA metabolism. Significant sex-based differences were observed in the expression levels of genes involved in Ox Phos at 78 wks (19%); higher expression levels were noted in female rats compared to males. Membrane transporters showed significant sex differences at 8 wks (21%), 21 wks (40%) and 78 wks (13%). Genes involved in FA metabolism also showed sex based differences at 8 (34%), 21 wks (29%) and 78wks (10%); most of the genes had higher expression in females than males. These findings may provide important insights into understanding the role of mitochondria in cardiovascular diseases in terms of sex based differences or altered susceptibility with age.

### PS 1124 Assessment of Postmarket Cardiac Adverse Events in Patients Treated with Antipsychotic Drugs.

D. Bi, R. Benz, J. Kerner, J. Willard and T. Colatsky. *Center for Drug Evaluation and Research, US FDA, Silver Spring, MD.*

This study assessed the cardiac adverse events (cAEs) induced by antipsychotic drugs, and evaluated their relationship to hERG affinities, clinical drug exposure and the magnitude of clinical QTc prolongation. Data were collected from public regulatory documents (e.g. Summary Basis for Approvals) and supplemented with published literature data. The incidence of each cardiac toxicity endpoint was calculated using the total number of all adverse events reported for each drug as a denominator. The incidence of QT prolongation was 5.1, 3.4, 0.5, 1.0, 0.9 and 1.9% for thioridazine, ziprasidone, quetiapine, risperidone, olanzapine, and haloperidol, respectively, which were correlated to the magnitude of QTc change from baseline (dQTc) of 40.7, 26.4, 19.5, 15.8, 12.7 and 11.3 msec, respectively. The incidences of Torsade de pointes (TdP) were 0.9, 0.7, 0.1, 0.2 and 0.1% for thioridazine, ziprasidone, quetiapine, risperidone and olanzapine, respectively, which were highly correlated to the dQTc. Furthermore, the incidence of QT prolongation was correlated to the ratio of total plasma C<sub>max</sub>/hERG IC<sub>50</sub> for the same group of drugs. Pimozide, one of the most potent hERG blockers (hERG IC<sub>50</sub> = 18 nM), had the highest incidences in causing QT prolongation (7.2%), TdP (3.4%), long QT syndrome (0.7%), syncope (3.4%) and sudden cardiac death (0.3%). The incidences of ventricular arrhythmia and cardiac arrest were greater than or equal to 5% in patients receiving diazepam, imipramine, thioridazine, haloperidol, amitriptyline, pimozide, or trazodone. The incidences of sudden death were more than 1% in pa-

tients treated with desipramine, thioridazine, ziprasidone or pimozide. In conclusion, relatively high incidences of potentially serious cardiac side effects, including QT prolongation, TdP, and lethal outcomes occurred in patients treated with the antipsychotics. The hERG affinities combined with the levels of clinical drug exposure may serve as one of the predictors for drug-induced cardiac toxicity by antipsychotics.

## PS 1125 Ozone Coexposure Modifies Cardiac Function Responses to Fine and Ultrafine Particulate Matter in Mice.

R. McIntosh-Kastrinsky<sup>1</sup>, H. Tong<sup>2</sup>, N. Kurhanewicz<sup>1</sup>, L. Walsh<sup>2</sup>, A. K. Farraj<sup>2</sup> and M. S. Hazari<sup>2</sup>. <sup>1</sup>University of North Carolina at Chapel Hill, Chapel Hill, NC; <sup>2</sup>Environmental Public Health Division, US EPA, Research Triangle Park, NC.

There is growing evidence from epidemiological studies that show acute exposure to particulate matter (PM) increases the risk of cardiovascular morbidity and mortality. Although the data supporting these findings are increasingly more convincing, the immediate impact of PM inhalation on cardiac function needs to be further clarified; this is particularly true of multipollutant exposures. Thus, this study was designed to evaluate the cardiac effects of concentrated ambient fine (PM<sub>2.5</sub>) and ultrafine (UFP) particles with and without ozone (O<sub>3</sub>) co-exposure. Based on previous findings, we hypothesized that UFP would cause the greatest decrement in cardiac function and that O<sub>3</sub> co-exposure would worsen the response. Mice were exposed by whole-body inhalation to either 200 µg/m<sup>3</sup> PM<sub>2.5</sub> or 100 µg/m<sup>3</sup> UFP with or without 0.3 ppm O<sub>3</sub>; separate groups were exposed to either filtered air or O<sub>3</sub> only. Twenty-four hours after exposure, cardiac function was assessed using a Langendorff cardiac perfusion preparation. Coronary flow, left ventricular developed pressure (LVDP) and contractility were measured before and after cardiac ischemia/reperfusion (I/R) injury. PM<sub>2.5</sub> or O<sub>3</sub> alone, or co-exposure to UFP+O<sub>3</sub> caused a significant decrease in baseline LVDP and contractility. Interestingly, UFP alone or PM<sub>2.5</sub>+O<sub>3</sub> did not cause significant decrements in cardiac function when compared to controls, nor were there significant differences in recovery LVDP or contractility between any group after I/R injury. These data suggest that the cardiac effects of PM inhalation are dependent on particle size and that O<sub>3</sub> interacts with PM<sub>2.5</sub> and UFP differently, resulting in varied cardiac impacts. Thus, these findings indicate that the cardiovascular effects of particle and gas co-exposures are not simply additive or generalizable, which increases the complexity of risk assessment. (This abstract does not reflect EPA policy)

## PS 1126 An Integrative Approach to Identify Functional, Structural and Pathological Biomarkers of Doxorubicin-Induced Cardiotoxicity.

H. R. Mellor<sup>1</sup>, L. Cove-Smith<sup>2</sup>, J. Kirk<sup>1</sup>, A. Hargreaves<sup>1</sup>, S. Price<sup>1</sup>, C. Betts<sup>1</sup>, C. Dive<sup>2</sup>, P. Hockings<sup>1</sup> and N. Woodhouse<sup>1</sup>. <sup>1</sup>Global Safety Assessment/PHB Imaging Group, AstraZeneca R&D, Macclesfield, United Kingdom; <sup>2</sup>The Paterson Institute For Cancer Research, University of Manchester, Manchester, United Kingdom. Sponsor: R. Roberts.

Doxorubicin is an anthracycline antibiotic commonly used in treatment regimens for a wide range of malignancies, including hematological cancers, many types of carcinoma and soft tissue sarcomas. Cardiotoxicity is a major safety complication associated with the clinical use of doxorubicin, several other marketed anti-cancer drugs and with many pre-clinical drug candidates. There is a need for novel, translational biomarkers to aid cardiac structural and functional monitoring in both patients at risk of cardiotoxicity and in pre-clinical species administered early drug candidates. In the present study, a detailed characterization of the effects of chronic doxorubicin treatment on rat heart structure and function has been performed using a range of approaches. A rat model of doxorubicin-induced cardiomyopathy was developed, involving 8 weekly intravenous boluses of doxorubicin hydrochloride followed by a 4 week 'washout' period. A timecourse assessment of cardiac function using multiple MRI biomarkers was performed under recovery anaesthesia, prior to dosing, on days 1 (baseline), 15, 29, 43, 57 and under terminal anaesthesia prior to necropsy on day 78. Reductions in cardiac output and ejection fraction were observed in treated animals from day 15. Peak myocardial enhancement was observed at day 57 onwards and correlated with serum cardiac troponin I elevations. A detailed immunohistochemical cardiac assessment is currently being performed to provide an understanding of the relationship between the development of pathological and functional MRI changes, serological biomarker elevations and cardiac pathological lesions. The ultimate aim is to apply the learning to pre-clinical drug discovery in order to support safety validation of drug targets, to optimize chemical design and to ultimately progress the safest molecules into later pre-clinical and clinical testing.

## PS 1127 Both Vitamin D Excess and Deficiency Increase Blood Pressure, but Only Excess Increases Arterial Stiffness.

N. Z. Mirhosseini<sup>1</sup>, K. Bohaychuk<sup>1</sup>, H. Vatanparast<sup>2</sup>, G. George<sup>3</sup> and L. P. Weber<sup>1</sup>. <sup>1</sup>Veterinary Biomedical Sciences, University of Saskatchewan, Saskatoon, SK, Canada; <sup>2</sup>Nutrition and Pharmacy, University of Saskatchewan, Saskatoon, SK, Canada; <sup>3</sup>Geology Department, University of Saskatchewan, Saskatoon, SK, Canada.

Vitamin D deficiency has been linked to an increased risk of hypertension, myocardial infarction and stroke. Recently, the Tolerable Upper Intake Level of 1, 25-dihydroxyvitamin D (D<sub>3</sub>) has been increased to 4000 IU/d, but levels of 10,000 IU/d for treatment of inflammatory conditions and 50,000 IU/week for short-term supplementation in deficient individuals have been suggested. High doses of D<sub>3</sub> may cause arterial calcification and cardioneurosis, but the velocity of the adverse events related to regular D<sub>3</sub> intake in doses higher than 10,000 IU/d, threshold for these changes and links to arterial calcification or hypertension are unclear. The objective of this study was to examine the effect of dietary doses of D<sub>3</sub> equivalent to recommended human doses after 1 month in male rats (n = 4/group): 0 IU/d (deficiency), 600 (recommended daily intake; control), 10,000 (upper therapeutic dose), 30,000 & 150,000 IU/d on cardiovascular function. Blood pressure telemetry and carotid artery Doppler ultrasonography were done at the baseline and weekly during diet testing. After 4 weeks, both systolic and diastolic blood pressure increased significantly (~15 mmHg; p<0.05, 1-way ANOVA, Duncan's Post-hoc test) in both D<sub>3</sub> deficiency and groups receiving ≥30,000 IU/d compared to the 10,000 IU/d group. Carotid artery luminal diameter was significantly smaller in 0 and ≥30,000 IU/d D<sub>3</sub> compared to control, which could indicate either increased arterial wall thickness or contractility. Pulse wave velocity and peak acceleration decreased over time in control and D<sub>3</sub> deficiency, but increased in groups receiving ≥30,000 IU/d D<sub>3</sub> indicating increased arterial stiffness. In conclusion, based on increased blood pressure, caution needs to be taken with D<sub>3</sub> supplementation ≥30,000 IU/d. Future studies will be directed at confirming the dose threshold and examining mechanisms for D<sub>3</sub>-induced arterial stiffness and hypertension.

## PS 1128 Fatty Acids Down Regulate and Inhibit Secretion of Adiponectin in Adipocytes through Oxidative Stress.

S. R. Kotha, T. O. Gurney, A. B. Shelton, S. I. Sherwani, U. J. Magalang and N. L. Parinandi. Division of Pulmonary, Allergy, Critical Care, and Sleep Medicine, The Ohio State University College of Medicine, Columbus, OH.

Adipose tissue is not merely a storage depot for the fat, but has emerged as a vital organ capable of synthesizing and releasing adipokines which act as regulators of diverse physiological functions. Adiponectin (30 kDa) protein, an important member of the adipokine family is known to regulate insulin action, NADPH oxidase activity, and lipid mobilization. Adiposity, release of free fatty acids from the adipose fat, and adiponectin secretion by the adipocyte are interconnected. These phenomena appear as crucial factors in cardiovascular and sleep disorders. Reports have been made on decreased circulating adiponectin levels in obese individuals, suggesting a link between fat load in adipose tissue and decrease in adiponectin release by adipose tissue. However, polyunsaturated fatty acids (PUFA) have been established as essential dietary fats and recently n-3 fatty acids (Omega-3) have gained importance in health, nutrition and disease. Having this as the premise, here, we hypothesized that PUFA load would modulate adiponectin secretion by adipocytes. To test our hypothesis, we loaded the 3T3 differentiated adipocytes with different PUFAs including linoleic (C18:2), linolenic (C18:3), arachidonic (C20:4), eicosapentaenoic (20:5; EPA), and docosahexaenoic (22:6; DHA) acids for 24 h and then analyzed the secreted adiponectin, intracellular adiponectin, fatty acid composition, triglyceride accumulation, cytotoxicity, and extent of lipid peroxidation (formation of 4-hydroxy-2-nonenal, 4-HNE) in the cells. Our results revealed that PUFA loading suppressed both adiponectin release by the cells and intracellular adiponectin, increased cellular PUFA content and triglyceride accumulation, and induced lipid peroxidation (intracellular formation of 4-HNE). Overall, our results suggested that the essential PUFAs suppressed secretion and synthesis of adiponectin in adipocytes through elevated lipid peroxidation and oxidative stress.

**PS 1129 Diesel Exhaust-Induced Cardiac Dysfunction Is Mediated by Sympathetic Dominance in Heart Failure-Prone Rats.**

A. P. Carll<sup>1,2</sup>, M. S. Hazari<sup>2</sup>, C. M. Perez<sup>3,2</sup>, Q. Krantz<sup>2</sup>, C. King<sup>2</sup>, D. W. Winsett<sup>2</sup>, D. L. Costa<sup>4</sup> and A. K. Farraj<sup>2</sup>. <sup>1</sup>Gillings School of Global Public Health, University of North Carolina-Chapel Hill, Chapel Hill, NC; <sup>2</sup>Environmental Public Health Division, US EPA, Research Triangle Park, NC; <sup>3</sup>Curriculum in Toxicology, University of North Carolina Chapel Hill, Chapel Hill, NC; <sup>4</sup>ORD, US EPA, Research Triangle Park, NC.

Short-term exposure to vehicular emissions is associated with adverse cardiac events. Diesel exhaust (DE) may provoke cardiac events through defective co-ordination of the two main autonomic nervous system (ANS) branches. We exposed heart failure-prone rats once to DE (500 µg/m<sup>3</sup> PM<sub>2.5</sub>, 4 h, whole-body inhalation) and tested for ANS-mediation of cardiotoxicity by several interventions, including post-DE sympathetic agonism (dobutamine) before and after parasympathetic ablation (vagotomy) and, separately, sympathetic or parasympathetic inhibition (atenolol or atropine) during- and treadmill exercise after-DE exposure. Left ventricular pressure (LVP), heart rate (HR), HR variability (HRV), and blood pressure (BP) were measured to determine cardiac function and autonomic balance. During exposure hour 2, DE markedly increased HR, BP and contractility in saline-pretreated rats, and atenolol entirely inhibited these effects, indicating DE caused mid-exposure sympathetic excitation. DE increased body temperature regardless of pretreatment. Upon exercise recovery at 4 h post-exposure, HRV and HR indicated that DE increased parasympathetic influence. Conversely, during exercise recovery at 21 h post-exposure, DE increased sympathetic influence in saline-pretreated rats, while it impaired contractility and decreased systolic BP in saline- and atropine-pretreated rats. Atenolol inhibited all of these effects. LVP at 1 d post-DE indicated systolic and diastolic dysfunction and changes in diastolic and chronotropic responses to dobutamine mediated partly through sympathetic dominance. Thus, DE-induced autonomic dysregulation of the heart involves time-dependent oscillations between sympathetic and parasympathetic dominance, with the former mediating DE's cardiotoxic effects. (Does not reflect EPA policy. Funded by EPA/UNC CR-83515201-0)

**PS 1130 Remote Subcutaneous and Intravenous Administration in Large Animals: Impact on Cardiovascular Safety Pharmacology Data and Sensitivity.**

R. Mikaelian<sup>1</sup>, S. Authier<sup>1,2</sup>, A. Ascah<sup>1</sup>, M. Pouliot<sup>1</sup>, E. Troncy<sup>2</sup> and R. Forster<sup>1</sup>. <sup>1</sup>CIToxLAB North America, Laval, QC, Canada; <sup>2</sup>Faculty of Veterinary Medicine, University of Montréal, St-Hyacinthe, QC, Canada.

The regulatory guideline S7A supports the use of unrestrained models for safety pharmacology assays. Parenteral bolus administrations including the intravenous (IV) and subcutaneous (SC) routes are associated with CMax achieved immediately or within minutes of dosing for some compounds. In this context, animal handling can constitute a major interference to data quality and can obscure pharmacodynamic responses. The current investigation compared cardiovascular changes after remote SC and IV delivery in telemetered cynomolgus monkeys and Beagle dogs with restrained administration in the same species. Remote parenteral administrations were associated with a substantial decrease in data variance and consequently improved minimum detectable differences. Mean heart rate variations from baseline in the first 30 min after restrained IV saline dosing reached a maximum of 27% compared to 9.7% for remote administration. Baseline systolic arterial pressure following remote SC saline dosing in cynomolgus monkeys ranged from 93.7 and 116.4 mmHg while post-dose values in the initial 60 min post-dose ranged from 94.0 and 116.3 mmHg. Recovery of cardiovascular parameters to baseline levels after animal handling was 25 to 120 minutes in both species which can constitute a major confounder to evaluation of short half-life drug candidates. Remote dosing presented optimal results when the animals remained completely undisturbed (i.e. no staff present in the animal room). Remote IV dosing is generally recognized to improve telemetry data quality but the current investigation also demonstrate beneficial effects of remote SC injections on sensitivity of cardiovascular investigations in safety pharmacology studies using telemetry in cynomolgus monkeys and Beagle dogs.

**PS 1131 Acute Silver Nanoparticle Exposure Increases Cardiac Ischemic/Reperfusion Injury in Sprague-Dawley Rats.**

C. J. Wingard<sup>1</sup>, R. Urankar<sup>1</sup>, J. Shananhann<sup>2</sup>, A. K. Vidanapathirana<sup>1</sup>, L. C. Thompson<sup>1</sup>, S. Sumner<sup>3</sup>, T. Fennell<sup>3</sup>, J. M. Brown<sup>2</sup> and R. M. Lust<sup>1</sup>. <sup>1</sup>Physiology, East Carolina University, Greenville, NC; <sup>2</sup>Pharmacology & Toxicology, East Carolina University, Greenville, NC; <sup>3</sup>RTI International, Research Triangle Park, NC.

The expanding use and production of silver nanoparticles (AgNP) as anti-bacterial/fungal agents is raising concerns regarding their safety to human health. The diversity of nanosized silvers (AgNP) and coatings for dispersion may produce combinations that minimize potential toxic effects on the cardiovascular system. We hypothesized that acute intratracheal (IT) exposure to 20 nm (S; small) or 110 nm (L; Large) AgNP coated with either polyvinylpyrrolidone (P) or citrate (C) would increase the susceptibility of cardiac tissue to a regional ischemic reperfusion (I/R) injury. Young male Sprague Dawley rats were exposed to 200 µg of AgNP. 24 hrs post-exposure, cardiac ischemia was induced for 20 mins followed by 2 hrs of reperfusion in situ. Hearts were sectioned stained with Evans blue to demarcate Area at Risk (AAR) and counter stained with TTC to determine % of AAR infarcted. Bronchoalveolar lavage fluid (BALF) and serum was collected post I/R injury to evaluate pulmonary injury and circulating markers of injury. Neither P (22 ± 2% Infarct/AAR) nor C (24 ± 1% Infarct/AAR) altered the extent of infarcted cardiac tissue as compared to naive (22 ± 2% Infarct/AAR). However, the installation of all forms of AgNP significantly increased the extent of cardiac I/R injury. As a group the P-coated AgNP developed larger infarcts than C-coated. The 20 nm were more effective at enhancing I/R Injury (SP 43 ± 2.0 % Infarct/AAR, SC 37 ± 3 % Infarct/AAR) than the 110 nm size (LP 37 ± 3 % Infarct/AAR, LC 31 ± 2 % Infarct/AAR). The opposite pattern was observed in the BALF endpoints with P and L AgNP having greater effects. Our results suggest IT exposure to AgNP have differential effects on pulmonary and cardiac tissues following the application of I/R injury. This work is supported by NIEHS U19 ES019525.

**PS 1132 Effect of Pulmonary Exposure to Welding Fumes on Cardiomyocyte Contractility.**

H. Kan<sup>1</sup>, J. M. Antonini<sup>1</sup>, M. Ye<sup>1</sup>, W. Zheng<sup>1</sup>, R. Salmen<sup>1</sup>, R. Popstojanov<sup>2</sup> and V. Castranova<sup>1</sup>. <sup>1</sup>PPRB, NIOSH, Morgantown, WV; <sup>2</sup>West Virginia University, Morgantown, WV.

Studies have found that pulmonary exposure to welding fumes is positively associated with a higher incidence of cardiovascular events. We reported previously that pulmonary exposure to welding fumes, manual metal arc-hard surfacing (MMA-HS), has a negative impact on cardiac function as evidenced by reduced heart contractility. However, the mechanisms underlying MMA-HS-induced depression of cardiac contractility remain unclear. To study the mechanisms, rats were given an intratracheal instillation of MMA-HS welding fumes (2 mg/rat) or saline once a week for seven weeks. Cardiomyocytes were isolated at 1 and 7 days post-exposure. Cardiomyocyte contractility and intracellular calcium level in response to increasing concentrations of adrenoceptor agonist isoprenaline and extracellular calcium were assessed using a Myocyte Calcium Imaging/Cell Length System. Pulmonary exposure to MMA-HS blunted contractile function in response to both isoprenaline and calcium at 1 day post-exposure (P < 0.01; P < 0.05, respectively). A blunted contractile response was also observed with welding fume treated rats at 7 days post-exposure in response to isoprenaline and calcium (P < 0.01). Intracellular calcium level in response to extracellular calcium stimulation was reduced at 7 days post-exposure (P < 0.05). These findings suggest that pulmonary exposure to welding fumes impairs cardiac function by decreasing cardiomyocyte contractility through a defect in the adrenergic signaling pathway and intracellular calcium handling.

**PS 1133 Silver Nanoparticle Exposure Increases Vasoconstrictor Response in Nonpregnant Female Sprague-Dawley Rats.**

J. O. Dawkins<sup>1</sup>, A. K. Vidanapathirana<sup>1</sup>, L. C. Thompson<sup>1</sup>, S. J. Sumner<sup>3</sup>, T. Fennell<sup>3</sup>, J. M. Brown<sup>2</sup> and C. J. Wingard<sup>1</sup>. <sup>1</sup>Physiology, East Carolina University, Greenville, NC; <sup>2</sup>Pharmacology & Toxicology, East Carolina University, Greenville, NC; <sup>3</sup>RTI International, Research Triangle Park, NC.

The use and production of silver nanoparticles (AgNP) is growing rapidly raising concerns regarding their safety to human health, particularly following translocation to the circulatory system. Previous findings from our lab have shown intravenous (IV) exposure to AgNP changes the vasoconstrictor response in both pregnant and male Sprague Dawley (SD) rats. We hypothesized, acute IV exposure to AgNP in non-pregnant females will increase vascular reactivity of arterial vessels

from mesenteric and uterine vascular beds and aortas and these changes will be influenced by NP size and coating. Female, non-pregnant, SD rats were intravenously exposed to 200  $\mu\text{g}$  of 20 or 110 nm AgNP coated with polyvinylpyrrolidone (PVP) or citrate and suspended in water. 24 hrs. post-exposure, wire myography tested the vasomotor responses in aortic, first order mesenteric and main uterine artery vessel segments. Cumulative dose response curves were created for phenylephrine (PE), angiotensin II (ANGII), and endothelin 1 (ET1). Segments of uterine artery and aorta from AgNP exposed animals generated larger stress when compared to vehicle controls. No significant differences were observed in the mesenteric artery responses. Maximum stress values in the uterine artery were greater ( $p < 0.05$ ) in response to ET1 and ANGII stimulation following exposure to 110 nm PVP AgNP ( $16.4 \pm 2.7$  and  $14.5 \pm 2.2$  mN/mm<sup>2</sup>, respectively) as compared to 110 nm citrate AgNP ( $8.0 \pm 1.0$  and  $6.9 \pm 0.8$  mN/mm<sup>2</sup>, respectively). Conversely, maximum stress in response to PE in aortic segments was greater ( $p < 0.01$ ) following exposure to 20 nm PVP AgNP ( $1.3 \pm 0.2$  mN/mm<sup>2</sup>) as compared to 20 citrate nm AgNP ( $2.8 \pm 0.3$  mN/mm<sup>2</sup>). Our results suggest IV exposure to AgNP has differential effects on increasing the vasoconstrictor responses that are dependent on the vascular bed, size of the NP and type of coating. This work is supported by NIEHS U19 ES019525.

### PS 1134 Intravenous vs Intratracheal Administration of C60 Differentially Promotes Constriction or Impairs Relaxation of the Isolated Coronary Artery.

N. A. Holland<sup>1</sup>, L. C. Thompson<sup>1</sup>, A. K. Vidanapathirana<sup>1</sup>, J. O. Dawkins<sup>1</sup>, S. J. Sumner<sup>3</sup>, A. Lewin<sup>3</sup>, T. Fennell<sup>3</sup>, J. M. Brown<sup>2</sup> and C. J. Wingard<sup>1</sup>.  
<sup>1</sup>Physiology, East Carolina University, Greenville, NC; <sup>2</sup>Pharmacology & Toxicology, East Carolina University, Greenville, NC; <sup>3</sup>RTI International, Research Triangle Park, NC.

The potential uses of C60 fullerenes have grown to include roles in both commercial industry and medicine, but the impacts on human health are not completely understood. Data from our lab suggests that C60 may exacerbate cardiac ischemia/reperfusion injury. We hypothesized that exposure to C60 would promote enhanced vasoconstriction and impaired endothelial-dependent relaxation responses of the coronary artery. Male Sprague-Dawley rats were exposed to a single 93.3  $\mu\text{g/kg}$  dose of intravenous (IV) or intratracheal (IT) C60 or polyvinylpyrrolidone vehicle. Twenty-four hours following exposures, coronary artery segments were isolated and evaluated using wire myography. Cumulative dose responses to serotonin (5-HT), acetylcholine (ACh), or sodium nitroprusside (SNP) were constructed. We found that IT exposure to C60 resulted in a leftward shift ( $P = 0.05$ ) of the 5-HT EC50 ( $558.4 \pm 104.5$  nM) compared to vehicle ( $870.7 \pm 129.7$  nM), but that IV exposure to C60 did not significantly shift the 5-HT EC50 values (C60:  $762 \pm 112.3$  nM vs. vehicle:  $669.3 \pm 59.4$  nM). Conversely, IV exposure to C60 led to a rightward shift ( $P = 0.09$ ) in the EC50 for ACh ( $232.5 \pm 68.9$  nM) compared to vehicle ( $100.9 \pm 48.8$  nM), but IT C60 exposure did not produce any differences in ACh EC50 (C60:  $245.7 \pm 37.4$  nM compared to vehicle:  $222.4 \pm 31.6$  nM). The relaxation responses to SNP were not different between any groups. The route of exposure to C60 appears to influence an enhancement of smooth muscle contraction by IT and impaired endothelial relaxation by IV administration. Based on these data we conclude that C60 exposure could enhance coronary vascular tone, possibly compromising dilatory flow during reperfusion, and thus exacerbating myocardial infarction. This work is supported by NIEHS U19 ES019525.

### PS 1135 Intratracheal Exposure to Silver Nanoparticles Promotes Enhanced Coronary Vascular Tone.

L. C. Thompson<sup>1</sup>, A. K. Vidanapathirana<sup>1</sup>, J. O. Dawkins<sup>1</sup>, S. J. Sumner<sup>3</sup>, T. Fennell<sup>3</sup>, J. M. Brown<sup>2</sup> and C. J. Wingard<sup>1</sup>. <sup>1</sup>Physiology, East Carolina University, Greenville, NC; <sup>2</sup>Pharmacology & Toxicology, East Carolina University, Greenville, NC; <sup>3</sup>RTI International, Research Triangle Park, NC.

Silver nanoparticles (AgNP) have physicochemical and antimicrobial properties that make them useful in both industrial and biomedical applications. In regard to human exposures, little is known about the way AgNP may impact physiological systems. We tested the hypothesis that coronary responsiveness to serotonin (5-HT) and acetylcholine (ACh) would be augmented 24 hrs following exposure to AgNP, and be dependent on particle sizes and the dispersants used to coat the particles. We used male Sprague-Dawley rats (10-12 weeks old) and delivered AgNP (1 mg/kg), of either 20 nm (SS) or 110 nm (LS) diameters, and suspended in either polyvinylpyrrolidone (PVP) or citrate (Cit), by intratracheal (IT) instillation or intravenous (IV) injection. After 24 hrs we isolated segments of the left anterior descending coronary artery for wire myography analysis of 5-HT and ACh dose-responses. Our data indicate no differences in coronary responses from AgNP groups

compared to their vehicle groups. We did observe some unique dispersant- and AgNP size-dependent comparisons in the coronary responses. Maximal 5-HT stresses were higher ( $P < 0.05$ ) in the SSCit-IT group ( $4.3 \pm 0.5$  mN/mm<sup>2</sup>) compared to the SSPVP-IT group ( $2.9 \pm 0.3$  mN/mm<sup>2</sup>) or the LSCit-IT group ( $3.2 \pm 0.4$  mN/mm<sup>2</sup>). ACh responses were impacted in a dispersant-dependent manner, shifting the EC50 from  $106.6 \pm 16.6$  nM in the LSPVP-IT group to  $50.4 \pm 19.9$  nM in the LSCit-IT group. We found no significant differences between coronary responses from rats exposed intravenously to AgNP or their vehicles. We conclude that pulmonary exposure to AgNP activates biological response pathways that are sensitive both the dispersant and AgNP size. This work is supported by NIH U19 ES019525.

### PS 1136 Environmental Predictors of Oxidized Ldl Cholesterol (oxLDL) in Navajo Populations Exposed to Uranium-Contaminated Mining Sites.

M. E. Harmon<sup>1</sup>, C. Miller<sup>2</sup>, M. J. Campen<sup>1</sup>, C. Shuey<sup>3</sup>, M. Cajero<sup>2</sup>, B. Pacheco<sup>2</sup>, E. Erdei<sup>1</sup>, J. DeGroat<sup>2</sup>, G. Stark<sup>2</sup>, S. Henio-Adeky<sup>3</sup>, S. Ramone<sup>3</sup>, T. Nez<sup>3</sup> and J. Lewis<sup>2</sup>. <sup>1</sup>College of Pharmacy, University of New Mexico, Albuquerque, NM; <sup>2</sup>Community Environmental Health Program, University of New Mexico, Albuquerque, NM; <sup>3</sup>Southwest Research and Information Center, Albuquerque, NM.

Numerous abandoned mines within the Navajo Nation contribute uranium, arsenic and other heavy metals to the soil and groundwater. Environmental exposure to heavy metal contaminants may promote or exacerbate cardiovascular disease. The prevalence of type 2 diabetes, a risk factor for cardiovascular disease, has increased among the Navajo community. Evidence is emerging that pre-existing metabolic disease may increase an individual's susceptibility to vascular toxicity of heavy metal contaminants. To assess the potential impact of these contaminants on cardiovascular health of exposed individuals, we examined traditional (IL-6, CRP) and novel (oxLDL, LOX-1 receptor) plasma biomarkers in a large community of the Navajo Nation. Samples and data were obtained through a culturally appropriate community-based participatory approach, incorporating data collection and outreach by Navajo community staff. Biomarker data were linked to geospatial data on contamination sites using traditional linear regression and Bayesian models. When we used a binary model for uranium and arsenic drinking water levels, we observed that the estimated annual intake of arsenic was a significant predictor of oxLDL; age, the occupational exposure score, and the distance-environmental exposure score were also significant predictors. Diabetes, based on glycated hemoglobin, was a significant predictor of oxLDL. No environmental factors were correlated with LOX-1, CRP, or IL6. In summary, oxLDL does not seem to trend with environmental exposure to abandoned uranium mines or their heavy metal contaminants, but oxLDL does seem to trend with arsenic in drinking water. While still preliminary, these results indicate that arsenic intake may increase markers of cardiovascular risk.

### PS 1137 Pulmonary Nanoparticle Exposure Enhances Cardiac Parasympathetic Signaling.

T. L. Knuckles, J. Yi and T. R. Nurkiewicz. Center for Cardiovascular and Respiratory Sciences, West Virginia University, Morgantown, WV.

Pulmonary nanoparticle exposure has been associated with alterations in autonomic signaling in the peripheral microcirculation. One possible mechanism linking pulmonary nanoparticle exposure to remote effects is modulation of autonomic influences. Several studies have indicated an increase in parasympathetic signaling in the heart following particle exposure. We have recently reported that nanoparticle exposure alters microvascular responses to sympathetic nerve stimuli. Thus, we developed a model of baroreceptor function reflexes to determine the relative autonomic contributions. Rats were exposed to titanium dioxide (nano-TiO<sub>2</sub>) for 4 hr for 1 day at 9 mg/m<sup>3</sup>. 24-hours post-exposure, baroreflex sensitivity was determined by i.v. infusion of sodium nitroprusside (SNP; 5-20  $\mu\text{g/kg}$ ) or phenylephrine (PE; 1-16  $\mu\text{g/kg}$ ), with or without atropine (1 mg/kg) to diminish parasympathetic signaling. Nano-TiO<sub>2</sub> exposure did not alter PE-induced (4  $\mu\text{g/kg}$ ) changes in mean arterial pressure ( $\Delta\text{MAP}$ ;  $25 \pm 5$  mm Hg Sham,  $26 \pm 3$  mm Hg Exposed). However, nano-TiO<sub>2</sub> exposure increased the magnitude of  $\Delta\text{heart rate}$  in beats per minute ( $\Delta\text{BPM}$   $-20 \pm 2$  control vs.  $-26 \pm 3$  exposed), suggesting an enhanced parasympathetic response. When these experiments were repeated in the presence of atropine, PE-induced  $\Delta\text{BPM}$  was diminished in both groups; however, atropine significantly altered  $\Delta\text{BPM}$  in nano-TiO<sub>2</sub> compared to sham ( $-18 \pm 1$  Sham,  $-12 \pm 2$  Exposed), suggesting an enhanced sensitivity to muscarinic receptor blockade. Atropine treatment did not significantly alter  $\Delta\text{MAP}$  in either group. Nano-TiO<sub>2</sub> exposure did not significantly alter SNP-induced changes in  $\Delta\text{MAP}$  ( $-36 \pm 5$  mm Hg control vs.  $-41 \pm 2$  mm Hg exposed), or heart rate ( $\Delta\text{BPM}$   $18 \pm 7$  control vs.  $26 \pm 7$  exposed). Because parasympathetic projections in cardiovascular system are largely confined to the heart, these data suggest that nano-TiO<sub>2</sub> exposure

alters cardiac vagal tone, perhaps as a compensatory mechanism to enhanced sympathetic influence. Future work will focus on mechanisms that precipitate alterations in autonomic function. NIH RO1-ES015022 (TRN)

**PS 1138 Cigarette Smoke Induces Ventricular Remodeling through Activation of the Aryl Hydrocarbon Receptor.**

J. Bradley, M. C. El Hajj and J. D. Gardner. *Louisiana State University, Health Science Center, New Orleans, LA.*

Cigarette smoking is the major cause of preventable morbidity and mortality, with 5 million deaths annually worldwide. Cigarette smoke (CS) increases the risk of cardiovascular disease, including myocardial infarction and coronary artery disease. Of the 4700 identified components in CS, 60 are known carcinogens with polycyclic aromatic hydrocarbons (PAH) the most abundant carcinogenic agent. Chronic exposure to PAH can lead to ventricular dilation and dysfunction. Previously, we found the 5 wks of exposure to diesel exhaust particulates (DEP), which contain a high level of PAH similar to that in CS, induced ventricular dilation and dysfunction. DEP exposure impaired ventricular remodeling through activation of the aryl hydrocarbon receptor (AHR). Because of the similarities in chemical composition, we hypothesized that chronic exposure to CS would activate the AHR pathway inducing ventricular extracellular (ECM) remodeling. Male Sprague Dawley rats were exposed to six cigarettes per day (Kentucky 2R4F) for 12 wks using a modified version of the Griffith snout exposure method. CS exposure resulted in increased expression of AHR in the left ventricle. Furthermore, these animals had increased cardiac expression of cytochrome P450 1A1, an enzyme upregulated by AHR activation. CS exposure reduced cardiac collagen as assessed through decreased levels of hydroxyproline. In addition, CS increased the expression of MMP-9, a key regulator in collagen turnover. These in vivo findings were confirmed in isolated cardiac fibroblasts, where 10% CS extract reduced the secretion of collagen by cardiac fibroblasts. In all, our findings indicate that CS alters ventricular ECM remodeling through the reduction of myocardial collagen by an AHR dependent mechanism.

**PS 1139 The Association of Vascular Disease with Exposure to Diesel Exhaust.**

M. Peterson<sup>1</sup>, P. Valberg<sup>2</sup> and C. Long<sup>2</sup>. <sup>1</sup>Gradient, Seattle, WA; <sup>2</sup>Gradient, Cambridge, MA.

Cardiovascular disease (CVD) includes numerous heart- and circulatory-system related conditions, many of which are related to the buildup of plaque in the walls of coronary (heart) arteries, in which case the disease is called coronary artery disease (CAD). CVD is the leading cause of mortality in the US, with about 25% of all deaths related to some form of this disease. While the majority of research on the health effects of exposure to disease exhaust (DE) has focused on pulmonary endpoints, there is a growing body of research on the cardiovascular effects of DE particulate inhalation. Because DE exposure in the US is widespread, both occupationally and regionally, possible cardiovascular effects from DE could have significant public health implications. We performed a weight-of-evidence evaluation of the potential for DE to cause CAD, considering the mechanistic, toxicological, and epidemiological aspects of DE. Based on our research and analysis, we find little evidence to support an association of CAD with DE exposure at low (ambient) exposure levels. In particular, the occupational epidemiology studies fail to provide consistent evidence of increased risk. We identified twelve studies of diesel-exposed worker populations in which cardiovascular health endpoints were studied. Several of these studies found significantly increased risks of one or two endpoints (or in one or two subpopulations), while other studies reported significantly decreased risks for some endpoints/subpopulations. Overall, there was not a consistent effect observed across the literature. Moreover, because of a lack of dose-response between DE particulate levels and CVD mortality, the results of our evaluation also have implications for assigning cardiovascular mortality risk to ambient air PM<sub>2.5</sub>, as is often done in assessing monetary value of PM<sub>2.5</sub> reductions.

**PS 1140 FGF21 Expresses in Diabetic Hearts and Protects from Palmitate- and Diabetes-Induced Cardiac Cell Death In Vitro and In Vivo via Erk1/2-Dependent p38 MAPK/AMPK Signaling Pathway.**

C. Zhang<sup>1,2</sup>, X. Li<sup>1,2</sup> and L. Cai<sup>1,2</sup>. <sup>1</sup>University of Louisville, Louisville, KY; <sup>2</sup>Wenzhou Medical College, Wenzhou, China.

The present study examined whether fibroblast growth factor (FGF) 21 expresses in the heart of diabetic mice and also protects from fatty acid (palmitate)- and diabetes-induced cardiac apoptosis. Streptozotocin (STZ) induced type 1 diabetes increased FGF21 expression about 40 fold at 2 months and 1.5 fold at 6 months. To

define if the up-regulated cardiac FGF21 expression offers a protective effect on fatty acid- or diabetes-induced cardiac damage, H9C2 cells were exposed to palmitate at 62.5  $\mu$ M for 15 h, which significantly increased apoptosis. Pre-incubation of palmitate-treated cells with FGF21 significantly reduced the apoptosis, examined by DNA fragmentation and cleaved caspase-3. Mechanistically FGF21 inhibited palmitate down-regulated phosphorylation levels of Erk1/2, p38 MAPK and AMPK. Via application of inhibitor of each kinase and Erk1/2 siRNA, FGF21 was found to prevent palmitate-induced cardiac apoptosis via up-regulating Erk1/2-dependent p38 MAPK/AMPK signaling pathway. To confirm these in vivo, STZ-induced diabetic mice were treated with FGF21 for 10 days, which significantly prevented diabetes-induced cardiac apoptosis along with up-regulation of Erk1/2, p38 MAPK and AMPK phosphorylation. The cardiac protection of FGF21 was completely blocked by Erk1/2 inhibitor. FGF21 also protected cardiac apoptosis in acute fatty acid-treated mice via the same signaling pathway. More importantly, compared to wild-type mice, FGF21 gene knock-out mice are highly susceptible to diabetes-induced cardiac cell death and inhibition of Erk1/2, p38 MAPK and AMPK phosphorylation, which could be prevented by FGF21 treatment. These results strongly suggest that the early stage increase in FGF21 mRNA expression may represent an early protective mechanism; Application of FGF21 to diabetic mice or acute fatty acid-treated mice can prevent cardiac cell death via ERK1/2-dependent p38 MAPK and AMPK signaling pathway.

**PS 1141 Effects of Nicotine on Cardiovascular Remodeling in a Mouse Model of Systemic Hypertension.**

E. S. Colombo<sup>1,2</sup>, J. Davis<sup>1</sup>, M. Makvandi<sup>1</sup>, M. Aragon<sup>1</sup>, M. Paffett<sup>1</sup> and M. J. Campen<sup>1</sup>. <sup>1</sup>College of Pharmacy & Internal Medicine, University of New Mexico Health Science Center, Albuquerque, NM; <sup>2</sup>Internal Medicine, University of New Mexico, Albuquerque, NM.

The association of cigarette smoking and hypertension with the development of heart disease and aortic aneurysms is clear. The use of nicotine-alone formulations, such as the nicotine patch, gum or 'smokeless' electric cigarettes is increasing, as they are perceived as healthier alternatives to traditional cigarettes. Unfortunately, there is little data available on the effect of isolated nicotine on myocardial and aortic remodeling in healthy subjects or in the setting of hypertension. We hypothesized that nicotine would exacerbate the effects angiotensin-induced hypertension, as evidenced by reduced left ventricular wall thickness and aortic wall remodeling. For this study we utilized subcutaneous osmotic minipumps to administer angiotensin II, nicotine, nicotine plus angiotensin II (Ang-II) or saline to C57Bl/6 (n=6) mice for a total of 4 weeks. Ventricular wall thickness, activity of matrix metalloproteinase 2 and 9 (MMP2/9) and presence of type 1 collagen was assessed as evidence of cardiac remodeling. Heart weights were increased by treatments, with control<nicotine<ang-II<nicotine+ang-II, but a statistical interaction of nicotine x ang-II was not noted. Activity levels of MMP-2 mirrored these changes and demonstrated clear additivity between nicotine and ang-II. Additionally, histopathological analysis of aortas revealed that combined nicotine and ang-II treatment induced significant hypertrophy compared to all other groups. This pilot project reveals possible cardiotoxic interactions between nicotine and angiotensin-II induced hypertension. These data indicate that in the presence of hypertension, nicotine alone can drive development of cardiovascular, which has important implications on labeling and marketing of nicotine replacement therapy. These data also raise the possibility that angiotensin inhibitors may be specifically efficacious in prevention of cardiovascular disease among hypertensive individuals using nicotine.

**PS 1142 Metallothionein Preservation of Akt2 Function by Down-Regulating TRB3 Restores Diabetic Inhibition of Cardiac Insulin Signaling.**

Y. Tan<sup>1,2</sup>, Y. Wang<sup>3,1</sup>, X. Li<sup>2</sup> and L. Cai<sup>1,2,3</sup>. <sup>1</sup>Pediatrics, University Louisville, Louisville, KY; <sup>2</sup>CARIDC, Wenzhou Medical College, Wenzhou, China; <sup>3</sup>Jilin University, Changchun, China.

Cardiac insulin resistance is a key pathogenic factor for diabetic cardiomyopathy, but its mechanism remains largely unclear. Here we demonstrated that streptozotocin-induced diabetes significantly inhibited protein kinase B (Akt) Ser473 and Thr308 phosphorylation from 2 weeks to 2 months. In cardiac-specific metallothionein-transgenic (MT-TG) diabetic mice, both Akt phosphorylation sites were preserved normally at all time-points. Analysis of Akt isoforms revealed that Akt2, but not Akt1, expression and phosphorylation were decreased at all time-points in wide-type (WT) mice, but not MT-TG mice. Diabetes also increased Akt negative regulator tribbles (TRB)3 expression only in WT mice, suggesting possible contribution of MT prevention of diabetic up-regulation of Akt negative regulator to

Akt2 function preservation. For mechanistic study, cardiac H9c2 cells with and without forced MT overexpression (MT-H9c2) were treated with tert-butyl hydroperoxide (tBHP, an organic oxidant). tBHP did not affect basal Akt phosphorylation, but significantly inhibited insulin-stimulated total Akt phosphorylation and increased TRB3 expression only in H9c2 cells. Furthermore, tBHP reduced Akt2 phosphorylation in the basal and insulin-stimulating conditions, which were significantly, but not completely, attenuated in MT-H9c2 cells. Silencing TRB3 expression with its siRNA completely blocked tBHP-induced inhibition of insulin-stimulated Akt2 phosphorylation, while overexpression of TRB3 in MT-H9c2 cells transfected with recombinant TRB3 plasmid completely abolished MT preservation of insulin-stimulated Akt2 phosphorylation in response to tBHP. These results suggest that oxidative stress-attenuated cardiac Akt, especially Akt2, function via up-regulating Akt negative regulator plays a critical role in diabetic inhibition of insulin signaling in the heart. MT preservation of Akt2 function by inhibition of Akt negative regulator prevents diabetic inhibition of cardiac insulin signaling.

#### **PS 1143 Development of an Ultrasound Imaging Biomarker of Drug-Induced Vascular Injury.**

T. A. Swanson<sup>1</sup>, M. P. Lawton<sup>2</sup>, S. Portugal<sup>2</sup>, L. Obert<sup>2</sup>, J. Kreeger<sup>2</sup> and B. E. Enerson<sup>2</sup>. <sup>1</sup>*Comparative Medicine, Pfizer Worldwide Research, Groton, CT;* <sup>2</sup>*Drug Safety Research, Pfizer Worldwide Research, Groton, CT.*

Acute drug-induced vascular injury (DIVI) is caused by several classes of drugs, including Phosphodiesterase (PDE) inhibitors and dopamine agonists. The finding of DIVI in preclinical toxicity studies presents a significant challenge for pharmaceutical companies, with many compounds terminated from development because of the inability to monitor DIVI in the clinic. Ultrasound imaging is a non-invasive technique that can be used to measure blood flow and vessel diameter in multiple tissues and across species, and therefore has the potential to be a translatable biomarker of DIVI. Our objective was to demonstrate the utility of high-frequency ultrasound imaging for measuring hemodynamic changes in mesenteric arteries of male Sprague Dawley rats treated with fenoldopam and CI-1044 (PDE4 inhibitor). Blood flow and vessel diameter were measured in the superior mesenteric arteries and right renal arteries at 4, 8 and 24 hours after dosing and the rats were subsequently necropsied at each time point. Microscopic observations consistent with DIVI were found in animals treated with fenoldopam at 24 hours and included mild to moderate perivascular accumulations of mononuclear cells, neutrophils in tunica adventitia and superficial tunica media as well as multifocal hemorrhage and necrosis in the tunica media. Animals dosed with both drugs show marked increases in flow and shear stress as early as 4 hours after dosing, with the fenoldopam-treated rats exhibited the large changes in these parameters. Vessel diameter and blood flow were used to calculate shear stress and regression analysis was used to model the relationship between the presence of lesions and various hemodynamic parameters and indicated that peak blood flow velocity was the best predictor of lesion formation. This data suggests that ultrasound imaging may provide a translatable and non-invasive functional biomarker for localized hemodynamic changes that may correlate with acute vascular lesion formation in specific target tissues.

#### **PS 1144 Environmentally-Persistent Free Radicals (EPFRs) Exacerbate Cardiac Dysfunction during Ischemia-Reperfusion (I-R) Injury.**

B. Burn, S. Mahne, V. Subramaniam and K. Varner. *Pharmacology, Louisiana State University Health Sciences Center, New Orleans, LA.*

EPFRs have been identified in the particulate matter (PM) milieu at Superfund sites. These EPFRs, capable of redox cycling and the continual generation of radical species, form during combustion processes as halogenated hydrocarbons chemisorb to transition metal-oxide-containing particles. We showed that short-term nose-only inhalation of EPFRs decreased stroke volume (SV) and cardiac output (CO) in rats secondary to increased pulmonary resistance and decreased ventricular filling. EPFRs also increased markers of oxidative stress and inflammation both systemically and in the left ventricle. Epidemiological studies link PM exposure to increased cardiac morbidity and mortality from ischemic events. Therefore, the current study sought to determine if prior exposure to EPFRs would increase cardiac vulnerability to I-R injury. The EPFRs (0.2 µm diam) tested were surrogates consisting of 1,2-dichlorobenzene chemisorbed to a silica/CuO particle at 230°C (DCB230). Rats were exposed via nose-only inhalation to DCB230 (171 µg), silica particles or vehicle for 20 min/day for 7 days. Ventricular function was measured in vivo using pressure-volume catheters. I-R injury was induced by ligating the left anterior descending coronary artery for 20 min followed by 60 min of reperfusion.

Compared to controls, baseline CO, stroke work and SV were significantly reduced by exposure to DCB230. These parameters were further reduced during ischemia and remained below control throughout reperfusion. Although not significantly different from controls, end diastolic volume and heart rate trended lower in DCB230 treated rats throughout, possibly contributing to the reduced ventricular function. Indices of contractility and diastolic function were not different between the groups. These data show that EPFRs reduce baseline ventricular function and exacerbate the decrease in ventricular function elicited during I-R injury. Supported by NIH P42-ES013648 (subaward 61365).

#### **PS 1145 The Role of Nickel in Systemic Inflammation and Blood Coagulative Effects Induced by PM2.5.**

F. Deng, P. Xia and X. Guo. *Occupational & Environmental Health Sciences, Peking University School of Public Health, Beijing, China.*

Exposure to fine particles (PM2.5) is associated with adverse cardiopulmonary health effects; however, the causative components in PM2.5 are limited. Nickel is one of the major elements of ambient particulate matters. This study was designed to investigate the acute cardiovascular systemic toxicity induced by PM2.5 on Wistar rats and the role of nickel sulfate in it. Male Wistar rats were exposed by intratracheal instillation to blank membrane (control), fine particles with the doses of 7.5, 15 and 30mg/kg body weight and balanced saline (control), Nickel sulfate at dosages of 7.5, 75 and 750µg/kg Ni; The rats were sacrificed after 24h, blood samples were collected and parameters of inflammation, cytokines, coagulative effects and the nickel levels in serum were measured to estimate the cardiovascular injury. The results showed that both of PM2.5 and Nickel sulfate induced a significant increase of serum C-reactive protein, IL-6 and TNF-α, PT levels in the plasma decreased significantly in PM2.5-treated rats compared with the control group. Plasma fibrinogen increased significantly at 15 mg/kg and 30 mg/kg PM2.5 groups. The PT and APTT showed no changes in NiSO4-treated rats, Plasma fibrinogen levels increased significantly at 750 µgNi /kg NiSO4-treated rats. The TF concentrations in plasma increased significantly at 75 µgNi/kg and 750 µgNi/kg dosage groups (P<0.05), there was a slight increase at low dosage (7.5 µgNi/kg) group. To be compared with the corresponding concentration of NiSO4, the acute effects of PM2.5 were more stronger. Our results suggest that water-soluble nickel in PM2.5 may play an important role in PM2.5 toxic effects on animal cardiovascular system.

Key words: PM2.5; Nickel sulfate ; Cardiovascular Toxicity

Note: This experiment was carried out in accordance with the Peking University Society's criteria for the care and use of animals in research.

#### **PS 1146 Involvement of Shear Stress in Fenoldopam and Dopamine-Induced Mesenteric Medial Arterial Necrosis.**

D. Dalmas, K. Frazier, H. Thomas and M. Scicchitano. *Safety Assessment, GlaxoSmithKline, King of Prussia, PA.*

Extrapolation and relevance of drug-induced rat vascular injury to humans has hampered drug development due to lack of understanding of the pathologic mechanisms involved. Although vasodilatation and increased shear stress (SS) have been hypothesized to be involved in the pathogenesis of these lesions, the exact role of SS on primary target cells, vascular smooth muscle (VSMC) and endothelial cells (EC) in vivo remain unclear. Dopaminergic DA1 agonists such as Fenoldopam and Dopamine reproducibly induce mesenteric medial arterial necrosis (MAN) in rats following single vasotoxic doses. To investigate the involvement of SS in the development of MAN, rats were given vehicle, Dopamine or Fenoldopam for 4 days. Yohimbine, a alpha-2 adrenoreceptor antagonist, also vasoactive but lacking MAN was given to rats for 4 days for comparison. To evaluate the timecourse of lesion development, rats were also given vehicle or a single vasotoxic dose of Fenoldopam and necropsied 1-, 4-, 6-, 12- or 24 hours postdose. Mesentery from each rat was collected and frozen in OCT, then EC and VSMC were microdissected from rat mesenteric arteries, and RNA was amplified and analyzed. Regulations of 37 shear stress responsive genes were evaluated using TaqMan® gene expression profiling. Many of the genes evaluated were confirmed to be differentially expressed by Dopamine and Fenoldopam in EC- and/or SMC-enriched samples as compared to controls and Yohimbine following 4 daily doses. A number of SS responsive genes were also shown to be differentially regulated beginning 1- and/or 4-hours post-Fenoldopam treatment and prior to histological evidence of MAN (which was initially observed beginning at 12-hours). Evaluation of this panel of genes has provided evidence of the involvement and regulation of SS responsive genes in both EC and VSMC during the development of Dopamine and Fenoldopam-induced vascular injury.

**PS 1147 Direct Interaction between Multiwalled Carbon Nanotubes and the Coronary Microcirculation.**

T. R. Nurkiewicz<sup>1</sup>, B. T. Chen<sup>2</sup>, D. Frazer<sup>2</sup>, R. R. Mercer<sup>2</sup>, J. F. Scabilloni<sup>2</sup>, V. Castranova<sup>2</sup> and P. G. Stapleton<sup>1</sup>. <sup>1</sup>Physiology and Pharmacology, West Virginia University, Morgantown, WV; <sup>2</sup>National Institute for Occupational Safety and Health, Morgantown, WV.

Recently our collaborative group identified multi-walled carbon nanotube (MWCNT) translocation from the lung to the heart, liver, and kidneys within 24 hours after pulmonary exposure. From this finding, we continued to examine the microvascular ramifications associated with this direct interaction. To model drug delivery platforms, as well as lung migration, MWCNT were injected into the tail vein of rats (25-900 µg, suspended in 900 µL normosol). 24-hours later, coronary arterioles (<170 µm in diameter) from the left anterior descending artery distribution were isolated for reactivity assessments based on responses to transmural pressure (myogenic responsiveness), intraluminal flow (shear stress), phenylephrine (10-9-10-4 M), acetylcholine (10-9-10-4 M), A23187 (10-9-10-5 M), and spermineNONOate (10-9-10-4 M). Myogenic responsiveness was not altered after MWCNT injection. However, MWCNT injection at all concentrations robustly attenuated reactivity. The coronary microvascular dysfunction associated with MWCNT injection is significant, impacting endothelium-dependent, -independent, adrenergic, and flow-mediated dilation pathways. These alterations, in combination with previous findings, indicate that the microvascular impairments that follow MWCNT injection are more severe than those observed after ingestion or inhalation exposure. Studies are currently underway to further evaluate mechanistic differences between these routes of exposure. NIH-RO1-ES015022 and RC1-ES018274 (TRN)

**PS 1148 Phosgene-Induced Lethal Lung Edema Correlate with Persistent Stimulation of Cardiopulmonary Reflexes.**

W. Li<sup>1</sup> and J. Pauluhn<sup>2</sup>. <sup>1</sup>Department of Toxicology, Fourth Military Medical University, Xi'an, China; <sup>2</sup>Toxicology, Bayer Pharma AG, Wuppertal, Germany.

Phosgene gas is a lower respiratory tract irritant. As such, it stimulates nociceptive vagal C-fiber related reflexes in a dose-rate and concentration x exposure duration (Cxt)-dependent manner. In rats this reflex is characterized by extended apnea time periods, bradycardia, and hypothermia. While inhalation exposures at non-lethal Cxt products show rapid reversibility of reflexively induced changes in respiratory patterns, lethal Cxt products seem to cause their prolonged stimulation after discontinued exposure to phosgene. This observation has been taken as indirect evidence that phosgene-induced lethal lung edema is likely to be caused by dysfunctional neurogenic control of cardiopulmonary and microvascular physiology. In order to verify this hypothesis, data from respiratory function measurements during and after the inhalation exposure to phosgene gas were compared with time-course measurements of respiratory and cardiac function over 20 hours post-phosgene exposure. These data were complemented by time-course analyses of nitric oxide (NOe) and carbon dioxide in exhaled breath, including time-dependent changes of extravasated protein in bronchoalveolar lavage fluid (BALF) and hemoglobin in blood. The nitric oxide synthetase inhibitors L-NAME and L-NIL were used to further elucidate the role of NOe in this type of acute lung injury and whether its analysis can serve as an early biomarker of pulmonary injury. Collectively, the sequence and time-course of pathological events in phosgene-induced lung edema appear to suggest that over-stimulated, continued sensorimotor vagal reflexes trigger changes in cardio-pulmonary hemodynamics. In the absence of any successful intervention, this imbalance progresses eventually to a refractory, self-perpetuating and self-amplifying acute lung edema within 24 hours post-phosgene exposure. The continued excessive parasympathetic tone appears to be the major etiopathology in this type of high permeability lung edema following acute high-level exposures to phosgene gas.

**PS 1149 Role of Nrf2 Antioxidant Defense in Mitigating Cadmium-Induced Oxidative Stress in the Olfactory System of Zebrafish.**

L. Wang and E. P. Gallagher. Department of Environmental and Occupational Health Sciences, University of Washington, Seattle, WA.

Exposure to trace metals can disrupt olfactory function in fish leading to a loss of behaviors critical to survival. Cadmium (Cd) is an olfactory toxicant that elicits cellular oxidative stress as a mechanism of toxicity while also inducing protective cellular antioxidant genes via activation of the nuclear factor (erythroid-derived 2)-like 2 (Nrf2) pathway. However, the molecular mechanisms of Cd-induced olfactory injury have not been characterized. In the present study, we investigated the role of

the Nrf2-mediated antioxidant defense pathway in protecting against Cd-induced olfactory injury in zebrafish. A dose-dependent induction of Nrf2-regulated antioxidant genes associated with cellular responses to oxidative stress was observed in the olfactory system of adult zebrafish following 24 h Cd exposure. Zebrafish larvae exposed to Cd for 3 h showed increased glutathione S-transferase pi (*gst pi*), glutamate-cysteine ligase catalytic subunit (*gclc*), heme oxygenase 1 (*hmox1*) and peroxiredoxin 1 (*prdx1*) mRNA levels indicative of Nrf2 activation, and which were blocked by morpholino-mediated Nrf2 knockdown. The inhibition of antioxidant gene induction in Cd-exposed Nrf2 morphants was associated with disruption of olfactory driven behaviors, increased cell death and loss of olfactory sensory neurons (OSNs). Nrf2 morphants also exhibited a downregulation of OSN-specific genes after Cd exposure. Pre-incubation of embryos with sulforaphane (SFN) partially protected against Cd-induced olfactory tissue damage. Collectively, our results indicate that oxidative stress is an important mechanism of Cd-mediated injury in the zebrafish olfactory system. Moreover, the Nrf2 pathway plays a protective role against cellular oxidative damage and is important in maintaining zebrafish olfactory function. This work was supported by the University of Washington Superfund Research Program (NIEHS P42ES004696).

**PS 1150 Cadmium Enhances Instability of Lysyl Oxidase Messenger RNA.**

Y. Zhao, S. Gao, P. Toselli and W. Li. Biochemistry, Boston University School of Medicine, Boston, MA.

Lysyl oxidase (LO), a copper-dependent enzyme, catalyzes crosslinking of collagen and elastin essential for tissue and organ morphogenesis and repair. Our previous studies have shown the critical role of downregulation of LO in cadmium (Cd)-induced emphysema pathogenesis *in vitro* and *in vivo*. The present studies further investigate Cd effects on posttranscriptional modification of the LO gene in rat fetal lung fibroblasts (RFL6). Treatment of cells with Cd (1-5 µM) inhibited levels of LO steady-state mRNAs in a dose-dependent manner. RFL6 cells displayed a relatively stable LO mRNA stability as assessed by the actinomycin D (an inhibitor of mRNA synthesis, 5 µg/ml) chase assay with the  $t_{1/2} = 24$  h. In contrast, in cells treated with 5 µM Cd plus actinomycin D, the  $t_{1/2}$  for LO mRNA decay was reduced to 0.75-h (45 min). Thus, Cd facilitates the LO mRNA decay. Rat LO mRNA contains two AU-rich elements (ARE, AUUUA), the stability determinant, at 174/178 and 200/204 downstream of the translation stop codon in the 3'-UTR. We cloned the entire LO 3'-UTR (1/229) and the ARE fragment (152/229) into the pGL3-Promoter vector after the coding region of the SV40 promoter-driven luciferase gene. The LO 3'-UTR or the ARE fragment strongly stabilized the reporter mRNAs manifested by increased luciferase activities in transfected cells. Mutation of two AREs abolished the enhancement of reporter mRNA stabilities by the LO 3'-UTR or the ARE fragment. Notably, luciferase activities driven by the LO 3'-UTR or ARE in recombinant constructs were significantly inhibited in cells treated with 5 µM Cd, indicating Cd enhancement of the decay of LO 3'-UTR or ARE-driven reporter mRNAs. HuR, a major ARE binding protein, enhances the mRNA stability. RNA immunoprecipitation (RIP) assay indicated that Cd effectively blocked the binding of HuR into the LO mRNA AREs. Thus, Cd targeting the HuR may be a critical mechanism for LO mRNA instability by this metal ion (supported by the grant of NIEHS 011340).

**PS 1151 Involvement of Inhibition of UBE2D Family Gene Expressions on Cadmium-Induced p53 Dependent Apoptosis in Human Proximal Tubular Cells.**

M. Tokumoto<sup>1,2</sup>, J. Lee<sup>2</sup>, Y. Fujiwara<sup>2</sup> and M. Satoh<sup>2</sup>. <sup>1</sup>Showa Pharmaceutical University, Machida, Japan; <sup>2</sup>School of Pharmacy, Aichi Gakuin University, Nagoya, Japan.

Cadmium (Cd), known to be a causative agent of *Itai-itai* disease, produces severe toxic effects in the kidney, liver, lung and bone. Particularly, chronic exposure to Cd causes renal dysfunction. Recently, we have found that overaccumulation of p53 may relate to Cd-induced apoptosis and may be due to the suppression of p53 degradation through the inhibition of gene expressions of Ube2d family in rat proximal tubular cells (NRK-52E cells). In this study, we examined the effects of Cd on the expressions of UBE2D family, accumulation of p53 and apoptosis in human proximal tubular cells (HK-2 cells). TUNEL positive cells, indicators of apoptosis, were increased by treatment with 20 µM Cd for 18 h. Moreover, using real-time RT-PCR, we demonstrated that Cd caused significant decrease of UBE2D2 mRNA levels from 6-h treatment, and UBE2D4 mRNA levels from 12-h treatment. Western blot analysis showed that Cd drastically increased p53 protein levels in HK-2 cells, even though the mRNA levels of p53 were decreased by Cd. Additionally, knockdown of UBE2D family genes by siRNA increased cellular protein levels of p53. These results indicate that Cd induces apoptosis through p53 accumulated by suppressions of UBE2D family gene expressions, in human proximal tubular cells as well as in rat proximal tubular cells.

**PS 1152 Serum and Hepatic Alkaline Phosphatase Activity in Rats Exposed Chronically to Cadmium.**

E. Brambila, S. Treviño-Mora, A. Andrade-García, B. León-Chávez and P. Aguilar-Alonso. *Clinical Chemistry Research Laboratory, Facultad de Ciencias Químicas, Benemérita Universidad Autónoma de Puebla, Puebla, Mexico.*

Changes of serum and hepatic alkaline phosphatase activity in rats administered with 65 ppm of Cd<sup>2+</sup> in drinking water were studied during a 3 months period. After metal administration, Cd<sup>2+</sup> in rat livers showed an accumulation of 21 µg/g tissue. Serum alkaline phosphatase activity decrease in 3 months Cd-exposed rats. Liver alkaline phosphatase activity increased after 1 month Cd-exposed rats, however, later enzymatic activity decreased in the rats exposed to the metal by 3 months. In order to determine if Cd accumulated in liver had an inhibitory effect on enzyme activity, hepatic alkaline phosphatase from non-exposed and 3-month exposed rats to Cd was isolated and apo-alkaline phosphatase was prepared using chelex-100. Apo-alkaline phosphatase was reactivated with Zn<sup>2+</sup> and Mg<sup>2+</sup>. Reactivation assays shown that liver alkaline phosphatase isolated from Cd-exposed rats had 2-fold more activity as compared with the enzyme isolated from Cd-non-exposed rats. Protein alkaline phosphatase did not show changes between non-exposed and metal-exposed rats as determined by western-blot and ELISA assays. Results of this work suggest that chronic Cd-exposure has an inhibitory effect on serum and hepatic alkaline phosphatase activity, and the mechanism of inhibition can involve the substitution of native zinc in the enzyme by the Cd progressively accumulated in the tissue.

**PS 1153 The Cadmium-Responsive Genes *Numr-1* and *Numr-2* Are Regulated by Multiple Pathways.**

Q. Ding and J. H. Freedman. *NIEHS, Research Triangle Park, NC.*

Exposure to the carcinogenic metal cadmium can activate multiple signaling pathways to affect the expression of hundreds of genes. However, the molecular mechanism by which cadmium affects transcription is not completely understood. Whole genome microarray studies in the nematode *C. elegans* showed nuclear metal-responsive gene-1 (*numr-1*) mRNA levels increased 7-fold following a 24h cadmium exposure. Subsequent genomic analysis identified a second gene, *numr-2*, that is 99% identical to *numr-1*, in both coding and regulatory regions. Both *numr*'s are developmentally regulated and expressed in identical cells: constitutively in a subset of neurons in the head, vulva and tail; and in intestinal and pharyngeal cells following metal exposure. Metals and calcium, but not other environmental stressors, induce *numr-1/2* transcription. Bioinformatic analysis identified 25 putative, upstream regulatory elements in the *numr* promoters. The roles of the cognate DNA binding proteins on *numr-1* expression in the absence and presence of cadmium was examined in loss of function mutants or by RNAi. Among the tested genes, two alleles of *osm-9* (TRPV channel protein), *ok1677* and *ky10*, showed significant gene-cadmium interactions, suggesting *osm-9* regulates cadmium-induced *numr-1/2* transcription. Three other genes may also be involved in *numr-1/2* transcriptional regulation: *ceb-20* (homeodomain protein), *unc-86* (POU-type homeodomain protein) and *gem-4* (calcium-dependent phosphatidylserine binding protein). In addition to *osm-9*, *unc-86* and *ceb-20* are expressed in neurons, suggesting a link between neuronal activity and metal-inducible *numr-1/2* transcription. The four candidate genes are present in independent signaling pathways, which suggest that cadmium-induced *numr-1/2* transcription is regulated by multiple signaling pathways. Further analyses disrupting these signal transduction pathways will be used to define the role of these genes in cadmium-induced *numr-1/2* transcription.

**PS 1154 SRC Kinase Participation in MT-II Production and Acetylation STAT3 in Mouse Hepatocytes Exposed to Cadmium.**

K. Martínez<sup>1</sup>, V. Souza<sup>1</sup>, A. López<sup>1</sup>, A. López-Reyes<sup>2</sup>, D. Clavijo<sup>1</sup>, L. Bucio<sup>1</sup>, L. Gómez-Quiroz<sup>1</sup> and M. Gutiérrez-Ruiz<sup>1</sup>. <sup>1</sup>Ciencias de la Salud, Universidad Autónoma Metropolitana, Mexico City, Mexico; <sup>2</sup>Dirección de Investigación, Instituto Nacional de Rehabilitación, Mexico City, Mexico.

Cadmium(Cd), a toxic metal initially accumulated in the liver, forms high affinity complexes with metallothionein-II (MT-II). This protein requires the activation of transcription factors such as STAT3. Phosphorylation is crucial to regulate the activity of several proteins, as well as acetylation, has been linked in gene expression processes giving greater affinity for the transcription factors to DNA. This process has been reported in STAT3 to form more stable dimers. There is evidence that this modification is carried out by the p300 coactivator protein, which is characteristic

because of its histone acetyltransferase activity and its Stat3 C-terminal affinity. MT-II production also has been associated with Src; however, molecular mechanisms induced by Cd have not been yet fully understood. The aim was to evaluate the participation of Src in Stat3 activation and its relation with MT-II production and acetylation in hepatocytes treated with 5µM CdCl<sub>2</sub>. Primary mouse hepatocytes were treated with different Cd concentrations determining phosphorylation of STAT3, Src, ERK1/2 and the induction of p300 and MT-II by Western-blot. A pretreatment for 30 min with Src inhibitor SU6656 was performed to evaluate the relationship between STAT3 activation and MT-II content; the same approach was done with the ERK1/2 inhibitor PD98059, used to correlate STAT3 activation and ERK signaling. We proved that Cd induced STAT3 acetylation. Cd increased activation of STAT3, Src, ERK1/2, p300, and MT-II. STAT3 phosphorylation and ERK1/2 were significantly reduced by Src, ERK1/2 inhibitors. MT-II expression diminished with Src inhibitor. Our results suggest that Cd induces STAT3 phosphorylation by a mechanism dependent of Src and ERK1/2, while STAT3 induces acetylation by p300 likely to increase production of MT-II as a biological response to Cd. SEP-CONACYT.CB-2008-106194

**PS 1155 Overaccumulation of p53 and Induction of Apoptosis in Renal Tubules of C57BL/6 Mice Chronically-Exposed to Cadmium.**

J. Lee<sup>1</sup>, M. Tokumoto<sup>1,2</sup>, Y. Fujiwara<sup>1</sup> and M. Satoh<sup>1</sup>. <sup>1</sup>School of Pharmacy, Aichi Gakuin University, Nagoya, Japan; <sup>2</sup>Showa Pharmaceutical University, Tokyo, Japan.

Long-term exposure to cadmium (Cd) affects adversely to renal tubules. We have recently demonstrated that Cd induces p53-dependent apoptosis through the inhibition of gene expression of Ube2d family in rat proximal tubule cells (NRK-52E cells). In this study, we examined the effect of chronic exposure to Cd on the localization of p53-dependent apoptosis in kidney of mice. Five weeks old female C57BL/6 mice were fed diet containing 300 ppm Cd without restraint for 12 months. After 6- and 12-month feeding, we evaluated renal toxicities, and measured mRNA levels of Ube2d family and protein levels of p53 in kidney. In order to examine the localization of p53, we used immunostaining with anti-p53 antibody. Localization of apoptosis was examined by TUNEL staining. Although exposure of mice to Cd induced mild renal toxicity, significant decreases of mRNA levels of Ube2d family and accumulation of p53 were detected in kidney. Interestingly, not only overaccumulation of p53 proteins but also induction of apoptosis was triggered specifically in renal tubules of mice by Cd exposure. These results indicate that Cd may induce apoptosis through p53 accumulated by suppressions of Ube2d family expressions, specifically in renal tubules.

**PS 1156 Effects of Cadmium on the Urinary Excretion and Localization of Cystatin C in Kidney.**

W. C. Prozialeck<sup>1</sup>, A. Van Drael<sup>1</sup>, S. Zawdzka<sup>1</sup>, J. Edwards<sup>1</sup>, C. D. Ackerman<sup>1</sup> and V. S. Vaidya<sup>2</sup>. <sup>1</sup>Department of Pharmacology, Midwestern University, Downers Grove, IL; <sup>2</sup>Renal Division, Brigham and Women's Hospital, Harvard Medical School, Boston, MA.

Cadmium (Cd) is a nephrotoxic environmental pollutant for which there is an urgent need for improved biomarkers of toxicity. Cystatin C is a low molecular weight protein that has been shown to be a sensitive biomarker for ischemic, and some types of toxic, kidney injury. The objective of the present study was to determine if cystatin C might be a useful early biomarker of Cd nephrotoxicity. Adult male rats were given subcutaneous injections of Cd (0.6 mg/kg, 5 days per week). At 6, 9 and 12 weeks, urine samples were collected and analyzed for cystatin C, protein, creatinine and kidney injury molecule-1 (Kim-1). Serum was analyzed for creatinine and cystatin C, and kidneys were processed for histopathologic analyses. Cd caused a 1-2 fold increase in urinary excretion of cystatin C and larger increases in Kim-1 excretion that were evident at 6, 9 and 12 weeks. No change in urinary protein was evident until 12 weeks. Cd had no effect on urinary creatinine or serum levels of creatinine and cystatin C. Histochemical analyses revealed evidence of proximal tubule injury in the Cd-treated samples, along with alterations in the pattern of cystatin C distribution. Control samples showed a speckled pattern of cystatin C labeling beneath the apical surface of the proximal tubule cells, whereas, Cd treated samples exhibited diffuse labeling in the cytoplasm and on the cell surface. The pattern of cystatin labeling paralleled that of the brush border transport protein megalin, which has been implicated as a mediator of cystatin C uptake in the proximal tubule. These results indicated that Cd increases the urinary excretion of cystatin C, and they suggest that this effect may involve disruption of megalin-mediated uptake of cystatin C by epithelial cells of the proximal tubule. Supported by Midwestern University and NIH Grant RO1 ES006478 to WCP.

**PS 1157 Cadmium Exposure Affects Insulin Signaling in *Caenorhabditis elegans*.**

Y. Sun and J. H. Freedman. *BSB, DNTP, NIEHS, Research Triangle Park, NC.*

Diabetes mellitus (DM) and diabetes-related kidney disease are serious, world-wide health problems. Although there is no direct evidence linking cadmium (Cd) to DM, Cd exposure alters blood glucose levels and potentiates diabetic nephropathy. The insulin/insulin-like growth factor signaling (IIS) pathway regulates multiple biological functions including glucose metabolism and longevity. The model organism *C. elegans*, which has an IIS pathway homologous to that of mammalian species, was used to investigate mechanistic links among Cd, transcription, and insulin signaling. The focus of this investigation was the *C. elegans* Cd-responsive gene *cdr-1*, whose transcription is up-regulated almost 800-fold exclusively by Cd. To identify regulatory factors and pathways that control *cdr-1* transcription, an integrated transgenic strain of *C. elegans* containing GFP under the control of the 5'-regulatory region of *cdr-1* was constructed. Following cadmium exposure (10  $\mu$ M, 24 h) in the transgenic strain, GFP expression increases in intestinal cells. In a candidate screen, genes involved in various stress response pathways were tested for their potential role in controlling *cdr-1* expression. Genes were knocked out either by genetic crosses to known loss-of-function *C. elegans* mutants or by RNAi. Changes of *cdr-1* transcription were then determined by measuring GFP expression or qRT-PCR. The expression of *cdr-1*, in both the absence and presence of Cd (100  $\mu$ M, 5 h) was suppressed when genes in the IIS pathway; *daf-2*, *age-1*, *daf-18*, *pdsk-1*, *akt-2*, *sgk-1* and *daf-16*; were knocked down. Statistically significant interactions between Cd and IIS pathway genes were observed. Furthermore, knocked down of IIS pathway-related genes; *skn-1*, *hsf-1*, *pha-4*, *pop-1*, *lin-14*, *tor-2*, *ras-1*, *wnk-1*; also inhibited *cdr-1* expression in response to Cd. These results suggest that the IIS pathway mediates Cd-inducible transcription. In addition, they support a model where Cd exposure could induce elevated blood glucose levels by directly affecting the IIS pathway. The mechanism by-which Cd activates the IIS pathway is currently being investigated.

**PS 1158 Investigating a Protective Role of the Antioxidant N-Acetylcysteine against Cadmium-Induced Damage to Bone Extracellular Matrix.**

D. D. Wright, W. S. Wright and S. J. Heggland. *Biology, The College of Idaho, Caldwell, ID.*

Environmental pollution of cadmium, a heavy metal commonly utilized in electronics, is a global human health concern. Bone is a known target site for cadmium. One mechanism to protect against cadmium-induced osteotoxicity and bone loss is by reducing oxidative stress. Our lab previously demonstrated that n-acetylcysteine (NAC) rescues osteoblasts from cadmium-induced apoptosis. Others have shown that reactive oxygen species generated through oxidative stress decreases bone mineral density, in part, through targeting the collagen component of the extracellular matrix (ECM). We hypothesize that the antioxidant NAC will protect against cadmium-induced damage to ECM produced by osteoblasts. Saos-2 cells were induced to mineralize and treated with 1mM NAC or 5 $\mu$ M CdCl<sub>2</sub> only or in combination for 6 or more days. Upon termination cell viability, phosphate ECM deposition, and collagen secretion and distribution in the ECM were evaluated using MTT, von Kossa, SircolTM collagen assay, and immunofluorescence, respectively. Treatment with CdCl<sub>2</sub> for 6 days resulted in increased phosphate deposition, which was restored to that of control in the presence of NAC. We also examined collagen, the main organic component of the ECM. When osteoblasts were induced to form an ECM, treatment with CdCl<sub>2</sub> led to significantly less collagen secretion which was reflected in less collagen deposition into the ECM; these effects were reversed in the presence of NAC. Further, NAC and NAC combined with CdCl<sub>2</sub> significantly increased cell viability compared to control, leading us to also investigate cell cycle progression. These studies provide further evidence that antioxidants promote bone health by reducing the toxic effects of cadmium. Research funded by NIH-INBRE P20 RR016454 and P20 GM103408 and NIH R15ES015866 grants.

**PS 1159 Cadmium Causes Injury to Pancreatic Islets That Is Associated with Caspase-3 Labeling.**

J. Edwards and Y. Bahrami. *Pharmacology, Midwestern University, Downers Grove, IL.*

Diabetes is a growing worldwide epidemic. There is increasing interest in how environmental contaminants can contribute to the onset of type II diabetes. Impaired insulin release is a hallmark of type I diabetes and is key in the progression of type II diabetes. Multiple epidemiological and experimental studies show that exposure

to the metal cadmium (Cd), is associated with diabetes and reduced serum insulin. To examine the cytotoxic effects of Cd within pancreatic islets, male Sprague Dawley rats were injected subcutaneously with either saline (control) or Cd (0.6 mg Cd/kg/day, 5 days per week). After 6, 9 and 12 weeks of Cd treatment, pancreatic tissue samples were removed then fixed in formalin. Pancreata were sectioned and H&E stained to identify islets then examined for changes in islet histology. A trained veterinary pathologist scored each sample for cytoplasmic vacuolization and signs of necrosis and apoptosis. All pancreata from Cd treated animals had elevated scores for signs of vacuolization, apoptosis and necrosis. However, these changes in cell viability did not appear to change with longer Cd exposure times. In another study using the same pancreas samples, tissue was labeled for the apoptosis indicator, active caspase 3. In this study, pancreatic samples were counter stained with hematoxylin so that immuno-labeled islets could be identified. This study resulted in similar findings. Islets from Cd-treated animals had greater caspase-3 labeling and as before, the intensity of labeling appeared to be time independent. These preliminary results show that Cd acts to injury pancreatic islets which may result in diminished insulin release.

**PS 1160 Regulation of Glutathione Synthesis in Cadmium-Treated Cultured Choroid Plexus.**

S. Francis Stuart, R. Young and A. Villalobos. *Interdisciplinary Faculty of Toxicology and Nutrition & Food Science, Texas A&M University, College Station, TX.*

In primary cultures of rat choroid plexus we have shown that exposure to cadmium (Cd) induces oxidative stress, stimulates apical choline uptake, and alters glutathione (GSH) synthesis. Our aim is to characterize the regulation of GSH availability and synthesis in response to low dose exposure to Cd and assess the significance of GSH in cellular adaptation to Cd. We treated choroid plexus primary cultures with 0 or 500 nM CdCl<sub>2</sub> in serum free medium (SFM) for 12 h and collected samples at 3, 6, 9, and 12 h. Induction of heme oxygenase-1 (HO-1), heat-shock protein 70 (HSP70), and metallothionein-1 (MT-1) in Cd-treated cells was compared to time-matched controls by immunoblot and qRT-PCR analyses. HO-1 protein was induced at 3 h and gradually increased through 12 h. HO-1 gene expression was maximally induced by 70-fold at 6 h and was sustained through 12 h. HSP70 protein was maximally induced by 5-fold at 12 h. MT-1 gene expression was induced by 50-fold at 12 h. Cd induced the catalytic and modifier subunits of glutamate-cysteine ligase (GCL), the rate-limiting enzyme in GSH synthesis. GCLC protein levels peaked at 6 h while GCLM peaked at 9 h. Gene expression of GCLC and GCLM increased by 5-fold and 4-fold at 12 h. To elucidate the effects of Cd on GSH concentration, cells were pretreated (12 h) without or with buthionine sulfoximine (BSO, 100  $\mu$ M) then treated with 0 or 250 nM CdCl<sub>2</sub>  $\pm$  BSO in SFM for 12 h. Intracellular GSH and oxidized glutathione (GSSG) concentrations were assayed and compared to control. Cd increased GSH by 2-fold and increased GSSG by 30-fold. In Cd-treated cells, BSO reduced GSH concentrations by 92% but increased GSSG concentrations by 15-fold above controls. Inhibiting GSH synthesis with BSO augmented induction of HO-1, HSP70, and MT-1 and enhanced stimulation of apical choline uptake in Cd-treated cells. These data indicate that Cd stimulates GSH synthesis at points of transcription and translation, and the inhibition of GSH synthesis accentuates cellular stress.

**PS 1161 Stable Expression of FRET-Based Cd(2<sup>+</sup>) Biosensor for Advanced Research of Cytotoxic Cd(2<sup>+</sup>).**

D. Yang<sup>1,2</sup> and T. Chiu<sup>2,1</sup>. <sup>1</sup>Department of Medical Research & Education, Taipei Veterans General Hospital, Taipei, Taiwan; <sup>2</sup>Institute of Biophotonics & Biophotonics and Molecular Imaging Research Center (BMIRC), National Yang-Ming University, Taipei, Taiwan.

Cadmium ion (Cd<sup>2+</sup>) causes lots of human tissue damages. Several ion channels and transporter proteins as the molecular gateway of different ions have been previously proposed to be the cytotoxic entry mechanism(s) of Cd<sup>2+</sup>. However, the solid conclusions have not been made. Here we tried to explore this issue through establishing human cell line stably expressing the fluorescent resonance energy transfer (FRET)-based Cd<sup>2+</sup> biosensor for monitoring content of intracellular Cd<sup>2+</sup>. This newly constructed Cd<sup>2+</sup> sensor Met-cad 1.57 contains part of Cd<sup>2+</sup>-binding protein CadR originated from bacteria *Pseudomonas putida* as the Cd<sup>2+</sup> sensing key. Through G418 selection, the HEK293 line stably expressing Met-cad 1.57 HEK-MCD157 cells have been archived. The spectral patterns and sensing ranges of Met-cad 1.57 for intracellular Cd<sup>2+</sup> sensing were characterized in vivo under 96-well plate. Under both a fluorescence spectroscopy and a FRET microscopic ratio imaging, the contents of Cd<sup>2+</sup> were than monitored within living HEK-MCD157 cells. The dynamic range of Met-cad 1.57 from 0 to 100  $\mu$ M of Cd<sup>2+</sup> is 2–4.4 (2.2

fold) with a dissociation constant  $K_d$  around 271 nM. The role of voltage-gated  $Ca^{2+}$  channels as the candidate of  $Cd^{2+}$  entry gateway was further explored with the HEK-MCD157 cells. In summary, a human embryonic kidney cell line HEK-MCD157 stably expressed FRET-based  $Cd^{2+}$  biosensor Met-cad 1.57 was constructed for both reliable and convenient investigations on content measurement of  $Cd^{2+}$  within live-cell including the identification of  $Cd^{2+}$  entry pathway and subcellular sequestration.

## PS 1162 Blood Cadmium Level of Residents Living near the Abandoned Metal Mines in Korea.

D. Kim<sup>1</sup>, S. Ahn<sup>1</sup>, J. Ryu<sup>1</sup>, S. Yu<sup>1</sup> and D. Park<sup>2</sup>. <sup>1</sup>*Environmental Health, National Institute of Environmental Research, Incheon, Republic of Korea;* <sup>2</sup>*Environmental Health, Korea National Open University, Seoul, Republic of Korea.*  
Sponsor: J. Park.

**Introduction:** Preliminary biological exposure monitoring study selected 38 among 906 metal mines abandoned in Korea as the relative high risk areas for national surveillance subjects. They were surveyed from 2008 to 2011 under the environmental health policy by Ministry of Environment. The purpose of this study is to assess the blood cadmium levels from people living around a total of 38 abandoned metal mine areas and to determine if those areas have influenced exposure to cadmium of residents.

**Methods:** Blood cadmium levels were quantified using graphite furnace atomic absorption spectrometry (AAS) through appropriate blood collection, storage and pretreatment procedure. People living less than 3 km from the abandoned mine area were classified as the exposure group ( $n=4,687$ ). Control group ( $n=2,643$ ) was selected from people living in non-mining areas.

**Results:** Blood cadmium level from exposure group was found to be 1.59 ug/L as geometric mean (GM) (95 % CI: 1.56 - 1.62 ug/L) and 1.91 ug/L as arithmetic mean (AM) (95 % CI = 1.88-1.94 ug/L). Those levels were significantly higher than those from control group (GM=1.28 ug/L, 95 % CI=1.25-1.31 ug/L, AM= 1.52 ug/L, 95 % CI = 1.49-1.56 ug/L) ( $p<0.0001$ ). In addition, 79.5% ( $n=3,728$ ) of exposure group and 69.6% ( $n=1,840$ ) of control group exceeded the reference value (1.0 ug/L) derived by German human biomonitoring commission. Multiple regression model found that exposure group was significantly higher than that of control group after age, gender and smoking status were all adjusted (adjusted  $R^2=16.5\%$ ,  $p<0.0001$ ).

**Conclusions:** We found that blood cadmium level of people residing near abandoned metal mine area was significantly high, compared with those of control group. Our findings suggested that the abandoned mine areas may have elevated blood cadmium level of people in the vicinity of those areas.

## PS 1163 One-Week and Four-Week Inhalation Toxicity Studies of Nickel Sulfate and Nickel Subsulfide in Rats.

D. E. Dodd<sup>1</sup>, H. J. Clewell<sup>1</sup>, M. A. Sochaski<sup>1</sup>, H. G. Wall<sup>2</sup>, G. A. Willson<sup>2</sup> and A. R. Oller<sup>3</sup>. <sup>1</sup>*The Hamner Institutes for Health Sciences, Research Triangle Park, NC;* <sup>2</sup>*Experimental Pathology Laboratories, Inc., Research Triangle Park, NC;* <sup>3</sup>*NiPERA, Inc., Durham, NC.*

Inhalation toxicity studies of nickel sulfate ( $NiSO_4$ ) and Ni subsulfide ( $Ni_3S_2$ ) were conducted in F344 rats to evaluate cellular pathway responses in lung distal airways using gene expression analysis. Supportive data included lung histopathology, bronchoalveolar lavage (BAL) fluid analysis, and total Ni lung burden analysis. Groups of 5 to 8 male F344 rats were exposed to 0 (control), 0.125, 0.25, 0.5, or 1.0 mg/m<sup>3</sup>  $NiSO_4$  hexahydrate aerosol (0.8-1.2  $\mu$ m MMAD) or 0, 0.04, 0.08, 0.15, or 0.6 mg/m<sup>3</sup>  $Ni_3S_2$  aerosol (2.2-3.2  $\mu$ m MMAD) for one or four weeks duration (6 hr/day, 5 days/week).  $NiSO_4$ -exposed rats showed the following BAL results at 4 weeks: decrease in macrophage percentage, increases in neutrophil and lymphocyte percentages ( $\geq 0.5$  mg/m<sup>3</sup>); increases in LDH, total protein, and NAG, with a decrease in ALP levels (1.0 mg/m<sup>3</sup>). Minimal to slight/mild bronchial epithelial degeneration/hyperplasia and slight/mild alveolus inflammation were observed in the 1.0 mg/m<sup>3</sup> rats. Total Ni in lungs of exposed rats could not be directly measured due to interference with RNAlater solution. Ni concentrations were estimated at 0.7 to 1.0 ug Ni per g lung following 0.5 or 1.0 mg/m<sup>3</sup>  $NiSO_4$ . In the  $Ni_3S_2$  study, BAL results were similar to those for  $NiSO_4$ . Macrophage percentage was decreased, neutrophil and lymphocyte percentages were increased ( $\geq 0.15$  mg/m<sup>3</sup>), and increases in LDH, total protein, and NAG, with a decrease in ALP were observed. Minimal peribronchiolar/perivascular inflammation and alveolus inflammation were observed in the 0.6 mg/m<sup>3</sup> rats following one week exposure. Minimal to slight/mild alveolus inflammation was observed at 4 weeks ( $\geq 0.15$  mg/m<sup>3</sup>). Quantitative results of total Ni in lung indicated a range of 1.6 to 14.4 ug Ni per g

lung following 4 weeks  $Ni_3S_2$  exposure (0.04 to 0.6 mg/m<sup>3</sup>). These data will be integrated with results of gene expression analysis to evaluate mode of action pathways of Ni toxicity.

## PS 1164 Gene Expression Profiles in Peripheral Blood Mononuclear Cells of Chinese Nickel Refinery Workers with High Exposures to Nickel and Control Subjects.

A. B. Munoz<sup>1</sup>, A. Arita<sup>1</sup>, J. Niu<sup>1</sup>, Q. Qu<sup>1</sup>, N. Zhao<sup>2</sup>, Y. Ruan<sup>2</sup>, K. Kiok<sup>1</sup>, T. Kluz<sup>1</sup>, H. Sun<sup>1</sup>, Y. Chervona<sup>1</sup>, H. A. Clancy<sup>1</sup>, M. Shamy<sup>3</sup> and M. Costa<sup>1</sup>. <sup>1</sup>*Environmental Medicine, New York University Graduate School of Arts and Sciences, New York, NY;* <sup>2</sup>*Lanzhou University School of Public Health, Lanzhou, China;* <sup>3</sup>*Environmental Sciences, King Abdulaziz University, Jeddah, Saudi Arabia.*

**Background:** Occupational exposure to nickel (Ni) is associated with an increased risk of lung and nasal cancers. Ni compounds exhibit weak mutagenic activity, alter the cell's epigenetic homeostasis, and activate signaling pathways. However, changes in gene expression associated with Ni exposure have been only investigated in vitro. This study was conducted in a Chinese population to determine whether occupational exposure to Ni was associated with differential gene expression profiles in the peripheral blood mononuclear cells (PBMCs) of Ni-refinery workers when compared to referents.

**Methods:** Eight Ni-refinery workers and ten referents were selected. PBMC RNA was extracted and gene expression profiling was performed using Affymetrix exon arrays. Differentially expressed genes between both groups were identified in a global analysis and findings were validated using real-time PCR.

**Results:** A total of 2167 differentially expressed genes displayed a greater than 1.25 fold-change in Ni-refinery workers. DNA repair and epigenetic genes were significantly overrepresented ( $p<0.0002$ ). Of 31 DNA repair genes, 29 were repressed in the high exposure group and two were overexpressed while these genes were not repressed in the control group. Of the 16 epigenetic genes 12 were repressed in the high exposure group and 4 were overexpressed.

**Conclusions:** The results of this study indicate that occupational exposure to Ni is associated with alterations in gene expression profiles in PBMCs of subjects.

**Impact:** Gene expression may be useful in identifying patterns of deregulation that precede clinical identification of Ni-induced cancers.

## PS 1165 Differential Severity of Chromium-Induced Hepatotoxicity in a Day.

N. Miura<sup>1</sup>, M. Togawa<sup>2</sup> and T. Hasegawa<sup>2</sup>. <sup>1</sup>*National Institute of Occupational Safety and Health (NIOSH), Kawasaki, Japan;* <sup>2</sup>*Yamanashi Institute Environmental Science, Yamanashi, Japan.*

The diurnal variation of cadmium-induced mortality is our topic (*J Toxicol Sci*, 37, 191, 2012). We presented further evidences for the Cd-induced diurnal variation and considered the mechanism of these in SOT 2012 meeting. In this study, we report the diurnal susceptibility of chromium-induced toxicity in mice. Male C57BL/6J mice adapted for 14 days with assigned to 6 groups of 5 animals were administered intraperitoneally (i.p.) with hexavalent chromium ( $K_2Cr_2O_7$ , 35 mg/kg) at different hours in the day (10:00, 14:00, 18:00, 22:00, 2:00 and 6:00 h), describing as zeitgeber time (ZT); ZT2, ZT6, ZT10, ZT14, ZT18 and ZT22. In case of dark period (ZT14, ZT18 and ZT22), administrations were performed under red light. The mortality was determined during 14 consecutive days. Mice were most sensitive to Cr administered at ZT10, while least sensitive at ZT22. In contrast, the susceptibility to Cd-induced mortality was higher at ZT6 but lower at ZT18. Therefore, the daily fluctuation of metal sensitivity differed depending on metal compounds, probably depending on the valence of metal ion. The GPT value, an index of hepatotoxicity, also showed higher at ZT10 injection of Cr. The hepatic levels of Cr determined by ICP-MS were not significantly different between both time (ZT10 and ZT22), thus Cr accumulation in the liver was not a determination factor for this diurnal variation. Our results clearly indicate the susceptibility of metal-induced toxicity is markedly different in a day. We believe this viewpoint should be introduced into toxicology as "chronotoxicology" becoming indispensable in the future toxicology.

## PS 1166 Speciation of Chromium Released from Metal-On-Metal Hip Implants.

K. Thuet<sup>1</sup>, B. L. Finley<sup>1</sup>, P. K. Scott<sup>2</sup> and D. J. Paustenbach<sup>1</sup>. <sup>1</sup>*ChemRisk, LLC., San Francisco, CA;* <sup>2</sup>*ChemRisk, LLC., Pittsburgh, PA.*

Increased blood chromium (Cr) concentrations have been measured in many patients with hip prosthetic devices containing cobalt-chromium-molybdenum alloy. To date, no studies have attempted to analytically distinguish between non-toxic

trivalent Cr, Cr(III), and potentially harmful hexavalent Cr, Cr(VI), in these patients. However, it is known that Cr(VI) preferentially accumulates in red blood cells (RBCs), while Cr(III) remains largely confined to the serum compartment of the blood. Hence, the relative distribution of Cr into RBCs and serum is often used as an indirect measure of Cr valence. We reviewed 231 blood samples from six different studies involving patients with Cr-containing hip implants. Samples were generally collected pre-implant and then at three or six month intervals post-implant for up to two years. The ratio of serum to RBC Cr concentrations was highly consistent. Post-implant serum Cr concentrations (median values of 0.17-2.39 µg/L) typically increased by several fold over pre-implant concentrations (median value of approximately 0.2 µg/L), but the RBC concentrations did not increase over time. Specifically, the RBC Cr concentrations did not change pre- vs. post-implant (median values of 0.26 to 2.5 µg/L). These data indicate that the Cr released from the implants is in the form of Cr(III).

**PS 1167 E162 Protects against Chromium (VI)-Induced Cytotoxicity and Genotoxicity in Human Lung Fibroblast Cells.**

M. Braun<sup>1,2</sup>, J. Lechner<sup>2</sup> and J. Wise<sup>1,2,3</sup>. <sup>1</sup>Wise Laboratory of Environmental and Genetic Toxicology, University of Southern Maine, Portland, ME; <sup>2</sup>Maine Center for Toxicology and Environmental Health, University of Southern Maine, Portland, ME; <sup>3</sup>Department of Applied Medical Science, University of Southern Maine, Portland, ME.

Hexavalent chromium [Cr(VI)] is a ubiquitous environmental toxicant. Studies show that Cr(VI) induces many forms of DNA damage that may lead to cancer if they are not repaired. Nutraceuticals, because of their antioxidant properties, have the potential to decrease toxicity. The purpose of this study was to assess the protective effects of E162, a soluble powder made from crushed beets, on Cr(VI)-induced toxicity. We compared the levels of damage generated after co-treatment with Cr(VI) and E162 in human lung fibroblasts to those after Cr(VI) treatment alone for both acute and chronic exposures. Sodium chromate was used as a representative soluble Cr(VI) compound. After a short-term exposure, there was no protective effect of E162. After chronic exposure, however, E162 had a noticeable protective effect on sodium chromate-induced cytotoxicity and genotoxicity. For example, at 1 µM sodium chromate, only 19 percent of cell colonies survived compared to control, while E162 co-exposure increased that number to 35. 1 µM sodium chromate generated 23 total chromosomal aberrations, while E162 co-exposure decreased the number of lesions to 6. There were 49 percent of aneuploid metaphases at 1 µM sodium chromate but only 35 percent after the addition of E162. Uptake studies were performed, indicating that the protective effect of E162 was not a result of decreasing Cr(VI) uptake. Therefore, E162 may have a direct protective effect on cells against sodium chromate-induced toxicity. This work was funded by the NIEHS grant ES016893 (J.P.W.), the Maine Center for Toxicology and Environmental Health (JPW), and the Maine Space Grant Consortium (MB).

**PS 1168 Method: Measuring Protein-Bound and Free Cobalt(II) in Human Serum—Size Exclusion Liquid Chromatography with ICP-MS.**

B. D. Kerger<sup>1</sup>, B. L. Finley<sup>2</sup> and D. J. Paustenbach<sup>2</sup>. <sup>1</sup>ChemRisk, LLC., Aliso Viejo, CA; <sup>2</sup>ChemRisk, LLC., San Francisco, CA.

Cobalt (Co) ions are known to have a strong affinity for sulfhydryl proteins and amino acids in the blood and tissues, and sufficiently high concentrations of free ionic Co(II) can lead to adverse health effects in humans and animals. We describe a method using size exclusion liquid chromatography (SEC) to resolve protein-bound Co fractions from cyanocobalamin and free Co(II) after direct injection of serum samples stabilized with 0.1M acetic acid. Highly sensitive detection using ICP-MS was coupled with SEC to provide a method detection limit of 0.12µg/L in human serum for one higher molecular weight protein-bound Co peak (likely Co(II) bound to human serum albumin (66 kDa) and other large serum proteins), as well as for cyanocobalamin (1.3 kDa) and for free Co(II). Validation studies show that this novel method demonstrates good accuracy with >98% mean recovery and 10.4% relative percent deviation. Good precision was demonstrated for matrix spikes at 0.5 µg Co/L with 92.7% mean recovery and 4% relative percent deviation. Other metal cations known to compete with Co(II) for protein binding sites (Fe(II), Zn(II), Mn(II), Cd(II), Cu(II), Ni(II), Pb(II)) did not significantly alter Co(II) quantitation in the stabilized acetate solution. The sum of protein-bound and free ionic Co species provided >90% mass balance when compared to total Co measurements analyzed by acid digestion and ICP-MS in the same human serum samples. We conclude that this method complies with the method performance criteria outlined by the U.S. Depart. of Health and Human Services guidance for industry bioanalytical method validation. These measurements focusing on

identifying protein-bound and free Co(II) concentrations are likely to be more informative with respect to understanding blood and tissue Co concentrations associated with adverse health effects in people with workplace Co exposures, dietary Co supplement users, and patients with elevated Co blood levels due to cobalt-chromium alloy prosthetic devices.

**PS 1169 Chronic Exposure to Particulate Chromate Induces Persistent DNA Double-Strand Breaks in Human Lung Cells.**

Q. Qin<sup>1,2,3</sup>, H. Xie<sup>1,2,3</sup>, A. Holmes<sup>1,2,3</sup>, S. Wise<sup>1,2,3</sup> and J. Wise<sup>1,2,3</sup>. <sup>1</sup>Wise Laboratory of Environmental and Genetic Toxicology, University of Southern Maine, Portland, ME; <sup>2</sup>Maine Center for Toxicology and Environmental Health, University of Southern Maine, Portland, ME; <sup>3</sup>Department of Applied Medical Science, University of Southern Maine, Portland, ME.

DNA double strand breaks (DSB) are one of the most deleterious lesions that are induced by particulate chromate. If left unrepaired or misrepaired, DSB can cause mutations or chromosomal aberrations leading to genomic instability. The aim of this study is to determine the genotoxicity of particulate chromate and investigate cellular responses of repair proteins after chronic exposure. We found chromate exposure induced concentration-dependent increases in DSB and with longer exposure time, the amount of breaks remained constant. To address whether this reflected a cycle of breakage and repair or deficient repair, we developed a human lung cell line that stably express GFP-53BP1 and generated time-lapse videos of chromate treated cells. 53BP1 forms discrete nuclear foci at sites of DSB. By monitoring foci kinetics of these cells treated with chromate, we observed residual foci after 24 h, indicating some breaks persist presumably due to deficient repair. Therefore, we investigated the repair proteins involved in homologous recombination (HR) and non-homologous end joining (NHEJ) repair. We found that the nuclear fraction of phosphorylated ATM and Rad51 increased in 24 hours indicating HR is active. However, it largely decreased over time. We also observed concentration- and time-dependent decrease in Rad51 foci formation, which confirms that HR was inhibited. In contrast, protein expression of Ku80 and DNA-PKcs increased during chronic exposure to chromate. These results suggest that there is a signaling switch between HR and NHEJ during chronic exposure to chromate. Future work will focus on identifying key proteins that regulate the transitions between two repair pathways. This work was supported by NIEHS grant ES016893 (J.P.W.) and the Maine Center for Toxicology and Environmental.

**PS 1170 Repeated Particulate Chromate Exposure Induces Chromosome Instability, a DNA Double-Strand Break Repair-Deficient Phenotype, and Neoplastic Transformation in Human Lung Cells.**

S. Wise<sup>1,2,3</sup>, A. Holmes<sup>1,2,3</sup>, H. Xie<sup>1,2,3</sup>, W. Thompson<sup>2,3</sup> and J. Wise<sup>1,2,3</sup>. <sup>1</sup>Wise Laboratory of Environmental and Genetic Toxicology, University of Southern Maine, Portland, ME; <sup>2</sup>Maine Center for Toxicology and Environmental Health, University of Southern Maine, Portland, ME; <sup>3</sup>Department of Applied Medical Science, University of Southern Maine, Portland, ME.

One leading hypothesis for the carcinogenicity of hexavalent chromium (Cr(VI)) posits that Cr(VI) causes a DNA double strand break (DSB) repair deficiency which leads to chromosome instability and neoplastic transformation. However, no studies have been done to determine if Cr(VI) can cause DSB deficiency in human lung cells. To begin to test this possibility, we exposed human lung cells to lead chromate for three sequential 24 h periods, each separated by about a month. After each treatment, cells were seeded at colony forming density, cloned, expanded and retreated. Each generation of clones was tested for chromium sensitivity, chromosome complement, DNA repair capacity and ability to grow in soft agar. We found that after the first treatment, lead chromate-treated cells exhibited a normal chromosome complement though a few clones showed a repair deficient phenotype. After the second exposure, more than half of the clones acquired an abnormal karyotype including numerical and structural alterations and many showed deficient DNA DSB repair. The third treatment resulted in more abnormal clones, previously abnormal clones acquiring additional abnormalities, and most clones were repair deficient. Further investigation revealed that some clones were unable to form Rad51 foci in response to radiation, suggesting a defect in the homologous recombination repair pathway. Finally, clones from the third generation were able to form colonies in soft agar suggesting that the cells have neoplastically transformed. This work was supported by NIEHS grant ES016893 (J.P.W.) and the Maine Center for Toxicology and Environmental Health.

**PS 1171 Fin Whale Cells Are More Resistant to Particulate Chromate Cytotoxicity Than Human Cells.**

C. Wise<sup>1,2</sup>, S. Wise<sup>1,2,3</sup>, A. Holmes<sup>1,2,3</sup> and J. Wise<sup>1,2,3</sup>. <sup>1</sup>Wise Laboratory of Environmental and Genetic Toxicology, University of Southern Maine, Portland, ME; <sup>2</sup>Maine Center for Toxicology and Environmental Health, University of Southern Maine, Portland, ME; <sup>3</sup>Department of Applied Medical Science, University of Southern Maine, Portland, ME.

Hexavalent chromium (Cr(VI)) is present in the marine environment and is a known human carcinogen and skin irritant. Cr(VI) is the form of chromium that is well absorbed through the cell membrane. It is also the most prevalent form in seawater. We compared the cytotoxicity of Cr(VI) in fin whale and human skin cells. Our data show that particulate chromium is cytotoxic to human and fin whale cells in a concentration-dependent manner. Specifically, data show that Cr(VI) is less cytotoxic to fin whale skin cells than human skin cells. For fin whale cells, we found that concentrations of 0.1, 1.0, 5, 10 and 20 µg/cm<sup>2</sup> lead chromate induced 91, 72, 55, 40 and 38 percent relative survival, respectively. In human cells we found that concentrations of 0.1, 0.5, 1.0, 5 and 10 µg/cm<sup>2</sup> lead chromate induced 64, 28, 10, 0 and 0 percent relative survival, respectively. These data indicate that fin whale skin cells were 7.2 times more resistant to Cr(VI) than human skin cells. When corrected for intracellular ion uptake fin whale skin cells remained more resistant. We considered whether this effect was due solely to the chromate ion. Our data show that soluble chromium was also cytotoxic to human and fin whale cells in a concentration-dependent manner. They also indicate that fin whale skin cells were more resistant to soluble Cr(VI) than human skin cells. However, these soluble Cr(VI) differences were accounted for by intracellular ion uptake, which indicates that the difference cytotoxic effects are due to something other than the chromium ion by itself. Further investigations will look into the genotoxic effects of hexavalent chromium on these two species. This research is supported by The Environmental Protection Agency's Undergraduate Research Opportunities Fellowship (CFW), NIEHS grant ES016893 (JPW) and the Maine Center for Toxicology and Environmental Health (JPW).

**PS 1172 Cellular Defense against Telomere Dysfunction Induced by Hexavalent Chromium.**

H. C. Pope-Varsalona, F. Liu and P. L. Opreko. *Environmental and Occupational Health, University of Pittsburgh, Pittsburgh, PA.*

Dysfunctional telomeres, the protective caps at chromosome ends, contribute to a variety of pulmonary diseases. Our previous work established that DNA replication stress induced by the environmental pollutant hexavalent chromium Cr(VI) causes telomere loss and aberrations. Chronic inhalation of Cr(VI) leads to a variety of lung diseases, including fibrosis, and cancers. Cr(VI) forms DNA lesions that impede DNA replication and can cause collapse of the replication fork and chromosomal breakage. Telomeres are fragile DNA sites prone to breakage during replication stress. Cells have mechanisms for bypassing lesions that block replication forks called translesion synthesis (TLS). We hypothesize that Cr(VI)-induced DNA replication stress activates TLS DNA polymerase  $\eta$  (pol $\eta$ ) that suppress Cr(VI)-induced mutagenesis and telomere dysfunction. Our research is investigating several endpoints of telomere dysfunction in human cells proficient and deficient in pol $\eta$ . We observe that cells deficient in pol $\eta$  are 53 fold more sensitive to low levels of Cr(VI) compared to isogenic controls. Using a combination of immunofluorescence and telomere fluorescence in situ hybridization (IF-teloFISH), quantification of replication stress at genomic and telomeric DNA show a severely reduced recovery from Cr(VI)-induced replication stress in cells lacking functional pol $\eta$ . Moreover, we observe that Cr(VI) induces pol $\eta$  mobilization to stalled DNA replication sites at genomic and telomeric regions in human cells. Post Cr(VI) exposures, we identify telomeric aberrations in senescent cells, a critical endpoint of telomere dysfunction, by staining metaphase chromosomes with a fluorescent telomeric probe using teloFISH. Currently, we are assessing cellular senescence through various biomarkers. Our study attests to one mechanism by which Cr(VI) directly interacts with the genome, alters telomere integrity, and the cellular pathways that protect telomeres in the face of genotoxic replication stress.

**PS 1173 Reactive Oxygen Species Regulate PI3K/AKT-Dependent Activation of GSK-3 $\beta$ /Catenin and mTOR signaling in Cr(VI)-Induced Carcinogenesis.**

Y. Son, J. Lee, P. Poyil, L. Wang and X. Shi. *Graduate Center for Toxicology, University of Kentucky, Lexington, KY.*

Cr(VI) compounds are known human carcinogens that especially target lungs. Reactive oxygen species (ROS) are well produced by Cr(VI), however, the relevance of ROS and the underlying signaling pathways in Cr(VI)-induced carcinogenesis

remain to be elusive. The present study reports that chronic exposure of human bronchial epithelial cells to Cr(VI) at the low nanomolar range (10 - 100 nM) for 2 months induced cell transformation, as evidenced by anchorage-independent growth in soft agar and clonogenic assays. Chronic Cr(VI) treatment also increased the potential of these cells to invade and migrate. Injection of Cr(VI)-stimulated cells into nude mice resulted in the formation of tumors. In contrast, the Cr(VI)-mediated increases in colony formation, cell invasion, migration, and xenograft tumors were prevented by transfection with catalase, superoxide dismutase-1 (SOD1), or SOD2. In particular, chronic Cr(VI) exposure led to activation of signaling cascades involving PI3K/ AKT/GSK-3 $\beta$ /catenin, and PI3K/ AKT/mTOR and transfection with each of the above antioxidant enzymes markedly inhibited Cr(VI)-mediated activation of these signaling proteins. Inhibitors specific for AKT or  $\beta$ -catenin almost completely suppressed the Cr(VI)-mediated increase in total and active  $\beta$ -catenin proteins and colony formation. In addition, Cr(VI) inhibited autophagy under nutrition deprivation condition. Moreover, there was a marked induction of AKT, GSK-3 $\beta$ ,  $\beta$ -catenin, mTOR, and carcinogenic markers in tumor tissues formed in mice after injection with Cr(VI)-stimulated cells. Collectively, our findings suggest that ROS is a key mediator of Cr(VI)-induced carcinogenesis, and it activates PI3K/AKT dependent GSK-3 $\beta$ /catenin and inhibits autophagy through upregulation of mTOR signaling in this process.

**PS 1174 Instability of Metallothionein Inhibits Mitochondrial Activities following Exposure to Silver Nitrate in Human Bronchial Epithelial Cells.**

T. Miyayama<sup>1</sup>, Y. Arai<sup>2</sup>, N. Suzuki<sup>2</sup> and S. Hirano<sup>1,2</sup>. <sup>1</sup>Risk Center for Environmental Risk, National Institute for Environmental Studies, Tsukuba, Japan; <sup>2</sup>Graduate School of Pharmaceutical Sciences, Chiba University, Chiba, Japan.

Silver (Ag) has been reported to generate reactive oxygen species (ROS) and to bind sulfhydryl groups in metabolic enzymes and non-enzymatic proteins such as metallothionein (MT). In the present study, we assessed toxicity of AgNO<sub>3</sub> in human bronchial epithelial cells (BEAS-2B) focusing on the intracellular Ag distribution and ROS production. The cells were exposed to 0 - 100 µmol/l AgNO<sub>3</sub> for 0 - 24 h and cytotoxicity was assayed with a modified MTT method. The cell viability was decreased by AgNO<sub>3</sub> in a dose-dependent manner (IC<sub>50</sub> = 2.5 µmol/l). Concentration of Ag in culture media decreased with time and stabilized at 12 h after exposure. Concentrations of Ag and Ag-bound MT in the soluble fraction of cells were sharply increased up to 3 h and then decreased, indicating that cytosolic Ag relocated to the insoluble fraction of cells shortly after Ag exposure. mRNA levels of major human MT isoforms, MT-IA and MT-IIA, paralleled concentrations of Ag, Cu and Zn-MT. The ROS-derived fluorescence intensity appeared to be elevated at mitochondria after treatment of the cells with Ag. To evaluate effects of Ag on mitochondrial respiration and activities of electron transport chain complex, mitochondria were obtained from rat liver tissues. The electron transport activities of all mitochondrial complexes (I to IV) were inhibited by Ag. We observed that a concentration of cytosolic H<sub>2</sub>O<sub>2</sub> was increased up to 11.6 pmol per 1.0 x 10<sup>6</sup> cells. Ag as well as Cu and Zn were released from isolated MT by H<sub>2</sub>O<sub>2</sub> at concentrations as low as 0.001%. In conclusion, exposure to Ag increased MT synthesis and Ag was sequestered immediately by MT. 3 h after exposure, MT was decomposed by cytosolic H<sub>2</sub>O<sub>2</sub>. Ag released from MT relocated to insoluble cellular fractions and inhibited electron chain transfer of mitochondrial complexes, which eventually led to cell damage.

**PS 1175 Development and Optimization of a Procedure for the Determination of Indium-Tin Oxide Particle Size and Concentration in Cellular Media.**

K. Levine<sup>1</sup>, L. Han<sup>1</sup>, W. M. Gwinn<sup>2</sup>, D. L. Morgan<sup>2</sup>, A. S. Essader<sup>1</sup>, R. A. Fernando<sup>1</sup>, C. S. Smith<sup>2</sup> and V. G. Robinson<sup>2</sup>. <sup>1</sup>RTI International, Research Triangle Park, NC; <sup>2</sup>Division of National Toxicology Program, NIEHS, Research Triangle Park, NC.

Indium-tin oxide (ITO) is a solid mixture often comprised of approximately 90% indium oxide (In<sub>2</sub>O<sub>3</sub>) and 10% tin oxide (SnO<sub>2</sub>) by weight. ITO is employed as a transparent conductive coating for flat panel, liquid crystal, and plasma displays and is typically deposited after sintering as a thin film on the desired substrate through a variety of technologies. Fatal cases of interstitial pneumonia and alveolar proteinosis have been reported for workers exposed to ITO particles. *In vitro* studies of ITO are planned in order to better understand the toxicity of this compound. Comprehensive characterization of ITO test materials is required prior to toxicity testing. Characterization of ITO particle size under the conditions of laboratory testing is important because this physicochemical parameter can significantly impact bioavailability and cellular toxicity.

In these studies we developed, optimized, and applied a dynamic light scattering (DLS) sample preparation and measurement protocol for determining hydrodynamic particle size in a suite of sintered/non-sintered ITO samples. ITO samples were prepared in cellular growth media at doses ranging from 0.3 – 0.4 mg/mL. Sonication times of particle suspensions were evaluated from 15 – 90 minutes. Times ranging from 30 – 60 minutes yielded the most stable suspensions with respect to hydrodynamic particle size over a 24-hour period. Resulting suspensions from samples with 30 – 60 minute sonication times were stable for 10 – 24 hours after sonication, with respect to hydrodynamic particle size. Throughout the 24-hour DLS measurement period, suspensions were analyzed for indium content by inductively coupled plasma mass spectrometry (ICP-MS) to confirm ITO concentrations. The developed protocol enabled investigators to use ITO suspensions of known particle size and concentration in their *in vitro* cellular studies.

## PS 1176 Tungsten Exposure Increases Lung Metastases in an Orthotopic Murine Breast Cancer Model.

A. M. Bolt<sup>2,1</sup>, V. Sabourin<sup>2,1</sup>, J. Janiak<sup>2,1</sup>, A. Kelly<sup>2,1</sup>, G. Ursini-Siegel<sup>2,1</sup> and K. K. Mann<sup>2,1</sup>. <sup>1</sup>McGill University, Montréal, QC, Canada; <sup>2</sup>The Lady Davis Institute for Medical Research, Montréal, QC, Canada.

Tungsten is a strong, flexible metal that until recently had been thought to be an “inert” metal. These properties led to its incorporation into the manufacturing of medical devices. In a recent clinical trial, a tungsten-based shield was used in the treatment of breast cancer patients undergoing intraoperative radiotherapy. Following the procedure, the women were left with residual tungsten in their breasts. Elevated tungsten levels in the blood and urine indicate that tungsten is not remaining in the breast tissue. Tungsten was detected in the urine of patient even 8 months after mastectomy, indicating another reservoir has been created. Based on previous data, we hypothesize this reservoir to be the bone. Animal studies suggest that tungsten may contribute to carcinogenesis and can alter development and increase DNA damage in the immune system. In order to evaluate the effect of tungsten on breast cancer, female Balb/C mice were exposed to 15 ppm of sodium tungstate for 1 month followed by injection of 66cl4 cancer cells into the mammary fat pad. The size of primary tumor, the extent of lung metastases and immune parameters were evaluated. Tungsten did not alter the growth of the primary tumor. However, the number and average size of lung metastases was significantly greater in the tungsten-exposed animals. This model is not known to metastasize to the bone, but we found that tumor-bearing mice had 3-fold more tungsten in the bone than non-tumor bearing mice. Tungsten increased the peripheral blood leukocyte count in non-tumor bearing mice, but decreased the massive granulocytosis associated with tumor growth. These data suggest that tungsten increases the extent of breast cancer metastasis to the lung, which could have a significant impact on individuals who have cancer and are also exposed to tungsten. The levels of tungsten deposition within the bone and immune cell parameters were also altered, which could also impact metastasis in this model.

## PS 1177 Genetic Variation of Iron Metabolism in Mice.

K. E. Page<sup>1</sup>, D. W. Killilea<sup>2</sup>, E. Eskin<sup>3</sup>, A. J. Lusis<sup>3</sup> and C. Vulpe<sup>1</sup>. <sup>1</sup>Nutritional Sciences and Toxicology, University of Berkeley, Berkeley, CA; <sup>2</sup>Children's Hospital Oakland Research Institute, Oakland, CA; <sup>3</sup>David Geffen School of Medicine, University of California Los Angeles, Los Angeles, CA.

Iron deficiency is the most common disease in the world with an estimated 4-5 billion affected persons. Debilitating fatigue, altered immune function, decreased work capacity and anemia are among the deleterious consequences of this pervasive disorder. Similarly, liver iron overload is a significant health concern. Multiple genetic disorders of iron metabolism in man, rodents and other vertebrates suggest multiple loci can contribute to the susceptibility of iron deficiency and severity of iron overload. Previous studies have shown genetic variation in iron metabolism between inbred strains of mice. We hypothesize that this genetic variation underlies the differences seen in iron metabolism between inbred mice. Our aim is to map the quantitative trait loci responsible for the strain specific differences in iron metabolism. To do this we will use high resolution SNP analysis to “in silico” map the genetic loci responsible for the divergent iron related phenotypes using the hybrid mouse diversity panel (HMDP) [1]. Here we show the phenotypic analysis of the variation in iron metabolism for these mice, and how the overall elemental profiles change for each strain.

### References

1. Bennett BJ, Farber CR, Orozco L, Min Kang H, Ghazalpour A, et al. (2010) A high-resolution association mapping panel for the dissection of complex traits in mice. *Genome Research* 20: 281-290.

## PS 1178 ICP-MS Determination of Tissue Iron Levels in the Rat.

J. Bouchard<sup>1</sup>, C. Sabadie<sup>1</sup>, J. Decorde<sup>1</sup>, L. Jaillet<sup>1</sup>, P. Elford<sup>2</sup> and R. Forster<sup>1</sup>. <sup>1</sup>CiToxLAB, Evreux, France; <sup>2</sup>Azad Pharmaceuticals, Bern, Switzerland.

Iron is an essential trace element associated with toxicities when present in excess, as for example in conditions such as heterochromatosis. We have developed and validated a reliable and rapid quantitative method for the exploration of endogenous levels of total iron in rat plasma, heart, liver, spleen, kidney, stomach, lung and bone marrow. The analysis by ICP-MS (Inductively Coupled Plasma Mass Spectrometry) was selected among all other techniques, because of its easy handling of simple or complex matrices requiring very little sample preparation. The method was evaluated for accuracy, precision, linearity, matrix effect and instability derived from adsorption on container walls. Precision and accuracy for all matrices ranged from >4.3% to <7.9% and >1.5% to <12.2% respectively. Matrix effect was negligible and the assays for the evaluation of instability showed no adsorption of iron on container walls, either in glass, polypropylene or polyethylene. Iron levels were determined over a 28-day period, on 145 rats aged 7 to 8 weeks at the beginning of the study. In general a low to moderate inter-animal variability of endogenous iron levels was observed. The levels of total iron in plasma, heart, liver, stomach and bone marrow were stable over time with concentrations <5000 ng/mL in plasma and <18.0 µg/g (heart), <70.0 µg/g (liver), <8.00 µg/g (stomach), <140 µg/g (bone marrow) respectively. In spleen and kidney, the concentrations increased over time, from <80.0 µg/g to <400 µg/g in spleen and <15.0 µg/g to <30.0 µg/g in kidney and this was attributed to the ageing of the animals. A moderate to marked inter-animal variability was observed in lung, ranging from 5.00 µg/g to 40.0 µg/g. In conclusion, a reliable and rapid quantitative ICP-MS method was used to determine endogenous levels of total iron in rat plasma and tissues. This method can readily be adapted for the study of endogenous iron levels in other laboratory animal species.

## PS 1179 Development of a Transportable Neutron Activation Analysis System to Quantify Manganese in Bone *In Vivo*—Feasibility and Methodology.

Y. Liu<sup>1</sup>, D. S. Koltick<sup>2</sup>, P. Byrne<sup>1,3</sup>, W. Zheng<sup>1</sup> and L. Nie<sup>1</sup>. <sup>1</sup>Health Sciences, Purdue University, West Lafayette, IN; <sup>2</sup>Physics, Purdue University, West Lafayette, IN; <sup>3</sup>Medical Physics Consultants, Indianapolis, IN.

Manganese (Mn) is a vital element in human body for growth and other functions. However, overdose to Mn compounds can lead to many adverse health effects. An important issue in assessing Mn exposure is to select a proper biomarker. Over 40% of Mn in human body is stored in bone and bone Mn represents long term chronic Mn exposures. Hence it is attractive to develop a technology to quantify the concentration of Mn in human bones. *In vivo* neutron activation analysis (IVNAA) is a promising non-invasive technique which can determine the concentrations of various elements in the human body. In our study, we investigated the possibility and feasibility of developing a transportable IVNAA system for Mn quantification in hand bone by Monte Carlo (MC) simulations using a portable deuterium-deuterium (DD) neutron generator as neutron source. Experiments were conducted with a deuterium-tritium (DT) generator available in our lab to validate the MC simulation results. The count rates calculated from MC simulations were in agreement with those obtained from the experiments for the DT generator system setup. Different types of moderator and reflector for DD setups were simulated and paraffin was selected as the best material for both of the moderator and reflector. Then the optimal thicknesses for the reflector and moderator were determined. Assuming normal concentration of Mn in bone is about 1 µg/g and neutron yield is 4×10<sup>8</sup>/sec, the count rate is 0.324 counts/sec if we use a 4π NaI detector with 100% efficiency. The corresponding dose to the hand for 10 minutes irradiation time is about 43.704 mSv from MC simulation, which corresponds to about 48.64 µSv total body equivalent dose. In conclusion, it is feasible to develop a transportable NAA system to quantify Mn in bone *in vivo* with a minimum radiation dose exposure to the subject.

## PS 1180 Relative and Absolute Quantification of Metallothionein Isoforms in Human Kidney Cells Using Stable Isotope Labeling of Cysteines and MALDI-TOF/TOF Mass Spectrometry.

A. Mehush<sup>1,2</sup>, J. B. Shabb<sup>2</sup>, W. W. Muhonen<sup>2</sup>, S. H. Garrett<sup>1</sup>, S. Somji<sup>1</sup>, M. Sens<sup>1</sup> and D. A. Sens<sup>1</sup>. <sup>1</sup>Pathology, University of North Dakota, Grand Forks, ND; <sup>2</sup>Biochemistry, University of North Dakota, Grand Forks, ND.

Human metallothioneins (MTs) are known to chelate the naturally accumulated heavy metal pollutant cadmium in the renal cortex and their expression has been shown to be altered in different types of cancers. The current study was initiated to

develop analytical means to measure each isoform of this diverse protein family. The twelve human MT isoforms share 70 to 90% amino acid sequence identity which hampers antibody-based methods of isoform-specific quantification at the protein level. Trypsin digestion yields an N-terminal MT peptide that has a unique mass for each MT isoform. Each of these peptides contains five Cys residues, is N-terminally acetylated, and once alkylated is relatively hydrophilic. The human kidney HK-2 epithelial cell line expressing stably transfected MT-3 was used as a model system. Cytosol was prepared from control cells and cells exposed to 9  $\mu$ M cadmium for 3 days. The cytosol was then denatured with urea, reduced with DTT, and alkylated with either 14N- or 15N- iodoacetamide. For absolute quantification, ~145 pmols of MT isoform-specific 15N-labeled N-terminal acetylated peptides was added to the samples. The light and heavy-labeled samples were combined and digested with trypsin. Strong cation exchange (SCX) and C18 reverse-phase liquid chromatography (rp-HPLC) successively enriched the N-terminal MT peptides followed by MALDI-TOF/TOF MS and MS/MS. The ratio of light (control) vs. heavy (induced) MT peak intensities were calculated for each MT isoform detectable in both the control and Cd-induced samples. Seven MT isoforms were detected and quantified in the HK-2 MT-3 cells. MT-1F showed the largest induction (10-fold) from 9  $\mu$ M Cd treatment. Metallothionein 3 was induced 2-fold. This study describes an iodoacetamide stable isotope-labeling mass spectrometry-based method for simultaneous relative and absolute quantification of human metallothionein isoforms.

### PS 1181 Identification of Metallothionein-3 Interacting Proteins in the Human Proximal Tubule Cells.

A. Slusser<sup>1,2</sup>, C. Bathula<sup>1</sup>, J. R. Dunlevy<sup>1</sup>, J. B. Shabb<sup>2</sup>, D. A. Sens<sup>1</sup>, S. Somji<sup>1</sup> and S. H. Garrett<sup>1</sup>. <sup>1</sup>Pathology, University of North Dakota, Grand Forks, ND; <sup>2</sup>Biochemistry, University of North Dakota, Grand Forks, ND.

Metallothionein 3 (MT-3) is a small, cysteine-rich protein that binds to essential metal ions required for normal cellular processes, as well as heavy metals that have the potential to exert toxic effects on cells. MT-3 is expressed by epithelial cells of the human kidney, including the cells of the proximal tubule. This laboratory has previously shown that the mortal cultures of human proximal tubule (HPT) cells express MT-3 and could form domes in the cell monolayer, a morphological feature indicative of vectorial active transport. However the immortalized proximal tubular cell line HK-2 lacked the expression of MT-3 and failed to form domes. Transfection of the HK-2 cells with the MT-3 gene restored dome formation in the cells suggesting that MT-3 may have a role in vectorial active transport. Recent in vivo and in vitro studies have reported that MT-3 is interacting with other proteins and these interactions are thought to be playing an important role in execution of some of its functions. Thus the goal of this study was to identify the binding partners of MT-3, which would allow us to understand the mechanism through which MT-3 is regulating vectorial active transport and cell differentiation in HPT cells. For this purpose cell extracts were prepared using the immortalized human proximal tubule cell line HK-2. MT-3 pull-down experiments were performed followed by SDS-PAGE and mass spectrometry analysis. Data analysis revealed an interaction between MT-3 and myosin 9, gelsolin, beta-actin, and tropomyosin 3. Immunofluorescence studies further confirmed that MT-3 co-localizes with these proteins. These studies demonstrate that MT-3 is interacting with proteins that are involved in cytoskeleton reorganization of the cell and thereby regulating vectorial active transport and cell differentiation.

### PS 1182 The Unique N and C-Terminal Domains of Metallothionein-3 Influence the Growth and Differentiation of MCF-7 Breast Cancer Cells.

B. Voels, D. A. Sens, S. H. Garrett and S. Somji. Pathology, University of North Dakota, Grand Forks, ND.

Toxic insult from the heavy metal cadmium ( $\text{Cd}^{2+}$ ) is known to induce the expression metallothioneins (MT) which are heavy metal binding proteins. Previous work from our laboratory has shown that over-expression of MT-3 in breast cancers is associated with poor patient outcome. Furthermore, MT-3 has shown to inhibit the growth of breast cancer and prostate cancer cell lines. Studies have shown that the MT-3 protein contains 7 additional amino acids that are not present in any other member of the MT gene family, a 6 amino acid C-terminal sequence and a Thr in the N-terminal region. The unique N-terminal sequence is responsible for the growth inhibitory activity of MT-3 in the neuronal system. The goal of this study was to characterize the function of the N and C-terminal domains of MT-3 in the breast cancer cell line, MCF-7. For this purpose six different constructs of MTs were prepared which were as follows: wild type (WT) MT-3, MT-3 N-terminal deletion (MT-3 NT), MT-3 C-terminal deletion (MT-3 CT), WT MT-1E, and MT-1E mutated to contain the N-terminal of MT-3 or the C-terminal or both the

N- and the C-terminal of MT-3. Each of these constructs was transfected into MCF-7 cells and the growth rates and the transepithelial resistance (TER) was measured. The data obtained suggests that the N-terminal region of MT-3 is involved in growth inhibitory activity whereas the C-terminal region is involved in vectorial active transport which is indicated by the formation of domes in cell culture and an increase in TER. In conclusion, this study further characterizes the unique properties of the N- and the C-terminal domain of MT-3 and the potential role that it may play in the differentiation of certain breast cancers.

### PS 1183 Fluoride, Aluminum, and Mixtures: Histological Changes in the Liver of Mouse, *Mus norvegicus albinus*.

A. Vijaya Bhaskara Rao. Ecology and Environmental Sciences, Pondicherry University, Puducherry, India. Sponsor: I. Rusyn.

Fluoride is one of the chemical contaminants of water causing several health problems in man and animals. Aluminum is one of the most abundant metals in the environment. Although aluminum has been historically considered as a non toxic metal, which is toxic in its trivalent ( $\text{Al}^{3+}$ ) form. Earlier studies exhibited fluorosis and aluminosis when fluoride and aluminum exposed individually. However, it is important to study two different toxicants in combination to know whether they can act as synergistic or antagonistic. In this study the toxic effects exerted by the accumulation of fluoride, aluminum and their mixtures were studied in the liver of mice. Six different doses were tested for a period of 30 days and 60 days for their toxic effect in the liver. Microscopic study of liver tissue revealed interesting pathological changes in all the fluoride treated mice. The damage to the tissue was dose- and time dependent. The aluminum treated mice showed conspicuous histopathological changes in higher dose, which was more significant with the increase in period of exposure. Whereas, the histopathological changes, were not much conspicuous in lower dose groups, and also decreased with period of exposure. In the mixture of fluoride and aluminum treated mice, mild to severe changes were observed in the higher dose of fluoride with aluminum, whereas very mild and insignificant changes were observed in the mice exposed to lower dose of fluoride with aluminum.

### PS 1184 Both the Metal Moiety and the Organic Backbone of Ethylene Bisdithiocarbamate Fungicides Maneb and Mancozeb Contribute to Toxicity in Human Colon Cells.

L. Hoffman and D. Hardej. Pharmaceutical Sciences, St. John's University, Queens, NY.

Ethylene bisdithiocarbamate (EBDC) pesticides are used primarily as broad range contact fungicides on a wide variety of crops. A subset of the metal containing EBDC pesticides include Maneb (MB), Mancozeb (MZ), and Zineb (ZB), which are complexed with the transition metals manganese, zinc, or in the case of MZ, both manganese and zinc. While these agents are reported to possess low human toxicity, previous testing in our laboratory has established the toxicity of these compounds to transformed colon cells, HT-29 and Caco2, and to normal colon cells, CCD-18Co. Significant decreases in viability were observed with MB and MZ in HT-29 and CCD-18Co (80-260 $\mu$ M), and Caco2 cells (40-180 $\mu$ M). ZB exposure however, produced no significant decrease in cell viability in all cell types up to 800 $\mu$ M. Therefore, the purpose of this study was to determine if the metal moieties of MB and MZ contributes to the generation of toxicity. To determine if the manganese and zinc can accumulate within HT-29 and Caco2 cells and initiate toxicity, inductively coupled plasma-optical emission spectroscopy was performed. MB exposure resulted in a dose dependent increase in intracellular manganese levels within HT-29 and Caco2 cells (20-200 $\mu$ M). MZ exposure also resulted in a significant accumulation of zinc within HT-29 and Caco2 cells (40-200 $\mu$ M). To investigate whether manganese and/or zinc was a critical factor in the cytotoxic process, HT-29, Caco2, and CCD-18Co cells were treated with manganese chloride ( $\text{MnCl}_2$ ) and zinc chloride ( $\text{ZnCl}_2$ ).  $\text{MnCl}_2$  and  $\text{ZnCl}_2$  exposure produced no significant loss of viability in all cell types up to 400 $\mu$ M. The lack of toxicity observed following treatment with ZB within the same concentration range as MB and MZ suggests that the manganese portion of these agents may play a key role in generating the effects seen upon exposure. However, the lack of differences in the cytotoxicity of  $\text{MnCl}_2$  and  $\text{ZnCl}_2$  treated cells indicates that the EBDC backbone may act in conjunction with the metal moiety to cause toxicity.

**PS 1185 Signalling Pathways and Oxidative Stress Involved in Metal-Induced Cytokine Responses in Human Epithelial Lung Cells.**

M. Låg, J. Øvrevik, E. M. Lilleaas, A. Thormodsrø, A. I. Totlandsdal, J. A. Holme, P. E. Schwarze and M. A. Røfnes. *Department of Air Pollution and Noise, Norwegian Institute of Public Health, Oslo, Norway.* Sponsor: M. Løvik.

Inhalation of metals is associated with development and aggravation of lung and cardiovascular diseases, and inflammation is considered to be a central pathological mechanism. In this study we have investigated expression of inflammation-related genes in human bronchial epithelial cells (BEAS-2B) exposed to cadmium (Cd), zinc (Zn), arsenic (As), vanadium (V), manganese (Mn) and nickel (Ni), metals often found in polluted air. As measured by real-time PCR array, Cd, Zn and As induced cytokine expression patterns differing from V, Mn and Ni, with higher levels of CXCL8, CXCL5, IL-6 and CCL26. Furthermore, Cd, Zn and As, but not V, Mn and Ni, induced increased levels of 1-heme oxygenase indicative of oxidative stress. Thus, the mechanisms of Cd-, Zn- and As-induced cytokine responses were investigated further. In line with the gene-expression data, Cd, Zn and As also induced high levels of CXCL8 and IL-6 protein-release, and addition of antioxidants reduced the metal-induced cytokine responses. Moreover, the metals activated the mitogen activated protein kinases (MAPK) p38, JNK and ERK and the p65 subunit of NF-κB, measured as protein-phosphorylation by Western blotting after 2 and 4 hr. Use of MAPK-inhibitors and siRNAs against p65 revealed that these signalling pathways were involved in the cytokine responses. The p38 pathway seemed most important for both IL-6 and CXCL8 release induced by all three metals, whereas JNK seemed to be mainly involved in As-induced CXCL8 and ERK in As-induced IL-6 and CXCL8 releases. In conclusion, among the tested metals Cd, Zn, As were potent inducers of inflammatory responses and oxidative stress in epithelial lung cells. NF-κB and p38 signalling seemed central to metal-induced IL-6 and CXCL8 responses, whereas the relative involvement of JNK and ERK differed depending on the metal and cytokine.

**PS 1186 Development of an Immortalized Urothelial Cell Line to Study Metal-Induced Bladder Carcinogenesis.**

A. Holmes<sup>1,2,3</sup>, M. Hebert<sup>1,2</sup>, C. Case<sup>4</sup> and J. Wise<sup>1,2,3</sup>. <sup>1</sup>Wise Laboratory of Environmental and Genetic Toxicology, University of Southern Maine, Portland, ME; <sup>2</sup>Maine Center for Toxicology and Environmental Health, University of Southern Maine, University of Southern Maine, Portland, ME; <sup>3</sup>Department of Applied Medical Science, University of Southern Maine, University of Southern Maine, Portland, ME; <sup>4</sup>Musculoskeletal Research Unit, University of Bristol, Bristol, United Kingdom.

Numerous metals are well-known human bladder carcinogens. Despite the significant occupational and public health concern of metals and bladder cancer, the carcinogenic mechanisms remain largely unknown. In order to fully understand how metals transform a normal urothelial cell into a cancerous cell, it is important to study the process in a normal human urothelial cell line. Primary urothelial cells are insufficient for this purpose because of their very short lifespan, but currently, the effects of metals in a near-normal urothelial cell line with an extended lifespan are unknown. The objective of this study was to characterize chromate toxicity in primary human urothelial cells and to determine if an hTERT-immortalized human urothelial cell line exhibited a similar response to metals as primary cells. Hexavalent chromium (Cr(VI)) induced a concentration- and time-dependent increase in chromosome damage with the hTERT-immortalized cells exhibiting more chromosome damage than the primary cells. Chronic exposure to Cr(VI) also induced a concentration-dependent increase in aneuploid metaphases in both cell lines which was not observed after a 24 h exposure. Aneuploidy induction was higher in the hTERT-immortalized cells. When we correct for uptake, Cr(VI) induces a similar amount of chromosome damage and aneuploidy suggesting that the differences in Cr(VI) sensitivity between the two cell lines was due to differences in uptake. Therefore, the hTERT-immortalized cell line had a similar response to metals and will be a good tool for studying metal-induced bladder carcinogenesis. This work was supported by NIEHS grant ES016893 (J.P.W.) and the Maine Center for Toxicology and Environmental Health.

**PS 1187 Metallothionein Transcriptional Regulation, Aging, and the Insulin Signaling Pathway.**

J. Hall<sup>1</sup>, M. McElwee<sup>2</sup> and J. H. Freedman<sup>1,2</sup>. <sup>1</sup>BSB, DNTP, NIEHS, Research Triangle Park, NC; <sup>2</sup>LTP, NIEHS, Research Triangle Park, NC.

Metallothioneins (MTs) are highly conserved, cysteine-rich metal-binding proteins that function in metal homeostasis and detoxification, as well as free-radical scavenging. To better understand the role of MT in cadmium-associated cellular re-

sponses, regulatory factors and pathways that control the expression of the *C. elegans* MT gene, *mtl-1*, were identified through genetic screens. A mutagenesis screen identified a mutant, JF99 that harbored a mutation affecting *atf-7*, a negative transcription factor involved in the JNK/p38 pathway. In both JF99 and an *atf-7* deletion mutant, steady-state *mtl-1* mRNA levels were identical but significantly greater than levels in wild type nematodes in the absence of cadmium. In addition to *atf-7*, mutations in *pmk-1* caused a decrease in *mtl-1* expression, suggesting that PMK-1 regulated ATF-7 activity. A candidate gene screen identified three insulin signaling pathway genes (PDK-1 and the AKT-1/AKT-2 complex) that functioned independently of this pathway. Further genetic analysis confirmed that these genes act upstream of PMK-1 and ATF-7 to regulate *mtl-1* transcription. Based on our genetic pathway data and previous work, we propose that ATF-7 resides on the promoter region of *mtl-1* to inhibit the constitutively active transcription factor ELT-2, which is important for intestinal cell specific transcription. In the presence of cadmium, upstream factors signal PDK-1 and the AKT-1/2 complex to phosphorylate PMK-1 causing it to translocate to the nucleus and phosphorylate ATF-7, allowing ELT-2 to initiate transcription. The activation of this pathway results in an increase in MT, which scavenges cadmium and free radicals. In mammalian cells, knock-down of PDK1 and ATF7 resulted in changes in MT-1 expression, suggesting that this pathway was not unique to *C. elegans*. The insulin signaling pathway affects the aging process, thus an association between cadmium exposure and the activation of portions of the insulin signaling pathway provides a mechanistic link between metal homeostasis, ROS and aging.

**PS 1188 Metal-Regulatory Transcription Factor-1 Regulates Metal-Responsive Transcription of *Fosl1*.**

E. Braithwaite and J. H. Freedman. *NIEHS, Research Triangle Park, NC.*

The transcription factor fos related antigen-1 (*fosl1*) is an AP-1 protein whose expression is often elevated in tumors and transformed cells. Previous studies show that *fosl1* is transcriptionally regulated through the activity of the fos transcription factor and the MAPK pathway. In addition, *fosl1* is induced after exposure to cadmium; however, the mechanism by which this induction occurs has not been elucidated. Metals, such as cadmium, are able to induce the expression of a wide variety of genes through the activation of metal-regulatory transcription factor 1 (MTF-1). Upon activation, MTF-1 translocates to the nucleus and binds to metal responsive elements (MREs) in the promoters of metal-inducible genes. To determine if MTF-1 participates in cadmium-inducible *fosl1* regulation, a five kilobase region upstream of the transcription start site and the coding region of *fosl1* were analyzed for MRE sequences. Seven MREs were identified and chromatin immunoprecipitation (ChIP) analysis performed to determine if MTF-1 had the ability to bind the *fosl1* promoter after metal exposure. ChIP assays showed that MTF-1 localized to the *fosl1* promoter and bound each MRE sequence to varying degrees. To assess the biological impact of this binding, MTF-1 null (dko7) cells and dko7 cells transduced with MTF-1 (dko7 + MTF-1) were exposed to cadmium and RNA was isolated at various time periods to evaluate steady state mRNA levels of *fosl1* by real-time PCR (RT-PCR). These studies showed a biphasic increase in *fosl1* mRNA in dko7 + MTF-1 cells up to 12 hours after exposure to 5 μM cadmium after which the mRNA levels declined to background levels at 24 h. In contrast, dko7 cells showed a steady increase in *fosl1* mRNA accumulation for the duration of the study. These data suggest that MTF-1 is recruited to the *fosl1* promoter and may be a negative regulator of *fosl1* mRNA expression.

**PS 1189 Visualization of Reactive Oxygen Species (ROS) Using High-Content Image Analysis (HCA) in Undifferentiated Human Embryonic Stem Cells Exposed to Methyl Parathion (MP).**

J. S. Madren-Whalley and J. W. Sekowski. *ECBC, US Army RDECOM, Gunpowder, MD.*

Organophosphate (OP) pesticides represent a threat to soldiers, first responders and other civilians since they are highly toxic and widely accessible chemicals used in crop, industrial, and home applications. However, for many OP pesticides such as MP, there is incomplete toxicological data in humans. Most of the reports are epidemiological studies, adult and juvenile animal studies, or in vitro studies using transformed cell lines. Since undifferentiated human embryonic stem cells (hESC) maintain the ability to differentiate into any somatic cell in the body, they offer a unique vantage point to measure the effect of toxicants on the very early human development and cell repair system.

From our earlier metabolomics work examining the secretome of hESCs following exposure to MP, we hypothesized that ROS is generated during the toxic response to MP. In this follow-on work, we chose to visualize and quantitate: 1) the presence

and location of ROS, and 2) cell and nuclear morphology in MP-exposed WA09 hESC using the Cellomics Oxidative Stress I Assay on a Thermo Scientific Cellomics® ArrayScan® HCA System.

While low levels of oxidative stress are necessary for normal cell metabolism, high levels are associated with cellular dysregulation and pathologies such as cancer. As expected, our imaging data indicated that the cells did not change structurally, nor did they undergo senescence or apoptosis in response to the MP exposures we examined. While we were able to measure cellular oxidative stress (fluorescent conversion of dihydroethidium, DHE), the amount measured in the nuclei was much less than we had predicted. All other DHE was scattered and punctuate throughout the cell. These data, combined with other studies suggesting that hESC lose their robust ROS nuclear protection mechanism as they become more differentiated, opens up a new avenue of investigation to define the point in embryonic differentiation when cells become more vulnerable to the ROS-induced toxic effects of MP.

## PS 1190 Pluripotency Factors Silence Expression of the Aryl Hydrocarbon Receptor in Embryonic Stem Cells.

C. Ko, Q. Wang and A. Puga. *Environmental Health, University of Cincinnati, Cincinnati, OH.*

OCT4, SOX2, and NANOG are transcription factors that maintain pluripotency and self-renewal of embryonic stem cells (ESC) in culture: on the one hand, they activate expression of self-renewal genes, and on the other hand they prevent differentiation by silencing the expression of developmental genes. Unlike DNA methylation, polycomb group (PcG) proteins are chromatin modulators that repress the expression of developmentally important genes, such as those in the Hox family. PcG-mediated repression represents a plastic and dynamic way to keep genes poised to be reactivated during development. Promoters of developmental genes in ESC are often bivalently marked by trimethylation on lysine-4 (H3K4me3) and lysine-27 (H3K27me3) of histone H3, with PcG-mediated repression allowing these genes to be ready for reactivation upon differentiation. The aryl hydrocarbon receptor (AHR) has long been believed to mediate xenobiotic toxicity; increasing evidence suggests that it also plays a role during embryogenesis. To study AHR functions during early development, we have analyzed the regulation of AHR expression in C57Bl/6 mouse ESC and their in vitro differentiated progeny. In ESC, Ahr expression is silenced through bivalent marks in its promoter. Specifically, H3K27 is trimethylated in both distal and proximal promoter regions (dpr and ppr) and H3K4 is trimethylated in the ppr. We also detect the specific binding of pluripotency factors and PcG proteins in the dpr. RNA polymerase II appears to be paused in the ppr, producing short aborted Ahr transcripts. Upon differentiation, the Ahr promoter resolves into a H3K4me3 monovalent state and recruits Sp factors, leading to transcription activation. These results define an ESC-specific silencer domain located 2kb upstream of the Ahr gene transcription start site, responsible for the low, if any, Ahr expression in ES cells. Directed silencing, resulting from cooperation between pluripotency and PcG-repressive factors suggests that the Ahr may play a significant role in maintenance of pluripotency. Supported by NIH Grant 5R01ES06273

## PS 1191 Hypersensitivity of Stem Cells and Cancer Stem Cells to Cadmium Toxicity.

E. J. Tokar, M. Rogers and M. P. Waalkes. *NTP, NIEHS, NIH, Research Triangle Park, NC.*

Stem cells (SCs) generally are resistant to toxicants compared to mature cellular counterparts. Normal SCs (NSCs) can be malignantly transformed to cancer SCs (CSCs) which then likely drive the carcinogenic process. Cadmium (Cd), a known human carcinogen, can also be an effective anti-tumor agent in rodents, selectively destroying advanced tumors but leaving normal tissue intact, implying cancer cell sensitivity. CSCs likely are key to cancer maintenance, propagation, metastasis and repopulation. Thus, to help explain this paradox with Cd, we examined the effects of Cd on the human prostate NSC line, WPE-stem, and its isogenic mature parental cell line (PCL), RWPE-1, and a malignant CSC transformant from NSCs, As-CSC. The untransformed lines had similar LC50 values (NSC = 12.2  $\mu$ M; PCL = 13.9  $\mu$ M). However, the NSCs were much more sensitive to sub-chronic Cd exposure (90% cell loss at 1 week) compared to the mature PCL (15% loss). This is unusual as SCs are typically toxicant resistant. Various factors involved in Cd toxicity were then assessed. Anti-apoptotic *BCL2* decreased in NSCs (50%) but increased in the PCL (225%), and pro-apoptotic *BAX* increased in the NSCs (216%) but was unchanged in the PCL suggesting enhanced apoptosis was involved in this Cd hypersensitivity. The transport protein *ZnT1* effluxes zinc, which protects against Cd toxicity, while *ZIP8* aides in zinc and Cd uptake. Cd exposure increased *ZnT1* transcript 650% in NSCs but only 200% in the PCL. *ZIP8* levels increased 248% in NSCs but showed no change in the PCL. These data support a biokinetic

basis to higher Cd toxicity in NSCs. To define sensitivity in CSCs, we exposed the As-CSC and found them even more sensitive to Cd (LC50 = 6.0  $\mu$ M) than NSCs (12.2  $\mu$ M). Similar apoptotic and/or Cd uptake/efflux factors seen in the untransformed cells were involved in CSC hypersensitivity. Thus, Cd sensitivity may be related to differentiation stage and increased Cd sensitivity in SCs helps explain the initial loss of SCs during Cd transformation. Further, CSC hypersensitivity to Cd may be a major factor in Cd's ability to destroy certain cancers.

## PS 1192 Recruitment of Normal Stem Cells into an Oncogenic Phenotype by Noncontiguous Carcinogen-Transformed Malignant Epithelia Is Dependent on the Transforming Carcinogen.

Y. Xu, E. J. Tokar, R. J. Person, R. Orihuela and M. P. Waalkes. *NTP, NIEHS, NIH, Research Triangle Park, NC.*

Cancer stem cells (CSCs) are likely key to carcinogenesis. In prior work we found that arsenic-transformed malignant epithelial cells (MECs) recruit nearby, but non-contiguous normal stem cells (NSCs) into a CSC-like phenotype. Here, we tested if this recruiting effect on NSCs occurs with MECs transformed by other carcinogens. Normal human prostate epithelial SCs (WPE-stem) were co-cultured via transwell dishes that separate cells but not secreted factors with isogenic MECs derived from normal human prostate epithelial RWPE-1 cells by cadmium or N-methyl-N-nitrosourea (MNU) exposure (called Cd-MECs or MNU-MECs, respectively). SCs co-cultured with normal RWPE-1 cells served as control. After 2 weeks of Cd-MEC co-culture, SCs showed high secretion of metalloproteinase-9 (MMP-9, 3.6-fold of control) and MMP-2 (2.2-fold), increased colony formation (1.8-fold) and invasion (2.5-fold), formation of aggressive ductal structures in Matrigel and loss of tumor suppressor gene, *PTEN*, expression (62% of control), all indicative of cancer phenotype. MNU-MEC co-culture had no such effects on SCs. Epithelial-to-mesenchymal transition occurred in Cd-MEC co-cultured SCs, as shown by cell morphology and *VIMENTIN* over-expression, but not in MNU-MEC co-cultured SCs. During Cd-MEC co-culture, loss and regain of SC-related gene expression (*ABCG-2*, *OCT-4* and *WNT3*) occurred, likely as a key to MEC recruitment of NSCs into CSCs. Overall, the data indicate SCs gain a cancer phenotype with Cd-MEC co-culture but not with MNU-MECs. Analysis showed Cd-MECs secreted high levels of the tumor microenvironmental related factor, TGF $\beta$ -1. Direct TGF $\beta$ -1 treatment of NSCs duplicated most responses from Cd-MEC co-culture. Since recruitment of NSCs into CSCs can also occur with arsenic-transformed MECs, we conclude that the effects of nearby MECs on NSCs are not carcinogen specific but apply to some, but not all, carcinogens. This phenomenon may be important in chemically-induced tumor extension and dissemination.

## PS 1193 Aberrant microRNA Expression Correlates with RAS Activation in Malignant Transformation of Human Prostate Epithelial and Stem Cells by Arsenic.

N. N. Ngalame, E. J. Tokar and M. P. Waalkes. *NTP, NIEHS, NIH, Research Triangle Park, NC.*

Inorganic arsenic (iAs) is a human carcinogen probably targeting the prostate and can malignantly transform the human prostate epithelial cell line, RWPE-1 (to CAsE-PE cells) and a derivative stem cell (SC) line, WPE-stem (to As-CSC cells) by unclear mechanisms. MicroRNAs (miRNA) are non-coding but exert negative control on expression by degradation or translational repression of target mRNAs. Aberrant miRNA expression is likely a key factor in carcinogenesis. By miRNA array of 84 miRNAs in CAsE-PE and As-CSC cells, for 29 and 13 miRNAs respectively, expression changed by >1.5 fold of control, and 7 were common in both cells. Target gene expression correlated with miRNA changes (suggested by TargetScan and microRNA.org) in transformants with shared pathways like oncogenesis, miRNA biogenesis, SC differentiation, and metastasis and invasion. KRAS oncogene was induced in CAsE-PE but not by mutation or promoter hypomethylation. Overexpression of KRAS protein was very intense in As-CSC cells. In both cell types, iAs transformation decreased miRNAs targeting KRAS and RAS superfamily members. Reduced miR-134 (15 fold), miR-373 (11 fold), miR-155 (4 fold), miR-138 (4 fold), miR-205 (4 fold), miR-181d (3 fold), and miR-181c (2 fold) in CAsE-PE cells correlated with increased target RAS oncogenes, *RAN*, *RAB27A*, *RAB22A* mRNAs and KRAS protein. Reduced miR-143 (5 fold), miR-34c-5p (3 fold), and miR-205 (2 fold) in As-CSC cells correlated with increased target *RAN* mRNA, and KRAS, NRAS, and RRAS proteins. The RAS/ERK signaling pathway helps control cell survival, differentiation, and proliferation, and if

dysregulated promotes a cancer phenotype. Within the RAS/ERK pathway iAs transformation increased expression of RAF kinase protein, and ERK kinase mRNA in CAsE-PE cells, and MEK1/2, ERK and MAP4K4 kinase mRNAs in AsCSC cells. Thus, dysregulated miRNA expression appears to impact RAS activation in both iAs transformants, and appears key to iAs-induced acquired cancer phenotype in these human prostate cells.

**PS 1194 Aryl Hydrocarbon Receptor Contributes to Mouse Embryonic Stem Cell-Derived Cardiomyocyte Differentiation.**

Q. Wang, C. Ko, Y. Fan, Y. Wang and A. Puga. *University of Cincinnati, Cincinnati, OH.*

2,3,7,8-tetrachlorodibenzo-p-dioxin (TCDD) is a ubiquitous toxicant persistent in the environment. It is a prototypic ligand for the aryl hydrocarbon receptor (AHR), a ligand-activated transcription factor whose activation upon ligand binding regulates the expression of many xenobiotic detoxification genes. Besides being a critical mediator of gene-environment interactions, AHR has functions beyond those of a xenobiotic interacting protein. Studies in Ahr-/- mice have shown that AHR has physiological roles in hematopoiesis and heart development. To characterize these roles and the consequences of TCDD exposure in cardiomyocyte specification, we studied the effects of TCDD exposure during mouse embryonic stem cells (mESCs) differentiation into cardiomyocytes. mESCs were allowed to spontaneously differentiate via embryo-like aggregates (embryoid bodies, EB) into contracting cardiomyocytes. Immunocytochemistry on contracting EBs indicates that AHR colocalizes with the cardiac markers cardiac troponins T and I and NKX2.5. ShRNA knockdown of AHR during differentiation or TCDD treatment significantly decreased the percentage of contracting EBs. A time series of TCDD treatment revealed that the time between day 0 and day 3 of mESC differentiation was the most critical window for TCDD toxicity. An ESC clone containing a stably integrated plasmid bearing a Cyp1a1 promoter-driven puromycin-IRES2-eGFP was allowed to differentiate in the presence of TCDD followed by puromycin selection. Real-time PCR analyses of the puromycin resistant selected cells showed that many mesoderm marker genes were up-regulated while both endoderm and ectoderm markers were down-regulated, indicating that early AHR activation might be committed to mesodermal lineages. Our data suggest that AHR is involved in the regulation of cardiomyocyte differentiation during embryonic development and that TCDD exposure during early differentiation is toxic to cardiomyocyte development. Supported by NIH Grant 5R01ES06273.

**PS 1195 Exposure to Concentrated Air Particles Depletes Bone Marrow Hematopoietic Stem Cells.**

T. O'Toole, W. Abplanalp, J. Lee, D. J. Conklin and A. Bhatnagar. *Diabetes and Obesity Center, University of Louisville, Louisville, KY.*

Results from several epidemiological and laboratory studies suggest that exposure to airborne particulate matter (PM) is associated with an increase in cardiovascular disease (CVD) risk. While acute PM exposures have been linked to arrhythmias, thrombosis, inflammation, endothelial dysfunction, myocardial infarction and stroke, long term exposures increase the risk of mortality due to heart failure, cardiac arrest, and ischemic heart disease arrhythmias. Despite these associations however, relatively little is known about the molecular mechanisms linking exposures to CVD risk. In previous studies we have shown that circulating endothelial progenitor cells (EPCs) were depleted in humans exposed to natural variations in fine particulate matter (PM<sub>2.5</sub>) and in mice exposed to concentrated air particles (CAPS). However the effects of exposure on other progenitor cell types remains unknown. Hence, to examine how PM affects other stem cell populations we exposed mice to CAPS generated from downtown Louisville, Kentucky air using a versatile aerosol concentration enrichment system (VACES) for 9 days and examined levels of bone marrow-derived hematopoietic stem cells (HSCs) and mesenchymal stem cells (MSCs) using colony forming assays. In CAPS-exposed mice we observed an approximate 35% decrease in CFU-GM (colony forming unit-granulocyte, macrophage) colonies compared to filtered air-exposed, control mice. However the absolute number of colonies and the relative decrease versus air controls varied directly with CAPS levels. Flow cytometry-based phenotypic analysis of these colonies suggested a uniform decrease of multiple hematopoietic lineages rather than a decrease in a specific subset. In contrast no change was observed in BFU-E (burst forming unit-erythroid) colonies between the filtered air and CAPS treatments, or in the number of bone marrow-derived MSCs. These results suggest that HSC depletion may contribute to the cardiovascular complications resulting from chronic PM exposure by affecting immune responses to injury and dysfunction.

**PS 1196 Cadmium Concurrently Affects Cell Cycle, Total Histone Protein Production (THP) and H3 Histone Modification Pathways in Mouse Embryonic Stem Cells.**

S. R. Gadha and F. A. Barile. *Pharmaceutical Sciences, St. John's University College of Pharmacy and Health Sciences, Queens, NY.*

The fetal basis of adult disease (FEBAD) theorizes that embryonic challenges initiate pathologies in adult life through epigenetic modification of gene expression. We previously reported (2012) that cadmium (Cd) exerts differential toxicity in mouse embryonic stem cells (mESC) by targeting THP production and H3 (a core histone protein) early in stem cell development, while H3K27 mono-methylation (H3K27me1, associated with transcriptional activation) is affected in later stages of differentiation. Thus, low dose acute Cd exposure selectively disrupts chromatin structure, an effect not seen in differentially mature cells. In this study we tested the effects of Cd on cell cycle progression (flow cytometry), chromatin structure and epigenetic pathways (THP and H3K27me1 analysis, respectively) in undifferentiated mESC after 1-h and 24-h exposures plus recovery. The data suggest that mESC do not recover from Cd insult at 0.032 mM (IC<sub>50</sub> for MTT assay), whereas cells recovered from 1-h exposure at 0.01 mM (IC<sub>25</sub> for MTT assay). This confirms our previous results that maximum cytotoxicity is seen during the first few hours of exposure at low concentrations. Additionally, THP production is suppressed to a greater extent than cell proliferation at 0.01 mM (24-h). Interestingly, 1-h exposure plus recovery resulted in a significant increase in THP production. Furthermore, 24-h exposure (with recovery) suppressed both cell proliferation and THP production, indicating that Cd targets THP production at longer exposure times and disrupts repair mechanisms. Flow cytometry data demonstrates that 0.01 mM Cd, for 24- and 48-h, increases DNA synthesis and percent of cells in G1 phase as well as percent of cells in mitosis; differentiation is affected at 72-h only. Thus presently we report that low dose acute Cd toxicity is cumulative and disrupts DNA repair, while concurrently affecting cell cycle progression, repair mechanisms, chromatin structure and transcriptional state in mES cells.

**PS 1197 Cadmium Induces Up-Regulation of Genes Associated with Early Embryonic Development in Mouse Embryonic Stem Cells.**

A. Aliberti and F. A. Barile. *Pharmaceutical Sciences, St. John's University College of Pharmacy and Health Sciences, Queens, NY.*

Cadmium (Cd) alters gene expression and increases cell proliferation, but the exact mechanism of its nongenotoxic effect has yet to be elucidated. Previously we reported that exposure to low concentrations of Cd (80 nM to 5 µM) causes a toxicologically relevant increase in cell proliferation, as determined by [<sup>3</sup>H]-thymidine incorporation, in undifferentiated pluripotent mouse embryonic stem cells (mESC). Since epigenetic mechanisms are important during early embryonic development, we evaluated the potential of Cd to disrupt normal epigenetic processes in these cells. Using trypan blue exclusion, exposure of cells to Cd (up to 75 µM for 24 hours) resulted in inhibitory concentrations 50% (IC<sub>50</sub>) and 25% (IC<sub>25</sub>) of 40 and 20 µM, respectively. Real-time PCR analysis of genes associated with epigenetic chromatin modification during early embryonic development indicates that treatment of cells with IC<sub>50</sub> and IC<sub>25</sub> concentrations results in a greater than 2-fold up-regulation of *Aurke*, *Setd1b*, and *Smyd1*. *Aurke*, a member of the Aurora kinase family, has a significant influence on cell proliferation of the pre-implantation blastocyst. *Setd1b* is a component of the histone methyltransferase complex that trimethylates H3K4 (histone 3, a core histone protein, at position lysine 4), resulting in downstream expression of *Oct-4*. *Smyd1* is involved early in embryonic development of cardiac progenitor cells. The results suggest that Cd up-regulates genes that are important in early mitosis and blastocyst formation, methyltransferase activity, and cellular differentiation, the consequences of which implicate the potential role of the metal to alter the normal processes that are coupled with embryonic development *in vivo*.

**PS 1198 Colony-Forming Cell (CFC) Assays Predict for Increased Clinical Neutropenia Resulting from Combination Therapies.**

E. Clarke, A. Mergaert and G. Dos Santos. *ReachBio LLC, Seattle, WA.*

Combination therapy can be more efficacious than monotherapy in preventing progression of certain diseases. Unfortunately, this increased therapeutic efficacy often comes with increased hemotoxicity. In a randomized study of 646 patients with Multiple Myeloma, Orłowski et al. (2007) saw clinical neutropenia in 20% of patients receiving Bortezomib alone as compared to 35% of patients receiving Bortezomib and Doxorubicin. Shah et al. (2007) reported clinical neutropenia in

25% of patients receiving Imatinib and Hydroxyurea in patients with recurrent malignant glioma. Some myelotoxic combinations may be unintentional: Hachem et al. (2003) reported myelosuppression in bone marrow transplant patients treated with Linezolid that also happened to be on selective serotonin reuptake inhibitors (SSRIs). To see if in vitro CFC assays could predict the clinical neutropenia observed with these combinations, we tested the compounds alone and in combination on CFU-GM inhibition. Normal bone marrow cells and single compounds (range of concentrations) were mixed in methylcellulose-based media (ColonyGel 1102) and plated in 35mm dishes (3 replicates/concentration). CFU-GM were enumerated on day 14. Compound IC50 values were: Bortezomib (B) 12µM; Doxorubicin (D) 28 µM; Imatinib (I) 2.6 µM; Hydroxyurea (H) 31 µM; Linezolid (L) 109 µM; and the SSRI Fluoxetine (F) 27 µM.

Drug pairs (B+D; I+H; and L+F) were then tested using a matrix design. When compounds were combined at their IC50 equivalent values, there was an additional inhibition of CFU-GM: 69% with B+D, 84% with I+H and 75% with F+L. These data suggest that the CFU-GM assay may be a useful tool to evaluate drug combinations and predict for clinical neutropenia in a variety of circumstances: when concern of increased hemotoxicity with a strategic therapeutic combination exists; when there is limited information on the drug combinations to be employed; when a drug is to be used on pre-treated patient populations. CFC assays may also be useful in evaluating compounds with potential myeloprotective effects in combination with myelotoxic compounds.

### PS 1199 The Effect of TCDD on the Development of Human Hematopoietic Stem Cells to Lineage-Committed B Cells.

J. Li<sup>1,2</sup>, A. Phadnis<sup>1,2</sup>, R. B. Crawford<sup>2,3</sup> and N. E. Kaminski<sup>1,2,3</sup>. <sup>1</sup>Genetics Program, Michigan State University, East Lansing, MI; <sup>2</sup>Center for Integrative Toxicology, Michigan State University, East Lansing, MI; <sup>3</sup>Department of Pharmacology and Toxicology, Michigan State University, East Lansing, MI.

2,3,7,8-Tetrachlorodibenzo-p-dioxin (TCDD) is an ubiquitous environmental contaminant that exhibits a broad spectrum of toxicity. Epidemiological studies have identified an association between exposure to TCDD and B cell disorders, such as suppression of humoral immunity and increased incidence of B cell leukemia. Although extensive studies have been dedicated to explicate the mechanism underlying suppression of mature B cell function by TCDD, little is known whether TCDD will alter the sequential progression of human hematopoietic stem cells (HSC) to lineage-committed B cells. To address this question, we established a co-culture system using irradiated human marrow stromal cells as a supportive microenvironment to drive the differentiation of human cord blood CD34+ HSC in the presence of cytokines (IL-3, IL-7, SCF and Flt3L). In three weeks of culture, we observed increased expression of IL-7R, which is a hallmark of lymphopoiesis. Furthermore, generation of lineage-committed B cells was detected by the co-expression of B220 and CD19 in 20% of the cell population. To test the effect of TCDD on B cell development, we treated CD34+ HSC with 1nM, 10nM and 30nM TCDD. Compared to the vehicle control, the cell proliferation was remarkably arrested by TCDD in a concentration-dependent manner. We also observed a significant decrease of IL-7R expression in TCDD-treated cells. These data illustrate establishment of an in vitro model system to drive the development of cord blood HSCs to lineage-committed B cells. Preliminary studies showing downregulation of IL-7R suggest a role by TCDD in altering early B cell development.

### PS 1200 New Methodology for the Production of Thin-Layered Cardiomyocyte Tissue from Human-Induced Pluripotent Stem Cells (hiPSCs) Derived Cardiomyocytes for Use in High-Throughput Electrophysiological Platforms and High-Content Imaging Systems.

S. Yoshida<sup>1</sup>, K. Tsuzaki<sup>2</sup>, S. Tomizawa<sup>2</sup> and Y. Asai<sup>1</sup>. <sup>1</sup>ReproCELL Inc., Kanagawa, Japan; <sup>2</sup>Drug Safety Testing Center Co., Ltd., Saitama, Japan.

We have been developing functional cardiomyocytes derived from human iPS cells for many years. We have previously reported on cryopreserved cardiomyocytes, ReproCardio 2, derived from human iPS cells that demonstrate stable cardiac characteristics such as αMHC, cTnT, MLC-2a, MLC-2v, and Cx43. Using ReproCardio 2 clumps on electrophysiological assay systems, we have further developed our QTempo® assay (on the MEA platform) to better predict the drug induced QT interval prolongation (DIQTIP).

The use in cardio-toxicity assays requires the reliable assay platform like tissue. We have been developing this technology to make functional thin layered cardiac tissue, which has improved beating synchronization and stability, and better reliability for use in cardio toxicity assays. The thin-layer tissue derived from ReproCardio 2 stained positive for cTnT especially around the synchronized beating cell area. We

have developed a calcium flux assay (inotropic assay) using the thin layered cardiomyocytes that demonstrate a robust and synchronized calcium flux (Fluo8) and high content imaging technologies. Furthermore, the thin-layer showed advantages over monolayers, especially its robust signal with changes in serum concentration, which is preferable for high throughput screening (HTS) platforms. When using electrophysiology platforms, ReproCardio 2 thin-layer also demonstrated a more robust electrophysiological output similar to that seen with beating cardiomyocyte clumps especially the dose response to DIQTIP causing compounds such as E-4031 and Cisapride. In fact, the results were similar to that obtained in the clinical. The thin-layer cardiomyocytes have shown to be the preferred format giving rise to a robust and sustainable platform for measuring prolonged QT-interval and other cardiotoxic parameters such as calcium flux, and in turn will produce a more predictive format for toxicity assays in drug discovery.

### PS 1201 Proteomic Analyses of Human Primary Hepatocytes and Stem Cell-Derived Hepatocytes Identifies Hepatocyte Maturity Markers and Shows Improved Phenotype Maintenance in an Air-Liquid Interface Culture Model.

C. Rowe<sup>1</sup>, C. Goldring<sup>1</sup>, D. Gerrard<sup>2</sup>, N. Hanley<sup>2</sup>, M. Storm<sup>3</sup>, D. Tosh<sup>3</sup>, K. Piper Hanley<sup>2</sup> and B. Park<sup>1</sup>. <sup>1</sup>MRC Centre for Drug Safety Science, University of Liverpool, Liverpool, United Kingdom; <sup>2</sup>Centre for Endocrinology & Diabetes, University of Manchester, Manchester, United Kingdom; <sup>3</sup>Centre for Regenerative Medicine, University of Bath, Bath, United Kingdom. Sponsor: D. Mendrick.

Failure to predict hepatotoxic drugs in pre-clinical testing makes it imperative to develop better liver models with a stable cultured phenotype. Stem cell-derived models offer promise with hepatocyte-like cells currently considered to be 'fetal-like' in their maturity. This is based on limited biomarkers and lacks the required proteomic datasets that directly compares fetal and adult hepatocytes. Here, we quantitatively compare the proteomes of human fetal liver, adult hepatocytes, HepG2 cells and ES-derived hepatocyte-like cells. In addition, we investigate the changes in human fetal and adult hepatocytes when cultured in an air-liquid interface format and in extracellular matrix sandwich culture. The proteomes were qualitatively similar across all samples but hierarchical clustering showed that each sample type had a distinct quantitative profile. Hepatocytes cultured at the air-liquid interface retained a proteome more closely clustered to fresh cells than conventional culture, which acquired myofibroblast features. Principal component analysis extended these findings and identified sets of proteins as specialized indicators of hepatocyte differentiation. Our quantitative datasets are the first that directly compare multiple human liver cells, define a model for enhanced maintenance of hepatocytes in culture and provide new protein markers for determining human hepatocyte phenotype and maturity.

### PS 1202 Scalable, HTS/HCI-Amenable and NURR1-Expressing Dopaminergic Progenitor Cells Derived from Human Embryonic Stem Cells.

J. Chilton<sup>1</sup>, B. R. Culp<sup>1</sup>, K. L. Galland<sup>1</sup>, J. N. Le<sup>1</sup>, J. A. McCabe<sup>2</sup>, Z. Lin<sup>2</sup>, N. M. Filipov<sup>2</sup> and S. L. Stice<sup>1,2</sup>. <sup>1</sup>Aruna Biomedical, Inc., Athens, GA; <sup>2</sup>University of Georgia, Athens, GA.

One of the most common neurodegenerative diseases, Parkinson's disease (PD) affects approximately 1-2% of the population over age 65. The lack of an appropriate and scalable cell type hinders progress in PD drug discovery and elucidating disease mechanisms. Our goal was to generate human dopaminergic progenitor cells, derived from human embryonic stem cells (hESCs), which are homogeneous, expandable for high throughput screening (HTS) and high content imaging (HCI) assays and demonstrate a propensity for dopaminergic differentiation. We isolated cells exhibiting > 95% immunoreactivity for nuclear receptor related 1 protein (NURR1 or NR4A2), a transcription factor essential for generating midbrain dopaminergic neurons. We refer to these cells as DopaPro™ cells, which display normal karyotype, form adherent monolayers and proliferate over multiple passages. DopaPro™ cells were differentiated with leukemia inhibitory factor (LIF), brain derived neurotrophic factor (BDNF), glial derived neurotrophic factor (GDNF), transforming growth factor beta 3 (TGF-β3), forskolin and ascorbic acid (AA). By 3 weeks, differentiated DopaPro™ cells showed tyrosine hydroxylase (TH) expression. We asked whether DopaPro™ cells, as putative midbrain progenitor cells, required regionalization signals such as Sonic Hedgehog (SHH) or fibroblast growth factor 8 (FGF8), which are normally used in directed differentiation of hESCs to dopaminergic neurons. DopaPro™ cells did not require, nor was their differentiation to TH positive populations significantly enhanced, when cultures were exposed to SHH and FGF8 for 2 weeks prior to LIF, BDNF, GDNF,

TGF- $\beta$ 3, forskolin and AA. SHH and FGF8 were also not required for dopamine production. Here, hESC-derived progenitor cells poised for potential dopaminergic cell derivation were generated, thus reducing time and need for midbrain induction factors. Results show DopaPro™ cells are a unique, renewable and scalable cell source for PD research.

## PS 1203 Conditions for Isolation and Maintenance of Rat Hepatic Stem/Progenitor Cell Colonies.

J. A. Harrill<sup>1</sup>, J. Rowlands<sup>2</sup>, R. S. Thomas<sup>1</sup> and L. M. Reid<sup>3</sup>. <sup>1</sup>ICSS, The Hamner Institutes for Health Sciences, Research Triangle Park, NC; <sup>2</sup>TERC, The Dow Chemical Company, Midland, MI; <sup>3</sup>University of North Carolina at Chapel Hill, Chapel Hill, NC.

Hepatic stem cells, hepatoblasts, and committed hepatocytic and biliary progenitors constitute a stepwise maturational lineage which produces all mature cells of the liver. Hepatic stem/progenitors are localized to the Canals of Hering: periportal ductular structures derived from ductal plates in fetal and neonatal livers. These periportal stem cell niches are enriched in a variety of extracellular matrix molecules including certain types of collagens (III, IV and V) and hyaluronans, non-sulfated polymers of D-gluronic acid + D-N-acetylglucosamine. We have compared the ability of hyaluronans, as well as type III and type IV collagens, to support the proliferation of hepatic stem/progenitors isolated from neonatal and adult rat livers. Cells were isolated either by suspension digestion (neonates) or perfusion digestion with collagenase (adult) and cultured in a serum-free medium (Kubota's Medium) designed to culture-select endodermal stem/progenitors. Cells from either age seeded onto collagen III or IV (5 ug/cm<sup>2</sup>) yielded hepatic stem/progenitor cell colonies which expanded for 5-7 days of culture, at which time the mesenchymal cell components overgrew the plating surface. By contrast, a substratum of hyaluronans (5 – 100 ug/cm<sup>2</sup>), in combination with Kubota's Medium, promoted coordinated attachment and growth of discrete hepatic stem/progenitors and their mesenchymal cell progenitor partners. Colonies consisted of hepatic stem /progenitors growing on top of mesenchymal cell progenitors. Neonatal liver-derived colonies had large expansion potential, increasing in area by more than 100-fold by 10 days in culture. It is hypothesized that the expansion potential of adult-derived cells was more limited due to the need for an alternate method of isolation or addition of exogenous growth factors. This novel culture system provides an opportunity to study the effects of hepatotoxicants on early lineage stages consisting of rat hepatic stem/progenitor cells.

## PS 1204 The *In Vitro* Human CFU Assay Combined with Automated Image Analysis of Colony Morphology Markedly Improves Assessment of Hematopoietic Toxicity of AZT and Other Nucleoside Inhibitors.

M. Huber<sup>1</sup>, D. Raj<sup>1</sup>, C. Grande<sup>1</sup>, J. Parrott<sup>1</sup>, O. Egeler<sup>1</sup>, K. Tse<sup>1</sup>, C. Farzim<sup>1</sup>, A. Eaves<sup>1,2</sup> and J. Damen<sup>1</sup>. <sup>1</sup>STEMCELL Technologies Inc, Vancouver, BC, Canada; <sup>2</sup>Terry Fox Laboratory, BC Cancer Agency, Vancouver, BC, Canada.

Antiviral nucleoside analogs target viral polymerases but can also inhibit cellular polymerases, leading to a decrease in cell proliferation and ultimately suppression of hematopoiesis, resulting in anemia and neutropenia. For assessment of hematotoxicity in this compound class, the FDA's *Guidance for Industry: Antiviral Product Development – Conducting and Submitting Virology Studies to the Agency* recommends the use of the colony-forming unit (CFU) assay, which utilizes primary hematopoietic stem and progenitor cells. In 2003, the European Centre for the Validation of Alternative Methods (ECVAM) published a standardized CFU assay methodology that is validated for the prediction of the maximum tolerated dose (MTD) of myelosuppressive compounds (Pessina *et al.*, Tox Sci. 2003. 75:355-367). This *in vitro* assay is a key tool for assessing toxicity prior to initiation of costly *in vivo* studies and human clinical trials. Unfortunately, in these standardized CFU assays, nucleoside inhibitors such as azidothymidine (AZT) do not exhibit high toxicity (IC<sub>50</sub> = 100-200  $\mu$ M), despite the fact that they are well known to perturb hematopoiesis in patients. Although AZT does not strongly reduce the number of hematopoietic colonies in the CFU assay, it does have a dramatic effect on their morphology. To quantitate changes in colony morphology, we utilized the STEMvision™ platform for automated advanced image analysis in conjunction with the CFU assay. Our results indicate that IC<sub>50</sub> values for AZT based on the quantitation of morphological changes such as colony size were ~20-fold lower (5-10  $\mu$ M) than the IC<sub>50</sub> based on colony numbers (100-200  $\mu$ M). These data suggest that quantitation of colony morphology is a key parameter to predict drug potency and *in vivo* toxicity in this drug class.

## PS 1205 Investigation of a Redox-Sensitive Predictive Model of Mouse Embryonic Stem Cell Differentiation via Quantitative Nuclease Protection Assays and Glutathione Redox Status.

K. J. Chandler<sup>1</sup>, J. M. Hansen<sup>2</sup>, E. S. Hunter<sup>1</sup> and T. B. Knudsen<sup>1</sup>.

<sup>1</sup>NHEERL/NCC, US EPA, Research Triangle Park, NC; <sup>2</sup>Department of Pediatrics, Emory University School of Medicine, Atlanta, GA.

Mouse embryonic stem cells (mESCs) recapitulate developmental signals that occur *in vivo* and are amenable to high-throughput profiling of chemical-induced effects. *In silico* models of impaired mESC differentiation identified 19 ToxCast™ assays that distinguished chemical effects on cardiomyocyte differentiation versus cytotoxicity (Wilcoxon rank sum, p=0.03). Taken together, these assays connect a redox-sensitive pathway(s) as a likely target of a chemical set that impaired mESC differentiation. To evaluate this predictive model, a custom quantitative nuclease protection assay (qNPA) array (HTG Molecular Diagnostics) of 41 redox-sensitive targets and differentiation markers was designed. The concentration-dependent effects of twelve ToxCast chemicals were evaluated using the qNPA array. The highest concentration produced AC 20 cytotoxicity in mESCs and the remaining were half logarithmic decrements. Cells were harvested on days 4 and 9 of culture. The prediction model correctly identified that pyridaben would disrupt redox signaling in mESCs. Expression of the redox-responsive transcription factors Nrf2, Hif1 $\alpha$  and Mtf2 increased upon exposure. Pyridaben showed significant concentration-dependent effects on markers for endoderm, ectoderm and mesoderm differentiation on day 4 of culture (decreased Fgf5, Otx2, and Fgf8 expression and increased Tbx3 expression) without producing a 50% decrease in cardiomyogenesis in the standard assay on day 9. Preliminary data evaluated the redox status (glutathione/glutathione disulfide) of mESCs at 3, 6, 9 and 24 hours following chemical exposure and indicated a unique pattern of redox status for predicted redox disrupting chemicals. These experiments document the importance of using multiple differentiation endpoints and support the linkage of our predictive model to altered differentiation in chemical profiling. This abstract does not reflect EPA policy.

## PS 1206 Arsenic Trioxide Alters Regulation of Differentiation in Mouse Embryonic Stem Cells.

T. Lee and F. A. Barile. *Pharmaceutical Sciences, St. John's University College of Pharmacy and Health Sciences, Queens, NY.*

Arsenic trioxide (As<sub>2</sub>O<sub>3</sub>) is a known human carcinogen yet it is currently approved by the Food and Drug Administration as a chemotherapeutic agent for the treatment of acute promyelocytic leukemia. As<sub>2</sub>O<sub>3</sub> alters cellular differentiation by mechanisms of which are yet not clearly understood. Thus, in the current study, we investigated the influence of As<sub>2</sub>O<sub>3</sub> on differentiation of mouse embryonic stem cells (mESC). These pluripotent stem cells are derived from the inner cell mass of the blastocyst, and are capable of continuous proliferation, self-renewal and differentiation into the three germ layers. Undifferentiated cells express early specific stem cell markers, including *Oct-3/4*, *Nanog*, and *Sox-2*, which have an important role in developmental regulation and differentiation. In our initial studies, 1.0  $\mu$ M to 6  $\mu$ M As<sub>2</sub>O<sub>3</sub> reduced cell viability over 24-h with increasing concentrations, whereas significant reductions were observed at or below 1  $\mu$ M only with 48-h exposures, a concentration which is equivalent to therapeutic administration. End point PCR analysis revealed that increasing concentrations of As<sub>2</sub>O<sub>3</sub> reduced gene expression of stem cell markers. This supports the western blot results, protein levels decreased with decreased in gene expression. Western blot analysis for *Oct-3/4* and *Sox-2* protein expression at the same concentrations indicated that protein levels were decreased by As<sub>2</sub>O<sub>3</sub> in a dose- and time-dependant manner. While *Oct-3/4* and *Sox-2* protein expression levels are crucial for maintaining mESC in their undifferentiated state, the reductions in the presence of arsenic imply the loss of "stemness". Consequently, it appears that As<sub>2</sub>O<sub>3</sub> exposure reduces the ability of the stem cells to maintain proper state of differentiation.

## PS 1207 Vascular Endothelial Cells Exposed to PCB 153 Show Increased Expression of Stem Cell Markers.

J. K. Das and Q. H. Felty. *Environmental & Occupational Health, Florida International University, Miami, FL.*

The contribution of PCB exposure to the development of vascular disease is an area of research that has received little attention. The stability of these chemicals has allowed them to persist in the environment and consequently continues to expose the general population to PCBs. Since PCBs have been reported in human blood; vascular toxicity from PCB exposure is a public health concern. Vascular lesions from the lung of patients with severe PAH have been characterized with excessive EC proliferation and markers of angiogenesis. The exact cell type from where vascular

lesions originate from is not clear. However, our studies have focused on ECs as the origin of vascular lesions because EC stem-like cells have been reported to be involved in vascular injury. The theory that malignancies depend on stem-like cells for proliferation has received much attention, but there have been few studies which support a pathogenic role for stem cells in vascular disease. Thus, the objective of this study was to determine whether exposure to the PCB congener 153 can increase the level of stem cell markers in vascular ECs. ECs overexpressing ID3 were used to study the effects of PCB153 in 3D spheroid cultures. Co-culture model of EC with SMCs and fibroblasts was used to study the expression of stem cell markers in a monolayer by confocal microscopy. The effect that PCB153 had on cell cycle progression was also determined by flow cytometry. We observed PCB153 significantly increased expression of stem cell markers CD34+, CD133+, VEGFR-3 in spheroids overexpressing ID3. ECs exposed to PCB153 showed stable sphere formation in B27 medium at 10 days. ECs exposed to PCB153 in co-cultures showed increased expression of stem markers CD34+ and Nanog as well as increased angiogenic phenotype. Cell cycle analysis confirmed that more stem like cells exposed to PCB153 were in G1 phase. Our results show that PCB153 exposure increased expression of stem cell markers and may be related to mechanisms by which vascular disease depends on stem-like cells for proliferation.

**PS 1208 Evaluation of Iontropic and Chronotropic Compounds In Vitro Using Human iPS-Derived Cardiomyocytes and Impedance-Based Contractility Assay.**

X. Zhang, B. Xi, X. Wang, X. Xu and Y. A. Abassi. *Acea Biosciences, San Diego, CA.*

The  $\beta$ -adrenergic receptor ( $\beta$ AR) signaling system is one of the most powerful regulators of cardiac ionotropic and chronotropic function.  $\beta$ AR antagonists, commonly known as beta-blockers ( $\beta$ -blockers) have been used for decades to treat hypertension, ischemic heart disease, some arrhythmias, and more recently to treat congestive heart failure. Up to date, 3 types of  $\beta$ -blocker drugs have been developed for therapeutic purpose. In order to better understand the cardiac effects of different types of  $\beta$ -blockers, we have developed an in vitro assay using human iPS-derived cardiomyocytes in conjunction with impedance measurement. We evaluated the activities of six  $\beta$ -blocker drugs and compounds including (1) non-selective  $\beta$ -blockers; (2) cardioselective  $\beta$ -blockers; and (3) nonselective  $\alpha$  and  $\beta$ -blockers. The data as measured by impedance readout revealed that the  $\beta$ -blockers from different classes displayed subtle but unique profile of acute impedance changes post compound addition. With the exception of atenolol and metoprolol, pindolol, alprenolol, propranolol and carvedilol significantly decreased the cell beating rate (BR) and even temporally led to beating arrest at the highest tested concentration (3  $\mu$ M). In addition, the 1 hour pretreatment with all these four compounds at higher doses abolished the isoproterenol-induced positive chronotropic effects on BR. Carvedilol was the only drug that appeared to profoundly reduce cell beating amplitude (CA) in a dose-dependent manner. The in vitro assay used here indicates that human iPS-derived cardiomyocytes respond similarly to the  $\beta$ -blockers from the same group. However, each type of  $\beta$ -blockers generates distinct profiles and do have different chronotropic and ionotropic effects which we will summarize in the current poster.

**PS 1209 Selection of CYP3A4<sup>+</sup> hESC-Derived Hepatocytes for Drug Metabolism and Toxicity Assays.**

K. Bonham<sup>1</sup>, R. Rodriguez<sup>1</sup>, S. Ogawa<sup>2</sup>, C. Blanco<sup>1</sup>, H. Xian<sup>1</sup>, R. Stull<sup>3</sup>, G. Keller<sup>2</sup> and R. Snodgrass<sup>1</sup>. <sup>1</sup>VistaGen Therapeutics, Inc., South San Francisco, CA; <sup>2</sup>McEwen Centre for Regenerative Medicine, Toronto, ON, Canada; <sup>3</sup>Stem CentRx, South San Francisco, CA.

The ability to produce human hepatocytes that express adult levels of drug metabolizing enzymes including CYP3A4 in a stable and reproducible system will greatly benefit the drug development process by decreasing costs, reducing animal studies, and increasing drug safety. Many groups are trying to develop hepatocytes from human stem cells to address the lack of availability, quality, and reproducibility of primary hepatocytes, however, most protocols produce immature hepatocytes with minimal expression of the adult enzymes related to drug metabolism. Since CYP3A4 is the most abundant P450 expressed in adult liver and metabolizes 50% of drugs on the market, it is imperative that assay systems express relevant levels of this enzyme. To this end, we previously reported the generation of a hESC reporter line (3A4BLA) containing humanized beta-lactamase (hBLA) inserted in frame with the CYP3A4 gene. Here we show that 3A4BLA-hepatocytes can be used to: 1) monitor the differentiation of mature hepatocytes; 2) sort for mature hepatocytes; 3) monitor drug induction of CYP3A4; and 4) develop in vitro assays for drug metabolism and toxicity. Using an optimized protocol for hES-hepatocyte differentiation, we demonstrate CYP3A4 in 25-40% of the cells and show that these cells produce levels of CYP3A4 mRNA approaching primary hepatocytes, express high

levels of ALB, and store glycogen. More importantly, they metabolize testosterone and midazolam and respond properly to inducers of CYP3A4 like Rifampicin and Phenobarbital. With this system we can obtain a relative measure of CYP3A4 expression on a per cell basis in response to compounds and correlate those data with cell metabolism, CYP3A4 activity, and secretion of albumin and urea. Taken together, these data demonstrate development of a robust system with the potential of purifying human hepatocytes with more mature functions, as well as assaying drug effects on CYP3A4 expression, activity, and metabolism.

**PS 1210 Adapting the MTT Assay for Use with Human Embryonic Stem Cells (hESC).**

R. Z. Behar, V. Bahl, Y. Wang, J. Weng, S. Lin and P. Talbot. *University of California Riverside, Riverside, CA.*

hESC are difficult to adapt to 96-well plate assays because they survive best when plated as colonies, which are difficult to count and plate accurately. To address this problem, two protocols were developed to perform the MTT assay using hESC. In the first protocol, plating was done with Rho-associated kinase inhibitor (ROCKi), which allows accurate counting and plating of single hESC. The second protocol involved plating hESC as small colonies without ROCKi but with adaptations to allow accurate counting and plating of small colonies. In the ROCKi protocol, 5,000 cells/well are counted using a hemocytometer then plated and incubated for 96-hours, while the small colony method calls for 20,000-30,000 cells/well followed by 72-hours of incubation. To enable rapid and uniform plating of small hESC colonies, we developed a spectrophotometric method to accurately determine hESC concentration. The percent transmittance for multiple readings of the same sample produced a coefficient of variation (COV) of 1.5%. Next, we determined the cell concentration needed to carry out an experiment in a 96-well plate by plating various cell concentrations and determining the optimal concentration needed for a 72-hour experiment. Finally, to confirm that the correct cell number was pipetted accurately into each well, control wells were subjected to the MTT assay and used to calculate the COV, which ranged from 0.7 to 8.5%, showing that pipetting of small colonies was uniform. The small colony protocol was validated using the NIH Plate Uniformity and Signal Variability Assessment, which tested for signal separation, drift and edge effects. When comparing the ROCKi protocol to the small colony protocol, it was found ROCKi caused a shift in the IC50 from 1.34e-3 to 1.45e-4 M. In addition, hESC morphology was altered with ROCKi treatment, which appeared to stress the cells, while cells in the small colony protocol appeared healthier, tightly packed, and cobblestone-like. Both protocols allow the MTT assay to be carried out rapidly and accurately with high reproducibility between replicate experiments using hESC.

**PS 1211 Differential Regulation of Pluripotency Maintenance and Differentiation Genes in Undifferentiated Human Embryonic Stem Cells (hESC) Exposed to Methyl Parathion (MP) and Its Active Metabolite Methyl Paraaxon (MPO).**

J. W. Sekowski and J. S. Madren-Whalley. *ECBC, US Army RDECOM, Gunpowder, MD.*

Given their wide spread use, ease of procurement, and potential for serious health consequences if deployed by terrorists, toxic industrial chemicals (TICs) represent a real threat to warfighters and civilians at home and abroad. Unfortunately, for a vast number of TICs, including the widely-used organophosphate insecticide, MP, there is incomplete knowledge regarding the basic molecular consequences of exposure in humans. Although the literature suggests diverse toxicological consequences for MP exposure during early fetal development, it is primarily based on human epidemiological studies, in vivo animal studies, or in vitro studies using immortal, transformed cell lines. Furthermore, the relative contribution and the molecular mechanism(s) of action of the parent compound, MP, versus the active metabolite, MPO, has not yet been elucidated in an early developmental system. In an in vivo model, the MP is converted by hepatic and extra hepatic phase I and II metabolism to MPO, and the relative ratios can vary depending on the in vivo system. Given that undifferentiated hESCs do not produce the enzymes necessary to carry out the conversion of MP to MPO, they provide a unique opportunity to examine the individual influence of the parent and active metabolite on molecular pathways influencing very early human development.

In this study we compared the expression of 84 genes known to be important in the maintenance of pluripotency and differentiation in hESCs cells following a 24 hour exposure of cells to either MP or MPO. These RT-PCR data indicate several key differences in the expression of genes following exposure to MP and MPO. The results of this study have opened a new avenue toward understanding how MP and its active metabolite MPO specifically interfere with some of the earliest steps in human embryonic development.

**PS 1212 IQ-PSLG Nonclinical to Clinical Translational Safety Database Initiative.**

T. Monticello<sup>1</sup>, V. Kadambi<sup>2</sup>, M. Graziano<sup>3</sup>, M. Sommer<sup>4</sup>, K. Blanchard<sup>5</sup>, Q. Zhu<sup>5</sup> and M. Liu<sup>6</sup>. <sup>1</sup>Angen, Thousand Oaks, CA; <sup>2</sup>Millennium: The Takeda Oncology Company, Cambridge, MA; <sup>3</sup>Bristol-Myers Squibb, Princeton, NJ; <sup>4</sup>Pfizer, Groton, CT; <sup>5</sup>Boehringer Ingelheim, Ridgefield, CT; <sup>6</sup>IQ, Washington DC.

The International Consortium for Innovation and Quality in Pharmaceutical Development (IQ) is a science-focused organization of pharmaceutical and biotechnology companies. The mission of the Preclinical Safety Leadership Group (PSLG) of the IQ is to advance science-based standards for nonclinical development of pharmaceutical products and to promote high quality and effective non-clinical safety testing and human risk assessment. The IQ-PSLG is creating an industry-wide database to determine accuracy with which the interpretation of nonclinical safety assessments in animal models correctly predicts human risk in the early clinical development of biopharmaceuticals. This initiative aligns with the 2011 FDA strategic plan to advance regulatory science and modernize toxicology to enhance product safety. Eighteen member companies will contribute datasets from over 150 molecules. Though similar in concept to the initial industry-wide concordance dataset conducted by HESI/ILSI (Olson, et al. 2000 Reg Tox Pharmacol 32:56), the IQ-PSLG database will include both large and small molecules, be contemporary (circa 2005-2011) and will proactively track concordance from recently completed Phase I clinical studies. Database details, preliminary dataset results and the individual queries to be mined from the dataset will be presented. In summary, the output from this work will help identify actual human and animal adverse event data to define both the reliability and potential limitations of nonclinical data and testing paradigms in predicting human safety in Phase I clinical trials.

**PS 1213 Target Organ Toxicities in Studies Conducted to Support First Time in Human Dosing: An Analysis across Species and Therapy Areas.**

R. Roberts, D. Ryan, R. Callander, K. Stamp, S. Horner and S. Robinson. *Global Safety Assessment, AstraZeneca, Macclesfield, United Kingdom.*

Before a new chemical entity can enter human clinical trials, safety and tolerability must be assessed in non-clinical rodent and non-rodent toxicology studies. We conducted an analysis of target organ toxicities identified for 77 AstraZeneca candidate drugs (CDs) in these studies across a range of therapy areas and targets. Our analysis showed that in the rodent, the most frequently affected organ was the liver followed by the adrenal glands, kidney, spleen, bone marrow and thymus. In the non-rodent, the liver and thymus were the most frequently affected organs, followed closely by the testis and GI tract. This pattern was largely similar across intended therapy areas with the exception of oncology and infection where a larger range of organs was affected with higher incidences for adrenal glands, femur, spleen and thymus. Of those CDs for which no target organ toxicity was seen in one or both pre-clinical species, the majority were from the CNS/pain therapy area. Another important consideration is the need for a second species in toxicology testing. For the 75 CDs where both rodent and non-rodent studies were conducted, 1 or more new target organs were identified in rodents for 52 CDs (69%) and 1 or more new target organs were identified in non-rodents for 40 CDs (53%). Notably, the changes seen only in non-rodents included tissues of high relevance for human risk assessment such as the male reproductive tissues. There was only a single CD in our data set for which the target organ profile was identical in both preclinical species. In summary, our data show that liver, thymus, adrenal gland, spleen, kidney, bone marrow and lymph nodes are the most frequent target organs in preclinical studies. This profile is largely similar across therapy areas except for oncology and infection CDs, where a higher incidence of target organ toxicities across a wider range of organs was seen. The data additionally demonstrate the value of a second species in toxicity testing to support human safety.

**PS 1214 Quantitative Protein Expression Profiling of HepG2 Cells Treated with Compounds Implicated in Drug-Induced Liver Injury (DILI).**

A. Tavendale, C. Vazquez-Martin, D. Lamont and P. Ajuh. *Dundee Cell Products Ltd., Dundee, United Kingdom.* Sponsor: C. Elcombe.

Drug induced liver injury (DILI) is the single most common reason for removing approved drugs from the market, or issuing warnings and modifications of use. However, there is little knowledge of the key cellular mechanisms at the molecular level that underlie DILI. Insight into these mechanisms and the cellular pathways involved will enable the design of predictive assays to remove compounds that pose a toxicity risk early on in the drug discovery and development process.

In this study, we used a "toxicoproteomics" approach and SILAC (Stable Isotope Labeling with Amino acids in Cell culture) to study the changes in the proteome of the human hepatocellular carcinoma cell line HepG2 following treatment with a set of seven compounds (Labetalol, Nicotinic Acid, Diclofenac, Amoxicillin, Cefaclor, Rifampin and Tacrine) previously reported to be involved in DILI. We identified over 4,000 proteins by high-resolution mass spectrometry with a false discovery rate of 1%. We used MaxQuant software for protein identification and the quantitative analysis of data from mass spectrometry and DAVID Bio-informatics - GO (gene ontology) analysis tools to determine protein changes and biological processes/pathways affected by the treatment of cells with the drugs. Our results indicate that the levels of some enzymes with potential effects in drug toxicity were reduced when treated with the compounds. These include carnitine O-acyltransferase activity (involved in the metabolism of fatty acids), nucleotide-excision repair (DNA repair function) and Glutathione S-transferase A1 (detoxification of electrophilic compounds). Biological processes generally affected as determined by the GO analysis include the response to metal ion and nitrogen compound biosynthetic processes. These results provide further insight into possible cellular mechanism(s) linked to the toxic activities of the drugs analysed. Undoubtedly, quantitative proteomics could play a pivotal role in deciphering toxicity mechanisms at the molecular level.

**PS 1215 Demonstration of a Unique *In Vitro* to *In Vivo* to Clinical Correlation of Drug-Induced Phototoxicity.**

T. Su, P. Stetsko, J. Gong, W. Washburn, S. C. Griffen and T. Reilly. *Research & Development, Bristol-Myers Squibb, New Brunswick, Hopewell, and Lawrenceville, NJ.*

Drug-induced phototoxicity, which occurs when undesirable effects are elicited after exposure of the skin or eyes to ultraviolet (UV) light, has been an impediment to therapeutic use of a variety of drugs and can negatively impact pharmaceutical research and development. Moreover, proposed screening strategies often over predict in vivo hazards. Herein we report an example where in vitro data not only predicts in vivo animal effects but these effects are further translated to humans. As part of the toxicologic evaluation of a drug candidate for obesity, BMS-819881 ('881) absorbed UV light in the 290-310 nm range and was thus screened in an in vitro mouse fibroblast 3T3 cell assay. The compound had a phototoxicity factor  $\geq 18$  ( $>5$  indicates phototoxic potential). In a subsequent rat tissue distribution assay, '881 and its metabolites were found to distribute to the skin. In a definitive single-dose study in pigmented Long-Evans rats, '881 (given as a prodrug) induced various degrees of erythema, edema and/or flaking of the skin in a dose-dependent fashion after exposing to UV light at  $\geq 150$  mg/kg [AUC<sub>0-24h</sub>  $\geq 327$   $\mu\text{g}\cdot\text{h}/\text{mL}$ , C<sub>max</sub>  $\geq 21.7$   $\mu\text{g}/\text{mL}$ ; 5x margin to clinical exposures at 600 mg in a multiple ascending dose (MAD) study]. To investigate its potential mechanism of phototoxicity, '881 was tested for photostability and reactive oxygen species (ROS) production, a common causation for photosensitivity. BMS-819881 and its ketone metabolite were photolabile ( $\leq 85\%$  degraded) resulting in substantial production of singlet oxygen after exposure to UV light. Furthermore, in a 4-week MAD trial with '881 (given as a prodrug at  $\leq 600$  mg) in obese subjects, symptoms consistent with photosensitivity reactions (eg, sustained redness and itching) were reported in a dose-dependent manner. These data support a unique nonclinical prediction of clinical photosensitivity and suggest the potential added utility of photostability and ROS production assays in phototoxicity testing, at least in some circumstances.

**PS 1216 Preclinical Profiling and Computational Differentiation of Human Vascular Response to 95 Drugs Using Next-Gen RNAseq Transcriptomics.**

R. Figler, M. J. Lawson, A. J. Mackey, E. L. Berzin, J. C. Anstey, P. D. Schoppe-Bortz, R. W. Tilghman, B. R. Blackman and B. R. Wamhoff. *HemoShear, LLC, Charlottesville, VA.* Sponsor: A. Dash.

**BACKGROUND:** The ability to de-risk and validate preclinical compounds for on- or off-target vascular response is critical for drug development. Animal models and static cell culture systems are poor predictors of the human response. METH-ODS: We have established a human primary vascular endothelial and smooth muscle cell co-culture system which recapitulates hemodynamic forces and restores cell biology and responsiveness to drugs at physiologically relevant levels. We assayed 95 clinically relevant drugs at concentrations consistent with plasma levels following therapeutic dosing. Therapeutic areas included: dyslipidemia, inflammation, depression, diabetes, hypertension, thrombosis, and obesity, among others. Using RNAseq, we profiled the transcriptional responses observed in both cell types, across 5 biological replicates, to each drug versus its vehicle control. **RESULTS:**

Our analysis detected and corrected for small but persistent batch effects related to sample processing and employed multi-dimensional methods for differential statistics in >1000 samples. Each transcriptomic drug response profile differentiates drug-specific on- and off-target activities between cell types, within drug classes, and between drug classes, as well as estimating relative molecular pathway activity between drugs within a class. For example, preliminary analysis of TZD-class responses ranked the on-target "insulin receptor signaling pathway" for pioglitazone at 6th, but rosiglitazone at 159th, and troglitazone at 259th, while off-target "cancer" and "cell remodeling" pathways dominated the top 10 signaling pathways for troglitazone and rosiglitazone, consistent with clinical history of these drugs. **CONCLUSIONS:** Methods combining human-relevant systems with mining drug-specific profiles in conjunction with external drug annotation databases (FDA's AERS, Altman's OFFSIDES, EPA's ToxCast, Broad's Connectivity Map) serves to enhance ability to make broader human vascular drug response predictions.

**PS 1217 Towards a Platform of BAC-GFP Transgenomics-Based Pathway of Toxicity Reporters for Automated High-Content Imaging-Based Chemical Safety Assessment.**

S. Wink, B. Herpers, S. Hiemstra and B. van de Water. *Toxicology, LACDR, Leiden, Netherlands.*

Adaptive cellular stress responses are paramount in the healthy control of cell and tissue homeostasis after cell injury during hypoxia, oxidative stress or unanticipated side-effect of medications and other chemical exposures. Genome-wide transcriptomics analysis has revealed the detailed cellular stress response landscape and thereby the diversities of organelles and cell functions that are being affected upon exposure to diverse chemicals. Individual toxicological relevant stress responses have also been termed pathways of toxicity (PoT). We find that activation of PoT occur well before the typical ultimate outcome of chemical cell injury: cell death by necrosis or apoptosis. Understanding the activation of PoT caused by chemicals is complex because many simultaneous biochemical cellular perturbations may occur thereby affecting different PoT in parallel or a defined order. To increase our understanding of chemically-induced PoT activation and its contribution to safety assessment we believe that a time-resolved, sensitive and multiplex readout of chemical-induced toxicological relevant PoT will be essential.

For that purpose, we are currently developing a automated live-cell high-content imaging-based platform containing a panel of distinct PoT reporter cell lines. To conserve the endogenous regulation we tag selected target genes with GFP using BAC-transgene-omics approaches. So far we have generated 23 different human hepatoma HepG2 reporter cell lines that define autophagy, mitochondrial organization, Golgi structure, nucleosomes, ER morphology and stress, oxidative stress response and DNA damage responses.

Here we report the current status of our BAC-GFP PoT reporter platform and demonstrate that individual reporter cell lines are sensitive to their corresponding model stress responses. We anticipate that ultimately a phenotypic PoT profiling platform will allow a high throughput and time-resolved classification of chemical-induced stress responses in the safety assessment of chemicals.

**PS 1218 High-Throughput Respirometric Assay Identifies Predictive Toxicophore of Mitochondrial Injury.**

L. P. Wills<sup>2</sup>, G. Beeson<sup>1,2</sup>, R. Trager<sup>1</sup>, C. Lindsey<sup>1</sup>, Y. Peterson<sup>1</sup>, C. Beeson<sup>1,2</sup> and R. G. Schnellmann<sup>1</sup>. <sup>1</sup>Medical University of South Carolina, Charleston, SC; <sup>2</sup>MitoHealth, Charleston, SC.

Many environmental chemicals and drugs negatively affect human health through deleterious effects on mitochondrial function. Currently there is no chemical library of mitochondrial toxicants, and no reliable methods for predicting mitochondrial toxicity. We hypothesized that discrete toxicophores defined by distinct chemical entities can identify previously unknown and future mitochondrial toxicants. We used a respirometric assay to screen 1760 compounds (5  $\mu$ M) from the LOPAC and ChemBridge DIVERSet libraries. Thirty-one of the assayed compounds decreased uncoupled respiration, a stress test for mitochondrial dysfunction, prior to a decrease in cell viability and were toxic to isolated mitochondria. The mitochondrial toxicants were grouped by chemical similarity and two clusters containing four compounds each were identified. Cheminformatic analysis of one of the clusters identified previously uncharacterized mitochondrial toxicants from the ChemBridge DIVERSet. This approach will enable the identification of mitochondrial toxicants and advance the prediction of mitochondrial toxicity for both drug discovery and risk assessment. This project was funded through grant numbers GM084147, F32 ES020103-01, and 2R44-ES019378-02.

**PS 1219 Nonclinical Toxicology Profiling of the First-In-Class Sodium-Glucose Co-Transporter 2 (SGLT2) Inhibitor Dapagliflozin.**

M. Tirmenstein<sup>1</sup>, A. Bergholm<sup>2</sup>, E. Janovitz<sup>1</sup>, D. Hagan<sup>1</sup>, J. Whaley<sup>1</sup> and T. Reilly<sup>1</sup>. <sup>1</sup>Bristol-Myers Squibb Research & Development, Princeton, NJ; <sup>2</sup>AstraZeneca Research & Development, Mölndal, Sweden.

Dapagliflozin (Dapa) is a novel SGLT2 inhibitor that directly increases urinary glucose excretion as a mechanism for treating diabetes. To support its safe use during clinical development, Dapa was evaluated in a rigorous battery of in vitro and in vivo nonclinical safety studies. In vitro screening of >300 diverse targets indicated no significant off-target activities for Dapa or its primary metabolite. The complete set of in vivo safety studies included dosing up to 12-months in dogs and a lifetime (~2 years) in mice and rats. As expected, most of the effects were related to Dapa-induced pharmacology (i.e. SGLT2 inhibition) such as glucosuria with osmotic diuresis and mild loss of electrolytes, and limited body-weight gains despite increased food consumption. At extremely high doses, Dapa also caused intestinal glucose malabsorption. This effect only occurred in rats at extremely high doses (> 2000x clinical exposures) and was related to increased intestinal calcium absorption, a consequence of exacerbated carbohydrate fermentation in the rodent gut related to SGLT1 inhibition, which ultimately contributed to thickened trabeculae in long bones and soft tissue mineralization. Of particular importance, chronic Dapa treatment at >600x clinical exposures did not result in hyperplasia or any adverse effect on the kidneys or urinary tract nor at > 100x clinical exposures any increases in the incidence of or shortening in the latency period for tumor development. There was also no indication that SGLT2-/- mice had adverse urinary tract morphology or function when compared to their wild type counterparts in a 15-month observational study. Thus, the pharmacologic activity of Dapa in nonclinical species and the rigorous attempts to test supra- and off-target pharmacology allowed us to thoroughly evaluate its potential toxicity profile, providing us with confidence in its safety in patients with diabetes.

**PS 1220 Bone Assessments in Enhanced Pre-Postnatal Toxicity Study in Pregnant Cynomolgus Monkeys with up to 6-Months Postnatal Evaluation.**

A. Varela<sup>1</sup>, S. Y. Smith<sup>1</sup> and G. Chellman<sup>2</sup>. <sup>1</sup>Bone Research, Charles River, Montréal, QC, Canada; <sup>2</sup>Charles River, Reno, NV. Sponsor: M. Vézina.

Assessment of potential test article-related bone liability is becoming increasingly important, not only in the mature skeleton but also in the developing skeleton. Skeletal assessments were developed to evaluate potential liability in pregnant monkeys and offspring in an enhanced pre postnatal development (ePPND) toxicity study. Assessment in mothers during gestation and lactation included bone markers C-telopeptide (CTx), tartrate-resistant acid phosphatase active isoform 5b (TRAP5b), osteocalcin (OC), and bone specific alkaline phosphatase (bALP). In infants, assessment included bone markers, radiology, ex vivo bone densitometry (pQCT) and biomechanical testing.

Control mothers had generally high values of bone markers during early pregnancy and lactation. At GD20, most had OC levels above the upper limit of quantification then decreased at other time points during gestation, and increased during lactation. bALP and CTx increased at the end of the gestation and during lactation. TRAP-5b increased during pregnancy but decreased during lactation. In control infants, OC, bALP and TRAP-5b were increased up to 2, 4 or 10 fold, respectively, compared to historical data for 3-4 year-old animals. Radiographs were evaluated for skeletal abnormalities and bone length: age-related changes in epiphyseal mineralization, growth plate morphology, and increases in bone length were noted over time. Femur and lumbar vertebra geometry (pQCT) changed with increasing age with lower increases in density. Femur 3-point bending and vertebral compression showed increases in strength parameters with age (2-fold between BD1 and BD 180).

Skeletal changes were consistent with gestation and lactation in mothers, and with development and growth in infants. These data support the use of bone markers, densitometry, radiology, and biomechanical testing in toxicology studies, including ePPND studies, to provide a comprehensive evaluation of the maternal and developing skeleton in nonclinical drug development.

**PS 1221 Characterization of Batracylin-Induced Renal and Bladder Toxicity in Rats.**

L. Rausch<sup>1</sup>, D. Bunin<sup>1</sup>, K. Altera<sup>1</sup>, S. Samuelsson<sup>1</sup>, R. Kinders<sup>2</sup>, M. Davis<sup>3</sup> and T. Parman<sup>1</sup>. <sup>1</sup>SRI International, Menlo Park, CA; <sup>2</sup>SAIC-Frederick, Frederick, MD; <sup>3</sup>National Cancer Institute, Bethesda, MD.

Batracylin (NSC-320846; BAT) is an investigational anticancer agent that reached Phase I clinical trials. BAT is a dual inhibitor of DNA topoisomerases I and II and induces histone gamma-H2AX, a biomarker of DNA damage in vitro. Hemorrhagic cystitis was one of the dose limiting toxicities observed during clinical trials, and bladder and kidney were postulated to be responsible for the hematuria observed in the clinic. We investigated the mechanism of bladder and renal toxicity in Fisher 344 rats, a physiologically relevant model. The studies were designed to 1) examine the effect of BAT administration on rat bladder histology, 2) further characterize the previously reported renal toxicity of BAT, and 3) measure DNA damage in the kidney and bone marrow after BAT administration in rats using gamma-H2AX immunofluorescence. Once daily oral administration of 16 or 32 mg/kg BAT to Fisher 344 rats for 4 days caused overt toxicity. Abnormal clinical observations, adverse effects in clinical pathology, urinalysis, kidney and bladder were seen. Gamma-H2AX immunofluorescence indicated DNA damage in kidney and bone marrow. Furthermore, after administration of BAT, defects in the superficial and intermediate urothelial layers were observed using scanning electron microscopy. The maximum tolerated dose is estimated to be <16 mg/kg/day. Mesnex<sup>TM</sup> is known to reduce the incidence of hemorrhagic cystitis induced by ifosfamide or cyclophosphamide, but BAT toxicity in rats was not alleviated by twice daily intraperitoneal administrations of 80 mg/kg mesna. Thus, the mechanism of BAT-induced bladder and renal toxicity was not mediated by urotoxic mechanisms similar to those of ifosfamide or cyclophosphamide. These studies show that BAT causes renal and urothelial damage in rats that may be related to DNA damage, a previously identified mechanism of action for BAT. Work supported by NCI Contract N01-CM-42203 and N0-CM-2011-00028.

**PS 1222 NKTR-181, a Novel Opioid Agonist, Demonstrates Mu-Opioid Agonist Effects and Minimal CNS Side Effects in Both Rat and Dog.**

E. Tonkin, A. Odinecs and T. D. Sweeney. *Nektar Therapeutics, San Francisco, CA.*

NKTR-181 is a novel orally available mu-opioid agonist designed using Nektar's advanced polymer conjugate technology to achieve slower kinetics of entry into the brain relative to other opioids, while still producing analgesic efficacy. Previous studies of NKTR-181 in rodent models have demonstrated a clear separation of analgesia from unwanted CNS side effects compared with oxycodone. To assess the safety of this novel opioid, NKTR-181 was evaluated after daily oral dosing for 2 and 13 weeks in rats and dogs at doses up to 600 and 75 mg/kg/day, respectively. Clinical observations, body weights, clinical chemistry, and histopathology were performed and NKTR-181 plasma concentrations were analyzed by LC-MS/MS. Findings in both species were consistent with the pharmacology of a mu-opioid agonist; no off-target toxicity was observed. In rats, the major clinical sign was foot sores due to increased paw chewing at 200 to 600 mg/kg/day, a known opioid effect in rodents. Mild to moderate gait and activity changes were noted at 600 mg/kg/day in a neurobehavioral assessment in the 2-week study. The incidence of clinical findings diminished with repeated dosing. Decreased mean body weights relative to controls was observed in males at ≥200 mg/kg/day and in females at 600 mg/kg/day. In dogs, major clinical signs were post-dose emesis at doses ≥15 mg/kg/day and mild, transient hypoactivity at 75 mg/kg/day. Accommodation to both emesis and hypoactivity was observed. Decreased mean body weights relative to controls were observed at 75 mg/kg/day in the 13-week study. No adverse clinical pathology or histopathological changes were noted in the rat or the dog. The NOAEL was determined to be 200 mg/kg in rats and 75 mg/kg in dogs (human equivalent doses of 32 and 42 mg/kg, respectively). Plasma levels (AUC) at the NOAEL after 13 weeks of dosing were 170,034 hr\*ng/mL in rats and 33,026 hr\*ng/mL in dogs. These studies demonstrate that NKTR-181 is well tolerated and produces minimal CNS side effects in both rat and dog.

**PS 1223 Safety Assessment of NU100 in a 6-Month Cynomolgus Monkey Study.**

H. Hu<sup>1</sup>, V. Tammara<sup>2</sup>, D. Hobson<sup>3</sup>, E. Shaw<sup>2</sup>, D. Zeng<sup>2</sup> and A. M. Brooks<sup>1</sup>. <sup>1</sup>Covance Laboratories Inc., Madison, WI; <sup>2</sup>Nuron Biotech Inc., Exton, PA; <sup>3</sup>LoneStar PharTox LLC, Boene, TX.

NU100 is recombinant human interferon beta-1b (IFN beta-1b) being developed for treating multiple sclerosis. NU100 has a better purity profile (aggregate-free and HAS free) compared to other marketed products. A GLP monkey study for NU100

safety assessment was conducted which was originally planned as a 6-month subcutaneous injection study with a 28-day recovery. Male and female cynomolgus monkeys were assigned to 5 groups (4 or 6 animals/sex/group), and were dosed once daily or every other day with NU100, Betaferon and placebo at dose levels of 0, 0.01, 0.06, or 0.28 mg/kg/dose. Animals were monitored clinically, and blood samples were collected for evaluation of serum levels of IFN beta-1b, neopterin (a biomarker for IFN beta-1b pharmacodynamics), and anti-drug antibodies (ADA). No NU-100-related adverse clinical findings were noted during the study. IFN-beta-1b serum concentration peaked in circulation within 2 to 4 hours after administration of NU100 on Days 1 and 15 with a higher level on Day 15; however, by Weeks 18 and 22, IFN beta-1b level returned to the baseline levels. Similarly, neopterin concentrations increased on Day 1 following administration of NU100 in a dose-dependent manner. Mean predose neopterin concentrations remained slightly elevated on Day 15 compared with Day 1 baseline levels. Nevertheless, no further induction of neopterin was noted on Day 15. By Weeks 18 and 22, neopterin concentrations returned to predose levels. At week 2, 12.5% animals treated with NU100 and 37.5% treated with Betaferon were confirmed positive for ADA. All NU100 treated primates were confirmed positive for ADA at weeks 2, 4, 8, 12, and 18 during the study. Due to the loss of IFN-beta-1b activity resulting from the generation of anti-IFN beta-1b antibodies, the dosing phase of the monkey study was terminated one month earlier than planned, following discussion with and approval from the FDA. In conclusion, NU100 was well tolerated by monkeys in this chronic toxicology study.

**PS 1224 BPM31510 Is a Novel Regulator of Mitochondrial Function That Mitigates/Rescues Drug-Induced Toxicity—Evidence in Drug-Induced Cardiotoxicity and Cancer Chemotherapy Using *In Vitro* and *In Vivo* Models.**

R. Sarangarajan<sup>1,2,3</sup>, T. Walshe<sup>2</sup>, A. Lee<sup>2</sup>, R. Ouro-djubo<sup>2</sup>, L. M. Mauro<sup>4</sup>, V. Vishnudas<sup>1,2</sup>, J. J. Jimenez<sup>4</sup> and N. R. Narain<sup>1,2,3</sup>. <sup>1</sup>Berg Pharma LLC, Natick, MA; <sup>2</sup>Berg Biosystems, Natick, MA; <sup>3</sup>Berg Diagnostics, Natick, MA; <sup>4</sup>University of Miami, Miller School of Medicine, Miami, FL.

In a large cohort of drugs routinely used in clinical practice, disruption of mitochondrial function represents a common thread associated with incidence of organ specific toxicities. An example is the incidence of cardiotoxicity associated with anti-diabetic drugs, cancer chemotherapeutics and anti-retroviral agents. Ubidecarenone is a mitochondrial resident molecule with multiple functionalities including electron transport and generation of ATP. The delivery of ubidecarenone to the mitochondria is a challenge due to its physiochemical properties. BPM31510 is a nanodispersion formulation containing ubidecarenone incorporated into a novel lipid mixture with improved ability to deliver ubidecarenone with ability to influence mitochondrial function. The effect of BPM31510 on the toxicity profiles of several cancer chemotherapeutic agents was tested in cell cultures and animal models of cancer and on the cardiotoxicity potential of an anti-diabetic drug in primary cultures of normal human cardiomyocytes. BPM31510 significantly enhanced the efficacy of multiple chemotherapeutic agents used for treatment of cancers of the pancreas, prostate, breast and colon in in-vitro and in-vivo models. In addition, BPM31510 mitigated chemotherapy induced toxicity in primary cultures of normal human liver, fibroblast and prostate cells. Furthermore, BPM31510 reversed mitochondrial dysfunction resulting from exposure to an anti-diabetic drug. BPM31510 represents a novel technology effectuating a multimodal physiological response in which it does not interfere with the normal therapeutic mechanism of action of chemotherapy drugs, yet confers protection to normal tissues. BPM31510 is currently in clinical trial as a mono-therapy for solid-tumors with no reported adverse effects.

**PS 1225 Etirinotecan Pegol Nonclinical Toxicology Studies Establish a Margin of Safety to Support an Every Three-Week Clinical Dosing Schedule.**

T. D. Sweeney, E. Tonkin, U. Hoch and C. Ji. *Nektar Therapeutics, San Francisco, CA.*

Background: Etirinotecan pegol, formerly NKTR-102, is a unique targeted topoisomerase I inhibitor designed for prolonged tumor cell exposure. Etirinotecan pegol has demonstrated a favorable tolerability profile in nonclinical and clinical studies with improved safety over irinotecan. Toxicology studies were conducted in dogs to further evaluate etirinotecan pegol safety and establish dose-related toxicities. Methods: Etirinotecan pegol was administered as an IV infusion to dogs for 3 months using a q14d schedule at doses up to 30 mg/kg (600 mg/m<sup>2</sup>) irinotecan equivalents. Direct comparison to irinotecan was evaluated in dogs using a q7dx4 schedule (Persson et al, 2008). Clinical observations, clinical chemistry, and histopathology were performed and toxicokinetic samples were collected and assayed by LC-MS/MS for etirinotecan pegol, irinotecan, SN38, SN38-Glucuronide,

and APC. Results: Etririnecan pegol-treated dogs (25 mg/kg, 500 mg/m<sup>2</sup>) had reduced neutropenia and diarrhea and no mortality compared to irinotecan-treated animals at the same dose when given q7dx4. When given q14d for 3 months, etirinecan pegol-treated dogs (30 mg/kg, 600 mg/m<sup>2</sup>) had no neutropenia and minimal diarrhea at SN38 exposure levels up to 5-fold above those in patients given 145 mg/m<sup>2</sup> etirinecan pegol on a q21d schedule. Body weight gain suppression and decreased food intake were the primary side effects observed at this etirinecan pegol dose and schedule. No test-article related alopecia was noted in animals treated with etirinecan pegol in any of the toxicology studies in contrast to literature reports of alopecia in both humans and in animals treated with irinotecan. Conclusions: Nonclinical toxicology studies show that etirinecan pegol produces markedly less neutropenia and diarrhea with no mortality when directly compared to irinotecan. Etririnecan pegol is well-tolerated for 3 months at doses that provide a good safety margin (based on SN38 exposure) to support a clinical regimen of 145 mg/m<sup>2</sup> given every 3 weeks.

**PS 1226 Transient Thrombocytopenia without Coagulopathy in Rats following Single IV Bolus of Oxycyte®, a Perfluorocarbon (Pfc) Based Oxygen Carrier.**

S. Anderson<sup>1</sup>, L. Bernard<sup>2</sup>, J. Szabo<sup>2</sup> and T. Bradshaw<sup>1</sup>. <sup>1</sup>*Oxygen Biotherapeutics, Morrisville, NC;* <sup>2</sup>*Ricerca Biosciences, Concord, OH.*

Oxycyte®, a 60% w/v perfluoro(t-butylcyclohexane)[FtBu] intravenous emulsion, is being developed for treatment of traumatic brain injury (TBI). Transient thrombocytopenia (TTP), a known class effect of PFCs, may pose a risk for TBI patients. A rat model of intracranial hemorrhage (ICH) is under development to ascertain whether TTP subsequent to Oxycyte administration exacerbates ICH and whether platelet transfusion will ameliorate TTP associated ICH. As part of model development, studies were conducted to determine hematology, coagulation, cytokine, and PK profiles following Oxycyte administration. Male rats received a single IV bolus of Oxycyte at 3, 6, or 12 mL/kg. Blood was collected via jugular cannula (n=3/group) at 10 post administration time points and analyzed for FtBu concentration. Additional rats (n=5/group/time point) were sacrificed on Study Days (SD) 2, 3, 4, 5, 7, 10, 14, and 30 for hematology and blood cytokine analyses. Blood T1/2 following 3, 6, or 12 mL/kg was 4.2, 3.9, and 6.3 hours respectively. AUC was 12- and 48-fold higher for rats receiving 6 and 12 mL/kg compared to 3 mL/kg. There was a 30-40% decrease in PLT counts on SD3-5 in rats receiving 3 or 6 but not 12 mL/kg suggesting Oxycyte-induced PLT sequestration (TTP) rather than PLT destruction. Mean platelet volumes were increased in all Oxycyte groups through SD7 with a decrease in reticulocyte (RTC) counts and elevated fibrinogen levels through SD5. Except for elevated fibrinogen concentrations, there were no significant changes in coagulation parameters. No elevations in IL-6, TNF- $\alpha$ , and IL-1 $\beta$  levels were detected. Liver and spleen weights were elevated at all time points. RTC changes were considered a pharmacologic response to Oxycyte with no concurrent changes in erythrocyte counts. Increased liver and spleen weights were expected effects due to removal of Oxycyte by the reticuloendothelial system, the known mechanism for clearing PFC particles.

**PS 1227 Immunomodulatory Activity of Orphan Drug Elmiron® in Female B6C3F1/N Mice.**

S. Thakur<sup>1</sup>, N. Abraham<sup>2</sup>, K. L. White<sup>3</sup>, M. J. Smith<sup>3</sup>, W. Auttachoat<sup>3</sup> and D. R. Germolec<sup>1</sup>. <sup>1</sup>*Division of National Toxicology Program, NIEHS, NIH, Research Triangle Park, NC;* <sup>2</sup>*Integrated Laboratory Systems, Research Triangle Park, NC;* <sup>3</sup>*Virginia Commonwealth University, Richmond, VA.*

Interstitial cystitis/painful bladder syndrome (IC/PBS) is a chronic disorder characterized by bladder discomfort and urinary urgency in absence of identifiable infection. Elmiron® (EMR; sodium pentosan polysulfate) is the only approved oral therapy for treatment of IC/PBS. Based on the lack of chronic toxicity data and potential for long term use in the treatment of IC/PBS, NTP conducted 90-day and 2-year toxicity studies for EMR. The results suggested that EMR could potentially modulate the immune system. Therefore, this study was conducted to evaluate the immunomodulatory effects of EMR when administered for 28-days via oral gavage to female B6C3F1/N mice, at doses of 63, 125, 250, 500 or 1000 mg/kg. Mice treated with EMR had a significant increase in absolute liver weights (500 and 1000 mg/kg). The absolute numbers of splenic macrophages (63, 500 and 1000 mg/kg) and natural killer (NK) cells (250 and 1000 mg/kg) were significantly increased. EMR treatment did not affect the humoral immune response (antigen specific antibody response to sheep red blood cells [SRBC]) or cell-mediated immunity (mixed leukocyte response). However, innate immune responses such as phagocytosis of radiolabelled SRBC by liver macrophages (1000 mg/kg) and NK

cell activity were enhanced (500 and 1000 mg/kg). Further analysis using a disease resistance model showed that EMR-treated mice demonstrated significantly increased anti-tumor activity against B16F10 melanoma cells at the 500 and 1000 mg/kg doses, where the numbers of tumor nodules were decreased by 55% and 68%, respectively. Collectively, we conclude that EMR administration stimulates the immune system, increasing numbers of specific cell populations and enhancing phagocytosis and NK cell activity in female B6C3F1/N mice.

**PS 1228 Assessment of Long-Term Preclinical Safety of Inhaled Technosphere® Particles and Afrezza® Inhalation Powder.**

S. Greene<sup>1</sup>, K. Nikula<sup>2</sup>, D. Poulin<sup>3</sup>, K. McNally<sup>4</sup> and J. Reynolds<sup>5</sup>. <sup>1</sup>*MannKind Corp, Valencia, CA;* <sup>2</sup>*Seventh Wave Laboratories, Chesterfield, MO;* <sup>3</sup>*Charles River Laboratories, Montréal, QC, Canada;* <sup>4</sup>*ITR Laboratories, Montréal, QC, Canada;* <sup>5</sup>*JA Reynolds & Associates, Madison, CT.*

The inhalable insulin, AFREZZA® inhalation powder and novel excipient, FDKP (fumaryl diketopiperazine which self assembles into Technosphere® Particles), were evaluated in nonclinical safety studies for the treatment of diabetes. Daily doses of either Technosphere particles or AFREZZA inhalation powder were administered by nose-only route in chronic repeat dose and carcinogenicity studies in rats or oronasal route in dogs. With the exception of transient exaggerated pharmacological effects of insulin, inhalation administration for up to 104 weeks in rats and 39 weeks in dogs was well-tolerated. There were no adverse effects on body weight, food consumption, ophthalmoscopy, clinical pathology parameters or electrocardiography (dogs). There were no indications of carcinogenic potential or proliferation related to AFREZZA inhalation powder in pulmonary tissues by immunostaining using proliferating cell nuclear antigen assay. Non-proliferative lesions were limited to minimal goblet cell hyperplasia and eosinophilic accumulation in the olfactory/respiratory epithelium in rats; and minimal neutrophil infiltration in lung in dogs. Maximum systemic concentrations of insulin and FDKP were rapidly attained. Terminal half life was approximately 20 and 60 min for insulin and FDKP, respectively. In dogs, systemic exposure of FDKP and insulin was generally dose proportional with no sex differences or accumulation. In rats, insulin exposures were generally higher in females compared to males. Exposure to insulin was inversely related to dose-dependent decreases in serum glucose levels. Based on the data from these chronic inhalation studies, the no adverse effect level was established as the highest studied doses for AFREZZA inhalation powder and Technosphere particles in both species.

**PS 1229 NF- $\kappa$ B Activation in the Hippocampus during Multiple Subthreshold Exposures to Seizurogenic Compounds.**

J. A. Miller<sup>1</sup>, K. S. Kirkley<sup>1</sup>, Y. H. Rao<sup>2</sup>, M. Patel<sup>3</sup>, R. A. Bialecki<sup>4</sup> and R. B. Tjalkens<sup>1</sup>. <sup>1</sup>*Center for Environmental Medicine, Colorado State University, Fort Collins, CO;* <sup>2</sup>*Department of Pediatric Neurology, University of Colorado, Denver, CO;* <sup>3</sup>*Department of Pharmaceutical Sciences, University of Colorado, Denver, CO;* <sup>4</sup>*Safety Assessment, AstraZeneca, Boston, MA.*

Drug-induced seizures have been documented for broad classes of pharmaceuticals including CNS and Non-CNS targeted drugs. A better understanding of the early molecular signaling events involved in promoting seizures is necessary to identify potential proconvulsive liability of new pharmacologic agents earlier in the development process. The NF- $\kappa$ B pathway is involved in regulating a number of stress genes and its activation may conceivably be an early indicator of potential seizure liability. Presently, we employed a NF- $\kappa$ B-dependent GFP reporter mouse to investigate the role of NF- $\kappa$ B signaling in rendering hippocampal neurons hyperexcitable. Utilizing EEG recordings and video documentation we established a sub-threshold dose level of the seizurogenic compound kainic acid (KA). Transgenic reporter mice were exposed to multiple sub-threshold doses of KA and regional and cell specific NF- $\kappa$ B activity was assessed after each dose. Under control levels reporter expression was absent in the hippocampus except for a slight basal expression in the CA3 pyramidal layer. Upon multiple exposures to KA, a pronounced expression of the GFP reporter was observed in the stratum moleculare, dentate gyrus molecular layer and in the dentate hilus. Additionally we exposed reporter mice to multiple low levels of a different seizurogenic compound, pentylenetetrazole (PTZ). After multiple doses of PTZ, a global increase in GFP expression was observed. Comparison of the two compounds suggests a regionally selective expression consistent with the distinct mechanisms of action for each compound. Utilizing cultured slices from the reporter mice we observed similar selective GFP expression in response to the two compounds demonstrating the potential utility of this method for the assessment of proconvulsive properties of new pharmacologic compounds.

**PS 1230 Starting Dose Selection for First-in-Human Trials Using Model-Based Approaches.**

V. Kadambi, S. Palani, A. Lynn, J. Senn, S. Ottinger, J. Mettetal, S. Chong, E. Fedyk, W. Shyu and A. Chakravarty. *Millennium: The Takeda Oncology Company, Cambridge, MA.*

Selection of the safe starting dose (SSD) in oncology represents a critical decision point in the drug development process, as under- or over-prediction of the SSD can have serious consequences in Phase I, exposing patients to doses that are either sub-therapeutic or unsafe.

The SSD is commonly estimated by determining if 1/10th the severely toxic dose in rodents (STD10) is tolerated by non-rodents, and if so, using 1/10th of the rodent STD10 dose as the SSD. In general, the STD10 is estimated from GLP toxicology studies where relatively large numbers of animals are divided into a few dose groups to increase statistical power within a group.

Here, we propose an alternative method to estimate the STD10 based on logistic regression curve-fitting, (a standard technique for modeling binary outcomes in the clinical setting) with mortality as a binary endpoint. To this end, we simulated mortality data based on 400 different sigmoidal dose-mortality curves with a probabilistic model, and predicted STD10 by logistic regression, comparing this approach to the traditional dose-picking methodology for the same datasets. Model-predicted STD10 values outperformed the traditional method, with better accuracy (absence of downward bias) and precision relative to the true STD10. Additionally, this approach was resistant to the effect of outliers (unexplained mortality). More importantly, the superior accuracy and precision of the STD10 values determined by logistic regression could be achieved with fewer animals used in the conventional approach. A retrospective analysis of an anticancer compound currently in Phase I clinical trials demonstrated potential to narrow the gap between the human Maximum Tolerated Dose and SSD from 110-fold to 10-fold.

By using the information from all animals in a study, logistic regression curve-fitting provides the potential for a more robust and less biased SSD, while at the same time decreasing the number of animals utilized.

**PS 1231 Application of Electrorretinography (ERG) in Early Drug Development for Assessing Ocular Toxicity in Rats.**

W. W. Collette, M. Twamley, Q. Peng, S. Aguirre, W. Huang, A. Saccaan and A. John-Baptiste. *Worldwide Safety Sciences, Pfizer Inc., La Jolla, CA.*

Retinal ocular toxicity is among the leading causes of drug development attrition in the pharmaceutical industry. Electrorretinography (ERG) is a non-invasive functional assay used to assess neuro-retinal physiological integrity by measuring the electrical responses of various retinal cell types. When applied in the pre-clinical setting, ERG may be utilized to evaluate potential ocular toxicity of drug candidates. Studies were designed to assess the sensitivity and specificity of ERG to detect ocular toxicity in Wistar Han rats using several drugs with varied activity in the retina ranging from no evidence to those with demonstrated microscopic retinal degeneration. To directly assess the utility of ERG, these studies were conducted following a single intravitreal injection (IVT). Doses were selected based on an in-vitro retinal pigment epithelium (RPE) cytotoxicity assay and compound solubility limit. Serial collections of ERG assessments were conducted over a two week period. In addition, EDTA blood samples were obtained for miRNA retinal toxicity biomarker analysis, in-direct ophthalmic examinations were performed, and eyes were collected at the end of the study for histopathology evaluation. Here we report IVT administration of AG-012986 resulted in decreases in b-wave amplitude correlating with increases in plasma levels of retinal toxicity biomarkers (miR-124a and miR-183) as well as marked retinal degeneration as revealed by microscopic evaluation. By contrast, administration of vehicle or acetaminophen did not result in any changes in b-wave amplitude. This work suggests that ERG assessment of retinal toxicity following a single IVT treatment may be a sensitive and reliable screening tool in rodents to identify compounds that have a potential risk for ocular toxicity.

**PS 1232 Absolute Quantitation of Low-Abundance Protein Adducts Using a Novel Accelerator Mass Spectrometry Liquid Sample Interface.**

B. Stewart<sup>1</sup>, A. T. Thomas<sup>2</sup>, T. Ognibene<sup>2</sup>, K. W. Turteltaub<sup>1</sup> and G. Bench<sup>2</sup>. <sup>1</sup>Biosciences and Biotechnology Division, Lawrence Livermore National Laboratory, Livermore, CA; <sup>2</sup>Center for Accelerator Mass Spectrometry, Lawrence Livermore National Laboratory, Livermore, CA.

Drug characterization studies including the detection and quantitation of protein adducts arising from reactive drug metabolites provide important information about a drug candidate's potential to cause adverse reactions. Current methods for

characterizing protein adducts are limited by low sensitivity and difficulty identifying modified proteins. We report the use of a novel accelerator mass spectrometry (AMS) liquid sample interface for absolute quantitation of protein modification by <sup>14</sup>C-iodoacetamide and identification of peptide modification patterns. Competitive binding experiments showed that covalent adducts of cysteine residues in bovine serum albumin can be quantified at the attomole level in microgram-size samples of intact protein. Tryptic digestion and HPLC separation of albumin peptides followed by peptide analysis using the liquid sample interface and electrospray ionization and tandem mass spectrometry (ESI-MS/MS) showed reproducible patterns of adduct formation, with modifications localized to specific regions of the protein corresponding to regions predicted by known chemical reactivity. Measurements of whole protein adducts using the liquid sample interface were comparable to values measured by standard graphitization with AMS analysis. This technology presents an important novel method for absolute quantitation of <sup>14</sup>C-labeled proteins and peptides. Potential applications include microdosing studies using <sup>14</sup>C-labeled protein therapeutics and investigation of post-translational and chemical modifications of proteins.

**PS 1233 Evaluation of Respiratory Function in the Conscious, Nonrestrained Cynomolgus Monkey Using Respiratory Inductive Plethysmography.**

J. Le Bigot, J. Maucotel, F. El Amrani, S. Loriot, A. El Amrani, J. Legrand and R. Forster. *CiToxLAB France, Evreux, France.*

Evaluation of the potential alteration of respiratory function is mostly performed in rodents using whole body plethysmography, while cardiovascular telemetry studies are usually conducted in large animals. The purpose of the present study was to evaluate the use of respiratory inductive plethysmography (RIP) as a method that might be suitable for routine evaluation of respiratory function in primates.

Four monkeys were equipped with jacketed external telemetry devices including abdominal and thoracic belt sets (JET, DSI). Thoracic and abdominal signals were recorded and analysed using Ponemah software. After an acclimation period, animals received theophylline (100 mg/kg, p.o), clonidine (100 µg/kg, i.m) and corresponding vehicle (0.5% methylcellulose, p.o or NaCl 0.9%, i.m). Respiratory rate (RR), tidal volume (TV) and minute volume (MV) were recorded continuously over 24 hours.

Theophylline induced increases in TV, MV and RR when compared to vehicle (Emax: +55%, +118% (p < 0.01) and + 41% (p < 0.01), respectively). Clonidine produced significant decreases in TV and MV and RR (Emax: -12%, -29 % (p < 0.01) and -27% (p<0.05)).

The results demonstrate the validity of the RIP method for the assessment of respiratory function in the monkey for a long period (24 hours). These findings support the use of the RIP method for combined assessment of potential effects of drug candidates on cardiovascular and respiratory functions. The methodology could allow the integration of respiratory investigations into regulatory toxicology studies in primates. Such an approach is particularly applicable for the safety evaluation of biotechnology-derived products, for which rodents are often not applicable models.

**PS 1234 Impact of Food and Fecal Contamination on Dog Urinalysis Data.**

M. Felix, V. Allegret, N. Oleas, S. Y. Smith and F. Poitout. *Charles River, Montréal, QC, Canada.* Sponsor: *M. Vézina.*

Suspected aberrant urinalysis results were observed in dogs urinating limited urine volumes, or presenting clinical diarrhea, prompting an investigation to determine potential causes of contamination. Diet consumed and feces were identified as potential sources. Dietary effects on blood urine contents were determined using two laboratory diets: Certified Canine Chow No. 5007 and Harlan Teklan Certified 25% Lab Dog Diet (2025). Urine was collected from animals deprived of food and water, previously fed either diet during a 5 hour period as well as following an overnight collection period. Each diet was mixed with saline to mimic contamination. Five hour small urine samples collected from animals fed diet 5007, and 5007 diet-saline suspensions, both tested positive for moderate (3+) to large (4+) amounts of blood measured semi-quantitatively with urine dipsticks (Multistix 10SG, Siemens). 2025 diet-saline suspensions tested positive for traces of blood. Larger volumes and more dilute urine collected following overnight collection tested negative for blood indicating levels were below the detection threshold. The effect of fecal contamination, in dogs presenting diarrhea, on several markers of kidney function was also evaluated. Varying amounts of feces, from 1 to 5 grams were added to approximately 8 mL urine to mimic contamination. Contaminated and uncontaminated samples were analyzed for N-Acetyl-B-D-glucosaminidase (NAG), Gamma-glutamyl-transferase (GGT) and protein, with values corrected for urinary creatinine concentration. Increases in kidney markers were proportional

to the amount of fecal contamination, with the highest amount of fecal contamination tested showed NAG/creatinine ratio was increased by 38 fold, GGT/creatinine ratio by 24 fold and protein/creatinine ratio by 8 fold. In conclusion, the type of diet and feces were demonstrated as sources that may impact data obtained from contaminated and/or small urine samples. Optimally, urine should be collected from dogs deprived of food but with access to water (plus a water catcher), or by cystocentesis or bladder catheterization to minimize contamination.

**PS 1235 High-Resolution Isotope Dilution (HRID) Quantitative Analysis: Metabolites in Safety Testing (MIST) Application to Diclofenac.**

J. Vrbanc<sup>1</sup>, A. Hilgers<sup>1</sup>, B. Shilliday<sup>1</sup>, T. Dubnicka<sup>1</sup>, D. Humphries<sup>2</sup> and R. Hayes<sup>2</sup>. <sup>1</sup>ADME, MPI Research, Mattawan, MI; <sup>2</sup>Analytical Sciences, MPI Research, Mattawan, MI.

During early clinical development it is important to understand the identity and amount of circulating metabolites in man. Are there human specific metabolites? Guidelines have been issued by regulatory agencies to address this question (CDER, 2008). We are interested in applying the metabolism of isotope labeled drugs [<sup>14</sup>C alone or both <sup>14</sup>C and <sup>13</sup>C] and HRID to accurately determine MIST liability in the clinic in a manner that is both rapid and not excessively expensive (e.g., involve AMS, de novo synthesis and bioanalytical method development for relevant drug metabolites). Simplicity and ruggedness are also important aspects of these efforts. This work investigated diclofenac (D). Diclofenac, [<sup>14</sup>C]D (62.7 mCi/mmol) and [<sup>13</sup>C<sub>6</sub>]D were purchased. Human hepatocytes were purchased from Life Technologies, Grand Island, NY. Incubations were conducted following Life Technologies procedures. Chromatographic separation was achieved using an Agilent 1200 HPLC system and detection of radioactivity was by an IN/US β-Ram Model 3. MS analysis was by Thermo LTQ Orbitrap Discovery MS (+ ESI). No special tuning was done for D metabolite analysis. Since the specific activity of the label was known and fixed, the amount of drug metabolite/parent drug in the incubates at 60 minutes were determined using LC-RAM. Assuming that the amounts of drug metabolites produced from [<sup>13</sup>C<sub>6</sub>]D was similar to the amount produced for the [<sup>14</sup>C<sub>6</sub>]D allowed for the construction of standard curves for all drug-related material within the limits of detection. This allowed for the quantitative analysis of drug-related material including, 4-hydroxy-D and D-glucuronide. The method resulted in acceptable linearity, sensitivity and reproducibility for all analytes. A second key concept is that using HRMS compared to MS-MS using tandem quadrupole affords considerable advantages in simplicity and ruggedness, a key objective.

**PS 1236 12-Week Intrathecal Administration Study in Port Catheterized Juvenile Cynomolgus Monkeys.**

S. H. Korte<sup>1</sup>, C. B. Rose<sup>1</sup>, M. Niehoff<sup>1</sup> and M. Butt<sup>2</sup>. <sup>1</sup>Covance Laboratories GmbH, Muenster, Germany; <sup>2</sup>Tox Path Specialists, Frederick, MD. Sponsor: G. Weinbauer.

The cynomolgus monkey is the predominant NHP species when it comes to pre-clinical safety evaluation of new medical products. Assessment of juv. toxicity within this species represents an emerging field, requiring established techniques for 12 month or younger monkeys. The objective of the study was to determine the feasibility of bi-weekly bolus delivery in an intrathecally implanted port catheter system to the juv. monkey for 12 wks and to assess the feasibility of CSF collection. Vehicle or PBS was administered to 6 implanted (between L2-L5) monkeys (8-13.5 months; ~800 g). Clinical signs, bw, neurological examinations, CSF, and clinical pathology data were obtained. Perfusion necropsy, spinal cord brain trimming and pathology were conducted. There were no indications for procedural-related clinical signs, bw development, clinical pathology or neurological findings. Increased AST was observed on day 2, most likely related to manual restraint of the animals on day 1. Necropsy confirmed the placement of the catheter tips at T11/T12 in 4/6 animals. There were no adverse effects noted at the site of the catheter in the intrathecal space and in particular, no evidence of pronounced reactions at the catheter tips. At the catheter tip, tissue reactions were consistent with those reported to occur with the placement of intrathecal catheters in multiple species (M Butt, 2011). Changes at the catheter tip included slight to minimal fibrosis, adhesion to the overlying dura, and slight compression of the spinal cord (no cord damage). Overall lumbar CSF sampling through the port was only possible in 1/6 animals. However, spinal lumbar CSF sampling under sedation using a Pencan Paed® needle proved to be successful on all occasions. Obtained CSF indicated a low level of white blood cells after surgery, and minimum of red blood cells contamination. In conclusion, lumbar intrathecal administration of juvenile cynomolgus monkeys for up to 12 wks using a surgically implanted port catheter system is considered feasible.

**PS 1237 BMS-964210, a Pegylated Bispecific Adnectintargeting EGFR and IGF-1R, Demonstrates Improved Class-Specific Toxicity Profile in Cynomolgus Monkeys.**

M. Guha<sup>1</sup>, R. W. Lange<sup>1</sup>, J. Gokemeijer<sup>2</sup>, R. White<sup>1</sup>, B. Silver<sup>2</sup>, N. Marsh<sup>2</sup>, K. Manson<sup>2</sup>, T. P. Sanderson<sup>1</sup> and R. T. Bunch<sup>1</sup>. <sup>1</sup>Drug Safety Evaluation, Bristol-Myers Squibb, Mount Vernon, IN; <sup>2</sup>Early Candidate Assessment, Adnexus, Waltham, MA.

Simultaneous modulation of epidermal growth factor receptor [EGFR] and insulin like growth factor receptor 1 [IGF-1R] signaling, as an oncology therapeutic strategy, is based on cross talk between the two signaling pathways to overcome resistance developed if only a single pathway is targeted. However, evidence of class-related adverse effects of individual anti-EGFR and anti-IGF-1R agents in humans including diarrhea, acne form skin rash and interstitial pneumonitis (EGFR-specific) and hyperglycemia, thrombocytopenia and cardiovascular toxicities (IGF-1R-specific) has emerged in clinical and non-clinical toxicity studies. In contrast to marketed anti EGFR monoclonal antibodies which bind to domain III of the extracellular portion of EGFR, BMS 964210 binds with high affinity to domain I and overlaps the EGF and TGFα binding pocket of both human and cynomolgus monkey EGFR and IGF 1R. In a 4 week intravenous (2QW) toxicology study with BMS-964210 in cynomolgus monkeys (6, 12 and 25 mg/kg), pharmacodynamic elevation of plasma biomarkers of EGFR and IGF 1R blockade (TGFα, amphiregulin, and IGF 1) were observed. Despite the generation of anti BMS 964210 antibodies, systemic exposures following first dose were dose proportional and elimination was linear. No evidence of rash, pulmonary findings, hyperglycemia or thrombocytopenia was noted, and there were no drug related deaths or effects on neurologic, respiratory, or ophthalmologic endpoints. At the highest dose, two female monkeys suffered body weight loss and dehydration that required fluid administration for 3 days. Based on the highest non-severely toxic dose (HNSTD) of 12 mg/kg, there is sufficient safety margin to the proposed clinical starting dose of 0.5 mg/kg (QW). These preliminary data suggests that BMS-964210 may have an improved tolerability profile compared to marketed anti-EGFR mAb and deserves further evaluation in clinical studies.

**PS 1238 Subcutaneous Injection Sites: Is the Quality of the Diagnosis Improved When More Than One Tissue Section Is Examined?**

J. Briffaux, C. Thuilliez, C. Clément and M. Perron Lepage. *Ricerca Biosciences SAS, St. Germain sur l'Arbresle, France.*

At our Laboratory, the microscopic examination of subcutaneous injection sites involves the evaluation of three longitudinal sections per tissue sample. We conducted a retrospective study to evaluate the relevance of the diagnoses in subcutaneous injection sites if only one section is examined.

Two rat studies and three primate studies were reviewed. All animals received saline or test item injected subcutaneously in the dorsum. At necropsy, 3 pieces, each 3 mm wide, were trimmed from each site. Piece 1 was in the middle, piece 2 lateral to it and piece 3 medial to it. The original study pathologists formulated overall diagnoses for each site, taken from evaluation of each of the 3 pieces.

One pathologist reviewed the three sections from each site with reference to the findings recorded by the original study pathologists and attributed each of the original diagnoses to the section(s) where it was observed. In each species, animals receiving saline or test item were evaluated separately. Statistical analysis was performed, comparing section 1 with the other two sections and with the original overall diagnosis.

In the rat, section 1 had a statistically significantly higher number of findings when compared to other sections, in control and treated animals. In the primate, section 1 did not differ from the other sections in control and treated animals. In both species, however, section 1 had a statistically significantly lower number of findings when compared with the original overall diagnosis.

Contrary to the results we obtained in a previous study concerning intramuscular sites, this retrospective study reveals that examination of three sections of subcutaneous injection sites improves the quality of diagnosis. For microscopic changes induced by subcutaneous injections, particularly in primates, one middle piece is not considered to be sufficiently representative of the whole site.

**PS 1239 Internal Exposure of Common Environmental Pollutants in a Chinese Population.**

S. Chen<sup>1</sup>, Y. Lei<sup>1</sup>, S. Zhang<sup>1</sup>, A. Wang<sup>2</sup> and W. Shi<sup>1</sup>. <sup>1</sup>Pharmacology & Toxicology and Biochemical Pharmaceutics, Zhejiang University, Hangzhou, China; <sup>2</sup>Hangzhou EPIE Bio-detection Technology Limited, Hangzhou, China. Sponsor: D. Thomas.

Studies indicated that exposure to environmental pollutants could increase the potential risk of human's health. Many efforts have been made to detect the environmental pollutions, but, such data cannot be of concern to ordinary people for no one knows how many environmental pollutants and at what amounts were exposed to themselves. In order to provoke the attention of public and point out the individual who is at risk mostly, it is necessary to measure the internal exposure of environmental pollutants instead of external exposure of environmental pollutants. These data can directly reflect the exposure of those pollutants to ordinary people. In present study, we measured the total urinary concentrations of eleven common pollutants in a Chinese population by GC, GC-MS, HPLC and ELISA. We found the percentage of people with detectable levels of an individual chemical ranged from 13% to 100%. Cotinine (COT) was detected in 88% of the persons (n=2100), dibutyl phthalate (DBP) was detected in 97% of the persons (n=800), the detection rate of aflatoxin (AFT) and toluene (TOL) were 85% and 13%, respectively (n=600), organophosphorus (Org-p) was detected in 49% (n=400), tartrazine (TAR) was detected in 78% (n=351), the detection rate of diethylstilbestrol (DES), methanoic acid (MA), Styrene (STY), tetrachlorodibenzo-p-dioxin (TCDD) and nonyl phenol (NP) were 100%, 100%, 96%, 32% and 21%, respectively (n=100). The 95th percentiles of COT, DBP, AFT, TOL, Org-p, TAR, DES, MA, STY, TCDD and NP were 44 ng mL<sup>-1</sup>, 9 ng mL<sup>-1</sup>, 0.73 ng mL<sup>-1</sup>, 39 ng mL<sup>-1</sup>, 0.28 ng mL<sup>-1</sup>, 33.92 ng mL<sup>-1</sup>, 22, 000 ng mL<sup>-1</sup>, 23, 000 ng mL<sup>-1</sup>, 930 ng mL<sup>-1</sup>, 1,600 ng mL<sup>-1</sup> and 0.33 ng mL<sup>-1</sup>, respectively. The present data show that people in China are widespread exposure to multiple pollutants. Therefore, in order to describe the real risk of individual, a well designed study is needed to evaluate the associations between internal exposure of those pollutants and potential adverse health consequences.

**PS 1240 Occurrence of Gaseous Pesticides and Other Hazardous Volatiles in Sea Containers Arriving in Sweden.**

G. Johanson<sup>1</sup> and U. Svedberg<sup>2</sup>. <sup>1</sup>Work Environment Toxicology, Karolinska Institute, Stockholm, Sweden; <sup>2</sup>Occupational and Environmental Medicine, Sundsvall Hospital, Sweden.

Individuals who enter containers for inspection, unloading or cleaning may be exposed to gaseous pesticides (fumigants) and other volatiles. Previous reports from Hamburg and Rotterdam, as well as a few incidents in Sweden, have raised concerns about the exposure situation in Swedish container terminals. Since systematic studies in Sweden are missing, we performed a pilot study to investigate the occurrence of hazardous volatile chemicals in import containers. Air was sampled from 101 randomly selected containers in the port of Gothenburg. Air samples were drawn without opening the containers, as they passed and briefly halted at the import inspection station, and analysed by FTIR spectrometry. One container (1%) contained detectable residues of fumigant (1 ppm carbonyl sulphide), although none was labeled as fumigant treated. As in the two previous studies, a number of other volatile chemicals were detected. The most common ones were methanol (78%) and carbon monoxide (45%), with all readings below the occupational short term excursion limits (STEL). These substances are likely degradation products from the plywood flooring as they were also detected in empty containers. Other frequently detected chemicals include hydrocarbons (unspecified, 47%) and ammonia (15%), with some readings above or well above the STELs or ceiling limits (CL). In our judgement, based on the present and two previous studies, the probability of life-threatening exposure is low. However, violations of STELs and CLs do occur, thus prolonged or repeat visits in unchecked containers may constitute a significant health hazard. In conclusion, extensive and systematic investigations of import and export containers are greatly needed as basis for risk management measures. Methods for rapid and efficient ventilation should be developed. Prior to entering it should be ensured, by adequate measurements and/or ventilation, that the container is safe.

**PS 1241 Interactions between Urinary 4-Tert-Octylphenol Levels and Metabolism Enzyme Gene Variants on Idiopathic Male Infertility.**

Y. Qin<sup>1</sup>, M. Chen<sup>1</sup>, W. Wu<sup>1</sup>, B. Xu<sup>1</sup>, G. Du<sup>1</sup>, C. Lu<sup>1</sup>, J. D. Meeker<sup>2</sup>, Z. Zhou<sup>1</sup>, Y. Xia<sup>1</sup> and X. Wang<sup>1</sup>. <sup>1</sup>Nanjing Medical University, Nanjing, China; <sup>2</sup>University of Michigan School of Public Health, Ann Arbor, MI.

Background: Octylphenol (OP) and Trichlorophenol (TCP) are the representative members of alkylphenols and chlorophenols, which act as endocrine disruptors and have effects on male reproductive function.

Objectives: We studied the interactions between 4-tert-Octylphenol (4-t-OP), 4-n-Octylphenol (4-n-OP), 2,3,4-Trichlorophenol (2,3,4-TCP), 2,4,5-Trichlorophenol (2,4,5-TCP) urinary exposure levels and polymorphisms in selected xenobiotic metabolism enzyme genes among 589 idiopathic infertile male patients and 396 controls in a Han-Chinese population.

Methods: Ultra high performance liquid chromatography-tandem mass spectrometry (UPLC-MS/MS) was used to measure alkylphenols and chlorophenols in urine. Polymorphisms were genotyped using the SNPstream platform and the Taqman method. We used likelihood ratio tests (LRT) to explore these gene-environment interactions in idiopathic male infertility, and used false discovery rate (FDR) to adjust for multiple testing.

Results: Among four phenols that were detected, we found that only exposure to 4-t-OP increased the risk of male infertility (Ptrend=1.70×10<sup>-7</sup>). The strongest interaction was between 4-t-OP and rs4918758 in CYP2C9 (Pinter=6.05×10<sup>-7</sup>). It presented a significant monotonic increase in risk estimates for male infertility with increasing 4-t-OP exposure levels among men with TC/CC genotype (low level compared with non-exposed, odds ratio (OR) =2.26, 95% confidence intervals (CI) =1.06, 4.83; high level compared with non-exposed, OR=9.22, 95% CI=2.78, 30.59; but no associations observed among men with TT genotype). We also found interactions between 4-t-OP and rs4986894 in CYP2C19, and between rs1038943 in CYP1A1, on male infertile risk (Pinter=8.09×10<sup>-7</sup>, 3.73×10<sup>-4</sup>, respectively). Conclusions: We observed notable interactions between 4-t-OP exposure and metabolism enzyme gene polymorphisms on idiopathic infertility in Han-Chinese men.

**PS 1242 Smartphone Technologies Coupled with Environmental Models Allow for Large Scale Community Outreach and Risk Assessment.**

A. J. Larkin<sup>1,2,3</sup>, S. K. Krueger<sup>3,4</sup>, D. E. Williams<sup>1,3,4</sup> and W. M. Baird<sup>1,3</sup>. <sup>1</sup>Environmental and Molecular Toxicology, Oregon State University, Corvallis, OR; <sup>2</sup>Statistics, Oregon State University, Corvallis, OR; <sup>3</sup>Superfund Research Center, Oregon State University, Corvallis, OR; <sup>4</sup>Linus Pauling Institute, Oregon State University, Corvallis, OR.

Chronic exposure to several air pollutants has been identified by the EPA as a major source of concern for human health. Environmental models have been created to predict spatial distributions of air pollutants, but are unable to account for daily travel among the general US population. Several GPS-based methods of tracking a person's movement through areas of concern have been developed, but require expensive or bulky GPS units, have limited ability to provide timely results to participants, and are dependent on user compliance. Smartphones are widely popular across all demographic groups, with more than 100 million US smartphone users. We developed iPhone and Android applications with GPS functionality to predict personal and population-wide exposures to fine particulate matter (PM<sub>2.5</sub>), coarse particulate matter (PM<sub>10</sub>), and ozone. Environmental distribution models were created using Kriging algorithms with MODIS satellite imagery and Oregon Department of Environmental Quality hourly PM<sub>2.5</sub>, PM<sub>10</sub>, humidity, ozone, and temperature measurements. Geographic locations were sampled from four smartphone devices at 30 minute intervals (n>10000 sampling events). Locations and corresponding times were sent to a database running the environmental modeling software. Predicted exposure levels, times, and locations were returned to corresponding smartphones and were anonymously added to a data set of predicted exposures collected from all participants. Personal exposure levels were presented to participants as interactive smartphone maps and graphs. Hotspot exposure sites were predicted by partitioning Oregon into 10 km<sup>2</sup> regions and mapping daily group exposure levels within each region. This project was created with open-source software and can be scaled to larger groups with minimal cost. This research was supported by NIH P42 ES014465.

**PS 1243 A High-Throughput Analytical Method for Enhanced Toxicological Studies.**

C. Y. Usenko, E. M. Robinson, E. D. Bruce and S. Usenko. *Baylor University, Waco, TX.*

Toxicology studies are moving to high-throughput methodologies, however, often times the chemical concentrations are not analyzed or verified. Historically, analytical methods capable of measuring organics in aqueous solutions (including fish water and cell media) often relied on more complicated techniques. The technique presented here has reduced 99% of the historically used sample preparation. Thereby reducing the time per sample associated with preparation from ~90 minutes to <1 minute. This technique essentially eliminates the chance for target analyte loss during sample preparation and therefore eliminates the need for surrogate standards, such as <sup>13</sup>C-labeled, which is typically used to correct for analyte loss during sample preparation. This method utilizes an innovative liquid-liquid extraction, where ~10-25 µL of cell media or water is transferred to a gas chromatography (GC) vial with 1 mL of hexane and 50 mg of sodium sulfate. Target analytes partition from the water to hexane and the water is captured by the sodium sulfate. Overall extraction efficiency is ~100%. The utility of the novel method was demonstrated with a proof of concept experiment that evaluated BDE 47 water concentrations overtime from glass and plastic (48-well plate) wells. BDE 47 concentrations measured in the glass well remained consistent over 24 hrs; however there was a rapid decrease in BDE 47 water concentrations (~80%) within the first 8 hrs in the plastic well. These results demonstrate that this method is simple and useful for both water and cell media studies and offers the ability to monitor the same well over time. Many exposures in toxicology studies start at concentrations above solubility and are used in plastic plates. While this has been an acceptable method of rapidly obtaining LC and IC50 values, it may not be an accurate representation of the actual water concentration. By accurately analyzing the concentration and determining the uptake, more accurate results may be obtained and used for risk assessment and mechanistic determinations, while adding increased study to study comparability.

**PS 1244 Evaluating High-Throughput Exposure Models with NHANES Data.**

W. Setzer and J. F. Wambaugh. *National Center for Computational Toxicology, US EPA, Research Triangle Park, NC.*

Prioritizing screening and testing for large sets of chemicals for potential risk requires rapid exposure assessment, ideally based on chemical properties that are easily measured or computed. There are currently few such approaches, but like any predictive methodology these need to be evaluated against real exposure data. We evaluated two models, "Risk Assessment, Identification and Ranking" (RAIDAR; [www.arnotresearch.com/index.html#!/page\\_RAIDAR\\_DL](http://www.arnotresearch.com/index.html#!/page_RAIDAR_DL)) and USEtox™ ([www.usetox.org](http://www.usetox.org)) against the National Health and Nutrition Examination Study (NHANES) 2005 and 2011 data on urine concentrations of xenobiotics. Using NHANES to evaluate exposure models requires addressing several issues: chemicals measured in urine need to be linked back to potential exposures, and there may be multiple relationships between parent chemicals to which people are exposed and the product chemicals measured in urine; many chemicals were below limits of quantitation for a large fraction of the sampled subjects; variation among chemicals is a function of variation of exposure, pharmacokinetic (PK) variability, and the distribution of relative times of exposure and sampling. Steady state PK assumptions and a Bayesian statistical framework were used to infer parent exposures from NHANES urine products. We further use Bayesian statistical methods to evaluate the regression of median population exposure to the parent chemicals on RAIDAR and USEtox predictions, estimated production volume, and simple indicators of household use. Household use was the single most important factor. Among those chemicals with a consumer use, median exposure was correlated with production volume, but there was little evidence of a relationship between estimated exposure and any of the predictors among chemicals with no household use. The resulting model can be used for predicting exposure potential for new chemicals, along with the uncertainty of that prediction. Refining what constitutes 'household exposure', as well as including more exposure datasets, should reduce the uncertainty of the current model. [This abstract does not necessarily reflect EPA policy.]

**PS 1245 Haematology and Erythrocyte Osmotic Fragility Indices in Domestic Chicken following Exposure to a Polyvalent Iodophorous Disinfectant in Water Treatment.**

O. I. Azeez<sup>1</sup>, A. A. Oyagbemi<sup>1</sup> and O. T. Iji<sup>2</sup>. <sup>1</sup>Department of Veterinary Physiology, Biochemistry and Pharmacology, University of Ibadan, Ibadan, Nigeria; <sup>2</sup>Federal College of Animal Health and Production Technology, Moor Plantation, Apata, Ibadan, Nigeria.

The effect of prolonged use of Iodosteryl, a polyvalent iodophorous compound, as water disinfectant, on the hematology and erythrocyte osmotic fragility of the domestic chicken was investigated. Twenty-eight adult male domestic chickens of the Nera black strain were divided into four groups of seven birds per group. Birds in groups B-D were given potable water containing 1 mL, 2 mL and 4 mL/l Iodosteryl respectively for six weeks. Group A served as the control. Blood samples were collected from each bird after six weeks and analyzed immediately. No significant changes were observed in the packed cell volume (PCV), haemoglobin (Hb), mean corpuscular volume (MCV), mean corpuscular haemoglobin (MCH), mean corpuscular haemoglobin concentration (MCHC), platelet total and differential leucocytes values. However, red blood cells (RBC) were slightly lower while erythrocyte osmotic fragility and erythrocyte sedimentation rate (ESR) was higher in those birds exposed to Iodosteryl compared with control. This study confirms that prolonged use of Iodosteryl is stressful and may lead to intravascular haemolysis as indicated by the higher erythrocyte fragility and ESR values, respectively. The damage observed, may be due to peroxidation of erythrocyte membrane lipids, proteins by generation of free radicals induced by iodine.

**PS 1246 How Inaccurate Are Serum-Lipid Unadjusted Organochlorine Levels?**

S. Koifman, C. Freire, R. J. Koifman, A. S. Rosa and P. N. Sarcinelli. *National School Public Health/ FIOCRUZ, Rio de Janeiro, Brazil.* Sponsor: E. Silbergeld.

Introduction. Organochlorine pesticides (OCs) have been banned by many countries, but they are still detected in human and animal tissues worldwide. An empiric assessment comparing serum lipid adjusted and unadjusted OC levels has been, so far, not reported in the literature. Objective. To estimate how inaccurate are lipid-unadjusted OCs serum levels compared to adjusted ones. Methods. In a survey carried out in a rural population in Brazil exposed to OCs since early 1960's, blood samples were obtained from 995 residents of both sexes and all ages. Serum concentrations of 19 OCs were determined by gas chromatography with electron-capture detection and were further adjusted by triglyceride and cholesterol content. Pearson correlation coefficients and determination coefficients (R<sup>2</sup>) of serum lipid-adjusted and unadjusted concentrations of p,p'-DDE, beta-HCH and aldrin were calculated. Results. Among male and female adults (> 14 yr.), median (1st and 3rd quartiles) of serum-lipid adjusted concentrations were, respectively: 8.32 (2.86-21.9) and 9.64 (3.45-28.9) for p,p'-DDE; 6.0 (2.08-15.4) and 6.98 (2.81-17.6) for beta-HCH; 1.89 (0.73-11.0) and 2.44 (0.77-14.1) for aldrin. Determination coefficients of serum lipid-adjusted and unadjusted OCs were R<sup>2</sup>= 0.91 for p,p'-DDE, R<sup>2</sup>= 0.90 for beta-HCH, and R<sup>2</sup>= 0.93 for aldrin. Correlation between serum lipid-adjusted and unadjusted concentrations was indeed higher for those OCs with serum levels < 50 ng/mL. Conclusion. When serum lipid content is unavailable, unadjusted OC levels can be reasonably used to estimate internal dose of these chemicals, particularly when concentrations are < 50 ng/mL.

**PS 1247 Revised Methods for Estimating Potential Re-Entry Exposure Associated with Indoor Crack and Crevice Application.**

J. H. Driver<sup>1</sup>, J. H. Ross<sup>2</sup>, S. Selim<sup>3</sup>, J. Sharp<sup>4</sup> and M. Pandian<sup>5</sup>. <sup>1</sup>risksciences.net, LLC, Manassas, VA; <sup>2</sup>risksciences.net, LLC, Sacramento, CA; <sup>3</sup>Selim & Associates, Inc., Fresno, CA; <sup>4</sup>McLaughlin Gormley King Company, Minneapolis, MN; <sup>5</sup>infoscientific.com, Inc., Henderson, NV.

Surface deposition of insecticides applied as indoor residential foggers, baseboard or perimeter sprays, spot sprays and crack-and-crevice sprays represent pathways of unintentional, and unavoidable post-application exposure of children and adults. Estimation of the magnitude of this exposure following an application event is associated with uncertainty due to many factors including 1) surface residue deposition and distribution, 2) access to and the nature of contact with treated surfaces based on time-activity patterns of residents, and 3) the role of residue removal mechanisms such as cleaning treated surfaces, pesticide degradation or redistribution, hand washing and bathing following contact. A comparative spatial deposition study was conducted involving broadcast, perimeter and crack and crevice application methods. Residues measured using a spatial grid of deposition dosimeters on floor surfaces demonstrated significantly lower residue concentrations in readily

accessible areas following crack and crevice and perimeter applications, versus broadcast treatment. Analyses of other monitoring studies support this finding. The implications of these findings are discussed for both screening-level and higher tier probabilistic post-application, residential exposure assessment. In addition to surface deposition studies, published biomonitoring data from adults and children support  $\geq 9$ -fold lower estimates of exposure for perimeter and crack and crevice applications than EPA's default of 2-3 fold lower than broadcast. We propose an alternative "random walk" algorithm to provide an alternative to professional judgment when evaluating exposure in rooms where only a fraction of the room has been treated.

**PS 1248 Derivation of Biomonitoring Equivalents for Chlorpyrifos Using a Pharmacokinetic/Pharmacodynamic Model of Oral Exposures.**

S. M. Arnold<sup>1</sup>, A. Morriss<sup>2</sup>, J. Velovitch<sup>3</sup>, D. R. Juberg<sup>3</sup>, P. Price<sup>1</sup>, C. Burns<sup>1</sup>, M. Bartels<sup>1</sup>, A. T. McCoy<sup>1</sup>, M. Aggarwal<sup>2</sup> and T. Poet<sup>4</sup>. <sup>1</sup>The Dow Chemical Company, Midland, MI; <sup>2</sup>Dow AgroSciences, Milton Park, United Kingdom; <sup>3</sup>Dow AgroSciences, Indianapolis, IN; <sup>4</sup>Battelle, Richland, WA.

Blood chlorpyrifos (CPF) and its main urinary metabolite (3,5,6-trichloro-2-pyridinol, TCPy) are often included in general population-based biomonitoring data. Methods that put human internal dose measurements in a health-risk context have been lacking. The concept of Biomonitoring Equivalents (BEs) seeks to address this shortfall. BEs incorporate pharmacokinetic models to calculate biomarker levels consistent with continuous exposure at exposure guidance values (e.g., USEPA reference doses). BEs rely upon the underlying toxicological endpoints used in setting the guidance values and reduced uncertainty factors (UFs). Here, we calculate BE values for blood CPF and urinary TCPy using a physiologically based pharmacokinetic/pharmacodynamic (PBPK/PD) model. The model allows the direct determination of CPF blood concentration associated with a 10% inhibition in red blood cell cholinesterase (RBC ChE), the USEPA regulated endpoint, for oral exposures. This model also predicts age-specific individual human variability of blood levels associated with a 10% inhibition in RBC ChE using Monte Carlo analysis, which allows determination of blood levels protective of sensitive humans. Thus, no additional UFs are required to derive the BE. The preliminary blood BE value for CPF in adults is 3.5 µg/L. This level is about 1000 fold higher than the current reported blood levels in US pregnant women. The preliminary urinary BE for TCPy is 2,000 µg/L. The 95th percentile urinary TCPy in the general US adult population was 12.4 µg/L (CDC exposure years 2001-2002). Assuming that 10% of the reported levels occur from CPF exposure (the remainder is assumed direct exposure to environmental TCPy in non-worker populations), then the BE for TCPy will also be about 1000 fold larger than current levels. These findings suggest that current US adult dietary exposures to CPF are well below levels that could cause 10% inhibition of RBC ChE.

**PS 1249 Gene Expression of sFLT1 Links Prenatal Arsenic Exposure to Increased Risk on Small for Gestational Age.**

S. Remy<sup>1,3</sup>, E. Govarts<sup>1</sup>, B. Wens<sup>1,3</sup>, L. Bruckers<sup>2</sup>, M. Paulussen<sup>1</sup>, E. Den Hond<sup>1</sup> and G. Schoeters<sup>1,3</sup>. <sup>1</sup>Flemish Institute for Technological Research (VITO), Mol, Belgium; <sup>2</sup>Hasselt University, Hasselt, Belgium; <sup>3</sup>Antwerp University, Antwerp, Belgium. Sponsor: P. Hoet.

In the Flemish Environment and Health Study (2007-2011) we aimed: 1) to explore the relationship between prenatal arsenic exposure and the resulting effect on prenatal growth, and 2) to obtain more insight in the molecular basis of these relationships. Levels of arsenic were measured in cord blood samples of 255 newborns and the transcriptome of cord blood mononuclear cells was determined by Agilent whole human genome microarrays.

Arsenic levels ranged from 0.01 to 8.20 µg/L. Logistic regression analyses showed that a higher exposure to arsenic was statistically significantly associated with an increased risk for having a Small for Gestational Age (SGA)-baby, adjusted for a priori fixed confounders and statistically significant covariates ( $p < 0.05$ ). The odds of having an SGA-baby was multiplied with 1.65 (95% CI: 1.15-2.37) for an interquartile range increase of 0.93 µg/L arsenic.

To identify gene transcripts that link prenatal arsenic exposure to increased risk on SGA, we focused on the subset of most extreme samples (i.e. a group of lowest arsenic exposure ( $n=30$ ) and a group of highest arsenic exposure ( $n=30$ )). The list of transcripts that discriminate both groups was screened for genes involved in embryonic growth regulation. As such sFLT1 (soluble fms-like tyrosine kinase-1) was detected, a protein known to inhibit placental angiogenesis. This gene was significantly higher ( $p = 0.004$ ) expressed among high exposed individuals. Moreover, 75% of SGA-babies were found to show expression levels above median.

Our data suggest that disturbed placental angiogenesis, via upregulation of sFLT1, may link prenatal arsenic exposure to increased risk on SGA.

The studies of the Flemish Center of Expertise on Environment and Health are commissioned, financed and steered by the Ministry of the Flemish Community (Department of Economics, Science and Innovation; Flemish Agency for Care and Health; and Department of Environment, Nature and Energy).

**PS 1250 Plasma Polybrominated Diphenyl Ethers (PBDEs) in Californian Women at High Risk for Birthing an Autistic Child.**

Y. Lin<sup>1</sup>, I. Hertz-Picciotto<sup>2</sup>, D. Tancredi<sup>2</sup>, I. N. Pessah<sup>1</sup> and B. Puschner<sup>1</sup>. <sup>1</sup>Department of Molecular Biosciences, School of Veterinary Medicine, University of California Davis, Davis, CA; <sup>2</sup>Department of Public Health Sciences, School of Medicine, University of California Davis, Davis, CA.

Exposure to the polybrominated diphenyl ethers flame retardants (PBDEs) is a major preventable health concern. Little is known about the extent and patterns of PBDE exposures during pregnancy, especially in populations susceptible to heritable neurodevelopmental disorders. We measured plasma PBDE levels in Californian women participating MARBLES (Markers of Autism Risk in Babies-Learning Early Signs) who are at high risk for birthing an autistic child. BDE-28, -47, -49, -52, -95, -99, -100, -136, -153, and -183 were measured using GC/MS/MS in plasma samples collected from 79 women at each trimester and at delivery (215 samples total). PBDEs were normalized to plasma volume (ng/ml) and total lipids (ng/g). The concentrations of maternal PBDEs in MARBLES were compared to data from the National Health and Nutritional Examination Survey (NHANES 2003-2004). All ten congeners were detectable in the maternal samples from MARBLES, with BDE-100 ( $0.792 \pm 0.540$  ng/ml,  $163.5 \pm 117.5$  ng/g) and BDE-47 ( $0.661 \pm 0.458$  ng/ml,  $141.1 \pm 117.6$  ng/g) contributing the highest abundance. Compared to NHANES, women enrolled in MARBLES had significantly higher mean concentrations of BDE-47 (23.9 versus 141.1 ng/g), -99 (5.51 versus 92.3 ng/g), -100 (6.06 versus 163.5 ng/g) and -153 (9.90 versus 28.7 ng/g). Plasma PBDE (ng/ml) in women 25 to 35 years of age increased during gestation, but decreased if they were older than 35 years. Because of the increase of total plasma lipids during gestation, PBDE expressed on an ng/g lipid basis decreased in all age groups with gestational stage. Fluctuations in maternal plasma PBDE levels during pregnancy illustrate the importance of gestational age and underscore the non-linear relationship between volume- and lipid-corrected PBDE concentrations.

**PS 1251 Estimation of Dietary Lead Exposure for US Children Using a New Method: Implications for the Integrated Exposure Uptake Biokinetic Model for Lead in Children.**

M. Follansbee<sup>1</sup>, M. Ballew<sup>2</sup>, J. Brown<sup>2</sup>, M. Burgess<sup>2</sup>, M. Stifelman<sup>2</sup> and B. Thayer<sup>1</sup>. <sup>1</sup>SRC, Inc., East Syracuse, NY; <sup>2</sup>US EPA, Washington DC. Sponsor: G. Diamond.

In addition to site-specific inputs, the Integrated Exposure Uptake Biokinetic Model for Lead in Children (IEUBK model) uses national defaults that are recommended when site-specific information is not available. As part of a periodic evaluation of inputs to the IEUBK model, the methodology underlying the basis for default calculations of dietary lead intake has been updated. Previously, the food consumption values in the IEUBK model were based on information reported by Pennington (1983) and the lead in food values were based on food residue data from the ongoing FDA Total Diet Study; the latter are updated periodically as new data become available from FDA.

Recent advances in methods for estimating dietary intake provide a current and scientifically sound basis to develop nationally-representative, age-group specific values for food consumption. The dietary component of NHANES, called the What We Eat in America (WWEIA) Dietary Survey, includes two 24-hour dietary recall interviews during which each respondent reports the amount of all foods they consumed during the prior day. The food consumption values (grams/day) were estimated using a non-linear mixed model developed by the National Cancer Institute (the NCI method). The NCI method uses information on meal sizes and frequency (probability) with which specific food items are consumed to estimate daily consumption rates.

The NCI method produced estimates of dietary lead intake that were 18 to 219% higher than the previously estimated values, depending on the food item. Further analysis revealed the increase in the dietary lead intake values was largely due to an increase in the estimated daily consumption values rather than higher lead concentrations in food.

**PS 1252 Using Doubly-Labeled Water Energy Data for Estimating Ventilation Rates for the Integrated Exposure Uptake Biokinetic Model for Lead in Children.**

B. Thayer<sup>1</sup>, M. Follansbee<sup>1</sup>, J. Brown<sup>2</sup>, M. Burgess<sup>2</sup> and M. Stifelman<sup>2</sup>. <sup>1</sup>SRC, Inc., East Syracuse, NY; <sup>2</sup>US EPA, Washington DC. Sponsor: G. Diamond.

The default values in the IEUBK model (Version 1.1, Build 11) are based on values reported in the Office of Air Quality Planning and Standards report (U.S. EPA, 1989) and the IEUBK Model Technical Support Document (U.S. EPA, 1994). More recent data provide a more scientifically sound basis to further develop nationally-representative, age-group specific values for ventilation rates in children. The default values in the IEUBK model were derived based on body size in combination with smoothed data from Phalen et al. (1985). EPA's (2008) Child-Specific Exposure Factors Handbook provides recommendations for long-term (> 30 days) ventilation rates that are based on the average of several studies (Arcus-Arth and Blaisdell, 2007; Brochu et al., 2006; Stifelman, 2007).

Because Arcus-Arth and Blaisdell (2007) used indirect measures of ventilation rates based on dietary and activity survey responses, it was not considered acceptable for derivation of default values for the IEUBK model. Brochu et al. (2006) and Stifelman (2007), however, were based on the doubly-labeled water (DLW) energy data from the Institute of Medicine. DLW energy data are recognized as the gold standard for energy expenditure and an improvement over ventilation estimates based on dietary recall or activity survey data.

Ventilation rate was calculated from total energy expenditure using Layton's approach as described by Stifelman (2007). The analysis was on pooled data for males and females. More detailed analysis of ventilation rates as a function of age and gender showed the estimated ventilation rates to be parallel and 7% greater in males than females. The resulting ventilation rate values are between 19-66% higher than the existing IEUBK model defaults. Because these values are derived from energy expenditure information, they provide a more scientifically defensible basis for the default values in the IEUBK model.

**PS 1253 Conducting Probabilistic Reverse Dosimetry Calculations to Estimate Exposure Concentrations from Biomarker Data—An Example of Perchlorate.**

M. B. Phillips<sup>1</sup>, C. M. Grulke<sup>1</sup>, Y. Yang<sup>2</sup>, K. Holm<sup>1</sup>, D. T. Chang<sup>1</sup>, R. Goldsmith<sup>1</sup>, R. Tornero-Velez<sup>1</sup>, C. C. Dary<sup>3</sup> and C. Tan<sup>1</sup>. <sup>1</sup>US EPA ORD NERL, Research Triangle Park, NC; <sup>2</sup>The Hammer Institutes for Health Sciences, Research Triangle Park, NC; <sup>3</sup>US EPA ORD NERL, Las Vegas, NV.

Given the growing number of population-based biomonitoring surveys, there is an escalating interest in converting biomarker measurements (chemical/metabolite concentrations) to exposure concentrations (e.g., daily dose) to help support risk assessment. The conversion involves two steps: (1) formulating a model that describes the dose-biomarker relationship (forward dosimetry); and (2) solving for the plausible doses that are consistent with observed biomarker concentrations (reverse dosimetry). The objective of this study is to use probabilistic reverse dosimetry to estimate the distribution of average daily doses of perchlorate based on the National Health and Nutrition Examination Survey (NHANES) urinary biomarker data. Perchlorate was selected for its abundance in both exposure and biomarker data. First, Monte Carlo simulations of a physiologically based pharmacokinetic (PBPK) model for perchlorate were performed to account for variability/uncertainty in exposure factors and PK. Next, the simulated exposure-biomarker relationship was used to convert urinary perchlorate concentrations to a distribution of daily doses. The conversion was conducted using a web-based tool, Probabilistic Reverse dosimetry Estimating Exposure Distribution (PROCEED), with two methods: the Exposure Conversion Factor and Discretized Bayesian methods. The means of the estimated dose distributions were comparable to average daily doses estimated using other methods (point estimates), such as food concentrations multiplied by consumption rate. Probabilistic reverse dosimetry, however, also provides the distribution of dose estimates to represent the variability/uncertainty in exposure factors and PK.

[This abstract has been cleared by the EPA but solely expresses the view of the authors]

**PS 1254 The Effect of Clothing Care Activities on Textile Formaldehyde Content.**

R. Novick, M. G. Lew, M. A. McKinley, G. L. Anderson and J. J. Keenan. ChemRisk, San Francisco, CA.

Textiles are commonly treated with formaldehyde-based finishing agents that can potentially cause allergic contact dermatitis in sensitive individuals. There is limited data on the current formaldehyde content in textiles and the potential for reduction

through clothing care activities. This study sought to provide information on the formaldehyde content in clothing specifically focusing on 100% cotton permanent press shirts and pants, a clothing category that is generally treated with formaldehyde-based resins. Textiles were purchased and tested for formaldehyde content using the Japanese method 112. Several items (~20%) exhibited measurable levels of formaldehyde (> 20 ppm). Textile samples with the greatest formaldehyde content were hand or machine washed in hot or cold water, dried on a line or in a dryer, and ironed. Ironing did not appear to affect the textile formaldehyde content. The washing and drying procedures reduced formaldehyde content between 28 and 74% compared to the control. Differences in the temperature or type of washing and drying did not result in a clear trend in the formaldehyde content data. Understanding the formaldehyde content in commercially available permanent press clothing and the potential reduction through clothing care activities may be useful for manufacturers and sensitive individuals.

**PS 1255 Exposure Associated with Power Stripping of Asbestos Containing Insulation from Electrical Cable.**

C. L. Blake<sup>1</sup>, A. Jurkowski<sup>1</sup>, G. Johnson<sup>2</sup> and R. D. Harbison<sup>2</sup>. <sup>1</sup>Bureau Veritas North America, Inc., Kennesaw, GA; <sup>2</sup>Environmental and Occupational Health, University of South Florida, Tampa, FL.

Efforts to recycle copper from electrical conductors have led to the development of specialized machines which automatically remove insulating covers from wires and cable products. In the past, certain wire and cable products were insulated using chrysotile asbestos. This research was undertaken to determine the asbestos fiber exposure risks associated with power stripping machinery to remove asbestos-containing insulation materials from electrical wire or cable. A Rigby Machinery, Inc., Model 4H electric powered wire/cable insulation stripping machine was acquired along with approximately 42 m of asbestos insulated cable. During two separate, but nearly identical, test sessions, a laborer used the wire stripper to remove the asbestos-containing insulation from the subject cable. This work took place within a closed metal building with a total interior volume of 2,500 m<sup>3</sup>. Industrial hygiene personal and area air samples were collected for airborne fibers throughout all wire stripping periods. Collected air samples were analyzed using phase contrast microscopy (PCM) and transmission microscopy (TEM). The results of analysis using PCM for personal samples (n=3) taken during periods of continuous cable stripping activity showed test period airborne fiber exposures ranging from 0.034 to 0.068 (mean 0.056 f/ml). Follow-up analysis of these personal samples using TEM indicated asbestos adjusted PCM exposures ranging from 0.017 to 0.045 (mean 0.033 f/ml). Area air samples taken at distances ranging from 2 to 9 meters from the wire stripper (n=16) showed asbestos adjusted PCM concentrations ranging from less than 0.0001 to 0.041 f/cc (mean 0.007 f/ml). The process of power stripping asbestos-containing insulation from electrical wires and cables can cause exposure to airborne asbestos fibers. However, the levels of such exposure are not expected to exceed the current day occupational exposure limits for asbestos of 0.1 f/ml as an 8-hr TWA or 1.0 f/ml averaged over a 30-minute exposure period.

**PS 1256 N, N'-Di-Tert-Butylacetamide: Integrated Toxicity Testing Approach to Establish an Occupational Exposure Guideline.**

J. A. Hotchkiss, R. Sura, S. M. Krieger, J. Thomas and L. Andrews. The Dow Chemical Company, Midland, MI.

N,N' di-tert-butylacetamide (AMD; CAS # 54838-72-1) is a raw material and principal hydrolysis product of a new metalorganic molecule. An integrated testing strategy involving the assessment of multiple hazard endpoints was used to provide essential toxicologic data to set an occupational exposure guideline for AMD. The acute oral LD<sub>50</sub> was estimated to be 341.4 mg/kg (95% C.I. = 280-550 mg/kg). In a 28-day dietary study no target organ toxicity was identified. A no adverse effects level (NOAEL) of 150 mkd was based on decreased food consumption and body weight gains at 500 and 1000 mkd. A modified acute inhalation toxicity study with scheduled necropsies 1- and 14-d post-exposure and analysis of bronchoalveolar lavage, airway epithelial cell proliferation, and histopathology of the respiratory tract was conducted to determine the LC<sub>50</sub> and to assess airway epithelial injury and repair. The 4-h LC<sub>50</sub> was 388 ppm (506 mg/kg) and 404 ppm (527 mg/kg) AMD for male and female F344/DuCrI rats, respectively. Histopathologic changes were concentration-dependent and restricted to the olfactory, respiratory and transitional epithelium lining the anterior nasal airways. Increased cell proliferation was evident 1- and 14-d post-exposure. Epithelial regeneration was incomplete 14-d post-exposure. An RD<sub>50</sub> assay was conducted to assess the sensory irritation potential of inhaled AMD. Based on the concentration-dependent decrease in respiration rate the RD<sub>50</sub> was calculated to be 123.4 ppm (95% C.I. = 59-188). Based on these data an 8-h time-weighted average (TWA) occupational exposure level of 5 ppm with a 15 ppm short-term exposure limit (STEL) was established. These exposure limits are similar to ACGIH threshold limit values of 5-10 ppm for short-chain

aliphatic amines and suggest that the toxicity of AMD is similar to other alkyl amines such as dimethyl- and diethyl-amine. The integrated testing strategy used in this study represents an important approach for reducing animal use and rapidly adopting exposure guidelines for new materials to assure worker safety.

## PS 1257 Lipidomics of Subchronic Low Level Cadmium Exposure in the Rat.

O. O. Ogunrinola, O. Ademuyiwa, A. D. Wusu, O. K. Afolabi, E. O. Abam, D. O. Babayemi, E. A. Balogun and O. O. Odukoya. *Biochemistry, University of Agriculture, Abeokuta, Nigeria.*

Epidemiological studies suggest an association between cadmium in drinking water and vascular diseases. However, the precise cadmium mechanism of action remains enigmatic. This study was undertaken to investigate the effect of cadmium on lipid metabolism of Wistar male albino rats by exposing the animals to 100, 200 and 300 ppm cadmium doses for 12 weeks in their drinking water. Control animals received distilled water for the same period. At the end of 12 weeks, dyslipidemia induced by the cadmium doses exhibited different patterns. Dose-dependent hypocholesterolemia and hypotriacylglyceridemia characterised the effect of cadmium exposure at all doses whereas plasma free fatty acid (29%) was increased by cadmium exposure. Reverse cholesterol transport was inhibited by all the cadmium doses as evidenced by 65% decreased HDL cholesterol concentrations whereas hepatic cholesterol was decreased by 55%. Renal and brain cholesterol (46%, 65%) and triacylglyceride (62%, 50%) were dose-dependently decreased by cadmium exposure respectively; on the other hand, exposure to cadmium depleted cardiac cholesterol by 45%, but enhanced/balanced triacylglyceride content. Cadmium at all doses of exposure inhibited both hepatic and brain HMG CoA reductase by 49% and 61% respectively. We observed positive association between tissue cadmium levels and plasma FFA, and negative associations between tissue cadmium levels and HDL cholesterol. Our findings indicate that in contrast to strengthening a dose-dependent effect phenomenon as observed with many other compounds, cadmium up- or down-regulate different pathways in the lipid metabolism spectrum at "low" or "high" doses and this might be responsible for the insidious vascular effects.

## PS 1258 Serum Great Lakes Pollutant Levels in Lake Ontario Fish and Wildlife Consumers.

E.D. Stephen<sup>1</sup>, L. A. Georger<sup>1</sup>, M. R. Bonner<sup>3</sup>, P.J. Kostyniak<sup>2</sup>, J.R. Olson<sup>2,3</sup>, M. S. Bloom<sup>4</sup> and J. E. Vena<sup>3</sup>. <sup>1</sup>Math & Natural Sciences, D'Youville College, Buffalo, NY; <sup>2</sup>Pharmacology & Toxicology, SUNY Buffalo, Buffalo, NY; <sup>3</sup>Social & Preventive Medicine, SUNY Buffalo, Buffalo, NY; <sup>4</sup>Environmental Health Sciences, SUNY Albany, Albany, NY; <sup>5</sup>Epidemiology and Biostatistics, University of Georgia, Athens, GA.

Industrialization of the Great Lakes region resulted in the discharge of many halogenated aromatic hydrocarbons (HAHs) into the Lake Ontario basin. Due to their persistence and lipophilicity, HAHs can biomagnify in the food chain and are a potential source of human exposure to polychlorinated biphenyls (PCBs), polychlorinated dibenzo-p-dioxins (PCDDs), dibenzofurans (PCDFs) and pesticides. Consumption of Lake Ontario fish and wildlife is one factor that contributes to higher serum levels of persistent HAHs and potentially greater risk of adverse human health effects. The New York State Angler Cohort Study (NYSACS) is a large prospective cohort of licensed anglers from 16 New York counties in close proximity to Lake Ontario, 18 to 40 years of age established in 1991. Previously, 394 members of the NYSACS donated blood and were screened for serum PCB and pesticide levels. For this analysis, participants with the highest serum PCB153 levels (n=27) and with self reported consumption of Lake Ontario fish were chosen, and matched to subjects having never consumed Lake Ontario fish by age, sex and geographic area (n=16). We examined serum levels of PCBs, PCDDs, PCDFs and pesticides by GC/ECD and GC/MS. The consumer group had significant elevated levels of 20 PCBs, including PCB 126, 153, 138, 180 and 170. The consumer group also had a 1.6-fold increase in 2,3,7,8-TCDD, a 1.4-fold increase in 1,2,3,7,8-PentaCDD, a 1.54-fold increase in 2,3,4,7,8-PentaCDF, a nine-fold increase in mirex, a 2.5-fold increase in DDE and a two-fold increase in t-nonachlor relative to the non-consumer group (all values p<0.05). Together, the results indicate that consumption of fish and wildlife from Lake Ontario is a source of exposure to mirex and other HAHs. (Supported in part by ATSDR, Grant H75-ATH 298338)

## PS 1259 Exposure to Environmental Tobacco Smoke Causes Endotoxin Tolerance.

T. Muthumalage<sup>2</sup>, K. Hunter<sup>3,2</sup>, D. Redelman<sup>4</sup>, K. Pritsos<sup>1</sup> and C. A. Pritsos<sup>1,2</sup>. <sup>1</sup>Agriculture, Nutrition and Veterinary Sciences, University of Nevada, Reno, Reno, NV; <sup>2</sup>Environmental Sciences Program, University of Nevada, Reno, Reno, NV; <sup>3</sup>Microbiology and Immunology, University of Nevada, Reno, Reno, NV; <sup>4</sup>Physiology and Cell Biology, University of Nevada, Reno, Reno, NV.

Exposure to cigarette smoke is known to increase susceptibility to and severity of pulmonary diseases such as bronchitis and emphysema. During tobacco manufacturing processes, in which the temperature and humidity are brought to an optimum level for fermentation, tobacco is colonized by fungi and bacteria. Lipopolysaccharide (LPS), a gram negative bacterial component, has been found in tobacco smoke. In this study, we wanted to assess whether acute exposure to environmental tobacco smoke (ETS) could alter the immune response caused by exposure to the bacterial endotoxin, LPS. Using a C57BL/6 mouse model, we compared the inflammatory cytokine levels secreted by LPS stimulated alveolar macrophages in ETS exposed and unexposed (control) groups. Tumor necrosis factor-alpha (TNF-α) levels were significantly attenuated in the ETS exposed groups after ex-vivo exposure to LPS in comparison to the control group. We observed that whether the ex-vivo LPS exposure was performed immediately after the ETS exposure or a full day post-exposure, the TNF-α cytokine level was decreased by 30-40%. No significant difference was observed in alveolar macrophage recovery between the two groups. Also, no significant difference was found in cell viability between the two groups. This suggests that TNF-α attenuation in ETS exposed groups resulted from endotoxin tolerance caused by LPS or LPS-like constituents in ETS. This endotoxin tolerance resulting from acute ETS exposure can suppress the immune function and subsequently increase susceptibility to bacterial infections. These results provide insights into the weaker immune defense observed in smokers and secondhand smokers. This study was supported by the Flight Attendants Medical Research Institute grant 072083.

## PS 1260 Mitochondrial-K<sup>+</sup>-ATP Channel Activation Rescues of Phosgene-Induced Toxic Inhalational Lung Injury.

A. Senft<sup>1</sup>, J. D. McDonald<sup>1</sup>, W. Weber<sup>1</sup>, L. Fredenburgh<sup>2</sup>, G. Southan<sup>3</sup> and A. P. Salzman<sup>3</sup>. <sup>1</sup>Lovelace Respiratory Research Institute, Albuquerque, NM; <sup>2</sup>Harvard Brigham and Womens College, Boston, MA; <sup>3</sup>Radikal Therapeutics, Boston, MA.

To determine whether R-801, a mitochondrial-K<sup>+</sup>-ATP channel activator, is effective in rescuing acute lung injury (ALI) induced by phosgene (COCl<sub>2</sub>), C57/BL6 mice were exposed to COCl<sub>2</sub> (5 ppm) or filtered air (FA) for 20 min. Animals were administered intraperitoneal (IP) R-801 (80 mg/kg/dose) or vehicle (hydroxypropyl cyclodextrin, HPCD) at 2 and 6 h after COCl<sub>2</sub>. Animals were tracheostomized, bronchoalveolar lavage (BAL) performed, and lungs harvested at 24 and 48 h. COCl<sub>2</sub>-exposed animals developed severe lung injury compared to controls, with interstitial and alveolar edema, hemorrhage, and recruitment of inflammatory cells. Treatment with R-801 led to significant reduction in histologic lung injury and near normalization of lung histology. Immunostaining for Ly-6G (Gr-1) at 48 h demonstrated significant neutrophil (PMN) accumulation around bronchovascular bundles in COCl<sub>2</sub>-exposed animals which was profoundly attenuated in R-801-treated COCl<sub>2</sub>-exposed animals. Furthermore, levels of the pro-inflammatory cytokines and BALF protein were dramatically reduced compared with controls. Treatment with R-801 restored epithelial barrier integrity after COCl<sub>2</sub> with striking attenuation in BALF protein levels 48 h after COCl<sub>2</sub>. Taken together, our findings demonstrate that selective mito-K<sup>+</sup>-ATP channel opening with R-801 is highly effective at rescuing COCl<sub>2</sub>-induced ALI via attenuation of inflammation, restoration of epithelial tight junction barrier integrity, and induction of endogenous surfactant protein expression.

## PS 1261 Systematic Review of BPA "Low Dose" Literature in the Context of Human Dosimetry Exposes a Need to Set Standards for Responsible Communication of Both Toxicity and Exposure Data.

S. Hanson-Drury and J. G. Teeguarden. *Systems Toxicology and Exposure Science, Pacific Northwest National Laboratory, Richland, WA.*

BPA is a weakly estrogenic monomer used for making polycarbonate plastics and food packaging liners. At sufficient exposures, BPA is toxic in rodent non-human test systems. Uncritical reference to many toxicity studies as "low dose" has led to the belief that exposure levels in these studies are similar to human exposure levels,

implying that BPA is toxic to humans at current exposures. However, a comprehensive comparison of exposures in humans and test systems has not been conducted. Applying the fundamental principles of biomonitoring, exposure assessment and dosimetry, we conducted a systematic review of BPA exposure levels in 130 peer-reviewed *in vivo* and *in vitro* BPA toxicity studies self-referring as "low-dose." Total daily human exposure to BPA is ~ 0.03 µg/kg/day. In contrast, >90% of "low dose" BPA toxicity studies were conducted at doses exceeding human exposure by 10-1000,000 fold. Human blood concentrations from a single oral bolus dose of BPA equal to total daily BPA exposure are in the low pM range. In comparison, concentrations used in >90% of *in vitro* "low dose" studies were 10 to 1000,000 higher. We conclude that the use of the "low dose" descriptor is largely inconsistent with the state of our knowledge of human exposure. Looking forward, as human exposure data continue to emerge from large biomonitoring studies, we believe that there is a need to adopt standards for the conduct and reporting of toxicity studies that include objective comparisons to human exposures.

**PS 1262 Secondary Particulate Health Effects Research (SPHERES)**  
**Program: Secondary Organic Aerosol Effects on the Cardiovascular System.**

A. Rohr<sup>2,1</sup>, E. Knipping<sup>2</sup>, A. K. Lund<sup>1</sup>, M. J. Campen<sup>3</sup>, M. Doyle-Eisele<sup>1</sup> and J. D. McDonald<sup>1</sup>. <sup>1</sup>LRRI, Albuquerque, NM; <sup>2</sup>EPRI, Palo Alto, CA; <sup>3</sup>University of New Mexico, Albuquerque, NM.

The SPHERES research program was created to examine the role of inhaled secondary organic aerosol (SOA) on cardiovascular outcomes in mice, benchmarking effects against those observed from motor vehicle emissions (MVE). SOA was generated in a reaction chamber with either alpha-pinene or toluene, combined with (1) NO<sub>x</sub>; (2) NO<sub>x</sub> + SO<sub>2</sub>; (3) NO<sub>x</sub> + NH<sub>3</sub>; or (4) NO<sub>x</sub> + NH<sub>3</sub> + SO<sub>2</sub>. To examine the effects of these mixtures on progression of atherosclerosis, 8 wk old male Apo E<sup>-/-</sup> mice, on a high fat diet were exposed for 7 days, and resulting vascular oxidative stress and expression of molecular markers were assayed. Exposure to MVE resulted in enhanced vascular oxidative stress, measured by vascular TBARS and HO-1 levels. SOA caused a milder response than MVE, and the biological responses that were observed differed depending on the composition of the mixture. The only SOA exposure in which a statistical increase in TBARS was measured, compared to controls, was the "neutral" α-pinene (e.g. α-pinene reacted with NO<sub>x</sub>). All other SOA exposure conditions yielded only slight, or no, increase in TBARS expression, which is consistent with other studies in the literature (Lemos et al., 2011; rev. in Godleski et al., 2011). Several of the SOA exposure conditions yielded significant increases in expression of vascular HO-1 transcript. The "acidic" α-pinene mixture, as well as α-pinene + NH<sub>3</sub> (both neutral and acidic) and the neutral toluene exposure all resulted in statistically significant increases in HO-1 mRNA. Conversely, both the acidic and neutral toluene + NH<sub>3</sub> exposures showed significant decreases in vascular HO-1 expression. In aggregate, the results suggest that SOA causes mild cardiovascular responses that are dependant on composition. Research Funded by the Electric Power Research Institute.

**PS 1263 Pulmonary Toxicity of Oxygen and Carbon Dioxide Degraded Amines Used for Carbon Capture and Storage.**

D. Kracko<sup>1</sup>, C. Wegerski<sup>1</sup>, J. D. McDonald<sup>1</sup>, M. Doyle-Eisele<sup>1</sup>, S. Shaw<sup>2</sup>, E. Knipping<sup>2</sup> and A. Rohr<sup>2</sup>. <sup>1</sup>Lovelace Respiratory Research Institute, Albuquerque, NM; <sup>2</sup>Electric Power Research Institute, Palo Alto, CA.

Carbon dioxide (CO<sub>2</sub>) adsorption with aqueous amine solvents is among the leading candidates for use in carbon capture and sequestration (CCS) techniques aimed at reducing greenhouse gas emissions from flue gases (coal-fired power plants, refineries, etc). The environmental consequences from utilizing this technology have been poorly characterized. A concern is that amines or by-products that may occur due to interaction with flue gases are emitted creating unintended human exposure. This study evaluated the inflammatory response associated with inhalation exposure to amines and amine degradation products. Three model amines (monoethylamine (MEA), methyldiethanolamine (MDEA), piperazine (PIP)) and their laboratory-generated degradation products formed via addition of CO<sub>2</sub> and O<sub>2</sub> were evaluated. C57BL/6N mice were exposed for three days by whole-body inhalation to 6-25 ppm amine or the equivalent concentration of degraded amines. Inflammatory response in lungs was assessed by counting inflammatory cells in bronchoalveolar lavage fluid and measurement of cytokine expression in lung tissue. Inhalation exposure to O<sub>2</sub>-degraded MEA showed significant increases in total cells, neutrophils, and lymphocytes compared to control mice. Significant increases in inflammatory cytokine expression were seen in mice exposed to the O<sub>2</sub> degraded MDEA atmosphere, and minimal inflammation was observed with piperazine or

degraded piperazine. CO<sub>2</sub> degraded amines overall showed only mild inflammatory response. Characterization of the degraded amines showed numerous degradation products including carbonyl compounds, such as formaldehyde, and nitrosamines, a class of compound of which some species are carcinogenic. These are the first known studies to evaluate the potential inhalation hazard of amine degradation products. Research supported by the Electric Power Research Institute.

**PS 1264 Volatile Organic Compounds Released from Expanded Polystyrene.**

N. Pajaro-Castro, J. Perez-Romero and J. Olivero-Verbel. *Environmental and Computational Chemistry Group Pharmaceutical Sciences, University of Cartagena, Cartagena, Colombia.*

The importance of plastic materials for different applications in everyday life has continuously increased over the years. Manufactured goods made of polymers are generally complex materials. These are composed of polymers or copolymers themselves, together with a variety of additives with different volatilities. Currently, polystyrene is among the most widely used plastic in the form of foam containers. However, under certain conditions polystyrene foam may liberate residual styrene monomers, and other compounds, with well-known toxic properties. The aim of this study was to analyze the release of chemicals from expanded polystyrene (EPS) commercially available in Colombia. Headspace solid-phase micro-extraction with a 100 µm carboxen-polydimethylsiloxan fiber was utilized to capture organic compounds volatilized by heating EPS at different temperatures (55-85 Celcius). Volatiles were characterized by GC/MS after thermal desorption. The results demonstrated that for different EPS products, such as lunch carriers, dishes and soup containers, there is a temperature-dependent emission of several compounds, including styrene, benzaldehyde, ethylbenzene, (2-phenylcyclobutyl)benzene and tetradecane, among others. Data mining suggested these molecules possess a broad spectrum of toxicities. Taken together, these findings should encourage citizens to be careful while using EPS containers as carriers for hot foods or beverages. Vice-Rectoria for Research. UniCartagena. 2011-2012. Colciencias-UniCartagena, Colombia. Grant 110749326186 (2009).

**PS 1265 Assessment of Biomarkers of Benzene Exposure and Effect in Petrochemical Workers.**

S. Inayat-Hussain<sup>1,2</sup>, M. Sabtu<sup>2</sup>, F. S. Chin<sup>2</sup> and M. K. Chan<sup>1</sup>. <sup>1</sup>Environmental Health and Industrial Safety Program, Faculty of Health Sciences, Universiti Kebangsaan Malaysia, Kuala Lumpur, Malaysia; <sup>2</sup>UKM Medical Molecular Biology Institute, Universiti Kebangsaan Malaysia, Kuala Lumpur, Malaysia.

This study was conducted to assess biomarkers of benzene exposure and effect, and the relationship between these parameters in petrochemical plant workers during a major turnaround. Pre and post shift blood and urine samples were obtained from 35 workers including smokers and non-smokers who were potentially exposed to low air level of benzene. Air monitoring results showed that the benzene level in air samples was less than the Permissible Exposure Level (PEL) which is 0.5 ppm. Interestingly, there was a 2.1 fold increase of the biomarker of exposure namely urinary S-phenylmercapturic acid (SPMA) in workers as assessed by ELISA. There were 18 out of 35 workers who had levels of post-shift SPMA higher as compared to the pre shift data. Specifically, 6 workers showed levels of SPMA above the Biological Exposure Index (25µg/g creatinine). In workers who were smokers, there was an increase of 2.1 fold in the level of DNA strand breaks as assessed by Alkaline Comet assay whereas the increase of oxidized base (8-OHdG) was 1.1 fold as measured using ELISA. However, the non-smokers demonstrated a significant increase in 8-OHdG level (1.3 fold) but not significant for the DNA strand breaks (1.2 fold) (p<0.05). Notably, a strong correlation between SPMA and 8-OHdG (r=0.709) was observed in the post shift data for non-smokers. Taken together, these results suggest that biomonitoring of workers during exposure to low level of benzene may be important to protect workers' health.

**PS 1266 Identification of Sulfated Metabolites of 4-Chlorobiphenyl (PCB3) in the Serum and Urine of Male Rats.**

K. Dhakal<sup>1,4</sup>, L. Hans-Joachim<sup>1,4</sup>, L. M. Teesch<sup>2</sup>, M. W. Duffel<sup>1,3</sup> and L. W. Robertson<sup>1,4</sup>. <sup>1</sup>Interdisciplinary Graduate Program in Human Toxicology, The University of Iowa, Iowa City, IA; <sup>2</sup>High Resolution Mass Spectrometry Facility, The University of Iowa, Iowa City, IA; <sup>3</sup>Department of Pharmaceutical Sciences and Experimental Therapeutics, The University of Iowa, Iowa City, IA; <sup>4</sup>Department of Occupational and Environmental Health, The University of Iowa, Iowa City, IA.

Polychlorinated biphenyls (PCBs) are legacy pollutants that exert toxicity of various mechanisms. Lower chlorinated or lighter PCBs (LC-PCBs) are semi-volatile, and air-borne. In the old public school building in New York City, the EPA in 2012 has

estimated that students are inhaling six times more PCBs than they are receiving from dietary sources. However, LC-PCBs or metabolites have been rarely reported in the serum of population at risk. LC-PCBs are bioactivated to phenols and further to quinone electrophiles with genotoxic/carcinogenic potential. We hypothesized that phenolic LC-PCBs are subject to phase II conjugation and excretion via urine. Our objective was to identify the final metabolites in the urine that could be potentially employed in the exposure analysis of LC-PCBs. Male Sprague Dawley rats (150-175 g) were housed in metabolism cages and received a single intraperitoneal injection of 600  $\mu\text{mol/kg}$  body weight of PCB3. Control animals received corn oil only. Urine was collected every four hours, euthanized at 36 h, and serum was collected. The LC-MS analysis showed that PCB3 sulfates were the major metabolite in both urine and serum. Approximately 3% of the dose excreted in the urine as sulfate; with peak excretion occurring at 10-20 h of post-exposure. The major metabolites were 4'PCB3sulfate, 3'PCB3 sulfate, 2'PCB3 sulfate and presumably a catechol sulfate. Serum level of 4'PCB3 sulfate was  $6.18 \pm 2.16 \mu\text{g/mL}$  while 4'OH-PCB3 was only  $0.095 \pm 0.055 \mu\text{g/mL}$ . This is the first report that sulfated metabolites of PCBs are formed in vivo.

## PS 1267 Significant Megacluster of Total Cancer Mortality among the US Non-White Population.

J. Beaubier<sup>1</sup> and L. Russell<sup>2</sup>. <sup>1</sup>US EPA, Washington DC; <sup>2</sup>US EPA, Washington DC. Sponsor: J. Murphy.

NCI and EPA collaborated to describe the U.S. population cancer mortality experience for the 1950's, 60's and 70's. All mortality data are official statistics including 8 million records. For the 30 years, for all anatomic cancer sites, there was a significant difference in the percentage rate of increase between White and Non-white U.S. males. The White male increase was 17 %. For the same period, Non-white males experienced a 46 % increase. For both White and Non-white males highest rates of increase were in the Southeastern United States. The project also examined lung cancer. For White male lung cancer mortality, all ~3050 U.S. counties were ranked by percentile of their absolute rates. The counties were marked as red (99-98 percentile of absolute rates), orange (97-95 %), yellow (94-90 %), tan (89-75 %) and blue background (74-1 %). In the 1970s a significant megacluster of White male lung cancer mortality emerged in the Southeastern U.S. The counties show up as strings along rivers. But the important unit of analysis is not the rivers, but U.S. Geological Survey (USGS) hydrologic units. Principal component analysis showed some USGS hydrologic units were more informative: USGS Region 08-02 St. Francis river valley experienced a 300% increase in White male lung cancer mortality in the 1970s, or a 10 % increase per year. The heavily forested, rich bottom lands of the river valley were cut down and planted in cotton sprayed with DDT. DDT induces male rat lung cancers. The strings of high rate White male lung cancer counties lie predominately in the USGS Coastal Plains physiographic domain. During late Cenozoic and Tertiary Eras the Coastal Plains filled in with unconsolidated gravels and sands, porous to pollutants leaching into shallow wells and aquifers. Relative risk of a red county being within the Coastal Plains was 5.3 times greater than being in another part of the U.S. Color coded counties showed a "dose-related" effect - the higher the county rate, the more likely it was located in the Coastal Plains. Authors solely responsible for conclusions herein and do not reflect authors' institutions.

## PS 1268 Airborne Diacetyl from Cooking and Consumption of Microwave Popcorn: Estimation of Consumer Exposure with a Two-Zone Near-Field/Far-Field Model.

H. M. Bolstad<sup>1</sup>, K. M. Unice<sup>2</sup>, J. R. Maskrey<sup>2</sup>, D. M. Hollins<sup>1</sup>, B. D. Kerger<sup>3</sup> and D. J. Paustenbach<sup>1</sup>. <sup>1</sup>ChemRisk, San Francisco, CA; <sup>2</sup>ChemRisk, Pittsburgh, PA; <sup>3</sup>ChemRisk, Orange County, CA.

Diacetyl is a volatile diketone used to impart a butter flavor to foods such as microwave popcorn. Occupational exposure to airborne diacetyl has been reported to be associated with obstructive lung disease, and recent concerns have emerged regarding exposures to diacetyl by consumers. Given the absence of data on the airborne concentrations in the home, we estimated consumer exposure using a two-zone near-field/far-field model in which the near-field is a hemisphere above the microwave popcorn bag, and conducted Monte Carlo uncertainty and sensitivity analyses. A recent study revealed that an average of  $778.9 \pm 135 \mu\text{g}$  diacetyl was emitted during the popping, opening, and 40 minutes following opening. As part of the input to the model, we estimated that diacetyl is released into the breathing zone over a 40 minute period (a typical consumption duration) comprised of popping (2.5 min), opening (15 sec), and consumption (37.25 min). Based on available information, we estimated that 98.9% of the total diacetyl emitted was re-

leased during opening. The popcorn and the bag were assumed to be an arm length away from the nose of the consumer and present for the duration of the scenario. The estimated mean airborne diacetyl concentration in the breathing zone from one bag of microwave popcorn was 0.0030 ppm, whereas the 5th and 95th percentile concentrations were 0.0018 and 0.0048 ppm, respectively. Assuming complete absorption following inhalation and a breathing rate associated with light activity (0.6 m<sup>3</sup>/hr), the estimated mean total intake by inhalation per bag was 5.3  $\mu\text{g}$ . By comparison, the daily intake associated with occupational exposure at the eight hour TWA and 15 minute STEL Threshold Limit Values set by ACGIH (0.01 and 0.02 ppm, respectively) are 66 and four-fold greater, respectively.

## PS 1269 Examination of Specificity of Retinoid-Like Compounds for RXRs, RARs and RORs.

P. P. Albrecht<sup>1</sup>, K. Toyokawa<sup>1</sup>, E. Maddox<sup>1</sup>, P. Cramer<sup>1</sup>, B. Sher<sup>1</sup> and J. Vanden Heuvel<sup>1,2</sup>. <sup>1</sup>Indigo Biosciences, State College, PA; <sup>2</sup>Department of Veterinary and Biomedical Sciences, Pennsylvania State University, University Park, PA.

Vitamin A (retinol) and its metabolites play many physiological roles including cell differentiation, cell proliferation, energy homeostasis, circadian rhythm and immune response. Vitamin A and its metabolites are known to act through retinoid acid receptors (RARs), retinoid-related orphan receptors (RORs) and retinoid x receptors (RXRs). These receptors are also important drug targets, although the specificity of many retinoid-like compounds for the retinoid receptors has not been carefully explored due to the lack of robust and selective assays. In the present work we examined the retinoid-like compounds 4-hydroxyphenylretinamide, 4-hydroxyretinoic acid, 9-cis retinoic acid (9CRA), 13-cis retinoic acid (13CRA), AC-55469, Acitretin, Adapalene, AM-580, All-trans retinoic acid (ATRA), BMS961, Docosahexanoic acid (DHA), EC23, Eicosapentaenoic acid (EPA), ER50891, HX531, HX630, Methoprene, Methoprene acid, MM11253, Puerarin, RO 41-5253, SR1001, TO901317, TTNPB, and Ursolic acid for their ability to regulate RAR $\alpha$ ,  $\beta$ ,  $\gamma$ , RXR $\alpha$ ,  $\beta$ ,  $\gamma$ , and ROR $\alpha$ ,  $\beta$ ,  $\gamma$ . The compounds were tested for agonistic as well as antagonistic activities towards these receptors. Additionally cytotoxicity assays were performed to assess true antagonistic activity. Many of these compounds show a broad range of receptor activity (for example, EC23 shows agonistic activity for all three RARs) while others were highly selective. The data further illustrate the need to test new retinoic acid like drugs across the panel of RXRs, RARs and RORs to limit untoward effects.

## PS 1270 Oxidative Formation of the High Affinity Endogenous Aryl Hydrocarbon Receptor Ligand 6-Formylidolo(3, 2-B)Carbazole (FICZ).

U. Rannug<sup>1</sup>, A. Smirnova<sup>1</sup>, L. Vikström Bergander<sup>2</sup>, E. Wincent<sup>2</sup>, T. Alsberg<sup>3</sup> and A. Rannug<sup>2</sup>. <sup>1</sup>Department of Genetics, Microbiology & Toxicology, Stockholm University, Stockholm, Sweden; <sup>2</sup>Institute of Environmental Medicine, Karolinska Institutet, Stockholm, Sweden; <sup>3</sup>Department of Applied Environmental Science, Stockholm University, Stockholm, Sweden.

The endogenous high affinity aryl hydrocarbon receptor agonist FICZ is formed upon irradiation of tryptophan with UV or visible light. To elucidate the mechanisms in more detail photooxidation products were analyzed by HPLC and LC/MS. The results revealed that the formation of FICZ was dependent on H<sub>2</sub>O<sub>2</sub> since additions of catalase inhibited the reaction. It was also evident that indole-3-acetaldehyde (I-3-A) was a precursor that spontaneously generated FICZ. Monoamine oxidases (MAOs) catalyze the oxidative deamination of monoamines resulting in the corresponding aldehydes. Human recombinant MAO A and MAO B were therefore incubated with tryptamine to yield I-3-A. After the reaction and a post treatment period the amounts of I-3-A and FICZ were measured. Both enzymes generated I-3-A, which was then spontaneously converted to FICZ. Subsequently, tryptophan was incubated with H<sub>2</sub>O<sub>2</sub> at 37 °C in the dark. The mixture was concentrated on Sep-Pak C18, and HPLC and MS analyses confirmed the formation of FICZ from tryptophan by H<sub>2</sub>O<sub>2</sub>. From these and other experiments it can be concluded that tryptophan can give rise to FICZ in an oxidative environment, i.e. containing or producing reactive oxygen species. In addition, whenever I-3-A is formed there is a possibility for spontaneous formation of FICZ. Altogether, this implies that there are several different conditions under which the endogenous Ah receptor ligand FICZ can be formed in the body. Of great interest in this respect is a recent demonstration of FICZ in the skin of vitiligo patients characterized by a massive epidermal oxidative stress and high levels of H<sub>2</sub>O<sub>2</sub> (Schallreuter et al., FASEB J, 2012). It therefore seems likely that FICZ is ubiquitous in the human body but expected to be present at low steady state levels under normal conditions.

**PS 1271 The Aryl Hydrocarbon Receptor Regulates the Expression of Multiple Growth Factors in Highly Metastatic Head and Neck Squamous Cell Carcinoma Cell Lines.**

K. John<sup>1,2</sup>, J. Hughes<sup>1</sup>, T. S. Lahoti<sup>1</sup>, K. Wagner<sup>1</sup> and G. H. Perdew<sup>1</sup>. <sup>1</sup>Center for Molecular Toxicology and Carcinogenesis, Pennsylvania State University, University Park, PA; <sup>2</sup>DuPont Haskell Global Centers for Health and Environmental Sciences, Newark, DE.

The aryl hydrocarbon receptor (AHR) is a ligand activated transcription factor implicated in the regulation of diverse cellular processes. Previous studies in head and neck squamous cell carcinoma cell lines (HNSCC) have revealed considerable constitutive and ligand inducible AHR transcriptional activity. Antagonism of AHR activity through AHR antagonist treatment was found to greatly attenuate the highly metastatic and proliferative phenotype of these cells, suggesting that AHR plays a significant role in contributing to the 'aggressive' phenotype of these cells. Therefore, this study sought to use expression profiling to identify putative novel targets of the AHR repressed by AHR antagonist treatment that are associated with cancer cell survival and tumor invasiveness. Three growth factor targets were considered; amphiregulin (AREG), epiregulin (EREG) and platelet-derived growth factor A (PDGFA) identified by expression profiling and from previous studies. Quantitative PCR analysis revealed an attenuation of basal and/or induced gene expression levels of these growth factors in two HNSCC lines after AHR antagonist treatment. ELISA analysis revealed attenuation of both basal and induced protein levels of the growth factors examined in these cell lines. In addition, siRNA-mediated knock down of AHR exhibited attenuation of growth factor expression. In silico analysis revealed these growth factors possess dioxin-like response elements. Additionally, two other AHR ligands, 6-formylindolo[3,2-b]carbazole and benzo(a)pyrene also exhibited induction of the AHR target genes examined. In conclusion, AREG, EREG and PDGFA were identified as three key growth factor targets of the AHR associated with metastatic phenotype of head and neck cancers.

**PS 1272 Hepatocarcinogenesis Induced by a Potent, High Affinity Human PPAR $\alpha$  Agonist Is Diminished in PPAR $\alpha$ -Humanized Mice.**

J. E. Foreman<sup>1</sup>, T. Koga<sup>1</sup>, O. Kosyk<sup>2</sup>, L. R. Kramer<sup>1</sup>, F. J. Gonzalez<sup>3</sup>, I. Rusyn<sup>2</sup> and J. M. Peters<sup>1</sup>. <sup>1</sup>Pennsylvania State University, University Park, PA; <sup>2</sup>University of North Carolina at Chapel Hill, Chapel Hill, NC; <sup>3</sup>National Cancer Institute, Bethesda, MD.

PPAR $\alpha$ -null mice and PPAR $\alpha$ -humanized mice are both resistant to hepatocarcinogenesis induced by a PPAR $\alpha$  agonist Wy-14,643, a compound that has higher affinity towards the mouse PPAR $\alpha$  as compared to the human PPAR $\alpha$ . While the studies demonstrating these differences suggest that the mouse PPAR $\alpha$  is a key mediator in the hepatocarcinogenic effects of PPAR $\alpha$  agonists and that species differences exist, it was noted the duration of the studies was limited to ~1 year, and the PPAR $\alpha$  agonist has higher affinity for the mouse PPAR $\alpha$  as compared to the human PPAR $\alpha$ . Thus, the present study examined the effect of a potent, high affinity human PPAR $\alpha$  agonist (GW7647) on hepatocarcinogenesis in wild-type, PPAR $\alpha$ -null, or PPAR $\alpha$ -humanized mice. Dietary administration of GW7647 for up to 18 months caused severe hepatomegaly in wild-type mice. This effect was not found in similarly treated PPAR $\alpha$ -null mice and was diminished in humanized-PPAR $\alpha$  mice. Mortality prior to 18 months of treatment was generally found in greater proportion in wild-type mice fed GW7647 as compared to similarly treated PPAR $\alpha$ -null or PPAR $\alpha$ -humanized mice. Administration of GW7647 for up to 18 months caused close to 100% incidence of hepatocarcinogenesis in wild-type mice, but this effect was largely diminished in PPAR $\alpha$ -null mice and PPAR $\alpha$ -humanized mice. Tumors were present in some PPAR $\alpha$ -null and PPAR $\alpha$ -humanized mice, but they occurred in both control and treated animals at frequencies well below those found in wild type mice. Gross examination and results from additional molecular analysis suggests a difference in mechanism between these tumors and those induced by GW7647 in wild-type mice, but further analysis will be important for determination of mode of action. Results from these studies provide further mechanistic evidence for the species difference in the hepatocarcinogenesis of a high affinity human PPAR $\alpha$  agonist. (Supported by CA124533, CA140369, FES017568A)

**PS 1273 Arsenic Inhibits 3T3-L1 Adipogenesis and Suppresses Induction of Nuclear Receptors during the Earliest Stages of Differentiation.**

F. Zandbergen<sup>1</sup>, A. Adebayo<sup>1,2</sup>, M. M. Vantagoli<sup>1,2</sup>, V. Chatikavanij<sup>1</sup> and J. W. Hamilton<sup>1,2</sup>. <sup>1</sup>Marine Biological Laboratory, Woods Hole, MA; <sup>2</sup>Brown University, Providence, RI.

Chronic environmental exposure to inorganic arsenic (As) is associated with an increased risk of serious illnesses, including type 2 diabetes and cardiovascular disease (CVD), which in turn are often associated with aberrant blood lipid levels and excess adipose tissue. Since we had previously shown that inorganic arsenite (As) can suppress activation of steroid and other nuclear hormone receptors we hypothesized that it might also affect adipose lipid metabolism by targeting these or other members of the nuclear receptor family. Treatment of mouse 3T3-L1 cells with As during their differentiation into adipocytes resulted in reduced lipid content and suppressed induction of the master adipogenic transcription factors PPAR $\gamma$  and C/EBP $\alpha$  and their target genes. Transient As exposures showed that final lipid content was reduced most in cultures that had been exposed during the initial induction phase of adipogenesis. As did not decrease protein and phosphorylation levels of C/EBP $\beta$  - the transcriptional regulator of PPAR $\gamma$  and C/EBP $\alpha$ . C/EBP $\beta$  acquires its transactivation activity when growth-arrested 3T3-L1 preadipocytes re-enter the cell cycle and undergo a couple of mitoses in response to a combination of hormones, an event required for their differentiation into adipocytes. Interestingly, As increased protein expression of the cell cycle inhibitor p27, suggesting it blocks mitotic clonal expansion, and this may be the proximal event resulting in a cascade of downstream effects. Interference of As with differentiation of adipocytes and/or adipocyte-regulated lipid metabolism in vivo might lead to pathophysiological changes in plasma lipid levels and regulation of lipid storage in adipose tissue and liver, which in turn may contribute to the known association between As exposure and increased risk of type 2 diabetes, CVD and other metabolic disorders. (Funded by NIH-NIEHS SRP (P42 ES007373), and NIH-NRSA (2 T32 ES 7272-21))

**PS 1274 Liver X Receptor and Pregnane Xenobiotic Receptor Crosstalk on Direct Repeat 4 (DR4) Response Elements Is Sequence Dependent.**

K. Falkner<sup>1</sup>, B. Wahlang<sup>1</sup>, H. Bellis-Jones<sup>1</sup>, H. Clair<sup>1</sup>, R. Prough<sup>3</sup> and M. Cave<sup>1,2</sup>. <sup>1</sup>Department of Medicine/GI, University of Louisville, Louisville, KY; <sup>2</sup>Louisville VAMC, Louisville, KY; <sup>3</sup>Biochemistry, University of Louisville, Louisville, KY.

As both the human Liver X-Receptor  $\alpha$  (LXR) and the human Pregnane Xenobiotic Receptor (PXR) bind to a Direct Repeat 4 (DR4) response elements (RE), we compared the effects of co-transfection of either LXR, PXR or a combination of both receptors on their ability to transactivate different DR4 response elements containing reporter genes. Animal studies suggested that over-expression/activation of either of these receptors results in steatosis. Both reporters contained the same hexa-nucleotide (AGTTCA) core repeat but vary in the sequences in the immediate 5' and 3' positions. HepG2 cells were transfected with plasmids expressing human PXR and human LXR; receptor-responsive reporter plasmid, pGL3-PXRE-luciferase and tk-LXR-RE-luciferase. Cells were treated with known positive ligands for the respective receptors. The first reporter, optimized for PXR binding, was activated by co-transfection of PXR treated with 10 $\mu$ M rifampicin and known LXR ligand T0901317 (100nM), demonstrating that T0901317 is a PXR agonist. This reporter was also activated by LXR in the presence of T0901317. In combination, co-transfection resulted in increased fold induction of this reporter with both rifampicin and T0901317. Our LXR selective DR4 reporter was activated by T0901317 when LXR was co-transfected. The reporter was not activated by PXR either in the presence of rifampicin or T0901317. In contrast to the PXR optimized DR4 construct, co-transfection of both receptors resulted in a loss of LXR dependent activation of the reporter by T0901317. These results suggest that both positive and negative interactions are possible between these receptors and therefore, the response of target genes may vary considerably, based in part on minor differences in the nucleotide sequence of the DR4 response elements. Major crosstalk should be anticipated between the predominantly endobiotic LXR $\alpha$  and the predominantly xenobiotic receptor, PXR.

**PS 1275 Selective Activation of Human Pregnane X Receptor, Vitamin D Receptor, and Glucocorticoid Receptor by Flavonols.**

A. Lau and T. K. Chang. Faculty of Pharmaceutical Sciences, The University of British Columbia, Vancouver, BC, Canada.

Pregnane X receptor (PXR), vitamin D receptor (VDR), and glucocorticoid receptor (GR) regulate the expression of many genes, including those involved in the bioactivation and detoxification of drugs, toxicants, and endogenous chemicals.

Naturally occurring flavonols have been reported to possess paradoxical biological activities in vitro and in rodents; e.g. chemoprevention and exacerbation of estrogen-induced tumorigenesis. Previously, quercetin, kaempferol, and tamarixetin were reported to activate human PXR (hPXR). However, it is not known whether there is a structure activity relationship in the activation of hPXR by flavonols and whether they activate human VDR (hVDR) and human GR (hGR). In the present study, we compared the effects of structurally related flavonols (i.e. flavonol, galangin, datiscetin, kaempferol, morin, quercetin, isorhamnetin, tamarixetin, myricetin, and syringetin) on the activity of hPXR, hVDR, and hGR. Only flavonol, galangin, isorhamnetin, tamarixetin, and quercetin activated hPXR, whereas none of them activated hGR or hVDR, as determined in dual-luciferase reporter gene assays in transfected HepG2 human hepatoma cells. Dose-response experiments indicated that the minimum effective concentration for hPXR activation by these flavonols was 10-30  $\mu$ M. Flavonol and galangin, but not isorhamnetin, tamarixetin, or quercetin, recruited steroid receptor coactivator-1 (SRC-1), SRC-2, and SRC-3 to the ligand-binding domain of hPXR, as assessed by mammalian two-hybrid assays. Flavonol and galangin bound to the ligand-binding domain of hPXR in a time-resolved fluorescence resonance energy transfer competitive ligand-binding assay. Overall, flavonols activate hPXR in a receptor-selective and chemical-dependent manner. The addition of OH or OCH<sub>3</sub> group at C2' and C5' positions in Ring B of flavonol appears to be unfavorable. Therefore, a minor change in chemical structure leads to abolishment of hPXR activation, implying that flavonols may have differential impact on hPXR-mediated effects. [Supported by CIHR and MSFHR]

### PS 1276 A Novel Aryl Hydrocarbon Receptor 1 Sequence from Rainbow Trout (*Oncorhynchus mykiss*) Brain.

A. M. Kalinoski, J. M. Preslar, M. M. DeRocher, D. M. Hollis and E. V. Hestermann. *Biology Department, Furman University, Greenville, SC.*

The aryl hydrocarbon receptor (AhR) is a cytosolic protein receptor that mediates the toxic effects of polynuclear aromatic hydrocarbons, polychlorinated biphenyls, and other halogenated aromatic hydrocarbons. Two isoforms of AhR (AhR2 $\alpha$  and AhR2 $\beta$ ) have been described in rainbow trout (*Oncorhynchus mykiss*). However, AhR1 (the presumed ortholog of mammalian AhR) has yet to be sequenced. A novel AhR sequence was obtained through Rapid Amplification of cDNA Ends (RACE) of *O. mykiss* whole brain cDNA. Comparison of amino acid sequence in the conserved bHLH and PAS regions and phylogenetic analysis revealed that the new sequence is an AhR1. Tissue-specific expression of all three AhR forms was studied by qRT-PCR. AhR2 $\alpha$  and 2 $\beta$  showed similar patterns of expression and were found in the highest concentration in the heart, gill, and bulbus arteriosus. AhR1 was found in the highest concentration in the white muscle, heart, and brain. These results suggest that the newly sequenced AhR1 is functionally distinct from the previously described AhR2 forms.

### PS 1277 Ginsenosides Are Novel AH Receptor Ligands.

Q. Hu<sup>1</sup>, G. He<sup>2</sup>, J. Zhao<sup>2</sup>, A. Soshilov<sup>2</sup>, M. S. Denison<sup>2</sup>, H. Yin<sup>3</sup>, Q. Xie<sup>1</sup> and B. Zhao<sup>1</sup>. <sup>1</sup>State Key Laboratory of Environmental Chemistry and Ecotoxicology, Research Center for Eco-Environmental Sciences, Beijing, China; <sup>2</sup>Department of Environmental Toxicology, University of California Davis, Davis, CA; <sup>3</sup>Xiyuan Hospital, China Academy of Chinese Medical Sciences, Beijing, China.

The aryl hydrocarbon receptor (AhR) is a ligand-dependent transcription factor that mediates many of the biological and toxicological actions of structurally diverse chemicals. In this study we have examined the ability of a series of ginsenosides extracted from ginseng, a traditional Chinese medicine, to bind to and activate/inhibit the AhR signal pathway. The ability of the ginsenosides to stimulate/inhibit AhR-dependent luciferase gene expression was examined using a recombinant guinea pig adenocarcinoma (G16L1.1c8) cell line containing a stably integrated DRE-driven firefly luciferase reporter plasmid pGudLuc1.1. Our data show that the ginsenosides Rc and Rh1 are not only relatively weak inducers of AhR dependent gene expression compared to that of TCDD, but we demonstrated their ability to compete with [3H]TCDD for binding to and stimulate transformation and DNA binding of the guinea pig cytosolic AhR in vitro by utilizing a combination of ligand and DNA binding assays. The overall ability of these ginsenosides to stimulate AhR signal transduction demonstrates that these ginsenosides are a new class of naturally occurring AhR agonists. The weaker activity of these compounds may be due to their relatively large size, which results in steric hindrance within the AhR ligand binding pocket, although it remains to be determined whether the entire compound fits into the binding pocket. Considering the currently large consumption of ginseng, further studies into the molecular mechanisms of ginsenosides action, including involvement of the AhR pathway, are needed in order to better understand the diverse effects of these chemicals.

### PS 1278 Comparison of Serum Chemistry and Tissue Phenotypes in Aryl Hydrocarbon Receptor Knockout Rats and Mice.

R. Budinsky<sup>2</sup>, J. A. Harrill<sup>1</sup>, R. Hukkanen<sup>2</sup>, J. Rowlands<sup>2</sup> and R. S. Thomas<sup>1</sup>. <sup>1</sup>ICSS, The Hammer Institutes for Health Sciences, Research Triangle Park, NC; <sup>2</sup>TERC, The Dow Chemical Company, Midland, MI.

An aryl hydrocarbon receptor knockout (AHR-KO) rat was generated on a Sprague-Dawley outbred background in order to investigate the mode-of-action of 2,3,7,8-tetrachlorodibenzo-dioxin (TCDD) tumorigenesis. Aside from its role as a xenobiotic receptor, there is evidence that the aryl hydrocarbon receptor (AHR) plays a critical role in the development of some tissues. Previous reports describe a variety of tissue abnormalities in the liver, heart and kidney in AHR-KO mice. We conducted a comparative study of gross tissue pathology, histology and serum chemistry in AHR-KO rats and mice, and corresponding wild-types at 1, 6 and 12 weeks of age (n = 5 / sex / genotype / species) in order to evaluate the role of the AHR in tissue development across species. Adult AHR-KO mice, but not AHR-KO rats, had alterations in many serum chemistry markers associated with compromised liver function as compared to wild-type. Similarly, in adult AHR-KO mice, decreased liver-to-body weight and increased kidney- and heart-to-body weight ratios were observed. Similar changes were not observed in AHR-KO rats, save increased kidney-to-body weight ratios in females. Hepatic developmental abnormalities including portal hypercellularity, biliary reduplication, hepatocellular vesiculation and increased extramedullary hematopoiesis were observed in 1 week old AHR-KO mice and gradually dissipated across 6 and 12 week time points. Adult AHR-KO mice also had patent ductus venosus. None of these histological or gross morphological liver phenotypes were observed in AHR-KO rats. In contrast, AHR-KO rats had severe urinary tract pathology including hydronephrosis, hydronephrosis with secondary renal pelvic dilation, epithelial hyperplasia and mineralization leading to degenerative and inflammatory changes in cortical nephrons. Renal pathology was not observed in AHR-KO mice. Overall, these data indicate that the endogenous role of AHR in tissue development differs significantly between rats and mice.

### PS 1279 Selective AhR Modulator-Mediated Suppression of Acute Joint Edema Associated with Gouty Arthritis.

I. Murray, T. S. Lahoti, G. Krishnegowda, S. G. Amin and G. H. Perdew. *Pennsylvania State University, University Park, PA.*

Gouty arthritis is an inflammatory condition associated with the joints of subjects with high circulating levels of uric acid. Multiple factors promote the deposition of uric acid salt crystals within the synovium, which initiates an immune response resulting in a proinflammatory cytokine cascade and subsequent acute joint inflammation. Here, we examine the topical efficacy of the selective AHR modulator (SAHRM) SGA360 as an antiinflammatory therapy to suppress biomarkers associated with the *in vivo* monosodium urate (MSU) crystal model of gouty arthritis in C57BL/6J mice. Intraarticular (i.a.) injection of MSU into the ankle joints of subjects prompted a dose dependent increase in joint edema over sham controls, as determined through micrometry. Peak inflammation was manifest 24-36 h post injection and resolved over time. Edema was associated with significantly enhanced gene expression of the inflammatory mediators *Il1b*, *Cxcl1*, *Saa3*, *Ptgs2* and *Sphk1*, as assessed by quantitative PCR. Topical application of SGA360 at 6 h intervals after i.a. injection of MSU identified an attenuation of joint edema at 24 h when compared to controls. *Ahr* null mice revealed no significant difference in the level of MSU-induced edema when compared to wild-type. MSU-dependent edema in *Ahr* null mice proved to be refractory to the effects of SGA360 and thus established a requirement for AHR to mediate its antiinflammatory potential. Substitution of SGA360 with an AHR antagonist failed to inhibit MSU-induced edema in wild-type mice suggesting the action of SGA360 is independent of competition with endogenous AHR agonists. Analysis of MSU-induced gene expression in the context of SGA360 revealed a suppression of the mediators *Il1b*, *Cxcl1*, *Saa3*, *Ptgs2* and *Sphk1*. Furthermore, exposure to SGA360 following the establishment of edema revealed an increased rate of inflammatory resolution when compared to controls. These studies indicate that SAHRMs such as SGA360 may provide an effective topical therapy against acute inflammation associated with gouty arthritis.

**PS 1280 Aryl Hydrocarbon Receptor (AHR) Regulates Growth Factor Expression, Proliferation, Protease-Dependent Invasion and Migration in Primary Fibroblast-Like Synoviocytes from Rheumatoid Arthritis Patients.**

T. S. Lahoti<sup>1</sup>, K. John<sup>1,2</sup>, J. M. Hughes<sup>1</sup>, B. Zhu<sup>1</sup>, I. Murray<sup>1</sup>, J. M. Peters<sup>1</sup> and G. H. Perdew<sup>1</sup>. <sup>1</sup>Veterinary Sciences, Pennsylvania State University, University Park, PA; <sup>2</sup>DuPont Haskell Global Centers for Health and Environmental Sciences, Newark, DE.

Rheumatoid arthritis (RA) is a chronic autoimmune disease. It is characterized primarily by proliferation of cells in the synovial lining such as fibroblast-like synoviocytes (FLS). Under non-RA settings, FLS are a highly differentiated unicellular cell type. However, under inflammatory milieu, they become hyperplastic, invasive and highly migratory. Epidemiological studies have identified a positive correlation between cigarette smoking, a source of agonistic AHR ligands, and the progressive phenotype of RA. Thus, under inflammatory conditions, we hypothesize the AHR plays an important role in the expression of several growth factors in FLS. Our AHR gene knockdown data in IL-1B activated primary FLS suggest a positive link between ablation of AHR protein activity and suppression of inducibility of vascular endothelial growth factor-A (*VEGF-A*) and epiregulin (*EREG*) mRNA levels. GNF351, a potent AHR antagonist, was also shown to suppress cytokine-mediated upregulation of *VEGF-A*, *EREG* and basic fibroblast growth factor (*FGF-2*) expression, further validating the AHR dependency. ELISA was performed on supernatants collected from FLS-RA cells pre-exposed to GNF351, followed by stimulation with IL-1B, which revealed AHR antagonist-mediated suppression of VEGF-A activity. Cytokine dependent activation of growth factors has been shown to enhance FLS cell proliferation, which was attenuated by GNF351 pretreatment. Upon activation by cytokines, FLS have been shown to become invasive and highly migratory. Treatment of FLS with GNF351 mitigated cytokine-mediated expression of matrix metalloproteinases (MMP) -2 and -9 mRNA levels and also diminished FLS invasive phenotype. Overall, these results suggest that the AHR may be a viable therapeutic target in amelioration of disease progression in rheumatoid arthritis.

**PS 1281 Pregnane X Receptor and Cytochrome P450 CYP2 and CYP3 Gene Responses to Potential Agonists for PXR and AhR2 in Developing Zebrafish.**

A. Kubota, J. Goldstone, B. Lemaire, M. Takata, B. Woodin and J. Stegeman. Biology Department, Woods Hole Oceanographic Institution, Woods Hole, MA.

We addressed responses of developing zebrafish to potential agonists for the pregnane X receptor (PXR; also Steroid Xenobiotic Receptor SXR) and the aryl hydrocarbon receptor (AHR) to determine involvement and interaction of PXR and AHR signaling pathways in regulation of genes in cytochrome P450 subfamilies CYP2 and CYP3. Zebrafish embryos were exposed to 5-pregnen-3 $\beta$ -ol-20-one (pregnenolone; 1-10  $\mu$ M) or to carrier (DMSO) for 24 h, starting at 48 hours post-fertilization (hpf), and then harvested at day 3. We also exposed one-day-old embryos to 3,3',4,4',5-pentachlorobiphenyl (PCB126) or DMSO for 24 h and then held in clean water until day 4. Expression of PXR and selected CYP genes that are potential targets in the PXR signaling was assayed. Pregnenolone caused a concentration-dependent increase in mRNA expression of PXR, some CYP2AAs, CYP3A65 and CYP3C1, all of which peaked at 3  $\mu$ M and then declined. An AHR agonist PCB126 also upregulated the transcript levels of those genes in most cases in a concentration-dependent manner. We next sought to examine the role of the PXR and AHR in the modified expression of those potential target genes by using morpholino antisense oligonucleotides (MO or morpholino) to block initiation of translation of the PXR or AHR. Treatment of embryos with the PXR-MO, but not the control morpholino, partially inhibited pregnenolone-induced expression of PXR, CYP2 and CYP3 genes. Similarly, AHR2-MO treatment blocked PCB126-induced transcript expression of PXR and some CYP2 and CYP3 genes. The present study shows that PXR is not only self-upregulated, but also upregulated via activation of AHR2 in developing zebrafish. Selected zebrafish CYP2 and CYP3 genes appear to be in part under the regulation of PXR and AHR2. They include some CYP2AAs that were first identified in zebrafish. [Support: JSPS Postdoctoral Fellowships for Research Abroad no. 820 (A.K.), and NIH Superfund Research Program grant P42ES00738 (J.S.)]

**PS 1282 Aryl Hydrocarbon Receptor Reduces Cholesterol Absorption by Regulating NPC1L1 Expression.**

R. Tanos, A. Kusnadi and G. H. Perdew. Pennsylvania State University, University Park, PA.

Activation of Ah receptor (AHR) by an exogenous ligand such as dioxin is known to mediate the expression of target genes (e.g. CYP1A1), by binding to dioxin response element (DRE) sequences in their promoter region. We have previously demonstrated the ability of the receptor to attenuate the hepatic expression of cholesterol synthesis genes in a DRE-independent manner in mice and humans without affecting the levels of SREBP2. We opted to look at any changes in the levels of the NPC1L1 protein, a transcriptional target of SREBP2. NPC1L1 is known to mediate the intestinal absorption of dietary cholesterol and is clinically targeted by the drug Zetia, usually used in combination treatment with statins. NPC1L1 is also expressed in the liver although its exact function in this tissue has not been determined conclusively. To examine the effect of AHR activation on NPC1L1 expression, C57BL/6J mice and primary human hepatocytes were exposed to the AHR agonist B-naphthoflavone or selective ligand SGA 360 and results revealed a dramatic repression in the hepatic gene expression of NPC1L1. Attenuation of the expression levels of this gene was also confirmed in the intestine of C57BL/6J mice and a human intestinal cell line (Caco-2 cells). Additionally, activation of the receptor was capable of overcoming the statin-induced increase in NPC1L1 gene expression. Through mutagenesis experiments targeting the two DRE sequences present in the promoter region of the NPC1L1 gene, we established that the repression does not require functional DRE sequences; while knock-down experiments demonstrated that this regulation is AHR-specific and independent of the co-factor p300 and the transcription factor YY1. Finally, cholesterol absorption was shown to be reduced in human intestinal cells following AHR activation. These observations clearly establish a role for the AHR as a key regulator of cholesterol absorption and indicate the potential use of this receptor as a target for the treatment of metabolic diseases.

**PS 1283 Generation and Characterization of a Hairless Mouse Model to Study the Role of Aryl Hydrocarbon Receptor Activation in Response to Ultraviolet Light Exposure.**

K. J. Smith, T. S. Lahoti, J. A. Boyer, K. Wagner, I. Murray and G. H. Perdew. Center for Molecular Toxicology and Carcinogenesis, Pennsylvania State University, University Park, PA.

The aryl hydrocarbon receptor (AHR) is a ligand-activated transcription factor known to be a mediator of biological responses to external stimuli. Reports suggest that endogenous ligands of the AHR include tryptophan photoproducts generated upon exposure to ultraviolet (UV) light, such as 6-formylindolo[3,2-*b*]carbazole (FICZ), linking the AHR to cellular processes occurring in response to UV light. Despite advances in treating UV-related pathologies, the prevalence of detrimental health effects due to UV light indicate that novel therapies are needed. To determine the *in vivo* role of the AHR in UV-mediated inflammation, mouse strains expressing the high affinity ligand binding allele (*Ah<sup>b</sup>*) and low affinity ligand binding allele (*Ah<sup>h</sup>*) of the AHR were generated on an SKH1 hairless mouse background. These strains were characterized using genotyping, AHR proteotyping, and saturation ligand binding assays. The *Ah<sup>b</sup>* allele hairless strain was functionally characterized by the application of FICZ to the ears and compared to SKH1 mice, which exhibit the *Ah<sup>h</sup>* allele, to determine levels of *Cyp1a1* induction, an indicator of AHR transcriptional activity. The *Ah<sup>b</sup>* hairless mice showed greater induction of *Cyp1a1* when compared to the SKH1 mice upon FICZ treatment. *Ah<sup>b</sup>* and *Ah<sup>h</sup>* hairless mouse strains were exposed to UV (360 mJ/cm<sup>2</sup>), followed by skin treatment with a selective AHR modulator (SAhRM), to determine the level of induction of inflammatory genes, and the role of selective activation of the AHR in decreasing inflammatory gene expression. Similar induction of inflammatory genes (e.g., *Ptgs2*, *Il6*, *Il1b*) in untreated skin exposed to UV was seen in both mouse strains, but preferential repression of *Il1b* upon SAhRM treatment was observed only in the *Ah<sup>b</sup>* hairless mice. These strains will be useful in determining how the activity of the AHR can be pharmacologically modified to reduce inflammation upon UV exposure.

**PS 1284 Inhibition of Heat Shock Protein-90 Prevents the Transactivation and Translocation of Human Constitutive Androstane Receptor.**

T. Chen, E. M. Laurenzana, D. M. Coslo, F. Chen and C. J. Omiecinski. *Center for Molecular Toxicology and Carcinogenesis, The Pennsylvania State University, University Park, PA.*

17-(Dimethylaminoethylamino)-17-demethoxygeldanamycin (17-DMAG) is currently in clinical trials for cancer treatment. 17-DMAG is a hydrophilic derivative of geldanamycin (GA), and its analog, 17-(allylamino)-17-demethoxygeldanamycin (17-AAG), all inhibitors of the molecular chaperone, heat shock protein-90 (HSP90). 17-DMAG offers a potential advantage over 17-AAG and GA due to its increased bioavailability, limited metabolism and reduced in vivo toxicity. HSP90 inhibition results in defective protein folding, conformation and assembly of its client proteins, promoting their destabilization and degradation. Client proteins of HSP90 include transmembrane tyrosine kinases (e.g., HER2, EGFR), intermediary signaling kinases (e.g., AKT, p53) and nuclear receptor family members (e.g., AHR, PXR). Previous reports demonstrated that HSP90 is a cytosolic tethering partner of the constitutive androstane receptor (CAR). The present investigation evaluated the potential effects of 17-DMAG on human CAR transcriptional activation and nuclear translocation. 17-DMAG treatments repressed CAR-mediated CYP450 induction in cultured human primary hepatocytes. Cell-based gene reporter assays verified that 17-DMAG inhibited hCAR in a dose-dependent manner. Intracellular localization studies revealed that phenobarbital-stimulated nuclear translocation of hCAR in hepatocytes was completely blocked by 17-DMAG, as well as GA. Immunoprecipitation analyses indicated that the suppression of hCAR activity by 17-DMAG resulted from an enhanced interaction between hCAR and HSP90. Mammalian two-hybrid assays further demonstrated that 17-DMAG disrupted the interaction of hCAR with the nuclear co-activator, SRC1. Together, the data indicate that these targeted HSP90 inhibitors markedly disrupt normal hCAR function, suggesting that their clinical use may potentially impact CAR-mediated drug metabolism and clearance.

**PS 1285 Activation of Transient Receptor Potential Ankyrin-1 by Wood Smoke Particulate Material.**

D. Shapiro, C. E. Deering-Rice, E. G. Romero, G. S. Yost, J. M. Veranth and C. A. Reilly. *Pharm/Tox, University of Utah, Salt Lake City, UT.*

Exposure to wood smoke particulate matter (WSPM) has been linked to exacerbation of asthma, development of chronic obstructive pulmonary disease (COPD), and premature death. Combustion-derived PM (cdPM) such as cigarette smoke (CS), diesel exhaust (DEP), and WSPM, activate transient receptor potential ankyrin-1 (TRPA1) which promotes neurogenic inflammation/edema and airway irritation/cough. The mechanism of TRPA1 activation by DEP and CS involves the electrophilic/oxidant binding (3CK) and menthol-binding (ST) sites, and a novel mechanosensitive site. We hypothesized that WSPM would activate TRPA1 through one or more of these sites similar to other cdPM. Pine and mesquite PM were generated in the laboratory. Both types of WSPM particles activated TRPA1 in human TRPA1 over-expressing HEK-293 and primary mouse trigeminal (TG) neurons. WSPM also activated TRPA1 in A549 cells, a human alveolar adenocarcinoma cell line, which has recently been shown to express TRPA1. HC-030031, a TRPA1 specific antagonist, attenuated the calcium flux due to WSPM treatment in both human A549 cells and mouse primary TG neurons. Several known chemical components of WSPM, including 3,5-di-tert-butylphenol and agathic acid were TRPA1 agonists. Both WSPM and agathic acid activated TRPA1 primarily via binding the 3CK site, based on inhibition of calcium flux by glutathione and mutation of the 3CK site. Conversely, 3,5-di-tert-butylphenol activated TRPA1 through the ST site. This study established the mechanism by which WSPM and associated chemical components activated TRPA1 which may help tailor effective therapeutic treatments for WSPM pneumotoxicity. Support: NIEHS ES017431 and the University of Utah Undergraduate Research Opportunities Program.

**PS 1286 Exploratory Phenotype and Molecular Analysis Study in ROR-Gamma Knockout Mice.**

M. J. Horner<sup>1</sup>, R. Guzman<sup>1</sup>, C. Karbowski<sup>1</sup>, J. Schroeder<sup>1</sup>, C. DiPalma<sup>2</sup>, Y. He<sup>2</sup> and C. Afshari<sup>1</sup>. <sup>1</sup>Amgen Inc, Thousand Oaks, CA; <sup>2</sup>Amgen Inc., Seattle, WA.

Retinoid-related orphan receptor  $\gamma$  (ROR $\gamma$ ) is an orphan nuclear hormone receptor that is widely expressed in several tissues including liver and skeletal muscle. Previous gene expression profiling of liver from ROR $\gamma$  knockout (KO) mice suggested a possible role for ROR $\gamma$  in metabolism of steroids, bile acids, and xenobiotics (Jetten et al. 2007). ROR $\gamma$  has also been shown to regulate several metabolism

genes in skeletal muscle cells. The current study was designed to investigate the effects on pathology and genomics of knocking out the ROR $\gamma$  nuclear receptor in mice with a focus on liver and skeletal muscle tissues. Male and female wild type, heterozygote, or homozygote ROR $\gamma$  KO mice (10/group) were assessed at 10 weeks of age. Study endpoints included clinical observations, body weights, organ weights, gross and microscopic examination of tissues, and gene expression evaluation using RNA isolated from liver, skeletal muscle, and spleen. There was no impact with respect to clinical observations, body weight, and pathology on the phenotype of the heterozygous animals when compared with controls. Although no differences in clinical observations or body weights were observed in the homozygous animals, significant microscopic lesions were present in the thymus (thymic hyperplasia and lymphoma), spleen (increased cellularity), and lymph node (absent). These findings were not unexpected and are in line with established literature (Eberl and Littman 2003; Ueda et al. 2002). Pathway analysis of gene expression changes indicated that a majority of the altered pathways were related to immune response, an expected outcome. Skeletal muscle gene changes suggested a possible role for ROR $\gamma$  in energy homeostasis. However, no perturbations in pathways relevant to toxicological consequences were noted. Taken together, the data showed that knocking out of ROR $\gamma$  in mice led to expected changes in immune-associated pathology and gene expression, but did not reveal any additional phenotypic or genotypic toxicologically relevant effects.

**PS 1287 Estrogen Receptor  $\alpha$  and Aryl Hydrocarbon Receptor Are Not the Sole Determinants of Aminoflavone-Mediated Growth Inhibition.**

A. M. Brinkman<sup>1,2</sup> and W. Xu<sup>1,2</sup>. <sup>1</sup>Molecular and Environmental Toxicology Center, University of Wisconsin Madison, Madison, WI; <sup>2</sup>Department of Oncology, University of Wisconsin Madison, Madison, WI.

Numerous studies have suggested that the aryl hydrocarbon receptor (AhR) may be a potential therapeutic target for several human diseases, including estrogen receptor  $\alpha$  (ER $\alpha$ ) positive breast cancer. Aminoflavone (AF), an activator of AhR signaling that is structurally related to phytochemicals called flavonoids, is currently in clinical trials for the treatment of solid tumors. It has been hypothesized that ER $\alpha$  may be a predictor for response to AF-mediated growth inhibition, with ER $\alpha$ -positive cell lines being sensitive to the drug, and ER $\alpha$ -negative cell lines being resistant. However, the scope of cell lines tested in the literature is limited. Here, we show that ER $\alpha$ -negative human breast cancer cell lines express greater amounts of AhR protein compared to ER $\alpha$ -positive human breast cancer cell lines, giving reason to further characterize AF's efficacy in these models. Using cell counting assays to measure GI<sub>50</sub> values, we show that two ER $\alpha$ -negative breast cancer cell lines, MDA-MB-468 and Cal51, exhibit sensitivity to AF (GI<sub>50</sub> < 1 $\mu$ M), suggesting that ER $\alpha$  is not the sole predictor of responsiveness to AF. To examine the mechanism of AF-mediated growth inhibition, a doxycycline-inducible AhR knockdown system was created in these two cell lines. We show that there is no significant difference in growth inhibition caused by AF treatment in cells where AhR is knocked down and cells with endogenous levels of AhR. This suggests that a portion of the mechanism involved in AF-mediated growth inhibition in MDA-MB-468 and Cal51 cells is AhR-independent, or that compensatory mechanisms may exist. Overall, this work suggests that while ER $\alpha$  is not the sole determinant of sensitivity to AF, this compound may also be inhibiting cell growth in an AhR-independent fashion. Supported by NIEHS Predoctoral Training Grant T32 ES007015.

**PS 1288 Understanding the Physiological Role of Aryl Hydrocarbon Receptor Repressor (AhRR) Using Gene Knock-Down and Targeted Mutagenesis in Zebrafish.**

N. Aluru<sup>1</sup>, S. I. Karchner<sup>1</sup>, M. J. Jenny<sup>1,2</sup> and M. E. Hahn<sup>1</sup>. <sup>1</sup>Biology, Woods Hole Oceanographic Institution, Woods Hole, MA; <sup>2</sup>Biological Sciences, University of Alabama, Tuscaloosa, AL.

The aryl hydrocarbon receptor repressor (AhRR) is a transcriptional repressor of the aryl hydrocarbon receptor (AHR) and is regulated by an AHR-dependent mechanism. In humans, AhRR has been linked to tumorigenesis and reproductive defects. Zebrafish have two AhRR genes; AhRRa regulates constitutive AHR signaling during development, while AhRRb regulates polycyclic aromatic hydrocarbon-induced gene expression. The goal of this study was to elucidate the endogenous role of AhRRs during zebrafish development using two loss-of-function approaches: morpholino oligonucleotide (MO) knock-down and zinc finger nuclease (ZFN)-based gene targeting (knock-out). Zebrafish embryos were microinjected with MOs against AhRRa or AhRRb to knock down the expression of these proteins, followed by microarray analysis of gene expression in embryos at 72 hours post-fertilization. In AhRRa-MO injected embryos, 97 genes were upregulated and 182 genes were downregulated. The latter included cone type photoreceptor-specific

genes, suggesting a role for AHRRa in photoreceptor development. In addition, AHRRa knock-down caused upregulation of embryonic hemoglobin (hbbe3), suggesting a role in hematopoiesis. Knock-down of AHRRb caused upregulation of 31 genes and downregulation of 85 genes, without enrichment of genes related to any specific biological process. These results suggest that AHRRa plays an important endogenous role in development. To understand the role of AHRRa beyond development, we targeted *ahrra* using ZFNs. Microinjection of ZFN mRNA into zebrafish embryos caused a 7 base pair frame shift mutation at the *ahrra* locus. We screened for germline mutants and identified a founder fish that was outcrossed to generate heterozygous mutant offspring. Heterozygous mutants were crossed to generate *ahrra* mutant homozygotes. Using these homozygotes we are investigating the role of AHRRa in normal physiology and toxicology. [Supported by NIH R01ES006272]

**PS 1289 Tissue-Specific Expression of Cytokines and Chemokines in TCDD-Treated B6 and Aryl Hydrocarbon Receptor Repressor Transgenic Mice.**

C. Vogel<sup>1,2</sup>, D. Wu<sup>2</sup>, J. Baek<sup>2</sup>, S. Kado<sup>2</sup>, T. Singh<sup>2</sup>, G. Yang<sup>3</sup>, P. Leung<sup>3</sup>, E. Gershwin<sup>3</sup>, T. Herrmann-Stemmann<sup>4</sup> and E. Matsumura<sup>1,2</sup>. <sup>1</sup>*Environmental Toxicology, University of California Davis, Davis, CA*; <sup>2</sup>*Center for Health and the Environment, University of California Davis, Davis, CA*; <sup>3</sup>*Division of Rheumatology, Allergy and Clinical Immunology, University of California Davis, Davis, CA*; <sup>4</sup>*Institute for Environmental Research, University of Duesseldorf, Duesseldorf, Germany*.

The aryl hydrocarbon receptor (AhR) has been identified as an important transcription factor regulating the responses of immune cells including T cells and dendritic cells but the role of the AhR Repressor (AhRR) is less clear. The AhRR has been first described to suppress AhR activity as an inducible negative feedback loop, then again, there are many unanswered questions, as we know now that the basal or induced cytochrome P450 1A1 (CYP1A1) mRNA level rarely correlates with AhRR expression. To gain insight into the function of AhRR in vivo we developed a transgenic AhRR B6 mouse (AhRR Tg). These transgenic mice express significantly higher levels of AhRR mRNA in all tissues examined such as liver, lymph-node, kidney, spleen, and thymus. Treatment of B6 and AhRR Tg mice with TCDD causes significant induction of AhRR and CYP1A1 in most tissues examined. However, TCDD-induced expression of CYP1A1 was not significantly suppressed in most of the tissues of AhRR Tg mice. The most consistently observed trend in AhRR Tg mice was a repressed induction of several inflammatory markers induced by TCDD as compared to B6 mice. The TCDD-mediated induction in B6 mice as well as the repression in AhRR Tg mice of markers such as IL-1 $\beta$ , IL-6, KC, and COX-2 was tissue-specific. Results show that the AhRR may suppress AhR-mediated induction of inflammatory marker genes and that the AhRR may control AhR activity in the immune system. The cross-talk of AhR with other transcription factors including NF- $\kappa$ B has been well described. Therefore, this study suggests that AhRR interacts especially with alternative AhR pathways rather than simply blocking the classical AhR/ARNT pathway.

**PS 1290 Caloric Restriction Induces Nrf2-Dependent Effects on Lipid Metabolism.**

L. Armstrong, S. R. Kulkarni, J. Xu and A. L. Slitt. *Biomedical and Pharmaceutical Sciences, URI, Kingston, RI.*

Toxcast screening has identified the Nrf2 transcriptional pathway as being highly correlative to chemical promiscuity. Nrf2 is classically defined to have a role in mediating cytoprotection against oxidative stress, but recent work points to a more fundamental metabolic role in lipid metabolism. Studies have indicated that the Nrf2-Keap1 pathway is inducible in adipose tissue, and Nrf2 may have a role in mediating the beneficial effects of caloric restriction (CR). CR promotes the utilization of fat depots and fatty acid mobilization by altering fatty acid synthesis and  $\beta$ -oxidation through modulating Ppar- $\alpha$  and Ppar- $\gamma$  signaling. The potential role of Nrf2 in regulation of lipid metabolism during CR is essential in understanding the metabolic response of white adipose tissue (WAT) to low nutrient conditions. The purpose of the study was to determine the role of Nrf2 in the regulation of lipid metabolism during CR. Adult female lean (C57/BL6) mice and Nrf2KO mice were fed ad-libitum (AL) or placed on a 25% (kCal) reduced diet for 5-7 weeks. Body weight and blood glucose concentrations were monitored. Serum, liver, and white adipose tissues were collected. Hepatic triglycerides, serum free fatty acids, and lipogenic mRNA gene expression in WAT were determined. Overall, CR C57/BL6 mice had a greater percent weight loss (21%) and greater decrease in WAT mass (84%) compared to AL than CR Nrf2KO (11%, 49% respectively). CR C57/BL6

had a 4-fold lower liver triglyceride concentration than AL and 2.5-fold lower concentration compared to CR Nrf2KO. Further analysis of lipogenic genes in adipose tissue supported a dysregulation of the lipogenic pathway in Nrf2KO mice that leads to the resistance of fat utilization during CR. CR increased both Ppar- $\gamma$  and - $\alpha$  along with downstream gene expression (Lpl, Cd36, Scd-1, and Acc-1) in WAT from C57BL/6 mice compared to Nrf2KO mice. Determining whether Nrf2 has a role for mediating beneficial effects for lipid oxidation in WAT could have impact in multiple research areas—including toxicological studies that focus on obesogenic mechanisms.

**PS 1291 Electrophilic Metabolites of Aromatic Hydrocarbons Cause AhR Activation and Up-Regulation of CYP1A1 in HepG2 Cells: Involvement of S-Arylation of Cellular Proteins.**

Y. Abiko<sup>1,2</sup>, A. Puga<sup>2</sup> and Y. Kumagai<sup>1</sup>. <sup>1</sup>*Environmental Medicine Section, University of Tsukuba, Tsukuba, Japan*; <sup>2</sup>*Environmental Health, University of Cincinnati Medical Center, Cincinnati, OH.*

It is well established that aromatic hydrocarbons with 1 or 2 benzene rings and without chlorine substituents are not ligands of the arylhydrocarbon receptor (AHR), a cytosolic ligand activated transcription factor, the main factor responsible for the induction of the *CYP1A1* gene following nuclear translocation. We have recently found that *tert*-butyl-1,4-quinone (TBQ) and 1,2-naphthoquinone (1,2-NQ), electrophilic metabolites of *tert*-butylated hydroxyanisole and naphthalene, respectively, activate NRF2 through S-arylation of its negative regulator, KEAP1. To our knowledge there have not been any reports to indicate that electrophiles that covalently bind to cellular proteins might activate the AHR. In this study, we addressed this question by exposing cells in culture to several of these agents and using immunocytochemistry 12 hours later to determine AHR nuclear translocation. Exposure of HepG2 cells to TBQ, 1,2-NQ, 1,4-NQ or 1,4-benzoquinone, resulted in AHR translocation and *CYP1A1* induction, whereas both measures of AHR activation were negative after treatment with BHA, or naphthalene. Similar results were seen in A459 cells and RAW264.7 cells. TBQ treatment also enhanced the interaction of AHR with ARNT. Interestingly, pretreatment with BSO and NAC to modulate cellular GSH levels enhanced and suppressed 1,2-NQ-mediated activation of AHR, respectively, suggesting that covalent modification of these cellular proteins, possibly through S-arylation of cysteine residues, contributes to the activation. These results suggest that electrophilic metabolites of aromatic hydrocarbons can serve as bifunctional inducers through activation of both AHR and NRF2.

**PS 1292 AhR-Independent Gene Regulation by TCDD in Mouse Liver and Kidney.**

T. M. Seibel<sup>1</sup>, C. Lohr<sup>1</sup>, K. Andresen<sup>2</sup> and D. Schrenk<sup>1</sup>. <sup>1</sup>*Food Chemistry and Toxicology, University of Kaiserslautern, Kaiserslautern, Germany*; <sup>2</sup>*Institute of Biotechnology and Drug Research, Kaiserslautern, Germany.*

Arylhydrocarbon receptor (AhR)-deficient mice have been shown to be resistant to a variety of adverse effects of 2,3,7,8-tetrachlorodibenzo-p-dioxin (TCDD). Furthermore, AhR-deficient mice of various origins exhibit various phenotypes although the physiological function(s) of the AhR still await(s) elucidation. Here, we investigated the effects of TCDD on liver and kidney gene expression in adult female wild-type (wt) and AhR-deficient mice (originating from Finnish Public Health Institute, Kuopio, Finland) from our own breeding five days after treatment with either TCDD, single dose, 25  $\mu$ g/kg body weight, or with corn-oil (vehicle) given by oral gavage. Subsequently, RNA was isolated and Microarray analysis was performed using Agilent Whole Mouse Genome Oligo Microarray 4x44k. In wt mice, 282 genes were more than 2-fold up-regulated by TCDD in the liver including some of well-known AhR target genes like cytochrome P450 (CYP) 1A1, 1A2 and 1B1; 152 genes were up-regulated in the kidney. In AhR-deficient mice, 242 hepatic and 90 renal genes showed an increased expression after TCDD treatment. Among those, 15 hepatic and 13 renal genes were up-regulated in both wt and AhR-deficient animals. None of the core genes of the 'AhR gene battery' except CYP1B1 was up-regulated in AhR-deficient mice. The AhR-independent, TCDD-regulated genes comprise genes involved in lipid, carbohydrate, and amino acid metabolism, and in immune regulation. In wt mice, 203 hepatic and 20 renal genes were more than 2-fold down-regulated. In AhR-deficient mice, 234 hepatic genes including CYP1A2 and CYP3A44 and 235 renal genes showed a decreased expression. In addition, 18 hepatic genes were down-regulated in both wt and AhR-deficient animals. Our results demonstrate that TCDD can cause a broad spectrum of alterations in gene expression in mouse liver and kidney in an AhR-independent manner.

**PS 1293 Coexposure to Aryl Hydrocarbon Receptor and Thyroid Receptor Agonists Enhances Induction of Responsive Genes in Cultured Frog Cells and Prometamorphic Frogs.**

J. D. Taft and W. H. Powell. *Biology, Kenyon College, Gambier, OH.*

Amphibian metamorphosis is a postembryonic developmental process driven by thyroid hormone (TH) and mediated by the thyroid receptor (TR). 2,3,7,8-tetrachlorodibenzo-*p*-dioxin (TCDD) can disrupt TH function in humans and other species. Toxicity of dioxin-like compounds is mediated by the aryl hydrocarbon receptor (AHR). Here we used the African Clawed Frog (*Xenopus laevis*) as a model to probe the interaction of TR and AHR signaling. We quantified relative mRNA expression of both TR and AHR target genes in prometamorphic tadpoles and in XLK-WG cells following exposure to both TR and AHR agonists. Tadpoles (NF 53-55) were exposed to 5 nM TCDD and/or 10 nM T3 for 18 hours. TR targets *BTEB*, *TRβa*, and *TRβb* were not strongly induced by TCDD alone, and AHR target *CYP1A6* was not responsive to T3. However, exposure to both compounds resulted in elevated transcriptional responses of both transcript classes. Compared with T3-exposed animals, *BTEB*, *TRβa*, and *TRβb* mRNAs were 40-70% more abundant following co-exposure with TCDD. Similarly, *CYP1A6* mRNA was ~50% more abundant in tadpoles following T3 co-treatment than with exposure to TCDD only. Comparable patterns were observed in XLK-WG cells. The effect of TCDD on circulating TH varies with species and can differ for T4 and T3. While the superinduction of TH-responsive frog genes could involve TCDD-related alteration of TH levels, the requirement for co-treatment and the effect in cultured cells suggest the possibility of a transcriptional mechanism. We examined the promoter regions of *BTEB*, *TRβb*, and *CYP1A6*, finding potential cognate binding elements for each receptor. Overall, our results suggest some degree of co-regulation of the expression of several genes by both AHR and TR. Frogs display great insensitivity to TCDD toxicity, and frog AHRs bind TCDD with low affinity. We hypothesize that the induction of TR-regulated genes by AHR may represent an additional mechanism for protection of metamorphosis from disruption by xenobiotic or endogenous AHR agonists. (NIH: R15 ES011130)

**PS 1294 A Global Genomic Screening Strategy Reveals Diverse Activators of Constitutive Activated Receptor (CAR).**

K. Oshida<sup>1</sup>, N. Vasani<sup>1</sup>, B. Chorley<sup>1</sup>, S. Hester<sup>1</sup>, W. Ward<sup>1</sup>, R. S. Thomas<sup>2</sup>, D. Applegate<sup>3</sup>, L. M. Aleksunes<sup>4</sup>, C. D. Klaassen<sup>5</sup> and C. Corton<sup>1</sup>. <sup>1</sup>US EPA, Research Triangle Park, NC; <sup>2</sup>Hammer Institute, Research Triangle Park, NC; <sup>3</sup>Regenomed, Inc, San Diego, CA; <sup>4</sup>Rutgers University, New Brunswick, NJ; <sup>5</sup>KUMC, Kansas City, KS.

A comprehensive survey of conditions that activate CAR in the mouse liver has not been carried out but would be useful in understanding their impact on CAR-dependent liver tumor induction. A gene signature dependent on CAR activation was identified by comparing the transcript profiles after exposure to three CAR activators (phenobarbital, TCPOBOB, CITCO) in wild-type and CAR-null mice. In independent experiments using transcript profiles from the livers of chemically-exposed male or female mice, the signature correctly predicted activation of 3 CAR activators but not 9 activators of other pathways. The signature was used with 5 classification methods (e.g., support vector machines, K-nearest neighbors) to identify conditions in which CAR was activated in an Affymetrix compendium of ~750 mouse liver transcript comparisons encompassing a broad range of chemical, dietary and genetic perturbations. We found that CAR is activated by a large number of chemicals, dietary regimens and genetic mutations. Specific and novel findings include activation by 1) two PXR activators in a PXR-dependent manner indicating crosstalk between CAR and PXR, 2) 12 out of 15 chemical and triglyceride activators of PPARα to greater levels in PPARα-null mice than in wild type mice indicating that most PPARα activators are also CAR activators and there exists antagonism between CAR and PPARα, and 3) null mutations in a number of transcription factors (AhR, Fxr, Hnf1a, Pxr) that control expression of genes involved in metabolism of exogenous and endogenous chemicals. The findings increase our understanding of the factors that impact CAR activation and that could contribute to increases in CAR-dependent liver tumors. This abstract does not represent EPA policy.

**PS 1295 Effects of Munitions Compounds on Xenobiotic-Activated Nuclear Receptors and Cell Signaling Pathways.**

D. R. Johnson<sup>1</sup>, C. Y. Ang<sup>2</sup>, T. Habib<sup>2</sup> and E. J. Perkins<sup>1</sup>. <sup>1</sup>Environmental Laboratory, US Army Engineer Research & Development Center, Vicksburg, MS; <sup>2</sup>Badger Technical Services, Vicksburg, MS.

Exposure to certain munitions compounds is known to alter physiological functions in test organisms, however little is known about their molecular and cellular effects. The objective of this study to characterize the effects of new and existing

munitions compounds on xenobiotic-activated nuclear receptors and cell signaling pathways. Munitions compounds (0.01-10 mg/l) (e.g., nitroaromatics, cyclic nitramines, and new insensitive munitions) were added to wells containing transfected cells containing high constitutive levels of nuclear receptors for 24 h, then examined for nuclear activation according to in-house and commercially available kits. In general, nitroaromatic compounds had greater effects on nuclear receptor activity decreased nuclear receptor activity than other munitions compounds. Nitroaromatic munitions decreased activation of constitutive androstane receptor (CAR), peroxisomal proliferator activated receptors (PPAR), liver x receptor (LXR) at higher concentrations examined, whereas some nitroaromatic compounds activated the Ah receptor. Effects on 45 cell signaling pathways were examined using the Signal Finder multi-pathway reporter array kit that reverse-transfected transcription factor-firefly luciferase reporter plasmids into HepaRG liver cells. Cells were then exposed to munitions compounds for 24 h, then examined for signal pathway activation. Trinitrotoluene (TNT) and its environmental byproducts differentially activated cell signaling pathways, with at least two pathways commonly shared (AhR and Nrf2/Nrf1). 2,4-Dinitroanisole, a new TNT replacement munitions, activated fewer cell signaling pathways than TNT. These results create a more comprehensive picture of munitions effects within cells and potential down-stream effects within organisms. Furthermore, rapid nuclear bioassays, such as the ones described above, may help material scientist predict biochemical pathways that may be impacted by newly developed munitions earlier in the development process.

**PS 1296 The Aryl Hydrocarbon Receptor Depletion in Human MDA-MB-231 Breast Cancer Cell Line Attenuates *In Vivo* Tumor Growth and Pulmonary Metastasis in a Nude Mouse Model.**

G. Goode and S. E. Eltom. *Biochemistry and Cancer Biology, Meharry Medical College, Nashville, TN.*

The aryl hydrocarbon receptor (AhR) is a ligand activated transcription factor that is best characterized for its role in mediating the toxic responses elicited by environmental poly aromatic hydrocarbons (PAH). However there is compelling evidence for a PAH-independent role of AhR in breast cancer. AhR is overexpressed and constitutively activated in several human breast carcinoma cell lines and shows strong correlation with the degree of the tumor malignancy. In the present study we examine the effect of depleting AhR expression in the highly metastatic MDA-MB-231 human breast cancer cell line on tumor growth and experimental pulmonary metastasis in a nude mouse model. The AhR was stably knocked down using shRNA targeting AhR gene. Clonal cell line of MD231 HBC with approximately 80% depletion of AhR and its scramble control cells were transfected to stably and constitutively express luciferase gene for the purpose of *in vivo* bioluminescence imaging of tumors. Cells were injected either orthotopically in the mammary fat pad for monitoring the primary tumor growth, or intravenously in the lateral tail vein, for monitoring pulmonary experimental metastasis. Results showed that knock down (KD) of AhR expression significantly reduced incidence of mice with tumor growth, prolonged the latency and reduced tumor size in those mice which developed tumors compared to controls. Mice with AhR KD in the experimental metastasis group showed a significant reduction in the number of animals with lung metastasis compared to control, and decreased numbers and sizes of pulmonary metastasis in those, which manifested metastasis. Global gene expression profiling identified sets of genes associated with tumor growth and metastasis that have been altered subsequent to depletion of AhR, and are likely to account for these phenotypes. Our data provide the first *in vivo* evidence for the role of AhR in regulating breast cancer metastasis and identified it as a therapeutic target for metastatic breast cancer.

**PS 1297 Species Specificity of the Peroxisome Proliferator Response in Primary Hepatocytes.**

P. D. McMullen, S. Bhattacharya, C. G. Woods, R. A. Clewell, E. L. LeCluyse, K. M. Yarborough, L. Pluta, P. Lu, J. Dong, J. Pi and M. E. Andersen. <sup>1</sup>Clinical Research Program, NIEHS, Durham, NC; <sup>2</sup>Cell Adhesion Group, NIEHS, Durham, NC; <sup>3</sup>Pharmacology and Toxicology, East Carolina University, Greenville, NC; <sup>4</sup>National Toxicology Program (NTP), NIEHS, Durham, NC.

Perturbations induced by environmental chemicals often lead to different physiological outcomes in humans and rodents, calling into question the applicability of animal-based toxicity testing for human risk assessment. For example, peroxisome proliferators, which include several purported endogenous fatty acids as well as a number of synthetic ligands, induce lipid metabolism enzymes in humans and have been used successfully as therapeutic strategies for various dyslipidemias and diabetes. For rodents, in addition to their role in regulating fatty acid metabolism, peroxisome proliferators also influence peroxisome assembly, inflammatory responses,

and cellular proliferation. Understanding the basis for differences in clinical repercussions across species is essential to translating information from animal models to human health.

Here we present a genomic characterization of the response of human and rat primary hepatocytes to the PPAR $\alpha$ -specific agonist GW7647. We used gene expression microarray experiments to compile a highly resolved time- and dose-response characterization of the difference of the PPAR $\alpha$ -mediated response in these two species. Consistent with the qualitative differences in the response to peroxisome proliferators, we identified a substantially larger set of differentially expressed genes in rat cells compared to human. These additional genes include a suite of developmental processes that may account for the increased toxicity of peroxisome proliferators in rodents. Surprisingly, in both species, we found that the canonical nuclear receptor response mechanism accounts for only a small fraction of detected response, suggesting a larger role for non-genomic mechanisms than was previously thought.

## PS 1298 Development of a Rapid, Cell-Based Screen for Disruptors of the Retinol (Vitamin A) Signaling Pathway.

Y. Chen and D. H. Reese. *OARSA/CFSAN, US FDA, Laurel, MD*. Sponsor: T. Flynn.

A central goal in the 2007 National Research Council's vision for Toxicity Testing in the 21st Century is the development of a comprehensive suite of in vitro tests covering the major signaling pathways (toxicity pathways) in mammals that can be used for evaluating chemical toxicity while reducing or eliminating the use of animals. Our research focuses on the development of in vitro screens for detecting chemicals in food additives, supplements, and contaminants that can disrupt the major cellular signaling pathways in mammals. One of these pathways, the retinol (vitamin A) signaling pathway, is essential for life in all mammals. It is required for both normal embryonic development and maintenance of cellular phenotype in adult organisms; chemicals that cause even minor interference with its normal function and output are potential fetal and adult toxicants. We have developed a rapid (24 h) screen for detecting chemicals that disrupt this essential signaling pathway. It uses the mouse pluripotent P19 stem cell line and a medium-throughput 96-well format gene-expression assay to detect disrupting chemicals. It has detected all known retinol signaling pathway disruptors and some chemicals that are closely related, structurally, to known disruptors. Significantly, it also has detected members of a class of chemicals, the endocrine disruptors, which have not been associated previously with disruption of this pathway; chemicals that caused disruption included xenoestrogens (DES, BPA, 4-n-nonylphenol, and genistein and phthalate esters (dibutyl phthalate and diphenyl phthalate but not bis(2-ethylhexyl) phthalate). The effects of members of this class of chemicals on the pathway suggest the existence of an additional non-genomic mechanism of action by which some endocrine disrupting chemicals cause toxicity.

## PS 1299 Asian Ginseng (*Panax ginseng*) Potentiates Ethanol-Induced Cardiovascular Dysfunction in Medaka Embryogenesis (*Oryzias latipes*).

M. H. Haron<sup>2,1</sup>, L. A. Walker<sup>1,2</sup>, I. A. Khan<sup>1</sup> and A. K. Dasmahapatra<sup>1,2</sup>.  
<sup>1</sup>National Center for Natural Product Research, University of Mississippi, University, MS; <sup>2</sup>Department of Pharmacology, University of Mississippi, University, MS.

Alcohol is a teratogen, induces fetal alcohol spectrum disorder (FASD) which has serious central nervous system (CNS), cardiovascular, and craniofacial defects affecting the entire lifetime of an individual. Prevention of FASD, other than women abstaining from drinking alcohol during pregnancy, is not known. The synthetic drugs recommended for the treatment of alcoholism cannot be used by women during pregnancy which led us to investigate on natural products. Due to ethical constraints FASD studies in humans are very limited and several animal models are used to understand the molecular mechanisms. We have observed that developmental ethanol exposure of medaka (*Oryzias latipes*) embryos generates features which are analogous to human FASD phenotypes. We hypothesize that ethanol metabolism generates oxidative stress which can disrupt embryonic development of medaka. In the present experiment, we have used root extracts of Asian ginseng (*Panax ginseng*) as a preventive agent of FASD. Fertilized medaka eggs within 4 h post fertilization (hpf) were exposed to methanolic extracts (50-100  $\mu$ g/ml) of ginseng root (PG) or ethanol (300 mM) either alone or in combination. After 48 h of treatment the viable embryos were transferred to clean hatching solution and on 6 dpf the embryos were examined for vessel circulation followed by mRNA analyses of enzymes related to ethanol metabolism and oxidative stress. It was observed that ethanol (300 mM) alone was able to disrupt vessel circulation and cotreatment of PG (50-100  $\mu$ g/ml) with ethanol was able to enhance the effect; PG (100  $\mu$ g/ml) alone has no effect. mRNA analysis of alcohol metabolizing enzymes or oxidative

stress-related enzymes did not show any significant alterations in any of these treatment conditions. It is therefore concluded that potentiation of ethanol-induced cardiovascular deformities in medaka by PG may be mediated through a different mechanism rather than oxidative stress.

## PS 1300 Toxicology Profile of Virginia Cedarwood Oil Delivered via Dermal Application.

I. Surh<sup>1</sup>, R. A. Herbert<sup>2</sup>, G. S. Travlos<sup>2</sup>, M. Vallant<sup>3</sup>, L. M. Fomby<sup>4</sup>, M. R. Hejtmancik<sup>4</sup> and P. Chan<sup>1</sup>. <sup>1</sup>Toxicology Branch, Division of the National Toxicology Program, NIEHS, Research Triangle Park, NC; <sup>2</sup>Cellular and Molecular Pathology Branch, DNTP, NIEHS, Research Triangle Park, NC; <sup>3</sup>Program Operations Branch, DNTP, NIEHS, Research Triangle Park, NC; <sup>4</sup>Battelle, Columbus, OH.

Virginia cedarwood oil (CWO), which is extracted from *Juniperus virginiana* trees, is widely used as an insect repellent and a fragrance in cosmetic formulations resulting in human exposure. To investigate the toxicological effects of CWO, 90-day studies in F344 N rats and B6C3F1/N mice were conducted. CWO was administered by dermal application to male and female rats and mice at concentrations of 0, 6.25, 12.5, 25, 50% (v/v) in 95% ethanol or 100% daily (excluding weekends) for up to 14 weeks with an untreated control included. In rats, there were no effects on survival or body weights except in the 100% males in which 2 rats were terminated on day 79 due to severe skin lesions and a 13% lower group final mean body weight than that of the untreated control. All male and female mice in the 100% group were terminated during week 10 due to the severity of skin lesions. Final group mean body weights for females given 12.5, 25 or 50% and males given 50% were less than 90% of the controls. At the site of application, treatment related irritation, thickened skin, and ulcer formation were observed in all treated groups of rats and mice, except the 6.25% groups in rats. Clinical pathology showed an inflammatory leukogram secondary to dermal ulcers/inflammation in both rats and mice; mice also had a decreased erythron. In rats and mice there were dose-dependent increases in incidences and severity of skin lesions at the site of application, and bone marrow hyperplasia. In rats, there were dose-dependent increases in incidences and severity of kidney lesions in males. Male mice demonstrated increased incidences of kidney nephropathy and thymus atrophy.

## PS 1301 Novel Antiplatelet Activity of Protocatechuic Acid through Inhibition of High Shear Stress-Induced Platelet Aggregation.

K. Kim<sup>1</sup>, K. Lim<sup>1</sup>, J. Noh<sup>1</sup>, S. Kang<sup>1</sup>, K. Chung<sup>2</sup>, O. Bae<sup>3</sup> and J. Chung<sup>1</sup>.  
<sup>1</sup>College of Pharmacy, Seoul National University, Seoul, Republic of Korea; <sup>2</sup>School of Pharmacy, Sungkyunkwan University, Suwon, Republic of Korea; <sup>3</sup>College of Pharmacy, Hanyang University, Ansan, Republic of Korea.

Bleeding is the common and serious adverse effect of currently available antiplatelet drugs. Many efforts are being made to develop novel anti-thrombotic agents without bleeding risks. Shear stress-induced platelet aggregation (SIPA) which occurs under abnormally high shear stress plays a crucial role in the development of arterial thrombotic diseases. Here we demonstrated that protocatechuic acid (PCA), a bioactive phytochemical from *Lonicera* (honeysuckle) flowers, selectively and potently inhibits high shear (>10,000 s<sup>-1</sup>)-induced platelet aggregation. In isolated human platelets, PCA decreased SIPA and attenuated accompanying platelet activation including intracellular calcium mobilization, granule secretion and adhesion receptor expression. Anti-SIPA effect of PCA was mediated through blockade of von Willebrand factor (vWF) binding to activated GPIb, a primary and initial event for the accomplishment of SIPA. Conspicuously, PCA did not inhibit platelet aggregation induced by other endogenous agonists like collagen, thrombin or ADP that are important both in pathological thrombosis and normal haemostasis. Anti-thrombotic effects of PCA were confirmed in vivo in rat arterial thrombosis model, where PCA significantly delayed the arterial occlusion induced by FeCl<sub>3</sub>. Of a particular note, PCA did not increase bleeding time in rat tail trans-section model, while conventional anti-platelet drugs, aspirin and clopidogrel substantially prolonged it. Collectively, these results suggest that PCA may be a novel antiplatelet agent which can prevent thrombosis without increasing bleeding risks.

## PS 1302 The Soy-Associated Phytoestrogen, Genistein, Does Not Protect Against Alcohol-Induced Osteoporosis in Male Mice.

C. Yang<sup>1</sup>, K. Mercer<sup>1</sup>, L. Suva<sup>1</sup>, T. M. Badger<sup>2,1</sup> and M. Ronis<sup>2,1</sup>. *The Hamner Institutes for Health Sciences, Research Triangle Park, NC.*

Alcohol abuse acts as a risk factor for osteoporosis by increasing osteoclast activity and decreasing osteoblast activity in bone. These effects can be reversed by estradiol. Soy diets are also suggested to have protective effects on bone loss in men and

women, as a result of the presence of soy protein-associated phytoestrogens such as genistein and daidzein. In this study, male mice were pair fed (PF) a control diet, an EtOH diet or EtOH diet supplemented with genistein (250 mg/kg) for 8 weeks. Ex vivo microCT analyses of formalin fixed tibias from each group revealed a significant decrease in trabecular bone in the EtOH group in comparison with the pair-fed control in regards to bone volume (BV/TV), trabecular number (Tb.N), and trabecular separation (Tb.Sp), ( $p < 0.05$ ). No protective effect by genistein was observed in the EtOH+genistein group compared to the EtOH group in BV/TV, Tb.N, and Tb.Sp. Interestingly, there was an increase in trabecular thickness (Tb.Th) in the PF+genistein group compared to the PF ( $P < 0.05$ ), suggesting genistein can affect bone remodeling. In ex vivo bone marrow cultures, EtOH exposure decreased the number pre-osteoblasts compared to PF controls. In contrast, exposure to EtOH+genistein increased pre-osteoblast numbers compared to the EtOH-treated group, ( $p < 0.05$ ). These findings suggest that genistein has a partial protective effect on bone formation. In conclusion, genistein does not protect against ethanol induced bone loss despite increasing osteoblastogenesis. Supported in part by R01 AA18282 (M.J.R.) and UAMS INBRE award 8 P20 GM103429-11.

### PS 1303 Toxicological Safety Assessment of a Hydroethanolic Extract of *Caralluma fimbriata*.

J. R. Endres<sup>1</sup>, N. Deshmukh<sup>2</sup> and A. G. Schauss<sup>1</sup>. <sup>1</sup>AIBMR Life Sciences, Inc., Puyallup, WA; <sup>2</sup>INTOX Pvt. Ltd., Pune, India.

A toxicological safety assessment was conducted on a hydroethanolic extract of *Caralluma fimbriata*, an ingredient marketed as an appetite suppressant, to predict safety with oral consumption by humans. *Caralluma fimbriata* extract (CFE) is standardized to contain no less than 25% pregnane glycosides and no less than 10% saponin glycosides. The extract is >98% soluble in water. CFE is currently sold as the trademarked ingredient Slimaluma™. Two genotoxicity studies were conducted and no evidence of mutagenicity or genotoxicity was observed in the presence or absence of a rat liver S9 metabolic activation system at concentrations up to 5,000 µg of extract/plate (Ames Bacterial Reverse Mutation Assay) or 5,000 µg of extract/mL in a chromosomal aberration assay. Studies conducted in Wistar rats included a 14-day acute oral toxicity study, and a 90-day repeated oral toxicity study. A 6-month repeated oral toxicity study was conducted in Sprague-Dawley rats. In the 14-day study, the NOAEL was determined to be 5 g/kg bw. While a few statistically significant ( $p < 0.05$ ) findings were observed in the 90-day Wistar rat study, it was considered to be a sound basis for conducting a 6-month study. In the 6-month Sprague-Dawley rat study, the no observed effect level (NOEL) was concluded as 1,000 mg/kg bw/d, the highest dose group tested. Finally, in a developmental toxicity study in Sprague-Dawley rats no fetal abnormalities related to administration of the test article were observed.

### PS 1304 The Antidiabetic Activities of the Soft Drink Leaf Extract of *Phyllanthus amarus* (Order Euphorbiales; Family Euphorbiaceae) in Laboratory Animals.

A. A. Adedapo and S. O. Ofuegbi. *Veterinary Physiology, Biochemistry and Pharmacology, University of Ibadan, Ibadan, Nigeria.*

*Phyllanthus amarus* Schum (Family Euphorbiaceae) is an annual herbal shrub which has been used in traditional medicine in Nigeria to treat some disease conditions. This study evaluated the soft drink extract (SDE) of the plant for anti-diabetic activities in rats.

SDE was prepared by dissolving fresh aerial parts of the plant in 7up soft drink for 48 h, filtered, lyophilized and then used for the pharmacological investigations. Standard phytochemical methods were used to test for the presence of phytoactive compounds in the plant. Acute toxicity was carried out in mice to determine safe doses for this plant extract. The anti-diabetic activities of the SDE of the plant were assessed using some standard tests as well as histological changes in liver, kidney and pancreas. Diabetes mellitus was induced in rats using alloxan while glibenclamide at 0.2mg/kg was the reference drug used in this study.

The SDE at 200 and 400mg/kg body weight caused a significant reduction of fasting blood glucose, significant change in the oral glucose tolerance test, marked effect in the hypoglycaemic activity test, and pronounced reduction on the glucose, cholesterol and triglyceride levels of diabetic rats. The haemograms of all treated diabetic rats experienced recovery. Histopathologically, the liver of the diabetic non-treated and glibenclamide-treated groups showed widespread vacuolar change in the hepatocytes but there was no visible lesion seen in the kidney and pancreas of extract-treated and glibenclamide-treated groups. No lesion was also seen in the liver of SDE-treated group.

In conclusion, the results from this study may have validated the traditional basis for the use of *Phyllanthus amarus* as antidiabetic agent. The pharmacological activities noted in this study may be attributed to the presence of flavonoids and other phenolics contained in this plant. At the doses used, SDE also appeared safer than glibenclamide even though the latter is more potent.

### PS 1305 Protective Effects of Methanolic Root Extract of *Balanites aegyptiaca* (L.) Delile on Carbon Tetrachloride (CCl<sub>4</sub>)-Induced Hepatotoxicity in Rats.

O. A. Salawu<sup>1</sup>, F. Tukur<sup>2</sup>, A. Y. Tijani<sup>1</sup>, J. Ejiofor<sup>2</sup> and S. Ahmed<sup>3</sup>.

<sup>1</sup>Pharmacology and Toxicology, National Institute for Pharmaceutical Research and Development (NIPRD), Abuja, Nigeria; <sup>2</sup>Pharmacology and Therapeutics, Ahmadu Bello University, Zaria, Nigeria; <sup>3</sup>Pathology, Ahmadu Bello University Teaching Hospital, Zaria, Nigeria.

Objective: *Balanites aegyptiaca* (BA), a widely grown desert tree found in Africa and Asia is used as a remedy for several ailments including liver and spleen diseases. This study evaluated the protective activity of the methanol extract of BA root by direct (curative and prophylactic models) and indirect (barbiturate-induced sleep model) methods in CCl<sub>4</sub>-induced hepatotoxic rats.

Methods: In the curative study, 0.5 ml/kg CCl<sub>4</sub> was given intraperitoneally (ip) on alternate days, for 5 days, followed by 100, 200 and 400mg extract/kg orally daily, for 7 days. Other groups received the vehicle only, CCl<sub>4</sub> and the vehicle, and CCl<sub>4</sub> and the standard drug, silymarin (100 mg/kg/day) respectively. In the prophylactic study, all the rats received the treatment respectively for the first 7 days followed by CCl<sub>4</sub> as above. Degree of liver protection was measured in the rats by biochemical parameters (serum alanine transaminase, aspartate transaminase, alkaline phosphatase, albumin, bilirubin, triglycerides and cholesterol levels) monitoring, physical (weight) and histopathological changes in the liver. The indirect method was same as in prophylactic study but on the 13th day, the rats were given 25mg pentobarbitone sodium/kg ip and observed for onset and duration of sleep.

Results: Pre-treatment with the extract significantly ( $P < 0.05$ ) decreased CCl<sub>4</sub>-induced elevation of serum levels of the biochemical parameters, better than silymarin. In the curative study, its effect was comparable with that of silymarin. It also significantly decreased pentobarbitone sleeping time. There was improved tissue histopathology in both studies.

Conclusion: These results showed that BA root has significant hepatoprotective activities and could be useful as 'lead' in the development of new hepatoprotective agent.

### PS 1306 The Effects of Citrus Auraptene in Combination with All-Trans Retinoic Acid on Human Squamous Cell Carcinoma in a Xenograft Model.

H. E. Kleiner<sup>1</sup>, E. R. Lane<sup>1</sup>, J. Mathis<sup>2</sup>, J. McLarty<sup>3</sup>, M. S. Prince<sup>1</sup>, S. R. Crooks<sup>1</sup>, J. L. Clifford<sup>4</sup> and E. A. Orchard<sup>1</sup>. <sup>1</sup>Department of Pharmacology Toxicology & Neuroscience, Louisiana State University Health Sciences Center, Shreveport, LA; <sup>2</sup>Anatomy and Cellular Biology, Louisiana State University School of Health, Shreveport, LA; <sup>3</sup>Medicine, Louisiana State University Health Sciences Center, Shreveport, LA; <sup>4</sup>Biochemistry & Molecular Biology, Louisiana State University Health Sciences Center, Shreveport, LA.

Over 2,000,000 new cases of non-melanoma skin cancer (NMSC) are expected in the United States in 2012. Our group has previously demonstrated that citrus auraptene (AUR), combined with all-trans retinoic acid (ATRA), can inhibit the growth of human skin squamous cell carcinoma (SCC) tumors from the cell line SRB12-p9 (P9WT) in SCID/bg mice. ATRA is known to inhibit the STAT3 pathway, whereas AUR suppresses the activation of NF-κB and induces antioxidant enzymes such as glutathione S-transferase (GST). NF-κB and STAT3 are both hyperactivated in cancer. We hypothesize that suppressing both pathways by these compounds will produce a greater chemopreventive effect than by using either agent alone. Groups of 10 each female SCID/bg mice were injected with  $1 \times 10^6$  P9WT cells, s.c. Mice were dosed with AUR (0, 100, 200, 400 mg/kg bw) ± ATRA (2 mg/kg bw), p.o., beginning 4 days prior to tumor cell injection and 4 days/wk for the duration of the study (48 days). Tumor volumes were estimated by caliper. At the end of the tumor study, necropsies were performed, and tissues taken for further analyses. Statistical analyses revealed no effect of AUR by itself on tumor volumes. ATRA alone suppressed tumor volume by 16-fold. However, ATRA was so effective at blocking tumor volume that any additional effects of AUR may have been masked. ATRA also caused a loss of body weight, but the liver/body weight ratios were not different across groups, and the activity index of the mice was within range. In conclusion, this study will be repeated using lower doses of ATRA, in combination with AUR to determine the minimum effective dose of ATRA, (known to be toxic) while assessing the effect of the AUR. (SR21CA149761-02)

**PS 1307 Toxicological Evaluation of the Aqueous Extract of *Morinda morindoides* Root Bark.**

M. O. Abatan<sup>1,2</sup>, J. O. Olukunle<sup>2</sup>, O. L. Ajayi<sup>3</sup>, M. O. Olaniyi<sup>3</sup> and O. T. Adenubi<sup>2</sup>. <sup>1</sup>Veterinary Physiology, Biochemistry and Pharmacology, University of Ibadan, Ibadan, Nigeria; <sup>2</sup>Veterinary Physiology and Pharmacology, University of Agriculture, Abeokuta, Abeokuta, Nigeria; <sup>3</sup>Veterinary Pathology, University of Agriculture, Abeokuta, Abeokuta, Nigeria.

Toxicological evaluation of *Morinda morindoides* root bark was carried out using hematological and serum biochemical changes accompanying prolonged administration of the aqueous leaf extract of the plant in Wistar rats. Twenty rats were randomly but equally divided into four groups. Rats in groups I were administered with 0.9% physiological saline (10ml/kg b.w) as the control animals, while rats in groups II, III and IV were administered with aqueous extract at 400, 800 and 1600 mg/kg body weight respectively once daily for 28 days according to the acute toxicity study carried out. Parameters evaluated were complete blood count, serum protein, metabolites and enzymes. Samples from liver, spleen, heart, and kidney were processed for histopathology. Data were expressed as mean  $\pm$  Standard Error of Mean and analyzed using one way ANOVA. Difference of means are considered statistically significant at  $p < 0.05$ .

There were no significant changes in the hematological parameters between the treated groups and the control group. Rats in group IV exhibited significant increase in the serum levels of alkaline phosphatase, aspartate amino transaminase, alanine amino transferase and creatinine. Histopathology revealed mild diffuse degeneration of the liver, mild tubular nephrosis and mononuclear cellular infiltration in the heart. It was concluded that ethnomedicinal application of *Morinda morindoides* is quite safe at lower doses but it is hepatotoxic, nephrotoxic and cardiotoxic at higher doses.

**PS 1308 Antidiarrheal Evaluation of Aqueous and Ethanolic Leaf Extracts of *Acacia sieberiana* DC (*Fabaceae*) in Albino Rats.**

C. J. Dawurung, I. L. Elisha, N. V. Offiah, J. G. Gotepe, O. O. Oladipo, M. S. Makoshi, S. Makama and D. Shamaki. *Drug Development Unit, Biochemistry Division, National Veterinary Research Institute (NVRI) Vom, Jos, Nigeria.*

Sequel to reports on the use of *Acacia sieberiana* leaves in the management of animal diarrhea in some parts of Plateau State Nigeria, the anti diarrheal activity of aqueous and ethanolic extracts of the leaves of *A. sieberiana* were evaluated in albino rats. Studies were carried out on castor oil induced diarrhea and gastrointestinal transit at doses of 300, 600, and 1200 mg/Kg body weight. Both extracts did not show any significant ( $P > 0.05$ ) inhibitory effect in both assays when compared to the negative controls. The standard drugs, loperamide (10 mg/Kg) and atropine sulphate (3 mg/Kg) significantly ( $P < 0.05$ ) inhibited diarrhea and reduced the distance travelled by the activated charcoal in the intestine respectively. Phytochemical screenings of the extracts revealed the presence of saponins, cardiac glycosides, and flavonoids in both extracts, while tannins were present only in the ethanolic extract. In the toxicity test (limit test), no deaths or any apparent signs of toxicity or side effects were observed in the animals following the oral administration of both extracts at 2000 mg/Kg. The traditional use of *A. sieberiana* leaves in the management of diarrhea could not be justified by this study. Further work to assess the antibacterial, antiviral, anthelmintic and antiprotozoal activity of the leaves and antidiarrheal evaluation of other parts of the plant is necessary to verify the folkloric claims for its use in diarrheal management.

**PS 1309 Protection by Fish Oil against D-Galactosamine-Induced Hepatic Injury and Biochemical Alterations in the Plasma and Liver of Rats.**

Y. Shen, M. C. Parikh and C. A. Lau-Cam. *Pharmaceutical Sciences, St. John's University, Flushing, NY.* Sponsor: B. Billack.

The present study has investigated the actions of fish oil (FO) on D-galactosamine (GalN)-induced changes in plasma glucose (GLC), bilirubin, total proteins (TP) and enzymatic indices of hepatic damage; and in the levels of plasma and hepatic triglycerides (TG) and cholesterol (CHOL). Groups of 6 male Sprague-Dawley rats, 220-50 g in weight, were treated for 3 consecutive days with a 600 mg/kg oral dose of FO, as an emulsion in 0.9% NaCl-tween 20. On day 4, the rats received a single intraperitoneal, 400 mg/kg, dose of GalN in 0.9% NaCl. Additional rats received only the vehicles of the treatment solutions (control group), only GalN or only FO. All the rats were sacrificed by decapitation under isoflurane anesthesia 24 hr after receiving GalN, and their blood and livers were collected. The plasma fraction was analyzed for GLC, TG, CHOL, total (TB) and direct (DB) bilirubin, TP,

alanine transaminase (ALT), aspartate transaminase (AST) and alkaline phosphatase (ALP). A portion of liver was made into a 1:20 (w/v) homogenate in phosphate buffered saline pH 7.5 which was analyzed for its contents in TG and CHOL. Relative to control values, GalN increased the plasma GLC (41%), ALT (>200%), AST (>110%), ALP (+ 54%), TB (6.3-fold), DB (46-fold), TG (5.3-fold) and CHOL (1.6-fold) while decreasing those of TP (by 59%) (all at  $p \leq 0.01$ ). In addition, GalN increased the liver weight to body weight ratio (35%) and the levels of TG (61%) and CHOL (400%) significantly ( $p \leq 0.01$  vs. control). A pre-treatment with FO was able to attenuate the changes in plasma and liver components as well as in the liver weight to body weight ratio to a significant extent ( $p \leq 0.05$ ). By itself, FO was found to raise the plasma (98%) and liver TG (23%) and the liver CHOL (33%) significantly ( $p \leq 0.05$ ), but not as much as GalN. In conclusion, FO is found to protect the liver against GalN-induced hepatic injury, dysfunction and fat buildup and to attenuate accompanying changes in circulating GLC, TP, TG and CHOL.

**PS 1310 The Phototoxicity of Tagetes Oil and Absolute Evaluated Utilizing a Human Epidermal Model and Patch Testing.**

J. F. Lalko and A. Api. *Research Institute for Fragrance Materials Inc., Woodcliff Lake, NJ.*

Tagetes essential oil and absolute (*Tagetes minuta* L.) are utilized as fragrance ingredients in a variety of consumer and personal care products. Spectral analysis shows that the materials absorb UV wavelengths in the critical region of 290 – 700nm, and therefore have the potential to be photoactivated. In order to determine the potential for phototoxic effects, both materials were assessed in a phototoxicity test on a three dimensional human epidermal model (EST1000). This assay is based upon a comparison of the cytotoxic effects of the test material following exposure to a non-toxic dose of UV light. Cytotoxicity is expressed as a reduction in the mitochondrial conversion of MTT [(3-4,5-dimethyl thiazole 2-yl) 2,5-diphenyl-tetrazoliumbromide] to formazan. A material is considered to have a phototoxic potential if one or more concentrations +UVA (60 min with 6 J/cm<sup>2</sup>) results in a decrease in relative cell viability of  $\geq 30\%$ , when compared to the identical concentration –UVA. Tagetes essential oil and absolute were tested at concentrations ranging from 0.1% to 10% (v/v) in 1:3 ethanol:diethyl phthalate (EtOH:DEP). A confirmatory phototoxicity patch test was then conducted in a group of human volunteers, at a concentration identified to be non-phototoxic. In the EST1000 model, no phototoxicity was observed to Tagetes essential oil over the range of concentrations tested. However, within this same model, phototoxic effects were observed following exposure to Tagetes absolute at concentrations as low as 0.1%. Based on the dose-response in these *in vitro* assays, a concentration of 0.01% was identified as being non-phototoxic. This concentration (0.01% in 1:3 EtOH:DEP) of Tagetes essential oil and absolute was confirmed as having no phototoxic effects in humans following the phototoxicity patch test.

**PS 1311 Saponins from *Platycodon grandiflorum* and Its Constituent Platycodin D Regulates Fatty Acid Metabolism via an AMP-Activated Protein Kinase Dependent Signaling Pathway.**

H. Pil<sup>2,1</sup>, J. Choi<sup>1</sup>, H. Kim<sup>1</sup>, K. Tilak<sup>1</sup>, Y. Chung<sup>2</sup> and H. Jeong<sup>1</sup>. <sup>1</sup>Pharmacy, Chungnam National University, Daejeon, Republic of Korea; <sup>2</sup>International University of Korea, Jinju, Republic of Korea.

The saponins from the roots of *Platycodon grandiflorum* (CKS) have a variety of pharmacological properties, including antioxidant and hepatoprotective properties. This study was conducted to suggest the role of AMP-activated protein kinase (AMPK) pathway in the anti-obesity effect of CKS. We evaluated body weight, liver histology, and hepatic triglyceride content in high-fat diet (HFD)-fed mice treated with CKS. In addition, we characterized the underlying mechanism of CKS's effects in HepG2 cells by Western blot and RT-PCR analysis. CKS administration attenuated fat accumulation and induction of lipogenic genes such as sterol regulatory element binding protein-1c (SREBP-1c) and fatty acid synthase in the liver of HFD-fed mice. We also found that CKS suppressed high glucose-induced lipid accumulation in HepG2 cells. CKS inhibited the high glucose-induced fatty acid synthase (FAS) and sterol regulatory element binding protein-1c (SREBP-1c) expression. Blood biochemical analyses and histopathologic examinations showed that CKS prevented liver injury. Moreover, the using pharmacological AMPK inhibitor revealed that AMPK is essential to suppression of SREBP-1c expression in CKS-treated cells. These results indicate that CKS prevents high glucose-induced lipogenesis in HepG2 cells by blocking the expression of SREBP-1c, FAS through AMPK activation, suggesting that CKS is a novel AMPK activator with a potential role in the prevention and treatment obesity.

**PS 1312** *Platycodi radix* Attenuates Dimethylnitrosamine-Induced Liver Fibrosis in Rats.

J. Choi<sup>1</sup>, S. Jin<sup>1</sup>, Y. Hwang<sup>2</sup>, C. Choi<sup>3</sup>, Y. Chung<sup>2</sup>, Y. Lee<sup>4</sup> and H. Jeong<sup>1</sup>.  
<sup>1</sup>Pharmacy, Chungnam National University, Daejeon, Republic of Korea;  
<sup>2</sup>International University of Korea, Jinju, Republic of Korea; <sup>3</sup>Natural Resources Research Institute, Jangheung-gun, Republic of Korea; <sup>4</sup>Jangsaeng Doraji Research Institute of Biotechnology, Jinju, Republic of Korea.

Liver fibrosis is a wound healing response to a variety of chronic stimuli, including alcohol intake, viral infection, drugs, and metabolic disease. This study investigated the anti-fibrotic effects of the aqueous extract of the *Platycodi Radix* root (Changkil: CK) on dimethylnitrosamine (DMN)-induced liver fibrosis in rats by inducing Nrf2-mediated antioxidant enzymes. Repeated DMN exposure causes chronic liver injury with necrosis, fibrosis, and nodular regeneration through metabolic activation of CYP2E1 in experimental animals. CK inhibited DMN-induced increases in serum ALT and AST activities, fibrosis score, and hepatic malondialdehyde and collagen content. CK also inhibited DMN-induced reductions in rat body and liver weights. CK inhibited DMN-induced increases in MMP-13, TIMP-1, and TNF- $\alpha$  mRNA, and collagen type I and  $\alpha$ -smooth muscle actin protein. DMN-induced COX-2 expression and NF- $\kappa$ B activation was reduced by CK treatment. Furthermore, CK induced activation of Nrf2-mediated antioxidant enzymes such as  $\gamma$ -glutamylcysteine synthetase ( $\gamma$ -GCS), heme oxygenase-1 (HO-1), NAD(P)H quinone oxidoreductase 1 (NQO1), and glutathione-S-transferase (GST) in HepG2 cells. These results demonstrated that CK attenuates DMN-induced liver fibrosis through the activation of Nrf2-mediated antioxidant enzymes.

**PS 1313** Protective Effects of Saponins Isolated from the Root of *Platycodon grandiflorum* against Ovalbumin-Induced Airway Inflammation in a Mouse Allergic Asthma Model.

Y. Chung<sup>2</sup>, J. Choi<sup>1</sup>, H. Kim<sup>1</sup>, Y. Lee<sup>3</sup> and H. Jeong<sup>1</sup>. <sup>1</sup>Pharmacy, Chungnam National University, Daejeon, Republic of Korea; <sup>2</sup>International University of Korea, Jinju, Republic of Korea; <sup>3</sup>Jangsaeng Doraji Research Institute of Biotechnology, Jinju, Republic of Korea.

Bronchial asthma is a chronic airway disorder characterized by airway inflammation, mucus hypersecretion, and airway hyperresponsiveness. This study investigated the protective effects of saponins isolated from the root of *Platycodon grandiflorum* (Changkil saponins: CKS) on airway inflammation induced by allergic reaction in mice. Mice were sensitized and challenged with ovalbumin (OVA) developed inflammation and remodeling in airway. CKS inhibited OVA-induced number of inflammatory cells and levels of TNF- $\alpha$ , INF- $\gamma$ , IL-4, IL-5, IL-13, monocyte chemoattractant protein-1 (MCP-1) and OVA-specific IgE in bronchoalveolar lavage fluid. Also, CKS attenuated OVA-induced mucus hypersecretion in lung histopathological studies. CKS inhibited OVA-induced mRNA expression level of MMP-2, MMP-9, and MUC5AC in lung tissues. Furthermore, CKS blocked NF- $\kappa$ B p65 nuclear translocation in the nuclear extracts from lung tissues of OVA-challenged mice. These results suggest that CKS ameliorates OVA-induced inflammation and remodeling in airway.

**PS 1314** Topical Application of Cultivated Ginseng Suppresses 2, 4-Dinitrochlorobenzene-Induced Atopic Dermatitis in NC/Nga Mice.

J. Choi<sup>2</sup>, J. Choi<sup>1</sup>, S. Jin<sup>1</sup>, Y. Chung<sup>2</sup> and H. Jeong<sup>1</sup>. <sup>1</sup>Pharmacy, Chungnam National University, Daejeon, Republic of Korea; <sup>2</sup>International University of Korea, Jinju, Republic of Korea.

Atopic dermatitis (AD) has been known to be related with local and systemic immunologic dysfunction that leads to Th1/Th2 response as well as being related to environmental factors. This study examined the inhibitory effects of 1-chloro-2,4-dinitrobenzene (DNCB)-induced AD by cultivated ginseng (CG) (Panax ginseng C.A. Meyer) in NC/Nga mice. CG, an herb used in Korean herbal medicine, has been widely used in China and Japan to treat fatigue and to enhance resistance to many diseases. CG ameliorates DNBCB-induced skin dermatitis severity, serum level of IgE and TARC, and mRNA expression of T helper (Th)1 and Th2 cytokines in mice. In addition, CG reduced thickness of the dermis and dermal infiltration of inflammatory cells in histopathological examination. These results indicate that CG inhibits allergic contact dermatitis through the modulating of Th1 and Th2 responses and diminishing the inflammatory cells in the skin lesions in NC/Nga mice.

**PS 1315** *Pleurotus eryngii* Extracts Inhibits 2, 4-Dinitrochlorobenzene-Induced Atopic Dermatitis in NC/Nga Mice by the Regulation of Th1/Th2 Balance.

S. Chun<sup>2</sup>, J. Choi<sup>1</sup>, S. Jin<sup>1</sup>, J. Choi<sup>2</sup>, Y. Chung<sup>2</sup> and H. Jeong<sup>1</sup>. <sup>1</sup>Pharmacy, Chungnam National University, Daejeon, Republic of Korea; <sup>2</sup>International University of Korea, Jinju, Republic of Korea.

Atopic dermatitis (AD) is a chronic, relapsing and inflammatory skin disease in humans and animals, caused by a complex interrelationship among genetic, environmental, pharmacologic, psychological, immunologic and skin barrier dysfunction factors. This study investigated the inhibitory effect of the *Pleurotus eryngii* extracts (PEE) on 2,4-dinitrochlorobenzene (DNCB)-induced atopic dermatitis (AD)-like skin lesions. *Pleurotus eryngii* has been used in traditional medicine for nutritional and medicinal food that enhances the host immune system as a response to various diseases. This study evaluated skin dermatitis severity, ear thickness, histopathological examination, and cytokines level in DNBCB-applied mice treated with PEE. Continuous treatment of PEE inhibited the development of the AD-like skin lesions. PEE attenuates DNBCB-induced skin dermatitis severity, serum level of IgE and TARC, and mRNA expression of TNF- $\alpha$ , INF- $\gamma$ , IL-4, IL-5, and IL-13 in mice. Also, PEE reduced thickness of the dermis and dermal infiltration of inflammatory cells and mast cells in histopathological examination. These results suggest that PEE inhibits allergic contact dermatitis through the modulating of T helper (Th)1 and Th2 responses and diminishing the inflammatory cells and mast cells infiltration in the skin lesions in NC/Nga mice.

**PS 1316** Chronic Oral Toxicity Study of the Extracts from Herbs in Phikud Navakot.

K. Kanchana<sup>1</sup>, K. Chaimongkolnukul<sup>1</sup>, S. Cherdyu<sup>1</sup>, S. Ampawong<sup>2</sup> and T. Ketjareon<sup>2</sup>. <sup>1</sup>Academic Services Office, National Laboratory Animal Center, Mahidol University, Nakorn Pathom, Thailand; <sup>2</sup>Veterinary Medical Office, National Laboratory Animal Center, Mahidol University, Nakorn Pathom, Thailand. Sponsor: - NA.

Phikud Navakot is commonly used as Thai traditional medicine for alleviation hyperlipidemia, cardiovascular diseases, and cerebrovascular diseases. Chronic toxicity effects of the extracts from herbs in Phikud Navakot were performed because there were no 6-month toxicological studies reported in the literature. The repeated dose as 10, 100, 1,000 mg/kg/day of the extracts were randomly administered to both male and female Sprague Dawley rats as described in the OECD code 452 guideline. 183 rats survived to the end of the study while 20 rats died. The cause of death was considered to be related to the gavage technical error which positively correlated to high dose concentration. Mean body weights of dosed rats were similar to those of the control group. No differences in feed consumption, relative organ weights, and hematology and blood clinical chemistry were noted. Significant proportionally increased incidences of transitional cell hyperplasia of the renal pelvis in both sexes dosed rats. Therefore our obtained results suggested that Phikud Navakot is a relatively nontoxic herb for repeated oral administration. However the contraindication of the usage of Phikud Navakot is related to induce transitional cell hyperplasia of the renal pelvis after prolong high dose oral administration.

**PS 1317** Plum Consumption Modulate Gut Microbiota and Obesity in Zucker Rats.

G. Noratto<sup>1</sup>, J. Garcia-Mazcorro<sup>2</sup>, H. Martino<sup>3</sup>, D. Byrne<sup>4</sup>, M. Markel<sup>5</sup>, J. Suchodolski<sup>3</sup>, J. Steiner<sup>3</sup> and S. U. Mertens-Talcott<sup>6</sup>. <sup>1</sup>School of Food Science, Washington State University, Pullman, WA; <sup>2</sup>Facultad de Medicina Veterinaria y Zootecnia, Universidad Autónoma de Nuevo León, Monterrey, Mexico; <sup>3</sup>Department of Nutrition and Health, University of Vicos, Vicos, Brazil; <sup>4</sup>Horticulture, Texas A&M University, College Station, TX; <sup>5</sup>Gastrointestinal Laboratory, Texas A&M University, College Station, TX; <sup>6</sup>Nutrition and Food Science, Texas A&M University, College Station, TX.

The role of peach and plum polyphenols on the modulation of gut microbiota and the possible relationship with obesity is unknown. We investigated how peach and plum consumption can modulate metabolic syndrome and relative proportions of gut microbiota populations in feces of obese Zucker rats. Experimental groups received peach or plum juice ad libitum during 11 weeks, the control and lean groups received water with same amount of glucose than fruit juices. At the end of the study blood was analyzed for glucose, insulin triglycerides, cholesterol and LDL oxidation levels. DNA in feces was analyzed using 454-pyrosequencing and qPCR. Results showed that only plum juice consumption prevented weight gain and modulated microbiota populations in feces; this was related to the higher content of polyphenols in plum juice (3X of peach). However, both peach and plum juice exerted similar protective effects on metabolic syndrome and inflammatory markers

in blood as confirmed by a component score coefficient analysis in which peach and plum groups were overlapped and located in between the control and lean groups. Pyrosequencing data from DNA in feces showed that plum group had higher abundance of Bacteroidetes, Ruminococcaceae, and Lactobacillus. qPCR data showed that plum group had higher Faecalibacterium, Lactobacillus, and Turicibacter than all other groups. The abundance of Bifidobacterium in plum group was similar to the lean group and higher than peach and control groups ( $p < 0.05$ ). These results suggest that polyphenols-rich foods can alter the composition of the distal intestinal microbiota in obese rats and modulate metabolic syndrome and obesity.

**PS 1318 Kolaviron, a Biflavonoid of *Garcinia kola* Seed Offered Cardioprotection against Ischaemic/Reperfusion Injury by Up-Regulation of Prosurvival and Down-Regulation of Apoptotic Signaling Pathways.**

A. A. Oyagbemi<sup>1,2,3</sup>, J. D. Bester<sup>2,3</sup>, A. J. Esterhuyse<sup>2,3</sup> and O. E. Farombi<sup>3,2</sup>.  
<sup>1</sup>Veterinary Physiology, Biochemistry and Pharmacology, University of Ibadan, Ibadan, Nigeria; <sup>2</sup>Biochemistry, University of Ibadan, College of Medicine, Ibadan, Nigeria; <sup>3</sup>Department of Biomedical Sciences, Faculty of Health and Wellness Sciences, Cape Peninsula University of Technology, Bellville, Cape Town, South Africa.

Possible cardioprotective effect of Kolaviron (KV) administration and the molecular mechanism (s) involved in ischaemic/reperfusion injury of isolated rat hearts were assessed. Twenty rats were used for this study. They were grouped into ten rats of group of two. Rats in group I received 2ml/kg of corn oil (vehicle) while animals in groups II received 200 mg/kg body weight of Kolaviron (KV) for four weeks respectively. Isolated rat hearts were stabilized for 5 minutes on Langendorff, perfused on working heart model for 10 minutes and subjected to global ischaemia for 15 minutes followed by 25 minutes reperfusion. Antioxidant enzymes, markers of oxidative stress and western blot analyses were carried out on snap-frozen heart tissues. There was significant ( $p < 0.05$ ) increase in superoxide dismutase (SOD), catalase (CAT) and glutathione peroxidase (GPx), oxygen radical absorbance capacity (ORAC) and concomitant significant ( $p < 0.05$ ) decrease in malondialdehyde (MDA) and intracellular reactive oxygen species (ROS) in isolated rat hearts of animals that received KV compared to the control. Western blot analysis revealed significant up-regulation of Akt/PKB, p-Akt/PKB, HSP27, p-HSP27 and down-regulation of p38 MAPK, Caspase 3, cleaved Caspase 3 and cleaved PARP. Taken together, KV offered cardioprotection by enhancing the expression of pro-survival signaling pathway and abrogation of apoptotic pathway in isolated rat hearts subjected to ischaemic/reperfusion injury.

**PS 1319 Antimalarial Activity of Methanolic Fraction of *Clerodendrum violaceum* Leaf Extract.**

J. O. Adebayo, A. Zailani and E. A. Balogun. Biochemistry, University of Ilorin, Ilorin, Nigeria.

Malaria is a parasitic disease with devastating impact in Africa. Decoction of *Clerodendrum violaceum* leaf is indigenously used in Nigeria for the treatment of the disease. In this study, the methanolic fraction of *Clerodendrum violaceum* leaf extract was evaluated in *P. berghei*-infected mice in a 4-day suppressive test. Also, its effects on the activities of antioxidant enzymes in the infected mice were also evaluated. The results revealed that the methanolic fraction of *Clerodendrum violaceum* leaf extract possesses antimalarial activity, causing 42.69% and 79.42% reduction in parasitemia at the doses of 125 and 250 mg/Kg body weight on day 5 post-inoculation. It also caused 61.78% and 87.57% reduction in parasitemia at the doses of 125 and 250 mg/Kg body weight on day 8 post-inoculation. The extract fraction however caused a significant increase ( $P < 0.05$ ) in superoxide dismutase and catalase activities and a significant decrease ( $P < 0.05$ ) in glutathione peroxidase activity in erythrocyte and liver in a dose-dependent manner compared to controls on day 5 post-inoculation. The results of this study suggest that *Clerodendrum violaceum* leaf may be a potential source of cheaper antimalarial drug.

**PS 1320 Effect of Probiotics (*Lactobacillus* and *Bifidobacterium*) on Growth Performance and Haematological Profile of *Clarias gariepinus* Juveniles.**

S. O. Ayoola<sup>1</sup>, E. K. Ajani<sup>1,2</sup> and O. F. Fashae<sup>1</sup>. <sup>1</sup>Marine Sciences, University of Lagos, Akoka, Lagos, Nigeria; <sup>2</sup>Aquaculture and Fisheries, University Ibadan, Oyo State, Ibadan, Nigeria.

This study was carried out to evaluate the use of probiotic (a mixture of *Lactobacillus* and *bifidobacterium* species) on growth performance and haematological parameters of *Clarias gariepinus* juveniles. Fifteen tanks were used and 10

*Clarias gariepinus* juveniles (mean weight  $14.9 \pm 0.83$  g) per tank, each in triplicate. Five treatment tanks were fed a diet containing 40% crude protein supplemented with varying inclusion of probiotic comprising about 109 colony-forming units per gram of diet (the probiotic diet). Diet T0 contain 0g probiotic (control diet) while the other group contain 0.5 g, 1.0 g 1.5 g and 2.0 g probiotic diet. Results shows that Fish fed with diet T1 (0.5 g probiotic) had the best growth performance. There was no significant difference ( $P > 0.05$ ) in the Mean Corpuscular Volume, Mean Corpuscular Haemoglobin and Mean Corpuscular Haemoglobin Concentration, of fish fed different concentration of probiotic. All blood parameter obtained were between the range of recommended fish blood. It is concluded that using probiotic (especially at 0.5 g) as supplementary feed on *Clarias gariepinus* showed a slight increase in the haematological parameters compare with the control diet but it has no negative impact on the health status of the species. However, probiotic (*Lactobacillus* and *bifidobacterium*) can be used as a probiotic agent in aquaculture, to enhance fish health, survival and growth performance.

**PS 1321 Antifungal and Insecticidal Activities of Five Essential Oils from Plants of the Colombian Caribbean Coast.**

B. E. Jaramillo<sup>1</sup>, E. Duarte Restrepo<sup>1</sup> and W. Delgado Ávila<sup>2</sup>. <sup>1</sup>Chemistry Program, University of Cartagena, Cartagena, Colombia; <sup>2</sup>Chemistry Program, National University of Colombia, Bogotá, Colombia. Sponsor: B. Jaramillo.

Plants have developed chemical mechanisms of self-protection to avoid being attacked by insects fungi, bacteria and viruses. The diseases caused by these pests are controlled with fumigants, which have a high toxicity, and this necessitates the use of alternative compounds like essential oils. These are botanical sources of compounds potential alternative fumigants currently used, due to its low mammalian toxicity, high volatility and toxicity to stored grain pests and microorganisms.

**OBJECTIVE:** This study determined the insecticidal, antifungal, activities of essential oils isolated from *Chenopodium ambrosioides* L., *Triphasia trifolia*, *Eryngium foetidum*, *Bursera graveolens*, and *Swinglea glutinosa* collected in colombian caribbean coast.

**METHODS:** The essential oils (EO) were obtained from leaves of plants by hydrodistillation. The insecticidal activity assay was performed against *Sitophilus zeamais*. EO were also evaluated as fumigants against phytopathogenic fungi *Fusarium oxysporum* f. sp. *dianthi*.

**RESULTS:** *C. ambrosioides* was more active against *Fusarium oxysporum* than other EO evaluated, with a percentage of mycelial inhibition of 97.3% at 176.5  $\mu$ L EO/L air after 72 h of exposure; followed by *Eryngium foetidum* (65.4%); *Bursera graveolens* (60.0%); *Piper marginatum* (41.7%) and *Swinglea glutinosa* (14.7%). *C. ambrosioides* and *Eryngium foetidum* essential oils showed the best fumigant activity against *Sitophilus zeamais* (100% at 500  $\mu$ L/L air after 24 h of exposure); *Piper marginatum* oil had weak fumigant toxicity (86.7%  $\mu$ L/L air after 24 h of exposure).

**CONCLUSIONS:** This study demonstrated that essential oils exhibit important fungicidal activity on *F. oxysporum* and fumigant on *S. zeamais*, which could become an alternative to synthetic fungicides and insecticides.

**PS 1322 Protein Binding Effects the Cellular Uptake of Silver Nanoparticles in Human Cells.**

N. A. Monteiro-Riviere<sup>1,2,3</sup>, A. O. Inman<sup>1,2</sup>, M. E. Samberg<sup>2,3</sup>, S. Oldenburg<sup>4</sup> and J. E. Riviere<sup>1,2</sup>. <sup>1</sup>Nanotechnology Innovation Center of Kansas State, Kansas State University, Manhattan, KS; <sup>2</sup>Center for Chemical Toxicology Research and Pharmacokinetics, North Carolina State University, Raleigh, NC; <sup>3</sup>Joint Department of Biomedical Engineering at the University of North Carolina at Chapel Hill and North Carolina State University, North Carolina State University, Raleigh, NC; <sup>4</sup>nanoComposix, Inc, San Diego, CA.

Nanoparticles (NP) absorbed in the body will come in contact with blood proteins and form NP/protein complexes termed protein coronas, which may modulate NP cellular uptake. This study quantitated human epidermal keratinocyte (HEK) uptake of silver (Ag) NP complexed to different human serum proteins. Prior to HEK dosing, AgNP (20nm and 110nm citrate BioPure™; 40nm and 120nm silica-coated) were incubated for 2h at 37°C without (control) or with physiological levels of albumin (44mg/ml), IgG (14.5mg/ml) or transferrin (3mg/ml). HEK were exposed to the protein incubated AgNP for 3h, rinsed with medium and incubated for 48h, rinsed in buffer and lysed. Ag was assayed by inductively-coupled plasma optical emission spectrometry. Uptake of Ag in HEK was <4.1% of applied dose with proteins suppressing citrate, but not silica coated, Ag uptake into HEK two fold relative to controls. IgG dramatically reduced 110nm citrate AgNP uptake. In contrast, greatest uptake of 20nm silica AgNP was seen with IgG incubation, while 110nm silica AgNP showing similar uptake profiles across all exposures. Electron microscopy confirmed cellular uptake of all particles but showed differences in the

appearance and agglomeration state of the NP within HEK vacuoles. This suggests that NP association with serum proteins purportedly form different protein coronas that significantly modulates Ag uptake compared to native NP uptake, suggesting caution in extrapolating *in vitro* uptake data to predict behavior *in vivo* where the nature of the protein corona may determine patterns of cellular uptake, biodistribution, biological activity and toxicity. (Supported by NIH RO1 ES016138)

### PS 1323 Relationship between Silver Nanoparticle Intracellular Accumulation and Cytotoxicity in L-929 Fibroblasts.

B. E. Wildt<sup>1</sup>, E. I. Maurer<sup>2</sup>, G. Kumar<sup>1</sup>, H. A. Degheidy<sup>1</sup>, S. M. Hussain<sup>2</sup> and P. L. Goering<sup>1</sup>. <sup>1</sup>US FDA, Silver Spring, MD; <sup>2</sup>711 HPW/RHDJ, AFRL, Wright-Patterson AFB, Dayton, OH.

Medical devices containing silver nanoparticles (AgNPs) may release NPs or leach silver (Ag) ions, both of which are cytotoxic *in vitro* at high concentrations. Given the complexities of NP *in vitro* dosimetry, proper assessment of AgNP cytotoxicity requires a better understanding of intracellular Ag concentration and observed bio-effects. Therefore, the objective of this study was to measure time-dependent AgNP cell internalization in L-929 fibroblast cells, a cell line that is commonly used for medical device biocompatibility testing, while simultaneously assessing cell viability. These endpoints were assessed following exposure of cells to 50 µg/mL AgNPs (10, 50, 100 and 200 nm) and to equimolar Ag ions. Intracellular uptake of AgNPs and Ag concentrations in L-929 cells were assessed using time-lapse confocal microscopy, flow cytometry and ICP-MS at 4, 16 and 24 hrs after treatment. Metabolic activity and plasma membrane integrity of the cells were assessed at 4, 16 and 24 hrs after treatment using the MTT assay and ethidium homodimer-1 dead cell indicator, respectively. A time-dependent, linear increase in intracellular accumulation of AgNPs and Ag concentrations were observed using confocal microscopy and ICP-MS. Flow cytometric evidence of AgNP uptake and accumulation in cells was also observed from changes in side scatter characteristics vs. forward scatter characteristics dot plots. The results of the MTT assay suggest that Ag ions and 10 nm NPs are highly toxic, compared to 50, 100 and 200 nm NPs. Membrane integrity analysis of time-lapse images revealed that 10 nm AgNPs are cytotoxic within 1 hr after dosing and all cells are dead after 10 hrs. In contrast, equimolar concentrations of Ag ions kill all cells within an hour. This study demonstrated that the size-dependent *in vitro* cytotoxicity of AgNPs to L-929 fibroblasts correlated with intracellular Ag accumulation, and underscores the value of using multiple analytical methods when determining NP accumulation and cytotoxicity.

### PS 1324 Role of Sample Preparation in *In Vitro* Cytotoxicity Responses to Silver Nanoparticles.

A. N. Clendaniel<sup>2,1</sup>, G. Kumar<sup>1</sup>, H. A. Degheidy<sup>1</sup>, B. J. Casey<sup>1</sup> and P. L. Goering<sup>1</sup>. <sup>1</sup>CDRH, US FDA, Silver Spring, MD; <sup>2</sup>Richard Stockton College of New Jersey, Galloway, NJ.

Metallic nanoparticles readily agglomerate in aqueous media and this effect can influence their physical properties and *in vitro* biological responses. The goal of this study was to: 1) compare effects of cell culture medium containing 10% FBS and DI water as suspension vehicles on AgNP size and agglomeration, and 2) compare effects of pre-mixing of medium and AgNPs on their biological responses in L-929 fibroblasts compared to direct addition of nanoparticles to the cells. To assess the effects of premixing on agglomeration, AgNPs were pre-mixed with cell culture medium or DI water for 1 min, or 1, 5, 24, or 120 hr. Results of dynamic light scattering analysis showed that pre-mixing AgNPs with medium maintained particle dispersion better than DI water. The hydrodynamic diameter of AgNPs increased proportionally to the pre-mixing time. AgNP agglomeration was size-dependent; 10 nm AgNPs agglomerated more readily than 100 nm and 200 nm particles. To assess the effects of premixing on biological responses, AgNPs pre-mixed with cell culture medium for 1 min, or 1, 5, or 24 hr were added to L-929 fibroblasts, or were added to the cells without premixing. After 24 hr exposure, cell viability was assessed by using the standard MTT assay. After 4 and 24 hr exposures, the degree of cell necrosis (via 7-AAD dye) and apoptosis (via Annexin V dye) was assessed using flow cytometry. AgNPs produced a mass concentration (µg/ml) dependent decrease in MTT reduction. Pre-mixing of AgNPs with cell culture medium did not affect cell viability compared to controls; however, AgNPs added directly to the media without pre-mixing were cytotoxic. The degree of necrosis and apoptosis of L-929 cells when exposed to AgNPs depended on mass concentration, exposure time, and size of AgNPs. Cells treated with 10 nm particles at 50 µg/ml showed 22-fold and 33-fold increases in the percentage of apoptotic and necrotic cells, respectively, after 24 hr. Thus, the data show that different sample preparation for AgNPs can affect particle agglomeration and biological responses.

### PS 1325 Flow Cytometry Evaluation of Cell Cytotoxicity Induced by Silver Nanoparticles.

G. Kumar<sup>1</sup>, A. N. Clendaniel<sup>2,1</sup>, H. Degheidy<sup>1</sup>, B. E. Wildt<sup>1</sup> and P. L. Goering<sup>1</sup>. <sup>1</sup>CDRH, US FDA, Silver Spring, MD; <sup>2</sup>The Richard Stockton College of New Jersey, Pomona, NJ.

Particles possess unique properties in the nanoscale, e.g., enhanced catalytic activity, high surface area and surface energy, and light emission/absorption properties, which might result in interference with colorimetric *in vitro* cytotoxicity assays such as MTT, LDH release, and Neutral Red. Alternatively, assays that do not use spectrophotometric detection, such as trypan blue exclusion or flow cytometry (FC) based assays, are less likely to be influenced by nanoparticle interference. The aim of this study was to evaluate FC assays to assess the cytotoxicity of three different sizes (10, 100, or 200 nm) silver nanoparticles (AgNPs) at different mass concentrations (1, 25, or 50 µg/ml) in L-929 fibroblast cells. After 4 hrs and 24 hrs exposure, cell necrosis and apoptosis were assessed using 7-AAD and Annexin V dyes, respectively, with FC. Multiple FC controls (including cells alone, AgNPs alone, and single fluorophore controls and their combinations) were used to optimize the experiment and eliminate background autofluorescence and fluorochrome overlap. The data show that cell necrosis and apoptosis in AgNP-exposed fibroblasts depend on dose, exposure time, and AgNPs size. Cells treated with 10 nm particles at 50 µg/ml showed 7- to 22-fold increases in percentage of apoptotic cells and 2- to 33-fold increases in percentage of necrotic cells after 4 hrs and 24 hrs, respectively. Cells treated with 200 nm particles at 50 µg/ml showed only up to 6 fold increases in degree of apoptosis after 24 h. The data show that AgNPs produced a dose- and time-dependent decrease in cell viability; however, 200 nm AgNPs were significantly less toxic than smaller sized particles. Thus, standard FC assays can be utilized to assess apoptosis and necrosis in response to nanomaterial exposure.

### PS 1326 Incorporation of Silver Nanoparticles into a Degradable Poly(L-Lactide-Co-Epsilon-Caprolactone) Copolymer Scaffold for Skin Regeneration.

M. E. Samberg<sup>1</sup>, P. Mente<sup>1</sup>, T. He<sup>2</sup>, M. W. King<sup>2</sup> and N. A. Monteiro-Riviere<sup>1,3</sup>. <sup>1</sup>Joint Department of Biomedical Engineering at the University of North Carolina at Chapel Hill and North Carolina State University, North Carolina State University, Raleigh, NC; <sup>2</sup>College of Textiles, North Carolina State University, Raleigh, NC; <sup>3</sup>Nanotechnology Innovation Center of Kansas State, Kansas State University, Manhattan, KS.

The development of an antibacterial, degradable scaffold system that utilizes patient-derived cells would improve upon current skin grafting techniques which often result in severe scarring, aesthetically undesirable mismatches in skin tones, and are susceptible to surgical site infection. The objective of this study was to characterize and assess the toxicity of an electrospun scaffold of poly(L-lactide-co-epsilon-caprolactone) (PLCL) incorporating antibacterial 20nm silver nanoparticles (AgNP). The content and distribution of 20nm AgNP incorporated within the PLCL scaffold was optimized to maximize their biocompatibility and antimicrobial activity. The toxicity of the scaffold to human epidermal keratinocytes (HEK) was assessed using Live/Dead and alamarBlue viability assays following 7 days and 14 days. No significant decreases in cell viability were noted at either time point and cell proliferation increased 120% by 7 days and 200% by 14 days on both control and AgNP incorporated scaffolds. After 14 days, scanning electron microscopy revealed a confluent layer of HEK on the surface of the scaffolds, and fluorescent microscopy confirmed cell migration into the scaffold interior. The antibacterial efficacy of the scaffold was evaluated against *Escherichia coli* and *Staphylococcus aureus*. The mechanical properties of the PLCL scaffold were assessed via uniaxial tensile testing to failure. A slight decrease in the modulus of elasticity was observed following AgNP incorporation compared to control, while cellular attachment increased the modulus of elasticity significantly. (Supported by NIH RO1 ES016138)

### PS 1327 Formation of a Protein Corona on Silver Nanoparticles Mediates Cellular Toxicity via Scavenger Receptors.

J. Shannahan<sup>1</sup>, R. Chen<sup>2</sup>, T. Fennell<sup>3</sup>, C. J. Wingard<sup>1</sup>, P. Ke<sup>2</sup> and J. M. Brown<sup>1</sup>. <sup>1</sup>East Carolina University, Greenville, NC; <sup>2</sup>Clemson University, Clemson, SC; <sup>3</sup>RTI International, Durham, NC.

Addition of a protein corona (PC) on the surface of nanomaterials can modify their activity, bio-distribution, cellular uptake, clearance and toxicity. As silver nanoparticles (AgNP) are incorporated into many products as anti-bacterial/fungal agents, the risk of human exposure escalates. We hypothesize that AgNPs will associate with proteins commonly found in human serum and cell culture media forming PCs which will impact cell activation and cytotoxicity. Furthermore, we believe that

activation of scavenger receptor B (SR-B) mediates this toxicity. Citrate- or PVP-coated AgNPs were incubated with human serum albumin (HSA), bovine serum albumin (BSA), high-density lipoprotein (HDL), or water (control). AgNPs associated with each protein (HSA, BSA, HDL) forming PCs by TEM, UV-vis spectroscopy and altered Z-potential and hydrodynamic size. Rat aortic endothelial (RAEC) and rat lung epithelial (RLE) cells were exposed to increasing concentrations of AgNPs (0, 6.25, 12.5, 25 or 50 µg/ml) with or without PC for 3h or 6h. All PC-coated AgNPs demonstrated a dose-response relationship in cytotoxicity in both cell types. To determine the role of SR-B in the observed cytotoxicity, cells were exposed to AgNPs with or without PCs for 3h in the presence of a SR-B antagonist. Treatment with the SR-B antagonist inhibited cytotoxicity in RAEC but not RLE. Lastly, cell activation was assessed at 1h by measuring interleukin-6 (IL-6) mRNA expression. All PC-coated AgNPs induced IL-6 mRNA expression at 1h in both cell types whereas treatment with the SR-B antagonist was found to inhibit expression. Differences in the induction of IL-6 were found between PC-coated AgNPs based upon suspension (citrate or PVP). This study characterizes a PC on AgNPs using proteins found in human serum and cell culture media. The presence of these PCs influenced cytotoxicity and cell activation through SR-B leading to altered cell responses. This work was supported by the U19 ES019525 and R01 ES09311.

**PS 1328 Importance of p38MAPK and pmk-1 a *Caenorhabditis elegans* Homologue, in Silver Nanoparticles-Induced DNA Damage Response and Apoptosis.**

J. Choi, N. Chatterjee, H. Eom and J. Ahn. *Faculty of Environmental Engineering, College of Urban Science, Seoul, Republic of Korea.* Sponsor: D. Ryu.

Silver nanoparticles (AgNPs) have recently received much attention for their possible applications in new material design, biotechnology and other commercial purposes. Our previous studies conducted in Jurkat T cells and *Caenorhabditis elegans* displayed that AgNP exposure caused dose and time dependent increase in only p38MAPK and pmk-1 expression among all other stress responsive proteins and DNA damage in Jurkat T cells. These findings motivated to ask whether and how p38MAPK and pmk-1 is involved in AgNP induced DNA damage response and eventually in mode of cell death. Our approach was comparative and we used the wild type (wt) and p38MAPK knocked down Jurkat T cells (siRNA transfection) as in vitro model system and wild type (N2) and pmk-1 (KU25) mutant strains of *C. elegans* as in vivo model system. The result showed that p38MAPK siRNA knocked down (KD) Jurkat T cells and pmk-1 mutant worms were more sensitive to AgNP and posed higher DNA damage response by activating sensors (hus-1, γH2AX) and effectors (cep-1 and p53) but preferred necrosis rather than DNA damage mediated apoptosis which is attested by egl-1 and ced-3 expression in *C. elegans* and in the same way, Bax/caspases in KD cells. Moreover, loss of p38MAPK and pmk-1 displayed impairment with the expression and activation of DNA damage repair systems (Rad-51, Lig-4). The mode of choosing of cell death pattern ultimately affects longevity and survival which in turn, support the idea that apoptosis actually play a defense against AgNP induced toxicity. On the whole, p38MAPK and pmk-1 play an evolutionarily conserved role in AgNP induced DNA damage response and cell death.

**PS 1329 Cytotoxicity and Genotoxicity of Silver Nanoparticles and Silver Ions to CHO K1 Cells.**

X. Jiang<sup>1</sup>, R. Foldbjerg<sup>2</sup>, T. Mclaus<sup>3</sup>, C. Chen<sup>1</sup>, H. Autrup<sup>2</sup> and C. Beer<sup>2</sup>. <sup>1</sup>National Center for Nanoscience and Technology, Chinese Academy of Science, Beijing, China; <sup>2</sup>Environmental and Occupational Medicine, Aarhus University, Aarhus, Denmark; <sup>3</sup>Interdisciplinary Nanoscience Center (iNANO), Aarhus University, Aarhus, Denmark.

Silver nanoparticles (Ag NPs) are used in a variety of commercial products due to their antimicrobial activity. As both in vitro and in vivo studies have demonstrated toxic effects of Ag NPs, there is an urgent need to explore the toxicity of Ag NPs. Here we studied the cytotoxicity and genotoxicity of Ag NPs (BSA coated, 15.9±7.6 nm) and silver ions (Ag<sup>+</sup>) to Chinese hamster ovary (CHO K1) cells. To analyse the cytotoxic effects the mitochondrial activity was determined by the MTT assay, intracellular reactive oxygen species (ROS) and the cell cycle were analyzed by flow cytometry. Fluorescence microscopy and flow cytometry based micronucleus assays were applied to qualify and quantify the number of micronuclei induced by Ag NPs and Ag<sup>+</sup>. P32 postlabeling was performed to detect DNA adducts. In addition, inductively-coupled plasma mass spectrometry (ICP-MS) and transmission electron microscope (TEM) were applied to study the uptake and intracellular distribution of Ag NPs, respectively.

A time and dose dependent decrease in mitochondrial activity and increase of intracellular ROS level in CHO K1 cells was observed after exposure to Ag NPs and Ag<sup>+</sup> (0-20 µg/ml) for 24h and 48h. Ag NPs and Ag<sup>+</sup> induced a cell cycle arrest in the G2/M phase. Micronucleus assay and P32 postlabeling revealed that both Ag NPs and Ag<sup>+</sup> induced micronuclei and DNA adducts. Using TEM observations Ag NPs were found to be located in endosomes/ lysosomes suggesting that Ag NPs are taken up by receptor mediated endocytosis. However, no Ag NPs were found in the nucleus suggesting that Ag NPs are presumably dissolved into Ag<sup>+</sup> in the endosomes/ lysosomes and released to the cytoplasm. From here they can enter mitochondria and /or the nucleus leading to an increased intracellular ROS level and the induction of DNA damage.

**PS 1330 Chronic Exposure to Realistic Doses of Silver Nanoparticles Demonstrated Differential Cellular Responses Than Acute Exposure in Human Keratinocytes.**

K. K. Comfort<sup>1,2</sup>, L. Braydich-Stolle<sup>1</sup> and S. M. Hussain<sup>1</sup>. <sup>1</sup>Molecular Bioeffects Branch, Human Performance Wing, Air Force Research Laboratory, Wright-Patterson AFB, OH; <sup>2</sup>Chemical and Materials Engineering, University of Dayton, Dayton, OH.

One obstacle plaguing the field of nanotoxicology is the development of a mechanism to translate acute exposure data to an accurate prediction of real world implications of nanomaterials (NM). In an effort to enhance the efficacy of information gathered from an in vitro environment, a chronic NM exposure scenario was designed and implemented in which human keratinocyte cells (HaCaT) were dosed with 50 nm silver nanoparticles (Ag-NP) 8 h a day, 5 days a week, for 3 months. Working concentrations were based off the permissible exposure limits set by OSHA and were 0.4, 4, and 400 pg/ml. The HaCaT stress response of the chronically treated cells was directly compared to a 24 h acute exposure at a concentration equal to the cumulative Ag-NP dosage encountered over the 3 months. Cellular endpoints evaluated include activation of Heat shock protein-27 signal transduction, ki67 expression, pro-inflammatory cytokine secretion, actin inflammation, and alterations in gene regulation. Results indicated that the chronically dosed HaCaT cells were functioning under sustained, augment cellular stress: as seen with increased reactive oxygen species levels, HSP-27 signaling, cytosolic ki67 expression, and actin inflammation and disorganization. Furthermore, considerable IL-6 secretion was observed throughout the experiment, indicating a continuous inflammatory response. Most notably, these stress indicators were all significantly higher in chronically dosed cells vs. their acute counterparts, demonstrating a more severe response. Additionally, chronically dosed cells demonstrated a vastly higher modification to gene regulation, again representing the potential for a serious long-term impact. In conclusion, this study identified a significant variation in the HaCaT stress response following chronic exposure of Ag-NPs vs. an acute scenario and offers a novel approach to nanotoxicology research.

**PS 1331 Evaluation of Uptake and Cytotoxicity of Citrate Stabilised Gold Nanoparticles in Chinese Hamster Ovary (CHO) Cells prior to the *In Vitro* Mammalian Mutation Test.**

M. Vetten<sup>1,2</sup> and M. Gulumian<sup>1,2</sup>. <sup>1</sup>Toxicology and Biochemistry Section, National Institute for Occupational Health, Johannesburg, South Africa; <sup>2</sup>School of Pathology, University of the Witwatersrand, Johannesburg, South Africa.

The health risk assessment of engineered gold nanoparticles (AuNPs) requires the generation of hazard identification data. Currently the Organisation for Economic Co-operation and Development (OECD) has released a guidance manual for the testing of manufactured nanomaterials. Within this document various established toxicological endpoints have been proposed for study, including the *in vitro* mammalian cell gene mutation test (OECD TG476) for genotoxicity assessment. Prior to this mutation study, preliminary experiments were required to assess the cytotoxicity and uptake of the AuNPs into the cells. Chinese Hamster Ovary (CHO) cells were treated with 14 nm, 20 nm, and 40 nm citrate stabilised gold nanoparticles. The Roche xCELLigence RTCA system was used to determine cytotoxicity of the particles using cell impedance. The nanoparticles were non-toxic for the duration of the period tested. The use of this technology eliminated any potential interference of the nanoparticles with the assay. The uptake of the particles into the cells was visualised using the CytoViva Hyperspectral Imaging system and showed a time-dependent uptake of the particles into the cells. This preliminary data confirms lack of toxicity of the particles prior to use in the mutation assay, and confirms uptake of the particles into the cells. Mutagenicity studies using this cell line will be conducted to measure mutation at hypoxanthine-guanine phosphoribosyl transferase (HPRT). Although gold nanoparticles have been shown in literature to induce some DNA damage; to our knowledge, the genotoxicity of gold nanoparticles has not been assessed using the HPRT mutation assay to date.

**PS 1332 Bioavailability of Silver Nanoparticles in Artificial Physiological Fluids: Coating and pH Impact on Degree of Ionic Dissociation.**

L. Braydich-Stolle, E. Breitner, E. I. Maurer, B. Stacy and S. M. Hussain. 711 HPW/RHDJ, Wright-Patterson AFB, Dayton, OH.

The majority of studies have focused on nanoparticle (NP) fate and their induced damage with limited information on the physiological environment's role in altering NP properties. Artificial fluids (AFs) have been used to test the bioavailability of metallic compounds (difference between the amount of a substance a person is exposed to and the amount of substance the body receives). Literature has demonstrated that inhaled NPs accumulated in lungs and clearance was hindered during chronic exposure indicating the observed effects should become more pronounced over time due to impeded clearance. Based on these findings, this study examined the impact of artificial interstitial, alveolar, lysosomal, and gastric fluid on the physical properties of hydrocarbon coated silver (Ag-HC) and polysaccharide coated silver (Ag-PS) NPs and the associated changes in toxicity. Since inhalation exposure is of concern, the toxicity of the Ag-NPs exposed to the AFs was evaluated in alveolar macrophages and doses represent a week or year of exposure (0.5 ng/ml and 25 ng/ml) based on the concept that this delayed clearance will result in macrophages continually be recruited to engulf the NPs. For all the AFs, the Ag-HC NPs demonstrated large agglomeration, limited ionic dissociation, and no changes in cell viability. Ag-PS NPs exposed to alveolar and interstitial fluid demonstrated a similar trend, in addition to a loss of the PS coating. For the gastric fluid, large agglomerates were observed but these were rare and most likely due to the Ag NPs precipitating out as AgCl. Interestingly, the Ag-PS NPs exposed to lysosomal fluid demonstrated a loss of coating, less agglomeration, and significant decreases in cell viability. Since NPs are most likely taken up via endocytosis in cell cultures or by phagocytic cells in an in vivo system, the interactions of the NP with the lysosomal environment has critical implications on mediating the NP cellular consequences. Based on this study, the lysosomal environment has the potential to make a NP more toxic over time. (88ABW-2012-5185)

**PS 1333 Cytotoxic and Inflammatory Responses to Silver Nanoparticles in Hepatocyte-Kupffer Cell (HC-KC) Coculture and HepG2 Cells.**

M. W. Betz, B. E. Wildt, B. J. Casey and P. L. Goering. CDRH, US FDA, Silver Spring, MD.

Nanoparticles accumulate in several organs following in vivo exposure, notably the liver. Numerous studies have assessed effects of nanoparticles on liver cells *in vitro*, but it is unclear whether it is preferable to conduct these studies using a physiologically-relevant cell culture model or if using an established liver-derived cell line is adequate. To address this question, we compared cellular responses to AgNPs in a primary rat HC-KC coculture with those in HepG2 cells. Metabolic activity (MTT reduction) was assessed 24 hr after exposure of cells to 10, 50, or 100nm AgNPs administered at 1, 10, 25, or 50 µg/mL and 0.25, 0.5, 1, 2, 3, 4 cm<sup>2</sup>/mL. Calcium homeostasis and flux were investigated after exposure to AgNPs by mass concentration. Inflammatory responses were assessed by measuring TNF-α and IL-6 levels in HC-KCs and monocultures of hepatocytes and Kupffer cells after 6 and 24 hr exposure to 50nm AgNPs ± lipopolysaccharide. Metabolic activity results showed that HC-KCs are more sensitive to AgNPs than HepG2 cells on the basis of both mass and surface area. Calcium homeostasis and flux levels also demonstrated that HC-KCs were more sensitive to AgNPs than HepG2 cells. Using confocal microscopy, AgNPs appeared to localize in the cytoplasm of both HC-KC cell types; however, a greater density of particles was observed in Kupffer cells compared to hepatocytes. Kupffer cells and HC-KCs both produced strong inflammatory responses (TNF-α and IL-6) to AgNPs by 6 hr, which remained unchanged at 24 hr, while hepatocytes alone did not produce TNF-α or IL-6. Thus, the data show that inflammatory responses in HC-KCs are dependent on the presence of Kupffer cells. Additionally, with increasing AgNP concentrations, TNF-α and IL-6 levels remained constant in HC-KCs but decreased in Kupffer cells suggesting the KCs are more sensitive in monoculture and protected by hepatocytes in the coculture. This study demonstrates the value of using a more physiologically-relevant cell culture system for the *in vitro* investigation of nanoparticle toxicity on liver.

**PS 1334 Evaluation of Genotoxicity of Silver Nanoparticles with *In Vitro* and *In Vivo* Standard Assays.**

Y. Li<sup>1</sup>, J. Yan<sup>1</sup>, N. Mei<sup>1</sup>, Y. Chen<sup>1</sup>, M. G. Pearce<sup>1</sup>, W. Ding<sup>1</sup>, C. Candice<sup>2</sup>, P. C. Howard<sup>2</sup>, P. Rice<sup>3</sup>, T. Zhou<sup>4</sup>, R. K. Elespuru<sup>5</sup>, M. M. Moore<sup>1</sup> and T. Chen<sup>1</sup>. <sup>1</sup>Division of Genetic and Molecular Toxicology, US FDA/National Center for Toxicological Research, Jefferson, AR; <sup>2</sup>Nanotechnology Core Facility, US FDA/National Center for Toxicological Research, Jefferson, AR; <sup>3</sup>Center for Food Safety and Applied Nutrition, US FDA, College Park, MD; <sup>4</sup>Center for Veterinary Medicine, US FDA, Rockville, MD; <sup>5</sup>Center for Devices and Radiology Health, US FDA, Silver Spring, MD.

Many publications are available on genotoxicity of nanomaterials. However, it is difficult to compare these results objectively due to conflicting results from different test methods, most of which were not the standard assays. In this study, both *in vitro* and *in vivo* standard genotoxicity assays including the Ames test, the *in vitro* and *in vivo* micronucleus assay and the mouse lymphoma gene mutation assay were applied to assess the genotoxicity of 5 nm uncoated and PVP coated silver nanoparticles (AgNPs). Mutagenic evaluation of uncoated AgNPs with the Ames test showed negative results possibly due to lack of cell uptake of the nanoparticles and strong cytotoxicity of AgNPs to bacteria. The AgNPs, however, induced mutations in a dose-dependent manner in mouse lymphoma cells via an oxidative stress mechanism evidenced by the results from loss of heterozygosity analysis of the Tk mutants, oxidative Comet assay and gene expression analysis. Micronuclei in TK6 cells were also increased by AgNPs in a dose-dependent manner. At a concentration of 30 µg/ml, uncoated AgNPs caused around 50% cytotoxicity (relative population doubling) and induced a significant, 3.17-fold increase over the vehicle control while PVP-coated AgNPs induced 50% cytotoxicity and 2.25-fold increase of micronuclei over the control at only 1.75 µg/ml. Although AgNPs can reach the bone marrow, they were negative in *in vivo* micronucleus assay. Our results demonstrate that the AgNPs are genotoxicity in *in vitro* mammalian assays, but not in *in vivo* mouse micronucleus assay.

**PS 1335 DNA-Dependent Protein Kinase Reduces Toxicity of Silver Nanoparticles in Mammalian Cells through JNK and Telomerase Pathways.**

H. Lim and H. Manoor Prakash. *Physiology, Yong Loo Lin School of Medicine, National University of Singapore, Singapore, Singapore.* Sponsor: S. Sawant.

Silver nanoparticles (Ag-np) are distinctively reported to be toxic to mammalian cells. Less is known about the signalling response triggered in cells to counteract such toxicity. This study was initiated to enhance our mechanistic insight on correlation between, DNA-dependent protein kinase catalytic subunit (DNA-PKcs) and toxicity of Ag-np. The toxicity of polyvinyl alcohol (PVA)-coated Ag-np was studied in normal human lung fibroblast and human breast cancer and brain cancer cells. DNA-PKcs inhibition was carried out to investigate impact of DNA-PKcs on influencing toxicity of Ag-np. The toxicity was evaluated using changes in cell survival, DNA damage and repair and telomeres length. We observed concurrent activation of DNA-PKcs and JNK pathway in cancer cells upon Ag-np treatment, which were anticipated as physiologic responses to DNA damage and repair. JNK pathway was insufficiently activated in DNA-PKcs inhibited cancer cells, abolishing the signalling events required for mediating DNA repair. Further investigation on genotoxic effect of Ag-np indicated that Ag-np causes telomere attrition and dysfunction in human cancer cells by disrupting shelterin complex integrity and telomerase expression. Recruitment of activated DNA-PKcs to damaged telomeres signifies the importance of DNA repair machinery at damaged telomeres. DNA-PKcs inhibition potentiates the damaging effect of Ag-np at telomeres in human cancer cells. Abrogation of JNK mediated DNA repair and substantial damages at telomeres lead to higher cell death in DNA-PKcs inhibited, Ag-np treated cancer cells. Altogether, presence of DNA-PKcs effectively reduces the toxic effects of Ag-np in human cancer cells by triggering the activation of JNK pathway and telomeres length maintenance. This study suggests that the potentially detrimental combination of Ag-np with DNA-PKcs inhibition can however be applied as a better strategy in cancer therapy.

**PS 1336 Determination of Nanosilver Dissolution Kinetics and Toxicity in an Environmentally Relevant Aqueous Medium.**

A. Harmon, A. J. Kennedy, A. R. Poda, A. J. Bednar, M. A. Chappell and J. A. Steevens. *US Army Corps of Engineers, Vicksburg, MS.*

The dissolution potential of citrate capped silver nanoparticles (AgNPs) in laboratory test media and in the environment is critical for determining toxicity. In the present study, the ion-release kinetics from citrate capped 20, 50, and 80 nm

AgNPs in dilutions of an environmentally relevant freshwater (30µS/cm and 150µS/cm reconstituted water) was examined and related to the associated impact on an aquatic organism (*Daphnia magna*). Diluted suspensions of nanoparticles were placed on a multi-tube vortexer and orbital shaker for 0, 1, 2, 3 and 7 days. The acute toxicity of the AgNPs suspensions was then assessed with *D. magna* at 0 and 7 days post interaction between the particles and test media. An increase in hydrodynamic diameter measured by dynamic light scattering and field flow fractionation over time was observed at a relatively higher specific conductivity of 150 µS/cm in 20nm particles (3.3 fold increase) and only a small increase in 50 and 80nm particles (1.4 and 1.2 fold increase, respectively). At a lower conductivity of 30 µS/cm a 1.7, 1.0, and 1.2 fold increase was observed in 20, 50 and 80nm, respectively. Results showed that although the total concentration of silver in solution decreased with time, there was a consistent spike in dissolved concentration after 2-3 days interaction, followed by a steady decrease in dissolved silver in 150µS/cm and 30 µS/cm medium. This suggests that the concentration of dissolved silver in environmentally relevant ionic strength media increases over time after the introduction of citrate capped AgNPs which may have implications on aquatic organisms. When exposed *D. magna* was exposed to 150µS/cm and 30µS/cm test media, 30µS/cm test media induced more toxicity than 150µS/cm test media. Toxicity increased with longer *nAg* interaction time with smaller particles inducing more toxicity than larger particles.

### PS 1337 Silver Nanoparticles Induce Mast Cell Degranulation via Scavenger Receptors.

A. Aldossari, J. Shannahan, S. Hilderbrand and J. M. Brown. *Pharmacology and Toxicology, East Carolina University, Greenville, NC.*

Silver nanoparticles (AgNPs) are increasingly incorporated into a variety of consumer and industrial products such as water filters and cosmetics for their antimicrobial properties. This has increased human exposures to AgNPs and therefore the possibility of adverse health effects. Mast cells are well known to orchestrate allergic immune responses through degranulation and release of pre-formed mediators such as histamine. Furthermore, mast cells have been shown to mediate pulmonary inflammation following exposure to nanoparticles in a murine model. We therefore examined whether AgNP could induce mast cell degranulation. Bone marrow derived mast cells (BMMCs) were generated from femoral bone marrow of C57BL/6 mice. BMMCs were exposed to either citrate- or polyvinylpyrrolidone (PVP)-coated AgNPs (20 nm or 110 nm diameter) at increasing concentrations (6.25, 12.5, 25, or 50 µg/ml) for 3, 6, or 24 h. Exposure to 20 nm AgNPs, but not 110 nm AgNPs, was found to cause concentration-dependent degranulation of BMMCs at 1 h. TNF-α gene expression was increased in BMMCs following AgNP exposure while TNF-α protein levels were increased only after exposure to citrate-coated AgNPs at 50 µg/ml. To determine the mechanism of BMMC degranulation following exposure to 20 nm AgNPs, we examined scavenger receptors which have been shown to mediate nanoparticle uptake in macrophages. PCR and flow cytometry demonstrated the presence of scavenger receptor class B1 (SR-B1) on the surface of cultured BMMCs. To determine the role of SR-B1, BMMCs were treated with two different SR-B1 antagonists (blt-1 or blt-2). Treatment with either SR-B1 antagonist was found to prevent AgNP-induced degranulation of BMMCs. These *in vitro* findings suggest that AgNPs may induce an inflammatory response via mast cell degranulation *in vivo*, which is dependent upon nanoparticle size and scavenger receptor activation. Therefore mast cell degranulation may be considered as an indicator of nanomaterial toxicity. This work was funded by NIEHS R01 ES019311 and U19 ES019525.

### PS 1338 High-Throughput Methods for Assessing the Molecular Toxicity of Nanomaterials in Bacteria.

C. Kaweeteerawat<sup>1,2</sup>, A. Ivask<sup>2</sup>, C. Low-Kam<sup>2,3</sup>, P. Holden<sup>2,4</sup> and H. A. Godwin<sup>1,2</sup>. <sup>1</sup>Molecular Toxicology, University of California Los Angeles, Los Angeles, CA; <sup>2</sup>University of California Center of Environmental Implication of Nanotechnology, University of California Los Angeles, Los Angeles, CA; <sup>3</sup>Department of Biostatistics, University of California Los Angeles, Los Angeles, CA; <sup>4</sup>Donald Bren School of Environmental Science and Management, University of California Santa Barbara, Santa Barbara, CA.

Synthesis and use of nanoparticles has skyrocketed during the past decade. To ensure that nanotechnology is safely and sustainably developed, rapid, cost-effective methods are needed to determine the toxicity of nanoparticles. Here, we report the application of a suite of sub-lethal assay as well as a growth inhibition assay to a series of silver and metal oxide nanoparticles in bacteria (*Escherichia coli*). Sub-lethal effects such as perturbation of membrane integrity (using PI/SYTO) disruption of membrane potential (using DiBAC) and reduction of respiration rate (using XTT) were used to identify toxic nanoparticles. To further look into mechanism of toxicity, intracellular Reactive Oxygen Species (ROS) and the intrinsic property of

nanoparticles to oxidize electron (abiotic ROS generation) were measure by using H2DCFDA and DCFH respectively. These studies revealed that toxicity of the silver particles studied correlates with size and surface charge, with smaller particles and particles with a more positive surface charge being more toxic. By contrast, the toxicity of the metal oxide particles studied correlates most significantly with their ability to oxidize biomolecules, although dissolution of some of the particles also plays an important role.

### PS 1339 Role of microRNA in Toxicity of Silver Nanoparticles in Jurkat T Cells.

H. Eom<sup>1</sup>, J. Choi<sup>1</sup> and J. Lee<sup>2</sup>. <sup>1</sup>Faculty of Environmental Engineering, College of Urban Science, Seoul, Republic of Korea; <sup>2</sup>National Instrumentation Center for Environmental Management, Seoul, Republic of Korea. Sponsor: D. Ryu.

In this study, in order to identify whether miRNAs are involved in toxicity of silver nanoparticles (AgNPs), we investigated miRNA expression in AgNPs treated Jurkat T cells using mRNA and miRNA microarrays. Surprisingly small numbers of genes were affected by both silvers exposure (19 up- and 2 down-regulated mRNA by AgNPs exposure, and 2 up- and 1 down-regulated mRNA by Ag ion exposure). More important numbers of differentially expressed (DE) miRNAs than DE mRNAs were revealed by miRNA microarray, such as, 31 up- and 51 down-regulated miRNAs by AgNPs exposure, whereas 11 up- and 27 down-regulated miRNAs by Ag ion exposure. The most dramatic alteration was observed in hsa-miR-1238 (a decrease of 67 folds) by AgNPs exposure. An integrated analysis of mRNA and miRNA expression was conducted on DE mRNA and DE miRNA by AgNPs and Ag ion exposure, which revealed that the expression of miRNA, hsa-miR-219-5p, was negatively correlated with that of mRNA, metallothionein 1F (MT1F) and tribbles homolog 3 (TRIB3), in the cells exposed to AgNPs; whereas, the expression of hsa-miR-654-3p was negatively correlated with the expression of mRNA, endonuclease G-like 1 (EDGL1) in the cells exposed to Ag ions. However no mRNA regulated by hsa-miR-1238 was identified. Individual validation was followed on these 3 miRNA-mRNA pairs using qPCR. Bioinformatics analysis was further conducted using Pathway Studio, which suggests hsa-miR-219-5p - MT1F and -TRIB3 pairs play an important role in AgNPs toxicity in Jurkat T cells by regulating the genes in important stress response pathways, such as, cell survival, cell death and oxidative stress. Overall results suggest that compared to serious toxicity, only limited genes were affected by AgNPs at transcriptomic level, whereas more important number of miRNAs were identified, which suggests fine regulation with miRNA may play important role in AgNPs toxicity.

### PS 1340 Assessing the Influence of Gold and Silver Nanoparticles on Conventional In Vitro Cytotoxicity Assays.

K. Boodhia<sup>1,3</sup>, L. Koekemoer<sup>1,3</sup>, C. Andros<sup>1,2</sup> and M. Gulumian<sup>1,2</sup>. <sup>1</sup>Toxicology, National Institute for Occupational Health, Johannesburg, South Africa; <sup>2</sup>Hematology and Molecular Medicine, University of Witwatersrand, Johannesburg, South Africa; <sup>3</sup>Biochemistry, University of Johannesburg, Johannesburg, South Africa.

Gold nanoparticles (AuNPs) and silver nanoparticles (AgNPs), due to their optical properties are used in optics and biomedical applications. A principal property of these NPs is their enhanced surface plasmon resonance which enables them to scatter and absorb light with great efficiency. When assessing NP toxicity, there are many challenges as conventional methods are optically based and make use of absorbance, luminescence and fluorescence. The objective of this work was to assess if AuNPs and AgNPs are capable of interfering with currently accepted *in vitro* cytotoxicity assays. Changes in the endpoints of the XTT, ATP, LDH and MitoPT-JC-1 assays was assessed in the absence and presence of cells, after the addition of AuNPs and AgNPs, to assess interference. Results obtained from XTT, ATP and LDH assays in the presence of cells showed toxicity. In the absence of cells, the XTT and ATP assays showed significant changes in their absorbance and luminescence; this could be explained by product adsorption to the NP or interference of NPs with the readings of the products assessed. On the other hand, the LDH assay showed little or no change in fluorescence. When using the MitoPT-JC-1, evaluation of cell treated with the NPs showed viable mitochondria, however in the absence of cells there is a decrease in the fluorescence which too can be explained by product adsorption to the NP. In conclusion, NPs have the ability to interfere in *in vitro* toxicity assays, skewing results. For this reason when assessing NP toxicity using these assay systems, their reliability and sensitivity needs to be determined. To overcome this interference of the gold and silver NPs a non invasive system such as the xCELLigence RTCA system, which does not use absorbance luminescence, and fluorescence, can be used to determine the viability of cells by measuring the cell index, a dimensionless parameter, which is an expression of cell adherence.

**PS 1341 Realistic Assessment of Nanomaterial Toxicity *In Vitro* Using a Nanoaerosol Exposure Chamber.**

C. Grabinski<sup>1,2</sup>, M. Sankaran<sup>2</sup> and S. M. Hussain<sup>1</sup>. <sup>1</sup>Molecular Bioeffects Branch, Air Force Research Laboratory, Wright-Patterson AFB, OH; <sup>2</sup>Department of Chemical Engineering, Case Western Reserve University, Cleveland, OH.

Traditional *in vitro* toxicology methods require dispersion of nanomaterials (NMs) in biological media for administration to cells, which does not depict realistic inhalation exposure. The objective of this work is to design and optimize a system to mimic inhalation exposure by delivering well-characterized NM aerosols to cells grown at the air-liquid interface. Gold or silver NMs were drawn into the gas phase from an aqueous dispersion using electrospray. The aerosolized NMs were introduced into a chamber and deposited onto cells using electrostatic deposition. The deposition of NMs in the chamber was assessed by evenly placing copper grids throughout the chamber and imaging particle deposition using transmission electron microscopy (TEM). NM deposition on cells grown in the chamber was quantified by digesting the samples and measuring gold or silver content using inductively coupled plasma – mass spectrometry (ICP-MS). A human nasal epithelial cell-line was grown in the chamber, and the viability was assessed using the Alamar Blue assay. Results showed that gold and silver NMs could be deposited uniformly in the chamber and that the dose could be controlled by varying the electric field strength and frequency used for electrostatic deposition. Additionally, the dose was found to be relevant compared to NM deposition in the respiratory tract predicted by the Multiple Path Particle Dosimetry model. The results of the Alamar Blue assay showed that the cells could be sustained in the chamber, and the application of electric fields did not have an effect on cell viability. This study demonstrates a promising step forward in the development of a standardized realistic exposure method for assessing NM toxicity *in vitro*.

**PS 1342 Influences of Capping Agent and Cell Type on Cellular Uptake of Silver Nanoparticles.**

F. Zhang, B. L. Lau and E. D. Bruce. *The Institute of Ecological, Earth and Environmental Sciences, Baylor University, Waco, TX.*

The usage of engineered silver nanoparticles (AgNPs) in catalysts, sensors, drug carriers, and personal care products is growing because of their unique physicochemical and biological activities. Consequently both occupational and consumer exposure to these AgNPs is likely to increase in proportion to the production and usage in the market. Meanwhile, there are increasing concerns that exposure to these NPs may cause potential adverse effects on human health as well as the environment. Capping agents are selected organic or inorganic material applied to the surface of nanoparticles as stabilizer to prevent aggregation. However, little is known about the effect of capping agents on the NPs-cell interaction and the mechanisms behind it. Experiments were carried out to quantitatively and mechanistically investigate the role of capping agents of AgNPs on cellular uptake by two different cell lines, human bronchoalveolar carcinoma derived cells (A549) and human colon adenocarcinoma derived cells (Caco-2). *In vitro* studies were used to quantify the uptake kinetics and the extent of internalized AgNPs and to investigate the uptake mechanism among five capping agents (citrate, polyvinylpyrrolidone (PVP), tannic acid, silica and penetratin) by two cell lines. Preliminary results on A549 cells showed that 34% of the penetratin-coated AgNPs were internalized, followed by tannic acid-coated AgNPs, 25%, while the silica-coated AgNPs showed the least uptake, only 4% internalized content. Penetratin is a cell-penetration peptide designed to translocate across the cell membrane, which explains why penetratin-coated AgNPs were more readily internalized than other capping agents. These results demonstrated that capping agents play an important role in cellular uptake of AgNPs. Further experiments on Caco-2 cell line are currently underway and will expand our knowledge on nanoparticle-cell interactions. The combined results can be applied to manage the risk associated with occupational and consumer exposure to AgNPs.

**PS 1343 Comparative Cytotoxicity of Silver Nanomaterials in a Murine Macrophage Cell Line.**

T. D. Green<sup>1</sup>, A. Badawy<sup>2</sup>, T. Tolaymat<sup>3</sup> and D. J. Thomas<sup>1</sup>. <sup>1</sup>ISTD, NHEERL, ORD, US EPA, Research Triangle Park, NC; <sup>2</sup>Department Civil & Environmental Engineering, University of Cincinnati, Cincinnati, OH; <sup>3</sup>LRPCD, NRMRL, ORD, US EPA, Cincinnati, OH.

Manufactured silver nanomaterials (AgNPs) are used as antimicrobials in many consumer products. Although increased use of AgNPs increases risk of exposure by inhalation or ingestion, there are few data on human health risks associated with exposure. Here, we evaluated the toxicity of AgNPs in the murine macrophage J774A.1 cell line. Macrophages play a key role in the inflammatory response by

phagocytosis of pathogens, debris, and particles. Phagocytosis of AgNPs by macrophages could expose cells to Ag and alter cell structure and function. We used two *in vitro* cytotoxicity assays, lactate dehydrogenase (LDH) and reduction of 3-(4,5-dimethylthiazol-2-yl)-2,5-diphenyltetrazolium bromide (MTT), to compare cytotoxic effects of ionic Ag, polyvinylpyrrolidone PVP coated-AgNPs (MHD=13 nm), hydrogen reduced H<sub>2</sub>-AgNPs (14 nm), and citrate-AgNPs (12 nm). Cells were exposed to Ag, PVP-coated AgNPs, H<sub>2</sub>-AgNPs, or citrate-AgNPs, either in media alone or media supplemented with 1% fetal bovine serum (FBS) for 1, 4, or 24 hours before assessment. Each AgNP diminished MTT reduction capacity of J774A.1 cells with 50% reductions in activity in the low parts per million of Ag concentration range. Compared with AgNPs, Ag was a more potent cytotoxicant. LDH leakage increased after exposure to Ag and AgNPs indicated that all compounds produced damage to cell membranes. In MTT assays, addition of 1% FBS to media mitigated cytotoxic effects of all forms of Ag. In LDH assays, addition of FBS did not affect Ag-dependent membrane damage. These results indicate AgNPs affect integrity of cell membranes and metabolic competency of cells, although it is yet unclear whether these effects are mediated by phagocytosis of AgNPs or by accumulation of Ag solubilized from nanoparticles. Future studies that examine the disposition, fate, and effects of AgNPs will provide more information for assessment of bioavailability and potential human health risks. (This abstract does not reflect U.S. EPA policy.)

**PS 1344 Dispersion and Dissolution Behavior of Silver Nanoparticles in Artificial Biological Fluids.**

A. M. Mayo<sup>1</sup>, D. R. Johnson<sup>2</sup>, A. J. Bednar<sup>2</sup> and J. A. Steevens<sup>2</sup>. <sup>1</sup>Badger Technical Services, Vicksburg, MS; <sup>2</sup>Environmental Laboratory, US Army Engineer Research & Development Center, Vicksburg, MS.

Nano-sized silver (nAg) is the most widely used engineered nanoparticle in consumer products, so much attention is being given to environment, health, and safety (EHS) risk associated with nAg exposure. The purpose of this study was to evaluate the agglomeration and dissolution of engineered nAg in artificial biofluids to better understand nAg stability throughout the body. Twenty-four hour time-course evaluations of 1 mg/L nAg in artificial biological fluids (alveolar, interstitial, gastric [pH 1.5], and intestinal fluid) were conducted using field flow fractionation-inductively coupled plasma-mass spectrometry (FFF-ICP-MS), dynamic light scattering (DLS), spectrophotometry, and dissolution methods. Silver nitrate (AgNO<sub>3</sub>) was used as a positive control. Citrate- and PVP-Ag (20 nm) in alveolar fluid and intestinal fluid showed similar settling patterns, with absorbance levels decreasing only 10% from t=0 to t=24h, likely due to the presence of surfactants. In contrast, these same particles in interstitial fluid and gastric fluid (pH 1.5) show a 40% decrease in absorbance at 24 h. Rapid agglomeration of coated-nAgs appeared to be occur, as indicated by the sudden formation of black particulates upon addition of the coated-nAgs to all artificial biofluids tested. nAg showed marked size increases over 24 h in interstitial, intestinal, and gastric fluids. The decrease in surface area resulting from this agglomeration may also have an effect on Ag dissolution rates. Citrate- and PVP-coated nAg dissolution, as well as AgNO<sub>3</sub>, suggests the loss of Ag<sup>+</sup>, when compared with Ag<sup>+</sup> concentrations in water. The high concentration of chloride ions in many artificial biofluids may lead to the rapid formation of AgCl during nAg dissolution. These studies demonstrate that nAg is likely to undergo several dissolution and agglomeration changes as the particle moves through different organ systems. Furthermore, these data can be used to generate prediction models of nAg dispersion throughout the body.

**PS 1345 Correlating *In Vivo* Agglomeration State with Oral Bioavailability of Gold Nanoparticles.**

G. K. Hinkley<sup>1</sup>, S. M. Roberts<sup>1</sup> and K. W. Powers<sup>2</sup>. <sup>1</sup>Center for Environmental and Human Toxicology, University of Florida, Gainesville, FL; <sup>2</sup>Particle Engineering Research Center, University of Florida, Gainesville, FL.

Particle size is thought to be a critical factor affecting the bioavailability of nanoparticles (NPs) following oral exposure. Nearly all studies of NP bioavailability focus on characterization of the primary particle size of the material as supplied or as dosed, and not on the effective particle size within the gastrointestinal tract (GIT), which is presumably most relevant for absorption. In the study reported here, agglomeration behavior of gold nanospheres was evaluated *in vivo* throughout the gastrointestinal tract (GIT) using transmission electron microscopy (TEM). Agglomeration state within the GIT was then correlated with bioavailability as indicated by tissue levels of Au detected using inductively coupled plasma mass spectrometry (ICP-MS). Mice were dosed (10mg/kg) with either 22nm PEG-coated or uncoated Au NPs. Previous work done by this group using dynamic light scattering in simulated gastric fluid (SGF) has shown that uncoated Au NPs quickly agglomerate in this environment while PEG-coated Au NPs remain well dispersed after 24 hours in SGF. Samples were taken from various regions of the GIT at varying times

after dosing for TEM analysis. Images from these samples are consistent with predicted agglomeration behavior in that PEG-coated Au NPs can be observed as primary (22nm), non-agglomerated NPs in the stomach, small intestine (SI), cecum, large intestine (LI) and feces of dosed animals. In contrast, uncoated Au NPs were observed to form agglomerates of several hundred nanometers in the stomach and remain agglomerated in the SI, cecum, LI and feces. At 12 hours post-gavage there was significantly more gold detected in the blood and liver ( $p < 0.05$ ) of animals dosed with PEG-coated vs. uncoated Au particles. The characterization of these particles in vivo supports our hypothesis that differences in ICP-MS tissue levels of Au between animals dosed with PEG-coated vs. uncoated Au NPs is due to the particle size being presented to absorptive surfaces in the GIT.

### PS 1346 Comparison of Acute and Chronic Toxicity and Effects of Nanoparticles *Ceriodaphnia dubia*.

A. J. Kennedy<sup>1</sup>, A. Harmon<sup>1</sup>, J. G. Laird<sup>1</sup>, A. J. Bednar<sup>1</sup>, C. Detzel<sup>2</sup> and J. A. Steevens<sup>1</sup>. <sup>1</sup>US Army Corps of Engineers, Vicksburg, MS; <sup>2</sup>NanoSafe, Blacksburg, VA.

In recent years, the usage of nanoparticles has grown tremendously, and their potential to exert toxicity in aquatic environments is an increasing concern. This study evaluated the toxicity of 20 and 100nm nanosilver and nanogold to *Ceriodaphnia dubia* in soft reconstituted water. The selected nanoparticles were chosen for nanosilver ability to dissolve in environmentally relevant solution and nanogold for its slow dissolution in environmentally relevant solution. Standard toxicity test have shown that *Ceriodaphnia dubia* are less sensitive to silver chronically than they are acutely. This is most likely a result of the addition of food binding to the silver reducing bioavailability. An altered testing procedure adding food after 8 hours from water renewal alongside standard testing procedures was evaluated acutely and chronically. This window of time will allow for the uptake of nanoparticles by the organisms that would otherwise not be available. In acute and chronic test *Ceriodaphnia dubia* were less sensitive to nanogold than nanosilver. When comparing acute and chronic 20nm nanogold tests, 100% mortality was shown in the highest concentration 75 mg/L chronically with 60% survival acutely in the highest concentration. This would suggest the possibility that toxicity is occurring by different mechanisms. In 20nm nanosilver chronic testing the altered testing procedure showed an increase in mortality and delayed reproduction compared to standard testing procedures confirming that the addition of food decreases sensitivity to the organism. Future work will include the testing of 100nm nanosilver and nanogold. Further studies are needed to indicate that toxicity is occurring by different mechanisms when comparing acute-to-chronic ratios and testing of different aquatic organisms.

### PS 1347 Silver Nanoparticles Impair Neuronal Synaptic Function and Alter Neurotransmitter Content in the Brain.

K. Sriram, J. R. Roberts, G. X. Lin, J. M. Antonini, A. Kenyon and A. M. Jefferson. CDC-NIOSH, Morgantown, WV.

Silver nanoparticles (AgNPs) find application in the manufacturing of industrial, household and diagnostic products, besides its extensive antimicrobial use. While the economic benefits of manufacturing such materials are highly promising, their adverse environmental and health effects are yet to be fully realized. The unique physico-chemical properties of AgNP influence its ability to aerosolize, and thus occupational or environmental exposure is of major concern. To determine if AgNPs pose a neurological risk, we evaluated its effects in a rodent model. Well characterized AgNP (primary particle size = 20-50 nm) suspensions were prepared in dispersion medium (DM; mean particle aggregate size in DM = 180 nm). Adult male Sprague-Dawley rats were intra-tracheally instilled with a single dose of either DM, 37.5, 112.5 or 450 µg AgNP. At 1, 7, 28, or 84d post-exposure, various indices of neural dysfunction were examined in discrete brain areas. By 7d post-exposure, AgNPs caused a partial loss (35-40%) of striatal synaptosomal-associated protein 25 (Snap25) and syntaxin binding protein 1 (Stxbp1), critical molecular regulators of synaptic neurotransmission. Levels of Snap25 decreased further (~85%) by 84d post-exposure. AgNP also decreased (~25%) striatal tyrosine hydroxylase (Th) protein content. Further, AgNP caused a time-dependent increase (16-45%) in striatal norepinephrine, while lowering (25%) serotonin content by 28d post-exposure. However, AgNP did not alter striatal dopamine content, although it reduced striatal Th. Reactive astrogliosis, as evidenced by increased (30%) expression of glial fibrillary acidic protein (Gfap) was observed in the striatum, 7d following exposure. The persistent reduction of synaptic proteins 84d following cessation of exposure suggests that AgNPs can potentially be neurotoxic. Whether such abnormalities can culminate in neurodegeneration remains to be investigated. Our findings call for extensive safety evaluation to better understand the risks associated with AgNPs and avert any adverse neurological health effects.

### PS 1348 A Study of Mice Inhalation Exposures to Silver Nanoparticles Generated by Nebulization and Electrospray Methods.

A. Lao<sup>1</sup>, M. Zhong<sup>1</sup>, K. Galdanes<sup>1</sup>, D. Chen<sup>2</sup>, T. Gordon<sup>1</sup> and L. Chen<sup>1</sup>.

<sup>1</sup>Environmental Medicine, New York University, Tuxedo, NY; <sup>2</sup>Energy, Environmental and Chemical Engineering, Washington University in St. Louis, St. Louis, MO.

Many forms of engineered nanomaterials are currently being used in industrial and medical applications in the advanced field of nanotechnology. One of the major routes of human exposure to nanomaterials is inhalation. Silver nanoparticles or nanosilver in particular, are prevalent in consumer products and many other applications as antibacterial agents, yet there are relatively limited nanosilver toxicity data in the literature. A series of rodent exposures were conducted to assess the lung inflammatory response. The nanoparticles were generated via a Collision nebulizer and an electrospray aerosol generator using suspensions composed of citrate stabilized nanosilver or polyvinylpyrrolidone (PVP) stabilized nanosilver. The primary size of both nanosilvers was 20 nm in diameter. Particle size distributions of aerosolized citrate stabilized nanosilver and PVP stabilized nanosilver were also characterized. Count median diameters (CMD) of citrate nanosilver and PVP nanosilver were between 50 and 60 nm, while their volume median diameters (VMD) were between 80 and 100 nm, respectively. The CMD and VMD of citrate stabilized nanosilver generated by electrospray were found to be about 2-fold and 3-fold lower, respectively, than that generated by Collision nebulizer. Acute nose-only exposures were conducted on male BALB/c mice using the nebulizer and lung inflammatory responses were examined following 4-h exposure to citrate stabilized nanosilver at a concentration of 1.0 mg/m<sup>3</sup>. At 24-h and 7-d post exposure, there were little change in the number of polymorphonuclear neutrophils and protein concentrations in bronchoalveolar lavage fluid as compared to filtered air control. Our results showed that citrate and PVP coated nanosilver elicited minimal pulmonary inflammatory response in mice at the concentration tested in this experiment.

### PS 1349 Estimation of Human Equivalent Exposure from Rat Inhalation Toxicity Study of Silver Nanoparticles Using Multipath Particle Dosimetry Model.

J. Ji and L. Yu. Institute of Nanoproduct Safety Research, Hoseo University, Asan, Republic of Korea.

Respiratory tract dosimetry is a useful tool to estimate the exposure concentrations of an inhaled substance that will produce the same result at a target site of the respiratory tract in both rats and humans. Thus, to enable the results of animal inhalation studies to be extrapolated to human equivalent exposure levels, the MPPD (multi-path particle dosimetry) model was used to estimate the differences in the respiratory dosimetry of rats and humans. In our previous study, when animals were subchronically exposed to silver nanoparticles over a period of 90 days, a no observable adverse effect level (NOAEL) of 100 µg/m<sup>3</sup> was suggested. Therefore, this study used results from a previous animal study, including the test aerosol information and estimated clearance rate of silver nanoparticles after a 90-day inhalation toxicity test. As a result, the human equivalent workplace exposure concentration of silver nanoparticles was estimated as 59 µg/m<sup>3</sup> compared to the rat NOAEL of 100 µg/m<sup>3</sup>.

### PS 1350 Alterations in Lung Host Defense after Pulmonary Exposure to Silver Nanoparticles in Rats.

B. M. Yingling<sup>1,2</sup>, C. McLoughlin<sup>2</sup>, J. M. Antonini<sup>2,1</sup>, R. I. MacCuspie<sup>3</sup>, V. A. Hackley<sup>3</sup>, B. T. Chen<sup>2</sup>, D. Schwegler-Berry<sup>2</sup> and J. R. Roberts<sup>2,1</sup>. <sup>1</sup>WVU, Morgantown, WV; <sup>2</sup>NIOSH, Morgantown, WV; <sup>3</sup>NIST, Gaithersburg, MD.

Silver nanoparticles (AgNP) are among the fastest growing categories of manufactured nanomaterials, and there is a need to investigate the risk for potential adverse effects of respiratory exposure in workers. The goal of the current study was to characterize susceptibility to lung bacterial infection following AgNP exposure *in vivo*. AgNP, 20 nm in diameter with a 0.3% wt polyvinylpyrrolidone coating (NanoAmor, Inc.), were suspended in a physiological dispersion medium (DM) and sonicated. On day 0, rats were intratracheally (IT) instilled with 37.6 (Ag Low) or 449 (Ag High) µg of AgNP in DM or DM alone. On day 3, rats were inoculated IT with 5x10<sup>5</sup> *Listeria monocytogenes* (LM). Rats were euthanized on day 3 (pre-infection), and on days 4, 6, 8, and 10. Bronchoalveolar lavage (BAL) was performed on the right lung. The left lung was cultured to assess LM burden, and the lung-associated lymph nodes (LALN) were harvested. BAL cells and fluid were retained for analysis of injury, inflammation and oxidant production, and LALN lymphocytes were counted to assess immune response. On day 3 pre-infection, increased BAL albumin levels (lung injury) neutrophil influx (inflammation), LALN lymphocytes, and

BAL cell oxidant production were measured in the Ag High group when compared to the Ag Low and DM groups. Following infection, LM lung burden increased significantly in the DM and Ag Low groups as compared to the Ag High group, peaking on day 6, with the highest burden in the DM group. LALN lymphocytes and BAL neutrophils, lymphocytes, and cellular oxidant production were elevated in the Ag High group on days 4 and 6 compared to DM and Ag Low groups. By day 8, LM lung burden, and BAL and LALN cell counts were similar for all groups. Induction of an early inflammatory response and oxidant burst in conjunction with increased lymphocyte proliferation in the lungs of the high dose AgNP group prior to infection enhanced the innate immune response and led to an increased clearance rate of bacteria from the lungs.

**PS 1351 Exposure to Inhaled Silver-Nanoparticles Results in the Induction of Gene Expression Alterations in Oxidative Stress Pathway Components, in a Time-Dependent Manner.**

M. A. Popovech, K. Galdanes, E. L. Saunders, M. N. Hernandez, L. Chen and T. Gordon. *Environmental Medicine, New York University School of Medicine, Tuxedo, NY.*

The use of silver nanoparticles (AgNPs) is ubiquitous, and they are now commonly employed in pharmaceuticals, medical imaging, medical devices, cosmetics, clothing, and other consumer products. Due to the commonality of AgNPs, along with a general lack of toxicity and safety testing, AgNPs have been deemed safe by default. However, legitimate concerns exist, and a number of recent studies suggest that AgNPs pose a threat to human health. This study was conducted in order to examine the hypothesis that inhaled nano-sized Ag particles cause lung and extrapulmonary organ dysfunction via oxidative stress pathways. Male and female FVB/NJ mice were exposed to either 0.5 mg/m<sup>3</sup> or 1 mg/m<sup>3</sup> of AgNPs generated from metal rods, using a Palas spark generator, via nose only inhalation for 4 hrs. An n=5 animals were used in each treatment group, and all treated animals were compared to air exposed controls. At 2hr, 24hr, 48hr, 72hr, and 7d post-exposure, animals were euthanized and blood, lavage and tissue were collected. RNA was isolated from lung and liver tissue and mRNA expression levels, of key oxidative stress genes, were quantified by real-time RT-PCR. A number of significant alterations in gene expression of key oxidative stress genes were observed in response to AgNP exposure. At 2 hours post exposure, Hmx1 and Keap1 expression increased ~2.75 fold in lung tissue, and modestly decreased to ~2.5 fold at 24 hours post exposure. Whereas in liver tissue, Keap1 expression changed from a 2.5 fold increase to a 3.5 fold increase in liver tissue, at 2 and 24 hours post exposure, respectively. Similarly, in liver tissue, Txnrd1 expression increased from 0.5 fold to a 2.5 fold increase at 2 and 24 hours post exposure, respectively. These experiments have suggested that exposure to inhaled AgNPs results in the induction of gene expression alterations in oxidative stress pathway components. Further, these alterations occur in a time-dependent manner.

**PS 1352 Genetic Influence of Pulmonary Response to Silver Nanoparticles Exposure.**

M. N. Hernandez, E. L. Saunders and M. Popovech. *Environmental Medicine, New York University, Tuxedo, NY.*

Within the last decade, nanotechnology has seen a boost in commercial, medical and industrial applications. However, there is great uncertainty in terms of the biomolecular activity nanoparticles (NPs) may have on biological systems. In particular, this study sought out to determine the genetic influence on the pulmonary response to silver NPs. Murine models were employed to evaluate the variation of inter-strain response. Differences were quantitated by measuring inter-strain variability in terms of polymorphonuclear neutrophil (PMN) infiltration in bronchoalveolar lavage fluid. Initially, three mouse strains (C57BL/6J, FVB/NJ, and BALB/cJ) representing resistant, moderate, and sensitive responders, respectively, were exposed to 0.5 µg/g body weight of 20 and 110 nm citrate or PVP stabilized silver NPs by oropharyngeal aspiration. Bronchoalveolar lavage was performed 24 hr post exposure to measure PMN number and protein concentration. All three strains were found to be more sensitive to 20 nm silver citrate (40-85% PMN response) and 20 nm silver PVP (15-85% PMN response). We then performed a similar exposure in 8 strains of mice (DBA/2J, C57BL/6J, AKR/J, 129SI/SvJ, A/J, FVB/NJ, C3H/HeJ, Balb/cJ) at a lower dose of 0.25 µg/g body weight of 20 nm silver citrate. PMN responses between 1.5% and 60% were observed. In addition, temporal pulmonary response was measured in C57BL/6J, FVB/NJ, and BALB/cJ mice at 24 hrs and 7 days. At 24 hours, PMNs were found to be strain dependent, between 14-46%, and the response at 7 days was found to be between 0-15% PMN response. Based upon these initial findings on inter-strain response variation, it can be concluded that these mouse models show a susceptibility pattern among strains, and can help to elucidate sensitivity mechanisms in terms of exposure assessment and innate inter-species responses.

**PS 1353 Short- and Long-Term Effects of Commercially Available Gold Nanoparticles in Rodents.**

J. Bahamonde<sup>1</sup>, B. Brenseke<sup>1</sup> and M. R. Prater<sup>1,2</sup>. <sup>1</sup>*Biomedical Sciences and Pathobiology, Virginia Tech, Blacksburg, VA;* <sup>2</sup>*Biomedical Sciences, Edward Via College of Osteopathic Medicine, Blacksburg, VA.*

Gold nanoparticles (GNPs) have physical and chemical properties that place them as top candidates for biomedical uses, including promising alternatives for targeted drug delivery, cancer therapy, and diagnostic contrast imaging. Their characteristics and behavior depend largely on their size, shape, and coating, making their uniformity an important aspect to consider, and making comparisons among studies a great challenge. We acquired 15 nm GNPs commercially available for *in vivo* contrast imaging, characterized them, and exposed female BALB/c mice, female F344 rats, and female and male C57BL/6 mice to either 1g/kg of GNPs, or phosphate buffered saline (PBS) via tail vein injection. Blood, urine, and feces collection, euthanasia and necropsy were performed at 24 hours, 1, 2, 3, 4, and 18 weeks post exposure. GNPs were found to be polydispersed, polyethylene glycol-coated, and varied in size from about 4 to 30 nm. Three out of the 19 rats exposed to GNPs died unexpectedly within 24 hours of exposure, with no deaths registered in any other group. GNPs were detected in urine for up to 1 week post exposure, and in feces for up to 2 weeks in mice and 4 weeks in rats. On gross inspection, GNPs caused immediate and persistent darkening of all tissues, and stayed in blood for up to 1 week. Histological examination demonstrated accumulation of GNPs in macrophages and endothelial cells of all tissues examined up to the end of the study, with increased numbers of activated macrophages in GNPs exposed animals compared to PBS exposed animals. Serum levels of interleukin-18, a pro-inflammatory cytokine secreted by macrophages, were significantly higher in animals exposed to GNPs in comparison to those exposed to PBS. Main conclusions of this study are that commercially available GNPs are not necessarily standardized, may cause acute death in rats, accumulate in macrophages and endothelial cells, incite granulomatous inflammation, and persist in the body indefinitely.

**PS 1354 Assessment of Genotoxicity of Silver Nanoparticles in Myh-Deficient and Wild Type Mice.**

R. Reliene, P. Kovvuru, P. E. Mancilla and A. Shirode. *University at Albany, State University of New York, Albany, NY.*

Silver nanoparticles (AgNPs) are extensively used in consumer products due to their antimicrobial properties. AgNPs are released from textile fabrics under regular wash conditions and were detected in sewage sludge of a municipal wastewater treatment plant, suggesting a potential for widespread exposures to AgNPs. However, genotoxicity and underlying molecular mechanisms of AgNPs are poorly understood. We studied DNA double strand breaks (DSBs) and chromosomal damage by γ-H2AX assay and micronucleus assay, respectively, in mice after 5-day treatment with AgNPs by oral application. AgNPs treatment resulted in a 2-fold induction in γ-H2AX foci in both bone marrow and peripheral blood. In addition, AgNPs increased the frequency of micronucleated cells in bone marrow erythroblasts and peripheral blood erythrocytes. Myh is a DNA glycosylase involved in both base excision repair and mismatch repair. We speculated that Myh is involved in AgNP-mediated DNA damage, which predisposes Myh deficient mice to DSBs and/or chromosomal damage. We observed a similar number of γ-H2AX foci and about 2-fold more micronuclei in AgNP treated Myh deficient compared to wild-type controls, suggesting a potential role of Myh in the repair of AgNP-mediated damage. We further investigated the effect of AgNPs on changes in the expression levels of 84 genes involved in DNA repair using PCR array profiler. In total, 25 genes were downregulated and 12 genes were upregulated as a function of AgNP treatment (1.5-fold cutoff). Most downregulated genes play a role in base excision and nucleotide excision repair, while upregulated genes are part of different DNA repair pathways. In summary, AgNP exposure by oral ingestion induces DSBs and chromosomal damage and alters expression of DNA repair genes, suggesting a potential hazard to genetic integrity. Further studies are needed to understand the effect of AgNP on DNA damage signaling, DNA repair efficiency, genomic instability and carcinogenicity.

**PS 1355 Comparative Hepatotoxicity Study of Two Different Diameter Size Silver Nanoparticles in Sprague-Dawley Rats.**

A. Patlolla<sup>1</sup> and P. Tchounwou<sup>2</sup>. <sup>1</sup>*Biology, Jackson State University, Jackson, MS;* <sup>2</sup>*Biology, Jackson State University, Jackson, MS.*

The antibacterial effect of silver nanoparticles (Ag-NPs) has resulted in their extensive application in health, electronic, and household products. Due to the intensive commercial application of Ag-NPs, their health risk assessment is of great importance. The previous *in vitro* studies demonstrated that AgNPs caused toxicity in

various cell-lines. However, the data on the toxicity of Ag-NPs in vivo is largely lacking. The main objective of this study was to determine the effect of two different diameter sizes (6nm, 10nm) silver nanoparticles on certain liver enzymes (alanine ALT, aspartate AST and alkaline phosphatase ALP) in serum and analysis of liver damage in Sprague-Dawley rats. Four groups of five male rats, each weighing approximately 80 + 2 g, were administered orally, once a day for five days with doses of 5, 25, 50, 100, mg/kg body weight (BW) of Ag-NPs. A control group was also made of five rats. Serum was collected following standard protocols, and the activity of the liver enzymes (ALT, AST and ALP) was determined by colorimetric method. The results demonstrated that Ag-NPs exposure increased the activities of the liver enzymes (ALT, AST, ALP) and damage in liver tissue in exposed groups compared to control. The increase in the activity was larger in 6nm size AgNPs compared to 10nm size. Only the highest two concentrations 50 mg/kg and 100 mg/kg showed statistically significant increases in ALT and ALP in both diameter size AgNPs compared to control. AST activity showed an increase; however, it was not statistically significant compared to control. Furthermore, the smallest sized AgNPs (6nm size) had a greater ability to induce hepatic damage in Sprague-Dawley rats than the other sized AgNPs (10 nm). These data suggest that the AgNPs-induced hepatotoxic effects against tissue cells are particle size-dependent, and thus, the particle size needs careful consideration in the design of the nanoparticles for biomedical uses.

### PS 1356 Increased Mucus Production and Histopathological Gill Alterations after Exposure to Nanosilver and Silver Nitrate.

A. D. Hawkins<sup>1</sup>, C. Thornton<sup>1</sup>, A. Harmon<sup>2</sup>, A. J. Kennedy<sup>2</sup>, J. A. Stevens<sup>2</sup>, N. G. Reyero Vinas<sup>2</sup>, K. Bu<sup>3</sup>, J. Cizdziel<sup>3</sup> and K. L. Willett<sup>1</sup>. <sup>1</sup>Pharmacology/Environmental Toxicology Research Program, University of Mississippi, Oxford, MS; <sup>2</sup>Environmental Lab, ERDC, Vicksburg, MS; <sup>3</sup>Chemistry, University of Mississippi, University, MS.

Silver nanoparticles are among the most widely used nanomaterials because of their antibacterial and antifungal properties. Despite their extensive use, information is now becoming available on the toxicity and fate of nanosilver formulations within living organisms. Mucus has both increased and decreased the toxicity of different xenobiotics by either concentrating the xenobiotic on the gills and body or encapsulating toxicants to prevent exposure. In order to understand the relationship between mucus, toxicity and silver exposure, zebrafish (ZF) and fathead minnows (FHM) were exposed for 36 or 96 hr to nominally 20 nm PVP- or citrate-coated silver nanoparticles (PVP-AgNPs; citrate-AgNPs) or silver nitrate (AgNO<sub>3</sub>) at 2 nominal concentrations (20 and 200 µg/L) or (2 and 6 µg/L), respectively. After 4 hr, ZF produced significantly more mucus secretion in every treatment than the control fish in a dose-dependent manner as measured by a phenol-sulfuric acid method. FHM gill RNA was extracted for microarray analyses. To quantitate distribution of silver, skin, liver and GI were digested for ICP-MS. FHM gills were also paraffin embedded, sectioned and examined for histopathological lesions to phenotypically anchor the molecular and chemical endpoints. The highest AgNO<sub>3</sub> and both citrate-AgNPs concentrations caused significant atrophy in gill mucus goblet cells. Every silver treatment also had a significantly higher histopathological alterations index compared to control. Citrate-AgNPs (20 and 200 µg/L) had the highest incidence of alterations (3.5 and 3.25 times higher than control, respectively). The results suggest that mucus production and mucus-related cells are impacted by silver exposure. This research is supported by US Army ERDC grant: W912HZ-09-C-0033.

### PS 1357 Impact of Silver Nanoparticles (AgNP) on Bacteria Species Isolated from Gastrointestinal (G.I.) Tract of Sprague-Dawley (SD) Rats.

M. S. Imam<sup>1</sup>, S. Khare<sup>2</sup>, A. M. Paredes<sup>3</sup> and M. D. Boudreau<sup>1</sup>. <sup>1</sup>Division Biochemical Toxicology, NCTR, Jefferson, AR; <sup>2</sup>Division of Microbiology, NCTR, Jefferson, AR; <sup>3</sup>Office of Scientific Coordination, NCTR, Jefferson, AR.

The food industry is incorporating AgNP into a growing number of products, which suggests that consumers are being exposed orally to increasing amounts of these nanoparticles. The absorption of AgNP from the G.I tract has been demonstrated; however the potential effects from the interactions of AgNP with bacteria of the G.I. tract are largely unknown. We investigated the bactericidal effects of AgNP on *Lactobacillus* sp. (G+) and *Bacteroides* sp. (G-) isolated from the G.I. tract of SD rats. Three sizes of AgNP (10, 75, and 110 nm) at (0.1, 0.5, 1, 2, 5, 10 µg/ml) were incubated with cultures of bacteria (in triplicate), and the bactericidal effects at 60, 120, and 180 min were assessed using colony forming unit (CFU) and adenosine triphosphate (ATP) release assays. There were no CFUs in cultures of *Lactobacillus* sp. or *Bacteroides* sp. when incubated for 120 min or longer in the presence of 75 or 100 nm AgNP at concentrations of ≥2 µg/ml or in the presence of 10 nm AgNP at concentrations of ≥1 µg/ml, suggesting enhanced bactericidal

effects by 10 nm AgNP. Both bacterial species showed a significant decrease in ATP release when exposed to AgNP (10, 75, or 107 nm) at concentrations > 1 µg/ml. At equivalent number of cells (10<sup>3</sup> cells/ml), *Bacteroides* sp. were more sensitive than *Lactobacillus* sp to the bactericidal properties of AgNP (10, 75, or 110 nm), likely reflecting differences in cell wall composition between species. Scanning electron microscopy showed that AgNP were attached to bacterial cells at the surface, suggesting that protein binding or cell wall distortion by AgNP might result in cellular toxicity or death. These results provide new insights into the bactericidal properties of AgNP and how the consumption of AgNP might disrupt the normal balance of microorganisms in the healthy G.I. tract. Supported by interagency agreements 224-12-0003 and AES12013 between the NCTRFDA and NIEHS/NTF

### PS 1358 Influence of Dose, Size and Chemical Composition on Persistence of Silver Nanoparticles in the Rat Lung.

D. S. Anderson, R. Silva, D. Lee, P. C. Edwards, K. E. Pinkerton and L. S. Van Winkle. University of California Davis, Davis, CA.

Silver nanoparticles (AgNPs) have antimicrobial activity and unique electrical properties, resulting in increasing use. While there have been studies of the biological effects of AgNPs, including persistence and clearance of AgNPs from the lung, an examination of the effect of AgNP size and surface coating (used to stabilize these materials when in solution) has not been fully investigated. We investigated lung deposition, retention and clearance of 20nm and 110nm spherical AgNPs coated with citrate or polyvinylpyrrolidone (PVP). Rats were instilled intratracheally with 0.1, 0.5 or 1.0 mg/kg of either one of the AgNP solutions or a vehicle control and were assessed at 1, 7 and 21-days post treatment. Ag was quantified in tissue using inductively coupled plasma mass spectrometry. At one day postinstillation, lungs dosed with 1.0 mg/kg AgNPs had 0.25 to 0.51 mg Ag/g dry tissue and these amounts did not differ by surface coating or particle size. Sham controls had no detectable Ag. Total leukocytes and neutrophils in bronchoalveolar lavage fluid increased in a dose dependent manner 1-day after exposure to all AgNPs with significant increases in the 1.0mg/kg dose compared to all other doses for all 4 particle types. This increase persisted at the 7-day time point in all AgNP groups except for 20nm PVP. Distribution of Ag in the lung was determined using autometallography and semiquantitative scoring on paraffin-embedded lung sections to demonstrate Ag was preferentially localized to the bronchoalveolar duct junction at the 1-day time point. At 7-days post exposure, Ag was localized to the subepithelial extracellular matrix of the terminal bronchioles. Uptake of Ag by alveolar macrophages was also observed. These findings suggest Ag can persist in the lungs over time and alveolar macrophages have a role in the clearance. Supported by U01ES02027 and P42ES004699. Nanomaterials supplied by the NIH NCNHR consortium.

### PS 1359 Subtle Surface Variations Influence Biological Compatibility of Gold Nanoparticles.

K. Kim<sup>1</sup>, T. Zaikova<sup>2</sup>, J. E. Hutchison<sup>2</sup> and R. L. Tanguay<sup>1</sup>. <sup>1</sup>Environmental and Molecular Toxicology, Oregon State University, Corvallis, OR; <sup>2</sup>Chemistry, University of Oregon, Eugene, OR.

To better understand the nanoparticle physicochemical properties that influence biological compatibility, we investigated how subtle ligand variation on the surface of gold nanoparticles (AuNPs) influences biological responses. The zebrafish embryos were exposed to four distinct, well-defined ligand-stabilized 1.5 nm spherical AuNPs. The ligand shells for each AuNP contain: (1) only anionic 2-mercaptoethanesulfonic acid (MES), (2) only cationic N,N,N trimethylammoniumethanethiol (TMAT), (3) a mixed ligand shell containing MES and a small amount of triphenylphosphine (TPP), and (4) a mixed ligand shell containing TMAT and a small amount of TPP. Small-angle X-ray scattering (SAXS) confirmed the core size of the particles and that there was no agglomeration in the embryonic test medium. The only difference between partial and full functionalization was the P/Au ratio as determined by XPS analysis. The MES/TPP coated particles caused higher mortality and malformation than those fully functionalized with MES, and in TMAT/TPP coated particles a higher incidence of smaller size and pale gray eyes was observed. In the gene expression profiles of transcription factors for apoptosis (p53 and bax), eye development (pax6a, otx2 and rx1) and pigmentation (sox10 and mitfa), the gene expression of embryos were significantly disrupted in both mixed ligand particles in a concentration-dependent manner, consistently with the observed developmental toxicity. In addition, laser ablation ICP-MS analysis revealed that biological absorption and distribution of AuNPs in exposed embryos were closely related to the toxicity phenotype and gene expression caused by differential surface functionalization. These data provide new insights into the understanding of how subtle surface changes impact biological compatibility and further emphasize the importance of material characterization. This research is supported by NIEHS P3 ES000210, ES016896 and Air Force Research Laboratory #FA8650-05-1-5041.

**PS 1360 Gold Nanoparticles in Central Nervous System of Mice: Localization and Inflammatory Markers.**

F. Fallahi<sup>1,2</sup>, S. M. Hussain<sup>1,2</sup>, I. E. Pavel<sup>1</sup>, J. P. O'Callaghan<sup>3</sup>, M. Sharma<sup>1,2</sup>, R. Saadawi<sup>4</sup> and M. Morris<sup>1</sup>. <sup>1</sup>Pharmacology & Toxicology, Wright State University, Dayton, OH; <sup>2</sup>711 HPW/RHDJ, AFRL, Wright-Patterson AFB, Dayton, OH; <sup>3</sup>CDC-NIOSH, Morgantown, WV; <sup>4</sup>Chemistry, University of Cincinnati, Cincinnati, OH.

Gold nanoparticles (GNPs) possess unique physicochemical properties that may facilitate entry into the central nervous system (CNS) where they may act therapeutically. There is little information on GNPs biodistribution in specific brain regions or extent of inflammation induction. Experiments determined the localization and neuroinflammatory response of spherical GNPs (10 nm) after IV injection in male C57Bl mice. As a supplement, a known inflammogen, lipopolysaccharide (LPS, 2 mg/kg, sc), was tested. To determine the optimal buffer concentration to maintain GNP solubility, we measured aggregation of GNPs using various PBS concentrations (10, 1, 0.1, 0.01 X). 0.01X PBS produced the least amount of GNP aggregation and was used in all studies. The next experiment verified entry of GNPs into CNS. Mice were IV injected using the tail vein (200 µg/ml 10 nm GNPs in 0.01X PBS). After 24 hrs mice were perfused transcardially with 2 % glutaraldehyde/paraformaldehyde and brains were collected. GNPs were measured using inductively coupled plasma mass spectrometry in whole brain homogenates. To specifically localize accumulation of GNPs in brain, septum, caudate, hippocampus, hypothalamus, cortex, frontal cortex, and spinal cord were dissected. Hypothalamus, hippocampus, and septum had the highest levels of GNPs (6.7, 6.2, and 4.6 µg Au/g, respectively). To evaluate brain inflammation, we used q-PCR analysis of frozen brain regions for study of pro-inflammatory mediators, LIF, CCL2 and IL1β. GNPs did not affect cytokine/chemokine expression in cortex, frontal cortex or hippocampus. LPS, as expected, caused a marked (100-fold) increase in the same cytokines. Results show that GNPs enter brain and concentrate in specific regions without eliciting an inflammatory response. Data raise the possibility of usefulness of GNPs in drug delivery and therapeutic treatment of CNS diseases.

**PS 1361 Dissolution Kinetics of Inhaled Metal Nanoparticles in a Murine Model.**

E. L. Saunders, E. Bartnick, K. Galdanes, M. Popovech, M. N. Hernandez, L. Chen and T. Gordon. *Environmental Medicine, New York University, Tuxedo Park, NY.*

Previous work has established that Ag, Ni, and Ce nanoparticle (NP) inhalation induces a defined dose/inflammatory-response relationship. Adverse responses to each metal were found to vary by size, shape (TEM analysis) and chemistry (XPS analysis). This study was conducted to delineate the inflammatory responses generated by exposure to Ag, Ni, and Ce NP's in a murine model, as marked by the polymorph neutrophil response (PMN), and examine absorbed kinetics associated with NP exposure. PMN response for the larger sized particles (100-130nm) did not exceed 4% across three doses (1mg/m<sup>3</sup>, 0.5mg/m<sup>3</sup>, and 0.25mg/m<sup>3</sup>), and ranged from 4% to 32% for smaller sized particles (30-45nm) in a concentration dependant manner. To further investigate the inflammatory response and extrapulmonary translocation, synthetic body fluids were used to establish dissolution rates; specifically, synthetic phagolysosomal fluid (PSF, pH 4.6), and synthetic lung surfactant (LS, pH 7.5). NP's were dispersed directly into the fluids using a fritted bubbler and the dissolved fraction was subsequently separated from the particles using centrifugation of spin column filters (1-2nm pore size). The metal concentrations were then analyzed using ICP-MS and expressed as percentage of dissolved vs. total. Surprisingly results of Ag showed similar trends in both fluid types, with larger particles dissolving more rapidly than smaller particles. The percent difference between 130nm and 30nm particles in LS was 18% at 15 min, 9% at 30 min, and 0% at 1 hr. In contrast, percent differences between these two Ag NP's in PSF were 42% at 15 min, 26% at 30 min, and 6% at 1 hr. To assess the effect of size on kinetics, mice were exposed to Ag NP's of 4 sizes (20, 30, 90, and 130nm) with liver, kidney, lungs, and brain, digested for ICP-MS analysis. Our results clearly showed that, for those NP's that dissolve within 48 hrs, the NP's with the lower dissolution rate (e.g., the smaller Ag NP's produce a greater inflammatory response.

**PS 1362 Utility of the Greenscreen™ for Nanoscale Hazard Assessments: Nanosilver Case Study.**

N. A. Linde, T. L. McGrath, B. J. Lampe and J. C. English. *NSF International, Ann Arbor, MI.*

A project employing GreenScreen™ methodology was undertaken to assess the chemical hazards of selected manufactured nanomaterials. The GreenScreen™ methodology provides a basis for clear and transparent communication of potential

human health and environmental hazards. It is being adopted by businesses, governments, and others seeking to identify safer chemical replacements. The purpose of the present investigation was to evaluate the utility of the GreenScreen™ for assessing the hazards of nanoscale substances and to recommend changes to the method to accommodate the properties specific to nanomaterials. An independent Science Advisory Team was assembled and tasked with providing technical guidance from project onset through ongoing implementation, including the selection of nanomaterials and identification of reliable data. In the initial stage of the project, chemical hazard assessments were undertaken for nanoscale silver and a silica-silver nanocomposite, AGS-20, used to confer antimicrobial properties to textile fabrics, thereby inhibiting the growth of odor-causing bacteria in the treated textile. The scope of each assessment was defined with respect to chemical entities, particle size and shape, use of ligands, stabilizers or capping agents, and potential transformation products. Modifications to the GreenScreen™ method and template to accommodate nanomaterial applications were developed and incorporated. Recognizing that the methodology fundamentally assesses only hazard, not risk, this exercise demonstrated that a GreenScreen™ assessment of nanoscale materials can reveal hazard characteristics and concern levels that differ among different nanoscale forms and conventional forms. The availability of data on adequately characterized materials and the identification and use of relevant analogs to address data gaps remains a challenge. Potential confounds in the application of the results for product comparisons are described. Hazard assessments for several additional nanoscale materials are planned or underway, to further evaluate the utility and limitations of this approach.

**PS 1363 The Role of Macrophage Scavenger Receptor A in the Disposition of Silver Nanoparticles.**

J. N. Smith<sup>1</sup>, M. H. Littke<sup>1</sup>, J. A. Klein<sup>1</sup>, C. W. Frevert<sup>2</sup>, B. D. Thrall<sup>1</sup> and J. G. Pounds<sup>1</sup>. <sup>1</sup>Systems Toxicology, Battelle Memorial Institute, Pacific Northwest Division, Richland, WA; <sup>2</sup>University of Washington, Seattle, WA.

The role of macrophage scavenger receptor A (SR-A) in the disposition and biological response of silver nanoparticles was investigated using cellular and animal models. Bone marrow derived macrophages from wild-type C57BL/6J and SR-A deficient mice were exposed to silver nanoparticles (20 and 110 nm, primary size) coated with citrate and polyvinylpyrrolidone (PVP). Macrophages from wild-type mice demonstrated higher rates of silver binding/uptake compared those from SR-A<sup>-/-</sup> mice (0.5 vs. 0.003 hr<sup>-1</sup>, respectively), which led to increased levels of cell associated silver (~10 fold at 24 hr) after exposure to 20 nm silver nanoparticles measured by inductively coupled plasma mass spectrometry (ICP-MS). In contrast, no significant differences in total cell binding/uptake or cytotoxicity with 110 nm silver particles were observed between wild-type and SR-A<sup>-/-</sup> macrophages. After administration of 20 nm particles by oropharyngeal aspiration *in vivo*, wild-type mice and SR-A<sup>-/-</sup> mice demonstrated similar silver clearance from lungs, bronchoalveolar lavage (BAL) fluid, and BAL cells (half-life: 15.5 vs. 23.8 d, respectively in lungs) after 28 d measured by ICP-MS. However, wild-type mice had increased levels of silver in liver (area under the curve [AUC]: 0.06 vs. 0.02 g<sup>-1</sup>xd, respectively) and spleen (AUC: 0.16 vs. 0.03 g<sup>-1</sup>xd, respectively) driven by higher silver levels in liver and spleen at day 7, indicating increased uptake of silver by wild-type mice. After retro-orbital injection, *in vivo* biokinetics of silver in wild-type and SR-A<sup>-/-</sup> mice were very similar. Overall, these results support the conclusion that SR-A plays a significant role in silver nanoparticle uptake at both the cellular and whole animal levels, but its role may be size-dependent.

**PS 1364 Nanosilver-Induced Lung Inflammation Is Mouse Strain Dependent.**

D. Botta<sup>1</sup>, S. C. Schmuck<sup>1</sup>, D. K. Scoville<sup>1</sup>, C. C. White<sup>1</sup>, C. M. Carosino<sup>1</sup>, C. M. Schaupp<sup>1</sup>, W. C. Griffith<sup>1</sup>, E. M. Faustman<sup>1</sup>, T. Gordon<sup>2</sup> and T. J. Kavanagh<sup>1</sup>. <sup>1</sup>Department of Environmental and Occupational Health Sciences, University of Washington, Seattle, WA; <sup>2</sup>Department of Environmental Medicine, New York University, New York, NY.

Silver nanoparticles (NanoAg) have found many uses in electronics, medical diagnostics and as microbicides. While ionic silver (Ag<sup>+</sup>) is acknowledged to have relatively low toxicity toward mammals, the particulate nature of NanoAg has raised concerns, especially in the context of potential occupational exposures. Because human genetic variability can influence susceptibility to many toxicants, we used multiple inbred mouse strains to determine if genetics could influence NanoAg induced lung toxicity and inflammation. We exposed the Collaborative Cross (CC) parental mouse strains (C57BL/6J, 129S1/SvJ, A/J, NOD/LtJ, and NZO/HILtJ) and 3 wild derived strains (CAST/EiJ, PWK/PhJ, and WSB/EiJ) to citrate-stabilized 20 nm NanoAg at a dose of 0.25 µg/gm BW via oropharyngeal aspiration. Mice were sacrificed either 1 or 21 days after exposure. Lung injury and inflammation were assessed by examining total protein and lactate dehydrogenase activity,

and the presence of leukocytes and inflammatory cytokines in bronchoalveolar lavage fluid (BALF). One day after exposure, none of the strains exhibited differences in total protein or LDH activity compared to saline vehicle controls. However, there were marked strain-dependent differences in lung inflammation, with C57BL/6 mice showing a 3-6 fold lower response compared to other strains. Evidence to date indicates that neutrophilic inflammation was attenuated by 21 days, suggesting a transient effect for these nanoparticles. Because C57BL/6 mice were not very responsive, relying on this strain alone to assess NanoAG-induced inflammation may not adequately assess their safety. This work is done in collaboration with the NCNHR Consortium and supported by NIH/NIEHS grants U19ES019545, P30ES07033 and T32ES07032.

### PS 1365 Characterization and Toxicity of Silver Nanowires.

A. Tagmount<sup>1</sup>, B. Gilbert<sup>2</sup>, L. Scanlan<sup>1</sup>, C. Tran<sup>1</sup>, C. Clark<sup>1</sup> and C. Yulpe<sup>1</sup>.  
<sup>1</sup>Nutrition Science and Toxicology, University of California Berkeley, Berkeley, CA;  
<sup>2</sup>Earth Science Division, LBNL, Berkeley, CA.

Metal and semiconductor nanowires (NW) have a diverse range of anticipated applications in electrical devices, sensors, catalysts and composite materials but there is very limited information on the fate of NW in the environment or the effect of NW on organisms. We are studying the environmental fate and biological toxicity of silver nanowires (Ag NW), a representative metal NW, to (1) *Daphnia magna*, an aquatic eco-indicator and (2) cell lines of different species representing potential target organs, including a cell line from fathead minnow, another eco-indicator species. LC50 values were determined in *D. magna* exposed to Ag NW and different end-points of cytotoxicity were investigated using cell based imaging assays (high content screening) and other cell assays. Transcriptomic response to Ag NW was also studied in *Daphnia* and in a macrophage cell line using high throughput RNA sequencing. We characterized the physicochemical properties of Ag NW to determine how their chemistry relates to cytotoxicity. We studied the colloidal stability and oxidation rates of Ag NW with two lengths and two coatings in different aqueous solutions, including conditions relevant to studies of toxicity to *D. magna*, and cell media. While poly(vinylpyrrolidone) (PVP) and aluminosilica (SiO<sub>2</sub>) coatings prevent NW aggregation in ultrapure water, rates of aggregation and settling were greatly increased in the presence of dissolved inorganic and ionic ions. In stirred anaerobic solutions, morphological changes, including fusing of multiple nanowires, was the dominant transformation. In aerobic solutions, Ag oxidation to release dissolved Ag<sup>+</sup> occurred for all coating types. Rates of Ag<sup>+</sup> release cannot explain observed differences in Ag NW toxicity to *Daphnia*, suggesting that toxicity is controlled by a complex mixture of colloidal and chemical processes in solution. Also, in parallel to this physicochemical study, cell internalization, sub-cellular localization as well as in situ localization of Ag NW in *Daphnia* were carried out

### PS 1366 Examining Mechanisms of Toxicity and Uptake of Gold Nanoparticles to *Caenorhabditis elegans*.

O. Tsyusko<sup>1</sup>, J. M. Unrine<sup>1</sup>, R. M. Nass<sup>2</sup> and B. Collin<sup>1</sup>. <sup>1</sup>Plant and Soil Sciences, University of Kentucky, Lexington, KY; <sup>2</sup>Stark Neuroscience Research Institute, Indiana University, Indianapolis, IN.

Background: Gold nanoparticles (Au-NPs) have been used in previous studies as a particle-specific probe in nanotoxicity studies due to their resistance to oxidative dissolution. Objectives: To examine the particle-specific toxicity of Au-NPs to *C. elegans* using a toxicogenomic approach and to explore possible mechanisms of defense against toxicity of Au-NPs using gfp strains, mutants and RNAi. Methods: The LC10 of 5.9 mg/L Au-NPs was used for 12hr exposure in microarray experiments using Affymetrix whole genome microarrays. qRT-PCR was used to confirm results for six selected genes. Selected mutant and gfp *C. elegans* strains were used for toxicity testing to Au-NPs. Differences in distribution of Au in endocytosis mutants were examined using synchrotron-based X-ray microfluorescence spectroscopy. Results: 797 significantly differentially expressed genes identified from whole genome microarray analyses were linked to seven common biological pathways. Significant up-regulation was observed for 26 pgn/abu genes from non-canonical unfolded protein response (UPR) pathway and molecular chaperones (hsp-16.1, hsp-70, hsp-3 and hsp-4). There was significant increase in sensitivity to Au-NPs in non-canonical UPRs (pgn-5 and abu-11) knockouts. Au-NPs induce gfp expression of the vesicular GABA transporter homologue in GABA neurons. Significant up-regulation by Au-NPs of FOXO transcription factor daf-16 was confirmed by microarrays and through using daf-16::gfp strains. Differences in distribution of Au among endocytosis mutants (chc-1 and rme-2) and wild type nematodes were correlated with differences in toxicity. Conclusions: Our results suggest possible involvement of genes from endocytosis and UPR pathways in uptake and detoxification mechanisms, respectively. Au-NPs may also induce stress response through insulin signaling pathway. Support: US NSF EPA CEINT, University of KY microarray core Pilot grant.

### PS 1367 Mouse Neural Progenitor Cells As a Functional Model for Developmental Neurotoxicity Testing: Intracellular Calcium Signaling.

M. M. Dingemans, M. de Groot and R. H. Westerink. Neurotoxicology Research Group, Toxicology Division, Institute for Risk Assessment Sciences (IRAS), Faculty of Veterinary Medicine, Utrecht University, Utrecht, Netherlands.

Developmental neurotoxicity (DNT) is often investigated in a traditional manner (*in vivo* using large numbers of experimental animals), while development of *in vitro* methods for DNT reduces animal use and increases insight into cellular and molecular mechanisms of DNT. Neural progenitor cells (NPCs) are particularly suited for the investigation of neurodevelopmental processes as they are pre-programmed to differentiate into nervous system-specific cell types: neurons and glia.

The intracellular calcium concentration ([Ca<sup>2+</sup>]<sub>i</sub>) plays an essential role in neurotransmission, plasticity and neurodevelopment and can therefore be used as a functional readout for DNT [1]. We therefore investigated changes in [Ca<sup>2+</sup>]<sub>i</sub> evoked by a set of neurotransmitters in primary mouse NPCs using the Ca<sup>2+</sup>-responsive dye Fura-2. Calcium responses were measured at a single-cell resolution at various differentiation durations. Calcium responses could be evoked by depolarization, acetylcholine, and adenosine triphosphate (ATP), indicating the expression and functionality of the respective neurotransmitter receptors and related calcium signaling pathways.

The data demonstrate that this model allows for the investigation of possible effects of (suspected) developmental neurotoxins on the development of neuronal characteristics, such as intracellular signaling in response to neurotransmitters. As investigation of chemical-induced effects on the development of functional neuronal characteristics is underrepresented in DNT testing, we argue that biochemical and morphological approaches should be complemented with investigations of neuronal (network) functionality, including network formation, inter- and intracellular signaling and neuronal network function.

Funding: EU (DENAMIC-FP7282957); ZonMW NL (85300003).

[1] de Groot et al. Toxicol Sci in press [doi: 10.1093/toxsci/kfs269].

### PS 1368 Ketamine-Induced Neuronal Damage and Altered N-methyl-D-aspartate (NMDA) Receptor Function in Rat Primary Forebrain Culture.

N. Sadovova<sup>1</sup>, F. Liu<sup>2</sup>, M. G. Paule<sup>2</sup>, W. Slikker<sup>3</sup> and C. Wang<sup>2</sup>. <sup>1</sup>Toxicologic Pathology Associates, Jefferson, AR; <sup>2</sup>Division of Neurotoxicology, National Center for Toxicological Research/US FDA, Jefferson, AR; <sup>3</sup>Office of Director, National Center for Toxicological Research/US FDA, Jefferson, AR.

Ketamine, a noncompetitive NMDA receptor antagonist, is used in pediatric general anesthesia and causes neuronal cell death during the brain growth spurt. To understand the underlying mechanisms associated with ketamine-induced neuronal toxicity and search for approaches or agents to prevent such adverse effects, a primary cell culture system was utilized. Neurons harvested from the forebrain of newborn rats were maintained under control conditions or exposed to either ketamine (10 μM), or ketamine plus L-carnitine (1, 30 and 100 μM) for 24 hours, followed by a 24-hour withdrawal period. Ketamine exposure resulted in elevated NMDA receptor (NRI) expression, increased generation of reactive oxygen species (ROS) as indicated by higher levels of 8-oxoguanine production, and enhanced neuronal damage. Co-administration of L-carnitine significantly diminished ROS generation and provided near complete protection of neurons from ketamine-induced cell death. NMDA receptors regulate channels that are highly permeable to calcium. Calcium imaging data demonstrated that neurons exposed to ketamine had a significantly elevated influx of calcium and higher intracellular free calcium concentrations ([Ca<sup>2+</sup>]<sub>i</sub>) evoked by NMDA (50 μM), compared to control neurons. These findings suggest that prolonged ketamine exposure produces an increase in NMDA receptor expression (compensatory up-regulation) which allows for a higher/toxic influx of calcium into neurons once ketamine is removed from the system, leading to elevated ROS generation and neuronal cell death. L-carnitine appears to be a promising agent in preventing ketamine toxic effects on neurons at an early developmental stage.

### PS 1369 L-Carnitine Ameliorates Propofol-Induced Toxicity in Rat Embryonic Neural Stem Cells.

M. G. Paule<sup>1</sup>, F. Liu<sup>1</sup>, C. M. Fogle<sup>1</sup>, N. Sadovova<sup>2</sup>, W. Slikker<sup>1</sup> and C. Wang<sup>1</sup>. <sup>1</sup>Division Neurotoxicology, National Center Toxicological Research US FDA, Jefferson, AR; <sup>2</sup>Toxicology Pathology Associates, Inc., National Center Toxicological Research US FDA, Jefferson, AR.

Propofol is a widely used general anesthetic. A growing body of data suggests that perinatal exposure to general anesthetics can result in long-term deleterious effects on brain function. In the developing brain there is evidence that general anesthetics

can cause cell death, synaptic remodeling, and altered brain cell morphology. Acetyl-L-carnitine (aLc), an anti-oxidant dietary supplement, has been reported to prevent neuronal damage from a variety of causes. To evaluate the ability of aLc to protect against propofol-induced neuronal toxicity, neural stem cells were isolated from gestational day 14 rat fetuses and on the 8th day in culture were exposed for 24 hr to propofol at 10, 50, 100, 300 and 600  $\mu$ M, with or without aLc (10  $\mu$ M). Markers of cellular proliferation (EdU), mitochondrial health (MTT), cell death/damage (LDH) and oxidative damage (8-oxo-dG) were monitored to determine: 1) the effects of propofol on neural stem cell proliferation; 2) the nature of propofol-induced neurotoxicity; 3) the degree of protection afforded by aLc; and 4) to provide information regarding possible mechanisms underlying protection. After propofol exposure at a clinically-relevant concentration (50  $\mu$ M), the number of dividing cells was significantly decreased and oxidative DNA damage was increased. There was also a significant dose-dependent reduction in mitochondrial health as evidenced by decreases in MTT metabolism. No significant effect on LDH release was observed at propofol concentrations up to 100  $\mu$ M. The oxidative damage at 50  $\mu$ M propofol was blocked by aLc. Thus, clinically-relevant concentrations of propofol induce dose-dependent adverse effects on rat embryonic neural stem cells by slowing or stopping cell division/proliferation and causing cellular damage. Elevated levels of 8-oxo-dG suggest oxidative damage and aLc effectively blocks at least some of the toxicity of propofol, presumably by scavenging oxidative species and/or reducing their production.

### PS 1370 Determination of Neurotoxicity in the Developing Rat Induced by Dexmedetomidine.

J. Liu. *Anesthesia, Harvard Medical School, Boston, MA.*

Anesthetic, sedative and analgesic drugs are used for diagnostic studies and surgery procedures in infants and children, but little is known about their impact on the developing nervous system. Dexmedetomidine is a selective  $\alpha_2$ -adrenergic agonist, and has been used many clinical applications including the reduction of postoperative delirium and has many protective effects on cell damage in animal models. However, dexmedetomidine induced human neutrophil apoptosis by activation of caspases-3, 7, -8 and -9. Based on these, we hypothesize how dexmedetomidine affects neuroapoptosis in the developing rat brain.

**Material and Methods:** Sprague-Dawley postnatal day 7 (P7) rat pups were used for this study. Rats were divided into three doses of 10, 25, and 50  $\mu$ g/kg body weight of dexmedetomidine and one control group. Each rat pup received 5 intraperitoneal doses of either saline, or Dex at 90 minutes intervals over 6 hours. After the 6 hour treatment period, the animals were deeply anesthetized with pentobarbital (100 mg/kg, IP). Parts of the brain tissues were extracted and flash frozen in liquid nitrogen for western blotting analysis. The other parts were fixed in 4% paraformaldehyde for immunohistochemical assay. Apoptosis such as cleaved-caspase-3, TUNEL, and other protein expression such as GSK-3 $\beta$  were determined by immunohistochemistry and western blotting assays.

**Results and Conclusion:** Dexmedetomidine increased neuroapoptosis by increasing apoptosis and cleaved caspase-3 expression in the rat brain tissues. Dexmedetomidine also increased the p-GSK-3 $\beta$  / GSK-3 $\beta$  ratio, indicating a reduction in GSK-3 $\beta$  activity. These findings suggest that dexmedetomidine may induce neuroapoptosis by regulating GSK-3 $\beta$  in the developing rat brain.

### PS 1371 Nicotine-Induced Toxicity in Rat Embryonic Neural Stem Cells.

F. Liu<sup>1</sup>, N. Sadovova<sup>2</sup>, C. M. Fogle<sup>1</sup>, M. G. Paule<sup>1</sup>, W. Slikker<sup>1</sup> and C. Wang<sup>1</sup>.  
<sup>1</sup>Division of Neurotoxicology, National Center for Toxicological Research NCTR/US FDA, Jefferson, AR; <sup>2</sup>Toxicologic Pathology Associates, Jefferson, AR.

Maternal smoking substantially increases the risk of learning disabilities, behavioral problems, and attention deficit/hyperactivity disorder in offspring. Nicotine is the main pharmacologically active component of tobacco smoke. Prenatal exposure to nicotine is capable of causing fetal brain damage. To evaluate nicotine's effects on the developing nervous system and explore potential mechanisms underlying such toxicity, rat embryonic neural stem cells were used.

Brain cortices were collected from fetal rats (gestational day14, GD14) for neural stem cell isolation and subsequent culture in commercial rat growth medium. On the 8th day in vitro (DIV), confluent neural stem cells were exposed to nicotine at concentrations of 0.5, 1.0, 2.0, 5.0 and 10  $\mu$ M for 24 hours. Neural stem cells were identified using monoclonal anti-*nestin* antibody. Markers of cellular proliferation (EdU), mitochondrial health (MTT), cell death/damage (LDH) and immunohistochemical staining of activated caspase 3 were monitored to determine the nature of nicotine-induced neurotoxicity.

Nicotine treatment resulted in a substantial dose-dependent reduction in mitochondrial function as evidenced by significant decreases in the metabolism of MTT. No significant effect of nicotine on LDH release was observed. 1  $\mu$ M nicotine significantly increased the expression of activated caspase 3, suggesting that nicotine induced neural stem cell apoptosis.

These results suggest that nicotine decreased neural stem cell viability, and nicotine-induced cell death is probably apoptotic in nature.

### PS 1372 Consequences of Nicotine Exposure on Larval Zebrafish Circadian Rhythms.

M. E. Wolter and K. R. Svoboda. *Joseph J. Zilber, School of Public Health, UWM, Milwaukee, WI.*

Cigarette smokers often report having problems associated with disrupted sleep. One potential mechanism underlying sleep disruption could be related to alterations in an individual's circadian rhythm. Nicotine from cigarettes can activate neuronal nicotinic acetylcholine receptors (nAChRs) throughout the nervous system including structures important for maintaining the circadian rhythm. We have utilized oscillations in larval zebrafish locomotor activity as a model to study circadian rhythms. Initially, the circadian rhythm in embryos reared on a 14/10 light/dark (L/D) cycle was evaluated. Of 257 larvae examined, 76.6% exhibited a typical rhythm where locomotor activity was high in the initial hours of the cycle, declined to a minimum, and then became elevated again at the end of the cycle. We then determined the consequences of raising embryos in constant dark or constant light conditions from 0-127 hours post fertilization (hpf) as well as being exposed to nicotine. At 127 hpf, 23.5% of the larvae reared in constant dark exhibited a typical circadian rhythm and 12.5% of embryos reared in constant light exhibited a typical circadian rhythm. Moreover, the locomotor activity of larvae reared in constant light was reduced and remained at a constant level for the duration of the cycle. Since nAChRs are expressed in the zebrafish pineal gland and retina (two structures that influence circadian rhythms in fish) early in development, we hypothesized that nicotine exposed fish would have a pattern of activity similar to those reared in constant light. Zebrafish reared in 15  $\mu$ M nicotine from 36-96 hpf and then evaluated at 127 hpf indeed lacked the normal circadian rhythm. The locomotor activity pattern of the nicotine-exposed zebrafish was similar to the pattern of zebrafish reared in constant light; the activity was reduced and remained at constant level for the duration of the cycle. These results indicate that nicotine is capable of disrupting vertebrate circadian rhythms and could be involved with the disrupted sleep pattern of smokers.

### PS 1373 Ethanol Pretreated Astrocytes Increase Synapses in Hippocampal Neurons.

P. J. Roque<sup>1</sup>, G. Giordano<sup>1</sup>, A. Barria<sup>2</sup>, M. Guizzetti<sup>3</sup> and L. G. Costa<sup>1</sup>.  
<sup>1</sup>DEOHS, University of Washington, Seattle, WA; <sup>2</sup>Physiology & Biophysics, University of Washington, Seattle, WA; <sup>3</sup>Department of Psychiatry, University of Illinois, Chicago, IL.

In children exposed to alcohol *in utero*, problems with learning and memory suggest hippocampal involvement and effects on synapse formation and function. Astrocytes may contribute to synaptogenesis by releasing specific factors. The present study investigated how ethanol influences the ability of astrocytes to modulate synapse formation *in vitro*. Using immunocytochemical labeling of synaptic proteins, confocal imaging and 3-dimensional object analysis, we found that astrocytes pre-treated with ethanol (50 mM) and co-cultured with primary hippocampal neurons (14 days in culture) for 24 hours, induce a 4.5-fold increase in synaptic structure formation. To corroborate that this is reflected in increased functionality, we used whole cell patch clamp techniques to measure spontaneous miniature excitatory post-synaptic currents. In neurons co-cultured with ethanol pre-treated astrocytes, we observed a higher frequency of events, relative to neurons co-cultured with control astrocytes, suggesting more functional synapses in the ethanol group. However, a second population of neurons in the same treatment group was observed to have a lower frequency than control astrocytes. No amplitude differences were observed, suggesting no difference in the number of post-synaptic receptors between groups. Ethanol increases the efflux of cholesterol-containing lipoproteins (CCL) from astrocytes, and cholesterol appears to play a role in synapse formation. Direct treatment of hippocampal neurons with high-density lipoproteins induced a 3.2-fold increase in synaptic structures. When cholesterol release from astrocytes was induced by LXR/RXR agonists, through the over-expression of cholesterol transporters, this also resulted in an increase in synapses, suggesting a role for astrocytic CCLs in the observed synaptic increase after ethanol pre-treatment (Supported by F31AA019869, AA008154).

**PS 1374 PCB 95 and IFN-gamma Exert Opposing Effects on Dendritic Growth in Cultured Rat Sympathetic Neurons.**

P. E. Goines and P. J. Lein. *Molecular Biosciences, University of California Davis School of Veterinary Medicine, Davis, CA.*

There is credible evidence that environmental factors interact with genetic susceptibilities to determine risk for neurodevelopmental disorders such as autism spectrum disorders (ASD). PCBs and IFN $\gamma$  are implicated as environmental risk factors for ASD. Increased levels of both have been documented in ASD, and both interfere with neuronal connectivity in central neurons via effects on dendritic growth. Recent reports indicate that PCBs upregulate inflammatory cytokines, but the combined effects of these factors on neuronal connectivity have not been explored. Because of emerging awareness of autonomic dysfunction in ASD, which may link the triad of behavioral deficits, gastrointestinal disturbances, and immune dysfunction often observed in ASD, we are quantifying independent and combined effects of PCB95 and IFN $\gamma$  on dendritic morphology in cultured sympathetic neurons. Sympathetic neurons were dissociated from superior cervical ganglia of perinatal rat pups and grown in serum-free defined medium in the absence of glial cells. Under these conditions, these neurons do not extend dendrites unless treated with BMP7 (10 ng/ml). After 5 d of exposure to BMPs in the absence of presence of PCBs (1 pM-1  $\mu$ M) and/or IFN $\gamma$  (30 ng/ml), cultures were fixed and immunostained for MAP2b to visualize dendrites. PCB 95 increased the number and length of dendrites in a concentration-dependent manner in the absence or presence of BMP7 and these effects were inhibited by pharmacological block of ryanodine receptor calcium channels. IFN $\gamma$  reduced dendritic growth in PCB 95-treated cultures in the absence or presence of BMP7. These findings illustrate a novel interaction between PCBs and cytokines in the autonomic nervous system, and suggest that exposure to these factors during critical windows of neurodevelopment may interfere with normal patterns of neuronal connectivity in sympathetic neurons and contribute to neuronal, immune and GI dysfunction in ASD. Support provided by NIEHS (R01 ES014901 to PJJ) and a Hartwell Biomedical Research Fellowship (to PEG)

**PS 1375 PCB 95 Stimulates Synaptogenesis via Ryanodine Receptor-Mediated miR132 Upregulation.**

H. Chen<sup>1</sup>, A. Lesiak<sup>2</sup>, M. Zhu<sup>2</sup>, S. M. Appleyard<sup>2</sup>, S. Impey<sup>3</sup>, D. Bruun<sup>1</sup>, G. A. Wayman<sup>2</sup> and P. J. Lein<sup>1</sup>. <sup>1</sup>Department of Molecular Biosciences, University of California Davis, Davis, CA; <sup>2</sup>Program in Neuroscience, Washington State University, Pullman, WA; <sup>3</sup>Vollum Institute, Oregon Health and Sciences University, Oregon Health and Sciences University, Portland, OR.

Polychlorinated biphenyls (PCBs) are widespread environmental pollutants linked to developmental neurotoxicity in children. Recent evidence suggests that non-dioxin-like (NDL) PCBs interfere with neuronal connectivity via interactions with ryanodine receptors (RyRs) which are calcium release channels broadly expressed in the nervous system. NDL PCBs stabilize RyRs in the open configuration and this triggers a calcium-dependent signaling pathway that mediates activity-dependent dendritic growth via CREB activation. CREB activation is also linked to increased formation of dendritic spines and synapses via upregulation of miR132, which suppresses the translation of p250GAP, a negative regulator of synaptogenesis. This suggests the possibility that NDL PCBs modulate these signaling events to influence synaptogenesis. To test this, we quantified dendritic spine and synapse formation in primary dissociated hippocampal cultures and organotypic hippocampal slice cultures treated with PCB 95, a NDL congener with potent activity at the RyR. Nanomolar concentrations of PCB 95 significantly increased spine density and the frequency of miniature excitatory post-synaptic currents. These effects were coincident with upregulation of miR132 and were blocked by inhibiting RyR or CREB, suppressing miR132 or expressing a mutant p250GAP, translation of which is not suppressed by miR132. These data demonstrate that PCB 95 sensitization of the RyR modulates synaptogenesis via activation of a CREB-miR132-p250GAP signaling pathway, and provide further evidence of mechanisms by which NDL PCBs may interfere with normal patterns of connectivity in the developing brain. Supported by NIH grants R01 MH086032, R01 ES014901, P42 ES04699, and the Hope for Depression Research Foundation.

**PS 1376 Developmental PCB 95 Exposure Affects Spatial Memory in Weanling Mice.**

C. Barnhart<sup>1</sup>, D. Yang<sup>1</sup>, H. Chen<sup>1</sup>, L. Qi<sup>2</sup> and P. J. Lein<sup>1</sup>. <sup>1</sup>Molecular Biosciences, University of California Davis, Davis, CA; <sup>2</sup>Public Health Sciences, University of California Davis, Davis, CA.

Polychlorinated biphenyls (PCBs) are ubiquitous environmental contaminants that have been linked to behavioral deficits in children and experimental animals. We previously reported that developmental exposure to Aroclor 1254 interferes with

spatial memory in weanling rats coincident with decreased experience-dependent dendritic plasticity. We hypothesize that non-dioxin-like (NDL) PCBs mediate this phenomenon via interactions with ryanodine receptor (RyR) Ca<sup>2+</sup> channels. To test this hypothesis, we are comparing the effects of developmental exposure to NDL PCB 95, a potent RyR sensitizer, on spatial memory in wildtype (WT) versus mice heterozygous (HET) for the human R163C-RyR1 mutation that enhances sensitivity to halogenated hydrocarbons. RyR1<sup>WT</sup> dams were exposed to 0, 0.1, 1, or 6 mg PCB 95/kg/day in the diet for 2 weeks prior to mating with RyR1<sup>HET</sup> males, and throughout gestation and lactation. Offspring were weaned at P21 and trained in the Morris water maze from P24-P29. Preliminary analyses shows that developmental PCB 95 exposure affects latency, percentage of time (PT) and distance (PD) in the training quadrant, and average distance to the target (ADT) during training and these effects are both sex- and genotype-dependent. Within dose groups, RyR<sup>HET</sup> weanlings have higher PT and PD and lower ADT than RyR<sup>WT</sup> littermates during the probe test. There are no treatment, sex or genotype differences in latency, time in walls, or path length during the visual cue test. There are also no differences in dam or pup body weight across experimental groups. These experiments suggest that developmental exposure to a RyR-active NDL PCB congener alters spatial learning and memory and the magnitude of this effect is influenced by sex and by expression of the R163C-RyR1 mutation. This work supported by NIH (grants R01 ES014901, T32 ES007059 and P42 ES04699) and the ARCS Foundation.

**PS 1377 Optimizing Methods to Quantify CYP1A Enzyme Activity in Mouse Brain following Developmental PCB Exposure.**

A. Ashworth and C. P. Curran. *Biological Sciences, Northern Kentucky University, Highland Heights, KY.*

Polychlorinated biphenyls (PCBs) are developmental neurotoxins and endocrine disruptors that remain widespread in the human food supply. Children exposed during gestation and lactation are at highest risk of neurotoxicity. Genetic differences can influence how these chemicals are metabolized, so we use a mouse model in an effort to identify genes which affect human susceptibility to developmental PCB exposure. Coplanar PCBs activate the aryl hydrocarbon receptor (AhR) in high-affinity AhR mice and increase cytochrome P450 (CYP1) expression, including CYP1A2 protein which can sequester PCBs in the liver. Our work and the work of others have shown that this sequestration is protective. However, our previous research also found an increase in CYP1A1 mRNA in the brains of our most susceptible mouse line with the AhR<sup>Cyp1a2(-/-)</sup> genotype at postnatal day 28 when PCB tissues levels were highest. Other researchers have reported differential expression and regulation of CYP1A1 and CYP1A2 in the brain. So, we are now assessing CYP1A protein levels and activity in various brain regions. We used the EROD assay as a test for CYP1A1 activity and the MROD assay for CYP1A2 activity. Liver from PCB-treated AhR<sup>Cyp1a2(+/-)</sup> was used as a positive control whereas Cyp1a1<sup>(-/-)</sup> and Cyp1a2<sup>(-/-)</sup> knockout mice served as the respective negative controls. We compared traditional methods used for liver tissue (microsome purification) and a modified EROD protocol assay developed for smaller tissue volumes which uses a whole tissue homogenate. Both methods yielded sufficient protein for enzyme activity assays in all tissues tested: cortex, cerebellum, and hypothalamus. We found that 100mM potassium phosphate was an optimal buffer to homogenize the tissue, compared with 50mM Tris buffer. As expected, we also found higher enzyme activity in microsomes compared with whole tissue homogenates. Confirming previous reports, we also detected significant MROD activity in liver microsomes from Cyp1a2<sup>(-/-)</sup> mice, indicating this is a non-specific test for CYP1A2 activity.

**PS 1378 Selective Dieldrin Toxicity to Differentiating Dopaminergic Neurons.**

S. Schildknecht, B. Zimmer and M. Leist. *University of Konstanz, Konstanz, Germany.*

Parkinson's Disease (PD) is characterized by the selective loss of dopaminergic neurons of the Substantia nigra. Epidemiological observations have suggested a causative role of environmental pollutants such as heavy metals and pesticides in idiopathic forms of PD. Dieldrin is an insecticide for which adverse effects on the dopaminergic system have been reported. However, the underlying selective neurotoxicity is not fully characterized yet. In a model of murine embryonic stem cell-derived neurons, we observed a selective degeneration of dopaminergic neurons while other types such as GABA neurons, were not affected by dieldrin. Based on these observations with mixed neuronal types, a human dopaminergic cell line (LUHMES) was used for all further studies. LUHMES cells are conditionally immortalized human fetal mesencephalic cells that acquire a dopaminergic phenotype following differentiation for 6 days. Exposure to dieldrin during early differentiation (day 0-2) lead to an inhibition of normal differentiation and ultimately cell death. The same concentrations of dieldrin (0.5-1  $\mu$ M) did not show any adverse

effect when added to fully differentiated LUHMES or other, non-neuronal cell types. By using an alternative differentiation protocol, LUHMES can be differentiated into neurons without tyrosine hydroxylase (TH), the central enzyme in dopamine synthesis. When exposed during early differentiation (day 0-2), these TH-negative cells were less sensitive to dieldrin compared with normally differentiated LUHMES, indicating that components of the dopaminergic phenotype are responsible for the selective degeneration observed.

**PS 1379 Differential Gene Expression in the Neonatal Rat Brain following Combined Maternal Exposure to Chlorpyrifos and Nicotine.**

T. V. Damodaran<sup>1,2</sup>, J. Bradley<sup>2</sup> and M. B. Abou-Donia<sup>2</sup>. <sup>1</sup>Biology, NCCU, Durham, NC; <sup>2</sup>Pharmacology and Cancer Biology, DUMC, Durham, NC.

Environmental exposure to toxic chemicals during early fetal development has been known to manifest long lasting adverse effects for several decades. We hypothesized that combined exposures to pesticides used in households and to nicotine in cigarettes may have adverse synergistic outcome in both the mother and developing fetus. We studied the effects of combined exposure to chlorpyrifos (0.2 mg/kg) and nicotine (1mg / kg) with appropriate controls on the developing rats. Following parturition from exposed mothers, the brains of the new born litters were dissected out to isolate different tissues from the brain. Total RNA from the cerebellum was isolated and global gene expression analysis was done using cell cycle specific super arrays from Qiagen, employing standard molecular techniques. Some of the major findings include the following: A) There were a number of cell cycle genes altered in various treatment groups. B) cdc25b was significantly up-regulated in nicotine treatment group, but was down-regulated in both chlorpyrifos and combined treatment groups. C) cdk5 was up-regulated in chlorpyrifos alone and combined treatment groups. D) Up-regulation of p27kit1 and p15ink4b were noted in combined treatment group and not in nicotine or chlorpyrifos alone groups. This data indicates complex pathways of inhibition and acceleration of cell cycle. Further studies with those genes identified as biomarkers from this study can be useful for developing molecular tools for diagnostics and therapeutics for toxicities involving chlorpyrifos and nicotine

**PS 1380 The Effect of Embryonic Exposure to Deltamethrin on the Dopaminergic System and Swim Activity in the Zebrafish.**

T. S. Kung, J. Richardson, K. R. Cooper and L. A. White. Rutgers University/UMDNJ, New Brunswick, NJ.

Pyrethroids are commonly used insecticides that are generally considered to pose little risk to human and environmental health. However, there is increasing concern that children are more susceptible to the adverse effects of pesticides. We developed the zebrafish model to test the hypothesis that developmental exposure to low doses of pyrethroid pesticide deltamethrin alters dopaminergic gene expression and leads to persistent behavioral alterations. Zebrafish embryos were treated with deltamethrin at doses below the LOAEL (0.25-0.5 µg/L), during the embryonic period (3-72hpf) using a static non-renewal water exposure. After 72hpf, embryos were either harvested for RT-qPCR or reared in pesticide free water until adulthood. At 72hpf, deltamethrin treated embryos had significant increased expression of the dopamine transporter (DAT) and dopamine receptors D1 and D2. We quantified the swim activity of 2-week old zebrafish (larvae) and 1-year old zebrafish (adults) using the Noldus Ethovision system and observed significant increases in swim activity in both larvae and male adults that had been developmentally exposed to deltamethrin. To determine if the increased swim activity at the 2-week stage is mediated by deltamethrin's effect on dopaminergic system, we treated deltamethrin exposed and control larvae to methylphenidate, a DAT agonist. Methylphenidate had a significant stimulating effect on control larvae and a significant suppressive effect on larvae developmentally exposed to deltamethrin. To further investigate the role of the DAT, embryos were injected with a DAT morpholino to transiently reduce mature DAT transcript levels during the developmental period. DAT knockdown alone results in significant increases in swim activity at 2-weeks of age which is significantly reduced in deltamethrin treated embryos. Our data suggest that exposure to deltamethrin during the embryonic period results in persistent behavioral changes and is likely due to an interaction between deltamethrin and the dopaminergic system. NIEHS R56ES018863, T32ES007148, R01ES015991

**PS 1381 Dysregulation of Redox Homeostasis by Paraquat in Rat Developing Brain.**

M. Rathinam, L. Chen, A. Fowler, A. Riar, M. Narasimhan, L. Mahimainathan and G. I. Henderson. Pharmacology and Neuroscience, Texas Tech University Health Sciences Center, Lubbock, TX.

Immature brain is susceptible to paraquat (PQ) induced oxidative stress resulting in neuron damage. We hypothesize that dysregulation of glutathione (GSH) homeostasis is a key factor in these neurotoxic responses. To test this, postnatal day 4 (PN4) rat pups were chosen as the period between birth and PN10 includes active brain development equivalent to that in the human 3rd trimester. Initially, LD50 levels on PN4 were evaluated. Sprague Dawley rat pups were grouped as control, vehicle control, and PQ was administered (I.P) at 10, 25 and 50 mg/kg. At 24h post-treatment, declines in viability by 45% and 100% were observed in the 25 and 50 mg/kg PQ groups, respectively. During the 24h period, a decline in motor activity was also noticed in these two high dose groups. For subsequent studies the 10 mg/kg dose was used for all time points (2-24 hours). Body weight was unchanged compared to both controls (p<0.05) Brain PQ levels peaked at 4h (140µg/mg protein) as assessed by HPLC. In brain, a significant (p<0.05) increase in reactive oxygen levels (ROS) was observed by DCF-DA fluorimetry as early as 6h which persisted to 24h. Increased oxidized form of GSH (GSSG) was observed at all time points (2, 4, 6, 8 and 24h) while decreased reduced glutathione (GSH) was noted only at 24h. These changes were reflected in decreased GSH/GSSG ratios with an associated increase in brain PARP-1 levels (50%) at 24h. These results indicate altered redox homeostasis and DNA damage in PQ exposed brain. The studies have established a role for oxidative stress in PQ induced neurotoxicity in developing brain and a model for studying PQ neurodevelopmental toxicity.

**PS 1382 Neonatal Bisphenol A (BPA) Exposure Alters Sex-Specific Estrogen Receptor 2 (ERβ) mRNA Expression in the Postnatal Rat Brain.**

J. Cao, L. Joyner and H. B. Patisaul. Biology, North Carolina State University, Raleigh, NC.

Perinatal life is a critical window for sexually dimorphic brain organization, which is profoundly influenced by endogenous steroids, most notably estrogen. Exposure to endocrine disrupting compounds may disrupt this process, resulting in compromised reproductive physiology and altered sociosexual behavior in adult life. To test the hypothesis that Bisphenol A (BPA) exposure specifically confined to the neonatal critical period impacts ESR expression through weaning, the present study assessed the impact of exposure (on the first three days of life) to 10 µg estradiol benzoate (EB), 50 µg/kg BPA (LBPA) or 50 mg/kg BPA (HBPA) on ESR2 expression in the bed nucleus of the stria terminalis (BNST), the paraventricular nucleus (PVN) and the anterior medial amygdala (MeA) in the postnatal rat brain. In unexposed animals, ESR2 expression decreased in the BNST and increased in the PVN from postnatal day (PND) 0 to 19 in both sexes. Sexually dimorphic ESR2 expression was transient in the neonatal BNST and PVN. EB decreased ESR2 expression in females in the BNST, and in both sexes in the PVN. In the BNST, ESR2 expression was decreased in males by LBPA and in females by HBPA on PND 10. LBPA increased ESR2 expression in females but decreased it in males on PND 10, thus reversing the sexually dimorphic expression pattern observed in the vehicle controls. In the MeA, BPA mimicked the EB effect and decreased ESR2 expression levels on PND 4. Collectively, these data demonstrate that the neonatal period is vulnerable to BPA exposure, and BPA does not simply mirror the impacts of EB, but rather, disrupted ESR2 expression in a dose, temporal, and region specific manner. The functional significance of this altered ESR2 expression may underlie reported disruptions of adult reproductive deficiencies and abrogated sex differences in sociosexual behavior across the lifespan. Further work will also be needed to establish if these effects can be induced via exposures which recapitulate human exposure conditions and doses.

**PS 1383 Effects of Different Endocrine Disruptor Mixtures on Gene Expression in Neonatal Rat Brain Regions: Focus on Developing Excitatory Synapses.**

W. Lichtensteiger<sup>1</sup>, C. Bassetti-Gaille<sup>1</sup>, O. Faass<sup>1</sup>, J. Boberg<sup>2</sup>, S. Christiansen<sup>2</sup>, U. Hass<sup>2</sup>, A. Kortenkamp<sup>3</sup> and M. Schlumpf<sup>1</sup>. <sup>1</sup>GREEN Tox and Institute of Anatomy, University of Zurich, Zurich, Switzerland; <sup>2</sup>National Food Institute, Technical University of Denmark, Søborg, Denmark; <sup>3</sup>Institute for the Environment, Brunel University, Uxbridge, United Kingdom. Sponsor: T. Slotkin.

Brain development is regulated by sex hormones. In mammals, estradiol is thought to control male sexual brain differentiation, but recent data also indicate a role for androgen receptor-mediated mechanisms. Female brain development is dependent

on estrogens. It is not known how these processes are affected by real-world mixtures of endocrine disruptors (EDCs). We investigated effects of a mixture of 13 EDCs (T-Mix) and of mixtures of its estrogenic (E-Mix) and anti-androgenic (A-Mix) components, administered by oral gavage to rat dams from gestational day 7 until weaning. The mixture ratio was chosen to reflect high end human intakes (S. Christiansen et al., 2012). At postnatal day 6, during the last part of sexual brain differentiation, exon microarray analyses were performed in medial preoptic area (MPO) of both sexes in the highest dose group, and real time RT-PCR of selected mRNA species in MPO and ventromedial hypothalamus (VMH) of all dose groups. Microarray analyses in MPO revealed sex-specific effects on gene expression patterns that differed between all three EDC mixtures. Real time RT-PCR of individual mRNA species demonstrated treatment- and sex-dependent differences between MPO and VMH; effects were dose-dependent. Prominent are effects of all three EDC mixtures on the expression of genes encoding for proteins involved in excitatory glutamergic synapse formation and function, including a number of genes identified as risk factors for autism spectrum disorders. Our study demonstrates differential responses of the developing brain to different types of EDC mixtures and points to excitatory synapse development as a new, potentially relevant focus. Supported by EU FP7 Framework Programme (CONTAMED).

### PS 1384 The Effect of Prenatal Exposure to Amorphous Nanosilica Particles on Neonatal Memory.

Y. Morishita<sup>1</sup>, Y. Yoshioka<sup>1</sup>, K. Takao<sup>2,3</sup>, Y. Ago<sup>4</sup>, H. Satoh<sup>1</sup>, N. Nijori<sup>1</sup>, T. Tanaka<sup>1</sup>, K. Takuma<sup>4</sup>, T. Yoshida<sup>1</sup>, H. Nabeshi<sup>5</sup>, T. Yoshikawa<sup>1</sup>, S. Tsunoda<sup>6,7</sup>, T. Matsuda<sup>4</sup>, T. Miyakawa<sup>2,3</sup>, K. Higashisaka<sup>1</sup> and Y. Tsutsumi<sup>1,6,7</sup>.  
<sup>1</sup>Laboratory of Toxicology and Safety Science, Graduate School of Pharmaceutical Sciences, Osaka University, Suita, Japan; <sup>2</sup>Division of Systems Medicine, Institute for Comprehensive Medical Science, Fujita Health University, Toyoake, Japan; <sup>3</sup>Section of Behavior Patterns, Center for Genetic Analysis of Behavior, National Institute for Physiological Sciences, Okazaki, Japan; <sup>4</sup>Laboratory of Medicinal Pharmacology, Graduate School of Pharmaceutical Sciences, Osaka University, Suita, Japan; <sup>5</sup>National Institute of Health Science, Setagaya-ku, Japan; <sup>6</sup>Laboratory of Biopharmaceutical Research, National Institute of Biomedical Innovation, Ibaraki, Japan; <sup>7</sup>MEI Center, Osaka University, Suita, Japan.

Nanomaterials (NMs) are increasingly being used in various fields for their unique functions. Therefore, it is important to ensure the safety of NMs to take advantage of their usefulness. Previously we identified the hazard that intravenous injection of several NMs to pregnant mice might induce intrauterine growth retardation (IUGR). IUGR children are known to have high risks of contracting some diseases, such as neurological disorders. Thus, it is important to assess postnatal effects of prenatal exposure to NMs. In this study, we examined neonatal memory after in utero exposure to amorphous nanosilica particles (nSP), as one of the typical NMs. Pregnant mice were intravenously injected nSP. The body weight of pups were measured weekly. Working memory, reference memory, and context memory of pups were measured by eight-arm radial maze test, Barnes maze test, and fear conditioning test. Pups of nSP treated mice (nSP pups) had smaller body weight than control mice from birth to 30 weeks old. On the other hand, no difference was found on the scores of memory tests between nSP pups and control mice. These results suggest that in utero exposure to nSP might result in growth disorder of pups but have little effect on memory of pups.

### PS 1385 Sex-Dependent Impairment of Learning due to Exposure to Concentrated Ambient Particles.

J. L. Allen, D. Weston, K. Conrad, G. Oberdorster and D. A. Cory-Slechta.  
*Environmental Medicine, University of Rochester Medical School, Rochester, NY.*

Multiple studies link air pollution to impaired cognition in humans and experimental animals. Our study sought to determine the effects of ultrafine (<100nm) concentrated ambient particles (CAPS) on learning in C57BL/6 mice exposed to CAPS or filtered air for 2 weeks during early postnatal life with and without CAPS re-exposure as adults. Behavioral testing begun at 2-3 mos of age using a repeated learning and performance paradigm that housed a series of three response levers (left, center, right) was located on the front wall of the chamber. During the repeated learning component of the paradigm, the required sequence changed with each session, whereas a constant sequence was used in the performance component. Both male and female mice showed significant sequence-dependent learning impairments, but no alterations in the performance component, consistent with selective learning deficits. Postnatal female CAPS-exposed mice showed significant learning impairment in sequences requiring a right-center-left order, whereas male adult CAPS-exposed mice were impaired on learning sequences requiring a left-center-right order. Assessment of brain pathology in non-behaviorally tested littermates showed CAPS-related evidence of sex and brain-region dependent microglial

activation, astrogliosis, and neurochemical changes even several months post termination of exposure, the importance of which will be determined by histopathological examination and neurochemical analysis of the brains from CAPS-exposed mice that underwent behavioral testing. Collectively, these findings demonstrate long-lasting brain and behavioral toxicity in response to CAPS exposures, with impairments on the repeated learning and performance paradigm that are sex-, sequence-, and exposure period-dependent. They support the need for broader assessment of the role of CAPS exposure in nervous system diseases and disorders. Supported by T32ES007026, R21ES019105, P30ES01247.

### PS 1386 Effects of Maternal Inhalation of Gasoline Evaporative Condensates on Sensory Function in Rat Offspring.

L. L. Degn<sup>1</sup>, D. F. Lyke<sup>1</sup>, T. E. Beasley<sup>1</sup>, P. A. Evansky<sup>2</sup>, S. A. Martin<sup>1</sup>, W. K. Boyes<sup>1</sup>, P. J. Bushnell<sup>1</sup> and D. W. Herr<sup>1</sup>. <sup>1</sup>TAD/INB, US EPA, Durham, NC; <sup>2</sup>EPHD, US EPA, Durham, NC.

In order to assess potential health effects resulting from exposure to ethanol-gasoline blend vapors, we previously conducted neurophysiological assessment of sensory function following gestational exposure to 100% ethanol vapor (Herr et al., *Toxicologist*, 2012). For comparison purposes, the current study investigated the same measures after gestational exposure to 100% gasoline evaporative condensates (GVC). Pregnant Long-Evans rats were exposed to 0, 3K, 6K, or 9K ppm GVC vapors for 6.5 h/day over GD9 – GD20. Sensory evaluations of male offspring began around PND106. Peripheral nerve function (compound action potentials, NCV), somatosensory (cortical and cerebellar evoked potentials), auditory (brainstem auditory evoked responses), and visual evoked responses were assessed. Visual function assessment included pattern elicited visual evoked potentials (VEP), VEP contrast sensitivity, and electroretinograms (ERG) recorded from dark-adapted (scotopic) and light-adapted (photopic) flashes, and UV and green flicker. Although some minor statistical differences were indicated for auditory and somatosensory responses, these changes were not consistently dose- or stimulus intensity-related. Scotopic ERGs had a statistically significant dose-related decrease in the b-wave implicit time. All other parameters of ERGs and VEPs were unaffected by treatment. All physiological responses showed changes related to stimulus intensity, and provided an estimate of detectable levels of change. The results show that gestational exposure to GVC vapors did not result in large decrements in peripheral nerve, somatosensory, auditory, or visual function when the offspring were assessed as adults. However, the alterations in ERG b-waves may indicate subtle changes in retinal function. Additional studies are in progress to evaluate the effects of exposure to the evaporative condensate vapors from a blend of ethanol (15%) and gasoline (85%). *This is an abstract of a proposed presentation and does not necessarily reflect EPA policy.*

### PS 1387 Abnormality in Fear-Related Emotional Function in Mice Perinatally Exposed to a Low Dose of TCDD.

S. Benner<sup>1</sup>, A. Haijima<sup>1</sup>, Y. Zhang<sup>1</sup>, R. Kobayakawa<sup>2</sup>, K. Kobayakawa<sup>2</sup>, M. Kakeyama<sup>1</sup> and C. Tohyama<sup>1</sup>. <sup>1</sup>Laboratory of Environmental Health Sciences, Center for Disease Biology and Integrative Medicine, Graduate School of Medicine, University of Tokyo, Tokyo, Japan; <sup>2</sup>Osaka Bioscience Institute, Osaka, Japan.

An increasing trend of prevalence of developmental disorders, psychiatric illnesses and associated pathological behaviors has been suspected of being induced at least partly by environmental chemical exposure during development. We have previously reported the lasting consequences of perinatal exposure to a low dose of 2,3,7,8-tetrachlorodibenzo-p-dioxin (TCDD) in brain functions, such as cognitive and social-emotional defects in mice. Nevertheless, the effects on emotional function have not yet been clearly defined. The current study thus aimed to examine whether a perinatal TCDD-exposure at an oral dose of 0.6 µg TCDD/kg on GD 12.5 in C57BL/6 dams affects emotional function in offspring. Eleven brain regions were microdissected by the punch out technique for determination of the basal monoamine contents using HPLC-ECD. Behavioral responses toward acquired and innate fear were analyzed using fear conditioning and olfactory-based fear stress tests. A depression-like behavior was assessed using forced swim test. It was found that the TCDD-exposure enhanced dopamine level in the ventral tegmental area and ventral hippocampus. These mesolimbic structures are thought to regulate behavioral responses toward external stimuli by processing internal information, such as memory and emotion. A mesolimbic dopaminergic balance is particularly sensitive to aversive stimuli such as fear. Accordingly, the TCDD-exposed mice exhibited abnormal behavioral responses to both acquired and innate fear. However, no apparent alterations in the basal serotonin levels were found in the examined regions. In correlation, no abnormalities associated with serotonergic emotional behavior emerged under the forced swim test. The present results suggest that a perinatal low-dose TCDD exposure persistently disrupts dopamine balance in brain regions involved in regulating fear-related emotion.

**PS 1388 Neonatal Exposure to Perfluorohexane Sulfonate (PFHxS) in Mice Alters Neuroprotein Levels Essential for the Developing Brain.**

I. Lee and H. Viberg, *Environmental Toxicology, Uppsala University, Uppsala, Sweden.*

Perfluorohexane sulfonate (PFHxS) is a perfluorinated compound (PFC) used as an industrial additive. The chemical properties of PFCs make them suitable as surfactants and oil- and water repellents, and they are frequently used in products for packaging and as protective coatings. However, the same properties account for their extreme physico-chemical stability, making them practically non-biodegradable, which has generated a worldwide environmental spread and concern. Since we recently have seen that other PFCs, like perfluorooctane sulfonate (PFOS) and perfluorooctanoic acid (PFOA), can induce developmental neurotoxic effects, the purpose of the present study was to explore if neonatal exposure to PFHxS can affect specific neuroprotein levels e.g. calcium/calmodulin-dependent kinase II (CaMKII), growth-associated protein-43 (GAP-43), synaptophysin and tau, in the mouse brain. Male and female NMRI-mice were exposed, on postnatal day 10, to a single oral dose of 6.1 or 9.2 mg PFHxS/kg bw and control animals received a 20% fat emulsion vehicle. The animals were euthanized 24h or 4 months after PFHxS exposure and the neuroprotein levels in hippocampus and cerebral cortex were analyzed. 24h after exposure there were significant differences seen in the neuroprotein levels compared with control and the neurotoxic effects differed between hippocampus and cerebral cortex. Increased levels of CaMKII, synaptophysin and tau in the hippocampus and decreased levels of GAP-43 in the cerebral cortex were measured for both sexes. The effects on the protein levels in adult animals were less pronounced than in the neonates. The results from the present study show that a single oral exposure to PFHxS during a critical period of brain development can cause developmental neurotoxic effects. The neurotoxic effects are similar to previous studies done with other PFCs such as PFOS and PFOA. Further investigations on the developmental neurotoxic effects of PFHxS are needed as there still is very limited knowledge about the neurotoxicity of PFCs.

**PS 1389 Prenatal Exposure to 1-Bromopropane Changes Basic Excitability of the Hippocampus and Inhibits the Behaviors Induced by Kainic Acid and Pentylenetetrazole in the Rat Offspring during Lactation Period.**

Y. Fueta<sup>1</sup>, S. Ueno<sup>1</sup>, T. Ishidao<sup>1</sup>, M. Kanemitsu<sup>2</sup> and H. Hori<sup>1</sup>. <sup>1</sup>University of Occupational and Environmental Health, Kitakyushu, Japan; <sup>2</sup>Kyushu Institute of Technology, Kitakyushu, Japan.

1-Bromopropane (1-BP), a substitute for specific chlorofluorocarbons, is mainly used for degreasing agents and spray adhesives. 1-BP exhibits central neurotoxicity in adult humans. Animal studies have shown reproductive/developmental toxicity as well as neurotoxicity. However, developmental neurotoxicity remains unclear. We aimed to clarify whether prenatal exposure to 1-BP affects development of neuronal excitability and behaviors in the juvenile offspring. 1-BP was inhalationally exposed to pregnant Wistar rats from day 1 to 20 (6 h/day) with the concentration of 0, 400, or 700 ppm. On the days of PND 13, 14 and 15, field potentials were recorded from the CA1 area of hippocampal slices obtained from the control and 1-BP groups. At PND14, kainic acid (KA, 0, 0.1, 0.5 and 2.0 mg/kg) or pentylenetetrazole (PTZ, 60 mg/kg) was injected to the control and 1-BP groups. Stimulation/response curves of field excitatory postsynaptic potential and those of population spike (PS) enhanced, and the ratios of paired-pulse responses of PS decreased in the 1-BP groups at PND14. PTZ or KA injection to the PND14 offspring resulted in a significant inhibition of the drug-induced behaviors in the 1-BP groups. Our results provide the evidence that prenatal exposure to 1-BP/metabolites affects the central nervous system (CNS) of the offspring during lactation period, suggesting developmental modification of neuronal networks and changes in the excitability of the CNS during the lactation period.

**PS 1390 Neonatal Exposure to a Single Low Dose of Ionising Radiation Causes Persistent Disruptions in Cognitive Abilities and Increased Levels of Tau in Mice.**

S. Buratovic<sup>1</sup>, B. Stenéröw<sup>2</sup>, S. Sundell-Bergman<sup>3</sup>, A. Fredriksson<sup>1</sup>, H. Viberg<sup>1</sup> and P. Eriksson<sup>1</sup>. <sup>1</sup>Environmental Toxicology, Organismal Biology, Uppsala, Sweden; <sup>2</sup>Radiology, Oncology and Radiation Science, Biomedical Radiation Sciences, Uppsala, Sweden; <sup>3</sup>Soil and Environment, Uppsala, Sweden.

Ionising radiation (IR) is extensively used in the medical field for treatment and diagnostics. Concern has been raised about possible negative consequences from low dose exposure to IR during critical phases of perinatal and/or neonatal brain devel-

opment. The brain growth spurt, which is characterized by maturation of axonal and dendritic outgrowth, establishment of neural connections and acquisition of new motor and sensory abilities, occurs perinatally in humans and neonatally in mice. By using the neonatal mouse as an animal model we are able to study the effect of IR during early periods of brain development and which consequences it has for the adult animal.

Neonatal NMRI mice were irradiated (0; 0.35 and 0.5 Gy) at one single occasion on postnatal day 10. At 2- and 4-months of age, spontaneous behaviour was tested in a novel home environment and parameters observed were locomotion, rearing and total activity. Analyses of important neuroproteins in cerebral cortex were performed 24h following irradiation (0 and 0.5 Gy) and at 6-months of age.

Observations of spontaneous behaviour revealed a significantly deranged behaviour in 2- and 4-month old mice of both sexes irradiated with 0.35 or 0.5 Gy in a dose response related manner. The observed reduced activity during the beginning of the test period and increased activity at the end of the test period indicates a lack of habituation capacity and disrupted cognitive functions. Neuroprotein analyses of cerebral cortex 24h after irradiation and at 6-months of age showed a significantly increased level of tau in mice irradiated with 0.5 Gy compared to controls. This demonstrates that a single dose of IR, given at a defined critical period during brain development, is sufficient to cause persistently reduced cognitive functions and increased levels of tau in mice.

**PS 1391 CYP1A1\_CYP1A2(-/-) Double Knockout Mice Exhibit Impaired Motor Function.**

A. Lang, H. Garber, C. Strohmaier, K. Taylor and C. P. Curran. *Biological Sciences, Northern Kentucky University, Highland Heights, KY.*

CYP1A1 and CYP1A2, members of the cytochrome P450 superfamily, are key detoxifying enzymes normally expressed in the liver. Though they are also reportedly expressed in the cortex and cerebellum of the brain, their physiological function in the brain remains unknown. Previous work in our lab uncovered motor deficits in Cyp1a2(-/-) knockout mice. To confirm those findings, we obtained Cyp1a1\_1a2 (-/-) double knockout mice which had the Cyp1a2 gene deleted using a different genetic strategy. We compared Cyp1a1\_1a2 (-/-) double knockout mice with wild-type Cyp1a1\_Cyp1a2 (+/+) mice using a battery of four behavior tests: The rotarod test primarily identifies deficits in cerebellar function related to balance and motor coordination. Gait analysis, adhesive removal, and pole climbing tests primarily identify impairments in the nigrostriatal pathway, which is a major dopaminergic pathway related to motor function. We found significant impairments in Cyp1a1\_1a2 (-/-) double knockout mice in rotarod testing and adhesive removal. Male knockouts demonstrated the greatest impairment in adhesive removal compared with females. Interestingly, Cyp1a1\_1a2 (-/-) double knockout mice had shorter latencies in the pole-climbing test. This might be explained by a difference in motivation or anxiety, because the animals climb down a 50cm pole to return to their home cage. There were no significant differences in the gait test for stride length, stride width or stride differential. Together, these data suggest a novel function for CYP1A2 in brain regions important to normal motor function.

**PS 1392 Aryl Hydrocarbon Receptor (AhR) Deletion in Cerebellar Granule Neuron Precursors Impairs Motor Function and Neurogenesis.**

D. P. Dever, K. Conrad, D. A. Cory-Slechta and L. Opanashuk. *Environmental Med, University of Rochester, Rochester, NY.*

The AhR is a ligand-activated member of the basic-helix-loop-helix (bHLH)/PER-ARNT-SIM transcription superfamily that regulates the toxicity of 2,3,7,8-tetrachlorodibenzo-p-dioxin (TCDD). Increasing evidence suggests that AhR influences the development of many tissues, including the central nervous system. In particular, the AhR has been reported to be involved in regulating critical stages of neurogenesis. Our previous data suggest that inappropriate and/or sustained AhR activation by TCDD disrupted granule neuron precursor (GNP) development. Moreover, studies in AhR knockout mice suggested that GNP maturation was abnormal. This study tested the hypothesis that the AhR endogenously controls GNP maturation in the developing cerebellum. We created a GNP-specific AhR knockout mouse (AhR<sup>fx</sup>/Math1<sup>CRE</sup>/+) utilizing the Cre-LoxP conditional knockout strategy, then examined motor function and GNP maturation. GNPs in AhR<sup>fx</sup>/fx/Math1<sup>CRE</sup>/+ exclusively expressed Cre recombinase in the developing mouse cerebellum and the intrachromosomal recombination of AhR alleles by Cre recombinase resulted in decreased AhR protein expression. Behavioral studies revealed that AhR<sup>fx</sup>/fx/Math1<sup>CRE</sup>/+ mice displayed repetitive motor activity and abnormal rotarod performance. Additionally, DNA content, a surrogate measure of

cell number, was reduced at PND10, PND21, and PND60 in AhR $\alpha$ /f $\alpha$ /Math1CRE/+ mice compared to controls, suggesting that cell numbers were diminished. Following AhR excision, there were fewer proliferating GNP in the external germinal layer of the cerebellum at PND10, which resulted in a reduction of granule neurons reaching their final destination in the adult cerebellum. These results suggest that AhR activity plays a role in regulating granule neuron number, possibly by promoting GNP cell cycle activity, which ultimately impacts cerebellar function. These studies will provide novel insights for understanding mechanisms of dioxin-mediated neurotoxicity in the developing cerebellum.

**PS 1393 Assessment of Brain Morphometry Data Using Multivariate Statistical Analysis Methodology.**

W. Miner, T. J. Vidmar and L. Freshwater. *BioSTAT Consultants, Portage, MI.*

As required by EPA guidelines, brain morphometry is an area of interest in screening chemicals for developmental neurotoxicity. Brain morphometry data includes multiple measurements from the same animal such as brain weight, brain width, and brain length. These measurements are typically resource intensive and costly and therefore often made on a small subset of animals. Univariate statistical methodology (eg. ANOVA) treats these measurements as independent of one another and analyzes each separately. By contrast, using multivariate analysis of variance, the potential error resulting from conducting multiple univariate tests can be avoided. Multivariate statistical analysis evaluates all measurements simultaneously, taking advantage of the correlation between those measurements. In this simulated study, female brain morphometry data were generated in SAS® using the means, standard deviations, and correlations between measurements observed in an actual study. Three dose groups (control, low, and high) were created. The simulation was designed such that individual brain morphometry components suggested the presence of dose-related increasing trends. A univariate analysis of variance was performed on each of the components: brain weight, brain width, and brain length. The univariate analysis showed no significance for any of the three brain measurements at the 5% significance level. Performing a multivariate analysis of variance yielded an overall significant treatment effect ( $p < .05$ ). Pairwise comparisons provided evidence that brain morphometry for both the low and high dose groups was significantly higher when compared to the control group. In the simulated study, the univariate analysis of variance fails to detect biologically relevant treatment effects in brain morphometry measurements. The multivariate analysis, which addresses the measurements concurrently, identifies statistically significant differences among the dose groups. These results suggest a multivariate analysis should be used to analyze brain morphometry data.

**PS 1394 Mother's Environmental Tobacco Smoke Exposure during Pregnancy and Externalizing Behavior Problems in Children.**

J. Liu<sup>1</sup>, P. Leung<sup>2</sup>, L. McCauley<sup>3</sup> and J. Pinto-Martin<sup>1</sup>. <sup>1</sup>*School of Nursing, University of Pennsylvania, Philadelphia, PA;* <sup>2</sup>*Chinese University of Hong Kong, Hong Kong, China;* <sup>3</sup>*Nell Hodgson School of Nursing, Emory University, Atlanta, GA.*

**Background:** While the impact of active maternal smoking during pregnancy on child health has been well investigated, the association between maternal passive smoking, or environmental tobacco smoke (ETS), and behavioral development of offspring is less clear. This study examines the association between maternal ETS exposure during pregnancy and child behavior problems.

**Methods:** As part of the Jintan China Cohort Study, mother-child pairs ( $n=646$ ) were included in the analyses. Maternal ETS exposure at home, the workplace, and other places during pregnancy was retroactively assessed when children were 5-6 years old. Behavior was assessed via the Child Behavior Checklist when children were 5-6 years old. Logistic regression models were constructed to examine associations between maternal exposure to ETS during pregnancy and internalizing and externalizing behavior problems, adjusting for potential cofounders including child sex and parental characteristics.

**Results:** 37% of mothers reported ETS during pregnancy. Children of mothers exposed to ETS during pregnancy had higher scores for externalizing and total behavior problems with 25% of children whose mothers were exposed to ETS, compared to 16% of children of unexposed mothers. After adjusting for potential cofounders, ETS exposure was associated with a higher risk of externalizing behavior problems in offspring of exposed mothers (OR=2.08, 95% confidence interval [CI] 1.27-3.43). Analysis after multiple imputations and sensitivity analysis further verified the association, but no dose-response relationship was found. ETS exposure, however, was not associated with internalizing or total behavior problems.

**Conclusion:** This study suggests that maternal ETS exposure during pregnancy may impact child behavioral development, particularly externalizing behaviors.

**PS 1395 Patterns of Clinical Bioindicators in Rat Serum following Acute Exposure to Pesticides of Different Chemical Classes.**

D. W. Herr<sup>1</sup>, N. A. Stewart<sup>2</sup>, D. F. Lyke<sup>1</sup>, K. L. McDaniel<sup>1</sup> and V. C. Moser<sup>1</sup>. <sup>1</sup>*TAD/NB, US EPA, Durham, NC;* <sup>2</sup>*Contractor, Durham, NC.*

There is interest in bioindicators of adverse outcomes in safety assessment and translational research. Chemically-induced neurological effects may be reflected in specific neuronal changes and/or by general stress-like responses, and such bioindicators may be useful for measuring health impacts. We examined differential profiles of clinical bioindicators after acute treatment (po) with different pesticides (permethrin, deltamethrin, fipronil, imidacloprid, carbaryl, triadimefon). These same rats were evaluated for EEG changes (Lyke *et al.*, *Toxicologist*, 2010, 2011, 2012, 2013). Rats were sacrificed after EEG testing. Serum samples were processed by Myriad RBM using their RodentMAP® and Rat MetabolicMAP® assays. Depending on the pesticide, 2-18 of 78 analytes were altered, and each pesticide produced a different pattern of changes. Discriminant analysis indicated that these alterations differed in a dose-related manner for each chemical. The data show that acute exposure to different classes of pesticides produced different patterns of changes in clinical bioindicators, which may be analyzed for linkages to biological pathways. *This is an abstract of a presentation and does not necessarily reflect EPA policy.*

**PS 1396 Acute Triadimefon-Induced Changes in the EEG of Long-Evans Rats.**

D. F. Lyke, K. L. McDaniel, V. C. Moser and D. W. Herr. *TAD/NB, US EPA, Durham, NC.*

We have reported that the non-stimulus driven EEG is altered differently by acute treatment with deltamethrin, permethrin, fipronil, or imidacloprid (Lyke and Herr, Lyke *et al.*, *Toxicologist*, 2010, 2011, 2012) in non-restrained animals. In the current study, we examined the ability to detect changes in EEG activity produced by triadimefon, a triazole pesticide which inhibits sterol synthesis in fungal cell membranes and inhibits dopamine re-uptake in the mammalian nervous system. Adult male Long-Evans rats were implanted with epidural screw electrodes. After about 1 week recovery, non-restrained animals were gavaged with corn oil (vehicle) and tested for 2 days for acclimation. On day 3, the rats were dosed with 1 ml/kg corn oil, 75, or 150 mg/kg triadimefon and tested 1 h later. EEG was recorded as 30 segments of 2 s durations, transformed using a Fast Fourier Transformation, and the spectra averaged. These dosages have increased motor activity in Long-Evans rats in previous studies. Treatment with 150 mg/kg triadimefon increased the amplitude associated with Theta activity compared to controls (31% increase), and compared to 75 mg/kg triadimefon (27% increase), when recorded between the visual cortex and cerebellum. These results were different from the decreased gamma activity resulting from treatment with fipronil, increased gamma activity following treatment with permethrin, slightly decreased alpha activity with deltamethrin, and lack of changes after dosing with imidacloprid. The data show that triadimefon can alter CNS activity as measured by EEG, and the alterations may differ from some other pesticides. *This is an abstract of a proposed presentation and does not necessarily reflect EPA policy.*

**PS 1397 In Vitro Assessment of Parkinsonian Neurodegeneration by Dinitrophenolic Herbicides in PC12 Cells.**

H. J. Heusinkveld<sup>1</sup>, A. C. van Vliet<sup>1</sup>, P. C. Nijssen<sup>2</sup> and R. H. Westerink<sup>1</sup>. <sup>1</sup>*Neurotoxicology Research Group, Institute for Risk Assessment Sciences, Faculty of Veterinary Medicine, Utrecht University, Utrecht, Netherlands;* <sup>2</sup>*Department of Neurology, Elisabeth Hospital, Tilburg, Netherlands.*

Parkinson's disease (PD) is the most prevalent human neurodegenerative disorder after Alzheimer's disease affecting 1-2% of the population over 65 years of age. In several epidemiologic studies, chronic exposure to environmental pollutants, in particular pesticides, has been linked to neurodegeneration and the development of PD, though the underlying mechanisms are largely unknown.

Research directed by neurologist Dr Peter Nijssen encountered PD patients clustered in a remote rural area in the Netherlands, both occupationally and non-occupationally involved in agriculture, with relatively high exposure to pesticides. Among the pesticides, (dinitrophenolic) herbicides, were identified as common denominator. Since this class of herbicides is known as mitochondrial uncouplers, we assessed the potential role of dinitrophenolic herbicides in dopaminergic neurodegeneration.

Using a battery of in vitro tests, including measurements of cell viability, oxidative stress, single-cell fluorescence calcium imaging and protein analysis, the effects of dinitrophenolic herbicides on different pathways of neurotoxicity were assessed in PC12 cells as a model for mature dopaminergic neurons. Our results demonstrate

that dinitrophenolic herbicides induce moderate cytotoxicity via calcium-dependent activation of caspase-mediated apoptosis as well as activation of key proteins characteristic for Parkinsonian neurodegeneration in surviving dopaminergic cells. This leads to the hypothesis that human exposure to dinitrophenolic herbicides may be linked to the pathophysiology of PD. Funding: EU (ACROPOLIS, KBBE-245163) and the Dutch "International Parkinson Fonds" (PAGES).

### PS 1398 Protein Cysteine Oxidation and Dopaminergic Cell Death Induced by Pesticides.

J. Navarro-Yepes<sup>1,2</sup>, L. M. Del Razo<sup>1</sup>, R. Franco<sup>2</sup> and B. Quintanilla-Vega<sup>1</sup>.  
<sup>1</sup>Toxicology Department, CINVESTAV-IPN, Mexico City, Mexico; <sup>2</sup>Redox Biology Center, University of Nebraska-Lincoln, Lincoln, NE.

Parkinson's disease (PD) is characterized by the loss of dopaminergic neurons in the substantia nigra, which is linked to mitochondrial dysfunction, oxidative stress, protein aggregation and impairment in protein degradation pathways. Epidemiological studies suggest that chronic exposure to pesticides is associated with an increased risk of developing PD. However, the underlying mechanisms have not been precisely elucidated. Oxidative protein modifications can modulate the activation of cell death pathways. Thus, we explored the role of oxidative cysteine modifications in dopaminergic cell death induced by pesticides. Human neuroblastoma cells (SK-N-SH and SH-SY5Y) and the fetal human mesencephalic cell line (LUHMES, Lund human mesencephalic) were exposed to paraquat (PQ), rotenone and dieldrin. Compared to neuroblastoma cells, LUHMES cells exhibited greater sensitivity to all pesticides independent from their differentiation state. Apoptotic cell death induced by pesticides was paralleled to oxidative stress and a decrease in glutathione content. Cell death was prevented by glutathione ethyl ester. PQ induced protein alterations in both sulfenic acid (PSOH) and glutathionylation profiles (PSSG). Mass spectrometry of immunoprecipitated PSOH/PSSG proteins identified several proteins from the ubiquitin/proteasome degradation system and molecular chaperones as being modified by PSOH and PSSG in response to PQ, including E3 ubiquitin-protein ligases (SIAH1, TRIM13, RNF25, RNF139, HERC2, BRE1B), ubiquitin hydrolases (USP47, USP24), ubiquitin conjugating enzymes (UBE20), and Hsp40 co-chaperones (DNAJB4, DNAJC11). The expression of the protein DNAJC11 was down-regulated in a concentration dependent manner by PQ. Results suggest a role for protein cysteine oxidation (sulfenylation and/or glutathionylation) in the regulation of the ubiquitin/proteasome and chaperone-mediated folding systems in response to pesticide exposure. Supported by CONACYT-Mexico (Grant #104316).

### PS 1399 Aldehyde Dehydrogenase Dysfunction Increases Parkinson's Disease Risk via Gene-Environment Interactions.

A. G. Fitzmaurice<sup>1,2</sup>, S. L. Rhodes<sup>3</sup>, M. Cockburn<sup>4</sup>, B. Ritz<sup>3</sup> and J. M. Bronstein<sup>1,2,5</sup>. <sup>1</sup>Neurology, David Geffen School of Medicine at University of California Los Angeles, Los Angeles, CA; <sup>2</sup>Molecular Toxicology, University of California Los Angeles, Los Angeles, CA; <sup>3</sup>Epidemiology, University of California Los Angeles Fielding School of Public Health, Los Angeles, CA; <sup>4</sup>Preventive Medicine, Keck School of Medicine of University of California Los Angeles, Los Angeles, CA; <sup>5</sup>Greater Los Angeles Veterans Administration Medical Center, Los Angeles, CA.

Parkinson's disease (PD) is a neurodegenerative disorder characterized by the loss of dopaminergic neurons in the substantia nigra. We recently reported that exposure to the fungicide benomyl resulted in dopaminergic neuronal loss, aldehyde dehydrogenase (ALDH) inhibition, and an epidemiologic association with increased PD occurrence. Since the dopamine metabolite 3,4-dihydroxyphenylacetaldehyde (i.e., DOPAL) is highly toxic and an ALDH substrate, ALDH inhibition might contribute to the particular vulnerability of dopaminergic neurons. To investigate the potential relevance of this mechanism, we developed a novel ex vivo neuronal assay to screen pesticides for ALDH inhibitory activity. All dithiocarbamates tested (e.g., mancozeb, maneb, ziram), two dicarboximides (captan, folpet), and two imidazoles (benomyl, triflumizole) inhibited ALDH activity, potentially via metabolic byproducts (e.g., carbon disulfide, thiophosgene). We developed a geographic information system method employing state-mandated commercial pesticide use reports to estimate patient exposures to specific pesticides from 1974-1999. Exposures to ALDH-inhibiting pesticides (i.e., from the screen) were associated with dose-dependent twofold to fourfold increases in PD risk. Patients were genotyped for variation in the mitochondrial ALDH2 gene, and haplotypic analyses of six single nucleotide polymorphisms revealed that ALDH2 variation potentiated PD risk for people working where ALDH-inhibiting pesticides were sprayed liberally. This ALDH model for PD etiology might help explain the selective vulnerability of dopaminergic neurons in PD and provide a potential new mechanism through which environmental toxicants contribute to PD pathogenesis.

### PS 1400 Pesticide-Linked Parkinson's Disease: Using *Drosophila* to Build a Novel *In Vivo* Model of Paraquat, Maneb and Ziram Exposure.

C. A. Martin<sup>1</sup>, A. Barajas<sup>2</sup> and D. Krantz<sup>1,2</sup>. <sup>1</sup>Molecular Toxicology, University of California Los Angeles, Los Angeles, CA; <sup>2</sup>Neurobiology, University of California Los Angeles, Los Angeles, CA.

The vast majority of Parkinson's disease (PD) cases are sporadic and environmental exposure to pesticides have long been suspected to contribute to PD development, though the disease etiology remains poorly understood. Recently, epidemiological data has supported this and revealed that individual exposures to the pesticides ziram, maneb, and paraquat increase PD risk. Interestingly, it appears that these pesticides interact synergistically and exposure to all three pesticides increases PD risk up to three-fold. We are using the model organism *Drosophila melanogaster* to study the connection between pesticide exposures and the neuronal dysfunction and dopaminergic cell loss characteristic of PD. We find that combined, but not individual, chronic exposures to maneb and paraquat leads to significant dopaminergic neuron loss. To understand how neuronal dysfunction may contribute to a PD phenotype, we complement this approach by utilizing the *Drosophila* neuromuscular junction. This powerful tool has allowed us to explore the way pesticide exposures may more subtly affect neuronal physiology and behavior in an intact synapse. We report that ziram exposure significantly alters synaptic vesicle fusion and reuptake, processes that are essential for proper neuronal signaling. Ziram has been shown to inhibit the E1 ligase, which is required for targeting proteins to the proteasome for degradation. We find that inhibiting the proteasome increases synaptic vesicle fusion in a similar manner to ziram, implying a shared mechanism of action. However, it remains unclear if it is ziram's inhibition of E1 itself or ziram's downstream effect on the proteasome that is responsible for this synaptic phenotype. Ongoing investigations are exploring these possible neurotoxic mechanisms of action and may help elucidate the interrelationship between ziram, neuronal dysfunction, and early neurotoxic mechanisms that could initiate a PD phenotype.

### PS 1401 High i.p. Doses of Paraquat Do Not Result in a Loss of Dopaminergic Neurons in the Substantia Nigra of the Mouse.

M. Butt<sup>3</sup>, P. Botham<sup>1</sup>, C. Breckenridge<sup>2</sup>, L. Smith<sup>1</sup>, N. Sturgess<sup>1</sup> and J. Wolf<sup>4</sup>.  
<sup>1</sup>Syngenta, Bracknell, United Kingdom; <sup>2</sup>Syngenta, Greensboro, NC; <sup>3</sup>Tax Path Specialists, Frederick, MD; <sup>4</sup>EPL, Sterling, VA.

A number of publications have reported that the i.p. administration of paraquat (PQ) to rodents (normally male C57Bl/6 mice; up to 3 x 10 mg/kg) results in a loss of dopaminergic neurones from the substantia nigra pars compacta (SNpc), which is the primary area of neuropathological damage in Parkinson's disease (PD). We have conducted studies in the male C57Bl/6 mouse examining the effect of high i.p. doses (up to the maximum tolerated dose of 3 x 25 mg/kg) of PQ looking not only for neuronal cell loss, but also for evidence of striatal neurochemical changes and pathological changes using stains to detect disintegrating neurones and neuronal processes and the expected astrocyte/microglial activation in response to neuronal cell damage. Mice were administered paraquat dichloride on 1, 2 or 3 occasions (separated by one week) at doses of 10, 15 or 25 mg/kg. A relatively low dose of N-1-methyl-4-phenyl-1,2,3,6-tetrahydropyridine (MPTP; 10 mg/kg administered i.p. 4 times in a single day at 2 hr intervals) was dosed to a separate group as a positive control. Studies were conducted to GLP and assessment of toxicological endpoints was by individuals blinded to treatment group. No consistent stereological evidence for a loss of tyrosine hydroxylase positive (TH+) dopaminergic neurones in the SNpc was observed in the PQ treated mice. PQ did not alter the concentration of striatal dopamine or its metabolites. Over a range of time points (4-168 hrs post-dose), there was no evidence of PQ-induced neuronal degeneration in the SNpc, degenerating processes in the striatum or apoptotic cell death; astrocytes and microglia were not activated. In the MPTP treated mice the number of TH+ dopaminergic neurones in the SNpc was reduced, striatal dopamine was reduced and significant pathological changes, including necrotic neurones and astrocyte/microglial activation in the SNpc, were consistently observed. These results bring into question the use of PQ mouse studies as a robust model for PD/parkinsonism.

**PS 1402 Repeated Exposure to Paraquat Affects the Neural Behavior in Male C57BL/6 Mice.**

D. Lou<sup>1</sup>, Q. Zhao<sup>2</sup>, M. Huang<sup>3,1</sup> and Z. Zhou<sup>1</sup>. <sup>1</sup>Department of Occupational Health Sciences and Toxicology, Fudan University, Shanghai, China; <sup>2</sup>Center of Disease Control in Minhang District, Shanghai, China; <sup>3</sup>Department of Environmental and Occupational Health Sciences, Ningxia Medical University, Yinchuan, China.

Epidemiological studies have revealed that neural degenerative diseases such as Parkinson disease are typically influenced by genetic and environmental factors, while little is known about the environmental factors. The broad application of paraquat (PQ) has given rise to wide public concern on its potential to damage the nigrostriatal dopaminergic (DA) system because its chemical structure closely resembles that of the well-known DA neural toxicant MPP<sup>+</sup>. We used male C57BL/6 mice (aged 8 weeks and weight 20 ± 2 g) to examine the effects of PQ oral exposure on neural behavior. The Society's criteria for the care and use of laboratory animals were used for all the experiments in this study. After treated with normal saline (vehicle) and PQ (5mg/kg, 10 mg/kg or 20mg/kg) daily for 30 consecutive days, no significant differences in the body weight gain as well as the brain coefficient were observed among different dose groups. The transmission electron microscope showed that the subcellular structures of DA neurons were impaired when exposed to the high dose of PQ. The Open Field test revealed reduced locomotor activity and exploratory drive with the increase of PQ concentrations. Cognitive assessments were conducted in all the groups of mice via Morris Water Maze, no statistically significant difference among treatment groups was shown in the avoidance latency, although a trend toward less learning can be observed. On probe trial, PQ-treated mice did show a significant preference for the correct quadrant. Together, the functional observational battery showed treatment-related, but not necessarily dose-related changes in the mice's reactivity and activity. Thus, we proposed that repeated exposure to PQ can induce neurochemical and persistent neurobehavioral changes.

(Supported by NSFC81072324)

**PS 1403 Protective Effect of Edaravone Pretreatment against Mancozeb Cytotoxicity in Rat Hippocampal Astrocytes.**

L. D. Trombetta and N. Ruparel. *Pharmaceutical Sciences, St. John's University, Queens, NY.*

Mancozeb [manganese-zinc ethylenebis(dithiocarbamate)] is a polymeric dithiocarbamate fungicide that has been used commercially for decades. A number of studies have shown this agent to cause neurotoxicity that is linked to oxidative stress. The purpose of this experiment was to study the protective effects of edaravone (3-Methyl-1-phenyl-2-pyrazoline-5-one) on rat hippocampal astrocytes after mancozeb insult. Edaravone has been demonstrated to be a free radical scavenger and inhibits cerebral edema and infarction after brain ischemia. Rat hippocampal astrocytes maintained in Dulbecco's modified Eagle's medium with 10% FBS were exposed to a range of concentrations of Mn-Zn dithiocarbamate for one hour at 37°C. Viabilities 23hrs post-treatment with 4uM, 8uM, 16uM, and 24uM doses were 94%, 82%, 34%, and 20%, respectively. The LC50 was found to be 14.7 uM. For further experiments, treatment with 12uM mancozeb was chosen. Cells pretreated with edaravone (10uM, 80uM, 160 uM, 320uM) for 24 hours, and then treated with 12uM mancozeb for 1 hour showed significant increases in viability at all doses of edaravone. The 320uM pretreatment of edaravone increased the viability by 63.7% when compared to the group treated with 12uM mancozeb alone. GSH studies showed that 12uM mancozeb treatment for 1 hr. decreased the GSH/GSSG ratio by 45.87%, however, when astrocytes were pretreated with 320uM Edaravone the GSH/GSSG ratio was significantly different from the group with mancozeb alone with a decrease of 36.84%. Edaravone pretreatment was shown to be protective against mancozeb cytotoxicity and this protection may involve a reduction in oxidative stress.

**PS 1404 Role of Alpha-Synuclein and Its Mutants on Dithiocarbamates Cytotoxicity.**

A. Stoll and S. Cheng. *Science, John Jay College of Criminal Justice, New York, NY.*

Mn-containing dithiocarbamates, such as maneb (MB) and mancozeb (MZ), often seen in the agricultural industry, have been known to increase the toxicity of neurotoxin MPTP on dopaminergic neurons, which can lead to cell death and Parkinson-like symptoms. Dopamine transporter (DAT) is a key protein in MPTP's toxicity by transporting the active metabolite (MPP<sup>+</sup>) into dopaminergic neurons; increasing the cell surface expression of DAT raises the uptake of MPTP. Alpha-synuclein, a protein that interacts with the dopamine transport, can regulate DAT trafficking and the DAT cell surface expression. Alpha-synuclein (wt) and its mutants (A30P and A53T) have been associated with Parkinson's disease.

The aim of this study is elucidate the role of the alpha-synuclein and its mutants on dithiocarbamate cytotoxicity. HEK 293 cells transfected with DAT and either alpha-synuclein or its mutants were treated with dithiocarbamates for 1hour. Cell lysates from these treated groups and the control group, treated with phosphate buffered saline (PBS), were used for co-immunoprecipitation using anti-DAT antibody. The co-immunoprecipitated proteins were subjected to Western blot analysis, probed with alpha-synuclein and DAT antibodies. The integrated density values (IDV) of the alpha-synuclein were normalized to the IDV of the DAT. The PBS control was taken as 1.

We report roughly a 30% decrease in the DAT/alpha-synuclein interaction in the presence of the A53T mutant versus wild-type, but not in the presence of the A30P mutant. With dithiocarbamates, the interaction of DAT and alpha-synuclein (wt) was enhanced, with increases ranging from 50% to 200%. Cells transfected with A53T mutants respond to pesticides more dramatically than cells transfected with A30P mutants in increasing the interaction between the DAT and the alpha-synuclein.

**PS 1405 The Role of RTP801 in Maneb and Mancozeb-Induced Cytotoxicity.**

S. Cheng, C. Ta, A. A. Calderone and S. Oh. *Sciences, John Jay College of Criminal Justice, New York, NY.*

Environmental factors, such as pesticide exposure, have been implicated in the pathogenesis of neurodegenerative diseases such as Parkinson's disease (PD). Manganese (Mn)-containing ethylene-bis-dithiocarbamate compounds, maneb (MB) and mancozeb (MZ) have been extensively used for pesticides over the past 50 years. Exposure to MB lowers the threshold for dopaminergic damage triggered by MPTP, which is a human Parkinson's disease inducing neurotoxin. Preliminary data from Cheng's lab demonstrate that MB and MZ enhance 1-methyl-4-phenylpyridium (MPP<sup>+</sup>)-induced cell death in rat pheochromocytoma (PC12) cells. However, the neurotoxic molecular mechanisms and the signal transduction pathways involved in the action of these dithiocarbamate toxins in PD are still not clear. Neuron death, regardless of initiating causes, generally requires proapoptotic gene activation. Studies showed RTP801 is dramatically increased by oxidative stresses. A sequential mechanism (induction of RTP801, suppression of mTOR signaling, and then depletion of phosphorylated/activated Akt) has been suggested to be the mechanism of neurotoxins-induced cell death. In this study we observed no change in RTP801 protein expression after 4 h diethyldithiocarbamate (DDC) and MB treatments. But for MZ, RTP801 was twice the PBS control. After 8 h treatment, all chemicals showed significant increase of RTP801 protein expression (about 3 to 4 fold). This observation proved that the RTP801 protein expression has been regulated by Manganese (Mn)-containing ethylene-bis-dithiocarbamate compounds. Then, the transcriptional activation was studied by real time RT-PCR for 2 h, 4 h, and 8 h treatments. At 2 h, the transcription of RTP801 was increased for MB and MZ (2 and 3.5 fold), but not very significant for DDC. At 2 h, the transcription appeared the highest comparing to other time periods, and gradually decreased at 4 h and 8h. This observation showed that the up-regulation of RTP801 is due to the increase in RTP801 mRNA transcript. RTP801 shRNA will be used to further confirm the involvement of RTP801 in MB and MZ induced cytotoxicity.

**PS 1406 Nrf2 Protects Hippocampus against Oxidative Stress Caused by Maneb.**

D. Kurzatkowski and L. D. Trombetta. *Pharmaceutical Sciences, St. John's University, Queens, NY.*

Maneb is an ethylene(bis)dithiocarbamate fungicide that has been used to treat diseases of vegetables, fruits, and field crops. This study investigated the neurotoxic effects of maneb on the hippocampus of C57BL/Nrf2 (-/-; knockout) and C57BL/Nrf2 (+/+; WT) mice. The mechanism by which maneb exerts its neurotoxicity is unclear; however, a number of effects have been observed both in vitro and in vivo, which suggest a link between exposure to maneb and an increase in oxidative stress. Genes that are regulated by the ARE help control the redox status of the cell and protect it against oxidative injury. The Nrf2-ARE pathway can be found in most tissue types and is responsible for the control of expression of many genes that are involved in the protection of cells such as γ-GCS light subunit, peroxiredoxin, glutathione peroxidase, glutathione reductase, superoxide dismutase, and heme-oxygenase 1. The activation of Nrf2 has been linked to neural cell protection against numerous toxicants; therefore, Nrf2-/- mice treated with pro-oxidants such as maneb would be expected to show increased neurologic damage. Animals were injected I.P., twice a week for 30 days, at 0, 15, 30 and 60 mg of maneb/kg body weight. Levels of TBARS were not increased in hippocampal tissue in Nrf2+/+ animals at any dose of maneb but were significantly increased in the Nrf2-/- animals at the 30 and 60 mg dose. The TUNEL technique demonstrated

the presence of positive cells in the hippocampus of Nrf2<sup>-/-</sup> mice treated with 60 mg/kg maneb. Of 84 antioxidant pathway genes included in an oxidative stress and antioxidant defense array, qPCR demonstrated that the only gene mediated by the Nrf2 transcription pathway significantly modulated by at least 1.5-fold was glutathione peroxidase 4 (GPX4). This enzyme was significantly upregulated in Nrf2<sup>+/+</sup> mice treated with 30 mg/kg maneb and significantly downregulated in Nrf2<sup>-/-</sup> mice treated with the same concentration. It was concluded that maneb exposure causes oxidative stress mediated by the Nrf2 pathway and that GPX4 plays an important role in this protection.

**PS 1407 Neurotoxicity of the Dithiocarbamate Fungicide Ziram Is Dependent on Synuclein in Zebrafish: Implications for Parkinson's Disease.**

A. Lulla<sup>1,2</sup>, L. Barnhill<sup>1,2</sup>, M. Stahl<sup>2</sup>, A. G. Fitzmaurice<sup>1,2</sup>, S. Li<sup>2</sup> and J. M. Bronstein<sup>2,1</sup>. <sup>1</sup>Toxicology, University of California Los Angeles, Los Angeles, CA; <sup>2</sup>Neurology, University of California Los Angeles, Los Angeles, CA.

Parkinson's disease (PD) is a neurodegenerative disorder characterized by dopaminergic (DA) neuronal death and  $\alpha$ -synuclein ( $\alpha$ -syn) accumulation. Epidemiological studies reveal that exposure to the dithiocarbamate fungicide ziram is associated with increased risk of PD. We have previously found that ziram causes selective toxicity to DA neurons, ubiquitin proteasome system (UPS) inhibition, and  $\alpha$ -syn accumulation in primary neuronal cultures. Here, we use developing zebrafish (ZF, *Danio rerio*) embryos as an in vivo model to investigate mechanisms of ziram toxicity and its dependence on endogenous synuclein.

ZF embryos exposed to environmentally relevant of ziram were deformed, had altered swimming behavior, and premature death with a LD50 of approx. 50 nM at 7 days post fertilization (dpf). Transgenic ZF expressing green fluorescent protein (GFP) driven by vesicular monoamine transporter protein (VMAT) were used to identify aminergic neurons in ZF embryos. Ziram exposure (50nM) resulted in a 35% reduction in VMAT-GFP-expressing neurons in anterior DA clusters and 26% reduction in posterior clusters (noradrenergic) but was not toxic to non-DA sensory neurons.

ZF express 3 synucleins similar to mammalian  $\beta$  and  $\gamma$  synucleins. Overexpression of ZF  $\gamma$ 1-syn in neurons led to ZF-syn aggregates and neuronal death in a similar manner as overexpression of human  $\alpha$ -syn. ZF embryos exposed to ziram also showed accumulation and aggregation of endogenous ZF  $\gamma$ 1-syn. This accumulation appears to confer some of ziram's neurotoxicity since knockdown of ZF  $\gamma$ 1-syn expression improved survival. Furthermore, treatment with CLR01, a molecular tweezer that mitigates  $\alpha$ -syn toxicity, also attenuated ziram toxicity. The mechanism/s by which ziram increases ZF  $\gamma$ 1-syn appear to involve inhibition of protein degradation since ziram at concentrations as low as 10 nM inhibited the UPS in ZF embryos. These studies add further insight into the mechanism of pesticide neurotoxicity relevant to the risk of PD.

**PS 1408 Linking Developmental Atrazine Exposure in Zebrafish to Long-Term Neurotransmission Alterations.**

C. Xiao, G. J. Weber, S. E. Watson, J. L. Freeman and J. R. Cannon. School of Health Sciences, Purdue University, West Lafayette, IN.

Atrazine is an agricultural herbicide widely used to prevent pre- and post-emergence of broadleaf and grassy weeds in major crops. It is a major environmental contaminant, commonly present in potable water supplies. Recent work has suggested that atrazine exposure may affect behavior and neurotransmitter systems in rodents. However, rodent studies have typically utilized exposures many magnitudes above environmentally relevant levels and produced conflicting data. The role of early-life exposures in the development of late-life neurodegenerative diseases has recently received much attention. In an effort to assess the immediate and late-life effects of atrazine on neurological function, zebrafish embryos were exposed to environmentally relevant doses of atrazine (0, 0.3, 3, 30ppb) from 1-72 hours post fertilization. Following the developmental exposure, larvae were changed to atrazine-free water and allowed to mature under normal conditions to assess lifespan impacts. Neurotransmitter levels were assessed using HPLC with electrochemical detection. Adult female zebrafish (9 months) exhibited statistically significant decreases in 5-hydroxyindoleacetic acid (5-HIAA), the primary metabolite of serotonin, as well as a reduction in 5-HIAA/serotonin turnover. Interestingly, larvae evaluated at 7 days post fertilization did not show significant alterations in neurotransmitters levels, indicating that deficits arise over time, many months after the initial exposure. In addition, microarrays performed on adult female brain tissue revealed alterations in genes that are enriched in neurological, psychological and developmental diseases. Thus, after short-term atrazine exposure during development, persistent neurotransmitter disruptions are observed, indicating long-term disruption of brain function. Future experiments are focused on elucidating mechanisms of neurologic dysfunction and neurodegeneration elicited by toxicant exposure during critical development stages.

**PS 1409 Effects of the Long-Term Coexposure to the Herbicide Atrazine and Inorganic Arsenic (IAs) in the Nigrostriatal Dopaminergic System of the Albino Rat.**

U. Bardullas, M. Giordano and V. Rodríguez. Departamento de Neurobiología Conductual y Cognitiva, Instituto de Neurobiología, Universidad Nacional Autónoma de México, Queretaro, México.

The herbicide atrazine (ATR) and the metalloid arsenic (As) are substances widely distributed in the environment. In recent years interest has grown regarding the toxicity of these substances on the nigrostriatal dopaminergic system. To date, no study has evaluated the effects of chronic and simultaneous exposure to ATR and As, substances that may share the same neuronal target. In order to study the effects of the coexposure As+ATR, six groups of rats were given atrazine (10 mg ATR/kg), arsenic (0.5 or 50 mg As/L of drinking water) or their combinations (ATR+0.5 mg As/L or ATR+50 mg As/L) daily for one year. Behavioral tests showed hypoactivity in the 50 mg As/L group, and hyperactivity in the ATR group. All treatments decreased motor coordination. Striatal DA content was significantly reduced in ATR, 0.5 mg As/L, ATR+0.5 mg As/L and ATR+50 mg As/L groups, compared to controls. The number of mesencephalic TH<sup>+</sup> cells was significantly reduced in ATR and ATR+0.5 mg As/L groups, compared to controls. Furthermore, the assessment of cell integrity in the substantia nigra showed decreases in cytochrome oxidase reactivity in all treatment groups, but no changes in malondialdehyde immunoreactivity. In summary, the nigrostriatal dopaminergic system appears to be a target for the toxic effects of As and ATR. Our results indicate that when combined, ATR + As act independently, and ATR has more severe effects on dopaminergic neurons. We appreciate the technical assistance of Biol. Soledad Mendoza. This work was sponsored by PAPIIT 214608-19 and CONACYT 60662, 103907 and 152842.

**PS 1410 Glyphosate Treatment Suggests Offspring and Reproductive Toxicity in *Caenorhabditis elegans*.**

R. Negga, M. B. Johnson, K. A. McVey, I. B. Snapp and V. A. Fitsanakis. Biology, King College, Bristol, TN.

Herbicides are widely used in both agricultural and residential areas; therefore, pesticide users, as well as family members, may be routinely exposed to these potentially harmful chemicals. Epidemiological studies have shown pesticide exposure may lead to decreased fetus viability in exposed versus non-exposed females. A significant gap in the literature exists as to whether these observations are applicable to exposures of glyphosate-containing herbicides. To further examine this question, we utilized the model organism, *Caenorhabditis elegans*, to test our hypothesis that exposure to the glyphosate-containing herbicide, TouchDown (TD), results in decreased numbers of offspring in wild-type (N2) worms. Furthermore, this exposure could render surviving offspring more susceptible to neurodegeneration. Based on concentrations (LC50 and LC75) from previous data, eggs were removed from gravid adults and chronically (24 hours) exposed to TD. The numbers of hatched offspring were counted to determine whether TD adversely affected embryo viability. One-way ANOVA indicated a statistically significant decrease ( $p < 0.05$ ) in the number of hatched eggs from treated compared to control worms. Our second study was designed to determine whether eggs exposed to TD would result in general neuronal degeneration. Eggs from NW1229 worms (a green fluorescent protein (GFP)::neuron construct) were treated as described. Data suggested potential neuronal degeneration in treated worms compared to control ( $p < 0.05$ ), as determined by fluorescence photomicrograph analysis. Lastly, we chronically exposed eggs from strain CL2166 (GFP::glutathione-S-transferase) to varying concentrations of TD. Fluorescence between control and treated groups, however, did not vary, suggesting that large increases in oxidative stress are not responsible for the observed changes in the nervous system. Taken together, these results suggest that TD decreases the number of viable offspring in the nematode, and that neurodegeneration may be present in those that survive.

**PS 1411 Effects of the Subchronic Exposure to the Herbicide Glyphosate on Behavior and the Nigrostriatal and Mesolimbic Dopaminergic Areas of the Albino Rat.**

I. Hernandez-Plata<sup>1</sup>, M. Diaz-Muñoz<sup>2</sup>, M. Giordano<sup>1</sup> and V. M. Rodríguez<sup>1</sup>. <sup>1</sup>Neurobiología Conductual y Cognitiva, Instituto de Neurobiología, Queretaro, México; <sup>2</sup>Neurobiología Celular y Molecular, Instituto de Neurobiología, Queretaro, México.

Glyphosate (Glyph) is the active ingredient of several herbicide formulations widely used to eliminate weeds. Although it has been described that the Glyph formulations are slightly toxic for mammals, reports of human exposure and studies using animal models suggest that Glyph formulations may be neurotoxic. In order to evaluate the effects of Glyph on the nervous system, male Sprague-Dawley rats received six i.p injections of 50, 100 or 150 mg Glyph/kg or saline (n=10) during 2

weeks (3 injections/week). We recorded locomotor activity 15 min before and 3 h immediately after each injection. Also, the locomotor activity was recorded during 24 h, 16 days after the last injection. The subchronic exposure to Glyph caused decreases in locomotor activity immediately after each injection, as well as 48 h after the Glyph injection. This hypoactivity was maintained until the 16th day post-treatment. We did not detect changes neither in monoamine concentrations nor in the levels of TH in NAcc or STR at 2 and 16 days after the last Glyph injection. However, specific binding to D1 dopamine receptors in NAcc decreased dose-dependently when measured 48-h after the last Glyph injection. These results indicate that subchronic exposure to Glyph has acute as well as long-term effects on locomotor activity, and that these effects may be related to a decrement in specific binding to D1 dopamine receptors in NAcc. We thank Soledad Mendoza for her technical assistance. Supported by CONACYT 60662, 152842 and 103907 and PAPIIT grants 214608-19 and 211709-21; IHP received a fellowship from CONACYT 164300.

**PS 1412 Relationship between Administered Dose, Target Tissue Levels and Thermoregulatory Response Alterations after Acute Oral Exposure to the Potent Tremor-Inducing Pyrethroid Bifenthrin in Rats.**

M. Mosquera-Ortega<sup>1</sup>, A. Pato<sup>3</sup>, C. Sosa-Holt<sup>3</sup>, A. Ridolfi<sup>2</sup>, M. J. Wolansky<sup>1</sup> and E. Villaamil Lepori<sup>2</sup>. <sup>1</sup>*Biological Chemistry, IQUIBICEN (CONICET); University of Buenos Aires, Buenos Aires, Argentina;* <sup>2</sup>*Toxicology, Pharmacy and Biochemistry, University of Buenos Aires, Buenos Aires, Argentina;* <sup>3</sup>*Biological Chemistry, University of Buenos Aires, Buenos Aires, Argentina.*

In toxicological studies, potency estimates for pyrethroid insecticides (PYRs) in rats may depend on the exposure and testing conditions. This experimental factor may challenge present efforts to reconsider the health risks posed to humans by exposure to PYRs. We are using exposure-dose-effect studies to explore the influence of the testing conditions on the qualitative toxicological classification of, and relative potencies for, these insecticides. Four PYRs (tefluthrin, bifenthrin [BIF], deltamethrin, alpha-cypermethrin) are evaluated in Wistar adult rats. Body temperature is measured using microchip-like transponders implanted in rat backs 5-7 days before testing. Subcutaneous temperature (T-SC) is then monitored by radiotelemetry at 30 min intervals for 5 h after oral dosing of PYRs in corn oil. Basal T-SC is recorded before the test day, and 30 min before dosing (i.e., physiological T-SC). The maximal difference in T-SC compared to the pre-dosing baseline (i.e.,  $\Delta T_{\text{max}}$ ) is here used as a measure of peak response. Soon after the thermoregulation assay, target tissues are dissected out. Blood, liver and brain (striatum, cortex, cerebellum) are collected at 6 h post-dosing for posterior determination of PYR residues using a SPE-GC-ECD protocol. Results for BIF are shown in this first presentation. 0, 0.5, 3, 9 and 12 mg BIF/Kg (N=4-8) produced dosage-related increases in temperature and  $\Delta T$ . Dose-related increases in both BIF levels in target tissues and  $\Delta T_{\text{max}}$  were observed. R-squared values were +0.6 in all pairwise relationships. These results are mostly consistent with previous BIF studies carried out using motor activity and rectal temperature as endpoints (Wolansky et al., 2006, 2007), and a toxicokinetic study (Scollon et al., 2011).

**PS 1413 Interactions of a Promoter/Potentiator of Neuropathy and Esterases of Membrane and Soluble Fractions of Brain.**

I. Mangas, J. Estévez and E. Vilanova. *Unit of Toxicology and Chemical Safety Institute of Bioengineering, University Miguel Hernández, Elche, Spain.*

Phenylmethyl sulfonyl fluoride (PMSF) is a protease and esterase inhibitor causing protection or potentiation/promotion of the organophosphorus induced delayed neuropathy if dosed before or after the organophosphate inducer. The molecular target/s of potentiation/promotion has not yet been elucidated. The analysis of the kinetic of inhibition of PMSF on chicken brain esterases (using a kinetic model which considers the spontaneous hydrolysis of inhibitor) allowed to discriminate the following esterase components: In soluble fraction, a resistant component E $\alpha$  (28%) and two sensitive components, E $\beta$  (61%) and E $\gamma$  (11%) with I50 (20 min) of 70 and 447  $\mu$ M; in membrane fraction two resistant components EP $\alpha$  and EP $\delta$  (14%) and two sensitive, EP $\beta$  (41%) and EP $\gamma$  (44%) with I50 (20 min) of 138 and 23  $\mu$ M. The enzymatic components discriminated correspond to the previously observed in experiments with mipafox and paraoxon in these fractions. E $\alpha$  becomes 6-fold more resistant to mipafox after the pre-incubation with 5  $\mu$ M PMSF and 50-fold with 4000  $\mu$ M PMSF. E $\gamma$  becomes totally resistant after pre-incubation with 10  $\mu$ M PMSF or more and it becomes resistant to PMSF after pre-incubation with 20 nM mipafox. However none of the membrane esterases changed their sensitivity. The data suggest that these effects might be due to an irreversible interaction of PMSF and mipafox at sites other than the substrate catalytic center. Such interactions should be considered to interpret the potentiation/promotion phenomenon of PMSF and to understand the effects of multiple exposures to chemicals.

**PS 1414 In Vitro Inhibition and Aging of Neuropathy Target Esterase (NTE) Caused by Fenamiphos and Acephate.**

G. L. Emerick, L. S. Fernandes, N. G. Santos and A. C. Santos. *Departamento de Análises Clínicas, Toxicológicas e Bromatológicas, Universidade de São Paulo, Ribeirão Preto, Brazil.*

Organophosphorus-induced delayed neuropathy (OPIDN) is a neurodegenerative disorder characterized by ataxia progressing to paralysis with concomitant central and peripheral distal axonopathy. Symptoms of OPIDN in people include tingling of the hands and feet. These symptoms appear about 8–14 days after exposure. One of the criteria for acceptance of organophosphates pesticides (OPs) in Brazil is if the compound does not cause OPIDN. Guidelines for evaluating OPIDN require the observation of dosed animals over several days and the sacrifice of at least 48 hens. Adhering to these protocols in tests with analytical standards of OPs is difficult because large quantities of the compound are needed and many animals must be sacrificed. Thus, developing an in vitro screening protocol to evaluate if the OP is able to induce or not delayed neuropathy is important. This study aimed to evaluate in SH-SY5Y human neuroblastoma cell culture samples the potential of some OPs, which are widely used in Brazil, to induce delayed neurotoxicity. The relations between the inhibition and aging of neuropathy target esterase (NTE) by the fenamiphos and acephate were evaluated as indicator of the compound ability to induce OPIDN. Mipafox was used as inducer of OPIDN and paraoxon was used as non-inducer. The compounds were diluted in ethanol and the cells were incubated with the OPs for 24 hours in a 96-well microplate. Paraoxon exhibited an inhibitory concentration of 50% of enzyme activity (IC50) value approximately 47 times greater than that of the mipafox. Fenamiphos and acephate exhibited IC50 values 117 and 124 times, respectively, greater than that of the mipafox in the SH-SY5Y human neuroblastoma cells. Considering the esterases inhibition and aging results, fenamiphos and acephate would not be expected to have a great ability to induce OPIDN in humans compared with the ability of mipafox. Financial support: Fapesp grant # 2012/00168-6.

**PS 1415 Inhibition and Aging of Neuropathy Target Esterase (NTE) in SH-SY5Y Human Neuroblastoma Cells As Screening for Inducers of Delayed Neuropathy.**

L. S. Fernandes, G. L. Emerick, N. G. Santos and A. C. Santos. *DACTB, Universidade de São Paulo, Ribeirão Preto, Brazil.*

Organophosphorus-induced delayed neuropathy (OPIDN) is characterized by a central-peripheral distal axonopathy and Wallerian-type degeneration that develops 8–14 days after poisoning by a neuropathic organophosphate (OP). The current Organisation for Economic Co-operation and Development (OECD) guidelines for evaluating organophosphorus-induced delayed neuropathy (OPIDN) require the observation of dosed animals over several days and the sacrifice of at least 48 hens. Adhering to these protocols in tests with analytical standards of OPs is difficult because large quantities of the compound are needed and many animals must be sacrificed. Thus, developing an in vitro screening protocol to evaluate if the OP is able to induce or not delayed neuropathy is important. This study aimed to evaluate in SH-SY5Y human neuroblastoma cell culture samples the potential of some OPs, which are most utilized in Brazil, to induce delayed neurotoxicity. The relation between the inhibition and aging of neuropathy target esterase (NTE) by the trichlorfon was evaluated as a possible indicator of the compound ability to induce OPIDN. Mipafox was used as inducer of OPIDN and paraoxon was used as non-inducer. The compounds were diluted in ethanol and the cells were incubated with the OPs for 24 hours. Paraoxon exhibited an inhibitory concentration of 50% of enzyme activity (IC50) value approximately 47 times greater than that of the mipafox. Trichlorfon exhibited an IC50 value 48 times greater than that of the mipafox in the SH-SY5Y human neuroblastoma cells. Considering the esterases inhibition and aging results, trichlorfon would not be expected to have a great ability to induce OPIDN in humans compared with the ability of mipafox.

**PS 1416 Use of a Human Haploid Cell-Based Loss of Functional Genetic Screening Model to Identify Human Susceptibility Genes for Chlorpyrifos Toxicity.**

A. Dubois, J. R. Olson and X. Ren. *Pharmacology & Toxicology, University at Buffalo, The State University of New York, Buffalo, NY.*

Chlorpyrifos (CPF), one of the most widely used organophosphorus pesticides, has been known to cause neurotoxicity through the inhibition of cholinesterase activity. However, other neurobehavioral deficits, unrelated to cholinesterase inhibition, have been linked to chlorpyrifos exposure. The mechanisms behind these effects are not fully known or understood. High-throughput loss-of-function genetic

screening tools in yeast or other non-mammalian model systems have been successfully used to study human susceptibility to chemical exposure and decipher chemical compounds mode of action. We recently obtained a newly developed human haploid cell based loss of functional genetic screening model and adopted this haploid cell model in our laboratory. We treated the cells with 200  $\mu$ M CPF, a dose causing 30% death of haploid cells after 3 days of treatment. After 21-days of treatment, we were able to identify cells carrying genes with deficient functions that play a role in the resistance to CPF-induced toxicity. We are currently conducting functional tests to validate their association with CPF toxicity. Ultimately, this approach will help identify novel susceptibility genes and gain insight into potential mechanisms of CPF-induced toxicity. (This work was supported by Startup funds to X.R. provide by SUNY Buffalo).

**PS 1417 Pharmacological Modulation of Endocannabinoid Signaling Differentially Affects Acute Toxicity of Paraoxon and Chlorpyrifos Oxon in Rats.**

J. Liu and C. Pope. *Physiological Sciences, Oklahoma State University, Stillwater, OK.*

Organophosphorus anticholinesterases (OPs) elicit acute toxicity by inhibiting acetylcholinesterase, increasing acetylcholine levels at cholinergic synapses throughout the nervous system. This leads to excessive/prolonged activation of cholinergic receptors and resulting signs of toxicity including increased parasympathetically-mediated secretions (SLUD signs) and involuntary movements (e.g., tremors). Endocannabinoids (eCBs, e.g., anandamide [AEA] and 2-arachidonoyl glycerol [2-AG]) are released from membrane lipids upon neuronal activation. AEA, 2-AG and potentially other putative eCBs can regulate neurotransmission by activating presynaptic CB1 receptors to inhibit neurotransmitter release. We hypothesized that pharmacological modulation of eCB signaling will influence the expression of anticholinesterase toxicity. The comparative effects of WIN 55,212-2 (WIN, a CB1 receptor agonist, 1.5 or 5 mg/kg), AM251 (a CB1 receptor antagonist, 3 mg/kg), URB597 (an inhibitor of AEA degradation, 3 mg/kg) and capsazepine (a TRPV1 endovanilloid antagonist, 10 mg/kg) on the toxicity of paraoxon (PO) and chlorpyrifos oxon (CPO) were evaluated. Involuntary movements were induced by both OPs in a dose-related manner (PO: 0.4,0.5,0.6 mg/kg, sc; CPO: 8,10,12 mg/kg, sc), whereas somewhat less consistent dose-related effects were noted with SLUD signs. WIN partially reduced signs of toxicity following PO exposure, but had little effect on toxicity following CPO. The CB1 receptor antagonist AM251 had no effect on CPO toxicity, but substantially increased lethality following PO exposure (6/12 vs 1/9). URB597 had no effect on PO toxicity, or on involuntary movements following CPO, but increased SLUD signs following CPO. Similar to effects of URB597, capsazepine had little effect on PO toxicity, but increased SLUD signs following CPO. These results suggest that pharmacological modulation of eCB and/or endovanilloid signaling may differentially influence selected toxic responses to anticholinesterases in an OP-related manner. (Supported by NIEHS R01ES009119).

**PS 1418 Hippocampal Changes Induced by Noncholinergic Diisopropylfluorophosphate (DFP) Exposure in Fischer 344 Rat Brain.**

D. A. Mahle<sup>1</sup>, A. Soto<sup>1</sup>, V. T. Chan<sup>1</sup> and N. V. Reo<sup>2</sup>. <sup>1</sup>711 HPW/RHDJ, Wright-Patterson AFB, OH; <sup>2</sup>Wright State University, Fairborn, OH.

The mechanism of organophosphate (OP) induced inhibition of acetylcholinesterase and subsequent excitotoxicity is well described. However, exposure to OPs at non-cholinergic doses has been reported to cause deficits in cognitive behavior and spatial memory, though little is known about the mechanisms of action. Here an integrated approach using both metabolomic and transcriptomic techniques was used to reveal some of the non-cholinergic effects of DFP in rat hippocampus. Adult male Fischer 344 rats were administered 1 mg/kg DFP or saline (control) via subcutaneous injection at 10 mL/kg. Time points for hippocampal collection were 0.5, 1, 2, 12, 24 and 48 hr post dose. AChE activity reached a minimum of 55% at 2 hr post dose. Total RNA was isolated from hippocampus for differential gene expression analysis using the Affymetrix 1.0 ST gene array at 1 hr post dose. Lipid and aqueous extracts were prepared from each hippocampus at 2 hr post dose, and profiles of small molecule metabolites, lipids and phospholipids were measured using multinuclear NMR spectroscopy. The amino acids valine, isoleucine and alanine were increased 4-5 fold, while cis-aconitate and fumarate were increased 2-3 fold after exposure to DFP. Succinate and  $\gamma$ -aminobutyric acid (GABA) were decreased approximately 57%. No change was detected in any of the

lipid metabolites measured. Differential gene expression and pathway analysis revealed that the I-kappaB/NF-kappaB and the Wnt signaling pathways were down-regulated. By evaluating the impact of low level OP exposure on the metabolic and transcriptomic profile of the hippocampus, we hope to gain a greater understanding of the noncholinergic mechanisms of action and sensitive target areas of OPs.

**PS 1419 Dose-Dependent Behavioral Deficits in Egyptian Agricultural Workers with Chronic Organophosphorus Pesticide (OP) Exposures.**

W. K. Anger<sup>1</sup>, F. M. Farahat<sup>2</sup>, P. J. Lein<sup>3</sup>, J. R. Olson<sup>4</sup>, M. Lasarev<sup>1</sup> and D. Rohlman<sup>1</sup>. <sup>1</sup>Oregon Health & Science University, Portland, OR; <sup>2</sup>Menoufia University, Shebin Elkom, Egypt; <sup>3</sup>University of California Davis, Davis, CA; <sup>4</sup>University at Buffalo, Buffalo, NY.

Chronic exposure to OPs is consistently associated with deficits on neurobehavioral tests in workers using pesticides. While years of work have correlated with degree of effect in a few studies, a dose-effect relationship has not been identified, leading some to doubt the association. We identified a population of pesticide application teams in Egypt primarily exposed to one OP, chlorpyrifos (CPF). Teams include engineers (who do not typically enter the fields during applications), technicians (who walk side-by-side with the applicators in the fields), and applicators (who are typically seasonal workers and have the highest exposures). TCPy levels in urine confirmed the pattern of lower to higher exposures across these job categories. Trailmaking, a test of complex visual scanning, motor speed and agility, consists of two test components, A and B that differ in complexity. The test was administered to 54 engineers, 59 technicians, 31 applicators, and 150 controls 3 times during the OP application season and 1.5 months after applications had ended. While time to complete Trailmaking A and B improved across sessions, a consistent dose-response relationship was seen in performance speed: Controls had the best (fastest) performance throughout the application season on Trailmaking A ( $p < 0.04$ ) and B ( $p < 0.001$ ). Applicators had slower performance than engineers ( $p = 0.015$ ) and technicians ( $p = 0.032$ ) on Trailmaking A. On the more complex Trailmaking B test, applicators and technicians had comparable performance that was significantly slower ( $p = 0.003$  and  $p = 0.012$  respectively) than performance of engineers. Test performance at 1.5 months after applications ended revealed that differences between the groups were persistent. Ongoing studies are evaluating relationships between neurobehavioral performance and genetic polymorphisms of enzymes that metabolize CPF. (NIH R01 ES016308; MPI: WKA & PJJ)

**PS 1420 Chlorpyrifos Exposure and Self-Reported Neurological Symptoms in Adolescent Pesticide Applicators.**

D. Rohlman<sup>1</sup>, K. Khan<sup>1</sup>, A. A. Ismail<sup>2</sup>, G. Abdel Rasoul<sup>2</sup>, M. R. Bonner<sup>3</sup>, M. R. Lasarev<sup>1</sup>, A. L. Crane<sup>4</sup>, S. T. Singleton<sup>4</sup> and J. R. Olson<sup>3,4</sup>. <sup>1</sup>Occupational and Environmental Health, University of Iowa, Iowa City, IA; <sup>2</sup>Community Medicine & Public Health, Menoufia University, Shebin El-Kom, Egypt; <sup>3</sup>Social & Preventive Medicine, State University of New York at Buffalo, Buffalo, NY; <sup>4</sup>Pharmacology & Toxicology, State University of New York at Buffalo, Buffalo, NY.

Although studies with adults have demonstrated associations between organophosphorus (OP) pesticide exposure and neurological symptoms, the change in symptom reporting across an application season and the relationship between symptoms and biomarkers of exposure is poorly understood and few studies have examined adolescents. The prevalence of neurological symptoms across the chlorpyrifos (CPF)-application season was examined in adolescent pesticide applicators ( $n = 57$ ) and environmentally exposed adolescents ( $n = 38$ ) in Egypt. Self-reported symptom data at 32 time points over a 7-month CPF-application season were collected. Associations of symptoms with the urine CPF biomarker, trichloro-2-pyridinol (TCPy) and blood cholinesterase inhibition were also investigated. Increased reporting of neurological symptoms were observed among both applicators and non-applicators after several weeks of repeated exposure. Applicators demonstrated a greater percentage of neurological symptoms relative to baseline than the non-applicators at all subsequent time intervals. Cumulative TCPy, an estimate of overall seasonal exposure, was positively associated with average percentage of symptoms only among the applicators in the adjusted models. No associations were found between acetylcholinesterase (AChE) and butyrylcholinesterase (BChE) inhibition and self-reported symptoms after accounting for covariates. Results of the study demonstrate that adolescent applicators and non-applicators experience a greater percentage of neurological symptoms due to repeated exposure. Reduction of CPF exposure among the adolescent applicators should be a public health priority since neurological symptoms remained elevated even after the cessation of CPF application. Supported by NIEHS ES017223.

**PS 1421 Differential Antagonism of Tetramethylenedisulfotetramine-Induced Seizures by Agents Acting at NMDA and GABAA Receptors.**

M. Shkarjian<sup>1,2</sup>, J. Velíšková<sup>3,4,6</sup>, P. Stanton<sup>3,6</sup> and L. Velíšek<sup>3,5,6</sup>.  
<sup>1</sup>Environmental Health Science, New York Medical College, Valhalla, NY; <sup>2</sup>Medicine, UMDNJ-RWJMS, Piscataway, NJ; <sup>3</sup>Cell Biology & Anatomy, New York Medical College, Valhalla, NY; <sup>4</sup>Obstetrics & Gynecology, New York Medical College, Valhalla, NY; <sup>5</sup>Pediatrics, New York Medical College, Valhalla, NY; <sup>6</sup>Neurology, New York Medical College, Valhalla, NY. Sponsor: D. Heck.

Tetramethylenedisulfotetramine (TMDT) is a highly lethal neuroactive rodenticide responsible for many accidental and intentional poisonings in mainland China. Ease of synthesis, water solubility, potency, and difficulty to treat make TMDT a potential terrorist weapon. We characterized TMDT-induced seizures and mortality in male C57BL/6 mice. TMDT (ip) produced a syndrome of twitches, clonic, and tonic-clonic seizures decreasing in onset latency and increasing in severity with increasing dose; 0.4 mg/kg was 100% lethal. The NMDA antagonist, ketamine (KET, 35 mg/kg) injected ip after the first TMDT-induced seizure, did not reduce lethality, but increased the number of clonic seizures. Doubling the KET dose decreased tonic-clonic seizures and eliminated lethality through a 60 min observation period. Treating mice with another NMDA antagonist, MK-801, 0.5 or 1 mg/kg ip, showed similar effects as low and high doses of KET, respectively, and prevented lethality, converting continuous (status epilepticus) EEG activity to isolated interictal discharges. Treatment with these agents 15 min prior to TMDT administration did not increase their effectiveness. Post-treatment with diazepam (5 mg/kg; GABAA allosteric enhancer) reduced seizure manifestations and prevented lethality 60 min post-TMDT, but ictal events were evident in EEG recordings and, hours post-treatment, mice experienced status epilepticus and died. Thus, TMDT is a highly potent and lethal convulsant for which single-dose benzodiazepine treatment is inadequate in managing EEG seizures or lethality. Repeated benzodiazepine dosing or combined application of benzodiazepines and NMDA receptor antagonists are more likely to be effective in treating TMDT poisoning. Supported by NIH NS056093, NS072966, NS044421, DOD PR100634P1 & NYMC

**PS 1422 Postexposure Administration of Diazepam Blocks TETS-Induced Tonic Seizures and Death but Does Not Prevent Neuroinflammation.**

D. Bruun<sup>1</sup>, S. Vito<sup>2</sup>, B. Inceoglu<sup>2</sup>, B. D. Hammock<sup>2</sup> and P. J. Lein<sup>1</sup>. <sup>1</sup>VM Molecular Bioscience, University of California Davis, Davis, CA; <sup>2</sup>Entomology, University of California Davis, Davis, CA.

Tetramethylenedisulfotetramine (TETS) is a potent convulsant rodenticide that is considered a credible chemical threat agent. There is no approved therapy for TETS poisoning, although clinical reports suggest that generally-used anticonvulsants, including diazepam, keep patients alive when administered soon after exposure. Our goal was to identify the therapeutic window for diazepam when administered after TETS exposure, and to determine whether post-exposure administration of diazepam would attenuate the delayed neuroinflammation associated with acute TETS intoxication. In adult male mice administered a lethal dose of TETS (0.15 mg/kg, i.p.), a relatively high dose of diazepam (5 mg/kg, i.p.) blocked tonic seizures and death when administered 3 min after the second clonic seizure (approximately 20 min after TETS injection). Administration of diazepam at later times did not significantly reduce tonic seizures and death relative to TETS-exposed animals that did not receive diazepam. However, animals protected by diazepam from tonic seizures and death still exhibited significant and persistent region- and time-dependent activation of astrocytes and microglia, as determined by GFAP and Iba-1 immunoreactivity and microglia morphology. Thus, we next determined whether combined administration of diazepam with an anti-inflammatory agent would mitigate post-TETS neuroinflammatory responses. Inhibition of soluble epoxide hydrolase (sEH) has been shown to exert potent anti-inflammatory effects. Combined administration of diazepam and the sEH inhibitor 1709 (1 mg/kg, i.p. every 24 h after TETS injection) significantly decreased microglial activation but enhanced astrocyte activation. While the functional significance of this combined treatment has yet to be determined, these data suggest that combinatorial therapy may be necessary to mitigate long-term neurological sequelae of acute TETS intoxication. Support provided by the NIH NINDS CounterAct Program (R21 NS072094 and U54 NS072022).

**PS 1423 THC-Mediated Immunosuppression Leads to Decreased Th1 Response to Allogeneic Cells by Triggering Induction of MDSCs.**

J. M. Sido, M. Nagarkatti and P. Nagarkatti. Pathology, Immunology & Microbiology, University of South Carolina School of Medicine, Columbia, SC.

Host versus graft disease (HvGD) is a model for transplant rejection, wherein the recipient mounts an immunological response to donor cells causing T-cell driven destruction of the graft. The host immune response involves activation of T-cells, up-regulation of Th1 cytokines, and cellular proliferation in lymphoid organs. Δ-9-Tetrahydrocannabinol (THC) is a cannabinoid (CB) associated with anti-inflammatory and immunosuppressive properties, and is a known ligand for CB receptors 1 and 2 (CB1 and CB2). Our lab recently published that administration of THC recruits myeloid derived suppressor cells (MDSCs) which are innate regulatory cells, CD11b+Gr1+ in mice, that have been shown to reduce inflammation. To this end, we used THC (20mg/kg) pretreatment to ameliorate HvGD in C57BL/6 mice administered C3H/HeJ splenocytes (2.2x10<sup>7</sup> cells). Our studies show that THC treatment was able to reduce clinical symptoms of HvGD dependent on the presence of the CB1 receptor. THC-treated mice had significantly reduced lymphoid organ proliferation, Th1 cytokine levels, and T-cell activation. Using CB knockout mice as well as antagonists, we found that THC treatment was unable to reduce HvGD in the absence of CB1 receptor. Furthermore, THC treatment led to induction of MDSC resulting in a microenvironment that allowed graft cells to persist without eliciting graft versus host disease. The mechanism of CB1-dependent THC-mediated reduction in T cell proliferation and in Th1-mediated inflammation by induction of MDSCs, suggests a novel role for THC to induce a state of homeostasis that results in elevated host immunosuppression and reduced toxicity associated with transplantation (Support in part by NIH P01AT003961, R01AT006888, R01ES019313, R01MH094755, P20RR032684 and VA Merit Award BX001357).

**PS 1424 Mechanistic Comparison of Asbestos-Associated Autoantibodies.**

K. Serve, A. Santin and J. Pfau. Biological Sciences, Idaho State University, Pocatello, ID.

Chrysotile and amphibole asbestos are structurally distinct silicate fibers that cause a range of respiratory tract diseases, though Libby amphibole (LA) exposure is associated with diffuse pleural fibrosis and chrysotile with localized pleural plaquing. LA-associated disease seems to progress more rapidly, suggesting additional factors in disease manifestation. Examination of serum antibodies revealed mesothelial cell autoantibodies (MCAAs) in both LA and chrysotile exposed subjects. However, MCAA presence was significantly correlated with pleural disease only in LA exposed subjects, suggesting a role of MCAAs in driving pleural fibrosis on-set and/or progression. We hypothesized that LA and chrysotile associated MCAAs interact with mesothelial cells in mechanistically distinct ways, resulting in the different disease phenotypes observed within each asbestos-exposed cohort. We compared the ability of LA and chrysotile-associated MCAAs to induce cellular changes indicative of fibrotic disease, including collagen deposition and matrix metalloproteinase (MMP) expression. Results revealed that both LA and chrysotile MCAAs induce deposition of insoluble collagen proteins by cultured human pleural mesothelial cells. However, only LA MCAAs required MMP activity for collagen deposition. Immunoblot analysis revealed increased levels of MMP-8 in the supernatants of cells exposed to LA MCAAs whereas chrysotile MCAAs inhibited MMP-8 expression. These data, coupled with differences in cytokine profiles, indicate mechanistically distinct routes of MCAA-induced collagen deposition. We additionally determined that LA MCAAs are predominantly an IgG3 subtype whereas chrysotile MCAAs are mixed IgG1, 3, and 4 subtypes. This suggests that LA and chrysotile MCAAs differ in their potential for receptor binding and complement activation, which may contribute to distinct modes of pathogenicity. The mechanistic dissimilarities between LA and chrysotile MCAAs may help explain the disparate disease phenotypes and fibrosis progression noted in clinical observations of asbestos-exposed subjects.

**PS 1425 Cannabidiol-Induced Myeloid-Derived Suppressor Cells Lead to Amelioration of Experimental Autoimmune Encephalomyelitis.**

D. M. Elliott, P. Nagarkatti and M. Nagarkatti. Pathology, Microbiology and Immunology, University of South Carolina School of Medicine, Columbia, SC.

Multiple sclerosis (MS) is an autoimmune disease of the CNS with heterogeneous symptoms and progression. According to the National Multiple Sclerosis Society, roughly 400,000 people are affected in the US today and current therapies include

immunosuppressive agents with harsh side effects. Cannabinoids, which are a group of compounds derived from the marijuana plant (*Cannabis sativa*), are known to mediate their signals through the cannabinoid receptors, CB1 and CB2, and have been effective as treatment for cancer associated pain, nausea and appetite loss. Recently, their anti-inflammatory properties have been studied. Moreover, the use of cannabinoid therapy for MS has also been exploited. However, the proposed mechanism of action needs to be explored further. We used experimental autoimmune encephalomyelitis (EAE), a murine model of MS, to explore the anti-inflammatory role of cannabidiol (CBD) and its effects on myeloid-derived suppressor cells (MDSCs). EAE disease paradigms were consistently reduced with CBD treatment, as a significant reduction in clinical scores of paralysis and decrease in cellular infiltration, marked improvement of CNS tissue integrity, and reduced demyelination via histopathological analysis were observed. In addition, CBD treatment led to a reduction in the percentage and absolute number of T cells particularly the CD4<sup>+</sup> T cells infiltrating the CNS (spinal cord and brain), which were significantly increased in the untreated EAE mice. However, there was a profound increase in MDSC induction in the spleens, CNS, and peritoneal wash of CBD treated EAE mice as compared to the untreated EAE controls. Both granulocytic and monocytic MDSCs were increased in CBD treated EAE mice. Together, these studies demonstrate that CBD treatment may ameliorate EAE via the induction of MDSCs which suppress the aberrant autoimmune response. (Supported by NIH grants R01 AT006888, R01 ES019313, R01 MH094755, P01 AT003961, P20 RR032684 and VA Merit Award BX001357).

### PS 1426 Attenuation of Trichloroethene-Mediated Autoimmune Response in iNOS-null MRL<sup>+/+</sup> Mice.

G. Wang<sup>1</sup>, M. Wakamiya<sup>2</sup>, J. Wang<sup>1</sup>, G. Ansari<sup>1</sup> and M. Khan<sup>1</sup>. <sup>1</sup>Pathology, University of Texas Medical Branch, Galveston, TX; <sup>2</sup>Institute for Translational Sciences and Animal Resource Center, University of Texas Medical Branch, Galveston, TX.

Exposure to trichloroethene (TCE), a ubiquitous environmental contaminant, is associated with an autoimmune response both in humans and animal models. However, mechanisms underlying TCE-mediated autoimmunity remain largely unknown. Previous studies from our laboratory in MRL<sup>+/+</sup> mice suggest that reactive oxygen and nitrogen species (RONS) may contribute to TCE-induced autoimmunity. The current study was undertaken to further assess the role of oxidative and nitrosative stress in TCE-induced autoimmunity by using iNOS-null MRL<sup>+/+</sup> mice. iNOS-null mice were backcrossed to MRL<sup>+/+</sup> mice for 10 generations and then N10 heterozygous mutants were intercrossed to obtain homozygous mutants. Female MRL<sup>+/+</sup> and iNOS-null MRL<sup>+/+</sup> mice were given TCE (10 mmol/kg, i.p., every 4th day) for 6 weeks; their respective controls received corn oil only. TCE treatment led to significant induction of anti-malondialdehyde (MDA)- and anti-4-hydroxynonenal (HNE)-protein adduct antibodies along with increased iNOS in sera, and increased nitrotyrosine (NT) in sera, livers and kidneys in MRL<sup>+/+</sup> mice, suggesting an overall increase in oxidative and nitrosative stress. The TCE-induced oxidative stress was also associated with significant increases in serum anti-nuclear antibodies (ANA) and anti-double stranded DNA antibodies (anti-dsDNA) levels. Interestingly, iNOS and NT levels were negligible in both controls and TCE-treated iNOS-null MRL<sup>+/+</sup> mice. However, TCE treatment in iNOS-null mice still led to significant increases in serum anti-MDA/HNE-antibodies along with increases in serum ANA and anti-dsDNA compared to controls. Remarkably, the increases in serum ANA and anti-dsDNA induced by TCE in the iNOS-null mice were significantly less pronounced compared to that in MRL<sup>+/+</sup> mice. Our results provide further evidence for a role of oxidative/nitrosative stress in TCE-induced autoimmune response, and iNOS elimination attenuates this autoimmune response. Supported by NIH ES016302.

### PS 1427 Mouse Model of Halogenated Platinum Salt Hypersensitivity.

W. Williams<sup>1</sup>, E. H. Boykin<sup>1</sup>, C. Copeland<sup>1</sup>, L. Copeland<sup>1</sup>, S. J. Quell<sup>3</sup>, S. H. Gavett<sup>1</sup>, M. Selgrade<sup>2</sup> and D. M. Lehmann<sup>1</sup>. <sup>1</sup>US EPA, Research Triangle Park, NC; <sup>2</sup>ICF International, Durham, NC; <sup>3</sup>Independent, Research Triangle Park, NC.

Occupational exposure to halogenated platinum salts can trigger the development of asthma. Concern for increased asthma risk exists for the general population due to the use of platinum (Pt) in catalytic converters and its emerging use as a diesel fuel additive. To investigate airway responses to Pt, we developed a mouse model of Pt hypersensitivity. Previously, we confirmed the dermal sensitizing potency of ammonium hexachloroplatinate (AHCP) using an ex vivo [3H]methyl thymidine labeling version of the local lymph node assay in BALB/c mice. Here, we investigated the ability of AHCP to induce airway responses in mice sensitized by the dermal route. Mice were sensitized through application of 100 µL 1% AHCP in DMSO to

the shaved back on days 0, 5 and 19, and 25 µL to each ear on days 10, 11 and 12. Unsensitized mice received vehicle. On day 24, mice were challenged by oropharyngeal aspiration (OPA) with 0 or 100 µg AHCP in saline. Before and immediately after dosing, airway responses were assessed using whole body plethysmography (WBP). A dose dependent increase in immediate airway responses (IAR) was observed in AHCP sensitized and challenged mice. On day 26, changes in ventilatory responses to methacholine (Mch) aerosol were assessed by WBP; dose-dependent increases in Mch responsiveness occurred in sensitized mice. Bronchoalveolar lavage fluid harvested from sensitized mice contained an average of 7.5% eosinophils compared to less than 0.5% in control mice ( $p < 0.05$ ); significant increases in total serum IgE was observed for all sensitized mice. This model will be useful for assessing both relative sensitizing potency and cross-reactivity between different halogenated Pt salts and for investigating the possible adjuvant effects of diesel exhaust particles. This abstract does not represent EPA policy.

### PS 1428 Effect of Analgesic Administration on the Guinea Pig Maximization Test.

D. W. Rice, L. C. Anderson and J. H. Gass. Department of Toxicology, Baxter Healthcare Corporation, Round Lake, IL.

Guinea pig maximization tests have been associated with inflammation at cutaneous induction sites due to the use of 1-chloro-2, 4-dinitrobenzene (DNCB) as a positive control and Complete Freund's Adjuvant (CFA). CFA enhances the sensitization potential of the test substances and its use is required by ISO 10993-10. To alleviate the potential for pain and distress, we evaluated the use of the analgesic, buprenorphine hydrochloride (HCl). Analgesics can modulate the inflammatory response and may interfere with the detection of contact sensitization. The purpose of this study was to determine if the administration of buprenorphine HCl, as a refinement to reduce the potential for pain and distress, would affect the results of the guinea pig maximization test. DNCB and Rubbercare® Gloves were used as the test articles. The experimental design was consistent with the procedures described in ISO 10993-10 and the guinea pig maximization test (Magnusson and Kligman), with additional parameters evaluated. The experimental design consisted of 10 groups with each group receiving different concentrations of the test articles with or without analgesic treatment. Twenty-four to 30 hours after topical induction, the groups treated with buprenorphine HCl were given 0.006 mg/kg every 12 hours for a total of three doses. Three animals per group were terminated on study day 10 for hematology, coagulation and histologic evaluation of treatment sites. The remaining animals were terminated after completion of the sensitization test. Body weight gain, clinical observations, pain assessment, and sensitization potential were evaluated. Clinical observations, hematology, coagulation or histopathology of treatment sites were similar in groups that received analgesics compared to groups that did not. At least 60% to 100% of animals in each group were sensitized with no difference between corresponding groups with or without analgesic treatment. Based upon the results of this study, the use of the analgesic, buprenorphine HCl, did not interfere with the evaluation of the results of the guinea pig maximization test.

### PS 1429 Chemical Assessment of "In-Use" Allergic Contact Dermatitis Patch Test Reagents from Dermatology Clinics.

P. D. Siegel<sup>1</sup>, J. F. Fowler<sup>2</sup>, B. F. Law<sup>1</sup>, E. M. Warshaw<sup>3</sup> and J. S. Taylor<sup>4</sup>. <sup>1</sup>NIOSH/CDC, Morgantown, WV; <sup>2</sup>University of Louisville, Louisville, KY; <sup>3</sup>University of Minnesota, Minneapolis, MN; <sup>4</sup>Cleveland Clinic, Cleveland, OH.

Epicutaneous patch tests (EPT) are commonly used to identify chemical agents of allergic contact dermatitis in dermatology patients. Test validity and assessment of allergic reaction severity are highly dependent on the use of reliable chemical allergen test reagents. The purpose of the present study was to measure the actual concentration of nickel sulfate (NiSO<sub>4</sub>), methyl methacrylate (MM), formaldehyde (FA) and glutaraldehyde (GA) compared to the labeled concentrations of commercial reagents found in dermatology clinics where patch testing is routinely performed. The commercial reagents, NiSO<sub>4</sub>, MM and GA are supplied either dissolved or suspended in petrolatum (usually in syringe, multiuse containers) while FA is diluted in water. Participating clinics submitted in-date and out-dated reagents to the laboratory for analyses. Both NiSO<sub>4</sub> and FA levels were at or above the labeled concentration. NiSO<sub>4</sub> particulate was uniformly distributed throughout the petrolatum. In contrast, MM was low and variable in commercial allergen reagents. "In-use" MM reagent syringes were all ≤56% of the 2% label concentration with no observable relationship to expiration date. One MM syringe purchased directly from the manufacturer was 70% of the labeled concentration. Lower MM levels in syringes were consistently measured at the tip vs. plunger end

of the syringe suggesting loss due to MM's volatility. GA patch test reagents concentrations ranged from 27 to 45% of the labeled (1% in petrolatum) amount, independent of expiration date. No GA concentration pattern between tip and plunger was observed. These data suggest that false negative EPT results may be due to instability of volatile or self-polymerizing chemical allergens in the test reagents.

#### **PS 1430 Adjuvant Effect of Dibutyl Phthalate (DBP) in an Animal Model of Contact Hypersensitivity.**

A. S. Lourenço<sup>2</sup>, R. M. Zaia<sup>2</sup>, A. Prudente<sup>2</sup>, M. F. Otuki<sup>2</sup> and A. J. Martino-Andrade<sup>1,2</sup>. <sup>1</sup>Fisiologia, Universidade Federal do Paraná, Curitiba, Brazil; <sup>2</sup>Farmacologia, Universidade Federal do Paraná, Curitiba, Brazil. Sponsor: E. Silbergeld.

Recent studies have demonstrated that certain phthalates can have adjuvant effects in contact hypersensitivity models, exacerbating inflammatory responses. According to human exposure estimates, perfumes containing DBP can result in topical applications as high as 0.4 mg DBP/day. The aim of the present study was to investigate the adjuvant effect of DBP in the oxazolone-induced contact hypersensitivity model using human relevant doses. Adult male Balb/c mice were divided into 5 different groups (n=6/group). These animals received oxazolone (75 µg/animal) in hairless abdomen (induction). After five days, mice received oxazolone (75 µg/ear; positive control and DBP exposed groups) or vehicle (negative control group) in the right ear (sensitization). In addition, in the sensitization day and in the two subsequent days, DBP groups received three different doses (0.04, 0.4 and 4 mg DBP/ear) twice a day, while positive and negative controls received vehicle (acetone). All exposures were topical. For three subsequent days after sensitization ear thickness (edema) was measured with the use of a micrometer. After the last measurement, animals were decapitated and the ears were collected for the determination of N-acetyl-β-D-glucosaminidase (NAG) and Myeloperoxidase (MPO) activity. The study was in accordance to the ethics committee of the Federal University of Paraná. Ear thickness was increased in positive control when compared to vehicle only (negative control) group. No difference was seen between positive control and the lowest DBP dose group. However, oxazolone-induced edema was increased in the groups treated with 0.4 and 4 mg DBP/ear when compared to positive control. Similar results were found in MPO and NAG activity. The groups treated with the two highest DBP doses displayed significantly higher enzymatic activity when compared to positive control group. These results indicate that human relevant doses of DBP can have adjuvant effects in the oxazolone-induced contact hypersensitivity in mice.

#### **PS 1431 Characterization of the Mouse Allergy Model to Understand Mechanisms of Drug Allergy.**

X. Zhu, S. Cole, T. Kawabata and J. Whritenour. Pfizer Inc. Immunotoxicology CoE, Drug Safety Research and Development, Groton, CT.

Developed as a modification of the Lymph Node Proliferation Assay, the mouse allergy model (MAM) appears to be a promising tool for predicting the potential of drug development candidates to produce hypersensitivity reactions (HR). In this model, drugs associated with HR in the clinic produce a marked increase (compared to controls) in the cellularity of the draining lymph nodes (LN). The objective of this study was to characterize the phenotype of draining LN cells to identify new parameters that can be used to enhance the sensitivity and specificity of the MAM and to better understand the mechanism(s) for the response. Drugs that are associated with HR in the clinic (abacavir and amoxicillin) were selected as positive controls for this study. Negative control drugs (metformin and cimetidine) were selected based on the low number of reported HR for these compounds. Groups of 5 mice per group were injected subcutaneously with drug (100 mg/kg) or vehicle once daily for three consecutive days. After a two day rest, cells from the draining brachial LN were isolated and analyzed by flow cytometry. A significant increase in total LN cell number (compared to vehicle) was observed for mice treated with the positive control drugs. Compared to vehicle and negative control animals, an increase in CD4+ and CD8+ T cells and B cells was observed in the draining LN of abacavir and amoxicillin treated animals. Positive control drugs produced significant decreases (~25% compared to control) in the percentage of naïve T cells and increases (~27% compared to control) in the percentage of L-selectin (CD62L) and CD44 double-negative T cells. The negative control drugs induced slight, but statistically insignificant, changes in the expression of these markers. Drugs associated with HR in the clinic produced changes in draining LN cellularity and phenotype that are not observed for negative control drugs. Changes observed in adhesion molecule expression may suggest an effect of positive control drugs on lymphocyte trafficking.

#### **PS 1432 Characterization and Comparison of Methylene Diphenyl Diisocyanate Haptenated Human Serum Albumin and Hemoglobin.**

M. Mhike<sup>1,2</sup>, J. M. Hettick<sup>1</sup>, I. Chipinda<sup>1</sup>, R. H. Simoyi<sup>2</sup> and P. D. Siegel<sup>1</sup>. <sup>1</sup>Health Effects Laboratory Division, NIOSH/CDC, Morgantown, WV; <sup>2</sup>Department of Chemistry, Portland State University, Portland, OR.

Methylene diphenyl diisocyanate (MDI) is widely used as a cross-linking agent in the manufacture of polyurethane products. Exposure to diisocyanates (dNCO), such as MDI, is known to cause occupational asthma. MDI haptenation of proteins is central to dNCO immunological sensitization, however, the resultant protein conjugates are complex and difficult to characterize. The objective of the present study was to characterize hemoglobin (Hb) and human serum albumin (HSA) following conjugation to different molar concentrations of MDI. MDI-protein conjugates were acid digested to obtain free methylene dianiline (MDA). MDA was extracted, derivatized with fluorescamine and analyzed by HPLC-fluorescence. MDI-Hb was also digested with trypsin and specific amino acid conjugation sites determined by ultra-performance liquid chromatography-quadrupole-tandem time-of-flight mass spectrometry. The trinitrobenzene sulfonic acid assay (TNBS) and denaturing gel electrophoresis were used to determine the extent of cross-linking. MDI conjugation was observed to be dependent on the MDI: protein ratio and the concentration of protein. Greater binding to HSA than Hb was observed and MDI bound to only eight binding sites on Hb compared to twenty for HSA (at 40:1 molar ratio of MDI: protein). Self-polymerization of MDI onto protein was observed on some amino acids at higher MDI concentrations. The TNBS assay was used to confirm cross linking in MDI-HSA with approximately 60% loss of amine reactivity at 40:1 MDI: HSA. More cross-linking was observed at 0.5 mg/ml HSA than at 5mg/ml at 40:1 MDI: HSA. It is concluded that MDI has a greater reactivity toward HSA than Hb with respect to the number of residues haptenated and amount of MDI bound per mole of protein.

This work was supported by an Interagency agreement with the NIEHS (Y1-ES-0001).

#### **PS 1433 Dimethylfumarate: Potency Prediction and Clinical Experience.**

I. R. White<sup>2</sup>, D. Basketter<sup>1</sup>, F. G. Burleson<sup>3</sup>, G. Burleson<sup>3</sup> and I. Kimber<sup>4</sup>. <sup>1</sup>DABMEB Consultancy Ltd., Sharnbrook, United Kingdom; <sup>2</sup>Department of Cutaneous Allergy, St. John's Institute of Dermatology, London, United Kingdom; <sup>3</sup>BRT - Burleson Research Technologies, Morrisville, NC; <sup>4</sup>Faculty of Life Sciences, University of Manchester, Manchester, United Kingdom.

Dimethylfumarate (DMF) was the cause of a major outbreak of allergic contact dermatitis as a consequence of its use as an antifungal agent in leather products, particularly when used in furniture. This became known, as "toxic sofa dermatitis". However, what has not previously been established is why the risks to human health had not been assessed adequately for this chemical. The purpose of these investigations was, therefore, to determine whether the frequency and severity of reactions to DMF arose as a function of its intrinsic skin sensitizing potency and/or the nature and extent of exposure. The intrinsic sensitizing potency of DMF was measured using the standard local lymph node assay (LLNA) with determination of an EC3 value; the threshold in the LLNA and which serves as an indicator of relative skin sensitising potency in humans. The EC3 value for DMF was 0.35% when tested in dimethylformamide as a vehicle, indicating that this chemical is a strong, but not an extreme, skin sensitizer in this mouse model. DMF was found therefore to have a relative sensitising potency that is comparable with formaldehyde, also a strong human skin sensitizer. The conclusion is drawn that the frequency and intensity of allergic contact dermatitis reactions to DMF suggest that it was the prolonged, repeated and occlusive exposure over large skin areas to this chemical, combined with strong sensitising potency, that together generated the "perfect storm" conditions that caused the DMF epidemic.

#### **PS 1434 Characterization of the Allergenic Potential of Proteins: An Assessment of the Kiwifruit Allergen Actinidin.**

L. Beresford<sup>1</sup>, S. McClain<sup>2</sup>, I. Kimber<sup>1</sup> and R. J. Dearman<sup>2</sup>. <sup>1</sup>Faculty of Life Sciences, Manchester University, Manchester, United Kingdom; <sup>2</sup>Syngenta Crop Protection, Durham, NC.

Assessment of the potential allergenicity (IgE-inducing properties) of novel proteins is an important component of the overall safety assessment of foods. Resistance to digestion with pepsin is commonly measured to characterize allergenicity, although the association is not absolute. We have shown previously that the measurement of specific IgE antibody production induced by systemic (intra-peritoneal) exposure of BALB/c strain mice to a range of proteins correlates with

allergenic potential. The purpose of the present investigations was to explore further the utility of these approaches using the kiwifruit allergen, actinidin. During the past 10 years, kiwifruit has become an important allergenic foodstuff, coincident with its increased consumption, particularly as a weaning food. The ability of actinidin to stimulate antibody responses has been compared with the reference allergen ovalbumin, and with the non-allergenic protein bovine hemoglobin. Hemoglobin was rapidly digested by pepsin whereas actinidin was relatively resistant unless subjected to prior chemical reduction (conditions more closely reflecting intracellular digestion). Hemoglobin stimulated detectable IgG antibody production at relatively high doses (10%), but failed to stimulate IgE. In contrast, actinidin was both immunogenic and allergenic at relatively low doses (0.25% to 1%). Vigorous IgG and IgG1 antibody production and relatively high titer IgE antibody responses were recorded, similar to those provoked by ovalbumin. Thus, actinidin displays a marked ability to provoke IgE, consistent with allergenic potential. These data provide further encouragement that in tandem with analysis of pepsin stability, the assessment of IgE antibody production following systemic (intraperitoneal) exposure of BALB/c strain mice provides an informative approach for the prospective identification of protein allergens.

## PS 1435 Risk of Allergic Reaction to Undeclared Milk Proteins in a Dietary Supplement.

J. Fleischer and M. H. Whittaker. *ToxServices LLC, Washington DC.*

In food allergic individuals, the immune system is sensitized to food proteins and mounts a damaging inflammatory response. As a major food allergen, milk and milk-derived ingredients must be declared on food labels under the U.S. Food Allergen Labeling and Consumer Protection Act. Individuals with cow's milk allergy (CMA) may be at risk from a single exposure to undeclared milk, and may experience hives, swelling, vomiting, diarrhea, and/or asthma. Life-threatening anaphylaxis may occur.

We assessed the risk of allergic reaction due to consumption of undeclared milk proteins in a dietary supplement in adults with CMA by calculating acceptable daily intake (ADI) thresholds for the milk proteins lactoglobulin and casein. ADIs are the lowest exposures that would elicit only mild symptoms in adults with CMA. We compared these ADIs with estimated intake (EI) levels for the two proteins, based on analytical evaluation of the supplement and recommended serving size.

We conducted benchmark dose (BMD) modeling on data from published double- or single-blind, placebo-controlled milk challenge studies in individuals with CMA. Dichotomous modeling (presence/absence of allergic response) was conducted using EPA's BMD Software 2.1.2. BMDs and BMDLs (lower 95% confidence interval for the BMD) at a benchmark response (BMR) of 10% for allergic response to milk challenge were modeled. BMDLs were adjusted for milk lactoglobulin and casein content (10% and 83% of total milk protein, respectively) and divided by an UF of 10 (individual variation) to obtain the ADIs. ADIs were 0.3 mg/person for lactoglobulin and 2.1 mg/person for casein, compared to respective EIs of 0.47 mg/person and 0.02 mg/person. The ADI for lactoglobulin was exceeded at an EI of 0.47 mg/person, suggesting that levels of undeclared milk protein in a dietary supplement are sufficient to increase the risk of allergic reaction in adults with CMA. The potentially severe and life-threatening nature of allergic reaction suggests the need for immediate risk management action and highlights the importance of GMPs for dietary supplements.

## PS 1436 Allergenic Antibiotics (Blactams and Sulfonamides) Induce Oxidative Stress in Keratinocytes.

B. E. Lucas<sup>1</sup>, A. E. Asangba<sup>1</sup>, S. Mohammad<sup>1</sup>, M. Gande<sup>1</sup>, K. L. Voie<sup>2</sup>, K. L. Campbell<sup>2</sup> and S. N. Lavergne<sup>1</sup>. <sup>1</sup>Comparative Biosciences, University of Illinois, Urbana, IL; <sup>2</sup>Veterinary Clinical Medicine, University of Illinois, Urbana, IL.

Drugs can induce hypersensitivity reactions (drug allergies). Delayed drug hypersensitivity occurs after >5 days of drug exposure. Surprisingly, delayed reactions usually target the skin although most drugs are not administered per-cutaneously. "Danger" signals such as necrotic cell debris, oxidative stress or inflammation, are key elements in the events leading to the sensitization of the immune system against an environmental toxicant or a therapeutic drug. We hypothesized that allergenic antibiotics would induce oxidative stress in keratinocytes in vitro. We therefore measured levels of intracellular glutathione (reduced and total GSH) and reactive oxygen species (ROS) in a canine keratinocyte cell line (CPEK cells) exposed to 2 Blactams (amoxicillin or cephalixin) 2 sulfonamides (sulfamethoxazole and sulfadimethoxine). Amoxicillin, cephalixin, sulfadimethoxine and sulfamethoxazole decreased levels of GSH in CPEK cells after 2h compared to the negative control; at 8h, levels were similar to the negative control with the 2 Blactams, but higher with the 2 sulfonamides; there was no difference between conditions at 24h. These effects affected total GSH rather than reduced or oxidized GSH. Sulfadimethoxine

was the only antibiotics that increased hydrogen peroxide levels compared to the media control at 2h/8h/24h. When measuring a larger range of ROS (hydroxyl, peroxide, superoxide), amoxicillin started to increase ROS levels at 4h; these ROS levels were further increased by amoxicillin and cephalixin at 24h compared to the media control. The effects were dose-dependent over a 2-2000uM range. Our data on these canine keratinocytes confirm results published on sulfonamides and human keratinocytes; they also expand them to Blactams.

## PS 1437 Activities of Xenobiotic Metabolizing Enzymes in Cell Lines Used for Skin Sensitization Testing *In Vitro*.

D. Vogel<sup>1,3</sup>, E. Fabian<sup>1</sup>, T. Eltze<sup>1,2</sup>, T. Ramirez<sup>1</sup>, S. N. Kolle<sup>1</sup>, B. van Ravenzwaay<sup>1</sup> and R. Landsiedel<sup>1</sup>. <sup>1</sup>Experimental Toxicology and Ecology, BASF SE, Ludwigshafen am Rhein, Germany; <sup>2</sup>Product Safety Paper Chemicals, BASF SE, Ludwigshafen am Rhein, Germany; <sup>3</sup>Food Chemistry and Toxicology, Technical University of Kaiserslautern, Kaiserslautern, Germany.

Skin sensitization is caused by repeated contact with an allergen. An early step in the sensitization process is the interaction of haptens with proteins. In some cases the hapten is formed from pro-haptens by enzymatic reactions in the skin (1). Several in vitro methods are currently in the validation process as alternative methods to test for skin sensitization (2,3).

The metabolic activities of selected enzymes were assayed in keratinocyte-like cells Keratinosens® (Givaudan, Switzerland) and LuSens (BASF, Germany) as well as in the dendritic-like cell U937 (used for the MUSST assay) and THP-1 (used for the h-CLAT). Protein and cytochrome c reductase contents as well as activities of oxidizing enzymes (CYP, FMO, ADH, AIDH), hydrolysing enzymes (esterase) and conjugating enzymes (NAT and UGT) were measured in subcellular fraction of the cells by monitoring metabolic transformation of model substrates. CYP, FMO, UGT and ADH activities were below the detection limit for all investigated cells. NAT1 and esterase activities were detectable in all cell lines. AIDH activities were detected in the keratinocyte-like cells Keratinosens® and LuSens but not in U937 or THP-1 cells.

These results demonstrate that potential pro-haptens can be metabolically activated during sensitization testing in vitro. The xenobiotic metabolizing enzymes of the respective cells need, however, to be compared to those of native skin.

1 Jäckh C et al. (2012) Relevance of xenobiotic enzymes in human skin in vitro models to activate pro-sensitizers. *J Immunotoxicol.* [Epub ahead of print]

2 Mehling A et al. (2012) Non-animal test methods for predicting skin sensitization potentials. *Arch Toxicol.* 86:1273

3 Bauch C et al. (2012) Putting the parts together: combining in vitro methods to test for skin sensitizing potentials. *Regul Toxicol Pharmacol.* 63:489

## PS 1438 Interleukin 17 Expression by Chemical Allergen-Activated Lymph Node Cells: Selectivity for Contact Allergens.

I. Kimber, A. Metryka, M. D. Hayes and R. J. Dearman. *Faculty of Life Sciences, Manchester University, Manchester, United Kingdom.*

Chemical allergens can cause skin sensitization resulting in allergic contact dermatitis, or sensitization of the respiratory tract associated with occupational asthma. The immunological mechanisms resulting in sensitization, and the contributions made by the innate immune response are not fully understood. The interleukin (IL)-17 cytokine family, originally described as Thelper (Th)17 cytokines, are now known to be expressed by cells of the innate immune system. It has been shown previously that topical exposure of mice to 2,4-dinitrochlorobenzene (DNCB), a potent contact allergen, is able to provoke the rapid (within 6-16 hours) production of IL-17 by components of the innate immune system in regional lymph nodes. Here we have examined whether this rapid elaboration of IL-17 cytokines is selective for contact allergens. BALB/c mice were exposed on the dorsum of both ears to various allergens (DNCB, dinitrofluorobenzene, oxazolone, 2-methyl-4-isothiazolin-3-one and 5-chloro-2-methyl-4-isothiazolin-3-one, or  $\alpha$ -hexylcinnamaldehyde), to the irritants sodium lauryl sulfate and benzalkonium chloride or to the appropriate vehicle control. At various times thereafter cells from draining lymph nodes were isolated and cultured, and supernatants analyzed for IL-17A, IL-17F, IL-17A/F and IL-22 expression. Expression of IL-17 cytokines and IL-22 was selective for contact allergens with no significant increase in response to skin irritants. A chemical respiratory allergen (trimellitic anhydride; TMA) also induced IL-17 and IL-22, but with substantially delayed kinetics compared with contact allergens. Enhancing the dendritic cell migration kinetics in response to TMA to match those induced by contact allergens did not impact on the tempo of lymph node IL-17 expression. Collectively these data suggest that the rapid elicitation of IL-17 cytokines in draining lymph nodes is a potentially selective biomarker of exposure to contact allergens, and may provide a platform for the development of a novel approach to the characterization of skin sensitizing activity.

**PS 1439 Interleukin 17 Responses Induced in Mice by Chemical Allergens: A Functional Role for Gammadelta T Cells.**

R. J. Dearman<sup>1</sup>, M. D. Hayes<sup>1</sup>, B. Hunt<sup>2</sup>, A. Hayday<sup>2</sup> and I. Kimber<sup>1</sup>.

<sup>1</sup>Manchester University, Manchester, United Kingdom; <sup>2</sup>London Research Institute, London, United Kingdom.

Interleukin (IL)-17 cytokines, expressed by T helper (Th)17 cells, play pivotal roles in adaptive immune responses. They have been implicated in autoimmune and allergic diseases and have roles in bacterial and fungal clearance. Importantly, IL-17 is produced not only by adaptive immune cells but also by cells of the innate immune system including the nonconventional  $\gamma\delta$  T cell subset. It has been shown recently that IL-17 expressing  $\gamma\delta$  T cells are required for the development of adaptive Th17 responses that mediate experimental autoimmune encephalomyelitis, a murine model of multiple sclerosis. We have examined whether IL-17 influences sensitization to chemical allergens. BALB/c strain mice were exposed topically to the contact allergen 2,4-dinitrochlorobenzene (DNCB), the respiratory allergen trimellitic anhydride (TMA), or to vehicle alone. At selected time points single cell suspensions of draining lymph nodes were cultured and analyzed for cytokine secretion or for mRNA following enrichment/depletion using magnetic beads. A single exposure to either allergen resulted in transient up-regulation of IL-17 from  $\gamma\delta$  T cells. Maximal levels of secretion were observed at 6h and 48h following exposure to DNCB and TMA, respectively. After repeated exposure under conditions where DNCB and TMA stimulate polarized Th1 and Th2 cytokine phenotypes, respectively, DNCB, but not TMA, was shown to induce the expression of IL-17. IL-17 production by DNCB-activated cells was shown by complement depletion to reside only in the CD4<sup>+</sup> population. In subsequent experiments, responses were explored in  $\gamma\delta$  T cell null mice and C57BL/6 wild type (WT) controls. A similar pattern of IL-17 production to that provoked in BALB/c strain mice was seen in the WT mice following prolonged exposure to DNCB. However, in the  $\gamma\delta$  T cell null mice the adaptive Th17 response was completely abrogated. These data suggest strongly that the lack of IL-17 production by  $\gamma\delta$  T cells during the acute (innate) response affects the subsequent adaptive Th17 response to contact allergens.

**PS 1440 IL-18 Secretion in Human 3D Organotypic Skin Models for the Identification of Contact Sensitizers.**

E. Corsini<sup>1</sup>, S. Gibbs<sup>2</sup>, V. Galbiati<sup>1</sup>, S. Spiekstra<sup>2</sup>, H. Kandarova<sup>3</sup>, P. Hayden<sup>4</sup>, C. Seaman<sup>4</sup> and E. L. Roggen<sup>5</sup>. <sup>1</sup>DiSeFeB, Università degli Studi di Milano, Milan, Italy; <sup>2</sup>Vrije Universiteit Medical Center, Amsterdam, Netherlands; <sup>3</sup>MatTek Corporation, Ashland, MD; <sup>4</sup>GSK, Hertfordshire, United Kingdom; <sup>5</sup>3Rs Management and Consultancy, Kongens Lyngby, Denmark.

Over the last decade, several in vitro methods have been proposed to identify potential of contact sensitizers, but no accepted in vitro method yet available. Keratinocytes play a key role in all phases of skin sensitization. Interleukin-18 (IL-18) production in keratinocyte was identified as a potentially useful endpoint for determination of contact sensitizers. Limitations of traditional submerged cell culture include chemical solubility, stability in water and metabolic competence. To overcome these problems, experiments were performed to test the possibility to use commercially available 3D organotypic skin models to exploit the possibility to use the secretion of IL-18 for the identification of contact sensitizers. A protocol was developed using different 3D skin models, including EpiDerm TM, EST1000TM. Preliminary experiments were conducted to determine chemical toxicity profiles using the MTT viability assay. Additional doses were then chosen for IL-18 secretion experiments. Following topical exposure for 24 h to several contact allergens (including benzocaine, cinnamaldehyde, citral, DNCB, eugenol, isoeugenol, 2-mercaptobenzothiazole, oxazolone, etc.) and irritants (including chlorobenzene, lactic acid, octanoic acid, phenol, salicylic acid, SDS, Tween 20, etc.) a robust increase in IL-18 release was observed only after exposure to contact allergens. The method could be easily transferred to naïve laboratories. Using a cut-off of 2-fold increase of IL-18 above vehicle control and 40% cell viability, depending from the laboratory 85-100 % sensitivity and 88-100 % specificity were obtained. This model appears to be very promising, additional testing with a larger chemical set is required to fully evaluate the utility of this assay.

**PS 1441 Animal Strains Usable to the LLNA: brdU-ELISA (OECD 442B).**

T. Anzai<sup>1,2</sup>, Y. Nozaki<sup>3</sup>, M. Kaminishi<sup>1,2</sup>, H. Takagi<sup>3</sup>, T. Satoh<sup>1</sup>, R. Guest<sup>4</sup> and K. Sato<sup>2</sup>. <sup>1</sup>Harlan Laboratories Co., Ltd., Tokyo, Japan; <sup>2</sup>School of Medicine, Showa University, Tokyo, Japan; <sup>3</sup>Japan SLC, Hamamatsu, Japan; <sup>4</sup>Harlan Laboratories (UK), Derby, United Kingdom.

The murine local lymph node assay (LLNA) is a widely accepted alternative test to assess the skin sensitizing potential of chemical substances. The original LLNA was designed to quantify lymph cell proliferation in the draining auricular lymph nodes

by incorporation of radiolabeled thymidine analogues. To avoid use of the radioisotope in the tests, some modified LLNA protocols were developed. One of the modified methods utilizes the nucleus (uridine) analogue of 5-Bromo-2'-deoxyuridine (BrdU). In this method, the incorporated BrdU is measured by ELISA, using anti BrdU antibody. This modified LLNA:BrdU-ELISA has been validated and adopted as OECD test guideline 442B. In this guideline, the CBA/J or CBA/JN strains are recommended, since researchers had used these strains during the validation. Previously, we noted differences in response in the LLNA with different strains of mouse. In this study, we used mice of several CBA strains to compare the reactivity against several skin sensitizers and a non sensitizer. It is confirmed that the mouse strains, CBA/CaOlaHsd and CBA/N Slc showed similar but not equal response to CBA/JN.Crlj, the preferred strain in the LLNA:BrdU-ELISA.

**PS 1442 Elucidation of the Reason Underlying the Incorrect Sensitization Evaluation Results for Methyl Methacrylate, Methyl Salicylate and 2-Mercaptobenzothiazole by Nonradioactive Local Lymph Node Assay.**

W. Jang<sup>1</sup>, K. Jung<sup>1</sup>, Y. Lee<sup>2</sup>, Y. Yum<sup>2</sup>, Y. Heo<sup>3</sup> and K. Lim<sup>1</sup>. <sup>1</sup>Amorepacific R&D Center, Yong-in, Republic of Korea; <sup>2</sup>Korea FDA, Cheong-won, Republic of Korea; <sup>3</sup>Catholic University of Daegu, Daegu, Republic of Korea.

The non-radioisotopic local lymph node assay (LLNA) using bromodeoxyuridine (BrdU) with flow cytometry (FCM) has been developing as an alternative test for identifying skin sensitizers. We previously performed pre-validation with recommended reference substances in the OECD Test Guideline 429 using Balb/c mice. Our results by non-radioactive LLNA were similar to those of traditional LLNA. However, a weak sensitizer, methyl methacrylate (MM), a non-sensitizer, methyl salicylate (MS) and a moderate sensitizer, 2-mercaptobenzothiazole (MBT) were wrongly identified by non-radioisotopic LLNA:BrdU-FCM as a non-sensitizer, a weak sensitizer and a non-sensitizer, respectively. Therefore, we tried to clarify the reason underlying the wrong prediction by LLNA:BrdU-FCM. First, we compared strain difference of Balb/c mice from CBA mice that are recommended strain in the OECD Test Guideline 429 with several test materials including the 3 chemical substances described above. Mice received topical application of the test material or vehicle on both ears for consecutive 3 days. Mice were sacrificed 24 hr after intraperitoneal injection of BrdU. Ear thickness and ear weight were measured for evaluating irritation and auricular lymph nodes were used for determining BrdU incorporation into lymph node cells. All of test materials including positive control showed similar stimulation index and ear thickness between two mice strains suggesting that strain difference may not be the reason for the wrong prediction by LLNA:BrdU-FCM. Interestingly, MBT was correctly identified as a moderate sensitizer when AOO was used as a vehicle while it was a non-sensitizer when DMF was used as recommended in the OECD guideline suggesting that vehicle selection may profoundly affect the prediction for MBT by LLNA:BrdU-FCM.

**PS 1443 Polarized Immune Responses Induced by Chemical Allergens Display Differential DNA Methylation Patterns.**

V. Chapman<sup>1</sup>, J. Moggs<sup>2</sup>, R. Terranova<sup>2</sup>, T. Zollinger<sup>2</sup>, I. Kimber<sup>1</sup> and R. J. Dearman<sup>1</sup>. <sup>1</sup>Manchester University, Manchester, United Kingdom; <sup>2</sup>Novartis, Basel, Switzerland.

There is increasing evidence that epigenetic regulation of gene expression plays a pivotal role in the orchestration of immune responses. It has been demonstrated previously that chemical allergens can be divided into two categories; contact allergens (such as dinitrochlorobenzene; DNCB), that cause type 1/type 17 polarized responses and respiratory allergens (such as trimellitic anhydride, TMA) that induce a preferential type 2 response. Such polarization occurs upon repeated (13 day) topical exposure. In order to explore the regulation and maintenance of such responses at the molecular level, the genome wide pattern of DNA methylation following treatment with the reference allergens DNCB and TMA was characterized. Mice (n=5 per group) were exposed to DNCB, TMA or vehicle alone for 13 days, and draining auricular lymph nodes excised. DNA was extracted, sonicated and processed for methylated DNA immunoprecipitation (MeDIP) followed by hybridization to a high resolution DNA promoter array (Roche) representing 28,000 probe ranges, covering promoter regions and known CpG islands. Changes in DNA methylation profiles for allergen-activated tissues were compared with the vehicle-treated control samples, with a cut off of p<0.01. More differentially methylated regions (DMR) were recorded for DNCB tissue than for TMA tissue (6319 versus 2178), although approximately half those identified for TMA were in common with DNCB. Direct comparisons between DNCB and TMA-treated tissue revealed 268 DMR that were differentially regulated between the two different classes

of allergens. The 15 most significant genes identified were associated with hypermethylation and hypomethylation for DNCB and TMA exposure, respectively. Thus, topical exposure to different classes of chemical allergen under polarizing conditions results in characteristic patterns of DNA methylation indicative of epigenetic regulation of the developing allergic response. Furthermore, DNCB and TMA are associated with more silencing and activating epigenetic marks, respectively.

**PS 1444 Chemicals Acute Toxicity Testing and Evaluation Based on Nematode *Caenorhabditis elegans* Model.**

Y. Li, K. Yang, S. Gao, H. Jing, L. Qi, J. Ning, Z. Tan, C. Zhao, L. Ma and G. Li. *Institute for Toxicology, Beijing Centers for Disease Control and Prevention, Beijing Research Center for Preventive Medicine, Beijing, China.*

The toxicity assessment and risk management of chemicals is highly associated with the safety of human health. At present, the conventional model of which rodent tests were greatly characterized, can no longer meet the increasing requirements of chemical toxicological evaluation. Studies on the non-rodent in vivo assay by using model organisms are becoming a potential perspective and frontiers in the research field of chemicals toxicity risk assessment. Nematode *Caenorhabditis elegans* (*C. elegans*) has great potential value in the chemical rapid toxicity screening and complying with principles of "3R" for its short life cycle, easy operation and low cost. However, the fact that how the acute toxicity in rodents and even health risks in human being can be predicted through toxicity in *C. elegans*, is still a key scientific problem that remains to be solved. In this pilot study, we assayed 50% lethal concentration (LC50) and 50% lethal time (LT50) of 20 selected chemicals using *C. elegans* as an in vivo model organism in 96-well plate for 24h, analyzed the correlation between LC50 of *C. elegans* and LD50 of rat/mouse. The results indicated that the estimated toleration of chemical pH for *C. elegans* was greater than 2.75. There was a positive correlation between LC50 of *C. elegans* and LD50 of rat/mouse ( $R > 0.83$ ,  $P < 0.01$ ). LC50 and LT50 of chemicals in *C. elegans* have positive correlation as well. Taking together, there is an intrinsic relationship between LC50 of *C. elegans*, LD50 of rat/mouse. LC50 and LT50 are recommended as toxic effect index for further study on acute toxicity test of chemicals using *C. elegans*. *C. elegans* will be a potential valuable in vivo pre-screening toxicity model in the new chemical's predictive toxicity test and assessment prior to the conventional rodent model (partly supported by NSFC Grant in China #81273108, Capital Development Project 2011-1013-03, and Beijing Health Bureau Project-2011. Corresponding author: Guojun J. Li: guojunli88@yahoo.com).

**PS 1445 Predicting Developmental Neurotoxicity in Rodents from Larval Zebrafish—and Vice Versa.**

V. C. Moser, R. C. MacPhail, P. M. Phillips, M. E. Culbreth, K. L. McDaniel, K. A. Jarema and S. Padilla. *TAD & ISTD, NHEERL, US EPA, Research Triangle Park, NC.*

The complexity of standard mammalian developmental neurotoxicity tests limits evaluation of large numbers of chemicals. Less complex, more rapid assays using larval zebrafish are gaining popularity for evaluating the developmental neurotoxicity of chemicals; there remains, however, a pressing need to determine the utility of the model for predicting adverse neurobehavioral outcomes. We are undertaking studies to compare the developmental effects of chemicals in both larval zebrafish and rats. Zebrafish studies show that transitions between light and dark periods can produce robust changes in activity that may be differentially altered by chemicals; an analogous behavior pattern is being studied in rats. Developmental heptachlor in rats increased motor activity in addition to altering righting reflex ontogeny, and impairing learning and memory in adult offspring. In zebrafish, developmental heptachlor produced marked increases in dark-induced activity and dysregulation of the light-dark patterning of activity. Preliminary studies with dimethyl phthalate (DMP) in zebrafish showed reduced habituation only during the dark period, perhaps reflecting changes in anxiety or cognitive behaviors. We evaluated developmental effects of DMP in rats using light-dark transition activity measures in addition to standard neurobehavioral toxicity tests including anxiety. Alterations were observed on several of these endpoints; however, the results were not always dose-related and were confounded by maternal toxicity at high doses. While these results suggest concordance between outcomes of two chemicals from different classes, considerably more comparisons with positive and negative controls are needed to understand the predictability of the larval zebrafish assay. Further exploration of analogous/homologous behavioral tests in both species may be beneficial in evaluating neurotoxic outcomes from developmental exposures, and in assessing the conformity of results.

This is an abstract of a proposed presentation and does not reflect US EPA policy.

**PS 1446 Developmental and Reproductive Toxicity of Fusarium Mycotoxins in the Nematode *Caenorhabditis elegans*.**

Z. Yang<sup>2,1</sup>, L. Tang<sup>1</sup>, G. Qian<sup>1</sup> and J. Wang<sup>1</sup>. *Toxicology and Environmental Research & Consulting, The Dow Chemical Company, Midland, MI.*

Developmental and reproductive toxic effects of some naturally occurring Fusarium mycotoxins were shown in certain animal models. In this study we used the nematode *Caenorhabditis elegans* (*C. elegans*), as an alternative model for mechanistic studies, to investigate the developmental and reproductive toxic effects of T-2 toxin (T-2), zearalenone (ZEN), and deoxynivalenone (DON). *C. elegans* (N2) at 1-day or 3-day old were exposed to various concentrations of these toxins for up to 72 hrs. The development arrested rate (DAR) and the reproduction arrested rate (RAR) were outcomes used to assess the overall effects on the development and reproduction of the exposed *C. elegans*. T-2 has the most potent suppressive effects on the development and growth, concentrations from 0.5- to 8-mg/L caused averaged DAR from 12.01% to 41.6%; exposure to ZEN from 5- to 80-mg/L caused averaged DAR from 11.14% to 35.56%; exposure to DON from 50- to 800-mg/L caused averaged DAR from 12.71% to 32.77%. The concentration ratio for inducing significant DAR (10%) is approximate to 1:10:100 for T-2, ZEN, and DON, respectively. T-2 also has the most potent toxic effect on the reproduction, concentrations from 0.5- to 8-mg/L caused averaged RAR from 28.97% to 72.43% with an EC50 at 3.57-mg/L; exposure to ZEN from 5- to 80-mg/L caused averaged RAR from 26.15% to 90% with an EC50 at 12.02-mg/L; exposure to DON from 50- to 800-mg/L caused averaged RAR from 23.83 to 52.33% with an EC50 at 585.85-mg/L. The concentration ratio for EC50 is approximate to 1:3.4:164.1 for T-2, ZEN, and DON, respectively. These results suggest that T-2 and ZEN have more significant toxic effects than DON on development and reproduction in *C. elegans* and that *C. elegans* is an excellent model, due to its short life cycle and easy genetic manipulation of genes, for studying molecular mechanisms of developmental and reproductive toxic effects caused by food-borne mycotoxins.

**PS 1447 Zebrafish As a Complementary Model in Toxicology.**

A. Menke<sup>2</sup>, A. Wolterbeek<sup>1</sup>, A. Beker<sup>1</sup>, C. Snel<sup>2</sup> and D. de Groot<sup>1</sup>. <sup>1</sup>TNO, Zeist, Netherlands; <sup>2</sup>TNO Triskelion BV, Zeist, Netherlands. Sponsor: R. Woutersen.

Growing awareness to apply the principles of Replacement, Refinement and Reduction (3Rs) of animals in regulatory testing drives the need for alternatives identifying potential toxic agents with accuracy, speed, reliability and respect for animal welfare. So far, for complex endpoints like reproduction and developmental toxicology, animal-free in vitro models are limited and cover only a restricted part of the reproductive cycle. Various characteristics warrant the Zebrafish (embryos and/or larvae) as an ideal non-mammalian whole organism model that could bridge gaps between in vitro cell systems and complex reproduction studies in mammals, e.g. small size, ease of obtaining high number of progeny, external fertilization, transparency and rapid development of embryo, and a basic understanding of its gene function and physiology.

Macroscopical examination of zebrafish embryos/larvae predicted toxicity of chemical and pharmaceutical agents with high certainty and proved to form a reliable total organism approach to study embryo- and developmental (neuro)toxicity. More in depth analysis and interpretation of the locomotor data in the developing zebrafish larvae relative to (nervous system) development increases the use of the zebrafish model in developmental neurotoxicity research. A full histopathological survey of the embryo's combined with high-end analytical methods appeared to further increase the applicability domain of zebrafish into toxicity screening studies. Further refinement with respect to the physical and chemical properties of test compounds that determine the body burden and tissue distribution increases the predictability of the assay. For translation to other toxicity models and man, there is an urgent need to research on responsible toxicity pathways.

This research is supported by the Dutch Ministry of Health, Welfare and Sport and the Dutch Ministry of Social Affairs and Employment.

**PS 1448 Using Yeast Functional Toxicogenomics to Decipher the Toxicity of the Dieldrin Organochlorinated Pesticide.**

B. Gaytan<sup>1</sup>, A. Loguinov<sup>1</sup>, S. Lantz<sup>1</sup>, N. Denslow<sup>2</sup> and C. Vulpe<sup>1</sup>. <sup>1</sup>University of California, Berkeley Berkeley, CA; <sup>2</sup>University of Florida, Gainesville, FL.

Exposure to organochlorinated pesticides (OCPs) has been linked to neurotoxicity, endocrine disruption, and cancer, but the cellular mechanisms of toxicity remain largely unknown. It was hypothesized that a chemical genomics approach using a *Saccharomyces cerevisiae* gene deletion library could help elucidate the cellular mechanisms by which various OCPs induce toxicity. In this study, pools of deletion

strains were exposed in triplicate for five and fifteen generations to the IC20, 50% IC20, and 25% IC20 dieldrin OCP concentrations. The oligo sequences unique to each deletion strain were PCR-amplified and hybridized to TAG4 arrays to identify sensitive, unaffected, and resistant strains. The overrepresented biological terms within the data assisted in the selection of individual deletion strains for confirmation experiments. Analyses indicate that amino acid sensing and components of the pyruvate dehydrogenase complex are critical for cell survival under dieldrin exposure. Exogenous amino acids rescue dieldrin toxicity, while lower concentrations of amino acids in the media exacerbate toxicity. Finally, it was demonstrated that dieldrin inhibits amino acid uptake in yeast cells. Future investigations will examine whether amino acid status is tied to dieldrin toxicity in human cell lines. Additionally, the development of an automated high-throughput system to screen the yeast deletion library for altered growth in various toxicants may be discussed.

**PS 1449 Evaluation of Epigenetic and Developmental Effects in *Danio rerio* Zebrafish Embryos following Diethylstilbestrol, 17 $\beta$ -Estradiol And/or 5-Azacytidine Treatment.**

R. G. Ellis-Hutchings, R. A. Alyea, V. A. Marshall, M. J. LeBaron, R. Sura, N. P. Moore, B. Gollapudi and R. J. Rasoulpour. *Toxicology and Environmental Research & Consulting, The Dow Chemical Company, Midland, MI.*

The fundamental mechanisms that regulate epigenetic modifications as well as embryo development are highly conserved amongst vertebrates. *Danio rerio* (zebrafish) potentially may be used to examine epigenetic alterations during stages of early development. Zebrafish embryos were treated with estrogenic molecules (17 $\beta$ -estradiol (E2) or diethylstilbestrol (DES) (0.001, 0.01, 0.1, 1, 1.5, 2, 2.5, 3, 5, 7, and 10 $\mu$ M) in the presence or absence of a DNA methyltransferase inhibitor 5-azacytidine (5-azaC, 1-100 $\mu$ M) and evaluated daily for lethality. On test day 5, morphological abnormalities were assessed using a quantitative scoring system: somites, notochord, tail, fins, heart, face, brain, arches and jaw. Treatment with 25 $\mu$ M 5-azaC prior to the period of DNA re-methylation (2-cell stage) caused >80% lethality whereas starting treatment shortly after the onset of DNA re-methylation ( $\geq$  16 cell stage) resulted in <10% lethality. Regardless of developmental stage, treatment with 50 and 100 $\mu$ M 5-azaC caused >90% lethality. Treatment with >2 $\mu$ M DES caused significant mortality whereas treatment with 1 or 1.5 $\mu$ M increased the incidence of developmental variations. Treatment with >7 $\mu$ M E2 significantly impacted survival, while 5 $\mu$ M caused a generalized slight increase in developmental abnormalities; however, 1, 1.5, 2, 2.5 and 3 $\mu$ M E2 caused slight developmental effects on the heart, face and brain. Overall, E2 had a wide developmental dose response curve while DES caused significant mortality within a narrow region. Morphological characterization of embryos and larvae following exposure to these compounds indicated that within the chosen dose response range, clear apical end point no-observed-adverse-effect levels (NO(A)ELs) and lowest-observed-adverse-effect levels (LO(A)ELs) can be determined thereby providing a useful model to establish associations between apical and epigenetic end points.

**PS 1450 A High-Throughput Mechanism-Based Toxicity Screen Using *C. elegans*.**

R. B. Goldsmith<sup>2</sup>, J. R. Pirone<sup>3</sup>, W. A. Boyd<sup>2</sup>, M. V. Smith<sup>3</sup> and J. H. Freedman<sup>1</sup>. <sup>1</sup>NIH, Research Triangle Park, NC; <sup>2</sup>NTP, NIEHS, Research Triangle Park, NC; <sup>3</sup>SRA International, Durham, NC.

To quantitatively assess the effects of chemical exposures on transcription, an automated high-throughput *in vivo* toxicity assay was developed to measure changes in the levels and cell-specificity of specific gene expression in *C. elegans*. Transcriptional responses were measured in individual strains of transgenic *C. elegans* that express fluorescent proteins under the control of archetypal stress-inducible genes: *ced-3*, *cyp-35A2*, *gcs-1*, *gst-38*, *gst-4*, *hsp-16.2*, *hsp-16.41*, *hsp-17*, *hsp-4*, *hsp-6*, *hsp-60*, *mtl-2*, *ugt-1* and *ugt-13*. As part of assay development, transgenic nematodes with large dynamic ranges (i.e., low constitutive levels of expression) and sensitivity (high response at low concentrations) were identified following exposure to juglone, an oxidative stressor; N-methyl-N'-nitro-N-nitrosoguanidine, a DNA damaging agent; cadmium, a heavy metal; chlorpyrifos, an organophosphate neurotoxin; tunicamycin, an endoplasmic reticulum stressor; and heat shock, a protein denaturant. Concomitant with chemical exposure, fluorescence data were measured from images acquired using a high content imager and subsequently analyzed using CellProfiler's WormToolbox, a high-throughput imaging analysis program designed for use with nematodes. For some of the stress-inducible genes high levels of constitutive expression limited their dynamic range and utility in this assay. As expected, not all of the chemicals affected all of the genes; however, the chemicals generally affected the stress-inducible genes that corresponded to their known mechanisms of action. For example, nematodes containing the *hsp-4* transgene, which responds to endoplasmic reticulum stress, showed increased fluorescence after tunicamycin treatment. In addition, strong correlations were observed between chemical concentration and fluorescent signal. The results obtained using the

transgenic *C. elegans* were verified by measuring changes in the cognate steady-state mRNA levels by qRT-PCR. These results show that this assay can be used to assess the effect of toxicants on gene expression *in vivo*.

**PS 1451 The Effects of Microcystin-LR on the Chemotaxis Indexes of *Caenorhabditis elegans***

C. Moore and B. Puschner. *Molecular Biosciences, University of California Davis School of Veterinary Medicine, Davis, CA.*

The blue green algae toxins microcystins (MCs) are known ubiquitous hepatotoxins found in fresh and marine waters. The World Health Organization has established a drinking water guideline of 1  $\mu$ g/L total MCs based on MC-LR liver toxicity data after oral exposure. MCs inhibit serine/threonine protein phosphatases (PP1 and 2A), a mechanism extensively studied in the liver; yet the effects of MCs on the nervous system are poorly understood. To study MCs' effects on the nervous system, a 24-hour exposure assay using the neurotoxicity model *Caenorhabditis elegans* (*C. elegans*) was established. *C. elegans* have remarkable genetic and neurobiochemical conservation with humans, and with all 302 neurons extensively studied, key sensory neurons have been linked to specific behaviors. It is well known the AWA and AWC sensory neurons detect diacetyl and benzaldehyde, respectively, and sensory neuron function can be quantified using a chemotaxis index (CI). Wildtype (N2) adult nematodes were exposed for 24 hours to 0, 1, 10, 40, 80, 160 and 320  $\mu$ g/L MC-LR before determining CIs. No significant changes in CIs for benzaldehyde were observed. At MC-LR concentrations of 40  $\mu$ g/L and above, CIs for diacetyl decreased significantly. The unchanged CIs for benzaldehyde suggest that AWC is not affected. The decreased CIs for diacetyl suggest that AWA is targeted by MC-LR. PP2A inhibitor okadaic acid and PP1 inhibitor autamycin were used in the same 24-hour exposure model to evaluate whether PP1 or PP2A inhibition result in changes in AWA function. Results of CI indexes suggest that the AWA chemosensory neuron is affected by MC-LR resulting in neurotoxicity.

**PS 1452 Quantitative Assessment of Phase II ToxCast™ Chemical Toxicity in *C. elegans*.**

W. A. Boyd<sup>1</sup>, M. V. Smith<sup>2</sup>, J. R. Pirone<sup>2</sup>, J. R. Rice<sup>1</sup> and J. H. Freedman<sup>1,3</sup>. <sup>1</sup>DNTP, NIEHS, NTP, Research Triangle Park, NC; <sup>2</sup>SRA International, Research Triangle Park, NC; <sup>3</sup>LTP, NIEHS, NIH, Research Triangle Park, NC.

The Tox21 community is working to prioritize thousands of chemicals for further toxicity testing and to develop prediction models for human toxicity. To integrate the large amounts of high throughput *in vitro* and *in vivo* toxicity and develop these models, better quantitative methods are necessary. To develop quantitative assessments of *in vivo* toxicity data, the U.S. EPA's ToxCast Phase II library, which contains 676 unique chemicals including failed drugs, food additives and industrial products, was screened using the *C. elegans* growth assay. This assay uses the COPAS Biosort to measure size changes in individual nematodes after 48-h exposures. Over the seven concentrations tested (0.5-200  $\mu$ M), >50% of the chemicals caused a decrease in growth. To rank their toxicity in *C. elegans*, a concentration-response curve for each chemical was described using isotonic regression and the statistical significance of the curve assessed. For significant concentration-response curves, the fitted isotonic regression model calculated three parameters that characterized the efficacy and potency of each chemical: 1) change in response between control and highest concentration (R); 2) concentration of chemical at which half of R is reached (ECR50); and 3) slope of the curve at the ECR50. Chemicals were also ranked by computing a toxicity score, which is a weighted sum of the change in response at each dose relative to the control. The top 5% most active compounds included several organic pollutants (e.g., DDT, PFOS), which have been banned from use due to their toxicity and bioaccumulation. Excellent reproducibility was observed for eight chemicals replicated in the library: seven were active and one was inactive for all replicates. The application of this new method for the quantitative assessment of chemical toxicity in *C. elegans* could be applied to other *in vitro* and *in vivo* toxicity screens, thus allowing for better comparisons among various assays, and the development of predictive models of toxicity.

**PS 1453 Triazole-Induced Gene Expression Changes in the Zebrafish Embryo.**

S. A. Hermesen<sup>1,2</sup>, T. E. Pronk<sup>1</sup>, E. van den Brandhof<sup>1</sup>, L. T. van der Ven<sup>1</sup> and A. H. Piersma<sup>1,3</sup>. <sup>1</sup>Health Protection, RIVM, Bilthoven, Netherlands; <sup>2</sup>Toxicogenomics, University, Maastricht, Netherlands; <sup>3</sup>IRAS, University, Utrecht, Netherlands. Sponsor: H. van Loveren.

The zebrafish embryo is a promising alternative test for developmental toxicity. The classical read-out is via morphological assessment. Microarray analyses may increase sensitivity and predictability of the test by detecting more subtle and mechanistic

responses. We have shown earlier that with transcriptomics data we could discriminate between two chemical classes, glycol ethers and triazoles, in a concentration-response design. It is time-consuming and expensive to perform concentration-response analysis for many compounds. Thus, we studied the possibility of relating gene expression profiles of structurally related chemicals tested in a single concentration, to a complete transcriptomic concentration-response of the triazole antifungal flusilazole (FLU). We tested five other triazoles, hexaconazole (HEX), cyproconazole (CYP), triadimefon (TDF), myclobutanil (MYC), and triticonazole (TTC) at equipotent concentrations based on morphological evaluation. Results showed that compounds differed in their regulation of major anti-fungal and developmental toxicity pathways, steroid biosynthesis and retinol metabolism, respectively. Assuming that the ratio between these pathways is relevant for efficacy compared to developmental toxicity, we found TTC was more efficacious and CYP was more toxic compared to the other triazoles. MYC showed a different response similar to the high toxic concentrations of FLU. We here demonstrated that gene expression data allow more comprehensive assessment of compound effects by discriminating relative potencies using these specific gene sets. The zebrafish embryo model can therefore provide information on relative pathway sensitivity related to intended mechanism of action and toxicological activity of compounds.

**PS 1454 Early-Life Exposure to Methylmercury and Multiple Stressors: *Daphnia pulex* As an Alternative Model System to Evaluate Long-Term Effects.**

D. Doke and J. M. Gohlke. *Environmental Health Sciences, University of Alabama at Birmingham, Birmingham, AL.*

While human populations are exposed simultaneously to chemical stressors and physical factors including temperature and differing nutrition, safe limits of exposure are based primarily on tests using single chemicals. Due to the high cost and time required to test mixtures in traditional animal models, development of novel model systems are of critical importance. We are currently evaluating *Daphnia pulex*, a standardized USEPA and OECD ecotoxicology model system and an NIH model organism for biomedical research, as a tool for assessing long-term effects of early life exposures to multiple stressors. As a case study, we are examining the interaction between MeHg exposure and varying temperature regimes and nutrition. We hypothesize that: Early life exposures in high temperature or a low food regime will increase MeHg toxicity as measured by reproduction and lifespan in *Daphnia pulex*. *D. pulex* were exposed to a matrix of three temperature regimes emulating standard laboratory conditions versus natural environment daily fluctuations, three feed rates and five concentrations (200ng/l to 1000ng/l) of MeHg as methylmercury (II) chloride. Data evaluating lifespan and fecundity across the temperature regimes suggest that although there are no significant differences in time to first reproduction, *D. pulex* lifespan and fecundity were increased in daily fluctuating versus constant temperature regimes. This indicates that subtle differences in lifespan can be detected across standard laboratory thermal conditions and those that would be experienced in a natural environment. Subsequent work will evaluate interactions. Since current alternative model systems are not designed to evaluate long-term effects of early life exposures, our research is designed to evaluate the utility of *D. pulex* as a complementary model system.

**PS 1455 A Rapid Chemical Screening Platform in *C. elegans* for Assessing Environmental Germline Disruption.**

P. Allard<sup>1</sup>, N. Kleinstreuer<sup>3</sup>, T. B. Knudsen<sup>3</sup> and M. Colaiacovo<sup>2</sup>. <sup>1</sup>*Environmental Health Sciences, UCLA, Los Angeles, CA;* <sup>2</sup>*Genetics, Harvard Medical School, Boston, MA;* <sup>3</sup>*NCCT, US EPA, Research Triangle Park, NC.*

Despite the developmental impact of errors in chromosome segregation, we lack the tools to comprehensively assess environmental effects on meiotic integrity in animals. Here, we report the development of an assay in *C. elegans* that fluorescently marks aneuploid embryos following chemical exposure. We qualified the predictivity of the assay against chemotherapeutic agents as reference compounds, as well as environmental compounds with comprehensive mammalian in vivo endpoint data. The assay was highly predictive of mammalian reproductive toxicities with a maximum specificity of 78%. Finally, we validated selected compounds from the screen by analyzing germline maintenance following exposure. With this novel approach, we provide the first high-throughput screening strategy for the assessment of environmental effects on the germline.

**PS 1456 Cytotoxic Effects of Methyl-Mercury in Whole Worms and Pan-Neuronal GFP-Expressing Embryonic Cultures of *Caenorhabditis elegans*.**

K. Breithaupt<sup>1</sup>, R. K. Hajela<sup>1,2</sup> and W. D. Atchison<sup>1,2</sup>. <sup>1</sup>*Neuroscience Program, Michigan State University, East Lansing, MI;* <sup>2</sup>*Pharm/Tox, Michigan State University, East Lansing, MI.*

*Caenorhabditis elegans* (*C. elegans*) strain KC136 was used to study whole worm viability in response to methylmercury (MeHg) toxicity in a semifluid gellan gum medium. Stage L3 KC136 whole worm viability is reduced by exposure to 0.5-25  $\mu$ M MeHg ( $p=0.0001$ ) for 24-48 hrs. At the highest [MeHg] tested, cytotoxicity was 54% and time of exposure (24 and 48 hrs) did not have an effect ( $p=0.15$ ). *C. elegans* strain NW1229, which expresses pan-neuronal Green Fluorescent Protein (GFP), was used to prepare primary cell cultures from eggs to test the ability of the nemadipine-A to reduce the cytotoxicity of MeHg in worm neurons. Nematodipine-A is a novel dihydropyridine (DHP) L-type voltage gated  $Ca^{2+}$  channel antagonist and we hypothesize it has a similar effect as we have previously reported for the non-DHP-type antagonist verapamil. At [MeHg] of 0.4-1.2  $\mu$ M, cytotoxicity in neurons was both concentration and time dependent as determined by ethidium homodimer viability assay. Thus the results obtained in whole worms differ somewhat from those of isolated neurons relative to time-dependence of cytotoxicity. As previously reported, verapamil reduced MeHg-induced cytotoxicity by ~10% at 1 hr of exposure, however, lost its protective effect at 3 hrs ( $p=0.08$ ). Similarly, nemadipine-A (0.25-1  $\mu$ M) protected neurons against MeHg toxicity at 1 hr ( $p=0.033$ ), but not 3 hrs of exposure. The reduction of MeHg-induced cytotoxicity by L-type  $Ca^{2+}$  channel antagonists at early stages of exposure suggests that L-type  $Ca^{2+}$  channels contribute to MeHg mediated neuronal cell death in *C. elegans*, just as they do in mammalian neurons. The lack of correlation between time and exposure to MeHg may result from upregulation of genes for proteins involved in metal detoxification. Using *C. elegans* neuronal cultures as a model system for MeHg neurotoxicity may help uncover why certain neurons are more susceptible to MeHg-induced cell death furthering our understanding of the underlying mechanisms.

**PS 1457 MTBE Disrupts HIF1-Vegf Regulated Angiogenesis in Zebrafish (*Danio rerio*).**

J. A. Bonventre<sup>1,2</sup>, T. S. Kung<sup>2</sup>, L. A. White<sup>2</sup> and K. R. Cooper<sup>2</sup>. <sup>1</sup>*EMT, Oregon State University, Corvallis, OR;* <sup>2</sup>*JGPT, Rutgers University, New Brunswick, NJ.*

Understanding the sensitivity of developing vascular networks to toxic insult is important to advancing vascular biology. Methyl tert-butyl ether (MTBE) induces vascular lesions in the zebrafish embryo, including pooled blood in the common cardinal vein (CCV), cranial hemorrhages (CH), and abnormal intersegmental vessels (ISV). The transcript levels of two isoforms of vascular endothelial growth factor, *vegfa* and *vegfb*, as well as a primary receptor, *vegfr2*, are significantly decreased during the critical period (6-somites to Prim-5). The vascular lesions were hypothesized to be a result of the MTBE-induced down-regulation of *vegfa*. An over-expression study was conducted to rescue MTBE-induced vascular lesions. Over-expression of zebrafish *vegfa* resulted in 46% fewer animals exhibiting MTBE-induced CH and 35% fewer embryos exhibiting abnormal ISV, while no rescue was observed for the CCV lesion. Global gene expression changes during the critical period, assayed with the Affymetrix GeneChip® and analyzed with Ingenuity Pathway Analysis®, identified the cardiovascular system as a primary pathway altered by MTBE exposure, as well as other pathways associated with hypoxia inducible factors (HIFs). Two further rescue studies were designed to block HIF1 $\alpha$  degradation to test the hypothesis that MTBE toxicity was HIF1 $\alpha$ -dependent. Chemical inhibition of HIF1 $\alpha$  degradation, by blocking prolyl-4-hydroxylase activity with N-oxalylglycine, rescued both the CCV lesion (24%) and CH (32%). Knockdown of a ubiquitin ligase component, von Hippel-Lindau protein, with an anti-sense morpholino rescued only the CCV lesion (35%). Rescue of MTBE-induced vascular lesions by over-expression of *vegfa* and inhibition of HIF degradation demonstrated that MTBE toxicity is mediated by a down-regulation of HIF driven Vegf at a critical period during the developing cardiovascular system. Chemicals with anti-angiogenic properties, such as MTBE, can be used to advance the science of angiogenesis in both a disease state and during development. Funding: ES07148, ES05022

**PS 1458 An In Vitro Placental Model Using BeWo Cells for the Prediction of Placental Transfer of Compounds.**

H. Li<sup>1</sup>, B. van Ravenzwaay<sup>1,2</sup>, I. Rietjens<sup>1</sup> and J. Louisse<sup>1</sup>. <sup>1</sup>*Division of Toxicology, Wageningen University, Wageningen, Netherlands;* <sup>2</sup>*Experimental Toxicology and Ecology, BASF SE, Ludwigshafen, Germany.*

The use of reverse dosimetry for in vitro-in vivo extrapolation (IVIVE) enhances the use of in vitro toxicity data for risk assessment (Louisse et al., 2010). With reverse dosimetry, in vitro toxic effect concentrations are translated to in vivo doses using physiologically based kinetic (PBK) modelling. For the PBK models needed for reverse dosimetry, parameter values for kinetic processes need to be obtained, such as for intestinal absorption, metabolism and placental transfer. The present study aims to assess whether an in vitro model for the placental barrier, consisting of human placental BeWo cells, could be used to predict the placental transfer kinetics of compounds. To this end, BeWo cells were grown on transwell inserts to form a confluent monolayer, thereby separating an apical maternal compartment from a basolateral fetal compartment. For a set of 9 compounds the transport velocity from the apical to the basolateral compartment was determined in this model. Relative transport rates obtained in this model were compared with the relative transport rates of these compounds calculated from data of ex vivo human placental perfusion studies reported in the literature (Hewitt et al., 2007). The relative transport rates in the BeWo model were in good correlation ( $R^2=0.95$ ) with the relative transport rates calculated for the ex vivo model (Li et al., submitted). This indicates that the BeWo model can be useful in the prediction of the transplacental transfer of compounds and for obtaining model parameter values for PBK that can be used for reverse dosimetry.

**PS 1459 Controlled Hemodynamics and Transport in Primary Hepatocytes Shift Induction and Toxic Responses to Drugs Closer to In Vivo Concentrations.**

A. Dash, T. Deering, J. Thomas, B. R. Blackman and B. R. Wamhoff. *Liver Surrogate Systems, Ajit Dash, Charlottesville, VA.*

Preclinical in vitro drug screening systems exhibit efficacy and toxicity responses to concentrations very different from corresponding clinical or in vivo plasma C<sub>max</sub> levels, contributing to poor in vitro-in vivo correlations. We established a primary hepatocyte system using controlled hemodynamics and transport that retains polarized morphology and metabolic function more stably than traditional static cultures. We tested the hypothesis that restoring these critical parameters could achieve in vitro hepatocyte drug response at concentrations closer to in vivo levels. Fresh rat hepatocytes were cultured under controlled hemodynamics alongside static controls for 5 days before treating with various concentrations of test drugs (dexamethasone, acetaminophen, chlorpromazine) for 2 days. Cytotoxic response was evaluated by MTT and ATP assays and cytochrome p450 activity by standard kits. Under controlled hemodynamics, dexamethasone was significantly more toxic to primary hepatocytes at concentrations used for induction studies in static cultures ( $93.31 \pm 5.26\%$  vs.  $32.8 \pm 9.5\%$  at  $50 \mu\text{M}$ ,  $p < 0.01$ ). Induction responses of Cyp3A activity equivalent to  $50 \mu\text{M}$  of dexamethasone in static cultures were seen at  $2.5 \mu\text{M}$  under controlled hemodynamics. Cytotoxic dose response curves of acetaminophen demonstrated a leftward shift with IC<sub>50</sub> values at  $10 \mu\text{M}$  in devices compared to  $30 \mu\text{M}$  in static cultures. A similar shift in cytotoxic response was seen with chlorpromazine with induction of Cyp1A activity in a dose dependent manner at sub lethal concentrations. We demonstrate that control of transport and hemodynamics in a primary hepatocyte system results in induction and toxicity responses to drugs at concentrations significantly lower than static systems and closer to in vivo levels. The retention of in vivo-like hepatocyte phenotype and metabolic function coupled with drug response at more physiological concentrations emphasizes the importance of restoring in vivo physiological transport parameters in vitro.

**PS 1460 Validation of In Vitro Systems to Explore Mechanisms of Striated Muscle Toxicity.**

W. Dott<sup>1</sup>, J. Wright<sup>2</sup>, P. Mistry<sup>2</sup> and K. Herbert<sup>1</sup>. <sup>1</sup>*Cardiovascular Sciences, University of Leicester, Leicester, United Kingdom;* <sup>2</sup>*Product Safety, Syngenta, Bracknell, United Kingdom.* Sponsor: P. Botham.

The validation of in vitro cardiac and skeletal muscle models of toxicity may find a utility in predicting toxicity early within the research and development process. The primary aim of this project was to investigate the extent of translation from an in vivo to an in vitro, system, using a toxicogenomics approach. Female Han Wistar rats were dosed daily via the diet with sulfonyl isoxazoline (SI) chemistries for 4 or 28 days. Histopathological evaluation revealed a dose-dependent myositis and myodegeneration in striated muscle. Gene expression profiling of cardiac and skeletal

muscle tissues taken from sub-toxic doses identified a number of perturbed cellular pathways including: mitochondrial dysfunction, altered energy metabolism, oxidative stress, cell cycle and apoptosis. This data provided a plausible hypothesis which suggested mitochondrial toxicity as a principle mechanism of SI-induced striated muscle toxicity. To investigate the translation of this toxicity to an appropriate in vitro system cardiac (H9c2) and skeletal muscle (L6) cell lines were selected. A cell based assay was developed in which the cardiac and skeletal muscle cells were adapted to use mitochondrial oxidative phosphorylation rather than glycolysis. This system identified the SI compounds as mitochondrial toxicants. In addition there was a significant increase in mitochondrial reactive oxygen species, which provided further evidence of mitochondrial perturbation. SI treatment also induced cellular hypertrophy, accompanied by cell cycle arrest, and subsequent caspase-mediated apoptosis. These in vitro results were consistent with the transcriptomics data, providing further validation that the cell systems models may have utility for predicting striated muscle toxicity. Future work will be aimed at exploring tissue-specific toxicity using higher tier in vitro models (liver, muscle bioreactor flow through systems) which might better represent the in vivo system.

**PS 1461 3D Liver Models for Investigating Drug-Induced Hepatotoxicity.**

E. Jain<sup>1</sup>, M. Ehrlich<sup>2</sup>, T. Murali<sup>3</sup> and P. Rajagopalan<sup>1</sup>. <sup>1</sup>*Department of Chemical Engineering, Virginia Tech, Blacksburg, VA;* <sup>2</sup>*Virginia-Maryland College of Veterinary Medicine, Blacksburg, VA;* <sup>3</sup>*Department of Computer Science, Virginia Tech, Blacksburg, VA.*

Testing the toxic effects of chemicals has traditionally relied on large-scale animal studies. In addition to being extremely expensive, this strategy has come under scrutiny for its over-reliance on laboratory animals, and the need to extrapolate results from animals to humans. In vitro tissue mimics are a promising avenue for studying the effects of toxicants. Such systems can serve as reliable models of in vivo structures and can be systematically probed with a wide range of cues. Since they are engineered, experimentation on these mimics is considerably less complex than those needed to probe tissues and organisms in vivo. We have designed a novel 3D organotypic liver model assembled with three cell types (hepatocytes, liver sinusoidal endothelial cells and Kupffer cells) and a polyelectrolyte multilayer (PEM) that mimics the Space of Disse. We have established a dose range ( $20\text{--}40\text{mM}$ ) for acetaminophen in 3D liver models that is non-lethal yet is capable of perturbing hepatic function. When acetaminophen was administered 4 days after hepatocytes were obtained from rat livers, conventional monolayer, collagen sandwich and 3D liver model cultures showed a small decrease in cell viability. When the drug was administered at day 12, only the 3D liver models showed a decrease in viability. All cultures exhibited a decrease in albumin production and urea secretion. The 3D liver models exhibited better urea secretion than monolayer and collagen sandwich cultures. Intracellular glutathione levels were measured for all three cultures. 3D liver models exhibited approximately 40% decrease in glutathione in comparison to monolayer and collagen sandwich cultures that exhibited greater than 60% decrease. These trends suggest that the inclusion of non-parenchymal cells in the 3D liver model may impart cytoprotective effects and present an in vivo like environment.

**PS 1462 In Vitro Cell Models: Moving from Tumor Cell 'Monsters' to Differentiating Immortalized- or Stem Cells.**

D. Gerhold, D. Kuo, Z. Tong, J. Braisted, M. Xia, A. Simeonov and C. P. Austin. *Tox21 Consortium, NIH-National Center for Advancing Translational Sciences (NCATS), Rockville, MD.*

The Tox21 Consortium aims to develop in vitro quantitative High Throughput Screening (qHTS) using human cells and targets to replace animal testing. In screening for cytotoxicity, primary human cells make useful models, but results from primary cells are irreproducible and the cells are problematic to obtain. At the other extreme, transformed cell lines are readily available and reproducible, but are often poor representations of normal human tissues. Between these extremes, immortalized cells or differentiated stem cells provide reliable phenotypic models for neurons, kidney proximal tubule epithelial cells or podocytes, cardiomyocytes, vascular endothelial cells, and hepatocytes. We are evaluating cell models for these cell types by evaluating susceptibilities to toxicants that are organ-selective in vivo. Efforts are also underway to adapt such cells that require differentiation to qHTS in 1536-well plate format. Gene expression profiling is being leveraged to dissect the modes of cytotoxicity, and to determine why in vitro models succeed for some compounds and fail for others. We will present the evaluation of several such toxicological models vis-à-vis: differentiated phenotypes, cytotoxicity assays, and gene expression profiling.

**PS 1463 Potential Cholestatic Compounds Assessed by Membrane Transport Vesicle Assays As Well As Bile Canaliculi Inhibition in Primary Hepatocytes in Both Human and Rat.**

L. Qiu<sup>1</sup>, M. Taimi<sup>2</sup>, C. Strock<sup>2</sup>, J. Gilbert<sup>2</sup> and Y. Will<sup>1</sup>. <sup>1</sup>Compound Safety Prediction, Pfizer Global Research & Development, Groton, CT; <sup>2</sup>Apredica, Watertown, MA.

BSEP (Bile Salt Export Pump) inhibition has been proposed as a mechanism for drug-induced cholestasis, a subtype of drug induced liver injury (DILI). Screening systems for BSEP inhibition have been established in membrane vesicles from Sf9 insect cells over-expressing rat or human BSEP transporter. However, as any cell-free assay, the data from vesicle assays might not reflect true BSEP inhibition profile due to lack of biotransformation and metabolism. In addition, the contribution of MRP2 (Multidrug resistance-associated protein 2) to drug induced liver cholestasis also needs to be considered.

In this study, we examined 18 potential cholestatic compounds, which were either known to be BSEP inhibitors, dual inhibitors for BSEP and MRP2 or glutathione depleters, in both human and rat BSEP and MRP2 vesicle assays. Moreover, a high-content imaging assay using fluorescent selective substrates for BSEP and MRP-2 transporters including CMFDA and CLF, was used to examine these compounds in inhibition of bile canaliculi excretion in both human and rat sandwich-cultured hepatocytes. In addition, CMFDA and CLF were characterized for their ability as uptake substrates for BSEP and MRP2 transporters.

We found that both, CMFDA and CLF were not selective for BSEP transport since they were also potent MRP2 substrates. Vesicle and hepatocyte canaliculi inhibition data showed no substantial species difference between human and rat, for either transporter.

Furthermore the vesicle data correlated well with the hepatocyte canaliculi data. However, for a few compounds the vesicle data did not translate into hepatocyte canaliculi data probably due to impact of cell-based effects such as metabolism or permeability.

In conclusion, to better predict drug-induced cholestasis, a larger set of compounds with known clinical DILI outcomes need to be tested in both vesicle and hepatocyte canaliculi assays in order to elucidate the mechanisms involved in liver toxicity.

**PS 1464 Development of Alternative *In Vitro* Methods to Screen for Pulmonary Toxicities—Characterization of Epithelial-Macrophage Coculture and *In Vitro* Assay Conditions at the Air-Liquid Interface (ALI).**

S. P. Ng and D. B. Warheit. DuPont Haskell Global Centers for Health & Environmental Sciences, Newark, DE.

The successful development of *in vitro* assays with cultured pulmonary cells and aerosols is instrumental for creating toxicity/screening tests for use during product development. To optimize for future *in vitro* aerosol exposures using the Nano-Aerosol Chamber for In Vitro Toxicology system, rat lung epithelial L2 cells and NR8383 macrophages (MØ) were co-cultured on an ALI system and cell metabolism (XTT), cytotoxicity (LDH), and cytokine (IL-6) release assays were developed as endpoints to assess cell toxic effects following particle exposures. Co-cultures were exposed to 0-80 µg/cm<sup>2</sup> ZnO fine particles in supplemented growth medium for 2 hrs followed by 24-hr maintenance of cultures at ALI. Results showed that both XTT and LDH assays performed with cells co-cultured at the ALI were able to detect toxicity in a dose-response manner. Cytotoxic effects measured following 20 µg/cm<sup>2</sup> ZnO particle exposures (i.e., -LC<sub>50</sub>) increased with epithelial cell:MØ (L2:NR8383) ratios, revealing that the seeding ratio strongly affects the assay sensitivity. In a separate study, optimization for cytokine release assay performed with different cell seeding densities and L2:NR8383 ratios showed the highest IL-6 release (~2.5 ng/mL) from cultures seeded at 0.5E5/cm<sup>2</sup> in a 2:1 ratio and maintained at ALI for 1 day. Maximum stimulation of IL-6 release was detected from the optimized cultures 4- and 24-hr post-exposure to low dose (2.5 µg/cm<sup>2</sup>) ZnO (200-300% of medium-exposed controls); IL-6 release was suppressed to 0-50% of controls after relatively high-dose ZnO (>10 µg/cm<sup>2</sup>) exposures. In conclusion, these studies are useful in characterizing and optimizing the co-culture and *in vitro* assay conditions with ALI which could better simulate *in vivo* exposure of lung cells to inhaled materials (when compared to a submerged exposure system) and ultimately should facilitate the development of reliable *in vitro* cell exposure systems and cell-based lung toxicity/screening tests.

**PS 1465 Predicting Heart-Specific Toxicity Using Two Cell Models: Human iPS-Derived Cardiomyocytes and Human Liver Cells (HepaRG).**

P. C. Wilga, D. Keller, B. Franz and J. M. McKim. CeeTox, Inc., Kalamazoo, MI.

A major reason for the failure of new drugs is due to adverse effects in the cardiovascular system. An *in vitro* model capable of identifying heart-specific liabilities would be of considerable value. To differentiate heart toxicity from liver toxicity, a dual cell model was developed that utilizes changes in cell health and function following exposure to a test drug. Human cardiomyocytes and normal human liver cells were used as the test system. Cardiomyocytes were derived from induced pluripotent stem cells (iPS) obtained from Cellular Dynamics International. Terminally differentiated bi-potent HepaRG cells were from Life Technologies. Each cell type was established in a 96-well format and prepared in triplicate wells for each concentration. Markers of cell health (ATP, LDH leakage, and GSH) were monitored in both cell types. Additional information was collected for beat rate (BR) in heart cells and endpoints were monitored over concentration and time. The concentration-response curves were compared using mean IC<sub>50</sub> values. Beat rate (BR) was measured using the xCelligence RTCA Cardio system (ACEA). To test the model, hepatotoxic (camptothecin (CAMP), rotenone (ROT)) or cardiotoxic (doxorubicin (DOX), mitoxantrone (MTX)) compounds were used. These were added to cells at concentrations of 0, 0.1, 1, 10, and 100 µM and exposed for 24 hr. In addition, drugs known to produce QT prolongation (Terfenadine (T) and verapamil (V)) were included and the BR determined. T and V significantly reduced BR at a concentration of 0.3 µM. To determine heart (H) or liver (L) specificity, average IC<sub>50</sub> values were obtained for each cell type and the H-to-L ratio calculated. H-to-L ratios were MTX = 0.5, DOX = 2.6, ROT = 0.02 and CAMP undetermined. Ratios < 1.0 indicate cardiotoxicity, those >1.0 but < 3 indicate toxicity in both models, while ratios >3 indicate hepatotoxicity. BR data was used to improve these predictions. The combined data provided better resolution and enabled cardiac toxicity to be determined with greater confidence.

**PS 1466 Predicting Respiratory Sensitization Using Activation of Nrf2/ARE Genes in a Human Reconstructed Airway Model.**

J. A. Willoughby, D. Keller, P. C. Wilga and J. M. McKim. CeeTox, Inc., Kalamazoo, MI.

Current *in vitro* methods for determining sensitization have focused on skin sensitization and provide data on hazard, but are unable to predict potency. The aim of this study was to determine if a new method known as SenCeeTox®, originally developed to detect skin sensitizers, could also identify respiratory sensitizers and provide potency. The EpiAirway™ model from MatTek Corp. was used as the test system. Viability, test article reactivity, and the expression of genes controlled by Nrf2/ARE (NADPH Quinone oxidoreductase (NQO), aldoketoreductase (AKR), interleukin-8 (IL8), aldehyde dehydrogenase (ADH), heme oxygenase-1 (HMOX1), and glutamate cysteine-ligase catalytic subunit C (GCLC)) were monitored. CYP1A1 was monitored to identify proallergens. Test solutions of p-benzoquinone (BQ), benzoic acid (BA), glycerol (Gly), cinnamic aldehyde (CA), toluene diisocyanate (TDIC), and oxazolone (OX) were prepared in DMSO. Each test agent was evaluated in a glutathione depletion assay (GSH) and then applied apically to the tissue at concentrations of 0, 100, 250, 500, and 2500 µM. Following 24 hr incubation, total RNA was isolated and changes in gene expression determined by qRT-PCR. Tissue viability was monitored by MTT. BQ reduced viability to 73% at 2500 µM, depleted GSH by 70% and induced NQO, AKR, CYP1A, ADH, HMOX1 and GCLC. Oxazolone reduced viability to 56% at 2500 µM, depleted GSH by 92% and induced GCLC. TDIC had no effect on viability, depleted GSH by 26% and induced GCLC. CA had no effect on viability, depleted GSH by 22% and induced GCLC. Glycerol and benzoic acid had no effect on viability or GSH depletion, but did produce a positive response on GCLC. These data provided a rank order of potency from highest to lowest of BQ > OX > TDIC > CA >> BA and Glycerol. This ranking is consistent with reported sensitization potency categories for these chemicals. In conclusion, Nrf2/ARE signaling pathways are intact in the EpiAirway™ tissue and that this model may provide a means of accurately identifying respiratory sensitizers.

**PS 1467 Measurement of Phagocytic Activity in Rats with the Phagotest® Kit.**

J. Legrand<sup>1</sup>, C. Mimouni<sup>1</sup>, M. Valin<sup>1</sup>, N. Pearson<sup>1</sup>, R. Forster<sup>1</sup> and J. Descotes<sup>2</sup>. <sup>1</sup>CiToxLAB, Evreux, France; <sup>2</sup>Poison Center, Lyon, France.

Very few tools are available to assess phagocytosis, a major functional component of the innate immune system, during nonclinical immunotoxicity studies. The objective of the present study was to evaluate the feasibility of the Phagotest® in rats.

Phagotest® (Glycotope Biotechnology, Berlin, Germany) is routinely used in clinical immunology laboratories to assess phagocytosis in humans. It allows the quantitative determination of leukocyte phagocytosis by measuring the percentage of phagocytes that have ingested bacteria and the number of ingested bacteria per cell. In the present study, 2 ml samples taken from 6 male and 6 female Sprague-Dawley rats onto heparin lithium tubes were incubated with FITC-labeled *E. coli* bacteria at +37°C. Thereafter, phagocytosis was stopped by placing the samples on ice and adding a quenching solution. After washing and erythrocyte lysis, a DNA staining solution was added prior to flow cytometry analysis using a XL MCL flow cytometer with the Expo 32 ADC software (Beckman Coulter, France). The percentage of phagocytizing cells (granulocytes and monocytes, differentiated by side scatter and forward scatter) and their mean fluorescence intensity (number of ingested bacteria) were determined in four independent runs. The mean  $\pm$  SD of the percentage of phagocytizing granulocytes was found to be  $84.4 \pm 5.0$  for males and  $86.2 \pm 11.02$  for females, and the mean  $\pm$  SD of the percentage of phagocytizing monocytes,  $51.6 \pm 8.3$  for males and  $55.5 \pm 11.7$  for females. Intra-individual precision (CV%) was between 10.4% and 13.6% for males, and between 18.1% and 24.2% for females. These results demonstrate that the Phagotest® kit can be used to assess phagocytosis in rats as it is in humans.

### PS 1468 Thirdhand Smoke: Extraction and Cytotoxicity.

V. Bahl<sup>1,2</sup>, P. Jacob<sup>3</sup>, C. Havel<sup>3</sup>, S. Schick<sup>3</sup>, T. Mao<sup>3</sup> and P. Talbot<sup>1</sup>. <sup>1</sup>Department of Cell Biology and Neuroscience, University of California Riverside, Riverside, CA; <sup>2</sup>Environmental Toxicology Graduate Program, University of California Riverside, Riverside, CA; <sup>3</sup>University of California San Francisco, San Francisco, CA.

Thirdhand smoke (THS) consists of chemicals that remain in indoor environments after secondhand smoke has cleared. The purpose of this study was to develop an extraction protocol for THS and evaluate its cytotoxicity using terrycloth exposed to cigarette smoke for 110 hours over 334 days and stored at room temperature (RT). THS was extracted in DMEM culture medium at different temperatures and for different lengths of time, and concentrations of nicotine, and related chemicals in the extracts were measured. Highest concentrations of nicotine, cotinine, nicotilline, anataline, N-formynornicotine, 2,3'-bipyridine, N'-nitrosornicotine (NNN) and 4-(methylnitrosamino)-1-(3-pyridyl)-1-butanone (NNK) were present in the extracts made at RT for 1 hr. However, highest concentrations of 1-(N-methyl-N-nitrosamino)-1-(3-pyridinyl)-4-butanal (NNA) and myosmine were in the 1 hr extract made at 4°C. The 1 hour, RT extract had 144 µg of nicotine per gram of terrycloth. A terrycloth bathrobe, weighing 450 g and similarly exposed to smoke, would contain 64 mg of nicotine, which is higher than the LD50 dose for humans. Cytotoxicity was assayed using mouse neural stem cells. The extract made at RT for 1 hr was more cytotoxic than that made for 2 hrs. However, when extracted at 4°C, the 2 hr extract was more cytotoxic. Prolonging the extraction time to 24 hours at RT caused complete loss of cytotoxicity, whereas extracting for 24 hours at 4°C helped to preserve some activity. Extracts made with lower headspace volume were more cytotoxic than when the headspace volume was large, presumably due to better preservation of volatile chemicals. In general, the extract made for 1 hr at RT was most cytotoxic, killing cells at the full strength and 30% dose. These data are consistent with the interpretation that cytotoxicity of THS extracts resides in the volatile fraction and that extraction conditions are critical when quantifying chemicals in THS.

### PS 1469 Prevalidation of the Ex Vivo Model Precision Cut Lung Slices (PCLS) for the Prediction of Respiratory Toxicology.

K. Sewald<sup>1</sup>, L. Lauenstein<sup>1</sup>, S. Vogel<sup>2</sup>, A. Hess<sup>2</sup>, X. Schneider<sup>3</sup>, C. Martin<sup>3</sup>, R. Pirow<sup>4</sup>, M. Liebsch<sup>4</sup>, R. Landsiedel<sup>2</sup> and A. Braun<sup>1</sup>. <sup>1</sup>Fraunhofer ITEM, Hannover, Germany; <sup>2</sup>BASF Ludwigshafen, Germany; <sup>3</sup>RWTH, Aachen, Germany; <sup>4</sup>BfR ZEBET, Berlin, Germany. Sponsor: C. Dasenbrock.

**Introduction:** For acute inhalation toxicity studies, animals inhale chemicals. At the beginning it is difficult to estimate non-toxic doses for *in vivo* inhalation. In the context of REACH and the principle of 3Rs, there is a public demand for alternative methods. The goal of this BMBF-funded project is the pre-validation of PCLS as a suitable *ex vivo* alternative model to replace pre-studies of inhalation toxicology. The project is conducted in three independent laboratories. BfR provides support in biostatistics.

**Methods:** In all participating laboratories, PCLS were prepared and exposed to 5 concentrations of industrial chemicals in DMEM under standard culture conditions for 1 hour. After post-incubation, chemical-induced toxicity was assessed by LDH and WST-1 assay. In addition, PCLS protein content and pro-inflammatory cytokine IL-1 $\alpha$  were measured by BCA assay and ELISA, respectively. For all endpoints a sigmoid dose-response model was fitted to the data and EC<sub>50</sub> values were calculated. Test acceptance criteria were established for each endpoint.

**Results:** This study shows the results of the first 6 tested substances out of 20. In all laboratories, concentration dependent toxicity could be shown for aniline, glutaraldehyde, triton X-100 and paracetamol, but not for lactose and methyl methacrylate. EC<sub>50</sub>-values obtained for the WST-1, LDH and BCA data were very similar in all participating laboratories. No increase in IL-1 $\alpha$  was observed for these chemicals.

**Conclusion:** Local respiratory toxicity induced by chemicals could be tested with comparable results in the PCLS model without *in vivo* experiments in three independent laboratories. The standardization of the PCLS method was successful and the reproducibility of the results is very promising after testing of the first 6 substances.

### PS 1470 High-Content Analysis of Drug-Specific Neurotoxic Effects on Rat Dorsal Root Ganglion Cells.

H. P. Behrsing<sup>1</sup>, F. M. Cutuli<sup>1</sup>, M. Davis<sup>2</sup> and R. E. Parchment<sup>1</sup>. <sup>1</sup>Laboratory of Investigative Toxicology, Applied/Developmental Research Directorate, SAIC-Frederick, Frederick National Lab. for Cancer Research, Frederick, MD; <sup>2</sup>Division of Cancer Treatment and Diagnosis, National Cancer Institute, Bethesda, MD.

The incidence of chemotherapy-induced peripheral neuropathy (CIPN) is increasing because more neurotoxic drugs are being developed and these are increasingly administered in combinatorial regimens to longer living cancer patients. To evaluate neurotoxic drugs, a high content analysis (HCA) strategy was developed to assess response differences of exposed rat dorsal root ganglion cells (DRG). DRG microculture wells were exposed to CIPN-inducing drugs (up to 1 µM) for 24 hr. After exposure, treatment medium was removed and cells were fixed, or were given fresh culture medium and allowed to "recover" for 24 or 72 hr prior to fixation. DRG were fluorescently stained for nuclei, acetyl- $\alpha$  tubulin, and Nissl bodies. Four of the six drugs evaluated caused concentration-specific changes in acetyl- $\alpha$  tubulin staining (AATS) and total neurite area (TNA) after 24 hr exposure. Eribulin and colchicine were most potent, reducing TNA by 50% at <10 nM, but only colchicine effects were reversible after drug removal (AATS intensity doubled in value and TNA increased >5-fold during the 72 hr recovery period). Taxol moderately decreased TNA (~65% of control), but increased AATS intensity to >150% at 1 µM. Initially, bortezomib notably increased AATS intensity but a later effect included loss of AATS, TNA, and increased cell loss after drug removal. Evaluation of Nissl staining areas also showed drug-specific changes in response to exposure and "recovery". Cisplatin and thalidomide had no effect on the parameters measured. Evaluating cellular response is confounded by low level cytotoxicity and loss of viability over time. The use of HCA has identified several morphological endpoints and biomarkers of rat DRG that may serve as indicators of drug-specific neurotoxic risk. Funded by NCI Contract No. HHSN261200800001E.

### PS 1471 Testing Nanomaterials in Precision-Cut Lung Slices: In Vitro-In Vivo Comparisons.

S. Vogel<sup>1</sup>, A. Aumann<sup>1</sup>, W. Wohlleben<sup>3,1</sup>, S. Treumann<sup>1</sup>, U. G. Sauer<sup>4</sup>, K. Wiench<sup>2</sup>, S. Gröters<sup>1</sup>, B. van Ravenzwaay<sup>1</sup> and R. Landsiedel<sup>1</sup>. <sup>1</sup>Experimental Toxicology and Ecology, BASF SE, Ludwigshafen am Rhein, Germany; <sup>2</sup>Product Safety, BASF SE, Ludwigshafen am Rhein, Germany; <sup>3</sup>Polymer Physics, BASF SE, Ludwigshafen am Rhein, Germany; <sup>4</sup>Scientific Consultancy - Animal Welfare, Neubiberg, Germany.

The usefulness of precision-cut lung slices (PCLuS) in assessing nanomaterial (NM) respiratory toxicity was investigated. The data from testing 16 OECD reference NM (rutile and anatase TiO<sub>2</sub>, CeO<sub>2</sub>, SiO<sub>2</sub>, Ag, coated and uncoated ZnO NM, and different multi-walled carbon nanotubes) in rat PCLuS were related to published *in vivo* acute inhalation toxicity data, and the influence of different test system parameters on test results was evaluated.

After 24-hour exposure to the test substances indicators of oxidative stress (glutathione levels), inflammatory reactions (induction of cytokines: CINC-1/IL-8, MCSF, OSP, TNF alpha, MCP-1 and intracellular IL-1 alpha), cytotoxicity (membrane integrity by LDH release, mitochondrial activity by WST-1 metabolism), and apoptosis (caspase 3/7 activity) were measured in the PCLuS. No concentration-dependent oxidative stress or apoptosis was observed with any NM. Cytokines were induced by most of the NM, with varying. ZnO and Ag induced severe cytotoxicity, whereas the remaining NM induced no or only slight cytotoxicity in the tested concentrations. Histopathological evaluation of the PCLuS revealed only particle uptake into macrophages for most of the NM.

The observed effects in PCLuS by most of the NM not always reflected NM size, NM class, or pulmonary inflammatory reactions *in vivo*. The relevance of the different effects measured in PCLuS for respiratory toxicity *in vivo* needs further investigations.

**PS 1472 A Transcriptomic Comparison between the Neural and Cardiac Embryonic Stem Cell Tests (ESTn and ESTc).**

P. T. Theunissen<sup>1,2</sup>, J. L. Pennings<sup>1</sup>, D. A. van Dartel<sup>3</sup>, J. F. Robinson<sup>1,2</sup>, J. C. Kleinjans<sup>2</sup> and A. H. Piersma<sup>1,4</sup>. <sup>1</sup>Health Protection, RIVM, Bilthoven, Netherlands; <sup>2</sup>Toxicogenomics, University, Maastricht, Netherlands; <sup>3</sup>Human and Animal Physiology, University, Wageningen, Netherlands; <sup>4</sup>IRAS, University, Utrecht, Netherlands.

In vitro screening assays may increase testing efficiency and reduce animal use in developmental toxicity testing. The cardiac mouse embryonic stem cell test (ESTc) is a promising in vitro assay in this field, in which the effect of developmental toxicants on cardiomyocyte differentiation is assessed. To increase prediction of the EST approach, we developed a neural differentiation variant of the stem cell test (ESTn). In both ESTn and ESTc, we performed a series of transcriptomic studies to characterize gene expression changes 1) across time during normal differentiation and 2) in response to a series of developmental toxicants in the ESTn and ESTc. In the present study, gene expression profiles of ESTn and ESTc over time as well as model-specific changes induced by seven compounds are compared. Time-related gene expression profiles showed that specific genes changed over time differently in each model, related to the two specific lineages of differentiation. Interestingly, compound-induced gene-expression changes were generally model-specific, particularly for methylmercury and flusilazole, which were predicted better in ESTn and in ESTc, respectively. Valproic acid-induced gene expression changes were most comparable between ESTn and ESTc. Direct transcriptomic comparisons between the ESTn and ESTc models indicate that both assays support and complement each other. Therefore, a combined transcriptomics approach, incorporating ESTc and ESTn, may result in improved developmental toxicant detection over individual assays.

**PS 1473 In Vitro Proliferation in Human and Rat Urothelial Cells.**

E. L. Bowen<sup>1</sup>, J. Southgate<sup>1</sup>, S. Baker<sup>1</sup> and P. Rawlinson<sup>2</sup>. <sup>1</sup>Jack Birch Unit for Molecular Carcinogenesis, University of York, York, United Kingdom; <sup>2</sup>Syngenta, Bracknell, Berkshire, United Kingdom. Sponsor: R. Peffer.

Despite the regular use of the rat in toxicity studies, which are used for human risk assessment, the extrapolation from rat to humans is often difficult. This study set out to explore the utility of cell culture systems to better understand species differences. As urine is a main route of chemical excretion from the body, the epithelial barrier lining of the bladder (urothelium) may be exposed to higher concentrations of xenobiotics, with the potential for adverse findings. Methods have been successfully developed to culture normal human urothelial (NHU) cells in vitro, with subsequent differentiation to form a functional barrier. With this in mind, equivalent normal rat urothelial cell culture systems were grown from Wistar (NRU-W) and Homozygous Scottish (NRU-HS) rats. They were compared to human cell cultures by exploring their regulation and capacity for proliferation. NHU cells could be propagated beyond passage 6 in serum-free medium, whilst NRU-W could only be maintained up to passage 1, and NRU-HS cells required serum to grow to passage 1. By immunofluorescence, NHU cells were shown to express nuclear Ki67 and cyclin D1, but the same proliferation markers were cytoplasmic in NRU cells. In contrast, Ki67 was virtually negative in histological sections of human and HS rat urothelium, but strongly expressed (nuclear) in Wistar. The results for human urothelium reflect the fact it is mitotically-quiet, and has a low rate of turnover in vivo, but has a large capacity for regeneration, which can be seen in culture. It appears that there may be fundamental differences in the way in which rat urothelium is regulated, with cells maintained in the cell cycle in vivo and with a less proliferative phenotype observed in vitro. Future work will aim to further characterise these differences, and to understand the consequence of these findings for the development of a comparative model.

**PS 1474 In Vivo-In Vitro Comparison of Respiratory Tract Toxicity Using Human 3D Airway Models and Human A549 and Mouse 3T3 Monolayer Cell Systems.**

U. G. Sauer<sup>3</sup>, S. Vogel<sup>1,2</sup>, A. Hess<sup>1</sup>, S. N. Kolle<sup>1</sup>, L. Ma-Hock<sup>1</sup>, B. van Ravenzwaay<sup>1</sup> and R. Landsiedel<sup>1</sup>. <sup>1</sup>Experimental Toxicology and Ecology, BASF SE, Ludwigshafen am Rhein, Germany; <sup>2</sup>Performance Chemicals - Master Data, Product Safety, Product Stewardship, BASF SE, Ludwigshafen am Rhein, Germany; <sup>3</sup>Scientific Consultancy - Animal Welfare, Neubiberg, Germany.

Four in vitro systems to predict acute inhalation toxicity were evaluated. 19 substances (lactose, paracetamol, methylmethacrylate, aniline, acetic- and trimellitic anhydride, N-hexylchloroformate, octanoyl chloride, isophorone and toluene diisocyanate, zinc oxide, paraquat, glutar- and formaldehyde, acetone, ethanol, dimethylformamide, ammonium hexachloroplatinate and sodiumdodecylsulfate)

were tested in 3D human airway epithelial models, EpiAirway™ and MucilAir™, and in A549 and 3T3 monolayer cell cultures. Cytotoxicity was assessed by determining LDH release and MTT or WST reduction.

IC50 values were compared to literature rat 4-hour LC50 values classified according to the US EPA and GHS hazard categories. Best results were achieved with a prediction model identifying non-toxic substances (determination of LDH release in 3T3 cells: sensitivity 1.00 and specificity 0.89).

Further predictions of in vivo hazard categories based on four in vitro hazard categories resulted in mediocre correlations: 9 of 19 test substances were classified concordantly in the MucilAir™ system determining MTT reduction and 8 of 19 in A549 cells determining WST reduction. Concordance could be improved by excluding substances leading to pulmonary edema and emphysema in vivo.

None of the test systems was outstanding; and there was no evidence that the use of 3D or monolayer systems using respiratory tract cells provide an added value to simple 3T3 monolayers. However, the test systems only reflected bronchiole epithelia and alveolar cells and only investigated cytotoxicity so that effects occurring in other cells by other mechanisms were not recognized.

**PS 1475 Neurotoxicity In Vitro: Assessment of the Predictivity of Neuronal Networks Coped to Microelectrode Arrays for Identification of Neurotoxicants.**

H. Hüner, T. Ramirez, T. Weisschu, N. Stein, B. van Ravenzwaay and R. Landsiedel. *Experimental Toxicology and Ecology, BASF SE, Ludwigshafen am Rhein, Germany.*

A challenging aspect to assure the safety of a product is the assessment of its neurotoxic hazard potential. Currently, only in vivo methods are regulatorily accepted and so far, no in vitro model has been fully validated. The majority of the test systems are reduced to the analysis of cytotoxicity in immortalized cell lines, without including unique characteristics of the nervous system, such as axonal transport, synaptic transmission or its electrophysiology. Recently, with the advance in technology and the ability to maintain neuronal models for prolonged periods, a test system emerged, combining the use of microelectrode arrays (MEAs) and in vitro culture of 2D neuronal networks (NN). Herein, we report on the in-house validation of the NN MEA assay using a set of 43 compounds with known neurotoxic and non-neurotoxic potential with the aim to use it for screening of compounds under development. The results demonstrate that the methods presents a sensitivity of 71%, while the specificity is still an aspect for optimization, since in its current status, it cannot distinguish specific neurotoxicity from unspecific cytotoxicity. In order to increase the sensitivity and predictivity, we are currently working on the combination of the electrophysiological assessment with a panel of cytotoxicity assays.

**PS 1476 A Human 3D Myocardial Microtissue Model for Cardiotoxicity Testing.**

C. Zuppinger<sup>1</sup>, I. Agarkova<sup>2</sup>, W. Moritz<sup>2</sup> and J. M. Kelm<sup>2</sup>. <sup>1</sup>University of Bern, Bern, Switzerland; <sup>2</sup>InSphero, Zürich, Switzerland. Sponsor: A. Wolf.

Cardiomyocytes (CMs) are terminally differentiated cells in the adult organism and regeneration is limited. This is a worrisome fact, since insults such as ischemia and cardiotoxic compounds can lead to cell death and irreversible reduction of cardiac function. As testing platform, isolated organs and primary cells from rodents have been the standard in research and toxicology so far, but due to a very limited cell supply there is a strong need for better in vitro models. Hence, an in vitro model comprising the advantages of 3D cell culture and the availability of induced pluripotent stem cells (iPSC) from human origin was developed and characterized. Myocardial microtissues (MTs) were generated by self-assembly in multi-well hanging drop cultures. iPSC-derived CMs were evaluated regarding cardiac features and toxicological response. Prior use of the iPSC-derived cells, CMs were characterized after 10 days in standard culture which showed highly differentiated myofibrils positive for sarcomeric proteins such as myomesin, myosin, cardiac actin and desmin. The cells showed spontaneous contractile activity and connexin-43 positive gap junctions. In the hanging drop cultures, iPSC-derived CMs formed MTs within 4 days, contracting up to 3 weeks recorded by optical motion tracking. Excited by electrical field pacing they complied to the external stimulus up to 2Hz. Effects of a cardiotoxic cancer therapeutics such doxorubicin on iPSC-derived CMs in 2D- and 3D-culture were further evaluated with respect to caspase activation, LDH release and cellular ATP levels. Adult human CMs are a very rare and hard to handle cell source. New concepts have to be developed to create cardiac models systems to be used for cardiotox testing, ideally in a standard multi-well format. Within this "proof-of-concept" study a novel 3-dimensional human myocardial MT model was developed and characterized based on iPSC-derived CMs. Morphological and functional characterization underline that this model might become a valuable tool for substance safety testing in the future.

**PS 1477 Use of An *In Vitro* Flow Cytometric Method As a Replacement for Live Animal Experimentation.**

J. Godin-Ethier<sup>1</sup>, S. Th  baud<sup>1</sup>, J. Leiva<sup>1</sup>, C. L  vesque<sup>1</sup>, A. Nelson<sup>1</sup> and W. Lee<sup>2</sup>.  
<sup>1</sup>Immunology, ITR International, Baie d'Urfe, QC, Canada; <sup>2</sup>Toxicology, ITR International, Baie d'Urfe, QC, Canada.

**Scope:**

Animal welfare guidelines place more and more emphasis on the 3 Rs principle as a way to achieve excellence in animal care and use. In that objective, we have developed an *in vitro* flow cytometry method that allows us to quantify the immune response to IL-2 stimulus in a lymphocyte population thus replacing the use of live monkeys.

We have evaluated the potency of test items to phosphorylate stat5 in lymphocyte subsets expressing or not the IL-2 high affinity receptor subunit (CD25).

**Experimental Procedures and Results:**

Cynomolgus monkey peripheral blood mononuclear cells (PBMC) were stimulated with increasing doses of the test items under evaluation. The PBMCs were then stained using conjugated monoclonal antibodies specific to different lineage markers such as CD3, CD4, CD8 and CD25 to allow distinction between the different T lymphocyte subsets. In addition, in order to evaluate the potency of the test items to differentially stimulate CD25+ and CD25- lymphocytes, we have evaluated the activation of a downstream mediator of the IL-2 receptor signaling by measuring the phosphorylation of the Signal Transducer and Activator of Transcription (Stat5). Intracellular staining using a Phospho-Stat5 (pStat5) specific antibody was thus performed and data was acquired by flow cytometry. The pStat5 signal fold-increase was plotted against the test items concentration and the half maximal effective dose (EC50) was determined. The results obtained showed that the calculated EC50 for the CD4+CD25+ was of approximately 100 to 1000 times lower compared to CD4+CD25- cells and CD8+ cells. In addition, when comparing the potency to the two test articles to stimulate CD4+CD25+ cells, a 2-log difference was observed between calculated EC50.

**Conclusions:**

This innovative approach enables us to replace animal experimentation by an *in vitro* assay. Our method assesses the potency of test items to signal through the IL-2 receptor in different lymphocyte subsets.

**PS 1478 The Role of Facilitated Transport by Serum Protein in *In Vitro* Intrinsic Clearance.**

B. J. Blaauwboer, J. Moulin and N. Kramer. *Institute for Risk Assessment Sciences, Utrecht University, Utrecht, Netherlands.*

When a chemical is exposed to an *in vitro* cell assay in culture medium with serum protein, the effect (e.g. clearance) observed may be lower than when the chemical is exposed in culture medium without serum protein. This is because the chemical can bind to serum protein, which reduces the unbound free concentration of the chemical available for uptake into cells. Therefore, it is better to determine *in vitro* intrinsic clearance (CL<sub>int</sub>) based on unbound fractions of chemicals. However, a few studies have suggested that serum protein may also facilitate the transport of chemicals through aqueous media (facilitated transport). Thus the presence of serum protein may increase the uptake rate of chemicals into cells and solid phase microextraction (SPME) fibers. If the uptake rate determines clearance, then the presence of serum protein may increase clearance, thus hampering the extrapolation of *in vitro* CL<sub>int</sub> to *in vivo* clearance when clearance assays use varying concentrations of serum. Therefore, the uptake rate and clearance of the strongly-albumin bound, quickly cleared chemical testosterone was measured in HepaRG, HepG2 and H4IIE hepatoma cell lines at varying concentrations of bovine serum albumin using the substrate depletion approach. To measure the free fraction, mimic uptake of testosterone in cells, and facilitate the modeling of the transport into cells, a SPME method was developed for extracting the unbound chemical from the exposure medium. Results indicate that *in vitro* CL<sub>int</sub> of testosterone increases with increasing albumin concentration when using the unbound fraction. SPME was successfully applied to determine the free concentration and study the uptake rate of unbound testosterone into cells.

**PS 1479 Screening of Cosmetics Ingredients for Phototoxic Potential Using the *In Vitro* 3T3 Neutral Red Uptake Phototoxicity Test.**

R. Labib<sup>1</sup>, E. Gilberti<sup>1</sup>, S. Gettings<sup>1</sup> and H. Raabe<sup>2</sup>. <sup>1</sup>Product Safety & Integrity, Avon Products, Suffern, NY; <sup>2</sup>Institute for *In Vitro* Sciences, Gaithersburg, MD.

Phototoxicity is an acute toxic response after exposure to a phototoxicant and either UV radiation or visible light (UV/VIS). Phototoxicity from substances applied topically typically occurs at the site of photo-irradiation. Phototoxicity is the result of

direct cellular damage caused by a nonimmunological inflammatory response. Clinically, phototoxicity resembles an exaggerated sunburn (erythema, increased skin temperature, pruritis and edema). Phototoxicity reactions have been reported for both synthetic substances and those which occur naturally (eg., botanical extracts). Although symptoms generally subside quickly, the potential for substances used in topical products to cause phototoxicity is clearly of concern for manufacturers of cosmetics, personal care and other consumer products. Historically, the potential to cause phototoxicity from substances applied topically was evaluated by utilizing various animal models; however in 1997 the 3T3 Neutral Red Uptake Phototoxicity Test (3T3 NRU PT) was validated by ECVAM's Scientific Advisory Committee as an *in vitro* method for evaluating the phototoxic potential of chemicals shown to absorb in the UV/VIS range. To illustrate the utility of the 3T3 NRU PT as a useful screening tool in the safety evaluation of potential cosmetic ingredients, the results of the evaluation of 42 botanical extracts and 25 synthetic chemicals found to absorb in the UV/VIS range are reported. Most substances evaluated were found not to be phototoxic *in vitro*; however, 9 substances were identified as potentially/probably phototoxic in the 3T3 NRU PT and were eliminated from further consideration for use as cosmetic ingredients. Several substances found to be non-phototoxic in the 3T3 NRU PT were formulated with other ingredients in a prototype cosmetic formulation and subject to clinical testing. No manifestations of phototoxicity were observed in any of the test subjects in the prototype formulation containing any of the substances identified as non-phototoxic *in vitro*.

**PS 1480 Validation of a Cell Microelectronic Sensing Technique for Semi-Quantification of Cyanobacterial Toxins (Microcystins) in Recreational Water.**

V. Charoensuk<sup>1</sup>, D. Y. Huang<sup>1</sup>, W. Zhang<sup>2</sup>, S. Gabos<sup>3</sup> and D. W. Kinniburgh<sup>1</sup>.  
<sup>1</sup>Physiology & Pharmacology, Alberta Centre for Toxicology, Calgary, AB, Canada;  
<sup>2</sup>Protection Branch, Family and Population Health, Alberta Health, Edmonton, AB, Canada; <sup>3</sup>Office of the Chief Medical Officer of Health, Alberta Health, Edmonton, AB, Canada.

Microcystins (MCYSTs) are hepatotoxins produced by cyanobacteria (blue-green algae) commonly found in fresh water. There are a few semi-quantitative and quantitative detection methods available including protein phosphatase inhibition assay (PPI), enzyme-linked immunosorbent assay (ELISA) and liquid chromatography tandem mass spectrometry (LC/MS/MS).

Our laboratory recently developed a novel assay using a cell microelectronic sensing technology known as RTCA (Real-Time Cell Analyzer, Roche xCELLigence system) for detecting MCYSTs cytotoxicity. The assay is based on the fact that MCYSTs toxicity requires the active uptake of MCYSTs into the cytoplasmic membrane which is mediated by the organic anion transporting polypeptides (OATPs). By comparing the 48-hour cytotoxic effects of MCYSTs in wild type Chinese hamster ovarian cells (CHO/WT) and in CHO with OATP1B3 expression (CHO/OATP1B3), we semi-quantified MCYSTs cytotoxicity in recreational water using standard curves prepared from MCYST-LR, the most common MCYST analogue. MCYSTs levels in water samples were compared with results from PPI, ELISA and LC/MS/MS. The RTCA directly demonstrated MCYSTs total toxicity and the semi-quantitative results have high correlation to those from other methods (p-value < 0.0001), particularly at the Canadian recreational water guideline level (20 µg/L) or greater.

In summary, we have validated a semi-quantitative assay for cytotoxic testing of MCYSTs in recreational water by observing real-time toxic response at microgram per litre concentrations.

**PS 1481 Human Intestinal Microflora Reduces Butyl Paraben Toxicity in HepG2 Cell Cultures.**

W. Kang<sup>2</sup>, T. Khanal<sup>1</sup>, H. Kim<sup>1</sup>, T. Jeong<sup>2</sup> and H. Jeong<sup>1</sup>. <sup>1</sup>Pharmacy, Chungnam National University, Daejeon, Republic of Korea; <sup>2</sup>Pharmacy, Yeungnam University, Gyeongsan, Republic of Korea.

Parabens are alkyl esters of p-hydroxybenzoic acid, including methyl paraben, ethyl paraben, propyl paraben, and butyl paraben. In the present study, possible role of metabolism by fecalase in BP-induced cytotoxicity was investigated in HepG2 cell cultures. As an intestinal bacterial metabolic system for butyl paraben, human fecal preparation containing intestinal microflora (fecalase) was employed. Initially, among the parabens tested, cytotoxicity of butyl paraben was most severe. When butyl paraben was incubated with fecalase, it rapidly disappeared, in association with reduced cytotoxicity in HepG2 cells. In addition, butyl paraben-incubated with fecalase reduced cytotoxicity of HepG2 cells in a concentration-dependent manner. Moreover, butyl paraben-incubated with fecalase significantly caused an increase in Bcl-2 expression together with a decrease in Bax expression and cleaved Caspase-3. Furthermore, anti-apoptotic effect by the incubation of butyl paraben

with fecalase was also confirmed by the terminal deoxynucleotidyltransferase-mediated dUTP-biotin nick-end labeling assay. Taken all together, the findings suggested that metabolism of butyl paraben by human fecalase might have protective effects against butyl paraben-induced toxicity in HepG2 cells.

## **PS 1482 Characterization of Cellular and Molecular Markers of Toxicity in C6-Glioma Cells Exposed to Modern Pyrethroids.**

D. M. Romero, M. J. Wolansky and M. L. Kotler. *Biological Chemistry, IQUIBICEN (CONICET); School of Sciences, University of Buenos Aires, Buenos Aires, Argentina.*

Pyrethroids (PYRs) are insecticides increasingly used in various pest control applications. Low levels of PYR residues have been detected in diverse environmental samples, food and human urine. In vitro systems may be useful to characterize the diversity of primary and secondary toxicogenic pathways that may account for the pyrethroid-type specific divergence in clinical syndromes observed in small rodents. We use C6-glioma cell cultures to identify toxicologically relevant PYR exposures that may require cumulative risk assessment efforts in animals in vivo. Four compounds (bifenthrin, tefluthrin,  $\alpha$ -cypermethrin, deltamethrin) were examined after 24 h of PYR exposure. We also evaluated pyrethroid actions in C6 cells treated with sodium butyrate (NaBu) which induce an astrocyte-like phenotype. Threshold dose and EC15(24h) estimates were obtained after modeling MTT test data. In order to study subcellular integrity and signaling pathways with greater specificity and sensitivity, Mitotracker-Red and Neutral Red staining (informing on mitochondrial and lysosomal status, respectively), caspases and p53 (cell death related markers), AchE (an insecticide neurotoxicity related target) and GFAP (glia-specific xenobiotic response) were then examined. Low  $\mu$ M exposures induced dose-related declines in cell viability in both cell systems. We further found dose-related increases in fragmented mitochondria and mitochondrial membrane potential disruption in C6 cells. Increase in cell death related proteins and drop of GFAP levels were also observed in NaBu-treated cells. In addition, cholinesterase inhibition was not evident below EC15 levels for general cell viability for any test chemical. These results confirm that  $\mu$ M exposures affect cell viability markers unrelated to the proposed primary mode of action of pyrethroids, and that the classically proposed target cell for pyrethroids, the neuron, is not the only cell type that may be susceptible of cytotoxicity and severe cell damage in mammals.

## **PS 1483 DNA Damage-Induced by Goldenseal Constituents.**

S. Chen<sup>1</sup>, L. Wan<sup>1,2</sup>, H. Lin<sup>1</sup>, L. Couch<sup>1</sup>, N. Mei<sup>1</sup> and L. Guo<sup>1</sup>. <sup>1</sup>NCTR, Jefferson, AR; <sup>2</sup>Shanghai Institute for Food and Drug Control, Shanghai, China.

Goldenseal is used for the treatment of gastrointestinal disturbances, urinary disorders and inflammation. The major alkaloid constituents in goldenseal are berberine, hydrastine, and canadine. Because it is one of the most widely used herbal dietary supplements in the United States and the lack of carcinogenicity data, goldenseal was nominated to the National Toxicology Program (NTP). The NTP conducted 2 year bioassay on goldenseal and reported that goldenseal increased the incidence of liver tumors in rodents. However, the mechanisms of goldenseal-associated liver carcinogenesis are unclear. In this study, we compared genotoxicity of five goldenseal constituents and studied the underlying mechanisms. Five goldenseal constituents tested (berberine, palmatine, hydrastine, hydrastinine, and canadine) did not induce mutagenicity in the salmonella mutation assay. Berberine and palmatine at high concentrations showed positive results in the mouse lymphoma assay. Berberine and palmatine also caused DNA strand breaks in cultured hepatic cells whereas the rest three did not. The expression of the  $\gamma$ -H2AX, a biomarker of double strand breaks, was induced in a dose-dependent manner in response to berberine treatment. In addition, berberine and palmatine suppressed that activities of both topoisomerase I and II, indicating that the inhibitory effect may contribute to berberine- and goldenseal-induced genotoxicity and tumorigenicity.

## **PS 1484 DNA Adduct Formation and Mutation Induction by Aristolochic Acid in Rat Spleen.**

N. Mei, X. Guo, P. McDaniel and T. Chen. *Division of Genetic and Molecular Toxicology, National Center for Toxicological Research, Jefferson, AR.*

Aristolochic acid (AA) is a potent human nephrotoxin and carcinogen. We previously reported that AA treatment resulted in DNA damage and mutation in the kidney and liver of rats. In the present study, we have determined the DNA adducts and mutations induced by AA in rat spleen. Big Blue transgenic rats were gavaged

with 0, 0.1, 1.0 and 10.0 mg AA/kg body weight 5-times/week for 3 months. Three DNA adducts, [7-(deoxyadenosin-N6-yl)-aristolactam I, 7-(deoxyadenosin-N6-yl)-aristolactam II and 7-(deoxyguanosin-N2-yl)-aristolactam I], were identified by P32-postlabeling. Over the dose range studied, there were strong linear dose-responses for AA-DNA adduct formation in the treated rat spleens, ranging from 4.6 to 217.6 adducts/ $10^8$  nucleotides. Spleen cII mutant frequencies (MFs) also increased in a dose-dependent manner, ranging from 32.7 to 286.2  $\times 10^{-6}$  in the treated animals. Mutants isolated from the different treatment groups were sequenced; there were significant differences between the spectra of 1 mg/kg AA-treated and control groups, and between the 10 mg/kg AA-treated and control groups. A:T  $\rightarrow$  T:A transversion was the major type of mutation in AA-treated rats, while G:C  $\rightarrow$  A:T transition was the main type of mutation in the vehicle controls. These results indicate that AA is genotoxic in the spleen of rats exposed under conditions that result in DNA adduct formation and mutation induction in kidney and liver.

## **PS 1485 In Vitro Genotoxicity of Ginkgo biloba Extract and Two of Its Major Components, Quercetin and Kaempferol.**

H. Lin, X. Guo, S. L. Dial, C. E. Schulte, M. G. Manjanatha, M. M. Moore and N. Mei. *DGMT, NCTR/US FDA, Jefferson, AR.*

Ginkgo biloba (ginkgo), one of the world's oldest living tree species, has been used for many years for a variety of medicinal purposes. The NTP 2-year bioassays on ginkgo extract found an increased incidence of liver cancer in mice and thyroid gland cancer in both mice and rats. In this study, the mouse lymphoma assay (MLA) was used to evaluate the in vitro mutagenicity of ginkgo extract and two of its major constituents, quercetin and kaempferol. L5178Y/Tk+/-3.7.2C mouse lymphoma cells were treated with different concentrations of ginkgo extract (0.2-1.2 mg/ml), quercetin (3-30  $\mu$ g/ml) and kaempferol (2.7-57.2  $\mu$ g/ml) in the absence of metabolic activation. Ginkgo extract, quercetin, and kaempferol significantly increased the mutant frequency in the MLA. Loss of heterozygosity (LOH) analysis for mutants induced by quercetin and kaempferol were also examined at five microsatellite loci spanning the entire mouse chromosome 11. The results indicated that the mutational spectrum from the quercetin and kaempferol treatment were significantly different from that of the negative control. In addition, the neutral comet assay conducted in the mouse lymphoma cells with quercetin and kaempferol also demonstrated a dose-dependent increase in the DNA double-strand breaks (DSBs). Western blot analysis showed that quercetin increased the phosphorylation of ATM, and consequently increased expression of  $\gamma$ -H2AX, phosphorylated Chk1 and Chk2 in the cells; while kaempferol increased expression of  $\gamma$ -H2AX and phosphorylated Chk1. These results suggest that ginkgo extract and two of its major constituents, quercetin and kaempferol, are genotoxic in the mouse lymphoma cells.

## **PS 1486 Loss of Heterozygosity Analysis of the Tk Mutants Induced by Cigarette Smoke Condensates in Mouse Lymphoma Cells.**

X. Guo, M. M. Moore and N. Mei. *Division of Genetic and Molecular Toxicology, National Center for Toxicological Research, Jefferson, AR.*

Cigarette smoke condensate (CSC) is a set of sticky particles comprised of thousands of chemicals created by burning cigarette. Our previous study on 11 cigarette smoke condensates (CSCs) using the mouse lymphoma assay (MLA) has demonstrated that all these CSCs resulted in a dose-dependent increase of both cytotoxicity and mutagenicity in the mouse lymphoma cells. To elucidate the underlying mutagenic mechanism, we examined the mutational types of CSC-induced Tk mutants by analyzing loss of heterozygosity (LOH) using the allele-specific PCR at five microsatellite loci (Tk1, D11Mit42, D11Mit36, D11Mit20 and D11Mit74) spanning the entire chromosome 11. For each CSC treatment, 48 large and 48 small mutant colonies were randomly collected from the cultures of the highest acceptable concentrations. The statistical analysis demonstrated that the mutational spectra of all colonies induced in CSC-treated mouse lymphoma cells were significantly different from those of the vehicle control, although the most common type of all the mutations including CSC-treated and control samples was LOH involving the Tk and D11Mit42 locus. A larger proportion of LOH at Tk and D11Mit 42 loci was observed in the CSC-induced small colonies, whereas the large colonies showed different LOH patterns among the 11 CSCs. These results suggest that CSCs are mutagenic in mouse lymphoma cells with a clastogenic mode-of-action, and the induction of large and small colony mutants may result from different mechanisms.

**PS 1487 Evaluation of Genotoxicity of Cyproterone Acetate in Both Sexes of Rats.**

W. Ding<sup>1</sup>, M. E. Bishop<sup>1</sup>, M. G. Pearce<sup>1</sup>, G. A. White<sup>2</sup>, L. Lyn-Cook<sup>1</sup> and M. G. Manjanatha<sup>1</sup>. <sup>1</sup>Division of Genetic and Molecular Toxicology, FDA/NCTR, Jefferson, AR; <sup>2</sup>Toxicology Pathology Associates, FDA/NCTR, Jefferson, AR.

Cyproterone acetate (CPA), a hormone therapy drug with anti-androgenic activity, is commonly used for androgenisation symptoms in women and treatment of prostate cancer in men. CPA is known to produce liver tumor in rats, with a higher incidence in females. In standard genotoxicity assays, such as Ames test, HGPRT assay, chromosomal aberration assay and *in vivo* micronucleus assay, negative responses were observed. However, more recent studies have demonstrated that CPA induces a sex-specific genotoxicity, forming DNA adducts in female rats but not in male rats. To investigate the genotoxicity of CPA, and to answer the question if it is sex-specific, we evaluated the genotoxicity of CPA through *in vivo* Comet assay in both sexes of rats. hOGG1- and Endo III-modified *in vivo* Comet assay were performed to measure CPA induced oxidative DNA damage. Groups of 5 seven-week old male F344 rats were treated with olive oil or 10, 25, 50 or 100 mg/kg bw CPA in olive oil at 0, 24, and 48 hr. Animals were sacrificed at 48 hr, 3 hr after the last treatment. Liver, testis, kidney and blood were collected for Comet assay. CPA treatment resulted in an increase in DNA strand breaks in the liver of male rats with significant ( $p \leq 0.05$ ) increases detected in rats treated with 50 and 100 mg/kg CPA. There were near-linear dose responses for EndoIII-sensitive and hOGG1-sensitive DNA damages in CPA-treated rat livers, both with significant ( $p \leq 0.05$ ) increases detected in all the dose groups, suggesting a possible role of reactive oxygen species for CPA-induced genotoxicity. To evaluate the genotoxicity of CPA in female rats, groups of 5 seven-week old female F344 rats will be treated identically with CPA. Liver, mammary gland, uterus, ovary, kidney and blood will be collected for Comet assay and the responses will be compared with the males. This study will provide a further understanding of the cancer mode of action of CPA and if there is any sex-specific genotoxic response in rats.

**PS 1488 Assessment of Dosimetry and Biological Responses *In Vitro* Using a Vitrocell® Smoke Exposure System.**

D. Thorne<sup>1</sup>, J. Kilford<sup>2</sup>, B. Payne<sup>2</sup>, K. Scott<sup>1</sup>, J. Adamson<sup>1</sup>, A. Dalrymple<sup>1</sup>, C. Meredith<sup>1</sup> and D. M. Dillon<sup>1</sup>. <sup>1</sup>Group R&D, British American Tobacco, Southampton, United Kingdom; <sup>2</sup>Covance Laboratories Ltd., Harrogate, United Kingdom.

Routine toxicological assessment of tobacco smoke commonly uses the particulate fraction of the smoke aerosol. The particulate phase of cigarette smoke makes up a small percentage of the total aerosol, approximately 5-9% by weight. The remaining ~91% is associated with the vapour phase of cigarette smoke and is not routinely evaluated. Whole smoke exposure systems are capable of capturing the full interactions of both the particulate and vapour phase together and offer unique potential for toxicological assessment.

In this study we used a Vitrocell® VC10 smoking robot to expose cell cultures at the air-liquid interface to ISO mainstream 3R4F cigarette smoke. All experiments were independent and completed a minimum of three times. For biological assessment we developed the Neutral Red Uptake (NRU) assay with a Balb/c cell line, and the Ames assay using bacterial strain YG1042. We also used a novel quartz crystal microbalance (QCM) tool for real-time *in situ* deposition analysis. For the Ames assay we observed a mean fold increase of 5.9 at the highest concentration of smoke tested (1L/min), which correlated with a  $2.29 \mu\text{g}/\text{cm}^2$  increase in particulate deposition. Clear differences were seen at all doses; for example, 12, 8 and 4L/min produced a 2.1, 2.3, 3.8 and 0.04, 0.09, 0.50 fold increase and deposited mass ( $\mu\text{g}/\text{cm}^2$ ) respectively. The NRU assay showed a complete cytotoxic dose response (12-1L/min), with a calculated dilution  $\text{IC}_{50}$  and deposited mass  $\text{IC}_{50}$  of approximately 6.5 L/min and  $1.7 \mu\text{g}/\text{cm}^2$  respectively.

We conclude that the VC10 can be used in conjunction with routine toxicological assays for the assessment of cigarette smoke toxicity, as demonstrated by consistent responses in two independent *in vitro* test systems. Furthermore, QCM measurements *in situ* of exposure have enabled us to present biological data as a function of deposited mass. QCMs have also acted a important QC tool for smoke exposure and provide valuable information on the exposure system itself.

**PS 1489 Evaluation of the Results of Several Genotoxicity Tests in Carvacrol and Thymol.**

J. Scognamiglio, V. T. Politano and A. Api. Research Institute for Fragrance Materials, Woodcliff Lake, NJ.

Carvacrol (CAS499-75-2) and thymol (89-83-8) are fragrance ingredients that have been studied in bacterial and mammalian genotoxicity assays *in vitro* and in an *in vivo* chromosome aberration test. These materials have antibacterial and anti-

fungal properties and are cytotoxic. Their cytotoxicity needs to be considered when evaluating the results of genotoxicity assays using mammalian cell cultures because cytotoxicity is the most important confounding factor in analyzing these results. To avoid the occurrence of secondary (indirect) modes of clastogenic activity, the highest concentrations tested in these assays should lead to sufficient levels of cytotoxicity within the guidelines, but not cause extreme cytotoxicity. In published literature, there are inconsistent results of the genotoxicity tests on these two materials, where positive results correlate with cytotoxicity, indicating that positive results can be explained by secondary effects. An SOS Chromotest was less prone to false positives than the Ames test and was negative with both carvacrol and thymol. A positive chromosomal aberration test in rats on both carvacrol and thymol was further evaluated to clarify the cause of the chromosomal aberration observed. Thus an *in vitro* micronucleus test in human peripheral blood lymphocytes was conducted with careful selection of doses based on cytotoxicity to determine if these materials were potential clastogens or a spindle poison. Both assays yielded negative results, supporting the hypothesis that the previous positive genotoxic outcomes were the result of high cytotoxic activity in the test system and that carvacrol and thymol are likely not genotoxic agents.

**PS 1490 No Direct Genotoxic Potential of Different Radiofrequency Electromagnetic Fields in MRC-5 Cells and B6C3F1 Mice.**

C. Dasenbrock<sup>1</sup>, T. Tillmann<sup>1</sup>, A. Oertel<sup>1</sup>, H. Brockmeyer<sup>1</sup>, M. Murbach<sup>2</sup>, M. Capstick<sup>2</sup>, N. Kuster<sup>2</sup> and C. Ziemann<sup>1</sup>. <sup>1</sup>Fraunhofer ITEM, Hannover, Germany; <sup>2</sup>IT'IS Foundation, Zurich, Switzerland.

Public exposure to electromagnetic fields in the radiofrequency spectrum (RF-EMF) has increased dramatically, attracting notice to health risk evaluation. RF-EMF was classified as possibly carcinogenic to humans (Group 2B) by the IARC in 2011. But clear risk assessment is still limited by data gaps and contradictory data, not only for mobile phones but also for wireless network devices. As there are some indications for disturbance of DNA-integrity by RF-EMF exposure, we evaluated the *in vitro* and *in vivo* genotoxic potential of different RF-EMF signals by using well established and standardized genotoxicity.

*In vitro*, normal human MRC-5 lung fibroblasts were exposed intermittently (5 min ON, 10 min OFF) in a 1950 MHz exposure system for 1, 4, and 24 h to various RF-EMF signals (continuous wave (CW), UMTS, WiFi, GSM-basic, RFID) at specific absorption rates (SAR) up to  $4.92 \text{ W}/\text{kg}$ . DNA-strand break (SB) induction and oxidative DNA-damage were subsequently evaluated in an enzyme (hOGG1)-modified comet assay.

*In vivo*, male B6C3F1 mice were whole-body exposed to CW, UMTS, WiFi, or RFID signals at SAR of 1.6, 4.0 and  $10 \text{ W}/\text{kg}$  for 14 d, 20 h/d (5 min ON, 10 min OFF) using a reverberation chamber. Micronucleus (MN) frequency was determined in peripheral blood, immature bone marrow erythrocytes and keratinocytes. Irrespective of signal type, SAR-value, and exposure duration RF-EMF did not mediate significant cytotoxicity, induction of DNA-strand breaks, or oxidative DNA-damage in MRC-5 cells, compared to concurrently sham-exposed cells. In addition, no increase in MN formation was observed in B6C3F1 mice. In conclusion, none of the tested signal modulations revealed evidence for a direct DNA-damaging or cytotoxic potential of RF-EMF.

This study was part of the SEAWIND project, funded by the European Union's Seventh Framework Programme ([FP7/2007-2013]) under grant agreement No. 244149.

**PS 1491 *In Vitro* Evaluation of Cytotoxic and Genotoxic Effects of Ofloxacin.**

V. Sekeroglu<sup>1,2</sup>, Z. Atli Sekeroglu<sup>1,2</sup>, M. Aksoy<sup>2</sup> and S. Kontas<sup>2</sup>. <sup>1</sup>Applied Medical Sciences, University of Southern Maine, Portland, ME; <sup>2</sup>Biology, University of Ordu, Ordu, Turkey. Sponsor: J. Wise Sr.

Ofloxacin (OFX), the second-generation of quinolones, is a broad-spectrum fluoroquinolone antibiotic used in the treatment of various bacterial infections. In this study, the genotoxic and cytotoxic effects of OFX in cultured human peripheral blood lymphocytes were investigated by measuring chromosome aberrations (CAs), sister chromatid exchange (SCE) assay, mitotic index (MI) and proliferation index (PI). Cultures were treated with three doses of OFX (30, 60 and  $120 \mu\text{g}/\text{ml}$ ) at 48 h exposure period for all assays. An untreated culture (negative control) and a positive culture treated with MMC (positive control) were established, as well. Although the frequency of SCE slightly increased in a concentration-dependent manner, dose-dependent increases were not observed in the CAs. But, these increases were statistically not significant, compared to negative control ( $P < 0.05$ ). With respect to the cytotoxic effects of the test compound on lymphocyte cultures, as measured by MI and PI, a concentration-dependent reduction in cell proliferation was also observed. The highest dose of OFX ( $120 \mu\text{g}/\text{ml}$ ) significantly reduced the MI values compared to negative control ( $P < 0.05$ ), whereas decreases in PI values were not found significant compared to negative control.

The results of this study indicate that OFX can exert a cytotoxic effect especially at the higher doses because of statistically significant decreases in MI, but has no genotoxic activity in both CA and SCE assays in human peripheral blood lymphocyte cultures.

## PS 1492 Genotoxic Effects in Children Environmentally Exposed to Particulate Matter.

M. Sánchez-Guerra<sup>1,2</sup>, A. Araujo<sup>3</sup>, L. Serrano-García<sup>3</sup>, L. Hernández-Cadena<sup>4</sup>, R. Montero-Montoya<sup>1</sup>, I. Alvarado-Cruz<sup>1</sup>, A. De Vizcaya-Ruiz<sup>1</sup>, L. Rafael-Vázquez<sup>1</sup>, E. Jiménez-Mendoza<sup>1,5</sup>, J. Torres-Arellano<sup>1,5</sup>, V. Mugica<sup>6</sup> and B. Quintanilla-Vega<sup>1</sup>. <sup>1</sup>Toxicology Department, CINVESTAV-IPN, Mexico City, Mexico; <sup>2</sup>Exposure Epidemiology and Risk Program, Harvard School of Public Health, Boston, MA; <sup>3</sup>Instituto de Investigaciones Biomédicas, UNAM, Mexico City, Mexico; <sup>4</sup>INSP, Cuernavaca, Mexico; <sup>5</sup>FÉZ-Iztacala, UNAM, Mexico City, Mexico; <sup>6</sup>UAM-Azcapotzalco, Mexico City, Mexico.

Ecatepec County is considered one of the most contaminated counties in the Metropolitan Area of Mexico City. There are reports about the high levels of particulate matter (PM) in this area related to the high traffic and industrial activity. PM is associated with several health problems including genotoxic effects. Children are considered one of the most susceptible populations to air pollution. The aim of this study was to evaluate the DNA damage related to the exposure to PM in the air. We conducted an air monitoring study and an epidemiological survey in schoolchildren from 6 to 10 years (n=86) of both genders in an area of Ecatepec County and the following was evaluated: concentrations of PM<sub>10</sub> and PM<sub>2.5</sub> in the air, as well as the organic and elemental carbon content (CO and CE, respectively), the presence of micronucleus (MN), apoptotic cells (AC) and necrotic cells (NC), and the nuclear division index (NDI) in peripheral lymphocytes by the cytokinesis-block micronucleus test in 1000 cells. The geometric average age was 8.4 years; 41% of children showed at least 1 MN (range 1-6), 27% showed 1-49 AC and 16% had 1-9 NC, some children showed exceptionally high AC or NC values. We found a significant association between CO-PM<sub>10</sub> and the presence of MN, AC and NC, and a decrease in the NDI, while CE-PM<sub>10</sub> was associated with MN and NC. Regarding PM<sub>2.5</sub>, the CO content was associated only with the presence of MN. These preliminary data suggest that both the CO and CE contents of PM from Ecatepec County are involved in the genotoxic effects observed in schoolchildren. Study supported by CONACYT-México (Grant #106034).

## PS 1493 Bariatric Surgery Reduces Intestinal Toxicity in Man.

A. Alkandari, Q. Wu, H. Ashrafian and N. J. Gooderham. *Surgery and Cancer, Imperial College London, London, United Kingdom.*

Obesity is a global epidemic. Worldwide 500 million people are classified as obese with a global prevalence that continues to rise. Obesity and its co-morbidities are amongst the leading causes of global mortality and morbidity and pose substantial socioeconomic burdens on health services worldwide. Bariatric surgery is a form of gastrointestinal surgery that leads to sustained weight loss, resolution of type 2 diabetes and a decrease in cancer risk. These operations alter gut microbial composition which is reflected in the bacterial composition of faeces. We hypothesise that the protective effect of bariatric surgery is due to a decrease in diet-derived intestinal toxic burden. Here, we determined the effect of bariatric surgery on intestinal cytotoxicity and genotoxicity in man. Aqueous dimethyl sulfoxide faecal extracts were obtained from preoperative and 2 month postoperative samples from 5 individuals undergoing Roux-en-Y gastric bypass. Human MCL5 cells, a lymphoblastoid cell line expressing CYP1A1, 1A2, 2E1 and 3A4 and epoxide hydrolase, were used to assess faecal extract toxicity and genotoxicity was determined at the TK and HPRT loci using benzo(a)pyrene as a positive control. We found a trend of decreased cytotoxicity postoperatively, as assessed by relative total growth (20% decrease compared to preoperative faecal extracts). Furthermore, the genotoxicity of the faecal extracts decreased postoperatively at both the TK and HPRT loci (30% and 70% respectively, whereas the BaP control induced mutation frequency more than 50 fold). These results support the hypothesis that bariatric surgery leads to a decrease in diet-derived intestinal toxicity burden, which in turn may contribute to the health beneficial effects associated with surgery.

## PS 1494 The Tobacco-Specific nitrosamine 4-(methylnitrosamino)-1-(3-pyridyl)-1-butanone (NNK) Induces Mitochondrial and Nuclear DNA Damage in *Caenorhabditis elegans*.

R. K. Bodhicharla<sup>1</sup>, P. Gaddamanugu<sup>2</sup> and J. N. Meyer<sup>1</sup>. <sup>1</sup>Nicholas School of the Environment, Duke University, Durham, NC; <sup>2</sup>R.J. Reynolds Tobacco Company, Winston-Salem, NC.

The metabolites of the tobacco-specific carcinogen NNK form DNA adducts in animal models. One report indicates that NNK could cause damage to the mitochondrial as well as nuclear genome in rats (Stepanov and Hecht, 2009 *Chem. Res. Toxicol.* 22: 406-414). Using a different DNA damage detection technology, we tested whether this could be repeated in the nematode *Caenorhabditis elegans*; we also evaluated whether mitochondrial function would be affected. We treated N2 strain (wild-type) nematodes with NNK in liquid culture. Quantitative PCR was applied to analyze NNK-induced nuclear and mitochondria DNA damage. This assay has the advantage of measuring all DNA lesions that inhibit the DNA polymerase, and normalizes results to mitochondrial DNA copy number (Hunter *et al.*, 2010 *Methods* 51:444-451). Our results confirm that NNK causes both nuclear and mitochondrial DNA damage, but surprisingly nuclear DNA damage was greater than mitochondrial DNA damage in *C. elegans*. To test whether the mitochondrial DNA damage was associated with mitochondrial dysfunction, we used a transgenic nematode strain that permits *in vivo* measurement of ATP levels and found lower levels of ATP in NNK-exposed animals when compared to the unexposed controls. To test whether the lower levels of ATP were due to the inhibition of respiratory chain components we investigated oxygen consumption in whole *C. elegans* and found reduced oxygen consumption in exposed animals when compared to the unexposed controls. Our data suggest a model in which NNK causes damage to both nuclear and mitochondrial genomes, and support the hypothesis that the mitochondrial damage is functionally important. These results also represent a first step in developing this genetically tractable organism as a model for assessing NNK toxicity.

## PS 1495 Meta-Analysis Evaluating the Association between Diseases Linked to Asbestos and Genetic Polymorphisms.

L. Lievense<sup>1</sup>, C. J. Ronk<sup>2</sup>, S. A. Gross<sup>3</sup> and C. A. Barlow<sup>3</sup>. <sup>1</sup>ChemRisk LLC, Chicago, IL; <sup>2</sup>ChemRisk LLC, San Francisco, CA; <sup>3</sup>ChemRisk LLC, Boulder, CO.

Asbestos is a ubiquitous, naturally occurring mineral fiber that has been linked to the development of malignant and fibrotic lung diseases. Numerous studies have shown that a polymorphism in the genes involved in xenobiotic and oxidative metabolism or in DNA repair processes may play an important role in the pathogenesis of many, if not most, diseases. Unlike some other neoplastic diseases, no association with mesothelioma risk has been consistently demonstrated for polymorphic genes involved with oxidative stress, metabolism, or DNA repair. To evaluate the association between diseases linked to asbestos and genetic variability, we performed a meta-analysis combining the available data on the presence of polymorphisms in GSTM1, GSTT1, NAT2, mEH, XRCC1, and XRCC3 from Italian (n = 57) and Finnish (n = 48) populations with pleural mesothelioma in which the relative magnitude of asbestos exposure was classified. Meta-relative risk statistics were estimated through fixed effects modeling using SAS software. Our analysis found that the GSTM1 null genotype, NAT2 fast acetylator genotype, mEH low activity genotype, and the T/M variant allele of XRCC3-T241M were significantly associated with having an increased risk of pleural mesothelioma. When mesothelioma patients were stratified by asbestos exposure (high vs. low), the association between mesothelioma and GSTM1, NAT2, and mEH was not statistically significant for the high exposure group. The association between the T/M variant allele of XRCC3-T241M and mesothelioma was significantly increased, regardless of asbestos exposure. The R/Q variant allele of XRCC1-R399Q appeared to be confined to those mesothelioma patients with a history of high exposure to asbestos, although the confidence interval includes parity. The results from the present analysis strengthen the hypothesis that intensity of asbestos exposure combined with the presence of certain genetic polymorphisms may increase individual mesothelioma risk.

## PS 1496 Evaluation of the Mutagenicity of Dyed Fabrics with Direct Black 38.

G. A. Oliveira<sup>1</sup>, D. M. Leme<sup>1</sup>, T. C. Santos<sup>2</sup>, M. B. Zanoni<sup>2</sup> and D. P. Oliveira<sup>1</sup>. <sup>1</sup>Faculty of Pharmaceutical Sciences of Ribeirão Preto, University of São Paulo (USP), Ribeirão Preto, Brazil; <sup>2</sup>Institute of Chemistry, University Estadual Paulista (UNESP), Araraquara, Brazil.

There are several information on toxicity of textile dyes, but data of colored fabrics are still limited. Although a dye itself may be toxic, its presence in the finished material may not be harmful. Direct Black 38 (DB38) is a benzidine-based azo dye,

commonly used in textile industry. It is known that, under conditions of perspiration, dyes migrate from colored fabrics and penetrate into human skin. Objective: Evaluate the mutagenicity of DB38 extracted from dyed cotton fibers using artificial sweat solutions. Methodology: Pieces of cotton fabric were dyed with DB38 and washed with and without rinsing (bath with a colloid dispersant). DB38 was extracted from the dyed fabric with artificial sweat solutions (pH 5.5, 6.5, 8.0) at 37°C and 42°C for 2, 8 and 12 h. HPLC-DAD analysis was performed to determine the concentration of dye extracted in each sweat extract. Both original dye and sweat extracts were evaluated by the Salmonella/microsome assay using the strains TA98 and TA100 with and without S9 mix in order to compare with the higher dye concentration extracted with sweat. Results: Original DB38 dye showed positive mutagenic response for TA98 and TA100 with S9. The migration of DB38 dye into artificial sweat resulted in 5.9 µg/mL (dyeing without rinsing, pH 8.0, 42°C, 8 h). Sweat extracts with DB38 did not induce mutagenic effects under the conditions tested. Discussion: Original dye induces mutagenicity by both base-pair substitution and frameshift mutations in presence of S9. However, these effects could no longer be observed after its extraction from dyed fabric using artificial sweat as extracting agent. Our findings showed that DB38 dye can migrate from colored fabrics to artificial sweat, however the concentration of dye extracted does not cause mutagenicity. Thus, as important as the toxicological information of textile dyes, is an investigation of the toxic effects of fabrics which contain these dyes in order to avoid human health problems.

**PS 1497 Characterizing the Genotoxicity of the Trichloroethylene Metabolite Dichlorovinyl Cysteine.**

J. B. Asfaha, V. De La Rosa and C. Vulpe. *University of California Berkeley, Berkeley, CA.*

Trichloroethylene (TCE) is an industrial solvent and common environmental contaminant. TCE is metabolized via the glutathione conjugation (GSH) pathway where the reactive metabolite, dichlorovinyl cysteine (DCVC) is formed. Previous work in the field has shown DCVC as the penultimate metabolite resulting in renal toxicity. Our studies using a functional genomics approach in yeast suggest DNA damage and repair pathways play a role in DCVC toxicity. Specifically, we identified the error-prone translesion synthesis (TLS) repair pathway and nucleotide excision repair (NER) as important for response to DCVC exposure. Preliminary work in human fibroblast cells shows initiation of translesion synthesis repair after DCVC exposure. Studies to identify potential DCVC-DNA lesions were conducted using liquid chromatography mass spectrometry (LCMS) analysis. Results indicate the potential for DCVC to cause direct DNA damage via DNA adducts with specific nucleotides. Our data suggests DCVC is genotoxic and has the potential to lead to cell death.

**PS 1498 Coexposure to LA Sweet Crude Oil and Dispersant Alters Genomic DNA Damage Occurrence in the Gulf Killifish.**

K. E. Germ and G. D. Mayer. *Environmental Toxicology, The Institute of Environmental and Human Health, Texas Tech University, Lubbock, TX.*

The BP-Deepwater Horizon event in the Gulf of Mexico unleashed an unprecedented environmental disaster where more than 650 miles of Gulf coastline was littered with Louisiana Sweet Crude oil. During this event Corexit 9500, a surfactant designed to disperse and emulsify crude oil and expedite microbial breakdown, was used to mitigate damage. However, surfactant additives can increase membrane permeability and biological uptake of exogenous compounds including components of crude oil. Recent studies indicate that although visible traces of weathered crude oil have long been absent in the estuarine environments, particular toxic mutagens persist in organisms and sediments that were once co-exposed to oil and dispersant. This research focuses on the notion that toxic components of crude oil may persist and adversely affect genomic integrity. We examined genomic DNA coding sequences, cytochrome c oxidase-subunit I and cystic fibrosis transmembrane conductance receptor for lesion analysis. Here we show that killifish, *Fundulus grandis*, exposed to crude oil and dispersant have increased amounts of genetic damage in both mitochondrial and nuclear templates, relative to killifish exposed to each individual compound. Additionally, DNA lesion formation in the mitochondrial genome was increased in the co-exposures, compared to singular exposures of contaminants.

**PS 1499 Absence of Genotoxicity in a Series of 2'-O-Methyl Phosphorothioate Oligonucleotides.**

Y. Ponstein, C. den Besten and S. de Kimpe. *Prosenza, Leiden, Netherlands.*  
Sponsor: E. van Doesum-Wolters.

PRO044, PRO045 and PRO053 are 2'-O-methyl phosphorothioate RNA antisense oligonucleotides (AON) that are in development for the treatment of Duchenne Muscular Dystrophy (DMD), a lethal orphan disease for which no disease modifying therapy exists. The fundamental cause of this disease is mutations in the dystrophin gene leading to out of frame transcripts for the corresponding muscle protein. AON-induced exon skipping of exon 44, 45 and 53, respectively, in human dystrophin pre-mRNA results in the restoration of the reading frame and an internally deleted but functional dystrophin protein. The mutagenic and clastogenic potential of PRO044, PRO045 and PRO053 was assessed using in vitro tests in bacteria and mammalian cells and an in vivo rodent assay. The bacterial reverse mutation assay (i.e. Ames test using *Salmonella typhimurium* TA98, TA100, TA102, TA1535 and TA1537) showed that the mentioned AONs have no mutagenic activity at concentrations up to 5,000-10,000 µg per plate, in the presence or absence of an in vitro metabolic activation system (S9-mix). The Chinese hamster ovary (CHO) chromosomal aberration assay showed that PRO044, PRO045 and PRO053 did not induce structural aberrations in the presence or absence of S9-mix, with tested concentration up to 5,000 µg/mL. In addition, PRO044, PRO045 and PRO053 did not induce any polyploidy or give indications of mutagenic properties in the presence or absence of S9-mix at 5,000 µg/mL. In the in vivo micronucleus assay, no genotoxic effect was observed in the bone marrow of mice following repeated subcutaneous administrations of PRO044, PRO045 and PRO053 at dose levels ranging between 80 and 1,000 mg/kg on days 1, 3, 5, and 8, resulting in a weekly dose of 320 to 4,000 mg/kg. In conclusion, results from these experiments demonstrate that PRO044, PRO045 and PRO053 are not mutagenic nor clastogenic. This is in accordance with the EMA's reflection paper indicating that phosphorothioate nucleotides (as potential degradation products/metabolites of phosphorothioate oligodeoxynucleotides) are unlikely to pose a genotoxic hazard.

**PS 1500 Different Extraction Strategies to Evaluate the Genotoxicity of the Water Soluble Fraction of Air Particulate Matter.**

I. C. Palacio<sup>2,1</sup>, R. L. Franklin<sup>1</sup>, C. F. Suzuki<sup>1</sup>, I. F. de Oliveira<sup>1</sup>, D. A. Roubicek<sup>1</sup> and S. B. Barros<sup>2</sup>. <sup>1</sup>*Departamento de Análises Ambientais, Companhia de Tecnologia de Saneamento Ambiental, São Paulo, Brazil;* <sup>2</sup>*Departamento de Análises Clínicas e Toxicológicas, Universidade de São Paulo, São Paulo, Brazil.*

Exposure to contaminated airborne particulate matter (PM) as a consequence to urban air pollution has adverse effects on human health and the ecosystem. In most air pollution studies, only the genotoxic potential of the organic fraction is evaluated and the toxic effects of the soluble metals are not usually verified. In order to determine an appropriate extraction method for assessing the mutagenicity of the water-soluble fraction of PM, we performed microwave assisted (MW) and ultrasonic bath (UT) extractions, using water as the only solvent, in 10 different air samples (Total particulate matter-TPS- and PM10- fraction of particles with diameter of 10µm or less), from the state of São Paulo, Brazil. Mutagenicity and extraction performances were evaluated using the Salmonella/microsome assay with strains TA98 and TA100, followed by chemical determination of soluble metals (ICP). Except for one sample, the mutagenic potential of TPS was significantly higher in the samples extracted with MW than those with UT. The PM10 samples extracted with MW showed mutagenic activity only with TA98, with and without metabolic activation, and in those with UT there was no biological response. Of the metals analyzed (Ni, Cu, Zn, Cr, Fe, Pb, Mn, Co, V and Ti), only vanadium (in the samples extracted with MW) and copper (in the UT extracted samples) were above detectable levels. Our results demonstrate the importance in determining an efficient extraction method for evaluating genotoxicity, especially at low concentrations of water-soluble contaminants in the air particulate matter. The MW represented a powerful tool to evaluate the genotoxicity of those samples, and additionally has methodological advantages against UT, allowing more reproducibility of the test conditions and improving the analysis precision. Supported by CAPES Ph.D. fellowship Isabel Palacio

**PS 1501 Time Course Study of Sulphur Mustard-Induced DNA Damages in Hairless Skh-1 Mice.**

M. Batal<sup>1,2</sup>, I. Boudry<sup>2</sup>, C. Cléry-Barraud<sup>2</sup>, S. Mouret<sup>2</sup> and T. Douki<sup>1</sup>. <sup>1</sup>CEA, Grenoble, France; <sup>2</sup>IRBA, La Tronche, France. Sponsor: J. McDonough.

A major target for sulphur mustard (SM) is DNA. DNA alkylation leads to the formation of monoadducts, mainly at the N7 position of guanine (HETE-N7Gua: N7 hydroxyethylthioethyl-guanine) and in a lesser extent at the N3 position of adenine (HETE-N3Ade: N3 hydroxyethylthioethyl-adenine), and biadducts (N7Gua-ETE N7Gua: bis[N7guanin-ethyl]sulphide). It is a critical step to explain SM cytotoxicity. Therefore, we have developed a high performance liquid chromatography coupled to tandem mass spectrometry (HPLC-MS/MS) method to quantify the three main SM-DNA adducts. The assay was applied to SKH-1 mice exposed to liquid SM on the dorsal skin at 2, 6 and 60 mg/kg during 4h and were sacrificed at 6h, d1 (day 1), d3, d7, d14 and d21 after exposure. SM exposed skin, skin adjacent to exposed skin and skin being located at 2 cm apart of this latter were removed. The maximum of DNA lesions in SM exposed skin was obtained at 6h post-exposure. The contribution of HETE-N3Ade to SM DNA adducts in skin was much lower than that found in isolated and cellular DNA in previous experiments. Adducts frequencies decreased from d1 likely as the result of DNA repair. Yet a relatively important persistence of SM-DNA adducts was observed since HETE-N7Gua and N7Gua-ETE N7Gua were still detected at d21 after 60 mg/kg exposure. For each exposure dose, SM-DNA adducts were also measured, in skin adjacent to the exposed zone, although in lower amounts. They were quantified until d14 after 60 mg/kg exposure. For the highest dose, SM-DNA adducts were detected at 2 cm of the burn but only at d1. These results show a limited radial diffusion of SM in skin but a significant persistence in time. They also demonstrate the reliability of our method to quantify SM-DNA adducts which could be monitored as part of therapeutic tests.

**PS 1502 Accurate Assessment for the *In Vitro* CB Micronucleus Test by Comparison of Two Different Protocols Using Human Lymphocytes.**

S. Bohnenberger, A. Poth and W. Voelkner. *Genotoxicity and Alternative Toxicology, Harlan Cytotest Cell Research, Rosdorf, Germany.*

The OECD Guideline 487 for the *In Vitro* Mammalian Cell Micronucleus Test (MNvit) became effective in July 2010. The objective of the test is to identify micronucleus formation via clastogenic and aneugenic mechanisms in cells that have completed mitosis. This work presents the assessment of various test parameters for the performance of the assay with human lymphocytes with regard to the above mentioned Guideline. With respect to the *In Vitro* Mammalian Cell Micronucleus Test (MNvit) aneugenic and clastogenic reference chemicals (colcemid/demecolcin, mitomycin C (MMC) and cyclophosphamide (CPA). were tested for their potential to induce micronuclei in cultured human peripheral blood lymphocytes. The protocol given by the current OECD Guideline 487 was compared to a slightly modified protocol allowing the cells to have a recovery period between end of treatment and addition of the cytokinesis blocker cytochalasin B. Lymphocyte proliferation was studied in response to stimulation with phytohemagglutinin and the normal cell cycle time was assessed by bromodeoxyuridine uptake. The presented data show difficulties in the detection of an aneugenic compounds in binucleate cells and marked differences in the induction of micronuclei in the micronucleus *in vitro* by the two different test protocols employed by using the four different reference chemicals. Reproducible results were obtained with the clastogenic reference chemical MMC, regardless of the protocol used. With both aneugenic compounds robust and adequate results could be obtained by including the evaluation of micronucleated cells and using the pulse treatment. Robust data were obtained with CPA when using a time schedule including a recovery period.

**PS 1503 Clastogenicity and Mutagenicity Testing of Gaseous Compounds.**

C. S. Farabaugh<sup>1</sup>, J. Randazzo<sup>2</sup>, M. M. Wells<sup>1</sup>, M. L. Moy<sup>1</sup> and M. J. Schlosser<sup>1</sup>. <sup>1</sup>WIL Research, Skokie, IL; <sup>2</sup>WIL Research, Ashland, OH.

WIL Research evaluated methods for genetic toxicology testing with gaseous compounds in both the *In Vitro* Chromosome Aberration (CA) assay using human peripheral blood lymphocytes (HPBL) and the Bacterial Reverse Mutation assay (Ames assay). In the CA assay, 10 mL HPBL cultures were initiated with S9 (3-hour exposure) and without S9 (3- and 22-hour exposures) in flasks and were sealed in airtight Tedlar bags using a heat sealer. The air was evacuated and a mixture of ambient air, ~5% CO<sub>2</sub>, and the appropriate concentration of Chloroethane (CE) up to 30% v/v for the 22-hour exposure or Propylene Oxide (PO) up to 10% v/v

for the 3-hour exposures were added via a septum into the bag. The cultures in the bags were then incubated at 37°C in a humidified atmosphere with 5% CO<sub>2</sub>. For the 3-hour exposure periods, cultures were removed from bags and washed before being returned to the humidified incubator until a single harvest time of ~22 hours. Statistically significant, dose related increases in cells with aberrations when compared to the vehicle control cultures were observed with responses of up to 42% of cells for the 22-hour exposure (at a dose level of 5% v/v), 14.5% for the 3-hour exposure with S9 (2.5% v/v), and 30% for the 3-hour exposure without S9 (2.5 % v/v).

In the Ames assay, *Salmonella* tester strains TA98, TA100, TA1535, and TA1537 and *E. coli* tester strain WP2uvrA were exposed using the preincubation method to various concentrations of CE up to 25% v/v and incubated at 37°C for ~30 minutes in sealed Tedlar bags. The air was evacuated and a mixture of ambient air and the appropriate concentration of CE were added via a septum into the bag. Following exposure, the cultures were removed from the bags, plated, and incubated at 37°C for ~48 hours. Dose related increases in the mean number of revertants when compared to the vehicle control cultures were observed.

Results indicate that gaseous exposures using Tedlar bags are appropriate for producing positive responses with and without S9 with known clastogenic and mutagenic compounds in the CA and Ames assays.

**PS 1504 Quantitative Analysis of Specific DNA Adducts and *In Vivo* Mutagenicity following Exposure to the Hepatocarcinogen Estragole.**

Y. Ishii<sup>1</sup>, S. Takasu<sup>1</sup>, K. Matsushita<sup>1</sup>, K. Kuroda<sup>1</sup>, T. Nohmi<sup>2</sup>, K. Ogawa<sup>1</sup>, A. Nishikawa<sup>1</sup> and T. Umemura<sup>1</sup>. <sup>1</sup>Pathology, National Institute of Health Sciences, Tokyo, Japan; <sup>2</sup>Research and Development Promotion, National Institute of Biomedical Innovation, Osaka, Japan.

DNA modifications are considered a trigger for somatic mutations. However, factors such as DNA repair and cell proliferation are known to contribute to DNA modification processes, promoting gene mutations. We previously reported that specific DNA adducts are formed in the livers of rats following treatment with estragole (ES), a hepatocarcinogen in rodents. ES caused formation of the DNA adducts, ES-3'-N<sup>2</sup>-dG, ES-3'-C8-dG, and ES-3'-N<sup>6</sup>-dA, in rat livers, as determined by LC-MS/MS analysis. To clarify associations between the number of modified bases and the mutant frequencies (MFs) in the same animal and organ, we quantified ES-specific DNA adducts and performed reporter gene mutation assays in livers, kidneys, and lungs of 6-week-old F344 *gpt* delta rats given ES at doses of 0, 3, 30, and 300 mg/kg/day by gavage for 4 weeks. Relative liver and kidney weights were significantly increased in rats given high-dose ES. Mitosis, single-cell necrosis in hepatocytes, and oval cell proliferation were seen in high-dose group livers. Three ES-specific DNA adducts were detected in a dose-dependent manner beginning with the low-dose group. *gpt* MF was significantly increased only in the high-dose group. In lungs and kidneys, DNA adducts were detected only in the high-dose group, but their frequencies were almost identical to those in the low-dose group livers. These results suggest that the site specificity observed in ES carcinogenicity may depend on the number of modified bases. In addition, the fact that ES-specific DNA adducts were detected to some extent in the livers of rats treated with moderate doses, despite *gpt* MF being unchanged, suggests involvement of micro-environmental factors, such as cell proliferation and DNA repair enzymes, in the progression from DNA modification to gene mutation. Some of these factors will be presented, along with results of *gpt* mutation assays in the lungs and kidneys.

**PS 1505 Mutagenic Activity of Allura Red AC and Tartrazine in *Salmonella typhimurium*.**

R. Narayananeni, S. Sharma, S. Visram, G. Lo and R. D. Mehta. *Genetic Toxicology, PBR Laboratories Inc, Edmonton, AB, Canada.*

Allura Red AC (Red 40) and Tartrazine (Acid yellow 23) are two of the most commonly used artificial color additives (azo dyes) in food, drug and cosmetic industries. Allura Red and Tartrazine are nitrous derivatives which are the focus of studies on mutagenesis and carcinogenesis because of their transformation into aromatic amines after being metabolized by the gastrointestinal microflora. We investigated the mutagenic activity of Tartrazine and Allura Red against TA98, TA100, YG1041 and YG1042 strains of *Salmonella Typhimurium* using the protocol described by Prival and Mitchell (1981). Both YG1041 and YG1042 strains, derived from TA98 and TA100, respectively carry a plasmid with genes for higher levels of nitroreductase and O-acetyltransferase involved in the break down of azo dyes to mutagenic aromatic amines. These strains have been shown to detect mutagenic activity of azo dyes in the effluents from textile industries, eliciting a higher mutagenic response compared to TA98 and TA100 (Umbuzeiro et al, 2003). We used six dose levels (4mM, 2mM, 1mM, 0.5mM, 0.25mM, 0.125mM) of Allura Red and Tartrazine for testing the mutagenic activity. The assay was performed

under hamster S9-activated and non-activated conditions. In our study, none of the four tester strains showed toxicity or an increase in the mutation frequency at the dose levels tested. Whereas, Tartrazine has been reported to have cytotoxic effect in mammalian cells (Patterson and Butler, 1982) and Allura Red has been found to cause DNA damage when tested with the comet assay (Shuji et al, 2001). European Food Safety Authority (2009) has also reported that Allura Red was negative in *in vitro* genotoxicity as well as long term carcinogenicity studies. Our results demonstrate that the salmonella strains even with high level of nitroreductase and O-acetyltransferase activities failed to show mutagenic activity in both, Tartrazine and Allura Red.

## PS 1506 Genotoxicity of 2-Bromo-3'-Chloropropiophenone.

F. Meng<sup>1</sup>, J. Yan<sup>1</sup>, Y. Li<sup>1</sup>, P. Fu<sup>2</sup>, L. Fossum<sup>3</sup>, R. Sood<sup>3</sup>, D. Mans<sup>3</sup>, P. Chu<sup>3</sup>, M. M. Moore<sup>1</sup> and T. Chen<sup>1</sup>. <sup>1</sup>Division of Genetic and Molecular Toxicology, NCTR/FDA, Jefferson, AR; <sup>2</sup>Division of Biochemical Toxicology, NCTR/FDA, Jefferson, AR; <sup>3</sup>CDER, FDA, Silver Spring, MD.

Impurities are generally an integral part of any drug substance or drug product. They can be either process-related impurities that are not completely removed during purification or formed due to the degradation of the drug substance over the product shelf-life. Unlike the drug, they do not provide health benefits. Therefore, their amount should be minimized. 2-Bromo-3'-chloropropiophenone (BCP) is an impurity of bupropion, a second-generation antidepressant and a smoking cessation aid. The US Pharmacopeia recommends an acceptable level for BCP that is not more than 0.1% of the maximum dose of bupropion. Recently a qualitative structure-activity analysis (DEREK for Windows version 13) has shown that BCP is likely genotoxic. The genotoxicity of BCP, however, has not been tested based on a search of the available public literature. Because the US FDA limits genotoxic impurities to much lower levels than non-genotoxic impurities, it is important to determine whether or not BCP is genotoxic. Therefore, in this study the Ames test and the *in vitro* micronucleus assay were conducted to evaluate the genotoxicity of BCP. BCP was mutagenic with S9 metabolic activation, increasing the mutant frequencies in a concentration-dependent manner, up to 22- and 145-fold induction over the controls in Salmonella strains TA100 and TA1535, respectively. BCP was also positive in the *in vitro* micronucleus assay, resulting in up to 3.3- and 5.1-fold increase of micronucleus frequency for treatments in the absence and presence of S9, respectively; and 9.9- and 7.4-fold increase of hypodiploids without and with S9, respectively. The addition of N-acetyl-L-cysteine, an antioxidant, reduced but not eliminated the genotoxicity of BCP in both assays. The results suggest that BCP is mutagenic, clastogenic, and aneugenic, and these activities are possibly mediated via generation of reactive metabolites.

## PS 1507 Comparison of Mainstream Smoke (Mss) Cytotoxicity and Clastogenicity from Filtered Cigars with the Corresponding Data for the Mss from the KY3R4F Reference Cigarette.

J. H. Lauterbach<sup>1</sup>, E. Z. Sheabar<sup>2</sup>, D. Muldoon<sup>2</sup>, G. Nelluru<sup>2</sup>, T. Oshunwusi<sup>2</sup> and D. Powell<sup>2</sup>. <sup>1</sup>Lauterbach & Associates, LLC, Macon, GA; <sup>2</sup>Arista Laboratories, Richmond, VA.

Filtered cigars, dimensionally similar to 100s cigarettes, have become popular smoking articles. Unlike cigarettes, the tobacco column is wrapped with a single ply of paper-type reconstituted tobacco. The blends in filtered cigars range from light-air cured tobaccos to tobaccos with more cigar-like character. Since filtered cigars have been reported to be popular with younger smokers, concern has been raised about the toxicity of the smoke relative to cigarette smoke. Rickert et al., 2011, reported that on a per unit smoke nicotine basis the toxicity of the mainstream smoke (MSS) from filtered cigars was no less than that of the MSS from cigarettes. However, the Rickert work used the Health Canada Intensive (HCI) smoking regimen and used king-size like products that are no longer popular or available commercially. In this research, we have used ISO smoking regimen and three contemporary 100 mm filtered cigars, one of which (FC1) had a more traditional cigar blend than did the other two (FC2, FC3). On a unit TPM basis, there was little difference in the Neutral Red cytotoxicity of the MSS from the three filtered cigars and the cytotoxicity of the MSS of the KY3R4F reference cigarette. However, when the results were put on a per unit smoke nicotine basis, the MSS from two of the three filtered cigars (FC2, FC3), which had low MSS nicotine concentrations, were more cytotoxic than the MSS from the KY3R4F. On a per unit nicotine basis, the cytotoxicity of the MSS from FC1 was similar to that of the MSS of the KY3R4F. Genotoxicity was determined with the *in vitro* micronucleus assay. On a unit TPM basis, toxicity rankings (-S9) were FC1=FC3>FC2>>KY3R4F and (+S9) were FC3>FC2>FC1>>KY3R4F. On a unit nicotine basis, toxicity rankings (for both -S9, +S9) were FC3>FC2>FC1>>KY3R4F. Our results were similar to those reported by Rickert et al. and showed that the ISO smoking regimen was better able to show product differences than was the HCI regimen.

## PS 1508 Effects of Obesity on Spontaneous Reporter Gene Mutations in *Gpt* Delta Mice Fed a High-Fat Diet.

S. Takasu<sup>1</sup>, Y. Ishii<sup>1</sup>, K. Matsushita<sup>1</sup>, K. Kuroda<sup>1</sup>, Y. Kodama<sup>2</sup>, K. Ogawa<sup>1</sup>, A. Nishikawa<sup>3</sup> and T. Umemura<sup>1</sup>. <sup>1</sup>Division of Pathology, National Institute of Health Sciences, Tokyo, Japan; <sup>2</sup>Division of Toxicology, National Institute of Health Sciences, Tokyo, Japan; <sup>3</sup>Biological Safety Research Center, National Institute of Health Sciences, Tokyo, Japan.

Epidemiologically, obesity has been suggested to be associated with increased risk of several human cancers, including cancers of the liver, kidneys, and colon. In several rodent models, genetically induced obesity or high-fat diet (HFD) induced obesity has been shown to enhance carcinogenesis in the liver and colon after treatment with a regimen of respective tumor initiators. However, the factors responsible for the obesity-related progression of carcinogenesis, especially the initiation phase, are not fully elucidated. To reveal the effects of obesity induced by an HFD on spontaneous gene mutations, we performed reporter gene mutation assays in liver, kidney, and colon tissues from obese mice fed an HFD. Six-week-old male and female C57BL/6 *gpt* delta mice were fed either an HFD or a standard diet (STD) for 13 or 26 weeks. At the end of the experimental period, all mice were sacrificed, and reporter gene mutation assays were performed. Final body weights of male and female mice fed an HFD for 13 weeks were significantly increased compared with those fed an STD. *gpt* and *Sp1* mutant frequencies in the liver, kidneys, and colon of male mice fed an HFD for 13 weeks were not significantly different from those fed an STD. These results implied that HFD-induced obesity does not influence the spontaneous frequencies of somatic gene mutations, indicating that obesity may affect the tumor promotion phase rather than the tumor initiation phase to enhance carcinogenesis. Further data from the organs of mice fed an HFD for 26 weeks will be presented to evaluate the effects of long-term consumption of an HFD on spontaneous mutagenicity *in vivo*.

## PS 1509 Community Lead (Pb) Domains and Exposure Disparities: Case Study of Pre- and Post-Katrina New Orleans.

H. W. Mielke<sup>1,2</sup>, C. R. Gonzales<sup>3</sup>, E. T. Powell<sup>3</sup> and P. W. Mielke<sup>4</sup>. <sup>1</sup>Pharmacology, Tulane University School of Medicine, New Orleans, LA; <sup>2</sup>Chemistry, Tulane University, New Orleans, LA; <sup>3</sup>Lead Lab, Inc., New Orleans, LA; <sup>4</sup>Statistics, Colorado State University, Fort Collins, CO.

We sought to gain insight into the Pb toxicity characteristics of communities in New Orleans. Based on previous soil Pb mapping we divided New Orleans census tracts into two soil Pb domains, high (median  $\geq 100$  mg/kg) and low (median  $< 100$  mg/kg). Soil samples from four locations represented each of the domains: busy streets, residential streets, house sides, and open spaces (away from streets and houses). Blood and soil Pb concentrations within the high and low Pb domains of New Orleans were analyzed by permutation statistical methods (Multi-Response Permutation Procedures). The children's blood Pb prevalence  $\geq 5$   $\mu\text{g/dL}$  for the high and low Pb domains were 58.5% and 24.8%, respectively, pre-Katrina vs. 29.6% and 7.5% in post-Katrina New Orleans. In the high Pb domain median soil Pb was 367, 313, 1228, and 103 mg/kg, respectively, busy streets, residential streets, house sides, and open space locations; in the low Pb domain median soil Pb was 64, 46, 32, and 28 mg/kg, respectively (p-Values  $< 10E-16$ ). After Katrina relatively small decreases in soil Pb were observed, and elevated soil Pb permeates the high Pb domain; children living there generally lack Pb safe areas for outdoor play. The low Pb domain was safer by factors ranging from 3 to 38 depending on specific location. Patterns of lead deposition from decades of Pb accumulation have not been transformed by renovations conducted post-Katrina. We expect that all large cities will exhibit the same characteristics as observed in New Orleans. Low Pb soils are available outside of cities to remedy soil Pb contamination. Mapping soil Pb delineates Pb deposition and assists with planning to improve primary prevention of Pb exposure.

## PS 1510 Portable XRF Technology to Quantify Lead and Strontium in Bone *In Vivo*—Calibration and Validation.

A. J. Specht<sup>1</sup>, M. Weisskopf<sup>2</sup> and L. Nie<sup>1</sup>. <sup>1</sup>Health and Human Sciences, Purdue University, West Lafayette, IN; <sup>2</sup>Public Health, Harvard University, Boston, MA.

Concentrations of lead and strontium in bone can serve as a long-term indicator of exposure levels, and can be more easily correlated to their respective health effects. Lead adversely affects almost all the systems in the body. High levels of strontium, on the other hand, have been correlated to skeletal abnormalities in animal and human populations. We have previously shown the viability of a portable XRF system in detection of lead in bone *in vivo*. This system has since been improved to include a larger detector with an improved geometry. In this project, the new instrument was calibrated and validated to quantify lead and strontium in bone *in vivo*.

The system was effectively calibrated for bone lead quantification with lead doped bone-equivalent phantoms. However, it is difficult to calibrate the system for bone strontium quantification using strontium doped phantoms because most of the bone equivalent materials are severely contaminated with strontium. Therefore, a new calibration method was developed, which made use of a Monte Carlo (MC) simulation model developed specifically for this instrument. In this new method, net strontium signals were obtained for different soft tissue thicknesses using MC simulations and the signals were plotted against corresponding concentrations of the strontium. The concentrations of strontium for in vivo measurements can then be calculated from the calibration lines generated from MC simulation. Three main results were obtained from this study: a) An agreement between the experimental and simulated spectra of approximately 13% were shown with the MC simulation model; b) the detection limit for bone lead and strontium is improved by a factor of 2 with the improved instrument; c) it is valid to calibrate the system with the calibration lines created by MC simulations. In conclusion, the new system with improved detection limit, combined with the use of Monte Carlo simulations for calibration can be applied to accurately quantify lead and strontium in bone in vivo.

## PS 1511 The Effect of Environmental Exposure to Lead on Blood Pressure in Korean Adults.

J. Park<sup>1</sup>, S. Choi<sup>1</sup>, S. Eom<sup>2</sup>, D. Kim<sup>1</sup>, H. Kim<sup>2</sup>, B. Choi<sup>1</sup>, K. Park<sup>3</sup>, H. Pyo<sup>3</sup>, Y. Hong<sup>4</sup>, S. Sohn<sup>5</sup> and H. Kwon<sup>6</sup>. <sup>1</sup>Chung-Ang University, Seoul, Republic of Korea; <sup>2</sup>Chungbuk National University, Cheongju, Republic of Korea; <sup>3</sup>Korea Institute of Science and Technology, Seoul, Republic of Korea; <sup>4</sup>Dong-A University, Busan, Republic of Korea; <sup>5</sup>Chonnam National University, Gwangju, Republic of Korea; <sup>6</sup>Dankook University, Cheonan, Republic of Korea.

General population is exposed to chronic and low level of lead (Pb). Previous studies reported that blood Pb is possibly related to the blood pressure. However, the effect of environmental exposure to Pb on blood pressure is not clear yet. This study was performed to estimate the representative blood Pb level and to assess whether blood pressure is affected by chronic and low Pb exposure in Korean adults. The total study subjects of 2,090 people (male: 908, female: 1,182) were nationwide sampled by multi-staged, sex- and age- stratified probability method, who had not been exposed to Pb occupationally. The geometric mean concentration of Pb in blood was 2.22 ug/dL. The level of blood Pb was significantly higher in males (2.60 ug/dL) than in females (1.97 ug/dL). The level of blood Pb was increased with age-dependent pattern which was the highest in the group of 50-59 years old. Also, blood Pb level was affected by individual behavioral patterns such as smoking and drinking. The mean concentration of blood Pb was higher in rural or urban inhabitants than in metropolitan, respectively. The positive relations were observed between blood Pb concentrations and systolic/diastolic blood pressure in males and in females, both. However, blood Pb was significantly correlated with systolic and diastolic blood pressure after adjustment for covariates in males, but not in females. In summary, the findings from this study suggest that chronic Pb exposure under the environment might be increase blood pressure, systolic and diastolic, both, in males.

## PS 1512 Induction of Autophagy and Aberrant MHC Class II Surface Expression in Lead-Exposed Murine Macrophage Raw 2674 Cells: Dysregulation in Mhc-II<sup>+</sup> Compartment Exocytosis.

R. M. Gogal<sup>1</sup>, R. P. Kerr<sup>1</sup>, T. M. Krunkosky<sup>1</sup>, D. J. Hurley<sup>2</sup>, B. S. Cummings<sup>3</sup> and S. D. Holladay<sup>1</sup>. <sup>1</sup>Department of Biosciences and Diagnostic Imaging, University of Georgia, Athens, GA; <sup>2</sup>Department of Population Health, University of Georgia, Athens, GA; <sup>3</sup>Department of Pharmaceutical and Biomedical Sciences, University of Georgia, Athens, GA.

Aberrant major histocompatibility complex class II (MHC-II) surface expression on antigen presenting cells (APCs) is associated with dysregulated immune homeostasis. Lead (Pb) is known to increase MHC-II surface expression on murine peritoneal macrophages ex vivo at concentrations exceeding 25  $\mu$ M. Little data exist examining this effect at physiologically relevant concentrations. To address this deficit, we examined the effects of Pb on MHC-II surface expression, secondary T-cell activation markers (CD80, CD86, CD40), cell viability, cellular metabolic activity, and  $\beta$ -hexosaminidase activity in RAW 267.4 macrophage cell lines, with changes in cell ultrastructure evaluated by electron and confocal microscopy. Pb induced a bi-phasic, dose dependent increase in MHC-II, CD86, and lysosome-associated LAMP-1 and LAMP-2 surface expression during one cell doubling cycle (17 hr), which was mirrored by increased  $\beta$ -hexosaminidase activity. Although cell viability was unaffected, cellular metabolism was inhibited. Electron microscopy revealed evidence of lipid vacuolization, macroautophagy and myelin figure formation in cells cultured with either Pb or LPS. Confocal microscopy with antibodies

against LC3B showed a punctate pattern consistent with the presence of mature autophagosomes. Collectively, these data suggest that 2.5-5.0  $\mu$ M Pb increased MHC-II surface expression by inhibiting metabolic activity, inducing autophagy, and increasing MHC-II trafficking in a macrophage cell line.

## PS 1513 Exposure to Cobalt Causes Changes in Gene Expression and Protein Abundance in Two Rat Liver-Derived Cell Lines.

M. Permenter<sup>2</sup>, W. E. Dennis<sup>1</sup>, J. A. Lewis<sup>1</sup> and D. A. Jackson<sup>1</sup>. <sup>1</sup>USACEHR, Fort Detrick, MD; <sup>2</sup>Excet, Inc., Fort Detrick, MD.

Cobalt is an essential component of the diet, but in large doses it is acutely toxic, and chronic exposures can injure multiple organ systems. While the toxic effects of cobalt have been widely studied, the exact mechanisms of toxicity remain unclear. In order to further elucidate these mechanisms in liver, we exposed two rat liver-derived cell lines, H4-II-E-C3 and MH1C1, to sublethal concentrations of cobalt chloride to eliminate cell-line specific effects. We chose the treatment concentrations based on a novel qPCR assay using a panel of genes developed from previous metal toxicity studies, as opposed to traditional cytotoxicity assays, to more accurately predict gene expression endpoints at sublethal concentrations. We examined changes in gene expression using DNA microarrays and also examined changes in secreted and cytoplasmic protein abundance using mass spectrometry. We performed both gene-level and functional analyses of the results and observed changes in pathways that are involved in the Nrf2-mediated response, protein degradation, glutathione production, Hif-1 signaling, and energy metabolism. These results are consistent with the known effects of cobalt toxicity, including oxidative stress and hypoxic responses. The changes in protein abundance closely resemble and validate our conclusions drawn from the microarray analysis. This work offers key insights into the role specific genes, proteins, and pathways play in cobalt toxicity mechanisms, and provides leads, which upon validation, may characterize novel toxic effects.

Opinions, interpretations, conclusions, and recommendations are those of the authors and are not necessarily endorsed by the U.S. Army. The research described herein was sponsored by the U.S. Army Medical Research and Materiel Command, Military Operational Medicine Research Program.

## PS 1514 Dose-Response Relationships for Blood Cobalt Concentrations and Associated Health Effects.

A. Monnot, S. Gaffney, D. J. Paustenbach and B. L. Finley. ChemRisk, San Francisco, CA.

Cobalt (Co) is an essential component of vitamin B12. As with all metals, at sufficiently high doses, Co can have detrimental effects on different organ systems, and adverse responses have been observed in patients on Co therapy, workers handling Co-containing powders, and other Co-exposed groups. Although blood Co concentrations are thought to be the most accurate indicator of ongoing Co exposure, little is known regarding the dose-response relationships between blood Co concentrations and adverse health effects. In this analysis, we reviewed the animal toxicology and epidemiology literature to identify blood Co concentrations at which effects have, and have not, been reported. Where necessary, a biokinetic model was used to convert oral doses to blood Co concentrations. Our results indicate that blood Co concentrations in humans of approximately 300  $\mu$ g/L and higher have been associated with certain hematological and reversible endocrine responses (polycythemia and reduced iodide uptake, respectively), while blood Co concentrations of 700-800  $\mu$ g Co/L and higher have been consistently associated with a risk of more serious neurological, reproductive, or cardiac effects. Although there are some anecdotal reports to the contrary, the weight of evidence from the many available studies suggest that blood Co concentrations of 300  $\mu$ g/L and less have not been associated with adverse responses in healthy humans. This suggests that certain populations known to have blood Co concentrations of < 100  $\mu$ g/L, such as some patients with Co-containing hip implants and those who ingest Co vitamin supplements, are unlikely to be at risk due to Co exposure.

## PS 1515 Loss of Hypoxia-Inducible Factor (HIF)-1 $\alpha$ , and Not HIF-2 $\alpha$ , in the Lung Alveolar Epithelium of Mice Leads to Enhanced Eosinophilic Inflammation in Cobalt-Induced Lung Injury.

S. P. Proper, K. Greenwood, J. Harkema and J. J. LaPres. Michigan State University, East Lansing, MI.

Cobalt is a known hypoxia mimic and stabilizer of hypoxia-inducible factors (HIFs). HIF-1 $\alpha$  contributes to cobalt toxicity in vitro and previous work in our lab has shown that loss of HIF-1 $\alpha$  in the alveolar epithelial cells led to a switch from a

neutrophilic to eosinophilic response. While HIF-1 $\alpha$  and HIF-2 $\alpha$  have known overlapping gene targets, HIF-2 $\alpha$  is the predominant HIF isoform in the adult lung, and little is known about HIF-2 $\alpha$  in the context of cobalt-induced lung injury. We therefore hypothesized that HIF-2 $\alpha$  could be playing a more active role in cobalt toxicity. To compare the roles of HIF-1 $\alpha$  and HIF-2 $\alpha$  in cobalt-induced lung injury, we used mice deficient in either HIF-1 $\alpha$  (HIF-1 $\alpha$  $\Delta/\Delta$ ), HIF-2 $\alpha$  (HIF-2 $\alpha$  $\Delta/\Delta$ ) or both HIF-1 $\alpha$  and HIF-2 $\alpha$  (HIF-1/2 $\alpha$  $\Delta/\Delta$ ) in alveolar type II epithelial cells. Mice were exposed to cobalt (60  $\mu$ g/day) or saline via oropharyngeal aspiration for five consecutive days, and sacrificed on day six. Bronchoalveolar lavage (BAL) cellularity, qRT-PCR, and histopathologic analyses were performed. Results confirm previous data showing that loss of HIF-1 $\alpha$  leads to enhanced eosinophilic inflammation, and an enhanced T-helper type 2 (Th2) response. In contrast, inflammation in HIF-2 $\alpha$  mice resembled that of control mice following cobalt exposure. HIF-1/2 $\alpha$  $\Delta/\Delta$  mice showed similar cobalt-induced eosinophilic inflammation seen in HIF-1 $\alpha$  $\Delta/\Delta$  mice. Together, data suggest that loss of HIF-1 $\alpha$  in lung epithelium plays the dominant role in determining the response to cobalt-induced lung injury, and that HIF-2 $\alpha$  does not play an active role in cobalt-induced lung injury. Coupled with other experiments performed in our lab, this indicates that epithelial HIF-1 $\alpha$  in the postnatal developmental period plays a central role in guiding immune responses in the airway.

**PS 1516 Can Zinc Reverse Uranium Toxicity? Potential for a Community-Based Intervention.**

L. G. Hudson, K. L. Cooper, R. Tsosie, D. Begay and J. L. Lewis.  
*Pharmaceutical Sciences, University of New Mexico, Albuquerque, NM.*

Many Navajo people have been, and continue to be, exposed to uranium through the legacy of uranium mining. 1100 abandoned Cold War uranium waste sites remain within Navajo communities and numerous wells exceed maximum contaminant levels for uranium and other metals such as arsenic. Certain metals can disrupt protein function by interacting with zinc finger structures and thus inhibit important cellular processes including DNA repair. Based on this mechanism, many metals are now viewed as co-carcinogens and amplify the DNA damaging capacity and tumorigenicity of other carcinogens even at levels where the metals alone are not carcinogenic. The carcinogenicity of uranium is well established in the literature, but there is little known regarding uranium interaction with zinc finger protein structures. Published reports demonstrating that uranium exposure leads to deficiency in DNA repair processes suggest that uranium may interfere with zinc finger DNA repair proteins. Our work with arsenic demonstrates that very low levels of arsenic causes zinc depletion from target zinc finger DNA repair proteins leading to increased DNA damage and mutagenesis that can be reversed by zinc. Based on these findings, we investigated the effect of uranium on DNA repair and the activity of a specific zinc finger DNA repair protein target (PARP-1). Uranium in the form of uranyl acetate (UA) demonstrated little cytotoxicity in an immortalized human embryonic kidney cell line (HEK293) at concentrations at or below 10  $\mu$ M. UA at concentrations of 10 or 100  $\mu$ M inhibited the DNA repair protein PARP-1 and caused retention of ultraviolet radiation-induced DNA lesions (CPDs and pH2Ax). The addition of zinc ameliorated PARP-1 inhibition and partially decreased the retention of DNA damage. These findings suggest that one mechanism of uranium toxicity may rely on disruption of zinc finger protein function, so this work will inform a planned assessment of the potential for zinc to block uranium toxicity as an additional component of the Navajo Birth Cohort Study.

**PS 1517 Toxicological Properties of PM<sub>1</sub> from Pellet Combustion—Role of Zn.**

O. Uski<sup>1,2</sup>, P. Jalava<sup>2</sup>, M. Happonen<sup>2</sup>, T. Kaivosoja<sup>2</sup>, H. Lamberg<sup>2</sup>, J. Leskinen<sup>2</sup>, T. Torvela<sup>2</sup>, J. Tissari<sup>2</sup>, O. Sippula<sup>2</sup>, J. Jokiniemi<sup>2,3</sup> and M. Hirvonen<sup>2,1</sup>.  
<sup>1</sup>*Department of Environmental Health, National Institute for Health and Welfare, Kuopio, Finland;* <sup>2</sup>*Department of Environmental Science, University of Eastern Finland, Kuopio, Finland;* <sup>3</sup>*Technical Research Centre of Finland, Espoo, Finland.*  
Sponsor: M. Viluksela.

Biomass combustion is important source of ambient air fine particulate matter (PM<sub>2.5</sub>), which has been associated with a substantial health burden. Thus, it is important to reveal the effect of used fuel in induced adverse health effects. In search for causative constituents, we studied the role of Zn on toxicity of combustion emission PM<sub>1</sub>. PM<sub>1</sub> samples were produced in complete combustion using a pellet boiler (25 kW). Untreated reference pellet fuel (including 11 mg/kg Zn) was used as control sample. The same pellets were doped with Zn in different concentrations; 170, 480 and 2300 mg Zn/kg fuel. PM<sub>1</sub> samples were collected on PTFE-filters from diluted flue gas by using Dekati® gravimetric impactor, and subsequently extracted from filters

by using methanol. Mouse macrophages (RAW264.7) were exposed for 24 h to four doses (15, 50, 150 and 300 mg/ml) of emission samples. Markers for cytotoxicity (MTT), inflammation (MIP-2 and TNF- $\alpha$ ) and cell cycle analysis (DNA content analysis) were measured.

All the studied emission samples induced significant dose-dependent decrease in cell viability when compared to control. However, with the samples where Zn was added the toxicity was more severe. Moreover, significant increase in S-G<sub>2</sub>/M-phase in the cell cycle was detected after exposure to emissions from all Zn doped pellets, but not with reference pellet. Instead, only minor inflammatory responses were seen by all the samples.

The present results indicate that in very good combustion conditions, high Zn content of fuel induces significant changes in the cell cycle and increases cytotoxicity of PM<sub>1</sub>. Combustion particles toxicity is affected not only by the appliances design or the combustion conditions but also of the fuel and fuel quality.

**PS 1518 A Preliminary Study on Analytical Methodology for Determination of Zinc in Liver of Laboratory Rats, by ICP-QMS.**

L. V. Saldivar<sup>1</sup>, H. Garcia<sup>1</sup>, R. Leon<sup>1</sup>, T. Rodríguez Salazar<sup>1</sup>, M. G. Espejel<sup>1</sup> and T. I. Fortoul<sup>2</sup>. <sup>1</sup>*Analytical Chemistry, UNAM Faculty of Chemistry, Mexico City, Mexico;* <sup>2</sup>*Cellular and Tisular Biology, UNAM Faculty of Medicine, Deleg Coyoacán, México City, Mexico.* Sponsor: D. Acosta.

Zinc is an essential micronutrient for living organisms. It plays a specific role in the synthesis and stabilization of proteins. Its deficiency is characterized by growth retardation, and impaired immune function. While the excess of Zn results in fever and pathological changes in some tissues. Excessive absorption of zinc suppresses copper and iron absorption. Therefore Zn, Cu and Fe can be utilized as pathological indicators. The determination of these elements is of interest in the biomedical area, where laboratory rats are used as model animals, because of their physiological similarities to the human body.

The Inductively Coupled Plasma-Quadrupole Mass Spectrometry (ICP-QMS) has been applied to the analysis of trace elements in biological samples due to its characteristics: low detection limit, multielemental analysis and low sample volume. In this work, analytical methodology was optimized to determine total Zn concentration in livers of laboratory rats. Samples were dried and homogenized, and digested in a microwave oven using HNO<sub>3</sub> and H<sub>2</sub>O<sub>2</sub> mixture. Analytical quantification of the isotopes <sup>66</sup>Zn using <sup>74</sup>Ge as internal standard, was performed using an Elan DRC-e spectrometer (Perkin-Elmer). The dynamic reaction cell was not employed. Results for three replicates of certified reference material (NIST SRM 1577c, National Institute of Standards and Technology) were in good agreement with certified values: 0.21 % (mean relative error, accuracy), and 0.2 % RSD (precision). The range of Zn total concentrations found in samples of livers of rats were: 37-163 mg/kg. This study belongs to a research where it is included the determination of Zn/Cu ratio in several tissues.

The authors thank the financial support of DGAPA-PAPIIT IN229911 and PAL 3400-02.

**PS 1519 Effects of Tungsten Chemical Species on Biochemical Pathways and Mineralization in Bone.**

C. Y. Ang<sup>1</sup>, D. R. Johnson<sup>2</sup>, J. M. Seiter<sup>2</sup>, A. R. Osterburg<sup>3</sup>, G. F. Babcock<sup>3</sup>, P. G. Allison<sup>2</sup> and A. J. Kennedy<sup>2</sup>. <sup>1</sup>*Badger Technical Services, Vicksburg, MS;* <sup>2</sup>*Environmental Laboratory, US Army Engineer Research & Development Center, Vicksburg, MS;* <sup>3</sup>*Cincinnati Shriners Hospital for Children and the University of Cincinnati, Cincinnati, OH.*

Tungsten (W) is a metal that has numerous civil and military applications. When W enters the environment, it is rapidly oxidized and speciates based on the environmental matrix it is embedded in. Bone is the long-term storage organ for W—and presumably W chemical species if present—when taken up by organisms. It is unknown what long-term effects W has in bone, therefore, we evaluated the effects of W species on biochemical pathways in hFOB 1.19 osteoblastic cells exposed to water (control) or W chemical species (sodium tungstate, phosphotungstate [PW], poly tungstate [polyW], and tungstosilicic acid [TSA]) at 0-10,000  $\mu$ M for 24 h at 37 degrees C. W species did not affect adenosine triphosphate (ATP) concentrations except at the highest concentration. PW, polyW, and TSA, but not tungstate, significantly increased protein tyrosine kinase activity at 10,000  $\mu$ M after 4 h exposure. Tungstate and PT increased cellular cyclic adenosine monophosphate (cAMP) at  $\geq$  100  $\mu$ M, while TSA decreased cellular cAMP at 10,000  $\mu$ M. Preliminary analyses also demonstrate an effect on alkaline phosphatase, the enzyme involved in bone mineralization. Synchrotron analysis of bone from female rats exposed to 200

mg/kg/d sodium tungstate in drinking water ad libitum for 90 d showed W incorporation into bone as calcium poly-tungstate (77% total W in bone) and calcium tungstate (23%). These data demonstrate that W chemical species generally only affect phosphate-dependent cell signaling and secondary messenger pathways in hFOB 1.19 cells, and may also affect bone mineralization enzymes, resulting W species incorporation into bone in animals. Follow-up studies will analyze the effects on bone mineralization and strength associated with W incorporation due to chronic exposure.

**PS 1520 Accumulation of Manganese (Mn) in Rat Brain Ventricular Region following *In Vivo* Subchronic Mn Exposure: Effect on Copper (Cu) Status.**

S. L. O'Neal, L. Hong and W. Zheng. *School of Health Sciences, Purdue University, West Lafayette, IN.*

Welders and smelters occupationally exposed to high levels of Mn have an increased risk for developing manganism, a disease similar to Parkinson's. Existing human and animal studies indicate that Mn accumulates mainly in the striatum, the area adjacent to the brain ventricular region (BVR) which houses cells implicated in adult neurogenesis. The neural stem cells in BVR are capable of migrating to striatum and hippocampus en route to the olfactory bulb. This group has previously shown Mn exposure results in Mn accumulation in the choroid plexus (CP), cerebrospinal fluid (CSF) and increases intracellular Cu concentration. This study was undertaken to test the hypothesis that a high Mn level in the CP and CSF may influence the surrounding ventricular structure and interfere with the homeostasis of other essential elements. Adult male rats received daily ip injections of MnCl<sub>2</sub> at the doses of 6 and 15 mg Mn/kg as the low and high dose groups, respectively, or saline as the control, 5 days per week for 4 weeks. Twenty-four hr after the last injection, BVR, femur bone and liver tissues were dissected and quantified by atomic absorption spectroscopy for concentrations of Mn, Cu, iron (Fe) and zinc (Zn). Data analysis by Student's t-test showed that levels of Mn in BVR of the low- and high-dose groups increased by 94.8% and 218.5%, respectively, as compared to controls (n=4-6, p < 0.01). In femur, Mn concentration increased by 278.2% and 1237.4% in the low- and high-dose groups, respectively (p < 0.01). Interestingly, Cu concentrations in BVR decreased significantly for low- and high-dose groups (p < 0.05). In contrast, Cu levels in bone increased by 23.2% and 51.2% for low- and high-dose groups, respectively (p < 0.05). Taken together, our data provide the initial evidence that Mn accumulates in brain ventricular area following *in vivo* exposure. Mn's potential impairment of this region in the disease progression of Mn Parkinsonism deserves further investigation. (Supported in part by NIH RO1 ES008146)

**PS 1521 Methylmercury-Induced Dopaminergic Neurotoxicity in *Caenorhabditis elegans*.**

E. Martinez-Finley and M. Aschner. *Vanderbilt University Medical Center, Nashville, TN.*

Mercury is a persistent environmental contaminant that exerts its toxic effects on the nervous system through molecular mechanisms that remain unknown. Parkinson's disease (PD) is a neurodegenerative disorder characterized by the slow progression and irreversible loss of the dopaminergic (DAergic) neurons. The etiology of PD remains elusive, with aging, environmental toxicant exposure and genetic mutations contributing to the disease. Epidemiological studies have pointed to the contribution of methylmercury (MeHg) to DAergic vulnerability and the predisposition to PD. We examined the impact of early-life exposure to MeHg on DAergic neurodegeneration in *Caenorhabditis elegans* (*C. elegans*) with emphasis on gene-environment interactions. SKN-1, orthologue of mammalian Nrf2, is a major stress-activated cytoprotective transcription factor. We hypothesized that MeHg's toxicity is dependent on an intact SKN-1 response and skn-1 knockout (KO) worms would show heightened toxicity compared to wildtype (N2). We also tested the effect of MeHg in a pdr-1KO worm, ortholog to the human parkin gene (mutated form found in juvenile PD), under the premise that these worms would show heightened sensitivity to MeHg. We identified the impact of early-life MeHg exposure on MeHg content, stress reactivity and measures of DAergic neurodegeneration in N2, skn-1KO and pdr-1KO worms exposed to 0-30μM MeHgCl for 30 minutes following synchronization. Our data suggests that skn-1KO (LD50=19μM) and pdr-1KO (LD50=17μM) are more sensitive to MeHg than N2 controls (LD50=25μM). MeHg uptake was higher in the pdr-1KO strain compared to the N2 strain. DAergic morphology observed via fluorescent analysis at adult life-stage revealed presence of puncta at 20μM MeHg in skn-1KOs and loss of cell body fluorescence in pdr-1KO. Dopamine (DA)-dependent behavioral

analysis revealed alterations in DA following MeHg exposure, corroborated by decreased DA levels, measured via HPLC. Taken together this data suggests that exposure to MeHg early in the lifespan can have detrimental effects on DAergic neurons. Supported by RO1ES07731 and EST32007028.

**PS 1522 Lactational Exposure to Mercury (Hg) and Evidence of Oxidative Stress.**

I. Al-Saleh, M. Abdel Jabbar, R. Al-Rouqi, R. Elkhatib, A. Alshabbaheen and N. Shinwari. *Environmental Health Section, Biological & Medical Research Department, King Faisal Specialist Hospital & Research Centre, Riyadh, Saudi Arabia.*

The objective of this work was to assess exposure to Hg in mothers and their breast-fed infants. We also evaluated urinary 8-hydroxy-2-deoxyguanosine (8-OHdG) and malonaldehyde (MDA) in both the mothers and infants as biomarkers of oxidative stress. The mean urinary Hg (UHg) levels in 155 mothers and 102 infants was 1.47 and 7.9μg/g-Cr, respectively with significant correlation between the two (r=0.36, P=0). UHg levels > 5μg/g-Cr (background level in unexposed population) found in 3.3% mothers and 50.1% infants. The mean concentration of Hg in breast milk was 1.19μg/L (range: 0.012-6.44μg/L) with only one mother had Hg > 4μg/L, the ATSDR upper limit. This corresponds to approximately a daily intake of 1.02μg Hg (0.13-5.47μg). Based on the average infant's body weight in this study (7.7Kg) and the EPA reference dose of Hg (0.3 μg/Kg/day), this brings the highest daily intake to 2.31μg. There were 7 infants exceeded this limit. None of the mothers had total blood Hg > the EPA reference dose of 5.8μg/L. Probably, this might be due to the low exposure to organic in comparison to inorganic Hg. Furthermore, no correlation was noted between UHg in infants and Hg in breast milk (P>0.05). On the other hand, Hg in breast milk was associated with total Hg in blood (r=0.53, P=0) suggesting the efficient transfer of organic form of Hg from blood to milk. Both urinary MDA (r=0.2, P=0.015) and 8-OHdG (r=0.24, P=0.003) levels increased with the mother's UHg levels. Infant's UHg levels in infants were positively associated with urinary levels of MDA (r=0.31, P=0.003) and 8-OHdG (r=0.43, P=0) in infants. There was also an association between Hg in breast milk and increased urinary MDA levels in infants (r=0.35, P=0). Our results clearly showed the transfer of Hg from the mother to infant through breastfeeding, and its role in inducing oxidative stress, that can be of potential health risk. Nevertheless, breastfeeding should not be discouraged; and instead efforts should be made to identify and eliminate the source of Hg exposure in the present population.

**PS 1523 Methylmercury Toxicity in KK-Ay Obese Type 2 Diabetic Mice.**

M. Yamamoto<sup>1</sup>, R. Yanagisawa<sup>1,2</sup>, E. Motomura<sup>1</sup>, M. Nakamura<sup>1</sup>, M. Sakamoto<sup>1</sup>, M. Takeya<sup>3</sup> and K. Eto<sup>4</sup>. <sup>1</sup>National Institute Minamata Disease, Minamata, Japan; <sup>2</sup>National Institute Environment Studies, Tsukuba, Japan; <sup>3</sup>Kumamoto University, Kumamoto, Japan; <sup>4</sup>Jushindai, Tamana, Japan.

We examined the toxic effects of methylmercury (MeHg) exposure on the brain, kidney, pancreas and spleen of KK-Ay type 2 diabetic mice to clarify how the metabolic changes associated with type 2 diabetes mellitus (T2DM) affect MeHg toxicity. MeHg (5 mg Hg/kg/day p.o.) was given to male KK-Ay and C57BL/6J (BL/6) mice three times per week for 6 weeks beginning at 4 weeks of age. Average of body weights (BW) of vehicle-treated BL/6 and KK-Ay mice were 16.3 g and 16.4 g on the first day, and 24.8 g and 42.3 g on the last day of the experiment, respectively. BW gain in MeHg-treated KK-Ay mice stopped 4 weeks after MeHg-administration, and these mice began to lose weight around 5 weeks. Six of 7 MeHg-treated KK-Ay mice showed neurological symptoms such as hind limb crossing in the final stage of the experiment. Alternatively, no obvious symptoms and decrease in body weight were observed in vehicle-treated and MeHg-exposed BL/6 mice. The mean blood mercury level of KK-Ay mice administered MeHg increased constantly throughout the administration of MeHg and reached a maximum of about 8 μg/ml. On the other hand, the average blood mercury level of BL/6 mice administered MeHg was 2.8 μg/ml after 10 days of MeHg administration. The average kidney weights of vehicle-treated and MeHg-exposed KK-Ay mice were 542 mg and 408 mg, and those of BL/6 mice were 357 mg and 413 mg, respectively. The average spleen weights of vehicle-treated and MeHg-exposed KK-Ay mice were 91 mg and 135 mg, and those of BL/6 mice were 65 mg and 71 mg, respectively. The average total mercury concentrations in the cerebrum, kidney, pancreas, spleen and epididymal fat pad of KK-Ay mice were 27, 51.7, 40.9, 32 and 1.6 μg/g, respectively. The average total mercury concentrations in these organs of BL/6 mice were 7.4, 51.9, 10.4, 6.9 and 0.57 μg/g, respectively. These results indicate that body fat gain in T2DM and low accumulation of mercury in adipose tissue can increase organ accumulation of MeHg accompanied by toxicity in KK-Ay mice.

**PS 1524 The Palmitoylation of Meh1, a Component of EGO Complex, Has an Important Role in the Reduction of Methylmercury Toxicity in Budding Yeast.**

G. Hwang, Z. Zhang and A. Naganuma. *Graduate School of Pharmaceutical Sciences, Tohoku University, Sendai, Japan.*

Methylmercury (MeHg) is an environmental pollutant that causes the severe central nervous system disorder. However, the molecular mechanism underlying MeHg toxicity remains to be clarified. We have found that deletion of the Akr1, one of palmitoyl transferase, causes hypersensitivity to MeHg in budding yeast.

In this study, we found that yeast cells lacking Meh1, one of substrates for Akr1, exhibit hypersensitivity to MeHg. Palmitoylation of Meh1 was not detectable by a deletion of Akr1, suggesting that Akr1 is the main palmitoyl transferase for Meh1. We also found that the palmitoylation of Meh1 by Akr1 is essential for the protective effect of Meh1 against MeHg toxicity. Meh1 has been identified as a component of the EGO complex that is involved in the regulation of microautophagy. We found an increased susceptibility to MeHg in yeast cells with deletion of Meh1 or the other EGO complex components (Gtr2 and Ego3). Moreover, Meh1/Gtr2- or Meh1/Ego3-double deletion mutants did not exhibit further increase in the susceptibility to MeHg when compared to Meh1 deletion mutant. These results suggest that Meh1 might reduce MeHg toxicity as a component of the EGO complex. It has been reported that Meh1 forms an EGO complex by binding with Ego3 on vacuole membrane. Interestingly, Meh1 with a mutation in the palmitoylation site was defective in its ability to bind with Ego3. Moreover, normal Meh1-GFP was localized in the vacuolar membrane, but the mutant Meh1-GFP was widely distributed in the cytoplasm and not in the vacuolar membrane. These phenomena proposed that the palmitoylation of Meh1 has an important role in its cellular distribution and formation of the EGO complex.

As for our result, the palmitoylation of Meh1 by Akr1 is related to the formation of the EGO complex through its localization into the vacuolar membrane, and this action is important for the reduction of MeHg toxicity.

**PS 1525 Involvement of AAT Transporters in Methylmercury Toxicity in *Caenorhabditis elegans*.**

S. W. Caito and M. Aschner. *Department of Pediatrics/Pediatrics Toxicology, Vanderbilt University Medical Center, Nashville, TN.*

*Caenorhabditis elegans* (*C. elegans*) is a powerful genetic model for the investigation of neurotoxicity of metals, such as methylmercury (MeHg). MeHg has been shown to accumulate in *C. elegans*, leading to decreased survival, reproductive and developmental defects, and neurodegeneration. It is unknown how MeHg is transported in the worm. In mammals, MeHg complexes with cysteine, which functionally resembles methionine; and the complex is transported into cells via a molecular mimicry mechanism involving the large neutral amino acid transporter LAT1. It is unknown if MeHg can enter cells without being complexed to cysteine or if there are additional uncharacterized MeHg transport mechanisms. *C. elegans* can be used to quickly identify MeHg transport mechanisms due to their ease of genetic manipulability and high degree of homology to mammals. Herein we tested the hypothesis that LAT1 homologues (AATs) are responsible for MeHg transport in *C. elegans*. Worms were pre-treated with 1 mM methionine to assess whether MeHg toxicity could be attenuated by increasing a competitor for AAT transporters. Treatment with MeHg resulted in decreased survival of *C. elegans* (LD50 = 22.91  $\mu$ M), however methionine pre-treatment showed significantly less toxicity to MeHg (LD50 = 47.54  $\mu$ M,  $p < 0.0001$ ), implicating the AAT amino acid transport systems in MeHg toxicity. Using RNAi feeding protocols we selectively knocked down expression of the *aat-1*, *aat-2* and *aat-3* genes, and assayed for MeHg induced-lethality. Knockdown of each gene individually resulted in a significant right hand shift in the dose-response lethality curve (*aat-1*: LD50 = 118.1  $\mu$ M,  $p < 0.001$ ; *aat-2*: LD50 = 102.1  $\mu$ M,  $p < 0.001$ ; *aat-3*: LD50 = 44.65  $\mu$ M  $p < 0.001$ ), suggesting these genes may be involved in MeHg transport. As lethality of MeHg was not completely blocked by methionine pre-treatment or *aat* gene knockdown, there is a possibility that additional MeHg transport mechanisms may be identified in *C. elegans*.

**PS 1526 Effects of Methylmercury on Heart Rate Variability in the Rat.**

M. Sasaki, M. Yamamoto and M. Fujimura. *Department of Basic Medical Sciences, National Institute for Minamata Disease, Minamata, Japan.*

Analysis of heart rate variability (HRV) in humans has revealed that methylmercury (MeHg) exposure decreases parasympathetic nerve function or increases sympathetic nerve function. However, limited information is available on such effects in

experimental animals. In the present study, 5 rats were treated 2 times per week for 5 weeks with MeHg (4 mg/kg) or vehicle orally. Several weeks before and after treatment, telemetry recordings of ECG were acquired. HRV and its power spectrum parameters were determined from 1-hour segments (approximately 16,000 to 20,000 beats) of ECG data during the day by LabChart and its HRV Module. With 4 mg/kg MeHg treatment, a decrease in body weights and the hind limb crossing sign and an increase in the heart rate (HR) were observed from the analysis of the ECG. HRV analyses showed a decrease in the coefficient of HRV (CVRR) and low frequency (LF) and high frequency (HF) HRV. A slight increase in the LF/HF ratio was observed due to the decrease in HF. These results suggest that a decrease in the CVRR, LF, and HF and an increase in the HR indicate the suppression of parasympathetic nervous system activities after repeat treatments with MeHg in rats. These findings also suggest similar effects of MeHg on the autonomic nervous system of humans and animals.

**PS 1527 Sex Differences in Paraoxonase Activity in Subchronic Inorganic Mercury Exposure.**

A. D. Wusu<sup>1</sup>, O. Ademuyiwa<sup>1</sup>, O. O. Ogunrinola<sup>1</sup>, O. K. Afolabi<sup>1</sup>, E. O. Abam<sup>1</sup>, D. O. Babayemi<sup>1</sup>, E. A. Balogun<sup>1</sup> and O. O. Odokoya<sup>2</sup>.

<sup>1</sup>Biochemistry, University of Agriculture, Abeokuta, Nigeria; <sup>2</sup>Chemistry, University of Agriculture, Abeokuta, Nigeria.

Epidemiological evidences suggest an increased risk of cardiovascular diseases (CAD) as a result of inorganic mercury exposure. The underlying mechanisms underpinning this risk, as well as sex differences in response to mercury exposure, are not yet understood. Paraoxonase (PONase), an enzyme located in the high-density-lipoprotein (HDL) has been shown to protect against CAD. In order to investigate the association between inorganic mercury exposure and CAD, male and female rats were exposed to mercury (0.5, 1.0 and 1.5mg/kg) for 12 weeks. PON activities towards paraoxon (PONase) and phenylacetate (AREase) in plasma, lipoproteins, hepatic and brain microsomal fractions were determined using standard methods. Inhibition of PONase and activation of AREase in plasma and HDL characterised the effects of inorganic mercury in both sexes. Inorganic mercury exposure inhibited PONase by 63% (plasma) and 67% (HDL) respectively in male animals, whereas the female enzyme was inhibited by 80 and 47% respectively. AREase activity was activated by 55 and 53% in male, whereas the activation in female amounted to 25 and 49% respectively. In the VLDL, inorganic mercury inhibited PONase in both sexes whereas AREase was activated in female animals but inhibited in male. In the hepatic microsomal fractions, only the PONase enzyme was inhibited in male animals whereas in female, activation was observed in both enzymes at the highest dose of inorganic mercury. Brain microsomal cholesterol was increased in male but decreased in female by inorganic mercury resulting in altered cholesterol/phospholipid ratios. Our findings indicate that inorganic mercury exposure exerts an inhibitory effect on PONase but activated AREase. Modulation of PON activity may be an early biochemical step in the induction of CAD by mercury. This may also be mediated through changes in membrane fluidity brought about by changes in the concentration of cholesterol in the microsomes.

**PS 1528 Ethylmercury Induces ER Stress and Mitochondria Dysfunction Mediated Autophagy.**

M. Dong and J. Choi. *School Lifesciences and Biotechnology, Korea University, Seoul, Republic of Korea.* Sponsor: B. Lee.

Mercury is one of the most important environmental and industrial pollutants throughout the world. Exposure to mercury causes strong damage to organs including the brain, blood, liver, bone and kidneys. Renal proximal tubular cells represent the primary target site. We previously investigated the cytotoxicity of seven kinds of mercury compounds in human renal proximal tubule (HK-2) cells. Ethylmercury chloride (EMC) was shown the strongest cytotoxicity among them with 2.4 and 0.76  $\mu$ M of IC50 values exposed for 24 h and 48 h in HK-2 cells, respectively. In this study, we explored the mechanism of EMC induced cytotoxicity in HK-2 cells. EMC was increased the accumulation of JC-1 monomers in mitochondria from 0.5 to 2  $\mu$ M concentrations in a dose-dependent manner. The expression of MT-I and Hic-5, which were related to oxidative stress, was also induced by EMC treatment. In addition, calcium is a well-known regulator of many intracellular processes, including apoptosis and autophagy. Interestingly, EMC was increased in cytosolic [Ca<sup>2+</sup>], which was the tendency appears unlikely that the increased after 2  $\mu$ M A23187 treatment. EMC was up-regulated the expression of UPR target genes and proteins such as transcription factor, CHOP, XBP-1, ERdj4 and GRP 78. After the exposure of EMC to cells, LC3II formation was dose- and time-dependently increased. When cells were treated with ER inhibitor 4-Pheylbutyric acid, they blocked the formation of autophagosome compared with untreated cells. However, cleaved of caspase-9, caspase-12 and PARP were weakly activated. To test whether ER stress by EMC can occur in vivo, EMC was treated to

male C57BL/6 mice with 1, 2, 5 and 10 mg/kg/day. The expression of ER stress related marker genes were increased by immunoblot analysis. LC3-II was significantly increased in the kidneys of EMC treated mice. Together, these results suggest that EMC induced autophagy via ER stress and mitochondrial dysfunction not only in human renal proximal tubule (HK-2) cells but also in mice kidneys.

## PS 1529 Protective Role of Quercetin against Mercury-Induced Nephrotoxicity in Sprague-Dawley Rats.

J. Kim<sup>1</sup>, Y. Kim<sup>2</sup>, W. Kim<sup>3</sup>, Y. Shin<sup>4</sup>, A. Won<sup>4</sup>, E. Park<sup>4</sup>, E. Lee<sup>4</sup>, M. Yoo<sup>4</sup>, Z. Lan<sup>4</sup>, T. Kim<sup>4</sup> and H. Kim<sup>4</sup>. <sup>1</sup>College of Pharmacy, Pusan National University, Busan, Republic of Korea; <sup>2</sup>Gorton School, Farmers Row, Groton, MD; <sup>3</sup>The Hockaday School, Dallas, TX; <sup>4</sup>Sehwa High School, Seoul, Republic of Korea.

Mercury chloride (HgCl<sub>2</sub>) is a well-known nephrotoxicant. HgCl<sub>2</sub> preferentially accumulates in the kidneys and causes nephrotoxicity as a result of oxidative stress. The aim of this study was to investigate the possible protective role of quercetin against HgCl<sub>2</sub>-induced acute renal damage. Quercetin, a naturally occurring phenolic compound found in fruits and vegetables, has gained considerable attention for its antioxidant properties. In this study, quercetin (250 mg/kg) was administered orally to Sprague-Dawley male rats for 3 days prior to HgCl<sub>2</sub> (20 mg/kg) treatment. All animals were sacrificed 24 h after the last treatment and various urine or blood biomarkers associated with renal damage were measured. Significant increases in urinary volume and decreases in urinary pH were observed in the HgCl<sub>2</sub>-treated group. Blood urea nitrogen (BUN) and serum creatinine (sCr) levels were significantly increased in the HgCl<sub>2</sub>-treated group when compared to control group. In the HgCl<sub>2</sub>-treated group, the urinary excretion of BUN, sCr, lactate dehydrogenase (LDH) and total protein were all markedly lower than those of the control group. These adverse effects were ameliorated by pretreatment with quercetin. Compared to the HgCl<sub>2</sub>-treated group, quercetin pretreatment led to a significant decrease in the amounts of KIM-1, NAGL, HMGB1, and Netrin-1 in the urine. Furthermore, histopathological examinations indicated that quercetin had a protective effect against HgCl<sub>2</sub>-induced proximal tubular damage. These results suggest that quercetin may be a promising agent to protect against HgCl<sub>2</sub>-induced acute kidney injury.

## PS 1530 Selenium Protects against the Toxic Effects of Methylmercury in Sperm Whale (*Physeter macrocephalus*) Skin Cells.

L. C. Savary<sup>1,2,4</sup>, A. Holmes<sup>1,2,3</sup>, M. Braun<sup>1,2</sup>, D. Evers<sup>5</sup>, I. Kerr<sup>2,4</sup>, R. Payne<sup>2,4</sup>, W. Thompson<sup>2,3</sup>, C. Perkins<sup>6</sup>, T. Zheng<sup>7</sup>, C. Zhu<sup>7</sup> and J. Wise<sup>1,2,4</sup>. <sup>1</sup>Wise Laboratory of Environmental and Genetic Toxicology, University of Southern Maine, Portland, ME; <sup>2</sup>Maine Center for Toxicology and Environmental Health, University of Southern Maine, Portland, ME; <sup>3</sup>Department of Applied Medical Sciences, University of Southern Maine, Portland, ME; <sup>4</sup>Ocean Alliance, Gloucester, MA; <sup>5</sup>Biodiversity Research Institute, University of Southern Maine, Portland, ME; <sup>6</sup>Center for Environmental Sciences and Engineering, University of Connecticut, Mansfield, CT; <sup>7</sup>Yale School of Public Health, New Haven, CT.

Mercury (Hg) persists, bioaccumulates and is toxic to the marine environment posing risks to the marine ecosystem. Selenium (Se), an essential element, antagonizes Hg toxicity when present in equimolar amounts. The sperm whale, a toothed whale, is a sentinel of ocean health. We biopsied skin from 343 free-ranging sperm whales in 17 regions around the globe during the voyage of the Odyssey, between 2000-2005 analyzing them for total Hg and Se levels. Hg was detected in 340 samples with a global mean of 2.4 ug/g ww ranging from 0.1 to 16 ug/g. Se was detected in all samples with a global mean of 33.0 ug/g ww ranging from 2.5 to 179.0 ug. The global mean Se:Hg molar ratio was 59:1 ranging from 3:1 to 1719:1. This excess Se may mitigate the toxic effects of Hg. Hg is known to cause cytotoxicity, altered mitotic index and aneuploidy in cells. The aim of this study was to determine if Se protects sperm whale skin cells from Hg-induced toxicity at similar concentrations found in the skin biopsies. Sperm whale skin cells developed from the biopsies were cotreated with 72 h exposure to 2, 3, 4 or 5 uM methylmercury (MeHg) and 10 uM sodium selenite, and cytotoxicity, mitotic index and genotoxicity was measured. Our findings show MeHg induces cytotoxicity, alters mitotic index and causes aneuploidy in sperm whale skin cells, and Se protects against MeHg induced toxicity compared to control.

## PS 1531 Selenium Compounds Cause Apoptosis and GSH Depletion in Rat Hippocampal Astrocytes.

S. Roy and D. Hardej. Pharmaceutical Sciences, St. John's University, Queens, NY.

Selenium (Se) is a required trace element in mammalian systems. While generally accepted to play a protective role, exposure to high levels of Se have been associated with neurotoxicity. Previous work in our laboratory has demonstrated toxicity of Te

and Se compounds in rat hippocampal astrocytes. The purpose of this study was to evaluate the mechanism of cell death of diphenyl diselenide (DPDS) and selenium tetrachloride (SeCl<sub>4</sub>) and to investigate their effects in the functioning of mitochondrial complexes III and IV and depletion of the antioxidant GSH. Rat hippocampal astrocytes were used as a model system. The LC50 of both compounds had been previously found to be 7.8 μM. For the present study, concentrations of both compounds ranging from 1.9-15.625 μM were tested. Phase-contrast microscopy was used to study the morphological changes in the cells following treatments. Micrographs of cells exposed to high concentrations of either compound (15.625 and 7.8 μM) showed decreases in cell number and increases in rounded cells with loss of processes. Micrographs of cell exposed to low concentrations (3.9 and 1.9 μM) appeared similar to control astrocytes. Inductively Coupled Plasma-Optical Emission Spectrometry (ICP-OES) demonstrated that treatments with both compounds resulted in a dose-related increase of Se in the cells that is significantly greater than amounts seen in the controls. Caspase 3/7 activities were assessed and significant increases in activity were observed at the 7.8 μM and 15.625 μM concentrations with both Se compounds confirming apoptotic activity. ELISA assays were used to investigate the activities of complexes III and IV of the mitochondrial respiratory chain. There were no significant changes in the activities of the two enzymes in any treatment group. GSH/GSSG ratios were significantly decreased at 7.8 and 15.625 μM of each compound indicating oxidation of sulfhydryl groups. These results suggest that selenium compounds cause cytotoxicity in rat hippocampal astrocytes resulting in apoptosis but mitochondrial complexes III and IV are not involved.

## PS 1532 Heavy Metal Hazards of Smokeless Tobacco in Nigeria.

O. Orisakwe<sup>2</sup>, Z. N. Igweze<sup>1</sup> and K. O. Okoro<sup>1</sup>. <sup>1</sup>Department of Pharmacology College of Health Sciences, University of Port Harcourt, Rivers State, Nigeria, Nigeria; <sup>2</sup>Toxicology Unit, Department of Experimental Pharmacology & Clinical Pharmacy, University of Port Harcourt, Rivers State, Nigeria, Nigeria.

Smokeless tobacco (ST) or snuff prepared by grinding tobacco leaves into a very fine powder with addition of salt petre and other ingredients has been in use in Nigeria for a very long time. ST is marketed for oral and nasal use. Recently there has been an upsurge in the use of ST even amongst the younger generation. Information on the public health implication and heavy metal hazards of ST in Nigeria is sparse. This study was carried out to determine the extent of heavy metal contamination in ST used in Nigeria. Concentration of five heavy metals, Lead(Pb), Cobalt(Co), Cadmium(Cd), Nickel(Ni), and Chromium(Cr) were determined in smokeless tobacco by wet digestion using HNO<sub>3</sub> and analysis with AAS 205A Spectrophotometer. Thirty samples of smokeless tobacco sourced from six geographical regions in Nigeria were used. Our results showed that the level of contamination with all the metals was ≤10 μg/g, 11-30 μg/g, ≤10 μg/g, 20-70 μg/g and 2770-11400 μg/g for Pb, Co, Cd, Ni and Cr. These concentrations are higher than acceptable limits. Health risks associated with ST snuffing have received little or no attention in Nigeria in spite of wide spread use. This study underscores the importance of elaborate human risk assessment of ST in Nigeria and indeed Sub Saharan Africa.

## PS 1533 Tobacco Cigarettes: A Source of Metals (Al, Cd, Co, Cr, Mn, Ni, Pb, Sr) for Humans.

C. Rubio<sup>1</sup>, T. Garcia<sup>1</sup>, A. Soler<sup>1</sup>, D. Glez-Weller<sup>1</sup>, A. J. Gutiérrez<sup>1</sup>, A. Hardisson<sup>1</sup> and A. Anadon<sup>2</sup>. <sup>1</sup>Toxicology, Universidad de La Laguna, La Laguna, Spain; <sup>2</sup>Farmacología y Toxicología, Universidad Complutense de Madrid, Madrid, Spain.

Every six seconds a smoker dies, the victim of an addiction that causes a high degree of toxicity.

Al, Cd, Co, Cr, Mn, Ni, Pb and Sr were determined in 33 tobacco samples randomly obtained in Tenerife using Inductively Coupled Plasma Spectrometry by previously treating the samples according to the standard procedure, that is, by adding HNO<sub>3</sub> at 65% to the sample and burning it in a muffle oven for 50 hours at 450 degrees Celsius.

With respect to results, 428 mg Al/kg, 0.810 mg Cd/kg, 0.558 mg Co/kg, 1.442 mg Cr/kg, 112.026 mg Mn/kg, 2.238 mg Ni/kg, 0.602 mg Pb/kg and 82.206 mg Sr/kg. Al was the metal with the greatest concentration while Co had the lowest. The tobacco was also classified according to the type of tobacco (Virginia vs Dark), type of cigarette (Normal vs Light) and manufacturer. The amount of Al in Virginia tobacco was 423 mg/kg while in Dark this was 478 mg/kg. Cd concentrations were 0.807 mg/kg for Virginia and 0.844 mg/kg for Dark, Co values were 0.56 mg/kg for Virginia and 0.533 mg/kg for Dark, Cr values were 1.487 mg/kg for Virginia and 1 mg/kg for Dark, Mn was determined to be 113.362 mg/kg for Virginia and 98.667 mg/kg for Dark, Ni values were 2.242 mg/kg for Virginia and 2.199 mg/kg

for Dark, Pb afforded 0.607 mg/kg for Virginia and 0.556 mg/kg for Dark, and Sr gave values of 77.982 mg/kg for Virginia and 124.444 mg/kg for Dark. Regarding the differences between Light and Normal tobacco, the following values were obtained in Light: 412.4 mg Al/kg, 0.873 mg Cd/kg, 0.553 mg Co/kg, 1.64 mg Cr/kg, 120.02 mg Mn/kg, 2.4 mg Ni/kg, 0.873 mg Pb/kg and 78.627 mg Sr/kg; while in Normal tobacco the values determined were 434.783 mg Al/kg, 0.783 mg Cd/kg, 0.559 mg Co/kg, 1.366 mg Cr/kg, 108.56 mg Mn/kg, 2.168 mg Ni/kg, 0.484 mg Pb/kg and 83.762 mg Sr/kg.

Exposure to metals through the inhalation of cigarette smoke represents a significant source of metal contamination to smokers, adding to the dietary intake of these same metals.

**PS 1534 Metal Mobilization from Retained Embedded Fragments in a US Veteran: Biomonitoring Correlates with Fragment Content.**

J. Gaitens<sup>1,2</sup>, K. Squibb<sup>1,2</sup>, J. Centeno<sup>3</sup>, M. Condon<sup>1</sup> and M. McDiarmid<sup>1,2</sup>.  
<sup>1</sup>VA Medical Center, Baltimore, MD; <sup>2</sup>School of Medicine, University of Maryland, Baltimore, MD; <sup>3</sup>Joint Pathology Center, Silver Spring, MD.

Recent clinical findings implicate the potential for local and systemic long-term health effects from embedded metal fragments associated with injuries from improvised explosive devices in soldiers serving in military conflicts. In the past, fragments embedded in muscle tissue were thought to be relatively inert; however, evidence has shown that soldiers with embedded depleted uranium fragments have elevated urine U levels 20 years after exposure. To understand the potential health risks associated with embedded fragments from blast injuries, the Department of Veterans Affairs has established a medical surveillance program which integrates fragment composition data, surrounding tissue analyses, and urine biomonitoring results that characterize systemic and local tissue exposure to: Al, As, Cd, Cr, Co, Cu, Fe, Mn, Ni, Pb, U, W and Zn. These metals were chosen based on available fragment composition data and known toxicity of individual metals. We present here results from a Veteran who had 3 fragments removed several years after injury. Using EDXRF, the removed fragments were determined to be an Al-Cu alloy. Chemical analysis of adherent tissue showed levels of Al and Cu consistent with mobilization of these elements from the fragment to the surrounding tissue. Histology showed focal foreign body-type giant cell reaction and chronic inflammatory cell infiltrates, but no evidence of neoplastic changes. Prior to fragment removal, biomonitoring results showed a urine Al level 1.5 fold higher than the reference range, but below levels associated with adverse health effects. Concentrations of all other metals were within established reference ranges. These results provide further evidence that metal fragments in the body are not inert and materials released from fragments can enter systemic circulation over time, thus warranting long-term biomonitoring and medical surveillance of Veterans with embedded fragments. Supported by the Department of Veterans Affairs.

**PS 1535 Baseline Blood Levels of Manganese (Mn), Lead (Pb), Cadmium (Cd), Copper (Cu), and Zinc (Zn) in Residents of Beijing Suburb.**

L. Zhang<sup>1</sup>, L. Lu<sup>1</sup>, Y. Pan<sup>2</sup>, C. Ding<sup>2</sup>, D. Xu<sup>1</sup>, J. Zhao<sup>1</sup>, W. Zheng<sup>3</sup> and H. Yan<sup>2</sup>.  
<sup>1</sup>Occupational Disease Control, Fengtai CDC, Beijing, China; <sup>2</sup>Institute of Occupational Health, China Center for Disease Control and Prevention, Beijing, China; <sup>3</sup>School of Health Science, Purdue University, West Lafayette, IN.

The baseline blood concentrations of heavy metals are important for monitoring metal exposure in the general population. The data can be used to evaluate the current environmental pollution and also serve as the references for exposure assessment in local residents as well as in occupational settings. The purpose of this study was to determine the blood levels of Mn, Pb, Cd, Cu, and Zn among the residents (aged 12-60 years old) living in the suburb southwest of Beijing, China. Blood samples were drawn from a total of 648 subjects from March 2009 to February 2010. Metal concentrations in the whole blood were measured by ICP-MS. The geometric means of the blood levels of Mn, Pb, Cd, Cu and Zn were 11.4, 42.6, 0.6, 802.4 and 4,665 ug/L, respectively. Blood Mn level of all participants is similar to the reports by Korean (Lee et al. Int J Hyg Env Health 2012;215:449) and Canadian (Clark et al. Chemosphere 2007;70:155) studies in literature. Blood Pb level was higher in Chinese residents than those of Korea's and Czech's (Batarlova et al. Int J Hyg Env Health 2006;209:359). Blood Pb levels in the all participants were higher among Chinese than those of Korean and Czechs; the magnitude of increase became more evident when compared with Korean data. Blood Cd levels in this Chinese cohort were within the same range as Czech's, but were significantly higher

than German's (Heitland & Koster J Trc Elem Med Biol 2006;20:253). Blood Cu levels were significantly lower in Chinese than those of Germany and Canadian, while blood Zn levels were significantly lower than those of Czechs. Based on the data of the 95th percentile, we estimate the normal reference values for the whole blood Mn to be 21.7 ng/mL, Pb 10.3 ug/dL, Cd 5.3 ng/mL, Cu 1.36 ug/mL, and Zn 9.03 ug/mL in Chinese resident living in Beijing suburb. These baseline values will be useful for occupational and environmental exposure assessment.

**PS 1536 Effect of Long-Term Exposure of Heavy Metals on the Expression Profile of Cytoprotective Genes among Individuals Living in Mining Areas.**

I. M. Attafi, S. A. Albakheet and H. M. Korashy. *Pharmacology and Toxicology, King Saud University, Riyadh, Saudi Arabia.*

Environmental exposure to heavy metals is one of the most global concerns, particularly among whom living around the polluted areas. These heavy metals are known to generate oxidative stress species, and induce of oxidized DNA adduct formation, and DNA repair genes causing disease induction. The aim of this study is to evaluate the effects of long-term exposure to environmental heavy metals in the expression profile of some cytoprotective genes and the level of oxidized DNA adduct formation among individuals living around mining areas. Sixty healthy volunteers were divided to two groups; exposed group consisted of 40 male residents in a heavy metal-polluted area, whereas the control group consisted of 20 male residents in a non-polluted area. Whole blood concentrations for heavy metals, particularly lead, cadmium, and mercury, were determined using ICP-MS. Total RNA was isolated using PAXgene Blood RNA kits and the mRNA levels of heavy metals biomarker genes: NQO1, HO-1, and MT-1 and DNA repair genes: OGG1 and APE1 were determined by RT-PCR. Plasma levels of 8-OHdG were evaluated by ELISA technique. The results showed a significant increase in blood levels of heavy metals among exposed group. RT-PCR results revealed significant inhibitions of NQO1 mRNA level in group which were highly contaminated with lead, whereas the group of highly contaminated with cadmium showed the highest inhibitory effect on MT-1 mRNA level and significant induction of OGG1 mRNA level. Furthermore, mercury contaminated group showed a significant inhibition of APE1 mRNA level. The level of 8-OHdG was well correlated with the level of OGG1 mRNA. We conclude that long-term exposure to environmental heavy metals differentially altered the expression of cytoprotective and DNA repair genes. Therefore, they may be used as biomarkers for early prediction of disease risk among individuals living around polluted areas.

**PS 1537 Phytotoxicity and Trace Metal Accumulation from Long-Term Chicken Litter Amendment in Wilkes County, North Carolina: A Field Study.**

A. K. Hastings, S. Mouro, M. Brower and S. Tuberty. *Biology, Appalachian State University, Boone, NC.* Sponsor: G. LeBlanc.

Arsenic, zinc and copper are commonly integrated in chicken feeds to ensure increased weight gain in chickens and prevent chicken house diseases. These metals ultimately become part of the litter that is spread by farmers over crop fields as an alternative to expensive fertilizers. Massive growth in industrial chicken production across Wilkes County, NC has resulted in increased concentrations of phytotoxic metals in farmland soils and loss of copper sensitive crops such as peanuts. Using *Zea mays* as a representative crop species, our research objective was to evaluate the long-term sustainability of this practice by measuring adverse effects on corn in fields that have received a varied number of poultry litter amendments. Three agricultural fields receiving chicken litter amendment ranging from less than 10 yrs to more than 30 yrs within Wilkes County were selected as sampling areas for trace metal analysis. Soils were collected prior to and after annual litter application dates and corn tissue samples were collected in thirty day intervals (30, 60 & 90 days post planting) from each field. Nearly 400 corn tissue and soil samples were lyophilized and homogenized; 0.5g samples were nitric acid digested with a microwave reactor (USEPA Method 3051); and analyzed using ICP-OES to quantify levels of Cu and Zn. ICP-OES analysis indicated that industrial broiler chicken litter contains considerably elevated Cu (~388 ppm) and Zn (~481 ppm) concentrations. Thirty day corn seedling Cu and Zn burdens correlate closely with soil metal levels and with significantly delayed seedling emergence time and reduced growth rates (e.g., mean leaf height and area). No correlation was observed between soil metal levels and mature plant burdens. Continued chicken litter application may result in significantly reduced *Zea mays* productivity due to elevated Cu and Zn levels and therefore is not sustainable at the maximum application rates currently practiced in NC.

**PS 1538 Association of 25-Hydroxyvitamin D and 1, 25-Dihydroxyvitamin D with Metals in a Cohort of Adolescents in Torreon, Mexico.**

R. D. Zamoiski<sup>1</sup>, E. Guallar<sup>2,3</sup>, G. G. Garcia-Vargas<sup>4</sup>, M. Rubio-Andrade<sup>4</sup>, P. J. Parsons<sup>5</sup>, A. J. Steuerwald<sup>5</sup>, S. J. Rothenberg<sup>6</sup>, A. Navas-Acien<sup>1,2</sup>, C. Resnick<sup>1</sup>, V. Weaver<sup>1</sup> and E. K. Silbergeld<sup>1</sup>. <sup>1</sup>*Environmental Health Sciences, Johns Hopkins Bloomberg School of Public Health, Baltimore, MD*; <sup>2</sup>*Epidemiology, Johns Hopkins Bloomberg School of Public Health, Baltimore, MD*; <sup>3</sup>*Cardiovascular Epidemiology and Population Genetics, National Center for Cardiovascular Research, Madrid, Spain*; <sup>4</sup>*Facultad de Medicina, Universidad Juárez del Estado de Durango, Gómez Palacio, Mexico*; <sup>5</sup>*Inorganic and Nuclear Chemistry, Wadsworth Center, Albany, NY*; <sup>6</sup>*Centro de Investigación en Salud Poblacional, Instituto Nacional de Salud Pública, Cuernavaca, Mexico*.

**Background:** Data suggest that nephrotoxic metals may disrupt vitamin D metabolism and inhibit production of 1,25(OH)2D, the active vitamin D metabolite, from 25(OH)D in the kidney. Prior studies support this but are few in number and limited by small sample sizes. We sought to describe this association in a much larger sample.

**Methods:** Cross-sectional study of 512 adolescents in Torreon, a smelter town in Mexico. BPb was measured using atomic absorption; urine As, Cd, Mo, W, Sb, Tl, and U using ICP-MS. Vitamin D was measured using radioimmunoassay and chemiluminescent assay. Multivariate linear models with vitamin D as the outcome measured effect of metal on vitamin D level, controlling for age, sex, smoking, SES, and time outdoors.

**Results:** 25(OH)D was positively associated with Mo, Tl, and U ( $\beta=2.25, 1.46$ , and  $0.89$ , respectively). 1,25(OH)2D was positively associated with As and U ( $\beta=3.64, 2.25$ ), even after controlling for 25(OH)D ( $\beta=3.45, 1.90$ ).

**Conclusions:** No evidence that metals are inhibiting production of 1,25(OH)2D. Exposure to U or As may upregulate 1,25(OH)2D, perhaps in response to proximal tubule damage. Nephrotoxic metals such as U and As may cause a sub-threshold Fanconi syndrome, wasting phosphorus, and upregulating 1,25(OH)2D to maintain homeostasis.

**PS 1540 Broad Spectrum Safety of LOWAT: A Novel Weight Management Ingredient.**

E. Lau<sup>1</sup>, Z. M. Saiyed<sup>1</sup>, J. Lugo<sup>1</sup>, G. Trimurtulu<sup>2</sup>, A. V. Krishnaraju<sup>2</sup> and K. Sengupta<sup>2</sup>. <sup>1</sup>*R&D, Interhealth Nutraceuticals, Benicia, CA*; <sup>2</sup>*Laila Nutraceuticals, Vijayawada, India*.

LOWAT is a novel formulation consisting of extracts from Piper betle leaves and Dolichos biflorus seeds. Clinical research demonstrated that LOWAT is effective and well-tolerated in weight management. The current study evaluated the broad spectrum safety of LOWAT in a battery of animal and in vitro studies including acute oral, acute dermal, primary dermal irritation, primary eye irritation, mammalian erythrocyte micronucleus and chromosomal aberration tests. A sub-chronic repeated-dose 28-day toxicity study was conducted to determine the no-observable-adverse-effect-level (NOAEL) of LOWAT.

The LD50 levels of LOWAT in Sprague-Dawley (SD) rats, as determined by the acute oral and acute dermal toxicity studies, were  $>5,000$  and  $>2,000$  mg/kg body weight, respectively. Primary skin and eye irritation studies done on New Zealand rabbits classified LOWAT as non-irritating to the skin and as mildly irritating to the eye. Genotoxicity studies showed that LOWAT was non-mutagenic.

In a repeated-dose 28-day oral toxicity study, SD rats were administered orally with LOWAT at 0, 50, 250 or 2,500 mg/kg body weight daily dose. Rats were sacrificed at 28 days after supplementation. Body weight, food and water consumption, select organ weights, ocular health, hematology, blood chemistry, clinical chemistry and histopathology were assessed. No morbidity, mortality, or significant adverse events were observed at 28 days. Based on these findings, NOAEL of LOWAT was determined to be at least 2,500 mg/kg body weight in male and female SD rats.

These results, combined with the tolerability of LOWAT in the human clinical trial, demonstrate the broad spectrum safety of LOWAT.

**PS 1541 Evaluation of Nose-Only Inhalation Exposure to Aerosolized Linalool in Sprague-Dawley Rats.**

J. Randazzo<sup>1</sup>, D. Vitale<sup>2</sup>, D. Kirkpatrick<sup>1</sup>, F. G. Burleson<sup>3</sup> and M. Singal<sup>2</sup>. <sup>1</sup>*WIL Research, Ashland, OH*; <sup>2</sup>*Research Institute for Fragrance Materials, Woodcliff Lake, NJ*; <sup>3</sup>*Burleson Research Technologies, Morrisville, NC*.

Linalool is a commonly used fragrance material that has been associated with skin sensitization. The study objective was to understand the effects of inhalation exposure in Sprague-Dawley (SD) rats when aerosolized linalool when administered to rats by nose-only inhalation at 0.1, 1, and 10 ppm (0.63, 6.3, 63 mg/m<sup>3</sup>) for 2 weeks (6 hours/day, 5 days/week). Standard endpoints evaluated included: clinical observation; body and organ weights; hematology and serum chemistry evaluation; macroscopic/microscopic examination of selected organs; and bronchoalveolar lavage fluid (BALF) analysis for cellular markers of inflammation (i.e., cytokines). As a positive control to validate the utility of cytokine measures as indicators of pulmonary inflammation, a nose-only inhalation pilot was conducted with 25 mg/m<sup>3</sup> amorphous silica (0, 1, 2, 5 or 10 exposures). At all exposure levels, linalool was well tolerated with test substance-related effects limited to non-adverse microscopic findings in the nasal cavity. Therefore, the no-observed-adverse-effect level (NOAEL) was considered to be 10 ppm (equivalent to 63 mg/m<sup>3</sup>), the highest exposure concentration tested.

**PS 1542 Evaluation of Nose-Only Inhalation Exposure to Aerosolized Cinnamal in Sprague-Dawley Rats.**

D. Vitale<sup>1</sup>, J. Randazzo<sup>2</sup>, D. Kirkpatrick<sup>2</sup>, F. G. Burleson<sup>3</sup> and M. Singal<sup>1</sup>. <sup>1</sup>*Research Institute for Fragrance Materials, Woodcliff Lake, NJ*; <sup>2</sup>*WIL Research, Ashland, OH*; <sup>3</sup>*Burleson Research Technologies, Morrisville, NC*.

Cinnamal is a commonly used fragrance material that has been associated with skin sensitization. The study objective was to understand the effects of inhalation exposure in Sprague-Dawley (SD) rats when aerosolized cinnamal when administered to rats by nose-only inhalation at 1, 10, and 100 ppm (5.4, 54.1, 540.5 mg/m<sup>3</sup>) for 2 weeks (6 hours/day, 5 days/week). Standard endpoints evaluated included: clinical observation; body and organ weights; hematology and serum chemistry evaluation; macroscopic/microscopic examination of selected organs; and bronchoalveolar lavage fluid (BALF) and serum analysis for cellular markers of inflammation (i.e., cytokines). As a positive control to validate the utility of cytokine measures as indicators of pulmonary inflammation, a nose-only inhalation pilot was conducted with 25 mg/m<sup>3</sup> amorphous silica (0, 1, 2, 5 or 10 exposures). Exposure to cinnamal at 100 ppm was not tolerated as evidenced by adverse clinical observations and substantial body weight loss coupled with histologic changes in the upper and lower respiratory tract and clinical chemistry alterations suggestive of hepatotoxicity. Exposures were terminated for the 100 ppm group following the 5th exposure and the animals were sacrificed on study day 7. Exposures at 1 and 10 ppm (equivalent

**PS 1539 Is Genotoxic Metal Exposure Part of the Toxic Legacy of the Deepwater Horizon Oil Crisis?**

J. J. Wise<sup>1,2,4</sup>, J. Wise<sup>1,2,4</sup>, W. Thompson<sup>2,3</sup>, C. Perkins<sup>5</sup> and J. Wise<sup>1,2,4</sup>. <sup>1</sup>*Wise Laboratory of Environmental and Genetic Toxicology, University of Southern Maine, Portland, ME*; <sup>2</sup>*Maine Center for Toxicology and Environmental Health, University of Southern Maine, Portland, ME*; <sup>3</sup>*Department of Applied Medical Science, University of Southern Maine, Portland, ME*; <sup>4</sup>*Ocean Alliance, Gloucester, CT*; <sup>5</sup>*Center for Environmental Sciences and Engineering, University of Connecticut, Storrs, CT*.

In the wake of the Deepwater Horizon oil disaster of 2010, we collected tissue samples from sperm whales in order to determine the effects of the oil and chemical dispersants on their population. We focused on whales because they are at the top of the food chain and they are biologically similar to humans. Sperm whales live and feed at the same depth as the Deepwater Horizon well head, placing them at high risk to this disaster. After it became apparent the spewing oil was going to be the worst incident in US history, concern largely focused on oil and dispersants while the potential threat of genotoxic metals in the oil has gone largely overlooked. Genotoxic metals, such as chromium and nickel, damage DNA and bioaccumulate in organisms resulting in longer exposures. Analysis of sperm whale skin samples showed mean levels of Ni and Cr at significantly higher levels than those found in whales collected around the world prior to the spill. We found Cr and Ni levels ranged from 0.4-94.63 ppm in tissue collected from Gulf of Mexico whales in the wake of the crisis, with mean Ni and Cr levels of 14.9 and 12.00 ppm, respectively. In addition, we found Cr and Ni levels ranged from 0.24-8.46 ppm in crude oil from the riser, oil slicks from surface waters and tar balls from Gulf beaches. Maps of where we collected our samples showed the highest metal levels in whales closest to the epicenter. Given the capacity of these metals to break DNA, their presence in the oil and their elevated levels in whales, we believe metal exposure is an important overlooked concern for the Deepwater Horizon oil disaster. Further analysis is underway to determine the impact of this disaster on the genetic health of the whales and the long term impact in years following.

to 5.4 or 54.1 mg/m<sup>3</sup>, respectively) did not result in any adverse findings and show a clear threshold of response for lung and liver. Therefore, the no-observed-adverse effect concentration (NOAEC) was determined to be 10 ppm (equivalent to 54.1 mg/m<sup>3</sup>).

## PS 1543 Evaluation of Nose-Only Inhalation Exposure to Aerosolized Isoeugenol in Sprague-Dawley Rats.

M. Singal<sup>1</sup>, J. Randazzo<sup>2</sup>, D. Kirkpatrick<sup>2</sup>, F. G. Bursleson<sup>3</sup> and D. Vitale<sup>1</sup>.  
<sup>1</sup>Research Institute for Fragrance Materials, Woodcliff Lake, NJ; <sup>2</sup>WIL Research, Ashland, OH; <sup>3</sup>Bursleson Research Technologies, Morrisville, NC.

Isoeugenol is a commonly used fragrance material that has been associated with skin sensitization. The study objective was to understand the effects of inhalation exposure in Sprague-Dawley (SD) rats when aerosolized when administered to rats by nose-only inhalation at 0.15, 1.5, and 14.9 ppm (1, 10, and 100 mg/m<sup>3</sup>) for 2 weeks (6 hours/day, 5 days/week). Prior to the main study, a preliminary 3-day exposure (6 hours/day) was run at 89.4 and 44.7 ppm to allow selection of appropriate doses. At both concentrations, the animals were observed to have decreased body weight over the 3 day exposure period. Therefore, a third of the lowest dose tested, 14.9 ppm, was chosen as the high exposure level for the main study. Standard endpoints evaluated included: clinical observation; body and organ weights; hematology and serum chemistry evaluation; macroscopic/microscopic examination of selected organs; and bronchoalveolar lavage fluid (BALF) and serum analysis for cellular markers of inflammation (i.e., cytokines). As a positive control to validate the utility of cytokine measures as indicators of pulmonary inflammation, a nose-only inhalation pilot was conducted with 25 mg/m<sup>3</sup> amorphous silica (0, 1, 2, 5 or 10 exposures). Exposure of SD rats to  $\geq 0.15$  ppm isoeugenol resulted in adverse histologic changes indicative of dose dependent epithelial irritation. These were the only findings noted following isoeugenol exposure up to 14.9 ppm. There were no test substance-related microscopic effects in the lower respiratory tract tissues (lungs, trachea or larynx), liver, or kidneys. There were no toxicologically significant effects on BALF or serum cytokine levels. Therefore, neither a no-observed-adverse-effect level (NOAEC), nor a no observed effect level (NOEC) could be determined for this study regarding upper airway irritation. For the lower airway the NOEL was considered to be 14.9 ppm.

## PS 1544 Toxicological Evaluation of 4, 4, 5, 5, 6, 6, 7, 7, 8, 8, 8-Undecafluoro Octanoic Acid (5:3 Acid).

S. MacKenzie<sup>1</sup>, T. L. Serex<sup>1</sup>, C. Carpenter<sup>1</sup>, D. L. Nabb<sup>1</sup>, R. Hoke<sup>1</sup>, S. A. Gannon<sup>1</sup>, D. Hoban<sup>1</sup>, M. Donner<sup>1</sup> and R. C. Buck<sup>2</sup>. <sup>1</sup>DuPont Haskell Global Centers for Health and Environmental Sciences, Newark, DE; <sup>2</sup>E.I. du Pont de Nemours & Company, Inc., Chemicals and Fluoroproducts, Wilmington, DE.

Studies were conducted to evaluate mammalian and aquatic toxicity of 4,4,5,5,6,6,7,7,8,8,8-undecafluoro octanoic acid (5:3 acid) (CAS# 914637-49-3). 5:3 acid is a metabolite of 6:2 fluorotelomer alcohol (6:2 FTOH). 6:2 FTOH is a raw material for fluorotelomer-based products. Rat oral and dermal LD50 values were 2950 mg/kg and >5000 mg/kg, respectively. 5:3 acid produced no dermal irritation but irreversible eye irritation in rabbits, while a weak dermal sensitization response was observed in mice (LLNA), with an EC3 of 23%. A bacterial reverse mutagenicity assay and an in vivo rat micronucleus assay were negative. A 2-week rat gavage study identified red blood cells (anemia), liver (hypertrophy, focal necrosis, and increased beta-oxidation), kidney (tubular vacuolation), stomach (ulceration), and thyroid (follicular hyperplasia; of questionable relevance to humans) as target organs. Rats dosed at 600/900 mg/kg/day were euthanized in extremis. The NOAEL was <30 and 30 mg/kg bw/day in males and females, respectively. In vitro metabolism was evaluated in male and female rat hepatocytes and predicted half-life in males and females of 430 and 2573 min., respectively, and identified several metabolites. Preliminary evaluations (single dose and repeat dose exposures) demonstrated that 5:3 acid exhibits biphasic pharmacokinetics. Studies demonstrated low to moderate toxicity in aquatic organisms with the following results: 72-hour EbC50 in *Pseudokirchneriella subcapitata* was 22.5 mg/ml; 90-day NOEC in rainbow trout was 9.14 mg/L; 48-hour EC50 in *Daphnia magna* was >103 mg/L; 21-day NOEC in *Daphnia magna* was 1.25 mg/L. The 90-day bioconcentration factor (BCF) measured in rainbow trout was 2.25-5.85, which supports a lack of predicted bioaccumulation in fish. 5:3 Acid is not expected to be harmful to human health or the environment at environmentally relevant concentrations.

## PS 1545 A 28-Day Toxicity Study of PSOA by Oral Gavage in Rats Followed by a 14-Day Recovery Period.

T. O'Brien<sup>1</sup>, N. Pechacek<sup>1</sup>, W. Aulmann<sup>2</sup> and K. Laidlaw<sup>3</sup>. <sup>1</sup>Ecolab, St. Paul, MN; <sup>2</sup>Ecolab, Düsseldorf, Germany; <sup>3</sup>Charles River, Edinburgh, United Kingdom.

The objective of this study was to determine the potential repeat dose toxicity and reversibility of any findings over a 14 day recovery period for a peroxy sulfonated fatty acid (PSOA). The study design followed OECD Guideline 407. Sprague-Dawley (CrI:CD(SD)) rats were given PSOA once daily via gavage for 28 days at doses of 0, 5, 15 and 50 mg/kg/day. The highest PSOA concentration used was 0.5%. On completion of the dosing period, designated recovery animals were retained for a 14 day recovery period. The following parameters and end points were evaluated in this study: clinical signs, body weights, body weight changes, food consumption, ophthalmology, functional observations, clinical pathology parameters, gross necropsy findings, organ weights, and histopathology. No early deaths were observed in the dose groups. At the end of the treatment period, gross and microscopic findings observed were of the nature and incidence commonly seen in rats of this age and strain for studies of this type, and/or were of similar incidence in control and treated animals. Differences in the incidence of dark foci in the lungs, observed in male rats sacrificed on Day 29, were shown to correlate with alveolar hemorrhage which showed no biologically significant difference in incidence between treated animals and controls. The increased incidence of minimal hemorrhage in the thymus of treated animals which were sacrificed after the recovery period on Day 43 is considered incidental, as this is a common background lesion. Overall, no test article-related findings were observed for this study. Also no impairment of the mucous membranes of the gastrointestinal tract was observed up to the highest concentration of 0.5 %, which can be regarded as a No-Observed-Effect-Concentration (NOEC) in terms of local toxicity after 28 days repeated exposure. In conclusion, administration of PSOA by once daily oral gavage was well tolerated in rats at levels of 5, 15 and 50 mg/kg/day. Based on these results, the No-Observed-Effect Level (NOEL) was considered to be 50 mg/kg/day.

## PS 1546 Smokeless Tobacco (Guthka)-Induced Toxicological Effects in a Mouse Model: A Nicotine Twist.

D. Willis<sup>1</sup>, M. A. Popovich<sup>1</sup>, E. Gany<sup>2</sup>, C. Hoffman<sup>1</sup>, J. L. Blum<sup>1</sup> and J. T. Zelikoff<sup>1</sup>. <sup>1</sup>Environmental Medicine, New York University, Tuxedo Park, NY; <sup>2</sup>Memorial Sloan Kettering Cancer Center, New York, NY.

The popularity of smokeless tobacco (ST), usually placed within the mouth to be chewed, sucked, or swallowed, is growing rapidly and its prevalence of use is rising globally, due (in part) to greater convenience and stricter smoking laws. Guthka, an addictive form of ST that contains areca nut, catechu, cardamom, lime, flavored chewing tobacco, and natural and artificial flavoring materials, is particularly common amongst Southeast Asian communities throughout the world, including the US. This study seeks to determine the generalized toxic effects of Guthka and to determine the role of nicotine in producing Guthka-associated toxicity. Ten-week-old B6C3F1 male mice were divided randomly into three groups and treated for 3-wk (5 d/wk) via the oral mucosa with equal volumes of water (control), a water-soluble nicotine solution, containing 0.24 mg of nicotine, or a water-soluble, 21 mg lyophilized Guthka solution. Serum cotinine, used as the exposure metric, was measured weekly in all three groups and was similar in both the Guthka- and nicotine-treated mice (36 vs. 48 ng/mL, respectively). At sacrifice, liver, heart, spleen, tongue, kidneys, thymus, and testes were collected, weighed, and evaluated histologically; serum testosterone (T) and hepatic CYP 2A5 (equivalent to human CYP2A6 in humans and the major nicotine and cotinine oxidase in mouse liver) was also measured. Heart weight (relative to body weight) was significantly decreased following either nicotine or guthka exposure, while normalized liver/body weight and serum T levels were significantly decreased in the Guthka-treated group only. These findings suggest that repeated Guthka use adversely impacts body weight, organ weight, and circulating T levels and that Guthka toxicity may be driven by toxic components other than nicotine. As the use of Guthka rapidly increases worldwide, future studies are needed to further delineate its toxicological implications. MSK Cancer Center and NIEHS Center Grant ES000260.

## PS 1547 Safety Assessment of Dicamba Monooxygenase from the Biotechnology-Derived Soybean MON 87708.

M. Koch, L. Burzio, J. Finnessy, T. Kaempfe, H. Kang, A. Silvanovich, C. Wang and E. Bell. Monsanto Company, St. Louis, MO.

Monsanto has developed a soybean, MON 87708, which is tolerant to dicamba herbicide. It contains a gene, *dmo*, that expresses dicamba monooxygenase (MON 87708 DMO). A safety evaluation of the MON 87708 DMO protein was conducted, it examined: 1) the source of the gene; 2) its function and a history of safe use for structurally similar proteins; 3) its homology to known allergens, toxins, or

other proteins known to have adverse effects in mammals; 4) its stability to heat treatment; 5) its digestibility in simulated gastrointestinal fluid; and 6) its potential toxicity *in vivo*. The *dmo* gene was obtained from a strain of *Stenotrophomonas maltophilia*, a bacterium that is found in a variety of foods (i.e., "ready to eat" salads, vegetables, frozen fish, milk, and poultry), is widespread in the home environment, and has not been reported to be allergenic. Accordingly, the gene was considered to come from a safe source. Structurally, MON 87708 DMO is classified as a Rieske-type non-heme iron oxygenase (RO), as such it shares structural and functional similarities with related proteins in plants - including crops like corn, rice, and soybean. Thus, there is a history of safe use of RO proteins that are structural homologs of MON 87708 DMO. Similarly, protein homology searches conducted with MON 87708 DMO indicate no biologically relevant sequence similarities to allergens (including 8 amino acid epitopes), toxins, or other proteins with adverse biological activities. When subjected to temperatures approximating soybean processing, MON 87708 DMO demonstrates a loss of enzymatic activity and a change in structural stability. The protein also rapidly digests in simulated GI fluids. As well, field trial data indicates low MON 87708 DMO expression levels *in planta*. Taken together, dietary exposure to intact/active MON 87708 DMO is anticipated to be negligible. MON 87708 DMO was also administered to mice in acute and 28-day toxicity studies, and the protein was not associated with signs of toxicity. The weight of evidence demonstrates that MON 87708 DMO is safe for food and feed.

## PS 1548 A 14-Day IV Infusion Exploratory Toxicity Study of Hydroxylamine in Rats.

J. Zhou, R. Giovannelli, W. J. Reagan and M. D. Aleo. *Drug Safety R&D, Pfizer Worldwide Research and Development, Groton, CT.*

Hydroxylamine (HA) is an important industrial reducing agent with little therapeutic value. However, it may be formed as a by-product when drugs containing hydroxamic acid functional groups are used, and thus exhibit hemotoxicities. As many of these compounds are developed as intravenously (IV) administered (infusion) drugs, understanding the dose-toxicity relationship of HA by IV infusion becomes important in risk mitigation and management. In this study, we investigated if, at the same daily doses (12, 24 or 36 mg/kg/day), either by continuous infusion (CI) or by twice daily 1-hour intermittent infusions (II), HA produced the same level of toxicity. As systemic toxicities of HA are well-known, the focus of this study was on toleration and hematologic effects. Clinical signs, body weight and quantitative food consumption were assessed. Blood samples were taken at various times to evaluate methemoglobin (metHb) and total hemoglobin (Hb) levels. Hematology parameters and morphology were evaluated in blood samples taken on Days 3, 9 and 15. Dose-dependent increases in the metHb level were observed in both CI- and II-treated animals, however, a higher level of metHb was generally observed in II animals at the same daily doses. The metHb level increased within the first 4-6 days of dosing and then declined in the remaining course of study. Clinically, administration of HA up to 36 mg/kg/day (CI or II) was well-tolerated, with only pale appearance observed in the high-dose animals (CI and II) during the second week. No significant effect of HA on the body weight was observed although food consumption at 36 mg/kg (CI and II) was significantly reduced. Multiple hematology parameters demonstrated HA induced a dose- and time-dependent hemolytic anemia with the formation of Heinz bodies in both CI and II animals. The reduction of total Hb worsened with daily dosing and appeared to reach a plateau after 6-9 days of dosing. These data provided useful information on the choice of infusion regimen and risk management of some hydroxamic acids by infusion.

## PS 1549 Increased Hypothalamic Dopaminergic Neuron Tyrosine Hydroxylase Expression in Lean Wistar Rats.

S. M. Plummer<sup>1</sup>, M. Beltran<sup>2</sup>, M. Millar<sup>2</sup>, R. Wiegand<sup>3</sup> and J. Wright<sup>4</sup>. <sup>1</sup>MicroMatrices Associates Ltd., Dundee, United Kingdom; <sup>2</sup>MRC Centre for Reproductive Health, Edinburgh, United Kingdom; <sup>3</sup>MRC Centre for Inflammation Research, Edinburgh, United Kingdom; <sup>4</sup>Syngenta Ltd., Bracknell, United Kingdom.

Caloric restriction in Wistar rats has been reported to show a decrease in mammary and pituitary tumours and an increase in uterine tumours (1, 2) associated with delayed hypothalamic dopaminergic neuronal senescence (3). This study was designed to assess the effects of reduced body weight gain on hypothalamic dopaminergic neurons using FFPE tissue obtained from 100 female Wistar rats (50 controls; 50 with >30% body weight gain reduction) from a 2 year bioassay. A combination of immunostaining (IHC) and RNAscope™ *in situ* hybridisation (ISH) was used to examine expression of tyrosine hydroxylase (TH), a rate limiting enzyme for dopamine synthesis.

TH protein expression was detected in both the paraventricular (PVH)/periventricular (PeVH) nuclei and the median eminence (ME). TH RNA expression was also detected in these regions, but there was a disparity in the strength and location of

TH RNAscope™ staining compared to TH protein staining. TH protein staining was strongest in the ME, whereas TH RNA staining was strongest in the PVH/PeVH nuclei. To examine the relationship between TH protein vs RNA staining in more detail dual fluorescence IHC/ISH was performed. This analysis showed coincident TH protein and RNA staining in some neuronal cell bodies and axons; however, some neurons displayed TH protein staining in the absence of TH RNA staining and vice versa. Qualitative assessment indicated that rats with reduced bodyweight gain showed an increase in the number and intensity of TH RNA and TH protein positive neurones in the PVH/PeVH nuclei and the ME, respectively. These results indicate a disparity between the expression of TH RNA and TH protein in the rat hypothalamus, and suggest that chronic reduction in bodyweight gain may alter regulation of TH expression at the RNA and protein levels in hypothalamic nuclei.

- (1) Roe et al 1995;
- (2) Keenan et al 1995;
- (3) Harlemann et al 2012

## PS 1550 Proposition 65 and Cancer Incidence in California.

L. Haighton, H. Fikree, A. Pais, S. Prasad and J. W. Card. *Intertek Cantox, Mississauga, ON, Canada.*

Proposition 65 has been in effect in California (CA) for 25 years. It requires businesses to notify consumers if products they buy contain chemicals that are known to the State of CA to cause cancer and birth defects or other reproductive harm. This study determined the tumor types reported to be associated with the 71 carcinogens that were first added to the Proposition 65 list in 1987 and evaluated the incidence rates for these tumor types in males (M) and females (F) in CA through to 2009. Corresponding incidence rates in Washington State (WA; geographically similar) and New York State (NY; as a diverse East coast regional control) were evaluated as comparators. Of the 71 chemicals added as carcinogens to the Proposition 65 list in 1987, >10 have each been reported to be associated with urinary bladder and breast tumors and >20 each with liver and lung tumors. Between 1988 and 2009, there was a modestly decreased trend in bladder cancer incidence in CA [linear slope = 0.19 (M) and 0.06 (F); R<sup>2</sup> = 0.75 (M) and 0.77 (F)]. Less robust decreases were observed in WA [slope = 0.05 (M and F); R<sup>2</sup> = 0.01 (M) and 0.18 (F)], while a modestly increased trend was observed in NY. Over the same time period, there was a modestly increased trend in breast cancer incidence (slope = 0.15 to 0.41; R<sup>2</sup> = 0.02 to 0.18) and an approximate doubling of liver cancer incidence in both sexes in all 3 states (slope = 0.07 to 0.41; R<sup>2</sup> = 0.80 to 0.99). A substantial and comparable decrease in lung cancer incidence was observed in males in all 3 states (slope = 1.18 to 1.80; R<sup>2</sup> = 0.90 to 0.99). For females, lung cancer incidence decreased in CA (slope = 0.36; R<sup>2</sup> = 0.79) but increased in WA and NY. The results of this preliminary assessment indicate that since Proposition 65 came into effect 25 years ago, liver cancer incidence in CA has approximately doubled but consistent and robust decreases in incidence rates have been observed for bladder cancer in both sexes and for lung cancer in females. The contribution of Proposition 65 to these observed changes is unclear and warrants further investigation.

## PS 1551 Alternatives to Bisphenol A in Thermal Paper: Analysis of Substitution Options and Trade-Offs.

C. Baier-Anderson<sup>1</sup>, J. Rhoades<sup>2</sup>, M. Kawa<sup>2</sup> and J. Tunkel<sup>2</sup>. <sup>1</sup>US EPA, Washington DC; <sup>2</sup>SRC, Inc, Syracuse, NY.

The U.S. Environmental Protection Agency (US EPA) Design for Environment (DfE) Program undertook a chemical alternatives assessment for the use of bisphenol A (BPA) in thermal paper, including cash register receipts, as part of the Action Plan for BPA in March 2010. The purpose of the alternatives assessment is to identify and compare alternative chemicals to inform decision-making. The alternatives assessment was conducted via a multi-stakeholder partnership that identified 19 functional alternatives to BPA. The hazard assessment for BPA and the alternatives used the DfE hazard evaluation criteria to assign hazard designations for human health toxicity, ecological toxicity and environmental fate endpoints. Some alternatives were well characterized for all endpoints. Other alternatives were poorly characterized, wherein analog data, predictive models, structural alerts and expert judgment were used to make hazard designations for data gaps. Trends for human health, ecological toxicity and fate characteristics were indicated in a number of the alternatives due to particular molecular size ranges and/or molecular structures. In general, all alternatives have important trade-offs although if used with appropriate control measures, some of the alternatives could provide incremental benefits. Effective hazard assessment approaches, coupled with decision-making protocols that are practical tools for businesses to use in materials selections, will lead to more sustainable product development when human health or ecological toxicity concerns exist. The resulting hazard profiles should be of value to manufacturers making substitution decisions and facilitate reductions in environmental releases and subsequent exposures.

**PS 1552 Body-Residue Based Environmental Safety Assessment of Personal Care Product Ingredients: A Case Study with Benzophenone-3.**

F. Liu<sup>1</sup>, V. Tu<sup>1</sup> and N. Y. Wang<sup>2</sup>. <sup>1</sup>Revlon Research Center, Edison, NJ; <sup>2</sup>Environmental Assessment Scientist Serving in a Personal Capacity, Cincinnati, OH.

Personal care product (PCP) ingredients are released into aquatic ecosystem via wastewater discharge and potentially affect environmental health. The environmental safety assessment (ESA) is an important component of overall ingredient safety evaluation. We presented here an exploratory effort in applying the body-residue based approach in ESA of PCP ingredients. The traditional water-concentration based ESA has been used to evaluate the environmental impact of PCP ingredients. Compared with the water-based concentration, body residue concentration represents an internal dose, takes chemical disposition into account and provides an integrated assessment of the exposure an organism receives over space and time. With advancement of computational toxicology, critical body residues (CBRs) corresponding to toxicity endpoints and chemical bioaccumulation levels can be modeled as an alternative to animal testing. Organic UV filters are widely used in PCPs to offer sunscreen benefit. Environmental occurrence of various organic UV filters has been documented in both abiotic and biotic media. As a lipophilic UV filter, benzophenone-3 bioaccumulates in fish and concerns have been raised due to its *in vitro* antiestrogenic and antiandrogenic activities. The CBR and body residue level of benzophenone-3 were predicted using QSAR models. Information on environmental occurrence of benzophenone-3 was compiled and analyzed. The modeled tissue levels were comparable with the measured tissue levels in the environment. Our ESA analysis indicated that the CBR was significantly higher than the tissue level of benzophenone-3 in various fish species habituated in different aquatic ecosystems. The result was in good agreement with water-concentration based approach obtained by comparing the measured water concentration with the predicted no effect concentration (PNEC). As a result of this work, an alternative approach based on available *in silico* methods was developed for conducting screening level ESA of PCP ingredients.

**PS 1553 Evaluation of the Potential for Establishing a Threshold for Chemical Ocular Irritation Using a Model of Repeated Topical Ocular Administration in Albino Rabbits.**

K. G. Eckles, J. Amin, K. Krenzer and M. E. Richardson. *Nonclinical Safety, Bausch & Lomb, Rochester, NY.*

**Rationale:** The qualification of low levels of impurities in topical ophthalmic products is often hampered by a lack of ocular safety data at levels relevant to the products; establishing a threshold would be valuable in safety assessments. Therefore, the goal of this study was to explore the possibility of a threshold level for ocular irritation from repeated topical exposure to agents in solution.

**Methods:** Ten compounds from 8 chemical families (acids, acrylates, alcohols, aldehydes, alkalis, amines, anionic surfactants, and cationic surfactants), were identified which resulted in severe ocular irritation or corrosive effects when administered as a single drop on the rabbit eye at high concentrations. Each chemical was prepared in an appropriate vehicle (saline or sesame seed oil) to give concentrations of 20 and 100 ppm. One eye of albino rabbits (5/dose group) was administered 50  $\mu$ L of the test article 4 or 6 times daily (oil- or saline-vehicle, respectively) for 3 days. The contralateral eye served as a vehicle control. Draize scoring was performed before the first daily dose and after the final daily dose and biomicroscopy was performed pre-dose and on Days 2 and 3.

**Results:** None of the 10 chemicals resulted in notable ocular irritation at either 20 or 100 ppm after repeated ocular administration.

**Conclusion:** Despite being severe irritants or corrosives when dosed as a single drop at high concentrations, the favorable ocular irritation results observed with up to 100 ppm concentrations of severe irritants or corrosives suggest that it may be possible to establish a threshold for ocular irritation.

**PS 1554 Human Health Assessment of Scented Candle Emissions.**

T. Petry<sup>2</sup>, D. Vitale<sup>1</sup>, L. Cruse<sup>3</sup>, F. J. Joachim<sup>4</sup>, R. Mascarenhas<sup>5</sup>, S. Schneider<sup>6</sup>, B. Smith<sup>7</sup> and M. Singal<sup>1</sup>. <sup>1</sup>Research Institute for Fragrance Materials, Woodcliff Lake, NJ; <sup>2</sup>ToxMinds BVBA, Brussels, Belgium; <sup>3</sup>Procter & Gamble, Cincinnati, OH; <sup>4</sup>SC Johnson & Son, Racine, WI; <sup>5</sup>Reckitt-Benckiser, Hull, United Kingdom; <sup>6</sup>Firmenich SA, Princeton, NJ; <sup>7</sup>Firmenich SA, Geneva, Switzerland.

Airborne compounds in the indoor environment arise from a wide variety of sources such as environmental tobacco smoke, heating & cooking, dusts, emissions from furniture and construction materials as well as outdoor sources. One product

category which has received recent attention as a source of indoor airborne substances is scented candles. The potential impact of airborne candle emissions on the quality of the indoor air is highly dependent on the type and concentrations of chemical substances released. To better understand the potential of scented candles to contribute to the indoor load of airborne substances, a comprehensive candle emission testing program initiated by the consumer products and fragrance industry was undertaken to investigate the emissions of volatile and semi-volatile organic compounds (VOC; SVOC) and particulate matter (PM). Associated human exposures scenarios were derived and computer models used to estimate exposure of these materials to consumers. Measured chamber concentrations of VOC, SVOC and PM were used to predict their respective, cumulative indoor air concentrations in a standard EU-based dwelling using 2 models - the well-known and widely accepted ConsExpo 1-Box inhalation model and the recently developed, refined RIFM 2-Box indoor air dispersion model. The output from both models has been used to estimate realistic yet conservative consumer exposure to scented candle emissions measured under this program. The potential consumer health risks associated with the exposure to these materials was compared to existing air quality guideline values and established safe exposure levels. This investigation concluded that even under the conservative assumptions, potential human exposures are a minimum of one order of magnitude below established regulatory indoor air guideline values and/or published safe exposure levels.

**PS 1555 Cobalt Whole Blood Concentrations in Healthy Adult Volunteers following Two Weeks of Ingesting a Cobalt Supplement.**

B. L. Finley<sup>2</sup>, B. E. Tvermoes<sup>1</sup>, K. M. Unice<sup>3</sup>, J. M. Otani<sup>2</sup>, D. J. Paustenbach<sup>2</sup> and D. A. Galbraith<sup>2</sup>. <sup>1</sup>ChemRisk, Boulder, CO; <sup>2</sup>ChemRisk, San Francisco, CA; <sup>3</sup>ChemRisk, Pittsburgh, PA.

Recently, there has been an increase in the marketing and sales of dietary supplements, energy drinks, muscle builders and other consumer products that may contain relatively high concentrations of essential elements. Cobalt-containing supplements are readily available in the U.S. and have been marketed to consumers as energy enhancers. However, little information is available regarding cobalt (Co) body burden and steady-state blood concentrations following the intake of Co dietary supplements. We assessed Co whole blood concentrations in four healthy adult male volunteers who ingested a commercially available Co supplement (0.4 mg Co/day) for 15 or 16 days. Pre-supplementation blood Co concentrations were less than the reporting limit of 0.5  $\mu$ g/L, consistent with background concentrations reported to range between 0.2 to 0.4  $\mu$ g/L. The mean whole blood Co concentration in the volunteers after 15 or 16 days of dosing was 3.6  $\mu$ g Co/L and ranged from 1.8 to 5.1  $\mu$ g Co/L. The mean observed concentration in the study group was approximately 9 to 18 times greater than background concentrations. Further studies of Co whole blood concentrations following supplementation over longer time periods with additional monitoring of physiological parameters may provide useful information for evaluating the health of persons who take various doses of Co.

**PS 1556 Multiparameter *In Vitro* Toxicity Testing of Crizotinib, Sunitinib, Erlotinib, and Nilotinib in Human Cardiomyocytes.**

K. Doherty<sup>1</sup>, R. L. Wappel<sup>1</sup>, D. R. Talbert<sup>1</sup>, P. B. Trusk<sup>1</sup>, D. M. Moran<sup>1</sup>, J. W. Kramer<sup>2</sup>, A. M. Brown<sup>2</sup>, S. A. Shell<sup>1</sup> and S. Bacus<sup>1</sup>. <sup>1</sup>Quintiles, Westmont, IL; <sup>2</sup>ChanTest, Cleveland, OH.

Targeted therapy has greatly improved the treatment and prognosis of multiple types of cancer. However, unexpected cardiotoxicity has arisen in a subset of patients for some of the tyrosine kinase inhibitors (TKi). For these TKi, the cardiotoxicity was not wholly predicted by pre-clinical testing, which centers around the inhibition of the *human Ether-à-go-go-Related Gene* (hERG) channel. Therefore, we sought to determine whether a multi-parameter panel of tests that assesses a drug's effect on cellular, molecular, and electrophysiological endpoints would more accurately predict cardiotoxicity. To do so, we examined how 4 FDA-approved drugs impacted cell viability, apoptosis, reactive oxygen species (ROS) generation, metabolic status, impedance, and ion channel function in human cardiomyocytes. The 3 drugs with known associated cardiac adverse events (crizotinib, sunitinib, and nilotinib) all proved to be cardiotoxic in our series of *in vitro* tests while erlotinib, a cardiac-safe drug, did not show any indications of toxicity. Crizotinib, an ALK/ MET inhibitor, was the most cardiotoxic by our panel, leading to increased ROS production, caspase activation, cholesterol accumulation, and a significant disruption in cardiac cell beat rate and blockage of ion channels. The multi-targeted TKi sunitinib also demonstrated severe cardiotoxicity in our tests, showing decreased cardiomyocyte viability, inhibition of AMPK, increased lipid droplet accumulation, disrupted beat pattern, and hERG block. Nilotinib, a second

generation Bcr-Abl inhibitor, led to increased ROS generation, caspase activation, hERG block, and an arrhythmic beat pattern. Thus, each drug showed a unique toxicity profile, demonstrating that a multi-parameter approach allows for a more complete assessment of the potential for drug-induced cardiotoxicity and may allow for earlier detection in the drug development process.

## PS 1557 Safety Assessment of Chemicals in Toys.

M. Whitehead, J. Doran, G. Goodfellow and J. Daniels. *Intrinsic Health Sciences Inc., Mississauga, ON, Canada.*

Numerous countries have enacted laws and regulations to protect children from the potential health hazards associated with exposures to chemicals used in the manufacture of toys, including the United States, Canada and the member states of the European Union. Assessing the risk posed to children from exposure to chemicals in toys poses a special challenge, due to the particular vulnerability of this population to both adverse effects and chemical exposure. Examples of chemical categories used in toys that may be of concern include metals, boron-containing substances, pigments and colorants, preservatives, and allergenic fragrances. The aim of this study was to evaluate the risk of substances flagged as potential chemical hazards when included as ingredients in child-intended products in various jurisdictions. Results of toxicological studies indicate that metal-containing pigments, certain azo dyes, and boric acid and its salts are associated with toxicity concerns such as reproductive, developmental, mutagenic, and carcinogenic effects. Product formulation data collected in a proprietary database over a two-year period was analyzed in order to determine the levels and frequency of use of these substances in various categories of toys. Exposure considerations and scenarios designed to specifically address the enhanced risk to children from chemical exposures as a result of the intentional use and reasonably anticipated misuse of different categories of toys were developed. Using the results of the toxicological studies and exposure scenarios developed by our group, we analyzed the margin of safety for the use of these chemicals of concern with respect to toxicity effects in toys. The results of our studies suggest that restricted chemicals are still being used to formulate toys at levels that indicate potential concern for this sensitive population.

## PS 1558 Health-Based Framework for Evaluating the Safety of Hydraulic Fracturing Products.

D. Wikoff<sup>1</sup>, L. Fitzgerald<sup>1</sup>, L. C. Haws<sup>1</sup> and M. Harris<sup>2</sup>. <sup>1</sup>ToxStrategies, Austin, TX; <sup>2</sup>ToxStrategies, Houston, TX.

Hydraulic fracturing has made it possible to extract natural gas from dense shale rock formations and has become the fastest-growing source of gas in the U.S. Because the process involves drilling through groundwater formations, there has been concern that drinking water aquifers could become contaminated – a concern compounded by a lack of information regarding the composition and safety of the products used. In an effort to address these concerns, we developed a quantitative framework to characterize potential safety of hydraulic fracturing products. The framework consists of four evaluation criteria that are applied to each of the product components: composition and use, toxicity, exposure, and risk of release. Each of the criteria has specific requirements associated with scores ranging from 1-5 (with 1 being the best and 5 being the worst) that are based on USEPA guidelines and standard risk assessment practices. A final composite product score is calculated based on scores for each of the criteria for each of the components and this score is used to place the product into a category of use relating to its safety (not recommended for use, use with caution/specialized conditions, or acceptable for designated use). Importantly, if any component of the hydraulic fracturing product does not achieve a score below the STOP point for any of the four criteria (indicative a minimum level of knowledge or safety), the product is automatically placed into the not recommended for use category. This framework allows health experts to tailor the evaluation to any type of product used in the fracturing process and can be consistently conducted by independent parties. Because this process focuses on human health risk and environmental exposures, it is different than those currently available in the natural gas industry and is more in line with standard risk assessment practices. Most importantly, this framework allows for transparency in the evaluation process and provides a quantitative method upon which experts can make decisions.

## PS 1559 Novel Methodology in Hazard Assessment: Chemical Clustering for Read Across—The Phthalate Alternatives Case Study.

M. Kawa<sup>1</sup>, J. Rhoades<sup>1</sup>, C. Baier-Anderson<sup>2</sup>, T. Webb<sup>1</sup>, K. Mayo-Bean<sup>3</sup> and J. Tunkel<sup>1</sup>. <sup>1</sup>SRC, Inc., East Syracuse, NY; <sup>2</sup>US EPA, DFE, Washington DC; <sup>3</sup>US EPA, OPPT, Washington DC.

Phthalates are a class of compounds produced in high volume in the U.S. and are found in many products, primarily as plasticizers. The U.S. EPA published an initial Action Plan for eight phthalates in 2010 due to concern about the toxicity of phthalates and the evidence of pervasive human and environmental exposure. As indicated in the Action Plan, a Design for the Environment (DfE) alternatives assessment (AA) will be performed for these chemicals. The DfE Program publishes AAs to help industries identify safer chemicals and provide a comparison of potential human health and environmental impacts of chemical alternatives. DfE hazard criteria are used to assign hazard designations for human health toxicity, ecological toxicity and environmental fate endpoints. Over 70 substances were identified as potential alternatives to the eight action plan phthalates. Some alternatives are well characterized for all endpoints, while others are data poor. In the absence of experimental data, DfE assessment methodology designates hazards based on a read across approach to structurally similar compounds. This poster describes a novel technique for green chemistry and hazard screening that uses the EPA's Office of Pollution Prevention and Toxics ChemACE program to cluster the alternatives based on common structures, functional groups, and molecular architectures. The ChemACE program automates chemical clustering based on structural similarities and generates reliable and organized results. Using this methodology, read across (analog) data from data-rich chemicals was used to assist in assigning and justifying hazard designations for data poor chemicals within a cluster. This allows for the determination of hazard designations for as many endpoints as possible including human health endpoints that often lack experimental data and methods for estimation. The resulting AAs should be of value to manufacturers making substitution decisions and facilitate reductions in potential human health impacts.

## PS 1560 Transdermal Toxicity of the Phorbol Ester Isolated from Biodiesel Feedstock, Jatropha Curcas.

M. Nakao, S. Kinoshita and Y. Ishihara. *Kurume University, Kurume, Japan.*

[Purpose] *Jatropha curcas* attracts rising attention as a biodiesel feedstock in the world. However, *Jatropha* contains various toxic components, generating concerns about its health effects. One of toxic components is potential tumor promoter, phorbol esters. Toxicity of *Jatropha* phorbol esters has not been fully described. In this study, transdermal toxicity of main component of *Jatropha* phorbol esters was assessed in mice.

[Experimental procedures] One of the *Jatropha* phorbol esters, 12-deoxy-16-hydroxyphorbol-4'-[12',14'-butadienyl]-6'-[16',18',20'-nonatrienyl]-bicyclo [3.1.0] hexane-(13-*O*)-2'-[carboxylate]-(16-*O*)-3'-[8'-butenoic-10'] ate (DHPB) (1 – 10 µg), was applied onto skin of mice. As a positive control, 12-*O*-Tetradecanoylphorbol 13-acetate (TPA) (1 – 10 µg) a known tumor promoter was applied. Transformation activity of test compound was assayed using Bhas42 cells. Autopsy was conducted on the dead mice to observe the lesions. All survived mouse were sacrificed at 8 weeks from the beginning of the study and hematological tests and splenic lymphocyte measurement using flow cytometer were carried out.

[Results] 2.5 µg of DHPB led to weight loss and over 5 µg of DHPB caused death during 3 weeks observation. There were no such symptoms in the mice treated with the same dose of TPA. Gastrointestinal bleeding and splenic atrophy was observed in the dead mice. The NOAEL of DHPB was considered to be 2 to 2.5 µg. No papilloma on the skin was observed in DHPB group in contrast to TPA which developed papilloma when the dose exceeded 1 µg. There was no significant difference in splenic lymphocyte composition among DHPB, TPA, and control groups. Hematological analyses showed that the number of red blood cells, platelet, and lymphocyte was markedly decreased in DHPB treated mice at 8 weeks.

[Conclusion] DHPB, on the contrary to TPA, showed no tumor promotion in this experiment but showed acute toxicity which was not seen in the mice treated with TPA. These results suggest that DHPB has different characteristics in transdermal toxicity in comparison with those of TPA.

**PS 1561 Identifying No Observed Effect Levels (NOEL) and No Observed Adverse Effect Levels (NOAEL) through Metabolomics.**

G. Montoya<sup>1</sup>, V. Strauss<sup>1</sup>, H. G. Kamp<sup>1</sup>, W. Mellert<sup>1</sup>, T. Walk<sup>2</sup>, R. Looser<sup>2</sup>, M. Herold<sup>2</sup>, G. Krennrich<sup>2</sup>, E. Peter<sup>2</sup> and B. van Ravenzwaay<sup>1</sup>. <sup>1</sup>Experimental Toxicology and Ecology, BASF SE, Ludwigshafen am Rhein, Germany; <sup>2</sup>metanomics, Berlin, Germany.

A key quantitative element in toxicity studies is the identification of the NO(A)EL – no observed (adverse) effect level. With the introduction of omics into toxicology, questions have been raised concerning the sensitivity of these methods. BASF's Experimental Toxicology and Ecology unit and metanomics developed the MetaMap® Tox database with more than 500 reference compounds obtained from rat studies (OECD 407 design). Metabolome analysis in plasma was performed after 7, 14 and 28 days and relative levels of endogenous metabolites in treated rats versus controls were analyzed. We have obtained metabolome data at toxicological NO(A)EL doses.

Recent advances in metabolic profiling technologies together with expert judgment offer the possibility of identifying whether differences from control values are treatment related and to discriminate between those that are adverse and those that are not. To obtain a measure of sensitivity of metabolomics vs. classical toxicology, we have used these data to analyze metabolomics changes at toxicological NO(A)EL doses. We have done this considering the number of statistically significant metabolite changes ( $p < 0.05$ ), the false-positive rate and the correlation with defined patterns for diverse modes of action (approximately 100 defined in MetaMap®Tox). Results show that in most cases where there are no toxicological effects (NOEL) there are also only few metabolomics changes (at/below the level of the false positive rate and without a match to the predefined MoA patterns). In some cases in which the study demonstrated a NOAEL (only effect noted being liver weight increase) metabolomics changes are often present and identify the liver as target organ. Following this analysis, it would seem that metabolomics is generally not more sensitive than classical toxicology, with respect to the identification of a NO(A)EL.

**PS 1562 Metabolic Profile of Rats in Repeated Dose Toxicological Studies after Oral and Inhalative Exposure.**

E. Fabian<sup>1</sup>, N. Bordag<sup>2</sup>, M. Herold<sup>2</sup>, H. G. Kamp<sup>1</sup>, G. Krennrich<sup>2</sup>, R. Looser<sup>2</sup>, L. Ma-Hock<sup>1</sup>, W. Mellert<sup>1</sup>, E. Peter<sup>2</sup>, A. Prokoudine<sup>2</sup>, M. Spitzer<sup>2</sup>, V. Strauss<sup>1</sup>, T. Walk<sup>2</sup>, J. Wiemer<sup>2</sup> and B. van Ravenzwaay<sup>1</sup>. <sup>1</sup>Experimental Toxicology and Ecology, BASF SE, Ludwigshafen am Rhein, Germany; <sup>2</sup>Metanomics, Berlin, Germany.

BASF and metanomics, in a joint effort, developed the MetaMap®-Tox application containing metabolic profiles attained from administration of over 500 toxicants. The toxicants were administered to five Wistar rats for each sex and each of the two dose levels for a total duration of four weeks following a standardized protocol, in accordance with OECD 407. Metabolome analysis of plasma samples was performed after one, two and four weeks. The ratios of the metabolites from treated rats versus untreated rats (control) were transferred to MetaMap®-Tox for data assessment.

In this study, metabolic profiles after oral and inhalative exposure were compared for six selected model compounds: aniline (A), chloroform (CL), ethylbenzene (EB), 2-methoxyethanol (ME), N,N-dimethylformamide (DMF) and tetrahydrofuran (THF). The toxicants were dosed inhalatively for six hours/day, five days a week and orally each day via the feed (DMF) and by gavage (A, CL, EB, ME, THF). Statistical evaluation (pairwise comparison in MetaMap®-Tox as well as principle component analyses) showed similar metabolic changes for DMF, EB, CL and ME, indicating a comparable systemic toxicity after oral and inhalative exposure. In contrast, metabolic profiles of A and THF showed differences between the tested exposure routes. Metabolic profiles were sufficient for the identification of test substance related toxicological modes of action using MetaMap®Tox. In conclusion, our results indicate the potential of metabolic profiling for generating fingerprints of systemic toxicity following different exposure scenarios.

**PS 1563 Percellome Toxicogenomics Application to Sick Building Syndrome-Level Inhalation Toxicity.**

J. Kanno, K. Aisaki, K. Igarashi, Y. Taquahashi and S. Kitajima. *Division of Cellular and Molecular Toxicology, National Institute of Health Sciences, Tokyo, Japan.*

Toxicity of low concentration formaldehyde (FA) corresponding to the level of Sick House/Building Syndrome (SHS) is difficult to assess by the ordinary inhalation animal studies; histopathological endpoints are negative for toxicity at such concentration. However, transcriptomic responses are captured at this exposure level.

Here we applied our Percellome Toxicogenomics Project. This project has been launched to develop a comprehensive gene network for the mechanism-based predictive toxicology. For this purpose, a normalization method designated as "Percellome" is developed (BMC Genomics 7:64, 2006) to generate mRNA expression values in "copy numbers per one cell" from microarrays and Q-PCR. The time- and dose-dependent alteration of gene expression induced by various exposure protocols in mice (4 time points x 4 dose levels, triplicate) are studied on more than 100 chemicals. Data are expressed in 3-D graphs (time x dose x mean copies per cell +/- sd); 45,000 surfaces corresponding to the probe sets of the Affymetrix Mouse Genome 430 2.0 Array.

FA at concentrations close to the "Indicative indoor exposure value of SHS (Ministry of Health Labour and Welfare, Japan)" of 0.08 ppm was applied to the 22hr/day x 7 day exposure protocol (0, 0.1, 0.3 and 1.0ppm, 4 time points, triplicate). C57Bl/6J mice were exposed and lung, liver and hippocampus were analyzed. As a result, strong suppression of gene expression related to neuronal activity in hippocampus, i.e. the immediate early genes including Arc, Nr4a1, Fos, Junb and Egr4 were shown. This study indicated that the comprehensive transcriptomic analysis will become useful for prediction of the effect on central nervous system of the very low concentration of toxicants. Our finding may be considered as a first substantial data that would explain the indefinite or unidentified complaint by this SHS-level exposure of FA. (Supported by Health Sciences Research Grants from the Ministry of Health, Labour and Welfare, Japan)

**PS 1564 Ten-Year Retrospective Assessment of the Food Contact Notification Program.**

A. P. Neal-Kluever, J. Cooper, T. Zebovitz and K. Butts. *Division of Food Contact Notifications, US FDA, College Park, MD.*

The Food Contact Notification (FCN) Program is FDA's premarket review system for evaluating the safety of packaging and other materials that contact food. Additionally, FCN notifiers can take advantage of a pre-notification consultation (PNC) program designed to provide guidance in advance of FCN filing. To assist program development and improve program transparency we performed a retrospective assessment of the FCN program. We analyzed the first 10 years of program performance, which included 924 FCNs and 980 PNCs. Overall, 76% of FCNs become effective, 23% were withdrawn, and 1% received not-accepted status. Some trends were observed which influenced the likelihood of an FCN becoming effective, such as whether the FCN was a resubmission, received a time extension, proposed a new use, or proposed the use of a novel or polymeric FCS. Company size as determined by the Small Business Association influenced whether an FCN was likely to become effective, with larger companies exhibiting a higher effective outcome rate. Smaller companies were more likely to withdraw FCNs, but experienced very high effective outcome rates with resubmitted and extended FCNs. There were some differences between the outcomes of notifiers utilizing and not utilizing the PNC program. Interestingly, 78% of the PNCs in the study period were not associated with an FCN.

**PS 1565 Development of a Regulatory Value for the Carcinogenic Potential of Isoprene via Inhalation Exposure.**

T. D. Phillips<sup>1</sup>, R. L. Sielken<sup>2</sup> and C. Valdez-Flores<sup>2</sup>. <sup>1</sup>Toxicology Division, Texas Commission on Environmental Quality, Austin, TX; <sup>2</sup>Sielken & Associates Consulting, Inc., Bryan, TX.

Isoprene is the 2-methyl analogue of 1,3-butadiene, a known human carcinogen. While isoprene is synthesized and used in the manufacturing of substances such as synthetic rubber, it is also produced naturally by plants, animals, and bacteria and is one of the main endogenous compounds found in human breath. Following the Texas Commission on Environmental Quality (TCEQ) Guidelines for the development of toxicity factors, a preliminary review and characterization of the carcinogenic potential of isoprene was conducted. Three key studies provided adequate data for the dose-response assessment of isoprene's carcinogenic potential. In order to determine URFs for study endpoints assuming exposure for 24h/d, 7d/wk, for a lifetime, the dose levels and numbers of animals at risk in the data sets were adjusted for differences between the exposure durations and times of response observation. The doses were adjusted to the constant lifetime environmental dose that is equivalent to the time-dependent doses in the studies, based on the multistage theory of carcinogenesis using the Armitage and Doll (1954) mathematical description of carcinogenesis with the number of stages being  $m = 1, 2, \text{ or } 3$ . Similarly, the number of subjects at risk of developing the specified response by necropsy time in the study was adjusted to the equivalent number of animals at risk if the time to necropsy were equal to the nominal animal lifetime. The adjusted parameters were used to carry out 171 model fits. The EC10 for each endpoint was identified using the estimated multistage models, and from there a URF for each endpoint was calculated. Based on the TCEQ Guidelines, only malignant endpoints considered relevant to humans and showing a statistical significance were considered for the draft

URF. The chosen draft URF was  $9.1\text{E-}04$  per ppm for liver carcinoma in a one stage carcinogenic process ( $m=1$ ). From the draft URF, a draft air concentration at the  $1\text{E-}05$  excess cancer risk level is calculated to be 11 ppb.

**PS 1566 Evaluation of Selected Nitrosamines As Candidates for Regulatory Determination Using a Group Approach.**

J. Donohue<sup>1</sup>, M. Simic<sup>1</sup>, Z. Bain<sup>1</sup>, A. Gebhart<sup>2</sup>, S. Goldhaber<sup>2</sup> and R. Howd<sup>2</sup>.  
<sup>1</sup>Office of Water, US EPA, Washington DC; <sup>2</sup>ToxServices, Washington DC.

In May 2011, EPA Administrator, Lisa Jackson announced the Drinking Water Strategy, a new cost-efficient approach to protecting public health that included broadening the traditional regulatory framework for chemicals by addressing groups of contaminants. Common physical and/or toxicological properties are features to be considered in determining group composition. The six nitrosamines, recently monitored nationally at public water systems (PWSs) under the Second Unregulated Contaminant Monitoring Rule (2009–2011), meet the grouping criteria based on a common mutagenic mode of action plus their chemical, and metabolic properties. Their toxicological data and co-occurrence at PWSs have been integrated to evaluate the practicality of considering a group of toxicologically similar chemicals in a Regulatory Determination context. The nitrosamines evaluated include N-Nitrosodi-n-butylamine, N-Nitrosodiethylamine, N-Nitrosodimethylamine, N-Nitrosodi-n-propylamine, N-Nitrosomethylethylamine, and N-Nitrosopyrrolidine. [The views expressed in this abstract are those of the authors and do not necessarily reflect the views or policies of the U.S. EPA.]

**PS 1567 Key Decisions in Establishing National Ambient Air Quality Standards.**

L. Fraiser<sup>1</sup> and L. J. Bradley<sup>2</sup>. <sup>1</sup>Environment, AECOM, Austin, TX; <sup>2</sup>Environment, AECOM, Chelmsford, MA.

This paper provides an evaluation of key decisions made by the US Environmental Protection Agency (EPA) in establishing more stringent short-term National Ambient Air Quality Standards (NAAQS) and provides an opinion on whether the supporting science suggests that their implementation will result in additional public health protection. Although EPA states that the NAAQS are based on evaluation of all relevant scientific evidence, they routinely are not. Despite many epidemiology studies that found no association between particulate matter (PM) exposure and mortality, EPA based the recent 24-hr PM<sub>2.5</sub> NAAQS on only two studies reporting associations between PM<sub>2.5</sub> reductions and health benefits. Only one controlled sulfur dioxide (SO<sub>2</sub>) study caused a significant response in the range used as the point of departure in establishing the 1-hr SO<sub>2</sub> NAAQS and neither clinical nor epidemiological studies support clinically-relevant lung decrements at this level. EPA used a consistent definition for moderate decrements in the lung function of asthmatics in establishing 1-hr NAAQS for nitrogen dioxide (NO<sub>2</sub>) and SO<sub>2</sub> but used a slightly different categorization in the latest review of the 8-hour ozone NAAQS. EPA included human exposures to NO<sub>2</sub> by mouthpiece in establishing the NO<sub>2</sub> NAAQS, but excluded mouthpiece exposure studies in developing the 1-hr SO<sub>2</sub> NAAQS because of the potential for increased pollutant delivery and altered distribution/deposition of pollutant that can occur. This evaluation of recently promulgated NAAQS reveals inconsistency in the way that EPA uses health effects studies to support its decisions, emphasizing the need to define key criteria/concepts, such as "adverse" effect, "sensitive" populations and principles of cause-effect relationships. It also highlights the need for guidelines on incorporating negative study results into weight-of-evidence evaluations. When all relevant data are considered, particularly in the context of other contributing factors, they do not support that the recent ratcheting down of NAAQS will result in additional health public protection.

**PS 1568 Development of a Proposed 24-Hour Health-Protective Air Monitoring Comparison Value for Formaldehyde for Comparison to 24-Hour Monitoring Data in the Barnett Shale Area.**

A. L. Curry, J. T. Haney and D. McCant. Toxicology Division, Texas Commission on Environmental Quality (TCEQ), Austin, TX.

The Barnett Shale is a large natural gas reserve encompassing more than 5,000 square miles and covering approximately 26 counties in North Texas. Due to public concern that natural gas compressor stations emit high formaldehyde concentrations, formaldehyde has been of increased public and regulatory interest in recent years. It has also been detected in 24-h carbonyl samples collected by the TCEQ in

the Barnett Shale. However, use of these data for evaluating potential health effects is typically limited to calculating long-term annual means for comparing to chronic, health-protective air monitoring comparison values (AMCVs). For evaluation of acute exposures, the agency generally uses 1-hr AMCVs, which are not designed to evaluate 24-h results. Thus, the development of a 24-h AMCV would allow the TCEQ to evaluate 24-h formaldehyde data for possible health concerns. Critical effect dose-response data for irritation (e.g., eyes, upper respiratory tract) from acute (~400 ppb) and chronic (~200 ppb) human studies suggest a narrow range for the lowest reported effect levels, indicating these irritant effects are primarily concentration dependent. The TCEQ conservatively used the same point of departure (POD) that its chronic noncarcinogenic AMCV is based on (NOAEL of 70 ppb) because the exposure duration (8 h/d) is more similar to the 24-h duration of interest than the 2–4 h exposure durations for the acute studies. Because the 8 h/d exposure was repeated 5 d/wk for 10 yrs, and irritation appears to be primarily concentration dependent, an 8-to-24-h exposure duration adjustment was judged not to be necessary. Dividing the POD of 70 ppb by an intrahuman uncertainty factor of 3 results in a proposed 24-h, health-protective AMCV of 23 ppb. The 24-h AMCV falls between TCEQ's 1-h (41 ppb) and chronic (8.9 ppb) noncarcinogenic AMCVs. To date, there has been only 1 exceedance in 1999 of the proposed formaldehyde 24-h AMCV when compared to Barnett Shale monitored data.

**PS 1569 Use of Other Scientifically-Relevant Information to Satisfy Tier 1 Testing Requirements in US EPA's Endocrine Disruptor Screening Program.**

P. L. Bishop<sup>1</sup> and C. Willett<sup>2</sup>. <sup>1</sup>People for the Ethical Treatment of Animals, Norfolk, VA; <sup>2</sup>The Humane Society of the United States, Washington DC.

The Endocrine Disruptor Screening Program (EDSP) has been designed to determine whether certain substances may have effects on the estrogen, androgen and thyroid hormonal systems. EPA is using an initial Tier 1 screening battery consisting of five in vitro and six in vivo assays to evaluate a chemical's potential to interact with the hormone systems in mammals and other animals. By order of the Office of Management and Budget, EPA must also consider Other Scientifically Relevant Information (OSRI) that is directly or functionally equivalent to data gathered in Tier 1, in lieu of developing new test data. This study characterizes the types of OSRI submitted by recipients of the first 67 test orders issued by EPA and reviews EPA's approach to acceptance of OSRI. It also assesses the impact of OSRI acceptance on reducing the number of animals used in screening this first round of chemicals. Companies submitted OSRI in lieu of some or all Tier 1 assays for 47 chemicals and sought waivers for 412 assays. EPA granted only 94 waivers, an overall acceptance rate of 23%; of these, 50 were for in vivo tests. For 20 of the 47 chemicals, EPA denied all OSRI and required the entire battery of assays to be performed. In most instances, the OSRI accepted was either identical to data that would have been generated by the Tier 1 test or indicated a positive response by the chemical in question. Although identified as potential sources of OSRI in EPA's guidance to test order recipients, guideline studies for pesticide registration, such as the mammalian two-generation reproductive toxicity study and 90-day rodent or dog studies, were all consistently rejected by EPA as satisfying Tier 1 data requirements. The 50 in vivo waivers EPA granted saved about 2,800 animals; however, nearly 26,000 were killed in the Tier 1 assays EPA required. The study concludes with a discussion of the implications for future use of OSRI in the EDSP.

**PS 1570 A New Approach to Academic and Guideline Research: The CLARITY-BPA Research Program.**

A. F. Johnson<sup>2</sup>, J. Aungst<sup>4</sup>, J. R. Bucher<sup>3</sup>, C. Luisa<sup>5</sup>, K. Delclos<sup>5</sup>, J. J. Heindel<sup>1</sup>, P. C. Howard<sup>5</sup>, D. Keefe<sup>4</sup>, R. Newbold<sup>3</sup>, W. Nigal<sup>3</sup> and T. T. Schug<sup>1</sup>. <sup>1</sup>Division of Extramural Science, NIEHS, Durham, NC; <sup>2</sup>Program Evaluation, MDB, Durham, NC; <sup>3</sup>NTP, NIEHS, Durham, NC; <sup>4</sup>Office of Food Safety, US FDA, College Park, MD; <sup>5</sup>Division of Biochemical Toxicology, National Center for Toxicological Research, US FDA, Jefferson, AR.

Recently, medical research has seen a strong push toward translational research, or "bench to bedside" collaborations, which strive to enhance the utility of laboratory science for improving medical treatment. The success of that paradigm supports the potential application of the process to other fields, such as risk assessment. Close collaboration among academic, government, and industry scientists may facilitate the application of scientific findings to regulatory decision making. The National Toxicology Program (NTP), National Institute of Environmental Health Sciences (NIEHS), and U.S. Food and Drug Administration (FDA) developed a consortium-based research program to more effectively link academic and guideline-compliant research. An initial proof-of-concept collaboration, the Consortium Linking Academic and Regulatory Insights on BPA Toxicity (CLARITY-BPA), uses bisphenol A (BPA) as a test chemical. The CLARITY-BPA program combines a core perinatal guideline-compliant 2-year chronic toxicity study with mechanistic

studies/endpoints led by academic investigators. Twelve extramural grantees were selected by NIEHS through an RFA-based initiative to participate in the overall study design and conduct disease-relevant investigations using tissues and animals from the core study. While the study is expected to contribute to our understanding of potential effects of BPA, it also has ramifications beyond this specific focus. Through CLARITY-BPA, NIEHS has established an unprecedented level of collaboration among extramural grantees and regulatory researchers. The CLARITY-BPA represents a potential new model for filling knowledge gaps, informing chemical risk assessment, and identifying new methods or endpoints for regulatory hazard assessments.

## PS 1571 How Consistent Are the Derived No-Effect Levels (DNELs) in the European REACH Legislation?

L. Schenk<sup>1,2</sup>, U. Deng<sup>1</sup> and G. Johanson<sup>1</sup>. <sup>1</sup>Work Environment Toxicology, Karolinska Institute, Stockholm, Sweden; <sup>2</sup>Division of Philosophy, Royal Institute of Technology, Stockholm, Sweden.

The new European REACH regulation places more responsibility than hitherto on manufacturers and importers of chemicals ("industry") to provide safety information. An important part of the development of a REACH Chemical Safety Report is derivation of Derived No-Effect Levels (DNELs) which represent "the level of exposure above which humans should not be exposed". In order to study the consistency, we compared DNELs presented by industry at the website of the European Chemicals Agency (ECHA) with those derived by us in our interpretation of the REACH guidance (Chapter R.8: Characterisation of dose [concentration]-response for human health, [http://echa.europa.eu/documents/10162/13632/information\\_requirements\\_r8\\_en.pdf](http://echa.europa.eu/documents/10162/13632/information_requirements_r8_en.pdf)). There are various DNELs, e.g. representing short-term, long-term, inhalation and dermal exposure, as well as workers and the whole population. We limited our study to "worker-DNELs long-term" for inhalation route as they resemble occupational exposure limits (OELs). We found 24 substances for which (1) such DNELs were given in the ECHA chemical database (<http://echa.europa.eu/web/guest/information-on-chemicals/registered-substances>) and (2) a scientific basis for OEL had been published by the Swedish Criteria Group within the last 15 years in the serial Arbete och Hälsa (<https://gupea.ub.gu.se/handle/2077/3194?locale=en>). The results were startling, as the DNELs given by industry were 2.4 to 1,100 times higher than ours for 23 substances and 260,000 times higher for trimellitic anhydride. Some of the discrepancy is explained by different choice of key studies/points of departure (PODs). However, the choice of assessment factors (AFs) also differed markedly, as industry's total AFs (calculated implicitly from the POD and the DNEL) were 1-230 times lower than ours. We conclude that although the REACH guidance is relatively detailed, many arbitrary choices remain that will influence the DNEL. A major problem is that little advice is given on when and how to depart from default AFs.

## PS 1572 Animal Use for Testing Involving Unrelieved Pain and Distress.

M. Paris<sup>1</sup>, L. Rinckel<sup>1</sup>, W. Casey<sup>2</sup> and W. Stokes<sup>2</sup>. <sup>1</sup>ILS, Inc., Research Triangle Park, NC; <sup>2</sup>NTP/NICEATM, NIEHS, Research Triangle Park, NC.

Each facility in the United States that uses live animals for research, tests, experiments, or teaching must submit an annual report to the U.S. Department of Agriculture (USDA) that includes "the common names and the numbers of animals upon which experiments, teaching, research, surgery, or tests were conducted involving accompanying pain or distress to the animals and for which appropriate anesthetic, analgesic, or tranquilizing drugs were (or were not) used" (9 CFR, Chapter 1 Part 2, Section 2.36). In accordance with the definitions in §2132 of the Animal Welfare Act (7 U.S.C. 54), it is not necessary to report birds, rats of the genus *Rattus* and mice of the genus *Mus* bred for use in research, or fish, amphibians and livestock or poultry used in agricultural research. In the 2010 USDA annual report on animal usage, a total of 1,134,693 animals were reported, with 97,123 of those reported as experiencing unrelieved pain and distress. Based on an analysis of these data by the National Toxicology Program Interagency Center for the Evaluation of Alternative Toxicological Methods (NICEATM), 95% (91,997/97,123) of the animals reported to the USDA as experiencing unrelieved pain and distress were used for testing. Of these animals, 57% (54,889/97,123) were used for vaccine testing, and 38% (37,108/97,123) were used for toxicity testing. Most of the animals used for toxicity testing were used for safety testing and drug efficacy testing. NICEATM is currently investigating and promoting alternative test methods to further reduce the number of animals used in painful procedures. Supported by ILS staff under NIEHS Contract N01-ES-35504.

## PS 1573 A Reference Database for the Evaluation of Alternative Tests for Acute Dermal Systemic Toxicity.

J. Strickland<sup>1</sup>, F. Stack<sup>1</sup>, M. Paris<sup>1</sup>, L. Rinckel<sup>1</sup>, W. Casey<sup>2</sup> and W. Stokes<sup>2</sup>. <sup>1</sup>ILS, Inc., Research Triangle Park, NC; <sup>2</sup>NTP/NICEATM, NIEHS, Research Triangle Park, NC.

Alternatives for acute systemic toxicity testing are one of the highest priorities of ICCVAM and NICEATM. These are the most commonly performed product safety tests worldwide and are required by multiple U.S. Federal agencies. Acute toxicity testing can involve large numbers of animals and result in significant unrelieved pain and distress to test animals. High quality reference data are needed to evaluate alternative toxicity tests that may reduce, refine (enhance animal well-being and lessen or avoid pain and distress), and replace the use of animals for acute dermal systemic toxicity testing. To identify appropriate reference data for the acute dermal systemic toxicity test, NICEATM collected and analyzed data for 1897 substances. Rabbits were used for 28% (526) of the studies, and rats were used for 72% (1371). Of the 1897 substances, 84% (1598/1897) had data for both male and female animals, and 98% (1561/1598) of those substances were in the same GHS dermal hazard category. For the 37 substances that showed a different dermal hazard category between the sexes, female values were more often in a higher hazard category (21 for females vs. 16 for males). Two hundred forty six studies reported day of death. Approximately two thirds of the deaths (67% of male deaths [513/761]; 63% of female deaths [463/733]) occurred by Day 2 after a 24-hour dermal treatment on Day 0. Eighty-five substances had sufficient data to calculate dermal dose-mortality slopes. Dose-mortality slopes did not vary by species, sex, or GHS hazard category. As expected, the dermal dose-mortality slopes were lower than acute oral dose-mortality slopes. These data were used to design a proposed sequential test for acute dermal systemic toxicity, the dermal up-and-down procedure, to reduce the number of animals tested for acute dermal hazard classification. Supported by ILS staff under NIEHS Contract N01-ES-35504.

## PS 1574 Regulatory Acceptance of the BG1Luc Estrogen Receptor Transactivation Test Method.

W. Casey<sup>1</sup>, P. Ceger<sup>2</sup>, J. Strickland<sup>3</sup>, L. Rinckel<sup>2</sup>, E. Grignard<sup>3</sup>, S. Bremer<sup>3</sup>, H. Kojima<sup>4</sup>, S. Han<sup>5</sup> and W. Stokes<sup>1</sup>. <sup>1</sup>NTP/NICEATM, NIEHS, Research Triangle Park, NC; <sup>2</sup>ILS, Inc., Research Triangle Park, NC; <sup>3</sup>EUROL ECVAM, Ispra, Italy; <sup>4</sup>JaCVAM, Tokyo, Japan; <sup>5</sup>KoCVAM, NIFDS/KFDA, Cheongwon-gun, Chungcheongbuk-do, Republic of Korea.

NICEATM coordinated an international interlaboratory validation study of the BG1Luc estrogen receptor transactivation test method (BG1Luc ER TA, LumiCell®) developed by Xenobiotic Detection Systems, Inc. In 2010, the validation study completed its goal to evaluate the usefulness and limitations of the BG1Luc ER TA test method to screen for substances with in vitro ER agonist or antagonist activity. The international validation study was sponsored by NICEATM, with participation from the European Centre for the Validation of Alternative Methods, and the Japanese Center for the Validation of Alternative Methods. In 2012, NICEATM-ICCVAM released a test method evaluation report on the usefulness and limitations of the BG1Luc ER TA test method. ICCVAM recommended the use of the BG1Luc ER TA as a screening test to identify substances with in vitro ER agonist and antagonist activity and recommended that the BG1Luc ER TA test method could be considered as an alternative to the existing ER TA test guideline (EPA OCSP 890.1300/OECD TG 455). All 15 ICCVAM member agencies, including the US Environmental Protection Agency, concurred with the ICCVAM recommendations. NICEATM sponsored the new method for evaluation by the Organisation for Economic Co-operation and Development (OECD), which approved the BG1Luc test method and added the BG1 agonist protocol to the existing Test Guideline 455. The BG1 antagonist method has been adopted as OECD Test Guideline 457. Acceptance of the BG1Luc ER TA test method by U.S. and international agencies is an example of increased cooperation and collaboration to support the international adoption of scientifically valid test methods that will protect people, animals, and the environment while reducing, refining, and replacing animal use. Supported by ILS staff under NIEHS Contract N01-ES-35504.

## PS 1575 Quantitative Risk Assessment As the Basis for a Proposed NIOSH Recommended Exposure Limit for Hexavalent Chromium Compounds.

K. MacMahon, R. Park, F. Rice and K. Ashley. NIOSH, Cincinnati, OH. Sponsor: D. Dankovic.

To update the National Institute for Occupational Safety and Health (NIOSH) recommendations for protecting workers with occupational exposure to Cr(VI) compounds, all aspects of occupational exposure to and control of hexavalent

chromium compounds (Cr(VI); e.g., chromic acid, CAS No. 1333-82-0; sodium dichromate, CAS No. 7789-12-0) were evaluated including epidemiology, toxicology, risk assessment, analytical methods, and industrial hygiene practices. Derivation of a proposed Recommended Exposure Limit (REL) was one component of the updated risk management recommendations. The NIOSH proposed REL was derived based on the results of a quantitative risk assessment (QRA) of lung cancer in chromate production workers. The NIOSH REL was previously based on the quantitative limitation of the 1975 analytical method; at that time NIOSH recommended that occupational carcinogens be controlled to the lowest feasible concentration. Data from a cohort of Baltimore chromate production workers were selected for analysis due to the availability of extensive exposure assessment data, information about smoking histories, strong statistical power, and relative lack of confounding exposures. Excess lifetime risk at the REL of 1 µg Cr(VI)/m<sup>3</sup> was estimated as 6 (95% confidence limits=3-12) lung cancer deaths per 1000 workers. Based on these results, NIOSH proposed a REL of 0.2 µg Cr(VI)/m<sup>3</sup> 8-hour time-weighted average exposure during a 40-hour workweek. The proposed REL has an estimated working lifetime (45 years) excess risk of lung cancer mortality of approximately one in 1000. NIOSH, Occupational Safety and Health Administration, and international consensus standard analytical methods can accurately quantify workplace exposures at the proposed REL. Recommending the control of occupational Cr(VI) exposures to below the proposed REL is intended to reduce the incidence of work-related lung cancer.

### PS 1576 The Dermal Up-And-Down Procedure: An Alternative Test Method for Acute Dermal Systemic Toxicity Testing.

W. Stokes<sup>1</sup>, J. Strickland<sup>2</sup>, R. Morris<sup>3</sup>, L. Ho<sup>3</sup>, J. Wilkerson<sup>3</sup>, F. Stack<sup>2</sup>, M. Paris<sup>2</sup>, L. Rinckel<sup>2</sup> and W. Casey<sup>1</sup>. <sup>1</sup>NTP/NICEATM, NIEHS, Research Triangle Park, NC; <sup>2</sup>ILS, Inc., Research Triangle Park, NC; <sup>3</sup>SRA International, Research Triangle Park, NC.

Acute dermal systemic toxicity testing is required to identify chemicals and products that have the potential to cause life-threatening or fatal toxicity following skin exposures. Such testing is one of the five most commonly conducted safety tests and requires up to 20 or more animals per test. A dermal up-and-down procedure (UDP) was developed to estimate acute dermal toxicity hazard classification categories with fewer animals. The UDP incorporates an efficient experimental design using sequential testing to estimate LD50 rather than the simultaneous testing of multiple groups of animals at multiple doses, as specified by current regulatory test guidelines. In the dermal UDP, individual animals are dosed sequentially, and the response of each animal after 48 hours is used to determine the dose applied to the next animal. If a dose produces significant toxicity, the next animal is tested at a lower dose. Conversely, if no significant toxicity is observed, the next animal is tested at a higher dose, with the highest dose not to exceed a pre-specified limit dose. Unless there is a basis for a lower starting dose, the initial dermal UDP starting dose is the appropriate limit test dose (2000 or 5000 mg/kg). The default dose-progression factor for subsequent doses is 4.2. If the expected LD50 is less than the default starting dose, testing is started at one dose below the closest default dose. Using a starting dose of 5000 mg/kg, default doses are 5000, 1200, 300, 70, 15, and 4 mg/kg, while the default doses for a starting dose of 2000 mg/kg are 2000, 500, 100, 25, and 5 mg/kg. The dermal UDP provides LD50 point estimates and confidence limits for dermal hazard classifications while using up to 85% fewer animals. The proposed dermal UDP can support accurate hazard identification while significantly reducing animal use. Supported by ILS staff under NIEHS Contract N01-ES-35504 and SRA staff supported by NIEHS Contract GS-23F-9806H.

### PS 1577 Fatal Misuse of Humidifier Disinfectants in Korea: Importance of Screening Risk Assessment and Implications for Management of Chemicals in Consumer Products.

J. Lee<sup>1</sup>, J. Kwon<sup>2</sup> and Y. Kim<sup>3</sup>. <sup>1</sup>Institute of Environmental Safety and Protection, NeoEnBiz Co., Bucheon, Republic of Korea; <sup>2</sup>Department of Environmental Engineering, Ajou University, Suwon, Republic of Korea; <sup>3</sup>Korea Institute of Toxicology, Daejeon, Republic of Korea. Sponsor: K. Park.

The Korea Centers for Disease Control and Prevention (KCDC) reported on August 31, 2011 that the unidentified fatal lung disease found in Korea might have been caused by chemical disinfectants used with household humidifiers. Among them, four patients passed away because of the rapid development of pulmonary fibrosis after long exposure to the disinfectants over several months. A provisional conclusion by an epidemiological investigation that active ingredients of disinfecting products (polyhexamethyleneguanidine (PHMG) and oligo(2-(2-ethoxy)ethoxyethyl guanidinium chloride (PGH)) caused this disease was reinforced by a subsequent inhalation toxicological study using rats. In Korea, humidifier disinfectants have been put in the water tanks of humidifiers for the prevention of germs, mold, and/or algae. The disinfectants were manufactured and

sold on the market without any data on inhalation toxicity being submitted and without risk evaluation on an industrial or government level. We conducted a screening-level risk assessment for the disinfectants. With these high values of the risk quotients for PHMG and PGH containing the guanidine moiety, it should have been possible to screen the chemicals with potential health concerns before their introduction to the market. Precautionary measures such as "premarket registration and evaluation" and "significant new use notice and re-evaluation" need to be complemented by post-market control systems such as product recall and health surveillance systems to screen the health hazards of chemicals.

### PS 1578 Multiple Federal Hazard Assessment Programs—A Relevant Information or Redundant Efforts?

N. B. Beck<sup>1</sup>, B. A. Richard<sup>1</sup> and A. Twardowski<sup>2</sup>. <sup>1</sup>American Chemistry Council, Washington DC; <sup>2</sup>Concordia College, Moorhead, MN.

Much interest, at both the Executive and Legislative levels, is currently directed towards evaluating how to reform and streamline government to improve efficiencies and decrease costs. In Jan. 2010, President Obama, acknowledging challenging economic times, began an effort to decrease waste and inefficiencies in the government. Similarly, Public Law 111-139 (2010) required the Government Accountability Office to identify federal programs with duplicative goals and activities. Regarding the evaluation of hazards associated with environmental contaminants, there are at least three Federal programs that have seemingly overlapping, although not perfectly aligned goals. Our question was: Do these government programs provide novel information or are the efforts redundant? While the EPA Integrated Risk Information System (IRIS) evaluates risk information for chronic non-cancer and cancer effects, the Agency for Toxic Substances and Disease Registry (ATSDR), in its Toxicological Profiles, evaluates non-cancer effects at acute, sub-chronic and chronic exposures. The National Toxicology Program's Report on Carcinogens (RoC) provides cancer descriptors, as does the IRIS Program, although NTP does not develop quantitative risk values. The IRIS Reference Values and the ATSDR Chronic Minimal Risk Levels were examined. Additionally, the IRIS and NTP cancer classifications for substances were also reviewed. If the same substance was evaluated by two programs, we also compared the final Agency recommendations. Significant findings will be presented. For example, the analyses show that even though the IRIS program has evaluated over 550 chemicals there are only 85 chemicals with Reference Concentrations (RfC) and since 1995 EPA releases, on average, 3 new RfCs a year. Similarly, although ATSDR has evaluated over 170 chemicals, there are only 42 with chronic inhalation values and approximately half of these chemicals are the same ones EPA evaluated. The full analysis of results will help the agencies and stakeholders assess the value in supporting three separate programs.

### PS 1579 Utilization of Benzene Chromosomal Biomarkers by US Courts in Adjudicating Causation.

G. E. Marchant. College of Law, Arizona State University, Tempe, AZ.

This study evaluates the utilization of chromosomal biomarkers in court cases that involved benzene exposure, one of the first major set of cases to rely on biomarker data. The methodology involved searching the Westlaw database for all toxic tort cases involving plaintiffs allegedly injured by benzene exposure in which evidence of chromosomal aberrations was offered. The judicial decisions in these cases were evaluated to determine whether the judges properly understood and applied the scientific information on biomarkers, and to determine how useful the biomarker data was to the ultimate outcome of the case. A standardized multi-criteria analysis sheet was used to evaluate each case. A total of 17 U.S. court cases decided in the period from 1995 to 2012 that involved benzene chromosomal biomarker evidence were identified and evaluated in this study. The analysis identifies several problems in how judges and juries in these cases dealt with biomarker evidence, including: (i) some courts treat the evidence as deterministic rather than probabilistic, incorrectly concluding that biomarker evidence alone proves or disproves causation, or in other cases holding that the biomarker data is completely irrelevant and thus inadmissible; (ii) different courts treated the same biomarker evidence differently, resulting in inconsistent decisions; and (iii) individual judges made statements in specific cases indicating a poor understanding of biomarkers. Notwithstanding these limitations, the overall results of using chromosomal biomarker evidence in these toxic tort cases was beneficial, as the evidence was instrumental in helping to prove or disprove causation in appropriate cases. This analysis demonstrates that biomarker data can provide effective and useful evidence in toxic tort litigation, and are likely to be used increasingly frequently in such cases. At the same time, the problems identified in this analysis with handling of biomarker data by some courts provide important lessons for judges, attorneys, and scientific experts.

**PS 1580** **In Vitro Episkin Skin Corrosion As a Reference Test Method in OECD TG431 for the Assessment of Skin Corrosion in Subcategories 1A, 1B, and 1C.**

N. Alépée, M. H. Grandidier and J. Cotovio. *L'Oréal Research & Innovation, Aulnay sous Bois, France.* Sponsor: *E. Dufour.*

Skin corrosion or irritation refers to the production of irreversible or reversible damage to the skin following the application of a test substance, respectively. An effective way of predicting test substance toxicity is to make use of testing strategies which incorporate a range of alternative test methods. For the determination of skin irritation and corrosion, hazard assessments for both endpoints could be conducted using in vitro test methods that have been regulatory accepted (OECD TG431 & TG439). In the present study, skin irritation and corrosion evaluations were performed on Reconstructed human Epidermis (RhE) models i.e. EpiSkin and SkinEthic RHE. In the case of skin corrosion, GHS guidelines differentiate between non corrosive (NC) to corrosive (C) substances with 3 subcategories: 1A, 1B and 1C. The current evaluation of the test method was performed on 81 test substances from a wide range of chemical for each subcategory class (38 NC, 31 Cat1B/1C and 12 Cat1A) enlarging the evidence base associated with this method. Using the EpiSkin test method, within-laboratory variability (>87%) was assessed in 3 runs. Therefore a sensitivity of 98% and overall accuracy of 89% (with an accuracy of 1A, 1B/1C, NC of 79%) were obtained. The test method able to discriminate 1A, from 1B and 1C classes with the highest well -prediction rate for sub-categorize the substances in comparison with the others validated methods, was submitted to OECD for scientific review and adoption. Adoption of the EpiSkin seems sufficient to fill the gaps in terms of sub-categorisation predictions leading to a significant impact on the sub-group transport package labeling.

**S 1581** **Application of Systems Biology to Identify Molecular Mechanisms and Biomarkers of Lead (Pb) Neurotoxicity: Implications in a Developmental Origin of Alzheimer's Disease.**

*J. L. Freeman. Health Sciences, Purdue University, West Lafayette, IN.*

The heavy metal lead (Pb) can induce a wide-range of adverse health effects depending on dose and duration of exposure. During development the nervous system is most sensitive to Pb toxicity with epidemiological studies linking neurological deficits at and below the previous CDC blood Pb level of concern. Although the toxicity of Pb is extensively studied, the underlying genetic, epigenetic, and molecular mechanisms of Pb neurotoxicity are not completely understood. Moreover, recent studies link developmental Pb exposure with latent effects that do not appear until late in life, indicating a developmental origin of adult neurodegenerative disorders. More specifically, the latent overexpression of hallmark genes and proteins in Alzheimer's disease (AD) are reported in these studies. This session brings together a group of investigators that are actively applying systems biology (transcriptomics and epigenomics) and targeted approaches to define the mechanisms and identify biomarkers of both the developmental and late-life neurological alterations associated with a developmental Pb exposure in a variety of model systems and in human populations. Topics cover a study with the zebrafish model on the genetic mechanisms of developmental Pb neurotoxicity with an emphasis on transcriptomic alterations to a human comparative transcriptomic study in young adults aiming at establishing biomarkers between early-life Pb exposure and AD. The session also addresses the transcriptomic and epigenomic pathways of the developmental origin of Pb-induced neurodegenerative alterations with a specific focus on AD in rodent and primate models. Furthermore, the mechanism by which Pb increases the formation of amyloid  $\beta$  plaques in a transgenic mouse model is discussed. Overall, this session highlights the latest findings on the genetic, epigenetic, and molecular mechanisms of Pb neurotoxicity linking neurodevelopmental and later life impacts to further deduce the developmental origin of Pb-induced neurodegenerative disease with a specific focus on AD.

**S 1582** **Genetic Mechanisms of Developmental Lead Neurotoxicity and Links to Adult Neurodegenerative Disease Pathogenesis.**

*J. L. Freeman. Health Sciences, Purdue University, West Lafayette, IN.*

It is well established that lead (Pb) exposure is detrimental to neurological development, but the underlying mechanisms of Pb developmental neurotoxicity are not clearly elucidated. Furthermore recent evidence supports the hypothesis that a developmental Pb exposure results in later lifespan effects including pathological features characteristic of Alzheimer's disease (AD) proposing a developmental origin of Pb-induced adult neurological disease. The genetic and epigenetic mechanisms underlying and linking the immediate adverse effects of the developmental Pb exposure and the lasting impacts of the developmental exposure throughout the lifespan

are yet to be determined. In this study, global gene expression analysis using the zebrafish vertebrate model system demonstrated that developmental Pb exposure results in immediate altered expression of genes associated with axon guidance, neurogenesis, and neurodegeneration. Furthermore, gene expression alterations were correlated to functional changes in the form of altered protein levels and a delay in axonal growth. While being an established developmental model, characterization of the adult zebrafish is limited and is just beginning to be explored for application in neurodegenerative disease pathogenesis research. Studies utilizing zebrafish embryos show that many genes with direct roles in AD are highly conserved in terms of sequence and function supporting the application of the adult zebrafish brain as a model to investigate the role of a developmental Pb exposure in the pathogenesis of neurological disease. To further our understanding of these genes, protein sequence analysis and gene expression characterization was conducted. This study demonstrates that a strong degree of conservation occurs in regards to the presence and orientation of specific functional domains and in expression patterns. This study provides a framework for assessment of the influence of a developmental Pb exposure on late life neurological disease pathogenesis.

**S 1583** **Prenatal Lead Exposure and Biomarkers for Alzheimer's Disease in Humans.**

*M. Mazumdar<sup>1,2</sup>. <sup>1</sup>Environmental Health, Harvard School of Public Health, Boston, MA; <sup>2</sup>Neurology, Children's Hospital Boston, Boston, MA.* Sponsor: *J. Freeman.*

Animal studies suggest that early life lead (Pb) exposure influences gene expression and production of proteins associated with Alzheimer's disease (AD). This presentation will discuss recent studies in humans implicating early-life Pb exposure in the pathogenesis of AD. Aggregation of  $\beta$ -amyloid (A $\beta$ ) is a hallmark of AD pathology and plasma concentrations of A $\beta$  are biomarkers that potentially could predict the risk of AD prior to the clinical manifestation of dementia. To evaluate the association between early-life Pb exposure and AD risk, the mean plasma A $\beta$  concentration was measured in young adults and compared among those that had high umbilical cord blood Pb concentrations and those with lower cord blood Pb concentrations. Expression of genes whose products affect A $\beta$  production and deposition was evaluated and was inversely correlated with umbilical cord blood Pb concentrations. Gene network analysis suggested enrichment in gene sets involved in nerve growth and general cell development. These data suggest that prenatal Pb exposure may influence A $\beta$ -related biological pathways that are implicated in AD. Challenges in designing studies that investigate the contribution of early-life environmental exposures to adult disease will also be reviewed in this presentation.

**S 1584** **Do Epigenetic Pathways Initiate Late Onset Alzheimer's Disease (LOAD)?: Towards a New Paradigm.**

*N. H. Zawia. Biomedical and Pharmaceutical Sciences, University of Rhode Island, Kingston, RI.*

Cognitive decline and many of the hallmark pathological features of Alzheimer's disease (AD) such as amyloid plaques and tau tangles are present in normal aging individuals and pose a challenge for distinguishing AD from normal aging. The majority of AD cases occur in the elderly; however, it is still unresolved whether AD is a disease of old age or whether it has earlier beginnings. The development of early onset AD (EOAD) seems to be largely genetic; however, late-onset AD (LOAD) may be influenced by epigenetic factors acquired during early developmental stages. LOAD exhibits numerous non-Mendelian anomalies that suggest an epigenetic component in disease etiology. The sporadic nature of >90% of AD cases, the differential susceptibility and course of illness, as well as the late age onset of the disease suggest that epigenetic and environmental components play a role in the etiology of LOAD. In this presentation, the evidence derived from primates and rodents (genomic and epigenomic as well as biomarker-specific) that AD has a developmental origin and that early life exposure can reprogram gene expression in old age through epigenetic pathways rendering the brain more susceptible to neurodegenerative diseases will be provided.

**S 1585** **CNS Homeostasis of  $\beta$ -Amyloid, Plaque Formation, and Lead Toxicity.**

*W. Zheng. Health Sciences, Purdue University, West Lafayette, IN.*

The hallmark of Alzheimer's disease (AD) pathology is aggregation of  $\beta$ -amyloid (A $\beta$  or A $\beta$ ). Previous studies in this laboratory have established that the brain barrier systems are actively engaged in regulation of the homeostasis of A $\beta$  in

brain extracellular milieu (Crossgrove et al., *Exp Biol Med* 2005;230:771) and that lead (Pb) exposure can alter the property of the Abeta transport protein (LRP1) leading to abnormal accumulation of Abeta in brain tissues (Behl et al., *TAAP* 2009;240:245; *Neurotox* 2010;31:524). In the current study, we used transgenic PDAPP mice which over-express amyloid precursor protein (APP) and exhibit amyloid plaques in brain tissues to investigate if in vivo Pb exposure shortened the onset of amyloid plaque formation and increased the plaque aggregation. Our data show that in vivo Pb exposure resulted in an increased deposition of amyloid plaques in these transgenic mouse brains. Mechanistic investigation revealed that Pb reduced Abeta clearance from the central nervous system by inhibiting LRP1 at brain barriers. Pb also directly participated in physiochemical reaction with Abeta molecules in the test tube. Moreover, Pb increased the concentrations of other metals (i.e., Fe, Zn) in amyloid plaques in the mouse brain by synchrotron X-ray fluorescent (XRF) quantitation. Within the plaques, Pb concentrations were found to be significantly correlated with those of Fe and Zn. Our data support a role of Pb in the formation of amyloid plaques; how these findings may relate to human AD etiology deserves further investigation (Supported in part by NIH/NIEHS ES008146 and ES017055).

## **S 1586 Bone As a Target Tissue for Environmental Toxicants.**

J. Schlezinger, *Environmental Health, Boston University School of Public Health, Boston, MA.*

Bone brings to mind the strong, but light, organ that provides the skeleton for vertebrates. However, bone is more than just inert, osseous tissue. The bone marrow is a multifunctional organ that supports not only ongoing bone remodeling, but also provides the microenvironmental niche for hematopoiesis and regulates whole body energy homeostasis and as such, represents a significant target for environmental toxicants. Critical cell types in the bone marrow include multipotent mesenchymal stromal cells (MSCs) and hematopoietic stem cells (HSCs). MSCs are the source of both adipocytes and osteoblasts. HSCs are the source of all blood cell lineages and the bone-resorbing osteoclasts. The interaction between osteoblasts and osteoclasts creates a balance of bone formation and resorption, which is essential for maintenance of bone quality. There also is essential crosstalk between the mesenchymal and hematopoietic compartments that supports lifelong blood cell generation. Lymphocyte development, in particular, requires stromal cell support/interaction. Understanding how environmental toxicants disturb the interplay of bone marrow compartments requires attention given the rapidly aging population who are already at risk for loss of bone quality and immune suppression. We will explore new data suggesting that bone is responsive to many environmental toxicants, which may perturb the delicate balance between bone marrow cell types. A series of presentations will define interactions within both the mesenchymal and hematopoietic compartments and how exposure to toxicants may impact bone biology. Presentations will move from a broad, multispecies analysis of the effects of persistent organic pollutants on bone to more focused analyses of effects of ethanol and metals (lead, organotin, and tungsten) on bone and the bone marrow microenvironment.

## **S 1587 Bone Tissue As a Target for POPs Acting As EDCs (an Overview from Wild Animals to Humans).**

M. Lind, *Occupational and Environmental Medicine, Uppsala University, Uppsala, Sweden.*

Since World War II, there has been an increase in age-standardized incidence rates of osteoporotic bone fractures in industrialized countries, with the Nordic countries taking the lead. The reason for this increase is unknown but the idea that exposure to endocrine-disrupting chemicals (EDCs) could be involved has been put forward. The consequences of environmental contaminant-induced bone toxicity is evident across many species. Exposure to persistent organic pollutants (POPs) acting as EDCs, has been shown to negatively affect the bone tissue (e.g. leads to an osteoporotic phenotype) in laboratory models (monkeys, rats, mice, frogs, goat, sheep, bone cells), as well as wild-life (polar bears, seals, alligators and herring gulls). Important signaling pathways such as the estrogen receptor and aryl hydrocarbon receptor pathways have been suggested to contribute to the observed effects. Importantly, epidemiological studies on humans also support this hypothesis since they show a relationship between exposure to endocrine disrupting POPs and decreased bone mineral density or increased risk of bone fractures. The literature on this topic is, however, rather small and prospective studies on in utero or early EDC exposure and future osteoporotic bone fractures do not exist. The mechanisms behind the deleterious effects of EDCs on bone tissue also need to be a focus of study.

## **S 1588 Lead Exposure and Skeletal Dysregulation: A Molecular Mechanism of Toxicity That Contributes to Osteoporosis and Other Bone Diseases.**

J. Puzas and E. Beier, *Center for Musculoskeletal Research, University of Rochester, Rochester, NY.*

**Rationale and Scope:** Lead exposure and osteoporosis represent two of the most widespread health issues affecting humans. Our recent investigations provide evidence that these entities are linked. We have also identified a molecular mechanism by which lead can adversely affect bone forming cells.

**Experimental Procedures:** We used a small animal rodent model as well as isolated cell experiments to evaluate the effect of lead exposure. The animals were treated with lead in their drinking water. The cell studies were performed in culture media with added lead acetate. All treatments achieved lead levels relevant to human exposures. Bone mass parameters were measured with micro CT analysis, histology and Raman infrared spectrometry. Cell effects and signaling pathways in osteoblasts were measured with molecular methods for mRNA and protein.

**Results:** Our findings indicate that lead exposure induces an osteoporotic-like phenotype in the animal model. Bone volume, bone formation rates, bone quality and bone cell number were all significantly depressed in the treated animals. Lead also induced a strong adipogenic response in the marrow space. Data from exposure of cells to lead indicate that all parameters of osteoblastic bone formation were also markedly inhibited. Immunohistochemical assays as well as a molecular analysis of in vitro cell signaling pathways indicate that the effect of lead is, at least partially, due to a strong depression of the TGFbeta and Wnt pathways. The mechanism for this depression appears to be related to an up regulation of the bone formation inhibitor, sclerostin.

## **S 1589 Role of NADPH Oxidases and Reactive Oxygen Species in Regulation of Bone Turnover and the Skeletal Toxicity of Alcohol.**

M. Ronis<sup>1,2</sup>, K. Mercer<sup>1</sup>, L. Suva<sup>2</sup>, T. M. Badger<sup>1,2</sup> and J. Chen<sup>1,2</sup>. <sup>1</sup>*Arkansas Children's Nutrition Center, Little Rock, AR;* <sup>2</sup>*University of Arkansas for Medical Sciences, Little Rock, AR.*

Recent studies with genetically modified mice and dietary antioxidants have suggested an important role for superoxide derived from NADPH oxidase (NOX) enzymes and other reactive oxygen species (ROS) such as hydrogen peroxide in regulation of normal bone turnover during development and also in the responses of the skeleton to toxicants such as ethanol (EtOH) which generate excess ROS in bone tissue. We have shown that EtOH causes bone loss as a result of NOX generated ROS, reduced bone formation via impaired Wnt-β catenin signaling and increased RANKL-dependent osteoclastogenesis. Buffering of anti-oxidant capacity through administration of the glutathione precursor N-acetylcysteine, completely prevented EtOH-induced loss of bone mineral density, inhibiting both suppression of bone formation and increases in bone resorption. There was no apparent bone phenotype associated with genotype at age 3 mo., in mice lacking the NOX co-factor p47<sup>phox</sup> and thus with impaired capacity to generate excess superoxide in response to EtOH. However, these mice were only protected from alcohol-stimulated increases in bone resorption. This was accompanied by inhibition of EtOH-associated increases in osteoclastogenesis and induction of RANKL. In mice where hydrogen peroxide concentration in bone is reduced as a result of transgenic expression of catalase, whereas 6 wk old mice had increased trabecular bone, 3 mo. old mice had reduced trabecular bone and impaired osteoblastogenesis compared to wild type mice and were unprotected against ethanol actions. These data suggest that ROS signaling involving hydrogen peroxide is important in regulation of adult bone formation but that excess production of superoxide via NOX as a result of exposure to toxicants such as EtOH can stimulate RANKL-dependent increases in bone resorption. Supported in part by R01 AA018282 (M.J.R.).

## **S 1590 Organotins: Unique Modulators of Bone Quality and the Bone Marrow Microenvironment.**

J. Schlezinger<sup>1</sup>, A. Baker<sup>2</sup> and L. Gerstenfeld<sup>3</sup>. <sup>1</sup>*Environmental Health, Boston University School of Public Health, Boston, MA;* <sup>2</sup>*Medicine, Boston University School of Medicine, Boston, MA;* <sup>3</sup>*Orthopaedic Surgery, Boston University School of Medicine, Boston, MA.*

Bone marrow multipotent mesenchymal stromal cells (BM-MSC) are critical for osteogenesis, as well as for creating the supportive niche for lymphopoiesis. PPARγ is a central mediator of BM-MSC differentiation, traditionally thought to promote adipogenesis while suppressing osteogenesis. A growing number of environmental contaminants (e.g. phthalates, organotins) have been shown to activate PPARγ and increase adipogenesis, and thus recently have been termed environmental obesogens. Organotins are unique in their ability to bind and activate both PPARγ and

RXR, opening the possibility that they may activate multiple permissive nuclear receptor pathways. We investigated the hypothesis that tributyltin (TBT) is a potent modifier of BM-MSC differentiation and thus a negative regulator of bone quality and lymphopoiesis. *In vivo* TBT exposure results in decreased cortical bone and increased marrow adiposity without significantly altering bone resorption. B cell populations are altered in both the bone marrow and the spleen of TBT-treated mice. In primary BM-MSC cultures, TBT potently induces adipogenesis and suppresses osteogenesis. Surprisingly, female-derived BM-MSCs are significantly more sensitive to TBT-mediated suppressive effects than male-derived cells. In addition to activating a PPAR $\gamma$ -mediated gene expression pathway (FABP4 and adiponin) and suppressing a Runx2-mediated pathway (osterix and osteocalcin), TBT activates the LXR *in vivo* and *in vitro*, another nuclear receptor that contributes to bone homeostasis. Finally, TBT completely suppresses the development of hematopoietic cells in culture. Given its potency and ubiquitous environmental presence, TBT presents a risk to bone health and may accelerate the accumulation of adipocytes and loss of lymphopoiesis that occurs during aging.

## **S** 1591 **Tungsten: Effects on Bone Marrow and Lymphocyte Development.**

K. K. Mann. *Oncology, McGill University, Montréal, QC, Canada.*

Very little is known about the toxicity of tungsten. Recently, increased environmental tungsten levels were found near sites of pediatric leukemia clusters. These leukemia cases were predominantly of the preB lymphocyte subtype of acute lymphocytic leukemia. While no data link tungsten exposure to leukemogenesis, tungsten is known to accumulate within the bone, the site of B cell development. This important hematopoietic compartment is likely the site where leukemogenic events occur. We have explored the effects of tungsten exposure on developing B lymphocytes using *in vitro* and *in vivo* models. *In vitro*, B lymphocytes are more sensitive to tungsten-induced DNA damage and growth inhibition than the supporting mesenchymal stromal cells. In wild-type mice, we have shown that tungsten concentrations rapidly increase in the bone and reach a plateau after approximately 4 weeks of exposure. Removal of tungsten results in a slow release of tungsten from the bone with a much slower "off" rate. In addition, we see alterations in bone mineral content and density following tungsten exposure. Tungsten exposure alters B lymphopoiesis, increases DNA damage within the bone marrow B cells, and increases preB-colony forming units. Any of these could provide a leukemogenic hit, and thus, tungsten could act as a tumor promoter. Although we did not observe development of leukemia in wild-type mice, current data in pre-leukemic mouse models, as well as murine breast cancer models, will be discussed.

## **S** 1592 **Nonmonotonic Dose-Response Curves and Endocrine-Disrupting Chemicals: Fact or Falderal?**

L. E. Gray<sup>1</sup> and P. M. Foster<sup>2</sup>. <sup>1</sup>RTB, US EPA, Research Triangle Park, NC; <sup>2</sup>NTP, NIEHS, Research Triangle Park, NC.

"All substances are poisons. It's the dose that makes the poison," (Paracelsus, 1493–1541) is a fundamental tenet in toxicology: the severity of a response to a toxicant increases proportionally to the dose. Furthermore, it is generally assumed that dose-response curves for noncancer effects display a threshold below which there is no effect. Currently these assumptions are being challenged by claims that endocrine-disrupting chemicals (EDCs) often display U-shaped or inverted U-shaped nonmonotonic dose-response curves (NMDRCs) at low, environmentally-relevant exposure levels; levels below traditional NOAELs ("Current Chemical Testing Missing Low-Dosage Effects of Endocrine-Disrupting Chemicals" Endocrinology Society, 2012). In addition, the US EPA's Endocrine Disruptor Screening program (EDC program) has been severely criticized, sometimes unfairly. This symposium will review the state of the science on EDCs concerning the shape of the dose-response curve in the low-dose range and the prevalence of NMDRCs. Talks will initially discuss mechanisms of action, the biological plausibility for NMDRCs, and then focus on chemicals that disrupt the estrogen and androgen signaling pathways and the prevalence of *in vitro* and *in vivo* NMDRCs. Presentations will also discuss the shape of the dose-response curves from "case studies" of estrogenic chemicals. These "case studies" are robust, multigenerational studies conducted in a government laboratory using a protocol that had been "enhanced" to include several estrogen-sensitive endpoints in addition to the standard endpoints. Finally, we will discuss how some governmental agencies are addressing the NMDRC-low dose issue and views on how this might impact the risk assessment of EDCs and other chemicals. Changing how EDCs are tested to accommodate NMDRCs would significantly increase the resources need for testing as it would require the addition of several "low" dose groups and if NMDRCs are prevalent, then this would significantly impact several of the default assumptions used in risk assessment, including noncancer health effects displaying a threshold, and that adverse effects do not occur below the NOAELs.

## **S** 1593 **Molecular Pharmacology of Steroid Hormone Action: Nonmonotonic Dose-Responses.**

W. R. Kelce. *Nonclinical Development, Novan Therapeutics, Durham, NC.*

The basic biology of steroid hormone (SH) synthesis and action is reviewed to provide a molecular pharmacology basis for typical monotonic and nonmonotonic dose-response observations. Examples illustrate the molecular pharmacology basis for observed *in vitro* and *in vivo* effects. As the level of biological organization increases (from cell-free binding to transcription to *in vivo* adverse effects), the opportunity for complex nonmonotonic dose-responses emerge. Full strong receptor agonists and antagonists *in vitro* provide the highest level of predictability whereas weak agonists and antagonists are affected by ambient ligand levels. Agonist or antagonist activity can be passive (competition for receptor binding and subsequent direct receptor activation or inactivation) or active (influenced by co-activator and/or co-repressor preference and/or availability which can be cell type and tissue specific). *In vitro* cytotoxicity, cofactor squelching and substance metabolism can confound data interpretation. SH ligands can also have rapid nongenomic effects leading to receptor/co-regulator phosphorylation and nonmonotonic responses. Similar to SH receptors, inhibition of rate limiting steroidogenic enzymes (delivery of cholesterol to the inner mitochondrial membrane and P45017 $\alpha$ ) are more predictive than enzymes whose activity can be reduced by 95% or more without altering the rate of SH production. The intact animal leads to an even higher order of biological complexity where interactions with the hypothalamic-pituitary-gonadal axis can logically lead to nonmonotonic dose responses. Exogenously administered androgens and the maintenance of spermatogenesis will be used as an example. Low levels of testosterone have little effect, physiological levels reduce GnRH and LH production leading to reduced intratesticular levels of testosterone and the consequent inhibition of spermatogenesis and supraphysiological levels restore intratesticular testosterone and maintain spermatogenesis. Discussion of the molecular pharmacology of SH action will provide the mechanistic basis for examples discussed by the other speakers.

## **S** 1594 **Mechanistic Requirements for Nonmonotonic Dose-Response.**

R. B. Conolly<sup>1</sup>, L. E. Gray<sup>1</sup> and G. T. Ankley<sup>2</sup>. <sup>1</sup>US EPA, Research Triangle Park, NC; <sup>2</sup>US EPA, Duluth, MN.

Conolly and Lutz (Toxicol. Sci. 77, 151-157, 2004) noted that "Dose-response curves for the first interaction of a chemical with a biochemical target molecule are usually monotonic; i.e., they increase or decrease over the entire dose range." Nonmonotonic dose response (NMDR) thus reflects more complex behaviors. Examples of such complexity include the regulation of cAMP levels in the striatum of the rat brain by the combined action of adenosine A1 and A2 receptors, dimerization of ligand-bound steroid hormone receptors prior to the promotion of gene expression, and induction of DNA repair in response to a DNA damaging xenobiotic, where the repair activity acts on previously formed endogenous adducts and on exogenous adducts due to the xenobiotic. Computational models will be used to illustrate how these relatively simple systems can give rise to NMDR. Interestingly, for each example, the models show that quantitative adjustments of key parameters allow for transitions from nonmonotonicity to monotonicity, with an intermediate, threshold-like behavior. The models that will be described are supported to varying degrees by relevant data. Full consideration of the ecotoxicological and human health significance of NMDR will require, among other things, understanding of the extent to which (1) the frequency with which NMDR occur is a function of the level of biological organization involved, (2) the nonmonotonic behaviors are wholly or partially aspects normal homeostatic regulation and, (3) the dose ranges over which NMDR occur in the laboratory are relevant to actual exposures in the real world. This work was reviewed by the U.S. EPA and approved for publication but does not necessarily reflect Agency policy.

## **S** 1595 **Nonmonotonic Dose-Response Curves (NMDRCs) Are Common after Estrogen or Androgen Signaling Pathway Disruption—Fact or Falderal?**

L. E. Gray. *Reproductive Toxicology Branch, NHEERL, US EPA, Research Triangle Park, NC.*

The shape of the dose response curve in the low dose region has been debated since the 1940s, originally focusing on linear no threshold (LNT) versus threshold responses for cancer and noncancer effects. Recently, it has been claimed that endocrine disruptors (EDCs), which act via high affinity, low capacity receptors, commonly induce adverse effects displaying NMDRCs at low doses. Effects that would be missed in standard EDC screening and multigenerational testing protocols.

Case studies of chemicals that disrupt reproductive development and function via the androgen and estrogen signaling pathways were reviewed, including in vitro and in vivo multigenerational studies for LNT, threshold and NMDRCs responses. In vivo studies selected included comprehensive, robust, well designed studies that administered the chemical via a relevant route of exposure over a broad dose response range, including low doses. The chemicals include ethinyl estradiol, estradiol, genistein, bisphenol A, trenbolone, finasteride, flutamide, phthalate esters, selective estrogen receptor modulators and inhibitors of aromatase.

Current conclusions are: 1) EDCs appear to induce some LNT effects. 2) NMDRCs are biologically plausible and occur frequently in vitro, but the points of inflection occur at high concentrations that are not relevant in vivo. 3) NMDRCs appear to be more common a) in short- versus long-term exposures and b) with upstream, mechanistic events vs. downstream phenotypic effects. 4) A few adverse effects of EDCs are non-monotonic, but other effects in these studies displayed monotonic responses at lower dose levels. 5) A number of robust multigenerational studies of estrogens and antiandrogens showed NMDRCs were uncommon at low dose levels. 6) Multigenerational Test guidelines can be enhanced on a case-by-case basis to improve the sensitivity to low dose effects of some EDCs. 7) Additional data needs to be examined from robust, multigenerational studies using a broad range of dosage levels for other toxicity pathways. This abstract does not reflect USEPA policy

## **S 1596 Comprehensive Studies Addressing Critical Questions in the Dose-Response Assessment of Endocrine-Active Compounds.**

K. Delclos, D. R. Doerge, S. M. Lewis, M. M. Vanlandingham and L. Camacho. *NCTR, US FDA, Jefferson, AR.*

It has been strenuously argued that standard guideline-compliant screening and testing protocols used to assess reproductive and developmental toxicants are inadequate to detect endocrine-active agents due to unique characteristics of the dose response. In particular, it has been proposed that potentially adverse effects may be missed by not including low doses that are closer to exposures in the general human population. Over the past decade, our laboratory has been conducting studies, including both multigenerational and chronic exposures, in Sprague Dawley rats that attempted to address this and other issues (e.g., long term cross generational effects). Articles tested include the potent estrogen ethinyl estradiol (EE<sub>2</sub>), the soy isoflavone genistein, *p*-nonylphenol, and the weak and ubiquitous estrogen bisphenol A. In addition to covering a range of doses within or close to human exposure ranges, these studies covered a broad range of endpoints and, importantly, included measures of internal doses. Knowledge of the serum levels of the test article and its metabolites allows better understanding of the relationship between the method and window of exposure and the observed effects. Clear effects on estrogen-sensitive endpoints were observed, but were largely confined to the high end of the dose range and there was no evidence for unique effects at low doses. Genistein induced estrogenic effects at an internal dose range achievable in humans. In the case of EE<sub>2</sub>, there appeared to be opposite effects on the age of vaginal opening, a marker of puberty, due to low (acceleration) or high (delay) neonatal doses. These studies were largely focused on endpoints that are typically considered as indicative of adverse effects for risk assessments. However, questions of whether molecular or other non-standard endpoints are altered at lower doses or with a different dose response are also being explored with the goal of evaluating whether such endpoints can enhance safety assessments of endocrine-active agents. Support: NIEHS/FDA IAG # 224-12-0003(FDA)/AES12013(NIEHS).

## **S 1597 Low Dose and Nonmonotonic Dose-Response Curves for Endocrine Disruptors.**

L. S. Birnbaum. *NIEHS, Research Triangle Park, NC.*

The incidence of conditions such as diabetes, obesity, asthma, neurodevelopmental, and reproductive problems has increased substantially in the past 20 years. The human genome has not changed in that period of time, which leads to the hypothesis that the environment is likely the cause of much of this increase. The endocrine system is a highly organized system of glands and hormones that regulates vital functions such as growth, response to stress, sexual development and behavior, production and utilization of insulin, metabolism, intelligence and behavior, and the ability to reproduce. This system can be perturbed by environmental chemicals that were designed for one effect but have been shown to interfere with endocrine signaling.

To date, there are over 800 identified endocrine disrupting chemicals (EDCs) and they are found in many everyday products. Recent evidence shows that the mechanisms by which EDCs, as well as endogenous hormones, act are much more intricate than originally recognized.

One aspect of endocrine disruptors is their ability to cause effects at low doses. Just as tiny amounts of hormones can have large effects on physiological systems, tiny amounts of chemicals that mimic hormones can have similar large effects. A feature related to low dose effects is the non-monotonic dose-response behavior of EDCs. In the past, basic toxicology focused on the simple dichotomy of toxic versus nontoxic, which implies that all substances can be harmful at high doses while at some lower dose, no harm is done. However, we now know that EDCs can create physiologically relevant effects at low doses, and these effects can have a substantial impact on our health. These effects may be beneficial at certain doses and deleterious at others. This modern understanding of non-monotonic effects is critical to understanding the behavior of chemical agents and also how resulting health effects may differ based on various exposures.

## **S 1598 Understanding Toxicities of Abnormal Lipid Metabolism: Alcoholic, Nonalcoholic, and Toxicant-Induced Fatty Liver Disease.**

M. S. Mitra<sup>1</sup> and M. You<sup>2</sup>. <sup>1</sup>*Drug Safety Evaluations, Bristol-Myers Squibb, Mt. Vernon, IN;* <sup>2</sup>*Department of Molecular Pharmacology and Physiology, University of South Florida, Tampa, FL.*

Accumulation of excess neutral lipids in the liver, referred to as fatty liver disease (FLD), is a major metabolic disorder and risk factor for development of hepatotoxicity. It is a progressive disease that initially manifests as reversible fatty liver, which upon infliction of inflammation advances to a nonreversible steatohepatitis, and finally leading to hepatic cirrhosis. FLD is generally categorized on the basis of its etiology, the two main types being alcohol-induced steatohepatitis (ASH) and obesity-induced (nonalcoholic steatohepatitis, NASH). Another class of FLD, drug/toxicant-induced FLD (TASH), is a major cause of pharmaceutical candidate attrition. The underlying pathogenic mechanisms of hepatic lipid accumulation and their implications are not completely understood. In this symposium, recent advances in the pathogenic role of microRNAs in the development of FLD will be introduced. The molecular mechanisms by which fatty liver promotes liver injury will be discussed using examples of drug overdose, hepatic ischemia-reperfusion, and obstructive cholestasis. Further, the implications of excess hepatic lipid accumulation in regards to altered drug metabolism and cellular uptake will be presented. The symposium will end with a comparative analysis of novel clinical biomarkers of ASH, NASH, and TASH. Students, as well as toxicologists working in academia, federal, and pharmaceutical industries interested in animal models, pathogenic mechanisms, biomarkers, and drug metabolism and toxicity of ASH, NASH, and TASH will benefit from this symposium.

## **S 1599 Symposium Introduction—Pathogenesis of Hepatic Fat Accumulation.**

M. S. Mitra. *Drug Safety Evaluations, Bristol-Myers Squibb, Mt. Vernon, IN.*

The introductory talk will focus on presenting a high level overview of FLD by providing background information on its pathogenesis. This will include presentation of epidemiology of FLD and the mechanisms of development of FLD that includes two stage model of development and progression of fatty liver to steatohepatitis to cirrhosis. Further, the molecular mechanisms of pathogenesis of FLD in regards to hepatic lipid uptake and esterification, de novo lipogenesis, fatty acid oxidation, and export of VLDL-triglyceride will be presented. The presentation will also include pathology of FLD and review the current scoring systems. The presentation will also describe the available biomarkers for diagnosis and monitoring FLD.

## **S 1600 miR-217-SIRT1 Signaling and Alcoholic Fatty Liver Disease.**

M. You. *Department of Molecular Pharmacology and Physiology, University of South Florida, Tampa, FL.* Sponsor: M. Mitra.

Alcohol-mediated inhibition of hepatic sirtuin 1 (SIRT1) plays a central role in the pathogenesis of alcoholic fatty liver disease. Our group has investigated the underlying molecular mechanisms of this inhibition by identifying a new hepatic target of alcohol, microRNA-217 (miR-217). We have found that, in cultured hepatocytes and in mouse livers, chronic alcohol administration dramatically and specifically induced miR-217 levels and caused excess fat accumulation. Our studies have further revealed that overexpression of miR-217 in hepatocytes promoted ethanol-mediated impairments of SIRT1 signaling. More importantly, miR-217 impairs lipin-1, a vital lipid regulator, in hepatocytes. Taken together, our novel findings suggest that miR-217 is a specific target of alcohol in the liver and may present as a potential therapeutic target for treating human alcoholic fatty liver disease. This presentation will discuss the results and implications of these novel findings in the pathogenesis of alcoholic fatty liver disease.

**S 1601 Enhanced Susceptibility of Fatty Livers to Drug Hepatotoxicity and Innate Immune Responses.**

H. Jaeschke. *Department of Pharmacology, Toxicology & Therapeutics, The University of Kansas Medical Center, Kansas City, KS.*

Steatosis is a risk factor for enhanced liver injury during drug hepatotoxicity and sterile inflammation. However, the mechanisms of this aggravated liver damage can vary dependent on the degree of steatosis and the pathophysiology. Steatosis can trigger microcirculatory disturbances, mitochondrial dysfunction and cause inflammation, which are important contributing factors for the increased susceptibility to liver cell death. The molecular mechanisms by which fatty liver promotes liver injury in genetic versus diet-induced steatosis models will be discussed in detail using examples of drug overdose (acetaminophen), hepatic ischemia-reperfusion and obstructive cholestasis.

**S 1602 Increased Risk of Drug Toxicity due to Altered Pharmacokinetics in Nonalcoholic Steatohepatitis.**

N. J. Cherrington. *Pharmacology and Toxicology, University of Arizona, Tucson, AZ.*

Many severe adverse drug reactions occur when a patient is unable to metabolize and eliminate the standard dose of a drug due to alterations in drug metabolizing enzymes or transporters. Sources for this inter-individual variability include genetic polymorphisms or environmental factors such as inflammatory diseases that directly or indirectly alter the function of the enzymes and transporters that determine the pharmacokinetics of the drug. This presentation will discuss obesity-related and other possible sources of inter-individual variation in the transcriptional regulation, post-translational modification, and sub-cellular localization of specific drug metabolizing enzymes and transporters, thereby altering the pharmacokinetics and toxicity of drugs in patients that are at greater risk of adverse drug reactions

**S 1603 Biomarkers and Mechanisms for Steatohepatitis.**

C. McClain. *Pharmacology and Toxicology, University of Louisville, Louisville, KY.*

Steatohepatitis may be caused by toxicants (TASH), obesity (NASH), or alcohol (ASH) among other causes. Mechanistic similarities and differences appear to exist between different types of steatohepatitis. We compared serum adipocytokines, cytokerin 18 (CK18), and antioxidants in human subjects with ASH, NASH, and TASH. All forms of steatohepatitis were associated with reduced serum antioxidants and insulin resistance (although adipokine levels differed by etiology). ASH and TASH were characterized by higher levels of pro-inflammatory cytokines. Likewise, ASH and TASH were associated with increased hepatocellular necrosis:apoptosis ratios compared with NASH which had a similar ratio to healthy controls. Lastly, complementary studies in mice showed major interactions between diet (high fat) and environmental toxins. This presentation will describe these findings and highlight the similarities and differences of novel clinical biomarkers of TASH, NASH, and ASH.

**W 1604 "Air"-ing on the Side of Caution: Anticipating Impacts of Emerging Issues in the Health Effects of Air Pollution.**

A. K. Farraj. *EPHD, NHEERL, US EPA, Durham, NC.*

Dramatic reductions in air pollution over the last three decades have largely been driven by the enactment of federal regulations (e.g., the Clean Air Act in the United States). Today, policymakers and air quality managers rely on cutting-edge science to reduce and control air pollution. Toxicology is at the fore-front of this effort providing critical input on health effects of air pollution including dose-dependence, the role of constituents and size, mode of action, and relative toxicity of air pollution sources. Despite these advances, serious adverse health effects including cardiopulmonary mortality are still measurable at ambient air levels to which millions of people are currently exposed. Risk assessment of these air sheds is likely to get further complicated in light of the uncertainty posed by several emerging issues that intersect air quality and health. Climate change is one such issue that may affect health via direct effects of weather (i.e., heat and precipitation) and indirectly through increasing concentrations in ground-level ozone and particulate matter, two key air pollutants linked to adverse health effects. The burgeoning increase in obesity and associated metabolic disorders, groups with exaggerated sensitivity to the adverse effects of air pollution, is likely to aggravate health outcomes. With the implementation of new fuel standards and increasing popularity of alternative fuels, it is unclear what impact these changes may have on health effects of traffic-related emissions. Finally, several methods of power generation, including modern coal

technology, nuclear energy, and hydrofracking have recently captured public interest, yet their impacts on air quality are unknown. This workshop discusses the current state of the science including key toxicological findings and recent innovations as well as challenges in the study of these emerging issues. The workshop concludes with a prospective look at air pollution research with a discussion session that engages the audience in an effort to define data gaps and potential mitigation strategies.

**W 1605 Health Impacts from Climate Change through Atmospheric Systems: Recent Findings and Challenges.**

M. Bell. *Environmental Health, Yale University, New Haven, CT* Sponsor: [A. Farraj](#).

Climate change is anticipated to exacerbate many existing human health burdens such as through an increase in the duration and intensity of heat waves and through accelerated formation of tropospheric ozone. However, many questions on the nature of these impacts remain. This presentation discusses case studies of research on how atmospheric systems (air pollution, weather) could be impacted by climate change, thereby affecting human health, and will explore the challenges of this type of research. The case studies involve linking air quality, meteorological, and climate modeling to estimate the health consequences from changes in ozone levels in 50 U.S. cities and the mortality impacts from changes in heat waves in Chicago, Illinois, U.S. Challenges and assumptions of approaches to estimate health impacts from a changing climate include uncertainty in the various modeling systems (e.g., air quality models, climate change models), the use of current day relationships for weather or pollution and health for future scenarios, the changing distribution of susceptible subpopulations (e.g., elderly), and adaptive measures (e.g., air conditioning).

**W 1606 Environmental Factors and Cardiometabolic Disease: Signals in the Air.**

S. Rajagopalan. *Cardiovascular Medicine, Ohio State University, Columbus, OH.* Sponsor: [A. Farraj](#).

Cardiometabolic diseases represent a pandemic, with the World Health Organization (WHO) projecting that more than 2.3 billion people will be overweight/obese by 2015. Technology innovations, globalization with its free movement of food and services, seismic shifts in agrarian practices coupled with rural-urban migration, nutritional transition to freely available high-caloric diets have irrevocably altered energy expenditures during work and leisure. These and other factors are helping to foster the continued "epidemiological transition" occurring across the globe. Scientific effort over the last few decades has focused on components of urbanization such as inactivity and dietary factors. More recent observations provide additional links between chronic exposure to environmental factors in air/water and propensity to diseases. This issue is of importance given the extraordinary confluence of high levels of airborne and water pollutants in urbanized environments. Multiple studies in China, India and other rapidly urbanizing economies demonstrate a steep gradient in urban-rural prevalence. This presentation summarizes recent evidence on how air pollution may represent an under-appreciated yet critical linkage between urbanization and the emergence of cardiometabolic diseases, with a focus on diabetes mellitus.

**W 1607 Implications of New Fuel Standards and Alternative Fuels on Traffic Emissions: Insight from the Chemistry and Health Effects of Soy Biodiesel Emissions.**

M. S. Hazari. *Environmental Public Health Division, US EPA, Research Triangle Park, NC.*

The environmental impacts of combustion-derived vehicular emissions are well-established. In an effort to reduce greenhouse gas (GHG) emissions, improve fuel economy, and expand the nation's renewable fuel sector, new standards detailing the minimum volume of renewable fuel, which includes cellulosic biofuel, biomass-based diesel, advanced biofuel and total renewable fuel, contained in transportation fuel sold in the United States were recently proposed. Although it is assumed that these alternative energy sources will provide a "greener" fuel option, it is still largely unknown how their combustion emissions will impact human health, particularly when combined with traditional sources such as gasoline or diesel. Each biofuel has a unique chemical makeup, which will impact emissions characteristics and potential toxicity. Thus, this presentation highlights the new 2012 standards for renewable fuel, addresses the complexity of emissions arising from the combustion of various biofuel types, and examines the potential human health implications of incorporating biofuels into the transportation fuel sold in the U.S. For this last point, many of the health effects of vehicular air pollution in the last 10 years have

focused on particulate matter (PM). Recent studies suggest that certain biodiesel blends contain less PM and may be less toxic. Hence, a recent soy biodiesel study is discussed with respect to chemical composition and component analysis, and toxicological effects, including cardiovascular, pulmonary and carcinogenic endpoints, in several rodent models.

**W 1608 Fracking, Coal, and Nuclear Energy: Impacts of Contemporary Methods of Power Generation on Air Quality and Remediation Efforts.**

J. D. McDonald. *Toxicology, Lovelace Respiratory Institute, Albuquerque, NM.*

The complexity of the world's power production needs requires that a number of approaches be used to generate and distribute power. Natural gas, coal, nuclear, and other sources are all in play. Each of these energy sources are subject of intense regulation targeted at mitigating potential air and other contamination, recently including mitigation of carbon dioxide. The increase in demand for natural gas has led to new methods for harvesting and obtaining it, including the controversial techniques such as fracking. Carbon capture and sequestration offers a number of engineering challenges, and methods for capturing include potential approaches that may initiate additional environmental concerns. Of course nuclear energy, especially considering the recent events in Fukushima, has its own environmental concerns. This presentation focuses on emerging considerations related to the impact of power generation on air quality. The emphasis will be on coal emissions (modern vs traditional), carbon capture and sequestration (CCS), and natural gas (including fracking). Some mention of nuclear concerns will be considered. The presentation includes recent toxicology data on the health effects of inhaled amines and their degradation products used in CCS, and data on emissions from coal after they are atmospherically transformed in the environment and on air contaminants associated with fracking.

**W 1609 Predicting the Future: Getting Ahead of Problems—A Presentation and Discussion.**

D. L. Costa. *Office of Research & Development, US EPA, Research Triangle Park, NC.*

Despite dramatic reductions in air pollution since 1970, the impact of pollutants on health and the environment remains a concern to both regulators and the general public. Studies have not been able to show thresholds of effect for prominent "criteria" pollutants like particulate matter (PM) and ozone (O<sub>3</sub>) and much uncertainty remains with air toxic air pollutants that vary across sources. Millions of people are exposed to the criteria pollutants, but there are subpopulations which are at risk due to unusual exposure circumstances or underlying biologic susceptibility or increasing age. Science continues to chip away at these concerns through human population studies, and human and animal toxicological studies. But as we look to the future with increasing national demand for energy and global population and industrial growth, there is increasing pressure on resources and the atmospheric reservoir for pollutants. Climate change with its impacts on air pollution chemistry as well as regional weather is widely thought to be undermining the gains we've seen in reducing the national air pollution burden through challenging environmental complexities. New technologies, fuels, and ambient pollutant profiles require systematic assessments and innovative tools if we are to dissect these many interrelated issues to ensure optimal strategies to protect human and environmental health. This presentation attempts to draw on what we know and speculate on what we need to know from our science to forecast both emerging issues and solutions—preferably preventative—that have been discussed in this workshop. The audience will be engaged to embellish and enhance this discourse.

**W 1610 Breaking the Routine: Is There Room for Modern Techniques of Neuropathology Assessment in Routine Preclinical Safety Studies?**

C. D. Toscano<sup>1</sup> and J. P. O'Callaghan<sup>2</sup>. <sup>1</sup>FDA/CDER/OND/DNP, Silver Spring, MD; <sup>2</sup>CDC/NIOSH/Neurotoxicology Laboratory, Morgantown, WV.

Neurotoxicity in routine preclinical safety studies is traditionally assessed with three H&E-stained brain sections; an approach that is not optimal, considering the brain's complex neuroanatomy. The need to increase the sensitivity of this approach is supported by the finding that routine neuropathology assessments would fail to detect MPTP, ethanol and carbonyl sulfide induced-CNS lesions. Increasing the number of brain sections sampled and inclusion of additional histology stains have been recommended but there is no expert consensus on the feasibility of incorporating modern methods of assessment into routine preclinical safety studies. We will explore and comment on the adequacy of the traditional approach to neuropathology assessment in routine preclinical safety studies. We will also examine

the current regulatory guidance on neurotoxicity assessment in routine preclinical safety studies and discuss the feasibility of changing the current approach. Examples of emerging methods, such as MRI-directed histology and detection of circulating biomarkers of CNS damage, along with strategies for incorporating these techniques into standard preclinical safety studies will also be discussed. Finally, we will attempt to build consensus on appropriate approaches for improving the sensitivity of neurotoxicity assessment in routine preclinical safety studies by fostering a discussion between the audience and panel members. This discussion will focus on the feasibility of employing the proposed new markers, endpoints, and approaches and potential issues with interpretation of results of these studies. In conclusion, we believe that by examining the adequacy of current approaches of neuropathology assessment, discussing possible improvements to regulatory guidance and presenting emerging approaches of neurotoxicity assessment that this workshop will allow for a much needed dialogue on the need and feasibility of improving the current methods of neuropathology assessment in routine preclinical safety studies.

**W 1611 Routine Neuropathology Analysis for Nonclinical General Toxicology Studies.**

B. Bolon. *Veterinary Biosciences, Ohio State University, Columbus, OH.*

Microscopic neuropathological evaluation in Good Laboratory Practice (GLP)-type nonclinical general toxicology studies is one component of a battery of assays performed to assess potential nervous system toxicity of new chemical entities. Strategies for neuropathological assessment in such studies vary by species and among different industries and regulatory bodies. A Society of Toxicologic Pathology (STP) Working Group has recommended the following neuropathological strategy as suitable for all GLP-type nonclinical general toxicology studies. Selected brain areas should be examined routinely: caudate / putamen; cerebellum; cerebral cortex; hippocampus; hypothalamus; medulla oblongata; midbrain; olfactory bulb (in rodents only); pons; and thalamus. In rodents, these regions can be assessed in 6-7 full coronal sections on 2 standard-size slides; in non-rodents, they may be evaluated unilaterally in 6-7 standard slides each bearing 1 coronal hemisection. Spinal cord (cervical, thoracic, and lumbar regions) and peripheral nerve (sciatic and/or tibial) should be viewed in longitudinal / oblique and transverse sections. Current neurohistology practices—immersion fixation in 10% formalin, embedding in paraffin, and initial analysis only of H&E-stained sections—is acceptable for nonclinical general toxicology studies. These recommendations slightly expand current practice (i.e., analysis of 3-4 transverse brain sections in rodents) to improve sampling consistency using available technology. These recommendations affirm the importance of consistent routine neuropathological evaluation in GLP-type nonclinical general toxicology studies while acknowledging that histopathology is only one component of neural safety testing in such studies. Therefore, institutions should retain flexibility in devising the neuropathology portion of GLP-type nonclinical general toxicology studies as long as major nervous system regions are evaluated systematically.

**W 1612 A Regulatory Perspective on the Current State of Neuropathological Assessments in Drug Development.**

R. Mellon. *FDA/CDER/OND/DAAAP, Silver Spring, MD.* Sponsor: C. Toscano.

Neurotoxicological assessment of drug products is currently accomplished in preclinical studies by evaluation of central nervous system (CNS) safety pharmacology studies and general toxicology studies, which include simple behavioral observations and histopathological evaluation of the brain. Histopathological assessments in routine toxicology studies have identified adverse findings not detected by behavioral observation and therefore generate critical safety data. The scientific community has raised concern that histopathology in routine toxicology studies lacks adequate granularity for such a complex organ as the brain and therefore may not be appropriate for initial evaluations nor do they adequately identify when detailed "second tier" neurotoxicology studies are necessary. For example, the standard sampling and staining approach used in general toxicology studies may not be sufficient to detect certain CNS lesions (e.g. "Olney" lesions associated with NMDA receptor antagonists). Adopting an expanded sampling routine, such as the recently proposed Society of Toxicologic Pathology recommendations for the sampling and assessment of the brain in routine safety into Tier 1 testing, would increase the sensitivity of these studies. As there is currently no official CDER guidance on the assessment of the neurotoxicity of drug candidates, many approaches have been taken to addressing and reviewing the neurotoxicity of drug candidates; examples of these approaches and the level of success of such approaches will be provided. A regulatory perspective of the limitations of the current standard approach and feasibility of including modern methods of neuropathology assessment will be discussed. Overall, incorporation of modern methods of neuropathology assessment and improving the documentation of procedures used into the final study reports would provide greater confidence in the quality of the assessment. Such changes have the

potential to impact the safety assessment of a drug candidate prior to first-in-human clinical studies, throughout drug development and as part of post-market-ing safety assessments.

## **W** 1613 Utilization of MRI Imaging to Optimize the Selection of Brain Sections for Assessment by Classical Neurohistopathology.

J. P. Hanig<sup>1</sup>, M. G. Paule<sup>2</sup>, J. Ramu<sup>2</sup>, L. Schmued<sup>2</sup> and S. Liachenko<sup>2</sup>. <sup>1</sup>OTR, FDA/CDER, Silver Spring, MD; <sup>2</sup>Neurotoxicology, NCTR/FDA, Little Rock, AR.

Sampling of 3 coronal brain sections for morphological assessment in routine pre-clinical toxicology studies is clearly insufficient to reliably characterize all potential neuropathologies that may be caused by new drug candidates. It has been estimated that 60 coronal sections would be required to adequately insure that this can be accomplished. This is never done in routine safety studies. Using a panel of classical neurotoxins, including kainic acid, trimethyltin, domoic acid and nitropropionic acid that target different brain areas and structures and that exhibit effects varying from the massive to the subtle, a method has been developed for using MRI imaging to complement routine preclinical toxicology studies by allowing for a focused targeting and selection of candidate sections for histology in the rat. Proof of concept involves in-vivo MRI scanning to create files that can be compared and registered with coronal sections of the same brain sample after it has been fixed and stained appropriately for traditional neuropathology. Validation involves the establishment of concordance between the loci of pathological manifestation in each of these imaging approaches. Issues of comparability with respect to sensitivity, temporal equivalence of damage detection and whether MRI signals always predict morphological damage will be discussed. Successive in vivo MRI scans also allow subjects to be used as their own controls and for establishing time of onset, development and repair of morphologic damage. The MRI information may be used to optimize time of sacrifice for maximal visualization of traditional neurohistopathology. Most importantly, this method, when qualified, could provide guidance on where in the brain 3 "smart" sections should be taken for classical neuropathology in support of preclinical drug safety studies. Overall, we show that low resolution MRI imaging in the intact rat, may represent a powerful biomarker that can inform classical neurohistopathology assessment, but is not a substitute for it.

## **W** 1614 Translational Safety Biomarker Assessment of Neurotoxicity.

A. Jeromin. *NextGen Sciences DX, Boston, MA.* Sponsor: *C. Toscano.*

Neurotoxic effects of drugs pose a significant hurdle in the drug development process. Traditionally, neurotoxicity is assessed pre-clinically by classical histopathology, which has limited translational value for clinical development. Recent advances in imaging, functional assessment and the identification of fluid-based biomarkers of neurotoxicity might allow for the nomination of novel translational safety in neurotoxicity. Ideally, fluid based biomarkers of neurotoxicity detected in either CSF or blood could be combined with histopathology, high-resolution structural MRI and PET imaging, and other methods to assess neurotoxicity. We have assessed protein-based biomarkers of necrosis and apoptosis in addition to glial fibrillary acid protein (GFAP), ubiquitin C-terminal hydrolase L1 (UCH-L1), a biomarker of cell body injury and member of the ubiquitin proteasome system, myelin basic protein (MBP), a demyelination marker, and microtubule-associated protein (MAP-2), a biomarker of dendritic injury, in pilot studies with known neurotoxins, including kainate. We developed and employed sensitive and qualified ELISAs to assess this panel of biomarkers. In addition, this data will be supplemented by existing multiplexed solutions for cytokines to incorporate inflammatory components in addition to these brain injury biomarkers. Along with the ELISAs, we have developed and applied multiple-reaction monitoring (MRM)-based panels of brain biomarkers. These MRM-type assays have shown significant improvement in sensitivity and allow for the multiplexed assessment of hundreds of proteins for targeted discovery with a follow-up verification studies on validated assays. These multiplexed biomarker panels comprise markers of different pathways, ranging from inflammation to synaptic changes and have proven to be useful in identifying neurotoxicity.

## **W** 1615 Drug Safety Assessment and Regulatory Landscape in Emerging Markets.

P. Mu<sup>1</sup> and G. Krishna<sup>2</sup>. <sup>1</sup>TeamedOn LLC, Rockville, MD; <sup>2</sup>Supernus Pharmaceuticals, Inc., Rockville, MD.

With 85% of world's population and rapid economic growth, the emerging market countries are up and coming, and are now actively courted by large global pharmaceutical industries. Within the next decade, Asia is expected to overtake Europe in

pharmaceutical sales. For example, China is predicted to be the second largest pharmaceutical market after the United States by 2015 (Nature Reviews Drug Discovery, 2010). Many large pharmaceutical companies have increased their presence in emerging markets for research and discovery, and are seeking to market their products locally. Due to the short history of innovative pharmaceutical research and development, many of the emerging countries have limited experience of first hand review of new drugs applications, hence rely mostly on the review decisions taken elsewhere to grant the approval in local markets. However, regulatory agencies of the emerging countries are working diligently to catch up with the international standards and in the process establishing the regulations that address their country specific needs to promote innovation and bring drugs that are appropriately tested to demonstrate safety for their own population. The establishment and expansion of regulatory agencies functions is creating local job opportunities for people with specialized skills, to help with the review of various components of the new drug applications while at the same time presenting challenges never experienced before due to the nature of innovation. This has sometimes led to regulations that are not well defined and open to interpretation. The drug safety assessment and regulatory landscape in China, India, Korea, and Brazil will be introduced during the presentations. The similarity and difference of the regulatory environment in the emerging countries will be compared with the major ICH guidelines. The challenges and possible solutions for companies seeking regulatory approval in emerging markets will be discussed. This will also provide an open forum for regulators from emerging markets to exchange ideas on how to tackle unique situation they experience.

## **W** 1616 Framing the Workshop Theme.

S. Goel. *Supernus Pharmaceuticals, Inc., Rockville, MD.*

Countries in emerging markets are gaining increased focus regarding research and development activities and regulatory filings to market drugs due to an increase in consumer demand and rapid growth of their economies. To this end, it is essential to understand the progress and the intricacies in the regulatory filings among emerging markets. The speakers of this workshop will address several common questions on regulatory filing in their respective countries, including 1) The overall structure of the regulatory agencies and divisions under which various classes of drugs applications are submitted for reviews, 2) Comparison of various milestones in regulatory review process, preIND meeting, IND, SPA, end of Phase 2 meeting, and NDA, 3) Discovery and nonclinical safety studies required to support various stages of drug development and general comparison with ICH guidelines, 4) Requirements for country of origin of data, 5) Expertise and composition of non-clinical reviewers, 6) State of GLP compliance in contract research organizations within their countries, 7) Language used in regulatory submissions, 8) Regulatory outcomes and issue resolution.

## **W** 1617 Current Status of Preclinical Safety Assessment of Drugs in China.

J. Jiang. *State FDA (SFDA), Beijing, China.* Sponsor: *P. Mu.*

In China, Ministry of Health had regulated new drug registration and evaluation from 1949 to 1998. Starting from 1998, State Food and Drug Administration (SFDA) took over this function. There are three laws in China regulating the drug evaluation and registration process. In addition, SFDA has published 17 technical guidance for safety assessment of chemical drugs or biologics and 12 for traditional Chinese herbal medicines. Currently, in China chemical drugs or biologics are divided into 6 different registration categories. They are (1) investigational drug never marketed in any country, including synthesis or semi-synthesis; natural sources or by fermentation; optical isomer; new combination of products, (2) drug with changed administration route, not marketed both domestically and internationally, (3) drug marketed outside of China, but not in Chinese market, (4) raw materials and formulations of drugs with changed acid or alkaline radicals or metallic elements, but no changes of pharmacology, (5) drug with changed dosing form, but not administration route, and (6) raw materials and formulations of drugs fitting in Chinese national standard. Moreover, there are 11 registration categories for traditional Chinese herbal medicines. Preclinical safety assessments vary according to the registration categories of new drugs. During early development, investigator develops strategies to determine safety of investigational drug according to the registration category. In 2003, SFDA officially issued the "Good Laboratory Practice (GLP) for Non-clinical Laboratory Studies" and required all preclinical safety assessments of drug to be conducted in GLP accredited labs. China has developed its own unique drug evaluation system, which ensures safe and effective drug products for patients.

## **W** 1618 Regulations and Developments in Safety Assessment of New Drugs in India.

Y. K. Gupta. *All India Institute of Medical Sciences, New Delhi, India.* Sponsor: G. Krishna.

India is emerging as a major center for research and development of new chemical entities for therapeutic use. The Drug and Cosmetic Rules, 1945 and all its amendments set the foundation for manufacture and sale of drugs. The "Schedule Y" of the above rule specifies the studies that must be done in animals to establish safety and efficacy of new drugs prior to trials in humans. However, until recently India has been a center for manufacture of generic drugs. The Government of India Ministry of Health and Family Welfare established the Office of Central Drugs Standard Control Organization (CDSCO) headed by the Drugs Controller General (India) [DCG(I)] to regulate drug development. The current and up to date information on CDSCO can be found at <http://www.cdscn.in>. In March 2011, the DCG(I) formed 12 New Drug Advisory Committee (NDAC) based on broad categorization of use of drugs on various systems in the body, such as Reproductive & Urology, Cardiovascular & Renal, Ophthalmology, Vaccines, Dermatology and Allergy, etc. The NDAC's consists of expert members to advise on the matters of review and regulatory approval of clinical trials & new drugs. The charter for NDACs specifies that the drugs under development should consider relevance to population, innovation, and un-met medical need in India. India is unique in that it officially recognizes the development and marketing of traditional medicines (Ayurvedic, Siddha, and Unani drugs) for therapeutic use. India also prohibits certain drugs for manufacture and sale that it considers detrimental to its populations health. In India, the regulatory compliance of non-clinical studies is monitored by National Good Laboratory Practices (GLP) Compliance Monitoring Authority in Department of Science and Technology of Government of India. The Indian GLPs are based on the OECD guidelines due to initial close working relation between OECD countries in audit and GLP certification of Indian CROs.

## **W** 1619 Safety Assessment and Regulatory Landscape in Korea.

S. Han<sup>1</sup> and I. J. Yu<sup>2</sup>. <sup>1</sup>Korea FDA, Osong, Republic of Korea; <sup>2</sup>Hoseo University, Asan, Republic of Korea.

Korea is another major emerging center for research and development of new pharmaceuticals. The 2011 Pharmaceutical Affairs law had changed the regulations for manufacture, application, review, and approval of drugs. Korea Food and Drug Administration (KFDA), similar to US FDA, is a sole regulatory agency governing manufacture, application, review, approval, and surveillance of drugs. Within KFDA, the Pharmaceutical Safety Bureau with the Drug Evaluation Department is responsible for establishment of safety control system for drugs, promotion/support of the pharmaceutical industry, establishment of standards for the production of drugs and quality management, approval screening for drugs, and collection and evaluation of information on the side effects of drugs. Biopharmaceutical & Herbal Medicine Bureau and Medical Device Safety Bureau have similar roles in the relevant areas. As the research and development institute under KFDA, NIFDS (National Institute of Food and Drug Safety Evaluation) has played the key role in comprehensive research that is necessary for food and drugs regulation in Korea. It has been instrumental in the development and evaluation of toxicological and pharmaceutical methods. Center for Drug Development Assistance in KFDA supports for new drug R&D and regulatory affairs. The nonclinical safety studies at various stages of development are required according to ICH guidelines. Korean GLPs are based on the OECD GLP principles as a member country of OECD and Korean CROs have been frequently monitored jointly by three GLP authorities: KFDA, Rural Development Administration (RDA), and National Institute of Environmental Research (NIER).

## **W** 1620 Regulatory Developments in Brazil to Address Market Needs.

D. Barbano. *Brazilian Health Surveillance Agency (ANVISA), Brasilia, Brazil.* Sponsor: S. Goel.

In Brazil, for registration purposes, the medicines are classified in different categories, such as synthetics, biologics, phytotherapeutics. Synthetic medicines are classified as new, generic and similar. Each category of medicine is regulated by specific resolution, and its registration is granted for five years. The registration must be renewed by resubmitted the drug for evaluation at the end of each five year period. The registration of biological products is regulated by ANVISA since 2002. Due to the recent expiration of several patents for innovative biotechnology products, the interest in the production and sale of copies of these products is growing in Brazil. The regulatory framework for registration of biological products, (including new molecules or copies), was established in Brazil in December 2010 with the

publication of RDC No. 55/2010. For development of this technical regulation, the regulatory frameworks and guidance's of different agencies in the world were considered, including Health Canada (Canada), European Medicines Agency (EMA, Europe), CECMED (Cuba), and WHO Similar Biotherapeutic Products (SBP) guidelines. New Biological Products must be registered by the classic and regular manner, with the presentation of complete dossier, containing all the production, quality, non-clinical and clinical data. The non-innovative biological products can be registered with reduced information. ANVISA is actively developing new resolutions to fill old regulatory gaps to support development of biological products. The regulatory developments at ANVISA in relation to emerging needs of Brazil will be presented.

## **W** 1621 Workshop Summarization and Question and Answer Session.

G. Krishna. *Supernus Pharmaceuticals, Inc., Rockville, MD.*

Drug safety assessment around the globe is evolving. With the introduction of International Conference on Harmonization (ICH) guidelines, most emerging regions are trying to learn and adapt to the new expectations and processes. Drug industry scientists and the regulatory agencies are coming together and working diligently in the hopes of making a difference in the "waiting" patient. To this end, the workshop on Drug Safety Assessment and Regulatory Landscape in Emerging Markets is expected to answer multiple questions on the dynamics of evolving science, regulations, and processes based on the experiences from the more established markets/regions versus the individual interpretation and application of guidelines in the emerging markets. The Question and Answer session would provide an opportunity to deliberate current thinking on the subject and summarize the thoughts.

## **PL** 1622 Cell-Level Model of Morphogenetic Tissue Fusion for Computational Toxicology.

M. Hutson<sup>1</sup> and T. B. Knudsen<sup>2</sup>. <sup>1</sup>Physics & Astronomy, Vanderbilt University, Nashville, TN; <sup>2</sup>NCCT, EPA, Research Triangle Park, NC.

Vertebrate development is replete with instances of tissue fusion in which two tissues – each with its own complement of mesenchymal and epithelial cells – meet, adhere and eventually fuse into a seamless mesenchyme and epithelium. Such fusion is critical for proper morphogenesis of multiple organs, with failure implicated in several developmental defects: cleft lip/palate; closure defects of the neural tube; omphalocele (body wall); coloboma (optic cup); and hypospadias (urethra). Some of these defects are context-dependent – e.g., instances of cleft palate caused by failure of the palatal shelves to elevate, or hypospadias concomitant with impaired growth of the genital tubercle. Nonetheless, there is mounting evidence for fusion-specific defects (e.g., Pallister-Killian syndrome and VACTERL association). Furthermore, a predictive model built from ToxCast Phase-I data and ToxRefDB mapped cleft palate to Gene Ontology terms for diverse biological processes (balanced accuracies of 0.66-0.76): negative regulation of epithelial cell proliferation; epithelial-mesenchymal transitions (EMT); TGFβ2 production and type-II TGFβ receptor binding; and neural crest migration. We have thus constructed a cell-level computational model of tissue fusion that incorporates cellular adhesion and viscoplasticity with paracrine/juxtacrine control of proliferation, apoptosis, EMT and cell migration. The model includes three growing tissues – only two of which normally fuse – to explicitly model failures of both fusion competence and specificity. As a first demonstration, we model secondary palate fusion by tuning the relative contributions of apoptosis, EMT and cell migration to match dissolution of the midline epithelial seam. This flexible model is a platform for computational toxicology that can elucidate the varying interplay of such cell behaviors in the normal course of different tissue fusion events and their role in differential susceptibility to chemical disruption. [This work does not reflect EPA policy].

## **PL** 1623 Investigating Adverse Outcome Pathway Models for Mitochondrial Toxicity.

M. L. Patel, S. Canipa and D. Portinari. *Lhasa Limited, Leeds, United Kingdom.* Sponsor: C. Marchant.

Adverse Outcomes Pathways (AOPs) are used to describe the steps of a chemical interacting with a biological system from the subcellular to population level of observation. We investigated the published literature to develop qualitative AOPs for oxidative phosphorylation by mitochondria. Literature searches were carried out to identify chemicals and potential mechanisms of inhibition for each of the complexes of the electron transport chain (ETC) and for ATP synthase. Compounds for which sufficient experimental data could be located were then used to build plausible mechanistic pathway maps.

A dataset of over 200 compounds covering experimental data in a number of relevant screens (measuring individual complex activity, cellular ATP levels, reactive oxygen species (ROS) generation, oxygen consumption, mitochondrial membrane potential and cytotoxicity) was constructed. Seven model compounds were identified as having sufficient data and plausible mechanistic evidence to construct AOPs. The compounds used were: Rotenone, Thenoyltrifluoroacetone, 3-Nitropropionic acid, Antimycin A, Myothiazol, and Cyanide for mapping the ETC pathway, and Oligomycin A for ATP synthase. Using these representative model compounds an AOP was mapped for each complex from the molecular initiating event (MIE) to effects at the cellular level. The AOPs for inhibition of complexes of the ETC were then combined to create a single pathway.

We report the construction of AOPs for oxidative phosphorylation in mitochondria and their speculative extrapolation to in vivo endpoints such as cardiotoxicity, neurotoxicity and hepatotoxicity. The AOP maps are described in terms of the normal physiological pathway processes and potential intervention points, with reference to experimental in vitro assays which were used to support the elucidated steps. Not all compounds with mitochondrial effects may go on to display in vivo toxicology. An AOP view of such pathways is an useful construct in providing information in a form suitable for assessing outcomes relevant to risk assessment.

**PL 1624 Interactive Data Mining of Toxicogenomics and In Vivo Toxicity Databases Using Chemotypes to Improve Chemical-Disease Prediction Inferences and Mode-of-Action QSAR Models.**

A. Mostrag-Szlichtyng<sup>1</sup>, C. Yang<sup>1</sup>, J. Rathman<sup>1,2</sup>, C. Mattingly<sup>3</sup>, A. Davis<sup>3</sup>, A. Planchart<sup>3</sup> and A. M. Richard<sup>4</sup>. <sup>1</sup>Altamira, LLC, Columbus, OH; <sup>2</sup>The Ohio State University, Columbus, OH; <sup>3</sup>North Carolina State University, Raleigh, NC; <sup>4</sup>US EPA, Research Triangle Park, NC.

The Comparative Toxicogenomics Database (CTD, <http://ctdbase.org>) aims to shed light on the connection between chemical exposures and human health outcomes by inferring relationships via integration of curated chemical-gene, gene-disease and chemical-disease data from the scientific literature. Independent of CTD, structural knowledge via chemotypes, features linking chemicals to phenotypes, has been developed based on in vivo studies from toxicity databases, including regulatory sources at the US EPA and the US FDA. A chemotype is defined as a chemical substructure annotated with atom/bond properties that carry biological activity information. We explored whether the chemical-disease links in CTD could contribute to the further development of chemotypes, and whether mode-of-action Quantitative Structure Activity Relationship (QSAR) models for toxicity endpoints built around chemotypes could be used to validate CTD disease inferences or further delineate phenotypic effects. We applied a set of previously developed MOA models and chemotypes, e.g., for cleft palate, to the data found in CTD. Many of the same chemotypes (representing attributes of glucocorticoids, retinoids, conazoles, dioxanes, and phthalic esters) were found to be associated with cleft palate in CTD, either by direct curation or inferred via common interacting genes. The structural feature space enriched with cleft palate chemotypes was highly populated by the chemicals deemed associated with this condition in CTD. This work demonstrated how interactive data mining between CTD and in vivo toxicity databases with chemotype probes can improve the predictive power of gene-disease and chemical-disease associations, as well as the MOA models; also described is how these associations can be tested experimentally. This abstract does not reflect EPA policy.

**PL 1625 Cheminformatics Analysis of Compound-Cytochrome P450 Interaction Profiles.**

D. Fourches<sup>1</sup>, M. Elias<sup>2</sup>, E. Muratov<sup>1</sup>, L. Sheppard<sup>3</sup>, P. Bradley<sup>3</sup>, J. Reed<sup>3</sup> and A. Tropsha<sup>1</sup>. <sup>1</sup>University of North Carolina at Chapel Hill, Chapel Hill, NC; <sup>2</sup>The Hebrew University of Jerusalem, Jerusalem, Israel; <sup>3</sup>Instem Scientific, Cambridge, United Kingdom. Sponsor: L. Rusyn.

Only five isoforms (1A2, 2C9, 2C19, 2D6, and 3A4) of Cytochrome P450 (CYP) enzymes are responsible for the metabolism of the vast majority of drugs. Beyond knowing what drugs are metabolized by a specific isoform and the subsequent metabolites, it is of critical importance to evaluate the CYP inhibition potency of a compound for predicting its most likely CYP-related adverse effects. In this study, our objective was to integrate, analyze, and model the growing compendium of publicly-available CYP-related datasets for these five isoforms using cheminformatics approaches: INSTEM (4,676 compounds) was obtained as assertional meta-data generated from MEDLINE abstracts; SUPERCYP (678 compounds) extracted from the online webportal; NCGC (16,142 compounds) is a compilation of qHTS screening results released by the NIH Center for Translational

Technologies. After chemical curation and duplicates' analysis, we have analyzed these datasets using cheminformatics approaches and addressed questions pertaining to: (i) the chemical concordance between the different isoforms illustrating the singularity of 1A2 and the tight 2C9:2C19 coupling, (ii) the identification of compounds being simultaneously potent and selective for a particular CYP isoform; compounds with selective CYP profiles found in the INSTEM database were experimentally confirmed in the NCGC screening, and (iii) the detection of erroneous database entries by performing neighborhood analysis using chemical similarity calculations. We have aimed to achieve and test robust predictors of CYP interaction profiles by building Quantitative Structure-Activity Relationships (QSAR) models for each isoform. To further benchmark our QSAR models (solely based on two-dimensional structures of chemicals), we docked our integrated CYP database into the CYP binding pockets using their crystal structures. We show how QSAR models and docking approaches can be used in synergy to predict CYP interaction profiles of drug candidates.

**PL 1626 Mechanistic Analysis of Welding Aerosol Toxicity Using Ingenuity Pathway Analysis (IPA).**

S. Tugendreich<sup>1</sup>, N. Ng<sup>1</sup>, P. C. Zeidler-Erdely<sup>2</sup>, J. M. Antonini<sup>2</sup>, M. L. Kashon<sup>2</sup> and A. Erdely<sup>2</sup>. <sup>1</sup>Ingenuity Systems, Redwood City, CA; <sup>2</sup>NIOSH, Morgantown, WV.

Welding involves occupational exposure to an aerosol containing gases and metal-rich particulates that induce adverse physiological effects including inflammation, immunosuppression, and cardiovascular dysfunction. To develop a deeper mechanistic understanding of these adverse effects, mice were exposed by inhalation to gas metal arc-stainless steel (GMA-SS) welding fume at 40 mg/m<sup>3</sup> for 3 hr/d for 5 d a week for 2 weeks followed by gene expression analysis of whole blood cells, aorta, and lung at 4 hr and 28 d post-exposure. New features in Ingenuity Pathway Analysis (IPA) were used to analyze the expression data. The analysis results establish the importance of interferons and the IRF-family of transcription factors, predicting that they are activated at 4 hours and maintained through 28 days in both blood and lung. The IPA Upstream Regulator Analysis also predicted involvement of several toxicants, such as nickel and ozone, which have been detected in welding aerosol thereby highlighting the utility of Upstream Regulator Analysis for toxicogenomics applications. In addition, as an important drug discovery tool, IPA predicted several compounds that might be useful to ameliorate the inflammatory phenotype. One such compound was LY294002, a PI3K inhibitor that has already been shown to be efficacious in a mouse model of asthma. The new Mechanistic Network Analysis in IPA was used to computationally construct a plausible hypothesis that TRIM24 inactivation may lead to activation of IRF7 and STAT1 and other upstream regulators to drive the gene expression profile after the first exposure. Finally, Downstream Effects Analysis in IPA predicted large increases in proliferation, chemotaxis, and trafficking of immune cells in the lung after 4 hours. In summary, IPA has a unique new set of capabilities to enhance the mechanistic understanding of toxicological datasets and to provide support for new hypotheses that can be tested in the lab.

**PL 1627 Insights into the TBX2 Role in Cellular Senescence in COPD: A Bayesian Structure Learning Approach.**

U. Tran and G. Acquaaah-Mensah. Massachusetts College of Pharmacy and Health Sciences, Worcester, MA.

COPD ranks among the top leading causes of death worldwide. The transcriptional factor T box 2 (TBX2) plays an important role in the COPD molecular etiology. A senescence hypothesis for the etiology of COPD has emerged. TBX2 and related genes have anti-senescence activity. Their expressions are suppressed in COPD, but elevated in many cancers. The purpose of this study was to identify the directionality of regulatory relationships between TBX2 and other genes involved in cellular senescence. From a compendium of lung epithelium cell microarrays generated using the Robust Multi-Array Average procedure, a subset of genes of interest was used for structure learning. The Bayesian Network Structure Learning approach was then used to learn the regulatory relationships. The Bayesian Network Inference with Java Objects toolkit (Banjo) was used, in each instance, to generate the single best-scoring direct acyclic network, given the gene expression data. In order to focus the large search space, an initial network of genes that TBX2 interacts with including ANF, NKX2-5, NDRG1, CDKN1A, PML, E2F, CDKN2A, and CDKN2B was identified. Simulated Annealing and Greedy Search were the network search algorithms used. The results predicted that TBX2 regulates both COL4A3 and PML. Reports in the literature confirm that TBX2 interacts with both COL4A3 and PML. Subsequently, the original known network was updated with these two interactions, and a new iteration of the learning procedure initiated.

As part of this new iteration, the compendium subset with expression data of genes of interest was updated to include senescence related genes. The results identified new TBX2 interaction partners including WNT3, WNT6, WNT7B, WNT11, IL12RB1, IL13, IL13RA1, IL27RA, CTNND1, E2F4, and FOXO3. The published literature, a functional map scoring relationships based on microarrays from over 15000 publications (HEFaLMP), as well as entries in a cis-regulatory elements database (cREMag) were utilized to validate the results. Thus, the results affirm the importance of TBX2 in the COPD etiology.

## PL 1628 Prediction of Metabolites Using Computational Approaches.

M. Kansy<sup>1</sup>, L. T. Anger<sup>1</sup>, U. Gundert-Remy<sup>2</sup> and A. Brigo<sup>1</sup>. <sup>1</sup>Non-Clinical Safety, F. Hoffmann-La Roche Ltd., Basel, Switzerland; <sup>2</sup>Institute of Clinical Pharmacology and Toxicology, Charité University Medical School Berlin, Berlin, Germany.

An increasing number of computational tools are nowadays available, which are claimed to predict drug metabolism. Those tools could most probably be used in an extended way to consider potential drug metabolites earlier in toxicity prediction of for example genotoxicity or carcinogenicity. Therefore it's important to understand the quality and limitations of metabolism prediction tools if applied in a broader context. However, to date, the software packages used in metabolism prediction have only been validated with relative small datasets containing limited number of compounds. Hence, they require a more comprehensive and explorative evaluation. Aim: Meteor (Lhasa Ltd., Leeds, UK), an available prediction tool, has been used to predict the metabolites of 325 drugs in therapeutic use. The results of the prediction were compared to the known human metabolites.

Methods: The WHO ATC index was used to extract drugs for the therapeutic classes of anti-infectives (A07E, M01A, S01BA, G02CC, M02AA, S01BC), central nervous system drugs and muscle relaxants (N, M03), cardiovascular drugs (C), oncologic substances (L01) and virostatics (J05, D06BB, S01AD). Additional information was received by queries in the DrugBank database. PharmaPendium and DrugBank were the sources to obtain information on the human metabolites of the therapeutic drugs observed in clinical studies.

Meteor (version 13.0.0, Lhasa Ltd.) is a so called knowledge-based expert system. As such it uses structured expert knowledge and its output offers the structures of metabolites with a guess on the probability of the occurrence of the metabolite.

The evaluation shows that the reliability of the prediction of human metabolites is presently limited. Hence, further development is necessary to improve the prediction potential.

## PL 1629 Comparison of Microarray and RNA-Seq for Gene Expression Analyses of Dose-Response Experiments.

M. B. Black<sup>1</sup>, E. Healy<sup>1</sup>, B. B. Parks<sup>1</sup>, L. Pluta<sup>1</sup>, T. Chu<sup>2</sup>, R. D. Wolfinger<sup>2</sup> and R. S. Thomas<sup>1</sup>. <sup>1</sup>The Hamner Institutes for Health Sciences, Research Triangle Park, NC; <sup>2</sup>SAS Institute, Cary, NC.

Relative to microarrays, differential gene expression analysis using RNA-Seq data has been reported to offer higher precision estimates of transcript abundance, a greater dynamic range of transcript detection, and detection of novel transcripts. However, appropriate methods of analyzing RNA-Seq data and the number of reads required to match the sensitivity of microarrays are still a subject of debate. Moreover, comparisons of the two technologies have not covered dose-response experiments that are relevant to toxicology. Male F344 Rats were exposed for 13 weeks to 5 concentrations of bromobenzene. RNA was extracted from livers of five animals per dose level and used for measuring gene expression changes using both Affymetrix HT RG-230 PM microarrays and ABI SOLiD 50bp single read RNA-Seq. Sequencing produced an average of 9.3M reads per sample mapping to exons. The sequencing data was normalized using RPKM (Reads Per Kilobase per Million) and the microarray data was normalized using RMA. A standard one-way ANOVA was used to analyze the data across doses. Results were compared based on statistical significance (FDR < 0.05) and fold change (FC  $\geq \pm 1.5$ ) for 5,906 genes which had read counts > 10 and matched unambiguously to genes on the microarray. The results showed that paired fold-change values were highly correlated between microarrays and RNA-Seq, while the -log p-values showed little correlation. Random sampling at different read depths showed that RNA-Seq and microarrays produced similar numbers of significant genes based on fold-change (FC  $\geq \pm 1.5$ ) at ~6-8M mapped reads per sample. However, RNA-Seq produced significantly less significant genes based on p-value (FDR < 0.05) at even the highest read depth of 9.3M mapped reads per sample. Among the significant genes, ~50% overlapped between RNA-Seq and microarrays at each dose. The results highlight the need for additional studies examining the use of RNA-Seq data in toxicology.

## EC 1630 The Symbiosis of Mentoring: Getting the Most out of the Mentor-Mentee Relationship.

B. Hannas<sup>1</sup>, N. J. Walker<sup>2</sup>, S. H. Safe<sup>3</sup>, E. W. Carney<sup>4</sup> and O. Olivero<sup>5</sup>. <sup>1</sup>Reproductive Toxicology Branch, US EPA, Research Triangle Park, NC; <sup>2</sup>NTP, NIEHS, Research Triangle Park, NC; <sup>3</sup>Molecular & Cellular Medicine, Texas A&M University, College Station, TX; <sup>4</sup>The Dow Chemical Company, Midland, MI; <sup>5</sup>Laboratory of Cancer Biology & Genetics, National Cancer Institute, Bethesda, MD.

Mentoring is a critical element in the career development of all toxicologists, both in terms of making the most of potential mentors and developing effective mentoring skills. Whether through involvement in academia, or helping to develop the expertise of an early-career scientist, most toxicologists will provide mentoring at some point in their career. The mentor role serves to transfer knowledge, give advice and provide support to a trainee or developing scientist, while the mentee is relied upon by the mentor to provide active participation and input into the relationship. According to national polls, as well as SOT-specific surveys, one of the resounding topics of interest for developing scientists is mentoring from the broad perspectives of choosing the right mentor, down to developing the skills to become a sound mentor. Therefore, this session was designed to complement existing mentor matching opportunities offered through SOT. Speaker presentations will focus on: (1) the fundamentals of mentoring, including the different situations and roles in which the mentee-mentor dynamic may be encountered; (2) an introduction to the most commonly used mentoring techniques; (3) identifying characteristics of a strong mentor-mentee relationship; and (4) mentoring towards the future of science and the challenge to overcome more complex scientific problems. Speaker perspectives will address the mentorship role within academia, government, and industry. Attendees of this session will learn to identify a healthy mentor-mentee relationship and understand the benefits to each member of the collaboration. Mentoring topics discussed in this session will be applicable to scientists at every career stage through highlighting the basics behind a strong, mutually-beneficial mentoring relationship.

## S 1631 Role of Systems Biology in Characterizing Risk of Developmental Origins of Disease.

D. T. Szabo<sup>1</sup> and T. L. Palenski<sup>2</sup>. <sup>1</sup>National Center for Environmental Assessment, US EPA, Arlington, VA; <sup>2</sup>Molecular and Environmental Toxicology, University of Wisconsin Madison, Madison, WI.

Systems biology is the study of complex interactions of biological components, such as nucleic acids, proteins, chemical reactions, cells, and whole organisms, at multiple levels of organization. The National Research Council recommends implementing the use of systems biology approaches in the risk assessment process. While recent advances have been made to prioritize chemicals for further screening, to better understand mode of action, strengthen weight-of-evidence, and eventually replace traditional *in vivo* animal model data with *in vitro* and *in silico* methods, these data have not been systematically considered in mainstream approaches for risk assessment which also largely focuses on adult populations. The goal of this symposium is to consider emerging knowledge and information from systems biology to inform risk assessment and decision making in the arena of developmental origins of disease. Growing evidence suggests that chemical exposures in early life can have immediate and long-term effects on the structure and function of organ systems, leading to the development of disease later in life. Systems biology approaches can aid in understanding molecular, cellular, metabolic, and morphological changes resulting from such exposures. These approaches, which include analysis of complex data sets from multiple experimental sources, interdisciplinary 'omics tools, and computer simulation modeling, are increasingly being applied to better understand developmental origins of disease. We will present current systems biology approaches on how to better identify developmental origins of disease and its implications to the risk assessment process through several case studies.

## S 1632 Predictive Models of Developmental Toxicity.

N. S. Sipes and T. B. Knudsen. National Center for Computational Toxicology, US EPA, Research Triangle Park, NC.

Environmental chemical exposure during development can lead to birth defects which can have lasting effects through adulthood. *In vivo* data from both rodent and non-rodent species gathered using standardized prenatal guidelines are used in risk assessments to determine developmental toxicity potential; however these studies may not indicate the underlying complex mechanisms which lead to developmental toxicity. We used a systems biology approach to develop predictive models

that link in vivo outcomes (including malformations, fetal weight reductions, and prenatal loss) with potential mechanisms of toxicity. This approach uses in vivo data from guideline and literature studies and over 3 million in vitro data points from high-throughput and high-content screening techniques on chemical-biological interactions. Specifically, these assays are obtained from biochemical, cell-free and cell culture assays, along with embryonic stem cells and zebrafish embryos. The predictive models developed confirm known pathways, such as retinoic acid receptor and transforming growth factor, and suggest novel pathways such as G-protein-coupled receptors and inflammatory pathways to be important pathways involved in developmental toxicity of environmental chemicals. These models have the potential to aid in the prioritization of chemicals for further targeted toxicity testing and risk assessment, to generate hypotheses about mechanistic pathways leading to adverse developmental outcomes, and to reduce cost and increase throughput of chemical testing.

### **S** 1633 Multiple Organ-Omic Integration for HBCD Developmental Neurotoxicity Hazard Identification.

D. T. Szabo<sup>1</sup> and L. S. Birnbaum<sup>2</sup>. <sup>1</sup>National Center for Environmental Assessment, US EPA, Arlington, VA; <sup>2</sup>NIEHS/NCI, Research Triangle Park, NC.

Exposure to environmental chemicals during critical windows of development has shown to disrupt adult neurobehavioral function; however, the mode-of-action is not always well understood. A systems biology approach was taken to identify toxicity pathways after exposure to the major brominated flame retardant mixture, hexabromocyclododecane (HBCD), along with the individual chemicals that make up the commercial mixture to better characterize developmental neurotoxicity, strengthen its overall weight-of-evidence, and support its hazard identification for risk assessment. Short-term disruptions to the developmental profile of genes, proteins, and metabolites in the hippocampus, liver, and systemic circulation were identified after exposure to the commercial mixture and individual stereoisomers. Different molecular pathway profiles generated in several organs suggest the necessity to assess the effects from the individual isomers as well as the mixture when evaluating HBCD and can be used as a model for other environmental mixtures for chemical risk assessment. This presentation will demonstrate the utility of an omics and systems biology strategy to capture information on various facets of brain development that can be altered after environmental exposures and to provide focus for further toxicity studies in determining possible modes-of-action including methods to prioritize individual chemicals in mixtures for chemical risk assessments.

### **S** 1634 Assessing Antiandrogenic Effects of *In Utero* Exposure to Dibutyl Phthalate and Other Xenobiotics.

D. Spade and K. Boekelheide. Department of Pathology and Laboratory Medicine, Brown University, Providence, RI.

The rates of male reproductive tract malformations such as cryptorchidism and hypospadias have increased in the United States throughout the latter half of the 20th century. These disruptions in androgen-sensitive development may be influenced by early life exposures to environmental anti-androgens. However, determining the impact of exposure on human fetal development is hindered by species differences and a lack of human data. Using a fetal testis xenograft model, we have shown that human fetal testis is more resistant than fetal rat testis to the anti-androgenic effects of dibutyl phthalate (DBP). We are expanding this analysis to determine how environmental anti-androgens affect human fetal testis, particularly through alterations in gene expression and DNA methylation. To provide a baseline for this analysis, 12 unimplanted human fetal testis samples aged 14 to 23 weeks gestation have been evaluated using Affymetrix Human Gene 1.0 ST gene expression microarrays and the Illumina Infinium 450k methylation arrays to reveal developmental trends in fetal testis gene expression and DNA methylation. This will provide a baseline for ongoing analysis of xenografted tissues after exposure to anti-androgens. During this window, global testis DNA methylation increases significantly, although not at all genes. DNA methylation at imprinted sites consistently increases throughout this time frame, and there are significant changes in DNA methylation of genes related to testosterone biosynthesis, cell cycle, and transcriptional control. Therefore, reprogramming of testis DNA methylation during this developmental time period aligns with the existing data in mouse, and suggests that this window may be sensitive to disruption by xenobiotics. Assessing the anti-androgenic effect of various environmental compounds in human systems is essential for determining the risk that environmental chemicals pose for the in utero development of the male reproductive system, including understanding the fetal origins of disorders of the male reproductive tract.

### **S** 1635 Mechanistic Pathways Underlying Low-Dose PFOA Effects on Mammary Gland Growth.

M. B. Macon<sup>1</sup> and S. E. Fenton<sup>2</sup>. <sup>1</sup>Curriculum in Toxicology, University of North Carolina at Chapel Hill, Chapel Hill, NC; <sup>2</sup>National Toxicology Program, NIEHS, Research Triangle Park, NC.

Perfluorooctanoic acid (PFOA) is a synthetic surfactant and, in areas of high contamination in the US, has recently been found to have a probable link to several human diseases. Prenatal exposure to PFOA causes delayed mammary gland growth in female mice. Exposure to low levels of PFOA throughout gestation results in persistent mammary gland abnormalities in female offspring that remain until late in life. Although activation of peroxisome proliferator activated receptor alpha (PPAR $\alpha$ ) is thought to mediate PFOA-induced liver toxicity, the role of this transcription factor in the mammary gland is unclear. Genome-wide microarray analysis, protein expression approaches, and morphological analysis were used to identify molecular mechanisms involved in mammary gland delays following prenatal PFOA exposure. Our studies followed female mice exposed to environmentally relevant levels of PFOA in utero spanning neonatal time-points to late adolescence. Through analysis of whole mammary tissues and isolated cell types, it was found that PFOA altered pathways involved in epithelial-stromal interactions, including endocrine disruption, leaving the mammary gland more susceptible to the development of disease. The dosing levels of PFOA used in our studies produce body burdens in mice that are similar to those found in humans living in highly contaminated areas, therefore, these findings have implications related to the human risk assessment of PFOA.

### **S** 1636 Molecular Mechanisms Linking Maternal Diet-Induced Obesity to Offspring Metabolic Syndrome.

M. Alfaradhi and S. Ozanne. Metabolic Research Laboratories, University of Cambridge, Cambridge, United Kingdom. Sponsor: D. Szabo.

Population studies have suggested that the maternal nutritional status during key stages of development is able to influence offspring risk of metabolic diseases. Recent focus has been on maternal over-nutrition and obesity in programming metabolic disorder in offspring. This stems from human data which has correlated maternal body-mass index (BMI), maternal weight gain during pregnancy, and gestational diabetes to offspring BMI and risk of metabolic disorders such as type 2 diabetes. A large number of studies have reported dysregulation of key organs involved in glucose homeostasis and feeding regulation in the offspring of obese mothers. We have utilized a mouse model in which dams are fed a western-style diet (highly palatable, high-fat, high-sugar diet) during gestation and lactation and taken a whole systems approach to establish mechanisms through which metabolic disease in the offspring arises. Our studies incorporate analysis at the whole body, tissue and cellular level. Offspring of these dams are hyperphagic from a young age, leading to increased body weight and the development of type 2 diabetes later in life. Hyperinsulinaemia is an early observation in these offspring compared to offspring in the control group fed regular chow and we have associated this with impaired insulin signaling protein expression, especially in adipose tissue. We have employed both candidate and genome-wide mRNA and microRNA array approaches to explore the mechanisms by which the programmed changes in insulin signaling protein expression occurs and to identify novel genes and regulatory elements that are associated with metabolic disorders in the offspring. These findings have important implications for the identification of markers of disease risk and identification of susceptible populations to adverse effects resulting from sub-optimal early life exposures.

### **S** 1637 Toxicopigenomics, Disease Susceptibility, and Implications for Risk Assessment.

K. Kutanzi<sup>1</sup> and M. Verma<sup>2</sup>. <sup>1</sup>Biochemical Toxicology, National Center for Toxicological Research, US FDA, Jefferson, AR; <sup>2</sup>Division of Cancer Control and Population Sciences, National Cancer Institute, NIH, Bethesda, MD.

In the past, classical toxicology has largely focused on the genotoxic effects of environmental toxicants and chemicals. Recent studies have clearly indicated that environmental chemicals, along with their genotoxic abilities, can cause epigenetic alterations that, in concert, may lead to the development of a number of pathological states. The field of toxicopigenomics has since emerged from the combination of epigenetics, which studies the methylation of DNA, histone modifications, and chromatin condensation, and toxicology. During the last few years, excellent progress has been made in detecting altered epigenomic profiles in response to various chemical insults. Future investigations, however, are needed to link chemical

exposure to epigenetic alterations which develop over time, and, in turn, may increase the risk of disease. Although whole populations may be exposed to toxic substances, only a few people develop the disease, which may, in part, be due to the different epigenomic backgrounds of individuals. That is why the potential role of epigenetics in disease susceptibility, along with the potential opportunities for epigenetic biomarkers in the assessment of toxicity and carcinogenicity of chemicals have received a lot of attention recently. Specifically, the following key aspects need to be addressed: 1) How stable are the epigenetic alterations induced by environmental toxicants?; 2) What periods of development across the lifespan are windows of vulnerability and/or opportunity for an altered epigenome?; 3) How can exposure to toxicants *in utero* affect the epigenome and predispose individuals to various diseases throughout life?; 4) Are there methodological and measurement gaps to be filled to advance our understanding of toxicopigenomics?; and 5) How can we develop risk prediction models? Evidence that epigenetic alterations can be potentially reversed may be helpful in developing treatment and preventative strategies.

### **S 1638 Epigenetic Alterations in Response to Exposure to Environmental Toxicants.**

I. Koturbash. *Department of Environmental and Occupational Health, College of Public Health, University of Arkansas for Medical Sciences, Little Rock, AR.*

Epigenetics is the study of heritable changes in gene expression that are not associated with alterations in DNA sequence. Epigenetic mechanisms include DNA methylation, post-translational histone modifications, and nucleosome positioning along DNA, and are important for maintenance of normal cellular homeostasis. Disruption of epigenetic mechanisms may compromise the balance of the cellular epigenome and lead to development of various pathological states, including cancer. Accumulating evidence clearly indicates that various environmental toxicants, independently of their genotoxic abilities, can cause epigenetic alterations. These changes in the cellular epigenome are exhibited as decreases in global DNA methylation, aberrant gene-specific DNA methylation, changes in histone modifications, as well as associated alterations in chromatin status. Importantly, epigenetic alterations can be detected long before the occurrence of genetic changes; and are stable, persisting after the initial exposure-related DNA damage has been repaired. These findings highlight the significance of epigenetic alterations in the mechanisms of toxicity and carcinogenicity.

### **S 1639 Application of Cancer Toxicopigenomics in Identifying High-Risk Populations.**

M. Verma. *National Cancer Institute, NIH, Rockville, MD.* Sponsor: K. Kutanzi.

The epigenome is dynamic and very susceptible to environmental changes. Toxicopigenomic studies are conducted to explain the epigenetic effects of environmental exposures. Epigenetic programming occurs during development and reflects altered gene expression in disease states. This programming differs from genetic polymorphisms or mutations because genetic changes are reflected in all cells, whereas epigenetic changes are cell- and tissue-specific. Studies that involve the measurement of epigenetic changes that occur at the genome-wide level and their association with disease are called epigenome-wide association studies (EWAS). Epigenetic alterations respond quickly to environmental changes, and technologies are available to measure these changes. During the last 5 years, excellent progress has been made in the field of altered epigenomic profiling in response to toxins and environmental. It now is possible to use high-throughput technologies to measure epigenetic patterns that are altered by toxin exposure. Different environmental exposures, including toxins, affect different components of the epigenetic machinery and alter the methylation and acetylation equilibrium. Epidemiologic studies help to identify the etiology of a disease, especially factors that contribute to disease development. In the case of cancer, such factors include toxic substances, radiation, infectious agents, specific dietary components, tobacco, alcohol, and environmental factors. It makes sense to identify epigenetic markers in normal and exposed populations. The advantages of identifying epigenetic biomarkers of exposure include improved exposure assessment, documentation of early alterations preceding cancer development, and identification of high-risk populations. Examples of interaction between toxic substances and cancer initiation and progression will be discussed.

### **S 1640 Changes in Histone Tail Modifications and Gene Expression in PBMC from Subjects Exposed to Nickel and Arsenic.**

M. Costa. *Environmental Medicine, New York University School of Medicine, Tuxedo Park, NY.*

A major target of Nickel (Ni) ions in cells is the iron- and ascorbic acid-dependent dioxygenase enzymes. The family of histone H3 demethylases is an example of these enzymes. Since Fe binding is required for catalytic activity and Ni ions readily displace the Fe from all of these enzymes, Ni exposure results in inactive enzyme which increases global levels of the activating mark H3K4 trimethylation (H3K4me3) and the silencing mark H3K9 dimethylation (H3K9me2). Arsenic (As) induces oxidative stress in cells and will deplete reduced ascorbate which is required for the activity of these histone demethylases. *In vitro* exposure to Ni or As increases the levels of posttranslational modifications of histone tails. Here we show changes in global levels of histone modifications in peripheral blood mononuclear cells (PBMCs) of subjects with occupational exposure to Ni by inhalation in a Nickel refinery in China and subjects from Bangladesh exposed to As in their drinking water. Occupational exposure to Ni was associated with an increase in H3K4me3 and decrease in H3K9me2. A global increase in H3K9me2 and decrease in H3K9ac was found in subjects exposed to As. Additionally, exposure to As resulted in opposite changes in a number of histone modifications in males compared to females in the As exposed population. We also analyzed the gene expression changes in PBMC in a smaller subset of individuals exposed to Ni and As. Hierarchical clustering revealed that several thousand genes were similarly changed across subjects highly exposed to Ni, and there was similar clustering with low Ni exposure and with controls. With As the results were more complex because of the strong effect of gender. With As there were genes that changed in a gender dependent manner and also with As exposure independent of gender. The results of these two studies suggest that exposure to Ni or As compounds, and possibly other carcinogenic metal compounds, can induce changes in global levels of posttranslational histone modifications and gene expression in PBMC.

### **S 1641 Chromatin Remodeling As a Driver and Target for Lung Cancer.**

S. A. Belinsky. *Lovelace Respiratory Research Institute, Albuquerque, NM.* Sponsor: K. Kutanzi.

Epigenetic silencing of genes and microRNAs (miRs) via chromatin remodeling and cytosine methylation has emerged as a major mechanism in lung cancer etiology. The reversal of gene and miR silencing using pharmacological agents and potentially dietary supplements (e.g., omega-3 polyunsaturated fatty acids [n-3 PUFA]) by affecting cytosine-DNA methyltransferases (DNMTs), histone methyltransferases (HMTs), or histone deacetylases (HDACs) offers new strategies for prevention and intervention for lung cancer. We have developed an *in vitro* model using hTERT/cdk4 immortalized human bronchial epithelial cell lines (HBECs) that identifies molecular changes driving transformation of preneoplastic lung epithelial cells during exposure to carcinogens found in mainstream and environmental tobacco smoke. Our studies provided a mechanistic link between increased DNMT1 protein, *de novo* methylation of genes, and reduced DNA repair capacity that together seemed causal for transformation. Our recent studies show that the exposure of HBECs to carcinogens for 4 wks induces a persistent and irreversible, multifaceted dedifferentiation program characterized by the epithelial-to-mesenchymal transition (EMT). EMT induction was epigenetically driven, initially by chromatin remodeling involving H3K27me3 enrichment, with ensuing DNA methylation sustaining the silencing of miR-200b, -200c, and -205 implicated in this developmental program and persisting in malignant tumors. Overexpression of these miRs reversed transformation. Genome-wide profiling has identified >300 genes with a promoter CpG island whose expression is reduced after only 4 wks of treatment. The polycomb repressive complex PRC2 regulated many of these genes. While ensuing promoter methylation after 8 wks of further exposure to the carcinogens is seen in a small subset of these genes, many of these genes show dense methylation in tumor-derived cell lines and primary tumors. These findings implicate chromatin remodeling mediated by HMTs whose expression increases during carcinogen exposure and in primary tumors, as important initiators of epigenetic gene silencing (Supported by R01 ES008801).

### **S 1642 Molecular Basis for Dioxin-Induced Cardiovascular Disease.**

A. Puga. *Environmental Health, University of Cincinnati College of Medicine, Cincinnati, OH.*

Interactions between genetic and environmental factors are responsible for several forms of human congenital cardiovascular malformations. Of these, valvular stenosis and hypoplastic left heart syndrome are the most common forms of birth defects

in humans, occurring in eight newborns from every 1000 live births and constituting 25–30% of all cases of human cardiovascular malformation. These two congenital heart defects are the leading cause of neonatal and infant death and, underscoring the fetal origin of adult disease concept, are also a major cause of adult cardiac insufficiency, linking fetal and adult cardiovascular disease. The main known risk factors for these abnormalities in cardiac development are genetic inheritance and maternal exposure to hazardous chemicals, but their precise molecular etiology remains elusive. We have recently found that treatment of differentiating mouse ES cells with dioxin represses Nkx2.5 gene expression and other cardiac markers as a consequence of AHR activation. By following the expression trajectories of cardiomyocyte markers during ES cell differentiation we found that dioxin silenced the expression of Nkx2.5 and other cardiomyocyte-specific genes, including the genes coding for cardiac troponin-T and  $\alpha$ - and  $\beta$ -myosin heavy chains, and inhibited the formation of beating cardiomyocytes, a characteristic phenotype of differentiating mouse ES cells. The key mediator of these effects was the aryl hydrocarbon receptor (AHR), epigenetically silenced in pluripotent ES cells and activated during differentiation. Our work with ES cells may unravel molecular and epigenetic mechanisms responsible for human cardiac malformations due to environmental (organochlorinated compounds) or genetic (NKX2.5 mutations) causes. NKX2.5 repression by dioxin-mediated AHR activation may help us identify the regulatory loops controlling the NKX2.5 functions that determine embryonic identity and progression of cardiac tissue differentiation, and how these functions are silenced by the activated AHR. (Supported by NIH grants 5R01ES006273 and 5P30ES06096).

### **W** 1643 Dietary Arsenic—Forms, Hazards, and Risks.

P. M. Bolger. *Exponent, Annapolis, MD.*

Arsenic, particularly inorganic arsenic, is a well known and ubiquitous environmental contaminant, particularly in drinking water, and it originates from both anthropogenic and natural sources. It demonstrates a myriad of toxicological effects across a broad spectrum of organ systems. It has generally been believed that arsenic in food occurs in organic forms that demonstrate minimal, if any, toxicological activity. This is particularly the case with the forms found in seafood (e.g., arsenosugars). However, there has been concern for some time that organic forms may not be the predominant forms in certain foods, like rice, where concentrations of inorganic forms in certain cultivars may be significant. In addition, other organic forms, like tri- and penta- mono- and dimethyl forms, may be found, and at levels that are not insignificant, and could potentially pose a health hazard. These organic forms may not be as innocuous as the organic forms found in seafood. This session will explore the current state of knowledge regarding the occurrence of various forms of arsenic found in foods, as well as their potential exposures, hazards (e.g., toxicological, epidemiological) and risks to public health, and what risk management options may be available.

### **W** 1644 Noncancer Disease Risk Promoted by Low Level Arsenic Exposures.

A. Barchowsky. *Environmental and Occupational Health, University of Pittsburgh, Pittsburgh, PA.*

Exposure to arsenic through drinking water and diet increases risk for a number of cancers and non-cancer diseases. Cardiovascular diseases contribute to a large portion of non-cancer arsenic-promoted morbidity and mortality, and may occur at relatively low levels of arsenic exposure that were considered safe based on cancer risk. While epidemiological studies have established the disease risk to low level exposures, basic studies have lagged in demonstrating mechanism for disease. However, recent low level exposure studies in mice and cultured human cells suggest novel receptor mediated and reactive oxygen species-dependent modes of action for arsenic induced pathogenic vascular and tissue remodeling, as well as metabolic dysfunction. This talk will review the current state of understanding of arsenic-induced cardiovascular disease risk and potential modes of action.

### **W** 1645 Exposure Assessment Methods for Dietary Arsenic.

L. Barraj and N. Tran. *Exponent, Washington DC.*

A brief overview of types of dietary exposure assessments and discusses the associated data requirements will be presented. Existing food consumption data sources that can be used for estimating dietary exposure to arsenic are reviewed and their strengths and limitations are discussed. Algorithms and models typically used are presented and their applicability to the various exposure scenarios (e.g., short term versus long term) are discussed.

### **W** 1646 Recent Epidemiologic Studies of Arsenic and How They Apply to the Health Evaluation of Arsenic in Food.

H. J. Gibb. *Tetra Tech Sciences, Arlington, VA.* Sponsor: P. Bolger.

The association of arsenic in drinking water with an increased risk of skin, lung, bladder, and kidney cancer has been known for several decades. In addition to the association of arsenic with increased risks of various forms of cancer, studies have found an association of arsenic in drinking water with a variety of noncancer effects including skin lesions, cardiovascular disease, diabetes, liver damage, and kidney disease. Some of these effects have been reported to occur at drinking water concentrations lower than 100  $\mu\text{g As/L}$ . Several studies indicate that exposures at younger ages have a disproportionately greater effect than exposures at older ages. Recent reports of arsenic in brown rice syrup and apple juice have raised concern whether arsenic in food products may also present a health problem, particularly for infants. The development of an epidemiologic database that focuses primarily on recent studies and how such studies may affect the risk assessment of arsenic in food will be presented.

### **W** 1647 Potential Risks to Human Health from Arsenic in the Diet: A European Food Safety Authority (EFSA) Perspective.

J. R. Schlatter. *Federal Office of Public Health (retired), Zurich, Switzerland.*

In 2010, the Panel on Contaminants in the Food Chain (CONTAM Panel) of the European Food Safety Authority (EFSA) assessed the risks to human health related to the presence of arsenic in food. More than 100,000 occurrence data on arsenic in food were considered with approximately 98 % reported as total arsenic. Making a number of assumptions for the contribution of inorganic arsenic to total arsenic, the inorganic arsenic exposure from food and water across 19 European countries was estimated for average consumers, for 95th percentile consumers and for children. The CONTAM Panel modeled the dose-response data from key epidemiological studies and selected a benchmark response of 1 % extra risk. A range of benchmark dose lower confidence limit (BMDL01) was identified for cancers of the lung, skin and bladder, as well as skin lesions. The estimated dietary exposures to inorganic arsenic for average and high level consumers in Europe as well as for children are within the range of the BMDL01 values identified, and therefore there is little or no margin of exposure and the possibility of a risk to some consumers cannot be excluded.

### **W** 1648 Pulmonomics, the Exposome, and Microbiomes in Immunotoxicology.

M. A. Williams. *US EPA, Research Triangle Park, NC.*

The exposome has revealed itself to be a powerful approach for assessing environmental exposures and their influences on human diseases. As we explore the origins of human disease, and the contributions made by environmental pollutants, a comprehensive understanding of systems biology is needed. This requires an integrated understanding of how environmental chemicals and other stressors of gene and protein expression are not only linked to a toxicological outcome but which may impact on chronic inflammatory diseases such as allergic asthma, COPD, and even lung cancer. Perturbations in normal cell cycle kinetics, apoptotic cell-death pathways, immune dysfunction, and a recent appreciation of the consequences of inadvertent dysregulation of the gut and lung microbiomes collectively distort normal systems biology homeostasis and the advent of adverse health effects. For the first time, this symposium presents emerging critical issues and paradigms that discuss the contributions and interplay of systems biology, the exposome, and microbiomes as they relate to immunotoxicology, dysregulation of inflammatory pathways, and chronic diseases. Invited speakers will place in context and share state-of-the-art approaches for advancing our understanding of the interplay of gene and environment and of the exposome in initiating and prolonging chronic inflammatory disease.

### **W** 1649 Breath Biomarkers from Viable Pulmonary Aerosols: Discovery of Human Microbiome Contributions.

J. Pleil. *Methods Development and Applications Branch, National Exposure Research Laboratory (NERL), US EPA, Research Triangle Park, NC.*

Exhaled breath and exhaled breath condensate (EBC) are two human biological fluids collected non-invasively to assess previous exposures to exogenous compounds and to evaluate metabolic (or health) effects. Although expression of volatile organic compounds (VOCs) in exhaled breath is considered a window into the circulating blood representing external exposures and human metabolism, it also represents contributions from the life cycles of the human microbiome. We have

developed methodology for distinguishing between human and bacterial contributions via collection of human generated aerosols in EBC, culturing them in growth media, and analyzing headspace with gas-chromatography – mass spectrometry. We have cataloged a series of VOCs from both aerobic and anaerobic conditions to inform human biomonitoring efforts for the assessment of in-vitro and in-vivo studies of the safety of manufactured chemicals.

## **W** 1650 Experimental Exposure of Mice to House Dust Alters Gut Microbiome and Attenuates Allergic Pulmonary Responses.

N. Lukacs. *Pathology, University of Michigan Medical School, Ann Arbor, MI.*

Sponsor: M. Williams.

Atopic asthma is more common in clean Western countries and its prevalence has increased greatly during the last century, along with improved hygiene and housing conditions. Exposure to a more diverse microbiome during childhood correlates with a lower risk of developing asthma during later life. Recent data has suggested that a diverse microbiome is associated with growing up with older siblings and pets. Dietary sampling from the environment can directly impact the gut microbiome. Interaction between intestinal microbiome and Gut Associated Lymphoid Tissue (GALT) not only directs local immune responses but also appears to affect the outcome of antigen-driven responses in the respiratory system. Using 2 different mouse models of allergic asthma (using the model-antigen ovalbumin –OVA – and the clinically relevant cockroach allergen – CRA), we set out to study pulmonary immune responses after dietary supplementation with household dust collected from homes with or without pets. Daily dosing of sieved dust administered to 6-8 week old BALBc mice via oral gavage for 2 weeks was used for controlled exposure. Following the dust treatment, mice were sensitized and challenged with CRA, or alternatively received a transfer of OVA-specific DO11.10 T-cells and a subsequent OVA challenge. In the dust exposed animals a significant decrease in Th2 cytokine protein expression and total IgE levels was observed in pet dust-treated animals exposed to allergen. Moreover, these mice showed reduced mucus hypersecretion in the lung, as determined by PAS staining and RT-PCR for gob5. Interestingly, phylochip analysis of the cecal content of these mice revealed that the pet dust treatment altered the microbiome in favor of *Lactobacillus* species. Altogether these data demonstrate that short-term oral sampling of dust from homes with pets, but not without pets, significantly alters the gut microbiome and can subsequently attenuate pulmonary allergen-induced immune responses.

## **W** 1651 Translating the Airway Transcriptome into Biomarkers of Tobacco-Related Lung Disease.

A. Spira. *The Pulmonary Center, Boston University School of Medicine, Boston, MA.*

Sponsor: M. Williams.

While cigarette smoke exposure is associated with lung cancer, COPD and a number of chronic inflammatory diseases of the lungs, only a fraction of smokers develop these diseases and there are currently no effective tools for identifying those smokers at highest risk for disease. Furthermore, we lack biomarkers for measuring the host response to inhaled toxins like cigarette smoke. This talk will focus on applying whole-genome gene-expression studies to airway epithelial cells in order to gain insights into the physiological responses to tobacco smoke exposure. The goal of the presentation will be to explore how individual variability in the airway genomic response to tobacco smoke associates with risk of tobacco-related lung diseases and how this information can be leveraged to serve as clinically-relevant biomarkers of disease activity in both lung cancer and COPD. This talk will be of broad interest to the biomedical research community including those with expertise in genomics, molecular biology, and epidemiology related to tobacco exposure and pulmonary disease.

## **W** 1652 Immune-Mediated Adverse Effects of Drugs and Environmental Agents.

J. Uetrecht. *Pharmacy, University of Toronto, Toronto, ON, Canada.*

Many adverse effects of drugs and environmental agents are immune-mediated. Exposure to drugs is easier to determine than most environmental agents, and most drugs can cause idiosyncratic (i.e. specific to an individual) adverse reactions (IDRs) such as skin rash, liver injury, bone marrow injury, and autoimmunity, most of which are immune-mediated. This provides a clear example of how different people can be affected by agents in different ways. Most drugs associated with a significant risk of IDRs form chemically reactive metabolites, which suggests that a major factor is the ability of the drug to form a hapten. However, this observation

is also consistent with the danger hypothesis because reactive metabolites can also cause cell injury leading to the release of danger signals that promote an immune response. There are also environmental agents that form reactive intermediates and lead to an immune response, e.g. poison ivy and hair dyes can cause contact hypersensitivity. However, not all drugs that cause IDRs form reactive metabolites so there must be other possible mechanisms. Other apparent mechanisms involve epigenetic changes, reactivation of viruses and direct binding to MHC. One example of an environmental agent that binds to MHC leading to an immune response is beryllium, which binds to HLA-DPB1 that has a glutamic acid at AA 69, and very low exposures to beryllium can lead to severe chronic lung disease in patients with this genotype. Other agents such as vinyl chloride can lead to autoimmunity. Although IDRs are frequently referred to as dose independent, this is not true; drugs given at a dose of 10 mg/day are associated with a very low risk of IDRs. This may reflect a threshold in hapten density required to induce an immune response. This suggests that most environmental agents are unlikely to cause immune-mediated adverse reactions; however, beryllium is an exception, and this threshold may be significantly lower for agents that act more directly to modulate immune responses. Environmental agents such as benzene can also lead to immunosuppression. Funded by grants from CIHR.

## **W** 1653 Targeted 'Omics Research in the Regulatory Environment.

J. Sobus. *Exposure Measurements and Analysis Branch, US EPA, Research Triangle Park, NC.*

The US EPA's Office of Research and Development (ORD) has recently implemented the "Chemical Safety for Sustainability" (CSS) research program. Much of this program is dedicated to "facilitating faster, more efficient, more certain, and sustainable chemical assessments and management decisions". Achieving these goals will require high-throughput and multi-chemical assessments of environments, living intact organisms, and surrogate (in vitro) systems. Single chemical assessment strategies alone cannot support these requirements, and will be supplemented using 'omic-based approaches to exposure- and health-based assessments. This presentation will highlight opportunities to integrate cutting-edge 'omics approaches into existing regulatory-based research frameworks. Special attention will be given to biomarker-based 'omics tools that can be used to link across environmental, biological (in vivo), and in vitro sample environments.

## **W** 1654 Standard and Nonstandard Animal Models for Evaluation of Drug Abuse Potential for Pharmaceutical Compounds with Novel Mechanisms.

C. G. Markgraf<sup>2</sup> and M. Guha<sup>1</sup>. <sup>1</sup>*Drug Safety Evaluation, Bristol-Meyers Squibb Co., Mt Vernon, IN;* <sup>2</sup>*DSS, Merck, Kenilworth, NJ.*

Preclinical assessment of abuse liability potential for new drugs with central nervous system (CNS) activity has been a recent focus of both regulatory and industry interest. The standard animal models used for evaluation of abuse potential for these pharmaceutical candidates are self-administration and drug discrimination. These models have been well characterized in both rats and monkeys with known drugs of abuse. However, unique challenges encountered when evaluating drugs with novel mechanisms or with difficult pharmaceutical properties raise questions: How can reinforcing properties be evaluated if there is no acceptable IV formulation? What comparator drug is appropriate for a candidate compound with a novel CNS-active mechanism? In these situations, using a nonstandard model may offer an attractive alternative. The promise of such alternative animal models is balanced by the challenge in data interpretation and in incorporation of the data into a comprehensive risk assessment. This workshop will start with a discussion of the regulatory requirements and standard data collected for a preclinical abuse potential assessment, followed by presentations on conditioned place preference (CPP) and intracranial self stimulation (ICSS)—both nonstandard animal models of drug abuse potential in a regulatory setting. The scientific rationale for their use, how each compares to standard animal models, and the use of their data in risk assessment and in an abuse potential package for submission to health authorities will be discussed.

## **W** 1655 Current Challenges in Abuse Liability Assessment of Drugs with Novel Mechanisms of Action.

K. H. Horn. *Drug Safety Evaluation, Bristol-Meyers Squibb, Mt Vernon, IN.*

Preclinical data from abuse liability assessments are required to support the registration and scheduling of new drugs with central nervous system activity. Despite the availability of a standard set of well characterized animal models (self administration and drug discrimination), there may be circumstances for compounds with

novel mechanisms of action where the standard models are not suitable or cannot be utilized for the lack of suitable comparators for training or due formulation issues. In these cases, investigators may wish to turn to alternative approaches to understand the abuse liability potential for drugs under development. The purpose of this presentation is to highlight the complexity and challenges associated with designing an abuse liability package for drugs with novel or unknown mechanisms of action where the use of standard assays may not be appropriate or when pharmaceutical properties prevent the use of standard assays. The first part of the presentation will focus on the standard pre-clinical models of abuse liability (self-administration, drug discrimination, and withdrawal/dependence). Following this introduction, the presentation will discuss specific circumstances, situations, and/or challenges that investigators may encounter during drug development which may require consideration of unconventional approaches.

#### **W 1656 The Assessment of Abuse Liability: The Regulatory Perspective.**

S. N. Calderon-Gutkind. *CDER, FDA, Silver Springs, MD.* Sponsor: M. Guha.

The assessment of the abuse liability of a drug is part of the evaluation performed by FDA, according to the requirements of the Federal Food, Drug and Cosmetic Act.

Issues concerned with the assessment of potential for abuse and with scheduling a drug under the U.S. Controlled Substances Act (CSA) are the responsibilities of the Office of the Center Director, Controlled Substance Staff.

When a new drug has structural or pharmacological similarity to a known drug of abuse, sponsors are required to thoroughly characterize its abuse potential and submit study results for scientific review. A drug's abuse potential is determined relative to a pharmacologically similar or other appropriate comparator drug. The abuse liability assessment is based upon comprehensive evaluation of chemistry, pharmacology (preclinical and clinical), pharmacokinetics, and pharmacodynamic profiles of the drug, and adverse events observed in clinical trials, as well as anticipated public health risks that may follow introduction of the drug on the market.

This presentation will focus on the current guidance for industry on the assessment of the abuse potential of drugs, and on the particular challenges encountered when assessing the abuse potential of drugs with novel mechanisms of action or pharmacological profiles.

#### **W 1657 Conditioned Place Preference As a Tool for Assessing Abuse Liability.**

C. L. Cunningham. *Behavioral Neuroscience, Oregon Health & Science University, Portland, OR.* Sponsor: C. Markgraf.

The conditioned place preference (CPP) procedure is commonly used to assess the rewarding and aversive effects of drugs in laboratory animals. This procedure is also used to study the role of learning in the control of drug seeking and relapse as well as the brain mechanisms underlying drug-induced learning and reward. However, the CPP procedure has not been used systematically in the assessment of abuse potential. This presentation will focus on important issues that should be considered when using the CPP procedure for such assessments. The basic procedure and its parametric determinants will be briefly described, followed by a review of its advantages and limitations as a tool for assessing abuse potential. This review will focus on relevant theoretical, methodological, empirical and practical issues that arise when comparing the CPP procedure to the most commonly used tool for assessing abuse potential, i.e., drug self-administration. For example, consideration will be given to the use of these procedures for assessing "reinforcement" vs. "reward" and to the conceptual issue of whether these procedures simply offer different strategies for measuring a common biological process. Literature showing similarities and differences in drug effects between these procedures will be briefly reviewed along with examples showing a positive effect of a known abused drug in one procedure but not in the other. Although a more systematic evaluation of its utility for predicting drug abuse liability in humans is needed, CPP might have significant value as an additional tool for assessing abuse potential in laboratory animals.

#### **W 1658 Use of Intracranial Self-Stimulation for Abuse Liability Assessment.**

T. J. Hudzik. <sup>1</sup>*Neuroscience Research, Abbott, Ludwigshafen, Germany;* <sup>2</sup>*Institute of Pharmacology, Pavlov Medical University, St. Petersburg, Russian Federation.* Sponsor: C. Markgraf.

All drugs entering the CNS may initially be viewed as having a potential risk for abuse. As there is no single test or assessment procedure likely to offer an ultimate characterization of abuse liability, preclinical abuse liability assessment is based on

using several experimental approaches that focus on establishing pharmacological equivalency to known drugs of abuse, ability to induce physical dependence, and reinforcing effects. This report discusses intracranial self-stimulation (ICSS; brain stimulation reward) as a tool that could complement existing assessment strategies. Many drugs of abuse facilitate ICSS in laboratory animals prepared with electrodes implanted into brain "reward" areas. In addition to fairly robust predictive validity, ICSS has a number of important advantages in studying: i) drug-drug interactions; ii) quantitative comparisons among drugs; iii) complex drug formulations, especially those intended to be abuse-resistant; and iv) multiple, repeated drug exposures. This report limits a review of the ICSS literature to that pertinent to its usefulness as a procedure predictive of the abuse liability of drugs, and argues for the standardization of experimental protocols to enable a more final assessment of its usefulness in this regard.

#### **W 1659 Impact of Nonstandard Animal Models on Preclinical Study Design for Meeting Regulatory Requirements.**

M. Kallman. *Discovery and Translational Services, Covance, Greenfield, IN.*

Although most pharmaceutical companies have transitioned to provide non-clinical data to address regulatory requirements for scheduling decisions on new drugs these studies have typically been the traditional dependence, drug discrimination, and self-administration studies. Alternative models of conditioned place preference and intracranial self-administration have been available as scientific tools for sometime but they have only rarely been conducted to support the regulatory environment. The reasons for the emphasis on the traditional models will be considered. In addition, a discussion of the advantages and potential applications of the non-standard models for scheduling decision making may provide insight into the utility of these models. The emphasis of the talk will be what the future environment might be and how we can develop scientific data packages using these non-standard models to meet the future decisions for scheduling.

#### **W 1660 The Placenta in Toxicology: Target or Travel Agent?**

C. J. Bowman<sup>1</sup> and W. Foster<sup>2</sup>. <sup>1</sup>*Developmental & Reproductive Toxicology, Pfizer Inc., Groton, CT;* <sup>2</sup>*Department of Obstetrics & Gynecology, McMaster University, Hamilton, ON, Canada.*

The placenta is a fascinating organ in its dynamic form and function appearing as a transient and critical tissue in the reproductive cycle. It is a collaboration of maternal and zygotic cellular layers whose major function is a conduit between mother and fetus focused on the growth and viability of the next generation whilst preserving maternal well-being. The unique physiology of biodistribution and metabolism of the placenta also render it sensitive as a target of toxicity. The human placenta is a complicated organ and understanding the comparative physiology of nonclinical species can be a critical component for drug and chemical safety assessment; both as a potential target of toxicity and as a presumed barrier to undesirable xenobiotics. As in much of toxicology, it is important to appreciate different perspectives including clinical, epidemiological, basic research, industry, and regulatory. It is only when this information is integrated and applied that we can appreciate the value and importance of basic research and the views of regulatory and industrial sciences.

#### **W 1661 How Predictive Are Animal Studies in Detecting Fetal Risks in Humans?**

G. Koren<sup>1,2</sup>. <sup>1</sup>*The Hospital for Sick Children, The University of Toronto, Toronto, ON, Canada;* <sup>2</sup>*Molecular Toxicology, The University of Western Ontario, Toronto, ON, Canada.* Sponsor: C. Bowman.

Every year scores of new molecules enter the market. Because half of all pregnancies are unplanned, fetal exposure to these drugs is inevitable. Unfortunately, due to wide variability and differences between and human placenta in anatomy and physiology, making animal models of placental transfer difficult to interpret. There is an urgent need for non human models to predict human risk/safety. The placenta is the only human organ that can be ethically harvested and kept alive *ex vivo* for 4-6 hr. By cannulating maternal and fetal vessels, the perfusion model can be used to study rates and extent of drug transfer across the human placenta, as well as placental functions such as oxygen consumption, hCG secretion etc. Using placental perfusion, we have established a model of predicting *in vivo* drug transfer, correlating it with results of *in vivo* fetal and neonatal sampling (Hutson et al, Clin Pharmacol Ther, 2011). Implementation of this model can revolutionize the prediction of fetal exposure to drugs *in vivo*.

## **W** 1662 Environmental Factors in Placental Toxicology and Women's Health.

M. M. Veras<sup>1,2</sup> and P. Saldiva<sup>1,2</sup>. <sup>1</sup>*Pathology, University of São Paulo, São Paulo, Brazil;* <sup>2</sup>*National Institute of Integrated Analysis of Environmental Risk, São Paulo, Brazil.* Sponsor: C. Bowman.

Environmental pollution is shown to affect reproductive functions in humans. In some situations exposures are unavoidable, such as traffic-derived air pollution in urban areas. The relationship between gestational exposure to air pollution and fetal outcomes is receiving progressively greater attention. Epidemiological findings correlate low birth weight, higher frequency of preterm birth, neonatal mortality and compromised specific reproductive endpoints such as infertility with air pollution. The limitations of epidemiological studies are associated with difficulties of identifying individual exposure levels as well as the presence and management of many cofounder factors such as nutritional and social status and smoking that challenges the establishment of causal relationships. To overcome these factors our group conducted experimental studies (murine model) using realistic concentrations of air pollutants, which "mimic" human exposures. Experimentation using real-world exposures to air pollutants provided corroboration of epidemiologic data and was used to identify the pathophysiological mechanisms involved. Changes in estrous cyclicity, fertility, number of ovarian follicles, embryonic implantation index, fetal development and placentation were some of the outcomes observed. In summary this session will provide an overview of the effects of environmental air pollution on reproductive functions; in particular, adverse effects on pregnancy outcome and placentation.

## **W** 1663 The Placenta As Therapeutic Border Patrol for Unintended Populations.

C. J. Bowman. *Developmental & Reproductive Toxicology, Pfizer Inc., Groton, CT.*

For most bio/pharmaceuticals the placenta and developing conceptus is not the target of therapy so effects on these tissues would generally be undesirable and should be addressed in the safety assessment and benefit-risk considerations of the intended therapy. In addition to direct placental toxicity and/or altered placental function, placental transfer of bio/pharmaceuticals may permit direct effects on the developing embryo, including teratogenicity. The most important placental transfer mechanism of small molecule pharmaceuticals is simple passive diffusion, but there are other mechanisms such as facilitated and active transport, phagocytosis/pinocytosis, membrane discontinuity and electrochemical gradient. The emerging class of large molecule therapies have brought new attention to the currently held dogma that all drugs cross the placenta to some extent (some more than others). These large molecule biopharmaceuticals are generally too big to passively cross plasma membranes and thus may offer a safety advantage (lower risk of teratogenicity) due to limited exposure to the unintended embryo. Antibody-like biopharmaceuticals have a unique placental transfer mechanism that is normally reserved for transport of maternal antibodies to protect the conceptus before and after birth. There is limited data regarding this mechanism of transfer and its timing as it pertains to antibody-like biopharmaceuticals and how it may impact the interpretation of nonclinical developmental toxicity data for human risk assessment to minimize the potential for birth defects. Recent data in the rodent indicates that antibody-like biopharmaceuticals cross the placenta during organogenesis in this species. This potential for embryo exposure during rat organogenesis, even at low levels, merit additional attention to placental transfer in nonclinical species and their concordance to human and how best to use nonclinical data to inform human developmental toxicity risk assessment.

## **W** 1664 The Placenta As a Target Organ in Toxicology—A Case Study.

B. van Ravenzwaay. *Experimental Toxicology and Ecology, BASF SE, Ludwigshafen, Germany.*

Triazole fungicides are known to cause changes in the placenta and they are known to cause late post implantation losses in prenatal studies in rats. Studies were initiated to investigate if there is a connection between these effects and the general mode of action of triazole fungicides, aromatase inhibition, causing a reduction of circulating estradiol. In prenatal studies, estradiol was co-administered with the triazole fungicide during rat prenatal development to test whether estrogen could prevent triazole late fetal resorptions. Co-treatment with estradiol reduced post implantation loss to 9%, compared to 48% without estradiol. Placental changes (labyrinth and trophospongium degeneration) were also less severe with estradiol treatment, indicating that these changes are secondary to reductions in estradiol. Thus, placental pathology may be the cause of late fetal resorptions. Expert pathological evaluation indicated that placental pathology could not support late fetal development; a quantitative evaluation suggested that degeneration of at least 70% of

the labyrinth correlated well with late fetal resorption. As rat placenta is histologically and biochemically different from human placenta, while guinea-pig placentas are quite similar, we studied the effect of the triazole fungicide using guinea-pigs. In this model, prenatal triazole treatment did not result in an increase in the incidence of late fetal resorptions, despite a profound reduction in circulating estradiol levels. Similarly, no placental changes were noted. These differences can be explained by the fact that the rat placenta is unable to produce estradiol whereas the placenta is the main source of estradiol maintaining pregnancy following implantation in guinea-pigs and humans. Despite the triazole fungicide-induced decrease in total circulating estrogen production, the local concentration of estradiol in the guinea pig placenta is sufficiently high to support normal maintenance and development in the fetal compartment. Therefore, the guinea-pig is a better model to assess prenatal toxicity of compounds inhibiting aromatase activity.

## **W** 1665 Regulatory Perspectives on Embryo-Fetal Developmental Studies: The Placenta in Pharmacological Studies and Toxicological Assessments.

L. Leshin. *US FDA, Silver Spring, VA.* Sponsor: C. Bowman.

In the safety assessment of bio/pharmaceuticals, a gross examination of the placenta is included as part of the *in vivo* embryo-fetal developmental toxicity study. Data from this study contribute to the risk assessment of drugs for use by patients of childbearing potential and during pregnancy. A more thorough evaluation of the placenta has the potential to contribute mechanistic information that could substantially inform the interpretation of study outcomes. Our knowledge of placental transport, metabolism, and immunology has increased dramatically since the development of the currently used regulatory practices and requirements. Closer examination of the placenta using various *in vitro* and *in vivo* approaches could provide a more complete understanding of drug effects on embryo-fetal development. With the progress made in understanding placental biology this critical multifunctional tissue can take on a more prominent role for improved pregnancy risk assessment.

## **IS** 1666 K-12 Toxicology Outreach Activities: Regional Chapter Successes and Resources.

C. E. Sulentic<sup>1</sup> and R. Ponce<sup>2</sup>. <sup>1</sup>*Pharmacology & Toxicology, Wright State University, Dayton, OH;* <sup>2</sup>*Amgen Inc, Seattle, WA.*

K-12 activities are a vital component in our mission to educate the community regarding hazards and hazard communication. Several regional SOT chapters have very active K-12 community outreach programs and others are interested in establishing these programs within their communities. Facilitating this type of outreach across all regional chapters is a tactical goal of the Regional Chapter Collaboration and Communication Committee (RCCCC) and the Education Committee. This goal ties directly into the SOT strategic plan of promoting recognition of toxicology and communicating the benefit of toxicology to external audiences. The 2011 Education Summit sponsored by SOT underscored the need for enhancing the perception of toxicology as a valuable discipline among scientists and nonscientists alike, which is vital to maintaining the discipline of toxicology and the pipeline of future toxicologists. Community outreach at the K-12 level is an important component in increasing the visibility and perceived importance of toxicology. Regional SOT chapters can be and have been a vital resource in facilitating outreach activities among the membership-at-large. This session will highlight some of the successful K-12 outreach activities supported by regional chapters and will include hands-on demonstrations, one organized and implemented by graduate students, as well as an overview of efforts to update website resources for K-12 activities. This session will also provide pedagogical insights helpful to those new to educational outreach. Promoting and facilitating K-12 activities by regional chapters has the added potential of greater graduate student and postdoc engagement and therefore increased opportunities for skill development and pedagogical background for those trainees considering academic careers.

## **IS** 1667 Totally Toxic! A K-12 Outreach Program Based on the 5E Model of Science Education.

C. P. Curran. *Biological Sciences, Northern Kentucky University, Highland Heights, KY.*

The Ohio Valley SOT (OVSOT) chapter developed an outreach program called "Totally Toxic!" to introduce middle and high school students to the fundamentals of toxicology. The program uses the Biological Sciences Curriculum Study (BSCS) 5E Model to Engage, Explore, Explain, Elaborate and Evaluate student understanding. Working in teams, students identify common toxins and toxicants in

their homes, learn about historic and recent poisonings then solve a toxic mystery. The "Strange Case of Jennifer Strange" is based on the true story of the water intoxication death of a California mother. The activities will be demonstrated, and the pedagogical advantages of the 5E model for science education will be discussed.

### **IS** 1668 Inspector Tox Outreach Activity.

D. Hardej<sup>1</sup> and A. Schatz<sup>2</sup>. <sup>1</sup>Department of Pharmaceutical Sciences, St. John's University, Jamaica, NY; <sup>2</sup>Merck & Co., Whitehouse Station, NJ.

Inspector Tox was developed by the Mid-Atlantic SOT (MASOT) chapter as a means of introducing the basic concepts of toxicology to school aged children. This program includes Inspector Tox an investigator of harmful or toxic events and helps guide the audience through determining if several "toxic scenes" set in the house, backyard, and at the beach are relatively safe or dangerous. The various scenes are devised to introduce a mix of potentially toxic compounds including chemicals (pesticides), natural toxins (bee sting, poison ivy), UV radiation (sunlight), social/behavioral toxicants (alcohol, cigarette smoking, and poor diet), and even includes components that the audience might not initially recognize as toxic, such as food allergies (peanuts) and dust.

### **IS** 1669 Silly Science and Other Activities for K-12 Outreach.

M. M. Bourgeois. EOH, University of South Florida, CPH, Tampa, FL.

Activities to explore dose, toxicity and therapeutic windows of drugs will be demonstrated and include describing dosages using familiar measurements (i.e. tablets, teaspoons, medicine cups, glasses, buckets and kiddie pools) that are toxic by showing children the different amounts of specific household substances (water, salt, sugar, baby aspirin, etc.) necessary to do them harm.

### **IS** 1670 Exploring Toxicology: Designing Learning Goals and Evaluation Strategies for Outreach Activities.

E. Shanle and K. L. Blanke. Molecular and Environmental Toxicology Center, University of Wisconsin Madison, Madison, WI.

Molecular & Environmental Toxicology Center (METC) graduate students at the University of Wisconsin-Madison participate in toxicology outreach events to promote a better understanding of toxicology to the local community. METC currently has 37 graduate students, and 15 students (41%) have participated in at least one educational outreach activity over the past year. Two activities graduate students use to teach about toxicology are Carnation Intoxication and Tox Land. Carnation Intoxication uses colored dye added to the water of white carnations to show that plants can take up toxins from their environment along with water and nutrients. Learning goals for this activity are age dependent and include a basic understanding of toxicology and the concepts of bioaccumulation and experimental design. Tox Land is a game that takes participants on a path through global events related to toxicology while also highlighting local daily activities that have positive or negative effects on people, animals, and the environment. The learning goals for Tox Land are that participants are informed about global/local toxicologically relevant events. Both Carnation Intoxication and Tox Land are evaluated using survey questions that reflect the learning goals to assess what participants learn. Evaluations are used to improve activities in order to better inform the public about toxicology.

### **IS** 1671 Resources for Toxicology K-12 Education Outreach: Updating the SOT K-12 Website.

M. R. Gwinn. Office of Research & Development, US EPA, Washington DC.

The Society of Toxicology's Education K-12 Sub-Committee is updating the SOT website to increase support for K-12 education activities, share resources across the membership and with the public, and increase effectiveness in interacting with educators, parents and students. One main goal is to work with the Society membership to create the most useful resource website to help support excitement for toxicology through K-12 education outreach. Ideally, this website would be accessible to the public, easily searchable and contain hands-on activities, PowerPoint presentations and recommendations for increasing K-12 education outreach. Many SOT members are active in toxicology outreach, and many more would like to be but

don't know where to start. Working with Society members, the K-12 Sub-Committee will include links to successful activities, including past Annual Meeting activities and ongoing Regional Chapter outreach activities. This resource website will serve as a tool for those interested in getting involved in K-12 education outreach, as well as for those interested in learning more about what toxicologists do.

### **IS** 1672 The Regulatory Framework for Cosmetics: Current Status, Recent Science, and Future Prospects.

P. Wexler. Toxicology and Environmental Health Information Program, National Library of Medicine, Bethesda, MD.

Cosmetic products represent an immense global industry. It has been estimated that the \$60 billion cosmetics industry uses some 12,500 unique chemical ingredients in personal care products. These products and their chemical components are subject to varying degrees of regulation globally. In the US, the US FDA's regulatory authority over cosmetics is relatively minimal and different from that of other products regulated by the Agency, such as drugs, biologics, and medical devices. Although the US FDA can inspect cosmetic manufacturing facilities, respond to complaints of adverse reactions, and conduct research on cosmetics and their ingredients to address safety concerns, the Food, Drug, and Cosmetic Act does not subject cosmetics to US FDA premarket approval. The regulation of cosmetics in the European Union is considerably more stringent. A Safe Cosmetics Act of 2011 was introduced in the US House of Representatives in June, 2011, with the aim of ensuring that all personal care products are safe. It would establish labeling requirements and a safety standard, and issue guidance prescribing good manufacturing practices for cosmetics and ingredients. People, largely though not exclusively women, are exposed to vast quantities of cosmetics over their lifetimes. Compared with the safety of most other products, cosmetics are commonly believed to present a minimal, if any, risk, and are overlooked in discussions of hazardous substances. Are the regulations currently in place adequate? What is the US government's viewpoint? What is the stance of industry and advocacy groups on the cosmetics regulatory framework? How does the European Union handle issues involving the safety of cosmetics? Recent scientific issues surrounding production, safety, and testing of cosmetics could well influence the regulatory arena in years to come. These include 1) the increasing use of nanomaterials in cosmetic products and 2) computational and high-throughput alternative test methodologies. Both these topics will offer a backdrop to current and future regulatory approaches.

### **IS** 1673 Safety Evaluation of Nanoparticles and Skin.

N. A. Monteiro-Riviere. Anatomy and Physiology, Kansas State University, Manhattan, KS.

This presentation will review the physicochemical properties such as size, shape, coatings, vehicles and charge on skin penetration of nanoparticles (NP) that may enhance or prevent toxicity. There are properties of a chemical/ NP that determines its propensity to cause dermatotoxicity, which is the ability to penetrate skin and subsequently interact with biological components that could elicit a toxicological response. Recent advances of NP in consumer products such as cosmetics indicate safety concerns. Penetration of NP in skin is a controversial subject, partly because many factors that influence absorption were not studied and opinions of some investigators were generalized and based on limited studies of a few NP, many on large particles and not nanosize. Discrepancies may relate to differences in NP composition, surface chemistry, vehicles or solvents, techniques and methods of exposure, and analytical analysis, and duration of the experiment. This review will show how formulation, surface chemical alterations and mechanical stressing of skin and species can modulate the results.

### **IS** 1674 US EPA Computational Toxicology Predicting Cancer and Noncancer Outcomes for Cosmetics and Industrial Chemicals.

N. Kleinstreuer. National Center for Computational Toxicology, US EPA, Research Triangle Park, NC.

EPA's Computational Toxicology Research Program (CompTox), part of the broader Chemical Safety for Sustainability Research Program, is at the forefront of a major transformation in the field of toxicology in how chemicals are evaluated for potential effects on human health and the environment. EPA is partnering with the cosmetics company L'Oréal, pharmaceutical companies, European regulatory authorities, and other U.S. government agencies to research ways CompTox can decrease the cost of testing large numbers of chemicals, reduce animal use, identify

targeted testing strategies, and understand potential mechanisms of toxicity. Broad compound libraries may be screened and prioritized using rapid, automated high-throughput screening (HTS) assays with human gene and protein targets. Multiple HTS assay targets, e.g. chemokine expression in human primary skin cells, are highly relevant to cosmetics safety assessments. CompTox has already screened more than 1,000 chemicals in over 650 HTS assays in the ToxCast ("toxicity forecaster") research program, including many key ingredients in personal care products, fragrances, and cosmetics. The L'Oréal partnership provides collaborative research funding and access to existing cosmetics ingredients safety data, which are compared to the ToxCast results to determine the utility of CompTox tools in the safety assessment of chemicals in cosmetics. CompTox research has also developed predictive models for cancer and non-cancer toxicity endpoints, with a focus on the molecular and cellular pathways that are the targets of chemical interactions. Using computational approaches, EPA is building decision support tools based on ToxCast in vitro HTS results to help prioritize cosmetics chemicals for further investigation, as well as applying and refining predictive models for a number of adverse health outcomes. This abstract does not necessarily represent EPA policy.

## **IS 1675 Cosmetics—US FDA Regulatory Perspectives.**

P. A. Hansen. *Office of Cosmetics and Colors, US FDA, College Park, MD.* Sponsor: P. Wexler.

The two most important laws pertaining to cosmetics marketed in the United States are the Federal Food, Drug, and Cosmetic Act (FD&C Act) and the Fair Packaging and Labeling Act (FPLA). The presentation will cover the specific legal authorities granted to FDA under these two laws and the regulatory tools FDA uses to implement them. These regulatory tools include regulations, guidance, inspections, import monitoring, and other programs. The presentation will also cover other activities important to the oversight of cosmetic safety, such as FDA's Voluntary Cosmetic Registration Program, the agency's adverse event monitoring systems, outreach to consumers and health professionals, and more. The role of FDA's research and other scientific efforts will be discussed. Examples of recent activities in areas important to cosmetic safety will be highlighted. Additional authorities that have been suggested for strengthening FDA's monitoring of cosmetic safety and labeling will also be presented.

## **IS 1676 Assessing the Safety of Cosmetics in the US.**

H. Breslawec. *Personal Care Products Council, Washington DC.* Sponsor: P. Wexler.

Cosmetics in the United States have been regulated under the same legal framework for almost 75 years. The Cosmetic Safety Amendments Act of 2012 proposes to modernize the existing regulatory framework, and the proposed provisions in that legislation will be discussed. The responsibility for the pre-market assessment of the safety of cosmetics prior in the US, as in the EU, rests with the manufacturers. This presentation compares the US regulatory system with that in the EU and discusses how the industry assesses the safety of cosmetic ingredients and products. The Cosmetic Ingredient Review (CIR) Expert Panel, an independent group of dermatologists, toxicologists and other scientists who have, for over 35 years, assessed the safety of cosmetic ingredients in an open and public manner. The CIR is funded by the industry, but operates independently in a transparent manner. Current issues of interest in safety evaluation of cosmetic ingredients and products, will be discussed.

## **IS 1677 Safety Evaluation of Cosmetics and Their Ingredients in Europe: New Challenges Ahead.**

V. Rogiers. *Toxicology, Dermato-Cosmetology and Pharmacognosy, Vrije Universiteit Brussel, Brussels, Belgium.* Sponsor: P. Wexler.

Cosmetic products present on the European market must be safe for the consumer. In Europe, product safety is based on the safety of the ingredients (chemical structure, toxicological profile, exposure) and is the responsibility of the manufacturer, first importer or marketer. In July 2013, the EC Regulation n°1223/2009 will replace in all Member States the well-known Cosmetic Directive 76/768/EEC with its important sixth and seventh amendments. Under this RECAST, a so-called responsible person gets a key function in the follow-up of the safety of the products under consideration. This is not an easy task as the safety of cosmetics and their ingredients has to be guaranteed by the use of in vitro methods, replacing experimental animal testing. In the EU, during the last years the 3R principle (Refinement, Reduction, Replacement) of Russell and Burch has been implemented in the specific legislation of several types of products, including chemicals, pesticides, pharmaceuticals, food additives, ... but the cosmetics legislation is the only one in the world allowing only replacement methods, which additionally need to be validated.

Therefore, complete banning of animal testing of cosmetics and their ingredients has a tremendous impact with far reaching consequences. This presentation will cover the safety assessment process of cosmetics and their ingredients and the changes that have been introduced by shifting from legislation to a regulation (including special considerations for CMRs, nanomaterials...). Also, the actual status of validated in vitro methods will be given and the prospective for the near future will be discussed.

## **IS 1678 Cosmetics: Health Risks, Choices, and Opportunities for Change.**

S. Lunder. *Environmental Working Group, Washington DC.* Sponsor: P. Wexler.

The \$60 billion cosmetics industry relies on over 8,000 unique ingredients to produce tens of thousands of products sold in the U.S. Women use an average of 12 products daily, with an average of 167 ingredients, and men use about half that. Products go on skin, lips, hands and around eyes. Consumers ingest, inhale, and dermally absorb ingredients, in various amounts. Biomonitoring studies have established that cosmetic chemicals are common pollutants in blood and urine. Are these exposures safe? FDA regulates the cosmetic industry, but lacks the authority to require premarket testing, review products before they are sold, or recall products known to pose risks. Lacking a mandatory safety standard for cosmetics, the industry makes its own determinations about what is safe enough for consumers. But recent studies have detected lead, formaldehyde and other hazardous compounds in some everyday cosmetic products. And many other ingredients are poorly tested, or show no toxicity information at all in the public scientific literature. With the industry under growing scrutiny and pressure, change is in progress. Consumer awareness is on the rise, some companies are removing ingredients of greatest concern, and Congress has introduced legislation to modernize cosmetics safety regulations.

## **PL 1679 The DNT-EST: A Predictive Embryonic Stem Cell Test for Developmental Neurotoxicity Testing In Vitro.**

A. E. Seiler, K. Gulich, K. Hayess, R. Pirow, B. Slawik, M. Steinfath, C. Riebeling, A. Visan and A. Luch. *ZEBET, Federal Institute for Risk Assessment, Berlin, Germany.* Sponsor: E. Fritsche.

Disturbances and diseases of the brain and nervous system such as attention-deficit hyperactivity disorder, dyslexia, sensory deficits, mental retardation, autism-like disorders, learning disabilities, and cerebral palsy has also put the vulnerability of the developing human brain to environmental chemicals exposure into the focus of public awareness. Most of the chemicals on the market have not been evaluated for their toxic potency, an issue now being addressed by the registration, evaluation and authorization of chemicals (REACH) legislation of the European Union. In order to answer the increasing need for toxicity testing, the development of reliable methods ensuring a higher throughput than the currently available test guidelines became a main issue of risk assessment. One of the key aspects in this context is the application of alternative, non-animal approaches including in vitro test methods. Recently, we developed a new in vitro assay using mouse embryonic stem cells (mESC) to predict adverse effects of chemicals and other compounds on neural development - the so-called DNT-EST. After treatment of differentiating stem cells for 48 h or 72 h at two key developmental stages, endpoints for neural differentiation, viability and proliferation were assessed. As a reference we treated undifferentiated stem cells 2 days after plating for 48 h or 72 h in parallel to the differentiating stem cells, also measuring viability and proliferation. Here, we show that chemical testing of a training set comprising nine substances (six substances of known developmental toxicity and three without specific developmental neurotoxicity) enabled a mathematical prediction model to be formulated that can discriminate positive from negative DNT compounds with an in vivo - in vitro concordance of 100%. Thus, the mESC model introduced here might represent a useful tool for predicting adverse health effects of exogenous agents that affect brain development.

## **PL 1680 Identification of Pathways of Developmental Neurotoxicity for High-Throughput Testing by Metabolomics.**

H. T. Hogberg<sup>1</sup>, M. Bouhifd<sup>1</sup>, T. Dao<sup>1</sup>, A. Kleensang<sup>1</sup>, S. J. Nolan<sup>1</sup>, S. Odwin-DaCosta<sup>1</sup>, L. Smirnova<sup>1</sup>, E. van Vliet<sup>2</sup>, H. Welles<sup>1</sup>, L. Zhao<sup>1</sup> and H. Thomas<sup>1</sup>.  
<sup>1</sup>The Johns Hopkins University, Bloomberg School of Public Health, Baltimore, MD;  
<sup>2</sup>University of Barcelona, August Pi i Sunyer Biomedical Research Institute, Barcelona, Spain.

Tox-21c proposed a paradigm shift in the field of toxicology. Instead of relying on traditional animal experiments, the report proposes the application of the latest advances in science and technology to develop more relevant test strategies. An area of

toxicology where Tox-21c could have a significant impact is developmental neurotoxicity (DNT). There is concern that exposures to environmental chemicals contribute to the increasing incidence of neurodevelopmental disorders in children. However, due to lack of DNT studies only very few substances have been identified as developmental neurotoxicants.

This study aimed to develop an *in vitro* approach using metabolomics and gene expression for DNT assessment. A 3D rat primary neuronal organotypic model was exposed from day 7 up to 21 to suspected (developmental) neurotoxicants including pesticides (carbaryl, chlorpyrifos, lindane maneb), drugs (fluconazole, isotretinoin, phenytoin, terbutaline, valproic acid) and metals (CaCl<sub>2</sub>, PbCl<sub>2</sub>). Mass spectrometry based metabolomics measurements and quantitative measurement of genes expressed in different cell types (neural precursor cells, neurons and glial cells) were performed. Treatment with the different compounds significantly modified the expression of selected genes, related to the different stages of neuronal and/or glial cell development and maturation. Moreover, the mass spectrometry analysis showed differences in metabolite levels between control and treated cells. Further analysis of the altered metabolites could give mechanistic insight into the DNT of these compounds. This study demonstrates that gene expression and metabolomic analysis can be sensitive endpoints for DNT assessment. Funded by the Swedish Research Council and the FDA

#### **PL 1681 Reduced Nrf2 Signaling Contributes to Human Neuroprogenitor Cell (hNPC) Aging.**

E. Fritsche, J. Schuwald, S. Giersiefer and K. Gassmann. *IUF, Duesseldorf, Germany.*

During the normal brain aging process, neural progenitor cells (NPC) lose their capacities to proliferate and differentiate into neurons, which is associated with age-related impairment of cognitive functions. Molecular mechanisms causing NPC aging are unknown and also effects of chemicals, which might induce extrinsic brain aging are so far enigmatic. One common mechanism, however, well known to be involved in cellular aging processes, is oxidative stress. As a wide variety of toxicants cause cell damage through their ability to elicit oxidative stress, this study tests the hypothesis if changes in the oxidative stress response contributes to NPC aging. Therefore, young (1-2 months in culture (MIC)) and aged (3-9 MIC) human NPCs, which grow as neurospheres, were studied for their abilities to proliferate and differentiate into neurons. Moreover, their capabilities to activate the nuclear factor erythroid 2-related factor2 (Nrf2) pathway and thus respond towards oxidative stress were investigated. Finally, Nrf2 was knocked down via lentiviral transduction.

Our data indicate that aged neurospheres reproduce the aging phenotype observed in brains *in vivo*: NPC proliferation and the potential to differentiate into neurons is decreased. Moreover, 'old' NPC accumulate beta-galactosidase, which is an established aging marker. With regard to the antioxidant defense, young and old NPCs express mRNA for the transcription factor (Nrf2). However, Nrf2 protein is not induced in old NPCs challenged with H<sub>2</sub>O<sub>2</sub> or tetrachlorohydroquinone (TCHQ) like it is in young cells. As a consequence, the Nrf2 downstream targets superoxide dismutase (SOD), catalase (CAT) and glutathione peroxidase (GPx) are not up-regulated in aged NPCs either. Knocking down Nrf2 indicates that NPC proliferation and neuronal differentiation are dependent on sufficient Nrf2 signaling.

#### **PL 1682 Effect of Organophosphorus Flame Retardants on Neuronal Development *In Vitro*.**

W. Mundy<sup>1</sup>, T. Freudenrich<sup>1</sup>, K. Wallace<sup>1</sup> and M. Behl<sup>2</sup>. <sup>1</sup>ISTD, US EPA, Research Triangle Park, NC; <sup>2</sup>Kelly Government Solutions, NTP/NIEHS, Research Triangle Park, NC.

The increased use of organophosphorus compounds as alternatives to brominated flame retardants (BFRs) has led to widespread human exposure. There is, however, limited information on their potential health effects. This study compared the effects of nine organophosphorus flame retardants (OPFs) with the BFR tetrabromobisphenol A and the known developmental neurotoxicants Pb and t-retinoic acid on neuronal proliferation and neurite outgrowth *in vitro*. Proliferation was assessed in human stem cell-derived neuroprogenitor (hNP1) cells after a 24 hr exposure by counting the number of cells incorporating BrdU. Neurite outgrowth was assessed in human stem cell-derived (hN2) neurons and rat primary cortical neurons after 48 hr of exposure by measuring the length and branching of neurites labeled with  $\beta$ III-tubulin antibody. Cytotoxicity was estimated by total cell counts. Cells were cultured and exposed to chemicals (0.003 to 30  $\mu$ M) in 96-well plates and endpoints quantified using the Cellomics ArrayScan high content imager. In hNP1 cells, Pb, t-retinoic acid, tetrabromobisphenol A and a majority of the OPFs were cytotoxic at concentrations > 3  $\mu$ M; however, tricresyl phosphate and triphenyl phosphate both decreased proliferation at 30  $\mu$ M in the absence of cytotoxicity. In

hN2 cells OPFs, tetrabromobisphenol A and t-retinoic acid decreased neurite outgrowth only at cytotoxic concentrations, while Pb decreased neurite outgrowth in the absence of cytotoxicity. Rat neurons were less sensitive than hN2 cells in that no chemical was cytotoxic at the concentrations tested; however, tricresyl phosphate, t-butylphenyl diphenyl phosphate, isodecyl diphenyl phosphate, and isopropylated phenyl phosphate decreased neurite outgrowth at 30  $\mu$ M. These data suggest that some OPFs have the ability to affect neurodevelopmental processes *in vitro* at micromolar concentrations, and that human neurons may be more sensitive compared to rats. *This abstract does not necessarily reflect U.S. EPA policy.*

#### **PL 1683 PCB 95-Induced Dendritic Growth in Primary Cultures of Rat Hippocampal Neurons Is Dependent on mTOR Activation.**

G. W. Miller, H. Chen and P. J. Lein. *Molecular Biosciences, University of California Davis, Davis, CA.*

Despite being banned since the late 1970s, polychlorinated biphenyls (PCBs) remain persistent environmental toxicants that pose significant risk to the developing nervous system. We recently demonstrated that the non-dioxin-like PCB 95 alters neuronal connectivity by promoting dendritic arborization in cultured hippocampal neurons via ryanodine receptor (RyR)-mediated, transcriptionally driven mechanisms. PCB 95 sensitizes RyR and this interaction requires FKBP12. Interestingly, FKBP12 also regulates mammalian target of rapamycin (mTOR), and the mTOR signaling pathway enhances dendritic growth via increased protein synthesis. Based on these observations, we hypothesize that mTOR signaling contributes to the dendrite promoting activity of PCBs. To test this hypothesis, primary cell cultures dissociated from hippocampi of wildtype (Sprague Dawley) postnatal rats were plated at high density and exposed to PCB 95 (2,2',3,5'-pentachlorobiphenyl, 20 pM – 2 nM) in the absence or presence of rapamycin. Exposure to PCB 95 from days 7 to 9 *in vitro* increased dendritic growth in pyramidal hippocampal neurons in a concentration-dependent manner. Simultaneous exposure to rapamycin at 20 nM, a concentration that inhibits mTOR activation, ameliorated the dendrite promoting activity of PCB 95. Ongoing studies are confirming that PCB 95 activates the mTOR signaling pathway implicated in dendritic growth, and determining whether these effects are RyR-dependent. These findings identify a novel mechanism by which low level exposures to non-dioxin-like PCBs cause developmental neurotoxicity, and perhaps dysfunction of other cell types, such as immune cells, whose function is heavily dependent on mTOR signaling. Supported by NIH grants R01 ES014901 and P42 ES04699.

#### **PL 1684 Diazinon and Diazoxon Impair Glial-Neuronal Interactions and Production of Neuritogenic Proteins in Primary Astrocytes.**

D. M. Pizzurro<sup>1</sup>, G. Giordano<sup>1</sup> and L. G. Costa<sup>1,2</sup>. <sup>1</sup>Department of Environmental and Occupational Health Sciences, University of Washington Seattle, Seattle, WA; <sup>2</sup>Department of Neuroscience, University of Parma Medical School, Parma, Italy.

Many organophosphorus insecticides (OPs) are increasingly recognized as developmental neurotoxicants. However, the mechanisms by which they exert their neurotoxicity remain unclear. This project focuses on a widely-used OP, diazinon (DZ), and its active metabolite, diazoxon (DZO), and their potential to impair astrocytes' ability to foster neuronal development. We have previously shown that astrocytes play a major role in fostering neurite outgrowth in neurons; in this project, a 50% decrease in the longest neurite length was observed in primary hippocampal neurons incubated with primary astrocytes previously exposed to 10  $\mu$ M DZ or DZO. We have also shown that this effect is largely mediated by increased oxidative stress in astrocytes that results from exposure to DZ or DZO. To further elucidate how these compounds adversely affect astrocytes and disrupt normal glial-neuronal interactions, levels of the pro-neuritogenic extracellular matrix proteins fibronectin and laminin were evaluated by Western blot analysis and confocal microscopy. Fibronectin and laminin have been extensively shown to play a vital role in a variety of neurodevelopmental processes, including neurite outgrowth and differentiation. At the same concentrations that significantly inhibit neurite outgrowth, both DZ and DZO cause a 30-40 % decrease in fibronectin and laminin protein levels in astrocytes. These decreases are prevented by astrocyte pre-treatment with the antioxidants melatonin and N-t-butyl-alpha phenylnitron (PBN), further supporting the role of oxidative stress in the mechanism of neurotoxicity. These findings were confirmed by confocal microscopy analysis of extracellular fibronectin expression, which showed a 40% decrease after exposure to DZ or DZO. These results suggest that DZ and DZO impair neuronal development by adversely affecting astrocyte production and secretion of important neuritogenic factors.

**PL 1685 Increased Oxidative Stress and Mitochondrial Dysfunction in a PARK2-Mutant iPSC Model of Environmental Risk in Parkinson's Disease.**

A. Aboud<sup>1</sup>, A. M. Tidball<sup>1</sup>, K. K. Kumar<sup>1</sup>, B. Han<sup>1</sup>, G. G. Li<sup>1</sup>, K. M. Erikson<sup>2</sup>, P. Hedera<sup>1</sup>, M. Neely<sup>1</sup>, K. C. Ess<sup>1</sup> and A. B. Bowman<sup>1</sup>. <sup>1</sup>Neurology, Vanderbilt University, Nashville, TN; <sup>2</sup>University of North Carolina Greensboro, Greensboro, NC.

Interactions of environmental and genetic risk factors for Parkinson's disease (PD) are believed to modify disease onset and progression in a patient-specific manner. We sought to examine such interactions by assessing sensitivities of neural progenitor cells (NPCs) differentiated from human induced pluripotent stem cells (iPSCs) to PD-relevant environmental toxicants. These iPSCs were derived from a patient (SM) with biallelic PARK2 mutations and preclinical PD as assessed by DaTScan, and from healthy control subjects (CA and CB). Mn exposure resulted in significantly higher ROS generation in SM than CA NPCs, but no difference in cytotoxicity or mitochondrial fragmentation was observed. Moreover, we found that SM NPCs accumulate significantly less intracellular Mn than CA NPCs. These results indicate heightened susceptibility of SM NPCs to Mn given the higher rate of ROS generation and the comparable cytotoxicity and mitochondrial fragmentation in the presence of significantly less intracellular Mn. While the accumulation of Cu was not different between SM and CA NPCs, it induced significantly greater ROS generation, loss of mitochondrial function and cytotoxicity in SM than CA NPCs. These differences in Cu exposure-associated phenotypes were not observed in the primary fibroblasts used to generate the iPSC lines. Given the role of PARK2 in mitochondrial integrity, heightened sensitivity of SM NPCs to manganese and copper may be due to suboptimal mitochondrial function in cells that lack functional PARK2. Our results support the hypothesis that genetic alterations may increase sensitivity to specific toxicants. We demonstrate here that iPSC technology can detect patient-specific and cell type-specific differences in vulnerability to PD environmental risk factors. Support: NIH ES016931 and NS078289

**PS 1686 Evaluation of the Ames II and 96-Well *In Vitro* Flow Micronucleus (MN) Assay Using 25 ToxCast™ Chemicals.**

M. Aardema<sup>1</sup>, A. D. Kligerman<sup>2</sup>, K. Houck<sup>1</sup>, R. R. Young<sup>3</sup>, L. F. Stankowski<sup>3</sup>, K. Pant<sup>3</sup> and T. E. Lawlor<sup>3</sup>. <sup>1</sup>Marilyn Aardema Consulting; Chief Scientific Advisor Toxicology BioReliance by SAFC, Fairfield, OH; <sup>2</sup>US EPA Office of Research and Development, Research Triangle Park, NC; <sup>3</sup>BioReliance by SAFC, Rockville, MD.

ToxCast™ is a multi-year effort to develop a cost-effective approach for the US Environmental Protection Agency to prioritize thousands of chemicals that need toxicity testing. Initial evaluation of more than 650 high-throughput, robotic, microwell-based endpoints with little or no metabolic activation showed that most of these assays lacked specificity and sensitivity for detecting direct-acting genotoxins. In an attempt to understand how to improve this approach for genotoxicity testing, we evaluated the specificity and sensitivity of 25 selected Phase I and Phase II chemicals from the ToxCast™ program using standard genotoxicity endpoints. These chemicals were chosen because of their known genotoxicity, their responses in specific ToxCast™ assays, or available data from the literature and databases. The tests used were the medium throughput Ames II and in vitro flow MN assays conducted ±S9. Results to date indicate that, as expected, the Ames II assay showed an excellent correlation with published data and industry submissions. Overall concordance was 89 and 82% (with and without S9, respectively). The MN assay also had good concordance of 78 and 73% (with and without S9, respectively); however, the number of conclusive calls was significantly smaller mainly due to concentrations limits and cytotoxicity. Chemicals were also tested in a 96-well in vitro single cell gel electrophoresis (Comet) assay though there were insufficient data from the literature to evaluate performance of this assay. Taken together, these studies offer a promising approach to higher throughput genotoxicity testing. [This is an abstract of a proposed presentation and does not necessarily reflect US EPA policy.]

**PS 1687 The Role of DNA Polymerase Eta in Oxidative Stress Response and Mutagenesis.**

K. N. Herman and S. D. McCulloch. Toxicology, North Carolina State University, Raleigh, NC.

Oxidative stress is induced by exposure to chemicals and radiation such as heavy metals, pesticides and ultraviolet exposure from sunlight. Oxidative stress leads to elevated levels of reactive oxygen species (ROS), which in turn can produce DNA lesions including 8-oxoguanine (8-oxoG). 8-oxoG has been linked to mutagenesis, cancer and aging. One way cells respond to this damage is translesion synthesis

(TLS), most often by Y family DNA polymerases. Y-family polymerases have open active sites, allowing them to copy past DNA adducts that otherwise block replication. DNA polymerase eta (pol η) is known to bypass cyclobutane pyrimidine dimers (CPD); more recently, pol η has been shown to bypass 8-oxoG. Intriguingly, while in vitro bypass of 8-oxoG by pol η appears to occur with nearly 50% error rate, in vivo experiments suggest it acts to suppress mutagenesis, similar to CPD. This apparent discrepancy has not been fully explained.

Due to the ability of pol η to bypass 8-oxoG very efficiently but with poor fidelity in vitro, we investigated pol η response in cells to oxidative-stress-induced DNA damage. We have demonstrated that pol η acts as a suppressor of oxidative stress-induced mutagenesis, likely due to bypass of 8-oxoG. We examined both pol η-expressing and -deficient cells and evaluated cell responses to various ROS-inducing treatments. We evaluated the cytotoxicity of these treatments and found that while pol η did not greatly alter cell survival, the mutation rate of surviving cells was markedly decreased when measured using hypoxanthine phosphoribosyl transferase (HPRT) mutation assay; showing the presence of pol η suppresses mutations compared to deficient cells. The measured mutation rates varied depending on the treatment used, possibly due to variation in the types and levels of different lesions generated by each. In total, the results demonstrate that pol η acts to suppress oxidative stress-induced mutations, suggesting that polymerase fidelity in vitro data is only part of the larger picture of lesion bypass.

**PS 1688 Different Micronucleus Induction of Mice Exposed to N-Ethyl-N-Nitrosourea at Light and Dark Dosing Times.**

K. Ito<sup>1,2</sup>, S. Masumori<sup>1</sup>, M. Nakajima<sup>1</sup>, M. Hayashi<sup>1</sup>, H. Sakakibara<sup>3</sup> and K. Shimoi<sup>2,4</sup>. <sup>1</sup>Public Interest Incorporated Foundation Biosafety Research Center, Iwata, Japan; <sup>2</sup>Graduate School of Integrated Pharmaceutical and Nutritional Sciences, University of Shizuoka, Shizuoka, Japan; <sup>3</sup>Graduate School of Agriculture, University of Miyazaki, Miyazaki, Japan; <sup>4</sup>Institute for Environmental Sciences, University of Shizuoka, Shizuoka, Japan.

Mammals, including human beings, have a circadian clock system to regulate behavioral and physiological processes. In this study, we investigated the effect of dosing time on micronucleus induction in the bone marrow by evaluating the frequencies of micronucleated peripheral reticulocytes (MNRETs) in mice exposed to N-ethyl-N-nitrosourea (ENU) to assess any difference in genotoxic sensitivity to chemicals between light and dark periods (inactive phase/sleep phase for rodents and active phase/awake phase for rodents). Nine-week-old male C3H/HeJ mice were treated intraperitoneally with ENU (12.5 or 25 mg/kg body weight) at zeitgeber time (ZT) 3 in the light period or ZT15 in the dark period, and then the time courses of the frequencies of the MNRETs were determined. The frequencies of the MNRETs induced by ENU increased time-dependently and peaked at 48 hr after treatment for ZT3 and ZT15, and were obviously higher in the ZT15 treatment group than the ZT3 treatment group. The MNRETs were measured at 48 hr after treatment with ENU (25 mg/kg body weight) at various dosing times (ZT0, 3, 6, 12, 15 and 18). The frequencies of the MNRETs in mice treated at ZT0, 15 and 18 were significantly higher than those in mice treated at ZT3, 6 and 12. These results suggest that genotoxic sensitivity to ENU in mouse bone marrow is different between light and dark periods maybe due to different biological responses (detoxification, cell cycle, DNA repair, etc.) related to circadian rhythms. The results in this study also suggest that varying treatment time points may change the toxicological activity of chemicals.

**PS 1689 The Use of Immunofluorescent Techniques in the CB Human Lymphocyte Micronucleus Test for Discrimination of Clastogenic and Aneugenic Compounds.**

A. Poth and S. Bohnenberger. Genotoxicity and Alternative Toxicology, Harlan Cytotest Cell Research, Rossdorf, Germany.

The micronucleus assay in human lymphocytes was developed as a short term screening test for the detection of both clastogenic and aneugenic chemicals. For human lymphocytes it is recommended to score micronuclei by the cytokinesis block (CB) method using cytochalasin B. The original method developed by Fenech and Morley, 1985, focusses exclusively on binucleated cells. However, recent studies suggest that micronuclei in mononucleated cells could provide complementary information. Results obtained with aneugenic compounds show a dose-dependent increase of micronuclei in mononucleated cells. At present, the underlying mechanism has not been clearly identified. In order to obtain more information a immunofluorescence technique was employed involving CREST analysis for detection of kinetochore proteins. As reference positive controls, Ethylmethanesulfonate (EMS) and Mitomycin C (MMC) were used as clastogenic

compounds and Colcemide as an aneugenic compound. Both, MMC and EMS exert a clastogenic activity which lead to a dose-dependent increase in micronucleus-positive binucleates only. In contrast treatment with colcemide resulted in an increase in micronuclei in both mononucleated and binucleated cells. The high level of CREST+ micronuclei in mononucleated cells suggest that polyploid cells which have undergone an incomplete endomitosis might be the case. Our results suggest that micronuclei in mononucleated cells can be used to investigate the aneugenic activity of chemicals in a fast and easy way, and can be included in the CB assay with human lymphocytes.

## PS 1690 Induction of Nucleotide Excision Repair Is Diminished in Heterozygous p53 Knockout Mice following Chronic Dietary Exposure to Aflatoxin B<sub>1</sub>

J. E. Mulder<sup>1</sup>, R. Mehta<sup>2</sup>, G. S. Bondy<sup>1</sup> and T. E. Massey<sup>1</sup>. <sup>1</sup>Pharmacology and Toxicology, Queens University, Kingston, ON, Canada; <sup>2</sup>Toxicology Research Division, Health Canada, Ottawa, ON, Canada.

Aflatoxin B<sub>1</sub> (AFB<sub>1</sub>) is produced by *Aspergillus* species, moulds that grow on grains, oilseeds and spices. AFB<sub>1</sub> is biotransformed *in vivo* into a highly reactive metabolite that binds to DNA, forming DNA adducts that may induce cancer if not repaired. p53 is a tumour suppressor gene implicated in both AFB<sub>1</sub> carcinogenesis and the regulation of DNA repair. Male heterozygous p53 knockout mice (p53 (+/-); B6.129-*Trp53*<sup>tm1Brd</sup>/N5, Taconic) and their wild type controls were exposed to 0, 0.2 or 1.0 ppm AFB<sub>1</sub> in AIN 93M semi-purified diet for 26 weeks. Nucleotide excision repair (NER) activity of lung and liver nuclear protein extracts was assessed with an *in vitro* assay, using adducted plasmid DNA as a substrate. In wild type mice, repair of AFB<sub>1</sub>-N<sup>7</sup>-Gua adducts was 124% and 96% greater than control in lung extracts from mice exposed to 0.2 ppm or 1.0 ppm AFB<sub>1</sub> respectively, and 224% greater than control in liver extracts from mice exposed to 0.2 ppm AFB<sub>1</sub> (p<0.05). In p53(+/-) mice, repair of AFB<sub>1</sub>-N<sup>7</sup>-Gua was only 45% greater than control in extracts from lungs of mice exposed to 0.2 ppm AFB<sub>1</sub> (p<0.05), and no difference was observed in extracts from lungs of mice treated with 1.0 ppm AFB<sub>1</sub> or extracts from livers of mice treated with either AFB<sub>1</sub> concentration. When comparing AFB<sub>1</sub> effects on NER activity after normalizing to untreated tissue, the induction of NER activity was significantly attenuated in p53(+/-) mice compared to wild type controls in both lung and liver, and AFB<sub>1</sub> dose had a significant effect in p53(+/-) mice. In conclusion, the increase in NER activity seen in wild type mice following chronic AFB<sub>1</sub> exposure indicates a homeostatic response to DNA damage. This homeostatic response was diminished or lost in p53(+/-) mice, which is consistent with p53 having a key role in regulating NER. (Supported by CIHR Grant No. MOP- 89698 and GRDI)

## PS 1691 XPC Haplotypes Alter Nucleotide Excision Repair and Levels of UV-Induced Genetic Damage.

C. M. Rondelli<sup>1,2</sup>, C. J. Etzel<sup>3</sup>, C. E. Cross<sup>2</sup>, M. Xu<sup>2</sup> and S. Z. Abdel-Rahman<sup>2</sup>. <sup>1</sup>Cell Biology & Environmental Toxicology, University of Texas Medical Branch, Galveston, TX; <sup>2</sup>Obstetrics and Gynecology, University of Texas Medical Branch, Galveston, TX; <sup>3</sup>Epidemiology, MD Anderson Cancer Center, University of Texas, Houston, TX.

The XPC protein encoded by the polymorphic XPC gene is essential for initiating global genome nucleotide excision repair (NER). Over 90 single nucleotide polymorphisms (SNPs) have been reported in XPC, but only a few were evaluated as disease risk modifiers with conflicting results. SNPs do not exist as independent variants in the genome but as combinations forming specific haplotypes due to linkage disequilibrium (LD) between them. The impact of XPC haplotypes on DNA repair capacity (DRC) is not known. Using bioinformatics, we recently determined the haplotype structure of XPC and found a correlation between XPC haplotypes and genetic damage in smokers. In this study we test the hypothesis that XPC haplotypes influence DNA damage by altering NER capacity through modifying transcription and/or translation. To test this hypothesis, we exposed human lymphoblastoid cell lines representing different XPC haplotypes to low UV dose to induce pyrimidine-6-4-pyrimidone photoproducts (6-4PPs) and cyclopuridine dimers (CPDs) formation. Levels of these adducts (reflecting DNA damage) and their rate of removal over time (representing DRC of the cells) were determined to evaluate the effect of XPC haplotypes on NER. We found that XPC haplotypes do not only influence NER, but that the haplotype influence is affected by the adduct being repaired. To provide a mechanistic explanation to our findings, we determined XPC mRNA and protein expression levels in different cell lines as a function of time after exposure. Our data indicate that XPC haplotypes significantly influence the rate of translation and transcription. Additional in-depth mechanistic

studies examining the effects of haplotypes on XPC transcription, translation, and function are currently in progress to clarify the role of XPC haplotypes in disease risk. (Supported by F31-019053; T32-07454; P30-006676; K07-CA093592; CA123208.)

## PS 1692 Evaluation of High-Throughput Mutation Test with Proprietary Pharmaceutical Candidates.

H. Adachi, K. Kijima, T. Yamada, J. Kimura and H. Funabashi. Dainippon Sumitomo Pharma Co., Ltd., Osaka, Japan.

[Background] High-Throughput Fluctuation Test (HTFT) is a bacterial gene mutation assay in *Salmonella typhimurium* with the same endpoint as that of the Ames assay. HTFT requires only a few mg of a test sample for the assay, which makes it possible to incorporate the assay into an early drug developmental stage. It is reported that the results in HTFT have a high concordance with the Ames assay results for well-known positive and negative control compounds. In the present study, to assess the availability of the test to early drug screening, we tested our proprietary pharmaceutical candidates in HTFT.

[Method] HTFT was performed for 47 our proprietary pharmaceutical candidate compounds in TA100 and TA98 with and without metabolic activation system prepared from rat liver (S9). Most of the compounds tested in this study were predicted as not having any obvious structural alerts for mutagenicity by a commercially available *in silico* system, DEREK for Windows. Microplates were used during the pre-incubation and incubation period, and mutation was detected with a pH indicator, which reflects the bacterial growth in medium. All the test compounds were also evaluated in the conventional Ames assay using five strains and the results were compared with HTFT results.

[Results and Discussion] The sensitivity (the proportion of positives in Ames assay correctly identified by HTFT), specificity (the proportion of negatives in Ames assay correctly identified by HTFT) and the concordance between the both assay results for a total of 47 test compounds were 88% (23/26), 86% (18/21) and 87% (41/47), respectively. In conclusion, the results of the present study indicate that HTFT is a reliable assay with a high sensitivity and specificity for detecting genotoxic compounds even among pharmaceutical candidates without obvious mutagenic structural alerts as well. Considering the advantages with respect to the amount of required sample and potential throughput capacity, HTFT is therefore thought to be a good screening tool for genotoxicity in the earlier drug screening.

## PS 1693 Establishment of the Comet Assay and Micronucleus Test Using Chimeric PXB-Mice® with Humanized Liver.

C. Tateno<sup>1,2</sup>, Y. Ishida<sup>1,2</sup>, M. Kakuni<sup>1</sup>, M. Fukumuro<sup>3</sup>, J. Tanaka<sup>3</sup>, S. Masumori<sup>3</sup>, M. Nakajima<sup>3</sup> and M. Hayashi<sup>3</sup>. <sup>1</sup>PhoenixBio Co., Ltd., Higashihiroshima, Japan; <sup>2</sup>Liver Research Project Center, Hiroshima University, Hiroshima, Japan; <sup>3</sup>Public Interest Incorporated Foundation, Biosafety Research Center, Iwata, Japan.

Genotoxicity studies have been performed as *in vitro* screening tests to predict carcinogenesis and genetic disorders in humans. Notably, the comet assay and micronucleus test may be used to detect the *in vivo* genotoxicity of test compounds and their metabolites in rodents. However, metabolic activities differ between humans and rodents. Thus, we developed humanized chimeric PXB-mice®—whose liver retains human-type metabolic activities—by using albumin enhancer/promoter-driven urokinase plasminogen activator transgenic/severe combined immunodeficiency disease (uPA/SCID) recipient mice. Using the PXB-mice, we performed a comet assay and micronucleus test of N-ethyl-N-nitrosourea (ENU). At the SOT 2012 Annual Meeting, we presented that a dose-dependent increase in the number of positive cells was observed (i) in the comet assay using liver, (ii) in the micronucleus test using bone marrow, but not (iii) in the micronucleus test using liver, which is probably because of insufficient mitotic condition in the liver. In the present study, we established a new type of PXB-mice by using cDNA-uPA/SCID recipient mice, which would be expected to supply a higher mitotic condition for human hepatocytes. Cryopreserved human hepatocytes from a 2-year-old Hispanic were transplanted into cDNA-uPA/SCID mice. The 7- or 9-week-old male new PXB-mice were orally treated daily with ENU at 25 mg/kg body weight for 2 or 4 weeks. The liver and femur bone marrow were collected from the PXB-mice and employed in the comet assay and micronucleus test. The number of positive cells significantly increased (i) in the comet assay using hepatocytes and also in the micronucleus test using (ii) bone marrow or (iii) hepatocytes from the 7-week-old male PXB-mice treated orally with ENU for 4 weeks. In conclusion, we established comet assays and micronucleus tests using a new type of PXB-mice to predict human genotoxicity *in vivo*.

**PS 1694 Reconstructed 3D Human Skin Micronucleus Assay: Preliminary Prevalidation Results.**

R. Fautz<sup>1</sup>, S. Pfuhler<sup>2</sup>, M. Aardema<sup>3</sup>, G. Ouedraogo<sup>4</sup>, B. Barnett<sup>2</sup>, B. Faquet<sup>4</sup>, G. Mun<sup>5</sup>, N. J. Hewitt<sup>6</sup>, S. Hoffmann<sup>7</sup>, R. Curren<sup>5</sup> and J. Barroso<sup>8</sup>. <sup>1</sup>Kao Germany GmbH, Darmstadt, Germany; <sup>2</sup>Procter & Gamble Company, Cincinnati, OH; <sup>3</sup>Marilyn Aardema Consulting LLC, Fairfield, OH; <sup>4</sup>L'Oréal, Paris, France; <sup>5</sup>IIVS Inc., Gaithersburg, MD; <sup>6</sup>Hewitt Consulting, Erzhhausen, Germany; <sup>7</sup>seh Consulting+Services, Koeln, Germany; <sup>8</sup>Cosmetics Europe, Brussels, Belgium.

The skin is the main route of exposure of many chemicals and cosmetic ingredients; therefore, Cosmetics Europe (formerly COLIPA) has funded projects to establish and evaluate more realistic models for genotoxicity using 3D reconstructed skin (RS) tissues. The aim is to use these to follow-up on positive results from the in vitro genotoxicity battery[1], which has been criticized for its low specificity. The RS model, EpiDerm™, was combined with the micronucleus (MN) assay and the resulting "RSMN" assay exhibited good intra- and inter-laboratory reproducibility[2], and correctly identified 3 coded chemicals as being either positive or negative[3]. A detailed protocol for the RSMN assay was published, together with a harmonized scoring atlas for micronuclei[4]. We have extended the number of coded chemicals to 29 as part of the pre-validation process. Eight of these were true positives, 11 were false positives and 10 were negatives. There was an excellent specificity (88%), demonstrating that the RSMN has a good potential to improve the specificity of in vitro genotoxicity assays as a whole. Of the 8 carcinogens with a suggested genotoxic mode of action, 5 were correctly predicted. While this indicates that the model shows decent sensitivity, the total number of true positives was considered too low to draw a final conclusion about the sensitivity of this assay. Therefore more coded compounds will be tested in a next project phase with a focus on genotoxic carcinogens. Overall, these data support the use of the 3D skin EpiDerm™ model for genotoxicity testing of dermally applied chemicals. [1] Pfuhler et al. 2010, Reg Pharm Tox; [2] Hu et al. Mutat Res. 2009, 673(2):92; [3] Aardema et al. 2010, Mutat Res. 2010, 701(2):123, [4] Dahl et al. Mutat Res. 2011, 720(1-2):42. Sponsored by CosEur and ECVAM

**PS 1695 Reduction of Ataxia telangiectasia Associated Death Rates in ATM KO Mice with Yel002.**

M. J. Davoren and R. H. Schiestl. *Environmental Health Science, University of California Los Angeles, Los Angeles, CA.*

Ataxia Telangiectasia is a devastating disease that affects 1 in every 40,000–100,000 individuals worldwide. 1% of Americans carry a copy of a compromised Ataxia Telangiectasia Mutated (ATM) gene, an important signaling protein involved in both DNA repair and apoptosis. Having two copies of defective or null alleles leads to the disease, symptoms including motor defects (ataxia), extreme sensitivity to ionizing radiation, immunodeficiency, and predisposition to cancer. Lymphoma rates, in particular, occur at nearly 100 times the normal. Despite all of the defects, patients with AT are mentally normal, and many promising young high school and college graduates have their lives cut short by 22, the median age of death. The only treatments are palliative, focused on treating infections that result due to the compromised immune system.

The Schiestl Lab investigates the nature of DNA damage and its repair. During a yeast based high-throughput screen for agents that mitigate the damaging effects of radiation, the candidate drug Yel002 was identified. In later trials on healthy mice subjected to lethal radiation doses, Yel002 was found to significantly increase survival, even when administered a day after the insult. As radiation induces damage largely via strand breaks in DNA, it was thought to act by upregulating the DNA repair process. As AT patients symptoms result from DNA repair deficiency, we decided to treat ATM KO mice with the drug weekly in a long term study to cut death rates. Previous data on this same mouse strain showed that these mice usually die of cancer in the sterile facility by 50 weeks on average. Mice treated with a weekly injection of 75mg/kg Yel002 show far lower death rates – over 80% are still alive at week 60, and survival looks promising as it continues.

**PS 1696 Classification of Genotoxic Mode of Action in TK6 Cells via a High Content, Flow Cytometric In Vitro Micronucleus Assay.**

S. Bryce, S. Avlasevich, J. Weber, E. Beha and S. Dertinger. *Litron Labs, Rochester, NY.*

This laboratory has previously described a high content flow cytometric method for scoring micronuclei (In Vitro MicroFlow®) in CHO-K1 cells that is capable of discriminating aneugenic from clastogenic modes of action (MoA). It would be useful to capture MoA information when studying other cell lines, for instance the human

cell line TK6. Previous reports suggested that the proportion of metaphase cells represents a signature that can effectively discriminate between clastogenic and aneugenic MoA. We therefore set out to combine a flow cytometric micronucleus scoring method with a technique for enumerating metaphase cells and evaluate the multiplexed assay's ability to differentiate clastogenic and aneugenic responses. In order to accomplish metaphase scoring, the fluorescent reagent anti-histone H3 (pS28) antibody (anti-H3-P), which recognizes the phosphorylated form of the histone, was incorporated into the flow cytometric micronucleus assay procedure. TK6 cells were treated in a continuous exposure design with each of ten reference clastogens and seven reference aneugens. At the time of harvest (24 to 27 hrs after treatments were initiated), cells were processed according to In Vitro MicroFlow kit instructions; with the exception that anti-H3-P was incorporated into the sample processing. Data acquisition occurred for 4 mins per sample and provided approximately 2,000 metaphase cells per replicate. Each of the genotoxins was observed to cause increased MN frequencies and relative survival values to decrease in a concentration-dependant manner. Whereas the proportion of metaphase cells to total cells (as well as the proportion of metaphase cells to G2/M cells) were decreased by each of the ten reference clastogens, they were elevated by each of the seven aneugens. These data indicate that automated and multiplexed micronuclei and metaphase cell-scoring of TK6 cells provide strong aneugenic versus clastogenic MoA signatures that effectively discriminate between these classes of genotoxic agents.

**PS 1697 Qualification of 96-Well High-Throughput In Vitro Micronucleus and Comet Assays.**

T. E. Lawlor<sup>1</sup>, K. Pant<sup>1</sup>, M. Aardema<sup>2</sup> and L. F. Stankowski<sup>1</sup>. <sup>1</sup>BioReliance by SAFC, Rockville, MD; <sup>2</sup>Marilyn Aardema Consulting, Fairfield, OH.

We recently qualified 96-well high throughput versions of the in vitro micronucleus (MN) assay in CHO cells, and the Comet assay in TK6 cells. The MN assay evaluated the ten reference compounds in OECD TG 487 using MicroFlow™ kits (Litron Laboratories; 10 independent trials), while the Comet assay evaluated six reference compounds using the Japanese Center for Validation of Alternative Methods (JaCVAM) Comet validation protocol (version 6.2; four independent trials). All trials were performed, using 7-10 concentrations in duplicate cultures with and/or without exogenous metabolic activation (S9), to assess inter- and intra-experimental variability, as well as sensitivity and specificity. Using an empirical analysis of the results, it was possible to reduce the criteria for a positive response for micronuclei and hypodiploidy to 2- and 6-fold concurrent vehicle control values, respectively, thereby increasing sensitivity without an appreciable loss of specificity. Mitomycin C and cytosine arabinoside were reproducibly positive without S9, as were benzo(a)pyrene and cyclophosphamide with S9; all four compounds produced a clastogenic signature. Colchicine and vinblastine were positive with and/or without S9, and both produced a significant increase in micronuclei and hypodiploid cells, indicative of an aneugenic mechanism of action. In contrast, di(2-ethylhexyl)phthalate, nalidixic acid, pyrene and sodium chloride were all negative in all trials and at all dose levels with and without S9 except for one concentration of pyrene in one trial +S9. Reproducible positive results were observed in the Comet assay for the genotoxins 2-aminoanthracene +S9, and 9-aminoacridine, ethyl methanesulfonate and methyl methanesulfonate –S9, while reproducible negative results were observed for the nongenotoxins cycloheximide and triton-X ±S9. These results support the utility of these high throughput assays for genotoxicity screening in general and are being employed in the US EPA ToxCast program.

**PS 1698 Integration of Pig-a and Micronucleus Endpoints into a 28-Day Rodent Toxicity Assay with Urethane.**

L. F. Stankowski<sup>1</sup>, M. Aardema<sup>2</sup>, T. E. Lawlor<sup>1</sup>, S. E. Miller<sup>1</sup>, S. Roy<sup>1</sup>, Y. Xu<sup>1</sup> and R. H. Elbekai<sup>1</sup>. <sup>1</sup>BioReliance by SAFC, Rockville, MD; <sup>2</sup>Marilyn Aardema Consulting, Fairfield, OH.

Urethane is a rodent carcinogen (by po, ip, sc and inhalation routes) and is mutagenic and clastogenic in vivo, but generally considered non-genotoxic in vitro. Thus, it is an important chemical to evaluate the utility of the Pig-a in vivo gene mutation assay. As part of the Pig-a international validation trial, we examined the induction of CD59-negative reticulocytes and total red blood cells (RET<sup>CD59-</sup> and RBC<sup>CD59-</sup>) in the peripheral blood of male Sprague Dawley® rats treated with urethane for 29 consecutive days (25.0, 100 and 250 mg/kg/day, po). Animals also were evaluated for micronucleated reticulocytes (mnRET) in peripheral blood on Days 4, 15 and 29. Ethylmethane sulfonate (EMS; 200 mg/kg/day on Days 3, 4, 13, 14, 15, 27, 28 and 29) and sterile saline (daily) were evaluated as positive and vehicle controls, respectively (all n = 6). All animals survived to Day 29, no animals exhibited overt signs of toxicity due to urethane, and there were no significant differences in body weight gain between urethane and control groups. Significant,

dose dependent increases ( $p < 0.05$ ) were observed for urethane, up to 74- and 24-fold vehicle control values for RET<sup>CD59</sup>, up to 4.2- and 8.1-fold for RBC<sup>CD59</sup> (each on Days 15 and 29), and up to 6.6-, 4.0- and 5.3-fold for mnRET (Days 4, 15 and 29). EMS also induced significant 31- and 18-fold increases in RET<sup>CD59</sup>, 4.5- and 5.7-fold increases in RBC<sup>CD59</sup> (Days 15 and 29), and up to 2.8-, 11- and 16-fold in mnRET (Days 4, 15 and 29). These results compare favorably with earlier in vivo observations, and demonstrate the utility and sensitivity of the Pig-a in vivo gene mutation assay. Samples also were collected for evaluation of chromosome aberrations in peripheral blood lymphocytes; micronucleus induction in bone marrow; and DNA damage in peripheral blood and various organs using the Comet assay (the 29th dose being required for the Comet endpoint at terminal sacrifice). However, these latter analyses are ongoing.

## PS 1699 Reconstructed Skin Micronucleus (RSMN) Assay in Normal Human 3-Dimensional (NHu-3D) Skin Model.

M. Klausner, Y. Kaluzhny, V. Karetsky and J. DeLuca. *MatTek Corporation, Ashland, MA*. Sponsor: P. Hayden.

Safety assessment of new products for human use requires genotoxicity testing. Current in vitro assays have low specificity resulting in a high rate of false positives that may be due to use of transformed cell lines, non-physiological exposures, and lack of normal metabolism. Furthermore, the 7th amendment to the Cosmetics Directive banned in vivo genotoxicity testing in 2009.

EpiDerm is a 3D normal human cell-based epidermal model that is highly reproducible, contains a skin-like barrier, and possesses biotransformation capabilities including CYP450, GST, and UDP enzymatic activity. The RSMN assay utilizes topical application of test materials in a similar fashion to actual human contact. Test materials are dosed 2 to 4 times every 24 h in the presence of Cytochalasin-B and cells are harvested from the EpiDerm tissues 24 hours after the last dose. Altogether, 50 materials (24 direct genotoxins, 14 non-genotoxins, and 12 genotoxins that require metabolic activation) have been analyzed in the RSMN assay. Analysis of the complete set of chemicals resulted in 93.3% Sensitivity, 100% Specificity, and 95.5% Accuracy. In addition, a co-culture system that utilized a lymphoblast cell line TK6 cultured beneath of the EpiDerm tissues was used as a target to expand the relevance of dermally applied compounds to systemic carcinogenicity. Micronucleus induction in TK6 cells was assessed after treatment of the EpiDerm with MitomycinC,  $\beta$ -Propiolactone, and Ethyl Methanesulfonate. The TK6 cells, as well as the EpiDerm tissue itself, were found to be positive. However, exposure to the genotoxin, Benzidine, was negative in EpiDerm but positive in TK6 cells.

In conclusion, the RSMN assay that utilizes the EpiDerm skin model is more specific in identifying dermal human carcinogens than existing in vitro assays. The approach of using the human reconstructed skin together with a human lymphocyte target cell line appears to be a good method of detecting genotoxic effects for hard to predict chemicals and expanding the relevance of dermally applied compounds to systemic carcinogenicity.

## PS 1700 The Use of 3D Human Dermal Equivalents to Assess Genotoxicity of Textile Dyes.

D. M. Leme<sup>1</sup>, F. L. Primo<sup>2</sup>, A. Tedesco<sup>2</sup> and D. P. Oliveira<sup>1</sup>. <sup>1</sup>*Faculdade de Ciências Farmacêuticas de Ribeirão Preto (FCFRP/USP), Ribeirão Preto, Brazil;* <sup>2</sup>*Faculdade de Filosofia, Ciências e Letras de Ribeirão Preto (FFCLR/USP), Ribeirão Preto, Brazil.*

**Introduction:** The use of 3D-human reconstructed skin seems to be promising for safety assessment of chemicals. Compared to traditional 2D in vitro systems, which basically represent one cell type, this model can provide organ-specific toxicity, mechanical/biochemical signaling and cell-cell communication. Humans are daily exposed to textile dyes through skin contact with colored garments. Studies have pointed that some textile dyes can be hazard to human beings. Considering that dyes, under conditions of perspiration, can migrate from clothes and penetrate into human skin, identification of safe textile dyes, related to dermal exposure, is relevant to avoid human health problems. **Objective:** Genotoxicological assessments of Reactive Green 19 (RG19), Reactive Blue 2 (RB2) and Disperse Red 1 (DR1) using the Comet assay with in vitro human dermal equivalents. **Methodology:** The dermal equivalent models were constructed in 3D-collagen matrix, using human gingival fibroblasts isolated from adult donors, at a density of  $3 \times 10^5$  cell/cm<sup>2</sup>, into 60 mm cell culture dishes, containing collagen type-I and D-MEM supplemented with 10% BFS and other nutrients (Primo et al., 2011). The alkaline Comet assay was carried out according to Tice et al. (2000), with slight modifications. **Results:** RB2 and DR1 did not induced DNA damage, whereas RG19 showed weak genotoxic response. **Discussion:** Our data are not in agreement with previous genotoxicological assessments of these dyes using 2D cell cultures. Genotoxicity was reported to DR1 using in vitro hepatocarcinoma cells. However, here this dye showed

to be non-genotoxic. RG19 did not induce DNA damage in in vitro human dermal fibroblasts, but a weak genotoxicity was here observed. **Conclusion:** This difference might be related to the test systems used in each study (2D and 3D cell cultures). 3D-human reconstructed skin affords better cellular environment, which could provide more reliable data of the genotoxicity of chemical (e.g. textile dyes).

## PS 1701 Comparison of Two High-Throughput Methods for In Vitro Micronucleus Assessment Comparison of Two High-Throughput Methods for In Vitro Micronucleus Assessment.

B. Goodwin<sup>1</sup>, J. Bemis<sup>2</sup>, Z. Liu<sup>3</sup>, S. Bryce<sup>2</sup>, K. Luu<sup>3</sup>, K. L. Witt<sup>4</sup>, C. P. Austin<sup>1</sup>, R. R. Tice<sup>4</sup> and M. Xia<sup>1</sup>. <sup>1</sup>*NCGC, NCATS, NIH, Rockville, MD;* <sup>2</sup>*Litron Laboratories, Rochester, NY;* <sup>3</sup>*IntelliCyt Corporation, Albuquerque, NM;* <sup>4</sup>*Division of the National Toxicology Program, NIEHS/NIH, Raleigh, NC.*

Identification of compounds with the potential to induce DNA damage is an important component of the chemical safety evaluation process. Micronuclei (MN), a frequently used endpoint for genotoxicity studies, are formed by clastogens inducing acentric chromosome fragments or aneugens disrupting anaphase during cell division. The traditional in vitro micronucleus (IVMN) test uses trained individuals to manually count MN, which is both labor intensive and time consuming. Here, we compare the performance of two automated high throughput methods for MN detection using CHO-k1 cells in 384-well format. Method 1 is a high-content MN assay using the Thermo Scientific ArrayScan VTi. Method 2 is the IntelliCyt Corp high capacity flow (HCF)-based High Throughput Flow Cytometry (HTFC) Screening System® using the In Vitro MicroFlow® kit (Litron Laboratories). For this comparison, cells were exposed to 10 compounds (20 dilutions, selection based on solubility, cytotoxicity, dose range finding, or 100  $\mu$ M limit concentration) for 24h, and processed on both systems, or incubated with cytochalasin B (CB) for another 24h prior to Arrayscan analysis. The compounds used included clastogens (etoposide, camptothecin, methyl methanesulfonate, bleomycin), aneugens (colchicine, griseofulvin, vincristine, geldanamycin), and non-genotoxic ones (nalidixic acid, sodium chloride). Both platforms correctly identified the known MN-inducing compounds and the 2 non-genotoxic compounds. Scoring of a 384-well plate required ~3h for the ArrayScan and 30m for the HTFC; the latter platform was also able to distinguish aneugens from clastogens. These data show that the throughput of the IVMN assay can be increased dramatically to permit screening large chemical libraries on a robotic platform. Supported by NIEHS Interagency Agreement Y3-ES-7020-01.

## PS 1702 Genome Profiling of Carcinogen Resistance in Budding Yeast Expressing Human P450 Genes.

M. Fasullo<sup>1,3</sup>, P. Egner<sup>2</sup> and T. Begley<sup>1,3</sup>. <sup>1</sup>*Nanobiosciences, College of Nanoscale Sciences and Engineering, Albany, NY;* <sup>2</sup>*Bloomberg School of Public Health, Johns Hopkins University, Baltimore, MD;* <sup>3</sup>*Biomedical Sciences, State University of New York, Albany, NY.*

Human susceptibility to environmental carcinogens is highly variable. Epidemiological studies have identified genes that confer resistance; however, these studies are limited due to small sample sizes. We use *Saccharomyces cerevisiae* (yeast) to profile eukaryotic genes that confer resistance to environmental carcinogens, such as the potent hepatocarcinogen, aflatoxin B1 (AFB1). A yeast collection is available containing ~5,000 diploid strains homozygous for individual gene knock-outs. Each gene knock-out is bar-coded and can be identified by high-throughput DNA sequencing. Since many carcinogens require P450-mediated activation, we introduced human CYP1A2, constitutively expressed on a high-copy expression vector, in the yeast diploid collection. We verified P450 expression in selected mutants by Western blots. To identify which strains are AFB1 sensitive, cells were inoculated in 96 well plates and growth was measured in a plate reader. To expedite results, we switched to high-throughput DNA sequencing of bar code sequences using an illumina platform. Results indicate the importance of the recombinational and excision repair pathways in conferring AFB1 resistance, and the accumulation of AFB1-N7-guanine DNA adducts in nucleotide excision repair (NER) mutants. The functional importance of recombination is further indicated by the presence of carcinogen-associated DNA repair foci that appear in AFB1-exposed cells, and the extreme sensitivity of double mutants lacking both recombinational and nucleotide excision repair. **Conclusions:** We have modified the yeast diploid strain collection to profile the genome resistance to P450-activated carcinogens, and identified genes in the recombinational and NER pathways that confer resistance. Further studies will identify orthologous human genes that confer carcinogen resistance. The yeast strain collection will be valuable in monitoring resistance to additional P450-activated chemicals and drugs.

**PS 1703 Roles for Telomeric Proteins in Regulating Nucleotide Excision Repair at Telomeres.**

D. Parikh and P. Opresko. *University of Pittsburgh, Pittsburgh, PA.*

Ultra-violet (UV) irradiation is the most ubiquitous environmental inducer of skin cancer and melanomas. UV exposure creates DNA photoproducts primarily cyclobutane pyrimidine dimers (CPD) and 6-4 photoproducts (6-4 PP). These cause mutations and block DNA replication, unless repaired by nucleotide excision repair (NER). Thymine repeats (TT) on G-rich strands of telomeric DNA are hotspots for CPD formation. Telomeres are DNA-shelterin protein complexes at ends of chromosomes, reported to lack a defined NER pathway for CPD repair. Diminished binding or loss of shelterin proteins TRF1 and TRF2 at telomeres cause telomere deprotection and end-to-end fusions directly leading to genomic instability. Also TRF2 binds to the key NER protein XPF-ERCC1 and recruits it to telomeres. Our working hypothesis is that telomeric photoproducts are repaired at slower rates compared to genomic lesions and that this repair inhibition involves interactions between XPF-ERCC1 with TRF2.

We measured photoproduct formation and repair in telomeres purified from human osteosarcoma (U2OS) cells exposed to UVC via a novel dot blot assay. We report a method for direct quantification of photoproducts formed *in vivo* and ensuing repair based on a standardized qPCR assay for DNA damage. Photoproducts were detected in genomic and telomeric DNA using specific antibodies following exposure of cells to 10 J/m<sup>2</sup> UVC and after recovery times of 0 to 12 hours. CPDs decreased in genomic DNA after 12 hours but persisted in telomeric DNA. Southern blot assays using radio-labeled oligonucleotides that bind to telomeric DNA confirmed enrichment of telomeres in purified fractions. To investigate possible mechanisms for repair inhibition, we tested directly effect of TRF2 on NER protein XPF-ERCC1 via enzyme activity assays. We discovered that nuclease cleavage activity of purified XPF-ERCC1 on a stem-loop DNA substrate was completely abolished by TRF2. Our results provide the first direct biochemical evidence towards quantifying critical UV damage at telomeres and elucidating NER pathway regulation by shelterin.

**PS 1704 Oxidative Stress-Induced PIGO Mutations in DT40 Cells: Critical Role of NHEJ and TLS Repair Pathways in ROS-Induced Mutations.**

V. Sharma<sup>1</sup>, L. B. Collins<sup>1</sup>, J. A. Swenberg<sup>1,2</sup> and J. Nakamura<sup>1</sup>. <sup>1</sup>*Department of Environmental Sciences and Engineering, University of North Carolina at Chapel Hill, Chapel Hill, NC;* <sup>2</sup>*Curriculum in Toxicology, University of North Carolina at Chapel Hill, Chapel Hill, NC.*

A major mechanism resulting in the genetic alterations that can lead to cancer is through the induction of mutations in genes controlling vital cellular functions. Genotoxic chemicals cause chemically specific DNA adducts that can result in gene mutations, whereas non-genotoxic carcinogens can exert their effects through oxidative stress. The cells in animals, humans, and cell culture are subjected to continuous endogenous DNA damage arising mainly from oxidative stress and depurination. To understand mechanisms by which oxidative stress causes mutations, hydrogen peroxide (H<sub>2</sub>O<sub>2</sub>) was chosen as a model compound. 8-oxo-dG, a major DNA lesion generated during oxidative DNA damage showed non-linear increases following H<sub>2</sub>O<sub>2</sub> treatment. Similarly, H<sub>2</sub>O<sub>2</sub> caused a significant increase in PIGO gene mutations in parental DT40 cells. In addition, to study the critical DNA repair pathways associated with the oxidative stress, DNA damage response analyses were performed in different repair protein deficient DT40 cells. Hypersensitivity of RAD18, REV1, Rad54, RAD51c, Fen1, POLK, POLη, Ku70, Lig4 deficient cells to H<sub>2</sub>O<sub>2</sub> suggests that homologous recombination (HR), non-homologous end joining (NHEJ), translesion synthesis (TLS), and base excision repair (BER) are essential for tolerance to oxidative DNA damage. Due to the error prone nature of NHEJ and TLS repair pathways, we hypothesize that H<sub>2</sub>O<sub>2</sub> induced mutation levels may be decreased in NHEJ and TLS deficient cells. As we expected, Ku70 (NHEJ) and REV1 (TLS) deficient cells revealed a significant decrease in PIGO mutation frequency which might be due to the lack of these error prone pathways in the cells. This indicates that NHEJ and TLS pathway may play an important role in the mutagenesis observed during oxidative stress.

**PS 1705 Evaluating the Role of p53 in Cellular Fate and Micronucleus Induction following Exposure to Etoposide and Mms.**

R. A. Clewell<sup>1</sup>, B. Sun<sup>1</sup>, S. M. Ross<sup>1</sup>, A. Scott<sup>2</sup>, Y. Adeleye<sup>2</sup> and M. E. Andersen<sup>1</sup>. <sup>1</sup>*The Hammer Institutes, Research Triangle Park, NC;* <sup>2</sup>*Unilever, Colworth, United Kingdom.*

Etoposide (ETP) and methyl methanesulfonate (MMS) represent genotoxic chemicals with direct and indirect mechanisms of DNA damage. ETP inhibits binds topoisomerase II, leading to double strand breaks (DSBs). MMS is an alkylating agent that induces single strand breaks and DSBs. To evaluate the role of p53 in downstream protein response and cell fate with ETP and MMS exposure, we generated p53 knockdown (KD) HT1080 cells and utilized HCT116 p53 knockout (KO) cells for comparison with wild-type human HT1080 fibrosarcoma and HCT116 colon carcinoma cells. In WT cells, MMS and ETP induce DSBs (p-H2AX), (s15)p-p53, and p53 protein at 100 μM and 0.2 μM, respectively. Despite similar induction of p53, cellular response was different for the chemicals: ETP induced apoptosis, M-phase arrest, and a large increase in micronuclei (MN), while MMS induced S-phase arrest and showed little induction of apoptosis or MN. p53 regulated protein MDM2, p21 and Wip1 responses were reduced in KD HT1080s and completely abolished in KO HCT116s. Apoptosis was also significantly reduced in p53 KD/KO cells. Cell cycle arrest, however, was similar in WT and p53 KD/KO cells. Basal MN levels were approximately 1.8-fold higher in p53 KO cells than WT cells at 27 and 40 hr. However, chemical induction of MN in WT and p53 KO HCT116 cells showed notable time-dependencies. MN were slower to form in p53 KO cells; only the 40 hr time point showed a strong increase in MN induction in KO cells compared to WT cells after ETP or MMS treatment. While the total frequency of MN 40 hours after treatment was higher in KO cells than WT. Interestingly, the ratio of MN in p53 KO cells to WT cells remained constant across doses (KO:WT ~ 2:1) and chemicals. It appears that the efficiency of DSB break repair is similarly affected by p53 in the naïve and chemical treated cell at the tested doses (≤ 1 μM ETP, ≤ 200 μM MMS). Mechanistic studies of the relationship between DSBs, p53 function and MN are important in assessing the value of MN as functional marker of DNA damage.

**PS 1706 AZT-Induced Aneuploidy Is Mediated by Aberrant Sathmin1 Expression.**

A. Rivera-Rodriguez, M. Poirier, O. Olivero and V. Sanchez. *NCI, NIH, Bethesda, MD.*

Previous studies have shown that the antiretroviral nucleoside reverse transcriptase inhibitor (NRTI) zidovudine (AZT) causes cell cycle anomalies resulting in aneuploidy. In addition, we demonstrated a decrease in β-tubulin polymerization in normal human mammary epithelial cells (NHMECs) exposed to 100 μM AZT for 24 hours. Polymerized β-tubulin is a critical component of normal chromosome segregation, the lack of which causes improper spindle formation and chromosome misalignment. MicroRNA analysis of AZT-exposed NHMECs revealed downregulation of hsa-miR-770-5p, which has multiple cellular targets including Sathmin 1 (STMN1). Active STMN1 (non-phosphorylated) inhibits the polymerization of α- and β-tubulin required for normal cellular functions. Because hsa-miR-770-5p is downregulated in AZT-exposed cells, we hypothesized that AZT exposure would produce upregulation of STMN1, and result in decreased levels of polymerized/functional tubulins. Here we exposed human breast MCF-10A cells to 100 μM AZT for up to 3 passages (p), and quantified total STMN1 (tSTMN1) and phosphorylated (inactive) pSTMN1 by Western Blot. At p1 there was an increase in tSTMN1 (1.49 ± 0.3 fold) and a decrease in pSTMN1 (0.66 ± 0.3 fold) in AZT-exposed cells compared to unexposed cells. At p2 a consistent increase in tSTMN1 (1.46 ± 0.0003 fold), and an increase in pSTMN1 (1.78 ± 0.05 fold) was observed. At p3, no change was detected for tSTMN1 while a decrease was observed in pSTMN1 (0.51 ± 0.5 fold). The data are consistent with the conclusion that AZT induces aneuploidy by inhibition of hsa-miR-770-5p followed by upregulation of STMN1, decreased polymerization of tubulin, spindle abnormalities, and misdistribution of chromosomes into daughter cells at replication.

**PS 1707 Dose Response and Temporality of Ethylene Oxide-Induced Macromolecular Changes and Genotoxicity in Mice.**

M. R. Schisler<sup>1</sup>, M. J. LeBaron<sup>1</sup>, F. Zhang<sup>1</sup>, Y. C. Jeong<sup>1</sup>, M. Bartels<sup>1</sup>, R. Sura<sup>1</sup>, J. A. Hotchkiss<sup>1</sup>, D. R. Geter<sup>1</sup>, B. Gollapudi<sup>1</sup> and N. P. Moore<sup>2</sup>. <sup>1</sup>Toxicology & Environmental Research & Consulting, The Dow Chemical Company, Midland, MI; <sup>2</sup>Toxicology & Environmental Research & Consulting, The Dow Chemical Company, Horgen, Switzerland.

Ethylene oxide (EO), a reactive industrial chemical, induced alveolar/bronchiolar adenomas and carcinomas in the lungs of B6C3F1 male mice at atmospheric concentrations of 50 and 100 ppm. The purpose of the current study was to characterize the mode of action (MoA) for lung tumors induced by EO. Male B6C3F1 mice were exposed by inhalation (6 hours/day, 5 consecutive days/week) to 0, 10, 50, 100, or 200 ppm (4 weeks) or 0, 100, or 200 ppm (8 or 12 weeks) and examined for incidence of micronuclei in the peripheral blood (MNT), DNA damage (Comet assay), histopathology of the lung, and characterization of DNA- and glutathione-adducts and lipid peroxidation in the tumor target and non-target tissues. In general, reactive oxygen species-related adducts (8-OHdG, CrotondG, M1dG) were only minimally affected, whereas alkylated DNA adducts (O<sup>6</sup>-HEdG, N1-HEdA, N6-HEdA, and N7-HEG) were increased more robustly. There was a dose-dependent increase in glutathione adducts (HESG) in all tissues, although severe GSH depletion was not noted. There were no treatment-related changes in the MN-RET (reticulocyte) frequency or %RET. Comet analysis of the lung revealed a dose-dependent, statistically significant increase in DNA damage at 50 ppm and above. There was no treatment-related histopathology in the lung, although a slight decrease in the proportion of Ki-67 positive cells was observed at 4 and 8 weeks in the terminal bronchioles. In summary, these observations reveal a complex sequela of biomarkers of exposure and effect following inhalation exposure to EO with a clear NOEL for all apical endpoints studied.

**PS 1708 Cii Mutant Frequencies and Types of Mutations in the Lung of Big Blue Mice Exposed to Ethylene Oxide for up to 12 Weeks by Inhalation.**

M. G. Manjanatha<sup>1</sup>, S. D. Shelton<sup>1</sup>, Y. Chen<sup>1</sup>, B. L. Parsons<sup>1</sup>, B. Gollapudi<sup>2</sup>, N. P. Moore<sup>3</sup>, L. T. Haber<sup>4</sup> and M. M. Moore<sup>1</sup>. <sup>1</sup>Genetic and Molecular Toxicology, FDA/NCTR, Jefferson, AR; <sup>2</sup>Toxicology & Environmental Research and Consulting, Midland, MI; <sup>3</sup>Dow Europe GmbH, Horgen, Switzerland; <sup>4</sup>TERA, Cincinnati, OH.

Ethylene oxide (EO) is a direct acting mutagen and many in vitro and in vivo data in rodents support its role as a mutagen and carcinogen, but whether EO is carcinogenic through a mutagenic mode of action remains unclear. To investigate this question, male Big Blue B6C3F1 mice (10 mice/group) were exposed to EO by inhalation, six hours/day, five days/week for 4 (0, 10, 50, 100, or 200 ppm EO), 8 or 12 weeks (0, 100, or 200 ppm EO). Lung DNAs were analyzed for induction of *cII* mutant frequencies (MFs) at 4, 8 and 12 weeks of exposure and 428 mutants derived from 4-12 wk control and 200 ppm EO treatments were analyzed to determine the mutational spectra. The background *cII* MFs increased with age from  $17.4 \pm 2.2 \times 10^{-6}$  at 4 weeks to  $29.6 \pm 4.1 \times 10^{-6}$  at 12 weeks. Although EO-induced *cII* MFs were 1.5-2.75-fold higher than the concurrent controls, significant increases in the *cII* MF were found only after 8 and 12 weeks of exposure to 200 ppm EO ( $p \leq 0.05$ ). DNA sequencing of *cII* mutants showed a significant shift in the mutational spectra between control and 200 ppm EO following 8 and 12 wk exposures ( $p \leq 0.035$ ), consistent with the significant increases in the EO-induced MFs at these weeks. The predominant types of EO-induced mutations in lung were G→T and A→T transversions; the role of EO-induced DNA adducts in the etiology of these mutations needs further elucidation. These results indicate that EO is likely to be a weak mutagen at high exposure concentrations in the lung, a tumor target tissue.

**PS 1709 Gain and Loss of K-Ras Mutations in Mouse Lungs following Inhalation Exposure to Ethylene Oxide.**

B. L. Parsons<sup>1</sup>, M. G. Manjanatha<sup>1</sup>, M. B. Myers<sup>1</sup>, K. L. McKim<sup>1</sup>, Y. Wang<sup>1</sup>, B. Gollapudi<sup>2</sup>, N. P. Moore<sup>3</sup>, L. T. Haber<sup>4</sup> and M. M. Moore<sup>1</sup>. <sup>1</sup>Division of Genetic and Molecular Toxicology, US FDA-NCTR, Jefferson, AR; <sup>2</sup>Toxicology & Environmental Research and Consulting, The Dow Chemical Company, Midland, MI; <sup>3</sup>Dow Europe GmbH, Horgen, Switzerland; <sup>4</sup>TERA, Cincinnati, OH.

K-ras codon 12 GGT→GAT mutation is the most prevalent K-ras mutation in spontaneous mouse lung tumors, whereas K-ras codon 12 GGT→GTT mutation was detected in 21/23 (91%) of mouse lung tumors induced by ethylene oxide (EO) [Hong et al. (2007) Toxicologic Pathology 35:81-85]. To investigate whether EO drives G→T transversion through a mechanism involving oxidative damage

and induction of 8-oxo-2'-deoxyguanosine at the second position of K-ras codon 12, allele-specific competitive blocker PCR (ACB-PCR) was used to measure the levels of three different K-ras codon 12 mutations (codon 12 GGT→GAT, GGT→GTT, and GGT→TGT) in lung DNAs of male Big Blue B6C3F1 mice exposed to EO. Ten mice per group were exposed to EO by inhalation, six hours/day, five days/week for 4 (0, 10, 50, 100, or 200 ppm EO), 8 or 12 weeks (0, 100, or 200 ppm EO). Four weeks of exposure to 100 ppm EO caused a significant increase in K-ras codon 12 GGT→GTT mutant fraction (MF) relative to controls, and 50, 100, and 200 ppm EO caused significant increases in K-ras codon 12 GGT→GAT MF. Surprisingly, 8 weeks of exposure to 100 and 200 ppm EO caused significant decreases in K-ras codon 12 GGT→GAT and GGT→GTT MFs relative to controls. The increases and subsequent decreases in K-ras MF may be interpreted as mutant cell proliferation, followed by selective killing of K-ras mutant cells, mediated by EO dose-dependent production of reactive oxygen species. Therefore, the shift in K-ras mutation spectrum observed in EO-induced mouse lung tumors may be due to effects on intracellular signaling pathways and selection of preexisting mutant cells, rather than direct mutagenesis of the K-ras gene by EO.

**PS 1710 Genotoxic and Epigenetic Effects of Tamoxifen Exposure in Mouse Liver.**

A. de Conti, V. Tryndyak, M. Churchwell, F. A. Beland and I. P. Pogribny. FDA-NCTR, Jefferson, AR.

Tamoxifen is a widely used non-steroidal anti-estrogenic drug for treatment and prevention of breast cancer in women; however, there is sufficient evidence that tamoxifen is hepatocarcinogenic in rats, but not in mice. Currently, there is insufficient knowledge to clarify the absence of hepatocarcinogenic effect of tamoxifen in mice. In light of this, the goal of the present study was to investigate the mechanism of mouse resistance to tamoxifen-induced liver carcinogenesis. Feeding female WSB/Eij mice a 420 p.p.m. tamoxifen-containing diet for 12 weeks resulted in substantial accumulation of tamoxifen-DNA adducts, e.g., (E)-α-(deoxyguanosin-N<sup>2</sup>-yl)-tamoxifen (dG-Tam) and (E)-α-(deoxyguanosin-N<sup>2</sup>-yl)-N-desmethyltamoxifen (dG-DesMeTam), in the livers as assessed by electrospray ionization tandem mass spectrometry coupled with high-performance liquid chromatography. The levels of hepatic dG-Tam and dG-DesMeTam DNA adducts in tamoxifen-treated mice were 261 adducts/10<sup>8</sup> nt and 340 adducts/10<sup>8</sup> nt, respectively. In contrast, the degree of global DNA methylation and extent of histone modifications, including trimethylation of histone H4 lysine 20 and histone H3 lysine 9 and lysine 27 in the livers of tamoxifen-exposed mice did not differ from their values in control mice. Previously, we demonstrated that hepatocarcinogenic activity of tamoxifen in rats is associated with its ability to induce, in addition to genotoxic alterations, extensive epigenetic abnormalities. In contrast, in mice tamoxifen-treatment induced only genotoxic alterations without affecting the cellular epigenome. These results provide additional evidence that carcinogenic process requires genotoxic and non-genotoxic alterations and latter are indispensable events in carcinogenesis.

**PS 1711 Acinar Cell Autophagy in Experimental Pancreatic Injury: Immunolocalization and Response of Relevant Proteins.**

L. W. Zhang, J. Zhang, K. I. Shea, G. A. Tobin, A. Knapton and R. L. Rouse. CDER, US FDA, Silver Spring, MD.

Drug-induced pancreatitis (DIP) is an under-diagnosed condition that lacks sensitive and specific biomarkers. In vivo and in vitro studies were designed to identify models and potential biomarkers for DIP. As a part of these studies, experimental pancreatitis was created in male C57BL/6 mice by intraperitoneal injection of caerulein (10 or 50 µg/kg) at one hour intervals for a total of seven injections. Pancreata from caerulein-treated mice exhibited consistent acinar cell autophagy and apoptosis with sporadic necrosis. Both serum amylase and lipase showed significant caerulein dose-dependent increases. TUNEL staining detected significant dose-dependent acinar cell apoptosis. By light microscopy, autophagy was characterized by the formation of autophagosomes and autolysosomes within the cytoplasm of acinar cells. Immunohistochemical (IHC) studies with specific antibodies for proteins related to autophagy and pancreatic stress were used to evaluate the role of acinar cell autophagy in the response to pancreatic injury. Western blots were used to confirm IHC results using pancreatic lysates from control and treated animals. Autophagy was identified as a contributing process in caerulein-induced pancreatitis and proteins previously associated with autophagy were impacted by caerulein treatment. Autophagy identified by autophagosomes and autolysosomes was found to be a common pathway, in which cathepsins, LAMP2, VAMP1, LC3, ATG9, Beclin1, and pancreatitis-associated proteins were simultaneously engaged. Regenerating islet-derived 3 gamma (Reg3γ), a pancreatic acute response protein, was dose-dependently changed in caerulein-treated mice and co-localized with the autophagosomal marker, LC3. These data suggest a role for autophagy in DIP and supports Reg3γ as an IHC marker of pancreatic injury.

**PS 1712 Deciphering the Role of Trail in Altering Spermatogenesis by Controlling Germ Cell Apoptosis.**

Y. Lin and J. Richburg. *The University of Texas at Austin, Austin, TX.*

TRAIL (TNFSF10/Apo2L) is a member of the tumor necrosis factor (TNF) superfamily of proteins, expressed in human and rodent testis. TRAIL is known to induce apoptosis via binding to its receptors DR4 (TRAIL-R1/TNFRSF10A) and DR5 (TRAIL-R2/TNFRSF10B) in humans, and TRAIL-R (MK/mDR5) in mice. TRAIL is found in Leydig cells and germ cells during development and TRAIL-R is predominantly expressed in post-meiotic germ cells in the rat. The major role of TRAIL in male reproduction is still unclear. In this study, we investigated TRAIL-/- mice and evaluated the possible role of TRAIL in germ cell development by measuring testis weight, germ cell apoptosis, and spermatid head count in peripubertal (28 day-old) or young adult animals (44 day-old). Our results revealed that there was a significant difference in testis to body weight ratio between C57 and TRAIL-/- mice. Also, peripubertal TRAIL-/- mice show a dramatic increase in the basal germ cell apoptotic index (A.I., 21.54%) as compared to the C57BL/6J wild-type strain (5.16%). The A.I. in adult C57 mice had dropped to 1.5%, but remained elevated in adult TRAIL-/- mice (20.2%); indicating a sustained high incidence of germ cell apoptosis. Spermatid head counts in adult TRAIL-/- mice were dramatically reduced compared with C57 (39%), indicating these animals suffer a marked decline in the production of mature spermatozoa. We hypothesize that TRAIL is an important factor for maintaining germ cell homeostasis during germ cell development via a death receptor-dependent mechanism.

**PS 1713 Investigation of Sex-Dependent Toxicity of Cysteinyl Leukotriene Receptor 1 Antagonist Zafirlukast.**

Q. Shi and Z. Weng. *Division of Systems Biology, US FDA, NCTR, Jefferson, AR.*  
Sponsor: X. Yang.

The FDA-approved prescription drug label states zafirlukast, a cysteinyl leukotriene receptor 1 (CysLT1) antagonist, induces adverse hepatic events "predominantly in females." To model this possible sex-dependent toxicity, we examined suspension cultured hepatocytes from male and female rats. Concentrations ranging from 1-200  $\mu$ M were tested at multiple time points (1-4 hr). Three parameters were examined: cytotoxicity (lactate dehydrogenase (LDH) leakage), energy level (cellular adenosine triphosphate (ATP)) and cellular respiration ( $O_2$  consumption). Hepatocytes from female rats were more sensitive than male rats in all three parameters. Changes in ATP and cellular respiration were seen as early as 1 hr while cytotoxicity was not observed until 2 hr. Additional studies are underway and include two pharmacological counterparts to zafirlukast (montelukast and pranlukast). With such studies we hope to identify drugs that exert sex-dependent toxicity and their mechanisms.

**PS 1714 1, 3-Dinitropyrene (1, 3-DNP)- and 1, 8-DNP-Induced DNA Damage and Cell Death: Possible Link to Carcinogenic Effects.**

J. A. Holme<sup>1</sup>, H. E. Nyvold<sup>1</sup>, V. M. Arlt<sup>2</sup>, R. Becher<sup>1</sup>, K. B. Gutzkow<sup>1</sup>, A. Solhaug<sup>3</sup>, L. Ekeren<sup>1</sup>, M. Låg<sup>1</sup>, P. E. Schwarze<sup>1</sup>, M. A. Refsnes<sup>1</sup> and J. Øvreik<sup>1</sup>. <sup>1</sup>Division of Environmental Medicine, Norwegian Institute of Public Health, Oslo, Norway; <sup>2</sup>King's College London, London, United Kingdom; <sup>3</sup>Norwegian Veterinary Institute, Oslo, Norway. Sponsor: M. Lovik.

Nitro-polycyclic aromatic hydrocarbons (nitro-PAHs) are found on particulate matter from diesel and gasoline exhaust. Often they are found to have greater mutagenic and carcinogenic potencies when compared with their parent PAHs. In the present study we have compared the genotoxic and cytotoxic effects of two closely related carcinogenic dinitropyrenes (DNPs); 1,3-DNP and the more potent 1,8-DNP.

In human lung BEAS-2B cells, both compounds induced reactive oxygen species ( $H_2O_2$ ; flow cytometry), oxidative DNA damage (comet assay), and a DNA damage response measured as phosphorylation of p53 (Western blotting) at non-cytotoxic concentrations (3-30  $\mu$ M). In mu-rine hepatoma Hepa1c1c7 cells 1,3-DNP (>3  $\mu$ M) induced cell death (a mixture of apoptosis and necrosis), while 1,8-DNP had no cytotoxic effects. The compounds caused little/less  $H_2O_2$ , and oxidative DNA damage than in BEAS-2B. Interestingly, 1,8-DNP was overall more potent than 1,3-DNP with regard to the induction of single-strand DNA breaks (comet) and the formation of DNA adducts (32P-postlabelling). Furthermore, 1,8-DNP gave a stronger DNA damage response (phosphorylation of H2AX and p53) than 1,3-DNP in Hepa1c1c7 cells. Thus, there was no apparent link between the induction of cell death and early increases in ROS-formation or DNA damage/DNA damage responses in the two cell lines. 1,3-DNP-induced apoptosis in Hepa1c1c7

cells was specifically associated with mitochondrial damage (increased formation of superoxide anion; flow cytometry), but was also dependent on the p53-linked transcriptional apoptotic pathway (inhibitors and siRNA).

We suggest that the stronger carcinogenic potency of 1,8-DNP compared to 1,3-DNP is due to its greater DNA damage properties, which in combination with its lower potency to induce cell death increases the probability of causing mutations.

**PS 1715 Role of NOX Mediated Autophagy in Reducing Cytotoxic Effects of Erlotinib in Head and Neck Cancer Cells.**

A. Sobhakumari<sup>1,2</sup>, E. V. Fletcher<sup>1,2</sup>, A. Raeburn<sup>2</sup>, L. Love-Homan<sup>2</sup> and A. L. Simons<sup>2,1</sup>. <sup>1</sup>Human Toxicology, University of Iowa, Iowa City, IA; <sup>2</sup>Department of Pathology, University of Iowa, Iowa City, IA.

Most head and neck squamous cell carcinomas (HNSCC) overexpress Epidermal Growth Factor Receptor (EGFR) which makes it an attractive candidate for molecular targeted therapies. A combination of surgery, radiation and chemotherapeutic agents like EGFR inhibitors are routinely used in the treatment, however, many HNSCC tumors become resistant to EGFR inhibitors. The cellular self-degradation process autophagy is activated by oxidative stress and has recently been reported to reduce the efficacy of chemotherapy. Previous work in our lab has shown that the EGFR inhibitor Erlotinib induces oxidative stress via NADPH Oxidase 4 (NOX4) in HNSCC cells. The purpose of this study is to determine if Erlotinib induces autophagy in HNSCC cells via NOX4 and if autophagy is a pro-survival or pro-death mechanism. Erlotinib induced cytotoxicity (as determined by clonogenic assay) in FaDu and Cal-27 HNSCC cells compared to control treated cells. Erlotinib induced the expression of the autophagy marker LC3B-II in both cell lines as determined by western blot and immunofluorescence assays. Knockdown of autophagy genes Beclin-1 and Atg5 sensitized both cell lines to the cytotoxic effect of Erlotinib, suggesting that autophagy may be a pro-survival mechanism. Erlotinib increased NOX4 mRNA and protein levels in FaDu and Cal-27 cells. Treatment with DPI (diphenyleneiodonium) and a p38 inhibitor in the presence of Erlotinib suppressed the increase in LC3B-II expression in FaDu and Cal-27 cells. Finally, knockdown of NOX4 using adenoviral siNOX4, partially suppressed the activation of LC3B-II in FaDu and Cal-27 cells. These results suggest that Erlotinib may activate autophagy in HNSCC cells as a pro-survival mechanism, and NOX4 may play a role in mediating this effect. In conclusion, NOX4-induced autophagy may play a role in reducing the efficacy of Erlotinib. [Supported by NIH grant K01-CA134941 and ACS grant IRG-77-004-34].

**PS 1716 The Aryl Hydrocarbon Receptor (AhR) Suppresses Apoptosis in UVB-Irradiated Keratinocytes and May Serve As a New Target for Chemoprevention.**

T. Haarmann-Stemmann<sup>1</sup>, K. Fraenstein<sup>1</sup>, J. Tigges<sup>1</sup>, F. Engel<sup>1</sup>, C. Wiek<sup>2</sup>, H. Hanenberg<sup>2</sup>, E. Fritsche<sup>1</sup> and J. Krutmann<sup>1</sup>. <sup>1</sup>Leibniz Research Institute for Environmental Medicine, Duesseldorf, Germany; <sup>2</sup>Otorhinolaryngology, Heinrich Heine University, Düsseldorf, Germany.

Exposure of keratinocytes to ultraviolet (UV) radiation results in the initiation of apoptosis, a protective mechanism that eliminates cells harbouring irreparable DNA damage. Hence, a modulation of this process may significantly influence the initiation and progression of UV-induced skin cancer. We have found that the aryl hydrocarbon receptor (AHR), a ligand-activated and UVB-sensitive transcription factor, serves an anti-apoptotic function in UVB-irradiated human keratinocytes. Chemical and shRNA-mediated disturbance of AHR signaling significantly enhanced UVB-induced apoptosis. This effect was due to a loss of expression of E2F1 and its downstream target checkpoint kinase-1 (CHK1), two factors critical for cell-cycle control and DNA damage response. Ectopic overexpression of E2F1 in AHR-knockdown keratinocytes restored CHK1 expression and diminished the observed sensitization to UVB-induced apoptosis. Accordingly, experimental CHK1 recovery alone was also sufficient to attenuate UVB-induced apoptosis in AHR-knockdown keratinocytes, indicating that the loss of proper checkpoint control drives damaged keratinocytes into programmed cell death. Our results demonstrate for the first time an interplay between AHR, E2F1 and CHK1 and identify this signaling axis as a novel anti-apoptotic pathway in keratinocytes, which may represent a putative target for chemoprevention of non-melanoma skin cancer.

**PS 1717 Role of Secretory Phospholipase A<sub>2</sub> in the Toxicity of Bile Acids to Prostate Cancer Cells.**

S. L. Wilding and B. S. Cummings. *University of Georgia, Athens, GA.*

Bile acids mediate the digestion and absorption of fats and fat-soluble vitamins; however, pathological increases are associated with cholestasis and cell death. Recent studies show that high concentrations of bile acids can induce apoptosis in

several cells, including cancer cells, by mechanisms that are not fully understood. The goal of this study was to determine the toxicity of three different bile acids (chenodeoxycholic acid, deoxycholic acid, and lithocholic acid) in prostate cancer cell lines (PC-3, LNCaP, and DU-145). Treatment of cells with bile acids induced time- and concentration-dependent decreases in MTT staining, a marker of cytotoxicity, with IC50 values of approximately 100-200  $\mu$ M after 72 hr. In general, lithocholic acid was more potent than chenodeoxycholic acid, followed by deoxycholic acid. Further, LNCaP cells tended to be more susceptible to bile acid-induced toxicity, than either DU-145 or PC-3 cells. Based on reports that bile acids increase the expression of inflammatory enzymes called secretory phospholipase A<sub>2</sub> (sPLA<sub>2</sub>), we tested the hypothesis that these enzymes regulate the mechanisms of bile acid-induced cell death. Analysis of sPLA<sub>2</sub> expression using quantitative PCR showed that several sPLA<sub>2</sub> isoforms were expressed in PC-3, LNCaP and DU-145 cells, including Group IB, IIA, V and X sPLA<sub>2</sub>. Nevertheless, treatment of cells with the sPLA<sub>2</sub> inhibitor LY311727, prior to exposure to bile acids, did not alter MTT staining compared to cells exposed to bile acids alone. Similar results were seen with the calcium-independent PLA<sub>2</sub> (iPLA<sub>2</sub>) inhibitor bromenol lactone. Collectively, these data show the novel finding that bile acids can induce toxicity to prostate cancer cells and suggest the neither sPLA<sub>2</sub> nor iPLA<sub>2</sub> activity mediate the mechanisms of cytotoxicity.

**PS 1718 Etoposide-Induced Mitochondria-Dependent Apoptosis through C-Jun N-Terminal Kinases, Extracellular Signal-Regulated Kinases, and Glycogen Synthesis Kinase-3 $\alpha$ / $\beta$  Pathway in Pancreatic  $\beta$ -Cells.**

K. Lee<sup>1</sup>, S. Hsieh<sup>1</sup>, C. Su<sup>2</sup>, D. Hung<sup>3</sup>, K. Chen<sup>4</sup>, T. Tseng<sup>5</sup>, T. Lu<sup>6</sup>, S. Liu<sup>7</sup>, Y. Chen<sup>6</sup> and C. Huang<sup>8</sup>. <sup>1</sup>Department of Emergency, Buddhist Tzu Chi General Hospital, Taichung, Taiwan; <sup>2</sup>Department of Otorhinolaryngology, Head and Neck Surgery, Changhua Christian Hospital, Changhua, Taiwan; <sup>3</sup>Toxicology Center, China Medical University Hospital, Taichung, Taiwan; <sup>4</sup>Department of Urology, China Medical University Hospital, Taichung, Taiwan; <sup>5</sup>Department of Anatomy, China Medical University, Taichung, Taiwan; <sup>6</sup>Department of Physiology and Graduate Institute of Basic Medical Science, China Medical University, Taichung, Taiwan; <sup>7</sup>Institute of Toxicology, National Taiwan University, Taipei, Taiwan; <sup>8</sup>School of Chinese Medicine, China Medical University, Taichung, Taiwan.

Etoposide, a semisynthetic derivative of podophyllotoxin, is an important chemotherapeutic agent and widely used to treat human cancers. Etoposide also can produce the severe side effects and cause cell damages and the physiological dysfunctions. However, the toxicological effects of etoposide-induced pancreatic  $\beta$ -cell death remain unclear. Here, we investigate the cytotoxic effect and its possible mechanisms of etoposide on pancreatic  $\beta$ -cells. Treatment of pancreatic  $\beta$ -cell-derived RIN-m5F cells with etoposide (1-100 M) for 24 h significantly reduced cell viability and underwent apoptosis, accompanied with mitochondrial dysfunctions. Moreover, etoposide triggered the protein phosphorylation of glycogen synthesis kinase (GSK-3 $\alpha$ / $\beta$ ) at 8 h treatment and maintained to 24 h, which could be reversed by lithium chloride (LiCl, a specific inhibitor of GSK-3 $\alpha$ / $\beta$ ). In addition, etoposide (20  $\mu$ M) markedly increased the phosphorylation of JNK and ERK1/2, but not p38. Pharmacological inhibitors SP600125 and PD98059 effectively attenuated etoposide-induced caspase-3 activity and JNK and ERK1/2 activation, but LiCl could not reverse the phosphorylation of JNK and ERK1/2 induced by etoposide. In conclusion, these results suggest that etoposide exerts its cytotoxicity on pancreatic  $\beta$ -cells by inducing the mitochondria-dependent apoptosis through JNK/ERK activation-regulated GSK-3 $\alpha$ / $\beta$  signaling pathway.

**PS 1719 Berberine Induces Human Tongue Squamous Carcinoma Cell Apoptosis through PI3K-Regulated ER Stress Pathway.**

C. Su<sup>1</sup>, T. Lu<sup>2</sup>, D. Hung<sup>3</sup>, K. Chen<sup>4</sup>, T. Tseng<sup>5</sup>, C. Huang<sup>6</sup> and Y. Chen<sup>2</sup>. <sup>1</sup>Department of Otorhinolaryngology, Head and Neck Surgery, Changhua Christian Hospital, Changhua, Taiwan; <sup>2</sup>Department of Physiology and Graduate Institute of Basic Medical Science, China Medical University, Taichung, Taiwan; <sup>3</sup>Division of Toxicology, Trauma and Emergency Center, China Medical University Hospital, Taichung, Taiwan; <sup>4</sup>Department of Urology, China Medical University Hospital and China Medical University, Taichung, Taiwan; <sup>5</sup>Department of Anatomy, China Medical University, Taichung, Taiwan; <sup>6</sup>School of Chinese Medicine, China Medical University, Taichung, Taiwan.

Until now, oral cavity squamous cell carcinoma (OSCC) is the most common head-and-neck cancer, which accounts for approximately 3% of all newly diagnosed cancer cases. Despite of recent advances in surgical, radiotherapy, and chemotherapy treatment protocols, it has been discussed that OSCC could not be eradicated. Berberine is a natural alkaloid. Recently, berberine has been showed to

inhibit metastasis in lung cancer cells, and cytotoxic in glioma, prostate and nasopharyngeal cancer cells. However, the therapeutic effects and the possible mechanisms of berberine in OSCC are still unclear. Results found that berberine significantly decreased cell viability in human tongue squamous carcinoma derived SAS cells line. Besides, berberine increased the ER-stress signals, including Grp94, CHOP, Xbp-1 mRNAs and proteins. Further, the pro-caspase-12 protein level was decreased, and the caspase-12 mRNA level was increased. In mitochondrial pathway, berberine increased Bax, Bak, Bid mRNAs and proteins levels and decreased Bcl-2 mRNAs and proteins levels. Besides, the pro-caspase-9, pro-caspase-7, and pro-caspase-3 proteins level was decreased. We also found that phospho-AKT protein level was decreased after berberine treatment in cells. Besides, LY294002, the inhibitor of phosphoinositide 3-kinases (PI3Ks), promoted ER-stress and mitochondrial related apoptosis signals. Through this study, suggested that berberine may a useful compound in inhibition of OSCC through PI3K-AKT regulated ER-stress and mitochondrial pathways.

**PS 1720 Amiodarone-Induced Autophagy Protects Lung Epithelial Cancer Cells from Death.**

K. Lee<sup>1</sup>, S. Oh<sup>1</sup>, S. Oh<sup>2</sup>, B. Lee<sup>1</sup>, Y. Yang<sup>3</sup>, M. Yang<sup>3</sup> and K. Lee<sup>3</sup>. <sup>1</sup>College of Pharmacy and Research Institute of Pharmaceutical Sciences, Seoul National University, Seoul, Republic of Korea; <sup>2</sup>Research Center for Resistant Cells, Chosun University, Gwangju, Republic of Korea; <sup>3</sup>Inhalation Toxicology Center, Korea Institute of Toxicology, Jeongseup, Republic of Korea.

Amiodarone-induced toxicities in various off-target organs including cornea, liver, skin, thyroid and lung often limit the use of this drug especially in the case of long-term treatment. Despite low incidence rate, amiodarone-induced pulmonary toxicity is the one of greatest concern and leading cause for discontinuation. In the present study, we investigated the induction of autophagy following amiodarone treatment in vitro and the relevance of autophagy to the pulmonary toxicity. Amiodarone treatment caused morphological change in H460 cells. Increased numbers of cytoplasmic vacuoles as well as round and floating cells were observed. Amiodarone-induced autophagy was demonstrated by increased LC3-II conversion, upregulation of Atg5 and Atg7 and degradation of p62 protein. Autophagic flux as determined by lysosomal inhibitor bafilomycin A1 was also increased by amiodarone. The phosphorylation of AMP-activated protein kinase at Thr172 was increased and that of Akt at Ser473 was decreased by amiodarone which resulted in the reduction of mTOR and p70S6 kinase phosphorylation. To determine the role of autophagy in amiodarone toxicity, amiodarone-induced cell death was evaluated in the presence of 3-methyladenine or by knocking down autophagy related genes, Atg5 or Atg7. Inhibition of autophagy decreased the cell viability and increased apoptosis significantly. In conclusion, amiodarone-induced autophagy functions to rescue stressed cells from death. The findings have important implications in developing further strategy to minimize drug-induced toxicity in human.

**PS 1721 Paraquat Causes Hepatocytes Death via Oxidative Stress-Induced JNK/ERK Activation Regulated Mitochondria-Dependent Apoptosis Pathway.**

D. Hung<sup>1</sup>, T. Tseng<sup>2</sup>, C. Su<sup>3</sup>, K. Lee<sup>4</sup>, K. Chen<sup>5</sup>, S. Hsieh<sup>4</sup>, T. Lu<sup>6</sup>, L. Tsai<sup>6</sup>, S. Liu<sup>7</sup>, Y. Chen<sup>6</sup> and C. Huang<sup>8</sup>. <sup>1</sup>Division of Toxicology, Trauma & Emergency Center, China Medical University Hospital, Taichung, Taiwan; <sup>2</sup>Department of Anatomy, China Medical University, Taichung, Taiwan; <sup>3</sup>Department of Otorhinolaryngology, Head and Neck Surgery, Changhua Christian Hospital, Changhua, Taiwan; <sup>4</sup>Department of Emergency, Buddhist Tzu Chi General Hospital, Taichung, Taiwan; <sup>5</sup>Department of Urology, China Medical University Hospital and China Medical University, Taichung, Taiwan; <sup>6</sup>Department of Physiology and Graduate Institute of Basic Medical Science, China Medical University, Taichung, Taiwan; <sup>7</sup>Institute of Toxicology, National Taiwan University, Taipei, Taiwan; <sup>8</sup>School of Chinese Medicine, China Medical University, Taichung, Taiwan.

Paraquat (1,1'-dimethyl-4,4'-bipyridium dichloride, PQ), a common herbicide used all over the world, is toxic to human beings and causes severe injuries to multiple organs, including lung and liver. However, the toxicological effects and molecular mechanisms of PQ-induced on hepatocytes are mostly unclear. In this study, we found that PQ significantly reduced the cell viability in rat hepatocytic cell line H4-II-E cells. Treatment of H4-II-E cells with PQ also induced several features of mitochondria-dependent apoptotic signals, including loss of mitochondrial membrane potential (MMP), increase in cytosolic cytochrome c release, activation of PARP and caspase-3/-7, and increased oxidative stress injuries such as reactive oxygen species (ROS) generation and glutathione depletion. These PQ-induced apoptotic-related signals could be effectively reversed by antioxidant NAC. Moreover, PQ increased the phosphorylation of JNK and ERK1/2, but not p38. Pharmacological inhibitors SP600125, PD98059, and NAC significantly attenuated PQ-induced cytotoxicity, caspase-3/-7 activation, MMP loss, and inhibited

the phosphorylation of JNK and ERK1/2. Taken together, these results suggest that PQ exerts its cytotoxicity on hepatocytes by inducing apoptosis via an oxidative stress-induced JNK and ERK1/2 activation regulated mitochondria-dependent signaling pathway

## **PS** 1722 Oxidative DNA Damage and Apoptosis Induction after Enniatin B Exposure in Caco2 Cells.

M. Ruiz, A. Prosperini, A. Juan Garcia and G. Font. *Preventive Medicine, University of Valencia, Burjassot Valencia, Spain.*

Enniatin (EN) B is a cyclohexadepsipeptidic mycotoxin produced by *Fusarium* spp. often found in cereals and cereal-based products. Its cytotoxic potential have been reported but the mechanisms involved in its toxicity remain to be elucidated. Since the oxidative pathway could be implicated in mycotoxin's toxicity, in this study the generation of reactive oxygen species (ROS) and lipid peroxidation (LPO) have been investigated in human colorectal adenocarcinoma (Caco-2) cells. Subsequently the induction of oxidative stress have been assumed to be directly related to DNA damage and apoptosis. Cells were exposed to EN B at sub-cytotoxic concentration of 1.5 and 3  $\mu$ M. A significant increase ( $p \leq 0.05$ ) in ROS production was observed by the fluorescent probe H<sub>2</sub>-DCFDA after 3  $\mu$ M exposure in Caco-2 cells from 10 up to 120 min. LPO was determined by thiobarbituric acid reactive substances (TBARS) after 24 h of exposure. Significant increase of malondialdehyde (MDA) was observed after the highest (3  $\mu$ M) concentration tested of 48% ( $p \leq 0.05$ ), as compared to control. Genotoxicity was evaluated through the alkaline Comet assay after 2 and 24 h of exposure. Median tail moment ( $\mu$ M) was significantly high respect to the control with a dose-dependent relationship ( $p \leq 0.05$ ) after short and longer exposure. The induction of apoptosis and necrosis was assessed by flow cytometry. Annexin V coupled to FITC in combination with PI was used to determine different apoptotic phases after 24 h of exposure to EN B (1.5 and 3  $\mu$ M). Both concentrations induced apoptosis and necrosis in a dose-dependent manner. These findings show that 3  $\mu$ M concentration of EN B caused oxidative damage, by means of ROS generation that could be responsible of LPO, DNA damage and triggers apoptosis in Caco2 cells.

Acknowledgements: The Science and Innovation Spanish Ministry (AGL2010-17024/ALI). A. Prosperini thanks "Santiago Grisolia" fellowship (Conselleria de Educaci3n, Comunitat Valenciana)

## **PS** 1723 Mevalonate Pathway Plays a Major Role in Adriamycin Resistance.

T. Takahashi, S. Nakashima, T. Masuda, S. Yoneda and A. Naganuma. *Graduate School of Pharmaceutical Sciences, Tohoku University, Sendai, Japan.*

In a search for novel mechanisms of resistance to adriamycin, an anthracycline anti-tumor antibiotic used in cancer chemotherapy, we have previously screened a ORF library derived from budding yeast for genes related to adriamycin resistance and found that overexpression of the gene for HMG-CoA synthase, an enzyme in mevalonate pathway, confers resistance to adriamycin in budding yeast. We have also found that promotion of mevalonate pathway decreased the toxicity of adriamycin in yeast cells.

In this study, we examined the relationships between enzymes involved in mevalonate pathway and the adriamycin resistance, and found that deletion of the gene for Ram1, a farnesyltransferase, reduced the degree of adriamycin resistance induced by overexpression of HMG-CoA synthase. These results suggest that overexpression of HMG-CoA synthase might decrease the adriamycin toxicity through promotion of farnesylation of proteins. Moreover, overexpression of HMG-CoA synthase or addition of mevalonate to culture medium decreased the toxicity of adriamycin in human breast MCF7 cells, suggesting that mevalonate pathway plays a key role in mechanism of adriamycin resistance not only in yeast cells but also in human cells.

## **PS** 1724 Carbamazepine Suppresses Ischemia/Reperfusion Injury to Mouse Livers by Enhancing Autophagic Flux.

J. Kim, J. Wang and K. E. Behrns. *Surgery, University of Florida, Gainesville, FL.*

**BACKGROUND:** Onset of the mitochondrial permeability transition (MPT) plays a causative role in ischemia/reperfusion (I/R) injury, a pathological event occurring during organ transplantation, cardiac failure and hemorrhagic shock. Current therapeutic strategies for reducing reperfusion injury remain disappointing. As autophagy selectively and timely eliminates abnormal or damaged cellular constituents and organelles such as dysfunctional mitochondria, this lysosome-mediated catabolic process confers cytoprotection against I/R injury and various diseases. We have shown that calpain-dependent depletion of autophagy-related proteins (Atg) causes the MPT and hepatocyte death after I/R. Carbamazepine (CBZ),

an FDA approved anticonvulsant drug, has recently been reported to increase autophagy. The AIM of this study was to investigate the effects of CBZ on hepatic I/R injury.

**METHODS:** Hepatocytes and livers from male C57BL/6 mice were subjected to simulated and *in vivo* I/R, respectively. Cell death, intracellular calcium, calpain activity, changes in Atg, autophagic flux, MPT and mitochondrial membrane potential after I/R were analyzed in the presence and absence of 20  $\mu$ M CBZ.

**RESULTS:** CBZ significantly increased hepatocyte viability after reperfusion, as judged by propidium iodide fluorometry. Confocal microscopy of rhod-2, fluo-4, calcein and tetramethylrhodamine methylester revealed that CBZ prevented reperfusion-induced mitochondrial calcium loading, onset of the MPT and mitochondrial depolarization. Immunoblotting and fluorometric analysis showed that CBZ blocked calpain activation, Atg6 depletion, and loss of autophagic flux after reperfusion. Intravital multiphoton imaging of anesthetized mice demonstrated that CBZ substantially reversed autophagic defects and mitochondrial dysfunction after I/R *in vivo*.

**CONCLUSION:** CBZ protects hepatocytes against I/R injury by preventing a temporal sequence of calcium overloading, calpain activation, Atg6 depletion, defective autophagy, onset of the MPT, and cell death.

## **PS** 1725 A Multiplexed Assay for Differentially Examining Cytostatic and Cytotoxic Effects.

A. L. Niles<sup>2</sup>, M. Zhou<sup>1</sup>, T. L. Riss<sup>2</sup> and D. Lazar<sup>2</sup>. <sup>1</sup>Promega Biosciences, San Luis Obispo, CA; <sup>2</sup>Promega, Madison, WI.

We have developed a multiplexed assay which can conveniently differentiate between cytostatic and cytotoxic effects produced in cell culture under standard compound screening conditions. The assay first employs a pro-fluorescent, cell impermeant, DNA probe which changes fluorescent intensity only with changes in membrane integrity due to cytotoxicity. Second, an ATP detection chemistry is applied to examine the relative number of viable cells after treatment. We examined the utility of this multiplex by dosing a suspension cancer cell line (K562) and attachment-dependent cancer line (HeLa) with serially diluted compounds for a period of 72hrs. We chose the antimetabolite compounds, 6-aminomercaptopurine and methotrexate, because of their anti-neoplastic properties and mechanistic relevance in halting cell growth and division. Here we show that by coupling two convenient biomarkers for viability and cytotoxicity, we can define the differences between anti-proliferative and cytotoxic effects. The distinction between cytostatic and cytotoxic effects on particular target cell populations may ultimately help direct prioritization of oncology drug development efforts or offer insight into rational combinations during chemosensitivity testing.

## **PS** 1726 Amiodarone-Induced Perturbations in Rat Pleural Mesothelial Cells.

S. Chappidi and J. M. Cerreta. *PHS, St. John's University, Queens, NY.* Sponsor: L. Trombetta.

Amiodarone (AM) is an anti-arrhythmic drug whose clinical use is often limited due to its toxic effect on the lungs. AM's pulmonary toxicity is mediated in part through apoptosis of the epithelial cells and their replacement with fibrotic tissue. Our laboratory has previously determined that Caspase 8 and 9 levels are increased in cells exposed to AM. Such increases suggest that both the extrinsic and intrinsic pathways have a role in AM induced apoptosis. The current study was carried out to further examine the pathway of AM induced cell injury and determine cellular changes caused by such injury in rat pleural mesothelial cells (RPMC's). RPMC's were grown to confluence in Ham's F-12 medium containing 15% FBS at 37 °C in a humidified, 5% CO<sub>2</sub> environment. Cultures were treated with increasing concentrations (12.5, 25, 50, or 100  $\mu$ g/ml) of AM for 1, 6, 12, or 24 hours. Cytotoxicity of AM was determined by MTT assay. Cell membrane integrity was observed indirectly by measuring the levels of LDH released into the supernatant after 24hr of treatment with AM. To examine activation of the apoptotic pathway, translocation of BAX protein from cytosol to mitochondria was measured by Western Blot analysis following exposure to the 50  $\mu$ g/ml of AM. Cell extracts of both control and AM treated (50 $\mu$ g/ml) cultures were examined to determine cellular GSH/GSSG levels. AM exposed cultures had a time and concentration dependent cytotoxicity at all points tested. At 24 hrs, cell viability was found to be 96%, 72%, 47% or 13% respectively with increasing concentrations of AM. The LDH levels were found to increase (275%, 550%, 1575%, 2075%) following treatment with increasing concentrations of AM. Cultures exposed to 50 $\mu$ g/ml AM had a 330% increase in levels of BAX present in the mitochondrial fraction. Cells exposed to various concentrations (as above) of AM had a concentration dependent decrease (72%, 85%, 68% or 26%) in the levels of GSH/GSSG ratio when compared to the control. Such results suggest that amiodarone is triggering multiple pathways leading to cell death.

**PS 1727 Characterization of Cigarette Smoke and Menthol on Human Alveolar Adenocarcinomic (A549) Cells.**

E. R. Esposito, B. Greene, M. L. Coronel and H. Tran. *Pharmaceutical Sciences, Sullivan University College of Pharmacy, Louisville, KY.*

**Purpose:** Menthol provides local anesthesia to nerve endings, allowing smokers to take deeper, longer inhalations, thus giving longer exposure to carcinogenic elements found in cigarette smoke. There are few cellular studies addressing evidence concerning the risk of developing lung cancer between mentholated and non-mentholated cigarettes. We would like to determine if an association exists between mentholated cigarettes and incidence of lung cancer in the smoker population. Using an in vitro model, we aimed to characterize the effects of cigarette smoke, with or without menthol, in human alveolar adenocarcinomic (A549) cells and determine if the rate of cell proliferation and cell death is altered.

**Methods:** Dose response studies were conducted to determine appropriate concentrations of cigarette smoke condensate (CSC) and menthol for cell viability assays. Cells were treated for 24 hours with either: CSC, menthol, or CSC + menthol compared to vehicle controls. Several techniques were applied to measure cell death and apoptosis. Cell viability was measured using Trypan blue, while intracellular caspase activation was determined using a fluorescein-conjugated antibody designed for flow cytometric applications. Early and late indicators of apoptosis were assessed using Annexin-V and propidium iodide detection assay.

**Results:** Data suggest that menthol alone decreased cell viability and increased Annexin positive cells while co-treatment with CSC + menthol did not affect cell viability. Pan-caspase activation was not significantly altered for CSC, menthol, or CSC + menthol treated cells. Interestingly, cells treated with CSC only appeared to emit a source of auto fluorescence. Future studies are required to address the issue. Data are the average of three independent experiments  $\pm$  standard error of the mean (S.E.M.) Statistical significance is determined  $p < 0.05$ .

**PS 1728 Induction of Late-Apoptosis on Chinese Hamster Ovary Cells by Sandalwood (*Santalum album*) Essential Oil.**

C. M. Ortiz-Sanchez, L. Morales-Torres and J. L. Matta. *Physiology, Pharmacology and Toxicology, Ponce School of Medicine and Health Sciences, Ponce, Puerto Rico.*

Essential oils (EOs) are volatile aromatic compounds that can be extracted from any part of a given medicinal or aromatic plant. EOs have a wide range of applications in the pharmaceutical, food, and cosmetic industries. Recently, there has been an increased interest regarding the pharmacological properties of EOs. Among the large diversity of commercially available EOs, sandalwood essential oil (SEO) is used in food industry as a flavoring ingredient with a daily consumption of 0.0074 mg/kg. It is also used in perfumery and other cosmetic products. SEO has antiviral and antimicrobial properties. However, its pharmacological activity on mammalian cells is largely unknown. The aim of this study was to determine the effect of SEO on Chinese hamster ovary cell (CHO-K1) proliferation and viability. These cells were exposed to concentrations of SEO ranging from 1 – 600  $\mu$ g/mL for 24, 48, 72, and 96 hours. Cell viability was measured by Trypan blue exclusion using the Cellometer Auto T4, while cell proliferation was determined by the tetrazolium salt (MTT) assay. Apoptosis detection was performed by flow cytometry using Annexin-V-PE (a marker for early apoptosis) and 7-AAD (a marker for late apoptotic/necrotic cells). Among all exposure times studied, the same tendency was seen at 24, 48, 72, and 96 hours; SEO decreased cell proliferation in a dose-dependent manner to around 80%. The inhibitory concentration (IC50) was approximately 31  $\mu$ g/mL. Apoptotic effects were studied in concentrations above and below the IC50 using three doses: 25, 30 and 35  $\mu$ g/mL. An increase of 3% and 15% in late apoptotic cells was detected with increasing SEO concentration at 30 and 35  $\mu$ g/mL, respectively ( $p < 0.05$ ). In conclusion, SEO has the potential to decrease cell proliferation by inducing late apoptosis in CHO-K1 cells. However, further analyses are needed to elucidate the pathways involved in this process. Research supported by the NIGMS-NIH Award # R25GM082406.

**PS 1729 Investigating the Role of HO-1/BVR Expression on Apoptosis Regulation.**

C. George and M. J. Jenny. *Department of Biological Sciences, University of Alabama, Tuscaloosa, AL.*

Cadmium (Cd)-resistant cells, when exposed to a variety of chemicals capable of inducing oxidative stress, exhibit significantly lower occurrences of apoptosis compared to non-resistant cells, suggesting that Cd-resistance is in part an adaptation to oxidative stress. Previous studies have attributed this adaptation to increased expression of metallothionein genes and genes involved in the glutathione synthesis/recycling pathway. However, recent studies over the last several years have demonstrated

novel anti-oxidant and anti-apoptotic properties with members of the heme oxygenase-1 (HO-1)/biliverdin reductase (BVR) pathway. To investigate the role of HO-1/BVR in resistance to Cd-toxicity we established a Cd-adapted human hepatocellular liver (HepG2) Ter-On cell line by continuously culturing the cells in 5 $\mu$ M Cd for 16 weeks, with routine media change and cell passage every 3-4 days. After 16 weeks, control and Cd-adapted cells were dosed with additional 0.1, 0.5, 1, 10 and 20 $\mu$ M Cd concentrations and real-time PCR was used to compare gene expression of HO-1, BVRa, BVRb and glutathione reductase (GSR). Interestingly, basal expression of GSR was significantly down-regulated while HO-1, BVRa and BVRb was up-regulated in the Cd-adapted cell line. In addition, there was greater induction of BVRa and BVRb expression in the Cd-adapted cells after additional Cd treatment as compared to control cells. Custom PCR arrays (QIAGEN Inc) were used to analyze expression of genes related to stress and toxicity when control and Cd-adapted cells were dosed with 10 $\mu$ M Cd. The Cd-adapted cells displayed significant alterations in other genes related to oxidative stress, DNA repair and cell division/apoptosis signaling pathways, including many pathways linked to BVRa/ERK regulation, such as tumor necrosis factor (TNF), TNF receptor, lymphotoxin alpha, early growth response 1, insulin-like growth factor 1, interferon alpha and interferon beta 1. Future studies will investigate the direct role of HO-1 and BVR in regulating the potential anti-apoptotic properties of these Cd-adapted cells. [Supported by R00ES017044]

**PS 1730 Role of BCL-2 Proteins in Heat Shock-Induced Apoptosis.**

I. M. Mahajan<sup>1,2</sup>, M. Chen<sup>1,2</sup>, I. Muro<sup>2</sup>, C. W. Wright<sup>2</sup> and S. B. Bratton<sup>1,2</sup>.

<sup>1</sup>Molecular Carcinogenesis, UT Austin/MD Anderson Cancer Center, Smithville, TX;

<sup>2</sup>Pharmacology and Toxicology, University of Texas at Austin, Austin, TX.

Apoptosis is a programmed form of cell death executed by caspases (cysteine proteases) that cleave substrates exclusively after aspartic acid residues. In response to stress, cells often activate the intrinsic apoptotic pathway, wherein mitochondrial outer membrane permeabilization (MOMP) initiates the release of proapoptogenic proteins, such as cytochrome c and Smac, into the cytosol. In particular, cytochrome c promotes formation of a caspase-activating complex known as the Apaf-1-caspase-9 apoptosome. Heat shock (HS) is an ancient stress that activates both prosurvival (thermotolerance) and prodeath cellular responses, and we have previously shown that HS induces apoptosis through pathways that involve MOMP and downstream effector caspase-3 activation, but do not require activation of the apoptosome. HS-induced MOMP is strictly controlled by BCL-2 family members, which include both pro-apoptotic (e.g. Bax, Bim, Bid, etc.) and anti-apoptotic (e.g. Bcl-2, Mcl-1, etc.) proteins. Other studies suggest that HS initiates MOMP following cleavage of Bid by caspase-2. However, we observe that mouse embryonic fibroblasts (MEFs), lacking either caspase-2 or Bid, remain sensitive to HS. In contrast, we find that bim<sup>-/-</sup> MEFs are highly resistant to HS-induced apoptosis and exhibit significantly decreased levels of MOMP. Thus, our findings indicate that Bim is essential for HS-induced death, while caspase-2 and Bid function as part of an amplification loop. Interestingly, Bim is known to induce MOMP through direct activation of Bax and/or Bak, but we find that bax<sup>-/-</sup>/bak<sup>-/-</sup> MEFs are only partially resistant to HS-induced cell death, implying the existence of a Bim-dependent, Bax/Bak-independent pathway. We speculate that another proapoptotic Bcl-2 family member, namely Bok, may functionally substitute for Bax and Bak, or alternatively that Bim may directly permeabilize lysosomal membranes, resulting in the release of proapoptotic cathepsins. (These studies were supported by grants, CA129521 and GM096101, from the NIH.)

**PS 1731 SDF-1 $\beta$  Protects High Fat-Induced Cardiac Cell Apoptosis through Its Receptor CXCR7-Mediated AMPK Activation.**

Y. Zhao<sup>1,2</sup>, L. Cai<sup>2,1</sup> and W. Li<sup>1</sup>. <sup>1</sup>Cancer Center, First Bethune Hospital of Jilin University, Changchun, China; <sup>2</sup>KCHRI, University of Louisville, Louisville, KY.

Hyperlipemia often occurs in the patients with obesity and type 2 diabetes, and is also primary trigger for cardiac remodeling and dysfunction. Stromal cell-derived factor-1 $\beta$  (SDF-1 $\beta$ ) was cardiac protective, but whether it also protects the cardiac cells from high fat-induced apoptosis remains unknown. By using H9c2 cardiac muscle cell line, we observed the effect of SDF-1 $\beta$  on saturated free fatty acid-induced its apoptotic response. Exposure of H9c2 cells to palmitate at 62.5 nM for 15 h caused a significant apoptotic effect, shown by up-regulation of cleaved-caspase3. Pretreatment with SDF-1 $\beta$  significantly prohibited palmitate-induced apoptosis along with significant increases in AMPK-mediated IL-6 production. AMPK activator (AICAR) significantly prevents palmitate-induced cardiac apoptosis while AMPK inhibitor (compound C) prohibited SDF-1 $\beta$ 's protective effect. Direct addition of recombinant human IL-6 to cell cultures prevented palmitate-induced

apoptosis whereas IL-6 siRNA abolished the protective effect of SDF-1 $\beta$ . CXCR7 siRNA, but not CXCR4 antagonist abolished SDF-1 $\beta$ 's protective effect and above related signal transduction. These in vitro results suggest that SDF-1 $\beta$  prevents palmitate-induced cardiac apoptosis via its receptor CXCR7 and further activating AMPK-mediated IL-6 excretion. In vivo studies, by using type 2 diabetes models, we confirmed that high fat diet induced cardiac apoptosis, and that SDF-1 $\beta$  prevented high fat diet-induced cardiac apoptosis along with its activation of AMPK. This important finding opens a new road for the research of SDF-1 $\beta$ 's cardiac protection that is irrelevant with its well-known function of stem cell mobilization.

### PS 1732 Paraoxon Induces Cell Death by the Activation of Caspases in Cultured Human Pulmonary Cells.

D. J. Angelini<sup>1,2</sup>, R. A. Moyer<sup>3</sup>, A. Hajjaj<sup>1,4</sup>, S. Cole<sup>1,2,3</sup>, K. L. Willis<sup>1,2,3</sup>, J. Oyler<sup>5</sup>, R. M. Dorsey<sup>1</sup> and H. Salem<sup>1,6</sup>. <sup>1</sup>Edgewood Chemical Biological Center, Aberdeen Proving Ground, MD; <sup>2</sup>National Research Council, Washington DC; <sup>3</sup>Defense Threat Reduction Agency, Fort Belvoir, VA; <sup>4</sup>Science Applications International Corporation, Abingdon, MD; <sup>5</sup>US Army Medical Research Institute of Chemical Defense, Aberdeen Proving Ground, MD; <sup>6</sup>Department of Homeland Security, Chemical Security Assessment Center, Aberdeen Proving Ground, MD.

**INTRODUCTION:** Organophosphate chemicals are known to induce pulmonary toxicity in both humans and experimental animals. To elucidate the mechanism of organophosphate-induced cytotoxicity, we examined the effects of parathion and paraoxon on primary cultured normal human bronchial epithelial cells (NHBEs) as well as small airway cells (SAECs).

**METHODS:** We evaluated the viability/cytotoxicity of primary NHBEs and SAECs following exposures to the organophosphate chemicals parathion and paraoxon. Since caspases have a major role in the regulation of apoptosis and cell death, we evaluated paraoxon-induced cell death in the presence of the caspase inhibitor Z-VAD.

**RESULTS:** Parathion failed to induce losses in cellular viability at concentrations known to cause toxicity in vivo following a 24 hour treatment (IC50 >9mM) in either NHBEs or SAECs. Its toxic metabolite, paraoxon, produced a dose-dependent decrease in cell viability following a 24 hour treatment period for both pulmonary cell types (IC50 ~0.5mM). Treatment with paraoxon also induced caspase activation in these cells. Pharmacological inhibition of caspases with Z-VAD during paraoxon treatment protected against paraoxon-induced cell death.

**CONCLUSIONS:** These combined data suggest that paraoxon induces cell death in NHBEs and SAECs, at least in part, through the activation of caspases.

### PS 1733 BDE-154 Decrease Cell Proliferation, Viability and Mitochondrial Membrane Potential Leading to HepG2 Cell Death.

A. O. Souza<sup>1</sup>, L. C. Pereira<sup>2</sup>, M. Tasso<sup>1</sup>, D. P. Oliveira<sup>2</sup> and D. J. Dorta<sup>1</sup>. <sup>1</sup>Química, FFLRP-USP, Ribeirão Preto, Brazil; <sup>2</sup>Análises Clínicas, Bromatológicas e Toxicológicas, FCFRP-USP, Ribeirão Preto, Brazil.

**INTRODUCTION:** Polybrominated diphenyl ethers (PBDEs) are a class of flame retardants composed by 209 different congeners with evidences of several toxic potential on the organisms. Toxic damages of lower and higher brominated congeners have been widely reported but more information about other congeners to clarify of risk of PBDEs class on the health is still necessary. **OBJECTIVE:** The aim of this work was to investigate the effects of the BDE-154 on HepG2, because it had showed growth levels of bioaccumulation on the biotic compartments.

**METHODOLOGY:** We performed a cell proliferation test using SRB colorimetric assay in order to evaluate its inhibitory effects on cell proliferation and then we did a cell viability test by MTT assay, that was performed to investigate relationships between the inhibitory potential of cell growth with the induction of cell death. Subsequently, the effect on the mitochondrial membrane potential (MPP) using TMRM dye was performed to evaluate a possible effect on the cell mitochondria and finally the exposure of phosphatidylserine on the outer membrane using Annexin V and propidium iodeto (PI) staining was evaluated. In all tests, the cells were exposure at concentrations ranging from 0.1 to 25 $\mu$ M for 24 and 48 hours.

**RESULTS:** Our results shown that BDE-154 are capable of inhibiting cell proliferation at doses starting at 10 $\mu$ M ( $p < 0.05$ ) after 48 hours of exposure, although the results of MTT assay had shown a significant decrease in cell viability on lower doses in both times of incubation. Changes on cell proliferation and viability were followed by decrease of MPP and an increase of phosphatidylserine exposure at the cell membrane. **CONCLUSIONS:** According to our results, BDE-154 presents a significant potential to interfere with the mitochondrial homeostasis of HepG2 cells which can lead to apoptosis in the concentration of 25  $\mu$ M.

### PS 1734 Computational Dosimetry Driven Hazard Ranking of 25 Metal Oxide Nanomaterials Using Low- and High-Throughput In Vitro Toxicity Data.

D. Telesca<sup>2</sup>, J. G. Teeguarden<sup>1</sup>, T. Xia<sup>3</sup>, H. Zhang<sup>3</sup>, A. Nel<sup>3</sup>, J. G. Pounds<sup>1</sup> and B. D. Thrall<sup>1</sup>. <sup>1</sup>Biological Sciences, Pacific Northwest National Laboratory, Richland, WA; <sup>2</sup>Biostatistics, University of California Los Angeles, Los Angeles, CA; <sup>3</sup>Nanomedicine, California Nanosystems Institute, University of California Los Angeles, Los Angeles, CA.

Seeking to integrate broad sets of mechanistic and more traditional dose-response data across in vitro and in vivo systems, and between species, the nanotoxicology field faces the challenge of translating these data into knowledge that will impact public health policy for this emerging class of materials. Using a rich data set on in vitro toxicity of 25 metal oxides as an example, we present framework for nanomaterial risk assessment and hazard ranking based on a paradigm for nanomaterial dosimetry in vitro and in vivo that is consistent with current practice for chemical risk assessment. Integrating cytotoxicity and high-throughput data on 25 metal oxide nanoparticles with cellular dosimetry data derived from in vitro and in vivo models of nanoparticle dosimetry, we demonstrate the impact of cellular dosimetry on hazard ranking schemes. Specifically, the dosimetry hazard ranking approach showed that on a cellular dose and tissue-dose basis, the relative toxicity of the metal oxides is fundamentally different than those bases solely on exposure measures ( $\mu$ g/ml). For example, Co<sub>3</sub>O<sub>4</sub> was ranked #10 based on in vitro studies, but scaled based on tissue doses in exposed humans, Co<sub>3</sub>O<sub>4</sub> was the most hazardous material. Human exposure equivalents calculated using ISDD and MPPD models for each nanomaterial ranged from 0.1 to 10,000 mg/m<sup>3</sup>, indicting some but not all might pose a hazard for exposed humans. Making dosimetry corrections for iron oxide particles, we also show good correspondence between in vitro and in vivo inflammatory responses. The framework, along with high-throughput in vitro data, can clearly be used to rank nanomaterial hazards for broad classes of particles, though it remains an untested hypothesis that such approaches accurately reflect risk in exposed humans.

### PS 1735 Ranking and Profiling Nanomaterial (NM) Bioactivity by ToxCast High-Throughput Screening (HTS).

A. Wang<sup>1</sup>, E. Berg<sup>2</sup>, M. A. Polokoff<sup>2</sup>, J. Yang<sup>2</sup>, A. El-Badawy<sup>3</sup>, D. Reif<sup>1</sup>, N. Kleinstreuer<sup>1</sup>, S. Marinakos<sup>4</sup>, A. Badireddy<sup>4</sup>, S. H. Gavett<sup>1</sup>, D. Rotroff<sup>1</sup>, S. Gangwal<sup>5</sup>, J. Rabinowitz<sup>1</sup>, C. W. Matson<sup>6</sup>, T. Tolavmat<sup>3</sup>, M. Wiesner<sup>4</sup> and K. Houck<sup>1</sup>. <sup>1</sup>ORD, US EPA, Research Triangle Park, NC; <sup>2</sup>BioSeek, LLC, San Francisco, CA; <sup>3</sup>ORD, US EPA, Cincinnati, OH; <sup>4</sup>CEINT, Duke University, Durham, NC; <sup>5</sup>Xanofi, Raleigh, NC; <sup>6</sup>Environmental Sciences, Baylor University, Waco, TX.

HTS allows for rapid examination of large numbers of chemicals for biological effects and the results can be used to prioritize them for further assessment and provide mechanistic insight. To prioritize NMs for further testing, we screened NMs (Au, Ag, CeO<sub>2</sub>, CNT, CuO, TiO<sub>2</sub>, SiO<sub>2</sub>, or ZnO core) and their ion and micro counterparts for cytotoxicity, transcription factor activation, and cellular protein expression. We ranked samples by promiscuity (the number of assays affected) and potency. Two ranking methods produced very similar results and high promiscuity was coupled with high potency. Ag, Cu, and Zn samples were ranked highest priority for further testing. Sample replicates, screened in different test runs, had the same rankings, indicating consistency in data among test runs. To research potential mechanisms of bioactivity, we tested ion contribution to Cu NM bioactivity and compared CNT to asbestos in 8 BioMAP® human primary cell systems for tissue and inflammatory responses. 3 Cu stocks (micro-CuO, nano-CuO, fungicide A containing nano-Cu(OH)<sub>2</sub>) were split and one half was repeatedly washed until the wash liquid had the same electrical conductivity as pure H<sub>2</sub>O, indicating very few released ions. This wash decreased, but did not eliminate, bioactivity, suggesting released ions contribute to bioactivity. The bioactivity profiles of micro-CuO, nano-CuO, and washed nano-CuO were more similar to each other than to other Cu samples, including washed micro-CuO, implying micro- and nano-CuO were affected by the wash differently. The 3 asbestos had similar profiles but only minimal overlap with CNTs. One CNT had a similar profile with Cu, suggesting Cu was present in this sample. Thus HTS can be used to prioritize NMs and provide info on potential mechanism of bioactivity including chemical composition of the samples.

**PS 1736 Coating Nanoporous Alumina: Cellular Responses to Surface Layers of Zinc and Titanium Oxides.**

P. E. Petrochenko<sup>2,1</sup>, G. Kumar<sup>1</sup>, W. Fu<sup>3</sup>, S. A. Skoog<sup>2,1</sup>, Q. Zhang<sup>1</sup>, J. Zheng<sup>1</sup>, C. Liang<sup>3</sup>, P. L. Goering<sup>1</sup> and R. J. Narayan<sup>2</sup>. <sup>1</sup>CDRH, US FDA, Silver Spring, MD; <sup>2</sup>Joint Department of Biomed Engineering, University of North Carolina at Chapel Hill, Chapel Hill, NC; <sup>3</sup>Chemical Sciences Division, Oak Ridge National Lab, Oak Ridge, TN.

Nanoporous anodic aluminum oxide (AAO) membranes have applications in skin wound repair; the surface topography of these materials has been shown to modulate wound healing. Previous work by our group has shown that coating titanium dioxide (TiO<sub>2</sub>) onto nanoporous AAO does not affect cell viability and that zinc oxide (ZnO)-coated AAO membranes exhibit antimicrobial activity against several bacterial strains associated with skin infection. In this study, the nanoporous structure of 20, 100, or 200 nm pore diameter AAO membrane substrates was maintained by depositing nm-thick layers of TiO<sub>2</sub> or ZnO using an atomic layer deposition (ALD) process involving alternative adsorption/hydrolysis of Ti isopropoxide or diethyl Zn, respectively. X-ray spectroscopy (EDX) confirmed the presence of ZnO or TiO<sub>2</sub> on AAO membranes. Cell viability and inflammatory responses were evaluated on ZnO- and TiO<sub>2</sub>-coated AAO membranes. RAW 264.7 macrophages cultured on ZnO-coated AAO exhibited a significant decrease in metabolic activity (MTT reduction) after 24 or 48 h exposure; however, no changes were observed in lactate dehydrogenase (LDH) release or reactive oxygen species (ROS) production. L929 fibroblasts grown on TiO<sub>2</sub>-coated AAO had higher viability (MTT assay) than controls (uncoated AAO) after 48 hrs; no change in viability was observed using the Neutral Red assay. No significant increase in fibroblast cell proliferation (DNA assay) was observed. No TNF- $\alpha$  production or decrease in viability was seen in RAW 264.7 macrophages grown on TiO<sub>2</sub>-coated membranes. The total adsorbed protein per unit area on uncoated and TiO<sub>2</sub>-coated AAO was up to 12-times greater than that on tissue culture polystyrene. The results show that nm-thick ALD coatings maintain the nanoporous structure of AAO membranes. Further, antimicrobial ZnO coatings decrease cell viability and TiO<sub>2</sub> coatings appear to be more biocompatible *in vitro*.

**PS 1737 Potential Phototoxicity of Aged Al(OH)<sub>3</sub>-Coated TiO<sub>2</sub> Nanoparticles in Retinal Pigment Epithelial Cells.**

J. N. Ortenzio<sup>1</sup>, L. L. Degen<sup>2</sup>, R. Zucker<sup>2</sup>, J. Virkutyte<sup>3</sup>, S. R. Al-Abed<sup>4</sup>, H. Ma<sup>5</sup>, S. Diamond<sup>6</sup>, K. Dreher<sup>2</sup> and W. K. Boyes<sup>2</sup>. <sup>1</sup>Contractor, Research Triangle Park, NC; <sup>2</sup>US EPA, Research Triangle Park, NC; <sup>3</sup>Contractor, Cincinnati, OH; <sup>4</sup>US EPA, Cincinnati, OH; <sup>5</sup>Contractor, Duluth, MN; <sup>6</sup>US EPA, Duluth, MN.

Titanium dioxide (TiO<sub>2</sub>) nanoparticles (NPs) exposed to UVA radiation generate reactive oxygen species (ROS). As a component of sunscreen formulations, TiO<sub>2</sub> NPs may be coated with Al(OH)<sub>3</sub> to prevent ROS from causing oxidative damage to tissues. Simulated swimming pool water (SSPW) degrades the Al(OH)<sub>3</sub> coating which could reduce the coating's protective function. We examined the potential phototoxicity of 25 nm, Al(OH)<sub>3</sub>-TiO<sub>2</sub> NPs that had been aged in SSPW for 0 min, 45 min, 1 day, 3 days, 10 days, or 14 days. In two non-cellular assays, measuring methylene blue degradation or thiobarbituric acid reactive species, aged Al(OH)<sub>3</sub>-TiO<sub>2</sub> showed substantially less photocatalytic activity than the positive control: uncoated Aeroxide P25, 31 nm. In a cellular assay, a human-derived retinal pigment epithelium cell line (ARPE-19) was used as a site of photoreactivity. Cells were split into 24-well culture plates, incubated for 24h, then treated with 0, 3, 10, 30, or 100  $\mu$ g/ml of each aged NP or 30  $\mu$ g/ml of positive control. After treatment, the cells were either exposed to 1.5h UVA radiation or no light. 24h later, cell viability was assessed by live/dead assays (calcein-AM/propidium iodide). Flow cytometry and dark field microscopy verified that the TiO<sub>2</sub> NPs entered the cells. Flow cytometry showed dose-related increased side-scatter signal consistent with uptake of NPs, and dark field microscopy showed TiO<sub>2</sub> accumulation along the nuclear envelope and near the endoplasmic reticulum of ARPE-19 cells. No difference in cytotoxicity was observed after UVA irradiance among the SSPW-aged groups. The positive control yielded 100% cytotoxicity under UVA irradiation. The lack of phototoxicity observed with SSPW-aged Al(OH)<sub>3</sub>-TiO<sub>2</sub> suggests that degradation of the particle coating did not increase the risk of phototoxic reactions under the conditions tested.

This abstract does not reflect EPA policy.

**PS 1738 Silica and Gold Nanoparticle Exposure Decreases Phagocytosis in Mouse Raw 264.7 Cells.**

S. Bancos and K. M. Tyner. US FDA, Silver Spring, MD.

Silica (SiO<sub>2</sub>) and gold (Au) nanoparticles (NPs) have been proposed for various therapeutic and diagnostic applications. It has been previously shown *in vivo* that administration of NPs leads to particle accumulation in macrophages of the reticu-

loendothelial system independent of NP core composition, size, or mode of administration. There is, however, little to no information on whether NP accumulation affects macrophage function. Using a panel of *in vitro* assays, we assessed the proliferation, activation, cytokine production and phagocytosis ability of RAW 264.7 cells in response to non-toxic concentrations of SiO<sub>2</sub> NPs (~10 nm) and Au NPs (~10 nm) during a 6h-48h time course. There was a 50-60% reduction in cell number in SiO<sub>2</sub> NP-treated cells that was associated with an increase in the percentage of cells arrested in G0/G1 phase and a decrease in the percentage of cells in the S phase; there were no significant changes in the expression of CD40, CD80 and CD86 markers. Au NP-treated cells showed a 14- 40% decrease in cell number; neither the cell cycle status of Au NP-treated cells nor the expression of surface markers could be assessed due to Au NP interference with the flow cytometry assay. Among the cytokines analyzed, TNF- $\alpha$  levels increased only in cells treated with 0.01 g/L SiO<sub>2</sub> NP, whereas IL-6 and IL-10 levels did not change in SiO<sub>2</sub> NP- or Au NP-treated cells. The ability of SiO<sub>2</sub> NP- and Au NP- treated cells to phagocytose FITC-E. coli bioparticles was evaluated by flow cytometry and confocal microscopy. The results show that phagocytosis was reduced by ~50% in both SiO<sub>2</sub> NP- and Au NP- treated macrophages. Overall, the results indicate that 10 nm SiO<sub>2</sub> NP and Au NP exposure can impact macrophage phagocytosis *in vitro*, but does not appear to impact cytokine production or the expression of activation markers. A decrease in phagocytosis may lead to decreased immunity and diminished response to bacterial infections.

**PS 1739 Comprehensive Assessment of Property-Dependent Bioimpact of Engineered Nanomaterials Using Novel 'Bench-Top' Human Tissue Screening Platforms.**

R. Iyer<sup>1</sup>, J. Gao<sup>2</sup>, A. Nagy<sup>2</sup>, S. Iyer<sup>2</sup>, J. Hollingsworth<sup>3</sup>, J. Drocco<sup>4</sup>, J. Song<sup>2</sup>, T. Sanchez<sup>2</sup> and H. Wang<sup>5</sup>. <sup>1</sup>Defense Systems and Analysis, Los Alamos National Lab, Los Alamos, NM; <sup>2</sup>Biosciences Division, LANL, Los Alamos, NM; <sup>3</sup>MPA-CINT: Center for Integrated Nanotechnologies, LANL, Los Alamos, NM; <sup>4</sup>Theoretical Division, Los Alamos National Laboratory, Los Alamos, NM; <sup>5</sup>Chemistry Division, LANL, Los Alamos, NM.

The core focus of our effort was to develop human three-dimensional (3-D) *in vitro* tissue models to serve as a realistic representation of human exposures and for assessing NM toxicity to decisively rank what physico-chemical parameters can drive toxicity. Core NM parameters including composition, size, shape, redox activity, functionalization and charge were all tested by investigating a multitude of NMs. Kinetics of bioresponses such as necrosis, apoptosis, oxidative stress, cytokine secretion and changes in gene and protein expression were all evaluated in response to nanomaterial exposure. We also developed novel computational analytics to differentiate bioresponses as a factor of NM property. Network-inference-based methods, such as context-likelihood of relatedness (CLR), as well as clustering-based methods, such as principal component analysis (PCA) were used to identify a set of known regulons as well as other co-regulated transcripts potentially unique to nanotoxicity. Further investigation revealed that NM composition, followed closely by charge, were parameters which significantly influenced NM-driven toxicity. Moreover, we found significant differences between the molecular mechanisms of NMs toxicity in monolayer cell culture models versus our complex, more physiologically relevant tissue models. As such, we conclude that further development of human 3-D tissue models is warranted in order to gain accurate information regarding the risk and consequences of NM exposure.

**PS 1740 Genotoxicity of TiO<sub>2</sub> Anatase Nanoparticles in B6C3F1 Male Mice *Pig-A* and Flow Cytometric Micronucleus Assays.**

J. Yan<sup>1</sup>, R. Sadiq<sup>2,1</sup>, J. A. Bhalli<sup>1</sup>, R. S. Woodruff<sup>3</sup>, M. G. Pearce<sup>1</sup>, Y. Li<sup>1</sup>, T. Mustafa<sup>4</sup>, F. Watanabe<sup>4</sup>, L. M. Pack<sup>5</sup>, A. S. Biris<sup>4</sup>, Q. M. Khan<sup>2</sup> and T. Chen<sup>1</sup>. <sup>1</sup>Division of Genetic and Molecular Toxicology, National Center for Toxicological Research, US FDA, Jefferson, AR; <sup>2</sup>National Institute for Biotechnology and Genetic Engineering, Faisalabad, Pakistan; <sup>3</sup>Division of Microbiology, Arkansas Regional Laboratory, US FDA, Jefferson, AR; <sup>4</sup>Nanotechnology Center, University of Arkansas at Little Rock, Little Rock, AR; <sup>5</sup>Nanotechnology Core Facility, National Center for Toxicological Research, US FDA, Jefferson, AR.

*In vivo* micronucleus and *Pig-a* (phosphatidylinositol glycan, class A gene) mutation assays were conducted to evaluate the genotoxicity of 10 nm titanium dioxide anatase nanoparticles (TiO<sub>2</sub>-NPs) in mice. Groups of five 6- to 7-week-old male B6C3F1 mice were treated intravenously for three consecutive days with 0.5, 5.0, and 50 mg/kg TiO<sub>2</sub>-NPs for the two assays; mouse blood was sampled one day before the treatment and on Day 4, and Weeks 1, 2, 4, and 6 after the beginning of the treatment; *Pig-a* mutant frequencies were determined at Day -1 and Weeks 1, 2, 4 and 6, while percent micronucleated-reticulocyte (%MN-RET) frequencies were measured on Day 4 only. Additional animals were treated intravenously with three

daily doses of 50 mg/kg TiO<sub>2</sub>-NPs for the measurement of titanium levels in bone marrow after 4, 24, and 48 hrs of the last treatment. The measurement indicated that the accumulation of the nanoparticles reached the peak in the tissue 4 hrs after the administration and the levels were maintained for a few days. No increase in either *Pig-a* mutant frequency or the frequency of %MN-RETs was detected, although the %RETs was reduced in the treated animals on Day 4 in a dose-dependent manner indicating cytotoxicity of TiO<sub>2</sub>-NPs in the bone marrow. These results suggest that although TiO<sub>2</sub>-NPs can reach the mouse bone marrow and are capable of inducing cytotoxicity, the nanoparticles are not genotoxic when assessed with *in vivo* micronucleus and *Pig-a* gene mutation tests.

#### PS 1741 Comparative Assessment of Nanomaterial Definitions and Considerations for Implementation.

R. David<sup>4</sup>, D. R. Boverhof<sup>1</sup>, J. H. Butala<sup>2</sup>, S. Clancy<sup>3</sup>, M. Lafronconi<sup>5</sup> and J. West<sup>6</sup>. <sup>1</sup>The Dow Chemical Company, Midland, MI; <sup>2</sup>Ferro Corp, Cleveland, OH; <sup>3</sup>Evonik Degussa, Parsippany, NJ; <sup>4</sup>BASF Corp, Florham Park, NJ; <sup>5</sup>Procter & Gamble, Cincinnati, OH; <sup>6</sup>American Chemistry Council, Washington DC.

The use of nanomaterials is bringing promising new advances to science and technology. In concert have come calls for increased regulatory oversight to ensure their appropriate identification and control. If nanomaterial-specific regulations are implemented, it will be critical that they are accompanied by definitions that are clear, consistent and practical to apply. Numerous definitions for nanomaterials have been proposed by various government, industry, and standards organizations; however, these definitions differ in their core elements and scope. A comprehensive comparative assessment was conducted on existing nanomaterial definitions with the goal of identifying elements essential for a sound regulatory definition. Common elements across definitions included size and dimensions; however, size limits were inconsistent and several important elements were not captured consistently including: consideration of agglomerates and aggregates, distributional thresholds, novel properties and solubility. Other important differences included number size distributions versus weight distributions and natural versus intentionally-manufactured materials. Accordingly, this analysis was extended to identify the critical elements to clearly define the materials subject to a nanomaterial regulation. The analysis also evaluated the extent of characterization required to determine whether a material falls within current nanomaterial definitions and found that some are not aligned with currently available analytical capabilities. Overall, this analysis highlights the similarities and differences in currently proposed nanomaterial definitions as well as the technical constraints that will need to be addressed for the successful implementation of a regulatory nanomaterial definition.

#### PS 1742 Cytotoxicity and Genotoxicity Studies in A549 Cells Cultured with Metal Oxide Nanoparticles.

A. Miyajima-Tabata<sup>1</sup>, K. Sakai<sup>1</sup>, T. Kawakami<sup>2</sup>, R. Kato<sup>1</sup>, A. Matsuo<sup>1</sup> and K. Isama<sup>2</sup>. <sup>1</sup>Division of Medical Devices, National Institute of Health Sciences, Tokyo, Japan; <sup>2</sup>Division of Environmental Chemistry, National Institute of Health Sciences, Tokyo, Japan. Sponsor: A. Hirose.

Nanomaterials are now widely used in various fields of science, technology and medicine. However, there are many unclear safety issues because they are new materials. An *in vitro* cellular toxicological study using well-characterized nanoparticles is conducted for the evaluation of the biological effects of nanoparticles. In this study, we compared the sensitivity of human lung-derived epithelioid-like cell line A549 cells and Chinese hamster lung fibroblast (CHL) cells to nanoparticles. This study also evaluated the cytotoxicity and the genotoxicity of ten kinds of metal oxide nanoparticles (MNs; primary diameter: <50 nm) in A549 cells.

A549 and CHL cells were treated with ZnO or polystyrene as typical nanoparticles and the cytotoxicity and the genotoxicity were examined. A549 cells were treated with MNs and the cytotoxicity and the genotoxicity of MNs were evaluated. The cytotoxicity was evaluated with colony formation and MTT assays, and the genotoxicity test was evaluated with an *in vitro* micronucleus test. The physicochemical properties, such as the hydrodynamic diameter of secondary MNs, the zeta potential etc., were determined in both suspension and 10%FBS-MEM.

No remarkable difference was observed between A549 and CHL cells in the cytotoxicity and the genotoxicity when treated with ZnO or polystyrene. The hydrodynamic diameter of MNs observed in suspension and 10%FBS-MEM were 41.0 to 256.8 nm and 152.9 to 1388.6 nm, respectively. Although the zeta potentials of MNs measured in suspension were positive (+41.6 to +62.1 mV), except SiO<sub>2</sub> and ZnO (-54.4 and -7.5 mV), all of the zeta potentials of MNs measured in 10%FBS-MEM were negative (-22.7 to -10.7 mV). Cytotoxicity was observed following treatment with CuO, NiO, ZnO, ITO, and Y<sub>2</sub>O<sub>3</sub> in the colony formation assay and with CuO, NiO, and ZnO in the MTT assay. The results of the genotoxicity study will be discussed.

#### PS 1743 In Vitro Toxicity Evaluation of Chemical Biological Defense (CBD) Nanomaterials.

C. J. Cao, A. O'Neill, L. C. Crouse and M. S. Johnson. *Toxicology Portfolio, US Army Institute of Public Health, Aberdeen Proving Ground, MD.*

Nanomaterials are gaining in commercial and military applications which yield new capabilities applicable to CBD. US Army Public Health Command (US-APHC) and Office of the Surgeon General (OTSG) have made efforts in chemical, biological, radiological and nuclear incident response for protecting the work force, civilian and military, from the unintended consequences of nanotechnology processes and materials exposures. The study used the Microtox® Toxicity Test System and Neutral Red Uptake (NRU) assay to fast evaluate four CBD nanomaterials for their aquatic toxicity in marine organisms, *Vibrio fischeri*, and basal cytotoxicity in human liver cells in support of the ongoing USAPHC/OTSG efforts. Four nanomaterials: RNP-212 and FAST-ACT®, proprietary formulation of nanocrystalline metal oxides used for neutralizing a wide range of toxic chemicals and chemical warfare agents; PhotoScrub™, a fiberglass cloth coated with TiO<sub>2</sub> that uses UV light induced catalytic ionization of TiO<sub>2</sub> to destroy chemical/biological warfare agents; Nano SBC, a nanosized sodium bicarbonate being investigated as a replacement fire extinguishing agent in hand held fire extinguishers of Army Aviation Weapons Systems, were selected for these tests. Microtox toxicity (EC50 15min; mg/L) shows FAST-ACT (13.78) > RNP-212 (362) > Nano SBC (1394) > PhotoScrub (>2500). Using US Fish and Wildlife Service aquatic toxicity criteria, FAST-ACT and RNP-212 are considered "slightly toxic" and "practically nontoxic", respectively; both Nano SBC and PhotoScrub are considered "relatively harmless". The Microtox study fills the data gap for aquatic toxicity information for the new nanomaterials. Neither FAST-ACT, RNP-212, PhotoScrub at 1250 µg/mL, nor Nano SBC at 2500 µg/mL were found toxic to human cells with NRU assay. The human basal cytotoxicity data and predicted LD50 are comparable with the results from animal studies. Both *in vitro* and *in vivo* studies assessed these four nanomaterials as low hazard.

#### PS 1744 Inhibition of Adipogenic Differentiation of Human Mesenchymal Stem Cells by TiO2 Nanoparticles.

Y. Zhang<sup>1</sup>, L. Guo<sup>2</sup>, L. Yu<sup>2</sup>, Y. Gao<sup>2</sup>, Y. Jones<sup>1</sup>, A. Keasling<sup>1</sup>, B. Green<sup>2</sup>, D. Hansen<sup>2</sup>, A. Inselman<sup>2</sup>, L. Shi<sup>2</sup>, P. C. Howard<sup>1</sup> and B. Ning<sup>2</sup>. <sup>1</sup>NCTR/ORANanotechnology Core Facility, Office of Scientific Coordination, NCTR/FDA, Jefferson, AR; <sup>2</sup>Division of Systems Biology, NCTR/FDA, Jefferson, AR.

Nanotechnology has resulted in the creation of many new materials and devices with a vast range of applications. TiO<sub>2</sub> has historically been used as a pigment with many applications, and nanoscale TiO<sub>2</sub> is additionally appearing in human consumer products, raising safety issues of human health and environmental concerns. Stem cells are proposed to be attractive tools for toxicity testing because of their sensitivity to external stimuli during differentiation. The physical and chemical properties of TiO<sub>2</sub> nanoparticles were characterized using transmission electron microscopy (TEM), nanoparticle tracking analysis, dynamic light scattering, Brunauer-Emmett-Teller, Raman and X-ray fluorescence spectroscopy. We examined the impact of TiO<sub>2</sub>, and other nanomaterials, on cytotoxicity and differentiation of human mesenchymal stem cells (hMSC). TiO<sub>2</sub> nanoparticles induced cytotoxicity in a concentration-dependent manner in hMSCs. Additionally, the differentiation of hMSCs to adipocytes, determined using imaging and Oil Red O staining, was inhibited in a concentration-dependent manner. Moreover, uptake of the TiO<sub>2</sub> nanoparticles by hMSCs was confirmed using TEM, suggesting a possible endocytosis pathway. The mRNA expression for the adipogenic markers adiponectin, aP2, and LPL were significantly reduced to 61%, 53%, and 61% of control levels following exposure to TiO<sub>2</sub> nanoparticles. Furthermore, incubation of the TiO<sub>2</sub> with the mesenchymal stem cell lysate resulted in the identification of 208 proteins associated with the nanoparticles using proteomic and mass spectrometry analyses. These results indicate (i) the interaction and impact of nanoparticles with stem cells is selective (other nanoparticles did not induce this effect), (ii) TiO<sub>2</sub> nanoparticles inhibited differentiation of mesenchymal stem cells, and (iii) further work is needed to elucidate the mechanism of action of TiO<sub>2</sub> in this cell population.

**PS 1745 Comparison of Toxicity of Bare- and Phospholipid-Coated Iron Oxide Nanoparticles in Different Cell Lines.**

E. Park<sup>1</sup>, D. Choi<sup>1</sup>, H. Umh<sup>2</sup>, J. Kim<sup>1</sup>, D. Kim<sup>1</sup>, S. Kim<sup>1</sup> and Y. Kim<sup>2</sup>.  
<sup>1</sup>Department of Molecular Science and Technology, Ajou University, Suwon, Republic of Korea; <sup>2</sup>Department of Chemical Engineering, Kwangju University, Seoul, Republic of Korea. Sponsor: E. Park.

We pursue a better quality of life as well as a rich life through the development of science and technology. However, the scientific principles and its application threaten our health sometimes. In this study, we compared the toxicity of phospholipid coated-iron oxide nanoparticles (PLC-FeNPs) and bare-FeNPs in different cell lines. PLC-FeNPs showed higher negative charge than that of bare-FeNPs in the vehicle, but not in the cell culture media containing fetal bovine serum. In addition, the trend of uptake in each cell lines was very similar between both types of FeNPs, despite differences in their diameters. However, cell cycle changes varied according to the cell line and the type of FeNPs. We performed further study using two macrophage cell lines. At 1 h after exposure, MH-S cells exposed to both types of FeNPs showed a strong correlation between gene expression changes despite the uptake process was different, but RAW264.7 cells exposed to both types of FeNPs showed a weak correlation between gene expression changes despite the uptake process was similar. At 24 h after exposure, two macrophage cells exposed to PLC-FeNPs and RAW264.7 cells exposed to bare-FeNPs induced the increase in the number of autophagosome-like vacuoles. While, the cytosolic component of MH-S cells exposed to bare FeNPs completely disappeared, although the membrane remained intact. The predominant gene in MH-S and RAW264.7 cells was also different. Furthermore, when treated with both types of FeNPs, RAW264.7 cells secreted TNF $\alpha$  only, whereas MH-S cells secreted IL-1 $\beta$  and IL-6 along with TNF $\alpha$ . Based on these results, choice of cell line is very important to improve the reliability of in vitro toxicity data. Further, we think that the increase of autophagosome-like vacuoles may be an important cause of cell death which is caused by nanoparticles.

**PS 1746 Mechanisms of Silica Nanoparticle-Induced Interleukin-8: Requirement of p38/TACE/TGF- $\alpha$ /EGFR-Cascade and NF- $\kappa$ B Signalling in Lung Epithelial Cells.**

M. A. Refsnes, T. Skuland, J. Øvrevik, P. E. Schwarze and M. Låg. Department of Air Pollution and Noise, Norwegian Institute of Public Health, Oslo, Norway. Sponsor: M. Løvik.

Nanoparticles (NPs) of non-crystalline (amorphous) silica particles (SiNPs) are used in a large range of products. Inhalation of NPs represents a potential health hazard and may induce inflammation in lung tissues. We have previously shown that SiNPs induced marked cytokine responses independently of particle uptake in human bronchial epithelial cells (BEAS-2B). In the present study the mechanisms involved in SiNP-induced IL-8 responses were further examined. SiNP-exposure induced an early increase in phosphorylation of p65 (NF- $\kappa$ B) as well as the three main MAP-kinases ERK1/2, p38 and JNK, concurrent with an early up-regulation of IL-8 mRNA. SiNP also induced a time-dependent increase in phosphorylation of the epidermal growth factor receptor (EGFR) and release of the EGFR-ligand transforming growth factor (TGF)- $\alpha$ . SiNP-induced IL-8 responses were attenuated by the p38-inhibitor SB202190, the NF $\kappa$ B-inhibitor PDTC-p65 and siRNA against p65, as well as the EGFR-inhibitor AG1478, a TGF- $\alpha$ -neutralizing antibody and TAPI-1 (inhibitor of the metalloprotease TACE which cleaves pro-TGF- $\alpha$  to TGF- $\alpha$ ). However, inhibitors of ERK and JNK did not exert any effect on SiNP-induced IL-8. Moreover, SiNP-induced EGFR-phosphorylation was inhibited by AG1478 and TAPI-1, and SB202190 reduced the SiNP-induced TGF- $\alpha$  response. The SiNP-induced phosphorylations of p38 and p65 were not affected by TAPI-1 or AG1478. Thus, SiNP appeared to induce EGFR-phosphorylation through a p38- and TACE-dependent cleavage/release of TGF- $\alpha$ . Interestingly, EGF and TGF- $\alpha$  induced little effect on IL-8 release compared to SiNP, suggesting that EGFR-signalling alone is an insufficient stimuli for IL-8 induction. In conclusion, SiNP-induced IL-8 responses seemed to require activation of p38/TACE/TGF- $\alpha$ /EGFR-cascade, presumably acting in concert with the classical NF- $\kappa$ B pathway in BEAS-2B cells.

**PS 1747 Role of Tungstate Nanoparticles in the Production of ROS and Induction of Cellular Damage.**

K. M. Dunnick<sup>1,2</sup>, M. A. Badding<sup>1</sup>, N. R. Fix<sup>1</sup>, J. M. Patete<sup>3</sup>, S. S. Wong<sup>3,4</sup>, V. Castranova<sup>1</sup> and S. S. Leonard<sup>1,2</sup>. <sup>1</sup>HELD, National Institute for Occupational Safety and Health, Morgantown, WV; <sup>2</sup>Pharmaceutical and Pharmacological Sciences, West Virginia University, Morgantown, WV; <sup>3</sup>State University of New York at Stony Brook, Stony Brook, NY; <sup>4</sup>Brookhaven National Laboratory, Upton, NY.

Alkaline-earth metal tungstate AWO<sub>4</sub> (A= Ca, Ba, Sr) nanoparticles are currently being used in a variety of applications including use as components of medical equipment, optical fibers, gas sensors, and scintillator detectors. Due to tungstate nanoparticle versatility, their manufacturing is expected to increase within the next 10 years. Our ongoing study is designed to examine the effects of tungstate nanoparticle exposure in order to develop safe workplace practices to limit exposure. Electron Spin Resonance (ESR) was used to measure hydroxyl radical ( $\cdot$ OH) production of tungstate nanoparticles following incubation with either hydrogen peroxide (H<sub>2</sub>O<sub>2</sub>) or RAW 264.7 cells. Additionally, enhanced dark field microscopy was used to assess nanoparticle association and engulfment by RAW cells over multiple time points up to 3 hours. Assays measuring H<sub>2</sub>O<sub>2</sub> production, oxygen consumption, DNA damage and lipid peroxidation were used to assess possible cellular injury following RAW cell incubation with tungstate nanoparticles. Data showed that tungstate nanoparticles are capable of producing  $\cdot$ OH in the presence of H<sub>2</sub>O<sub>2</sub> and RAW cells. Further, tungstate nanowires produced significantly greater  $\cdot$ OH compared to nanospheres as shown through ESR measurements. Initial dark field microscopy data showed an increase in association between tungstate nanoparticles and cells and a decrease in non-specific binding after 3 hours of exposure. Cellular damage results in conjunction with ESR data will promote an understanding of tungstate nanoparticle toxicity. It is important to understand the damaging effects and free radical production produced by tungstate nanoparticle exposure in order to ensure that accurate toxicity models are developed and to promote proper training in nanoparticle inhalation prevention.

**PS 1748 Comparative *In Vitro* Toxicity Study of Bismuth and Bismuth-Derivatives Nanoparticles.**

A. De Vizcaya-Ruiz<sup>1</sup>, M. Esquivel-Gaón<sup>1,6</sup>, O. C. Barbier<sup>1</sup>, M. Uribe-Ramirez<sup>1</sup>, J. Narváez-Morales<sup>1</sup>, J. Muñoz-Saldaña<sup>2</sup>, S. Velumani<sup>3</sup>, Y. Matsumoto<sup>3</sup>, D. Diaz<sup>4</sup>, E. Berea<sup>5</sup>, K. A. Dawson<sup>6</sup> and S. Anguissola<sup>6</sup>. <sup>1</sup>Toxicology, Cinvestav, Mexico City, Mexico; <sup>2</sup>Unidad Queretaro, Cinvestav, Queretaro, Mexico; <sup>3</sup>Electrical Engineering Department, Cinvestav, Mexico City, Mexico; <sup>4</sup>Facultad de Química, UNAM, Mexico City, Mexico; <sup>5</sup>Farmaquímica, Mexico City, Mexico; <sup>6</sup>CBNI, University College Dublin, Dublin, Ireland.

Bismuth and bismuth-derived nanoparticles (Bi-NP) were developed for safer consumer applications as bioprobes, photocatalysts, piezoelectrics and contrast agents. A comparative in vitro study was performed to test the biointeraction and toxicity of Bi-NP - bismuth trioxide (Bi<sub>2</sub>O<sub>3</sub>), bismuth vanadate (BiVO<sub>4</sub>), bismuth antimony (Bi-Sb), bismuth-sodium-barium-titanate (BNT-BT), and zero-valent colloidal Bi (ZV-Bi). Dispersion and stability in biological fluids and in vitro toxic effects in target cells (liver-HepG2, kidney-LLCPK1, lung-A549 and brain-SHSY5Y) were evaluated using a nanometer fractionized suspension (<200 nm) achieved through sonication, centrifugation, and addition of bovine serum albumin (BSA) to reduce agglomeration. Scanning electron microscopy (SEM) confirmed morphological analysis and dispersion of Bi-NP. Cytotoxicity was observed at high concentrations (100  $\mu$ g/ml) at 24 to 72 h, using well established LDH and MTT assays and High Content Analysis. Lung and brain cells were more susceptible, the main form of cell death was necrosis without involving reactive oxygen species (ROS) generation. Cell cycle analysis showed arrest at G0-G1 phase with BNT-BT and Bi-Sb. With BiVO<sub>4</sub> treatment an increase in S-phase and significant DNA damage assessed with the comet assay, were observed. No relevant acute cytotoxicity was observed in the exposed cell systems from the initial screening of Bi-NP. The severity of biological outcomes of Bi-NP in descending order were BiVO<sub>4</sub>>Bi<sub>2</sub>O<sub>3</sub>>Bi-Sb>BNT-BT>ZV-Bi. Further work is underway to elucidate the mechanisms and nuclear effects, and to connect the biological effects with the physicochemical properties of the Bi-NP. Funding from the European Community Seven Framework Programme and CONACYT (Grant agreements #263878 and 12514).

**PS 1749 Long-Term Inhalation Study with Nanomaterials: Characterization of As-Produced Properties and Persistence Simulation Assays.**

W. Wohlleben<sup>3,1</sup>, L. Ma-Hock<sup>1</sup>, J. Keller<sup>1</sup>, K. Wiench<sup>2</sup> and R. Landsiedel<sup>1</sup>.  
<sup>1</sup>Experimental Toxicology and Ecology, BASF SE, Ludwigshafen am Rhein, Germany;  
<sup>2</sup>Product Safety, BASF SE, Ludwigshafen am Rhein, Germany; <sup>3</sup>Polymer Physics, BASF SE, Ludwigshafen am Rhein, Germany.

The most urgent knowledge gap in nanosafety research concerns the long-term fate and effects of nanomaterials that may have been released into the air or the environment. BASF and the German Ministry for the Environment (BMU) have initiated a chronic inhalation study as part of the EU project NanoREG. Here we report whether the materials chosen can be regarded as representatives of poorly soluble biopersistent (PSB) particles.

The original batch of CeO<sub>2</sub> distributed as NM212 from the OECD sponsorship program and an identical reproduction of the BaSO<sub>4</sub> distributed as NM220 were characterized by 20 physical-chemical endpoints according to the nanospecific REACH guidance R7.1, benchmarked against TiO<sub>2</sub> (NM105) and the non-persistent SiO<sub>2</sub> (Aerosil 150). The as-tested solubility was simulated by incubation for 28d in buffer (PBS) or phagolysosomal fluid (PSF), or 1d in stomach (0.1N HCl). Analysis included released ions by atom spectroscopy, agglomeration by analytical ultracentrifugation and laser diffraction, morphology by electron microscopy (TEM, SEM) and selected area electron diffraction (SAD).

The re-characterization of CeO<sub>2</sub> NM212 and BaSO<sub>4</sub> NM220 confirms their conformity with earlier work on the OECD batches by PROSPECT and NanoCare projects. The solubility of CeO<sub>2</sub> NM212 is as low as TiO<sub>2</sub> NM105. The positive control SiO<sub>2</sub> dissolves as expected. The solubility of BaSO<sub>4</sub> NM212 in all media, including PSF, is vanishing against the positive control, and noticeable only in 0.1N HCl. All materials, incl. TiO<sub>2</sub>, undergo morphological changes by Ostwald ripening and recrystallization in PSF and HCl, but retain their crystallinity.

Dissolution is 0 to 0.1% per month; extrapolated on the chronic inhalation study, CeO<sub>2</sub> NM212 and BaSO<sub>4</sub> NM220 remain 99% persistent.

**PS 1750 Intracellular Generation of Reactive Oxygen Species As a Central Parameter for the Interaction of Manganese Oxide Nanoparticles with Lung Epithelial Cells.**

U. Sydikl<sup>1</sup>, C. Bieschke<sup>1</sup>, D. Ströckmann<sup>1</sup>, M. Gotic<sup>2</sup>, S. Music<sup>2</sup> and K. Unfried<sup>1</sup>. <sup>1</sup>IUF, Dueseldorf, Germany; <sup>2</sup>Institute Ruder Boskovic, Zagreb, Croatia. Sponsor: T. Haarmann-Stemmann.

Nanoparticles consisting of manganese oxide have been suggested for several innovative technological approaches, including the use in nanomedicine and diagnostics. Therefore, the interaction of such nanoparticles with human target cells is of particular interest for the success of nanomedical approaches but also with regard to unintended side effects. To address this problem, we tested different kinds of manganese nanoparticles (MnNP) in an in vitro system which we earlier evaluated for proliferative, apoptotic, and pro-inflammatory endpoints induced by poorly soluble nanoparticles.

MnNP were synthesized and the biological and toxic effects of the generated particles were studied in comparison to carbon nanoparticles (CNP) in dose response experiments with rat and human lung epithelial cell lines. After physico-chemical characterization, a set of three MnNP consisting of Mn<sub>3</sub>O<sub>4</sub> or MnO<sub>2</sub> with significant differences in size and shape were selected. According to the different oxidation stages of manganese, the particles showed significant differences in Fenton reactivity in the cell free system. These data, however, did not reflect the capacity of the particles to induce intracellular oxidative stress. However, quantitative differences in intracellular reactive oxygen species (ROS) correlated with the capacity to trigger membrane-dependent signaling processes. Furthermore, the metabolic activity (WST-Assay) was negatively correlated with intracellular ROS, indicating a link between mitochondrial activity and ROS generation. None of the particles had effects on the membrane integrity of the cells. The data clearly demonstrate that the intracellular generation of ROS by MnNP, probably determined by particle size and shape, has more relevance for nanoparticle cell interaction than the oxidative capacity of the particles themselves.

**PS 1751 The Effects of Ceria Nanoparticles on Primary Human Monocyte-Derived Macrophages and Bronchial Macrophages.**

J. D. Marshburn<sup>1</sup>, A. B. Rice<sup>1</sup>, M. D. George<sup>1</sup>, S. M. Anderson<sup>1</sup>, N. J. Walker<sup>2</sup>, S. Garantzotis<sup>1</sup> and S. Hussain<sup>1</sup>. <sup>1</sup>Clinical Research Program, NIEHS/National Institute of Health, Durham, NC; <sup>2</sup>National Toxicology Program, NIEHS, Durham, NC.

Cerium dioxide (CeO<sub>2</sub>) nanoparticles (NPs) are used in various industrial and consumer product applications and are of significant environmental health interest. The health effects of CeO<sub>2</sub> NPs on primary human cells are poorly understood. We have previously shown that CeO<sub>2</sub> NPs are toxic to primary human peripheral blood monocytes at relatively low doses, which led to apoptosis and autophagy. Now we aimed at deciphering the cytotoxic effects of CeO<sub>2</sub> NPs in mature macrophages (human peripheral blood monocyte-derived macrophages) and bronchial macrophages. CD14<sup>+</sup> cells were isolated from peripheral blood samples of healthy volunteers and matured ex-vivo over a 7 day period to obtain macrophages. Bronchial macrophages were isolated from sputum inductions of healthy volunteers. Cells were exposed to 0, 1, 5, 10, or 20 µg/mL CeO<sub>2</sub> NPs for over a period of 24 or 48 hours. Transmission electron microscopy analysis revealed that both, blood and bronchial macrophages were internalizing CeO<sub>2</sub> NPs and were found either in vesicles or free cytoplasm. No significant change was observed in the viability of both types of cells after exposure to CeO<sub>2</sub> NPs. Moreover, we did not observe any increase in caspase 3/7 activity after exposure to CeO<sub>2</sub> NPs. We found that this increased resistance to NPs as compared to monocytes was due to decreased apoptosis and autophagy induction in mature cells. In conclusion we demonstrate that mature antigen presenting cells are resistant to the cytotoxic effects of environmentally relevant CeO<sub>2</sub> NP exposures.

**PS 1752 Structural Basis for the Toxic Potential of Cellulose Nanocrystals.**

F. L. Sinche<sup>1</sup>, J. Simonsen<sup>3</sup> and S. Harper<sup>1,2</sup>. <sup>1</sup>Environmental and Molecular Toxicology, Oregon State University, Corvallis, OR; <sup>2</sup>Chemical, Biological and Environmental Engineering, Oregon State University, Corvallis, OR; <sup>3</sup>Wood Science & Engineering College of Forestry, Oregon State University, Corvallis, OR.

Cellulose nanocrystals (CNCs) are a renewable nanomaterial that holds promise for an array of nano-related applications such as drug delivery and reinforcing nanocomposites. Although the core material of CNC is widely believed to be biocompatible, some of its intrinsic features such as geometrical ratio (L/d) and its high strength and stiffness are reminiscent of other fiber-like nanomaterials such as carbon nanotubes and metal oxides crystals, which have been reported to induce toxicity. Despite these similarities, we still lack knowledge of how those features of CNC may affect biological responses in vivo. Following acid hydrolysis of cellulose fibers to obtain CNC, we further used surface modifications and a wide range of concentrations to study the influence of fibrous and spherical shapes of CNC on the biological responses using zebrafish embryos as a model organism. We account for the surface modifications of CNC and differentiate between the responses elicited by embryos exposed to nanofibrillated cellulose (NFC) synthesized via TEMPO (T) and mechanical homogenization (H). We found chemical modifications of CNC yielded homogenous dispersion and the conversion of surface functional groups for charge modifications was high. Using morbidity and mortality measures in embryonic zebrafish exposed to the CNC formulations, our findings suggest relatively low toxicity from both CNC and surface-modified CNCs compared to hundreds of other nanomaterials that have been tested in our model system (nbi.oregonstate.edu). However, NFC-T and NFC-H influenced the toxicity in a concentration-dependent manner. Our results give insight into the biological responses from in vivo exposures using cellulosic nanomaterials with fiber-like and modified-charge features.

**PS 1753 Identification of Metal and Silicate Particles Including Nanoparticles in Electronic Cigarette Fluid and Aerosol.**

M. T. Williams<sup>1</sup>, A. Villarreal<sup>1</sup>, K. Bozhilov<sup>2</sup>, S. Lin<sup>1</sup> and P. Talbot<sup>1</sup>. <sup>1</sup>Cell Biology and Neuroscience, University of California, Riverside, Riverside, CA; <sup>2</sup>Central Facility for Advanced Microscopy, University of California Riverside, Riverside, CA.

Electronic cigarettes (EC) deliver aerosol by heating fluid containing nicotine, flavorings, and a humectant. EC cartomizers combine the fluid chamber and heating element in a single unit. Because EC do not burn tobacco, they may be safer than conventional cigarettes. Their use is rapidly increasing worldwide with little prior testing of their aerosol. We hypothesized that EC aerosol contains metals derived from the various components. Cartomizer contents and aerosols were analyzed

using microscopy, cytotoxicity testing, x-ray microanalysis, particle counting, and inductively coupled plasma optical emission spectrometry. A nickel-chromium filament was coupled to a thicker silver coated copper wire. The silver coating was sometimes missing. Four tin solder joints attached the wires to each other and coupled the copper/silver wire to the air tube and mouthpiece. All cartomizers had evidence of use before packaging (burn spots on the fibers and electrophoretic movement of fluid in the fibers). Fibers in two cartomizers had green deposits that contained copper. Centrifugation of the fibers produced large pellets containing tin. Tin particles and tin whiskers were identified in cartridge fluid and outer fibers. Cartomizer fluid with tin particles was cytotoxic in assays using human pulmonary fibroblasts. The aerosol contained particles >1µm comprised of tin, silver, iron, nickel, aluminum, and silicate and nanoparticles (< 100 nm) of tin, chromium, and nickel. Of 22 elements identified, 12 were present in concentrations higher than the minimum risk level. Many of the elements identified in EC aerosol are known to cause respiratory distress and disease. The presence of metal and silicate particles in cartomizer aerosol, often above minimal risk levels, demonstrates the need for improved quality control in EC design and manufacture and studies on how EC aerosol impacts the health of users and bystanders.

#### PS 1754 Does Nanostructured Synthetic Amorphous Silica Disintegrate after Oral Uptake?

M. Maier<sup>1</sup>, F. Babick<sup>2</sup>, R. R. Retamal Marin<sup>2</sup> and M. Stintz<sup>2</sup>. <sup>1</sup>Evonik Industries AG, Hanau, Germany; <sup>2</sup>Technical University Dresden, Dresden, Germany. Sponsor: D. Warheit.

The interest in manufactured nanomaterials with potential new properties has led to increasing concern about their potential systemic uptake and fate as well as the associated risk to humans. Materials applied in processed food are of special interest. Synthetic amorphous silica (SAS) is a nanostructured material formed by flame hydrolysis or precipitation that has been used for decades. In commercial products, basic structural elements are submicron aggregates (fused nanosized primary particles) that themselves form micrometer (or even larger) agglomerates. SAS is employed in a variety of products, e.g. as free-flow agent in soup powders. As to risk evaluation, it is important to understand whether structural changes may occur during the further processing or after oral uptake.

In a first step, we addressed possible effects of heating in water (modeled processing of soup powder) and acid environment (pH of gastric juice) on the structure and size distribution of SAS. Methods for the reproducible dispersion of SAS and the reliable determination of the volume weighted particle size distribution of SAS suspensions were developed and validated. Two food grade SAS types were studied: precipitated SAS and pyrogenic (fumed) SAS. SAS was first heated in water (100 °C) and then poured into HCl to reach pH=1.3 (paddle apparatus). During both steps time dependent changes in the volume weighted size distribution were monitored using laser diffraction (LD).

LD with validation, e.g. by comparison to microsieving analysis, proved as a reliable technique to characterize the dispersity of SAS suspensions and to evaluate the volume fraction of fine particles. Heating of SAS in water is only a weak dispersion leading to size distributions well above 1 µm. In acid environment (2 hours, pH=1.3) no significant changes in dispersity of SAS – neither agglomeration nor erosion of agglomerates or aggregates – was observed. In separate animal studies (rats, oral, repeated dose), no isolated nanosized primary particles of SAS were detected in the blood or organs.

#### PS 1755 In Situ Characterization of Nanoparticles: Surface Properties Affecting Agglomeration and Particle's Corona.

A. Haase<sup>1</sup>, M. D. Driessen<sup>1</sup>, C. Schulze<sup>2</sup>, M. Wiemann<sup>3</sup>, H. Galla<sup>4</sup>, M. Lehr<sup>2,5</sup>, A. Luch<sup>1</sup> and W. Wohlleben<sup>6</sup>. <sup>1</sup>Federal Institute for Risk Assessment (BfR), Berlin, Germany; <sup>2</sup>Saarland University, Saarbrücken, Germany; <sup>3</sup>IBE, Münster, Germany; <sup>4</sup>University of Münster, Münster, Germany; <sup>5</sup>Helmholtz Institute for Pharmaceutical Research, Saarbrücken, Germany; <sup>6</sup>BASF SE, Ludwigshafen, Germany. Sponsor: M. Pallardy.

In situ characterization of 'as-tested' nanoparticles is essential to understand their toxic effects and to develop Nano-QSARs. The national project nanoGEM correlates as-produced with as-tested and as-released properties, and further to uptake and effects in-vitro and in-vivo.

Here we report on lipid and protein interactions of 16 nanoparticles in a) serum containing cell culture medium, b) pure phospholipids vs. CuroSurf vs. native lung surfactant.

The surface of suspended nanoparticles with sizes of 10nm (ZrO<sub>2</sub>), 15nm (SiO<sub>2</sub>) and 50nm or 200nm (Ag) was furnished either with acidic, amino-functional, PEG, acrylic and electro-steric functionalities. Characterization followed the

nanospecific REACH guidance R7.1, benchmarked against OECD reference materials TiO<sub>2</sub>, ZnO, BaSO<sub>4</sub>, AlOOH. We assessed in situ agglomeration by light scattering, nanoparticle tracking and analytical ultracentrifugation; protein corona by 1D/2D gel electrophoresis with mass spectrometry; lipid interaction by secondary ion mass spectrometry (SIMS), phosphate assays and film balances.

In protein containing media, only nanoparticles with electro-steric functionalities remained dispersed, partially due to negative charge; all nanoparticles attracted a corona with BSA as main component that often decreased during 1h to 24h. Astonishingly, phospholipids had a low affinity to nanoparticles. Only few functionalities attracted lipids and then agglomerated afterwards. The presence of proteins in CuroSurf or native surfactant may induce lipid binding in some cases but not vice versa.

The surface coating controls the dispersability and the corona of proteins and lipids by kinetic properties. However, nanoparticles behave completely different in lung lining fluid compared to serum containing cell culture media. This has implications for the validity of toxicity testing.

#### PS 1756 Possible Adjuvant Role of Manufactured Nanoparticles in Chemical-Induced Sensitization.

B. Baré<sup>1</sup>, N. Lambrechts<sup>1</sup>, P. Hoer<sup>2</sup> and I. Nelissen<sup>1</sup>. <sup>1</sup>Environmental Risk and Health Unit, Flemish Institute for Technological Research (VITO NV), Mol, Belgium; <sup>2</sup>Lung Toxicology Unit, Catholic University Leuven (KULeuven), Leuven, Belgium.

The adjuvant activity of air pollution particles on allergic airway sensitization is well known, but a similar role of manufactured nanoparticles in allergic sensitization following chemical exposure has not been clarified. Such mixed exposure situations may be relevant to daily life activities.

The goal of our study is to assess the possible adjuvant effect of manufactured nanoparticles (NPs) on a chemical-induced sensitization response in vitro.

Human cord blood-derived CD34+ progenitor cells that are differentiated into immature myeloid dendritic cells (CD34-DC) are used as in vitro antigen-presenting cell model. These are exposed to sensitizing model chemicals, such as nickel sulphate, and spherical Au-NPs (5, 50 and 250 nm) for 6 and 24 hours, either as separate inducers or as a mixture. Concentration-response series of the chemicals are used. Cytotoxic effects of the chemicals and NPs are assessed using flow cytometric analysis of propidium iodide incorporation. Triggering of antigen-presenting properties of the exposed CD34-DC is assessed by expression analysis of the VI-TOSSENS® genes CCR2 and CREM (Lambrechts et al., Toxicol. Lett. 2011) on mRNA samples of lysed cells after 6 hours of exposure using RT-qPCR. Additionally, maturation of CD34-DC is assessed by quantifying cell surface expression of HLA-DR and the co-stimulatory molecules CD80, CD86, and CD83 after 24 hours using flow cytometry.

The results that are obtained in this study, clarify whether gold nanoparticles operate as adjuvants for allergenic responses and as such enhance our insight in the risks that nanoparticle exposure may pose to our health.

#### PS 1757 Zinc Oxide Particles Induced Migration of Monocytes and Increased Macrophage Cholesterol Uptake.

Y. Suzuki<sup>1</sup>, S. Tada-Oikawa<sup>1</sup>, G. Ichihara<sup>2</sup> and S. Ichihara<sup>1</sup>. <sup>1</sup>Graduate School of Regional Innovation Studies, Mie University, Tsu, Japan; <sup>2</sup>Department of Occupational & Environmental Health, Nagoya University Graduate School of Medicine, Nagoya, Japan.

Background: Metal oxide nanoparticles have been widely used in industry, cosmetics, as well as biomedicine. However, the correlation between exposure to metal oxide nanoparticles and the increased incidence of cardiovascular disease remains elusive. The present study investigated the migration of monocytes and macrophage cholesterol uptake that are essential for atherosclerotic progression induced by nano-sized metal oxide particles.

Methods and results: Human umbilical vein endothelial cells (HUVECs) were cultured and exposed to nano-sized TiO<sub>2</sub> and ZnO. Exposure to ZnO for 6 hours reduced the cellular viability in a dose-dependent manner and increased the production of reactive oxygen species (ROS) whereas there were no changes by the exposure to TiO<sub>2</sub>. Exposure to ZnO for 21 hours increased the level of monocyte chemoattractant protein-1 (MCP-1) in HUVECs, and cell migration of human monocytic leukemia (THP-1) was observed after incubation with HUVEC supernatants. We also investigated the effect of nano-sized metal oxide particles on cholesterol uptake in THP-1 macrophages after stimulation with acetylated-LDL. The exposure to ZnO up-regulated the expression of membrane scavenger receptors of modified LDL particles and increased cholesterol uptake.

Conclusion: The exposure to ZnO reduced the cellular viability in a dose-dependent manner and increased the production of ROS in HUVECs. The exposure to ZnO also induced THP-1 cell migration and increased macrophage cholesterol uptake. The study indicates that nano-sized ZnO particles accelerate foam cell formation in THP-1 macrophages.

## PS 1758 Comparison of Cellular Uptake of Titanate Nanomaterials by Human Monocytes.

S. Boonrungsiman, W. Suchaoin and R. Maniratanachote. *National Nanotechnology Center, National Science and Technology Development Agency, Pathum Thani, Thailand.*

Titanate nanomaterials (TiNMs) have been applied in various industrial products, including cosmetics, dye sensitized solar cells, and photocatalytic materials. There is also increasing concern on human health risk due to exposure to these nanomaterials during production and application of the products. Therefore, safety assessment of TiNMs is required. Several studies have been focused on toxicity and biological interactions of titanate nanoparticles (TiNPs), but less is known for titanate nanofibers (TiNFs). The aim of this study was to investigate the uptake patterns and toxicity of two TiNFs with different dimensions (about 50 and 70 nm in diameter and 500 and 1500 nm in length, respectively) compared with a spherical TiNP (about 170 nm in diameter) in human monocytes, THP-1 cells. The uptake of TiNMs into the cells was observed over the time for up to 24 hours using side scatter cytometry (SSC), which reflect internal cellular complexity, and electron microscopy. The results showed that all of TiNMs were immediately absorbed on plasma membrane when they exposed to the cells as observed by SEM and SSC. Engulfment of both TiNFs and TiNPs by THP-1 cells occurred within 10 minutes exposure. Interestingly, SSC profile may suggest the different uptake patterns between TiNFs and TiNPs. In addition, the results from SSC and SEM suggested that TiNFs were taken up by the cells which took longer time than that of TiNPs because of their length. TiNFs with concentrations up to 100 µg/ml did not reduce cell viability, while TiNPs significantly reduced cell viability at concentration of 100 µg/ml. None of TiNMs (with concentrations up to 100 µg/ml) significantly trigger intracellular ROS generation. This information on cellular uptake and response might be useful for risk assessment of nanomaterials.

## PS 1759 Air-Liquid Interface Exposure of Lung Cells to Metal Nanoparticles Generated by a Spark Discharge System.

J. Kim, J. Park, T. M. Peters and P. S. Thorne. *Occupational and Environmental Health, The University of Iowa, Iowa City, IA.*

Metal-based nanoparticles (NPs) are generated from a variety of processes including welding, cutting and brazing. Airborne NPs are of particular concern over human exposure, as they can readily move in ambient air and enter the body through inhalation. The objective of this study was to investigate toxic effects on human alveolar type-II cells (A549) after air-delivery of various metal NPs. We used a spark discharge system (SDS) capable of generating and depositing airborne NPs directly onto cells at an air-liquid interface (ALI). The generated NPs (from various source materials including Cu, Zn electrodes and welding rods) were characterized by using a scanning mobility particle sizer, inductively coupled plasma-mass spectrometer and electron microscopes (SEM, TEM). To better model *in vivo* repeated-low dose protocols we sequentially exposed lung cells to NPs *in vitro* (4 h exposure-2 h rest in an incubator-4 h exposure) and cell viability was determined by Alamar Blue assay at 4 h post-exposure. The SDS produced stable NP aerosols for 4 h (Cu,  $8 \times 10^6$ ; Zn,  $6 \times 10^6$ ; welding rods,  $7 \times 10^6$  particles/cm<sup>3</sup>). Particle size distribution indicated the geometric mean diameter of the generated particles to be average 15 (Cu), 25 (Zn) and 16 nm (welding rods) with a geometric standard deviation of 1.5, 1.7 and 1.4, respectively. SEM and TEM results confirmed the deposition of nano-sized particles on cell-free transwells. The cellular concentration of Cu NPs was 5.9 µg Cu/transwell (4.7 cm<sup>2</sup>) and a substantial amount of Cu was released to the basolateral medium (0.3 µg) during air-delivery of Cu NPs in 4 h. Viability for cells exposed to Cu NPs was significantly reduced to 79% ( $p < 0.05$ ) at 4 h post-exposure compared to cells maintained in an incubator. Our results demonstrated that the SDS can be useful for generating metal NPs and simulating welding fumes for their toxicity assessment. In addition, integrated ALI exposures of human lung cells with SDS can provide screening data to aid prediction of toxicity of metal NPs.

## PS 1760 Engineered Nanoparticles Enhanced CD8<sup>+</sup> T Cell Cytokine Production.

B. L. Kaplan<sup>1,4</sup>, W. Chen<sup>2,4</sup>, Q. Zhang<sup>3</sup>, G. L. Baker<sup>3</sup> and N. E. Kaminski<sup>1,4</sup>.  
<sup>1</sup>Pharmacology and Toxicology, Michigan State University, East Lansing, MI;  
<sup>2</sup>Microbiology and Molecular Genetics, Michigan State University, East Lansing, MI;  
<sup>3</sup>Chemistry, Michigan State University, East Lansing, MI; <sup>4</sup>Center for Integrative Toxicology, Michigan State University, East Lansing, MI.

Engineered nanoparticles are being used in various commercial products; however, a significant concern is the potential of these particles to cause adverse effects on human health, as evidenced by exacerbation of allergic airway disease. The objective of this interdisciplinary research is to investigate the putative adjuvant properties of

engineered nanoparticles on biological responses at the animal, cell, and membrane levels. Silica nanoparticles (SNPs) were modified with alkyne-terminated surfaces and appended with polyethylene glycol azides via "click" chemistry. At the cell level, *in vitro* mouse models were utilized to examine the effect of modified SNPs on dendritic cell (DC)-induced T cell effector function. Ovalbumin (OVA)-derived peptides OVA<sub>257-264</sub> or OVA<sub>323-339</sub> were presented by endogenous antigen presenting cells in splenocytes or a mouse DC line, DC2.4. IFNγ and IL-2 production by CD8<sup>+</sup> or CD4<sup>+</sup> T cells in response to OVA peptides was measured by flow cytometry. At modest peptide stimulation levels, modified SNPs (up to 10 µg/ml) enhanced the proportion of CD8<sup>+</sup>, but not CD4<sup>+</sup>, T cells that produced cytokines. Various functional groups (-COOH, -NH<sub>2</sub>, -OH) on modified SNPs enhanced cytokine production to different levels, with -COOH SNPs being the most effective. Furthermore, 50 nm -COOH SNPs exhibited greater enhancement effect on CD8<sup>+</sup> T cell response than the other sizes. Importantly, modified SNPs did not aggregate in *in vitro* culture media, demonstrating their effect at the true nanoscale. Collectively, our results demonstrated the potential adjuvant effect of modified SNPs on CD8<sup>+</sup> T cell function and will also complement other studies being conducted by the team at the membrane and the intact animal level. (Supported by NIH Grant RC2 ES018756)

## PS 1761 Biological Impacts of Ferroelectric Nanoparticles: Comparison between Lead and Bismuth.

M. Esquivel-Gaón<sup>1,3</sup>, M. Uribe-Ramirez<sup>1</sup>, E. Herrera-Jimenez<sup>2</sup>, J. Muñoz-Saldaña<sup>2</sup>, L. M. Del Razo<sup>1</sup>, M. Monopoli<sup>3</sup>, K. A. Dawson<sup>3</sup>, S. Anguissola<sup>3</sup> and A. De Vizcaya-Ruiz<sup>1</sup>. <sup>1</sup>Toxicology, Cinvestav, Mexico City, Mexico; <sup>2</sup>Unidad Queretaro, Cinvestav, Queretaro, Mexico; <sup>3</sup>CBNi, University College Dublin, Dublin, Ireland.

The risk posed by lead during manufacturing of ferroelectric ceramics has led to efforts to develop lead-free options, bismuth sodium titanate with barium titanate (BNT-BT) nanoparticles (NP) have become a strong candidate to replace lead zirconate titanate (PZT)-based ceramics. In order to evaluate the biological effects generated by PZT and BNT-BT NP we investigated their interaction with biomolecules adsorbed on the NP surface, which defines the interface with cellular membranes, the uptake and potential toxicity in human cell lines. The NP were dispersed, stabilized with bovine serum albumin (BSA) and characterized in complete cell culture medium showing an average size of 188 nm (BNT-BT) and 168 nm (PZT), as measured by differential centrifugal sedimentation. The analysis of the proteins adsorbed with high affinity to the NP surface (hard corona) after the incubation with FBS showed prevalently BSA and complex protein profiles dependent on the concentration of FBS. Uptake studies in cell cultures rely on fluorescently labeled NPs; we generated BNT-BT and PZT NP showing fluorescent properties by labeling BSA used to stabilize the dispersions. The NP were tracked through the endolysosomal pathway using a time lapse live cell imaging approach. For cytotoxicity assessment, cell membrane damage and mitochondrial activity were measured in Hep G2, LLC-PK1, A549 and SH-SY5Y cells after exposure to increasing concentrations of BNT-BT and PZT NP for 24 or 48 h. The integrity of the cell membrane was not significantly affected; however the mitochondrial activity decreased after 48 h with 100 µg/ml for both NP being more evident for the PZT NP in neuroblastoma cells. Our results suggest that BNT-BT showed lower levels of toxicity compared to PZT thus it could be a good replacement for PZT-based ceramics. Funding from the European Community Seven Framework Program and CONACYT (Grant agreements #263878 and 12514) and Epitope Map Program.

## PS 1762 Role of Lung Surfactant Lipid and Protein Corona in Airborne Positively Charged Nanoparticle Exposure.

Y. Xie, A. Tolic, W. Chrisler, C. Mihai, C. Szymanski, D. Hu and G. Orr. *Pacific Northwest National Laboratory, Richland, WA.*

Airborne nanoparticles (NPs) that reach the alveolar region are likely to be presented to alveolar epithelial cells coated with a corona of lung surfactant lipids and proteins. However, the effect of the corona on airborne NP toxicity is still unclear, mainly because most studies were conducted in cells exposed to NPs in growth media, limiting the corona to molecules found in the media. Furthermore, accumulating observations support a role for positive surface charge in NP toxicity, but the impact of the corona, which shifts the NP surface charge to more negative values, is unclear. To understand the role of coronas in airborne NP exposure, we exposed alveolar epithelial cells at the air-liquid interface (ALI) to aerosolized NPs that were pre-incubated with a natural surfactant lipid and protein (Infasurf®) or BSA solution. Bare polystyrene (PS) NPs, showing no toxicity, were compared with aminated or carboxylated PS NPs, showing high or low level of toxicity, respectively. Cellular response was compared between NPs at the same cellular dose, measured as µg/cm<sup>2</sup> using a quartz crystal microbalance. We found that the lowest dose required to induce toxicity by aminated NPs with no corona was 3 folds lower than the dose required to induce toxicity by aminated NPs with a surfactant co-

rona, and 1.8 folds lower than the dose required by aminated NPs with a BSA corona. In contrast, BSA corona eliminated toxicity of carboxylated NPs at all measured doses. With no corona, the level of aminated NPs at the cell surface or inside the cytoplasm was significantly higher than the level of carboxylated NPs. To evaluate the possibility that the observed protective effect of surfactant or BSA coronas from aminated or carboxylated NP toxicity, respectively, is due in part to a decrease in NP-cell interaction and internalization, we currently quantify any changes in these processes that might be induced by the coronas. This work was funded by NIEHS grant 1RC2ES018786-01 to GO.

### PS 1763 Metastatic Capacity Induced by Cells Exposed to Titanium Dioxide Nanoparticles.

A. Déciga-Alcaraz<sup>1</sup>, V. Freyre-Fonseca<sup>1,2</sup>, E. I. Medina-Reyes<sup>1</sup>, N. L. Delgado Buenrostro<sup>1</sup> and Y. I. Chirino<sup>1</sup>. <sup>1</sup>Facultad de Estudios Superiores Iztacala, Universidad Nacional Autónoma de México, México City, México; <sup>2</sup>Departamento de Graduados e Investigación en Alimentos, Escuela Nacional de Ciencias Biológicas, Instituto Politécnico Nacional, México City, México.

**Background.** Titanium dioxide nanoparticles (TiO<sub>2</sub> NPs) have been classified as a possibly carcinogenic to humans (Group 2B) by the International Agency for Research in Cancer. In this regard, its potential carcinogenic effects have been under research. However, less has been investigated about the effects of cells exposed to TiO<sub>2</sub> NPs when they reach bloodstream, especially if TiO<sub>2</sub> NPs exposed cells could proceed from a tumor.

**Aim.** We hypothesized that tumor cells exposed to TiO<sub>2</sub> NPs could promote a metastatic events. To test this hypothesis, lung adenocarcinoma cells were exposed to TiO<sub>2</sub> NPs (1, 5 and 10 µg/cm<sup>2</sup>) for 7 days and 30,000 cells of each concentration were injected into bloodstream of chicken chorioallantoic membrane (CAM) of free pathogens fertilized eggs previously incubated during 11 days at 37°C and 80% humidity. Analysis of morphological changes was performed at 16th day.

**Results.** TiO<sub>2</sub> NPs were characterized by transmission electronic microscopy (TEM) suspended in F12K medium with 10% Serum Fetal Bovine (SFB) and zeta potential was -20.98±0.75, and TiO<sub>2</sub> NPs agglomerate size was 212.3 ±4.417nm, 630.2±20.94 nm and 588.3±43.11 nm for 1, 5 and 10 µg TiO<sub>2</sub>/mL respectively. Images showed that there is an increase in distance between blood vessels and a decrease in number of nodes in CAM treated with cells exposed to 10 µg/cm<sup>2</sup> of TiO<sub>2</sub>. In addition, there were observed cell clusters on the CAM treated with cells exposed to 1 and 5µg/cm<sup>2</sup> of TiO<sub>2</sub> NPs.

**Conclusion.** TiO<sub>2</sub> NPs exposure (10 µg/cm<sup>2</sup>) to lung adenocarcinoma cells induced an increase in blood vessel distance and a decrease the number of nodes, which seems to be a downregulation effect in angiogenesis. However, pre-exposed lung adenocarcinoma cells to 1 and 5 µg/cm<sup>2</sup> of TiO<sub>2</sub> NPs provided a capacity to form clusters, which could represent a higher metastatic effect.

### PS 1764 Phenotypic Polarization and Attenuation of Toll Receptor Signaling Functions in Macrophages Exposed to Engineered Nanoparticles.

V. K. Kodali<sup>1</sup>, M. H. Littke<sup>1</sup>, S. C. Tilton<sup>2</sup>, J. G. Teeguarden<sup>1</sup>, L. Shi<sup>1</sup>, C. W. Frevert<sup>3</sup>, W. Wang<sup>4</sup>, J. G. Pounds<sup>1</sup> and B. D. Thrall<sup>1</sup>. <sup>1</sup>Systems Toxicology, Pacific Northwest National Laboratory, Richland, WA; <sup>2</sup>Computational Sciences Division, Pacific Northwest National Laboratory, Richland, WA; <sup>3</sup>Department of Comparative Medicine, University of Washington, Seattle, WA; <sup>4</sup>Bioscience Division, Oak Ridge National Laboratory, Oak Ridge, TN.

Although macrophages play a critical role in scavenging engineered nanoparticles (ENPs) from tissue, relatively little is known about how their normal innate immune function is impacted. We investigated how pretreatment of macrophages with 33 nm superparamagnetic iron oxide (SPIO) or 50 nm amorphous silica modulated the transcriptional response of macrophages to the toll 4 receptor (TLR4) ligand LPS. Affymetrix microarray analysis showed over 5000 mRNAs were differentially regulated (>1.5 fold, p<0.05) in response to LPS (10 ng/ml, 6 hrs). SPIO pretreatment (25 µg/ml) alone altered expression of a smaller set of genes (1029 total), but modulated expression of nearly 500 LPS regulated genes in a greater than additive manner. In contrast to SPIO, relatively few LPS regulated genes were modulated by silica pretreatment. Pathway analysis showed that pretreatment with SPIO suppressed LPS activation of several key cellular functions like chemotaxis, interferon and Jak-Stat inflammation signaling while enhancing cell adhesion and oxidative/nitrate stress responses. Pretreatment of macrophages with SPIO also caused a dose dependent decrease in phagocytosis of *S. pneumoniae* and *S. typhimurium*, whereas silica pretreatment had no effect. Flow cytometry studies using fluorescent LPS or antibodies against TLR4 revealed that SPIO exposure caused dose-dependent down regulation of cell surface TLR4 level while silica had no effect. Our results demonstrate that macrophages exposed to some ENPs are polarized toward an anti-inflammatory phenotype which attenuates pro-inflammatory signaling by TLR4, and suppresses their phagocytic activity against pathogens.

This work was supported by NIEHS Grant U19-ES019544.

### PS 1765 Intracellular Trafficking and Accumulation Dynamics of Zinc Ions in Alveolar Epithelial Cells Exposed to Airborne ZnO Nanoparticles at the Air-Liquid Interface.

C. Mihai, W. Chrisler, Y. Xie, C. Szymanski, A. Tolic, D. Hu, B. Tarasevich and G. Orr. Pacific Northwest National Laboratory, Richland, WA.

Airborne nanoparticles (NPs) that enter the respiratory tract are likely to reach the alveolar region. Accumulating observations support a role for zinc oxide (ZnO) NP dissolution in toxicity, but the majority of the studies were done in cells exposed to NPs in growth media, where large doses of dissolved ions are shed into the exposure solution. To better represent the exposure in the respiratory tract and focus on the dissolution of airborne NPs in the cellular environment, we exposed alveolar epithelial cells to aerosolized NPs at the air-liquid interface (ALI). Using a fluorescent indicator for zinc ions (Zn<sup>2+</sup>) and organelle-specific fluorescent proteins, we quantified Zn<sup>2+</sup> in single cells and organelles over time and correlated these values with toxicity. We found that intracellular Zn<sup>2+</sup> in cells exposed at the ALI peaked 3 h post exposure and decayed to normal levels by 24 h, which was in contrast to exposures in submersed cultures where intracellular Zn<sup>2+</sup> continued to increase over time. For the lowest toxic dose at 24 h, the peak at the ALI was ~3 folds lower than the 24 h value in submersed cells, and ~8 folds lower than the 24 h value in submersed cells exposed to Zn<sup>2+</sup> only. At the ALI, 45% of intracellular Zn<sup>2+</sup> was found in endosomes at 1 h post exposure, decreasing to 24% by 3 h. In contrast, 20% of intracellular Zn<sup>2+</sup> was found in lysosomes at 1 h, increasing to 42% by 3 h. Interestingly, exposure of submersed cells to Zn<sup>2+</sup> only, led to a minimal accumulation of ions in either the endosomes or lysosomes, with the majority of ions found in larger vesicles. Our observations indicate that airborne ZnO NPs induce toxicity at the ALI at intracellular Zn<sup>2+</sup> levels that are significantly lower than those detected when toxicity is induced in submersed cultures, and the localized dissolution and trafficking of Zn<sup>2+</sup> in endosomes following with their accumulation in lysosomes play critical roles in airborne NP toxicity. This work was funded by NIEHS grant 1RC2ES018786-01 to GO.

### PS 1766 Aggregation Dynamics and Structure Measurements of Nanomaterials in Biologically Relevant Conditions.

N. B. Saleh<sup>1</sup>, S. M. Hussain<sup>2</sup> and A. Afroz<sup>1</sup>. <sup>1</sup>Civil and Environmental Engineering, University of South Carolina, Columbia, SC; <sup>2</sup>Wright-Patterson AFB, US Air Force, Dayton, OH.

Nanomaterial dosimetry for in vitro studies continued to be debated in nanotoxicology literature, particularly due to the propensity of aggregation of highly diffusive nano-scale materials. In classical nanotoxicology literature, average particle size and surface charge are the typical measured parameters either initially or at the end of exposure time period; with no information on the dynamic behavior throughout the process. Moreover, aggregate structural information is mostly ignored. This study focuses on monitoring dynamic aggregation behavior of metallic and carbonaceous nanoparticles under biological (i.e., in exposure media with added penicillin streptomycin, at 37 °C) exposure conditions. The aggregation dynamics is monitored by employing state-of-the-art ALV goniometer system. Suspension-phase fractal dimension was measured with angle-dependent static light scattering for an angular range of 12°-120°. Aggregation dynamics results indicate that electrostatic interaction serves as the key interfacial force to providing stability to nanomaterials. In addition, continuous measurements of aggregate size in physiological condition show network formation. Furthermore, time dependent fractal dimension results indicate that aggregate structure remains unchanged over time; however, were significantly altered by the background solution chemistry. The key implications of the study include: consideration of intermediate time-endpoint (instead of 24 hr); aggregation dynamics and network formation can minimize size-effects on nanotoxicology; aggregation dynamics with aggregate structure information can better determine nanomaterial dosimetry.

### PS 1767 Targeting Alternatively Activated Rat Macrophages Using Mannose Functionalized Nanocarriers.

P. Chen<sup>1</sup>, X. Zhang<sup>1</sup>, A. Venosa<sup>2</sup>, Z. Szekely<sup>1</sup>, D. L. Laskin<sup>2</sup> and P. J. Sinko<sup>1</sup>. <sup>1</sup>Pharmaceutical Science, Rutgers University, Piscataway, NJ; <sup>2</sup>Department of Pharmacology & Toxicology, Rutgers University, Piscataway, NJ.

In response to inflammatory signals generated at sites of injury, macrophages are activated into two main phenotypes: classically activated M1 cells and alternatively activated M2 cells. Whereas M1 macrophages release cytotoxic/proinflammatory

mediators that contribute to tissue injury, M2 macrophage-derived mediators suppress inflammation and initiate wound repair. Mannose receptor (MR) is known to be expressed at high levels on M2 macrophages. In these studies, a mannose functionalized nanocarrier (NC) was designed and developed with the goal of selectively targeting M2 macrophages. Mannose functionalized NC (FITC-Gaba-Ser(Man)-PEG12-Ser(Man)-Gaba-Gaba-Cys) were prepared using solid phase synthesis and their identity confirmed by MALDI-TOF/MS and HPLC analysis. Rat peritoneal macrophages (PMs) were incubated for 24-48 h with IFN- $\gamma$  (20ng/ml) or IL-4/IL-13 (10ng/ml), to induce M1 or M2 activation, respectively. mRNA levels of the M1 marker, inducible nitric oxide synthase (iNOS) and the M2 marker, arginase (Arg)-1 were quantified by RT-PCR, and protein levels by western blotting. Treatments of PMs with IFN- $\gamma$  resulted in increased expression of mRNA and protein for iNOS, whereas IL-4/IL-13 upregulated Arg-1 expression. After incubating for 60 min, NC binding to macrophages was quantified by confocal microscopy. Confocal microscopy showed that uptake of mannosylated NC into M2 PMs was 2.4 fold greater than control PMs, and 11.8 fold greater than M1 PMs. M2-macrophage phenotype-specific uptake was completely abolished by mannan, suggesting MR-mediated targeting. NCs were co-localized with rhodamine-dextran, a general fluid phase endocytosis marker, indicating that the NCs were internalized by PMs. The present studies demonstrate that mannosylated NCs are specific for macrophages expressing mannose receptor. These NC may be useful for delivery of drugs to sites of injury and infection. Support: NIH AI51214, AR055073, CA132624, ES004738, ES005022, and GM034310

**PS 1768 Synthesis, Characterization and Toxicological *In Vitro* Activity of Nanomaterials Containing Active Ingredients of *Matricaria chamomilla* L.**

A. Vera<sup>1</sup>, L. A. Flores<sup>1</sup>, F. M. Mercado<sup>1</sup>, R. Vazquez<sup>1</sup>, J. A. Soriano<sup>1</sup>, R. L. Ortega<sup>1</sup>, A. Jain<sup>2</sup>, P. Sengar<sup>2</sup>, G. A. Hirata<sup>3</sup>, R. E. Cachau<sup>4</sup>, R. Hernandez<sup>5</sup>, U. Pal<sup>6</sup>, Z. N. Juarez<sup>1</sup>, M. C. Miranda<sup>1</sup> and **T. D. Palacios-Hernandez<sup>1</sup>**. <sup>1</sup>Ciencias Biológicas, UPAP, Puebla, Mexico; <sup>2</sup>School of Biosciences and Technology, VIT, Vellore, India; <sup>3</sup>Centro de Nanociencias y Nanotecnología, UNAM, Ensenada, Mexico; <sup>4</sup>Frederick National Laboratory for Cancer Research, Frederick, MD; <sup>5</sup>Ciencias Químico-Biológicas, UDLAP, Puebla, Mexico; <sup>6</sup>Instituto de Física, BUAP, Puebla, Mexico.

In this contribution, the synthesis, characterization and biological activity of polymeric nanocapsules (PNC) and iron oxide nanoparticles (NPs) containing active ingredients of *Matricaria chamomilla* L., is being evaluated. *M. chamomilla* L. specimens were collected and dried, to obtain the chloroform, hexane and water extracts. Iron oxide NPs were prepared by a co-precipitation method using FeCl<sub>3</sub>, Na<sub>2</sub>SO<sub>3</sub> and NH<sub>4</sub>OH. PNC were prepared by emulsion method using aqueous solutions of sodium alginate containing the active principle, calcium chloride and dioctyl sodium sulfosuccinate. Characterization of all the materials was done by dynamic light scattering (DLS), transmission electron microscopy (TEM), phase contrast microscopy, RAMAN spectroscopy, X-ray diffraction (XRD) and Fourier Transformed Infrared spectroscopy (FTIR). Plant extracts are being purified by column chromatography and were characterized by proton (1H) and carbon (13C) Nuclear Magnetic Resonance (NMR). TEM analysis confirmed the presence of nanoparticles in a size range of 6-10 nm, XRD and RAMAN showed the magnetite phase at SPION and FTIR showed the characteristic vibrations for OH in magnetite NPs and organic groups at PNC. A high particle size distribution (93-200 nm) was obtained in polymeric nanocapsules by DLS and confocal microscopy, due the presence of aggregates. NMR showed in the hexane extract the presence of flavonoids, sugars and phenols. At this moment we are still working on the purification of *M. chamomilla* L. extracts and the evaluation of biological activity upon bacterial cultures, to determine ecotoxicity of all the materials synthesized.

**PS 1769 Comparative *In Vitro* Cell Uptake of Bismuth and Bismuth-Derivatives Nanoparticles in Lung Cells.**

L. M. Del Razo<sup>1</sup>, B. Quintanilla-Vega<sup>1</sup>, O. C. Barbier<sup>1</sup>, M. Esquivel-Gaón<sup>1,2</sup>, M. Uribe-Ramírez<sup>1</sup>, A. Barrera-Hernández<sup>1</sup>, L. C. Sanchez-Peña<sup>1</sup>, K. A. Dawson<sup>2</sup>, S. Anguissola<sup>2</sup> and **A. De Vizcaya-Ruiz<sup>1</sup>**. <sup>1</sup>Toxicology, Cinvestav-Instituto Politécnico Nacional, Mexico, City; <sup>2</sup>CBNI, University College Dublin, Dublin, Ireland.

Bismuth (Bi) has exceptionally low magnetic susceptibility and very low thermal conductivity which favors their use as a thermoelectric material. Therefore, low-dimensional Bi compounds are good candidates as nanomaterials. In this study, the physicochemical properties of Bi-derived nanoparticles (Bi-NP) – Bi trioxide (Bi<sub>2</sub>O<sub>3</sub>), Bi vanadate (BiVO<sub>4</sub>), and zero valent Bi in colloidal form (ZV-Bi) – and uptake in A549 lung cells were evaluated. The properties include the dispersion and

stability, elemental composition and uptake in lung cell cultures. Testing for biocompatible dispersants for biological and toxicological evaluations was performed using sonication and centrifugation steps, combined with stabilization of the NP surface with bovine serum albumin (BSA; 10mg/ml) to reduce agglomeration. Its dispersion properties and elemental composition were confirmed using dynamic light scattering and energy dispersive X-ray spectroscopy. Average size of Bi<sub>2</sub>O<sub>3</sub>, BiVO<sub>4</sub>, and ZV-Bi was 9.2 nm (0.34 pdl), 49.9 nm (1 pdl) and 3.3 ± 1nm, respectively. Elemental content was in 67.6%-Bi, 32.4%-O in Bi<sub>2</sub>O<sub>3</sub>, 55.5%-Bi, 25.9%-V and 18.6%-O in BiVO<sub>4</sub> and 49.9%-Bi, 33.7%-O and 16.4%-Na in ZV-Bi. From a parallel cytotoxicity study of the exposure to Bi<sub>2</sub>O<sub>3</sub>, BiVO<sub>4</sub>, and ZV-Bi the 50 µg/ml non-cytotoxic level was chosen to assess the cellular uptake of Bi at 6, 24 or 48 h in lung cells by atomic fluorescence spectrophotometry by hydride generation. A differential uptake of Bi was observed, BiVO<sub>4</sub> was internalized in cells in 86.6% while Bi<sub>2</sub>O<sub>3</sub> and ZV-Bi in 27.8 and 26.1%, respectively. Our results suggest that Bi-NP cellular internalization is dependent of the physicochemical properties, where a more conductive NP such as BiVO<sub>4</sub> was more effectively internalized; therefore, NP transport and uptake is a relevant process that needs to be thoroughly investigated. Funding from the European Community Seven Framework Programme and CONACYT (Grant agreements #263878 & 12514).

**PS 1770 Oxidative Stress, Cell Viability and Types of Cell Death Induced by Transition Metal Oxide Nanoparticles Depend on Surface Charge, Available Surface Binding Site, and Ion Dissolution.**

Y. Huang<sup>1</sup>, C. C. Chusuei<sup>2</sup>, C. Wu<sup>1</sup>, S. Mallavarapu<sup>2</sup>, J. G. Winiarz<sup>3</sup> and R. S. Aronstam<sup>1</sup>. <sup>1</sup>Biological Sciences, Missouri University of Science and Technology, Rolla, MO; <sup>2</sup>Chemistry, Middle Tennessee State University, Murfreesboro, TN; <sup>3</sup>Chemistry, Missouri University of Science and Technology, Rolla, MO.

We investigated physicochemical properties of nano-sized oxides of Fourth Period transition metals that contribute to cytotoxicity. The cytotoxicity (i.e., cell killing) of nanoparticles (NPs) TiO<sub>2</sub>, Cr<sub>2</sub>O<sub>3</sub>, Mn<sub>2</sub>O<sub>3</sub>, Fe<sub>2</sub>O<sub>3</sub>, NiO, CuO, and ZnO increases as atomic number increases. This trend is not cell type specific, as it is observed in nontransformed human lung (BEAS-2B) and adenocarcinomic human alveolar basal (A549) epithelial cell lines. We assessed physicochemical properties of NPs to discover the determinants of cytotoxicity: 1) the point-of-zero charge (PZC) (i.e., isoelectric point) describes the surface charge of NPs in cytosolic and lysosomal compartments; 2) the relative number of available binding sites on the NP surface was used to estimate the probability of biomolecular interactions on the particle surface; 3) band-gap energy predicts electron abstraction from NPs which might lead to oxidative stress and subsequent cell death; and 4) ion dissolution. Our results indicate that that cytotoxicity is a function of particle surface charge, relative number of available surface binding site, and metal dissolution from NPs. These NPs are capable of inducing oxidative stress that is consistent with the trend of cell killing; however, H<sub>2</sub>DCFDA is not a suitable dye to accurately assess oxidative stress due to quenching effect. Ratio of apoptosis and necrosis also follows the trend of cell killing. Our findings provide a basis for both risk assessment and the design of safer nanomaterials.

**PS 1771 Cytotoxic and Antitumor Effect of Vitamin E Analogues Functionalized to Magnetite Nanoparticles.**

A. Angulo Molina<sup>1,2,3</sup>, J. Reyes Leyva<sup>3</sup>, J. Hernández<sup>1</sup>, **T. D. Palacios-Hernández<sup>2,4</sup>**, M. A. Méndez Rojas<sup>2</sup>, M. Cerro López<sup>2</sup>, J. Flores<sup>3</sup>, F. Ruiz<sup>5</sup>, O. Contreras<sup>5</sup> and G. A. Hirata<sup>5</sup>. <sup>1</sup>Centro de Investigación en Alimentación y Desarrollo, CIAD, AC, Hermosillo, Mexico; <sup>2</sup>Universidad de las Américas Puebla, UDLAP, Puebla, Mexico; <sup>3</sup>Centro de Investigaciones Biomédicas de Oriente CIBIOR, IMSS, Metepec, Puebla, Mexico; <sup>4</sup>Universidad Popular Autónoma del Estado de Puebla, UPAP, Puebla, Mexico; <sup>5</sup>Centro de Nanociencias y Nanotecnología, CNYN, Ensenada, Mexico.

**BACKGROUND:** Magnetite nanoparticles (Nps) can be used as nanocarriers to enhance and improve the efficiency of delivery of vitamin E analogues. Herein we report the cytotoxic and antitumor effect of magnetite Nps functionalized with alpha tocopheryl succinate (α-TOS), the most effective analogue of vitamin E in inducing death in cancer cells. One problem with α-TOS is its vulnerability to esterases, making impossible its oral use or in cancer cells with high levels of esterases. **OBJECTIVE:** To investigate the cytotoxicity and antitumor effect of magnetite Nps functionalized with α-TOS (Nps-α-TOS).

**METHODS:** Magnetite Nps-α-TOS were functionalized mixing Nps, silane agents and α-TOS under vigorous stirring (40oC) for 4 h. The Nps-α-TOS were characterized by FTIR, EDS, TEM, SEM and DLS. Then a human cervix cancer cell line (SiHa) high in esterases was treated with the various concentrations by 72 h. Its effects on cytotoxicity and antitumor effect were evaluated using confocal microscopy and MTT assay.

**RESULTS:** Electronic microscopy studies revealed an average Nps size of 130 nm ( $\sigma = \pm 32.7$  nm) and irregular spherical in shape. IR, EDS and DLS results support the formation of Nps detecting mineral and organics constituents respectively with high stability. The in vitro tests shows by first time the Nps- $\alpha$ -TOS can be internalized and are more cytotoxic and effective that  $\alpha$ -TOS alone and inhibits the growth of resistant cervix cancer cell.

**CONCLUSION:** In this study we found that magnetite Nps can work as nanocarriers of  $\alpha$ -TOS. This composite protect the anticancer activity of  $\alpha$ -TOS and enhances the anti-tumor effect in resistant cancer cells.

**PS 1772 Cellular Internalization and Trafficking of Individual Nanoparticles Investigated with Nanometer Resolution Using Super Resolution Fluorescence Microscopy.**

G. Orr, D. Hu, A. Tolic, Y. Xie, C. Mihai, C. Szymanski, M. Markillie, L. Cosimbescu and B. Tarasevich. *Pacific Northwest National Laboratory, Richland, WA.*

The cellular internalization mechanism of engineered nanoparticles (NPs) and their intracellular trafficking govern the cellular interactions of the particles, which ultimately determine their impact on the cell. These cellular mechanisms largely depend on the size of the NPs or the aggregates that are often formed. To identify mechanisms specific to individual NPs or small nano-scale aggregates, we used stochastic optical reconstruction microscopy (STORM) to resolve the intracellular location of individual NPs within organelles and in respect to subcellular structures with 10-20 nanometer resolution. Using FastLime, a photo-switching derivative of green fluorescent protein, we created fluorescent chimeras for clathrin, caveolin and actin, and expressed the proteins in alveolar epithelial cells. The transfected cells were exposed to amorphous silica NPs, tagged with a photo-switching dye, and imaged at 2 h and 16 h post exposure. We found NPs within clathrin- and caveolin-coated vesicles in both time-points, suggesting a preferential binding of the NPs to molecules found in clathrin-coated pits and caveolae at the cell surface. A significant number of NPs were found aligned along actin filaments at 16 h post exposure. The distance between the NPs and the filaments was calculated for more than 1100 NPs, and the distribution of the distances in the range of 0 to 100 nm was significantly different from the distribution expected to occur if the NPs were randomly placed in the cytoplasm. Together, our observations suggest a mechanism for the internalization and trafficking of amorphous silica NPs in alveolar epithelial cells that occurs through interactions with molecules found in caveolae and clathrin-coated pits, followed by internalization via vesicles that eventually are shuttled along actin filaments within the cytoplasm. This work was funded by NIEHS grant 1RC2ES018786-01 to GO.

**PS 1773 Signaling Pathways and microRNA Changes in Nano-TiO<sub>2</sub> Treated Human Lung Epithelial (BEAS-2B) Cells.**

S. Thai, C. P. Jones, K. Wallace, H. Ren, R. Y. Prasad, W. O. Ward, M. J. Kohan and C. F. Blackman. *US EPA, Research Triangle Park, NC.* Sponsor: C. Corton.

The effect of titanium dioxide nanoparticles (nano-TiO<sub>2</sub>, Degussa p25, 86% anatase and 14% rutile) treatment of human lung epithelial cells (BEAS-2B) was examined by analyzing changes in messenger [mRNA] and microRNA [miRNA]. BEAS-2B cells were treated with 0, 3, 10, 30 or 100 ug/ml nano-TiO<sub>2</sub> for 1 day (for mRNA analysis) or 3 days (for miRNA analysis). Differentially expressed mRNA and miRNA were analyzed using Affymetrix microarrays (human U133 Plus 2.0) and Affymetrix miRNA microarrays, respectively. Although, the tested doses were not cytotoxic, there were alterations in both mRNA and miRNA expression. The expression of mRNA/miRNA changes were examined in MetaCore (GeneGo) and IPA (Ingenuity Pathway Analysis) to delineate associated signaling pathways. Signaling pathways altered by nano-TiO<sub>2</sub> treatments included: cell cycle regulation, apoptosis, calcium signaling, translation, NRF2-mediated oxidative response, IGF1 signaling, RAS signaling, PI3K/AKT signaling, cytoskeleton remodeling, cell adhesion, BMP signaling, and inflammatory response. Many of the genes in these signaling pathways are known to be regulated by the miRNAs that were altered by the nano-TiO<sub>2</sub> treatment. The miRNA 17-92 cluster and let-7 miRNA family that are reportedly involved in lung cancer formation were altered by nano-TiO<sub>2</sub> treatment. The miR-17-92 cluster, an oncogenic microRNA cluster, is induced while the tumor suppressor microRNA, let-7 family, is suppressed. The observed changes in miRNA expression introduces an additional mechanistic dimension that supports the significance of the observed mRNA expression changes, and demonstrated that the nano-TiO<sub>2</sub> treatment can cause diverse but coordinated pathway alterations associated with changes in in vivo response to tumorigenes. [This abstract does not necessarily reflect the policies of the U.S. EPA.]

**PS 1774 In Vitro Co-Culture System to Examine the Effects of Inhaled Nanoparticles.**

K. B. Donohue<sup>1</sup>, A. M. Mayo<sup>2</sup>, D. R. Johnson<sup>1</sup>, R. Nellums<sup>3</sup>, S. F. Son<sup>3</sup> and J. A. Stevens<sup>1</sup>. <sup>1</sup>Environmental Laboratory, US Army Engineer Research & Development Center, Vicksburg, MS; <sup>2</sup>Badger Technical Services, Vicksburg, MS; <sup>3</sup>Purdue University, West Lafayette, IN.

Engineered nanoparticles (NPs) possess numerous potential benefits to society in fields as diverse as electronics, textiles, medicine, energy and construction. The respiratory system represents a unique target for the potential toxicity of NPs. Due to their dimensions, inhaled NPs can reasonably be expected to penetrate to the deepest part of the lungs, the alveolar sacs. Completed inhalation studies in laboratory rats have demonstrated that some NPs induce oxidative stress, inflammation and fibrosis. In this study, we examine the effects of nanothermite and parent nano-materials (bismuth oxide [Bi<sub>2</sub>O<sub>3</sub>] and copper oxide [CuO] spheres and rods) on an alveolar co-culture model consisting of human type II pneumocytes and alveolar macrophages. Co-cultures were set up with a ratio of 3:1 of type II pneumocytes to each alveolar macrophage 24 h prior to treatment. Media was then removed and co-cultures were treated with 0.001 100 mg/l NPs for 24 h. Cell viability was only affected by CuO at 100 mg/l; CuO spheres and rods had similar effects. These studies demonstrate that only high concentrations of raw Bi<sub>2</sub>O<sub>3</sub> and CuO NPs affect respiratory co-cultures and that CuO NP size does not affect respiratory co-cultures. Additional phagocytosis studies and cytokine analysis studies (intracellular and secreted concentrations) are being conducted to evaluate inflammatory effects of these NPs in the respiratory co-culture immune cells.

**PS 1775 Metabolomic Studies of the Nanotoxicity of TiO<sub>2</sub> and CeO<sub>2</sub>.**

K. T. Kitchin<sup>1</sup>, B. Robinette<sup>1</sup>, B. Castellon<sup>1</sup> and R. Michalek<sup>2</sup>. <sup>1</sup>US EPA, Durham, NC; <sup>2</sup>Metabolon, Durham, NC.

Nanomaterial exposures to humans and wildlife pose unknown degrees of risk to major organ systems including the liver. TiO<sub>2</sub> and CeO<sub>2</sub> nanomaterial exposures (3 or 30 ug/ml for 3 days) were performed in cultures of human liver HepG2 cells. TiO<sub>2</sub> and CeO<sub>2</sub> nanomaterial exposures altered the concentrations of biochemicals associated with arginine metabolism, lipids and fatty acids, TCA cycle and glutathione. Some metabolites that were significantly altered in 4 or more of the 8 TiO<sub>2</sub> or CeO<sub>2</sub> nanomaterial treatments were cysteine, GSH, asymmetric dimethylarginine and gamma-glutamyl amino acids. Asymmetric dimethylarginine (a competitive inhibitor of nitric oxide synthase) was significantly increased by many nanomaterial exposures, particularly by CeO<sub>2</sub> exposures. One CeO<sub>2</sub> nanomaterial with smaller primary particle size caused increases in many lipids, including long chain fatty acids, lysolipids, membrane sphingolipids, monacylglycerols and diacylglycerols; six other nanomaterial exposures did not. With respect to the TCA cycle, nanomaterial exposures sometimes decreased the concentrations of glutamate, glutamine, malate, fumarate and succinate. In 5 nanomaterial treatment groups, hepatocyte glutathione depletion reached 13 to 34% of control levels. Overall, our nanotoxicology studies have shown (a) many biochemical effects in HepG2 cells and (b) major differences in the biochemical and biological responses between different TiO<sub>2</sub> and CeO<sub>2</sub> nanomaterials and (c) oxidative stress (major GSH depletion) was caused by exposure to both TiO<sub>2</sub> and CeO<sub>2</sub> of different primary particle sizes. Disclaimer: [This is an abstract or a proposed presentation and does not necessarily reflect EPA policy. Mention of trade names or commercial products does not constitute endorsement or recommendation for use.]

**PS 1776 Neurotoxicity of Au-NPs in an In Vitro Blood Brain Barrier (BBB) Model.**

M. Sharma<sup>1,2</sup>, C. E. Sulentic<sup>2</sup>, J. J. Schlager<sup>1</sup> and S. M. Hussain<sup>1,2</sup>. <sup>1</sup>711 HPW/RHDJ, AFRL, Wright-Patterson AFB, Dayton, OH; <sup>2</sup>Department of PharmTox, WSU, Dayton, OH.

Gold nanoparticles (Au-NPs) have demonstrated great potential in the development of a variety of tools with applications ranging from biomedical to military fields. Biodistribution studies indicate differential uptake of NPs depending on their functionalization, treatment conditions, and location in the body. Unlike other organ systems, brain vasculature is comprised of endothelial cells that form an anatomical and physiological barrier that protects neurons from metabolic fluctuations and toxins. The cost and extent of expertise required for in vivo studies, pose limitations, and therefore, better in vitro models are pursued to study toxicophysiological aspects of the BBB. The main aim of this study is to modify a previously described static in vitro BBB model by adding a constant flow of media containing NPs and then studying the NP trafficking across the endothelial cells. Murine brain endothelial cells (bEnd3) and astrocytes (C8D1A) were cultured on the luminal

and abluminal sides, respectively, of a transwell membrane. Permeability studies using Fluorescein isothiocyanate-tagged dextran and polyethylene glycol (PEG) confirmed a tight layer of bEnd3 cells with transendothelial resistance of  $122 \pm 3 \Omega\text{cm}^2$ . This culture set up was treated with citrate and PEG-coated Au-NPs (50  $\mu\text{g/ml}$ ) for 24 hr to quantify non-specific leakage of substrates across the cell barrier and to evaluate the association of NPs with astrocytes, with and without flow of media. Inductively coupled plasma mass spectrometry results show fewer NPs on the abluminal side confirming a tight cell barrier and transmission electron microscopy imaging suggest endosomal localization of NPs in bEnd3 cells. Unlike the static set up, brightfield imaging suggested less aggregation of NPs with flow and citrate-coated NPs associate more with astrocytes in comparison to PEGylated NPs. These data demonstrate that surface properties influence passage of NPs across bEnd3 cells. This multicell model could be applied as a rapid screening technique to analyze uptake and toxicity of NMs across the BBB.

## PS 1777 Effect of Surface Modification of Metal Oxide Nanoparticles upon Cell Viability and Genotoxicity of Epithelial Breast Cells.

T. D. Palacios-Hernandez<sup>1</sup>, E. Gonzalez<sup>2</sup>, M. A. Mendez<sup>3</sup>, G. A. Hirata<sup>4</sup>, D. Momot<sup>5</sup>, E. E. Hernandez<sup>5</sup>, A. Marogi<sup>5</sup>, M. Poirier<sup>5</sup>, O. Olivero<sup>5</sup> and R. E. Cachau<sup>6</sup>. <sup>1</sup>Biological Sciences, UPAEP, Puebla, Mexico; <sup>2</sup>Chemistry Center, ICUAR, Puebla, Mexico; <sup>3</sup>Chemical and Biological Sciences, UDLAP, Puebla, Mexico; <sup>4</sup>Nanosciences and Nanotechnology Center, UNAM, Ensenada, Mexico; <sup>5</sup>National Cancer Institute, NIH, Bethesda, MD; <sup>6</sup>Frederick National Laboratory of Cancer Research, Frederick, MD.

In this work, the biological activity of different metal oxide nanoparticles (Fe<sub>3</sub>O<sub>4</sub>, Co<sub>3</sub>O<sub>4</sub>, CuO) upon epithelial breast cells MCF-10A have been evaluated. The first step is the fabrication and characterization of the metal-oxide nanoparticles (MONPs) followed by the functionalization with folic acid, L-arginine and L-cysteine which is confirmed by Fourier Transform Infrared Spectroscopy (FTIR) and Low Voltage Electron Microscopy (LVEM) measurements. In order to determine real time cell viability, semi-confluent cells were exposed to either 0, or 0.2 mg/mL of particles with and without functionalization.  $2 \times 10^3$  cells/well were grown in a gold wired 16-well plate for 15 hours, with readings of impedance collected every 15 minutes to monitor cell proliferation. To determine cell-nanoparticle interactions, cells were grown during 24 hours, exposed to 0.2 mg/mL of particles and allowed to grow for additional 48 hours. After that, cells were fixed and stained with DAPI to evaluate apoptosis necrosis and characterization of normal nuclear morphology. Additionally a dose-response growth curve using Fe<sub>3</sub>O<sub>4</sub> nanoparticles, presumably, the less toxic exposure, free and functionalized with folic acid (Fe-AF) was carried out. Results indicate that the most toxic treatment was Fe<sub>3</sub>O<sub>4</sub> and the less toxic was Fe<sub>3</sub>O<sub>4</sub> functionalized with folic acid, although all the MONPs evaluated didn't cause a strong toxic response due the values of cell index obtained by impedance evaluation. However, the presence of particles interacting with the cell and nucleus showed the possibility of genotoxic effects, and for that reason, in an attempt to explore this condition, the micronucleus assay employing Cytochalasin B (Cytome assay) is being conducted as a follow up.

## PS 1778 Synthesis, Characterization and Evaluation of Biological In Vitro Activity of Eu<sup>3+</sup> Doped Hydroxyapatite.

J. Delgado-Jimenez<sup>1</sup>, T. D. Palacios-Hernandez<sup>2</sup>, A. Angulo Molina<sup>1</sup>, J. L. Varela<sup>3</sup>, R. Agustin<sup>3</sup> and E. Rubio-Rosas<sup>3</sup>. <sup>1</sup>Ciencias Químico-Biológicas, UDLAP, Puebla, Mexico; <sup>2</sup>Ciencias Biológicas, UPAEP, Puebla, Mexico; <sup>3</sup>Centro de Vinculación Universitaria y Transferencia de Tecnología, BUAP, Puebla, Mexico.

In this work, the synthesis, characterization and biological in vitro activity of Eu<sup>3+</sup>-doped hydroxyapatite (Eu-HAp) is being evaluated. Hydroxyapatite synthesis is being carried out by microwave-hydrothermal techniques, modifying parameters such as temperature, power, pH and calcium precursors. In a typical process, the synthesis was carried out by the mixture of CaCl<sub>2</sub> or Ca(NO<sub>3</sub>)<sub>2</sub>·4H<sub>2</sub>O and Eu(NO<sub>3</sub>)<sub>3</sub>·5H<sub>2</sub>O. After that, a solution of (NH<sub>4</sub>)<sub>2</sub>HPO<sub>4</sub> was added. The full mixture was alkalized and transferred into a Milestone START D Microwave Digestor System. Power and temperature measurements were adjusted regarding the literature, and after that the product was purified and dried. The products obtained, as powders, were grinded and characterized by X-Ray Diffraction (XRD), Scanning and Transmission Electron Microscopy (SEM, TEM), Atomic Force Microscopy (AFM) and Fourier-Transformed Infrared Spectroscopy (FTIR). As preliminary results, infrared spectroscopy showed the signals corresponding to O-H stretching at approximately 3500 cm<sup>-1</sup>. Regarding PO<sub>4</sub> vibrations, we found approximately at 400, 550, a small signal at 600, 1000 and 1100 cm<sup>-1</sup> the characteristic vibration of this group. Regarding XRD, we have obtained nanocrystals at a size range of 37-50 nm, and the crystalline phase corresponding to hydroxyapatite

was confirmed in the samples obtained by the most alkaline pH ranges (above 10), while at pH 9 we obtained a mixture between hydroxyapatite and monetite phases. To evaluate the biological in vitro activity of our materials, MTT assay is being performed upon mouse fibroblasts that are treated with representative samples of Eu-HAp nanoparticles previously synthesized by our group.

## PS 1779 Interactive Toxicity of Usnic Acid and Lipopolysaccharide in Human Liver HepG2 Cells.

S. C. Sahu, M. W. O'Donnell and R. L. Sprando. *Toxicology, US FDA, Laurel, MD.*

Usnic acid (UA), a natural botanical product, is a constituent of some dietary supplements used for weight loss. It has been associated with clinical hepatotoxicity leading to liver failure in humans. The present study was undertaken to evaluate the interactive toxicity, if any, of UA with lipopolysaccharides (LPS), a potential contaminant of food, at low nontoxic concentrations. The human hepatoblastoma HepG2 cells were treated with the vehicle control and test agents, separately and in combination (UA+LPS) at concentrations of UA 1.0  $\mu\text{M}$  and LPS 1.0 ng/ml, for 24 h at 37.0 °C in 5% CO<sub>2</sub>. Following the treatment period, the cells were evaluated by the traditional biochemical endpoints of toxicity in combination with the toxicogenomic endpoints that included cytotoxicity, oxidative stress, mitochondrial injury and changes in pathway-focused gene expression profiles. Compared to the controls, low nontoxic concentrations of UA and LPS separately showed no effect on the cells as determined by the biochemical endpoints. However, the simultaneous mixed exposure of the cells to their mixture resulted in increased cytotoxicity, oxidative stress and mitochondrial injury. The pathway-focused gene expression analysis resulted in the altered expression of several genes out of 84 genes examined. Most altered gene expressions induced by the mixture of UA and LPS were different from those induced by the individual constituents. The genes affected by the mixture were not modulated by either UA or LPS. The results of this study suggest that the interactions of low nontoxic concentrations of UA and LPS produce toxicity in HepG2 cells.

## PS 1780 Dihydroartemisinin Inhibits PMA-Induced Cyclooxygenase-2 Expression through Downregulating AKT and MAPK Signaling Pathways in Murine Macrophages.

E. Han<sup>1</sup>, H. Kim<sup>1</sup>, J. Choi<sup>1</sup>, Y. Hwang<sup>2</sup> and H. Jeong<sup>1</sup>. <sup>1</sup>Pharmacy, Chungnam National University, Daejeon, Republic of Korea; <sup>2</sup>Korea International University, Jinju, Republic of Korea.

Dihydroartemisinin (DHA), a semi-synthetic derivative of artemisinin isolated from the traditional Chinese herb *Artemisia annua* L., has recently been shown to possess antitumor activity in various cancer cells. However, the effect of anti-inflammatory potentials of DHA in murine macrophage RAW 264.7 cells has not been studied. The present study investigated the effect of COX-2 and molecular mechanisms by DHA in phorbol 12-myristate 13-acetate (PMA)-stimulated RAW 264.7 cells. DHA dose-dependently decreased PMA-induced COX-2 expression and PGE<sub>2</sub> production, as well as COX-2 promoter-driven luciferase activity. Additionally, DHA decreased luciferase activity of COX-2 regulation-related transcription factors including NF- $\kappa$ B, AP-1, C/EBP and CREB. DHA also remarkably reduced PMA-induced p65, C/EBP $\beta$ , c-jun and CREB nuclear translocation. Furthermore, DHA evidently inhibited PMA-induced phosphorylation of AKT and the MAP Kinases, such as ERK, JNK and p38. These data indicated that DHA effectively attenuates COX-2 production via down-regulation of AKT and MAPK pathway, revealing partial molecular basis for the anti-inflammatory properties of DHA. These findings demonstrate that DHA effectively attenuates COX-2 production, and provide further insight into the signal transduction pathways involved in the anti-inflammatory effects of DHA.

## PS 1781 Protective Role of Silymarin against Oxidative Stress Induced in Human Neuroblastoma Cell Line SH-SY5Y.

A. Anadon, M. A. Martinez, E. Ramos, V. Castellano, I. Ares, M. Martinez, M. R. Martinez-Larrañaga and A. Romero. *Toxicology & Pharmacology, Complutense University, Madrid, Spain.*

Silymarin (SM) is a mixture of bioactive flavonolignans isolated from *Silybum marianum* (L.) Gaertn., employed usually in the treatment of alcoholic liver disease and as anti-hepatotoxic agent in humans. The essential activity of SM is an antioxidant

effect of its flavonolignans. Because of the importance of oxidative stress and mitochondrial dysfunction in causing neuronal death, prompted us to investigate the effects of SM against an in vitro model of reactive oxygen species (ROS) production in the human neuroblastoma cell line SH-SY5Y. We selected two cytotoxic stimuli, for one hand, hydrogen peroxide (H<sub>2</sub>O<sub>2</sub>) (500  $\mu$ M), and on the other hand the combination of 30  $\mu$ M rotenone plus 10  $\mu$ M oligomycin-A (R/O) that inhibit mitochondrial respiration complexes I and V, respectively. Cell viability, measured as MTT reduction, was decreased to 70% in cells treated with H<sub>2</sub>O<sub>2</sub> and to 60% in cells exposed to R/O. Cell incubation with increasing concentrations of SM (1-1000  $\mu$ M) for 24 hr, followed by a 24-hr period with H<sub>2</sub>O<sub>2</sub> (extracellular ROS) or R/O (intracellular ROS). Maximum protection was achieved with 300  $\mu$ M SM (30% protection). Our results showed that R/O and H<sub>2</sub>O<sub>2</sub>-induced cytotoxicity in SH-SY5Y cells was suppressed by treatment with SM. Because, it is recently reported that SM crosses the blood-brain barrier and enters the CNS and it is non-toxic even at higher doses, this flavonoid may be useful in diseases known to be aggravated by reactive oxygen species and in the development of novel treatments for neurodegenerative disorders. This work was supported by projects Ref. BSCHGR58/08(UCM), Ref. No. S2009/AGR-1469(CAM) and Consolider-Ingenio 2010 No.CSD2007-063(MEC), Spain.

**PS 1782 Thymoquinone, a Bioactive Component of *Nigella sativa*, Modulates Redox Status and Insulin Secretion from Pancreatic Beta Cells.**

J. P. Gray<sup>1,3</sup>, R. Follmer<sup>1</sup>, R. Rebar<sup>1</sup>, N. Seeram<sup>2</sup> and E. Heart<sup>3</sup>. <sup>1</sup>Science, US Coast Guard Academy, New London, CT; <sup>2</sup>Bioactive Botanical Research Laboratory, University of Rhode Island, Kingston, RI; <sup>3</sup>Cellular Dynamics, Marine Biological Laboratory, Woods Hole, MA.

*Nigella Sativa* is a traditional medicine that has been used in the Mediterranean to treat a variety of disorders, including type 2 diabetes. A primary component of *Nigella sativa* extract is thymoquinone which, like *Nigella sativa* extract, attenuates diabetes symptoms. The molecular targets and interactions of thymoquinone with metabolic pathways relevant to glucose-stimulated insulin secretion (GSIS) from pancreatic  $\beta$ -cells have not yet been identified. Our laboratory previously demonstrated that low (nM- $\mu$ M) doses of various quinones such as menadione stimulate insulin secretion from  $\beta$ -cells, and this action was coupled to the generation of low levels of H<sub>2</sub>O<sub>2</sub>, a putative mediator of GSIS. Here we compared the mechanism of action of thymoquinone to that of menadione in  $\beta$ -cells. Like menadione, thymoquinone induced a dose-dependent increase in the production of H<sub>2</sub>O<sub>2</sub>. Unlike menadione, the redox cycling of thymoquinone was not dependent on the glucose concentration. Both NADPH and NADH supported the redox cycling of thymoquinone in cytosolic and mitochondrial fractions. This was consistent with the ability of thymoquinone to decrease NADH/NAD<sup>+</sup> and NADPH/NADP<sup>+</sup> ratios, thus reducing intracellular redox poise. Thymoquinone-dependent redox cycling activities were inhibited by diphenylene iodonium, an inhibitor of flavin-containing oxidoreductases. Dicoumarol and MAC220, NQO1 inhibitors previously shown to inhibit menadione-dependent redox cycling, failed to inhibit thymoquinone-dependent redox cycling. Unlike menadione, thymoquinone was found to potentiate GSIS in a dose-dependent manner at stimulatory glucose (concentrations which potently stimulate insulin secretion). These data suggest that while the mechanisms of thymoquinone redox cycling are different than those of menadione, thymoquinone retains the ability to regulate both redox status and insulin secretion from  $\beta$ -cells.

**PS 1783 Antioxidant and DPPH-Scavenging Activities of Compounds and Ethanolic Extract of the Leaf and Twigs of *Caesalpinia bonduc* L. Roxb.**

O. O. Olubanke<sup>1</sup>, O. E. Ogunlana<sup>2</sup>, A. T. Lawa<sup>1</sup>, J. O. Olagunju<sup>3</sup>, A. A. Akindahunsi<sup>4</sup> and N. H. Tan<sup>5</sup>. <sup>1</sup>Biological Sciences, Covenant University, Ota, Nigeria; <sup>2</sup>Biological Sciences, Crawford University, Igbesa, Nigeria; <sup>3</sup>Medical Biochemistry, College of Medicine, Lagos State University, Ikeja, Nigeria; <sup>4</sup>Biochemistry, Federal University of Technology, Akure, Nigeria; <sup>5</sup>State Key Laboratory of Phytochemistry and Plant Resources, Kunming Institute of Botany, Kunming, China.

Antioxidant effects of ethanolic extract of *Caesalpinia bonduc* and its isolated bioactive compounds were evaluated *in vitro*. The compounds included two new cassane diterpenes, 1 $\alpha$ ,7 $\alpha$ -diacetoxyl-5 $\alpha$ ,6 $\beta$ -dihydroxyl-cass-14(15)-epoxy-16,12-olide (1) and 12 $\alpha$ -ethoxyl-1 $\alpha$ ,14 $\beta$ -diacetoxyl-2 $\alpha$ ,5 $\alpha$ -dihydroxyl-cass-13(15)-en-16,12-olide (2); and others, bonducellin (3), 7,4'-dihydroxy-3,11-dehydrohomoisoflavanone

(4), daucosterol (5), luteolin (6), quercetin-3-methyl ether (7) and kaempferol-3-O- $\alpha$ -L-rhamnopyranosyl-(1 $\rightarrow$ 2)- $\beta$ -D-xylopyranoside (8). The antioxidant properties of the extract and compounds were assessed by the measurement of the total phenolic content, ascorbic acid content, total antioxidant capacity and 1-1-diphenyl-2-picryl hydrazyl (DPPH) and hydrogen peroxide radicals scavenging activities. Compounds 3, 6, 7 and ethanolic extract had DPPH scavenging activities with IC<sub>50</sub> values of 186, 75, 17 and 102  $\mu$ g/ml respectively when compared to vitamin C with 15  $\mu$ g/ml. On the other hand, no significant results were obtained for hydrogen peroxide radical. In addition, compound 7 has the highest phenolic content of 0.81 $\pm$ 0.01 mg/ml of gallic acid equivalent while compound 8 showed the highest total antioxidant capacity with 254.31 $\pm$ 3.54 and 199.82 $\pm$ 2.78  $\mu$ g/ml gallic and ascorbic acid equivalent respectively. Compound 4 and ethanolic extract showed a high ascorbic acid content of 2.26 $\pm$ 0.01 and 6.78 $\pm$ 0.03 mg/ml respectively. The results obtained showed the antioxidant activity of the ethanolic extract of *C. bonduc* and deduced that this activity was mediated by its isolated bioactive compounds.

**PS 1784 Selective Elimination of Malignant Melanomas through Autophagic and Mitochondria-Based Mechanisms by the Antitumor Agent Osw-1.**

K. Riaz Ahmed, C. Garcia-Prieto, L. Feng and P. Huang. *Molecular Pathology, University of Texas MD Anderson Cancer Center, Houston, TX.* Sponsor: M. Smith.

Drug resistance and lack of therapeutic selectivity are two of the biggest challenges to successful melanoma therapy. Constitutive activation of Extracellular Signal Regulated Kinase 1/2 (ERK1/2) and subsequent chemoresistance has been reported in malignant melanomas. ERK1/2 has also been implicated in activation of mitochondrial gene expression and regulation of autophagy thus making it an important therapeutic target.

The natural product, OSW-1, isolated from the bulbs of ivory coast lily, has been shown to be highly cytotoxic in numerous cancer cell lines with yet undefined mechanisms of action. Herein, we report our results on the anticancer activity and selectivity of OSW-1 in malignant melanoma cells and its potential mechanisms of action.

Our preliminary results demonstrated that OSW-1 was highly effective in killing tumor cells that are resistant to most of the currently available anticancer drugs, with IC50 values in sub-nM concentrations. Importantly, OSW-1 preferentially killed melanoma cells and exerted much lower toxicity to normal melanocytes in culture. Biochemical analysis revealed that OSW-1 treatment caused damage of the mitochondrial membrane integrity, leading to a decrease in transmembrane potential and subsequently initiating cell death, apparently through autophagy. Further study demonstrated that OSW-1 inhibited ERK1/2 expression in melanoma cells and caused a significant disturbance of cellular calcium homeostasis, leading to aberrant calcium-mediated processes including mitochondrial impairment. Based on these results, we postulate that OSW-1 inhibits ERK1/2 mediated signaling and triggers mitochondrial damage in cells leading to a significant disturbance of cellular calcium and cell death through autophagy. This study is of great significance since ERK1/2 signaling is important to melanoma cell survival and inhibition of ERK1/2 expression and induction of autophagic cell death by OSW-1 will be critical to combat therapeutic resistance and enhance drug selectivity.

**PS 1785 3-Caffeoyl, 4-Dihydrocaffeoylquinic Acid from *Salicornia herbacea* Attenuates High Glucose-Induced Hepatic Lipogenesis in Human HepG2 Cells.**

H. Chun<sup>2</sup>, Y. Hwang<sup>3,1</sup>, J. Choi<sup>1</sup>, H. Kim<sup>1</sup>, Y. Chung<sup>3</sup> and H. Jeong<sup>1</sup>. <sup>1</sup>Pharmacy, Chungnam National University, Daejeon, Republic of Korea; <sup>2</sup>Korea Research Institute of Bioscience and Biotechnology, Jeongseup, Republic of Korea; <sup>3</sup>International University of Korea, Jinju, Republic of Korea.

3-Caffeoyl, 4-dihydrocaffeoylquinic acid (CDCQ) from *Salicornia herbacea* has a variety of pharmacological properties, including antioxidant and anti-inflammatory and hepatoprotective properties. The aims of our study were to provide new data on the molecular mechanisms underlying the role of CDCQ in prevention of high glucose-induced lipid accumulation in human HepG2 cells. We found that CDCQ suppressed high glucose-induced lipid accumulation in HepG2 cells. CDCQ strongly inhibited the high glucose-induced FAS expression by modulating SREBP-1c activation. Moreover, the use of a specific inhibitor or liver kinase B1 (LKB1)-siRNA transfected HepG2 cells showed that CDCQ activated AMP-activated protein kinase (AMPK) via silent information regulator T1 (SIRT1) or LKB1 in HepG2 cells. These results indicate that CDCQ prevents lipid accumulation by

blocking the expression of SREBP-1c and FAS through LKB1/SIRT1 and AMPK activation in HepG2 cells, suggesting that CDCQ is a novel AMPK activator with a potential role in the prevention obesity.

**PS 1786 Effects of Saponins from the Roots of *Platycodon grandiflorum* on TGF- $\beta$ 1-Induced Epithelial-Mesenchymal Transition in A549 Cells.**

C. Ho<sup>1</sup>, H. Kim<sup>1</sup>, Y. Hwang<sup>2</sup>, Y. Chung<sup>2</sup> and H. Jeong<sup>1</sup>. <sup>1</sup>Pharmacy, Chungnam National University, Daejeon, Republic of Korea; <sup>2</sup>International University of Korea, Jinju, Republic of Korea.

Epithelial to mesenchymal transition (EMT) is a key event in the progression of cancer. EMT is characterized by the loss of epithelial and the gain of mesenchymal features. Previous studies have revealed that treatment with CKS, saponins from the roots of *Platycodon grandiflorum*, significantly reduces metastasis and tumorigenesis, but the underlying mode of action has not been elucidated. In this study, we investigated the inhibitory effect of CKS on transforming growth factor (TGF)- $\beta$ 1-induced alterations characteristic of EMT in human lung carcinoma cells. We found that CKS-treated cells displayed inhibited TGF- $\beta$ 1-mediated E-cadherin down-regulation and Vimentin up-regulation and also retained epithelial morphology. Furthermore, TGF- $\beta$ 1-increased Snail expression was reduced by CKS. Pretreatment of cells with CKS blocked TGF- $\beta$ 1-induced Smad2/3 phosphorylation and Smad7 down-regulation. CKS inhibited TGF- $\beta$ 1-mediated phosphorylation of Akt, ERK1/2, and glycogen synthase kinase-3 $\beta$  (GSK-3 $\beta$ ). Furthermore, TGF- $\beta$ 1-increased Snail expression was reduced by pharmacology inhibitors of Akt, ERK1/2, and GSK-3 $\beta$ . These results indicate that pretreatment with CKS inhibits the TGF- $\beta$ 1-induced EMT process and prevents TGF- $\beta$ 1-induced transdifferentiation via activation of Akt and ERK1/2 and inactivation of GSK-3 $\beta$  in A549 cells.

**PS 1787 Platycodin D Regulates Hepatic Lipogenesis via an AMP-Activated Protein Kinase Dependent Signaling Pathway in Human HepG2 Cells.**

H. Lee<sup>2</sup>, Y. Hwang<sup>3,1</sup>, J. Choi<sup>1</sup>, H. Kim<sup>1</sup>, Y. Chung<sup>3</sup> and H. Jeong<sup>1</sup>. <sup>1</sup>Pharmacy, Chungnam National University, Daejeon, Republic of Korea; <sup>2</sup>Korea Research Institute of Bioscience and Biotechnology, Daejeon, Republic of Korea; <sup>3</sup>International University of Korea, Jinju, Republic of Korea.

Platycodin D, the saponins from the roots of *Platycodon grandiflorum* (CKS), has a variety of pharmacological properties, including anti-hyperlipidemic, antioxidant and hepatoprotective properties. This study was conducted to suggest the role of AMP-activated protein kinase (AMPK) pathway in the anti-obesity effect of platycodin D. We characterized the underlying mechanism platycodin D's effects in HepG2 cells by Western blot and RT-PCR analysis. Platycodin D increased the phosphorylation of AMPK and acetyl-CoA carboxylase (ACC) in HepG2 cells. Use of a specific inhibitor showed that platycodin D activated AMPK via SIRT1/calmodulin-dependent kinase kinase (CaMKK) in HepG2 cells. Taken together, these data suggest that platycodin D exert improving effects on high glucose-induced lipogenesis by reducing of SREBP-1c and FAS expression via AMPK activation.

**PS 1788 Rutaecarpine Suppresses LPS-Induced Inflammation in Mouse Macrophages: A Possible Pathway through the Induction of Heme Oxygenase-1 Expression.**

S. Jin<sup>1</sup>, Y. Hwang<sup>2</sup>, H. Kim<sup>2</sup>, J. Choi<sup>1</sup>, H. Kim<sup>1</sup>, Y. Chung<sup>2</sup> and H. Jeong<sup>1</sup>. <sup>1</sup>Pharmacy, Chungnam National University, Daejeon, Republic of Korea; <sup>2</sup>International University of Korea, Jinju, Republic of Korea.

Rutaecarpine, a quinazolinocarboline alkaloidal compound, is a natural product isolated from *Evodia rutaecarpa* and has various biological and pharmacological effects, including anti-inflammatory and anti-oxidative properties. In the present study, we investigated the effect of rutaecarpine against lipopolysaccharide (LPS)-induced inflammation in RAW264.7 macrophages. Treatment with rutaecarpine suppressed inducible nitric oxide synthase expression and nitric oxide (NO) production by downregulating NF- $\kappa$ B activity in lipopolysaccharide (LPS)-stimulated RAW264.7 macrophages. Rutaecarpine acts by inducing the expression of heme

oxygenase-1 (HO-1) in a dose- and time-dependent manner. The signaling pathway involved in rutaecarpine-mediated HO-1 induction included Ca<sup>2+</sup>/calmodulin-dependent protein kinase II (CaMKII) and extracellular signal regulated kinase 1/2 (ERK1/2). Furthermore, the CaMKII-ERK1/2 cascade targets the transcription factor, NF-E2-related factor-2 (Nrf2). Taken together, our results demonstrate that rutaecarpine-induced expression of HO-1 is mediated by the Ca<sup>2+</sup>-CaMKII-Nrf2-HO-1 pathway and inhibits LPS-induced inflammation in RAW264.7 macrophages.

**PS 1789 Cultivated Ginseng Inhibits Tarc Expression by Suppressing the Activation of NF- $\kappa$ B and STAT1 in Human Keratinocyte Cells.**

B. Park<sup>1</sup>, J. Choi<sup>1</sup>, J. Choi<sup>2</sup>, Y. Chung<sup>2</sup> and H. Jeong<sup>1</sup>. <sup>1</sup>Pharmacy, Chungnam National University, Daejeon, Republic of Korea; <sup>2</sup>International University of Korea, Jinju, Republic of Korea.

Atopic dermatitis (AD) is associated with the paradigm of an allergic T helper (Th) 2-mediated disease, characterized by abnormal IgE production, peripheral eosinophilia, mast cell activation, as well as Th2 and Th1 cytokine up-regulation in chronic skin lesions. This study examined the inhibitory effects of cultivated ginseng (CG) (*Panax ginseng* C.A. Meyer) on atopic dermatitis in HaCaT cells. CG, an herb used in Korean herbal medicine, has been widely used in China and Japan to treat fatigue and to enhance resistance to many diseases. CG suppressed TNF- $\alpha$ /IFN- $\gamma$ -induced TARC, CTACK, and MDC mRNA expression in HaCaT cells. Additionally, CG inhibited TNF- $\alpha$ /IFN- $\gamma$ -induced activation of NF- $\kappa$ B and STAT1. These results indicate that CG inhibits chemokine expression in keratinocytes by suppressing of NF- $\kappa$ B and STAT1 activation.

**PS 1790 Mollugin Inhibits Proliferation and Induces Apoptosis by Inhibiting HER2 Expression in HER2-Overexpressing Breast and Ovarian Cancer Cells.**

M. Do, T. Tran, M. Na and H. Jeong. Pharmacy, Chungnam National University, Daejeon, Republic of Korea.

Overexpression of the HER2 gene causes many cancer types and has been reported to enhance cell proliferation, tumor growth, angiogenesis, and metastasis. This study investigated the molecular mechanisms by which mollugin exerts anti-tumor effect in HER2-overexpressing breast and ovarian cancer cells. Mollugin exhibited potent inhibitory effects on cancer cell proliferation, especially in HER2-overexpressing SK-BR-3 human breast cancer cells and SK-OV-3 human ovarian cancer cells in a dose- and time-dependent manner. Additionally, caspase-3 activity and PARP cleavage were significantly upregulated in HER2-overexpressing SK-BR-3 and SK-OV-3 cells treated with mollugin. Mollugin treatment caused a dose-dependent inhibition of HER2 gene expression at the transcriptional level, potentially in part through suppression of NF- $\kappa$ B activation. Moreover, mollugin inhibits cyclin D1 expression by downregulating HER2 activation and consequently reducing PI3K/Akt signaling. These results suggest that mollugin is a novel modulator of the HER2 pathway in HER2-overexpressing cancer cells with a potential role in the treatment and prevention of human breast and ovarian cancer with HER2 overexpression.

**PS 1791 Multiple Signaling Pathways Involved in Suppression of MDR1 by Mollugin from *Rubica cordifolia*.**

T. Tran, H. Kim, M. Do, S. Jin, E. Shim, H. Han, M. Na and H. Jeong. Pharmacy, Chungnam National University, Daejeon, Republic of Korea.

Multidrug resistance (MDR) is known to be a serious problem in cancer treatment and has been identified as a negative prognostic factor in malignancies. This study investigated mollugin, purified from roots of *Rubica cordifolia* L., down-regulated MDR1 expression in MCF-7/adriamycin (MCF-7/adr) cells, human breast multidrug-resistant cancer cell. Mollugin treatment significantly inhibited MDR1 expression by blocking MDR1 gene transcription. Mollugin treatment also significantly increased intracellular accumulation of the fluorescently-tagged P-gp substrate, rhodamine-123. The suppression of MDR1 promoter activity and protein expression was mediated through mollugin-induced activation of AMP-activated protein kinase (AMPK) and inhibited NF- $\kappa$ B as well as CREB activation.

These results suggest that mollugin treatment enhanced suppression of P-gp expression by inhibiting the NF- $\kappa$ B signaling pathway and attenuating CRE transcriptional activity through AMPK activation.

**PS 1792 Liver Kinase B1 Is Required for Phillyrin-Induced AMPK Activation in Human HepG2 Hepatocytes.**

H. Han, M. Do, H. Kim, T. Khanal, T. Tran, M. Na and H. Jeong. *Pharmacy, Chungnam National University, Daejeon, Republic of Korea.*

Phillyrin, an active constituent found in certain functional foods, has anti-obesity activity in vivo. This study investigated the ability of phillyrin to induce AMP-activated protein kinase (AMPK) in human HepG2 hepatocytes. Phillyrin strongly activated the phosphorylation of AMPK $\alpha$  at Thr172 in HepG2 cells under normal glucose condition. Additionally, the phosphorylation of AMPK $\alpha$  at Thr172 and ACC at Ser79 was significantly suppressed in cells treated with high glucose, phillyrin dose-dependently recovered the phosphorylation of AMPK $\alpha$  at Thr172 and the downstream target acetyl-CoA carboxylase (ACC) phosphorylation at Ser79 in HepG2 cells pretreated by phillyrin. Moreover, phillyrin significantly stimulated the phosphorylation of liver kinase B1 (LKB1) at Ser428 in a time-dependent manner, with a time course matching that of AMPK $\alpha$  phosphorylation at Thr172. In addition, the defeat of phillyrin-stimulated AMPK $\alpha$  activation in HeLa cells deficient in LKB1 or in siRNA LKB1-transfected HepG2 cells, suggesting that LKB1 is required for phillyrin-induced AMPK activation. These results indicate that anti-obesity effects are mediated, at least in part, by the activation of LKB1/AMPK.

**PS 1793 Prevention of Free Fatty Acid-Induced Hepatic Steatosis by S-Allyl Cysteine through AMPK Pathways.**

H. Jeong<sup>1</sup>, Y. Hwang<sup>2</sup>, H. Kim<sup>1</sup>, J. Choi<sup>1</sup> and Y. Chung<sup>2</sup>. <sup>1</sup>Pharmacy, Chungnam National University, Daejeon, Republic of Korea; <sup>2</sup>Korea International University, Jinju, Republic of Korea.

S-allylcysteine (SAC) is the most abundant organosulfur compound in aged garlic extract (AGE), which has been used to standardize commercial aged extracts. SAC has been reported to have antioxidant, anti-cancer, anti-hepatotoxic and neurotrophic properties. In this study, we provide evidence that SAC prevented free fatty acid (FFA)-induced lipid accumulation and lipotoxicity in hepatocytes. SAC significantly reduced FFA-induced generation of reactive oxygen species, caspase activation, and subsequent cell death. Also, SAC mitigated total cellular lipid and TG accumulation in steatotic HepG2 cells. SAC significantly increased the phosphorylation of AMP-activated protein kinase (AMPK) and acetyl-CoA carboxylase (ACC) in HepG2 cells. Additionally, SAC down-regulated the levels of sterol regulatory element binding protein-1 (SREBP-1) and its target genes, including ACC and fatty acid synthase (FAS). Use of a specific inhibitor showed that SAC activated AMPK via calcium/calmodulin-dependent kinase kinase (CaMKK) and SIRT1. Our results demonstrate that SAC activates AMPK through CaMKK and inhibits SREBP-1-mediated hepatic lipogenesis. The results indicate that SAC inhibit lipogenesis in cultured human hepatocytes, and further suggest that SAC impair triglyceride synthesis in part due to decreased de novo fatty acid synthesis resulting from inhibition on AMPK-dependent FAS and SREBP-1c.

**PS 1794 Cyto-/Genotoxic Effect of Extract from *Bufo bufo* gargarizans Cantor in Human T Cell Leukemia Cells.**

S. Lee, Y. Lee, Y. Choi and H. Chung. *School of Public Health, Seoul National University, Seoul, Republic of Korea.* Sponsor: J. Chung.

Cinobufacini (Huachansu), an extract from the skins of *Bufo bufo* gargarizans Cantor and has been widely used as an oriental medicine for cancer therapy. Although numerous experimental studies on cinobufacini have been investigated its anti-cancer properties, there is no information whether cinobufacini has anti-cancer effects on human leukemia. The genotoxicity of cinobufacini has not been determined. The aim of the present study was to examine the cyto-/genotoxic effect of cinobufacini in human T cell leukemia (Jurkat T-cells) and human normal lymphocytes.

Jurkat T-cells and normal lymphocytes were treated for 24 or 48 hours with various concentrations of cinobufacini. Cytotoxicity was evaluated by Trypan blue exclusion assays. Apoptotic cell death was detected by propidium iodide (PI) staining, and intracellular reactive oxygen species (ROS) was determined by fluorescent dye 5-(and 6)-141 carboxy-2, 7-dichlorodihydrofluorescein diacetate (DCF-DA;

Molecular Probes) using flow cytometry analysis. The genotoxicity of cinobufacini in Jurkat-T cells was measured by comet assay and cytokinesis-block micronucleus assay.

Cinobufacini significantly inhibited cell viability in Jurkat-T cells but not in normal lymphocytes in dose- and time- dependent manner. Jurkat T-cells treated with cinobufacini induced significantly higher levels of sub-diploid cells compared with control. The DNA content in the sub-G1 region increased from 3.35 % to 22.2 % and from 6.13 % to 42.25 %, when Jurkat-T cells treated with cinobufacini for 24 or 48 hours, respectively. Cinobufacini treatment resulted in significantly higher levels of intracellular ROS. Cinobufacini also induced significant DNA damage determined by comet assay and cytokinesis-block micronucleus assay. In conclusion, these findings suggest that an extract from *Bufo bufo* gargarizans Cantor may be effective for treatment of leukemia.

**PS 1795 Potentially Toxic Minerals Used in South African Traditional Medicine.**

R. Street and M. P. Cele. *University of KwaZulu-Natal, Durban, South Africa.* Sponsor: A. Ndfor.

The World Health Organization recognizes the incorporation of plant, animal and/or mineral based products in traditional medicines. Millions of South Africans rely on traditional medicines for their primary health care needs. Heavy metal toxicity related to the use of traditional medicine has been reported worldwide. Although minerals are widely available at South African traditional medicine markets, there is insufficient pragmatic information regarding them. Thus the aim of this study was to identify the commonly used crude metal and crystalline salts in the South African traditional medicine trade. Premarket surveys indicated commonly available minerals. These minerals were then purchased from a rural traditional medicine market. Information regarding the colloquial name, mode of administration as well as the price and weight were recorded. Scanning electron microscopy-energy dispersive X-ray was used to determine the composition of the unknown medicinally used powdered products. The elemental spectra was viewed using a Leo 1450 SEM. Mineral salts identified included ammonium chloride, calcium sulphate and sulphur powder. If not handled correctly, such salts can cause numerous infirmities including eye irritation and dermal toxicity. Among the available metal salts were potassium dichromate, a Class 1 carcinogen, which is routinely taken both orally and as an enema, and potassium permanganate. Also very concerning was the finding of liquid mercury documented as being ingested for female reproductive complaints. This study is the first to classify and document the commonly available minerals used in South African traditional medicine. Identifying such products has revealed actual and present hazards in the South African traditional medicine trade. Training programmes are underway to alert traditional healers to the risks involved in handling and consuming such potentially harmful substances as well as to provide healthcare workers with algorithms for metal poisonings.

**PS 1796 Safety Assessment of Botanical Extracts in Cosmetics.**

J. Song and Y. Yang. *L'Oreal R&I, Shanghai, China.*

It's a worldwide trend that customers prefer to use personal care products (PCP) containing natural and organic ingredients from botanicals. However natural does not equal safe. In fact, various preparations and complex compositions of plants have great potential to cause adverse effects such as irritation, sensitization and systemic toxicity. The current dilemma is that there is no official guideline to evaluate botanicals in PCP and the chemical assessment cannot be easily adapted to the safety assessment of botanic substances. In line with the guideline issued by Scientific Committee on Consumer Safety in EU, we proposed a strategy to guide the safety evaluation of botanical extracts. The first and foremost is a good characterization of the botanicals which include species, geographic origin, growing and harvesting conditions, manufacturing process, profile of macro and micronutrients, analytical markers, chromatographic fingerprint, known toxins, etc. Other commonly checked points are UV absorptive capability, 26 major allergens, residual solvents, and additives. For botanical ingredients from food or herbal medicines with a safe history of use, the assessment should be carefully made by taking into consideration of all factors such as parts of plants used, genetic modifications, safety files for registration, and exposed population etc. The focus is to assure that botanicals intended to be used as a cosmetic ingredient is similar to its traditional counterpart used as food and / or herbal drugs in terms of composition, specifications, quality, and safety. After identifying the potential hazard, the exposure analysis will cover all relevant toxicological endpoints. Special attention should be paid to the type I allergy and local tolerance i.e., skin/mucous irritation, phototoxicity/photoallergy, and

Type IV sensitization. In risk assessment, besides in vitro, in vivo and clinical tests, the threshold of toxicological concern (TTC) is a popular and robust tool to support safety of the concerned or unknown partition in composition.

**PS 1797 Effects of Crocetin and Safranal, Constituents of Saffron, in 22Rv1 Prostate Cancer Cells.**

F. F. Albaqami and K. L. Willett. *Department of Pharmacology and ETRP, University of Mississippi, University, MS.*

Saffron extracts have induced apoptosis, cell cycle arrest, inhibited cellular proliferation, and tumor progression in various cancer cell lines. We are interested in studying the potential chemopreventative effects of saffron especially as it relates to prostate cancer. Recognized active constituents of saffron are crocetin and safranal. Cytotoxicity of safranal was investigated using the androgen responsive 22Rv1 prostate cancer cell line. The cytotoxicity IC50 of safranal at 24 hr was 141  $\mu$ M using the tetrazolium dye assay (XTT). The assay was incompatible with crocetin. Using the Caspase-Glo® 3/7 assay system, it appears that apoptotic mechanisms were involved in safranal's cytotoxicity because after 6 hr of exposure, the EC50 of apoptosis was similar to the cytotoxicity IC50. Safranal's antioxidant activity as measured by a 2',7'-dichlorodihydrofluorescein diacetate assay indicated decreased reactive oxygen species formation. Ongoing studies are investigating the potential of saffron to also inhibit prostate cell invasion and migration in vitro. (Supported by Saudi Arabian Ministry of Higher Education and Salman bin Abdulaziz University)

**PS 1798 Kahweol Induces Apoptosis Through Inhibition of STAT3 Phosphorylation in Human Lung Adenocarcinoma A549 Cells.**

H. Kim<sup>1</sup>, J. Choi<sup>1</sup>, K. Tilak<sup>1</sup>, Y. Hwang<sup>1,2</sup> and H. Jeong<sup>1</sup>. <sup>1</sup>Pharmacy, Chungnam National University, Daejeon, Republic of Korea; <sup>2</sup>International University of Korea, Jinju, Republic of Korea.

Epidemiological studies have shown that unfiltered coffee consumption is associated with a low incidence of cancer. Kahweol, the coffee-specific diterpene, has been reported to have anti-carcinogenic properties. Animal data support such a chemopreventive effect of coffee. However, the precise underlying protective mechanisms are poorly understood. In this study, the apoptotic effect of kahweol in human lung adenocarcinoma A549 cells was investigated. In cell viability assays and cell proliferation assays, kahweol exhibited anti-proliferative and pro-apoptotic effects on A549 cells in a time- and dose-dependent manner. Kahweol considerably inhibited the expression of Bcl-2 but increased that of Bax; it also stimulated the cleavage of caspase-3 and poly ADP-ribose polymerase. In addition, kahweol-induced apoptosis was confirmed by TUNEL assays. Furthermore, kahweol inhibited dose-dependent phosphorylation of signal transducer and activator of transcription 3 (STAT3). An overexpression in STAT3 led to resistance to kahweol-induced apoptosis, suggesting that STAT3 was a critical target of kahweol. These findings suggest that kahweol inhibited A549 cell growth and induced apoptosis via down-regulation of STAT3 signaling pathway. These data may contribute to the explanation of the reported antitumoral effects of kahweol, including the recent epidemiological meta-analysis showing that drinking coffee could decrease the risk of certain cancers.

**PS 1799 In Vitro Antioxidant Activities of Fractions of Clerodendrum violaceum Leaf Extract.**

E. A. Balogun, A. Zailani and J. O. Adebayo. *Biochemistry, University of Ilorin, Ilorin, Nigeria.*

Many diseases are mediated by reactive oxygen species. Clerodendrum violaceum is a medicinal plant used indigenously in Nigeria for the treatment of some of such diseases. In this study, the antioxidant activities of the hexane, ethyl acetate and methanolic fractions of Clerodendrum violaceum leaf extract were evaluated in vitro using 2,2-diphenyl-1-picryl-hydrazyl-hydrate (DPPH), superoxide anion and hydrogen peroxide scavenging assays. The antioxidant components of the extract fractions were also determined. The results showed that the methanolic fraction had the highest concentrations of vitamin C, vitamin E, selenium, phenols and flavonoids. Moreover, the methanolic fraction of the extract had the highest free

radical scavenging activities against DPPH, superoxide anion and hydrogen peroxide with EC50 values of 0.08, 0.45 and 0.60 mg/ml respectively. It also had the highest reducing power against ferric ion. The results of the study suggest that the methanolic fraction of Clerodendrum violaceum leaf extract may be a potent source of antioxidant compounds which may be useful for the prevention and treatment of reactive oxygen species-mediated diseases.

**PS 1800 Comparative Pharmacodynamic Effects of Rituximab-EU (MabThera®) and Rituximab-Pfizer in Cynomolgus Monkeys.**

A. M. Ryan<sup>1</sup>, S. Sokolowski<sup>1</sup>, M. Collinge<sup>1</sup>, A. Shen<sup>1</sup>, J. Arrington<sup>2</sup>, T. Cummings<sup>1</sup>, S. Ploch<sup>2</sup>, S. Stephenson<sup>2</sup>, N. Tripathi<sup>2</sup>, S. Hurst<sup>1</sup>, G. Finch<sup>1</sup> and M. Leach<sup>1</sup>. <sup>1</sup>Pfizer WRD, Groton, CT; <sup>2</sup>Covance, Madison, WI.

Background: Rituximab-Pfizer is in Phase 1/2 in RA patients as a potential biosimilar. Analytical and functional characterization has demonstrated in vitro similarity to the licensed rituximab products. Methods: The pharmacodynamic effects of rituximab-Pfizer and rituximab-EU were compared in sexually-mature cynomolgus monkeys in single-dose PK and repeat-dose toxicity studies; both had a 13-week postdose observation period to assess B cell repletion. Peripheral blood lymphocytes were evaluated by flow cytometry, and spleen and axillary and mesenteric lymph nodes (repeat-dose only) were examined microscopically by CD20+ immunohistochemistry. Results: B cell effects were similar in magnitude and time course between rituximab-Pfizer and rituximab-EU. Marked to complete depletion of peripheral blood B cells occurred on Day 4 (the first time point evaluated) in both studies. In the single-dose study, repletion of B cells began on Day 15 (2 mg/kg) and Day 29 (10 and 20 mg/kg) and continued through Day 92, with a subset of animals in each group near or above the pre-dose values at the end of the 13-week observation period. In the repeat-dose study, peripheral B cell depletion persisted through Day 30 of the dosing phase and was associated with lower splenic weights, decreased lymphoid follicle cellularity and decreased CD20+ cells in lymphoid tissues. After repeat-dosing, partial repletion of peripheral blood B cells was noted in recovery animals by Day 92 of the recovery phase. Complete histopathologic recovery occurred in 3 recovery animals (2 rituximab-Pfizer and 1 rituximab-EU). Lymphoid cellularity and CD20+ cells were increased in the remaining 9 recovery animals (relative to the dosing phase results), indicating partial recovery. Conclusion: The magnitude and time course of B cell depletion and repletion were similar between rituximab-Pfizer and rituximab-EU and were consistent with the expected pharmacology of anti-CD20 monoclonal antibodies and the reported innovator data.

**PS 1801 Brain Microhemorrhage Assessment of an Antiamyloid Beta Peptide (A $\beta$ ) Monoclonal Antibody (mAb) Using a Transgenic Mouse Model of Alzheimer's Disease (AD).**

L. A. Buckley<sup>1</sup>, D. Hall<sup>1</sup>, J. Douville<sup>2</sup>, W. H. Jordan<sup>3</sup>, D. Koger<sup>1</sup>, W. H. Anderson<sup>1</sup>, D. G. Waters<sup>1</sup> and R. B. DeMattos<sup>1</sup>. <sup>1</sup>Eli Lilly & Co., Indianapolis, IN; <sup>2</sup>Charles River Laboratories, Montréal, QC, Canada; <sup>3</sup>Vet Path Services, Inc., Mason, OH.

Solanezumab (SLZ), a humanized mAb against A $\beta$  peptide, is being developed for the treatment of AD. SLZ recognizes a mid domain epitope of the A $\beta$  peptide with high affinity and selectivity to soluble monomer. The potential to cause cerebral amyloid angiopathy (CAA)-associated microhemorrhage (MH) was studied in an aged transgenic mouse (APPV717F) model of AD using a murine surrogate of SLZ, m266.2. Critical study design factors included the use of: 1) age-optimized mice (>21 months) known to have established cerebral amyloid prior to treatment and thus potentially susceptible to CAA-MH; 2) sufficient numbers ( $\geq 25$ ) of mice/group; 3) a dose projected to achieve a near-maximal pharmacologic response; 4) a positive control mAb against an N-terminal epitope of A $\beta$  peptide (3D6); 5) meticulous attention to brain collection and processing; 6) expanded brain sectioning and specialized microscopy; and 7) examinations by primary and peer-review pathologists experienced in neuropathologic assessments. Groups of mice received either vehicle control, 50 mg/kg m266.2, or 50 mg/kg 3D6 by weekly ip injection for 4 months (curtailed from the original 6-month duration due to age-related mortality). Plasma exposure to m266.2 and 3D6 was demonstrated at the end of the study. Multiple histologic brain sections stained with Perl's Prussian Blue/DAB-enhanced Perls from each animal were evaluated to score siderophages resulting from hemorrhage, and multiple H&E stained slides were examined with both brightfield and epifluorescent illumination for the presence of other changes in the brain. While the positive control 3D6 elicited the expected robust microhemorrhage response associated with vascular degeneration, the brains of mice given

m266.2 were not different from those of vehicle control mice. In conclusion, m266.2 did not induce CAA-MH or microscopic evidence of any inflammatory or degenerative changes in the brain.

**PS 1802 Safety Assessment of REGN1001 a Monoclonal Antibody Against Angiopoietin-Like 4 (AngPTL4) in Cynomolgus Monkey Toxicology Studies Under Normal and High-Fat Diet Feeding Regimens.**

J. Trejors<sup>1</sup>, R. Soltys<sup>1</sup>, T. Daly<sup>1</sup>, T. O'Neill<sup>2</sup>, K. Mozzachio<sup>2</sup> and A. Arulanandam<sup>1</sup>. <sup>1</sup>Drug Safety, Regeneron Pharmaceuticals, Tarrytown, NY; <sup>2</sup>General Toxicology, WIL Research, Ashland, OH.

REGN1001 is an antibody directed against Angiopoietin-like 4 (AngPTL4) and blocks its ability to inhibit lipoprotein lipase (LPL), an enzyme that hydrolyzes triglycerides (TG) and hence leads to a reduction in plasma TG levels. Evidence for the role of AngPTL4 as a regulator of TG metabolism has been obtained in AngPTL4 gene knockout studies in which profound decreases in TG levels were observed. Several studies have also indicated that AngPTL4 ablation in rodents either via AngPTL4 gene KO or Ab inhibition during high-fat diet (HFD feeding) regimens can lead to the prominent appearance of foamy macrophages and severe inflammatory changes in mesenteric lymph nodes (MLN). To better predict the safety profile of REGN1001 in hyperlipidemic patients (prone to ingest a high fat diet), a toxicology program evaluating REGN1001 intravenous dosing under normal diet and high-fat diet conditions was undertaken in 2 separate 13-week cynomolgus monkey toxicology studies. The first study utilized a normal (high-fiber) feeding regimen; the second study used a HFD regimen that closely resembles a western diet. Consistent with the data described in rodents, only the HFD regimen resulted in foamy macrophages in the MLN in monkeys. After a 15-week treatment free recovery period, during which half the animals were withdrawn from HFD, the incidence/severity of foamy macrophages in MLN was decreased relative to those maintained on the HFD regimen. These studies for the first time demonstrate in primates that AngPTL4 inhibition under HFD fed conditions can result in the presence of foamy macrophages in the MLN. In addition, these toxicology studies demonstrate the importance of incorporating human disease factors in to animal models for safety testing. Given these data, the likelihood of a similar, clinically-relevant toxicity occurring in hyperlipidemic humans receiving REGN1001 or other ANGPTL4 inhibitors cannot be discounted.

**PS 1803 13-Week Toxicity Study of an Anti-Interleukin-6 Antibody (MEDI5117) by Every Other Week Intravenous or Subcutaneous Injection to Cynomolgus Monkeys.**

T. S. Manetz<sup>1</sup>, P. C. Ryan<sup>1</sup>, R. Faggioni<sup>2</sup>, Z. Yao<sup>2</sup>, R. Lee<sup>2</sup>, A. Schneider<sup>2</sup>, I. Vainstein<sup>2</sup>, C. Nhan<sup>2</sup>, K. Mojica<sup>2</sup>, C. Chavez<sup>2</sup>, K. McKeever<sup>1</sup> and R. Dixit<sup>1</sup>. <sup>1</sup>Translational Sciences, MedImmune, LLC, Gaithersburg, MD; <sup>2</sup>Translational Sciences, MedImmune, LLC, Hayward, CA.

MEDI5117 is a human immunoglobulin G1 (IgG1)-YTE (triple mutation) monoclonal antibody that binds to interleukin 6 (IL-6) with sub-pM affinity and neutralizes it by preventing binding to the interleukin 6 receptor (IL-6R). The Fc domain of MEDI5117 contains the YTE mutation that increases MEDI5117 Fc-binding to the neonatal Fc receptor (FcRn) at pH 6.0 and thus increases the antibody half-life. To support the first in human clinical study, the nonclinical safety of MEDI5117 was assessed in a GLP repeat IV or SC administration study in cynomolgus monkeys when given by IV bolus injection (15 or 100 mg/kg) or SC injection (15 or 50 mg/kg) every other week for 13 consecutive weeks (7 total dose administrations). Administration of MEDI5117 by SC injection did not result in adverse findings. Administration of MEDI5117 by IV bolus injection resulted in the unscheduled euthanasia of one 15 mg/kg animal that had apparent and treatable anaphylactic reactions to the two previous MEDI5117 dose administrations. There were no similar findings for the other 15 mg/kg IV animals or for animals administered the higher 100 mg/kg IV dose level, and the data demonstrated decreased observed pharmacodynamic and toxicokinetic profiles from this animal as compared to other 15 mg/kg IV animals, as well as the presence of anti-drug antibodies. Since this was most likely related to the formation of anti-drug antibody that has been recognized by regulatory agencies as not predictive of immunogenicity in humans and there was a lack of any other findings which is consistent with the toxicology profiles reported for other anti-IL-6 antibodies (Martin et al., 2004 and Femta Pharmaceuticals IND Submission Press Release), this adverse event was not factored into the NOEL determination. Therefore, the NOEL from the GLP study was 100 mg/kg for animals dosed IV and 50 mg/kg for animals dosed SC, the highest doses tested.

**PS 1804 Mavrilimumab (CAM-3001): A Novel Anti-GM-CSF Receptor Alpha Monoclonal Antibody for the Treatment of Rheumatoid Arthritis.**

P. C. Ryan<sup>1</sup>, M. Sleeman<sup>2</sup>, M. Rebelatto<sup>1</sup>, B. Wang<sup>3</sup>, H. Lu<sup>3</sup>, X. Chen<sup>3</sup>, C. Wu<sup>3</sup>, L. Roskos<sup>3</sup>, D. Close<sup>2</sup>, H. Towers<sup>2</sup>, K. McKeever<sup>1</sup> and R. Dixit<sup>1</sup>.

<sup>1</sup>Biologics Safety Assessment, MedImmune, Gaithersburg, MD; <sup>2</sup>Research and Development, MedImmune, Cambridge, United Kingdom; <sup>3</sup>Clinical Pharmacology and DMPK, MedImmune, Hayward, CA.

Rheumatoid arthritis is a progressive and disabling autoimmune disease characterized by inflammation of the joints, with subsequent long term structural damage, chronic pain, and limited daily activity. Despite the availability of a variety of effective therapies, a significant portion of patients fail to achieve optimal outcomes including clinical remission and ongoing low disease activity. MedImmune is currently pursuing development of mavrilimumab (CAM-3001), a human monoclonal antibody (mAb) targeting GM-CSF receptor alpha, as a novel treatment for RA. GM-CSF plays a central role in the pathogenesis of rheumatoid arthritis (RA) through the activation, differentiation, and survival of macrophages and neutrophils. The nonclinical safety of mavrilimumab was evaluated in several studies in cynomolgus monkeys as the pharmacologically relevant species. Overall, the nonclinical safety results supported the continued clinical development of mavrilimumab. In clinical studies in RA patients, mavrilimumab has demonstrated good clinical activity with adequate safety to support further clinical development. A Phase 2b study of mavrilimumab in subjects with RA is in progress.

**PS 1805 Preclinical Safety and Pharmacodynamics of an Anti-GM-CSF Monoclonal Antibody in Cynomolgus Macaques.**

D. Blanset, E. Musvasva, A. Avakian, S. van Tongeren, J. Phillips, C. Grimaldi and S. Cannan. Boehringer-Ingelheim, Ridgefield, CT.

Administration of anti-GM-CSF monoclonal antibodies (mAb) have been proposed as potential therapeutics for inflammatory diseases. In addition to its role in immunity and inflammation, GM-CSF is required for proper maintenance of surfactant catabolism by pulmonary alveolar macrophages (PAM). In humans, loss of GM-CSF signalling results in deregulated surfactant turnover and can manifest as pulmonary alveolar proteinosis (PAP). Therefore, specialized assessments were included in a toxicology study to assess the potential for an anti-GM-CSF mAb to affect surfactant catabolism. The mAb was given intravenously at 0.25 or 50 mg/kg once weekly for 4 weeks or subcutaneously at 0.25, 5 or 50 mg/kg for 13 weeks. In addition to standard toxicity endpoints, bronchoalveolar lavage fluid (BALF) was assessed for cell differentials, intracellular lipids and surfactant protein-D (SP-D) levels. Serum SP-D levels were also evaluated. The mAb was well tolerated with no clinical signs of toxicity. There were no adverse effects on clinical or anatomic pathology. Non-adverse effects in the lung included a dose related increase in the percentage of enlarged PAM, increased numbers of lipid containing PAM and increased BALF SP-D levels. These minor changes may be related to changes in surfactant catabolism but were not accompanied by clinical or histopathological findings indicative of PAP. Serum SP-D values were comparable across groups, consistent with absence of PAP as determined by histopathology. In ex vivo assays, GM-CSF induced CD11b, pStat5 and proliferation of TF-1 cells were inhibited in a dose related manner consistent with the expected pharmacology. Exposure at 0.25 mg/kg was significantly decreased by the formation of anti-drug antibodies which correlated with decreased activity in the ex vivo assays. In conclusion, anti-GM-CSF mAb was well tolerated by cynomolgus monkeys and produced expected pharmacological effects that were reversible upon treatment cessation.

**PS 1806 Nonclinical Safety Evaluation of Anti-PD-L1 (MDPL3280A) in Mice and Cynomolgus Monkeys.**

R. Prell, R. Fuji, R. Deng, R. Pai, N. Ma and J. McBride. Genentech, S. San Francisco, CA.

Programmed cell death 1 (PD-1) is a receptor expressed on T cells following activation and binding to its ligand, PD-L1, down-regulates the quality and magnitude of T-cell responses. Many neoplastic cells express PD-L1 and evade destruction by the immune system. MPDL3280A, an effectorless (FcγR-binding deficient) human IgG1 mAb that blocks PD-1/PD-L1 interactions, is in development as a potential therapy for solid tumors. The nonclinical safety program included an in vitro cytokine release assay with human PBMCs, a tissue cross reactivity study, an exploratory 15-day repeat-dose study in C57BL/6 and CD-1 mice, and an 8 week repeat dose toxicity study in monkeys. MPDL3280A did not induce cytokine release from human PBMCs. MPDL3280A-specific staining was detected in the lymph node of monkey tissues and the placenta, lymph node, tonsil, and thymus of

human tissues. In vivo, no adverse drug related changes in immunologic endpoints were observed in either species. Drug-related findings were consistent with the expected pharmacology following PD-1/PD-L1 pathway inhibition. In mice, this included reversible increases in splenic weights in both strains, attributed to an enhanced immune response to a heterologous mAb. Minimal sciatic neuropathy with inflammation was observed in C57BL/6 mice only, a strain expressing the MHC H-2b haplotype that in PD-1-deficient mice, develops spontaneous autoimmune peripheral neuropathy. In monkeys, arteritis/periarthritis in parenchymal and/or tubular organs was observed, which is a recognized spontaneous inflammatory condition in this species, and may reflect an MPDL3280A-related enhancement of a pre-existing condition. A high incidence of anti-therapeutic antibodies (50/56 (89%)), which had no consistent impact on exposure, and minimal SC injection sites reactions were also attributed to MPDL3280A-enhanced immune responses. These findings are consistent with PD-1/PD-L1 inhibition and identify heightened immune responses and the potential to increase autoimmune liabilities in predisposed individuals as possible safety risks in patients.

## PS 1807 Investigation of the Potential Role of Immunogenicity in Abatacept-Related Lymphocytic Inflammation in Adult and Juvenile Rats.

J. Li<sup>1</sup>, J. Mysore<sup>1</sup>, D. A. DeVona<sup>1</sup>, M. Abbott<sup>2</sup>, M. P. Bernard<sup>1</sup>, S. Eble<sup>1</sup>, W. J. Freebern<sup>1</sup> and H. G. Haggerty<sup>1</sup>. <sup>1</sup>Drug Safety Evaluation, Bristol-Myers Squibb, New Brunswick, NJ; <sup>2</sup>Drug Safety Evaluation, Bristol-Myers Squibb, Syracuse, NY.

Abatacept is a fusion protein of a human IgG1 Fc and the extracellular domain of human CTLA-4 that inhibits T-cell activation. Species specific lymphocytic inflammation of the thyroid and pancreatic islets was observed in adult and juvenile rats treated with abatacept subcutaneously (SC) every 3 days for 3 months at pharmacologic doses of 65 and 20 mg/kg/day respectively. Studies in adult and juvenile rats were performed to assess a potential relationship of immunogenicity to lymphocytic inflammation observed in juvenile and adult rats. Abatacept was administered SC at 0 (control) or 0.03 mg/kg (a subpharmacologic dose) to adult rats (20/sex/group) on Days 1 and 29, or to juvenile rats (20/sex/group) on Days 1 (postnatal day 28), 15, 29, and 43. Anti-drug antibodies (ADA) were measured pretest, on Days 29, 43, 57, and 85. Additional criteria for evaluation included survival, toxicokinetics, clinical observations, body weights, food consumption, T cell-dependent antibody response (TDAR), peripheral blood T-regulatory cell phenotyping, selected organ weights, gross and microscopic pathology analyses. Scheduled necropsies were conducted 3 months following study initiation. Abatacept was clinically well tolerated in both adult and juvenile rats with no abatacept-related toxicologic effects. There were no effects on TDAR or the percentage of CD4+CD25+Foxp3+ lymphocytes (a T-regulatory cell population) in abatacept-treated rats consistent with a lack of pharmacologic activity. Robust and persistent ADA responses were detected in all abatacept-treated rats, with no evidence of lymphocytic inflammation of the thyroid or pancreatic islets. Thus, the lymphocytic inflammation previously observed in abatacept-treated adult and juvenile rats at pharmacologic doses was most plausibly due to pharmacologic immunosuppression and not a consequence of immunogenicity.

## PS 1808 Assessment of Biocomparability of NU100 and Betaferon in Cynomolgus Monkeys.

A. M. Brooks<sup>1</sup>, V. Tammara<sup>2</sup>, D. Hobson<sup>3</sup>, E. Shaw<sup>2</sup>, D. Zeng<sup>2</sup>, F. G. Burleson<sup>4</sup> and H. Hu<sup>1</sup>. <sup>1</sup>Toxicology, Covance Laboratories Inc., Madison, WI; <sup>2</sup>Nuron Biotech Inc., Exton, PA; <sup>3</sup>LoneStar PharmTox LLC, Boerne, TX; <sup>4</sup>Burleson Research Technologies, Morrisville, NC.

Betaferon is a marketed recombinant human interferon beta-1b (IFN beta-1b) for treatment of relapsing-remitting multiple sclerosis (RRMS). NU100 is an improved recombinant human IFN beta-1b produced using proprietary manufacturing technology. NU100 is aggregate-free and HSA-free in its formulation. In a GLP monkey study for NU100 safety assessment, male and female cynomolgus monkeys were assigned to 2 groups (4 animals/sex/group), and received once every other day NU100 or Betaferon at a dose level of 0.06 mg/kg/dose for 15 days. Animals were monitored for safety; blood samples were collected to determine serum levels of IFN beta-1b, neopterin (a biomarker for IFN-beta-1b pharmacodynamic profile), and anti drug antibodies (ADA). No NU-100- or Betaferon-related adverse safety signs occurred within these 15 days. IFN-beta-1b levels peaked approximately 3 hours postdose; Cmax and AUCall for NU100 and Betaferon were 23.7 (CV 49.1%) and 14.3 (CV 48.0%) ng/mL and 225 (CV 51.6%) and 157 (CV 40.6%) h\*ng/mL at steady state, respectively, and were not statistically significantly different. Neopterin levels peaked 24 hours postdose on Day 1; Emax and EAUCall for NU100 and Betaferon were 5.4 (CV

41.4%) and 6.29 (CV 31.7%) nMol/L and 65.9 (CV 45.2%) and 75.7 (CV 39.5%) h\*nMol/L, respectively; whereas Neopterin concentrations reached steady state on Day 15; Emax and EAUCall for NU100 and Betaferon were 1.71 (CV 78.1%) and 1.03 (CV 107.2%) nMol/L and 21 (CV 77.3%) and 35.6 (CV 7.9%) h\*nMol/L, respectively, and were not statistically significantly different. This reduced response on Day 15 to treatment was likely due to the production of anti-drug antibody (ADA), with 3 of 8 animals in the Betaferon group and 1 of 8 animals in the NU100 group positive for ADA. In conclusion, NU100 and Betaferon had comparable safety, toxicokinetic, and pharmacodynamic profiles in cynomolgus monkeys.

## PS 1809 Preclinical Development and Safety Assessment of the First Inhaled Nanobody ALX-0171.

S. Jacobs<sup>1</sup>, E. Depla<sup>1</sup>, S. Rossenu<sup>2</sup>, S. Priem<sup>1</sup>, E. Vanheule<sup>1</sup>, A. Schoolmeester<sup>1</sup>, K. Allosery<sup>1</sup>, S. De Boever<sup>1</sup>, L. Detalle<sup>1</sup>, V. H. Chen<sup>3</sup> and J. Baumeister<sup>1</sup>. <sup>1</sup>Ablynx NV, Zwijnaarde, Belgium; <sup>2</sup>MSD BV, Oss, Netherlands; <sup>3</sup>Boehringer Ingelheim, Ridgefield, CT.

Nanobodies are therapeutic proteins based on the smallest functional fragments of naturally occurring heavy chain only antibodies. The trivalent Nanobody ALX-0171 targets the respiratory syncytial virus (RSV) with high specificity and potency. It has the potential to be effective in prevention and treatment of RSV infection, a cause of severe upper and lower airway inflammation in susceptible populations. The medical need is high in young children, with 0.3million patients younger than 5 years hospitalised every year. ALX-0171 is formulated as a nebulizer solution for pulmonary inhalation as clinical route of administration. Using a vibrating mesh nebulizer, a droplet size  $\leq 3.4 \mu\text{m}$  (MMAD) was achieved, while the drug's stability was maintained. The preclinical package consisted of 2-week repeated dose toxicity studies via iv administration or inhalation in adult rats, a respiratory safety pharmacology study in rats via single inhaled dose and a cardiovascular safety pharmacology study in dogs (iv, single ascending dose). No drug- or immunogenicity-related safety findings were observed. A standard BCOP assay demonstrated the non-corrosive nature of the compound. In addition, a cotton rat disease model was performed to assess safety, tolerability and efficacy of ALX-0171 (intratracheal delivered). A dose-dependent reduction of viral transcripts following viral re-challenge in lung tissue of RSV-infected cotton rats was demonstrated as efficacy marker. A significant improvement of infection-related events (body weight stagnation, organ weight, BALF inflammatory cell counts) was demonstrated without signs of immune-induced events upon ALX-0171 administration. Treatment-induced anti-drug antibodies were measured in BALF and plasma and results indicated a mild immunogenicity response. It can be concluded that ALX-0171 was well-tolerated in safety assessments in preclinical species. ALX-0171 successfully completed a phase I clinical trial.

## PS 1810 The Occurrence of Microscopic Vacuoles in Toxicology Studies with Marketed Pegylated Proteins Is Associated with High Doses, High Clinical Multiples, and Accumulation.

L. S. Kaufman<sup>1</sup>, C. Conover<sup>2</sup> and A. Buchbinder<sup>2</sup>. <sup>1</sup>PDS, Mt Arlington, NJ; <sup>2</sup>Enzon Pharmaceuticals, Piscataway, NJ.

To obtain a more complete understanding of the clinical significance of microscopic vacuoles observed in toxicology studies with marketed pegylated proteins, nonclinical programs were reviewed from FOI data (publicly available BLA reviews) for Omontys, Krystexxa, Cimzia, Mircera, Macugen, Somavert, Pegasys, Neulasta, PegIntron, and Adagen. Cumulative toxicology doses for conjugate, PEG, and protein were calculated for each study and compared with cumulative recommended clinical doses over the same interval. None of the studies included PEG control groups. Microscopic pathology evaluations across programs were part of GLP toxicology studies and were performed on formalin/immersion-fixed tissues. There was no indication of whole-body perfusion techniques. Microscopic vacuoles were noted in toxicology studies with Omontys, Krystexxa, Cimzia, Macugen (IV but not intravitreal), Somavert, and Neulasta but not for Mircera, Macugen (intravitreal), Pegasys, PegIntron or PEG12kD. Across programs, their appearance and reversibility were dose-related and associated with large cumulative PEG/conjugate doses, short inter-dose intervals, longer study durations, drug accumulation, and large clinical multiples. At high cumulative doses (up to 14,000-fold the recommended clinical dose based on mg/m<sup>2</sup> and PEG doses of 2720 mg/m<sup>2</sup>), vacuoles were noted in the macrophage phagocyte system and, in some instances, choroid plexus, uterus, ovary, pituitary, and adrenal cortex. Nearly all of the high doses associated with vacuoles exceeded high-dose guidelines per ICH S6 Addendum. In conclusion, the appearance of microscopic vacuoles in toxicology studies with marketed pegylated proteins appears related to high cumulative doses

and associated drug accumulation, which is not present at recommended clinical doses. This review does not address the potential for vacuole formation in pegylated proteins associated with toxicities in excess of those appropriate for marketed products.

**PS 1811 TAS-116, an Orally Highly Potent HSP90 $\alpha/\beta$  Selective Inhibitor, Leads Minimized Ocular Toxicity in Both Albino and Pigmented Rats.**

H. Hitotsumachi<sup>1</sup>, Y. Kodama<sup>2</sup>, S. Ohkubo<sup>2</sup>, K. Yonekura<sup>2</sup>, K. Besshi<sup>1</sup>, F. Morita<sup>1</sup> and T. Hayashi<sup>1</sup>. <sup>1</sup>*Tokushima Research Center, Taiho Pharmaceutical Co., LTD., Tokushima, Japan;* <sup>2</sup>*Tsukuba Research Center, Taiho Pharmaceutical Co., LTD., Tsukuba, Japan.* Sponsor: *M. Takahashi.*

**BACKGROUND:** Heat Shock Protein 90 (HSP90) is a key chaperon which has a critical role for cancer cell growth and survival. Several HSP90 inhibitors have been developed clinically, however, visual symptoms have limited the ability to maximize drug exposure in patients. TAS-116 is an orally available HSP90 $\alpha/\beta$  selective inhibitor showing high antitumor activity in various human tumor xenograft models. To evaluate the effect of TAS-116 to the optic organ, we confirmed the safety profiles of TAS-116 in both albino and pigmented rat.

**RESULTS:** When TAS-116 administered orally for 14 days, no dose-related change was revealed in ophthalmological examination in albino rat. In histopathology, reference HSP90 inhibitors (AUY922 and 17-DMAG) caused degeneration and/or disarrangement of photoreceptor cells and increase in TUNEL positive apoptotic cells in retinal outer nuclear layer (ONL). On the other hand, TAS-116 demonstrated no histological changes or increase in TUNEL positive cells in ONL in albino rat. When all compound administered intravenously in albino rat, AUY922 and 17-DMAG showed greater exposure in retina compared to plasma, whereas TAS-116 showed less distribution in retina than in plasma. In addition, oral administration of TAS-116 demonstrated less retinal distribution and did not accumulate in retina after 2-week repeated dosing. In contrast, TAS-116 indicated a much higher distribution in subcutaneously implanted tumor over retina in rat model. Furthermore, TAS-116 had no melanin affinity because TAS-116 did not induce the retinal toxicity and also showed less distribution in retina in pigmented rat.

**CONCLUSION:** TAS-116 does not induce ocular toxicity in both albino and pigmented rat. This is probably due to less distribution in retinal tissue of TAS-116. These unique profiles of TAS-116 indicate that TAS-116 has a potential to be a best-in class HSP90 inhibitor with minimized ocular toxicity.

**PS 1812 ETEC Vaccines: An 85-Day Intradermal Repeat Dose Toxicity Study of Three Candidates in Guinea Pigs.**

C. S. Godin<sup>1</sup>, M. Maciel<sup>2</sup> and S. Savarino<sup>2</sup>. <sup>1</sup>*AVANZA Laboratories, Gaithersburg, MD;* <sup>2</sup>*Naval Medical Research Center, Silver Spring, MD.*

A vaccine against enterotoxigenic *E. coli* (ETEC) is being developed to protect travelers and young children that are at risk from this disease. The purpose of this study was to evaluate the potential toxicity and immunogenicity of three vaccine candidates, proteins 1, 2 and adjuvant, when administered either alone or in combination to guinea pigs by the intradermal route on Days 1, 22, 43, and 64 at a dose of 100  $\mu$ g. Animals were dosed with saline, proteins 1, 2, and adjuvant alone, a combination of protein 1 and adjuvant, or a combination of protein 2 and adjuvant. Evaluations included mortality, physical examinations, body weights, body temperatures, dermal Draize scores/induration measurements, gross pathology, organ weights, and histopathology. On Day 3, punch biopsies were collected from the first injection site. Punch biopsies of the remaining vaccination sites, from all vaccination sites of the remaining animals, and from a naïve site distant from the sites of vaccination, were collected at necropsy. Administration of protein 1 alone, protein 2 alone, adjuvant alone, protein 1 with adjuvant, and protein 2 with adjuvant in guinea pigs was well tolerated as all animals survived to termination with no adverse clinical signs. There were no test article-related effects upon the following parameters: mortality, physical examinations, body temperature, and body weights. Dermal erythema and induration were more significant when the vaccines were in combination with adjuvant than when administered alone or when adjuvant was administered alone. However, these observations resolved over time. On Days 3 and 63, but not at other intervals, total protein and/or albumin were increased in some treated groups suggesting immune stimulation correlating with inflammation at the injection site. Increased incidence and severity of cellular infiltrate, edema, and hemorrhage in the dermis and subcutis were noted in biopsy sites collected on Days 3 and 66. Following recovery, all findings had either resolved or would be expected to resolve.

**PS 1813 The Inhibin B Response to a Motilin Receptor Agonist in Male Rats.**

M. K. Ziejewski<sup>1</sup>, J. D. Vidal<sup>2</sup>, D. J. Stanislaus<sup>1</sup>, A. R. Apostoli<sup>1</sup>, P. Chowdhury<sup>3</sup> and S. B. Laffan<sup>1</sup>. <sup>1</sup>*Safety Assessment - Reproductive Toxicology, GlaxoSmithKline, King of Prussia, PA;* <sup>2</sup>*Safety Assessment - Pathology, GlaxoSmithKline, King of Prussia, PA;* <sup>3</sup>*Safety Assessment - Toxicology, GlaxoSmithKline, Ware, United Kingdom.*

**Background:** In a repeat oral dose toxicity study, 16/16 male rats given 100 mg/kg/day GSK1322888 sustained testicular injury after 4 weeks of treatment; the findings were not reversible after 12 weeks off-dose. A subsequent study was conducted to further characterize testicular toxicity and to explore the possible relationship between onset of lesions and, changes in circulating hormone levels. **Methods:** Male Sprague-Dawley rats (11 weeks old at study start) were orally administered 30 or 100 mg/kg/day GSK1322888 for 2 weeks with a 4 week off-dose period. Blood was collected via tail vein twice during the treatment period (Day 4 and 11) and three times during the off-dose period (Day 28, 36 and 42) for measurement of serum testosterone (T), dihydrotestosterone (DHT), and inhibin B (InhB), luteinizing hormone (LH), and follicle stimulating hormone (FSH) concentrations. A histopathologic examination of testes was performed at the end of the treatment and off-dose periods. **Results:** At 100 mg/kg/day, microscopic findings of the testis (degeneration of the germinal epithelium) were evident for 9/10 male rats on Day 14 and 10/10 rats at the end of the 4-week recovery period. There was no testicular toxicity observed at 30 mg/kg/day. During all stages of evaluation, there was no apparent difference among control and treated animals in hormone concentrations. **Conclusion:** There was poor correlation between changes in serum levels of InhB and testis histopathology. Based on these observations, the utility of InhB as a hormonal marker for germ cell toxicity is limited.

**PS 1814 Preclinical Safety Evaluation of JNJ-35815208, a Selective Estrogen-Related Receptor Alpha Modulator.**

J. Zhou, F. Selan, L. Hall, R. Mamidi, M. Duvall and C. Loudon. *Drug Safety Sciences, Janssen Research & Development, LLC, Raritan, NJ.*

Estrogen-related receptor- $\alpha$  (ERR $\alpha$ ) is an orphan nuclear receptor that has emerged as a novel therapeutic target for the treatment of type II diabetes and cancer. Here we describe non-clinical safety evaluation in rats and dogs of a novel and selective ligand, JNJ-35815208, for ERR $\alpha$  as a potential anti-diabetic agent. Following single oral administration in rats, mortality was observed at  $\geq$  1000 mg/kg. Repeated dose for 14 days to rats at 8, 40, and 200 mg/kg/day was well tolerated at doses up to 40 mg/kg. At 200 mg/kg/day, microscopic findings were observed in the testes and epididymides, characterized by mild bilateral degeneration/atrophy of the seminiferous tubules, minimal bilateral degeneration of the germ cells, luminal cellular debris, and oligospermia in the epididymides. In the 4-week rat study at 1, 6, or 40 mg/kg/day, there were no toxicological findings. In dogs, following single-dose administration at 50 and 250 mg/kg, as well as during the 5-day repeat dose at 150 and 250 mg/kg/day, the primary finding was emesis noted at all dose levels. In the four-week dog study at 2, 16 and 75.5/100 mg/kg/day, microscopic findings were noted in the female reproductive organs and the mammary glands at all doses. That resulted in reductions in the size of the ovaries, uterus, and vagina as well as atrophy of the mammary glands. These effects were associated with a persistent anestrus of the reproductive cycle. In male dogs, multifocal atrophy of the glandular epithelium of the prostate gland was observed at the mid- and high doses and small testes accompanied by mild degeneration of the germinal epithelium and vacuolated Sertoli cells at the high dose. Erythroid hypocellularity in the bone marrow was noted in males at 16 mg/kg/day and in both sexes at 75.5/100 mg/kg/day, with corresponding decreases in RBC, hemoglobin, hematocrit and reticulocyte counts at the high dose. Overall, these data suggest ERR $\alpha$  may play a role in both male and female reproductive organs as well as in the bone marrow.

**PS 1815 Humanized Mice: A New Animal Model for Risk Assessment of Biologics.**

K. E. Howard<sup>1</sup>, X. H. Li<sup>1</sup>, C. M. Gonzalez<sup>1</sup> and J. A. Ragheb<sup>2</sup>. <sup>1</sup>*CDER/OTR, US FDA, Silver Spring, MD;* <sup>2</sup>*CDER/OBP, US FDA, Bethesda, MD.* Sponsor: *J. Weaver.*

Testing of biological drug products for safety and efficacy in animal models has been difficult to assess because common models such as rodents, canines and non-human primates do not necessarily share common biological receptors with humans. A new animal model, the humanized mouse, has recently emerged in widespread use for infectious disease pathogenesis and vaccine testing research. Humanized mice are made via ablation of the bone marrow followed by surgical

implantation of human liver and thymic tissue underneath the kidney capsule and CD34+ hematopoietic stem cell transplantation. Approximately 12-16 weeks following surgery, the mice have an engrafted functional human immune system, achieve 20-25% humanization in peripheral blood and are suitable for studies. This approach potentially offers the ability to test for efficacy and safety of drug products in an in vivo model of the human immune system. If proven reliable via testing of commercially available biologics, this animal model could be a powerful tool in drug testing.

In order to begin assessing the ability of this model to predict uniquely human immune responses, we tested two forms of interferon- $\beta$  (IFN- $\beta$ ) currently marketed in the USA using clinically relevant dosing regimens and routes. Humanized mice were initially given IFN- $\beta$ -1a subcutaneously (sc) at doses 0.6  $\mu$ g, 1.5  $\mu$ g or 3.0  $\mu$ g once weekly or IFN- $\beta$ -1b sc at doses of 2.5  $\mu$ g, 12.5  $\mu$ g or 25  $\mu$ g three times weekly for four weeks to determine if acute toxicity would result. A follow-up study using doses of 0.3  $\mu$ g of IFN- $\beta$ -1a or 5  $\mu$ g of IFN- $\beta$ -1b for eight weeks assessed serum drug levels, immunogenicity and immune responses. The results of these studies demonstrated that (1) standard drug doses used in IFN- $\beta$  studies in transgenic IFN $\beta$  mice can be toxic to mice with a human immune system, as humanized mice can respond to the drug in a clinically relevant manner; (2) presence of the appropriate human receptors makes drug level assessment possible in humanized mice; and (3) humanized mice respond immunologically to IFN $\beta$ .

### PS 1816 Evaluation of Antisense Oligonucleotides in Human Pbmcs and Association of Release of IL-6 *In Vitro* to Constitutional Symptoms.

H. S. Younis, T. Machemer, D. A. Norris and S. P. Henry. *Preclinical Development, ISIS Pharmaceuticals, Carlsbad, CA.*

Oligonucleotide based therapeutics produce low-grade non-specific proinflammatory responses that manifest as increased cytokine/chemokine production, splenomegaly and/or lymphohistiocyte cell infiltrates in multiple tissues in animal models of toxicity. In humans, antisense oligonucleotides are well tolerated and may produce constitutional effects such as flu-like symptoms and injection site erythema that are typically self-limiting. The objective of this research was to determine if in vitro cytokine production from human peripheral blood mononuclear cells (PBMC) may be used to determine the potential for antisense oligonucleotides (ASO) to produce constitutional symptoms in humans. Fresh PBMC (n=50 donors) were cultured with a selected list of ASOs (ISIS 104838, ISIS 113715, ISIS 325568 and ISIS 353512; 0-80uM) that have been evaluated in humans and produced a broad range of constitutional symptoms (none to moderate). By 24 hr of treatment, the culture supernatant was harvested for measurement of cytokine (IL-6 and IL-10) release. A sigmoidal Emax model was used to determine the Emax and EC50 for the IL-6 response of each ASO. Dose-dependent increases in IL-6 were consistently greater (0.3uM EC50) for ISIS 353512 (the ASO that produced the most pronounced constitutional symptoms in humans) than for the other evaluated ASOs (1.3-3uMEC50 range). The IL-6 Emax/EC50 ratio was 10-fold greater for 353512 than the least responding ASO ISIS 104838, and provided the best term for differentiating ISIS 353512 from the ASOs generating lesser responses. The release of IL-10 was also greater for ISIS 353512 but was more difficult to quantify given the lack of a dose response and relative low magnitude of change. Collectively, the results suggest that human PBMC may be a viable in vitro model to rank order ASOs for their potential to produce constitutional symptoms in humans and to investigate the mechanisms of ASO mediated proinflammation.

### PS 1817 Mechanistic Basis of the Species-Specific Complement Activation in Cynomolgus Monkeys with Oligonucleotide Treatment.

L. Shen<sup>1</sup>, A. Frazer-Abel<sup>2</sup>, P. C. Giclas<sup>2</sup> and S. P. Henry<sup>1</sup>. <sup>1</sup>Isis Pharmaceuticals, Inc., Carlsbad, CA; <sup>2</sup>National Jewish Health, Denver, CO.

Antisense oligonucleotide (ASO)-mediated alternative pathway of complement (APC) activation is a common class effect in macaque monkeys at high doses. Activation is due to the interaction between ASO and complement Factor H (CFH), the inhibitory protein of the APC. Transient reduction of circulating CFH protein is observed after each dosing in monkeys, and is correlated with peak ASO plasma concentration. While common across multiple ASO sequences in macaque monkeys, there is no evidence of APC activation in rodents, dogs, or humans. The mechanistic basis of the sensitivity for macaque monkeys to ASO-induced APC activation was studied using an in vitro model with serum from various species. Dose-dependent increase in C3a was found in cynomolgus monkey serum after incubation with ISIS 104838, replicating the phenomena seen in vivo. No evidence of complement activation was observed in human serum under the same conditions. Serum collected from the new world monkeys, such as marmoset and squirrel monkeys, also showed no ASO-induced APC activation. There is 88% amino acid sequence homology found between cynomolgus and human CFH proteins, and

CFH gene single nucleotide polymorphisms (SNP) in human have been associated with functional change of the protein. Therefore, the relative inhibitory effect of cynomolgus and human CFH proteins in ASO-induced APC activation was evaluated by supplementing the purified CFH proteins in cynomolgus serum followed by ASO challenge. Dose-dependent inhibition in C3a formation was observed with CFH from both species, however, the IC<sub>50</sub> for the human CFH protein was about 3-fold lower than the monkey protein, suggesting stronger fluid phase inhibition to its substrate. Collectively, the results suggest a species and possible strain-specific complement effect with ASO in cynomolgus monkeys that likely due to the difference in regulatory function of the CFH protein and the result of interaction with ASO.

### PS 1818 Perturbation of Autophagy by Basic Lipophilic Compounds: Correlation of LC3 and P62 Abundance Employing U2OS-GFP Cells.

R. L. Yafawi, S. Lu, B. Jessen and A. John-Baptiste. *Drug Safety, Pfizer Global Research and Development, San Diego, CA.*

Many psychotropic compounds possess weakly basic lipophilic properties, with lysosomal trapping being an important mechanism of their distribution. Weakly basic lipophilic compounds accumulate in acidic intracellular organelles (i.e. lysosomes, endosomes, and phagosomes) via pH partitioning which may result in cytotoxicity. Multiple mechanisms regulate autophagy, with the lysosome being the major component of the autophagic pathway. Recognizing the potential toxicity caused by modulation of autophagy is critical, and understanding possible factors attributing to its dysfunction is necessary. We hypothesized that psychotropic agents with lysosomotropic properties have the potential to disrupt autophagy. We examined the link between lysosomal accumulation and autophagic dysfunction in osteosarcoma cells (U2OS), by examining the effects of eleven weakly basic lipophilic compounds known to accumulate in lysosomes. Their effects on autophagy were determined by using specific autophagy markers (Microtubule Associated Protein 1 Light Chain 3 (LC3), Sequestosome 1 (p62), and p70S6K). LC3 and p62 were employed to measure either the induction of autophagy, or the inhibition/perturbation of autophagolysosomal degradation. To gain greater insight regarding the pathway regulating autophagy, p70S6K (phosphorylation) a downstream marker of the Mammalian Target of Rapamycin (mTOR) activity was examined. All compound treatments resulted in at least a 3-fold increase in LC3 immunofluorescence and p62 abundance relative to controls. Treatment with compounds did not inhibit phosphorylation of p70S6K as observed via immunofluorescent staining. The data presented indicates lysosomotropic compounds may contribute to the perturbation of autophagy. However, mTOR activity did not seem to play a part in altering the autophagic process.

### PS 1819 Effects of Tyrosine Kinase 2 Inhibitors on Megakaryocyte Development.

H. Uppal<sup>1</sup>, D. Danilenko<sup>1</sup>, E. Harstad<sup>1</sup>, J. Tarrant<sup>1</sup>, E. Clarke<sup>2</sup>, P. Dhawan<sup>1</sup>, A. Kauss<sup>1</sup>, B. McCray<sup>1</sup>, D. Misner<sup>1</sup> and J. Singh<sup>1</sup>. <sup>1</sup>Safety Assessment, Genentech Inc., San Ramon, CA; <sup>2</sup>ReachBio LLC, Seattle, WA.

Background: Tyrosine Kinase 2 (Tyk 2) is a member of the Janus Activated Kinase (Jak) family. Tyk 2 is associated with signaling of pro-inflammatory cytokines, IL-12 and IL-23. Therefore, inhibition of Tyk 2 may potentially treat inflammatory diseases such as inflammatory bowel disease (IBD), rheumatoid arthritis, and psoriasis. Tyk 2 is also activated during thrombopoietin signal transduction, a pathway necessary for megakaryocyte development and platelet production. Studies were conducted in vitro and in vivo with potent Tyk 2 inhibitors with varying levels of JAK-family and general kinase selectivity to understand potential effects of these Tyk 2 inhibitors on platelet development.

Methods: Tyk 2 inhibitors were evaluated in vitro in human, mouse and cynomolgus monkey megakaryocyte colony forming cell assays. General cytotoxicity was evaluated by measuring cellular ATP levels. Direct effects of Tyk 2 inhibitors on platelet function (aggregation), energetics (oxygen consumption), and viability (ATP levels) were also evaluated in vitro. The effect of Tyk 2 inhibitors on platelet number was evaluated in short term (5-10 day) mouse studies. Tyk 2 and Jak mRNA expression was evaluated in human megakaryocytes by quantitative PCR to understand target expression.

Results: Tyk 2 inhibitors caused a comparable reduction in the number of colony forming cells and the viability of megakaryocytes from human, mouse and non-human primates. There were no direct effects of Tyk 2 inhibitors on the aggregation capacity, oxygen consumption, or ATP levels of human platelets in plasma. Tyk 2 inhibitors caused platelet reduction in mice. Tyk2 and Jak 1, 2, and 3 were comparably expressed in human megakaryocytes.

Summary: The in vitro and in vivo findings demonstrate that platelet reductions caused by multiple Tyk 2 inhibitors (with varying selectivity against other Jak family kinases) are likely due to effects on megakaryocyte development.

**PS 1820 Application of Canine Kidney Tissue Slices to Detect the Toxicity of Prototypical Nephrotoxic Agents.**

K. Kowalkowski, M. Klapczynski, D. J. Cugier, E. A. Blomme, W. R. Buck and M. J. Liguori. *Cellular and Molecular Exploratory Toxicology, AbbVie, Abbott Park, IL.*

Precision-cut renal tissue slices retain the multicellular, structural, and functional features of their original organ and offer a more relevant approach to interrogate toxicity compared to traditional cell-based in vitro systems. Here, we sought to evaluate the utility of this system to detect toxicity induced by prototypical kidney tubular toxicants, including cadmium chloride (CdCl<sub>2</sub>) and cisplatin. Kidneys from male beagle dogs were cut into 300 µm slices, and cultured at 37°C in an O<sub>2</sub> rich atmosphere for 24 to 48 h. Initial experiments optimized the culture conditions to maintain viability to at least 48 h. The slices were immediately treated after isolation with multiple doses of CdCl<sub>2</sub>, cisplatin, or vehicle. Multiple endpoints of toxicity were evaluated including H&E stained sections, intracellular ATP content, LDH release, total RNA integrity, and a novel endpoint for this type of system, kidney injury molecule-1 (Kim-1) mRNA levels via in situ hybridization. There was a significant elevation of LDH leakage at all doses tested for both compounds. The intracellular level of ATP also declined significantly at 100 µM CdCl<sub>2</sub> and 100 µM cisplatin, indicative of substantial cellular damage. Mild to marked degeneration and necrosis of renal tubules was evident beginning at 24 h upon microscopic examination. Kim-1, which has been previously demonstrated as a promising in vivo kidney injury biomarker and is not normally expressed in normal tissue, was clearly overexpressed in CdCl<sub>2</sub> treated slices, but not vehicle treated slices, especially along the tubular epithelium. In severely necrotic slices, Kim-1 was undetectable, likely due to RNA destabilization as later confirmed using integrity assessments. These data demonstrate that a renal slice in vitro model can be used to detect potent nephrotoxicants and that Kim-1 should be further explored as a novel in vitro biomarker to monitor toxicity in renal slice systems.

**PS 1821 Investigation of Protein Kinase C Inhibitor-Induced Steroid Hormonal Perturbation in Rat.**

H. Schadt, M. Schwald, D. Ledieu, U. Junker Walker, F. Spence, S. Chibout, A. Wolf and F. Pognan. *Preclinical Safety, Novartis Pharma AG, Basel, Switzerland.*

Steroid hormones are crucial endogenous mediators synthesized and secreted into the bloodstream by endocrine glands, such as the adrenal cortex and gonads. They mediate a wide variety of physiological functions. Altered steroid hormone status may affect the progression of various types of cancer. For instance, prepubertal ovariectomy in BFU/Mna rats accelerated the growth of spontaneous thymoma, which could be mitigated by intraperitoneal injection of estrogens. In azaserine-treated rats, the rate of spontaneous pancreatic tumors in males is increased, while orchidectomy reduced the incidence of such neoplasms compared to intact animals.

In a 104-week oral carcinogenicity study in rat with a protein kinase C inhibitor, a treatment related increased incidence of pancreatic acinar adenoma in males and thymoma in females were observed at dosages  $\geq$  100 mg/kg/day. Since changes in steroid hormones are considered to potentially affect the development of pancreatic and thymus neoplasia in rodents, a 2-week oral mechanistic follow-up study was conducted in rats to investigate this hypothesis. For this purpose, a mass spectrometry method previously developed in our lab for the quantification of steroid hormones in plasma, was further applied to analyze 17 steroids in adrenal, testicular and ovarian tissues. Aldosterone was increased in plasma and adrenals in treated males with a concomitant and pronounced decrease of androstenedione and testosterone in plasma, adrenals and testes. In female rats, progesterone, together with corticosterone, showed a trend towards increased concentrations in adrenals and ovaries after treatment, whereas ovarian androstenedione and estrogen levels tended to be reduced. This correlated with a circulating luteinizing hormone decrease in both sexes. In conclusion, the reduction in ovarian estrogen levels might be connected to the thymus neoplasias of the previous study. As androgen levels were found to be decreased, a direct connection to the previously reported pancreatic tumors is unlikely.

**PS 1822 Comparison of In Vivo Central Corneal Thickness (CCT) Measurements in Dogs, Rabbits, and Nonhuman Primates Using a Handheld Ultrasound Pachymeter or Specular Microscope.**

M. Vézina<sup>1</sup>, S. Wise<sup>1</sup>, K. Tenneson<sup>1</sup> and M. Bussi res<sup>2</sup>. <sup>1</sup>Charles River, Montr al, QC, Canada; <sup>2</sup>V&O Services, St. Lazare, QC, Canada.

The cornea is responsible for 2/3 of light refraction in the eye and thus is a critical tissue for clear vision. Alterations in corneal thickness have a direct effect on visual acuity and can be caused by alterations in the function of the corneal endothelium,

aqueous humor composition, drainage or formation rate, or in the glands producing the tear film. There has been an increase in the number of topical ocular therapeutics as this method is deemed one of the simplest clinically. As the formulations are in direct contact with the cornea, it can be an intended or unintended target tissue. In non-clinical topical ocular studies, serial in-vivo measurement of corneal thickness can provide a rapid empirical insight into the health of the cornea during study conduct and whether or not any changes in corneal thickness are reversible. There are several ways to obtain central corneal thickness measurements, two of which are ultrasound pachymetry (UP) that requires contact with the corneal surface and specular microscopy (SM) which is a non-contact procedure. The data presented represent background thickness measurements and precision between the 2 methods. In most cases, animals required sedation in order to reduce eye movements. CCT measurements by UP and SM were: dogs (n=10) 548.5±33 µm and 583.5±27 µm; rabbits (n=12) 378±27 µm and 394±16 µm; NHPs (n=10) 422±21 µm and 440±19 µm. Direct comparison showed a difference of 6% between the 2 methods for dogs, 4% for rabbits and 4% for NHP, with the SM values consistently higher. Precision as determined by 2 separate measurement occasions in dogs was 0.6% for SM and 0.1% for UP. In conclusion, both specular microscopy and ultrasound pachymetry provide reproducible, precise CCT data in dogs, rabbits and non-human primates allowing for repeat measures during the course of a study when corneal changes are of concern. Care should be taken for interpretation if data are acquired using both methods considering the 4-6% lower results using UP.

**PS 1823 In Vivo Evaluation of the Corneal Endothelial Cell Layer Using Specular Microscopy.**

K. Tenneson and M. V zina. *Ocular and Neuroscience, Charles River, Montr al, QC, Canada.*

The corneal endothelium is a monolayer of specialized cells whose primary physiological function is to maintain the health and transparency of the corneal stroma. In preclinical ocular and non-ocular studies, pharmacological and/or toxicological effects of a test compound may produce changes in the structure and function of the corneal endothelium. Additionally, intraocular surgery (including induced disease models) or implanted devices can compromise the endothelium and cause corneal edema. Specular microscopy (SM) enables a rapid, minimally invasive, direct evaluation of the cornea, and can provide supplemental information on corneal endotheliopathies, alone or in combination with direct slit-lamp examination on pre-clinical toxicology studies. SM provides three primary endpoints: number of cells/unit area (density), shape of cells (pleomorphism) and size of cells (polymegathism). When the endothelium is disrupted, there can be an overall shift in the number of cells, proportion of cell shapes (pleomorphism) and sizes (polymegathism). In order to characterize the endothelial layer in species regularly used on ocular toxicology studies, dogs, rabbits and non-human primates (NHP) were subjected to SM. Overall, cell density was similar across species (rabbits: 2769 cells/mm<sup>2</sup>; dogs: 2635 cells/mm<sup>2</sup>; NHPs: 3058 cells/mm<sup>2</sup>). Normal endothelial cells have a hexagonal shape, and account for the majority of cells (rabbits: 75%; dogs: 65%, NHPs: 71%). Average cell sizes were 364 µm<sup>2</sup> for rabbit, 384 µm<sup>2</sup> for dog, and 328 µm<sup>2</sup> for NHP. In conclusion, SM is a sophisticated tool that can complement the standard endpoints performed on specialized ocular preclinical studies and the data presented provides background data in rabbits, dogs and NHPs to facilitate the recognition of compound-related changes.

**PS 1824 Therapeutic Effect of MG132 on Diabetic Cardiomyopathy Is Associated with the Suppression of Proteasome Activities: Roles of Nrf2 and NF- B.**

W. Sun<sup>1</sup>, Y. Fu<sup>2</sup> and L. Cai<sup>1</sup>. <sup>1</sup>University of Louisville, Louisville, KY; <sup>2</sup>Jilin University, Changchun, China.

MG132, a proteasome inhibitor, can up-regulate nuclear factor erythroid 2-related factor 2(Nrf2)-mediated anti-oxidation and down-regulate nuclear factor-(NF)- B-mediated inflammation. The present study was to define whether through above two mechanisms MG132 can provide a therapeutic effect on diabetes-induced cardiomyopathy. To this end, transgenic OVE26 type 1 diabetic mice were used. OVE26 mice develop hyperglycemia at 2 – 3 weeks after birth and exhibit albuminuria and cardiac dysfunction at 3 months of age. Therefore starting at 3 months of age OVE26 diabetic mice were treated intraperitoneally with MG132 at 10 µg/kg body-weight daily for 3 months. At 3 and 6 months of age, cardiac function was measured with M-mode echocardiography. At 6 months, cardiac tissues were subjected to pathological and biochemical examination. OVE26 diabetic mice, but not MG132-treated OVE26 diabetic mice, showed significant cardiac dysfunction, including increased left ventricular systolic diameter and wall thickness and a decreased left ventricular ejection fraction with an increase of heart weight/tibia length ratio. Hearts of OVE26 diabetic mice exhibited structural derangement and remodeling (fibrosis and hypertrophy). In OVE26 diabetic mice,

there was also increased cardiac oxidative damage and inflammation. All of these pathogenic changes were reversed by MG132 treatment, which is associated with a significant suppression of diabetic increase in proteasome activity. In addition, MG132 treatment also significantly up-regulated Nrf2 expression and transcription (shown by increased expression of Nrf2 down-stream antioxidant genes) and down-regulated Ik-B expression and NF- $\kappa$ B nuclear accumulation. These results suggest that MG132 provided a therapeutic effect on diabetic cardiomyopathy in OVE26 diabetic mice possibly via the up-regulation of Nrf2-dependent anti-oxidation and the down-regulation of NF- $\kappa$ B-mediated inflammation.

**PS 1825 MG132 Prevents the Progression of Diabetes-Induced Pathological Damage to Aorta Is Associated with Its Up-Regulation of Nrf2 and Its Down-Stream Antioxidant Proteins.**

X. Miao<sup>1,2</sup>, G. Su<sup>2</sup> and L. Cai<sup>1</sup>. <sup>1</sup>University of Louisville, Louisville, KY; <sup>2</sup>Jilin University, Changchun, China.

Endothelial damage and dysfunction are manifested in diabetic cardiovascular complications. Nuclear factor-erythroid 2-related factor 2 (Nrf2) is one of the most important cellular defense mechanisms against oxidative stress by up-regulation of several antioxidants, phase II detoxifying enzymes, and other proteins that detoxify xenobiotics and neutralize reactive oxygen and/or nitrogen species. Deletion of Nrf2 gene significantly enhances the susceptibility of cardiomyocytes to high-level glucose-induced reactive oxygen species generation and cell death. The present study was to define whether induced Nrf2 by MG132 can provide a therapeutic effect on diabetes-induced aortic pathogenic changes. To this end, transgenic OVE26 type 1 diabetic mice and age-matched control mice were used. OVE26 mice develop hyperglycemia at 2–3 weeks after birth and exhibit renal and cardiac dysfunction at 3 months of age, suggesting the induction of diabetic complications. Therefore starting at 3 months of age, OVE26 diabetic mice were intraperitoneally treated with MG132 at 10  $\mu$ g/kg body weight daily for 3 months. At the end of MG132 treatment, aortas from these mice were morphologically and immunohistochemically examined. Significant increases in the wall thickness and structural derangement of aorta were found in OVE26 diabetic mice, which was accompanied by significant increases in aortic oxidative and/or nitrosative damage (4-HNE as lipid peroxidation and 3-NT as protein nitration), inflammation (TNF- $\alpha$  and PAI-1), and remodeling (CTGF and TGF- $\beta$ 1). These pathological changes were not observed in MG132-treated OVE26 diabetic mice, which was also associated with a significant increase of aortic Nrf2 expression and transcription function. These results suggest the therapeutic effect of MG132 on diabetes-induced aortic pathogenic damages and its association with Nrf2 expression and function.

**PS 1826 Characterization of miR-208a Responses in Isoproterenol-Induced Cardiac Injury in Sod2<sup>-/-</sup> and C57BL/6J Mice.**

L. Liu. Pfizer, San Diego, CA.

The present investigation aimed to characterize miR-208a as a putative biomarker for early cardiac injury in isoproterenol (ISO)-induced acute myocardial damage in mice and to investigate potential strain-dependent effects in response to ISO administration. Plasma from age-matched male C57BL/6J and Sod2<sup>-/-</sup> mice treated with a single intraperitoneal (IP) administration of ISO was collected for measuring cardiac troponin I (cTnI) and miR-208a at 3, 6, and 24 hours post injection. Administration of ISO led to increases in both cTnI and miR-208a at all time points tested. However, the magnitude of increase and the temporal release profiles of these biomarkers were different between the two strains. In C57BL/6J mice, cTnI and miR-208a tracked with each other in both magnitude and time, the highest values were seen at 3 hours. By contrast, in Sod2<sup>-/-</sup> mice, the magnitude of miR-208a was much greater than that of cTnI with the highest values of both biomarkers observed at 6 hours. Similar to C57BL/6J mice, the temporal profile of miR-208a followed that of cTnI in Sod2<sup>-/-</sup> mice. Histopathologic examination of hearts treated with ISO revealed myocardial degeneration at  $\geq$  3 hours in C57BL/6J mice and  $\geq$  6 hours in Sod2<sup>-/-</sup> mice which correlated with the highest concentration of the biomarkers in each strain. The higher systemic exposure of ISO in C57BL/6J mice compared to that in Sod2<sup>-/-</sup> mice may have contributed to the observed earlier response in C57BL/6J mice compared to Sod2<sup>-/-</sup> mice.

**PS 1827 Polybrominated Diphenyl Ethers Exposure and Intrauterine Growth Restriction: A Case-Control Study in Chinese Newborns.**

Y. Zhang<sup>1</sup>, Y. Zhao<sup>1</sup>, H. Ao<sup>1</sup> and X. Meng<sup>2</sup>. <sup>1</sup>Fudan University, Shanghai, China; <sup>2</sup>Tongji University, Shanghai, China. Sponsor: Z. Liu.

**BACKGROUND:** Intrauterine growth restriction (IUGR) is associated with perinatal morbidity and mortality. It has multifactorial etiology. Along with malnutrition and psychosocial, environmental pollutants, including polybrominated diphenyl ethers (PBDEs), have also been considered to be involved in the etiology of this disease.

**OBJECTIVES:** This case-control study was performed to assess maternal-fetal exposure to PBDEs and investigate whether in utero PBDEs exposure is associated with IUGR.

**METHODS:** A total of 29 newborn-mother pairs residing in Wenzhou were enrolled in this study during December 2010 and February 2011. Maternal blood and umbilical cord blood (UCB) samples were collected and analyzed for PBDEs by the method of Gas chromatography-mass spectrometry (GC-MS). Conditional logistic regression and Spearman correlation were used to analyze the association between PBDEs exposure and IUGR.

**RESULTS:** All PBDE congeners in serum were detected except for BDE 138, 183, and 190. BDE 209 was the most abundant congener followed by BDE 207, 208, and 66, with the detection frequencies of 50%, 83%, 74%, and 74%, respectively. The concentrations of BDE 66, BDE 209, BDE 183-209 and 19 PBDEs in UCB are significantly higher in newborns with IUGR than those in controls. BDE 183-209 and 19 PBDEs levels in UCB were inversely associated with birth weight and Quetelet's index ( $p=0.008$ ,  $0.020$  respectively). After controlling for potential confounders, dose-response relationships were observed between IUGR and BDE 183-209 and 19 PBDEs levels in UCB.

**CONCLUSION:** Only one UCB sample from the control group did not detect PBDEs which might indicated that newborns in China were ubiquitously exposed to PBDEs. Significantly higher PBDEs levels were detected in IUGR cases compared with those in controls. In utero PBDEs (especially high-brominated BDE congeners) exposures were associated with IUGR in a dose-dependent manner. Prenatal PBDEs exposure may be a risk factor for IUGR.

**PS 1828 Maternal and Child Polybrominated Diphenyl Ether (PBDE) Levels in US National Children's Study (NCS) Formative Research.**

A. J. Schecter<sup>1</sup>, D. Cherry<sup>2</sup>, L. S. Hyman<sup>3</sup>, D. Cheng<sup>1</sup>, N. Imran<sup>1</sup>, M. Hommel<sup>1</sup>, K. Kannan<sup>4</sup>, L. Wang<sup>4</sup>, S. H. Yun<sup>4</sup>, N. Thiex<sup>5</sup>, B. Spector<sup>5</sup>, J. Moye<sup>6,7,8</sup> and L. S. Birnbaum<sup>9,8,10</sup>. <sup>1</sup>The University of Texas School of Public Health, Dallas, TX; <sup>2</sup>The University of Texas, Tyler, TX; <sup>3</sup>The University of Texas Southwestern Medical Center, Dallas, TX; <sup>4</sup>New York Health Department, Albany, NY; <sup>5</sup>South Dakota State University, Brookings, SD; <sup>6</sup>NCS, Bethesda, MD; <sup>7</sup>NICHD, Bethesda, MD; <sup>8</sup>NIH, Bethesda, MD; <sup>9</sup>NIEHS, Research Triangle Park, NC; <sup>10</sup>NCI, Bethesda, MD.

The NCS is a prospective health study of 100,000 children (birth to 21 years) and their mothers. We report on a nested, formative study involving measurement of lipid soluble persistent PBDE flame retardants. PBDEs have been associated with various health effects. This study involved 20 mother-child pairs; 20 samples each of maternal third trimester blood, maternal blood at birth, cord blood, and breast milk were tested individually for nine PBDE congeners. Total PBDE was the sum of nine PBDE congeners when quantifiable. Some PBDE congeners were detected in maternal blood samples and breast milk samples at all time points. In infant cord blood samples, only BDE 47, BDE 100, BDE 99 and BDE 153 were detected in  $\geq$ 40% of samples. BDE 183 and BDE 209 levels were below detectable levels in all samples. Lipid normalized PBDE levels were higher in maternal birth serum and one month postpartum breast milk than in infant cord blood. Across all congeners, medians for maternal third trimester plasma were highest. Further investigation of PBDE compartmentalization during the prenatal and postpartum periods is warranted to understand fetal and infant exposure. The views expressed in this abstract are those of the authors and do not necessarily reflect the views of the National Institutes of Health or the Department of Health and Human Services. Funded by the Eunice Kennedy Shriver National Institute of Child Health and Human Development, contracts number HHSN 275201100004C and HHSN275200800035C.

**PS 1829 Effect of Body-Weight Loading onto the Articular Cartilage on the Occurrence of Quinolone-Induced Chondrotoxicity in Juvenile Rats.**

K. Goto, M. Imaoka, M. Goto, I. Kikuchi, T. Suzuki, T. Jindo and W. Takasaki. *Medicinal Safety Research Laboratories, DaiichiSankyo Co., Ltd., Tokyo, Japan.*

Quinolone antibacterial agents have been reported to induce chondrotoxicity in juvenile animals, and the mechanism has not yet been clarified. We have reported that gene expression of tumor necrosis factor receptor superfamily, member 12a (Tnfrsf12a, cell death-related gene), prostaglandin-endoperoxide synthase 2 (Ptgs2, inflammatory response-related gene), plasminogen activator, urokinase receptor (Plaur, stress response-related gene), and matrix metalloproteinase 3 (Mmp3, proteolysis-related gene) was involved in the induction of cartilage lesions of the distal femoral articular cartilage in juvenile rats treated orally with ofloxacin (OFLX). In the present study, the effect of body-weight loading onto the articular cartilage on the occurrence of the cartilage lesions was investigated in male juvenile Sprague-Dawley (SD) rats given OFLX orally once at 900 mg/kg. Just after dosing of OFLX, hindlimb unloading was performed for 0 h, 2 h, 4 h, and 8 h by a tail-suspension method. Animals were sacrificed at 8 h post-dose, and then the distal femoral articular cartilage was subjected to a histological examination and an investigation for gene expression of Tnfrsf12a, Ptgs2, Plaur, and Mmp3 by qRT-PCR analysis. As a result, cartilage lesions and up-regulations of these 4 genes that were seen in rats without the tail suspension were not observed in rats with the 8-h tail suspension, and a tendency to decrease in the incidence of the cartilage lesions and the gene expression was noted in a tail-suspension time dependent manner. Our results clearly indicate that body-weight loading onto the cartilage is necessary to induce cartilage lesions and gene expression of Tnfrsf12a, Ptgs2, Plaur, and Mmp3 in juvenile rats treated with OFLX.

**PS 1830 Effects of Maternal Exposure to Phthalates and Bisphenol A on Neonates.**

A. M. Vetrano<sup>1</sup>, F. E. Archer<sup>1</sup>, S. W. Marcella<sup>2</sup>, B. Buckley<sup>3</sup>, D. Wartenberg<sup>1,3</sup>, M. G. Robson<sup>3,4</sup>, L. Wang<sup>5</sup>, D. Q. Rich<sup>5</sup> and B. Weinberger<sup>1</sup>. <sup>1</sup>UMDNJ-Robert Wood Johnson Medicine School, New Brunswick, NJ; <sup>2</sup>UMDNJ-School of Public Health, Piscataway, NJ; <sup>3</sup>Environmental and Occupational Health Sciences Institute - UMDNJ and Rutgers University, Piscataway, NJ; <sup>4</sup>School of Biological and Environmental Sciences - Rutgers University, New Brunswick, NJ; <sup>5</sup>Univ. of Rochester, Rochester, NY.

**RATIONALE:** Phthalate and bisphenol A (BPA) metabolites may have anti-androgenic and pro-inflammatory effects. We hypothesized that maternal exposure to phthalates and BPA in pregnancy is associated with decreased anogenital index in infants and shortened gestation.

**METHODS:** Urinary concentrations of phthalate and BPA metabolites were measured from 72 pregnant women enrolled in a high-risk obstetric clinic, at the last clinic visit prior to delivery, using high-performance liquid chromatography-tandem mass spectrometry. Anogenital index (AGI) was calculated by normalizing anogenital distance to weight. Gestational age was determined by either sonographic dating or date of implantation. Using linear regression models, we estimated the change in gestational age and anogenital index associated with each interquartile range (IQR) increase in phthalate and BPA metabolite concentration.

**RESULTS:** IQR increases in urinary mono(2-ethyl-5-hydroxyhexyl) phthalate (MEHHP) and total BPA concentrations were associated with 4.2 and 1.1 day decreases in gestation, respectively. When stratifying by gender, these alterations were found only in male infants. Levels of monoethyl phthalate (MEP) were associated with lower AGI in males, but this difference (0.2 mm) is not likely to be clinically significant.

**CONCLUSIONS:** MEHHP and total BPA were associated with small reductions in gestation, and MEP with a small reduction in AGI, with effects only in males. Increased sensitivity of males to the effects of phthalates and BPA may be related to the roles of androgen precursors in both genital differentiation and in the initiation of labor.

Supported by NIH P30ES005022, R21HD058019 and NJ Dept. of Environmental Protection

**PS 1831 Intravenous Dose Range-Finding Toxicity of Allopregnanolone (ALLO) in Neonatal Dogs.**

K. L. Steinmetz<sup>1</sup>, L. Rausch<sup>1</sup>, M. Patrick<sup>1</sup>, J. M. Brune<sup>1</sup>, S. H. Mellon<sup>2</sup> and P. S. Terse<sup>3</sup>. <sup>1</sup>SRI Intl, Menlo Park, CA; <sup>2</sup>Department OB GYN, University of California San Francisco, San Francisco, CA; <sup>3</sup>NCATS, NIH, Bethesda, MD.

Treatment with allopregnanolone (ALLO), a GABA-ergic neurosteroid, may be useful treating Niemann-Pick Type-C (NP-C) disease. NP-C is a rare autosomal recessive neurodegenerative disease caused by genetic mutations, resulting in lysosomal accumulation of unesterified cholesterol and glycolipids. Treatment of neonatal NIH NPC1 mice with a single sc dose of ALLO resulted in increased life span, onset delay of neurological symptoms, survival of cerebellar Purkinje and granule cell neurons, and reduced cholesterol and ganglioside accumulation. Previous toxicity studies with ALLO suggested that the presence of isoflurane anesthesia may have contributed to a relatively low MTD of <3 mpk bolus intravenous (IV) injections to unconscious neonatal Beagle dogs. The current study determined the tolerability of ALLO administered IV with extended infusion or bolus injections in conscious pups. Indwelling IV catheters were placed under isoflurane anesthesia. Animals were allowed to recover from anesthesia for ALLO/vehicle treatment. Pups (1-2 per dose, age: postnatal day (PND) 17-PND59) received vehicle 20% hydroxypropyl  $\beta$ -cyclodextrin (HPBCD) up to 10 hr with no notable clinical signs. After 3 days washout between dose administration, pups received up to 20 mpk (7.5, 15, and 20 mpk) ALLO by IV infusion, which extended up to 4-8 hr. Dose-dependent sedation was observed at all IV infusion dose levels. After determining that ALLO was well tolerated by extended infusion, bolus IV doses were escalated up to 50 mpk in 1-2 pups (age range PND27-59) per dose level. Hematology and clinical chemistry values were within normal ranges. In summary, ALLO can be administered as IV bolus or extended infusion (>8hr) to conscious neonatal dogs. Pups tolerated ALLO in 20%HPBCD vehicle up to the highest doses tested; 20 mpk (PND17) by infusion and 50 mpk (PND59) by bolus. Conscious neonatal pups appear to tolerate higher doses of ALLO as compared with ALLO administered under isoflurane anesthesia suggesting additive and/or synergistic sedative effects.

**PS 1832 Oxidative and Genetic Damage in School Children from a Heavily Polluted City.**

I. Alvarado-Cruz<sup>1</sup>, M. Sánchez-Guerra<sup>1,2</sup>, L. Hernández-Cadena<sup>3</sup>, L. Espinosa-Juárez<sup>1</sup>, N. Pelallo-Martínez<sup>1</sup>, L. Rafael-Vázquez<sup>1</sup>, R. Angulo-Olaiz<sup>1</sup>, M. J. Solís-Heredia<sup>1</sup>, A. De Vizcaya-Ruiz<sup>1</sup>, V. Mugica<sup>4</sup> and B. Quintanilla-Vega<sup>1</sup>. <sup>1</sup>Toxicology Department, CINVESTAV-IPN, Mexico City, Mexico; <sup>2</sup>Public Health School, Harvard University, Boston, MA; <sup>3</sup>INSP, Cuernavaca, Morelos, Mexico; <sup>4</sup>UAM-Azcapotzalco, Mexico City, Mexico.

Ecatepec County is one of the most industrialized, populated and polluted counties in Mexico. Particulate matter (PM<sub>10</sub> and PM<sub>2.5</sub>) concentrations in this area are frequently above the air quality Mexican standards. Other contaminants, such as lead (Pb) are present. PM and Pb are associated with adverse effects, including oxidative and genetic damage. A cross-sectional study was conducted in 185 schoolchildren (7-10 years of both genders) from two regions of Ecatepec; an industrialized area with heavy traffic (Zone 1; n=94) and a zone with moderate vehicular traffic (Zone 2; n= 91). PM was obtained by air sampling, blood lead (PbB) levels were determined by atomic absorption spectroscopy, plasma malondialdehyde (MDA) as oxidative stress indicator by colorimetry and the DNA damage in mononuclear cells by the comet assay; parents answered a structure questionnaire. PM<sub>10</sub> and PM<sub>2.5</sub> levels, as well as the organic and elemental carbon content (CO and CE, respectively) were higher in Zone 1. Children from this zone showed significantly higher PbB (62% showed >5  $\mu$ g/dL) and MDA levels, but similar DNA damage compared to Zone 2 children. We observed positive associations between PM<sub>10</sub> and PM<sub>2.5</sub> and OTM values ( $p<0.05$ ); while a positive association between CO in PM<sub>10</sub> and PM<sub>2.5</sub> and OTM ( $p<0.05$ ) was also found. MDA levels were associated with PM<sub>10</sub>, PM<sub>2.5</sub> and PbB levels, as well as with CO and CE content in both particles ( $p<0.05$ ). Results suggest that children from Ecatepec are exposed to high PM concentrations and that CO and CE content in PM as well as Pb are involved in the genetic and oxidative damages observed in children living in this highly polluted area. Supported by CONACyT-Mexico (Grant #106034).

**PS 1833 Developmental Immunotoxicity Testing for Hazard Identification.**

E. C. Tonk<sup>1,2</sup>, A. Verhoef<sup>1</sup>, E. R. Gremmer<sup>1</sup>, H. van Loveren<sup>1,2</sup> and A. H. Piersma<sup>1,3</sup>. <sup>1</sup>RIVM, Bilthoven, Netherlands; <sup>2</sup>Health Protection, RIVM, Bilthoven, Netherlands; <sup>3</sup>Toxicogenomics, University, Maastricht, Netherlands.

The inclusion of parameters to assess developmental immunotoxicity (DIT) is an important and critical step forward in regulatory toxicity testing of chemicals. We have performed multiple juvenile and generation studies in rats using various study

designs and test compounds (methylmercury, di-octyltin dichloride (DOTC), di(2-ethylhexyl) phthalate, alcohol, nonylphenol) and the results demonstrate the relatively high sensitivity of immune parameters compared to developmental parameters. Specifically, functional immune parameters appeared affected at relatively low doses. An expanded T cell dependent antibody response (TDAR) parameter set and evaluation of LPS-stimulated NO and TNF- $\alpha$  production by adherent splenocytes were identified as sensitive functional immune parameters. For example, in a juvenile exposure study DOTC affected KLH-induced lymphocyte proliferation at BMD 0.29 mg/kg whereas body weight was affected at 57.7 mg/kg. In a generation study design, alcohol affected splenocyte proliferation at BMD 0.49 % whereas developmental delay was noted at 1.2 %. These results support the OECD TG 443 extended one-generation reproductive toxicity study (EOGRS) guideline, including its cohort for DIT assessment. It provides substantial insight in the immunotoxic potential of chemical. Our research thus identified complementary immune parameters as potentially useful additions to the EOGRS guideline which can be easily added to the study protocol. Furthermore, our research demonstrated the relative sensitivity of the juvenile immune system (postnatal day 10-50) and the significance of the juvenile window in DIT testing. The comparisons of various scenarios have provided important lessons about parameter assessment and exposure protocols, which will feed into the definition of a preferred approach to regulatory developmental immunotoxicity testing for chemicals.

### PS 1834 Feasibility of Continuous Intravenous Infusion in Postweaning Juvenile Rats.

L. Allais, J. Briffaux, C. Gerhardy, P. Vignand, S. David and P. Fant. *Ricerca Biosciences SAS, St. Germain sur l'Arbresle, France.*

Juvenile animals are increasingly requested in nonclinical safety studies to contribute to the commercialization of pediatric therapeutics. The main objectives when conducting Pivotal Toxicology studies in juvenile animals are to ensure a complete evaluation of potential adverse effects of the drug at the relevant target pediatric age and additionally to detect any potential delayed toxicity during animal development, regardless of the treatment period duration. The rat is still the most commonly used species in Juvenile Toxicology studies, hence enabling extensive background data starting from birth.

Various administration routes have been investigated in the juvenile rat and are mostly technically feasible from the early days after birth. However, increasing challenging requirements in terms of dosing procedures implies that juvenile study designs need to be adapted taking into account animal welfare recommendations.

We investigated the suitability of a continuous intravenous infusion method for use in a juvenile toxicity study in pups surgically implanted on Post-Natal Day (PND) 21. A polyurethane catheter was implanted into the posterior vena cava via the femoral vein and then tunneled subcutaneously to exit at the nape of the neck. The pups were continuously infused (24 h/day) with sterile physiological saline for 4 weeks and all possible technical challenges with respect to the growth of the animal were investigated. We assessed standard toxicology endpoints (including clinical observations, growth, food intake and clinical pathology) and compared the results with background data from non infused animals at a similar age.

The results of the present evaluation demonstrated that continuous intravenous infusion using adapted equipment is feasible in young pups and did not interfere with the animal growth from PND 21 to the age of 7 weeks.

### PS 1835 Lung Function in Children Chronically Exposed to Arsenic in Drinking Water.

R. Recio-Vega<sup>1</sup>, E. Olivas-Calderon<sup>1</sup>, T. Gonzalez-Cortes<sup>1</sup>, C. Gonzalez-De Alba<sup>1</sup>, G. Ocampo-Gomez<sup>1</sup>, J. A. Gandolfi<sup>2</sup> and R. Lantz<sup>3,4</sup>. <sup>1</sup>Environmental Health, University of Coahuila, Torreon, Mexico; <sup>2</sup>Pharmacology and Toxicology, College of Pharmacy, University of Arizona, Tucson, AZ; <sup>3</sup>Cell Biology and Anatomy, University of Arizona, Tucson, AZ; <sup>4</sup>Southwest Environmental Health Science Center, University of Arizona, Tucson, AZ.

#### Introduction

Arsenic level in drinking water at the Comarca Lagunera in Mexico surpassed (50-120  $\mu\text{g/l}$ ) the permitted levels by the Mexican Official Norms (25 $\mu\text{g/l}$ ) due to the intense over-exploitation of the aquifers.

Arsenic exposure through drinking water has been associated with different cancers. Additionally negative effects over human lung function have been described.

Experimental animal studies have reported pathological changes in pulmonary development as well as bronchial hyperresponsiveness and disturbances in pulmonary tissue repair proteins. Clinical human studies have shown diminishment in spirometric values and higher bronchiectasis and chronic obstructive pulmonary disease frequencies. These findings have been reported in adults but not in children.

#### Objective

To evaluate the relationship between lung function and arsenic levels in children chronically exposed to arsenic.

#### Results

At present, 390 children have been included. The mean age is 9.0 years and 98% have lived in the community all their life. 77.6 % of the children were conceived in their current communities. From the studied population, 6.3% reported chronic cough for more than 2 years and 2.9% for 7-12 years. In addition, 12.1% have been treated for bronchiolitis. The mean urinary arsenic level was 155.4 ppb (range of 14.6-893.8). In all subjects spirometric values of FVC, FEV1 and FEV1/FVC ratio were lower with respect to reference values.

#### Conclusion

A high incidence of lung diseases and a reduction in the lung function were recorded in children chronically exposed to arsenic in drinking water.

### PS 1836 Blood and Urine Cadmium Concentrations and Micronucleus Frequency in Buccal Epithelium from Children in Three Populations in Yucatan, Mexico.

N. Pérez-Herrera<sup>1</sup>, J. Perera-Rios<sup>1</sup>, A. Rodriguez-Uc<sup>1</sup>, J. Gordillo-Mena<sup>1</sup>, J. Uicab-Ventura<sup>1</sup>, J. Alvarado-Mejía<sup>1</sup>, L. González-Navarrete<sup>1</sup>, L. Fargher<sup>2</sup>, R. Moo-Puc<sup>3</sup>, L. Yañez-Estrada<sup>4</sup> and F. Arcega-Cabrera<sup>5</sup>. <sup>1</sup>Faculty of Medicine, Autonomous University of Yucatán, Mérida, Mexico; <sup>2</sup>Human Ecology Department, CINVESTAV, Mérida, Mexico; <sup>3</sup>Research Unit, Mexican Institute of Social Security, Mérida, Mexico; <sup>4</sup>Faculty of Medicine, Autonomous University of San Luis Potosí, San Luis Potosí, Mexico; <sup>5</sup>Faculty of Chemistry, National Autonomous University of Mexico, Mérida, Mexico. Sponsor: B. Quintanilla-Vega.

Buccal epithelium represents the first boundary against inhalation or ingestion of toxicants. Micronucleus (MN) tests of buccal epithelium have been effectively used in epidemiological studies in adult populations exposed to genotoxins; yet, its use in juvenile populations has been limited. A transversal study was conducted in children from the cities: Merida, Progreso and Ticul, in the Yucatan Peninsula to evaluate the MN frequency in exfoliated buccal epithelium and cadmium concentrations in blood and urine from children exposed to different scenarios. Ten children (6 and 8 years of both genders) were selected from each city (n=30). MN frequency was analyzed by microscopy after a Shift staining and Cd concentrations by atomic absorption spectroscopy. MN frequency was similar in the three populations (p=0.7451), Merida 0.33 (0-1.33/1000 cells), Progreso 0.33 (0-1/1000 cells), and Ticul 0.66 (0-2.33/1000 cells). Cadmium levels in urine were higher (p=0.043) in children from Merida (State Capital) compared to the other cities (1.30 vs 1.09 and 0.73  $\mu\text{g/l}$ ). However, urine Cd concentrations did not correlate with MN frequencies (p=0.505). Blood Cd levels were similar in the three populations (p=0.6021), and a significant and positive correlation between MN frequency and blood Cd levels was observed (rs =0.4583, p=0.0484). Our preliminary results emphasize the importance of conducting biomonitoring of metals and early detection of genotoxic effects in children. Supported by CONACYT-México, Grant # FOSEC-Salud 139738.

### PS 1837 Orellanine, a Bipyridyl Mycotoxin, Induces Apoptosis in a Cell Culture Model of Parkinson's Disease.

P. Anantharam<sup>1</sup>, B. Taiwo<sup>1</sup>, J. Luo<sup>2</sup>, V. Anantharam<sup>2</sup>, A. Kanthasamy<sup>2</sup>, A. G. Kanthasamy<sup>2</sup>, E. Whitley<sup>3</sup> and W. K. Rumbleha<sup>1</sup>. <sup>1</sup>VDPAM, Iowa State University, Ames, IA; <sup>2</sup>Biomedical Sciences, Iowa State University, Ames, IA; <sup>3</sup>Pathology, Iowa State University, Ames, IA.

Parkinson's disease (PD) affects over one million people in the U.S. alone and more than 6 million people worldwide. Potential risk factors for PD include aging, genetic alterations, and environmental neurotoxicant exposures. Although incompletely understood, the etiology and pathological mechanism of PD is characterized by a profound degeneration of dopaminergic neurons in the substantia nigra pars compacta. The majority of PD patients do not know the specific trigger of their disease although exposures to environmental factors are believed to contribute to or influence the development and progression of the disease. We have identified a novel environmental bipyridyl mycotoxin similar to Paraquat (PQ) and MPTP. Like PQ and MPTP, orellanine (OR) is a bipyridyl molecule and we hypothesized that OR will induce apoptosis in N27 cells. Here, we investigated the neurotoxic effects of OR (3,3',4,4'-tetrahydroxy-2,2'-bipyridine-1,1'-dioxide) on mesencephalic dopaminergic neuronal cell line (N27 cells), an in vitro model of PD. Using an MTT assay, OR induced a dose-dependent decrease in the viability of N27 cells with an EC50 of 44.9  $\pm$  15.3  $\mu\text{M}$  (six times lower than that of PQ or MPP+), suggesting that OR is more potent than PQ or MPP+ on N27 cells. To explore the

mechanisms of cell death, we investigated the effect of OR on mitochondrial-dependent apoptotic pathway in N27 cells. The results showed that OR (100  $\mu$ M) induces mitochondrial cytochrome C release followed by sequential activation of caspase-9 and caspase-3, and subsequently DNA fragmentation in a dose- and time-dependent fashion, with peak activation occurring 12 h after OR exposure. Co-treatment with caspase-3 specific inhibitor, Z-DEVD-FMK (50 mM) significantly attenuated OR-induced caspase-3 and DNA fragmentation. Together, this study demonstrates that OR induces cytotoxicity in mesencephalic N27 dopamine-producing cells via the caspase-3-dependent apoptotic pathway.

**PS 1838 Trichostatin A (TSA), a Histone Deacetylase Inhibitor, Mediates Dopaminergic Cell Death via an NF- $\kappa$ B Dependent Mechanism.**

V. Lawana, N. Singh, G. Huh, P. Chandramani-Shivalingappa, H. Jin, V. Anantharam, A. G. Kanthasamy and A. Kanthasamy. *Biomedical Science, Iowa State University, Ames, IA.*

Trichostatin A (TSA) is a potent, reversible inhibitor of histone deacetylase (HDACi) that functions through hyperacetylation of core histones. A previous study from our lab has linked histone hyperacetylation to dopaminergic neurodegeneration. TSA has been shown to induce profound dopaminergic neuronal cell death, but the cellular mechanisms underlying HDACi-mediated apoptotic cell death remains unclear. Herein, we show that TSA treatment induced dose dependent apoptotic cell death in the dopaminergic neuronal cell culture model (N27 cells). In order to better define the apoptotic cell death, we investigated the role of caspases including caspase-2, caspase-8, caspase-9, and caspase-3. The caspases (2, 8, 9, and 3) activation coincided with ROS generation and proteasomal dysfunction and was found to occur early and prior to cell death. Additionally, TSA induced apoptotic cell death was preceded by PKC delta activation, upregulation of p44/42 MAP kinase, nuclear translocation of p-65 and hyperacetylation of histone (H3). Conversely, downregulation of I $\kappa$ B $\alpha$  and survivin levels was also observed as revealed by Western blot and immunohistochemical analyses. Notably, pharmacological inhibition of NF- $\kappa$ B and caspases via SN-50 and ZVAD, respectively, conferred resistance against TSA induced apoptotic cell death in dopaminergic neuronal cells. These results suggest that NF- $\kappa$ B mediated and caspase dependent cell death signaling events may be critically linked to TSA induced dopaminergic neuronal degeneration. Further investigation of the mechanistic link between oxidative stress and proteasomal dysfunction in TSA-induced dopaminergic neuronal cell death may enhance our understanding on the influence of histone modifications on the nigrostriatal dopaminergic degeneration (supported by NIH grants ES10586 and NS65167).

**PS 1839 Chemically-Induced Aging of PC12 Cells to Study *In Vitro* Neurodegeneration.**

M. de Groot and R. H. Westerink. *Neurotoxicology Research Group, Institute for Risk Assessment Sciences, Faculty of Veterinary Medicine, University of Utrecht, Utrecht, Netherlands.*

Neurodegenerative diseases, e.g. Parkinson's disease, are multifactorial and the mechanisms underlying these disorders are often unknown. *In vitro* models can increase insight into the cellular and molecular mechanisms by reducing multifactorial diseases to a more controllable set of parameters. A well-known cell model in *in vitro* neurotoxicology is the pheochromocytoma (PC12) cell line. PC12 cells have been used for decades to study the effects of environmental stressors on important processes of neuronal development, function and degeneration, including differentiation and neuritogenesis, the synthesis, storage and release of neurotransmitters and the regulation and function of different ion channels. However, the use of PC12 cells to investigate neurodegeneration *in vitro* is debated as this tumor-derived cell line is rather resistant against environmental insults.

In this study we therefore induced different degrees of aging in PC12 cells by altering their oxidative status to investigate if this would increase the susceptibility to environmental stressors, such as pesticides. The characteristics of these 'aged' PC12 subtypes and their sensitivity to an environmental stressor were investigated using different (functional) assays, i.e. measurements of cell viability, measurements of oxidative stress using the ROS-sensitive dye H<sub>2</sub>-DCFDA, and single cell measurements of [Ca<sup>2+</sup>]<sub>i</sub> using the Ca<sup>2+</sup>-sensitive dye Fura-2.

Our data demonstrate that the different aged PC12 models show a clearly different Ca<sup>2+</sup>-homeostasis as compared to naïve PC12 cells. This altered homeostasis is accompanied by a change in ROS production over time and by an increased sensitivity to an environmental stressor as compared to naïve PC12 cells. As such, these aged PC12 models with increased vulnerability can be used to gain mechanistic insight in *in vitro* neurodegeneration studies.

Funding: ZonMW NL (85300003).

**PS 1840 Differential Alternate Splicing of L-Type Calcium Channel in Brain Regions: Implication in Parkinson's Disease.**

A. Verma and V. Ravindranath. *Centre for Neuroscience, Indian Institute of Science, Bangalore, India.* Sponsor: B. Moorthy.

Parkinson's disease (PD) is a movement disorder characterized by resting tremors, bradykinesia and rigidity caused by death of dopaminergic neurons in substantia nigra pars compacta (SNpc) of the brain. An intriguing question in the pathogenesis of PD is the selective degeneration of SNpc neurons and their terminals in striatum, while the adjacent dopaminergic neurons in ventral tegmental area (VTA) are affected only in later stages of the disease. Among the several hypotheses that have been put forth to address cell death, mitochondrial dysfunction, oxidative stress and accumulation of misfolded proteins in the cytosol (Lewy body) have been studied extensively. More recently it has been shown that SNpc neurons exhibit L-type calcium channel, Cav1.3, mediated autonomous pace-making, which could potentially result in increased cytosolic calcium resulting in neurotoxicity. While the VTA neurons also exhibit pace-making, it is driven by sodium conductances thereby ensuring that cytosolic calcium levels are not elevated. Thus, Cav1.3 channels could play a role in the selective susceptibility of SNpc neurons in PD. A short splice variant of Cav1.3, Cav1.3-42A has been shown to promote calcium influx into the cell in contrast to the long variant Cav1.3. Thus the presence of greater amounts of Cav1.3-42A relative to Cav1.3 could lead to increased intracellular calcium. We measured the relative levels of Cav1.3 and the short splice variant Cav1.3-42A in brain regions and found that the expression of Cav1.3-42A was 4-fold higher in the ventral midbrain compared to striatum or cortex. Concomitantly, levels of Cav1.3 were significantly less in ventral midbrain. These results indicate that the presence of Cav1.3-42A in significantly higher concentration in ventral midbrain, could contribute not only to amplified pace-making but also result in increased cytosolic calcium levels in neurons thus contributing to the degeneration of these neurons.

**PS 1841 Development of a Cellular Model to Assess Catecholamine Transport and Toxicity.**

K. Stout, A. I. Bernstein and G. W. Miller. *Environmental Health, Emory University, Atlanta, GA.*

Environmental exposure to neurotoxins can lead to catecholaminergic degeneration and subsequent Parkinson's disease (PD) development. Historically, dopamine neurons have been the primary focus of neurotoxicological research in PD though the importance of noradrenergic degeneration is becoming increasingly evident. Our laboratory recently developed a cellular model to assess dopaminergic transport and toxicity. Here we demonstrate the development of a novel noradrenergic cellular model for assessing catecholamine transport and toxicity. Many neurotoxic compounds act as inhibitors of the vesicular monoamine transporter 2 (VMAT2) within monoaminergic neurons. The primary role of VMAT2 is to sequester monoamines into vesicles, protecting them from cytosolic metabolism, and readying them for release upon stimulation. Inhibition of vesicular packaging results in increased metabolism of neurotransmitter. NE metabolites inhibit mitochondrial complex I, thereby reducing ATP synthesis and likely inducing toxicity. To investigate noradrenergic transport and toxicity we are utilizing a monoamine-like fluorescent substrate (Molecular Devices) to investigate VMAT2 function in HEK cells stably transfected with the human norepinephrine transporter (NET) and mCherry-tagged human VMAT2. These cells model physiological NE uptake within NE neurons. NET localizes to the cell membrane and VMAT2 forms intracellular vesicle-like structures. The fluorescent substrate we are utilizing mimics the action of NE in these cells. It is transported into the cell via desipramine-sensitive NET uptake (IC<sub>50</sub> = 113.9 nM). Within the cell, the dye is sequestered into vesicles by VMAT2, evidenced by co-localization of fluorescence between the substrate and mCherry. Tetrabenazine, a VMAT2 inhibitor, inhibits co-localization in a dose-dependent manner (IC<sub>50</sub> = 382.8 nM). Both co-localization and inhibition are detectable by microscopy and analyzed with IDEV (Cellomics). This cellular model allows investigation of both normal and altered transporter function in response to toxicants in a noradrenergic cellular model.

**PS 1842 Alpha-Synuclein Protein Aggregates Activate Microglia and Contribute to Neurotoxicity in the Nigral Dopaminergic System through a Fyn Kinase Dependent Mechanism.**

N. Panicker<sup>1</sup>, K. Kanthasamy<sup>2</sup>, D. Harischandra<sup>1</sup>, H. Saminathan<sup>1</sup>, R. Gordon<sup>1</sup>, V. Anantharam<sup>1</sup>, A. G. Kanthasamy<sup>1</sup> and A. Kanthasamy<sup>1</sup>. <sup>1</sup>Biomedical Sciences, Iowa State University, Ames, IA; <sup>2</sup>Biochemistry & Cell Biology, Rice University, Houston, TX.

Abnormal protein aggregation and chronic neuroinflammation are recognized as key pathophysiological hallmarks of many neurodegenerative diseases including Parkinson's disease (PD). Aggregates of the presynaptic protein  $\alpha$  synuclein are the

major component of Lewy bodies, the histological marker of PD. Aggregated  $\alpha$  synuclein is known to stimulate resident brain microglia, leading to their chronic activation and subsequent production of neurotoxic factors and proinflammatory cytokines. Identification of the molecular signaling events perpetuating  $\alpha$ -synuclein mediated microglial activation could unravel glial neuronal crosstalk mechanisms that lead to persistent gliosis and neurodegeneration in PD. In the present study, we examined the role that Fyn, a major non-receptor tyrosine kinase, plays in aggregated  $\alpha$  synuclein induced microglial activation. Immunocytochemical and Western blot analyses revealed that Fyn was expressed in primary murine microglia as well as in BV2 microglial cells. Stimulation of the cells with  $\alpha$  synuclein aggregates rapidly activated Fyn within 30 minutes of exposure. The time course activation of Fyn also paralleled PKC $\delta$  Y311 phosphorylation. Interestingly, the  $\alpha$ -synuclein induced PKC $\delta$  Y311 phosphorylation was suppressed in primary microglia isolated from Fyn knockout (Fyn  $-/-$ ) mice, implicating Fyn as the kinase that carries out this event. The  $\alpha$ -synuclein induced activation of p44/42 (Erk1/2) and p38 map kinases was diminished in both Fyn, as well as PKC $\delta$  knockout microglia. Notably, the Fyn knockout primary microglia showed attenuated release of cytokines TNF $\alpha$ , IL-10 and IL-12 in response to  $\alpha$  synuclein aggregate stimulation when compared to wild type microglia. Collectively, our results demonstrate a non receptor tyrosine kinase mediated pro-inflammatory signaling pathway that may mediate neuroinflammation in PD (supported by NIH grants ES19276 and NS65167).

### PS 1843 Loss of NF- $\kappa$ B p50 Enhances LPS-Induced Systemic Inflammation and Early Microglial Activation.

T. Taetzsch, S. Levesque, C. McGraw, M. Surace and M. L. Block. *Anatomy & Neurobiology, VCU, Richmond, VA.*

Inflammation associated with chronically activated microglia has been implicated in the progressive degeneration of nigral dopaminergic (DA) neurons in Parkinson's disease (PD), but the mechanisms are not well understood. NF- $\kappa$ B p50 is an important regulator of the pro-inflammatory response with both inhibitory and initiating roles in the production of cytokines. Importantly, reduced NF- $\kappa$ B p50 expression has been observed in the substantia nigra (SN) of patients suffering dementia with lewy bodies, supporting a potential role for NF- $\kappa$ B p50 in PD-like neurodegeneration. To examine the consequences of loss of NF- $\kappa$ B p50 function in microglial activation in vivo, NF- $\kappa$ B p50 $^{+/+}$  and NF- $\kappa$ B p50 $^{-/-}$  mice were injected with 5mg/kg LPS IP and sacrificed after 3 hours. Expression of the pro-inflammatory genes TNF $\alpha$  and IL-1 $\beta$  were significantly higher while iNOS expression was lower and COX2 expression was unchanged in the midbrain of LPS treated NF- $\kappa$ B p50 $^{-/-}$  mice, as compared to NF- $\kappa$ B p50 $^{+/+}$  mice. Analysis of microglia morphology in the SN using unbiased stereology revealed significantly higher numbers of microglia with activated morphology in LPS treated NF- $\kappa$ B p50 $^{-/-}$  mice versus NF- $\kappa$ B p50 $^{+/+}$  mice. In addition, LPS-treated NF- $\kappa$ B p50 $^{-/-}$  mice had significantly elevated serum levels of TNF $\alpha$  when compared to LPS-treated NF- $\kappa$ B p50 $^{+/+}$  mice. In vitro kinetics studies demonstrated that TNF $\alpha$  and iNOS expression is significantly increased at 6 and 12h, but not 3h post-LPS treatment in NF- $\kappa$ B p50 $^{-/-}$  mixed glia cultures, suggesting a possible role of NF- $\kappa$ B p50 in resolution of the glial pro-inflammatory response. These studies underscore that loss of NF- $\kappa$ B p50 function amplifies systemic inflammation, increases neuroinflammation, enhances microglial activation, and may impede glial resolution of the pro-inflammatory response.

### PS 1844 Fungal Volatile Organic Compound(s): Potential Environmental Agent(s) for the Pathogenesis of Parkinson's Disease?

A. A. Inamdar<sup>1</sup>, M. M. Hossain<sup>2</sup>, J. Richardson<sup>2</sup> and J. Bennett<sup>1</sup>. <sup>1</sup>*Plant Bio and Pathology, Rutgers, The State University of New Jersey, New Brunswick, New Jersey;* <sup>2</sup>*EOHSI, Rutgers, The State University of New Jersey, Piscataway, NJ.*

Parkinson's disease (PD) is the most common movement disorder and possesses multifactorial etiology. Recently, environmental contaminants including mold exposure are implicated in PD-like movement disorders in epidemiological studies. Although the exact fungal component responsible to such movement disorder is under speculation, fungal volatile organic compounds (VOCs), a class of fungal secondary metabolites has been reported to be associated with the adverse health effects in the human population. There are few in vitro and human studies demonstrating the biological activity of these fungal VOCs; however, the plausible studies elucidating the mechanism of action of these VOCs are lacking. Our lab has pioneered invertebrate *Drosophila* model to study the neurotoxic effects of common fungal VOCs (Inamdar et al., 2010). We have reported that exposure to chemical standards of 1-octen-3-ol and other fungal VOCs cause loss of dopaminergic neurons and movement deficits in *Drosophila* suggesting that these tested fungal

VOCs has potential to induce Parkinson's disease like symptoms. To determine the mechanism of toxicity of fungal VOCs, we focused on 1-octen-3-ol. Employing the available genetic and molecular tools in our *Drosophila* model, we demonstrate the modulatory effect of 1-octen-3-ol on dopamine regulatory pathway. We show that 1-octen-3-ol inhibits the vesicular monoamine transporter, VMAT thereby causing the induction of oxidation of dopamine and loss of dopaminergic neurons. Furthermore, we show that 1-octen-3-ol alters regulation of JNK and Akt signaling pathways in flies. In conclusion, our data present strong cues in support of Parkinson-mimetic activity of 1-octen-3-ol and provide insights into neurological problems especially movement disorders associated with damp indoor environments.

### PS 1845 Mutations in *pink-1* and *pdr-1* Result in Reduced Dopaminergic Neurodegeneration after Chemical Insult in *Caenorhabditis elegans*.

C. P. Gonzalez, R. K. Bodhicharla and J. N. Meyer. *Nicholas School of the Environment, Duke University, Durham, NC.*

Mitochondrial dysfunction has been linked to neurodegenerative diseases including Parkinson's disease. Neurons are cells with a high energy demand, and as a result are hypothesized to be particularly vulnerable to disturbances to mitochondrial homeostasis. We investigated how knocking out two genes involved in mitochondrial dynamics, *pink-1* and *pdr-1*, affected dopaminergic neuron viability after chemical insult in *Caenorhabditis elegans*. *pink-1* and *pdr-1* are the nematode homologs of the human genes PINK1 and PARK2 which when mutated cause familial Parkinson's disease. We induced neurodegeneration with 6-hydroxydopamine (6-OHDA) and assessed damage 48 hours post-exposure using the BY250 (*dat-1::GFP*) strain in which the four cephalic dopaminergic neurons are visualized with GFP. We used the BY250 strain as wild-type for *pink-1* and *pdr-1*. The strain BY250 was generously provided by Michael Aschner (Vanderbilt University) and the strains *pink-1*; *dat-1::GFP* and *pdr-1*; *dat-1::GFP* were kindly provided by Guy Caldwell (University of Alabama). Each neuron was scored from 0 to 2.5, with zero representing an intact dendrite and 2.5 representing the highest level of neurodegeneration observed, utilizing fluorescent microscopy. Our preliminary results indicate that after exposure to 15 mM 6-OHDA, the wild-type worm had a higher level of neurodegeneration than the *pink-1* knockout ( $p < 0.0001$ ) and the *pdr-1* knockout ( $p = 0.0052$ ). These counterintuitive results might be explained by the fact that loss of *pink-1* promotes mitochondrial fusion, which in turn could protect from 6-OHDA damage through mitochondrial functional complementation. Because 6-OHDA generates reactive oxygen species within the cell, it may cause lipid peroxidation and mitochondrial DNA damage, possibilities that we are currently testing. Future studies will explore the effect of these mutations on mitochondrial homeostasis and neurodegeneration after exposure to 6-OHDA and other toxicants associated with Parkinson's disease including rotenone and paraquat.

### PS 1846 Identification of Novel Genes and Epigenetic Mechanisms in *C. elegans* Models of Idiopathic Parkinson's Disease and Manganism.

R. M. Nass<sup>1</sup>, S. Ghosh<sup>2</sup>, K. Shah<sup>2</sup>, J. Trinidad<sup>3</sup> and N. VanDuyn<sup>1</sup>. <sup>1</sup>*Pharmacology and Toxicology, Indiana University School of Medicine, Indianapolis, IN;* <sup>2</sup>*Chemistry, Purdue University, West Lafayette, IN;* <sup>3</sup>*Chemistry, Indiana University, Bloomington, IN.*

Background: Idiopathic Parkinson's disease (PD) and manganism are oxidative stress-related disorders that result in abnormal dopamine (DA) signaling and cell death. Both neurological disorders involve basal ganglia and mitochondrial dysfunction, and suggest overlapping epidemiology, yet the origin of the pathogenesis and the molecular determinants common to both disorders are ill-defined. Recently we have shown that the PD-associated transcription factor SKN-1/Nrf2 is expressed in *C. elegans* DA neurons and inhibits PD-associated DA neurodegeneration. Aims/Objectives: In this study we asked what are the common genes, molecular pathways, and mechanism involved in DA neuron vulnerability to PD-associated toxicants. Methods: We utilized reverse genetics, biochemical assays, immunofluorescence, transgenic *C. elegans*, RT-PCR, Western analysis, behavioral and neuronal morphology analysis to characterize expression, localization and the role that SKN-1, IDN-1, and post-translational modifications play in 6-OHDA-, rotenone-, and manganese (Mn)-induced neuronal death. Results: In this study we demonstrate that IDN-1 mutants render DA neuron up to 15-fold more resistant to the neurotoxins relative to WT. We show that IDN-1 is expressed in DA neurons, and IDN-1 overexpression results in a 2-fold increase DA neuron vulnerability. We also show that DA neuron vulnerability is affected by transcriptional and

post-translational modifications of involving these and other proteins identified using RNAi affects DA neuron vulnerability. Conclusions: This study identifies novel genes and molecular pathways involved in DA neuron vulnerability in PD and manganism, and provides the first *in vivo* evidence that a common epigenetic mechanism likely plays a significant role in both disorders. Support: NIEHS ES014459 and ES003299 to RN, and EPA STAR Graduate Fellowship to NVD.

**PS 1847 Decreased Mitochondrial Biogenesis and Suppression of Mitochondrial Gene Expression Induced by Environmental Toxicants in *Caenorhabditis elegans* Model of Parkinsonism.**

S. Zhou, Z. Wang and J. E. Klaunig. *Indiana University, Bloomington, IN.*

Mitochondrial alterations have been documented in the brains of subjects with Parkinson's disease (PD), a disorder characterized by the selective loss of dopamine (DA) neurons. Recent studies demonstrating that PD-associated proteins are either in the mitochondria or translocated into mitochondria in response to stress. Pesticides and heavy metals have been suggested to be risk factors for PD. While, environmental agents can modulate mitochondrial function, the mechanism of this alteration has not been defined in the context of the development and progression of PD. The complexity of the mammalian neurological system has made it difficult to dissect the molecular components involved in the pathogenesis of PD. In the present study we used *C. elegans* as the model of neuron degeneration and investigated the effect of Mn<sup>2+</sup> and rotenone on mitochondrial biogenesis and gene regulation. Exposure to rotenone (2 or 4  $\mu$ M) resulted in significant loss of dopamine (DA) neuron in *C. elegans*. We then determined if the rotenone-induced neuron degeneration is accompanied by a change in mitochondria biogenesis. Analysis of mitochondrial genomic replication showed a dramatic decrease in mitochondrial DNA (mtDNA) copies in rotenone-treated *C. elegans* compared to control. This decreased mitochondrial biogenesis occurred prior to the development of loss of DA neurons, and was persistent. The inhibition of mtDNA replication was also found in *C. elegans* exposed to neuron toxicant Mn<sup>2+</sup> at the concentration 50 or 100 mM. We further examined the mitochondrial gene expression and found significant lower level of mitochondrial complex IV subunits COI and COII in *C. elegans* exposed to rotenone. These results demonstrated that environmental chemicals cause persistent suppression of mitochondrial biogenesis and mitochondrial gene expression, and suggest a critical role of modifying mitochondrial biogenesis in toxicants-induced neuron degeneration in *C. elegans* model.

**PS 1848 A Genome-Wide RNAi-Based Screen for Enhancers and Suppressors of Manganese Toxicity in *Caenorhabditis elegans*.**

P. Chen<sup>1,2</sup>, T. T. Nguyen<sup>2,3</sup> and M. Aschner<sup>1,2,3</sup>. <sup>1</sup>*Pediatric Toxicology, Vanderbilt University, Nashville, TN;* <sup>2</sup>*Neuroscience, Vanderbilt University, Nashville, TN;* <sup>3</sup>*Pharmacology, Vanderbilt University, Nashville, TN.*

Environmental or occupational exposure to manganese (Mn) causes a neuropathy resembling idiopathic Parkinson's disease (PD). Exposure to excessive Mn levels has been linked to mitochondrial dysfunction, oxidative stress, protein aggregation and disruption of iron homeostasis. However, the mechanisms behind these impairments remain unknown, partially due to limited knowledge about genetic factors associated with Mn toxicity. The complexity of the vertebrate brain and the difficulties associated with vertebrate models of PD has hindered the understanding of molecular mechanisms associated with this disorder. The nematode, *Caenorhabditis elegans* (*C. elegans*) and mammals share a highly conserved genetic code, and offers an innovative and powerful platform to evaluate the genetic factors associated with Mn-induced toxicity. Taking advantage of the RNA interference (RNAi) technique and the available RNAi library, we are able to evaluate the impact of ~ 87% of *C. elegans* genes on Mn toxicity, individually. By feeding the worms with a specific strain of RNAi bacteria, we have successfully knocked down (quantified by qRT-PCR) three selected genes (*smf-2*, *smf-3* and *dpy-7*) in *C. elegans*. In vertebrate, the divalent metal transporter 1 (DMT1) has been shown to regulate Mn transport; its nematode homologs (*smf-1*, 2 and 3) have also been proved to be involved in Mn induced toxicity. We hypothesized that knocking down *smf-1*, 2 or 3 would affect worms' survival after exposure to Mn. Consistent with our hypothesis, knocking down of SMF-1 significantly increases the survival rate of *C. elegans* by 2 fold ( $P < 0.01$ ) and SMF-3 by 1.5 fold ( $P < 0.05$ ) after Mn treatment at the larval (L4) stage; *smf-2* knockdown did not cause to a significant change in Mn-induced survival rate. Taken together, our studies establish that a genome-wide RNAi based screen could be carried out using the survival assay to identify genetic enhancers and suppressors of Mn induced toxicity in *C. elegans*.

**PS 1849 Loss of *Pdr-1/Parkin* Alters Manganese Homeostasis in *C. elegans*.**

S. Chakraborty<sup>1,2</sup> and M. Aschner<sup>2,3</sup>. <sup>1</sup>*Neuroscience Graduate Program, Vanderbilt University, Nashville, TN;* <sup>2</sup>*Center for Molecular Toxicology, Vanderbilt University, Nashville, TN;* <sup>3</sup>*Pediatrics, Vanderbilt University, Nashville, TN.*

Environmental overexposure to the essential trace element manganese (Mn) can result in an irreversible, toxic condition known as manganism. This disorder shares similar neuropathology with Parkinson's disease (PD), exhibiting overt dopaminergic (DAergic) cell loss associated with the presentation of motor and cognitive deficits. However, the mechanisms behind the pathophysiology of both disorders remain unclear. Many PD genes have been identified to explain a subset of cases, including the *parkin/PARK2* gene that encodes for an E3 ubiquitin ligase. Using *Caenorhabditis elegans* (*C. elegans*) as a model that contains the necessary DAergic machinery, we hypothesize that a loss-of-function mutation in *pdr-1*, the worm homolog of *parkin*, would increase vulnerability to Mn toxicity compared to wildtype (WT) worms by altering proper Mn homeostasis. Synchronous L1 worms from WT N2 and *pdr-1(gk448)* mutant strains were acutely exposed to MnCl<sub>2</sub> for 30 minutes, followed by lethality scoring of approximately 40-50 worms 24 hours post-treatment. Here, we show that a loss of *pdr-1* increases Mn-induced lethality compared to WT worms ( $p = 0.0005$ ), as seen with a leftward shift in the dose-response curve. Moreover, *pdr-1* mutants show higher, dose-dependent Mn accumulation compared to WT worms ( $p < 0.001$ ), suggesting overall impaired Mn homeostasis in *pdr-1* mutants. Interestingly, *pdr-1* mutants show altered mRNA expression levels of key *C. elegans* Mn importers, including up-regulation of *smf-1* and *smf-3*, and down-regulation of *smf-2*. However, *pdr-1* mutants do not show any difference in mRNA levels of *ferroportin* (*fpn-1.1* in worms) at baseline, indicating a lack of regulation at the export level. Finally, upon exposure, *pdr-1* mutants show altered total glutathione (GSH) levels compared to WT animals ( $p < 0.05$ ). Such changes indicate a role of *pdr-1* in modulating Mn import through altered transporter expression, implicating a novel role of the PD-associated gene in metal homeostasis and increased oxidative stress.

**PS 1850 Manganese Accumulations in Gill Mitochondria of *Crassostrea virginica*.**

A. Nuhar, B. Boissette, M. A. Carroll and E. J. Catapane. *Biology, Medgar Evers College, Brooklyn, NY.*

Manganese is a neurotoxin causing Manganism in people chronically exposed to elevated levels in their environment. Manganese targets dopamine neurons in basal ganglia. Oxidative stress has been implicated as a factor of manganese toxicity and dopamine dysfunction. Mitochondria play a role as cause and target of oxidative stress damage. The mechanisms of damage is attributed to manganese's capacity to produce toxic levels of free radicals and induce mitochondrial dysfunction. Others report manganese accumulates in mitochondria and represent the primary pool of manganese in cells. Controversy exists to the extent of manganese accumulation in mitochondria. Others report manganese accumulates within nuclei and cytoplasm, but not mitochondria. Our lab is using the oyster, *Crassostrea virginica*, as a test animal to study manganese neurotoxicity. We found manganese disrupts the dopamine system as well as mitochondrial respiration. To study if manganese accumulates within mitochondrial of gill cells of *C. virginica* we used differential centrifugation and atomic absorption spectrometry. Gills were homogenized and centrifuged to isolate nuclear, mitochondrial and post-mitochondrial fractions. Each fraction was analyzed for manganese. To determine if isolated mitochondria accumulate manganese we prepared treated mitochondrial suspensions with up to 300 mM manganese. Results show a dose dependent accumulation of manganese in mitochondria of up to 5000%. Two day treatments of animals with 500 and 1000  $\mu$ M Mn increased manganese ( $\mu$ g/gdw) in gill from a baseline of 5.8 to 41.6 and 133.8, respectively, and centrifugation revealed Manganese accumulations were primarily in nuclear and mitochondrial fractions. The study shows mitochondria accumulate manganese. In vivo treatments reveal accumulations with both the nuclear and mitochondrial fractions.

**PS 1851 Manganese Treatments Decreases Immunofluorescence Emissions of Postsynaptic Dopamine D2 Receptors.**

Y. Chekayev, R. Opoku, M. A. Carroll and E. J. Catapane. *Biology, Medgar Evers College, Brooklyn, NY.*

Manganese a neurotoxin causing Manganism, a Parkinsons-like disease, disrupts dopamine neurotransmission. Gill lateral cell cilia of *Crassostrea virginica* are controlled by serotonergic-dopaminergic innervations. Dopamine causes cilio-inhibition, serotonin cilio-excitation. Our lab showed post-synaptic dopamine receptors in gill cells are D2 type and manganese blocks cilio-inhibitory effects of dopamine

by blocking dopamine post-synaptic receptors. Questions exist in the literature if manganese decreases the number of D2 receptors in brain. To test that we used antibody-antigen histoimmunofluorescence techniques to visualize dopamine D2 receptors in gill and ganglia of *C. virginica*. We used a primary antibody against D2 receptors followed by FITC linked secondary antibody. Animals were treated with 500  $\mu$ M of manganese for 5 days. Gill, cerebral and visceral ganglia were excised and exposed to primary and secondary antibodies. Paraffin embedded sections were viewed with a phase contrast Zeiss epilume fluorescence microscope with a ProgRes C3 Peltier cooled camera. Antibody treated sections showed bright FITC fluorescence in lateral ciliated cells and other areas of gill and ganglia. Sections lacking primary antibody treatment did not display similar fluorescence. We analyzed fluorescence intensity of 120 control and 80 gill lateral cells from animals treated with manganese using ImageJ software. Intensity of manganese treated cells was 70% less than controls. The study identifies dopamine D2 receptors in gill cells and cerebral and visceral ganglia, and shows a negative correlation between fluorescence intensity of dopamine D2 receptors in manganese treated animals and controls. The question if the decrease in intensity is due to decrease in actual number of receptors or if manganese alters protein conformation of D2 receptor and D2-ligand binding sites needs to be further explored.

**PS 1852 Chelating Agents Reverse Neurotoxic Effects of Manganese on Dopaminergic Innervation of Gill of the Bivalve Mollusc *Crassostrea virginica*.**

C. Ojo, K. Rogers, T. Adams, E. J. Catapane and M. A. Carroll. *Biology, Medgar Evers College, Brooklyn, NY.*

Lateral cilia of gill of *Crassostrea virginica* are controlled by a serotonergic-dopaminergic innervation. Dopamine is an inhibitory transmitter at gill causing cilio-inhibition. Manganese is a neurotoxin causing Manganism in people exposed to high levels in the atmosphere. Clinical interventions for Manganism have not been successful. Recently, p-aminosalicylic acid (PAS) was reported to provide effective treatment of severe Manganism in humans. PAS is an anti-inflammatory drug which has been used to treat tuberculosis. It also has chelating properties. Previously, we showed treatments of *C. virginica* with Mn disrupts dopaminergic innervation of gill. Pre- or co-treatments with PAS or calcium disodium EDTA prevented the neurotoxic effects of manganese. We hypothesized chelating agents would be effective in reversing neurotoxic effects of manganese when applied to gills after manganese. We used gills of *C. virginica* to measure lateral cilia beating rates of preparations treated first with manganese followed by treatments with either PAS, calcium disodium EDTA or DMSA (meso-2,3-dimercaptosuccinic acid). Beating of cilia were measured by stroboscopic microscopy. Dose responses of PAS, calcium disodium EDTA and DMSA ( $10^{-11}$  -  $10^{-4}$  M) against beating were conducted after 100  $\mu$ M of manganese was added to gill. All 3 drugs reversed the neurotoxic effects of manganese in a dose-dependent manner. DMSA was the most potent. The study demonstrates these chelators are effective in reversing acute neurotoxicity of manganese. This information should be of interest to those designing therapeutic drug treatments for Manganism.

**PS 1853 Effects of Antioxidants and Anti-Inflammatory Agents on Neurotoxic Effects of Manganese on Dopaminergic Innervation of Gill of the Bivalve Mollusc *Crassostrea virginica*.**

K. LaFleur, M. Rotibi, E. J. Catapane and M. A. Carroll. *Biology, Medgar Evers College, Brooklyn, NY.*

Lateral cilia of the gill of *Crassostrea virginica* are controlled by a serotonergic-dopaminergic innervation. Dopamine acts as an excitatory neurotransmitter within the ganglia, but an inhibitory neurotransmitter at gill, causing cilio-inhibition. The mechanism of action of manganese toxicity is not fully understood, but may be due to oxidative damage. We found several chelators, including p-aminosalicylic acid (PAS) prevented neurotoxic effects of manganese in *C. virginica*. The therapeutic actions of PAS are thought to be due to chelation, but PAS is also anti-inflammatory. We sought to determine if anti-inflammatory agents and/or antioxidants are effective in preventing neurotoxic actions of manganese in gill of *C. virginica*. Indomethacin, an anti-inflammatory agent with antioxidant abilities, and ascorbic acid, an antioxidant with possible anti-inflammatory abilities were tested. We examined acute and short term (3 - 5 days) treatment of indomethacin and ascorbic acid on manganese toxicity on dopaminergic innervation. Beating rates of lateral cilia in gill epithelial cells were measured by stroboscopic microscopy. Acute or short-term treatments of indomethacin or ascorbic acid (25 - 100  $\mu$ M) and had no effect on the cilio-inhibitory effects of dopamine (10-6 - 10-3 M). When acute or short-term manganese treated animals (25 - 100  $\mu$ M) were pretreated with indomethacin or ascorbic acid (25 - 100  $\mu$ M), both drugs effectively prevented the

neurotoxic effects of manganese, with ascorbic acid being more effective than indomethacin. The study demonstrates antioxidants and anti-inflammatory agents can block the neurotoxic actions of manganese and may be possible therapeutic agents in the treatment of Manganism.

**PS 1854 Neurotoxic Effects of Manganese on GABAergic Innervation in the Bivalve Mollusc *Crassostrea virginica*.**

J. Ogunnoiki, K. Jackson, E. J. Catapane and M. A. Carroll. *Biology, Medgar Evers College, Brooklyn, NY.*

High levels of airborne manganese cause Manganism, a neurotoxic, Parkinsons-like disease in humans by interfering with dopaminergic neurotransmission in brain. Recent studies are showing GABAergic neurons also are damaged by manganese. *C. virginica* contains a dopaminergic and serotonergic innervation of its gill. It is a simple system to study manganese toxicity. Previously we showed manganese disrupts dopaminergic innervation. We also showed the cerebral ganglia of *C. virginica* contains GABA and within the cerebral ganglia GABA inhibits serotonergic innervation of gill lateral cell cilia. Here we studied if ganglia and peripheral tissues contain GABA receptors, and if manganese has effects on GABA neurons within cerebral ganglia of *C. virginica*. We used primary antibodies (GABAA Ra1-6 ) and secondary antibodies (IgG-FITC) to detect GABA receptors with paraformaldehyde fixed, paraffin embedded tissues using a Zeiss epilume fluorescence microscope and ProgRes C3 Peltier cooled camera. We found fluorescence due to GABA receptors in cerebral ganglia, visceral ganglia, palps and digestive tract. We also examined effects of manganese treatments on GABAergic inhibition of serotonin neurons in cerebral ganglia. Beating of lateral cilia in gill cells were measured by stroboscopic microscopy. Applying serotonin to cerebral ganglia caused a dose-dependent increase in cilia beating. Applying GABA prior to serotonin prevented the increase. Acute applications of manganese (50 and 500  $\mu$ M) prior to GABA prevented GABA from inhibiting serotonin. The study is showing GABA receptors are present in ganglia and peripheral tissues in *C. virginica*, and acute manganese treatments damage GABA neurons. *C. virginica* preparations are good, simple test preparation to study the GABAergic system and the mechanism underlying the neurotoxic effects of manganese.

**PS 1855 Optimization of Fluorescence Assay of Cellular Manganese Status for High-Throughput Screening.**

K. K. Kumar<sup>1,3</sup>, A. Aboud<sup>1</sup>, D. K. Patel<sup>1</sup>, M. Aschner<sup>2</sup> and A. B. Bowman<sup>1,2</sup>. <sup>1</sup>Department of Neurology, Vanderbilt University, Nashville, TN; <sup>2</sup>Department of Pediatrics, Vanderbilt University, Nashville, TN; <sup>3</sup>Medical Scientist Training Program, Vanderbilt University, Nashville, TN.

The advent of high throughput screening (HTS) technology permits identification of compounds that influence various cellular phenotypes. However, screening for small molecule chemical modifiers of neurotoxicants has been limited by the scalability of existing phenotyping assays. Furthermore, the adaptation of existing cellular assays to HTS format requires substantial modification of experimental parameters and analysis methodology to meet the necessary statistical requirements. Here we describe the successful optimization of the Cellular Fura-2 Manganese Extraction Assay (CFMEA) for HTS. By optimizing cellular density, manganese (Mn) exposure conditions, and extraction parameters, the sensitivity and dynamic range of the fura-2 Mn response was enhanced to permit detection of positive and negative modulators of cellular manganese status. Finally, we quantify and report strategies to control sources of intra- and inter-plate variability by batch level and plate-geometric level analysis. Our goal is to enable HTS with the CFMEA to identify novel modulators of Mn transport. Support: NIH ES016931 and ES010563.

**PS 1856 Manganese Exposure Alters Mitochondrial Biogenesis in Dopaminergic Neuronal Cells.**

M. Ay, A. Kanthasamy, H. Jin, D. Kim, V. Anantharam and A. G. Kanthasamy. *Iowa State University, Ames, IA.*

Excessive manganese (Mn) exposure causes a movement disorder commonly referred to as manganism in humans. Mn mainly accumulates within mitochondria and adversely affects mitochondrial structure and function both in vivo and in vitro. Over the past decades, mitochondrial dependent biochemical processes such

as oxidative stress, Ca<sup>2+</sup> dysregulation and apoptotic signaling have been identified as possible mechanisms of Mn neurotoxicity. However, mitochondrial dynamics and the molecular mechanisms that govern the mitochondrial biogenesis during Mn neurotoxicity are yet to be determined. Since the transcriptional co-activator peroxisome proliferator-activated receptor gamma coactivator 1-alpha (PGC-1alpha) is the master regulator of mitochondrial biogenesis, herein, we examined the effect of Mn on PGC-1alpha dependent mitochondrial biogenesis in dopaminergic neuronal cells. The MN9D dopaminergic neuronal cell model was exposed to 100-500  $\mu$ M of manganese, and the mRNA expression levels of several mitochondrial biogenesis markers, including PGC-1alpha, mitochondrial transcription factor A (TFAM), and cytochrome B (CytB), were measured using qRT-PCR analysis. Interestingly, the results revealed a dose-dependent induction of PGC-1alpha, TFAM, and CytB mRNA levels following 24 h of manganese exposure, whereas short-time manganese exposure (3-6 h) did not result in any significant induction of PGC-1alpha mRNA. Since PKD1 serves as a key compensatory anti-apoptotic kinase, we measured PKD1 phosphorylation, and the kinase phosphorylation was significantly decreased at 24 h with 500  $\mu$ M Mn exposure. A decreased level of Bcl-2 (a pro-survival protein) was also observed at 24 h. Importantly, overexpression of PGC-1 alpha protein significantly protected the cells against Mn-induced neurotoxicity. Taken together, our data indicate that Mn exposure induces mitochondrial biogenesis through PGC-1 alpha transcription to counter metal induced neurotoxic stress (NIH grants ES19267, ES10586, and NS074443).

### PS 1857 Manganese Exposure Induces Release of $\alpha$ -Synuclein and Promotes Exosome Mediated Cell to Cell Transmission of Synuclein Aggregates in Neurotoxicity Models.

D. Harischandra, H. Jin, A. Kanthasamy, V. Anantharam and A. G. Kanthasamy. Biomedical Science, Iowa State University, Ames, IA.

Chronic manganese exposure is a well-known occupational and environmental hazard considered to be a potential risk factor for environmentally linked Parkinsonism.  $\alpha$ -Synuclein ( $\alpha$ -syn) is a major presynaptic protein in CNS, and aggregation of  $\alpha$ -syn has been implicated in the pathophysiology of Parkinson's disease. Previously, we showed that  $\alpha$ -syn protects dopaminergic neuronal cells against metal neurotoxicity during early exposure. In the present study, we further characterized the effect of long-term manganese exposure on  $\alpha$ -syn metabolism. A 300  $\mu$ M manganese exposure to human  $\alpha$ -syn stably expressing N27 dopaminergic cells for 24-48 hr induced a time-dependent increase in  $\alpha$ -syn immunoreactive aggregates in the cells. Further analysis of the protein aggregation by inclusion body specific fluorescence probes revealed formation of aggregates in a time-dependent manner. We were also able to detect enhanced accumulation of protein oligomers in manganese treated dopaminergic cells. Studies conducted with MN9D cells stably expressing human  $\alpha$ -syn showed that the  $\alpha$ -syn is secreted out of the cells into extracellular media following manganese exposure, in a time-dependent manner. Further characterization of extracellular media by ultracentrifugation followed by electron microscopic analyses revealed that manganese treatment induces exosome vesicle formation in  $\alpha$ -syn cells. Interestingly, we also observed manganese increased the expression of prion in  $\alpha$ -syn expressing cells as compared to vector control cells. Furthermore, manganese treatment increases GRP 78 and caspase 12 levels, suggesting that manganese induces ER stress in  $\alpha$ -syn expressing cells. Collectively, these results demonstrate that prolonged manganese exposure promotes  $\alpha$ -syn protein aggregation and secretion into extracellular milieu by forming exosomal vesicles, which may contribute to propagation of protein aggregation by a prion-like mechanism in dopaminergic neuronal cells. (NIH grants ES19267, ES10586, and NS65167)

### PS 1858 Trp73 Gene in Dopaminergic Neurons Is Highly Susceptible to Manganese Neurotoxicity.

D. Kim, H. Jin, V. Anantharam, R. Gordon, A. Kanthasamy and A. G. Kanthasamy. Biomedical Science Department, Iowa State University, Ames, IA.

Chronic exposure to elevated levels of manganese has been linked to a Parkinson's disease like movement disorder, resulting from dysfunction of the extrapyramidal motor system within the basal ganglia. However, the exact cellular and molecular mechanisms of manganese-induced neurotoxicity remain elusive. Since oxidative stress and apoptosis are considered to be prime mechanisms of manganese neurotoxicity, we sought to identify genes that are susceptible to manganese-induced neurotoxic insult using the Qiagen mouse apoptosis RT<sup>2</sup> Profiler<sup>TM</sup> PCR array system. C57 black mice were treated with 10 mg/kg manganese via oral gavage for 30 days. The nigral tissue was collected and RT-PCR based gene expression was performed for 84 genes associated with apoptotic signaling. Interestingly, we found significant

down-regulation of a tumor repressor gene, namely Trp73, in manganese treated nigral tissue, as compared to control. To further determine the molecular mechanism of manganese-induced Trp73 down-regulation, we treated N27 dopaminergic cells with 300  $\mu$ M manganese and examined the gene expression. Consistent with our animal study, we found reduced expression of Trp73 at mRNA levels in N27 dopaminergic cells. We further determined the Trp73 protein levels during manganese treatment. Trp73 protein level was also reduced in manganese treated N27 cells as well as in manganese treated nigral lysate. Furthermore, manganese treatment in primary striatal culture down-regulated Trp73 protein level in a dose dependent manner. After confirming Trp73 down-regulation during manganese toxicity in three different models, we have begun additional mechanistic studies in cell culture models of manganese neurotoxicity. Taken together, our results demonstrate Trp73 is a gene susceptible to manganese neurotoxicity, and further characterization of the role of Trp73 in cell survival/cell death will improve our understanding of the molecular underpinnings of manganese neurotoxicity (supported by NIH grants ES10586 and ES19267).

### PS 1859 Mechanism of Manganese-Induced Inhibition of Glutamate Transporter GLAST Function.

A. North<sup>1</sup>, A. Webb<sup>1</sup>, D. Son<sup>1</sup>, M. Aschner<sup>2</sup> and E. Lee<sup>1</sup>. <sup>1</sup>Physiology, Meharry Medical College, Nashville, TN; <sup>2</sup>Pediatrics, Vanderbilt University Medical Center, Nashville, TN.

Manganese (Mn) is an essential trace element required for normal growth, development and homeostasis; however, chronic overexposure to elevated levels of Mn induces a Parkinson's disease-like symptoms referred to as manganism. It has been reported that manganism is associated with excitotoxicity, resulting from the dysfunction of the astrocytic glutamate transporters (GLAST and GLT-1), which take up ~80% of synaptic glutamate. However, the mechanism by which Mn disrupts glutamate transporter function has yet to be elucidated. Our previous studies have shown that Mn suppressed transcriptional activity of astrocytic GLAST by decreasing its mRNA and protein levels. Accordingly, herein, we seek to understand the molecular mechanism of Mn-induced GLAST suppression at transcriptional levels, testing whether Mn induces a modulatory effect on astrocytic GLAST promoter activity. The experiments were conducted by assessing EAAT1 (human form of GLAST) luciferase activity in astrocytes transiently transfected with EAAT1 vectors. We hypothesized that Ying-Yang 1 (YY1) and NF- $\kappa$ B pathways play a critical role in repressing the GLAST gene expression, and that Mn modulates the activities of these transcriptional factors. The results revealed that Mn activates the YY1 promoter (p<0.05), and overexpression of YY1 decreases EAAT1 promoter activity. We have also found that CBP (CREB binding protein) acts as a co-regulator of YY1 on the EAAT1 promoter. NF- $\kappa$ B also regulates EAAT1 promoter activity. Overexpression of NF- $\kappa$ B p65 increases the EAAT1 promoter activity (10 folds, p<0.001), whereas mutation on NF- $\kappa$ B binding sites at -533 or -163 of EAAT1 promoter represses EAAT1 promoter activity (p<0.001) and reduces p65 effects on EAAT1 promoter activity (3 folds, p<0.001). Mn activates NF- $\kappa$ B reporter activity and produces TNF- $\alpha$  which decreases EAAT1 activity via NF- $\kappa$ B activation. Taken together, our results indicate that the YY1 and NF- $\kappa$ B pathways play critical roles in Mn-induced repression of EAAT1 promoter activity.

### PS 1860 Analysis of Brain Mn Distribution Influenced by Disease Stage in Mouse Models of Huntington's Disease.

T. V. Bichell<sup>1,2</sup>, M. Wegrzynowicz<sup>1,2</sup>, M. S. Cardone<sup>1</sup>, M. Uhouse<sup>1</sup>, M. Aschner<sup>1,2,3</sup> and A. B. Bowman<sup>1,2,3</sup>. <sup>1</sup>Department of Neurology, Vanderbilt University, Nashville, TN; <sup>2</sup>Center for Molecular Toxicology, Vanderbilt University, Nashville, TN; <sup>3</sup>Department of Pediatrics, Vanderbilt University, Nashville, TN.

Huntington's disease (HD) is a genetic neurodegenerative disorder primarily affecting the striatum. There is considerable variability in age of onset in HD strongly influenced by environmental factors. We have previously reported a disease-toxicant interaction between HD and manganese (Mn) exposure, wherein the pathogenic HD mutation is associated with a striatal specific defect in net Mn uptake. For example, there is decreased Mn accumulation in the striatum of FVB-YAC128 mice at 13 weeks of age after 7 day subcutaneous Mn exposure with 3 total injections at 50mg Mn chloride tetrahydrate/kg. To determine if increased exposure duration influenced this phenotype we measured striatal Mn after a 9 day exposure with a total of 5 injections. At this age (13 weeks), prior to the onset of neurodegenerative phenotypes, the higher exposure strengthened the difference in striatal Mn accumulation between wildtype and mutant mice. To determine if this Mn phenotype was progressive over the course of disease, we examined striatal Mn levels at 12 months of age. Unexpectedly, no difference in striatal Mn accumulation between wildtype

and HD mice was observed using the 7 day paradigm. This alteration in Mn accumulation may be related to disease processes, or to changes due to normal aging, or it may be that the Mn transport defect diminishes with disease progression. To examine this in more detail we will measure and image regional brain Mn accumulation using Inductively Coupled Plasma Mass Spectroscopy (ICPMS), laser ablation ICPMS and other novel methods in HD mouse models. In addition, we will examine primary cultured glia and neurons for cell-type differences in the HD-Mn phenotype. Our ultimate goal is to determine whether disease progression influences brain Mn deposition in HD, and if so, what role glia and neurons play in this process. Supported: NIH ES016931, T32 ES007028

**PS 1861 Verification of Manganese-Related Choroid Plexus Differentially Expressed Proteins *In Vitro*.**

G. J. Li, Y. Dong, J. Liu, Y. Liu, H. Jing, C. Zhao and L. Ma. *Institute for Toxicology, Beijing Centers for Disease Control and Prevention, Beijing Research Center for Preventive Medicine, Beijing, China.*

The regulation of brain manganese (Mn) depends largely on the blood-brain barrier and blood-cerebrospinal fluid barrier (BCB). The latter is constituted by choroid plexus (CP) epithelial cells, which is specialized for cerebrospinal fluid (CSF) production, has been considered as a primary target in Mn-induced neurotoxicity. In our previous study, a total of 32 Mn-related differentially expressed proteins were identified by 2D-PAGE combined with Nano-LC-MS/MS in an *in vivo* Mn-toxicity rat model, of which 27 were up-regulated, 5 were down-regulated. This study aims to further verify the 7 selected proteins (PHB1, VDAC,  $\beta$ -actin, HSP70, STIP1, TTR, Vimentin) at transcriptional and translational level respectively in immortalized choroid epithelial Z310 cells *in vitro* under manganese chloride (MnCl<sub>2</sub>) exposure. The expressed level of 7 proteins and their mRNA were detected by Western Blot and Real Time RT-PCR, following MnCl<sub>2</sub> (0, 50, 100, 200  $\mu$ mol/l) exposure for 24h or 12h in Z310 cells. The results demonstrated that PHB1,  $\beta$ -actin and STI1 were up-regulated and TTR was down-regulated at both transcriptional and translational levels as compared to controls, which are in accordant with results in *in vivo* study. Whereas VDAC, HSP70 and Vimentin were down-regulated at both transcriptional and translational levels as compared to controls, which are opposite to the results in *in vivo* study. Taking together, this study validated that Mn toxic effects on PHB1,  $\beta$ -actin, STIP1 and TTR in CP are accurate and reliable, which provide the valuable clue for elucidating the molecular mechanism of Mn toxicity on choroid plexus epithelial cells (partly supported by NSFC Grant in China #81273108, Capital Development Project 2011-1013-03, and Beijing Health Bureau Project-2011. Corresponding author: Guojun J. Li, guojunli88@yahoo.com).

**PS 1862 Expression and Aggregation of a-Synuclein in the Blood-CSF Barrier: New Evidence for the Effects of Toxic Intracellular Manganese and Copper Levels.**

C. A. Bates<sup>1</sup>, X. Fu<sup>1</sup>, D. Ysselstein<sup>2</sup>, J. Rochet<sup>2</sup>, H. Gu<sup>3</sup>, Y. Du<sup>3</sup> and W. Zheng<sup>1</sup>. <sup>1</sup>Health Sciences, Purdue University, West Lafayette, IN; <sup>2</sup>Medicinal Chemistry and Molecular Pharmacology, Purdue University, West Lafayette, IN; <sup>3</sup>Neurology, Indiana University School of Medicine, Indianapolis, IN.

The blood-cerebrospinal fluid barrier (BCB) is responsible for maintaining the homeostasis of a variety of molecules in the brain and cerebrospinal fluid (CSF) including alpha-synuclein (a-Syn). a-Syn plays an integral role in the pathobiology of Parkinson's disease. Little is known about the role of the BCB in the transport and regulation of a-Syn in the brain and CSF. Previous findings in this lab provided evidence that a-Syn was endogenously expressed in our immortalized Z310 choroid epithelial cell model, and 100  $\mu$ M MnCl<sub>2</sub> exposure for 24 and 48 hours induced a-Syn aggregation in these cells. The current studies test the hypothesis that the increased a-Syn aggregation in Z310 cells may result from Mn interacting with a-Syn expression and/or its aggregation. qPCR was used to quantify a-Syn expression in Z310 cells after 100  $\mu$ M MnCl<sub>2</sub> incubation for 24 hr. Our data revealed that Mn treatment did not affect a-Syn mRNA expression in Z310 cells. Using the Thioflavin T fibril aggregation assay, 70  $\mu$ M recombinant a-Syn was incubated with 2 mM MnCl<sub>2</sub> and CuCl<sub>2</sub> for 7 days *in vitro*. a-Syn aggregation increased significantly (530% and 634%, respectively) as compared to controls (n=3, p<0.05). Finally, we found that 24 hr incubation with 50 and 100  $\mu$ M CuCl<sub>2</sub> induced a-Syn aggregation in Z310 cells. These findings support the hypothesis that cellular aggregation of a-Syn in the BCB is facilitated by exposure to heavy metals. More specifically, Mn exposure induces this effect by two pathways: 1) direct interaction with cellular a-Syn within the cell and/or 2) increasing intracellular Cu levels, shown by our data in literature, leading to Cu-accelerated a-Syn aggregation. (Support by NIH/NIEHS ES08146-S2 Minority Supplemental Award)

**PS 1863 Reduced Copper (Cu) Efflux across the Blood-CSF Barrier (BCB) following Manganese Exposure: Effect on Cu Transporters ATP7A and ATP7B.**

X. Fu, Y. Zhang, W. Jiang and W. Zheng. *School of Health Sciences, Purdue University, West Lafayette, IN.*

Increased Cu levels in blood, saliva and brain are found in Mn-exposed animals and humans. However, the underlying mechanism is unknown. ATP7A and ATP7B are Cu-ATPases that function to maintain intracellular Cu homeostasis by exporting excess Cu from the cytosol to extracellular space. This study was designed to test the hypothesis that Mn exposure disrupted the Cu transport across the BCB by interrupting the intracellular trafficking of ATP7A and ATP7B. Rats received ip injections of 6 mg Mn/kg as MnCl<sub>2</sub> or saline, 5 d/wk for 4 wks. Increased Cu and Mn levels in serum and CSF were observed following Mn exposure. An *in situ* ventriculo-cisternal perfusion by infusing [64Cu] and [14C]-sucrose into brain ventricle was conducted to determine Cu clearance by the BCB. Mn exposure significantly increased [64Cu] radioactivity by 2.6 fold in the CSF outflow, as compared to controls, suggesting a reduced Cu removal by the choroid plexus. Confocal images exhibited both Cu-ATPases distributed in perinuclear region in normal plexus tissues and Z310 cells. Incubation of plexus tissues with Mn or Cu caused translocation of ATP7A from the cytosol toward the apical membrane facing the CSF, whereas ATP7B relocated toward the basal membrane facing the blood. Exposing Z310 cells to 100  $\mu$ M MnCl<sub>2</sub> for 24 hr led to a significant decrease in ATP7A and ATP7B fluorescent intensities, which was consistent with their significant mRNA and protein expression reductions in tissue and Z310 cells. The two-chamber Transwell transport studies showed a reduced Cu efflux from the CSF to the blood following Mn exposure or when ATP7A or ATP7B expression were knocked down by siRNA. Collectively, these data suggest that Mn exposure reduces Cu efflux by the BCB which appears to be due to the reduction of ATP7A and ATP7B. A decreased clearance of Cu by Mn exposure may result in the buildup of Cu in the brain. Opposite translocation of ATP7A vs. ATP7B is interesting, yet how this may help interpret a decreased Cu efflux via the BCB remains uncertain. (Supported by NIH/RO1-ES008146)

**PS 1864 Bone Manganese (Mn) Concentrations in Sprague-Dawley Rats following Subchronic Manganese Exposure.**

L. Hong, S. O. Neal, L. Nie and W. Zheng. *Purdue University, West Lafayette, IN.*

Occupational exposure to Mn causes a Parkinson-type disorder called Manganism, a neurodegenerative disease currently without reliable biomarkers for body burden estimation and for pre-symptomatic toxicity assessment. Data in literature suggest that Mn deposited in bone accounts for 43% of total body Mn. The objective of this study was to determine if bone Mn levels were parallel to Mn concentrations in brain regions known to be the targets of Mn toxicity. Groups of rats (6-7 each) received daily dose of 50 mg Mn/kg as MnCl<sub>2</sub> PO for 0, 2, 4, 6, 8 or 10 weeks before tissue dissection. The metal concentrations of Mn, zinc (Zn), iron (Fe), and copper (Cu) in bone tissues, body fluids, brain tissues, as well as other organs were analyzed by atomic absorption spectrophotometry. Following Mn exposure, bone tissues including femur, tibia, humerus and skull bones showed a dose-time-dependent increase in Mn concentrations, with 1.0-1.6  $\mu$ g/g of bone mass at week 10, which were about 2.3-3.6 fold higher than those in controls (-0.4  $\mu$ g/g) at day 0 (p<0.01). A statistically significant relationship exists between bone Mn concentrations and Mn levels in brain tissues such as striatum (r=0.755, p<0.001), hippocampus (r=0.782, p<0.001) and choroid plexus (0.652, p<0.001), and in brain fluid such as cerebrospinal fluid (r=0.720, p<0.001). Interestingly, *in vivo* exposure to Mn also led to significantly increased Fe (152-372%) and Zn (194-230%) concentrations in bone tissues except the skull bones, with no statistically significant effect on bone Cu (58-95%). These results suggest that bone is a significant storage site for body Mn; the good correlation between bone Mn and brain Mn alludes to bone Mn being an internal source of Mn long-term exposure. Further experimentation for noninvasive quantitation of Mn in bone is well warranted for Mn neurotoxicological research. (Supported in part by R21 OH010044, and RO1 ES008146)

Keywords:

Manganese, Manganism, Biomarker, Bone, Correlation, Pharmacokinetics

**PS 1865 Effects of Chronic Manganese Exposure on Cognitive Functioning in Nonhuman Primates.**

J. Schneider<sup>1</sup>, C. Williams<sup>1</sup>, M. Ault<sup>1</sup> and T. R. Guilarte<sup>2</sup>. <sup>1</sup>Thomas Jefferson University, Philadelphia, PA; <sup>2</sup>Columbia University, New York, NY.

Exposure to elevated levels of manganese (Mn) can result in neurological dysfunction in humans including effects on cognitive functioning, particularly those that depend on the integrity of frontal cortex. Our group is performing longitudinal

studies assessing cognitive and motor function consequent to Mn exposure along with measures of in vivo brain chemistry in non-human primates to better define the neurological consequences and molecular mechanisms of chronic Mn exposure. Adult cynomolgus monkeys were trained to perform cognitive tasks including tests of attention (5 choice serial reaction time (5-CRT)), executive functioning (spatial and non-spatial working memory (self-ordered spatial search (SOSS) and delayed matching-to-sample (DMTS)), and visuospatial learning (paired associate learning (PAL)). After these (and other) tasks were learned to criterion (using the monkey CANTAB test system) and performance was stable, animals received Mn (1.66 - 2.5 mg Mn/kg per injection, 2x/wk) or vehicle (2x/wk) with an intended total exposure period of 1.5 yrs. Through 8 mos. of exposure, the PAL task, a sensitive index of mild cognitive impairment (MCI) in humans, showed consistent deficits beginning in the second mo. of Mn exposure. Deficits in SOSS and DMTS performance became obvious at 4 and 6 mos. of Mn exposure and attentional impairments, suggested by increased reaction times in the 5-CRT task, were observed consistently at approx. mo. 5. Over the same period of time, performance of the control group either did not change significantly or in some instances, improved. These data show that using a sensitive cognitive assessment battery based on monkey versions of human neuropsychological tests, deficits in several cognitive domains are associated with Mn exposure and in particular, Mn disrupts performance of the PAL task, highly sensitive to detecting early Alzheimer's disease and MCI, and in particular, disrupts frontal-related functions. Supported by NIH RO1 ES010975.

**PS 1866 Neurochemical Alterations in the Nonhuman Primate Brain during Chronic Exposure to Manganese: A 1H MRS Study.**

S. Dharmadhikari<sup>1,2</sup>, J. L. McGlothlan<sup>3</sup>, R. Edden<sup>4,5</sup>, P. Barker<sup>4,5</sup>, J. Schneider<sup>6</sup>, U. Dydak<sup>1,2</sup> and T. R. Guilarte<sup>3</sup>. <sup>1</sup>*School of Health Sciences, Purdue University, W Lafayette, IN;* <sup>2</sup>*Department of Radiology, Indiana University School of Medicine, Indianapolis, IN;* <sup>3</sup>*Department of Environmental Health Sciences, Columbia University Mailman School of Public Health, New York, NY;* <sup>4</sup>*Russell H. Morgan Department of Radiology and Radiological Science, Johns Hopkins University, Baltimore, MD;* <sup>5</sup>*F.M. Kirby Center for Functional Brain Imaging, Kennedy Krieger Institute, Baltimore, MD;* <sup>6</sup>*Department of Pathology, Anatomy and Cell Biology, Thomas Jefferson University, Philadelphia, PA.*

Alterations in brain chemistry upon chronic manganese (Mn) exposure can be studied non-invasively using 1H Magnetic Resonance Spectroscopy (MRS). In this longitudinal Mn exposure study, 1H MRS was used for the detection of brain metabolite changes that are associated with chronic Mn exposure in non-human primates. A total of 7 adult male cynomolgus monkeys underwent MRS on a 3 T Philips Achieva MRI scanner before Mn exposure and after 8 months of Mn exposure (n=3, 1.66-2.5 mg Mn/kg per injection, 2x/wk). Short echo-time PRESS single voxel MRS data was obtained from frontal cortex (FC), parietal cortex (PC), thalamus, and putamen, and gamma-aminobutyric acid (GABA)-edited MRS data was obtained from FC and striatum using MEGA-PRESS. The quantification of metabolites including N-Acetyl-aspartate (NAA), Glutamate (Glu), Glutamine (Gln), mI (myo-Inositol), total creatine (tCr), choline (tCho) and GABA was done using LCModel. A significant decrease in NAA/tCr (p=0.035) and mI/tCr (p=0.013) and a significant increase in Glu+Gln (p=0.03) from baseline was measured in the PC. The thalamus showed a significant increase in tCr (p=0.041) and a significant decrease in mI/H<sub>2</sub>O (p=0.022). No significant changes were measured in any metabolites in the FC and in GABA levels in any region. The significant differences in major metabolites are quite robust despite the small number of animals and changes in NAA/tCr in the PC are in agreement with our previously published results (Guilarte et al., Toxicol Sci 94: 351-358, 2006). (Supported by NIH ES010975)

**PS 1867 What Is the Mechanistic Evidence for Trichloroethylene As a Cause of Parkinson's Disease?**

D. G. Dodge<sup>1</sup> and B. D. Beck<sup>2</sup>. <sup>1</sup>*Gradient, Bend, OR;* <sup>2</sup>*Gradient, Cambridge, MA.*

Parkinson's Disease (PD) is a type of movement disorder characterized pathologically, in part, by the progressive and selective loss of dopaminergic neuron cell bodies within the substantia nigra pars compacta (SNpc) and associated deficiency of the neurotransmitter dopamine in the striatum. Mitochondrial dysfunction (i.e., Complex I inhibition), oxidative stress, and abnormal protein aggregation (with intracellular  $\alpha$ -synuclein accumulation) have been strongly implicated in PD pathology. A number of recent papers have suggested a causal role for trichloroethylene (TCE) in PD, either directly or via its role in the endogenous formation of 1-trichloromethyl-1,2,3,4-tetrahydro- $\beta$ -carboline (i.e., the TaClo hypothesis). We assess, from a toxicological perspective, the evidence for TCE as a cause or substantial

contributor to PD in humans. With regard to the TaClo hypothesis, in vitro studies in a number of different cell systems have provided evidence that TaClo causes changes in mitochondria and dopaminergic neurons but is not preferentially selective towards dopaminergic cells. In vivo studies in rats have shown that high doses of TaClo injected directly into the brain cause only modest decreases in dopamine neurons; intraperitoneal (i.p.) administration of TaClo was not selective towards dopaminergic neurons; and i.p. and oral exposure of TaClo caused locomotor changes that were not consistent in direction or with dose. Furthermore, there is no experimental or credible human evidence that TaClo is formed in vivo after exposure to TCE. In animal studies conducted to evaluate TCE directly as a potential cause of PD, relatively high i.p. or oral doses have resulted in findings that are both consistent and inconsistent with mechanistic and motor effects thought to be important in PD. Compared to other well-developed models of PD, the TCE model is poorly characterized. Overall, we conclude that TCE as a causal factor in PD has not been demonstrated and remains speculative.

**PS 1868 Neuroprotective Efficacy and Pharmacokinetics of Novel Para-Phenyl Substituted Diindolylmethanes in a Model of Parkinson's Disease.**

B. Trout<sup>1</sup>, J. A. Miller<sup>1</sup>, R. Hansen<sup>1</sup>, S. H. Safe<sup>2</sup>, D. Gustafson<sup>1</sup> and R. B. Tjalkens<sup>1</sup>. <sup>1</sup>*Center of Environmental Medicine, Environmental Radiological and Health Science, Colorado State University, Fort Collins, CO;* <sup>2</sup>*Center for Environmental and Genetic Medicine, Institute of Biosciences and Technology, Texas A&M Health Science Center, Houston, TX.*

There are no approved therapeutics that block the chronic inflammatory component of neurodegenerative diseases such as Parkinson's. This is partly because of poor distribution to the central nervous system for compounds with demonstrated efficacy in vitro. This study examined selected para-phenyl substituted diindolylmethane (C-DIM) compounds, which we previously demonstrated to be effective at decreasing glial-derived inflammatory gene expression in vitro. We postulated that the pharmacokinetic properties of C-DIM compounds would positively correlate with neuroprotective efficacy in a progressive model of Parkinson's disease (PD) in vivo. Pharmacokinetics and metabolism of 1,1-bis(3'-indolyl)-1-(p-methoxyphenyl)methane (C-DIM5), 1,1-bis(3'-indolyl)-1-(p-hydroxyphenyl)methane (C-DIM8), and 1,1-bis(3'-indolyl)-1-(p-chlorophenyl)methane (C-DIM12) were determined in plasma and brain of C57Bl/6 mice. Intravenous (1 mg/kg) and oral (10 mg/kg) doses were given to determine the optimal route of administration and putative metabolites were measured in plasma, liver, and urine. Oral dosage of C-DIM compounds displayed greater AUC, C<sub>max</sub>, and T<sub>max</sub> levels than intravenous administration. C-DIM12 exhibited distinguished pharmacokinetics of the selected C-DIMs, with an oral bioavailability of 42% in comparison of C-DIM8 (6%). Following pharmacokinetic studies, efficacy of C-DIM5, C-DIM8, and C-DIM12 (50 mg/kg, oral gavage) was established using a progressive, neuroinflammatory PD model employing MPTP and probenecid (MPTPp) over a period of 14 days. By first creating a lesion in the region of the brain affected in PD (substantia nigra) and then treating with anti-inflammatory C-DIMs, we determined that C-DIM5 and C-DIM12 demonstrated the greatest efficacy in attenuating the progressive loss of dopamine neurons.

**PS 1869 Neurotoxicity Study of Lipopolysaccharide (LPS) Induced Mouse Model of Parkinson's Disease.**

Z. Nan<sup>1</sup>, W. Wang<sup>2</sup> and W. Low<sup>1</sup>. <sup>1</sup>*Neurosurgery, University of Minnesota, Minneapolis, MN;* <sup>2</sup>*Global Regulatory, HB Fuller, St. Paul, MN.*

Parkinson's disease (PD) is a debilitating neurodegenerative disease characterized by gradual and progressive loss of dopaminergic (DA) neurons in substantia nigra pars compacta (SNc). 95% of PD may be attributed to multi-variant etiology; among them, inflammation is getting more attention. Current understanding is that inflammation in the central nervous system can produce large amount of pro-inflammatory factors such as tumor necrosis factor  $\alpha$ , interleukin-1 $\beta$ , interleukin-6, proteinases, and glial activation; the subsequent interaction among these factors and host cells leads to progressive death of dopaminergic neurons in SNc, resulting in PD. Lipopolysaccharide (LPS) is an endotoxin derived from gram-negative bacteria and is widely used as an inflammation inducer. In this preliminary study, we wanted to know what dose level of LPS can effectively induce PD in C57Bl/6 mice by direct brain injection at the SNc site. Six groups of mice were injected with low dose LPS (200 microgram/Kg), high dose LPS (400microgram/Kg) and normal saline as control, respectively, into one side of the SNc site or the target it projects to (striatum of the same side). The surviving DA neurons in the SNc site were shown and counted by immunohistochemistry method using rabbit anti-tyrosine

hydroxylase and visualized by diaminobenzidine staining at 1st and 3rd week after injection. We compared the number of surviving DA neurons at SNc with DA neurons at SNc on the contralateral side. We found significant loss of DA neurons at SNc in both injection sites of SNc and striatum in the high dose groups at 1st and 3rd week. No significant loss of DA neurons was observed in the low dose and the control groups. We concluded that LPS at the dose level of 400microgram/kg can effectively and rapidly induce PD in C57Bl/6 mice through direct brain injection, and the pathological change resembles the neurodegenerative characteristics found in PD. The dose response relationship and the pro-inflammatory characteristics associated with the DA neuron loss may need further investigation.

## PS 1870 Neuroinflammation and Microglial Dysfunction.

M. Entezari<sup>1</sup> and M. Javdan<sup>2</sup>. <sup>1</sup>Natural Sciences, LaGuardia Community College, Long Island City, NY; <sup>2</sup>Biological Sciences and Geology, Queensborough Community College, Bayside, NY.

Neuro-inflammation and accumulation of A $\beta$ -containing amyloid plaques are critical components in the pathogenesis of Alzheimer's disease (AD). Microglia are the brain tissue macrophages that play critical roles in the inflammatory aspects of AD by releasing proinflammatory cytokines. Activated microglia are also able to migrate to the sites of A $\beta$  deposition and eliminate A $\beta$  by phagocytosis. Thus, the impairment of microglia migration and A $\beta$  phagocytosis appear to be closely involved in the progression of AD. The underlying molecular mechanisms responsible for disease progression are still unclear. Previously we have shown that elevated levels of high-mobility group box 1 (HMGB1), a ubiquitous DNA binding protein that promotes inflammatory tissue injury impairs the peritoneal macrophages' functions. Therefore, we hypothesized that HMGB1 contributes to microglial dysfunction in neuro-inflammation. In this study we demonstrate that HMGB1 levels were significantly elevated in the extracellular space of cultured BV2 macroglia cells 24 hours after exposure to 1  $\mu$ g/ml Lipopolysaccharide (LPS) compare to untreated control cells. Exposure to 1  $\mu$ g/ml LPS also resulted in significant suppression of microglia's ability to migrate and to phagocytose. Simultaneous treatment of BV2 cells with LPS and anti-HMGB1 antibody significantly improved the migration and phagocytic ability of these cells. Moreover, treating BV2 cells with recombinant HMGB1 not only induced impairment in migration and phagocytosis but also accompanied by the expression of Toll-like receptor 4 (TLR4) on these cells. These results suggest that activation of the LPS-induced HMGB1/TLR4 signaling pathway contributes to the microglia dysfunction. Thus, inhibiting of HMGB1 may provide a therapeutic target for enhancing of microglia's ability to migrate and phagocytose in AD.

## PS 1871 Translocator Protein 18 KDa (TSPO) in Sandhoff Disease: An Update on a Preclinical Biomarker of Neurodegeneration.

M. Loth<sup>1</sup>, J. Choi<sup>1</sup>, J. L. McGlothlan<sup>1</sup>, H. Wang<sup>2</sup>, M. Pomper<sup>2</sup> and T. R. Guilarte<sup>1</sup>. <sup>1</sup>EHS, Columbia University, NYC, NY; <sup>2</sup>Radiology, Johns Hopkins University, Baltimore, MD.

Translocator protein 18 kDa (TSPO) is extensively used as a biomarker of active brain disease and neuroinflammation (Chen & Guilarte, Pharm Ther 118: 1-17, 2008). Sandhoff disease, which is clinically similar to Tay-Sachs's disease, is a neurodegenerative condition in which a deficiency in the enzyme lysosomal  $\beta$ -hexosaminidase leads to accumulation of gangliosides and glycolipids in the brain, resulting in progressive and widespread neurodegeneration. We previously reported the longitudinal expression of TSPO in a mouse model of Sandhoff disease at the later stages of the disease (2 and 3 months). Now we report TSPO expression at early disease time points (1 and 1.5 months) in order to assess the temporal expression of TSPO and its relationship to behavioral and neuropathological endpoints. Using TSPO quantitative autoradiography with the TSPO specific ligands [125I]iodo-DPA-713 and [3H]-DPA-713, we show that TSPO levels are increased as early as 1 month in relevant brain regions concurrent with behavioral expression of disease. We also demonstrate that the temporal increase in TSPO levels is associated with ongoing neurodegenerative changes and activation of microglia and astrocytes using silver staining (marker of active degeneration) and immunohistochemistry of Mac-1 (microglia) and GFAP (astrocytes). Triple labeled immunofluorescent confocal imaging confirmed that TSPO colocalized with microglial markers as well as with the gp91phox subunit of NADPH oxidase at an age when brain tissue is undergoing neurodegeneration. These results further strengthen the evidence that TSPO can be used as an early and sensitive preclinical biomarker of brain injury and inflammation [Supported by NIEHS grant ES007062 to TRG].

## PS 1872 Characterization of Mice with Overexpression of the Vesicular Monoamine Transporter 2 (VMAT2; Slc18a2).

K. Lohr<sup>1</sup>, A. I. Bernstein<sup>1</sup>, T. Guillot<sup>1</sup>, K. Stout<sup>1</sup>, E. Heath<sup>1</sup>, M. Wang<sup>1</sup>, Y. Li<sup>1</sup>, A. Salahpour<sup>2</sup> and G. W. Miller<sup>1</sup>. <sup>1</sup>Environmental Health, Emory University, Atlanta, GA; <sup>2</sup>University of Toronto, Toronto, ON, Canada.

The vesicular monoamine transporter 2 (VMAT2) is responsible for packaging monoamines for rapid release at neuronal synapses. VMAT2 is also responsible for sequestering toxicants away from their sites of action in the cell. Despite previous evidence suggesting that decreased levels of VMAT2 can contribute to cellular dysfunction, it was not known if an increase in VMAT2 protein would result in increased function in vivo. We generated C57BL6 BAC transgenic mice with increased VMAT2 expression to determine the effects of increased vesicular monoamine filling on associated neurochemical and behavioral outcomes. Our VMAT2-HI mice show robust VMAT2 overexpression, proper localization of VMAT2, increased whole brain synaptic vesicle [3H]-dopamine uptake, and a measurable behavioral phenotype. These data show the effects of elevated VMAT2 levels on neurochemistry and behavior, suggesting that increased vesicular dopamine storage mediated by increased VMAT2 levels can alter the neurochemical and behavioral output of the monoaminergic system. Finally, as VMAT2 acts as a neuroprotective mechanism in monoaminergic neurons, these VMAT2-HI mice serve as a valuable tool to investigate resistance to toxicant exposure.

## PS 1873 Background Survival of Transgenic Mouse Models of Alzheimer's Disease in Our Laboratories.

J. Douville and C. Copeman. Charles River, Montréal, QC, Canada. Sponsor: M. Vézina.

Transgenic mouse models of Alzheimer's disease are of great value for evaluating efficacy and/or toxicology of drug therapies. These models typically present hallmarks of the disease between 12 and 20 months of age; however, age-related attrition represents a challenging issue that may impair the statistical significance of the data generated. We present survival data of three different transgenic Alzheimer mouse models when housed under our optimized laboratory conditions. The homozygous strain of PDAPP mouse (STOCK-TgN(APP)<V717F> (line number 6042M)) showed mortality rates of 13 (males) and 21% (females), between the ages of 7 to 12 months and of 70 (males) and 60% (females), between the ages of 12 to 21 months. Heterozygous PDAPP mice (STOCK-TgN(APP)<V717F> (line number 6042T)) showed greater survival with only 6.4 and 16.8% mortality for males and females, respectively at 14 to 20 months of age and 16% and 42% mortality for males and females, respectively, between 20 to 26 months of age. Young Tg2576 mice (B6; SJL-Tg (APPswe) 2576Kha) presented a survival rate comparable to wild type mice with 100 and 90% survivors between the ages of 9 and 14 weeks. When survival is calculated for older Tg2576 mice, 79 and 75 % of males and females, respectively, survive over the age of 13 to 22 months. As the survival rates vary between the different strains and the age-related attrition is relatively high, consideration for increased population should be given accordingly in study designs using these transgenic mouse models.

## PS 1874 Oxidative Damage and Age-Related Alterations in Kainic Acid-Induced Excitotoxicity.

R. C. Gupta<sup>1</sup>, S. Zaja-Milatovic<sup>2</sup> and D. Milatovic<sup>3</sup>. <sup>1</sup>Toxicology, Murray State University, Hopkinsville, KY; <sup>2</sup>University of Virginia, Charlottesville, VA; <sup>3</sup>Vanderbilt University Medical Center, Nashville, TN.

Recent research findings in brain have highlighted increased excitatory stimulation as a contributor to aging as well as neuronal damage that accompanies multiple neurodegenerative diseases. Findings from patients and animal models have widely supported the hypothesis that neuronal oxidative/nitrosative damage is a major effector contributing to neurodegeneration. Therefore, the present study investigated antioxidative and neuroprotective effects of the antioxidant vitamin E ( $\alpha$ -tocopherol) and the NMDA receptor antagonist memantine in age-related excitotoxicity induced by kainic acid (KA). Mice exposed to KA (1 nmol/5  $\mu$ l, icv) showed significant increases in cerebral oxidative biomarker F2-isoprostanes (F2-IsoPs, 158%) and nitrosative biomarker citrulline (249%) formation when determined at 30 min after exposure. At the same time, pyramidal neurons in the hippocampus of young and old mice showed significant reductions in dendritic length (60%) and spine density (40%) compared to controls (100%). Pretreatment with vitamin E (100 mg/kg, ip/day for 3 days) and memantine (5 mg/kg, ip, but not 1 mg/kg) attenuated the KA-induced increases in cerebral F2-IsoPs and citrulline and decrease in

spine density of hippocampal pyramidal neurons in young mice. However, vitamin E (100 mg/kg, ip/day for 3 days) and memantine (5 mg/kg, ip) were not effective in suppressing KA-induced oxidative stress and a decrease in the dendritic length of hippocampal pyramidal neurons in aged mice. These data strongly suggest that different mechanisms are involved in cerebral neuroprotection of aged mice compared to young mice. Elucidation of these mechanistic changes has important clinical implications for therapeutic strategies in both normal aging and neurodegenerative disease.

## PS 1875 Rapid Immunoassay Development and Evaluation of ICAM-1 and E-Selectin As Potential Biomarkers of Vascular Injury in Rats.

M. J. Cameron<sup>1</sup>, H. W. Smith<sup>2</sup>, J. L. Weaver<sup>4</sup>, N. King<sup>5</sup>, N. Vansell<sup>3</sup> and B. E. Enerson<sup>3</sup>. <sup>1</sup>Immunology, MPI Research, Mattawan, MI; <sup>2</sup>Investigative Toxicology, Eli Lilly and Company, Indianapolis, IN; <sup>3</sup>Drug Safety Research and Development, Pfizer Inc, Groton, CT; <sup>4</sup>DDSR/OTR/OPS/CDER, FDA, Silver Spring, MD; <sup>5</sup>Predictive Safety Testing Consortium, Critical Path Institute, Tucson, AZ.

To qualify biomarkers of vascular injury in support of the Predictive Safety Testing Consortium's (PSTC) Vascular Injury Working Group (VIWG) we developed biomarker immunoassays on the Gyros platform for rat ICAM-1 and E-Selectin using a fit-for-purpose approach. ICAM-1 (Intercellular Adhesion Molecule 1), also known as CD54, is a cell surface glycoprotein typically expressed on endothelial cells. E-Selectin, also known as CD62 and endothelial leukocyte adhesion molecule 1, is typically expressed on activated endothelial cells. The assays were developed using commercially sourced reagents. Rats (n=5/group) were treated with either 60 mg/kg of CI-1044 (oral gavage) or 100 mg/kg of fenoldopam (subcutaneous). Both drugs are known to cause vascular injury. Samples were taken at 4, 8, 16, 24, 48, 72 hours and recovery for CI-1044 and at 0.5, 2, 6, 24, 72 hours and recovery for fenoldopam and serum was evaluated for levels of ICAM-1 and E-Selectin. Histopathologic examination indicated vascular lesions were present from the CI-1044 rats starting at 16 hours post dose consisting of perivascular inflammation of the mesenteric arteries and progressing to fibrinoid necrosis at later time points. The mesenteric vascular lesions in fenoldopam-treated rats consisted of arterial necrosis/apoptosis observed at 24 hours post dose, followed by perivascular inflammation and fibrinoid necrosis at later time points. There was no significant change noted in the circulating levels of ICAM-1 in CI-1044 or fenoldopam treatment groups. There was a significant decrease in serum E-Selectin levels in both CI-1044 and fenoldopam treated groups after 48 hours. E-Selectin has the potential to become a valuable biomarker in the evaluation of vascular injury for preclinical drug safety studies.

## PS 1876 Synthesis and Characterization of PEG-Ylated Meso-Porphyrins for Targeting the Epidermal Growth Factor Receptor in CRC.

R. J. Ledet<sup>1</sup>, K. R. Fontenot<sup>2</sup> and G. H. Vicente<sup>2</sup>. <sup>1</sup>Chemistry and Biology, Southern University and A&M College, Baton Rouge, LA; <sup>2</sup>Chemistry, Louisiana State University and A&M College, Baton Rouge, LA. Sponsor: W. Gray.

This project introduces a novel macrocycle conjugated to polyethylene glycol linker, which we hypothesize will serve as the template for a selective molecule with high fluorescence yields that greatly increases earlier detection of CRC by utilizing the EGFR as a biomarker. Our targeted remedy is a porphyrin that is conjugated to a peptide with an affinity for the Epidermal Growth Factor Receptor (EGFR). Porphyrins are characteristically aromatically stable, contain trademark absorption bands in the visible and near-IR range, and have fluorescence quantum yields much above the current fluorophores. This makes the macrocycle optimal for confocal laser endomicroscopy (CLE) agent production. Consequently, we use a polyethylene glycol linker in order to increase water solubility, retain low toxicity, and to achieve high fluorescence quantum yields, as well as high conjugation yields. In this research, we were able to produce both precursors to the porphyrin-peptide conjugate, MesoPOR-(mono)-3PEG and MesoPOR-(di)-3PEG. These molecules were synthesized successfully with the use of peptide conjugation mechanisms. Molecular weights were confirmed using Matrix Assisted Laser Desorption Ionization Mass Spectrometry (MALDI-MS). Characterization was performed using <sup>1</sup>H Nuclear Magnetic Resonance (<sup>1</sup>H-NMR) and Ultraviolet-Visible Spectroscopy (UV-Vis) of the intended molecules. The synthesized molecules, MesoPOR-(mono) 3PEG and MesoPOR-(di) 3PEG, will be useful in peptide conjugation that targets EGFR. These peptide ligands will increase selectivity and detect CRC via CLE.

## PS 1877 Multiplex Analysis of Urinary Protein Biomarkers for the Detection of Vancomycin Induced Sub-Acute Nephrotoxicity.

W. Zheng<sup>1</sup>, T. C. Fuchs<sup>2</sup>, I. Yoon<sup>1</sup>, D. Droll<sup>1</sup>, X. Qiang<sup>1</sup> and P. Hewitt<sup>2</sup>. <sup>1</sup>R&D, EMD Millipore, St. Charles, MO; <sup>2</sup>Non-Clinical Safety R&D, Merck Serono, Darmstadt, Germany.

In pharmaceutical and chemical industries the kidney is routinely assessed during preclinical safety evaluations. The importance of the kidney as a central detoxification organ leads to a high exposure of renal tissue to drugs, reactive metabolites or environmental compounds. Traditional markers for assessing renal toxicity, such as blood urea nitrogen (BUN) and serum creatinine (SCR), are insensitive. Although both are direct measurements of renal function, increases in serum concentrations of these biomarkers occur only after substantial renal injury. For improved detection of acute nephrotoxicity a panel of novel urinary kidney biomarkers has been approved by the FDA, EMA and PMDA. However, limited data regarding the performance of these acute markers after sub-acute or sub-chronic treatment are publicly available. To increase the applicability of these markers, it is important to evaluate the ability to detect these markers after 28 days or even longer. In this study, Wistar rats were treated with three doses of Vancomycin to induce renal damage and studied for 28 days. Urine was collected under cooled conditions on an 18-hour cycle on days 4, 8, 15 and 29. Luminex® xMAP® based MILLI-PLEX® Rat Kidney Toxicity Magnetic Bead Assays were used to measure 14 candidate protein biomarkers simultaneously from the urine samples. Vancomycin treatment resulted in a dose-dependent increase in urinary biomarkers, specific for the observed areas within the nephron, determined histopathologically. Several biomarkers were found promising in this study, which includes NGAL, Cystatin C, KIM-1, Osteopontin, Clusterin and Albumin. The simultaneous measurement of these proteins with multiplex technology offered a robust and convenient method to study these biomarkers. Taken together, our data demonstrate the high accuracy and predictivity of some of these new markers to detect sub-acute treatment with one well described nephrotoxin, Vancomycin.

## PS 1878 Association of the Cumulative Body Burden of Estrogen-3, 4-Quinone with Body Mass Index and Breast Cancer Risk Using Albumin Adducts As Biomarkers.

P. Lin<sup>1</sup>, D. Chen<sup>2</sup>, C. Lin<sup>1,2</sup>, W. Hsieh<sup>3</sup>, W. Yu<sup>3</sup>, C. Lin<sup>1</sup>, M. Go<sup>1</sup> and C. Juan<sup>1</sup>. <sup>1</sup>Environmental Engineering, National Chung Hsing University, Taichung, Taiwan; <sup>2</sup>Comprehensive Breast Cancer Center, Changhua Christian Hospital, Changhua, Taiwan; <sup>3</sup>Department of Laboratory Medicine, Da-Chien General Hospital, Miaoli, Taiwan.

Both 17 $\beta$ -estradiol-2,3-quinone (E2-2,3-Q) and 17 $\beta$ -estradiol-3,4-quinone (E2-3,4-Q) are reactive metabolites of estrogen. Elevation of E2-3,4-Q to E2-2,3-Q ratio is thought to be an important indicator of estrogen-induced carcinogenesis. Our current study compared the cumulative body burden of these estrogen quinones in serum samples taken from Taiwanese women with breast cancer (n=152) vs healthy controls (n=140) by using albumin (Alb) adducts as biomarkers. Results clearly demonstrated the presence of cysteinyl adducts of E2-2,3-Q-4-S-Alb and E2-3,4-Q-2-S-Alb in all study population at levels ranging from 61.7-1330 and 66.6-1590 pmol/g, respectively. Correlation coefficient between E2-2,3-Q-4-S-Alb and E2-3,4-Q-2-S-Alb was 0.610 for controls and 0.767 for breast cancer patients (p<0.001). We also noticed that in subjects under age 50 with body mass index (BMI) less than 27, background levels of E2-3,4-Q-2-S-Alb was inversely proportional to BMI with about 25% increase in E2-3,4-Q-2-S-Alb per 5 kg/m<sup>2</sup> decrease in BMI (p<0.001). In addition, we confirmed that mean levels of E2-3,4-Q-2-S-Alb in breast cancer patients were ~5 fold greater than in those of controls (p<0.001). Overall, this evidence suggests that disparity in estrogen disposition and the subsequent elevation of cumulative body burden of E2-3,4-Q may play a role in the development of breast cancer. (This work was supported by the National Science Council, Taiwan, through Grants NSC99-2314-B-005-001-MY3)

## PS 1879 Biomarker-Based Evaluation of Diesel Exhaust Emissions from 2007-Compliant Engines in Rats and Mice Exposed for Defined Time Periods.

L. M. Hallberg<sup>1</sup>, J. L. Parks<sup>1</sup>, C. M. Norton<sup>2</sup>, C. Hernandez<sup>1</sup>, J. B. Ward<sup>1</sup>, B. T. Ameredes<sup>1</sup> and J. K. Wickliffe<sup>2</sup>. <sup>1</sup>University of Texas Medical Branch, Galveston, TX; <sup>2</sup>Tulane University Health Sciences Center, New Orleans, LA.

In 2001 the USEPA adopted new air quality standards for diesel fuels and emissions; the health impact was not established. Diesel exhaust (DE) is associated with adverse health effects, including cardiovascular, lung cancer, and neurological

deficits. Proposed mechanisms include damage to DNA and lipids through exposure to reactive oxygen, toxic DE particulates, and inflammation. Our objective is to determine if engineering changes in 2007 diesel engines significantly reduces DNA and lipid damage.

To determine the extent of oxidative and genotoxic damage caused by inhaled DE, biomarkers of lipid peroxidation (LP) and DNA damage were employed being assessed by the Comet assay (DNA damage), serum levels of 8-OHdG, and LP.

In rats (1 month exposure), no significant differences (NSD) were noted by Comet assay (exposure level vs air control  $p < 0.53$  Low(L), 0.92 Mid(M), 0.77 High(H) nor were there gender effects in either tail moment (TM) or tail length (TL) ( $p < 0.59$  L, 0.90 M, 0.42 H, 0.16 gender effects). After 3 months exposure, NSD were noted in TM or TL in rats. NSD in mice (1 month,  $p < 0.56$  L, 0.20 M, 0.61 H, 0.79 gender effects) in TM or TL ( $p < 0.60$  L, 0.21 M, 0.63 H, 0.73 gender effects). After 3 months, NSD in TM or TL ( $p < 0.15$ ,  $p < 0.16$ ) nor gender were observed.

In serum (8-OHdG ELISA) NSD were observed in rats ( $p < 0.86$ ) or mice ( $p < 0.46$ ) among 1 and 3 month groups. In rodent hippocampus (L P-T-Bars assay), significant differences were observed in rats between L and M groups ( $p < 0.02$ ) but NSD among other groups. NSD were observed among mice ( $p < 0.92$ ) treatment groups. In mouse, 1 month was significantly higher than 3 months ( $p < 0.01$ ).

In conclusion, NSD was evident comparing air controls to 3 treatment groups. Based on the endpoints evaluated, we conclude that 2007-compliant engines did not produce any significant, persistent, oxidatively-induced DNA damage (lung) or exposure-dependent lipid peroxidation in (hippocampus) from these exposures.

## PS 1880 Investigation of Early Biomarkers of Doxorubicin (DOX)-Induced Cardiac Tissue Injury in B6C3F1 Mice.

V. Desai<sup>1</sup>, E. Herman<sup>2</sup>, C. Moland<sup>1</sup>, S. Lewis<sup>3</sup>, K. Davis<sup>4</sup>, N. George<sup>5</sup>, S. Kerr<sup>6</sup> and J. C. Fuscoe<sup>1</sup>. <sup>1</sup>Division of Systems Biology, NCTR, US FDA, Jefferson, AR; <sup>2</sup>Division of Applied Pharmacology Research, CDER, US FDA, Silver Spring, MD; <sup>3</sup>Division of Scientific Coordination, NCTR, US FDA, Jefferson, AR; <sup>4</sup>Toxicologic Pathology Associates, NCTR, US FDA, Jefferson, AR; <sup>5</sup>Division of Bioinformatics and Biostatistics, NCTR, US FDA, Jefferson, AR; <sup>6</sup>Arkansas Heart Hospital, Little Rock, AR.

Cardiac troponins (cTn) are widely used as biomarkers for assessing cardiac injury in preclinical and clinic testing. Here we report a study that was designed to identify early biomarkers of cardiac injury in male B6C3F1 mice. Mice were treated weekly for 2, 3, 4, 6, and 8 weeks with (a) 3 mg/kg DOX given intravenous (i.v.) via tail vein, resulting in cumulative doses of 6, 9, 12, 18, and 24 mg/kg, respectively, (b) an equivalent volume of saline (SAL) given i.v. via tail vein, (c-d) 60 mg/kg dexrazoxane (DXZ), a cardioprotective drug, given intraperitoneal (i.p.) 30 min before i.v. injection of DOX or SAL, and (e) SAL given i.p. 30 min before i.v. injection of SAL. At necropsy, which was performed a week after the last dose, blood samples were collected for measurements of cTnT and hematological parameters. Also, hearts were collected for evaluations by light and electron microscopy, genomics, proteomics, and metabolomics. Preliminary results showed a release of cTnT in plasma in 8% of mice at 6 mg/kg, 17% of mice at 9 and 12 mg/kg, and 92% of mice at 18 and 24 mg/kg cumulative DOX doses, indicating a dose-related increase in cardiac injury. Plasma cTnT levels were also elevated in 16%, 58%, and 55% of mice treated with DXZ+DOX for 3, 6, and 8 weeks, respectively. Microscopic examination of hearts revealed the presence of cardiac lesions only in mice exposed to 24 mg/kg cumulative DOX dose, suggesting that DXZ provided cardioprotection against irreversible damage. The presence of histological damage in the heart of only mice exposed to the highest cumulative DOX dose yet some elevation in cTnT at lower cumulative DOX doses suggests that our ongoing evaluation of molecular changes may reveal more sensitive biomarkers of cardiac injury.

## PS 1881 Investigation on Plasma Bile Acids As Biomarkers of Cholestasis Induced by Bsep Inhibition in Preclinical Animals.

M. Miyake<sup>1</sup>, T. Shimizu<sup>1</sup>, M. Kobayashi<sup>1</sup>, M. Yamazaki<sup>2</sup>, H. Satou<sup>1</sup>, T. Honda<sup>1</sup>, T. Tomari<sup>1</sup> and N. Masutomi<sup>1</sup>. <sup>1</sup>Safety Research Laboratories, Research Division, Mitsubishi Tanabe Pharma Corporation, Chiba, Japan; <sup>2</sup>Advanced Medical Research Laboratories, Research Division, Mitsubishi Tanabe Pharma Corporation, Saitama, Japan. Sponsor: J. Sugimoto.

[Purpose] The bile salt export pump (BSEP) is a bile acid efflux transporter, the inhibition of which has been proposed to play a role in drug-induced cholestasis. However, there are no known biomarkers (BMs) to detect BSEP inhibition. We previously performed metabolomics analyses on rat plasma treated with cyclosporin A, a well-known BSEP inhibitor, and found that plasma bile acids (PBA) could be BMs for BSEP inhibition. To further evaluate the usefulness of PBA, we characterized the specificity and time-course changes of PBA in rats and dogs. [Methods and

Results] PBA were measured by LC/MS in rats dosed rifampicin (a BSEP inhibitor), methapyriline (a hepatocellular toxicant), 2,3,5,6-tetramethyl-1,4-phenylenediamine (a muscular toxicant) and dexamethasone (a hepatic glyconeogenesis inducer). Increase of cholic acid and taurocholic acid, accompanied by decrease of glycocholic acid and chenodeoxycholic acid were specific to rifampicin treatment, confirming the reproducibility of the previous analyses. Next, single dosing studies were conducted in rats and dogs to investigate the time-course changes of PBA. In rats, PBA were increased maximally at 6-9 hrs after cyclosporin A dosing and tended to return to the normal level at 24 hrs after dosing, which corresponded to the toxicokinetics of cyclosporin A. On the other hand, PBA were detected only after feeding in untreated dogs, and rifampicin intensified the rise in PBA concentration induced by meal. [Conclusion] The results show that PBA can be specific BMs of BSEP inhibition in preclinical animals. Since PBA showed time-course changes associated with plasma drug concentrations and were also affected by meal in dogs, plasma sampling time point would be critical to evaluate changes in PBA induced by BSEP inhibition.

## PS 1882 Kidney Injury Biomarkers Lipocalin-2, Clusterin and Albumin, but Not Kidney Injury Molecule 1, Are More Sensitive Than Traditional Markers of Gentamicin-Induced Kidney Injury in Beagles.

M. Wagoner<sup>1</sup>, L. Cheatham<sup>1</sup>, D. Eisinger<sup>2</sup>, E. Sace<sup>3</sup>, K. M. Lynch<sup>4</sup>, J. McDuffie<sup>5</sup>, M. Sonce<sup>5</sup>, K. Marshall<sup>2</sup>, M. Damour<sup>2</sup>, L. Stephen<sup>1</sup>, Y. P. Dragan<sup>1</sup>, J. Fikes<sup>1</sup> and L. B. Kinter<sup>1</sup>. <sup>1</sup>Safety Assessment, AstraZeneca Pharmaceuticals, Waltham, MA; <sup>2</sup>Myriad RBM, Saranac Lake, NY; <sup>3</sup>Pfizer, San Diego, CA; <sup>4</sup>GlaxoSmithKline, King of Prussia, PA; <sup>5</sup>Janssen Pharmaceuticals, La Jolla, CA.

A panel of 8 novel urinary protein biomarkers were recently qualified by the FDA for the detection of acute kidney injury (AKI), significantly improving the sensitivity and specificity with which renal injury may be detected in rat. However, the translation of these biomarkers to dogs, one of the most common species used in preclinical drug development, remains unknown yet must be established prior to broad implementation in toxicity screens. Here, we monitored AKI biomarkers kidney injury molecule 1 (Kim-1), lipocalin-2 (NGAL), clusterin and albumin in urine from male beagles infused once daily for 10 days with the nephrotoxic antibiotic gentamicin. Histological examination of the kidneys following treatment revealed severe epithelial degeneration, necrosis and regeneration alongside tubular dilation in gentamicin-treated dogs only. In gentamicin-treated dogs, significantly elevated urinary protein levels of albumin, clusterin and NGAL were measurable as early as 3 days after start of treatment with peak levels >100-fold above background. Both the speed and magnitude of response detected with these new biomarkers were superior to traditional AKI biomarkers, blood urea nitrogen (BUN) and serum creatinine (sCr), which did not increase until day 8. Urinary Kim-1 levels peaked around 2-fold, an order of magnitude lower than published levels from a similar 10-day rat study. Further analysis of samples for Kim-1 mRNA and protein will tell whether the canine Kim-1 response is markedly different from that observed in rats. These data indicate that three of four novel biomarkers qualified in rat (NGAL, clusterin and albumin) translate to canine and represent a substantial improvement over traditional AKI biomarkers in preclinical drug development.

## PS 1883 Bio-Monitoring of Multimycotoxin Exposure in Human Urine Samples from Cameroon Using a Multibiomarker Approach.

W. A. Abia<sup>1,2</sup>, B. Warth<sup>2</sup>, M. Sulyok<sup>2</sup>, R. Krska<sup>2</sup>, A. T. Chana<sup>1</sup>, P. B. Njobeh<sup>3</sup>, P. C. Turner<sup>4</sup>, C. Kouanfack<sup>5</sup>, M. M. Dutton<sup>3</sup> and P. F. Moundipa<sup>1</sup>. <sup>1</sup>Biochemistry, University of Yaounde I, Yaounde, Cameroon; <sup>2</sup>Department for Agrobiotechnology (IFA-Tulln), University of Natural Resources and Life Sciences, Vienna, Austria; <sup>3</sup>Food, Environment and Health Research Group (FEHRG), University of Johannesburg, Doornfontein, South Africa; <sup>4</sup>MIAEH, School of Public Health, University of Maryland, College Park, MD; <sup>5</sup>Day Hospital, Central Hospital, Yaounde, Cameroon.

Mycotoxins are secondary metabolites of fungi that contaminate food, but bio-monitoring of human exposure has mostly been limited to a few individually measured mycotoxin biomarkers, mainly aflatoxin. The aim of this study was to determine frequency of exposure and level of multi-mycotoxin in urine samples obtained from Cameroonian adults, mostly from HIV infected individuals. 175 urine samples (145/175; 83% from HIV positive individuals) as well as food frequency questionnaire responses were collected from consenting Cameroonians, and analyzed for 8 parent mycotoxins and 7 key metabolites using liquid chromatography separation and tandem mass spectrometry detection. In total, 11 mycotoxin biomarkers [e.g. aflatoxin M1 (AFM1), fumonisin B1 (FB1), ochratoxin A and total deoxynivalenol] and bio-measures [FB2, nivalenol and total zearalenone] were recovered,

individually or in combinations, in 110/175 (63%) samples; from HIV positive (64%) and HIV negative (57%), with additional 4 analytes present only in HIV positive samples. AFM1 (10%; mean 0.5, range <LOQ-1.4µg/L) and FB1 (3%; mean 0.6, range 0.5-15µg/L) were detected in the HIV subpopulation whilst low levels (<LOQ) were found in one sample each from HIV negative group. One HIV positive individuals' urine contained 6 metabolites. Levels of these metabolites were generally similar to those reported elsewhere in Africa. For the first time in Africa and elsewhere, this study has reported on 11 mycotoxin biomarkers/bio-measures quantified in human urine. Mycotoxin exposures in HIV individuals may require particular attention. The findings may constitute a major step towards mycotoxin exposure assessment and national mycotoxin regulations in Cameroon.

#### **PS 1884 Development of a New Oxidative Stress Biomarker Dityrosine ELISA.**

K. Sakai<sup>1</sup>, M. Takeuchi<sup>1</sup>, T. Ochi<sup>1</sup>, R. Rathnam<sup>2</sup> and Y. Kato<sup>3</sup>. <sup>1</sup>Japan Institute for the Control of Aging, Fukuroi, Japan; <sup>2</sup>Genox Corporation, Baltimore, MD; <sup>3</sup>School of Human Science and Environment, University of Hyogo, Himeji, Japan. Sponsor: K. Rao.

Accumulating evidence indicates that oxidative stress plays an important role in various diseases such as cancer, diabetes and hypertension. Recently it is also reported that oxidative stress is involved in toxicity of chemical substances such as arsenic, asbestos, diesel exhaust micro particles and antineoplastic drugs, and monitoring of oxidative stress inside human body may be informative for toxicological study. Oxidative stress may cause oxidative damages to biomolecules such as nucleic acids, lipids, proteins and enzymes, and oxidized products of such biomolecules have been used for the assessment of oxidative stress in the living bodies. Although protein is one of the most important biomolecules, only limited number of reports about the oxidized proteins has been published. Tyrosine is one of the major targets of protein oxidation, and dityrosine is known to be formed by oxidative stress. In this presentation, development of a new dityrosine ELISA is reported. A competitive dityrosine ELISA is established using anti-dityrosine monoclonal antibody (clone 1C3) which was developed by Kato et.al. 50 µL of diluted samples or standards are poured into micro plate wells which is pre-coated by dityrosine antigen, and incubated at 4 degree C overnight. After washing by PBS-tween buffer, 100 µL of HRP-conjugated anti mouse antibody is poured, and incubated for 1 hour at room temperature. TMB is used for color development. Assay range of dityrosine ELISA is 0.05 to 12 µmol/L, and shows good linearity and reproducibility. Dityrosine concentration in human urine ranges between 0.12 and 3.95 µmol/L (mean 1.44 µmol/L), and urinary dityrosine concentration measured by ELISA significantly correlated with that measured by LC-MS/MS. In conclusion, dityrosine ELISA may be useful for the assessment of oxidative stress in the living bodies.

#### **PS 1885 Method Development of Serum Canine Inhibin B Enzyme-Linked Immunosorbent Assay (ELISA).**

R. Kuk<sup>1</sup>, D. Kumar<sup>2</sup> and S. B. Laffan<sup>1</sup>. <sup>1</sup>Reproductive Toxicology, Safety Assessment, GlaxoSmithKline, King of Prussia, PA; <sup>2</sup>Assay Development, Bristol-Myers Squibb, Syracuse, NY.

Inhibin B (INH-B) is a heterodimeric glycoprotein consisting of an alpha and a beta-B subunit linked by disulphide bridges. INH-B is produced by the testes as well as the ovaries, and is responsible for the selective negative feedback control of follicle stimulating hormone. In males, INH-B is synthesized by the sertoli cells in the testis, and can be used as a marker of sertoli cell function and spermatogenesis in adult males. Hence, it is being considered a biomarker for detecting testicular damage. INH-B has been quantified in humans, rats and non-human primates, but not in canines due to lack of availability of reagents. Here, we report the methods development of the canine INH-B ELISA from Cusabio Biotech Co. (Wuhan, China). Assay standard curve is ranged from 4 to 1000 pg/mL with serum requirement of 50 µL. Assay optimization included modification of the procedure to include sample mixing followed by prolonged primary antibody-antigen incubation time to ensure saturation. Two custom quality controls were prepared at levels that are on the sensitive part of the standard curve. Qualification criteria included assessment of the standard curve, quantification range, reproducibility (precision) and dilutional linearity (% recovery). Standard curve was made more robust by adding more points on the sensitive part of the curve. Lower limit of quantification was qualified to be statistically above the variance of the blank value. Reproducibility was good (%CV≤30%) among assays. Linearity was acceptable for kit standards diluted with castrated dog serum or commercially available serum matrix, also, for intact serum diluted with its respective castrated serum (R<sup>2</sup>>0.9). This assay can detect >8 fold INH-B difference between intact and castrated canine

serum samples. Other parameters like frozen storage, freeze/thaw and lot-to-lot stability are pending. We conclude that this canine INH-B assay can consistently quantify INH-B levels in canine serum under the modified procedures.

#### **PS 1886 Mitigation of Fumonisin Biomarkers by Green Tea Polyphenols.**

K. Xue<sup>1</sup>, L. Tang<sup>1</sup>, Q. Cai<sup>2</sup>, L. Xu<sup>1</sup>, J. Su<sup>3</sup> and J. Wang<sup>1</sup>. <sup>1</sup>University of Georgia, Athens, GA; <sup>2</sup>Texas Tech University, Lubbock, TX; <sup>3</sup>Guangxi Cancer Institute, Nanning, China.

Fumonisin B1 (FB1) is a carcinogen and a strong tumor promoter in animal models. Green tea polyphenols (GTP) are highly effective in inhibition of a variety of carcinogen-induced tumorigenic effects in many model systems. In this study we assessed mitigative effects of GTP on FB1-biomarkers in blood and urine samples collected from a randomized, double blinded, and placebo controlled intervention trial, which recruited a total of 124 people aged 20-55 who exposed FB1 via their corn-based diet. These participants were consented, randomly divided into 3 groups, and daily treated with either low-dose (GTP 500 mg, n=42), high-dose (1,000 mg, n=41) or placebo (n=41) for 3 months. Urinary levels of free FB1 at baseline were comparable (medium at 560.73, 574.56, and 559.09 pg/mg creatinine) for all three groups (p=0.162). Levels at urine samples collected at 1-month of the intervention was significantly decreased in the high-dose group (medium: 364.94 pg/mg creatinine; p<0.01) as compared with level in the placebo group (medium: 575.25 pg/mg creatinine). The inhibition rate is 18.95% in low-dose group and 33.62% in high-dose group. Levels of free FB1 at samples collected at 3-month of the intervention showed significant decrease in both low-dose (medium: 319.45pg/mg creatinine; p<0.01) and the high-dose (medium: 215.83pg/mg creatinine; p<0.01) groups as compared with the levels of the placebo group as well as the baseline levels. The inhibition rate is 40.18% in low-dose GTP group and 52.6% in high-dose GTP group. Levels of sphinganine (Sa), sphingosine (So), and their ratio in urine and serum samples were also evaluated in this study. These results demonstrate that supplement of GTP effectively mitigates urinary excretion of free FB1 via to be specified pathways in humans.

#### **PS 1887 Variation of Urinary Creatinine.**

H. Na and M. Yang. Sookmyung Women's University, Seoul, Republic of Korea.

Urinary creatinine has been commonly used for adjusting dilution status of urine species in biological monitoring. However, it can vary according to sex, age, race, BMI, meat intake, etc. The purposes of our study are to investigate the intra- and inter-individual variations of urinary creatinine in a sex, age and race matched subjects, and to study the impact of meat intake on the variations of urinary creatinine. We designed a diet-controlled study among the subjects who were Korean healthy females (N=9, age= 20±4 yrs, BMI 19.7±2.4 kg/m<sup>2</sup>) and measured urinary creatinine at 5 intervals during 24 hours with and without meat consumption. As results, diverse intra- and inter-variations of creatinine levels were shown in the subjects: When subjects did not take meat, the largest and smallest intra-variations in urinary creatinine ranges were detected in the subject C and G, i.e. 0.34-2.97 (Δ2.63)g/L and 0.93-1.63 (Δ0.7) g/L, respectively. In addition, creatinine levels at 5-intervals were significantly different between the highest and lowest average levels-subjects, i.e. 2.13±0.73 g/L of the subject I and 0.86±0.52 g/L of the subject A (p<0.05), respectively. With intake of meat (charcoal-grilled Korean beef tenderloin), the trend of intra-variation of urinary creatinine in each subject was not different (p=1.00 by Fisher exact test). It suggests that meat intake had little influence on intra- and inter-variation of urinary creatinine. In conclusion, our data re-emphasize that urinary creatinine must be measured in each spot urine even among the subjects who have similar age, sex, race and BMI due to its intra- and inter-variation. In the near future, the causes of intra- and inter-individual variations of urinary creatinine should be further studied.

#### **PS 1888 Cardiolipin As a Biomarker of Mitochondrial Dysfunction Associated with Parkinson's Disease.**

Y. Tyurina<sup>1,2</sup>, D. Winnica<sup>1,2</sup>, V. Kapralova<sup>1,2</sup>, V. Tyurin<sup>1,2</sup> and V. Kagan<sup>1,2</sup>. <sup>1</sup>Department of Environmental and Occupational Health, University of Pittsburgh, Pittsburgh, PA; <sup>2</sup>Center for Free Radical and Antioxidant Health, Pittsburgh, PA.

A commonly used pesticide, rotenone, is a mitochondrial respiratory complex I inhibitor capable of selective oxidation of mitochondrial phospholipid, cardiolipin (CL). Given that rotenone exposure is associated with the development of

Parkinson disease (PD), we hypothesized that CL peroxidized molecular species accompanying mitochondrial dysfunction may represent a new biomarker of PD. In this study, we used circulating lymphocytes isolated from human blood and found that rotenone (50-250 $\mu$ M, 12-18h) caused apoptosis (phosphatidylserine externalization, caspase 3/7 activation), reactive oxygen species production (superoxide, H<sub>2</sub>O<sub>2</sub>), mitochondrial dysfunction (inactivation of complex I, decrease of mitochondria membrane potential, depletion of ATP) and activation of peroxidase activity of mitochondria. Using an oxidative lipidomics approach, we found that treatment of lymphocytes with rotenone resulted in accumulation of monolysio-CL and oxygenated free fatty acids. In addition we were able to detect oxygenated molecular species of tetra-linoleyl CL, a major CL molecular species in lymphocytes. Notably, molecular species of oxygenated CL formed in human lymphocytes were similar to those formed in cyt c driven reaction in the presence of H<sub>2</sub>O<sub>2</sub> – in line with the known participation of cytochrome as a catalyst of CL peroxidation during apoptosis. Using the combination of lipidomics and oxidative epitope-targeted enzymatic digestion of oxidized tetralinoleoyl-CL we found that its oxygenated LA species were represented by hydroxy- and hydroperoxy-derivatives. Thus, we conclude that CL and its oxygenation products and metabolites may represent a new biomarker of rotenone-induced mitochondrial dysfunction associated with PD. Supported by NIOSH OH008282; NIH ES020693, U19 AI068021, HL70755.

**PS 1889 Evaluation of Insulin-Like Growth Factor Acid-Labile Subunit As a Novel Biomarker of Effect to the Mycotoxin Deoxynivalenol.**

B. Flannery<sup>1,2</sup>, C. J. Amuzie<sup>2</sup> and J. Pestka<sup>1,2,3</sup>, <sup>1</sup>Food Science and Human Nutrition, Michigan State University, East Lansing, MI; <sup>2</sup>Center for Integrative Toxicology, Michigan State University, East Lansing, MI; <sup>3</sup>Microbiology and Molecular Genetics, Michigan State University, East Lansing, MI.

Deoxynivalenol (DON) is a trichothecene mycotoxin produced from *Fusarium* species frequently found in grain products due to its recurrent contamination and resistance to food processing treatments. In growing experimental animals, chronic low-level DON exposure has resulted in anorexia, weight suppression and growth hormone axis perturbations. As a result, children are thought to be especially sensitive to DON. Though a biomarker of exposure exists to measure DON exposure in humans, no biomarker of effect is currently available to predict the adverse negative weight effects of DON, thereby hindering complete risk assessment of this mycotoxin. Two studies were conducted to assess the potential of plasma insulin-like growth factor acid-labile subunit (IGFALS) to be used as an effect biomarker for DON. In the first study, a 9 wk dietary DON exposure was employed in mice to test the hypothesis that depression in plasma IGFALS occurs at toxicologically relevant doses prior to significant weight suppression. Results showed that the 1) NOAEL for depressed plasma IGFALS and weight was 2.5 ppm DON and 2) decreased plasma IGFALS was detectable before significant weight suppression was evident. In the second study, the specificity of reduced plasma IGFALS to DON, rather than DON-induced anorexia, was assessed using a dietary restriction study. Mice were fed ad-lib control diet, restricted control diet or identical amounts of restricted 15 ppm DON diet. Mice fed restricted DON diet exhibited significantly less plasma IGFALS than the restricted control indicating the specificity of plasma IGFALS reductions to DON. Thus, plasma IGFALS might be one suitable biomarker for predicting DON's adverse growth effects in animals and humans.

**PS 1890 Validation of a Meso Scale Discovery Immunoassay for KIM-1 Renal Biomarker in Cynomolgus Monkey (*Macaca fascicularis*) Urine.**

D. Fix and W. J. Reagan. *Drug Safety, Pfizer, Groton, CT.* Sponsor: J. Aubrecht.

The purpose of this study was to validate an immunoassay for detection of Kidney Injury Molecule 1 (KIM-1) in the urine of cynomolgus monkeys (NHP). Monkeys were treated with escalating doses of a compound that induced tubular degeneration/regeneration as determined by histopathology. Urine was collected pre-dose, 16 days post dose and 21 days post dose and urine with low, medium and high values of KIM-1 were used to validate the Meso Scale Discovery (MSD) Human KIM-1/TIM-1 (single-plex) immunoassay kit as this kit cross reacts with NHP KIM-1. Additional urine from older colony monkeys as well as normal younger NHPs were also used to establish a preliminary observed range (<0.01ng/mL). We determined intra-assay (7.7% CV) and inter-assay precision (24.5% CV), limit of blank (0.000331ng/mL), limits of quantitation (0.01ng/mL to 10ng/mL), dilutional linearity (not linear when diluted), recovery (84.8% - 122.8%), preliminary quality control range evaluation (0.438ng/mL/ CV 18.7%; 0.615ng/mL/ CV 16.8%), freeze/thaw (F/T) stability out to 4 F/T cycles (95.5% - 112.5%), and sample storage stability out to 10 weeks. There was also a good biologic correlation with time and dose-dependent increases in KIM-1 for the toxicity

study samples. All parameters measured showed acceptable immunoassay assay performance except dilutional linearity. Based on this assay performance and the other results obtained, the validated method is robust and can be performed under good laboratory practice conditions to support nonclinical studies to assess for renal toxicity.

**PS 1891 Evaluation of a Three-Dimensional Oral Cell Model for the Assessment of Tobacco Products.**

W. Fields, K. Fowler and B. R. Bombick. *R. J. Reynolds Tobacco, Company, Winston-Salem, NC.* Sponsor: S. Theophilus.

Oral disease is frequently associated with viral and environmental exposures as well as oral hygiene. The goals of this study were to evaluate the impact of smokeless tobacco extracts (STE) and cigarette total particulate matter (TPM) on cell survival, oxidative stress, inflammatory response and tissue integrity using three-dimensional cultures of human buccal (EpiOral™) cells.

EpiOral™ cells were treated with extracts of 1S2 (reference dry snuff), 2S3 (reference moist snuff) and a smokeless tobacco blend prepared in complete artificial saliva (CAS) as well as with TPM from Kentucky Reference 3R4F cigarette (DMSO-based) for time points through 24 hours. Toxicity was assessed with the lactate dehydrogenase (LDH) assay. Glutathione (GSH) measurement and histological analyses were used to assess oxidative stress and changes in tissue integrity, respectively. Gene expression analyses were also conducted via QRT/PCR and multiplex cytokine testing.

Dose- and time-dependent release of LDH was observed for all test articles. The optimal exposure time appears to be 12 hours where 3R4F TPM elicited up to a 3-fold increase in LDH release; the 1S2 and 2S3 extracts yielded a 2-fold increase while no increase was observed for the smokeless tobacco blend. Tissue integrity was slightly disrupted by TPM exposure, while no impact was observed for the STEs.

Oxidative stress as measured by GSH analysis was not apparent for any of the test articles; however, altered inflammatory response was observed by changes in IL-1 $\alpha$  and G-CSF cytokine release and modulations in at least one of the following genes, IL-1 $\alpha$ , TNF $\alpha$  or COX-2. The test articles also induced increases in cellular stress and xenobiotic metabolism as determined by changes in HO-1, HSP-70, CYP1A1 and CYP1B1.

Collectively, the data suggest that the EpiOral™ three-dimensional human cell culture model may be useful in evaluating tobacco extracts.

**PS 1892 Assessment of Cardiac Biomarkers in Cynomolgus Macaques.**

T. Parman, N. Chini, D. Vuong, M. Patrick, B. Schneider, K. Tinajero, L. Tang, D. Fairchild, K. Lopez and J. C. Mirsalis. *SRI International, Menlo Park, CA.*

A number of new cardiac biomarkers have recently been developed for use in rodents; however, there are no validated cardiac biomarkers suitable for use in nonhuman primate (NHP) studies. We previously reported results of cardiac markers in African green monkeys (AGM) and Rhesus macaques (RM). In the current study we have extended these evaluations to Cynomolgus macaques (CM), the most widely used NHP species for toxicity studies. Two CM/sex were given a single subcutaneous (sc) injection of isoproterenol (IPT; 4 mg/kg); 1 CM/sex received sc saline. Cardiac effects of IPT were observed within 1 hr postdose and included hypotension, ventricular premature complexes, ventricular bigeminy, atrial premature complexes, with or without aberrant conduction and ST segment elevation. Blood samples were collected prestudy and at 1, 4, 24, 48 and 72 hr postdose, and evaluated with MSD MIP-1 muscle injury kits (rat: cTnI, cTnT, FABP3, Myl3, sTnI; human: TNI). IPT produced significant increases in the level of most cardiac biomarkers: cTnT, FABP3, Myl3, sTnI and human cTnI were increased over predose levels by 4.2-, 2.5-, 25-, 28- and 23-fold, respectively, with peak times ranging from 4 to 48 hours. Similar results were seen in females, though rat cTnI was not increased in males, but a 4.9-fold increase was seen in females. At 72 hr postdose, there were still elevations in Myl3 and sTnI. IPT plasma levels at 1 hr postdose were higher in males (708 ng/ml) than in females (324 ng/ml) and fell to 324 and 102 ng/ml at 4 hr in males and females, respectively. Heart histopathology 3 days postdose revealed minimal to moderate cardiac myofiber degeneration, myofiber karyomegaly and leukocyte infiltration in all treated animals. These results indicate that the MSD rat and human muscle injury panel provides excellent sensitivity for assessing cardiac effects in CMs, and these data are consistent with the utility of these kits previously reported in RM and AGM. Work supported by NIAID Contract N01-AI-70043.

**PS 1893 A Comparative Study on Renal Toxicity of Industrial Chelates Using Novel Urinary Protein Biomarkers As Early Predictors of Nephrotoxicity.**

R. Krishnaraj<sup>1</sup>, E. C. Bisinger<sup>1</sup>, N. Edgerton<sup>2</sup>, D. E. Dodd<sup>2</sup> and J. Mapes<sup>3</sup>.  
<sup>1</sup>AlzoNobel Services, Inc., Chicago, IL; <sup>2</sup>The Hamner Institutes for Health Sciences, Research Triangle Park, NC; <sup>3</sup>Myriad RBM, Inc., Austin, TX.

Toxicogenomic approaches have identified protein biomarkers of renal cell injury/repair as early predictors of renal toxicity prior to changes in renal histopathology. We used these novel biomarkers to determine if rats orally dosed with industrial chelates exhibited altered urinary biomarker levels that preceded histopathologic changes in kidney. The nephrotoxicant/renal carcinogen, nitrilotriacetic acid (NTA), is known to cause rat proximal tubule cell injury/repair (3–7 weeks) followed by renal tumors (2 years) after oral dosing. A new, readily biodegradable chelate, L-glutamic acid diacetic acid (GLDA), previously which showed no significant microscopic renal changes (90-day, oral), and EDTA, known non-carcinogen (oral bioassay) were also included in our study. Male Wistar rats were gavaged daily (oral, 28 days, 1000 mg/kg/day; n=10/group) with Na<sup>+</sup> salts of these chelates. As expected, mean urinary levels of Na<sup>+</sup> & Zn<sup>2+</sup> were elevated in all chelate-treated groups. Two rats in NTA group were euthanized as moribund on Day 13. The surviving NTA group showed decreases in mean body weights, food and water consumption, and urine Mg<sup>2+</sup>, and increases in the mean levels of urine Ca<sup>2+</sup>, total protein, lactate dehydrogenase, kidney injury molecule-1 (Kim-1), Clusterin (CLU) and increased proximal tubule cell proliferation (BrdU). No such changes were seen with GLDA. Kim-1 and CLU are inducible kidney proteins and are approved by FDA as predictive, early and noninvasive urinary biomarkers of kidney cell injury/repair. At necropsy, bilateral kidney enlargement (mean relative kidney weights) was noted with NTA, but not GLDA. In conclusion, our study showed that NTA, but not GLDA or EDTA, caused significant early renal cell toxicity when evaluated with urinary protein biomarkers as early predictors of nephrotoxicity.

**PS 1894 Identifying Biomarkers of Kidney and Liver Toxicity by Integrating Toxicogenomics Datasets with Biological Networks.**

P. Hewitt<sup>1</sup>, T. C. Fuchs<sup>1</sup>, R. B. Russell<sup>2</sup>, D. Mitic<sup>2</sup> and G. Apic<sup>2</sup>. <sup>1</sup>Merck KGaA, Darmstadt, Germany; <sup>2</sup>Cambridge Cell Networks Ltd., Cambridge, United Kingdom.

The aim of this study was to identify candidate biomarkers of kidney toxicity by interrogating transcriptome profiles from hundreds of publicly available toxicogenomics datasets and to test the findings with additional *in vivo* studies. We manually annotated 34,837 toxicogenomics observations from over 345 articles. Additionally, raw transcriptomics datasets from the EU PredTox and Japanese TG-GATEs projects were assessed. We ranked biomarkers by a combination of scores: 1) presence of the datasets where biomarkers were sought (e.g. nephrotoxicity); 2) absence in control datasets (e.g. other toxicities); 3) network centrality within the dataset (by exploiting, curated dataset of interactions between protein, gene and chemicals, which considers the nature of the interaction and its confidence; 4) previously observed presence of the protein coded by the gene in urine or blood samples. Application of these approaches to the three datasets identifies 43 significant candidates (of 1273 genes identified at least once in a kidney array) including NGAL, HAVCR1 (Kim-1) and clusterin and several new candidates. These findings correspond to tests performed on model nephrotoxic compounds (cisplatin (0.3 and 0.6 mg/kg), vancomycin (50 and 300 mg/kg) and puromycin (10 and 30 mg/kg)) using whole genome expression profile experiments [Illumina RefSeq] both *in vivo* (Rat; 3, 7, 14 and 28 days) and *in vitro* (rat NRK cells; 24 and 72h), and a battery of biomarker detection assays in urine. Four of the six best kidney toxicity biomarker candidates identified by these experiments were among the 43 candidates above. Overall, the results demonstrate that our *in silico* approach can greatly enrich candidates for those likely to be true biomarkers when given large datasets of dysregulated genes.

This project was funded by the German Federal Ministry of Education and Research (BMBF) under the BioRhine-Neckar Spitzencluster (BioRN-BMC-TP08).

**PS 1895 Evaluation of Novel Biomarkers of Nephrotoxicity in Monkeys Treated with Gentamicin.**

J. Gautier<sup>1</sup>, X. Zhou<sup>2</sup>, Y. Yang<sup>3</sup>, T. Gury<sup>1</sup>, Z. Qu<sup>2</sup>, J. Léonard<sup>1</sup>, J. Wang<sup>2</sup>, P. Detilleux<sup>1</sup> and B. Li<sup>2</sup>. <sup>1</sup>Preclinical Safety, Sanofi, Vitry-sur-Seine, France; <sup>2</sup>National Center for Safety Evaluation of Drugs, Beijing, China; <sup>3</sup>Preclinical Safety, Sanofi, Shanghai, China.

Most studies to evaluate renal safety biomarkers have been performed in rats. This preliminary study was conducted in cynomolgus monkeys to define the optimal conditions to evaluate the potential usefulness of novel biomarkers of nephrotoxicity in this species. Groups of 3 males were given daily intramuscular injections of 10, 25, 50 mg/kg/day gentamicin, a known nephrotoxic agent, for 10 days and 75 mg/kg/day for 9 days and were sacrificed on Day 10 or 11. Blood samples and 16-hour urine samples were collected on Days -7, -3, 2, 4, 7 and at the end of the dosing period. In parallel to conventional parameters, the novel urinary renal biomarkers evaluated (after normalization to urinary creatinine) included  $\alpha$ 1-microglobulin, microalbumin, clusterin and calbindin. Kidney microscopic findings consisted in dose dependent increase in tubular cell degeneration/necrosis from minimal to mild at 10 mg/kg/day, moderate at 25 mg/kg/day, to severe at 50 and 75 mg/kg/day gentamicin. Serum creatinine was slightly increased at 10 mg/kg/day on Day 11 (less than 25% increase as compared to pre-test values in each individual animals), moderately increased (2-fold) at 25 mg/kg/day on Day 11, and markedly increased (more than 2-fold) at 50 and 75 mg/kg/day from Day 7. Parallel increases were observed with BUN. Urinary  $\alpha$ 1-microglobulin was increased by 4.5-fold and microalbumin, clusterin, calbindin were increased by more than 20-fold as compared to pre-test values in each individual animals at 10 mg/kg/day on Day 11. Marked increases in these urinary biomarkers were also observed at higher doses of gentamicin from Day 7. These first results indicate that the urinary biomarkers  $\alpha$ 1-microglobulin, microalbumin, clusterin and calbindin may be useful sensitive biomarkers of nephrotoxicity in monkeys and potentially in humans.

**PS 1896 Restricted Diet Prevents Negative Effects of OVX on Soft Tissue Composition.**

R. Samadfam and S. Y. Smith. Bone Research, Charles River, Montréal, QC, Canada. Sponsor: M. Vézina.

Ovariectomy (OVX) in rats is associated with weight gain and loss of bone mass. The increased body weight is in part attributed to increases in growth, consistent with OVX-induced hyperphagia. The objective of this study was to determine the effects of OVX on body composition in aged rats (over 6 months of age) with or without food restriction. PMI Nutrition International diet was used for all animals with animals assigned to the restricted diet groups receiving 21 g/day. Body composition was evaluated at baseline and at 4, 8, 12 and 19/20 weeks post surgery using DXA (Dual Energy X-ray Absorptiometry) and/or pQCT (Peripheral Quantitative Computed Tomography). DXA evaluation showed increases in whole body area and BMC for OVX rats on both restricted and unrestricted diet compared to their corresponding sham controls, with greater increases for animals fed *ad libitum*. Overall, BMD for OVX groups were comparable to baseline values whereas increases up to 2 and 6% were noted for sham controls respectively on the restricted and fed *ad libitum*. Significant increases were noted over the study period in muscle mass for rats on restricted diet, with trends for increases in fat mass. For *ad libitum* fed rats, although an increase in muscle mass was noted 4 weeks following surgery compared to sham controls, muscle mass gradually declined over the remaining study period with lower values 20 weeks post surgery. Fat mass increased for this group. When muscle mass and fat mass values were adjusted for body weight, no significant differences were noted between OVX and sham controls for animals on the restricted diet, indicating that the increased body weight is the result of proportional increases in muscle and fat mass, likely related to the effect of OVX on skeletal growth. For animals fed *ad libitum*, significant decreases in lean mass with significant increases in fat mass were noted when adjusted for body weight, compared to sham controls, indicating negative effects on soft tissue composition. Data from the restricted diet group suggest that calorie restriction prevents OVX-induced muscle loss and fat gain.

**PS 1897 3, 3', 4, 4', 5-Pentachlorobiphenyl (PCB 126) Decreased the Ratios of Epoxide Metabolites to Their Corresponding Diols in Male Rodents.**

X. Wu<sup>1</sup>, J. Yang<sup>2</sup>, C. Morisseau<sup>2</sup>, L. W. Robertson<sup>1</sup>, B. D. Hammock<sup>2</sup> and H. Lehmler<sup>1</sup>. <sup>1</sup>Department of Occupational and Environmental Health, University of Iowa, Iowa City, IA; <sup>2</sup>Department of Entomology, University of California Davis, Davis, CA.

Oxylipins are oxygenated metabolites of certain fatty acid species. Changes in the homeostasis of these regulatory lipid mediators are of interest as markers of exposure to certain toxicants, including the aryl hydrocarbon receptor agonist 3,3',4,4',5-pentachlorobiphenyl (PCB 126). Here we test the hypothesis that chronic exposure to PCB 126 alters the levels of regulatory lipid mediators (oxylipins) in rats. Male Sprague-Dawley rats (5 weeks old) were treated biweekly with injections of PCB 126 in corn oil over a period of 3 months, representing cumulative PCB doses of 0, 0.06, 0.3, and 1.2 µg/kg body weight. PCB 126 treatment caused a dose-dependent reduction in growth and relative thymus weight, while relative liver weight was increased with PCB dose. PCB 126 levels in the liver increased in a dose-dependent manner, while PCB 126 levels in plasma were below the detection limit. The ratios of epoxide/diol metabolites displayed a dose-dependent decrease in plasma for oxylipins derived from arachidonic acid (ARA), eicosapentaenoic acid (EPA), docosahexaenoic acid (DHA) and linoleic acid (LA), as determined by metabolomics profiling of oxylipins with liquid chromatography-tandem mass spectrometry. Similarly, the epoxide/diol ratios for ARA and DHA derived oxylipins decreased in a dose-dependent manner in the liver. The effects of PCB treatment on epoxide/diol ratios were associated with significantly increased activities of soluble epoxide hydrolase (sEH) in cytosol and peroxisomes in the liver at the highest PCB 126 dose. Since increased sEH activity and decreased epoxide/diol metabolites ratios have been linked to cardiovascular disease and inflammation, our results suggest that changes in oxylipin plasma levels may be useful biomarkers of human exposure to PCB 126 and other dioxin-like compounds [supported by NIH grants ES04699 and ES013661].

**PS 1898 Identification of Neural Biomarkers of Altered Sexual Differentiation following Gestational Exposure.**

G. W. Louis<sup>1,2</sup>, D. R. Hallinger<sup>1</sup> and T. E. Stoker<sup>1</sup>. <sup>1</sup>Endocrine Toxicology Branch, Toxicity Assessment Division, US EPA, Research Triangle Park, NC; <sup>2</sup>ORISE Program, Department of Energy, Oak Ridge, TN.

Sexual differentiation of the brain occurs during late gestation through the early postnatal period. The development of the phenotypical male brain is dependent on the aromatization of circulating testosterone to estradiol. Exposure to endocrine disrupting chemicals (EDCs) during early-life alters sexual maturation of the rat hypothalamic-pituitary-gonadal axis and subsequently, the timing of puberty and adult reproductive behavior. We set out to identify predictive neuronal biomarkers for use in evaluating the effect of EDCs on sexual differentiation in the male and female. We examined changes in gene expression in the rat hypothalamus [(specifically, in the anteroventral periventricular nucleus (AVPV) and arcuate nucleus (ARC)] after in utero exposure to the aromatase inhibitor, letrozole. Pregnant dams were gavaged with vehicle or letrozole (0.1mg/kg) on gestational days 20 and 21. The AVPV and ARC were microdissected from male and female offspring on several pre-, peri-, and post-pubertal postnatal days (PND) and were evaluated for changes in expression of a number of neuropeptides that have sex specific patterns during development. These genes include those that encode for kisspeptin (Kp) and tachykinin-2 (Tac2). We identified an increase with age in the expression of Kp in the AVPV of the genetic female, but not the genetic male. Kp expression in the AVPV of the letrozole-exposed genetic male was increased to the same level observed in the genetic female on PND 14, 25 and 49. However, Kp expression in the male ARC was not altered by letrozole. ARC Tac2 expression in the male was also not changed by letrozole. This work will provide optimal time points for these measures, but additional studies are needed to determine whether these, and other CNS biomarkers, are predictive of altered puberty and/or sexual behavior due to early-life EDC exposure. *This abstract does not necessarily reflect EPA policy.*

**PS 1899 Biomarkers of Exposure and Effect in Long-Term Smokers and Moist Snuff Consumers.**

B. A. Jones<sup>1</sup>, G. L. Prasad<sup>1</sup>, P. Chen<sup>1</sup> and D. W. Graff<sup>2</sup>. <sup>1</sup>R & D, RJ Reynolds Tobacco Co., Winston-Salem, NC; <sup>2</sup>Celerion, Lincoln, NE. Sponsor: G. Krautner.

To assess the effects of chronic exposure to combustible and non-combustible tobacco product use, a single site, cross-sectional clinical study was conducted. Three cohorts of healthy males (40/cohort, 35-60 years) were enrolled: long-term smokers

and moist snuff consumers (MSC), and non-tobacco consumers (NTC). Select biomarkers of exposure (BioExp) and potential biomarkers of effect (BioEff) indicating oxidative stress, inflammation and metabolomic changes, among others, were investigated. Blood biomarkers were measured in subjects abstaining overnight from both food and tobacco, and urinary biomarkers were measured in ambulatory collections of 24h urine samples. Nicotine (and its metabolites) and total tobacco specific nitrosamines (TSNAs) were higher in MSC followed by smokers and NTC. Tobacco combustion-related BioExp (polycyclic aromatic hydrocarbons, aromatic amines and mercapturic acid metabolites) were significantly higher in smokers, with no difference observed between MSC and NTC cohorts. Compared to NTC and MSC, smokers exhibited significantly elevated levels of biomarkers associated with oxidative stress, inflammation, and platelet activation. Smokers also exhibited significantly higher levels of apolipoprotein B100 and oxidized low-density lipoprotein relative to NTC and MSC. Thus, alterations in BioEff suggesting inflammation, oxidative stress and altered lipid metabolism were detected in smokers compared to the non-smoking cohorts. In summary, our findings are in agreement with existing epidemiological data which show the reduced harm from smokeless tobacco consumption compared to smoking, with no-tobacco-use being the least risky. The BioExp and BioEff evaluated in this study are likely to be useful in future assessments of the health effects of new tobacco products.

**PS 1900 Mechanistic Biomarkers Provide Early Detection of Acetaminophen-Induced Acute Liver Injury at First Presentation.**

D. Antoine<sup>1</sup>, C. Goldring<sup>1</sup>, P. Starkey-Lewis<sup>1</sup>, J. Dear<sup>2</sup>, J. Moggs<sup>3</sup>, V. Platt<sup>1</sup> and B. Park<sup>1</sup>. <sup>1</sup>MRC Centre for Drug Safety Science, University of Liverpool, Liverpool, United Kingdom; <sup>2</sup>NPIS Edinburgh, University of Edinburgh, Edinburgh, United Kingdom; <sup>3</sup>Preclinical Safety, Novartis Institutes for Biomedical Research (NIBR), Basel, Switzerland. Sponsor: D. Mendrick.

We investigated the potential of a panel of novel biomarkers - which demonstrate either enhanced liver expression or are linked to the mechanisms of toxicity - to identify patients with paracetamol (acetaminophen)-induced acute liver injury at first presentation to hospital when current liver injury markers are normal. In plasma samples from patients (n=129), at first presentation to hospital following paracetamol overdose, we measured microRNA-122 (miR-122; high liver specificity), High Mobility Group Box-1 (HMGB1; marker of necrosis), full length and caspase-cleaved Keratin-18 (K18; markers of necrosis and apoptosis, respectively) and glutamate dehydrogenase (GLDH; marker of mitochondrial dysfunction). In all patients, the biomarkers at first presentation significantly correlated with peak ALT/INR (International Normalized Ratio). In patients with normal ALT/INR at presentation, miR-122, HMGB1 and necrosis K18 identified the development of liver injury (n=15) or not (n=84) with a high degree of accuracy, and significantly outperformed ALT activity, INR and plasma paracetamol concentration for the prediction of subsequently liver injury (n=11) compared with no injury (n=52) in those patients presenting within 8 hours of overdose. Elevations in plasma miR-122, HMGB1, and necrosis keratin-18 identify subsequent development of acute liver injury in patients on admission to hospital, soon after paracetamol overdose, and in patients with ALTs in the normal range. The clinical development of such a biomarker panel could improve the speed of clinical decision making, both in the treatment of acute liver injury and in the design/execution of new treatment strategies that aim to refine the management of this common poisoning.

**PS 1901 Lead Concentrations Correlation between Fingernails and Whole Blood.**

K. P. Olympio<sup>1</sup>, C. A. Cardoso<sup>2</sup>, M. C. Rodrigues<sup>2</sup>, I. Ramires<sup>2</sup>, M. S. Luz<sup>3</sup>, L. G. Albuquerque<sup>3</sup>, F. Barbosa<sup>4</sup>, M. A. Cardoso<sup>1</sup>, P. V. Oliveira<sup>3</sup>, W. R. Günther<sup>1</sup> and M. A. Buzalaf<sup>2</sup>. <sup>1</sup>Faculdade de Saúde Pública - USP, São Paulo, Brazil; <sup>2</sup>Faculdade de Odontologia de Bauru - USP, Bauru, Brazil; <sup>3</sup>Instituto de Química - USP, São Paulo, Brazil; <sup>4</sup>Faculdade de Ciências Farmacêuticas - USP, Ribeirão Preto, Brazil.

Whole blood has been the biological fluid of choice to assess lead exposure. Other biomarkers need to be studied deeply, and the analysis of trace metals concentrations in nails is a non-invasive and simple collection procedure. The aim of this study was to investigate possible correlations between blood lead levels (BLL) and washed and non-washed fingernails lead levels (FLL) in 55 adults living in a lead contaminated area. Venous blood and fingernails (thumbs and forefingers) samples were collected. The nails of the left hand were washed with acetone and HCl 0.1 mol/L and the nails from right hand were not submitted to any pre-analytical procedure. Samples were analyzed by GF AAS and pairwise correlations were used to correlate lead concentrations between: BLL and FLL; nails from fingers from the

same hand and between washed and non-washed fingernails. It was found a non-significant correlation between BLL and washed forefinger nails lead ( $r=0.219$ ,  $p=0.112$ ) and between BLL and thumb nails lead ( $r=0.182$ ,  $p=0.191$ ). Comparing fingernails from the same hand (thumb and forefinger), lead concentrations of non-washed nails varied largely, even when transversal fragments from the same nail were analyzed. Lead concentrations in non-washed forefingers nails were not found to be correlated with non-washed thumb nails ( $r=0.169$ ,  $p=0.219$ ). On the other hand, for washed nails, thumb and forefinger nails were found to be correlated ( $r=0.39$ ,  $p=0.003$ ). In conclusion, the results showed that non-washed nails are not a reliable biomarker for lead exposure. However, although washing up the nails may diminish the lead external contamination, the correlation between fingers is still weak to consider fingernail as a biomarker to lead exposure. In addition, even the washed nails were not found to be significantly correlated to BLL.

## PS 1902 Detecting and Quantifying Endogenous and Exogenous Formaldehyde Adducted Hemoglobin Utilizing Selected Reaction Monitoring.

G. L. Andrews Kingon<sup>1</sup>, B. C. Moeller<sup>1</sup> and J. A. Swenberg<sup>1,2</sup>. <sup>1</sup>Curriculum in Toxicology, University of North Carolina at Chapel Hill, Chapel Hill, NC; <sup>2</sup>Environmental Sciences and Engineering, University of North Carolina at Chapel Hill, Chapel Hill, NC.

Widely recognized as a highly toxic compound, formaldehyde (FA) is considered to be a known animal and human carcinogen. It is ubiquitously present through normal cellular metabolism as well as from environmental pollutants. This compound is highly reactive towards macromolecules, forming diverse protein adducts and DNA damage that can be employed as biomarkers of chemical exposures. In particular, hemoglobin and red blood cells (RBCs) exposed to FA have been shown in laboratory studies to form an imidazolidone-type structure on the N-terminal peptides of hemoglobin alpha and beta chains. This data and the long lifetime of hemoglobin in RBCs (63 days in rats and 120 days in humans) afford investigation of the formation of endogenous and exogenous FA-hemoglobin adducts and the accumulation and loss of adducts. Monitoring this biomarker may reveal if inhaled FA enters the systemic circulation and reaches distant sites. In order to differentiate the origin of FA (endogenous versus exogenous), 10 ppm [<sup>13</sup>CD<sub>3</sub>]-FA rat inhalation exposures of 6 hours/day for 1 or 5 days were performed and globin was isolated from the washed RBCs. Stable isotope labeled peptides for the alpha and beta chains of hemoglobin were synthesized and purified then reacted with FA to achieve the imidazolidone modification. These internal standards were then spiked into the globin samples prior to trypsinization and off-line fractionation. Utilizing protein cleavage isotope dilution mass spectrometry and selected reaction monitoring, methods were developed for quantification of the N-terminal valine FA hemoglobin adduct peptides. In vitro reactions of RBCs and FA are ongoing to determine penetration of the chemical into the RBCs and biomarker stability following exposure. Additional globin samples from exposed and control rats and nonhuman primates have been collected and analyses are in progress.

## PS 1903 Assessment of the Relative Performance of Ten Urinary Biomarkers for Renal Safety across Twenty-Two Rat Toxicology Studies.

Z. Erdos, K. Vlasakova, H. Jin, K. McNulty, L. Phadtare, V. Chapeau, N. Mokrzycki, S. P. Troth, N. Muniappa, E. Wang, D. Holder, W. J. Bailey, F. D. Sistare, W. E. Glaab and Y. Gu. Safety Assessment and Laboratory Animal Resources, Merck Research Laboratories, West Point, PA.

Novel kidney injury markers have been recently identified which may outperform or add value to the conventional kidney injury biomarkers blood urea nitrogen (BUN) and serum creatinine. To assess the relative performance of the growing list of these novel biomarkers, a comprehensive evaluation was conducted for 10 urinary biomarkers in 22 rat studies including both kidney toxicants and compounds with toxicities observed only in other organs. Furthermore, these kidney toxicity studies included proximal tubule toxicants as well as glomerular toxicants. The ten urinary biomarkers evaluated included Kim-1, Clusterin, Osteopontin, Osteoactivin, Albumin, Lipocalin-2, GST-alpha,  $\beta$ 2-Microglobulin, Cystatin C, and Retinol Binding Protein 4 using novel immuno-based assays developed on the MesoScale platform. Receiver operator characteristic (ROC) curves were employed as the main criteria to compare the performance of this panel of biomarkers in individual study animals against the microscopic histomorphologic changes observed. Of the kidney toxicity studies analyzed, Kim-1, Clusterin, and Albumin showed the highest overall sensitivity for detecting tubular injury, while Albumin exceeded all other markers in detecting glomerular injury. The data presented here represents a comprehensive parallel analysis of the performance of leading renal biomarker candidates, and further demonstrates that this multiplexed approach enhances the ability to monitor drug-induced renal injuries as well as provide insight to linkages between individual biomarkers and specific histopathologic processes.

## PS 1904 Drug-Induced Kidney Injury Urinary Biomarker Response in Rats after Treatment with Nonnephrotoxicants.

L. Besenhofer, M. Wagoner, L. Cheatham, F. McGrath, P. Bentley, J. Fikes and L. B. Kinter. Safety Assessment US, AstraZeneca, Waltham, MA.

Drug induced kidney injury (DIKI) biomarkers are important tools with which to monitor and diagnose acute and chronic kidney injury. Qualification of the biomarkers for use in nonclinical studies requires an understanding of the DIKI biomarker profile after treatment with nephrotoxicants and non-nephrotoxicants to fully understand the potential for false positives in future studies. Renally-acting pharmacotherapies were used in this study to investigate the renal biomarker profile of non-nephrotoxicant drugs. Diuretic drugs were chosen to target specific nephron segments including furosemide (Loop of Henle), hydrochlorothiazide (distal tubule), spironolactone (collecting duct), and erythritol (pan-nephron). Male and female Han-Wistar rats ( $n=10$ ) were treated orally for 14 days and biomarker excretion was measured on days 1, 8, 15 and 22 (recovery groups,  $n=5$ ). Data were normalized to urine creatinine and then to control levels. There were no significant differences between controls and treated rats in excretion of any of the eight biomarkers assessed including: alpha-glutathione-s-transferase ( $\alpha$ GST), mu-GST, renal papillary antigen-1 (RPA-1), clusterin, albumin, lipocalin-2, osteopontin and kidney injury molecule-1 (KIM-1). Osteopontin excretion in female rats and clusterin excretion in male rats were the most variable with up to 19.1 and 9.9 fold differences from controls, respectively, despite mean values being roughly equivalent to vehicle controls. The results from this study indicate that diuretic treatment affecting different portions of the nephron does not result in increased biomarker signal. As such, the likelihood of obtaining false positive results due to physiological differences in animals in nonclinical safety screening studies is minimal.

## PS 1905 Urinary Biomarker Response to Hepsera-Induced Kidney Toxicity in Rats.

Y. Yang, S. Morgan, C. Thompson, D. Desmond, D. Zhao, R. Yeager and E. Blomme. Abbott Laboratories, Abbott Park, IL.

Hepsera (adefovir dipivoxil) is an acyclic nucleoside phosphonate analog approved for treatment of hepatitis B infection. It is associated with renal tubular toxicity in rats and monkey, and has dose-limiting nephrotoxicity in the clinic. The purpose of this study was to evaluate urinary biomarker response for Hepsera-induced kidney toxicity in rats. Male Sprague-Dawley rats were first administered Hepsera at 20, 40 and 60 mg/kg/day orally for 14 days. Minimal to mild tubular degeneration was observed at 20 mg/kg/day with increased severity at 40 and 60 mg/kg/day. There were no changes in BUN or serum creatinine. In contrast, urinary biomarkers (KIM1, albumin, NAGL, and osteopontin) were dose-dependently elevated. To further investigate the time-course of the biomarker changes, male and female rats were treated with 20 mg/kg/day Hepsera for 1, 2, 4 weeks with 4 weeks of recovery. Tubular degeneration was observed with males more affected than females. This was first observed on Day 8 (minimal) and increased in incidence and severity with longer duration of dosing. Renal histopathology was still present at the end of recovery in males. There were no changes in BUN, while serum creatinine was slightly increased in males on Days 16 and 29. In males, urinary KIM1, beta2-microglobulin (B2M), albumin, and NGAL were increased (2.5-37 fold) on Days 16 and 29. NGAL and B2M levels were still elevated after 29 days of recovery in contrast to KIM1 and albumin levels. Similar changes were observed in females on Day 29, but not on Days 8, 16 or recovery Day 29. These results indicate that urinary biomarkers can be more sensitive for Hepsera-induced kidney toxicity than BUN and serum creatinine.

## PS 1906 Novel Noninvasive Biomarker of Irradiation-Induced Gastro-Intestinal Injury.

A. Banerjee<sup>1</sup>, N. Sieracki<sup>2</sup>, A. Zakharov<sup>1</sup>, M. Bonini<sup>2</sup> and A. Lyubimov<sup>1</sup>. <sup>1</sup>Toxicology Research Laboratory, UIC, Chicago, IL; <sup>2</sup>Pharmacology, UIC, Chicago, IL.

A non-invasive early marker of radiation induced gastro-intestinal (GI) injury continues to be in high demand. Hence, our aim was to establish a novel fecal biomarker of GI damage in mouse models which can be further extrapolated for use in non-human primates as well as in humans. A Reactive Nitrogen Species (RNS)-detector compound NMAA-1 was established as a novel GI irritation/oxidative stress biomarker in an irradiated mouse model. NMAA-1 is a small molecule, which upon reaction with peroxynitrite (ONOO<sup>-</sup>) produces cleaved NMAA-1. The ability of NMAA-1 to detect ONOO<sup>-</sup> selectively and in a concentration-dependent manner in aqueous solution and in living cells is known. We exploited this selectivity in the quantification of NMAA-1 and cleaved NMAA-1 in feces of mice with irradiation-induced GI damage. C57Bl/6 mice were irradiated at a high lethal dose of

13Gy or at a LD<sub>70/30</sub> of 8.1Gy in two independent experiments using a Cs<sup>137</sup> source. NMAA-1 was administered at 40-60 µM per animal via oral gavage without any signs of toxicity. Fecal samples were collected from the irradiated and non-irradiated control mice at different time points (pre-dose, 4, 6 and 8 hr post dose) prior to irradiation and also on days 1, 5 and 7 post irradiation from all animals. NMAA-1 and cleaved NMAA-1 levels were measured in the feces using LC-MS/MS method. Up to a three-fold increase in the level of the marker was noted in the fecal samples collected between days 5 to 7 in mice irradiated at 13Gy as compared to the control levels with C<sub>max</sub> at about 6 hrs post dose. In case of 8.1Gy irradiation, two-fold or more increase in NMAA-1 and % cleaved NMAA-1 levels was seen in the feces until day 7. It was also observed that post irradiation the appearance of the fecal marker was moved to later time points probably due to decreased GI motility. NMAA-1 has proven to be very distinctive in its role as an indicative marker of GI damage due to radiation-induced toxicity. This promises to be an extremely important diagnostic tool for such condition and further optimization is ongoing.

**PS 1907 Exploring Challenges in Reconstructing Doses or Estimating Blood Concentrations from Urinary Biomarker Data Using a Pharmacokinetic Model for Perchlorate.**

C. Tan, M. B. Phillips and J. Sobus. *US EPA ORD NERL, Research Triangle Park, NC.*

Many human biomarkers of current-use environmental chemicals are measured in urine. While urinary biomarkers are easier to collect than others (e.g., blood markers), reconstructing doses from urinary biomarkers is challenging. In many cases there exists a complicated relationship between dose and biomarker, for example, when a common biomarker for several chemicals exists and the concentration/relative proportion of the exposures from the environment are unknown. Even when there is a simple dose-biomarker relationship, many factors can impact the interpretability of urinary biomarker data, including urine volume, time between voids, and time between dose(s) and sample collection. In this study, a physiologically based pharmacokinetic (PBPK) model of perchlorate was used to examine how these various factors impact our ability to reconstruct doses from urinary biomarkers. The selection of perchlorate was based on its simple dose-biomarker relationship: 100% oral bioavailability and 100% excretion of the parent compound in urine. First, synthetic exposure profiles (varying daily intake doses, time of exposure, etc.) were generated and used as inputs to the PBPK model for simulating three biomarker sampling protocols: random spot voids, first voids, and 24 h cumulative voids. Correlations between simulated urinary concentrations and intake doses were calculated at both the individual- and population-level to determine which sampling protocol provides a more accurate and precise intake estimate. The strongest correlations were observed between the 24 h cumulative concentrations and average daily intake. Additional considerations for the impacts of changing urine volume, time between voids, and time between exposure and sample collection showed that random spot urine samples were highly sensitive to all three factors whereas 24 h cumulative samples were less sensitive.

[This abstract has been cleared by the EPA but solely expresses the view of the authors]

**PS 1908 Fecal and Blood Biomarkers for Gastrointestinal Injury and Subsequent Recovery.**

A. Lyubimov<sup>1</sup>, Y. Chen<sup>2</sup>, J. Anwer<sup>2</sup>, A. Zakharov<sup>1</sup> and A. Banerjee<sup>1</sup>. <sup>1</sup>*Toxicology Research Laboratory, UIC, Chicago, IL;* <sup>2</sup>*Center for Biomedical Testing, Chicago, IL.*

The search for reliable, non-invasive biomarkers of gastro-intestinal (GI) injury/recovery is ongoing but so far no biomarkers as reliable as histopathology have been identified in animal models. Our aim was to establish such biomarkers in non-human primates (NHPs). Previously we established ELISA and MSD methods for lactoferrin and calprotectin measurements in NHPs feces. These methods are currently being improved by multiplexing on one MSD platform. Two new markers including intestinal and liver fatty acid binding protein (I-FABP) and L-FABP were established as markers of intestinal epithelial integrity. These are released rapidly from GI enterocytes into the blood after cellular damage. I-FABP was assayed on a MSD standard plate with a specific antibody (LLOD=5.95 pg/mL), whereas L-FABP was analyzed using ELISA (LLOD=102 pg/mL). Our MSD method for I-FABP has about 10 times lower LLOQ (9.7 pg/mL) as compared to its ELISA method (94 pg/mL). Normal ranges in NHPs plasma were established and found to be above the LLOD for both methods. These biomarkers proved to be helpful for assessment of drug therapeutic effect and potentially survival prognosis after irradiation GI damage. Additionally an LC-MS/MS method was established to estimate the systemic citrulline levels as a marker of GI injury. Citrulline is an amino acid released in circulation predominantly by the intestine enterocytes and is considered a

marker of intestinal integrity. The LC-MS/MS method works in the dynamic range of 125-125000 ng/mL (-0.7-700 µM) of citrulline concentration in plasma. The L-FABP and I-FABP changes correlated well with the citrulline levels as well as histopathology findings based on the analysis of the samples obtained from a NHP irradiation study. Further optimization of the MSD, ELISA and LC-MS/MS methods are being undertaken to provide more sensitive assays from smaller sample volume (including dried blood spot measurements) for these fecal and/or circulating biomarkers of gastro-intestinal inflammation, injury, and recovery.

**PS 1909 Clearance Rates of Organophosphate Metabolites in an Occupationally-Exposed Cohort of Farmworkers.**

W. C. Griffith<sup>1</sup>, Z. N. Guerrette<sup>1</sup>, B. Thompson<sup>2</sup>, G. D. Coronado<sup>2</sup>, D. B. Barr<sup>3</sup>, E. M. Vigoren<sup>1</sup> and E. M. Faustman<sup>1</sup>. <sup>1</sup>*Institute for Risk Analysis and Risk Communication, University of Washington, Seattle, WA;* <sup>2</sup>*Fred Hutchinson Cancer Research Center, Seattle, WA;* <sup>3</sup>*Rollins School of Public Health, Emory University, Atlanta, GA.*

Our studies in the Yakima valley of Washington state follow a cohort of 99 farmworkers (orchard workers) and 95 non-farmworkers to investigate potential exposures to organophosphate pesticides (OPs) by assaying urine samples for the 6 di-alkyl non-specific metabolites of OPs. Urine samples were collected April-June 2005 on three dates spaced two days apart when OP pesticides were being applied and workers were in the orchards. The most commonly used OP in this time period was azinphos-methyl and one of its metabolites, DMTP, had the highest concentration in urine compared to other metabolites of OPs for both farmworkers and non-farmworkers. We used a Bayesian Markov chain Monte Carlo method to estimate the joint distribution of the metabolites and clearance rates in a mixed effects model. The farmworker levels of DMTP were 19 times non-farmworkers. The clearance half-life of DMTP had a geometric mean (95% confidence interval) of 3.6 (2.5,6.0) days across all of the farmworkers (fixed effects), whereas non-farmworkers showed no clearance. The half-lives for individual farmworkers (random effects) varied between 1.5 days and no clearance. The shorter half-lives occurred in farmworkers who had higher first day concentrations of DMTP and farmworkers with no clearance with those who had lower first day concentrations. These results are consistent with a continuing variable level of occupational exposure of the farmworkers but some of the farmworkers having a higher exposure before our collection of urine. The pattern in the non-farmworkers is consistent with exposures to metabolites of OPs through diet and other routes of non-occupational exposure. Similar results were also found for DMP. (Supported by grants P01 ES009601, P30 ES007033 from NIEHS and RD-834514, RD-831709, RD-832733 from US EPA. Contents are authors' responsibility.)

**PS 1910 Assessment of MMP-3 and MMP-9 As Preclinical Biomarkers of Drug-Induced Vascular Injury.**

R. J. Gonzalez, B. Bednar, S. Lin, B. Connolly, S. Patel, G. Mesfin, T. Johnson, H. Miyazaki, W. E. Glaab and F. D. Sistare. *Merck & Co., West Point, PA.*

Drug-induced vascular injury (DIVI) continues to be a major obstacle in drug development. Attempts to correlate this observation in preclinical toxicity studies with hemodynamic changes are not always successful. Additionally, no accessible and specific biomarkers of DIVI exist, making risk assessment and monitoring in humans a challenge during drug development and regulatory approval. It has been previously reported that circulating levels of matrix metalloproteinases (MMPs), specifically MMP-3 and MMP-9, were able to distinguish between patients with active antineutrophilic cytoplasmic antibody (ANCA)-associated vasculitis (AAV) and remission. In order to determine whether MMPs are involved in the arterial pathology associated with DIVI observed in animal toxicology studies, a fluorescent imaging probe, MMPSenseTM, was used to measure activity of MMPs along with a fluorescent blood pooling agent, AngioSenseTM, ex-vivo in the mesenteric arteries of rats following administration of fenoldopam. Increased fluorescence in the mesenteric arteries from both imaging probes correlated well with vascular injury, as determined histologically, and was in agreement with increases in both MMP-3 and -9 expression in the affected arteries using immunohistochemical staining. To assess whether changes to circulating levels of MMP-3 and -9 respond to incidence and severity of DIVI, we compared their levels in plasma from several models of DIVI in rat, dog and monkey. Circulating levels of MMP-3 appear to correlate well with DIVI and the response is conserved across our pre-clinical species. In summary, MMPs appear to have a role in the arterial pathology associated with DIVI seen in animal toxicology studies, which is reflected in circulating levels of MMP-3 in pre-clinical species, and provide a potential accessible biomarker to monitor for DIVI in animals and in the clinic.

**PS 1911 Molecular, Cellular, and Histological Changes in Mice Living on Sand Contaminated with Coal Dust under Laboratory Conditions.**

K. Caballero-Gallardo, L. Carranza-Lopez and J. Olivero-Verbel. *Environmental and Computational Chemistry Group Pharmaceutical Sciences, University of Cartagena, Cartagena, Colombia.*

Coal mining is one of the most important economical activities in Colombia. However, few data have been gathered concerning the impact of these activities on human and ecosystem health. During coal mining and transport, different types of dust material are formed. The aim of this work was to evaluate the toxic effects associated with the exposure to total suspended particle matter fraction of coal dust (<38 µm), from a sample collected in the Loma mine, Cesar, Colombia. Washed and sterilized sand was contaminated with coal dust to obtain concentrations ranging from zero (control) to 4%. Six different mice per group were allowed to live in boxes with this bed for eight weeks with ad libitum water and food. At the end of the experiment, animals were euthanized and blood and tissues collected. Mice in contact with coal dust did not evidence significant weight or hepatosomatic changes compared to control. However, animals in the 4% coal dust group grew faster. Real Time PCR analysis revealed an increase in Cyp1A1 mRNA for animals living on sand with concentrations greater than 2% coal dust. Unexpectedly, for mice on polluted sand, SOD and MT1 hepatic mRNA were downregulated, and no changes were observed on Myc expression. The results of comet assay in peripheral blood cells, and the micronucleus test in blood smears revealed significant potential genotoxic damage at the greatest tested coal dust level. Histopathological analysis showed a dose-response relationship for the presence of hepatic necrosis, steatosis, vacuolization and nuclei enlargements in exposed animals. These results suggest that soil contaminated with coal dust induces several molecular, cellular and histopathological changes in mice. Accordingly, it is necessary to revise the current legislation on mining practices in Colombia in order to prevent health problems derived from these particles. Vice-Rectoría for Research. UniCartagena. 2011-2012. Colciencias-UniCartagena, Colombia. Grant 110749326186 (2009).

**PS 1912 Advancing Adoption of Novel Safety Biomarkers into Drug Development through Voluntary Submission of Data at US FDA, EMA, and PMDA.**

E. G. Walker, M. Brumfield and E. H. Dennis. *Critical Path Institute, Tucson, AZ.*

Regulatory science, the science of developing new tools, standards, and approaches to assess the safety, efficacy, quality, and performance of regulated medical products, has advanced over time due to a number of factors. However, many safety biomarkers used in nonclinical and clinical safety assessment in drug development have not changed in decades. Recently established channels for FDA, EMA, and PMDA to receive and evaluate scientific data supporting novel tools for use in drug development are now better defined in guidances, e.g. FDA's Draft Guidance for Industry "Drug Development Tool Qualification" and EMA's "Evaluation of novel methodologies for use in drug development." The outcome of a qualification submission to one of these regulatory agencies is a formal opinion regarding the utility of a novel drug development tool (DDT) for a particular and well-circumscribed application in the drug development process, defined within a "context of use." While recognizing that other mechanisms exist within the research community for driving scientific consensus on novel biomarkers, this study focuses on the formal regulatory qualification process. This study compares the procedure, volume and types of submissions, and proposes a framework for assessing success at FDA, EMA, and PMDA. Safety biomarkers comprise over half of the sixteen unique biomarkers qualified thus far, and are highlighted. Qualification of new safety biomarkers by regulatory agencies and subsequent adoption by drug developers is anticipated to speed therapeutic development for patients in need, build scientific consensus as to the usefulness and readiness of novel tools for understanding disease and therapeutic development, and decrease uncertainty between the regulators and sponsors regarding their appropriate application.

**PS 1913 Growth Hormone and IGF-1 Measurements in Beagle Dogs by ELISA: Assay Implementation and Variations in Baseline Levels.**

C. Gauthier, J. Leiva, G. Gonzalez and A. Nelson. *Immunology, ITR International, Baie d'Urfe, QC, Canada.* Sponsor: W. Ruddick.

Scope :

Measurements of GH and IGF-1 in Beagle dogs are complicated by several technical and biological issues. In this poster, we present data from ELISA methods that were specially adapted and qualified at our facility for the quantification of GH & IGF-1 in canine serum. During assay implementation and routine use, several observations have been made with these hormone baseline levels and some biological & technical parameters.

**Experimental Procedures & Results :**

Beagle dog serum was obtained from males and females, originating from two different breeders; Marshall and Covance. Samples were tested from dogs housed at three different preclinical testing facilities; ITR Laboratories Canada Inc. ("ITR") and two other undisclosed facilities ("Lab B" & "Lab C"). A commercial GH ELISA kit designed for rat/mouse GH and another commercial human IGF-1 kit were adapted for use with dog serum samples. Typical basal GH levels in Beagle dogs vary from < 6.25 to 40 ng/mL. No significant differences were observed in the GH basal level between different genders, breeding source or test facility. However, GH levels generally increased with higher body weight and age. GH varied between individuals of the same study. Typical basal IGF-1 levels in Beagle dogs varied greatly, from < 42 to 150 ng/mL (ex. from Marshall-bred dogs housed at ITR), while the normal range increase to 150-500 ng/mL with Covance-bred dogs housed at "Lab C". Age and body weight only had minor impact on the IGF-1 basal levels, while a gender difference was only seen within the Covance-bred dogs housed at "Lab C".

**Conclusions :**

The GH/IGF-1 data gathered internally from several preclinical studies with Beagle dogs of various origins have shown that basal IGF-1 levels can vary significantly depending on the dog breeding source and housing facility, in addition to age and body weight. It was also found that due to the natural cyclic activity of GH, multiple pre-dose samplings are useful, with the last pre-dose sample being ideally taken as close as possible to dosing with the test item.

**PS 1914 Evaluation of Iodide Deficiency in the Lactating Rat and Pup Using a Biologically-Based Dose Response (BBDR) Model.**

J. W. Fisher<sup>1</sup>, S. Li<sup>2</sup>, K. Crofton<sup>3</sup>, R. Zoeller<sup>4</sup>, E. D. McLanahan<sup>3</sup>, A. Lumen<sup>1</sup> and M. E. Gilbert<sup>3</sup>. <sup>1</sup>FDA/NCTR, Jefferson, AR; <sup>2</sup>Georgia Health Sciences University, Augusta, GA; <sup>3</sup>EPA/ORD, Research Triangle Park, NC; <sup>4</sup>University of Massachusetts, Amherst, MA.

A biologically-based dose response (BBDR) model for the hypothalamic-pituitary thyroid (HPT) axis in the lactating rat and nursing pup was developed to describe the perturbations caused by iodide deficiency on the HPT axis. Model calibrations, carried out by adjusting key model parameters, were used as a technique to evaluate HPT axis adaptations to dietary iodide intake in euthyroid (4.1 -39 µg iodide/d) and iodide deficient (0.31 and 1.2 µg iodide /d) conditions. Iodide deficient conditions in both the dam and pup were described with increased blood flow to the thyroid gland, TSH-mediated increase in thyroidal uptake of iodide and binding of iodide in the thyroid gland (organification), and in general, reduced thyroid hormone production and metabolism. Alterations in thyroxine (T4) homeostasis were more apparent than for triiodothyronine (T3). Model predicted average daily area-under-the-serum- concentration-curve (AUC, nM\*day) values for T4 at steady-state in the dam and pup decreased by 14-15% for the 1.2 µg iodide /d iodide deficient diet and 42 to 52% for the 0.31 µg iodide /d iodide deficient diet. In rat pups that were iodide deficient during gestation and lactation, these decreases in serum T4 levels were associated with synaptic response suppression in the hippocampal region of the brain, while other measures of neurotoxicity were unaltered.

**PS 1915 An Animal Model of Marginal Iodine Deficiency during Development: The Thyroid Axis and Neurodevelopmental Outcome.**

M. E. Gilbert<sup>1</sup>, J. M. Hedge<sup>1</sup>, L. Valentin-Blasini<sup>2</sup>, B. C. Blount<sup>2</sup>, K. Kannan<sup>3</sup>, J. Tietge<sup>4</sup>, R. Zoeller<sup>5</sup>, K. Crofton<sup>1</sup>, J. Jarrett<sup>2</sup> and J. W. Fisher<sup>6</sup>. <sup>1</sup>US EPA, Research Triangle Park, NC; <sup>2</sup>CDC, Atlanta, GA; <sup>3</sup>SUNY, Albany, NY; <sup>4</sup>US EPA, Duluth, MN; <sup>5</sup>University of Massachusetts, Amherst, MA; <sup>6</sup>FDA, Jefferson, AR.

Thyroid hormones (TH) are essential for brain development and iodine is required for TH synthesis. Environmental chemicals that perturb the thyroid axis result in modest reductions in TH, yet there is a paucity of data on the neurological impairments associated with low level TH disruption. This study examined the dose-response characteristics of marginal iodine deficiency (ID) on parameters of thyroid function and neurodevelopment. ID diets were prepared by adding varying concentrations of iodine to a casein-based diet producing 5 nominal iodine levels ranging from ample (1000 µg iodine/kg chow) to deficient (25 µg iodine/kg chow).

Female Long Evans rats were maintained on these diets beginning 7 wk prior to breeding until the end of lactation. Dams were sacrificed on gestational days 16 and 20, or when pups were weaned on postnatal day (PN) 21. Fetal tissue was harvested with sacrifice of the dams, pups were sacrificed on PN14 and PN21. Blood, thyroid gland, and brain were analyzed for iodine, TH, TH precursors and metabolites. Serum and thyroid gland iodine and TH were reduced in the two most deficient diets. T4 was reduced in the fetal brain but was not altered in the neonate. Cognitive function, assessed by acoustic startle, water maze learning and fear conditioning, was unchanged in adult offspring, but excitatory synaptic transmission was impaired in the dentate gyrus by the two most deficient diets. A 15% reduction in cortical T4 in the fetal brain was sufficient to induce permanent reductions in synaptic function in the adult. These findings have implications for regulation of TH-disrupting chemicals, and suggest that standard behavioral assays do not readily detect neurotoxicity induced by modest developmental TH disruption. (Does not reflect EPA or CDC policy).

## PS 1916 Association of Paraoxonase-1 Activity and Gene Polymorphisms with Type 2 Diabetes Mellitus.

P. Eden<sup>1,2</sup>, E. Olsen<sup>3</sup>, J. Watt<sup>3</sup> and J. E. Chambers<sup>2</sup>. <sup>1</sup>711th Human Performance Wing, Wright-Patterson AFB, OH; <sup>2</sup>Mississippi State University, Starkville, MS; <sup>3</sup>81st Medical Group, Keesler AFB, MS.

Paraoxonase-1 (PON-1) is an HDL-associated lactonase that hydrolyses organophosphates such as paraoxon and diazoxon, the active metabolites of the insecticides parathion and diazinon, as well as affords protection against LDL oxidation. There is evidence that Type 2 diabetes mellitus (T2DM) patients display lower PON-1 activity. This study examined plasma from 150 T2DM and 150 non-diabetic subjects to evaluate PON-1 activity and relevant genetic variations associated with changes in PON-1 activity. PON-1 activity was measured spectrophotometrically using the substrates paraoxon, diazoxon, and phenyl acetate. Two significant genetic polymorphisms (PON-1192 and PON-155) were also determined using real-time polymerase chain reaction melting curve analysis. The PON-1192 genotype displayed an average melting curve peak at  $61.1^{\circ}\text{C} \pm 1.1$  (SD) for the (R) homozygous allele while the (Q) homozygous allele showed a peak of  $66.3^{\circ}\text{C} \pm 0.6$ . The PON-155 genotype had an average melting curve peak at  $61.9^{\circ}\text{C} \pm 0.9$  for the (L) homozygous allele and  $66.3^{\circ}\text{C} \pm 0.9$  for the (M) homozygous allele. A prevalence of the PON-1192RR polymorphism was found between T2DM subjects and non-diabetics (odds ratio = 2.3; 95% confidence interval = 1.25- 4.21,  $p = 0.01$ ). The substrate diazoxon demonstrated lower plasma PON-1 activity in T2DM subjects ( $7469 \pm 140$  U/L) compared to non-diabetics ( $8287 \pm 151$  U/L),  $p = 0.02$ . In addition, African-Americans in this study demonstrated a higher association with the PON-1192RR genotype (51.5%) than did Caucasians (9.1%) ( $p < 0.001$ , odds ratio = 10.66). The genetic and plasma PON-1 activity results suggest that the PON-1192RR polymorphism is less protective against development of T2DM and that decreased PON-1 activity is associated with increased development of T2DM.

## PS 1917 Effect of Dioxin on the Nursing Behavior of Dams and the Growth of Pups: A Study for the Mechanism Focusing on Damage to Maternal Prolactin and Fetus/Infant Growth Hormone.

M. Fujii<sup>1</sup>, T. Takeda<sup>1</sup>, J. Taura<sup>1</sup>, Y. Hattoni<sup>1</sup>, Y. Ishii<sup>1</sup>, H. Uchi<sup>2</sup>, K. Tsukimori<sup>3</sup>, M. Furue<sup>2</sup> and H. Yamada<sup>1</sup>. <sup>1</sup>Graduate School of Pharmaceutical Sciences, Kyushu University, Fukuoka, Japan; <sup>2</sup>Kyushu University Hospital, Fukuoka, Japan; <sup>3</sup>Fukuoka Children's Hospital, Fukuoka, Japan. Sponsor: Y. Kumagai.

Maternal exposure to 2,3,7,8-tetrachlorodibenzo-p-dioxin (TCDD) causes a number of developmental disorders including growth retardation in the pups. Although our previous studies have demonstrated that TCDD imprints defects in gender-specific phenotypes through a reduction in gonadotropin production in perinatal pups (1,2), the mechanism for growth retardation by TCDD remains unknown. In this study, we investigated a hypothesis that maternal exposure to TCDD damages to maternal prolactin, a regulator of milk secretion and maternal care to the pups, and growth hormone (GH) in the pups to disturb the growth of offsprings. As has been reported so far, oral administration of TCDD (1  $\mu\text{g/kg}$ ) to pregnant Wistar rats at gestational day 15 attenuated the body weight and height of infants and their short-term memory examined 5 weeks after birth. In addition, we observed that TCDD reduced the number of pups after birth, whereas the same was not seen at fetal stages. In relation to this finding, TCDD reduced not only maternal expression of prolactin in a nursing period-specific manner, but also the frequency of licking, one of the maternal nursing behaviors. Furthermore, maternal exposure to

TCDD attenuated the serum concentration of GH in perinatal pups. Such attenuation may be an outcome due to the reduced expression of a receptor for GH-releasing hormone (GHRH), a regulator of GH biosynthesis, because a lowered expression of GHRH receptor cause by TCDD also appeared during the same period. Taken together, it is suggested that maternal exposure to TCDD produces its developmental toxicity on pups by a combination of a reduction in the expression of maternal prolactin and pup GH.

References: 1) Takeda, T., et al., J. Pharmacol. Exp. Ther., 329, 1091 (2009); 2) Takeda, T., et al., J. Biol. Chem., 287, 18440 (2012).

## PS 1918 Effects of Perfluorooctane Sulfonate (PFOS) on the Hypothalamic-Pituitary-Testicular Axis Activity in Adult Male Rat.

M. A. Lafuente and N. Pereiro. Laboratory of Toxicology, University of Vigo, Orense, Spain.

Perfluorooctane sulfonate (PFOS) is considered such as an endocrine disruptor. This study was designed to evaluate the possible alterations induced by PFOS on the hypothalamic-pituitary-testicular axis activity. For this purpose, male Sprague-Dawley rats were orally treated for 28 days with PFOS, at the doses of 0.5, 1.0, 3.0 and 6.0 mg/kg/day. Control rats received 0.5% Tween-20 vehicle. Twenty four hours after the last dose of PFOS, rats were killed by decapitation and the hypothalamus was removed in order to determine in this brain region both neuropeptide Y (NPY) and gonadotropin-releasing hormone (GnRH) concentration by specific enzyme-linked immunoabsorbent (ELISA) assays. Serum luteinizing hormone (LH), follicle stimulating hormone (FSH) and testosterone levels were measured by specific commercial kits. In addition, the relative gene expression of NPY and GnRH in hypothalamus, of GnRH receptor in pituitary and of LH receptor and FSH receptor in testis was determined by quantitative real time PCR. Serum LH and testosterone levels and relative gene expression of GnRH and of FSH receptor were decreased in rats treated with PFOS. Serum FSH concentration and relative gene expression of LH receptor in testis were increased in these same animals. Hypothalamic concentration of NPY and GnRH was decreased with the doses of 1.0 and 3.0 mg/Kg/day, but GnRH levels were increased with the dose of 6.0mg/Kg/day. Relative gene expression of NPY was diminished with the dose of 0.5mg/Kg/day, but it was increased with the dose of 6.0mg/Kg/day. Finally, relative gene expression of GnRH receptor was not modified in pituitary by PFOS. The obtained results suggest that PFOS exposure can modify the hypothalamic-pituitary-testicular axis activity at several levels, and these alterations seem to be dependent of the administered dose. This work was supported by a grant from the Ministry of Education and Science, Spain (AGL2009-09061).

## PS 1919 Conditional Knockout of the Aryl Hydrocarbon Receptor in the Liver Alters Mouse Phenotype As Well As Glucose and Lipid Homeostasis.

D. Carter and C. Elferink. Pharmacology and Toxicology, UTMB, Galveston, TX.

The aryl hydrocarbon receptor (AhR) is a ligand activated transcription factor historically known for its role in the adaptive metabolism of xenobiotics. However, generation of the AhR knockout mouse (AhR-KO) has provided evidence of physiological roles for the AhR. To study the physiological role of AhR in the liver, AhR conditional knockout (AhR-CKO) mice were utilized by crossing AhR  $\text{fx}/\text{fx}$  (control) mice with mice that express Cre recombinase under the control of the albumin promoter, resulting in loss of AhR expression specifically in the liver parenchyma. Our experiments indicate a novel sex dependent phenotype wherein, AhR-CKO females exhibited reduction in body weight, loss of adipose tissue and increased basal glucose levels ( $218 \pm 19.73$  mg/dl). Therefore, our goal is to characterize the AhR-CKO mouse phenotype and identify potential AhR-dependent mechanisms responsible for lipodystrophy and abnormal glucose homeostasis. AhR-CKO and control mice were subjected to glucose and insulin tolerance tests. Our data suggests decreased glucose tolerance and increased insulin sensitivity in AhR-CKO females compared to their controls. Plasma analyses also suggest alterations in leptin (control  $3.227 \pm 0.27$  vs CKO  $1.028 \pm 0.129$ ), FFA (control  $0.3630 \pm 0.026$  vs CKO  $0.594 \pm 0.02$ ) and insulin levels (control  $0.495 \pm 0.008$  vs CKO  $0.253 \pm 0.004$ ). Immuno-Histochemical staining for insulin revealed reduced insulin content and smaller pancreatic islets in AhR-CKO mice. We also conducted histopathological analysis using Oil red O staining, which revealed decreased lipid content in AhR-CKO mice livers compared to controls. Our experiments strongly suggest that AhR activity in the liver communicates with extra-hepatic tissues and alters their function. AhR-CKO mice may offer an elegant model to study the link between endogenous AhR activity in the liver and clinically relevant metabolic disorders such as diabetes, lipodystrophy and obesity.

**PS 1920 Endocrine Modulatory Effects of Cadmium and Activation of MAPK Signaling.**

I. Ali<sup>1</sup>, P. Damdimopoulou<sup>2</sup>, S. I. Mäkelä<sup>3</sup>, M. Berglund<sup>1</sup>, U. Stenius<sup>1</sup>, A. Adamsson<sup>4</sup>, A. Åkesson<sup>1</sup>, H. Håkansson<sup>1</sup> and K. Halldin<sup>1</sup>. <sup>1</sup>Institute of Environmental Medicine, Karolinska Institute, Stockholm, Sweden; <sup>2</sup>Department of Biosciences and Nutrition, Karolinska Institute, Huddinge, Sweden; <sup>3</sup>Department of Cell Biology and Anatomy and Turku Center for Disease Modeling, Institute of Biomedicine, University of Turku, Turku, Finland; <sup>4</sup>Department of Physiology, Institute of Biomedicine, University of Turku, Turku, Finland.

Research on endocrine modulatory effects of Cadmium (Cd) started over a decade ago, when this metalloestrogen was found to interact with the estrogen signaling pathway. Since then, several independent in vitro as well as in vivo reports have emerged on this topic. Our objective has been to characterize the details of molecular mechanisms of action for the endocrine modulatory effects of Cd. We applied a combined in vivo and in vitro approach by using transgenic ERE-luc reporter mice model as well as hepG2, MCF-7 and ECC-1 cell lines. After 3-days s.c. exposure to CdCl<sub>2</sub>, we did not detect reporter gene activation in the dose ranges 5-500 µg/kg bw and 0.5-500 µg/kg bw in female and male mice respectively. Nevertheless, we observed significant thickening of the uterine epithelium in the absence of uterine weight increase in females, and detected activation of Raf, Erk1/2 MAPK in the liver of both genders in low dose groups. Further, in our in vitro settings, low doses of CdCl<sub>2</sub> (1nM-100nM) also activated Raf, Erk1/2 MAPK and this effect disappeared with the inhibition of GPR30 and EGFR receptors. Our data shows that the molecular markers that are modulated by Cd differ depending on the exposure level; i.e. low doses relevant to human exposure via diet stimulate cytoplasmic kinases, while higher doses induce cellular stress responses. We conclude that CdCl<sub>2</sub> affects cellular signaling pathways that can produce physiological effects reminiscent of bona fide estrogen stimulation. However, CdCl<sub>2</sub> does not activate canonical estrogen signaling.

**PS 1921 Bisphenol A (BPA) Levels Were Associated with Increased Estrogen.**

M. Lind<sup>1</sup>, T. Naessen<sup>2</sup>, J. Bergquist<sup>3</sup>, M. M. Kushnir<sup>3,4</sup> and L. Lind<sup>5</sup>. <sup>1</sup>Occupational and Environmental Medicine, Uppsala University, Uppsala, Sweden; <sup>2</sup>Department of Women's and Children's Health, Section for Obstetrics and Gynecology, Uppsala University, Uppsala, Sweden; <sup>3</sup>Analytical Chemistry/Department of Physical and Analytical Chemistry, Uppsala University, Uppsala, Sweden; <sup>4</sup>ARUP Institute for Clinical and Experimental Pathology, Salt Lake City, UT; <sup>5</sup>Department of Medical Sciences, Acute and Internal Medicine, Uppsala University, Uppsala, Sweden.

**BACKGROUND:** The plastic associated compound bisphenol A (BPA) is a known estrogen-receptor agonist. Since background exposure to BPA could be detected in most individuals, we explored the relationships between BPA levels in serum and levels of endogenous sex hormones and their precursors in a population-based sample.

**METHODS:** 1,016 subjects all aged 70 years were investigated in the Prospective Investigation of the Vasculature in Uppsala Seniors (PIVUS) study. BPA was measured in serum at ALS Canada using an API 4000 liquid chromatograph/ tandem mass spectrometer, and sex hormones were measured at ARUP Institute for Clinical and Experimental Pathology, Salt Lake City, by high-specificity liquid chromatography-tandem mass spectrometry.

**RESULTS:** In men, BPA levels were related to estrone (E1,  $p < 0.00001$ ) and estradiol (E2,  $p = 0.02$ ) levels. BPA levels were also related to levels of the precursors pregnenolone and 17-OH-pregnenolone ( $p < 0.05$ ) and estimated aromatase activity ( $p < 0.05$ ), indicating an increased formation of estrogens from androgen precursors. In women, only weaker relationship compared with E1 was found ( $p < 0.05$ ).

**IN CONCLUSION:** increased levels of BPA were associated with increased estrogen levels in elderly males, indicating endocrine disrupting activity in the elderly.

**PS 1922 A Comparison of RIA and LC-MS/MS Methods to Quantify Steroids in Rat Serum and Urine following Exposure to an Endocrine Disrupting Chemical.**

B. W. Riffle<sup>1,2</sup>, S. C. Laws<sup>1</sup> and W. M. Henderson<sup>3</sup>. <sup>1</sup>ETB, TAD, NHEERL, ORD, US EPA, Research Triangle Park, NC; <sup>2</sup>ORISE, US Department of Energy, Oak Ridge, TN; <sup>3</sup>ERD, NERL, ORD, US EPA, Athens, GA.

Commercially available radioimmunoassays (RIA) are frequently used in toxicological studies to evaluate effects of endocrine disrupting chemicals (EDCs) on steroidogenesis in rats. Currently there are limited data comparing steroid concentrations in rats as measured by RIAs to those obtained using liquid chromatography coupled with tandem mass spectrometry (LC-MS/MS). This study evaluates the

concordance of serum and urine steroid concentrations as quantified by both RIA and LC-MS/MS following exposure to a known EDC, atrazine (ATR). Adult male rats were dosed with ATR (200 mg/kg/d) or methylcellulose (solvent control) by oral gavage for 5 days. Animals were decapitated 2 hours after the final dose. Serum was collected and separated into 2 aliquots for analysis. Serum was assayed by RIA for androstenedione (A), corticosterone (CORT), estradiol (E2), estrone (E1), progesterone (P4), and testosterone (T). Serum was extracted via solid phase extraction prior to LC-MS/MS analysis with positive electrospray ionization in multiple-reaction monitoring mode for A, CORT, P4, and T. E1 and E2 serum concentrations were quantified similarly by LC-MS/MS, following derivatization with dansyl chloride. To compare CORT values from urine, pregnant adult rats were dosed with either ATR (100 mg/kg/d) or methylcellulose by oral gavage for 5 days (i.e., gestational days 14-18). Urine samples were collected daily for 2 consecutive 6 hour intervals following dosing and assayed for CORT by RIA and LC-MS/MS as described above. Data analyses demonstrated a high degree of correlation between the two detection methods ( $R^2 = 0.88 - 0.92$ ). No statistically significant differences were observed between RIA and LC-MS/MS means for any of the steroids assayed. These findings indicate that steroids may be reliably measured in rat biological media using RIAs or LC-MS/MS in toxicological studies. This abstract does not reflect U.S. EPA policy.

**PS 1923 Exposure of Pregnant Fischer 344 Rats to Low Levels of Dietary Zearanol Induces Precocious Puberty and Decreased Mammary Tumor Latency in F1 and F2 Progeny.**

C. Lewis<sup>1</sup>, J. T. Barrett<sup>1</sup>, M. A. Gallo<sup>1,2</sup> and H. Zarbl<sup>1,2</sup>. <sup>1</sup>Environmental and Occupational Medicine, Robert Wood Johnson Medical School, UMDNJ, Piscataway, NJ; <sup>2</sup>Environmental and Occupational Health Sciences Institute, Robert Wood Johnson Medical School, Piscataway, NJ.

Zearanol (Zer) is a synthetic derivative of zearalenone (Zea), a potent myco-estrogen produced by several species Fusarium that contaminate grain. Zer has estrogenic activity comparable to that of DES and is ~1000 times more estrogenic than Bisphenol A. After its growth promoting effects on livestock were noted in the early 1970's, Zer replaced diethylstilbestrol (DES) in implants to enhance meat production and quality. Accidental and occupational exposures were associated with precocious puberty and gynecomastia. Banned in Europe and Asia, Zer is introduced into livestock in the Americas, can be detected in the finished product, and is stable at cooking temperatures. Our recent studies in prepubescent girls indicate that human exposure is primarily via the consumption of beef and corn, and urinary levels of unconjugated Zer were associated with differences in the onset of puberty, height and weight (Bandera et al., Science of the Total Environment 409(24):5221-5227, 2011). Our studies in rats indicated that exposure to non-toxic doses of Zer in utero (between prenatal day 7 to term) via the mother's diet (0.1µg/day in safflower oil), results in precocious puberty in females F1 progeny, defined by a three day decrease in age at vaginal opening. F1 male progeny showed feminization as assessed by a decreased ano-genital distance. F1 female treated with a single carcinogenic dose of N-Nitroso-N-methylurea (NMU) showed a decrease in latency and an increase in the incidence of mammary tumors. Similar effects on puberty and carcinogenesis were also observed in the F2 progeny, but only if both the dam and the sire were exposed to Zer in utero. Together these studies suggest that in utero exposure to the Zer may produce transgenerational effects on sexual maturation and carcinogenesis.

Supported by grants from The NJCCR and the NIEHS (ES005022).

**PS 1924 P-p-DDE Levels Are Associated with Reduced Testosterone Levels in Elderly Males.**

L. Lind<sup>1</sup>, T. Naessen<sup>2</sup>, J. Bergquist<sup>3</sup>, M. M. Kushnir<sup>3</sup> and M. Lind<sup>2</sup>. <sup>1</sup>Department of Medicine, Uppsala, Sweden; <sup>2</sup>Uppsala University, Uppsala, Sweden; <sup>3</sup>ARUP Institute for Clinical and Experimental Pathology, Salt Lake City, UT.

**Background:** The DDT metabolite p-p-DDE is a known androgen-receptor agonist. Since background exposure to p-p-DDE still could be detected in most individuals, we explored the relationships between p-p-DDE levels in serum and levels of endogenous sex hormones and their precursors in a population-based sample.

**Methods:** 1,016 subjects all aged 70 years were investigated in the Prospective Investigation of the Vasculature in Uppsala Seniors (PIVUS) study. p-p-DDE was measured in plasma by a high-resolution chromatography coupled to high resolution mass spectrometry (HRGC/HRMS), and sex hormones by high-specificity liquid chromatography-tandem mass spectrometry.

**Results:** In men, p-p-DDE levels were related to both reduced testosterone ( $p = 0.006$ ) and SHBG levels ( $p = 0.008$ ). Furthermore, also reduced levels of the precursors pregnenolone and 17-OH-pregnenolone were related to high p-p-DDE levels ( $p < 0.05$ ), indicating a general reduction in endogenous sex hormone synthesis in subjects with high p-p-DDE levels. Similar tendencies, but less pronounced, were seen in women.

In conclusion, increased levels of p-p-DDE levels were associated with both reduced testosterone and SHBG levels in elderly males, indicating endocrine disrupting activity by DDT in the elderly.

## **PS** 1925 *In Utero* Bisphenol A (BPA) Exposure, the Developing Immune System and Memory.

J. N. Franklin, Q. Hu and J. DeWitt. *Pharmacology and Toxicology, East Carolina University, Greenville, NC.*

Exposure to exogenous agents during susceptible stages of neurodevelopment may be associated with the onset of neurological disorders. The emerging contaminant bisphenol A (BPA) is a widely used ingredient in the production of plastics and resins utilized in food and beverage packaging. Our hypothesis is that developmental exposure to BPA induces neural and behavioral alterations and that these alterations will be associated with developmental immunotoxicity. C57BL/6 female mice were given 0, 25, 50, or 100 mg/kg of BPA in a corn oil vehicle by gavage, beginning at pairing with males and ending at weaning of pups. Littermates were assessed on a Barnes maze at postnatal day 21 (PND21), PND42, and PND60. Splenic lymphocytes, including B cells, natural killer cells (NK cells) and T cells (CD3, CD4, CD8, and CD25 subclasses), were immunofluorescently labeled to determine the immunophenotype of offspring from each treatment group. The Barnes maze is a reliable indicator of hippocampal-dependent learning and memory that has been used to link immune dysfunction with altered neurodevelopment. On the Barnes maze, the time to initially reach the escape hole did not significantly differ among treatment groups. A significant interaction between sex and dose was detected in offspring immunophenotype, indicating that immune cell subpopulations responded differently between sexes by dose. Liver weights increased in adult offspring by dose, though this trend was not statistically significant. Our data indicate that developmental exposure to BPA does not alter aspects of learning and memory as evaluated by the Barnes maze, but may induce differences in immunophenotype between sexes that may confound behavioral responses. Additional work is ongoing to evaluate changes to hippocampal neurons induced by developmental BPA exposure.

## **PS** 1926 Low-Dose Evaluation of the Antiandrogen Flutamide in a 28-Day Toxicity Study in the Rat.

A. Sarabay<sup>1</sup>, H. Tinwell<sup>1</sup>, O. Blanck<sup>1</sup>, F. Schorsch<sup>1</sup>, M. Pallardy<sup>2</sup>, R. Bars<sup>1</sup> and D. Rouquié<sup>1</sup>. <sup>1</sup>Bayer CropScience, Sophia Antipolis, France; <sup>2</sup>Faculty of Pharmacy, University Paris-Sud, INSERM UMR 996, Châtenay-Malabry, France.

The dose-response characterization of endocrine mediated toxicity is an on-going debate which is controversial when exploring the nature of the dose-response curve and the effect at the low end of the curve. Therefore, to contribute to this debate we have assessed the effects of a wide range of dose levels of the antiandrogen flutamide (FM) on male rats using omic and traditional tools. Flutamide was administered to Wistar rats at the doses of 0, 0.001, 0.01, 0.1, 1 and 10 mg/kg/day for 28 days. The highest dose level corresponds to a therapeutic dose in humans and it is also known to induce changes in male reproductive tissues in rodents. At necropsy, blood samples were collected for testosterone measurements. Male reproductive tissues were weighed. The testes were collected for histopathological assessment in addition to the evaluation of gene expression changes. Results showed that testicular lesions (Leydig cell hyperplasia) were detected from 1 mg/kg/day whereas the testosterone levels were only increased at 10 mg/kg/day. A preliminary molecular investigation of targeted genes by qPCR shows changes at 1 and 10 mg/kg/day. Based on the available results, only monotonic responses were observed based on gravimetry, microscopic examination, hormonal analyses and gene expression using qPCR analyses. Full genome gene expression evaluation using DNA microarrays is on-going to evaluate the shape of the global gene expression dose response curves.

## **PS** 1927 Investigation of Vinclozolin at Environmentally-Relevant Concentrations.

S. Gröters<sup>1</sup>, S. Schneider<sup>1</sup>, K. C. Fussell<sup>1</sup>, V. Strauss<sup>1</sup>, M. Frericks<sup>2</sup>, S. Melching-Kolmuss<sup>2</sup>, B. Siddeek<sup>3</sup>, M. Benahmed<sup>3</sup> and B. van Ravenzwaay<sup>1</sup>. <sup>1</sup>Experimental Toxicology and Ecology, BASF SE, Ludwigshafen am Rhein, Germany; <sup>2</sup>Product Safety, BASF SE, Ludwigshafen am Rhein, Germany; <sup>3</sup>U895, équipe 5, Bâtiment Universitaire Archimède, Centre Méditerranéen de Médecine Moléculaire (C3M), Inserm, Nice, France.

Endocrine disruption has become an important topic of public concern. Despite an increasing amount of attention, little is understood about if environmentally relevant doses of endocrine disrupting chemicals (EDCs) affect homeostasis.

Furthermore, there are often knowledge gaps in the studies used to assess EDCs. To address these concerns, we performed a pre-/post-natal reproductive toxicity study of vinclozolin as part of a larger BASF and CEFIC funded project to measure the developmental toxicity of low single- and mixture-doses of anti-androgens. The tested doses were selected to mimic a low-effect level, the no observed adverse effect level (NOAEL) for endocrine effects, and the acceptable daily intake (ADI). At the LOAEL dose, female offspring developed normally, while the male offspring showed effects known for anti-androgens. No effects at all were noted at the lowest two doses, the NOAEL and the ADI. At the top dose, an increase was noted in nipples and/or areolas in male animals on PND 12. This effect was transient, as all had regressed by PND 21. In both of these dose groups, male offspring which were reared to young adulthood displayed additional anti-androgen effects including, delayed sexual maturation and reduced male sex organ sizes and weights. However, no significant decrease in anogenital distance on PND 1 was noted in the animals of this dose group. Similarly, assessment of sexual steroid hormones and their precursors revealed no effects at any of the dose levels. Taken together, the weight of evidence of the clinical and pathological findings suggests a lack of a non-monotonic dose-response curve.

## **PS** 1928 Investigation of Flutamide at Environmentally-Relevant Concentrations.

S. Melching-Kolmuss<sup>2</sup>, S. Schneider<sup>1</sup>, K. C. Fussell<sup>1</sup>, S. Gröters<sup>1</sup>, V. Strauss<sup>1</sup>, B. Siddeek<sup>3</sup>, M. Benahmed<sup>3</sup>, M. Frericks<sup>2</sup> and B. van Ravenzwaay<sup>1</sup>. <sup>1</sup>Experimental Toxicology and Ecology, BASF SE, Ludwigshafen am Rhein, Germany; <sup>2</sup>Product Safety, BASF SE, Ludwigshafen am Rhein, Germany; <sup>3</sup>U895, équipe 5, Bâtiment Universitaire Archimède, Centre Méditerranéen de Médecine Moléculaire (C3M), Inserm, Nice, France.

Endocrine disruption has become an important topic of public concern. Despite an increasing amount of attention, little is understood about if environmentally relevant doses of endocrine disrupting chemicals (EDCs) affect homeostasis. Furthermore, there are often knowledge gaps in the studies used to assess EDCs. To address these concerns, we performed a pre-/post-natal reproductive toxicity study of flutamide as part of a larger BASF and CEFIC funded project to measure the developmental toxicity of low single- and mixture-doses of anti-androgens. The tested doses were selected to mimic a low-effect level, the no observed adverse effect level (NOAEL) for endocrine effects, and the acceptable daily intake (ADI). While female offspring developed normally, the male offspring showed effects known for anti-androgens. No effects were noted at the lowest dose, the ADI. Significant decreases in anogenital distance on PND 1 were noted in animals exposed to the top dose. An increase in nipples and/or areolas in male animals on PND 12 was noted at the top two doses. This effect was partially transient, as all had regressed by PND 21, except at the flutamide top dose. In both of these dose groups, male offspring which were reared to young adulthood displayed additional anti-androgen effects including, delayed sexual maturation and reduced male sex organ sizes and weights; however, offspring from the top dose group also had an increased incidence of developmental sexual defects including hypospadias, short penis, and cryptorchidism. Assessment of sexual steroid hormones and their precursors revealed no effects at any dose level. Taken together, the weight of evidence of the clinical and pathological findings suggests a lack of a non-monotonic dose-response curve.

## **PS** 1929 The Effects of 2, 3, 7, 8-Tetrachlorodibenzo-p-dioxin (TCDD) on Hypothalamus-Pituitary-Gonadal (HPG) Axis in Female Rat Primary Cultures.

K. Solak, F. Wijnolts, B. J. Blaauboer, M. van den Berg and M. B. van Duursen. *Institute for Risk Assessment Sciences, Utrecht University, Utrecht, Netherlands.*

2,3,7,8-tetrachlorodibenzo-p-dioxin (TCDD) belongs to a group of structurally persistent, highly lipophilic compounds, that exerts a variety of adverse effects on the development and physiology of the reproductive system. TCDD and other dioxin-like PCBs act as endocrine disruptive compounds (EDCs) on the hypothalamus-pituitary-gonad (HPG) reproductive axis, mainly through the activation of aryl hydrocarbon receptor (AHR) signaling. Females are believed to display higher sensitivity to TCDD mainly due to the sex differences in adipose tissue percentage and thus higher accumulation of TCDD in female tissues, including ovaries. The present study was designed to explore the mechanisms of endocrine disrupting properties of TCDD on female adult rat hypothalamus-pituitary-gonadal axis (HPG axis) in vitro by employing primary hypothalamus, pituitary and ovaria cultures. In all HPG axis compartments, TCDD elevated its sensitive markers CYP1a1 and AhR after 24 hours. No changes in gonadotropin-releasing hormone (GnRH) and gonadotropins mRNA and protein levels were observed after 10nM TCDD treatment. TCDD exerted its anti-estrogenic effects by alteration of the crucial enzymes in ovarian steroidogenesis. Significant down-regulation of CYP17 and

CYP19 mRNA levels were observed with a slight decrease of estradiol levels after 24 hours. Furthermore, the FSH receptor was significantly down-regulated by TCDD, indicating that TCDD may disturb the HPG axis via this receptor by modulation of ovarian response to gonadotropins. This process may which further lead to ovarian desensitization. To investigate the AhR involvement in these enzyme and receptor mRNA observed changes, siRNA against AhR was applied. The results suggest a key role of the AhR in CYP19 gene regulation in the regulation of female reproductive tract.

### PS 1930 BPA and TBBPA Target ATP Binding Cassette Transporters in the Blood-Testis Barrier and Impair Leydig Cell Steroidogenesis.

M. J. Roelofs<sup>1</sup>, A. C. Dankers<sup>2</sup>, A. H. Piersma<sup>1,3</sup>, F. G. Russel<sup>2</sup>, R. Masereeuw<sup>2</sup> and M. B. van Duursen<sup>1</sup>. <sup>1</sup>Institute for Risk Assessment Sciences, Utrecht University, Utrecht, Netherlands; <sup>2</sup>Department of Pharmacology and Toxicology, Radboud University Nijmegen Medical Centre (RUNMC), Nijmegen, Netherlands; <sup>3</sup>Center for Health Protection, National Institute for Public Health and the Environment (RIVM), Bilthoven, Netherlands.

Disturbances of androgen production in Leydig cells and/or androgen function in Sertoli cells in the (fetal) testis have been shown to cause a wide variety of male reproductive abnormalities in experimental animals. Drug transporters in the blood-testis barrier (BTB) prevent entry and accumulation of xenobiotics in the testis, but are also involved in local transport of steroid hormones. Among these are the ATP-binding cassette (ABC) transporters, P-glycoprotein (P-gp/ABCB1), breast cancer resistance protein (BCRP/ABCG2), multidrug resistance protein 1 (MRP1/ABCC1) and 4 (MRP4/ABCC4). We studied the interaction of Bisphenol A (BPA) and Tetrabromobisphenol A (TBBPA) with human P-gp, BCRP, MRP1 and MRP4-mediated transport using membrane vesicles of human embryonic kidney (HEK293) cells overexpressing these transporters. Also, the effects of these compounds on testosterone production and expression of steroidogenic genes (Star, Cyp11A1, 3 $\beta$ -HSD, 17 $\beta$ -HSD, Ins13, Cyp17A, Cyp19, LH receptor, Srd5a1) in mouse Leydig MA-10 cells were determined. BPA and TBBPA concentration-dependently induced testosterone secretion by MA-10 cells and expression of testis-specific mRNAs of 17 $\beta$ -HSD and Srd5a1 (5 $\alpha$ -reductase 1) were upregulated. BPA and TBBPA differentially inhibited P-gp, BCRP, MRP1 and/or MRP4 activity. Blocking P-gp using PSC833, increased testosterone secretion upon BPA and TBBPA exposure. The MRP inhibitor MK571 completely blocked testosterone secretion elicited by BPA and TBBPA. Our data suggest that EDCs might disrupt local androgen production and androgen transport from the Leydig into Sertoli cells thus affecting normal germ cell development.

### PS 1931 Effects of GPER Activation on (Xeno) Estrogen-Induced Cellular Responses.

L. C. Smith<sup>1</sup>, K. Ralston-Hooper<sup>2</sup>, P. Ferguson<sup>2</sup> and T. Sabo-Attwood<sup>1</sup>. <sup>1</sup>Department of Physiological Sciences, Environmental & Global Health and Center for Environmental and Human Toxicology, University of Florida, University of Florida, Gainesville, FL; <sup>2</sup>Department of Civil and Environmental Engineering and Nicholas School of the Environment, Duke University, Durham, NC.

Estrogen can exert cellular effects through both nuclear (ESR1 and ESR2) and membrane-bound receptors (GPER). It is unclear if these receptors act independently or engage in crosstalk to influence hormonal responses. To investigate each receptor's role in proliferation, activation of reporter genes and protein phosphorylation in breast cancer cells (MCF-7), we employed ESR1 (PPT), ESR2 (DPN) and GPER (G1) selective agonists. As anticipated, 17 $\beta$ -estradiol (E2), PPT and DPN, enhanced cell proliferation, whereas G1 had no impact. However, E2, PPT- and DPN-induced proliferation was repressed when cells were co-exposed with G1. Similar results were observed for activation of an estrogen response element (ERE)-driven luciferase reporter gene where G1 elicited a dose-dependent decrease in E2-, PPT- and DPN induced activity. As membrane receptors typically initiate a series of phosphorylation events, we performed global cytosolic phosphoproteome analysis by HPLC-MS/MS on cells exposed to E2 or G1. Of the 238 phosphorylated proteins identified only 10 sites were shared between E2 and G1 whereas 31 and 13 events were specific for each ligand, respectively. Using pathway analysis we developed a putative network of proteins that are influenced by GPER activation and have identified 'central nodes' (i.e. NDRG2) which highlights a possible role for these proteins as targets of GPER activity. As xenoestrogens, such as bisphenol-A and genistein, bind to ESRs and GPER we are currently investigating the impact these compounds have on nuclear and membrane estrogen receptor signaling networks. Overall, our proteomic and mechanistic approaches will lead to the identification and sorting of GPER networks and the potential interplay with ESRs that will illuminate the role of these receptors in cellular responses to E2 and xenoestrogens.

### PS 1932 Antiproliferative, Antiandrogenic, and Cytotoxic Effects of Novel Synthetic Derivatives of Caffeic Acid in LNCaP Human Androgen-Dependent Prostate Cancer Cells.

T. Sanderson<sup>1</sup>, H. Clabault<sup>1</sup>, C. Patton<sup>1</sup>, L. M. LeBlanc<sup>2</sup>, M. Hébert<sup>2</sup> and M. Touaibia<sup>2</sup>. <sup>1</sup>INRS-Institut Armand-Frappier, Laval, QC, Canada; <sup>2</sup>Département de Chimie et Biochimie, Université de Moncton, Moncton, NB, Canada.

Caffeic acid and its naturally occurring derivative caffeic acid phenethyl ester (CAPE) have antiproliferative and cytotoxic properties in a variety of cancer cell lines, but little is known about their effects on prostate cancer cells. We evaluated the effects of caffeic acid, CAPE and 18 novel synthetic derivatives on cell proliferation, subcellular localisation and expression of androgen receptor (AR) and secretion of prostate-specific antigen (PSA) in LNCaP human hormone-dependent prostate cancer cells. LNCaP cells cultured in steroid-free medium were exposed to 0.1 nM dihydrotestosterone (DHT) in combination with various concentrations of caffeic acid derivatives (0.3-100  $\mu$ M) for 24-72 h during which cell proliferation was followed using an xCELLigence cell monitoring system (Roche). Cytoplasmic and nuclear levels of AR were determined by immunoblotting and PSA secretion using a commercial ELISA. Cytotoxicity was measured by assessing mitochondrial function using a WST-1 assay. Seven synthetic derivatives of CAPE were strong, concentration-dependent inhibitors of androgen-stimulated LNCaP cell proliferation with up to 3-fold greater potencies (IC<sub>50</sub>=8-24  $\mu$ M) than CAPE (IC<sub>50</sub>=28.9 $\pm$ 4.5  $\mu$ M); caffeic acid had no effect. Concomitant with inhibition of cell proliferation, DHT-stimulated PSA secretion was reduced by CAPE and the 7 derivatives. The most potent derivative MT-30 (IC<sub>50</sub>=7.9  $\pm$  2.4  $\mu$ M) inhibited DHT-stimulated cell proliferation and PSA secretion significantly at 0.3  $\mu$ M. Exposure to 10 nM DHT increased cytoplasmic and nuclear AR levels and co-treatment with increasing concentrations of MT-30 and CAPE, interestingly, further increased these levels. In conclusion, a number of synthetic derivatives of caffeic acid are potent inhibitors of androgen-dependent prostate cancer cell growth, acting via an antiandrogenic mechanism that involves increased nuclear accumulation of (possibly inactive) AR.

### PS 1933 Cadmium Content in Human Pancreatic Insulin Producing Beta Cells.

M. El Muayed<sup>1</sup>, K. W. MacRenaris<sup>2</sup> and W. L. Lowe<sup>1</sup>. <sup>1</sup>Division of Endocrinology, Northwestern University Medical School, Chicago, IL; <sup>2</sup>The Chemistry of Life Processes Institute, Northwestern University, Chicago, IL. Sponsor: J. Bolton.

Evidence suggests that chronic low level cadmium exposure impairs the function of insulin producing beta cells and may be associated with type 2 diabetes mellitus. We previously reported that insulin producing beta cells accumulate Cd avidly and gradually in a dose and time dependent manner over prolonged time periods, leading to impaired beta cell function at environmental Cd exposure concentrations. This is likely due to the high beta cell Zn turnover and the significant overlap between Zn and Cd transport and buffering mechanisms. In the present study we compared the content of cadmium (Cd) and Mercury (Hg) between native human islets with that of liver samples (10 human subjects living in the USA). The content of Cd and Hg in these tissues lysates was measured by ICP-MS. All studies were approved by our institutional review board. The cadmium (Cd) content in islets from 10 human non-diabetic subjects ranged from 7.4 to 71.92 nM/g protein (average 28.80  $\pm$  6.73 nM/g protein). The concentration of mercury (Hg) was significantly lower ranging from undetectable (detection threshold 4 nM/g protein) to 5.05 nM/g protein. In comparison, human liver lysates contained significantly less Cd (9.04  $\pm$  1.99 nM/g protein). No Hg was detected in any of the liver samples (detection threshold 4 nM/g protein). We conclude that human islets accumulate measurable, and likely relevant quantities of Cd that are higher than those of Hg under normal environmental exposure conditions. In comparison, the Cd concentration in Liver samples was significantly lower, likely due to the significantly lower Zn turnover rate in liver cells compared to that in beta cells.

### PS 1934 Formulation Development and Analysis Methods for Bisphenol AF in 5K96 Verified Casein Feed.

K. Aillon<sup>1</sup>, V. Ault<sup>1</sup>, A. Sullivan<sup>1</sup>, R. Mathias<sup>1</sup>, J. Algaier<sup>1</sup>, R. Harris<sup>1</sup>, B. Collins<sup>2</sup> and S. Waidyanatha<sup>2</sup>. <sup>1</sup>MRIGlobal, Kansas City, MO; <sup>2</sup>National Toxicology Program, NIEHS, Research Triangle Park, NC.

Bisphenol AF (BPAF), a perfluorinated BPA homologue, is a cross linking agent in fluoroelastomers used in food and pharmaceutical processing equipment. Due to inadequate toxicity data, occupational and potential consumer exposure, and structural similarity to bisphenol A, BPAF was selected for evaluation by the National Toxicology Program (NTP). MRIGlobal supported the NTP by formulating BPAF

into a phytoestrogen-free rodent diet, LabDiet 5K96 Verified Casein diet, developing the associated formulation analysis methods, and evaluating homogeneity and storage stability in the formulated diet.

The analysis method involved the extraction of BPAF from feed using acetonitrile/acetic acid (99/1 v/v). The method covered a formulation range of ~200 to ~10,000 µg/g with dilution into the curve up to 15,000 µg/g. The method was linear, accurate, and precise with BPAF recoveries ≥ 99%.

Homogeneity evaluation of 937.5 and 15,000 µg/g formulations showed recoveries ≥ 99% with RSD values ≤ 0.9%. Long-term BPAF stability for the 937.5 µg/g formulation showed the formulation was stable for 42 days (recovery ≥ 94.5%) when stored under refrigerated or freezer conditions.

When the 937.5-µg/g formulation was stored under simulated dosing conditions, in the presence of rat urine and feces, the ACN/acetic acid extraction resulted in an 68% BPAF recovery after 7 days, indicating possible BPAF instability or extensive binding to feed under these conditions. To investigate this, several solvents with different polarity and pH were tested. ACN/acetic acid 99/1 extraction resulted in 79% BPAF recovery after 8 days storage in the presence of rat urine and feces. Adding an additional acid-digestion and extraction step, in which the formulation was digested with 8.3N HCl at ~ 75°C and extracted with ethyl ether:petroleum ether (1:1), BPAF recovery increased to 90% in Day 7 samples. This suggests that BPAF is stable but exhibits non-covalent binding to feed components.

### PS 1935 Silencing of Testisin through CpG Methylation from Exposure to Phthalates in Ntera-2 Cells.

J. Gomes, J. Kapongo, B. Nguyen and D. Krewski. *University of Ottawa, Ottawa, ON, Canada.*

Di (2-ethylhexyl) phthalate (DEHP) is one of the most highly produced and frequently studied phthalates. Its metabolite, monoester mono (2-ethylhexyl) phthalate (MEHP) is reported to be a testicular toxicant. Following toxicity pathway analyses we identified Testisin, GSTP1 and MGMT genes to study their expression in testicular germ cells (Ntera-2). Testisin present in normal tissue but absent in neoplastic tissue and regulates proteolytic reactions in testicular germ cells; GSTP1 inactivates carcinogens and is a member of glutathione-S-transferase; and Methylguanine DNA methyltransferase (MGMT) provides defense against neoplasm. Testicular cells under laboratory conditions were exposed to MEHP in a dose- and time-dependent manner at concentrations of 1µM, 10µM, and 100µM at 24, 48, 72 and 96hr time points. The control was made by exposure of MEHP to 5'aza (demethylating agent) for hypermethylation. After exposure, those genes were analyzed by Quantitative Real Time PCR (qRT-PCR). The results revealed an overall down regulation for each gene as the concentration and/or time increased. The expression of Testisin, GSTP1 and MGMT was downregulated but not significantly in the last two cases. Following exposure to 5-aza treatment and coexposure, there was a significant up-regulation and restoration of the expression of the Testisin gene. This suggests that MEHP may down-regulate Testisin gene expression by DNA methylation. These findings provide evidence that MEHP can alter the expression of Testisin, GSTP1 and MGMT, genes. Testisin which is associated with testicular germ cell tumors and its downregulation and subsequent restoration may be caused by DNA methylation following exposure to MEHP. The expression of GSTP1 which is a xenobiotic metabolizing enzyme gene and the DNA repair enzyme gene suggests that the toxicant is fairly active in these cells exposed to MEHP. The investigation of DNA methylation at the CpG islands of the promoter region of Testisin is described.

### PS 1936 An Examination of the Effects of Methyltriclosan on Early-Embryonic Development in the South African Clawed Frog (*Xenopus laevis*).

M. Cromie<sup>1</sup>, M. Wages<sup>2</sup>, B. Perafan<sup>1</sup>, E. Smith<sup>2</sup> and J. Carr<sup>1</sup>. <sup>1</sup>*Biological Sciences, Texas Tech University, Lubbock, TX;* <sup>2</sup>*The Institute of Environmental and Human Health, Texas Tech University, Lubbock, TX.* Sponsor: [W. Gao](#).

Triclosan (5-chloro-2-(2,4-dichlorophenoxy)phenol) is a commonly used bactericide present in many personal care products such as detergents, liquid hand soaps, deodorants, cosmetics, lotions, mouthwash, and toothpaste, and it can be integrated with fabrics, plastics, carpets, and toys. Methyltriclosan is a derivative that is formed from triclosan via biological methylation at an unknown interval during waste water treatment. Methyltriclosan is more abundant in the environment, more lipophilic than triclosan, and has a greater potential to accumulate in fatty tissues. The global decline of amphibian populations has raised awareness surrounding the possible effects of poor water quality on the health of habitats. Since metamorphosis and reproductive development in amphibians is highly regulated by thyroid hormone (TH), and the structure of triclosan is similar to that of TH, there is the possibility that triclosan and methyltriclosan may act on TH receptors to alter

metamorphosis and reproductive development. Standard 96-hour Frog Embryo Teratogenic Assay-Xenopus protocols were followed using South African Clawed Frog (*Xenopus laevis*) embryos. After measuring the larvae the data revealed that early embryonic exposure to environmentally relevant concentrations of methyltriclosan resulted in statistically significant alterations in total body length, snout-to-vent length and crown width. Furthermore, molecular studies were performed to identify the effects of methyltriclosan exposure on the TH-responsive gene, TH/bZIP. The results of the quantitative real-time polymerase chain reaction did not support the induction of TH/bZIP gene expression after exposure to environmentally relevant concentrations of methyltriclosan. However, the expression of other TH-responsive genes may be altered upon exposure. Collectively, these data are the first to report on the responsiveness of vertebrate embryos to methyltriclosan exposure.

### PS 1937 No Evidence of Endocrine Disruption by Glyphosate in Male and Female Pubertal Assays.

J. Bailey<sup>1,2</sup>, J. Hauswirth<sup>2</sup> and D. Stump<sup>3</sup>. <sup>1</sup>*Dow AgroSciences, LLC, Indianapolis, IN;* <sup>2</sup>*Joint Glyphosate Task Force, Raleigh, NC;* <sup>3</sup>*WIL Research Laboratories, LLC, Ashland, OH.*

The Food Quality Protection Act and Safe Drinking Water Act amendments (1996) required the USEPA to develop the Endocrine Disruptor Screening Program (EDSP), which currently consists of 11 Tier 1 screening assays to evaluate the potential for a chemical to interact with the endocrine system. Glyphosate was included in the first list of 67 compounds subject to the EDSP, which were selected for screening based on their potential for exposure rather than suspected interference with the endocrine system.

The potential for glyphosate (G) to induce endocrine disruption has now been evaluated in the male and female Pubertal assays, the two most apical mammalian EDSP Tier 1 assays.

The female pubertal assay evaluates potential effects on pubertal development and thyroid function in the juvenile female. Four groups of fifteen juvenile female rats were dosed with the following: 0, 100, 300 and 1000 mg/kg/d G once daily via oral gavage from postnatal day (PND) 22 to 42. There was no evidence of any direct test substance-related estrogenic or anti-estrogenic effects, nor was there any evidence of direct test substance-related effects on pubertal development or thyroid function in the juvenile female rat following oral administration of glyphosate at any dosage level tested.

The male pubertal assay evaluates potential effects on pubertal development and thyroid function in the juvenile males. Four groups of fifteen juvenile male rats were dosed with the following: 0, 100, 300 and 1000 mg/kg/d G once daily via oral gavage from PND 23 to 53. There was no evidence of any direct test substance-related androgenic or anti-androgenic effects, nor was there any evidence of direct test substance-related effects on pubertal development or thyroid function in the juvenile male rat at any dosage level tested.

Based on these results, glyphosate does not exhibit endocrine disruption in the male and female pubertal assays.

### PS 1938 Exposure to G-1, a Selective Agonist for G Protein-Coupled Estrogen Receptor 1 (GPER), Results in Elevated Levels of Vitellogenin in Adult Fathead Minnows (*Pimephales promelas*).

S. Jayasinghe<sup>1</sup>, K. Kroll<sup>1</sup>, N. Denslow<sup>1</sup> and T. Sabo-Attwood<sup>2</sup>. <sup>1</sup>*Department of Physiological Sciences, Center for Environmental and Human Toxicology, University of Florida, Gainesville, FL;* <sup>2</sup>*Department of Environmental and Global Health, Center for Environmental and Human Toxicology, University of Florida, Gainesville, FL.*

Several research groups have shown that G protein-coupled estrogen receptor-1 (GPER) mediates 17β-estradiol (E2) activation through non-genomic membrane initiated pathways. Estrogens play critical roles in a variety of biological processes, including reproduction and development in vertebrates. In fish, hepatic synthesis of vitellogenin (VTG), a precursor egg yolk protein that is vital to successful reproduction, is controlled by E2 via nuclear estrogen receptors (ESR). However, the involvement of GPER in vitellogenesis has not been investigated. As the GPER is not a well characterized in fish the aims of our study are to: (1) assess the tissue-specific expression of GPER in adult fathead minnows (FHM) and (2) determine the effect of GPER activation on VTG synthesis in FHM males and females using a selective GPER agonist (G-1) and antagonist (G-15). Using qRT-PCR we show that GPER mRNA is detectable in numerous organs, and is most highly expressed in the brain followed by gall bladder, trunk kidney, intestine, liver, heart, ovary and muscles. Aqueous exposure to G-1 (5, 30 and 100 ng/L) for 48 hours resulted in a dose dependent increase of hepatic VTG expression compared to vehicle control in both

males and females. In efforts to block GPER-mediated induction of VTG expression, we co-exposed male fish to G-1 and the GPER antagonist G-15. Preliminary results were surprising as the combination of G-1/G-15 enhanced VTG expression compared to each agent singly. Overall, these data suggest that control of VTG synthesis likely involves both nuclear and membrane receptors that are sensitive to E2 activation. We are currently investigating the impact of xenoestrogens on GPER activation in control of VTG synthesis.

**PS 1939 Study on the Subchronic Oral Toxicity of the Circuit Board Powder in Rats.**

N. Wu. Institute of Hygiene, Zhejiang Academy of Medical Sciences, Hangzhou, Zhejiang, China.

**Objective** To investigate the subchronic oral toxicity of the circuit board powder in SD rats. **Methods** Male and female SD rats were randomly divided into four groups named A, B, C and D, A and D group had 16 rats, B and C group had 14 rats, A and D group retained 4 rats for a 45d recovery experiment after the 90d subchronic experiment. A group was given normal diet as control, B, C and D groups were given mixed feed which was made from adding the circuit board powder 10, 20, 50g per kg to the normal diet. All of the groups were ate and drank freely under natural light. After 90 days' feeding, each group calculated the major organ coefficient, measured the blood biochemical parameters, and determined the content of serum triiodothyronine (T3), thyroxine (T4) and testosterone (T) after 45d, 90d and 45d recover. **Results** Compared with the control group, each dose group of the circuit board powder have no significant difference in body weight. There were significant differences between the high-dose group and control group of female rats in some blood biochemical parameters. The organ coefficient of liver in the medium- and high-dose groups of female rats was also significant increase. The content of serum T3, T4 and T in each dose group were significantly higher than that of the control group after 45d and 90d, each index had the most obviously increase in the low-dose group. There was no significant difference between the high-dose group and control group in serum T3, T4 and T after 45d recovery. **Conclusion** subchronic oral exposure to the circuit board powder can cause liver damage in rats, and elevated the content of serum T3, T4 and T.

**PS 1940 Activation of the Hypothalamic-Pituitary-Adrenal (HPA) Axis following Extended Exposure to Atrazine (ATR).**

S. C. Laws<sup>1</sup>, R. Cooper<sup>1</sup> and B. W. Riffle<sup>1,2</sup>. <sup>1</sup>ETB, TAD, NHEERL, ORD, US EPA, Research Triangle Park, NC; <sup>2</sup>ORISE, US Department of Energy, Oak Ridge, TN.

While it is known that adrenal steroids impact reproduction and a variety of other physiological and behavioral functions, disruption of the HPA-axis is not typically considered in toxicological studies. Here we characterize changes in basal corticosterone (CORT) and progesterone (P4) over a 21- day exposure to the chlorotriazine herbicide, ATR. Adult Wistar male rats were dosed by oral gavage with 0, 5, 25, 75, or 200 mg/kg/d given either as a single dose or multiple daily doses (7, 14, or 21 doses) at 0900 hrs (nadir of circadian CORT rhythm) and were decapitated 30 minutes after the last dose (n=10/group). Necropsy body weight was significantly lower than controls (p < 0.05) only in the 200 mg/kg group dosed for 21 days. Adrenal weights were unaffected by ATR at any time point. Serum CORT was elevated in response to a single dose of ATR (LOEL=5mg/kg). Serum CORT was also increased following 7 (LOEL=75mg/kg), 14 (LOEL=25mg/kg), and 21 (LOEL=75mg/kg) daily doses. A similar profile was observed for serum P4 following a single dose (LOEL=25 mg/kg), or 7 (LOEL=75 mg/kg), 14 (LOEL=75 mg/kg), and 21 (LOEL=200 mg/kg) doses of ATR. Urinary CORT (ratio of CORT/urinary creatinine), measured over a 6 hr period after dosing, was significantly increased in the ATR groups (e.g., LOEL for one dose =75 mg/kg, LOEL for 21 doses =75 mg/kg). These data demonstrate a HPA response after daily doses of ATR (e.g., 75 and 200 mg/kg) for up to 21 days. Further work is needed to evaluate the effects of ATR on the circadian CORT rhythm and to discern any impact on reproductive function. This abstract does not reflect U.S. EPA policy.

**PS 1941 2-Isopropylthioxantone (ITX) Induces Endocrine Disrupting Effects and Increases Liver Weight during Puberty in Male Wistar Rats.**

P. Hendriksen, E. Kramer, M. Groot, J. C. Rijk, R. L. Hoogenboom and A. A. Peijnenburg. Toxicology, RIKILT Institute of Food Safety, WUR, Wageningen, Netherlands. Sponsor: S. Rangarajan.

2-isopropylthioxantone (ITX) is a photo-initiator used in the printing process of many materials. ITX has been detected as contaminant in food such as milk and fruit beverages. Previous in vitro studies revealed ITX acting agonistic on the aryl

hydrocarbon receptor (AhR) and antagonistic on both the androgen receptor and estrogen receptor. In addition, ITX increases aromatase activity in vitro. To validate these findings in vivo, male rats were treated daily with 50, 150 or 500 mg/kg/day ITX during their puberty period from PND 23 to 53. For comparison, rats were treated with 50 ng/kg/day TCDD (AhR agonist), 30 mg/kg/day Casodex (AR antagonist) or 50 mg/kg/day flutamide (both AhR agonist and AR antagonist). ITX, from the lowest dose onwards, exerted a decrease in weight of the ventral prostate, and the highest dose of ITX decreased the weight of the seminal vesicles and coagulating gland, and reduced the number of spermatozoa in the cauda. The same effects, but more severe, were induced by flutamide and Casodex. Epididymal weight, caput sperm counts and preputial separation were negatively affected by Casodex and flutamide and not by ITX. ITX reduced testosterone and increased estrogen levels confirming the in vitro finding on increased aromatase activity. 500 mg/kg/day ITX-500 reduced the body weight, while it increased liver weight with 20% and relative liver weight with 38%. Whole genome mRNA expression profiling of the liver revealed a striking similarity of genes affected by ITX and flutamide. Furthermore, many TCDD-affected genes, including many known AhR target genes, were regulated by ITX as well. Taken together, these results convincingly demonstrates ITX to be an endocrine disruptor that exerts AhR agonistic and AR antagonistic activities both in vitro and in vivo.

**PS 1942 In Vivo Human Pharmacokinetics of Dibenzo[DEF, P]Chrysene (DBC) following Microdosing—Bridging the Gap between High-Dose Animal Data and Environmentally-Relevant Human Exposures.**

E. P. Madaan<sup>1,4</sup>, R. Corley<sup>3</sup>, K. W. Turteltaub<sup>2</sup>, T. Ognibene<sup>2</sup>, M. Malfatti<sup>2</sup>, M. Garrard<sup>1,4</sup>, K. Sudakin<sup>1,4</sup>, T. Mcquistan<sup>1,4</sup> and D. E. Williams<sup>1,4</sup>. <sup>1</sup>Oregon State University, Corvallis, OR; <sup>2</sup>Lawrence Livermore National Lab, Livermore, CA; <sup>3</sup>Pacific Northwest National Lab, Richland, WA; <sup>4</sup>Linus Pauling Institute, Corvallis, OR.

Polycyclic Aromatic Hydrocarbons (PAHs) comprise environmental mixtures of toxicants resulting from the combustion of carbonaceous material, of which some high molecular weight constituents are carcinogens in animal models. There is little data currently available on the pharmacokinetics or pharmacodynamics of any PAHs, especially the higher molecular weight, carcinogenic PAHs, in humans. Utilizing the sensitivity of accelerator mass spectroscopy (AMS), <sup>14</sup>C- labeled PAHs can be studied at environmentally relevant concentrations, below the average daily exposure and at levels regulatory agencies have determined from animal studies to be safe daily exposures over a lifetime. The 30 ng DBC dose utilized in this study has an EPA estimated B(a)Peq of 300-900 ng, falling within the U.S. daily dietary estimate of an average B(a)P exposure of 40-2800 ng/person . Over 90% of exposure to carcinogenic PAHs is through the diet. <sup>14</sup>C-DBC was detected in blood and urine post ingestion of a 5 nCi (30ng) <sup>14</sup>C- DBC dose given by capsule to healthy male and healthy, infertile female volunteers (n=9). Blood was collected at 15 time points over 72 hours with 11 collections during the first 8 hours post-dosing. Urine was collected in 5 pools over 72 hours with 3 pools in the first 24 hours. Plasma concentrations of <sup>14</sup>C reached maximal concentrations of 11 to 68 fg DBC eq./ml within 1.5-4 hr after consumption with an alpha phase half-life for <sup>14</sup>C clearance that averaged 3.5 ± 2.3 hr across all volunteers. A more prolonged beta-elimination phase was also observed. These results are the first available human pharmacokinetic data from a high molecular weight, probable human (IARC class 2A) carcinogenic, PAH. This unique dataset can be used to enhance the confidence of human health risk assessments to PAH exposures.

**PS 1943 Evaluation of Tumor Pathology Concordance between Epidemiological and Rodent Studies.**

J. Wan<sup>1</sup>, J. W. Card<sup>1</sup>, H. Fikree<sup>1</sup>, L. Haighton<sup>1</sup>, V. Lee-Brotherton<sup>1</sup> and B. Sangster<sup>2</sup>. <sup>1</sup>Intertek Cantox, Mississauga, ON, Canada; <sup>2</sup>ASAT Foundation, Leidschendam, Netherlands.

To assist with evaluating human cancer risk from chemical exposures, an investigation was conducted to assess concordance at the tissue level between tumors reported in epidemiological investigations and rodent bioassays for a selected group of chemicals. This investigation focused on chemicals that were considered to be probable human carcinogens (Group 2A) by IARC or "Reasonably Anticipated" carcinogens by the US NTP, and for which there was evidence of tumor concordance at the organ level. The 7 chemicals identified for this evaluation, and the organ-level tumor concordances for each, were as follows: 1-amino-2,4-dibromanthraquinone (lung), tetrachloroethylene (liver, kidney), trichloroethylene (liver, kidney), inorganic lead compounds (lung, kidney, brain), 2,4,6-trichlorophenol (lymphoma), polychlorinated biphenyls (liver, gastrointestinal), and benzyl chloride (lung). Based on pathology, concordance between rodent and human tumors for at least 1 tumor type was identified for 4 of the 7 compounds (tetrachloroethylene, trichloroethylene, inorganic lead compounds, and polychlorinated biphenyls);

however, the strength of the concordance was considered weak in all cases. For the same 4 compounds, there were a large number of tumors which lacked concordance between animal and epidemiological studies. Of the remaining compounds, insufficient data were available for an evaluation of tumor pathology (1-amino-2,4-dibromoanthraquinone and 2,4,6-trichlorophenol) or there was an absence of concordance at the tissue level (benzyl chloride). In conclusion, this investigation of concordance between animal and human tumors reported to be caused by specific compounds shows that, even when chemically-induced tumors are identified to be occurring in the same organ in both rodents and humans, there is no strong evidence of concordance of these tumors at the level of the affected tissue.

## PS 1944 Benchmark Dose Models for Benzene Genotoxicity Using the Diversity Outbred Mouse.

K. L. Witt<sup>1</sup>, G. E. Kissling<sup>1</sup>, D. L. Morgan<sup>1</sup>, K. R. Shockley<sup>1</sup>, D. M. Gatti<sup>2</sup>, G. A. Churchill<sup>2</sup> and J. E. French<sup>1</sup>. <sup>1</sup>DNTP, NIEHS, Research Triangle Park, NC; <sup>2</sup>Center for Genome Dynamics, The Jackson Laboratory, Bar Harbor, ME.

The genetic basis for inter-individual variation in response to toxicant exposure is poorly understood. The Diversity Outbred (DO) mouse is a new model that can be used to explore population based response variation. DO mice were derived from a set of eight inbred founders and are maintained by random breeding as an heterozygous population containing over 38 million SNPs and 5 million indels (CNV). The genetic diversity and a fine recombination haplotype structure allow high mapping resolution. In experiments reported here, J:DO male mice were exposed to benzene (0, 1, 10, 100 ppm; 75 mice/group) by inhalation, 6 hr/day, 5 days/wk for 28 days in two independent cohorts (300 mice each). Samples of pre- and post-exposure peripheral blood (PB) or post-exposure for bone marrow (BM) were evaluated for frequency of micronucleated reticulocytes (MN-RET) using flow cytometry. MN-RET showed significant increasing trends in response to benzene exposure ( $p < 0.0001$ ) in both cohorts and were significantly higher than controls in both the 10 ppm ( $p = 0.013$ ) and the 100 ppm ( $p < 0.0001$ ) groups. Genotoxicity was highly variable within the 100 ppm groups. Linkage analysis identified quantitative trait loci (QTL) on chromosome 10 (Chr10) between megabase 26 and 35 (LOD=14.6). We identified benzene resistant and susceptible Chr10 QTL genotypes from the lowest and highest quartiles of the BM MN-RET response in the 100 ppm group. Animals in the 0, 1, and 10 ppm groups having these genotypes were placed into the resistant or susceptible groups for modeling. The benchmark concentration (BMC) and its 95% lower confidence limit (BMCL) were estimated from the best-fit model for the most resistant (BMCL = 5.9 ppm) and most susceptible (BMCL = 0.01 ppm) animals, a 590-fold difference between subpopulations. These data suggest that an uncertainty factor of 100 for interspecies and intraspecies variation may not be sufficient for calculation of a human benzene reference concentration based on benzene genotoxicity.

## PS 1945 Is There a Subset of Susceptible Individuals in Controlled Air Pollution Studies?

M. Seeley and J. E. Goodman. *Gradient, Cambridge, MA.*

To establish primary National Ambient Air Quality Standards for criteria air pollutants such as nitrogen dioxide (NO<sub>2</sub>), ozone (O<sub>3</sub>) and sulfur dioxide, US EPA evaluates results from epidemiology, controlled human exposure, and animal studies. For the controlled human exposure studies, which focus on individuals with asthma, there is concern that there may be a subset of susceptible individuals who respond to lower concentrations than the average individual with asthma, but whose response is obscured by evaluating group-level data. To address this, we identified controlled human exposure studies with more than one exposure concentration that provided individual-level data for airway hyper-responsiveness. We identified three studies involving exposure to NO<sub>2</sub> (including data for 38 subjects), and one study each for ozone (O<sub>3</sub>) and sulfuric acid (each including data for 10 subjects). For each study, we compared individual data across exposures to determine whether there were individuals who were consistently more or less responsive, defined by having a response that differed by more than two standard deviations from the group mean response. To determine whether evaluating group-level responses might obscure responses for potentially susceptible individuals, we compared the concentration-response function (CRF) for all subjects to the CRF for a subset that excluded less responsive subjects and the CRF for only more responsive subjects. Among the five studies, we identified only one subject, in one study, who was considerably more responsive at both exposure levels in the study. The shapes of the CRFs, however, were similar for the group as a whole and the more responsive subject. We also identified one subject, in one study, who was less responsive at all exposure levels in the study. Exclusion of data for this subject did not qualitatively change the shape of the CRF. Our analysis of these five studies indicates that evaluating group-level responses to air pollutants does not obscure CRFs for potentially susceptible individuals.

## PS 1946 Concordance of Transcriptional and Apical Benchmark Dose Levels for Conazole-Induced Liver Effects in Mice.

V. S. Bhat<sup>1</sup>, S. Hester<sup>2</sup>, S. Nesnow<sup>2</sup> and D. A. Eastmond<sup>1</sup>. <sup>1</sup>Environmental Toxicology, University of California Riverside, Riverside, CA; <sup>2</sup>NHEERL, US EPA, Research Triangle Park, NC.

The ability to anchor chemical class-based gene expression changes to phenotypic lesions and to describe these changes as a function of dose and time can inform mode of action and improve quantitative risk assessment. Previous research identified a 330-gene cluster commonly responsive to three hepatotumorigenic conazoles (cypro-, epoxi- and propiconazole) at 30 days. Extended to two more conazoles (triadimefon and myclobutanil), the present assessment encompasses four tumorigenic and one non-tumorigenic conazole. Transcriptional benchmark dose levels (BMDL<sub>T</sub>) were estimated for a subset (~50 genes) of the gene cluster that had a ≥5-fold change in signal intensity at the tumorigenic dose and demonstrated dose-responsive behavior. The modeled genes primarily encompassed pathways involved in Phase I/II or lipid metabolism, oxidative stress, MAP kinase signaling, and/or apoptosis (such as Cyp2b10, Lcn13, Abcc4, Akr1b7, Gadd45b). The median BMDL<sub>T</sub> estimates from the gene subset were concordant (within a factor of 0.8 to 1.2) with the apical benchmark dose (BMDL<sub>A</sub>) for increased liver weight at 30 days for the four tumorigenic conazoles. The 30-day median BMDL<sub>T</sub> estimates were within one-half order of magnitude (generally more sensitive) of the chronic BMDL<sub>A</sub> for liver tumors. Discordant 30-day BMDL<sub>T</sub> and BMDL<sub>A</sub> values were obtained for the non-tumorigenic conazole (myclobutanil). Potency differences seen in the dose-responsive transcription of some of these biomarker genes, particularly those involved in Phase II metabolism and bile acid transport (such as Gstm3, Gstm3, Abcc4, Akr1b7), mirrored each conazole's tumorigenic potency. The 30-day BMDL<sub>T</sub> and BMDL<sub>A</sub> estimates corresponded to tumorigenic potency on a mg/kg-day basis with cyproconazole > epoxiconazole > propiconazole > triadimefon > myclobutanil (non-tumorigenic). These initial results support the utility of measuring short-term gene expression changes to inform quantitative risk assessments from long-term exposures. This abstract does not reflect EPA policy.

## PS 1947 Assessment Factors for Susceptible Populations—Analysis of Airway Response during Short-Term Exposure to Volatile Chemicals.

M. Johansson, G. Johanson and M. Öberg. *Institute of Environmental Medicine, Stockholm, Sweden.*

Health-based guidance values for short-term exposure to airborne hazardous chemicals are developed to support the protection of the general population, including susceptible sub-groups such as asthmatics, in the case of sudden release of chemicals. The Acute Exposure Guideline Level (AEL) program is one of the most well-known set of short-term values. Our analysis of AEL documents reveals that only 8% include data on asthmatics. A comparison of documents in nine additional sets of short-term values shows that data on asthmatics are frequently disregarded. The aim of the present study was to investigate the experimental support of a general difference in airway response between healthy and asthmatic individuals during short-term exposure. We performed a review of experimental data from 108 studies including both asthmatic and healthy subjects exposed to airborne chemicals during identical experimental conditions. In total, experimental data for 19 chemicals and 9 mixtures were identified. Thresholds for airway response and the difference between asthmatic and healthy subjects were calculated in each study. The difference between subgroups was compared to the general assessment factors applied for susceptible populations in the derivation of guidance values. In addition, dose-response relationships of four high volume chemicals were calculated for healthy and asthmatic individuals, separately, to identify threshold concentrations for effects on lung function. Our results show that asthmatic individuals generally are more susceptible than healthy individuals. An inter-individual assessment factor of three may not be sufficiently protective for all chemicals.

## PS 1948 Thermal Constraints and Chemical Exposure in the Workplace: Prioritization of Occupations for Better Prevention.

A. Adam-Poupart<sup>1</sup>, G. Truchon<sup>2</sup>, M. Lévesque<sup>1</sup>, M. Busque<sup>2</sup>, P. Duguay<sup>2</sup>, R. Bourbonnais<sup>3</sup> and J. Zayed<sup>1,2</sup>. <sup>1</sup>Environmental and Occupational Health, Université de Montréal, Montréal, QC, Canada; <sup>2</sup>Institut de recherche Robert-Sauvé en santé et sécurité du travail (IRSST), Montréal, QC, Canada; <sup>3</sup>ROH Consultant, Laval, QC, Canada.

Chemicals and heat exposure are common hazards found in the workplace and their coexposure may lead to increased health risk due to potential interactions: some chemicals can affect the thermoregulatory mechanisms and reduce the

worker's capacity to adapt to heat, while heat exposure can modify physiological parameters and increase the absorption of some chemicals. Therefore, the aim of this research was to identify the occupations at risk of concomitant exposure to heat and chemicals in Quebec (Canada). To achieve this goal, a list of occupations from all industry sectors of Quebec was built from national employment data, and occupations at risk of heat stress were determined with a risk rating matrix based on the probability of occurrence and the severity of health effect. For occupations judged as having significant and critical heat stress risk, the presence of chemicals that may be found at work was documented (solvents, dust, pesticides, polycyclic aromatic hydrocarbons, toxic gases, heavy metals, asbestos/silica and reagents/other chemicals) and a list of occupations with high potential of simultaneous exposure to heat and chemicals was produced and submitted to a panel of experts for prioritization. From an initial set of 1010 occupations, 257 were judged as having significant and critical heat stress risk and 136 of these were included in the list of occupations with high potentially simultaneous exposure. Experts identified 22 priority occupations grouped in metal manufacturing, non-metallic mineral product, construction and public administration sectors. This innovative approach, based on a matrix analysis and judgment of experts, served as a useful tool to identify sectors/occupations where health risk assessments, preventive interventions and regulatory practices should be conducted or developed.

#### PS 1949 Acute and Chronic Noncancer Inhalation Toxicity Factors for Acrylonitrile.

J. Lee, R. L. Grant and S. Shirley. *Toxicology, TCEQ, Austin, TX.*

Acrylonitrile (AN) is used extensively in the production of plastics, synthetic rubber, nitrile elastomers, resins, and acrylic fibers. The USEPA indicates that Texas contributes 11% of the nations reported ambient AN emissions annually. Inhalation of AN vapors can cause respiratory irritation, and at higher levels, neurological symptoms including dizziness, weakness, headache, and impaired judgment. To ensure that the general public in Texas is protected against potential inhalation effects from AN exposure, the Texas Commission on Environmental Quality (TCEQ) has developed acute and chronic reference values (ReVs). An acute ReV (1-hr exposure duration) of 1100 µg/m<sup>3</sup> was derived based on no signs or symptoms observed in human volunteers exposed to AN for up to 8 hours. A chronic ReV of 2.2 µg/m<sup>3</sup> was derived based on benchmark dose modeling for increased nasal lesions observed in female rats. The chronic ReV is comparable to the California EPA reference exposure level of 5 µg/m<sup>3</sup>. Effects Screening Levels (ESLs) were calculated from ReVs by applying a target hazard quotient of 0.3, to account for possible cumulative exposure. ESLs are used to evaluate modeled ground level concentrations due to emissions from facilities during air permit reviews. The corresponding acute and chronic ESLs were 330 and 0.7 µg/m<sup>3</sup>, respectively. Reproductive/developmental animal and epidemiological data were not used to derive ReVs since AN is not expected to be a developmental or reproductive toxicant in the absence of significant maternal toxicity. Furthermore, the overall carcinogenic weight-of-evidence shows that while AN is capable of causing tumors in rats and mice at high doses, AN does not appear to contribute to the development of cancerous tumors in humans. Thus, no inhalation unit risk factor was derived. The derived chronic ESL, however, is within the range of the concentrations at 1 x 10<sup>-5</sup> cancer risk estimated by USEPA and thus, is expected to be protective against potential cancer risk.

#### PS 1950 Hexavalent Chromium Carcinogenicity: Use of a Nonlinear-Threshold Assessment to Develop a Cancer-Based Chronic Inhalation Reference Value.

N. Erraguntla<sup>1</sup>, J. T. Haney<sup>1</sup>, R. L. Sielken<sup>2</sup> and C. Valdez-Flores<sup>2</sup>. <sup>1</sup>*Toxicology Division, Texas Commission on Environmental Quality, Austin, TX;* <sup>2</sup>*Sielken & Associates Consulting, Bryan, TX.*

It is important to conduct up-to-date chemical assessments for known human lung carcinogens such as hexavalent chromium (CrVI). An updated carcinogenic assessment has been conducted for CrVI, which has been the subject of recent scientific debate. In addition to default linear low-dose extrapolation methods used to calculate an inhalation unit risk factor (URF), the study authors believe epidemiological data supported by data relevant to the mode of action (MOA) are sufficient to justify considering the results of a nonlinear-threshold carcinogenic assessment for comparison to URF-based de minimis excess risk (e.g., 1 in 100,000) air concentrations. The intent of the current study is not to perform an exhaustive weight of evidence evaluation of all data potentially relevant to the MOA (or MOAs), but rather to present available summary MOA information and statistical evidence interpreted as supporting a potential practical threshold for CrVI-induced carcinogenicity and the results of the consequential nonlinear-threshold inhalation carcinogenic assessment. Relevant epidemiological studies available in the scientific

literature were reviewed and additional statistical dose-response analyses conducted to identify potential carcinogenic thresholds and points of departure (PODs). Occupational-to-environmental dosimetric adjustment of the "sub-threshold" cumulative exposure POD selected (0.195 mg CrVI/m<sup>3</sup>-yr) resulted in a POD<sub>HEC</sub> of 0.0071 mg CrVI/m<sup>3</sup>. Uncertainty factors (total UF of 30) were then applied to derive a cancer-based chronic inhalation reference value (ReV) of 0.24 µg CrVI/m<sup>3</sup>. The margin of exposure is ≈16,000-475,000 based on the ratio of the "sub-threshold" cumulative exposure POD to cumulative exposures estimated based on annual average CrVI ambient air concentrations measured at various sites in Texas (5.9E-06 to 1.7E-04 µg CrVI/m<sup>3</sup>), which are ≈1,400-41,000 times lower than the calculated cancer-based chronic ReV.

#### PS 1951 Hypothesis-Based Weight-of-Evidence Evaluation of the Human Carcinogenicity of Toluene Diisocyanate.

R. L. Prueitt<sup>1</sup>, J. E. Goodman<sup>2</sup> and L. R. Rhomberg<sup>2</sup>. <sup>1</sup>*Gradient, Seattle, WA;* <sup>2</sup>*Gradient, Cambridge, MA.*

Humans are exposed to toluene diisocyanate (TDI) primarily through inhalation in workplaces where it is produced or used. It is classified as a possible human carcinogen, based primarily on increased tumor incidences in rodents treated with TDI by oral gavage. We used the hypothesis-based weight-of-evidence (HBWoE) method to conduct a novel evaluation of all the evidence regarding the hypothesis that TDI is a human carcinogen. We weighed the available data from epidemiology, animal toxicity, and mechanistic studies in terms of quality and relevance to humans, allowing each data set to inform one another. We then evaluated all of the data together to determine whether TDI carcinogenicity is plausible in humans. Our analysis determined that the epidemiology data are not sufficiently robust to support TDI as a human carcinogen; the few positive associations are more likely attributable to alternative explanations than causation. The experimental animal studies indicate that inhalation exposure to TDI does not induce tumors in rats or mice. Tumors observed after oral gavage exposure are most likely due to the conversion of a small amount of the administered TDI to toluene diamine (TDA), which also causes tumors in rats and mice when administered through this physiological exposure route. Further, TDA is formed in *in vitro* TDI genotoxicity assays. While TDI is genotoxic in these assays, it is not genotoxic in rodents or humans *in vivo* after inhalation exposure (during which TDA is not formed). Our HBWoE analysis indicates that the conversion of TDI to TDA is necessary for carcinogenesis to occur, but it does not occur in mammalian species under physiological exposure conditions. Thus, our analysis demonstrates that a causal association between TDI exposure and carcinogenic effects is not plausible in humans. This analysis not only provides insight about TDI carcinogenicity, but it addresses the larger issue of combining human, animal, and mechanistic data for risk assessment.

#### PS 1952 Evaluation of Toxic Effects of 3-MCPD and Associated Esters in Rats.

S. Onami<sup>1</sup>, Y. Cho<sup>1</sup>, T. Toyoda<sup>1</sup>, Y. Ishii<sup>1</sup>, T. Umemura<sup>1</sup>, M. Yoshida<sup>1</sup>, K. Horibata<sup>2</sup>, M. Honma<sup>2</sup>, T. Nohmi<sup>3</sup>, A. Nishikawa<sup>3</sup> and K. Ogawa<sup>1</sup>. <sup>1</sup>*Pathology, NIHS, Tokyo, Japan;* <sup>2</sup>*Genetics and Mutagenesis, NIHS, Tokyo, Japan;* <sup>3</sup>*Biological Safety Research Center, NIHS, Tokyo, Japan.*

3-Monochloropropane-1,2-diol (3-MCPD) is regarded as a rodent renal and Leydig cell carcinogen. Furthermore, 3-MCPD esters may be generated in various foods and food ingredients as a result of food processing. Since there are limited reports about toxicity of these compounds, we conducted the following two studies. 1) *In vivo* genotoxicity study (Pig-A and *gpt* gene mutation assays in the kidneys and testes, micronucleus assay) with male F344 *gpt* delta transgenic rats carrying reporter genes for mutations, treated by gavage with a carcinogenic dose of 3-MCPD (3.6×10<sup>-4</sup> mol/kg body weight) or its esters, i.e., 3-MCPD palmitate diester (PD), 3-MCPD palmitate monoester (PM) and 3-MCPD oleate diester (OD) at the molar equivalents for 4 weeks. 2) 13-Week subchronic toxicity study of these compounds with F344 rats at three doses where the highest was the same as that in the genotoxicity study. In the first study, no clear *in vivo* genotoxicity of 3-MCPD or its esters was observed in the three assays. In the 13-week study, the absolute and relative kidney weights were significantly increased in rats treated with 3-MCPD at a carcinogenic dose and the esters at high and medium doses. Relative liver weights were significantly increased in the 3-MCPD-treated rats and the high dose ester-treated rats, except for female rats treated with PM. By 4 weeks, 1 male and 5 females of 3MCPD group died from the renal tubular necrosis. On histopathological analysis, a significantly increased incidence of renal mineralization in all high dose ester-treated females and of apoptotic epithelial cells in the epididymis of 3-MCPD and high dose ester-treated male were observed as compared to vehicle control. The results suggest 3-MCPD fatty acid esters may be non-genotoxic but have potential toxicity for kidneys and epididymis of rats. NOAELs of PD, PM and OD were suggested to be 14, 8 and 15 mg/kg/day, respectively.

**PS 1953 A Simulation Study Investigating the Risk of Obtaining BMDs Which Are Higher Than the "True" BMD.**

J. Ringblom, G. Johanson and M. Öberg. *Karolinska Institutet, Institute of Environmental Medicine, Stockholm, Sweden.*

A central aspect of quantitative health risk assessment of chemicals is the derivation of the point of departure (POD). Historically, calculating NOAELs has been the most common way to obtain the POD. However, Benchmark Dose (BMD) analysis has been recommended as a more robust alternative, as it uses data from all dose groups in the study to derive the POD. An important step in the BMD approach is the identification of the BMDL, i.e. the lower limit of the confidence interval for the BMD. The aim of this study was to investigate how often the estimated BMDL corresponds to an effect greater than the critical effect, thereby underestimating the risk in the derivation of guidance values.

In this simulation study we assume a known sigmoidal dose-effect curve (and hence a known BMD) and examine how often the BMDL is higher than the "true" BMD. Effects were generated by Monte Carlo simulations using 5 different dose placement scenarios. All scenarios used 4 dose groups (control, low, medium and high dose) and logarithmic dose spacing. Each scenario was simulated using 5, 10, 20 or 50 animals per group, assuming dose-effect curves typically seen in continuous data from experimental studies. The BMD and the BMDL values were calculated using a set of 5 nested exponential models implemented in available BMD-software (BMDs and PROAST).

The results suggest that the risk of obtaining a BMDL which is higher than the true BMD can be considerably larger than normally expected. In one scenario the BMDL was higher than the true BMD in 74% of the simulations. This occurs because the second model in the nested set of models lacks the ability to level off at higher doses.

It is therefore suggested that the second model in the nested set ( $y = a \cdot e^{bx}$ ) should be used with caution. It is also important to visually inspect the dose effect curve and the individual data points.

**PS 1954 Characterizing the Impacts of Uncertainty and Scientific Judgment in Exposure Limit Development.**

A. Maier<sup>1</sup>, R. Sussman<sup>2</sup>, B. Naumann<sup>3</sup> and R. Roy<sup>4</sup>. <sup>1</sup>*Toxicology Excellence for Risk Assessment, Cincinnati, OH;* <sup>2</sup>*SafeBridge Consultants, Inc., New York, NY;* <sup>3</sup>*Merck and Co., Whitehouse Station, NJ;* <sup>4</sup>*Corporate Toxicology, 3M, St. Paul, MN.*

There is a misperception by some that exposure limits are precise estimates. In the eyes of risk managers, one discrete value is often considered to be "correct" and all others considered "incorrect." Exposure limits should be evaluated based on whether the value is derived in a manner "consistent with current principles" or "not consistent." An analysis of current risk assessment methods was conducted to identify the bases for variability in exposure limits for individual chemicals. The role of scientific judgments, risk policy perspectives, and evolving science methods were evaluated in the context of exposure limit setting methods. A systematic methods analysis shows that important drivers to be considered in evaluating acceptability of an exposure limit include: thoroughness of the review of available data, interpretation of results according to current scientific principles under the regulatory framework being used, and consideration of sufficient sources of variability and uncertainty. Sources of variability that may be encountered in risk assessments performed by different industrial hygienists or toxicology professionals using identical data sets include: selection of the point of departure, uncertainty factors used for data extrapolation, and use of adjustments for toxicokinetics, among others. These and related considerations form the basis of a "quality evaluation" process proposed for assessing the robustness of an exposure limit. Transparency in methods to assure robustness is a core principle embedded in risk assessment methods harmonization. Application of a systematic quality evaluation process provides for more informed use of exposure limits for risk management. A clear understanding of the basis for disparate values can provide useful information regarding the current level of uncertainty in the science and the level of confidence appropriate in using different exposure limits to characterize risk.

**PS 1955 Chemical-Induced Methemoglobin Formation and Exploration on Its Biological Threshold.**

Z. Yan<sup>1</sup> and Q. Zhao<sup>2</sup>. <sup>1</sup>*ORISE, Cincinnati, OH;* <sup>2</sup>*NCEA, US EPA, Cincinnati, OH.*

Methemoglobin (metHb) is hemoglobin with the iron oxidized from Fe<sup>2+</sup> to the Fe<sup>3+</sup> state. An accumulation of metHb in the blood (methemoglobinemia) is often observed in response to exposure to many chemical agents, such as aniline and aniline derivatives like dapsone, and is often used as the basis for the derivation of non-cancer risk values. Therefore, an understanding of the relative sensitivity of com-

mon laboratory animals compared to humans to these metHb-forming agents is important. In this research, we compared the relative sensitivities to dapsone, a metHb-forming agent in rats, mice, and humans based on the data from in vitro and in vivo studies. In vivo data indicate that humans are more sensitive to dapsone than rats, followed by mice. However, in vitro results are inconsistent in terms of metHb formation. The inconsistency can be explained by differences in liver metabolism among species. In vitro comparisons between the parent compound (dapsone) and its metabolite (hydroxylamine) also suggest that the metabolite is more potent than the parent compound to induce metHb. Due to a higher sensitivity in vivo, the rat might be a more suitable animal model than the mouse for predicting metHb-forming effects in humans. In addition to the relative sensitivities, we further examined the background levels of metHb to explore the potential for identifying the biologically significant threshold of metHb formation after exposure to metHb-forming agents. F344 rats were used as an example. We identified a 100% increase above the control mean as a benchmark response (BMR) based on the collected metHb background levels. A comparison of the identified BMR and one standard deviation from the control mean, as commonly used in benchmark dose modeling, suggests that the new BMR generates lower or comparable benchmark dose lower confidence limits (BMDLs). Therefore, a 100% increase above the control mean could be another way to establish a BMR for methemoglobinemia in F344 rats. The views expressed in this abstract are those of the authors and do not necessarily reflect the views or policies of the U.S. EPA.

**PS 1956 Analysis of Possible Changes to the Levels of Concern for Polycyclic Aromatic Hydrocarbons in Seafood.**

R. E. Weil, L. D. Stuchal, A. S. Kane and S. M. Roberts. *University of Florida, Gainesville, FL.*

Anthropogenic contamination of coastal regions with oils from drilling operations, spills and tanker leaks has impacted coastal communities and seafood safety for decades, and will likely continue based on our oil-based economy. Federal and state agencies suspend commercial and recreational harvests in oil-affected regions based on testing for petrogenic toxicants, including polycyclic aromatic hydrocarbons (PAHs). Criteria for re-opening affected fisheries are dependent on human health risk-based levels of concern (LOCs) developed by the US Food and Drug Administration (FDA) for specific petroleum-related contaminants in seafood, including seven carcinogenic PAHs. As with the Deepwater Horizon oil spill and other oil spill events, FDA cancer-based risk assessment for seafood consumption applies the US Environmental Protection Agency (EPA) cancer slope factor for benzo[a]pyrene (BaP), and relative potency factors (RPFs) for the remaining six PAHs relative to BaP. Use of LOCs in risk assessment is based on numerous assumptions. Here we examine how LOCs for PAHs change with modifications based on: (1) variable seafood consumption rates using data reflective of high-end seafood consumers in affected regions, (2) an expanded list of carcinogenic PAHs and changes in relative potency factors as described in the EPA draft document "Development of a Relative Potency Factor Approach for Polycyclic Aromatic Hydrocarbon Mixtures," (3) the proposed change in the EPA cancer slope factor for BaP (the index carcinogenic PAH), and (4) exposure assumptions relevant to children, including incorporation of an age-dependent adjustment factor for PAH carcinogenicity. Analyses provide an indication of both direction and magnitude of changes in LOCs associated with each possible modification. This study suggests that LOCs for PAHs in seafood from the Gulf of Mexico may be more numerous and markedly lower than the suite currently applied relative to the Deepwater Horizon oil spill.

**PS 1957 The Use of Genetically Modified Mice in Cancer Risk Assessment: Challenges and Limitations.**

S. V. Vulimiri<sup>1</sup>, D. A. Eastmond<sup>2</sup>, J. E. French<sup>3</sup> and B. Sonawane<sup>1</sup>. <sup>1</sup>*National Center for Environmental Assessment, US EPA, Washington DC;* <sup>2</sup>*Cell Biology & Neuroscience, University of California Riverside, Riverside, CA;* <sup>3</sup>*NIHES, Research Triangle Park, NC.*

The use of genetically modified (GM) mice to assess carcinogenicity is playing an increasingly important role in the safety evaluation of chemicals. While progress has been made in developing and evaluating models such as the *Tsp53+/-*, the *Tg.AC* and the *nash2* models, the suitability of these models as replacements for the conventional rodent cancer bioassay and for assessing human health risks remains uncertain. The objective of this research was to evaluate the prospective use of GM mice and the recently developed accelerated cancer bioassays in evaluating the potential health risks associated with exposure to carcinogenic agents. We compared the published results from the GM bioassays with those obtained using the National Toxicology Program's conventional chronic mouse bioassay for their potential use in risk assessment. To date, the GM models have shown moderate success in distinguishing carcinogens from non-carcinogens. Analysis of information

from different studies indicates that the GM models are less efficient in detecting carcinogenic agents but more consistent in identifying non-carcinogenic agents. We identified several issues of concern related to the assay design of GM models (e.g., sample size, study duration, genetic stability, and reproducibility) as well as pathway-dependent effects, and different carcinogenic mechanisms operable in GM and non-GM animals. The use of the GM models for dose-response assessment is particularly problematic as these models are, at times, much more or less sensitive than the conventional cancer bioassays. Thus, the existing GM mouse models may be useful for hazard identification, but will be of limited use for dose-response assessment. Hence, caution should be exercised when using GM mouse models to assess the carcinogenic risks of chemicals.

Disclaimer: The views expressed in this abstract are those of the authors and do not necessarily reflect the views or policies of the USEPA or the NIEHS.

**PS 1958 Integrating Local Communities in the Health Risk Assessment Process following the Deepwater Horizon Oil Spill—A Focus on Vietnamese-Americans.**

M. J. Wilson<sup>1</sup>, S. Frickel<sup>4</sup>, D. Nguyen<sup>5</sup>, J. Howard<sup>1</sup>, B. R. Simon<sup>3</sup> and J. Wickliffe<sup>1,2</sup>. <sup>1</sup>Pharmacology and Toxicology, Rutgers University, Piscataway, NJ; <sup>2</sup>Environmental and Occupational Medicine, UMDNJ-Robert Wood Johnson Medical School, Piscataway, NJ.

Vietnamese-American populations in southeast Louisiana consist largely of commercial and subsistence fisherfolk and represent one of the highest seafood consuming groups in the Gulf South. We collected targeted survey data from a Vietnamese-American fishing community in Orleans Parish Louisiana, to determine shrimp consumption rates, body weights, ages, and genders in order to conduct deterministic and probabilistic health risk assessments tailored to this unique population. Cancer risk estimates and levels of concern (LOCs) for several polycyclic aromatic hydrocarbons were determined using GC/MS in SIM mode on a sample of white shrimp collected from the Gulf with shrimpers from this community. Our approach also developed health risk assessments using LOCs, oral slope factors, and risk levels used by the Food and Drug Administration and the Natural Resources Defense Council. Our results demonstrate the need to include key populations in the risk assessment process and measure risk model parameters in such populations rather than rely solely on generic exposure assumptions.

**PS 1959 Challenges in Safety Assessment of Botanicals in Cosmetics: A Possible Risk Assessment Strategy.**

B. Mukerji, P. Hepburn, E. Antignac, T. Ashikaga, D. Chavez, K. Khoo, P. Sinhaseni and A. Khaiat. *Safety and Toxicology, Asean Cosmetic Association, Singapore, Singapore.*

There is a growing trend of using botanical raw materials in personal care products, such as those used in traditional medicine or those from the many exotic plants which may be part of local folklore or food use. These materials present a challenge to both the Product Developer and Regulator alike, in assuring the development of safe cosmetic products, from the complex composition of the materials through to the lack of documented data on history of use and safety.

This paper presents a strategy for the safety assessment of these botanicals used in cosmetics, based on various risk assessment concepts. A critical first step in the risk assessment is the characterisation of the botanical raw material, with key measurements being identified. A complete understanding of "what is known?" about the material should then be developed from both literature sources as well as traditional knowledge. It may then be possible to determine whether a history of safe use (HOSU) can be established and if the material can be considered safe at that stage for particular cosmetic applications. If not then further risk assessment approaches (ie comparative approach, threshold of toxicological concern (TTC)) are proposed. Finally, in order to complete the risk assessment there may be a need to fill gaps in the hazard profile and/or potential consumer exposure scenarios, by conducting some further testing.

**PS 1960 Simulation of Acute Reference Dose (ARfD) Setting for Pesticides in Japan.**

M. Yoshida<sup>1</sup>, D. Suzuki<sup>1</sup>, K. Matsumoto<sup>2</sup>, K. Inoue<sup>1</sup>, M. Takahashi<sup>1</sup>, T. Morita<sup>3</sup>, M. Shirota<sup>4</sup> and A. Ono<sup>5</sup>. <sup>1</sup>Department of Pathology, National Institute of Health Sciences, Tokyo, Japan; <sup>2</sup>Research Center for Human and Environmental Sciences, Shinshu University, Nagano, Japan; <sup>3</sup>Division of Safety Information on Drug, Food and Chemicals, National Institute of Health Sciences, Tokyo, Japan; <sup>4</sup>Laboratory of Comparative Toxicology, School of Veterinary Medicine, Azabu University, Kanagawa, Japan; <sup>5</sup>Division of Risk Assessment, National Institute of Health Sciences, Tokyo, Japan.

We conducted simulations of Acute Reference Dose (ARfD) setting, based on review documents of 208 pesticides published by Food Safety Commission (FSC) in Japan. These pesticides were evaluated in FSC during last 8 years. We applied the conceptual framework of Solecki, et al.(2005) to create and implement a conceptual framework adapted to current assessment needs in Japan. Through this process, we were able to set the ARfDs for over 90% of those 208 pesticides. The studies that provided the rationale for ARfD setting were primarily reproductive and developmental toxicity studies, acute neurotoxicity studies, and pharmacology studies. It was not necessary to establish ARfDs for approximately 30% of the pesticides simulated in the present study. Some of the simulated ARfDs might be conservative, and some endpoints for ARfD setting might not be proper, because the published data obtained in the present study were written for acceptable daily intake (ADI) setting. We were unable to set an ARfD for 14 pesticides because of insufficient data on acute toxicities. This could be improved by more complete record-keeping (for example, the type of changes observed immediately after administration, and the duration of the observation period). Furthermore, we categorized the 208 pesticides by mechanism of action or chemical structure. In comparison of absolute ARfDs or relative ARfDs to ADI among the categories, considerable number of pesticides with similar mechanisms of action or similar chemical structure also showed similar ARfDs.

**PS 1961 Tumour and In-Life Data from CD-1 Mouse Dietary and Oral Gavage Tumorigenicity Studies, Completed over the Period of 1995 to 2011.**

W. N. Hooks<sup>1</sup> and I. Taylor<sup>2</sup>. <sup>1</sup>Safety Assessment, Huntingdon Life Sciences, Huntingdon, United Kingdom; <sup>2</sup>Pathology, Huntingdon Life Sciences, Huntingdon, United Kingdom. Sponsor: D. Mitchell.

A previous review (1) of Crl:CD-1 ® (ICR) BR mouse tumorigenicity studies indicated terminal (Week 104) mortality values of 53±10.2% for males and 57±7.7% for females, with no major differences between the dietary and oral gavage routes of administration. Expanding on this, the aim of this review was to establish if the in-life data and tumour profile had changed over time and if there were any differences between the routes of administration. Data was analysed from over 60 mouse studies terminated at or about 2 years and completed over the period of 1995 to 2011. Analysis of bodyweight gain and food consumption over the first year revealed lower values for oral gavage studies (both sexes) when compared with dietary studies. The analyses over time (Period 1, 1995-2001 against Period 2, 2002-2011), performed for oral gavage studies only, did not show any remarkable differences. The most prevalent tumours were hepatocellular adenoma/carcinoma and adrenal adenoma (males), bronchioalveolar adenoma/carcinoma, Harderian gland adenoma and haemopoietic tumours (males and females), and uterine polyps (females). Generally, excluding the latter, these tumours were also the major pathological factors contributory to death (FCTD). Other major FCTD included urinary tract lesions (males) and ovarian haemorrhagic cysts (females). The most prominent difference between dietary and oral gavage studies was a lower incidence of hepatocellular tumours (males) in the latter. Analyses over time (for oral gavage studies only), indicated a lower incidence of hepatocellular tumours (males) and Harderian gland adenoma (both sexes) in Period 2. In conclusion, although there were some differences in the mortality patterns, in-life parameters, tumour profile and FCTD between the alternative oral routes and between the time periods, the CD-1 mouse has a well-defined tumour profile and continues to be suitable strain for use in tumorigenicity bioassays.

(1) W. Hooks, Abstract 2301, *The Toxicologist* CD, Vol. 126, Issue 1, March 2012.

**PS 1962 Factors Influencing the Outcome of Developmental Neurotoxicity Studies of Bisphenol A—Implications for Regulatory Testing and Risk Assessment.**

A. Beronius<sup>1</sup>, N. Johansson<sup>1</sup>, C. Rudén<sup>2</sup> and A. Hanberg<sup>1</sup>. <sup>1</sup>*Institute of Environmental Medicine, Karolinska Institutet, Stockholm, Sweden;* <sup>2</sup>*Department of Applied Environmental Science, Stockholm University, Stockholm, Sweden.* Sponsor: G. Johansson.

Developmental neurotoxicity (DNT) of bisphenol A (BPA) has been investigated in a large number of studies. However, there are discrepancies in the results reported between these studies. This investigation aims to identify and analyze factors that have contributed to these differences and to assess whether there are sex-differences in the sensitivity of certain endpoints or tests used in DNT-studies.

Forty-four DNT studies of BPA were identified in the open literature. Details about study design and results from each study, as well as the criteria for DNT testing according to the standardized OECD test guideline (TG) 426, were collected in a data base. This enabled systematic and detailed comparisons between studies as well as to the TG criteria. Multivariate analyses of the compiled data were applied in order to investigate how different factors of the study design contribute to differences in outcomes between studies.

The results from this investigation indicate that the choice of behavioral endpoints and the behavioral test methods used seem to have the largest impact on study outcome. In general, the most sensitive endpoints were the ones not required according to the standard OECD TG 426. Interestingly, non-standard endpoints seem to be especially important to detect effects in females.

One main conclusion from this investigation is that non-standardized studies seem to provide information that could be pivotal for the risk assessment of BPA, especially in the identification of effects in females. There is a need to develop tools that improve the usability of non-standardized studies in risk assessment of chemicals, particularly with regard to endocrine disrupting compounds, and that can facilitate the evaluation of data obtained from such studies.

**PS 1963 Development of Human Health Benchmarks for Pesticides.**

S. Ramasamy<sup>1</sup>, E. Doyle<sup>1</sup>, B. Behl<sup>1</sup>, B. May<sup>2</sup>, M. Goodis<sup>2</sup> and S. Knizner<sup>3</sup>. <sup>1</sup>*Office of Water, US EPA, Washington DC;* <sup>2</sup>*Office of Pesticide Programs, US EPA, Arlington, VA;* <sup>3</sup>*Office of Environmental Information, US EPA, Washington DC.*

On March 22, 2010, EPA Administrator, Lisa P. Jackson announced a new drinking water strategy that outlines four principles to expand public health protection. One of these principles is to use the authority of multiple laws to more effectively protect drinking water, by sharing data collected under different statutes. Under this principle, the Office of Water (OW) and the Office of Pesticide Programs (OPP) collaborated to develop the human health benchmarks for approximately 350 pesticides (HHBPs) that are currently registered to be used on food crops. These HHBPs are levels of certain pesticides in water at or below which adverse health effects are not anticipated from one-day or lifetime exposures. EPA derived the HHBPs using toxicity studies conducted on laboratory animals submitted to EPA under the Federal Insecticide, Fungicide and Rodenticide Act (FIFRA) the Federal Food Drug and Cosmetics Act (FFDCA) as amended by the Food Quality Protection Act (FQPA), with the typical methods used for developing drinking water health advisories under the Safe Drinking Water Act (SDWA). Specifically, EPA used the acute or chronic reference doses established for human dietary assessment for the most sensitive population and applied standard exposure assumptions used in calculating drinking water health advisories based on gender, age, body-weight, and water consumption of target populations. For the acute benchmark, the entire exposure is assumed to occur from drinking water (100 percent). For the chronic benchmark, EPA applied a default relative drinking water source contribution (20 percent), assuming additional exposure may arise from other sources. The HHBPs are not enforceable. EPA is providing the benchmarks for informational purposes for use by states, water systems and the public to help understand monitoring data for pesticides that have no drinking water standards or health advisories. The HHBPs can be found on EPA's website at: <http://www.epa.gov/pesticides/hhbp>

**PS 1964 Differences between US EPA Iris Inhalation Reference Concentrations (RfCs) and European Chemicals Agency (ECHA) Long-Term Inhalation Derived No Effect Levels (DNELs) for the General Population.**

M. Jackson<sup>1</sup>, R. Lemus-Olalde<sup>2</sup>, C. Inhof<sup>2</sup>, Z. Yin<sup>2</sup>, B. Locey<sup>1</sup>, B. H. Magee<sup>3</sup> and K. T. Connor<sup>3</sup>. <sup>1</sup>*ARCADIS, Brighton, MI;* <sup>2</sup>*ARCADIS, Cincinnati, OH;* <sup>3</sup>*ARCADIS, Chelmsford, MA.*

ECHA previously released manufacturer/importer REACH (Registration, Evaluation, Authorization and Restriction of Chemicals) chemical registration files, making available the Derived No Effect Levels (DNELs) for hundreds of substances. The DNEL is defined as "the level of exposure above which humans should not be exposed" and needs to reflect the likely route(s), duration and frequency of exposure. Typically, DNELs are developed by Industry using ECHA's guidance; the registrant has the final decision on the selection of the key studies, endpoints of concern, and the assessment factors to account for sources of uncertainty, instead of a regulatory agency such as the U.S. EPA for the IRIS program. Considering this major difference, we have conducted a comparison analysis between REACH's long-term inhalation DNEL for non-carcinogenic effects for the general population and IRIS' chronic RfC, which is defined as "an estimate (with uncertainty spanning perhaps an order of magnitude) of a continuous inhalation exposure to the human population (including sensitive subgroups) that is likely to be without an appreciable risk of deleterious effects during a lifetime." Overall, despite being defined similarly, many of the current U.S. EPA IRIS inhalation RfCs for which long-term inhalation DNELs were available are lower by a factor of at least 10. The differences between these RfCs and DNELs may be a result of differences in the processes by which they are derived, including differences in the availability of toxicity data, as unpublished data or ECHA-required data may be used in the REACH assessments [ECHA requires the registrant to conduct toxicity testing (when data for a required endpoint are not available)], the entity (industry versus regulatory agency) responsible for generating the reference values, the methodologies and selection of default values used in the derivation, and the process by which the final values are accepted.

**PS 1965 Assessment Factors in Human Health Risk Assessment and Their Associated Level of Safety.**

S. Escher<sup>2</sup>, S. Hoffmann-Doerr<sup>1</sup>, M. Batke<sup>2</sup> and I. Mangelsdorf<sup>2</sup>. <sup>1</sup>*BASF Personal Care and Nutrition GmbH, Duesseldorf, Germany;* <sup>2</sup>*Fraunhofer Institute for Toxicology and Experimental Medicine - ITEM, Hannover, Germany.* Sponsor: K. Wiench.

Human health risk assessment requires solid information on adverse effects after long-term exposure. Because of ethical considerations, human data or long-term studies with animals are in general scarce. Consequently, reliable assessment factors (AF) are needed in risk assessment to overcome differences between short-term animal studies and the human situation.

In human health risk assessment, traditional AF are established, e.g. a factor of 100 (10 x 10) for interspecies/intraspecies extrapolation. Some of these AF were substantiated by either deterministic or probabilistic approaches, whereas other factors lack a scientific rationale. Furthermore, the level of safety achieved with the application of more than one AF has remained an open question so far. Our analyses aimed therefore at the derivation of AF and their corresponding level of safety when applied solely or in combination in human health risk assessment.

The toxicological database RepDose(TM) (containing appr. 2500 repeated dose studies on appr. 700 chemicals) served as the basis for the derivation of AF. Pairs of NOEL ratios - e.g. obtained from two studies with the same chemical and species, but different application durations if time AF were analyzed - were plotted in a distribution curve. Distribution curves for interspecies and time extrapolation were evaluated. All distribution functions were best described by lognormal curves. Furthermore, the combinations of these distributions were analyzed in probabilistic approaches by means of Monte Carlo simulations. On the basis of the resulting distribution curves, overall AF were determined, for which the corresponding percentile indicates the associated level of safety. Our results demonstrate that the probabilistic approach is well suited to derive AF, provided that the database is comprehensive and contains studies of good quality.

RepDose: Trademark of the Fraunhofer Gesellschaft zur Foerderung der angewandten Forschung e.V., 80686 München, DE

**PS 1966 Associations between Carcinogenic and Immune Suppression Activities of PAHs: Insights into Improving Cancer Risk Assessment for PAH Mixtures.**

K. Zaccaria and P. McClure. *SRC, Inc., Syracuse, NY.*

Multiple studies have noted that many carcinogenic polycyclic aromatic hydrocarbons (PAHs) also demonstrate immunosuppressive effects. Here, we have tested the strength of this association by deriving both cancer and immunotoxic relative potency factors (RPFs) for multiple PAHs, using the well-studied carcinogenic and immunotoxic compound benzo(a)pyrene (BaP) as the index PAH. Our quantitative analysis demonstrated a correlation between the immunosuppressive and carcinogenic potential of PAHs. As evasion of immune destruction has been identified as an "emerging hallmark of cancer" (Hanahan and Weinberg, 2011 Cell 144: 646-674), we propose that this association between carcinogenic and immune suppression activities of PAHs offers an opportunity to improve cancer risk assessment for PAH mixtures. While current assessments of cancer risks from PAH-containing fractions of environmental mixtures rely on a component-based RPF approach, we hypothesize that a more scientifically defensible whole mixtures approach would be advanced not only by a battery of inexpensive, short-term tests of different modes of carcinogenic action (e.g., genotoxic and non-genotoxic), but also a battery of tests for immunosuppressive activity. The addition of immunotoxicity tests may improve the ability to discern the similarity of an untested environmental mixture with reference mixtures that have cancer slope factors. Therefore, we performed a comprehensive review of the immunotoxic effects of BaP, and developed an integrated knowledge map illustrating immunosuppressive effects of BaP and, when known, tissue-specific mechanistic information. Our analysis revealed that research to date has not yet identified a transcriptional signature(s) for immune suppression to aid in the development of a specific battery of short-term in vitro test for immunotoxicity. Thus, future directed research to develop and validate a battery of tests for immunotoxicity is warranted and could find widespread use in assessing cancer risk from environmental PAH-containing mixtures.

**PS 1967 Potential Involvement of Oxidative Stress and Iron Disturbance in the Development of Oral Cavity Tumors in Rats Exposed to Hexavalent Chromium.**

M. Suh<sup>1</sup>, C. T. Thompson<sup>1</sup>, G. Hixon<sup>1</sup>, M. A. Harris<sup>1</sup>, C. R. Kirman<sup>2</sup>, S. M. Hays<sup>2</sup>, L. C. Haws<sup>1</sup> and D. M. Proctor<sup>1</sup>. <sup>1</sup>*ToxStrategies, Katy, TX*; <sup>2</sup>*Summit Toxicology, Allenspark, CO.*

In the NTP 2-year Cr(VI) drinking water study, the incidence of oral cavity tumors was significantly increased in male and female rats of the highest dose group (516 mg/L sodium dichromate dihydrate [SDD]). We investigated the potential involvement of iron (Fe) disturbance and oxidative stress in rat oral cavity tumor formation because Cr(VI) has been shown to compete with Fe uptake and causes microcytic anemia at high doses. Also, Fe deficiency can cause oxidative stress. We measured the GSH/GSSG ratios in rat oral mucosa and plasma following 90-days of treatment, and observed a significantly decreased ratio in oral mucosa at exposures  $\geq 60$  mg SDD/L, and in plasma at  $\geq 170$  mg SDD/L. We also found that Fe levels were significantly decreased in rat liver at  $\geq 60$  mg SDD/L, in bone marrow at  $\geq 170$  mg SDD/L, and in the duodenum at 520 mg SDD/L. A statistical mediation analysis using the NTP data on rat oral cavity tumor incidence and that for chronic liver inflammation, bone marrow hyperplasia, and salivary gland atrophy—all of which may be caused by Fe disturbance—was conducted to assess the association between Fe disturbance and oral cavity tumors in treated rats. The link from Cr(VI) exposure to these three endpoints combined was significant, as well as the link from these endpoints combined to oral tumors,  $t(498)=3.985$ ,  $p<1\times 10^{-4}$ . When each endpoint was analyzed separately, only the link from Cr(VI) exposure to salivary gland atrophy, and that from salivary gland atrophy to tumors were significant,  $t(498)=4.282$ ,  $p<1\times 10^{-4}$ . Taken together, these findings suggest that Fe metabolic disruption, oxidative stress and salivary gland atrophy may contribute to tumor formation in Cr(VI)-exposed rats. Further, these cancers may be species-specific as rats are generally more susceptible to oral cancers than mice, oral tumors were not observed in the NTP Cr(VI) treated mice, and no increase in oral cavity tumors have been reported in Cr(VI)-exposed workers.

**PS 1968 Estimating the Relative Bioavailability of Polycyclic Aromatic Hydrocarbons (PAHs) from Soil at Environmentally-Relevant Concentrations.**

J. W. Munson<sup>1</sup>, Y. W. Lowney<sup>2,1</sup>, M. V. Ruby<sup>3</sup> and S. M. Roberts<sup>1</sup>. <sup>1</sup>*CEHT, University of Florida, Gainesville, FL*; <sup>2</sup>*Exponent, Boulder, CO*; <sup>3</sup>*Integral Consulting, Louisville, CO.*

Polycyclic aromatic hydrocarbons (PAHs) are common soil contaminants at a variety of sites, including industrial facilities, military bases, and former skeet ranges. The risk from exposure to PAHs in soil is driven primarily from incidental ingestion of carcinogenic PAHs, and as with many other soil contaminants, is dependent in part upon their oral bioavailability. Most previous studies attempting to understand PAH bioavailability from soil have used PAH concentrations well above the range of greatest environmental interest. We report here a method by which the relative oral bioavailability (RBA) of 3H-benzo[a]pyrene (BaP) in vivo in constructed, weathered soils and PAH source materials can be measured at BaP concentrations in the ppb range. A suite of these materials is being used to examine the BaP-soil interactions that may control in vivo RBA, as well as for the development of in vitro PAH RBA estimation methods. Soil was spiked with 3H-BaP in varying concentrations and allowed to weather for up to two months. No loss of BaP or 3H label was observed as a result of weathering. Rats were administered a single dose of soil or PAH source material by gavage, and blood samples were taken via jugular cannula for up to six days after the dose. For comparison, in order to estimate RBA, other rats were given a comparable gavage dose of 3H-BaP added to food. The area under the curve (AUC) for total radioactivity in blood was used to indicate absorbed BaP dose for each animal, and the ratio AUCs for soil versus food doses was used to estimate RBA for the soil or PAH source material. AUCs could be measured without difficulty for soil/food BaP concentrations as low as 200 ppb, facilitating study of critical factors controlling bioavailability at environmentally relevant concentrations. Supported in part by a grant from the Strategic Environmental Research and Development Program (SERDP).

**PS 1969 Mode-of-Action Evaluation for Lung Tumors in Mice Exposed to Ethylene Oxide via Inhalation.**

L. T. Haber<sup>1</sup>, B. L. Parsons<sup>2</sup>, N. P. Moore<sup>3</sup>, B. Gollapudi<sup>4</sup>, M. G. Manjanatha<sup>2</sup>, M. J. LeBaron<sup>4</sup> and M. M. Moore<sup>2</sup>. <sup>1</sup>*Toxicology Excellence for Risk Assessment (TERA), Cincinnati, OH*; <sup>2</sup>*Division of Genetic and Molecular Toxicology, National Center for Toxicological Research, US FDA, Jefferson, AR*; <sup>3</sup>*Dow Europe GmbH, Horgen, Switzerland*; <sup>4</sup>*Toxicology & Environmental Research and Consulting, Dow Chemical Company, Midland, MI.*

Ethylene oxide (EO) is a direct acting mutagen and a rodent carcinogen, but it is uncertain whether EO is carcinogenic through a mutagenic mode of action (MOA). To address the MOA for mouse lung tumors, an integrated study was conducted evaluating a variety of biomarkers related to oxidative stress, DNA reactivity/ breakage, mutations in a reporter (cII) and endogenous (K-ras) gene, and cell proliferation as putative key events, in the target tissue. The dose response and temporality for these key events was assessed in male B6C3F1 mice exposed to 0, 10, 50, 100, or 200 ppm EO (4 weeks) or 0, 100, or 200 ppm EO (8 or 12 weeks) by inhalation (6 hours/day, 5 consecutive days/week). Results indicate that: (1) EO does not appear to cause the lung tumors primarily via its DNA reactivity, since a sustained increase in cII MF was not seen at 100 ppm (which produced substantial increases in lung tumors in the mouse NTP study), and the increase at 200 ppm was only weak. (2) Oxidative stress is likely to play a multifaceted role in the tumorigenic process, in light of the absence of an effect on 8-OHdG adducts, and the observed mutation spectra of K-ras codon 12 and cII. The role of EO-induced DNA adducts in the etiology of the observed mutations needs further elucidation. (3) The available data on cell proliferation and K-ras mutations support a MOA that includes effects on intracellular signaling pathways and selection of preexisting K-ras mutant cells, as well as an interplay between oxidative stress and RAS activation. These results suggest a complex multi-faceted MOA, potentially involving EO action at multiple steps along the pathway to tumor development.

**PS 1970 Challenges in Estimating Safe Levels of Nanomaterials for Humans from Animal Toxicology Experiments.**

A. Bacom<sup>1</sup>, M. Odin<sup>1</sup>, P. McClure<sup>1</sup>, K. Salinas<sup>1</sup>, P. Wood<sup>2</sup>, D. Bottimore<sup>2</sup> and T. Thomas<sup>3</sup>. <sup>1</sup>*SRC, Inc., East Syracuse, NY*; <sup>2</sup>*Versar, Inc., Springfield, VA*; <sup>3</sup>*US Consumer Product Safety Commission, Bethesda, MD.* Sponsor: *G. Diamond.*

The use of nanosized particles in commercial products is increasing, leading to greater exposure of people to these materials. Exposure is most likely to occur through inhalation and dermal routes, but oral exposure may also occur. We evaluated published toxicity data for 3 different nanomaterials: nanosilver (nAg), nanotitanium dioxide (nTiO<sub>2</sub>), and carbon nanotubes (CNT), as a preliminary step for

deriving safe exposure levels for these materials. Each of these materials comes in a multitude of forms, varying in size, shape, structure, purity, and surface coating, which affect chemical properties, such as solubility, reactivity, and propensity for agglomeration. All 3 nanomaterials have multiple repeated exposure inhalation studies available, suitable for use in dose-response assessment, but only nAg has repeated dose oral studies, and none of the materials has a suitable dermal study. The lung was the critical target in the inhalation studies of all 3 materials, with pulmonary inflammation being the most sensitive endpoint. For nAg, the liver was also identified as a target by both inhalation and oral exposure (bile duct hyperplasia). Using these data, it is possible to derive safe exposure levels for long-term exposure to the specific forms of nAg, nTiO<sub>2</sub>, and CNT tested in these studies. It is, however, unclear to what extent these levels may apply to other forms of nAg, nTiO<sub>2</sub>, and CNT. Mechanistic data for all 3 nanomaterials show that the specific physical and chemical characteristics of the particles can influence toxicity in defined ways. However, the relationships are complex, and as yet, only partially understood, making the task of estimating safe levels of a particular nanomaterial challenging. Toxicity assessments for nanomaterials must take these additional uncertainties into account. (The views expressed in this abstract are those of the authors only and do not necessarily reflect the views or policies of the U.S. CPSC).

## PS 1971 Quality Assurance and Quality Control for an xCelligence High-Throughput Risk Assessment Assay.

M. Stampfl<sup>1</sup>, F. Ackah<sup>2</sup>, V. Charoensuk<sup>3</sup>, T. Pan<sup>4</sup>, C. Jin<sup>1</sup>, Y. A. Abassi<sup>1</sup>, X. Xu<sup>1</sup>, X. Wang<sup>1</sup>, B. Huang<sup>4</sup>, D. Kinniburgh<sup>3</sup>, W. Zhang<sup>2</sup> and S. Gabos<sup>2</sup>.  
<sup>1</sup>Acea Biosciences, Inc, San Diego, CA; <sup>2</sup>Alberta Health and Wellness, Edmonton, AB, Canada; <sup>3</sup>Alberta Centre for Toxicology, University of Calgary, Calgary, AB, Canada; <sup>4</sup>University of Alberta, Edmonton, AB, Canada.

Taking advantage of impedance based non-invasive, real time cell analysis (RTCA) technology, and human cell lines with different organ origins, a High Throughput Risk Assessment (HTRA) assay is under development to meet 21st century toxicity testing requirement for hazard identification, chemical mode of action understanding, and eventually human health risk assessment. The HTRA assay is run on an fully automated system, composed of 4 xCELLigence RTCA HT stations running 384 well EPlates, liquid handler, and compound/cell culture hotels. Impedance signal derived from adherent cells in the EPlate 384 are continuously monitored for 100 hours to reflect cell growth and responses to testing chemicals. To assess and validate the usefulness of this new in vitro screening system for identifying general toxicity of environmental hazards, 14 chemicals with known in vivo LD50 values were tested with 11 different concentrations in duplicate or quadruplicate, and repeated in 2 separate experiments. The quality assurance program includes the generation of SOPs for experiments and data analysis. Specifically, experimental plate layout to reduce false responses is discussed. The quality control system includes variability and reproducibility analysis. Coefficient of variation, signal to noise ratio and Z factor were calculated to evaluate variability. The analysis excluded one cell line from the cell panel. Intra-plate reproducibility of impedance signals was within acceptable range. Intra-plate reproducibility based on LC50 values from different cell lines, was acceptable. Inter-laboratory validation is in progress. In summary, results from HTRA assay system showed good screening quality and reproducibility. Together with its higher throughput, rich real-time information, HTRA assay system could effectively provide biologically relevant cytotoxicity information for human health risk assessment.

## PS 1972 Advancing Human Health Risk Assessment: Charting a Course through Committee Recommendations.

M. Dourson<sup>1</sup>, R. Becker<sup>2</sup>, L. T. Haber<sup>1</sup>, L. H. Pottenger<sup>3</sup>, T. Bredfeldt<sup>4</sup> and P. Fenner-Crisp<sup>5</sup>. <sup>1</sup>Toxicology Excellence for Risk Assessment, Cincinnati, OH; <sup>2</sup>American Chemistry Council, Washington DC; <sup>3</sup>The Dow Chemical Company, Midland, MI; <sup>4</sup>Texas Commission on Environmental Quality, Austin, TX; <sup>5</sup>Independent Consultant, North Garden, VA.

Over the last dozen years, many national and international expert groups have weighed in on specific improvements to risk assessment. Many of their stated recommendations are mutually supportive, but others appear conflicting, at least in an initial assessment. This effort synthesizes these opinions, identifies areas of consensus and sources of differences, and recommends a biological-centric, practical course forward for risk assessment, which includes: (1) Incorporating a clear problem formulation process at the outset of the assessment to ensure the level of complexity in design of the risk assessment is appropriate for informing the relevant risk management decision; (2) Use of mode of action (MOA) information and an understanding of the relevant biology as the key, central organizing principle for dose-response assessment; (3) Integrating MOA information into dose-response assessments using existing guidelines for noncancer and cancer assessments, and applying this knowledge with toxicokinetics to enable interpretation of human biomonitoring data in a risk context; (4) Using the tiered, iterative approach developed by the

World Health Organization International Programme on Chemical Safety as a scientifically robust, fit-for-purpose approach for risk assessment of combined exposures (chemical mixtures). While scientifically-based defaults will remain important and useful when data on MOA or other data to refine an assessment are absent or insufficient, assessments should always strive to achieve the ultimate goal—to use 21st century knowledge of biological processes, dose-response, and chemical interactions at the molecular, cellular, organ and organism levels to minimize the need for extrapolation and reliance on default approaches.

## PS 1973 Assessment on Health Risk and Risk Factors Related to Lead Exposure by Ingestion of Aquatic Animals from the Overflow Marsh.

S. Chaiklang<sup>1</sup> and S. Kiatsayomphu<sup>2</sup>. <sup>1</sup>Environmental Health Science, Faculty of Public Health, Khon Kaen University, Muang, Thailand; <sup>2</sup>Central Laboratory, Faculty of Public Health, Khon Kaen University, Muang, Thailand.

The previous study identified that aquatic animals in Loeng Puay marsh were lead polluted. The lead concentrations in River snails were exceeded the food standard. This survey research aimed to determine health risk on ingestion of lead-contaminated aquatic animals from Loeng Puay marsh and the adverse health effects. The interviews of 75 residents at Loeng Puay on the consumptions of the aquatic animals and adverse health effects related to lead toxicity were conducted. The lead concentrations in aquatic animals (n=100) i.e. Nile tilapia, Common silver barb, River snail and Golden apple snail were analyzed by using Atomic Absorption Spectrophotometry. Health risk assessment was performed according to the US EPA guideline (2004). The correlated factors with the adverse health effects were identified by the univariate analysis.

The highest lead concentration in all kind of aquatic animals was found in River snail and was used as represent concentration for health risk assessment on the acute effect. By considering the total intake rate of all aquatic animal consumption in the day, the maximum dose of lead exposure was 26.46 g/kg/day which was higher than the provisional tolerable weekly intake (PTWI=25 g/kg). The adverse health effects related to lead toxicity were reported from 46.67% of residents. Most of symptoms were disorders of joints and skeleton, numbness, and acroanesthesia, respectively. The univariate analysis identified that the fishermen had the higher risk on lead exposure (justified by adverse health effect) when compared to other occupations (OR=7.07, 95% CI: 2.20-23.81, p<0.001). The findings indicated the health risk from high dose ingestion of lead-contaminated aquatic animals. However, the potential health risk depends on amount of food ingestion and personal factors. There should be continuously environmental monitoring of the lead accumulation in this overflow marsh for the safety of food chain and the health surveillance program.

## PS 1974 Integrating Hazard Characterization Approaches for Evaluating the Potential of Consumer Products to Cause Asthma.

J. Patterson, A. Maier, M. J. Vincent and B. K. Gadagbui. TERA, Cincinnati, OH.

Concerns have been raised regarding the potential for consumer products, including cleaning products to cause or exacerbate asthma or asthma-like responses. Although many forms of asthma are inflammation-based, some low-molecular-weight chemicals have been shown to trigger immunoglobulin E (IgE) independent occupational asthma. Single exposures to high concentrations of chemical irritants are also known to elicit an asthma-like response: reactive airways dysfunction syndrome (RADS). RADS can occur within hours of the initial exposure and may continue, as non-specific bronchial hyper-responsiveness, for extended durations. Exposure to irritants may be a trigger for respiratory symptoms in individuals with pre-existing asthma. Current methods cannot adequately assess the potential for consumer product ingredients to trigger asthma or asthma-like responses; epidemiological studies can only measure possible effects associated with a multitude of chemicals and products, and no single animal model can reliably replicate the complexity of an asthma-like response in humans. In order to characterize asthma and respiratory related hazards associated with consumer products, a decision system is needed that incorporates existing guidance, frameworks, and models. To develop such a tool, we compiled and evaluated in vivo, in vitro, and in silico methods that may provide data, or insight, to predict potential asthma or asthma-like responses (e.g., respiratory sensitization) and noted strengths and weaknesses associated with each method. We collaborated with asthma research experts to refine our findings and approach. Despite the wealth of information on asthma, current guidelines, bioassays, and computer models cannot definitively identify whether a particular ingredient, or chemical, causes or exacerbates asthma or asthma-like responses. However, possible predictors of allergy-induced asthma, such as respiratory sensitization, are useful to assess the likelihood that a particular chemical, ingredient, or product may be associated with asthma induction.

**PS 1975 Assessment of the Impacts of Changes in Regulatory Toxicology of Polycyclic Aromatic Hydrocarbons on Site Assessments.**

J. H. Salatas<sup>1</sup>, M. R. Garry<sup>1</sup> and Y. W. Lowney<sup>2</sup>. <sup>1</sup>Exponent, Bellevue, WA; <sup>2</sup>Exponent, Boulder, CO.

Polycyclic aromatic hydrocarbons (PAHs) are common soil contaminants at many industrial facilities, military bases, and other sites. For PAH mixtures, the U.S. Environmental Protection Agency (EPA) and other regulatory agencies use relative potency factors (RPFs) to assess the potential toxicity of individual PAHs. EPA currently provides RPF values for cancer risks for seven individual PAHs, but is considering RPFs for 25 individual PAHs, spanning values of potency relative to benzo[a]pyrene (BaP) from 0.009 to 60. As part of a larger study aimed at tying together research on soil PAH chemistry with *in vivo* measures of bioavailability across diverse soil types and contaminant sources for the purpose of improving remedial decisions for soil PAHs at U.S. Department of Defense (DOD) sites, we investigated the potential impacts of proposed changes in regulatory toxicology of PAHs on regulatory decision-making. Specifically, we investigated the degree to which changes in PAH RPFs could alter conclusions about health-based screening at DOD sites. Using EPA's Records of Decision database for Superfund sites, we identified 11 DOD sites with 22 exposure units in which PAHs were identified as chemicals of concern in surface or subsurface soil. Site data were evaluated for exceedances of health-based soil screening levels using current and proposed RPFs. Results indicate that the percentage of sites exceeding a screening level would increase; up to twice as many sites for some individual PAHs (e.g., chrysene). In addition, the magnitude of exceedance would increase for all sites. The results suggest that both the number of sites and the areal extent of individual sites requiring remediation could increase with the proposed changes in RPFs. Additional issues include lack of background data for PAHs newly added to the risk assessment paradigm and methods for assessing undetected PAHs. This work was supported in part by a grant from the Strategic Environmental Research and Development Program.

**PS 1976 Rapid Risk-Based Response to a Crude Oil Spill.**

K. Philipps and D. B. Davies. *Intrinsic Environmental Sciences Inc., Calgary, AB, Canada.*

Issues surrounding pipeline safety and the potential health and environmental impacts that can result from pipeline accidents and malfunctions have led to considerable debate lately across North America. A number of recent high-profile oil spills in areas that are populated highlight the need for risk assessment to be completed rapidly to inform risk-based decision making. An example of such an assessment was completed in response to a break at an underwater pipeline crossing in which a sweet crude oil was released in a watercourse, upstream of several residences, active livestock farming operations, recreational properties and a municipal drinking water intake. Within 24-hours, a clean-up and contaminant sampling strategy was developed and implemented, and continued over several weeks. Preliminary evaluation and interpretation of the contaminant data was completed to aid in community consultation, to identify the need for further monitoring, and to provide risk-based decision making strategies to local authorities managing drinking water and recreational use access. The conclusions of an initial risk assessment completed two weeks after the spill served to provide reassurance to regulators and the general public regarding the safety of drinking water for residents and livestock, resulting in the re-opening of some drinking water intakes in the impacted area. The assessment considered the nature and levels of the contaminants that were determined to be present in the water column and sediments, the results of toxicity studies for the various contaminants, and the opportunity for exposure of people and animals to the contaminants. Following the analysis of additional sampling results, a more comprehensive risk assessment was completed. The final results of the assessment revealed that the clean-up efforts had successfully mitigated risk to human health and the local ecosystem.

**PS 1977 Validation Oral Slope Factors for Benzo(a)pyrene Using Whole Mixture Results.**

K. T. Connor and B. H. Magee. *Risk Assessment, ARCADIS, Chelmsford, MA.*

EPA's draft Integrated Risk Information System Assessment of Benzo(a)pyrene (BaP) is due to be released for public review in 2013. The document will present an Oral Slope Factor (OSF) that will replace the current value of 7.3 (mg/kg-day)<sup>-1</sup>. The OSF will be coupled with new Relative Potency Factors (RPFs) when EPA finalizes the PAH Mixtures guidance document. A literature search identified the available studies that meet EPA's study quality criteria and OSFs were derived using EPA's benchmark dose model software (BDMs) in accordance with standard EPA

policy and guidance. The OSFs and the proposed RPFs have been validated against the results of rodent mixture studies to determine if the BaP OSF in conjunction with EPA's proposed RPFs properly estimate PAH mixture effects. Benchmark dose modeling Culp et al. (1998) data results in two BaP OSFs with reasonable model fits: forestomach – 1.23 (mg/kg-day)<sup>-1</sup> and esophagus – 0.19 (mg/kg-day)<sup>-1</sup>. Culp et al. (1998) also tested two coal tar samples in the same study. BaP-Toxic Equivalents were calculated for the coal tar mixtures using the EPA proposed RPFs. A nominal concentration of 100 ppm was assumed for unusual PAHs for which concentrations were unknown. When compared to the whole mixture OSFs for two separate coal tar mixtures, the current BaP OSF overestimates carcinogenic risk by 20 to 31-fold. The BaP OSF based on forestomach tumors in Culp et al. (1998) overestimates risk by 3 to 5-fold, whereas the BaP OSF based on esophagus tumors in the same study gives no overestimation. If the unusual PAHs with new RPFs are present in coal tar at concentrations significantly higher than the assumed 100 ppm, then the BaP OSF based on esophagus tumors will overestimate the coal tar tumorigenic risks observed in the whole mixture studies. This validation exercise demonstrates that the EPA proposed RPFs have to be implemented side-by-side with an OSF for BaP that is less than 1 (mg/kg-day)<sup>-1</sup> to ensure that risks from real world PAH mixtures are not overestimated by the RPF risk assessment approach.

**PS 1978 Cytotoxicity Test for Hazardous Substances by Using the RTCATM High-Throughput Assay.**

Y. Li<sup>1</sup>, D. Y. Huang<sup>1</sup>, W. Zhang<sup>2</sup>, S. Gabos<sup>3</sup> and D. Kinniburgh<sup>1</sup>. <sup>1</sup>Alberta Centre for Toxicology, University of Calgary, Calgary, AB, Canada; <sup>2</sup>Health Protection Branch, Family and Population Health, Alberta Health, Edmonton, AB, Canada; <sup>3</sup>Canadian Institute of Public Health Inspectors - Alberta Branch, Edmonton, AB, Canada.

Most current toxicity tests require the use of laboratory animals and involve exposure by various routes and monitoring whether animals die or exhibit any clinical signs of toxicity. Increasing societal concerns about animal use have led to the development of alternative *in vivo* test methods that can significantly reduce and refine the use of mammals for this purpose. The emerging *in vitro* cell based assays endeavor to provide information about the mode or mechanism of action that causes cytotoxicity and use such information to develop cell-based *in vitro* tests that can adequately model and predict *in vivo* toxicity. A non-invasive biophysical approach for the detection of cellular changes, the RTCATM instrument was developed for screening hazardous substances. In the present study, 6 chemicals (sodium arsenate, cadmium chloride, colchicine, verapamil, propranolol and mercury chloride) were applied to human renal adenocarcinoma cell line (ACHN) at 11 serial diluting working concentrations, respectively. The net cellular responses (the Cell Index) were recorded for 72 hours after adding chemicals. The real-time and unique time-concentration-dependent response curves (TCRC) were obtained. The experimental design composed two stages: initial screening test (range finder test) and definitive test (more defined test concentrations). The better TCRC patterns were observed in the latter. The patterns were associated with some toxicity pathways or mode of action for these chemicals. The lethal concentrations could be calculated, which could be used to predict the starting lethal doses *in vivo* test. Based on these preliminary findings, other 8 substances in other 6 cell lines will be tested in the future. This work will facilitate cellomic based test development and achieve the replacement of animals in acute oral toxicity testing.

**PS 1979 Advancements in Arsenic Research Suggest a Dose-Dependent Transition Concentration for Cancer Endpoints.**

R. Gentry<sup>1</sup>, H. J. Clewell<sup>2</sup>, P. Balbuena<sup>2</sup>, A. Efremenko<sup>2</sup>, M. B. Black<sup>2</sup> and J. W. Yager<sup>3</sup>. <sup>1</sup>ENVIRON International Corporation, West Monroe, LA; <sup>2</sup>The Hamner Institutes for Health Sciences, Research Triangle Park, NC; <sup>3</sup>University of New Mexico, Albuquerque, NM.

Recent *in vitro* studies have been conducted in both animal and human primary bladder cells to investigate the potential mode of action for bladder cancer following exposure to arsenic compounds. Results from 24 hour *in vitro* gene expression studies with human uroepithelial cells treated in culture with mixtures of inorganic arsenic and its pentavalent or trivalent metabolites provide evidence of a common suite of gene changes consistently identified for a number of key signaling pathways: oxidative stress, protein folding, growth regulation, metallothionein regulation, DNA damage sensing, thioredoxin regulation, and immune response. Lowest observed effect levels (LOELs) ranged from 0.6 – 6.0  $\mu$ M total arsenic and no observed effect levels (NOELs) ranged from 0.18 – 1.8  $\mu$ M total arsenic. Benchmark dose modeling of the responses indicated lower confidence limits (BMDLs) ranging from 0.09 – 0.58  $\mu$ M total arsenic for the eight genes most commonly significantly expressed across individual samples for the trivalent arsenical mixture, and from 0.35– 1.7  $\mu$ M for total arsenic in the pentavalent arsenical mixture. These studies

provide the first evidence of no effect levels for arsenical-induced cell signaling perturbations in normal human cells exposed to biologically plausible concentrations of arsenic. Results from longer term exposures, again in primary human cells, provide consistent results that also suggest a dose-dependent transition for arsenic. Results of these *in vitro* studies, in combination with evidence from epidemiological studies, provide the basis for a shift in the approach for conducting a cancer risk assessment for arsenic. It also provides support for a concentration demonstrating a dose-dependent transition in responses from those representing adaptive change to those that may be key events in the development of cancer endpoints.

## PS 1980 Refining the Application of a Database Uncertainty Factor in Human Health Risk Assessment.

C. Fleming<sup>1</sup>, Z. Yan<sup>1</sup>, J. Lambert<sup>2</sup> and Q. Zhao<sup>2</sup>. <sup>1</sup>ORISE, Cincinnati, OH; <sup>2</sup>US EPA, Cincinnati, OH.

In human health risk assessment (HHRA), lack of information on a chemical is typically accounted for by the use of uncertainty factors (UFs). Typically, UFs are applied to account for five major areas of uncertainty: interspecies variation, intraspecies variation, extrapolation from subchronic to chronic exposure duration, extrapolation from a LOAEL to a NOAEL, and an incomplete database. To reduce uncertainty inherent in HHRA, methods are needed to replace or better assign values to these UFs. In this preliminary analysis, we analyzed all chemicals from the USEPA's Toxicity Reference Database (ToxRefDB) with complete databases (i.e., general toxicity studies in two species, developmental toxicity studies in two species, and a multigeneration reproductive study) to assess whether a database UF (UFD) of 3 or 10 is sufficient to account for missing data. A subtractive approach was employed in which the points of departure (PODs) based on reported LOAELs and NOAELs in the ToxRefDB were compared for the complete database and following removal of selected studies. Removal of developmental toxicity studies from the database increased the POD by >3-fold in 12/186 (6.5%) chemicals and by >10-fold in only 1 chemical. Removal of multigeneration reproductive toxicity studies from the database increased the POD by >3-fold in 18/186 (9.7%) chemicals and by >10-fold in 4/186 (2.2%) chemicals. Removal of general toxicity studies from the database increased the POD by >3-fold in 59/186 (31.7%) chemicals and by >10-fold in 27/186 (14.5%) chemicals. This analysis will need to be supplemented with studies from a broader spectrum of chemical types (ToxRefDB is composed almost entirely of pesticides). When completed, this analysis could provide a method to systematically and empirically select the UFD in cases where chemical-specific information to inform selection of the UFD is lacking. The views expressed in this abstract are those of the authors and do not necessarily reflect the views or policies of the U.S. EPA.

## PS 1981 Short-Term Exposure to Perfluoroalkyl Acids Causes Increase of Hepatic Lipid and Triglyceride in Conjunction with Liver Hypertrophy.

K. P. Das<sup>1</sup>, C. R. Wood<sup>1</sup>, M. B. Rosen<sup>2</sup>, C. Lau<sup>1</sup> and B. D. Abbott<sup>1</sup>. <sup>1</sup>Toxicity Assessment Division, ORD, NHEERL, US EPA, Research Triangle Park, NC; <sup>2</sup>Integrated Systems Toxicology Division, ORD, NHEERL, US EPA, Research Triangle Park, NC.

Persistent presence of perfluoroalkyl acids (PFAAs) in the environment is due to extensive use of industrial and consumer products. These chemicals activate peroxisome proliferator-activated receptor- $\alpha$  (PPAR $\alpha$ ) in liver and alter lipid metabolism. The current study was designed to evaluate liver toxicity of perfluorooctanoic acid (PFOA), perfluorononanoic acid (PFNA), perfluorohexane sulfonate (PFHxS), and perfluorophosphonic acid (PFPA), with emphasis on hepatocellular hypertrophy and steatosis. SV129 wild-type (WT) and PPAR $\alpha$ -null (Null) adult male mice were dosed for 7 days with vehicle, PFOA, PFNA, PFHxS (10 mg/kg), and PFPA (20 mg/kg); and WY14643 (50 mg/kg) was a positive control. Mice were killed 24 h after the last treatment. Liver samples were collected for biochemical analysis of triglyceride (TG) and DNA content. Frozen 6  $\mu$ m sections of liver were stained with Oil Red O for lipid and used for morphometric analysis. Liver weights were elevated in both WT and Null mice in all of the treatment groups, except in Null mice of the PFPA and WY groups. Morphometric analysis revealed an increase in cell size in WT and Null livers exposed to PFOA, PFNA, PFHxS or PFPA, except for the PFPA and WY groups in Null mice. This pattern of change is consistent with the reduced DNA content per mg liver. In the Oil Red O stained sections, WT liver showed increased lipid accumulation in all treatment groups; whereas in Null livers, this was seen only after PFNA and PFHxS treatment. Similarly, elevated TG level was found in PFAA-exposed WT but not in WY-exposed mice, and increased TG was seen in Null mice only after PFNA treatment. Null livers had more lipid and TG than WT livers, both in control and treated mice. These results indicate that PFAAs induce liver hypertrophy and steatosis in WT; and the involvement of PPAR $\alpha$  is suggested by observations in Null mice. (This abstract does not necessarily reflect US EPA policy.)

## PS 1982 Structure-Activity Relationships for Perfluoroalkane-Induced Interference with Rat Liver Mitochondrial Respiration.

K. B. Wallace<sup>1</sup>, G. E. Kissling<sup>2</sup>, R. Melnick<sup>3,4</sup> and C. R. Blystone<sup>3</sup>. <sup>1</sup>Biochemistry & Molecular Biology, University of Minnesota Medical School, Duluth, MN; <sup>2</sup>Biostatistics Branch, NIEHS, Research Triangle Park, NC; <sup>3</sup>National Toxicology Program, NIEHS, Research Triangle Park, NC; <sup>4</sup>Ron Melnick Consulting, LLC, Chapel Hill, NC.

Perfluorinated alkanes (PFAAs) represent a broad class of commercial products detected primarily for the coatings industry. Unfortunately, residues have been detected in a variety of species world-wide prompting aggressive toxicity testing. Although some effects of PFAA exposures are linked to activation of the PPAR $\alpha$  nuclear receptor, interference with mitochondrial bioenergetics has been implicated as an alternate and possibly important mechanism of cytotoxicity. The current investigation was designed to explore structure-activity relationships for the various modalities by which PFAAs interfere with mitochondrial respiration. Freshly isolated rat liver mitochondrial were incubated with one of 16 different PFAAs. The effects of each PFAA on mitochondrial respiration was measured at five different concentrations and dose-response curves generated. All PFAAs tested inhibited mitochondrial respiratory control, mostly by stimulating state 4 and inhibiting state 3 respiration with the EC20 ranging from 1  $\mu$ M to 413  $\mu$ M. The perfluoroalkyl sulfonamides were most potent with an EC20 between 1 and 11  $\mu$ M. The results are consistent with evidence that the perfluorinated carboxylic acids stimulate the mitochondrial permeability transition whereas the sulfonamides act as protonophoric uncouplers of oxidative phosphorylation. In all cases, there was a pronounced increase in potency with increasing carbon number, with a prominent inflection in potency between the six and eight carbon congeners. The results provide a foundation for classifying PFAAs according to specific modes of mitochondrial toxicity and establishing structure-activity evidence-based initial estimates of safety for PFAA congeners for which minimal *in vivo* toxicity testing currently exists. (This work was funded by NIEHS NTP contract 273200620005C).

## PS 1983 Determination of Polychlorinated Biphenyls (PCBs) and Hydroxylated Metabolites (OH-PCBs) in Human Blood Serum from Two Populations in East Chicago, IN and Columbus Junction, IA.

W. Koh<sup>1</sup>, R. Marek<sup>2</sup>, J. DeWall<sup>3</sup>, P. S. Thorne<sup>1,3</sup> and K. C. Hornbuckle<sup>1,2</sup>. <sup>1</sup>Interdisciplinary Graduate Program in Human Toxicology, The University of Iowa, Iowa City, IA; <sup>2</sup>Department of Civil and Environmental Engineering, The University of Iowa, Iowa City, IA; <sup>3</sup>Department of Occupational and Environmental Health, The University of Iowa, Iowa City, IA. Sponsor: L. Robertson.

PCBs are persistent and bioaccumulating toxic pollutants which pose health risk to humans and organisms. Although commercial production of these compounds was reduced and then banned in the 1970s, they are still present in our environment and found in human blood serum. In this study, we determined PCBs and their metabolites in human blood serum in these two populations. Human blood serum samples were collected as part of the Airborne Exposure to Semi-Volatile Organic Pollutants (AESOP) study from East Chicago, an industrialized area with known high PCBs exposure in the past, and Columbus Junction, a rural area with no recognized historical PCB contamination. Our methods, which emphasize rigorous quality assurance and control (QA/QC), enabled us to evaluate all 209 PCB congeners and a sub-set of OH-PCBs congeners. After a series of extraction and cleanup procedures, samples were analyzed using gas chromatography with tandem mass spectrometry (GC-MS/MS) for PCBs and gas chromatography with electron capture detection (ECD) for OH-PCBs. Our results show that the sum of PCB congeners ranged from non-detect to 658 ng/g l.w. (median = 33.5 ng/g l.w.) and the sum of the four major OH-PCB congeners ranged from non-detect to 1.2 ng/g f.w. (median = 0.07 ng/g f.w.). We conclude that PCBs and OH-PCBs are detected in human blood serum from populations living in East Chicago, IN and Columbus Junctions, IA.

## PS 1984 Associations among Polychlorinated Biphenyls (PCBs) and Chlorinated Pesticides and Serum Lipids in Residents of Anniston, Alabama.

M. Pavuk<sup>1</sup>, Z. Aminov<sup>2</sup>, R. Haase<sup>2</sup>, D. O. Carpenter<sup>3,2</sup> and W. E. Turner<sup>4</sup>. <sup>1</sup>ATSDR/CDC, Atlanta, GA; <sup>2</sup>School of Public Health, University at Albany, Rensselaer, NY; <sup>3</sup>Institute for Health and the Environment, University at Albany, Rensselaer, NY; <sup>4</sup>NCEH/CDC, Atlanta, GA. Sponsor: N. Karch.

Associations among total cholesterol, triglycerides, and high density lipoprotein cholesterol (HDL) and serum polychlorinated biphenyls (PCBs) and chlorinated pesticides concentrations were examined in a sample of residents of Anniston, Alabama, participants of the Anniston Community Health Survey (ACHS).

For this analysis, nine PCBs with different number of chlorines (in brackets) and toxicological characteristics were selected: PCBs 74 (4), PCB 99 (5), PCB 118 (5), 153 (6), 170 (7), 187 (7), 196-203 (8), 206 (9), and 209 (10) were included. Four chlorinated pesticides were also included in the analyses:  $\beta$ -HCH, Oxychlorane, trans-Nonachlor, and p,p'-DDE.

Study includes 765 subjects with PCBs and lipid measurements. We wanted to minimize the effect of altered lipid levels due to presence or progression of disease(s) in studying the associations. Persons on lipid lowering medications, with dyslipidemia, diabetes, and coronary heart disease were excluded from the statistical analyses. Multiple linear regression models adjusted for age, race, gender, and BMI were used to analyze the data. Other major CHD risk factors such as smoking, exercise, and family history of heart disease were also examined.

Only higher chlorinated PCBs 206 and 209 were related to total cholesterol. Seven out of 9 PCBs were related to triglycerides; PCBs 99, 118 were not associated with triglycerides. Oxychlorane and p,p'-DDE were related to both total cholesterol and triglycerides; trans-Nonachlor was associated with triglycerides only. No association with PCBs or pesticides was found for HDL.

Interpretations of these results are limited. In particular, potential sequence of events relating lipid levels and PCB exposure is complex and uncertain and can only be elucidated with longitudinal study design.

## PS 1985 Persistent Organic Pollutants and Transthyretin-Bound Thyroxine in Plasma of Inuit Women of Childbearing Age.

Y. Audet-Delage<sup>1</sup>, R. Dallaire<sup>1</sup>, N. Ouellet<sup>1,2</sup>, <ls>Dewailly<sup>1</sup> and P. Ayotte<sup>1,2</sup>. <sup>1</sup>Axe en Santé des Populations et Environnementale, Centre de Recherche du CHUQ, Québec, QC, Canada; <sup>2</sup>Laboratoire de Toxicologie, Institut National de Santé Publique du Québec, Québec, QC, Canada.

The Inuit population of Nunavik (Northern Quebec, Canada) is highly exposed to persistent organic pollutants (POPs) through their traditional diet which comprises fatty tissues from marine mammals. Some POPs – i.e. hydroxylated metabolites of polychlorinated biphenyls (HO-PCBs), pentachlorophenol (PCP) and perfluorooctane sulfonate (PFOS) – are known to compete with thyroxine (T4) for binding sites on transthyretin (TTR), a T4 transport protein located in plasma and cerebrospinal fluid. Displacement of T4 from TTR could result in decreased T4 delivery to the developing fetus and in turn delayed growth and impaired neurodevelopment in infants. We set out to test the hypothesis that POPs or their metabolites decrease circulating concentrations of T4 bound to TTR (T4-TTR) in Inuit women of reproductive age. We measured T4-TTR concentrations in archived plasma samples obtained from 120 Inuit women (18-39 year old) by combining native polyacrylamide gel electrophoresis and liquid chromatography-tandem mass spectrometry (LC-MS/MS) techniques. Total T4 concentration was measured by LC-MS/MS, while those of TTR and thyroxine binding globulin (TBG) were determined by gel densitometry and an ELISA assay, respectively. POPs levels had been previously determined in those samples. The mean T4-TTR concentration was 8.4 nmol/L (SD = 2.4) with values ranging from 2.9 to 14.4 nmol/L, representing on average 6% of total T4 circulating concentration. Plasma levels of HO-PCBs, PCP or PFOS were not correlated to T4-TTR concentrations. Linear regression analysis revealed that TTR, TBG and total T4 concentrations were significant predictors ( $p < 0.001$ ) of T4-TTR levels (adjusted R-square = 0.26,  $p < 0.001$ ), but not POPs levels. Our results suggest that actual circulating levels of POPs in Inuit women of childbearing age are not high enough to affect TTR-mediated thyroid hormone transport.

## PS 1986 Effect of TCDD on Peripheral Hormones Regulating Feed Intake and Energy Balance in Rats.

R. Pohjanvirta<sup>1</sup>, S. Lensu<sup>2</sup> and J. Lindén<sup>1</sup>. <sup>1</sup>Department of Food Hygiene and Environmental Health, University of Helsinki, Helsinki, Finland; <sup>2</sup>Department of Biology of Physical Activity, University of Jyväskylä, Jyväskylä, Finland. Sponsor: M. Viluksela.

A lethal dose of 2,3,7,8-tetrachlorodibenzo-*p*-dioxin (TCDD) brings about a drastic body weight loss dubbed the wasting syndrome in rats. The decline of body weight primarily results from severe hypophagia but at present next to nothing is known about the factors underlying the reduced feed intake. The most important peripheral hunger signal in the body is ghrelin, mainly secreted into blood by stomach cells, whereas the principal satiety hormone is leptin produced by the white adipose tissue. Practically no data exist on the impact of TCDD on these hormones. In the present study, we exposed TCDD-sensitive Long-Evans (*Turku/AB*; L-E) and TCDD-resistant Han/Wistar (*Kuopio*; H/W) rats to 100 µg/kg TCDD ig. and euthanized the rats at days 1, 4 or 10. The dose selected is lethal to all L-E rats but sublethal to H/W rats. A feed-restricted control (FRC) group of L-E rats was included in the study to help distinguish between primary and secondary effects. In addition to leptin and ghrelin, also glucagon was determined in serum samples with

the Bio-Plex Suspension Array System. By 10 days, body weight dropped by about 30% in TCDD-treated and FRC L-E rats but only by some 5% in TCDD-treated H/W rats. Concurrently, serum leptin decreased to non-detectable levels in FRC. It diminished also in TCDD-treated L-E and H/W rats but less prominently. Serum ghrelin was elevated by TCDD in L-E rats at all time-points, and in H/W rats on day 10; in FRC, the increase was lesser on day 4 and comparable on day 10. Glucagon took an upward course in TCDD-treated L-E rats alone reaching a nine-fold increase vs. control on day 10. These data reveal that the major peripheral signals of energy balance remain intact and change appropriately in lethally TCDD-treated L-E rats. However, they do not lead to the normal behavioural response (i.e. feeding) to rectify the tilted energy status.

## PS 1987 Effects of Developmental PCB Exposure on Energy Metabolism in Adult and Aged Mice.

A. Brown, A. Ashworth, K. Smith and C. P. Curran. *Biological Sciences, Northern Kentucky University, Highland Heights, KY.*

Polychlorinated biphenyls (PCBs) are known to cause learning, memory, and behavioral deficits in the developing human brain. Our previous work showed that allelic differences at the *Ahr* and *Cyp1a2* loci alter susceptibility to developmental PCB neurotoxicity. While exploring behavioral differences in aged animals, we discovered a significant divergence in weights dependent on sex, genotype and treatment. The experiments described here were designed to see if gestational and lactational PCB exposure could alter energy metabolism in adult and aged mice. We compared blood glucose, triglycerides and cholesterol in PCB-treated and corn oil-treated control mice with the following genotypes: *AhrbCyp1a2*(+/+), *AhrbCyp1a2*(-/-) and *AhrdCyp1a2*(-/-). The knockout lines were both backcrossed onto a C57BL/6J background which was our wild type control. Pregnant dams were exposed to an environmentally relevant PCB mixture during gestation and lactation. One male and one female per litter were tested at 6 months and 13 months of age. There was a significant effect of genotype and a significant gene x treatment x sex interaction for fasting blood glucose levels. For glucose tolerance testing, mice were fasted overnight, then injected with 2 mg/kg glucose and blood collected over two hours. There was a significant main effect of sex and genotype in glucose tolerance at 6 months. We observed a significant main effect of genotype and sex for plasma cholesterol and a significant genotype x sex interaction for triglycerides. At 13 months, there was a significant genotype x treatment interaction for triglycerides, but only a main effect of sex for cholesterol with male mice having significantly higher levels. We replicated our prior weight trends with PCB-treated male *AhrbCyp1a2*(-/-) mice weighing significantly less than their corn oil-treated controls. These mice also had significantly lower triglyceride levels compared with the corn oil-treated controls. Our results indicate that the metabolic effects of developmental PCB exposure are persistent, but vary depending on both sex and genotype.

## PS 1988 Parent PBDEs and the Hydroxylated Congeners Alter Normal Thyroid Activity.

E. D. Bruce and C. Y. Usenko. *Biology, Baylor University, Waco, TX.*

Polybrominated diphenyl ethers (PBDEs) are brominated flame retardants that have been used for over 30 years. In recent years, the different technical mixtures have been banned or phased out, however there are still significant environmental concentrations. Due to the similarity in chemical structure between PBDEs and thyroid hormones, it has been postulated that PBDEs act through an endocrine disruption pathway by mimicking thyroid hormone. In this study, embryonic zebrafish are used to investigate the interaction of PBDEs on thyroid hormone homeostasis. Thyroid hormone levels were increased following exposure to BDEs 47, 99, and 100. Furthermore, co-exposure with propylthiouracil, a thyroid hormone inhibitor, exacerbated the effects of BDE 47 exposure on spontaneous movement. Additionally, alterations in gene transcription of thyroid-related genes to several different PBDE congeners (BDE 28, BDE 47, BDE 99, and BDE 100) were compared. There was limited alteration in gene expression for most of the genes examined. Deiodinase 1 and the sodium-iodide symporter (SLC5r) were upregulated following exposure to all congeners. Additionally, a hydroxylated PBDE was also investigated for disruption of thyroid-related gene expression. Thyroid transcription factor (NKX2.1) was downregulated by exposure to BDEs 28, 99, and 100; however it was significantly increased following exposure to 6-OH-BDE 47. Exposure to 6-OH-BDE 47 induced the greatest amount of induction, even at concentrations 4-fold below the parent PBDE exposure concentrations. Hydroxylated PBDEs have an even greater similarity to thyroid hormone structure and may be primarily responsible for the adverse effects of PBDE exposure. These results demonstrate that PBDEs do affect thyroid homeostasis; however hydroxylated PBDEs may pose the greatest risk of exposure.

**PS 1989 Search for the Basis of PCB126-Triggered Disruption of Hepatic Metal Homeostasis in Rodents.**

W. D. Klaren<sup>1,2</sup>, I. K. Lai<sup>1,2</sup> and L. W. Robertson<sup>1,2</sup>. <sup>1</sup>Interdisciplinary Graduate Program in Human Toxicology, University of Iowa, Iowa City, IA; <sup>2</sup>Occupational and Environmental Health, College of Public Health, University of Iowa, Iowa City, IA.

PCBs, industrial chemicals and persistent environmental pollutants, are found in many rural and urban settings. Previous studies have shown that the treatment of rats with PCB126 causes a significant disruption of hepatic metal homeostasis that could potentially alter antioxidant defenses. The current study is focused on this metal disruption, in particular on Cu, Zn and Se. Two copper-containing proteins were investigated, tyrosinase (TYR) and cytochrome c oxidase (COX), along with metal chaperones ceruloplasmin (CP), selenoprotein p (SeP) and metallothionein (MT). These proteins cover a wide range of functions from intra- and extracellular metal trafficking (MT, SeP and CP), pigment production (TYR) and electron transport (COX). An animal study was conducted where 56 rats were fed one of three AIN diets containing levels of copper (2, 6 & 10 ppm). After three weeks, animals were given a single IP injection of PCB126 (1 µmol/kg or 5 µmol/kg in corn oil) and euthanized two weeks later. The expression levels of these proteins were investigated by qRT-PCR, ELISA, and western blot. Metals analysis showed a decrease of Zn and Se, but an increase of Cu in the liver. Serum CP concentration and hepatic mRNA levels were increased with dietary copper and PCB treatment (although the latter not significantly). TYR was expressed in the liver both transcriptionally and translationally a new finding. COX was decreased with PCB126 exposure and had no statistical association with dietary copper. SeP was unchanged either by PCB126 or dietary copper, not reflecting the decrease of hepatic Se. MT was highly increased by PCB126 at the 1 µmol/kg dose. The increase of metallothionein seen along with the higher binding affinity of Cu potentially explains the changes seen with Zn. Although metallothionein may contribute to the disruption of hepatic metal homeostasis, it fails to fully explain the Se and Cu changes. (P42 ES 013661)

**PS 1991 Adduction of Cytochrome C by Quinoid Metabolites of Polychlorinated Biphenyls (PCBs).**

M. Li<sup>1</sup>, L. Teesch<sup>3</sup>, D. Murry<sup>1,4</sup>, L. W. Robertson<sup>1,2</sup> and G. Ludewig<sup>1,2</sup>. <sup>1</sup>Interdisciplinary Graduate Program in Human Toxicology, University of Iowa, Iowa City, IA; <sup>2</sup>Department of Occupational and Environmental Health, University of Iowa, Iowa City, IA; <sup>3</sup>High Resolution Mass Spectrometry Facility, University of Iowa, Iowa City, IA; <sup>4</sup>College of Pharmacy, University of Iowa, Iowa City, IA.

PCBs, a group of 209 individual congeners, were widely used as industrial chemicals and are ubiquitous and persistent human and environmental contaminants. Even though PCBs are carcinogens in rodents, they are still in use in closed applications. Lower chlorinated biphenyls can be metabolized to dihydroxy metabolites and further oxidized to quinoid metabolites both *in vitro* and *in vivo*. Quinoid metabolites may form adducts at nucleophilic sites of proteins like cytochrome c, an essential component in the mitochondrial electron transport chain. We hypothesized that the PCB-quinones covalently bind to cytochrome c thereby causing defects in mitochondrial function. LC-MS was used to detect adducts of cytochrome c with selected PCB-quinones *in vitro*. SDS PAGE gel electrophoresis followed by NBT staining was employed to separate the adducted proteins. Trypsin digestion and LC-tandem MS were applied to identify the amino acid binding sites on cytochrome c. SYBYL-X was employed to simulate the conformation change of cytochrome c after binding with PCB3-*para*-Q. We found that more than one molecule of PCB-quinone can bind to one molecule of cytochrome c. In addition, cross-linking of cytochrome c was observed on the SDS PAGE gel. Different conditions, such as pH, incubation time and concentrations of PCB quinones, influence the formation of cross links. Lysine (K27, K39, K54/56, K73/74) and glutamic acid (E61, E62) were identified as binding sites by LC-tandem MS. Software simulation showed conformation changes of adducted cytochrome c. These preliminary data provide evidence that covalent binding of PCB quinone metabolites to cytochrome c, may be included among the toxic effects of PCBs. (Supported by NIEHS Superfund Program P42 ES013661.)

**PS 1990 Aroclor 1254-Induced Modulation of Osteoblast Differentiation Is Predominantly AhR-Dependent.**

M. Herlin<sup>1</sup>, M. Korkalainen<sup>2</sup>, J. Ringblom<sup>1</sup>, M. Öberg<sup>1</sup>, M. Viluksela<sup>2</sup> and H. Håkansson<sup>1</sup>. <sup>1</sup>Institute of Environmental Medicine, Karolinska Institutet, Stockholm, Sweden; <sup>2</sup>National Institute of Health and Welfare, Kuopio, Finland.

Exposure to food-derived mixtures of persistent organic pollutants modulates developing bone tissue properties. To further clarify details in the mode-of-action involved in the *in vivo* findings, this study used a comparative approach to elucidate qualitative and quantitative details in the modulations of osteoblast differentiation *in vitro*. MC3T3-E1 cells were exposed to Aroclor 1254 (A1254) or 2,3,7,8-tetrachlorodibenzo-p-dioxin (TCDD), the model compound for high affinity ligands of the aryl hydrocarbon receptor (AhR). Following A1254 exposure, the expression of the matrix maturation and mineralization marker genes ALP and OCN, were decreased, while no effects were seen on the proliferation marker gene RUNX2. These results suggest that the late phases of osteoblast differentiation were affected, which is in accordance with observations following TCDD exposure. However, higher doses of A1254, as compared to TCDD, were required to achieve significant effects and the maximal effects were lower. The AhR-dependent genes, CYP1A1 and AhRR, were induced by A1254 and TCDD at doses comparable to those where the differentiation markers were affected. Taken together, these results show that A1254, which is a technical mixture of dioxin-like and NDL-PCB congeners predominantly, exhibits dioxin-like modulations on osteoblast differentiation, suggesting that, in accordance with the *in vivo* findings, the A1254 induced effects are mainly AhR-dependent. We further evaluated the relative potency (REP) of A1254 as compared to TCDD. The REP values for OCN, CYP1A1 and AhRR expression were a magnitude higher as compared to the estimated toxic equivalent dose based on the chemical composition of A1254, while the REP value for ALP expression was at the same level as the estimated equivalent chemical dose. Therefore, on a quantitative basis the higher than expected REP values in this study might indicate a contribution also of NDL-PCB congeners to the observed *in vitro* responses.

**PS 1992 Alterations in Xenobiotic Metabolizing Enzyme and Immune Relevant Genes following Administration of Brominated and Chlorinated Dioxins and Furans in Female B6C3F1 Mice.**

R. Frawley<sup>1</sup>, M. Smith<sup>2</sup>, K. White Jr<sup>2</sup>, N. J. Walker<sup>1</sup>, L. S. Birnbaum<sup>1,3</sup>, T. Maynor<sup>4</sup>, M. DeVito<sup>1</sup> and D. R. Germolec<sup>1</sup>. <sup>1</sup>DNTP NIEHS, Research Triangle Park, NC; <sup>2</sup>VCU, Richmond, VA; <sup>3</sup>NCI, Research Triangle Park, NC; <sup>4</sup>ILS, Inc, Research Triangle Park, NC.

Increased use of brominated flame-retardants and incineration of bromine-containing materials has lead to an increase in the presence of polybrominated dibenzo-p-dioxins and dibenzofurans (PBDD/Fs) in the environment. Measurable amounts of PBDD/Fs have been detected in sediment, seafood, and human serum. Previous studies indicated that an acute single exposure to 2,3,7,8-tetrachlorodibenzo-p-dioxin (TCDD), 2,3,7,8-tetrabromodibenzofuran (TBDF), 2,3,7,8-tetrachlorodibenzofuran (TCDF), 1,2,3,7,8-pentabromodibenzofuran (1PeBDF), 1,2,3,7,8-pentachlorodibenzofuran (1PeCDF), 2,3,4,7,8-pentabromodibenzofuran (4PeBDF), 2,3,4,7,8-pentachlorodibenzofuran (4PeCDF), and 2,3-dibromo-7,8-dichlorodibenzo-p-dioxin (DBDCDD) suppressed antigen-specific antibody forming cell (AFC) responses in B6C3F1/N mice, and that the brominated compounds were more potent than their chlorinated analogs. In addition, we evaluated expression of xenobiotic metabolizing enzyme (XME) and immune-relevant genes in the livers from these mice. Gene expression was measured using qRT-PCR. TCDD, TBDF, TCDF, 1PeBDF, 1PeCDF, 4PeBDF, 4PeCDF, and DBDCDD up-regulated the phase I XME genes Cyp1a1 and Cyp1a2. Based on estimated ED50, the rank order of potency for Cyp1a1 was TCDD>TBDF>4PeBDF>1PeBDF>TCDF>4PeCDF>1PeCDF, and for Cyp1a2 was TCDD>TBDF>1PeBDF>4PeCDF>4PeBDF>TCDF>1PeCDF. TCDD, 4PeBDF, TBDF, TCDF, and DBDCDD altered expression of phase II XME, phase III XME, and the thyroid transport protein transthyretin (Ttr) genes. 4PeCDF and 1PeBDF altered a phase II XME and Ttr genes. Additionally, 4PeBDF, TBDF, TCDF, and DBDCDD downregulated several genes that have been associated with antibody production and/or inflammation. Collectively these changes in gene expression are consistent with previously reported suppression of the AFC response and induction of aryl hydrocarbon-mediated and thyroid hormone responses. This abstract does not necessarily reflect the policies or views of NIH.

**PS 1993 PBDE-100 Induces Mitochondrial and HepG2 Impairment.**

L. C. Pereira<sup>1</sup>, A. O. Souza<sup>2</sup>, M. J. Tasso<sup>2</sup> and D. J. Dorta<sup>2</sup>. <sup>1</sup>FCFRP, Faculdade de Ciências Farmacêuticas de Ribeirão Preto, Ribeirão Preto, Brazil; <sup>2</sup>FFCLRP, Faculdade de Filosofia, Ciências e Letras de Ribeirão Preto, Ribeirão Preto, Brazil.

**INTRODUCTION:** Polybrominated diphenyl ethers (PBDEs) have been used in diverse products and are ubiquitous contaminants in sediments, in biota and are also found in human tissues, raising concerns about its toxicity. Many studies have reported liver toxicity and induction of apoptosis by mitochondrial dysfunction. **OBJECTIVE:** The aim of this work was to investigate the mechanisms of toxicity using HepG2 cells and isolated rat liver mitochondria. **METHODS:** Briefly, the effects of BDE-100 (0,1-50  $\mu\text{mol/L}$ ) was assessed on the mitochondrial respiration; Mitochondrial Membrane Potential ( $\Delta\psi$ ); mitochondrial swelling; interaction with membrane using 1-anilino-8-naphthalene sulfonate (ANS) and 1,6-diphenyl-1,3,5-hexatriene (DPH);  $\text{Ca}^{2+}$  release and mitochondrial ATP levels with the luciferin-luciferase system using isolated rat liver mitochondria. Furthermore, cytotoxic effect was investigated by testing cell viability with (4,5 dimethylthiazol-2-yl) - 2,5 diphenyltetrazolium bromide dye (MTT) assay and cell proliferation with Sulphorhodamine B. **RESULTS:** In higher concentrations BDE-100 was able to induce mitochondrial alterations, and interact with the mitochondrial membrane, inhibiting the phospholipidation; leading to dissipation of the  $\Delta\psi$ , deregulation of calcium homeostasis and mitochondrial swelling add a reduction in mitochondrial ATP content. In addition, it was observed inhibition the proliferation and reduce viability of the cells showing its cytotoxic action. **CONCLUSIONS:** These results suggest the formation of pores in the mitochondrial membrane and alteration in mitochondrial structure and function, leading to cell death due to cytotoxic effects in HepG2, perhaps through mitochondrial pathway. **Word Keys:** Mitochondria; HepG2; BDE-100 Supported by: FAPESP

**PS 1994 Genomic Plasticity and Polychlorinated Biphenyls: Telomerase Reactivation and AhR Desensitization in Human Keratinocytes after Long-Term Exposure to PCB126.**

S. Pk, L. W. Robertson and G. Ludewig. *Human Toxicology, The University of Iowa, Iowa City, IA.*

Polychlorinated biphenyls (PCBs) are environmental pollutants and dioxin-like PCB126 (3,3',4,4',5-pentachlorobiphenyl) is classified by IARC as a human carcinogen. Chromosome ends have 'telomeres' which shorten with age in somatic cells. Lengthening of telomeres and high telomerase activity, the telomere maintaining enzyme, are key steps in carcinogenesis. To examine if PCB126 carcinogenicity is mediated through this mechanism, we exposed immortalized human skin keratinocytes (HaCaT) for 90 days to 5  $\mu\text{M}$  PCB126. Every sixth day cells were re-seeded and telomerase activity, telomere length, cMyc, hTERT and hTR (telomerase components), TRF1 and TRF2 (reduce telomerase access to telomeres) mRNA, CYP1A1 mRNA and activity, superoxide and  $\text{H}_2\text{O}_2$  levels were determined. PCB126 caused an increase in CYP1A1 mRNA and activity, TRF1/2 mRNA, and superoxide and  $\text{H}_2\text{O}_2$  and a reduction of telomerase activity (50%), hTERT and hTR mRNA (10%), telomere length (40%), and cell growth from Days 6 to 48. From Day 54 on, an increase in cell growth, cMyc, hTERT, and hTR mRNA levels (to 130%), reactivation of telomerase activity (to 100%), elongation of telomere length (to 90%), and a decrease in TRF1 and TRF2 mRNA were observed. In addition, from Day 78 PCB126 no longer activated the AhR response (CYP enzymes) and no mutation were found on the AhR ligand binding region. Microarray results confirmed an increase in expression of cell growth genes on Day 54 and desensitization of AhR-response on Day 78. This study shows for the first time a telomerase reactivation, telomere lengthening, and increased cell growth after telomeres were significantly shortened by PCB-exposure in human cells. Possible mechanisms include de novo cMyc amplification (telomerase) and/or selection of a small subpopulation of cells. Either way, this work adds a new toxicity pathway for PCBs and a possible mechanism of carcinogenesis for this and related contaminants to be considered in their safety evaluation and risk assessment.

**PS 1995 Exposure to PCB 126 Triggers Antioxidant Defense through Cross-Talk of Caveolae and Nrf2 Signaling.**

M. C. Petriello, B. Hennig and S. Han. *Toxicology, University of Kentucky, Lexington, KY.*

Environmental toxicants such as polychlorinated biphenyls have been implicated in the promotion of multiple inflammatory diseases including cardiovascular disease, but information regarding mechanisms of toxicity and cross-talk between relevant signaling pathways is lacking. We have reported that coplanar PCBs promote endothelial cell activation through the lipid microdomain caveolae, and the loss of

caveolin-1 (Cav-1) ameliorates these detrimental effects. We have also shown that PCB 126 can activate the antioxidant transcription factor Nrf2 resulting in upregulation of antioxidant genes and downregulation of inflammatory markers. Normally, Nrf2 is sequestered in the cytoplasm and degraded through inhibitory action of Keap1, but upon activation via toxicants such as PCBs, can enter the nucleus and activate the transcription of a battery of protective genes. Our previous data suggests downregulation of Cav-1 and upregulation of Nrf2 protects against PCB-induced cellular dysfunction, but here we show for the first time an intimate example of cross-talk between these two cellular signaling pathways. To examine the cross-talk between Cav-1 and Nrf2 pathways in PCB-induced inflammation we silenced cav-1 in vascular cells. Importantly, Cav-1-silenced cells treated with PCB126 resulted in increased levels of Nrf2-ARE binding determined by EMSA. Also, in cells treated with PCB 126, silencing of Cav-1 resulted in decreased protein levels of both inhibitory Keap1 and Fyn kinase, which both have been shown previously to be implicated in Nrf2 deactivation. We also show that Keap1 levels were significantly decreased in livers from Cav-1 KO mice when compared to control C57BL/6 mice. Finally, Cav-1 silencing allowed for a more effective antioxidant response, as observed by higher levels of the antioxidant genes glutathione S-transferase (GST) and NADPH dehydrogenase quinone 1 (NQO1) in cells exposed to PCB 126. Ultimately, these data introduce novel cross-talk between Cav-1 and Nrf2 and implicates the ablation of Cav-1 as a protective mechanism of PCB-induced cellular dysfunction and inflammation.

**PS 1996 Fibroblast Growth Factor 21 (FGF21) Is a Target Gene of the Aryl Hydrocarbon Receptor (AhR).**

X. Cheng<sup>1,2</sup> and C. D. Klaassen<sup>2</sup>. <sup>1</sup>Pharmaceutical Sciences, St. John's University, Queens, NY; <sup>2</sup>Internal Medicine, KU Medical Center, Kansas City, KS.

Dioxins, such as 2, 3, 7, 8-tetrachlorodibenzo-p-dioxin (TCDD), are environmental pollutants. The toxic effects of TCDD are well documented mainly through activating the aryl hydrocarbon receptor (AhR). However, the underlying mechanisms for TCDD's adverse effects, such as the wasting syndrome, are not well understood. Fibroblast growth factor (Fgf) 21 plays critical roles in metabolic adaptation to fasting by increasing lipid oxidation and ketogenesis in the liver. The present study was performed to determine whether activation of the aryl hydrocarbon receptor (AhR) induces Fgf21 expression. In mouse liver, TCDD increased Fgf21 mRNA in both a dose- and time-dependent manner. Moreover, TCDD increased Fgf21 mRNA levels in livers of wild-type mice, but not of AhR-null mice. Chromatin immunoprecipitation assays indicate that TCDD increased AhR protein binding to the Fgf21 promoter (-105/+1 base pair). Diethylhexylphthalate (DEHP) decreased Fgf21 mRNA expression and DEHP pretreatment attenuated TCDD-induced Fgf21 expression, which may explain a previous report that DEHP pretreatment decreases TCDD-induced toxicities. In mouse liver, TCDD increased the mRNA of fatty acid uptake protein CD36 but decreased mRNA of de novo fatty acid biosynthesis enzyme fatty acid synthase (FAS). In addition to these findings in liver, TCDD induced Fgf21 mRNA in mouse white adipose tissue. In conclusion, TCDD induces Fgf21 expression via activation of the AhR-signaling pathway. Pharmacological manipulation of Fgf21 expression by AhR activators may provide an effective strategy for treating obesity, diabetes, and the metabolic syndrome. (Supported by NIH grants DK-081461, ES-09649, ES-019487, and RR-021940.)

**PS 1997 Human Transcription Factor Activation by Polychlorinated Biphenyls and Organochlorine Pesticides.**

B. Wahlang<sup>1</sup>, L. Al-Eryani<sup>1</sup>, K. Falkner<sup>1</sup>, H. Bellis-Jones<sup>1</sup>, H. Clair<sup>1</sup>, R. Prough<sup>3</sup> and M. Cave<sup>1,2</sup>. <sup>1</sup>Department of Medicine/GI, University of Louisville, Louisville, KY; <sup>2</sup>Louisville VAMC, Louisville, KY; <sup>3</sup>Biochemistry, University of Louisville, Louisville, KY.

**Introduction:** Polychlorinated Biphenyls (PCBs) are persistent environmental toxins, present in 100% of the US adult population and theoretically predicted to act as ligands for transcription factors involved in xenobiotic/endobiotic detoxification, obesity and steatosis. These human receptors include pregnane xenobiotic receptor (PXR), arylhydrocarbon receptor (AhR) and possibly the liver-X-receptor- $\alpha$  (LXR). This study evaluates a PCB mixture, Aroclor 1260, and selected individual PCB congeners, as potential ligands for these receptors. Additionally, we also look at PXR activation by selected organochlorine pesticides. **Methods:** MTT assay was performed to determine acutely toxic concentrations for Aroclor 1260. HepG2 cells were transfected with plasmids expressing human LXR or human PXR; and receptor-responsive plasmids including tk-LXR-RE-luciferase, pGL3-PXR-RE-luciferase or pGL3-AhR-RE-luciferase. Transfected cells were treated with ligands for LXR (T0901317:100nM), PXR (Rifampicin:10 $\mu\text{M}$ ) and AhR

(Benanthracene:50µM); varying concentrations of Aroclor 1260 or individual congeners and organochlorine pesticides. Results: The toxicity threshold of Aroclor 1260 in HepG2 cells was 26.0±3.7µg/mL. Aroclor 1260 did not activate the LXR/LXR-RE system and had no effect on LXR-dependent induction by T0901317. Aroclor 1260 induced the PXR reporter system in a simple monotonic fashion with significant inductions being observed at concentrations of 10µg/mL or greater. Amongst congeners tested, 126 and 196 activated PXR. Aroclor 1260 did not activate AhR but as expected, individual congeners 126 and 118 were potent inducers of AhR. Organochlorine pesticides including dieldrin and chlordane activated PXR. Conclusion: Aroclor 1260 is a direct agonist of human PXR but not LXR. This mixture did not significantly activate AhR. PCB 126 activated both PXR and AhR and 196 activated PXR only.

**PS 1998 Validation of QuEChERS-Based Extraction for the Determination of Organochlorine Pesticides in Liver and Serum Using GC-MS/MS.**

M. Bokhart<sup>1</sup>, A. Lehner<sup>2</sup>, M. Johnson<sup>2</sup> and J. P. Buchweitz<sup>2,3</sup>. <sup>1</sup>Chemistry, Michigan State University, East Lansing, MI; <sup>2</sup>Diagnostic Center for Population and Animal Health, Michigan State University, East Lansing, MI; <sup>3</sup>Pathobiology and Diagnostic Investigation, Michigan State University, East Lansing, MI.

Organochlorine (OC) pesticides are chemically stable, have low volatility, and low rates of degradation which lead to their persistence in the environment and classification as persistent organic pollutants (POP). OC pesticides bioaccumulate and biomagnify to greater extents in animals at higher trophic levels due to their high lipid solubility. These compounds generally affect the nervous system of the target organism. The mechanism of action involves the disruption of chemical ion movement in neurons but the major pathologic changes are observed in the liver and reproductive systems. Michigan State University Diagnostic Center for Population & Animal Health (MSU DCPAH) has developed and validated a quantitative QuEChERS approach for 24 organochlorine analytes in liver and blood serum. Identification and quantitation of the extracted compounds is by capillary gas chromatography interfaced to a tandem quadrupole mass spectrometer (GC-MS/MS). The QuEChERS approach utilizes an acetonitrile extraction, partitioning facilitated by the addition of salts and a dispersive solid phase extraction cleanup. Depending on compound and matrix, the limits of detection (LOD) vary from 0.002-2.4 ppb and limits of quantification (LOQ) vary from 0.01-7.4 ppb. Compared to other multiresidue methods for trace pesticide detection, the QuEChERS extraction method has many advantages including less sample size required, faster throughput time of samples, and less solvent used per sample leading to a reduction in overall cost, a lower carbon footprint and improved lab safety.

**PS 1999 Development of Weighted Distributions of Relative Potency Estimates for Dioxin-Like Compounds.**

L. C. Haws<sup>1</sup>, G. Hixon<sup>1</sup>, M. DeVito<sup>2</sup>, N. J. Walker<sup>2</sup>, L. Kuriakose<sup>3</sup>, L. S. Birnbaum<sup>4</sup>, M. Harris<sup>3</sup> and D. Wolkoff<sup>1</sup>. <sup>1</sup>ToxStrategies, Austin, TX; <sup>2</sup>NIEHS, Research Triangle Park, NC; <sup>3</sup>ToxStrategies, Houston, TX; <sup>4</sup>NCI, Research Triangle Park, NC.

Potential human health risks associated with exposure to dioxin-like compounds (DLCs) are evaluated using toxic equivalency factors (TEFs). TEFs are single point estimates even though they are based on relative estimates of potency (REPs) that often span several orders of magnitude. One potential improvement to the TEF methodology would be to use the full distributions of REP values for each congener. WHO recognized the value of such an approach during their most recent review of the TEF methodology but expressed concern that all REP values are not of equivalent quality or relevance. As such, we previously established a consensus-based framework that weights REPs based on REP quality and relevance and to develop a numerical approach for quantitatively weighting each REP using machine learning. Since that time, we have applied the quantitative weighting framework to the REP database to develop a numerical weight for each REP value, which in turn has been used to develop a weighted distribution of REPs for each congener, and have also developed 95% confidence intervals (CIs) around the percentile associated with the TEF values using the R statistical programming environment. The weighted distributions were generally tighter than were the unweighted distributions. Additionally, when examining where the current WHO TEFs fell on the weighted distributions for each congener, we found a lack of consistency across congeners, with values percentiles ranging from the 1st-99th percentiles. The CIs for many of the congeners were also quite broad. For example, the TEF for 12378 PeCDF fell on the 47th percentile of the weighted distribution, but the CI ranged from the 29th to the 68th percentile. These calculations improve characterization

of the variability and uncertainty inherent in the health risk estimates for this class of compounds, demonstrating that reliance on the point estimate TEFs could significantly under- or over-estimate risk. (This abstract does not reflect the policies or views of NIEHS or NCI).

**PS 2000 Uptake and Systemic Relative Effect Potencies of 4-PECDF, PCB-126, PCB-118 and PCB-156 in Female Mice after Acute Exposure.**

K. I. van Ede<sup>1</sup>, P. Andersson<sup>2</sup>, K. P. Gaisch<sup>1</sup>, M. van den Berg<sup>1</sup> and M. B. van Duursen<sup>1</sup>. <sup>1</sup>Institute for Risk Assessment Sciences, Utrecht University, Utrecht, Netherlands; <sup>2</sup>Faculty of Science and Technology, Umeå University, Umeå, Sweden.

Risk assessment of mixtures of chlorinated dioxins (PCDDs), furans (PCDFs) and biphenyls (PCBs) is performed using Toxic Equivalency Factors (TEFs) that are derived from multiple relative effect potencies (REPs) linking administered dose levels to toxic/biologic effects. Increasing evidence suggests that using administered dose levels instead of systemic levels (e.g. liver or plasma concentrations), may lead to misinterpretation of risk. In this study, REPs of 4-PeCDF, PCB-126, PCB-118 and PCB-156 were determined in female mice three days after a single oral dose. REPs were calculated relatively to TCDD, based on cytochrome P450 1A1 (EROD) activity in liver and gene expression of CYP1A1, 1A2 and 1B1 in liver and peripheral blood lymphocytes (PBL) using administered dose, liver levels and plasma levels. Using the administered dose, REPs for the various endpoints ranged between 0.01 – 0.2 for 4-PeCDF (WHO-TEF 0.3), 0.005 – 0.04 for PCB-126 (WHO-TEF 0.1), 0.000005 – 0.00003 for PCB-118 (WHO-TEF 0.00003) and 0.00001 – 0.00003 for PCB-156 (WHO-TEF 0.00003). Recalculating the REPs using plasma levels increased REPs 4- to 9-fold for 4-PeCDF and 2-fold for PCB-126. In contrast, plasma-based REPs for PCB-118 and PCB-156 were slightly lower than the REPs based on administered dose. Recalculating the REPs using liver levels resulted in a decrease in REPs for 4-PeCDF and PCB-126 and an increase for PCB-118 and PCB-156. In general, deviation in REPs using either administered or systemic levels were seen for all tested congeners. However, most administered and systemic REPs were within or below one order magnitude uncertainty of WHO-TEFs. Only liver REPs for PCB-118 and PCB-156 based on liver concentration were higher. Even though, tissue specific REPs might give a more accurate value of the potency of a single compound. Additional rat and human in vitro data will be used to further confirm and/or explore these findings.

**PS 2001 Phenylethyl Isothiocyanate and Dithiocarbamate Restore Proangiogenic Properties of Cyp1b1-Deficient Vascular Cells through Decreased NF-κB Activity and Oxidative Stress.**

T. L. Palenski<sup>1</sup>, C. M. Sorenson<sup>2</sup> and N. Sheibani<sup>1</sup>. <sup>1</sup>Ophthalmology & Visual Sciences, University Wisconsin-Madison, Madison, WI; <sup>2</sup>Pediatrics, University Wisconsin-Madison, Madison, WI.

**Purpose:** Cytochrome P450 1B1 (Cyp1B1) is expressed in the vasculature and loss of its expression/activity is associated with increased oxidative stress, increased thrombospondin-2, and NF-κB activation. This is concomitant with attenuation of angiogenesis in vivo and in vitro. Both phenylethyl isothiocyanate (PEITC), found in cruciferous vegetables, and pyrrolidine dithiocarbamate (PDTC) inhibit NF-κB activity. The objective of this study was to determine if inhibition of NF-κB by PEITC or PDTC restores the reductive and proangiogenic properties of Cyp1B1-deficient vascular cells.

**Methods:** Primary cultures of retinal endothelial (EC) and pericytes (PC) were prepared from Cyp1B1+/+ and Cyp1B1-/- mice. Cyp1B1-/- retinal vascular cells were incubated with either 1 µM PEITC or 10 nM PDTC for 24 h, unless indicated otherwise. NF-κB expression and activity were determined by Western blot analysis and luciferase reporter activity. Immunofluorescence staining was performed to visualize p65 localization. Oxidative stress was measured using dihydroethidium staining. The ability of Cyp1B1+/+ and Cyp1B1-/- vascular cells to undergo capillary morphogenesis in Matrigel was also determined after 8 h incubation with PDTC or PEITC. Rates of cell migration were compared using a transwell assay. **Results:** PEITC and PDTC both inhibited NF-κB p65 expression and activity. NF-κB inhibition decreased p65 staining and nuclear localization in Cyp1B1-/- retinal vascular cells. Inhibition of NF-κB restored capillary morphogenesis and migration of retinal vascular cells. Oxidative stress in Cyp1B1-/- retinal vascular cells was relieved with incubation with PEITC and PDTC.

**Conclusion:** Cyp1B1 expression/activity is essential for maintaining the normal proliferative, migratory, and reductive state of the vascular cells, and its alteration has significant impact on vascular development and angiogenesis.

**PS 2002 Cyp1b1-Deficiency Alters Structure and Function of Trabecular Meshwork via Increased Oxidative Stress.**

Y. Zhao<sup>1</sup>, S. Wang<sup>1</sup>, C. M. Sorenson<sup>2</sup>, D. M. Peters<sup>1,3</sup>, L. Teixeira<sup>5</sup>, R. R. Dubielzig<sup>5</sup> and N. Sheibani<sup>1,4</sup>. <sup>1</sup>Departments of Ophthalmology and Visual Sciences, University of Wisconsin-Madison, Madison, WI; <sup>2</sup>Pediatrics, UW-Madison, Madison, WI; <sup>3</sup>Pathology, UW-Madison, Madison, WI; <sup>4</sup>Pharmacology, UW-Madison, Madison, WI; <sup>5</sup>Comparative Ocular Pathology Laboratory of Wisconsin, UW-Madison, Madison, WI.

Cytochrome P450 1b1 (Cyp1b1) is a member of the cytochrome P450 super family of proteins with mono-oxygenase activity. Although mutations in Cyp1b1 gene have been reported in patients with congenital glaucoma, the role Cyp1b1 plays in the development and function of trabecular meshwork (TM) remains unknown. Here we determined the impact of Cyp1b1 deficiency on the development and function of TM tissue in C57Bl/6 mice. The intraocular pressures (IOPs) of Cyp1b1<sup>+/+</sup> and Cyp1b1<sup>-/-</sup> mice were measured non-invasively with a commercially available tonometer. The integrity of TM tissues of 1-week to 8-month-old Cyp1b1<sup>+/+</sup> and Cyp1b1<sup>-/-</sup> mice were assessed by electron microscopy (EM). Oxidative stress in the TM tissues was evaluated by immunostaining for 4-hydroxyl-2-noneal (HNE). N-Acetylcysteine (NAC; 1.5 mg/g body weight, once every three days for three weeks, IP) was administered in 3-day-old Cyp1b1<sup>-/-</sup> mice and the morphology of TM was assessed by EM. Our results showed a modest but significant increase in diurnal IOP of Cyp1b1<sup>-/-</sup> mice at 6-12 weeks of age. The 2-week-old Cyp1b1<sup>-/-</sup> mice presented ultra structural irregular collagen distribution in the TM tissue, which became more severe as mice aged. Increased HNE staining was observed in TM tissue of Cyp1b1<sup>-/-</sup> mice in vivo. Administration of NAC prevented the postnatal formation of lesions in Cyp1b1<sup>-/-</sup> TM. These results were consistent with our previous in vitro findings that TM cells prepared from Cyp1b1<sup>-/-</sup> mice exhibit increased oxidative stress and cellular defects, which are reversed when incubated with NAC. Thus, the metabolic activity of Cyp1b1 contributes to oxidative homeostasis and integrity of ultra-structure and function of TM.

**PS 2003 Macrophage Toxicity in Response to Particles Collected from Indium-Tin Oxide Production.**

M. A. Badding<sup>1</sup>, N. R. Fix<sup>1</sup>, K. M. Dunnick<sup>1</sup>, K. J. Cummings<sup>2</sup>, V. Castranova<sup>1</sup> and S. S. Leonard<sup>1</sup>. <sup>1</sup>Health Effects Laboratory Division, National Institute for Occupational Safety and Health, Morgantown, WV; <sup>2</sup>Division of Respiratory Disease Studies, National Institute for Occupational Safety and Health, Morgantown, WV.

Occupational exposure to indium compounds has recently been associated with lung disease among workers in the indium-tin oxide (ITO) industry. Previous studies have suggested that autoantibodies and reactive oxygen species (ROS) may play a role in the development of pulmonary lesions following indium compound exposures. However, the molecular mechanisms behind indium compounds' toxicity remain largely unknown. Thus, we aim to uncover how compounds encountered in the ITO production process affect cultured macrophages and ultimately, contribute to the pathogenesis of indium lung disease. The indium compounds used in this study were collected from different process stages at an ITO production facility. Darkfield microscopy has revealed that various indium compounds interact with the cells as early as 5 minutes post-exposure, suggesting that cellular reactions to the ITO compounds may be occurring very rapidly. Indeed, using electron spin resonance (ESR) to measure ROS generation, we found that various collected indium compounds produce free radicals in the presence and absence of RAW 264.7 mouse macrophages within 5 minutes. We also hypothesize that indium compound particle uptake by macrophages leads to subsequent cellular damage, which could be contributing to lung pathology. Therefore, various imaging techniques are being used to observe particle association with and uptake by macrophages over a time course. Current studies are underway to evaluate the effects of the collected indium compounds on intracellular ROS production, lipid peroxidation, DNA damage, and cell proliferation over the same time course. These findings will provide a foundation for the molecular basis behind an emerging occupational health issue and assist in the prevention indium lung disease.

**PS 2004 Role of Cytochrome P450 (CYP)1A Enzymes in Sex-Specific Differences in Hyperoxic Lung Injury.**

K. Lingappan, W. Jiang, L. Wang, X. Couroucli and B. Moorthy. *Pediatrics, Baylor College of Medicine, Houston, TX.*

Preterm male infants have a higher incidence of chronic lung disease (CLD) compared to females and hyperoxia contributes to its pathogenesis. Cytochrome P450(CYP)1A enzymes attenuate hyperoxic lung injury. The mechanisms responsible for sex differences in hyperoxic lung injury and the role of CYP1A enzymes remain largely unknown. We tested the hypothesis that mice will display sex-specific

differences in hyperoxic lung injury and that this phenomenon will be altered in mice lacking the genes for CYP1A1 or 1A2. Male (M) and Female (F) (8-10 wk) wild type (WT) (C57BL/6J), Cyp1a1-null, and Cyp1a2-null mice were exposed to hyperoxia (FiO<sub>2</sub>>0.95). Lung injury was estimated by lung-weight/body-weight (LW/BW) ratios, histopathology and immunohistochemistry for quantitation of neutrophil infiltration. Levels of 8-iso PGF<sub>2</sub>α (lung) were determined by LC-MS/MS and apoptosis was assessed by TUNEL (terminal deoxynucleotidyl transferase-mediated dUTP nick end-labeling) staining. Measurement of cytokine protein expression levels in lung homogenates was done using suspension bead array. CYP1A1 and A2 expression was quantified in the lungs and liver at the enzyme, protein and mRNA level. Upon exposure to hyperoxia, WT males showed a greater increase in LW/BW ratios, displayed greater perivascular and alveolar injury, neutrophil infiltrates and TUNEL+ cells than females. The suspension bead array assay revealed increases in mouse lung tissue homogenate levels of IL-6 (F>M) and VEGF (M>F). WT females showed higher hepatic and pulmonary CYP1A level and activity compared to males. Strikingly, the sex-based differences were lost in mice lacking Cyp1a1 or 1a2. The increased susceptibility of WT males to hyperoxic lung injury suggests modulation by sex-specific factors like reactive oxygen species, inflammatory cytokines, and factors that regulate apoptosis. Further studies to elucidate the mechanistic role of CYP1A in the sex specific modulation of hyperoxic injury could lead to the development of strategies to prevent or treat CLD in the premature infant.

**PS 2005 Towards Elucidating the Pathophysiological Role of Reactive γ-Ketoaldehydes Formed through the Isoprostane Pathway of Lipid Peroxidation.**

T. T. Nguyen<sup>1,2</sup>, P. Chen<sup>2,3</sup>, M. Aschner<sup>1,2,3</sup> and L. Roberts<sup>1,4</sup>. <sup>1</sup>Pharmacology, Vanderbilt University Medical Center, Nashville, TN; <sup>2</sup>Pediatrics, Vanderbilt University Medical Center, Nashville, TN; <sup>3</sup>Neuroscience, Vanderbilt University Medical Center, Nashville, TN; <sup>4</sup>Medicine, Vanderbilt University Medical Center, Nashville, TN.

Numerous environmental toxins cause oxidative damage to lipids, proteins, and DNA. Lipid peroxidation leads to the formation of reactive aldehydes amongst which the γ-ketoaldehydes formed via the isoprostane pathway of lipid peroxidation, termed isoketals (IsoKs), are the most reactive and injurious. Selective scavengers of IsoKs have been developed which have shown remarkable protection against oxidative damage in animal models of oxidative stress. However, the precise molecular processes preserved due to scavenging IsoKs have not been defined. This can, however, be elucidated studying the highly tractable organism, *Caenorhabditis elegans* (*C. elegans*). Accordingly, to identify the pathophysiological roles of IsoKs in oxidative injury, *C. elegans* are exposed to oxidative insult in the absence and presence of salicylamine. A fluorescent *C. elegans* strain containing a GFP transcriptional reporter for the SKN-1 target gene *gst-4* (*P<sub>gst-4</sub>::GFP*) was utilized for detection of altered gene expression in order to determine processes protected by reactive γ-ketoaldehyde scavengers. Late-stage L4 worms were dosed with a submaximal dose of a SKN-1 activating xenobiotic, juglone, for one hour and plated for recovery for one hour. Current studies show a nearly 4-fold increase in fluorescent intensity after a submaximal (LD<sub>20</sub>) dose of juglone (p-value = 0.02). These results demonstrate that a brief exposure to the xenobiotic juglone is sufficient in activating SKN-1 in *C. elegans*, and can be used in oxidative and xenobiotic stress studies. (Supported by T32ES007028-38 [T.T.N.]).

**PS 2006 High-Content Imaging Assay to Detect Drug-Induced Reactive Oxygen Species Generation.**

Y. Will, R. Swiss and S. Nadanaciva. *Pfizer Inc, Groton, CT.*

The disruption of cellular redox circuits can lead to an increase in reactive oxygen species (ROS) within cells, causing oxidative stress and eventually cell damage. Mitochondria are the main producers of ROS in the form of superoxide anion. Two of the electron transport chain complexes, Complex I and Complex III, are thought to be responsible for most of the ROS generated in mitochondria. Several drugs associated with oxidative stress have been shown to contribute to toxicity in the liver, heart, kidney and central nervous system. Thus, it is important to be able to screen new chemical entities that may cause an increase in ROS production in order to reduce compound attrition at the early drug discovery stage. Hence, we developed a 384-well format high content imaging assay that measures superoxide production. The effect of 60 compounds including thiazolidinediones, antipsychotics, antidepressants and anticancer agents was measured in this assay in transformed human liver epithelial cells (THLE) using the fluorescent dyes, Dihydroethidium (for superoxide levels) and Hoechst (for cell number). In a separate 384-well format high content imaging assay, we tested the effect of the compounds on the mitochondrial membrane potential (MMP) of the cells using the

fluorescence dye, TMRM. Quantitative image analysis showed that the compounds could be grouped into four categories: (a) those that caused superoxide formation and a loss in MMP at similar concentration ranges (for example, astemizole, sorafenib), (b) those that caused superoxide production but had no effect on MMP (dasatinib), (c) those that caused a loss in MMP but had no effect on superoxide formation (tamoxifen, sertraline), and (d) those that had no effect either on superoxide formation or on the MMP over 24 hours (pioglitazone, risperidone). Both high content imaging assays were robust and rapid and can be implemented within a screening paradigm to identify compounds that modulate oxidative stress and mitochondrial membrane potential.

## PS 2007 The Antioxidant Lipoic Acid Exacerbates Paraquat-Induced Cytotoxicity.

Z. Suntutres<sup>1,2</sup>, R. Pycko<sup>2</sup> and J. Coccimiglio<sup>2</sup>. <sup>1</sup>Northern Ontario School of Medicine, Thunder Bay, ON, Canada; <sup>2</sup>Biology, Lakehead University, Thunder Bay, ON, Canada.

In several countries the use of herbicides has become important in the preservation of sustainable agriculture. A widely used herbicide for broadleaf weed control is paraquat (PQ) known to be toxic to humans and animals. The treatment against PQ poisoning remains supportive with no antidotes or specific treatments available. Recognizing that PQ induces its toxicity primarily via oxidative stress-mediated mechanisms, modulating the levels of cellular antioxidants seems to serve as a potential treatment strategy. We studied the in vitro effects of the thiol-containing antioxidant lipoic acid (LA) in a human lung adenocarcinoma epithelial cell line. Incubation of control A549 cells with PQ resulted in time- and concentration-dependent increases in intracellular PQ levels with concomitant decreases in cell viability and mitochondrial membrane permeability (MMP) and increases in intracellular calcium concentrations [Ca<sup>2+</sup>]<sub>i</sub>. Challenge of cells with LA alone did not cause any changes in any of the biochemical parameters measured with the exception of the MMP being significantly decreased. Co-treatment of A549 cells with LA and PQ potentiated the PQ-induced cytotoxicity as evidenced by the further exacerbation of PQ-induced decreases in MMP and increases in DNA fragmentation and [Ca<sup>2+</sup>]<sub>i</sub>. Chromatographic analysis (GC/MS/MS) showed that LA was primarily associated with cell membranes. These data suggest that LA does not offer any protective effects against PQ-induced toxicity. The mechanism(s) for its ability to modulate cell survival/death by modulating the cellular redox-regulated signal transduction in PQ-challenged cells is under investigation. This research project was supported by Natural Sciences and Engineering Research Council of Canada (NSERC).

## PS 2008 Lipid Droplets with Oxygenated Fatty Acids and Triglycerides in Dendritic Cells: Possible Role in Antigen Presentation in Cancer.

V. Tyurin<sup>1,2</sup>, W. Cao<sup>3</sup>, J. Loomen<sup>3</sup>, V. Kagan<sup>1,2</sup> and D. Gabrilovich<sup>3</sup>. <sup>1</sup>Department of Environmental and Occupational Health, University of Pittsburgh, Pittsburgh, PA; <sup>2</sup>Center for Free Radical and Antioxidant Health, University of Pittsburgh, Pittsburgh, PA; <sup>3</sup>Department of Immunology, H. Lee Moffitt Cancer Center, Tampa, FL.

Immuno-surveillance plays a critical role in control of tumor progression whereby dendritic cells (DC) are the most potent antigen presenting cells responsible for the development of immune responses. Our previous work has identified lipid droplets as potent regulators of DC's immune functions. Notably, DCs isolated from tumor-bearing mice or treated with tumor explant supernatants (TES) accumulated lipid droplets containing considerable amounts of PUFA (C18:2, C18:3, C20:4 and C22:6). Among those, the amounts of C18:2 were significantly higher compared to other PUFA species. Since accumulation of lipid droplets in DCs in cancer was mediated via Msr1 receptor, which is primarily responsible for the uptake of oxidatively modified lipids, we performed analysis of oxidized lipids in DCs using LC-ESI-MS. To investigate possible role of oxidized fatty acid in antigen presentation we used a model system where DCs from naïve mice were grown in the presence of C18:2. Treatment of DCs with C18:2 in combination with a hydrophobic free radical generator, an azo-initiator AMVN, - but not with C18:2 alone - resulted in accumulation of oxygenated lipid droplets and caused significant decrease in antigen presentation. Oxygenated FFA containing one, two and three oxygens as well as oxygenated triacylglycerols, TAGs, including truncated TAGs with m/z 766 [M+NH<sub>4</sub>]<sup>+</sup>, containing acyl corresponding to 9-oxo-nonanoic acid, were observed in DC grown in the presence of TES and DC treated with C18:2 and AMVN. Given that lipid droplets can directly co-localize with cellular compartments involved in antigen processing and formation of pMHC complexes, it is likely that accumulation of oxygenated FFAs and TAGs in DC may be responsible for the loss of their immune-regulatory functions in cancer. Supported by grant with CA165065, NIOSH OH008282, NIH U19 AI068021, HL70755.

## PS 2009 Mitochondrial Cardiolipin As a Substrate for Cytochrome C-Catalyzed Production of Oxygenated Lipid Mediators.

V. Kagan<sup>1</sup>, V. Tyurin<sup>1</sup>, S. Poloyac<sup>2</sup>, M. Epperly<sup>3</sup>, J. Greenberger<sup>3</sup>, H. Bayir<sup>4</sup> and Y. Tyurina<sup>1</sup>. <sup>1</sup>Department of EOH, University of Pittsburgh, Pittsburgh, PA; <sup>2</sup>Pharmaceutical Science, University of Pittsburgh, Pittsburgh, PA; <sup>3</sup>Radiation Oncology, University of Pittsburgh, Pittsburgh, PA; <sup>4</sup>Critical Care Medicine, University of Pittsburgh, Pittsburgh, PA.

Lipid mediators - central to the normal homeostasis and responses to stress and disease - are generated through oxygenation of polyunsaturated fatty acids (PUFA), such as linoleic acid (LA), arachidonic acid (AA) and docosahexaenoic acid. Their regulatory effects are believed to depend on a fine balance between PUFA esterification/reacylation of phospholipids and on their hydrolysis by phospholipases A (PLA). We suggested that mitochondrial cardiolipins (CLs) can be a source of bioactive lipid mediators generated with the catalytic participation of cytochrome c (cyt c). In this study we employed models of rat traumatic brain injury (TBI) and mouse total body irradiation (TIR). Using oxidative lipidomics approach and MS/MS analysis, we found that TBI resulted in oxidation of polyunsaturated molecular species of CL and accumulation of its hydrolysis products such as oxygenated LA, AA and monolysio-CL. Similar, a significant increase of oxidized CLs in small intestine of TIR mice (9.5 Gy) was accompanied by accumulation of CL hydrolysis products. To generate oxygenated CL in vitro we utilized brain CL, with its highly diversified polyunsaturated molecular species, and cyt c. We found that incubation of brain CL with cyt c in the presence of H<sub>2</sub>O<sub>2</sub> yields a rich assortment of oxygenated CL species, hydrolysis of which by PLA1 and A2 generated multiple oxygenated fatty acids similar to those that were formed in vivo in brain after TBI and small intestine after TIR. An oxidation-specific lipoprotein lipase A2, was able to utilize peroxidized tetralinoleoy-CL to yield different oxygenated species of linoleic acid and lyso-CLs. Thus, mitochondrial CL/cyt c represents a novel mechanisms involved in lipid mediators-generating pathways. Supported by NIH ES020693, ES021068, U19 AI068021, HL70755; NIOSH OH008282, NS076511, NS061817.

## PS 2010 Development of a Mitochondria-Targeted Nano-Complex of Imidazole-Substituted Oleic Acid As a Radiomitigator.

A. Star<sup>1,3</sup>, A. Kapralov<sup>2,3</sup>, A. Amoscatto<sup>2,3</sup>, V. Tyurin<sup>2,3</sup>, W. Seo<sup>1,3</sup>, M. Epperly<sup>4,3</sup>, J. Greenberger<sup>4,3</sup>, Y. Tyurina<sup>2,3</sup> and V. Kagan<sup>2,3</sup>. <sup>1</sup>Department of Chemistry, University of Pittsburgh, Pittsburgh, PA; <sup>2</sup>Department of Environmental and Occupational Health, University of Pittsburgh, Pittsburgh, PA; <sup>3</sup>Center for Medical Countermeasures against Radiation, University of Pittsburgh, Pittsburgh, PA; <sup>4</sup>Radiation Oncology, University of Pittsburgh, Pittsburgh, PA.

Increasing likelihood of intended or accidental exposure to ionizing radiation dictates the necessity to develop effective medical countermeasures of radiation injury as has been recognized as a high priority both in the US and worldwide. No effective medical radiation countermeasures of acute and delayed radiation injuries are currently known. Based on newly discovered mechanisms of radiation damage - oxidation of cardiolipin by cytochrome c in mitochondria as a required stage in radiation-induced apoptosis - we designed and synthesized mitochondria-targeted triphenylphosphonium-conjugated imidazole-substituted oleic (TPP-IOA) which prevented/mitigated cell death induced by irradiation and protected C57BL6 mice against total body irradiation. To improve therapeutic efficiency of TPP-IOA we chose to employ branched polyethylene glycol (PEG) functionalized single walled carbon nanotubes (SWCNT) and use it as a carrier to deliver mitochondria-targeted TPP-IOA to tissues. We found that loading of PEG-SWCNT with TPP-IOA caused a marked extension of the life-span of TPP-IOA in circulation. Moreover we showed that TPP-IOA-nano-complex was more effective as radiomitigator than free TPP-IOA. While the dose of TPP-IOA in TPP-IOA-nano-complexes was two times lower compared with free TPP-IOA the mitigating effect of TPP-IOA-nano-complexes was higher than that of TPP-IOA alone. Importantly, we were able to detect TPP-IOA nano-complexes in radiosensitive tissue such as small intestine. These data warrant further studies aimed at the development of radioprotectors/radiomitigators with broad spectrum of applications in biomedicine and biodefense. Supported by NIOSH OH008282; NIH U19 AI068021, HL70755, ES019304.

## PS 2011 XBP1, SYVN1 and Nrf2: At the Crossroads of ER Stress and Oxidative Stress.

T. Wu and D. D. Zhang. College of Pharmacy, University of Arizona, Tucson, AZ.

Transcription Factor Nrf2 has long time been revealed as the master regulator of intracellular redox homeostasis. As an adaptive response to oxidative stress, Nrf2 activates transcription of a battery of genes encoding antioxidant protein, detoxification

enzymes and xenobiotic transporters by binding to the cis-antioxidant response elements in the promoter region of these genes. Previous works by our lab and others demonstrated that Nrf2 is subject to poly-ubiquitin-mediated proteasomal degradation in a Keap1-dependent manner. Here we report that active form of XBP1, XBP1s suppresses Nrf2 and its downstream signal under ER stress condition, through activation transcription of synovial apoptosis inhibitor 1 (SYVN1). SYVN1, also known as Hrd1, is an ER-associated degradation (ERAD) ubiquitin ligase. We have determined that SYVN1 directly interacts with the Neh4 and Neh5 domain within Nrf2. Overexpression of SYVN1 attenuates Nrf2 signaling, whereas knockdown of SYVN1 enhances expression of Nrf2 and its downstream genes. Furthermore, SYVN1 accelerates the clearance of Nrf2 protein through promoting ubiquitination of Nrf2. These findings demonstrate that XBP1 and SYVN1 are involved in regulating the Nrf2 pathway in a new Keap1-independent mechanism. Moreover, our data revealed a possible crosstalk between ER stress pathway and oxidative responses via UPR and Nrf2 signaling pathway in order to protect cells against environmental stress.

**PS 2012 Sulforaphane Stimulates Basal but Inhibits Glucose-Stimulated Insulin Secretion in Beta-Cells: Role of Reactive Oxygen Species and Induction of Endogenous Antioxidants.**

J. Fu<sup>1</sup>, Q. Zhang<sup>1</sup>, C. G. Woods<sup>1</sup>, H. Zheng<sup>1</sup>, B. Yang<sup>1,2</sup>, M. E. Andersen<sup>1</sup> and J. Pi<sup>1</sup>. <sup>1</sup>Institute for Chemical Safety Sciences, The Hamner Institutes for Health Sciences, Durham, NC; <sup>2</sup>College of Basic Medical Science, China Medical University, Shenyang, China.

Excessive oxidative damage by reactive oxygen species (ROS) is a major contributor to pancreatic  $\beta$ -cells dysfunction. Interestingly, ROS are also involved as a second messenger in glucose-stimulated insulin secretion (GSIS) in  $\beta$ -cells. This paradox obscures the regulatory role of antioxidants in insulin secretion. In the present study, we used an integrated mathematical modeling and in vitro approach to understand the effects of antioxidant sulforaphane (SFN) on insulin secretion. Experiments with INS-1(832/13) cells and isolated mouse islets showed that 30-min SFN treatment stimulated basal insulin secretion in a concentration-dependent manner at low glucose conditions (3 mM). This acute stimulatory effect resulted from an initial SFN-elicited increase of ROS, and when suppressed with cell-permeable ROS scavenger N-acetylcysteine or glutathione ethyl ester, SFN-stimulated insulin secretion was diminished. Due to the negative feedback and incoherent feedforward loops comprising the redox homeostatic control circuit, cells can adapt to prolonged SFN treatment and settle to a steady state exhibiting strong induction of antioxidants but only marginally increased ROS levels. This adapted state slightly increased basal insulin secretion in INS-1(832/13) cells. More importantly, the model predicted that the elevated antioxidant capacity at the adapted state attenuates glucose-stimulated ROS signal and GSIS. This effect was validated in INS-1(832/13) cells exposed to low, non-cytotoxic concentrations of SFN. Despite suppressing GSIS, prolonged exposure to SFN protected INS-1(832/13) cells from cytotoxicity induced by exogenous H<sub>2</sub>O<sub>2</sub>. Taken together, our studies demonstrated that SFN has divergent effects on basal and glucose-stimulated insulin secretion in  $\beta$ -cells. Although the adaptive induction of endogenous antioxidants by SFN enhances  $\beta$ -cell survival, it suppresses GSIS.

**PS 2013 Generation of Reactive Oxygen Species by Process Materials from Indium-Tin Oxide Production.**

N. R. Fix<sup>1</sup>, K. M. Dunnick<sup>1</sup>, M. A. Badding<sup>1</sup>, A. B. Stefaniak<sup>2</sup>, K. J. Cummings<sup>2</sup>, V. Castranova<sup>1</sup> and S. S. Leonard<sup>1</sup>. <sup>1</sup>Health Effects Laboratory Division, National Institute of Occupational Safety and Health (NIOSH)/CDC, Morgantown, WV; <sup>2</sup>Division of Respiratory Disease Studies, National Institute of Occupational Safety and Health (NIOSH)/CDC, Morgantown, WV.

The transition metal indium has been used for decades for various applications including electronics, fusible alloys, and solar cells. Indium compounds usage has increased dramatically based on the rise in demand of touch screens and flat panel displays (LCD's). With this growth of industry, there is potential for increase of indium lung disease among workers who produce, use, or reclaim indium-tin oxide (ITO). Inhalation exposure of indium samples can occur during various times of manufacturing. Materials from different process stages were collected from an ITO production facility. While the pathogenesis of indium lung disease is unknown, previous work has suggested a role for reactive oxygen species (ROS). Chemical characteristics of the process materials will aid in determination of reactivity differences between compounds. Electron spin resonance (ESR), a common tool used for measuring ROS, was used in both acellular and cellular exposures. Acellular samples were evaluated by combining 10 mg/mL process material, phosphate buffered saline (PBS), 10mM hydrogen peroxide (H<sub>2</sub>O<sub>2</sub>), and 100mM DMPO (spin trap). RAW 264.7 mouse monocyte macrophages, DMPO, and the same concentration

of composite were used in the cellular samples conducted in ESR. Scavengers and chelators were used to define radical mechanisms. Results indicated that ventilation dust (VD), tin-oxide (SnOX), and unsintered ITO (UITO) cause a greater increase in ROS production than the other process material. H<sub>2</sub>O<sub>2</sub> and O<sub>2</sub> consumption measurements were used to determine the source of the ROS. ESR studies combined with investigation of ROS production will help to determine the mechanisms behind indium lung disease. Data from this study will be used to determine possible hazards in occupational exposure of indium process material while increasing the understanding of indium lung disease.

**PS 2014 Lower Expression of Nrf2 Promotes Proliferation, Migration and Invasion of Prostate Cancer Cells.**

R. Khatri and A. K. Jaiswal. *Pharmacology and Experimental Therapeutics, University of Maryland Baltimore, Baltimore, MD.*

The nuclear factor Nrf2 is known to play a critical role in cellular protection against oxidative stress and cellular transformation. However, unabated nuclear accumulation of Nrf2 is also known to reduce apoptosis, promote cancer cell survival and drug resistance. Mutations in INrf2 and Nrf2 leading to nuclear accumulation of Nrf2 in many cancers including prostate and breast cancer are known. These also raise interesting questions regarding the role of Nrf2 in cancer metastasis and/or metastasis progression that remains elusive. In this study we have investigated the hypothesis that loss of Nrf2 is associated with metastasis/metastasis progression. We used less metastatic LNCaP and highly metastatic LNCaP derived C4-B2 prostate cancer cell lines to test our hypothesis. The analysis revealed that highly metastatic C4-B2 cells expressed higher INrf2 and lower Nrf2 levels as compared to less metastatic LNCaP cells. We used control, INrf2 and Nrf2 shRNA to generate C4-B2 and LNCaP derived cells with altered levels of INrf2 and Nrf2 to determine the role of Nrf2 in metastasis and metastasis progression in Soft agar colony formation and X-CELLigence proliferation, migration and invasion assays. C4-B2-INrf2shRNA cells expressing inhibited levels of INrf2 and higher levels of Nrf2 showed fewer colonies in soft agar and proliferated faster but did not migrate as compared to C4-B2-Control shRNA cells. Similarly, LNCaP-Nrf2shRNA cells expressing inhibited levels of Nrf2 in less metastatic LNCaP cells demonstrated significantly higher number of colonies in soft agar, proliferated faster and showed greater migration and invasion as compared to LNCaP-Control shRNA cells. These results together suggest that lower Nrf2 levels are associated with higher proliferation, migration and invasion or metastatic progression. Currently, we are investigating the mechanism of the role of Nrf2 in metastasis progression and plan in vivo experiments to test our hypothesis of the association of lower Nrf2 with metastasis progression in mice.

**PS 2015 Mechanisms of Oxidative Stress Promoted by 1, 4-Diamino-2-Butanone in Trypanosoma cruzi and Mammalian Cells.**

E. J. Bechara<sup>1,2</sup>, C. O. Soares<sup>2</sup>, W. Colli<sup>2</sup> and M. M. Alves<sup>2</sup>. <sup>1</sup>Ciências Exatas e da Terra, Universidade Federal de São Paulo, Diadema, Brazil; <sup>2</sup>Bioquímica, Universidade de São Paulo, São Paulo, Brazil.

The putrescine analogue 1,4-diamino-2-butanone (DAB) is highly toxic to pathogenic microorganisms, including various fungi and Trypanosoma cruzi. Similar to other  $\alpha$ -aminocarbonyl metabolites such as aminoacetone and 5-aminolevulinic acid, DAB exhibits pro-oxidant properties. DAB reportedly undergoes metal-catalyzed oxidation in aerobic medium yielding H<sub>2</sub>O<sub>2</sub>, NH<sub>4</sub><sup>+</sup> ion, and 4-amino-2-oxobutanal, a highly toxic  $\alpha$ -oxoaldehyde. Administered to mammalian cell cultures, DAB decreases the cell viability which was shown to be associated with changes in redox balance. Thus, treatment of RKO cells derived from human colon carcinoma or cultured LL-MK2 Rhesus epithelial cells with millimolar DAB caused significant decline in cell viability, which was inhibited by pre-addition of catalase, aminoguanidine (an  $\alpha$ -oxoaldehyde trap), N-acetyl cysteine or reduced glutathione. Now we explore the mechanisms by which DAB exhibits pro-oxidant effects on trypanostigotes and on intracellular T. cruzi amastigotes. DAB (0.05-5.0 mM) exposure in trypanostigotes, the infective stage of T. cruzi, leads to a decline in parasite viability (IC<sub>50</sub> c.a. 0.2 mM DAB; 4 h incubation), changes in morphology, thiol redox imbalance, and increased TcSOD activity. Medium supplementation with catalase (2.5  $\mu$ M) protects trypanostigotes against DAB toxicity, while host cell invasion by trypanostigotes is hampered by DAB. Additionally, intracellular amastigotes are susceptible to DAB toxicity. Furthermore, pre-treatment with 100-500  $\mu$ M buthionine sulfoximine (BSO) of LLC-MK2 potentiates DAB cytotoxicity, whereas 5 mM N-acetyl-cysteine (NAC) protects cells from oxidative stress. Together, these data support the hypothesis that redox imbalance, not only the long reported DAB-promoted inhibition of polyamine metabolism, contributes to its cytotoxicity in both T. cruzi and mammalian host cells.

**PS 2016 Receptor-Mediated Reactive Oxygen Species Contribute to Impaired Coronary Vasodilation following Acute Ozone Exposure in Rat.**

M. Paffett<sup>1</sup>, S. Robertson<sup>1</sup>, S. Lucas<sup>1</sup>, T. Anderson<sup>2</sup>, M. Nysus<sup>2</sup>, J. Norenberg<sup>2</sup> and M. J. Campen<sup>1</sup>. <sup>1</sup>Pharmaceutical Sciences, University of New Mexico, Albuquerque, NM; <sup>2</sup>Radiopharmaceutical Sciences, University of New Mexico, Albuquerque, NM.

Ozone (O<sub>3</sub>) exposure in both humans and rodents leads to elevations in alveolar and peripheral inflammation, believed to promote endothelial dysfunction. Although pulmonary inflammation is a well-defined response to inhaled O<sub>3</sub>, little is known regarding acute effects of O<sub>3</sub> exposure on the mechanisms responsible for impaired coronary vasodilation. We hypothesized that a single, whole-body O<sub>3</sub> exposure will induce pulmonary inflammation and the transference of pulmonary inflammatory elements will contribute to reactive oxygen species (ROS)-induced endothelial dysfunction. We tested this hypothesis by assessing pulmonary immune infiltrates from bronchial alveolar fluid lavage (BALF), circulating WBCs and coronary artery endothelial function 24 hrs following O<sub>3</sub> exposure (4h at 1ppm) or filtered air (FA). BALF total protein, cell number, macrophage/neutrophil counts and circulating WBC differentials were assessed. Furthermore, experiments assessing the effects of O<sub>3</sub> on the endothelial-dependent vasodilator, acetylcholine (ACh), in coronary arteries pre-constricted (~50%) with a thromboxane mimetic (U46619) in the presence or absence of luminal administration of the superoxide dismutase mimetic (PEG-SOD). Parallel experiments were performed where rodents were injected (i.p.) with inhibitory antibodies directed against lectin-like oxidized low density lipoprotein receptor-1 (LOX-1). Our results demonstrate significant increases in BALF total protein and cell number were evident in O<sub>3</sub> exposed rats, specifically neutrophils, compared to FA controls. Systemic increases in circulating neutrophils were also evident following O<sub>3</sub> exposure. Moreover, ACh-mediated vasodilation was restored in vessels loaded with PEG-SOD and partially restored in rodents pretreated with the LOX-1 inhibitor. Our data suggest that that O<sub>3</sub>-induced pulmonary inflammation contributes to increased ROS-mediated endothelial dysfunction downstream of LOX-1.

**PS 2017 In Vitro Modification of Plasminogen by Methylglyoxal Disrupts Normal Zymogen Activation.**

O. R. Kinsky, M. J. Kimzey, T. J. Monks and S. S. Lau. Southwest Environmental Health Sciences Center, Department of Pharm/Tox, College of Pharmacy, University of Arizona, Tucson, AZ.

Reactive dicarbonyls such as methylglyoxal (MG) are present in blood and react with arginines (R) of target proteins, leading to diabetic micro- and macrovascular complications. Normal MG plasma concentrations are estimated to reach 4.5 μM, with these values tripling as diabetic complications progress. Dicarbonyls irreversibly modify R residues, resulting in a net loss of positive charge via hydroimidazolone formation. Previous shotgun LC/LC-MS/MS proteomics analysis of human serum reacted with MG (18 hrs at 37°C) indicated that plasminogen (PLG) was readily modified at multiple sites. Subsequent studies in our laboratory determined that modification at R561 of PLG resulted in drastic energy-of-interaction changes between PLG and tissue plasminogen activator (tPA). The model revealed that a MG-adduct formed at R561 decreased the interaction energy by up to 410.4 kcal/mol, 164-fold higher than the minimum energy change necessary for an altered interaction. Modified R561 in PLG is of particular biological interest because of its role in the thrombolytic cascade, R561 being the site of cleavage from PLG to plasmin. In an effort to determine functional consequences of this adduction, MG-modified PLG and its activation by both exogenous and endogenous activators was studied. The activation of MG-modified PLG by streptokinase (STK) was altered in both a time (0-60 min) and concentration (1-500 μM MG) dependent manner. Unmodified PLG (90-100 kDa) was cleaved by STK, with the concurrent formation of angiostatin (ANG; 38 kDa) and plasmin light chain (PLC; 25 kDa). In contrast, such effects were diminished in MG-modified PLG, with reduced accumulation of ANG and PLC, and reduction in the disappearance of PLG. Similar studies are underway with tPA and urokinase. The findings indicate that MG-modification of PLG may disrupt the thrombolytic cascade thereby contributing to vascular complications associated with diabetes. (R24DK083948, ABRG, ES016652, T32ES007091, P30ES006694).

**PS 2018 Oxidative Stress-Dependent Destruction of Cdc25C As a Novel Chemotherapeutic Strategy for the Targeted Induction of Cell Cycle Arrest.**

S. Qiao<sup>1,2</sup> and G. T. Wondrak<sup>1,2</sup>. <sup>1</sup>Pharmacology and Toxicology, University of Arizona, Tucson, AZ; <sup>2</sup>Arizona Cancer Center, University of Arizona, Tucson, AZ. Sponsor: W. Klimecki.

Cellular oxidative stress is an established causative factor in carcinogenesis. Recent research suggests that elevated oxidative stress in cancer cells represents a phenotypic vulnerability that can be targeted by redox intervention. Multiple myeloma is a redox sensitive hematological malignancy characterized by dysregulation of cell cycle progression and checkpoint control. Guided by a phenotypic drug screen for novel leads that display antiproliferative activity through induction of oxidative stress, we have identified the FDA-approved antimicrobial thiostrepton (T) as multiple myeloma-directed experimental chemotherapeutic. In RPMI-8226 multiple myeloma cells, major hallmarks of hyperproliferation including hyperphosphorylation of retinoblastoma (pRb; Ser 780, Ser807/811) and overexpression of c-myc and cyclin D1 were fully suppressed at both mRNA and protein levels at submicromolar concentrations of T. Moreover, T-induced G2/M cell cycle arrest was characterized by inhibitory phosphorylation of cyclin-dependent kinase 1 (CDK1; Tyr15), dephosphorylation of histone H3 (Ser10), and cyclin B1 accumulation as revealed by immunodetection. Flow cytometric analysis indicated rapid induction of cytotoxic oxidative stress followed by destruction of the redox-sensitive oncogenic phosphatase cdc25C (cell division cycle 25C), known to abrogate the G2/M checkpoint by activation of dephosphorylation of cyclin B-CDK1 (Tyr15). Strikingly, hydrogen peroxide treatment mimicked T-induced destruction of cdc25C. Vice versa, antioxidant pretreatment (N-acetyl-L-cysteine) prevented cdc25C depletion, inhibitory phosphorylation of CDK1, and enrichment of the G2/M fraction, further substantiating the causative role of ROS in T-induced cell cycle arrest. Taken together, these data suggest feasibility of T-based prooxidant intervention targeting the oncogenic redox-sensitive G2/M regulator cdc25C and its downstream effectors for experimental chemotherapy of multiple myeloma.

**PS 2019 Selective Detoxification of Hypothiocyanite by Mammalian Thioredoxin Reductase, the Missing Link in Lung Innate Immunity and Antioxidant Defense.**

J. D. Chandler<sup>1,2</sup>, R. J. Hondal<sup>3</sup> and B. J. Day<sup>1,2</sup>. <sup>1</sup>Pharmaceutical Sciences, University of Colorado Denver, Denver, CO; <sup>2</sup>Medicine, National Jewish Health, Denver, CO; <sup>3</sup>Biochemistry, University of Vermont, Burlington, VT.

Haloperoxidases metabolize thiocyanate (SCN) in the presence of hydrogen peroxide (H<sub>2</sub>O<sub>2</sub>) producing the thiol-selective oxidant hypothiocyanite (OSCN). OSCN has been implicated in innate immunity through its ability to inhibit the growth of multiple pathogens. Paradoxically, SCN has been shown to protect cells from promiscuous oxidizing species such as hypochlorite (OCl) by a direct reaction forming OSCN, suggesting its selective detoxification by mammalian cells. Mammalian thioredoxin reductase (TR) is distinguished from lower order TRs by its C-terminal selenocysteine (Sec) redox couple and broader substrate specificity. Recombinant rat TR1, recombinant mouse TR2 and purified rat TR metabolized OSCN with high affinity but do not metabolize OCl. Mutant forms of mouse TR2 lacking Sec had significantly higher Km for OSCN. Recombinant E. coli TR did not metabolize OSCN or OCl. Lysates from human lung epithelial cells (16HBE) readily metabolized OSCN but lysates from E. coli and P. aeruginosa were inactive. Auranofin, a TR inhibitor, decreased OSCN metabolism in 16HBE lysates. 16HBE cells and P. aeruginosa were exposed to an oxidase-peroxidase coupled system that generated a 100 μM steady state exposure of OSCN or OCl for 2 hours. OCl was highly toxic to both 16HBE and P. aeruginosa, but OSCN was only toxic to P. aeruginosa. Inhibition of mammalian TR with auranofin increased OSCN toxicity in 16HBE cells. These findings implicate mammalian TR as the major detoxification pathway for OSCN and suggest a novel mechanism of innate immunity and antioxidant defense in mammals wherein OSCN formation simultaneously results in pathogen inhibition while preventing damage to host tissue. This study was funded by NIH Grant HL084469 and a Cystic Fibrosis Foundation Research Grant.

**PS 2020 GRP78 Contributes to the Selective Cytoprotection Afforded by All-Trans-Retinoic Acid against Renal Injury.**

J. Sapiro, A. C. Gallegos, I. Y. Rojas, A. B. Romans, R. D. Canatsey, T. J. Monks and S. S. Lau. SWEHSC, Pharm/Toxicol, University of Arizona, Tucson, AZ.

Chemical-induced nephrotoxicity is a major cause of acute kidney injury. Pretreatment of LLC-PK<sub>1</sub> cells with all-trans-retinoic acid (ATRA) affords cytoprotection against chemical nephrotoxins. ATRA pretreatment (25 μM, 24 hrs)

protected against p-aminophenol (PAP, 150  $\mu$ M, 3 hr), iodoacetamide (25  $\mu$ M, 2 hr), and  $H_2O_2$  (250  $\mu$ M, 3 hr)-induced cytotoxicity as assessed by the MTS assay. Moreover, ATRA suppressed tumor necrosis factor- $\alpha$  (TNF- $\alpha$ , 30 ng/mL, 2 hr)-induced caspase-3 cleavage by 4-fold, indicative of a reduction in apoptosis. In contrast, pretreatment of cells with ATRA had no effect on cisplatin (25  $\mu$ M, 24 hr)-induced caspase-3 cleavage. The data reveal that ATRA selectively protects against toxicants that induce necrotic and death receptor-mediated (extrinsic) apoptotic cell death but not against mitochondrial-mediated (intrinsic) apoptotic cell death. Although the molecular mechanism(s) underlying the cytoprotective effects of ATRA remain unclear, the endoplasmic reticulum (ER) molecular chaperone Grp78 is a pivotal contributor to the cytoprotective/adaptive response to cell stress. Therefore, we subsequently used Grp78 non-inducible cells to explore the relationship between the ER stress response and ATRA signaling. LLC-PK<sub>1</sub> cells, in which the induction of grp78 expression was disrupted via stable expression of an antisense grp78 RNA (pKASgrp78), were more sensitive to the cytotoxic effects of PAP relative to control cells transfected with an empty vector (PKNEO). Furthermore, although ATRA itself induced Grp78 in naive LLC-PK<sub>1</sub> and PKNEO cells, it was unable to do so in the pKASgrp78 cells. Thus, Grp78 may contribute to ATRA-mediated cytoprotection and ATRA may provide an effective therapeutic intervention for chemical-induced renal injury or other pathological conditions. (ES006694, ES016578).

## PS 2021 Sulfur Dioxide Modulates Oxidative Stress Responses in IL-10-Deficient Mice with Airway Inflammation.

A. L. Reno<sup>1</sup>, L. M. Hallberg<sup>2</sup>, W. C. Spear<sup>1</sup>, J. L. Parks<sup>1</sup>, A. P. Chaparro<sup>3</sup>, E. G. Brooks<sup>3</sup> and B. T. Ameredes<sup>1</sup>. <sup>1</sup>Internal Medicine, University of Texas Medical Branch, Galveston, TX; <sup>2</sup>Preventive Medicine and Community Health, University of Texas Medical Branch, Galveston, TX; <sup>3</sup>Pediatrics, University of Texas Health Science Center, San Antonio, TX.

**RATIONALE:** Inhaled sulfur dioxide (SO<sub>2</sub>) at low concentrations (1-5 ppm) can produce bronchospasm in asthmatics, linked to increased oxidative stress and airway inflammation (AI), potentially due to a deficiency in IL-10 production. We tested this hypothesis in IL-10-sufficient C57Bl6 (C57), and IL-10 knockout (-/-) mice, with experimentally-induced AI.

**METHODS:** AI was induced by sensitization and challenge with ovalbumin (OVA, O/O), with and without inhaled SO<sub>2</sub> (1 ppm for 6 hr/day over 10 days). Bronchoalveolar lavage fluid (BALF) was analyzed for leukocyte counts; a pro-oxidant/anti-oxidant balance (PAB) assay provided an index of oxidative stress, and interleukin-4 (IL-4) levels in lung homogenates were measured by ELISA, as an indicator of AI. Nitrite levels were measured in BALF by Griess assay, as an index of iNOS activity.

**RESULTS:** Respective mean eosinophil counts ( $\times 10^3$ /g mouse) for C57 and IL-10-/- mice ( $P < 0.05$ ) were: O/O-SO<sub>2</sub> (3.1 vs. 1.4; n.s.), and O/O+SO<sub>2</sub> (3.0 vs. 4.3; n.s.), indicating eosinophilia in mice with mild AI alone, and those that inhaled SO<sub>2</sub>, as compared to saline-challenged controls having no eosinophils. SO<sub>2</sub> shifted the PAB toward pro-oxidative in C57 mice with AI, whereas the opposite was found for their IL-10-/- counterparts ( $P < 0.05$ ). IL-4 levels in the O/O+SO<sub>2</sub> C57 mice were significantly increased compared to their IL-10-/- counterparts. BALF nitrite levels ( $\mu$ M/kg body weight) were decreased in the C57 O/O+SO<sub>2</sub> group (61 $\pm$ 5; n.s.) as compared to O/O-SO<sub>2</sub> (86 $\pm$ 15). A similar trend was seen for the IL-10-/- mice (62 $\pm$ 7 vs. 80 $\pm$ 10; n.s.).

**CONCLUSIONS:** The results indicate there is a robust inflammatory response in the lungs of mice exposed to OVA allergen attenuated by SO<sub>2</sub> inhalation, perhaps via an anti-oxidant promotion mechanism.

## PS 2022 Statin-Induced Cytotoxicity in C2C12 Myoblasts Is Accompanied by Mitochondrial Dysfunction and Excessive ROS Production.

T. Schirris<sup>1,3</sup>, J. J. Nabers<sup>1,3</sup>, J. D. Beyrath<sup>2,3</sup>, J. A. Smeitink<sup>2,3</sup> and F. G. Russel<sup>1,3</sup>. <sup>1</sup>Pharmacology and Toxicology, Radboud University Nijmegen Medical Centre, Nijmegen, Netherlands; <sup>2</sup>Pediatrics, Radboud University Nijmegen Medical Centre, Nijmegen, Netherlands; <sup>3</sup>Centre for Systems Biology and Bioenergetics, Nijmegen, Netherlands.

Statins are widely used cholesterol-lowering drugs that are generally well-tolerated. The most important adverse effects are muscle pain and inflammation of muscle cells. The mechanism is not fully understood, although for some statins a direct effect on mitochondrial function has been found. Here, we systematically studied the effect of a series of sixteen different statin drugs on mitochondrial function and cytotoxicity in a mouse myoblast cell line (C2C12). A high-content method was developed to measure the viability and ROS production of C2C12 cells using a 384-well microscopy assay. Furthermore, mitochondrial function was assessed using

high-resolution oxygen consumption measurements in comparison with maximal ATP production rates. Nine of the sixteen statins studied induced cell death after 24h, including cerivastatin, simvastatin, atorvastatin and rosuvastatin, which are most frequently associated with clinical cases of myopathy. Of these nine statins, rosuvastatin lactone had the highest potency (IC<sub>50</sub> 22 $\pm$ 10  $\mu$ M) and atorvastatin the lowest (IC<sub>50</sub> 182 $\pm$ 36  $\mu$ M). After 8h treatment at IC<sub>50</sub> concentrations, all nine statins showed increased ROS levels; itavastatin lactone gave the largest increase of 4300 $\pm$ 36AU compared to control (585 $\pm$ 99AU,  $P < 0.001$ ). Moreover, these nine statins reduced the ATP production, most potently by cerivastatin lactone (16 $\pm$ 8% of control,  $P < 0.05$ ). These results were further confirmed by a reduced malate-, glutamate-, and succinate-driven oxygen consumption by all nine statins. In conclusion, a series of clinically relevant statins affected mitochondrial function and viability of C2C12 myoblasts with different potencies. Further research is needed to investigate the link between the observed mitochondrial dysfunction and the inflammatory and the apoptotic hallmarks of statin-induced myopathies.

## PS 2023 Screening and Characterization of Aldehydes on the Basis of Protein Carbonylation.

H. Dhot<sup>1,2</sup> and P. J. O'Brien<sup>2</sup>. <sup>1</sup>Institute of Environmental Medicine, Karolinska Institutet, Stockholm, Sweden; <sup>2</sup>Faculty of Pharmacy, University of Toronto, Toronto, ON, Canada.

Proteins are easily susceptible to Post Translational Modifications (PMT) where protein carbonylation is the most common type that plays a pivotal role in etiology and/or progression of lethal diseases like neurodegenerative diseases, cancers, aging, diabetes and sepsis. Since, ROS and secondary by products of oxidative stress can induce the protein carbonylation and this type of protein oxidation is regarded as a well-known biomarker of oxidative stress with different susceptibility for different amino acids. In this study, we studied the protein carbonylation caused by different aliphatic (formaldehyde to decanal i.e. aldehydes from carbon 1 to carbon 10) and aromatic (benzaldehyde and its derivatives) aldehydes by applying BSA Protein carbonylation assay. Taking into account the ED 50 values of the aliphatic aldehydes, 2mM and 4mM concentrations of aldehydes were used. Among aliphatic aldehydes, only first two aldehydes (HCHO and CH<sub>3</sub>CHO) showed the highest protein carbonylation in a dose dependent manner. On the other hand, aromatic aldehydes showed the following trend: 4Chlorobenzaldehydes (max at 120 mins) > Cinnamaldehyde (max at 120 mins) > benzaldehyde (max at 120 mins) > p-Tolualdehyde (max at 60 mins) > m-Tolualdehyde (max at 40 mins). GSH was found effective against protein carbonylation. Protein carbonylation increased with increase in dose except in case of cinnamaldehyde and benzaldehyde where high dose decreased the carbonylation. So, our result suggests that aliphatic aldehydes can be characterized as less reactive towards protein carbonylation reaction than aromatic aldehydes. Among aromatic aldehydes, cinnamaldehyde and 4-chlorobenzaldehyde can be regarded as fast reacting aldehydes, m-tol and p-tol as slowly reacting with or without lag phase respectively, ortho substituted aldehydes as causing no protein carbonylation.

## PS 2024 Autophagy Is Protective against CYP2E1-Dependent Arachidonic Acid, Buthionine-Sulfoximine, and Carbon Tetrachloride Cytotoxicity in E47 HepG2 Cells through Preventing Mitochondrial Dysfunction.

D. Wu and A. I. Cederbaum. *Pharmacology & Systems Therapeutics, Mount Sinai School of Medicine, New York, NY.* Sponsor: Y. Lu.

The goal of this study was to evaluate if autophagy promotes or is protective against CYP2E1 toxicity. E47 HepG2 cells express CYP2E1 and control C34 cells which do not express CYP2E1 were treated with arachidonic acid (AA), or buthionine-sulfoximine (BSO), or carbon tetrachloride (CCl<sub>4</sub>), in the presence or absence of 3-methyladenine (3MA) or rapamycin. All three compounds reduced cell viability in E47 cells but not in C34 cells. 3MA further reduced cell viability while rapamycin increased it. These results suggested that autophagy prevented against AA, BSO and CCl<sub>4</sub> cytotoxicity in E47 cells. These compounds induced oxidative stress in E47 cells as TBARS increased and GSH decreased. 3MA enhanced TBARS and decreased GSH while rapamycin prevented these changes. Flow cytometry suggested that these compounds mainly induced necrosis and 3MA enhanced necrosis but not apoptosis; rapamycin prevented the necrosis. These compounds induced mitochondrial membrane swelling, cytochrome c release, reducing mitochondrial ATP production, 3MA enhanced but rapamycin prevented these changes. Mitochondrial ROS production was enhanced by rapamycin but decreased by 3MA. E47 cells were transfected with Atg7 siRNA which enhanced AA cytotoxicity, increased oxidative stress. The decline in viability was restored and oxidative stress was blocked in the presence of rapamycin. The antioxidant N-acetyl-L-cysteine prevented the AA or Atg 7 siRNA-induced oxidant stress and loss of E47 cell viability.

and the potentiation of these effects by 3MA. Treating the E47 cells with AA induced p38 MAPK, 3MA enhanced the activation and rapamycin inhibited it. This study shows that autophagy is protective against AA, BSO and CCl<sub>4</sub> induced CYP2E1 dependent cytotoxicity. This protection may be due at least in part through prevention of mitochondrial dysfunction to maintain cell survival.

## PS 2025 Absence of Upstream Consensus Regulatory Element Sequences for Nrf2 in Human Glutathione S-Transferase Genes.

C. M. Schaupp<sup>1</sup>, T. K. Bammler<sup>2</sup>, R. P. Byer<sup>2</sup>, T. J. Kavanagh<sup>1,2</sup> and D. L. Eaton<sup>1,2</sup>. <sup>1</sup>Environmental and Occupational Health Sciences, University of Washington, Seattle, WA; <sup>2</sup>Center for Ecogenetics & Environmental Health, University of Washington, Seattle, WA.

Nuclear factor erythroid-derived 2-like 2 (NFE2L2, or NRF2) is involved in antioxidant response to cellular stress. In response to oxidative or electrophilic stimuli, NRF2 binds its target genes containing an antioxidant response element (ARE), upregulating expression of detoxifying/antioxidant enzymes. Numerous studies have demonstrated that some rodent liver GSTs are highly inducible via activation of the Keap1/Nrf2/ARE antioxidant response pathway by prototypical Nrf2 activators such as BHA, sulforaphane and oltipraz. Thus, these chemicals may have therapeutic value based on their putative ability to activate NRF2-mediated antioxidant pathways. However, human studies in vitro and in vivo have not generally seen a robust induction of GSTs following administration of Nrf2 activators, suggesting that human liver GSTs are less responsive to ARE-mediated induction. To identify the potential basis for a possible inter-species difference in GST inducibility, we used the web-based oPOSSUM software to identify ARE sequences up to 10,000 base pairs upstream of the transcriptional start sites of antioxidant enzymes putatively regulated by NRF2 in murine and human genomes. Only three out of 19 human GST genes (GSTM2, GSTO2, and GSTZ1) contained an ARE consensus sequence within 10kb of the transcriptional start site, whereas ARE sequences were present in 11 of 17 murine GSTs analyzed. Notably, none of the common, highly expressed human alpha or mu class GSTs contained consensus NRF2 elements, whereas 2 of 4 alpha class, and 5 of 7 mu class, mouse GSTs contained one or more Nrf2 response elements. Our data suggest that inter-species differences in GST inducibility may result from differences in the presence and location of ARE consensus sequences upstream of murine and human GST genes—a conclusion which may have major implications in the clinical setting.

## PS 2026 Pharmacological Inhibition of Thioredoxin Reductase I Attenuates Hyperoxic Lung Injury by Augmenting Glutathione Synthesis.

L. K. Rogers<sup>1,3</sup>, R. D. Britt<sup>1</sup>, T. E. Tipple<sup>1,3</sup> and M. Velten<sup>1,2</sup>. <sup>1</sup>Center for Perinatal Research, The Research Institute at Nationwide Children's Hospital, Columbus, OH; <sup>2</sup>Anesthesiology and Intensive Care, Rheinische Friedrich-Wilhelms University, Bonn, Germany; <sup>3</sup>Pediatrics, The Ohio State University, Columbus, OH.

Inflammation and oxygen toxicity increase free radical production and contribute to the development of acute respiratory distress syndrome (ARDS). We have previously shown increased glutathione (GSH) levels in lung epithelial cells in vitro and attenuated adult murine hyperoxic lung injury in vivo following thioredoxin reductase-1 (TrxR1) inhibition with auranofin and aurothioglucose (ATG), respectively. The present studies tested the hypothesis that ATG treatment increases pulmonary GSH levels, decreases lung injury, and improves survival. Adult male mice were given a single IT dose of 0 or 0.375 µg/g E. coli LPS. After 12 h, an injection of 0 or 25 mg/kg ATG or a combination of ATG and 800 mg/kg buthionine sulfoximine (BSO) were administered, i.p. Mice were then exposed to room air (RA) or >95% hyperoxia (O<sub>2</sub>). After 3 d exposure, bronchoalveolar lavage (BAL) and lung tissues were collected. BAL protein concentrations were significantly greater in LPS/O<sub>2</sub>-exposed mice when compared to PBS/RA controls. In LPS/O<sub>2</sub>-exposed mice, ATG treatment significantly decreased BAL protein concentrations, increased lung GCLM expression, GSH levels, and GSH/GSSG ratios, and improved survival compared to PBS-treated LPS/O<sub>2</sub>-exposed mice. BSO treatment dramatically decreased the survival of ATG-treated LPS/O<sub>2</sub>-exposed mice. In summary, ATG enhances GSH levels, decreases lung injury, and improves survival in a GSH-dependent manner in a murine model of ARDS. If enhancement of pulmonary GSH levels can be accomplished via drug-mediated TrxR1 inhibition, which seems to be without detrimental effects, this approach could constitute a novel strategy to improve outcomes in patients with oxidant-mediated lung injury. This work was supported by the National Institutes of Health (RDB F31HL097619, TET K08HL093365, and LKR R01AT006880).

## PS 2027 Aniline Up-Regulates Cyclins via Induction of Oxidative Stress in Rat Spleen.

J. Wang, G. Wang, H. Ma and M. Khan. University of Texas Medical Branch, Galveston, TX.

Aniline exposure is associated with toxicity to the spleen leading to splenomegaly, fibrosis and a variety of sarcomas of the spleen. In earlier studies, we have shown that aniline exposure leads to iron overload, oxidative and nitrosative stress and activation of redox-sensitive transcription factors, which could regulate various genes leading to a tumorigenic response in the spleen. However, molecular mechanisms leading to aniline-induced cellular proliferation in the spleen remain largely unknown. This study was undertaken to further assess the role of oxidative and nitrosative stress in the regulation of cell cycle proteins (cyclins) following aniline exposure. Groups of male SD rats were treated with aniline (1 mmol/kg/day by gavage), aniline plus N-acetylcysteine (NAC, an antioxidant, 300 mg/kg/day, i.p.), aniline plus aminoguanidine (AG, an iNOS inhibitor, 200 mg/kg/day, i.p.) or aniline plus zinc protoporphyrin (ZP, a heme oxygenase inhibitor, 50 µmol/kg/day, i.p.) for 7 days (controls received drinking water only), and mRNA expression of cyclins A, B, D3 and E were measured in spleen. Aniline treatment resulted in significant increases in the expression of cyclin A (7.9-fold), cyclin B (7.3-fold), cyclin D3 (3.7-fold) and cyclin E (5.4-fold) as compared to the controls. Interestingly, all of the three inhibitors significantly reduced the aniline-induced overexpression of cyclins. Specifically, NAC reduced the expression of cyclins A, B, D3 and E by 61%, 48%, 38%, and 41%, AG reduced cyclins A, B, D3 and E by 60%, 63.0%, 51%, and 37%, whereas ZP reduced cyclins A, B, D3 and E by 30%, 61%, 62%, and 44%, compared to aniline only treated rats, respectively. Our data suggest that oxidative and nitrosative stress play a role in aniline-induced overexpression of cyclins which could be critical in cell proliferation, and may contribute to aniline-induced tumorigenic response in the spleen. Supported by NIH ES06476.

## PS 2028 Understanding the Role of UCP2 in Fatty Acid Beta-Oxidation and Drug-Induced Liver Injury.

J. E. Montanez<sup>1</sup>, P. B. Smith<sup>2</sup> and A. D. Patterson<sup>1,2</sup>. <sup>1</sup>Veterinary and Biomedical Science, The Pennsylvania State University, University Park, PA; <sup>2</sup>Center for Molecular Toxicology and Carcinogenesis, The Pennsylvania State University, University Park, PA.

UCP2, originally described as a mitochondrial uncoupling protein, has been reported to serve many other functions including regulation of glucose and lipid metabolism as well as regulation of ROS in cancerous cells. We recently reported that under hepatotoxic conditions such as that induced by acetaminophen, UCP2 expression was found to protect against liver damage in a PPARα-dependent fashion. Interestingly, polymorphisms in the coding sequence of the UCP2 gene have been found to be associated with obese and/or diabetic individuals further implicating UCP2 in the fatty acid beta-oxidation pathway. However, the precise mechanism by which UCP2 exerts these salubrious effects is unknown. In this study, the metabolic functions of UCP2 and UCP2 (A55V) variant were compared using a gas chromatography coupled with mass spectrometry-based metabolomics approach. COS-7 cells were transfected with myc/flag-tagged UCP2 and UCP2 (A55V). After confirming expression of the constructs via Western blotting (no difference was observed between UCP2 and UCP2 (A55V)), the cells were extracted, metabolites derivatized using methoxamine and MSTFA, and the samples ran on an Agilent 5975C Series GC/MSD. Principal component analysis of the data show distinct separation of the UCP2 transfected cells from the control and UCP2 (A55V) transfected cells. Among others, palmitic acid was found to be dramatically decreased (~2.3 fold) in the UCP2-transfected cells compared to control and UCP2 (A55V) transfected cells. Further, palmitic acid is thought to induce UCP2 expression through PPARα activation. This study illustrates the utility of the metabolomics approach for elucidating and/or clarifying the metabolic function of UCP2.

## PS 2029 Real-Time Monitoring of Xenobiotic-Induced Intracellular Redox Changes Using Ozone As a Model Oxidant.

E. A. Gibbs-Flournoy<sup>1</sup>, S. O. Simmons<sup>2</sup>, P. A. Bromberg<sup>3</sup> and J. M. Samet<sup>4</sup>. <sup>1</sup>Curriculum in Toxicology, University of North Carolina at Chapel Hill, Chapel Hill, NC; <sup>2</sup>ISTD/NHEERL, US EPA, Research Triangle Park, NC; <sup>3</sup>Center for Environmental Medicine, Asthma, and Lung Biology, University of North Carolina at Chapel Hill, Chapel Hill, NC; <sup>4</sup>EPHD/NHEERL, US EPA, Chapel Hill, NC.

Oxidative injury is often cited as a key feature in the toxic action of many xenobiotics; however, unambiguous indices of xenobiotic-induced oxidative stress have proven elusive. A new generation of sensors capable of reporting intracellular redox

status has shown much promise. However, their use in toxicological assessments involving strong electrophiles remains to be validated. Exposure to ozone ( $O_3$ ), a highly reactive oxidant gas, induces pulmonary function decrements and inflammatory responses in the airways through oxidative mechanisms. An important unresolved toxicological question concerns the effect of  $O_3$  exposure on intracellular redox status. Using live-cell microscopy, we addressed this issue directly with the novel application of roGFP2, a genetically-encoded fluorescent reporter of the intracellular glutathione redox potential,  $E_{GSH}$ . BEAS-2B human bronchial epithelial cells transduced to stably express cytosolic roGFP2 were exposed to concentrations of  $O_3$  ranging from 0.15 - 1.0 ppm. Cells were imaged in real-time during  $O_3$  exposure in a custom-built stage-top exposure chamber.  $O_3$  exposure induced a dose- and time- dependent increase of the cytosolic  $E_{GSH}$ . Modulation of glutathione system components confirmed that roGFP2 is not directly oxidized but properly equilibrates with the oxidation status of the glutathione pool. Exposure to  $O_3$  induces a substantial increase in  $E_{GSH}$  in BEAS-2B cells that is indicative of an oxidant-dependent impairment of redox homeostasis. Moreover, this study demonstrates the utility of using redox reporters in making reliable assessments of cells undergoing exposure to xenobiotics with potent oxidizing properties. THIS ABSTRACT OF A PROPOSED PRESENTATION DOES NOT NECESSARILY REFLECT EPA POLICY.

**PS 2030 Formation 4-Hydroxynonenal, an Electrophilic Lipid Peroxidation End Product, in Rabbit Corneal Organ Cultures Treated with Nitrogen Mustard.**

A. T. Black<sup>1</sup>, R. Zheng<sup>1</sup>, I. Po<sup>1</sup>, D. E. Heck<sup>2</sup>, D. L. Laskin<sup>1</sup>, D. R. Gerecke<sup>1</sup>, M. K. Gordon<sup>1</sup> and J. D. Laskin<sup>3</sup>. <sup>1</sup>Pharmacology & Toxicology, Rutgers University, Piscataway, NJ; <sup>2</sup>Environmental Science, New York Medical College, Valhalla, NY; <sup>3</sup>Environmental & Occupational Medicine, UMDNJ-Robert Wood Johnson Medical School, Piscataway, NJ.

Sulfur mustard (SM, bis (2-chloroethyl) sulfide) and nitrogen mustard (NM, mechlorethamine) are cytotoxic vesicants that can cause ocular injury. The cornea is particularly sensitive, developing opacity and ulcerations following SM exposure. In these studies we used an air-liquid interface (air lifted) organ culture model in which vesicants are applied directly to the central cornea to assess mustard-induced oxidative stress. Three and six hr post treatment (100 nmol NM in 10  $\mu$ l PBS), the corneal epithelial layer was found to express proteins containing the lipid peroxidation product 4-hydroxynonenal (4-HNE). This was associated with expression of the antioxidant hemeoxygenase-1 (HO-1). To assess molecular mechanisms underlying this response, we analyzed the effects of 4-HNE on human corneal epithelial cells (HCEC) in culture. 4-HNE (0.03 mM) was found to cause a time-dependent induction of HO-1 mRNA and protein; optimal expression of the enzyme was evident after 10 hr. HO-1 is known to be regulated by both MAP kinases and phosphatidylinositol (PI)-3 kinase (PI3K)/Akt signaling. Treatment of corneal cells with a p38 MAP kinase inhibitor (SB203580, 10  $\mu$ M) blocked upregulation of HO-1 protein by 4-HNE. Inhibitors of the MAP kinases Erk1/2 (PD98059, 10 $\mu$ M) and JNK (SP600125, 20 $\mu$ M), and PI-3K (Wortmannin, 100 nM), partially suppressed HO-1 expression. These data indicate that NM is an effective inducer of oxidative stress in corneal epithelial cells, as measured by the formation of 4-HNE protein adducts. Moreover, induction of HO-1 is regulated by 4-HNE in a process dependent on MAP kinase and PI3K/Akt signaling. Countermeasures that target oxidative stress may be effective countermeasures for SM-induced corneal injury. Supported by NIH grant U54AR055073.

**PS 2031 Isoniazid-Induced Cellular Challenge in HL-60 Cells: An In-Depth Proteomic Perspective.**

M. R. Khan<sup>1</sup>, A. Baghdasarian<sup>1</sup>, R. P. Fahlman<sup>2</sup> and A. Siraki<sup>1</sup>. <sup>1</sup>Pharmacy & Pharmaceutical Sciences, University of Alberta, Edmonton, AB, Canada; <sup>2</sup>Biochemistry, University of Alberta, Edmonton, AB, Canada.

**INTRODUCTION:** Isoniazid (INH) is the first line therapy to combat tuberculosis. However, its use is associated with potent clinical toxicity, particularly liver damage. However, the rare but important side-effect of INH-induced agranulocytosis is an idiosyncratic drug reaction for which the toxicity mechanism is unclear. Since INH forms various reactive metabolites, we hypothesized that intracellular protein modification by INH could reveal a possible mechanism of INH-induced agranulocytosis. **METHODS:** HL-60 (promyelocytic leukemia) cells were used for these studies. Trypan Blue exclusion was performed for cytotoxicity. Immunoblot assays were conducted by using anti-INH and anti-DMPO antibodies to identify INH-covalently bound proteins and INH-induced protein radicals, respectively. Later, these modifications were confirmed by MALDI-TOF MS. For quantitative proteomics, we performed SILAC (stable isotope labelling by amino acids in cell culture). **RESULTS:** 5 mM INH had no significant cytotoxicity after 48 hrs. Anti-DMPO (protein radicals) showed a prominent protein radical at 50 kDa, however,

multiple INH covalent protein adducts were found by anti-INH immunoblotting. In SILAC experiments, we found changes in 101 proteins (very high confidence limits) of which 38 were upregulated and 63 were downregulated. We observed a significant down regulation of ribosomal proteins, transcriptional factors and splicing factors. But at the same time, factors associated with protein stability were up-regulated. Pro-apoptotic signals were counterbalanced by anti-apoptotic signals, and cell growth factors were upregulated. **CONCLUSION:** Our result showed that INH is acutely non-toxic to HL-60 cells, and is unlikely to possess direct toxicity to neutrophils or bone marrow precursors. INH treatment appeared to induce cellular energy conservation through downregulation of protein synthesis and enhanced protein stability. Further pathways will be elucidated once INH-induced protein radicals and covalent adducts are identified.

**PS 2032 Attenuation of Experimental Retinopathy of Prematurity by Vitamin A in the Newborn Rat.**

X. Courouclis<sup>1</sup>, Y. Liang<sup>1</sup>, G. Zhou<sup>2</sup>, W. Jiang<sup>1</sup> and B. Moorthy<sup>1</sup>. <sup>1</sup>Pediatrics, Baylor College of Medicine, Houston, TX; <sup>2</sup>Institute of Biosciences and Technology, Texas A&M University Health Science Center, Houston, TX.

Supplemental oxygen administration is frequently encountered in the treatment of premature infants suffering from respiratory distress. However, hyperoxia contributes to the development of chronic lung disease [bronchopulmonary disease (BPD)] and retinopathy of prematurity (ROP). In this investigation, we tested the hypothesis that exposure of newborn rats to vitamin A and hyperoxia would attenuate retinopathy and abnormal neovascularization compared to those exposed to hyperoxia alone. Newborn Fisher 344 rats were maintained in room air or exposed to hyperoxia ([gt] than 95% O<sub>2</sub>) for 7 days. Some animals were treated i.p. with vitamin A [2 mg/kg], once daily for the first 5 days of hyperoxic exposures. Animals were sacrificed at selected time points after termination of hyperoxia. Retinal vascular densities of flat mounted retinas were assessed. Protein expression of HIF-1 $\alpha$  was determined by Western blotting. Oxidative DNA damage in retinal tissue was determined by 32P-postlabeling. Immediately after 7 days of exposure to hyperoxia alone, we observed constricted retinal vessels, compared to those given vitamin A + hyperoxia. Seven to thirty days after termination of hyperoxia alone, the animals displayed formation of abnormal retinal vessels and capillaries, compared to the vitamin A + hyperoxia group. At the 7 day time point, the HIF-1 $\alpha$  protein expression in the hyperoxia + vitamin A group was much higher than the hyperoxia alone group. On the other hand, at later time points, the HIF-1 $\alpha$  protein levels were higher in the hyperoxia group. Interestingly, oxidative DNA adducts were significantly decreased in the retinas of animals given vitamin A + hyperoxia. Our study supports the hypothesis that vitamin A protects retina from oxygen-induced abnormal neovascularization, and this is the first report that shows oxidative DNA damage to contribute to experimental ROP.

**PS 2033 Systemic Nerve Growth Factor Modulates the Transcription of Amino Acid Transporters and Glutathione (GSH) Synthesis in Mice Striatum.**

C. Valdovinos-Flores and M. E. Gonssebatt. Universidad Nacional Autonoma de Mexico, Mexico City, Mexico.

Nerve growth factor (NGF) is a member of structurally related proteins, named neurotrophins (NTs), that regulate neuronal survival, development, function, and plasticity. Moreover, NGF is an important activator of antioxidant mechanisms. These functions of NGF are mediated by the tropomyosin-related kinase receptor A (TrkA). There is evidence that NTs and their receptors are expressed also in visceral tissues. Physical exercise and stress increase levels of NGF in plasma. Using a murine model we have shown that systemic inhibition of GSH synthesis with L-buthionine-S-R-sulfoximine (BSO) increased brain GSH content and induced the transcription of ngfb in liver. Murine striatum cholinergic neurons express TrkA receptors thus, we investigated if an i.p. injection of BSO or of sodium arsenite (iAs) modulate the transcription of ngfb and trka as well TrkA phosphorylation in mice striatum. Both agents induced the activation of the NGF/TrkA pathway which correlated with an increased transcription of xCT, LAT1, EAAC1 amino acid transporters system genes that provide L-cys / L-cys2 to central nervous system and of GCLm which participates in the de novo synthesis of GSH. The inhibition of TrkA phosphorylation by K252a or anti-NGF neutralizing antibody abrogated the BSO and iAs induced transcription of xCT, LAT1, EAAC1 and GCLm suggesting the participation of this pathway in the *in vivo* antioxidant response at least in striatum. Furthermore, since anti-NGF neutralizing antibodies would not cross the blood-brain barrier, our results suggest that NGF functions as a systemic redox-sensor in both CNS and peripheral tissues and that the NGF/TrkA pathway plays a critical role in the antioxidant response in the striatum in our murine model. Supported by CONACYT 102287

**PS 2034 HMGB1 Mediates Hyperoxia-Induced Impairment of *Pseudomonas aeruginosa* Clearance and Inflammatory Lung Injury in Mice.**

V. S. Patel<sup>1</sup>, R. Sitapara<sup>1</sup>, A. Gore<sup>1</sup>, B. Phan<sup>1</sup>, L. Sharma<sup>1</sup>, V. Sampat<sup>1</sup>, J. Li<sup>2</sup>, H. Yang<sup>2</sup>, S. Chavan<sup>2</sup>, H. Wang<sup>2</sup>, K. Tracey<sup>2</sup> and L. Mantell<sup>1,2,3</sup>.

<sup>1</sup>Pharmaceutical Sciences, Saint John's University, Fresh Meadows, NY; <sup>2</sup>Center for Inflammation and Immunology, The Feinstein Institute for Medical Research, North Shore-LIJ Health Science, Manhasset, NY; <sup>3</sup>Center for Heart and Lung Research, The Feinstein Institute for Medical Research, North Shore-LIJ Health Science, Manhasset, NY.

Mechanical ventilation with supraphysiological concentrations of oxygen (hyperoxia) is routinely used to treat patients with respiratory distress. However, a significant number of patients on ventilators have enhanced susceptibility to infections and develop ventilator-associated pneumonia (VAP). *Pseudomonas aeruginosa* (PA) are one of the most common bacteria found in these patients. Previously, we demonstrated that prolonged exposure to hyperoxia can compromise the ability of alveolar macrophages (AM), an essential part of the innate immunity, to phagocytose PA. The objective of this study was to investigate potential molecular mechanisms underlying hyperoxia-compromised innate immunity against bacterial infection in a mouse model of PA pneumonia. Here, we show that exposure to hyperoxia ( $\geq 99\%$  O<sub>2</sub>) led to a significant elevation in levels of airway HMGB1 and an increased mortality in C57BL/6 mice infected with PA. Treatment of these mice with neutralizing anti-HMGB1 monoclonal antibody (mAb) resulted in a reduction in bacterial counts, injury, and number of neutrophils in the lung and an increase in leukocyte phagocytic activity compared to mice receiving control mAb. This improved phagocyte function was associated with reduced levels of airway HMGB1. The correlation between phagocytic activity and levels of extracellular HMGB1 was also observed in cultured macrophages. These results indicate a pathogenic role for HMGB1 in hyperoxia-induced impairment in host ability to clear bacteria and inflammatory lung injury. Thus, HMGB1 may provide a novel molecular target for improving hyperoxia-compromised innate immunity in patients with VAP.

**PS 2035 Exposure to Perfluorooctanoic Acid (PFOA) Causes Oxidative Stress in the Mouse Pancreas.**

Q. Wu, A. A. Bond, L. M. Kamendulis and B. A. Hocevar. *Environmental Health, Indiana University School of Public Health, Bloomington, IN.*

Perfluorooctanoic acid (PFOA), a perfluoroalkyl compound used in the manufacture of many industrial and commercial products, does not readily decompose in the environment, and is biologically persistent in fish, animals and humans. Human exposure to PFOA occurs through both environmental and occupational exposures. Due to the long half-life of PFOA in humans (3.8 yrs), the potential exists for PFOA exposure to participate in chronic diseases. Chronic PFOA exposure in rodents induces pancreatic acinar cell tumors (PACTs), and human epidemiologic studies also suggest that PFOA exposure may have adverse effects on the pancreas. While multiple animal studies have examined PFOA-mediated liver toxicity, very little is known about the effects of PFOA on pancreatic function. To assess the role of PFOA on the pancreas, we treated C57BL/6 mice with vehicle, or PFOA at doses of 0.5, 2.5 or 5.0 mg/kg BW/day for 28 days. In addition, mice were treated with cerulein, which induces mild pancreatitis and produces an oxidative stress in the pancreas. We found significant accumulation of PFOA in the serum, liver and pancreas of PFOA treated animals, which was associated with induction of oxidative stress, as measured by the lipid peroxidation products malondialdehyde and F2 $\alpha$ -isoprostanes, as well as the oxidatively modified DNA base, 8OHdG. The serum, liver and pancreatic ratio of reduced to oxidized glutathione decreased with increased PFOA dose, again indicating the stimulation of oxidative stress in the liver and pancreas. For both of these responses, the pancreas was more severely affected in comparison to the liver. As a further response to oxidative stress, induction of anti-oxidant genes was also evaluated. While mitochondrial superoxide dismutase mRNA levels were induced to comparable levels in both liver and pancreas, the pancreas failed to upregulate either glutathione peroxidase or catalase genes. These results suggest that the pancreas may be highly susceptible to oxidative damage elicited by exposure to perfluoroalkyl compounds.

**PS 2036 Chronic Over-Expression of Receptor Tyrosine Kinase ErbB2 in the Heart Alters Redox-Sensitive Molecules in the Mitochondria.**

F. Belmonte<sup>1,2</sup>, S. Das<sup>3</sup>, V. Sivakumaran<sup>3</sup>, P. Sysa Shah<sup>2</sup>, C. Steenbergen<sup>3</sup> and K. Gabrielson<sup>2</sup>. <sup>1</sup>Environmental Health Sciences-Molecular and Translational Toxicology, Johns Hopkins University, Baltimore, MD; <sup>2</sup>Molecular and Comparative Pathology, Johns Hopkins University, Baltimore, MD; <sup>3</sup>School of Medicine, Johns Hopkins University, Baltimore, MD.

Previous studies on cardiac-specific over-expression of epidermal growth factor receptor 2 (ErbB2) demonstrated that ErbB2 activates protective signaling pathways (pro-survival) and induces a hypertrophic phenotype that does not progress to heart failure. To explore this interesting phenomenon, we used the ErbB2 transgenic murine model to determine whether the observed phenotypes are due to redox-sensitive molecules in the mitochondria that alter mitochondrial function by regulating reactive oxygen species (ROS) formation. Microarray data that compare the transgenic mice to wild type mice suggest that ErbB2 alters various oxidative stress genes. We found that ErbB2 over-expression in the heart upregulates glutathione reductase (Gsr), glutathione peroxidase 1 (Gpx1), and peroxiredoxin 5 (Prdx5) proteins. We measured ROS production and found that the transgenic mitochondria produce less ROS than the wild type mitochondria. Total glutathione (GSH) levels and glutathione peroxidase activity are higher in the transgenic mice compared to the wild type group. We measured the mitochondrial Ca<sup>2+</sup> retention capacity and found that the transgenic group has less Ca<sup>2+</sup> uptake than the wild type group. The mitochondrial membrane potential ( $\Delta\Psi$ ) was measured with the fluorescent dye tetramethylrhodamine ethyl ester (TMRE) and we found that the transgenic group has a higher baseline  $\Delta\Psi$  than the wild type group. Our data suggest that ErbB2 over-expression alters redox-sensitive genes that regulate ROS production through pro-survival and mitochondrial pathways to ultimately prevent heart failure.

**PS 2037 The Role of NO and the Glutathione Pathway in Menadione-Induced Oxidative Stress.**

P. Venkatakrishnan, B. Masters and L. J. Roman. *Biochemistry, UTHSCSA, San Antonio, TX.*

Skeletal muscle cells undergo frequent oxidative challenges due to rapid changes in energy demand, high metabolic activity, and high levels of heme-proteins. The induction of oxidative stress and resulting protective responses involves many pathways. Among them are the products of oxygen metabolism by flavoproteins, hemo-proteins, Fe-S-center-containing proteins and other oxidation-reduction centers. Nitric oxide synthases (NOSs) reduce redox-cycling compounds such as menadione (MD), forming superoxides, which in the presence of nitric oxide (NO) reacts to form peroxynitrite, both of which cause oxidative injury. Therefore, we examined the mechanistic role of NO for cell survival during MD-induced oxidative stress under NOS inhibition using a NOS inhibitor, L-NAME. Dose viability studies performed with various amounts of MD +/- L-NAME for 24 hrs allowed us to choose 10  $\mu$ M MD for further studies and also showed that NOS inhibition did not significantly affect the cell viability at any concentration. Increased nNOS protein expression and increased 3-nitrotyrosine formation, a biomarker for peroxynitrite formation was observed with MD and MD + L-NAME over the controls alone by both Western blotting and Immunocytochemistry, suggesting that the cells compensate for decreased bioavailable NO by increasing nNOS. We examined the major antioxidant involved in cellular protection mechanism at 24 hours. Glutathione peroxidase1 protein levels was decreased with MD+L-NAME treatment which was reversed in the presence of NO donor deta-NONOate with MD+L-NAME. On the other hand, SOD1 and PRDX6 levels remain unchanged. Interestingly, at 24 hrs, GSH assays and stable isotope labeling of amino acids with cell culture along with LC-MS analysis also reveal that proteins in glutathione homeostasis are modulated by NO under oxidative stress as a mechanism of cell survival. Current studies are aimed to dissect the relationship between NO and glutathione under MD-induced oxidative stress.

**PS 2038 Synthesis and Crystal Structure of N-Acetyl-5-Chloro-3-Nitro-L-Tyrosine Ethyl Ester.**

T. T. Mutahi<sup>1</sup>, B. J. Edagwa<sup>2</sup>, F. R. Fronczek<sup>2</sup> and R. M. Uppu<sup>1</sup>. <sup>1</sup>Environmental Toxicology, Southern University and A&M College, Baton Rouge, LA; <sup>2</sup>Chemistry, Louisiana State University, Baton Rouge, LA.

3-Nitro-L-tyrosine and 3-chloro-L-tyrosine are widely regarded as markers of peroxynitrite (PN) and HOCl formation (respectively) *in vivo*. A question that follows naturally but never addressed in detail is what happens when PN and HOCl that are co-produced at the inflammatory sites react simultaneously with tyrosine

residues in proteins. The significance of these combined oxidations on the issue of biomarker validation could be overwhelming given the report by Whiteman and Halliwell (*Biochem. Biophys. Res. Commun.* 258,168–172,1999) wherein it was shown that the 3-nitro-L-tyrosine was lost to some unknown product(s) following oxidation with HOCl. Another important consequence could be that we need additional biomarkers and their validation. Herein, we report the synthesis and characterization of the oxidation product of HOCl reaction with N-acetyl-3-nitro-L-tyrosine ethyl ester (NANTEE), a model for protein-bound 3-nitro-L-tyrosine. When HOCl was a limiting reagent (HOCl < NANTEE), the major product at pH 7.2 was found to be N-acetyl-5-chloro-3-nitro-L-tyrosine ethyl ester (NACNTEE). Following purification (reversed phase HPLC) and characterization (<sup>1</sup>H-NMR; 400 MHz, CD<sub>3</sub>OD: δ 1.23 (t, J = 7.1 Hz, 3H), 1.92 (s, 3H), 2.92 (dd, J = 14.1, 8.7 Hz, 1H), 3.12 (dd, J = 14.1, 5.8 Hz, 1H), 4.16 (q, J = 7.0 Hz, 2H), 4.63 (dd, J = 8.6, 5.8 Hz, 1H), 7.60 (d, J = 2.1 Hz, 1H), 7.86 (d, J = 2.1 Hz, 1H), 8.43 (s, 1H)), single crystals of NACNTEE obtained in methanol were used for the determination of crystal structure using KappaCCD (charge-coupled device) diffractometer. It was found that the OH group forms an intramolecular O—H...O hydrogen bond to the nitro group and the N—H group forms an intermolecular N—H...O hydrogen bonds to an amide O atom, linking the molecules into chains along [1 0 0]. The crystal studied was a non-merohedral twin, with a 0.907 (4):0.093 (4) domain ratio. [Support from NSF (HRD-1043316) and the US DoED (PO31B040030) is acknowledged. Corresponding author's email: rao\_uppu@subr.edu].

### PS 2039 Oxidative Stress Mediates Chlorpromazine-Induced Cholestasis in Human HepaRG Cells.

A. Guilloze<sup>1</sup>, S. Antherieu<sup>1</sup>, P. Bachour-El Azzi<sup>1,2</sup>, J. Dumont<sup>1</sup>, Z. Abdel-Razzak<sup>2</sup>, C. Guguén-Guilloze<sup>1</sup>, B. Fromenty<sup>1</sup> and M. Robin<sup>1</sup>. <sup>1</sup>Inserm 991, University of Rennes, Rennes, France; <sup>2</sup>Lebanese University, EDST-PRASE and EDST-AZM Center-LBA3B, Hadath, Lebanon.

Intra-hepatic cholestasis represents a frequent manifestation of drug-induced liver injury in humans. However, the mechanisms involved are diverse and remain poorly understood. Early hepatic effects of chlorpromazine (CPZ), known for years to induce intra-hepatic cholestasis, have been analyzed using differentiated human HepaRG cells. Bile acids (BA) efflux was found to be inhibited as early as after 30min-CPZ treatment as shown by [H<sup>3</sup>]-taurocholic acid (TA) intracellular accumulation. This accumulation seemed to be mediated by reactive oxygen species generated by CPZ since it was mostly prevented by N-acetyl cysteine co-treatment. In addition, CPZ-induced ROS generation was accompanied by a disruption of the pericanalicular distribution of F-actin as well as an alteration of the inner mitochondrial membrane potential. Following 24 hour-treatment, CPZ inhibited the expression of the two main canalicular bile transporters BSEP and MDR3. Moreover, NTCP mRNA and activity as well as CYP8B1 mRNA were inhibited, while MRP4 was overexpressed. These alterations indicate that BA uptake and synthesis were decreased, whereas basolateral transport was enhanced. These alterations likely represent hepatoprotective mechanisms against BA toxicity. These data support the conclusion that among other mechanisms, oxidative stress plays a major role as both a primary causal and an aggravating factor in early CPZ-induced intra-hepatic cholestasis in human hepatocytes (This work was supported by the European Community, Contracts LIINTOP-STREP-037499 and Predict-IV-202222).

### PS 2040 Evaluation of Thiotaurine for Effects against Ethanol-Induced Oxidative Stress in the Presence and Absence of Inhibitors of Ethanol Metabolism in the Rat.

M. C. Parikh, Y. Shen and C. A. Lau-Cam. *Pharmaceutical Sciences, St. John's University, Jamaica, NY.* Sponsor: B. Blase.

The present study was undertaken to verify the in vivo effects of thiotaurine (TTAU), a sulfane compound reported to exhibit antiradical activity in vitro, against ethanol (EtOH)-induced oxidative stress. For this purpose, TTAU was given to male Sprague-Dawley rats (200–250 g) as a single, 2.4 mmol/kg, intraperitoneal (i.p.) dose 30 min before an oral, 4 g/kg, dose of EtOH (40% w/v). The same experiments were carried out with rats treated with the alcohol dehydrogenase inhibitor 4-methylpyrazole (4MP, 75 mg/kg, i.p.) and the aldehyde dehydrogenase inhibitor cyanamide (CYN, 60 mg/kg, i.p.), administered 30 min and 60 min, respectively, before EtOH. Control animals received only physiological saline. All the rats were sacrificed by decapitation at 1 hr after EtOH administration, and their blood and livers were collected for the assay of plasma and hepatic levels of malondialdehyde (MDA) and reduced (GSH) and oxidized (GSSG) glutathione and of corresponding activities of the antioxidant enzymes catalase (CAT), glutathione peroxidase (GPx) and superoxide dismutase (SOD). EtOH elevated the plasma

(+34%) and liver (+32%) GSH, lowered the plasma (–65%) and liver (–63%) GSH/GSSG ratio, and lowered the corresponding activities of CAT (–86% and –77%, respectively), GPx (–91% and –70%, respectively) and SOD (–45% and –54%, respectively). Both CYN and 4MP attenuated the alterations caused by EtOH, with the latter compound appearing more potent than the former. In contrast, the GSH/GSSG ratio seen with ethanol was lowered further by CYN but raised by 4MP. TTAU was not only more protective than 4MP against EtOH-induced alterations in the liver and plasma but in its presence the protective actions of CYN and 4MP became enhanced. The present results indicate that EtOH metabolism to acetaldehyde and beyond influences oxidative stress by EtOH to a greater extent than EtOH itself, and that such an event can be effectively counteracted by TTAU.

### R 2041 Skeptically Examining the Limits of Toxicology Evidence in the Courtroom.

G. B. Corcoran<sup>1</sup>, J. Norman<sup>2</sup>, M. J. Saks<sup>3</sup>, S. Bobst<sup>4</sup> and R. T. Kennedy<sup>5</sup>.

<sup>1</sup>Pharmaceutical Sciences, Wayne State University, Detroit, MI; <sup>2</sup>ExxonMobil Biomedical Sciences, Annandale, NJ; <sup>3</sup>Sandra Day O'Connor College of Law, Arizona State University, Tempe, AZ; <sup>4</sup>Nexeo Solutions, The Woodlands, TX; <sup>5</sup>New Mexico Court of Appeals, Albuquerque, NM.

The opposing orientation of toxicology experts and select evidence can skew the accuracy and value of testimony in court. Lawyers and judges are acquiring increasing skills to evaluate technical and scientific assertions with skepticism. Scholarly scientific approaches are required to establish whether techniques and methods asserted to be scientifically sound are valid and support justice. An introduction briefly covers topics helpful to understanding what happens to experts in litigation. This includes the law's theory of expert evidence, rules of evidence and procedure relating to expert testimony, alternative admissibility rules (Frye v Daubert trilogy), the NRC report and Canadian parallels, a law-science syllogism, the adversary process in theory and practice, ethical principles, clashes of ethics, data (especially quantitative), disclosure of evidence helpful to the other side, and for whom the litigation expert works. The toxicology expert must address relevant science in a fair, representative manner and communicate effectively. The use of Bradford-Hill Criteria (1964) has been promoted to address general causation in toxic torts. While comprehensive, it poses challenges including jargon and communication. Recently, a five question approach was introduced to address specific causation. Explanations and examples of causation will be reviewed. Finally, the 2009 National Academies report recommends that forensic sciences look to academic scientific models for reliable practice and technique validation to support court testimony. Lawyers and courts have become more skeptical of unsupported opinions and increasingly aware of how to combat them. Academic toxicology can offer much to advance the legitimacy of admitted evidence, including in the area of forensics. A discussion will include foibles and solutions.

### IS 2042 Harnessing Electronic Standards and Informatics to Transform the Use of Regulatory Toxicological Data.

L. P. Myers<sup>1</sup>, L. Burns Naas<sup>2</sup>, T. Kropp<sup>1</sup>, A. Nanzer<sup>3</sup> and T. Smyrniotis<sup>4</sup>. <sup>1</sup>Center for Drug Evaluation and Research, US FDA, Silver Spring, MD; <sup>2</sup>Gilead Sciences, Inc., Foster City, CA; <sup>3</sup>F. Hoffmann-La Roche Ltd., Basel, Switzerland; <sup>4</sup>MPI Research, Inc., Mattawan, MI.

One of the major efforts in nonclinical regulatory informatics has centered on the development and testing of the electronic data submission standard, also called SEND (Standard for Exchange of Nonclinical Data). This standard was developed by the Clinical Data Interchange Standards Consortium's (CDISC) SEND Team for nonclinical data collected from animal toxicology studies and allows for the electronic submission of tabulated toxicology data in an electronic format. The initial pilot project began in 2003 and was followed by a second pilot in 2007 focused on CDER-regulated projects. The production of the SEND 3.0 Implementation Guide in 2011 was a major step forward for the electronic submission and exchange of standardized data and enablement of data warehousing efforts that better support scientific review and regulatory science initiatives. However, it is recognized that data standards are simply enablers to support the broader goals of better exploring and exploiting diverse study data and metadata in order to answer important scientific review and regulatory science questions. The range of needs and challenges in the regulatory pharmacology and toxicology field can be daunting but many of the challenges are shared among key stakeholders (e.g., the US FDA, sponsors, and CROs). These challenges, which range from warehousing to analysis to QA/GLP ramifications, are laying the foundation for a compliant exchange of data and opportunities for collaboration through public/private partnerships. This session will discuss the current computational science initiatives at the US FDA and in industry, existing partnerships, challenges and successes, as well as the transformative effect on the CRO model.

## EC 2043 Regulatory Science and Risk Assessment: Lessons for Early-Career Scientists on What to Expect and How to Pursue This Career Path.

B. J. Lew<sup>1</sup>, J. A. Torres<sup>2</sup>, D. L. Bjerke<sup>1</sup>, J. C. Lipscomb<sup>3</sup>, A. Maier<sup>4</sup> and D. Jacobson Kram<sup>5</sup>. <sup>1</sup>PS&RA, Procter & Gamble Company, Cincinnati, OH; <sup>2</sup>Environmental Toxicology, Texas Southern University, Houston, TX; <sup>3</sup>NCEA, US EPA, Cincinnati, OH; <sup>4</sup>Toxicology Excellence for Risk Assessment (TERA), Cincinnati, OH; <sup>5</sup>CDER, US FDA, Silver Spring, MD.

During academic training, postdoctoral and graduate students generally are not provided with opportunities for interacting with toxicologists who are involved in risk assessment and regulatory affairs. The educational training mainly focuses on basic sciences or solving mechanistic problems and thus lacks the practical aspects of risk assessment and regulatory preparation. This concern was discussed at the Education Summit in October 2011, which was organized by the Education Committee of the SOT. Dr. John Doull's comment that, "toxicology is what we do, but risk assessment is why we do it," shows the importance for trainees to become aware of both. Unfortunately, when it is time for the trainee to make the decision on what will be the next step in their careers, they are well prepared on what we do, but fall short on why we do it. The objectives of this session are to provide postdoctoral and graduate students with basic understanding of approaches in risk assessment and regulatory affairs in some of the sectors and to educate them about necessary preparative steps in this field. In this 80-minute Education-Career Development Session, trainees will become more familiar with the routine job of toxicologists outside of the academic setting. Further, there will be a panel discussion on steps that can be taken during graduate school and postdoctoral training to improve the preparation for a career in risk assessment and regulatory fields. Thus, the participants are expected to gain a basic knowledge of risk assessment and regulatory preparation in the life of a toxicologist and how to pursue this field.

## PS 2044 Surgical Alternatives for Multiple CSF Sampling in Conscious Cynomolgus Monkeys: A Novel Approach.

J. Sternberg, S. H. Korte and C. B. Rose. Covance Laboratories GmbH, Muenster, Germany. Sponsor: G. Weinbauer.

Intrathecal infusion via the lumbar route represents an accepted while specialized clinical route for drug delivery in humans. Since primates are often required as relevant species for pre-clinical safety assessment, this dose route is well established in cynomolgus monkeys. However, for the majority of these studies, CSF (cerebrospinal fluid) for bioanalysis, clinical chemistry as well as cell counts needs to be collected at multiple time points within few days. Sampling using spinal needle (Pencan Paed®: 25G, 50 or 25 mm, B. Braun Melsungen AG, Melsungen, Germany) on sedated animals (Ketamin and Domitor; Antisedan as antidote) is limited to three occasions within the first 24 hours, hence limiting the ability for a detailed evaluation. In this study, three female cynomolgus monkeys (~3.5 kg) where implanted (L2-L3) using MID-LOVOL port (Solomon Scientific, USA), connected to a 3FR intrathecal PU catheter. To compare our established technique of s.c. port placement under the shoulder blade, the MID-LOVOL port was implanted in the established way (animal A), in the thoraco-lumbar region (animal B) and in the region of the sacrum (animal C). To ensure the patency of the system it was flushed every three days with 0.5 ml artificial CSF beginning on the day of surgery. On day 14, 17, 20 and 23 after surgery a Huber needle was used for CSF collection, while the animals were placed in a restraint chair. There were no adverse clinical signs, body weight changes, clinical pathology or neurological findings directly after surgery in all three animals. Successful CSF collection could only be performed in animal C. The port position of this animal proved to be an advantage for needle insertion/fixation hence CSF collection in the restraint chair. In conclusion, port implantation under the shoulder blade, in the thoraco-lumbar region as well as in the region of the sacrum is possible.

## PS 2045 Hydration with Saline Decreases Toxicity of Calcitriol-Injected Mice in Preclinical Studies.

A. Azari, M. Kanavi, S. Darjatmoko, V. Lee, H. Potter, L. Teixeira and D. Albert. Ophthalmology, University of Wisconsin Madison, Madison, WI.

Purpose: To study the effectiveness of saline injection in reducing the toxicity profile of calcitriol when coadministered in mice.

Design: Meta-analysis of published mice studies with calcitriol.

Methods: A comprehensive PubMed and ISI web of knowledge search was performed to identify all published case control articles of calcitriol injection in mice, and relevant articles were selected. Using mortality as an end point to study the toxic effects of calcitriol, the relative risk of mortality in mice given saline injections was evaluated for different calcitriol dosages, as well as mouse and tumor types.

Results: Coadministration with 0.25 ml of normal saline solution injected intraperitoneally is associated with a lower mortality rate than calcitriol given alone. The calculated relative risk of mortality was 0.1419 (95% CI 0.0093-2.2133, z-statistic 1.393, p-value = 0.1636) when saline is administered with calcitriol compared to calcitriol alone.

Conclusions: Hydration with saline is a common practice in patients receiving calcitriol, which appears to be pertinent in experimental studies of mice receiving calcitriol. It is important to note that results of preclinical studies form the basis for decisions in drug use in patient trials. Decreasing mortality in animal experiments will prove to be a meaningful contribution to the field of research. To avoid some mortality due to toxicity, a common practice for investigators was administering less than the target doses or even skipping doses in order to decrease calcitriol induced mortality in mice. Combination of high mortality in mice and administration of suboptimal dose in certain situations may impede evaluation of the potential therapeutic effects of calcitriol. The same problem is likely to exist with other drugs as well (e.g., chemotherapeutic agents). This preliminary data indicates that supplemental hydration should be kept in mind in evaluating drug toxicology.

## PS 2046 Identification of Behaviorally Active Doses of Morphine and Evaluation of Its Analgesic Effects in the Rhesus Monkey.

T. Wolinsky<sup>1</sup>, C. Cruz<sup>2</sup>, I. Hubert<sup>2</sup>, G. Froget<sup>1,2</sup>, M. Lemaire<sup>1</sup> and D. Virley<sup>1,2</sup>. <sup>1</sup>Porsolt SAS, Le Genest-St-isle, France; <sup>2</sup>Porsolt Inc. USA, San Antonio, TX.

Pain affects millions of people worldwide and is commonly treated with opioid analgesics, despite considerable safety/risk management concerns. The purpose of this study was two-fold: First, to establish a therapeutic index for morphine by determining the behaviorally active range in an operant responding procedure and second, to work within this dose range to evaluate the analgesic effects of morphine in the rhesus monkey (*Macaca mulatta*) in a thermal pain tail withdrawal procedure.

For the operant responding procedure, 2 monkeys were trained to lever-press for food on a fixed-ratio (FR30) schedule. The sessions lasted 120 minutes (8 cycles of 15 minutes) during which the rate of responding was recorded. Acute doses of morphine sulfate (0.3 – 3 mg/kg s.c.) were administered at the beginning of the session. For the tail withdrawal procedure, 4 monkeys were seated in restraint chairs and the lower section of the shaved tail was immersed into water at 40, 50, and 55 °C. Sessions began with a control tail withdrawal latency determination at each temperature followed by an acute dose of morphine sulfate (0.3 – 3 mg/kg s.c.). Temperatures were presented to the animals in a randomized order at 15, 30, 60, 90 and 120 minutes post-dose.

Morphine markedly decreased the rate of operant responding at 1 mg/kg and eliminated lever-pressing at 3 mg/kg. Analgesic effects of morphine in the tail-withdrawal assay were observed at all doses tested: The onset and duration of action were dose-dependent. The minimum effective dose was found to be 0.3 mg/kg, while 3 mg/kg produced the maximal effect in all 4 animals tested.

These results suggest that acute morphine has a narrow therapeutic index in the rhesus monkey. The selected behavioral test procedures could therefore provide appropriate efficacy and safety measures for assessing novel opioid and non-opioid based analgesics with high translational validity and relevance.

## PS 2047 Pharmacodynamic Glycemia Effects from Rapid and Long-Acting Insulins Administered at Mealtime to Alloxan-Induced Diabetic Miniature Yucatan Swine.

L. D. Brown<sup>1,2</sup>, T. J. Madsen<sup>1</sup>, E. C. Blair<sup>1</sup>, B. C. Hanks<sup>1,2</sup>, K. P. Horlen<sup>1</sup>, J. Hiemstra<sup>2</sup>, A. Stricker-Krongrad<sup>1</sup>, J. Liu<sup>1</sup> and G. F. Bouchard<sup>1,2</sup>. <sup>1</sup>Sinclair Research Center, LLC, Columbia, MO; <sup>2</sup>Sinclair BioResources LLC, Auxvasse, MO.

Pharmacodynamic effects from various insulins with known properties in humans were studied in the Yucatan miniature swine for comparative purposes. Yucatan miniature swine (*Sus scrofa*, at least 3 months, 20-60 kg) were made diabetic with intravenous alloxan and regulated on insulin. Animals were considered diabetic if they became hyperglycemic ( $\geq 150$  mg/dL) within 2-5 days following induction. All procedures were on overnight fasted animals (no feed or insulin for 18 hrs). Our diabetic miniswine average baseline bG of  $429 \pm 84.5$  (SD) mg/dL (N=148 measurements) while non-diabetics average  $58.7 \pm 8.2$  (SD) mg/dL (N=238 measurements). For this study, well-known prototypical marketed insulins (Apidra<sup>TM</sup>, Humalog<sup>TM</sup>, Lantus<sup>TM</sup>, 0.25 or 0.45 U/kg s.c.) were administered at mealtime, then blood glucose profiles recorded using handheld glucometer devices (One Touch Ultra<sup>®</sup>, Lifescan) over the next 8 hrs (rapid-acting) or 24 hrs (long-acting). Venous blood samples were collected from vascular access ports for bG readings. Blood glucose profile data in the diabetic Yucatan generally compared well to published human glucodynamic data for glycemia effects following insulin. These data suggest the Yucatan diabetic model has similar pharmacodynamic responses to the presentation of exogenous insulins for onset and peak effects but not duration for the rapid-acting insulins. The long-acting insulin (Lantus<sup>TM</sup>) peaked in swine

where no peak (same action throughout day) is normally reported in humans. These differences could be due to either the duration of the fasting, the relative high doses of insulin or the use of a small number of animals in this study.

#### **PS 2048 Toxicity Mechanisms of Anti-Inflammatory Kinase Inhibitors.**

E. Berg, M. A. Polokoff, A. O'Mahony, J. Melrose and D. Nguyen. *BioSeek LLC, South San Francisco, CA.* Sponsor: K. Houck.

Improving the safety of drug candidates that enter clinical development requires assays that are more predictive of human outcomes. The BioMAP® platform uses human primary cells to model complex aspects of disease and tissue biology and can be applied to better understand biological mechanisms that underlie drug adverse effects. Here we present the analysis of several anti-inflammatory kinase inhibitors, including inhibitors of p38 MAPK, Jak kinase (tofacitinib) and Syk kinase (fostamatinib) tested in a panel of 12 BioMAP® systems covering a broad range of human biology. Specific effects of these compounds in BioMAP® assays modeling aspects of wound healing and vascular biology appear to correlate with certain side effects of these drugs in patients, including skin rash (p38 MAPK), gastrointestinal perforations (Jak), and hypertension (syk). These *in vitro* effects may be useful in screening lead candidates prior to testing in animals or humans.

#### **PS 2049 Evaluation of PBPK Models for Medical Decision Making upon Acute Chemical Exposure: Dichloromethane (DCM) As an Example.**

R. Z. Boerleider<sup>1,2</sup>, C. C. Hunault<sup>1</sup>, J. C. van Eijkeren<sup>3</sup>, I. de Vries<sup>1</sup>, J. G. Bessems<sup>3</sup> and J. Meulenbelt<sup>1,2</sup>. <sup>1</sup>National Poisons Information Center, University Medical Center Utrecht, Utrecht, Netherlands; <sup>2</sup>IRAS, Utrecht University, Utrecht, Netherlands; <sup>3</sup>RIVM, National Institute for Public Health, Bilthoven, Netherlands.

**Rationale:** Assessing the risks of exposure to hazardous chemicals in emergency situations and decision-making on individual medical treatment is not straightforward. We therefore evaluated the use of physiologically based pharmacokinetic (PBPK) models in this context, taking DCM as an example. DCM is toxic by inhalation and can cause mild to serious health effects.

**Methods:** In a clinical trial approved by the Hospital Medical Ethical Board, six healthy volunteers were individually exposed to DCM for 1 hour. The volunteers had to apply a paint stripper to a surface without air mask, in a closed room. Eighteen blood samples were drawn ( $t = -1$  to 48h post-dose). Whole blood DCM concentrations and percentages of carboxyhemoglobin (% HbCO) were measured using GC. The DCM air concentration in the room was continuously monitored by a Miran 1B2 infrared spectrophotometer. Experimental blood DCM concentrations and % HbCO were subsequently compared to the predictions of a previously published PBPK DCM model.

**Results:** The DCM external dose (area under the exposure-time curves) ranged between 175 and 390 ppm\*h (equal to 608 - 1354 mg\*h/m<sup>3</sup>). DCM blood concentrations reached maximum levels at the end of the exposure ( $t = 1$ h) and ranged between 0.25 and 5.1 mg/L. Increase in % HbCO was delayed (maxima reached between 2 and 6 h) and ranged between 0.4 and 2.3 %. The predicted DCM blood concentration ranged between 1.55 and 4.20 mg/L at  $t = 1$  h and the predicted % HbCO ranged between 3.1 and 4.1 % at  $t > 1.5$  h. The general form of the concentration-time profiles was well predicted, especially in the elimination phase of DCM from blood.

**Conclusion:** The model was found to fit experimental DCM blood concentrations reasonably well but should be refined for % HbCO. Such a PBPK model might be helpful in case many individuals are acutely exposed to DCM and for whom HbCO monitoring is not available.

#### **PS 2050 Specificity Protein (Sp) 1 Transcription Factor Modulates Long Noncoding RNA Expression in Liver Cancer Cells.**

S. Gandhi<sup>1,2</sup> and S. H. Safe<sup>2,3</sup>. <sup>1</sup>College of Medicine, Texas A&M College of Medicine Health Sciences Center, Houston, TX; <sup>2</sup>Institute of Biosciences and Technology, Texas A&M College of Medicine Health Sciences Center, Houston, TX; <sup>3</sup>Department of Veterinary Physiology and Pharmacology, Texas A&M College of Medicine Health Sciences Center, Houston, TX.

Hepatocellular carcinoma is one of the most prevalent forms of cancer worldwide and it exhibits highly invasive and metastatic properties. Recent studies have shown that of the small proportion of the genome that is transcribed only about 1.4% encodes for protein-coding genes. Of the remaining vast majority of transcripts that do not encode protein, long noncoding RNAs (lncRNAs) have recently gained attention because of their pivotal role in disease. lncRNAs are a class of transcripts

longer than 200 nucleotides and have been characterized as having both tumor suppression and oncogenic functions in many types of cancers. Although their mechanisms of action remain largely unknown, many lncRNAs are regulated by transcription factors in a tissue-specific manner. Specificity protein (Sp) transcription factors Sp1, Sp3, and Sp4 are overexpressed in many tumors, and regulate expression of genes required for cancer cell and tumor growth, survival, angiogenesis, and inflammation. Sp proteins are the targets of many conventional and alternative chemotherapeutic drugs, and therefore further study of their functions is of great interest. In this study, we examined the role of Sp transcription factors in regulating lncRNAs in liver cancer cells. Using HepG2 and Huh-7 cells as models, we investigated the effects of Sp downregulation on the expression of several lncRNAs as well as cell growth and survival. Downregulation of Sp transcription factors by RNA interference or by drugs that target these proteins identified a set of lncRNAs in liver cancer cells that are modulated by Sp transcription factors. Further studies are underway to examine the specific functions of these lncRNAs in liver cancer growth and metastasis as well as their utility as diagnostic biomarkers.

#### **PS 2051 The Third Trimester: The Critical Phase of the Deleterious Effects of Cadmium in Pregnancy.**

J. I. Anetor, P. Tawari-Eebi, M. Charles-Davies and A. Arowojolu. *Chemical Pathology, College of Medicine, University of Ibadan, Ibadan, Nigeria.*

Environmental cadmium (Cd) is rising globally particularly in the developing countries. Reports indicate that the deleterious effects of Cd may occur at lower levels than hitherto thought. The effects of Cd on female reproduction particularly in pregnancy has received only measured attention and these reports did not delineate the phases of pregnancy at which adverse effects may be critical. One hundred and sixty subjects (125 pregnant; 35 non-pregnant), were studied. Pregnant subjects were classified into three trimesters: 1st (35), 2nd (35) & 3rd (55). Cadmium, Cu, Zn, Fe, Se, Serum proteins were determined in all subjects. Third trimester subjects were followed until delivery. Cadmium levels were similar in the 1st & 2nd trimesters but significantly increased in the 3rd trimester compared to controls and 1st & 2nd trimesters. Zinc level was significantly decreased in the 3rd trimester compared with the 1st & 2nd trimesters. Importantly, Cd was inversely related to Zn. Thirty-two (58%) subjects delivered normal weight babies, 19 (35%) delivered babies with low birth weight (LBW). Four (7%) delivered babies with high birth weight. Women with LBW babies had significantly higher Cd and lower Zn levels as well as low BMI. Cadmium, Zn, Se all correlated inversely with neonatal birth weight (NBW). Cadmium and Se strongly correlated inversely with NBW ( $r = -0.7$ ,  $p = 0.000$ ;  $r = -0.31$ ,  $p = 0.02$ ) respectively. Zinc also correlated directly with NBW. These data suggest that the third trimester with the lowest Zn level also had the highest Cd level (Cd is a metabolic antagonist of Zn). It appears the critical phase that Cd may elicit its toxic effect in pregnancy is the 3rd trimester and low Zn level may be the driving factor. The third trimester is therefore the phase to target in risk assessment, communication and management.

#### **PS 2052 Ethanol Is a Significant Cofactor in HAART-Induced Hepatotoxicity.**

H. Donde<sup>1</sup>, S. Ghare<sup>1</sup>, J. Zhang<sup>1</sup>, I. Kirpich<sup>1</sup>, S. Joshi-Barve<sup>1</sup>, C. McClain<sup>1,2</sup> and S. Barve<sup>1</sup>. <sup>1</sup>Department of Medicine/GI, University of Louisville, Louisville, KY; <sup>2</sup>Louisville VAMC, Louisville, KY.

Highly Active Antiretroviral Therapy (HAART) has led to a significant increase in the life expectancy of HIV patients; however, there are significant side effects including lipodystrophy and hepatotoxicity. Alcohol abuse is highly prevalent in HIV infected individuals and hence may be a significant negative cofactor in HAART induced hepatotoxicity.

The present study examines the mechanisms underlying HAART and alcohol induced hepatotoxicity. The effects of HAART drugs (azidothymidine, and Indinavir sulphate) in combination with alcohol were examined both *in vitro* (H4IIEC3- a rat hepatoma cell line) and *in vivo*. Individual treatments of H4IIEC3 cells with alcohol and AZT showed a certain level of hepatotoxicity which was significantly increased in combinatorial treatment of alcohol and AZT. These data indicate that alcohol can induce and further enhance HAART-induced cytotoxicity. Alcohol and HAART drug interactions and hepatotoxicity were also assessed *in vivo* using an animal model of chronic alcohol feeding. Mice were pair-fed liquid diets (Lieber DeCarli) containing 35% of calories as alcohol (alcohol-fed, AF) or as isocaloric maltose-dextrin (pair-fed, PF). HAART treatment groups received AZT (30mg/kg BW) and IDV (50mg/kg BW) by oral gavage for 5 weeks. Animals exposed to both alcohol and HAART developed increased visceral adiposity compared to pair-fed animals, suggesting disturbances in lipid metabolism in these mice. Lipodystrophy was also evidenced by macro and microvesicular steatosis in the livers; elevated liver triglycerides and free fatty acids. Additionally, animals receiving combinations of alcohol and HAART exhibited increased inflammation and greater hepatic neutrophil infiltration.

Overall, our data demonstrate that alcohol exacerbates HAART hepatotoxicity, and is a significant cofactor in the development of hepatic steatosis and liver injury.

**PS 2053 Acute Exposure to Acrolein, a Ubiquitous Environmental Pollutant, and Anti-HIV HAART Medication Leads to Hepatotoxicity.**

S. Ghare<sup>1</sup>, H. Donde<sup>1</sup>, S. Joshi-Barve<sup>1</sup>, C. McClain<sup>1,2</sup> and S. Barve<sup>1</sup>.

<sup>1</sup>Department of Medicine/GI, University of Louisville, Louisville, KY; <sup>2</sup>Louisville VAMC, Louisville, KY.

Highly Active Antiretroviral Therapy (HAART) is the current treatment for HIV infection. Although HAART leads to a significant increase in the life expectancy of patients with HIV; the prolonged use of HAART causes hepatotoxicity. This has become a significant clinical problem which leads to discontinuation of therapy in turn causing HIV virus reactivation and the development of AIDS. Additionally, environmental pollutants are known to significantly impact general health as well as therapeutic outcome; however their contribution to HAART therapy-induced liver toxicity is unknown. Acrolein is a common environmental, food and water pollutant and a major component of cigarette smoke. It is also produced endogenously via lipid peroxidation and cellular metabolism. The present study examines the potential impact of acute acrolein exposure on the hepatotoxic effects associated with HIV medication. A well characterized human hepatoma cell line (HepG2) model system was used to investigate the combined cytotoxic effects of acrolein along with HAART drug, azidothymidine (AZT). HepG2 cells were treated with various concentrations of acrolein and HAART drugs either individually or in combination. Our results showed that acute exposure to either acrolein or HAART drugs had minimal to no effect on hepatocyte survival. However acrolein exposure enhanced the AZT- induced apoptotic death in HepG2 cells. Acrolein also sensitized hepatocytes to AZT- induced mitochondrial dysfunction, as shown by mitochondrial membrane depolarization and ATP depletion. Notably, acrolein and AZT responsive epigenetic modifications at the FasL promoter were observed, leading to a marked enhancement in FasL gene expression, a known death ligand for hepatocyte and liver damage. Overall, the data suggest that exposure to environmental pollutant acrolein has the potential to exacerbate AZT- induced hepatotoxicity, and increase the severity of drug induced liver injury. This work was supported by NIH grants.

**PS 2054 Solubility Enhancement Studies for a Potential Cyanide Antidote.**

M. Negrito, K. Kovacs, M. Ancha, M. Jane, S. Lee, S. Angalakurthi, S. Rasheed and I. Petrikovics. *Chemistry, Sam Houston State University, Huntsville, TX.*

Present studies focused on the solubility enhancement for the sulfur donor methyl propyl trisulfide (MPTS) to develop an intramuscular formulation for treating cyanide (CN) intoxication. Various FDA approved co-solvents (ethanol, polyethylene glycols (PEG 200, PEG 300, PEG 400) and propylene glycol (PG)), and surfactants (Cremophor EL, Cremophor RH40, polysorbate 80, sodium cholate and sodium deoxycholate) and their combinations were applied to enhance the solubility of the lipophilic MPTS. For solubility determination GC-MS methods were developed. The maximum solubility of MPTS was found at 90% ethanol of over 170 mg/ml. The maximum solubility of over 40 mg/ml was achieved with 20 % Cremophor EL. The combination of the surfactant 20% Cremophor EL and the co-solvent 75% ethanol lead to a synergistic solubilizing effect with the solubility reaching over 400 mg/ml of MPTS.

The in vitro efficacy studies for the MPTS vs. thiosulfate (TS), determined by measuring the thiocyanate formation spectrophotometrically, showed that MPTS is a significantly superior sulfur donor than TS. Similarly, the preliminary in vivo efficacy studies, determined on a therapeutic mice model and expressed as Antidotal Potency Ratios (APR), the ratio of CN LD50 with and without the test antidote(s), showed that MPTS is superior to TS. The combination of MPTS + TS showed a synergistic effect (APR= 3.6).

**PS 2055 Chemical Hazards Emergency Medical Management (CHEMM): Chemical Specific Acute Patient Care Guidelines for Prehospital and Emergency Department/Hospital Management.**

P.J. Hakkinen<sup>1</sup>, D. Siegel<sup>2</sup>, A. Maier<sup>3</sup>, F. Chang<sup>1</sup>, A. Wullenweber<sup>3</sup>, J. Strawson<sup>3</sup>, A. Willis<sup>3</sup>, P. Nance<sup>3</sup>, O. Kroner<sup>3</sup> and R. Sandhu<sup>3</sup>. <sup>1</sup>National Library of Medicine (NLM)/National Institutes of Health (NIH), Bethesda, MD; <sup>2</sup>National Institute of Health (NIH)/National Institute of Child Health and Human Development, Bethesda, MD; <sup>3</sup>Toxicology Excellence for Risk Assessment, Cincinnati, OH.

Chemical Hazards Emergency Medical Management (CHEMM) is an online and downloadable interactive tool. It is designed to enable first responders, first receivers, other healthcare providers, and planners to plan for, respond to, recover from, and mitigate the effects of mass-casualty incidents involving chemicals. Content has been developed via NLM staff, CHEMM contractors, and Federal government and non-Federal government subject matter experts (SMEs). CHEMM includes chemical-specific, acute patient care guidelines for pre-hospital and emergency department/hospital management for exposures to selected groups of chemicals. The information is divided into sections for response in the Hot Zone, Decontamination Zone, and Support Zone/Treatment Area, and each chemical page includes chemical specific information on substance identification, rescuer protection, triage, pediatric/geriatric/obstetric vulnerabilities, clinical symptoms, antidotes, and more. The first version of CHEMM was released in mid-2011, with recent efforts including the addition of over 50 new chemicals with the types of information noted above.

**PS 2056 Manganese Accumulation in the Brain of Asymptomatic Welders and Its Functional Consequences.**

E. Lee<sup>1</sup>, M. R. Flynn<sup>2</sup>, G. Du<sup>1</sup>, M. Lewis<sup>1</sup> and X. Huang<sup>1</sup>. <sup>1</sup>Neurology, Pennsylvania State University, Hershey, PA; <sup>2</sup>Environmental Sciences and Engineering, University of North Carolina at Chapel Hill, Chapel Hill, NC.

Manganese, a neurotoxicant that is concentrated in welding fumes, may play a role in neurodegenerative processes such as Parkinsonism.

In the present study, we examined possible brain biomarkers of manganese exposure in asymptomatic welders using state-of-the-art MRI techniques and correlated imaging findings with functional measures (neuropsychological tests). Sixteen welders and 16 age- and education-matched controls comprised the current sample. For welders, increased welding hours were associated with higher T1 relaxation rates in amygdala, caudate nucleus, hippocampus, putamen, and orbitofrontal white matter in addition to traditionally reported globus pallidus, reflecting increased accumulation of manganese. The higher hours in welding were also associated with greater T1-weighted intensity values in caudate nucleus and hippocampus for welders. Subgroup analysis of welders who were highly exposed to welding compared to controls with no lifetime exposure to welding indicated that welders had higher T1 relaxation rates in globus pallidus and putamen consistent with current literature.

Correlation analyses of MRI results and neuropsychological tests revealed that performance on set shifting tasks (stroop and visual-verbal tests) were negatively correlated with T1-weighted intensity values in orbitofrontal white and grey matter for all subjects. In addition, executive function (the D-KEFS tower test) also was correlated negatively with T1-weighted intensity values in amygdala, caudate nucleus, hippocampus, putamen, and globus pallidus. Moreover, welders with high welding exposure showed decreased working memory performance and associated increased T1-weighted intensity values.

These results suggest that brain regions other than the globus pallidus, e.g., the caudate nucleus and/or hippocampus, also may reflect sensitively manganese exposure. In addition, there may be some cognitive decline associated with manganese deposition in brain.

**PS 2057 Ethanol-Induced Reductions of Antimicrobial Peptide LL-37 in THP-1 Cells and Bal Fluid of Ethanol Fed Mice.**

M. McCaskill, H. Hottor, M. Sapkota and T. Wyatt. *Department of Environmental, Agricultural, Occupational Health, University of Nebraska Medical Center, Omaha, NE.*

The most common infections plaguing the pulmonary system outside of common viral infections such as Rhinovirus and Influenza are Haemophilus influenzae, Klebsiella pneumonia, Burkholderia repacia, Bordetella pertussis, and Mycobacterium tuberculosis. Respiratory infection incidence has been directly correlated to circulating levels of vitamin D. Vitamin D is required for antimicrobial peptide LL-37 production and function in the lung. As a result, antimicrobial LL-37 production is correlated with respiratory function and health. C57Bl6 mice

were exposed to ethyl-alcohol via the Meadows-Cook model for 6 weeks. Mice were also fed Diallyl Disulfide (DADS) at 1uM/gram of feed, and 4000IU of cholecalciferol in their daily diet. THP-1 human acute monocytic cell line were pre-treated with 80mM alcohol for 24 hours, and treated with 1uM of DADS, and 100nM of 1,25 dihydroxy vitamin D for 6, 12, 24 hours. Eighty mM alcohol exposed THP-1 cells displayed a 53% reduction in the cellular supernatant of LL-37. The 6 hour exposure of DADS attenuated the alcohol induced reduction of cellular supernatant LL-37. The 6 hour treatment of 1,25 dihydroxyvitamin D also attenuated the reduction LL-37 in the supernatant of THP-1 cells. In the BALF of the 6 week alcohol fed mice, 1,25 dihydroxyvitamin D was reduced by 70%. In the in-vivo model DADS exposure completely abrogated the alcohol induced reduction of BALF LL-37. This data displays the propensity of alcohol to affect the ability of THP-1's (pre-monocyte cell model) to produce an antimicrobial peptide LL-37. This may be related to the disturbances in 1,25 dihydroxy vitamin D in the pulmonary epithelium as reflected by reductions of BALF of alcohol fed mice. The ability of DADS and vitamin D to attenuate this alcohol induced reduction of LL-37 in the THP-1 cells, and BALF of chronically alcohol fed mice may assist with novel treatment options for human chronic alcohol related respiratory infection severity and rates.

**PS 2058 Utility of Intranasal Fentanyl Powder Formulation: Pharmacokinetics-Pharmacodynamics Relationship in Rhesus Monkeys.**

K. Yunomae, N. Yanagida, M. Nishizono, T. Kamenosono, S. Haruta, Y. Ooshima, H. Sameshima, K. Fukuzaki and R. Nagata. *Shin Nippon Biomedical Laboratories (SNBL), Ltd., Kagoshima, Japan.*

The recent survey conducted by the American Pain Foundation revealed that breakthrough pain posed the greatest challenge to the quality of life (QOL) of cancer patients. The fentanyl buccal tablet, a self-administration formulation, is used at present to relieve breakthrough pain rapidly. However, a new formulation that possesses much quicker pain relief is required to improve the QOL. SNBL has developed an intranasal fentanyl powder formulation (TRF) with the applied "µco System", an intranasal drug delivery system technology. The purpose of this study was to investigate the utility of TRF by comparing the absorption properties and time of onset of action after administration of TRF with those of the commercial buccal tablet. [Methods] Six male rhesus monkeys with body weights 5.4-8.0 kg were used. The plasma fentanyl levels were analyzed by LC/MS/MS. The tail withdrawal latency (TWL) procedure using 50°C water was conducted to evaluate antinociception of fentanyl following administration (8 µg/kg) of fentanyl in 3 forms: TRF (intranasal), intravenously injectable formulation, and buccal tablet. [Results] T<sub>max</sub> and C<sub>max</sub> after administration of TRF were 12.8 min and 2.6 ng/mL, respectively, and were much quicker and higher than the corresponding values for the buccal tablet (50.8 min and 1.1 ng/mL). TRF prolonged the TWL. The effect continued for 25 min from just after nasal administration, similar to that of the intravenously injectable formulation. The effect of the buccal tablet on TWL was noted only at 45 min after buccal administration, suggesting a slow onset of action. [Conclusion] TRF showed a quicker nociceptive effect due to a more rapid nasal absorption of fentanyl in comparison with the buccal tablet. These results indicated that TRF would be a useful formulation for rapidly relieving breakthrough pain in cancer patients with self-administration.

**PS 2059 Better Prediction of Immunogenicity of Biopharmaceuticals, Is It Possible?**

G. M. van Mierlo<sup>3</sup>, F. J. Tielen<sup>2</sup>, R. Klein Entink<sup>1</sup>, A. Penninks<sup>3</sup>, M. Sauerborn<sup>3</sup>, S. Folkertsma<sup>1</sup>, E. Reefman<sup>2</sup> and B. Fabriek<sup>1</sup>. <sup>1</sup>*Quality and Safety, TNO, Zeist, Netherlands;* <sup>2</sup>*Metabolic Health Research, TNO, Leiden, Netherlands;* <sup>3</sup>*Toxicology Applied Pharmacology, TNO Triskelion, Zeist, Netherlands.* Sponsor: R. Woutersen.

A major drawback of biologicals is the possible induction of immunogenicity upon clinical use, that may result in a safety issue and/or a reduction of drug efficacy. Anti-drug antibodies (ADA) are determined as a measure of immunogenicity. Current preclinical models have proven lack of predictivity for clinical immunogenicity. Therefore, there is a need for better methods to predict which drugs are likely to induce immunogenicity in clinical trials.

Based on historical data of immunogenicity, information on structurally, therapeutically and/or 'mode-of-action' similar compounds can be obtained to establish the translational aspects these models. We selected interferon alfa, beta and TNF-inhibitors as model compounds (13 in total) for which the public domain (FDA reviews, BLA, NDA, EMEA, pubmed) was scavenged for immunogenicity related information. The Information consisted of physical chemical properties, formulation aspects (including stability data), preclinical animal toxicity data, clinical data (study specifics and ADA occurrences and effect).

Due to the lack of information on in vitro immunogenicity in literature, we decided to generate these data for the 13 selected compounds. We performed autologous ex vivo human T-DC co-cultures and established T cell proliferation and DC maturation as response markers.

A logistic regression model has been developed relating physical chemical, animal and in vitro information to immunogenicity, where immunogenicity has been defined as two dimensional: the prevalence in the general population and the potency of the substance (dose-response sensitivity). In a statistical analysis of the model, together with expert information, important predictive factors for immunogenicity were successfully identified.

In conclusion, retrospective analysis of various characteristics and preclinical data from on-market biological can provide us with insight in the mechanism of immunogenicity.

**PS 2060 Improved Efficacy of Delivery of Antigen Using a Novel Injection Device in the Rabbit.**

N. Hebert<sup>1</sup>, S. Garipey<sup>1</sup>, I. Brochu<sup>1</sup>, A. Caron-Laramée<sup>2</sup>, M. Brouillette<sup>2</sup> and C. Hébert<sup>2</sup>. <sup>1</sup>*Charles River, Sherbrooke, QC, Canada;* <sup>2</sup>*University of Sherbrooke, Sherbrooke, QC, Canada.* Sponsor: M. Vézina.

Needle-free injector devices show a novel, improved and safer alternative to more classical intramuscular injection immunization protocols.

Two routes of administration [intramuscular (IM) versus intradermal (ID) injection; with a gene-gun type needle-free injector device] were compared in rabbits and the immunogenicity response, together with any potential toxicity were evaluated following immunization with a plasmid coding for the Hepatitis B surface protein (HbSAg) when administered up to three times (Days 1 and 29 [and Day 43; intradermal only]).

Overall, there were no differences between routes of administration when body temperature, body weight, food consumption, selected coagulation and clinical chemistry parameters, and C-Reactive proteins were compared over a period of 43 days. At necropsy, there were no organ weight changes or any adverse macroscopic observations. Based on the magnitude of antibody response and the number of animals mounting a response, a more robust immune response was observed in animals immunized with the injector delivery method (ID). Only 17% of animals receiving the IM injection showed detectable levels of anti-HbSAg antibodies, compared to 50% of animals receiving the ID injection. Furthermore, anti-HbSAg levels in animals administered ID were generally higher than the IM responder. In conclusion, these results suggest that a needle-free injector device shows a safe alternative to intramuscular injection with an increased efficacy when using in immunization regimens.

**PS 2061 Development of a Protocol to Determine the T Cell Dependent Antibody Response (TDAR) to KLH in the Mouse—A Comparison between the CD-1 and C57BL/6N Strains.**

S. Kirk, A. Luccock and K. Troth. *Covance Laboratories Ltd., Harrogate, United Kingdom.*

Pre-clinical safety assessment of biopharmaceuticals may require testing in a specific strain of mouse, when this is the only species where the test material is pharmacologically active. This can present challenges when evaluating immunotoxicity due to known differences in immune responses that exist between different strains. In this study we developed a robust TDAR protocol in the CD-1 mouse then attempted to transfer a similar protocol for use in the C57BL/6N strain.

Initially CD-1 mice were immunised twice intravenously, 1 week apart, at KLH dose levels of 0.3 or 80 mg/kg/challenge. Cyclosporin was also tested at 20 and 100 mg/kg/day in order to establish a positive control. KLH and cyclosporin dose levels of 80 mg/kg and 100 mg/kg respectively, were not tolerated resulting in several premature decedents. A strong IgM and IgG response was observed at the 0.3 mg/kg dose level. Cyclosporin administration at 20 mg/kg/day was sufficient to suppress this response in females only. Cyclosporin administration was tested at 60 mg/kg/day, which proved adequate to suppress the immune response to KLH in both sexes. This protocol was tested in C57BL/6N mice, but failed to produce a robust antibody response. Based on a protocol provided by another lab, C57BL/6N mice were challenged subcutaneously with KLH at 0.1 mg/kg in alum on Day 1 then challenged with KLH only at 0.05mg/kg on Day 7. Control group mice were tested in parallel, without the use of alum. A strong IgM and IgG anti-KLH response was noted in both sexes, most notably in females. In the control group, only the females produced a robust anti-KLH response.

In conclusion, we have established a robust immunisation protocol to measure the TDAR response in CD-1 mice and a suitable positive control to suppress the response. An immunisation protocol in the C57BL/6N mouse was also established

however the use of an adjuvant was required to produce a strong anti-KLH response. Further work to establish a suitable dose level of cyclosporin in C57BL/6N mice is still required.

## **PS 2062 T Cell Dependent Antibody Responses in the Rat: Forms and Sources of Keyhole Limpet Hemocyanin Matter.**

H. Lebecq<sup>1</sup>, M. B. Hock<sup>2</sup>, J. Sundsmo<sup>3</sup>, D. Mytych<sup>2</sup>, H. Chow<sup>3</sup>, L. Carlock<sup>1</sup>, M. K. Joubert<sup>2</sup> and J. L. Bussiere<sup>2</sup>. <sup>1</sup>Amgen, Seattle, WA; <sup>2</sup>Amgen, Thousand Oaks, CA; <sup>3</sup>Stellar Biotechnologies, Port Hueneme, CA.

The T-cell dependent antibody response (TDAR) is a functional assay used in immunopharmacology and immunotoxicology to assess the ability to mount an antibody (IgM and/or IgG) response to immunization. Keyhole limpet hemocyanin (KLH) is extensively used as immunogen of choice both in nonclinical and clinical settings. Native KLH is comprised of high molecular weight (HMW) assemblies (>600-800 kDa) of KLH subunit dimers. It is not known how the different forms (HMW vs. subunit) and manufacturing processes (commercial sources) may impact the nature of anti-KLH immune responses (e.g., magnitude and inter-animal variability). Anti-KLH IgM and IgG responses were studied in female Sprague-Dawley rats immunized on days 1 and 22 with 100 µg of HMW KLH from two different sources or subunit KLHs from three different sources without co-injection with any adjuvant. Dose analysis and biophysical characterization of KLH formulations were conducted. Anti-KLH IgM and IgG responses were measured on days 1, 8, 15, 22, 29, 36, and 43 using a proprietary indirect electrochemiluminescence immunoassay. The two HMW KLH preparations showed a greater number of sub-visible particles (2-150 µm size range) than the three subunit KLHs. All HMW KLHs and all subunit KLHs were equivalent on SEC (hydrodynamic volume), PAGE (size and charge) and SDS-PAGE (molecular radius). Robust primary and secondary anti-KLH IgG and IgM responses were detected for both sources of HMW KLH. The subunit KLH immunizations resulted in lower IgG and IgM responses, with the exception of Stellar Biotechnologies subunit KLH which produced a robust secondary response. Inter-animal variability for IgM and IgG responses was lower with HMW KLH than with subunit KLHs. In conclusion, different forms and sources of KLH are associated with different magnitudes and inter-animal variabilities in IgM and IgG responses, a critical finding to take into consideration when designing TDAR studies for proper immunotoxicology or immunopharmacology testing.

## **PS 2063 Use of the T Cell-Dependent Antibody Response to Evaluate Immunostimulation.**

M. S. Piché<sup>1</sup>, J. Shenton<sup>2</sup>, C. Dumont<sup>1</sup>, R. Bourgeois<sup>1</sup>, I. Brochu<sup>1</sup>, A. J. Grenier<sup>1</sup>, E. Marcotte<sup>1</sup>, L. Durette<sup>1</sup>, M. Poirier<sup>1</sup>, L. de Haan<sup>2</sup> and L. LeSautour<sup>1</sup>. <sup>1</sup>Immunology, Charles River, Montréal, QC, Canada; <sup>2</sup>Medimmune, Cambridge, United Kingdom.

**Purpose:** The T-cell-dependent antibody response (TDAR) has traditionally been used to evaluate immunosuppression. The purpose of this study was to evaluate whether the TDAR following immunization with the T-dependent antigen (TDA) KLH, has utility for evaluating pharmacologically-mediated immunostimulation in cynomolgus monkeys. Recent advances in the development of immunostimulatory therapeutics, primarily T-cell stimulating biologics with cross-reactivity limited to the cynomolgus monkey, have presented a need for pharmacodynamic assays capable of measuring increased T-cell activation in monkeys.

**Methods:** Instead of immunizing the monkeys with 10 mg of KLH, an immunization dose used for evaluating immunosuppression, monkey were immunized twice (1 month apart) with either 0.1 mg or 1.0 mg of KLH in the presence or absence of adjuvants as model immunostimulants. The subsequent antibody response to KLH was measured in the serum following both immunizations, while the cellular response was measured by ELISpot following the second immunization after *ex vivo* challenge of peripheral blood cells with KLH.

**Results:** Immunostimulation by the adjuvant, defined as an increased magnitude of the TDAR, was more clearly demonstrated in monkeys dosed with 0.1 mg of KLH as compared to monkeys dosed with 1 mg of KLH. In addition, a strong KLH-induced IFN-γ response and a mild IL-5 response were elicited following KLH immunization in the presence of the model immunostimulants; however, the cytokine responses were not consistently observed across all animals.

**Conclusion:** Although further validation using known immunostimulatory therapeutics (as opposed to adjuvants) is required, it is clear that monitoring enhanced antibody responses and possible *ex vivo* cytokine responses following low dose immunization with KLH may present an opportunity to evaluate pharmacologically-mediated immunostimulation in cynomolgus monkeys.

## **PS 2064 Assessment of Hepatitis B Surface Antigen and Tetanus Toxoid-Specific T Cell-Dependent Antibody Responses in Cynomolgus Monkeys.**

B. Wang<sup>1</sup>, D. A. DeVona<sup>1</sup>, M. P. Bernard<sup>1</sup>, Q. Wang<sup>2</sup>, C. Gleason<sup>3</sup>, H. G. Haggerty<sup>1</sup> and W. J. Freebern<sup>1</sup>. <sup>1</sup>Immunotoxicology, Bristol-Myers Squibb, New Brunswick, NJ; <sup>2</sup>Rutgers University, New Brunswick, NJ; <sup>3</sup>Global Biometric Sciences, Bristol-Myers Squibb, Syracuse, NY.

Assessment of T-cell-dependent antibody responses (TDAR) is implemented in nonclinical safety testing to evaluate test article effect on immune function. Robust ELISA-based assays to analyze hepatitis B surface antigen (HBsAg)- and tetanus toxoid (TT)-specific antibodies in serum from cynomolgus monkeys immunized with HBsAg and TT were developed. Assay optimization included evaluation of vaccination doses (Engerix B [HBsAg] at 10 and 20 µg, human pediatric and adult doses; TT Adsorbed at 5 flocculation units) and dosing regimen, post-immunization blood collection times, capture reagents and concentrations thereof, initial test serum dilutions, detection antibody dilutions, and incubation times. HBsAg- and TT-specific IgG and IgM endpoint titers (EPT) were analyzed pretest and weekly up to 6 weeks post-immunization to evaluate antibody response kinetics to these antigens. In brief, HBsAg or TT (0.2 or 0.03 µg/well, respectively) is adsorbed overnight onto a 96-well microtiter plate followed by incubation with an initial test serum dilution of 1:5 or 1:50 and titrated 3x to final dilutions of 1:295245 or 1:2952450 for HBsAg or TT-specific antibody analyses, respectively. Bound HBsAg or TT specific-antibodies are detected using a 1:500 or 1:1000 dilution of alkaline phosphatase-conjugated goat anti-human Ig (total, IgM or IgG). After substrate addition and colorimetric analysis, an EPT is calculated. Following primary immunization, peak HBsAg IgM- and IgG-specific responses were observed 22 and 28 to 35 days post immunization, respectively. HBsAg-specific IgG EPT did not generally increase from primary peak response after a second challenge. Since the study monkeys were immunized with TT prior to purchase, a TT IgM-specific response was not detected. TT-specific IgG responses peaked 15 days post on-study immunization.

## **PS 2065 Development of a Delayed Type Hypersensitivity (DTH) Model in Cynomolgus Monkeys.**

G. Bannish<sup>1,5</sup>, H. Babbe<sup>2</sup>, A. Curran<sup>6</sup>, L. A. Coney<sup>5</sup>, L. Hall<sup>3</sup>, J. Zhou<sup>3</sup>, J. Ma<sup>4</sup>, M. Perpetua<sup>1</sup>, J. Doughty<sup>1</sup>, A. Beavis<sup>1</sup> and M. Scully<sup>2</sup>. <sup>1</sup>Biologics and Biomarker Analysis, Huntingdon Life Sciences, East Millstone, NJ; <sup>2</sup>Janssen R&D, LLC, Radnor, PA; <sup>3</sup>Janssen R&D, LLC, Raritan, NJ; <sup>4</sup>Janssen R&D, LLC, La Jolla, CA; <sup>5</sup>Group Strategic Marketing, Huntingdon Life Sciences, Huntingdon, United Kingdom; <sup>6</sup>Safety Assessment, Huntingdon Life Sciences, East Millstone, NJ. Sponsor: C. Auletta.

We have developed an improved delayed type hypersensitivity (DTH) model to assess the cellular immune response. Animals were sensitized with three antigens, keyhole limpet hemocyanin (KLH), *Candida Albicans* (CA), and Tetanus Toxoid (TT) emulsified in incomplete Freund's adjuvant (IFA). These antigens were administered subcutaneously on 3 to 5 occasions over 1 to 2 weeks, followed by a resting period of 1 month. Antigenic challenge was administered intra-dermally with reduced amounts of antigen and in the absence of IFA adjuvant, and at multiple sites with individual antigens or a combined cocktail. Specific IgG responses to each of the antigens were detected. Slight erythema and induration were observed at some sites and some animals, most prominent at 48 hours and with KLH or cocktail. Histological evaluations detected a more intense cellular response with KLH and the combination than TT or CA at both 48 and 72 hours post challenge. Mononuclear cell infiltration (CD3 labeled lymphocytes and CD68 labeled macrophages) was observed in biopsies from CA (3 of 4 animals), TT (3 of 4 animals), KLH (all animals) and the cocktail (all animals), with maximal responses occurring at the 48 and 72 hour time points. Flow cytometry was performed on samples from blood, bone marrow, spleen, and lymph nodes to assess regular and activated immune cell subsets, including evaluation of naïve T lymphocytes (CD95-CD28+) and central memory T lymphocytes (CD95+CD28+) throughout the course of the study. In summary, these findings are consistent with infiltration of cytotoxic T lymphocytes into the challenge site, which is a hallmark of a classical DTH response.

**PS 2066 Validation of a 7-Color Flow Cytometry Panel for Lymphocyte Phenotyping in Peripheral Blood from Cynomolgus Monkeys.**

S. Eble<sup>1</sup>, B. Wang<sup>1</sup>, D. A. DeVona<sup>1</sup>, C. Thompson<sup>1</sup>, C. Gleason<sup>2</sup>, H. G. Haggerty<sup>1</sup>, W. J. Freebern<sup>1</sup> and M. P. Bernard<sup>1</sup>. <sup>1</sup>Bristol-Myers Squibb, New Brunswick, NJ; <sup>2</sup>Global Biometric Sciences, Bristol-Myers Squibb, Syracuse, NY.

Standard peripheral blood immunophenotyping is often implemented in nonclinical safety testing to evaluate potential test article effects on specific lymphocyte population cell counts. The purpose of this study was to validate a robust, resource efficient, high throughput 7-color flow cytometry panel for the identification of T, B, and NK cells in cynomolgus monkey blood. In brief, whole blood was aliquoted into wells (2.2 mL capacity) of a 96-deep well block, washed with PBS, and incubated with fluorophore-conjugated, cell-marker specific antibodies. Following red blood cell lysis, subsequent paraformaldehyde fixation of leukocytes and addition of counting beads, detection of immunostaining was performed using a BD FACSCanto II flow cytometer. Total lymphocytes were identified by side light scatter and CD45 immunostaining and the CD45+ lymphocyte subpopulations were characterized as follows: total T cells (CD16-CD3+), helper T cells (CD16-CD3+CD4+CD8-), cytotoxic T cells (CD16-CD3+CD8+CD4-), double positive T cells (CD16-CD3+CD8+CD4+), double negative T cells (CD16-CD3+CD8-CD4-), B cells (CD16-CD20+), and NK cells (CD3-CD16+CD159a-, CD3-CD16-CD159a+, and CD3-CD16+CD159a+). The inter-assay, intra-assay, and inter-analyst precision estimates based on absolute numbers of lymphocyte subpopulations (calculated using counting beads) were all within 20% (%CV; coefficient of variation). Validation testing demonstrated antibody specificity and minimal fluorescence carryover between samples. Whole blood stability (ie prior to immunostaining) was demonstrated for up to 24 hours at ambient temperature and the fixed samples were determined to be stable for up to 24 hours at 5 ± 4°C prior to flow cytometric analysis. Based on the results from this validation study, it was determined that the 7-color flow cytometry panel described herein reliably and precisely identifies T, B, and NK cells in cynomolgus monkey whole blood.

**PS 2067 Testing the Use of CD107a and IFN-γ As Markers of Cynomolgus Cytotoxic T Lymphocyte Activation.**

L. Anest, A. Guerrero, M. Fort and P. Narayanan. *Discovery Toxicology*, Amgen, Seattle, WA.

Cytotoxic T lymphocytes (CTLs) are key effector cells, in the immune system, that play an important role in anti-viral host defense and cancer immune-surveillance. Non-human primates, especially cynomolgus macaques, are the closest surrogates for detecting immunosuppressive properties of targeted anti-inflammatory therapeutics in human. While qualified methods exist to measure CTL function in humans and rodents, there are few assays currently available for detection of changes in CTL function in response to drug exposure in cynomolgus macaques. Herein, we present an adaptation of a flow cytometry-based human CTL degranulation assay for characterization of cynomolgus macaque CTL function. This is based on detection of lysosomal-associated membrane protein 1 (CD107a) on the surface of degranulated CTL in conjunction with the secretion of IFN-γ which allows for the identification of fully activated CTL. Briefly, whole blood samples from cynomolgus macaques were stimulated in vitro with staphylococcal enterotoxin B (SEB) for six hours, then stained for the detection of intracellular IFNγ and surface expression of CD3, CD4, CD8 and CD107a prior to analysis on a flow cytometer. Whole blood samples from naïve cynomolgus macaques (n = 11) were tested to establish a range of dual positive CD107a+IFNγ+ CTL (0.04-1.58% of CD3+CD4-CD8+ T cells) in response to SEB stimulation. Next, a longitudinal study was completed to determine the intra-animal variation of CD107a+IFNγ+ CTL responses in 4 cynomolgus macaques by collecting samples at 2-3 week intervals over a two month period. CTL activation in response to SEB stimulation demonstrated a %CV of 31-57% over the course of the study. The direct addition of an immunosuppressive compound, cyclosporine A, to WB suppressed IFN-γ secretion but not degranulation of CTL in response to SEB in a concentration-dependent manner. The ability to quantify the CTL functional responses in cynomolgus macaques may be a useful tool for determining any immunomodulatory effects of drug candidates in pre-clinical safety studies on this important lymphocyte subset.

**PS 2068 Validation of Assays for Phagocytic Function of Polymorphonuclear Neutrophils and Monocytes in Whole Blood from Cynomolgus Macaque.**

M. Perpetua<sup>1</sup> and G. Bannish<sup>2,1</sup>. <sup>1</sup>Biologics and Biomarker Analysis, Huntingdon Life Sciences, East Millstone, NJ; <sup>2</sup>Group Strategic Marketing, Huntingdon Life Sciences, East Millstone, NJ.

Phagocytosis constitutes an essential arm of host defense against bacterial and fungal infections. The process can be subdivided into phagocyte chemotaxis to sites of inflammation, binding to foreign agents, ingestion of opsonized bacteria, and intracellular killing by oxygen-dependent and oxygen-independent mechanisms. We have assessed several of these functions in whole blood from cynomolgus macaque using commercially available kits designed for human use. Tests included intra-assay precision, inter-assay precision, processed stability, sample stability, and inter-analyst variability. The percent coefficient of variation was lower for granulocytes than monocytes, typically 1% versus 10% or less in the ingestion assay. Respiratory burst following stimulation with phorbol 12-myristate 13-acetate (PMA), opsonized bacteria, or the chemotactic peptide N-formyl-Met-Leu-Phe (fMLP) was within ranges established for human whole blood. The PMA stimulant was high and consistently > 95% above unstimulated negative control values, the fMLP was low (< 5%), and opsonized bacteria induced a high percentage of stimulated granulocytes (>95%) but lesser stimulated monocytes (~60%). The highest CV values occurred in tests of oxidizing monocytes for inter-assay (19%), processed stability (19%), and sample stability (15%), but were otherwise typically below 5%. Overall these results determine the ability to use these assays for analysis of phagocytic function in cynomolgus macaque under GLP conditions.

**PS 2069 Flow Cytometry Immunophenotyping of Lymphocyte Subsets in a Large Cohort of Beagle Dogs.**

J. Descotes<sup>2</sup>, C. Mimouni<sup>1</sup>, J. Legrand<sup>1</sup> and R. Forster<sup>1</sup>. <sup>1</sup>Marketing, CiToxLAB, Evreux, France; <sup>2</sup>Poison Center, Lyon, France.

Since the dog is a major non-rodent species used in regulatory drug safety studies, there is a growing need to generate historical immunological background data to interpret the results of nonclinical immunotoxicity studies in dogs. We have initiated the compilation of data on peripheral blood lymphocyte subsets in a large cohort of male and female naïve Beagle dogs of at least 6 months of age. Venous blood samples of approximately 0.5 ml were collected from fasted animals in the morning. Immunophenotyping analysis of B lymphocytes, total T lymphocytes, T CD4+ and CD8+ lymphocytes with commercial BD Pharmingen fluorescent antibody reagents (BD Biosciences, France) is performed using a Navios 10-color flow cytometer with the Navios v1 software (Beckman Coulter, France). Flow count® fluorospheres are added to each sample prior to flow cytometry analysis for direct determination of lymphocyte subset absolute counts. At writing, validated results are available on 40 males and 50 females. Results obtained in males and females, respectively, are presented as percentage of gated cells and mean (± standard deviation) of absolute count of each lymphocyte subset/μl: B lymphocyte percentage (21.3% & 18.5%) and absolute count (604.4±185.5 & 495.5±171.5); total T lymphocyte percentage (60.8% & 64.1%) and absolute count (1719.6±599.4 & 1728.5±334.9); T CD4+ lymphocyte percentage (41.0% & 43.6%) and absolute count (1180.4±399.7 & 1159.3±228.1); T CD8+ lymphocyte percentage (12.7% & 12.2%) and absolute count (360.2±136.6 & 324.6±106.9). Stored samples from additional animals (total of 100 animals from each sex) are being processed, which will very shortly constitute the largest cohort of data on peripheral blood lymphocyte subsets in the naïve Beagle dog.

**PS 2070 Development of Molecular Classifiers for Distinguishing between True Sensitizers and False Positives in the Local Lymph Node Assay.**

D. R. Boverhof<sup>1</sup>, D. Adenuga<sup>1</sup>, M. Woolhiser<sup>1</sup>, I. Kimber<sup>2</sup>, R. Dearman<sup>2</sup>, M. Black<sup>3</sup> and R. S. Thomas<sup>3</sup>. <sup>1</sup>The Dow Chemical Company, Midland, MI; <sup>2</sup>University of Manchester, Manchester, United Kingdom; <sup>3</sup>The Hamner Institutes for Health Sciences, Research Triangle Park, NC.

Recent publications have highlighted certain chemistries which yield false positive responses in the LLNA when compared with guinea pig and human data. Toxicogenomics was applied to provide molecular characterization of the LLNA responses with the goal of developing classifiers for predicting true skin sensitizers. Auricular lymph node gene expression responses were evaluated in female CBA mice exposed to equipotent doses of 9 known chemical sensitizers and 7 false positives per the standard LLNA dosing regimen. Lymph nodes were analyzed for 3HTdR incorporation on study day 6 and gene expression responses on study days

4 and 6. Subsequent to data filtering, a comprehensive cross-validation model comparison using 84 different statistical classification methods was performed to identify expression-based classifiers for each chemical class (sensitizers and false positives) and time point. The predictive performance of the models was evaluated using five-fold cross-validation. The gene lists from the top performing model for each chemical class and time point were subsequently confirmed and refined using quantitative RT-PCR. The top performing day 4 classifiers had AUC values of 0.904 and 0.926 for sensitizers and false positives, respectively, while the day 6 classifiers showed higher AUC values of 0.962 and 1.00 for sensitizers and false positives, respectively. The optimal day 6 classifier gene list included 44 and 30 genes for sensitizers and false positives, respectively, with 19 overlapping genes. The 55 total genes displayed functional relevance to sensitization and irritation responses and both classifiers are now being evaluated against a series of new chemistries to independently assess model performance. Overall these data highlight the potential utility of molecular classifiers for distinguishing between sensitizers and false positives.

**PS 2071 Development of an *Ex Vivo* BrdU-Labeling Procedure for the Murine LLna.**

D. M. Lehmann<sup>1</sup>, C. Copeland<sup>1</sup>, E. H. Boykin<sup>1</sup>, S. J. Quell<sup>2</sup>, L. Copeland<sup>1</sup> and W. C. Williams<sup>1</sup>. <sup>1</sup>NHEERL, US EPA, Research Triangle Park, NC; <sup>2</sup>Independent, Research Triangle Park, NC.

The murine local lymph node assay (LLNA) is widely used to identify chemicals that may cause allergic contact dermatitis. Exposure to a dermal sensitizer results in proliferation of local lymph node T cells, which has traditionally been measured by in vivo incorporation of [3H]methyl thymidine (3HTdR). A more recent non-isotopic variation of the assay utilizes bromodeoxyuridine (BrdU) incorporation in vivo. To eliminate the need for animal injections, we developed an ex vivo labeling procedure. BALB/c mice were dosed topically on the dorsum of both ears for 3 consecutive days with vehicle or one of 3 concentrations of eugenol (EUG), cinnamaldehyde (CA), hexyl cinnaminic aldehyde (HCA), nickel sulfate (NiS), isopropanol (IP) or lactic acid (LA). On day 5, lymph nodes were harvested, and single-cell suspensions were labeled ex vivo with 3HTdR or BrdU. Lymphocyte proliferation was determined by scintillation counting or BrdU ELISA, respectively. Concentration-dependent increases in ear thickness and lymphocyte proliferation were observed for EUG, CA and HCA, but none of the doses tested resulted in excessive skin irritation. The results of both the ex vivo 3HTdR and ex vivo BrdU assays correctly identified EUG, CA and HCA as dermal sensitizers according to the criteria outlined in the Globally Harmonized System for Classification and Labeling of Chemicals. As anticipated, non-sensitizers IP and LA did not induce a positive threshold response in either assay. Furthermore, a positive threshold response was not obtained for the false negative chemical NiS in either assay. The results of both ex vivo assays are in close agreement with those of the in vivo BrdU labeling procedure. We conclude that the ex vivo BrdU labeling method offers predictive capacity comparable to the other previously established LLNA protocols while eliminating animal injections and the use of radioisotope. This abstract does not represent EPA policy.

**PS 2072 A Proteomics Approach to Elucidate the Role of Nrf2 in Primary Bone-Marrow-Derived Dendritic Cells of Mice upon Activation by Contact Allergens.**

A. Haase<sup>1</sup>, F. Mussotter<sup>1</sup>, Z. El Ali<sup>2</sup>, S. Kerdine-Römer<sup>2</sup>, J. Tomm<sup>3</sup>, M. Pallardy<sup>2</sup>, M. von Bergen<sup>3</sup> and A. Luch<sup>1</sup>. <sup>1</sup>Federal Institute for Risk Assessment (BfR), Berlin, Germany; <sup>2</sup>University of Paris-Sud, INSERM UMR-996, Paris, France; <sup>3</sup>Department of Proteomics and Metabolomics, Helmholtz Centre for Environmental Research (UFZ), Leipzig, Germany.

Contact sensitizers are low molecular weight compounds, which can prompt dendritic cells in the skin to subsequently activate naïve T-cells in draining lymph nodes. Often these compounds are electrophilic and lead to activation of the Keap1/Nrf2 pathway. We aimed to further elucidate the underlying molecular mechanisms of skin sensitization and to identify putative biomarkers. We used bone marrow-derived dendritic cells (BMDC) from CD34+ progenitor cells from wild-type or Nrf2 -/- mice. Cells were treated for 8 h with different contact allergens: cinnamaldehyde (CA), 1-chloro-2,4-dinitrobenzene (DNCB), nickel sulfate (NiSO<sub>4</sub>) or with SDS as an irritant control. Analysis was done using 2D gels and ESI-MS/MS. Protein spots were considered as differentially expressed if they changed at least 1.5-fold ( $p < 0.05$ ). While treatment with 250 and 400 µM nickel and 100 µM SDS hardly had any effects, CA and DNCB led to significant changes in protein expression. We found 9 and 27 spots upregulated with 50 and 100 µM CA, respectively. For 5 and 10 µM DNCB 14 and 35 spots were upregulated, respectively. Some of those were not detected in Nrf2 -/- cells, indicating a Nrf2-dependent regulation. More than 90% of the proteins could be identified. Some of those have been already characterized as

Nrf2-dependent such as glutathione S-transferases, glutamate cysteine ligase, or catalase. We also identified other proteins involved in oxidative stress, signal transduction pathways, basic cellular pathways and also heat shock proteins. Some of them were not inducible in Nrf2 -/- cells and were not previously described as Nrf2-dependent. We could confirm Nrf2 activation in the response of mouse BMDC upon exposure to contact sensitizers. We could identify interesting potential biomarkers, some of which should be studied in more detail in the future.

**PS 2073 Nrf2-Dependent and -Independent Effects of tBHQ on Early T Cell Activation.**

C. E. Rockwell<sup>1</sup>, P. E. Fields<sup>3</sup>, C. D. Klaassen<sup>2</sup>, J. W. Zagorski<sup>1</sup>, A. E. Turley<sup>1</sup> and H. Dover<sup>1</sup>. <sup>1</sup>Pharmacology & Toxicology, Michigan State University, East Lansing, MI; <sup>2</sup>Pharmacology, Toxicology & Therapeutics, University of Kansas Medical Center, Kansas City, KS; <sup>3</sup>Pathology & Laboratory Medicine, University of Kansas Medical Center, Kansas City, KS.

Nrf2 is a transcription factor that is activated by cellular stress from various sources, including oxidative stress and electrophiles. In response to cell stress, Nrf2 upregulates a battery of cytoprotective genes. In addition to this role, Nrf2 has also been shown to have immunomodulatory effects, including anti-inflammatory effects in innate immune cells and effects on T cell differentiation. The purpose of the present studies was to determine the role of Nrf2 in cytokine production and other events associated with early T cell activation. The present studies demonstrate that the Nrf2 activator, tBHQ, causes a significant decrease in the early production of IFN $\gamma$  and IL-2 in anti-CD3/anti-CD28-activated splenocytes from both wild-type and Nrf2-null mice. Interestingly, splenocytes from Nrf2-null mice produced increased levels of IFN $\gamma$ , but decreased levels of IL-2, as compared to those from wild-type mice. In addition to IL-2 and IFN $\gamma$ , the effects of tBHQ on other genes that are upregulated after T cell activation were investigated. In contrast to IL-2 and IFN $\gamma$ , tBHQ caused only modest effects on the upregulation of CD25 and CD69, which are also induced during early T cell activation. Treatment of activated splenocytes with tBHQ also inhibited calcium influx. Collectively, the current studies suggest that tBHQ inhibits early production of IFN $\gamma$  and IL-2 and that this effect is at least partially Nrf2-independent. These studies also suggest that Nrf2 promotes IL-2, but inhibits IFN $\gamma$ , at early time points after T cell activation. (This work was funded by NIH grant: ES018885.)

**PS 2074 Activation of Nrf2 by TBHQ Inhibits IL2 Production, but Not CD69 Expression, in Human Jurkat T Cells.**

J. W. Zagorski<sup>1,2</sup>, A. E. Turley<sup>2</sup>, K. R. Vandenberg<sup>2</sup>, J. Compton<sup>2</sup>, H. E. Dover<sup>2</sup> and C. E. Rockwell<sup>2,1</sup>. <sup>1</sup>Cellular and Molecular Biology, Michigan State University, East Lansing, MI; <sup>2</sup>Pharmacology and Toxicology, Michigan State University, East Lansing, MI.

Nuclear factor erythroid 2-related factor 2 (Nrf2) is a transcription factor that is activated by cell stress, such as electrophilic and oxidative stimuli. Once activated, Nrf2 translocates to the nucleus and induces the transcription of its target genes, including HMOX and NQO1. Previously, it has been shown that Nrf2 skews CD4+ T cell differentiation in primary murine T cells, however the role of Nrf2 in human T cells is largely uncharacterized. Therefore, the purpose of the present studies was to determine the effects of Nrf2 activation upon early events of CD4+ T cell activation, in human Jurkat T cells. Treatment of Jurkat cells with the Nrf2 activator, tBHQ (5 µM), significantly decreased both transcript and protein production of IL-2. Similarly, a modest reduction of CD25 induction by tBHQ was observed, but CD69 expression remained unaffected. Nuclear translocation of c-fos and c-jun (transcription factors that regulate IL-2) was not affected by tBHQ treatment. In contrast, cells pretreated with 1 µM and 5 µM tBHQ showed both a delay of and decrease in Ca<sup>2+</sup> influx stimulated by anti-CD3/anti-CD28. Collectively, the current studies suggest a differential effect of tBHQ on early events of CD4+ T cell activation, and these effects are at least partially due to inhibition of Ca<sup>2+</sup> influx into the cell. (This work is supported by NIH grant: ES018885)

**PS 2075 Inhibition of Early Cytokine Production by the Nrf2 Activator, tBHQ, in Human Primary Blood Mononuclear Cells.**

A. E. Turley<sup>1,2</sup>, J. W. Zagorski<sup>1</sup> and C. E. Rockwell<sup>1,2</sup>. <sup>1</sup>Pharmacology and Toxicology, Michigan State University, East Lansing, MI; <sup>2</sup>Center for Integrative Toxicology, Michigan State University, East Lansing, MI.

tBHQ (tert-butylhydroquinone) is a common food preservative and a known Nrf2 (nuclear factor erythroid 2-related factor 2) activator. Nrf2 is a ubiquitously expressed transcription factor responsive to cell stress that regulates many cytoprotec-

tive and detoxification genes. In addition, Nrf2 has been shown to have anti-inflammatory properties and to modulate the activity of numerous immune cell types, including T cells. The purpose of the present studies was to characterize the role of Nrf2 during T cell activation in primary blood mononuclear cells isolated from human whole blood. The induction of several genes associated with early T cell activation, including IL-2, IFN- $\gamma$ , CD25 and CD69, was investigated in PBMCs treated with tBHQ prior to T cell activation. Treatment with tBHQ inhibited production of the early cytokines IL-2 and IFN- $\gamma$ , in a dose-dependent manner. Compared to the cytokines, induction of the cell surface markers CD25 and CD69 was less sensitive to tBHQ, with expression inhibited only at the highest concentration of tBHQ. The effects of tBHQ on protein expression of IL-2, IFN- $\gamma$ , CD25, and CD69 correlated with the mRNA expression of these genes. Consistent with Nrf2 activation, tBHQ treatment also caused induction of the Nrf2 target genes Hmox-1, Nqo1, and Gclc. Collectively, these studies demonstrate that tBHQ inhibits early cytokine production by anti-CD3/anti-CD28-activated PBMCs while only modestly decreasing CD25 and CD69 induction. Overall, these data suggest that Nrf2 may differentially modulate the early events of T cell activation in primary human T cells. (This work is supported by NIH grant ES018885)

**PS 2076 Diethylstilbestrol (DES)-Regulated microRNA-30a May Induce Autophagy by Regulating Beclin1 in Thymic Cells of Neonatal Mice.**

N. P. Singh, U. P. Singh, I. K. Abbas, P. Nagarkatti and M. Nagarkatti. *Pathology, Microbiology, and Immunology, University of South Carolina School of Medicine, Columbia, SC.*

Prenatal exposure to DES is known to cause changes in immune functions thereby increasing susceptibility to autoimmune diseases in humans. Experimental studies have also indicated that prenatal exposure to DES affects thymic T cells. Our laboratory has been investigating DES-regulated miR profile in fetal thymocytes following prenatal exposure. Of the 608 miRs examined by performing high-throughput miR arrays with thymocytes on gestational day 18 (GD18) of C57BL/6 mice exposed to DES, we observed more than 60 miRs that were up- or down-regulated (>1.5-fold) when compared to vehicle treated group. Upon further analyses, we observed significant downregulation (>2.0 fold) of miR-30a in fetal thymocytes post DES exposure. miR-30a has been shown to regulate Beclin 1 (BECN1) expression affecting autophagic activity. In the current study, therefore, we examined whether miR-30a that was down regulated in fetal thymocytes post DES exposure plays a role in autophagy vis a vis immune dysfunction in neonatal mice. Recent studies have suggested that autophagy in the thymic epithelium is dispensable for negative selection of autoreactive T cells. Upon analysis of miR-30a by Real-Time PCR, we observed significant (more than 2-fold) downregulated expression of miR-30a in fetal thymocytes but upregulated expression of BECN1. We further characterized miR-30a for its binding affinity with BECN1 3'UTR region. Our studies demonstrated significant blocking of BECN1 expression in the presence of miR-30a and the effect of miR-30a was reversed in the presence of DES. Together, these data demonstrate that prenatal exposure to DES can cause alterations in thymocyte differentiation through dysregulation in miR-30a leading to altered BECN1 expression that in turn may influence the mechanisms of autophagy in fetal thymocytes. (Supported in part by NIH grants P01AT003961, R01AT006888, R01ES019313, R01MH094755, P20RR032684 and VA Merit Award BX001357).

**PS 2077  $\Delta^9$ Tetrahydrocannabinol (THC) Rescues Mice from Staphylococcal Enterotoxin B (SEB)-Induced Acute Lung Injury (ALI) and Subsequent Mortality by the Induction of Regulatory T Cells and the Down-Regulation of microRNA-182.**

R. Rao, P. Nagarkatti and M. Nagarkatti. *University of South Carolina, Columbia, SC.*

Acute Lung Injury (ALI) is characterized by infiltration of lymphocytes in the lung, edema, Acute Respiratory Distress Syndrome (ARDS), and death. In this study, Staphylococcal Enterotoxin B (SEB) was used to induce ALI in mice. SEB is a superantigen that activates T cells expressing V $\beta$ 8, which leads to activation of ~20% of T-cells and massive release of pro-inflammatory cytokines leading to the induction of ALI/ARDS. We tested the hypothesis that  $\Delta^9$ Tetrahydrocannabinol (THC), a cannabinoid known for its anti-inflammatory properties can rescue mice from SEB induced mortality. Intranasal followed by intraperitoneal administration of SEB resulted in death of mice, while THC treatment rescued them from mortality. SEB exposure induced vascular leak in the lung, which was reduced by THC treatment. SEB administration resulted in the infiltration of lymphocytes (CD3 $^+$ , V $\beta$ 8 $^+$ ,

NK, NKT, MDSC and macrophages) in the lung and THC treatment led to the decrease in their absolute cell numbers. Interestingly, THC treatment caused an induction of CD4 $^+$ Foxp3 $^+$  T-cells in the lung, indicating a role for regulatory T-cells in the amelioration of SEB induced inflammation. Additionally, SEB exposure led to the induction of miR-182 that caused a downregulation in Foxo1 expression leading to clonal expansion of T-cells. THC treatment however, decreased miR-182 expression indicating that THC might mediate its effects in part through the down-regulation of miR-182. Cytokine analysis showed that while SEB exposure led to the increase of IL-2 and MCP-1 in the serum and IFN- $\gamma$  and IL-6 in the Bronchoalveolar lavage fluid (BALF), THC treatment resulted in a decrease in these cytokines. Together, our data demonstrates that THC can rescue mice from SEB induced ALI and death. (Supported in part by NIH grants P01AT003961, R01AT006888, R01ES019313, R01MH094755, P20 RR032684 and VA Merit Award BX001357)

**PS 2078 Identification of microRNA That Affect Multiple Pathways of TCDD-Induced T Cell Dysregulation.**

P. Mehrpouya, P. Nagarkatti and M. Nagarkatti. *Department of Pathology, Microbiology and Immunology, University of South Carolina School of Medicine, Columbia, SC.*

2, 3, 7, 8-Tetrachlorodibenzo-p-dioxin (TCDD), an environmental contaminant, is well known for inducing severe toxicity including immunosuppression. We examined the mechanisms by which TCDD affects the T cell response to Staphylococcal enterotoxin B (SEB). SEB, a superantigen, activates ~20% of T cells via V $\beta$ 8 T cell receptor, causes a robust release of pro-inflammatory cytokines. We injected C57BL/6 mice with SEB in footpads and treated i.p with vehicle or TCDD. Our studies showed that TCDD treatment of SEB-activated lymphocyte led to a decrease in V $\beta$ 8 $^+$  T cells in compare to vehicle and causes an increased induction of apoptosis in SEB-activated T cells. TCDD led to induction of FoxP3 $^+$  T regulatory cells (Tregs) and suppression of pro-inflammatory cytokines, IFN- $\gamma$ , TNF- $\alpha$  and IL-6 while increasing the expression of the anti-inflammatory cytokine, IL-10. Showing the role of microRNA (miR) in TCDD-induced immune dysregulation, we performed high throughput miR analysis. Following TCDD administration, 36 miRs were up-regulated while 50 were down-regulated. In silico analysis demonstrated that several pathways were affected including induction of apoptosis, cytochrome P450 expression and Treg differentiation. We validated the role of selected miR following vehicle or TCDD treatment of SEB-activated LN cells. miR-31, complementary to the 3'-UTR of the target gene Foxp3, was down regulated in the TCDD treated group which is validated by RT-PCR. miR-351 directed against the target gene CYP1A1, was down-regulated in the TCDD treated group which suggests that TCDD acts as an AhR ligand causing increased CYP1A1 expression as well as Tregs induction. miR-21 targets the pro-apoptotic targets, Fas and FasL was down-regulated, which results in TCDD-mediated toxicity. Our studies demonstrated that TCDD affects miR expression that acts through several mechanisms to cause immune dysregulation. (Supported by NIH grants P01AT003961, P20 RR032684, R01AT006888, R01ES019313, R01MH094755 and VA Merit Award BX001357)

**PS 2079 Quantitative Phosphoproteomic Analysis of the Dynamic Signaling Network Mediating Proinflammatory Response in the Spleen of Mice under Deoxynivalenol-Induced Ribotoxic Stress.**

X. Pan<sup>1,2</sup>, D. Whitten<sup>3</sup>, C. Wilkerson<sup>1,3</sup> and J. Pestka<sup>2,4</sup>. <sup>1</sup>Department of Biochemistry and Molecular Biology, Michigan State University, East Lansing, MI; <sup>2</sup>Center for Integrative Toxicology, Michigan State University, East Lansing, MI; <sup>3</sup>Proteomics Core Facility, Michigan State University, East Lansing, MI; <sup>4</sup>Department of Food Science and Human Nutrition, Michigan State University, East Lansing, MI.

The trichothecene mycotoxin deoxynivalenol (DON) is a widely-studied model ribotoxin that targets the innate immune system and has public health significance due to its common contamination of human and animal food. Induction of proinflammatory genes in the spleen by DON is known to involve activation of transcription factors mediated by rapid phosphorylation of mitogen-activated protein kinases (MAPKs). To further understand how phosphorylation of proteins leads to the onset of proinflammatory response, stable isotope dimethyl labeling-based proteomics was applied to quantitatively profile the immediate ( $\leq 30$  min) phosphoproteome changes in the spleen of mice orally exposed to a toxicologically relevant dose of DON. A total of 90 phosphoproteins indicative of novel phosphorylation events were significantly modulated by DON. In addition to critical branches and

scaffolds of MAPK signaling being affected, DON exposure altered phosphorylation of proteins that mediate PI3K/AKT, B cell receptor and T cell receptor-linked pathways and DNA methylation. Gene ontology analysis indicated that DON exposure affected biological processes such as cytoskeleton organization, regulation of apoptosis and immune system development, which could modulate cell adhesion and lymphocyte function, setting the stage for the proinflammatory response. Fuzzy c-means clustering analysis further revealed that DON evoked several distinctive temporal profiles of the regulated phosphopeptides. These results should shed light on mechanisms of the immunotoxicity of ribotoxins and could ultimately lead to novel strategies for countering the adverse actions of such agents.

## PS 2080 Targeted Proteomic Analysis of Phospho-Lyn in Hg Intoxicated B Cells.

J. A. Caruso<sup>1</sup>, P. M. Stemmer<sup>1</sup>, M. J. McCabe<sup>2</sup> and A. J. Rosenspire<sup>3</sup>. <sup>1</sup>Institute of Environmental Health Sciences, Wayne State University, Detroit, MI; <sup>2</sup>Environmental Medicine, University of Rochester, Rochester, NY; <sup>3</sup>Immunology and Microbiology, Wayne State University, Detroit, MI.

Network and key node analysis of proteins undergoing Hg(2+)-induced phosphorylation and dephosphorylation in Hg intoxicated mouse WEHI 231 B cells identified Lyn as the top scoring node. Lyn is a Src family protein tyrosine kinase known to be intimately involved in the B Cell Receptor (BCR) signaling pathway. Under normal signaling conditions the tyrosine kinase activity of (mouse) Lyn is controlled by phosphorylation, primarily of two well known canonical regulatory tyrosine sites, Y397 and Y508. However Lyn has multiple tyrosines, threonines and serines, which have not so far been determined to play a major role under normal signaling conditions, but are potentially important targets for phosphorylation following Hg(2+) exposure. In order to determine how Hg(2+) intoxication modulates the phosphorylation of additional residues in Lyn, a targeted MS assay was developed. Initial mass spectrometric surveys of purified Lyn identified seven phosphorylated amino acid residues (6 tyrosines and 1 serine). A targeted quantitative assay was then developed from these results using the multiple reaction monitoring (MRM) strategy. WEHI 231 cells were treated with Hg, pervanadate, or anti-mu antibody (to stimulate the BCR), and cell stimulation confirmed by anti-phosphotyrosine western blots. Whole cell lysates from these same samples were then separated by 1D SDS-PAGE and the regions containing Lyn were selected for analysis. In gel digestion produced tryptic peptides that were analyzed on a TSQ Vantage MS system using a Lyn-specific MRM method that targeted 11 peptides and 6 phosphopeptides. Data indicate that several Lyn sites are subject to Hg(2+)-induced phosphorylation. However Y117 and Y194 were especially susceptible, suggesting that their phosphorylations may be important mediators of Hg immunotoxicity. Supported by NIEHS: R21ES019228

## PS 2081 Penicillium Mycotoxins Alter the Expression of Genes Coding Enzymes That Regulate Epigenetic Programming in Bovine Macrophages.

S. Oh<sup>1</sup>, R. Cliff<sup>2</sup>, C. G. Balch<sup>1</sup>, B. S. Sharma<sup>1</sup>, H. J. Boermans<sup>2</sup>, S. Haladi<sup>3</sup> and N. A. Karrow<sup>1</sup>. <sup>1</sup>Animal & Poultry Science, University of Guelph, Guelph, ON, Canada; <sup>2</sup>Biomedical Sciences, University of Guelph, Guelph, ON, Canada; <sup>3</sup>Alltech Inc., Guelph, ON, Canada.

Penicillium mycotoxins (PM) are natural immunomodulatory contaminants that accumulate in grains, crops, fruits, and fermented products, especially during post harvest periods, due to improper storage and harvesting methods. In this study, the expression of genes coding key enzymes involved in epigenetic regulation was assessed using a bovine macrophage cell line (BoMac). BoMac were activated with bacterial lipopolysaccharide (LPS) and exposed for 6 hr to the following PM: citrinin (CIT), ochratoxin A (OTA), patulin (PAT), mycophenolic acid (MPA), penicillic acid (PA), or a combination of one of the above with OTA at the concentration that inhibits BOMAC cell proliferation by 25% (IC25). Messenger RNA was isolated and real-time PCR analysis was performed to assess mycotoxin-induced changes in the expression of DNA methyltransferases (DNMTs), histone demethylases (JMJD3 and UTX), histone acetylases (CBP/p300), histone deacetylases (HDACs), and histone ubiquitin ligase (BMI1). LPS-induced expression of DNMT3a was augmented by OTA+PA, while DNMT3b expression was reduced by PA, OTA+PA and CIT+OTA. JMJD3 expression was induced by PA but down-regulated by OTA+PA. CBP/p300 expression was reduced by all individual mycotoxins as well as OTA+MPA and OTA+PA, and BMI1 expression was reduced by MPA, OTA+MPA and OTA+PA. The expression of HDAC1 was reduced by CIT, MPA and PA, while HDAC2 expression was induced by CIT+OTA and OTA+PAT. Lastly, HDAC3 expression was reduced by MPA, PA, CIT+OTA,

OTA+PAT, OTA+MPA and OTA+PA. These findings propose a potential novel regulatory mechanism by which PM can modulate bovine macrophage gene expression and function.

## PS 2082 Genipin-Induces Cyclooxygenase-2 Expression through Upregulating NF-κB, C/EBP and AP-1 Signaling Pathways in Murine Macrophages.

T. Khanal, H. Kim, J. Choi and H. Jeong. Pharmacy, Chungnam National University, Daejeon, Republic of Korea.

Genipin, the aglycone of geniposide, exhibits anti-inflammatory and anti-angiogenic activities. Cyclooxygenase-2 (COX-2) acts as a link between inflammation and carcinogenesis through its involvement in tumor promotion. In the present study, we examined the effect of genipin on COX-2 gene expression and analyzed the molecular mechanism of its activity in murine RAW 264.7 macrophages. Furthermore, genipin dose-dependently increased the levels of COX-2 protein and mRNA. These results demonstrate that genipin induced COX-2 expression via NF-κB and AP-1 activation. Moreover, genipin increased the luciferase reporter gene activity in cells transfected with a COX-2 promoter. Transient transfections utilizing COX-2 promoter deletion constructs and COX-2 promoter constructs, in which specific enhancer elements were mutagenized, revealed that the NF-κB, C/EBP and AP-1, were predominant contributors to the effects of genipin. Together, these results suggest that genipin induces the expression of COX-2 in Raw 264.7 macrophages, and the induction is related with activation of NF-κB and AP-1 signaling pathway. Taken together, these findings suggest that genipin is related biological activities and induced inflammation.

## PS 2083 The Role of Transcription Factor FoxO1 in Asbestos-Induced Apoptosis of MT-2 Cells.

H. Matsuzaki<sup>1</sup>, S. Lee<sup>1</sup>, M. Maeda<sup>2</sup>, N. Kumagai-Takei<sup>1</sup>, Y. Nishimura<sup>1</sup> and T. Otsuki<sup>1</sup>. <sup>1</sup>Department of Hygiene, Kawasaki Medical School, Kurashiki, Japan; <sup>2</sup>Laboratory of Functional Glycobiology, Department of Biofunctional Chemistry, Division of Agricultural and Life Science, Graduate School of Environmental and Life Science, Okayama University, Okayama, Japan.

Asbestos is known to cause mesothelioma and lung cancer. We previously reported that asbestos affects not only mesothelial and lung epithelial cells, but also anti-tumor immune system. Regulatory T cells, Treg, produce inhibitory cytokines to suppress anti-tumor immune system. MT-2 cells were cultured with asbestos for 8 months and employed as Treg model exposed to asbestos. MT-2 cells exposed to asbestos showed higher viability after treatment with high concentration of asbestos than original MT-2 cells, and was designated as MT-2Rst. Total RNA were prepared from MT-2Rst and original MT-2 cells, respectively, and mRNA expressed in these cells were analyzed by using a micro array containing 41,000 human genes. FoxO1, forkhead transcription factor, was found to decrease in MT-2Rst cells. We generate FoxO1 knock-down MT-2 cells with shRNA. FoxO1 shRNA reduced population of apoptotic cells after treatment with asbestos, whereas did not alter basal apoptotic ratio. These results suggest that FoxO1 play a role in regulation of asbestos-induced apoptosis, and down-regulation of FoxO1 in MT-2Rst is involved in its resistance to asbestos.

## PS 2084 BCL-6 and SHP-1: Putative Regulators of TCDD-Mediated Impaired Human B Cell Activation.

A. Phadnis<sup>1,2</sup>, R. B. Crawford<sup>2,3</sup>, R. S. Thomas<sup>4</sup> and N. E. Kaminski<sup>2,3</sup>. <sup>1</sup>Genetics, Michigan State University, East Lansing, MI; <sup>2</sup>Center for Integrative Toxicology, Michigan State University, East Lansing, MI; <sup>3</sup>Department of Pharmacology and Toxicology, Michigan State University, East Lansing, MI; <sup>4</sup>Hamner Institute for Health Sciences, Research Triangle Park, NC.

The environmental contaminant 2,3,7,8-Tetrachlorodibenzo-p-dioxin (TCDD) is known to cause suppression of humoral immune responses. Evidence from epidemiological studies performed in dioxin-contaminated areas suggest associations between exposure to dioxin-like compounds and increased incidence of non-Hodgkin's lymphoma (NHL) in human subjects. We have observed that TCDD-treatment of CD40L and cytokine-activated human peripheral blood B cells leads to suppression of B cell activation. Hence, in order to elucidate the molecular mechanisms underlying impaired B cell activation by TCDD, we focused on two candidate genes – SHP-1, a protein tyrosine phosphatase that inhibits signaling in

activated B cells and BCL-6, a transcriptional repressor of B cell activation and differentiation also mutated in NHL. SHP-1 was identified through a genomic analysis of AHR binding in TCDD-treated mouse B cells. To evaluate the potential involvement of SHP-1 in this process, time-course measurements were performed and SHP-1 mRNA and protein levels were induced at day 3 in presence of TCDD. In several donors, we also observed a TCDD concentration-dependent increase in protein levels of SHP-1. With respect to BCL-6, we observed decreased downregulation of protein levels compared to control cells. When BCL-6 and SHP-1 levels were measured simultaneously in human B cells, an increase in the double positive (SHP-1hi BCL-6hi) population was seen in the presence of TCDD. This increase in SHP-1 and BCL-6 levels was observed in several TCDD-sensitive human donors and the changes were concentration-dependent. Collectively, these results suggest that the regulators, BCL-6 and SHP-1 may be involved in the TCDD-mediated suppression of human primary B cell activation. (Supported in part by NIH R01 ES002520 and P42 ES004911)

## PS 2085 Paradox of Epithelial Early Growth Response 1 in Epithelial Inflammatory Signaling under Ribosomal Insults.

K. Do, H. Choi, J. Kim, S. Park, C. Oh and Y. Moon. *Lab. of Mucosal Exposome and Biomodulation, Department Microbiology and Immunology, Pusan National University School of Medicine and Medical Research Institute, Yangsan, Republic of Korea.*

Regulation of gut epithelial NF- $\kappa$ B expression and activity are crucial for preventing overstimulation of pro-inflammatory response following exposure to commensal bacteria. To determine whether the EGR-1 modulates epithelial NF- $\kappa$ B signaling, we investigated the effects of epithelial EGR-1 on responses to bacterial NF- $\kappa$ B-activating lipopolysaccharide (LPS) in intestinal epithelial cells under ribosomal stress. Although nuclear translocation of NF- $\kappa$ B was observed in the cells exposed to LPS, chemokine expression was slightly affected. In contrast, simultaneous exposure to LPS and ribosomal insults decreased epithelial NF- $\kappa$ B activities, but chemokine expression was super-induced. Similar to our previous study, ribosomal insults-induced EGR-1 mediated induction of pro-inflammatory chemokines in the intestinal epithelial cells. Mechanistically, mucosal ribosomal insult-triggered EGR-1 mediated PPARG induction, which blocked NF- $\kappa$ B activation by LPS. Taken together, EGR-1 regulates pro-inflammatory NF- $\kappa$ B activation by LPS via EGR-1-induced PPARG although EGR-1 is a positive mediator of chemokine induction by mucosal ribosomal insult in gut epithelial cells (This study was carried out with the support of National Joint Agricultural Research Project of RDA (project number PJ008405032012) RDA, Republic of Korea).

## PS 2086 TCDD-Induced Modulation of Ig Expression in a Human B Lymphocyte Cell Line.

B. Johnson, J. Liu and C. E. Sulentic. *Pharmacology & Toxicology, Wright State University, Dayton, OH.*

2,3,7,8-tetrachlorodibenzo-p-dioxin (TCDD) is a potent environmental toxin known to inhibit immunoglobulin (Ig) gene expression in various animal studies. We have identified the mouse 3'Igh regulatory region (3'IghRR) as a sensitive transcriptional target of TCDD that may mediate inhibition of Ig expression. Interestingly, the hs1,2 enhancer of the human 3'IghRR is polymorphic and has been associated with a number of autoimmune diseases. In contrast to the inhibitory effects of TCDD on the mouse hs1,2, the human hs1,2 is activated by TCDD. Whether this species difference in hs1,2 modulation translates to the 3'IghRR and Ig expression is unknown. The sensitivity of the antibody response to TCDD-induced suppression in animal models suggests that human B-cells could be a sensitive target of TCDD; however, very few studies have evaluated the effect of TCDD on human B-cell function and Ig expression and none have evaluated the human 3'IghRR. The objective of this study was to characterize the CL-01 human B lymphocyte cell line as a potential human cellular model to determine the relationship between the AhR, 3'IghRR, Ig expression and class switch recombination. Our results support expression of a functional AhR in the CL-01 cells. TCDD treatment also induced transcriptional activity of luciferase reporters regulated by each allele of the polymorphic human hs1,2 enhancer. Additionally, the CL-01 cells can be activated to express Ig by ligands for the Toll-like receptor 9 (TLR9) and this activation appears to be sensitive to TCDD-induced modulation. Future studies will evaluate the role of the hs1,2 polymorphism in 3'IghRR activation, Ig expression and CSR and in the effects of TCDD on these processes. Since TCDD represents a large class of chemicals found in the environment, diet, and pharmaceuticals, understanding chemical-induced modulation of the human 3'IghRR and hs1,2 enhancer may provide a clue to the etiology of autoimmune diseases associated with the hs1,2 polymorphism. (Supported by NIEHS R01ES014676)

## PS 2087 Comparison of the Effects of Deoxynivalenol and Tributyltin Oxide to That of Model Compounds Inducing Endoplasmic Reticulum Stress, Ribotoxic Stress and T Cell Activation.

P. C. Schmeits<sup>1</sup>, M. R. Katika<sup>1</sup>, A. A. Peijnenburg<sup>1</sup>, H. van Loveren<sup>2</sup> and P. Hendriksen<sup>1</sup>. <sup>1</sup>Toxicology and Effect Monitoring, RIKILT Institute of Food Safety, Wageningen, Netherlands; <sup>2</sup>Laboratory for Health Protection Research, National Institute of Public Health and the Environment, Bilthoven, Netherlands.

Two common immunotoxicants, the mycotoxin deoxynivalenol (DON) and the organotin compound tributyltin oxide (TBTO), were previously studied for their effects on the human Jurkat transcriptome. DON induces ribotoxic stress and both DON and TBTO induces ER stress, oxidative stress, calcium mediated signalling, NFAT and NF $\kappa$ B pathways, T cell activation and apoptosis. The present study aimed to confirm this finding by comparing the effects of DON and TBTO on mRNA expression in Jurkat cells to that of positive controls inducing ribotoxic stress (anisomycin), ER stress (thapsigargin) and T cell activation (PHA and ionomycin).

Jurkat cells were exposed for 6 hours to subcytotoxic concentrations of DON, TBTO, anisomycin, thapsigargin, ionomycin and PHA. RNA was isolated and hybridised on Affymetrix U133 Plus 2.0 Arrays. Effects on mRNA expression were analysed on the level of individual genes or on the level of pathways.

The gene expression profiles of anisomycin and DON were almost identical confirming that DON and anisomycin both induce ribotoxic stress and act via the same mechanism. Anisomycin and DON upregulated the processes of ribosomal function, RNA biosynthesis, T cell activation and apoptosis. Genes were similarly affected by thapsigargin and TBTO confirming that both compounds induce ER stress. Both TBTO and thapsigargin upregulated genes involved in RNA biosynthesis, ER stress, T cell activation and oxidative stress, and downregulated ribosomal function. Another group of genes were upregulated by TBTO and not affected by the other compounds and are involved in DNA packaging and nucleosome assembly. As expected, ionomycin induced genes involved in T cell activation. In contrast, PHA did not affect any pathway. In conclusion we showed that DON induces ribotoxic stress and TBTO induces an endoplasmic reticulum stress response.

## PS 2088 Bidirectional Impact of Atrazine-Induced Elevations in Progesterone (P4) on the LH Surge in the Ovariectomized (OVX), Estradiol (E2)-Primed Rat.

J. M. Goldman<sup>1</sup>, L. K. Davis<sup>2</sup>, A. S. Murr<sup>1</sup> and R. L. Cooper<sup>1</sup>. <sup>1</sup>Endocrine Toxicology Branch, Toxicology Assessment Division, NHEERL, ORD, US EPA, Research Triangle Park, NC; <sup>2</sup>Impact Pharmaceutical Services, Research Triangle Park, NC.

Multiple daily exposures to the herbicide atrazine (ATRZ) have been reported to suppress the luteinizing hormone surge (LHS) in female rats. Exposure has also been found to elevate P4 concentrations, and an increase in P4 is known to have a different directional effect on LH depending on its temporal association to the surge. Consequently, the present study focused on the effects of ATRZ dose and exposure duration on the LHS in OVX, E2-primed Long-Evans rats. ATRZ was administered by gavage (1300h), and serial tail blood samples were taken at 1400, 1600, 1800 & 2000h following 1, 2 & 4 days of exposure. An initial study with 0 & 100 mg/kg (previously demonstrated to suppress the LHS after multiple treatments) significantly enhanced the afternoon LH surge peak & area under the curve (AUC) in response to a 1-day exposure, an effect consistent with kisspeptin genetic expression in the brain anteroventral periventricular region. In contrast, 4 daily treatments caused a significant suppression in both measures, whereas no effects were present following 2 days of dosing. After a 1-day treatment, prompt & marked elevations in serum P4 concentrations, attributable to adrenal secretion, were present at both 30 minutes & 1 hour, but by the 4th day a marked decline was present at 1 hour. A dose-response assessment was subsequently conducted with 0, 10, 30 & 100 mg/kg ATRZ for 1 & 4 days. At 1 day, 100 mg/kg caused similar elevations in circulating P4, the LH peak & AUC, whereas 4 daily exposures resulted in a shift to a reduced AUC. No effects on the surge were observed with 10 or 30 mg/kg at 1 or 4 days. This influence on the LHS indicates that the effectiveness of ATRZ in inducing P4-associated bidirectional shifts in LH depends on both the dosage administered and importantly on the temporal association of exposure to the appearance of the surge. (This abstract does not represent EPA policy.)

## PS 2089 Chloroethylaziridine: An Ovotoxic Metabolite of Cyclophosphamide?

J. A. Madden and A. F. Keating. *Iowa State University, Ames, IA.*

Phosphoramidate mustard (PM) has been implicated as the ultimate ovotoxic metabolite of the chemotherapeutic agent cyclophosphamide, however, studies suggest that in extra-ovarian tissues PM can spontaneously metabolize to a volatile

cytotoxic compound, chloroethylaziridine (CEZ). To our knowledge, CEZ toxicity has not been characterized directly in the ovary. Postnatal day 4 (PND4) Fisher 344 (F344) rat ovaries were cultured in media containing vehicle control (1% DMSO; CT) in the absence or presence of PM (60  $\mu$ M) or CEZ. CEZ-treated ovaries were those that were present in the same incubator as PM-treated (60  $\mu$ M) ovaries, thus receiving exposure to the volatile metabolite. Additionally, the requirement of ovarian tissue for CEZ formation was evaluated by adding PM (60  $\mu$ M) to wells that did not contain an ovary to determine any ovotoxic impact on ovaries that were in control media in the same incubator. Following 6 days of culture, follicle types were classified and counted in all treatments. Relative to control, PM and CEZ caused primordial follicle loss ( $P < 0.05$ ), with PM being more ovotoxic ( $P < 0.05$ ) than CEZ (CT -  $426.7 \pm 28.88$ ; PM -  $86.33 \pm 9.9$ ; CEZ -  $260 \pm 30.0$ ). Small primary follicle depletion only occurred following PM exposure ( $P < 0.05$ ), not CEZ, relative to CT (CT -  $103.3 \pm 16.95$ ; PM -  $3.67 \pm 1.45$ ; CEZ -  $83.67 \pm 7.8$ ). In the absence of ovarian tissue, CEZ spontaneously arose from PM, and depleted ( $P < 0.05$ ) both primordial (CT -  $377.5 \pm 53.24$ ; CEZ -  $82.75 \pm 29.93$ ) and small primary follicles (CT -  $85.0 \pm 21.91$ ; CEZ -  $24.5 \pm 6.4$ ), relative to control. Thus, ovarian tissue is not a requirement for CEZ generation from PM. This study supports that CEZ is a novel ovotoxicant that warrants further characterization in the ovary to understand its contributions to the detrimental effects of chemotherapy on female fertility. The volatility and toxicity of CEZ is particularly concerning for chemotherapy patients and their families as well as the medical professionals caring for these patients (Supported by ES016818).

**PS 2090 Role of Connexin Proteins during the Ovarian Response to 7, 12-Dimethylbenz[*A*]Anthracene Exposure in Rat Ovaries.**

S. Ganesan and A. E. Keating. *Animal Science, Iowa State University, Ames, IA.*

7,12-dimethylbenz[*a*]anthracene (DMBA) is an ovotoxic polycyclic aromatic hydrocarbon liberated through burning of organic matter. Connexin (CX) 43 and 37 are gap junction proteins providing granulosa:granulosa and granulosa:oocyte communication, respectively, and are essential for follicle survival. CX43 can inhibit chemical-induced apoptosis and low CX43 expression correlates with increased granulosa cell apoptosis. An acute single DMBA exposure to cultured postnatal day 4 (PND4) F344 rat ovaries caused loss of both large primary and secondary follicles at a concentration of 12.5 nM DMBA, while a higher concentration, 75 nM, resulted in only large primary follicle loss 8 days after exposure. This study investigated CX protein involvement during the ovarian response to DMBA exposure. PND4 F344 rat ovaries were cultured for 4 days followed by single exposures of vehicle control (1% DMSO) or DMBA (12.5 nM or 75 nM) and the culture was maintained for 4 or 8 days for Cx43 and Cx37 mRNA or protein quantification ( $n = 3$ ; 6-10 ovaries/pool) and localization ( $n = 3$ ). After 4 days, Cx37 mRNA was increased ( $P < 0.05$ ) by 12.5 nM (3.5-fold) and 75 nM (1.5-fold) DMBA exposures, while, conversely, Cx43 was decreased (12.5 nM - 0.94-fold; 75 nM - 0.70-fold;  $P < 0.05$ ). After 8 days, Cx37 and Cx43 mRNA decreased (12.5 nM - 0.99 and 0.95-fold; 75 nM - 0.85 and 0.95-fold;  $P < 0.05$ ), regardless of DMBA concentration, compared to control. CX43 protein was located between the granulosa cells of all follicle stages, while CX37 was present in the oolemma. After 8 days, decreased ( $P < 0.05$ ) CX37 (12.5 nM - 13%) and CX43 (12.5 nM - 8%; 75 nM - 23%) proteins were observed. These data support an initial increase in Cx37 and Cx43 mRNA as part of the ovarian protective response to DMBA exposure, while the decrease after 8 days of DMBA exposure is likely a reflection of the loss of follicular viability induced by DMBA. (Supported by ES016818 to AFK and AAUW fellowship to SG).

**PS 2091 Endocrine Modulation Potential of Steroids for Possible Applications in Contraception.**

K. Kim, A. Wang and K. L. Steinmetz. *SRI International, Menlo Park, CA.*

The objective of this study was to evaluate novel steroids for selective endocrine modulation potential using high-throughput in vitro screening cell-based and receptor binding systems. Steroids were tested for their potential to bind and modulate activity of the androgen receptor (AR), estrogen receptor (ER), progesterone receptor (PR), and glucocorticoid receptor (GR). For cell-based assays, a reporter gene construct of each hormone response element upstream of the luciferase reporter gene promoter was stably or transiently transfected into mammalian cells and luciferin used for light generation. Relative hormone-responsive activity was quantified by measuring light produced. In the cell-based system, the orally active androgens dimethandrolone (DMA, CDB-1321) and 11 $\beta$ -methyl-19-nortestosterone (CDB-4746) showed androgenic, progestational, anti-estrogenic, and anti-glucocorticoid activities. Their esterified prodrugs, DMAU (DMA-17 $\beta$ -undecanoate, CDB-4521) and 11 $\beta$ -methyl-19-nortestosterone 17 $\beta$ -dodecylcarbonate

(CDB-4754) were less progestational and anti-estrogenic than DMA and CDB-4746, respectively. In contrast, testosterone (CDB-0111) and testosterone 17 $\beta$ -undecanoate (CDB-3122) only showed androgenic activities. The AR binding system showed that the prodrugs have almost no receptor binding capacity compared with the parent drugs. Levonorgestrel (CDB-0107), a progestational compound used in emergency contraceptive pill, and its esterified prodrug, levonorgestrel-17 $\beta$ -butanoate (LB, CDB-1830) showed androgenic, strong progestational and anti-estrogenic, and weak anti-glucocorticoid activities. In conclusion, we have screened steroids for endocrine modulating activity. For esterified prodrugs, liberation of the parent drug by ester cleavage appears essential for biological activity. This work is supported by NICHD Contract N01-HD-9-0014.

**PS 2092 Dioxin-Produced Imprinting of Sexual Immaturity through Fixing the Status of a Reduction in the Hypothalamic Expression of Gonadotropin-Releasing Hormone.**

T. Takeda<sup>1</sup>, M. Fujii<sup>1</sup>, J. Taura<sup>1</sup>, M. Yamamoto<sup>2</sup>, M. Himeno<sup>2</sup>, Y. Ishii<sup>1</sup> and H. Yamada<sup>1</sup>. <sup>1</sup>Graduate School of Pharmaceutical Sciences, Kyushu University, Fukuoka, Japan; <sup>2</sup>Faculty of Pharmaceutical Sciences, Nagasaki International University, Sasebo, Japan. Sponsor: Y. Kumagai.

2,3,7,8-Tetrachlorodibenzo-*p*-dioxin (TCDD) causes a number of disorders in reproduction and development. Our previous studies have revealed that single treatment of pregnant Wistar rat with TCDD (1  $\mu$ g/kg, orally) reduces the pituitary synthesis of gonadotropin in perinatal pups, leading to not only a reduction in gonadal steroidogenesis but also the imprinting of sexual immaturity such as defects in sexual behaviors after growing up. However, the reason why the attenuation of pituitary gonadotropin imprints sexual immaturity remains largely unknown. To address this issue, we performed a DNA microarray analysis to identify target gene the altered expression of which is linked to dioxin-induced sexual immaturity, using the hypothalami of 70 days-old male pups. The result showed that TCDD causes alterations in the expression of many genes in the hypothalamus (up: 332, down: 283). Among them, we focused on a reduction in gonadotropin-releasing hormone (GnRH) gene, because this hormone plays a pivotal role in the regulation of sexual behaviors. Further analysis indicated that a reduction in GnRH mRNA emerges from postnatal day 4 which is involved in the critical period for the brain organization/differentiation stimulated by sex-steroids. The cerebral level of GnRH protein in the pups was also reduced by maternal exposure to TCDD, although the hypothalamic content remained unchanged. Intracerebroventricular infusion of GnRH into the TCDD-exposed pups after their growing up restored many defects in sexual behaviors. These results together with our previous findings suggest that maternal exposure to TCDD impairs the maturation of GnRH neurons in the offspring by reducing steroidogenesis at fetal and neonatal stage, and this is the origin for imprinted defects in sexual behaviors at adulthood owing to a permanent reduction in GnRH expression.

**PS 2093 Bisphenol A Down-Regulates Cytochrome P45011a1 prior to Inhibiting Steroidogenesis in Mouse Antral Follicles.**

J. Peretz and J. A. Flaws. *Comparative Biosciences, University of Illinois, Urbana, IL.*

Bisphenol A (BPA) is an endocrine disrupting chemical used in polycarbonate plastic products and the epoxy resin lining of food and beverage cans. Once released from these products, BPA readily enters the body and affects physiological processes such as steroidogenesis. Previous studies in our lab have shown that exposure to BPA decreases sex steroid hormone levels in mouse antral follicles. The current study was designed to expand these findings by testing the hypothesis that BPA first decreases the mRNA expression levels of cytochrome P45011a1 (side chain cleave; *Scx*), which then leads to decreased sex steroid hormone production. To test this hypothesis, antral follicles were mechanically isolated from adult cycling mice, individually cultured in supplemented  $\alpha$ -minimum essential medium, and treated with either vehicle control (DMSO) or various concentrations of BPA (1, 10, or 100  $\mu$ g/mL). Follicles and media were collected at various time-points between 6h and 96h. Exposure to BPA10  $\mu$ g/mL and 100  $\mu$ g/mL significantly decreased progesterone levels beginning at 24h and continuing throughout culture compared to DMSO (24h:DMSO:4.86 $\pm$ 2.25; BPA10:1.62 $\pm$ 0.82; BPA100:0.95 $\pm$ 0.06 ng/mL;  $n=5-6$ ;  $p \leq 0.05$ ). Exposure to BPA10  $\mu$ g/mL and 100  $\mu$ g/mL significantly decreased androstenedione, testosterone, and estradiol levels at 72h and 96h compared to DMSO. Further, exposure to BPA10  $\mu$ g/mL and 100  $\mu$ g/mL decreased expression of *Scx* beginning at 18h and continuing throughout culture compared to DMSO. These data suggest that BPA decreases expression of *Scx* as early as 18h and that this reduction in *Scx* leads to a decrease in progesterone production by 24h, followed by a decrease in androstenedione, testosterone, and estradiol production at

later time points. Therefore, BPA exposure targets *Sec* and thus, inhibits the conversion of cholesterol to pregnenolone, resulting in the decreased sex steroid hormone levels of BPA-exposed antral follicles.

Supported by National Institute of Health R01 ES019178 and P20 ES 018163

**PS 2094 Di(2-Ethylhexyl) Phthalate Alters the Expression of Phosphatidylinositol 3-Kinase Signaling Proteins Involved in Early Ovarian Folliculogenesis In Vivo.**

P. R. Hannon and J. A. Flaws. *Department of Comparative Biosciences, University of Illinois, Urbana, IL.*

Di(2-ethylhexyl) phthalate (DEHP) is a common plasticizer in consumer, building, and medical products containing polyvinyl chloride. Widespread production and use in everyday items represent a public health concern as humans are exposed to DEHP via ingestion, inhalation, and dermal contact. Large doses of DEHP harm ovarian function; however, the effects of DEHP on the ovary at environmentally relevant doses are unknown. Our group has shown that 30 day exposure to relatively low doses of DEHP accelerates recruitment of primordial follicles to the primary stage of development. Immature follicles at this stage rely on intrinsic ovarian factors and proper regulation of the phosphatidylinositol 3-kinase (PI3K) signaling pathway for primordial follicle survival, quiescence, and activation of folliculogenesis. Since DEHP accelerates primordial follicle activation, we tested the hypothesis that 30 day treatment with DEHP alters the expression of intrinsic ovarian factors, specifically those involved in the PI3K signaling pathway. To test this hypothesis, CD-1 mice (post-natal day 39) were orally dosed with tocopherol stripped corn oil (vehicle control) or DEHP (20 µg/kg/day, 200 µg/kg/day, 20 mg/kg/day, and 200 mg/kg/day) daily for 30 days. Whole ovaries and ovarian tissue with antral follicles removed were subjected to gene expression analysis by qPCR (n=4/group). In the whole ovary, DEHP increased the mRNA expression of *Kit* at the 20 µg/kg dose, and decreased the mRNA expression of *Pten* and *Foxl2* at the 20 mg/kg dose and *Kit*, *Pten*, *Rps6*, and *Tsc1* at the 200 mg/kg dose (e.g. *Tsc1* vehicle: 1.05±0.19; 200 mg/kg: 0.5±0.02; p≤0.05). In ovarian tissue with antral follicles removed, DEHP decreased the mRNA expression of *Mtorc1* at the 200 µg/kg and 20 mg/kg doses. These data suggest that DEHP alters the expression of factors involved in early folliculogenesis, specifically in PI3K signaling. Furthermore, the dysregulation of PI3K signaling could lead to adverse acceleration of early folliculogenesis. Supported by R01 ES019178.

**PS 2095 Humoral Immunity in Infant Cynomolgus Monkeys: Control Background Data.**

S. Oneda<sup>1</sup>, N. Lalayeva<sup>1</sup>, R. Watson<sup>1</sup>, N. Makori<sup>1</sup>, P. Franklin<sup>1</sup>, T. Beck<sup>1</sup>, K. Fukuzaki<sup>1</sup> and R. Nagata<sup>2</sup>. <sup>1</sup>SNBL USA, Ltd., Everett, WA; <sup>2</sup>Shin Nippon Biomedical Laboratories, Ltd., Tokyo, Japan.

**Background:** Developmental immunotoxicity (DIT) evaluations are performed to determine if the test article has an immunotoxic effect on the developing immune system. T-cell dependent antibody response (TDAR) to keyhole limpet hemocyanin (KLH) is one of the methods to assess DIT in the nonhuman primate. Differences in KLH-specific IgM and IgG responses within animal age and animal origin were evaluated in infant cynomolgus monkeys (*Macaca fascicularis*, hereafter Cynos).

**Methods:** KLH was administered by intramuscular injection to infant Cynos twice. The initial KLH injection (1st dose) occurred postnatal days (PND) 90, 120, 180, or 270. The second KLH injection (boost, 2nd dose) occurred 2 to 3 months after the 1st dose (PND180, 180, 240, and 330, respectively). The origins of the Cynos were Indonesian (Island, IL) and Cambodian (Mainland, ML). Serum samples were obtained prior to each KLH injection and once weekly for 4 weeks following each KLH injections. KLH-specific serum IgM and IgG levels were measured using ELISA methods.

**Results:** IgM elevated rapidly after the 1st and 2nd doses. The highest IgM in IL (69.2 and 73.6 µg/mL after the 1st and 2nd doses, respectively) was 24-27% lower than ML (95.2 and 96.4 µg/mL). IgG elevated gradually after the 1st dose but rapidly after the 2nd dose. The highest IgG after the 1st dose in IL (34.5 µg/mL) was 24% lower than ML (45.2 µg/mL). After the 2nd dose, the highest IgG in IL (1339.7 µg/mL) was 39% higher than ML (941.7 µg/mL). The profiles (patterns) of IgM and IgG were similar between IL and ML. IgM was clearly low on PND90/180 group when compared with PND120/180 while IgG was comparable. There were no notable differences in IgM and IgG between PND120/180 and PND180/240 groups. Both IgM and IgG were highest in PND270/DB330 group at most time points.

**Conclusion:** There were no remarkable differences in TDAR results between animal origins. It is recommended that TDAR assessment be conducted in 4 month or older infants.

**PS 2096 Bisphenol A Treatment of Cultured Mouse Ovarian Antral Follicles May Affect the Aryl Hydrocarbon Receptor Signaling Pathway.**

A. Ziv-Gal, Z. R. Craig, W. Wang and J. A. Flaws. *Comparative Biosciences, University of Illinois, Urbana, IL.*

Bisphenol A (BPA) is a commonly used plasticizer in the manufacture of polycarbonate plastics. Previous studies indicate that BPA exposure has toxic effects on the female reproductive system. For example, BPA (50-100 µg/ml) inhibits growth and steroidogenesis in cultured adult mouse antral follicles. Nevertheless, not much is known about the underlying mechanism. The aryl hydrocarbon receptor (AHR) is a ligand activated transcription factor that regulates cellular processes in the ovary including transcriptional activation of cytochrome P450, family 1, subfamily B, polypeptide 1 (*Cyp1b1*). Interestingly, previous studies have shown that *in-utero* BPA treatment alters expression levels of AHR signaling pathway related genes in mouse embryonic ovaries. Hence, our current study was designed to examine whether the toxic effects of BPA observed in adult mouse antral follicles are mediated by the AHR signaling pathway. We hypothesized that BPA treatment of cultured adult mouse antral follicles alters expression levels of *Ahr*, aryl hydrocarbon receptor nuclear translocator (*Arnt*), aryl hydrocarbon receptor repressor (*Ahrn*), and *Cyp1b1*. To test this hypothesis, we mechanically isolated antral follicles from mouse ovaries (C57BL/6) and cultured them in vehicle control or BPA (0.001-50 µg/mL) for 24 and 96 hours. At the end of the cultures, follicles were further processed for gene expression analyses. Our results indicate that at 24 hours, BPA 50 µg/mL treatment significantly decreased *Ahrn* and *Cyp1b1* expression levels compared to the control group (p≤0.05). At 96 hours, BPA treatment (0.001-10 µg/mL) did not alter expression levels of any of the examined genes compared to the control group. These data suggest that relatively low doses of BPA do not affect the expression levels of selected AHR related genes. A high dose of BPA (50 µg/mL) may affect the expression of selected genes in the AHR signaling pathway as early as 24 hours. Supported by: NIH ES019178 (JAF), NIH K99ES021467 (ZRC), the Environmental Toxicology Scholar Program (WW, AZG).

**PS 2097 Oral Two-Generation Reproduction Toxicity Study with Synthetic Amorphous Silica, NM200 in Wistar Rats.**

A. Wolterbeek<sup>1</sup>, S. Schneider<sup>2</sup>, R. Landsiedel<sup>2</sup>, D. de Groot<sup>1</sup>, I. Waalkens<sup>1</sup>, M. Wouters<sup>3</sup>, R. van Ee<sup>3</sup> and H. van de Sandt<sup>1</sup>. <sup>1</sup>TNO, Zeist, Netherlands; <sup>2</sup>BASF, Ludwigshafen, Germany; <sup>3</sup>TNO, Eindhoven, Netherlands. Sponsor: R. Woutersen.

Safety assessments must complement the technological progress in engineering of new nanomaterials.

Although the current test guidelines on developmental and reproductive toxicity are generally able to determine hazards, their specific application to nanomaterials needs to be evaluated. The results of a two-generation reproduction toxicity study (OECD 416) with NM200 are presented here.

Male and female Wistar Han rats (28 per group) were treated by oral gavage with NM-200 (supplied by Joint Research Centre, Italy) at dose levels of 0, 100, 300 and 1000 mg/kg body weight/day for two consecutive generations (premating 10 weeks, mating 2 weeks, gestation and lactation 3 weeks each). The nanostructured material was tested 'as delivered' and aggregates were not artificially broken down. The nanomaterial particle size distribution was characterized. Body weight and food consumption were measured regularly. Reproductive (including estrus cycle evaluation and sperm analysis) and developmental (including sexual maturation) parameters were measured and at sacrifice (reproductive) organs and tissues were sampled for histopathological analysis.

Oral administration of synthetic amorphous silica, NM-200 up to 1000 mg/kg bw/day had no adverse effects on the reproductive performance of rats or on the growth and development of the offspring into adulthood for two consecutive generations.

The systemic distribution of the silica particles will be studied in various target organs of F1-generation animals, both by chemical analysis and by electron microscopy. Measurement of uptake and organ burdens could be valuable additions to OECD standard test guidelines when applied to the hazard assessment of nanomaterials.

This study was sponsored by CEFIC (LRI-N3 project) and monitored by Monika Maier, Evonik Industries AG, Hanau, Germany on behalf of ASASP a CEFIC Sector group.

**PS 2098 Toxicological Profile and Tolerability of Pixantrone (Pixuvri) in Newborn Mice Comparative Study with Doxorubicin (DOX).**

A. M. Giusti<sup>1</sup>, P. A. Colombo<sup>1</sup>, M. Longo<sup>1</sup>, P. Della Torre<sup>1</sup>, A. Morisetti<sup>2</sup>, C. Allievi<sup>2</sup> and J. Singer<sup>3</sup>. <sup>1</sup>Accelera, Nerviano Milano, Italy; <sup>2</sup>CTI Advisor, Milano, Italy; <sup>3</sup>Cell Therapeutics, Seattle, WA.

Pixuvri at the doses of 15 and 27 mg/kg/day was given intraperitoneally to juvenile mice on Post Natal Days 10, 13, 17, 20, 35, 39 and 42 to assess its toxicological profile. Particularly, heart, bone marrow, liver and kidneys toxicity was evaluated for early and late onset.

DOX at 3 mg/kg/day was given as a comparator. Animals were sacrificed at the end of treatment and after 4- or 8-week of observation (DOX terminated after 4-week). Pixuvri up to 27 mg/kg/day was better tolerated than DOX at a dosage nine times lower (3 mg/kg/day) DOX induced a marked reduction in bodyweight gain and a cumulative mortality higher than 50% in pups, survivors being however sacrificed pre-term due to severe decay of their health conditions. Bone marrow toxicity was comparable between Pixuvri at low dose and DOX, whereas more pronounced effects were observed with Pixuvri 27 mg/kg/day, but recoverable after 4 or 8 weeks off-dose. Pixuvri was measurable in plasma up to 2 and occasionally to 6 h. after administration. After repeated treatments C<sub>max</sub> and AUC increased proportionally with the dose and no accumulation was seen. No significant gender difference was observed. Toxicity to thymus and reproductive organs was observed with both test items while no nephro- or hepatotoxicity was detected. Cardiotoxicity was negligible up to 27 mg/kg/day of Pixuvri in females, and quoted as minimal in high dose males at 4- and 8-week of recovery. The cardiotoxicity of DOX, assessed at the end of treatment and 4-week after, was lower than that of Pixuvri, although a significant reduction in heart weight was observed at the end of treatment sacrifice. Notably, for DOX it was not possible to assess the onset and severity of cardiotoxicity at the last timepoint of 8-week, that is definitely the most indicative of late cardiotoxicity. In conclusion, Pixuvri was better tolerated than DOX in newborn and young animals, all reaching adulthood, suggesting Pixuvri as a possible alternative to DOX for pediatric use.

**PS 2099 Murine Uterine Receptivity Markers Are Affected by Particulate Air Pollution in a Dose Response Manner.**

K. R. Castro<sup>1</sup>, G. Ribeiro Jr<sup>1</sup>, M. Peres<sup>1</sup>, P. Saldiva<sup>1</sup>, M. Matsuda<sup>2</sup> and M. M. Veras<sup>1</sup>. <sup>1</sup>Pathology - LIM05, University of São Paulo, São Paulo, Brazil; <sup>2</sup>Oftalmology - LIM33, University of São Paulo, São Paulo, Brazil. Sponsor: S. Barros.

It is of concern that exposure to air pollutants (AP) negatively affects reproductive function. Recently, we observed that AP is associated with increased rates of implantation failures (IF) in mice. The uterus requires a subtle collaboration of a variety of factors including: cytokines (LIF), adhesion and antiadhesion (MUC-1) molecules and hormonal induced morphological changes (e.g. decidualization, epithelial changes) to become receptive. The aim of this study was to investigate if increased IF due to chronic exposure to PM<sub>2.5</sub> could be related to changes in uterine receptivity. To test this, female mice (n=10/group) were continuously exposed (45 days) to either filtered air (AF) or 2 different daily exposure doses of concentrated ambient particles (600 and 1200 µg/m<sup>3</sup> of PM<sub>2.5</sub>). Estrous cyclicity was evaluated 2 weeks before mating and at 4.5 dpc females were euthanized and the following outcomes were evaluated: ovarian and uterine weight, number of corpora lutea, uterine histopathology and LIF and MUC-1 expression by qPCR and immunohistochemistry. We observed that the effects are dose dependent, being more pronounced in the higher dose. Results have shown that estrous cyclicity is affected by a reduction in the duration of the cycle accompanied by an extended diestrus. Ovarian weights are increased but there was no significant change in the number of CL. The histopathological evaluation of the uterus indicated a decrease in the volume and thickness of the endometrium. In both exposed groups, increased diameter and thickness of the glandular and luminal epithelium were seen. No significant alteration was observed in the expression of MUC-1 but there was significant suppression of LIF during the implantation window. In conclusion, exposure to PM<sub>2.5</sub> could have significant negative effects on endometrial receptivity by affecting the fine regulation of proliferation and differentiation (decidualization) of uterine cells mediated by LIF expression.

**PS 2100 Functional Assessment of Sexual Maturity in Female Cynomolgus Monkey (*Macaca fascicularis*).**

C. Luetjens and G. F. Weinbauer. Covance Laboratories GmbH, Muenster, Germany.

Selection of suitable criteria for assessing sexual maturity in the female long-tailed macaque (*Macaca fascicularis*) has yielded conflicting results. The present retrospective work investigates whether the presence of two consecutive menstrual bleedings hallmarks complete sexual maturation. Daily vaginal swabs were collected from 1175 Asian and 660 Mauritian origin animals and the records were used to assess the ovarian cycle pattern and seasonality. Animals were housed socially. The swabs were rated from no to heavy menstruation. Menstrual cycle length was categorized (C1, C2, and C3) depending on the cycle length difference between consecutive cycles to distinguish normal cycling females from females with prolonged cycle length. Data from 12446 cycles, comprising 1-38 cycles/animal were correlated with animal age and body weight. Mean cycle duration was 32.4 days. No seasonal differences were detected. The bleeding length for Mauritian animals (median 2.9 days) was significantly longer than for the Asian animals (median 2.6 days) and the bleeding severity differed also significantly (Mauritian animals: median 3.0; Asian animals: median 2.5). Among the 1835 females under study, 784 had single prolonged cycles and were in the category C2 or C3 whereby the Asian animals had three times more prolonged cycles. At arrival at our facility the average Mauritian origin animals were significantly heavier ( $3.75 \pm 0.62$  kg) than the Asian females ( $n=3.25 \pm 0.58$  kg) although the Asian animals were significantly older ( $4.74 \pm 1.18$  years) compared to Mauritian animals ( $4.01 \pm 0.58$  years). This investigation indicates that the onset of sexual maturity is different depending on female cynomolgus monkey origin. However, cycle lengths of the majority of cynomolgus monkeys appeared rather consistent and the cycle category was predictable. This information has to be taken into consideration in the planning phase of studies under the ICH guideline S6(R1) (ICH, 2011) in which the use of sexually mature animals have become part of toxicity studies.

**PS 2101 Air Pollution Accelerate Atherosclerosis Progression on Predisposed Mice.**

M. Peres<sup>1</sup>, K. R. Castro<sup>1</sup>, N. Costa<sup>1</sup>, G. Ribeiro Jr<sup>1</sup>, F. César<sup>2</sup>, M. Cavalcante<sup>2</sup>, D. Abdalla<sup>2</sup>, P. Saldiva<sup>1</sup> and M. M. Veras<sup>1</sup>. <sup>1</sup>Pathology, University of São Paulo, São Paulo, Brazil; <sup>2</sup>Toxicology, University of São Paulo, São Paulo, Brazil. Sponsor: S. Barros.

Exposure to urban particulate air pollution is linked to cardiovascular diseases including atherosclerosis. In this study we investigated if gestational (G) and/or post-natal (P) exposure to PM<sub>2.5</sub> is associated with aortic plaque formation in susceptible individual. LDLr<sup>-/-</sup> mice were exposed during pregnancy to either filter or polluted air (daily exposure dose=600 µg/m<sup>3</sup> of PM<sub>2.5</sub>) using a Harvard Particle Concentrator. After weaning, male pups were subdivided and 4 groups were formed according to the exposure period (G or PN). No hypercholesterolemic diet was given to the animals. After 20 weeks of exposure, we assessed non-invasively the size of atherosclerotic plaque (AP) in the aortic arch by ultrasound biomicroscopy. Then, aortic roots were collected and the expression of genes involved in plaque formation and progression was assessed by qPCR (VCAM, ICAM, PCAM, IL-1β, IL-6, IL-10, INFγ, MCP-1, CD36, MMP-1, MMP-9, TIMP-1 and TIMP-2). Birth weight was reduced in animals exposed to PM<sub>2.5</sub> during G period (less 11%). Groups exposed to PM<sub>2.5</sub> presented greater AP areas and there was an interaction effect ( $p<0.001$ ) between G and P exposures and the size the plaque ( $r=-0.43$ ,  $p<0.01$ ). Expression of IL-1β and IL-6 (proatherogenic cytokines) were higher in exposed groups and IL-10 expression (antiatherogenic cytokines) was reduced. Expression of adhesion molecules and genes involved in plaque destabilization were reduced (VCAM, MMP2, TIMP1 and 2). In most of the cases differences in genes expression were associated with G exposure to PM<sub>2.5</sub> but there were also interaction effects with P exposure. For other genes no differences were observed. Results demonstrate how environmental pollution can negatively influence intrauterine environment, impair fetal development and along with postnatal chronic exposure predispose susceptible individuals to atherosclerotic plaque formation later in life. Imbalance between pro- and anti-inflammatory cytokines might account for the progression of atherosclerosis due to PM<sub>2.5</sub> exposure.

**PS 2102 Brominated Diphenyl Ether-47 Induces Oxidative Stress-Stimulated Pro-Inflammatory Pathways in Human Extravillous Trophoblasts.**

H. Park and R. Loch-Carus. *Environmental Health Sciences, University of Michigan, Ann Arbor, MI.*

Preterm birth is associated with significant infant morbidity and mortality. Although the etiology of preterm birth is not fully determined, critical roles of oxidative stress and inflammation are implicated. Polybrominated diphenyl ethers (PBDEs) are widely used flame retardant compounds. Brominated diphenyl ether (BDE)-47 is one of the most prevalent PBDE congeners found in human breast milk, serum and placenta. Despite the presence of PBDEs in human placenta, the effects of PBDEs on pregnancy are poorly understood. The present study investigated BDE-47-induced oxidative stress and the role of oxidative stress on BDE-47-stimulated pro-inflammatory responses in a human extravillous trophoblast cell line, HTR-8/SVneo. HTR-8/SVneo cells were exposed to 5, 10, 15 and 20  $\mu$ M BDE-47 for 4 h and reactive oxygen species (ROS) generation was measured using the dichlorofluorescein (DCF) assay. Inhibition of ROS formation was measured after pre-treatment for 1 h with deferoximine (DFO), an iron-chelating antioxidant. To determine oxidative stress-mediated activation of inflammatory pathways by BDE-47, HTR-8/SVneo cells were pretreated with 1 mM DFO for 1 h prior to BDE-47 treatment for 24 h, or co-treated with 100  $\mu$ M ( $\pm$ )- $\alpha$ -tocopherol for 24 h. Cytokine release was analyzed by enzyme-linked immunosorbent assay. Treatment of HTR-8/SVneo cells with 15 and 20  $\mu$ M BDE-47 increased DCF fluorescence compared with solvent controls, indicating increased ROS formation. When cells were pretreated with DFO, BDE-47-stimulated DCF fluorescence was decreased. Pre- or co-treatment with DFO and ( $\pm$ )- $\alpha$ -tocopherol prevented BDE-47-induced interleukin-6 release. These data indicate that BDE-47-induced cytokine release in HTR-8/SVneo cells depended on ROS formation. Because inflammation occurring at gestational tissues during pregnancy has been associated with preterm birth, further research is needed to ascertain potential relevance of these findings to pregnancy and preterm labor.

**PS 2103 One-Generation Reproduction Study of Isobornyl Acetate in Rats, with an Evaluation through Sexual Maturity in the F1 Generation.**

V. T. Politano<sup>1</sup>, E. M. Lewis<sup>2</sup>, A. M. Hoberman<sup>2</sup>, R. M. Diener<sup>3</sup> and A. Api<sup>1</sup>.  
<sup>1</sup>Research Institute for Fragrance Materials, Inc., Woodcliff Lake, NJ; <sup>2</sup>Charles River Laboratories, Horsham, PA; <sup>3</sup>Argus International, Inc., Horsham, PA.

Isobornyl acetate, a widely used fragrance ingredient, was administered to male and female rats (25 rats/sex/dose) at dosages of 0, 30, 100, and 300 mg/kg/day. Administration via gavage of the test material or the vehicle, corn oil, began before the cohabitation period (83 days for males; 14 days for females), through cohabitation (maximum 14 days), until the day before sacrifice (males) or day 25 of presumed gestation (females that do not deliver) or day 22 of lactation. F1 generation rats selected for continued evaluation were sacrificed on day 60 ( $\pm$  3) postpartum. There were no treatment-related deaths at any dosage level tested. Excess salivation was observed in P generation male rats at 300 mg/kg/d and P generation females at 100 and 300 mg/kg/d. Mean body weights, body weight gains and feed consumption values were comparable among the dosage groups. There were 23, 22, 24, and 22 pregnant rats in the four dosage groups; all pregnant rats delivered litters. All natural delivery and litter observations were comparable. There were no treatment-related clinical signs, gross lesions or changes in body weight, body weight gains, feed consumption, or organ weights in the male and female F1 generation rats at any dosage level tested. Sexual maturation was unaffected in the F1 generation. Based on the results of this study, the no-observable-adverse-effect-level (NOAEL) for toxicity of isobornyl acetate is 300 mg/kg/day. The reproductive NOAEL in the P generation rats and the NOAEL for viability and growth of the F1 generation offspring is greater than or equal to 300 mg/kg/day. This dose is 2000 times greater than the conservatively calculated exposure (assuming 100% dermal absorption) to isobornyl acetate from fragrance use.

**PS 2104 Di (2-Ethylhexyl) Phthalate Is Not Genotoxic to Oocytes, but May Induce Apoptosis in Two-Cell Zygotes.**

S. Vargas-Marín, L. Vega, M. Solís-Heredia, B. Ramos-Robles, B. Quintanilla-Vega and I. Hernández-Ochoa. *Department of Toxicology, Cinvestav-IPN, Mexico City, Mexico.*

Di (2-ethylhexyl) phthalate (DEHP) is a phthalate found in food packaging, toys, medical equipment, among others. DEHP decreases the fertile capacity of the oocyte by interfering with its progression through meiosis and impairing embryo

development. Since DEHP is genotoxic to different cell types, we suggest that the decrease in the fertile capacity of the oocyte is also attributed to the genotoxic effect of DEHP. This study evaluated whether in vivo exposure to DEHP causes DNA damage in oocytes, and if this damage persists in the zygote. Female CD1 mice (n = 6 per group) were exposed orally to DEHP (20, 200 and 2000 mg/kg/d) or vehicle (corn oil tocopherol-stripped) every 24 h for 3 estrous cycles. The minimal dose of DEHP was based on the reference dose established by the Environmental Protection Agency (EPA). 5-fluorouracil (1  $\mu$ M) was used as positive control. Following treatments, mice on estrus received equine chorionic gonadotropin hormone (eCG; 5 IU) ip, 48 h later mice received hormone human chorionic gonadotropin (hCG; 5 IU) and 16 h post-hCG mice were either euthanized to collect eggs or bred with a fertile proved male mouse to collect zygotes. Oocytes were incubated with hyaluronidase to remove cumulus cells and then with Tyrode solution to remove the zona pellucida. Denuded oocytes were used to evaluate viability by staining with propidium iodide/Hoechst 33342 and DNA damage by comet assay. Viability was expressed as percentage live cells and DNA damage was assessed as the Olive Tail Moment (OTM). No significant differences in viability or OTM were observed among groups. Two-cell zygotes from mice exposed to 2000 mg/kg/d DEHP were used to assess the induction of micronuclei (MN) by staining with Hoechst 33342. DEHP did not induce MN in the zygote, however, intra-cytoplasmic prolongations resembling cell death by apoptosis were observed. These data suggest that DEHP is not genotoxic to oocytes, but it could elicit apoptosis in two-cell zygotes and thus contribute to reduced fertility. Conacyt-Mexico CB-167678.

**PS 2105 Inhaled Ambient Particulate Matter Induces Preterm Birth and Low-Birth Weight in a Mouse Model of Pregnancy.**

J. L. Blum, L. Chen and J. T. Zelikoff. *Environmental Medicine, New York University School of Medicine, Tuxedo, NY.*

Recent epidemiologic evidence has linked exposure to elevated levels of particulate matter (PM) in air pollution to preterm birth (PTB), low birth weight (LBW), and small for gestational age babies. However, several questions remain unanswered including mechanisms of action (MOA), gestational windows of vulnerability, and most active PM size and composition. To begin to better understand how PM exposure impacts fetal development, timed-pregnant B<sub>6</sub>C<sub>3</sub>F<sub>1</sub> mice were exposed whole body from gestational day (GD) 0.5 (morning of confirmed breeding) through GD17.5 to concentrated PM<sub>2.5</sub> (CAPs, at 15-times of ambient concentration) at our site in Tuxedo, NY or to filtered air (FA) for 6hr/day, 7days/wk. The daily average CAPs concentration throughout exposure was 163.8  $\pm$  99.6  $\mu$ g PM/m<sup>3</sup>. Based on EPA standards for PM<sub>2.5</sub> of 35  $\mu$ g/m<sup>3</sup>/24 hr, our 24 hr time-weighted average (i.e., 6.8  $\mu$ g/m<sup>3</sup>) is relevant for many U.S. urban centers. Exposure to CAPs in this study reduced the duration of gestation by 0.5 days (compared to FA controls), which is comparable to a 1 wk decrease in human pregnancy bringing birth close to the PT category (i.e., <37 wk). Concomitant with the observed PTB were both an 11.4% decrease in birth weight and 2.5% decrease in crown-to-rump length (CRL) at birth and at postnatal day 1. Neonates born to CAPs-exposed dams remained lighter than their filtered-air counterparts through the 21 days of nursing, though daily rates of weight gain were equal to that of FA controls. Exposure to airborne PM had no effect on conception rate, maternal weight gain during pregnancy, offspring anogenital distance, or sex ratio compared to FA control. These studies are the first to provide biological plausibility for the epidemiologic evidence demonstrating an association between PM exposure and PTB/LBW. The same recently-developed mouse model will be used in future studies to determine MOA and PM sensitive gestational "windows" of vulnerability. Supported by March of Dimes and NIEHS NYU Center ES000260.

**PS 2106 In Utero Exposure to Bisphenol A Increases Germ Cell Apoptosis in the Neonatal Mouse Ovary.**

W. Wang, Z. R. Craig, J. Peretz and J. A. Flaws. *Comparative Bioscience, University of Illinois, Urbana, Urbana, IL.*

Bisphenol A (BPA) is a known endocrine disruptor that is widely used as a synthetic plasticizer to harden polycarbonate plastics and epoxy resin. However, BPA can leach from plastic products into the food and water of consumers, leading to human exposure to BPA on a daily basis. The objective of this study was to examine the effects of prenatal BPA exposure on early ovarian development in mice. Pregnant dams (6 per treatment group) were orally dosed with tocopherol stripped corn oil (vehicle control) or BPA (0.5 and 50  $\mu$ g/kg/day) daily starting on gestation day 11 and continuing throughout pregnancy. After birth, neonatal ovaries were collected and subjected to histological evaluations and gene expression analyses. Our results show that the selected doses of BPA affected ovarian development differently. Specifically, compared to vehicle controls, BPA 0.5  $\mu$ g/kg/day treatment increased the number of healthy germ cells present in germ cell nests and increased

the number of primordial follicles, suggesting that BPA at this dose prevents apoptosis of germ cells, which is critical for the formation of the primordial pool. In contrast, BPA 50 µg/kg/day significantly increased the numbers of apoptotic germ cells, indicating BPA at this dose might accelerate germ cell apoptosis. To explore why the selected doses of BPA affect early ovarian development differently, we compared the expression of various apoptotic factors in the treatment groups. BPA 0.5 µg/kg/day increased the expression of the pro-apoptotic factor Bad and selected anti-apoptotic factors (Mcl-1, Bcl21), and the ratio of Bcl2/Bax, but decreased the expression of the pro-apoptotic factor Bik. In contrast, BPA 50 µg/kg/day significantly increased the expression of the pro-apoptotic factor Bak1. Collectively, these data suggest that in utero exposure to BPA affects early ovarian development, but that selected doses of BPA affect ovarian development differently. Supported by: NIH T32ES007326 (WW), NIH P20ES018193 (JAF), NIH K99ES021467 (ZRC).

**PS 2107 Enhanced Pre-Postnatal Toxicity Study of AMG 162 Administered by SC Injection to Pregnant Cynomolgus Monkeys with up to 6-Months Postnatal Evaluation.**

J. L. Bussiere<sup>1</sup>, R. Boyce<sup>1</sup>, I. Pyrah<sup>1</sup>, D. Branstetter<sup>2</sup>, M. Loomis<sup>1</sup>, C. Farmin<sup>3</sup>, L. Chouinard<sup>4</sup>, G. Elliott<sup>5</sup>, A. Varela<sup>4</sup> and G. Chellman<sup>5</sup>. <sup>1</sup>Amgen Inc., Thousand Oaks, CA; <sup>2</sup>Amgen Inc., Seattle, WA; <sup>3</sup>Genentech Inc., S. San Francisco, CA; <sup>4</sup>Charles River -PCS, Montréal, QC, Canada; <sup>5</sup>Charles River -PCS, Reno, NV.

AMG 162 is a fully human IgG2 monoclonal antibody that inhibits bone resorption by targeting RANKL, an essential mediator of osteoclast formation, function, and survival. Monthly SC injection of pregnant cynomolgus monkeys with 0 or 50 mg/kg AMG 162 from ~GD20 until parturition resulted in test article-related effects on the pregnant females and their offspring. In the pregnant females, there were reductions in biomarkers of bone turnover, increased stillbirths, one instance of dystocia, and one stillbirth following maternal signs of hypocalcemia. Lactation, mammary gland histomorphology, and fetal growth were comparable in controls and the AMG 162 group. In infants exposed in utero, there was increased postnatal mortality, decreased body weight gain, decreased growth/development, and decreased biomarkers of bone turnover from birth to 10 weeks of age. AMG 162-related effects in infants were present in bones (osteoclast hypoplasia, nonproliferative hyperostosis, physal hypertrophy, and decreased marrow space), normally erupted teeth (dysplasia and malalignment), lymph nodes (most absent), and in multiple tissues (extramedullary hematopoiesis). Signs of infection in multiple tissues were detected in 3 infants that underwent unscheduled necropsy. In infants necropsied at 6 months of age, there was full recovery from all bone-related changes observed earlier postpartum with some AMG 162-related effects persisting (absent/decreased size of lymph nodes, extramedullary hematopoiesis, dental dysplasia). One AMG 162-exposed infant, in which there had been recovery from pharmacological effects, had minimal to moderate mineralization of multiple tissues. In general, the effects observed in mothers and infants were consistent with the pharmacological action of AMG 162.

**PS 2108 Impact of Feed Choice When Performing Generational Reproduction Studies.**

A. Milius, R. Read, J. Waldschmidt and D. Dandekar. *Toxicology, Xenometrics, Stilwell, KS.*

The selection of an appropriate lab diet is extremely important for reproduction (repro) studies. In our lab, Purina Mills (PM) Rodent Diet 5002 has been the standard feed for all rodent repro studies for over 22 years. Our lab has not veered from this diet as a strong historical control exists with its utilization. A new diet, Harlan Teklad® (HT) Global 16% Protein Rodent Meal 2016CM, was recently introduced for use in an extended one-generation study. This feed was recommended by the supplier based on its use in other labs for repro studies and it meets the qualifications stated in guidelines of the Endocrine Disruptor Screening Program. Per guidelines, the Genistein-equivalent content of genistein plus daidzein (aglycone forms) of each batch of feed must be ≤ 300 µg/g vs. ~300 – 550 µg/g in the standard diet used in the past studies. During the delivery phase of the study, an increased incidence of pup mortality was noted in all groups including the control group. An increased incidence of pups with no milk in their stomach was also noted in all groups. Upon further evaluation, it was discovered that the feed was occluding the nostrils of many of the pups, thereby interfering with the suckling process. The general physical appearance of the HT feed was very similar to the PM, so feed-related differences due to physical form were not anticipated. However, after discovering the cause of mortalities relating to the feed, it was then noted that the texture of this feed was much finer (similar to talcum powder). Therefore, while a specific feed may be suitable for many repro & developmental study types, the same feed may not be suitable for those study types where offspring are reared. While the HT may be an excellent feed source for many repro & developmental study types, we did not consider this feed type to be suitable for our one-generation study.

Although, our findings are based on one experience in our lab, our findings demonstrate that a cautious approach should be taken when making changes in study design as any changes can be crucial to study outcome and interpretation of results.

**PS 2109 In Vitro Exposure to Di-n-Butyl Phthalate (DBP) Decreases the Expression of Cell Proliferation Transcripts in Cultured Mouse Ovarian Antral Follicles.**

Z. R. Craig, T. DelValle, W. Wang and J. A. Flaws. *Comparative Biosciences, University of Illinois, Urbana, IL.*

Di-n-butyl phthalate (DBP) is commonly found in consumer products such as plastics, cosmetics, insecticides and oral medications. We have shown previously that DBP (1000 µg/mL) inhibits growth and causes death of mouse antral follicles treated in vitro. Furthermore, we have shown that DBP may do so by altering the expression of important cell cycle regulators and causing an imbalance in the expression of key members of the *Bcl2* family, markers for the intrinsic apoptotic pathway. However, no studies have evaluated the effects of DBP on other cell proliferation markers or the extrinsic apoptotic pathway. The purpose of this study was to further investigate the mechanisms by which DBP inhibits follicle growth and causes antral follicle death. We hypothesized that DBP decreases the expression of cell proliferation genes such as *Mki67*, *Pcna*, and *Igf1*, and also increases the expression of *Fas*, a marker for the extrinsic apoptotic pathway. To test our hypothesis, antral follicles were isolated from adult CD-1 mice (32-37 days old) and individually exposed (n= 8-12/culture) to DBP (1-1000 µg/mL) or vehicle (dimethylsulfoxide, DMSO) for 24 h. Following culture, follicles were subjected to qPCR analysis for the expression of *Mki67*, *Pcna*, *Igf1*, and *Fas*. DBP treatment (100 and 1000 µg/mL) decreased the expression of *Mki67* and *Igf1* compared to control follicles (p<0.05). DBP treatment did not alter the levels of *Pcna* transcript when compared to control follicles, while *Fas* mRNA was undetectable in all treatment groups. Decreased expression of the cell proliferation genes *Mki67* and *Igf1* further supports that DBP-induced inhibition of antral follicle growth involves a defect in follicular cell proliferation. Also, undetectable *Fas* suggests that the extrinsic apoptotic pathway may not be involved under these conditions. Supported by NIH grants K99ES021467 (ZRC), R01ES019178 (JAF), T32ES007326 (WW) and the Billie Field Fellowship in Reproductive Biology (WW).

**PS 2110 Evaluating Benzo[a]pyrene Effects on Steroidogenesis and Reproduction.**

E. T. Booc<sup>1</sup>, C. Thornton<sup>1</sup>, X. Fang<sup>1</sup>, A. Lister<sup>2</sup>, D. MacLachy<sup>2</sup> and K. L. Willett<sup>1</sup>. <sup>1</sup>Pharmacology, University of Mississippi, University, MS; <sup>2</sup>Biology, Wilfrid Laurier University, Waterloo, ON, Canada.

Benzo[a]pyrene (BaP) is a polycyclic aromatic hydrocarbon (PAH) that has been implicated in modulating aromatase enzyme function. This effect has potential to interrupt normal reproductive function by causing imbalances in homeostatic androgen and estrogen levels. The aim of this study was to use a fish model, *Fundulus heteroclitus*, in order to assess whether BaP caused a significant change in steroid concentrations that could negatively alter additional reproductive biomarkers. Adult fish were exposed to waterborne BaP concentrations of (0, 1 or 10 µg/L) for 28 days. Males and females were combined for the second half of the exposure (days 14-28) in order to quantitate egg production and fertilization rates. BaP exposure did significantly reduce male gonad somatic index (GSI) and egg fertilization at 10 µg/L. Testosterone concentrations in males were significantly reduced at the high BaP dose averaging only 355 pg/mL plasma versus 2510 pg/mL in the controls. Also, estradiol concentrations in the females were significantly reduced at 1 and 10 µg/L BaP averaging 4070 and 3350 pg/mL plasma respectively compared to 7540 pg/mL plasma in the controls. Sperm concentrations, egg production, male liver somatic index (LSI), and female GSI and LSI were not altered. BaP exposure at these environmentally relevant concentrations caused negative alterations to both molecular and phenotypic biomarkers associated with reproduction. Our next goal is to assess if these parental effects will cause permanent changes in subsequent generations of progeny. (Supported by NIEHS R03 ES018962)

**PS 2111 Comparison of Estrogen Mixtures In Vitro vs In Vivo.**

B. Hannas, J. R. Furr, L. E. Gray and V. S. Wilson. *RTB, US EPA, Research Triangle Park, NC.*

Numerous sources contribute to widespread contamination of drinking water sources with both natural and synthetic estrogens, which is a concern for potential ecological and human health effects. In vitro screening assays are valuable tools for identifying mechanisms of toxicity but in vitro results cannot be directly extrapolated to in vivo exposures since most in vitro assays do not account for metabolism,

distribution and excretion or other systemic toxicities. In this study, we highlight some of the limitations associated with using *in vitro* estrogen transcriptional activation assays for predicting *in vivo* action of xenoestrogens. In particular, we compared the ability to predict the uterine growth response (uterotrophic assay, UA) to estrogens, administered to the rat orally either individually or as mixtures, using an *in vitro* estrogen transcriptional activation (TA) assay (T47D-kbluc cell line). We demonstrated that a binary mixture of bisphenol-AF (BPAF) + Methoxychlor in the UA conforms to dose additive (DA) estrogenicity, whereas the degree of estrogenicity of this mixture is underestimated by the TA assay. In contrast, the TA assay responded to a binary mixture of benzylbutyl phthalate (BBP) + BPAF in a DA manner, whereas, the UA displayed no estrogenic response to this mixture. These data illustrate the limitations associated with making *in vivo* predictions based on *in vitro* assay data for compounds that are metabolically inactivated *in vivo* in the liver, gut or other tissues or activated by the liver *in vivo*. Ongoing efforts related to this study include characterizing individual dose response curves and mixture estrogenicity for additional estrogens *in vitro* and *in vivo*. These data will be used to make predictions from the *in vitro* assay to the *in vivo* response to exposure to the compounds. This information is critical for valid interpretation of *in vitro* screening assay results. Disclaimer: Abstract does not necessarily reflect U.S.EPA policy.

**PS 2112 Bisphenol A May Affect the Fertilizing Ability of Mouse Oocytes via Mechanisms Involving Events from Sperm Penetration into the Oocyte to Formation of 1-Cell Zygote.**

B. Ramos-Robles<sup>1</sup>, M. Sánchez-Gutiérrez<sup>2</sup>, S. Vargas-Marín<sup>1</sup>, D. Acuña-Hernández<sup>1</sup>, B. Piña-Guzmán<sup>3</sup> and I. Hernández-Ochoa<sup>1</sup>. <sup>1</sup>Department of Toxicology, Cinvestav-IPN, Mexico City, Mexico; <sup>2</sup>Instituto de Ciencias de la Salud, UAEH, Pachuca, Mexico; <sup>3</sup>Departamento de Bioprocesos, UPIBI-IPN, Mexico City, Mexico.

The cumulus cells surrounding the oocyte expand before ovulation to allow oocyte maturation, and to facilitate sperm cell to penetrate the oocyte. It has been demonstrated that bisphenol A (BPA), a plasticizer that leaches from plastics into food and water, alters the expansion of cumulus cells. Since we have shown that BPA decreases the ability of oocytes, surrounded by cumulus cells, to be fertilized by sperm cells, this study examined whether BPA affects the fertilizing ability of oocytes through effects on cumulus cells, oocyte penetrability by sperm cells or zygote development to 8-cell stage. Female C57BL/6J mice (n = 6-8 per group) were exposed orally to BPA (50 µg/kg/d), diethylstilbestrol (10 µg/kg/d, positive control) or corn oil during 3 estrous cycles every 24 h. Following treatments, mice on estrus received equine chorionic gonadotropin hormone (5 IU) ip, 48 h later mice received hormone human chorionic gonadotropin (hCG; 5 IU) and 16 h post-hCG mice were either euthanized to collect oocytes and perform *in vitro* fertilization or bred with a fertility proven male mouse to collect zygotes. Percentage of fertilized oocytes decreased in BPA-treated mice compared to control regardless of the presence or absence of cumulus cells surrounding the oocyte. Percentage of penetrated oocytes by sperm cells decreased in BPA-treated mice compared to control, but additional independent experiments are needed to validate these last data. The numbers of 2-, 4- and 8-cell zygotes were similar in BPA-treated mice and control. Our data confirm the detrimental effect of BPA on the reproductive capacity of oocytes, and further suggest that BPA alters the fertilizing ability of oocytes via decreasing the oocyte penetrability and/or via mechanisms that involve events from sperm penetration into the oocyte to the formation of 1-cell zygote. Conacyt-Mexico CB-167678.

**PS 2113 Amphoteric Fluorotelomer-Based Surfactant: 28-Day Subchronic and One-Generation Reproductive Toxicity in Rats.**

J. O'Connor<sup>1</sup>, T. L. Serex<sup>1</sup> and R. C. Buck<sup>2</sup>. <sup>1</sup>Haskell, DuPont, Newark, DE; <sup>2</sup>Chemicals & Fluoroproducts, DuPont, Wilmington, DE.

An amphoteric fluorotelomer-based surfactant in glycol solvent mixture and water was evaluated in a 28-day oral gavage study (OECD 407) with a 28-day recovery subset and a one-generation reproduction study subset (OECD 422). Groups of 20 Crl:CD(SD) rats were dosed with vehicle (deionized water) containing 0, 10, 50, or 200 mg/kg/day test substance. Dams were allowed to deliver and rear their offspring until postnatal day (PND) 4. Litter examinations were determined at birth and on PND 4. For the subchronic and recovery evaluations, gross postmortem examinations were performed on selected rats and selected organs were weighed and/or retained for histopathological examination. There were no test substance related deaths or clinical observations, no effects on body weight or nutritional parameters, no effects on neurobehavioral endpoints, clinical pathology, reproductive performance, or on offspring at any dose. Test substance-related changes occurred at ≥ 50 mg/kg/day in the kidneys of male rats and in the nose of male and female rats. Increased hyaline droplets consistent with alpha2u globulin were noted at ≥ 50 mg/kg/day in the cortical tubules of males after 28 days of administration, and were

also observed in the P1 males after 45 days of test substance administration. Increased hyaline droplet accumulation was not present in the recovery males. Low incidences of nasal olfactory epithelium degeneration/atrophy were present in the 28-day and/or P1 rats at 200 mg/kg/day in males, and at ≥ 50 mg/kg/day in females. Olfactory lesions were reversible; the human relevance of this effect is unknown. No test substance-related changes were present in the nose of the 200 mg/kg/day recovery groups. Under these study conditions, the systemic toxicity NOAEL was 10 mg/kg/day based on histopathologic effects observed in the noses and kidneys of male rats at 200 mg/kg/day and in the noses of female rats at ≥ 50 mg/kg/day. The NOAEL for reproductive toxicity and effects on offspring was 200 mg/kg/day, the highest dose tested.

**PS 2114 Effects of Zearalenone with or without Proprietary Binders on Vaginal Morphology of Prepubertal Gilts.**

D. Bradley, T. J. Evans, D. Ledoux and G. Rottinghaus. University of Missouri, Columbia, MO.

The xenoestrogenic mycotoxin, zearalenone (ZEA), can cause hyperestrogenism in prepubertal gilts, resulting in changes in the size, structure, and, potentially, function of the female reproductive tract. Objectives of the present study were to: 1) evaluate ZEA-induced changes in the vaginal epithelium using morphologic parameters and 2) determine whether proprietary binders can ameliorate the xenoestrogenic effects of ZEA. Thirty prepubertal gilts were assigned to five treatment groups. The gilts were housed individually and fed either a control diet, the same control diet with an added 1.5 mg of ZEA per kg of feed, or the ZEA-contaminated diet with Binder A, B, or C added. Animals were humanely sacrificed on Day 21 and portions of the reproductive tracts were removed and fixed in formalin. Image analysis software was used to measure total vaginal lumen circumference, as well as the total length of vaginal epithelium exhibiting hyperplasia and/or squamous metaplasia. The mean vaginal luminal circumference of the cross sections was greater in ZEA-treated groups and the controls, with or without binder. Likewise, the mean percentage of hyperplastic vaginal epithelium was also higher in the ZEA-treated groups, regardless of the presence of binder. There was a tendency for two of the binders to have ameliorative effects on the percentage of vaginal epithelium undergoing ZEA-induced squamous metaplasia. It is clear that treatment with ZEA affected the morphometric parameters evaluated. While none of the binders appeared to ameliorate the ER-α estrogen receptor-mediated effects of ZEA, those effects of ZEA and its metabolites involving ER-β estrogen receptors, such as squamous metaplasia, were reduced by two of the binders. The results of this experiment demonstrated how morphometric parameters can be used to assess the effects of xenoestrogens, such as ZEA, and the potentially receptor-dependent ameliorative effects of proprietary binders.

**PS 2115 Effect of Bisphenol A (BPA) and Ethinyl Estradiol (EE2) in the Gene Expression of Estrogen Receptors (ER) and ER-Related Receptors in the Rat Prostate and Mammary Gland.**

L. Camacho, M. Basavarajappa, R. Prabhu, S. M. Lewis, M. M. Vanlandingham and K. Deldos. NCTR, US FDA, Jefferson, AR.

Tissue and temporal expression of receptors involved in estrogen signaling and their modulation by hormonally active agents are hypothesized to influence the long term effects of such agents; however, these expressions are poorly defined. NCTR Sprague-Dawley rats were dosed from gestation day 6 until parturition by oral gavage and their pups were directly dosed by the same route from postnatal (PND) 1 to 90. Dose groups included naïve and vehicle controls, BPA (2.5 µg-300 mg/kg body weight (bw)/day), and EE2 (0.5 and 5.0 µg/kg bw/day). The expression level of genes coding for nuclear ERs (Esr1 and 2), ER-related receptors (Esrra, b, and g), and G-protein-coupled ER (Gper) was analyzed in the whole prostate and female mammary gland at PND 4 and 90. Quantitative real-time RT-PCR was used and data was expressed as % Gapdh expression level. The most highly expressed receptor in PND 4 prostate was Esrra and its expression was also high in adult prostate (3 and 30% Gapdh, respectively). The expression of Esr2, which encodes ERβ, was only 0.1% Gapdh in PND 4 prostate, but increased to 40% Gapdh at PND 90. The expression of the other receptor genes was 1% Gapdh or less and was not affected by age (Esr1 > Esrrg > Gper > Esrrb). Neither BPA nor EE2 affected the expression of the receptor genes analyzed in the prostate under our conditions. In the mammary gland, the most expressed gene analyzed was ERα-coding gene Esr1 (6% Gapdh), while the least expressed gene was Esr2 (0.05% Gapdh), at both PND 4 and 90. At PND 4, Esrrg was slightly (<2x) induced by the low EE2 dose, relative to vehicle control. In the PND 90 mammary gland, both EE2 doses induced ~3x the expression of Esr2, while the expression of Esrrb was induced ~3.5x by the low, but not high, EE2 dose. BPA did not alter the expression of the genes analyzed in the mammary gland. Our data suggest that the expression of these receptors is tissue-specific and that BPA and EE2 differentially modulate their expression. IAG FDA 224-12-0003/NIH ES12013.

**PS 2116 A Combined Repeated Dose and Reproductive/Developmental Toxicity Screening Study of Perfluoroundecanoic Acid in Rats.**

A. Ono<sup>1</sup>, M. Ikeya<sup>2</sup>, T. Suzuki<sup>3</sup>, T. Nishimura<sup>4</sup>, T. Kawamura<sup>1</sup>, M. Takahashi<sup>1</sup>, M. Matsumoto<sup>1</sup>, H. Kato<sup>1</sup>, M. Hirata-Koizumi<sup>1</sup> and A. Hirose<sup>1</sup>. <sup>1</sup>Division of Risk Assessment, National Institute of Health Sciences, Tokyo, Japan; <sup>2</sup>Bozo Research Center Inc., Tokyo, Japan; <sup>3</sup>Tokyo Metropolitan Institute of Public Health, Tokyo, Japan; <sup>4</sup>Teikyo Heisei University, Chiba, Japan.

Perfluoroalkyl carboxylic acids are one of environmental contaminants which have received attention because of their possible effects on wild life and human health in recent years. In order to obtain the initial risk information on the toxicity of perfluoroundecanoic acid (PFUnA (C11)), we conducted the repeated dose and reproductive/developmental toxicity screening test. PFUnA was administered by gavage to rats at 0 (vehicle: corn oil), 0.1, 0.3 or 1.0 mg/kg/day. Males were dosed for 42 days beginning 14 days before mating and females were dosed from 14 days before mating to day 4 of lactation. During the dosing period, body weight gain was inhibited in both sexes at 1.0 mg/kg/day. In this group, there was a decrease in fibrinogen in both sexes and shortening of activated partial thromboplastin time in males. Blood biochemical examination revealed an increase in BUN and decrease in total protein in both sexes and increases in ALP and ALT and decrease in albumin in males at 1.0 mg/kg/day. The relative liver weight was increased in males at 0.3 mg/kg/day and above and in females at 1.0 mg/kg/day, and histopathologically, centrilobular hypertrophy of hepatocytes was observed in both sexes at 0.3 mg/kg/day and above. Focal necrosis and diffuse vacuolation of hepatocytes were also found in the 1.0 mg/kg/day group. Regarding the reproductive/developmental toxicity, the body weight of pups at birth was lowered and body weight gain for 4 days after birth was inhibited at 1.0 mg/kg/day while no dose-related changes were found in the other reproductive/developmental parameters. Based on these findings, the NOAELs for the repeated dose and reproductive/developmental toxicity are considered to be 0.1 mg/kg/day and 0.3 mg/kg/day, respectively.

**PS 2117 The Detrimental Effect of Bisphenol A on Mouse Two-Cell Zygote May Depend on the Dose.**

T. Moore-Ambriz<sup>1</sup>, D. Acuña-Hernández<sup>1</sup>, B. Ramos-Robles<sup>1</sup>, S. Vargas-Marín<sup>1</sup>, M. Sánchez-Gutiérrez<sup>2</sup> and I. Hernández-Ochoa<sup>1</sup>. <sup>1</sup>Department of Toxicology, Cinvestav-IPN, Mexico City, Mexico; <sup>2</sup>Instituto de Ciencias de la Salud, Universidad Autónoma del Estado de Hidalgo, Pachuca, Mexico.

Early development of the zygote begins with the first cleavage that forms diploid cells and it depends on the contribution of paternal gametes. Bisphenol A (BPA) is an environmental compound that may leach from plastics into food or water. Some studies have shown that BPA alters embryonic development but they mostly focus on effects at later stages of development. This study evaluated the effect of an *in vivo* exposure to different doses of BPA on the formation of two-cell zygotes. Female mice C57BL/6J (39 days old) (n = 6-16 per group) were orally exposed to BPA (0.05, 0.5 and 50 mg/kg/d) or corn oil (tocopherol-stripped, negative control) for 3 estrous cycles every 24 h. Following treatments, mice on estrus received equine chorionic gonadotropin hormone (5 IU) ip, 48 h later mice received hormone human chorionic gonadotropin (hCG; 5 IU) and 16 h post-hCG mice were bred with a fertility proven male mouse to collect two-cell zygotes. Zygotes were stained with Hoechst 33342 and classified for abnormalities such as cell lysing and cytoplasmic prolongations. Mice treated with all doses of BPA had lower percent of fertilized oocytes compared to control, but zygote abnormalities were observed from the dose of 0.5 mg/kg/d BPA. Specifically, two-cell zygotes from mice exposed to 0.5 mg/kg/d BPA had higher percent of cell lysing or cytoplasmic prolongations compared to control, and two-cell zygotes from mice exposed to 50 mg/kg/d BPA had higher cytoplasmic prolongations compared to control. Our data suggest that BPA alters the formation of 2-cell zygote causing abnormalities depending on the dose. Conacyt-Mexico CB-167678.

**PS 2118 Body Burden and Preliminary Effects in Rats following Low-Dose Drinking Water Exposure to a VOC Mixture during Pregnancy and Adolescence.**

A. J. Filgo<sup>1,3</sup>, D. M. Chambers<sup>2</sup>, E. M. Quist<sup>1,4</sup>, B. C. Blount<sup>2</sup> and S. E. Fenton<sup>1</sup>. <sup>1</sup>NTP Laboratory, DNTP, NIEHS, NIH, DHHS, Research Triangle Park, NC; <sup>2</sup>National Center for Environmental Health, Centers for Disease Control and Prevention, Atlanta, GA; <sup>3</sup>Curriculum in Toxicology, University of North Carolina at Chapel Hill, Chapel Hill, NC; <sup>4</sup>Comparative Biomedical Sciences, College of Veterinary Medicine, NC State University, Raleigh, NC.

Volatile organic compounds (VOCs) such as benzene, trichloroethylene, trans-1,2, dichloroethylene, tetrachloroethylene, and vinyl chloride are common industrial solvents used in a number of cleaning agents and solvents. Ingestion or inhalation

are the most common routes of reported environmental or occupational exposures to VOCs. In the US, spikes in birth defects, infant mortality, reproductive cancers and leukemia have occurred in areas where high levels of VOCs were detected in drinking water supplies. Here, time-pregnant Harlan Sprague Dawley rats and their offspring were given access to water containing mixtures of these 5 VOCs at concentrations 5, 10 and 50 times those detected in contaminated US drinking water (Sonnenfeld et al., 2001). Dams and pups were exposed from gestation day (GD) 10 until sacrifice. Blood was collected under hermetic conditions to determine VOC body burden in both dams (GD13, 15, 20 and postnatal day (PND)15, 21) and pups (PND15, 21, 28, 48). In exposed dams, low levels of VOCs were detected in the blood during pregnancy and increased during lactation. Dose dependent changes among each compound was also evident. Blood levels did not plateau, and differences in VOC body burden were attributed to the varying amounts of water consumed. Pup VOC levels also varied with changing body weight, milk and water consumption. At necropsy, pup body, liver and spleen weights were recorded and various tissues were collected for further analysis. VOC-exposure had no effect on selected organ weights or body/organ weight ratios. Morphological changes in the mammary gland were detected and were most prominent in male mammary tissue. Disclaimer: This abstract does not necessarily reflect NIEHS and CDC policy.

**PS 2119 The Inhibin B (InhB) Response to the Testicular Toxicants Mono-2-Ethylhexyl Phthalate (MEHP), 1, 3 Dinitrobenzene (DNB) or Carbendazim (CBZ) following Short-Term Repeat Dosing in the Male Rat.**

W. Breslin<sup>1</sup>, A. Paulman<sup>2</sup>, D. Sun-Lin<sup>1</sup>, K. M. Goldstein<sup>1</sup> and A. Derr<sup>2</sup>. <sup>1</sup>Eli Lilly and Company, Indianapolis, IN; <sup>2</sup>Covance Laboratories Inc., Greenfield, IN.

The objectives of this study were to evaluate the utility of plasma InhB as a biomarker of testicular injury in adult rats using the known Sertoli cell toxicants MEHP, DNB or (CBZ). The studies were run under conditions of short-term repeat dosing similar to that which would be used in early stage drug development to screen and prioritize drug candidates. The short-term high-dose exposure paradigm also allowed for assessment of changes in InhB as an early indicator of testicular injury. Following oral gavage administration of the compounds for 2 or 7 days, the rats were evaluated for clinical signs, body weight, food consumption, organ weights, plasma hormone levels, and gross and microscopic pathology of selected organs. MEHP, DNB, and CBZ produced a range of testicular toxicity characterized by minimal exfoliation of germ cells as demonstrated by increased cellular debris in the epididymis (MEHP) to more severe and dose/duration responsive Sertoli cell vacuolation, germ cell degeneration, and multinucleated giant cells of germ cell origin (DNB and CBZ). The slight to moderate Sertoli and germinal cell injuries did not correlate with significant changes in plasma InhB levels following 2 or 7 days of exposure. However, moderate to severe injury to germinal epithelium following up to 7 days of exposure, but not after a 2 day exposure, correlated with decreased in plasma InhB levels and less consistently with increases in plasma follicle stimulating hormone (FSH). In conclusion, under the conditions of these studies, changes in InhB were not an effective early onset marker of testicular toxicity or an effective marker for slight to moderate levels of acute injury and only reflected more severe disruption of spermatogenesis. Changes in plasma InhB and FSH were poorly correlated except in some instances of moderate to marked testicular toxicity.

**PS 2120 Poor Correlation between Rat Testis Histology and Serum Inhibin B after Treatment with Two Drug Candidates.**

W. J. Reagan<sup>1</sup>, R. E. Chapin<sup>1</sup>, J. A. Alvey<sup>1</sup>, R. A. Goldstein<sup>1</sup>, M. G. Dokmanovich<sup>1</sup>, K. Johnson<sup>2</sup> and F. J. Geoly<sup>1</sup>. <sup>1</sup>Drug Safety R&D, Pfizer, Inc, Groton, CT; <sup>2</sup>Arbor Analytics, Ann Arbor, MI.

Serum Inhibin B was measured in two studies of known-testis-toxic drug candidates. Study 1 was for a Hepatitis C candidate, and utilized a 10 week dosing period, followed by mating and necropsy of half of each group, and then a 12 week recovery period for the remaining 15 rats/group. At the end-of-dosing post-mating necropsy, 6 of 15 high-dose males had testis lesions (germ cell loss, degeneration); Inhibin B was significantly reduced in all animals in that group. The mid-dose group had no testis lesions but significantly reduced mean serum Inhibin B. After the 12 week recovery, 9/15 high-dose males showed damage in testes, and no mid-dose animals had testis lesions. Mean serum Inhibin B in all treated groups at recovery was not different from controls. Inhibin B appeared to both over-report and under-report testis damage in Study 1. Study 2 was an acute pathogenesis study for an antibacterial compound, using control and two dose levels and multiple time-points (days 5, 8, 15, 22, and then untreated until day 71). At each timepoint blood was sampled from all remaining rats and 5/group were killed for histologic evaluation. The low-dose group developed minimal to moderate lesions, while

serum Inhibin B was never changed. The high-dose animals progressed quickly from minimal lesions to being broadly and moderately affected (germ cell death, cell absence, disorganization); serum Inhibin B levels were reduced at days 8 and 15 only. In this study, Inhibin B appeared less sensitive than histology, except with marked testis damage, when Inhibin B was routinely low. Serum Inhibin B both over-reported damage (being reduced in the absence of lesions) and under-reported testis damage (being normal in the presence of testis lesions) in these two studies. We conclude that across both of these studies, there was a poor correlation between changes in serum levels of Inhibin B and testis histopathology.

**PS 2121 Assessment of Inhibin B As a Biomarker of Testicular Injury following Administration of Carbendazim, Cetrorelix, or 1, 2-Dibromo-3-Chloropropane in Wistar Han Rats.**

L. S. Her, A. M. Mineo, J. A. Phillips, M. S. Thibodeau and J. S. Moffit.  
*Nonclinical Drug Safety US, Boehringer Ingelheim Pharmaceuticals Inc., Ridgefield, CT.*

Although histopathology is considered the gold standard for assessing testicular toxicity in the nonclinical setting, identification of non-invasive biomarkers for testicular injury are necessary to improve safety monitoring capabilities for clinical trials. Inhibin B has been investigated as a potential noninvasive biomarker for testicular toxicity. The present study investigates the correlation of Inhibin B serum levels in Wistar Han rats with the onset and reversibility of testicular histopathology from classical testicular toxicants, carbendazim (CBZ), cetrorelix acetate (CTX), and 1,2-dibromo-3-chloropropane (DBCP). The dosing paradigm was selected with Interim (Day 8), Drug (Day 29), and non-dosing Recovery (Day 58) Phases. Monitoring of serum Inhibin B was not effective at predicting the onset of CBZ- or CTX-mediated testicular pathology in rats. Inhibin B level was reduced by DBCP administration at the end of the Drug Phase only, acting as a leading indicator of the onset of testicular toxicity, prior to the onset of germ cell depletion. However, since Inhibin B was decreased at the end of the Dosing Phase and the onset of testicular pathology occurred without any additional dosing in the Recovery Phase, it is unclear if monitoring Inhibin B would provide sufficient advanced warning of the onset of testicular pathology. Furthermore, FSH was decreased and the ratio of Inhibin B/FSH was increased with DBCP administration in the Interim Phase, but not in the Drug or Recovery Phases. Although the Inhibin B/FSH ratio was a leading indicator of testicular pathology, the effective window for monitoring may be narrow. Conclusion: Inhibin B has limited predictive capacity as a leading testicular biomarker in rats.

**PS 2122 The Inhibin B Response in Male Rats Treated with a GnRH Agonist and an Endothelin Receptor Antagonist.**

T. Mitchard, M. Coulson, S. Bickerton, J. Harris, C. Betts and J. Stewart.  
*Safety Assessment, AstraZeneca R&D, Macclesfield, United Kingdom. Sponsor: R. Roberts.*

The testis shows a moderate frequency as a preclinical toxicity target organ. This is primarily detected by histopathology and there is a need to identify circulating biomarkers to enable longitudinal monitoring and facilitate safe progression of compounds into the clinic. Inhibin B is primarily synthesized by the Sertoli cells and regulates pituitary FSH release through a negative feedback loop. This study was part of a HESI-sponsored initiative to evaluate inhibin B as a marker of spermatogenic dysfunction in the rat.

Inhibin B was measured in male Han Wistar rats (10 weeks old) administered vehicle or an endothelin receptor antagonist (ET-An) orally for 28 days or a GnRH agonist (GnRH-A) as a subcutaneous implant on Day 1. Ten animals/group/time point were killed on Days 4, 8, 15 and 29 (controls on Days 15 and 29), for testes weights and histopathology. In-life blood samples were taken on Days 4, 8, 15 and 29 to measure inhibin B, FSH and LH, and at necropsy for the same hormones plus testosterone.

Plasma inhibin B showed a wide concentration range in control animals (group means 76.4 to 184.2 pg/mL; individual animals 17.8 to 381 pg/mL). GnRH-A caused decreased testes weights plus degenerative testicular pathology from Day 4 with partial recovery by Day 29. Statistically significant reductions in inhibin B were observed at all time points and appeared to track the development and partial recovery of the pathology (generally <50 pg/mL on Days 4 to 15; group mean 92 pg/mL on Day 29). ET-An produced an increase in testes weights and a non-degenerative lesion of minimal tubular dilatation. There was a trend for lower inhibin B values (30 to 50%) at all time points, including on Day 4 when tubular dilatation was not yet evident. Overall, we conclude that following GnRH-A administration, inhibin B showed a good correlation with testicular pathology for GnRH-A, and following ET-An administration appeared to give a signal that might reflect changes in tubular function in the absence of degenerative pathology.

**PS 2123 Inhibin B As a Marker of Sertoli Cell Damage and Spermatogenic Disturbance in the Rat.**

T. Pfaff<sup>2</sup>, G. F. Weinbauer<sup>1</sup>, J. Rhodes<sup>3</sup> and M. Bergmann<sup>4</sup>. <sup>1</sup>Covance Laboratories GmbH, Muenster, Germany; <sup>2</sup>AiCuris GmbH & Co. KG, Wuppertal, Germany; <sup>3</sup>Covance Ltd., Harrogate, United Kingdom; <sup>4</sup>Department for Anatomy, Giessen, Germany.

This study was designed to determine the effects of Compound A on the fertility and early embryonic development in the male rat over a 15-19 weeks treatment and a 19 weeks treatment free period in control and 30, 60 and 180 mg/kg dose groups (n =22/group). Compound A in a dose-dependent manner induced various degrees of spermatogenic alterations compatible with Sertoli cells being the primary target, e.g. inter- and intracellular Sertoli cell vacuolization and altered cellular morphology followed by germ cell degeneration and marked reduction of epididymal sperm numbers. Blood-testis barrier remained intact (electron microscopy and hyperosmotic fixation test) until germ cells disappeared. Mating behaviour and weights of androgen-dependent prostate and seminal vesicles remained unaffected. Inhibin B levels correlated only with moderate to severe spermatogenic alterations. Ten animals with inhibin B levels below detection limit were encountered and five of these animals were fertile in week 19 but following another 15 weeks without treatment, animals were rendered infertile and inhibin B levels remained undetectable. In the rat, inhibin B only reflects major spermatogenic alterations and markedly reduced inhibin B levels might indicate irreversibility of these alterations and even infertility.

**PS 2124 The Inhibin B Response to Testicular Toxicants Ethylene Glycol Monomethyl Ether or Dibromoacetic Acid in Male Rats.**

B. Enright<sup>1</sup>, B. Torseni<sup>1</sup>, H. Lorenz<sup>2</sup> and K. Whitney<sup>1</sup>. <sup>1</sup>Abbott Laboratories, Abbott Park, IL; <sup>2</sup>Abbott GmbH & Co. KG, Ludwigshafen, Germany. Sponsor: R. Yeager.

This study was conducted as part of an ILSI-HESI consortium effort to assess the utility of circulating inhibin B as an early biomarker of testicular toxicity in rats. Two known testicular toxicants were selected for use in this study: ethylene glycol monomethyl ether (EGME) and dibromoacetic acid (DBAA). EGME (200 mg/kg/day), DBAA (250 mg/kg/day) or vehicle control (0.2% hydroxypropyl methylcellulose [HPMC]) were administered orally to male rats for 3, 6, or 14 consecutive days. On study days 4, 7, and 15, serum was collected for evaluation of inhibin B levels from all surviving animals and a subset of animals was necropsied from each of the control, EGME, and DBAA groups. Administration of EGME resulted in spermatocyte degeneration in late stage tubules and spermatocyte depletion to stage III on day 4, progressing to loss of spermatocytes and round spermatids to stage VI by day 7 and continued germ cell loss and degeneration of elongating spermatids by day 15. Inhibin B levels among EGME-treated animals progressively decreased relative to their respective controls at all time points. Administration of DBAA was associated with spermatid retention at all three time points and abnormal residual bodies at days 7 and 15. Inhibin B levels among DBAA-treated animals decreased progressively relative to their respective controls on days 7 and 15. The results of this study indicated that serum inhibin B levels in rats provided a signal of testicular toxicity for each of these known testicular toxicants administered at high levels; however, histopathology provided the earliest evidence of toxic effects.

**PS 2125 The Inhibin B Response to the Testicular Toxicant, 1, 3 Dinitrobenzene in Rats and the Analytical Evaluation of Inhibin B ELISA Kit.**

N. Bogdan<sup>1</sup>, M. Sonce<sup>1</sup>, M. Singer<sup>1</sup>, L. Hall<sup>1</sup>, S. Bryant<sup>1</sup> and P. Vinken<sup>2</sup>. <sup>1</sup>Drug Safety Sciences, Janssen Research and Development, LLC, Raritan, NJ; <sup>2</sup>Drug Safety Sciences, Janssen Research and Development, LLC, Beerse, Belgium.

**Background:** This work is part of an ILSI-HESI consortium effort to evaluate the analytical performance of a second generation ELISA kit and also to assess the utility of circulating inhibin B (InhB) as an early biomarker of testicular toxicity in rats. **Methods:** A commercially available InhB ELISA was used to assess for dilution linearity, frozen stability and serum/plasma comparison. Reference ranges were generated for male Sprague Dawley rats. To evaluate the biological utility of InhB, 1, 3-dinitrobenzene (DNB), a Sertoli cell toxicant, was orally administered to male rats for 2 or 5 consecutive days at 2 or 6 mg/kg/day. On Days 1 and 2, serum was collected for evaluation of InhB and follicle stimulating hormone (FSH) from all rats treated for 2 days, and on Days 1, 3 and 5 from all rats treated for 5 days. At the end of treatment, testes were weighed and examined histologically. **Results:** There

was no difference between serum or plasma InhB values and they were stable out to 12 weeks when stored at -20°C and -80°C. Dilution linearity was acceptable up to 32-fold. An age-related decline of InhB levels was seen between 6 and 9 weeks of age after which levels were stable up to 20 weeks. DNB caused a time-dependent increase in incidence and severity of testicular findings characterized by degeneration of the germinal epithelium, loss of pachytene spermatocytes and vacuolization of the Sertoli cells. InhB levels decreased only with the high dose treatment on Day 5 and without any associated changes in FSH. **Conclusions:** Overall, the InhB assay performed well under our conditions; however it is important to be aware of the biological variability and low control values observed by some other laboratories. In our study, a change in serum InhB levels was detected only in association with moderate/severe testicular toxicity, and is therefore considered of limited value as an early biomarker for Sertoli cell toxicity.

**PS 2126 The Inhibin B (InhB) Response to the Testicular Toxicants Hexachlorophene, Ethane Dimethane Sulfonate (EDS), Dibutylphthalate (DBP), Nitrofurazone, DL-Ethionine, 17-Alpha Ethinylestradiol, 2, 5-Hexanedione, or Carbendazim (CBZ) following Short-Term Dosing in the Male Rat.**

L. P. Saldutti<sup>1</sup>, Z. Erdos<sup>1</sup>, K. Pearson<sup>1</sup>, M. Goedken<sup>2</sup>, K. Menzel<sup>1</sup>, K. Turner<sup>3</sup> and W. E. Glaab<sup>1</sup>. <sup>1</sup>Merck Pharmaceuticals, West Point, PA; <sup>2</sup>Merck Pharmaceuticals, Kenilworth, NJ; <sup>3</sup>Research Triangle Institute, Research Triangle Park, NC.

**Background:** Inhibin B is a hetero-dimer glycoprotein that down regulates follicle stimulating hormone and is produced predominantly by the Sertoli cells. The potential correlation between changes in plasma Inhibin B and Sertoli cell toxicity was evaluated in male rats administered various testicular toxicants in 8 separate studies. Inhibin B fluctuations over 24 hours were also measured. **Methods:** For the testicular toxicity studies, five to eight Sprague-Dawley, Wistar, or Wistar-Han rats ranging from 8 to 13 weeks of age were administered 1 of 8 testicular toxicants for 1 to 29 days (depending on the compound). The 8 testicular toxicants were DL-Ethionine, dibutyl phthalate, nitrofurazone, 2,5-hexanedione, 17-alpha ethinylestradiol, ethane dimethane sulfonate, hexachlorophene, and carbendazim. For the 24-hour time period, plasma was collected by an automatic blood sampler. **Results:** Histomorphologic testicular findings were seminiferous tubule degeneration (STD), aspermatogenesis, and interstitial cell degeneration. Across the 8 testicular toxicants tested there were varying degrees of correlation between decreases in Inhibin B and STD and aspermatogenesis. In an ROC exclusion model analysis, where treated samples without histopathology were excluded, performed on all studies except EDS (Leydig cell toxicant), Inhibin B showed a sensitivity of 72% at 90% specificity, demonstrating the potential value of Inhibin B as a biomarker of testicular toxicity. **Conclusion:** Decreases in Inhibin B showed a good correlation with Sertoli cell toxicity. As anticipated, there was no correlation between decreases in Inhibin B and Leydig cell toxicity (interstitial cell degeneration). A pattern of Inhibin B secretion could not be identified over a 24 hour time period.

**PS 2127 Simvastatin and Dipentyl Phthalate Lower Testosterone Production and Exhibit Dose Additive Effects on the Fetal Testis via Distinct Mechanistic Pathways.**

B. Beverly<sup>1</sup>, C. Lambright<sup>1</sup>, J. R. Furr<sup>1</sup>, H. Sampson<sup>1</sup>, B. McIntyre<sup>2</sup>, P. M. Foster<sup>2</sup>, G. S. Travlos<sup>2</sup>, V. S. Wilson<sup>1</sup> and L. E. Gray<sup>1</sup>. <sup>1</sup>US EPA, ORD, NHEERL, TAD, Research Triangle Park, NC; <sup>2</sup>NIH, NIEHS, NTP, Research Triangle Park, NC.

Sex differentiation of the mammalian reproductive tract is a highly regulated process that is driven, in part, by fetal testosterone (T) production. In utero exposure to phthalate esters (PE) during sex differentiation can result in reproductive tract malformations in rats. PE alter the expression of genes associated with steroid synthesis/transport and cholesterol biosynthesis. Simvastatin (SMV) is a cholesterol-lowering drug that interferes with cholesterol biosynthesis. As cholesterol is a precursor for steroid biosynthesis, we proposed that like PE, maternal exposure to SMV during the critical period of sex differentiation would lower fetal T production and result in corresponding alterations in cholesterol- and androgen-mediated gene expression. Timed pregnant Sprague Dawley rats were dosed orally with 15.6, 31.25, or 62.5 mg/kg/d SMV from GD14-GD18. Testicular T production on GD18 was measured by RIA and changes in gene expression in fetal testes and livers were assessed by quantitative rt-PCR. Circulating lipid concentrations were also measured in dams and fetuses. SMV lowered fetal testicular T production and altered several genes involved in cholesterol biosynthesis in the fetal liver. Triglycerides, LDL, HDL, and total cholesterol were also lowered significantly in the fetal circulation, while lipids in the dam were not. Unlike PE, SMV did not

alter genes associated with sexual differentiation or development. In a second experiment, dams were dosed with 62.5 mg/kg/d SMV, 50 mg/kg/d dipentyl phthalate (DPeP, a PE), or a mixture of both. SMV and DPeP reduced fetal T production to 38.6 and 42.3% of the control values, respectively, but the SMV/DPeP mixture reduced T production to 20.9% of control. These studies suggest that although SMV and DPP affect two different pathways, they exhibit dose additive effects within the fetal testis.

Abstract does not reflect the views of the EPA. Support provided by USEPA/NTP IA# RW-75-92285501

**PS 2128 Postnatal Effects of Dipentyl Phthalate on Male Rat Reproductive Development.**

J. R. Furr and L. E. Gray. NHEERL, Toxicity Assessment Division, Reproductive Toxicology Branch, United States EPA, Research Triangle Park, NC.

We conducted several in utero, ex vivo and in vitro studies to characterize the relative potencies of a series of phthalates on fetal rat testis testosterone production and gene expression. Dipentyl phthalate (DPeP) was the most potent of the active chemicals in its effect on fetal testis endocrine function. Although these studies have pointed to the overall potency of DPeP, little literature exists defining its dose-response curve in vivo. The objective of this study was to determine if the potency of DPeP on fetal testis endocrine function was predictive of the ability of the chemical to induce reproductive tract malformations in male rats. We treated timed-pregnant Sprague-Dawley rats 0, 11, 33, 100 or 300 mg DPeP/kg/d, from GD 8-18 and examined the postnatal development of the male offspring. Male offspring of treated dams displayed decreased AGD, increased nipple retention, incomplete preputial separation, decreased sperm production, hypospadias, undescended testes, malformations of the testes, ventral prostate, and seminal vesicles, reduced body weight (300 mg/kg/day) and reduced postnatal survival. Phthalate syndrome (PS) malformations were seen in about 9%, 44% and 100% of the F1 male offspring at 33, 100 and 300 mg/kg/d, dosage levels that reduced fetal T production by 35%, 77% and 93% respectively. Also of note were skull malformations in highest treatment group in the form of malocclusions and incomplete zygomatic ossification. These results indicate the DPeP is about 3.5 fold more potent in inducing the PS in F1 male rats than is DEHP and demonstrate that the relative potencies for disrupting fetal testis endocrine function can be used to predict some the postnatal reproductive effects of this class of endocrine disruptors. **Disclaimer:** This abstract doesn't necessarily reflect USEPA policy. Supported in part by NTP/NIEHS IA# RW-75-92285501.

**PS 2129 Changes of Expression Levels of Oxidative Stress-Related Genes in Mouse Epididymides by Neonatal Exposure to Low-Dose Decabromodiphenyl Ether.**

M. Nakamoto<sup>1</sup>, H. Miyaso<sup>1</sup>, M. Komiyama<sup>1</sup>, Y. Matusno<sup>1,2</sup> and C. Mori<sup>1,2</sup>. <sup>1</sup>Department of Bioenvironmental Medicine, Graduate School of Medicine, Chiba University, Chiba-shi, Japan; <sup>2</sup>Center for Preventive Medical Science, Chiba University, Chiba-shi, Japan.

Decabromodiphenyl ether (decaBDE), one of polybrominated diphenyl ethers (PBDEs), is the most famous flame retardant and is used in worldwide. In a previous study, we identified adverse effects of neonatal decaBDE exposure on mouse epididymides, for example decrease of epididymal weight. On the other hand, neonatal exposure to diethylstilbestrol (DES), artificial estrogenic compounds, also causes several adverse effects on epididymides. DES exposure causes the decrease of epididymal weight, morphological abnormality, and the lasting change of expression levels of several genes. Molecular mechanisms for induction of harmful effects by decaBDE exposure remain unclear. Since many studies have reported that PBDEs have estrogenic activity, this activity may contribute to induction of adverse effects of decaBDE exposure. This study was carried out to examine how effects are caused in epididymides by neonatal decaBDE exposure, and elucidate molecular mechanisms of adverse effects by decaBDE exposure. Administration of decaBDE was performed subcutaneously at 0.25 mg/kg body weight/day, on postnatal days 1 to 5. At 12 weeks of age, epididymides were histologically examined and gene expression was analyzed using DNA microarray and real-time PCR. Our data showed that 1) no histological change was observed on epididymal tissues by neonatal decaBDE exposure, differently from that of DES, 2) decaBDE exposure could not induce the change of expression levels of genes which were affected by DES, but caused changes of expression levels of some oxidative stress related genes in mouse epididymides, 3) the expression level of Ubiquitin C (Ubc) increased in decaBDE-exposed mouse epididymides. Our presented data suggest the possibility that increase of oxidative stress is related to elicitation of harmful effects in decaBDE-exposed mouse epididymides.

## PS 2130 Structural Changes in Various Organs of Male Rats Caused by Long-Term Oral Administration of Chlorpyrifos.

S. Tripathi and A. K. Srivastav. *Department of Zoology, DDU Gorakhpur University, Gorakhpur, India.*

- Wistar rats (male) were divided into two groups — group A (GA) served as control and group B (GB) were daily administered orally chlorpyrifos (Anu Products Ltd., India) at a dose of 5 mg/kg b wt. Rats were sacrificed on 1st, 2nd, 4th, 6th, and 8th week after initiation of the experiment. Left testis and duodenum were excised and fixed in aqueous Bouin's solution. The tissues thus fixed were routinely processed for histological studies. Chlorpyrifos treatment caused degeneration in seminiferous tubules and thus inhibit the spermatogenesis in rats. Few seminiferous tubules lack the germinal epithelium. After exposure to chlorpyrifos the morphological observations of duodenum showed an increased mucous cell activity, disruption and sloughing of duodenal villar cells, lymphocytic infiltration and degeneration of cells. In conclusion the findings of the present study indicate that the organophosphate – chlorpyrifos can inhibit spermatogenesis and provoke degenerative features in the duodenum of rats and thus severely affect these organs.

## PS 2131 Assessment of Phthalate-Induced Changes in Fetal Rat Testis Gene Expression Using a rt-PCR Array.

C. Lambright<sup>1</sup>, H. Sampson<sup>2</sup>, J. R. Furr<sup>1</sup>, B. Hannas<sup>1</sup>, N. Evans<sup>1</sup>, L. E. Gray<sup>1</sup> and V. S. Wilson<sup>1</sup>. <sup>1</sup>ORD/RTD, US EPA, Research Triangle Park, NC; <sup>2</sup>ORISE/US EPA Fellow, Research Triangle Park, NC.

Phthalate esters (PE) such as diethyl hexyl phthalate (DEHP) produce reproductive malformations in male rodents by reduction of testosterone (T) production and gene expression after dams are exposed during the critical period of sexual differentiation. We investigated the effects of seven PE known to reduce fetal T production and further evaluated gene expression using novel SABiosciences PCR arrays. Each array tests for 84 genes either involved in phase one drug or lipoprotein transport and cholesterol metabolism/synthesis. Timed pregnant Sprague-Dawley rats were orally dosed with individual phthalates from gestational day (GD) 14-18. On GD 18, testes were collected from 3 fetuses per dam and cultured for 3 hours. Medium was collected and T values measured by RIA. Remaining testes were pooled by litter, RNA extracted, cleaned, quantified, and evaluated for gene expression using PCR arrays. PE were DiHP (750 mg/kg), Dihexyl (750 mg/kg), DPP (100 mg/kg), DiBP (900 mg/kg), DiNP (1500 mg/kg), DCHP (0, 100, 300, 600, or 900 mg/kg), and DEHP (750 mg/kg). Of the 84 genes on the Drug Metabolism arrays, four were significantly reduced: Cyp11b1, Cyp11a1, Cyp17a1, and ALDH2. Cyp11a1 and Cyp17a1 are involved in T synthesis, while Cyp11b1 aids in the production of cortisol and corticosterone. Using the lipoprotein/cholesterol arrays, we identified 10 genes that were significantly altered that are involved in cholesterol biosynthesis (such as APOC3, Dhcr24/7, EBP, MVK, Tm7sf2). These data support that PE effects in the fetal testis are not limited to alterations in androgen synthesis and include genes for other hormones (Insl3), growth factors, steroid transport proteins, and multiple genes involved in cholesterol synthesis. Disclaimer: This abstract doesn't necessarily reflect USEPA policy. Supported in part by NTP/NIEHS IA # RW-75-92285501-1 and fellowship administered jointly between EPA/DOE and the Oak Ridge Institute for Science and Education.

## PS 2132 Modulation by Antioxidants of Chemotherapeutic Drugs-Induced Alterations in Steroidogenic Enzyme Activities in the Testis.

N. Kilarkaje<sup>1</sup> and M. Al-Bader<sup>2</sup>. <sup>1</sup>Department Anatomy, Faculty of Medicine, Kuwait University, Safat, Kuwait; <sup>2</sup>Physiology, Faculty of Medicine, Kuwait University, Safat, Kuwait.

Combined treatment of bleomycin, etoposide and cisplatin (BEP) is a 'gold standard' therapy for several types of cancers. These drugs impair testicular functions, although the effects on Leydig cell steroidogenic enzymes are not known. We investigated the effects of the drugs on the enzymes and putative modulation by antioxidants of the drug effects. Male Wistar rats (13-15 week-old; N=5/group) were treated with either water (G1), or an antioxidant cocktail (AO; G2:  $\alpha$ -tocopherol [100 mg/kg], L-ascorbic acid [50 mg/kg], Zn [40 mg/L] and Se [100  $\mu$ g/L, po]), or BEP+AO (G4). In G3 and G4, E and P were given from day 1-5 and B on days 2, 9 and 16 of each cycle. The rats were anesthetized with ether and sacrificed by CO<sub>2</sub> asphyxiation the next day. The gene expressions were quantified by ReT-PCR by using specific primers. The expression of the proteins was evaluated by Western blotting and confocal microscopy. Data were compared by one way ANOVA and LSD test and p<0.05 was considered significant. The gene expressions of Cyp17a1,

P450scc, StAR and Scarb1 were up-regulated and that of Cyp19a1,  $\beta$ -hsd and 17 $\beta$ -hsd were down-regulated in G3 and G4. In G2, Cyp19a1,  $\beta$ -hsd, 17 $\beta$ -hsd and StAR expressions were down-regulated (p<0.05). The protein levels of LHR and  $\beta$ -HSD were unaffected, whereas that of StAR were up-regulated, and that of P450scc, 17 $\beta$ -HSD, Cyp17a, and Cyp19a were down-regulated in G2-G4 compared to G1 (p<0.05). No significant protective effects of the AO were observed, except on Cyp17a and Cyp19a. All proteins were localized in the cytoplasm. In conclusion, the drugs affect both gene and protein expressions of steroidogenic enzymes in Leydig cells and the antioxidants have limited protective effects (Supported by Kuwait University Grant # MA02/08, GM01/01 and GM01/05).

## PS 2133 Comparison of Fetal Testosterone Production in Various Tissues of the Male Sprague-Dawley Rat Dosed *In Utero* with Dipentyl Phthalate during the Critical Window of Sexual Differentiation.

K. R. Tatum-Gibbs<sup>1</sup>, J. R. Furr<sup>2</sup>, C. Lambright<sup>2</sup>, N. Evans<sup>2</sup>, B. Hannas<sup>2</sup>, B. W. Riffle<sup>1</sup>, H. Sampson<sup>1</sup>, A. K. Hotchkiss<sup>3</sup>, V. S. Wilson<sup>2</sup> and L. E. Gray<sup>2</sup>. <sup>1</sup>ORISE, US DOE, Oak Ridge, TN; <sup>2</sup>Reproductive Toxicology, US EPA, Research Triangle Park, NC; <sup>3</sup>NCEA, US EPA, Research Triangle Park, NC.

Phthalate esters are high-production volume chemicals used in the manufacture of numerous plastics and consumer products, which generates major concern for potential human exposure and environmental contamination. Several studies have demonstrated adverse effects associated with phthalate exposure administered during the critical window of sexual differentiation on the development of the male reproductive system, many of which can be attributed to a decrease in fetal testosterone (T) production. However, there is very little information regarding reduction in fetal T in tissues other than the testes and the "Point of Departure" as it relates to the relationship between reductions in fetal T levels and resultant postnatal male reproductive malformations. Therefore, the objective of the current study was to assess fetal T production in various tissues following in utero exposure to dipentyl phthalate (DPeP) to determine the relationship between reductions in fetal T with the postnatal reproductive male malformations. DPeP was given to timed pregnant Sprague-Dawley rats via oral gavage on gestation days (GDs) 14-18 at doses of 11, 33, 100, or 300 mg/kg/d (n=3); controls received the vehicle corn oil. At GD 18 dams were necropsied and fetal specimens (plasma, testes, reproductive tract, and whole body) were recovered for extraction of T using Solid Phase Extraction (SPE). We found the dose response curves for T production (media extraction) were very similar to the extracted T levels in the testes and serum. However, preliminary results suggest the dose response curves for the reproductive tract and whole body may be quite different from those of testes and serum T levels. This abstract does not reflect U.S. EPA policy. Supported by EPA/NTP IA # RW-75-922-85501

## PS 2134 Cumulative Effects of a 9 Phthalate Mixture on Charles River-Sprague-Dawley (CR-SD) Fetal Rat Testis Testosterone (T) Production and Gene Expression.

V. S. Wilson, J. R. Furr, C. Lambright, B. Hannas and L. E. Gray. *Reproductive Toxicology Branch, US EPA, ORD, NHEERL, TAD, Research Triangle Park, NC.*

*In utero* exposure to mixtures of 2 to 5 phthalate esters (PE) with similar modes of action have been shown to inhibit male reproductive development in a dose-additive fashion. Further when PE were administered to pregnant dams during the period of sexual differentiation, when reproductive malformations were observed in male offspring they correlated to significant reductions in fetal T levels. We have observed that a mixture of 9 PE administered on gestation day (GD) 14-18 to Harlan SD rats (dilutions of a fixed ratio mixture; top dose of 80 mg DEHP, DiHP, DiBP, DBP, BBP, DCHP, D(hexyl)P, D(heptyl)P, and 10 mg DPeP/kg/d) reduced fetal T production in a dose additive manner (Hannas et al, 2011). The current study compared the sensitivity of the fetal testis of CR-SD to the Harlan SD rat for disruption of testis T production and gene expression of the 9 PE mixture. A pilot postnatal study with Harlan SD rats (administered at the top dose and 67, 33, 17, and 8% of the top dose) the high dose group produced a high incidence of phthalate syndrome malformations accurately predicted by dose addition modeling, but far in excess of that predicted by response addition. The CR-SD rat (ED50 = 38% of top dose) was slightly less sensitive to disruption than the Harlan SD rat (ED50 = 26%) for fetal T production. Results demonstrate that mixtures of 9 PE behave in a manner accurately predicted by dose addition modeling. Thus considering PE hazard identification on an individual basis, without inclusion of other PE, could underestimate the risk posed by a mixture of PEs. Future postnatal 9 PE studies are planned in the CR-SD rats to determine the point of departure correlation between

reduced fetal T levels and the resultant postnatal male reproductive malformations. Disclaimer: This abstract does not necessarily reflect USEPA policy. Supported in part by NTP/NIEHS Interagency Agreement # RW-75-92285501.

## **PS 2135 Impact of Clinically Relevant Cisplatin Treatment on the Undifferentiated Spermatogonia Population and Niche.**

J. Harman and J. Richburg. University of Texas at Austin, Austin, TX.

A typical clinical cisplatin (CDDP) regimen consists of repeated cycles of 5-7 daily low dose injections followed 1-2 week recovery period; and while effective, often results in prolonged, sometimes permanent, infertility. Theoretically, undifferentiated spermatogonia (undiff-Sp), including spermatogonial stem cells (SSCs), should repopulate the testis after exposure has ceased. We hypothesize that SSC mitotic activity increases following the initial exposure to CDDP, rendering SSCs increasingly susceptible to CDDP-induced injury during subsequent cycles. We examined changes in the adult C57 undiff-Sp population and niche at days 1, 8 and 16 of the recovery period following a clinically-relevant course of 1 cycle (2.5 or 5.0 mg/kg/d) and 2 cycles (2.5 mg/kg/d) of intraperitoneal CDDP. Histological examination of the testis epithelium showed an increase in damage correlating with exposure dose and cycle number. Apoptosis was measured via TUNEL and found to increase during the recovery period following 1 cycle of 2.5mg/kg and 5.0mg/kg (300%), as well as 2 cycles of 2.5mg/kg (400%) CDDP compared to controls. Immunohistochemistry (IHC) was performed using antibodies specific for FOXO1 (undiff-Sp marker) and GDNF (critical SSC niche protein secreted by Sertoli cells). Analysis of FOXO1 showed a reduction in undiff-Sp during the recovery period following 1 cycle of 2.5 (50%) and 5.0mg/kg CDDP (66%), as well as 2 cycles of 2.5mg/kg CDDP compared with controls (50%); followed by a return to numbers equal with or surpassing controls at 16d recovery. IHC analysis of GDNF revealed a general increase in expression, prominently along the basal membrane, during the recovery period in all treatment groups. These data suggest that a greater dose of CDDP in a single cycle of exposure causes a greater impact on the functional stem cell pool and its niche and multiple cycles of exposure result in a still greater impact than an equivalent cumulative dose. Future experiments focus on whether CDDP exposure targets the SSCs, the Sertoli cells, or both.

## **PS 2136 Using a Rat Primary Epididymal Cell Model to Evaluate Drug-Induced Inflammation and Granulomas.**

K. Stachek<sup>2</sup>, W. Nowland<sup>1</sup>, T. Winton<sup>1</sup>, S. Kumpf<sup>1</sup>, S. N. Campion<sup>1</sup>, R. E. Chapin<sup>1</sup> and M. E. Hurtt<sup>1</sup>. <sup>1</sup>Drug Safety Research and Development, Pfizer Inc., Groton, CT; <sup>2</sup>College of Pharmacy, University of Rhode Island, Kingston, RI.

Epididymal inflammation and sperm granuloma formation have been detected in vivo in Sprague Dawley (SD) rats following various treatments. The objective of this in vitro primary rat cell model is to identify compounds that cause epididymal inflammation and granulomas using minimal compound and fewer animals. We had previously found that more potent granulomagens produced larger increases in transcript levels for the IL6 and GRO cytokines (3 to 10-fold increases), while less potent and negative compounds produced smaller (less than or equal to 2X) or no increases. We evaluated the marketed phosphodiesterase type 4 inhibitors, ibudilast (I), roflumilast (R), and the active metabolite roflumilast N-oxide (RNO), which are known to cause sperm granulomas in rats. Primary cultures of mixed epididymal epithelial cells were isolated and plated on Matrigel 24-well plates and exposed to increasing concentrations of test compounds. 24 hours post dosing, we measured mitochondrial metabolic activity using the MTS assay and cell lysates were evaluated for IL6, GRO, and IL10 gene expression by qRT-PCR at the IC20 (80% MTS activity). R and RNO were poorly soluble, which limited the in vitro exposure levels. Perhaps for this reason, modest increases in IL-6 and GRO were seen with R and RNO treatment (1.2- and 1-fold for R, 1.6- and 1.9-fold for RNO) while MTS activity was not reduced. However, treatment with ibudilast resulted in larger increases in IL-6 and GRO, 2.7- and 2.9-fold respectively at the IC20, consistent with its in vivo activity. The results of this study demonstrate that this primary epididymal culture model detects inflammatory signals that reflect the in vivo activity of at least one of these compounds in rats.

## **PS 2137 Evaluation of an In Vitro Model of Spermatogenesis for Predicting Testicular Toxicity.**

K. M. Goldstein<sup>1</sup>, M. Perrard<sup>2</sup>, P. Durand<sup>2</sup>, T. K. Baker<sup>1</sup> and D. E. Seyler<sup>1</sup>. <sup>1</sup>Investigative Toxicology, Eli Lilly & Co., Indianapolis, IN; <sup>2</sup>Kallistem, Lyon, France. Sponsor: C. Thomas.

Due to the complex physiology of the testes, *in vitro* models have been largely unsuccessful at predicting testicular toxicity *in vivo*. These models often bear limited resemblance to *in vivo* cellular organization. We evaluated an *in vitro* model (Hue et

al 1998) that forms tight junctions similar to the blood-testis-barrier (BTB), and supports spermatogenesis through meiosis II (secondary spermatocytes) and the formation of round spermatids. We used this *in vitro* model to evaluate the toxicity of four known testicular toxicants: Bisphenol A (BPA), 2-Methoxyacetic acid (MAA), 1,3-Dinitrobenzene (DNB), and Lindane in pre-pubertal rat seminiferous tubule cultures treated with compound for 28 days. Formation of the BTB (tight junctions) was measured by transepithelial electrical resistance (TEER) every 2 days. Cells were collected weekly for flow cytometric analysis to measure total viability and cell counts for each stage of spermatogenesis. Concentrations for each chemical were selected to approximate those shown to produce *in vivo* testicular effects. BPA and DNB decreased dramatically the TEER in a dose and time-dependent manner, whereas the effects of MAA and Lindane were less marked and transitory, even at the higher concentrations tested. Cell viability was slightly, if any, modified by the compounds; this was due most likely to the phagocytic activity of the Sertoli cells. All compounds induced dramatic dose-dependent diminutions of the populations of spermatocytes I and II, and round spermatids. It is important to note that the well-known specific toxic effects of MAA and DNB on pachytene spermatocytes were easily reproduced by this *in vitro* model. Combined, these assays not only predicted testicular toxicity *in vivo*, but also identified whether the compound directly targets the Sertoli cells or germ cells. With further validation, this cell model may be applicable as a screen to minimize running long-term live-phase studies.

## **PS 2138 Vinclozolin Alters the Testosterone Homeostasis by Regulating the Rat Liver Cytochrome P450.**

D. C. Escobar-Wilches, C. L. Zazueta-Beltran, M. L. Lopez-Gonzalez and A. Sierra-Santoyo. Toxicology, CINVESTAV-IPN, Mexico City, Mexico.

The Vinclozolin (V) is a well-characterized anti-androgenic fungicide in several species. The V is able to produce a complex pattern of induction, suppression and inhibition of cytochrome P450 (CYP) isoforms in mammals. The alteration of liver CYP expression can modify the testosterone biotransformation pattern. The objective of this work was to assess the effect of V on liver CYP expression and its repercussion on serum and urine levels of testosterone and its metabolites. Male Wistar adults rats were orally administered 100 mg/kg/d V for 7 d suspended in corn oil. After last dose the urine of 24 h was collected and animals were sacrificed and the blood was obtained by cardiac puncture. The liver was processed to obtain microsomes for enzyme assays and protein content analysis of different CYP isoforms. The testosterone and its metabolites were extracted from plasma and urine was processed by enzymatic hydrolysis using  $\beta$ -glucuronidase/sulphatase and analyzed by HPLC. V exposure increased 25% the liver relative weight and was accompanied by an increase of 40.3% of total CYP content. The liver immunoreactive protein content of CYP1A1, 1A2, 2A, 2B1 and 3A2 increased 6.5-, 16.4-, 2.3-, 6.5- and 1.5-fold, respect to the non-treated group. The protein content of CYP2E1 was not affected by V. Enzyme activities of EROD, MROD, PROD and PNPB significantly increased 3.0-, 6.4-, 64.3- and 1.6-fold, respectively. In V-treated animals testosterone levels increased 80-fold in serum and 150-fold in urine. V affected the testosterone biotransformation pattern, androstenedione levels increased in serum and urine 54- and 3.6-fold, respectively; 6-DHT increased 112-fold in urine. Other testosterone metabolites were not affected. These results indicate that V regulates liver CYP expression and alters the testosterone biotransformation pattern. In addition, they also suggest an alteration on testosterone homeostasis which may represent another mechanism of action for V. These results will provide further insight into the relationship between toxicity and V exposure.

## **PS 2139 Sperm mRNAs Are Molecular Markers of Testicular Injury in Rats.**

L. Anderson<sup>1</sup>, E. Dere<sup>2</sup> and K. Boekelheide<sup>1</sup>. <sup>1</sup>Department of Pathology and Laboratory Medicine, Brown University, Providence, RI; <sup>2</sup>Department of Urology, Rhode Island Hospital, Providence, RI.

Traditional endpoints used to measure male reproductive toxicity in humans, including semen and hormone analysis, are insensitive and unreliable; those used to monitor toxicity in animal studies, while sensitive, are not easily translatable to humans. It is therefore necessary to develop sensitive and reliable molecular biomarkers of testicular injury that can be used to both monitor human reproductive function and compare animal studies with human exposures.

**Objective:** This sub-chronic dose response study aimed to build on existing data that identified 12 mRNA transcripts that were altered in the sperm following exposure to single doses of the Sertoli cell toxicants 2,5-hexanedione (2,5-HD) or carbendazim (CBZ).

**Methods:** Adult male Fisher 344 rats were either exposed to 0, 0.14%, 0.21%, or 0.33% 2,5-HD in the drinking water for three months, or exposed by daily oral gavage to 0, 30, 50, or 70 mg/kg CBZ in corn oil for three months. Body and organ weights were obtained, and quantifiable histopathological parameters (homogenization resistant spermatid head counts and retained spermatid head counts) were measured. Sperm mRNAs were measured by qRT-PCR arrays.

**Results:** At doses that produced no-to-low levels of testicular injury, as assessed by organ weights and histopathology, a total of eight mRNA transcripts were altered in the cauda epididymal sperm. Four of the transcripts were significantly increased at the highest dose of HD, with clusterin increased in a dose responsive manner at all doses of HD. Six of the transcripts were significantly altered after exposure to CBZ, with clusterin also increased in a dose responsive manner at all doses of CBZ.

**Conclusions:** Our data indicate that sperm mRNA transcripts are sensitive markers of testicular toxicity. The clusterin transcript in particular may be a more sensitive indicator of Sertoli cell injury than the most sensitive histopathological endpoint.

## PS 2140 Effect of Neonatal Exposure to Decabromodiphenyl Ether on Transcript Levels of Splicing Factors in Mouse Testes.

H. Miyaso<sup>1</sup>, N. Nakamura<sup>2</sup>, Y. Matsuno<sup>3,1</sup>, M. Komiya<sup>1</sup> and C. Mori<sup>1,3</sup>.

<sup>1</sup>Department of Bioenvironmental Medicine, Graduate School of Medicine, Chiba University, Chiba, Japan; <sup>2</sup>Department of Pharmacology, Physiology and Toxicology, Marshall University, Huntington, WV; <sup>3</sup>Center for Preventive Medical Science, Chiba University, Chiba, Japan.

Decabrominated diphenyl ether (decaBDE) is one of flame retardants and is used in worldwide. Our previous study found postnatal exposure to decaBDE had adverse effect to male reproduction in mice. Mice were injected subcutaneously 0.025, 0.25, and 2.5 mg/kg decaBDE during postnatal day 1-5 and evaluated at 12 weeks of age. In 0.025, and 0.25 mg/kg dose groups, the number of Sertoli cells was reduced significantly. Thyroid hormones (THs) are key players for Sertoli cells development. We identified that the transcript levels of TH receptor  $\alpha$  (Thra) decreased significantly in testes of 0.025 mg/kg decaBDE dose group, while no change of TH levels was observed between control and all dose groups. Moreover, we found the ratio of Thra1/Thra2 level decreased in 0.025 and 0.25 mg/kg dose groups compared to control group. The ratio of Thra1/Thra2 level is known to be varied by the change physiologically, and the ratio of heterogeneous ribonucleoprotein (hnRNP) A1 (hnrnpa1): serine/arginine-rich splicing factor 1 (Srsf1) is related to Thra1/Thra2 level. However, no change was observed in hnrnpa1: Srsf1 level between control and dose groups. Therefore, we hypothesized other splicing factors may be involved in decrease of Thra1/Thra2 level. In this study, the transcript levels of hnRNP F (hnrnpf) and hnRNP H1 (hnrnp1) were examined by real-time PCR. Mice were dosed by above described method, and testes were collected at 12 weeks of age. Our data showed the decrease in transcript level of hnrnpf in 0.025 mg/kg dose group, and decrease of hnrnp1 level in 0.25 and 2.5 mg/kg dose groups compared to the control group. Our study suggests that hnrnpf and hnrnp1 are also involved in the decrease of Thra1/Thra2 ratio by neonatal decaBDE exposure.

## PS 2141 RSPOs Counteract TCDD Inhibition of Canonical Wnt Signaling during Fetal Mouse Prostate Development.

A. Branam<sup>1,2</sup>, N. M. Davis<sup>1,2</sup>, R. W. Moore<sup>1,2</sup>, A. J. Schneider<sup>1,2</sup>, C. M. Vezina<sup>1,3</sup> and R. E. Peterson<sup>1,2</sup>. <sup>1</sup>University Wisconsin-Madison, Madison, WI; <sup>2</sup>Pharmacy, UW-Madison, Madison, WI; <sup>3</sup>Comparative Biosciences, UW-Madison, Madison, WI.

Prostatic buds are derived from the urogenital sinus (UGS) and later form into the prostate ductal network in adult mammals. In utero TCDD exposure causes mispositioning and reductions in dorsal and lateral prostatic bud numbers and prevents formation of ventral buds leading to ventral prostate agenesis. Here we examined canonical Wnt signaling following TCDD exposure in vitro. We found multiple components of the pathway (Lef1, Tcf1, Wif1, Lgr5) to be downregulated by TCDD. R-spondins (RSPOs) are promoters of canonical Wnt signaling but their mechanism for activating the canonical Wnt pathway is not fully understood. Previously, we demonstrated RSPO2 and RSPO3 promote prostatic bud development and addition of these proteins can rescue the effects of TCDD on prostatic bud growth. We now further examined the mechanism of RSPO activation of the Wnt pathway in the UGS by studying the extracellular Wnt antagonists, DKKS, and determining their effects on budding in vitro and examining LGRs, which are putative RSPO receptors, by studying mRNA expression between vehicle and TCDD treated UGSs. Both mechanisms of Wnt activation by RSPOs have been demonstrated in other systems; however, it remains unclear if RSPOs preferentially

act through one mechanism over the other. Our results showed little effect on prostate bud number following treatment with DKK1 and DKK2. We found both Lgr4 and Lgr5 mRNA expression in the basal epithelium (BE) where prostatic buds form and additionally we found a decrease by TCDD in Lgr5 mRNA levels in vitro. These results suggest that RSPOs bind to LGRs located in the BE of the UGS to initiate prostate bud formation. Together, these data illustrate that TCDD inhibits multiple components of the Wnt signaling pathway and that the combined inhibition of these components significantly contributes to the inhibitory budding phenotype caused by TCDD. (Grant support: NIH ES01332, T32 ES007015)

## PS 2142 Sensitivity of Toxicological Endpoints to Detect Alterations in the Male Reproductive System of Nonhuman Primates.

G. D. Cappon<sup>1</sup>, D. Potter<sup>1</sup>, M. E. Hurr<sup>1</sup>, G. F. Weinbauer<sup>2</sup> and C. J. Bowman<sup>1</sup>. <sup>1</sup>Pfizer Worldwide Research & Development, Groton, CT; <sup>2</sup>Covance Laboratories GmbH, Muenster, Germany.

The assessment of the potential for a compound to cause toxicity to male reproductive processes relies heavily on histopathology and organ weights of the reproductive tissues. This is even more so with biologics where non-human primates (NHP) is the only relevant species and evaluation of functional fertility is impractical. To address this shortcoming ICH S6(R1) included a trigger for the addition of non-routine endpoints to NHP studies in cases where there is reproductive cause for concern. To determine the sensitivity of these endpoints to perturbation we performed a power analysis of routine and triggered endpoints. The analysis was done on control data from sexually mature Asian and Mauritian sourced NHP used in toxicity studies at Covance Laboratories GmbH. The power calculations were performed with a 2 sample two-sided T-test ( $\alpha=0.05$ ) assuming 3 NHP/group and the number of observations ranged from 98 to 472 per endpoint. For reproductive organ weights the power to detect a 50% change from control was 30%, 35%, 18% and 13% for testes, epididymides, prostate, and seminal vesicle, respectively. For testicular volume the power to detect a 50% change was ~ 30%, with slight differences depending on the method (caliper or ultrasound). For seminal analysis the power to detect a 50% change was 6%, 6%, 66% and 41% for ejaculate weight, sperm count, sperm motility, and sperm morphology (percent normal), respectively. For male hormone data the power to detect a 50% change was 10%, 30%, 7% and 78% for testosterone, inhibin B, luteinizing hormone, and follicle stimulating hormone, respectively. Given samples sizes of 3 per treatment group, and the magnitude of biological variability observed for these endpoints, the ability to draw conclusions about potential toxicity will be limited for most endpoints. Consequently, great care should be taken in the choice of endpoints added to general toxicity studies to assess the male reproductive system.

## PS 2143 Contribution of PI3K/Akt/DAF-16 Activity in *C. elegans* to Gene-Environment Interactions following MeHg Exposure.

S. J. Fretham and M. Aschner. *Pediatric Toxicology, Vanderbilt University Medical Center, Nashville, TN.*

Neither genetic nor environmental factors completely explain the etiology and progression of dopaminergic (DAergic) neurodegeneration in Parkinson's disease (PD). This study examines PI3K/Akt signaling as a mechanistic link between environmental and genetic factors known to contribute to PD. Specifically the interaction between methylmercury (MeHg) exposure, a ubiquitous neurotoxin, and PARK7 (DJ-1), an autosomal recessive PD gene. PI3K/Akt signaling is highly conserved and regulates many aspects of neuronal survival and function. MeHg exposure has been shown to activate PI3K/Akt signaling and DJ-1 modifies PTEN activity, an upstream regulator of PI3K/Akt. Mutant and transgenic *Caenorhabditis elegans* (*C. elegans*) strains were used to determine if PI3K/Akt responsiveness and loss of DJ-1 increases MeHg vulnerability. Strains used include: wild type (WT) Bristol N2; strains null for daf-16, age-1, daf-18, djr-1.1, and djr-1.2; and a strain overexpressing DAF16::GFP. Synchronous L1 populations were treated with 0-40  $\mu$ M MeHg for 30 minutes followed by assessment of survival and basal slowing (a dopamine-dependent feeding behavior). Compared to WT worms, increased PI3K/Akt activity resulting from genetic loss of daf-18 (PTEN homolog) and daf-16 (FOXO homolog) led to increased death and lower lethal dose (LD50) values following MeHg treatment while decreased PI3K/Akt activity through loss of age-1 (PI3K homolog) and overexpression of DAF-16::GFP increased survival. Loss of djr-1.1 or djr-1.2 (PARK7 homologs) did not affect survival. Basal slowing was significantly reduced in WT worms following 20  $\mu$ M but not 10  $\mu$ M MeHg treatment ( $p<0.01$ ). Basal slowing in worms lacking djr-1.1 but not djr-1.2, was decreased by 10  $\mu$ M and 20  $\mu$ M MeHg, suggesting that loss of djr-1.1 increases DAergic sensitivity to MeHg. Collectively, these findings demonstrate that MeHg-induced

PI3K/Akt activation contributes to toxicity and that MeHg impairs DAergic behavior, an effect that is enhanced by loss of *djr-1.1*. (Work supported by NIEHS R01-07331 and NIEHS T32-ES007028).

**PS 2144 Low-Dose Postnatal MeHg Exposure Alters mRNA Levels of Rat Brainstem Glutamate Receptors and Voltage Gated Calcium Channels.**

A. Colón-Rodríguez, R. K. Hajela, S. Escudero, Y. Yuan and W. D. Atchison. *Pharm/Tox, Michigan State University, East Lansing, MI.*

Methylmercury (MeHg) hastens the onset of motor paralysis in SOD-1 G93A mice, a genetic model of Amyotrophic Lateral Sclerosis (ALS), suggesting a gene-environment interaction in a genetically susceptible animal model. Associated with this are alterations in  $[Ca^{2+}]_i$  and glutamate receptor (GluR) function, both of which are suggested targets for MeHg toxicity. The goal of this study was to determine if MeHg alters mRNA levels of voltage gated  $Ca^{2+}$  channels (VGCCs), NMDA, or AMPA receptors. We measured mRNA levels of the pore forming  $\alpha_1$  subunit of L, N, P/Q and R type VGCCs, NR1 and NR2A subunits of NMDA receptors and GluR2 and GluR3 subunits of AMPA receptors. Determining if MeHg alters levels of these ion channels could contribute to understanding of MeHg-induced alteration in  $[Ca^{2+}]_i$  in motor neurons. Postnatal day 5 rats were treated sc with 0.75 or 1.5 mg/kg/day MeHg for 15 or 30 days (d), then stopped for a clearing period of 30 d. Quantitative real time PCR was performed on reverse transcript of RNA isolated from 10 mg of brainstem tissue, a region rich in motor neurons. MeHg treated animals had higher levels of GluR2, GluR3 and NR2A at 15 d in both 0.75 and 1.5 mg/kg/day exposure. MeHg induced an increase in the levels of all GluR subunits studied. It was highest at 30 d, and more pronounced in the 0.75 mg/kg/day exposure. GluR2 was the most affected subunit. At 60 d, levels of all GluR subunits were increased but at levels similar to those seen at 15 d of exposure. With the exception of  $\alpha_{1A}$ , levels of all VGCC  $\alpha_1$  subunits were higher at 0.75 mg/kg/day MeHg exposure on 15 and 30 d and lower at 60 d. At 15 d 1.5 mg/kg/day MeHg increased levels of all VGCC  $\alpha_1$  subunits except  $\alpha_{1E}$ . At 30 d the level was even higher for all of the  $\alpha_1$  subunits, but returned to levels similar to those at 15 d after the clearing period. The increase in the level of GluR subunits and most of the VGCCs could contribute to the alteration in  $Ca^{2+}$  homeostasis induced by MeHg on motor neurons. Supported by NIH grants R01ES03299 and R25NS065777.

**PS 2145 Effects of Chronic Postnatal Methylmercury Exposure on mRNA Expression of Calcium Regulatory Proteins in Adult Mouse Brain Stem.**

J. A. Musser<sup>1,2</sup>, A. Colón-Rodríguez<sup>1</sup> and W. D. Atchison<sup>1,2</sup>. <sup>1</sup>Department Pharmacology/Toxicology, Michigan State University, East Lansing, MI; <sup>2</sup>College of Veterinary Medicine, Michigan State University, East Lansing, MI.

Methylmercury (MeHg) causes marked alterations in neuronal  $[Ca^{2+}]_i$  homeostasis through its interaction with membrane ion channels such as voltage-gated  $Ca^{2+}$  channels (VGCCs), and  $Ca^{2+}$  permeable ligand-gated channels-NMDA (NMDAR) and AMPA receptors (AMPA). Chronic postnatal exposure to MeHg hastens the onset of Amyotrophic Lateral Sclerosis-like phenotype in the SOD1G93A genetically susceptible mouse model via glutamate-mediated excitotoxicity. The underlying mechanism of MeHg effects on brainstem motor neurons remains unclear. In this study we focused on examining the effects of chronic MeHg exposure on mRNA expression of the pore-forming  $\alpha_1$  subunits of the L ( $\alpha_{1L}$ ), N ( $\alpha_{1N}$ ), P/Q ( $\alpha_{1P/Q}$ ) and R-type ( $\alpha_{1R}$ ) VGCCs, NR1 and NR2 subunits of the NMDAR, GluR2 and GluR3 subunits of the AMPAR,  $Ca^{2+}$  binding proteins calbindin D28K and parvalbumin, and glutamate transporter EAAT2, all of which can modulate  $[Ca^{2+}]_i$  homeostasis. Eleven week old male ICR mice were exposed to 0, 0.5 or 5 ppm MeHg in drinking water *ad libitum* for 6 mos. Total RNA was extracted from 10 mg of brainstem and reverse transcription PCR performed. Quantitative real time PCR was performed on reverse transcript (cDNA) to measure expression of the target genes. Exposure to 0.5 ppm MeHg induced a decrease in the expression of the AMPAR subunits,  $Ca^{2+}$  binding proteins and the  $\alpha_1$  subunit of the N- and P/Q-type VGCCs. NMDAR expression at 0.5 ppm MeHg exposure was not altered for the NR1 subunit but was increased for NR2. At 5 ppm MeHg decreased expression of GluR2, EAAT2, calbindin D28K, parvalbumin, and all of the VGCC subunits. Expression of AMPAR subunit GluR3 was increased at 5ppm exposure. These results support the idea that MeHg-induced increase in  $[Ca^{2+}]_i$  on brainstem motor neurons is due to the glutamate receptors (greater GluR2 expression, and NR2 expression), or inefficient  $Ca^{2+}$  buffering (decrease in the  $Ca^{2+}$  binding proteins and EAAT2 transporter). VGCCs may not contribute to the alteration in  $[Ca^{2+}]_i$  induced by MeHg because their expression was decreased. Supported by NIH grants R01ES03299 and R25NS065777.

**PS 2146 Perinatal Exposure to Low-Dose Methylmercury Induces Dysfunction of Motor Coordination with Decreases in Synaptophysin Expression in the Cerebellar Granule Cells of Rats.**

M. Fujimura. *Basic Medical Sciences, National Institute for Minamata Disease, Minamata, Japan.* Sponsor: A. Naganuma.

Methylmercury (MeHg) is an environmental pollutant that is toxic to the developing central nervous system (CNS) in children, even at low exposure levels. Perinatal exposure to MeHg is known to induce neurological symptoms with neuropathological changes in the CNS. However, the relationship between the neurological symptoms and neuropathological changes induced in offspring as a result of exposure to low-dose MeHg is not well defined. In the present study, neurobehavioral analyses revealed that exposure to a low level of MeHg (5 ppm in drinking water) during developmental caused a significant deficit in the motor coordination of rats in the rotating rod test. In contrast, general neuropathological findings, including neuronal cell death and the subsequent nerve inflammation, were not observed in the region of the cerebellum responsible for regulating motor coordination. Surprisingly, the expression of synaptophysin (SPP), a marker protein for synaptic formation, significantly decreased in cerebellar granule cells. These results showed that perinatal exposure to low-dose MeHg causes neurobehavioral impairment without general neuropathological changes in rats. We demonstrated for the first time that exposure to low-dose MeHg during development induces the dysfunction of motor coordination due to changes of synaptic homeostasis in cerebellar granule cells.

**PS 2147 Striatal Synaptosome Mitochondrial Function Is Not Altered following a 6mo MeHg Treatment in Male BALB/c Mice.**

S. M. Fox<sup>1,2</sup> and W. D. Atchison<sup>1,2</sup>. <sup>1</sup>Pharmacology and Toxicology, Michigan State University, East Lansing, MI; <sup>2</sup>Center for Integrative Toxicology, Michigan State University, East Lansing, MI.

Methylmercury (MeHg) is a potent environmental neurotoxicant that causes cell-type specific damage in the cerebellum in a calcium ( $Ca^{2+}$ ) dependent manner. The developmental effects of MeHg have been widely explored. However, the effects of chronic exposure in adults have not been characterized. The ability of MeHg to cause cell-type specific damage due to alterations in  $Ca^{2+}$  regulation raises the possibility that other subsets of neurons with vulnerability that depends on  $Ca^{2+}$  regulation could be sensitive to MeHg. This study focused on investigating the effects of chronic MeHg treatment on the mitochondrial function of nigrostriatal dopamine (NSDA) neurons. These neurons exhibit a unique physiological phenotype; they autonomously generate action potentials in the absence of synaptic input. The spontaneous action potentials rely on the influx of  $Ca^{2+}$  through Cav1.3, L-type  $Ca^{2+}$  channels. We also investigated whether co-treatment with isradipine, a  $Ca^{2+}$  channel antagonist, would protect against MeHg-mediated damage. Beginning at 3mo, male BALB/c mice were given 5ppm Hg as MeHg in their drinking water alone or were co-treated with 2ppm isradipine in their food for 6mo. Following the 6mo treatment period mouse weight gain was normal and there were no phenotypic changes. Mitochondrial function was measured in synaptosome preparations from NSDA neurons using the Extracellular Flux Analyzer (Seahorse Biosciences). Mitochondrial basal respiration, ATP production rate, maximal respiration, and spare capacity were examined. No alterations were seen in any measure of mitochondrial function in animals treated with MeHg alone or in animals co-treated with isradipine ( $n \geq 4$ ,  $p$  values=0.8494, 0.1019, 0.9178, 0.8227 respectively). These studies have demonstrated that mitochondrial function of striatal synaptosomes is unchanged following a 6mo MeHg treatment. The effects of a 12mo MeHg treatment are currently being pursued. This work was supported by a ViCTER supplement to R01ES03299.

**PS 2148 Identification and Characterization of Plasma Membrane and Intracellular Transporters Involved in MeHg-Induced Whole Animal and DA Neuron Pathology.**

N. VanDuyn and R. M. Nass. *Pharmacology and Toxicology, Indiana University School of Medicine, Indianapolis, IN.*

Background: Methylmercury (MeHg) exposure from occupational, environmental, and food sources is a significant threat to public health. Recent epidemiological and vertebrate studies suggest that MeHg exposure may contribute to the propensity to develop Parkinson's disease (PD). We have developed a novel *C. elegans* model of MeHg toxicity and have shown that low, chronic exposure confers dopamine (DA) neuron degeneration, and that the toxicity is partially dependent on the phase II antioxidant transcription factor SKN-1/Nrf2. Aims/Objectives: In this study we

asked what genes are involved in MeHg-induced animal and DA neuron pathology. Methods: We utilized a reverse genetic screen, immunofluorescence, transgenic *C. elegans*, RT-PCR, ICP-MS, Western analysis, and neuronal morphology analysis to characterize expression, localization and the role that SKN-1, MPT-1, and MIT-1 play in MeHg-induced whole animal and DA neuronal death. Results: Over 17,000 genes were screened for whole animal sensitivity to MeHg, and 92 genes were identified (90% have strong human homologues) that affect whole animal and/or DA neuron pathology. Here we report detailed analysis of several transporters. Specifically, genetic knockdown of MPT-1 results in 40% of animals showing DA neurodegeneration relative to 0% in WT animals following 500 nM MeHg exposure for 4 days. Genetic knockdown of transporters MPT-1 and MIT-1 following high levels of MeHg exposure (10uM) results in 0% and 2% viability, respectively, compared to 100% in WT animals. Inductively Coupled Plasma Mass Spectrometry (ICP-MS) studies show that MPT-1 knockdown results in 2-fold higher Hg levels relative to WT, while MIT-1 contain 60% less than WT. We also provide evidence for differential cellular localization. Conclusions: This study describes a novel whole genome reverse genetic screen that has identified a number of molecular transporters and proteins involved in MeHg resistance. Support: NIEHS ES014459 and ES003299 to RN, and EPA STAR Graduate Fellowship to NVD.

## PS 2149 Biochemical Alterations of Rat Brain Mitochondrial Enzymes Induced by Aluminium Chloride.

R. Venugopal<sup>1</sup>, K. Arumugam<sup>1</sup>, V. Dhasal<sup>1</sup>, P. Subbarayalu<sup>2</sup> and S. Viswanadhapalli<sup>3</sup>. <sup>1</sup>Zoology, K.M. Centre for Post Graduate Studies, Puducherry, India; <sup>2</sup>Greehey Children's Cancer Research Institute, University of Texas Health Science Center at San Antonio, San Antonio, TX; <sup>3</sup>Medicine, University of Texas Health Science Center at San Antonio, San Antonio, TX.

Aim: The present study was planned to investigate the effect of aluminium chloride (AlCl<sub>3</sub>) on enzyme activities in the mitochondrial fractions of the brain of male albino rats. Methods: Adult male albino rats were administered AlCl<sub>3</sub> at two different doses, 50 mg and 100 mg/kg body weight, orally, daily for 45 days. At the end of the experimental period the animals were sacrificed, the brain was removed and mitochondrial fractions were isolated. Antioxidant enzymes like catalase, superoxide dismutase, glutathione peroxidase, glutathione reductase and glutathione-S-transferase were estimated in the brain extract. Other biochemical markers were also studied. Results: AlCl<sub>3</sub> administration had no effect on the body weight and brain weight. Almost all the antioxidant enzymes studied were markedly diminished in the brain of AlCl<sub>3</sub> treated animals. The lipid peroxidation and hydrogen peroxide were significantly increased. The activities of acid phosphatase and alkaline phosphatase were significantly increased. The activities of Ca<sup>++</sup> ATPase, Mg<sup>++</sup> ATPase and Na<sup>+</sup> K<sup>+</sup> ATPases were decreased by the AlCl<sub>3</sub> treatment in the brain. However, the influence was found to be more in 100 mg treated when compared to 50 mg AlCl<sub>3</sub> treated rats. The activity of acetylcholinesterase was diminished while the lactate dehydrogenase activity increased after aluminium treatment. Conclusion: The present study suggests the toxicity of aluminium by inducing the oxidative stress and adverse alterations in the brain metabolism and possible interference in brain coordination processes.

## PS 2150 Effects of Mercuric Chloride on Cell Surface Expression of Dopamine Transporter in PC12 Cells.

C. Hui, A. Carpi and S. Cheng, *Scicnes, John Jay College of Criminal Justice, New York, NY.*

Mercury compounds are known to have a ubiquitous nature due to their ability to move through the biogeochemical cycle and food web. Organic and inorganic forms of mercury generally target different organ systems of the body while biotransformation after exposure can result in the bioaccumulation of various species of the element. Divalent mercury (Hg<sup>2+</sup>) can be found within the brain following exposure to the mercury vapor of dental amalgams and after extended exposure to methyl mercury. Dopamine transporter protein (DAT) has been implicated as a link between neurotoxicity following exposure to 1-methyl-4-phenyl-1,2,3,6-tetrahydropyridine (MPTP). Increases in DAT expression on the cell membrane have been shown to result in amplified sensitivity to MPTP. The in vitro effect of mercuric chloride (HgCl<sub>2</sub>) on the cell surface expression of DAT in stably transfected DAT expressing PC12 cells was studied. Cell viability (MTT assay) following treatment with 0.5ppm HgCl<sub>2</sub> and 1-methyl-4-phenylpyridinium (MPP<sup>+</sup>) the active metabolite of MPTP, was observed to result in an additive increase in toxicity compared with treatment with MPP<sup>+</sup> alone. Using immunocytochemistry and Western blot, DAT surface expression was seen to increase following HgCl<sub>2</sub> (0.2-2.0ppm) exposure which exhibited a biphasic pattern with the maximum expression observed at 0.5 ppm when compared to the control. With null function DAT mutant, cell viability following exposure to HgCl<sub>2</sub> and MPP<sup>+</sup> showed an absence of the increase in toxicity observed at 0.5ppm originally observed in the wild

type control cells. The results show that HgCl<sub>2</sub> is able to increase DAT surface expression in a concentration dependent manner and as a result, exposure could trigger subsequent increased susceptibility to pesticides such as MPTP that use the DAT system as pathway of toxicity.

## PS 2151 Changes in Gene Induction Associated with Lead Acetate Mediated Oxidative Stress and Mitochondrial Dysfunction in Neuronal PC12 Cells.

H. Kim<sup>1</sup>, Z. Paras<sup>1</sup>, G. Tsai<sup>1</sup>, M. J. Kim<sup>1</sup>, M. Shakarjian<sup>1,2,3</sup> and D. E. Heck<sup>1</sup>. <sup>1</sup>New York Medical College, Valhalla, NY; <sup>2</sup>Medicine, UMDNJ-Robert Wood Johnson Medical School, Piscataway, NJ; <sup>3</sup>Environmental and Occupational Medicine, UMDNJ-Robert Wood Johnson Medical School, Piscataway, NJ.

Lead is a major environmental heavy metal toxin that affects brain development and impairs cognition in children and adults. Despite extensive research, molecular mechanisms underlying neurotoxicity mediated by lead are not well understood. Previous studies have shown that ROS production caused by lead exposure decreases cellular antioxidant defense networks in the brain. In the present studies, we evaluated lead-mediated alterations in oxidative stress pathways in PC12 cells. Using H2DCFDA in conjunction with flow cytometry, we found that lead exposure increased ROS production up to 2.7-fold (3 hr, 1 nM to 10 μM); this effect was associated with mitochondrial membrane potential changes which were 60% lower after 24 hour treatment with 1 μM PbAc<sub>2</sub>. Using QPCR, we observed that exposure to lead resulted in the induction of anti-oxidant genes including MnSOD, catalase, NQO1, HO-1 and GST-M1). QPCR analysis also revealed induction of genes that are indicators of Ca<sup>2+</sup> flux (TRPV1), inflammation (COX-2, IL-1 β, TNFα), and apoptosis (bcl-2, bax, caspase-3). Relative mRNA for signaling kinases ERK(p42/p44), SAPK/JNK and PKC-δ were increased while that for p38MAPK was decreased. Taken together our results suggest that lead treatment of PC12 cells enhances cellular ROS levels, negatively impacts the anti-oxidant gene profile and the mitochondrial membrane potential of PC12 cells, upregulates expression of genes critical for inflammation and apoptosis and alters expression of critical cellular signaling kinases. We speculate that changes in the expression of antioxidant enzymes and signaling kinases are important in lead-mediated neurotoxicity. (Supported by AR055073)

## PS 2152 Effects of Pb<sup>2+</sup> in the Neural Differentiation of Mouse Embryonic Stem Cells.

F. J. Sanchez-Martin and A. Puga, *Department of Environmental Health, University of Cincinnati, Cincinnati, OH.*

Exposure to environmental agents during embryonic life is suspected to modify the epigenetic mechanisms that regulate the gene expression patterns that control development. The resulting changes in gene expression may affect lineage differentiation and extend into adulthood, well beyond the time when the organism was exposed to the agents. This paradigm provides a testable molecular basis for the Barker hypothesis, which proposes that there is a fetal origin of adult disease. Lead (Pb) is a ubiquitous environmental toxicant whose possible effects, especially at early ages of development, include reduction of cognitive functions and IQ, behavioral effects, attention deficit and hyperactivity disorder. We are using neural differentiation of mouse embryonic stem cell (mESC) to determine the molecular changes taking place during embryogenesis and neurodevelopment as a consequence of long-term exposure to Pb<sup>2+</sup>. We find that after differentiation of mESC into neuronal cells, cultures express many neuronal markers, including *Tubb3*, *Syp*, *Gap43* and *Hud*, and do not express the glial marker *Gafp*. Furthermore, the cells express *Vglut1*, a marker of glutamatergic neurons. Incubation with Pb<sup>2+</sup> during differentiation reduces the expression of the calcium-dependent exon IV of *Bdnf* and alters the expression pattern of other neural genes but does not alter the morphology of the neuron and the expression of *Tubb3*. Thus, we conclude that after differentiation of mESC in vitro, we can obtain pure cultures of glutamatergic neurons whose gene expression patterns are changed by Pb<sup>2+</sup> exposure. These cells should provide an useful substrate to analyze the mechanisms of toxicity of environmental neurotoxicants. Supported by NIH grant R21 ES020048.

**PS 2153 Developmental Lead (Pb<sup>2+</sup>) Exposure and Mutant DISC1 Interact to Produce Schizophrenia-Like Neurobehavioral Abnormalities and Brain Volume Changes in Mice: A Gene-Environment Interaction Study.**

T. R. Guilarte<sup>1,3</sup>, J. L. McGlothlan<sup>1</sup>, B. Abazyan<sup>2</sup>, C. Yang<sup>2</sup>, K. Hua<sup>3</sup>, S. Mori<sup>3</sup> and M. Pletnikov<sup>3</sup>. <sup>1</sup>Environmental Health Sciences, Columbia University Mailman School of Public Health, New York, NY; <sup>2</sup>Psychiatry, Johns Hopkins School of Medicine, Baltimore, MD; <sup>3</sup>Radiology, Johns Hopkins School of Medicine, Baltimore, MD.

The glutamatergic hypothesis of schizophrenia suggests that hypoactivity of the NMDA receptor (NMDAR) is an important factor in the pathophysiology of schizophrenia and related mental disorders. The environmental developmental neurotoxicant lead (Pb<sup>2+</sup>) is a potent and selective antagonist of the NMDAR and two recent human studies have suggested an association between prenatal Pb<sup>2+</sup> exposure and the increased likelihood of expressing a schizophrenic phenotype later in life. Schizophrenia and other major mental disorders likely result from interactions between genetic risk factors and adverse environmental insults. We evaluated the neurobehavioral consequences of Pb<sup>2+</sup> exposure in mice with inducible expression of mutant Disrupted-in-Schizophrenia-1 (DISC1), a candidate gene for major psychiatric diseases. We hypothesize that mutant DISC1 and Pb<sup>2+</sup> exposure synergistically interact to produce an exaggerated phenotype in mutant mice. Mutant DISC1 and control mice born by the same dams were raised and maintained on normal or Pb<sup>2+</sup> diet. We tested animals in a series of behaviors associated with schizophrenia and performed volumetric MRI measurements of the brain. We found that the interaction between developmental Pb<sup>2+</sup> exposure and mutant DISC1 produced a significantly greater increase in locomotor activity, impaired pre-pulse inhibition of the acoustic startle that was abrogated by D-serine and exacerbated responses to MK-801, an NMDAR antagonist. Compared to control unexposed mice, mutant exposed animals had significantly larger lateral ventricles. Our data suggest that interactions between Pb<sup>2+</sup> and mutant DISC1 may synergistically produce schizophrenia-like behavioral alterations and brain volume changes in mice. [Supported by grant # ES06189-18S1 to TRG]

**PS 2154 Reduced Parvalbumin Expression in the Striatum, Frontal Cortex, and Hippocampus after Developmental Pb<sup>2+</sup> Exposure: Examining Early Life Pb<sup>2+</sup> Exposure As a Risk Factor for Schizophrenia.**

K. Stansfield<sup>1</sup>, K. Ruby<sup>2</sup>, J. L. McGlothlan<sup>1</sup> and T. R. Guilarte<sup>1</sup>. <sup>1</sup>EHS, Columbia University, NYC, NY; <sup>2</sup>Lake Erie College of Osteopathic Medicine, Erie, PA.

The calcium-binding protein, parvalbumin (PV), is expressed in GABAergic interneurons and is implicated in working memory and associative learning. Decreased PV expression is observed in schizophrenia patients and also in animal models of schizophrenia. N-methyl-D-aspartate receptor (NMDAR) antagonists are used to model certain aspects of schizophrenia in animal models and NMDAR antagonists decrease PV levels and the number of PV-positive interneurons, suggesting that NMDAR function plays a role in the expression of PV interneurons and in schizophrenia. Lead (Pb<sup>2+</sup>) is a potent NMDAR antagonist that has been implicated in the etiology of schizophrenia, therefore we examined the effect of developmental Pb<sup>2+</sup> exposure on PV cell density in the striatum and PV protein expression in the striatum, hippocampus and frontal cortex of rats developmentally exposed to Pb<sup>2+</sup>. A trend of decreased PV positive cell density was observed at all levels of the striatum, however a statistically significant decrease (t11=2.2; p = 0.005) in cell density was found in the caudal striatum of Pb<sup>2+</sup>-treated rats relative to controls. Additionally, PV protein expression measured by western blot was significantly reduced in the striatum (t22=3.3; p = 0.003), frontal cortex (t7 = 2.25, p = 0.05) and hippocampus (t10 = 2.31, p = 0.04) of rats developmentally exposed to Pb<sup>2+</sup>. Overall, these findings indicate that early life Pb<sup>2+</sup> exposure decreases the number of PV positive neurons in the striatum, and reduces the expression of PV in the striatum, frontal cortex and hippocampus. The data suggests a relationship between Pb<sup>2+</sup> induced NMDAR hypoactivity and PV expression, implicating a potential association between developmental Pb<sup>2+</sup> exposure and the expression of a schizophrenia phenotype later in life. [This work was supported by NIEHS grant # ES006189 to TRG]

**PS 2155 Effects of Developmental Lead Exposure on Associative Learning and Memory Are Modified by Sex, Developmental Window of Exposure, and Level of Exposure.**

D. Anderson, W. Mettill, S. Kidd and J. Schneider. Thomas Jefferson University, Philadelphia, PA.

Trace fear conditioning is a variant of fear conditioning in which a neutral conditioned stimulus (CS) is paired with an aversive unconditioned stimulus (UCS). Trace conditioning includes a "trace" interval of several seconds separating the CS and UCS. Learning the CS-UCS association across this interval and the consolidation of the memory requires participation of both the hippocampus and medial prefrontal cortex (mPFC). Long-term storage of information associating temporally disconnected events occurs in the mPFC in parallel with memory storage in the hippocampus. The current research investigated the extent to which these processes are affected by developmental Pb exposure. Long Evans dams were fed Pb-containing food (RMH 1000 with or without added Pb acetate: 0, 150, 375, 750 ppm) prior to breeding and stayed on the same diet through weaning at postnatal day 25 (perinatal exposure group (Peri)). Other animals were exposed to the same doses of lead but exposure started on postnatal day 1 and continued through postnatal day 25 (early postnatal exposure group (EPN)). Beginning at postnatal day 45, animals were placed in the trace fear conditioning apparatus. Conditioning trials (CS tone-UCS shock pairings) were repeated six times during an 18 min training period. Freezing behavior was measured during the trace period. Retention testing occurred 24/48 hrs and 10 days later to assess memory consolidation and long-term memory. At the lowest level of exposure, EPN-exposed females were more impaired at short and long-term retention than were Peri-exposed females; the opposite effect was observed in males. In females, the lowest level of exposure had the greatest disruptive effect on retention. In males, the highest level of exposure had the greatest disruptive effects on retention. These data suggest complex responses of the brain to developmental Pb exposure with likely different molecular effects in hippocampus and PFC that vary with sex and timing and level of exposure. Supported by NIH RO1-ES015295.

**PS 2156 Sex- and Hemisphere-Dependent Neurochemical Changes Produced by Lead, Prenatal Stress, and the Combination.**

D. A. Cory-Slechta, D. Weston, S. Liu and J. L. Allen. Environmental Medicine, University of Rochester Medical School, Rochester, NY.

Brain lateralization, important to mediation of cognition and 'multi-tasking', is disrupted in attention deficit disorder and schizophrenia. Altered brain lateralization could play a role in the corresponding cognitive and attention deficits associated with both low level lead (Pb) exposure and prenatal stress (PS). This study examined laterality of mesocorticolimbic (frontal cortex, nucleus accumbens, striatum, midbrain) monoamines and amino acids (frontal cortex only) that mediate such behavioral functions, both under normal (control) conditions, and in response to lifetime Pb (0 or 50 ppm), PS (restraint stress on gestational days 16-17) or Pb+PS in rats. Sex-dependent differences in brain laterality were seen even in control rats, as noted in frontal cortex, striatum and midbrain monoamines and frontal cortex amino acids. Hemispheric differences in Pb ± PS effects were most notable in males, as seen in frontal cortex and striatum, but particularly in midbrain, where Pb+PS, but neither alone, significantly reduced right hemispheric levels of homovanillic acid and norepinephrine, with similar trends in serotonin. In contrast, no Pb+PS effects were found in left hemisphere. Pb+PS, but neither alone, reduced frontal cortex dopamine and increased dopamine turnover in left hemisphere of males, whereas in the right hemisphere, Pb, PS and Pb+PS reduced frontal cortex dopamine and Pb alone increased dopamine turnover. The only suggestive Pb+PS hemispheric difference in females was increased right but not left hemisphere frontal cortex GABA. Thus Pb, PS and Pb+PS can differentially influence mesocorticolimbic neurotransmitter function both by hemisphere and sex. Such differences are likely to contribute to associated sex-related alterations in behavioral outcomes, such as our previously reported contrasting effects on learning accuracy produced by Pb+PS in males vs. females. The findings also underscore the significance of defining the hemisphere used for assay in experimental studies for evaluation of CNS mechanisms of behavior.

**PS 2157 Sex-Dependent Changes in the Effects of Lead and Prenatal Stress on Impulsivity and Neurochemical Substrate.**

H. Weston, D. Weston, S. Liu, J. L. Allen and D. A. Cory-Slechta. Environmental Medicine, University of Rochester Medical School, Rochester, NY.

Both lead (Pb) exposure and prenatal stress (PS) adversely affect cognition and attention. Impulsivity is one diagnostic component of attention deficit, and enhanced impulsivity has been related to multiple neuropsychiatric disorders. This

study examined whether combined Pb+PS would enhance impulsivity compared to either alone, as well as potential associated mechanisms using rats exposed to 0 or 50 ppm Pb from 2 mos prior to breeding through lactation with/without PS on gestational days 16-17. Impulsivity was assessed in a delay of reward paradigm that provides a choice between an immediate but small reward or a larger but delayed reward, with delay time increased across test sessions. Choice of the long delay typically declines with increasing delay time. In males, PS, particularly with Pb, delayed this transition, consistent with impulsivity of choice. A trend towards increased omission of trial initiation responding was also noted in males. Females showed no changes. Adverse effects in males may be related to reduced nucleus accumbens dopamine (DA) function and reduced frontal cortex, nucleus accumbens and striatal serotonergic (5HT) function, as found in 2 mos old male littermates of behaviorally-tested rats; effects less evident in females. The transitory nature of the behavioral changes in males may arise from the 'enriching' effects of behavioral testing: post-testing, Pb + PS increased levels of striatal DA and 5HT and metabolites, and of nucleus accumbens DOPAC, norepinephrine and 5HT in males, consistent with a reversal of pre-testing neurochemical changes. These findings demonstrate a preferential vulnerability of males to PS-induced impulsive choice that is enhanced by concurrent Pb exposure and which may arise from early reductions in mesocorticolimbic DA and 5HT function. As impulsivity is considered to play a central role in attention deficit, gambling, substance abuse and personality disorder, the findings have significant public health implications. Supported by EPA Grant RD 83457801.

**PS 2158 Investigation of the Combined Neurotoxicity of Developmental Iron Deficiency and Lead Exposure.**

A. Greminger<sup>1</sup>, D. A. Cory-Slechta<sup>1</sup> and M. Mayer-Proschel<sup>2</sup>. <sup>1</sup>Environmental Medicine, University of Rochester, Rochester, NY; <sup>2</sup>Biomedical Genetics, University of Rochester, Rochester, NY.

Iron deficiency (ID) and Lead (Pb) exposure are widespread public health problems that continue to affect women and children with similar risk factors, as well as produce similar neurotoxic effects on the developing CNS. Although studies of these insults singularly suggest a potential for enhanced neurotoxicity in their combination, previous work has failed to address this in relevant animal models, and consistent data from human cohorts are lacking. We utilized a maternal iron-deficient dietary model in the presence or absence of Pb-exposure to examine the possible synergism of ID and Pb during offspring neurodevelopment. Offspring of each exposure were assessed using hematologic parameters, as well as tissue Pb levels. Our data show that maternal Pb-only exposure did not cause anemia in either the dam or the offspring throughout development. In combination with ID, Pb did not decrease hematocrit levels in offspring beyond those of ID-only, arguing against the notion that Pb causes or worsens ID. However, the presence of ID significantly increased blood and tissue Pb levels by more than 50% in the dams and offspring compared to animals exposed to the same Pb levels in the absence of ID. Our data suggest that maternal non-anemic ID strongly increases absorption of Pb into the CNS of offspring underscoring the importance of non-anemic ID as a susceptibility factor to environmental Pb toxicity. To determine the functional impact of ID + Pb we measured overall brain maturation using the auditory brain stem response. We found significant decreases in neuronal conduction velocity in all three exposure groups (Pb-only, ID-only and ID + Pb) compared to control offspring at PND40. However, the combination of ID + Pb did not result in synergistic increases over either insult alone at this age or decibel level (70dB). Additional analysis at different ages and stimulation levels is required to determine if this lack of synergy may be due to compensatory mechanisms or is restricted to later in development.

**PS 2159 Bcl-xL-Mediated Remodeling of Rod and Cone Photoreceptor (PR) Synaptic Mitochondria (mt) After Postnatal Lead Exposure (PLE): Structure and Function.**

D. A. Fox<sup>1</sup>, G. A. Perkins<sup>2</sup>, M. H. Ellisman<sup>2</sup> and J. E. Johnson<sup>3</sup>. <sup>1</sup>Univ. Houston, Houston, TX; <sup>2</sup>Univ. California: San Diego, La Jolla, CA; <sup>3</sup>Univ. Houston-Downtown, Houston, TX.

PLE produces rod-selective apoptosis (blocked by Bcl-xL) and persistent scotopic-mesopic ERG and vision deficits in man and animals. Rod, but not cone, inner segment mt were considered the target: albeit PR synaptic mt were not examined. Thus, we determined the effects of PLE on these mt and if Bcl-xL provided protection. C57BL/6 mice pups had PLE during lactation by dams drinking Pb water. [BPb] was 10-20 µg/dL and at control level by 60 doa. EM, 3-D electron tomography, and oxygen consumption (QO2) studies were done at 70 doa: control, transgenics overexpressing Bcl-xL in PRs, PLE and Bcl-xL/PLE groups. In PLE, rod spherule and cone pedicle mt were swollen, cristae structure changed, and the no.

of segments/crista and fraction of cristae with multiple segments (branching) increased. In PLE, mt cristae surface area and volume (abundance) decreased in spherules and increased in pedicles. PLE remodeling of spherule mt produced smaller cristae with more branching, whereas pedicle mt had larger cristae with more branching and increased cristae junction diameter. PLE decreased dark-adapted PR and PR synaptic terminal QO2. In Bcl-xL/PLE, spherules still had decreased abundance; pedicles still had increased branching, crista segments/volume and crista junction diameter; and PR and synaptic QO2 only partially recovered. These findings reveal cellular and compartmental differences in the structure, vulnerability and remodeling of rod and cone inner segment and synaptic mt to PLE: consistent with findings that synaptic mt are more sensitive to calcium overload, oxidative stress and ATP loss than non-synaptic mt. These PLE alterations likely underlie the persistent scotopic-mesopic deficits, and stress the importance of examining synaptic dysfunction after developmental insults and preventing synaptic degeneration even if apoptosis is blocked.

Supported by NIH grants RO1 ES012482, T32 EY07024, P30 EY07551, P42 ES010337, RO1 DK54441, P41 RR004050 and P41 GM103412.

**PS 2160 Alpha-Synuclein-Mediated Activation of c-Abl and Dopamine Depletion in Dopaminergic Neuronal Cells Treated with Iron-Oxide Nanoparticles or Methamphetamine.**

S. Lantz<sup>1</sup>, Z. K. Binienda<sup>1</sup>, L. Mohammed Saeed<sup>1,2</sup>, B. Robinson<sup>1</sup>, M. G. Paule<sup>1</sup>, A. S. Burris<sup>2</sup>, S. F. Ali<sup>1</sup> and S. Z. Imam<sup>1</sup>. <sup>1</sup>FDA/NCTR, Jefferson, AR; <sup>2</sup>Nanotechnology Center, University of Arkansas, Little Rock, AR.

Mutations in the alpha-synuclein gene have been associated with autosomal dominant forms of Parkinson's disease (PD). Transgenic mice that over-express the human alpha-synuclein gene (primarily the point mutations A53T and A30P), develop neurological impairments similar to those of PD. Previous studies in our laboratory have shown that oxidative-stress-mediated activation of the tyrosine kinase, c-Abl, results in an increase in the phosphorylation of parkin, an important E3 ubiquitin ligase that assists in the clearance of proteins destined for proteasomal degradation. Here, we show that treatment with iron-oxide nanoparticles or methamphetamine results in activation of c-Abl, observed via the measurement of phospho-Abl. Additionally, an over-expression of alpha-synuclein protein in SHSY-5Y neuroblastoma cells was observed after these treatments. A 45% increase in the expression of alpha-synuclein was observed in SHSY-5Y cells treated with iron oxide nanoparticles (10 and 30 nanometers) at a concentration of 10 µg/ml. Similarly, a 55% increase in the expression of alpha-synuclein protein was observed 24 h after exposure to 500 µM methamphetamine. In addition, a significant depletion in dopamine was observed after treatment with either iron oxide nanoparticles or methamphetamine (55% and 65%, respectively), suggesting that both the over-expression of alpha-synuclein and excess dopamine might generate oxidative stress, which is one of the major pathways of c-Abl activation. These results suggest that the over-expression of alpha-synuclein and dopamine depletion after exposure to iron oxide nanoparticles or methamphetamine contribute to oxidative-stress mediated activation of c-Abl, thus initiating events that may lead to dopaminergic neuronal cell death.

**PS 2161 Identification of Iron Regulatory Proteins Differentially Expressed in Brains with Alzheimer Disease by Quantitative Proteomics.**

B. D. Minjarez<sup>1</sup>, L. Valero<sup>2</sup>, A. D. Rios-Perez<sup>4</sup>, M. Sanchez del Pino<sup>2</sup>, R. Mena<sup>3</sup> and J. P. Luna-Arias<sup>1</sup>. <sup>1</sup>Biología Celular, CINVESTAV, Mexico City, Mexico; <sup>2</sup>Proteómica, Centro de Investigación Príncipe Felipe, Valencia, Spain; <sup>3</sup>Fisiología, Biofísica y Neurociencias, CINVESTAV, Mexico City, Mexico; <sup>4</sup>Toxicología, CINVESTAV, Mexico City, Mexico.

Alzheimer's disease (AD) is the most common form of dementia affecting around 24.3 million people worldwide. As a consequence of the rapid demographic ageing, AD has become one of the most severe progressive socio-economical and medical burdens facing countries all over the world. AD brains are characterized by the presence of extracellular deposits of amyloid-β-containing plaques and intracellular neurofibrillary tangles (NFTs) composed of paired helical filaments of hyperphosphorylated Tau. AD is considered to be the result of complex events involving both genetic and environmental factors. Among them, two remarkable factors are oxidative stress and mitochondrial damage. Postmortem examinations of human brain tissue have demonstrated that iron concentrations are increased in the brains of AD patients compared to controls. The main goal of this study was the identification of proteins showing different expression levels in AD, using iTRAQ-protein labeling

and, identification and quantitation of peptides by tandem mass spectrometry. We identified more than 721 polypeptides, where some iron regulatory proteins were found up-regulated such as Ferritin light chain, Ferritin heavy chain and Melanotransferrin. In addition, several proteins involved in redox regulation also found such as Peroxiredoxin, Superoxide dismutase, Oxidation resistance protein 1, were up-regulated in AD brains in comparison to a normal brain. This approach will give us landscape of the proteome of AD brains that could be useful for the potential identification of AD biomarkers that may be involved in oxidative damage.

## PS 2162 Prediction of Drug-Induced Liver Injury Using High-Content Screening Assay of Rat Hepatocytes.

M. Chen<sup>1</sup>, T. Chun-Wei<sup>1</sup>, Q. Shi<sup>1</sup>, L. Guo<sup>1</sup>, H. Fang<sup>2</sup>, L. Shi<sup>1</sup> and W. Tong<sup>1</sup>. <sup>1</sup>US FDA, NCTR, Jefferson, AR; <sup>2</sup>ICF International at NCTR, US FDA, Jefferson, AR.

Drug induced liver injury (DILI) is a leading cause for drug failures in clinical trials and for post-approval drug withdrawals. This fact implies that the current animal-based approaches do not provide a sufficiently reliable assessment of DILI; therefore, there is an increased interest to develop new approaches for identifying hepatotoxicity, especially those that can be applied in the early drug discovery. In this study, we assessed the feasibility of using high content screening (HCS) assays of rat primary hepatocytes to predict the human specific hepatotoxicity of pharmaceuticals. We developed a predictive model using a commercial HCS assay on 8 cellular parameters that were relevant to hepatotoxicity mechanisms including cell loss, nuclear size, DNA damage, apoptosis, lysosomal mass, DNA fragmentation, mitochondrial potential, and steatosis. The model's performance was assessed both by internal cross-validations using a library of 108 drugs with human-specific hepatotoxicity annotations and by further external validation using an additional sixteen drugs. In the leave-one-drug-out cross-validation, the HCS assay-based predictive model yielded accuracy of 68% with sensitivity of 77% and specificity of 50%, which is significantly higher than that by chance and better than the quantitative structure-activity relationship (QSAR) model developed using the same set of drugs in accuracy. The results from the external validation showed that eight out of nine of the most-DILI-concern drugs (with 89% sensitivity) and four out of seven no-DILI-concern drugs (with 57% specificity) were correctly predicted. Our findings suggest that the HCS assay of rat hepatocytes can potentially approach useful for hepatotoxicity screening for drug discovery.

## PS 2163 Oral Toxicity Study of the Novel Optimized HCV Protease Inhibitor in Rats and Monkeys.

Z. J. Zhan<sup>1</sup>, H. Yan<sup>1</sup>, S. McPherson<sup>2</sup>, S. Neu<sup>3</sup> and Q. He<sup>2</sup>. <sup>1</sup>AB Pharma Ltd., Shanghai, China; <sup>2</sup>WuXi AppTec Co. Ltd., Suzhou, China; <sup>3</sup>Vet Path Services, Inc., Mason, OH.

ZN2007, a novel highly potent HCV-NS3 protease inhibitor with excellent PK and stability properties, was orally administered as sodium salt (ZN2007Na) to cynomolgus monkeys at 25, 500, or 1000 mg/kg/day for 14 days followed by a 7-day recovery period; and rats at 50, 500, or 1000 mg/kg/day for 28 days followed by a 14-day recovery period.

The monkeys were treated with ZN2007Na formulated in 20% (w/v) sulfolbutylether-B-cyclodextrin (SBECD) at 25, 500, and 1000 mg/kg/day for 14 days. No death occurred in 14-day study, and only some soft and/or watery stools were observed in all monkeys including both control and test article-treated groups through the dosing phase. This was considered to be related to the vehicle as it was seen in controls and has been reported in scientific publications (Stella and He, 2008). Abnormal stools were resolved from Day 16 through the recovery period. In rats, no death occurred in 28-day GLP study, and some mild to moderate salivation was the only test article-related finding in males at  $\geq 500$  mg/kg/day, and females at  $\geq 50$  mg/kg/day, respectively. There were no any test article-related changes in mortality, body weight, food consumption, ophthalmic examinations, clinical pathology parameters, electrocardiography (ECG), hematology, coagulation, serum chemistry, and also no any test article-related effects observed on both macroscopic and microscopic examinations for all tested animals at any dose levels (25, 50, 500, or 1000 mg/kg/day) in rats and monkeys, respectively. Moreover, there were no any side effects determined with other protease such as hERG, Cytochrome P450, etc. Based on the above findings, it is concluded that the NOAEL was 1000 mg/kg/day in rats. At NOAEL, the mean values of C<sub>max</sub> and AUC<sub>0-24h</sub> were 24350 ng/mL and 71400 h\*ng/mL in rats. So far, a number of toxicity studies were conducted at WuXi AppTec, and the preclinical safety data of inhibitor ZN2007Na in both rats and monkeys strongly support the safe use conditions for AB Pharma team to file IND for clinical trials in USA by the end of 2012.

## PS 2164 Physicochemical Properties and Compound Accumulation in Lysosomes and Mitochondria.

S. Lu<sup>1</sup>, A. Sista<sup>2</sup>, P. Hoerter<sup>2</sup>, B. Jessen<sup>1</sup> and Y. Will<sup>3</sup>. <sup>1</sup>Drug Safety Research & Development, Pfizer Inc, San Diego, CA; <sup>2</sup>Pharmaceutical Sciences, Pfizer Inc, San Diego, CA; <sup>3</sup>Compound Safety Prediction, Pfizer Inc, Groton, CT.

Eukaryotic cells are highly compartmentalized composing various functionally distinct, membrane-enclosed subcellular organelles such as lysosomes and mitochondria. Unwanted accumulation in nontarget sites can interact with organelle components, resulting in structural and functional changes, potentially leading to toxicity. Physicochemical properties have been shown to be a contributing mechanism for compound accumulation in cells and even organelles. In this study, we examined the relationship between physicochemical properties such as partition coefficient (logP) and acid dissociation constant (pKa) and lysosomal compound accumulation. Our data demonstrate a clear association of basic (basic pKa > 6) and lipophilicity (logP > 2) with lysosomal compound accumulation. We also showed this accumulation was derived by the low pH in the lysosomes. In addition our data revealed membrane perturbation by the compounds with similar physicochemical properties. In an effort to understand how physicochemical properties can contribute to mitochondrial compound accumulation we selected a set of basic compounds and measured their logD (partition coefficient) at neutral (7.4) and acidic (4.7) pH. The majority of basic compounds with acidic logD (at pH 4.7) > 0.3 induced more toxicity in HepG2 cells cultured in galactose than in cells cultured in high glucose-containing media, indicating mitochondrial liability associated with these compounds. This data supports the hypothesis that compounds with relatively pH-insensitive permeability selectively accumulate into mitochondria. Interestingly, certain compounds such as nefazodone and nicardipine were shown to carry both, lysosomal and mitochondria liabilities. In summary, our data indicate that physicochemical properties alone can contribute to both, lysosomal and mitochondrial compound accumulation. How this contributes to in vivo organ toxicity needs to be further elucidated.

## PS 2165 Lack of Retinal Pathology in a BACE1 Knockout Mouse or in Rats after Intravitreal Injections of BACE1 Inhibitors.

C. Somps, C. Houle, T. Brown, J. Harney, J. Brady and D. Karanian. Drug Safety, Pfizer Global R&D, Groton, CT.

The  $\beta$ -site amyloid precursor protein (APP)-cleaving enzyme 1 (BACE1) is a target of tremendous focus and development interest for the treatment of Alzheimer's disease. While initial characterization reports of BACE1 knockout (KO) mice suggest that BACE1 is a safe target for modulation (Roberds et al., 2001; Lou et al., 2001), more recent studies present evidence of retinal pathology (Cai, et al., 2012). Additionally, oral administration of a selective BACE1 inhibitor to rats has been associated with retinal changes after chronic dosing, including accumulation of auto-fluorescent material in the retinal pigment epithelium (RPE) and degeneration of photoreceptors in associated retina (May, et al., 2011). To address these concerns we evaluated the retinas in BACE1 homozygous KO mice from an in-house colony. With the goal of enabling a shorter duration screening paradigm for ocular toxicity, we also evaluated the retinas from rats after a single intravitreal injection of BACE1 inhibitors or non specific protease inhibitor at high (~10  $\mu$ M) intraocular concentrations. We found that 3-month old BACE1 KO mice are viable and without organ or clinical pathology distinctions from wild-type (wt) littermates. Ocular evaluation by H&E staining indicated that the retinas of the BACE1 KOs were unremarkable when compared to wt mice. Ophthalmic examinations, as well as light and fluorescent microscopy following intravitreal injections of BACE1 inhibitors, revealed no significant differences in the retinas or RPE between control and treated rats 1-8 days post-injection. In summary, our results support those of others indicating retinal pathologies reported with BACE1 inhibitors are not related to downregulation of BACE1 activity. Additionally, short duration intravitreal exposure to high concentrations of selective BACE1 inhibitors or nonspecific protease inhibition was not associated with detectable retinal pathology, and thus may not be a reliable model for predicting retinal toxicity of BACE1 inhibitors.

## PS 2166 Peptide Analysis Using Dry Blood Spot Technology Combined with Mass Spectrometry for Toxicology Studies: A Practical Approach for Minimizing Animal Use.

W. Ruddock, P. Aughton, J. Chapdelaine and G. Bain. ITR Laboratories Canada, Baie-D'Urfe, QC, Canada.

Scope: The amount of preclinical research based on peptides is constantly growing, however the difficulties of reliably analyzing this type of molecule leads to a major challenge in obtaining reliable toxicokinetic data. Combining the latest technology

related to dried blood spots and mass spectrometry provides many advantages even though the initial method development is more arduous than for typical small molecules of less than 1000 daltons.

**Experimental Procedures:** The peptide calcitonin-salmon was chosen based on it being readily available from Sigma Aldrich and that its molecular weight is higher than normally monitored by mass spectrometry since it consists of thirty-two amino acid linear polypeptide. The compound is dosed by oral gavage at 10 mg/kg to CD-1 mice, and 8 mL of blood collected by tail clipping every two minutes. The blood is immediately transferred to Whatman 903 filter paper and allowed to dry before placing with desiccant and refrigerating. The dry blood samples are then punched out, and calcitonin-salmon is extracted from the spots and injected. The chromatographic conditions were developed using reverse phase chromatography and detection using a triple quadrupole API 4000 mass spectrometer with electrospray ionization to monitor the parent and fragment ions of both calcitonin-salmon and its analog internal standard.

**Conclusions:** Results show that this approach provides a toxicokinetic profile with timepoints every two minutes whilst allowing a considerable reduction in mice required for a study and giving a full profile for each individual animal. This work shows that preliminary TK data may be obtained based on 3R principles even for peptide analysis, an area that still has room for much improvement using dry blood spot sample analysis.

## **PS 2167 Early and Progressive Changes in the Urinary Biomarker Profile of Cisplatin-Induced Kidney Injury in Cynomolgus Macaques.**

Y. Chen<sup>1</sup>, W. Luo<sup>2</sup>, H. Yu<sup>4</sup>, Q. Qin<sup>4</sup>, J. Qiao<sup>4</sup>, F. Chang<sup>1</sup>, D. Thurman<sup>1</sup>, M. Pinches<sup>3</sup>, S. Gales<sup>3</sup>, N. Barrass<sup>3</sup>, J. Valentin<sup>3</sup>, L. B. Kinter<sup>1</sup> and R. A. Bialecki<sup>1</sup>. <sup>1</sup>AstraZeneca R&D, Waltham, MA; <sup>2</sup>Discovery Statistics, Waltham, MA; <sup>3</sup>AstraZeneca R&D, Alderley Park, United Kingdom; <sup>4</sup>Shanghai Institute of Materia Medica, Shanghai, China.

Cisplatin-induced nephrotoxicity has been characterized in animals and humans. New urinary biomarkers may enable early or parallel detection of drug-induced kidney injury (DIKI) in non-rodent models. Our aims were to: 1) determine if a human renal biomarker panel can detect early DIKI when compared with traditional biochemical and histological indices; 2) monitor progressive cisplatin-mediated changes in DIKI biomarkers over 20 days in cynomolgus macaques. Animals (3M/3F per group) were treated with a single dose of cisplatin (2.5 mg/kg i.v. infusion; groups 1/2/4/5) or saline (groups 3/6) on day 1. Toxicokinetic profile was determined on day 1. Blood and urine samples were collected predose and postdose (days 1, 4, 9, 15, 20) for comparing changes in plasma chemistry, urinalysis and urinary DIKI biomarkers. Renal tissue was examined microscopically at different intervals. Results indicated cisplatin produced progressive renal histologic changes from subtle findings on day 2 to maximum effects on day 21. Traditional renal markers significantly increased in plasma creatinine (8-fold), BUN (3-fold), urinary glucose (5-fold), protein (3-fold) and enzymes (GGT, NAG) between day 4-9 but resolved by day 15 when renal pathology appeared more severe. Four new biomarkers (clusterin, calbindin, lipocalin, Tamm-Horsfall protein) changed progressively and significantly from day 4 to 20 days to parallel development of renal histologic injury. Importantly,  $\beta$ -2 microglobulin was significantly increased before subtle renal damage observed on day 2 and increased progressively over 20 days to parallel histologic changes, suggesting this is the most sensitive biomarker for detection of onset and potentially prodromal cisplatin-induced kidney injury in cynomolgus macaques.

## **PS 2168 A Case Study for Exploring Rodent Models to Assess Risk of Hypotension.**

M. Pannirselvam, D. Hodges, J. Jones, J. Prezioso, K. Tanner, H. Gao, E. Inett, F. Berlioz-Seux, C. Barnes, G. Smith, M. Sanders, U. Germann and D. Brewster. Vertex Pharmaceuticals, Cambridge, MA.

A cardiovascular (CV) safety pharmacology study in telemetered conscious dogs evaluating Compound-A (CPD-A), an anti-cancer agent, demonstrated a dose- and time-dependent decrease in mean arterial blood pressure (MAP), most likely attributable to off-target PDE3 inhibition. At 20 mg/kg p.o. CPD-A, MAP was reduced by ~30% from the baseline within 1-hour of dosing and this effect persisted ~12 hours. The objective of this study was to identify a rodent model that would best mimic the dog CV response to CPD-A. We investigated CPD-A (at doses up to 120 mg/kg, p.o.) in conscious, telemetered rats and detected no meaningful acute effects on MAP, although a moderate tachycardia was observed. Upon repeated daily dosing of 120 mg/kg QD to rats, CPD-A led to a mild decrease in MAP on Day 3 when compared to pre-dose baseline and time-matched vehicle controls. As

in the acute study, a moderate tachycardia was observed. To maximize exposure, a single intravenous bolus administration of 20 mg/kg CPD-A was investigated. This resulted in a significant MAP drop and a moderate reflex tachycardia. Based on these data, we hypothesized that a difference in sympathetic tone and baroreflex sensitivity between dog and rat may underlie the species difference in cardiovascular response observed after single oral administration of CPD-A. To explore this possibility, we also assessed CPD-A in isoflurane-anesthetized rat model to decrease sympathetic tone and baroreflex response. Continuous infusion of CPD-A at 10 and 20 mg/kg/hr led to a gradual decrease in MAP of up to 15 and 45%, respectively, and a mild bradycardia at the highest dose. As an alternative to the rat, we also evaluated a urethane-anesthetized guinea pig model. Infusion of 10 mg/kg CPD-A over 10 min resulted in a gradual drop in MAP accompanied by reflex tachycardia. These studies suggest the anesthetized rat or guinea pig offered good in vivo screening alternatives for this compound class.

## **PS 2169 MDR1, MRP2 and BCRP Transporter Gene Knockout in CACO-2 Cells.**

K. E. Sampson, J. Blasberg, A. Brinker, J. Pratt, N. Venkatraman, Y. Xiao, M. Bourner and D. C. Thompson. Sigma-Aldrich, St. Louis, MO.

**Purpose:** Membrane transporters P-glycoprotein (P-gp, MDR1), MRP2, and BCRP play a role in drug disposition and can mediate drug-drug interactions leading to safety/toxicity concerns. The goal of this study was to selectively knock out these drug transporter genes in a subclone of Caco-2 cells (C2BBE1) using zinc finger nuclease (ZFN) technology.

**Methods:** ZFN pairs targeting specific transporter genes were nucleofected into C2BBE1 cells. Stable clones were isolated and sequenced at gene target sites. Transport function in wild type (WT) and knockout (KO) cell lines was tested in bidirectional assays using probe substrates at 5  $\mu$ M for 2 hr at 37°C. Contents of both wells were analyzed for drug content using LC/MS-MS, and permeability was calculated for both directions. Lucifer yellow permeability was measured to verify monolayer integrity.

**Results:** ZFN-transfected clones were sequenced and the genotype was confirmed for disruptions in each allele. In bidirectional transport assays to confirm loss of transporter function, the efflux ratios (ER) for digoxin and erythromycin were reduced from 17.7 and 16.8 in the WT cells to 1.4 and 1.0 in the MDR1 KO cells, respectively. The ER for estrone 3-sulfate and nitrofurantoin were reduced from 22.7 and 13.2 in the WT to 1.8 and 1.7 in the BCRP KO cells, respectively. The ER for 5(6)-carboxy-2',7'-dichlorofluorescein was reduced to 2.0 in the MRP2 KO from 32.0 in the WT cells. Double knockout cell lines (MDR1/BCRP KO, MDR1/MRP2 KO, and MRP2/BCRP KO) were used to identify substrates of multiple transporters. Cimetidine was confirmed as a substrate of both P-gp and BCRP using the MDR1/BCRP KO cell line. Fexofenadine transport required P-gp and a basolateral MRP transporter such as MRP3, but not MRP2.

**Conclusions:** Stable single and double KO cell lines of human efflux transporters were successfully generated and characterized for loss of function using model substrates. These cell lines may be useful in clarifying complex drug-transporter interactions without reliance on the selectivity of chemical inhibitors.

## **PS 2170 Target Promiscuity and Physicochemical Properties Contribute to Pharmacologically-Induced ER-Stress.**

E. Koslov-Davino, X. Wang and T. Schroeter. Pfizer, Groton, CT. Sponsor: N. Greene.

In vivo toxicity of drug candidates remains a major problem in the pharmaceutical industry, and is a significant cause of late stage attrition. As a consequence predictive in vitro assays are developed and put in place early in the discovery pipeline to aid compound selection. Endoplasmic reticulum stress (ER-stress) has been implicated in many disease states, as well as compound-induced organ toxicities. We explored the role of ER-stress as a general mechanism of toxicity by utilizing a high-throughput in vitro assay to screen 318 chemically diverse Pfizer proprietary compounds with known in vivo toxicity outcome for nuclear accumulation of spliced X-Box Binding Protein 1 (XBP1s), a key transcription factor of the Unfolded Protein Response (UPR). We examined the correlation between physicochemical properties, such as molecular weight, pKa, lipophilicity, topological polar surface area, and passive permeability, as well as target promiscuity, between XBP1s hits and non-hits and found that lipophilicity, target promiscuity and low passive permeability significantly contributed to ER-stress. In addition, we have shown that compounds which cause ER-stress in the form of XBP1s activation at concentrations below 40  $\mu$ M have a more than four times greater chance of causing in vivo toxicity at 10  $\mu$ M plasma exposure.

**PS 2171 Enhancing the Safety of Antiviral Compounds by Assessing Mitochondrial and Nuclear Transcriptional Regulation Using a Multiplex Branched DNA Screen.**

M. Crosby and Y. P. Dragan. *Global Safety Assessment, AstraZeneca Pharmaceuticals LP, Waltham, MA.*

The development of antiviral therapeutics can be hindered by the fact that they can lead to liver, renal, and cardiac injury. One antiviral strategy focuses on inhibiting the transcription of viral nucleic acids via nucleoside analog reverse-transcriptase inhibitors (NRTIs). NRTIs may cause toxicity due to mitochondrial DNA incorporation (mtDNA) and/or inhibition of DNA polymerase  $\gamma$  (*Nature Rev Drug Disc* 2003, 2: 812-22; *Expert Opin Drug Metab Toxicol* 2010, 6:1493-604). Functionally, such types of therapeutics may affect mtDNA transcription and replication, resulting in downstream defects in oxidative phosphorylation and mitochondrial biogenesis, which can lead to compromised organ function. The strategies for ensuring mitochondrial safety include examining changes in mitochondrial biogenesis, metabolism, toxicity, and assaying for specific enzymatic activities in the electron transport chain. While these assays answer important functional questions, they may not necessarily pick up subtle changes with respect to DNA transcription and replication, which can lead to the downstream functional changes. The development of a multiplex, branched DNA (bDNA) assay to assess gene transcription in the mitochondria, as well as in the nucleus has the advantage of detecting a total of eight transcripts in a single lysate. This significantly reduces the cost, time, and consumables that would be needed for traditional qRT-PCR. Studies using human liver epithelial cells treated with a selected group of nucleoside reverse transcriptase inhibitors, including 2',3'-dideoxyinosine, 2',3'-dideoxy-3'-thiacytidine, and 3'-azido-3'-deoxythymidine indicate that this technology may be applied to support the selection of compounds in pharmaceutical programs interested in pursuing nucleoside reverse transcriptase inhibitors as a part of their antiviral strategy.

**PS 2172 Comparison of In Vitro Models for Prediction of Hepatotoxicity of Pharmaceutical Drug Candidates.**

C. McGinnis<sup>1</sup>, T. Sachnik<sup>1,2</sup>, X. Ang<sup>1,3</sup>, J. Johnson<sup>4</sup>, E. Viturro<sup>2</sup> and A. Odermatt<sup>3</sup>. <sup>1</sup>Non-Clinical Safety, Hoffmann-La Roche, Basel, Switzerland; <sup>2</sup>Technische Universität München, Munich, Germany; <sup>3</sup>Division of Molecular and Systems Toxicology, University of Basel, Basel, Switzerland; <sup>4</sup>Hepregen Corporation, Medford, MA.

Liver toxicity is one of the foremost reasons for failure of a drug candidate to reach the clinic. It is also a leading cause for market withdrawals, FDA warnings and modifications of use for current medications. As a result, In vitro hepatocyte-specific studies using cells from preclinical species and also human donors are being investigated to allow for prediction of DILI during the early phase of drug discovery. During this project several novel in vitro models were studied for their potential to detect liver toxic compounds. A high-throughput, 384-well based assay with two-dimensional monocultures of rat or human primary hepatocytes was validated and implemented with ATP depletion as a cellular endpoint. Data obtained from more than 30 commercial and proprietary compounds were compared to results obtained from 3T3 mouse fibroblasts as a non-metabolically competent model. Species-related, and cell type-dependent differences were determined and overall predictability compared to more advanced cell culture models such as a micropatterned hepatocyte co-culture model called HepatoPacTM, as well as a 3D hepatocyte spheroid culture using a Roche developed Hanging Droplet Culture Plate. In depth analysis of the species-, cell- and culture-dependent in vitro results were put into context with underlying mode of actions and dose-effect relationships. This work formed part of a B.Sc. project work carried out by Thomas Sachnik, and M.Sc. project work carried out by Xiaoman Ang.

**PS 2173 Bioassays to Explore Mitochondrial Functions and Anticancer Drug Toxicity.**

E. Robert, P. Picamal and N. A. Compagnone. *Department of Toxicology, ICDD, Meyreuil, France.* Sponsor: Y. Will.

The mitochondria have been identified as one of the major players in previously unrecognized drug-induced hepatic injuries. Hepatotoxicity is the main reason for drug withdrawal in clinical phases and post-marketing. Identifying early mitochondrial toxicities is thus essential to increase the chances of success in drug development. We have developed a panel of integrated functional bioassays aiming at measuring the different functions of the mitochondrial possibly associated with

mitochondrial toxicity in a high throughput and robust manner. Three major axes were explored using cell-based bioassays: the bioenergetics, the redox status and the mitochondrial DNA depletion. First, measurements of the dioxygen consumption, cellular ATP level, extracellular lactate release with regard to cell viability, were multiplexed using fluorescence and luminescence methods. The identification of mitochondrial liabilities associated to hepatotoxicity was largely improved compared to the literature. Secondly, considering that the redox status is associated to drug toxicity, we measured the modulation of the mitochondrial ROS production and antioxidant defenses in response to drugs. Finally, due to its proximity to the electron transport chain and its lack of histones, mitochondrial DNA constitutes a potential target for drug-induced damages. The mitochondrial DNA content was quantified using high content analysis. We performed all the bioassays on HepG2 cells. We tested a panel of drugs that have been marketed, known to be responsible or not for mitochondrial liabilities associated or not to liver and/or cardiac injuries. The tested compounds were classified according to mechanisms of toxicity we detected and compared to the literature. Mitochondrial liabilities can be identified with a predictivity of 84%. Coupling early indicators of mitochondrial dysfunction to late predictors of cytotoxicity provides more relevant and complete information on drug-induced mitochondrial injuries capable of reducing the large space of false negative left by existing methodologies.

**PS 2174 Glucose-Induced Gene Expression Changes Influence Barrier Function in Human Retinal Pigment Epithelial (RPE) Cells.**

G. L. Gong, L. Lecureux and L. D. Lehman-McKeeman. *BMS, Princeton, NJ.*

The RPE forms a blood-retinal barrier in the back of the eye, and alterations in this barrier can adversely affect vision. In the present work, ARPE-19 cells were cultured in physiologically-relevant glucose levels (5 mM) and high glucose conditions (25 mM) for a period up to 3 weeks. Permeability, assessed by apical-basolateral flux of FITC-labeled dextran, was  $10 \pm 1$  ng/ml/min in normal glucose and  $6 \pm 0.3$  ng/ml/min in high glucose, suggesting an increase in barrier function. High glucose also increased mRNA levels of pigment-epithelial-derived factor (PEDF) about 5-fold, while decreasing VEGF-A mRNA levels about 2-fold; these changes correlated with secreted levels of these growth factors, which increased 2.3-fold and decreased 2.8-fold, respectively, in culture medium. High glucose levels increased expression of sphingosine-1-phosphate receptor 1 (S1P1) in ARPE-19 cells more than 3-fold within 1 week of treatment, a change that was maintained during 3 weeks of exposure, whereas expression of S1P3 decreased in a time-dependent manner to nearly 7-fold lower levels after 3 weeks. mRNA levels of tight junction proteins zonula occludens-1 and claudin-1 were unchanged after 1 week of high glucose conditions, but decreased at 3 weeks by 2- and 8-fold respectively. The results of the present study indicate that, in ARPE-19 cells, high glucose conditions affect transcellular permeability and alter expression of proteins involved in tight junction regulation. Moreover, S1P1 and S1P3 genes, which are known to play critical roles in regulating the integrity of endothelial cell barrier function, may also contribute to the regulation of retinal barrier function in RPE cells.

**PS 2175 Towards an Integrated Risk Assessment of Hepatotoxic Drugs via Covalent Binding and Cellular Stress in Primary Hepatocytes.**

M. Teppner<sup>1</sup>, F. Boess<sup>1</sup>, B. Ernst<sup>2</sup> and A. Paehler<sup>1</sup>. <sup>1</sup>Non Clinical Safety, Hoffmann-La Roche Ltd., Basel, Switzerland; <sup>2</sup>Institute of Molecular Pharmacy, University of Basel, Basel, Switzerland.

**Introduction**

Idiosyncratic DILI is of concern to drug development as it occurs rarely but with severe outcome. Early biomarkers for DILI besides covalent binding (CVB) are warranted to classify problematic drugs in vitro. Here we present on complementary endpoints in primary hepatocytes that may early identify cellular damage.

**Methods**

Primary hepatocytes were treated with DILI drugs under attenuated oxidative stress via enzymatic in situ generation of H<sub>2</sub>O<sub>2</sub> up to 24 h. CVB was determined by <sup>14</sup>C binding, prostaglandins via quantification by LC-MS/MS in addition to ATP and LDH release. Expression profiles of Nrf2 regulated genes were created by qPCR analysis

**Preliminary Results**

In hepatocytes generating H<sub>2</sub>O<sub>2</sub>, CVB was significantly exaggerated (13-fold for troglitazone; 20-fold for diclofenac) as compared to controls indicating further peroxidase activation of initially formed reactive metabolites. Significant increase of prostaglandin isomers was observed at lower drug concentrations and at earlier time points than changes in ATP and LDH. In rat hepatocytes prostaglandins E<sub>2</sub> /

15(R) D2 increased by 3.3 / 2.3-fold for FeNTA and 3.0 / 2.0-fold for troglitazone at 6 h. In human hepatocytes, this increase was 3.6 and 3.8-fold respectively for troglitazone with no effect on LDH or ATP.

mRNA levels indicate the activation of several keap/Nrf2 regulated genes such as NAD(P)H dehydrogenase (7.7-fold) and GSH-S-transferase  $\alpha 2$  (6.1-fold) after 24 h for troglitazone. Heme oxygenase 1 (64.1-fold) as well as GSH-S-transferase  $\pi 1$  (12.3-fold) showed a transient induction after treatment with FeNTA.

#### Conclusions

The presented methods are useful for an early identification of DILI liabilities. Besides CVB, cellular stress in hepatocytes may contribute to development of DILI; here prostaglandins are sensitive biomarkers. mRNA levels give insight into the mechanism of toxicity. The in situ generation of H<sub>2</sub>O<sub>2</sub> provides a supportive tool by attenuating response that is specific to drug treatment.

### PS 2176 Aneugenicity Associated with Aurora Kinase Inhibition in a Novel Series of JAK1-Selective Kinase Inhibitors.

E. Harstad, K. Ford, M. Zak, R. Mendonca, S. Ubhayakar, G. Deshmukh, J. Kenny, W. Blair and D. Diaz. Genentech, South San Francisco, CA.

JAK1 inhibition imparts therapeutic benefit in inflammatory diseases, in particular rheumatoid arthritis. A novel series of JAK1-selective molecules was discovered eliminating anemia associated with JAK2 inhibition. In preclinical lead optimization screening, a metabolism-independent aneugenic micronucleus (MN) signal was discovered using a high-content micronucleus test (HC-MNT) in CHO cells. The objectives of this study were to: 1) determine the predictivity of the HC-MNT vs the manual MN assay in normal human mononuclear cells, 2) elucidate the mechanism of aneugenicity, and 3) develop an in silico toxicophore screen to eliminate MN formation. Over 80 JAK1 inhibitors were tested in the HC-MNT, and 20 were tested in the manual MN assay, with 89% positive predictive value in this series of molecules. Results from the HC-MNT indicated an aneugenic signature (based on cytotoxicity indices) that was confirmed via standard centromeric FISH staining in the manual assay. Bone marrow MN evaluations rats confirmed the in vivo relevance of the in vitro MN finding. Selected molecules tested also confirmed the lack of clastogenicity in vitro and in vivo. Aurora kinase inhibition was evaluated as a known microtubule-dysfunction mechanism leading to aneugenicity. In functional cellular assays, Aurora A inhibition was confirmed at high concentrations. Aurora A cellular IC<sub>50</sub>s were consistent with concentrations producing aneugenicity in vitro and in vivo, suggesting a relationship between Aurora A inhibition and aneugenicity exhibited by these compounds. In silico docking identified key interacting residues important for Aurora A binding, allowing Aurora A potency to be screened out prior to chemical synthesis. In summary, these experiments demonstrate the fidelity of the HC-MNT assay with the in vitro and in vivo MN assays for aneugenicity in this chemical series and enabled development of a toxicophore model to eliminate Aurora A liabilities.

### PS 2177 Evaluation of High Content Mechanism Screening As a Prediction Tool for Organ Toxicity.

W. Pennie<sup>2</sup>, S. Lu<sup>1</sup>, C. Stock<sup>3</sup>, J. Gilbert<sup>2</sup> and Y. Will<sup>2</sup>. <sup>1</sup>Drug Safety research and Development, Pfizer Inc, San Diego, CA; <sup>2</sup>Compound Safety Prediction, Pfizer Inc, Groton, CT; <sup>3</sup>Apredica, Watertown, MA.

Attrition due to drug safety remains a serious problem for the pharmaceutical industry. Extensive efforts are made to develop early predictive in vitro screens to assist in selecting compounds with a more desirable safety profile. Since cardiac and hepatic toxicity remain the top causes of compound attrition, much focus has been on building predictive assays for such toxicities. One platform is high content screening performed in an organ relevant cell line to assess a variety of mechanistic toxicity parameters. We have recently shown that general cytotoxicity screening such as ATP measurement in organ specific cell lines can not accurately predict specific organ toxicity. Here we wanted to understand if by choosing more mechanistic parameters we could differentiate compounds with different organ toxicities. In the current study we selected >50 compounds with known human hepatic or cardiac toxicity. These were tested in both H9C2 cells (cardiac panel) and primary rat hepatocytes (hepatic panel) using high content mechanism screening. We found that the majority of compounds, regardless of their designated organ toxicities, displayed similar effects on the two panels tested. Only a small number of compounds demonstrated differential activity in the two panels (eg. nimesulide was only toxic in the hepatic panel). Our results indicate that sophisticated high content mechanism screening in itself is still a poor predictor for differentiating cardiac and hepatic toxicity. More organ relevant endpoints, such as BSEP/MRP assessment for hepatotoxicity and ion channel pharmacology and beating changes for cardiac injury, might increase this prediction. Whether 3-dimensional tissues or stem cell approaches will provide more realistic cell models also remains to be seen. At this

point our high content screening approach can detect potential liabilities, identify mechanism of injury, and at the most provide a Therapeutic Index projection if exposure data are accurately projected.

### PS 2178 Consequences of Mrp2 Deficiency for Diclofenac-Induced Toxicity in Rat Intestine *In Vitro*.

X. Niu, D. van de Vegte, M. Langelaar, I. de Graff and G. Groothuis. Pharmacy, Groningen Research Institute of Pharmacy, Groningen, Netherlands.

Diclofenac (DCF), a widely used non-steroidal anti-inflammatory drug (NSAID), is associated with high prevalence of severe intestinal side-effects. The reactive metabolite diclofenac acylglucuronide (DAG) formed in the liver, and transported by bile into the intestine was reported to be involved in the intestinal injury, based on the observation that Mrp2 deficient (TR-) rat intestine was less sensitive to DCF toxicity due to the reduced biliary transport and intestinal exposure to DAG. However, it is not clear what are the direct consequences of Mrp2 deficiency in the intestine itself. Previously we reported that DCF was toxic in the rat intestine *in vitro* without the presence of liver metabolites. Therefore, using precision cut intestinal slices (PCIS), we compared wild type (WT) and Mrp2 deficient (TR-) rat intestine *in vitro*, by studying direct toxicity, DCF disposition and intracellular glutathione concentration.

PCIS from WT and TR- rats were incubated with a concentration range of DCF. DCF induced similar dose-dependent toxicity and 200  $\mu$ M DCF caused a significant decrease of ATP in both strains of rats indicating that the intestine from TR- rat is not intrinsically less sensitive to DCF toxicity.

As glutathione is a substrate of Mrp2, Mrp2 deficiency may influence its accumulation and thereby the DCF induced toxicity. Intestinal GSH level in the TR-rats was significantly lower than in WT rats but did not make the TR- rat intestine more vulnerable.

In both strains, hydroxyl DCF as well as DAG were detected as the main intestinal metabolites after 5 hours incubation, less amount was excreted into the medium by PCIS of the TR- rats. The study of DCF disposition is ongoing with using chamber.

In conclusion, the TR- rat intestine is not intrinsically less sensitive to DCF toxicity and the lower GSH level does not make it more vulnerable. Less intestinal metabolites are excreted by the PCIS of TR- rats, but whether this is due to lower production or lower excretion ability needs to be further validated.

### PS 2179 Effects of Nicotinamide Phosphoribosyltransferase (NAMPT) Inhibitors on Platelet Development.

J. Singh<sup>1</sup>, T. Zabka<sup>1</sup>, H. Uppal<sup>1</sup>, D. Diaz<sup>1</sup>, J. Tarrant<sup>1</sup>, E. Clarke<sup>2</sup>, T. Lin<sup>1</sup>, N. La<sup>1</sup>, B. McCray<sup>1</sup>, T. Nguyen<sup>1</sup>, P. Dhawan<sup>1</sup>, E. Doudement<sup>1</sup>, A. Kauss<sup>1</sup>, D. Dambach<sup>1</sup> and D. Misner<sup>1</sup>. <sup>1</sup>Safety Assessment, Genentech, South San Francisco, CA; <sup>2</sup>ReachBio, Seattle, WA.

BACKGROUND: Nicotinamide adenine dinucleotide (NAD) is an essential cofactor in glycolysis. Cancer cells have increased energy demands due to proliferation. Nicotinamide phosphoribosyltransferase (NAMPT) catalyzes the rate-limiting step of NAD synthesis, and is up-regulated in many cancer types. Thus, NAMPT inhibitors (NAMPTi) have the potential to treat cancer. Clinical trials with NAMPTi APO866 and GMX1778 failed to reach projected efficacious doses due to thrombocytopenia. We assessed the effects of NAMPTi on megakaryocyte development in vitro and evaluated hematopoietic effects including platelet production in rats. We also tested the hypothesis that nicotinic acid (NA), which replenishes NAD via a NAMPT-independent pathway, mitigates the hematopoietic effects of NAMPTi.

METHODS: Human megakaryocyte lineage cells were cultured from mononuclear cells (containing CD34+ progenitor cells) in vitro for 14 days in the presence of NAMPTi alone or with NA co-treatment. The differentiation, proliferation and survival of megakaryocytes were evaluated functionally (by colony formation) and cell viability was determined biochemically (by ATP levels). Rats were dosed for 4-14 days with NAMPTi alone or co-treated with NA. Bone marrow effects were evaluated by complete blood count with white cell differential and histopathology of hematopoietic tissues.

RESULTS: NAMPTi reduced the functional (colony forming) and biochemical (ATP) viability of megakaryocytes in vitro. This effect tracked with NAMPTi potency and was mitigated by NA co-treatment. NAMPTi caused cellular depletion of hematopoietic tissues and decreases in circulating reticulocytes, red blood cells and lymphocytes in rats. There was no significant reduction in circulating platelets. Hematopoietic effects in rats were partially mitigated by NA co-treatment. Thus, NA may mitigate NAMPTi-mediated thrombocytopenia in the clinic.

**PS 2180 Structural Optimization of the Rac GTPase Inhibitor EHOp-016.**

E. Velez, E. Hernandez and C. Vlaar. *University of Puerto Rico Medical Science Campus, San Juan, Puerto Rico.*

The Rho GTPase Rac family are intracellular signaling proteins that control gene expression and various cellular functions including invasion and metastasis, cell cycle progression and apoptosis. Furthermore, they have been reported to be implicated in cancer initiation and progression. Rac1 is a member of the Rho family GTPases associated with lamellipodia or invadopodia causing invading cells to migrate, and is activated via association with Guanine Exchange Factors (GEFs), among which Vav2. Increase Rac1 activation has been associated with increased breast and brain cancer cell proliferation and invasion. Therefore, one main goal is to focus on the design of novel Rac inhibitors for the development of anticancer drugs. Previously, our laboratory synthesized EHOp-016, which was demonstrated to be the first known inhibitor of Vav2-Rac1 interaction in MDA-MB-435 metastatic cancer cells at low micromolar concentrations. In order to reduce the toxicity and increase the potency, we utilized molecular docking to design novel EHOp-016 derivatives. The carbazole group of EHOp-016 appeared to be required for inhibitory activity, and thus was maintained as a core fragment in further design. It appeared from the docking experiments that replacement of the central pyrimidine ring with other building blocks that orient the potential inhibitors into a U-shaped conformation, provided the best docking results. Novel molecules, that according to docking results bind much better to Rac1 than EHOp-016 will be presented, and the specific interactions leading to increased binding will be discussed. As the compounds were designed to be easily accessible via laboratory synthesis, these proposed improved inhibitors of Rac activity could lead to novel antimetastatic cancer therapies.

**PS 2181 Role of Renal Cytochrome P450 Isozymes in the Bioactivation of 3, 5-Dichloroaniline *In Vitro*.**

C. Racine, T. Ferguson, S. Bakshi, D. Preston, D. Anestis and G. Rankin. *Pharmacology, Physiology and Toxicology, Marshall University, Huntington, WV.*

Chlorinated anilines are common intermediates in the production of agricultural chemicals, dyes, industrial compounds, and pharmaceuticals. Some chloroanilines can induce nephrotoxicity in vivo and in vitro. Previous studies have shown 3,5-dichloroaniline (3,5-DCA, 1.0 mM) induced nephrotoxicity in isolated renal cortical cells (IRCC) following 90 min exposure. Studies from our lab have also shown IRCC pretreated with non-selective cytochrome P450 (CYP) inhibitors [piperonyl butoxide (1.0 mM) and metyrapone (1.0 mM)] partially attenuated 3,5-DCA toxicity, suggesting that CYPs may play a role in 3,5-DCA bioactivation. The purpose of the present study was to further explore the role of CYP mediated 3,5-DCA bioactivation using an in vitro rat model. IRCC were obtained from male Fischer 344 rats. IRCC (4 x 10<sup>6</sup> cells/ml; 3mL) were incubated with shaking for 90 min with either dimethyl sulfoxide (DMSO) or 3,5-DCA (1.0mM). IRCC were pretreated with various CYP inhibitors [isoniazid (1.0 mM), ketoconazole (0.1 mM), omeprazole (0.01 mM), diethyldithiocarbamate (DEDTCa; 0.1 mM), oleanomycin triacetate (0.5 mM), or sulfaphenazole (0.1 mM)] and cytotoxicity was determined by measuring lactate dehydrogenase (LDH) release. Pretreatment with DEDTCa, omeprazole, and sulfaphenazole partially attenuated 3,5-DCA induced nephrotoxicity, while ketoconazole, isoniazid, oleanomycin triacetate did not alter 3,5-DCA induced nephrotoxicity. Studies in rats have shown that DEDTCa, omeprazole, and sulfaphenazole are effective inhibitors of the CYP2C family isozymes. These results suggest that 3,5-DCA is bioactivated via multiple pathways, one of which involves the CYP2C family. (Supported in part by NIH Grant 8P20GM103434 to the West Virginia IDeA Network for Biomedical Research Excellence)

**PS 2182 Studying Drug Effects on Renal Tubular Secretion of Creatinine with a Novel Cellular Model Coexpressing Major Creatinine Transporters OAT2, OCT2, OCT3 and MATE1.**

J. X. Zhang, M. S. Warren, J. Huang and Y. Huang. *Optivia Biotechnology Inc., Menlo Park, CA.*

Serum creatinine level is a commonly used surrogate measure for glomerule damage and kidney function evaluation. It is well known that creatinine clearance in the kidney is through free glomerular filtration and transporter mediated excretion in proximal tubule. Inhibiting these transporters can result in transient increase in plasma creatinine level, which can lead to false interpretation of glomerular damage.

Recently, we have identified that, in addition to OCT2 and MATE1, OAT2 and OCT3 can play major role on creatinine secretion. This finding led to development of a novel cellular model co-expressing all four transporters, for modeling active creatinine secretion in the kidney.

Using the model, we tested drugs with reported incidence of increasing serum creatinine. Most of these drugs inhibited B>A transcellular transport of [C14]Creatinine to different extent, suggesting they are able to block active tubular secretion of creatinine in vivo. It is noteworthy that Cimetidine, which has been previously demonstrated by us as a pan-inhibitor of all four transporters, was able to completely abolish creatinine transport; whereas trimethoprim, which is not an OAT2 inhibitor, only resulted in partial inhibition. These results are in good accordance with clinical studies that higher dosage of Cimetidine can completely block active creatinine secretion in proximal tubule whereas there is no statistically difference in serum creatinine level in patients under moderate- and high-dose of trimethoprim. Furthermore, salicylic acid, which was tested at clinically relevant concentrations, also exhibited a dose-dependent and substantial inhibitory effect on creatinine transport, which suggested that in addition to potentially causing damage to renal tubules, partial blockage of active creatinine secretion could also contribute to serum creatinine level increase caused by salicylic acid, possibly through inhibiting OAT2 and/or MATEs transporters.

**PS 2183 Proximal Tubular Transport of Mercuric Species following Compensatory Tubular Hypertrophy.**

C. Bridges<sup>1</sup>, D. W. Barfuss<sup>2</sup>, L. Joshee<sup>1</sup> and R. K. Zalups<sup>1</sup>. <sup>1</sup>*Division of Basic Medical Sciences, Mercer University, Macon, GA;* <sup>2</sup>*Department of Biology, Georgia State University, Atlanta, GA.*

Chronic kidney disease (CKD) is characterized by a progressive and permanent loss of functioning nephrons. As nephrons are lost, vascular, glomerular and tubular changes occur in remaining nephrons in an attempt to compensate for this loss. These changes lead to glomerular and tubular hypertrophy, hyperperfusion and hyperfiltration. We have hypothesized that tubular hypertrophy and hemodynamic changes resulting from CKD may increase the exposure of individual nephrons to nephrotoxins, such as mercury, and thus may increase the susceptibility of these nephrons to toxic compounds. To test this hypothesis we compared the transport of mercuric species in individually perfused proximal tubules isolated from normal (Sham) or uninephrectomized (NPX) rabbits. Kidneys of NPX rabbits undergo significant hypertrophy in the two weeks following surgery. Tubules isolated from NPX rabbits were larger in diameter than those from Sham rabbits. When the perfusion rate was increased in normal tubules, as a way in which to mimic hyperperfusion, we observed an increase in tubular accumulation of mercury. When tubules from Sham and NPX rabbits were perfused with cysteine-S-conjugates of mercury, we found that tubular accumulation of mercury was greater in tubules from NPX animals. Similarly, luminal disappearance flux ( $J_p$ ) of mercury was greater in tubules from NPX animals. Taken together, our data suggest that hypertrophic changes in proximal tubules may lead to an increased ability and/or tendency of proximal tubules to take up and accumulate nephrotoxins such as mercury.

**PS 2184 Suramin Attenuates Hyperglycemia-Induced Renal Oxidative Stress, Inflammation and Fibrosis in Rats.**

M. Korrappati<sup>1</sup>, B. E. Shaner<sup>1</sup>, B. A. Neely<sup>2</sup>, J. L. Alge<sup>2</sup>, J. M. Arthur<sup>2,3</sup> and R. G. Schnellmann<sup>1,3</sup>. <sup>1</sup>*Drug Discovery and Biomedical Sciences, MUSC, Charleston, SC;* <sup>2</sup>*Medicine, Division of Nephrology, MUSC, Charleston, SC;* <sup>3</sup>*Veterans Administration Medical Center, Charleston, SC.*

Hyperglycemia-induced oxidative stress, inflammation and fibrosis increase susceptibility of diabetic kidneys to nephrotoxic agents. Because development of novel agents that act early to prevent progression of hyperglycemia-induced changes is important, we examined the efficacy and mechanism(s) of suramin in hyperglycemia-induced renal injury before manifestation of overt histological damage. Two groups of male Sprague Dawley rats received streptozotocin (STZ) and one group, saline. Three weeks later one STZ group received suramin (10 mg/kg). All animals were euthanized one week later (4 weeks). While there was a decrease in creatinine clearance between controls and STZ ± suramin rats, there was no difference in creatinine clearance between STZ rats ± suramin intervention. LC-MS/MS-based analysis revealed increases in urinary proteins that are early indicators of diabetic nephropathy (DN) (e.g. cystatin C, clusterin, cathepsin B, and retinol binding protein 4 and peroxiredoxin-1) in the STZ group and were blocked by suramin. Endothelial intracellular adhesion molecule-1 (ICAM-1) activation, leukocyte infiltration and inflammation; transforming growth factor-β1 (TGF-β1) signaling; TGF-β1/SMAD-3-activated fibrogenic markers fibronectin-1, alpha-smooth muscle actin and collagen 1A2; activation of pro-inflammatory and pro-fi-

brotic transcription factors nuclear factor  $\kappa$ B (NF- $\kappa$ B) and signal transducer and activator of transcription factor-3 (STAT-3), respectively, were all increased in STZ rats and suramin blocked these changes. Therefore, delayed administration of suramin attenuated urinary markers of DN, inflammation by blocking NF- $\kappa$ B activation/ICAM-1-mediated leukocyte infiltration and fibrosis by blocking STAT-3-TGF- $\beta$ 1/Smad-3 signaling, supporting the potential use of suramin in development of diabetes-induced kidney injury.

## PS 2185 Resveratrol Alters Subcellular Changes in Oxidative Stress Mediated by Cisplatin in Rat Renal Tissue.

M. Valentovic<sup>1</sup>, J. G. Ball<sup>1</sup>, J. Wolfe<sup>1</sup>, S. Van Meter<sup>1</sup>, M. Wright<sup>1</sup>, B. Lamyathong<sup>2</sup> and B. Brown<sup>1</sup>. <sup>1</sup>Pharmacology, Physiology and Toxicology, Marshall University School of Medicine, Huntington, WV; <sup>2</sup>Wheeling Jesuit University, Wheeling, WV.

The cancer chemotherapeutic agent cisplatin is associated with a 33% incidence of diminished renal function. Interventions to reduce renal toxicity are important in improving patient outcome. Resveratrol (RES) is a phytochemical found in grapes, cranberries and nuts. RES has been recognized as a natural agent possessing anti-cancer and antioxidant properties. This study investigated RES attenuation of cisplatin renal in vitro toxicity and focused on differences between cytosolic and mitochondrial oxidative stress mediated by cisplatin. Male Fischer 344 rats (200-250 g) were anesthetized, with isoflurane and the kidneys were isolated. Renal cortical slices were prepared and pre-incubated with 30  $\mu$ l ethanol (VEH) or 30  $\mu$ g/ml resveratrol (RES, final concentration) for 30 min at 37°C. Tissue were subsequently incubated for a maximum of 120 min with 0, 75, or 150  $\mu$ g/mL cisplatin. Loss of membrane integrity was evaluated as leakage of lactate dehydrogenase (LDH). Oxidative stress and nitrosative stress was assessed in kidney homogenate as well as in subcellular fractions of mitochondria and cytosol. Oxidative stress was measured by protein carbonyl formation using an Oxyblot. Nitrosative alterations were assessed using 3-nitrotyrosine formation by western blot. LDH leakage required a 120 min exposure to cisplatin. An increase in protein carbonyls as detected by Oxyblot, was increased by cisplatin and totally prevented by RES. RES also decreased protein carbonyls in tissue not exposed to cisplatin. Our findings showed that a 30 min RES pre-incubation diminished cisplatin renal toxicity and that protein carbonyl and 3-nitrotyrosine and early changes in oxidative stress prior to the onset of loss of membrane integrity. (Supported by NIH Grants INBRE 3P20RR016477-09S4; 5P20RR016477 and 8P20GM103434 to the West Virginia IDeA Network for Biomedical Research Excellence).

## PS 2186 Diglycolic Acid Induces Cytotoxicity in Human Proximal Tubule Cells via Preferential Inhibition of Succinate Dehydrogenase and Oxidative Phosphorylation.

G. M. Landry, C. L. Dunning, T. V. Dupree, M. J. Hitt and K. McMartin. Pharmacology, Toxicology & Neuroscience, LSU Health Sciences Center, Shreveport, LA.

Diethylene glycol (DEG) is an organic solvent used in common consumer products, thus allowing for increased risk for exposure. DEG metabolism produces two primary metabolites, 2-hydroxyethoxyacetic acid (2-HEAA) and diglycolic acid (DGA). DGA, not DEG or 2-HEAA, produces proximal tubule cell necrosis leading to acute renal failure, the hallmark of DEG poisoning. Studies were designed to assess whether the mechanism for DGA-induced cytotoxicity involves disruption of cellular metabolic processes resulting in mitochondrial dysfunction. DGA induces severe ATP depletion in human proximal tubule (HPT) cells that occurs prior to significant cell death. HPT cells pretreated with increasing DGA concentrations showed significant decreases in oxygen consumption suggesting that DGA acts as an oxidative phosphorylation inhibitor, rather than a mitochondrial electron transport chain uncoupler. Co-incubation of DGA with the antioxidant,  $\alpha$ -tocopherol significantly reduced DGA-induced reactive oxygen species (ROS) formation, but did not reduce ethidium homodimer uptake or lactate dehydrogenase release, two measures of necrotic cell death, suggesting that ROS production is not a cause, but a consequence of DGA-induced cell death. DGA treatment also significantly and preferentially inhibits succinate dehydrogenase activity, but has no effect on other citric acid cycle enzyme activities. Intracellular transport studies utilizing DGA in competition with <sup>14</sup>C-succinate determined an approximate IC<sub>50</sub> value of 175 mmol/L. This value suggests that DGA-induced cytotoxicity is not due to substrate starvation of cells, but rather inhibition of metabolic processes, which occur at much lower DGA concentrations. These results indicate that DGA produces proximal tubule cell death by specific inhibition of mitochondrial-mediated processes resulting in decreased energy production and oxygen utilization.

## PS 2187 Chronic Ethanol Ingestion in Mice Induces Renal Inflammation and Injury through the Platelet-Activating Factor Receptor.

C. Latchoumycandane<sup>1</sup>, J. Liu<sup>1</sup>, L. E. Nagy<sup>2</sup> and T. M. McIntyre<sup>1</sup>. <sup>1</sup>Department of Cellular and Molecular Medicine, Lerner Research Institute, Cleveland Clinic, Cleveland, OH; <sup>2</sup>Department of Pathobiology, Lerner Research Institute, Cleveland Clinic, Cleveland, OH.

Ethanol exposure increases circulating oxidized phospholipids in rats and in alcoholic steatohepatitis patients, although the biological role of circulating oxidized phospholipids remains unclear. Platelet-activating factor (PAF), and some oxidized phospholipids, activate the Platelet-activating factor receptor (PAFR). We hypothesized that PAFR contributes to renal inflammation and injury after ethanol ingestion. In this study we find that mice fed a Lieber-DeCarli ethanol diet had increased levels of circulating PAF, and the pro-apoptotic oxidatively truncated phospholipid azelaoyl-PC. Most strikingly, PAFR-null mice had less infiltrating neutrophils, oxidized phospholipids and TUNEL positive cells in kidney as compared to wild-type (wt) mice fed with ethanol diet. Blood urea nitrogen and serum creatinine, renal functional markers, increased after ethanol exposure in wt mice but not in PAFR-null mice. The renal fibrosis marker,  $\alpha$ -smooth muscle actin was increased in ethanol-fed wt mice, but not in PAFR-null mice. Kidney injury molecule-1 (KIM-1), a marker for proximal tubular injury, is increased during acute renal injury, and we find higher expression of KIM-1 in the proximal tubules of ethanol fed wt mice as compared to PAFR-null mice. These results suggest that PAF and bioactive PAF-like oxidized phospholipids promote renal inflammation, acute injury, and renal fibrosis. These events completely depend on a functional PAFR. This demonstrates a novel mechanism of PAFR in alcoholic renal injury.

## PS 2188 Nephrotoxicity of Epigenetic Inhibitors Used for the Treatment of Cancer.

N. E. Scholpa, M. Moore and B. S. Cummings. Pharmaceutical and Biomedical Sciences, University of Georgia, Athens, GA.

Several studies exist investigating the anti-neoplastic activity of epigenetic inhibitors. In contrast, fewer studies have investigated the toxicity of epigenetic inhibitors in non-target organs, such as the kidney. Even fewer have investigated both the anti-neoplastic activity and toxicity of epigenetic inhibitors under similar conditions. This study determined the anti-neoplastic activity and nephrotoxicity of epigenetic inhibitors In Vitro. The therapeutic efficacy of epigenetic inhibitors was first determined in human prostate cancer cells (PC-3 and LNCaP) using the DNA methyltransferase inhibitor 5-azacytidine (5-Aza) and the histone deacetylase inhibitor trichostatin A (TSA). Cells were also treated with carbamazepine (CBZ), an anti-convulsant with histone deacetylase inhibitor-like properties. 5-Aza, TSA, or CBZ alone (0-100  $\mu$ M) did not induce decreases in MTT staining in PC-3 or LNCaP cells after 48 hr. In contrast, docetaxel, a frontline chemotherapeutic, did induce concentration-dependent decreases in MTT staining after just 24 hr. Treatment of prostate cancer cells with CBZ prior to docetaxel exposure decreased MTT staining in LNCaP cells, but neither TSA nor 5-Aza altered MTT staining compared to cells exposed to docetaxel alone. Treatment of normal rat kidney (NRK) and human embryonic kidney 293 (HEK293) cells with the same concentration of epigenetic inhibitors used in prostate cancer cells significantly decreased MTT staining after 48 hr. The epigenetic inhibitors were generally more toxic than the nephrotoxic bromate (0-400 ppm), and TSA and 5-Aza pretreatment increased the cytotoxicity of BrO<sub>3</sub><sup>-</sup> in NRK cells. Increased cytotoxicity in NRK cells correlated to alterations in epigenetic markers such as histone phosphorylation and to alterations in the methylation of the cyclin-dependent-kinase inhibitor protein p21. Collectively, these data suggest that epigenetic inhibitors can induce nephrotoxicity at doses that are therapeutically relevant in prostate cancer cells In Vitro.

## PS 2189 hTERT-Immortalized Renal Proximal Tubule Epithelial Cells: A Model for Testing Cadmium's Role in the Development of Renal Cancer.

B. R. Simon. Global Environmental Health Sciences, Tulane University, New Orleans, LA. Sponsor: J. Wickliffe.

The incidence of renal cell carcinoma (RCC) has steadily increased in the United States over the past three decades. Therefore, it is critical that scientists are better able to understand contributing factors. Cadmium (Cd) is a recognized carcinogen and widespread environmental contaminant. The kidney is a known target organ of Cd toxicity, however the mechanistic role(s) that Cd plays in the development of RCC has not been described. Renal proximal tubule epithelial cells (RPTECs) are specifically affected by Cd because of their propensity to reabsorb Cd from filtrate

leading to bioaccumulation. In order to elucidate the mechanisms by which Cd acts, we aim to characterize a newly developed cell line derived from renal proximal tubule epithelial cells of a healthy human male donor (RPTEC/TERT1). Our goal is to establish this new in vitro system for future toxicological and cancer research by characterizing the RPTEC/TERT1 cell line and utilizing them to conduct biologically relevant exposure studies. We will explore these goals through exposure experiments to binary mixtures of two common environmental contaminants, Cd and benzo(a)pyrene (B[a]P). Our preliminary results demonstrate that these cells are sensitive to both compounds separately over a wide range of exposure levels. Additionally, the characteristic Cd-interacting protein, metallothionein I/II, exhibits a Cd-specific protein response, which supports its ability to function as expected, based on in vivo evidence. The RPTEC/TERT1 cell line expresses metabolic biotransformation enzymes necessary for processing polycyclic aromatic hydrocarbons (PAHs) which is exemplified by their sensitivity to the representative PAH, B[a]P. Future experiments will further characterize DNA repair capacity of the RPTEC/TERT1 cell line and the development of mutagenic lesions when exposed to binary mixtures of sub-cytotoxic doses of Cd and B[a]P. This work will provide mechanistic support and augment current scientific knowledge regarding the development of RCC and exposure to xenobiotic mutagens and carcinogens.

**PS 2190 BUN and Serum CRE Alterations in Higa and BALB/c Mice after Subacute Administration of Fluoride via Drinking Water.**

T. Kido<sup>1,2</sup>, M. Tsunoda<sup>2</sup>, C. Sugaya<sup>2</sup>, H. Yanagisawa<sup>1</sup> and Y. Aizawa<sup>3</sup>. <sup>1</sup>Public Health and Environmental Medicine, The Jikei University School of Medicine, Tokyo, Japan; <sup>2</sup>Preventive Medicine, Kitasato University School of Medicine, Sagami-hara, Japan; <sup>3</sup>Kitasato University, Tokyo, Japan.

Fluoride (F) is known as an environmental pollutant. Because F is filtered by the kidney, mice with impaired renal function may be affected more significantly by F. IgA nephritis is the most common chronic glomerulonephritis. High IgA (HIGA) mice have been used as a model of IgA nephritis. The effects of fluoride on BUN and serum creatinine (CRE) of HIGA and BALB/c mice after subacute administration via drinking water were examined in this study to get basic information of the toxic effects of F on the mice with IgA nephritis. F was administered to HIGA and BALB/c mice, aged 11-12 weeks at 0, 50, 100, and 150 ppm in their drinking water for 4 weeks. The blood was sampled from the tail artery once a week. The BUN and CRE in the serum was determined by the kits. For the BUN levels in the HIGA mice, after one week from the beginning of the exposures, the mean BUN in the 50-ppm group was significantly higher than those in the 100- and 150-ppm groups. At 2 weeks, the mean value of BUN in the 100-ppm group was significantly higher than those in the 0- and 50-ppm groups. For the BALB/c mice, there were no significant differences among the groups. For the CRE in the serum of HIGA mice, after 1 week, the mean CRE in the 50-ppm group was significantly higher than those in the 100- and 150-ppm groups. For the BALB/c mice, after 3 weeks, the mean CRE in the 50-ppm group was significantly higher than those in the 0- and 100-ppm groups. The alterations in the BUN and CRE in the serum observed in the HIGA and BALB/c mice may indicate the toxic effects of F on the kidney. However, the alterations were not dose-dependent, and the effects of F on the kidney of HIGA mice were not as significant as those on kidney of the BALB/c mice. The toxic effects of F on the kidney were not enhanced in the HIGA mice at 11 to 12 weeks of age.

**PS 2191 Performance Evaluation of Urinary Complement Biomarker for the Immune-Mediated Glomerular Injury.**

M. Ko<sup>1</sup>, E. Nagiec<sup>2</sup>, D. Fix<sup>3</sup>, B. L. Homer<sup>2</sup> and A. John-Baptiste<sup>1</sup>. <sup>1</sup>Drug Safety, Research & Development, Pfizer, San Diego, CA; <sup>2</sup>Drug Safety, Research & Development, Pfizer, Cambridge, MA; <sup>3</sup>Drug Safety, Research & Development, Pfizer, Groton, CT. Sponsor: W. Huang.

With the increased focus on protein biotherapeutic development in recent years, glomerular injury has become a significant risk factor. In order to monitor this risk in preclinical and clinical drug development reliable, sensitive and specific biomarkers are greatly needed. Currently urinary albumin and total protein are the most commonly used diagnostic biomarkers for monitoring both tubular and glomerular injury. Rat passive Heymann nephritis (PHN) is a model of glomerular injury characterized by subepithelial immune complex deposits, along with deposition of C5b-9 and ensuing proteinuria (Pippin et al., 2009). Schulze et al. established that elevated urinary C5b-9 was associated with glomerular immune deposit formation in this model (1989, Kidney International, 35, 60-68). Consequently, we evaluated the performance of commercially available Quidel human and USCN rat C5b-9 ELISA kits on urine samples. Zymosan-activated plasma or serum samples from non-human primate (NHP) and rat, respectively, were used as positive

controls. The linear detection range of the standard curve, dilution effect, matrix effect, albumin interference, and inter-assay variability were assessed as performance parameters for the kits. In addition, a rat PHN study was conducted, and the urine samples were analyzed with USCN C5b-9 ELISA kits. The results showed poor performance of the kits, demonstrated by greater than  $\pm 30\%$  analytical recovery for dilution effects, urine matrix effects, albumin interference, and greater than 25% coefficient of variation for inter-assay variability. Moreover, using Urinary Stabilizing Buffer (Argutus Medical Ltd, Dublin, Ireland) did not improve the performance. Therefore, we could not demonstrate an association between the C5b-9 positively-stained glomeruli and urinary C5b-9 level in the rat PHN study. We concluded that Quidel and USCN kits performed poorly for the detection of urinary C5b-9 in rat and NHP urine.

**PS 2192 Miniaturized Multiplex Protein Nanoarray Assays for Early Detection of Drug-Induced Nephrotoxicity in Mice and Rats.**

A. W. Kherzai, R. G. Sanedrin, P. Han, N. A. Amro, R. Helfrich, S. Aziz, N. Patel, D. Mikos and H. Jamil. *Nano BioDiscovery, Nanoink INC, Skokie, IL.* Sponsor: S. Devi.

Drug-induced toxicity is the major cause of kidney damage. The previous methods for measuring drug induced injury, namely serum creatinine and blood urea nitrogen, have been found inadequate. Recently the FDA and EMEA have qualified a panel of biomarkers that is highly useful in the early identification and characterization of kidney injury.

Here we report the development of highly sensitive and small sample volume NanoArray multiplex assays for early detection of drug-induced nephrotoxicity in mouse and rat in-vivo models based on dip-pen nanolithography (DPNTM) using a NanoArrayer 3000TM. This instrument enables the production of highly reproducible micro- to nano-scale arrays of proteins which occupy an area approximately 100 times smaller than conventional microarrays. The reduced array area results in reduced reagent and sample requirement and increased sensitivity due to reduced analyte depletion. For a multiplexed sandwich ELISA, arrays of specific capture antibodies are printed on activated glass slides. Samples of as little as 2-4  $\mu$ l can be incubated over the arrays in 48 and 96 well format. The slides are then incubated with specific biotinylated detection antibodies followed by fluorescently labeled Streptavidin. The fluorescence is measured with a high resolution fluorescence scanner.

The multiplex assays were developed and validated for mouse (Albumin, Clusterin, Cystatin C, KIM-1, and EGF) and rat biomarkers panels (Albumin, Clusterin, Cystatin C, KIM-1, B2MG and TFF3) and showed high sensitivity and specificity. The assay was used to detect and quantify renal injury biomarkers in urine samples obtained from normal and drug compromised rats. The low volume sample requirements in conjunction with the extremely high sensitivity, selectivity, and reproducibility help enable longitudinal studies on individual rodents thus saving significant study costs and providing better toxicity data than other conventional methods used for preclinical and clinical safety and toxicity studies.

**PS 2193 Magnetic Resonance Imaging (MRI) Assessment of Renal Glomerular Filtration Rate (GFR).**

M. Uteng<sup>1</sup>, A. Mahl<sup>1</sup>, A. Piaia<sup>1</sup>, J. Cunliffe<sup>1</sup>, E. Persohn<sup>1</sup>, E. Tritto<sup>1</sup>, D. Leduc<sup>1</sup>, P. Moulin<sup>1</sup>, N. Shangari<sup>1</sup>, S. Chibout<sup>1</sup>, A. Wolf<sup>1</sup>, L. Li<sup>1</sup>, E. Pognan<sup>1</sup> and N. Beckmann<sup>2</sup>. <sup>1</sup>Novartis Institutes for BioMedical Research, Novartis, Basel, Switzerland; <sup>2</sup>Global Imaging Group, Novartis, Basel, Switzerland.

MRI of kidneys after administration of the contrast agent, gadolinium-tetra-azacyclo-dodecanetetra-acetic acid (Gd-DOTA), has been reported as a promising method for assessment of GFR. However, there is little literature on the sensitivity of this method compared to standard assessments in non-clinical trials of drug development. To this end, we have conducted a study with the aim to determine the sensitivity of MRI as a method for detection of GFR in rodents.

Sprague-Dawley rats were treated with Adefovir as positive control, and Telbivudine and Entecavir as negative controls for nephrotoxicity. The rats were treated daily by oral gavage for 4 weeks with 10X and 25X human equivalent exposure doses (HED) of compounds. After 3, 10 and 28 days treatment, GFR was assessed by MRI and creatinine clearance rate, while renal toxicity was assessed by urinary kidney biomarkers, clinical biochemistry parameters in blood and urine, histopathology, electron microscopy and gene expression profiling. Impairment of GFR was detected by MRI showing delayed time-to-peak signal of Gd-DOTA clearance in the renal cortex of animals treated with 25X HED Adefovir on day 28. These results correlated with histopathological observations of cortical tubular degeneration. Moreover, renal toxicity was also confirmed by urinary kidney biomarkers (e.g Kim1), and by down-modulation of renal tubular associated

genes. On the other hand, the creatinine filtration rate did not reveal any significant changes. Animals treated with Telbivudine and Entecavir showed neither renal impairment nor toxicity for the entire study duration. In conclusion, these results demonstrated that MRI is a sensitive method for non-invasive detection of GFR changes and that this technique may be a good alternative to the standard measurements of creatinine filtration in non-clinical investigative studies.

## PS 2194 Identification of 3-Indoxyl Sulfate As an Early Biomarker for Nephrotoxicant-Induced Acute Kidney Injury.

A. Won<sup>1</sup>, T. Kim<sup>1</sup>, Y. Shin<sup>1</sup>, B. Lee<sup>2</sup>, S. Kim<sup>3</sup> and H. Kim<sup>1</sup>. <sup>1</sup>College of Pharmacy, Pusan National University, PUSAN, Republic of Korea; <sup>2</sup>College of Pharmacy, Sungkyunkwan University, Suwon, Republic of Korea; <sup>3</sup>Department of Chemistry and Chemistry Institute for Functional Materials, Pusan National University, Busan, Republic of Korea.

The identification of new biomarkers of acute kidney injury (AKI) is important for the detection of drug-induced kidney damage. Various serum or urinary biomarkers have been used to detect AKI, but these biomarkers have shown poor sensitivity and specificity. In this study, we compared the sensitivity of a new metabolomic biomarker, 3-indoxyl sulfate (3-IS), with traditional biomarkers for the diagnosis of AKI using the area under the receiver operating characteristic (ROC) curve. Sprague-Dawley male rats were allocated to several groups. Each group was administered either a single dose of cisplatin (20 mg/kg, i.p.), continuous injection of cyclosporin A (10 mg/kg, i.p.), mercury chloride (1.5 mg/kg, i.p., and 7.5 mg/kg, i.p.), or gentamicin (60 mg/kg, s.c.). Urine and plasma samples were collected 1, 3, and 7 days after last injection of nephrotoxicants. Urine and blood biochemical parameters involved in kidney toxicity were measured. We also measured 3-IS levels in the serum, urine, and kidney using HPLC. In the nephrotoxicants-treated rats, blood urea nitrogen (BUN) and serum creatinine (sCr) levels were slightly increased. The 3-IS levels were significantly reduced in the urine of rats treated with cisplatin and other nephrotoxicants. In contrast, 3-IS levels were significantly elevated in the serum and kidneys of nephrotoxicants-treated rats. The 3-IS is produced by bacterial metabolism of tryptophan in the intestine, followed by oxidation and sulfation in the liver. The 3-IS is mainly excreted via active secretion by the organic anion transporter (OAT) in the proximal tubule. Thus, reduced urinary 3-IS levels can reflect proximal tubule injury. These results suggest that urinary 3-IS may be used as an alternative to traditional biomarkers to predict AKI.

## PS 2195 A Quantitative High-Throughput Screening Platform for Predictive Kidney Toxicity.

M. Adler<sup>1</sup>, E. Gottwald<sup>1</sup>, B. Goodwin<sup>2</sup>, M. Xia<sup>2</sup> and V. S. Vaidya<sup>1</sup>. <sup>1</sup>Renal Division, Department of Medicine, Brigham and Women's Hospital, Harvard Medical School, Boston, MA; <sup>2</sup>National Center for Advancing Translational Sciences, National Institutes of Health, Bethesda, MD.

Drug and environmental chemical-induced kidney toxicity plays an important role in the high incidence and prevalence of kidney injury in both hospitalized and non-hospitalized patients, which in many circumstances can be prevented or at least minimized by predictive toxicity screening. The goal of this study was to develop a cell-based quantitative high throughput screening (qHTS) platform with two aims: 1) to identify a more biologically relevant *in vitro* system for prediction of human kidney toxicity than currently used immortalized cells and 2) to identify a sensitive, specific, robust and translatable biomarker of kidney toxicity since *in vivo* biomarkers such as kidney injury molecule-1 do not respond *in vitro*. We used primary human proximal tubular epithelial cells (HPTEC) and observed that these cells in a monolayer possess human tubular epithelial characteristics like 1) formation of domes; 2) expression of zonula occludens-1, cytokeratin 18 by immunostaining; 3) a wide range of efflux and influx transporters including aquaporin 1, megalin, organic cation transporter 2, multidrug resistance protein 2, P-glycoprotein by semi-quantitative PCR and 4) activity of brush-border enzymes like alkaline phosphatase, and  $\gamma$ -glutamyl-transferase. We found that hemeoxygenase-1 (HO-1) mRNA and protein levels significantly increased in a concentration-dependent manner (tested over 6-point concentration curve) following exposure to structurally and mechanistically diverse kidney toxicants such as cisplatin, gentamicin, cyclosporin A and cadmium chloride and correlated well with cytotoxicity. HO-1 expression remained unchanged following treatment of HPTEC with non-kidney toxic compounds (e.g. carboplatin), demonstrating its specificity. Our results demonstrate the relevance and potential use of HPTEC in a qHTS platform using HO-1 as a biomarker for predictive safety assessment of drugs and environmental chemicals.

## PS 2196 Systems Biology Approach Identifies Transcriptional Regulator of Kidney Injury Molecule-1.

A. K. Ajay<sup>1,3</sup>, T. Kim<sup>2,3</sup>, P. J. Park<sup>2,3</sup>, V. Ramirez<sup>1,3</sup> and V. S. Vaidya<sup>1,3</sup>. <sup>1</sup>Renal Division, Brigham and Women's Hospital, Boston, MA; <sup>2</sup>Centre for Biomedical Informatics, Harvard Medical School, Boston, MA; <sup>3</sup>Department of Medicine, Harvard Medical School, Boston, MA.

Kidney injury molecule-1 (KIM-1) is the highest upregulated gene following kidney ischemic or toxic insult and functions as a phosphatidylserine receptor to internalize apoptotic cells. Owing to lack of information about regulation of KIM-1, we used genome-wide expression data following kidney ischemia reperfusion injury (IRI) in rats and utilizing ChIP enrichment analysis and kinase enrichment analysis we identified STAT3 and checkpoint kinase 1 (Chk1) as a potential transcription factor and kinase regulating KIM-1. Then we performed an extensive biological validation of the bioinformatics predictions and report that reactive oxygen species generation following IRI upregulates Chk1 that binds to STAT3 phosphorylating it at Ser727, which further binds to KIM-1 promoter for its transcription. We observed temporal association among pSTAT3, pChk1 and KIM-1 using immunoblotting and immunostaining in rat kidneys following IRI and in human kidneys from patients with kidney injury. To prove transcriptional regulation of KIM-1 by STAT3 we used i) primary human proximal tubular epithelial cells (HPTEC) and showed a significant increase (1.5 fold) in KIM-1 mRNA and protein following STAT3 activation. Conversely we used human renal carcinoma cell line (769 P) expressing high pSTAT3/KIM-1 and found 2-fold decrease in KIM-1 following STAT3 siRNA transfection. Furthermore, we confirmed that STAT3 binds on KIM-1 promoter in i) rat kidneys (10 fold by ChIP assay) following IRI; ii) HPTECs transfected with KIM-1-luciferase plasmid (3-fold by STAT3 activation) and iii) 769 P cells transfected with STAT3 siRNA (2-fold decrease). The binding of Chk1 to STAT3 was observed using immunoprecipitation in HPTEC by hydroxyurea (Chk-1 activator). These results reveal Chk1-STAT3 as one of the key pathways regulating KIM-1 transcription.

## PS 2197 Kidney miRNAs Show Age and Sex Differences in Expression during the Rat Life Cycle.

J. C. Kwekel, V. Desai, T. Han, C. L. Moland and J. C. Fuscoe. *Personalized Medicine Branch, US FDA, National Center for Toxicological Research, Jefferson, AR.*

Increasing evidence for epigenetic mechanisms of gene regulation has fueled interest in the role of miRNAs in toxicogenomics for biomarker discovery. While relatively immature in comparison to other genomic resources, the growing knowledge base of individual miRNAs and their putative gene targets allows for large scale inquiry into more comprehensive, genome-wide analysis of miRNA expression. Kidney tissues in the F-344 rat model system were examined over the life cycle for the purpose of evaluating miRNAs with putative roles in drug metabolism and kidney disease. miRNA expression was characterized at 2, 5, 6, 8, 15, 21, 78, and 104 weeks of age in both sexes using Agilent 8x15k rat miRNA microarrays containing multiple probes for 677 unique miRNAs. Five animals per sex and age were used for a total of 80 samples. Agilent's Feature Extraction software was used for initial analysis and processing of the raw data and 224 miRNAs were found to be expressed in the kidney in at least one age and sex. Combined filtering criteria of 1.5 fold change and  $p < 0.05$  (2-way ANOVA) revealed 105 miRNAs (47%) exhibiting differential expression by age or sex. Principal component analysis (PCA) showed PC1 accounted for 21% of the variability among the 105 differentially expressed miRNAs in a pattern consistent with age-specific effects. 12 miRNAs showed increased expression at 78 and 104 weeks, consistent with an aging-related effect (e.g. miR-142-3p, miR-223). Although no large scale, sex-related patterns were evident from the PCA, some miRNAs showed sex-specific patterns of expression (e.g. miR-204, miR-499, miR-183). miR-499 has been implicated in regulation of mitochondrial dynamics through direct targeting of calcineurin. Collectively, these results comprise one of the first large-scale characterizations of global miRNAs in the kidney over the entire rat life cycle and show age- and sex-related differences that may impact susceptibility to adverse effects in the kidney.

## PS 2198 Mice Deficient in microRNA-155 Have Greater Susceptibility to Cisplatin-Induced Kidney Toxicity.

K. L. Pellegrini, V. Bijol and V. S. Vaidya. *Renal Division, Department of Medicine, Brigham and Women's Hospital, Harvard Medical School, Boston, MA.*

Although originally identified as an oncogenic factor, microRNA-155 (miR-155) has also been found to be upregulated in macrophages and dendritic cells in response to a range of inflammatory stimuli and required for the activation of Th17 cells. We have previously shown miR-155 to be significantly upregulated following

ischemic or toxic insult to the kidney and the objective of this study was to further investigate the role of miR-155 in regulating kidney injury. Male miR-155<sup>-/-</sup> (KO) and wild type C57BL/6J (WT) mice were injected intraperitoneally with 20 mg/kg of cisplatin and sacrificed at 0, 24, 48, 72, 96 and 120 h (n = 5/timepoint) for the collection of blood and kidneys. Blood urea nitrogen (BUN) and serum creatinine (Scr) were measured to determine kidney function, and kidney injury molecule (KIM-1) mRNA, histopathology (necrosis) and TUNEL staining (apoptosis) were measured to determine the extent of proximal tubular injury.

The miR-155<sup>-/-</sup> mice had significantly higher kidney dysfunction as evidenced by more than 2-fold higher levels of BUN and Scr in the KO mice as compared to WT by 48 h. The KO mice also had significantly higher KIM-1 mRNA levels (3-fold) than the WT that remained higher than WT through to 120 h. Necrosis and apoptosis were significantly increased in the kidneys of KO mice as compared to WT mice throughout the time course, and mortality of approximately 60% was observed for the miR-155<sup>-/-</sup> mice as compared to 20% for the WT mice by 120 h. These results demonstrate that miR-155<sup>-/-</sup> mice are highly susceptible to cisplatin-induced kidney toxicity. Tumor protein 53 induced nuclear protein 1 (TP53INP1), which phosphorylates p53 to induce apoptosis, has previously been identified as a direct target of miR-155. We hypothesize that miR-155 is repressing the levels of TP53INP1 (and in turn, the induction of apoptosis) in the kidneys of C57BL/6J mice treated with cisplatin, and that the dysregulation of TP53INP1 in miR-155<sup>-/-</sup> mice promotes the induction of apoptosis, resulting in higher levels of kidney injury.

## PS 2199 Urinary microRNAs As Translational Biomarkers to Detect Acute Kidney Injury.

K. Ramachandran, J. Saikumar, S. S. Waikar and V. S. Vaidya. *Renal Division, Department of Medicine, Brigham and Women's Hospital, Harvard Medical School, Boston, MA.*

MicroRNAs (miRNAs) are a family of short, single stranded, non coding RNA molecules that direct the expression of nearly 60% of all protein coding genes. Extracellular miRNAs, identified in 14 different body fluids, have been proposed as biomarkers of disease and organ damage due to their stability, sensitivity, specificity and ease of detection. Previously, we identified 3 miRNAs (miR-21, -155 and -18a) that were upregulated following ischemic injury and gentamicin induced nephrotoxicity in rats. Human urinary levels of miR-21 and -155 were able to distinguish patients with and without acute kidney injury (AKI). The aim of our current study was to profile the human miRNome in the urine of patients with or without AKI to identify a panel of urinary miRNAs that can serve as sensitive and specific indicators for kidney injury. To estimate the fraction of miRNAs present in the urine, we used the Human miRNome miScript miRNA PCR Array from Qiagen (miRBase version 18 containing ~1900 miRNAs) on urines pooled from 6 patients with AKI and 6 healthy controls. Samples were collected from patients admitted in the Intensive Care Unit (ICU) with a rise in serum creatinine of 100% over baseline. Using a cycle threshold (Ct) range of 19-30, miRNAs that were expressed in both, or in either one of the diseased or healthy pools were selected. All miRNAs that had Ct values >30 in both the sample sets were considered as 'Not Expressed' and eliminated. Thus, we designed a customized array of the 378 detected miRNAs and analyzed the 12 urine samples (6 AKI and 6 healthy) individually. We found 52 miRNAs that were upregulated >5-fold in the AKI patients as compared to the controls and 33 candidate miRNAs (out of 52) were selected using a standard deviation cut-off of 1.5. Further evaluation of these candidate miRNAs for sensitivity, specificity, stability, reproducibility and robustness in an expanded cohort of patients with or without kidney damage will help in establishing the value of urinary miRNAs as non-invasive biomarkers for kidney injury.

## PS 2200 Genetic Reduction in Fibrinogen Protects from Progression of Acute Kidney Injury to Chronic Kidney Disease.

F. Craciun, A. K. Ajay and V. S. Vaidya. *Department of Medicine, Renal Division, Brigham and Women's Hospital, Harvard Medical School, Boston, MA.*

The incidence of acute kidney injury (AKI) is increasing and recent studies emphasize the significantly higher risk of developing chronic (CKD) and end-stage kidney disease for AKI survivors. We have shown that mRNA and protein expression in the kidney as well as urinary fibrinogen (Fg) is significantly increased following AKI in mice, rats and humans. Furthermore, we have demonstrated that Fg heterozygosity in mice reduces plasma Fg to 75% of the normal circulating levels, protecting from AKI and promoting faster resolution of kidney damage. Therefore, we hypothesized that Fg heterozygosity would protect from AKI to CKD progression. To test this we used a Folic acid (250 mg/kg, single sq injection) induced AKI to CKD progression model in wildtype (Fg+/+), heterozygous (Fg+/-) and Fg defi-

cient (Fg-/-) mice on Balb/c background and the mice were sacrificed at days 1 and 14 following administration (n=4-6/time point/group). At day 1 there was significant kidney dysfunction as assessed by blood urea nitrogen (112, 73 and 65 mg/dL for Fg+/+, Fg+/- and Fg-/- respectively) and serum creatinine (0.7, 0.6, 0.3 mg/dL for Fg+/+, Fg+/- and Fg-/- respectively), indicating protection in Fg+/- and Fg-/. Kidney mRNA levels of Kidney injury molecule-1 (marker of proximal tubular injury) were significantly higher for Fg+/+ (80 fold) than Fg+/- (46 fold) and Fg-/- (55 fold) as compared to uninjured mice. By day 14 these markers of acute injury reverted to normal but there was increased kidney mRNA expression of fibrosis markers fibronectin (9, 4 and 8 fold in Fg+/+, Fg+/- and Fg-/- respectively) and collagen (8, 3 and 9 fold in Fg+/+, Fg+/- and Fg-/- respectively) when compared to uninjured mice, with only Fg+/- showing protection. This was confirmed histologically by Masson's trichrome staining. We conclude that a lowered but not completely abolished level of Fg protects from AKI to CKD progression, providing a therapeutic target that could benefit AKI survivors.

## PS 2201 Urinary Levels of N-Acetyl-β-D-Glucosaminidase (NAG), Glutathione-S-Transferase (GST), Blood Lead and Plasma Creatinine As Early Indicators of Lead Nephropathy in Occupationally Exposed Subjects.

I. O. Omotosho<sup>1</sup> and G. O. Ademowo<sup>2</sup>. <sup>1</sup>Chemical Pathology, College of Medicine, University of Ibadan, Ibadan, Nigeria; <sup>2</sup>Institute of Advanced Medical Research, College of Medicine, University of Ibadan, Ibadan, Nigeria.

Lead (Pb) toxicity remains a public health problem. Although early diagnosis is paramount for meaningful intervention particularly in occupationally exposed subjects, the diagnosis of Pb poisoning at early stage remains a problem even in developed economies. This work addressed this issue by expressing urinary levels of NAG and GST as exponents of concentrations of conventional renal function markers (creatinine, urea and uric acid) and blood Pb. The result of exponential expression of these results showed a definite pattern particularly in occupationally exposed subjects relative to confirmed chronic renal failure subjects and control. When these figures were compared logarithmically, definite hyperboles for the control, the occupationally exposed and the CRF were observed; the importance of this in early diagnosis of lead nephropathy is to be discussed. Based on these, we propose hypothesis that can be used in the early identification of renal tubular damage especially in subjects occupationally exposed to lead using this logarithmic model.

## PS 2202 Early Postnatal Gentamicin Treatment Reduces Glomerular Number in Extra Uterine Growth Restricted Wistar Rats.

R. R. Bueters, A. Klaasen, L. P. van den Heuvel and M. F. Schreuder. *Pediatric Nephrology, Radboud University Nijmegen Medical Centre, Nijmegen, Netherlands.* Sponsor: F. Russel.

Introduction: Nephrogenesis is the process that leads to the formation of nephrons and ceases around the 36th week of gestation in man, without the possibility of additional formation later in life. A lower number of nephrons have been associated with an increased chance at chronic kidney disease development. In the Netherlands alone, almost 8% of all children are born preterm, and many are treated with drugs or suffer from extra uterine growth restriction (EUGR) that may potentially reduce nephron formation. In this study we investigated the impact of gentamicin and ceftazidime on kidney development w/o EUGR.

Methods: Wistar rats were allocated to either normal size litters (12 pups) or increased size litters (20 pups), the last resulting in EUGR. Both cohorts were divided in control and intervention groups where animals were administered 0.9% NaCl, 4 mg/kg gentamicin or 5 mg/kg ceftazidime via intraperitoneal route from post natal day 2-8. At day 8 and 35, animals were sacrificed and the kidneys were collected. Day 8 kidneys were examined for mRNA expression in a selection of targets, proliferation, apoptosis and general histopathology. Total glomerular count (estimated using stereology) and glomerular generation count were performed in kidneys collected at day 35.

Results: Gentamicin treatment in combination with EUGR resulted in 20% less glomeruli compared to sham treatment. EUGR animals had less body weight, but showed parallel growth compared to non-growth restricted animals, indicating a successful working model. No clear distinctions were noted in mRNA expression levels, glomerular generation count or general histopathology. The proliferation/apoptosis balance is currently under investigation.

Conclusion: Early postnatal gentamicin treatment in combination with EUGR tends to decrease the total glomerular number in Wistar rats, of which the pathways were not clarified yet. The long term clinical sequelae are still unclear.

**PS 2203 Resistance to Dioxin-Induced Hydronephrosis in a Mouse Strain Having Unresponsive Microsomal Prostaglandin E Synthase-1.**

K. Aida-Yasuoka, W. Yoshioka, T. Kawaguchi, S. Ohsako and C. Tohyama.  
*University of Tokyo, Tokyo, Japan.*

**Background:** The majority of dioxin toxicity is governed by aryl hydrocarbon receptor (AhR), and the degree of toxicity is affected by its allele type. It is known that AhRb1 and AhRb2 are responsible for marked manifestation of dioxin toxicity, but that AhRd is not. Our previous works 1, 2) showed that COX-2 and microsomal prostaglandin E synthase-1 (mPGES-1), an inducible form of PGE2 synthase, are critical factors in the pathogenesis of hydronephrosis (HN), and suggested the presence of the possible strain difference in the development of HN between C57BL/6J and BALB/c. Thus, we here examined the incidence of dioxin-induced hydronephrosis (HN) in mouse pups of these strains to clarify causative factors that bring out a strain difference in dioxin-induced HN.

**Methods:** Two strains of mice, C57BL/6J and BALB/c, harboring b1 and b2 alleles, respectively, were administered 2,3,7,8-tetrachlorodibenzo-p-dioxin (TCDD), at an oral dose of 15 µg/kg, 1 day after birth, to expose pups with TCDD via lactation. Kidneys were collected on postnatal day 7 for histology and gene expression analysis by quantitative RT-PCR.

**Results:** Incidence of HN was approx. 60% in C57BL/6J and 0% in BALB/c despite the comparable induction levels of CYP1A1 in the both strains. There was no strain difference in COX-2 mRNA abundance. A strain difference in mPGES-1 mRNA abundance was found comparable to the HN incidence. Gene expression of early growth response 1 (Egr-1), that activates mPGES-1 transcription, was increased in C57BL/6J, but not in BALB/c. In addition, mRNA of aquaporin 2, a water channel, that absorbs water at the collecting duct, was decreased in C57BL/6J and increased in BALB/c.

**Conclusions:** Although both C57BL/6 and BALB/c have dioxin-sensitive receptors, this study demonstrates that strain difference in the incidence of TCDD-induced HN in mouse pups can be partly explained by distinct expression differences in mPGES-1. It is also suggested that Egr-1 may modulate the induction of mPGES-1.

**References:** 1) Nishimura et al, 2008; 2) Yoshioka et al, 2012.

**PS 2204 Escape from Toxic Island: Learning Toxicology Concepts through Informational Posters and a Board Game.**

D. Hardej<sup>1,2</sup>, L. Hoffman<sup>1,2</sup> and A. R. Scharz<sup>1</sup>. <sup>1</sup>Mid-Atlantic Society of Toxicology (MASOT), Bordentown, NJ; <sup>2</sup>Pharmaceutical Sciences, St. John's University, Queens, NY.

Escape from Toxic Island is a program that was developed by the MASOT Education and Outreach Committee to teach toxicology concepts to school aged children. The program is composed of informational posters containing basic toxicology concepts followed by a board game with toxicology questions. Answers to many of the questions were contained in the posters and children were encouraged to use them to obtain correct answers as they moved along the game board. One of the informational posters contained basic definitions and toxicology concepts such as routes of exposure, signal words used in the labeling of toxic substances and government agencies that regulate toxicity. The second poster explored toxicity in and around the home and included information about cleaning products, pesticides, and car care products. The program was developed by the Chair of the MASOT Education and Outreach Committee. Review of the informational posters and game board was accomplished by Education and Outreach Committee members who represent academia, industry and government experts in toxicology to ensure relevancy and accuracy of information. In step with the success of the Inspector Tox program developed 2 years ago by this committee, island themed costumes and props were utilized. Toxic Island's resident pirate, Captain Tox, assisted with instruction and game play. Incorrect answers were cheerfully corrected after "walking the plank". The audience for the program resulted from a joint effort of St. John's University and the Afterschool All Stars Program. The Afterschool All Stars provides free programs to roughly 80,000 children in need in 13 different cities in the continental U.S. and Hawaii. Volunteers were recruited from MASOT, St. John's faculty, and graduate and undergraduate toxicology students. Learning outcomes for the program are based on responses made to questions posed on the game board. Respondents who answered incorrectly to game board questions were encouraged to explore the informational posters for correct answers.

**PS 2205 A C. elegans Dose-Response Protocol and Inquiry Lab in an Undergraduate Toxicology Course.**

M. J. Pomeroy-Black. *Biology, LaGrange College, LaGrange, GA.*

In order to prepare students for a multi-week research project, it is essential to allow them to practice the protocols that will be used in the project. Using *C. elegans*, students initially observed normal behavior and identified the developmental stages of the organisms. Students then practiced transferring *C. elegans* between plates and explored various endpoints that could be used in their research project, including avoidance, locomotion and feeding. During the next lab session pairs of students were given protocols for a dose-response lab activity in which they were assigned a compound, performed a dilution series, and used the dry drop test as a measure of avoidance. Data were compiled and statistically analyzed after the lab. After establishing this basis of knowledge the students designed and conducted their own experiment for the remainder of the semester. Student pairs wrote a research proposal based on a literature search, gathered preliminary data in the lab and embarked on several replications of their experiment. Students analyzed their data using an ANOVA and presented their research as a poster session to the broader community.

**PS 2206 The Best of the Worst: A Novel Approach to Teaching Environmental Toxicology.**

C. P. Curran. *Biological Sciences, Northern Kentucky University, Highland Heights, KY.*

Curriculum development for undergraduate toxicology courses taught is challenging, because of the varied preparation and background of students enrolled. Students are typically majoring in environmental science, chemistry, or biology, and each discipline has unique program requirements. Environmental toxicology courses present even greater challenges for students without a solid grounding in ecology or biochemistry. A novel course was developed at Northern Kentucky University, focused on problem-based learning and team-based learning to engage students in identifying and understanding environmental toxicology issues in their local communities and in a variety of ecosystems (polar, temperate and tropical). Sample activities such as "What is the Worst Environmental Problem in the World?" will be explained along with the pedagogical underpinnings of the curriculum design. Student satisfaction with the course was extremely high (4.8 on a 5.0 scale), indicating this course could be a model for other undergraduate educators.

**PS 2207 Risk Assessment Capstone Project for Seniors in an Undergraduate Toxicology Program.**

S. M. Ford. *College of Pharmacy & Allied Health Professions, St. Johns University, Jamaica, NY.*

Capstone projects are intensive, active learning exercises for seniors to apply their knowledge and skills to a complex problem in their discipline. The projects vary in form and function. They may be done in teams or by individual students; the tasks may be self-selected or assigned. Planning and implementation are student-directed under supervision of faculty. Outcome of the work may be a written document and/or an oral presentation. The scope should be substantial, utilize critical thinking, and draw upon the learning objectives of the major. In our BS Toxicology program, seniors are assigned a risk assessment in the course Regulatory Toxicology and Risk Assessment. They are given a hypothetical disaster, involving a population exposed to a chemical through air, water, food, soil, or medication. Ideally the chemical chosen is one for which the toxicological data is sparse, so that students must evaluate the agent based on its properties and chemical class. The scenario includes the amount released, the exposed population, and the media of exposure. The result of the project is a written risk analysis, a website, and presentation of their findings to the College. The capstone project requires the students to utilize the facts and concepts of toxicology in an analytical manner, and apply the skills of writing, oral communication, and teamwork to a realistic situation. The public presentation informs the larger university community on the process of toxic risk assessment.

**PS 2208 Development of a Summer Undergraduate Research Program in Toxicology and Environmental Health Sciences.**

L. M. Aleksunes<sup>1,3</sup>, L. Liang<sup>2,3</sup>, E. Caswell<sup>2</sup> and D. L. Laskin<sup>1,3</sup>. <sup>1</sup>Department of Pharmacology and Toxicology, Rutgers University, Piscataway, NJ; <sup>2</sup>Department of Health Systems and Policy, University of Medicine and Dentistry of New Jersey-School of Public Health, Piscataway, NJ; <sup>3</sup>NIEHS Center for Environmental Exposures and Disease, Piscataway, NJ.

Exposure to research opportunities in toxicology and environmental sciences is key to the development of the next generation of scientists. The Community Outreach and Engagement Core of the NIEHS Center for Environmental Exposures and Disease at the University of Medicine and Dentistry of New Jersey-Robert Wood Johnson Medical School and Rutgers University has developed a summer research fellowship program to promote toxicology and environmental sciences as careers in biomedical research. The program consists of 10-week basic science and translational research experiences for undergraduates and was also designed to include weekly events including laboratory safety and responsible conduct of research training, a field trip to a pharmaceutical company, career development and research seminars and student presentations. Participants of the 2012 summer research program ranked the field trip as the most valuable weekly activity followed by presentations from toxicologists and environmental health scientists. Based on pre- and post-survey results, over 60% of respondents reported that a career as a scientific researcher was most appealing based upon satisfaction from doing research, the perceived benefit of scientific knowledge to the community, and an overall interest in science. In addition, 87.5% of respondents will continue to pursue research after completion of the summer research program. This includes five students pursuing Ph.D. degrees beginning in 2012 or 2013. A summer research program engages undergraduate students in full-time research experiences and provides unique opportunities to promote toxicology and environmental sciences as research areas for the next generation of scientists and enhances career development skills. Supported by ES020721, ES005022, and ASPET SURF.

**PS 2209 Incorporation of Toxicology and Risk Assessment Principles into an Environmental Health Course.**

R. N. Phalen. *Health Science, CSUSB, San Bernardino, CA.* Sponsor: T. Dodd-Butera.

Environmental health deals with a multitude of public health issues ranging from sanitation to hazardous materials to air and water quality. Practitioners are largely involved in the regulatory side of protecting public health, which requires an intimate understanding of toxicology and risk assessment. However, many of the identified deficiencies with risk assessment are perpetuated by the educational curricula. For example, chemical hazards are introduced to students and evaluated by regulators on a case-by-case basis, often based on one toxicological endpoint alone. Strong emphasis is placed on making comparisons of reference doses to exposure estimates without regard to the effect of uncertainties associated with inadequate data. High uncertainty alone could result in selection of a more toxic substance over one less studied. A unique class project was created to give environmental health students, our future regulators, an improved perspective on how toxicological information can be used to make informed decisions that best protect human health and well-being. The multi-step exercise focuses on a decision made by the World Health Organization to bring DDT back into use to fight malaria. Students work in groups to collect chemical, toxicological, efficacy, and economic aspects of a common pesticide used for mosquito control. The class then comes together to compare and discuss the group results and select the best pesticide option for the impacted region. A semi-quantitative risk management tool is also used for a more objective determination. Lastly, a surprise change in one circumstance causes perspectives to change and the outcome is a completely different conclusion. The end result is a sophisticated interaction of ideas and concepts, which motivates students to start thinking about how there is more to toxicology than lethal doses and dose-response curves, and that there is more to risk assessment than hazard quotients. A detailed description of the project and handouts will be provided.

**PS 2210 Poisoning Principles: Clinical Toxicology and Undergraduate Nursing Education.**

T. Dodd-Butera<sup>1</sup> and M. Broderick Pritty<sup>2</sup>. <sup>1</sup>Nursing, CSU San Bernardino, College of Natural Sciences, San Bernardino, CA; <sup>2</sup>California Poison Control System, San Diego, CA.

According to the American Association of Poison Control Center's (AAPCC) annual report (2010), 601,197 human exposures to toxicants resulted in management in a health care facility. Therefore, education concerning clinical toxicology and

poisonings is essential in preparation of future healthcare professionals. This abstract describes an educational program for undergraduate nurses delivered through a collaboration with a regional Poison Control Center (PCC) and a local university. Undergraduate nursing students were assigned to a clinical toxicology rotation and were required to participate in didactic educational modules addressing principles of toxicokinetics, such as the ADME (absorption, distribution, metabolism, and exposure) model, prior to the PCC rotation. During the rotation, clinical toxicology approaches to the poisoned patient were reviewed. Attendance at a journal club at the poison center was included, covering topics such as: environmental exposures, chemicals, drug overdoses, and unintentional poisonings. A lecture on lead toxicity was then given to the entire class, including those undergraduate students in other rotations. The program culminated with all students participating in a poster session addressing clinical toxicology and other environmental health experiences. Students were required to evaluate the entire course, including the PCC rotation. Students reported an increase in knowledge and awareness about the role of toxicology and environmental health in their professional development. In addition, the knowledge gained could be applied to bedside nursing to evaluate the role of poisoning and antidote use, along with toxicology principles, for treatment and care of patients utilizing healthcare facilities. Recommendations for future programs include integrating toxicology into didactic and clinical experiences of undergraduate nursing students within all rotations, and across healthcare and scientific disciplines.

**PS 2211 Coal Ash Material Safety—A Health Risk-Based Evaluation of USGS Coal Ash Data from Five US Power Plants.**

L. J. Bradley. *AECOM, Chelmsford, MA.*

Over 42% of the estimated 130 million tons of coal ash produced annually in the US is put into beneficial use, and is material that is not placed in disposal facilities. However, these uses are threatened by USEPA's potential regulation of coal ash as a hazardous waste, and by constant references to "toxic coal ash" by the press in response to environmental groups' writings. Therefore, a detailed health-risk based evaluation was conducted of coal ash data released in a report by the US Geological Survey. Eight robust coal ash data sets were selected as representing material that could be put into beneficial use from five US power plants each utilizing a different source of coal. The evaluation was conducted by comparing constituent concentrations in coal ash to risk-based screening levels developed by the USEPA that are protective of a child's direct exposure to residential soils (including ingestion, dermal contact and inhalation routes of exposure). These screening levels are considered by the Agency to be protective for daily exposure by humans (including sensitive groups) over a lifetime. Coal ash percentiles (10th-90th) were compared directly to the screening levels, and in a more detailed evaluation, upper-bound exposure point concentrations were used in a cumulative risk screening process. Constituent concentrations in coal ash were also compared to USGS background concentrations in soils in the US. The results indicate that with few exceptions constituent concentrations in coal ash are below screening levels for residential soils, and are similar in concentration to background US soils. Because exposure to constituents in coal ash used in beneficial applications, such as concrete, road base, or structural fill would be much lower than assumed for a residential soil scenario, these uses should also not pose a direct contact risk to human health.

**PS 2212 Provisional Advisory Levels (PALs) for Chloroethanol (Ethylene Chlorohydrin).**

S. Milanez<sup>1</sup>, P. M. McGinnis<sup>2</sup>, L. Koller<sup>3</sup> and F. Adeshina<sup>4</sup>. <sup>1</sup>Oak Ridge National Laboratory, Oak Ridge, TN; <sup>2</sup>RG York and Associates, Syracuse, NY; <sup>3</sup>Environmental Health & Toxicology, Corvallis, OR; <sup>4</sup>US EPA, Washington DC.

PAL values developed for hazardous materials by the US EPA represent general public emergency exposure limits for oral and inhalation exposures corresponding to three different severity levels (1, 2, and 3) for 24-hour, 30-day, 90-day, and 2-year durations. PAL 1 represents the threshold for mild effects; PAL 2 represents the threshold for serious, irreversible or escape-impairing effects; PAL 3 represents the threshold for lethal effects. PALs have not been promulgated nor have they been formally issued as regulatory guidance, but are intended for use at the discretion of risk managers in emergency situations when site-specific risk assessments are not available. The PAL document for chloroethanol was developed based on the SOP and QAPP requirements.

Chloroethanol (2-chloroethanol; ethylene chlorohydrin), is a colorless, combustible liquid with a faint ether-like odor, and is soluble in water and organic solvents. It is a high production volume chemical that is used as an industrial solvent and a chemical manufacturing intermediate. It is formed when ethylene oxide is used to sterilize polyvinyl chloride plastics and to fumigate foods. Humans and animals exposed by inhalation or orally exhibited CNS, GI, and respiratory symptoms, and had post-mortem lesions in numerous internal organs. All PALs were derived using rat

data because the human data were not adequate; the animal data were generally consistent among species and with the limited human data. Developed PAL values for oral exposure are 35 mg/L as the PAL 1 for 24 hours; 110 mg/mL as the PAL 2 for 24 hours, and 30 and 90 days; 230 mg/L as the PAL 3 for 24 hours; and 160 mg/L as the PAL 3 for 30 and 90 days. PALs derived for inhalation exposure are 0.26 ppm and 0.78 ppm as the 24-hour PAL 2 and PAL 3, respectively. For 30 and 90 days, the inhalation PAL 1 is 0.0015 ppm and the PAL 2 is 0.015 ppm. Other oral and inhalation PAL values were not developed due to insufficient data.

#### **PS 2213 Provisional Advisory Level (PAL) Development for Lewisite and Sulfur Mustard.**

C. Bast<sup>1</sup>, R. Young<sup>2</sup>, P. M. McGinnis<sup>3</sup>, C. Baird<sup>4</sup> and F. Adeshina<sup>5</sup>. <sup>1</sup>Oak Ridge National Laboratory (ORNL), Oak Ridge, TN; <sup>2</sup>ORNL, Oak Ridge, TN; <sup>3</sup>RG York & Associates, Syracuse, NY; <sup>4</sup>US Army Public Health Command, Aberdeen, MD; <sup>5</sup>US EPA, Washington DC.

PAL values developed for hazardous materials by the US EPA represent general public emergency exposure limits for oral and inhalation exposures corresponding to three different severity levels (1, 2, and 3) for 24-hr, 30-d, 90-d, and 2-yr durations. PAL 1 represents the threshold for mild effects; PAL 2 represents the threshold for serious, irreversible or escape-impairing effects; PAL 3 represents the threshold for lethal effects. PALs have not been promulgated nor have they been formally issued as regulatory guidance. They are intended to be used at the discretion of risk managers in emergency situations when site specific risk assessments are not available. Application of PAL protocols has been performed for lewisite and sulfur mustard to estimate inhalation exposure limits; oral PAL values are not recommended (NR) due to insufficient data. PAL values for the vesicants, lewisite and sulfur mustard, are based on ocular effects in humans and animals or lethality thresholds in rodents.

Lewisite inhalation PAL 1, 2, and 3 values are NR, 0.01, and 0.037 mg/m<sup>3</sup>, respectively, for 24-hr; and NR for 30-/90-d and 2-yr.

Sulfur mustard inhalation PAL 1 values are 0.00083 mg/m<sup>3</sup> for 24-h and 0.00010 mg/m<sup>3</sup> for 30-d/90-d and 2-yr. PAL 2 values are 0.0042 mg/m<sup>3</sup> for 24-h, 0.0029 mg/m<sup>3</sup> for 30-d, and 0.00097 mg/m<sup>3</sup> for 90-d and 2-yr. PAL 3 values are 0.088 mg/m<sup>3</sup> for 24-h and NR for 30-d/90-d and 2-yr.

#### **PS 2214 Provisional Advisory Level (PAL) Development for Fentanyl.**

C. S. Wood<sup>1</sup>, C. Baird<sup>2</sup>, L. Koller<sup>3</sup> and F. Adeshina<sup>4</sup>. <sup>1</sup>Oak Ridge National Laboratory, Oak Ridge, TN; <sup>2</sup>US Army Public Health Command, Aberdeen, MD; <sup>3</sup>Environmental Health and Toxicology, Corvallis, OR; <sup>4</sup>US EPA, Washington DC.

PAL values developed for hazardous materials by the US EPA represent general public emergency exposure limits for oral and inhalation exposures corresponding to three different severity levels (1, 2, and 3) for 24-hr, 30-d, 90-d, and 2-yr durations. PAL 1 represents the threshold for mild effects; PAL 2 represents the threshold for serious, irreversible or escape-impairing effects; PAL 3 represents the threshold for lethal effects. Minimum data requirements must be met or a value may be considered NR (not recommended). PALs have not been promulgated nor have they been formally issued as regulatory guidance. They are intended to be used at the discretion of risk managers in emergency situations when site specific risk assessments are not available. Application of PAL protocols has been performed for fentanyl to estimate oral and inhalation exposure limits.

Fentanyl is a highly potent, synthetic opioid used clinically as an analgesic and anesthetic. Dose-response information from humans showed that effects were similar between children and adults. The magnitudes of sedation and analgesia were positively correlated with dose. Side-effects included pruritus, nausea, vomiting, headache, bradycardia, vertigo and respiratory depression leading to decreased oxygen saturation at higher doses. Oral PALs were based on adverse side-effects in humans. Oral PAL 1 and 2 values are 0.03 and 0.23 mg/L respectively, for 24-hr/30-d/90-d; oral PAL 3 and all 2-yr values are NR. Inhalation exposure resulted in sedation and respiratory depression. Inhalation PAL 1, 2, and 3 values are NR, 0.0037, and 0.11 mg/m<sup>3</sup> respectively, for 24-h. The 30-d/90-d/2-yr inhalation PALs are NR.

#### **PS 2215 Development of a Chronic Reference Concentration for Decalin.**

L. D. Stuchal, R. E. Weil and S. M. Roberts. Center for Environmental and Human Toxicology, University of Florida, Gainesville, FL.

Decalin is a naturally occurring dicycloalkane present in crude oil and produced as a product of combustion. Its ability to solubilize oils and fats makes it useful in paints, cleaning fluids, gasoline, and varnishes. Because of its widespread use in

many types of commercial products, decalin is ubiquitous in the environment and exposure by the general public is of concern. Neither oral nor inhalation toxicity values are currently available for decalin in published sources despite recurring point and non-point source releases. To derive a reference concentration (RfC) for decalin, inhalation toxicity studies were reviewed using a weight-of-evidence approach. A two-year mouse inhalation study conducted by the National Toxicology Program was chosen as the critical study for the derivation of the chronic RfC. In this study, a significant increase in the occurrence of hepatotoxicity was detected at the highest concentration tested (400 ppm) in male mice. Benchmark dose modeling was utilized to derive a point of departure for hepatic necrosis, syncytial alteration, and erythrophagocytosis. For data not amenable to modeling, a point of departure was derived using the no observable adverse effect level (NOAEL). The most sensitive adverse effect, syncytial alteration resulted in a BMDL<sub>10</sub> of 7.8 ppm using the Log-logistic model. A chronic RfC for decalin of 0.08 mg/m<sup>3</sup> was calculated by conversion of the BMDL<sub>10</sub> to a human equivalent continuous inhalation concentration of 1.4 ppm (7.9 mg/m<sup>3</sup>) using a dosimetric adjustment factor of 1 and application of a total uncertainty factor of 100. The chronic decalin RfC was derived despite several toxicity database limitations, including a small number of chronic inhalation studies and uncertainty regarding reproductive effects. Future research on decalin toxicity is needed to better characterize the adverse effects associated with its chronic inhalation.

#### **PS 2216 Weight-of-Evidence Evaluation of Methyl Methacrylate Olfactory Effects in Humans and Derivation of an Occupational Exposure Level.**

M. Pemberton<sup>1</sup>, L. A. Bailey<sup>2</sup> and L. R. Rhomberg<sup>2</sup>. <sup>1</sup>Systox, Cheshire, United Kingdom; <sup>2</sup>Gradient, Cambridge, MA.

Methyl methacrylate (MMA) causes olfactory effects in rodents that are considered relevant to humans. Recent scientific studies have focused on understanding the apparent lack of species concordance between the rodent and occupational studies. We have applied the hypothesis-based weight-of-evidence (HBWoE) approach to evaluate the concordance of the available data and the hypothesis that the observed difference in sensitivity between rats and humans may be the result of physiological and biochemical differences. Our WoE analysis integrated several lines of evidence [animal, human, mode of action (MoA), and toxicokinetics data] and found: 1) acute and chronic rat and mouse MMA inhalation studies consistently indicate degenerative lesions of the main olfactory region as the most sensitive endpoint; 2) numerous studies support an MoA for MMA involving high concentrations of carboxylesterase activity in nasal epithelial tissue that metabolizes MMA to methyl acrylic acid (MAA), an organic acid with irritative and corrosive properties; 3) carboxylesterases are a group of non-specific enzymes that are widely distributed throughout the body in animals and humans; 4) toxicokinetic studies and a physiologically based pharmacokinetic (PBPK) model describing inhalation dosimetry of MMA in the upper respiratory tract (URT) of rats and humans point to differences in nasal morphology and biochemistry that help reconcile these differences as species-specific manifestations of a common toxicological process, and predict a rat-to-human dosimetry adjustment factor (DAF) of 3 to 8, consistent with observed lower sensitivity in humans compared to rats; and 5) worker studies, although somewhat limited, consistently suggest a no observed adverse effect level (NOAEL) for URT irritation, including olfactory dysfunction, of 50 ppm. We derived MMA occupational exposure levels (OELs) from animal data (ranging from 28-118 ppm) and human data. Overall, our WoE analysis supports use of the human data for derivation of an MMA OEL of 50 ppm.

#### **PS 2217 An Updated Dose-Response Evaluation of Aldrin and Dieldrin.**

E. Hooker, H. J. Gibb and K. G. Fulcher. Tetra Tech Sciences, Arlington, VA.

The United States Environmental Protection Agency (USEPA) reviewed the cancer and non-cancer effects of the organochlorine insecticides, aldrin and dieldrin, in the late 1980's. The results of those assessments are reported by USEPA's Integrated Risk Information System (IRIS). These assessments include reference dose (RfD) values of 0.00003 and 0.00005 mg/kg-day and cancer slope factor values of 17 and 16 (mg/kg-day)<sup>-1</sup> for aldrin and dieldrin, respectively. The USEPA methods for dose-response analysis have changed in the decades since these evaluations were done. The dose-response analyses of cancer and non-cancer health effects of aldrin and dieldrin were re-evaluated using current methodology, including benchmark dose (BMD) analysis (BMDs Version 2.2 software) and current body weight scaling. A literature review was updated to determine the most appropriate adverse effect endpoints. Using current methodology and information, the cancer slope factors for aldrin and dieldrin were estimated to be 3.4 and 7.0 (mg/kg-day)<sup>-1</sup>, respectively (i.e., about 5 and 2.3 fold lower risk than previous assessments). The current analyses estimated RfD values of 0.0001 and 0.00008 mg/kg-day for aldrin

and dieldrin, respectively (both higher than previous assessments). Because aldrin and dieldrin are no longer used as pesticides in the United States, they are a low priority for additional review by the USEPA. However, because they are persistent and still detected in environmental samples, quantitative risk assessments based on the best available methods are required. Several national and international health assessment organizations (e.g., WHO) do not consider aldrin and dieldrin to be human carcinogens. Recent epidemiologic studies do not demonstrate a causal association between aldrin and dieldrin and human cancer risk. These re-evaluations, based on current methodologies and available data, suggest that these two compounds pose a lower human health risk than currently reported by USEPA.

**PS 2218 Benzene: Development of a 24-Hour, Health-Protective Comparison Value.**

J. T. Haney. *Toxicology Division, Texas Commission on Environmental Quality, Austin, TX.*

Texas has the most extensive volatile organic compound (VOC) ambient air monitoring network in the nation. As part of that network, the TCEQ collects every sixth-day, 24-hour canister VOC data. These data are used to calculate annual averages for comparison to chronic, health-protective Air Monitoring Comparison Values (AMCVs) (i.e., RfC-like values for noncarcinogenic effects, 1E-05 excess risk levels for cancer effects). In regard to acute exposure durations, however, the TCEQ typically has only 1-hour AMCVs, which while conservative are not designed to evaluate 24-hour sample results. Thus, the development of 24-hour, health-protective AMCVs would allow the TCEQ to more fully utilize 24-hour VOC data for the evaluation of potential public health concerns. The TCEQ has developed a proposed 24-hour AMCV for benzene since it is a ubiquitous VOC of both agency and public interest. Critical effect dose-response data for hematotoxicity from mouse studies indicate an effect level range of 10-100 ppm for subacute exposure (e.g., 6-8 hours per day, 5-10 days). A point of departure (POD) from these studies was used to develop the 24-hour value. The total number of exposure hours exceeds 24 hours for all these subacute studies and available toxicokinetic information indicates the time between the intermittent daily exposures would not allow for clearance of benzene's hematotoxicity-implicated metabolites (e.g., hydroquinone, hydroquinone glucuronide, catechol) from the bone marrow as evidence suggests they are not readily excreted. Using the same POD (LOAEL of 10.2 ppm) and uncertainty factors (total UF of 100) as the TCEQ used to derive its 1-hour AMCV (180 ppb) but without duration adjustment (based on toxicokinetic considerations) results in a conservative 24-hour, health-protective AMCV of 100 ppb. This value is well below even chronic human hematotoxicity observed adverse effect levels (e.g., 7.2-13.6 ppm). The proposed 24-hour AMCV is considered sufficiently conservative for the adequate protection of public health and would significantly complement TCEQ health effect evaluations of ambient air data.

**PS 2219 Derivation of a Guidance Limit for Cadmium in Children's Jewelry: Health Canada's Perspective.**

G. Barrett<sup>1</sup>, P. Chantal<sup>2</sup>, S. Wright<sup>3</sup>, P. Chowhan<sup>4</sup>, P. Pelletier<sup>1</sup>, H. Ryan<sup>1,2</sup> and J. Field<sup>1</sup>. <sup>1</sup>*Toxicology and Flammability Risk Assessment Unit, Consumer Product Safety Directorate, Health Canada, Ottawa, ON, Canada;* <sup>2</sup>*Product Safety Laboratory, Consumer Product Safety Directorate, Health Canada, Ottawa, ON, Canada;* <sup>3</sup>*Compliance and Enforcement Division, Consumer Product Safety Directorate, Health Canada, Ottawa, ON, Canada;* <sup>4</sup>*Risk Management Strategies Division, Consumer Product Safety Directorate, Health Canada, Ottawa, ON, Canada.* Sponsor: G. Chen.

It has been demonstrated that swallowed jewellery items may become lodged in the stomach, and morbidity and mortality have been associated with jewellery containing lead. Due to its inherent toxicity, the use of cadmium to make costume jewellery may pose an analogous threat. In the absence of reliable human toxicity data, the results from animal studies were used to derive an oral acute provisional minimal risk level (pMRL) of 0.0732 mg/kg bw for cadmium. Health Canada analyzed approximately 200 children's jewellery samples that were judged small enough to fit into a child's mouth for cadmium content. A subset of these samples were also subjected to migration testing, which revealed no consistency between the total amount of cadmium in a sample, and the amount that might be released in the simulated physiological environment of the stomach over an extended period (such as in the case of a piece of jewellery lodged in the stomach over several days). Since standardized migration testing cannot accurately predict the amount of cadmium that might leach out of a sample under such circumstances, the use of total cadmium content to derive a guideline is considered the most health-protective approach. Limiting total cadmium content to 130 ppm removes variables that interfere with migratable cadmium quantification (such as the thickness and composition of the surface plating, and elemental composition of the amalgam) and is protective of the scenario of an ingested piece of jewellery lodged in the stomach for an extended period of time.

**PS 2220 Assessment of Risks to the US Population Posed by Exposure to Gold and Ceramic Dental Restorations.**

R. E. Peters<sup>1</sup>, M. Richardson<sup>2</sup>, S. Clemow<sup>3</sup>, K. James<sup>1</sup> and S. D. Siciliano<sup>1</sup>. <sup>1</sup>*University of Saskatchewan, Saskatoon, SK, Canada;* <sup>2</sup>*Stantec Consulting Ltd., Ottawa, ON, Canada;* <sup>3</sup>*SNC-Lavalin Environment, Ottawa, ON, Canada.* Sponsor: L. Weber.

There is significant mercury exposure from dental amalgam used in restorative practice. However, little is known about the chemical exposures and risks of alternative dental restorative materials. Thus, it is difficult for clinicians to weigh the performance, risks, and benefits of dental amalgam to alternate restorative materials. Here we provide the first population-level risk assessment for gold alloy and ceramic restorative materials. Employing the US National Health and Nutrition Examination Survey (NHANES) data from 2001 to 2004, we assessed the exposure of adults to the components of gold alloy and ceramic dental restorations in the US general population. Three specific exposure scenarios were considered: 1) all restorations were either gold alloy or ceramic; 2) all crowns were gold alloy or ceramic; and 3) 11% of fillings were either gold alloy or ceramic, in 30% of the population. Silver appears to be the most problematic component of gold alloy restorations, due to a combination of relatively high toxicity and high proportional composition. Based on the toxicity of silver and its proportional content in gold dental alloys, it was estimated that adults could possess an average of 4 tooth surfaces restored with gold before exceeding the Reference Exposure Level (REL) for silver. Lithium appears to be the most problematic component of dental ceramics. All other ceramic components considered resulted in estimated daily doses well below their respective RELs. Based on the toxicity of lithium and its proportional content in dental ceramics, it was estimated that adults could possess an average of 16 tooth surfaces restored with ceramics before exceeding the REL for lithium. Relative to dental amalgam and gold alloys, ceramics present the fewest and lowest chemical exposures and risks.

**PS 2221 Development of an Oral Cancer Slope Factor for Acrylamide Based on Tumors Relevant to Humans.**

J. D. Urban<sup>1</sup>, C. M. Thompson<sup>2</sup>, R. Deskin<sup>3</sup>, M. Waite<sup>3</sup> and L. C. Haws<sup>1</sup>. <sup>1</sup>*ToxStrategies, Inc., Austin, TX;* <sup>2</sup>*ToxStrategies, Inc., Houston, TX;* <sup>3</sup>*Cytex Industries, Inc., Woodland Park, NJ.*

Acrylamide is an industrial chemical used mainly in the production of polyacrylamides. Acrylamide and polyacrylamides have many uses, including uses as flocculants and flow control agent for enhancing oil production from wells, in the production of dyes, organic chemicals, contact lenses, cosmetics and toiletries, in sugar refining, and as a chemical grouting agent and soil stabilizer. Acrylamide is also commonly present in fried foods and the primary route of human exposure in the general population is diet. In their most recent risk assessment for acrylamide, USEPA developed an oral cancer slope factor (OSF) of 0.5 (mg/kg-day)<sup>-1</sup> based on a 2-year drinking water study that reported increased incidences of thyroid tumors and tunica vaginalis mesotheliomas (TVMs) in male F344 rats. However, there is considerable evidence that F344 rats are particularly susceptible to TVMs, and therefore TVMs may not be relevant to humans. As such, our objective was to evaluate the overall weight of the evidence regarding each tumor type and to derive an OSF for acrylamide based on those tumors relevant to humans. Among the tumors induced by acrylamide (thyroid tumors, TVMs, mammary gland tumors, CNS tumors), thyroid and mammary gland tumors were considered most relevant to humans. Using the rat OSF for the combined increased incidences of thyroid and mammary gland tumors observed in female F344 rats, we derived a human OSF using a rat-to-human dose metric conversion factor based on serum levels of the primary acrylamide metabolite, glycidamide (widely considered to be the putative proximal carcinogen). The final human OSF for combined thyroid and mammary gland tumors was determined to be 0.09 (mg/kg-day)<sup>-1</sup>. This OSF suggests a lower cancer potency for acrylamide based on target tissues more relevant to humans. It should be noted however, the FDA and NTP just completed a 2-year, multi-species drinking bioassay and the results of this study may impact future OSF estimates for acrylamide.

**PS 2222 An Evaluation of the Human Carcinogenic Potency of Methyl Tert-Butyl Ether (MTBE): Considering New Data and Mode of Action.**

P. Sheehan and K. Bogen. *Exponent, Oakland, CA.*

The carcinogenic potency of MTBE was initially evaluated by State of California scientists in 1999 based on a gavage study with rats (Belpoggi et al. 1995, 1997, 1998) and inhalation studies with rats and mice (Bird et al. 1997). Potency was estimated at that time using a linearized multistage model. Since then, an additional

rodent cancer bioassay of MTBE in drinking water (Dodd et al. 2011), several genotoxicity and mutagenicity studies, evaluations of MTBE metabolites formaldehyde and tert-butyl alcohol (TBA), as well as other studies providing information on MTBE's mode of action have been reported. In addition, the U.S. Environmental Protection Agency (EPA) declared the data on lymphomas and leukemias from Belpoggi et al. (Ramazzini Institute) as unreliable for risk assessment raising additional uncertainty about California's potency estimate. The new data and remaining reliable historic rodent bioassay data were used to re-evaluate the cancer potency or slope factor (CSF) of MTBE considering mode of action (MOA). The overwhelming majority of studies indicate that neither MTBE nor TBA is genotoxic. In stark contrast, formaldehyde is clearly genotoxic, but when generated by MTBE metabolism is efficiently detoxified to preclude elevating background levels and associated genotoxic damage. Based on genotoxicity and MOA analyses, the most likely CSF for MTBE is zero, unless chronic exposures induce target-tissue toxicity including in sensitive individuals. A corresponding expected CSF value for MTBE conditional on a linear MOA was estimated to be 0.000018 per mg MTBE per kg body weight per day for a chronically exposed adult. If MTBE is carcinogenic to humans, then it is extremely weak relative to other chemical carcinogens evaluated by EPA.

**PS 2223 Development of a 24-Hour Air Monitoring Comparison Value (AMCV) for 1, 3-Butadiene and Comparison of 1-Hour, 24-Hour, and Chronic AMCVs to Observed Adverse Effect Levels.**

R. L. Grant and R. E. Jones. *Toxicology Division, Texas Commission on Environmental Quality (TCEQ), Austin, TX.*

The TCEQ develops AMCVs, which are considered safe concentrations of chemicals in air, to determine whether 1-hour (hr) or annual average chemical concentrations in ambient air exceed levels of potential concern for adverse health effects. Previously for 1,3-butadiene (BD), a 1-hr AMCV of 1,700 ppb was derived based on a mouse developmental study (6 hr/day exposures, gestational days 6-15). A chronic AMCV of 9.1 ppb was derived based on a 1 in 100,000 excess risk for leukemia mortality from an epidemiological study in styrene-butadiene workers. To calculate annual ambient air concentrations, the TCEQ collects a significant amount of 24-hr monitoring data that are not directly comparable to the 1-hr or chronic AMCV. Therefore, the TCEQ has developed a 24-hr AMCV for BD to evaluate the potential for health effects from 24-hr exposure. The same mouse study used for the 1-hr AMCV was judged to be the critical study for the 24-hr AMCV based on mode-of-action and toxicokinetic data. The 6-hr human equivalent point of departure (POD-HEC) of 51,300 ppb was duration adjusted (Haber's rule with  $n = 1$ ) to calculate the 24-hr POD-HEC of 12,800 ppb. The proposed 24-hr AMCV is 430 ppb after application of total uncertainty factors of 30. The TCEQ has developed guidelines to derive observed adverse effects levels (OAEs) based on available dose response data to better communicate to risk managers and the public the margin of safety between OAEs and AMCVs. For the 6- and 24-hr AMCVs, the acute OAE is 66,000 ppb (the central estimate POD-HEC for 5% decrease in fetal weight loss). The 1-hr AMCV of 1700 ppb is 39 times lower than the acute OAE and the 24-hr AMCV of 430 ppb is 150 times lower. The long-term OAE is 10,000 ppb (the lowest average occupational exposure concentration where the likelihood ratio test that slope = 0 was statistically significant for different maximum levels of cumulative BD ppm-years for leukemia deaths). The chronic AMCV of 9.1 ppb is 1,100 times lower than the chronic OAE.

**PS 2224 Health-Based 24-Hour Air Monitoring Comparison Value (AMCV) for Acrolein in Ambient Air: Comparison to Air Monitoring Data Collected in Texas.**

A. Jenkins. *Toxicology Division, Texas Commission on Environmental Quality, Austin, TX.*

Acrolein is of national and state interest because it is ubiquitous, is difficult to analyze in ambient air, and concentrations causing eye and respiratory irritation are low. In 2011, a follow-up special monitoring project for acrolein was conducted by the USEPA at a school near a building products manufacturing facility in Texas. Ten 24-hour (hr) ambient air samples were collected in canisters downwind of a facility known to emit acrolein and analyzed using an improved method. The follow-up project was done in response to finding that acrolein canister results can be affected by the canister cleaning method and calibration gas standards. The TCEQ has previously derived 1-hr and chronic health-protective AMCVs for acrolein in order to evaluate air monitoring data. In order to evaluate the 24-hr data collected at the school and at two other permanent monitoring sites in Texas, the TCEQ has developed a proposed 24-hr AMCV to better evaluate the potential for adverse health effects. Acrolein's toxicity is mainly concentration dependent and levels causing adverse effects are similar in humans and animals. The same rat study used to

develop the chronic AMCV was selected as the critical study for derivation of the 24-hr AMCV since interim histopathology was performed after various exposure durations (e.g., 6 hr/day for 4, 14, 30, and 65 days) which encompassed the 24-hr duration of interest. A no-observed-adverse-effect level of 200 ppb was identified from the key study for all exposure durations based on the absence of nasal epithelial hyperplasia. Based on a mode-of-action analysis, no duration adjustment was necessary. After correcting for animal-to-human dosimetric differences, the 24-hr human equivalent point of departure was 37.4 ppb. Total uncertainty factors of 30 were applied to calculate the 24-hr AMCV of 1.2 ppb. In comparison, the 1-hr AMCV for acrolein is 4.8 ppb and its chronic AMCV is 0.22 ppb. No concentrations exceeding the 24-hr AMCV using the improved canister method have been reported at monitoring sites in Texas.

**PS 2225 Protection against Toxic Effects of Arsenic by Vitamin E: Characterization of Transplacental Arsenic Species and Effects.**

A. Sampayo-Reyes<sup>1</sup>, R. Marcos<sup>2</sup> and A. Hernandez<sup>2</sup>. <sup>1</sup>*Departamento de Toxicogenética, Centro de Investigación Biomédicas del Noreste, Monterrey, Mexico;* <sup>2</sup>*Departament de Genètica i de Microbiologia, Universitat Autònoma de Barcelona, Bellaterra, Spain.*

Millions of people world-wide are exposed to arsenic (As) via drinking water. As is biotransformed for excretion, and the CH<sub>3</sub> groups necessary for such metabolism are also essential to DNA methylation. Pregnant women methylate As more efficiently to protect the fetus from immediate toxicity, but at the risk of later epigenetic deregulation. Thus, preventing early-life As exposure may be critical for the health of future generations. In order to evaluate early-life exposure to arsenic, pregnant hamsters were exposed to 50 and 100 ppm of arsenite via drinking water at the 0th and 8-9th day of gestation. Co-treatment with 8.5 mg/Kg/day of selenite or 6 mg/Kg/day of vit E was also carried out to assess whether those compounds exert any As-transplacental protective role. To characterize arsenic speciation during pregnancy, fetus development, unweaning and adulthood, As species were measured in the urine and/or organs by HPLC-ICP/MS. Teratogenic effects of transplacental arsenic were analyzed observing both reabsorptions and embryo anomalies, and in utero As-exposed litters were followed-up to evaluate tumor incidence at the adult stage. Characterization of arsenic species indicates that fetuses and unweaned offspring are As-exposed through placenta and milk, showing a speciation profile similar to that in mothers. Results demonstrate a teratogenic As effect in a dose and time-of-gestation dependent manner, and a noticeable protective effect of both selenite and vit E.

**PS 2226 Approaches for Deriving an OEL for Peracetic Acid and Occupational Risk Management Considerations.**

N. Pechacek<sup>1</sup>, A. Maier<sup>2</sup> and L. T. Haber<sup>2</sup>. <sup>1</sup>*Ecobal, St. Paul, MN;* <sup>2</sup>*Toxicology Excellence for Risk Assessment, Cincinnati, OH.*

To provide perspective on current and proposed occupational exposure limits (OELs) for peracetic acid (PAA; CAS 79-21-0) we evaluated PAA toxicity with the aim of understanding uncertainties and their implications for the resulting OEL. The database for PAA is limited and no single study is definitive. Two unpublished reports on human exposures to PAA provide some concentration-response data, indicating that a sensitive acute effect of PAA exposure is eye and respiratory tract irritation, but the studies differ quantitatively. These differences are not surprising, in light of the differences in exposures (apparently pure PAA vapor vs. an aerosol of a mixture), the subjective nature of the reporting, and the likely small sample sizes. The studies are also limited by the lack of clear concentration-duration-response data. Nonetheless, the studies provide a reasonable estimate of the threshold for the onset of irritation in humans in the range of 0.53 mg/m<sup>3</sup> for up to 3 hours and 1.56 mg/m<sup>3</sup> for up to 45 minutes. RD50 (concentration estimated to cause a 50% depression in respiratory rate) data in mice and rats provide additional information on the irritant potency of PAA. The RD50 in mice was 17 mg/m<sup>3</sup> for pure PAA vapor and 12 mg/m<sup>3</sup> for a commercial mixture. The rat RD50 was 21.5 to 24.1 mg/m<sup>3</sup>. Based on the array of human data and the RD50 values in rodents, we calculated potential TWA OELs ranging from 0.26 to 1.56 mg/m<sup>3</sup>. A similar range of 0.62 – 2 mg/m<sup>3</sup> is found among the published OELs, and any of these values could be justified as protective of worker health given the uncertainties in the data and the precision of the OEL methodology. More definitive sensory irritation studies would further clarify selection of a value in this range. Given the extant data, the ultimate OEL choice within a range of reasonable values is a policy-based risk management decision, not a scientific one. The optimal time averaging approach is also not clearly established by the data; however, a combination of a TWA with a STEL is the recommended risk management option.

**PS 2227 An Inhalation Risk Assessment for Measured Ambient Air Concentrations of 6:2 Fluorotelomer Alcohol.**

T. L. Serex<sup>1</sup>, M. W. Himmelstein<sup>1</sup>, R. C. Buck and M. H. Russell. *E.I. duPont de Nemours & Co. Inc., Wilmington, DE.*

6:2 Fluorotelomer Alcohol (CAS# 647-42-7, 1-Octanol-3,3,4,4,5,5,6,6,7,7,8,8,8, tridecafluoro-, 6:2 FTOH) is a raw material used for manufacturing surfactant and polymeric products. 6:2 FTOH vapor phase inhalation is a potential exposure route. The aim of the current investigation was to 1) compare the oral and inhalation repeated-exposure toxicity data to confirm systemic toxicity, target organs, and lack of an exposure route effect, 2) confirm similar metabolic and toxicokinetic profiles via both exposure routes, and 3) conduct an inhalation risk assessment for reported ambient air concentrations. In an inhalation range-finder (5-days) and a 28-day inhalation toxicity study, the profile of 6:2 FTOH and its metabolites in plasma under controlled inhalation exposure was investigated as well as the systemic toxicity and target organs. These studies provided a basis for toxicity comparison, plasma metabolites, and dosimetry between inhalation and oral dosing. Similar toxicity, metabolic and toxicokinetic profiles via both exposure routes was confirmed. Benchmark Dose Analysis (BMD) was conducted on the subchronic toxicity endpoints to determine the most sensitive effect and the corresponding BMD associated with this effect. Based on this analysis, the corresponding human equivalent dose (HED) was calculated to be 1.4 mg/kg bw/day. An additional assessment factor of 2 was applied to extrapolate from the subchronic exposure to a chronic exposure and resulted in a final HED of 0.7 mg/kg bw/day. An equivalent air concentration was determined using an allometric scaling factor to arrive at a human equivalent concentration (HEC) of 2.5 mg/m<sup>3</sup>. This HEC was then divided by the reported indoor and outdoor air concentrations to arrive at a margin of exposure (MOE). MOEs calculated for inhalation exposure to indoor or outdoor air ranged from 1.1E+05 to 2.5E+07. This assessment indicates there is no human health risk expected even at the highest ambient air concentrations of 6:2 FTOH reported.

**PS 2228 Derivation of an Occupational Exposure Limit for Inorganic Borates Using a Weight of Evidence Approach.**

M. J. Vincent<sup>1</sup>, A. Maier<sup>1</sup>, E. Hack<sup>2</sup>, P. Nance<sup>1</sup> and W. Ball<sup>3</sup>. <sup>1</sup>TERA, Cincinnati, OH; <sup>2</sup>The Henry Jackson Foundation, Bethesda, MD; <sup>3</sup>Rio Tinto Minerals, Greenwood Village, CO.

Inorganic borates are encountered in many settings worldwide, spurring international efforts to develop exposure guidance (U.S. EPA 2004; WHO 2009; ATSDR 2010) and occupational exposure limits (OEL) (ACGIH 2005, MAK 2011). We derived an updated OEL to reflect new data and current international risk assessment frameworks. We assessed toxicity and epidemiology data on inorganic borates to identify relevant adverse effects. International risk assessment frameworks (IPCS 2005; IPCS 2007) were used to evaluate endpoint candidates: reproductive toxicity, developmental toxicity, and sensory irritation. For each endpoint, a preliminary OEL was derived and adjusted based on consideration of toxicokinetics, toxicodynamics, and other uncertainties. Dose-response modeling supported selection of the point of departure for each endpoint. Developmental toxicity was the most sensitive systemic effect. An OEL of 1.6 mg B/m<sup>3</sup> was estimated for this effect based on a point of departure (POD) of 63 mg B/m<sup>3</sup> with an uncertainty factor (UF) of 40. Sensory irritation was considered to be the most sensitive effect for the portal of entry. An OEL of 1.4 mg B/m<sup>3</sup> was estimated for this effect based on the identified POD and an UF of 1. Reproductive effects are not the most sensitive basis for OEL derivation. An OEL of 1.4 mg B/m<sup>3</sup> was derived as an 8-hour TWA based on sensory irritation potential. The OEL is expected to protect from systemic toxicity endpoints.

**PS 2229 US EPA Decabromodiphenyl Ether Alternatives Hazard Assessment Results.**

J. Rhoades<sup>1</sup>, M. Kawa<sup>1</sup>, E. Lavoie<sup>2</sup>, C. Baier-Anderson<sup>2</sup> and J. Tunkel<sup>1</sup>. <sup>1</sup>SRC, Inc., East Syracuse, NY; <sup>2</sup>US EPA, OPPT, DfE, Washington DC.

The U.S. Environmental Protection Agency (US EPA) Design for Environment (DfE) Program undertook a chemical alternatives assessment for decabromodiphenyl ether (decaBDE) as part of the Action Plan for Polybrominated Diphenyl Ethers (PBDEs) published in December 2009. DfE convened a multi-stakeholder partnership to explore the human health and environmental profiles of functional and viable alternatives to decabromodiphenyl ether (decaBDE). The partnership identified ~ 30 functional alternatives to decaBDE. The hazard assessment for decaBDE and the alternatives used DfE hazard evaluation criteria to assign hazard designations for human health toxicity, ecological toxicity and environmental fate endpoints. The alternatives included a range of flame retardant

chemistries including both halogenated and non-halogen organic substances, inorganic materials, polymeric and non-polymeric substances and novel, new to market substances. Some alternatives were well characterized for all endpoints, while others were lacking data. Analog data, predictive models, structural alerts and expert judgment were used to make hazard designations for endpoints with data gaps. Trends for human health, ecological toxicity and fate characteristics were indicated in a number of the alternatives and are described in the poster. In general, molecular size ranges, molecular structures, and/or functional groups were found to be most influential on the hazard designations. A novel component of this assessment was the evaluation of higher molecular weight polymers for their human health and ecological toxicity based on their low potential for bioavailability and variability in low molecular weight components. Effective hazard assessment approaches of hazard criteria coupled with decision-making protocols are practical tools for businesses to use early in materials selection processes and will contribute to more sustainable product development. The resulting hazard profiles should be of value to manufacturers making substitution decisions in preparation for the upcoming decaBDE phase out.

**PS 2230 Predicting Bioavailability of Arsenic in Mining Soils.**

V. L. Mitchell<sup>1</sup>, N. T. Basta<sup>2</sup>, S. W. Casteel<sup>3</sup>, S. Whitacre<sup>2</sup>, L. E. Naught<sup>3</sup> and P. A. Myers<sup>1</sup>. <sup>1</sup>Toxic Substances Control, Cal EPA, Sacramento, CA; <sup>2</sup>Ohio State University, Columbus, OH; <sup>3</sup>University of Missouri, Columbia, MO.

Arsenic (As) is a naturally occurring element in soil and a key chemical of concern at former mine sites in California. Risk assessment calculations typically utilize default oral toxicity values, which are based on ingestion of readily soluble forms of As such as sodium arsenate (NaAs). However, mining soils in California are relatively high in iron hydroxide phases that bind As strongly, resulting in reduced solubility/bioavailability. The juvenile swine model is an approved, but often cost prohibitive, method for determining the relative bioavailability (RBA) of As in soils compared to that of NaAs. RBAs can be used to adjust toxicity criteria, resulting in a more accurate site-specific risk assessment. In vitro methodologies have proven to be useful surrogates for in vivo feeding studies in predicting bioavailability for other metals but lack precision for arsenic, particularly in high iron content soils. Six soil samples collected from Empire Mine State Historic Park (total As 302-12,041 mg/kg) were analyzed in the juvenile swine model. RBAs ranged from 4 to 20%. Gastrointestinal modeling correlated but underestimated RBA (1-9%). Sequential chemical extraction procedures (SEP) were applied to fractionate the As in soils into (F1) non-specifically sorbed; (F2) specifically sorbed; (F3) amorphous and poorly-crystalline oxides of Fe and Al; (F4) well-crystallized oxides of Fe and Al and residual As phases. The results of these extractions demonstrated that the sum of non-specifically sorbed and specifically sorbed arsenic (F1+F2) was similar to the predicted in vitro bioaccessibility while F1+F2+F3 is a conservative estimate of the in vivo RBA (10-50%). SEP could prove to be a cost-effective and valuable screening tool for estimating in vivo RBA. In summary, the assumption of 100% bioavailability of As in mining soils grossly overestimates exposure and risk to human health. Adjustments for As bioavailability in these materials and similar mining wastes provides a more accurate assessment of human exposure.

**PS 2231 A Quantitative Risk Assessment of 1-Bromopropane, Based on Tumor Data.**

D. A. Dankovic<sup>1</sup> and G. Dotson<sup>2</sup>. <sup>1</sup>Risk Evaluation Branch, CDC/NIOSH, Cincinnati, OH; <sup>2</sup>Document Development Branch, CDC/NIOSH, Cincinnati, OH.

The "green" movement has resulted in the introduction of several new "environmentally-friendly" substitutes into commerce, including 1-bromopropane (1-BP; CAS no. 106-94-5). Although use of 1-BP is intended to minimize ozone depletion, occupational exposure is of concern. Case studies, occupational exposure assessments, and epidemiological investigations have suggested that workplace exposure to 1-BP may be associated with neurological, reproductive, and hematological effects. Previous quantitative risk assessments of 1-BP have been based on toxicological studies of these and other non-cancer endpoints. This poster presents a quantitative risk assessment based on a NTP chronic bioassay, in which rats and mice were exposed to 125-500 or 62.5-250 ppm 1-BP, respectively, for up to 2 years. Inhalation of 1-BP produced alveolar/bronchiolar adenomas and carcinomas in female mice, adenomas of the large intestine in female rats, and keratoacanthoma/squamous cell carcinoma of the skin in male rats. Benchmark concentrations (BMC) and lower 95% confidence limits (BMCL) estimates at the 1 in 1000 response level (0.1%) were based on a previously published model average procedure. The BMC (BMCL) estimates were 0.85 (0.41) ppm for alveolar/bronchiolar adenoma + carcinoma; 13.5 (2.76) ppm for large intestine adenomas; and 3.73 (1.44) ppm for keratoacanthoma + squamous cell carcinoma of the skin. The BMC

(BMCL) estimates were extrapolated to humans on a (body weight)<sup>0.75</sup> basis, assuming a 45-year occupational exposure. Human-equivalent concentrations for a 1 in a 1000 lifetime added risk at the various tumor sites are 0.39 (0.19) ppm, for lung tumors; 6.17 (1.26) ppm for intestinal tumors; and 1.75 (0.68) ppm for skin tumors. These results suggest that even sub-ppm occupational exposures to 1-BP may pose an increased risk of cancer.

*The findings and conclusions in this report are those of the authors and do not necessarily represent the views of the National Institute for Occupational Safety and Health.*

## **PS** 2232 Human Health Risk Assessment of Inhaled Acudyne™ Shine Polymer in Hair Care Products.

S. M. Krieger, W. Shade, R. Sura, J. A. Hotchkiss and G. A. Hazelton. *The Dow Chemical Company, Midland, MI.*

ACUDYNE™ Shine is one of a family of acrylic polymers used in hair care product applications such as gels/mousses, and pump or aerosol sprays at concentrations up to 7 wt% to enhance the properties of the product. The pattern of use provides a potential for inhalation exposure to both consumers and salon workers. Sprague Dawley rats were exposed 6 h/day, 5 d/wk, for two- or 13-wks to ACUDYNE™ polymer concentrations of 0, 2, 11, and 100 mg/m<sup>3</sup> or 0, 1, 8, and 82 mg/m<sup>3</sup>, respectively, to provide toxicologic data for human risk assessment. A simulated consumer/occupational exposure monitoring study was conducted to determine typical breathing zone aerosol concentrations during product use. In the 13-wk study, no treatment-related changes in daily clinical observations, functional tests, ophthalmology, urinalysis, hematology, clinical chemistry, or coagulation parameters were observed. Males and females exposed to 82 mg/m<sup>3</sup> ACUDYNE™ had increased mediastinal and tracheobronchial lymph nodes, higher absolute and relative lung weights, and chronic-active bronchiolar-alveolar inflammation after 13-wks of exposure. Females also had decreased feed consumption and body weight gains. The No Adverse Effect Concentration was 8 mg/m<sup>3</sup> for males and females. Assuming 100% deposition, the inhaled dose of ACUDYNE™ polymer at an aerosol concentration of 8 mg/m<sup>3</sup> was estimated to be 0.47 mg/gm lung/day in rats. Based on a rat-to-human inhalation dosimetry factor of 24-32, the human equivalent inhaled dose at the same aerosol concentration was estimated to be 11.3 to 15.1 mg/gm lung/day. Results of the exposure monitoring study indicated breathing zone concentrations of respirable aerosol particles of 0.38 and 0.11 mg/m<sup>3</sup> and daily polymer lung deposition of  $\leq 0.19$  and  $\leq 0.44$   $\mu$ g/gm lung for consumer and occupational exposure scenarios, respectively. Based on the calculated human equivalent margin of exposure of  $> 25,000$  to  $150,000$  for all exposure scenarios, repeated daily inhalation exposure to ACUDYNE™ Shine polymer in hairspray formulations poses no significant human health risk.

## **PS** 2233 Derivation of Acceptable Drinking Water Levels for Bromine and Bromide-Releasing Antimicrobial Agents.

J. C. English, V. S. Bhat and C. J. McLellan. *NSF International, Ann Arbor, MI.*

Elemental bromine is the active ingredient in brominating cartridges, and is registered for disinfection of drinking water aboard ships and oil drilling platforms. Since bromine disproportionates in water to bromide (stable) and hypobromite (unstable) ions, this assessment applies specifically to inorganic bromide, whereas health-based guideline values for bromate and organic bromine compounds have been developed elsewhere. Repeated oral exposure in various mammalian species is associated with central nervous system effects expressed as behavioral and EEG changes. Repeated oral dosing also causes a hypothyroid effect that is specific to rats and not observed clinically. In a rat three-generation study with NaBr administered via the diet, the NOAELs for reproductive and parental effects were 48 and 12 mg Br/kg-day, respectively. In oral developmental toxicity studies, the NOAELs for both parental and developmental effects were 77 and 196 mg Br/kg-day, in rats and rabbits, respectively. Chronic administration of KBr or methyl bromide via the diet of rats did not result in treatment-related adverse findings. There is extensive clinical experience with various bromide salts based on their historical use as sedative-hypnotics and in treatment of seizure disorders. When male and female volunteers were administered NaBr capsules for 12 weeks, there was a small effect on EEGs that was reproducible but within normal limits. Serum T4, T3, and related hormone levels remained within normal limits. The most sensitive effect was gastric irritation expressed as nausea that occurred shortly after the ingestion of the capsules, but no longer occurred when the capsules were taken with a meal. Based on the absence of sedation and EEG changes within normal limits, the human systemic NOAEL was 7 mg Br/kg-day. Using a 10x uncertainty factor to account for intraspecies variability, an RfD of 0.7 mg/kg-day was determined for bromide, which corresponds to a Total Allowable Concentration of 12 mg/L in drinking water and accounts for exposure of the general population to bromide from the diet.

## **PS** 2234 Low-Level Arsenic in Drinking Water and Bladder Cancer Risk: Meta-Analysis Update and Risk Assessment Implications.

J. S. Tsuji<sup>1</sup>, D. D. Alexander<sup>2</sup> and V. Perez<sup>3</sup>. <sup>1</sup>Exponent, Bellevue, WA; <sup>2</sup>Exponent, Boulder, CO; <sup>3</sup>Exponent, Chicago, IL.

A published meta-analysis of relevant case-control and cohort studies was updated with two recent studies to further examine the association between low-level arsenic exposure and bladder cancer risk, and whether meta relative risks (mRR) differed significantly from bladder cancer risks predicted in a 2001 report by the National Research Council (NRC). Cancer risk estimates from NRC (2001), which are based on data from southwestern Taiwan, form the basis of the U.S. Environmental Protection Agency's 2010 proposed cancer slope factor for assessing arsenic cancer risks. Our updated meta-analysis of nine studies improved the precision of the previous estimate (mRR = 1.11; 95% CI: 0.95–1.30), with no significant association observed between low-level arsenic exposure and bladder cancer (1.07; 0.95–1.26; p-heterogeneity = 0.54). RRs for never-smokers in the individual studies and the mRR were consistently below 1.0 (0.83; 0.65–1.06; p-heterogeneity = 0.89). Thus, exposure misclassification/regression to the null cannot explain the lack of a significant positive relationship for never-smokers. The mRR was modestly elevated for ever-smokers, but not significantly, with heterogeneity among studies (1.19; 0.95–1.45; p-heterogeneity = 0.04). To evaluate the independent effect of arsenic in comparison to NRC (2001) risk estimates for the U.S., the mRR for bladder cancer in never-smokers was compared to RRs predicted by NRC (2001) at various water concentrations within the low-level studies and for less than lifetime exposures. The collapsed category mRR for never smokers was 0.82 (0.62–1.10) (using cut-points in individual studies near 50 ppb) and was compared to RRs calculated for non-smokers in the U.S. based on NRC (2001). The 95% CI did not include NRC predicted RRs at 20 or 50 ppb, even for half lifetime exposures (RRs of 1.14 and 1.31, respectively). Results of low-level studies differed significantly from, and were inconsistent with, risks predicted by NRC (2001) for non-smokers including those with less than lifetime exposure.

## **PS** 2235 A Chronic Oral Reference Dose for Hexavalent Chromium.

C. M. Thompson<sup>1</sup>, C. R. Kirman<sup>2</sup>, D. M. Proctor<sup>3</sup>, M. Suh<sup>4</sup>, S. M. Hays<sup>4</sup>, L. C. Haws<sup>5</sup> and M. A. Harris<sup>1</sup>. <sup>1</sup>ToxStrategies, Katy, TX; <sup>2</sup>Summit Toxicology, Orange Village, OH; <sup>3</sup>ToxStrategies, Rancho Santa Margarita, CA; <sup>4</sup>Summit Toxicology, Allenspark, CO; <sup>5</sup>ToxStrategies, Austin, TX.

Intestinal tumors have been observed in mice (but not rats) following chronic exposure to high concentrations of hexavalent chromium [Cr(VI)] in drinking water. Mice (but not rats) also exhibit histological lesions consistent with intestinal wounding, specifically villous blunting and crypt hyperplasia—collectively termed diffuse hyperplasia. Recent mode of action studies support that these tumors were indeed the result of chronic wounding and regenerative hyperplasia to repair the intestinal mucosa. Herein, we develop an oral reference dose (RfD) that is protective of the tumor precursor lesion (diffuse hyperplasia), and therefore is protective of intestinal cancer. A rodent physiologically based pharmacokinetic (PBPK) model was used to predict internal dose measures for chromium in the duodenum, jejunum, and ileum of mice under the conditions of the 2-year bioassay. These internal dose metrics together with corresponding incidences for diffuse hyperplasia in each intestinal segment were used to characterize the dose-response relationship for the small intestine in a single plot containing a robust dataset with as many as 24 data points. Points of departure (PODs) were derived using benchmark dose modeling and global nonlinear regression, with models providing acceptable fits differing  $< 3$ -fold. Human equivalent lifetime average dose values were estimated for each POD using two different methods of extrapolation with the human PBPK model for chromium. Dividing the PODs by uncertainty factors (UFs) of 10-30 yields a range of 8 RfD values (2 modeling approaches  $\times$  2 human equivalent dose methods  $\times$  2 UF values). The resulting RfD range is protective against diffuse hyperplasia, and is therefore protective of both noncancer and cancer effects in the small intestine. This range of RfD values leads to acceptable Cr(VI) concentrations in drinking water that are greater than those typically found in drinking water sources ( $\leq 5$   $\mu$ g/L).

## **PS** 2236 Mode-of-Action Evaluation for Hexavalent Chromium-Induced Lung Cancer.

D. M. Proctor<sup>1</sup>, M. Suh<sup>1</sup>, C. M. Thompson<sup>2</sup> and M. A. Harris<sup>2</sup>. <sup>1</sup>ToxStrategies, Rancho Santa Margarita, CA; <sup>2</sup>ToxStrategies, Katy, TX.

Inhalation of hexavalent chromium [Cr(VI)] has been associated with increased lung cancer risk among workers of certain industries, but no well recognized or published mode of action (MOA) exists. Although it has been suggested that

Cr(VI) acts by a mutagenic MOA because it damages DNA in vitro and in some in vivo tests, several recent reviews have concluded that Cr(VI) is only weakly mutagenic and that genetic/epigenetic changes resulting in genomic and/or microsatellite instability, inflammation, oxidative stress and deregulation of repair mechanisms play a role in carcinogenicity. Further, recent data for mouse small intestinal cancers caused by Cr(VI) in drinking water support a cytotoxic MOA involving chronic intestinal wound and healing. Using the modified Hill Criteria, we have reviewed kinetic, human, animal, and mechanistic data to develop a lung cancer MOA; evaluated plausibility, dose-response, and temporal concordance; and considered alternative MOAs. Among workers with an observed increase in lung cancer, respiratory tissue irritation and inflammation were common clinical findings, and in animal studies irritation and inflammation precede tumor formation in dose ( $\geq 50$   $\mu\text{g}/\text{m}^3$ ) and time (within 30 days), suggesting that cytotoxicity and inflammation are early key events. The overall evidence supports that Cr(VI) induces lung cancer by a non-mutagenic MOA involving oxidative stress, cytotoxicity, and inflammation, causing oxidative DNA damage, epigenetic DNA modifications and genomic instability, occurring at the high exposure concentrations. Further, extracellular Cr(VI) reduction in the lung limits absorption and may introduce non-linearity in the extrapolation of tissue dose from high to low exposures. Based on these findings, the risk assessment for inhalation exposure to Cr(VI) should consider intensity-based dose metrics and non-linear low dose extrapolation approaches.

**PS 2237 A Screening Level Assessment of the Health and Environmental Hazards of Organohalogen Flame Retardants.**

D. A. Eastmond, V. S. Bhat and K. Capsel. *Environmental Toxicology Graduate Program, University of California, Riverside, CA.*

Organohalogen flame retardants are extensively used in both industrial and consumer products. However, relatively little is known about the potential of many of these chemicals to cause adverse health and environmental effects. To address this, we conducted a health and environmental hazard screening of almost 100 brominated or chlorinated flame retardants based on the GreenScreen® or Quick Chemical Assessment Tool (QCAT®) methodologies. Priority consideration was given to human health hazards such as carcinogenicity (including mutagenicity and genetic toxicity), reproductive or developmental toxicity, endocrine disruption, and acute mammalian toxicity. Environmental hazards given priority consideration included acute aquatic toxicity, persistence, and bioaccumulation. Using publicly available information, each hazard category was assigned a concern level (low, moderate, high, or very high) based on pre-defined numerical ranges, such as no-observed adverse effect levels, and hazard classification schemes from authoritative sources, when available. Less than 10% of the screened chemicals had empirical data to assess each priority hazard category. Where empirical data were not identified, structure activity relationship (SAR) models were relied upon to predict hazard potential. After assigning concern levels for each priority health effect, each chemical received a score, similar to a report card (A, B, C, D, or F). The majority of the screened chemicals received either a D or F grade due to empirical data suggesting high hazard, SAR model predictions, and/or excessive data gaps. Carcinogenicity was the most prominent potential health hazard identified based on empirical data. The most prevalent data gap was endocrine disruption due to the lack of identified empirical data or computer models able to predict this hazard. This study highlights the limited toxicity information available for these widely used chemicals, and indicates that more testing and oversight is critically needed to identify safer alternatives for fire prevention.

**PS 2238 Air Quality and Human Health Risks Along the Texas Gulf Coast.**

T. Bredfeldt and D. McCant. *Toxicology, Texas Commission On Environmental Quality, Austin, TX.*

There are several urban and industrial regions along the Texas Gulf Coast that house some of the largest ports in the US, numerous refineries, thousands of chemical/petrochemical facilities and manufacturing plants. Given its dense population and industrial activity, monitoring and regulation of air quality in these regions is critical for protection of human health. The TCEQ has developed the largest ambient air monitoring network in the US to measure cumulative emissions in the area. In the coastal regions alone, there are more than 47 fixed-site air monitors (17 AutoGCs and 30 canisters), some of which have been operational for 20 years. Acrolein, benzene, 1,3-butadiene, and formaldehyde are considered air toxics of greatest concern. To evaluate risks associated with these air toxics, we collected site-specific concentrations of these four chemicals and evaluated them from both an acute and chronic health perspective by comparing them to TCEQ health-protective values called ambient air monitoring comparison values (AMCVs). We calculated average annual concentrations measured by 1-h AutoGC or 24-h canister and

found that concentrations of these air toxics have steadily declined. Using long-term average concentrations of these air toxics, we calculated long-term risks to be within our acceptable risk goal ( $< 1 \text{ E-5}$ ) or a hazard quotient ( $< 1$ ) for the majority of monitoring sites. The long-term average benzene concentration at Lynchburg Ferry and Huisache monitors reached concentrations that resulted in risk (1.8 and 1.1 E-5, respectively) slightly above our risk goal. To better understand dynamics of air toxics at sites with a history of exceeding the long-term AMCV, we used 1-h AutoGC data to characterize ambient conditions contributing to exceedances. We found exceedances of the respective acute AMCVs to be rare. Instead, a few ( $< 30\%$ ) hourly concentrations influenced the average concentration thereby causing long-term exceedances. The decline in air toxics concentrations due to improved monitoring and regulations has now resulted in air toxics at acceptable levels at all monitors in the coastal region.

**PS 2239 Assessment of Potential Perchlorate Exposures from the Use of Household Chlorine Bleach.**

T. Lewandowski<sup>1,2</sup>. <sup>1</sup>*Gradient, Seattle, WA;* <sup>2</sup>*Health and Nutrition Sciences, Brooklyn College/City University of New York, Brooklyn, NY.*

US Government surveys have indicated that perchlorate ( $\text{ClO}_4$ ) occurs at low levels (generally below 4  $\mu\text{g}/\text{L}$ ) in many U.S. public water supplies systems. Although small amounts of perchlorate in water may be due to natural processes, the higher concentrations of perchlorate found in some drinking water supplies (up to 100  $\mu\text{g}/\text{L}$ ) are believed to be the result of past use of  $\text{ClO}_4$  in aeronautics, explosives and/or fireworks, which subsequently affected nearby water bodies or watersheds. The potential health consequences of exposure to low concentrations of  $\text{ClO}_4$  in drinking water remain controversial, with disputed epidemiology findings and questions about the relevance of animal study data to humans. Because a small amount of  $\text{ClO}_4$  is produced by the normal decomposition of chlorate in household chlorine bleach, we examined whether the use of bleach under various scenarios could lead to exposures associated with possible health effects. We considered bleach of different ages and different label strengths and used a temperature- and time-sensitive model to estimate the decomposition of chlorate to  $\text{ClO}_4$ . Predicted  $\text{ClO}_4$  concentrations in bleach ranged from 1 to 34  $\text{mg}/\text{L}$ . The exposure scenarios considered addressed the use of bleach for household laundry, emergency water decontamination, "shock treatment" of private drinking water wells, and regular treatment of water in private swimming pools. In each case, our analysis indicated that potential exposures to  $\text{ClO}_4$  from the use of chlorine bleach would be well below levels associated with potential health effects. For example, the maximum  $\text{ClO}_4$  exposure of a pregnant woman drinking water sanitized with chlorine bleach in an emergency decontamination situation was estimated at 0.2  $\mu\text{g}/\text{kg}\cdot\text{day}$ , 35 times less than the dose associated with minimal effects on iodide uptake in humans. Thus the presence of  $\text{ClO}_4$  as a decomposition product in household bleach does not pose an adverse health risk for consumers.

**PS 2240 Derivation of a Reference Dose for Resorcinol.**

B. H. Magee. *Risk Assessment, ARCADIS, Chelmsford, MA.*

Resorcinol is a common chemical used in industry. US EPA has no final or provisional toxicological criteria for resorcinol. In 2004, a critical analysis of the toxicological database was performed with the purpose of deriving a scientifically reasonable Reference Dose (RfD). Key studies, critical effect(s) and associated doses (No Observed Adverse Effect Levels (NOAELs) and/or Lowest Observed Adverse Effect Levels (LOAELs) are identified and adjusted using uncertainty factors (UFs) to determine an oral RfD.

The analysis of available information from epidemiological studies and animal studies at the time established the one-generational dose range finding study conducted by WIL Research Laboratories (WIL, 2003) and sponsored by the Resorcinol Task Force (RTF) as the definitive study from which to derive the RfD. It identified thyroid toxicity as the critical effect of resorcinol exposure and 61  $\text{mg}/\text{kg}\cdot\text{day}$  as the NOAEL. The derived RfD was 2  $\text{mg}/\text{kg}\cdot\text{day}$ . The RfD was endorsed and approved by a Toxicology Excellence for Risk Assessment (TERA) Independent Peer Review Panel and approved by the Pennsylvania Department of Environmental Protection's (PaDEP's) Cleanup Standards Science Advisory Board ("CSSAB") in 2004.

Soon after that time, a full two-generational reproductive toxicity study was completed (WIL, 2005) and published (Welsch et al., 2008). The NOAEL from this definitive study for the same critical effect was 375  $\text{mg}/\text{kg}\cdot\text{day}$ , and the corresponding RfD is 13  $\text{mg}/\text{kg}\cdot\text{day}$  using the WIL (2005) results, thus indicating that the RfD of 2  $\text{mg}/\text{kg}\cdot\text{day}$  endorsed by the TERA Panel and approved by PaDEP in 2004 was health-protective.

Meanwhile, other regulatory regimes, such as REACH have focused on a more limited list of critical effects in order to derive the relevant Derived No Effect Levels (DNELs) for the development of Chemical Safety Assessments. This can lead to

outcomes which differ from those outlined above and are often even more conservative. This paper explores the background to these divergences and highlights that the context under which an RfD or DNEL is developed has a significant bearing on the final determination made.

**PS 2241 Risk Estimates for Dioxins, Furans, and PCBs in Edible Fish and Shellfish at the San Jacinto River Waste Pits, Texas, USA.**

E. S. Williams, S. Usenko and B. W. Brooks. *Environmental Science, Baylor University, Waco, TX.*

From the 1960s to the early 1980s, paper process wastes were disposed of at a pits site on the San Jacinto River. Eventually the pits subsided into the river, spreading polychlorinated dioxins, furans, and biphenyls into the adjacent aquatic ecosystem. Consumption advisories have been in place for local fish and shellfish since 1990. The San Jacinto River Waste Pits site was identified during a Total Maximum Daily Loads process, and was added to the National Priorities List in 2008. Previous efforts to characterize bioaccumulation of chlorinated compounds on the site included sampling of sediment and thirteen species of fish and shellfish. During the sampling period, numerous persons were observed fishing on or near the site. Important fish and shellfish consumed from the area appear to be clams (*Mercenaria* spp.), blue crabs (*Callinectes sapidus*), and black drum (*Pogonias cromis*). Mean TCDD concentrations in clams, crabs, and fish from the site were 28, 3.6, and 2.25 pg/g wet weight, respectively. TCDF was the only other dioxin/furan congener detected, but ten dioxin-like PCBs were observed in these samples. Excess lifetime cancer risk estimates posed by consumption of contaminated fish and shellfish were calculated using default exposure parameters; risk estimates for reasonable maximum exposures ranged from  $1.2 \times 10^{-5}$  to  $1.51 \times 10^{-4}$ . Risks in excess of  $10^{-4}$  under these parameters are associated only with consumption of clams from the site, and lower exposure frequency would be expected. Considerations of spatial sampling sufficiency, multiple exposure scenarios, associated risk estimates, and analysis of uncertainty will be presented.

**PS 2242 Evaluation of the Glyphosate Developmental Toxicity Database: Absence of Potential for Cardiovascular Malformations.**

A. Williams, G. Kimmel, C. Kimmel and J. DeSesso. *Exponent, Alexandria, VA.*

The herbicide glyphosate has undergone multiple safety tests for developmental toxicity in rats and rabbits. The European Commission's 2002 review of available glyphosate data (European Commission, 2002; BBA, 1998-2000) discusses, in particular, specific heart defects observed in individual rabbit developmental toxicity studies, but describes the evidence for a potential causal relationship as equivocal. The present assessment was undertaken to analyze the body of information generated from the seven unpublished rabbit studies submitted to European regulatory agencies in order to determine if glyphosate poses a risk for cardiovascular malformations. In addition, the results of six unpublished developmental toxicity studies in rats were considered. Five of the seven rabbit studies (dose range: 10-500 mg/kg/day) were GLP- and testing guideline-compliant for the era in which the studies were performed; a sixth study predated testing and GLP guidelines, but generally adhered to these principles. The seventh study was judged inadequate. In each of the adequate studies, offspring effects occurred at or above doses that caused maternal toxicity. An integrated evaluation of the six adequate studies, using conservative assumptions, demonstrated that neither the overall malformation rate nor the incidence of cardiovascular malformations increased with dose up to the point where severe maternal toxicity was observed (generally  $\geq 150$  mg/kg/day). Random occurrences of cardiovascular malformations were observed across all dose groups (including controls) and did not exhibit a dose-response relationship. In the six rat studies (GLP and testing guideline compliant; dose range: 30-3500 mg/kg/day), a low incidence of sporadic cardiovascular malformations was reported that was clearly not related to treatment. In summary, assessment of the entire body of the developmental toxicity data reviewed fails to support a potential risk for increased cardiovascular defects as a result of glyphosate exposure during pregnancy.

**PS 2243 Oral Risk Assessment for Isooctane—A Class-Based Approach Using the Surrogate n-Hexane.**

B. Wang<sup>1</sup>, P. Undesser<sup>2</sup> and M. Whittaker<sup>1</sup>. <sup>1</sup>ToxServices LLC, Washington DC; <sup>2</sup>Water Quality Association, Lisle, IL.

Isooctane is a volatile liquid commonly found in gasoline. It is principally released into the environment via the manufacture, use and disposal of products associated with the petroleum industry. Although the most likely route of human exposure to

this chemical is through inhalation, products such as polyethylene pipes used for distribution of drinking water can release it in water, and it has high oral absorption. NSF/ANSI 61 Annex A (2012) risk assessment guideline was used to determine an acceptable level of isooctane in drinking water. Weight of evidence indicates that isooctane is not mutagenic or carcinogenic. All the available repeated dose oral studies are short term in nature and the majority was designed to address the  $\alpha 2u$ -globulin-associated renal toxicity, which is specific to male rats and not relevant to humans. Thus, insufficient data are available to establish an oral reference dose (RfD) for isooctane. Since isooctane is categorized into the aliphatic EC5 (equivalent carbon) to EC8 fraction of petroleum hydrocarbons, a class based approach was taken. Most of the limited oral studies available for the chemicals in this fraction were performed on n-hexane. Relevant critical health effects with n-hexane exposure are peripheral neuropathy, reduced body weight and testicular atrophy. Many groups and agencies used n-hexane as a representative of this fraction, which is known to significantly overestimate the toxicity of these chemicals, and different RfD values were derived for n-hexane using different approaches. After comparing these assessments, we chose to use the most conservative, duration-adjusted lowest observed adverse effect level of 407 mg/kg/day established from a subchronic gavage study in rats, and a composite uncertainty factor of 3000 to calculate the RfD of 0.12 mg/kg/day for isooctane. Based on this value, a total allowable concentration of 840  $\mu\text{g/L}$  was derived. This drinking water action level is protective of public health since it used the more toxic n-hexane to fill the data gap, and it has a margin of exposure of over 15,000.

**PS 2244 Deriving Dermal Safe Harbor Levels for DEHP Relevant to Consumer Products for Adults.**

T. Jonaitis, J. W. Card and L. Haighton. *Intertek Cantox, Mississauga, ON, Canada.*

Di(2-ethylhexyl)phthalate (DEHP), a plasticizer in various consumer products, is listed as a chemical known to the State of California to cause cancer and reproductive toxicity. The Proposition 65 Safe Harbor Levels (SHL) for DEHP include a Maximum Allowable Dose Level (MADL) for DEHP, specific to the oral route, of 410  $\mu\text{g/day}$  for adults (58  $\mu\text{g/day}$  for infant boys; 20  $\mu\text{g/day}$  for neonatal boys). The No Significant Risk Level (NSRL) for cancer of 310  $\mu\text{g/day}$ , while not route-specific, was based on an oral study. While DEHP in children's toys is of concern due to mouthing behavior, most 60-day notices of violation for DEHP are related to consumer products intended for adults. Thus, there is a need for realistic, dermal-specific SHLs and accurate calculations of exposure. From studies on dermal absorption of DEHP from plastic film (present at 25.5 mg/cm<sup>2</sup> of film, or 40.37% w/w) applied to the skin of rats (used as a conservative estimate of migration of DEHP from a product into the human body since rats have a higher dermal absorption than humans), a maximum dermal absorption of 0.1% was determined. Comparatively, the reported oral bioavailability of DEHP is 25%. Using these values, the dermal MADL would correspond to 102,500  $\mu\text{g/day}$  for adults (410  $\mu\text{g/day} \times 0.25$  oral absorption fraction/0.001 dermal absorption) and the dermal NSRL would be 77,500  $\mu\text{g/day}$ . From the same study, a dermal absorption rate of DEHP from the plastic was calculated to be approximately 0.24  $\mu\text{g/cm}^2/\text{hour}$  for the rat which corresponds to 0.016  $\mu\text{g/cm}^2/\text{hour}$  for humans, given observed species differences. This value can be used to calculate dermal exposures with correction for differing concentrations. Also, a migration rate of 1.4  $\mu\text{g/cm}^2/\text{hour}$  can be used to determine the DEHP skin loading for estimating transfer of DEHP from a consumer product onto the hands, and then directly and indirectly to the mouth for comparison to the oral SHLs. In summary, route-specific SHLs are considered useful for realistically estimating risks associated with exposure of adults to DEHP from consumer products.

**PS 2245 Microfluidic Steroidogenesis Assays for *In Vitro* Toxicant Screening.**

A. B. Theberge<sup>1,2,3</sup>, E. Berthier<sup>4</sup>, C. J. Hedman<sup>5</sup>, B. P. Casavant<sup>2</sup>, N. P. Keller<sup>1,4</sup>, W. A. Bushman<sup>1,3</sup> and D. J. Beebe<sup>1,2</sup>. <sup>1</sup>Molecular and Environmental Toxicology, University of Wisconsin-Madison, Madison, WI; <sup>2</sup>Biomedical Engineering, University of Wisconsin-Madison, Madison, WI; <sup>3</sup>Urology, University of Wisconsin-Madison, Madison, WI; <sup>4</sup>Medical Microbiology and Immunology, University of Wisconsin-Madison, Madison, WI; <sup>5</sup>Institute for Clinical and Translational Research, University of Wisconsin-Madison, Madison, WI. Sponsor: C. Bradfield.

Many endocrine disrupting compounds act by interrupting steroidogenesis, thus disrupting subsequent processes that rely on steroids for signaling such as hormone-mediated pathways crucial for development. High-throughput in vitro assays are required to identify such compounds efficiently. Liquid chromatography-mass spectrometry (LC-MS) is a gold standard technique for steroid characterization and quantification, but traditional methods for steroid extraction with organic solvents, typically used to remove matrix components prior to LC-MS, require many manual

steps, thus presenting a bottleneck for steroid analysis. To expedite steroid extraction, we developed an integrated microfluidic device consisting of a bottom channel for cell culture and a top channel in which steroids are extracted directly from culture media into organic solvent. The top channel is accessible with a pipette or robot liquid handler, which can be used to transfer the sample to an LC-MS autosampler for analysis. We extracted cortisol solutions of known concentration to demonstrate consistent extraction over a range of biologically relevant concentrations spanning two orders of magnitude. We validated this microfluidic system with the human adrenocortical cell line H295A, demonstrating that these cells produce steroids in microculture and respond to cAMP, a known stimulant of steroidogenesis. Microfluidic extraction was used to isolate a panel of steroids including cortisol, cortisone, 11-deoxycortisol, and testosterone, which were quantified using LC-MS. In addition to high-throughput toxicant screening, the microfluidic platform holds great potential for steroidogenesis assays with limited samples, such as primary cells. Funded by NIH T32ES007015.

**PS 2246 An Improved *In Vitro* Method for Determining Chemical Effects on Steroidogenesis Using LC/MS/MS to Monitor Multiple Steroid Hormones Combined with Gene Expression.**

C. M. Toole<sup>1</sup>, H. Wagner<sup>1</sup>, K. Lewis<sup>2</sup> and J. M. McKim<sup>1</sup>. <sup>1</sup>*CeeTox, Inc., Kalamazoo, MI*; <sup>2</sup>*OpAns, LLC, Durham, NC*.

Steroid hormones play vital roles in development. Environmental compounds can impact the steroidogenic pathway producing a wide range of effects. Quantifying multiple steroids from a single biological sample, coupled with gene expression of the enzymes that form them, allows for a better evaluation of these effects. The human adrenal H295R cell line is currently used by the Environmental Protection Agency (EPA) to screen for chemical effects on steroidogenesis by evaluating production of Estradiol (E2) and Testosterone. Following EPA guidelines, 22(R)-hydroxycholesterol (22RHC) can be added (20–40  $\mu$ M) to the culture medium to increase basal production of E2. Addition of 22RHC to the H295R culture medium bypasses steroidogenic acute regulatory protein (StAR). To evaluate the induction mechanism of 22RHC, H295R exposures were conducted using both 22RHC and forskolin, a known inducer of steroidogenesis. 22RHC and forskolin were administered to cells at 0.4, 1, 4, 10, 20 and 40  $\mu$ M and 0.03, 0.2, 0.3, 1, 3 and 10  $\mu$ M, respectively for 48 hr. RT-PCR was used to quantitate the expression of 9 steroidogenic genes and LC/MS/MS was used to measure hormone levels of 12 steroids. Forskolin was found to upregulate mRNA of CYP11B2, HSD3B2, CYP21A2, CYP17A1, CYP19A1 in a dose-dependent manner. StAR mRNA was also increased at the highest exposure concentration. No significant upregulation of mRNA was observed in the 22RHC-exposed cells within the solubility limit. Steroid levels from LC/MS/MS displayed first and zero order enzyme kinetics. LC/MS/MS results showed that 22RHC exposures significantly increased early event markers (e.g., progesterone, pregnenolone, DOC, and 11 DOC), whereas forskolin exposures resulted in higher levels of most steroids. These results demonstrate that steroid genes are not regulated by a positive feedback loop in 22RHC exposed cells. This study shows that evaluation of multiple steroid levels combined with gene expression provides a more complete picture of steroidogenesis.

**PS 2247 Mapping Pathways of Endocrine Disruption in MCF-7 Cells: 2D and 3D Culture Systems.**

M. M. Vantangoli, S. Hall and K. Boekelheide. *Brown University, Providence, RI*.

It is becoming increasingly important to identify endocrine-active compounds early in toxicity testing, placing weight on the use of in-vitro screening. Currently, the pathways of endocrine disruption are being mapped in response to estrogenic compounds. In this study, human breast adenocarcinoma MCF-7 cells are being utilized to map pathways of endocrine disruption following exposure to estrogenic endocrine-active compounds. Our study utilizes two models, a 2-dimensional system representative of classical in-vitro studies, and a scaffold-free 3D culture system. Both systems follow a protocol that includes 72 hours of growth in media containing 10% FBS for 72 hours, followed by 48 hours in media containing 5% stripped serum. Treatments with compounds of interest begin following the 48 hours. Preliminary data shows that our 2D system is responsive to estrogenic compounds including estradiol, DES and BPA across several endpoints, including cell proliferation and protein expression. Over a range of concentrations of estradiol (0.01nM–100nM) and times (1, 3, 6, and 12 hours) analysis of gene expression showed increases in classical estrogen responsive genes including progesterone receptor (1.5–3.5 fold), cathepsin D (1.5–2 fold), estrogen-inducible pS2 (1.5–4 fold) and GREB1 (4–14 fold) at concentrations as low as 0.01nM estradiol. These results were also shown by Western blotting, with time-dependent increases in pS2 and

GPR30 following estradiol stimulation. Our 3D system exhibits cell-contacts and morphology that may play an important role in evaluating toxicities of estrogenic endocrine-active compounds. Here, we show the potential use of both 2D and 3D culture of MCF-7 cells to assess the estrogenic activities of suspected endocrine-active compounds.

**PS 2248 Cell-Specific Control of Estrogen Response Mechanisms in HeLa-9903 and T47D-KBluc Cell Lines.**

D. Blakeman, B. Meyer, A. Hulett, J. M. McKim and C. M. Toole. *CeeTox, Inc., Kalamazoo, MI*.

Estrogen signaling can be adversely affected by endocrine disrupting chemicals via agonism or antagonism. Cell lines capable of detecting agonism and antagonism are useful screening tools for determining estrogenic activity of chemicals. Transcriptional effects of the Estrogen Receptor (ER) are modulated by interactions with coregulatory proteins that function as either coactivators (agonism) or corepressors (antagonism). Selective ER modulators (SERMs), such as tamoxifen, favor recruitment of corepressors that inhibit transcriptional activity. In different tissues, tamoxifen can have partial-agonist-antagonist activities which may be related in part to the milieu of ER coactivators and corepressors in these tissues. To further elucidate effects of SERMs on transcriptional activity, agonism and antagonism was evaluated using reporter gene assays in two cell types, hER $\alpha$ -HeLa-9903, derived from a human cervical tumor, and T47D-KBluc, stably transfected breast cancer cells. Cells were acclimated in 96-well plates and exposed for 24 hr to tamoxifen (TAM), 4-OH tamoxifen (4HTAM), raloxifen (RALOX), estradiol (E2), dihydrotestosterone (DHT), corticosterone (CORT), or 17-methyltestosterone (MT). Cytotoxicity, luminescence, and solubility were measured. An agonist response was demonstrated for TAM, RALOX and 4HTAM in hER $\alpha$ -HeLa-9903 cells, but not T47D-KBluc. Antagonism also showed distinct results for the two cell types where T47D-KBluc cells demonstrated a potential additive effect with 4-HTAM and the maximal response was 4-fold higher than E2. RALOX and TAM also demonstrated enhanced responses in hER $\alpha$ -HeLa-9903 cells. Because T47D-KBluc cells have endogenous ER $\alpha$  and ER $\beta$ , and hER $\alpha$ -HeLa-9903 cells have exogenous ER $\alpha$ , coupled with the fact that corepressors and activators may be different in breast and cervical tissues, the resulting mechanisms controlling agonism and antagonism may be regulated, at least partially, by separate and distinct gene signaling mechanisms. These findings show that measuring estrogenic activity in two cell lines may provide a more accurate assessment of estrogen response.

**PS 2249 Profiling of ER $\alpha$ -Coregulator Binding As a Means for Functional Classification of Unknown Endocrine Disruptors.**

R. Houtman<sup>1</sup>, S. Wang<sup>2,3</sup>, J. M. Aarts<sup>2,3</sup>, W. Westerink<sup>4</sup>, B. J. Blaauboer<sup>5</sup>, T. Bovee<sup>2</sup> and R. van Beuningen<sup>1</sup>. <sup>1</sup>*PamGene International BV, Den Bosch, Netherlands*; <sup>2</sup>*RIKILT-Institute of Food Safety, Wageningen UR, Wageningen, Netherlands*; <sup>3</sup>*Division of Toxicology, Wageningen UR, Wageningen, Netherlands*; <sup>4</sup>*Wil Research, Den Bosch, Netherlands*; <sup>5</sup>*Division of Toxicology, Institute for Risk Assessment Sciences, Utrecht, Netherlands*.

Testing chemicals for their endocrine-disrupting potential, e.g. interference with estrogen receptor alpha (ER $\alpha$ ) signaling, is an important aspect of chemical safety profiling. Due to drawbacks of in vivo testing, the development of in vitro alternatives has a high priority. In a previous study, we have demonstrated an in vitro assay which profiles binding of (un)liganded nuclear receptors to a microarray of coregulator-derived peptides, as a good candidate. Here, a set of 13 model compounds, US-EPA recommended for ER $\alpha$  gene reporter assay proficiency testing, was used to assess reproducibility, robustness and added value of our assay. ER $\alpha$ -coregulator binding profiles in the presence of a concentration series of each compound were generated. With a median coefficient of variation of 5% and excellent correlation ( $R^2=0.99$ ) between duplicate measurements, the uncertainty level of the peptide microarray was well within the range observed for other commonly used in vitro ER functional assays. Per compound, a dose-response curve for each ER $\alpha$ -coregulator interaction was constructed. Our results show correct prediction of estrogenicity for 12 out of 13 tested compounds. The potency ranking for 9 out of the 10 ER-agonists exactly matched that for transcriptional activation as reported by ICCVAM and US-NIEHS with excellent correlation ( $R^2=0.98$ ). Moreover, unsupervised classification (Hierarchical clustering, Euclidean distance, average linkage) with the compound-characteristic ER $\alpha$ -coregulator binding profiles results in structurally related compounds to cluster together, whereas the steroid test compounds having an aromatic A-ring were separated from those with a cyclohexene A-ring. This latter feature should be exploited to build a prediction model to enable classification of unknown toxicants by comparison with pre-profiled references.

**PS 2250 Validation of the Yeast Estrogen and Yeast Androgen Screens for Endocrine Active Substances: Interlaboratory Ring Trial.**

C. Woitkowiak<sup>1</sup>, T. Ramirez<sup>1</sup>, H. Hüner<sup>1</sup>, C. Schönlau<sup>2</sup>, H. Hollert<sup>2</sup>, S. Broschke<sup>3</sup>, O. Zierau<sup>3</sup>, G. Vollmer<sup>3</sup>, M. Jäger<sup>4</sup>, A. Poth<sup>4</sup>, E. Higley<sup>5</sup>, M. Hecker<sup>5</sup>, B. van Ravenzwaay<sup>1</sup> and R. Landsiedel<sup>1</sup>. <sup>1</sup>Experimental Toxicology and Ecology, BASF SE, Ludwigshafen am Rhein, Germany; <sup>2</sup>RWTH, University of Aachen, Aachen, Germany; <sup>3</sup>Technical University Dresden, Dresden, Germany; <sup>4</sup>Harlan Cytotest Cell Research GmbH, Roßdorf, Germany; <sup>5</sup>University of Saskatchewan, Saskatoon, SK, Canada.

Endocrine disruptor compounds (EDCs) are a group of natural or synthetic compounds that have the capacity to interact with the endocrine system of living organisms and consequently causes adverse health effects in an intact organism, or its progeny, or (sub)populations. Due to the impact that this interaction could have on human health, there is an increasing interest in assessing the risk of the exposure to EDCs. Currently, several *in vitro* and *in vivo* assays have been developed and few of them validated and regulatory accepted. For instance, the US EPA developed the Endocrine Disruptor Screening Program, which has been recently implemented. For the program a large number of experimental animals will be still use used even for testing some of the *in vitro* assays. Herein, we performed the inter-laboratory validation of two robust models that addresses agonistic and antagonist effect at the human hormone receptor, the YES (Yeast Estrogen Screen) and the YAS (Yeast Androgen Screen). Both assays are non-animal alternatives to the estrogen and androgen receptor binding assays proposed in the EDSP and OECD Conceptual Framework. The ring trial is the final experimental part of the validation process at the European Center for Validation of Alternative Methods (ECVAM). A set of 24 blinded compounds (7 estrogens and 6 androgens of diverse potency, 3 anti-estrogens, 3 anti-androgens and 5 negative compounds) have been tested in five different laboratories. The analysis of the first phase of this ring-trial already demonstrates a high reproducibility for both methods among the different participating laboratories.

**PS 2251 Comparison of the Manual and Quantitative High-Throughput Versions of the BG1Luc Estrogen Receptor Transactivation Test Method.**

P. Ceger<sup>1</sup>, W. Casey<sup>2</sup>, J. Strickland<sup>1</sup>, L. Rinckel<sup>1</sup> and W. Stokes<sup>2</sup>. <sup>1</sup>ILS, Inc., Research Triangle Park, NC; <sup>2</sup>NTP/NICEATM, NIEHS, Research Triangle Park, NC.

NICEATM conducted an international validation study of the BG1Luc estrogen receptor (ER) transactivation (TA) test method. The test method evaluation report was reviewed and the method accepted by U.S. regulatory agencies and the Organisation for Economic Co-operation and Development. In 2011, NICEATM nominated the BG1Luc ER TA to Tox21 to be evaluated for adaptation into a quantitative high throughput screening (qHTS) assay. The Tox21 collaboration, an effort by the National Toxicology Program, NIH Chemical Genomics Center, Environmental Protection Agency, and Food and Drug Administration, was formed to advance toxicity testing by shifting from traditional *in vivo* tests to *in vitro* methods. A major goal of Tox21 is to prioritize chemicals for in-depth toxicity testing. One method for prioritization is the use of qHTS assays using cell- and biochemical-based assays to construct concentration-response curves for thousands of chemicals. The Tox21 consortium adapted the BG1Luc ER TA manual method to a qHTS format, making it the first assay validated for regulatory use to be adapted to Tox21. Data from qHTS assays have been generated for approximately 10,000 chemicals in both the agonist and antagonist versions of the qHTS assay. Seventy-six chemicals had been tested in both the manual and qHTS methods. Data from both methods were used to evaluate the degree to which classifications of test chemicals in the BG1 manual and qHTS methods matched reference classifications (accuracy) and the degree to which chemical classifications were identical between the two methods (concordance). Except for a few discrepancies attributable to different test concentrations used in the two methods, the BG1Luc ER TA manual and qHTS methods produced almost identical results in terms of accuracy, with a high degree of concordance. Supported by ILS staff under NIEHS contract N01-ES-35504.

**PS 2252 Reconstructed Vaginal-Ectocervical and Endocervical Tissue Models for HSV-2, Chlamydia, and Gonorrhea Infections.**

T. Landry<sup>1</sup>, K. LaRosa<sup>1</sup>, J. Pudney<sup>2</sup>, R. Ingalls<sup>2</sup>, D. Anderson<sup>2</sup>, P. Hayden<sup>1</sup>, M. Klausner<sup>1</sup> and S. Aychunie<sup>1</sup>. <sup>1</sup>MatTek Corporation, Ashland, MA; <sup>2</sup>Boston Medical School, Boston, MA.

Despite extensive efforts, limited success has been achieved in developing tissue models for sexually transmitted infections (STIs) such as herpes simplex virus 2 (HSV-2), Chlamydia trachomatis (Ct), and Neisseria gonorrhea (Ng). We devel-

oped highly differentiated, normal human 3-dimensional (NHu-3D) vaginal-ectocervical (EpiVaginal™) and endocervical tissues models for STI infections. Immunohistochemistry and quantitative real time PCR were used to characterize the ectocervical tissues to monitor HSV-2 infection. Infection of the endocervical tissue model by the infectious elementary body (EB) of Ct was assessed by quantitative cultures. ELISA assays were used to quantify TNF- $\alpha$  release in response to Ng and Toll-Like Receptor (TLR) ligands. Results showed that the EpiVaginal tissue expresses nectin-1, a receptor for HSV-2, and infection experiments showed that the tissue model was infectable with HSV-2. Similar to the *in vivo* situation, infection of the vaginal-ectocervical tissue model with HSV-2 caused a separation of the epithelium from the lamina propria layer ("blister formation"). The results were confirmed by DNA PCR. The data from Ct infected endocervical tissues showed a cyclic level of EBs which were: 1) present at 12 hrs, representing bacteria that failed to be taken up by the cells, 2) not detectable at 24 hrs, all intracellular EBs might have been converted to the replicative reticular bodies (RB) and are therefore are not cultivatable, and 3) present at 40 hr, RBs have been converted back to EBs completing the first cycle. Furthermore, the reconstructed endocervical tissues respond to Ng infection and TLR ligands by secreting TNF- $\alpha$  into the culture medium. In conclusion, new *in vitro* reconstructed ectocervical and endocervical tissue models have been developed for HSV-2, Ct, and Ng infections. The models can be used to study the safety and efficacy of candidate therapeutics aimed at preventing or neutralizing HSV-2, Chlamydia, or gonorrhea infections.

**PS 2253 Combining Pathway-Based *In Vitro* Assays to Prioritize 1848 Environmental Chemicals for Estrogenic Potential.**

D. Rotroff<sup>1,2</sup>, D. Reif<sup>1</sup>, N. S. Sipes<sup>1</sup>, T. B. Knudsen<sup>1</sup>, P. Kothia<sup>1</sup>, M. Martin<sup>1</sup>, K. Houck<sup>1</sup> and R. Judson<sup>1</sup>. <sup>1</sup>NCCT, EPA, Research Triangle Park, NC; <sup>2</sup>Environmental Sciences and Engineering, University of North Carolina at Chapel Hill, Chapel Hill, NC.

There are thousands of environmental chemicals subject to regulatory decisions for endocrine disrupting potential. Due to the resources required to perform traditional toxicity tests, high-throughput screening (HTS) assays have emerged as a viable tool for chemical prioritization. The ToxCast and Tox21 programs have tested 1848 chemicals in a broad screening panel of 19 assays for estrogen receptor (ER) agonist and antagonist activity. These assays screen for ER activity by profiling effects on ligand binding or cellular changes across a diverse array of assay types (e.g. receptor binding, protein complementation, transcriptional activation, and cell growth) and cell types (T47D, BG1, HEK293T, CHO-K1, HeLa). The protein complementation assays were run with and without S9 to determine metabolic potential. Assays were assigned to assay-groups to distinguish ER mechanisms (i.e. agonism, antagonism, metabolic activation/deactivation, ER $\alpha$ /ER $\beta$  activation). Concentration response data for each chemical was normalized to 17 $\beta$ -estradiol, scaled for differences in assay sensitivity, and fit to a Hill model. A composite concentration response curve for each chemical-group combination was created from curve fitting parameters to develop a weight-of-evidence metric for estrogenicity. Composite curve efficacy, potency, and "goodness of fit" were used to rank chemicals and distinguish putative partial agonists from discordant assay results. In a separate analysis, uterotrophic assay results (39 chemicals) were used to characterize composite curve predictivity using logistic regression. Overall, of the original 1848 chemicals 22 were active in at least 13 HTS ER agonist assays, including known ER agonists, 4-nonylphenol, and DES. 347 chemicals were active in at least 3 HTS ER agonist assays, indicating the need for assays measuring multiple biologically plausible ER mechanisms in order to confidently prioritize chemicals for estrogenicity. This abstract does not necessarily reflect Agency policy.

**PS 2254 Identification of Compounds That Activate Aryl Hydrocarbon Receptor Using a qHTS Platform.**

N. R. Miller<sup>1</sup>, R. Huang<sup>1</sup>, K. Houck<sup>2</sup>, M. S. Denison<sup>3</sup> and M. Xia<sup>1</sup>. <sup>1</sup>NCGC, NIH, Rockville, MD; <sup>2</sup>EPA, Research Triangle Park, NC; <sup>3</sup>Environmental Toxicology, University of California, Davis, Davis, CA.

The basic helix-loop-helix perARNT-SIM (bHLH-PAS) superfamily of transcription factors plays an important role in mediating the biological response to endogenous and xenobiotic small molecules. The Aryl hydrocarbon receptor (AhR) is a prominent member of the bHLH-PAS, and is crucial to adaptive responses to environmental changes. AhR mediates cellular responses to environmental pollutants such as aromatic hydrocarbons through induction of phase I and II enzymes but also crosstalks with other nuclear receptor signaling pathways. To identify potential AhR ligands as part of the Tox21 collaboration, we have optimized and miniaturized a cell-based AhR luciferase reporter gene assay in the recombinant human HepG2 cell line HG2L7.5c1 into a 1536-well plate format. We have validated this assay by screening a library of 1280 pharmacologically active compounds (LOPAC) plus 88 Tox21 chemicals in triplicate using a quantitative HTS (qHTS) platform.

From the primary screen, we have identified a group of relatively potent compounds including known AhR agonist indirubin-3'-oxime; CGS-15943, an adenosine receptor antagonist; the cyclin-dependent kinase inhibitor kenpaullone; the amiloride analogue phenamil; and the gastric proton pump inhibitor omeprazole. Validation of the cell-based assay on our integrated robotics system gave a signal to background ratio of 5 and average Z' factors of 0.4, that indicates this assay is suitable for qHTS of the Tox21 10K library. These findings support the utility of a cell-based AhR luciferase assay system for the high-throughput detection of compounds activating the AhR signal transduction pathway. Supported by EPA Interagency Agreement Y3-HG-7026-03.

**PS 2255 Comet and Nucleotide Postlabeling Results in the Chicken Egg Genotoxicity Assay.**

A. M. Jeffrey<sup>1</sup>, U. Deschl<sup>2</sup>, J. Duan<sup>1</sup>, K. D. Brunnemann<sup>1</sup>, E. Vock<sup>2</sup>, M. J. Iatropoulos<sup>1</sup> and G. M. Williams<sup>1</sup>. <sup>1</sup>Department of Pathology, New York Medical College, Valhalla, NY; <sup>2</sup>Boehringer Ingelheim Pharma GmbH & Co. KG, Biberach, Germany.

For the chicken egg genotoxicity assay, an *in vitro* alternative model for assessing genotoxicity, we used white leghorn chicken (*Gallus gallus*) egg fetal livers before full development of the nervous system. Injections were made on days 9, 10 and 11, the last 3 hours before termination. Livers were harvested for the COMET assay for DNA strand breaks and nucleotide postlabeling for DNA adducts. To deliver test substances, a variety of vehicles were evaluated, covering the range (from hydrophilic to hydrophobic) of solubility, using the endpoint of viability of the embryo-fetus. The following suitable vehicles were selected, i.e., 50 µl of deionized water, 50 µl of 0.5% aqueous methylcellulose, and 50 µl 20% Solutol HS15 for hydrophilic, amphiphilic, and hydrophobic substances, respectively. Test substances were injected with a 1 ml plastic BD syringe using a 0.4 mm x 13 mm needle. Following the injection into the air sac, the eggs were sealed with paper tape. Test compounds included diethylnitrosamine (hydrophylic) and 2-acetylaminofluorene (hydrophobic). The eggs were incubated and maintained at 37° ± 0.5° C and 60% ± 5% relative humidity. On day 11, the shells of viable eggs were opened at the blunt end, and the allantochorionic membrane was retracted to allow access to the entire anterior (visceral) aspect of the chicken fetus via the yolk sac. Fetal weights, were recorded after removal of the surrounding excess yolk. The abdominal cavity was opened and the entire liver was removed and weighed. Diethylnitrosamine (0.25 - 4.0 mg cumulative dose per egg) and 2-acetylaminofluorene (0.1-0.6 mg) were tested over a dose range and subsequent alkaline COMET assays were conducted on isolated liver cells. Both compounds gave a positive dose response with plateaus occurring at the higher doses. In addition, 2-acetylaminofluorene was positive in the nucleotide postlabeling assay and showed patterns of DNA adducts similar to those previously observed in turkey eggs and rats.

**PS 2256 Development of Hazard Evaluation Support System (HESS) and the Attached Database (HESS DB) for Repeated-Dose Toxicity of Chemical Substances.**

T. Yamada<sup>1</sup>, T. Abe<sup>1</sup>, R. Hasegawa<sup>1</sup>, Y. Sakuratani<sup>1</sup>, J. Yamada<sup>1</sup>, T. Yamashita<sup>2</sup>, Y. Yamazoe<sup>3</sup>, O. Mekenyan<sup>4</sup>, A. Hirose<sup>5</sup> and M. Hayashi<sup>6</sup>. <sup>1</sup>Chemical Management Center, National Institute of Technology and Evaluation, Tokyo, Japan; <sup>2</sup>BioIT Business Development Office, Fujitsu Limited, Chiba, Japan; <sup>3</sup>Graduate School of Pharmaceutical Sciences, Tohoku University, Sendai, Japan; <sup>4</sup>Laboratory of Mathematical Chemistry, University "Prof. Assen Zlatarov" Bourgas, Bourgas, Bulgaria; <sup>5</sup>Biological Safety Research Center, National Institute of Health Sciences, Tokyo, Japan; <sup>6</sup>BioSafety Research Center, Iwata, Japan.

Repeated-dose toxicity (RDT) is one of the key regulatory endpoints in the hazard assessment of chemical substances. The data is nationally and internationally utilized for the chemical management. On the other hand, reduced animal testing is desired for economic and animal welfare reasons. Herein, we developed Hazard Evaluation Support System database (HESS DB). HESS DB is a new toxicity database of RDT studies for about 500 chemicals, most of which have been conducted in accordance with Good Laboratory Practice Principles under Japanese Chemical Substance Control Law. Moreover, the DB includes available reference information on Absorption, Distribution, Metabolism, and Excretion (ADME) and toxicological mechanism for some of those chemicals. It is useful for checking the availability of toxicity test data and for setting the animal test conditions with related information of structural analogs. Additionally, chemicals showing similar histopathological changes can be efficiently searched with the DB. The DB is linked to simultaneously developed Hazard Evaluation Support System (HESS), which is compatible with OECD QSAR Toolbox and has a supportive function to group structural analogs with toxicity data. Combination use of HESS and HESS DB supports to perform category approach to predicting the primary toxicity of

untested chemicals in a transparent and interpretable manner. HESS and HESS DB are freely provided in the website of NITE (<http://www.safe.nite.go.jp/english/kasinn/qsar/hess-e.html>).

**PS 2257 Mitochondrial Bioenergetics and Drug-Induced Toxicity in a Panel of Mouse Embryonic Fibroblasts with Mitochondrial DNA Single Nucleotide Polymorphisms.**

C. V. Pereira<sup>1</sup>, P. J. Oliveira<sup>1</sup>, Y. Will<sup>2</sup> and S. Nadanaciva<sup>2</sup>. <sup>1</sup>CNC- Center for Neuroscience and Cell Biology, University of Coimbra, Coimbra, Portugal; <sup>2</sup>Pfizer Inc, Groton, CT.

Mitochondrial DNA (mtDNA) variations including single nucleotide polymorphisms (SNPs) have been proposed to be involved in idiosyncratic drug reactions. However, current *in vitro* and *in vivo* models lack the genetic diversity seen in the human population. Our hypothesis is that different cell strains with distinct mtDNA SNPs may have different mitochondrial bioenergetic profiles and may therefore vary in their response to drug-induced toxicity. Therefore, we used an *in vitro* system composed of four strains of mouse embryonic fibroblasts (MEFs) with mtDNA polymorphisms. We sequenced mtDNA from embryonic fibroblasts isolated from four mouse strains, C57BL/6J, MOLF/Eij, CZECHII/Eij and PERA/Eij, with the latter two being sequenced for the first time. The bioenergetic profile of the four strains of MEFs was investigated at both passage 3 and 10. Our results showed that there were clear differences among the four strains of MEFs at both passages, with CZECHII/Eij having a lower mitochondrial robustness when compared to C57BL/6J, followed by MOLF/Eij and PERA/Eij. Seven drugs (nefazodone, ketoconazole, tolcapone, flutamide, tamoxifen, imipramine and troglitazone) known to impair mitochondrial function were tested for their effect on the ATP content of the four strains of MEFs in both glucose- and galactose-containing media. Our results showed that there were strain-dependent differences in the response to some of the drugs. We propose that this model is a useful starting point to study compounds that may cause mitochondrial off-target toxicity in early stages of drug development, thus decreasing the number of experimental animals used.

**PS 2258 Assessment of Drug-Induced Inhibition of Fatty Acid Oxidation in Intact Cells.**

S. Nadanaciva, L. Qiu and Y. Will. Pfizer Inc, Groton, CT.

Fatty acid oxidation in mitochondria is an important metabolic pathway for energy generation in the heart and in organs such as the liver and muscle during fasting. Drug-induced inhibition of fatty acid oxidation in the liver can lead to microvesicular steatosis or macrovesicular steatosis and eventually to liver failure. Moreover, since the liver is the supplier of energy in the form of glucose (via gluconeogenesis) and ketone bodies to other organs, inhibition of fatty acid oxidation in the liver can lead to a deficiency in the energy supply for extra-hepatic tissues. Fatty acid oxidation in intact cells has traditionally been assayed by measuring the production of tritiated water from labeled fatty acids such as tritiated palmitate. In order to circumvent the use of radio-labeled material, we assessed fatty acid oxidation in intact cells by measuring the effect of palmitate, a long-chain fatty acid, on cellular oxygen consumption in an XF96 extracellular flux analyzer. We observed an increase in the oxygen consumption of cells such as c2c12 mouse myoblasts, HepG2 cells (a liver-derived carcinoma cell line) and hepatocytes upon palmitate addition. Etomoxir, an inhibitor of carnitine palmitoyltransferase-1 (an enzyme catalyzing the rate-limiting step of long-chain fatty acid entry into mitochondria) inhibited respiration. In a proof-of-concept study, we assessed the effect of drugs (amiodarone, tamoxifen, tianeptine and perhexiline) that are known to inhibit mitochondrial fatty acid oxidation. Our results showed that the measurement of drug-induced changes in cellular oxygen consumption in the presence of palmitate is a convenient method by which to assess inhibition of fatty acid oxidation in cells.

**PS 2259 Cytotoxicity and Genotoxicity of 2, 6-dichloro-3-methyl-1, 4-benzoquinone (DCMBQ) Involves Reactive Oxygen Species Production *In Vitro*.**

C. F. McGuigan, X. Li and X. Le. Division of Analytical & Environmental Toxicology, University of Alberta, Edmonton, AB, Canada.

Halobenzoquinones (HBQs) were recently identified as drinking water disinfection byproducts. Computational toxicity predictions have identified the HBQ 2,6-dichloro-3-methyl-1,4-benzoquinone (DCMBQ) as a potential carcinogen; however, little toxicity information is available. The normal BJ human fibroblast cell line (CRL-2522) was utilized to perform *in vitro* assays to examine the cytotoxicity, genotoxicity, and reactive oxygen species production capability of DCMBQ. Real-time cell electronic sensing (RT-CES) showed a concentration-dependent decrease

in cell index, indicative of cytotoxicity, after exposure to 12.5-50  $\mu$ M DCMBQ over a 72-hour period. Using the alkaline comet assay, a significant genotoxic effect (one-way ANOVA,  $p < 0.05$ ), indicated by increased tail moment, was observed in cells exposed to  $\geq 20 \mu$ M DCMBQ for 24 hours. To further determine the mechanism of toxicity, reactive oxygen species (ROS) production was measured using the fluorophore DCFDA (2',7'-dichlorofluorescein diacetate) in cells exposed to DCMBQ (5-50  $\mu$ M) for 2-72 hours. Significant time and concentration-dependent increases in ROS were observed (two-way ANOVA,  $p < 0.05$ ) for  $\geq 15 \mu$ M DCMBQ at 24 hours of exposure but as early as 4 hours of exposure for 50  $\mu$ M DCMBQ. This effect was significantly reduced by the addition of N-acetylcysteine (NAC), a ROS scavenger. Likewise, simultaneous addition of NAC to cells treated with highly genotoxic concentrations of DCMBQ in the alkaline comet assay reduced tail moment values to those comparable with untreated control groups. Based on these results, we conclude that DCMBQ is cytotoxic and genotoxic under these experimental conditions, and these effects are due at least in part to ROS production. As DCMBQ has been detected in finished drinking water samples, additional testing is urgently required to determine potential effects on human health.

## PS 2260 Intra- and Interlaboratory Validation Studies on Reactive Oxygen Species Assay for Photosafety Evaluation of Pharmaceuticals.

T. Toda<sup>1</sup>, S. Onoue<sup>2</sup>, Y. Seto<sup>2</sup>, H. Takagi<sup>3</sup>, N. Osaki<sup>3</sup>, S. Kawakami<sup>4</sup>, Y. Matsumoto<sup>5</sup>, Y. Iwase<sup>6</sup>, T. Yamamoto<sup>6</sup>, S. Wakuri<sup>7</sup>, K. Hosoi<sup>8</sup>, K. Nakamura<sup>1</sup> and H. Kojima<sup>9</sup>. <sup>1</sup>Shionogi & Co., Ltd., Osaka/Tokyo, Japan; <sup>2</sup>University of Shizuoka, Shizuoka, Japan; <sup>3</sup>Taisho Pharmaceutical Co., Ltd., Saitama, Japan; <sup>4</sup>Asahi Kasei Pharma Corporation, Shizuoka, Japan; <sup>5</sup>Aska Pharmaceutical Co., Ltd., Kanagawa, Japan; <sup>6</sup>Mitsubishi Tanabe Pharma Corporation, Saitama/Chiba, Japan; <sup>7</sup>Hatano Research Institute, Food and Drug Safety Center, Kanagawa, Japan; <sup>8</sup>Santen Pharmaceutical Co., Ltd., Nara, Japan; <sup>9</sup>National Institute of Health Sciences, Tokyo, Japan.

A reactive oxygen species (ROS) assay was previously developed for photosafety evaluation of pharmaceuticals. Although outcomes from the previous multicenter validation study were indicative of satisfactory transferability, reproducibility, and predictive capacity of the ROS assay using Atlas Suntest CPS/CPS plus solar simulators, the feasibility of different solar simulators for the ROS assay has never been elucidated. Herein, in 4 participating laboratories, 2 standards and 42 coded chemicals, including 23 phototoxins and 19 non-phototoxic drugs/chemicals, were assessed by the ROS assay using Seric SXL-2500V2 solar simulators with the aim of evaluating the compatibility of different solar simulators for the ROS assay. In the ROS assay on quinine (200  $\mu$ M), a typical phototoxic drug, the intra- and inter-day precisions (coefficient of variation; CV) were found to be 1.7–9.4% and 2.7–6.9%, respectively. The inter-laboratory CV for quinine averaged 13.2% for singlet oxygen and 7.1% for superoxide. The ROS assay on 42 coded chemicals (200  $\mu$ M) provided no false negative predictions as compared to the in vitro/in vivo phototoxicity, although several false positives appeared. These results were regarded as a convincing demonstration that the ROS assay is compatible with, and can be adapted to, other available suitable solar simulators without losing performance.

## PS 2261 Investigating the Role of Mitochondrial Dysfunction in Zoniporide Toxicity.

P. Rana, S. Rachel and Y. Will. *Compound Safety Prediction, Pfizer Global Research & Development, Groton, CT.*

Zoniporide, an inhibitor of the Na<sup>+</sup>-H<sup>+</sup> exchanger-1 was developed for the reduction of myocardial ischemic injury in acute coronary syndromes, in the high-risk surgical setting, and secondary for prevention in patients with ischemic diseases. A 28-days intravenous infusion rat study revealed target organ toxicity of the sciatic nerve, spinal cord, and stomach injury (Pettersen et al., 2008). Due to insufficient efficacy, zoniporide was discontinued after the phase 2 clinical trial. We have previously reported that zoniporide seems to affect mitochondrial function (Rana et al., 2011) here, we expand on our studies by investigating further mechanisms that could lead to this mitochondrial disturbance.

We tested zoniporide in rat liver mitochondria for its inhibition of mitochondrial respiration and conducted mitochondrial swelling experiments to study possible mitochondrial permeability transition pore (MPT) effects of zoniporide. We further tested this compound in H9c2 cells growing in glucose and galactose media and measured ATP depletion and Caspase 3/7 levels. Finally, we tested zoniporide on the flux analyzer and measured immediate effect on mitochondrial respiration and glycolytic rates. In the cell based assays, we tested zoniporide alone and in the presence of Cyclosporine A (CSA), which has been known to close the MPT. We observed that zoniporide did not inhibit mitochondrial respiration in rat liver isolated mitochondria. However, at 24 h, there was more than a 3-fold difference between glucose/galactose IC<sub>50</sub>, suggesting an effect on a mitochondrial target.

This was further confirmed using a flux analyzer, where there was decrease in oxygen consumption rate (OCR) which was accompanied by increase in extra cellular acidification rate (ECAR) suggesting that cell injury is primarily mitochondria targeted as cells switches respiration from mitochondrial OXPHOS to glycolysis. Co-incubation with CSA had a rescue effect on Caspase3/7 levels in galactose growing cells. In summary, we believe that zoniporide induced cell injury includes primarily mitochondria by causing MPT.

## PS 2262 Validation of an HTS-Amenable Assay to Detect Drug-Induced Mitochondrial Toxicity.

R. Swiss<sup>1</sup>, A. L. Niles<sup>2</sup>, J. J. Cali<sup>2</sup> and Y. Will<sup>1</sup>. <sup>1</sup>Compound Safety Prediction, Pfizer Global Research & Development, Groton, CT; <sup>2</sup>Promega, Madison, WI.

Drug-induced mitochondrial dysfunction has been shown to contribute to organ toxicity and late stage attrition. Therefore, testing for drug-induced mitochondrial dysfunction pre-clinically is vitally important and has the ability to greatly impact the success of a potential drug candidate. Several assays have been developed but are hampered for high-throughput screening because they either require special reagents, isolated mitochondria or specialized equipment.

Here we validate in 384-well format, a dual parameter assay that measures both cytotoxicity and mitochondrial toxicity simultaneously during very short exposure durations using standard detection methods. In this assay, cytotoxicity is measured by evaluating cell membrane integrity via the presence or absence of a distinct protease activity associated with necrosis.

For our initial evaluation, K562 cells were grown in both glucose-supplemented media and galactose-supplemented media and were tested in parallel. The objective was to see how many mitochondrial toxicants this cell-based assay would be able to detect.

We validated the assay using the classical mitochondrial toxicants antimycin A, CCCP and, oligomycin, as well as two drugs known to have mitochondrial liabilities (nefazodone, and flutamide) as well as the non-specific detergent digitonin, in a 384-well plate format with a 2 hour exposure.

We determined the assay to have excellent reproducibility with less than 3 fold differences between IC<sub>50</sub> values form day to day. Once the assay was validated, we screened a set of 75 commercial compounds that included compounds known to cause different organ toxicities and with known or unknown mitochondrial liabilities. Our screening data identified that compounds could be sorted into 7 different categories based on the calculated IC<sub>50</sub>s of each condition, the cytotoxicity measurement in both glucose and galactose-grown cells and the ATP measurement in both media conditions. Our results are currently evaluated for their sensitivity and specificity in comparison to other existing assays.

## PS 2263 Establishing a Link between Redox Cycling and Cell Death for Quinone and Flavin Chemotypes.

L. Jones, P. Rana, R. Swiss, R. Naven and Y. Will. *Compound Safety Prediction, Pfizer Global Research & Development, Groton, CT.*

Oxidative stress is one of the major mechanisms of drug induced toxicity. One electron reduction of oxidants generates reactive oxygen species (ROS) via redox cycling. In biological systems, the flavo enzymes mediate the transfer of electrons to the quinone by reducing it to the semiquinone. Recently, we evaluated flavin analogues for their ability to redox cycle and tried to establish their association to toxicity. We investigated menadione (a quinone analogue) and toxoflavin (a flavin analogue) for its attribution to its redox cycling activity that leads to oxidative stress which eventually leads to cell death.

In our proof of concept study, we investigated the redox cycling capability of menadione and toxoflavin by utilizing a biochemical assay that measures the H<sub>2</sub>O<sub>2</sub> produced through redox cycling of compounds. Next, we tested these compounds in THLE cells using high content imaging to assess the production of ROS using dihydro ethidium (DHE). In addition, we measured glutathione and ATP levels in THLE cells. Next, we wanted to know if we could rescue the detrimental effects of redox cycling on cell health, by incubation with two different antioxidants. One of them was catalase, which effectively dismantles hydrogen peroxide with water as a byproduct, the other was N-acetyl-cysteine (NAC), which minimizes oxidative stress.

Here, we report that both, menadione and toxoflavin redox cycle and produce hydrogen peroxide (ROS), both in the biochemical assay as well as in the cell based assay. Glutathione levels were also depleted with both of these compounds. Furthermore, the ROS formation and glutathione depletion lead to cell injury that is measured by ATP depletion. Catalase was able to dismantle H<sub>2</sub>O<sub>2</sub> in the biochemical assay. In the cell based assay, ROS, glutathione and ATP effects were recovered in the presence of NAC. In summary, we established the involvement of redox cycling of quinones and flavin chemotypes to toxicity in THLE cells

**PS 2264 Identification and Characterization of Potential Mitochondrial Liabilities Using a Multitiered *In Vitro* Rat Primary Hepatocyte Screening Paradigm.**

D. D. Baker, B. D. Jeffy and M. A. Breider. *Exploratory Toxicology, Celgene, Inc., San Diego, CA.*

A tier I rat primary hepatocyte multi-endpoint cytotoxicity assay (MECA) system is an effective tool to assess and rank order compounds on predicted potential to induce toxicity in repeat-dose *in vivo* rat toxicology studies. Our MECA system utilizes three primary biochemical endpoint assays: an ATP assay for cell viability, a lactate dehydrogenase (LDH) assay for membrane integrity and a WST-1 assay for mitochondrial function. A positive signal in the WST-1 assay should be further characterized with a Tier II specific assessment of sub-mitochondrial toxicity. To determine potential mitochondrial liabilities, our Tier II mechanistic assessment includes a JC-1 assay for Mitochondrial Pore Transition (MPT) status, a 2',7'-dichlorofluorescein diacetate (DCFDA) assay for reactive oxygen species (ROS) production, a Caspase 3/7 assay for apoptosis, and a Seahorse XF24™ assay system to determine functional oxidative phosphorylation (mitochondrial respiration). HMG-CoA reductase inhibitors (statins) are compounds that lower cholesterol and reduce cardiovascular disease. There has been increasing evidence that some statins may affect mitochondrial function, leading to adverse effects such as myopathy or rhabdomyolysis. We investigated the effects of multiple statins, including simvastatin, on various mitochondrial functional endpoints. Tier I screening of the statins in primary rat hepatocytes identified a general mitochondrial liability with a 50% decrease in WST-1 throughout the concentration range. In Tier II assays demonstrated that simvastatin treatment induced hepatocellular apoptosis at high concentrations and lowered both basal mitochondrial respiration and maximal respiration compared to control at non-cytotoxic concentrations. These data corroborate the decreased WST-1 reading and suggesting impaired electron transport chain function. A multi-tiered approach is essential to fully characterize potential mitochondrial dysfunction and add predictive value to *in vitro* toxicology screens in early phases of drug discovery.

**PS 2265 Impact of Exposure Profile on Toxic Response Using Hepatocytes (HepaRG) Cocultured with Intestinal Cells (Caco-2).**

K. Yuki, N. Ikeda, T. Kasamatsu and N. Nishiyama. *Kao Corporation, Haga-gun Tochigi, Japan.* Sponsor: *J. Avalos.*

[Background, Purpose] To develop an alternative method to *in vivo* toxicity studies, a general approach would be to extrapolate key markers identified in the early stage of the *in vivo* toxic response into an *in vitro* system. Under *in vivo* conditions, a test substance is absorbed, distributed, and/or metabolized before reaching target cells, whereas in an *in vitro* system, compounds are directly exposed to target cells and metabolic activation might or might not be involved. To address the impact of the significant difference of chemical exposure profiles between *in vivo* and *in vitro* systems, we have developed a co-culture system consisting of HepaRG cells and Caco-2 cells as a model for hepatocytes, where the system simulates intestinal absorption and liver metabolism processes.

[Methods] The toxic responses of the co-culture system toward four chemicals (acetaminophen, carbon tetrachloride, amiodarone, and EGCg) reported to have a hepatotoxic effect were compared to the single culture HepaRG system.

[Results] Co-culturing with Caco-2 cells increased ALB and CYP expression in HepaRG cells. Although treatment with each test chemical changed LDH and GSH activity in both culture systems, dosages of EGCg were very different for similar toxic effects. Monitoring of EGCg concentration and GSH activity revealed a two-fold lower EGCg Cmax, a 10-fold higher AUC (0-24), and reduction of GSH activity after 12 hr for the co-culture system.

[Discussion, Conclusion] This study demonstrated that the exposure profile of test substances may affect the toxic response of cultured cells. It is important to develop *in vitro* models that reflect the *in vivo* exposure conditions.

**PS 2266 Combinatorial High-Throughput Gene Transfection on a Chip for Metabolism-Induced Toxicity Screening.**

M. Lee<sup>4</sup>, S. Kwon<sup>1</sup>, D. Lee<sup>2</sup>, D. Shah<sup>1</sup>, B. Ku<sup>2</sup>, D. S. Clark<sup>3</sup> and J. S. Dordick<sup>1</sup>. <sup>1</sup>Department of Chemical and Biological Engineering, Rensselaer Polytechnic Institute, Troy, NY; <sup>2</sup>Central R & D Institute, Samsung Electro-Mechanics Co., Suwon, Republic of Korea; <sup>3</sup>Department of Chemical and Biomolecular Engineering, University of California Berkeley, Berkeley, CA; <sup>4</sup>Solidus Biosciences, Inc., San Francisco, CA.

Variation in metabolic enzyme expression among segments of the human population may cause deviations from the expected pharmacokinetic profile of a drug, resulting in idiosyncratic toxicity or a lack of efficacy. Cell lines that stably express

metabolic enzymes are emerging tools for prediction of these rare clinical events; however, it is difficult to create and maintain a library of stable cell lines that mimics the diversity of metabolic profiles. To address this need, we have developed a "Transfected Enzyme and Metabolism Chip" (or TeamChip) for high-throughput analysis of systematic drug metabolism and toxicology. The TeamChip is prepared by infecting an array of miniaturized 3-D cell cultures on a micropillar chip with varying concentrations of recombinant adenoviruses carrying genes for different metabolic enzymes in a microwell chip, which generates an array of cell cultures with differentiated metabolizing capabilities. As a proof of concept, we have demonstrated the controlled expression of individual drug-metabolizing enzymes (CYP3A4, 2D6, 2C9, 1A2, 2E1, and UGT1A4) in THLE-2 human liver cell line on the chip by altering the multiplicity of infection of the various recombinant adenoviruses. The expression levels of the metabolizing enzymes on the chip were determined by in-cell immunofluorescence assays and the activity of the expressed enzymes in THLE-2 cells were tested with fluorogenic dyes. By printing the 6 recombinant adenoviruses into the microwell chip in a combinatorial way, we were able to achieve 144 combinations of multiple metabolic enzymes expressed in THLE-2 cells on a single TeamChip. Finally, 6 model compounds that were shown to be hepatotoxic, in some cases idiosyncratically and withdrawn from the market, were tested to simulate enzyme-specific hepatotoxicity.

**PS 2267 Validation of High-Throughput and High-Content (HT/HC) Assays to Support 21st Century Toxicity Evaluations.**

R. Becker<sup>1</sup>, G. Patlewicz<sup>2</sup>, T. Simon<sup>3</sup>, K. Goyak<sup>4</sup>, R. Phillips<sup>4</sup>, J. Rowlands<sup>5</sup> and S. Seidel<sup>6</sup>. <sup>1</sup>American Chemistry Council, Washington DC; <sup>2</sup>DuPont Haskell Global Centers for Health and Environmental Sciences, Newark, DE; <sup>3</sup>Ted Simon LLC, Winston, GA; <sup>4</sup>ExxonMobil Biomedical Sciences Inc., Annandale, NJ; <sup>5</sup>The Dow Chemical Company, Midland, MI; <sup>6</sup>Dow Corning Corporation, Midland, MI.

Advances in high throughput and high content (HT/HC) methods have the potential to improve the efficiency and the effectiveness of toxicity evaluations and risk assessments. However, scientific confidence in these methods and their prediction models must be formally established before use in regulatory decision making. Traditional validation approaches that define relevance, reliability, sensitivity and specificity may not be readily applied since a number of these methods are proprietary; HT/HC methods may use one of a kind robotics; although run individually, these assays are likely to be used as a group or battery for decision making and, HT/HC methods are not exact replacements for *in vivo* testing. Building on the frameworks developed in the 2010 Institute of Medicine Report on Biomarkers and the OECD 2007 Report on (Q)SAR Validation, we present frameworks that can be adapted to address the validation challenges of HT/HC methods. These require explicit specification of context and purpose of use such that scientific confidence can be defined to meet different applications (e.g., a lesser degree of confidence may be acceptable for priority setting compared to that required to support hazard characterization, or classification/labeling). We recommend that a specific validation strategy be developed and implemented for HT/HC assays and their prediction models, focused on the specific biological response of interest. We discuss how anchoring the assays and their prediction models to Adverse Outcome Pathways should facilitate the interpretation of results and support scientifically defensible fit-for-purpose applications. To build scientific confidence, data should be publicly disseminated and assay results and prediction models should be subjected to independent scientific peer review.

**PS 2268 Performance Evaluation of Publicly Available QSAR Software Platforms for Toxicology Endpoints: Case Study Involving VEGA, OPENTOX, and OECD QSAR Toolbox.**

S. Bobst<sup>1</sup> and M. Vracko<sup>2</sup>. <sup>1</sup>Product Safety, Nexeo Solutions LLC, The Woodlands, TX; <sup>2</sup>Laboratory of Chemometrics, National Institute of Chemistry, Ljubljana, Slovenia.

Several Quantitative Structure Activity Relationship (QSAR) software methods are available for public use. QSAR methods are gaining greater acceptance as an alternative to animal testing, to fill data gaps for hazard communications (e.g. the U.N. Globally Harmonized System for chemical labeling) and data submissions for regulatory requirements (e.g. the European chemical regulation known as REACH). QSAR software models are constructed using data systems involving molecular descriptors, specific to toxic endpoints, and reference databases comparing known data references, with unknown data points. VEGA, OPENTOX, and OECD QSAR Toolbox are three software platforms widely known and publicly available. The analysis displays the performance of the software programs with a poly aromatic hydrocarbon (PAH) test data set. Variation in software performance, including specificity (false negatives), sensitivity (false positives), and strength of prediction (regression) is evaluated against the test case data. The comparative analysis provides insight into the criteria and requirements for determining which software

platform maybe most appropriate for specific endpoints for unique chemical categories. Such analysis assists industry stakeholders in planning the use of QSAR models for hazard communication, regulatory compliance, and sustainable life cycle management.

**PS 2269 Use of a Cell-Based Assay to Monitor the Stability of the Tox21 10K Compound Library.**

R. Huang<sup>1</sup>, J. Zhao<sup>1</sup>, M. Xia<sup>1</sup>, K. L. Witt<sup>2</sup>, K. Houck<sup>3</sup>, R. R. Tice<sup>3</sup>, D. Dix<sup>3</sup> and C. P. Austin<sup>1</sup>. <sup>1</sup>NCATS/NIH, Rockville, MD; <sup>2</sup>NTP, NIEHS/NIH, Research Triangle Park, NC; <sup>3</sup>NCCT, EPA, Research Triangle Park, NC.

In Tox21 Phase II, a collection of ~10K compounds ([http://www.epa.gov/ncct/dstox/sdf\\_tox21s.html](http://www.epa.gov/ncct/dstox/sdf_tox21s.html)) is being screened against a battery of nuclear receptor and stress response pathway assays. Knowing the identity and purity of each substance and its stability in dimethylsulfoxide (DMSO), the solvent of choice, is critical to the interpretation of assay results. In the screening protocol, a copy of the 10K library, maintained in the Tox21 robotics facility at room temperature (RT), is used in multiple assays over a 4-month period. In addition to an ongoing analytical analysis on the library at time 0 and 4 months, the complete results of which will not be available until mid 2013, we evaluated compound stability using the p53-beta lactamase reporter gene (p53-BLA) assay to monitor biological activity. This assay was selected because it is a highly reproducible (>95%) cell-based assay with a relatively high hit rate (16%). The library was tested 1 day, 2 weeks, 2, 4, and 6 months after being placed on the robot. The number of compounds that showed a significant change in activity (loss or gain) as an indication of compound degradation at each time point compared to the freshly thawed library (day one) reached a plateau of 1.7% of the 10K library at approximately 4 months. Most of the change in activity appeared to occur within the first 2 weeks and included compounds such as dinoterb, bithionol and captafol. Results show that the majority of compounds are relatively stable at RT for up to 6 months, with the caveat that the compounds inactive against p53 (i.e., the majority of the library) were not captured by this method. This study is the first attempt to use a cell-based assay to systematically monitor the stability of a large-scale, environmentally focused compound library. The results can be used to determine when to replace the library plates, and they also serve to validate the quality of the Tox21 production screen process – from compound storage and handling to robotic operations and assay performance.

**PS 2270 Application of Metabolomics *In Vitro* for Identification of Toxicological Modes of Action.**

T. Ramirez<sup>1</sup>, N. Bordag<sup>2</sup>, W. Mellert<sup>1</sup>, H. G. Kamp<sup>1</sup>, T. Walk<sup>2</sup>, R. Looser<sup>2</sup> and B. van Ravenzwaay<sup>1</sup>. <sup>1</sup>Experimental Toxicology and Ecology, BASF SE, Ludwigshafen am Rhein, Germany; <sup>2</sup>metanomics, berlin, Germany.

The demand for the use of alternatives to animal testing has increased in the last years, not only due to new regulations, such as REACH or the 7th Amendment of the cosmetic directive, but also because they can be used for toxicological screening during compound development. The use of state-of-the-art technologies combined with cellular *in vitro* models represents a new opportunity to obtain comprehensive information about the toxicological mode of action of compounds being in commerce and most importantly for compounds under development. Metabolomics is a versatile technology with multiple potential applications in safety profiling and has been considered as the alternative to elucidate the molecular basis of toxicity. Moreover, the combination of *in vitro* systems coped to this technology may on one hand enable the acquisition of quantitative information about the multi-parametric metabolic response of the cellular systems in normal and patho-physiological conditions and on the other hand, it represents a major step towards non-animal alternatives in toxicology. Herein, we report on the extracellular metabolic profile (secretome) of HepG2 cells after the exposure to chemicals compounds with well-known toxic profile and differ modes of action. The obtained metabolic fingerprint allowed for a clear distinction between the tested toxicological modes of action. These results may majorly contribute to the future elucidation of the biochemical events underlining the toxic modes of actions of chemical compounds without animal testing.

**PS 2271 Functional Genomics Approach in Yeast and the DT40 Avian Cell Line Identify Conserved Mechanisms of Trichloroethylene Toxicity.**

V. De La Rosa and C. Vulpe. University of California, Berkeley, Berkeley, CA.

Trichloroethylene (TCE) is an industrial solvent and a common drinking water contaminate. Previous studies have identified the TCE metabolite DCVC as responsible for increased kidney toxicity and renal cancer, yet the molecular events

mediating renal toxicity an cancer remain controversial. Our studies in yeast provide a foundation for identifying potential mechanisms of TCE renal toxicity and to establish an alternative model for identifying mechanisms of toxicity in humans. A functional genomics approach in yeast identified DNA damage and repair pathways important in response to DCVC exposure. Specifically, mutagenic translesion synthesis (TLS) and nucleotide excision repair (NER) pathways were found to play important roles in DCVC toxicity. This data suggests DCVC may cause direct DNA damage that elicits a mutagenic repair response. Follow-up studies were conducted in the DT40 avian cell to assess if the mutagenic DNA repair response is conserved in higher eukaryotes. The viability of DNA repair mutants was significantly decreased particularly for TLS and NER mutants. Furthermore, western blot analysis showed initiation of TLS repair after DCVC exposure. These results support a conserved DNA damage and mutagenic repair mechanism mediating DCVC renal toxicity. Additionally the results support a functional genomics approach in yeast as a viable model for identifying mechanisms of toxicity in higher organisms, including humans.

**PS 2272 The Value of Pharmacological Data to Support Systemic Acute Toxicity Evaluation of Compounds: A Profile Analysis.**

R. R. Note, H. Noçairi, L. Bourouf, G. Ouedraogo and J. Cotovio. *Department for The Development of Predictive Models and Methods, L'Oréal, Aulnay sous Bois, France.* Sponsor: E. Dufour.

Developing alternatives in the area of acute systemic toxicity implies combination of multiple parameters. We showed that integration of cell-death data, pharmacological profiles and physico-chemical properties resulted in a significant improvement of the LD50 prediction model originally developed by CeeTox. In order to reduce the false negative rate, correcting factors were applied to the model; this included considerations of a clear dose-response effect, the magnitude of the response and the number of receptors responding. A decrease of the LD50 parameter was expected the cited criteria were met. At a LD50 threshold of 500 mg/kg, the predictive performances of the so called V1 model were extremely encouraging with an overall concordance of 88%\*.

The purpose of the study is to get a better understanding of the data generated on the selection of 13 CNS and Heart receptors potentially playing a causative role in the toxic effect. The analysis of the profiles observed with the set of 73 public domain chemicals was completed as follows:

- Comparison of the LD50 values estimated via the different models (V0, V1, experimental)

- Toxicological categorization based upon the LD50 threshold of 500 mg/kg

- Identification of the receptors most responding and understanding of their biological relevance

No variation of the LD50 values was observed for 43 chemicals while an increase or a decrease was assigned to 10 and 20 chemicals respectively. As expected, the decrease in the LD50 value made the model more predictive for 16 out of the 20 compounds. With regards to the toxic compounds, the receptors most responding were a subset of 5 CNS and heart receptors (M2, alpha2, beta1, GABA, N neuronal). Next step will consist of checking the relevance of such receptors for a set of proprietary chemicals. As such, we could envisage the development of a more economical and pragmatic model that would be useful for early screening purposes.

\*SOT 2010, SOT 2011, SOT 2012

**PS 2273 Development of *In Vitro* Organotypic 3D Epithelial Models for High-Throughput Screening of Toxicological, Immunological and Developmental Signaling Pathways.**

C. Mankus, G. Jackson, J. Bolmarcich, P. Hayden and M. Klausner. *Mattek Corporation, Ashland, MA.*

Currently, there is a growing need for moderate to high-throughput toxicological assays that provide mechanistic information regarding cellular targets and signaling pathways. Here, we describe the development of *in vitro* organotypic 3D skin (EpiDerm™) and airway (EpiAirway™) models with the added feature of luciferase based transcription factor (TF) reporter functions. To produce the models, early passage normal human epidermal keratinocytes and tracheal epithelial cells were transduced with lentiviral vectors containing the TF response elements linked to luciferase. Stably transduced cells were selected by puromycin resistance, expanded several passages and cryopreserved to produce large pools of cells for organotypic model production. To date, reporters for 6 stress response pathways, including oxidative stress, DNA damage, metal stress, MAPK/inflammation, NFκB and xenobiotic stress have been developed in both the EpiDerm™ and EpiAirway™ models. Each model has demonstrated a dose response to positive control test articles including, TBHQ, Nutlin-3, ZnCl<sub>2</sub>, PMA, TNFα and TCDD, respectively, with an average induction of 3-15 fold over vehicle when luciferase activity in tissue

extracts was quantified using a microplate luminometer. TF reporters can be assembled in custom 96-well arrays for screening of unknown test compounds and monitoring of cell signaling pathway activity. Using this format, 3 test articles and a negative control (N=3) can be tested against 8 stress pathways in a single assay resulting in a heat map-like profile of pathway activation. The ultimate goal of the project is to develop a panel of 14 TF reporter models for both skin and airway models that can be assembled into custom 96-well high-throughput arrays as well as additional individual tissue formats. Results from these initial 6 models indicate that EpiDerm™ and EpiAirway™ reporter models will provide novel tools for conducting mechanistic human toxicological studies.

## PS 2274 *In Vitro* Predictive Toxicology for Breast Cancer.

R. Rudel<sup>1</sup>, J. Ackerman<sup>1</sup> and C. Vulpe<sup>2</sup>. <sup>1</sup>Silent Spring Institute, Newton, MA; <sup>2</sup>University of California, Berkeley, CA.

Identifying chemicals that increase breast cancer (BC) risk could help prevent BC, but rodent bioassays are expensive. In vitro and computational methods are being developed to predict adverse effects with limited in vivo testing. The present work aims to develop in vitro methods to predict chemicals that can increase BC risk. Animal and human studies suggest that both genotoxic carcinogens and certain hormone exposures increase BC risk. Our initial goal is to identify in vitro tests that predict mammary gland carcinogens (MCs) in rodent bioassays, since few breast carcinogens have been studied in humans. We have previously identified 208 chemicals causing mammary tumors in rodents in at least one study. We used the Chemical Carcinogenesis Research Information System (CCRIS) to compare genotoxicity profiles for MCs with 27 'non-carcinogens' (nonCs) that did not show increased tumors at any site in National Toxicology Program bioassays. We included five assay types: bacterial mutagenicity, and in vitro and in vivo micronuclei and chromosomal aberration. Data from at least one of these were available for 158 MCs and 22 nonCs. We found that most MCs are genotoxic: 87% were positive in >15% of CCRIS entries within any assay type, with or without metabolic activation (MA), while 10% were consistently negative (i.e., no study was positive). In comparison, 59% of nonCs were consistently negative. Since many in vitro predictive toxicity programs do not include MA, we also evaluated whether MA was needed for genotoxicity. Without MA, the MCs that were consistently negative for genotoxicity increased from 10% to 24%, and the number consistently positive (i.e., positive in >15% of entries in every assay type) dropped from 66% to 48%. In conclusion, a high percentage of MCs are consistently genotoxic but 10% are negative in all tests. Without activation almost 25% of the MCs would be consistently negative. The relationship between genotoxicity and cancer has been extensively discussed, but to our knowledge this is the first focus on breast cancer. Future work will extend to other in vitro endpoints.

## PS 2275 *In Vitro* to *In Vivo* Extrapolation Using Data from ToxCast.

M. DeVito<sup>1</sup>, S. S. Auerbach<sup>1</sup>, A. Merrick<sup>1</sup>, K. L. Witt<sup>1</sup>, K. Janardhan<sup>3</sup>, D. Malarkey<sup>1</sup>, H. Nagai<sup>1</sup>, I. Shah<sup>2</sup>, C. Corton<sup>2</sup> and R. Judson<sup>2</sup>. <sup>1</sup>NTP, NIEHS, Research Triangle Park, NC; <sup>2</sup>ORD, US EPA, Research Triangle Park, NC; <sup>3</sup>ILS, Research Triangle Park, NC; <sup>4</sup>Nihon Nohayaku Co. Ltd., Tokyo, Japan.

Using data from the USEPA ToxCast Phase I, a model was developed to predict non-genotoxic rat liver carcinogens. The model predicts that chemicals that activate PPAR $\alpha$ , increases in oxidative stress as measured by H2AX phosphorylation, decreases in MCP-1 or are anti-androgens in vitro are likely to induce rat liver tumors through non-genotoxic mechanisms. The present study evaluated the concordance of these in vitro responses to in vivo effects. The studied chemicals were either positive in the predictive model and were rat liver carcinogens (acetochlor, carbaryl, perfluorooctanoic acid (PFOA), 2,5-Pyridinedicarboxylic acid dipropyl ester (2,5-PCDA), simazine); positive in the model but were negative in a rat bioassay (bisphenol A, flusilazole) or were negative in the model and in vivo (triclosan). Using the highest dose from the cancer bioassay, male Sprague-Dawley rats were exposed by gavage to chemicals for 4d and euthanized 4h after the last dose. Livers were removed for gene array analysis. Serum MCP-1 levels were determined. In vitro and in vivo, PPAR $\alpha$  was activated by PFOA and acetachlor. Triclosan was positive in vivo, but not in vitro. None of the chemicals altered serum MCP-1 in vivo (2,5-PCDA and simazine, were positive in vitro). Carbaryl and bisphenol A induced H2AX phosphorylation in vitro but were not positive in vivo. Bisphenol A, acetochlor and flusilazole showed anti-androgen activity in vitro and in vivo. While negative in vitro, 2,5-PCDA, PFOA, carbaryl and triclosan altered androgen responsive genes in vivo. Carbaryl and acetochlor induced oxidative stress in vitro but not in vivo. In contrast, triclosan induced oxidative stress responsive genes in vivo but not in vitro. PPAR $\alpha$  pathway activation has a good concordance in vitro and in

vivo. Results for anti-androgenicity, MCP-1 and oxidative stress were much less concordant between in vitro and in vivo. This abstract does not necessarily reflect the policies or views of NIH or the USEPA.

## PS 2276 The *In Vitro* 3T3 Neutral Red Uptake Phototoxicity Test: What to Do with UVB Absorbers?

D. B. Learn, M. D. Schwartz, M. E. Dougherty and A. M. Hoberman. Center for Photobiology, Charles River Laboratories Preclinical Services, Horsham, PA.

The literature suggests and conventional wisdom holds that Ultraviolet B (UVB) is highly cytotoxic to the Balb C 3T3 fibroblast cell line used in the OECD 432 3T3 NRU Phototoxicity Test and thus the assay is not appropriate for test materials that absorb primarily in the UVB portion of the spectrum. The choice of an appropriate light source and filtering is always a critical factor in this or any assay, and, while this Guidance recommends an Ultraviolet A (UVA) dose of 5 J/cm<sup>2</sup>, the UVB dose (if any) or limit of exposure is not addressed. To define the sensitivity of the cells to UVB and evaluate if indeed their sensitivity precluded the use of UVB, we evaluated the Guidance-required cell viability, OD<sub>540</sub> absorption, and other endpoints with increased UVB (290 – 300 nm) exposure by removing the tissue culture plate lid during exposure using a xenon arc solar simulator. This direct (uncovered) exposure increased the UVB irradiance from approximately 19 mJ/cm<sup>2</sup> to approximately 32 mJ/cm<sup>2</sup>, concomitant with the recommended 5 J/cm<sup>2</sup> UVA dose. While cell survival was modestly reduced, the resulting IC<sub>50</sub>, OD<sub>540</sub> absorption, PIF, and MPE endpoints from this enhanced UVB exposure alone and response to Chlorpromazine indicate no adverse effect on the validity of the assay and acceptable Guidance-defined results under these exposure conditions. This additional ability to test UVB absorbers provides all the advantages of the assay to this subset of test materials, enhances this step in the preclinical process of drug discovery and further establishes the robustness of the assay as a valid step in preclinical drug development.

## PS 2277 Comparison of Multiple Assay Formats to Measure Kinase Inhibitor Activity.

K. Leach and D. Puppala. Compound Safety Prediction, Pfizer, Groton, CT.

Protein phosphorylation is a key mechanism for controlling cellular functions, and protein kinase inhibitors show good efficacy as oncology therapeutics. Currently there are 15 marketed kinase inhibitors, with many more in clinical trials. A key component of drug discovery efforts for these inhibitors is the optimization of kinase selectivity, since a greater degree of promiscuity is associated with a greater risk of safety concerns. A wide variety of biochemical and cellular kinase assays which utilize multiple technologies are available for testing compounds and determining kinase activity, and an important consideration is the translation across these assays. A set of 14 Pfizer kinase inhibitors with different primary kinase targets were profiled across three different types of assays: biochemical kinase assays measuring peptide substrate phosphorylation; ActivX technology, which measures specific binding to kinases within a cell lysate; and cell-based kinase assays, measuring endogenous substrate phosphorylation. The biochemical assays were conducted at Km levels of ATP, with nonphysiological peptide substrates, while the cellular assays utilized intact cells and cellular levels of ATP. A comparison of results across these platforms against three different kinases, aurora, abl or glycogen synthase kinase beta, was carried out and the results demonstrate a high degree of congruency with the cellular kinase activity and the Activ X technology. For this set of compounds, there was less agreement between the biochemical versus cellular kinase assays. These results suggest that utilization of high throughput biochemical assays can be used to provide an initial determination of kinase activity, but that followup testing under more physiological conditions using the ActivX technology, or cellular assays, is required to fully assess kinase inhibitor activity.

## PS 2278 Mouse Cecal Microbiota Converts Monomethylarsonic Acid (MMA) to an Array of Oxy- and Thio-Arsenical Metabolites.

M. J. Kohan<sup>2</sup>, D. J. Thomas<sup>2</sup>, T. Pinyavev<sup>1</sup>, M. Mantha<sup>1</sup>, K. M. Herbin-Davis<sup>2</sup> and J. T. Creed<sup>1</sup>. <sup>1</sup>MCEARD, NERL, US EPA, Cincinnati, OH; <sup>2</sup>ISTD, NHEERL, US EPA, Research Triangle Park, NC.

The metabolism of arsenicals markedly affects their tissue distribution and retention as well as the toxic and carcinogenic effects of this metalloid. Metabolism of arsenicals by the microbiota of the gastrointestinal tract has been shown to convert inorganic and dimethylated arsenicals to various methylated species. Here, anaerobic microbiota from ceca of adult female C57BL/6 mice was incubated with 20,

200, 1000, or 2000 parts per billion (ppb) MMA for up to 48 hours at 37°C. Samples of supernates from reaction mixtures were taken for arsenic speciation by HPLC-ICP-MS. MMA was converted to monomethylated mono- (MMMTA), di- (MMDTA), and tri- (MMTTA) thiolated species. In addition, MMA was also converted to dimethylated mono- (DMMTA) and di- (DMDTA) thiolated species. After 48 hours, DMDTA was the predominant metabolite in reaction mixtures containing 20, 200, or 1000 ppb MMA. In reaction mixtures containing 2000 ppb MMA, MMDTA was the predominant metabolite of MMA. These results show that anaerobic microbiota from mouse cecum includes organisms that efficiently methylate MMA and can convert oxyarsenicals into homologous thioarsenicals. The presumptive source of sulfur used for conversion of oxyarsenicals into thioarsenicals is hydrogen sulfide produced by the microbiota through dissimilatory sulfate reduction. Conversion of methylated oxyarsenicals into methylated thioarsenical during preabsorptive metabolism may influence the transport of ingested arsenic across the gastrointestinal barrier thereby affecting the systemic distribution, fate, and effects of arsenic. (This abstract does not reflect U.S. EPA policy).

## PS 2279 Paraoxonase Activity in Subchronic Low-Level Inorganic Arsenic Exposure.

O. Ademuyiwa<sup>1</sup>, O. K. Afolabi<sup>1</sup>, A. D. Wusu<sup>1</sup>, O. O. Ogunrinola<sup>1</sup>, E. O. Abam<sup>1</sup>, D. O. Babayemi<sup>1</sup>, E. A. Balogun<sup>1</sup> and O. O. Odukoya<sup>2</sup>.  
<sup>1</sup>Biochemistry, Federal University of Agriculture, Abeokuta, Nigeria; <sup>2</sup>Chemistry, Federal University of Agriculture, Abeokuta, Nigeria.

Epidemiological evidences indicate close association between inorganic arsenic exposure via drinking water and cardiovascular diseases. While the exact mechanism of this arsenic-mediated increase in cardiovascular risk factors remains enigmatic, studies indicate a role for paraoxonase (PON) in cardiovascular diseases. To study the association between inorganic arsenic exposure and cardiovascular diseases, rats were exposed to sodium arsenite (50, 100 and 150ppm) and sodium arsenate (100, 150 and 200ppm) in their drinking water for 12 weeks. PON activities towards paraoxon (PONase) and phenylacetate (AREase) in plasma, lipoproteins, liver and brain microsomal fractions were determined. Inhibition of PONase and AREase in plasma and HDL characterised the effects of the two arsenicals. While arsenite inhibited PONase by 33% (plasma) and 46% (HDL) respectively, arsenate inhibited the enzyme by 41 and 34% respectively. AREase activity was inhibited by 52 and 48% by arsenite; the inhibition amounted to 72 and 67% respectively by arsenate. The pattern of inhibition in plasma and HDL indicates that arsenite induced a dose-dependent inhibition of PONase whereas arsenate induced a dose-dependent inhibition of AREase. In the VLDL, arsenate inhibited PONase and AREase while arsenite inhibited PONase. In the hepatic and brain microsomal fractions, only the PONase enzyme was inhibited by the two arsenicals. The inhibition was more pronounced in the hepatic microsomes where a 70% inhibition was observed at the highest dose of arsenate. Microsomal cholesterol was increased by the two arsenicals resulting in increased cholesterol/phospholipid ratios. Our findings indicate that decreased PON activity observed in arsenic exposure may be an incipient biochemical event in the cardiovascular effects of arsenic. Modulation of PON activity by arsenic may also be mediated through changes in membrane fluidity brought about by changes in the concentration of cholesterol in the microsomes.

## PS 2280 Comparative Early Oncogenic Effects of Cadmium and Arsenic in Human Lung Epithelial Cells.

R. J. Person, E. J. Tokar and M. P. Waalkes. NTP, NIEHS, NIH, Research Triangle Park, NC.

Cadmium (Cd) and inorganic arsenic (iAs) are known human lung carcinogens. In this study, we compare development of in vitro cellular models of human lung cancer induced by Cd or iAs. We have shown chronic, low-level (5  $\mu$ M) Cd (as CdCl<sub>2</sub>) induces an acquired cancer phenotype in human lung epithelial cells (HPL-1D) after 20 weeks of continuous exposure. Here we compare an iAs model in development to this previously developed Cd model. The HPL-1D cells that were used are an immortalized, non-tumorigenic human peripheral epithelial cell and were used with both agents. HPL-1D cells were chronically exposed to non-toxic levels of Cd (5  $\mu$ M) or iAs (2  $\mu$ M) and over 20-26 weeks of chronic exposure signs of oncogenic transformation were assessed. Matrix metalloproteinase-2 (MMP-2) activity, colony formation in soft agar, invasion and expression of cancer relevant genes were used to assess oncogenic phenotype in these cell models. By 26 weeks of continuous iAs exposure, secreted MMP-2 significantly increased to 147% of control, near levels typical of a cancer phenotype. In comparison, after only 20 weeks of Cd exposure, MMP-2 levels increased to 358% of control and cell invasion and colony formation increased by more than 3-fold compared to control cells, all indicating an oncogenic phenotype. Following iAs exposure (26 weeks) increases were seen in MT-1A (768% of control) and MT-2A (614% of control) expression, similar to that

seen with Cd transformation. Expression of epithelial-to-mesenchymal transition marker *VIMENTIN* increased to 323% of control with chronic iAs exposure. High *VEGF* oncogene expression is often seen in lung adenocarcinomas and after 26 weeks of chronic iAs treatment expression increased to 4.3-fold above control. The SLC39A8 (ZIP 8) transporter, which is known to influx Cd, though increased by Cd transformation was unchanged in chronic iAs exposure. Thus, it appears that both Cd and iAs can induce early signs of transformation in human lung epithelial cells, although some gene expression is inorganic specific.

## PS 2281 Metallothionein Blocks Arsenic-Induced Oxidative DNA Damage.

W. Qu and M. P. Waalkes. NTP, NIEHS, NIH, Research Triangle Park, NC.

Metallothionein (MT) plays an important role in detoxication of inorganics. Inorganic arsenic is a toxic metalloid and a human carcinogen that may act, in part, by causing oxidative DNA damage (ODD). MT can limit ODD induced by other inorganic carcinogens, like cadmium. Although MT can mitigate arsenic toxicity *in vivo*, how MT impacts arsenic-induced ODD has not been defined. Here, we studied ODD induced by acute arsenic treatment *in vitro* and the effects of cellular MT using cells that poorly express MT (MT-I/II double knockout; called MT-null cells) compared to parental wild-type (WT) MT competent cells. MT-null and WT cell lines were first exposed to arsenite (NaAsO<sub>2</sub>) for 24 h to assess cytotoxicity. Arsenic was much less cytotoxic in WT cells (LC<sub>50</sub> = 11.0  $\pm$  1.3  $\mu$ M, mean  $\pm$  SEM) than MT-null cells (LC<sub>50</sub> = 5.6  $\pm$  1.2  $\mu$ M). Arsenic-induced ODD was measured by the immuno-spin trapping method which measures DNA radicals after conversion to stable DNA nitrones *in situ*. Arsenic treatment (1 or 5  $\mu$ M; 24 h) induced much less ODD in WT cells (121% and 141% of control, respectively) than in MT-null cells (202% and 260%). In WT cells arsenic caused concentration-related increases in MT expression (transcript and protein), and in metal-activated transcription factor 1 (MTF1), a requirement for induced MT gene expression by arsenic. In contrast, in MT-null cells, the basal levels of MT were very low and were not increased by arsenic. Transfection of MT-I into MT-null cells markedly reduced arsenic-induced ODD. Two important transport genes, *Mrp1* and *Mrp2*, showed increased expression in WT cells but not MT-null cells. Arsenic caused concentration-related increases in the oxidant defense genes, *HO-1* and *GSTA2* in both WT and MT-null cells, but to much higher levels in WT cells. Thus, MT protects against arsenic-induced ODD in MT competent cells potentially by multiple mechanisms including direct sequestration and scavenging oxidant radicals. MT-competent cells are more adept at activating metal transport systems and oxidant response genes, although the role of MT in these responses is unclear.

## PS 2282 Increase Blood Pressure, Changes of Left Ventricular Geometry, and Function in Children Environmentally Exposed to Inorganic Arsenic.

C. Osorio-Yañez<sup>1</sup>, J. Ayllon-Vergara<sup>2</sup>, L. Arreola-Mendoza<sup>3</sup>, G. Aguilar-Madrid<sup>4</sup>, E. Hernández-Castellanos<sup>1</sup>, A. Barrera-Hernández<sup>1</sup>, L. C. Sanchez-Peña<sup>1</sup> and L. M. Del Razo<sup>1</sup>. <sup>1</sup>Toxicology, Cinvestav-IPN, D.F., Mexico; <sup>2</sup>Español Hospital, D.F., Mexico; <sup>3</sup>CIEMAD-IPN, D.F., Mexico; <sup>4</sup>Health and Work, IMSS, D.F., Mexico.

Hypertension is a known cardiovascular risk factor to develop final cardiac events and epidemiologic studies in adults have been related hypertension with inorganic arsenic (iAs) exposure. Left ventricular mass (LVM) increase is a potent predictor of cardiovascular morbidity and mortality and it is stimulated by higher blood pressure as well as impaired myocardial contractile performance. Ejection fraction (EF) has been employed as a good index of global systolic function. The aim of this study was evaluate the association between iAs exposure, blood pressure, and echocardiographic parameters in children. In this cross-sectional study 170 children (3-14 years old) chronically exposed to iAs through drinking water were recruited in iAs-endemic area of central part of México. LVM and EF were derived from echocardiography and blood pressure was measured by standard protocols. Total arsenic in urine (UtAs) was significant associated with systolic ( $\beta$ =2.65;  $p$ =0.056) and diastolic ( $\beta$ =0.012;  $p$ =0.019) blood pressure in multivariate regression models adjusted by age, gender and body mass index. Indeed, diastolic blood pressure was associated with cumulative arsenic exposure ( $\Sigma$ AsE; ppb\*year) through drinking water ( $\beta$ =0.003;  $p$ =0.002). Notably, LVM (g) was significant associated with  $\Sigma$ AsE ( $\beta$ =15.43;  $p$ =0.002) in adjusted multivariate model. Diastolic prehypertension was present in 48%, concentric remodeling was presented in 60% [normal LVM and relative wall thickness (RWT)  $\geq$ 0.43] and LVM concentric hypertrophy defined as LVM  $>$ 88.9 g/m<sup>2</sup> and RWT  $\geq$ 0.43 were presented in 7% (11 children). Moreover, EF was inversely associated with UtAs  $>$  35ng/ml ( $\beta$ =-3.21;  $p$ =0.036) in adjusted multivariate analyses. In conclusion, iAs exposure would be able to cause diastolic prehypertension, increase of LVM and decrease of EF in children, given evidence of possible cardiovascular disease in early-life exposure.

**PS 2283 Reduction of Dimethylarsenate to the Supertoxic Dimethylarsenite by Rats and Rat Liver Cytosol.**

Z. Gregus and B. Némethi. *University of Pécs, Pécs, Hungary.*

Dimethylarsinic acid (DMA<sub>V</sub>) is the major urinary metabolite of inorganic arsenic in humans and most animals. DMA<sub>V</sub> is weakly cytotoxic, however, it is reduced to dimethylarsinous acid (DMA<sub>III</sub>) which is over 100 times more toxic. Although glutathione S-transferase omega 1 (GSTO1) catalyzes the reduction of DMA<sub>V</sub>, its role in DMA<sub>V</sub> reduction in vivo or in cell extracts is uncertain. We studied the reduction of DMA<sub>V</sub> to DMA<sub>III</sub> in rats and in rat liver cytosol to better understand its mechanism. To assess DMA<sub>V</sub> reduction in rats, we devised a novel procedure. This is based on following the time course of the accumulation in the blood of the RBC-bound dimethylarsenic (DMA<sub>s</sub>), which represents DMA<sub>III</sub>. Therefore, we serially measured the RBC-bound DMA<sub>s</sub> in the blood of DMA<sub>V</sub>-injected anesthetized rats with ligated renal pedicles. These studies indicated that reduction of DMA<sub>V</sub> to DMA<sub>III</sub> was rapid, as in 90 min 31% of the injected 50 µmol/kg DMA<sub>V</sub> dose was converted to DMA<sub>III</sub> that was sequestered by the circulating erythrocytes. Pretreatment of rats with glutathione (GSH) depletors (phorone or BSO) delayed the elimination of DMA<sub>V</sub> and the accumulation of RBC-bound DMA<sub>s</sub>, whereas the methyltransferase inhibitor PAD was without effect. Reduction of DMA<sub>V</sub> by rat liver cytosol was assayed by extraction of DMA<sub>III</sub> from the incubations of cytosol with DMA<sub>V</sub> and quantification by HPLC-HG-AFS. We found that reduction of DMA<sub>V</sub> required cytosolic protein and GSH and was inhibited by thiol reagents, GSSG and dehydroascorbate. Although thioredoxin reductase (TrxR) inhibitors (aurothioglucose and trivalent antimony) inhibited cytosolic DMA<sub>V</sub> reduction, TrxR plus NADPH alone or when added to the cytosol failed to support DMA<sub>V</sub> reduction. On ultrafiltration of the cytosol through a 3 kDa filter, the reducing activity in the retentate was lost but was largely restored by NADPH. Such experiments also indicated that the reducing enzyme was larger than 100 kDa, and was not GSTO1. In summary, reduction of DMA<sub>V</sub> to the supertoxic DMA<sub>III</sub> in rats and rat liver cytosol is rapid and GSH dependent, yet its mechanism is still elusive.

**PS 2284 Fibronectin Expression in Human Bladder Cells (UROtsa) Exposed to or Malignantly Transformed by Arsenic or Cadmium.**

A. R. Klinger<sup>1</sup>, M. E. Jenó<sup>1</sup>, K. J. Wilt<sup>1</sup>, H. M. Hewitt<sup>1</sup>, X. Zhou<sup>2</sup>, S. Somji<sup>2</sup>, S. H. Garrett<sup>2</sup>, D. A. Sens<sup>2</sup> and J. R. Dunlevy<sup>1</sup>. <sup>1</sup>Anatomy, University of North Dakota, Grand Forks, ND; <sup>2</sup>Pathology, University of North Dakota, Grand Forks, ND.

Fibronectin is an extracellular matrix glycoprotein that is present in nearly all connective tissues as well as a soluble protein within the blood. The main functions of fibronectin relate to cellular adhesion, cell migration, and cell signaling. In the bladder, fibronectin is found within the lamina propria, blood vessels, nerves, and smooth muscle basement membrane. Fibronectin is present at very low levels in the normal bladder epithelium but in bladder carcinomas it has been found to be substantially increased in expression and/or present in oncofetal alternatively spliced forms. This has led to several studies of fibronectin as a potential prognostic marker in bladder cancer. The purpose of the current study is to validate initial microarray studies that indicated strong differential expression of fibronectin in UROtsa bladder cells transformed with cadmium compared to non-malignant UROtsa cells. Fibronectin mRNA and protein were found to be increased in 6 of 7 cadmium transformed cell lines as well as in 5 of 6 arsenic transformed cell lines compared to the non-transformed parent cells. The ability of fibronectin expression to be altered epigenetically by histone acetylation or DNA methylation or directly by exposure to arsenic or cadmium was also examined. Fibronectin mRNA and protein was found to consistently decrease during 24-72 hours exposure to arsenic but was not consistently changed by short term exposure to cadmium. The results of this study show that alternations in fibronectin expression may correlate with transformation of bladder cells exposed to heavy metals.

**PS 2285 Gene Expression Changes Induced by Various Arsenicals In Vitro.**

P. R. Dodmane, L. L. Arnold, K. L. Pennington and S. M. Cohen. *Pathology and Microbiology, University of Nebraska Medical Center, Omaha, NE.*

Inorganic arsenic (IA) is a human urinary bladder, skin and lung carcinogen. The mechanism by which IA induces tumors is unknown. IA is metabolized to methylated arsenicals and excreted in urine. In vitro trivalent arsenicals are more cytotoxic than pentavalent forms. Multiple studies have documented a range of arsenic-induced gene changes in vivo and in vitro, but the dose response is unclear. In this

study, the dose response for IA and effects of various arsenicals for gene expression changes was evaluated in human bronchial epithelial cells (HBEC). Primary HBEC were exposed to 0.1, 1, 5 or 10 µM of As<sub>III</sub>, 1 µM MMA<sub>III</sub> and 1.4 µM DMA<sub>III</sub> for 24 h and 5.8 µM As<sub>III</sub> for 72 h. Increasing concentration of As<sub>III</sub> showed increasing number of differentially expressed genes (DEG) correlating with increasing cytotoxicity. The lowest As<sub>III</sub> used, 0.1 µM, did not induce any DEG, whereas there were 7, 101 and 1735 DEG at 1, 5 and 10 µM As<sub>III</sub>, respectively. Pathway analysis showed only IFN signaling and pattern recognition receptor pathways (PRRP) being altered with 1 µM As<sub>III</sub>. IFN signaling was also altered with 5 µM As<sub>III</sub> in addition to NRF2-mediated oxidative stress response (NOSR) and IL-17A signaling. Ten µM As<sub>III</sub> altered NOSR in addition to glutamate metabolism, cell cycle/G1/S check point regulation, p53 signaling and AhR signaling. DMA<sub>III</sub> induced 2 DEG and MMA<sub>III</sub> induced 268 DEG. DMA<sub>III</sub> induced lesser cytotoxicity compared to MMA<sub>III</sub>. MMA<sub>III</sub> induced canonical pathways of hepatic stellate cell activation, LXR/RXR activation, atherosclerosis signaling, PRRP and IFN signaling pathways. As<sub>III</sub> for 72 h induced 71 DEG that represented similar signaling pathways as observed at 24 h. These data suggest that arsenic at lower concentrations induces inflammatory and oxidative stress responses whereas at higher concentrations it altered multiple cellular pathways that control cell cycle and cell proliferation. NOAEL for As<sub>III</sub> appears to be between 0.1 to 1 µM. All arsenicals tested altered similar signaling pathways in HBEC and were similar to urothelial cells and keratinocytes.

**PS 2286 Effects of Treatment with Dimethylarsinous Acid (DMAIII) on the Urinary Bladder Epithelium of Female Arsenic Methyltransferase (As3mt) Knockout Mice and C57Bl/6 Mice.**

L. L. Arnold, P. R. Dodmane, K. L. Pennington and S. M. Cohen. *Pathology and Microbiology, University of Nebraska Medical Center, Omaha, NE.*

Chronic exposure to inorganic arsenic (InAs) is carcinogenic to the human urinary bladder. It produces urothelial cytotoxicity and proliferation in rats and mice. DMA<sub>V</sub>, a major methylated urinary metabolite of InAs, is a rat bladder carcinogen. DMA<sub>III</sub> was shown to be the likely urinary metabolite of DMA<sub>V</sub> inducing urothelial changes and is postulated to be one of the active metabolites of InAs. To evaluate potential DMA<sub>III</sub>-induced urothelial effects, it was administered to As3mt knockout mice which cannot methylate arsenicals. Female C57Bl/6 wild type and As3mt knockout mice (10/group) were administered DMA<sub>III</sub>, 77.3 ppm in water for four weeks. Urothelial effects were evaluated by light and scanning electron microscopy (SEM) and immunohistochemical detection of bromodeoxyuridine (BrdU). DMA<sub>III</sub> significantly increased the BrdU labeling index in the knockout group compared to control and to the treated wild type group. DMA<sub>III</sub> induced a greater increase in the incidence of simple hyperplasia in knockout mice (4/10) compared to wild type mice (2/10). All treated knockout mice had more and larger intracytoplasmic granules, compared to the treated wild type mice. Changes in SEM classification were not significant. In conclusion, DMA<sub>III</sub> induces urothelial toxicity and regenerative hyperplasia in mice and most likely plays a role in inorganic arsenic-induced urothelial changes. However, in mice, DMA<sub>V</sub> does not induce hyperplasia, suggesting that urinary concentrations of DMA<sub>III</sub> do not reach cytotoxic levels in DMA<sub>V</sub>-treated mice.

**PS 2287 Arsenite Inhibits DNA Repair through S-Nitrosation of Poly (ADP-Ribose) Polymerase 1.**

X. Zhou, K. L. Cooper, L. G. Hudson and K. Liu. *College of Pharmacy, University of New Mexico, Albuquerque, NM.*

Arsenic, a widely distributed carcinogen, is known to significantly amplify the impact of other carcinogens such as ultraviolet radiation and benzo(a)pyrene at low, non-cytotoxic concentrations. Evidence from our lab and others suggests inhibition of DNA repair could be an important mechanism of arsenic co-carcinogenesis. We recently demonstrated that reactive nitrogen species (RNS) induced by arsenic may play an important role in inhibition of PARP-1 activity, but the role of RNS in the mechanism of arsenic inhibition is not clear. In this work, we show that As(III)-induced RNS caused S-nitrosative modification on cysteine residuals of Poly(ADP-ribose) polymerase (PARP)-1, a key DNA repair protein in base excision repair. We found that similar to the effect of a NO donor, As(III) treatment in HaCat cells induced S-nitrosation on PARP-1 protein. This S-nitrosation of PARP-1 could be reduced by L-NAME (nitric oxide synthase inhibitor), c-PTIO (nitric oxide scavenger) or ascorbic acid. In addition, As(III) treatment lead to zinc loss and activity inhibition of PARP-1 protein isolated from cells. Importantly, we confirmed that S-nitrosation happened on zinc finger DNA binding domain of PARP-1 protein using biotin-switch assay. Taken together, these results show that arsenite induces S-nitrosation on zinc finger DNA binding domain of PARP-1 via generation of NO, leading to zinc loss and activity inhibition of PARP-1. These findings provide novel insight into the molecular mechanism of As inhibition of PARP-1.

**PS 2288 Paradoxical Effects of Ongoing Arsenic Exposure on an Arsenic-Transformed Bladder Cancer Model.**

F. Zhao, S. Pacheco, A. Gandolfi and W. T. Klimecki. *Pharmacology and Toxicology, University of Arizona, Tucson, AZ.*

Epidemiology studies have shown a strong link between chronic arsenic exposure and bladder cancer. An immortalized human urothelial cell line, UROtsa has been widely used as a model of arsenic-induced bladder toxicity. Chronic exposure to 1uM sodium arsenite transforms UROtsa to a cancerous cell line, URO-ASSC. This phenotype is stable with no further arsenite selection, and URO-ASSC is typically assayed for malignancy without arsenite exposure. In the absence of arsenite, we found that both UROtsa and URO-ASSC demonstrate constitutive autophagy. Recent evidence suggests that autophagy is a survival mechanism for cancer. This led us to hypothesize that disrupting autophagy could reduce malignant potential in URO-ASSC. We found that URO-ASSC accumulates LC3II protein levels 3.4 fold faster compared to UROtsa when autophagic flux was blocked with bafilomycin A1 in a 2-hour time course, suggesting a higher rate of autophagic turnover in URO-ASSC. Impairing autophagy in URO-ASSC by siRNA against ATG7 resulted in 65% reduction of anchorage-independent growth, a key phenotype of arsenic-induced malignant transformation. Surprisingly, when we reintroduced URO-ASSC cells to 1uM of arsenite exposure, LC3-II levels and autophagic flux were reduced by 50%, suggesting that ongoing exposure to arsenite impairs autophagy. This autophagy impairment was also associated with a 55% reduction in soft agar growth in the presence of 1uM arsenite. These *in vitro* experiments provide insight into the complex effect of arsenic exposure on the process of autophagy and its relationship to arsenite-induced malignancy. Furthermore, these studies raise the possibility that ongoing arsenic exposure may suppress malignant growth concurrently with establishing the malignant phenotype, perhaps in part through modulating the autophagic pathway. The translational impact of this finding could have bearing on human populations such as those in Chile, that transition from periods of sustained arsenic exposure to periods in which arsenic exposure has been mitigated.

**PS 2289 Effects of Arsenic on Expressions of Ube2d Family and Accumulation of p53 in Renal Tubular Cells and Vascular Endothelial Cells.**

M. Satoh<sup>1</sup>, J. Lee<sup>1</sup>, M. Tokumoto<sup>1,2</sup>, Y. Fujiwara<sup>1</sup> and C. Watanabe<sup>3</sup>. <sup>1</sup>*School of Pharmacy, Aichi Gakuin University, Nagoya, Japan;* <sup>2</sup>*Showa Pharmaceutical University, Tokyo, Japan;* <sup>3</sup>*Graduate School of Medicine, University of Tokyo, Tokyo, Japan.*

Arsenic is an environmental pollutant that induces apoptosis in various tissues. However, underlying molecular mechanisms of arsenic-induced apoptosis are not clear. Recently, we have found that apoptosis through the overaccumulation of p53 is involved in cadmium toxicity in rat proximal tubular cells (NRK-52E cells). Moreover, gene expressions of Ube2d family, which conjugate ubiquitin to p53 and drive p53 to be degraded, are suppressed by cadmium in NRK-52E cells. In this study, we examined the involvement of gene expressions of Ube2d family (Ube2d1, Ube2d2, Ube2d3 and Ube2d4) and accumulation of p53 in arsenic toxicity, using model cells of vascular endothelia and renal tubules. In NRK-52E cells, NaAsO<sub>2</sub> (As[III]) decreased mRNA levels of Ube2d family except Ube2d3 and increased protein levels of p53. Interestingly, although protein levels of p53 were markedly increased by As[III], mRNA levels of UBE2D family were not decreased by this metalloid in human brain microvascular endothelial cells (HBMECs). In human proximal tubular cells (HK-2 cells), As[III] slightly increased protein levels of p53 with low-dose treatment. However, mRNA levels of UBE2D family were not decreased by As[III] in HK-2 cells. Moreover, mRNA levels of p53 were decreased by As[III] in HBMECs and HK-2 cells. Our findings suggest that As[III] increases cellular protein levels of p53, mediating tissue- or cell-specific pathways for p53 stability.

**PS 2290 A Common Arsenic (+3 Oxidation State) Methyltransferase (AS3MT) Polymorphism Affects Urinary Metabolite Profiles of Arsenic in a US Population.**

D. J. Thomas<sup>4</sup>, Z. Drobna<sup>1</sup>, M. Styblo<sup>1</sup>, R. L. Calderon<sup>2</sup>, X. Lu<sup>3</sup>, X. Le<sup>3</sup> and E. E. Hudgens<sup>2</sup>. <sup>1</sup>*Nutrition, University of North Carolina at Chapel Hill, Chapel Hill, NC;* <sup>2</sup>*EPHD, NHEERL, US EPA, Research Triangle Park, NC;* <sup>3</sup>*Environmental Health Sciences, University of Alberta, Edmonton, AB, Canada;* <sup>4</sup>*ISTD, NHEERL, US EPA, Research Triangle Park, NC.*

AS3MT catalyzes methylation of inorganic arsenic (iAs) forming mono- (MAs) and di- (DMAs) methylated products that mediate some of the toxic and carcinogenic effects associated with chronic iAs exposure. Therefore, the catalytic efficiency of

AS3MT may be an important determinant of risk associated with chronic iAs exposure. Concentrations of iAs, MAs, and DMAs in urines from residents of Churchill County, Nevada, were used to calculate primary (MAs/iAs) and secondary (DMAs/MAs) methylation indices (MI). AS3MT genotypes were determined for 198 individuals selected on the basis of lowest and highest secondary MIs. The incidence of an AS3MT polymorphism (rs11191439) that replaces a methionyl residue in position 287 with a threonyl residue (M287T) affected the secondary MI. For the M287T polymorphism, median values for secondary MIs were 6.5 in 150 individuals homozygous for wild-type AS3MT, 2.8 in 43 individuals heterozygous for wild-type and mutant alleles, and 2.4 in 5 individuals homozygous for the M287T polymorphism. In contrast, median values for primary MIs were unaffected by this polymorphism. Two intronic variants (T35587C and G35991A) reported to alter the levels of MAs and DMAs in other studies did not alter primary and secondary MIs in this population. These results indicate that the common M287T polymorphism of AS3MT is associated with altered profiles of methylated arsenicals in urine from individuals chronically ingesting iAs in drinking water. Linkages among AS3MT genotype-dependent alterations in urinary arsenical profiles, the catalytic properties of AS3MT variants, and disease susceptibility require further examination. (This abstract does not reflect U.S. EPA policy).

**PS 2291 Arsenic Increases Atherosclerosis by LXR $\alpha$ -Dependent and LXR $\alpha$ -Independent Mechanisms.**

M. Lemaire<sup>1</sup>, C. A. Lemarié<sup>2</sup>, M. Flores Molina<sup>1</sup> and K. K. Mann<sup>1</sup>. <sup>1</sup>*Oncology, Lady Davis Institute for Medical Research, McGill University, Montréal, QC, Canada;* <sup>2</sup>*Medicine, Lady Davis Institute for Medical Research, McGill University, Montréal, QC, Canada.*

Arsenic exposure has been linked to atherosclerosis; however, molecular mechanisms involved in arsenic-enhanced atherosclerosis are unknown. Previously, we have shown *in vitro* and *in vivo* that arsenic inhibits transcriptional activation of the liver X nuclear receptors (LXR), key regulators of macrophage lipid homeostasis. Here, we evaluated the role of LXR $\alpha$  in arsenic-induced atherosclerosis using the ApoE<sup>-/-</sup> mouse model. In ApoE<sup>-/-</sup> mice, 200 ppb arsenic increased atherosclerosis plaque size after 13 weeks. In contrast, LXR $\alpha$ <sup>-/-</sup>ApoE<sup>-/-</sup> mice do not show increased plaque size following arsenic exposure, indicating that arsenic may enhance atherosclerosis in an LXR $\alpha$ -dependent manner. In the ApoE<sup>-/-</sup> mice, we saw significant changes in plaque composition, and thus in LXR $\alpha$ <sup>-/-</sup>ApoE<sup>-/-</sup>, we assessed plaque staining of: 1) lipid deposition and macrophage content and 2) collagen composition and smooth muscle cell content. Interestingly, arsenic decreases macrophages in LXR $\alpha$ <sup>-/-</sup>ApoE<sup>-/-</sup>, where no change was observed in ApoE<sup>-/-</sup> exposed mice. However, arsenic increased lipids in both genotypes, suggesting impaired macrophage cholesterol efflux capacity and subsequent lipid accumulation. Secondly, we observed that arsenic decreased collagen content in LXR $\alpha$ <sup>-/-</sup>ApoE<sup>-/-</sup> and ApoE<sup>-/-</sup> to the same extent, but arsenic increased smooth muscle cells, a major collagen producing cell type, in the LXR $\alpha$ <sup>-/-</sup>ApoE<sup>-/-</sup>, while they were decreased in ApoE<sup>-/-</sup>. This indicates that LXR $\alpha$  may be involved in maintaining matrix integrity. In fact, arsenic-exposed LXR $\alpha$ <sup>-/-</sup>ApoE<sup>-/-</sup> plaques had increased matrix metalloproteinase (MMPs) activity compared to both control LXR $\alpha$ <sup>-/-</sup>ApoE<sup>-/-</sup> and ApoE<sup>-/-</sup>, which could be responsible for both the decrease in plaque collagen and the smooth muscle cells invasion. Our observations suggest that arsenic may be increasing atherosclerosis formation through LXR inhibition, but it may alter plaque composition in a LXR independent manner.

**PS 2292 Induction of Cytochrome P450 1A1 (CYP1A1) by Pentavalent Methylated Arsenicals in Human Hepatoma HepG2 Cells.**

A. Anwar-Mohamed, O. Elshenawy and A. O. El-Kadi. *University of Alberta, Edmonton, AB, Canada.*

Arsenic (As[III]) is a worldwide environmental pollutant and a human carcinogen. It is well recognized that the carcinogenicity of As[III] is largely dependent on the methylation levels (monomethyl, dimethyl, and trimethyl) that are present during the process of metabolism in mammals. Oxidative methylation, is based on the findings that As[III] is sequentially converted to monomethylarsonic acid (MMA(V)), dimethylarsinic acid (DMA(V)), and trimethylarsine oxide (TMA(V)) in both humans and in laboratory animals such as mice and rats. Activation of the aryl hydrocarbon receptor (AhR) ultimately leads to the induction of the carcinogen activating enzyme cytochrome P450 1A1 (CYP1A1). Therefore, in this study we examined the effects of co-exposure to MMA(V), DMA(V), or TMA(V) in the absence and presence of the AhR ligand, 2,3,7,8-tetrachlorodibenzo-p-dioxin (TCDD), on the expression of CYP1A1 in HepG2 cells. Our results showed that

treatment of HepG2 cells with MMA(V), DMA(V), or TMA(V) alone significantly induces CYP1A1 mRNA, protein, and catalytic activity levels. Furthermore, when the cells were co-exposed to MMA(V), DMA(V), or TMA(V) in the presence of TCDD, there was further potentiation of the TCDD-mediated induction of CYP1A1 mRNA, protein, and catalytic activity levels. In addition, MMA(V), DMA(V), and TMA(V) in the absence and presence of TCDD induced the AhR-dependent XRE-driven luciferase reporter activity, suggesting an AhR-dependent mechanism. In conclusion, this is the first demonstration that As(III) metabolites, MMA(V), DMA(V), and TMA(V) induce CYP1A1 mRNA, protein, and catalytic activity levels in an AhR-dependent mechanism and represents a novel mechanism by which As(III) causes carcinogenicity. Supported by NSERC Discovery Grant RGPIN 250139-12.

**PS 2293 Comparative Oxidation State Specific Analysis of Arsenic by High-Performance Liquid Chromatography-Inductively Coupled Plasma-Mass Spectrometry and Hydride Generation-Cryotrapping-Atomic Absorption Spectrometry.**

J. Currier<sup>1</sup>, R. Saunders<sup>2</sup>, L. Ding<sup>2</sup>, W. M. Bodnar<sup>3</sup>, P. Cable<sup>3</sup>, T. Matoušek<sup>4</sup>, J. Creed<sup>5</sup> and M. Styblo<sup>2</sup>. <sup>1</sup>Curriculum in Toxicology, University of North Carolina at Chapel Hill, Chapel Hill, NC; <sup>2</sup>Department of Nutrition, University of North Carolina at Chapel Hill, Chapel Hill, NC; <sup>3</sup>Department of Environmental Sciences and Engineering, University of North Carolina at Chapel Hill, Chapel Hill, NC; <sup>4</sup>Institute of Analytical Chemistry of the ASCR, Brno, Czech Republic; <sup>5</sup>Microbiological and Chemical Exposure Assessment Research Division, NERL, US EPA, Cincinnati, OH.

Several methods are used for quantifying the toxic inorganic arsenic (iAs) metabolites, methylarsonous acid (MAs<sup>III</sup>) and dimethylarsinous acid (DMAs<sup>III</sup>), including reversed-phase high-performance liquid chromatography-inductively coupled plasma-mass spectrometry (HPLC-ICP-MS) and hydride generation-cryotrapping-atomic absorption spectrometry (HG-CT-AAS). While HG-CT-AAS has consistently detected these arsenicals in biological samples, HPLC-ICP-MS has provided contradictory results. Here, we compare the capacities of both methods to detect and quantify MAs<sup>III</sup> and DMAs<sup>III</sup> in an in vitro methylation system containing recombinant human arsenic (+3 oxidation state) methyltransferase (AS3MT), S-adenosyl methionine, a non-thiol reductant tris(2-carboxyethyl)phosphine, and arsenite (iAs<sup>III</sup>) or MAs<sup>III</sup> as substrates. HPLC separation of the in vitro methylation mixture resulted in significant losses of MAs<sup>III</sup> and DMAs<sup>III</sup> with total arsenic recoveries below 25%. Ultrafiltration showed that both MAs<sup>III</sup> and DMAs<sup>III</sup> are bound to AS3MT. Oxidation of the mixture with H<sub>2</sub>O<sub>2</sub> prior to HPLC separation increased arsenic recoveries to ~95% but oxidized MAs<sup>III</sup> and DMAs<sup>III</sup>, thus preventing quantification of these metabolites. In contrast, direct HG-CT-AAS analysis revealed large quantities of MAs<sup>III</sup> and DMAs<sup>III</sup> and high total arsenic recoveries (>72%) after cysteine treatment. These data suggest that HPLC-ICP-MS can provide false-negative results when used for analysis of MAs<sup>III</sup> or DMAs<sup>III</sup> in biological samples containing protein at concentrations as low as those commonly found in human urine.

**PS 2294 The Retention of Trivalent Arsenic Metabolites in Urothelial Cells Is Associated with Markers of As Exposure and Diabetes.**

M. Styblo<sup>5</sup>, J. Currier<sup>1</sup>, C. González-Horta<sup>2</sup>, L. M. Del Razo<sup>3</sup>, B. Sánchez-Ramírez<sup>2</sup>, L. Ballinas-Casarrubias<sup>2</sup>, G. G. García-Vargas<sup>4</sup>, M. C. Ishida<sup>2</sup>, R. Saunders<sup>2</sup>, Z. Drobna<sup>2</sup> and D. Loomis<sup>6</sup>. <sup>1</sup>Curriculum in Toxicology, University of North Carolina at Chapel Hill, Chapel Hill, NC; <sup>2</sup>Universidad Autónoma de Chihuahua, Chihuahua, Mexico; <sup>3</sup>CINVESTAV-IPN, Mexico City, Mexico; <sup>4</sup>Universidad Juárez del Estado de Durango, Durango, Mexico; <sup>5</sup>University of Nebraska Medical Center, Omaha, NE; <sup>6</sup>Department of Nutrition, University of North Carolina at Chapel Hill, Chapel Hill, NC.

Chronic exposure to inorganic arsenic (iAs) in drinking water has been linked to an increased prevalence of diabetes. Laboratory evidence suggests that methylarsonous acid (MAs<sup>III</sup>) and dimethylarsinous acid (DMAs<sup>III</sup>) that are formed in the course of iAs metabolism contribute to the diabetogenic effects of iAs exposure. However, no data are available on tissue concentrations of these toxic metabolites in humans. Here, we used a newly developed hydride generation(HG)-cryotrapping(CT)-inductively coupled plasma-mass spectrometry method with limits of detection of 0.04-2 pg As to examine the retention of tri- and pentavalent metabolites of iAs in urinary bladder exfoliated cells (BECs) isolated from urine of 343 residents of Chihuahua, Mexico who ingest drinking water contaminated with up to 400 ppb As. The urinary metabolites of iAs were measured by HG-CT-atomic absorption

spectrometry. The sum of As species in BECs ranged from 0.8 to 3,137 pg As/10,000 cells. Notably, iAs was the major species retained in BECs (~66% of total As). MAs<sup>III</sup> and DMAs<sup>III</sup> accounted for 8 and 2% of total As. We found positive statistically significant correlations between the concentrations of As species in BECs and in urine ( $r = 0.12-0.55$ ,  $p < 0.001$ ). When adjusted for age, sex, and BMI, trivalent arsenicals retained in BECs were significantly correlated with markers of diabetes, fasting plasma glucose (FPG) and 2-hour plasma glucose (2HPG) ( $r = 0.13-0.20$ ,  $p < 0.001$ ). Urinary iAs, MAs, and DMAs also correlated with FPG and 2HPG ( $r = 0.15-0.21$ ,  $p < 0.001$ ). Thus, both urinary metabolites of iAs and the metabolites retained in BEC can be used as biomarkers of the diabetogenic effects of iAs exposure.

**PS 2295 Oxidation State Specific Analysis of Arsenic Species in Tissues of Wildtype and Arsenic (+3 Oxidation State) Methyltransferase (As3mt) Knockout Mice.**

C. Douillet<sup>2</sup>, J. Currier<sup>1</sup>, R. Saunders<sup>2</sup>, Z. Drobna<sup>2</sup> and M. Styblo<sup>2</sup>. <sup>1</sup>Curriculum in Toxicology, University of North Carolina at Chapel Hill, Chapel Hill, NC; <sup>2</sup>Department of Nutrition, University of North Carolina at Chapel Hill, Chapel Hill, NC.

As3mt catalyzes the conversion of inorganic arsenic (iAs) to methylated metabolites, including methylarsonite (MAs<sup>III</sup>) and dimethylarsinite (DMAs<sup>III</sup>). While this enzyme is critical for the detoxification of ingested iAs, MAs<sup>III</sup> and DMAs<sup>III</sup> are more toxic than iAs. The As3mt-KO mice can thus be used to explore the role of MAs<sup>III</sup> and DMAs<sup>III</sup> in the adverse effects of iAs exposure. Wild-type (WT) C57BL/6 mice exposed to 50 ppm As as arsenite (iAs<sup>III</sup>) in drinking water developed diabetes characterized by impaired glucose tolerance without insulin resistance. Methylated arsenicals were detected in tissues maintaining glucose homeostasis, but the oxidation state of As was not determined. Our recently developed HG-CT-AAS method for the oxidation state specific speciation of As in complex biological matrices was used to compare retention of tri- and pentavalent As species in tissues of WT and As3mt-KO mice drinking water with iAs. As3mt-KO mice were exposed to 0, 15, 20, 25 or 30 ppm and WT mice to 50 ppm As as iAs<sup>III</sup> for 4 weeks. As3mt-KO mice retained almost exclusively iAs; iAs<sup>III</sup> was the most prevalent species in liver, pancreas, adipose, lung, heart, and kidney, ranging from 53 to 74% of total As. Methylated arsenicals did not exceed 10% of total As in any tissue. Tissues of WT mice retained iAs and methylated arsenicals; iAs<sup>III</sup>, MAs<sup>III</sup> and DMAs<sup>III</sup> represented 55-68% of the total As in the liver, pancreas, and brain. High levels of MAs<sup>III</sup> were found in the intestine and intestinal content of WT, but not As3mt-KO mice, suggesting that intestinal bacteria are not a major source of methylated As species. Our results indicate that internal total As doses in tissues critical to glucose homeostasis (liver, pancreas, skeletal muscle, adipose) equivalent to WT mice can be achieved in As3mt-KO mice after exposure to 25 and 30 ppm As. Future studies will compare the diabetogenic effects of iAs exposure in WT and As3mt-KO mice.

**PS 2296 Photo-Activatable GFP-Labeled Rat Glucocorticoid Receptor (paGFP-rGR) As Model to Study Effects of Arsenic on Endocrine Receptor Activation and Cellular Localization.**

S. K. Schmalig<sup>1,3</sup>, F. Zandbergen<sup>1</sup>, A. Adebayo<sup>1,2</sup>, C. M. Connolly<sup>1,4</sup>, V. Chatikavanij<sup>1</sup>, J. E. Bodwell<sup>5</sup> and J. W. Hamilton<sup>1,2</sup>. <sup>1</sup>Marine Biological Laboratory, Woods Hole, MA; <sup>2</sup>Brown University, Providence, RI; <sup>3</sup>Bridgewater State University, Bridgewater, MA; <sup>4</sup>Valdosta State University, Valdosta, RI; <sup>5</sup>Dartmouth Medical School, Lebanon, NH.

Exposure to arsenic (As) is associated with an increased risk of many serious illnesses including several types of cancer, type 2 diabetes, cardiovascular disease, and reproductive and developmental problems. Previous research showed that As can act as an endocrine disruptor, altering the regulation of gene expression by numerous nuclear hormone receptors, including the Glucocorticoid Receptor (GR). At very low doses (0.05-1  $\mu$ M) As enhanced hormone-mediated, GR-regulated gene expression by 2- to 3-fold. Conversely, at intermediate non-cytotoxic concentrations (1-5  $\mu$ M) As inhibits receptor-mediated gene expression. We have hypothesized that these differential effects reflect separate mechanisms with different targets and that the inhibited activation could be caused by 1) altered rate of hormone receptor translocation to the nucleus, 2) altered number of receptors that translocate, 3) altered steady-state nuclear levels of receptor (e.g., by decreases in nuclear export), 4) altered efficiency of receptor function, or some combination of these. To test this, we used HEK293 cells to generate a cell line stably expressing rat GR fused to photo-activatable Green Fluorescent Protein (HEK293-paGFP-rGR), allowing

for intracellular tracking of GR using microscopy. The paGFP-rGR behaves biochemically in a similar manner as native GR. PaGFP-rGR mediates hormone-induced gene expression and microscopy showed that the rate and extent of nuclear translocation of paGFP-rGR increase in a concentration dependent manner in response to synthetic glucocorticoid. We found that intermediate As concentrations reduce this translocation. (Funded by NIH-NIEHS SRP (P42 ES007373), NSF REU (0115378), and NIH-NRSA (2 T32 ES 7272-21))

## PS 2297 **In Utero Arsenic Exposure and Epigenetic Changes in the Mouse Liver: Comparisons with Transcriptional Modulation.**

K. Bailey<sup>1</sup>, D. Rojas<sup>2</sup>, Z. Drobna<sup>3</sup> and R. C. Fry<sup>1,2</sup>. <sup>1</sup>*Environmental Sciences and Engineering, University of North Carolina at Chapel Hill, Chapel Hill, NC;* <sup>2</sup>*Curriculum in Toxicology, University of North Carolina at Chapel Hill, Chapel Hill, NC;* <sup>3</sup>*Department of Nutrition, University of North Carolina at Chapel Hill, Chapel Hill, NC.*

Chronic exposure to high levels of iAs in drinking water is associated with cancers of the skin, urinary bladder, lung, liver, and prostate in humans. Exposure to iAs during fetal development has been of particular concern as this developmental time point is often particularly sensitive to the effects of environmental toxicants. In C3H and CD1 mice, iAs acts as a complete transplacental carcinogen in which male offspring born to pregnant CH3 and CD1 females exposed to 85 ppm iAs in drinking water during the latter part of gestation [gestational day (GD) 8-18] have an increased incidence of hepatocellular carcinomas (HCCs) in adulthood, a major form of cancer associated with chronic iAs exposure in humans. Analyses of normal-appearing liver tissue from transplacentally-exposed newborns and adults with liver tumors have previously reported perturbations in gene expression and/or global DNA methylation levels and suggested these alterations may contribute to iAs-associated liver carcinogenesis. Here, we examined the gene expression profiles of >35,000 transcripts and the DNA methylation levels of >15,000 CpG islands associated with gene promoters of fetal male CD1 mice (GD 18) transplacentally exposed to a hepatocarcinogenic dose (85 ppm) of iAs (GD 8-18). Compared to vehicle-exposed mice, we observed statistically significant changes in the transcriptome (308 transcripts) and DNA methylome (191 gene promoters) in gestationally-exposed fetal males ( $p < 0.05$ , 1.3-fold change vs. controls). Surprisingly, when using these same criteria for the identification of changes in DNA methylation and transcript levels, there were no common genes. These results suggest alterations in the DNA methylome may not necessarily be predictive of changes in gene expression and the relevance of these alterations in disease development warrant further study.

## PS 2298 **Arsenic Compromises Airway Epithelial Barrier Properties in Primary Mouse and Immortalized Human Cell Cultures.**

C. L. Sherwood<sup>1,4,5</sup>, A. Liguori<sup>1,4,5</sup>, C. Olsen<sup>1,4</sup>, C. Lantz<sup>2,4,5</sup>, J. L. Burgess<sup>4,6</sup> and S. Boitano<sup>1,3,4</sup>. <sup>1</sup>*Arizona Respiratory Center, AZ Health Sciences Ctr, Tucson, AZ;* <sup>2</sup>*Cell and Molecular Medicine, AZ Health Sciences Ctr, Tucson, AZ;* <sup>3</sup>*Physiology, AZ Health Sciences Ctr, Tucson, AZ;* <sup>4</sup>*Southwest Environmental Health Sciences Ctr, University of Arizona, Tucson, AZ;* <sup>5</sup>*Bio5 Institute, University of Arizona, Tucson, AZ;* <sup>6</sup>*Mel & Enid Zuckerman College of Public Health, University of Arizona, Tucson, AZ.*

Arsenic is a lung toxicant that can lead to respiratory illness through inhalation and ingestion. Lung effects from arsenic exposure include lung cancer and obstructive lung disease, as well as reductions in lung function and immune response. As a key player in innate immune defense, airway epithelial cells provide a barrier that protects underlying tissue from inhaled particulates, pathogens, and toxicants. In animal and human studies, arsenic ingestion can lead to altered lung function suggestive of epithelial barrier dysfunction. In this report, we evaluated the effects of a five-day exposure to environmentally relevant levels of arsenic (i.e.,  $< 4 \mu\text{M}$  as Na-arsenite; equivalent to  $\sim 300 \text{ ppb}$ ) on airway epithelial barrier properties. In a primary mouse tracheal epithelial (MTE) cell model we found that both micromolar ( $3.9 \mu\text{M}$ ) and sub-micromolar ( $0.8 \mu\text{M}$ ) arsenic concentrations reduced transepithelial resistance, a measure of barrier function. Immunofluorescent staining of arsenic-treated MTE cells showed altered localization patterns of barrier proteins claudin-1 and occludin at cell-cell contacts. In order to better quantify arsenic-induced changes in barrier molecular components we used the same arsenic exposure on an immortalized human bronchial epithelial cell line (16HBE14o-). We found that arsenic increased the protein expression of claudins -4, -5, and -7 as well as the mRNA levels of claudin-7 in 16HBE14o- cells. Additionally, micromolar levels of arsenic resulted in altered phosphorylation of occludin. In summary, exposure to environmentally relevant levels of arsenic can alter both the structure and function of airway epithelial barrier constituents and, consequently, basic innate immune defense in the airway.

## PS 2299 **Associations of Single Nucleotide Polymorphisms and Haplotypes in Arsenic [+3 Oxidation State] Methyltransferase (AS3MT) with Arsenic Metabolism: A Case Study in Arsenic Contaminated Areas from Vietnam.**

T. Agusa<sup>1</sup>, T. Kunito<sup>2</sup>, N. M. Tue<sup>1</sup>, V. M. Lan<sup>3</sup>, T. B. Minh<sup>4,5</sup>, P. K. Trang<sup>3</sup>, J. Fujihara<sup>6</sup>, H. Takeshita<sup>6</sup>, S. Takahashi<sup>1</sup>, P. H. Viet<sup>3</sup>, S. Tanabe<sup>1</sup> and H. Iwata<sup>1</sup>. <sup>1</sup>*Center for Marine Environmental Studies (CMES), Ehime University, Matsuyama, Japan;* <sup>2</sup>*Shinshu University, Matsumoto, Japan;* <sup>3</sup>*Center for Environmental Technology and Sustainable Development (CETASD), Vietnam National University, Hanoi, Vietnam;* <sup>4</sup>*Faculty of Chemistry, Vietnam National University, Hanoi, Vietnam;* <sup>5</sup>*United Nations Industrial Development Organization (UNIDO), Hanoi, Vietnam;* <sup>6</sup>*Shimane University Faculty of Medicine, Izumo, Japan.*

To understand associations of single nucleotides polymorphisms (SNPs) and haplotypes in arsenic [+3 oxidation state] methyltransferase (AS3MT) with arsenic metabolism, we investigated local residents from arsenic-contaminated areas of Vietnam. Analysis of 18 SNPs revealed that there were four haplotype (HT) groups (HT1; AS3MT 03963 – 06144 – 12390 – 14215 – 35587 – 37950, HT2; AS3MT 04602 – 35991, HT3; AS3MT 05913 – 09749 – 27215, HT4; AS3MT 358903 – 37853) in this population. Urinary monomethylarsonic acid (MMA)/inorganic As (IA) and MMA/dimethylarsinic acid (DMA) ratios were used as indicators of arsenic metabolism. AS3MT 12590 genotype and HT2 and 4 groups were significantly associated with MMA/IA. On the other hand, MMA/DMA was explained by AS3MT 07395, 08979, 12590, and 14458 genotypes. Because association of AS3MT 14458 with arsenic metabolism observed in this study was consistent with other populations in other previous studies, this SNP may significantly affect the metabolism regardless ethnicity.

## PS 2300 **Mechanism of Arsenic Carcinogenesis in Normal Human Lung Cells.**

H. Xie<sup>1,2,3</sup>, J. Wise<sup>1,2,3</sup>, S. Martin<sup>1</sup> and S. Huang<sup>1</sup>. <sup>1</sup>*Wise Laboratory of Environmental and Genetic Toxicology, University of Southern Maine, Portland, ME;* <sup>2</sup>*Maine Center for Toxicology and Environmental Health, University of Southern Maine, Portland, ME;* <sup>3</sup>*Applied Medical Sciences, University of Southern Maine, Portland, ME.*

Arsenic originates from both geochemical and numerous anthropogenic activities including mining, combustion of fossil fuels, wood preservation, agriculture and metallurgy. Exposure of the general public to significant levels of arsenic is widespread. Arsenic is a well-documented human carcinogen. Long-term exposure to low levels of arsenic in drinking water have been linked to bladder, lung, kidney, liver, prostate, and skin cancer. Among them, lung cancer is of great public concern. However, little is known about how arsenic causes lung cancer and few studies have considered effects in normal human lung cells. The purpose of this study was to determine the cytotoxicity and genotoxicity of arsenic in human primary bronchial fibroblast (NHBF) and epithelial cells (NHBE). Our data show that arsenic induces a concentration-dependent increase in cell death after short (24 h) or longer (120 h) exposures. Arsenic induces concentration-dependent but not time-dependent increase in chromosome damage in fibroblasts. No chromosome damage is induced after either 24 h or 120 h arsenic exposure in epithelial cells. Using comet assay and gamma-H2A.X foci forming assay, we found that 24 h or 120 h exposure to arsenic induces increases in DNA double strand breaks in both cell lines. These data indicate that arsenic is cytotoxic and genotoxic to human lung primary cells. However, the mechanism of arsenic-induced genotoxicity could be different in bronchial epithelial cells than that in fibroblasts. This work is supported by NIEHS grant R15ES021587 (H.X.) and by NIEHS grant ES016893 (J.P.W.). The content is solely the responsibility of the authors and does not necessarily represent the official views of the National Institutes of Health.

## PS 2301 **Gene Expression Alterations among Adults with Chronic Arsenic Exposure in Bangladesh.**

Y. Chervona<sup>1</sup>, A. Muñoz<sup>1</sup>, T. Kluz<sup>1</sup>, M. V. Gamble<sup>2</sup> and M. Costa<sup>1</sup>. <sup>1</sup>*Environmental Medicine, New York University School of Medicine, New York, NY;* <sup>2</sup>*Environmental Health Sciences, Mailman School of Public Health, Columbia University, New York, NY.*

Background: Exposure to arsenic (As) is associated with an increased risk of several cancers, as well as, cardiovascular disease, and childhood neuro-developmental deficits. Arsenic compounds are weakly mutagenic, but can alter DNA methylation and post-translational histone modifications (PTHMs) levels, as well, gene expression.

Methods: Water and urinary arsenic, as well as, gene expression profiles were analyzed in peripheral blood mononuclear cells (PBMCs) from a subset of participants (N=20) of a folate clinical trial in Bangladesh (FACT study). Gene expression profiling was performed using Affymetrix exon ST 1.0 arrays. Differentially expressed genes were identified in a global analysis and real-time PCR was used to validate the expression findings.

Results: Expression analysis revealed that a total of 561 and 1198 genes had a change in expression ( $p=0.05$ ) with increasing arsenic exposure, in males and females respectively. When examined together (N=20), 177 genes had a  $> 1.25$  fold change in expression. The analysis revealed that some genes appear to be gender specific (i.e. adenosylhomocysteinase (AHCY), oxoglutarate (alpha-ketoglutarate) dehydrogenase (lipoamide) (OGDH), lysine (K)-specific demethylase 5C/D (JARID1C/D), and SET domain containing (lysine methyltransferase) 7, while others changed in the same direction among both males and females (i.e. potassium voltage-gated channel, Isk-related family, member 3 (KCNE3), elongation factor, RNA polymerase II, 2 (ELL2), NADH dehydrogenase (ubiquinone) 1 beta sub-complex, 8 (NDUFB8), lactate dehydrogenase D (LDHD). Moreover, both males and females exhibited a decrease in the expression of DNA repair genes with increasing arsenic exposure.

Conclusion: Chronic exposure to As is associated with gender specific alterations in gene expression profiles of Bangladeshi adults.

## **PS 2302 Changes in Regulation of Lipid Metabolism from Low-Dose Arsenic Exposure.**

A. Adebayo<sup>1,2</sup>, F. Zandbergen<sup>2</sup> and J. W. Hamilton<sup>1,2</sup>. <sup>1</sup>Brown University, Providence, RI; <sup>2</sup>Marine Biological Laboratory, Woods Hole, MA.

Arsenic (As) is naturally present in the environment, and it can be found at various levels in drinking water resulting from contamination of groundwater. Exposure to As is a major health concern because it is associated with an increased risk of various diseases such as type II diabetes, cardiovascular disease (CVD), several types of cancer, and reproductive and developmental problems. Type II diabetes and CVD are in turn associated with altered blood lipid levels and obesity. Indeed, excess adipose tissue and altered blood lipid levels have been shown to be strong predictors for development of type II diabetes and CVD. Previous cell culture studies have shown that arsenic affects adipogenesis, and a recent *in vivo* study found that arsenic exposed dams displayed alterations in overall lipid metabolism and triglyceride levels. In the current study, we developed a model to investigate changes in transcription factors involved in regulating lipid metabolism. We exposed adult male C57BL/6J mice to 0, 10, or 100 ppb As in drinking water for 6 weeks, and then isolated various tissues from these mice in the fed or fasted state. We analyzed expression of genes and proteins involved in lipid metabolism and regulation in adipose tissue and liver using quantitative PCR and western blotting. Our results show alterations in expression of transcription factor SREBP-1c and its target genes, including diglyceride acyltransferase (DGAT2) and fatty acid synthase (FAS). These results indicate that arsenic can alter the expression of genes and proteins involved in fatty acid synthesis and triglyceride production, which may contribute to how arsenic exposure may cause metabolic imbalances in exposed individuals.

(Funded by NIH-NIEHS Superfund Research Program (P42 ES007373), and NIH-NRSA Training Grant (2 T32 ES 7272-21))

## **PS 2303 Survey of Arsenic in Drinking Water in the Southern Gobi Region of Mongolia.**

P. B. Olkhanud<sup>1</sup> and E. K. Silbergeld<sup>2</sup>. <sup>1</sup>Department of Environmental Health Sciences, HSUM, Ulaanbaatar, Mongolia; <sup>2</sup>Department of Environmental Health Sciences, JHSPH, Baltimore, MD.

Arsenic (As) is a naturally occurring toxicant of global concern. The extent of As content in ground water, however, has not been fully assessed in Mongolia, where all drinking water is sourced from groundwater. Mongolia is currently experiencing rapid mining development, especially in the southern region, which is triggering population growth that will drive increasing water demand for safe drinking water. Moreover, the high prevalence of As exposure and As related diseases just across the border in northern China further highlights the necessity for relevant studies in Mongolia. Thus, this study attempts to determine As concentrations in water sources near the Oyu Tolgoi mine in the Southern Gobi region of Mongolia and investigate its relationship with area, type and depth of the well, and develop a geo-statistical map describing the spatial pattern of As concentration in the drinking water sources. The results of our study show that the current and the potential future exposure to As in the Southern Gobi region of Mongolia is significant. In terms of current exposures, almost half of the Herder's wells that are currently in use and 16.4% of the Monitoring boreholes contain As levels above the World Health Organization's recommended level. The results also indicate different levels of As concentrations in the water from different types of tube-wells even in the same area

and a decreasing tendency of As concentration with increasing well depth suggesting different aquifers in that region. Overall, As in the drinking water sources in the Southern Gobi region of Mongolia is a critical public health issue, especially given the current mining boom in this region.

## **PS 2304 The Role of miRNA-29B in Dysregulation of Mesenchymal Stem Cell Differentiation to Adipocytes by Low-Dose Arsenic Exposure.**

K. Beezhold, L. R. Klei, Y. Garciafigueroa and A. Barchowsky. *Environmental and Occupational Health, University of Pittsburgh, Pittsburgh, PA.*

Human exposure to environmental toxicants is a well-known cause of disease and low chronic exposure may contribute significantly to longitudinal risk of chronic diseases. Pathogenic mechanisms for many environmental toxicants remain poorly defined, which limits development of effective interventions to protect against environmentally-derived chronic diseases. Low dose exposure to trivalent arsenic (AsIII) in drinking water is a major public health concern that contributes to a number of diseases and pathologies, including cardiovascular and metabolic diseases. While progress has been made in the understanding of the pathogenic signaling events contributing to arsenic-induced disease, many responsible mechanisms have not been elucidated. Control of miRNA expression and action presents a promising new means for understanding downstream effects of arsenic exposure; however, there are few reports of how arsenic regulates expression of miRNA and impacts their function. Our preliminary data indicated induction of miR-29 in white and brown adipose tissue isolated from arsenic exposed (100 µg/L in drinking water for 2 wk) mice and in human adipose-derived mesenchymal stem cells (hMSC) as arsenic inhibited adipocyte differentiation. Further analysis via real-time PCR revealed a 2-3 fold induction of miR-29b following arsenic exposure in hMSCs. The miR-29 family has been indicated by multiple studies to be involved in cardiovascular and metabolic diseases, with reduced stem or progenitor cell differentiation capacity believed to be a fundamental means for disease progression. Analysis of downstream proteins by western blot indicates that C/EBP- $\zeta$ , an inhibitor of adipogenesis, is upregulated in arsenic treated cells and this upregulation is diminished in cells stably expressing an inhibitor of miR-29b. These data show that exposure to low-dose arsenic effects expression of miRNA in hMSCs, negatively affecting their ability to properly differentiate into adipocytes. Supported by NIEHS grant R01ES013781.

## **PS 2305 Human Exposure to Arsenic in Drinking Water Is Associated with Increased Protein Halogenation in Blood and Sputum.**

R. Zangar<sup>1</sup>, R. Lantz<sup>2</sup>, R. B. Harris<sup>2</sup>, J. L. Burgess<sup>2</sup>, M. K. O'Rourke<sup>2</sup>, M. M. Montenegro<sup>3</sup>, M. M. Matzke<sup>1</sup>, B. Webb-Robertson<sup>1</sup> and J. G. Pounds<sup>1</sup>. <sup>1</sup>PNNL, Richland, WA; <sup>2</sup>University of Arizona, Tucson, AZ; <sup>3</sup>Instituto Tecnológico de Sonora, Tucson, Mexico.

Chronic arsenic exposure to environmentally high levels ( $> 200$  ppb) in geologically contaminated drinking water has been correlated with increased incidence of chronic lung disease, including cough, bronchitis, shortness of breath and obstructive or restrictive lung disease. However, the effects of chronic arsenic exposures at lower levels (e.g.,  $< 100$  ppb), which are prevalent in the United States and near the current EPA MCL of 10 ppb, have not been well studied. Eosinophils and neutrophils are associated with lung disease, and these granulocytes selectively secrete peroxidases that halogenate protein tyrosines. A custom ELISA microarray platform was used to measure the halogenation of 24 individual proteins in paired sputum and serum samples from 55 subjects in 4 Mexican cities with differing arsenic levels. Eighteen halogenated proteins were significantly correlated (Spearman's rank correlation,  $p < 0.05$ ) between the two fluids (highest  $r$  value  $-0.58$ ). Halogenated protein results were compared to total arsenic levels in urine using multiple linear regression, accounting for the study participants' age, BMI and resident city. The total urine arsenic was significantly associated ( $P \leq 0.05$ ) with the halogenation of 7 proteins in both plasma and serum (MMP1, 2 and 9, EGFR, VEGF, HBEGF, TGF $\alpha$ ) and 11 additional sputum-only proteins (PDGF, E-selectin, EGF, SP-A, leptin, HGF, CD14, IGF1, RANTES, TNF, ceruloplasmin) proteins. These results support the conclusion that environmental arsenic exposure is associated with elevated markers of pulmonary granulocyte activity. Replication in an independent study population is warranted to confirm our results. Supported by P42 ES4940, P30 ES006694, P50 CA095060, and U54 ES016015.

**PS 2306 Evaluating Arsenic Speciation in Fish, Shellfish, and Seaweed Using LC-ICPMS.**

B. D. Laird and L. Chan. *Department of Biology, University of Ottawa, Ottawa, ON, Canada.*

**Rationale & Objectives:** Risk due to dietary arsenic (As) exposure is speciation dependent. For example, although elevated As concentrations are commonly observed in fish, shellfish, and seaweed, the health risks are generally assumed to be low due to the predominance of organoarsenicals (e.g. arsenobetaine). However, little speciation data is available to support this assumption for many types of seafood. The objective of the research described in this poster is to fill this data gap by quantifying the relative contribution of various As species for a variety of store-bought seafood samples.

**Methodology:** Seafood samples were purchased from several supermarkets for As speciation analysis using Liquid Chromatography Inductively Coupled Plasma Mass Spectrometry (LC-ICP-MS). The samples included cherry stone clams, oyster shell clams, tiger prawn, halibut, mackerel, ling cod, marlin, snapper, yellow grouper, and Porphyra seaweeds. Extraction of As species was performed with a methanol-ammonium carbonate solution using a DigiPREP block digestion system. Quantified As species included As(III), As(V), arsenobetaine, arsenocholine, dimethylarsinic acid, and monomethylarsonic acid.

**Results:** Total As concentrations ranged between 6 (king mackerel) and 135 (ling cod)  $\mu\text{g g}^{-1}$  (d.w.). The main contributor to As concentrations tended to be arsenobetaine, which ranged between 35% (yellow grouper) and 100% (king mackerel). As(V) was not a significant contributor (<1%) to total As concentrations in any of the samples.

**Conclusions:** Arsenobetaine was the major As species in most of the seafood samples tested. Future work will be done to assess whether As speciation in foods is modified when digested in simulated gastrointestinal fluids.

**PS 2307 Reduction of Arsenite-Enhanced Ultraviolet Radiation DNA Damage by Supplemental Zinc.**

K. L. Cooper, B. S. King, M. M. Sandoval, K. Liu and L. G. Hudson. *Pharmaceutical Sciences, University of New Mexico, Albuquerque, NM.*

Arsenic is a recognized human carcinogen and there is evidence that arsenic augments the carcinogenicity of DNA damaging agents such as ultraviolet radiation (UVR) thereby acting as a co-carcinogen. Inhibition of DNA repair is one proposed mechanism to account for the co-carcinogenic actions of arsenic. We and others find that arsenic interferes with the function of certain zinc finger DNA repair proteins. Furthermore, we reported that zinc reverses the effects of arsenic in cultured cells and a DNA repair target protein, poly (ADP-ribose) polymerase-1. The study objective was to determine whether zinc ameliorates the effects of arsenite on UVR-induced DNA damage in human keratinocytes and in an in vivo model. In order to investigate the potential zinc effects, normal human epidermal keratinocytes (HEKn) and SKH-1 hairless mice were exposed to arsenite, zinc or both before solar-simulated (ss) UVR exposure. Poly (ADP-ribose) polymerase activity and DNA damage in each treatment group were measured in normal human keratinocytes by immunocytochemistry and mutation frequencies at the hprt locus were measured. DNA damage was assessed by immunohistochemical staining of skin sections isolated from SKH-1 hairless mice. Cell-based findings demonstrate that ssUVR-induced DNA damage and mutagenesis are enhanced by arsenite, and supplemental zinc partially reverses the arsenite effect. In vivo studies confirm that zinc supplementation decreases arsenite-enhanced DNA damage in response to ssUVR exposure. From this data we can conclude that zinc offsets the impact of arsenic on ssUVR-stimulated DNA damage in cells and in vivo. This suggests that zinc supplementation may provide a strategy to improve DNA repair capacity in arsenic exposed human populations.

**PS 2308 Arsenic-Stimulated Adipose Fat Metabolism Is Mediated by G-Protein Coupled Receptors.**

Y. Garciafigueroa, L. R. Klei and A. Barchowsky. *Environmental and Occupational Health, University of Pittsburgh, Pittsburgh, PA.*

Consumption of low to moderate levels of arsenic (As(III)) promotes a number of diseases that may stem from dysfunctional adipose tissue and glucose metabolism. As(III) inhibits adipocyte differentiation and insulin-stimulated glucose uptake. However, little is known of the impacts of As(III) on adipose lipid storage and lipolysis, as well as mechanisms through which As(III) affects lipolysis. We recently demonstrated that As(III)-inhibited human mesenchymal stem cell (hMSC) differentiation to adipocytes was mediated by G-protein coupled endothelin-1 receptors and hypothesized that a similar mechanism signals for As(III)-stimulated fat mobilization and utilization in mature adipocytes. To test this hypothesis, adipocytes

(identified by perilipin-coated, Nile red positive lipid droplets) derived from primary hMSC were exposed to 1  $\mu\text{M}$  As(III) for 24 to 72 h. As(III) stimulated lipolysis within 24 h relative to untreated adipocytes and caused a progressive loss of perilipin and lipid droplets over 72 h. As(III)-stimulated lipolysis was not associated with an increase in cAMP. However, pre-incubation of the adipocytes with the Gi-inhibitor, Pertussis toxin (Ptx), attenuated As(III)-stimulated lipolysis and lipid droplet loss. Selective inhibition of Gi-coupled endothelin-1 type A and B receptors (EDNRA/EDNRB) also attenuated the effects of As(III), but inhibition of other adipose Gi-coupled receptors involved in fat metabolism was ineffective. The endothelin receptors have different roles in the As(III) responses, since EDNRA inhibition was more effective in preserving lipid droplets and perilipin expression while blocking either endothelin receptor attenuated As(III)-stimulated lipolysis. These findings provide additional evidence that As(III) effects on adipogenesis, adipose cell function, and lipid metabolism are mediated through stimulation of specific G-protein coupled receptors. Supported by NIEHS grant R01ES013781 and R01ES013781-S1.

**PS 2309 Autophagy Is a Cell Self-Protective Mechanism against Arsenic-Induced Cell Transformation.**

G. Chen, T. Zhang and Y. Qi. *University of Kentucky, Lexington, KY.*

Subchronic exposure to arsenic increases the incidence of human cancers, such as skin, lung, colon and rectal cancer. The mechanism for arsenic-induced tumorigenesis is still not clear. It is generally believed that DNA damage and genomic instability, generated by arsenic-promoted oxidative stress, account largely for this process. The major sources of reactive oxygen species (ROS) are arsenic-damaged mitochondria. Autophagy is a catabolic process functioning in turnover of long-lived proteins and dysfunctional organelles such as mitochondria. Defects of autophagy under stress conditions promote genomic instability and increase the risk of tumorigenesis. In the present study using a human bronchial epithelial cell line, BEAS-2B cells, we investigated the role of autophagy in arsenic-induced cell transformation, an important step in arsenic tumorigenesis. Our results show that subchronic arsenic exposure induces BEAS-2B cell transformation accompanied with increased ROS generation and autophagy activation. However, the patterns for ROS and autophagy alteration are different. Arsenic exposure generated a prolonged and steady increase of ROS levels, while the activation of autophagy, after an initial boost by arsenic administration, decreases in response to subchronic arsenic exposure, although the activity is still higher than a non-treated control. Further stimulation of autophagy increases mitochondria turnover and decreases ROS generation as well as arsenic-induced cell transformation. Contrarily, inhibition of autophagy activity decreases mitochondria turnover and enhances arsenic-induced ROS generation and cell transformation. In addition, the mTOR signaling pathway is involved in arsenic-mediated autophagy activation. Our results suggest that autophagy is a cell self-protective mechanism against arsenic-induced cell transformation.

**PS 2310 In Utero Low-Level Arsenite Exposure Alters Blood Biochemistry in Adult Mice Predisposing for Liver Steatosis.**

P. Sanchez Soria<sup>1</sup>, S. Quach<sup>1</sup>, R. N. Hardwick<sup>1</sup> and T. D. Camenisch<sup>1, 2, 3</sup>.

<sup>1</sup>College of Pharmacy, University of Arizona, Tucson, AZ; <sup>2</sup>Steele Children's Research Center, University of Arizona, Tucson, AZ; <sup>3</sup>Southwest Environmental Health Sciences Center, University of Arizona, Tucson, AZ.

Chronic exposure to low levels of arsenic in drinking water has been strongly correlated to higher incidence of hypertension as well as other cardiovascular diseases. Additionally, recent animal studies have shown that chronic exposure to 100 parts per billion (ppb) sodium arsenite resulted in a significant increase in systolic blood pressure, and a similar increase was observed in diastolic blood pressure. Additionally, mice exposed to arsenic developed concentric left ventricular hypertrophy. In order to explore the mechanisms of arsenic-related adult disease, we wanted to evaluate how in-utero exposure contributes to the development of disease, later in adulthood. Mice were exposed to either 100 ppb in-utero, or sodium chloride (control) and were maintained for 34 weeks through adulthood. Blood biochemistry analysis was done, and organs were harvested for histological assessment, as well as protein and RNA studies. Results show that mice exposed to arsenic in-utero had significantly elevated blood glucose levels, as well as significantly higher cholesterol, LDL and HDL levels with no significant change in weight, when compared to control mice. Furthermore, liver enzymes alkaline phosphatase (ALP), alanine transaminase (ALT), and aspartate transaminase (AST) were elevated in the in-utero exposed mice, when compared to controls. Consistent with these results, oil red-o stain of liver sections show moderate steatosis and higher lipid content in the arsenic treated animals. Taken together, these results show that exposure to arsenic early in life may predispose for the development of metabolic diseases as well as cardiovascular ones.

## PS 2311 Arsenic Impairs Adult Muscle Stem Cells and Skeletal Muscle Integrity.

A. Roperti<sup>1</sup>, D. Stoltz<sup>2</sup>, B. Goodpaster<sup>3</sup>, E. Brown<sup>4</sup>, G. Distefano<sup>4</sup>, A. Barchowsky<sup>5</sup> and F. Ambrosio<sup>4</sup>. <sup>1</sup>Bioengineering, University of Pittsburgh, Pittsburgh, PA; <sup>2</sup>Cell Biology and Physiology, University of Pittsburgh, Pittsburgh, PA; <sup>3</sup>Medicine, University of Pittsburgh, Pittsburgh, PA; <sup>4</sup>Physical Medicine and Rehabilitation, University of Pittsburgh, Pittsburgh, PA; <sup>5</sup>Environmental and Occupational Health, University of Pittsburgh, Pittsburgh, PA.

Arsenic (As(III))-contaminated drinking water is a global health concern as chronic As(III) exposure increases risk for a number of cancers, diseases, and disabilities. As(III) exposure is associated with skeletal muscle weakness, impaired gait, and fatigue. While As(III) and other metals impact embryonic stem cells and development, it is not clear how As(III) impairs adult stem cell functions in tissue maintenance and regeneration. We hypothesized that As(III) exposure affects adult skeletal muscle stem cell (MuSC) metabolism and function to disrupt muscle maintenance and repair capacity. To investigate this hypothesis, we examined muscle integrity, MuSC metabolism, and phenotype in hind limb muscles isolated from mice exposed to 0 or 100 µg/L As(III) for 5 weeks. Histological analysis demonstrated disrupted muscle bundles with perivascular fatty inclusions and ultrastructural analysis revealed large, fused muscle cell mitochondria in As(III) exposed mice relative to control. MuSC isolated from the As(III) mice and cultured without As(III) for multiple doublings retained a phenotype with mitochondrial myopathy, autophagy, uncoupled oxidative phosphorylation, and impaired differentiation. This phenotype was a maladaptation to stress, as As(III) altered growth kinetics and resistance to oxidative stress. The phenotype and altered growth kinetics were reproduced in primary human MuSCs. These findings suggest that direct effects on MuSC mitochondrial phenotype, metabolism, and differentiation underlies muscle impairment observed following As(III) exposures. Supported by NIEHS grant R01 ES0136781, NIH K12 for Physical and Occupational Therapists (K12 HD055931) and NIA grant K01 1K01AG039477.

## PS 2312 Arsenic Induces Premature Senescence and Vascular Calcification *In Vivo* and *In Vitro*.

V. Sorribas, C. Sosa and A. Martin-Pardillos. *Laboratory of Molecular Toxicology, University of Zaragoza, Zaragoza, Spain.* Sponsor: A. Anadon.

Arsenic is a natural vasculotoxic agent with ubiquitous exposure to both, human and animals. Several mechanisms have been proposed to explain the vascular toxicity of arsenic. This work describes new mechanisms that affect the vascular smooth muscle cells (VSMC): stress-induced premature senescence (SIPS), dedifferentiation, and medial vascular calcification.

Rat aortic VSMC were treated with 1-100 µM of sodium arsenate (AsV), arsenite (AsIII), monomethylarsonic acid, or dimethylarsinic acid. None of the treatments induced VSMC calcification in the presence of 1 mM inorganic phosphate (Pi), but 1 µM AsIII increased calcification when induced with 2.5 mM Pi. Cytotoxicities of the four arsenic species were assayed with an LDH assay and acridine orange/ethidium bromide staining. Results revealed that the calcification increase with AsIII was accompanied by a rise in cytotoxicity due to simultaneous incubation with 2.5 mM Pi. This calcification increase was also observed in the aortas of an established vascular calcification model: 5/6 nephrectomized rats fed with a high Pi diet and treated with vitamin D3. Several known mechanisms that might explain arsenic toxicity in our experimental model were discarded: apoptosis, oxidative stress, and inflammasome activation. Nevertheless, both senescence-associated β-galactosidase (SA β-gal) activity and p21 expression were increased by AsIII, which reveals the induction of SIPS. AsIII also caused dedifferentiation of VSMC, as shown by the reduced expression of the VSMC markers SM22α and calponin. Senescence and similar patterns of gene expression were also observed in the aortas of healthy rats treated with 50 ppm AsV in drinking water for one month. In conclusion, both the premature senescence in aortic VSMC with phenotypic dedifferentiation and the increase of Pi-induced calcification are novel mechanisms of arsenic vasculotoxicity observed *in vitro* and *in vivo*.

## PS 2313 Prolonged iAs Exposure Leads to Aberrant Insulin Signaling in L6 Myocytes.

I. L. Druwe, J. J. Sollome, J. Gonzales and R. R. Vaillancourt. *Department of Pharmacology & Toxicology, The University of Arizona, Tucson, AZ.*

Diabetes mellitus is a metabolic syndrome characterized by inappropriate production of insulin or the inability of cells to respond to insulin. It is estimated that by the year 2050, 1 in 3 U.S. adults will have diabetes mellitus. Insulin is the principal hormone involved in lowering blood glucose and functions by suppressing liver

gluconeogenesis and glycogenolysis and by stimulating the glucose uptake in skeletal muscle and adipocytes. Recent epidemiological studies both in the USA and abroad have linked chronic ingestion of low levels of inorganic arsenic (iAs), an environmental toxicant, to the onset of diabetes mellitus. Although these observations have been met with some skepticism, there are few mechanistic studies to elucidate the mechanisms by which iAs perturbs insulin signaling. The few studies that have been performed have focused namely on adipocyte *in-vitro* models. Here we show that L6 myocytes, an insulin responsive cell line, exposed to low doses of iAs (0.25 to 2 µM) for 4 or 7 days showed a decreased insulin stimulated glucose uptake but no decrease in phospho-AKT or phospho-AS160. In addition, we found that phospho-ERK signaling decreased, while phospho-p38 MAPK signaling increased in response to prolonged iAs treatment. Interestingly enough increased p38 MAPK activity has been associated with insulin resistance. These data support the epidemiological evidence that chronic exposure to low, physiologically relevant levels of arsenite can contribute to insulin resistance and type 2 diabetes, and that the mechanisms involved are different than those produced by iAs in adipocyte cell models. And while the etiology of type 2 diabetes has yet to be elucidated these data show that in addition to pharmacological treatment and lifestyle modifications, environmental exposures should also be considered when evaluating the etiology of type 2 diabetes.

## PS 2314 Gene Expression Changes Associated with Chronic Low-Level Monomethylarsonous Acid Exposure in Human Urothelial Cells.

M. Medeiros<sup>1</sup>, T. Minh le<sup>1</sup>, D. J. Troup<sup>1</sup>, P. Novak<sup>2</sup> and A. Gandolfi<sup>1</sup>. <sup>1</sup>Pharmacology and Toxicology, University of Arizona, Tucson, AZ; <sup>2</sup>Biology Centre ASCR, Institute of Plant Molecular Biology, Ceske Budejovice, Czech Republic.

Bladder cancer has been associated with chronic arsenic exposure. Monomethylarsonous acid [MMA(III)] is a metabolite of inorganic arsenic and has been shown to transform a human urothelial cell line (UROtsa). It was used as a model arsenical to examine the mechanisms of arsenical-induced malignant transformation of urothelium. A microarray analysis was performed to assess the transcriptional changes in UROtsa from chronic 50 nM MMA(III) exposure that leads to transformation at three months. The analysis revealed only minor changes in gene expression at one and two months of exposure, contrasting with substantial changes observed at three months of exposure. To assess the changes occurring between 2 and 3 months of exposure, incremental analysis was performed for 29 genes, covering 7 distinct pathways (mitogenic, PI3K/AKT, apoptosis, JAK/STAT, oxidative stress, DNA repair, and inflammation), that were found changed at 3 months of exposure based on the gene array analysis. Between 2 and 3 months of exposure, progressive alterations in the expression of several genes (i.e., PDGFRA, COX2, XAF1) were observed. These alterations are being correlated with expected phenotypic changes (i.e., hyper-proliferation, colony formation in soft agar) in the transforming cells. Since short-term exposure (up to two months) has not been shown to induce transformation, the gene expression changes observed for cultures treated up to 3 months and beyond suggest that a stress-threshold exists. This study was supported by the Superfund Basic Research Program Grant (NIH grant ES04940) from National Institute of Environmental Health Sciences, and the Trainee in Toxicology and Toxicogenomics (NIEHS grant ES007091). Additional support from NIH grant CA23074, and NIEHS grant ES06694.

## PS 2315 Multidrug Resistance Protein 1 Confers Resistance to Organic Arsenic Compound in HL-60 Cells.

H. Narenmandula, S. Xu and Y. Zhang. *Department of Pharmacology, Toxicology, and Biochemical Pharmaceutics, Zhejiang University, Hangzhou, China.* Sponsor: D. Thomas.

Arsenic trioxide is established as one of most effective drugs for treatment of patients with acute promyelocytic leukemia (APL). However, non-promyelocytic leukaemia HL-60 cells is exhibit resistant to As2O3, and little is known about the underlying resistance mechanism for As2O3 and its biomethylation products, namely, monomethylarsonous acid (MMAIII) on the treatment of tumors. In the present study, we investigated the molecular mechanisms underlying iAsIII and its intermediate metabolite MMAIII-induced anticancer effects in the HL-60 cells. Here, we show that the HL-60 cells exhibit resistance to inorganic iAsIII (IC50=10 µM), but are relatively sensitive to its intermediate MMAIII (IC50=3.5 µM). Moreover, we found that the multidrug resistance protein 1 (MRP1), but not MRP2, are expressed in HL-60 cells, which reduced the intracellular arsenic accumulation, and conferred resistance to inorganic iAsIII and MMAIII. Pretreatment of HL-60 with MK571, an inhibitor of MRP1, significantly increased iAsIII and MMAIII-induced cytotoxicity and arsenic accumulations, suggesting that the expression of MRP1/4 may lead to HL-60 cells resistance to trivalent arsenic compounds.

## PS 2316 Integrative Toxicopathological Evaluation of Aflatoxin B1 Exposure in F344 Rats.

G. Qian<sup>1</sup>, F. Wang<sup>1</sup>, L. Tang<sup>1</sup>, M. E. Massey<sup>1</sup>, N. J. Mitchell<sup>2</sup>, J. Su<sup>1</sup>, J. H. Williams<sup>3</sup>, T. D. Phillips<sup>2</sup> and J. Wang<sup>1</sup>. <sup>1</sup>Environmental Health Science, University of Georgia, Athens, GA; <sup>2</sup>Veterinary Integrative Biosciences, Texas A&M University, College Station, TX; <sup>3</sup>Peanut Collaborative Research Support Program, University of Georgia, Griffin, GA.

An integrative evaluation of the toxicopathological effects of aflatoxin B1 (AFB1) was conducted in this study. Briefly, male F344 rats were orally exposed to a single-dose of AFB1 at 0, 50, 250 or 1000 µg/kg body weight (BW) or repeated-dose of AFB1 at 0, 5, 10, 25 or 75 µg/kg BW for up to 5 weeks. Biochemical and histological changes were assessed together with the formation of AFB1-lysine adduct (AFB-Lys) in serum and liver foci positive for placental form glutathione S transferase (GST-P+). In single-dose protocol, serum AST, ALT and ALP were dose-dependently elevated with maximal changes (> 100 folds) appeared at 3-day after treatment. Animal that received 250 µg/kg AFB1 showed concurrent bile duct proliferation, necrosis and appearance of GST-P+ hepatocytes at 3-day while the pre-neoplastic GST-P+ foci appeared after 1-week. Neither liver GST-P+ hepatocytes nor foci were induced by 50 µg/kg AFB1 treatment. In repeated-dose protocol, bile duct proliferation and liver GST-P+ foci co-occurred after 3-week, followed by proliferation foci formation after 4-week and dramatic ALT, AST and CK elevations after 5-week exposure in animals received 75 µg/kg AFB1. Liver GST-P+ hepatocytes and foci appeared in a dose- and time-dependent manner, low dose of AFB1 (5 µg/kg) did not induce liver GST-P+ foci formation throughout the experiment. Serum AFB-Lys increased temporally at low doses (5-25 µg/kg) and reached a maximum after 2-week exposure at 75 µg/kg group, consistent with liver histological changes that may affect the adduct formation. This integrative study demonstrates that liver GST-P+ cells and foci are sensitive biomarkers for AFB1 toxic effect and correlated with bile duct proliferation and biochemical alterations in F344 rats, which hold promise as potential target for future intervention strategies.

## PS 2317 Ethoxyquin Protective Effect against Aflatoxins Chronic Intoxication in Laying Hens.

A. G. Valdivia<sup>1</sup>, M. C. De Luna<sup>1</sup>, R. Ortiz<sup>1</sup>, A. Martinez de Anda<sup>1</sup>, T. Quezada<sup>1</sup>, F. Jaramillo<sup>2</sup> and J. Reyes<sup>3</sup>. <sup>1</sup>Agricultural Sciences Centre, Aguascalientes Autonomous University, Aguascalientes, Mexico; <sup>2</sup>Physiology and Toxicology, Basic Sciences Centre of UAA, Aguascalientes, Mexico; <sup>3</sup>Cellular Physiology, Research and Advanced Studies Centre of IPN, Mexico City, Mexico.

Ethoxyquin (EQ) is a synthetic compound used to prevent lipid oxidation and preserve the nutritional quality of feed. EQ can increase the expression of some enzymes detoxification system. Aflatoxins (AFs) are toxicogenic and carcinogenic common food contaminants that affect human health and productivity in poultry. The aim was to evaluate the EQ ability to decrease the toxic effect of AFs chronic dietary intake in laying hens. At 14 weeks age, 360 Leghorn Hy-Line hens were subjected to experimental chronic intoxication (0.00, 0.50, 1.00 and 1.50 mg AFs/kg BW) for 72 weeks, with and without EQ (500 mg/kg feed). The EQ feed was well accepted by hens and alone did not alter egg production, feed daily intake and feed efficiency index. Dietary AFs consumption decreased of performance of hens and produced pathological and biochemical alterations. However, EQ diminished the AFs induced changes in macro and microscopic architecture of liver and kidneys, plasma total protein, hepatic/renal reduced glutathione, specific enzyme activity of glutathione, gamma-glutamyl, alanine and aspartate transferases, which suggests the presence a EQ chemopreventive effect against AFs toxic effects in laying hens.

## PS 2318 Aflatoxin Exposure in Human Populations of Uganda.

M. Kang<sup>1</sup>, P. Nkurunziza<sup>2</sup>, R. Muwanika<sup>3</sup>, G. Qian<sup>1</sup>, L. Tang<sup>1</sup>, J. Seeley<sup>2</sup>, J. Williams<sup>1</sup> and J. Wang<sup>1</sup>. <sup>1</sup>University of Georgia, Athens, GA; <sup>2</sup>British Medical Research Council Uganda Unit, Entebbe, Uganda; <sup>3</sup>Rakai Health Science Program, Entebbe, Uganda.

Aflatoxins (AF) exposure and aflatoxicosis as well as chronic hepatocarcinogenic effects in human populations are serious global public health threats, especially for the developing world. In this study human serum samples (n=1931) from two existing cohort studies conducted in Uganda were measured for AFB1-lysine adduct. In samples (n=725) from the General Population Cohort (GPC), 90% (651/725) had detectable AFB1-lysine adduct with a median of 1.61 pg/mg albumin, ranged from 0.40 to 253.11 pg/mg albumin. In samples (n=1,206) from Rakai Community Cohort (RCC), 85% (1025/1206) had detectable AFB1-lysine adduct with a median of 3.19 pg/mg albumin, ranged from 0.41 to 167.04 pg/mg albumin. Levels of AFB1-lysine adduct in the RCC samples are significantly higher

than those in the GPC samples ( $p < 0.05$ ). Temporal patterns of AFB1-lysine adduct in these two distinct human populations were further evaluated in samples collected at 3-year interval since the initiation of the cohorts. Detection rates of AFB1-lysine adduct in GPC varied over time: 94% in 1989, 100% in 1992, 84% in 1995, 80% in 1998, 72% in 2001, 93% in 2004, 97% in 2007, and 94% in 2010 with median (range) of 1.77 (0.43-22.46), 2.44 (1.02-5.06), 0.83 (0.41-18.60), 0.89 (0.41-6.02), 1.15 (0.41-11.55), 1.77 (0.41-14.80), 1.92 (0.40-30.89), and 2.29 (0.47-253.11) pg/mg albumin, respectively. Detection rates of AFB1-lysine adduct in RCC also varied: 71% in 1994, 96% in 1996, 91% in 1999, 50% in 2002, 92% in 2005, 89% in 2008, and 90% in 2011 with median (range) of 2.44 (0.41-94.79), 1.16 (0.41-555.33), 1.19 (0.45-122.51), 5.08 (0.51-30.92), 3.58 (0.41-67.56), 3.22 (0.45-117.96), and 2.60 (0.43-167.04) pg/mg albumin, respectively. Levels of AFB1-lysine adduct in samples from these two cohort studies were further assessed with various demographic parameters. These results demonstrated the temporal patterns of AF exposure in rural human populations of Uganda.

## PS 2319 Immunological and Pathomorphological Study of Combined Effects of Fumonisin B1 and Ochratoxin A on Pigslets.

M. Mwanza<sup>1,2</sup>, M. M. Dutton<sup>2</sup> and S. D. Stoev<sup>3</sup>. <sup>1</sup>Animal Health, North West University, Mmabatho, South Africa; <sup>2</sup>Food, Environment and Health Research Group, Faculty of Health Science, University of Johannesburg, Johannesburg, South Africa; <sup>3</sup>Department of General and Clinical Pathology, Faculty of Veterinary Medicine, Trakia University, Trakia, Bulgaria.

In this study, two experiments (*in vivo* and *in vitro*) were carried out to study the effects on OTA and FB1 on pigs mononuclear cells as well as on live pigs to assess the effects of these mycotoxins on their health with particular reference to the immune system and pathomorphological changes. The *in vitro* study showed a time vs concentration decrease of pigs mononuclear cells were used the MTT assay and exposed to 5 and 40 ng/ml for ochratoxin A and 5 and 40 µg/ml of FB1 at 12, 24 and 48 hrs. While the *in vivo* study showed the ochratoxin A induced highest cell viability decrease as compared to FB1 when exposed singularly, whereas exposure to both mycotoxins simultaneously showed further reduction of cell viability. In the *in vivo* study was done with mycotoxic nephropathy induced in eighteen young pigs with mouldy diets containing 0.5 ppm ochratoxin A (OTA) and/or 10 ppm fumonisin B1 (FB1) for three months. The most obvious damage provoked by OTA was seen in the kidneys, as expressed by the strong degenerative changes in proximal tubules and fibrosis in kidneys, FB1 was found to induce an increase in permeability of vessels mainly in lung, brain, cerebellum or kidneys and slight to moderate degenerative changes in kidneys. The exposure to both mycotoxins simultaneously revealed synergistic pathomorphological changes characterized by the combination of the main lesions provoked by each mycotoxin alone, being stronger in their expression when administered together. In addition, Exposure to both mycotoxins and their combination showed induced humoral immune response in all experimental pigs shown by decrease in antibody titers.

## PS 2320 Deoxynivalenol (DON)-Induced Secretion of the Gut Satiety Hormone Cholecystokinin (CCK) in the STC-1 Enteroendocrine Cell Model Is Mediated by the Calcium Sensing Receptor (CaSR) and Transient Receptor Potential Ankyrin-1 (TRPA1).

H. Zhou<sup>1</sup> and J. Pestka<sup>1,2,3</sup>. <sup>1</sup>Food Science and Human Nutrition, Michigan State University, East Lansing, MI; <sup>2</sup>Center for Integrative Toxicology, Michigan State University, East Lansing, MI; <sup>3</sup>Department of Microbiology and Molecular Genetics, Michigan State University, East Lansing, MI.

The trichothecene mycotoxin deoxynivalenol (DON, vomitoxin) causes anorexia and emesis in part by inducing gut satiety hormone secretion by enteroendocrine cells of the gastrointestinal tract. To elucidate mechanisms for these effects, we employed the STC-1 enteroendocrine cell model, which can be induced by DON to secrete the gut satiety peptide cholecystokinin (CCK). We initially found that intracellular calcium mobilization was evoked in STC-1 cells by DON in a concentration- and time-dependent manner, generating sustained sinusoidal oscillations that preceded CCK secretion. Pretreatment with EGTA, a chelator of Ca<sup>2+</sup>, was found to block CCK secretion. Pretreatments with the CaSR (calcium sensing receptor) antagonists, NPS 2143 or Calhex 231 or TRPA1 (transient receptor potential ankyrin-1) antagonist HC 030031 were found to suppress DON-induced Ca<sup>2+</sup> mobilization and CCK release. Both sets of these inhibitors worked in an additive fashion. Furthermore, preincubation with 1) phospholipase C inhibitor, U73122, 2) inositol 1,4,5 triphosphate receptor (IP3R) blocker, 2-aminoethyl diphenylborinate, 3) the transient receptor potential melastatin-5 (TRPM5) inhibitor, triphenylphosphine oxide (TPPO), or 4) the L-type voltage-sensitive Ca<sup>2+</sup> channel (L-type VSCCs) blocker, nitrendipine could also significantly attenuate

DON-induced CCK release in STC-1 cells. The results suggest that DON might induce CCK release in enteroendocrine cells by increasing CaSR sensitivity to extracellular  $[Ca^{2+}]_0$  which mediates increased  $[Ca^{2+}]_i$  influx via L-type-VSCCs  $Ca^{2+}$  and TRPA1 cation channels. DON-induced calcium and hormonal responses demonstrated herein might ultimately contribute to anorexia and emesis potentially as a protective mechanism following ingestion of the toxin.

## PS 2321 Red Clover Exhibits Multifaceted Activity on Breast Cancer Cells.

B. M. Dietz, J. Eskra, M. Darji, S. Chen, G. F. Pauli and J. L. Bolton.  
*Medicinal Chemistry and Pharmacognosy, University of Illinois at Chicago, Chicago, IL.*

An increased breast cancer risk for postmenopausal women taking hormone therapy has been demonstrated by the Women's Health Initiative. Botanical dietary supplements, including red clover products, are commonly used to alleviate menopausal symptoms but still lack efficacy and safety studies. Red clover isoflavones, such as biochanin A and genistein, have been promoted for their cancer preventive activity, in part due to genistein's ER $\beta$  selective activity. Other studies suggested possible side effects in estrogen sensitive tissue due to genistein's ER $\alpha$  mediated estrogenicity. This study examines these controversial claims by performing several estrogenic assays with a well-characterized clinical red clover extract and pure isoflavones. Proliferation experiments in ER+ breast cancer cells (MCF-7) showed that the effect of the red clover extract on cell proliferation is highly concentration dependent and has a bell-shaped curve: Low- and high concentrations (30 - 100 ng/mL and > 5  $\mu$ g/mL, respectively) reduced cell proliferation, whereas intermediate amounts (300 ng/mL - 1  $\mu$ g/mL) increased it. The pure isoflavones, genistein and biochanin A, exhibited similar bell-shaped dose dependencies. Low- (10 nM) and high isoflavone concentrations (> 10  $\mu$ M) decreased cell proliferation, whereas cell survival increased at 300 nM - 1  $\mu$ M. These findings are in agreement with prior reports of genistein preferentially binding to ER $\beta$  at 6 - 20 nM and to ER $\alpha$  at ~300 nM, which may explain the dose-dependent effects of the isoflavones and the extract. Supporting the proliferation results, ERE-luciferase and gene induction assays showed that red clover extract at 300 ng/mL - 1  $\mu$ g/mL mimics estradiol and might, therefore, have similar adverse effects if consumed in higher quantities. These findings highlight the importance of correct dosing for isoflavone-containing products and the relevance of dose considerations to ensure safety of botanical dietary supplements.

## PS 2322 Occurrence of T-2 Toxin, HT-2 Toxin and Zearalenone in Retail Foods in Japan.

T. Yoshinari<sup>1</sup>, K. Aoyama<sup>2</sup>, M. Nakajima<sup>3</sup>, M. Taniguchi<sup>3</sup>, H. Takeuchi<sup>4</sup>, S. Hashiguchi<sup>5</sup>, S. Kai<sup>6</sup>, S. Tabata<sup>7</sup>, T. Tanaka<sup>8</sup> and Y. Sugita-Konishi<sup>1</sup>. <sup>1</sup>National Institute of Health Sciences, Tokyo, Japan; <sup>2</sup>Food and Agricultural Materials Inspection Center, Sendai, Japan; <sup>3</sup>Nagoya City Public Health Research Institute, Nagoya, Japan; <sup>4</sup>Mie Prefecture Health and Environment Research Institute, Mie, Japan; <sup>5</sup>Kawasaki City Institute for Public Health, Kawasaki, Japan; <sup>6</sup>Kanagawa Prefectural Institute of Public Health, Kanagawa, Japan; <sup>7</sup>Tokyo Metropolitan Institute of Public Health, Tokyo, Japan; <sup>8</sup>Kobe Institute of Health, Kobe, Japan.

Fusarium toxins are a group of mycotoxins produced by many kinds of Fusarium species, and frequently detected in field crops such as wheat, barley, maize and corn. They cause mycotoxicosis, a serious health hazard to humans and domestic animals. Therefore, collecting the information about fusarium toxin contamination in daily foods is crucial. Occurrence data of deoxynivalenol, a major fusarium toxin, have been collected in worldwide, but that of other toxins is limited. In this study, we examined foods from Japanese retail shops for contamination with three kinds of fusarium toxins, T-2 toxin, HT-2 toxin and zearalenone. Food samples were extracted with methanol-water (75 : 25). After filtration, the extract was diluted five times with phosphate buffered saline, and subjected to a DZT MS-PREP Immunoaffinity column. The toxins were quantified by LC-MS/MS. In 2011, a total of 196 samples of 12 different products were examined. In corn grits (20 samples) and tear grass (20 samples), more than 1 ng/g of T-2 toxin on average was detected. In barley, breakfast cereal, cookie, corn grits, tear grass and wheat, more than 1 ng/g of HT-2 toxin on average was detected (The sample sizes were 10, 10, 10, 20, 20 and 40, respectively). The maximum concentration of the sum of T-2 and HT-2 toxin was 48.9 ng/g in corn grits. In corn grits, red bean (10 samples) and tear grass, more than 5 ng/g of zearalenone on average was detected. These results showed that the highly toxic trichothecene mycotoxins, T-2 and HT-2 toxin were contaminated in retail foods in Japan. Especially contributors of these toxins are breakfast cereal, tear grass and wheat.

## PS 2323 In Vitro Metabolism and Interaction of Zearalenone and Its Metabolites in Mammalian Cells.

G. Font<sup>1</sup>, E. Tatay<sup>2</sup>, G. Meca<sup>3</sup> and M. Ruiz<sup>4</sup>. <sup>1</sup>Preventive Medicine, University of Valencia, Burjassot, Spain; <sup>2</sup>Preventive Medicine, University of Valencia, Burjassot, Spain; <sup>3</sup>Preventive Medicine, University of Valencia, Burjassot, Spain; <sup>4</sup>Preventive Medicine, University of Valencia, Burjassot, Spain.

Zearalenone (ZEA) is a non-steroidal estrogenic mycotoxin produced by Fusarium sp. fungi. ZEA is rapidly absorbed and metabolized to  $\alpha$ -Zearalenol ( $\alpha$ -ZOL) and  $\beta$ -Zearalenol ( $\beta$ -ZOL) in the liver; therefore mixtures of these mycotoxins may be simultaneously in biological systems and cause human health risk. The objectives of this study were: a) to compare the cytotoxicity of ZEA,  $\alpha$ -ZOL and  $\beta$ -ZOL alone or in combination in hamster ovary (CHO-K1) and human hepatoma (HepG2) cells using the MTT assay after 24, 48 and 72h of exposure, b) to evaluate the interactions of mycotoxins mixtures in both cell lines by the isobologram analysis and, c) to study the in vitro metabolism of ZEA in both types of cells using liquid chromatography coupled to the mass spectrometry detector-linear ion trap (LC-MS-LIT). The IC50 values obtained for individual mycotoxins range from 59.4 to >100.0  $\mu$ M, from 30.0 to 33.0  $\mu$ M and from 55.0 to >75.00  $\mu$ M in CHO-K1 cells and from 70.0 to >100.0  $\mu$ M, from 20.6 to 26.0  $\mu$ M and from 38.4 to >100.0  $\mu$ M in HepG2 cells for ZEA,  $\alpha$ -ZOL and  $\beta$ -ZOL, respectively. Isobologram analysis provides a combination index (CI) value to determine the type of interaction that occurs. The interactions of ZEA and its metabolites became slightly synergism at low levels (CI from 0.34  $\pm$  0.10 to 0.81  $\pm$  0.33) followed by additive effect (CI from 0.80  $\pm$  0.18 to 8.54  $\pm$  7.76) and turned into antagonism (CI from 1.41  $\pm$  0.16 to 26.17  $\pm$  20.72). The metabolism assays demonstrated that no conversion of ZEA in  $\alpha$ -ZOL and  $\beta$ -ZOL was detected. However, other metabolites products of ZEA,  $\alpha$ -ZOL and  $\beta$ -ZOL were generated in both cell lines.

Acknowledgement: The Science and Innovation Spanish Ministry (AGL2010-17024/ALI).

## PS 2324 Role of Peptide YY3-36 (PYY) and 5-Hydroxytryptamine (5-HT) in Emesis Induction by Deoxynivalenol (Vomitoxin).

M. Bates<sup>1</sup>, W. Wu<sup>1,5</sup>, S. Bursian<sup>3,2</sup>, B. Flannery<sup>1</sup>, H. Zhou<sup>1</sup>, J. Link<sup>3</sup>, H. Zhang<sup>5</sup> and J. Pestka<sup>1,2,4</sup>. <sup>1</sup>Food Science and Human Nutrition, Michigan State University, East Lansing, MI; <sup>2</sup>Center for Integrative Toxicology, Michigan State University, East Lansing, MI; <sup>3</sup>Animal Science, Michigan State University, East Lansing, MI; <sup>4</sup>Microbiology and Molecular Genetics, Michigan State University, East Lansing, MI; <sup>5</sup>College of Veterinary Medicine, Nanjing Agricultural University, Nanjing, China.

Deoxynivalenol (DON, vomitoxin), a trichothecene mycotoxin produced by Fusarium, frequently contaminates cereal grains causing reported outbreaks of human and animal food poisoning making it a relevant public health concern. Although these outbreaks have the rapid onset of emesis as a common hallmark, the mechanisms for this adverse effect are not fully understood. Recently, our laboratory has demonstrated that the mink (Neovison vison) is a suitable small animal model for investigating trichothecene-induced emesis. We employed the mink to determine the role of gut satiety hormone peptide YY3-36 (PYY3-36) and neurotransmitter 5-hydroxytryptamine (5-HT) in DON-induced vomiting. Emesis induction following intraperitoneal exposure to DON at 100 and 250  $\mu$ g/kg bw initiated within 15 to 30 min which persisted for up to 120 min. Measurement of DON in plasma by ELISA revealed that the emetic period correlated with distribution and clearance of the toxin. Significant elevations in both PYY3-36 (30 to 60 min) and 5-HT (60 min) were observed during emesis. Pretreatment with the Y2 receptor antagonist JNJ-31020028 attenuated PYY- and DON-induced emesis. The 5-HT3 receptor antagonist granisetron was found to completely suppress induction of vomiting by cisplatin, a known 5-HT inducer, as well as DON. Interestingly, granisetron pretreatment could partially block PYY3-36-induced emesis. Taken together, the results presented here suggest that both PYY3-36 and 5-HT play contributory roles in DON-induced emesis.

## PS 2325 Dietary Inclusion of Montmorillonite Clay Mitigates Bioavailability of Aflatoxin, Fumonisin and Aflatoxin/Fumonisin Mixtures in Fischer 344 Rats.

N. J. Mitchell<sup>1</sup>, K. Xue<sup>2</sup>, A. Marroquin-Cardona<sup>1</sup>, K. A. Brown<sup>1</sup>, S. E. Elmore<sup>1</sup>, S. Lin<sup>2</sup>, L. Tang<sup>2</sup>, J. Wang<sup>2</sup> and T. D. Phillips<sup>1</sup>. <sup>1</sup>College of Veterinary Medicine, Texas A&M University, College Station, TX; <sup>2</sup>Department of Environmental Health Sciences, University of Georgia, Athens, GA.

Aflatoxins (AFs) have been linked to hepatocellular carcinoma and mortality in humans and animals. Chronic AF exposure, particularly in developing countries, is a significant problem that continues to contribute to public health issues in communities burdened by poor economic status and food scarcity. One possible strategy to

improve food safety is to reduce exposures to AF using montmorillonite clay which binds AFs in the GI tract, and decreases bioavailability of these toxins. Our recent work in Ghana has shown that communities at risk for AF exposure are also at high risk for fumonisin (FB) exposure. In this study, montmorillonite clay was tested for FB<sub>1</sub> binding capacity in combination with AFB<sub>1</sub> in a rodent model. Fisher-344 rats were gavaged once with 0.125 mg AFB<sub>1</sub>/kg b.w. and/or 25 mg FB<sub>1</sub>/kg b.w. following an acclimation period with feed containing clay additive. Urine samples were collected at 12 hr time intervals for 72 hr following gavage and were analyzed for AF and FB biomarkers. Lower AFM<sub>1</sub> and FB<sub>1</sub> levels in the urine were indicative of reduced absorption of the parent compounds through the GI tract and into the circulation. AFM<sub>1</sub> and FB<sub>1</sub> excretion peaked between 12-24 hr and quickly declined by 36 hr. Addition of clay at 0.25%, 0.5% and 2% w/w feed decreased AFM<sub>1</sub> excretion by 88-97% at the 12 hr time point, indicating highly effective binding. Clay treated animals also had a reduction in FB<sub>1</sub> excretion, but to a lesser extent than the AFM<sub>1</sub> biomarker (i.e. 41-80%). When in combination both AFM<sub>1</sub> and FB<sub>1</sub> binding occurred, but capacity was decreased by almost half, suggesting that AFB<sub>1</sub> and FB<sub>1</sub> are competing for similar binding sites on the clay. This study indicates that inclusion of montmorillonite clay in contaminated diets can reduce bioavailability of both AFs and FBs in populations at high risk for mycotoxin exposure. (Supported by NIH/NCMHDR RO1-MD00519-01.)

### PS 2326 Development and Validation of an Analytical Method for Vomitoxin in Gavage Dose Formulations Used in Rodent Toxicology Studies.

J. C. Blake<sup>1</sup>, D. P. Coleman<sup>1</sup>, J. Gilliam<sup>1</sup>, M. A. Silinski<sup>1</sup>, R. A. Fernando<sup>1</sup>, C. S. Smith<sup>2</sup>, B. Collins<sup>2</sup> and V. G. Robinson<sup>2</sup>. <sup>1</sup>RTI International, Research Triangle Park, NC; <sup>2</sup>Division of National Toxicology Program, NIEHS, Research Triangle Park, NC. Sponsor: K. Levine.

Vomitoxin, also known as deoxynivalenol (DON), is a trichothecene mycotoxin produced by certain types of *Fusarium* fungi. It occurs predominantly in grains such as corn, wheat, barley, and rice, and has been shown to have great stability during storage, processing, and cooking of food. Because of the potential for widespread contamination of food and exposure to farmers through inhalation, the National Toxicology Program is investigating the toxicity of vomitoxin. Thus, the current study was undertaken to develop and validate a formulation analysis method for vomitoxin in deionized water as a gavage vehicle for use in toxicology studies. Important objectives of an analytical method for supporting a toxicological study are to insure that the correct test article is being administered at the specified dose concentrations and that the dose formulations are stable. To achieve these objectives, an Ultra Performance Liquid Chromatography (UPLC) method was developed and validated for analysis of vomitoxin in deionized water. Sample preparation involves a simple dilution with water and addition of an internal standard solution (2,6-dimethylphenol in acetonitrile). The method was successfully validated over the range 1.5 to 720 µg/mL. The limit of detection was estimated as 0.2 µg/mL and the limit of quantitation was estimated as 0.8 µg/mL. Assessment of formulation stability, at ambient and refrigerated storage conditions, over a 42-day period was evaluated. Dose simulation stability testing was also conducted to evaluate the formulations stability for at least three hours under simulated dosing conditions. In addition, analysis period stability of the analytical preparations was assessed. This method will be used to support toxicology studies of vomitoxin conducted by the National Toxicology Program.

### PS 2327 Comparative Hepatic Glutathione S-Transferase Mediated Detoxification of Aflatoxin B1 in Chickens.

B. R. Bunderson<sup>1</sup>, C. Rowe<sup>1</sup>, S. J. Lamont<sup>2</sup> and R. A. Coulombe<sup>1</sup>. <sup>1</sup>Toxicology Graduate Program, Utah State University, Logan, UT; <sup>2</sup>Department of Animal Science, Iowa State University, Ames, IA.

Efficiency of hepatic glutathione S-transferase (GST)-mediated conjugation of bioactivated aflatoxin B1 (AFB1) is critical to species resistance to this toxic and carcinogenic mycotoxin. Poultry are among the most susceptible animals, and domestic turkeys are especially susceptible, a condition we have shown to be associated with a deficiency of AFB1-detoxifying GSTs. Chickens are more resistant than domestic turkeys, yet little is known about their hepatic GST detoxification capabilities. In this study, we compared hepatic GST-mediated detoxification of prototype substrates 1-chloro-2,4-dinitrobenzene (CDNB), 1,2-dichloro-4-nitrobenzene (DCNB), ethacrynic acid (ECA), and cumene hydroperoxide (CHP) and toward the exo-AFB1-8,9-epoxide (AFBO) in livers of Broiler, Fayoumi, and Leghorn chickens. All breeds had equivalent GST activities, except Fayoumi, which was significantly lower toward CDNB. Broiler, Fayoumi, and Leghorn had similar GST-mediated conjugation activities toward AFBO (6.5 ± 0.2, 6.1 ± 0.6, 6.4 ± 0.2

pmol/min/mg, respectively). This level of hepatic AFB1 detoxification is substantially more than that in livers of domestic turkeys, which are more susceptible than chickens to AFB1. These data support previous findings that in vitro conjugation of AFB1 by GST is an accurate predictive marker species resistance to this mycotoxin. Supported in part by NRI Competitive grant 2007-35205-17880 from the USDA-NRI Animal Genome Project.

### PS 2328 Bisphenol A (BPA) Levels in Liquid Supernatants of Canned Foods Determined by Highly Sensitive BPA ELISA.

H. Kim<sup>1,2</sup>, A. Joiaim<sup>1</sup>, D. Kaplan<sup>1</sup>, K. Friedrich<sup>1</sup> and D. Putt<sup>1</sup>. <sup>1</sup>Detroit R&D, Inc., Detroit, MI; <sup>2</sup>Institute of Environmental Health Sciences, Wayne State University, Detroit, MI.

BPA [2,2-(4,4'-dihydroxydiphenyl)propane], an endocrine disruptor, mimics the action of 17β-estradiol (E2) in mammals, increasing the risk of hormone-related health problems such as early puberty, infertility, breast, ovarian and prostate cancers and insulin resistance. Fetuses and newborns are most vulnerable to the BPA toxicity. Recently, BPA levels of canned soup solids were measured by LC/MS/MS (detection limit, 2 ng/g) and it was found that the soup solids contained 10 to 80 ng/g BPA. A subsequent study revealed that the group that consumed a 12-ounce serving/day, for 5 days of canned soups, excreted 19-fold higher BPA in urine (mean, 21 ng/ml) compared with the control group that consumed same amounts of fresh soups (mean, 1.1 ng/ml). BPA in liquid supernatants of canned foods contain ~10-fold lower levels of BPA compared to the solids. To screen BPA in supernatants, a highly sensitive and facile BPA ELISA has been developed after production of BPA polyclonal antibodies by immunization of a goat with carboxylalkyl-derivatized BPA conjugated to KLH. The detection limit of the BPA ELISA was 1 pg. Whereas anti-BPA slightly cross-reacted with BPB, it did not cross-react with BPS, BPF or resveratrol, which are structurally similar to BPA. Ten-fold diluted supernatants of canned soups were applied to BPA ELISA. Supernatants obtained from 3 kinds of soups (3 cans/each kind of soup, 9 data points) produced by first company contained 9.56 ± 0.96 ng/ml, 9.07 ± 0.38 ng/ml and 10.38 ± 0.83 ng/ml of BPA, similar to ~8.70 ng/ml of BPA levels in supernatants from second company. A negative control, supernatants of canned vegetables from third company, contained extremely low levels of BPA (0.05 ± 0.02 ng/ml), suggesting use of BPA-free can linings. These results demonstrate that the competitive BPA ELISA is suitable for measurements of BPA leaching from the epoxy film-coated cans using liquid supernatants from canned foods.

### PS 2329 Perinatal BPA Exposure at Low Doses Impairs Oral Tolerance and Immunization to Ovalbumin in Offspring Rats at Adulthood.

S. Ménard, V. Braniste, M. Leveque, C. Lencina, M. Naturel, L. Moussa, S. Sekkal, C. Harkat, E. Gaultier, V. Theodorou and E. Houdeau. INRA, Toulouse, France. Sponsor: D. Zalko.

Aims: Bisphenol A (BPA) used in food packaging impacts gut epithelial barrier after perinatal exposure. Because antigen sampling by gut epithelium drives mucosal immune response, our aim was to address the consequences of perinatal BPA exposure at low doses on oral tolerance and immunization at adulthood. Methods: Dams were treated per os from gestation day 15 to pup weaning with BPA [0.5, 5 or 50 µg/kg/d] or vehicle (corn oil). Female offsprings (day 45) were used to assess para- and transcellular jejunal permeability by Ussing chambers, and immune response to ovalbumin (OVA) after either oral tolerance, immunization or oral challenge. Results: Perinatal BPA exposure decreased jejunal paracellular permeability by 2-fold at 0.5 and 50 µg/kg/d, and by 3-fold at all doses for transcellular permeability (p<0.05). BPA exposure at 5 and 50 µg/kg/d increased anti-OVA IgG titers after an oral tolerance protocol (116±62x103 and 86±29x103 respectively vs 7.2±2.2 x103 in controls; p<0.04). Anti-OVA IgG titers were only increased at 5 µg/kg/d after OVA immunization. Enhanced humoral response in rats exposed to 5 µg/kg/d was associated with higher IFNγ secretion by spleen in OVA-sensitized (2-fold) and MLN of OVA-tolerized (20-fold) rats (p<0.05). Finally, oral OVA challenge in BPA group increased MPO activity (316±34 vs 184±22 U/g protein in controls; p<0.05), IFNγ concentration (2-fold, p<0.05), and decreased TGFβ concentration (3-fold, p<0.05) in the colon, indicating inflammation. Conclusion: Perinatal exposure to low doses of BPA decreased jejunal paracellular and transcellular permeability, and impaired oral tolerance and immunization to dietary antigens at adulthood. BPA treatment during perinatal period affects intestinal homeostasis in a nonlinear dose-response relationship. These results suggest that perinatal period is a critical window for BPA exposure that may trigger food intolerance in later life.

**PS 2330 Perinatal BPA Exposure at Low Doses Impairs Immune Homeostasis and Promotes Intestinal Parasite Infection in Young Rats.**

V. Theodorou, S. Ménard, C. Lencina, M. Leveque, M. Olier, V. Braniste, M. Naturel, S. Sekkal, C. Harkat and E. Houdeau. *INRA, Toulouse, France.*  
Sponsor: *D. Zalko.*

**Aims:** Perinatal exposure to 5µg/kg/day of the food contaminant bisphenol A (BPA) impaired oral tolerance in adult rats (see Ménard et al, abstract 1). Herein, we aimed to address the consequences of BPA perinatal exposure on immune homeostasis in young rats at weaning, i.e. oral tolerance, systemic immunization with ovalbumin (OVA) and parasitic infection. **Methods:** Dams were given per os from gestational day 15 to pup weaning BPA [5µg/kg/d] or vehicle (corn oil). Weaned female offspring (day 25) were used to assess para- and trans-cellular jejunal permeability by Ussing chambers, and immune responses following oral tolerance or immunization to OVA, or after infection with a gut nematode *Nippostrongylus brasiliensis* (N bras). **Results:** Perinatal treatment with BPA did not affect intestinal permeability or humoral response (anti-OVA IgG titers) following either oral tolerance or immunization in D25 rats. However, a decrease of OVA-induced IFNγ secretion was observed in spleen of OVA-sensitized rats (53±15 vs 317±162 pg/ml; p<0.05) and in mesenteric lymph nodes of OVA-tolerized rats (3.9±2.3 vs 19±14 pg/ml; p<0.05). The lack of cellular response to food antigens questioned the ability of BPA-exposed rats to clear intestinal infections. A 3-fold increase in N bras living larvae was observed in the intestine of BPA-exposed rats compared to controls (2817±689 vs 757±291 larvae/g of faeces, respectively; p<0.05), but no significant change in myeloperoxidase activity into jejunal tissues. **Conclusion:** Perinatal exposure to low dose of BPA did not affect humoral response to the food antigen OVA in juvenile rats. However, a decrease of OVA-induced IFNγ secretion in BPA-exposed rats emphasized a lack of specific cellular response to food antigens. Finally, perinatal BPA treatment evoked an increased risk to intestinal parasitic infection without triggering an inflammatory response, demonstrating impaired immune defence in early life stages.

**PS 2331 Perinatal Peripubertal Exposure to Bisphenol-A Increases Hepatic Steatosis in Immature and Adult Mice.**

P. Shimpi<sup>1</sup>, A. Donepudi<sup>1</sup>, V. More<sup>1</sup>, M. Paranjpe<sup>2</sup>, S. DaFonte<sup>2</sup>, B. Rubin<sup>2</sup> and A. L. Slitt<sup>1</sup>. <sup>1</sup>*Biomedical and Pharmaceutical Sciences, University of Rhode Island, Kingston, RI;* <sup>2</sup>*Sackler School of Graduate Biomedical Sciences, Tufts University, Boston, MA.*

While diet and physical activity remain the predominant reason for development of obesity and obesity-related disease, there is some concern that environmental exposure to chemicals may be a predisposing factor. Bisphenol A (BPA), a component used in the manufacturing of certain plastics and plastic resins, can leach into food and/or drink from food and beverage containers. High urinary BPA levels have been positively associated with general and abdominal obesity in human populations. In rodents, developmental BPA exposure increases body weight and fatty liver (steatosis). The purpose of this study was to uncover potential mechanisms by which perinatal-peripubertal (PNPP) exposure to BPA increases liver steatosis. Pregnant CD-1 mice were administered 25 or 250 µg BPA/kg/day (BPA25, BPA250, respectively) via osmotic pump, and then after weaning on PND 20, the resulting daughters were exposed to BPA via drinking water up through PND 35. Tissues were collected at PND32 and at 39 weeks of age. Livers were analyzed for triglyceride content, stained with Oil Red O and relative mRNA expression was quantified by qPCR. At PND32, BPA25 and 250 increased liver Oil Red O staining compared to controls. BPA25, but not BPA250, increased protein expression for lipogenic enzymes, (Acc-1 and Fas) but did not significantly increase lipogenic gene expression. In adult mice, BPA25, but not BPA250, increased Oil Red O staining. BPA25 increased Acc-1 expression, whereas BPA250 increased Srebp1-c, Acc-1, and Fas. Protein expression was not changed. In conclusion, PNPP exposure to BPA had some effect in promoting steatosis and pro-steatotic gene expression in immature and adult female mice, but the exact mechanism by which BPA promotes steatosis remains unclear.

**PS 2332 Leaching of Chemicals with Estrogenic Activity from BPA-Free Materials after Common Use Stresses.**

G. D. Bittner<sup>2,1,3</sup>, C. Z. Yang<sup>2</sup>, M. Stoner<sup>2</sup> and D. Klein<sup>1</sup>. <sup>1</sup>*PlastiPure, Inc., Austin, TX;* <sup>2</sup>*CertiChem, Inc., Austin, TX;* <sup>3</sup>*University of Texas, Austin, TX.*

Since 2007, many consumer products are no longer made from polycarbonate (PC) plastics because of widespread concern about the estrogenic activity (EA) of bisphenol-A (BPA). However, BPA-Free plastics have not been thoroughly vetted by most

product manufacturers to ensure that they do not release other chemicals that have EA. We have used, robotized MCF-7 and BG1Luc assays currently undergoing validation by ICCVAM/NICEATM to quantify the total EA in chemicals leaching from a various widely-available plastic resins used to make consumer products and packaging. This study expands the prior work of Yang et al, 2011(EHP 119:989-998). We assayed the total EA in chemical mixtures leaching from unstressed and stressed polycarbonate (PC), polypropylene (PP), polyethylene (PE), cyclic olefin copolymer(COC), and polyethylene terephthalate glycol-modified (PETG - Tritan™) plastic resins. Plastic resins were subjected to simulated common-use stresses of dishwashing, microwaving, and sunlight, and then extracted for ~ 72 hours at 37 degrees Celsius by saline (hydrophilic) or ethanol (hydrophobic) solvents. The total EA in these leachates were then quantified and EA-specific responses were validated by conducting confirmation assays. EA positive determinations were made on samples with values 3 standard deviations or more higher than vehicle controls. Using these criteria, Tritan PETG and PC resins were consistently significantly positive for EA. PE and PP samples often tested positive for EA, but some consistently had no detectable EA. Most COC resins consistently had no detectable EA. Our data show that BPA-Free often does not mean EA-Free, i.e., that leaching of chemicals having EA from the plastic resins is often not addressed by simply choosing BPA-Free materials.

**PS 2333 Microsomal Metabolism of Asarone Isomers.**

A. T. Cartus and D. Schrenk. *Food Chemistry and Toxicology, University of Kaiserslautern, Kaiserslautern, Germany.*

The alkenylbenzenes alpha-asarone (aA; CAS 2883-98-9), beta-asarone (bA; CAS 5273-86-9), and gamma-asarone (gA; CAS 5353-15-1) are constituents of various plants, e.g. *Acorus calamus* (Sweet Flag) and some peppers. Both, aA and bA are carcinogenic to rodents and exhibit genotoxic effects in vitro. Neither genotoxicity nor carcinogenicity of gA have been evaluated so far. Several allylic alkenylbenzenes such as safrole, estragole and methyleugenol are well known genotoxic carcinogens, whereas their propenyl analogues are not. This suggests that an allylic side chain, and therefore the capability for the formation of an 1'OH metabolite, may be a basic prerequisite for the carcinogenicity of those compounds. However, the propenyl compounds aA and bA are an exception of that "allylic rule". We suggest the ortho-methoxy groups of aA and bA to be a key structural element for the mode of action of their carcinogenicity.

We investigated the metabolism of aA, bA and gA using liver microsomes from different species (including human). Identity of metabolites was confirmed by LC-MS/MS and 1H-NMR spectroscopy in comparison with synthesized reference standards.

Our results show that the side chain hydroxylation of aA and gA was the predominating metabolic step leading to E-3'OHA (from aA) and 1'OHA (from gA), respectively, together with the formation of side-chain dihydrodiols, for which the epoxides may be the precursors. To a smaller extent, we found enzymatically formed secondary metabolites derived from the alcohols like 3'oxoA and 1'oxoA, but no corresponding carboxylic acids. Furthermore, we found the corresponding mono-demethylated phenolic metabolites. These results are comparable to our prior results on phase I metabolism of methylisoeugenol and methyleugenol. In contrast, bA showed a more complex pattern of metabolites: in addition to Z-3'OHA, the unexpected direct formation of 1'OHA was proven. This metabolic step, possibly facilitated by steric attraction of the Z-configured bA side chain and the ortho-methoxy substituent, may explain the carcinogenicity of bA, but not of aA, where no 1'OH metabolite was found.

**PS 2334 Histamine in Scombrototoxin Fish Poisoning: Toxicology, Epidemiology and Dose-Response Analysis.**

Y. Zang and P. M. Bolger. *US FDA, College Park, MD.*

Histamine plays important physiological functions such as immune responses and gastric acid secretion. However, ingestion of fish containing large amounts of spoilage-originated histamine can result in scombrototoxin fish poisoning (SFP), a common chemical-originated food poisoning that affects cardiovascular, gastrointestinal and neurological systems. Fish importing countries have established various regulations and limits for histamine in fish and fishery products to protect consumers. However, many limits were established in a pre-quantitative risk assessment era. An assessment of toxicological and epidemiological data indicates that though other biogenic amines might also play a role in the etiology of SFP, histamine is the most significant causative agent. Due to limitations of the disease-reporting system, the epidemiology-based dose-response approach is not suitable in developing a safety limit of histamine in fish. Instead, a dose-response analysis was conducted

based on human oral challenge studies selected. Both the NOAEL and BMD assessments identified 50 mg of histamine per meal as the dose where either adverse effects were not noted or the estimate of additional risk (lower confidence level) was low. At this level healthy adults would not be expected to exhibit any of the symptoms associated with SFP. This dosage level will not apply to children and individuals with a specific sensitivity to histamine. In addition, this level was derived from data on small number of subjects. While the variation of response appears to be reflected in the study results, further studies would be most helpful in refining this threshold value. Using a conservative serving size of 250 g fish meat/meal, the maximum concentration of histamine in fish that should not cause an adverse effect was calculated as 200 ppm. Compliance sampling plan can be derived based on this threshold level to ensure a desirable level of protection of the public health.

**PS 2335 Carrageenan-Induced Disruption of Mucosal Barrier via Regulation of Proinflammatory NF- $\kappa$ B and Early Growth Response Gene 1: A Mechanistic Implication of Food-Borne Inflammatory Bowel Disease.**

J. Kim, H. Choi, K. Do, S. Park and Y. Moon. *Laboratory of Mucosal Exposome and Biomodulation, Department of Microbiology and Immunology, Pusan National University School of Medicine and Medical Research Institute, Yangsan, Republic of Korea.*

The widely used food additive carrageenan (CGN) has been shown to induce intestinal inflammation, ulcerative colitis-like symptoms, or neoplasm in the gut epithelia in animal models, which are also clinical features of human inflammatory bowel disease. In this study, the effects of CGN on pro-inflammatory transcription factors NF- $\kappa$ B and early growth response gene 1 product (EGR-1) were evaluated in terms of human intestinal epithelial barrier integrity. Both pro-inflammatory transcription factors were elevated by CGN and only NF- $\kappa$ B activation was shown to be involved in the induction of pro-inflammatory cytokine interleukin-8. Moreover, the integrity of the in vitro epithelial monolayer under the CGN insult was maintained by both activated pro-inflammatory transcription factors NF- $\kappa$ B and EGR-1. Suppression of NF- $\kappa$ B or EGR-1 aggravated barrier disruption by CGN, which was associated with the reduced gene expression of tight junction component zonula occludens 1 and its irregular localization in the epithelial monolayer (This work was supported by the Basic Science Research Program through the National Research Foundation of Korea, funded by Ministry of Education, Science, and Technology Grant 2012R1A1A2005837)

**PS 2336 Comparison of the Estrogenic Activity of Licorice Species with Hops in Botanical Dietary Supplement Formulations for Women's Health.**

A. Hajirahimkhan, C. Simmler, Y. Yuan, D. Nikolic, S. Chen, B. M. Dietz, G. F. Pauli, R. B. van Breemen and J. L. Bolton. *Medicinal Chemistry and Pharmacognosy, University of Illinois at Chicago, Chicago, IL.*

The Women's Health Initiative showed an increased risk of breast cancer for menopausal women taking hormone therapy. As a result, many women have turned to botanical supplements to manage menopausal symptoms, although there is limited data about their efficacy and safety. Our previous studies demonstrated estrogenic and chemopreventive properties for hops (*Humulus lupulus*). The goal of the current study was to compare the estrogenic effects of three common licorice species (*Glycyrrhiza glabra*, *Glycyrrhiza uralensis*, *Glycyrrhiza inflata*) with those of hops. Methanol extracts of the licorice species showed a dose-dependent induction of an estrogen responsive alkaline phosphatase in endometrial cancer cells with *Glycyrrhiza uralensis* being the most potent. Compared to hops, the activity of the licorice species was significant but less pronounced. Similar results were obtained in an estrogen response element (ERE)-luciferase reporter assay in breast cancer cells. The licorice constituent, liquiritigenin, was the major ligand of estrogen receptor (ER) in pulsed ultrafiltration mass spectrometry of the licorice extracts. Competitive binding assay using purified human ERs showed liquiritigenin as a selective ligand of ER $\beta$ . In comparison to 8-prenylnaringenin (8-PN), the major estrogenic principle of hops, liquiritigenin had lower affinity to both ERs. Liquiritigenin was less active than 8-PN in the induction of alkaline phosphatase and ERE-luciferase. Isoliquiritigenin, the precursor chalcone of liquiritigenin, demonstrated significant activity in these estrogenic assays, while xanthohumol, the precursor of 8-PN, did not exhibit estrogenic effects. The estrogenic activity of isoliquiritigenin was partially associated with its cyclization to liquiritigenin. These data suggest that licorice species are moderately estrogenic and are worthwhile further exploration as effective and safe dietary supplements to alleviate menopausal symptoms.

**PS 2337 Acrylamide and Acrolein: Heat-Induced Contaminants in Food.**

G. Eisenbrand<sup>1</sup>, N. Watzek<sup>1</sup>, D. Scherbl<sup>1</sup>, M. Baum<sup>1</sup>, F. Berger<sup>1</sup>, U. Fuhr<sup>2</sup>, O. Doroshenko<sup>2</sup>, D. Tomalik-Scharte<sup>2</sup> and E. Richling<sup>1</sup>. <sup>1</sup>*Chemistry, Division of Food Chemistry and Toxicology, Kaiserslautern, Germany;* <sup>2</sup>*Pharmacology, University Hospital of Cologne, Cologne, Germany.*

The genotoxic carcinogen (IARC class 2A) acrylamide (AA) is a food contaminant formed by thermal treatment of food. This applies as well to acrolein (AC) an  $\alpha,\beta$ -unsaturated aldehyde grouped into IARC group 3B. Whereas human dietary exposure levels to AA are well established and range between about 0.5-5  $\mu$ g/kg bw/d, exposure to AC is much less investigated. After uptake, AA is partly metabolised into the genotoxic glycidamide (GA). GA forms DNA adducts, primarily at N7 of guanine (N7-GA-Gua). AA, GA and AC are conjugated to glutathione (GSH) and excreted via urine as mercapturic acids (MA).

AA was given by gavage in single doses of 0.1-10,000  $\mu$ g/kg bw to female rats. Formation of urinary MAs and of N7-GA-Gua DNA adducts in liver, kidney and lung was measured 16 h after application using HPLC-MS/MS. At the lowest dosage (0.1  $\mu$ g AA/kg bw), N7-GA-Gua adducts were below the limit of detection in any organ tested. At 1  $\mu$ g/kg bw, enhanced adduct levels were found in kidney (~1 adduct/10<sup>8</sup> nucleotides) and lung (< 1 adduct/10<sup>8</sup> nucleotides), but not in liver. At 10 and 100  $\mu$ g/kg bw, adducts were found in all three organs not significantly different to those found at 1  $\mu$ g AA/kg bw (about 1-2 adducts/10<sup>8</sup> nucleotides). In two pilot intervention studies, MAs of AA and AC were monitored after ingestion of test meals of 150 g self-made potato chips (1 mg AA, 13 volunteers, study 1) and of 175 g commercially available potato chips (44  $\mu$ g AA and 5  $\mu$ g AC, 5 volunteers, study 2). Urinary MA contents were determined by HPLC-MS/MS for up to 72 h (study 1), respectively 24 h (study 2). Total excretion of AC-related MA exceeded that of AA-related MA by factors of about 12 (study 1) to 4 (study 2). These results suggest markedly higher exposure to AC than to AA from heat treated potato based foods representing a major source of dietary exposure to AA. They mandate further research to broaden the database on dietary AA and AC.

**PS 2338 Sex Hormone Modulation of Long-Term Induction and Short-Term Inhibition of CYP1A1/2 by Genistein in HepG2/C3A Cells.**

Y. Liu<sup>1,3</sup>, T. Flynn<sup>1</sup>, M. Ferguson<sup>2</sup> and M. Garcia<sup>1</sup>. <sup>1</sup>*Division of Toxicology, Center for Food Safety and Applied Nutrition, US FDA, Laurel, MD;* <sup>2</sup>*Division of Public Health and Biostatistics, Center for Food Safety and Applied Nutrition, US FDA, College Park, MD;* <sup>3</sup>*Oak Ridge Institute for Science and Education, Oak Ridge, TN.*

Genistein is widely consumed in soy products and dietary supplements for its reported beneficial health effects including cancer prevention. However, there have been conflicting data suggesting that genistein ingestion has both anticancer and cancer promoting activities. Cytochromes P4501As (CYP1A) play key roles in the metabolic activation of many carcinogens. Since genistein has both anti-estrogenic and estrogenic activities, sex-specific factors could also contribute to its biological activities. In the current study, human hepatoma HepG2/C3A cells were cultured in media with defined human sex hormone profiles to investigate CYP1As inhibition and induction by genistein. In male hormone supplemented cells, CYP1A1 and CYP1A2 gene expression and activities were induced to higher extent compared with female hormone supplemented cells after either  $\beta$ -naphthoflavone or genistein treatment. However, basal gene expression of CYP1A1 and CYP1A2 were higher in female- than in male-hormone supplemented cells. In the inhibition studies, CYP1A activities were significantly lower in the male-specific medium than in female specific medium. The results showed that genistein could exert both long-term (3-day) induction and short-term (1-hr) inhibition effects on CYP1A activities in vitro which could explain the inconsistent cancer-related reports. Furthermore, there were significant differences in both the inductive and inhibitory effects of genistein between the male- and female-specific media suggesting that sex hormones, in physiological concentrations and ratios, can modulate the effects of genistein on CYP1A gene expression and activities in a human liver cell line.

**PS 2339 Safety Evaluation of Optimash BG from T. Reesei for Use in Grain, Brewing, and Carbohydrate Processing.**

N. K. Muntean, V. Sewalt and Q. Bui. *DuPont Industrial Biosciences, Palo Alto, CA.*

Optimash BG is a cellulase enzyme used in grain processing (for the production of potable alcohol and brewing) and glucose production from starch. The enzyme, endoglucanase 2, is produced from a recombinant modified strain of *Trichoderma reesei*. A battery of toxicology studies was conducted to investigate its potential to

cause adverse effects in humans using methods complying with OECD guidelines. All studies were conducted according to OECD Principles of Good Laboratory Practice. Acutely, Optimash BG is not an eye irritant, a very mild skin irritant, and not toxic by ingestion with an oral LD50 greater than 2000 mg/kg bw. Optimash BG is not a mutagen, a clastogen, or an aneugen. In the *in vitro* cytogenetic test using cultured human lymphocytes cells, Optimash BG did not induce chromosomal aberrations (both structural and numerical) in the presence and absence of metabolic activation (S-9 mix) up to the highest concentration (5000 ug TP/ml). No mutagenic activity was noted in the Ames assay in the presence and absence of S-9 mix up to 5000 ug TP/plate. In a repeated 90 days oral (gavage) in Wistar rats, no biological or statistical differences were observed. Also, no treatment-related changes in the hematology and clinical chemistry were noted at study termination. The NOAEL was established at 80 mg total protein/kg bw/day (97.6 mg TOS/kg bw/day). Under the worst-case scenario that Optimash BG is applied at the maximum rate and the enzyme is neither destroyed nor removed during processing, the use of the enzyme in grain processing, carbohydrate processing and brewing is not expected to result in adverse effects to humans. With a margin of safety of 258 and a pADI of 39%, the use of Optimash BG is not of toxicological concern.

### PS 2340 A 13-Week Subchronic Toxicity Study of Glycidol Fatty Acid Esters in F344 Rats.

T. Toyoda<sup>1</sup>, Y. Cho<sup>1</sup>, S. Onami<sup>1</sup>, J. Akagi<sup>1</sup>, A. Nishikawa<sup>2</sup> and K. Ogawa<sup>1</sup>.  
<sup>1</sup>Division of Pathology, National Institute of Health Sciences, Tokyo, Japan; <sup>2</sup>Biological Safety Research Center, National Institute of Health Sciences, Tokyo, Japan.

Glycidol fatty acid esters (GEs) have been recently identified as food process contaminants in refined edible oils. Although there is toxicological concern arising from potential release of glycidol from parent esters during digestion in the gastrointestinal tract, little is known about *in vivo* toxicity of GEs. In the present study, subchronic toxicity of two types of GEs, oleate and linoleate esters, was investigated with administration at concentrations of 0, 225, 900 and 3600 ppm (equivalent molar concentration to 800 ppm glycidol) in drinking water for 13 weeks to male and female F344 rats. For comparison, treatment with 200 and 800 ppm of glycidol was also performed. Body weight gain of both sexes was markedly reduced with 800 ppm glycidol compared to the controls, and the cause was considered at least partly related to decreased water consumption. Hematological data showed significant increase of MCV in 800 ppm glycidol females and decrease of WBC in 3600 ppm oleate ester females. In serum biochemistry, increase of total cholesterol and potassium and decrease of ALT were detected in 800 ppm glycidol males, 3600 ppm linoleate ester males, and 800 ppm glycidol females, respectively. Serum creatinine levels in both sexes were decreased in the 800 ppm glycidol group. Relative weights of kidney and spleen were significantly increased in 200 and 800 ppm glycidol males and 800 ppm females. In addition, increase of relative kidney weights was also found in 3600 ppm oleate ester males. On histopathological assessment, increased cell debris was observed in the epididymal ducts of 800 ppm glycidol males, but not in ester groups. Although more detailed analysis will be needed to clarify any testicular toxicity of glycidol and *in vivo* genotoxicity of GEs, our results suggest that oleate and linoleate esters might be less toxic to F344 rats than glycidol itself.

### PS 2341 Modes of Action Underlying Citrinin-Induced Renal Carcinogenesis.

K. Kuroda<sup>1</sup>, M. Watanabe<sup>2</sup>, Y. Ishii<sup>1</sup>, S. Takasu<sup>1</sup>, K. Matsushita<sup>1</sup>, A. Kijima<sup>1</sup>, K. Ogawa<sup>1</sup>, T. Nomi<sup>3</sup>, A. Nishikawa<sup>3</sup>, Y. Sugita-Konishi<sup>2</sup> and T. Umemura<sup>1</sup>.  
<sup>1</sup>Division of Pathology, National Institute of Health Sciences, Tokyo, Japan; <sup>2</sup>Division of Microbiology, National Institute of Health Sciences, Tokyo, Japan; <sup>3</sup>Biological Safety Research Center, National Institute of Health Sciences, Tokyo, Japan.

Citrinin (CTN), a mycotoxin produced by *Penicillium* and *Aspergillus*, is known to induce renal tumors in rats; however, the involvement of genotoxic mechanisms remains unclear. To evaluate the genotoxic potential of CTN, reporter gene mutation, comet, and micronucleus assays were performed. For the reporter gene mutation assay, groups of 5 male *gpt* delta rats were given CTN at doses of 20 and 40 mg/kg by gavage for 28 days to extirpate the kidneys 3 days after the last dosing. For the comet and micronucleus assays, groups of 5 male F344 rats were treated with CTN at the same doses by gavage for 2 days to extirpate the kidneys or bone marrow, respectively. In the reporter gene mutation assay, the high dose (40 mg/kg) was decreased to 30 mg/kg on day 4 because of severe weight loss. The results of the reporter gene mutation and comet assays suggested that CTN did not induce DNA damage and subsequent gene mutations. Positive result was obtained only in the micronucleus assay, which might result from numerical chromosomal aberrations

due to microtubule dysfunction by CTN. Therefore, it seems likely that non-genotoxic mechanisms are involved in CTN-induced carcinogenesis. In kidney samples from *gpt* delta rats, increases in the labeling indices of proliferating cell nuclear antigen (PCNA)-positive cells and mRNA expression levels of cell cycle-related genes (i.e., *cyclin E1*, *cyclin A2*, *cyclin B1*, and *E2F1*) were observed at all doses, despite the fact that the low dose showed no toxicological effects. Accordingly, the promotion of cell cycle progression observed in the kidneys of CTN-treated rats may have resulted from a direct mitogenic function of CTN. Increased phospho-ERK levels observed at all doses indicated that CTN is a promising candidate trigger for induction of the cell cycle; however, further investigation of the detailed pathway appears warranted.

### PS 2342 The Dynamics of a Harmful Algal Bloom and Paralytic Shellfish Toxins in Juneau, Alaska.

D. W. Chamberlin<sup>1</sup>, G. L. Eckert<sup>2</sup> and S. L. Tamone<sup>3</sup>. <sup>1</sup>Department of Biology, Appalachian State University, Boone, NC; <sup>2</sup>School of Fisheries and Ocean Sciences, University of Alaska Fairbanks, Juneau, AK; <sup>3</sup>Department of Natural Sciences, University of Alaska Southeast, Juneau, AK. Sponsor: G. LeBlanc.

Paralytic shellfish poisoning (PSP) is a deadly neurological syndrome resulting from the ingestion of shellfish containing high levels of paralytic shellfish toxins (PSTs), and approximately seven cases of PSP are reported in Alaska annually. The main component of PSTs is the neurotoxin saxitoxin, which is produced by the dinoflagellate *Alexandrium* sp. In June and July 2012 during this summer undergraduate project at the University of Alaska Southeast, plankton tows, seawater samples, and bivalve samples revealed a significant bloom of *Alexandrium* and subsequent toxin event in seawater and bivalves. Saxitoxin was extracted from the water column by filtering 1L of seawater and sonicating the filter for one hour in diH<sub>2</sub>O. The concentration of saxitoxin in seawater, measured using ELISA, ranged from 26 ug/L to 230 ug/L during the bloom. Nine species of bivalves, *Saxidomus giganteus*, *Mytilus trossulus*, *Clinocardium nuttalli*, *Protothaca staminea*, *Mya truncata*, *Mya arenaria*, *Tresus capax*, *Mactromeris polynyma*, and *Hiatella artica*, were sampled for saxitoxins using ELISA following soft tissue homogenization and extraction. Two species, *Mytilus trossulus* and *Saxidomus giganteus*, exceeded the regulatory limit for saxitoxin, 80 ug/100g wet wt. *Mytilus trossulus* saxitoxin concentrations ranged from 67 to 215 ug/100g, while *S. giganteus* ranged from 143 to 279 ug/100g. After the bloom, concentration of saxitoxin in the seawater and *M. trossulus* decreased, at a rate of 5.7ug/day, but remained elevated in *S. giganteus*. The concentration of saxitoxin in *M. trossulus* was below the FDA regulatory limit of 80ug/100g wet wt. 26 days after the bloom of *Alexandrium* was detected. Recreational harvest of bivalves in Alaska is not regulated for PSP; however, these results suggest that PSP risk is very high, particularly for *S. giganteus*.

### PS 2343 Acute and 28-Day Oral Toxicity Evaluation of siRNAs and Longer Double-Stranded RNAs in Mice.

J. S. Petrick<sup>1</sup>, B. S. Wahle<sup>2</sup>, W. M. Moore<sup>1</sup>, R. Shah<sup>1</sup>, D. Eveleigh<sup>3</sup>, J. H. Sherman<sup>1</sup>, W. F. Heydens<sup>1</sup> and S. L. Lemke<sup>1</sup>. <sup>1</sup>Monsanto Company, St. Louis, MO; <sup>2</sup>Xenometrics, LLC, Stilwell, KS; <sup>3</sup>Asuragen, Inc, Austin, TX.

RNA interference is being used in agricultural biotechnology as a selective tool for developing crop traits. There are numerous biological barriers to uptake and activity of ingested nucleic acids that are ubiquitous components of animal diets. To evaluate the potential for adverse effects of dietary double stranded RNAs (dsRNAs), we conducted oral toxicity studies in mice with a pool of four 21-mer small interfering RNAs (siRNAs) and a 218 base pair dsRNA targeting the mouse ortholog of vacuolar ATPase (vATPase). When dsRNA targeting the insect ortholog of vATPase is expressed in corn plants, they are insecticidal against corn rootworm. Test materials were administered to CD-1 mice by oral gavage in a single dose acute toxicity study at 2000 mg/kg and in a 28 day repeat dose oral toxicity study at 1, 10, and 100 mg/kg. *Torula* yeast RNA was included as a control in both studies. There was no impact of treatment on body weight, food consumption, clinical observations, or gross pathology in the acute toxicity study. The acute NOAELs for both the siRNAs and dsRNA were 2000 mg/kg, the highest doses tested. In the 28-day study, there were no treatment-related adverse effects on body weight, food consumption, clinical observations, clinical chemistry, hematology, gross pathology, or micropathology. The NOAELs in the 28 day study for both the siRNAs and dsRNA were 100 mg/kg, the highest doses tested. In summary, siRNAs and longer dsRNAs with 100% sequence identity to mouse vATPase do not result in adverse effects when administered orally to mice in a large dose. These results are consistent with the current body of knowledge that exogenous dsRNA molecules in food, even those with sequences identical to human and/or animal genes, are safely consumed.

## PS 2344 The Global Burden of Disease Caused by Arsenic in Food.

S. Oberoi, A. Barchowsky and F. Wu. *Environmental and Occupational Health, University of Pittsburgh, Pittsburgh, PA.*

Arsenic is a ubiquitous, naturally occurring metalloid that poses a significant human cancer risk. While water consumption provides the majority of human exposure to arsenic, naturally occurring levels of arsenic in grains, vegetables, meats and fish, as well as through food processed with water containing arsenic (e.g. cooking rice) present a significant exposure to millions of individuals worldwide. To estimate the global burden of diseases attributable to toxic inorganic arsenic in food, we first evaluated the weight of evidence that supports a causal role for arsenic in a number of cancers and non-cancer disease endpoints. We determined that there was substantial evidence from large epidemiological studies that arsenic causes skin, lung, and bladder cancer in humans. The body burden of toxic arsenicals from foods is difficult to estimate and highly variable due to the natural distribution of arsenic in soils and water and the complication posed by multiple toxic inorganic and organic arsenicals, as well as non-toxic organic arsenicals contributing to total arsenic levels. Therefore we used GEMS/FAO-STAT estimates of food consumption in thirteen global clusters and JECFA reported measurements of total and inorganic arsenic in different foods to determine the upper and lower boundaries of foodborne inorganic arsenic exposures. We converted previously reported slope factors for arsenic related bladder, lung, and skin cancers that were based on water exposure to calculate the annual risk of the cancer incidence in males and females within each GEMS cluster. These cluster incidence estimates were summed to generate global estimates of 9,129 to 119,176 additional cases of bladder cancer, 11,844 to 121,442 of lung cancer, and 17,882 to 183,358 of skin cancer worldwide that are attributable to inorganic arsenic in food. These estimates indicate that foodborne arsenic contributes to a significant, but low level of global disease burden. *Supported by the WHO Foodborne Disease Burden Epidemiology Reference Group, Chemical Toxicology Task Force.*

## PS 2345 Hydrogen Peroxide Levels in Freshly Brewed Coffee and Effects on Storage.

S. N. Uppu<sup>2</sup>, B. London<sup>1</sup>, S. N. Murthy<sup>1</sup> and R. M. Uppu<sup>1</sup>. <sup>1</sup>*Environmental Toxicology, Southern University and A&M College, Baton Rouge, LA;* <sup>2</sup>*Science, Dutchtown High School, Geismar, LA.*

Coffee originating in the 15<sup>th</sup> century from Ethiopia is one of the heavily consumed beverages. Although there are studies on caffeine and other components of coffee such as cafestol, the presence of hydrogen peroxide (H<sub>2</sub>O<sub>2</sub>) in coffee was not known till recently as it was confined to scientific community and some informed public. It is a general belief that H<sub>2</sub>O<sub>2</sub> is formed only after long periods of storage or with certain roasting practices. The present study focused on dispelling the myths of H<sub>2</sub>O<sub>2</sub> in coffee. We first measured H<sub>2</sub>O<sub>2</sub> in freshly brewed coffee from different companies by ferrous oxidation-xylenol orange binding (FOX) method. Following this, we examined the time dependent accumulation of H<sub>2</sub>O<sub>2</sub> and its changes with temperature. Further, H<sub>2</sub>O<sub>2</sub> was estimated in coffee obtained from several local vendors. Contrary to the general belief that the accumulation of H<sub>2</sub>O<sub>2</sub> is an aging phenomenon of coffee, we found this toxicant even in freshly brewed coffee. This was true for all brands tested, and H<sub>2</sub>O<sub>2</sub> content increased upon storage. The highest increase was seen in coffee stored on the hot plate compared to the ones kept at room temperature/in cold. The H<sub>2</sub>O<sub>2</sub> content of coffee from different vendors ranged between 0.29 and 0.82 mM, which is 5- to 20-fold higher than the typical H<sub>2</sub>O<sub>2</sub> concentrations at which significant cytotoxic effects have been reported for assay systems using neuroblastoma and other cell types. Our findings shed new light on the probable toxic effects of a commonly consumed beverage like coffee, and the time and temperature dependent variations of keeping. While there are documented benefits of consumption of coffee, the H<sub>2</sub>O<sub>2</sub> mediated toxic effects are critical and have also to be borne in mind. Future studies are warranted to delineate the contribution of H<sub>2</sub>O<sub>2</sub> in the healthy well being of individuals who consume coffee extensively [Funding support from NSF (grant HRD-1043316) and the US Department of Education (grant PO31B040030) is acknowledged. Corresponding author's email: rao\_uppu@subr.edu].

## PS 2346 Toxicologic Evaluation of the Calcium Binding Protein Apoaquorin.

P. Marone<sup>1</sup>, M. R. Bauter<sup>1</sup>, H. Hofman-Huther<sup>2</sup> and D. Moran<sup>3</sup>. <sup>1</sup>*Toxicology, Eurofins Product Safety Laboratories, Dayton, NJ;* <sup>2</sup>*BSL Bioservice Scientific Laboratories GmbH, Planegg, Germany;* <sup>3</sup>*Quincy Bioscience, Madison, WI.*

The present study evaluated the mutagenic and toxicologic potential of a proprietary calcium binding jellyfish protein, Apoaquorin. The test article was investigated for its potential to induce gene mutations according to a plate incorporation

and pre-incubation test by Salmonella typhimurium strains TA98, 100, 1535, and 1537 and E.coli WP2uvrA at concentrations of 31.6, 100, 316, 1000, 2500, and 5000 µg/plate with and without metabolic activation. No toxic effects, precipitation or biologically relevant increases in revertant colony numbers of the test item were noted in any of the five tester strains used up to the highest dose group evaluated with and without metabolic activation in experiments I and II. Therefore, Apoaquorin did not cause gene mutation by base pair changes or frameshifts in the genome of the strains used and was considered to be non-mutagenic in the bacterial reverse mutation assay. In a 90-day oral gavage study including dose levels of 0, 92.6, 462.9, and 926.0 mg/kg/day in Sprague-Dawley rats, there were no adverse clinical, body weight, body weight gain, food consumption, food efficiency, or clinical- or histo-pathology changes associated with the administration of Apoaquorin. Therefore, the no-adverse-effect level (NOAEL) for Apoaquorin administered orally over 90 days was 926.0 mg/kg/day (666.7 mg/kg/day, based on an concentration of 722mg/g or 72% active ingredient) the highest dose tested, for male and female Sprague-Dawley rats.

## PS 2347 Toxicological Evaluation of a High-Purity Transresveratrol from an Alternative Synthetic Route.

J. A. Edwards, M. Beck and P. Beilstein. *Product Safety, DSM Nutritional Products, Kaiseraugst, Switzerland.* Sponsor: A. Davidovich.

trans-Resveratrol is a naturally-occurring, polyphenolic compound found predominantly in grapes. resVida (≥ 99.0% trans-resveratrol manufactured by DSM) has previously been assessed for safety based on toxicity studies (Williams et al, 2009) and obtained self-GRAS status in 2008. An alternative manufacturing process is now available in which trans-resveratrol is obtained with the same high purity of ≥ 99.0% but with different trace components to those in the original manufacturing process. Several of these new resveratrol-related by-products are found in nature (for example trans-pterostilbene). A safety assessment of the new process trans-resveratrol and its by-products was undertaken. The assessment process comprised:

- Identification of the new by-products
- Literature review for information on new by-products
- In silico analysis (DEREK) for toxic alerts of new by-products
- Structural analogue comparisons where appropriate
- In silico analysis (METEOR) for likely metabolism of newly identified by-products
- Ames tests (Salmonella Typhimurium Reverse Mutation Assays) with representative and spiked batches (to maximal specification level) of the new process material
- Definition of a new upper limit specification for newly identified by-products

Information presented from this process includes summarized data from the Ames test, which showed no mutagenic potential, with or without S9. From the assessment of all this information it was concluded that ≥ 99.0% trans-resveratrol produced from the alternative route is safe and suitable for use within the marketing limits defined in the GRAS evaluation of the original process material.

Williams LD, Burdock GA, Edwards JA, Beck M, Bausch J (2009) Safety studies conducted on high-purity trans-resveratrol in experimental animals, Food Chem Toxicol 47(9):2170-2182.

## PS 2348 A 28-Day Gavage Study of 2-Methylfuran in Male Fischer 344 Rats.

S. S. Gill<sup>1</sup>, M. Kavanagh<sup>1</sup>, W. Cherry<sup>1</sup>, M. Barker<sup>1</sup>, M. Weld<sup>2</sup> and G. M. Cooke<sup>1</sup>. <sup>1</sup>*TRD, Health Canada, Ottawa, ON, Canada;* <sup>2</sup>*Chemical Health Hazard Assessment Division, Health Canada, Ottawa, ON, Canada.* Sponsor: R. Mehta.

In thermally treated products, a series of alkylated furan derivatives have been found, in particular 2-substituted alkylfurans such as 2-methylfuran. These methyl analogues are metabolically activated in a similar fashion as the parent furan, yielding highly reactive unsaturated dialdehydes. There is limited toxicological data available for 2-methyl furan which makes conducting a risk assessment difficult. This pilot study was designed to determine the dose range of 2-methylfuran for future subchronic studies needed to determine a NOAEL. Male Fischer 344 rats 5-6 weeks of age were administered 2-methylfuran by gavage to final concentrations of 0, 0.4, 1.5, 3, 6, 12, or 25mg/kg bw/day. The animals were weighed daily prior to gavage. Food consumption was measured on a weekly basis. The liver was the primary target organ which developed dose-dependent toxicity. Relative liver weights were increased by 42% at 25 mg/kg bw/day. Histological changes in the liver were observed at 0.4, 1.5, 3, 6, 12 and 25 mg/kg bw/day. These changes were not accompanied by clinical changes in serum liver enzyme markers such as ALT, ALP and AST. Clinical biochemistry markers for kidney were altered but these were not accompanied by histological changes. At 25 mg/kg bw/day, spleen weights were increased and the prostate was significantly increased in size. Some hematological parameters were also altered. In this pilot study, the liver was the major target organ

for 2-methylfuran as indicated by changes in gross, histological and clinical parameters. Although there were changes in the weights of other organs including prostate, kidneys and spleen, these were not accompanied by histological changes. The results of this study will be used to conduct a future subchronic study to establish a NOAEL for risk assessment purposes.

**PS 2349 Characterization of Bacterial Mutagenicity QSAR Predictions of Food Additives to Support Safety Assessments in a Regulatory Setting.**

K. P. Cross<sup>1</sup>, G. J. Myatt<sup>1</sup>, K. Arvidson<sup>2</sup> and K. Muldoon-Jacobs<sup>2</sup>. <sup>1</sup>Leadscope, Inc., Columbus, OH; <sup>2</sup>Center for Food Safety and Applied Nutrition, US FDA, College Park, MD.

Assessment of food additive safety at the U.S. FDA has utilized quantitative SAR (QSAR) analysis models for endpoints ranging from genetic toxicity, reproductive and developmental toxicity to rodent carcinogenicity. However, many of the QSAR models in routine use were originally developed for drug and industrial chemical assessments. Consequentially a performance assessment on their use for compounds of interest to FDA CFSAN was undertaken. A set of approximately 4000 compounds of interest to CFSAN was assembled and used to characterize the performance of a QSAR model developed for predicting overall Salmonella mutagenicity. The test set was used to assess the suitability of the chemical space of the model for predicting food additive compounds. Overall performance statistics for accuracy, sensitivity, specificity and domain of applicability were measured. Structural classes were identified through compound clustering based on structural fingerprints that were well-predicted, poorly predicted, and not able to be predicted. Additionally, a set of public structural alerts that represent different mutagenic toxicophores was assembled and used to help more precisely quantify performance. Variation in performance was observed across different toxicophores, providing a detailed picture of the model's strengths and weaknesses from a structural perspective in assessing food additives.

**PS 2350 The Role of Palmitoylation in Chemical and Microbial Toxicity: Signal Pathways, Protein Binding and Trafficking.**

I. A. Ross and C. S. Kim. *Toxicology, US FDA, Laurel, MD.* Sponsor: T. Flynn.

Multicellular organisms use chemical messengers to transmit signals among organelles and to other cells. Relatively small hydrophobic molecules such as lipids are excellent candidates for this signaling purpose. In most proteins, palmitic acid and other saturated and some unsaturated fatty acids are esterified to the free thiol of cysteines and to the N-amide terminal. This process enhances the surface hydrophobicity and membrane affinity of protein substrates and play important roles in modulating protein trafficking, stability, and sorting. Protein palmitoylation has been involved in numerous cellular processes, including signaling, apoptosis, and neuronal transmission. The palmitoylation process is involved in diseases such as Huntington's disease, various cardiovascular and T-cell mediated immune disorders, and cancer. Our study on lipopolysaccharide and deoxynivalenol treatment to rats provides insights on the role of protein palmitoylation in chemical and microbial toxicity. In the liver of animals treated with 10 mg/kg DON, palmitic acid decreased by 22% between 3 and 24 hr and increased 24% between 24 and 72 hr as compared to the controls. LPS at 83 µg/kg caused 54% decrease in elaidic acid between 3 and 24 hr, and 7% between 24 hr and 72 hr while stearic acid decreased 33% between 3 and 24 hr and 60% between 24 and 72 hr as compared to the controls. Palmitate is a component of the LPS of Gram-negative bacteria. The bacterial outer membrane enzyme lipid A palmitoyltransferase PagP confers resistance to host immune defenses by transferring a palmitate chain from a phospholipid to the lipid A component of LPS. PagP is sensitive to cationic antimicrobial peptides (CAMP) which are included among the products of the Toll-like receptor 4 (TLR4) signal transduction pathway. This modification of lipid A with a palmitate appears to both protect the pathogenic bacteria from host immune defenses and attenuate the activation of those same defenses through the TLR4 signal transduction pathway.

**PS 2351 Compartment-Regulated Expression of Macrophage-Inhibitory Cytokine 1 under Mucosal ER Stress.**

S. Park, H. Choi, K. Do, J. Kim and Y. Moon. *Lab. of Mucosal Exposure and Biomodulation, Department Microbiology and Immunology, Pusan National University School of Medicine and Medical Research Institute, Yangsan, Republic of Korea.*

Endoplasmic reticulum (ER) stress causes global translational arrest during protein biosynthesis. In spite of global translational arrest, the critical stress responsive genes, including macrophage inhibitory cytokine 1 (MIC-1), are particularly

turned on. Functionally, MIC-1 played pivotal roles in ER stress-linked apoptotic death, which was also influenced by C/EBP homologous protein, a well known apoptotic mediator of ER stress. ER stress enhanced MIC-1 mRNA stability instead of transcriptional activation, and there were two mechanistic translocations critical for mRNA stabilization. First, C/EBP homologous protein triggered protein kinase C-linked cytosolic translocation of the HuR/ELAVL1 (Elav-like RNA-binding protein 1) RNA-binding protein, which bound to and stabilized MIC-1 transcript. As the second critical compartment-regulated modulation, ER stress-activated ERK1/2 signals contributed to enhanced stabilization of MIC-1 transcript by controlling the extended holding of the nucleated mRNA in the stress granules fusing with the mRNA-decaying processing body. Taken together, these two sequential compartment-associate modulation can account for stabilized transcription and subsequent re-initiation of translation of pro-apoptotic MIC-1 gene under mucosal ER stress (This study was carried out with the support of National Joint Agricultural Research Project of RDA (project number PJ008405032012) RDA, Republic of Korea).

**PS 2352 Azathioprine-Induced Hepatotoxicity in an In Vitro Inflammation-Immune Model.**

A. Maruf<sup>1</sup> and P. J. O'Brien<sup>1,2</sup>. <sup>1</sup>Pharmacology & Toxicology, University of Toronto, Toronto, ON, Canada; <sup>2</sup>Faculty of Pharmacy, University of Toronto, Toronto, ON, Canada.

Azathioprine (AZP) is widely used in clinical practice for preventing graft rejection in organ transplantations, various autoimmune and dermatological diseases with documented unpredictable hepatotoxicity. Several experimental models suggested that an episode of inflammation during drug treatment predisposes animals to tissue injury. Inflammation caused by infections or endotoxins markedly activates NADPH oxidase. In the phagosome, superoxide radicals spontaneously form hydrogen peroxide (H<sub>2</sub>O<sub>2</sub>) and other reactive oxygen species. The effect of inflammation on AZP using "Accelerated Cytotoxicity Mechanism Screening" technique was investigated in this study. The concentration of AZP required to cause 50% cytotoxicity in 2 hr towards isolated rat hepatocytes was found to be 400 µM. AZP (400 µM) significantly increased cytotoxicity compared to control hepatocytes. When a non-toxic H<sub>2</sub>O<sub>2</sub> generating system (glucose/glucose oxidase) was added to the hepatocytes prior to the addition of AZP, an increase in AZP cytotoxicity was observed. Because neutrophils or Kupffer cells release myeloperoxidase on activation, the effect of adding peroxidase to the hepatocytes exposed to H<sub>2</sub>O<sub>2</sub> on AZP was also investigated. AZP showed a significant increase in cytotoxicity compared to drug-control in presence of glucose/glucose oxidase with or without horseradish peroxidase. A significant increase was also observed with glutathione depleted and catalase inhibited hepatocytes. Furthermore, AZP increased reactive oxygen species (ROS) formation, lipid peroxidation and decreased %mitochondrial membrane potential with our inflammation-immune model indicating the involvement of oxidative stress by glutathione oxidation, lipid peroxidation and mitochondrial toxicity. Protection was achieved by a ROS scavenger, 4-hydroxy-2,2,6,6-tetramethylpiperidine-1-oxyl (200 µM) and an antioxidant N,N'-diphenyl-p-phenylenediamine (2 µM). These results raise the possibility that the presence or absence of inflammation may be another susceptibility factor for azathioprine-induced hepatotoxicity.

**PS 2353 Indole-3-Carbinol and 3, 3'-Diindolylmethane Decrease Histone Deacetylase 3 Which Plays an Important Role in the Promotion of Staphylococcal Enterotoxin B-Induced Immune Cell Activation.**

P. B. Busbee, M. Nagarkatti and P. Nagarkatti. *USC School of Medicine, Columbia, SC.*

Staphylococcal enterotoxin B (SEB) is an exotoxin produced by the *Staphylococcus aureus* bacterium. This toxin is classified as a "superantigen" because of its ability to directly bind T cell receptors with MHC II class receptors of antigen presenting cells, which activates a large proportion of T cells. SEB is commonly associated with classic food poisoning, and more recently gained attention as a potential biological warfare agent since it is easily aerosolized. We have shown that indole-3-carbinol (I3C) and one of its byproducts, 3,3'-diindolylmethane (DIM), which are found in cruciferous vegetables, is able to reduce the number of SEB-activated T cells both in vitro and in vivo. These compounds were also able to reduce immune cell activation, induce apoptosis, and decrease proinflammatory cytokine release. In the current study, we assessed the role histone deacetylases (HDACs) played in SEB-treated cells, as well as what effect I3C/DIM had on them. Using inhibitors specific for Class I or Class II HDACs, we showed that inhibition of Class I HDACs leads to decreased immune cell activation, increased apoptosis, and reduction in proinflammatory cytokine release in SEB-activated cells. However, inhibition of Class II

HDACs had opposite effects, suggesting a dual role of these HDAC classes in SEB stimulation, where Class I HDACs were important in SEB-mediated immune cell activation. Screening HDAC expression with western blots, we were able to determine that HDAC3 was the main HDAC upregulated after SEB stimulation, and I3C and DIM treatment was able to decrease this expression level. This research establishes for the first time the important role Class I HDACs, particularly HDAC3, play in SEB-induced stimulation. We were also able to provide more evidence for the effectiveness of I3C/DIM treatment in SEB through the downregulation of HDAC3. (Supported in part by NIH grants P01AT003961, R01AT006888, R01ES019313, R01MH094755, P20RR032684 and VA Merit Award BX001357).

**PS 2354 Quantification of Cytokines: Enzyme-Linked Immunosorbent Assay versus Cytometric Bead Array.**

M. van Tuyl, M. Stitzinger, M. Vloet, Y. Klijn-Pijnenborg and H. Emmen. *Toxicology, WIL Research Europe B.V., s-Hertogenbosch, Netherlands.*

Cytokines are important inflammatory mediators. Disturbance of the balance of pro- and anti-inflammatory cytokines may result in multiple organ toxicity. In this study, we compared two commonly used immunoassays for the detection of cytokines, i.e. Enzyme-Linked ImmunoSorbent Assay (ELISA) and Cytometric Bead Array (CBA).

BD OptEIA ELISA kits and BD CBA Flex Sets were used to determine interleukin 4 (IL-4), interleukin 10 (IL-10) and interferon gamma (IFN- $\gamma$ ) levels in serum of untreated rats and in assay diluent. The intra-assay variation was determined after spiking with the individual recombinant standard of an ELISA kit at concentrations within the ELISA standard range or spiking with the combined recombinant standards of the CBA sets at concentrations within the CBA standard range. In addition, inter-assay variation was determined by spiking at two concentrations within the range of both ELISA and CBA standards and by analyzing these spiked samples using both methods on the same day.

Both ELISA and CBA methods showed similar coefficients of variation for all cytokines, i.e. less than 15% for the majority of measurements. The accuracy of assay diluent spiked with one or more cytokines was within 75-125% for most measurements using both methods. Spiking of serum samples showed clearly that serum contains factors that interfered with the quantification of IL-4, IL-10 and IFN- $\gamma$  using the selected ELISA kits and CBA sets. For example, quantification of IL-10 in spiked serum showed an accuracy of approximately 30% using both methods and IFN- $\gamma$  analysis resulted in an accuracy of <30% using ELISA and an accuracy of 70-80% using CBA. The absolute values of cytokines in spiked serum samples may differ between both methods, like for IFN- $\gamma$ , but relative levels of cytokines always correlated with the spiked concentrations using either one of these methods.

In conclusion, both ELISA and CBA showed similar precision and consistency in relative cytokine levels.

**PS 2355 Aryl Hydrocarbon Receptor-Dependent Retention of Nuclear HuR Suppresses Cyclooxygenase-2 Expression Independent of DNA-Binding.**

M. Zago<sup>1</sup>, J. Sheridan<sup>1</sup>, P. Nair<sup>2</sup>, A. Rico de Souza<sup>1</sup>, I. E. Gallouzi<sup>1</sup>, S. Rousseau<sup>1</sup>, S. Di Marco<sup>1</sup>, Q. Hamid<sup>1</sup>, D. H. Eidelman<sup>1</sup> and C. J. Baglioni<sup>1</sup>. <sup>1</sup>McGill University, Montréal, QC, Canada; <sup>2</sup>McMaster University, Hamilton, ON, Canada.

**Rationale:** The aryl hydrocarbon receptor (AhR) has emerged an endogenous suppressor of cyclooxygenase-2 (Cox-2). Cox-2 is an immediate-early gene that is robustly increased by cigarette smoke exposure. We have published that the AhR suppresses cigarette smoke-induced Cox-2 protein but not mRNA, suggesting post-transcriptional regulation as a mechanism. The AhR may destabilize Cox-2 mRNA by retaining the RNA-binding protein (RBP) HuR in the nucleus. There is no known association between the AhR and HuR. Therefore, we investigated whether AhR-dependent retention of nuclear HuR is responsible for Cox-2 mRNA destabilization.

**Methods:** AhR<sup>-/-</sup>, AhR<sup>+/+</sup>, AhRDBD/DBD (harboring a mutant AhR unable to bind DNA) and AhRDBD/B6 mouse lung fibroblasts were exposed to cigarette smoke extract (CSE) for 3 h followed by Actinomycin D (ActD) for 30 minutes, 1 or 3 h. Cox-2 protein and mRNA were analyzed by western blot and qRT-PCR, respectively. HuR expression was assessed by western blot and immunofluorescence. AhR<sup>-/-</sup> cells were transfected with HuR siRNA and exposed to 1% CSE for 3 h with or without ActD for an additional 3 h. Cox-2 mRNA was then assessed by qPCR.

**Results:** Steady-state Cox-2 mRNA levels significantly declined upon ActD treatment in AhR<sup>+/+</sup> cells, AhRDBD/DBD and AhRDBD/B6 cells, suggesting that the AhR destabilizes Cox-2 mRNA by a DRE-independent mechanism. Cox-2 mRNA

instability was due to the nuclear retention of HuR. CSE did not alter HuR expression, but induced cytoplasmic HuR shuttling only in AhR<sup>-/-</sup> cells. Knockdown HuR in AhR<sup>-/-</sup> cells significantly decreased Cox-2 mRNA expression after exposure to ActD.

**Conclusions:** AhR-dependent retention of nuclear HuR suppresses cigarette smoke-induced Cox-2 protein by a mechanism that is independent of DNA-binding activity. These important findings open the possibility that a DRE-independent AhR pathway may be exploited therapeutically as an anti-inflammatory target.

**PS 2356 Ultraviolet Radiation (UVB)-Induced Migration of Skin Dendritic Cell Subsets Is Mediated through Transforming Growth Factor Beta Signaling.**

A. Ravindran<sup>1</sup>, J. Mohammed<sup>1</sup>, A. J. Gunderson<sup>1</sup>, M. C. Udey<sup>2</sup> and A. B. Glick<sup>1</sup>. <sup>1</sup>Center for Molecular Toxicology and Carcinogenesis, The Pennsylvania State University, State College, PA; <sup>2</sup>Dermatology Branch, National Cancer Institute, National Institutes of Health, Bethesda, MD.

Ultraviolet radiation (UVB) is the leading cause of skin cancer worldwide. UVB also modulates certain inflammation driven cutaneous pathologies such as contact hypersensitivity through actions on skin resident dendritic cell (DC) subsets. Transforming Growth Factor- $\beta$ 1 (TGF- $\beta$ 1) is a potent immunoregulatory cytokine in the skin microenvironment. Here, we show that TGF- $\beta$ 1 is required for UVB induced activation and migration of dendritic cells to the skin draining lymph nodes. We irradiated skin of Skin Hairless (SKH1) mice with UVB in the presence or absence of SB431542, a small molecule inhibitor of the TGF- $\beta$  type I receptor and measured lymph node migration of skin dendritic cell subsets at acute time points. Topical inhibition of TGF- $\beta$ 1 pathway with SB431542 suppressed the migration of skin dendritic cell subsets, primarily CD103<sup>+</sup> CD207<sup>+</sup> and CD207<sup>-</sup> DC populations to the lymph nodes in response to UVB irradiation. In addition, in an ex vivo, skin explant assay for the migration of dendritic cells, UVB induced DC migration into culture media was suppressed with topical inhibition with SB431542. In mice expressing a dominant negative receptor for TGF- $\beta$  in CD11c<sup>+</sup> dendritic cells (CD11c-T $\beta$ R1 DNR), UVB induced migration of the DC subsets was suppressed directly linking TGF- $\beta$  signaling in DCs to UVB induced migration of DCs. Treatment with SB431542 also suppressed UVB-induced Interferon  $\gamma$  (IFN $\gamma$ ) secretion as well as the effector differentiation of T lymphocytes within the lymph nodes. Consistent with decreased activation within the lymph nodes, SB431542 decreased UVB activation of the skin infiltrating CD4 and CD8 lymphocytes after acute treatments and in UVB-induced skin tumors. Together, these data show that the TGF- $\beta$ 1 signaling pathway is important for the initiation of the inflammatory response to UVB irradiation of the skin, mediated primarily through the dendritic cells.

**PS 2357 Alterations in the Hepatic Transcriptome during Live *Citrobacter Rodentium* Infection.**

M. D. Merrell and E. T. Morgan. *Pharmacology, Emory University, Atlanta, GA.*

Infection and inflammatory signaling can significantly alter drug metabolism enzyme expression (DME), thereby impacting the capacity of the liver to clear toxicants from the body. Previous work in our laboratory has detailed the modulation of gene expression of several hepatic DMEs during colonic infection with live *Citrobacter rodentium* (*C. rodentium*). These alterations included particularly strong downregulation of Fmo3 and Cyp4a family members, and appear to be largely independent of LPS-TLR4 signaling. In order to elucidate potential signaling networks and pathways involved in this downregulation, we examined the impact of *C. rodentium* infection on the hepatic transcriptome using the Illumina MouseRef-8 v2 expression BeadChip. HeJ mice (n=4) lacking toll-like receptor 4 (TLR4), along with appropriate wild type animals (HeOUJ), were orally inoculated with live *C. rodentium* in a sucrose solution or received sterile sucrose. After 7 days, animals were sacrificed, livers were harvested, and RNA was prepared and submitted for analysis. Genes showing differential expression during infection were identified and pathway analysis using gene-set enrichment was performed. Increased numbers of genes with altered expression were found in HeJ mice as compared to HeOUJ controls. Several DME genes not previously reported as being altered in *C. rodentium* infection were identified, comprising P450s, UGTs and GSTs. Ontology terms/pathways with high enrichment included *Drug Metabolism*, *Mitochondrion*, *Oxidation Reduction*, and *Inflammatory Response*. Other terms/pathways of interest include *Apoptosis*, *Glutathione Transferase Activity*, and *Lipid Metabolism*. An analysis of the potential transcription control pathways upstream of these observed gene expression changes was also performed. Potential upstream factors include Ahr-ARNT, Ekl-1, and Hnf3beta, among others. Taken together, these results demonstrate that drug metabolizing enzymes as a gene class are particularly sensitive to infection, and indicate several potential pathways that may be responsible for these effects. Supported by grant R01072372 from the NIH.

**PS 2358 Silencing of Keap1 in Macrophages Boosts Lipopolysaccharide-Induced Transcription of Interleukin 6 via IKK $\beta$  Activation.**

P. Lu, P. Xue, J. Dong, C. G. Woods, Q. Zhang, M. E. Andersen and J. Pi. *The Institute for Chemical Safety Sciences, The Hamner Institutes for Health Sciences, Research Triangle Park, NC.*

Interleukin-6 (IL6) is a multifunctional cytokine that regulates immune and inflammatory responses. Multiple transcription factors, including NF- $\kappa$ B and nuclear factor E2-related factor 2 (Nrf2), are implicated in the transcriptional regulation of IL6. Kelch-like ECH-associated protein 1 (Keap1) is a substrate adaptor protein for a Cullin 3-dependent E3 ubiquitin ligase complex, which regulates the degradation of various vital proteins, including Nrf2 and Ikk $\beta$ . In agreement with previous studies, stable knockdown of Nrf2 in RAW 264.7 mouse macrophages led to significantly attenuated antioxidant response and decreased expression of IL6 under basal and lipopolysaccharides (LPS)-treated conditions. However, Nrf2 activation alone (e.g. under tert-butylhydroquinone exposure) did not increase the expression of IL6, suggesting that Nrf2 is a necessary, but not sufficient, factor in regulating LPS-induced transactivation of IL6. In contrast, silencing of Keap1 in RAW cells and human monocyte THP1 cells markedly augmented the expression of IL6 under non-stressed and LPS-challenged conditions. The enhanced expression of IL6 in Keap1-knockdown (Keap1-KD) cells was significantly attenuated by silencing of Ikk $\beta$ , but not Nrf2, suggesting that stabilized Ikk $\beta$  resulting from Keap1 silencing is the major downstream event responsible for the transactivation of IL6. This finding was further confirmed by the enhanced protein levels of Ikk $\beta$  and subsequent increased expression and phosphorylation of NF- $\kappa$ B p65 in the Keap1-KD cells. Together, the present studies demonstrated that silencing of Keap1 in macrophages boosts LPS-induced transcription of IL6 via IKK $\beta$  activation. Given the importance of IL6 in inflammatory response, targeting Keap1 could be a novel approach in the treatment and prevention of inflammation and associated disorders.

**PS 2359 Potent Protection against PM2.5 Diesel Exhaust Particle-Caused ROS Generation and Vasculature Permeable through Regulation of Nrf2-Induced Pathways by Triterpenoids.**

C. Tseng<sup>1,2</sup>, C. Lin<sup>1</sup>, M. K. Gordon<sup>3</sup> and M. Chao<sup>1</sup>. <sup>1</sup>Bioscience Technology, Chung Yuan Christian University, Chung-Li, Taiwan; <sup>2</sup>Biomedical Engineering, Chung Yuan Christian University, Chung-Li, Taiwan; <sup>3</sup>Joint Program of Toxicology, Rutgers University, Piscataway, NJ.

Epidemiologies suggest that an increase of PM2.5 diesel exhaust particles (DEP) in ambient air corresponds to an increase in myocardial infarctions within 48 hours. To cause such disorder, the close association of capillaries and alveoli should allow inhaled DEP to get in close proximity to capillary endothelial tubes. However, the mechanism of how DEP travel from the alveolar space into bloodstream remains unclear. Our group has suggested that DEP might upregulate Nrf2 pathway and induce vascular permeability factor VEGF-A secretion. Once VEGF-A goes up, DEP may cause cell-cell adherent junction disruption and transmigrate into the circulation. In order to minimize the level that DEP traveling in the bloodstream, two triterpenoids (oleanic acid, ursolic acid) were used as antioxidant. After DEP  $\pm$  triterpenoids treatment, MTT was used to examine cell viability of 3D capillary-like endothelial cultures, Cm-H2DCFDA assays were used to determine the extent of ROS production in the model, and confocal microscopy was used to evaluate the endothelial junctional proteins in the cell-cell borders and localization of Nrf2 as well. At high dose DEP, 80% of the tube cells die within 24 hours. Cells treated with 25  $\mu$ g/ml DEP plus triterpenoids not only the translocation of Nrf2 and downstream HO-1 mRNA expression was reduced, but also ROS generation was inhibited. Additionally, Z-stacks images revealed that DEP not only accumulated on the surface of capillary tubes, but also penetrated into the lumen. VE-cadherin was observed to redistribute in response to DEP. Once combine with triterpenoids, endothelial tube cells were slightly affected only at high dose DEP, injuries caused by DEP-induced ROS were blocked. Our results suggest that triterpenoids might prevent DEP transmigration into bloodstream by inhibiting oxidative stress production and endothelial adherent junctions alternation.

**PS 2360 Differential Responses upon Inhalation Exposure to Biodiesel versus Diesel Exhaust on Oxidative Stress, Inflammatory, and Immune Outcomes.**

A. A. Shvedova<sup>1,2</sup>, N. V. Yanamala<sup>1</sup>, A. V. Tkach<sup>1</sup>, E. R. Kisin<sup>1</sup>, A. R. Murray<sup>1</sup>, T. Khaliullin<sup>1</sup>, M. Hatfield<sup>1</sup>, S. H. Gavett<sup>3</sup> and I. Gilmour<sup>3</sup>. <sup>1</sup>PPRB, HELD, NIOSH, Morgantown, WV; <sup>2</sup>Department of Physiology and Pharmacology, School of Medicine, WVU, Morgantown, WV; <sup>3</sup>Cardiopulmonary and Immunotoxicology Branch, US EPA, Research Triangle Park, NC.

Biodiesel (BD) exhaust may have reduced adverse health effects due to lower mass emissions and reduced production of hazardous compounds compared to diesel exhaust. To investigate this possibility, we compared adverse effects in lungs and liver of BALB/c mice after inhalation exposure (0, 50, 150 and 500  $\mu$ g/m<sup>3</sup>; 4 hr/day, 5 d/wk, for 4 wk) to combustion exhaust from 100% biodiesel (B100) and diesel (D100). Compared to D100, B100 exhaust caused a significant accumulation of oxidatively modified proteins (carbonyls), increase in 4-hydroxynonenal (4-HNE), reduction of protein thiols, depletion of antioxidant - glutathione (GSH), a dose-dependent increase in the levels of biomarkers of tissue damage (LDH) in lungs, and inflammation (myeloperoxidase, MPO) in both lungs and liver. B100 exposure also significantly enhanced expression of cytokines IL-6, and IL-12p70 (in a dose-dependent manner), along with IL-10, TNF- $\alpha$  and MCP-1 (increased compared to control) in both lung and liver tissues. Overall, the cytokine profiles in the lung and liver suggest that B100 and D100 exhaust elicit similar innate immune responses, predominantly involving T-cell independent pathways; however, the magnitude of inflammation was greater following B100 exhaust exposure. Interestingly, exposure to D100, but not B100 exhaust, induced a significant increase in the levels of IFN- $\gamma$  in the lungs, suggesting a broader engagement of Th1 component by D100 exhaust. Based on this, we hypothesize that the distinctive organic compounds and/or oxidative products formed as a result of increased oxidative stress upon B100 exposure, are capable of targeting biological/molecular pathways that are distinct from D100 exposure. (This abstract does not represent US EPA policy).

**PS 2361 THP-1 and HMC-1 Cell Interaction with Epithelial Cells in a 3D Tetraculture System of the Alveolar Barrier Modulates the Response to Oxidative Stress.**

S. G. Klein<sup>1,2</sup>, S. Tommaso<sup>1</sup>, L. Hoffmann<sup>1</sup>, B. Blömeke<sup>2</sup> and A. Gutleb<sup>1</sup>. <sup>1</sup>EVA, CRP - Gabriel Lippmann, Belvaux, Luxembourg; <sup>2</sup>Department of Environmental Toxicology, University of Trier, Trier, Germany.

Exposure to fine and ultra-fine ambient particles is still a problem of concern in many industrialised parts of the world and the intensified use of nanotechnology may further increase exposure to small particles. Among the various mechanisms, the production of oxidative stress is considered to be one of the key mechanisms how particles affect tissues. Complex in vitro coculture systems may be valuable tools to study related processes and to further evaluate the effects of particles on the lung (Klein et al., 2011). Therefore, a system consisting of four different human cell lines that should mimic the cell response of the alveolar surface in vitro was developed in order to be used with a native aerosol exposure system (Vitrocell<sup>TM</sup> chamber). It is composed of an alveolar type-II cell line (A549), differentiated macrophage-like cells (THP-1), mast cells (HMC-1) and endothelial cells (EA.hy 926), seeded in a 3D orientation on microporous membranes.

Oxidative stress was induced by incubating the cells with 2,2'-azobis-2-methylpropanimidamide, dihydrochloride (AAPH; 20 mM), and quantified as the oxidation of dichlorofluorescein diacetate (DCFH-DA) by measuring fluorescence. Results are reported as fold increase in ROS production relatively compared to untreated cells.

Single cell cultures of EA.hy 926 (11.8  $\pm$  1.4), THP-1 (11.5  $\pm$  1.3) and HMC-1 (14.7  $\pm$  2.9) showed significantly higher oxidative stress than the tetraculture (6.6  $\pm$  0.75). A549 cells alone show the lowest amount of oxidative stress (3.4  $\pm$  0.18) compared to other cultures. The interplay of model cell for the immune system (THP-1 and HMC-1) with A549 epithelial cells strongly influences the behaviour of our system, resulting in an alleviative effect for oxidative stress compared to the monocultures. The use of the tetraculture system may lead to a more realistic judgement about the hazard of new compounds in the future.

**PS 2362 ADME Studies on Nanoparticles Are So Far of Limited Use for PBPK Modeling.**

U. Carlander and G. Johanson. *Institute of Environmental Medicine, Work Environment Toxicology, Karolinska Institutet, Solna, Sweden.*

The health hazards with nanoparticles (NP) are largely unknown, and human data are unlikely to be generated to any great extent. Previous experience with xenobiotics shows that combined use of animal ADME studies and PBPK modeling is

useful in human health risk assessment and this approach should be useful also for NP. However, it requires that animal experiments are carried out and reported in an appropriate way. The aim of this study was to review published data on the biodistribution of intravenously injected NP. By this approach the additional complexity of absorption is avoided. Data were mainly retrieved for gold, silver, titanium dioxide, silica and polymeric NP. Very few of the 66 reviewed articles, covering 244 NP varieties, seem useful for PBPK modeling. The following major limitations were identified: (1) incomplete NP and dose characterization, (2) short follow-up post-dosing, (3) few samples per tissue, (4) few tissues/organs studied, and (5) failure to account for the mass balance, and (6) lack of confirmation of NP integrity in the tissues. These shortcomings make time course descriptions, half time calculations, estimates of bioaccumulation uncertain. Most studies present data for blood, liver and spleen, many also for lungs and kidneys. A few studies suggest that NP deposits in muscle, bone and carcass should not be neglected. Overall, our review indicates that it is difficult to draw general conclusions about NP biodistribution. With the limited data at hand, it seems that no individual factor such as size, coating, shape, charge, chemical composition or agglomerations status can explain the biodistribution. In conclusion, the ADME of NP is complex and additional studies are needed. To be useful in PBPK modeling, these studies should include more complete NP characterization, cover more organs and time points, have longer follow-ups, and account for the mass balance. It would be valuable to develop a standard protocol for ADME studies of NP. This study was financed by a grant from the Swedish Council for Working Life and Social Research.

### PS 2363 Copper Oxide Nanoparticle-Induced Acute Pulmonary Inflammation: Role of Dose Rate and Dissolution Rate.

B. L. Baisch, N. Corson, R. Gelein, P. Wade-Mercer, A. Walker, G. Oberdorster and A. Elder. *Environmental Medicine, University of Rochester Medical Center, Rochester, NY.*

Numerous studies in rodents use high doses and bolus delivery of nanoparticles (NPs) to the respiratory tract (RT) in order to identify potential hazards. Past data suggests differences in inflammatory responses following intratracheal instillation as compared to whole body inhalation exposure, indicating that bolus delivery may overestimate NP hazard. However, deposited doses to the lower RT are not always consistent in these studies and the impact of ions from soluble metal oxide NPs interacting with extracellular fluids and within cells is uncertain. We hypothesize that the delivered dose rate and dissolution rate are key determinants of the inflammatory response in the RT when the deposited dose is constant. F-344 rats (175-270g) were exposed to the same deposited dose (3µg) of CuO NPs (30-50nm; 13m<sup>2</sup>/g) by high dose rate (bolus) intratracheal instillation and low dose rate (aerosol) whole body inhalation (1mg/m<sup>3</sup> for 4h). Particle size distributions showed agglomerated structures for both intratracheal instillation (280-420nm, hydrodynamic diameter) and whole body inhalation (990nm, aerodynamic diameter) exposures. Dynamic dissolution of the NPs in simulated lung lining fluid (pH 7.4) showed substantial Cu<sup>2+</sup> release over 30h (67%). There were statistically significant increases in bronchoalveolar lavage fluid (BALF) neutrophils 8 and 24h after bolus delivery of CuO (4.43 ± 1.25 × 10<sup>5</sup>; 84.18 ± 18.53 × 10<sup>5</sup>) compared to saline controls (1.44 ± 0.41 × 10<sup>5</sup>) and 24h after aerosol exposure (48.34 ± 5.45 × 10<sup>5</sup>) compared to air controls (0.62 ± 0.14 × 10<sup>5</sup>). Within 7 days BALF neutrophils returned to control levels. The similar clearance pattern from the lower RT by both methods indicates that clearance was not affected by delivered dose rate. We conclude that both dose rate and dissolution rate should be considered when identifying NP hazard. This research was funded by NIH R01CA134218, P30ES01247, RC2ES018741, T32ES07026 and T32HL066988.

### PS 2364 Association between Neutrophilia and Inflammatory Responses for Ensuring Safety of Nanomaterials.

K. Higashisaka<sup>1</sup>, Y. Yoshioka<sup>1</sup>, T. Nagano<sup>1</sup>, A. Kunieda<sup>1</sup>, Y. Iwahara<sup>1</sup>, K. Tanaka<sup>1</sup>, K. Hata<sup>1</sup>, S. Tsunoda<sup>2,3</sup>, H. Nabeshi<sup>4</sup>, T. Yoshikawa<sup>1</sup> and Y. Tsutsumi<sup>1,2,3</sup>. <sup>1</sup>Laboratory of Toxicology and Safety Science, Graduate School of Pharmaceutical Sciences, Osaka University, Osaka, Japan; <sup>2</sup>Laboratory of Biopharmaceutical Research, National Institute of Biomedical Innovation, Osaka, Japan; <sup>3</sup>MEI center, Osaka University, Osaka, Japan; <sup>4</sup>National Institute of Health Science, Tokyo, Japan.

Recently, the development of nanomaterials is promoted extensively. These nanomaterials have been already used in various applications. Under this circumstance, the debate on safety of nanomaterials has expanded worldwide, because they have unique physicochemical properties and exert innovative functions. Therefore, it is urgent need to obtain more information to ensure the safety of nanomaterials. Previously, we demonstrated that some silica nanoparticles (nSP) might induce systemic inflammatory effects, whereas appropriate surface modification suppressed

these effects. However, association with neutrophil that are known to play an important role in inflammatory responses is hardly understood. Here, for clarifying the mechanism of inflammatory effects of nSP, we analyzed the changes of neutrophil proportion in mice. Initially, to evaluate systemic inflammation induced by nSP, we analyzed the changes of neutrophil proportion in mice after intravenous injection of nSP with diameters of 70 nm (nSP70) via tail vein. Flow cytometry analysis showed that the neutrophil proportion was elevated in peripheral blood of nSP70-treated mice. Furthermore, the plasma level of G-CSF was significantly elevated in nSP70-treated mice compared to that of control mice and anti-G-CSF antibody-treated mice exhibited a decrease in neutrophil proportion. These results suggested that the nSP70-induced increasing neutrophil proportion was dependent on G-CSF production. We are now trying to examine the association between neutrophilia and inflammatory responses. We believe that our findings provide useful information for ensuring the safety of nanomaterials.

### PS 2365 Differential Response of Brain and Liver Free Fatty Acids following Administration of Iron Nanoparticles in Rats.

Z. K. Binienda<sup>1</sup>, I. A. Ross<sup>2</sup>, B. Gough<sup>1</sup>, S. F. Ali<sup>1</sup>, S. Z. Imam<sup>1</sup> and C. S. Kim<sup>2</sup>. <sup>1</sup>Neurotoxicology, NCTR/FDA, Jefferson, AR; <sup>2</sup>Toxicology, CFSAN/FDA, Laurel, MD.

Intranasal treatment with ferric oxide nanoparticles (α-Fe<sub>2</sub>O<sub>3</sub> and γ-Fe<sub>2</sub>O<sub>3</sub> NPs), in rats caused microglial proliferation and activation in olfactory bulbs, hippocampus and striatum. Our in vitro studies with SHSY-5Y neuroblastoma cells exposed to 10 and 30 nm ferric oxide NPs showed over expression of alpha-synuclein protein, depletion of dopamine, and conditions for oxidative stress. Here, we examined the response of brain and liver free fatty acids (FFAs) in adult male Sprague-Dawley rats treated intraperitoneally (i.p.) either with saline (control) or ferric oxide (Fe<sub>2</sub>O<sub>3</sub>) – NPs at 25, 50 and 100 mg/kg. Rats were sacrificed 72 hrs after injection to harvest caudate nucleus and liver. Long chain FFAs were extracted with chloroform and methanol (4, 8 v/w) from tissue homogenates and the extracts were shaken, followed by centrifugation. The supernatants were reconstituted with Hepes, chloroform and methanol (3.2, 4, 8 v/w). The chloroform was then evaporated under nitrogen. The residue was reconstituted with ether-hexane (50:50, v/v) and eluted by column chromatography on acid-washed Florisil. FFAs were derivatized with BF<sub>3</sub>/methanol and fatty acid methyl esters were quantitated using gas chromatography. Concentrations of saturated FFAs (palmitic, stearic) in the liver and brain did not change following injection of the iron NPs. However, unsaturated brain FFAs (oleic, linoleic) were decreasing in a dose-related fashion in the CN (p<0.05). In the liver, the concentration of the unsaturated FFAs increased significantly at 25 and 50 mg/kg (p<0.05) but was no different from control at 100 mg/kg. These data indicate a differential response of liver and brain unsaturated fatty acids to iron nanoparticle exposure, suggesting different mechanisms in the liver and brain in response to oxidative stress.

### PS 2366 Effects of Cerium Oxide Nanoparticles on Fibroblast Function in Relation to Lung Fibrosis.

J. Y. Ma, B. Hines, M. Barger, R. R. Mercer and V. Castranova. *PPRB/HELD, NIOSH, Morgantown, WV.*

The emission of cerium oxide nanoparticles (CeO<sub>2</sub>) in the diesel exhaust, when cerium compounds were used as a diesel engine catalyst to lower the diesel exhaust particles, is a health concern. Our previous studies have shown that CeO<sub>2</sub> induced pulmonary inflammation and lung fibrosis. The objective of the present study is to investigate the modification of fibroblast function by CeO<sub>2</sub> in relation to fibrosis. Male Sprague Dawley rats were exposed to CeO<sub>2</sub> (0.15 to 7 mg/kg) by a single intratracheal instillation and sacrificed at various times post exposure. Alveolar macrophages (AM) were isolated by bronchoalveolar lavage (BAL), and lung fibroblasts were isolated from the lung tissues. The first BAL fluid and AM culture medium obtained after a 24 h incubation time were saved for further analysis. The results show that at 28 days after CeO<sub>2</sub> (3.5 mg/kg) exposure, lung fibrosis was evident by increased hydroxyproline content in lung tissues and enhanced Sirius Red staining collagen fibers in the lung. In addition, the presence of stress actin, expressed as α-smooth muscle actin (SMA), in fibroblasts was also significantly increased when compared to the control. Lung fibroblasts isolated from CeO<sub>2</sub>-exposed rats at 28 days post-exposure showed a dose-dependent decrease in proliferation rate using the MTT assay. Treating primary fibroblasts with CeO<sub>2</sub> in vitro, did not significantly affect cell proliferation rate; however, when treated with the first BAL fluid collected at 3- or 10-days after CeO<sub>2</sub> exposure, significantly increased cell proliferation when compared to the control. In vitro treatment of fibroblasts with TGF-β1 significantly increased α-SMA expression. These results

demonstrate that CeO<sub>2</sub> induces a diverse network of mediators that affects fibroblast proliferation and functional changes that may play a role in lung fibrosis. These findings suggest potential health effects of CeO<sub>2</sub> exposure.

## PS 2367 Toxicity of Nanoparticles Embedded in Paints Compared to Pristine Nanoparticles.

S. Smulders, K. Luyts, J. Vanoirbeek and P. Hoet. *Experimental Unit for Toxicology, KU Leuven, Leuven, Belgium.*

Nanomaterials are increasingly being used in the paint industry due to their unique physical and chemical properties. Nanoparticles often used in paints and coatings are TiO<sub>2</sub> (anti-UV, self-cleaning, air purification), Ag (anti-microbial) and SiO<sub>2</sub> (fire retardant, anti-scratch).

In this study, the toxic effects of 3 pristine nanoparticles (TiO<sub>2</sub>, Ag and SiO<sub>2</sub>), 3 aged paints containing nanoparticles (TiO<sub>2</sub>, Ag and SiO<sub>2</sub>) and control paints without nanoparticles were compared.

BALB/c mice were weekly oropharyngeally aspirated with nanoparticles or paint particles (20 µg/aspiration) for 5 weeks. Mice were sacrificed 2 or 28 days after the last aspiration. The local (lung/bronchoalveolar lavage fluid) and systemic (blood) toxicity was evaluated (cell counts, inflammatory cytokines, blood clotting parameters).

The pristine nanoparticles showed no effects in the blood and a subtle toxic effect in the lungs, which was most pronounced in the case of Ag nanoparticles (increase in neutrophils (7.8x10<sup>3</sup>), 2-fold increase in pro-inflammatory cytokines KC and IL-1β). The paints containing nanoparticles did not show significant toxicity.

In conclusion, we demonstrated that although pristine particles show some toxic effects, no significant toxicological changes were observed when they were embedded in a complex paint matrix.

## PS 2368 A 15-Day Oral Exposure to Dispersed TiO<sub>2</sub> P25 Particles Induces Epithelial Barrier Dysfunction and Bacterial Translocation in the Rat Intestine.

E. Houdeau<sup>1</sup>, E. Gaultier<sup>1</sup>, M. Nabila<sup>1</sup>, N. Naud<sup>1</sup>, A. Ait-Belgnaoui<sup>1</sup>, N. Thieriet<sup>2</sup>, M. Carrière<sup>3</sup>, J. Cravedi<sup>1</sup>, V. Theodorou<sup>1</sup> and F. Pierre<sup>1</sup>. <sup>1</sup>INRA Tolaim, Toulouse, France; <sup>2</sup>ANSES, Maisons-Alfort, France; <sup>3</sup>CEA-LAN, Grenoble, France. Sponsor: D. ZALCO.

**Aim:** Titanium dioxide (TiO<sub>2</sub>) has a long-standing use as food additive and is promised to broad use in food packaging as antimicrobial in biosourced films. Possible hazards of ingested TiO<sub>2</sub> particles for human digestive tract are under discussion. We addressed consequences for gut barrier function in rats orally exposed to TiO<sub>2</sub> P25 (85% anatase/15% rutile) at human level exposure. **Methods:** Male rats were orally given either vehicle (Ve) or TiO<sub>2</sub> P25 (provided by European Commission-Joint Research Center in the OECD sponsorship program) at 100, 1, 0.01 µg/kg BW/d in aggregated forms or ultrasonicated to obtain a stable dispersed submicron-sized TiO<sub>2</sub> commonly found in food. Particle size was measured by dynamic light scattering. Duodenal to colonic paracellular (4kD dextran) epithelial permeability was studied by Ussing chamber. Lipid peroxidation was assessed by Thiobarbituric Acid Reactive Substances (TBARS) assay, and inflammation through neutrophil myeloperoxidase activity (MPO). Bacterial translocation (BT) was assessed in mesenteric lymph nodes (MLN), liver and spleen. **Results:** Oral treatment with dispersed TiO<sub>2</sub> P25 particles (mean hydrodynamic diameter 630nm) at 100 or 1 µg/kg/d increased epithelial permeability (p<0.01) in the jejunum (+70±16% vs Ve) and colon (+57±19% vs Ve), and only in the jejunum at 10ng/kg/d (85%: 0.19±0.07 vs 0.10±0.03 nmol dextran.cm<sup>2</sup>.h<sup>-1</sup> in Ve; p<0.05). At all doses, dispersed P25 did not affect TBARS and MPO levels across the gut, whereas rats dosed with 100 µg/kg/d showed enhanced BT to MLN (14 rats/16 vs 4/16 in Ve; p=0.001) (10±0.2 vs 9.3±0.3 log10cfu/g of tissue, respectively), but not to liver and spleen. Neither gut permeability nor BT was affected in rats exposed to non-dispersed P25. **Conclusion:** Chronic oral exposure of rats with dispersed TiO<sub>2</sub> at human relevant dietary exposure alters intestinal barrier, with features of bacterial translocation suggesting enhanced risk of pathogen uptake.

## PS 2369 The Effect of Nanoparticles from Secondhand Cigarette Smoke on the Mouse Lung.

Z. Wu<sup>1</sup>, M. McCawley<sup>2</sup>, E. Kimani<sup>2</sup> and R. D. Dey<sup>1</sup>. <sup>1</sup>Neurobiology and Anatomy, West Virginia University, Morgantown, WV; <sup>2</sup>Community Medicine, West Virginia University, Morgantown, WV. Sponsor: T. Nurkiewicz.

Second hand cigarette smoke (also named Environmental tobacco smoke (ETS)) is an environmental trigger factor that leads to airway inflammation and airway hyperresponsiveness (AHR) in susceptible individuals and animals. The constituents

of ETS exist in the gas-phase and the aerosol particles which consist predominantly nanoparticles (two dimensions less than 100 nanometres). The purpose of this study is to characterize the role of nanoparticles on ETS-induced airway responses. The mice were exposed to side-stream tobacco smoke (SS), a surrogate to ETS, or 50 nm nanoparticles, or 80 nm nanoparticles, or gas-phase or filtered air (FA) for 3hrs. Lung function and inflammation in bronchoalveolar lavage (BAL) were measured following exposure. Methacholine (MCh) dose response for lung resistance (RL) was significantly elevated, and dynamic pulmonary compliance (Cdyn), was significantly decreased, in the SS, nanoparticles exposure groups compared with the FA and groups gas-phase exposure. At the same time, the total cells and neutrophils were significantly elevated in both SS and nanoparticles exposed mice. However, MCh dose-response curves for RL and Cdyn, inflammation were not significantly changed in the 50 nm nanoparticles and 80 nm nanoparticles exposure group. These results suggest that nanoparticles from second hand cigarette smoke play an important role in smoking-induced lung injury.

## PS 2370 The Comparative Immunotoxicity of Mesoporous Silica Nanoparticles and Colloidal Silica Nanoparticles in Mice.

S. Lee<sup>1</sup>, H. Yun<sup>2</sup> and S. Kim<sup>1</sup>. <sup>1</sup>Pharmacology, School of Medicine, Kyungpook National University, Daegu, Republic of Korea; <sup>2</sup>Engineering Ceramics, Powder & Ceramics Division, Korea Institute of Materials Science, Changwon, Republic of Korea.

Mesoporous silica (MPS) nanoparticles (NPs), which have unique pore structure, extremely high surface area and pore volume, have attracted attention for their potential biomedical applications, such as carriers for controlled drug delivery and matrix for tissue regeneration. To use MPS NPs for biomedical devices, their biocompatibility both in vitro and in vivo should be confirmed because the surface area of NPs is one of the important determinants of toxicity such as cellular uptake and immune response. We previously first reported that MPS NPs exhibited less cytotoxicity and inflammation potential than general amorphous colloidal silica (Col) NPs on macrophages. However, the low cytotoxicity does not guarantee high biocompatibility in vivo. In this study, we compared in vivo immunotoxicity of MPS and Col NPs in mouse model to define the influence of pore structural conditions of silica NPs. Both MPS and Col NPs (2, 20, 50 mg/kg/day) were intraperitoneally administered in female BALB/c mice for 4 weeks. There was no overt sign of clinical toxicity in both MPS and Col treated mice. Interestingly, the in vivo test showed opposite results from in vitro. MPS NPs significantly increased weight of liver and spleen, and proliferation of splenocytes. MPS NPs treated mice showed the altered lymphocyte population (CD3+, CD45+, CD4+ and CD8+) of spleen, increased serum IgG and IgM levels, and histological changes. In spite of the slight changes in lymphocytes population of spleen, Col NPs did not alter other immunological factors. Our results showed that in vivo exposure of MPS NPs causes more damages in systemic immunity than Col NPs by the immunoenhancement of spleen. The in vivo data showed opposite results from in vitro showing less cytotoxicity of MPS NPs. Our results suggest the importance of confirmation of biocompatibility both in vitro and in vivo during the design of new nanomaterials. These findings may provide useful information for the bioapplication of silica NPs.

## PS 2371 Evaluation of Intestinal Absorption of Amorphous Silica Nanoparticles.

K. Misato<sup>1</sup>, Y. Yoshioka<sup>1</sup>, M. Uji<sup>1</sup>, A. Uda<sup>1</sup>, T. Mori<sup>1</sup>, M. Yamaguchi<sup>1</sup>, T. Hirai<sup>1</sup>, T. Yoshida<sup>1</sup>, H. Nabeshi<sup>2</sup>, T. Yoshikawa<sup>1</sup>, S. Tsunoda<sup>3,4</sup>, K. Higashisaka<sup>1</sup> and Y. Tsutsumi<sup>1,3,4</sup>. <sup>1</sup>Laboratory of Toxicology and Safety Science, Graduate School of Pharmaceutical Sciences, Osaka University, Osaka, Suita, Japan; <sup>2</sup>National Institute of Health Science, Tokyo, Setagaya, Japan; <sup>3</sup>Laboratory of Biopharmaceutical Research, National Institute of Biomedical Innovation, Osaka, Ibaraki, Japan; <sup>4</sup>MEI center, Osaka University, Osaka, Suita, Japan.

With the recent development of nanotechnology, amorphous silica nanoparticles (nSP) with particle size below 100 nm have already been used in various foods as anticaking agents. Therefore, to ensure the safety of nSP, it is an urgent need to obtain safety information of nSP. However, there is little information about biodistribution of nSP after oral administration. In this study, we examined the biodistribution and absorption of nSP via oral route in vivo and in vitro. BALB/c mice were orally exposed to nSP with diameter of 70 nm (nSP70) or 1000 nm (mSP1000) at 2.5 mg/body for 28 days. After the last administration, we observed the localization of silica particles in tissues by transmission electron microscope. Both silica particles were observed in some tissues such as spleen and liver, although these results were qualitative analysis. Next, we evaluated the absorption of silica particles through intestine quantitatively by everted sac method. Although about 0.3% of mSP1000 in mucosal side was absorbed into serosal side, the level of absorbed nSP70 was about

1.7% in mucosal side. These results indicated that the particle size would be the major factor in permeability of intestine. Currently, we are trying to evaluate the relationship between physicochemical properties of nanomaterials and biodistribution, precisely. We believe that our study will contribute to create safer forms of nanomaterials.

**PS 2372 Indomethacin/Indomethacin Ester-Loaded Nanocapsules Reduce Brain Tumor in C57BL/6 Mice with No Observable Local Toxic Effect.**

S. F. Rodrigues<sup>1</sup>, L. Fiel<sup>2</sup>, N. Pereira<sup>1</sup>, I. Machado<sup>1</sup>, K. Elache<sup>1</sup>, S. S. Guterres<sup>2</sup>, A. R. Pohlmann<sup>2</sup> and S. H. Farsky<sup>1</sup>. <sup>1</sup>Clinical and Toxicological Analysis, University of São Paulo, São Paulo, Brazil; <sup>2</sup>Organic Chemistry, UFRGS, Porto Alegre, Brazil. Sponsor: S. Barros.

**Introduction:** Potentiation of the indomethacin (IndOH) cytotoxicity was demonstrated *in vitro* when IndOH was loaded combined with its ester (IndOEt) in poly( $\epsilon$ -caprolactone) nanocapsules (NC). **Objective:** To determine whether the antitumor activity of IndOH is kept *in vivo* when it is combined with IndOEt in NC and the capacity of those NC to cross the blood brain barrier (BBB). **Methodology:** Intravital microscopy was used in oral-, intraperitoneally- (i.p.) or intravenously- (i.v.) treated female C57BL/6 mice to visualize: 1) The intensity of red fluorescence within and outside cerebral (pial) venules after rhodamine-labeled NC treatment; 2) The interaction of leukocytes-rhodamine-labeled and platelets-FITC-labeled with the endothelial cells of pial venules. The BBB permeability was measured by the Evans blue extravasation assay. Effect of two week-IndOH/IndOEt-NC treatment on the volume of a brain tumor (induced by direct injection of glioblastoma cell line [GL261] into the brain) was measured. **Ethical Committee number:** CEUA/FCF/349. **Results:** The intensity of fluorescence outside the vessels dramatically increased 30 minutes following i.v. NC injection compared to 10 minutes time ( $P < 0.05$ ), and was maintained constant up to 2 hours. Higher intensity of fluorescence in the parenchyma was also observed 20 minutes, 1 and 2 hours ( $P < 0.05$ ) after i.p. injection, and 1, 2 and 4 hours after oral intake ( $P < 0.05$ ). No increase in leukocyte or platelet adhesion to endothelial cells, and Evans blue extravasation were noticed. IndOH/IndOEt-NC profoundly reduced the brain tumor. **Conclusion:** Antitumor activity of IndOH in brain is kept when it is combined to its ester into NC and may be due to a local effect once they cross the BBB. **Supported by:** FAPESP, CNPq.

**PS 2373 Isoprostanes As a Biomarker of Nanoparticle-Induced Toxicity In Vivo.**

L. Manzo<sup>1,2</sup>, T. Coccini<sup>1,2</sup>, E. Roda<sup>1</sup> and C. Signorini<sup>3</sup>. <sup>1</sup>University of Pavia, Pavia, Italy; <sup>2</sup>Maugeri Foundation IRCCS, Pavia, Italy; <sup>3</sup>University of Siena, Siena, Italy.

Oxidative stress was indicated as one of the main mechanisms associated with nanoparticle (NP)-induced toxicity. In this study, the validity of plasma F2-isoprostanes (F2-IsoPs), a proposed oxidative stress marker (Halliwell & Lee, Antioxid Redox Signal, 2010), was examined in rats treated intratracheally with a single dose of cadmium-doped silica nanoparticle (SiNP-Cd), a model nanoparticle previously shown to induce oxidative stress *in vivo* (Coccini et al, J Nanopart Res, 2012). The response to SiNP-Cd (1 mg/rat) was evaluated 24 hr, 7 and 30 days post-instillation by immunocytochemistry analysis of superoxide dismutase (SOD1), inducible nitric oxide synthase (iNOS) and cyclooxygenase type 2 (COX-2) expression in pulmonary tissue. Lung and plasma levels of F2-IsoPs were measured in parallel by GC/MS/MS analysis. Furthermore, the effects of SiNP-Cd were evaluated in comparison with those caused by equivalent amounts of CdCl<sub>2</sub> or SiNP. In the animals exposed to SiNP-Cd, pulmonary SOD1, iNOS, and COX-2 immunoreactivity was enhanced in a time-dependent manner (7 < 30 days). Pulmonary total F2-IsoPs were also increased significantly on thirty days post-exposure (46.7 ± 11 ng/g in SiNP-Cd vs 32.8 ± 7.8 ng/g in control). Pronounced elevation of free F2-IsoPs similarly occurred in plasma (54.6 ± 2 pg/ml in the SiNP-Cd group compared to 28 ± 8 pg/ml in controls). The increase in plasma F2-IsoPs was already detectable at day 7 and lasted until day 30 post-exposure. In the animals treated with silica nanoparticles no changes were observed regarding the immunological and biochemical parameters tested. The pulmonary response to CdCl<sub>2</sub> was less pronounced than that found with SiNP-Cd. These results indicate (i) the potential of SiNP-Cd to cause long-lasting oxidative tissue injury following pulmonary exposure in rat and (ii) a promising role for plasma F2-IsoPs as indicator of nanoparticle-induced oxidative insult (Grants: Italian Ministries of Health & University, and CARIPLO Foundation Rif. 2011 – 2096).

**PS 2374 Biokinetics of Nanoscaled Europium Oxide Particles following an Acute Inhalation in Rats.**

O. H. Creutzenberg, H. Kock and D. Schaudien. *Inhalation Toxicology, Fraunhofer Institute of Toxicology and Experimental Medicine, Hannover, Germany.* Sponsor: C. Dasenbrock.

Nanoscaled europium oxide (Eu<sub>2</sub>O<sub>3</sub>) particles were selected to investigate the biokinetics following inhalation. The rare earth Eu allowed a very high accuracy in analysis of potential translocation from lungs to remote organs. An aqueous dispersion of commercially available Eu<sub>2</sub>O<sub>3</sub> particles (0.1 w-%) was prepared in phosphate buffer (0.15 w-%) incl. bovine serum albumin (0.25 w-%). A suspension partially consisting of nanoscaled particles could be realized by mechanical homogenization and ultrasonic treatment and was aerosolized with pressurized air. Rats inhaled the dry aerosol for 6 hours in a single inhalation. Phosphate facilitated the disintegration of the Eu<sub>2</sub>O<sub>3</sub> particles in lung ambience after deposition. The potential translocation of Eu<sub>2</sub>O<sub>3</sub> particles was followed by chemical Eu analysis and transmission electron microscopy (TEM). Using chemical analysis, 36.8 µg/lung Eu<sub>2</sub>O<sub>3</sub> were detected 1 hour after inhalation in lungs. The amount declined slightly to 34.5 µg after 1 day and 35.0 µg after 5 days. The liver showed an increase of Eu<sub>2</sub>O<sub>3</sub> from 32.3 ng 1 hour up to 294 ng 5 days after inhalation. Additionally, lung-associated lymph nodes, thymus, kidneys, heart, and testes exhibited an increase of Eu<sub>2</sub>O<sub>3</sub> over the time period investigated. In the blood, the highest amount of Eu<sub>2</sub>O<sub>3</sub> was found after 1 hour whereas feces, urine and mesenteric lymph nodes revealed the highest amount after 1 day. In the other organs such as brain, spleen, adrenals and epididymides no changes of the Eu amount were detected. By TEM analysis, Eu<sub>2</sub>O<sub>3</sub> particles could be detected only in lungs, in liver, however, with one of the highest chemical Eu concentrations, no particles were detectable. In conclusion, mixed type metal oxide/phosphate particles are a suitable tool for biokinetic investigations after inhalative uptake. The use of Eu<sub>2</sub>O<sub>3</sub> combined with chemical and TEM analysis was a very suitable model to examine the translocation potential. Bioavailability was limited to soluble Eu<sub>2</sub>O<sub>3</sub>, a translocation of Eu<sub>2</sub>O<sub>3</sub> particles was not evident.

**PS 2375 NanoMiner—Resource for Human Transcriptomics Data in Nanoparticle Research.**

B. Fadeel<sup>1</sup>, L. Kong<sup>2,3</sup>, S. Tuomela<sup>3</sup>, L. Hahne<sup>2,3</sup>, H. Ahlfors<sup>3</sup>, O. Yli-Harja<sup>2</sup>, R. Lahesmaa<sup>3</sup> and R. Autio<sup>2,3</sup>. <sup>1</sup>Institute of Environmental Medicine, Karolinska Institutet, Stockholm, Sweden; <sup>2</sup>Department of Signal Processing, Tampere University of Technology, Tampere, Finland; <sup>3</sup>Turku Centre for Biotechnology, University of Turku and Åbo Akademi University, Turku, Finland.

The potential impact of nanoparticles on the environment and on human health has attracted considerable attention in recent years. Transcriptomics data generated from tissues or cells exposed to nanoparticles are being gathered at ever-increasing rates. In addition to the importance of the original findings, such data can have value if interpreted in a broader context and combined with other published results. To encourage the efficient use of the data, we have developed NanoMiner (<http://nanominer.cs.tut.fi/>), an integrative transcriptomics data resource for nanoparticle research. The data in NanoMiner is collected from public repositories, and the database currently contains 404 human transcriptomics samples of cells exposed to various types of nanoparticles. All samples in NanoMiner have been annotated, preprocessed and normalized using standard methods to ensure the quality of the data analyses and to enable systematic use of the database across different experimental setups and platforms. With NanoMiner, it is possible to: 1) search and plot the expression profiles of one or several genes of interest, 2) cluster the samples within the datasets, 3) find differentially expressed genes in various nanoparticle studies, 4) detect the nanoparticles causing differential expression of selected genes, 5) analyze enriched Kyoto Encyclopedia of Genes and Genomes (KEGG) pathways and Gene Ontology (GO) terms for the detected genes, and 6) search the expression values and differential expressions of the genes belonging to a specific KEGG pathway or Gene Ontology. The NanoMiner database is thus a valuable collection of microarray data and can also be used as a data repository for future analyses.

**PS 2376 Nano-Silica Aspiration Exposure Induces Endothelial Dysfunction in Diabetic Mice.**

S. A. Brenner<sup>3</sup>, M. Frame<sup>1</sup>, A. M. Dewar<sup>1</sup> and J. E. Vigilante<sup>2</sup>. <sup>1</sup>Biomedical Engineering, Stony Brook University, Stony Brook, NY; <sup>2</sup>Faculty of Medical Sciences, The University of The West Indies, Cave Hill, Barbados; <sup>3</sup>Nanobioscience, University of Albany College of Nanoscale Science and Engineering, Albany, NY. Sponsor: T. Nurkiewicz.

Silica (SiO<sub>2</sub>) nanoparticles are widely used in many diverse industries, such as polishing agents in semiconductor fabrication, as potential biomedical drug delivery agents, and in fabrics to make them wrinkle free. Our goal was to evaluate the ef-

fects of nano-silica (SiO<sub>2</sub>, longest dimension  $51.9 \pm 16.2$  nm, aspect ratio  $1.1 \pm 0.1$ ) on small arterioles in situ. First, a suspension of SiO<sub>2</sub> (in 1gm/ml albumin, saline) was directly applied to arterioles (micropipette, 137 pg total dose), using a hamster cheek pouch intravital microscopy model (isoflurane, N=6). Endothelial dysfunction (loss of dilation to acetylcholine, ACH 10-4M) was evident within minutes (dilation of  $78 \pm 14\%$  to constriction  $-3 \pm 5\%$ ,  $p < 0.05$ ), while dilation to adenosine was unaffected. Constrictor responses to phenylephrine were diminished by SiO<sub>2</sub> exposure (from  $-61 \pm 4\%$  to  $-1 \pm 2\%$ ); importantly, the baseline diameters were not altered by direct exposure to SiO<sub>2</sub>, and the vessels retained some responses. Next, mice were exposed to 20ug of SiO<sub>2</sub> via aspiration, and 24 hours later the cremaster m. model was examined (isoflurane). Db/db controls (N=6) have mild endothelial dysfunction seen as a diminished dilation to ACH (10-4M, dilation of  $43 \pm 14\%$  to  $10 \pm 6\%$ ). Exposure to SiO<sub>2</sub> (40gm wt, N=4) induced a profound endothelial dysfunction seen as constriction to ACH ( $-13 \pm 2\%$ ). Dilation to adenosine was unaffected. In C57BL/6, exposure to SiO<sub>2</sub> (25gm wt, N=2) did not significantly alter dilation to ACH or adenosine compared to controls (N=6). Further, in the aspiration model, constrictor responses to phenylephrine were not affected in either strain. Thus, direct exposure to 137 pg SiO<sub>2</sub> induced endothelial dysfunction immediately in healthy hamsters. Aspiration of 20ug induced a profound endothelial dysfunction in diabetics but not in the genetic background controls. (NIH DK68401, HL55492)

### PS 2377 Copper Nanoparticles or Ionic Copper (II) Causes Neurotoxicity and Cardiotoxicity in Zebrafish Embryos.

W. Trickler<sup>1,2</sup>, S. F. Ali<sup>1</sup>, M. G. Paule<sup>1</sup> and J. Kanungo<sup>1</sup>. <sup>1</sup>Division of Neurotoxicology, National Center for Toxicological Research, US FDA, Jefferson, AR; <sup>2</sup>Toxicologic Pathology Associates Inc., Jefferson, AR.

Copper oxide nanoparticles (Cu-NPs) are frequently used in medical devices, paints, fabrics or as antimicrobials. Their industrial applications may lead to the contamination of aquatic ecosystems. The toxicological and human health risks of NPs in the environment are hard to evaluate due to a lack of knowledge about the mechanisms by which NPs interact with biological systems. In this study, we investigated the toxicity of Cu-NPs and the ionic copper(II) form in wild-type (WT) zebrafish (Danio rerio, AB-strain) embryos and hb9-GFP transgenic zebrafish (Danio rerio, AB-strain) embryos by comparing bare Cu-NPs to the mass equivalent ionic form of copper(II) (CuCl<sub>2</sub>) at various concentrations (1.25-to-20 ug/ml). The toxicity was determined by phenotypic changes in the zebrafish embryos including survival, heart rate, motor neuron development and absorptive permeability. Both Cu-NPs and CuCl<sub>2</sub> were lethal to zebrafish embryos at 20 ug/ml (within 24-hrs) and 10 ug/ml (within 48-hrs), with CuCl<sub>2</sub> being more toxic at equivalent mass concentrations. Similarly, the heart rate was significantly reduced following exposure to either Cu-NPs or CuCl<sub>2</sub> in a concentration-time dependent manner. Additionally, the embryo permeability studies showed that exposure to either Cu-NPs or CuCl<sub>2</sub> (5 ug/ml) for 24-hrs significantly increased the topical absorption of the fluorescent tracer 6-coumarin (6CM). Furthermore, embryos treated with either Cu-NPs or CuCl<sub>2</sub> (2.5 ug/ml for 48-hrs) showed a significant reduction (nearly 2-fold) of spinal motor neurons. These results indicate that both CuCl<sub>2</sub> and Cu-NPs can be toxic to zebrafish embryos causing significant neurotoxicity and cardiotoxicity at exposure levels that do not cause lethality.

### PS 2378 Nickel Oxide Nanoparticles Provoke Intrinsic Apoptotic Pathway in HepG2 Cells, Male Wistar Rats and Tomato Seedling Roots.

Q. Saquib<sup>1</sup>, J. Musarrat<sup>1</sup>, A. A. Al-Khedhairi<sup>1</sup>, M. A. Siddiqui<sup>1</sup>, S. M. Attia<sup>3</sup>, M. Faisal<sup>2</sup>, J. A. Siddiqui<sup>1</sup>, S. Dwivedi<sup>1</sup> and S. T. Khan<sup>1</sup>. <sup>1</sup>Department of Zoology, King Saud University, Riyadh, Saudi Arabia; <sup>2</sup>Department of Botany, King Saud University, Riyadh, Saudi Arabia; <sup>3</sup>Department of Pharmacology, King Saud University, Riyadh, Saudi Arabia. Sponsor: M. Verma.

Many features of programmed cell death in plants resemble with those observed in human and animals. Therefore, this study has been done with a rationale to provide first evidence on the molecular toxicity of nickel oxide nanoparticles (NiO-NPs, <50 nm) in human hepatocellular carcinoma (HepG2) cells, male Wistar rats and tomato seedling roots. The cytotoxicity studies with NRU and MTT assays in HepG2 cells revealed 20.6 % and 18.4 % decline in the cell survival at the highest concentration of 100 µg/ml. Treated cells showed an increase in intracellular ROS generation and 30.5 % increase in flow cytometric sub-G1 apoptotic peak at 100 µg/ml NiO-NPs. Quantitative real-time PCR analysis of apoptotic pathway genes (P53, caspases 3 and 9) showed 2.0, 1.2 and 1.1-fold higher expression in HepG2 cells. Furthermore, western blot experiments also showed the greater activity of P53 and caspase 3 genes in cells exposed to 100 µg/ml NiO-NPs. Oral exposure of male

Wistar rats with 1, 2 and 4 mg/kg b.w of NiO-NPs for 48h and 14 days showed increased intracellular ROS generation, DNA damage, micronuclei formation and apoptosis in bone marrow cells. Tomato seeds exposed to NiO-NPs for 4 h, exhibited repression of root length, higher activities of antioxidant enzymes, and increased frequency of apoptotic and necrotic cells in comet assay. Flow cytometric analysis of 2 mg/ml treatment group revealed 122% higher ROS generation with alteration of mitochondrial membrane. Cell cycle data showed a shift of 65.5% cells towards apoptotic subG1 phase vis-à-vis control showed 16.5% cell in subG1. An increase in caspase-3 like protease activity validates the involvement of mitochondrial dependent intrinsic apoptotic pathway. Thus, this study has provided a new insight into the fundamental mechanism of NiO-NPs induced toxicity and signify its potential to induce cell death in animal and plant cells.

### PS 2379 Quantifying Quantum Dots in Frozen Tissue Sections Using Autometallography.

C. White<sup>1</sup>, C. M. Schaupp<sup>1</sup>, J. Herron<sup>1</sup>, D. K. Scoville<sup>1</sup>, L. A. McConnachie<sup>1</sup>, D. Botta<sup>1</sup>, J. Yu<sup>1</sup>, X. Yu<sup>1</sup>, X. Hu<sup>2</sup>, X. Gao<sup>2</sup>, J. Wilkerson<sup>1</sup> and T. J. Kavanagh<sup>1</sup>. <sup>1</sup>Environmental & Occupational Health Sciences, University of Washington, Seattle, WA; <sup>2</sup>Bioengineering, University of Washington, Seattle, WA.

Quantum dots (QDs) are engineered nanoparticles frequently composed of a CdSe core, ZnS shell, and an assortment of polymer coatings specific to their application. QDs are used in electronic systems because of their semiconductor properties and in biomedical research and medicine as imaging tools because of their unique fluorescent properties. Their widespread use and heavy metal core composition have raised concerns about their safety. An important consideration in evaluating QD toxicity is the accurate quantification of these nanoparticles within tissues. The current measurement methods favored include inductively coupled plasma mass spectrometry (ICP-MS) for the metal components of QDs, and QD fluorescence directly in tissue sections using microscopy. However, ICP-MS is expensive and cannot distinguish between metals present in QDs or free ions, and fluorescence microscopy is often difficult because of interfering tissue autofluorescence. We adapted a silver-enhanced autometallography technique for detecting QDs in frozen tissue sections. This technique is efficient and inexpensive, and quantification using digital imaging and densitometry correlates well with direct QD fluorescence measurements. The ability to efficiently measure QDs in tissues will provide important dose information that can be useful for evaluating the adverse health effects of QD exposures.

### PS 2380 Influence of Primary Particle Size and Agglomeration State of Inhaled Nano-TiO<sub>2</sub> on Rat's Pulmonary Response.

A. Noel<sup>1</sup>, M. Charbonneau<sup>2</sup>, Y. Cloutier<sup>3</sup>, R. Tardif<sup>1</sup> and G. Truchon<sup>3</sup>. <sup>1</sup>Environmental and Occupational Health, University of Montréal, Montréal, QC, Canada; <sup>2</sup>INRS-Institut Armand-Frappier, Université du Québec, Laval, QC, Canada; <sup>3</sup>Institut de Recherche Robert-Sauvé en Santé et en Sécurité du Travail, Montréal, QC, Canada.

The physico-chemical properties of nanoparticles (NP) and their agglomeration state influence their toxicokinetics, reinforcing the importance of the characterization of the exposure dose. The objective of this study was to evaluate the influence of initial particle size and agglomeration state of inhaled 20 mg/m<sup>3</sup> TiO<sub>2</sub> aerosols on rat's pulmonary response. Groups of rats (n=6) were exposed for 6 hr to aerosols composed of either 5; 10-30 or 50 nm TiO<sub>2</sub>. Two distinct agglomeration states were obtained. Aerosols were composed majorly of either large (LA) (>100 nm) or small agglomerates (SA) (<100 nm). A control group was exposed to compressed air. Exposures were characterized using weight measurement for mass concentration, an electrical low pressure impactor (Dekati) for size distribution and electron microscopy for agglomerates observation. Pulmonary response was analyzed 16 hr after the end of exposure through bronchoalveolar lavage fluids and lung histology. Total cell count, number of macrophages and neutrophils were increased statistically ( $p < 0.05$ ) compared to control for the 10-30 and 50 nm LA aerosols, while increases were significant only for total cell count and number of macrophages for the 5 and 10-30 nm SA aerosols. For each initial particle size, percentages of particle laden macrophages in LA aerosols were higher and statistically different from the SA ones. Morphological assessments of lung tissue showed that cellular infiltrates were more important in exposed groups compared to controls, with exemption of the 50 nm SA group. Our results indicate that higher increases in neutrophils number are related to LA aerosols, as for initial particle size, 10-30 nm TiO<sub>2</sub> NP seemed to induce more pronounced effects. Overall, this suggests that initial particle size and agglomeration state play a key role in the toxicity of TiO<sub>2</sub> aerosols.

**PS 2381 Silica Nanoparticles Induce Acute Pulmonary Toxicity in Mice.**

T. Lu<sup>1</sup>, D. Hung<sup>2</sup>, C. Su<sup>3</sup>, T. Tseng<sup>4</sup>, K. Chen<sup>5</sup>, C. Huang<sup>6</sup>, S. Liu<sup>7</sup> and Y. Chen<sup>1</sup>. <sup>1</sup>Department of Physiology and Graduate Institute of Basic Medical Science, China Medical University, Taichung, Taiwan; <sup>2</sup>Division of Toxicology, Trauma & Emergency Center, China Medical University Hospital, Taichung, Taiwan; <sup>3</sup>Department of Otorhinolaryngology, Head and Neck Surgery, Changhua Christian Hospital, Changhua, Taiwan; <sup>4</sup>Department of Anatomy, China Medical University, Taichung, Taiwan; <sup>5</sup>Department of Urology, China Medical University Hospital and China Medical University, Taichung, Taiwan; <sup>6</sup>School of Chinese Medicine, China Medical University, Taichung, Taiwan; <sup>7</sup>Institute of Toxicology, National Taiwan University, Taipei, Taiwan.

Silica nanoparticles (SiO<sub>2</sub>-NPs) are the one of most widely used and important nanomaterials in nanotechnology. Lung tissue is one of the main routes of entry nanoparticles, which may cause severe pulmonary toxicity. However, the toxicological effects and the precise mechanisms of SiO<sub>2</sub>-NPs on lung are still unclear. Here, we attempted to investigate the toxic injuries and the definite mechanism of SiO<sub>2</sub>-NPs on the acute pulmonary toxicity. The adult male ICR mice were exposed to intratracheal signal dose of 50 mg/kg SiO<sub>2</sub>-NPs and lung tissue were collected after 7 days. Our results found that SiO<sub>2</sub>-NPs increased 40% mortality rate and significantly induced pulmonary morphological and histological changes with neutrophils, macrophage and fibroblast cells from the terminal bronchial. The lung tissue weight/body weight ratio (LW/BW) increased 2-fold suggested that SiO<sub>2</sub>-NPs may trigger pulmonary edema. Meanwhile, the malondialdehyde (MDA) levels in the treated lung tissue were increased. Moreover, SiO<sub>2</sub>-NPs caused apoptosis-related signals, including up-regulation of Bax and down-regulation of Bcl-2 and activations of caspase cascades mRNA expression, which accompanied with triggered the endoplasmic reticulum (ER) stress identified through several key molecules, such as activating the CHOP, XBP-1, caspase-12, and increasing the GRP-78/-94 mRNA expression. These results suggest that SiO<sub>2</sub>-NPs induced an oxidative stress, and cause acute pulmonary toxicity through mitochondria and endoplasmic reticulum pathways.

**PS 2382 Biodistribution and Toxicity Profiling of Nanosilica in Rats after Subchronic Oral Exposure.**

M. van der Zande<sup>1</sup>, R. J. Vandebriel<sup>2</sup>, M. Groot<sup>1</sup>, E. Kramer<sup>1</sup>, K. Rasmussen<sup>3</sup>, P. Hendriksen<sup>1</sup> and H. Bouwmeester<sup>1</sup>. <sup>1</sup>RIKILT - Wageningen University & Research Centre, Wageningen, Netherlands; <sup>2</sup>The National Institute for Public Health and the Environment, Bilthoven, Netherlands; <sup>3</sup>Joint Research Centre, Ispra, Italy. Sponsor: S. Rangarajan.

Synthetic amorphous silica (SAS) is a conventional food additive. In earlier publications, we have shown that up to 43% of SAS in food products can be nanosized. Yet, the behavior and biological effects of ingested nanosized silicas are still largely unknown. We evaluated the biodistribution, accumulation, and toxicity of two nanostructured silicas: NM-202 from the OECD testing program, and a food grade SAS.

To this end, rats (n=5) were fed daily 0, 100, 500 or 1000 mg/kg bw NM-202, or 100, 1000 or 2500 mg/kg bw SAS during 28 days. Additional rats received 0 or 1000 mg/kg bw NM-202, or 2500 mg/kg bw SAS during 84 days. Using hydrodynamic chromatography ICP-MS, high fractions of nanosized silica (up to 100% of the total silica content) were detected in the gut contents of silica exposed rats. Nevertheless, ICP-MS data at day 29/85 show low, dose-independent distribution of both materials to the liver, kidney, spleen, brain, and testis, without organ specificity or accumulation. Analysis of blood biochemical markers and antibodies, NK-cell activity, and lymphocyte proliferation, did not indicate (immuno)toxicity. Contrarily, histopathology showed a significantly increased number of mononuclear cells per mm<sup>2</sup> up to 500% at day 29, and 200% at day 85, and an increase in apoptosis (cells/mm<sup>2</sup>) up to 200% at day 29 in livers of silica exposed rats vs. the controls. Also, the jejunal villus:crypt ratio of NM-202 exposed rats decreased significantly to ~90% vs. the controls after 29 days. However, whole genome liver and jejunal mRNA expression analysis did not indicate toxicity due to silica exposure. In conclusion, both silicas are non-accumulating and absorption is low. They appear to be generally non-toxic, but histopathological data suggest adverse effects on liver and gut tissue, which should be addressed in future research and considered in risk assessment of nanosilica.

**PS 2383 Oral Prenatal Developmental Toxicity Study with Synthetic Amorphous Silica NM-200 in Wistar Rats.**

S. Schneider<sup>1</sup>, W. Wohlleben<sup>2,1</sup>, R. Landsiedel<sup>1</sup>, A. Wolterbeek<sup>3</sup>, I. Waalkens-Berendsen<sup>3</sup> and H. van de Sandt<sup>4</sup>. <sup>1</sup>Experimental Toxicology and Ecology, BASF SE, Ludwigshafen am Rhein, Germany; <sup>2</sup>Polymer Physics, BASF SE, Ludwigshafen am Rhein, Germany; <sup>3</sup>Triskelion, Zeist, Netherlands; <sup>4</sup>Quality of Life, TNO, Zeist, Netherlands.

The engineering of new nanomaterials offers extraordinary opportunities in various technological fields, but safety assessments must complement the technological progress. Specifically, application of current developmental and reproductive toxicity test guidelines for hazard testing of nanomaterials must be evaluated. The results of the prenatal developmental toxicity study (OECD 414) are presented here.

Female Wistar rats received synthetic amorphous silica (NM-200, European Joint Research Centre, Ispra, Italy) by oral gavage at dose levels of 0, 100, 300 and 1000 mg/kg body weight/day from gestation day (GD) 6 through GD 19. The NM was dispersed in 10% fetal bovine serum in water and the particle size distribution was characterized. On GD 20, all females were assessed by gross pathology, including weight determinations of the uterus and the placentas. The corpora lutea were counted and the number and distribution of implants (resorptions, live and dead fetuses) were determined. The fetuses were removed from the uterus, sexed, weighed and investigated for external findings. Half of the fetuses of each litter were examined for soft tissue findings and the remaining fetuses for skeletal (and cartilage) findings.

No differences between the treatment groups and controls for clinical observations, body weights and food consumption of the dams were observed. No effects were observed on number of corpora lutea, implants, pre- and post-implantation losses as well as number and viability of offsprings. External, soft tissue and skeletal examination revealed no test-substance-related abnormalities.

This study was sponsored by CEFIC (LRI-N3 project) and is monitored by Monika Maier, Evonik Degussa GmbH, Hanau, Germany on behalf of CEFIC Sector group on Synthetic Amorphous Silica (ASASP).

**PS 2384 The T-Box Transcription Factor TBX21 (T-BET) Inhibits Airway Goblet Cell Hyperplasia Induced by Nickel Nanoparticles in Mice.**

E. E. Glista-Baker, B. C. Sayers, A. J. Taylor, E. A. Thompson and J. C. Bonner. *Environmental and Molecular Toxicology, North Carolina State University, Raleigh, NC.*

Engineered nanomaterials (ENMs), including metal nanoparticles, are increasingly used in many industrial applications, including electronics and engineering. Additionally, the human health risks that ENMs pose are of growing concern, especially in susceptible populations such as asthmatics. The T-box transcription factor TBX21 (T-bet) maintains Th1 cell development in the lung and loss of T-bet has been associated with the development of allergic airway inflammation characterized by Th2 cells. The purpose of this study was to determine if mice deficient in T-bet are susceptible to goblet cell hyperplasia caused by nickel nanoparticles (NiNP). Wild type (WT) and T-bet<sup>-/-</sup> mice were exposed to a NiNP (4 mg/kg) and lung tissues were collected at 1 or 21 days. The mucin-positive staining area (goblet cell hyperplasia) was quantified by morphometry using Alcian blue/PAS-stained lung sections. Whole lung mRNA levels for mucin genes (MUC5AC and MUC5B) were measured by Taqman real-time RT-PCR. Bronchoalveolar lavage fluid (BALF) was collected for differential cell counts and for measuring levels of secreted cytokines known to regulate goblet cell hyperplasia, namely IL-13 and CCL2. NiNP exposure caused a marginal increase in goblet cell hyperplasia in WT mice at 1 or 21 day post-exposure. However, NiNP caused a significant (p<0.001) increase in goblet cell hyperplasia in T-bet<sup>-/-</sup> mice and a significant (p<0.05) increase in MUC5AC and MUC5B mRNA levels at 21 days. Furthermore, IL-13 protein levels and eosinophilic infiltration were elevated (p<0.001) after 1 day in the BALF while CCL2 mRNA and protein levels were significantly increased at 1 and 21 days. These findings identify T-bet as a potentially important genetic susceptibility factor for NiNP exposure and suggest that individuals with pre-existing allergic airway disease are at a higher risk for environmental and occupational exposures to nanomaterials. (Funded by NIEHS RC2 ES018772 and R01 ES020897)

**PS 2385 Acute Toxicity Study of Nanoparticles of Bismuth Trioxide by Inhalation Exposure in Male Rats.**

O. C. Barbier<sup>1</sup>, B. Quintanilla-Vega<sup>1</sup>, L. M. Del Razo<sup>1</sup>, M. Cortés-Torres<sup>1</sup>, R. Angulo-Olais<sup>1</sup>, M. Uribe-Ramírez<sup>1</sup>, M. J. Solís-Heredia<sup>1</sup>, G. Martínez-Aguilar<sup>1</sup>, A. Barrera-Hernández<sup>1</sup>, L. C. Sanchez-Peña<sup>1</sup>, E. Berea<sup>2</sup> and A. De Vizcaya-Ruiz<sup>1</sup>. <sup>1</sup>Toxicology Department, CINVESTAV-IPN, Mexico City, Mexico; <sup>2</sup>Farmaquímica, Mexico City, Mexico.

Bismuth (Bi) compounds are widely used in several products, including metallurgical alloys and medical devices; Mexico is among the largest Bi producers. Bi toxicity is poorly studied, at micro scale it alters the kidney, nervous and reproductive systems, but little is known about the cytotoxicity of Bi nanoparticles (Bi-NP). Nanotoxicology has gained attention in the last decade due to the dramatically increase of nanomaterials in new appliances and their release to the environment. We conducted an in vivo study to evaluate the toxicity of Bi-NP by inhalation exposure. We exposed adult male Wistar rats (n=7) to an acute inhalatory dose (140 mg/kg, b.w, dispersed in 10 mg/ml BSA) of Bi<sub>2</sub>O<sub>3</sub> nanoparticles during 5 h using the InExpose SCIREQ® inhalation system by nebulization of 1.05 mL Bi<sub>2</sub>O<sub>3</sub> suspension/min. The control group (n=7) received nebulized phosphate buffer in BSA. Physiological parameters such as body weight and relative organ weights, and histopathology were determined. In addition, complete blood count (CBC) and blood chemistry were evaluated. Bronchoalveolar lavage (BAL) was performed to evaluate pulmonary inflammation by differential cell count. Relative weights of spleen, liver, kidney and testes were significantly higher (12-23% increase) in the exposed group, while the histopathology revealed alterations in lungs, liver, brain and spleen, and damage in the epithelium seminiferous. CBC, blood chemistry and BAL parameters were not affected by the acute inhalation exposure to Bi-NP. In our experimental conditions, Bi<sub>2</sub>O<sub>3</sub> nanoparticles showed moderate toxicity by inhalation exposure. Further studies are needed to evidence adverse effects due to the exposure to these NP; a subchronic study is underway to reach this objective. Funding from the European Community Seven Framework Program and CONACYT (Grant agreements #263878 and 12514).

**PS 2386 Pharmacokinetics and Biodistribution of Iron Oxide Nanoparticles Using Accelerator Mass Spectrometry.**

H. Enright<sup>1,3</sup>, P. D. Nallathambi<sup>2,3</sup>, V. Mikheev<sup>3</sup>, B. Forsythe<sup>3</sup>, W. Wang<sup>2,3</sup>, E. Kuhn<sup>1,3</sup>, S. T. Retterer<sup>2,3</sup>, K. W. Turteltaub<sup>1,3</sup> and M. Malfatti<sup>1,3</sup>. <sup>1</sup>Lawrence Livermore National Laboratory, Livermore, CA; <sup>2</sup>Oak Ridge National Laboratory, Oak Ridge, TN; <sup>3</sup>Battelle Center for Fundamental and Applied Systems Toxicology (B-FAST), Battelle Memorial Institute, Columbus, OH.

Nanoparticles (NP) and their use as diagnostic and therapeutic agents in the biomedical field are becoming increasingly more popular. However, to date, the toxicity and biological fate have not been thoroughly investigated. Iron oxide nanoparticles are utilized for many bio-applications, which include: imaging, as drug delivery vehicles and for cell tracking. In this work, Accelerator Mass Spectrometry (AMS), an ultrasensitive technique for quantifying rare isotopes, is used to quantify the biodistribution and pharmacokinetic properties of <sup>14</sup>C-labeled iron oxide NP in vivo.

<sup>14</sup>C-labeled carboxylated iron oxide NP (~10nm core size) were administered by nose only inhalation (0.175mg) or by a bolus intravenously (IV) (0.15mg) to male mice. For inhalation delivery, over 7 d, NP were observed to clear primarily from the lungs through the gastrointestinal system for excretion in the feces (t<sub>1/2</sub> = 1.42 d). Detectable levels were also observed in plasma and phagocytic organs such as the liver and spleen. Furthermore, accumulation in the olfactory bulb was also observed (1.05 ng/mg at 7d). After intravenous delivery, NP were observed to accumulate primarily in the liver, spleen and lungs over a 24 h period; the half-life in plasma was t<sub>1/2</sub> = 6.4 h. Taken together, these data indicate that once administered, carboxylated iron oxide NP are absorbed and distributed to major organs and are retained in tissue through 24 h for IV and through 7 d for inhalation. These observations may provide insight for assessment of potential toxicity upon exposure to iron oxide nanoparticles.

This work performed under the auspices of the U.S. Department of Energy by Lawrence Livermore National Laboratory under Contract DE-AC52-07NA27344 and supported by LLNL CRADA No. PNNL/284. LLNL-ABS-586092

**PS 2387 Zebrafish Xenograft Model of Glioblastoma to Identify Metal Oxide Nanoparticles with Anticancer Properties.**

L. Wehmas<sup>1,2</sup>, L. Truong<sup>1,2</sup>, J. A. Greenwood<sup>3</sup>, A. Punnoose<sup>4</sup> and R. L. Tanguay<sup>1,2</sup>. <sup>1</sup>Environmental and Molecular Toxicology, Sinnhuber Aquatic Research Laboratory and Environmental Health Sciences Center, Oregon State University, Corvallis, OR; <sup>2</sup>Safer Nanomaterials and Nanomanufacturing Initiative and Oregon Nanoscience and Microtechnologies Institute, Corvallis, OR; <sup>3</sup>Biochemistry and Biophysics, Oregon State University, Corvallis, OR; <sup>4</sup>Physics, Boise State University, Boise, ID.

Zinc oxide nanoparticles (ZnO-NPs) demonstrate selective cytotoxicity toward cancer cells in culture, and this effect may extend to other metal oxide nanoparticles (MO-NPs). Therefore, MO-NPs may possess unique qualities applicable to nanomedicine. To realize their potential as anticancer agents, we must identify safe and effective MO-NPs. We developed a screening approach that first utilizes cell culture assays to identify MO-NPs that preferentially inhibit cancer proliferation and determine the mechanism of selective toxicity. Then we assess the toxicity of the MO-NPs utilizing the embryonic zebrafish assay, an efficacious model for nano-safety assessment because of its high homology with humans and use of minimal test material. We prioritize MO-NPs that demonstrate relatively low toxicity to the zebrafish yet maintain preferential toxicity toward cancer cells in culture for assessment in a zebrafish xenograft model of glioblastoma. By xenotransplanting human glioblastoma cells into the cranium of zebrafish, we have developed an assay to identify MO-NPs that selectively inhibit cancer cell proliferation in vivo. We are testing four MO-NPs: zinc oxide, titanium dioxide, cerium dioxide, and tin dioxide. Preliminary results demonstrate that ZnO-NPs inhibit glioblastoma cell proliferation at 0.1 mM. Our screening paradigm holds promise for identifying physico-chemical traits which enhance the anti-cancer properties of MO-NPs while supporting safe NP design. Research support: NSF 134468, NIEHS P30 ES000210, ES 016896, T32 ES07060, and Air Force Research Laboratory #FA8650-05-1-5041.

**PS 2388 Toxicity of Zinc Oxide Nanoparticles: Role of Particle Dissolution and Photocatalytic ROS Production.**

H. Ma, L. Wallis, S. Li and S. Diamond. Mid-Continent Ecology Division, United States EPA, Duluth, MN.

Dissolution of zinc oxide nanoparticles (ZnO NPs) to ionic zinc has been recognized as an important mode of toxic action (MOA) due to their high solubility and high potency of ionic zinc to aquatic organisms. However, toxicity of ZnO NPs associated with their photocatalytic properties (generation of ROS under UV radiation) has been rarely reported. To understand the relative importance of these two MOAs, the current study investigated ZnO NP (30-50 nm) toxicity to *Daphnia magna* under simulated solar radiation (SSR) versus ambient laboratory light. *D. magna* immobilization, intracellular ROS production, and oxidative stress (lipid peroxidation) were used as toxicity endpoints. Particle dissolution was measured in a time-course manner using ICP-MS. Photocatalytic ROS production was measured by a fluorescent-based ROS assay and methylene blue photodegradation. Bulk ZnO (> 1µm) and ZnCl<sub>2</sub> were tested as reference toxicants. Concentration-dependent ROS production was detected for ZnO NPs under SSR, but not under laboratory light. Particle dissolution showed no significant differences between irradiation conditions, and both had a maximum dissolution rate of 20% within 24-h period. 48-h EC50s for *D. magna* immobilization under SSR and laboratory light were 0.069 mg/l (95% CI: 0.043, 0.109) and 0.109 mg/l (0.072, 0.171), respectively. Intracellular ROS production and lipid peroxidation in daphnids exposed under SSR were significantly greater than those under laboratory light, suggesting photo-induced toxicity associated with photocatalytic ROS production might have occurred. ZnCl<sub>2</sub> had EC50s of 1.2 mg/l under SSR and 1.1 mg/l under laboratory light. Bulk ZnO showed slightly lower toxicity than ZnO NPs. Our results suggest that photo-induced toxicity of ZnO NPs related to their photocatalytic properties should not be neglected when evaluating potential environmental hazards of these nanomaterials, and the relative importance of this MOA under different exposure scenarios and towards different environmental species warrants further investigation.

**PS 2389 Luminescent Lanthanide-Doped Metal Oxide Nanoparticles for Study of Deposition and Clearance in the Respiratory Tract.**

G. K. Das, D. S. Anderson, C. D. Wallis, A. D. Abid, L. S. Van Winkle and I. M. Kennedy. University of California Davis, Davis, CA.

Epidemiological studies have reported increased morbidity and mortality from respiratory and cardiovascular diseases which have close associations with exposure to airborne particulate matter (PM). Of the PM in the ambient air, ultrafine particles

have been well-demonstrated to be one of the key pathogenic factors for cardiorespiratory disorders. Previous studies investigating deposition and clearance have used mostly radiolabeled-PM, fluorescent labeling or specially engineered nanoparticles (NPs) with physical and chemical properties that are atypical of ambient PM. A low cost and high throughput alternative is needed that will permit direct measurement of PM deposition and clearance. Here, we have used luminescent trivalent europium ion-doped gadolinium oxide ( $Gd_2O_3:Eu^{3+}$ ) PM synthesized by a low cost spray flame synthesis to study the deposition and clearance of PM in rats. As rare earth elements, the lanthanides (i.e. Gd and Eu) exhibit very low natural abundance, and provide extremely good detection sensitivity in different organs with the use of inductively coupled plasma mass spectroscopy (ICP-MS). Moreover, the strong optical emission that arises from the intra-4f transition of the europium ions adds a powerful tool to detect the deposition site via fluorescence microscopy. ICP-MS data from the instillation study showed that 59% of the particles remained in the lung while a significant amount was detected in the feces (20.4%) after 24 hrs, suggesting a fast clearance mechanism. Dissolution of the NPs was investigated *in vitro* by monitoring the photoluminescence at physiological pH (7.0) and at a lysosomal pH (5.0) at 37°C up to 30 days; results confirmed that the lanthanides were transported as particles and not as soluble ions. The result with the instillation studies demonstrated the excellent sensitivity of this method. We have adapted our PM generator to a nose-only inhalation system for exposures of rodents. This work supported by NIEHS P42ES004699. We acknowledge the W. M. Keck Foundation for a research grant.

### PS 2390 Angiogenesis Alterations Caused by TiO<sub>2</sub> Nanoparticles.

V. Freyre-Fonseca<sup>1,2</sup>, A. Délica-Alcaraz<sup>1</sup>, E. M. Flores-Jiménez<sup>1</sup>, N. L. Delgado Buenrostro<sup>1</sup>, G. F. Gutiérrez-López<sup>1</sup> and Y. I. Chirino<sup>1</sup>. <sup>1</sup>Facultad de Estudios Superiores Iztacala, Universidad Nacional Autónoma de México, Mexico City, Mexico; <sup>2</sup>Departamento de Graduados e Investigación en Alimentos, Escuela Nacional de Ciencias Biológicas, Instituto Politécnico Nacional, Mexico City, Mexico.

Angiogenesis is a process by which the preexisting vascular tree of a tissue causes growing of new blood vessels. It plays a key role in tumor development and it has been demonstrated that titanium dioxide nanoparticles (TiO<sub>2</sub> NPs) exposure increases hypoxia and growth factors levels and these events are related to angiogenesis. However, the TiO<sub>2</sub> NPs effect in this process has been poorly explored. In this regard, chronic exposure to TiO<sub>2</sub> NPs could develop disorders in angiogenesis. The aim of this work was to study angiogenesis alterations caused by TiO<sub>2</sub> NPs exposure. Characterization of TiO<sub>2</sub> NPs was done using dynamic light scattering to measure nanoparticles size distribution and zeta potential. Chicken chorioallantoic membrane (CAM) model was used as following: fertilized eggs were incubated during 7 days at 37°C and 80% humidity and then exposed to 0, 5 and 10 µg of TiO<sub>2</sub> NPs previously suspended in MCDB-131 cell culture media and injected in blood vessels incubating for 7 days more. On 14th day, eggs were opened and digital analysis of images was done. Umbilical vein endothelial cells were obtained from embryos to measure VEGF expression by flow cytometry. Results showed that suspension of 5 and 10 µg of TiO<sub>2</sub> NPs had an agglomerated size of 535.2±9.35 nm and 503.1±1.069 nm, respectively. Zeta potential of agglomerates suspended in MCDB-131 was -17.36 ±1.18. Images of CAM showed structural differences between vessels of treated and untreated TiO<sub>2</sub> NPs eggs. An increase of 0.5 cm and of 1 cm between blood vessels was found in CAM of 5 µg and 10 µg TiO<sub>2</sub> NPs treated eggs, respectively. In addition, an increase in VEGF expression was observed in endothelial cells from TiO<sub>2</sub> NPs treated eggs. In conclusion, TiO<sub>2</sub> NPs exposure in CAM model induced and increase in the distance between blood vessels and in the VEGF expression in endothelial cells.

### PS 2391 Radiolabeled, Superparamagnetic, Nanoparticles for Bio-Distribution Studies in Life Sciences.

P. D. Nallathambay<sup>1,2</sup>, H. Enright<sup>1,3</sup>, M. Malfatti<sup>3</sup>, S. T. Retterer<sup>2</sup> and W. Wang<sup>2</sup>. <sup>1</sup>Health & Life Sciences, B-FAST, Battelle Memorial Institute, Columbus, OH; <sup>2</sup>BESD, Oak Ridge National Lab, Oak Ridge, TN; <sup>3</sup>Biosciences and Biotechnology Division, Lawrence Livermore National Lab, Livermore, CA.

Nanoscale drug delivery systems have generated considerable interest because they allow for the addition of cell specific targeting molecules and/or multiple therapeutic agents, while their bio-distribution in vivo displays molecular level kinetics. Iron based nanomaterials, with their inherent magnetic properties and an easily tailored surface chemistry, are of particular interest because of their simultaneous diagnostic and therapeutic potential. To determine how bio-distribution affects the biological efficacy of an iron based nano-carrier system, hydrophilic iron oxide nanoparticles (~10 nm) were synthesized, with either a carboxylic acid (-COOH) or an amine (-NH<sub>2</sub>) functional group. <sup>14</sup>C labels ( $t_{1/2}$ =5730 years) were incorporated into the organic functional groups on the surface of the nanoparticles. The radiolabeled, superparamagnetic, nanoparticles were then delivered intra-venously to mice and the

pharmacokinetic distribution in vivo was determined by Accelerator Mass Spectrometry (AMS); an ultrasensitive (10<sup>-18</sup> moles) quantitative spectrometric technique with small sample requirements. The radiolabeled nanoparticles were well distributed in plasma and also detected in different organs like the lungs, liver and spleen. The radiolabeling approach used in this study provides comparable bio-distribution data as the radio-labeled probes have the same chemical properties as the non-labeled probes. The synthesis approach described here is broadly applicable to the synthesis of nanoscale materials with multiple core and surface functionalities. The pharmacokinetic data, suggest that functionalized iron nanoparticles may have broad use as therapeutic, diagnostic or even theranostic agents in biological systems.

### PS 2392 Susceptibility to Quantum Dot-Induced Lung Inflammation Is Mouse Strain Dependent.

D. K. Scoville<sup>1</sup>, C. C. White<sup>1</sup>, D. Botta<sup>1</sup>, L. A. McConnachie<sup>1</sup>, M. E. Zadworny<sup>1</sup>, X. Hu<sup>2</sup>, X. Gao<sup>2</sup>, J. Yu<sup>1</sup>, R. Dills<sup>1</sup>, R. C. Zanger<sup>3</sup>, J. G. Pounds<sup>3</sup> and T. J. Kavanagh<sup>1</sup>. <sup>1</sup>Environmental and Occupational Health Sciences, University of Washington, Seattle, WA; <sup>2</sup>Bioengineering, University of Washington, Seattle, WA; <sup>3</sup>Systems Toxicology Group - Division of Biological Sciences, Pacific Northwest National Laboratory, Richland, WA.

Quantum dots (QDs) are nanoparticles typically composed of a CdSe core, a ZnS shell, and an assortment of polymer coatings specific to the application. Unique fluorescent and excellent semiconductor properties make QDs useful in biomedical imaging and electronics. However, due to their small size, large surface area, and heavy metal composition, there is concern over the safety of QDs. Using 8 genetically inbred mouse strains we have investigated susceptibility to QD induced lung inflammation using % neutrophils, total protein, and levels of inflammatory cytokines in bronchoalveolar lavage fluid (BALF) as biomarkers. Cadmium was measured as a marker of exposure and total glutathione (GSH) levels in frozen lung tissue were also measured. Significant treatment group and strain specific differences in the % neutrophils in BALF indicate that susceptibility to QD induced lung inflammation is mouse strain dependent. We also observed that the % neutrophils in BALF is correlated with lung Cd and GSH levels, as well as BALF cytokines. It is clear that strong relationships exist in some mouse strains and not in others. For example, the % neutrophils in BALF is highly correlated with macrophage inflammatory protein 1a (MIP1a) in A/J, C57BL/6J, WSB/Eij, NZO/HLtJ mice. However, CAST/Eij, NOD/ShiLtJ, PWK/PhJ, and 129S1/SvImJ mice do not show as strong a relationship. In future studies, recombinant inbred mouse strains will be used to map expression quantitative trait loci (eQTLs) associated with QD-induced lung inflammation. Analysis of such eQTLs could lead to insights regarding the molecular mechanisms responsible for QD toxicity and ultimately provide guidance on how to produce safer QDs. Supported by NIH grants R01ES016189, U19ES019545 and P30ES07033.

### PS 2393 Nrf2 Is a Positive Regulator of Cytokine Expression in Lung of Titanium Dioxide Nanoparticles Exposed Mice.

N. L. Delgado Buenrostro<sup>1</sup>, E. I. Medina-Reyes<sup>1</sup>, A. Cuadrado Pastor<sup>2</sup>, I. Lastres<sup>2</sup>, J. Pedraza<sup>3</sup>, R. Hernández<sup>4</sup> and Y. I. Chirino<sup>1</sup>. <sup>1</sup>Investigación y Posgrado UBIMED, Fesiztacala, UNAM, Mexico City, Mexico; <sup>2</sup>Investigación y Posgrado, Instituto Alberto Sols, Madrid, Spain; <sup>3</sup>Posgrado, Facultad de Ciencias UNAM, Mexico City, Mexico; <sup>4</sup>Investigación, Instituto de Nutrición, Mexico City, Mexico.

Background. Titanium dioxide nanoparticles (TiO<sub>2</sub> NPs) increase the generation of reactive oxygen species and the inflammatory response in lung tissue of exposed animals. As a result, the expression of Nrf2 acts a defense mechanism against ROS generation; however its role in inflammation remains unclear.

Aim. The goal of this work was to evaluate role of Nrf2 in inflammatory process induced by TiO<sub>2</sub> NPs in lung from exposed mice.

Methods. Male wild type mice (WT) and Nrf2 knockout mice (KO) were divided in the following groups: a) control-WT, b) TiO<sub>2</sub>-WT, c) control-KO and d) TiO<sub>2</sub>-KO. TiO<sub>2</sub> NPs were suspended in 50µl of SSI and received 5 mg/kg by oropharyngeal via twice a week/4 weeks. Then, mice were perfused with p-formaldehyde and lung tissue was obtained for histological and immunohistochemical analysis.

Results. Bronchioles, venules and interstitial space of TiO<sub>2</sub>-KO group showed higher inflammation and oxidative stress damage, than TiO<sub>2</sub>-WT group. On the other hand, Nrf2 was a positive mediator in the expression of IL-10, Interferon-gamma, TNF-alpha, and TGF-beta, and acts as a negative mediator of IL-4 expression in bronchial epithelium and alveolar space.

Conclusion. This work suggests that Nrf2 has a central role in up-regulation of cytokines released during inflammation induced by TiO<sub>2</sub> NPs in lung tissue.

**PS 2394 Distinct Expression Profiles of Stress Defense and DNA Repair Genes in *Daphnia pulex* Exposed to Cadmium, Zinc and Quantum Dots.**

S. Tang<sup>1</sup>, Y. Wu<sup>2</sup>, C. N. Ryan<sup>1</sup>, S. Yu<sup>1</sup>, D. Edwards<sup>1</sup> and G. D. Mayer<sup>1</sup>.  
<sup>1</sup>Environmental Toxicology, Texas Tech University, Lubbock, TX; <sup>2</sup>Biological Sciences, Texas Tech University, Lubbock, TX.

Use of nanocrystalline semiconductors (Quantum dots; QDs) is growing as new applications, especially in biomedical research, adopt this technology. More importantly, industrial and other mainstream uses of QDs seem likely to increase since QDs can theoretically more than double the efficiency of semiconductors in current photovoltaics. Often, with increased use comes increased appearance in the environment and, given the heavy metal composition of QDs, there exists a concern regarding the potential toxicity of these nanoparticulates on aquatic organisms. The freshwater invertebrate *Daphnia* is a ubiquitous dweller of ponds and lakes throughout North America, a keystone species in aquatic food chains, and an indicator species for environmental contaminants. In this study, we aimed to compare transcriptional responses of several key stress-mediated and DNA repair genes in *D. pulex* following exposure to QDs and the individual metallic components of which they are comprised. Exposure to both Cd and QDs led to induction of mortality and Cd accumulation, which was biologically supported by the increased expression of the heavy metal responsive gene, metallothionein (MT). Our study also revealed that Cd, Zn and CdSe/ZnS QDs induced a different pattern of gene expressions regarding stress defense and DNA repair, which furthered our knowledge regarding the different mechanisms of toxicity that are elicited by the nanoparticulate form of metals versus the ionic form.

**PS 2395 A Delphi Pilot Study in Brazilian Stakeholders About Nanotechnology, Nanomaterial, and Their Toxicological and Regulatory Implications.**

W. Waissmann<sup>1</sup>, R. S. Barros<sup>1</sup>, M. Moura<sup>1</sup>, E. Wilson<sup>2</sup>, A. S. Arcuri<sup>3</sup>, V. S. Pinto<sup>3</sup>, A. B. Veggi<sup>4</sup>, T. P. Silva<sup>4</sup> and L. Brickus<sup>1</sup>. <sup>1</sup>School of Public Health, Oswaldo Cruz Foundation, Rio de Janeiro, Brazil; <sup>2</sup>Law, Unisinos, Sao Leopoldo, Brazil; <sup>3</sup>Centro Nacional, Fundacao Jorge Duprat de Figueiredo, São Paulo, Brazil; <sup>4</sup>Nutricao, Universidade Gama Filho, Rio de Janeiro, Brazil.

**Abstract:**

We conducted an email study using Delphi method. In the first phase, 108 questionnaires (5 questions) were sent, 12 for each of the following groups: Researchers; Regulators, Personal from Funding Institutions (PFI), Public Health/Environmentalists, Producers, Workers/Unions Representatives, Consumers, Legislators, NGOs. Only two rounds were need. At the first, 43 (40%) questionnaires were completed. From the 43 sent, 33 (77%) were completed at the second round. We have no answers from legislators and NGOs. Only two answers have been changed, and this not modified the general results, which show: 60% of respondents considered the benefits equal or outweigh the risks, but recognize that population must better understand risks. More than 20% believe all research and production in nanotech should be suspended until the increase of nanorisk knowledge. Around 60% of the respondents believed Brazil is in a disadvantageous position in nanotech market products comparing to other developing countries, even though who agree that research is at a good level in the country. 80% consider inadequate and insufficient the legislation that deal with risks of nanotech, almost 100% understand consumers have insufficient information and more than 80% understand that even workers who deal with nanotechnology have little information on legislation and potential risks. It was used regular ways to send emails, similar for all categories. For next researches, the approach to NGOs and legislators should be modified.

**PS 2396 In Vitro/In Vivo Assessment of Engineered Nanomaterials Using a High-Content Analysis Platform.**

S. Anguissola<sup>1</sup>, L. Cooke<sup>1</sup>, D. Garry<sup>1</sup>, M. Esquivel-Gaón<sup>2</sup>, A. De Vyzcaia Ruiz<sup>2</sup>, M. Monopoli<sup>1</sup> and K. A. Dawson<sup>1</sup>. <sup>1</sup>Centre for Bionano Interactions, School of Chemistry and Chemical Biology, University College Dublin, Dublin, Ireland; <sup>2</sup>Department of Toxicology, Cinvestav, Mexico City, Mexico.

With increasing numbers of nanomaterials introduced on the market in consumer products, bio-medical and environmental applications it is of primary importance to assess, understand and manage their potential toxicity. To effectively assess and understand the mechanisms of toxicity induced by nanoparticles (NPs) we implemented a platform that correlates physico-chemical properties of nanomaterials with their biological effects in vitro on human cell lines and in vivo on zebrafish as a model of toxicity to aquatic species. Nanomaterials' physico-chemical characteristics were evaluated in the relevant exposure media for in vitro and in vivo exposure

and High Content Analysis (HCA) was employed to quantify several parameters of toxicity on exposed human cell lines and anatomical defects observed on exposed zebrafish larvae. To demonstrate the power of the platform the toxicological outcomes of surface-functionalized model nanoparticles (i.e. polystyrene Nanoparticles with carboxyl and amine surface modifications) are described along with Bismuth (Bi)-derived Nanoparticles designed for industrial applications developed within the EU/Mexico collaborative project Bisnano. The model NPs were well dispersed in either complete cell culture medium or zebrafish embryo medium; for Bi-derived NPs it was necessary to develop a dispersion protocol in order to isolate particles in the nanometer range from a heterogeneous powder which were subsequently stabilized with bovine serum albumin. The HCA approach was able to differentiate between apoptosis and necrosis induced in different cell models by amine-modified polystyrene (PS-NH<sub>2</sub>) NPs and highlighted lysosomal damage as the triggering mechanism of toxicity for both the PS-NH<sub>2</sub> NPs and the Bi-derived NPs. HCA analysis of zebrafish larvae quantified changes of anatomical features such as head/torso ratio, spine length and body curvature. The project was funded by QNano and Bisnano.

**S 2397 Biomarkers of Disease and Toxicity: Exploiting the Interconnections.**

D. L. Mendrick<sup>1</sup> and W. B. Mattes<sup>2</sup>. <sup>1</sup>Division of Systems Biology, NCTR, US FDA, Jefferson, AR; <sup>2</sup>Toxicology, PharmPoint Consulting, Poolesville, MD.

With the recent focus on (a) cellular pathways involved in toxicity sequelae and (b) translational biomarkers that may link animal and *in vitro* model observations with clinical reality, there is a need to broaden the understanding of how experimental models may replicate human toxicity and disease processes. Multicellular organisms may have large numbers of genes and proteins, but a relatively limited repertoire in terms of pathophysiology in response to disease or toxicant exposure. This fact allows research to improve and protect human health to be founded on the use of model systems that allow for tractable experimentation. Animal models and, more recently, *in vitro* systems have served as a means of both exploring mechanisms and identifying hazards in terms of disease and adverse events. However, the interconnections between disease and toxicity are rarely explored leaving the information in silos. This symposium will examine organ-based toxicity and disease processes, and compare lessons learned in biomarker identification and use across toxicity, disease, and species.

**S 2398 Introduction.**

D. L. Mendrick. US FDA, Jefferson, AR.

Biomarkers are needed that increase translation between *in vitro/in vivo* environments and across species. For clinical situations particularly, biomarkers that could distinguish a reaction to a toxin from a disease process would be valuable. However, since biomarkers arise due to perturbations of normal metabolic pathways, toxicity-specific biomarkers are scarce. The good news is that it means that research into toxicity or disease can yield biomarkers of interest in both fields. It is important that toxicologists and clinicians work together to select appropriate models to advance our understanding of biological processes.

**S 2399 Use of Biomarkers in Hepatology, Liver Disease, and Liver Toxicity.**

A. Regev. Global Patient Safety, Eli Lilly & Company, Indianapolis, IN. Sponsor: D. Mendrick.

Biomarkers in use today do not distinguish drug-induced liver injury (DILI) from other causes of hepatic damage such as viral hepatitis, alcoholic liver disease, and metabolic liver injury. Such specific biomarkers would be valuable to better manage patients. Currently available biomarkers fail to differentiate, during the early stages of live injury, between mild self-limiting hepatic abnormality and one that will progress to severe liver injury, liver failure and death. There is a clear need for new translational biomarkers to detect liver injury in animals and humans and to identify significant injury with more specificity than ALT. To enable the identification and qualification of translational biomarkers, better communication is needed between those that focus on preclinical safety testing and clinicians.

**S 2400 Fibrinogen: A New Kid on the Block of Translational Biomarkers for Kidney Damage.**

V. S. Vaidya. *Harvard Medical School, Boston, MA.*

Environmental contaminants and therapeutic substances contribute significantly to the high incidence and prevalence of acute kidney injury (AKI). Preclinical observations of kidney toxicity stops many compounds from entering later development due to the lack of early biomarkers of injury. In the clinic, morbidity and mortality with AKI remains unacceptably high. Our recent work has shown urinary as well as tissue fibrinogen levels increase significantly in mice, rats and humans following kidney injury/toxicity. We provide evidence that fibrinogen may function as a key molecular link between tubulo-vascular damage and regeneration in the kidney and provides new opportunities for its use in the diagnosis and prevention of kidney disease and enablement of the clinician to institute therapeutic interventions.

**S 2401 Cardiac Disease, Cardiotoxicity, and Translational Biomarkers.**

J. R. Turk. *CBSS, Amgen Inc, Thousand Oaks, CA.*

Heart disease is the leading cause of death in the United States. Cardiovascular health is a prime concern for both toxicologists and physicians. Interactions among genes and environmental factors including lifestyle and drugs, may negatively affect the cardiovascular system. Myocardial damage from ischemia, infectious and metabolic diseases, or cardiotoxic drugs may be followed with biomarkers such as the troponins, natriuretic peptides, and their combination in panels with multiple evolving biomarkers. These tools facilitate an understanding of the parallels between toxicity and background disease in animal models and human heart disease.

**S 2402 Links between Neurological Disease and Toxicity.**

D. L. Gerhold and C. P. Austin. *Division of Preclinical Innovation, National Center for Advancing Translational Sciences, NIH, Rockville, MD.* Sponsor: D. Mendrick.

It is well known that environmental agents, including self-administered drugs, are capable of causing neurological damage. Such agents may be used to create animal models of human disease, which may be useful in identifying drug targets, therapeutic strategies, and biomarkers. A well-known example is MPTP, a chemical contaminant in the illicit manufacture of a synthetic opioid which produced an acute Parkinsonian syndrome in users. MPTP has been extensively used in Parkinson's disease research as an investigative agent in both cultured cells and animals. A challenge remains that few good biomarkers exist for early neurological damage and thus there is an intensive focus on better predictive and diagnostic biomarkers. The combined use of models of neurological damage caused by drugs, toxicants, and disease may move the field forward faster in the identification and use of translational biomarkers.

**S 2403 Mechanistic Role(s) of Cytochrome(s) P450 in Oxidative Stress and Inflammation: New Opportunities for Drug Discovery.**

J. E. Manautou<sup>2</sup> and B. Moorthy<sup>1</sup>. <sup>1</sup>*Pediatrics, Baylor College of Medicine, Houston, TX;* <sup>2</sup>*Pharmaceutical Sciences, University of Connecticut, Storrs, CT.*

The major goal of this symposium is to discuss the molecular and cellular mechanisms by which cytochromes P450 (CYP) contribute to oxidative stress, which could in turn lead to inflammatory processes, ultimately leading to many human diseases including cancer, neurodegenerative diseases, bronchopulmonary dysplasia (BPD), acute respiratory distress syndrome (ARDS), and drug-induced hepatotoxicity. Although much is known about the functional role of CYPs in drug metabolism, their role in endobiotic metabolism, in relation to oxidative stress and inflammation, is understudied. The recent findings of the novel role of CYPs in oxidative stress and inflammation in the manifestation of multiple human diseases warrant the need for a symposium to discuss the latest mechanistic research in this area and its impact on human health. Specifically, the symposium will discuss: i) the role of CYP4f in neuroinflammation, which in turn contributes to neurodegenerative diseases such as Parkinson's and Alzheimer's diseases; ii) the role of the Ah receptor, oxidative stress, and inflammation in 2,3,7,8-tetrachlorodibenzo-p-dioxin (TCDD)-induced hepatotoxicity; iii) the functions of CYP1A1, 1A2, and 1B1 in the metabolism of eicosanoids, which in turn play mechanistic roles in TCDD toxicity; iv) the contribution of CYP4As in eicosanoid metabolism and the mechanism of down-regulation of CYPs during infection; and v) the novel protective role of

CYP1A1 and 1A2, and the pro-oxidant role of CYP1B1 in hyperoxic lung injury, in relation to BPD and ARDS. The symposium will also discuss new opportunities for drug discovery and their potential translatability in clinical settings.

**S 2404 Cytochromes P4504f, a Potential Therapeutic Target for Neuroinflammation.**

V. Ravindranath. *Center for Neuroscience, Indian Institute of Science, Bangalore, India.* Sponsor: B. Moorthy.

Inflammatory processes are involved in pathogenesis and progression of CNS disorders, such as infection, traumatic brain injury, and neurodegenerative diseases. Eicosanoids including leukotrienes, particularly leukotriene B4 (LTB4) mediate inflammatory response by initiating and amplifying generation of cytokines and chemokines. Cytochrome P450 (Cyp), a family of heme proteins mediate metabolism of xenobiotics and endogenous compounds, such as eicosanoids. We demonstrate that mouse brain Cyp4fs are expressed ubiquitously in several cell types in the brain including neurons and microglia, and modulate inflammatory response triggered by lipopolysaccharide (LPS), *in vivo* and in microglial cells, *in vitro* through metabolism of LTB4 to the inactive 20-hydroxy LTB4. Chemical inhibitor or shRNA to Cyp4fs enhance the inflammatory response, while the PPAR $\alpha$  agonist, fenofibrate induces Cyp4fs and attenuates it. Fenofibrate also confers neuroprotection against Japanese encephalitis (JE), *in vivo*, in a mouse model of JE viral infection through up-regulation of Cyp4fs, and could potentially be used for prophylaxis during JE epidemics to reduce mortality and morbidity. Thus, catalytic activity of Cyp4fs is a novel target for modulating neuroinflammation.

**S 2405 Metabolomics Identifies an Oxidative Stress-Mediated Signal Transduction Cascade Involved in Dioxin-Induced Hepatotoxicity.**

E. J. Gonzalez, T. Matsubara, N. Tanaka, K. W. Krausz, A. D. Patterson and Y. M. Shah. *Laboratory of Metabolism, National Cancer Institute, Bethesda, MD.*

A number of chemical contaminants that are highly prevalent in the environment, elicit some or all of their toxicity through the arylhydrocarbon receptor (AhR), a ligand-activated transcription factor. Activated AhR forms a heterodimer together with the AhR nuclear translocator (ARNT), and binds to xenobiotic response elements in the promoter regions of target genes resulting in induction or inhibition of expression. Among the AhR target genes are the cytochromes P450 CYP1A1, CYP1A2 and CYP1B1. 2,3,7,8-Tetrachlorodibenzo-p-dioxin (TCDD) is among the most potent environmentally toxic compounds. TCDD exposure alters serum metabolite profiles as a result of attenuating hepatic carboxylesterase 3, CES3 (also known as triglyceride hydrolase), expression in an AhR-dependent manner. Serum metabolomics identified azelaic acid-mono esters as significantly increased metabolites after TCDD exposure. The decreased CES3 expression was accomplished by TCDD-stimulated TGF $\beta$ -SMAD3 and IL6-STAT3 signaling, but not by direct TCDD-activated AhR induction of target genes. Proinflammatory cytokine activation was achieved by TCDD-mediated oxidative stress in the liver through TCDD-induction of xanthine dehydrogenase and NADPH oxidase expression in an AhR-dependent manner. Methionine- and choline-deficient diet-treated mice also showed enhanced serum azelaic acid ester levels following attenuation of hepatic CES3 expression, while genetically obese db/db mice did not, suggesting an association with steatohepatitis. These results support the view that azelaic acid-mono ester is an indicator of dioxin exposure and a possible diagnostic biomarker of steatohepatitis and indicate oxidative stress in the mechanisms of hepatotoxicity by TCDD.

**S 2406 Lipidomic Analysis Demonstrates That 2, 3, 7, 8-Tetrachlorodibenzo-p-dioxin Increases the Levels of Multiple Pro- and Anti-Inflammatory Cytochrome P450 Metabolites of Polyunsaturated Fatty Acids in Several Organs of the Mouse.**

O. Hankinson<sup>1,2</sup>. <sup>1</sup>*Pathology, UCLA, Los Angeles, CA;* <sup>2</sup>*Molecular Toxicology Program, UCLA, Los Angeles, CA.*

2,3,7,8-Tetrachlorodibenzo-p-dioxin (TCDD) adversely affects the immune system and many organs and tissues. These effects are mediated by the aryl hydrocarbon receptor (AHR). CYP1A1, CYP1A2 and CYP1B1 are upregulated by the liganded AHR. These cytochromes P450 are known to metabolize arachidonic acid and certain  $\omega$ -3 polyunsaturated fatty acids *in vitro*. Towards investigating a potential role of metabolism of these fatty acids in TCDD toxicity *in vivo*, we determined

the levels of 81 metabolites in several mouse organs/tissues of mice treated with TCDD. TCDD increased the levels of many hydroxides, epoxides and diols of arachidonic acid in the liver, lung, spleen and serum, but not the heart. That such increases occurred in serum, suggests that increases in these metabolites may be transferred from one organ to another via the blood. The changes in the levels of the metabolites correlated with changes in levels of CYP1A1, CYP1A2 and CYP1B1 in some organs but not others, suggesting that other enzymes may also be involved. TCDD increased the levels of the esterified forms of the eicosanoids in the liver in parallel with the corresponding free forms. The phospholipids so formed therefore represent a reservoir for these metabolites. Analysis of Ahr<sup>-/-</sup> null mice demonstrated that the changes in eicosanoid levels elicited by TCDD depend upon AHR. Many epoxides and diols of three  $\omega$ -3 unsaturated fatty acids, eicosapentaenoic acid {20:5(n-3)}, docosahexaenoic acid {22:6(n-3)}, and  $\alpha$ -linolenic acid {18:3(n-3)}, were also markedly increased in the liver, lung, but not the heart of mice treated with TCDD. Since many of the oxlipin metabolites that were increased by TCDD treatment exhibit potent biological activities, including both pro- and anti-inflammatory effects, these studies lay the foundation for future experiments addressing their potential role in mediating the toxic and other effects of TCDD and other ligands of the AHR.

## **S 2407 Regulation and Functions of Cytochromes P450 during Infection.**

E. T. Morgan and B. A. Nyagode. *Pharmacology, Emory University, Atlanta, GA.*  
Sponsor: B. Moorthy.

Activation of the innate immune system, whether by infection or aseptic stimuli, causes significant changes in hepatic cytochrome P450 (P450) enzyme expression, drug metabolism and clearance. This regulation has important consequences for drug administration and responses in disease states. Its reversal by therapeutic proteins targeting proinflammatory cytokines gives rise to a newly recognized drug-drug interaction mechanism. Understanding the regulatory pathways for the different enzymes is pivotal to predicting the clinical consequences of such regulation during disease and therapy. We have studied the regulation of hepatic P450 expression in various disease models in mice, including injection of bacterial lipopolysaccharide and infection with the colonic pathogen *Citrobacter rodentium*. The enzymes affected are dependent on the disease model, so that different drugs are likely to be affected in different human disease states. In the *C. rodentium* model, studies in cytokine or cytokine receptor-null mice indicate roles for interleukin-6 and tumor necrosis factor- $\alpha$  in the regulation of a small subset of P450 transcripts, including some members of the *Cyp3a* subfamily. Studies in SCID mice suggest that T cells or T-cell-derived cytokines might also be important in this model. However, the absence of cytokine signals fails to alter the down-regulation of the most profoundly suppressed liver enzymes i.e. *Cyp4a10*, *Cyp4a14* and flavin monooxygenase 3 (*Fmo3*), suggesting a different mechanism of regulation for these genes. To address whether or not *Cyp4a* enzymes play a role in the host-pathogen interaction, we infected *Cyp4a14*<sup>-/-</sup> and *Cyp4a10*<sup>-/-</sup> mice with *C. rodentium*, and compared their responses to those of wild-type mice. Results from these ongoing studies will be presented. Supported by National Institutes of Health grant R01DK072372.

## **S 2408 Mechanistic Role(s) of Cytochrome P4501A and 1B1 Enzymes in Hyperoxic Lung Injury: Implications for Bronchopulmonary Dysplasia (BPD) in Premature Infants and ARDS in Adults.**

B. Moorthy. *Pediatrics, Baylor College of Medicine, Houston, TX.*

Hyperoxia is routinely used in the treatment of pulmonary insufficiency and respiratory distress in preterm and term infants and in adults with acute respiratory disease (ARDS). However, in premature infants, hyperoxia contributes to the development of chronic lung disease (CLD), which is termed bronchopulmonary dysplasia (BPD). The molecular mechanisms of oxygen-mediated lung injury are not understood, but reactive oxygen species (ROS) are the most likely candidates. ROS-mediated reactions with biological macromolecules such as DNA, proteins, and lipids are also responsible for many other lung diseases such as acute respiratory distress syndrome (ARDS), asthma, emphysema, chronic obstructive pulmonary disease (COPD), and lung cancer induced by environmental pollutants. Results from our laboratory demonstrate a novel role for cytochrome P450 (CYP)1A enzymes in the detoxification of ROS-mediated lipid peroxidation products, e.g., F<sub>2</sub>-isoprostanes. Our major observations are that mice lacking the genes for CYP1A1 or 1A2 are more susceptible to hyperoxic lung injury than wild type mice, with *Cyp1a2*-null mice being the most sensitive. On the other hand, mice lacking the gene for CYP1B1, are less susceptible to lung injury, suggesting a pro-oxidant role for CYP1B1. Mice pre-treated with the CYP1A inducer  $\beta$ -naphthoflavone (BNF), followed by exposure to hyperoxia leads to protection against lung injury. We also found formation of bulky oxidative lesions (oxidative DNA adducts) in tracheal aspirates of premature infants and adults who received supplemental oxygen, and this

was associated with BPD and ARDS, thereby suggesting that these adducts could serve as novel biomarkers of these diseases. Future studies could lead to the development of rational strategies for the prevention/treatment of lung diseases associated with hyperoxia.

## **S 2409 Molecular Basis of Age-Related Susceptibility to Chemicals and Environmental Hazards: From Model Systems to Humans.**

J. S. Lee<sup>1</sup> and J. C. Fuscoe<sup>2</sup>. <sup>1</sup>US EPA, Durham, NC; <sup>2</sup>US FDA, Jefferson, AR.

The susceptibility of individuals to chemicals and environmental hazards at the extremes of the population age-distribution (the very young and the very old) is often not adequately assessed. By understanding genes expressed at the various life stages, the assessment of health risk versus benefit can be more rationally determined. Children are more susceptible to exposures to environmental toxicants compared to adults because intakes are increased, biologically-effective doses may differ, and early life stage exposure may lead to adverse health effects that are chronic in nature. Older adults are more susceptible to environmental toxicants because of pharmacokinetic and pharmacodynamic changes associated with aging. Altered absorption, distribution, metabolism, and excretion (ADME), along with decreased blood flow to the liver, decreased liver mass, and decreased content of specific cytochrome P450s (CYPs) could result in decreased clearance of chemicals in older adults. In addition to these factors, genetic and epigenetic changes that occur with age and chemical exposure may also increase susceptibility to environmental hazards. Our panel will examine genomic and epigenomic changes that occur with age using animal and human data. Rat liver and kidney data will be used to discuss age-related target organ vulnerabilities. Human relevance will be addressed using a longitudinal birth cohort study in Mexican-American children, two mother-child cohort studies in Mexico and the United States, and a cohort study of older men from the Normative Aging Study. Ultimately, understanding the implications of genetic and epigenetic changes related to age on the effects of chemical exposure will help to protect the health of children and older adults. Disclaimer: The views expressed are those of the authors and do not necessarily represent the views or policies of the US EPA or US FDA.

## **S 2410 Functional Genomic and Epigenomic Changes in the Liver and Kidney during the Rat Life Cycle.**

J. C. Fuscoe, T. Han, V. Vijay, V. Desai and J. C. Kwekel. *Division of Systems Biology, NCTR, US FDA, Jefferson, AR.*

The susceptibility of individuals at the extremes of the population age-distribution (the very young and the very old) and differences between sexes are often not adequately assessed. By understanding the genes expressed in each sex at the various life stages, the assessment of health risk versus benefit can be more rationally determined. Comprehensive analysis of the transcriptome, including miRNA, and the epigenome in the liver and kidney of Fisher 344 rats from 2 weeks to 2 years of age reveals substantial differences at various life-stages and between the sexes. In the liver and kidney, the expression of nearly 4000 genes was found to significantly vary with age and/or sex. Many of these genes are involved in xenobiotic metabolism and transport, processes that impact drug efficacy and safety. The expression of genes that code for some of the kidney injury protein biomarkers recently qualified by the FDA were found to vary substantially with age and sex, in some cases up to 100-fold. Such dramatic differences may impact the interpretation of biomarker results. Examination of miRNA expression in the liver showed nearly 200 miRNAs varied with age and/or sex. Notably, a group of 42 miRNAs was expressed at a relatively high level at 2 weeks of age in both sexes followed by low or no detectable expression at older ages. However, this 2 week-specific miRNA expression was not evident in the kidney. Analysis of potential target mRNAs for liver miRNAs suggests roles in disease susceptibility involving fibrosis as well as regulation of xenobiotic metabolism related genes. A similar number of kidney miRNAs also displayed sex and age-related changes which may be linked to gene regulation. These differences may be related to age- and sex-specific susceptibilities to adverse drug reactions or disease states. Understanding these differences should improve personalized medicine both in terms of disease prevention and management, and safer use of drugs.

## **S 2411 A Case-by-Case Approach to Pediatric Drug Safety Involving Multiage Juvenile Rat Models That Target Developmental Issues and Address Regulatory Concerns.**

P. Espandiar, W. Rodriguez and J. P. Hanig. *CDER, US FDA, Silver Spring, MD.*

The toxicity of drugs in pediatric populations may vary considerably from that seen in adults. Capacity to generate or inactivate the toxic moiety, issues of drug half-life, volume of distribution or specific target organ toxicity as well as hypersensitivity are

all critical factors. Vital organ systems mature at different times and present many challenges for selecting an appropriate model that captures the vulnerability necessary to characterize safety issues. One example of a multi-age pediatric model utilizes rats 10, 25, 40 and 80 days old roughly corresponding to human infants, toddlers, teenagers and young adults exposed to either the nephrotoxins gentamicin, or cisplatin or the hepatotoxin valproic acid. The differential effects across the various age groups were assessed by organometrics, histopathology, hematology, clinical chemistry, liver and kidney biomarkers, and metabolomics technologies to establish specific age-related target organ vulnerabilities. Each age group was shown, using principal component analysis, to be a distinctly separate entity in terms of treatment responses. This published model, representing a single possible approach, has potential for significant utility as a tool for pediatric safety evaluation, in comparison to dosing throughout the complete maturation process. The FDA Guidance for Nonclinical Safety Evaluation of Pediatric Drug Products (Feb., 2006) presents a wide variety of parameters involving juvenile/adult differences. These constitute many possible choices that may be incorporated into a pediatric preclinical model appropriate to address preclinical safety. The age of intended exposure, route, frequency and length of exposure are critical and will be discussed. In general the preclinical safety evaluation of new and approved drugs for pediatric use is handled on a case by case basis. This is reflected in some of the more recent EMA and ICH documents (2008, 2009) that allow for a multitude of choices based on the ultimate requirements of subsequent clinical trials.

### **S** 2412 Genetic and Epigenetic Mechanisms of Susceptibility to Environmental Exposures in Children.

N. Holland, P. Yousefi, K. Huen, K. Harley, V. Volberg, L. Barcellos, H. Quach, A. Bradman and B. Eskenazi. *SPH, CERCH, University of California Berkeley, Berkeley, CA*. Sponsor: [J. Lee](#).

Children are more susceptible to exposures to environmental toxicants than adults, and in utero exposures may result in developmental problems and chronic diseases. Some children can be particularly vulnerable due to their genetic makeup and age-related differences in protective enzyme levels such as paraoxonase (PON1). Results from the Center for the Health Assessment of Mothers and Children of Salinas (CHAMACOS) birth cohort study will be presented to illustrate complex relationships of the effects of prenatal exposure to pesticides, PON functional genomics and genome-wide DNA methylation in Mexican-American children. We determined PON1 genotypes and three PON1 enzyme activities in 450 mothers and their children. Although it was previously thought that children's PON1 levels reach adult ones by age 2, we found that PON1 levels and activities were the lowest in newborns and steadily increased with age. However, they remained below adult levels up to 7 years. Infants and young children, particularly those with PON1 genotypes encoding for lower PON1 levels and activities, have up to 65-fold lower levels of the protective PON1 enzyme than adults and may be especially susceptible to OP exposures. To assess DNA methylation in cord blood and peripheral blood (clots) of 9 year old CHAMACOS children we interrogated 485,577 CpG sites from >24,000 genes using the Illumina BeadChip platform. We found that ~15.5% of all CpG sites were differentially methylated between children at birth and 9 years of age. More than 2% of CpG sites investigated, in >1,900 genes, showed significant differences in methylation by sex, including 731 CpG sites located in autosomes. Candidate genes and pathways involved in response to environmental exposures during pregnancy have been identified. Unlike genetics, epigenetic mechanisms could be reversible and an enhanced understanding of their role may lead to better protection of pregnant women and children, and improved public health.

### **S** 2413 Prenatal Metal Exposure and Health Effects.

R. C. Fry. *Environmental Sciences and Engineering, University of North Carolina at Chapel Hill, Chapel Hill, NC*.

We will present data that we are collecting from two mother-child cohorts, one in Gómez Palacio, Mexico and one in North Carolina, USA. Both of the newborn cohorts are at risk for metal exposure. The research focuses on an arsenic endemic area of Mexico, Gómez Palacio, the study site for our newly established birth cohort. In this region we are assessing exposure to inorganic arsenic in pregnant women. Our results suggest that pregnant women in this region are at risk for high level exposure to arsenic, a finding that has implications both for the health of the women and also their children. In related research we show that exposure to inorganic arsenic is associated with changes in DNA methylation patterns. We are also examining changes in DNA methylation patterns in fetal DNA collected from the NC cohort which is at risk for prenatal exposure to cadmium. We demonstrate using genome-wide gene-specific DNA methylation analysis that there are significant differences in levels of promoter methylation in fetal or maternal samples. In addition, we

highlight that prenatal exposure to cadmium is associated with altered patterns of methylation of genes that play varied roles in the cell. Results from these cohort studies underscore the potential health effects of early life exposure to inorganic arsenic and cadmium, the potential for epigenetic alterations, short term health consequences, and potential relationships to detrimental health outcomes later in life.

### **S** 2414 Particulate Pollution, Susceptibility, and Epigenetic Pathways in an Elderly Cohort.

J. Madrigano<sup>1,2</sup>, A. Baccarelli<sup>2</sup>, M. A. Mittleman<sup>2,3</sup>, R. O. Wright<sup>2</sup>, D. Sparrow<sup>4</sup>, P. S. Vokonas<sup>4</sup>, L. Tarantini<sup>5</sup> and J. Schwartz<sup>2</sup>. <sup>1</sup>*Mailman School of Public Health, Columbia University, New York, NY*; <sup>2</sup>*Harvard School of Public Health, Boston, MA*; <sup>3</sup>*Beth Israel Deaconess Medical Center, Boston, MA*; <sup>4</sup>*Veterans Administration Boston Healthcare System and Department of Medicine, Boston University, Boston, MA*; <sup>5</sup>*Environmental and Occupational Health, University of Milan, Milan, Italy*. Sponsor: [J. Lee](#).

DNA methylation is a potential pathway linking environmental exposures to disease, and lower blood DNA methylation has been found in processes related to cardiovascular morbidity. Genetic and other host characteristics, such as psychological functioning, have been found to modify the association between air pollution and morbidity. In our study, DNA methylation of repetitive elements, as well as specific genes, was measured in 1406 blood samples from 706 elderly participants in the Normative Aging Study (NAS). We will discuss the changes in repetitive element DNA methylation, as well as two specific genes (the inducible nitric oxide synthase gene, iNOS, and the glucocorticoid receptor gene, GCR) associated with ambient particles (PM<sub>2.5</sub>) and black carbon (BC), estimated with mixed models. We will also discuss genotype and phenotype characteristic that may modify this association.

### **W** 2415 Challenging the Limits of Nonclinical Safety Assessment of Pediatric Medicines.

J. S. Moffit<sup>1</sup>, T. Ernest<sup>2</sup>, A. Mauz<sup>3</sup>, M. G. Paule<sup>4</sup>, J. Stewart<sup>5</sup> and P. Ji<sup>6</sup>. <sup>1</sup>*Nonclinical Drug Safety US, Boehringer Ingelheim Pharmaceuticals Inc, Ridgefield, CT*; <sup>2</sup>*Product Development, GlaxoSmithKline, Harlow, United Kingdom*; <sup>3</sup>*Nonclinical Drug Safety GER, Boehringer Ingelheim Pharma GmbH & Co. KG, Biberach an der Riß, Germany*; <sup>4</sup>*Division of Neurotoxicology, US FDA-National Center for Toxicological Research, Little Rock, AR*; <sup>5</sup>*Reproductive Toxicology Safety Assessment, AstraZeneca, Macclesfield, United Kingdom*; <sup>6</sup>*Division of Clinical Pharmacology II, US FDA-Office of Clinical Pharmacology, Silver Spring, MD*.

Pediatric safety assessments are a fundamental and integral part of drug development programs. Introduction of regulatory guidance in the last decade has formalized the inclusion of safety evaluations in juvenile animals, leading to a better understanding of potential drug effects on developmental processes and risks specific to pediatric age groups. Toxicology studies in juvenile animals have evolved to address inherent differences in susceptibility between mature and immature systems. Pediatric safety assessments are challenged by practical and interpretive complexities of conducting toxicity studies in immature animals against a background of increasingly diverse disease indications. This symposium will review a number of innovative approaches that challenge the current limits of the nonclinical safety assessment of new pharmaceuticals. Our panel of experts will discuss unique approaches and case studies dealing with the challenges of supporting pediatric formulations, nontraditional routes of administration, and the complexities of developmental neurotoxicity assessments. Furthermore, our experts will discuss how information from various sources such as in vitro experiments using neonatal tissue, pharmacokinetics, and clinical pharmacology work may be brought together to build a risk assessment specific for a young infant and pediatric dosing. These innovative approaches from industry and government challenge the limits of nonclinical safety assessment and provide reassurances of safety for pediatric medicines.

### **W** 2416 Safe and Effective Use of Established and Novel Excipients in the Development of Children's Medicines.

S. R. Maguire. *Product Development, GlaxoSmithKline R&D, Harlow, United Kingdom*. Sponsor: [J. Moffit](#).

Developing medicines for children is in some respects even more challenging than developing medicines for adults yet the range of excipients available for use in the development of children's medicines is likely to be significantly reduced without appropriate evidence of safe, tolerated excipient limits across the whole paediatric age range. Industry, with the support of academia, have the opportunity to work with

national regulatory agencies to raise awareness of the need to build a risk/benefit approach focused on the use of excipients in paediatric drug products; in particular the use of novel excipients in this population. Identification of key data should be determined together with an appropriate mechanism for this data to be shared to enhance access to medicines for children.

#### **W 2417 Technical Challenges and Data Interpretation Evaluating an Inhaled Long Acting $\beta$ 2-Agonist in Juvenile Dogs.**

A. Mauz. *Nonclinical Drug Safety Germany, Boehringer Ingelheim Pharma GmbH & Co. KG, Biberach an der Riß, Germany.*

Numerous inhaled medications are marketed to pediatric populations, but most of these products were registered prior to the regulated integration of juvenile toxicity studies in nonclinical safety programs. In order to initiate clinical trials in pediatric populations, safety assessments are conducted in juvenile animals to assess any potential toxicity effects during postnatal development, particularly with regard to lung development. This presentation will detail a case study for an inhaled, long acting  $\beta$ 2-agonist in juvenile dogs. Discussion will include insight into the pediatric safety strategy, technical challenges involved in dosing an inhaled medication to juvenile dogs, and data interpretation.

#### **W 2418 Modeling Pediatric Exposures to Neuroactive Agents: Developmental Neurotoxicology.**

M. G. Paule. *Division of Neurotoxicology, National Center for Toxicological Research, US FDA, Jefferson, AR.*

Given the obvious limitations, it is difficult to thoroughly explore the effects of pediatric neuroactive agents on neurons in human infants or children. Due to the complexity of the primate brain, the monkey is often the animal model of choice for developmental neurotoxicology experiments. Case studies will be presented on nonhuman primate models of pediatric exposures to general anesthetics and other neuroactive compounds. These examples will focus on translational endpoints involving cognitive functions such as learning and memory and in vivo imaging using PET. Strategies for neuroprotection will also be discussed.

#### **W 2419 Technical and Scientific Challenges in Risk Assessments for Neonates and Infants.**

T. Mitchard and J. Stewart. *Reproductive Toxicology, AstraZeneca, Macclesfield, United Kingdom.* Sponsor: J. Moffit.

Progression into clinical trials in neonates and infants often involves a risk assessment specific for that age group. The risk assessment is likely to include information from technically challenging bespoke studies in very young animals. However, these studies may not be limited to just repeat dose toxicity studies in young animals but may also include in vitro experiments using neonatal tissue (exploring pharmacodynamic endpoints), safety pharmacology and ADME work. This presentation will illustrate with case examples how information from various sources may be brought together to build a risk assessment specific for the young infant.

#### **W 2420 Pediatric Dosing Regimen Determination during Drug Development.**

P. Ji. *Division of Clinical Pharmacology II, US FDA, Office of Clinical Pharmacology, Silver Spring, MD.* Sponsor: J. Moffit.

In the past 10 to 15 years, the medical treatment options for Juvenile Idiopathic Arthritis (JIA) have greatly evolved and expanded due to a better understanding of the disease and the application of biologic agents. Regulations pertinent to pediatric clinical research have also helped provide a legal basis for investigating the effects of drugs and biologics in pediatric populations and facilitate pediatric drug development. The evaluation of clinical pharmacology, efficacy, and safety data has provided valuable labeling information for pediatric use. This presentation will discuss the application of clinical pharmacology, safety, and efficacy assessments in determining JIA pediatric dosing regimens.

#### **W 2421 Nanotoxicology: Computational Strategies, Advances, and Challenges.**

S. M. Hussain and J. J. Schlager. *Air Force Research Laboratory, US Air Force, Wright-Patterson AFB, OH.*

Engineered Nanomaterials (ENM), in the range of 1–100 nm, have been found to exhibit fascinating physicochemical properties making them suitable for numerous applications, extending into numerous military, industrial, medical, and scientific specialties. However, massive quantities of ENM would need to be produced for these applications to be realized, thereby increasing the potential risk of human exposure and raising additional concern about their short and long-term toxicological effects. Nanotoxicology has recently emerged as a new branch of toxicology which deals with toxicological ramifications of these ENMs based on their physicochemical properties, such as size, shape, surface coating, and charge. Conducting toxicological studies considering massive quantities of ENM already in the market would be time consuming and resource intensive. Therefore, there is a great need to develop computational models to predict toxicity and human health effects of ENMs. A recent report (Nature Nanotechnology Vol 6, 2011 P138) has demonstrated a computational model to predict the cytotoxicity of various metal-based nanoparticles. The main objective of this workshop is to discuss modeling techniques based on the electronic and structural complexity of ENMs to predict their biological effects.

#### **W 2422 Quantitative Nanostructure-Activity Relationships Modeling.**

A. Tropsha. *Eshelman School of Pharmacy, University of North Carolina at Chapel Hill, Chapel Hill, NC.* Sponsor: S. Hussain.

Evaluation of biological effects of Manufactured NanoParticles (MNP) (including toxicity and environmental fate) is of critical importance for the future of nanotechnology. Our group was among the first to assess the potential of modern cheminformatics methods such as Quantitative Structure – Activity Relationship modeling to develop statistically significant and externally predictive models that can accurately forecast biological effects of MNPs from the knowledge of their physical, chemical, and geometrical properties; we termed this approach Quantitative Nanostructure Activity Relationship (QNAR) modelling. We developed QNAR models for two different categories of MNP datasets: (i) those comprising MNPs with diverse metal cores and organic surface modifiers, in which experimentally measured properties were used as particle's descriptors, and (ii) those involving MNPs possessing the same core, but different surface-modifying organic molecules, for which descriptors can be calculated for a single representative of the surface-modifying molecule. In the former case, binary QNAR models with external predictive accuracy as high as 73% were developed for 44 MNPs tested for cellular bioactivity and characterized by experimental descriptors such as size, relaxivities, and zeta potential. For the latter case, we developed QNAR models for a library of 109 MNPs with CLIO-NH<sub>2</sub> core decorated with different synthetic small molecules that were tested for uptake in PaCa2 pancreatic cancer cells; models' external prediction power was shown to have an R<sup>2</sup> of 0.72 with a mean absolute error of 0.18 under 5-fold external validation procedure. Similar results were obtained for another dataset of 84 surface-modified Carbon Nanotube MNPs tested for protein binding and acute cellular toxicity; these models were used to design novel MNPs that were tested experimentally with the success rate of 80%. Our studies show that QNAR modelling can be used successfully for (i) predicting activity profiles of novel MNPs solely from their representative descriptors and (ii) designing and manufacturing safer nanomaterials with the desired properties.

#### **W 2423 Toxicity of Nanomaterials—Major Challenges for Theoretical Predictions.**

J. Leszczynski. *Department of Chemistry, Jackson State University, Jackson, MS.* Sponsor: S. Hussain.

Nanotechnology is expanding rapidly, but development of novel materials synthesized at the 'nano' scale should be always accompanied by a comprehensive assessment of risk to human health and to environmental ecosystems. It is vital to be able to predict possible environmental impact of new nanomaterials before their mass production and application. Computational Chemistry provides various tools to evaluate interaction of nanomaterials with biomolecules, shed a light on mechanisms of such phenomena, and predict toxicity of nano sized species. We believe that there is a strong need to develop "nano descriptors" i.e. novel and reproducible ways of representing the structures and/or physical properties of nanoparticles that are suitable for distinctive grouping these types of chemicals. This will facilitate development of QSARs that could reliably predict their characteristics and activities. A conceptual framework for grouping NPs should be considered as a first step in

identifying QSARs that are applicable within each group. Due to high variability in the molecular structure and different mechanisms of action, individual groups of nanoparticles should be modeled separately. In each case, according to the general QSAR rules, the applicability domain of the models should be carefully validated. Our recent *ab initio* study revealed details of interactions of gold clusters, carbon nanotubes and fullerenes with DNA bases and base pairs. Direct prediction of toxicity of unknown nanomaterials was done using QSAR models developed for a test set of compounds characterized experimentally. Based on experimental testing, we developed and tested novel interpretative nano-QSAR model describing cytotoxicity of 17 nano-sized metal oxides to bacteria *Escherichia coli*. The proposed model allowed us to formulate a hypothesis that mechanistically explained differences in toxicity between the individual oxides.

#### **W 2424 Biological Surface Adsorption Index (BSAI): A Molecular Signature for Nanomaterial Interactions.**

J. E. Riviere. *Institute of Computational and Comparative Medicine, Kansas State University, Manhattan, KS.*

Most characterization techniques available today for nanomaterials are based on hard physical-chemical properties of size, shape, and surface properties, often determined under very non-biological conditions. However, a major factor that determines biological interactions of nanomaterials *in vivo* are their surface properties related to forming interactions with molecules in the biological environment. We have developed the BSAI metric, which develops a signature of nanomaterial surface properties specifically related to biomolecular interactions. These properties are developed based on how a nanomaterial interacts with a series of probe compounds using a QSAR approach to generate five molecular descriptors that could be described as a multidimensional partition coefficient. This presentation will introduce the index and illustrate how it can be used to improve modeling of biological interactions.

#### **W 2425 Predictive Modeling on Nanoparticle-Biomolecular Interactions.**

R. Pandey. *Department of Physics, Michigan Technological University, Houghton, MI.*  
Sponsor: S. Hussain.

Nano-scale materials, such as semiconductor and metal quantum dots, carbon nanotubes, and graphene, exhibit novel optical, electrical, and magnetic properties that can be exploited for new generations of electronics and sensors. Nanoscale materials also exhibit unique affinity with biological molecules, such as nucleic acids and proteins, which can be utilized for a wide variety of biological diagnostics and sensing applications. In order to develop such application concepts, however, a fundamental understanding of the interactions between various nano and biological systems is critically important. This talk will present a brief overview of recent developments in the assembly and structure-property characterizations of hybrid nano-bio materials with a focus on the physical and chemical properties of their interface. Results obtained from recent theoretical and experimental investigations on optical protein-QD and nucleic acid base-nanotube (C, BN) interactions will be presented.

#### **W 2426 Toxicogenomics in Risk and Safety Assessment: Recent Advances and Continuing Challenges.**

C. Thompson<sup>1</sup> and M. D. Waters<sup>2</sup>. <sup>1</sup>*ToxStrategies, Inc., Katy, TX;* <sup>2</sup>*Integrated Laboratory Systems, Inc., Research Triangle Park, NC.*

Toxicogenomic studies can provide a vast amount of data with regard to the changes a chemical can have on a cell, tissue, or organism, and technological achievements continue to make it easier and cheaper to generate such data. However, the application of toxicogenomic data to environmental risk assessments and pharmaceutical safety assessments has progressed more slowly and, despite recent advances, challenges remain as to how best to harness and interpret these large and complex datasets to facilitate their practical application. This session will describe recent applications of toxicogenomics in environmental risk assessment with focus on assessing and predicting genotoxic modes of action and utilizing transcriptome changes from multidose and multi-endpoint animal bioassays in quantitative risk assessment. In addition, recent advances in the usage of toxicogenomics in pre-clinical pharmaceutical safety, clinical trial placement, and individualized medicine will be described.

#### **W 2427 Characterizing and Predicting Modes of Action of Carcinogenicity Based on Conventional and Toxicogenomics Methods.**

M. D. Waters. *Integrated Laboratory Systems, Inc., Research Triangle Park, NC.*

Predictive toxicogenomics uses global molecular expression data resulting from genomic perturbation (e.g., transcript profiles) to predict a toxicological outcome, such as carcinogenicity. In the context of risk assessment, the classification of carcinogens as genotoxic or nongenotoxic has become an essential and debatable issue because of the default assumption that drives regulatory decision-making regarding the presumed linearity of the dose-response curve for genotoxic carcinogens. In fact, the great majority of known human carcinogens are easily detected in conventional short-term tests for genotoxicity and induce tumors at multiple sites in rodents, thus provoking challenges as to the human relevance of nongenotoxic rodent carcinogens. Toxicogenomics studies appear quite useful in resolving this dichotomy and in pursuing mechanisms of action. In toxicogenomics studies, a strong DNA damage response at the gene expression level suggests direct DNA modification whereas increased expression of genes involved in cell cycle progression is more characteristic of the indirect-acting agents such as those that induce oxidative stress. Gene expression profiles have been demonstrated that discriminate nongenotoxic modes of action (e.g., cytotoxicity and regenerative proliferation, xenobiotic receptor agonists, peroxisome proliferator-activated receptors, or hormonal-mediated processes) and other profiles appear to delineate various paths to the formation of conventional cytogenetic alterations. The evidence accumulated to date suggests that toxicogenomics approaches will be useful in conjunction with conventional test methods in the dose and phenotype anchored assessment of chemical carcinogenicity. Case studies will be used to illustrate these points.

#### **W 2428 Case Studies of Dose-Response Genotoxicity and Toxicogenomic Studies Designed to Replace Default Assumptions Used in Carcinogenic Risk Assessments.**

L. Recio. *Integrated Laboratory Systems, Inc., Research Triangle Park, NC.*

Characterizing dose-response is a fundamental aspect of toxicology and can be used to determine and predict the potential adverse effects of chemicals to humans. Only recent genetic toxicology and toxicogenomic studies have adequately characterized dose-response over a range of exposures and have used these data for point-of-departure (POD) calculations needed in risk assessment, such as benchmark dose 10 (BMD10). Genotoxicity and toxicogenomic endpoints can be considered as biomarkers of 'key events' or adaptive responses that with robust experimental designs can provide the needed qualitative and quantitative dose-response information to establish chemical-specific modes-of-action that can be integrated into weight-of-evidence-based approaches for risk assessments. More recently genomic signatures for mode-of-action (MOA) (e.g., genotoxic vs nongenotoxic MOA) in target organs are emerging as mRNA biomarkers of effects. Low dose studies designed to identify exposure levels that do not cause alterations in basal genotoxicity or gene expression can be used to identify exposure levels (or dose) that represent the transition between the NOEL concentrations and other PODs such as BMD. Recent studies conducted at ILS with collaborators, represent case studies aimed at identifying the NOEL concentrations and other PODs using the *in vitro* micronucleus and mutagenicity studies in human cells for acetaldehyde, dose-response and impact of liver GSH detoxication on naphthalene genotoxicity, expression profiling studies to assess genotoxic vs nongenotoxic MOA in human TK6 cells, and an *in vivo* dose-response study conducted with the mouse liver carcinogen furan examining impact on the mouse genome and epigenome.

#### **W 2429 Application of Transcriptomic Data for Quantitative Chemical Risk Assessment.**

R. S. Thomas. *The Hamner Institutes for Health Sciences, Research Triangle Park, NC.*

Current challenges facing chemical risk assessment are the time and resources required to meet the data standards necessary for a published assessment and the incorporation of modern molecular biology information. The integration of transcriptomic data into the risk assessment paradigm may address both challenges by providing an efficient means to quantitatively and comprehensively evaluating the molecular changes resulting from chemical exposure. To assess the value of applying transcriptomics in quantitative chemical risk assessment, a series of studies was performed. In the first study, mice were exposed for 13 weeks to multiple concentrations of five chemicals that were positive in a two-year cancer bioassay. In a second study, rats were exposed in a time course to multiple concentrations of six chemicals with published risk assessments. In both studies, histological changes were evaluated and transcriptional microarray analysis was performed on the target tissues.

The histological and the tumor responses were analyzed using standard benchmark dose (BMD) methods to identify noncancer and cancer points-of-departure. The dose-related changes in gene expression were also analyzed using a BMD approach and grouped based on signaling pathways. The transcriptional BMD values showed a high degree of correlation with apical responses for specific pathways and many of the correlated pathways have been implicated in relevant disease pathogenesis. Importantly, transcriptional points-of-departure for even the most sensitive pathway were on average less than three-fold different than traditional apical points-of-departure for both cancer and non-cancer endpoints suggesting that transcriptomic changes in signaling pathways can be used to estimate noncancer and cancer points-of-departure for use in quantitative risk assessments.

## **W** 2430 **Challenges and Opportunities of Toxicogenomics Analyses in Safety Assessment during Preclinical Safety Studies.**

C. Karbowski. *Discovery Toxicology, Amgen, Thousand Oaks, CA.*

Microarray analysis is a key tool utilized in the biotechnology/pharmaceutical industry as part of a holistic approach to predicting and understanding mechanisms of toxicity of molecules in development. Historically, researchers have faced significant challenges in analyzing and interpreting these large datasets such as understanding the translation of molecular changes to phenotypic changes in an organism and the relevance of observed alterations to other species. However, progress in overcoming these challenges continues to be made. For example, contextualization of gene expression changes utilizing historical and publically available reference toxicant datasets coupled with recent advances in Systems Biology such as more comprehensive and toxicologically relevant content along with the incorporation of transcription factor analyses and gene directionality provides opportunities to understand the genesis and cross-species relevance of pre-clinical phenotypic changes. This presentation will provide an historical view of the utility of microarray analysis in preclinical safety assessment and then illustrate, through case examples, the added value provided when current state of the art tools are applied to help dissect molecular changes underlying phenotypic alterations.

## **W** 2431 **Role of Causal Reasoning in Patient Stratification from Efficacy and Safety Perspectives.**

A. Enayattallah. *Drug Safety Research & Development, Pfizer, Inc., Groton, CT.*

Advances in genomic technologies have led to the ability to rapidly generate extraordinary amounts of data. However, a lack of efficient tools to manage and interrogate such large amounts of data has limited the application of genomics in the pharmaceutical industry. Recently, we developed a computational platform we call the Causal Reasoning Engine (CRE) that is a powerful tool for transcriptomic data analysis. The CRE provides explanation of the observed transcriptomic changes in the context of prior biological knowledge, captured in a knowledge base of computable biological assertions. The platform was initially applied to investigative toxicology to provide mechanistic understanding of organ toxicities, including drug-induced liver injury (DILI) and drug-induced cardiac injury. More recent developments of the CRE platform indicate potential predictive power for evaluating compound responses and safety liabilities at the individual patient level, which would enable the stratification of patients in clinical trials. In the context of efficacy we will show a use case for patients with diseases known for their heterogeneity, such as systemic lupus erythematosus and inflammatory bowel disease. In this case individualized analysis using CRE clearly classifies patients based on their underlying disease mechanisms, and we will discuss the potential impact on patient and treatment selection in clinical trials. Finally, the results from the individualized analysis approach in patients with immune-mediated DILI will also be presented. Based on the examples presented here, we believe that the CRE approach shows great promise in being able to stratify patients to support the development of more effective and safer medicines.

## **RI** 2432 **Assessment of Environmental, Dietary, and Biological Risk Factors Impacting Liver Cancer Incidence in Texas.**

E. D. Bruce<sup>1,2</sup> and A. Romoser<sup>3</sup>. <sup>1</sup>*Institute of Biomedical Sciences, Baylor University, Waco, TX;* <sup>2</sup>*Institute of Ecological, Earth, and Environmental Science, Baylor University, Waco, TX;* <sup>3</sup>*Toxicology, Texas A&M University, College Station, TX.*

The increasing incidence of primary liver cancer in Texas is a result of multiple risk factors, including environmental and dietary exposures to carcinogens, as well as biological factors, such as hepatitis C infection. Texas has the highest liver cancer mortality rate in the United States, affecting the Hispanic portion of the population

most acutely. It is speculated that the increased incidence of primary liver cancer observed in these Hispanic communities is due to occupational exposures to pesticides, polycyclic aromatic hydrocarbons (PAHs), and dietary risk factors from contaminated maize. Current research and risk assessment in this field is focused on cancer epidemiology within these populations to determine those risk factors that are most hazardous to the community health of south Texas. Many pesticides used in farming and households are labeled as probable carcinogens and can cause many other negative health effects in people chronically exposed. Research and educational programs in Texas are striving to increase awareness of health effects from exposure and pesticide safety. PAHs are also known hepatic carcinogens, forming DNA adducts within the liver. Health effects observed in Texas from chronic PAH exposure through foods and poor air quality are being assessed. Additionally, mycotoxin occurrence is heightened in the southern portion of the state where drought conditions and excessive heat contribute to fungal growth on staple crops (i.e., maize). Specifically, aflatoxin and fumonisin exposures have been observed in various communities in San Antonio and along the Texas-Mexico border. These mycotoxins are known to both initiate and promote hepatocellular carcinoma. Understanding the risk factors for primary liver cancer in Texas is essential to developing future remediation, prevention, and treatment strategies, as well as identifying and establishing necessary changes in state regulations.

## **RI** 2433 **Liver Cancer Incidence Trends in Texas 1995–2009.**

J. F. Villanacci, C. Bowcock and A. Hackenwerth. *Texas Department of State Health Services, Austin, TX.* Sponsor: E. Bruce.

Liver cancer is the 12th most commonly diagnosed cancer in the US and the 6th most common cause of cancer deaths. Liver cancer incidence has been increasing in both Texas and the US. Although liver cancer only accounts for 1.3% of new cancer cases, it accounts for 2.6% of cancer deaths. Survival rates are poor with a five-year survival of 13 to 15 percent. In 2012, approximately 2,197 Texans are expected to be diagnosed with liver cancer and 1,768 are expected to die from the disease. Liver cancer incidence trends for Texas and the US were determined using data from the Department of State Health Services, Texas Cancer Registry and National Cancer Institute, Surveillance Epidemiology & End Results. For a 15-year period (1995 to 2009) age-adjusted incidence rates were computed by gender and race/ethnicity.

Texans experience higher liver cancer incidence rates than the US and the rates are increasing faster. From 1995 to 2009 Texas rates increased by an average annual rate of 5.7% compared to 3.9% for the US. The 15-year percent changes in incidence for Texas and the US were 126% and 77%, respectively.

In Texas, liver cancer incidence has been increasing in both men and women but faster in men. From 1995 to 2009 age-adjusted rates for men increased by 130%, while rates for women increased by 96%. In both Texas and the US, men of all race/ethnic groups are diagnosed two to four times as often as women. In Texas, Hispanics (any race) and Asian/Pacific Islanders have the highest rates but Blacks had the highest rate of change from 1995 forward with an annual percent increase of almost 7% and a 15-year increase of 141%. Texas Hispanics and Blacks have significantly higher liver cancer incidence rates than US Hispanics and Blacks. Hispanic men living in the 38 South Texas counties have the highest age-adjusted rate (25.7). Hispanic and Black men living in the remaining Texas counties have the next highest rates (19.4 and 19.1). From 1995 to 2005 there has been a downward shift in the age of diagnosis of liver cancer for both men and women of all race/ethnic groups.

## **RI** 2434 **A Lay Health Worker-Based Intervention for Reducing Families' Environmental Exposures.**

L. Cizmas<sup>1</sup>, J. Ross<sup>1</sup>, R. Rincon<sup>2</sup>, H. Tamez<sup>2</sup>, A. Ginez<sup>2</sup>, R. Perales<sup>2</sup>, C. Miller<sup>2</sup> and T. McDonald<sup>1</sup>. <sup>1</sup>*Texas A&M Health Science Center School of Rural Public Health, Texas A&M University, College Station, TX;* <sup>2</sup>*South Texas Environmental Education and Research Program, University of Texas Health Science Center, San Antonio, San Antonio, TX.*

In economically disadvantaged areas of San Antonio and Laredo, TX, poor living conditions and a hot climate increase the likelihood of pest infestations, leading to increased pesticide use. Promotoras (lay health workers) were employed to deliver a pesticide health education module to families with children between 6 months to 5 years of age. Assessments of attitudes and behaviors relating to pesticide use were given prior to and 6 months after module delivery. In Laredo, participants reported statistically significant changes in behavior and attitudes six months after the module. For example, the percent of participants reporting that they always had emergency numbers by the phone was 35% before the training and 86% six months

after the training, and the percentage reporting that they always used gloves when applying pesticides was 35% before the training and 84% six months after the training. Promotora-driven health education with local collaboration may improve family attitudes and practices relating to pesticide use, and may be explored as an option for addressing other environmental exposures as well.

#### **RI 2435 Early Obesity and Risk of Hepatocellular Carcinoma in USA.**

M. Hassan<sup>1</sup>, D. Li<sup>1</sup>, A. Kaseb<sup>1</sup>, J. L. Abbuzzese<sup>1</sup>, H. M. Hassabo<sup>1</sup>, M. Khalil<sup>1</sup>, I. Sahin<sup>1</sup>, J. Morris<sup>1</sup>, E. Hawk<sup>1</sup> and M. R. Spitz<sup>2</sup>. <sup>1</sup>The University of Texas MD Anderson Cancer Center, Houston, TX; <sup>2</sup>Baylor College of Medicine, Houston, TX. Sponsor: E. Bruce.

Despite the public health problem of obesity and increasing incidence of hepatocellular carcinoma (HCC) in the United States (US), the relationship between obesity and HCC has never been examined extensively in US population. At the University of Texas MD Anderson Cancer Center we conducted a case-control study aimed at examining HCC risk factors in the US. Cases were patients with pathologically confirmed diagnosis of HCC and US residency. The healthy control subjects were spouses of patients at MD Anderson who had cancers other than liver, gastrointestinal, lung, or head/neck cancer. Self-reported weight and body size (Stunkard pictograms) at ages 20, 30, 40, 50, 60, 70 was obtained from participants by personal interview. Between 2005 and 2011 we enrolled 403 cases and 661 controls. Body mass index (BMI) was classified as "underweight" (BMI < 18.5), "normal" (BMI range, 18.5-24.9), "overweight" (BMI range, 25-29.9), and "obese" (BMI ≥ 30.0). We found that individuals who were obese from the ages of 30 to 49 had a significant increased risk of HCC, independent of HCC established risk factors. The estimated odds ratio (OR) and 95% confidence interval (CI) was 4.1(1.6-10.5). The association was observed in men and women; the ORs (95% CIs) were 2.3(1.1-4.9) and 2.9(1.2-8.9) respectively. Moreover, individuals who were overweight or obese from the ages of 30 to 49 years had an earlier onset of HCC by 3 to 6 years (median age of onset was 65 years for patients with normal weight, 62 years for overweight patients [P=.02], and 59 years for obese patients (P <.001). Underlying evidence of cirrhosis was significantly observed in HCC patients with early obesity. We concluded that obesity is a significant risk factor for HCC in US where underlying cirrhosis can be a significant burden in disease management. Integration of obesity with other HCC risk factors into a risk model may lead to the development of a new scoring system to identify high-risk individuals who may benefit from HCC screening and prevention.

#### **RI 2436 Biomarkers of Hepatocellular Cancer Risk and Diagnosis.**

R. M. Santella. NIEHS Center for Environmental Health, Columbia University Mailman School of Public Health, New York, NY.

Hepatocellular carcinoma (HCC) incidence is increasing in the US and HCC has one of the fastest growing death rates of any cancer. There is wide geographic variation in HCC incidence around the world likely due to geographic differences in the prevalence of various etiologic factors. In Asia and Africa hepatitis B virus is the primary etiologic agent while in the US, hepatitis C virus is more common. Identified environmental/lifestyle risk factors include aflatoxin B1 (AFB1), a dietary mold contaminant, alcohol drinking, and cigarette smoking. We have used biomarkers in a prospective study in Taiwan to demonstrate that elevated baseline levels of AFB1 urinary metabolites, AFB1-albumin adducts, polycyclic aromatic hydrocarbon (PAH)-albumin adducts and urinary isoprostanes, a biomarker of oxidative stress, are associated with later development of HCC. We have also found AFB1- and PAH-DNA adducts in liver tissues of US HCC cases. Using a candidate gene approach, studies of liver tumor tissues have identified genes that are hypermethylated in tumors compared to adjacent tissues and found that this methylation was associated with elevated levels of AFB1-DNA adducts in the tissues. DNA isolated from plasma collected at the time of diagnosis contains these same methylated markers. More importantly, methylated DNA released from the tumor can be frequently found in plasma collected many years before clinical diagnosis suggesting their potential utility in screening high populations such as those with viral infection. More recently, we have used Illumina Infinium arrays that interrogate methylation of 27k or 450k CpG sites to more comprehensively identify regions with altered DNA methylation. These studies have found large numbers of hyper or hypomethylated regions in tumors compared to adjacent tissues and identified methylation markers that should enhance early diagnosis. Biomarkers of environmental exposure in combination with viral infection markers can identify populations at increased risk while methylation and microRNA markers may potentially be used for the early diagnosis of HCC.

#### **RI 2437 Mitigation of Aflatoxin Exposures Using a Clay-Based Enterosorbent.**

T. D. Phillips. Veterinary Integrative Biosciences, Texas A&M University, College Station, TX.

Concerns about the quality and safety of foods destined for human and animal consumption have evoked a growing awareness of the significant hazards associated with chemicals known as aflatoxins. The aflatoxin problem in foods is longstanding, unavoidable and seemingly inextricable. Aflatoxin exposure is often considered a risk factor for disease in countries where there is a lack of infrastructure for food safety regulation. However, aflatoxin exposure has been observed and is a cause for concern in underprivileged communities in Texas and the Southwest U.S. as well. Aflatoxin B1 (AFB1) is a direct acting mutagen and has been shown to disrupt genes involved in carcinogenesis and tumor suppression. Recent research with mycotoxin enterosorbent, NovaSil (NS), in an African population has shown the product to be safe and efficacious in reducing biomarkers of exposure to aflatoxin. Blood and urine samples were taken at Baseline, 1 Month, 3 Months and 4 Months. NS clay significantly reduced biomarkers for aflatoxin exposure in urine and blood and the treatment was well tolerated by participants. In a recent San Antonio study focusing on a population with a significantly elevated incidence of liver cancer, it was determined that biomarkers for aflatoxin correlated with ingestion of foods known to contain relatively higher levels of aflatoxin. Phase II of this study is underway to determine NS efficacy in reducing exposures to this toxin in Texas. Mitigating AFB1 exposure using NS represents an innovative, practical, sustainable and environmentally benign approach that will benefit more than 4.5 billion people living in climates conducive to the growth of fungi and production of mycotoxins in staple foods.

#### **RI 2438 Risk Factors Influencing the Incidence of Liver Cancer in San Antonio.**

F. A. Guerra. Department of Pediatrics, University of Texas Health Science Center San Antonio, San Antonio, TX. Sponsor: E. Bruce.

The incidence of hepatocellular carcinoma (HCC) is significantly elevated in Hispanic communities in Bexar County, Texas. Multiple factors including diet, environment, occupation, lifestyle, health status, and gender play a role in the etiology of HCC. Previous research with Texas A&M University has focused on defining the risk factors that may influence the high incidence of liver disease observed in San Antonio. Epidemiological and clinical intervention studies are ongoing in Bexar County, and have been successful in raising awareness in the community regarding environmental, dietary, and biological risk factors for disease. Ongoing studies with The University of Texas Health Science Center-San Antonio and Texas A&M University will investigate the impact of an intervention trial designed to decrease biomarkers of mycotoxin exposure and enhance public health in communities at high risk for HCC.

#### **PL 2439 A Novel Single Cell-Based High-Throughput Toxicity Study of Drugs.**

L. Ma, Y. Qiao and M. Su. NanoScience Technology Center, University of Central Florida, Orlando, FL. Sponsor: T. Lam.

Many anticancer drugs are genotoxic. The ability of tumor cells to repair drug induced DNA damage is indicative of therapeutic outcomes. But, tumors are heterogeneous in their ability to repair damaged DNA, and evaluation population response only gives a statistical average. Thus selection of drugs without knowing tumor response at single cell level can cause side effects due to toxicity of drugs. There is a need to screen drugs reliably and rapidly for individual patients. This paper describes a new single cell based HaloChip assay that can be used to detect and quantify DNA damage and repair capacity after exposing to genotoxic drugs, and examine drug response without population interference. After forming cell array, cells are embedded in agarose that provides an interconnected network for DNA diffusion, followed by exposure to NaOH and stained with ethidium bromide. Dimensions of halo and nucleus are derived from collected fluorescent image. In the case of repair, cells are washed after exposing to drug and incubated for different time before HaloChip assay. The level of DNA damage is quantified using relative nuclear diffusion factor (rNDF) derived from surface areas of halo and nucleus. The rNDFs increase from 0 to 6 as drug concentration increase from 0 to 50 μM, and reach plateau when drug concentration is over 10 μM. At same dosage, VP-16 induces more DNA damage in HeLa cells than that of other two drugs; CPT-11 induces more DNA damage in LNCaP cells than that of other two drugs. The bimodal repair curves are attributed to diversity of DNA lesions induced by drugs. The repair data are regressively fitted using first order exponential

equation. Longer repair time significantly reduces rNDF values. CPT-11 shows a slower reduction than the other two drugs for LNCaP cells. The time required to repair 50% DNA damage ( $t_{50}$ ) is derived within 0-24 hr repair time. In summary, HaloChip assay can be used to measure genotoxic drug induced DNA damage and its repair capacity. It is expected that the method will be useful in clinical, epidemiological, and experimental settings.

**PL 2440 New High-Throughput Version of the DEL Assay Detects Nonmutagenic Carcinogens.**

R. H. Schiestl, L. Parfenova, Y. Rivina, V. Kuteпова and D. Nguen. *Pathology; Environmental Health Sciences, Radiation Oncology, University of California Los Angeles, Los Angeles, CA.*

Genetic instability is a hallmark of carcinogenesis. Furthermore, cells from patients carrying mutations conferring cancer prone phenotypes show a higher level of genetic instability, including DNA deletions. In fact, the original yeast-based DEL (deletion) Assay with 100 chemicals shows an accuracy of 92% to detect carcinogens as compared to 62% detected with the Ames Assay. DEL events in all three formats are inducible by a wide variety of carcinogens including carcinogens that are negative in many other short-term tests. The DEL assay results also highly correlate with the clastogenicity of chemicals. Here we introduce the next generation DEL assay: a novel dual-read out *Saccharomyces cerevisiae* screen DEL-XG. DEL-XG simultaneously assesses the compound's genotoxicity and cytotoxicity properties. During an exposure to a genotoxic event the sequence is excised and the lacZ gene recombines to a functional beta-galactosidase genotype that with an addition of the X-Gal substrate produces a strongly positive indole (blue) product. The most important advance is that we can determine the effect of target gene expression on genotoxicity. Surprisingly and most importantly we found that the Ames negative carcinogens that were weakly positive in our standard His reversion assay, are 10 fold more potent in expressed DNA. This makes the new version of the DEL assay even more useful and makes sure that the Ames negative carcinogens will be positive even in the high throughput version. DEL-XG is a rapid and economical way to screen large chemical libraries for toxicity and potential carcinogenicity properties.

**PL 2441 In Vitro Genotoxicity Assays (Comet and Micronucleus) Using Engineered Skin.**

G. Ouedraogo<sup>1</sup>, F. Nessler<sup>2</sup>, S. Simar<sup>2</sup>, S. Talahari<sup>2</sup>, D. Lagache<sup>2</sup>, E. Vercauteren<sup>2</sup>, L. Nakab<sup>2</sup>, A. Mayoux<sup>2</sup>, N. Flamand<sup>1</sup>, G. Massin<sup>2</sup> and J. Cotovio<sup>1</sup>. <sup>1</sup>Predictive Model and Method Development, L'Oréal R&D, Aulnay sous bois, France; <sup>2</sup>Laboratoire de Toxicologie, Institut Pasteur de Lille, Lille, France. Sponsor: E. Dufour.

An in vitro micronucleus assay using human engineered skin and target cells grown beneath the tissues was developed. The purpose was to bring some information on exposure in in vitro genotoxicity assays for dermally applied compounds. Previous results have shown that this method was reproducible and could be transferred to other laboratories. The system has now evolved to combine both the comet assay and the micronucleus assay.

The approach is based on performing the comet assay in cells dissociated from the tissues, while the micronucleus assay was performed using the cells cultured beneath the reconstructed tissues. Four different time schedules were considered for this project: a 4 h treatment and a 27 h treatment period with or without an extra 27 h recovery period.

A set of 13 chemicals were tested with this approach. The results obtained show that the best prediction model was the long treatment period (27 h) without recovery for both the comet assay and the micronucleus assay.

Most of the "irrelevant positives" yielded negative in vitro results using this system.

**PL 2442 Development and Validation of a Toxicogenomics Signature to Differentiate Genotoxins vs Nongenotoxins.**

S. Beedanagari, S. Nicotra and L. Custer. *Bristol-Myers Squibb, East Brunswick, NJ.*

Genotoxicity testing has long been used to assess a compound's potential to induce genetic damage and hence its carcinogenic potential. The standard genotoxicity testing battery was designed to have high sensitivity but low specificity for detecting carcinogens that act by damaging DNA. As a consequence, positive genotoxicity test results require follow-up *in vitro* and/or *in vivo* testing to determine the biological relevance of the *in vitro* genotoxicity potential. Recent literature suggests that

Toxicogenomic approaches could serve as a useful tool to identify different mechanisms through which compounds/ chemicals exerts their genotoxic effects. Although multiple research groups to date have published papers listing several gene expression based molecular signatures *in vitro* using human and rodent cell lines, and *in vivo* using rodent models, there exists no consensus largely due to species differences and diverse "omics" technologies used. The broad objective of this study is to extend the work conducted by the ILSI-HESI technical committee on differentiating genotoxic and non-genotoxic carcinogens using real-time PCR (qPCR) based toxicogenomic approaches. In this study using a human lymphoblast TK6 cell line, we evaluated the utility of a qPCR technique to identify a molecular signature by studying gene expression profiles of twenty five genes. In our initial screening study we identified six genes that differentiated genotoxins vs non-genotoxins. However, in our validation study using ten model compounds per each group of aneugens, clastogens and non-genotoxins, we succeeded in reducing six gene signature to three gene signature. The proposed three genes that could effectively differentiate clastogens and aneugens from non-genotoxins with high specificity and sensitivity are Cyclin-dependent kinase inhibitor 1A (CDKN1A), Growth differentiation factor 15 (GDF15) and Tumor protein p53 inducible protein 3 (TP53I3).

**PL 2443 Characterization of Threshold Dose Response of Genotoxicity from Chemicals with Diverse Mechanisms of Damage.**

B. Sun<sup>1</sup>, S. M. Ross<sup>1</sup>, A. Scott<sup>2</sup>, Y. Adeleye<sup>2</sup>, M. E. Andersen<sup>1</sup> and R. A. Clewell<sup>1</sup>. <sup>1</sup>The Hamner Institute, Durham, NC; <sup>2</sup>SEAC, Unilever PLC, Bedfordshire, United Kingdom.

There is much debate regarding the existence of threshold dose-response for genotoxicity with DNA reactive chemicals. This study used in vitro high content imaging and flow cytometry assays together with Lutz threshold model (Lutz et al, 2009) to identify the threshold of dose-response for induction of double strand breaks (DSBs) and micronuclei (MN) in human p53-competent fibrosarcoma cells (HT1080). We evaluated 9 prototype chemicals: neocarcinostatin (NCS; direct DSB induction, mimics  $\gamma$ -irradiation), etoposide (ETP; topoisomerase II inhibitor), mitomycin C (MMC; DNA crosslinker), methyl methanesulfonate and ethyl nitrosourea (MMS, ENU; alkylating agents), hydrogen peroxide and *tert*-butylhydroquinone ( $H_2O_2$ , TBHQ; oxidative damage), quercetin and curcumin (QUE, CUR; oxidative polyphenols). All the oxidative agents  $H_2O_2$ , TBHQ, QUE and CUR induced a significant threshold response in both DSBs and MN, while the topo II inhibitor (ETP) and DNA crosslinker (MMC) induced non-threshold DSBs and MN response. The two alkylating agents showed different dose response trends: MMS exhibited threshold behavior of MN and DSBs, while ENU did not at the doses examined. Interestingly, NCS, a direct genotoxin and potent inducer of DSBs, induced a linear-like DSB response, but a threshold increase in MN, indicating that the DNA repair response prevents conversion of DSB to MN at low doses. We also assessed p-p53 (ser15) and total p53 induction by these chemicals. The shapes of the p-p53 curves are generally comparable to p-H2AX, demonstrating that dose-response relationship of p53 activation follows similar pattern as DSBs. Our results indicate that dose-response relationship for DNA damage and MN formation may exhibit threshold or non-threshold depending on the chemical. Whole genome transcriptomics and repair enzyme proteins induction are currently being measured to evaluate the role of chemical specific activation/inhibition of DNA repair in the determination of linear vs. nonlinear dose-dependency of genotoxic response.

**PL 2444 Concurrent Evaluation of General, Immune, and Genetic Toxicity Endpoints As Part of an Integrated Testing Strategy Approach.**

L. Sosinski, L. A. Murphy, M. R. Schisler, N. Visconti, R. Sura, M. J. LeBaron and D. R. Boverhof. *The Dow Chemical Company, Midland, MI.*

Integrated testing strategies involve the assessment of multiple endpoints within a single toxicity study and represent an important approach for reducing animal use and streamlining testing. The present study evaluated the ability to combine general, immune, and genetic toxicity endpoints into a single study. Specifically, this study evaluated the impact of sheep red blood cell (SRBC) immunization, as part of the T-cell dependent antibody response (TDAR) assay, on organ weights, RBC micronuclei formation, Comet response, and spleen T-cell immunophenotyping. Groups of female F344/DuCr1 rats were dosed with cyclophosphamide (CP) by i.p. injection for five consecutive days at 0, 1, 3, and 10 mg/kg bw/day. Six rats from each dose group were injected i.v. with SRBCs on the initial day of dosing, as per the TDAR assay, while an additional 6 rats per group did not receive SRBCs. A

sham control group was included to account for animal handling and an additional group was dosed with ethyl methanesulfonate by oral gavage as a positive control for the comet assay. For the TDAR assay, treatment with CP resulted in a dose-dependent decrease in the antibody response with a suppression of greater than 95% at the high dose. Injection with SRBC had no impact on evaluated organ weights. Analysis of micronuclei formation revealed a dose-dependent increase in response to CP treatment, with an induction of greater than 10-fold at the mid and high doses. Injection with SRBC had no impact on the level of micronuclei in control animals and did not alter the dose response to CP. There was no increase in liver DNA damage in response to CP as measured by the comet assay and injection with SRBCs did not alter this endpoint. Similarly, injection with SRBC did not alter the spleen T-cell profile in response to CP. Overall these data provide strong support for the concurrent assessment of general, immune, and genetic toxicology endpoints within a single study as part of an integrated testing strategy approach.

**PL 2445 Evaluation of Repeated Dose Liver Micronucleus Assay in Rats: Summary of Collaborative Study by CSGMT/JEMS-MMS.**

R. Takashima<sup>1</sup>, S. Hamada<sup>1</sup>, K. Shimada<sup>2</sup>, K. Matsumoto<sup>3</sup>, S. Kawakami<sup>4</sup>, J. Tanaka<sup>5</sup>, H. Matsumoto<sup>6</sup>, T. Nakai<sup>7</sup>, T. Imamura<sup>8</sup>, S. Matsumura<sup>9</sup>, H. Sanada<sup>10</sup>, Y. Terashima<sup>11</sup>, K. Inoue<sup>12</sup>, S. Mutou<sup>13</sup>, S. Hagio<sup>14</sup>, A. Hayashi<sup>15</sup>, T. Takayanagi<sup>16</sup>, Y. Ogiwara<sup>17</sup>, A. Maeda<sup>18</sup>, K. Narumi<sup>19</sup>, Y. Wako<sup>1</sup>, T. Morita<sup>20</sup>, H. Kojima<sup>20</sup>, M. Hayashi<sup>20</sup> and M. Honma<sup>20</sup>. <sup>1</sup>Mitsubishi Chemical Medicine, Ibaraki, Japan; <sup>2</sup>Astellas Pharma, Osaka, Japan; <sup>3</sup>Astellas Research Technologies, Osaka, Japan; <sup>4</sup>Asahi Kasei Pharma, Shizuoka, Japan; <sup>5</sup>Biosafety Research Center, Shizuoka, Japan; <sup>6</sup>Food and Drug Safety Center, Kanagawa, Japan; <sup>7</sup>Hokko Chemical Industry, Kanagawa, Japan; <sup>8</sup>Ina Research, Nagano, Japan; <sup>9</sup>Kao Corporation, Tochigi, Japan; <sup>10</sup>Kaken Pharmaceutical, Shizuoka, Japan; <sup>11</sup>Kissei Pharmaceutical, Nagano, Japan; <sup>12</sup>Maruho, Kyoto, Japan; <sup>13</sup>Mitsubishi Tanabe Pharma, Chiba, Japan; <sup>14</sup>Nissan Chemical Industries, Saitama, Japan; <sup>15</sup>Shin Nippon Biomedical Laboratories, Kagoshima, Japan; <sup>16</sup>Suntory Business Expert, Kyoto, Japan; <sup>17</sup>Taisho Pharmaceutical, Saitama, Japan; <sup>18</sup>Tonay Industries, Kanagawa, Japan; <sup>19</sup>Yakult Honsha, Tokyo, Japan; <sup>20</sup>National Institute of Health Sciences, Tokyo, Japan.

The repeated dose liver micronucleus (RDLMN) assay has a potential to detect genotoxic hepatocarcinogens that can be integrated into a general toxicological study. We have conducted a joint research in the Collaborative Study Group for the Micronucleus Test (CSGMT) to investigate the inter-laboratory variability and stable data acquisition in the RDLMN assay, which is supported by 19 Japanese facilities. In order to evaluate the performance of the assay, 28 chemicals including hepatocarcinogens were tested in 14- or 28-day RDLMN assays. As a result, the RDLMN assay detected the 9 chemicals positive out of 10 hepatocarcinogens, which were positive in the *in vitro* study while negative in the established bone-marrow micronucleus test. Also, the RDLMN assay detected the 2 hepatocarcinogens positive, which were positive in the short-term bone-marrow micronucleus test while negative in the 14- and 28-day repeated dose bone-marrow micronucleus tests. Accordingly, the RDLMN assay is not only useful in detecting genotoxic hepatocarcinogens but also appropriate for evaluation using a repeated low-dose regimen, and thus is considered ideal for integration into the general toxicity study.

**PL 2446 Acquisition of *In Vivo* Mutation and Cytogenetic Damage Information to Support Cancer Risk Assessment.**

S. Dertinger<sup>1</sup>, S. Phonethepswath<sup>1</sup>, J. Mereness<sup>1</sup>, S. Avlasevich<sup>1</sup>, D. Torous<sup>1</sup>, J. Bemis<sup>1</sup> and J. T. MacGregor<sup>2</sup>. <sup>1</sup>Litron Laboratories, Rochester, NY; <sup>2</sup>Toxicology Consulting Services, Arnold, MD.

Assessing the mode of action of carcinogenic chemicals is a critical component of cancer risk assessment. The US EPA's Cancer Risk Assessment Guidelines stress the importance of determining whether or not a chemical causes tumors through a direct DNA-reactive mechanism, particularly in respect to the choice of an appropriate quantitative model for the extrapolation of cancer risk to low doses. Weight of evidence (WoE) approaches that rely heavily on data from *in vitro* hazard identification assays are commonly used to address carcinogenic mode of action. *In vivo* data needed to improve the WoE include both concordance analysis of temporal mutation induction and dose-response concordance of mutation with tumor incidence (e.g., Moore *et al.*, Reg Toxicol Pharmacol 51:151-61, 2008). We used flow cytometric methods to acquire such data and thereby to test and extend this hypothesis. For example, male Sprague Dawley rats were treated for 28-consecutive days with the genotoxic carcinogen melphalan at 0, 0.031, 0.094, 0.28 and 0.75 mg/kg/day, which included dose levels corresponding to 0.33x, 1x, and 3x the tumorigenic dose rate 50 (TD50). We assessed two endpoints of genotoxicity *via* low

volume blood draws in order to efficiently obtain temporal data within the tumorigenic dosage range: MN-RET at days 4 and 29, and *Pig-a* gene mutation at days 15, 29, and 56. The earliest time points evaluated showed dose-related increases for both endpoints, long before tumors or pre-neoplastic lesions would be expected. These data illustrate the potential of these blood-based analyses to provide dose-response and temporality information that relates genetic damage to cancer induction. Continuing studies will include additional genotoxic and non-genotoxic carcinogens and non-carcinogens to provide a deeper understanding of the relationships between genetic damage and cancer induction.

**PL 2447 Axonal Degeneration of Chronic Organophosphate Ester-Induced Delayed Neurotoxicity (OPIDN) Has Different Features in Central and Peripheral Levels of the Nervous System.**

B. S. Jortner. Laboratory for Neurotoxicity Studies, Virginia PolyTech Inst State University, Blacksburg, VA.

OPIDN is considered one of the toxicant-induced central-peripheral distal axonopathies. The latter are characterized by degeneration of distal fibers in both the central and peripheral regions of the nervous systems. This has been noted in a rat model of long-term exposure to tri-ortho-tolyl phosphate (TOTP). In the present report we explore a difference in the nature of the axonopathy in the peripheral and central extensions of somatosensory fibers arising from neurons of dorsal root ganglia as seen in the sural nerve and spinal-medullary levels of the gracile fasciculus. As reported earlier (Jortner *et al.*, Toxicol. Pathol. 33:378) young adult male Long-Evans rats were administered 14 TOTP gavage doses at 75, 150 or 300 mg/kg, over a 63-day period. Sacrifice was on days 63 and 90 (after a 27 day recovery period). OPIDN was manifest by TOTP dose-related diminished activity of brain neurotoxic esterase on day 63, and distal gracile fasciculus and peripheral nerve (including sural nerve) myelinated fiber degeneration. In the present report we draw attention to a qualitative difference between lesions of central somatosensory myelinated fibers in the distal levels of the gracile fasciculus and those in peripherally directed sural nerve fibers. Axonopathy progressing to myelinated fiber degeneration was seen in both regions, and was more florid in the gracile tract. In addition, prominent dystrophic axons (Jellinger, Progr. Neuropathol. 1973) were seen in the central region, and were absent peripherally. Axon dystrophy is considered to reflect terminal degeneration with retrograde progression, possibly due to aberrant regeneration, synaptic dysplasia, failing terminal catabolism or transport. This varying pathological response of myelinated fibers from the same neuronal population is considered an effect of the differing (central vs. peripheral nervous system) environments on the evolution of axonal lesions in this chronic neurotoxic condition. Supported by USAMRMC DAMD17-99-1-9489.

**PL 2448 Maternal Paraoxonase (PON1) Status Modulates Fetal Effects Associated with Gestational Exposure of Mice to Chlorpyrifos Oxon.**

T. B. Cole<sup>1</sup>, W. Li<sup>1</sup>, A. Co<sup>1</sup>, J. Marsillach<sup>1</sup>, A. Hay<sup>1</sup>, R. Richter<sup>1</sup>, M. J. MacCoss<sup>1</sup>, L. G. Costa<sup>1,2</sup> and C. E. Furlong<sup>1</sup>. <sup>1</sup>Departments of Medicine, Environmental and Occupational Health Sciences, Genome Sciences, and Center on Human Development and Disability, University of Washington, Seattle, WA; <sup>2</sup>Department of Neuroscience, University of Parma, Parma, Italy.

Paraoxonase-1 (PON1) status (PON1 level and presence of the Q192R polymorphism) is an important determinant of toxicity for chlorpyrifos (CPF) and its metabolite, CPF-oxon (CPO). We examined whether maternal PON1 status influences fetal toxicity associated with gestational CPO exposure by comparing CPO toxicity among PON1<sup>-/-</sup>, wild type (WT), and humanized transgenic mice expressing tgHuPON1R192 or tgHuPON1Q192. Pregnant mice were exposed dermally to 0, 0.50, 0.75 or 0.85 mg/kg/d CPO from gestational days 6-17, and sacrificed on day 18 to measure enzyme inhibition in maternal and fetal tissues and gene expression in the GD18 fetal brain using Affymetrix microarrays. Fetal body weights from the PON1<sup>-/-</sup> dams exposed to 0.75 mg/kg/d CPO were significantly lower compared to vehicle controls. Pregnancy rate, number of resorptions and presence of fetal abnormalities were not significantly different among treatment groups in all genotypes. In the dams, repeated CPO exposure was associated with inhibition of RBC acylpeptide hydrolase (APH), plasma carboxylesterase (CES), plasma butyrylcholinesterase (BChE), and brain acetylcholinesterase (AChE). Maternal tgHuPON1 had protective effects on inhibition of fetal brain AChE and plasma CES, which were both inhibited only in PON1<sup>-/-</sup> fetuses. In fetal plasma, BChE was inhibited in PON1<sup>-/-</sup> and tgHuPON1Q192, but not WT or

tgHuPON1R192 mice, supporting the hypothesis that the R allele is more protective. The relatively high sensitivity of BChE to CPO inhibition is relevant for human exposures. Using a mass spectrometric (MS)-based approach to identify OP-adducted active-site serines in plasma BChE, we identified a monoethyl phosphoserine aged adduct in the plasma of exposed agricultural workers that is consistent with CPF exposure. Supported by NIEHS ES04696, ES09883, ES07033, ES09601/EPA-R826886.

**PL 2449 Comparative Effects of Parathion and Chlorpyrifos on Extracellular Endocannabinoids: Influence on Cholinergic Toxicity.**

C. Pope<sup>1</sup>, L. Parsons<sup>2</sup> and J. Liu<sup>1</sup>. <sup>1</sup>Physiological Sciences, Oklahoma State University, Stillwater, OK; <sup>2</sup>Committee on the Neurobiology of Addictive Disorders, Scripps Research Institute, La Jolla, CA.

Parathion (PS) and chlorpyrifos (CPF) are organophosphorus insecticides (OPs). Acute subcutaneous exposure to either can elicit extensive acetylcholinesterase inhibition but cholinergic signs are relatively minimal following CPF compared to PS. Endocannabinoids (eCBs, e.g., anandamide [AEA] and 2-arachidonoyl glycerol [2-AG]) inhibit neurotransmitter release via presynaptic cannabinoid CB1 receptors. Paraoxon and chlorpyrifos oxon, active metabolites of PS and CPF, can block CB1 receptor binding and inhibit eCB-degrading enzymes. We hypothesized that differential effects on eCB signaling play a role in selective toxicity. Male rats were treated with vehicle, PS (27 mg/kg, sc) or CPF (280 mg/kg, sc) and toxicity evaluated 2 and 4 d later, just prior to insertion of hippocampal microdialysis probes and dialysate collection. eCBs were evaluated by LC-MS/MS. PS-treated rats showed extensive toxicity while CPF elicited few signs. AEA levels were elevated 2 and 4 d following either CPF ( $\approx$  4-fold) or PS (2-3 fold), while 2-AG levels were unaffected. If eCB-mediated inhibition of neurotransmitter release influences OP toxicity, blockade of CB1 receptors should alter functional responses. The CB1 antagonist AM251 (3 mg/kg, ip, 1 or 3 daily doses) had no effect on CPF toxicity. In contrast, a single dose of AM251 reduced PS-induced signs, and 3 daily doses further reduced toxicity. Although both CPF and PS can increase extracellular AEA levels, eCB signaling only appears to influence the expression of PS toxicity. This interpretation assumes an essential role for the CB1 receptor, whereas a number of recent studies suggest non-classical cannabinoid receptors mediate some eCB actions. CPF may potentially influence eCB signaling through a CB1-independent pathway. Together, these results suggest that targeting the eCB signaling pathway may have selective actions in the treatment of acute poisoning by different organophosphorus toxicants. (Supported by NIEHS R01 ES009119)

**PL 2450 Developmental Exposure to Chlorpyrifos Increases Accumulation of the Endocannabinoid Anandamide in the Brain in the Absence of Cholinesterase Inhibition.**

R. L. Carr, C. A. Nail, L. C. Mangum and M. K. Ross. Center for Environmental Health Sciences, Mississippi State University, Mississippi State, MS.

Traditionally, chlorpyrifos (CPS) mediates its toxicity through inhibition of cholinesterase (ChE). However, in recent years, the toxicological effects of developmental CPS exposure have been attributed to an unknown non-cholinergic mechanism of action. We hypothesize that the endocannabinoid system may be an important target because of its vital role in nervous system development. We have previously reported that repeated exposure to CPS results in greater inhibition of the fatty acid amide hydrolase (FAAH), the enzyme that metabolizes the endocannabinoid anandamide (AEA), than inhibition of either ChE or monoacylglycerol lipase (MAGL), the enzyme that metabolizes the endocannabinoid 2-arachidonoylglycerol (2-AG). This exposure resulted in the accumulation of AEA in the forebrain of juvenile rats, but even at the lowest dosage level used (1.0 mg/kg) ChE inhibition was still present. Thus, it was not clear if FAAH activity will be inhibited as dosage levels that do not inhibit ChE. To determine this, 10 day old rat pups were exposed daily for 7 days to either corn oil or 0.5 mg/kg CPS by oral gavage. At 12 hrs post-exposure, the activities of ChE, MAGL, and FAAH were determined in the forebrain, as well as the levels of the endocannabinoids AEA and 2-AG. There was no significant inhibition of the activities of ChE or MAGL and no significant change in the amount of 2-AG. In contrast, FAAH activity was significantly inhibited resulting in a marked accumulation of AEA in the forebrain. Although it has not been determined whether this alteration of endocannabinoid signaling can impact brain maturation, it does suggest a potential candidate for the non-cholinergic mechanism of action of CPS.

**PL 2451 Prenatal Dexamethasone Augments Neurobehavioral Teratology of Chlorpyrifos.**

E. D. Levin, M. Cauley, J. E. Johnson, H. Sexton, K. Gordon, F. J. Seidler and T. A. Slotkin. Psychiatry, Duke University Medical Center, Durham, NC.

Interactive effects of environmental toxicants and therapeutic drugs have received little attention despite the fact that there is often simultaneous or sequential exposure to these compounds. We evaluated whether dexamethasone, which is widely used in preterm labor, augments the subsequent developmental neurotoxicity of the organophosphate insecticide, chlorpyrifos. Pregnant rats were administered dexamethasone on gestational days 17-19 at a dose (0.2 mg/kg) mimicking that used in preterm labor; after birth the pups were given 1 mg/kg chlorpyrifos on postnatal days 1-4, a regimen just above the threshold for barely-detectable cholinesterase inhibition. Dexamethasone and chlorpyrifos each caused significant locomotor hyperactivity in the figure-8 apparatus in male but not female offspring, assessed during adolescence at 5 weeks of age. However, the group that received the combined exposure showed greater hyperactivity than with either agent alone. In controls, females showed greater activity than males, and consequently, the elevation in males with the combined exposure abolished the normal sex difference in locomotor activity. Both dexamethasone and the combined treatment reduced habituation to approximately the same degree. The combined exposure also had a greater effect on novelty-suppressed feeding behavior, pointing to a greater level of anxiety. Our results indicate that prenatal exposure to glucocorticoids used in preterm labor could create a subpopulation with enhanced vulnerability to developmental neurotoxins. (Support: USPHS ES010356)

**PL 2452 Oxidative Stress: A Mechanism-Based Biomarker of Organophosphorus Pesticide (OP)-Induced Neurotoxicity?**

S. N. Levoe<sup>1</sup>, D. Bruun<sup>1</sup>, S. Y. Gyu<sup>1</sup>, E. Napoli<sup>1</sup>, D. Milatovic<sup>2</sup>, C. Giulivi<sup>1</sup>, M. Aschner<sup>2</sup>, K. M. Lattal<sup>3</sup> and P. J. Lein<sup>1</sup>. <sup>1</sup>Molecular Biosciences, University of California Davis, Davis, CA; <sup>2</sup>Pediatric Toxicology, Vanderbilt University, Nashville, TN; <sup>3</sup>Behavioral Neuroscience, Oregon Health & Science University, Portland, OR.

OPs are widely used in agriculture and industry, and their prevalence has prompted concern for public and worker safety. However, predicting individuals at risk is challenging because standard biomarkers of exposure (cholinesterase inhibition and urinary metabolites) do not correlate well with neurotoxicity following chronic low-level OP exposures. This may reflect the fact that mechanisms by which such exposures cause neurotoxicity are independent of or in addition to cholinesterase inhibition. We are testing the hypothesis that oxidative stress contributes to learning and memory deficits reported in individuals exposed occupationally to OPs. To test this hypothesis, we are determining whether biomarkers of oxidative stress correlate with learning and memory deficits caused by chronic exposure to the OP chlorpyrifos (CPF) and whether treatment with antioxidants protects against chronic CPF neurotoxicity. We are using a rat model based on exposure data collected from 255 Egyptian agricultural workers responsible for applying CPF to cotton fields. Our preliminary data indicate that exposure to CPF (10 mg/kg/d, s.c.) for 21 d causes deficits in performance in contextual fear conditioning. This exposure paradigm also causes decreased mitochondrial ATPase activity and increased expression of PGE2 in the brain of CPF animals that precede the onset of behavioral deficits. Preliminary studies also suggest that administration of the antioxidant 2-acetylcylopentanone (2-ACP) attenuated oxidative stress; ongoing studies are investigating whether 2-ACP protects against the behavioral deficits caused by chronic CPF exposure. If successful, these studies will not only identify a novel biomarker of effect for chronic OP neurotoxicity but also suggest novel approaches for protecting workers occupationally exposed to OPs. Supported by NIH R01 ES016308.

**PL 2453 Interactions between Paraoxon and Polyhydroxyfullerenes Chemically Defined.**

G. Magnin-Bissel<sup>1</sup>, Z. Zhou<sup>2</sup> and M. Ehrlich<sup>1</sup>. <sup>1</sup>Virginia Tech, Blacksburg, VA; <sup>2</sup>Luna Nano Works, Danville, VA.

Polyhydroxyfullerenes decrease organophosphate (OP)-induced inhibition of acetylcholinesterase (AChE) in vitro and moderate OP toxicity in vivo (Toxicol in Vitro 25, 301, 2011; SOT abstract 2576, 2011; SOT abstract 942, 2012). Mechanisms contributing to the interaction of OP compounds such as paraoxon (PON) and fullerenes were evaluated. Formation of a covalent bond was ruled out by monitoring the release of p-nitrophenol and the decrease in concentration of PON by HPLC. Nuclear Magnetic Resonance (NMR) was used because hydroxylated fullerenes are known to make aggregates in aqueous media and PON could be trapped in these aggregates by non-covalent bonding resulting in host-guest interactions. Complexation of PON with two hydroxylated fullerenes was examined

after 15 min incubation with the C80 derivative containing gadolinium (GdTMSOH) and a C70 derivative (C70-OH) without any metal. Proton-decoupled phosphorus (31P) NMR spectra were recorded on a Bruker Advance III 600 NMR instrument. The experiments with PON and the fullerenes were run in deuterium oxide with phosphoric acid 0.04% as an internal reference. Results for GdTMSOH demonstrated a small upfield change in the chemical shift as the concentration of fullerene increased. However, due to strong interferences from the metal, further studies were done with the C70-OH fullerene. Plotting the variation its chemical shift versus the concentration of fullerene resulted in a binding isotherm curve that reached a plateau at 0.03 mole/l. The binding constant (Kb) calculated by dividing the intercept by the slope from the double reciprocal plot was determined to be 19 (mole/l)<sup>-1</sup>. The results suggest that the fullerenes act in a manner much like cyclodextrins, which have previously been shown to chemically interact with OP compounds, decreasing their capability to inhibit AChE (Carbohydrate Res. 345, 141, 2010; Euro J Med Chem. 40, 615, 2005; Toxicology 265, 96, 2010). Supported by the CounterACT Program, NIH OD and NINDS, grant NS063723.

## PL 2454 Conditional Toxicity Value (CTV) Predictor for Generating Toxicity Values for Data Sparse Chemicals.

J. Wignall<sup>1</sup>, E. Muratov<sup>1</sup>, D. Fourches<sup>1</sup>, A. Tropsha<sup>1</sup>, T. J. Woodruff<sup>2</sup>, L. Zeise<sup>3</sup>, N. Wang<sup>4</sup>, D. Reif<sup>5</sup>, V. Coglian<sup>4</sup>, W. A. Chiu<sup>4</sup>, K. Guyton<sup>4</sup> and I. Rusyn<sup>1</sup>. <sup>1</sup>University of North Carolina at Chapel Hill, Chapel Hill, NC; <sup>2</sup>University of California San Francisco, San Francisco, CA; <sup>3</sup>California EPA, Oakland, CA; <sup>4</sup>National Center for Environmental Assessment, US EPA, Washington DC; <sup>5</sup>National Center for Computational Toxicology, US EPA, Durham, NC.

Chemical hazard assessments necessarily vary based on data availability and the type of risk management decision they support. While much recent attention has been on use of high-throughput toxicological data for screening and prioritization, assessments that support toxicity guidance values or standards still rely on epidemiological and in vivo experimental data. Such assessments, including Integrated Science Assessments and Integrated Risk Information System Toxicological Reviews, are highly data-, time-, and resource-intensive, and cannot be realistically expected for most environmental chemicals. Thus various stakeholders and expert groups, including the National Research Council in Science and Decisions, call for "default approaches to support risk estimation for chemicals lacking chemical-specific information." This project aims to address this challenge through the Conditional Toxicity Value (CTV) Predictor. This tool uses chemical properties and limited experimental data to predict toxicity values, such as the reference dose (RfD) and concentration (RfC), oral slope factor (OSF), inhalation unit risk (IUR), or cancer potency value (CPV). CTV predictions combine QSAR, regression, and hybrid modeling, rely on a new comprehensive database of existing guidance values and experimental data, and incorporate OECD principles for model building and external cross-validation. QSAR models for predicting existing RfD values (which span 7 orders of magnitude) had an R<sup>2</sup> up to 0.46±0.07 and Mean Absolute Error of 0.67±0.03 (Log10 mg/kg/day). A tool that can predict a toxicity value within an order of magnitude fills a critical gap in the current risk assessment /risk management paradigm.

Disclaimer: The views expressed here are the authors' and not necessarily those of the US or California EPA.

## PL 2455 Application of the Threshold of Toxicological Concern (TTC) Decision Support Approach to Antimicrobial Pesticides.

R. Canady<sup>2</sup>, T. McMahon<sup>1</sup>, M. Cheeseman<sup>7</sup>, C. Yang<sup>5</sup>, S. Felter<sup>6</sup>, A. Boobis<sup>4</sup>, M. Martin<sup>3</sup>, V. Dellarco<sup>1</sup>, P. Price<sup>8</sup>, M. Lauferweiler<sup>6</sup> and K. Jacobs<sup>9</sup>. <sup>1</sup>US EPA, Washington DC; <sup>2</sup>ILSI RF, Washington DC; <sup>3</sup>US EPA, Research Triangle Park, NC; <sup>4</sup>Imperial College London, London, United Kingdom; <sup>5</sup>Altamira llc, Columbus, OH; <sup>6</sup>Procter & Gamble Company, Cincinnati, OH; <sup>7</sup>Stephoe and Johnson, Washington DC; <sup>8</sup>Dow Chemical Company, Midland, MI; <sup>9</sup>CFSAN, US FDA, College Park, MD.

A tiered decision support approach has been developed to apply existing knowledge of antimicrobial pesticides (AMs) to new AMs being considered for use. The approach is intended to inform product development and regulatory review processes so that antimicrobial pesticides and pesticide products can be targeted early in development and so that animal testing can be focused on those chemicals that need the most attention. Expert groups were convened comprised of scientists from non-government organizations, industry, academia, and government. The experts have 1) collected high quality data from studies submitted to EPA's Office of Chemical Safety and Pollution Prevention and the U.S. Food and Drug

Administration's regulatory review files and entered the data into a publicly accessible data set using the structure and approach of EPA's ToxRef Database; 2) developed a tiered decision framework for estimating systemic dose from dermal exposures so that comparisons could be made to the oral toxicity data available; 3) applied chemoinformatics techniques to evaluate whether and how to bridge the AM data set to the 3 non-cancer TTC values of Munro et al (1996); 4) also used chemoinformatics techniques to define classes of AMs within a TTC decision framework, and 5) developed a decision tree to guide consideration of new AMs with respect to likely toxicity for anticipated systemic dose of a given formulation and the chemoinformatics class into which it falls. We will present the method for data curation, chemoinformatics, rationale for the decision approach, and case examples of the use of the approach. This work will advance the science and practical use of computational toxicology in support of risk management decision making.

## PL 2456 The Navigation Guide As an Evidence-Based Medicine Methodology to Evaluate Human Health Effects of Environmental Chemicals: Perfluorooctanoic Acid (PFOA) and Fetal Growth.

E. Koustas<sup>1</sup>, J. Lam<sup>1</sup>, P. Sutton<sup>2</sup>, P. Johnson<sup>2</sup>, D. Atchley<sup>2</sup>, S. Sen<sup>3</sup>, K. Robinson<sup>4</sup>, D. Axelrad<sup>1</sup> and T. J. Woodruff<sup>2</sup>. <sup>1</sup>Office of Policy, US EPA, Washington DC; <sup>2</sup>Program on Reproductive Health and the Environment, University of California San Francisco, Oakland, CA; <sup>3</sup>Epidemiology and Biostatistics, University of California San Francisco, San Francisco, CA; <sup>4</sup>Medicine, Epidemiology, and Health Policy & Management, Johns Hopkins University, Baltimore, MD.

Rationale: Evaluating environmental health literature and determining the weight of evidence are critical for informing policy and health recommendations. The National Academy of Sciences has called for an enhanced systematic and transparent approach to risk assessment and scientific decision-making. The Navigation Guide was developed through a collaboration of 22 scientists to improve methods of research synthesis in environmental health. The methodology is based on best practices in evidence-based medicine and environmental health sciences and aims to systematically and transparently synthesize the evidence from toxicology and observational epidemiology studies.

Approach: To establish proof of concept, we applied the Navigation Guide to the question of the impact of exposure to perfluorooctanoic acid (PFOA) on fetal growth. Steps include: (1) Specify the study question; (2) Select the evidence; (3) Rate the quality and strength of the evidence.

Findings: We identified 24 human observational and 21 animal toxicological studies relevant to the study question. Study quality was assessed using a modified version of the Cochrane Collaboration's Risk of Bias tool. Preliminary meta-analysis of combinable studies suggests there may be small reductions in birth weight with increased PFOA exposure in animals and humans.

Implication: The case study illustrates that the Navigation Guide can be used to apply the rigor of systematic review methodology to questions in environmental health. As has been demonstrated in the clinical field, the adoption of a systematic and transparent method to synthesize the scientific evidence in the environmental health field would speed incorporation of research into decision-making.

## PL 2457 Incorporating Population Variability and Susceptible Subpopulations into Dosimetry for High-Throughput Toxicity Testing.

B. A. Wetmore<sup>1</sup>, J. F. Wambaugh<sup>2</sup>, H. J. Clewell<sup>1</sup> and R. S. Thomas<sup>1</sup>. <sup>1</sup>The Hamner Institutes for Health Sciences, Research Triangle Park, NC; <sup>2</sup>National Center for Computational Toxicology, US EPA, Research Triangle Park, NC.

Xenobiotic clearance can vary widely across age-based or ethnic subpopulations due to differences in metabolic enzyme abundances and activities. A strategy to measure population-specific hepatic clearance values across a wide range of chemicals would allow pharmacokinetic variability due to age, ethnicity, and other factors to be incorporated into in vitro toxicity screening data. Metabolic clearance of ToxCast chemicals selected based on LC-MS method compatibility and exposure estimate availability were measured in vitro using 13 cytochrome P450 (CYP) and 5 UDP-glucuronosyltransferase (UGT) recombinantly expressed isoforms. Together with plasma protein binding, these isoform-specific clearance rates were then incorporated into an in vitro-to-in vivo extrapolation (IVIVE) modeling tool, Simcyp. The modeling tool accounts for known differences in isoform abundances among various age- or ethnic-based subpopulations to estimate the daily oral dose for each subpopulation, called the oral equivalent dose, necessary to produce steady-state in vivo blood concentrations equivalent to in vitro AC50 values across the ~600

ToxCast endpoints. CYPs 3A4, 3A5, 2C9, and 2C19 were the most active enzymes, contributing to the clearance of all of the chemicals tested. The subpopulation-specific oral equivalent dose values spanned ranges of 1.2 to 6.7-fold for the chemicals assessed. For most chemicals, the oral equivalent dose values for pediatric subpopulations fell closer to the estimated exposures than those derived for an adult population. Generation of these age-specific oral equivalents also affords direct comparison to age-specific exposure estimates in USEPA regulatory documents. This study demonstrates the feasibility and value of using isozyme-specific clearance data to tailor dosimetric values for a wide range of subpopulations. This abstract does not necessarily reflect EPA policy.

**PL 2458 Extrapolating *In Vitro* Embryotoxicity Data Toward *In Vivo* Exposure Levels Using a Combined *In Vitro*-Physiologically-Based Kinetic Modeling Approach.**

M. Strikwold<sup>1,2</sup>, R. Woutersen<sup>1,3</sup>, B. Spenkelink<sup>1</sup>, I. Rietjens<sup>1</sup> and A. Punt<sup>1</sup>.  
<sup>1</sup>Division of Toxicology, Wageningen University, Wageningen, Netherlands; <sup>2</sup>Van Hall Larenstein, University of Applied Sciences, Leeuwarden, Netherlands; <sup>3</sup>TNO Innovation for Life, Zeist, Netherlands.

*In vitro* assays play an important role in screening chemicals for their toxic potency and prioritizing them for further toxicity testing. Most of these *in vitro* assays are not suitable for a quantitative risk characterization as they lack *in vivo* kinetic processes. To overcome this limitation, the present research aimed at combining *in vitro* toxicity data with physiological based kinetic (PBK) modeling to predict *in vivo* exposure levels. In order to contribute to the 3Rs principle for the replacement, reduction and refinement of animal testing in the most optimal way the required PBK models were developed on the basis of only *in vitro* and *in silico* data and data available from literature. Phenol was selected as the model compound and the endpoint of interest concerns embryotoxicity. At first, the embryotoxicity of phenol was evaluated *in vitro* using the embryonic stem cell test (EST), revealing a concentration dependent inhibition of differentiation into beating cardiomyocytes. In a second step, PBK models were developed for rat and human using *in vitro* derived kinetic constants, *in silico* derived physico-chemical parameters and literature derived physiological data. After evaluating the performance of the PBK models, the *in vitro* concentration-response information from the EST served as an input in the PBK model, thereby generating an *in vivo* dose-response curve from which a Point of Departure for risk assessment could be derived. Finally, *in vivo* embryotoxic effect levels available from literature were used to evaluate this combined *in vitro*-PBK approach. In summary, this study shows how combining different alternatives to animal testing like *in vitro* toxicity testing and PBK modeling will enlarge their application from screening and prioritizing of chemicals toward deriving safe exposure levels for the risk assessment of chemicals.

**PL 2459 A Genomics-Based Determination of Relative Potencies of Dioxin-Like Compounds in Primary Human Hepatocytes.**

J. Rowlands<sup>1</sup>, R. Budinsky<sup>1</sup>, M. B. Black<sup>2</sup>, R. D. Wolfinger<sup>3</sup>, D. Cukovic<sup>4</sup>, S. Salagrama<sup>4</sup>, A. Dombkowski<sup>4</sup> and R. S. Thomas<sup>2</sup>. <sup>1</sup>The Dow Chemical Company, Midland, MI; <sup>2</sup>The Hamner Institutes for Health Sciences, Research Triangle Park, NC; <sup>3</sup>SAS Institute Inc., Cary, NC; <sup>4</sup>Institute of Environmental Health Sciences, Wayne State University, Detroit, MI.

Toxic equivalency factors (TEFs) for dioxin-like compounds are predominantly derived from relative potency (REP) determinations of endpoints such as enzyme activity from animal studies and *in vitro* studies in immortalized animal cells. Currently, REPs based on gene expression changes have not been considered when deriving TEF values. Moreover, data from humans and human cells are not included in the REP database for deriving TEF values. In this study, primary human hepatocytes were treated for 24 hours with 11 concentrations of 2,3,7,8-tetrachlorodibenzo-p-dioxin, 2,3,4,7,8-pentachlorodibenzofuran, or 2,3,7,8-tetrachlorodibenzofuran ranging from 0.00001-100 nM. Gene expression changes were analyzed using ANOVA to assess the relative contributions of concentration, congener, and the interaction between concentration and congener. A total of 1,443 genes showed significant changes with concentration (FDR < 0.05 and fold-change + 1.5 in at least one concentration for one congener). Of these, 399 were significant for both concentration and congener effects indicating parallel concentration response curves with differences in potency. Pathway enrichment analysis was performed on the 1,443 genes differentially expressed by concentration. The top 10 most enriched pathways included several nuclear receptors, immune response, and cell adhesion pathways. A focused assessment of the benchmark dose values for signaling pathways in the modes of action for DLC-induced effects can be used to determine more relevant REPs used by the World Health Organization (WHO) to

derive TEF values. The addition of human cells to the WHO database could provide meaningful measures of relative potency and provide quantitative data to reduce TEF uncertainty in human health risk assessments.

**PL 2460 Aryl Hydrocarbon Receptor Mode-of-Action and Human Relevance Framework for XDE-729 Methyl-Induced Rodent Liver Effects.**

D. L. Eisenbrandt<sup>2</sup>, L. A. Murphy<sup>1</sup>, N. J. Stagg<sup>2</sup>, M. J. LeBaron<sup>1</sup>, V. A. Marshall<sup>1</sup>, A. T. McCoy<sup>1</sup>, L. Kan<sup>1</sup>, D. R. Boverhof<sup>1</sup>, M. Bartels<sup>1</sup>, R. Billington<sup>2</sup> and R. J. Rasoulpour<sup>1</sup>. <sup>1</sup>The Dow Chemical Company, Midland, MI; <sup>2</sup>Dow AgroSciences LLC, Indianapolis, IN.

XDE-729 methyl, a novel herbicide in development, induces rodent liver enlargement, hypertrophy, and hyperplasia via an aryl hydrocarbon receptor (AhR) mediated mode-of-action (MoA) with the following key events: 1) presystemic liver exposure to XDE-729 methyl, 2) AhR activation with associated liver hypertrophy, leading to 3) hepatocellular proliferation. For key event 1, low levels of XDE-729 methyl are present in the liver after dietary exposure; however, XDE-729 methyl is rapidly metabolized in the liver to primarily XDE-729 acid, which is not an AhR activator, and excreted in the urine. For key event 2, AhR activation, measured by Cyp1a1 transcript induction occurred at dose levels of  $\geq 50$  mg/kg/day XDE-729 methyl and correlated with liver hypertrophy. For key event 3, hepatocellular proliferation was observed with exposure to 261 mg/kg/day XDE-729 methyl. A threshold for AhR activation and liver effects occurs at 10 mg/kg/day XDE-729 methyl, the no-observed-adverse-effect level (NOAEL) from the rat 90-day toxicity study. Collectively, the data provides a high level of confidence that XDE-729 methyl induces rodent liver effects through an AhR-mediated MoA at doses  $\geq 10$  mg/kg/day XDE-729 methyl. The AhR pathway is conserved across species and prototypical AhR ligands are activators of both human and rodent AhR; however, human AhR binding affinity for prototypical AhR ligands is quantitatively lower than rodent AhR. XDE-729 methyl is rapidly metabolized to XDE-729 acid, which does not activate AhR, and does not bioaccumulate in the rat liver. XDE-729 methyl exposure does not result in sustained activation of the AhR pathway and hepatic effects are transient and reversible. Based on the above, a margin of exposure risk assessment using the 10 mg/kg/day NOAEL from the rat 90-day toxicity study to derive the chronic reference dose/acceptable daily intake (cRfD/ADI) for XDE-729 methyl is protective of human health.

**PL 2461 Estimation of Cumulative Risk from Exposure to Phthalates Using NHANES Exposure Data and an *In Vitro* Potency Assay.**

P. Balbuena, J. Campbell, H. J. Clewell and R. A. Clewell. The Hamner Institutes for Health Sciences, Research Triangle Park, NC.

Endocrine active phthalates reduce testosterone synthesis in fetal rat testes, interfering with male sexual development at high doses. As they share the same mode of action, it is logical that a phthalate risk assessment should account for cumulative exposure. Lack of potency data *in vivo* limits the derivation of a cumulative risk estimate. We illustrate an approach using *in vitro* pharmacodynamic data together with NHANES exposure estimates to predict human risk from multiple phthalates. First, we developed a rat Leydig tumor cell line (R2C) *in vitro* assay to assess testosterone inhibition with several environmentally relevant phthalate metabolites: monobutyl (MBP), monoethylhexyl (MEHP), monoethyl (MEP), monomethyl (MMP), monoethyl (MOP), monobenzyl phthalate (MBzP) and two oxidative metabolites of MEHP (5-Ox-MEHP, 5-OH-MEHP). Effects of these chemicals on steroidogenesis *in vitro* were highly consistent with *in vivo* studies. *In vitro* IC50 values were used to derive relative potency factors (RPFs) in relation to MBP. These RPFs were used with the 2005 NHANES urine data to calculate relative risk estimates for each phthalate at the 50th or 95th percentile (exposure). Estimates for individual phthalates were then combined to obtain a dibutyl phthalate (DBP) equivalent risk estimate (mg DBP/kg/day). This *in vitro* predicted cumulative risk estimate was then compared to the USEPA *in vivo* derived reference dose (RfD) for DBP. At the 50th percentile DBP accounted for 8% of total exposure but represented 70% of the total risk of all phthalates. At the 95th percentile, the other phthalates contributed more to the cumulative risk. Cumulative potency weighted exposure for all phthalates was markedly lower than the USEPA RfD for DBP (0.1 mg/Kg BW/day), whether calculated for exposure at the 50th (0.0007 mg/kg/day) or 95th (0.004 mg/kg/day). Margin of exposure was 148.5 and 27.4 for the 50th and 95th percentile respectively. The analyses indicate the risk from exposure to phthalates is below current RfDs, even considering multiple phthalates.

## **R** 2462 Nonhuman Primate Sexual Maturity: What Is the Capacity to Endure Uncertainty?

D. Blanset<sup>1</sup>, D. M. Creasy<sup>2</sup>, G. F. Weinbauer<sup>3</sup>, J. L. Bussiere<sup>4</sup>, K. P. Hatfield<sup>5</sup> and J. S. Moffitt<sup>1</sup>. <sup>1</sup>Nonclinical Drug Safety US, Boehringer Ingelheim Pharmaceuticals Inc, Ridgefield, CT; <sup>2</sup>Huntingdon Life Sciences, East Millstone, NJ; <sup>3</sup>Covance Inc, Muenster, Germany; <sup>4</sup>Amgen Inc, Thousand Oaks, CA; <sup>5</sup>US FDA-CDER, Silver Spring, MD.

Evaluation of reproductive toxicity in regulatory studies relies on the use of sexually mature animals. This often involves the use of nonhuman primates (NHP) when lower order species are pharmacologically irrelevant. However, the decision on whether to utilize mature NHP and the criteria used to establish sexual maturity is anything but standardized. Several factors contribute to these differing opinions. Sexual maturity can occur over a wide range of ages and body weights and historical methods of predicting sexual maturity have not always correlated with the histopathological appearance of the gonads at necropsy. Evaluation of toxicity in the reproductive organs of pre/peripubertal animals is often difficult, given that the histology of the maturing reproductive organs may resemble the degenerative changes induced by reproductive toxicants in the sexually mature adult. Finally, there is a lack of consensus on the toxicological relevance and interpretation of the various possible reproductive endpoints. All of these factors result in a complicated balancing act: Ethically weighing the limited availability, high costs, and relevance of incorporating sexually mature NHP in toxicology studies against effective and meaningful evaluation of reproductive risks. This roundtable will discuss the challenges of assessing toxicity in immature vs. peripubertal vs. mature NHP, screening methods for identifying sexually mature NHP, factors that influence sexual maturity, and case studies where sexual maturity impacted the study interpretation. Overall, this session seeks to provide an opportunity for stakeholders to review the current state of the art and exchange views on appropriate paths forward to encourage ethical use of animals, while preserving appropriate risk assessments.

## **IS** 2463 Exposure Science in the 21st Century: Perspectives from the NAS and What It Means for Toxicology.

L. S. Birnbaum<sup>1</sup> and J. Orme-Zavaleta<sup>2</sup>. <sup>1</sup>NIEHS, Research Triangle Park, NC; <sup>2</sup>US EPA, Research Triangle Park, NC.

In 2010, US EPA with additional support from NIEHS, requested the National Academy of Sciences (NAS) to develop a long-range vision for exposure science in the 21st century and a strategy for implementing this vision over the next twenty years. Exposure science is the bridge between the sources of chemical, physical and biological agents and ecological and human health. Exposure science is critical for predicting, preventing, and reducing human health and ecosystem risks. The report, *Exposure Science in the 21st Century: A Vision and a Strategy*, was released September 7 by the NAS National Research Council. This report along with three other NAS reports, *Toxicity Testing in the 21st Century*, *Science and Decisions: Advancing Risk Assessment* and *Sustainability and the US EPA*, chart the future directions for using innovative technology and scientific advances to better understand environmental impacts on human and ecological health. The report outlines a framework for advancing exposure science to study how humans and ecosystems interact with chemical, biological, and physical agents in their environments. Key visions in the report in are to develop a universal exposure-tracking framework with a focus on preventing and mitigating adverse exposures. This will include the application of systems science to understand and characterize exposures across time, space, and biological scale.

## **IS** 2464 Regulatory-Based Nanotoxicology: Evolving National Strategies, and Research to Address Engineered Nanomaterial Health Risk Assessments.

W. K. Boyes<sup>1</sup>, S. Nadadur<sup>2</sup>, P. Sayre<sup>3</sup>, V. Castranova<sup>4</sup>, K. Dreher<sup>1</sup>, P. C. Howard<sup>5</sup> and D. B. Warheit<sup>6</sup>. <sup>1</sup>ORD, US EPA, Research Triangle Park, NC; <sup>2</sup>NIEHS, NIH, Research Triangle Park, NC; <sup>3</sup>ORD, US EPA, Washington DC; <sup>4</sup>NIOSH, CDC, Morgantown, WV; <sup>5</sup>NCTR, US FDA, Jefferson, AR; <sup>6</sup>Haskell Global Centers, DuPont, Wilmington, DE.

Engineered nanomaterials are increasingly being developed and incorporated into a variety of products and applications. However, the full development of nanotechnology is hampered by an uncertainty regarding their environmental, health and safety implications, and how these issues will be addressed by responsible regulatory agencies at the federal and state levels. Novel nanoscale materials present a number of scientific and technical challenges for assessing their potential health implications including: exposure and material characterization; adequacy of conventional toxicity testing methods/guidelines; dose metric(s) across the exposure-dose-effects

paradigm; and the role of alternative testing approaches to assess their toxicity. This session will bring together scientists from scientific advisory bodies, regulatory agencies and the private sector to present/discuss research needs, strategies, approaches and findings regarding the health effects testing of engineered nanomaterials and nano-enabled products as it relates to regulatory mission(s). Key topics include: assessing nanomaterial toxicity for regulatory and risk assessment applications; the status or role of alternative test methods to screen or prioritize nanomaterials for in vivo toxicity testing, and the extent to which harmonized testing can be achieved for these novel materials. Each speaker will have 10-12 minutes to highlight agency/institutional approaches and regulatory actions regarding the potential for health effects from engineered nanomaterials. The session will conclude with a 15 minute general discussion period. The overall goal is to provide participants with a view of the status of the development of nanomaterial toxicological assessments that would be sufficient to evaluate health and safety for regulatory agencies.

## **EC** 2465 Toxicological Writing for Industrial and Regulatory Audiences.

C. J. Amuzie<sup>1,2</sup> and M. La Merrill<sup>3</sup>. <sup>1</sup>Department of Pathology, MPI Research, Mattawan, MI; <sup>2</sup>Department of Pathobiology and Diagnostic Investigations, Michigan State University, East Lansing, MI; <sup>3</sup>Department of Preventive Medicine, Mount Sinai School of Medicine, New York, NY.

Excellence in scientific and technical writing leading to high-quality publications, a skill set developed and refined from graduate training through early career in toxicology, is one key trait that can lead to a successful career as a toxicologist. Some academic institutions have programs that support scientific and technical writing for their staff. However, the majority of toxicologists (80%) are employed outside academia, predominately within biopharmaceutical and chemical industries, government, and contract research organizations. Graduates from academic programs that train in writing might acquire skills related to preparation of dissertations, grant proposals, and manuscripts for scientific peer-reviewed journals. The skills acquired from this training, when existent, does not necessitate a smooth transition to a successful career outside academia. Thus early-career toxicologists are sometimes unaware of, or otherwise unprepared for, technical writing assignments that occur in industrial and regulatory toxicology. In addition, different writing skills are required for clear and concise communication of toxicological results to nontoxicologist stakeholders. Therefore, an interactive workshop that evaluates the challenges presented by, and the skills required for, toxicological writing outside academia will be of great use to the majority of graduate students, postdoctoral trainees, and early-career toxicologists. Four speakers from the pharmaceutical industry, the chemical industry, a government regulatory agency, and a contract research organization will review the type(s) of technical writing required within their setting. Notably, they will extensively highlight common mistakes and discuss valuable strategies and tools to avoid these mistakes through interactive exercises using provided writing examples.

## **S** 2466 From Immunotoxicity to Nanotherapy: The Effects of Nanomaterials on the Immune System.

M. J. Smith<sup>1,2</sup>, D. R. Germolec<sup>3</sup> and N. J. Walker<sup>3</sup>. <sup>1</sup>Pharmacology and Toxicology, Virginia Commonwealth University, Richmond, VA; <sup>2</sup>ImmunoTox, Inc, Richmond, VA; <sup>3</sup>National Toxicology Program, Research Triangle Park, NC.

The potential for human exposure to the diverse and ever-changing world of nanomaterials has raised concerns about the ability of these materials to influence health and disease. The small size of nanomaterials makes them a prime target for interaction with the cells of the immune system. Exposure to nanomaterials (inhalation, dermal, oral, parenteral) can affect multiple components of the immune system. For example, a single respiratory exposure to titanium dioxide nanoparticles can significantly increase the antibody-forming cell response to sheep erythrocytes, suggesting the possibility of nanomaterial interactions with lymphocytes and/or antigen-presenting cells. Furthermore, the cells of the innate immune system, including mast cells and the cells of the mononuclear phagocytic system, are also potential targets following nanomaterial exposure. A varied spectrum of effects, including inflammation, hypersensitivity, and immunomodulation, may then occur, via mechanisms which have yet to be elucidated. While incidental exposure may be undesirable, nanomaterials and nanomedicines engineered for various clinical applications provide opportunities to develop therapies that may or may not intentionally target the immune system. The interplay between nanomaterials and the immune system and the pharmacokinetic and phenotypic responses that result from these interactions are therefore critical factors that dictate the balance between toxicity and clinical efficacy of nanomedicines.

## **S** 2467 Overview of Concepts and Strategies Needed for Assessing the Safety of Nanoscale Materials.

N. J. Walker. *National Toxicology Program, NIEHS/NIH, Research Triangle Park, NC.*

In recent years there has been considerable research examining the potential utility of nanoscale materials and nanostructures in commercial and biomedical applications. Nanoscale materials (nanomaterials, nanoparticles), are a broadly defined set of substances that have at least one critical dimension less than 100 nanometers. The same novel chemical and physical properties that make nanomaterials useful also make their interactions with biological systems difficult to predict and evaluate in traditional toxicity models. The diversity in composition, size, surface coatings, and physico-chemical properties even within classes of "similar" nanomaterials can make translation of findings from one nanomaterial to another problematic. On the other hand though, testing of each nanomaterial individually and what change in a physicochemical property constitutes creation of a "new" material, remains uncertain. Over the past years there has been considerable effort looking at developing guidance for assessing safety of nanomaterials. Some of the key considerations include; effective characterization of physicochemical properties of nanomaterials not only in the bulk phase but also within the toxicological test system; use of in vitro biological responses and shorter term in vivo studies of panels of nanomaterials to develop structure activity relationships for predicting hazard and guide prioritizing further targeted in depth testing; development of best practices to reduce potential interference of a nanomaterial with the test systems.

## **S** 2468 Molecular Dynamics Simulations with Advanced Sampling Techniques to Study Nanoparticle-Membrane Interactions.

M. A. Philbert<sup>2</sup>, P. Elvati<sup>1</sup>, K. A. Russ<sup>2</sup> and A. Violi<sup>1</sup>. <sup>1</sup>Mechanical Engineering, University of Michigan, Ann Arbor, MI; <sup>2</sup>Toxicology Program, University of Michigan, Ann Arbor, MI.

Classical toxicology assessments consider bulk transport of particulate matter into discrete organelles of living cells as the primary means of nanoparticle (NP) toxicity. However, little is known about the potential of low-level exposure to alter biophysical functions (membrane form/function). Atomistic simulations, such as molecular dynamics (MD), can provide mechanistic information that is hard to measure experimentally. They may be used to validate theories derived from indirect experimental analysis, but the results of MD simulations are meaningful only if the run is long enough to visit all energetically relevant configurations. Well-tempered metadynamics can accelerate system dynamics allowing the analysis of processes that can take several seconds or hours to occur in real systems. Classically biased MD simulations were used to reconstruct the free energy landscapes of the mechanisms of NP entry into biological cells, thus accelerating the sampling of rare events and allowing exploration of potentially new biologically relevant reaction pathways. Results show that pristine C<sub>60</sub> resides preferentially in the aliphatic region of the lipid bilayers composed of POPC and cholesterol. With increasing cholesterol concentration, the minimum of the free energy profile moves towards the interface with water, showing a tendency of C<sub>60</sub> to move away from the membrane center. C<sub>60</sub> motility inside the hydrophobic region is not limited by any relevant thermodynamic barriers at body temperature, but the energetic cost to leave the membrane is system-dependent and varies from 10 to 20 k<sub>B</sub>T. Charges (C<sub>60</sub><sup>2-</sup>) or hydroxyl groups (C<sub>60</sub>(OH)<sub>24</sub>) make the region where the lipid heads are solvated by water the most favorable position for these species. These studies make plausible the potential for intramembranous mechanisms of NP toxicity in immune and other mammalian cells. Supported by ES08846, NIEHS NCNHR U01 (MAP), CBET 0644639 (AV), 1 U02 ES020128-01 (KR), T32-ES007062-26 (KR).

## **S** 2469 Evaluating the Local and Systemic Immunomodulatory Effects of Nanomaterials.

M. J. Smith<sup>1,2</sup>, D. R. Germolec<sup>3</sup>, C. E. McLoughlin<sup>1,4</sup>, W. Auttachoat<sup>1</sup> and K. L. White<sup>1,2</sup>. <sup>1</sup>Pharmacology and Toxicology, Virginia Commonwealth University, Richmond, VA; <sup>2</sup>ImmunoTox, Inc, Richmond, VA; <sup>3</sup>National Toxicology Program, Research Triangle Park, NC; <sup>4</sup>Biomedical Engineering, Virginia Commonwealth University, Richmond, VA.

The small size of nanomaterials (NM) makes them a prime target for interaction with the immune system following their uptake, processing, and presentation to lymphocytes by antigen-presenting cells. Traditional in vivo testing strategies have been used to evaluate NM-mediated immunotoxicity. The varied routes of exposure to NM (dermal, oral, inhalation, parenteral), as well as particle size, can produce differing immune effects, including contact hypersensitivity as well as local or systemic effects. For example, a single pharyngeal aspiration of anatase TiO<sub>2</sub> nanoparticles (< 25 nm) produced an enhanced antibody-forming cell response to

sheep erythrocytes, while TiO<sub>2</sub> microparticles (< 45 µm) produced no such effect. Subcutaneous, but not dermal, exposure to anatase nano-TiO<sub>2</sub> for 3 days increased cell proliferation in the draining lymph nodes, while oral exposure for 28 days was non-immunotoxic. Inhalation of 1.0 and 0.05 µm C60 fullerene for 13 weeks did not affect the systemic immune response, although inflammatory cytokines (MCP-1, MIP-1α) in the bronchoalveolar lavage fluid were increased for the 1.0 µm C60 only. Subcutaneous implantation of sub-micron electrospun biodegradable polycaprolactone materials in the ventral quadrant for 28 days had minimal effects on the immune system, suggesting that this material may have the potential for use in a variety of clinical applications. Nanomedicines intended for clinical applications unrelated to the immune system must be examined for the possibility that they might produce unintentional or unanticipated immune effects. However, depending upon the application (e.g. local anti-inflammatory drug delivery), effects on the immune system may be desirable.

## **S** 2470 Mast Cell Directed Nanomaterial Toxicity.

J. M. Brown<sup>1</sup>, X. Wang<sup>1</sup>, R. Urankar<sup>2</sup>, C. J. Wingard<sup>2</sup> and P. Karwa<sup>1</sup>. <sup>1</sup>Pharmacology & Toxicology, East Carolina University, Greenville, NC; <sup>2</sup>Physiology, East Carolina University, Greenville, NC.

Concern about the use of engineered nanomaterials (ENMs) has increased significantly in recent years due to potentially hazardous impacts on human health. Mast cells are critical for innate and adaptive immune responses, often modulating allergic and pathogenic conditions. Mast cells are well known to act in response to danger signals through a variety of receptors and pathways including IL-33 and the IL-1 like receptor ST2. We have examined the involvement of mast cells and the IL-33/ST2 axis in pulmonary and cardiovascular responses to ENMs including multi-walled carbon nanotubes (MWCNT) and silver nanoparticles (AgNP). We have utilized C57BL/6 mice, mast cell deficient mice (KitW-sh), KitW-sh mice reconstituted with wild-type or ST2-/- mast cells and ST2-/- mice to assess systemic and pulmonary inflammatory responses as well as cardiac ischemia-reperfusion (IR) injury responses following ENM exposure. In addition, we have used an in vitro mast cell model to screen for the ability of ENMs to directly induce mast cell degranulation. We have found that mice with normal mast cell populations (C57BL/6 and mast cell reconstituted KitW-sh), exhibit significant ENM directed systemic and pulmonary inflammation, fibrosis, altered lung function and exacerbated IR injury. In contrast, these toxicological effects of ENMs were not observed in mice deficient in mast cells (KitW-sh) or mice with mast cells unable to respond to IL-33 (ST2-/- mast cell reconstituted KitW-sh mice). Lastly, we have established that certain ENMs are capable of inducing mast cell activation in vitro. Our findings establish for the first time that mast cells and the IL-33/ST2 axis orchestrate adverse immune effects to ENMs giving insight into a previously unknown mechanism of toxicity and providing a realistic therapeutic target. The use of mast cells and the IL-33/ST2 axis as a screening tool for ENM toxicity and in the preclinical development of nanomedicines will be discussed.

## **S** 2471 Phenotypically Profiling the Factors Affecting the Pharmacokinetics and Pharmacodynamics of Nanoparticle Agents in Preclinical Models and in Patients.

W. Zamboni, W. Caron, G. Song, P. Kumar, J. Lay and P. Gehrig. *Eshelman School of Pharmacy, University of North Carolina at Chapel Hill, Chapel Hill, NC.* Sponsor: M. Smith.

Carrier-mediated agents consist of nanoparticles, nanosomes (nanoparticle sized liposomes) and conjugates. The theoretical advantages for using carrier-mediated drugs, including increased drug solubility, prolonged duration of exposure, selective delivery of entrapped drug to the site of action, and improved therapeutic index. Pegylated nanosomal formulations contain lipid conjugated to polyethylene glycol. The disposition of encapsulated drug is dictated by the composition of the carrier, thus altering the pharmacokinetic (PK) profile of the drug. A proposed clearance pathway of carrier agents is the monocytes and macrophages of the mononuclear phagocyte system (MPS). Our studies suggest there is a bi-directional interaction between nanosomal agents and the MPS. However, potential factors associated with clearance of carrier agents in patients and preclinical animal models have not been extensively evaluated. Standard allometric scaling approaches for nanosomal agents did not scale across all species. In addition, preliminary studies suggest that there is high variability in the function of the MPS in animal models and in patients. Thus, new methods for allometric scaling and measures of MPS function need to be developed for carrier-mediated agents. In addition, the most appropriate animal models for toxicology and pharmacology of carrier agents needs to be identified. Novel methods for phenotypically profiling the factors affecting the pharmacokinetics and pharmacodynamics of nanoparticle agents in preclinical models and in patients will be presented.

**S 2472 Modeling Human Genetic Variability and Susceptibility in the Laboratory.**

R. Woychik<sup>1</sup> and D. Threadgill<sup>2</sup>. <sup>1</sup>NIEHS, Research Triangle Park, NC; <sup>2</sup>North Carolina State University, Raleigh, NC.

Within a population of genetically heterogeneous individuals, a range of responses is observed for environmental exposures. The observed variability in response is attributable to extrinsic and intrinsic factors, including individual differences in exposure to environmental stressors and genetic/epigenetic heterogeneity, respectively. Current risk assessment practice is to account for interindividual variability with default uncertainty factors (e.g., a ten-fold decrease in allowable exposure to protect the most sensitive subpopulations), even though these defaults are seldom supported by scientific evidence. Advances in exposure science and molecular genetics are greatly increasing our ability to characterize intrinsic differences among individuals in their exposure and response to toxicants. This symposium highlights several novel and exciting approaches in safety evaluation that utilize recent advances in genetics. First, recent collaborative efforts in the complex traits community have led to the development of several new, powerful mouse resources that greatly facilitate the identification of allelic variants of genes associated with differential response to toxic exposure through genotype-phenotype associations. Second, several laboratories, including the National Toxicology Program, have begun applying these new mouse models of human population diversity to studies on the molecular mechanisms of interindividual variability in chemical metabolism and toxicity. Third, the ability to generate induced pluripotent stem (iPS) cells from population-derived human cell resources, as well as the availability of embryonic stem (ES) and iPS cells from mouse strains, makes it possible to conduct *in vitro* studies to investigate interindividual differences in resistance and susceptibility to xenobiotic exposures. Ultimately, these new approaches should greatly enhance our ability to characterize variability in response to toxicants and to identify those genes and pathways that contribute significantly to the observed differential responses to environmental exposures in humans.

**S 2473 Modeling Genetic Heterogeneity to Understand Susceptibility to Chemical Combinations: A Mouse Population-Based Study Using Trichloroethylene (TCE) and Inorganic Arsenic (iAs).**

D. Threadgill. North Carolina State University, Raleigh, NC.

Using the results of a recent mouse population-based study that investigated via dose response curves the differential toxicity to TCE and iAs singly and in combination, this presentation illustrates how genetic heterogeneity can be modeled to understand individual susceptibility to combinations of chemicals. The results demonstrate that these chemicals can elicit additive and synergistic toxicities in susceptible individuals. Furthermore, the target organs in the genetically heterogeneous mouse populations are similar to those in humans, indicating that susceptibility alleles in the mouse population model will inform on human susceptibility.

**S 2474 The Use of Population-Based Inbred Panels and Diversity Outbred Mouse Models to Explore Individual Variability and Toxicity to Benzene.**

J. E. French. Division of the National Toxicology Program, NIEHS, Research Triangle Park, NC.

Benzene is hematotoxic, genotoxic, and tumorigenic to the lymphohematopoietic systems in both laboratory animals and humans. Results from NTP population-based mouse model studies show significant individual variability in benzene ADME/TK and levels of DNA damage at human relevant exposures. The results of these studies illustrate how individual variability in genetically defined populations may be used to identify genetic variants associated with differences in toxicokinetics, resistance or susceptibility to a toxicant, and to identify causally related mechanisms of toxicity. Benchmark dose models can be used on quantitative data to determine a reference dose that will aid in the quantification of uncertainty factors and, possibly, eliminate default assumptions in risk assessment. In addition, by identifying multiple genetic variants through genotype-phenotype associations with significant size effects, networks and pathways may be predicted that are statistically anchored to toxicity phenotypes and functionally-validated through the use of recombinant inbred mice (Collaborative Cross) cell-based assays, *in vivo* targeted testing, and molecular biology using reverse genetics. Across species extrapolation is enhanced by identifying variants that are orthologous between mouse and human and if there are associated in orthologous networks or pathways. In combination with high-throughput and high content assays validated by *in vivo* targeted testing, these new tools will provide a new paradigm for toxicology and exposure related diseases.

**S 2475 Modeling Genetic Variability in Response to Environmental Toxicants Using Mouse ES Cells *In Vitro*.**

T. Choi. Predictive Biology, Inc., Carlsbad, CA.

A genetically diverse panel of ES cell lines have been produced from inbred, F1, and outbred mice, and this panel has been used to investigate the role of strain background on variable response to environmental toxicants. An example of such a study is an investigation of how genetic background and environmental factors interact in the onset or severity of arrhythmia, and how these interactions may be involved in the cardiotoxicity of environmental toxicants. The ultimate goal is to discover novel mechanisms, targets, and chemical structures underlying variability in cardiotoxic response. The approach is to conduct large scale, high throughput *in vitro* screens using cardiomyocytes derived from genetically diverse ES or iPS cells to interrogate gene x toxicant interactions *in vitro*. Toward this end, a large panel of genetically diverse mouse ES lines as well as an automated beating assay performed in 384 well plate format for time domain analysis of arrhythmia have been developed. Data based on testing reference compounds of known arrhythmogenic potential in ES derived cardiomyocytes support the validity of this approach.

**S 2476 The 1,000 Genomes *In Vitro* Toxicology Project: Quantitative High-Throughput Screening for Chemical Toxicity in a Population-Based *In Vitro* Model.**

I. Rusyn. University of North Carolina at Chapel Hill, Chapel Hill, NC.

A series of collaborative studies between the Tox21 consortium and the University of North Carolina have been conducted in which inter-individual variability in exposure response is being assessed in a population-wide human *in vitro* model. These experiments have generated quantitative high-throughput cytotoxicity data on about 200 chemicals in over 1000 cell lines representing 9 populations from 5 continents and all major racial groups. This rather simple toxicity phenotype of cytotoxicity can be leveraged with other molecular data (genotyping and transcript profiling) available on the same cell lines through the HapMap and 1000 Genomes consortia and applied to human health assessments.

**S 2477 Opportunities and Challenges to Incorporating Genetic Variability Data in Risk Assessment.**

W. A. Chiu. US EPA, Washington DC. Sponsor: R. Tice.

This presentation discusses how the new approaches and data sources on genetic variability described by the previous speakers will fit into a changing risk assessment landscape in the 21st Century. Key opportunities include the direct estimation how genetic variability contributes to susceptibility to toxicants and the identification of key biological pathways that confer differential susceptibility. However, some important challenges remain, such as inter-species and *in vivo-in vitro* extrapolation and, especially, the integration of genetic variability with other sources of human variability. [Disclaimer: The views in this presentation are those of the author, and do not necessarily reflect the views or policies of the U.S. Environmental Protection Agency.]

**S 2478 Role of Air Pollution As a Risk Factor for Central Nervous System Diseases and Disorders.**

D. A. Cory-Slechta. Environmental Medicine, University of Rochester Medical School, Rochester, NY.

Increasing evidence suggests that many of the adverse consequences of air pollutants extend beyond the lungs and indeed can target the brain where they produce many of the same types of inflammatory and other adverse consequences as documented in the lungs. Such findings have been variously described in experimental models for exposures such as the metal constituents of the ultrafine particulate matter of air pollution, for diesel exhaust and for ozone. Both direct effects via constituents of air contaminants translocated to the CNS and indirect effects via induction of systemic acute phase responses have to be considered. In addition, epidemiological studies have now begun to report associations of traffic- and combustion-related air pollutants with cognitive deficits in children. While our understanding of the extent of such impacts is still quite limited, these highly provocative findings could suggest that air pollution has been a greatly underappreciated risk factor for neurodevelopmental or neurodegenerative diseases. This symposium will present findings from experimental models describing the CNS toxicity of concentrated ultrafine particles in adults and in postnatally-exposed rodent models in relation to neurodevelopmental and neurodegenerative consequences, and of ozone in

the context of Parkinson's disease. In addition, recent epidemiological findings linking residential proximity to freeway with autism will be presented. The intent of the symposium is to stimulate discussion especially in the context of future research needs in this rapidly emerging area of neurotoxicology which requires a multidisciplinary approach involving expertise in the toxicology of the CNS, air pollution, mixtures, and nanoparticles in order to conduct appropriate risk assessment.

## **S** 2479 CNS Consequences of Postnatal Exposure to UFP.

D. A. Cory-Slechta and J. L. Allen. *Environmental Medicine, University of Rochester Medical School, Rochester, NY.*

Accumulating evidence suggests that air pollutants can induce inflammation and oxidative stress in the brain and that early development may be a period of particular vulnerability to such exposures. Epidemiological studies report associations between air pollutant exposure and impaired cognitive function in children and adults and attention deficit in children. Our studies seek to determine the effects of developmental and/or adult concentrated ambient particulate matter (CAPS) exposure on cognitive behaviors and their potential CNS mechanisms. C57Bl6 mice were exposed to AIR or CAPS during early postnatal life with or without adult challenge, yielding 4 groups: Air/Air, Air/CAPS, CAPS/Air and CAPS/CAPS. Behavioral measures included repeated learning, a fixed ratio wait for reward paradigm related to impulsivity (males only), Fixed Interval schedule-controlled behavior and locomotor behavior. Learning accuracy was significantly impaired after CAPS/Air and CAPS/CAPS exposures, particularly in females, even though ability to perform already-learned responses remained intact. In the fixed ratio wait for reward paradigm, CAPS/AIR and CAPS/CAPS decreased the time animals would wait for free reward deliveries, and thereby resulted in emission of a greater number of responses for reach reward earned. Response rates on the fixed interval schedule were reduced in CAPS/AIR males but increased in Air/CAPS females. Notably, as measured at the termination of behavioral testing, i.e., almost a full year after the adult exposures, histopathological hallmarks of CNS perturbation, namely astrogliosis and increased microglial presence, were seen in multiple brain regions, including dentate gyrus and ventral midbrain and increased glutamate and GABA was prevalent in frontal cortex of both sexes. Current efforts focus on understanding the relationships between inflammatory and neurotransmitter changes and behavioral outcomes. Exposure to CAPS appears to have long-term consequences for the CNS. As such, air pollutants may represent an underappreciated contribution to CNS disease and disorders.

## **S** 2480 Microglia and the Peripheral Immune Response in Diesel Exhaust-Induced Neuropathology.

M. L. Block. *Anatomy & Neurobiology, VCU, Richmond, VA.*

Air pollution has been linked to central nervous system (CNS) disease, but the mechanisms driving this response and the type of exposures responsible are largely unknown. To discern the early CNS response to diesel exhaust (DE), adult male rats were exposed to DE (2.0, 0.5, and 0 mg PM/m<sup>3</sup>) for one month by inhalation. DE exposure elevated markers of neuroinflammation (nitrotyrosine, IL-6, TNF $\alpha$ , and MIP-1 $\alpha$ ) in the midbrain, cortex, and olfactory bulbs, in addition to activation of microglia, as determined by morphology. The highest levels of neuroinflammation occurred in the midbrain, which also contained the highest level of the IBA-1 microglial marker. Neurotoxicity and early markers of neurodegenerative disease were unaffected. One month exposure to biodiesel exhaust revealed only changes in microglia morphology without any elevation of pro-inflammatory factors, demonstrating that neuroinflammation may be exposure specific. To reveal how DE might be causing neuroinflammation, rats were administered an IT bolus of DE particles (DEP, 20 mg/kg) where DEP exposure elevated serum and brain TNF $\alpha$ , suggesting a potential role for the particles in initiating peripheral inflammation capable of transferring to the brain. Microglia cultures treated with DEP (50 $\mu$ g/ml) failed to produce TNF $\alpha$ , indicating that brain TNF $\alpha$  production may not be due to the direct interaction of microglia with the particles. To explore the role of long-term exposure, we tested the effect of subchronic (6 month) DE (992, 311, 100, 35 and 0  $\mu$ g PM/m<sup>3</sup>) inhalation in rats and found elevated levels of the neurotoxic cytokine TNF $\alpha$  at lower exposures (DE, 100  $\mu$ g PM/m<sup>3</sup>) and early protein markers of neurodegenerative diseases (A $\beta$ 42,  $\alpha$  synuclein and phosphorylated tau) at higher levels (DE 992  $\mu$ g PM/m<sup>3</sup>), suggesting that subchronic DE exposure may impinge on common neurodegenerative disease pathways. Together, these findings demonstrate that the brain's immune system can detect and respond to DE and support that circulating cytokines (or another peripheral signal) may play a role in how neuroinflammation transfers to the brain.

## **S** 2481 Particle Translocation As an Explanation for the Adverse Effects of Inhaled Particulates in the CNS.

A. Elder. *Environmental Medicine, University of Rochester, Rochester, NY.*

The hypothesis that air pollution can adversely impact the central nervous system (CNS) is supported by the demonstration of gene-environment interactions for neurodegenerative disorders, such as Alzheimer's and Parkinson's diseases. The mechanisms by which this might occur are not fully understood, but may include transport of particulates into the brain, thus resulting in direct delivery of toxicants to the target tissue. Transport via the olfactory route, for example, has been demonstrated for poorly-soluble ultrafine or nanosized particles (<100 nm in diameter in at least one dimension) and for some soluble compounds following inhalation exposures. However, other pathways have been identified and the contribution of these to the overall accumulation in the CNS is unclear. Likewise, the contributions of particle physicochemistry and blood-brain barrier integrity are important to address in order to understand the long-term consequences to CNS health. Such consequences have been explored in recent research. Using a mouse model of Alzheimer's disease, we found that a 12-day inhalation exposure to poorly-soluble manganese oxide nanoparticle aerosols resulted in the activation of hippocampal microglia and astrocytes, suggesting activation of an innate immune response in the brain. Interestingly, this activation persisted for two months post-exposure. Increased immunostaining for amyloid beta and a loss of synaptophysin staining were also found. These data contribute to the growing evidence for an association between environmental exposures and neurodegenerative disease progression.

## **S** 2482 Does Air Pollution Exposure Increase Risk for Autism?

I. Hertz-Picciotto<sup>1</sup>, H. E. Volk<sup>2</sup> and R. S. McConnell<sup>2</sup>. <sup>1</sup>MIND Institute & Center for Children's Environmental Health, University of California Davis, Davis, CA; <sup>2</sup>Center for Children's Environmental Health, University of Southern California, Los Angeles, CA. Sponsor: D. Cory-Slechta.

Windham et al. (2006) reported that children with autism were more likely to live in census tracts with higher ambient levels of diesel, certain metals, and solvents. Traffic is a major source of air pollution, including particulates, polycyclic aromatic hydrocarbons, metals, sulfur dioxide and nitrogen oxides. Proximity to freeways and major roadways is highly correlated with ambient levels of such traffic-related air pollution. Using data from the CHARGE (CHildhood Autism Risk from Genes and Environment) Study, we examined the association between autism and proximity of residence to freeways and major roadways during pregnancy and near the time of delivery (Volk et al 2011). Using data from 304 autism cases and 259 typically developing controls, the mother's address recorded on the birth certificate and trimester-specific addresses obtained by questionnaire were geocoded, and measures of distance to freeways and major roads calculated with ArcGIS software. After adjustment for sociodemographic factors and maternal smoking, mothers of cases were more likely, at the time of delivery, to live within a quarter mile of a freeway as compared with mothers of controls: odds ratio (OR) = 1.86. At greater distances, risk was not elevated. Autism was also associated with residential proximity to a freeway during the third trimester (OR = 2.22). For each address, exposures to specific air pollutants from traffic and stationary sources were estimated with U.S. EPA's Air Quality System (Volk et al, in press). Exposures to nitrogen dioxide (NO<sub>2</sub>) and particulate matter less than 2.5 and 10  $\mu$  in diameter (PM<sub>2.5</sub> and PM<sub>10</sub>) in the first year of life were associated with about a two-fold increased risk for autism (NO<sub>2</sub> OR=2.06; PM<sub>2.5</sub> OR=2.12; PM<sub>10</sub> OR=2.14), with similar findings for gestational exposures. Given that many constituents in air pollution induce neurodevelopmental deficits in experimental rodent studies, a contribution from air pollution to autism susceptibility is plausible.

## **S** 2483 Ozone Pollution, Oxidative Stress, and Dysregulation of Inflammatory Responses in Rat Hippocampus.

S. Rivas-Arancibia. *Fisiología, Facultad de Medicina, Universidad Nacional Autónoma de México, México City, Mexico.* Sponsor: D. Cory-Slechta.

The oxidizing compounds contained in the air that we breathe in the large cities, is related to a large number of chronic degenerative diseases. To study the effects of ozone pollution on the brain, we developed a model consisting in a chronic exposure of rat to ozone doses, similar to total levels that occur in a day of high pollution in Mexico City. For this purpose, 84 male Wistar rats (250 to 300 gr) were randomly divided into 7 groups, each group received one of the following treatments: 1) control, 2) exposed to ozone free air for 30 days, 3) exposed to ozone for 7 days, 4) exposed to ozone for 15 days, 5) exposed to ozone for 30 days, 6) exposed to ozone for 60 days, and 7) exposed to ozone for 90 days. (0.25 ppm /4 hours daily). Two hours after the last exposure to ozone, each group was randomly divided into

two subgroups, hippocampus were dissected and afterward processed for immunohistochemistry. The second subgroup was used for western blot and spectrophotometric techniques (to determine lipid peroxidation, oxidized proteins, superoxide dismutase and glutathione). The results indicate that ozone, causes an increase in lipids and proteins oxidation after 15 days of exposure. After 30 days we found in the hippocampus damage and decrease of the neuroblasts, and neurons number, glial activation, increased of proinflammatory markers, together with changes in levels of antioxidant defenses and loss of its enzymatic activity. Results also showed accumulation of deposits of amyloid beta (A $\beta$ ) 1-42 at 90 days exposure. In conclusions: ozone lead to oxidative stress causing a neurodegenerative process in hippocampus, together with, dysregulation of immune responses, and loss of brain to capacity repair, and A $\beta$  1-42 plaques formation at 90day of ozone exposure. These experiments showed that chronic exposure to ozone at low doses, per se, is able to cause an oxidative stress state, which produces progressive cellular damage and cell death that resembling the damage described in the physiopathology of neurodegenerative diseases.

Grant DGAPA IN 219511

## **S** 2484 **Translational Methods to Assess the Safety of Natural Health Products, Including Traditional Medicines and Dietary Supplements.**

J. C. Griffiths<sup>1</sup> and S. A. Jordan<sup>2</sup>. <sup>1</sup>*Doc Standards, US Pharmacopeia, Rockville, MD;* <sup>2</sup>*Marketed Health Products, Health Canada, Ottawa, ON, Canada.*

Globally, ~80% of the world's population relies upon traditional medicines as part of standard healthcare; ~100 million Americans spend ~\$28 billion annually to consume herbals, vitamins, minerals, amino acids, and other naturally occurring products in the form of dietary supplements, botanical drugs, and natural health products. The complexity of mixtures with variance in composition and quality presents a challenge for risk practitioners. To address these issues, new methodologies and predictive technologies are being developed, tested and validated to mitigate risk of human toxicity and effectively increase the quality of information useful for application in safety assessments. Many of these methods are already reflected in multiagency government initiatives. Such methods are referred to as "translational" for making use of and extrapolating data from scientifically defensible approaches towards establishing human safety and use of viable products. In this symposium, various *in vitro*, *in vivo*, state-of-the-art *in silico* (computational), and 'omic methodologies will be presented. Discussion will cover case studies and regulatory science activities at US FDA/CDER and NCTR including conventional toxicological and computational assessments of individual chemical constituents and mixtures. Computational tools to deconvolute complexities and predict molecular targets for constituent phytochemicals will also be highlighted. Speakers will also address how the United States Pharmacopeia (USP) conducts evidence-based reviews on the safety of dietary supplements and how to couple data from *in silico* structure-based methods to complement and strengthen evidence and support committee-based human expert decision making regarding the suitability of dietary supplements for monograph development on product quality. Collectively, these presentations will provide a global picture of the state and utility of modern methods for assessing toxicity and safety of these products.

## **S** 2485 **Session Overview: The Promise of Translational and Integrative Safety Assessments of Dietary Supplements, Traditional Medicines, and Herbal Drugs.**

S. A. Jordan. *Marketed Health Products, Health Canada, Ottawa, ON, Canada.*

For thousands of years, herbs and other natural substances have been used in health care. Some traditional healing paradigms include knowledge of potential toxicity, and ways of preventing adverse effects. However, with modern use, a much larger and varied population now uses these products. In addition, commercial products may not be true to traditional use, indication, or form. A rise in use of these products with pharmaceutical drugs, resulting in possible herb-drug interactions, also has become an issue of concern. Potential safety concerns may also arise from quality issues. Regulators are often faced with a lack of quality information when making risk-based decisions on the safety of dietary supplements or traditional medicines, and an increase in these data allows for improved decision making. The development of translational methods, including omics, and computational models, has presented an opportunity to increase the amount of information, and to integrate novel data with traditional methods of assessing toxicity. The integration of all available data, including those derived from translational studies, can reduce uncertainty in decision making related to the potential hazard and risk associated with the use of these product types. Overall, this will benefit the public, the industry, and the regulatory community which is charged with licensing and monitoring the safety of dietary supplements and traditional medicines.

## **S** 2486 ***In Silico* Methods As Translational Tools for Supporting the Safety Assessment of Natural Health Products.**

L. G. Valerio. *CDER/Office of Pharmaceutical Science, US Food & Drug Administration, White Oak, MD.* Sponsor: J. Griffiths.

*In silico* methods including computational toxicology can serve to help address data gaps during safety evaluations for regulatory and industrial product safety. Natural health products including dietary supplements, botanicals, herbals, and related substances can benefit from the wide spectrum of scientific evidence produced by *in silico* toxicology analyses. Discussion will cover case studies and regulatory science activities in the application of structure-based computational assessments of individual chemical constituents derived from natural products and mixtures modeling. Translation of these data to support human safety and risk assessment processes will be presented. The *in silico* approach as a translational tool with emerging evidence-based predictive technologies and the use of these methods in applied safety science is of extraordinary heightened interest with the goal of meeting today's needs for protecting public health.

## **S** 2487 ***In Vitro* and *In Vivo* Approaches for Assessing the Safety of Natural Health Products.**

W. F. Salminen. *NCTR-Center for Hepatotoxicology, US Food & Drug Administration, Benton, AR.*

Dietary supplement use continues to increase as many people see these "natural" products as inherently safe alternatives to drugs. However, in the US and many other parts of the world, dietary supplements require none to minimal safety data before they are marketed. Many dietary supplements are complex mixtures of a wide variety of chemical compounds and the composition can vary greatly from manufacturer to manufacturer and even batch to batch making safety assessments very difficult. Various *in vitro* and *in vivo* approaches for assessing the safety of dietary supplements from classical toxicology studies to state-of-the-art toxicogenomics assessments will be reviewed. An overview of the US National Toxicology Program's (NTP) testing of dietary supplements will be presented and examples of potential drug-dietary supplement interactions will be discussed since these are likely to increase as people use dietary supplements in combination with approved drugs.

## **S** 2488 **Computational Methods Linking Traditional Chinese Medicine (TCM) and Western Therapeutics.**

D. E. Johnson. *Molecular Toxicology, University of California Berkeley, Berkeley, CA.*

Herbal remedies are widely used throughout the world with approximately 80% of the global population relying on traditional medicines as part of standard healthcare. In the US, an estimated 1 in 5 adults regularly consume herbal products and most of these are not included in patient records as "other medications", thereby limiting the understanding of potential herb-drug interactions to both the patient and health care professional. We have been using computational tools to deconvolute complex recipes and predict molecular targets for constituent phytochemicals with the goal of forming a comprehensive tool to help predict herb-drug interactions. This work will be illustrated using both open-source tools and commercial biological pathway mapping and predictive algorithms. Translational methodology will be introduced that proposes a chemical-disease category linkage between TCM and Western medicine for a rational integrative medicine approach.

## **S** 2489 **Herbogenomics As a Translational Method for the Safety Assessment of the Complex Mixtures in Traditional Chinese Medicines.**

Y. Kang. *Department of Pharmacology and Toxicology, University of Louisville School of Medicine, Louisville, KY.*

Natural health products, including traditional Chinese medicines (TCMs) are often complex mixtures. Assessing the safety of individual components of such products is problematic. The use of TCM has raised concerns of heavy metal contamination and toxicity. However, it has been known that metals and metalloids are essential components in some TCM preparations. For instance, mercury in cinnabar is irreplaceable for its therapeutic effect. Another scenario is that the TCM formulation is toxic to healthy population, but becomes remedy to seriously sick people. In this context, the dose regiment of arsenic trioxide used to treat acute promyelocytic leukemia (APL) is extremely toxic to general population, but is of high therapeutic efficacy for APL patients. It is difficult, if not impossible, to distinguish metal composition from metal contamination in TCM and their associated therapeutic or toxic effects. A novel approach of herbogenomics can provide

alternate perspectives on the active ingredients and toxic contaminations of TCM. The overall effects of TCM on target organs can be elucidated by functional genomics and proteomics, thus the addition or subtraction of heavy metals from TCM preparations would affect the outcome, which can be reflected by the genomic profile alterations. The information about metal composition and contamination is critical for general population considering the use of TCM as an alternative remedy.

**S 2490 Evidence-Based Reviews As a Method for Assessing the Safety of Dietary Supplements.**

M. L. Hardy. *Center for Integrative Medicine, University of California Los Angeles, Los Angeles, CA.* Sponsor: J. Griffiths.

Dietary supplement safety is one of the main regulatory concerns in the United States. Adverse events occur for a variety of reasons including contamination, misidentification or adulteration of plant based dietary supplements. However, even when a product is correctly made, adverse events in human subjects have been reported. Systematic review and meta-analysis of published clinical trials and adverse event case reports allow aggregation of disparate reports in order to improve the analytic strength of evaluations of potential harms. When adverse events are reported in properly randomized clinical trials, causality of the reported adverse event can be assumed. Clinical trials are almost always of insufficient power to detect any but the most common adverse events. Rare or serious adverse events are usually reported in as case reports or small case series. Attribution of risk in this case is limited by a number of factors including timing and duration of exposure to suspected offending substance as well as the clinical circumstances of the user. Although causality can rarely be attributed based on case reports, systematic review of aggregated cases can identify a suspicious signal. Additional limitations of all sources of adverse event reports are the result of incomplete information including very often poor characterization of the potential offending material. The application of these principles will be illustrated using an analysis of adverse events related to ephedra.

**W 2491 Are We Like Rodents, Rabbits, or Something Else? Mechanisms of Developmental and Reproductive Toxicity across Species.**

R. J. Rasoulpour<sup>1</sup>, K. Johnson<sup>3</sup>, S. N. Campion<sup>2</sup>, C. Timchalk<sup>4</sup> and J. E. Goodman<sup>5</sup>. <sup>1</sup>The Dow Chemical Company, Midland, MI; <sup>2</sup>Pfizer Global, Groton, CT; <sup>3</sup>Alfred I duPont Hospital for Children, Wilmington, DE; <sup>4</sup>Pacific Northwest National Laboratory, Richland, WA; <sup>5</sup>Gradient, Cambridge, MA.

Given the inherent complexity of embryo/fetal development and reproductive biology, developmental and reproductive toxicity (DART) hazard identification and research still heavily relies on animal models. Typically, this type of research is conducted in rodents (e.g., mouse and rat) as well as nonrodent species (e.g., rabbit and nonhuman primate), which, in the face of toxicity findings, raises the question of relevance to humans. Are we more like mice, rats, or other model organisms? Not surprisingly, answering this question is a challenge, and the scientific approach may be quite different depending upon the biological system and the level of mechanistic information available. However, within this challenge is an opportunity to understand the toxicokinetic and toxicodynamic differences between the species and provide the appropriate context for developmental and reproductive findings. Providing this context can directly impact the risk assessment and regulatory decision-making process. This workshop will highlight several different approaches to relate animal reproductive and developmental toxicity findings to human health. Speakers in fields of basic research, product safety testing, epidemiology, and physiologically-based pharmacokinetic modeling will address the central theme of the workshop, which is applying different experimental strategies to analyze cross-species toxicity. Within each presentation, potential regulatory implications and feedback from agencies, when available, will be addressed. The expected outcomes of the workshop are an increased understanding of the different approaches to dissect complex toxicity mechanisms and to take the next step towards cross-species comparisons that impact human relevance and regulatory decisions.

**W 2492 Challenges in Elucidating Developmental Toxicity Mechanisms in the Context of Guideline Safety Assessment Studies.**

R. J. Rasoulpour. *Developmental and Reproductive Toxicology, The Dow Chemical Company, Midland, MI.*

This presentation will provide a case study on unique challenges often posed by elucidating developmental toxicity mechanisms identified within guideline toxicity studies. The case study will focus on a recently identified novel mechanism of rat-

specific developmental toxicity induced by a developmental molecule, sulfoxaflo. At high doses, neonatal death and limb flexure effects occurred in rats, but not rabbits. The proposed mode-of-action was that these effects had a single mechanism mediated via the rat fetal isoform of the muscle nicotinic acetylcholine receptor. The studies included a combination of novel in vivo and in vitro mechanistic studies, which were integrated to identify agonism on this receptor as a critical event. Moreover, species comparison studies revealed that this initial event was isolated to sustained agonism on the rat fetal isoform of the nicotinic acetylcholine muscle receptor and did not occur in humans. Feedback on this project from global regulatory agencies will be presented and discussed. This stage-setting talk provides a clear example of how human relevance can be understood if the toxicity is mediated by a relatively simple mechanism (e.g., agonism at a single receptor).

**W 2493 Endocrine Disruption Mediated Developmental Toxicity in Mice versus Rats: Implications for Humans.**

K. Johnson. *Alfred I duPont Hospital for Children, Wilmington, DE.*

This presentation will examine the mechanisms behind phthalate-induced fetal testis endocrine disruption in mouse and rats and extrapolation of these rodent data to humans. It will analyze the species-sensitivity of phthalate endocrine disruption and compare these responses to those observed after phthalate exposure of human biological samples. In rats, gestational phthalate exposure produces male reproductive tract malformations (including hypospadias and cryptorchidism) via a phthalate-induced reduction of fetal testis insulin-like 3 and testosterone production. Although the phthalate molecular target is unknown, extensive molecular mechanistic studies in the rat have established reduced Leydig cell steroidogenic gene expression as causal for the inhibition of testosterone production. In contrast to the rat, available data for mouse gestational phthalate exposure indicate this species is resistant to inhibition of fetal testis hormone production. Despite mouse gestational phthalate exposure extensively altering the fetal testis gene expression profile and inducing fetal testis histopathology, no reductions in mouse fetal Leydig cell steroidogenic gene expression are evident. Because in vitro models do not recapitulate the fetal testis/Leydig cell endocrine disruption phenotype, the question of human susceptibility has been addressed with experiments using human fetal testis explants xenografted into rodent hosts. In these experiments, phthalate exposure of host animals harboring rodent fetal testis explants recapitulates the rodent in vivo phenotypes, and human fetal testis xenografts respond similarly to mouse fetal testis xenografts. While histopathology is observed in the human fetal testis xenografts, reductions in fetal testis testosterone production or steroidogenic gene expression are not seen. These xenografts data have important implications for current and future regulatory decisions but are not without caveats. The potential regulatory impact and caveats of these experiments will be presented.

**W 2494 Case Studies on Testis Toxicity in Rodent Models and Risk Management Strategies.**

S. N. Campion. *Pfizer Global, Groton, CT.*

This presentation will provide case examples of testis toxicity findings in regulatory studies for pharmaceutical development. For some of these examples, strategies used to elucidate the mechanisms of toxicity in order to put these findings into perspective for human risk assessment will be described. One of these case studies will focus on mechanistic work performed to determine that the adverse findings noted in rats were the result of a species specific mechanism that is not relevant in humans. A second case study will discuss work performed to elucidate the binding targets of a compound that elicits testis toxicity in rodents. While there are some examples of mechanistic work to de-risk testis issues with pharmaceuticals, mechanistic work is not commonly performed since the toxicity is often due to off-target effects of small molecules. In addition, the impact of the time required to perform mechanistic work to a program's timeline often makes this work unfeasible. Alternative approaches to understanding the impact of the toxicity in order to develop human health risk management strategies will be discussed, including evaluating the safety margin as well as the intended use of the drug (e.g., indication, patient population, duration of treatment). Marketed drugs with testicular toxicity findings in nonclinical studies will be discussed to provide a perspective of the tolerance of regulatory agencies to such findings. In general, there is a higher tolerance for male reproductive toxicity findings with pharmaceuticals relative to environmental chemicals because the benefit of the pharmaceutical exposure is considered relative to the risk when determining the impact of findings in preclinical studies.

**W 2495 Physiologically-Based Pharmacokinetic/Pharmacodynamic Modeling of Developmental Toxicity.**

C. Timchalk. *Pacific Northwest National Laboratory, Richland, WA.*

The developing brain is vulnerable to insults and evidence implicates low-level chemical exposures as potential developmental neurotoxins. Organophosphorus (OP) insecticides, like chlorpyrifos (CPF), inhibit cholinesterase (ChE) and are neurotoxic. PBPK/PD models have been exploited to enable cross-species extrapolation of CPF brain dosimetry and ChE inhibition and when linked with a dietary exposure model can predict response across populations. However, recent epidemiology studies suggest that OP neurotoxicity occurs at low-doses, even in the absence of significant brain ChE inhibition. The lack of quantitative cross-species brain dosimetry data associated with epidemiology results hampers any mechanistic based risk assessments. The implication of localized heterogeneous CYP450 brain metabolism has historically not been extensively investigated, but recent research suggests it is of key importance. To address these limitations, we are testing the hypothesis that low-dose exposures of preweanling rats to OP insecticides will result in differential brain region dosimetry, enhanced by localized brain bioactivation, potentially resulting in subtle changes in brain chemistry. Comparative in vitro metabolism studies in rats indicate that the overall brain microsomal metabolism was a fraction (~3%) of the liver. Following in vivo oral administration (1 and 5 mg/kg/day) of CPF to post-natal day-10 pups, CPF and its major metabolite were quantified in the brain with evidence of regional deposition and localized metabolism. The importance of localized brain metabolism is highly relevant for lipophilic pesticides that sequester in the lipid rich regions of the brain and can undergo localized metabolic activation to produce neurotoxic effects. This is particularly important in juvenile animals, and children, where there may be a disproportionate deposition of the parent pesticide in the brain. In this regard, these PBPK/PD modeling strategy have significant regulatory implications for assessing developmental neurotoxicity.

**W 2496 Using Epidemiology to Analyze Neurodevelopmental Toxicity across Species.**

J. E. Goodman. *Gradient, Cambridge, MA.*

The final presentation of the session will tackle cross-species analysis from a different angle by utilizing epidemiology data. This presentation will explore how epidemiology studies can address toxicity across species by estimating human exposures and/or outcomes with biomarkers and putting these into context with the animal model results. It will focus on how the effect of timing, selection choice, and measurement of biomarkers, as well as the results of toxicology studies, can influence the interpretation of results. Chlorpyrifos and neurodevelopmental effects will be used as a case study. US EPA assessed whether epidemiology data suggest that fetal or early-life chlorpyrifos exposure causes neurodevelopmental effects and, if so, whether they occur at exposures below those causing 10% inhibition of blood acetylcholinesterase (AChE), which is currently considered the most sensitive endpoint. We conducted a hypothesis-based weight-of-evidence analysis and found that a proposed causal association between chlorpyrifos exposure and neurodevelopmental effects in the absence of AChE inhibition does not have a substantial basis in existing animal or in vitro studies, and there is no plausible basis for invoking such effects in humans at their far lower exposure level. The epidemiology studies fail to show consistent patterns; the few associations are likely attributable to alternative explanations. The human data are inappropriate for a dose-response assessment because biomarkers were only measured at one time point, may reflect exposure to other pesticides, and many values are at or below limits of quantification. When considered with pharmacokinetic data, however, these biomarkers provide information on exposure levels relative to those in experimental studies and indicate a margin of exposure of at least 1,000. Because animal data take into account the most sensitive lifestages, the use of AChE inhibition as a regulatory endpoint is protective of adverse effects in sensitive populations.

**W 2497 Cumulative Risk: Toxicity and Interactions of Physical and Chemical Stressors.**

J. Simmons<sup>1</sup> and C. Rider<sup>2</sup>. <sup>1</sup>NHEERL, US EPA, Research Triangle Park, NC; <sup>2</sup>NTP, NIEHS, Research Triangle Park, NC.

Recent efforts to update cumulative risk assessment procedures and develop community-based risk assessment methods reflect increased interest in incorporating the totality of variables affecting human health into the risk assessment process. One key roadblock in advancement is uncertainty as to how nonchemical stressors behave in relationship to chemical stressors. An assumption that simplifies incorporation of nonchemical stressors into current risk assessment paradigms is that nonchemical stressors act in the same manner as chemicals. However, evidence is required to support this assumption. The term nonchemical stressors encompasses a

diverse set of variables including physical stressors, such as noise, temperature, disease, and radiation, as well as psychosocial stressors, which involve perception of circumstances. Physical stressors offer a reasonable starting place for measuring the effects of nonchemical stressors and their modulation of chemical effects (and vice versa), as they clearly differ from chemical stressors, present many diverse and highly-relevant stressors, and "doses" of many physical stressors are easily quantifiable. There is a commonly held belief that virtually nothing is known about the impact of nonchemical stressors on chemical-mediated toxicity or the joint impact of coexposure to chemical and nonchemical stressors. While generally true, there are several instances where a substantial body of evidence exists. The objective is to provide expert overviews, for those chemical and physical stressors that have been sufficiently studied to gain at least a limited understanding of their joint impact. In addition to providing the current state of knowledge, data gaps will be identified that should be addressed to facilitate inclusion of nonchemical stressors in risk assessment. (This abstract does not reflect US EPA or NIEHS policy.)

**W 2498 Cumulative Risk: Chemicals and Infectious Disease.**

M. Selgrade. *ICF International, Durham, NC.*

At least 4 types of mechanisms underlie potential interactions between toxic chemicals and infectious disease. 1) The best understood is suppression of immune responses, resulting in increased incidence/severity of infectious disease. For example, decreased alveolar macrophage function following exposure to several air pollutants enhances the risk of certain bacterial infections. Research on this model provides both qualitative and quantitative approaches to describe this risk. 2) Certain immune/inflammatory mediators that are activated during infection affect metabolic enzymes and transporters and have the potential to alter chemical toxicity as illustrated by the effects of murine cytomegalovirus on parathion poisoning, sodium pentobarbital induced sleeping time, and cyt P450. Infection and inflammation have also been shown clinically to affect the metabolism, distribution, and elimination of certain drugs. 3) Chemical exposure may enhance inflammation and immune pathology associated with an infection. This is best illustrated by effects of ozone, ultraviolet radiation, and TCDD on influenza infection. In all cases mortality is enhanced in the absence of increased virus titers in the lung or viral dissemination. Deaths appear to be due to increased inflammatory responses. Similarities exist between receptors and subsequently triggered signaling pathways for pathogen associated molecular patterns (PAMPs) and damage associated molecular patterns (DAMPs), which trigger inflammatory responses. A systems approach that examines the integration of these pathways is needed to better describe this phenomenon. 4) Infection enhances chemical induced lesions, e.g., p53 mutations, inflammation, cell proliferation. Such mechanisms might explain the interaction between hepatitis B virus infection and aflatoxin in the induction of liver cancer. These mechanisms are not necessarily comprehensive, distinct, or mutually exclusive and are imperfectly understood. However, they provide a useful framework to further explore the interactions between infectious disease and exposure to toxic chemicals with the ultimate goal of improving our understanding of cumulative risk.

**W 2499 Enhancement of Noise-Induced Hearing Loss by Chemicals.**

T. C. Morata. *Division of Applied Research & Technology, NIOSH, Cincinnati, OH.* Sponsor: J. Simmons.

The auditory effects of chemical toxicants have been investigated in the past two decades, in animal and human field and clinical studies. A number of studies demonstrated that some solvents, metals, asphyxiants, pesticides not only affect the sensory organ of the auditory system, as noise does, but also affect central auditory structures. Ototoxicity induces outer hair cell dysfunction in the cochlea (similar to the effects of noise), whereas neurotoxicity induces central auditory dysfunction. Audiological signs of neurotoxicity may or may not include poorer hearing thresholds, in addition to difficulties discriminating sounds such as speech, particularly in adverse listening conditions. The existing evidence prompted the proposal of new guidelines and standards on hearing loss prevention. In the U.S., the National Institute for Occupational Safety and Health has discussed specific research needs regarding the ototoxicity of chemicals used at work. The American Conference of Governmental Industrial Hygienists and the U.S. Army have proposed preliminary practical steps that employers and occupational health professionals can take to improve hearing loss prevention. Australia and New Zealand have developed standards recommending hearing tests for workers exposed to ototoxic agents. In the legislative arena, the European Parliament published a new noise directive (2003/10/EC), that requires employers to give attention to any effects on workers' health and safety resulting from interactions between noise and work-related ototoxic substances, when performing risk assessment of workplaces. Legislation regarding compensation has also changed in Australia and Brazil. In this presentation

the auditory effects of chemical alone or in combination with noise will be reviewed, and the recent guidelines, legislative developments and alternative strategies for the prevention of auditory effects resulting from exposure to chemicals in the workplace will be presented.

## **W** 2500 Exacerbation of Toxicity of Air Pollutants and Pesticides by Thermal Stress.

C. J. Gordon, C. Aydin and A. F. Johnstone. *Toxicity Assessment Division, US EPA, Research Triangle Park, NC.*

Considering the likelihood of global warming in the near future, it is important to understand how heat stress will alter the health effects of toxicants. The toxicity of pesticides and airborne toxicants is generally exacerbated in a warm environment. As air temperature increases, the pulmonary intake of air pollutants and absorption of pesticides applied to the skin is generally accelerated. Cellular toxicity is typically exacerbated when body temperature is elevated. This is primarily a result of a Q10 effect, meaning that the rate of a biochemical reaction doubles with a 10 °C increase in tissue temperature. The generation of reactive oxygen species is also exacerbated with warmer temperatures.

Since warmer temperatures worsen chemical toxicity, a thermoregulatory response to lower body temperature can be protective. Hyperthermia is most likely going to be detrimental in the recovery from toxicant exposure. Rodents and other small mammals have relatively large surface area:volume ratio. Following exposure to pesticides and air pollutants, metabolism is reduced and a rapid reduction in body temperature ensues. If given the opportunity to thermoregulate behaviorally, rodents seek colder temperatures, allowing body temperature to decrease quickly. Thus, the hypothermic response is a regulated response. This is thought to be an adaptive response because the hypothermic response is protective. Large mammals, including humans, have a greater thermal inertia and are unable to mount a hypothermic response as is seen in rodents. A warmer environmental temperature will thus impede the hypothermic response to toxicant exposure in rodents and will also be stressful to large mammals that are unable to undergo a significant cooling response. With the potential impact of global climate change on increased incident of heat stress in urban areas that are also rife with pollution, the topic of the thermoregulatory responses to environmental toxicants is timely. This is an abstract of a proposed presentation and does not reflect US EPA policy.

## **W** 2501 Modulation of X-Ray Mediated Testicular Toxicity by Chemical Exposure.

K. Boekelheide. *Brown University, Providence, RI.*

High density microarrays and a detailed bioinformatics analytical approach were used to demonstrate that an initial chemical exposure to 2,5-hexanedione (HD) altered the rat testis to ameliorate the response to a subsequent exposure to x-irradiation. Adult male rats were exposed to HD (0.33% or 1%) in the drinking water for 18 days followed by x-ray (2Gy or 5Gy), resulting in a total of 9 treatment groups. Testis samples were collected after 3 hr and gene array analysis was performed. Using a novel bioinformatic approach to summarize the effect of HD across all treatment groups, we focused on the modification of x-ray-induced gene alterations by HD co-exposure. Enrichment analysis was used to identify biological pathways where HD modification of gene expression was the greatest. HD exerted a significant influence on genes involved in Cell Cycle and DNA Replication, Recombination, and Repair. HD also had an antagonistic effect on x-ray-induced alterations of several apoptotic genes (Fas, BBC3, AEN). To further investigate the specific cell populations and stages in which these critical gene alterations occur, laser capture microdissection (LCM) samples were collected from the basal compartment of the seminiferous epithelium, enriching for those germ cells most susceptible to x-ray-induced apoptosis. Quantitative RT-PCR of the LCM samples confirmed the suppression of apoptotic genes by HD co-exposure. The co-exposure attenuation of germ cell apoptosis is the result of an adaptive response to the chemical exposure, causing altered paracrine signalling of the supportive cells in the seminiferous epithelium. These results suggest that toxicity pathway responses determine the outcome of co-exposures, whether chemical or physical in nature, and that complex paracrine interactions between cells modulate the extent of injury.

## **W** 2502 Sunlight Enhancement of the Toxicity of Air Pollutant Mixtures.

K. G. Sexton<sup>1</sup>, J. Zavala<sup>1</sup>, B. O'Brien<sup>1</sup>, W. Vizuete<sup>1</sup>, R. C. Fry<sup>1</sup>, I. Jaspers<sup>1,2</sup> and I. Rusyn<sup>1</sup>. <sup>1</sup>*Environmental Sciences & Engineering, University of North Carolina at Chapel Hill, Chapel Hill, NC;* <sup>2</sup>*Center for Environmental Medicine and Lung Biology, University of North Carolina at Chapel Hill, Chapel Hill, NC.*

Sunlight can significantly drive photochemical reactions of mixtures of air pollutants commonly observed in the atmosphere, producing many well known toxic compounds such as formaldehyde and other carbonyl containing products. These reactions also contribute to the formation of secondary organic aerosols as well as modifying the composition of existing aerosols or particulate matter (PM). Smog chambers can be used to prepare repeatable, controlled mixtures of simple to increasing complexity and be used to study photochemical atmospheric transformation with natural sunlight or simulated sunlight. Smog chambers can be interfaced with direct exposure to *in vitro* or *in vivo* models for toxicity studies including direct air-liquid-interface *in vitro* or *in vivo* inhalation exposures. Photochemical experiments have been conducted in smog chambers with industrial mixtures and complex mixtures of motor vehicle exhaust in urban atmospheres, often demonstrating enhanced toxicity as measured by markers of inflammation and other biological endpoints such as cytotoxicity. Modifications of experiments, exposure conditions and additional toxicological analyses can provide mechanistic and mode of action understanding. Novel genomic analyses of cells exposed to an urban-like mixtures showed transcriptional changes on a subset of genes, increasing the number of genes with altered expressions from 19 for the un-irradiated mixture, to 709 genes after a one-day sunlight irradiation. The implication is that toxicologists and those dependent on their findings, should consider studies that include mixtures resulting from natural atmospheric photochemical reactivity, transformation of air components, and the resulting enhancement of toxic effects of air pollutants and their products. Not considering such effects, could result in misinterpreting the mode of action and underestimating the potential risk of exposure to air pollution mixtures or its sources.

## **W** 2503 Mechanistic, Occupational, and Clinical Aspects of Lead Exposure.

A. Vale. *School of Biosciences, University of Birmingham, Birmingham, United Kingdom.*

The mechanisms of lead toxicity are increasingly being explained by the ubiquitous reactivity of the bivalent lead cation and its ability to substitute for essential cations, notably calcium and zinc. By these means, lead complexes with important functional groups including thiol and carboxyl groups, and damages many fundamental cell processes and structures including enzyme pathways, phospholipid integrity, ion channel specificity and control, and intrinsic protective systems including free radical scavengers and cellular repair mechanisms. Owing to the large sample sizes involved and its nationally-representative nature, NHANES has been the subject of a number of epidemiological analyses relating blood lead concentrations to a range of adverse outcomes such as blood pressure, renal function, auditory thresholds, and a host of other cardiovascular, neurobehavioral, and other developmental or adult outcomes. Some practitioners are now proposing that, as the NHANES data suggest that lead concentrations even less than 5 µg/dL (0.24 µmol/L) can have some health consequences, chelation should be performed at even very low lead concentrations. Is this an appropriate interpretation of these data? There is concern that the occupational intervention concentrations worldwide are not only unsupported scientifically and clinically but also have been set at concentrations that permit unsafe practices to continue. A group of experts has proposed that workers should be removed from occupational exposure if a single blood lead concentration exceeds 30 µg/dL (1.45 µmol/L), or if two successive blood lead concentrations measured over a four-week interval equal or exceed 20 µg/dL (0.97 µmol/L). Will these recommendations prevent clinically significant occupational lead exposure? Due to the paucity of clinical data, there is controversy about the lead concentration at which chelation therapy should be instituted in adults when exposure prevention has failed, the antidote to be used, and the most effective regimen to be employed.

## **W** 2504 Novel Mechanisms of Toxicity.

R. Lantz. *Cellular and Molecular Medicine, University of Arizona, Tucson, AZ.*

The broad spectrum of lead toxicity with adverse manifestations in developmental and functional aspects of many if not all organ systems are increasingly being explained by the ubiquitous reactivity of the bivalent lead cation and its ability to substitute for essential cations, notably calcium and zinc. By these means lead com-

plexes with important functional groups including thiol and carboxyl groups and damages many fundamental cell processes and structures including enzyme pathways, phospholipid integrity, ion channel specificity and control and intrinsic protective systems including free radical scavengers and cellular repair mechanisms. The ability for lead to substitute for calcium causes erroneous activation of calcium-dependent proteins and modulation of calcium-sensitive receptors. At its extreme, impaired regulation of calcium transport results in intracellular calcium accumulation which triggers apoptosis. Lead can activate protein kinase C to disrupt intracellular regulatory processes causing incorrect gene expression resulting in disordered cell proliferation and differentiation. Lead-mediated malfunction of the calcium sensitive N-methyl-D-aspartate (NMDA) receptor is recognized as one of, if not the most, important mechanism of lead-induced damage to neuronal development, learning and memory.

As the details of the molecular mechanisms of lead toxicity are unravelled, it is becoming clear that their complexity is increased by the fact that lead, like many toxins, acts not in isolation but as part of a multifactorial armoury of adverse influences including environmental factors, which together dictate the development, manifestations and progress of disease.

## **W** 2505 Threshold Toxic Dose: What Can We Learn from the NHANES Studies?

H. Hu. *Dalla Lana School of Public Health, University of Toronto, Toronto, ON, Canada.*

The National Health and Nutrition Examination Survey (NHANES) are cross-sectional surveys of the civilian noninstitutionalized population of the United States that have been administered by the National Center for Health Statistics and ongoing for decades. Subjects are selected based on a stratified multistage probability sampling of counties, blocks, households, and persons within households, with oversampling of some population subgroups (such as Mexican Americans, non-Hispanic blacks, and adults 60 years or older). Evaluations included the administration of extensive questionnaires, physical examination, and collection of urine and venous blood for a wide range of laboratory analyses. Lead levels have been measured in samples of venous blood since the 1970's. Owing to the large sample sizes involved (typically >10,000 individuals) and its nationally-representative nature, NHANES has been the subject of a number of epidemiologic analyses relating blood lead levels to a range of outcomes such as blood pressure, renal function, auditory thresholds, and a host of other cardiovascular, neurobehavioral and other developmental or adult outcomes. This presentation will provide an overview of these studies from the perspective of understanding dose-response relationships; it will also compare them with the parallel body of recent epidemiologic studies using other biomarkers of lead exposure (e.g., KXRF-measured bone lead levels as a marker of cumulative exposure) and/or other study designs (e.g., prospective or case-control studies).

## **W** 2506 Occupational Exposure Limits: Do They Protect Workers?

M. Kosnett. *Division of Clinical Pharmacology and Toxicology, University of Colorado Denver, Denver, CO.*

Research findings have heightened public health concerns regarding the hazards of low dose lead exposure to adults and children. In adults, studies have established the potential for hypertension, effects on renal function, cognitive dysfunction and adverse female reproductive outcome in adults with whole blood lead concentrations less than 40 µg/dL (1.93 µmol/L). However, in most nations worldwide, regulatory occupational exposure limits permit workers to maintain blood lead concentrations in excess of 40 µg/dL for a working lifetime. A group of experts has recently recommended that workers undergo removal from occupational lead exposure if a single blood lead concentration exceeds 30 µg/dL (1.45 µmol/L), or if two successive blood lead concentrations measured over a four week interval equal or exceed 20 µg/dL (0.97 µmol/L). Removal from lead exposure should be considered to avoid long-term risk to health if exposure control measures over an extended period do not decrease blood lead concentrations below 10 µg/dL (0.48 µmol/L), or if selected medical conditions exist that would increase the risk of continued exposure. In order to assure reductions in permissible blood lead concentrations, medical surveillance for lead exposed workers is recommended to include quarterly blood lead measurements for individuals with blood lead concentrations between 10 to 19 µg/dL (0.48 – 0.92 µmol/L), and semi-annual blood lead measurements when sustained blood lead concentrations are less than 10 µg/dL (0.48 µmol/L).

## **W** 2507 Chelation Therapy for Lead Poisoning: Unanswered Questions and Controversies.

S. M. Bradberry. *West Midlands Poisons Unit, City Hospital, Birmingham, United Kingdom.*

Intravenous edetate calcium disodium and oral succimer (dimercaptosuccinic acid; DMSA) are potent chelators of lead approved in many countries for the clinical management of lead poisoning. Both agents reduce the body burden of lead by the renal elimination of a lead-chelating agent complex but there remain unanswered questions regarding their precise pharmacokinetic and pharmacodynamic properties. These include the specific effects of each agent on tissue lead distribution and mobilization and how these parameters are affected by dose and duration of both lead poisoning and chelation. Edetate calcium disodium chelates by exchanging its central calcium ion for lead but the exact chemical nature of the succimer-lead chelate in man remains ill-defined. While assessment of efficacy of both agents is hampered by limited data, the inadequacy of blood lead as a marker of toxicity, variations in study design, species differences and, for clinical studies, the subjective nature of reporting changes in symptoms, available data overall suggest both drugs offer similar efficacy with regard to enhancing lead elimination, though this remains controversial. In addition, the indications for chelation in man remain ill-defined. The adequacy of treatment remains contentious both because of the paucity of efficacy data and because of increasing evidence that toxic effects of lead sustained during early development cannot be reversed by chelation. Moreover, even though most clinical toxicologists agree that where exposure prevention has failed, chelation should be considered in adults whose blood lead concentrations  $\geq 50$  µg/dL (2.4 µmol/L), the most effective regimen to employ in these circumstances is still controversial.

## **W** 2508 Ocular Medical Devices and Ocular Drug Delivery Systems: Challenges and Opportunities.

J. A. Render. *Toxicology, NAMS, Northwood, OH.*

The eye is a unique organ composed of many different structures working together to facilitate vision. The maintenance of clear vision during aging is threatened by various physiological changes (e.g., presbyopia) or diseases (e.g., age-related macular degeneration). The need for treatments is of increasing importance as the size of the aging population grows. The National Eye Institute predicts that by 2020, more than 50 million Americans will be impacted by age-related eye disease. Some of these conditions have been overcome through the use of medical devices. Ocular medical devices consist of instruments, apparatuses, appliances, and materials. Some devices are purely structural; whereas, other medical devices are a part of a delivery system that releases a drug. The five presentations in this program are designed to educate the audience on the therapeutic, safety, and regulatory challenges of developing ocular medical devices and drug delivery systems. The first presentation will cover the special requirements for developing contact lenses and contact lens solutions. The second presentation will describe the challenges associated with accommodative intraocular lenses (IOLs). The third presentation will discuss the ocular barriers (e.g., blood-eye-barrier) and how ocular medical devices and sustained release drug formulations have been designed to address these barriers with respect to developing protein therapeutics. Development of and regulatory challenges associated with a unique biodegradable small molecule ocular drug/injection applicator delivery system will be discussed in the fourth presentation. The symposium will conclude with a presentation that discusses the safety and regulatory requirements and complexities pertaining to ocular medical devices and ocular drug delivery systems.

## **W** 2509 Assessment of the Ocular Safety of Contact Lenses and Lens Solutions.

M. E. Richardson. *Nonclinical Safety, Bausch & Lomb, Rochester, NY.*

Contact lenses and lens care solutions are typically categorized as medical devices and therefore require biocompatibility testing per ISO standards and regional regulatory guidance documents. Recently evolving Regulatory Body expectations have significantly impacted the number and design of the biocompatibility studies required to clear an ocular medical device for marketing. The current 10993-1 (4th Edition) ISO guideline requires that medical device manufacturers utilize a risk management process as part of the design and implementation of a biological evaluation program for medical devices. ISO 10993-1 also requires that the choice of biocompatibility tests be based on, among other things, the end-use application, and take into account the chemical composition of the device, the conditions of exposure as well as the nature, degree, frequency and cumulative duration of exposure. These ISO requirements, along with those of the regional regulatory expectations, create a significant amount of complexity when designing the

biocompatibility testing strategies for contact lenses and solutions. For example, depending on the type of assay, the tested material may need to be the formulation itself, a lens extract or a lens/formulation combination. Further, it has been demonstrated that the selection of assays and individual study designs can influence the outcome of the study, which could potentially impact product registration. Testing protocols therefore need to be designed to account for the unique chemical and physical properties of the ocular medical device being tested in order to avoid potentially false positive outcomes. Consequently, a rational science-based approach should be used to develop and justify the biocompatibility testing strategy and study designs to ensure that the biological evaluation conducted is appropriate, robust and Regulatory-acceptable. This presentation will highlight some of the key challenges and case studies when conducting biocompatibility evaluations on contact lenses and solutions.

**W 2510 Accommodative Intraocular Lenses: A New Class of IOLs with a New Class of Challenges.**

A. Glasser. *College of Optometry, University of Houston, Houston, TX.* Sponsor: J. Render.

A new class of intraocular lenses (IOLs) is being developed with the goal of restoring the focusing ability of the eye (accommodation) for treating presbyopia (the age-related loss of near focusing ability). Although cataract surgery may be among the safest and most common of surgical procedures, these so called accommodative IOLs (A-IOLs) present new challenges as well as offer new opportunities. A-IOLs differ considerably from standard IOLs in that they are biomechanical devices designed to move or change shape in response to ciliary muscle contraction. A-IOLs are bulkier, made from different materials, may be implanted in different locations in the eye and have mechanisms of action that differ fundamentally from standard IOLs. The surgical procedures required to implant these devices are also more challenging, as they require new surgical devices. In addition, the safety considerations for A-IOLs are different. Pre-clinical animal testing that can be done is limited, complications that can arise are unique, and regulatory hurdles for demonstrating safety and effectiveness are higher. The ultimate success of A-IOLs will rely on solving significant biological challenges that still remain, such as resolving the post-operative healing response of the eye including prevention of post-operative lens epithelial cell proliferation and fibrosis of the lens capsule. This presentation will describe the challenges associated with the development A-IOLs. It will also introduce some future potential applications such as, the possibility of delivering drugs from A-IOLs to solve these biological challenges, as well as other unique surgical and pharmacological interventions aimed at resolving the problem of presbyopia.

**W 2511 Safety Assessment Strategies and Challenges for Developing Intravitreally Administered Biologics.**

E. A. Thackaberry. *Safety Assessment, Genentech, Inc, San Francisco, CA.*

The development of intraocular drugs to treat posterior segment disease, such as age-related macular degeneration, presents both advantages and challenges due to the unique aspects of ocular anatomy and physiology. While drug administration within the eye affords the promise of direct and local delivery, the reduction of systemic exposure and toxicity, and the availability of non-invasive tools allowing for real-time monitoring of the eye, there is an unmet need to reduce intravitreal injection frequency and treatment burden through sustained delivery formulations and devices. Adding to these complexities, developing antibody-based therapeutics presents additional challenges due to their inherent specificity (often limited to primates), which may limit the animal models available for assessing safety. Case studies on the safety assessment strategies and challenges encountered in developing protein therapeutics to the posterior segment of eye will be presented.

**W 2512 Development and Regulatory Considerations for an Ocular Drug Release System for Ocular Disease.**

A. Wiese. *Nonclinical Safety, Allergan, Irvine, CA.*

Delivering drugs to various compartments of the eye presents unique scientific and regulatory challenges. This presentation describes these challenges in the context of the development of Ozurdex®, a bioerodable drug delivery system containing dexamethasone delivered to the posterior segment of the eye. Key to the development of this drug was understanding the drug distribution and its effects in the eye, drug release characteristics and erosion profile of the implant, and evaluation of the toxicological profile of both drug and implant. Additionally, and in parallel, development and testing of the applicator and consideration of drug interactions was ongoing. Regional differences in regulatory agency expectations will be presented. Finally, general learnings and applicability of those learnings to the development of drug delivery systems to various compartments of the eye will be discussed.

**W 2513 Regulatory Considerations in Ocular Medical Device and Drug Delivery Systems Development.**

C. Ghosh. *Center for Drug Evaluation Research, US FDA, Silver Springs, MD.*

Ocular medical devices and drug delivery systems encompass a wide variety of products including solid devices (such as intraocular lenses, surgical instruments and contact lenses) and devices that are liquid-based (such as viscoelastics and contact lens solutions). This presentation will present the classification and regulatory requirements for major categories of ocular medical devices and drug delivery systems and discuss the regulatory decision making and implications pertaining to preclinical and clinical evaluations.

# Notes

A large rectangular area with horizontal ruling lines, intended for taking notes. The area is framed by a dark border on the top and sides, and a decorative floral pattern on the bottom.

# Author Index

## A

Aaronson, W	117	Ahn, S	1162	Ampawong, S	1316	Archer, F E	1830
Aardema, M J	792*, 1686*	Ahrenhoerster, L S	398*, 812	Amro, N A	2192	Arcuri, A S	2395
1697, 1694, 1698		Aiba, S	956	Amuzie, C J	1889, 2465*	Ares, I	592, 1781
Aarts, J M	2249	Aida-Yasuoka, K	2203*	Anadón, A	592, 1533, 1781*	Arias-León, J	603
Abadin, H G	479	Aillon, K	495, 581, 582, 1934*	Anand, S	895	Arima, A	1031
Abam, E O	1257, 1527, 2279	Aisaki, K	1563	Anand, S S	301, 488, 596, 922	Arita, A	1164
Abassi, Y A	1971, 1208	Ait-Belgnaoui, A	2368	Anantharam, P	1837*	Arlt, V M	1714
Abatan, M O	1307*	Aizawa, Y	736, 914, 2190	Anantharam, V	243, 729, 1837, 1838, 1842, 1856, 1857, 1858	Armer, L	756
Abazyran, B	2153	Ajani, E K	1320	Ancha, M	2054	Armstrong, L	1290*
Abbas, I K	2076	Ajay, A K	2196*, 2200	Andersen, M E	34*, 110, 474, 690, 726, 892, 897, 1297, 1705, 2012, 2358, 2443	Armstrong, R	219
Abbott, B D	557, 564, 1981	Ajayi, O L	1307	Anderson, C J	198	Arnett, D	848*
Abbott, M	1807	Ajuh, P	1214	Anderson, D	229, 532, 976, 2155*, 2252	Arnold, L L	1092, 2285, 2286*
Abbruzzese, J L	2435	Akagi, J	2340	Anderson, D S	1358*, 2389	Arnold, S M	1248*
Abdalla, D	2101	Åkesson, A	1920	Anderson, G	125	Aronson, S	440
Abdel Jabbar, M	1522	Akhiani, M	955	Anderson, G L	1254	Aronstam, R S	1770
Abdel Rasoul, G	1420	Akiba, S	475	Anderson, G	1254	Arowojolu, A	2051
Abdel-Rahman, S Z	195, 548, 1691	Akindahunsi, A A	1783	Anderson, K	335, 423, 424, 871	Arreola-Mendoza, L	2282
Abdel-Razzak, Z	1068, 2039	Akinwumi, K	164	Anderson, K L	416	Arrington, J	1800
Abdelmalak, M M	747	Aksoy, M	1491	Anderson, L	2139*	Arteel, G	646
Abdou, K A	281*	Al-Abed, S R	1737	Anderson, L C	1428	Arthur, J M	2184
Abdulla, A	652	Al-Bader, M	2132	Anderson, O S	807, 1007	Arulanandam, A	1802
Abe, T	2256	Al-Eryani, L	1997	Anderson, S	423*, 424, 1226*	Arumugam, K	2149
Abia, W A	1883*	Al-Fayoumi, S	501	Anderson, S E	416	Arvidson, K	857*, 859, 869, 2349
Abid, A D	2389	Al-Khedhairi, A A	2378	Anderson, S M	817, 1751	Arzuaga, X	1024
Abiko, Y	1291*	Al-Rouqi, R	1522	Anderson, T	2016	Asai, Y	1200
Abo, T	974*, 975	Al-Saleh, I	1522*	Anderson, W H	1801	Asaki, E	173
Abou-Donia, M B	1379	Aladjov, H	854	Anderson Thompson, E E	467*	Asangba, A E	1436
Aboud, A A	1685*, 1855	Alaniz, R	162	Andersson, P	2000	Ascah, A	757, 1130
Abplanalp, W	1195	Albakheet, S A	1536	Anderton, M	701	Aschner, M	245, 1521, 1525, 1848, 1849, 1855, 1859, 1860, 2005, 2143, 2452
Abraham, N	1227	Albaqami, F F	1797*	Ando, Y	938	Asfaha, J B	1497*
Ackah, F	1971	Albee, R	630	Andrade-Garcia, A	1152	Asgharian, B	607*
Ackerman, C D	1156	Albert, D	2045	Andreassen, T K	1029	Ashikaga, T	956, 969, 1959
Ackerman, J	2274	Alblas, M	240	Andresen, K	1292	Ashley, K	1575
Acon-Chen, C	347	Albores, A	182*, 451	Andrew, M	457	Ashrafian, H	1493
Acquaah-Mensah, G	134, 142, 696, 1627	Albrecht, P P	1269*	Andrews, D L	59, 61, 214, 241, 253	Ashworth, A	1377*, 1987
Acuña-Hernández, D	2112, 2117	Albuquerque, L G	1901	Andrews, L	849*, 966, 1256	Assaf, N	301, 593, 895
Adachi, H	1692*	Aldossari, A	1337*	Andrews Kingon, G L	1902*	Atchison, W D	1456, 2144, 2145, 2147
Adam-Poupart, A	1948*	Aleksunes, L M	645, 662, 1294, 2208*	Andros, C	1340	Atchley, D	2456
Adamo, M A	268	Alenius, H	453	Andrus, A K	1101	Atli Sekeroglu, Z	1491
Adams, R	549	Aleo, M D	1548	Aneskievich, B J	675, 689	Atobe, T	956*
Adams, T	1852	Alépée, N	970, 1037, 1580*	Anest, L	2067*	Atoni, A D	266
Adamson, G	267*, 1051	Alexander, D D	2234	Anestis, D	2181	Attafi, I M	1536*
Adamson, J	1488	Alexeeff, G V	878*	Anetor, J I	2051*	Attia, S M	2378
Adamsson, A	1920	Alfaradhi, M	1636*	Ang, C Y	515, 1295, 1519*	Atwa, S	143
Adebayo, A O	1273, 2296, 2302*	Alfi, M	141	Ang, X	2172	Aubrecht, J	929
Adebayo, J O	1319*, 1799	Algaier, J	495, 581, 582*, 1934	Angalakurthi, S	2054	Audet-Delage, Y	1985*
Adedapo, A A	1304*	Alge, J L	2184	Angelini, D J	1732*	Audouze, K	551
Adeleye, Y	690, 1705, 2443	Alharthy, K M	331*	Anger, L T	1628	Auerbach, S S	115, 514, 939*, 2275
Ademowo, G O	2201	Ali, I	1920*	Anger, W K	1419*	Aughton, P	2166
Ademuyiwa, O	1257, 1527, 2279*	Ali, M A	861*	Anguissola, S	1748, 1761, 1769, 2396*	Augsburger, A	749
Adenubi, O T	1307	Ali, S F	8, 91, 2160, 2365, 2377	Angulo Molina, A	1771*, 1778	August, L	878
Adenuga, D	1052*, 2070	Aliberti, A	1197*	Angulo-Olais, R	1832, 2385	Augustine, K	1026*
Adeshina, F	708, 2212, 2213, 2214	Alkandari, A	1493*	Anim, J A	203	Augustine-Rauch, K	1002, 1025
Adgate, J	767*	Allais, L	1834*	Ankley, G	265, 625, 1594	Aulmann, W	1545
Adkins, K	716, 1072	Allard, P	1455*	Annaka, N	973	Ault, M	1865
Adler, M	2195*	Allegret, V	1234	Ansari, G	1079, 1426	Ault, V	1934
Adunyah, S E	1110	Allen, J L	1385*, 2156, 2157, 2479	Ansari, M A	315	Aumann, A	1471
Adzemovic, T	435	Allen, K M	62*, 63, 235	Anselmo-Franci, J A	98	Aumsuwan, P	147*
Afolabi, O K	1257, 1527, 2279	Allen, K T	151	Anson, B D	85	Aungst, J	857, 1570
Afrooz, A	1766	Allievi, C	2098	Anstey, J C	1216	Austin, C P	1462, 1701, 2269, 2402*
Afshari, A	211	Allison, P G	1519	Antczak, P	555	Austin, E	501
Afshari, C	1286	Allosery, K	1809	Antherieu, S	2039	Authier, S	757, 758*, 1130
Afzali, M F	242*	Alpertunga, B	196*, 538	Antignac, E	1959	Autio, R	2375
Aga, D S	310	Alsberg, T	1270	Antoine, D	1900*	Autrup, H	1329
Agarkova, I	1072, 1476	Alshabbaheen, A	1522	Antonini, J M	211*, 465, 1107, 1132, 1347, 1350, 1626	Auttachoat, W	1227, 2469
Agarwal, C	365, 371	Altera, K	1221	Anwar-Mohamed, A	2292*	Avakian, A	1805
Agarwal, R	365, 366, 369, 371	Aluru, N	1288*	Anwer, J	1908	Avalos, J	972, 974
Aggarwal, M	594*, 719, 1248	Alvarado-Cruz, I	1492, 1832*	Anzai, T	178, 1441*	Avanasi, R	450
Aghaee, S	123*	Alvarado-Mejía, J	603, 1836	Ao, H	1827	Avila, D	646
Agina-Obu, D I	912	Alves, D A	354, 367	Aoki, K	428	Aylasevich, S	1696, 2446
Ago, Y	1384	Alves, M M	2015	Aoyama, K	2322	Axelrad, D	2456
Aguilar-Alonso, P	1152	Alvey, J A	2120	Api, A	1310, 1489, 2103	Ay, M	729, 1856*
Aguilar-Madrid, G	2282	Alyea, R A	537*, 1449	Apic, G	1894	Aydin, C	215, 2500
Aguirre, S	1231	Amano, I	1023	Apostoli, A R	1813	Ayehunie, S	623*, 2252
Agusa, T	2299*	Amantana, A	344	Applegate, D	557, 1294	Ayllon-Vergara, J	2282
Agustin, R	1778	Amaraneni, M	488*, 593, 596	Appleyard, S M	1375	Aylward, L	804*
Ahene, A	1020	Ambrosio, F	2311	Apte, U	632, 1097	Ayoola, S O	264, 1320*
Ahir, B	543	Ameredes, B T	1879, 2021	Aquirre, S	925	Ayotte, P	942, 1985
Ahlfors, H	2375	Amin, A	994	Aragón, M	223*, 1141	Azari, A	2045*
Ahmed, K I	281	Amin, J	1553	Arai, Y	1174	Azeez, O I	1245*
Ahmed, N S	599*	Amin, S G	181, 1279	Araki, D	974	Azeke, J	1046
Ahmed, S	1305	Aminov, Z	1984	Aranibar, N	1064	Aziz, S	2192
Ahn, J	1328	Ammenhauser, A	581	Araujo, A	1492		
Ahn, K	459	Amoako, A A	950	Arcaroli, J	172		
		Amoscato, A	2010	Arcega-Cabrera, F	1836		

The numerals following the author's names refer to the abstract numbers.  
The asterisk after the abstract number indicates the author is the first presenter.

# Author Index (Continued)

The numerals following the author's names refer to the abstract numbers.  
The asterisk after the abstract number indicates the author is the first presenter.

<b>B</b>			
Baan, R	1116	Bardullas, U	1409*
Babayemi, D O	1257, 1527, 2279	Baré, B	1756*
Babbe, H	2065	Barfuss, D W	2183
Babcock, G F	1519	Barger, M	815, 2366
Babendreier, J	702	Barile, F A	1196, 1197, 1206
Babick, F	1754	Barker, M	2348
Babin, M C	348, 353, 360	Barker, P	1866
Babin, P	559	Barks, A K	528, 1007*
Baccarelli, A	2414	Barlow, C A	1495
Bachour-El Azzi, P	1068, 2039	Barnaby, R	268, 385
Backos, D S	312	Barnes, C	2168
Bacom, A	721, 1970*	Barnes, E	634
Bacus, S	1556	Barnes, N	957
Badawy, A	1343	Barnett, B	1694
Badding, M A	1747, 2003*, 2013	Barnhart, C	1376*
Bader, J E	976, 982*	Barnhill, L	1407
Badger, T M	97, 1302, 1589	Barr, D B	1909
Badireddy, A	1735	Barraj, L	1645*
Badisa, V	652, 653	Barrass, N	2167
Bae, M	184	Barrera-Hernández, A	1769, 2282, 2385
Bae, O	913*, 1301	Barrett, G	2219*
Bae, Y	522	Barrett, J T	1114*, 1923
Baek, J	1289	Barria, A	1373
Baek, S	913	Barro, S	1040
Baeva, L	77*	Barron-Vivanco, B S	182
Baghdasarian, A	2031	Barros, R S	2395
Bagley, B D	201	Barros, S B	411, 1500
Baglole, C J	2355	Barros Vegailla, C	556*
Bahamonde, J	1353*	Barroso, J	1694
Bahl, V	1210, 1468*	Barrow, P	1028
Bahrami, Y	1159	Bars, R	809, 1099, 1926
Baier-Anderson, C	1551*, 1559, 2229	Bartels, M	269, 508*, 719, 811, 1248, 1707, 2460
Bailey, J	1937*	Barter, R A	709
Bailey, K	543, 2297*	Bartlett, M G	595
Bailey, L A	2216	Bartlett, R S	1014*
Bailey, N	759	Bartnick, E	1361
Bailey, S	1109	Barton, H A	884*
Bailey, W J	1903	Barve, S	646, 2052, 2053
Bain, G	2166	Basavarajappa, M	2115
Bain, Z	1566	Basketter, D	964*, 1036*, 1433
Baird, C	2213, 2214	Bass, V L	59*, 61, 213, 214
Baird, W M	554, 1242	Bassetti-Gaille, C	1383
Bais, P	1001	Bast, C	2213*
Baisch, B L	2363*	Basta, N T	2230
Bajaj, N	193*	Basu, N	530
Bajt, M	658, 1090	Bataille, A M	660*
Baker, A	1590	Batal, M	1501*
Baker, D D	2264*	Bates, C A	1862*
Baker, G L	1760	Bates, M	2324*
Baker, N A	787*	Bathula, C	1181
Baker, N C	126, 128, 863*, 864	Batke, M	1965
Baker, S	1473	Battelli, L A	20, 237, 452, 1457, 107
Baker, T K	2137	Baudet, S	1035*
Baksi, S	2181	Bauer, K	582
Balandaram, G	637*	Bauer, R N	224*
Balavenkatraman, K	1055*	Baum, M	2337
Balbuena, P	1979, 2461*	Bauman, M	979*
Balch, C G	2081	Baumeister, J	1809
Bale, A	714	Baumgartner, J	1074
Ball, J G	2185	Bauter, M R	2346
Ball, L M	289	Baxter, S A	526
Ball, W	1021*, 2228	Bayir, H	2009
Ballard, L	328	Baynes, R E	1038
Ballatori, N	1073	Bayona, M	482
Ballew, M	1251	Beach, A	149
Ballinas-Casarrubias, L	2294	Beach, S L	361
Balogun, E A	1257, 1319, 1527, 1799*, 2279	Beasley, T E	56, 1386
Bammler, T K	2025	Beaubier, J	1267*
Bancos, S	1738*	Beauchane, M P	198
Bandiera, S M	304, 314*	Beaulieu, S M	702
Banerjee, A	512, 1906*, 1908	Beavis, A	401, 2065
Banerjee, N	150*, 152	Bechara, E J	2015*
Banks, L D	306	Becher, R	1714
Bannish, G	401, 2065*, 2068	Beck, B D	206, 1867
Banton, M	307, 1091	Beck, M	2347
Barajas, A	1400	Beck, N B	1578*
Barba-Escobedo, P A	921	Beck, S	443
Barbano, D	1620*	Beck, T	759, 2095
Barbier, O C	1748, 1769, 2385*	Becker, R	1972, 2267*
Barbosa, F	1901	Beckmann, N	2193
Barcellos, L	2412	Beckord, H J	198
Barcelo, D	310	Bednar, A J	515, 1336, 1344, 1346
Barchowsky, A	1644*, 2304, 2308, 2311, 2344	Bednar, B	1910
		Beebe, D J	2245
		Beedanagari, S	2442*
		Beer, C	1329
		Beesley, L J	507
		Beeson, C	1218
		Beeson, G	1218
		Beezhold, D H	423
		Beezhold, K	423, 2304*
		Begay, D	1516
		Beger, R D	938*, 1086
		Beggs, K M	1077, 1078*
		Begley, T	1702
		Beha, E	1696
		Behar, R Z	1210*
		Behbod, F	672
		Behl, B	1963
		Behl, M	53*, 1682
		Behrns, K E	1724
		Behrsing, H P	1470*
		Beier, E	1588
		Beilstein, P	2347
		Bein, K J	227, 229
		Beker, A	1447
		Beland, F A	647, 1042, 1043, 1071, 1710
		Belanger, S	271
		Belinsky, S A	1641*
		Beliveau, M	344, 345*
		Bell, D A	529*
		Bell, E	1547
		Bell, M	1605*
		Bell, S	875
		Bellis-Jones, H	1274, 1997
		Bellmann, B	434
		Belmonte, F	2036*
		Belski, T	576
		Beltran, M	1549
		Bemis, J	1701, 2446
		Benahmed, M	105, 1927, 1928
		Benbrahim-Tallaa, L	1116*
		Bench, G	1232
		Bencic, D	625
		Benedetti, G	1067
		Benfenati, E	870
		Benitez, J	12
		Benner, S	1387*
		Bennett, J	1844
		Benskin, J P	275*
		Bentley, P	1904
		Benton, C	186
		Benz, D R	861
		Benzer, R	132, 1124
		Benzerdjeb, H	1089
		Bercu, J	842*
		Berdasco, N M	877*
		Berea, E	1748, 2385
		Beren, J	738
		Beresford, L	1434*
		Berg, E	1735, 2048*
		Berger, F	2337
		Bergfeld, D	714
		Bergholm, A	1219
		Bergin, I L	807
		Bergkvist, C	718
		Berglund, M	718, 1920
		Bergmann, M	2123
		Bergquist, J	1921, 1924
		Bergvall, C	569
		Berk, M	993*
		Berkson, J D	636, 733
		Berlioz-Seux, F	2168
		Bernard, L	1226
		Bernard, M P	1807, 2064, 2066
		Bernasconi, S	758
		Bernd, B	460
		Berninger, J	265
		Bernstein, A I	1841, 1872
		Bernstein, D I	189
		Beronius, A	1962*
		Berthier, E	2245
		Berthold, M R	858
		Bertschi, B	1055
		Berzin, E L	1216
		Besenhofer, L	1904*
		Bespalov, A	1658*
		Bessemers, J G	2049
		Besshi, K	1811
		Bester, J D	1318
		Bettencourt, B	411
		Betts, C	1126, 2122
		Betts, N P	922
		Betz, M W	77, 1333*
		Beverly, B	2127*
		Bexiga, C G	179
		Beyer, D	483
		Beyrath, J D	2022
		Bhalli, J A	1740
		Bhat, V S	1946*, 2233, 2237
		Bhatnagar, A	60, 1195
		Bhattacharya, S	635, 892*, 1297
		Bhattacharyya, S	938
		Bhavaraju, L	221*
		Bhusari, S	1094*
		Bhushan, B	632*
		Bi, D	1124*
		Bialecki, R A	1229, 2167
		Bichell, T V	1860*
		Bickerton, S	2122
		Bieschke, C	1750
		Bijol, V	2198
		Bilgesu, S A	458, 465
		Billack, B	351
		Billhimer, W	972
		Billings, D	896*
		Billington, R	594, 719, 811, 1108, 2460
		Binienda, Z K	2160, 2365*
		Birch, M E	465
		Bircsak, K M	662
		Biris, A S	1740
		Birnbaum, L S	484, 491, 1597*, 1633, 1828, 1992, 1999, 2463*
		Biscarrat, C F	879*
		Bishop, E L	120
		Bishop, M E	1487
		Bishop, P L	1569*
		Bishop, S	638
		Bisinger, E C	1893
		Bisson, W	333
		Biswas, R	259*
		Bittner, G D	111, 113, 2332*
		Bjerke, D L	2043
		Blaauboer, B J	1478*, 1929, 2249
		Black, A T	2030*
		Black, M	1052, 1979, 2070
		Black, M B	1629*, 2459
		Black, S	303, 308, 309*, 466
		Black, W M	93
		Blackman, B R	1216, 1459
		Blackman, C F	1773
		Blain, R	714
		Blair, E C	2047
		Blair, I A	292
		Blair, W	2176
		Blake, A	86
		Blake, C L	1255*
		Blake, J C	2326*
		Blakeman, D	2248*
		Blanchard, K	1212
		Blanck, O	809, 1099, 1926
		Blanco, C	90, 1209
		Blanke, K L	190*, 1670
		Blanset, D L	1805*, 2462*
		Blasberg, J	2169
		Blasi, E	1120*
		Blaszkevicz, M	188
		Block, M L	44*, 1843, 2480*
		Blömeke, B	293, 311, 1054, 2361
		Blomme, E A	640, 946, 1820, 1905
		Bloom, M S	1258
		Bloom, R	279
		Blossom, S	57*, 536
		Blount, B C	1915, 2118
		Blum, J L	1546, 2105*
		Blystone, C R	1982
		Boberg, J	1383
		Bobst, S	2041, 2268*
		Bodhicharla, R K	1494*, 1845
		Bodnar, W M	289, 953, 2293
		Bodwell, J E	2296
		Boekelheide, K	25*, 29*, 109, 573, 994, 1634, 2139, 2247, 2501*
		Boerleider, R Z	2049*
		Boermans, H J	2081
		Boess, F	2175
		Bogdan, N	2125*
		Bogen, K	2222

## Author Index (Continued)

- Bohaychuk, K ..... 1127  
 Bohnenberger, S ..... 1502\*, 1689  
 Boissette, B ..... 1850  
 Boitano, S ..... 2298  
 Boitier, E ..... 927  
 Bojang, P ..... 701\*  
 Bokhart, M ..... 1998\*  
 Bolger, P M ..... 843, 844\*, 1643\*, 2334  
 Bolmarcich, J ..... 2273  
 Bolon, B ..... 1611\*  
 Bolstad, H M ..... 1268\*  
 Bolt, A M ..... 1176\*  
 Bolton, J L ..... 2321, 2336  
 Bombick, B R ..... 1891  
 Bond, A A ..... 192, 2035  
 Bondy, G S ..... 448, 1690  
 Bonham, K ..... 1209\*  
 Bonifas, J ..... 293\*, 1054  
 Bonini, M ..... 1906  
 Bonner, J C ... 19\*, 24\*, 438, 439, 467, 2384  
 Bonner, M R ..... 1258, 1420  
 Bonventre, J A ..... 1457\*  
 Boobis, A ..... 2455  
 Booc, F T ..... 331, 2110\*  
 Boodhia, K ..... 1340\*  
 Boonungsiman, S ..... 1758\*  
 Boorman, G A ..... 670  
 Bordag, N ..... 1562, 2270  
 Bolders, R B ..... 75, 93  
 Borg, D ..... 570\*  
 Borghoff, S J ..... 102  
 Borgne-Sanchez, A ..... 1081\*  
 Borsay Horowitz, D ..... 277  
 Borude, P ..... 632, 1097  
 Botelho, D ..... 468\*  
 Botham, P ..... 55, 1401  
 Botta, D ..... 1364\*, 2379, 2392  
 Bottai, M ..... 569  
 Bottimore, D ..... 1970  
 Bouchard, D ..... 440  
 Bouchard, G F ..... 74, 750, 2047  
 Bouchard, J ..... 1178\*  
 Bouchard, M ..... 618, 942  
 Boudreau, M D ..... 1357  
 Boudry, I ..... 1501  
 Bouhifd, M ..... 109, 1680  
 Boule, L ..... 415\*  
 Boulet, J ..... 502  
 Bourbonnais, R ..... 1948  
 Bourdi, M ..... 636  
 Bourgeois, M M ..... 1669\*  
 Bourgeois, R ..... 2063  
 Bourner, M ..... 2169  
 Bourouf, L ..... 2272  
 Bousquet, R W ..... 226  
 Bouvard, V ..... 1116  
 Bouwmeester, H ..... 2382  
 Bovee, T ..... 2249  
 Boverhof, D R ..... 1052, 1741, 2070\*, 2444, 2460  
 Bowcock, C ..... 2433  
 Bowen, E L ..... 1473\*  
 Bowens, C M ..... 367  
 Bower, D ..... 870  
 Bowes, J ..... 1074  
 Bowman, A B ..... 6, 1685, 1855, 1860  
 Bowman, C C ..... 42  
 Bowman, C J ..... 1003, 1660\*, 1663\*, 2142  
 Boyce, R ..... 2107  
 Boyd, W A ..... 144, 1450, 1452\*  
 Boyer, J A ..... 1283  
 Boyer, S ..... 857  
 Boyes, W K ..... 606, 1386, 1737, 2464\*  
 Boykin, E H ..... 241, 253, 1427, 2071  
 Bozhilov, K ..... 1753  
 Bradberry, S M ..... 2507\*  
 Bradfield, C A ..... 169  
 Bradford, B U ..... 289  
 Bradley, D ..... 2114\*  
 Bradley, J ..... 89, 901\*, 1138\*, 1379  
 Bradley, L J ..... 1567, 2211\*  
 Bradley, P ..... 1625  
 Bradman, A ..... 783, 2412  
 Bradshaw, T ..... 1226  
 Brady, J ..... 2165  
 Braisted, J ..... 1462  
 Braithwaite, E ..... 1188\*  
 Brambila, E ..... 1152\*  
 Bramble, L ..... 62, 235  
 Branam, A ..... 2141\*  
 Branco, A ..... 680  
 Brandenberger, C ..... 62  
 Brandon, W ..... 75  
 Brandwein, D H ..... 959  
 Braniste, V ..... 2329, 2330  
 Brannen, K ..... 1025  
 Branstetter, D ..... 2107  
 Bratton, S B ..... 170, 1730  
 Braue, C R ..... 347  
 Braue, E ..... 1046  
 Braun, A ..... 444, 1469  
 Braun, M ..... 1167\*, 1530  
 Braydich-Stolle, L ..... 1330, 1332\*  
 Breckenridge, C ..... 1401  
 Bredfeldt, T ..... 768, 1972, 2238\*  
 Breen, M ..... 625\*  
 Breen, M S ..... 625  
 Breider, M A ..... 2264  
 Breithaupt, K ..... 1456\*  
 Breitner, E ..... 1332  
 Bremer, S ..... 1574  
 Brennan, A ..... 933  
 Brenner, S A ..... 2376\*  
 Brenseke, B ..... 1353  
 Breslawec, H ..... 1676\*  
 Breslin, W ..... 2119\*  
 Bressler, J P ..... 546  
 Brewster, D ..... 2168  
 Brian, R M ..... 75  
 Brickus, L ..... 2395  
 Bridges, C ..... 2183\*  
 Briffaux, J ..... 1017, 1035, 1238\*, 1834  
 Brighton, L ..... 224  
 Brigo, A ..... 1628  
 Brinker, A ..... 2169  
 Brinkman, A M ..... 1287\*  
 Britt, J ..... 481  
 Britt, R D ..... 2026  
 Brochu, I ..... 2060, 2063  
 Brock, K ..... 424  
 Brock, M ..... 89, 901  
 Brockmeyer, H ..... 434, 1490  
 Brocksmith, D ..... 74  
 Brockway, B ..... 68  
 Brockway, M ..... 68  
 Broderick Pritty, M ..... 2210  
 Brodsky, B ..... 245  
 Broich, K ..... 1041  
 Bromberg, P A ..... 2029  
 Bronstein, J M ..... 1399, 1407  
 Brooks, A ..... 1223  
 Brooks, A M ..... 1808\*  
 Brooks, B W ..... 288, 2241  
 Brooks, E G ..... 2021  
 Brooks, J ..... 131  
 Brooks, P ..... 62, 235  
 Broschk, S ..... 2250  
 Brouillette, M ..... 2060  
 Broussard, C ..... 393\*  
 Brouwer, K L ..... 881, 1059  
 Brower, M ..... 1537  
 Brown, A ..... 1987\*  
 Brown, A M ..... 72, 1556  
 Brown, B ..... 2185  
 Brown, E ..... 2311  
 Brown, J ..... 1251, 1252  
 Brown, J M ..... 433, 462, 1032, 1131, 1133, 1134, 1135, 1327, 1337, 2470\*  
 Brown, J S ..... 216  
 Brown, K A ..... 2325  
 Brown, L D ..... 74, 750, 2047\*  
 Brown, R D ..... 417  
 Brown, R P ..... 77, 200\*  
 Brown, T ..... 2165  
 Brown, T A ..... 454\*  
 Browne, E ..... 609  
 Bruce, E D ..... 610, 1243, 1342, 1988\*, 2432\*  
 Bruckers, L ..... 1249  
 Bruckner, J V ..... 488, 593, 595, 596  
 Bruening-Wright, A ..... 72  
 Brumfield, M ..... 1912  
 Brune, J M ..... 1831  
 Brunnemann, K D ..... 2255  
 Bruno, M E ..... 558\*  
 Brunström, B ..... 325  
 Bruun, D A ..... 1375, 1422\*, 2452  
 Bryant, M ..... 647  
 Bryant, S ..... 2125  
 Bryce, S ..... 1696\*, 1701  
 Bu, K ..... 1356  
 Buchbinder, A ..... 1810  
 Bucher, J R ..... 553, 1570  
 Büchse, A ..... 977  
 Buchweitz, J P ..... 1998  
 Bucio, L ..... 1154  
 Buck, R C ..... 493, 494, 1544, 2113, 2227  
 Buck, W R ..... 1820  
 Buck Louis, G M ..... 782\*  
 Buckley, B ..... 43\*, 1830  
 Buckley, L A ..... 1801\*  
 Buczynski, B W ..... 984\*  
 Budinsky, R ..... 1278\*, 2459  
 Bueters, R R ..... 2202\*  
 Buettner, C ..... 991  
 Bugel, S M ..... 52\*, 329, 333  
 Bui, Q ..... 2339  
 Bui-Nguyen, T ..... 588\*  
 Bull, R J ..... 615  
 Bunaciu, R ..... 693\*  
 Bunch, R T ..... 1237  
 Bunderson, B R ..... 2327\*  
 Bunin, D ..... 1221  
 Buratovic, S ..... 1390\*  
 Burch, D ..... 471  
 Burchiel, S W ..... 386  
 Burd, C ..... 700  
 Burgess, J L ..... 2298, 2305  
 Burgess, M ..... 1251, 1252  
 Burgoon, L D ..... 140, 265, 868, 875  
 Burke, M ..... 526  
 Burke, T ..... 246  
 Burkholder, A ..... 985  
 Burleson, F G ..... 1433, 1541, 1542, 1543, 1808  
 Burleson, G ..... 1433  
 Burlingham, J J ..... 96\*  
 Burn, B ..... 1144\*  
 Burns, C ..... 1248  
 Burns Naas, L ..... 1120, 2042  
 Buron, N ..... 1081  
 Burrier, R E ..... 1001  
 Burris, A S ..... 2160  
 Bursian, S ..... 2324  
 Burt, D ..... 929  
 Burzio, L ..... 1547  
 Bus, J ..... 307  
 Busbee, P B ..... 2353\*  
 Buschmann, J ..... 1027\*  
 Bushel, P ..... 258, 985  
 Bushman, W A ..... 251, 2245  
 Bushnell, P J ..... 56\*, 606, 1386  
 Busque, M ..... 1948  
 Bussiere, J ..... 2062  
 Bussiere, J L ..... 2107\*, 2462  
 Bussièrès, M ..... 1822  
 Butala, J H ..... 1741  
 Butenhoff, J L ..... 492, 629, 1004  
 Butt, M ..... 55, 1236, 1401\*  
 Butts, K ..... 1564  
 Butz, N ..... 186  
 Buzalaf, M A ..... 1901  
 Byer, R P ..... 2025  
 Byrne, D ..... 1317  
 Byrne, P ..... 1179  
 Caballero-Gallardo, K ..... 1911\*  
 Cabaton, N J ..... 550  
 Cabell, L ..... 576\*  
 Cable, P ..... 2293  
 Cachau, R E ..... 1768, 1777  
 Cai, C ..... 1024  
 Cai, L ..... 1140, 1142, 1731, 1824, 1825  
 Cai, Q ..... 313, 1886  
 Cai, X ..... 181\*, 540  
 Caito, S W ..... 1525\*  
 Cajero, M ..... 1136  
 Calderon, R L ..... 2290  
 Calderon-Gutkind, S N ..... 1656\*  
 Calderone, A A ..... 1405  
 Caldwell, D J ..... 203  
 Calhoun-Davis, T M ..... 170  
 Cali, J ..... 2262  
 Cali, J J ..... 1076, 1080\*  
 Calizo, B ..... 94  
 Callander, R ..... 1213  
 Camacho, L ..... 1596, 2115\*  
 Camenisch, T D ..... 2310  
 Cameron, D ..... 972\*, 974, 975  
 Cameron, M J ..... 1875\*  
 Campbell, A ..... 261  
 Campbell, J ..... 496, 897\*  
 Campbell, J A ..... 510  
 Campbell, J L ..... 2461  
 Campbell, K L ..... 1436  
 Campbell, M R ..... 529  
 Campen, M J ..... 45\*, 769, 222, 1136, 1141, 2016  
 Campion, S N ..... 2136, 2491, 2494\*  
 Canady, R ..... 2455\*  
 Cantsey, R D ..... 2020  
 Candice, C ..... 1334  
 Canet, M ..... 1065\*  
 Canipa, S ..... 1623  
 Canlet, C ..... 550\*  
 Cannan, S ..... 1805  
 Cannon, J R ..... 1408  
 Cao, C ..... 69  
 Cao, C J ..... 1743\*  
 Cao, J ..... 1382\*  
 Cao, L ..... 1020  
 Cao, W ..... 2008  
 Cappart, N ..... 992  
 Cappon, G D ..... 2142\*  
 Capsel, K ..... 2237  
 Capstick, M ..... 1490  
 Card, J W ..... 1550, 1943, 2244  
 Cárdenas-Marrufo, M ..... 603  
 Cardone, M S ..... 1860  
 Cardoso, C A ..... 1901  
 Cardoso, M A ..... 1901  
 Cardozo-Pelaez, F ..... 187  
 Carey, S A ..... 399\*  
 Carlander, U ..... 2362\*  
 Carll, A P ..... 65, 1129\*  
 Carlock, L ..... 2062  
 Carlson-Lynch, H ..... 721\*  
 Carney, E W ..... 537, 1630  
 Carolino, R G ..... 98  
 Caron, W ..... 2471  
 Caron-Laramée, A ..... 2060  
 Carosino, C M ..... 227\*, 1364  
 Carpenter, C ..... 1544  
 Carpenter, D O ..... 1984  
 Carpenter, S C ..... 494  
 Carpi, A ..... 2150  
 Carr, G ..... 549  
 Carr, J ..... 1936  
 Carr, R L ..... 2450\*  
 Carranza-Lopez, L ..... 1911  
 Carraway, M ..... 1122  
 Carreira, V S ..... 997\*  
 Carrière, M ..... 2368  
 Carroll, M A ..... 1850, 1851, 1852, 1853, 1854  
 Carroll Turpin, M A ..... 742\*  
 Carswell, G ..... 947  
 Carter, A L ..... 562  
 Carter, D ..... 1919\*  
 Carter, J ..... 212  
 Cartier, A ..... 189  
 Cartus, A T ..... 2333\*  
 Caruso, J A ..... 2080\*  
 Carvajal, I ..... 503  
 Casals, E ..... 816  
 Casati, S ..... 964  
 Casavant, B P ..... 2245  
 Cascio, W ..... 212, 828  
 Case, C ..... 1186  
 Casey, B J ..... 1324, 1333  
 Casey, W ..... 1572, 1573, 1574\*, 1576, 2251  
 Casida, J ..... 589  
 Casillas, R P ..... 336, 337, 341, 353, 355, 358  
 Cassee, F R ..... 826\*, 828, 830

The numerals following the author's names refer to the abstract numbers.  
 The asterisk after the abstract number indicates the author is the first presenter.

## C

# Author Index (Continued)

Cassisi, L A ..... 774\*  
 Castagné, V ..... 744  
 Castaneda, A ..... 227  
 Casteel, S W ..... 2230  
 Castellano, V ..... 592, 1781  
 Castellon, B ..... 1775  
 Castillo-Burguete, T ..... 603  
 Castranova, V ..... 19, 20, 23\*, 426,  
 427, 441, 449, 452, 457, 458, 465, 815\*,  
 1132, 1147, 1747, 2003, 2013, 2366, 2464  
 Castro, K R ..... 2099\*, 2101  
 Caswell, E ..... 2208  
 Catalán, J ..... 453\*  
 Catapano, E J 1850, 1851, 1852, 1853, 1854  
 Catlin, N ..... 573\*  
 Cauley, M ..... 2451  
 Causey, R D ..... 361  
 Cavagnaro, J ..... 851\*  
 Cavalcante, M ..... 2101  
 Cavallin, J ..... 265  
 Cave, M ..... 644, 940\*, 1274, 1997  
 Caverly-Rae, J M ..... 1004  
 Cearfoss, J ..... 560  
 Ceder, R ..... 870  
 Cederbaum, A I ..... 2024  
 Ceger, P ..... 1574, 2251\*  
 Cele, M P ..... 1795  
 Cendak, R ..... 878  
 Centeno, J ..... 1534  
 Cepa, S ..... 946  
 Cerignoli, F ..... 76  
 Cerreta, J M ..... 1726  
 Cerro López, M ..... 1771  
 Cervelli, J A ..... 353  
 Cerven, D R ..... 967, 978  
 César, F ..... 2101  
 Chadalapaka, G ..... 145\*, 159  
 Chae, M ..... 392  
 Chahoud, I ..... 1027  
 Chaiklang, S ..... 1973\*  
 Chaimongkolnukul, K ..... 1316  
 Chakraborty, M ..... 410, 636, 733\*  
 Chakraborty, S ..... 1849\*  
 Chakravarti, S ..... 860, 874\*  
 Chakravarty, A ..... 1230  
 Chalifour, L ..... 989\*  
 Chalker, L ..... 137  
 Chamberlin, D W ..... 2342\*  
 Chambers, D M ..... 2118  
 Chambers, H W ..... 340, 343  
 Chambers, J E ..... 83, 185,  
 340, 343, 508, 586, 1916  
 Chambliss, C K ..... 288  
 Champeroux, P ..... 71  
 Chan, C ..... 552  
 Chan, D ..... 77  
 Chan, E ..... 186  
 Chan, L ..... 2306  
 Chan, M K ..... 1265  
 Chan, M P ..... 717\*  
 Chan, P ..... 1300  
 Chan, V T ..... 1418  
 Chandler, J D ..... 2019\*  
 Chandler, K J ..... 1205\*  
 Chandramani-Shivalingappa, P ..... 1838  
 Chandrasekaran, Y ..... 885  
 Chang, C ..... 344  
 Chang, D ..... 799, 1253  
 Chang, D T ..... 321\*, 590  
 Chang, F ..... 2055, 2167  
 Chang, P ..... 887  
 Chang, S ..... 255\*, 492, 629, 1004  
 Chang, T K ..... 304, 314, 1275  
 Chang, X ..... 440, 600, 601, 883\*  
 Chang, Y ..... 355\*, 356  
 Chantal, P ..... 2219  
 Chao, M ..... 2359  
 Chaparro, A P ..... 2021  
 Chapdelaine, J ..... 2166  
 Chapeau, V ..... 1903  
 Chapin, R E ..... 25, 28\*, 2120, 2136  
 Chapkin, R ..... 672  
 Chapman, V ..... 1443\*  
 Chappell, M A ..... 1336  
 Chappidi, S ..... 1726\*  
 Charanek, A ..... 1068  
 Charbonneau, M ..... 2380

Charest-Tardif, G ..... 506, 622  
 Charles-Davies, M ..... 2051  
 Charoensuk, V ..... 1480\*, 1971  
 Chatikavanij, V ..... 1273, 2296  
 Chatterjee, N ..... 1328  
 Chatterjee, S ..... 635, 643  
 Chaudhuri, I S ..... 458  
 Chavan, H D ..... 663\*  
 Chavan, S ..... 2034  
 Chavez, C ..... 1803  
 Chavez, D ..... 1959  
 Chavez-Munguía, B ..... 451  
 Che, J ..... 204, 205  
 Chea, L S ..... 636, 733  
 Cheah, N ..... 671\*  
 Cheatham, L ..... 1882, 1904  
 Cheepala, S ..... 734  
 Cheeseman, M ..... 2455  
 Chekayev, Y ..... 1851\*  
 Chellman, G ..... 1220, 2107  
 Chelsky, D ..... 945  
 Chen, B ..... 465, 954  
 Chen, B T ..... 20, 211, 441\*, 457, 1147, 1350  
 Chen, C ..... 593, 596\*, 721, 1329  
 Chen, D ..... 1348, 1878  
 Chen, F ..... 1284  
 Chen, G ..... 2309\*  
 Chen, H ..... 1375\*, 1376, 1683  
 Chen, J ..... 1020, 1103\*, 1589  
 Chen, K ..... 1102\*, 1718, 1719, 1721, 2381  
 Chen, K H ..... 69  
 Chen, L ..... 66, 556, 597, 1348, 1351, 1361,  
 1381, 2105  
 Chen, L C ..... 238  
 Chen, M ..... 1241, 1730, 2162\*  
 Chen, P ..... 941, 1767\*, 1848\*, 1899, 2005  
 Chen, R ..... 1327  
 Chen, S ..... 320\*, 1239\*, 1483\*, 2321, 2336  
 Chen, T ..... 538, 650, 927,  
 1119\*, 1284\*, 1334, 1484, 1506, 1740  
 Chen, V H ..... 1809  
 Chen, W ..... 218, 419\*, 1760  
 Chen, X ..... 1804  
 Chen, Y ..... 172, 344, 461, 726, 1298\*, 1334,  
 1708, 1718, 1719, 1721, 1908, 2167\*, 2381  
 Chen, Z ..... 684  
 Cheng, D ..... 1828  
 Cheng, H ..... 78  
 Cheng, S ..... 1404, 1405\*, 2150  
 Cheng, W ..... 619\*  
 Cheng, X ..... 69\*, 1996\*  
 Cherdyu, S ..... 1316  
 Cherrington, N J ..... 511, 649,  
 1064, 1065, 1066, 1602\*  
 Cherry, D ..... 1828  
 Cherry, W ..... 2348  
 Chervona, Y ..... 1164, 2301\*  
 Chesné, C ..... 1068  
 Chesnut-Speelman, J ..... 1074  
 Chevalier, H J ..... 464  
 Chhabra, R S ..... 53  
 Chi, L ..... 591  
 Chiba, S ..... 445  
 Chibout, S ..... 1055, 1070, 1821, 2193  
 Chilton, J ..... 1202\*  
 Chin, F S ..... 1265  
 Chin-Sinex, H ..... 151  
 Chini, N ..... 1892  
 Chipinda, I ..... 1053, 1432  
 Chipman, K ..... 538  
 Chirino, Y I ..... 1763, 2390, 2393  
 Chishom, W P ..... 446  
 Chittiboyina, S ..... 192\*  
 Chiu, T ..... 1161  
 Chiu, W ..... 620, 710, 711, 876  
 Chiu, W A ..... 2454, 2477\*  
 Cho, C ..... 695  
 Cho, E ..... 204, 205\*  
 Cho, J ..... 207, 983  
 Cho, M ..... 695  
 Cho, S ..... 983\*  
 Cho, S M ..... 202\*  
 Cho, Y ..... 177\*, 1952, 2340  
 Choi, B ..... 459, 1511  
 Choi, C ..... 1312  
 Choi, D ..... 1745  
 Choi, H ..... 148\*, 220, 248, 2085, 2335, 2351

Choi, H M ..... 661  
 Choi, J ..... 1311, 1312\*, 1313,  
 1314\*, 1314\*, 1315, 1315, 1328\*, 1339,  
 1528, 1780, 1785, 1787, 1788, 1789, 1789,  
 1793, 1798, 1871, 2082  
 Choi, K ..... 496\*  
 Choi, S ..... 207, 228, 1511  
 Choi, T ..... 2475\*  
 Choi, Y ..... 202, 641, 1794  
 Cholanians, A B ..... 917  
 Chomysyn, E ..... 448  
 Chong, S ..... 1230  
 Chorley, B ..... 1294  
 Chotibut, T ..... 742  
 Chouinard, L ..... 2107  
 Chow, H ..... 2062  
 Chowdhury, I ..... 440  
 Chowdhury, P ..... 1813  
 Chowdhury, R ..... 685  
 Chowdhury, S ..... 469\*  
 Chowhan, P ..... 2219  
 Chrisler, W ..... 1762, 1765  
 Christensen, K Y ..... 1024  
 Christiani, D C ..... 15\*  
 Christiansen, S ..... 1383  
 Christine, G ..... 1039  
 Christoffersen, T E ..... 391  
 Chrysovergis, K ..... 724  
 Chu, C ..... 300  
 Chu, M T ..... 703\*  
 Chu, P ..... 1506  
 Chu, T ..... 1629  
 Chuang, G C ..... 80\*  
 Chun, H ..... 1785\*  
 Chun, S ..... 1315\*  
 Chun-Wei, T ..... 2162  
 Chung, F ..... 468  
 Chung, H ..... 1794  
 Chung, H J ..... 645  
 Chung, J ..... 1301  
 Chung, K ..... 1301  
 Chung, Y ..... 1311, 1312, 1313\*, 1314, 1315,  
 1785, 1786, 1787, 1788, 1789, 1793  
 Church, R J ..... 183\*  
 Churchill, G A ..... 1944  
 Churchwell, M ..... 1071, 1710  
 Chusuei, C C ..... 1770  
 Cicalese, L ..... 943  
 Cichocki, J A ..... 232\*, 233  
 Cienciewicz, J ..... 258\*  
 Ciganek, M ..... 563  
 Cisneros, B ..... 451  
 Ciurlionis, R ..... 640  
 Cizdziel, J ..... 1356  
 Cizmas, L ..... 2434\*  
 Clabault, H ..... 1932  
 Clair, H ..... 1274, 1997  
 Clancy, H A ..... 1164  
 Clancy, S ..... 1741  
 Clark, A ..... 576  
 Clark, B W ..... 323  
 Clark, C ..... 1365  
 Clark, D S ..... 2266  
 Clark, R S ..... 400\*  
 Clarke, E ..... 1198\*, 1819, 2179  
 Clarke, J ..... 649\*, 1066  
 Claude, N ..... 71  
 Clavijo, D ..... 1154  
 Clément, C ..... 1238  
 Clemow, S ..... 2220  
 Clendaniel, A N ..... 1324\*, 1325  
 Cléry-Barraud, C ..... 1501  
 Cleves, M ..... 97  
 Clewell, H J ..... 301, 474, 496, 616, 799,  
 895, 896, 897, 1163, 1979, 2457, 2461  
 Clewell, R A ..... 110, 690, 897,  
 1297, 1705\*, 2443, 2461  
 Cliff, R ..... 2081  
 Clifford, J L ..... 1306  
 Cline, H ..... 638  
 Clippinger, A ..... 854\*  
 Close, D ..... 803\*, 1804  
 Close, D M ..... 100  
 Cloutier, Y ..... 2380  
 Clynen, E ..... 949  
 Co, A ..... 2448  
 Coady, K K ..... 104, 112

Coccimiglio, J ..... 2007  
 Coccini, T ..... 2373  
 Cockburn, M ..... 1399  
 Coder, P S ..... 1003\*  
 Coffield, J A ..... 676  
 Coglian, V ..... 876, 2454  
 Cohen, S M ..... 1092, 2285, 2286  
 Cohrs, C ..... 311  
 Colagiovanni, D ..... 5  
 Colaiacovo, M ..... 1455  
 Colatsky, T ..... 1124  
 Cole, S ..... 1431, 1732  
 Cole, T B ..... 1010, 2448\*  
 Coleman, D P ..... 2326  
 Coleman, E ..... 270  
 Coleman, M ..... 291  
 Collette, W W ..... 925, 1231\*  
 Colli, W ..... 2015  
 Colli-Dula, R C ..... 944\*  
 Collin, B ..... 1366  
 Collinge, M ..... 1800  
 Collins, B ..... 495\*, 578, 581,  
 582, 1934, 2326  
 Collins, J L ..... 367  
 Collins, L B ..... 289, 620, 1704  
 Colombo, E S ..... 1141\*  
 Colombo, P A ..... 1034\*, 2098  
 Colon-Rodriguez, A ..... 2144\*, 2145  
 Comfort, K K ..... 1330\*  
 Compagnone, N A ..... 879, 2173  
 Composto, G M ..... 353  
 Compton, J ..... 2074  
 Conard, K R ..... 1001  
 Condon, M ..... 1534  
 Coney, L A ..... 401\*, 2065  
 Conklin, D J ..... 60, 769\*, 771\*, 987, 1195  
 Connolly, B ..... 1910  
 Connolly, C M ..... 2296  
 Connor, K T ..... 1964, 1977\*  
 Connors, R ..... 288\*  
 Connolly, R B ..... 619, 625, 1594\*  
 Conover, C ..... 1810  
 Conrad, K ..... 1385, 1392  
 Contreras, O ..... 1771  
 Cook, J C ..... 1092  
 Cook, N ..... 876  
 Cooke, G M ..... 2348  
 Cooke, L ..... 2396  
 Cooney, C ..... 536  
 Cooney, C A ..... 57  
 Cooper, G ..... 1024  
 Cooper, J ..... 1564  
 Cooper, K L ..... 1516, 2287, 2307\*  
 Cooper, K R ..... 1380, 1457  
 Cooper, R ..... 1940  
 Cooper, R L ..... 2088  
 Copeland, C ..... 1427, 2071  
 Copeland, L ..... 208, 1427, 2071  
 Copeland, L B ..... 241, 253  
 Copeman, C ..... 762, 1873  
 Coppie, B L ..... 639  
 Copple, I M ..... 654\*  
 Corbett, J ..... 643  
 Corcoran, G B ..... 2041\*  
 Corcoran, K ..... 174  
 Corley, R ..... 1942  
 Corley, R A ..... 299, 317, 894  
 Coronado, G D ..... 1909  
 Coronel, M L ..... 1727  
 Corrales, J ..... 328, 331  
 Correa, M C ..... 962  
 Corsini, E ..... 403, 1440\*  
 Corson, N ..... 2363  
 Cortés-Torres, M ..... 2385  
 Corton, C ..... 139, 557\*, 880, 891, 1294, 2275  
 Corvi, M M ..... 329  
 Cory-Slechta, D A ..... 1385, 1392,  
 2156\*, 2157, 2158, 2478\*, 2479\*  
 Cosgrove, J R ..... 275  
 Cosgrove, P A ..... 1060\*  
 Cosimbescu, L ..... 1772  
 Coslo, D M ..... 1284  
 Costa, D L ..... 65, 1129, 1609\*  
 Costa, L G ..... 260\*, 1010, 1373, 1684, 2448  
 Costa, M ..... 1164, 1640\*, 2301  
 Costa, N ..... 2101  
 Costin, G ..... 972, 976\*, 982

## Author Index (Continued)

Cote, I ..... 875  
 Cotovio, J ..... 1037, 1580, 2272, 2441  
 Cotruvo, J A ..... 615  
 Couch, L ..... 626\*, 1483  
 Coulombe, R A ..... 2327  
 Coulson, M ..... 25, 27\*, 2122  
 Coulter, J B ..... 546\*  
 Courrouli, X ..... 300, 316, 2004, 2032\*  
 Coutermarsh, B ..... 385  
 Couttet, P ..... 927, 1055, 1070  
 Cove-Smith, L ..... 1126  
 Cowie, D ..... 634\*  
 Cox, J A ..... 722  
 Cox, L ..... 494  
 Cozart, C ..... 647  
 Craciun, F ..... 2200\*  
 Cracknell, S ..... 225  
 Craig, M A ..... 85  
 Craig, Z R ..... 2096, 2106, 2109\*  
 Cramer, P ..... 1269  
 Crane, A L ..... 310, 1420  
 Cravedi, J ..... 2368  
 Crawford, J ..... 887  
 Crawford, R B ..... 395, 422\*, 612, 1199, 2084  
 Creasy, D M ..... 2462  
 Creech, N ..... 404  
 Creed, J ..... 2293  
 Creed, J T ..... 2278  
 Creppy, E E ..... 539\*  
 Creton, R ..... 322  
 Creutzenberg, O H ..... 2374\*  
 Crissman, K ..... 216  
 Crittenden, C ..... 86  
 Crofton, K ..... 714, 1914, 1915  
 Crofton, K M ..... 99, 103, 487, 863  
 Cromie, M ..... 1936\*  
 Cromwell, E F ..... 86  
 Cronin, M T ..... 858, 869, 889\*  
 Crooks, J ..... 213  
 Crooks, S R ..... 1306  
 Croom, E L ..... 507, 510  
 Crosby, M ..... 2171\*  
 Cross, C E ..... 195, 548\*, 1691  
 Cross, K P ..... 870, 2349\*  
 Crouse, L C ..... 1743  
 Crouch, C ..... 495  
 Crowell, S R ..... 299, 317, 865, 894\*  
 Cruse, L ..... 1554  
 Cruz, A ..... 482  
 Cruz, C ..... 2046  
 Cruz, W S ..... 390  
 Cruzan, G ..... 307\*  
 Csanaky, I L ..... 1082, 1083\*  
 Cuadrado Pastor, A ..... 2393  
 Cugier, D J ..... 640, 1820  
 Cukierski, M A ..... 1109  
 Cukovic, D ..... 2459  
 Culbreth, M E ..... 1445  
 Culp, B R ..... 1202  
 Cummings, B S ..... 488, 593, 595, 596, 615, 1512, 1717, 2188  
 Cummings, C A ..... 806  
 Cummings, K J ..... 2003, 2013  
 Cummings, T ..... 1800  
 Cumpston, A M ..... 237  
 Cumpston, J L ..... 441  
 Cunliffe, J ..... 2193  
 Cunningham, C L ..... 1657\*  
 Cunningham, F H ..... 120  
 Curran, A ..... 70, 401, 2065  
 Curran, C P ..... 832, 1377, 1391, 1667\*, 1987, 2206\*  
 Curran, I ..... 448  
 Curren, R ..... 1694  
 Currie, R ..... 634, 1069, 1102  
 Currier, J ..... 2293\*, 2294, 2295  
 Curry, A L ..... 1568\*  
 Cushing, L ..... 878  
 Custer, L ..... 2442  
 Cutuli, F M ..... 1470  
 Cyphert, J M ..... 230, 231\*, 241

## D

D'Amico, J L ..... 608  
 d'Argembeau-Thornton, L ..... 971, 980\*  
 Da Silva, M ..... 1028  
 Dachir, S ..... 346\*  
 Dadey, E ..... 401  
 DaFonte, S ..... 2331  
 Dahm, M ..... 465\*  
 Dahms, J K ..... 201  
 Daigle, A D ..... 747  
 Dail, M ..... 185\*  
 Dallaire, R ..... 1985  
 Dalmas, D ..... 936, 1146\*  
 Dalrymple, A ..... 1488  
 Dalton, C ..... 1046  
 Dalton, R ..... 187  
 Daly, T ..... 1802  
 Dambach, D ..... 887, 2179  
 Damdimopoulou, P ..... 1920  
 Damen, J ..... 1204  
 Dammann, M ..... 131  
 Damodaran, T V ..... 1379\*  
 Damour, M ..... 1882  
 Dan, M ..... 522\*  
 Dandekar, D ..... 2108  
 Daniels, J ..... 1557  
 Daniels, M E ..... 241  
 Daniels, M J ..... 253  
 Danielsen, P H ..... 437  
 Danilenko, D ..... 1819  
 Dankers, A C ..... 1930  
 Dankovic, D A ..... 2231\*  
 Danov, O ..... 444  
 Dantzer, W H ..... 511  
 Dao, T ..... 354, 1680  
 Dao, T L ..... 373  
 Dao, T T ..... 347  
 Darjatmoko, S ..... 2045  
 Darji, M ..... 2321  
 Darney, S P ..... 780\*  
 Dary, C ..... 799, 1253  
 Dary, C C ..... 321  
 Das, A ..... 886\*  
 Das, G K ..... 2389\*  
 Das, J K ..... 1207\*  
 Das, K P ..... 1981\*  
 Das, S ..... 643\*, 885\*, 2036  
 Das, S R ..... 329\*  
 Dasenbrock, C ..... 1490\*  
 Dash, A ..... 1459\*  
 DaSilva Pehl, A ..... 164  
 Dasmahapatra, A K ..... 147, 1299  
 Dassuncao, C ..... 138\*  
 Daston, G ..... 549  
 Daughtrey, W ..... 566  
 Dauzat, C ..... 1028  
 David, R ..... 571\*, 1741\*  
 David, S ..... 1834  
 Davidson, T ..... 503  
 Davies, D ..... 962  
 Davies, D B ..... 706, 1976  
 Davila-Borja, V M ..... 182  
 Davis, A ..... 1624  
 Davis, A P ..... 855, 867  
 Davis, J ..... 882, 1141  
 Davis, K ..... 1880  
 Davis, L K ..... 2088  
 Davis, M ..... 79, 631\*, 1221, 1470  
 Davis, N M ..... 2141  
 Davoren, M J ..... 1695\*  
 Dawkins, J O ..... 1032, 1133\*, 1134, 1135  
 Daws, L C ..... 920, 921  
 Dawson, K A ..... 1748, 1761, 1769, 2396  
 Dawurung, C J ..... 1308\*  
 Day, B J ..... 2019  
 De Boever, P ..... 816  
 De Boever, S ..... 1809  
 De Bont, H ..... 678  
 de Camargo, J V ..... 98  
 de Conti, A ..... 1710\*  
 de Dreu, M ..... 524  
 De Esch, C ..... 992  
 de Geyer d'Orth, T ..... 758  
 de Graauw, M ..... 1067  
 de Graff, I ..... 2178  
 de Groot, D ..... 1447, 2097

The numerals following the author's names refer to the abstract numbers.  
 The asterisk after the abstract number indicates the author is the first presenter.

de Groot, M ..... 992, 993, 1367, 1839\*  
 De Groot, D ..... 992\*, 993  
 de Haan, L ..... 2063  
 de Kimpe, S ..... 1499  
 De La Rosa, V ..... 555, 1497, 2271\*  
 De Luna, M C ..... 2317  
 de Oliveira, D ..... 1040  
 de Oliveira, I F ..... 1500  
 de Paula, V F ..... 179  
 De Vizcaya-Ruiz, A ..... 1492, 1748\*, 1761, 1769, 1832, 2385, 2396  
 De Vooght, V ..... 949  
 de Vries, I ..... 2049  
 De Vries, E ..... 992  
 DeAbrew, N ..... 549  
 DeAngelo, A B ..... 947  
 Dear, J ..... 1900  
 Dearman, R ..... 1052, 2070  
 Dearman, R J ..... 387, 1434, 1438, 1439\*, 1443  
 Debrauwer, L ..... 550  
 DeCaprio, A P ..... 295, 349  
 Déciga-Alcaraz, A ..... 1763\*, 2390  
 Deckert, R R ..... 367  
 Decorde, J ..... 1178  
 Deering, T ..... 1459  
 Deering-Rice, C E ..... 1285  
 DeGeorge, G L ..... 967  
 Degheidy, H ..... 1325  
 Degheidy, H A ..... 1323, 1324  
 Degn, L L ..... 606, 1386\*, 1737  
 DeGroot, J ..... 1136  
 DeKrey, G K ..... 388  
 Del Pino Sans, J ..... 998\*  
 Del Razo, L M ..... 1398, 1761, 1769\*, 2282, 2294, 2385  
 Delclos, K ..... 1570, 1596\*, 2115  
 Delgado Ávila, W ..... 1321  
 Delgado Buenrostro, N L ..... 1763, 2390, 2393\*  
 Delgado-Jimenez, J ..... 1778\*  
 Della Pasqua, O ..... 376  
 Della Torre, P ..... 2098  
 Dellarco, V ..... 2455  
 Dellinger, B ..... 80  
 DeLorme, M P ..... 464  
 Delrue, N ..... 794  
 DeLuca, J ..... 1699  
 DelValle, T ..... 2109  
 Delwig, A ..... 330  
 DeMarini, D M ..... 1113  
 DeMattos, R B ..... 1801  
 Demchuk, E ..... 703, 704  
 Demokritou, P ..... 815  
 den Besten, C ..... 1499  
 Den Hond, E ..... 1249  
 Deng, F ..... 1145\*  
 Deng, R ..... 1806  
 Deng, U ..... 1571  
 Deng, X ..... 412  
 Denison, M ..... 1277  
 Denison, M S ..... 2254  
 Dennell, S ..... 305  
 Denner, L ..... 943  
 Dennis, E H ..... 1912  
 Dennis, W ..... 588  
 Dennis, W E ..... 1513  
 Dennisova, N ..... 352  
 Denslow, N ..... 944, 1448, 1938  
 Depla, E ..... 1809  
 Der, K ..... 1020  
 Dere, E ..... 2139  
 Dereski, M ..... 62, 235  
 Derk, R ..... 426, 449  
 DeRocher, M M ..... 1276  
 Derr, A ..... 2119  
 Dertinger, S ..... 1696, 2446\*  
 Desai, P ..... 497  
 Desai, V ..... 527, 1123, 1880\*, 2197, 2410  
 Desbois, P ..... 71  
 Deschl, U ..... 2255  
 Descotes, J ..... 1467, 2069\*  
 DeSesso, J ..... 2242  
 Deshmukh, G ..... 2176  
 Deshmukh, N ..... 1303  
 DeSimone, M C ..... 737\*  
 Deskin, R ..... 2221  
 Desmond, D ..... 1905  
 DeSoi, D ..... 567  
 Desouky, S S ..... 599  
 Desrosiers, T A ..... 477  
 Detalle, L ..... 1809  
 Detilleux, P ..... 1895  
 Dettroyer, A ..... 859  
 Detzel, C ..... 1346  
 Devaraj, V ..... 320  
 Dever, D P ..... 1392\*  
 Devine, C K ..... 439  
 DeVito, M ..... 578, 1992, 1999, 2275\*  
 DeVito, M J ..... 487, 883  
 Devitt, N ..... 687  
 Devlin, R B ..... 216  
 DeVona, D A ..... 1807, 2064, 2066  
 Devorak, J ..... 354  
 Devorak, J L ..... 367  
 Dewailly, ..... 1985  
 DeWall, J ..... 1983  
 Dewar, A M ..... 94, 95\*, 469, 2376  
 DeWitt, J ..... 404\*, 1009, 1925  
 DeWoskin, R S ..... 128, 140\*, 608  
 Dews, A ..... 435  
 Dey, R D ..... 237, 2369  
 Dhakal, K ..... 1266\*  
 Dhar, D ..... 371  
 Dharmadhikari, S ..... 1866\*  
 Dhasal, V ..... 2149  
 Dhawan, P ..... 1819, 2179  
 Dhot, H ..... 2023\*  
 Di, Z ..... 678  
 Di Donato, L ..... 945  
 Di Giulio, R T ..... 323\*  
 Di Marco, S ..... 2355  
 Dial, S L ..... 1485  
 Diamond, G ..... 721  
 Diamond, S ..... 1737, 2388  
 Diaz, D ..... 1748, 2176, 2179  
 Diaz Ochoa, J G ..... 553\*  
 Diaz-Muñoz, M ..... 1411  
 Diaz-Sanchez, D ..... 212  
 Dicaire, C ..... 520\*  
 Dickerson, M T ..... 522  
 Dickey, R W ..... 48\*  
 Dickinson, S ..... 935  
 Diduch, L L ..... 431  
 Diehl, A ..... 643  
 Diener, R M ..... 2103  
 Dierolf, D ..... 1054  
 Dietz, B M ..... 2321\*, 2336  
 Diggs, D L ..... 306  
 Dillman, J F ..... 362, 363, 373  
 Dillon, C ..... 495  
 Dillon, D M ..... 120, 1488  
 Dills, R ..... 2392  
 DiLorenzo, A M ..... 228\*  
 Dimond, S ..... 483  
 Dinesdurage, H ..... 77, 200  
 Ding, C ..... 1535  
 Ding, L ..... 2293  
 Ding, Q ..... 1153\*  
 Ding, W ..... 1334, 1487\*  
 Ding, X ..... 283, 297, 319  
 Ding, Y ..... 117  
 Dingemans, M M ..... 1367\*  
 Dinkel, V ..... 1058\*  
 Dinu, C ..... 432  
 Dinu, D ..... 300\*  
 DiPalma, C ..... 1286  
 DiRenzo, F ..... 1008  
 Dirk, S ..... 460  
 Distefano, G ..... 2311  
 Ditewig, A C ..... 640  
 Dive, C ..... 1126  
 Dix, D ..... 2269  
 Dixit, R ..... 1803, 1804  
 Do, B N ..... 554  
 Do, K ..... 148, 2085\*, 2335, 2351  
 Do, M ..... 1790\*, 1791, 1792  
 Doak, S H ..... 35  
 Dobo, K ..... 839\*  
 Dodd, D A ..... 562  
 Dodd, D E ..... 230, 1163\*, 1893  
 Dodd-Butera, T ..... 2210\*  
 Dodge, D G ..... 1867\*

# Author Index (Continued)

Dodmane, P R ..... 2285\*, 2286  
 Doerge, D R ..... 486, 1596  
 Doherty, K ..... 1556\*  
 Doherty-Lyons, S P ..... 987\*  
 Doi, Y ..... 1091  
 Doke, D ..... 1454\*  
 Dokmanovich, M G ..... 2120  
 Dolinoy, D ..... 18\*, 396, 528, 530, 807, 1007  
 Domann, F E ..... 673  
 Dombkowski, A ..... 2459  
 Domoradzki, J Y ..... 617  
 Donaldson, K ..... 831  
 Donde, H ..... 2052\*, 2053  
 Donepudi, A ..... 2331  
 Dong, J ..... 1297, 2358  
 Dong, M ..... 1084, 1528\*  
 Dong, Y ..... 1861  
 Donley, E L ..... 1001  
 Donner, E ..... 684  
 Donner, M ..... 1544  
 Donohue, J ..... 1566\*  
 Donohue, K B ..... 1774\*  
 Dooley, G P ..... 242  
 Doran, J ..... 1557  
 Doran, R ..... 1030  
 Dordick, J S ..... 2266  
 Dorko, K ..... 692  
 Doroshenko, O ..... 2337  
 Dorsey, R M ..... 1732  
 Dorta, D J ..... 585, 1733, 1993  
 dos Santos, M T ..... 1040  
 Dos Santos, G ..... 1198  
 Dotson, G ..... 2231  
 Dott, W ..... 1460\*  
 Doucement, E ..... 2179  
 Dougherty, M E ..... 2276  
 Doughy, J ..... 401, 2065  
 Douglas, G ..... 794  
 Douillet, C ..... 2295\*  
 Douki, T ..... 1501  
 Dourson, M ..... 1972\*  
 Douville, J ..... 1801, 1873\*  
 Dover, H ..... 2073  
 Dover, H E ..... 2074  
 Downey, M ..... 972  
 Dowson, S ..... 865  
 Doyle, E ..... 1963  
 Doyle-Eisele, M ..... 500, 513, 514, 740, 743\*, 948  
 Dragan, Y P ..... 81, 82, 1882, 2171  
 Draganov, D ..... 483\*  
 Dragomir, A ..... 248, 249\*  
 Draper, R K ..... 443\*  
 Dreher, K ..... 820, 1737, 2464  
 Dreij, K ..... 569\*  
 Drewes, C C ..... 179\*  
 Driessen, M D ..... 1755  
 Driscoll, M V ..... 485\*  
 Driver, J H ..... 1247\*  
 Drobna, Z ..... 543, 2290, 2294, 2295, 2297  
 Drocco, J ..... 1739  
 Droll, D ..... 1877  
 Drummond, G ..... 720  
 Druwe, I L ..... 2313\*  
 Druzgala, P ..... 1075  
 Du, B ..... 288  
 Du, C ..... 95  
 Du, G ..... 1241, 2056  
 Du, Y ..... 1862  
 Du, Z ..... 958  
 Duan, J ..... 2255  
 Duarte, F V ..... 655  
 Duarte Restrepo, E ..... 1321  
 Dubetz, C ..... 275  
 Dubielzig, R R ..... 2002  
 Dubnicka, T ..... 1235  
 Dubois, A ..... 1416\*  
 Duché, D ..... 294  
 Duffel, M W ..... 1266  
 Dugas, T R ..... 87, 568, 742  
 Duguay, P ..... 1948  
 Dumais, A ..... 761\*  
 Dumas-Campagna, J ..... 506\*  
 Dumont, C ..... 2063  
 Dumont, J ..... 2039  
 Duncan, R ..... 411

Dunlevy, J R ..... 1181, 2284  
 Dunn, A R ..... 388  
 Dunn, K C ..... 554  
 Dunn, R T ..... 36\*, 37\*  
 Dunnick, K M ..... 1747\*, 2003, 2013  
 Dunning, C L ..... 2186  
 Dupree, T V ..... 2186  
 Durand, P ..... 2137  
 Durette, L ..... 2063  
 Durham, J ..... 617  
 Dutil, J ..... 482  
 Dutton, M M ..... 1883, 2319  
 Duvall, M ..... 1814  
 Dwivedi, S ..... 2378  
 Dydak, U ..... 1866  
 Dye, J ..... 208  
 Dzib-Cocom, L ..... 603  
 Dzierlenga, A L ..... 1066\*

## E

Eaddy, J ..... 716  
 Eaddy, J S ..... 183  
 Earley, S ..... 918  
 Earnhardt, N J ..... 1109  
 Easterling, M ..... 883  
 Eastmond, D A ..... 1946, 1957, 2237\*  
 Eaton, D L ..... 2025  
 Eaves, A ..... 1204  
 Ebersviller, S ..... 574  
 Eble, S ..... 1807, 2066\*  
 Eckert, G L ..... 2342  
 Eckles, K G ..... 1553\*  
 Edagwa, B J ..... 2038  
 Edden, R ..... 1866  
 Edelmann, W ..... 33\*  
 Eden, P ..... 185, 562, 1916\*  
 Edgerton, N ..... 1893  
 Edward, C ..... 549  
 Edwards, D ..... 2394  
 Edwards, G ..... 632, 1097  
 Edwards, J ..... 1156, 1159\*  
 Edwards, J A ..... 2347\*  
 Edwards, P C ..... 1358  
 Edwards, R J ..... 237  
 Edwards, S ..... 698  
 Efremenko, A ..... 895, 1979  
 Egele, O ..... 1204  
 Egnash, L A ..... 1001  
 Egner, P ..... 1702  
 Ehman, K ..... 483  
 Ehresman, D J ..... 492, 629, 1004  
 Ehrich, M ..... 1461, 2453  
 Eichinger-Chapelon, A ..... 516  
 Eidelman, D H ..... 2355  
 Eilstein, J ..... 294\*  
 Einhorn, S ..... 1063  
 Eisenbrand, G ..... 2337\*  
 Eisenbrandt, D L ..... 811, 1101, 1117, 2460\*  
 Eisenkraft, A ..... 346  
 Eisinger, D ..... 1882  
 Ejofo, J ..... 1305  
 Ekeren, L ..... 1714  
 Eklund, C ..... 613  
 Eklund, C R ..... 507  
 El Ali, Z ..... 2072  
 El Amrani, A ..... 1233  
 El Amrani, F ..... 1233  
 El Ghissassi, F ..... 1116  
 El Hajj, M C ..... 1138  
 El Muayed, M ..... 1933\*  
 El Sayed, K A ..... 568  
 El-Badawy, A ..... 1735  
 El-Kadi, A O ..... 2292  
 El-Masri, H A ..... 606, 880\*, 882, 891, 898  
 El-Sheikh, A A ..... 499  
 El-Tawil, O S ..... 633\*  
 Elache, K ..... 2372  
 Elbekai, R H ..... 1698  
 Eldasher, L ..... 662  
 Elder, A ..... 2363, 2481\*  
 Eldridge, S ..... 79\*, 631  
 Elespuru, R K ..... 1334  
 Elferink, C ..... 666, 943, 1919  
 Elford, P ..... 1178  
 Elias, M ..... 1625  
 Eling, T ..... 724

Elisha, I L ..... 1308  
 Elizabeth, B ..... 208  
 Eljarrat, E ..... 310  
 Elkhatib, R ..... 1522  
 Ellinger-Ziegelbauer, H ..... 927, 930, 931\*  
 Elliott, D M ..... 1425\*  
 Elliott, G ..... 2107  
 Ellis-Hutchings, R G ..... 537, 1449\*  
 Ellisman, M H ..... 2159  
 Elmore, S A ..... 53  
 Elmore, S E ..... 2325  
 ElSafty, A ..... 797  
 Elsass, K ..... 631  
 Elsebae, A H ..... 599  
 Elshenawy, O ..... 2292  
 Eltom, S E ..... 171, 1296  
 Eltze, T ..... 1437  
 Elvati, P ..... 435, 2468  
 Ema, M ..... 463  
 Embry, M ..... 271  
 Emerick, G L ..... 1414\*, 1415  
 Emmen, H ..... 748, 2354  
 Enayattallah, A ..... 2431\*  
 Endo, H ..... 914  
 Endo, M ..... 20, 427, 457  
 Endoh, S ..... 442  
 Endres, J R ..... 1303\*  
 Enerson, B E ..... 1121, 1143, 1875  
 Engel, F ..... 1716  
 Engel, G ..... 330  
 Engelward, B P ..... 30, 32\*  
 Engles, K ..... 996  
 English, J C ..... 1362, 2233\*  
 Engstrom, A ..... 260  
 Engwall, M ..... 1120  
 Enoch, S ..... 869  
 Enoch, S J ..... 858, 889  
 Enright, B ..... 2124\*  
 Enright, D ..... 477  
 Enright, H ..... 2386\*, 2391  
 Entezari, M ..... 1870\*  
 Eom, H ..... 1328, 1339\*  
 Eom, S ..... 1511  
 Epperly, M ..... 2009, 2010  
 Erdei, E ..... 1136  
 Erdely, A ..... 211, 458, 465, 791\*, 1107, 1626  
 Erdos, Z ..... 1903\*, 2126  
 Eriksen, G S ..... 391  
 Erikson, K M ..... 1685  
 Eriksson, P ..... 58, 1390  
 Ernest, T ..... 2415  
 Ernst, B ..... 2175  
 Ernstgård, L ..... 505\*  
 Erraguntla, N ..... 1950\*  
 Escalante, P ..... 393  
 Escalon, L ..... 559  
 Escher, S ..... 1965\*  
 Escobar-Wilches, D C ..... 298, 2138\*  
 Escudero, S ..... 2144  
 Eskenazi, B ..... 783\*, 2412  
 Eskin, E ..... 1177  
 Eskra, J ..... 2321  
 Espandiani, P ..... 2411\*  
 Espejel, M G ..... 1518  
 Espinosa-Juárez, L ..... 1832  
 Esposito, E R ..... 1727\*  
 Esquivel-Gaón, M ..... 1748, 1761\*, 1769, 2396  
 Ess, K C ..... 1685  
 Essader, A S ..... 1175  
 Esterhuyse, A J ..... 1318  
 Estévez, J ..... 1413  
 Ethridge, S ..... 768  
 Eto, K ..... 1523  
 Etzel, C J ..... 1691  
 Euling, S Y ..... 1024\*  
 Evans, D E ..... 465  
 Evans, K K ..... 511  
 Evans, M V ..... 507\*  
 Evans, N ..... 2131, 2133  
 Evans, T J ..... 2114  
 Evansky, P A ..... 56, 606, 1386  
 Eveleigh, D ..... 2343  
 Everds, N ..... 853\*  
 Evers, D ..... 1530  
 Ewart, L ..... 376

Eyre, R J ..... 501

## F

Faass, O ..... 1383  
 Fabian, E ..... 131, 1437, 1562\*  
 Fabrik, B ..... 2059  
 Fadeel, B ..... 2375\*  
 Fader, K A ..... 648  
 Fagan, M ..... 320  
 Faggioni, R ..... 1803  
 Fahlman, R P ..... 2031  
 Fairchild, D ..... 1892  
 Faisal, M ..... 2378  
 Falank, C ..... 156\*  
 Falciani, F ..... 555  
 Falkner, K ..... 644, 940, 1274\*, 1997  
 Fallahi, F ..... 1360\*  
 Fan, Y ..... 672, 688, 997, 1194  
 Fang, C ..... 319  
 Fang, H ..... 115, 2162  
 Fang, J ..... 626, 1042, 1043\*  
 Fang, M ..... 1093\*, 1114  
 Fang, X ..... 328, 2110  
 Fant, P ..... 1834  
 Faquet, B ..... 1694  
 Farabaugh, C S ..... 1503\*  
 Farahat, F M ..... 591, 1419  
 Fargher, L ..... 1836  
 Fargo, D ..... 985  
 Farin, F ..... 260  
 Farmin, C ..... 2107  
 Farombi, O E ..... 1318  
 Faroon, O ..... 138  
 Farooqui, M Y ..... 279\*  
 Farraj, A K ..... 65, 239, 1125, 1129, 1604\*  
 Farsky, S H ..... 390, 2372  
 Farsky, S P ..... 179  
 Farzim, C ..... 1204  
 Fashae, O F ..... 1320  
 Fauslo, M ..... 1702\*  
 Fattore, E ..... 718  
 Faugere, J ..... 970  
 Faulk, J ..... 528\*, 1007  
 Faust, J ..... 878  
 Faustman, E M ..... 780, 781\*, 1364, 1909  
 Fautz, R ..... 974, 1694\*  
 Fay, K ..... 746\*  
 Fedak, K ..... 471\*, 714  
 Fedan, J S ..... 211, 237  
 Fedyk, E ..... 1230  
 Feher, D ..... 247  
 Fehrenbach, H ..... 444  
 Felter, S ..... 2455  
 Felty, Q H ..... 1207  
 Felix, M ..... 1234\*  
 Feng, L ..... 1784  
 Feng, Y ..... 624  
 Fennell, T ..... 308\*, 466, 616, 1032, 1131, 1133, 1134, 1135, 1327  
 Fenner-Crisp, P ..... 1972  
 Fenton, S E ..... 806\*, 1015, 1635, 2118  
 Fenwick, S W ..... 654  
 Feo, M L ..... 310  
 Ferguson, M ..... 2338  
 Ferguson, P ..... 1931  
 Ferguson, S S ..... 1056  
 Ferguson, T ..... 2181  
 Fermini, B ..... 78  
 Fernandes, L S ..... 1414, 1415\*  
 Fernando, R A ..... 1019, 1175, 2326  
 Fernback, J E ..... 446  
 Ferreira, D ..... 665\*  
 Ferrell, B D ..... 746  
 Fiebelkorn, S A ..... 120\*  
 Fiel, I ..... 987  
 Fiel, L ..... 2372  
 Fiel, L A ..... 179  
 Field, J ..... 2219  
 Fields, P E ..... 2073  
 Fields, W ..... 1891\*  
 Figler, R ..... 1216\*  
 Fikes, J ..... 1882, 1904  
 Fikree, H ..... 1550, 1943  
 Filer, D L ..... 130\*  
 Filgo, A J ..... 806, 2118\*  
 Filipov, N M ..... 490, 1202

## Author Index (Continued)

Finch, G	1800	Francis Stuart, S	1160*
Fink, G	63	Franco, M F	585*
Finkelstein, Y	245	Franco, R	1398
Finley, B L	1166, 1168, 1514, 1555*	Franklin, C	723
Finn, J P	101	Franklin, J N	1925*
Finnessy, J	1547	Franklin, P	759, 2095
Firouzbakht, S	122*	Franklin, R L	1500
Fishbine, E	346	Franko, J	416, 423
Fisher, J W	486, 490, 615, 893, 1914*, 1915	Franz, B	1465
Fisher, P	594	Franzblau, A	530
Fitsanakis, V A	1410	Frauenstein, K	1716
Fitzgerald, L	1558	Frawley, R	1992*
Fitzmaurice, A G	1399*, 1407	Frazer, D	20, 211, 441, 457, 465, 815, 954, 1147
Fitzsimmons, P N	288	Frazer-Abel, A	1817
Fiumera, A C	583, 584	Frazier, K	1146
Fix, D	1890*, 2191	Fredriksson, A	58, 1390
Fix, N R	458, 818, 1747, 2003, 2013*	Fredriksson, L	678, 679*, 1067
Flake, G P	209	Freebern, W J	1807, 2064, 2066
Flamand, N	2441	Freed, T A	1019
Flannery, B	1889*, 2324	Freedman, J H	144, 1153, 1157, 1187, 1188, 1450, 1452
Flaws, J A	9, 2093, 2094, 2096, 2106, 2109	Freeman, E	547
Fleischer, J	1435*	Freeman, J	118
Fleming, C	1980*	Freeman, J L	324, 988, 1408, 1581*, 1582*
Fletcher, E V	1715	Freeman, K	1056
Flick, B	1008*	Freeman, M	750
Flint, O	1025	Freire, C	1246
Flor, S	106*	Freke, M	1006
Flores, J	1771	French, J E	1944, 1957, 2474*
Flores, L A	1768	Frericks, M	105, 1927, 1928
Flores Molina, M	2291	Freshwater, L	1393
Flores Torres, M	1069*	Fretham, S J	2143*
Flores-Jiménez, E M	2390	Freudenrich, T	1682
Flowers, L	721	Frevet, C W	1363, 1764
Flowers, R A	352	Freyre-Fonseca, V	1763, 2390*
Fluharty, K L	189, 237	Frick, A	186
Flynn, M R	2056	Frickel, S	1958
Flynn, T	2338	Friedman, M A	944
Foda, A M	478	Friedrick, K	2328
Foerster, I	1039	Friend, S	20, 237, 441
Foertsch, L	960*	Frisk, A	930
Fofaria, N M	161*	Fritsche, E	1039, 1681*, 1716
Fogle, C M	1369, 1371	Fritz, J M	813*
Foglio, N	981*	Froger-Colleaux, C	744
Foldbjerg, R	1329	Froget, G	744, 754, 2046
Foley, C	73	Fromenty, B	1081, 2039
Foley, J	1094	Fronczek, F R	2038
Foley, J F	209	Fry, R C	473, 477, 543, 698, 948, 2297, 2413*, 2502
Foley, J G	151	Fu, J	726, 2012*
Folkertsma, S	993, 2059	Fu, P	1506
Folkman, J K	437	Fu, W	1736
Follansbee, M	1251*	Fu, X	1862, 1863*
Follmer, R	1782	Fu, Y	1824
Fomby, L M	1300	Fuchs, A	974, 1013
Font, G	1722, 2323*	Fuchs, T C	1877, 1894
Fontaine, B R	1001	Fueta, Y	1389*
Fontenot, K R	1876	Fuhr, U	2337
Ford, J	606	Fuji, R	1806
Ford, K	2176	Fujihara, J	2299
Ford, S M	2207*	Fujii, M	1917*, 2092
Foreman, J E	1272*	Fujimoto, H	217*
Forgacs, A L	682*	Fujimura, M	667, 1526, 2146*
Forster, R	749*, 756, 757, 758, 761, 1028, 1130, 1178, 1233, 1467, 2069	Fujita, K	442*
Forsythe, B	2386	Fujiwara, R	157*
Fort, M	2067	Fujiwara, Y	1151, 1155, 2289
Fortoul, T I	1518	Fukuda, I	217
Fossom, L	1506	Fukuda, M	442
Foster, A J	1074	Fukuda, T	973
Foster, B	440	Fukumuro, M	1693
Foster, P M	784*, 1592, 2127	Fukuoka, K	383
Foster, W	1660	Fukushima, S	1091
Foulon, O	1028*	Fukuzaki, K	2058, 2095
Fourches, D	1625*, 2454	Fulcher, K G	2217
Fowler, A	1381	Funabashi, H	728, 1692
Fowler, J F	1429	Funhoff, R	1055
Fowler, K	1891	Furlong, C E	1010, 2448
Fox, D A	2159*	Furr, J R	2111, 2127, 2128*, 2131, 2133, 2134
Fox, J	876	Furue, M	1917
Fox, S M	2147*	Furukawa, F	1104
Fraiser, L	1567*	Fusco, J C	527, 1071, 1123, 1880, 2197, 2409, 2410*
Frame, A M	126, 605*, 862, 864	Fussel, K C	105*, 1927, 1928
Frame, M	94*, 95, 469, 2376		
Frame, S R	1004		
França, D D	98		
Francis, N	689*		

The numerals following the author's names refer to the abstract numbers.  
The asterisk after the abstract number indicates the author is the first presenter.

## G

Gabos, S	1480, 1971, 1978	Gassner, G T	318
Gabrielson, K	2036	Gasteiger, J	859
Gabrilovich, D	2008	Gato, W E	683*
Gadagbui, B K	723*, 1974	Gatti, D M	183, 1944
Gaddamanugu, P	1494	Gaultier, E	2329, 2368
Gadhia, S R	1196*	Gauthier, C	1913*
Gadson, M	412	Gautier, J	1895*
Gaehle, S	178	Gautier, R	550
Gaffney, S	1514	Gautrin, D	189
Gagne, G D	640	Gavett, S H	230, 231, 241*, 607, 1427, 1735, 2360
Gaisch, K P	2000	Gavina, J M	624
Gaitens, J	1534*	Gaytan, B	555, 1448*
Galbiati, V	403*, 1440	Ge, W	115, 1062
Galbraith, D A	478, 1555	Ge, Y	541*, 558
Galdanes, K	1348, 1351, 1361	Gearhart, J	509, 621
Gales, S	2167	Gearhart, J M	340, 343
Galla, H	1755	Gebhart, A	1566
Gallacher, D	76	Gehen, S C	104, 112, 1108*
Gallagher, E P	1149	Gehlhaus, M	721
Gallagher, J E	698	Gehrig, P	2471
Galland, F	665	Gelderblom, W	1105, 1106
Galland, K L	1202	Gelein, R	2363
Gallegos, A C	2020	Gennings, C	572
Galli, C L	403	Genter, M	290, 497
Galligan, J J	508	Gentry, R	1979*
Gallo, M A	352, 1923	Geoly, F J	2120
Gallouzi, I E	2355	George, C	1729*
Galloway, S	841*	George, G	1127
Gamble, M V	2301	George, I	208
Gamez, M	921	George, M D	1751
Gammon, D W	301, 488, 596, 602*	George, N	1880
Gan, D	957*	Georger, L A	1258
Gande, M	1436	Gerberick, F	960
Gandhi, A	498	Gerecke, D R	352, 353, 355, 356*, 2030
Gandhy, S	2050*	Gerhardy, C	1834
Gandolfi, A	2314	Gerhold, D	1462*
Gandolfi, A J	2288	Gerken, D K	53
Gandolfi, J A	1835	Gerlofs-Nijland, M E	830*
Ganesan, S	2090*	Gerlovina, I	555
Ganey, F	916, 987	Germ, K E	1498*
Ganey, P E	630, 656, 1057, 1077, 1078	German, H W	136*
Gangwal, S	1735	Germann, U	2168
Ganini, D	643	Germano, D	2107*
Gannon, S A	494, 1544	Germolec, D R	189, 1227, 1992, 2466, 2469
Gant, T W	534, 950	Gerrard, D	1201
Gany, F	1546	Gerrish, K E	209, 258, 1094
Gao, D	835	Gershwin, E	1289
Gao, H	2168	Gerstel, D	955
Gao, J	447*, 1739	Gerstenfeld, L	1590
Gao, S	1150, 1444	Geter, D	809, 1099
Gao, W	166, 313	Geter, D R	1707
Gao, X	470, 2379, 2392	Gettings, S	1479
Gao, Y	939, 1744	Gez, R	346
Garantziotis, S	433, 817, 1751	Gfeller, H	267
Garber, H	1391	Ghaemmaghami, A	1044
Garcia, H	1518	Ghare, S	2052, 2053*
Garcia, M	2338	Gharib, M	945*
Garcia, T	1533	Ghio, A	828
Garcia-Mazcorro, J	1317	Ghose, R	498
Garcia-Molina, P	603	Ghosh, A	729
García-Montes de Oca, F G	298*	Ghosh, C	2513*
Garcia-Prieto, C	1784	Ghosh, M	200
Garcia-Reyero, N	875	Ghosh, R N	963*
Garcia-Vargas, G G	473, 1538, 2294	Ghosh, S	1846
Garciafigueroa, Y	2304, 2308*	Ghouri, I	85
Gardella, K	167*	Gibb, H J	1646*, 2217
Gardner, C R	661*	Gibbs, S	489, 1440
Gardner, J D	1138	Gibbs-Flournoy, E A	2029*
Garipey, S	2060	Gibson, C J	645
Garner, C	500*, 513, 514	Giclas, P C	1817
Garner, E C	908	Giesel, N L	692*
Garofolo, F	518*, 519, 520, 521	Giersiefer, S	1681
Garrard, M	1942	Gift, J S	711
Garrett, S H	1180, 1181, 1182, 2284	Gilas, E	724
Garrigues-Mazert, A	294	Gilbert, B	1365
Garry, D	2396	Gilbert, J	89, 901, 1463, 2177
Garry, M R	1975	Gilbert, K	536*
Garshick, E	377	Gilbert, M E	54, 56, 714, 1914, 1915*
Garside, H J	1074	Gilberti, E	1479
Gascoin, E	754	Gilibili, R R	304*, 314
Gasiewicz, T A	1098	Gill, S S	2348*
Gasper, C	1020*	Gillespie, M E	934
Gass, J H	1428	Gilliam, J	2326
Gass, S	815	Gilmour, I	208*, 253, 2360
Gassmann, K	1681	Gilmour, M I	241, 1113

# Author Index (Continued)

Gilpin, S	972
Ginez, A	2434
Giordano, G	260, 1010*, 1373, 1684
Giordano, M	1409, 1411
Giovannelli, R	1548
Giuffrida, A	745
Giulivi, C	2452
Giusti, A M	2098*
Gjyshi, A	482
Glaab, W E	1903, 1910, 2126
Glasser, A	2510*
Gleason, C	2064, 2066
Glez-Weller, D	1533
Glick, A B	2356
Glista-Baker, E E	467, 2384*
Glover, K P	684*
Glover, M C	87
Glushakova, O Y	915*
Glynn, A	474, 718
Go, M	1878
Godin, C S	1812*
Godin-Ethier, J	1477*
Godwin, H A	1338
Goedken, M	2126
Goel, S	1616*
Goering, P L	1323, 1324, 1325, 1333, 1736
Goeritz, I	746
Gogal, R M	1512*
Gohlke, J M	1454
Goines, P E	1374*
Goins, A B	515*
Gokemeijer, J	1237
Golbraikh, A	144*
Gold, A	289
Goldberg, A	149*
Goldhaber, S	1566
Goldman, J M	2088*
Goldring, C	654, 932, 1201, 1900
Goldsmith, M	321
Goldsmith, M R	590
Goldsmith, R	799, 1253
Goldsmith, R B	1450*
Goldsmith, W	815
Goldsmith, W T	237
Goldstein, B	766*
Goldstein, K M	2119, 2137*
Goldstein, R A	2120
Goldstone, J	327, 1281
Golka, K	188*
Gollapudi, B	537, 796*, 1117, 1449, 1707, 1708, 1709, 1969
Gomes, A P	655
Gomes, C	970
Gomes, J	1935*
Gomez, C	957
Gomez-Acevedo, H	97
Gómez-Quiroz, L	1154
Gong, B	115*
Gong, G L	1002, 2174*
Gong, J	1215
Gong, P	875
Gonnerman, G	137
Gonsebatt, M E	2033
Gonzales, A	918
Gonzales, C R	1509
Gonzales, J	2313
Gonzalez, C M	1815
Gonzalez, C P	1845*
Gonzalez, E	1777
Gonzalez, F J	637, 734, 1272, 2405*
Gonzalez, G	1913
Gonzalez, R J	1910*
González, C	1121
Gonzalez Castillo, M	91*
Gonzalez-Cortes, T	1835
Gonzalez-De Alba, C	1835
González-Horta, C	2294
González-Navarrete, L	603, 1836
Good, K	722
Goodale, B C	333, 335*
Goode, G	1296*
Goode, J	200
Gooderham, N J	244, 571, 1069, 1102, 1493
Goodfellow, G	1557
Gooding, M	125
Goodis, M	1963
Goodman, J E	1945, 1951, 2491, 2496*
Goodpaster, B	2311
Goodrich, J	530*, 1007
Goodwin, B	1701*, 2195
Goodwin, D G	725, 926*, 1121
Gookin, G	64
Goravanahally, M P	237
Gordillo-Mena, J	1836
Gordon, C	59, 213
Gordon, C J	56, 215, 753, 2500*
Gordon, K	2451
Gordon, M K	352, 355, 356, 2030, 2359
Gordon, O	526
Gordon, R	1842, 1858
Gordon, T	212, 218, 1348, 1351, 1361, 1364
Gore, A	2034
Gorman, S	1073*
Gosset, J R	884
Goteb, J G	1308
Gotic, M	1750
Goto, K	1829*
Goto, M	1829
Gotti, A	798*, 805
Gottwald, E	2195
Gough, B	2365
Gould, G G	745*, 920, 921
Gould, J	503*, 981
Gould, M	146
Govarts, E	1249
Gow, A	468
Gow, A J	827
Goyak, K	118, 2267
Grabinski, C	1341*
Grace, C E	56
Graff, D W	1899
Grafström, R C	870
Graham, J S	346, 1046
Graham, S	741*, 1046
Grande, C	1204
Grandidier, M H	1037*, 1580
Grant, R L	1949, 2223*
Grasberger, H	255
Graudal, N	846*
Graves, S	489
Gray, J P	1782*
Gray, L E	1592*, 1594, 1595*, 2111, 2127, 2128, 2131, 2133, 2134
Graziano, M	1212
Green, B	1744
Green, K	227
Green, R	634
Green, T D	1343*
Greenberger, J	2009, 2010
Greene, B	1727
Greene, N	40*, 888
Greene, S	1228*
Greenhaw, J	627, 938, 1086
Greenwood, J A	2387
Greenwood, K	256*, 1515
Grégoire, S	1037
Gregus, Z	2283*
Greminger, A	2158*
Gremmer, E R	1833
Grenet, O	1055, 1070
Grenier, A J	2063
Greupink, R	499*
Griffen, S C	1215
Griffith, L	212
Griffith, W C	1364, 1909*
Griffiths, J C	2484*
Griffitt, J	575
Grignard, E	1574
Grimaldi, C	850*, 1805
Grodzki, A C	587*
Groetieck, I	930
Groot, M	1941, 2382
Groothuis, G	2178
Gross, M S	310
Gross, S A	1495
Grosse, Y	1116
Gröters, S	105, 814, 977, 1471, 1927*, 1928
Gruber, J	698*
Grulke, C M	321, 590, 799, 1253
Grulke, E A	819

The numerals following the author's names refer to the abstract numbers.  
The asterisk after the abstract number indicates the author is the first presenter.

Grunig, G	218*
Gu, H	1862
Gu, J	283
Gu, Q	899*
Gu, T	745
Gu, X	697*
Gu, Y	1903
Guallar, E	1538
Gudelsky, G	497
Guerra, F A	2438*
Guerrero, A	2067
Guerrette, Z N	1909
Guest, R	1441
Guguen-Guillouzo, C	1068*, 2039
Guha, M	1237*, 1654
Guha, N	1116
Guignat, M A	373
Guilarte, T	1871, 2154
Guilarte, T R	1865, 1866, 2153*
Guillot, T	1872
Guillouzo, A	1068, 2039*
Guilmette, R	740*
Guizzetti, M	1373
Gulich, K	1679
Gullick, D	488, 595*, 596
Gulumian, M	1331, 1340
Gunawan, R	480
Gunderson, A J	2356
Gundert-Remy, U	1628
Gunewardena, S	1097
Günther, W R	1901
Guo, J	202
Guo, L	626, 1483, 1744, 2162
Guo, T	417*
Guo, X	1145, 1484, 1485, 1486*
Gupta, P	677*
Gupta, R C	1874*
Gupta, Y K	1618*
Gurney, T O	1128
Gury, T	1895
Gust, K	143
Gustafson, D	1868
Guterres, S S	179, 2372
Guth, K	131*
Gutierrez, A	495
Gutiérrez, J	1533
Gutiérrez-López, G F	2390
Gutiérrez-Ruiz, M	1154
Gutkin, D	461
Gutleb, A	2361
Gutzkow, K B	1714
Guyton, K	620, 710, 876, 2454
Guzman, R	1286
Gwaltney, S	397
Gwinn, M R	1671*
Gwinn, W M	209, 226*, 1175
Gyu, S Y	2452

## H

Ha, C	124, 207
Haag, V	749
Haarmann-Stemmann, T	1039, 1716*
Haas, R	1058
Haase, A	1755*, 2072*
Haase, R	1984
Haber, L T	1708, 1709, 1969*, 1972, 2226
Haberzettl, P	60*, 771
Habib, T	1295
Hack, E	2228
Hackbarth, A	434
Hackenwerth, A	2433
Hackley, V A	1350
Haddad, S	506
Hadoke, P W	831
Hadrup, N	551
Haemel, M W	188
Haenen, S	949*
Hagan, D	1219
Hagenbuch, B	492
Haggard, D	137
Haggerty, H G	1807, 2064, 2066
Haggerty, H H	503
Hagio, S	2445
Hagiwara, A	1091
Hahn, M E	302, 694, 1288
Hahn, R A	352
Hahne, L	2375
Haidacher, S J	943
Haighton, L A	1550*, 1943, 2244
Hajjima, A	1023, 1387
Hajela, R K	1456, 2144
Hajirahimkhan, A	2336*
Hajjaj, A	1732
Håkansson, H	570, 718, 1920, 1990
Hakkinen, P J	364, 2055*
Haladi, S	2081
Halappanavar, S	448
Halder, M	271
Hales, B D	683
Hall, D	1801
Hall, J	1187*
Hall, L	1814, 2065, 2125
Hall, M L	247
Hall, P	222
Hall, S	2247
Hall, S J	994
Hallberg, L M	1879*, 2021
Hallidin, K	1920
Hallinger, D R	1898
Hamada, S	2445
Hamadeh, H K	37
Hamann, I	659*
Hamid, Q	2355
Hamilton, J W	1273, 2296, 2302
Hamilton, R	259
Hammock, B D	1422, 1897
Hammond, C	1073
Hammond, J A	877
Hampton, T	385
Han, B	1685
Han, E	1780*
Han, H	1791, 1792*
Han, L	1175
Han, P	2192
Han, S	1574, 1619*, 1995
Han, T	527*, 1071, 1123, 2197, 2410
Han, X	101, 684, 746
Hanberg, A	1962
Hanenberger, H	1716
Haney, J T	1568, 1950, 2218*
Hanig, J P	907, 908, 1613*, 2411
Hani, H	428*
Hankinson, O	2406*
Hanks, B C	74, 750, 2047
Hanley, N	932, 1201
Hannas, B	1630*, 2111*, 2131, 2133, 2134
Hanneman, W H	242
Hannon, P R	2094*
Hans-Joachim, L	1266
Hansen, D	1744
Hansen, J M	1205
Hansen, P A	1675*
Hansen, R	1868
Hansen, T	282, 444*
Hanson, G	73
Hanson-Drury, S	299*, 894, 1261*
Happo, M	1517
Haranosono, Y	129*
Harbeiter, R C	694
Harbell, J W	957
Harbison, R D	476, 1255
Harbison, S	476*
Hardej, D	1184, 1531, 1668*, 2204*
Hardisson, A	1533
Hardwick, R N	511, 649, 1065, 1066, 2310
Hardy, B	870
Hardy, M L	2490*
Hardy, P A	522
Hargreaves, A	1126
Harischandra, D	1842, 1857*
Harkat, C	2329, 2330
Harkema, J	62, 63, 235*, 236, 256, 399, 648, 1515
Harley, K	783, 2412
Harman, J	2135*
Harmon, A	1336*, 1346, 1356
Harmon, M E	1136*
Harney, J	2165
Haron, M H	1299*
Harper, R W	255

## Author Index (Continued)

- Harper, S ..... 786, 790\*, 1752  
Harrass, M ..... 1021  
Harrill, A H ..... 183, 716, 1089  
Harrill, J A ..... 1203\*, 1278  
Harris, A ..... 471, 765\*  
Harris, C ..... 1018  
Harris, J ..... 2122  
Harris, K L ..... 306\*  
Harris, M ..... 1558, 1999  
Harris, M A ..... 517, 1967, 2235, 2236  
Harris, P ..... 1120  
Harris, R ..... 495, 581\*, 582, 1934  
Harris, R B ..... 2305  
Harrop, J ..... 411  
Harrouk, W A ..... 1042, 1043  
Harry, G J ..... 832\*, 833\*  
Harstad, E ..... 1819, 2176\*  
Hartley, D P ..... 39\*  
Hartung, T ..... 109  
Haruta, S ..... 2058  
Hasegawa, G ..... 254  
Hasegawa, R ..... 2256  
Hasegawa, T ..... 1165  
Hashiguchi, S ..... 2322  
Hashimoto, H ..... 442  
Haskins, J R ..... 963  
Hass, U ..... 1383  
Hassabo, H M ..... 2435  
Hassan, M ..... 2435\*  
Hasselgren, C ..... 857  
Hassoun, E ..... 560\*  
Hastings, A K ..... 1537\*  
Hata, K ..... 2364  
Hatch, G E ..... 216\*  
Hatfield, K P ..... 2462  
Hatfield, M ..... 2360  
Hattori, Y ..... 1917  
Haugen, A ..... 986\*  
Haupt, T ..... 1051  
Hauswirth, J ..... 414, 1937  
Hautmann, M ..... 512  
Havel, C ..... 1468  
Hawk, E ..... 2435  
Hawkins, A D ..... 1356\*  
Hawley, E ..... 327  
Haws, L C ..... 517, 1558, 1967, 1999\*, 2221, 2235  
Hay, A ..... 2448  
Hayashi, A ..... 2445  
Hayashi, M ..... 795\*, 1688, 1693, 2256, 2445  
Hayashi, T ..... 974, 1811  
Hayday, A ..... 1439  
Hayden, P ..... 623, 971\*, 980, 1440, 2252, 2273  
Hayes, D ..... 87  
Hayes, E ..... 754\*  
Hayes, M D ..... 387\*, 1438, 1439  
Hayes, R ..... 1235  
Hayes, R L ..... 915  
Hayess, K ..... 1679  
Haykal-Coates, N ..... 65  
Haynes, L ..... 96  
Hays, M ..... 208  
Hays, S M ..... 517, 804, 1967, 2235  
Hazari, M S ..... 65, 239, 1125, 1129, 1607\*  
Hazelton, G A ..... 269, 2232  
He, G ..... 1277  
He, Q ..... 755, 2163  
He, T ..... 1326  
He, X ..... 446\*  
He, Y ..... 1286  
Healey, L ..... 870  
Healy, E ..... 186, 1629  
Heart, E ..... 1782  
Heath, E ..... 1872  
Hebert, M ..... 1186  
Hebert, N ..... 2060\*  
Hebert, V Y ..... 87\*, 742  
Hébert, C ..... 2060  
Hébert, M ..... 1932  
Hecht, S S ..... 169  
Heck, D E ..... 336, 337, 341, 353, 358, 2030, 2151  
Hecker, M ..... 2250  
Hedera, P ..... 1685  
Hedge, J ..... 1915  
Hedge, J M ..... 99, 103\*  
Hedman, C J ..... 2245  
Hedrich, W D ..... 181, 540  
Heerschap, A ..... 993  
Heggland, S J ..... 1158  
Heilman, J ..... 547\*  
Hein, N D ..... 906  
Heindel, J J ..... 986, 1570  
Heindel, N D ..... 352  
Heinonen, T ..... 1000  
Hejtmancik, M R ..... 53, 1300  
Helbing, C C ..... 275  
Helderman, C ..... 915  
Helfrich, R ..... 2192  
Helgen, H ..... 265  
Helma, C ..... 870  
Henderson, D ..... 670  
Henderson, G I ..... 1381  
Henderson, K A ..... 75\*, 93  
Henderson, W ..... 178, 1922  
Henderson, W M ..... 440\*  
Hendriks, H S ..... 902, 903\*  
Hendriksen, P ..... 1941\*, 2087, 2382  
Henges, K ..... 1030  
Hengstler, J G ..... 188  
Henio-Adeky, S ..... 1136  
Hennen, J ..... 311\*  
Henney, J ..... 845\*  
Hennig, B ..... 1995  
Hennings, L ..... 97  
Henriques, T ..... 176  
Henry, S P ..... 1816, 1817  
Hensler, J ..... 745, 920  
Hentges, S ..... 483  
Hentz, K L ..... 107\*  
Henwood, S M ..... 1013\*  
Heo, Y ..... 835, 1442  
Hepburn, P ..... 1959  
Heppenheimer, A ..... 975  
Her, L S ..... 2121\*  
Herbert, K ..... 1460  
Herbert, R A ..... 1300  
Herberz, I ..... 955  
Herbin-Davis, K M ..... 2278  
Herco, M ..... 1032  
Heredia-Ortiz, R ..... 618\*  
Herlin, M ..... 1990\*  
Herman, E ..... 1880  
Herman, K N ..... 1687\*  
Hermesen, S A ..... 1453\*  
Hernandes, C ..... 1879  
Hernandez, A ..... 1115\*, 2225  
Hernandez, E ..... 2180  
Hernandez, E E ..... 1777  
Hernandez, M N ..... 1351, 1352\*, 1361  
Hernandez, R ..... 1768  
Hernández, J ..... 1771  
Hernández, R ..... 2393  
Hernandez Ramon, E ..... 173\*  
Hernández-Cadena, L ..... 1492, 1832  
Hernández-Castellanos, E ..... 2282  
Hernández-Ochoa, I ..... 603, 2104, 2112, 2117  
Hernandez-Plata, I ..... 1411\*  
Herndon, J M ..... 917  
Herold, M ..... 1561, 1562  
Herpers, B ..... 678\*, 679, 1067, 1217  
Herr, D W ..... 1386, 1395\*, 1396  
Herrera-Jimenez, E ..... 1761  
Herring, A H ..... 477  
Herrmann-Stemmann, T ..... 1289  
Herron, J ..... 2379  
Hertz-Picciotto, I ..... 1250, 2482\*  
Hess, A ..... 1469, 1474  
Hester, S ..... 880, 891, 947\*, 1294, 1946  
Hestermann, E V ..... 1276  
Hettick, J M ..... 1432  
Heusinkveld, H J ..... 1397\*  
Hewitt, H M ..... 2284  
Hewitt, M ..... 858, 889  
Hewitt, N J ..... 1694  
Hewitt, P ..... 1877, 1894\*  
Heydens, W F ..... 2343  
Heylings, J ..... 10, 962\*  
Hezel, J Z ..... 562  
Hiemstra, J ..... 2047  
Hiemstra, S ..... 1217  
Higashisaka, K ..... 407, 409, 1384, 2364\*, 2371  
Higley, E ..... 2250  
Higuchi, M ..... 208, 626  
Hilberer, A ..... 975, 982  
Hilderbrand, S ..... 1337  
Hilgers, A ..... 1235  
Hill, F C ..... 515  
Hilty, C ..... 672  
Himeno, M ..... 2092  
Himmelstein, M W ..... 493\*, 494, 2227  
Hines, B ..... 815, 2366  
Hines, R N ..... 301, 692  
Hinkle, P ..... 1073  
Hinkley, G K ..... 1345\*  
Hirabayashi, Y ..... 668\*  
Hirai, T ..... 407\*, 409, 2371  
Hiramoto, M ..... 952  
Hirano, S ..... 445, 1174  
Hirata, G A ..... 1768, 1771, 1777  
Hirata-Koizumi, M ..... 2116  
Hirose, A ..... 1016, 2116, 2256  
Hirota, M ..... 956  
Hirota, R ..... 924, 952  
Hirvonen, M ..... 402, 1517  
Hisama, M ..... 973  
Hitotsumachi, H ..... 1811\*  
Hitt, M J ..... 2186  
Hixon, G ..... 1967, 1999  
Ho, C ..... 1786\*  
Ho, L ..... 1576  
Hoard-Fruchey, H ..... 347, 362, 363, 373\*  
Hoban, D ..... 1544  
Hobbie, K ..... 871  
Hoberman, A M ..... 1006, 2103, 2276  
Hobson, D ..... 1223, 1808  
Hocavar, B A ..... 192, 2035  
Hoch, U ..... 1225  
Hock, M B ..... 2062  
Hockings, P ..... 1126  
Hodges, D ..... 2168  
Hoenerhoff, M ..... 806, 1094  
Hoerter, P ..... 2164  
Hoet, P ..... 455, 949, 1756, 2367  
Hoffman, A D ..... 746  
Hoffman, C ..... 218, 916, 987, 1546  
Hoffman, L ..... 1184\*, 2204  
Hoffmann, L ..... 2361  
Hoffmann, S ..... 1694  
Hoffmann-Doerr, S ..... 1965  
Hofman-Huth, H ..... 2346  
Hogan, K ..... 1024  
Hogberg, H T ..... 109, 1680\*  
Hoglund, A ..... 738  
Hoke, R ..... 1544  
Holada, K ..... 429, 430  
Holden, P ..... 1338  
Holder, D ..... 1903  
Holian, A ..... 259  
Holladay, S D ..... 1512  
Holland, N ..... 783, 2412\*  
Holland, N A ..... 1134\*  
Hollert, H ..... 2250  
Hollingsworth, J ..... 1739  
Hollins, D M ..... 478, 1268  
Hollis, D M ..... 1276  
Holm, K ..... 321, 799\*, 1253  
Holme, J A ..... 391, 1185, 1714\*  
Holmes, A ..... 1169, 1170, 1171, 1186\*, 1530  
Holmes, R S ..... 312  
Holowiecki, A ..... 691  
Holzgrebe, F ..... 67\*  
Homer, B L ..... 2191  
Hommel, M ..... 1828  
Honda, K ..... 463  
Honda, T ..... 1881  
Hondal, R J ..... 2019  
Honeychurch, K ..... 344  
Honeycutt, M ..... 768\*  
Hong, H ..... 115, 866, 1094  
Hong, L ..... 1520, 1864\*  
Hong, P S ..... 93  
Hong, S ..... 489\*, 695\*  
Hong, X ..... 601  
Hong, Y ..... 303, 1511  
Honma, M ..... 1952, 2445  
Hood, D B ..... 400, 990, 995  
Hoogenboom, R L ..... 1941  
Hooker, E ..... 2217\*  
Hooks, W N ..... 1961\*  
Hooven, L A ..... 278\*  
Hope, E F ..... 201  
Hopfer, U ..... 1055  
Hori, H ..... 1389  
Horibata, K ..... 1952  
Horie, M ..... 442  
Horlen, K P ..... 2047  
Horn, K H ..... 1655\*  
Horn, T ..... 631  
Hornbuckle, K C ..... 1983  
Horner, M J ..... 1286\*  
Horner, S ..... 1213  
Hornung, M W ..... 99, 103  
Horvath, C ..... 852\*  
Horwitz, V ..... 346  
Hosoi, K ..... 2260  
Hosokawa, M ..... 736\*, 914  
Hossain, M M ..... 262\*, 916, 1844  
Hotchkiss, A K ..... 1024, 2133  
Hotchkiss, I ..... 62  
Hotchkiss, J A ..... 307, 1256\*, 1707, 2232  
Hottor, H ..... 2057  
Hou, Y ..... 726  
Houck, K ..... 114\*, 116, 130, 891, 900, 1735, 2253, 2254, 2269  
Houck, K A ..... 873, 1686  
Houdeau, E ..... 2329, 2330, 2368\*  
Houle, C ..... 2165  
Housen, M S ..... 281  
Houtman, R ..... 2249\*  
Houtzager, M ..... 240  
Hovorka, J ..... 561  
Howard, J ..... 1958  
Howard, K E ..... 1815\*  
Howard, P C ..... 1334, 1570, 1744, 2464  
Howard, W R ..... 580  
Howd, R ..... 1566  
Howell, B A ..... 881, 1059  
Howell, D ..... 712  
Howell, G E ..... 586  
Hristozov, D ..... 869  
Hruby, D E ..... 344  
Hsia, F K ..... 198\*  
Hsieh, J ..... 127\*  
Hsieh, S ..... 1718, 1721  
Hsieh, W ..... 1878  
Hsu-Sheng, Y ..... 475  
Hu, A ..... 69  
Hu, D ..... 1762, 1765, 1772  
Hu, H ..... 1223\*, 1808, 2505\*  
Hu, Q ..... 404, 1277\*, 1925  
Hu, X ..... 2379, 2392  
Hua, K ..... 2153  
Hua, M ..... 141\*  
Huang, B ..... 1971  
Huang, C ..... 1718, 1719, 1721, 2381  
Huang, D Y ..... 1480, 1978  
Huang, J ..... 1075, 2182  
Huang, M ..... 292\*, 600\*, 1402  
Huang, P ..... 1784  
Huang, R ..... 116, 127, 578, 2254, 2269\*  
Huang, S ..... 2300  
Huang, W ..... 1231  
Huang, X ..... 2056  
Huang, Y ..... 1075, 1770\*, 2182  
Huang, Z ..... 910  
Huard, L ..... 762  
Hubbard, A E ..... 16, 555  
Hubbs, A F ..... 20, 237\*, 416, 432, 452, 457  
Huber, M ..... 1204\*  
Hubert, I ..... 2046  
Hudson, A C ..... 306, 1110\*  
Hudgens, E E ..... 2290  
Hudsell, B ..... 995  
Hudson, L ..... 2287  
Hudson, L G ..... 386, 1516\*, 2307  
Huen, K ..... 2412  
Hueser, A ..... 594  
Hughes, J ..... 1271  
Hughes, J M ..... 1280  
Hughes, M F ..... 7\*, 487\*

# Author Index (Continued)

Huh, G ..... 1838  
 Hui, C ..... 2150\*  
 Hukkanen, R ..... 1278  
 Hulderman, T ..... 465  
 Hulett, A ..... 2248  
 Humphries, D ..... 1235  
 Hunault, C C ..... 2049  
 Hüner, H ..... 1475\*, 2250  
 Hung, D ..... 1718, 1719, 1721\*, 2381  
 Hunt, B ..... 1439  
 Hunter, E S ..... 1205  
 Hunter, K ..... 1259  
 Hunter, S ..... 128, 898  
 Hurley, D J ..... 1512  
 Hurst, S ..... 1800  
 Hurr, M E ..... 2136, 2142  
 Huse, S M ..... 573  
 Hussain, S ..... 433, 817\*, 1332, 1751  
 Hussain, S M ..... 8\*, 375\*, 1323, 1330, 1341, 1360, 1766, 1776, 2421\*  
 Hutchison, J E ..... 1359  
 Hutson, M ..... 1622\*  
 Hutson, P ..... 251  
 Huttunen, K ..... 402  
 Huynh, W ..... 609\*  
 Hwang, G ..... 952, 1524\*  
 Hwang, Y ..... 1312, 1780, 1785, 1786, 1787, 1788, 1793, 1798  
 Hyde, D M ..... 399  
 Hykal-Coates, N ..... 253  
 Hynan, L S ..... 1828  
 Hyunsu, J ..... 943

## I

Iatropoulos, M J ..... 2255  
 Ibanez, F ..... 970  
 Ibi, D ..... 910  
 Ichihara, G ..... 910, 1757  
 Ichihara, S ..... 910, 1757  
 Ichihashi, K ..... 407, 409  
 Ideker, T ..... 822\*  
 Idowu, A A ..... 264\*  
 Igarashi, K ..... 668, 1563  
 Ignacio, J S ..... 364  
 Iguchi, T ..... 271  
 Igweze, Z N ..... 1532  
 Iizuka, Y ..... 122  
 Iji, O T ..... 1245  
 Ijomone, O M ..... 266  
 Ikeda, H ..... 973  
 Ikeda, N ..... 2265  
 Ikeya, M ..... 2116  
 Ikonomou, M G ..... 275  
 Imai, N ..... 969, 1091  
 Imam, M S ..... 1357\*  
 Imam, S Z ..... 2160, 2365  
 Imamura, T ..... 2445  
 Imaoaka, M ..... 1829  
 Impey, S ..... 1375  
 Imran, N ..... 1828  
 Imse, J ..... 764\*  
 Inagaki, A ..... 973  
 Inamdar, A A ..... 1844\*  
 Inayat-Hussain, S ..... 1265\*  
 Inceoglu, B ..... 1422  
 Inett, E ..... 2168  
 Ing, B ..... 301  
 Ingalls, R ..... 2252  
 Ingber, S Z ..... 479\*  
 Ingermanson, R ..... 76  
 Inhof, C ..... 1964  
 Inman, A O ..... 1038, 1322  
 Inoue, K ..... 642\*, 808, 1960, 2445  
 Inoue, T ..... 668  
 Inselman, A ..... 1744  
 Inturi, S ..... 365\*, 366, 369, 371  
 Irie, K ..... 808  
 Irwin, J F ..... 347, 373  
 Irwin, K ..... 804  
 Isama, K ..... 1742  
 Ishida, M C ..... 2294  
 Ishida, Y ..... 1693  
 Ishidao, T ..... 1389  
 Ishihara, Y ..... 254\*, 1560  
 Ishii, Y ..... 752, 1504\*, 1508, 1917, 1952, 2092, 2341

Ismail, A A ..... 1420  
 Itai, K ..... 736  
 Ito, K ..... 1688\*  
 Ito, Y ..... 736  
 Itoh, T ..... 157  
 Ivask, A ..... 1338  
 Ivy, J ..... 800\*  
 Iwahara, Y ..... 2364  
 Iwasaki, T ..... 1023  
 Iwase, Y ..... 2260  
 Iwata, H ..... 178, 2299  
 Iyer, R ..... 1739\*  
 Iyer, S ..... 1739

## J

Jablonski, R ..... 712  
 Jack, J ..... 882  
 Jackson, B ..... 385  
 Jackson, B C ..... 312\*  
 Jackson, B P ..... 268  
 Jackson, D ..... 235  
 Jackson, D A ..... 588, 1513  
 Jackson, D P ..... 666  
 Jackson, F ..... 545  
 Jackson, G ..... 2273  
 Jackson, K ..... 1854  
 Jackson, M ..... 211, 1964\*  
 Jackson, M C ..... 237  
 Jackson-Humbles, D ..... 62, 256  
 Jacob, P ..... 1468  
 Jacobs, K ..... 2455  
 Jacobs, S ..... 1809\*  
 Jacobsen, M J ..... 478  
 Jacobson Kram, D ..... 837, 2043  
 Jägemann, N ..... 713  
 Jäger, M ..... 2250  
 Jahng, Y ..... 285  
 Jailliet, L ..... 1178  
 Jain, A K ..... 366, 369\*, 371, 1768  
 Jain, E ..... 1461\*  
 Jaiswal, A K ..... 153, 1100, 2014  
 Jakupoglu, C ..... 713  
 Jalava, P ..... 1517  
 Jalgama, S ..... 250\*, 568  
 Jalil, I ..... 75  
 Jamadar, S ..... 731\*  
 Jamei, M ..... 1047  
 James, K ..... 2220  
 James, M O ..... 747  
 James, R ..... 374, 481  
 James, S J ..... 57  
 James, T T ..... 169\*  
 Jamil, H ..... 2192  
 Jan, B ..... 412  
 Jan, Y ..... 336, 337\*, 358  
 Janardhan, K ..... 2275  
 Jane, M ..... 2054  
 Janes, Z ..... 327  
 Jang, W ..... 252, 1442\*  
 Janiak, J ..... 1176  
 Janouskova, O ..... 429\*, 430  
 Janovitz, E ..... 1219  
 Janssen, N A ..... 830  
 Janus, J ..... 950  
 Jarabek, A M ..... 230, 236\*, 607, 702  
 Jaramillo, B E ..... 1321\*  
 Jaramillo, F ..... 2317  
 Jardim, W F ..... 98  
 Jarema, K A ..... 59, 753, 1445  
 Jarrett, J ..... 1915  
 Järventausta, H ..... 453  
 Jarvis, I W ..... 569  
 Jaspers, I ..... 224, 574, 2502  
 Javdan, M ..... 1870  
 Javors, M ..... 920  
 Jayaraman, A ..... 162  
 Jayasinghe, S ..... 1938\*  
 Jayjock, M ..... 723  
 Jayne, W ..... 1102  
 Jayyosi, Z ..... 1089  
 Jedynska, A ..... 240  
 Jefferson, A M ..... 1347  
 Jeffery, C ..... 243  
 Jeffrey, A M ..... 2255\*  
 Jeffries, H E ..... 574

The numerals following the author's names refer to the abstract numbers.  
 The asterisk after the abstract number indicates the author is the first presenter.

Jeffy, B D ..... 2264  
 Jeliaskova, N ..... 870  
 Jeliaskova, V ..... 870  
 Jenkins, A ..... 2224\*  
 Jenkins, C A ..... 96  
 Jenkins, G J ..... 35  
 Jenner, J ..... 1046\*  
 Jenner, K J ..... 267  
 Jennings, S H ..... 737  
 Jenny, M J ..... 691\*, 1288, 1729  
 Jeno, M E ..... 2284  
 Jeon, K ..... 459  
 Jeong, H ..... 1311, 1312, 1313, 1314, 1315, 1481, 1780, 1785, 1786, 1787, 1788, 1789, 1790, 1791, 1792, 1793\*, 1798, 2082  
 Jeong, H Y ..... 645  
 Jeong, S ..... 535, 1011  
 Jeong, T ..... 285\*, 286, 287, 1481  
 Jeong, Y ..... 976  
 Jeong, Y C ..... 1707  
 Jeromin, A ..... 1614\*  
 Jespersen, L F ..... 437  
 Jessen, B ..... 1818, 2164  
 Jesseph, J M ..... 151  
 Jett, D ..... 348  
 Ji, C ..... 1225  
 Ji, J ..... 1349\*  
 Ji, P ..... 2415, 2420\*  
 Jia, K ..... 297  
 Jia, Z ..... 905  
 Jiang, M ..... 651, 997  
 Jiang, Q ..... 1009\*  
 Jiang, V ..... 1111  
 Jiang, W ..... 300, 316\*, 1863, 2004, 2032  
 Jiang, X ..... 1329\*  
 Jimenez, J J ..... 1224  
 Jiménez-Delgadillo, B ..... 603  
 Jiménez-Mendoza, E ..... 1492  
 Jiménez-Vélez, B D ..... 263, 405  
 Jin, C ..... 1971  
 Jin, H ..... 729, 1838, 1856, 1857, 1858, 1903  
 Jin, S ..... 1312, 1314, 1315, 1788\*, 1791  
 Jin, U ..... 162, 175\*  
 Jinchun, S ..... 938  
 Jindo, T ..... 1829  
 Jing, H ..... 1444, 1861  
 Jirova, D ..... 1036  
 Joachim, F J ..... 1554  
 Jocteur-Monrozier, A ..... 1035  
 Johanson, G ..... 133, 505, 622, 705, 1240\*, 1571, 1947, 1953, 2362  
 Johansson, M ..... 1947\*  
 Johansson, N ..... 1962  
 John, A ..... 311  
 John, K ..... 181, 1271\*, 1280  
 John-Baptiste, A ..... 925, 1231, 1818, 2191  
 Johnson, A F ..... 1570\*  
 Johnson, B ..... 2086\*  
 Johnson, D ..... 121, 122, 123, 124, 125, 214, 915  
 Johnson, D B ..... 59, 61\*  
 Johnson, D E ..... 2488\*  
 Johnson, D R ..... 515, 1295\*, 1344, 1519, 1774  
 Johnson, E A ..... 347, 373  
 Johnson, G ..... 476, 1255  
 Johnson, G E ..... 35\*  
 Johnson, J ..... 2172  
 Johnson, J D ..... 368  
 Johnson, J E ..... 2159, 2451  
 Johnson, K ..... 929, 1012, 2120, 2491, 2493\*  
 Johnson, M ..... 1998  
 Johnson, M B ..... 1410  
 Johnson, M S ..... 1743  
 Johnson, P ..... 2456  
 Johnson, R ..... 867  
 Johnson, T ..... 1910  
 Johnson, V J ..... 14\*, 189  
 Johnstone, A F ..... 54, 215\*, 2500  
 Joiakim, A ..... 2328  
 Jokiniemi, J ..... 1517  
 Jonaitis, T ..... 2244\*  
 Jones, B A ..... 941, 1899\*  
 Jones, C ..... 905

Jones, C P ..... 1773  
 Jones, H M ..... 884  
 Jones, J ..... 2168  
 Jones, L ..... 2263\*  
 Jones, R ..... 932  
 Jones, R E ..... 2223  
 Jones, R P ..... 654  
 Jones, Y ..... 1744  
 Jönsson, M E ..... 325\*  
 Jonynas, A ..... 414  
 Jordan, S ..... 219\*  
 Jordan, S A ..... 2484, 2485\*  
 Jordan, W H ..... 1801  
 Jortner, B S ..... 2447\*  
 Joseph, L ..... 353\*  
 Joseph, P ..... 954  
 Joshee, L ..... 2183  
 Joshi, A D ..... 666\*  
 Joshi, K ..... 572\*  
 Joshi, N ..... 422, 638, 639\*  
 Joshi-Barve, S ..... 646, 2052, 2053  
 Joubert, M K ..... 2062  
 Joyner, L ..... 1382  
 Juan, C ..... 1878  
 Juan Garcia, A ..... 1722  
 Juárez, Z N ..... 1768  
 Juárez-Pérez, E ..... 182  
 Juberg, D R ..... 508, 1248  
 Judson, P N ..... 861  
 Judson, R ..... 114, 116\*, 126, 605, 862, 864, 2253, 2275  
 Jugg, B J ..... 741  
 Jules, G E ..... 990\*  
 Juliar, B E ..... 1042  
 Julie, P ..... 1026  
 Jung, D ..... 268\*  
 Jung, K ..... 252, 1442  
 Junker Walker, U ..... 1821  
 Jurkowski, A ..... 1255  
 Jutooru, I D ..... 145, 159\*  
 Jye, Y ..... 641

## K

Kääriö, H ..... 402\*  
 Kabirow, K K ..... 512\*  
 Kadambi, V ..... 1212, 1230\*  
 Kadar, T ..... 346  
 Kadiiska, M ..... 643, 801\*  
 Kadir, T ..... 878  
 Kado, S ..... 1289  
 Kaempfe, T ..... 1547  
 Kagan, V ..... 461, 1888, 2008, 2009\*, 2010  
 Kai, S ..... 2322  
 Kaiser, R ..... 67  
 Kaivosoja, T ..... 1517  
 Kajita, A ..... 973  
 Kakehashi, I ..... 1091\*, 1095  
 Kakeyama, M ..... 1387  
 Kakiuchi-Kiyota, S ..... 1092\*  
 Kakuni, M ..... 1693  
 Kalaitzis, V ..... 802  
 Kalantari, F ..... 705, 718\*  
 Kale, V M ..... 250  
 Kalinoski, A M ..... 1276\*  
 Kallman, M ..... 12\*, 1659\*  
 Kaluzhny, Y ..... 971, 980, 1699  
 Kamendulis, L M ..... 192, 2035  
 Kamenosono, T ..... 2058  
 Kamholz, A ..... 1058  
 Kaminishi, M ..... 1441  
 Kaminski, N E ..... 395, 419, 421, 422, 612, 1199, 1760, 2084  
 Kammerer, A ..... 296  
 Kamp, H G ..... 1561, 1562, 2270  
 Kamus-Elimeleh, D ..... 346  
 Kan, H ..... 1132\*  
 Kan, H L ..... 1117  
 Kan, L ..... 2460  
 Kan, R K ..... 342, 347\*, 354, 367, 373  
 Kanakia, S ..... 469  
 Kanavi, M ..... 2045  
 Kanchana, K ..... 1316\*  
 Kandarova, H ..... 707, 971, 980, 1036, 1440  
 Kane, A S ..... 1956

## Author Index (Continued)

Kanemitsu, M	1389	Kimzey, M J	2017	Koch, M	1547*
Kang, B	204, 205	Kelly, C M	68*	Kock, H	2374
Kang, H	535*, 1011, 1547	Kelly, K A	350*	Kodali, V K	1764*
Kang, M	285, 286, 287, 1105, 1106, 2318*	Kelly, K M	191	Kodama, Y	642, 736, 808, 1508, 1811
Kang, S	1301	Kelly, L	932	Kodavanti, P S	912*
Kang, W	286, 1481*	Kelm, J M	1072, 1476	Kodavanti, U P	59, 61, 213*, 214, 231
Kang, Y	2489*	Kellsall, J	927	Koek, W	920
Kanki, M	924*, 927, 937, 952	Kenfield, J	759	Koekemoer, L	1340
Kannan, K	1828, 1915	Kenna, J G	1074	Koenderink, J B	499
Kanno, J	668, 1563*	Kennedy, A D	941	Koerner, J	376
Kanno, S	445*	Kennedy, A J	1336, 1346*, 1356, 1519	Koetzner, L	502*
Kansy, M	1628*	Kennedy, G L	1004	Koga, T	1272
Kanthasamy, A	243, 729, 729, 775, 1837, 1837, 1838, 1842, 1842, 1856, 1857, 1857, 1858, 1858	Kennedy, I M	2389	Koger, D	1801
Kanthasamy, A G	777*, 1838, 1856	Kennedy, R T	2041	Koh, W	1983*
Kanthasamy, K	243*, 1842	Kennedy, T P	257	Kohan, M J	1773, 2278*
Kanungo, J	2377	Kenneke, J F	321, 590*	Kohlgruber, A	291
Kaphalia, B S	1079	Kenny, J	2176	Kohonen, P	870
Kaplan, B L	378, 395, 419, 420, 421, 1760*	Kent, D R	198	Koibuchi, N	1023*
Kaplan, D	2328	Kenyon, A	458, 1347	Koifman, R J	1246
Kapongo, J	1935	Kenyon, E M	613*	Koifman, S	1246*
Kapralov, A	2010	Kerdine- Römer, S	2072	Koivisto, J	453
Kapralova, V	1888	Kerger, B D	1168*, 1268	Kojima, H	523, 973*, 1574, 2260, 2445
Karakitsios, S P	798, 802*, 805	Kermenidou, M	802	Kolisetty, N	615*
Karanian, D	2165	Kern, S	267	Kolle, S N	964, 965*, 966, 977*, 1437, 1474
Karbowsky, C	1286, 2430*	Kerner, J	1124	Koller, L	2212, 2214
Karchner, S I	694, 1288	Kerr, I	1530	Kollessery, G J	111, 113
Karetsky, V	1699	Kerr, R P	1512	Kolluri, S K	333
Karnaukhova, E	431	Kerr, S	1880	Koltick, D S	1179
Karrow, N A	2081	Kerzic, P	909	Komiyama, M	2129, 2140
Kasahara, T	969, 973	Ketelslegers, H	118	Komm, B	1109
Kasai, H	1095	Ketjareon, T	1316	Kondraganti, S	1079*
Kasaian, M	933	Kevin, B	670	Kong, L	2375
Kasamatsu, T	2265	Khayat, A	1959	Kong, M	286
Kaseb, A	2435	Khalil, M	2435	Kong, Q	755
Kashon, M L	189, 237, 416, 432, 457, 954, 1107, 1626	Khalullin, T	461, 2360	Kongsbak, K	551*
Kaski, S W	347	Khan, I A	147, 1299	Konje, J C	950
Kasper, P	838*	Khan, K	1420	Konstantinov, A	326
Kasperkovitz, P	411*	Khan, M	1426, 2027	Kontas, S	1491
Kassel, K M	638	Khan, M R	2031*	Kooter, I M	240*
Katagiri, R	1031	Khan, Q M	1740	Kopec, A	638, 1061*
Katika, M R	2087	Khan, S I	147	Kopf, J	444
Kato, H	428, 442, 1031*, 2116	Khan, S T	2378	Koplovitz, I	342
Kato, R	1742	Khan-Malek, R	931	Kopshinsky, J	73
Kato, Y	969, 1884	Khanal, T	1481, 1792, 2082*	Kopylev, L	711
Katoh, M	973	Khanna, A	885	Korashy, H M	315*, 1536
Katwa, P	2470	Khare, S	1357	Koren, G	1661*
Kaufman, L S	972, 1810*	Khatir, R	2014*	Koriyama, C	475
Kauss, A	1819, 2179	Kherzai, A W	2192*	Korkalainen, M	1990
Kavanagh, M	2348	Khoo, K	1959	Kormos, T	221
Kavanagh, T J	260, 1364, 2025, 2379, 2392	Kia, R	932	Korrapati, M	2184*
Kawa, M	1551, 1559*, 2229	Kiatsayomphu, S	1973	Korte, S H	923, 1236*, 2044
Kawabata, T	1431	Kidane, L	870	Kortenkamp, A	1383
Kawabe, M	1016, 1104	Kidd, S	532*, 2155	Kosak, J	724
Kawada, A	751	Kido, T	914, 2190*	Koslov-Davino, E	2170*
Kawada, T	389	Kiersma, M E	1088	Kosmet, M	2506*
Kawaguchi, T	2203	Kijima, A	752, 2341	Kostyniak, P J	1258
Kawai, K	1095*	Kijima, K	1692	Kosy, O	289, 1272
Kawakami, S	2260, 2445	Kikuchi, I	1829	Kotha, S R	1128*
Kawakami, T	1742	Kikura-Hanajiri, R	523	Kothia, P	116, 2253
Kawamoto, T	475	Kilarkaje, N	2132*	Kothiya, P G	862*
Kawamura, T	2116	Kilford, J	1488	Kotler, M L	1482
Kawana, M	157	Killilea, D W	1177	Koturbash, I	1638*
Kawashima, H	254	Kim, C S	2350, 2365	Kouanfac, C	1883
Kaweeteerawat, C	1338*	Kim, D	1162*, 1511, 1745, 1856, 1858*	Koufaris, C	1069, 1102
Ke, P	1327	Kim, H	150, 152*, 287, 1311, 1313, 1481, 1511, 1529, 1780, 1785, 1786, 1787, 1788, 1788, 1791, 1792, 1793, 1798*, 2082, 2194, 2151*, 2328*	Kouno, E	157
Keane, M	432, 1107	Kim, J	148, 285, 286, 287*, 459, 535, 724, 796, 983, 1529*, 1724*, 1745, 1759*, 2085, 2194, 2335*, 2351	Kousta, E	2456*
Keasling, A	1744	Kim, K	159, 1301*, 1359*, 2091*	Kouzuki, H	956
Keating, A F	2089, 2090	Kim, M	533*	Kovacs, K	2054
Kedderis, G L	290	Kim, M J	2151	Kovalova, N	612*
Keebaugh, A J	64*, 238	Kim, S	204, 205, 620, 904*, 1745, 2194, 2370	Kovovich, M	450*
Keefe, D	1570	Kim, T	1529, 2194, 2196	Kovvuru, P	1354
Keenan, J J	1254	Kim, W	1529	Kowalkowski, K	1820*
Kehe, K	357*	Kim, Y	204, 205, 207*, 207*, 1529, 1577, 1745	Koyama, K	427
Keith, L	579	Kimani, E	2369	Kozhich, A	503
Kelce, W R	1593*	Kimball, J	872	Kracke, K L	394*
Kelliipakaau, S	164	Kimber, I	387, 1052, 1433, 1434, 1438*, 1439, 1443, 2070	Kracko, D	1263*
Keller, D	1465, 1466	Kimmel, C	2242	Kraeling, M E	470*, 1049
Keller, G	1209	Kimmel, G	2242	Kraft, A D	710, 714, 1005*
Keller, J	814*, 1749	Kimura, J	728, 1692	Kramer, E	1941, 2382
Keller, N P	2245			Kramer, J W	72*, 1556
Kellner, R	1027			Kramer, L R	1272
				Kramer, N	1478
				Kramer, V J	104, 112
				Kransler, K M	709
				Krantz, D	1400

The numerals following the author's names refer to the abstract numbers.  
The asterisk after the abstract number indicates the author is the first presenter.

# Author Index (Continued)

Krantz, Q	1129
Krantz, T	208, 213, 214
Kraus, W	392
Krausz, K W	2405
Krawiec, L	976
Kreckler, L	73*
Kreeger, J	1143
Krennrich, G	1561, 1562
Krenzer, K	1553
Krewski, D	1935
Krieger, A	597
Krieger, R	597
Krieger, S M	1256, 2232*
Kriesky, J	766
Krishan, M	497*
Krishna, G	1615, 1621*
Krishnamurthy, P	663
Krishnan, P	629*
Krishnan, V	872
Krishnaraj, R	1893*
Krishnaraju, A V	1540
Krishnegowda, G	1279
Kristin, B	432
Kroenke, M	581, 582
Kroll, K	1938
Krolski, M	595
Kroner, O	364, 2055
Kropp, T	2042
Krouzek, J	561
Krska, R	1883
Krucoff, M	376
Krueger, S K	554, 1242
Kruhla, N L	132, 890*
Krunkosky, T M	1512
Krutmann, J	1039, 1716
Ku, B	2266
Ku, W W	837*
Kubota, A	302, 327, 1281*
Kubota, R	501, 1016
Kuhlman, C L	165*
Kuhn, E	291, 2386
Kuk, R	1885*
Kulkarni, S R	1290
Kumagai, Y	1291
Kumagai-Takei, N	380, 381, 382, 383*, 2083
Kumar, A	643
Kumar, D	371*, 1885
Kumar, G	1323, 1324, 1325*, 1736
Kumar, K K	1685, 1855*
Kumar, P	2471
Kumar, R	885
Kumpf, S	2136
Kung, T S	1380*, 1457
Kunieda, A	2364
Kunito, T	2299
Kuno, H	755*
Kuo, D	1462
Kuper, C	992
Kuper, F	699*
Kurata, H	973
Kurata, M	129
Kurhanewicz, N	239*, 1125
Kuriakose, L	1999
Kurita, H	525*
Kuroda, K	752, 1504, 1508, 2341*
Kurtz, C	716
Kuryshv, Y A	72
Kurzatowski, D	1406*
Kushida, M	928
Kushman, M E	710*
Kushnir, M M	1921, 1924
Kusnadi, A	1282
Kuster, N	1490
Kutanzi, K	1637*
Kutepova, V	2440
Kuwamura, M	928
Kwekel, J C	527, 1123, 2197*, 2410
Kwon, E	204, 205
Kwon, H	1511
Kwon, J	1577
Kwon, S	2266
Kyotani, D	969
Kyrlidis, A	458

## L

La, N	2179
La Merrill, M	991*, 2465
Labib, R	1479*
Lacerda, S	429, 430, 431*
Lacey, C	352
Lachenauer, E	121
Lacher, S	187*
LaFew, W	900
Laffan, S	1813
Laffan, S B	1885
LaFleur, K	1853*
Lafronconi, M	1741
Lafuente, M A	1918*
Låg, M	1185*, 1714, 1746
Lagache, D	2441
Lahesmaa, R	2375
Lahoti, T S	1271, 1279, 1280*, 1283
Lai, I K	1989
Lai, Y	884
Lai-Zhang, J	640
Laidlaw, K	1545
Laine, J E	473*
Laios, M D	398, 812*
Laird, B D	2306*
Laird, J G	1346
Lakatos, P A	398, 812
Lake, A D	649, 1064*, 1065
Lake, B G	301*, 895
Lalaye, N	759*, 2095
Lalko, J F	1310*
LaLone, C	265*
Lam, J	90, 2456
Lam, K	291
Lamb, J C	107, 810
Lamberg, H	1517
Lambert, A	1055
Lambert, J	1980
Lambert, J C	1024
Lambrechts, N	1756
Lambright, C	2127, 2131*, 2133, 2134
Lambroussis, C	228
Lamedin, J	114
Lamm, S	481*
Lamont, D	1214
Lamont, S J	2327
Lamore, S D	81, 82*
Lampe, B J	1362
Lamyathong, B	2185
Lan, Q	16
Lan, V M	2299
Lan, Y	869
Lan, Z	1529
Lance, W	502
Landis, R	906
Landolph, J R	164*
Landry, G M	2186*
Landry, T	623, 2252*
Landsiedel, R	131, 814, 964, 965, 966, 977, 1437, 1469, 1471, 1474, 1475, 1749, 2097, 2250, 2383
Lane, E R	1306
Lang, A	1391*
Lange, R W	1237
Langelaar, M	2178
Langley, M R	729*
Langrish, J P	831
Lantz, C	2298
Lantz, R	1835, 2305, 2504*
Lantz, S	899, 1448, 2160*
Lao, A	1348*
Laporte, J	503
LaPres, J J	256, 1515
Larkin, A J	554, 1242*
LaRosa, K	2252
Lasarev, M	1419
Lasarev, M R	1420
Laskin, D L	220*, 248, 249, 336, 337, 341, 353, 358, 359, 661, 1767, 2030, 2208
Laskin, J D	220, 248, 249, 336*, 337, 341, 353, 355, 356, 358, 359, 661, 2030
Lasley, S M	350
Lastres, I	2393
Latchoumycandane, C	2187*

Latendresse, J R	1071
Latham, J D	906
Latinwo, L M	652, 653
Lattal, K M	2452
Lau, A	1275*
Lau, B L	1342
Lau, C	557, 564, 1981
Lau, F	1540*
Lau, S S	165, 681, 917, 2017, 2020
Lau-Cam, C A	1309, 2040
Laue, H	267
Lauenstein, L	1469
Lauer, F T	386*
Laufersweiler, M	2455
Laumbach, R J	827
Laurenzana, E M	181, 1284
Lauterbach, J H	1507*
Lauterstein, D E	916*
Lavergne, S N	739, 1436
Lavoie, E	2229
Law, B F	1429
Lawa, A T	1783
Lawana, V	1838*
Lawlor, T E	1686, 1697*, 1698
Lawrence, B	392, 415
Lawrence, D A	835*
Lawrence, J W	1060
Lawrence, P	984
Lawrence, Q	581
Laws, S C	277, 1922, 1940*
Lawson, M J	1216
Lawton, M	1143
Lawton, M P	1121
Lay, J	2471
Lay, J M	867
Lazar, D	1725
Le, J N	1202
Le, V	397
Le, X	2259, 2290
Le Bigot, J	1233*
Le Sommer, C	110*
Lea, T	391
Leach, K	78, 2277*
Leach, M	1800
Learn, D B	2276*
Leavitt, S	558
LeBaron, M J	537, 1101, 1117*, 1449, 1707, 1969, 2444, 2460
LeBlanc, L M	1932
Leborfsky, M	628
Lebrec, H	2062*
Lechner, J	1167
LeCluyse, E L	496, 1056*, 1076, 1297
Lecureux, L	2174
Ledbetter, A D	59, 61, 65, 213
Ledet, R J	1876*
Ledieu, D	1821, 2193
Lednicki, J	436
Ledoux, D	2114
Lee, A	1224
Lee, B	641, 1720, 2194
Lee, C	208
Lee, D	285, 1358, 2266
Lee, E	1529, 1859, 2056*
Lee, G	459
Lee, H	1787*
Lee, I	58, 1388*
Lee, J	60, 459, 459, 696*, 1151, 1155*, 1173, 1195, 1339, 1577*, 1949*, 2289
Lee, J S	2409*
Lee, K	207, 210, 480, 641, 1718*, 1720*, 1721
Lee, M	1062, 2266*
Lee, M K	217
Lee, R	1803
Lee, R B	370
Lee, S	175, 380, 381, 382*, 383, 904, 934*, 1084*, 1118, 1794*, 2054, 2083, 2370*
Lee, T	1206*
Lee, V	2045
Lee, W	1477
Lee, Y	1312, 1313, 1442, 1794
Lee-Brotherton, V	1943
Leeds, J M	344
Lefebvre, D E	448*
LeFew, W R	606, 820

Leffel, E K	345
Legare, M E	242
Legrand, J	749, 1233, 1467*, 2069
Lehman, J G	361*
Lehman, P A	1045
Lehman, R M	268
Lehman-McKeeman, L D	821*, 1025, 1064, 2174
Lehmann, D M	1427, 2071*
Lehmann, M	188
Lehmier, H	296*, 1897
Lehner, A	1998
Lehr, M	1755
Lei, C	124*
Lei, Y	1239
Lein, P J	587, 1374, 1375, 1376, 1419, 1422, 1683, 2452
Leishman, D	376
Leist, M	1378
Leiva, J	1477, 1913
Lemaire, B	327, 1281
Lemaire, M	2046, 2291*
Lemarié, C A	2291
Leme, D M	1496, 1700*
Lemke, S L	2343
Lemos, B	680
Lemus-Olalde, R	1964
Lenberg, J L	388
Lencina, C	2329, 2330
Lennon-Hopkins, K	867
Lensu, S	1986
Leon, L S	507
Leon, R	1518
León-Chávez, B	1152
Leonard, H D	465
Leonard, S S	458, 818, 1747, 2003, 2013
Léonard, J	1895
Leonhardt, A	460
Lepage, M	754
Lereaux, G	294
Leroy, M	1017
LeSauteur, L	4*, 2063
Leshin, L	1665*
Lesiak, A	1375
Leskinen, J	1517
Lesmana, R	1023
Leszczynski, J	2423*
Letasiova, S	707*
Leung, M C	126*, 605
Leung, P	1289, 1394
Leung Liu, L	393
Leuschner, J A	347, 354, 373
Leveque, M	2329, 2330
Levesque, S	1843
Lévesque, C	1477
Lévesque, M	1948
Levin, E D	2451*
Levine, J L	51*
Levine, K	1175*
Levine, M	466
Levoe, S N	2452*
Lew, B J	2043*
Lew, M G	1254
Lewandowski, R	62, 235
Lewandowski, T	2239*
Lewin, A	466, 1134
Lewis, C	1923*
Lewis, E	397, 1006
Lewis, E M	2103
Lewis, J	1136
Lewis, J A	588, 1513
Lewis, J L	1516
Lewis, K	2246
Lewis, M	2056
Lewis, S	1880
Lewis, S M	1596, 2115
Lewis, S S	988
Li, B	670*, 1895
Li, C	735
Li, D	2435
Li, F	734
Li, G	16, 1103, 1444
Li, G G	1685
Li, G J	1861*
Li, H	1458*
Li, J	503, 1199*, 1807*, 2034

## Author Index (Continued)

- Li, L ..... 297\*, 2193  
 Li, M ..... 1991\*  
 Li, N ..... 556  
 Li, Q ..... 389\*  
 Li, R ..... 1068  
 Li, S ..... 443, 954, 1407, 1914, 2388  
 Li, W ..... 1148\*, 1150, 1731, 2448  
 Li, X ..... 1118\*, 1140, 1142, 2359  
 Li, X H ..... 1815  
 Li, Y ..... 291, 626, 1095, 1334\*,  
 1444\*, 1506, 1740, 1872, 1978\*  
 Li, Z ..... 290  
 Liachenko, S ..... 907\*, 908, 1613  
 Liang, C ..... 1736  
 Liang, L ..... 911, 2208  
 Liang, Y ..... 2032  
 Libalova, H ..... 563\*  
 Liberda, E N ..... 598\*  
 Licht, K M ..... 370, 372  
 Lichtensteiger, W ..... 1383\*  
 Lichtveld, K ..... 574  
 Lickfeldt, D W ..... 508  
 Lickteig, A J ..... 1082\*, 1083  
 Liebsch, M ..... 1469  
 Lievense, L ..... 1495\*  
 Liguori, A ..... 2298  
 Liguori, M J ..... 640\*, 1820  
 Lilleaas, E M ..... 1185  
 Lillcrap, A ..... 271  
 Lim, H ..... 1335\*  
 Lim, K ..... 252\*, 1301, 1442  
 Lin, C ..... 176, 1878, 1878, 2359  
 Lin, G X ..... 1347  
 Lin, H ..... 933\*, 1483, 1485\*  
 Lin, P ..... 1878\*  
 Lin, S ..... 1105, 1106, 1210, 1753,  
 1910, 2325  
 Lin, T ..... 2179  
 Lin, Y ..... 1250\*, 1712\*  
 Lin, Z ..... 84\*, 490\*, 1202  
 Linak, W P ..... 1113  
 Lind, L ..... 1921, 1924\*  
 Lind, M ..... 1587\*, 1921\*, 1924  
 Linde, N A ..... 1362\*  
 Lindén, J ..... 1986  
 Linderholem, A L ..... 255  
 Lindquist, I ..... 687  
 Lindquist, N ..... 570  
 Lindsay, J ..... 1058  
 Lindsey, C ..... 1218  
 Ling, L ..... 925  
 Lingappan, K ..... 2004\*  
 Link, J ..... 2324  
 Linney, E E ..... 691  
 Linthicum, A D ..... 1038\*  
 Lippmann, M ..... 212, 238  
 Lipscomb, J C ..... 290, 613, 2043  
 Lister, A ..... 2110  
 Little, M H ..... 1363, 1764  
 Little, M ..... 662\*  
 Liu, A ..... 1103  
 Liu, F ..... 1172, 1368, 1369, 1371\*, 1552\*  
 Liu, J ..... 74, 139\*,  
 750\*, 882, 891, 1087\*, 1370\*, 1394\*,  
 1417\*, 1861, 2047, 2086, 2187, 2449  
 Liu, K ..... 386, 2287, 2307  
 Liu, L ..... 676\*, 1826\*  
 Liu, M ..... 1212  
 Liu, S ..... 283\*, 1718, 1721, 2156,  
 2157, 2381  
 Liu, T ..... 133\*  
 Liu, Y ..... 597\*, 1179\*, 1861, 2338\*  
 Liu, Z ..... 602, 1062, 1701  
 Lizarraga, L E ..... 917\*  
 Lloyd, A L ..... 625  
 Lo, G ..... 1505  
 Lobach, A R ..... 408\*  
 Lobo-Mendez, F ..... 509  
 Loccisano, A E ..... 608\*  
 Locey, B ..... 1964  
 Loch-Carusio, R ..... 2102  
 Loeb, J ..... 436  
 Loft, S ..... 437  
 Loguinov, A ..... 1448  
 Lohr, C ..... 1292  
 Lohr, K ..... 1872\*  
 London, B ..... 2345  
 Long, C ..... 423, 424, 1139  
 Long, C M ..... 416\*  
 Longacre, S ..... 602  
 Longnecker, M P ..... 474  
 Longo, M ..... 1034, 2098  
 Lookingland, K J ..... 420  
 Loomen, J ..... 2008  
 Loomis, D ..... 1116, 2294  
 Loomis, M ..... 2107  
 Looser, R ..... 1561, 1562, 2270  
 Lopez, K ..... 1892  
 López, A ..... 1154  
 López-Campos, C ..... 182  
 Lopez-Gonzalez, M L ..... 298, 2138  
 López-Manzanero, G ..... 603\*  
 López-Reyes, A ..... 1154  
 Lorber, M ..... 1024  
 Lorentsen, H ..... 748  
 Lorenz, H ..... 2124  
 Lorenzo, C ..... 432  
 Lorge, E ..... 794  
 Lorient, S ..... 1233  
 Loth, M ..... 1871\*  
 Lou, D ..... 601, 1402\*  
 Loudon, C ..... 1814  
 Louha, S ..... 885  
 Louis, G W ..... 1898\*  
 Louise, J ..... 1458  
 Lounkine, E ..... 824  
 Lourdel, D ..... 762  
 Lourenço, A S ..... 1430\*  
 Love-Homan, L ..... 1715  
 Loveless, S E ..... 922  
 Low, W ..... 1869  
 Low, Y ..... 860  
 Low-Kam, C ..... 1338  
 Lowe, J A ..... 332  
 Lowe, W L ..... 1933  
 Lowney, Y W ..... 1968, 1975  
 Lowry, D ..... 432  
 Lowry, D T ..... 457  
 Lozano, R ..... 921\*  
 Løgsted, J ..... 1029  
 Lu, C ..... 166\*, 531, 1241  
 Lu, H ..... 1804  
 Lu, J ..... 985  
 Lu, L ..... 1535  
 Lu, P ..... 1297, 2358\*  
 Lu, S ..... 283, 1818, 2164\*, 2177  
 Lu, T ..... 1718, 1719, 1721, 2381\*  
 Lu, X ..... 2290  
 Lu, Y ..... 1086, 1087  
 Lucak, J ..... 500, 513\*  
 Lucas, B E ..... 1436\*  
 Lucas, L ..... 582  
 Lucas, S ..... 2016  
 Lucas, S N ..... 222  
 Luch, A ..... 1679, 1755, 2072  
 Luccock, A ..... 2061  
 Ludewig, G ..... 106, 155, 191, 1991, 1994  
 Luebke, R ..... 404  
 Luetjens, C ..... 1013, 2100\*  
 Lugo, J ..... 1540  
 Luisa, C ..... 1570  
 Luithardt, H ..... 89, 901  
 Lukacs, N ..... 1650\*  
 Luke, A M ..... 813  
 Lukomska, E ..... 416, 423, 424  
 Lulla, A ..... 1407\*  
 Lumen, A ..... 893\*, 1914  
 Lumley, L A ..... 370, 372  
 Lummus, Z L ..... 189  
 Lumpkin, M H ..... 604  
 Luna-Arias, J P ..... 2161  
 Lund, A K ..... 829\*  
 Lund, B ..... 570  
 Lunder, S ..... 1678\*  
 Lung, S ..... 261\*  
 Luo, J ..... 1837  
 Luo, W ..... 2167  
 Lusa, A J ..... 1177  
 Lust, R M ..... 1131  
 Luster, M I ..... 189  
 Luu, H ..... 202  
 Luu, K ..... 1701  
 Luvizutto, J L ..... 98  
 Luyendyk, J ..... 630, 638\*, 639, 1061  
 Luyts, K ..... 455\*, 2367  
 Luz, M S ..... 1901  
 Lyke, D F ..... 1386, 1395, 1396\*  
 Lyles, R L ..... 653\*  
 Lyman, E A ..... 367  
 Lyn-cook, L ..... 1487  
 Lynch, K M ..... 1882  
 Lynn, A ..... 1230  
 Lyon, K ..... 624  
 Lyons, M A ..... 800  
 Lyubimov, A ..... 512, 1906, 1908\*  
**M**  
 Ma, D ..... 1080  
 Ma, H ..... 1063, 1737, 2027, 2388\*  
 Ma, J ..... 75, 815, 1020, 2065  
 Ma, J Y ..... 2366\*  
 Ma, L ..... 738\*, 1444, 1861, 2439\*  
 Ma, N ..... 1806  
 Ma, Q ..... 446  
 Ma, Y ..... 1025  
 Ma-Hock, L ..... 814, 1474, 1562, 1749  
 Ma'ayan, A ..... 823\*  
 Maayah, Z H ..... 315  
 Macadam, D ..... 247\*  
 MacArthur, A G ..... 694  
 MacCoss, M J ..... 2448  
 MacCuspie, R I ..... 1350  
 MacGregor, J T ..... 2446  
 Machado, I ..... 2372  
 Machala, M ..... 563  
 Machemer, T ..... 1816  
 Maciel, M ..... 1812  
 MacKenzie, S ..... 1544\*  
 Mackey, A J ..... 1216  
 Mackman, N ..... 638  
 MacLachy, D ..... 2110  
 MacMahon, K ..... 1575\*  
 MacMillan, D ..... 606  
 Macon, M B ..... 1015\*, 1635\*  
 MacPhail, R C ..... 59, 215, 753\*, 819,  
 896, 912, 1445  
 MacRenaris, K W ..... 1933  
 Madanayake, T W ..... 687\*  
 Madden, J A ..... 2089\*  
 Madden, J C ..... 858, 869, 889  
 Madden, M ..... 221  
 Maddox, E ..... 1269  
 Maden, E P ..... 554, 894, 1942\*  
 Madhavan, S ..... 872  
 Madl, A K ..... 450  
 Madren-Whalley, J S ..... 1189\*, 1211  
 Madrigano, J ..... 2414\*  
 Madsen, T J ..... 74, 750, 2047  
 Maeda, A ..... 2445  
 Maeda, M ..... 380, 382, 383, 2083  
 Magalang, U J ..... 1128  
 Magaw, R I ..... 565  
 Magee, B H ..... 1964, 1977, 2240\*  
 Maggioni, S ..... 870  
 Maghezzi, S ..... 758  
 Magnin-Bissel, G ..... 2453\*  
 Maguire, M ..... 400, 995  
 Maguire, S R ..... 2416\*  
 Mahadevan, B ..... 792  
 Mahajan, I M ..... 1730\*  
 Mahapatra, C T ..... 330\*, 332  
 Maher, J M ..... 946\*  
 Mahimainathan, L ..... 1381  
 Mahl, A ..... 2193  
 Mahle, D A ..... 509, 621, 1418\*  
 Mahmoud, A S ..... 281  
 Mahne, S ..... 1144  
 Mahoney, R K ..... 231  
 Maier, A ..... 364, 723, 1954\*, 1974,  
 2043, 2055, 2226, 2228  
 Maier, M ..... 1754\*  
 Maisenbacher, H W ..... 747\*  
 Maisog, J ..... 782  
 Maitre, A ..... 618  
 Maiuri, A ..... 1057\*, 1077  
 Majid, A ..... 913  
 Makama, S ..... 1308  
 Mäkelä, S I ..... 1920  
 Makin, A ..... 1029\*  
 Makori, N ..... 759, 2095  
 Makoshi, M S ..... 1308  
 Makris, S ..... 710, 714, 1005  
 Makvandi, M ..... 1141  
 Malarkey, D ..... 806, 1092, 1094, 2275  
 Malaviya, R ..... 359  
 Maldonado Ortega, D ..... 91  
 Maldonado-Rojas, W ..... 180\*  
 Malek, D E ..... 199\*, 203  
 Malek, R L ..... 368  
 Malfatti, M ..... 291\*, 1942, 2386, 2391  
 Malik, H ..... 932  
 Malik, H Z ..... 654  
 Maliver, P ..... 809, 1099  
 Mallavarapu, S ..... 1770  
 Malley, L A ..... 922  
 Malloy, A ..... 538  
 Malo, J ..... 189  
 Mamidi, R ..... 1814  
 Man, S ..... 470  
 Manautou, J E ..... 233, 660, 664,  
 665, 697, 1085, 2403\*  
 Mancilla, P E ..... 1354  
 Mancuso, P ..... 396  
 Mandal, M ..... 220, 248\*  
 Mandyam, N ..... 885, 886  
 Manetz, T S ..... 1803\*  
 Mangas, I ..... 1413\*  
 Mangelsdorf, I ..... 1965  
 Mangum, L ..... 586\*  
 Mangum, L C ..... 83\*, 2450  
 Manikanthan, B ..... 397  
 Manimaran, R ..... 703, 704\*  
 Maniratanachote, R ..... 1758  
 Manjanatha, M G ..... 1485, 1487,  
 1708\*, 1709, 1969  
 Mankus, C ..... 2273\*  
 Mann, K K ..... 1176, 1591\*, 2291  
 Mann, T ..... 741  
 Manoor Prakash, H ..... 1335  
 Mans, D ..... 1506  
 Manson, K ..... 1237  
 Mantell, L ..... 2034  
 Mantell, L L ..... 257  
 Mantey, J A ..... 306  
 Mantha, M ..... 2278  
 Manzan, M ..... 612  
 Manzo, L ..... 2373\*  
 Mao, T ..... 1468  
 Mapes, J ..... 1893  
 Maraschiello, C ..... 178\*, 1041  
 Marcella, S W ..... 1830  
 Marcellin, M ..... 1055  
 Marchant, G E ..... 1579\*  
 Marchitti, S ..... 321  
 Marchitti, S A ..... 590  
 Marcoe, K F ..... 1074\*  
 Marcos, R ..... 1115, 2225  
 Marcotte, E ..... 2063  
 Marczylo, E L ..... 950\*  
 Marczylo, T H ..... 950  
 Marek, R ..... 1983  
 Maria-Engler, S ..... 1040  
 Marier, J F ..... 344, 345  
 Marinakos, S ..... 1735  
 Marinovich, M ..... 403  
 Markam, D ..... 483  
 Markel, M ..... 1317  
 Markell, L K ..... 101\*, 684  
 Markgraf, C G ..... 1654\*  
 Markillie, M ..... 1772  
 Marogi, A ..... 1777  
 Marone, P ..... 2346\*  
 Marroquin-Cardona, A ..... 2325  
 Marsden, E ..... 1017  
 Marsh, N ..... 1237  
 Marshall, K ..... 1882  
 Marshall, P ..... 741  
 Marshall, V A ..... 1449, 2460  
 Marshburn, J D ..... 817, 1751\*  
 Marsillach, J ..... 2448  
 Martin, A I ..... 1006  
 Martin, C ..... 1469  
 Martin, C A ..... 1400\*  
 Martin, M ..... 114, 116, 130, 864,  
 900, 2253, 2455  
 Martin, M T ..... 126, 139, 856, 862, 873

# Author Index (Continued)

Martin, S .....	2300	McBride, C R .....	996	McMullin, T .....	617*	Meyer, J .....	1494
Martin, S A .....	56, 606*, 898, 1386	McBride, J .....	1806	McNerney, M E .....	1033	Meyer, J N .....	1845
Martin, S S .....	153	McCabe, J A .....	1202	McNett, D A .....	617	Meyer, K .....	1020
Martin-Pardillos, A .....	88*, 2312	McCabe, M J .....	2080	McNulty, K .....	1903	Meyer, R E .....	477
Martinez, M .....	592, 1781	McCain, W C .....	1048*	McPherson, S .....	755, 2163	Meyer, S A .....	143, 250, 568*
Martinez, M A .....	592, 1781	McCallister, M M .....	995*	McQuerry, D .....	865	Meyer, W .....	977
Martinez, K .....	1154*	McCant, D .....	1568, 2238	Mcquistan, T .....	1942	Mhike, M .....	1432*
Martinez de Anda, A .....	2317	McCarthy, A .....	857	McVey, K A .....	1410	Miao, X .....	1825*
Martinez-Aguilar, G .....	2385	McCarthy, T J .....	962, 1045*	Meade, B J .....	416, 423, 424*	Michalek, R .....	1775
Martinez-Finley, E .....	1521*	McCaskill, M .....	2057*	Meade, M L .....	360*	Micheau, B .....	1037
Martinez-Larrañaga, M R .....	592*, 1781	McCauley, J .....	961*	Means, J C .....	683	Mcclaus, T .....	1329
Martino, H .....	1317	McCauley, L .....	1394	Meca, G .....	2323	Mielke, H W .....	1509*
Martino-Andrade, A J .....	1430	McCaw, Z .....	985	Medeiros, M .....	2314*	Mielke, P W .....	1509
Martinozzi-Teissier, S .....	970	McCawley, M .....	2369	Medina-Reyes, E I .....	1763, 2393	Mierke, D R .....	739
Martone, A .....	489	McClain, C .....	246, 644, 646, 650, 940, 1603*, 2052, 2053	Meehan, J .....	115	Mihai, C .....	1762, 1765*, 1772
Marty, M .....	508	McClain, S .....	1434	Meek, E C .....	185, 340, 343*	Mihaylova, D .....	413
Marty, S .....	104, 112*, 1101	McClellan, R O .....	377	Meek, M .....	2	Mikaelian, R .....	1130*
Maruf, A .....	2352*	McClure, P .....	721, 1966, 1970	Meeker, J D .....	1241	Mikheev, V B .....	789
Maruszczyk, J .....	859	McCluskey, J .....	476	Meerman, J .....	679	Mikheev, V .....	2386
Mary, D .....	208	McClymont, L .....	811	Mehrpuoya, P .....	2078*	Mikos, D .....	2192
Mascarenhas, R .....	1554	McConnachie, L A .....	2379, 2392	Mehta, J .....	134*	Milanes, C .....	878
Masereeuw, R .....	499, 1930	McConnell, E .....	875*	Mehta, R .....	1690	Milanez, S .....	2212*
Maskrey, J R .....	1268	McConnell, R S .....	2482	Mehta, R D .....	1505	Milasova, T .....	707
Mason, R P .....	643	McCoy, A T .....	719, 720*, 1248, 2460	Mehus, A .....	1180*	Milatovic, D .....	1874, 2452
Mason, S .....	755	McCracken, J .....	60	Mei, C .....	283	Milchak, L M .....	959*
Massey, M E .....	2316	McCray, B .....	1819, 2179	Mei, N .....	1334, 1483, 1484*, 1485, 1486	Milcova, A .....	561
Massey, T E .....	1690	McCulloch, S D .....	1687	Meier, R .....	828	Mili, M .....	249
Massin, G .....	2441	McDaniel, C .....	185	Meighan, T G .....	211, 426, 1107	Milius, A .....	2108*
Masters, B .....	2037	McDaniel, K L .....	56, 1395, 1396, 1445	Meinl, T .....	858	Millan, A .....	88
Mastovich, J .....	432	McDaniel, P .....	1484	Mekenyan, O .....	2256	Millar, M .....	1549
Mastuzaki, H .....	380	McDiarmid, M .....	1534	Melby, N .....	559	Miller, A .....	352
Masuda, T .....	1723	McDonald, F .....	930	Melching-Kolmuss, S .....	105, 1927, 1928*	Miller, C .....	137, 1136, 2434
Masumori, S .....	1688, 1693	McDonald, J D .....	377, 500, 513, 514, 743, 1260*, 1262, 1263, 1608*	Mellert, W .....	1561, 1562, 2270	Miller, D B .....	350
Masumura, K .....	751	McDonald, T .....	2434	Mellon, R .....	1612*	Miller, D J .....	614*
Masutomi, N .....	1881	McDonnell, B .....	216	Mellon, S H .....	1831	Miller, G W .....	778*, 1683*, 1841, 1872
Mathews, J .....	303, 308, 309	McDonnell, E V .....	994	Mellor, H R .....	1126*	Miller, J A .....	1229*, 1868
Mathias, N .....	503	McDonough, J .....	576	Melnick, J .....	114	Miller, L .....	999, 1022*
Mathias, R .....	495, 1934	McDougall, R .....	474, 622*, 799	Melnick, R .....	1982	Miller, M .....	831*
Mathijs, K .....	118*	McDowell, E .....	1012	Melnyk, S B .....	57	Miller, N R .....	2254*
Mathis, J .....	1306	McDuffie, J .....	1882	Melo, D .....	740	Miller, S .....	870
Matousek, T .....	2293	McElwee, M .....	1187	Melrose, J .....	2048	Miller, S E .....	1698
Matson, C W .....	323, 1735	McFadden, J .....	811	Mena, R .....	2161	Mills, L .....	277*
Matsubara, T .....	2405	McFadden, L G .....	719	Menard, A L .....	345	Mills, N L .....	831
Matsuda, M .....	2099	McFarland, C N .....	706*	Ménard, S .....	2329*, 2330	Mimouni, C .....	1467, 2069
Matsuda, T .....	1384	McGarrigle, B P .....	310, 591	Mendez, I B .....	64, 238*, 261	Minarchick, V C .....	92, 818*, 996
Matsuda, Y .....	428	McGarry, K G .....	368	Mendez, M A .....	1777	Mincey, B D .....	747
Matsumoto, H .....	427, 2445	McGee, S .....	326	Mendez Mancilla, A .....	91	Minck, D R .....	1109
Matsumoto, K .....	1960, 2445	McGill, M R .....	628, 658*, 1090	Méndez Rojas, M A .....	1771	Minema, D .....	595
Matsumoto, M .....	2116	McGinnis, C .....	2172*	Mendoca, M S .....	151	Mineo, A M .....	2121
Matsumoto, Y .....	1748, 2260	McGinnis, C L .....	273*	Mendonca, R .....	2176	Miner, W .....	1393*
Matsumura, F .....	475, 1289	McGinnis, P M .....	2212, 2213	Mendrick, D L .....	11*, 938, 1086, 2397*, 2398*	Mingoia, R T .....	101, 494*, 746
Matsumura, S .....	2445	McGlothlan, J L .....	1866, 1871, 2153, 2154	Menegola, E .....	1008	Minh, T B .....	2299
Matsumura, Y .....	2140	McGrath, F .....	1904	Meng, F .....	1119, 1506*	Minh le, T .....	2314
Matsuo, S .....	642, 808	McGrath, P .....	735	Meng, X .....	1827	Minjarez, B D .....	2161*
Matsuoka, A .....	1742	McGrath, T L .....	1362	Menguy-Vacheron, F .....	1089	Minnema, D .....	55, 593
Matsushita, K .....	752*, 1504, 1508, 2341	McGraw, C .....	1843	Menke, A .....	1447*	Minnema, D .....	132
Matsuzaki, H .....	381, 382, 383, 2083*	McGuigan, C F .....	2259*	Mente, P .....	1326	Miosse, I R .....	97
Matta, J L .....	482*, 1728	McGuinn, W .....	3	Menzel, K .....	2126	Miranda, M C .....	1768
Mattes, W B .....	2397	McHale, C .....	16*	Mercado, F M .....	1768	Mirhosseini, N Z .....	1127*
Matthews, E .....	857	McInally, K .....	1228	Mercado-Feliciano, M .....	308	Mirowsky, J E .....	212*
Mattie, D R .....	562*, 580, 893	McIntosh, L .....	945	Mercer, K .....	1302, 1589	Mirsalis, J C .....	1892
Mattingley, C .....	855, 867*, 1624	McIntosh-Kastrinsky, R .....	239, 1125*	Mercer, R R .....	20, 237, 452*, 458, 1147, 2366	Misato, K .....	2371*
Matusno, Y .....	2129	McIntyre, B .....	9*, 25, 26*, 303, 2127	Mercer, R R .....	20, 237, 452*, 458, 1147, 2366	Mishin, V .....	341
Matzke, M M .....	2305	McIntyre, T M .....	2187	Mercola, M .....	76	Mishra, A .....	426, 449*
Mauch, K .....	553	McKee, J .....	216	Meredith, C .....	120, 1488	Mislan, K .....	328
Maucotel, J .....	1233	McKee, R H .....	566*	Mereness, J .....	2446	Misner, D .....	887, 1819, 2179
Maujeul, M .....	754	McKeever, K .....	1803, 1804	Mergaert, A .....	1198	Mistry, P .....	1460
Maurer, E I .....	1323, 1332	McKiernan, K .....	78	Merk, H F .....	1039	Mitchard, T .....	2122*
Maurer, L .....	906*	McKim, J .....	496, 1077	Merrill, M D .....	2357*	Mitchell, G .....	602
Mauro, L M .....	1224	McKim, J M .....	1465, 1466, 2246, 2248	Merrick, A .....	2275	Mitchell, N J .....	1105, 1106, 2316, 2325*
Mauz, A .....	2415, 2417*	McKim, K L .....	1709	Merrick, B A .....	209, 526*, 939	Mitchell, V L .....	2230*
May, B .....	1963	McKinley, M A .....	1254	Merrill, E .....	621*	Mitic, D .....	1894
Mayeno, A N .....	800	McKinney, W .....	20, 211, 441, 457, 465, 815, 954	Mertens-Talcott, S U .....	150, 152, 1317	Mitkus, R J .....	611
Mayer, A M .....	247	McKinstry, K .....	237	Mesfin, G .....	1910	Mitori, H .....	924, 952
Mayer, G D .....	1498, 2394	McKone, J .....	121*	Messersmith, W .....	172	Mitra, M S .....	1598*, 1599*
Mayer-Proschel, M .....	2158	McLanahan, E D .....	606, 898*, 1914	Messina, M .....	1034	Mittleman, M A .....	2414
Maynor, T .....	545, 951, 1992	McLarty, J .....	1306	Messner, S .....	1072	Miura, N .....	1165*
Mayo, A M .....	1344*, 1774	McLaurin, K W .....	126, 856*	Metryka, A .....	1438	Miyajima-Tabata, A .....	1742*
Mayo-Bean, K .....	1559	McLellan, C J .....	2233	Mettetal, J .....	1230	Miyakawa, K .....	630*, 1078
Mayoux, A .....	2441	McLoughlin, C .....	1350	Mettit, W .....	2155	Miyakawa, T .....	1384
Mazué, G .....	1034	McLoughlin, C E .....	2469	Metushi, I G .....	732*	Miyake, M .....	1881*
Mazumdar, M .....	1583*	McMahon, T .....	2455	Metwally, F M .....	797*	Miyamae, Y .....	924, 952
Mazumder, A .....	146*	McMartin, K .....	2186	Meulenbelt, J .....	2049	Miyamoto, M .....	68, 70, 937
Mazur, C S .....	321, 590	McMullen, P D .....	110, 892, 1297*	Meunier, J .....	294	Miyaso, H .....	2129, 2140*
Mbiya, W .....	1053*			Meyer, B .....	2248	Miyata, K .....	928
McArthur, A .....	691			Meyer, D .....	67	Miyawaki, I .....	728

The numerals following the author's names refer to the abstract numbers.  
The asterisk after the abstract number indicates the author is the first presenter.

## Author Index (Continued)

Miyayama, T .....	1174*	Morris, M .....	1360	Musarrat, J .....	2378	Narayanan, L .....	509
Miyazaki, H .....	1910	Morris, R .....	1576	Muscato, Z .....	393	Narayanan, P .....	2067
Miyazawa, M .....	969	Morris, S .....	476	Music, S .....	1750	Narenmandula, H .....	2315*
Mizuta, Y .....	177	Morrison, J C .....	636, 733	Muskhelishvili, L .....	647	Narumi, K .....	2445
Mobley, L .....	576	Morriss, A .....	1248	Musser, J A .....	2145*	Narváz-Morales, J .....	1748
Moeller, B C .....	948, 953*, 1902	Morse, J .....	154*	Mussio, J .....	79	Nascarella, M A .....	206*
Moeller, T .....	305*	Mortensen, J .....	10*	Mussotter, F .....	2072	Nash, D G .....	1113
Moffett, M C .....	370	Morthole, V I .....	367	Mustafa, G M .....	943*	Nash, J R .....	976, 982
Moffit, J S .....	2121, 2415*, 2462	Morton, M J .....	567	Mustafa, T .....	1740	Nass, R M .....	731, 1366, 1846*, 2148
Moggs, J .....	1055, 1443, 1900	Mortuza, T .....	488, 593, 596	Musvasva, E .....	1805	Nassirpour, R .....	927
Mohamed, E A .....	633	Moscovitz, J E .....	645*	Mutahi, T T .....	2038*	Nath, S .....	872*
Mohammad, M .....	646*	Mosedale, M .....	716*	Muthas, D .....	1074	Natsch, A .....	267, 1051*
Mohammad, S .....	1436	Moser, G J .....	724*	Muthumalage, T .....	1259*	Naturel, M .....	2329, 2330
Mohammadi-Bardbori, A .....	669	Moser, J .....	712*	Mutlu, E .....	208, 1113*	Naud, N .....	2368
Mohammed, J .....	2356	Moser, V .....	896	Mutou, S .....	2445	Naufal, Z .....	763*
Mohammed Saeed, L .....	2160	Moser, V C .....	56, 1395, 1396, 1445*	Muwanika, R .....	2318	Naught, L E .....	2230
Mohl, B .....	918	Moses, M A .....	1098*	Mwanza, M .....	2319*	Nault, R .....	552*, 648
Mohler, R E .....	565	Mosquera-Ortega, M .....	1412*	Myatt, G J .....	72, 870*, 2349	Naumann, B .....	1954
Moiilanen, L H .....	201*	Mostert, V .....	713*	Myers, L P .....	2042*	Navarro-Yepes, J .....	1398*
Mojica, K .....	1803	Mostrag-Szlichtyng, A .....	1624*	Myers, M B .....	1709	Navas-Acien, A .....	1538
Mokrzycki, N .....	1903	Motomura, E .....	1523	Myers, P A .....	2230	Naven, R .....	2263
Moland, C .....	1123, 1880	Moukha, S .....	539	Myers, T M .....	342	Naya, M .....	463*
Moland, C L .....	527, 2197	Moulder, A .....	348	Mysore, J .....	1807	Neagu, D .....	869
Moller, P .....	437*	Moulin, J .....	1478	Mytych, D .....	2062	Neal, B H .....	810
Momot, D .....	1777	Moulin, P .....	2193			Neal, M .....	243
Mondello, S .....	915	Moundipa, P F .....	1883			Neal, S O .....	1864
Monks, T J .....	165, 681, 917, 2017, 2020	Mouneimne, R .....	672			Neal-Kluever, A P .....	1564*
Monnot, A .....	1514*	Moura, M .....	2395	Na, H .....	1887*	Neassen, T .....	1924
Monopoli, M .....	1761, 2396	Mourad, F .....	393	Na, M .....	1790, 1791, 1792	Neely, B A .....	2184
Montanez, J E .....	2028*	Mouret, S .....	1501	Nabb, D L .....	101, 746, 1544	Neely, M .....	1685
Monteiro, A .....	482	Mouro, S .....	1537	Nabers, J J .....	2022	Negga, R .....	1410*
Monteiro-Riviere, N A .....	197, 1038, 1322*, 1326, 1673*	Moussa, L .....	2329	Nabeshi, H .....	407, 409, 1384, 2364, 2371	Negrito, M .....	2054*
Monteleone, J P .....	480*	Moy, M L .....	1503	Nabila, M .....	2368	Nekhayeva, I .....	195
Montenegro, M M .....	2305	Moye, J .....	1828	Naciff, J M .....	549*	Nel, A .....	19, 21*, 1734
Montero-Montoya, R .....	1492	Moyer, R A .....	1732	Nadadur, S .....	2464	Nelissen, I .....	816*, 1756
Montes-Grajales, D .....	119*	Moyers, W B .....	237	Nadanaciva, S .....	2006, 2257, 2258*	Nellums, R .....	1774
Montgomery, B .....	1071	Mozzachio, K .....	1802	Naessen, T .....	1921	Nelluru, G .....	1507
Monticello, T .....	1212*	Mu, P .....	1615*	Nagai, H .....	2275	Nelms, M .....	889
Montoya, G .....	1561*	Mueller, L .....	224, 840*	Nagai, T .....	445, 910	Nelson, A .....	945, 1477, 1913
Montoya-Durango, D E .....	542*	Mugica, V .....	1492, 1832	Nagano, K .....	1091	Nelson, J .....	1058
Moo-Puc, R .....	1836	Muhonen, W W .....	1180	Nagano, R .....	442	Nemery, B .....	949
Moon, G .....	206	Mukai, T .....	445	Nagano, T .....	2364	Németi, B .....	2283
Moon, Y .....	148, 2085, 2335, 2351	Mukerji, B .....	1959*	Naganuma, A .....	952, 1524, 1723	Nemoto, S .....	129
Moore, C .....	1451*	Mukerji, P .....	922*	Nagari, A .....	392	Nesnow, S .....	1946
Moore, J .....	483	Mukherjee, B .....	63	Nagarkatti, M .....	657, 1423, 1425, 2076, 2077, 2078, 2353	Nesslany, F .....	2441
Moore, M M .....	794, 1334, 1485, 1486, 1506, 1708, 1709, 1969, 2188	Mukherjee, S .....	635*	Nagarkatti, P .....	657, 1423, 1425, 2076, 2077, 2078, 2353	Neu, S .....	2163
Moore, N P .....	537, 1449, 1707, 1708, 1709, 1969	Mukhi, S .....	602	Nagata, R .....	759, 1031, 2058, 2095	Newbold, R .....	1570
Moore, R W .....	2141	Mulder, J E .....	1690*	Nagie, E .....	2191	Newby, D E .....	831
Moore, S .....	219, 225*	Muldoon, D .....	1507	Nagie, E .....	2191	Newland, M .....	995
Moore, W .....	469	Muldoon-Jacobs, K .....	857, 2349	Nagy, A .....	1739	Nez, T .....	1136
Moore, W M .....	2343	Müller, P .....	824	Nagy, L E .....	2187	Nezu, Y .....	234
Moore-Ambriz, T .....	2117*	Müller, S .....	955	Nail, C A .....	2450	Ng, N .....	1626
Moormann, O .....	188	Müllerschön, H .....	966	Nair, P .....	2355	Ng, S P .....	1464*
Moorthy, B .....	300, 316, 2004, 2032, 2403, 2408*	Mumtaz, M .....	579*, 702	Naito, H .....	910	Ng, W .....	406*
Morales, L .....	482	Mummy, K L .....	562, 580*	Nakab, I .....	2441	Ngalame, N N .....	1193*
Morales-Torres, L .....	1728	Mun, G .....	979, 982, 1694	Nakahara, S .....	973	Ngateprutaram, T .....	421*
Moran, D .....	2346	Mundy, W .....	1682*	Nakai, T .....	2445	Ngo, C .....	142
Moran, D M .....	1556	Munichika, Y .....	973	Nakajima, M .....	973, 1688, 1693, 2322	Ngo, H .....	123
Morata, T C .....	2499*	Muniappa, N .....	1903	Nakamoto, M .....	2129*	Nguan, D .....	2440
More, V .....	2331	Munoz, A B .....	1164*	Nakamura, J .....	1704	Nguyen, A .....	472
Moreau, M .....	942*	Muñoz, A .....	2301	Nakamura, K .....	2260	Nguyen, B .....	142*, 1935
Moreno, A J .....	655	Muñoz, B .....	182	Nakamura, M .....	973, 1523	Nguyen, D .....	1958, 2048
Moreno, C .....	453	Muñoz-Saldaña, J .....	1748, 1761	Nakamura, N .....	2140	Nguyen, T .....	2179
Morgan, D L .....	209*, 226, 1175, 1944	Munro, T .....	237	Nakanishi, J .....	463	Nguyen, T T .....	1848, 2005*
Morgan, E T .....	2357, 2407*	Munson, J W .....	1968*	Nakano, T .....	383	Ngwa, A .....	243
Morgan, L J .....	372	Muntean, N K .....	2339*	Nakao, M .....	254, 1560*	Nhan, C .....	1803
Morgan, R E .....	27	Murali, T .....	1461	Nakasato, A .....	390	Nhan, K .....	137
Morgan, S .....	1905	Muralidhara, S .....	593, 596	Nakashima, H .....	1016	Nhan, M .....	124
Mori, C .....	2129, 2140	Muratov, E .....	144, 1625, 2454	Nakashima, S .....	1723	Niaz, M S .....	306, 1110
Mori, S .....	2153	Murbach, M .....	1490	Nakatsu, N .....	937	Nichols, A C .....	272*
Mori, T .....	2371	Muro, I .....	167, 1730	Nakazawa, K .....	523	Nichols, J .....	985*
Moriguchi, A .....	924, 952	Muro, Y .....	464	Nallathamby, P D .....	2386, 2391*	Nichols, J W .....	267, 288, 746
Morinaga, T .....	254	Murphy, C G .....	855*, 867	Nam, G .....	983	Nicholson, H D .....	146
Morisetti, A .....	2098	Murphy, G .....	354	Nan, B .....	63	Nicolich, M J .....	566, 709
Morishita, M .....	63	Murphy, L .....	2444	Nan, Z .....	1869*	Nicotra, S .....	2442
Morishita, Y .....	1384*	Murphy, L A .....	811*, 2460	Nance, J .....	54*	Nie, L .....	1510, 1864
Morisseau, C .....	1897	Murphy, R F .....	825*	Nance, P .....	723, 2055, 2228	Nie, L H .....	1179
Morita, F .....	1811	Murr, A S .....	2088	Nanzer, A .....	2042	Niehof, M .....	282*
Morita, T .....	1960, 2445	Murray, A R .....	2360	Napoli, E .....	2452	Niehoff, M .....	1236
Moritz, W .....	1476	Murray, E .....	579	Naquet, P .....	665	Nielsen, S J .....	927
Morris, D .....	73	Murray, H .....	479	Narain, N R .....	1224	Niemenen, J .....	402
Morris, J .....	631, 2435	Murray, I .....	1279*, 1280, 1283	Narasimhan, M .....	1381	Niessen, K V .....	339
Morris, J B .....	232, 233, 604	Murray, J A .....	537	Naravani, R .....	1505*	Nigel, W .....	1570
		Murray, J C .....	191	Narawa, T .....	157	Niggemann, B .....	760*, 923
		Murry, D .....	1991	Narayan, R J .....	1736	Nijmeijer, S M .....	524
		Murthy, S N .....	2345	Narayanan, B .....	66	Nijssen, P C .....	1397

The numerals following the author's names refer to the abstract numbers.  
The asterisk after the abstract number indicates the author is the first presenter.

## N

# Author Index (Continued)

Niklas, J ..... 553  
 Nikolic, D ..... 2336  
 Nikula, K ..... 1228  
 Niles, A L ..... 1076, 1725\*, 2262  
 Nilsen, A M ..... 413\*  
 Ning, B ..... 1744  
 Ning, J ..... 1444  
 Ning, Z ..... 64  
 Nishihara, K ..... 952  
 Nishijima, N ..... 407, 409  
 Nishikawa, A ..... 177, 752,  
 1504, 1508, 1952, 2340, 2341  
 Nishikawa, T ..... 254  
 Nishimaki, F ..... 1091  
 Nishimura, T ..... 2116  
 Nishimura, Y ..... 380, 381\*,  
 382, 383, 2083  
 Nishino, T ..... 217  
 Nishiyama, N ..... 974, 975, 2265  
 Nishizono, M ..... 2058  
 Niture, S K ..... 1100\*  
 Niu, J ..... 556, 1164  
 Niu, N N ..... 69  
 Niu, X ..... 2178\*  
 Nixon, M ..... 724  
 Njohbeh, P B ..... 1883  
 Nkurunziza, P ..... 2318  
 Nnodi, O U ..... 919\*  
 Noçairi, H ..... 2272  
 Noel, A ..... 2380\*  
 Noh, J ..... 1301  
 Nohmi, T ..... 751, 752, 1504, 1952  
 Nojiri, N ..... 1384  
 Nolan, S J ..... 1680  
 Nomi, T ..... 2341  
 Nomura, H ..... 428  
 Nong, A ..... 624\*, 804  
 Noratto, G ..... 1317\*  
 Nordberg, C M ..... 703  
 Norenberg, J ..... 2016  
 Norman, J ..... 2041  
 Norman, K ..... 957, 979, 982  
 Norppa, H ..... 453  
 Norris, D A ..... 1816  
 North, A ..... 1859\*  
 North, C M ..... 709\*  
 North, M ..... 555  
 Norton, C M ..... 1879  
 Norton, M G ..... 738  
 Norwood, J ..... 56  
 Notch, E ..... 385\*  
 Note, R R ..... 2272\*  
 Novak, M J ..... 136  
 Novak, P ..... 649, 1064, 2314  
 Novick, R ..... 1254\*  
 Nowland, W ..... 2136  
 Nozaki, Y ..... 751, 1441  
 Nugent, P ..... 5\*  
 Nuhar, A ..... 1850\*  
 Nukada, Y ..... 974, 975\*  
 Numano, T ..... 1016, 1104  
 Nunley, A N ..... 368  
 Nurkiewicz, T R ..... 92\*, 818, 996,  
 1137, 1147\*  
 Nwoha, P U ..... 266\*  
 Nyagode, B A ..... 2407  
 Nyland, J F ..... 394, 418  
 Nyska, A N ..... 214, 231  
 Nysus, M ..... 2016  
 Nyvold, H E ..... 1714

## O

O'Brien, B ..... 581, 2502  
 O'Brien, E ..... 396\*  
 O'Brien, T ..... 1545\*  
 O'Callaghan, J P ..... 350, 1360, 1610  
 O'Driscoll, C M ..... 546  
 O'Lone, R ..... 927  
 O'Mahony, A ..... 2048  
 O'Neal, S L ..... 1520\*  
 O'Neill, A ..... 1743  
 O'Neill, T ..... 1802  
 O'Reilly, K T ..... 565  
 O'Reilly, M A ..... 984  
 O'Shields, B ..... 691  
 O'Toole, T ..... 1195\*

O'Brien, K M ..... 639  
 O'Brien, P J ..... 2023, 2352  
 O'Donnell, M W ..... 1779  
 O'Rourke, M K ..... 2305  
 Obejero-Paz, C A ..... 72  
 Oberdorster, G ..... 1385, 2363  
 Öberg, M ..... 705\*, 1947, 1953, 1990  
 Oberoi, S ..... 2344\*  
 Obert, L ..... 1143  
 Ocampo-Gomez, G ..... 1835  
 Ochi, T ..... 1884  
 O'Connor, J ..... 2113\*  
 Odermatt, A ..... 2172  
 Odewumi, C ..... 652, 653  
 Odin, J ..... 987  
 Odin, M ..... 1970  
 Odinecs, A ..... 1222  
 Odukoya, O O ..... 1257, 1527, 2279  
 Odwin-DaCosta, S ..... 109, 1680  
 Oeda, S ..... 956  
 Oertel, A ..... 1490  
 Offiah, N V ..... 1308  
 Ofuegbie, S O ..... 1304  
 Ogata, K ..... 928\*  
 Ogata, S ..... 234\*  
 Ogawa, K ..... 177, 752, 1504,  
 1508, 1952, 2340, 2341  
 Ogawa, S ..... 1209  
 Ogiwara, Y ..... 2445  
 Ognibene, T ..... 1232, 1942  
 Ogunlana, O E ..... 1783  
 Ogunnoiki, J ..... 1854\*  
 Ogunrinola, O O ..... 1257\*, 1527, 2279  
 Ogunsola, O A ..... 470, 1049\*  
 Oh, C ..... 148, 2085  
 Oh, D ..... 285, 286\*, 287  
 Oh, M ..... 602  
 Oh, S ..... 1405, 1720, 1720, 2081\*  
 Ohkubo, S ..... 1811  
 Ohl, P ..... 858  
 Ohno, Y ..... 937  
 Ohsako, S ..... 2203  
 Ohta, H ..... 736  
 Ohtani, K ..... 194  
 Ojeda-Cuello, M ..... 180  
 Ojo, C ..... 1852\*  
 Okamoto, K ..... 969  
 Okamoto, M ..... 428  
 Okazaki, Y ..... 464  
 Okechukwu, C ..... 174\*  
 Okonkwo, N ..... 318\*  
 Okoro, K O ..... 1532  
 Okubo, S ..... 937\*  
 Oladipo, O O ..... 1308  
 Olagunju, J O ..... 1783  
 Olaniyi, M O ..... 1307  
 Oldenburg, S ..... 1322  
 Oldham, M ..... 567\*  
 Oleas, N ..... 1234  
 Olier, M ..... 2330  
 Olivas-Calderon, E ..... 1835  
 Oliveira, D P ..... 1496, 1700, 1733  
 Oliveira, G A ..... 1496\*  
 Oliveira, P J ..... 2257  
 Oliveira, P V ..... 1901  
 Olivera, D S ..... 367\*  
 Olivero, O A ..... 173, 1630, 1706, 1777  
 Olivero-Verbel, J ..... 119, 180, 1264, 1911  
 Olkhanud, P B ..... 2303\*  
 Oller, A R ..... 1163  
 Olsen, C ..... 2298  
 Olsen, E ..... 1916  
 Olsen, L ..... 391  
 Olshan, A F ..... 473, 477  
 Olson, G R ..... 1042  
 Olson, J R ..... 310\*, 541, 591,  
 1258, 1416, 1419, 1420  
 Olubambi, O T ..... 276\*  
 Olubanke, O O ..... 1783\*  
 Olukunle, J O ..... 1307  
 Olympio, K P ..... 1901\*  
 Omiecinski, C J ..... 181, 540\*, 1284  
 Omotosho, I O ..... 2201\*  
 Onami, S ..... 177, 1952\*, 2340  
 Oneda, S ..... 2095\*  
 Ono, A ..... 937, 1960, 2116\*

Onoue, S ..... 2260  
 Onua, E ..... 512  
 Onyije, F ..... 266  
 Ooshima, K ..... 974, 975  
 Ooshima, Y ..... 1031, 2058  
 Ootsuyama, A ..... 1095  
 Opanashuk, L ..... 1392  
 Opoku, R ..... 1851  
 Opperhuizen, A ..... 671  
 Opreko, P ..... 1703  
 Opreko, P L ..... 1172  
 Orchard, E A ..... 1306  
 Orecna, M ..... 429, 430\*, 431  
 Orihuela, R ..... 1192  
 Orisakwe, O ..... 1532\*  
 Orlicky, D J ..... 172, 366, 369  
 Orme, M ..... 501  
 Orme-Zavaleta, J ..... 2463  
 Orr, G ..... 1762, 1765, 1772\*  
 Ortega, R L ..... 1768  
 Ortenzio, J N ..... 1737\*  
 Ortiz, R ..... 2317  
 Ortiz-Martinez, M G ..... 263\*  
 Ortiz-Sanchez, C M ..... 1728\*  
 Ortwine, D ..... 887  
 Osaki, N ..... 2260  
 Oshida, K ..... 557, 1294\*  
 Oshiro, W M ..... 56, 606  
 Oshunwusi, T ..... 1507  
 Osimitz, T ..... 895  
 Osimitz, T G ..... 102, 301, 596  
 Osmitz, T ..... 488  
 Osorio-Yañez, C ..... 2282\*  
 Osterburg, A R ..... 1519  
 Otani, J M ..... 1555  
 Otsuki, T ..... 380\*, 381, 382, 383, 2083  
 Ott, V ..... 1063  
 Ottinger, S ..... 1230  
 Otuki, M F ..... 1430  
 Ouédraogo, G ..... 1694, 2272, 2441\*  
 Ouellet, N ..... 1985  
 Ouro-djobo, R ..... 1224  
 Overmann, G ..... 549  
 Ovesen, J ..... 688\*  
 Ovsiannikov, D ..... 188  
 Owens, E O ..... 42\*  
 Oyagbemi, A A ..... 1245, 1318\*  
 Oyler, J ..... 1732  
 Ozanne, S ..... 1636  
 Ozawa, S ..... 808  
 Ozden, S ..... 538\*  
 Ozhan, G ..... 196  
 Øvrevik, J ..... 1185, 1714, 1746

## P

Pacheco, B ..... 1136  
 Pacheco, S ..... 2288  
 Pack, L M ..... 1740  
 Padilla, S ..... 1445  
 Paehler, A ..... 2175  
 Paffett, M ..... 222, 1141, 2016\*  
 Page, K E ..... 1177\*  
 Pai, R ..... 887\*, 1806  
 Painter, K L ..... 868\*  
 Pais, A ..... 1550  
 Pajaro-Castro, N ..... 1264\*  
 Pakbin, P ..... 64  
 Pal, U ..... 1768  
 Palacio, I C ..... 1500\*  
 Palacios-Hernandez, T D ..... 1768, 1771,  
 1777\*, 1778  
 Palani, S ..... 1230  
 Palate, B ..... 1028  
 Palenski, T L ..... 1631, 2001\*  
 Palestino Escobedo, G ..... 91  
 Pallardy, M ..... 1926, 2072  
 Palmeira, C M ..... 655\*  
 Palmer, J A ..... 1001  
 Pan, T ..... 1971  
 Pan, X ..... 674, 2079\*  
 Pan, Y ..... 1535  
 Pandey, R ..... 2425\*  
 Pandian, M ..... 1247  
 Pandiri, A ..... 1094  
 Panicker, N ..... 243, 1842\*  
 Pannirselvam, M ..... 2168\*

Pant, K ..... 1686, 1697  
 Pantano, P ..... 443  
 Panzica-Kelly, J ..... 1002, 1025\*  
 Papagiannis, C ..... 176  
 Papineni, S ..... 104\*, 112, 1101, 1117  
 Paranjpe, M ..... 2331  
 Paras, Z ..... 2151  
 Parchment, R ..... 79  
 Parchment, R E ..... 1470  
 Paredes, A M ..... 1357  
 Parfenova, L ..... 2440  
 Parham, F ..... 578\*  
 Parikh, D ..... 1703\*  
 Parikh, M C ..... 1309, 2040\*  
 Parinandi, N L ..... 1128  
 Paris, M ..... 1572\*, 1573, 1576  
 Park, B ..... 654, 932, 1201, 1789\*, 1900  
 Park, D ..... 1162  
 Park, E ..... 1529, 1745\*  
 Park, H ..... 210, 641, 2102\*  
 Park, J ..... 1511\*, 1759  
 Park, K ..... 1511  
 Park, P J ..... 2196  
 Park, R ..... 1575  
 Park, S ..... 148, 218, 535,  
 641, 641, 1011, 2085, 2335, 2351\*  
 Park, Y ..... 252, 535, 1011  
 Parkins, R ..... 1057  
 Parks, A B ..... 702  
 Parks, B ..... 186  
 Parks, B B ..... 1629  
 Parks, J ..... 1879  
 Parks, J L ..... 2021  
 Parlapiano, A ..... 401  
 Parman, T ..... 1221, 1892\*  
 Parr-Dobrzanski, B ..... 594  
 Parrish, M L ..... 670  
 Parrott, J ..... 1204  
 Parsons, B L ..... 1708, 1709\*, 1969  
 Parsons, G N ..... 439  
 Parsons, L ..... 2449  
 Parsons, P J ..... 1538  
 Passage, J K ..... 537  
 Pastoret, A ..... 1115  
 Patel, B ..... 989  
 Patel, D K ..... 1855  
 Patel, M ..... 352, 911, 1229  
 Patel, M L ..... 861, 1623\*  
 Patel, N ..... 1047, 2192  
 Patel, P ..... 308, 1088\*  
 Patel, R ..... 905  
 Patel, R D ..... 698  
 Patel, S ..... 244\*, 1910  
 Patel, T ..... 1044\*  
 Patel, V ..... 257  
 Patel, V S ..... 2034\*  
 Patete, J M ..... 1747  
 Pathi, S ..... 163\*  
 Patisaul, H B ..... 1382  
 Patlewicz, G ..... 2267  
 Patlolla, A ..... 1355\*  
 Pato, A ..... 1412  
 Patri, A K ..... 470  
 Patrick, M ..... 1831, 1892  
 Patterson, A D ..... 629, 2028, 2405  
 Patterson, J ..... 364, 1974\*  
 Patton, C ..... 1932  
 Patton, R E ..... 1042  
 Paul, K B ..... 99\*, 103  
 Paule, M G ..... 899, 907, 908, 1368, 1369\*,  
 1371, 1613, 2160, 2377, 2415, 2418\*  
 Pauli, G F ..... 2321, 2336  
 Paulman, A ..... 2119  
 Pauluhn, J ..... 425\*, 1148  
 Paulussen, M ..... 1249  
 Paustenbach, D J ..... 478, 1166,  
 1168, 1268, 1514, 1555  
 Pavel, I E ..... 1360  
 Pavkovic, M ..... 930, 931  
 Pavuk, M ..... 1984\*  
 Pawsey, J ..... 96  
 Payne, B ..... 1488  
 Payne, H ..... 672  
 Payne, O ..... 1046  
 Payne, R ..... 1530  
 Peachee, V ..... 414

## Author Index (Continued)

- Pearce, B ..... 448  
 Pearce, M G ..... 1334, 1487, 1740  
 Pearson, K ..... 2126  
 Pearson, N ..... 1467  
 Peat, T ..... 1112\*  
 Pechacek, N ..... 1545, 2226\*  
 Peddada, S ..... 1094  
 Pedraza, J ..... 2393  
 Pfeffer, R ..... 634  
 Pegram, R A ..... 507, 510\*, 613  
 Pejnenburg, A A ..... 1941, 2087  
 Pekkanen, J ..... 402  
 Pelallo-Martínez, N ..... 1832  
 Pelch, K E ..... 526  
 Pellegrini, K L ..... 2198\*  
 Pelletier, P ..... 2219  
 Pellizzon, M A ..... 727\*  
 Peltier, R ..... 212  
 Peltier, R E ..... 609  
 Pemberton, M ..... 966, 2216\*  
 Pena, N ..... 865\*  
 Pence, L ..... 938  
 Peng, Q ..... 925, 1231  
 Pennie, W ..... 2177\*  
 Penning, T M ..... 292  
 Pennings, J ..... 671  
 Pennings, J L ..... 1472  
 Pennington, K L ..... 1092, 2285, 2286  
 Penninks, A ..... 2059  
 Perafan, B ..... 1936  
 Perales, R ..... 2434  
 Perdue, G H ..... 1271, 1279, 1280, 1282, 1283  
 Pereira, C V ..... 2257\*  
 Pereira, L C ..... 1733, 1993\*  
 Pereira, N ..... 2372  
 Pereiro, N ..... 1918  
 Perera-Rios, J ..... 1836  
 Peres, M ..... 2099, 2101\*  
 Peretz, J ..... 2093\*, 2106  
 Perez, C M ..... 65\*, 1129  
 Perez, V ..... 2234  
 Pérez-Herrera, N ..... 603, 1836\*  
 Pérez-Osorio, C ..... 603  
 Perez-Romero, J ..... 1264  
 Perkins, C ..... 1530, 1539  
 Perkins, E J ..... 143, 250, 559, 875, 1295  
 Perkins, G A ..... 2159  
 Perkins, M ..... 354  
 Perkins, R ..... 117  
 Permenter, M ..... 1513\*  
 Perpetua, M ..... 401, 2065, 2068\*  
 Perrard, M ..... 2137  
 Perras, R ..... 1006  
 Perron, J ..... 756\*  
 Perron Lepage, M ..... 1017\*, 1238  
 Perrott, R L ..... 741  
 Perry, R ..... 1109  
 Persohn, E ..... 2193  
 Person, R J ..... 1192, 2280\*  
 Pescara, I C ..... 98  
 Pessah, I N ..... 1250  
 Pestka, J ..... 391, 399, 1889, 2079, 2320, 2324  
 Peter, B ..... 748\*  
 Peter, E ..... 1561, 1562  
 Peters, D M ..... 2002  
 Peters, J M ..... 629, 637, 1004, 1272, 1280  
 Peters, M ..... 81\*, 82  
 Peters, R E ..... 2220\*  
 Peters, T M ..... 1759  
 Peters-Golden, M ..... 396  
 Petersen, J R ..... 943  
 Petersen, S ..... 998  
 Peterson, B ..... 368  
 Peterson, E ..... 871\*  
 Peterson, H M ..... 101, 746  
 Peterson, K E ..... 1007  
 Peterson, M ..... 1139\*  
 Peterson, R E ..... 2141  
 Peterson, S M ..... 324, 988  
 Peterson, Y ..... 1218  
 Petitclerc, K ..... 762  
 Petrick, J S ..... 2343\*  
 Petriello, M C ..... 1995\*  
 Petrikovics, I ..... 2054  
 Petrochenko, P E ..... 1736\*  
 Petry, T ..... 1554\*  
 Pfaff, T ..... 2123\*  
 Pfau, J ..... 379, 1424  
 Pfreder, M E ..... 274  
 Pfuhler, S ..... 1694  
 Pfund, W P ..... 496  
 Phadk, D ..... 939  
 Phadke, D P ..... 526  
 Phadnis, A ..... 1199, 2084\*  
 Phadtare, L ..... 1903  
 Phalen, R N ..... 2209\*  
 Phan, B ..... 2034  
 Philbert, M ..... 2468\*  
 Philbert, M A ..... 435, 906  
 Philipps, K ..... 1976\*  
 Phillips, J ..... 1805  
 Phillips, J A ..... 2121  
 Phillips, M B ..... 321, 799, 1253\*, 1907  
 Phillips, P M ..... 56, 753, 1445  
 Phillips, R ..... 118, 2267  
 Phillips, S ..... 545, 951\*  
 Phillips, T ..... 1105, 1106  
 Phillips, T D ..... 1565\*, 2316, 2325, 2437\*  
 Phonetheswath, S ..... 2446  
 Phueng, J ..... 126, 873\*  
 Pi, J ..... 726, 1297, 2012, 2358  
 Piaia, A ..... 2193  
 Picamal, P ..... 879, 2173  
 Piccirillo, V ..... 414  
 Piché, M S ..... 2063\*  
 Pierre, F ..... 2368  
 Piersma, A H ..... 1453, 1472, 1833, 1930  
 Pietila, M L ..... 963  
 Pietka-Ottlik, M ..... 351  
 Pike, J ..... 1012\*  
 Pike, S T ..... 395\*, 419  
 Pil, H ..... 1311\*  
 Pilcher, G ..... 1033  
 Pillai, A N ..... 352  
 Pimentel, R ..... 176  
 Piña-Guzmán, B ..... 2112  
 Pinches, M ..... 2167  
 Pinkerton, K E ..... 19, 22\*, 227, 229, 1358  
 Pino, M A ..... 351\*  
 Pinto, D J ..... 1022  
 Pinto, V S ..... 2395  
 Pinto-Martin, J ..... 1394  
 Pinyavev, T ..... 2278  
 Piper Hanley, K ..... 1201  
 Pique, C ..... 1035  
 Piroird, C ..... 970\*  
 Pirone, J R ..... 1450, 1452  
 Pirow, R ..... 1469, 1679  
 Pizzurro, D M ..... 1684\*  
 Pk, S ..... 155, 1994\*  
 Planchart, A ..... 1624  
 Platoff, G ..... 348  
 Platt, V ..... 1900  
 Pleil, J ..... 1649\*  
 Pletnikov, M ..... 2153  
 Ploch, S ..... 1800  
 Plotzke, K P ..... 617  
 Plummer, L E ..... 227  
 Plummer, S M ..... 1549\*  
 Plunkett, D W ..... 49\*  
 Plunkett, L M ..... 47\*  
 Pluta, L ..... 1297, 1629  
 Po, I ..... 2030  
 Poage, D ..... 176  
 Poblete-Naredo, I ..... 182, 451  
 Poda, A R ..... 1336  
 Podolefsky, L ..... 191\*  
 Podoll, T ..... 501\*  
 Poet, T ..... 1248  
 Pognan, F ..... 1055, 1070, 1821, 2193  
 Pogribna, M ..... 647  
 Pogribny, I P ..... 537, 647, 1071, 1710  
 Pohjanvirta, R ..... 1986\*  
 Pohl, H R ..... 479  
 Pohl, L ..... 410  
 Pohl, L R ..... 636, 733  
 Pohlmann, A R ..... 179, 2372  
 Poirier, M ..... 1706, 1777, 2063  
 Poirier, M C ..... 173  
 Poitout, F ..... 762, 1234  
 Polak, S ..... 1047\*  
 Polakoff, B ..... 547  
 Politano, V T ..... 1489, 2103\*  
 Polli, J R ..... 674\*  
 Polokoff, M A ..... 1735, 2048  
 Poloyac, S ..... 2009  
 Poltoratsky, V ..... 384\*  
 Pomeroy-Black, M J ..... 2205\*  
 Pomper, M ..... 1871  
 Ponce, R ..... 1666  
 Ponstein, Y ..... 1499\*  
 Pope, C ..... 1417, 2449\*  
 Pope-Varsalona, H C ..... 1172\*  
 Popovech, M ..... 1352, 1361  
 Popovech, M A ..... 1351\*  
 Popovich, M A ..... 1546  
 Popovich, P G ..... 836\*  
 Popstojanov, R ..... 1132  
 Porceddu, M ..... 1081  
 Porter, A ..... 468  
 Porter, D W ..... 19, 20\*, 427, 441, 452, 456, 457, 458, 465, 818  
 Porter, W ..... 672  
 Portinari, D ..... 1623  
 Portugal, S ..... 1143  
 Poth, A ..... 1502, 1689\*, 2250  
 Pottenger, L H ..... 31\*, 1101, 1972  
 Potter, D ..... 2142  
 Potter, H ..... 2045  
 Poulin, D ..... 1228  
 Pouliot, M ..... 757, 758, 1130  
 Poulsen, K L ..... 656\*, 1077  
 Pounds, J G ..... 789, 1363, 1734, 1764, 2305, 2392  
 Powell, D ..... 1507  
 Powell, E T ..... 1509  
 Powell, W H ..... 1293  
 Powers, K W ..... 1345  
 Powley, M W ..... 793\*  
 Poyil, P ..... 1173  
 Prabhakar, L ..... 872  
 Prabhur, R ..... 2115  
 Prasad, G L ..... 941\*, 1899  
 Prasad, R Y ..... 1773  
 Prasad, S ..... 1550  
 Pratap, S ..... 990  
 Prater, M R ..... 1353  
 Prats, E ..... 559  
 Pratt, J ..... 2169  
 Pratt, L F ..... 967  
 Pratt, M ..... 721, 1024  
 Pratt-Hyatt, M ..... 1082, 1083  
 Prefontaine, A ..... 762\*  
 Prell, R ..... 1806\*  
 Prescott, E ..... 501  
 Preslar, J M ..... 1276  
 Preston, D ..... 2181  
 Prezenger, J ..... 1077  
 Prezioso, J ..... 2168  
 Price, J ..... 76  
 Price, O T ..... 607  
 Price, P ..... 1248, 2455  
 Price, P S ..... 877  
 Price, R J ..... 301  
 Price, S ..... 1126  
 Price, S L ..... 100  
 Priem, S ..... 1809  
 Primakova, I ..... 1006  
 Primo, F L ..... 1700  
 Prince, M S ..... 1306  
 Pringle, R B ..... 340\*, 343  
 Pritsos, C A ..... 1259  
 Pritsos, K ..... 1259  
 Proctor, D M ..... 517, 1967, 2235, 2236\*  
 Proctor, W R ..... 410, 636\*, 733  
 Prokoudine, A ..... 1562  
 Pronk, T E ..... 1453  
 Proper, S P ..... 256, 1515\*  
 Proscura, E ..... 245  
 Prosperini, A ..... 1722  
 Prough, R ..... 1274, 1997  
 Prozialeck, W C ..... 1156\*  
 Prudente, A ..... 1430  
 Prueitt, R L ..... 1951\*  
 Pruet, S ..... 412  
 Pruet, S B ..... 397\*, 586  
 Przybylak, K ..... 858, 889  
 Przygoda, R T ..... 199, 203\*  
 Pudney, J ..... 2252  
 Puga, A ..... 525, 688, 997, 1190, 1194, 1291, 1642\*, 2152  
 Punnoose, A ..... 2387  
 Punt, A ..... 2458  
 Puentes, V ..... 816  
 Puppala, D ..... 78\*, 2277  
 Purkey, A ..... 172  
 Puschner, B ..... 1250, 1451  
 Pushett, D ..... 744\*  
 Putt, D ..... 2328  
 Puzas, J ..... 1588\*  
 Pyatt, D ..... 909\*  
 Pycko, R ..... 2007  
 Pyo, H ..... 1511  
 Pyrah, I ..... 2107  
 Pyrgiotakis, G ..... 815

## Q

- Qi, L ..... 1376, 1444  
 Qi, Y ..... 2309  
 Qian, G ..... 1105, 1106, 1446, 2316\*, 2318  
 Qian, Y ..... 776  
 Qiang, X ..... 1877  
 Qiao, J ..... 2167  
 Qiao, S ..... 2018\*  
 Qiao, Y ..... 2439  
 Qin, Q ..... 1169\*, 2167  
 Qin, S ..... 89\*  
 Qin, Y ..... 1241\*  
 Qiu, L ..... 1463\*, 2258  
 Qu, Q ..... 556, 1164  
 Qu, W ..... 226, 2281\*  
 Qu, Z ..... 1895  
 Quach, H ..... 2412  
 Quach, S ..... 2310  
 Quackenbush, K ..... 172  
 Quell, S J ..... 1427, 2071  
 Quesada, P ..... 1035  
 Quezada, T ..... 2317  
 Quinaglia, G A ..... 98  
 Quintanilla-Vega, B ..... 603, 1398, 1492, 1769, 1832, 2104, 2385  
 Quist, E M ..... 806, 2118

## R

- Ra, K ..... 885  
 Raabe, H ..... 957, 976, 979, 981, 982, 1479  
 Rabinowitz, J ..... 1735  
 Rachel, S ..... 2261  
 Racine, C ..... 2181\*  
 Radonjic, M ..... 699, 992  
 Raeburn, A ..... 1715  
 Rafael-Vázquez, L ..... 1492, 1832  
 Raffaele, K ..... 714  
 Ragavan, M ..... 672  
 Rager, J E ..... 543, 698, 948\*  
 Raghavan, S ..... 885  
 Ragheb, J A ..... 1815  
 Rahmer, H ..... 434  
 Raife, T J ..... 191  
 Raigneau, M ..... 519\*  
 Raimundo, C M ..... 98  
 Raj, D ..... 1204  
 Rajagopalan, P ..... 1461  
 Rajagopalan, S ..... 1606\*  
 Rajeswara, N ..... 885  
 Raldua, D ..... 559  
 Ralston, S ..... 1120  
 Ralston-Hooper, K ..... 1931  
 Ramachandran, A ..... 628  
 Ramachandran, K ..... 2199\*  
 Ramaiah, S ..... 933  
 Ramasamy, S ..... 1963\*  
 Ramesh, A ..... 306, 400, 990, 995, 1110  
 Ramirez, I ..... 1901  
 Ramirez, T ..... 1437, 1475, 2250, 2270\*  
 Ramirez, V P ..... 675\*, 2196  
 Ramirez Lee, M ..... 91  
 Ramone, S ..... 1136  
 Ramos, E ..... 592, 1781  
 Ramos, K S ..... 542, 701  
 Ramos-Robles, B ..... 2104, 2112\*, 2117  
 Ramu, J ..... 907, 908\*, 1613

# Author Index (Continued)

Rana, P	2261*, 2263
Rand, M D	330, 332*
Randazzo, J	1503, 1541*, 1542, 1543
Randles, K	878
Raney, S G	1045
Rankin, G	2181
Rannug, A	302, 325, 669*, 1270
Rannug, U	669, 1270*
Rao, N	257
Rao, R	2077*
Raol, Y H	1229
Rappaport, S M	16
Rasheed, S	2054
Rashi, I	447
Rashleigh, B	277
Rasmussen, K	2382
Rasoulpour, R J	537, 719, 811, 1101*, 1449, 2460, 2491*, 2492*
Rathfelder, N	1055
Rathnam, M	1381*
Rathman, J	857, 859, 869*, 1624
Rathnam, R	1884
Rau, J L	57
Rauma, M	133
Rausch, L	1221*, 1831
Rauscher, H	787
Rautenberg, M	870
Ravindran, A	2356*
Ravindranath, V	1840, 2404*
Rawat, S	321, 590, 610*
Rawlinson, P	1473
Ray, M	435
Ray, S D	1088
Read, R	2108
Reagan, W J	1548, 1890, 2120*
Reamon-Büttner, S	434
Rebar, R	1782
Rebelatto, M	1804
Recio, L	545*, 951, 2428*
Recio-Vega, R	1835*
Reddy, G	1048
Redelman, D	1259
Reed, J	1625
Reed, K L	464
Reefman, E	2059
Rees, B J	35
Reese, D H	1298
Reese, T M	515
Refsnes, M A	1185, 1714, 1746*
Regev, A	2399*
Reid, L M	1203
Reidel, B	690*
Reif, D	116, 130, 862, 864, 1735, 2253, 2454
Reigan, P	312
Reilly, C A	1285
Reilly, T	1215, 1219
Reily, M D	1064
Reisfeld, B	800
Rekhadevi, P V	306, 1110
Reliene, R	1354*
Remy, S	816, 1249*
Ren, H	213, 1773
Ren, X	541, 1416
Renaud, L	71*
Renault, E	539
Render, J A	2508*
Renne, R	217
Reno, A L	2021*
Reo, N V	1418
Resnick, C	1538
Retamal Marin, R R	1754
Retterer, S T	2386, 2391
Reuhl, K R	919
Reverdy, E E	198
Rey-Moreno, M	977
Reyero Vinas, N G	559*, 1356
Reyes, E S	598
Reyes, J	2317
Reyes Leyva, J	1771
Reynolds, J	1228
Reynolds, S H	432*, 457
Rhoades, J	1551, 1559, 2229*
Rhoades, R	995
Rhodes, J	2123
Rhodes, S L	1399
Rhomberg, L R	1951, 2216
Riar, A	1381
Riaz Ahmed, K	1784*
Ribeiro Jr, G	2099, 2101
Ricci, M R	727
Rice, A B	817, 1751
Rice, D W	1428*
Rice, E	270
Rice, F	1575
Rice, J R	1452
Rice, P	504, 1334
Rich, D Q	1830
Richard, A M	859, 862, 1624
Richard, B A	1578
Richards, J E	214, 912
Richards, J H	241, 253
Richardson, D	954
Richardson, J	262, 423, 779*, 916, 1114, 1380, 1844
Richardson, M	2220
Richardson, M E	1553, 2509*
Richarz, A	869
Richarz, A N	858*, 889
Richburg, J	1712, 2135
Richendrfer, H	322*
Richling, E	2337
Richter, R	2448
Rick, D L	269, 811
Ricke, W A	1098
Rico de Souza, A	2355
Rider, C	309, 489, 564, 578, 2497
Ridley, M	869
Ridolfi, A	1412
Riebeling, C	1679
Riediker, M	828*
Riefke, B	930*, 931
Riehl, T	483
Rieth, S	290
Rietjens, I	1458, 2458
Riffle, B W	277, 1922*, 1940, 2133
Rijk, J C	1941
Riley, R	1105, 1106
Rinckel, L	1572, 1573, 1574, 1576, 2251
Rincon, R	2434
Ringblom, J	705, 1953*, 1990
Ringeissen, S	859
Rios-Perez, A D	2161
Ripp, S	803
Risatti, C	981
Riss, T L	1725
Ritz, B	1399
Rivas-Arancibia, S	2483*
Rivera, P	228
Rivera-Rodriguez, A	1706*
Rivest, P	108
Riviere, J E	131, 1322, 2424*
Rivina, Y	338*, 2440
Robert, E	2173*
Roberts, C	1044
Roberts, J	433
Roberts, J R	458*, 954, 1347, 1350
Roberts, K	230
Roberts, L	2005
Roberts, R	701, 1213*
Roberts, S M	1345, 1956, 1968, 2215
Robertson, D	1064
Robertson, L W	1266, 1897, 1989, 1991, 1994
Robertson, S	222*, 2016
Robertson, S H	370, 372
Robichaud, A	757
Robin, M	2039
Robinet, B	1775
Robinson, B	2160
Robinson, C	742
Robinson, C N	87
Robinson, E M	1243
Robinson, J F	1472
Robinson, K	1006*, 2456
Robinson, P	509, 621
Robinson, S	1213
Robinson, V G	1019*, 1175, 2326
Robitaille, C	108*
Robson, M G	1830
Roche, B M	93
Rochester, G	117
Rochet, J	1862
Rockwell, C E	638, 2073*, 2074, 2075

The numerals following the author's names refer to the abstract numbers.  
The asterisk after the abstract number indicates the author is the first presenter.

Roda, E	2373
Rodrigues, A S	352*
Rodrigues, M C	1901
Rodrigues, S F	2372*
Rodriguez, A M	354, 367
Rodriguez, R	1209
Rodriguez, V M	1411
Rodriguez, W	2411
Rodriguez, R I	405*
Rodriguez, V	1409
Rodriguez Salazar, T	1518
Rodriguez Yanez, Y	451*
Rodriguez-Santiago, J	739*
Rodriguez-Uc, A	1836
Roelofs, M J	1930*
Rogers, A B	737
Rogers, J M	56
Rogers, K	1852
Rogers, L K	2026*
Rogers, M	1191
Roggen, E L	1440
Rogiers, V	1677*
Rohlman, D	1419, 1420*
Rohr, A	46*, 1262*
Rohrer, P	1085*
Rojanasakul, Y	426, 449
Rojas, D	543*, 2297
Rojas, I Y	2020
Rojas-Garcia, A E	182
Roland, K	936
Rolo, A P	655
Roman, L J	2037
Romans, A B	2020
Romero, A	592, 1781
Romero, D M	1482*
Romero, E G	1285
Romoser, A	2432
Rompion, S	754
Rondelli, C M	195, 548, 1691*
Ronis, M	97*, 1302, 1589*
Ronk, C J	478*, 1495
Roperti, A	2311*
Roponen, M	402
Roque, P J	1373*
Rosa, A S	1246
Rosado, A	78
Rosas, I O	743
Rose, C B	923*, 1236, 2044
Rose, F	1044
Rose, K	1056
Rose, T	305
Rosen, M B	577, 1981
Rosengren, R J	146
Rosenspire, A J	2080
Rosenstein, M C	867
Rosenzweig, B A	725, 926
Roskos, L	1804
Ross, D G	487
Ross, I A	2350*, 2365
Ross, J	75, 89, 900, 901, 2434
Ross, J B	93*
Ross, J H	597, 1247
Ross, M E	1001
Ross, M K	83, 586, 2450
Ross, N	448
Ross, P	876
Ross, S M	110, 1705, 2443
Rossenu, S	1809
Rossi, E	453
Rostami Hodjegan, A	1047
Roth, R A	630, 656, 1057, 1077*, 1078
Roth, W	504*
Rothenberg, S J	1538
Rothman, N	16
Rothwell, C	362*
Rotibi, M	1853
Rotroff, D	114, 116, 1735, 2253*
Rottinghaus, G	2114
Roubicek, D A	1500
Rountree, M R	128
Rouquie, D	809, 1099*, 1926
Roursgaard, M	437
Rouse, R L	725*, 926, 1711
Rousseau, S	2355
Roussel, C	1081
Rowe, C	654, 932*, 1201*, 2327
Rowland, A M	193, 686, 687
Rowlands, J	1203, 1278, 2267, 2459*
Roy, M	1072
Roy, R	1954
Roy, S	274*, 1531*, 1698
Roy, T	566
Royland, J E	912
Ruan, Y	1164
Ruark, C	621
Rubin, B	2331
Rubinstein, J	997
Rubio, C	1533*
Rubio-Andrade, M	473, 1538
Rubio-Rosas, E	1778
Ruby, K	2154
Ruby, M V	1968
Ruddock, W	2166*
Rudel, R	2274*
Ruden, C	1962
Rudraiah, S	664*
Ruff, A L	361
Ruffli, H	271
Ruillon, S	71
Ruiz, F	1771
Ruiz, M	1722*, 2323
Ruiz, P	138, 702
Rumbeih, W K	1837
Ruparel, N	1403
Russ, K A	435*, 2468
Russel, F G	499, 1930, 2022
Russell, L	1267
Russell, M H	493, 2227
Russell, R B	1894
Russell, S L	367
Russum, C	265
Rusyn, I	86, 289, 574, 620, 710, 876, 1272, 2454, 2476*, 2502
Rutter, S J	741
Ryan, A M	1800*
Ryan, C N	2394
Ryan, D	1213
Ryan, G	324*
Ryan, H	2219
Ryan, K	911*
Ryan, P C	410, 1803, 1804*
Ryu, J	1162

## S

Saadawi, R	1360
Sabadie, C	1178
Sabelli, R	521*
Sabo-Attwood, T	436, 1931, 1938
Sabolsky, E M	92, 818
Sabourin, V	1176
Sabtu, M	1265
Sacaan, A	1231
Sacco, J	190
Sace, F	925, 1882
Sacher, O	869
Sachnik, T	2172
Sadik, A M	484, 491
Sadiq, R	1740
Sadler, N	317*, 894
Sadovova, N	1368*, 1369, 1371
Sadowski, R N	739
Safe, S H	145, 149, 158, 159, 160, 162*, 163, 175, 242, 1118, 1630, 1868, 2050
Saffarini, C	994*
Sager, T M	456*, 458
Sahar, R	346
Sahin, I	2435
Sahu, S C	1779*
Saikhov, R	860, 874
Saikumar, J	2199
Saili, K S	329
Saini, Y	256
Saito, N	280*, 427, 428
Saiyed, Z M	1540
Sakaguchi, H	974, 975
Sakai, K	1742, 1884*
Sakaki, H	129
Sakakibara, H	1688
Sakamoto, K	973
Sakamoto, M	1523
Sakamoto, Y	642
Saks, M J	2041

## Author Index (Continued)

Sakuratani, Y .....	2256	Savarino, S .....	1812	Schulze, C .....	1755	Shadley, J D .....	692
Salagrama, S .....	2459	Savery, L C .....	1530*	Schuwald, J .....	1681	Shafer, T J .....	6*, 820, 900
Salahpour, A .....	1872	Saville, B M .....	344	Schwab, C .....	859, 869	Shah, D .....	2266
Salatas, J H .....	1975*	Savolainen, K .....	453	Schwald, M .....	1821	Shah, F .....	888*
Salawu, O A .....	1305*	Sawyer, M E .....	507	Schwander, S .....	468	Shah, I .....	139, 864, 880, 882, 891*, 2275
Salazar-García, S .....	91	Sayers, B C .....	467, 2384	Schwartz, J .....	2414	Shah, K .....	1846
Salcedo, T W .....	1*	Sayler, G .....	803	Schwartz, J E .....	372	Shah, P .....	498*
Saldiva, P .....	1662, 2099, 2101	Sayler, G S .....	100	Schwartz, M D .....	2276	Shah, R .....	144, 2343
Saldivar, L V .....	1518*	Sayre, P .....	2464	Schwarze, P E .....	1185, 1714, 1746	Shah, R R .....	526, 939
Saldutti, L P .....	2126*	Scabillon, J F .....	20, 452, 1147	Schwegler-Berry, D .....	20, 211,	Shah, Y M .....	2405
Saleh, N B .....	436, 1766*	Scandale, I .....	1034	441, 446, 458, 1350		Shaik, S .....	325
Salem, H .....	1732	Scanlan, L .....	1365	Sciaky, D .....	867	Shakarjian, M .....	341, 1421*, 2151
Salinas, K .....	1970	Scarlata, S .....	94	Scicchitano, M .....	936*, 1146	Shalaby, A A .....	633
Salisbury, J L .....	432	Scavello, M K .....	629	Scinicariello, F .....	479	Shamaki, D .....	1308
Salmen, R .....	1132	Schadt, H .....	1821*	Sciuto, A M .....	354, 367, 741	Shamy, M .....	1164
Salminen, W F .....	627, 938, 1086, 2487*	Schäfer-Korting, M .....	131	Scognamiglio, J .....	1489*	Shananhann, J .....	1131
Samadifam, R .....	1896*	Schaffner, C P .....	919	Scollon, E J .....	487	Shaner, B E .....	2184
Samala, P .....	164	Schatz, A .....	1668	Scott, A .....	690, 1705, 2443	Shangari, N .....	2193
Samberg, M E .....	197, 1322, 1326*	Schatz, A R .....	2204	Scott, A M .....	515	Shankar, K .....	97
Sameshima, H .....	2058	Schaudien, D .....	2374	Scott, C W .....	81, 82	Shankaran, H .....	708*
Samet, J M .....	619, 2029	Schaupp, C M .....	1364, 2025*, 2379	Scott, K .....	1488	Shanle, E .....	169, 1670*
Saminathan, H .....	1842	Schauss, A G .....	1303	Scott, M .....	301, 630	Shannahan, J .....	462, 1327*, 1337
Sampat, V .....	2034	Schechter, A J .....	1828*	Scott, M A .....	1078	Shao, K .....	711*
Sampayo-Reyes, A .....	2225*	Scheffler, B E .....	328	Scott, P K .....	1166	Shapira, E .....	245
Sampson, H .....	2127, 2131, 2133	Scheitza, S .....	1054*	Scoville, D K .....	1364, 2379, 2392*	Shapiro, A J .....	876*
Sampson, K E .....	2169*	Schenk, L .....	1571*	Scribner, K C .....	672*	Shapiro, A M .....	999*
Samuelsson, S .....	1221	Schepky, A G .....	955*	Scully, M .....	2065	Shapiro, D .....	1285*
Sanada, H .....	2445	Scherbl, D .....	2337	Seal, E .....	216	Sharapova, T .....	946
Sanchez, T .....	1739	Schick, S .....	1468	Seaman, C .....	1440	Sharits, B C .....	374
Sanchez, V .....	1706	Schiestl, R H .....	338, 1695, 2440*	Searfoss, G .....	927	Sharma, A .....	670, 894
Sanchez del Pino, M .....	2161	Schildknecht, S .....	1378*	Sebag, I A .....	989	Sharma, A K .....	181
Sanchez Soria, P .....	2310*	Schirris, T .....	2022*	Secretan-Lauby, B .....	1116	Sharma, A M .....	1050*
Sánchez-Guerra, M .....	1492*, 1832	Schisler, M R .....	1117, 1707*, 2444	Sedykh, A .....	127, 144, 860*	Sharma, B .....	602
Sánchez-Gutiérrez, M .....	2112, 2117	Schladweiler, M C .....	59, 61, 213, 214*, 231	Seeger, T .....	339	Sharma, B S .....	2081
Sanchez-Martin, F J .....	2152*	Schlager, J J .....	360, 375, 509, 1776, 2421	Seeley, J .....	2318	Sharma, L .....	257*, 2034
Sanchez-Peña, L C .....	1769, 2282, 2385	Schlatter, J R .....	1647*	Seeley, M .....	1945*	Sharma, M .....	1360, 1776*
Sánchez-Ramírez, B .....	2294	Schlezinger, J .....	1586*, 1590*	Seeram, N .....	1782	Sharma, N .....	97
Sand, S .....	718	Schlichting, A .....	460*	Segal, D .....	714*, 1005	Sharma, S .....	1505
Sanders, A P .....	477*, 543, 698	Schlick, K .....	470	Segner, H .....	746	Sharma, V .....	1704*
Sanders, J M .....	484, 491*, 500, 513, 514	Schlink, S .....	750	Seibel, T M .....	1292*	Sharp, J .....	1247
Sanders, M .....	2168	Schlosser, M J .....	1503	Seidel, A .....	311	Sharpe, M R .....	1090
Sanderson, T .....	108, 149, 1033, 1932*	Schlosser, P M .....	290, 604*, 608	Seidel, S .....	2267	Sharpless, N .....	700
Sanderson, T P .....	1237	Schlumpf, M .....	1383	Seidler, F J .....	2451	Shaw, E .....	1223, 1808
Sandhu, R .....	2055	Schmaling, S K .....	2296*	Seigel, P .....	1053	Shaw, J R .....	268
Sandoval, M M .....	2307	Schmeits, P C .....	2087*	Seiler, A E .....	1679*	Shea, K I .....	725, 1711
Sanedrin, R G .....	2192	Schmidt, A .....	66	Seillier, A .....	745	Sheabar, F Z .....	1507
Sangare-Tigori, B .....	539	Schmitt, G .....	516*	Seiter, J M .....	1519	Sheehan, J .....	70
Sangster, B .....	1943	Schmitt, T .....	938	Sekeroglu, V .....	1491*	Sheehan, P .....	2222*
Sankaran, G .....	597	Schmuck, S C .....	1364	Seki, J .....	952	Sheibani, N .....	2001, 2002
Sankaran, M .....	1341	Schmuczerova, J .....	561	Sekkal, S .....	2329, 2330	Sheik Mohideen, S .....	910
Sanpui, P .....	436*	Schmued, L .....	899, 907, 1613	Sekowski, J W .....	1189, 1211*	Shell, S A .....	1556
Sant, K E .....	1018*	Schnackenberg, L K .....	938	Selan, F .....	1814	Shelton, A B .....	1128
Santella, R M .....	2436*	Schneeweis, L .....	503	Selgrade, M .....	714, 1427, 2498*	Shelton, P M .....	153*
Santin, A .....	1424	Schneider, A .....	1803	Selim, S .....	1247	Shelton, S D .....	1708
Santos, A C .....	1414, 1415	Schneider, A J .....	2141	Selinski, S .....	188	Shen, A .....	1800
Santos, N G .....	1414, 1415	Schneider, B .....	1892	Sell, B E .....	181	Shen, J .....	866*
Santos, T C .....	1496	Schneider, J .....	73, 532, 1865*, 1866, 2155	Sellamuth, R .....	935*	Shen, L .....	1817*
Sapiro, J .....	2020*	Schneider, K J .....	295*	Sellamuthu, R .....	954*	Shen, Y .....	1309*, 2040
Sapkota, M .....	2057	Schneider, S .....	105, 1008,	Seemple, K .....	410*, 636, 733	Shenton, J .....	2063
Saquist, Q .....	2378*	1554, 1927, 1928, 2097, 2383*		Sen, S .....	2456	Sheppard, L .....	1625
Saraceni-Richards, C .....	867	Schneider, X .....	1469	Seng, W .....	735*	Sherer, J D .....	151
Sarang, S .....	307	Schnellmann, R G .....	1218, 2184	Sengar, P .....	1768	Sherf, B .....	1269
Sarangarajan, R .....	1224*	Schnoor, J L .....	155	Sengupta, K .....	1540	Sheridan, J .....	2355
Sarcinelli, P N .....	1246	Schnurbus, R .....	1034	Senn, J .....	1230	Sherman, J H .....	2343
Sargent, L .....	237, 432, 457*	Schoeny, R .....	794	Sens, D A .....	1180, 1181, 1182, 2284	Sherwani, S I .....	1128
Sarigiannis, D A .....	798, 802, 805*	Schoeny, G .....	1249	Sens, M .....	1180	Sherwood, C L .....	2298*
Sarkanen, R .....	1000	Schoeters, G .....	2188*	Sentz, J .....	70	Sheth, C .....	1024
Sarkar, S .....	635	Scholpa, N E .....	929*	Seo, J .....	535, 1011	Shetty, S .....	1072*
Sarker, S .....	468	Schomaker, S J .....	2250	Seo, W .....	2010	Shi, L .....	115, 1744, 1764, 2162
Sarrabay, A .....	1926*	Schönau, C .....	949	Sepulveda, M S .....	324, 988	Shi, Q .....	284, 627, 1713*, 2162
Sasaki, D .....	924, 952*	Schoofs, L .....	1809	Serex, T L .....	493, 1544, 2113, 2227*	Shi, W .....	1239
Sasaki, K .....	280	Schoolmeester, A .....	1216	Serrano-García, L .....	1492	Shi, X .....	1173
Sasaki, M .....	1526*	Schoppee-Bortz, P D .....	1216	Serve, K .....	1424*	Shi, Y .....	743
Sasso, A F .....	290*, 608, 1024	Schorsch, F .....	809, 1099, 1926	Sethi, P .....	488, 593*, 596	Shih, T .....	342*, 347
Satin, M .....	847*	Schrenk, D .....	1292, 2333	Seto, Y .....	969, 2260	Shilliday, B .....	1235
Sato, J .....	968	Schrettl, V .....	357	Settivari, R .....	549	Shim, E .....	1791
Sato, K .....	1441	Schreuder, M F .....	2202	Setzer, W .....	128, 882, 1244*	Shimada, A B .....	390*
Satoh, H .....	1384	Schreurs, M .....	499	Severson, M .....	265	Shimada, K .....	2445
Satoh, M .....	1151, 1155, 2289*	Schroeder, J .....	1286	Sewald, K .....	444, 1469*	Shimahara, M .....	736
Satoh, T .....	1441	Schroeter, T .....	2170	Sewalt, V .....	2339	Shimatani, W .....	973
Satou, H .....	1881	Schubauer-Berigan, M K .....	465	Sexton, H .....	2451	Shimizu, T .....	1881
Sauer, U G .....	1471, 1474*	Schuessler, T F .....	757*	Sexton, K G .....	574, 2502*	Shimoi, K .....	1688
Sauerborn, M .....	2059	Schuetz, J D .....	734	Seyler, D E .....	2137	Shimokawa, N .....	1023
Saunders, E L .....	1351, 1352, 1361*	Schug, T T .....	986, 1570	Shabb, J B .....	1180, 1181	Shimpi, P .....	2331*
Saunders, R .....	2293, 2294, 2295	Schuler, D .....	464*	Shack, A .....	397	Shin, H .....	535, 1011*
Savage, G M .....	206	Schulte, C E .....	1485	Shade, W .....	2232	Shin, J .....	459, 939
		Schultz, S T .....	745				

The numerals following the author's names refer to the abstract numbers.  
The asterisk after the abstract number indicates the author is the first presenter.

# Author Index (Continued)

Shin, K .....	641, 983	Singh, S .....	172*	Sokolowski, S .....	1800	Stanley, B .....	432
Shin, Y .....	1529, 2194	Singh, T .....	1289	Solak, K .....	1929*	Stanley, J .....	559
Shinoda, S .....	973	Singh, U P .....	2076	Solano, M M .....	98*	Stanley, S .....	461
Shinohara, N .....	442	Singhal, R .....	1089*	Soldatow, V .....	620*	Stanfield, K .....	2154*
Shinwari, N .....	1522	Singleton, S T .....	310, 591*, 1420	Solecki, R .....	1027	Stanton, B .....	385
Shiotsuka, R .....	483	Sinhaseni, P .....	1959	Soler, A .....	1533	Stanton, B A .....	268
Shipkova, P .....	1064	Sinko, P J .....	353, 1767	Solhaug, A .....	391*, 1714	Stanton, P .....	1421
Shipkowski, K A .....	438*	Sioutas, C .....	64	Soliman, S S .....	599	Stapleton, H .....	326
Shipp, E .....	50*	Sipes, N S .....	116, 126, 1632*, 2253	Solis-Heredia, M .....	2104	Stapleton, P A .....	92
Shirley, D L .....	394, 418	Sippula, O .....	1517	Solis-Heredia, M J .....	1832, 2385	Stapleton, P G .....	996*, 1147
Shirley, S .....	1949	Siraki, A .....	2031	Sollome, J J .....	2313	Star, A .....	461, 2010*
Shirode, A .....	1354	Sirenko, O .....	86*	Soltys, R .....	1802	Stark, G .....	1136
Shirota, M .....	1960	Sirin, G S .....	135*	Somji, S .....	1180, 1181, 1182, 2284	Starkey-Lewis, P .....	1900
Shirwaiker, R A .....	197*	Sistare, F D .....	1903, 1910	Sommer, M .....	1212	Starr, J M .....	487
Shivanna, B .....	300	Sistla, A .....	2164	Somps, C .....	2165*	Staska, L .....	457
Shmukler, A .....	675	Sitapara, R .....	257, 2034	Son, D .....	1859	Stavitskaya, L .....	132*
Shockley, K R .....	1094, 1944	Sitharaman, B .....	469	Son, S .....	535, 1011	Stedman, D B .....	1003
Sholtes, D .....	117	Sivakumaran, V .....	2036	Son, S F .....	1774	Steen, D .....	1080
Shpyleva, S .....	647*	Sivaraman, L .....	1033*	Son, Y .....	1173*	Steenbergen, C .....	2036
Shroods, A L .....	747	Six, C .....	305	Sonawane, B .....	710, 1957	Steenhof, M .....	240, 830
Shu, L .....	176	Sjögren, B .....	505	Sonee, M .....	1882, 2125	Steevens, J A .....	1336, 1344, 1346, 1356, 1774
Shuey, C .....	1136	Skagen, K .....	187	Song, C .....	207, 210	Stefaniak, A B .....	2013
Shurin, G .....	461	Skoog, S A .....	1736	Song, G .....	2471	Steffy, D A .....	272
Shurin, M .....	461*	Skuland, T .....	1746	Song, J .....	210*, 1739, 1796*	Stegeman, J .....	302, 327*, 1281
Shvedov, A A .....	461, 2360*	Slade, D .....	495	Song, K .....	459	Stein, N .....	1475
Shymonyak, S .....	289	Slade, R .....	216	Song, M .....	650*, 1095	Steinbach, T .....	456
Shyu, W .....	1230	Slavov, S .....	938	Soni, M G .....	843*	Steinberg, P .....	444
Sica, M .....	713	Slawik, B .....	1679	Sood, R .....	1506	Steiner, J .....	1317
Siciliano, S D .....	2220	Slaybaugh, K .....	87	Sorenson, C M .....	2001, 2002	Steinfath, M .....	1679
Siddeek, B .....	105, 1927, 1928	Sleman, M .....	1804	Soriano, J A .....	1768	Steinmetz, K L .....	1831*, 2091
Siddens, L K .....	554	Slikker, W .....	1368, 1369, 1371	Soriano, M .....	355	Steinritz, D .....	357
Siddiqui, J A .....	2378	Slitt, A L .....	13, 485, 1290, 2331	Sorrentino, J .....	700*	Stemmer, P M .....	2080
Siddiqui, M A .....	2378	Slotkin, T A .....	2451	Sorribas, V .....	88, 2312*	Stenerlöw, B .....	1390
Sido, J M .....	1423*	Slusser, A .....	1181*	Sosa, C .....	2312	Stenius, U .....	569, 1920
Sieber, M .....	1041*	Smeester, L .....	543	Sosa-Samper, I .....	747	Stepaniants, S .....	670
Siegel, D .....	2055	Smeitink, J A .....	2022	Sosa-Holt, C .....	1412	Stephen, F D .....	1258*
Siegel, P D .....	1429*, 1432	Smirnova, A .....	1270	Soshilov, A .....	1277	Stephen, L .....	1882
Siegrist, K .....	457	Smirnova, L .....	109, 1680	Sosinski, L .....	2444*	Stephenson, S .....	1800
Sielken, R L .....	1565, 1950	Smith, A .....	387	Soto, A .....	1418	Sternberg, J .....	2044*
Siemann, L .....	581, 582	Smith, A J .....	741	Soto, A M .....	550	Stintz, T R .....	562
Sieracki, N .....	1906	Smith, A M .....	1001*	Soufi, M .....	594	Stetsko, P .....	1215
Sierra-Santoyo, A .....	298, 2138	Smith, B .....	1554	Soukup, J .....	216	Steuerwald, A J .....	1538
Sievers, C K .....	169	Smith, C .....	372*	South, N .....	502	Stevens, Z .....	623
Siezen, K .....	1096	Smith, C J .....	373	Southgate, J .....	1473	Stewart, B .....	1232*
Signorini, C .....	2373	Smith, C S .....	1019, 1175, 2326	Souza, A O .....	1733*, 1993	Stewart, J .....	2122, 2415, 2419*
Siivola, K .....	453	Smith, E .....	1936	Souza, V .....	1154	Stewart, N A .....	1395
Silbergeld, E K .....	1538, 2303	Smith, G .....	85*, 2168	Spade, D .....	1634*	Stewart, S .....	1121
Siler, S Q .....	881, 1059	Smith, G J .....	232, 233*	Sparrow, D .....	2414	Stewart, S R .....	725
Silinski, M A .....	1019, 2326	Smith, H W .....	1875	Spasova, M A .....	614	Stice, S L .....	1202
Silkaitis, K .....	680*	Smith, J N .....	1363*	Spear, W C .....	2021	Stickney, J .....	721
Sills, R .....	1094	Smith, K .....	1987	Specht, A J .....	1510*	Stierum, R .....	699, 992
Silva, R .....	1358	Smith, K J .....	1283*	Specter, B .....	1828	Stifelman, M .....	1252
Silva, T P .....	2395	Smith, L .....	55, 1401	Speen, A .....	905*	Stifleman, M .....	1251
Silvanovich, A .....	1547	Smith, L C .....	1931*	Speirs, I .....	906	Stinchcombe, S .....	1008
Silver, B .....	1237	Smith, M .....	144, 1992	Spence, F .....	1821	Stintz, M .....	1754
Sim, W .....	641*	Smith, M A .....	674	Spencer, R .....	128	Stitzinger, M .....	2354
Simak, J .....	429, 430, 431	Smith, M J .....	1227, 2466*, 2469*	Spenkelink, B .....	2458	Stöckmann, D .....	1750
Simanek, E .....	470	Smith, M T .....	16	Spezia, F .....	1028	Stockton, P S .....	209
Simar, S .....	2441	Smith, M V .....	1450, 1452	Spiekstra, S .....	1440	Stoev, S D .....	2319
Simeonov, A .....	1462	Smith, P .....	435	Spira, A .....	1651*	Stoker, T E .....	1898
Simic, M .....	1566	Smith, P B .....	629, 2028	Spire, C .....	927	Stokes, W .....	502, 1572, 1573, 1574, 1576*, 2251
Simion, A F .....	972, 974	Smith, S .....	652*	Spitz, M R .....	2435	Stoll, A .....	1404*
Simkins, T J .....	420*	Smith, S Y .....	1220, 1234, 1896	Spitzer, M .....	1562	Stoltz, D .....	2311
Simmler, C .....	2336	Smith, T .....	253	Sprando, R L .....	470, 1779	Stone, M F .....	370
Simmons, J .....	891, 2497*	Smolik, C .....	745, 920*, 921	Squibb, K .....	1534	Stone, S .....	441
Simmons, S O .....	99, 103, 2029	Smulders, S .....	455, 2367*	Sram, R J .....	563	Stoner, M .....	113, 2332
Simon, B R .....	1958, 2189*	Smyrniotis, T .....	2042	Sreevalsan, S .....	158*	Storm, M .....	1201
Simon, C .....	1041	Snapp, I B .....	1410	Sriram, K .....	237, 1347*	Stout, K .....	1841*, 1872
Simon, T .....	2267	Snawder, J E .....	290	Srivastava, A K .....	2130	Stout, M .....	495
Simonich, M T .....	333*	Sneed, R .....	270*	Srivastava, D .....	885	Stoute, M .....	761
Simons, A L .....	1715	Sneed, S .....	856	Srivastava, S K .....	161, 677	Straif, K .....	1116
Simons, J B .....	367	Snel, C .....	1447	St-Amand, A .....	804	Strak, M .....	830
Simonsen, J .....	1752	Snider, T .....	368*	St. Claire, R .....	1059	Straus, V .....	814, 1561
Simoyi, R .....	1053	Snodgrass, R .....	90, 1209	Staal, Y .....	699	Strauss, V .....	105, 1562, 1927, 1928
Simoyi, R H .....	1432	Snow, S J .....	1122*	Stacey, G .....	870	Strawson, J .....	2055
Simpson, P M .....	692	Snow, T A .....	494	Stachelek, K .....	2136*	Street, R .....	1795*
Sinche, F L .....	1752*	Snyder, N .....	943	Stack, F .....	1573, 1576	Streeter, J .....	915
Singal, M .....	1541, 1542, 1543*, 1554	Snyder, R .....	303, 308, 466*, 616, 817	Stacpoole, P W .....	747	Streicker, M .....	724
Singer, J .....	2098	Snyder, R J .....	433*	Stacy, B .....	1332	Streifel, K .....	918*
Singer, M .....	2125	Soares, C O .....	2015	Stagg, N J .....	811, 2460	Stricker-Krongrad, A .....	74*, 750, 2047
Singer, T .....	516, 794	Sobhakumari, A .....	1715*	Stahl, M .....	1407	Strickland, J .....	964, 1573*, 1574, 1576, 2251
Singh, J .....	1819, 2179*	Sobol, M .....	1080	Stamatis, M .....	675	Strickland, J D .....	820*
Singh, K P .....	168, 544	Sobus, J .....	1653*, 1907	Stamp, K .....	1213	Strikwold, M .....	2458*
Singh, N .....	1838	Sochaski, M A .....	1163	Stampf, M .....	1971*		
Singh, N M .....	193, 686*	Soelberg, J .....	299, 894	Stanislaus, D J .....	1813		
Singh, N P .....	2076*	Sohn, S .....	1511	Stankowski, L F .....	1686, 1697, 1698*		

## Author Index (Continued)

- Ströbele, M ..... 444  
 Strock, C ..... 89, 901, 1463, 2177  
 Strohmaier, C ..... 1391  
 Strom, S C ..... 692  
 Struble, E B ..... 738  
 Strupp, C ..... 594  
 Stuchal, L D ..... 1956, 2215\*  
 Stueckle, T A ..... 426\*, 449  
 Stuhler, J ..... 1058  
 Stull, R ..... 1209  
 Stump, D ..... 1937  
 Sturgeon, J ..... 432  
 Sturgess, N ..... 55\*, 1401  
 Stweart, S R ..... 926  
 Styblo, M ..... 473, 2290, 2293, 2294\*, 2295  
 Su, C ..... 1718, 1719\*, 1721, 2381  
 Su, D ..... 529  
 Su, F ..... 125\*  
 Su, G ..... 1825  
 Su, J ..... 1105, 1106, 1886, 2316  
 Su, M ..... 2439  
 Su, S ..... 540  
 Su, T ..... 1215\*  
 Su, Z ..... 115  
 Suarez, E ..... 482  
 Suárez-Solis, V ..... 603  
 Subbarayalu, P ..... 2149  
 Subramaniam, V ..... 1144  
 Subramanian, K ..... 885, 886, 910  
 Suchaoin, W ..... 1758  
 Suchodolski, J ..... 1317  
 Suda, M ..... 194  
 Sudakin, K ..... 1942  
 Sugaya, C ..... 736, 914, 2190  
 Sugimoto, N ..... 1016  
 Sugita-Konishi, Y ..... 736, 2322, 2341  
 Suguro, M ..... 1104  
 Suh, M ..... 517, 1967\*, 2235, 2236  
 Suhonen, S ..... 453  
 Sulentic, C E ..... 378\*, 1666\*, 1776, 2086  
 Sullivan, A ..... 1934  
 Sullivan, B P ..... 638, 1061  
 Sulyok, M ..... 1883  
 Sumida, K ..... 928  
 Sumner, S ..... 466, 616, 1131  
 Sumner, S C ..... 1032  
 Sumner, S J ..... 1133, 1134, 1135  
 Sun, B ..... 690, 1705, 2443\*  
 Sun, G ..... 501  
 Sun, H ..... 1164  
 Sun, J ..... 1086\*  
 Sun, Q ..... 772\*  
 Sun, R ..... 249  
 Sun, S ..... 78  
 Sun, S L ..... 69  
 Sun, W ..... 620, 1824\*  
 Sun, Y ..... 1157\*  
 Sun-Lin, D ..... 2119  
 Sundaram, R ..... 782  
 Sundell-Bergman, S ..... 1390  
 Sundsmo, J ..... 2062  
 Sunesara, I ..... 143  
 Sung, J ..... 459\*  
 Sung, S ..... 641  
 Sunouchi, M ..... 523\*  
 Suntres, Z ..... 2007\*  
 Sura, R ..... 307, 537, 1256, 1449, 1707, 2232, 2444  
 Surace, M ..... 1843  
 Surh, I ..... 1300\*  
 Susanne, R ..... 460  
 Sussman, R ..... 1954  
 Sutton, P ..... 785, 2456  
 Suva, L ..... 1302, 1589  
 Suzuki, C F ..... 1500  
 Suzuki, D ..... 1960  
 Suzuki, M ..... 973  
 Suzuki, N ..... 1174  
 Suzuki, O ..... 186, 985  
 Suzuki, T ..... 194, 1829, 2116  
 Suzuki, Y ..... 1757\*  
 Svedberg, U ..... 1240  
 Svoboda, K K ..... 352  
 Svoboda, K R ..... 1372  
 Swank, A ..... 558  
 Swanson, A ..... 335  
 Swanson, T A ..... 1143\*  
 Swayze, S ..... 362  
 Sweeney, L M ..... 374  
 Sweeney, T D ..... 1222, 1225\*  
 Swenberg, J A ..... 948, 953, 1704, 1902  
 Swenson, T ..... 589\*  
 Swiss, R ..... 2006, 2262\*, 2263  
 Switzer, R C ..... 54  
 Sydlik, U ..... 1750\*  
 Synoweic, K A ..... 565  
 Sysa Shah, P ..... 2036  
 Szabo, D T ..... 1631\*, 1633\*  
 Szabo, J ..... 1226  
 Szekely, Z ..... 1767  
 Szymanski, C ..... 1762, 1765, 1772
- ### T
- Ta, C ..... 1405  
 Tabata, S ..... 2322  
 Tablin, F ..... 229  
 Tada-Oikawa, S ..... 1757  
 Taetzsch, T ..... 1843\*  
 Taft, J D ..... 1293\*  
 Tagmount, A ..... 1365\*  
 Taimi, M ..... 1463  
 Taiwo, B ..... 1837  
 Takada, M ..... 445  
 Takada, S ..... 234  
 Takagi, H ..... 751\*, 1441, 2260  
 Takahashi, H ..... 407, 409\*  
 Takahashi, M ..... 642, 808, 1960, 2116  
 Takahashi, S ..... 2299  
 Takahashi, T ..... 1723\*  
 Takala, V M ..... 399  
 Takami, K ..... 937  
 Takanashi, S ..... 428  
 Takano, S ..... 157  
 Takao, K ..... 1384  
 Takasaki, W ..... 234, 1829  
 Takashima, R ..... 2445\*  
 Takasu, S ..... 752, 1504, 1508\*, 2341  
 Takata, M ..... 1281  
 Takatsuru, Y ..... 1023  
 Takayanagi, T ..... 2445  
 Takebuchi, N ..... 968  
 Takeda, R ..... 973  
 Takeda, T ..... 1917, 2092\*  
 Takenouchi, O ..... 969\*  
 Takeshita, H ..... 445, 2299  
 Takeuchi, H ..... 2322  
 Takeuchi, K ..... 427  
 Takeuchi, M ..... 1884  
 Takeya, M ..... 1523  
 Taki, F A ..... 674  
 Takuma, K ..... 1384  
 Talahari, S ..... 2441  
 Talbert, D R ..... 1556  
 Talbot, P ..... 141, 1210, 1468, 1753  
 Talcott, S ..... 152  
 Tamez, H ..... 2434  
 Tammara, V ..... 1223, 1808  
 Tamone, S L ..... 2342  
 Tamura, A ..... 728\*  
 Tamura, K ..... 642, 808\*  
 Tan, C ..... 799, 1253, 1907\*  
 Tan, N H ..... 1783  
 Tan, W ..... 412\*  
 Tan, Y ..... 321, 531, 1142\*  
 Tan, Z ..... 197, 1444  
 Tanabe, S ..... 2299  
 Tanaka, J ..... 1693, 2445  
 Tanaka, K ..... 2364  
 Tanaka, N ..... 2405  
 Tanaka, T ..... 1384, 2322  
 Tancredi, D ..... 1250  
 Tang, D G ..... 170  
 Tang, L ..... 1105\*, 1106, 1446, 1886, 1892, 2316, 2318, 2325  
 Tang, L T ..... 597  
 Tang, S ..... 2394\*  
 Tanguay, R L ..... 52, 137, 329, 333, 334, 335, 871, 1359, 2387  
 Tani, Y ..... 234  
 Taniguchi, M ..... 2322  
 Tanner, K ..... 2168  
 Tanos, R ..... 1282\*  
 Taquahashi, Y ..... 1563  
 Tarantini, L ..... 2414  
 Tarasevich, B ..... 1765, 1772  
 Tardif, R ..... 506, 622, 2380  
 Tarkhov, A ..... 859  
 Tarrant, J ..... 1819, 2179  
 Taschwer, M ..... 1058  
 Tasso, M ..... 1733  
 Tasso, M J ..... 1993  
 Tatay, E ..... 2323  
 Tateno, C ..... 1693\*  
 Tatum-Gibbs, K R ..... 2133\*  
 Taura, J ..... 1917, 2092  
 Taurin, S ..... 146  
 Tavcar, R ..... 756, 761  
 Tavendale, A ..... 1214\*  
 Tawari-Eebi, P ..... 2051  
 Tayabali, A F ..... 448  
 Taylor, A J ..... 438, 439\*, 467, 2384  
 Taylor, I ..... 96, 1961  
 Taylor, J S ..... 1429  
 Taylor, K ..... 1391  
 Taylor, M M ..... 56  
 Taylor, V ..... 385  
 Tchana, A ..... 1883  
 Tchounwou, P ..... 1355  
 Teagarden, R E ..... 388\*  
 Tedesco, A ..... 1700  
 Teeguarden, J G ..... 708, 789\*, 865, 1261, 1734, 1764  
 Teesch, L ..... 1991  
 Teesch, L M ..... 1266  
 Tegegn, T ..... 429, 430, 431  
 Tegenge, M A ..... 611\*  
 Teixeira, L ..... 2002, 2045  
 Telesca, D ..... 1734\*  
 Teng, Q ..... 440  
 Tennant, A ..... 54  
 Tenneson, K ..... 1822, 1823\*  
 Teodoro, J S ..... 655  
 Teppner, M ..... 2175\*  
 ter Braak, B ..... 1096\*  
 Terashima, Y ..... 2445  
 Terranova, R ..... 1443  
 Terrones, M ..... 427  
 Terry, C ..... 719\*, 720  
 Terse, P S ..... 1831  
 Tewari-Singh, N ..... 365, 366\*, 369, 371  
 Thackberry, E A ..... 2511\*  
 Thai, S ..... 1773\*  
 Thakur, S ..... 1227\*  
 Thalacker, F ..... 1058  
 Thayer, B ..... 721, 1251, 1252\*  
 Thébaud, S ..... 1477  
 Theberge, A B ..... 2245\*  
 Theodorou, V ..... 2329, 2330\*, 2368  
 Theunissen, P T ..... 1472\*  
 Thibault, P ..... 945  
 Thibodeau, M S ..... 2121  
 Thienpot, B ..... 559  
 Thieriet, N ..... 2368  
 Thiermann, H ..... 339\*, 357  
 Thiex, N ..... 1828  
 Thillainadarajah, I ..... 856  
 Thomas, A D ..... 35  
 Thomas, A T ..... 1232  
 Thomas, D J ..... 1343, 2278, 2290\*  
 Thomas, H ..... 936, 1146, 1680  
 Thomas, J ..... 1256, 1459  
 Thomas, J A ..... 1003  
 Thomas, R ..... 16, 186, 555, 1052, 2070  
 Thomas, R F ..... 213, 214  
 Thomas, R S ..... 422, 557, 1203, 1278, 1294, 1629, 2084, 2429\*, 2457, 2459  
 Thomas, T ..... 1970  
 Thompson, B ..... 1909  
 Thompson, C ..... 1905, 2066, 2426\*  
 Thompson, C A ..... 1109  
 Thompson, C M ..... 517, 2221, 2235\*, 2236  
 Thompson, C T ..... 1967  
 Thompson, D C ..... 312, 2169  
 Thompson, E A ..... 2384  
 Thompson, J A ..... 211  
 Thompson, K ..... 927\*, 1033  
 Thompson, K L ..... 725, 926, 1119  
 Thompson, L C ..... 1032, 1131, 1133, 1134, 1135\*  
 Thompson, V R ..... 349\*  
 Thompson, W ..... 1170, 1530, 1539  
 Thompson-Iritani, S ..... 503  
 Thormodsæter, A ..... 1185  
 Thorne, D ..... 1488\*  
 Thorne, P S ..... 1759, 1983  
 Thornton, C ..... 328, 331, 1356, 2110  
 Thornton, C M ..... 877  
 Thorsrud, B ..... 1020  
 Thrall, B D ..... 789, 1363, 1734, 1764  
 Threadgill, D ..... 183, 737, 2472, 2473\*  
 Thuett, K ..... 1166\*  
 Thuilliez, C ..... 1017, 1238  
 Thurman, D ..... 2167  
 Thybaud, V ..... 794\*, 796  
 Tian, Y ..... 117  
 Tice, R R ..... 127, 526, 578, 939, 1701, 2269  
 Tichenor, S ..... 67  
 Tidball, A M ..... 1685  
 Tie, Y ..... 703  
 Tielen, F J ..... 2059  
 Tierney, N K ..... 1045  
 Tiesman, J ..... 549  
 Tietge, J ..... 265, 1915  
 Tiffany-Castiglioni, E ..... 775\*, 776\*  
 Tigges, J ..... 1039\*, 1716  
 Tijani, A Y ..... 1305  
 Tilak, K ..... 1311, 1798  
 Tilghman, R W ..... 1216  
 Tillmann, T ..... 1490  
 Tilton, S C ..... 329, 335, 554\*, 871, 1764  
 Timchalk, C ..... 2491, 2495\*  
 Timme-Laragy, A R ..... 302, 694\*  
 Tinajero, K ..... 1892  
 Tinwell, H ..... 809\*, 1099, 1926  
 Tipple, T E ..... 2026  
 Tirmenstein, M ..... 1219\*  
 Tissari, J ..... 1517  
 Titorenko, V I ..... 149  
 Tiwari, N ..... 886  
 Tiwary, A K ..... 565\*  
 Tjalkens, R B ..... 834\*, 918, 1229, 1868  
 Tkach, A V ..... 461, 2360  
 Tobin, G A ..... 1121\*, 1711  
 Toda, T ..... 2260\*  
 Todd, M ..... 849  
 Togawa, M ..... 1165  
 Tohyama, C ..... 1387, 2203  
 Toibero, D M ..... 738  
 Tokar, E J ..... 526, 643, 1191\*, 1192, 1193, 228  
 Tokumoto, M ..... 1151\*, 1155, 2289  
 Tolavmat, T ..... 1735  
 Tolaymat, T ..... 1343  
 Tolic, A ..... 1762, 1765, 1772  
 Tomalik-Scharte, D ..... 2337  
 Tomar, S ..... 657\*  
 Tomari, T ..... 1881  
 Tomaszewski, M J ..... 963  
 Tomizawa, S ..... 1200  
 Tomm, J ..... 2072  
 Tommaso, S ..... 2361  
 Ton, T ..... 1094  
 Tong, H ..... 1125  
 Tong, W ..... 115, 117, 866, 1062, 2162  
 Tong, Z ..... 1462  
 Tonge, D P ..... 534\*  
 Tonk, E C ..... 1833\*  
 Tonkin, E ..... 1222\*, 1225  
 Toole, C M ..... 2246\*, 2248  
 Topinka, J ..... 561\*, 563  
 Topping, V D ..... 470  
 Tornero-Velez, R ..... 321, 799, 1253  
 Tornesi, B ..... 2124  
 Torous, D ..... 2446  
 Torres, J A ..... 2043  
 Torres-Arellano, J ..... 1492  
 Torrie, C A ..... 1092  
 Torvela, T ..... 1517  
 Toscano, C D ..... 1610\*  
 Toselli, P ..... 1150  
 Tosh, D ..... 932, 1201  
 Totlandsdal, A I ..... 1185  
 Touaibia, M ..... 1932  
 Touart, L ..... 271

# Author Index (Continued)

Touissant, J	469
Toward, R	76
Towers, H	1804
Toyoda, A	969
Toyoda, T	177, 1952, 2340*
Toyokawa, K	1269
Tracey, K	2034
Trager, R	1218
Tran, C	1365
Tran, H	1727
Tran, N	1645
Tran, T	1790, 1791*, 1792
Tran, U	1627*
Trang, P K	2299
Trask, O	186
Travlos, G	2127
Travlos, G S	1300
Treas, J	168*, 544
Trejos, J	1802*
Tremblay-Franco, M	550
Trepanier, L	190
Treumann, S	1471
Treviño-Mora, S	1152
Trickler, W	2377*
Trimble, M W	670
Trimurtulu, G	1540
Trinh, M	344*
Trinidad, J	1846
Tripathi, D N	685*
Tripathi, N	1800
Tripathi, S	2130*
Tristan-Lopez, F	427
Tritto, E	2193
Troese, M	967*
Trombetta, L D	1403*, 1406
Troncy, E	757, 1130
Tropsha, A	144, 860, 1625, 2422*, 2454
Troth, K	2061
Troth, S P	1903
Troup, D J	2314
Trout, B	918, 1868*
Troyer, J T	345
Truchon, G	1948, 2380
Trudel, L J	685
Truong, L	137*, 333, 2387
Trusk, P B	1556
Tryndyak, V	1071*, 1710
Tsai, G	2151
Tsai, L	1721
Tsaioun, K	38*
Tsaprailis, G	165
Tse, K	1204
Tseng, C	2359*
Tseng, T	1718, 1719, 1721, 2381
Tsosie, R	1516
Tsuchiya, S	973
Tsuda, S	280
Tsuji, H	217
Tsuji, J S	2234*
Tsuji, L J	598
Tsuji, M	475*
Tsujita, K	956
Tsukimori, K	1917
Tsunoda, M	736, 914*, 2190
Tsunoda, S	407, 409, 1384, 2364, 2371
Tsuruoka, S	20, 427*, 457
Tsutsumi, H	1104*
Tsutsumi, Y	407, 409, 1384, 2364, 2371
Tsuzaki, K	1200
Tsyusko, O	1366*
Tu, V	1552
Tuberty, S	1537
Tue, N M	2299
Tugendreich, S	1626*
Tugwood, J D	534
Tukey, R H	320, 1111
Tukur, F	1305
Tunkel, J	1551, 1559, 2229
Tuomela, S	2375
Turgut Kara, N	538
Turk, J R	2401*
Turley, A E	2073, 2074, 2075*
Turner, A	471
Turner, K	2126
Turner, P C	1883
Turner, W E	1984
Turteltaub, K W	1232, 1942, 2386
Tvermoes, B E	1555
Twamley, M	1231
Twardowski, A	1578
Tyagi, T	168, 544*
Tyl, R	466
Tyler, H	443
Tyner, K M	1738
Tyurin, V	1888, 2008*, 2009, 2010
Tyurina, Y	1888*, 2009, 2010

## U

Ubhayakar, S	2176
Uchi, H	1917
Udaka, A	2371
Udasin, R G	341*
Udey, M C	2356
Ueno, S	1389
Uetrecht, J	406, 408, 732, 1050, 1652*
Uhlirva, K	563
Uhouse, M	1860
Uicab-Ventura, J	1836
Uji, M	2371
Ulman, E A	727
Umbright, C	954
Umbuzeiro, G A	98, 569
Umamura, T	752, 1504, 1508, 1952, 2341
Umeno, H	952
Umh, H	1745
Undesser, P	2243
Unfried, K	1750
Unice, K M	1268, 1555
Unrine, J	1366
Unrine, J M	819
Uppal, H	1819*, 2179
Uppu, R M	2038, 2345
Uppu, S N	2345*
Urakar, R	1131, 2470
Urano, K	1104
Urban, J D	4, 2221*
Urban, L	824*
Uribe-Ramirez, M	1748, 1761, 1769, 2385
Ursini-Siegel, G	1176
Urushidani, T	937
Usami, M	523
Usenko, C Y	1243*, 1988
Usenko, S	1243, 2241
Uski, O	1517*
Usui, Y	427, 428
Usuki, F	667*
Uteng, M	1070, 2193*

## V

Vaara, O	402
Vado-Solis, I	603
Vaidya, V S	11, 1156, 2195, 2196, 2198, 2199, 2200, 2400*
Vaillancourt, R R	1064, 2313
Vainshtein, I	1803
Vakil, S	443
Valberg, P	1139
Valdez, M F	745
Valdez-Flores, C	1565, 1950
Valdivia, A G	2317*
Valdivia, P	900*
Valdovinos-Flores, C	2033*
Vale, A	2503*
Valentin, J	376*, 2167
Valentin-Blasini, L	1915
Valentine, J	503
Valentovic, M	2185*
Valerio, L G	2486*
Valero, L	2161
Valin, M	1467
Vallanat, B	59, 213, 947
Vallant, M	1300
Van, A N	121
van Benthem, J	794
van Beuningen, R	2249
van Breemen, R B	2336
van Cott, A	977

The numerals following the author's names refer to the abstract numbers.  
The asterisk after the abstract number indicates the author is the first presenter.

van Darteel, D A	1472
van de Sandt, H	2097, 2383
van de Vegte, D	2178
van de Water, B	678, 679, 1067*, 1096, 1217
van Delft, J	118
van den Berg, M	524, 902, 1929, 2000
van den Brandhof, E	1453
van den Heuvel, L P	2202
Van den Heuvel, J J	499
van der Laan, J	1096
van der Ven, L T	1453
van der Zande, M	2382*
Van der Zwaag, G H	368
Van Dreel, A	1156
van Duijnhoven, E	748
van Duursen, M B	524*, 1929, 1930, 2000
van Ede, K I	2000*
van Ee, R	2097
van Eijkeren, J C	2049
van Erp, A M	377*
van Kleef, R G	902, 903
van Loveren, H	1833, 2087
Van Meter, S	2185
van Mierlo, G M	2059*
van Ras, M	240
van Ravenzwaay, B	105, 131, 814, 964, 965, 977, 1008, 1437, 1458, 1471, 1474, 1475, 1561, 1562, 1664*, 1927, 1928, 2250, 2270
Van Remmen, H	921
van Rozendaal, B	748
van Schooten, F J	671
Van Scoy, J	581
van Steensel, M	118
van Tongeren, S	1805
van Triel, J	240, 699
van Tuyl, M	748, 2354*
van Vliet, A C	1397
van Vliet, E	1680
van Wijk, H	730*, 1014
Van Winkle, L S	229*, 232, 1358, 2389
Vandebriel, R J	2382
Vanden Heuvel, J	1269
Vandenberg, K R	2074
VanDuyn, N	731, 1846, 2148*
Vanhala, E	453
Vanheule, E	1809
Vanlandingham, M M	1042*, 1043, 1596, 2115
Vanoirbeek, J	949, 2367
Vansell, N	1875
Vantangoli, M M	109, 1273, 2247*
Vantrease, J	97
Varela, A	1220*, 2107
Varela, A T	655
Varela, J L	1778
Vargas-Marín, S	2104*, 2112, 2117
Vargo, J	106
Varguaz-Villarrubia, Z	739
Varma, T K	1079
Varner, K	1144
Varner, K J	80
Varney, T R	367
Varsally, W	555
Vasani, N	557, 1294
Vasanthakumari, V	160*
Vasiliov, V	172, 312
Vatanparast, H	1127
Vaughan, J M	66*
Vazquez, R	1768
Vazquez-Martin, C	1214
Vega, H	597
Vega, L	2104
Vega, R	76
Veggi, A B	2395
Veith, G	854
Velasquez, N	71
Veldhoen, N	275
Velez, E	2180*
Velišek, L	1421
Velišková, J	1421
Velovitch, J	1248
Velten, M	2026
Veltien, A	993
Velumani, S	1748
Vena, J E	1258
Venkatkrishnan, P	2037*
Venkatraman, N	2169
Venosa, A	359*, 1767
Venugopal, R	2149*
Vera, A	1768*
Vera-Avilés, M	603
Veranth, J M	1285
Veras, M M	1662*, 2099, 2101
Vercauteren, E	2441
Verhoef, A	1833
Verma, A	1840*
Verma, J R	35
Verma, M	1637, 1639*
Vermeulen, J	671
Vermeulen, R	16
Verner, M	474*, 622
Verstraelen, S	816
Vesterdal, L K	437
Vertrano, A M	1830*
Vetten, M	1331*
Vezina, C M	2141
Vézina, M	1822*, 1823
Viberg, H	58*, 1388, 1390
Vicart, A	1055
Vicente, G H	1876
Vidal, J D	1813
Vidanapathirana, A K	1032*, 1131, 1133, 1134, 1135
Vidmar, T J	1393
Viet, P H	2299
Vigilance, J E	2376
Vignand, P	1834
Vigoren, E M	1909
Vijay, V	1123*, 2410
Vijaya Bhaskara Rao, A	1183*
Vikström Bergander, L	669, 1270
Vilanova, E	1413
Villaamil Lepori, E	1412
Villalobos, A	1160
Villanacci, J F	2433*
Villano, C	981
Villarreal, A	1753
Villeneuve, D L	265, 625
Villalba, J	743
Viluksela, M	1990
Vincent, M J	1974, 2228*
Vines, L L	391
Vinggaard, A	551
Vinken, P	2125
Violi, A	435, 2468
Virkutyte, J	1737
Virley, D	744, 2046
Visan, A	1679
Visconti, N	2444
Vishnudas, V	1224
Visram, S	1505
Viswanadhapalli, S	2149
Vitalde, D	1541, 1542*, 1543, 1554
Vitela, M	745
Vito, S	1422
Vitolo, M I	153
Vituro, E	2172
Vizuete, W	574, 2502
Vlaar, C	2180
Vlasakova, K	1903
Vloet, M	2354
Vock, E	2255
Voelkner, W	1502
Voels, B	1182*
Vogel, A R	584*
Vogel, C	475, 1289*
Vogel, D	1437*
Vogel, S	1469, 1471*, 1474
Vogl, W A	304
Vohr, H	964
Voie, K L	1436
Vokonas, P S	2414
Volberg, V	2412
Volk, H E	2482
Vollmer, G	2250
Volz, D	326*
von Bergen, M	2072
Vorrink, S U	673*
Vracko, M	2268
Vrbanc, J	1235*

## Author Index (Continued)

Vulimiri, S V ..... 1957\*  
 Vulpe, C ..... 555\*, 1177, 1365, 1448,  
 1497, 2271, 2274  
 Vuong, D ..... 1892

## W

Waalens, I ..... 993, 2097  
 Waalkens-Berendsen, I ..... 2383  
 Waalkes, M P ..... 7, 226, 526, 643,  
 1191, 1192, 1193, 2280, 2281  
 Wade-Mercer, P ..... 2363  
 Waechter, J ..... 483  
 Wages, M ..... 1936  
 Wagner, H ..... 2246  
 Wagner, J G ..... 62, 63\*, 235, 256  
 Wagner, K ..... 1271, 1283  
 Wagner, K A ..... 567  
 Wagoner, M ..... 1882\*, 1904  
 Wahlang, B ..... 1274, 1997\*  
 Wahle, B S ..... 2343  
 Waidyanatha, S ..... 303\*, 308, 309, 489,  
 495, 500, 513, 514, 581, 582, 1019, 1934  
 Waikar, S S ..... 2199  
 Waissmann, W ..... 2395\*  
 Waite, M ..... 2221  
 Wakamiya, M ..... 1426  
 Wako, Y ..... 2445  
 Wakuri, S ..... 2260  
 Waldschmidt, J ..... 2108  
 Walesky, C ..... 632, 1097\*  
 Walk, T ..... 1561, 1562, 2270  
 Walker, A ..... 2363  
 Walker, C L ..... 685  
 Walker, E G ..... 1912\*  
 Walker, L A ..... 147, 1299  
 Walker, M K ..... 773\*  
 Walker, N J ..... 433, 817, 1630,  
 1751, 1992, 1999, 2466, 2467\*  
 Wall, H G ..... 230, 1163  
 Wallace, K B ..... 558, 1682, 1773, 1982\*  
 Wallis, C D ..... 2389  
 Wallis, L ..... 2388  
 Walsh, L ..... 239, 1125  
 Walshe, T ..... 1224  
 Walters, G W ..... 574  
 Walters, J ..... 583  
 Wambaugh, J ..... 864, 891, 1244  
 Wambaugh, J F ..... 882\*, 2457  
 Wamhoff, B R ..... 1216, 1459  
 Wan, J ..... 1943\*  
 Wan, L ..... 1483  
 Wanda, B ..... 620  
 Wang, A ..... 788\*, 1239, 1735\*, 2091  
 Wang, B ..... 503, 531\*, 1804,  
 2064\*, 2066, 2243\*  
 Wang, C ..... 115, 1368, 1369, 1371, 1547  
 Wang, E ..... 1903  
 Wang, F ..... 2316  
 Wang, G ..... 1426\*, 2027  
 Wang, H ..... 1103, 1739, 1871, 2034  
 Wang, J ..... 925\*, 958\*,  
 1105, 1106\*, 1426, 1446, 1617\*, 1724,  
 1886, 1895, 2027\*, 2316, 2318, 2325  
 Wang, J D ..... 356  
 Wang, L ..... 316, 426, 449,  
 452, 1149\*, 1173, 1828, 1830, 2004  
 Wang, M ..... 526, 1872  
 Wang, N ..... 876, 2454  
 Wang, N Y ..... 1552  
 Wang, P G ..... 1049  
 Wang, Q ..... 1190, 1194\*, 2064  
 Wang, R ..... 194\*, 443, 875  
 Wang, S ..... 2002, 2249  
 Wang, W ..... 1764, 1869,  
 2096, 2106\*, 2109, 2386, 2391  
 Wang, X ..... 462\*, 529,  
 595, 1208, 1241, 1971, 2170, 2470  
 Wang, Y ..... 734, 1062\*,  
 1094, 1142, 1194, 1210, 1709  
 Wang, Z ..... 810\*, 935, 958, 1108, 1112, 1847  
 Wanibuchi, H ..... 1091, 1095  
 Wappel, R L ..... 1556  
 Ward, J B ..... 1879  
 Ward, W ..... 557, 1294  
 Ward, W O ..... 59, 1773  
 Warheit, D B ..... 464, 1464, 2464  
 Waritimi, G E ..... 266  
 Warner, G ..... 411  
 Warner, R ..... 929  
 Warren, M S ..... 1075\*, 2182  
 Warren, S H ..... 1113  
 Warrior, U ..... 1074  
 Warshaw, E M ..... 1429  
 Wartenberg, D ..... 1830  
 Warth, B ..... 1883  
 Washburn, W ..... 1215  
 Wason, S ..... 809, 1099  
 Watanabe, C ..... 2289  
 Watanabe, F ..... 1740  
 Watanabe, K H ..... 625  
 Watanabe, M ..... 973, 975, 2341  
 Watanabe, S ..... 969, 973  
 Watanabe, T ..... 234, 914  
 Waters, D G ..... 1801  
 Waters, K M ..... 329, 335, 554, 786\*, 871  
 Waters, M D ..... 545, 951, 2426, 2427\*  
 Watford, S ..... 864\*  
 Wathen, A ..... 1058  
 Watkins, A ..... 236  
 Watkins, J B ..... 151\*  
 Watkins, P B ..... 183, 716, 881, 1059, 1089  
 Watson, D E ..... 41\*  
 Watson, R ..... 2095  
 Watson, S ..... 303, 309  
 Watson, S E ..... 1408  
 Watson, W ..... 246\*  
 Watt, C ..... 305  
 Watt, J ..... 1916  
 Wattrelos, O ..... 71  
 Watzek, N ..... 2337  
 Wayman, G A ..... 1375  
 Weaver, J L ..... 1121, 1875  
 Weaver, V ..... 1538  
 Webb, A ..... 1859  
 Webb, J ..... 803  
 Webb, T ..... 1559  
 Webb-Robertson, B ..... 2305  
 Weber, G J ..... 324, 988\*, 1408  
 Weber, J ..... 1696  
 Weber, K ..... 178, 1041  
 Weber, L P ..... 1127  
 Weber, W ..... 740  
 Webster, T ..... 577\*  
 Wegerski, C J ..... 500, 513, 514\*  
 Wegrzynowicz, M ..... 1860  
 Wehmas, L ..... 2387\*  
 Wei, B ..... 887  
 Wei, Y ..... 297, 472\*  
 Weil, R E ..... 1956\*, 2215  
 Weinbauer, G F ..... 1013, 2100,  
 2123, 2142, 2462  
 Weinberg, J ..... 414\*  
 Weinberger, B ..... 1830  
 Weinhouse, C ..... 807\*  
 Weintraub, N ..... 770\*  
 Weisschu, T ..... 1475  
 Weisskopf, M ..... 1510  
 Weithardt, H ..... 1039  
 Weld, M ..... 2348  
 Weldy, C S ..... 260  
 Welles, H ..... 1680  
 Wells, M M ..... 1503  
 Wells, P G ..... 999, 1022  
 Wen, X ..... 662  
 Wenck, H ..... 955  
 Weng, J ..... 1210  
 Weng, Z ..... 194, 284\*, 1713  
 Wens, B ..... 1249  
 Wensler, H ..... 742  
 Wepener, V ..... 276  
 Werle-Schneider, G ..... 713  
 Wessinger, W D ..... 57  
 West, J ..... 1741  
 West, P R ..... 1001  
 Westerholm, R ..... 569  
 Westerink, R H ..... 902\*, 903,  
 1367, 1397, 1839  
 Westerink, W ..... 2249  
 Weston, D ..... 1385, 2156, 2157  
 Weston, H ..... 2157\*  
 Weswick, J ..... 114  
 Wetmore, B A ..... 2457\*  
 Wexler, A ..... 229  
 Wexler, A S ..... 227  
 Wexler, P ..... 1672\*  
 Whaley, J ..... 1219  
 Wheeler, B ..... 644\*, 940  
 Wheeler, J ..... 138  
 Whitacre, S ..... 2230  
 White, C ..... 2379\*  
 White, C A ..... 488, 593, 596, 615  
 White, C C ..... 1364, 2392  
 White, C W ..... 365, 366, 369, 371  
 White, G A ..... 1487  
 White, I R ..... 1433\*  
 White, K L ..... 1227, 2469  
 White, L A ..... 1380, 1457  
 White, M ..... 328  
 White, R ..... 566, 1237  
 White Jr, K ..... 1992  
 Whitebread, S ..... 824  
 Whitehead, M ..... 1557\*  
 Whitehurst, A ..... 174  
 Whitley, E ..... 1837  
 Whitmire, M T ..... 722  
 Whitney, K ..... 2124  
 Whittaker, M ..... 2243  
 Whittaker, M H ..... 1435  
 Whittaker, R ..... 76\*  
 Whitten, D ..... 2079  
 Whitten, K ..... 367  
 Whritenour, J ..... 1431  
 Whyte, T L ..... 494  
 Wible, D J ..... 170\*  
 Wickliffe, J ..... 1958  
 Wickliffe, J K ..... 1879  
 Wiegand, C ..... 713  
 Wiegand, R ..... 1549  
 Wieggers, T C ..... 867  
 Wiek, C ..... 1716  
 Wieland, W ..... 878  
 Wiemann, C ..... 594  
 Wiemann, M ..... 1755  
 Wiemer, J ..... 1562  
 Wiench, K ..... 814, 966\*, 1471, 1749  
 Wieneke, N ..... 713  
 Wiese, A ..... 2512\*  
 Wiesner, M ..... 1735  
 Wignall, J ..... 2454\*  
 Wijnoles, F ..... 1929  
 Wikoff, D ..... 1558\*, 1999  
 Wilbanks, M S ..... 143\*, 250  
 Wilding, S L ..... 1717\*  
 Wildt, B E ..... 1323\*, 1325, 1333  
 Wilga, P C ..... 1077, 1465\*, 1466  
 Wilhelm, C ..... 348\*  
 Wilkerson, C ..... 2079  
 Wilkerson, J ..... 1576, 2379  
 Will, Y ..... 36, 84, 1463, 2006\*,  
 2164, 2177, 2257, 2258, 2261, 2262, 2263  
 Willard, J ..... 1124  
 Willard, P A ..... 237  
 Wille, K ..... 1076\*  
 Willett, C ..... 271\*, 1569  
 Willett, K L ..... 328\*, 331, 1356,  
 1797, 2110  
 Williams, A ..... 221, 2242\*  
 Williams, A L ..... 107  
 Williams, C ..... 628, 658, 1865  
 Williams, C D ..... 1090\*  
 Williams, D E ..... 299, 317,  
 554, 894, 1242, 1942  
 Williams, E S ..... 2241\*  
 Williams, G M ..... 2255  
 Williams, J ..... 2318  
 Williams, J H ..... 2316  
 Williams, K J ..... 639  
 Williams, L R ..... 1048  
 Williams, M A ..... 241, 253\*, 1648\*  
 Williams, M T ..... 1753\*  
 Williams, P ..... 247, 1044  
 Williams, S ..... 670  
 Williams, W ..... 404, 1427\*  
 Williams, W C ..... 2071  
 Williamson, P T ..... 435  
 Willis, A ..... 2055  
 Willis, D ..... 1546\*  
 Willis, K L ..... 1732  
 Willoughby, J A ..... 1466\*  
 Wills, L P ..... 1218\*  
 Willson, G A ..... 230\*, 1163  
 Wilson, C A ..... 507  
 Wilson, D ..... 229  
 Wilson, D M ..... 13\*, 877  
 Wilson, E ..... 2395  
 Wilson, G A ..... 562  
 Wilson, M J ..... 1958\*  
 Wilson, S R ..... 666  
 Wilson, V S ..... 2111, 2127, 2131,  
 2133, 2134\*  
 Wilt, K J ..... 2284  
 Wilt, N ..... 972, 982  
 Wiltshire, T ..... 186\*, 985  
 Winans, B ..... 392\*  
 Wincent, E ..... 302\*, 1270  
 Wine, R ..... 433  
 Wingard, C J ..... 466, 1032, 1131\*,  
 1133, 1134, 1135, 1327, 2470  
 Winiarz, J G ..... 1770  
 Wink, S ..... 679, 1217\*  
 Winkler, D ..... 722\*  
 Winkle, L V ..... 297  
 Winnica, D ..... 1888  
 Winnik, W ..... 558  
 Winsett, D W ..... 65, 1129  
 Winton, T ..... 2136  
 Wisbech, C ..... 391  
 Wise, C ..... 1171\*  
 Wise, J ..... 156, 575\*, 575\*, 1167, 1169,  
 1170, 1171, 1186, 1530, 1539, 1539, 2300  
 Wise, J J ..... 1539\*  
 Wise, L M ..... 739  
 Wise, S ..... 575, 1169, 1170\*, 1171, 1822  
 Wiseman, J ..... 870  
 Witek, R P ..... 1056  
 Witriol, A M ..... 367  
 Witt, K L ..... 1701, 1944\*, 2269, 2275  
 Witters, H ..... 816  
 Wnorowski, G ..... 502  
 Wogan, G N ..... 685  
 Wohlers, D ..... 579  
 Wohlleben, W ..... 1471, 1749\*, 1755, 2383  
 Wohlman, I ..... 337, 358\*  
 Woitkowiak, C ..... 2250\*  
 Wolansky, M J ..... 487, 1412, 1482  
 Wolberg, A ..... 1122  
 Wolf, A ..... 1055, 1070, 1821, 2193  
 Wolf, C J ..... 564\*  
 Wolf, D C ..... 880  
 Wolf, J ..... 55, 1401  
 Wolfarth, M ..... 456, 458  
 Wolfarth, M G ..... 20  
 Wolfe, J ..... 2185  
 Wolfe, M L ..... 1063\*  
 Wolff, H ..... 453  
 Wolfinger, D ..... 978\*  
 Wolfinger, R D ..... 1629, 2459  
 Wolfson, J ..... 476  
 Wolinsky, T ..... 2046\*  
 Wolter, M E ..... 1372\*  
 Wolterbeek, A ..... 992, 993,  
 1447, 2097\*, 2383  
 Wolton, K ..... 1030\*  
 Womack, D S ..... 702\*  
 Won, A ..... 1529, 2194\*  
 Wondrak, G T ..... 2018  
 Wong, A W ..... 113  
 Wong, B ..... 354\*  
 Wong, B A ..... 374\*, 562, 580  
 Wong, L ..... 251\*, 1020  
 Wong, S S ..... 1747  
 Wong, V ..... 154  
 Wood, C ..... 139, 891  
 Wood, C E ..... 880, 947  
 Wood, C R ..... 1981  
 Wood, C S ..... 2214\*  
 Wood, P ..... 1970  
 Woodahl, E ..... 187  
 Woodall, G M ..... 140  
 Woodhead, J L ..... 881\*, 1059  
 Woodhouse, N ..... 1126  
 Woodin, B ..... 327, 1281  
 Woodruff, R S ..... 1740  
 Woodruff, T J ..... 785\*, 2454, 2456  
 Woods, C G ..... 726, 1297, 2012, 2358  
 Woolhiser, M ..... 1052, 2070  
 Wooten, J ..... 174  
 Worek, F ..... 339

The numerals following the author's names refer to the abstract numbers.  
 The asterisk after the abstract number indicates the author is the first presenter.

# Author Index (Continued)

Wormser, U ..... 245\*  
 Wortelboer, H ..... 499  
 Worth, A ..... 859  
 Wouters, M ..... 2097  
 Woutersen, R ..... 699, 992, 993, 2458  
 Woychik, R ..... 2472\*  
 Wright, A ..... 317, 894  
 Wright, C ..... 167, 418\*  
 Wright, C W ..... 1730  
 Wright, D D ..... 1158\*  
 Wright, D J ..... 1109\*  
 Wright, F ..... 620  
 Wright, G M ..... 526  
 Wright, J ..... 1030, 1044, 1069, 1460, 1549  
 Wright, L K ..... 370\*, 372  
 Wright, M ..... 2185  
 Wright, R O ..... 2414  
 Wright, S ..... 2219  
 Wright, S H ..... 511  
 Wright, W S ..... 1158  
 Wu, C ..... 1770, 1804  
 Wu, D ..... 1289, 2024\*  
 Wu, F ..... 2344  
 Wu, H ..... 541, 716, 895\*  
 Wu, J ..... 257  
 Wu, K C ..... 1087  
 Wu, M ..... 552  
 Wu, N ..... 20, 1939\*  
 Wu, P ..... 819  
 Wu, Q ..... 600, 1493, 2035\*  
 Wu, T ..... 2011\*  
 Wu, W ..... 1241, 2324  
 Wu, X ..... 296, 1897\*  
 Wu, Y ..... 2394  
 Wu, Z ..... 2369\*  
 Wullenweber, A ..... 2055  
 Wusu, A D ..... 1257, 1527\*, 2279  
 Wyatt, T ..... 2057

## X

Xi, B ..... 1208  
 Xia, K ..... 620  
 Xia, M ..... 116, 127, 578, 1462, 1701, 2195, 2254, 2269  
 Xia, P ..... 1145  
 Xia, T ..... 1734  
 Xia, Y ..... 1241  
 Xian, H ..... 90\*, 1209  
 Xiao, C ..... 1408\*  
 Xiao, P ..... 601  
 Xiao, Y ..... 2169  
 Xie, B ..... 939  
 Xie, H ..... 575, 1169, 1170, 2300\*  
 Xie, M ..... 583\*  
 Xie, Q ..... 1277  
 Xie, W ..... 651\*  
 Xie, Y ..... 628\*, 658, 1762\*, 1765, 1772  
 Xin, X ..... 155\*  
 Xu, B ..... 1241  
 Xu, D ..... 1535  
 Xu, J ..... 115, 1290  
 Xu, L ..... 601\*, 715, 866, 926, 1121, 1886  
 Xu, M ..... 195\*, 548, 1691  
 Xu, P ..... 476  
 Xu, R ..... 973  
 Xu, S ..... 2315  
 Xu, T ..... 100\*, 803  
 Xu, W ..... 169, 1287  
 Xu, X ..... 117, 1208, 1971  
 Xu, Y ..... 1192\*, 1698  
 Xue, K ..... 1886\*, 2325  
 Xue, P ..... 726\*, 2358  
 Xue, S ..... 87

## Y

Yacovino, L L ..... 662  
 Yafawi, R L ..... 925, 1818\*  
 Yager, J D ..... 109  
 Yager, J W ..... 1979  
 Yamada, A ..... 924  
 Yamada, H ..... 937, 1917, 2092  
 Yamada, J ..... 2256  
 Yamada, K ..... 910  
 Yamada, M ..... 751  
 Yamada, T ..... 728, 1692, 2256\*

Yamaguchi, F ..... 968\*  
 Yamaguchi, M ..... 254, 2371  
 Yamamoto, M ..... 1523\*, 1526, 2092  
 Yamamoto, S ..... 380  
 Yamamoto, T ..... 2260  
 Yamamoto, Y ..... 973  
 Yamashita, A ..... 667  
 Yamashita, T ..... 2256  
 Yamate, J ..... 928  
 Yamazaki, M ..... 1881  
 Yamazoe, Y ..... 2256  
 Yan, B ..... 556  
 Yan, H ..... 1535, 2163  
 Yan, J ..... 1119, 1334, 1506, 1740\*  
 Yan, K ..... 692  
 Yan, Z ..... 1955\*, 1980  
 Yanagiba, Y ..... 194  
 Yanagida, N ..... 2058  
 Yanagisawa, H ..... 2190  
 Yanagisawa, R ..... 1523  
 Yanamala, N V ..... 2360  
 Yañez-Estrada, L ..... 1836  
 Yang, B ..... 726, 2012  
 Yang, C ..... 857, 858, 859\*, 869, 1302\*, 1624, 2153, 2455  
 Yang, C S ..... 1103  
 Yang, C Z ..... 111, 113\*, 2332  
 Yang, D ..... 1161\*, 1376  
 Yang, G ..... 1289  
 Yang, H ..... 63, 210, 2034  
 Yang, J ..... 1735, 1897  
 Yang, K ..... 881, 1059\*, 1444  
 Yang, L ..... 531, 869  
 Yang, M ..... 184\*, 210, 533, 658, 1720, 1887  
 Yang, X ..... 486\*, 627\*, 938, 1086  
 Yang, Y ..... 207, 1253, 1720, 1796, 1895, 1905\*  
 Yang, Z ..... 1105, 1106, 1446\*  
 Yao, P ..... 1004\*  
 Yao, Y ..... 283  
 Yao, Z ..... 1803  
 Yarborough, K M ..... 726, 1297  
 Yauk, C ..... 545  
 Ye, M ..... 1132  
 Yeager, R ..... 176\*, 946, 1905  
 Yee, M ..... 984  
 Yego, E K ..... 363\*  
 Yen, A ..... 693  
 Yeung, D ..... 348  
 Yi, J ..... 996, 1137  
 Yin, H ..... 641, 1277  
 Yin, S ..... 16  
 Yin, Z ..... 1964  
 Yingling, B M ..... 458, 1350\*  
 Yli-Harja, O ..... 2375  
 Yokel, R A ..... 522, 819\*  
 Yokoyama, K ..... 736  
 Yoneda, S ..... 1723  
 Yonekura, K ..... 1811  
 Yoo, H ..... 289\*, 620  
 Yoo, M ..... 1529  
 Yoon, B ..... 668  
 Yoon, I ..... 1877  
 Yoon, J ..... 204\*, 205  
 Yoon, M ..... 301, 616\*, 799, 895, 896  
 Yoshida, M ..... 642, 808, 1952, 1960\*  
 Yoshida, S ..... 1200\*  
 Yoshida, T ..... 407, 409, 956, 1384, 2371  
 Yoshikawa, T ..... 407, 409, 1384, 2364, 2371  
 Yoshimura, H ..... 217  
 Yoshinari, T ..... 2322\*  
 Yoshioka, W ..... 2203  
 Yoshioka, Y ..... 407, 409, 1384, 2364, 2371  
 Yoshitake, Y ..... 973  
 Yost, G S ..... 1285  
 You, J ..... 204, 205  
 You, M ..... 1598, 1600\*  
 Young, B ..... 799  
 Young, R ..... 1160, 2213  
 Young, R R ..... 1686  
 Young, S ..... 352, 446, 954  
 Young, W ..... 887  
 Younis, H S ..... 1816\*

The numerals following the author's names refer to the abstract numbers.  
 The asterisk after the abstract number indicates the author is the first presenter.

Yourick, J J ..... 470  
 Yousefi, P ..... 2412  
 Ysselstein, D ..... 1862  
 Yu, H ..... 2167  
 Yu, I ..... 459, 1349  
 Yu, I J ..... 1619  
 Yu, J ..... 2379, 2392  
 Yu, K ..... 117\*, 509\*  
 Yu, L ..... 1744  
 Yu, S ..... 1162, 2394  
 Yu, W ..... 1878  
 Yu, X ..... 601, 715\*, 2379  
 Yuan, J ..... 449  
 Yuan, Y ..... 2144, 2336  
 Yucesoy, B ..... 14, 189\*  
 Yueh, M ..... 1111\*  
 Yuen, P ..... 927  
 Yuki, K ..... 2265\*  
 Yum, Y ..... 1442  
 Yun, H ..... 2370  
 Yun, S H ..... 1828  
 Yun, W ..... 287  
 Yunomae, K ..... 2058\*  
 Yuri, M ..... 952

## Z

Zabka, T ..... 2179  
 Zaccaria, K ..... 1966\*  
 Zacharewski, T R ..... 552, 648\*, 682  
 Zadworny, M E ..... 2392  
 Zago, M ..... 2355\*  
 Zagorski, J W ..... 2073, 2074\*  
 Zaia, R M ..... 1430  
 Zaikova, T ..... 1359  
 Zailani, A ..... 1319, 1799  
 Zair, Z M ..... 35  
 Zaja-Milatovic, S ..... 1874  
 Zak, M ..... 2176  
 Zakharov, A ..... 1906, 1908  
 Zalko, D ..... 550  
 Zalups, R K ..... 2183  
 Zamboni, W ..... 2471\*  
 Zambrano, C ..... 393  
 Zamoiski, R D ..... 1538\*  
 Zandbergen, F ..... 1273\*, 2296, 2302  
 Zang, Y ..... 2334\*  
 Zangar, R ..... 2305\*  
 Zanger, R C ..... 2392  
 Zanoncelli, S ..... 1034  
 Zandoni, T B ..... 1496  
 Zanonni, T B ..... 1040\*  
 Zappia, J ..... 959  
 Zarbl, H ..... 1093, 1114, 1923  
 Zargorski, J W ..... 2075  
 Zaroogian, G ..... 277  
 Zaslon, Z ..... 396  
 Zaugg, D ..... 516  
 Zavala, J ..... 574\*, 2502  
 Zawdzka, S ..... 1156  
 Zawia, N H ..... 1584\*  
 Zayed, J ..... 1948  
 Zazueta-Beltran, C L ..... 2138  
 Zebedeo, N ..... 379\*  
 Zebovitz, T ..... 1564  
 Zeidler-Erdely, P C ..... 211, 465, 791, 1107\*, 1626  
 Zeise, L ..... 876, 878, 2454  
 Zelikoff, J T ..... 66, 916, 987, 1546, 2105  
 Zemo, D A ..... 565  
 Zeng, D ..... 1223, 1808  
 Zhan, Z J ..... 2163\*  
 Zhang, C ..... 675, 689, 1002\*, 1025, 1140\*  
 Zhang, C X ..... 1026  
 Zhang, D D ..... 2011  
 Zhang, F ..... 269\*, 681\*, 1342\*, 1707  
 Zhang, H ..... 1734, 2324  
 Zhang, J ..... 646, 725, 926, 1121, 1711, 2052  
 Zhang, J X ..... 1075, 2182\*  
 Zhang, L ..... 16, 910\*, 1535\*  
 Zhang, L W ..... 1711\*  
 Zhang, P ..... 600, 738  
 Zhang, Q ..... 319, 726, 1736, 1760, 2012, 2358  
 Zhang, S ..... 1239

Zhang, T ..... 2309  
 Zhang, W ..... 1480, 1971, 1978  
 Zhang, W Q ..... 921  
 Zhang, X ..... 958, 1114, 1208\*, 1767  
 Zhang, Y ..... 135, 734\*, 835, 1087, 1387, 1744\*, 1827\*, 1863, 2315  
 Zhang, Z ..... 1524  
 Zhao, B ..... 1277  
 Zhao, C ..... 1444, 1861  
 Zhao, D ..... 1905  
 Zhao, F ..... 2288\*  
 Zhao, G ..... 144  
 Zhao, J ..... 1277, 1535, 2269  
 Zhao, L ..... 109\*, 1680  
 Zhao, N ..... 1164  
 Zhao, Q ..... 2\*, 601, 1402, 1955, 1980  
 Zhao, W ..... 492\*  
 Zhao, Y ..... 227, 1150\*, 1731\*, 1827, 2002\*  
 Zheng, H ..... 726, 2012  
 Zheng, J ..... 1736  
 Zheng, J F ..... 417  
 Zheng, R ..... 2030  
 Zheng, T ..... 1530  
 Zheng, W ..... 1132, 1179, 1520, 1535, 1585\*, 1862, 1863, 1864, 1877\*  
 Zhitkovich, A ..... 154  
 Zhong, G ..... 747  
 Zhong, L ..... 738  
 Zhong, M ..... 1348  
 Zhou, G ..... 316, 2032  
 Zhou, H ..... 2320\*, 2324  
 Zhou, J ..... 1548\*, 1814\*, 2065  
 Zhou, M ..... 1725  
 Zhou, N ..... 95  
 Zhou, S ..... 935, 1112, 1847\*  
 Zhou, T ..... 1334  
 Zhou, W ..... 1049  
 Zhou, X ..... 1895, 2284, 2287\*  
 Zhou, Z ..... 600, 601, 1241, 1402, 2453  
 Zhu, B ..... 1280  
 Zhu, C ..... 1530  
 Zhu, H ..... 144  
 Zhu, J ..... 472  
 Zhu, M ..... 1375  
 Zhu, Q ..... 1212  
 Zhu, W ..... 166, 313\*  
 Zhu, X ..... 890, 1431\*  
 Zhu, Y ..... 319\*  
 Ziegelhofer, T ..... 70\*  
 Ziejewski, M K ..... 1813\*  
 Ziemann, C ..... 434\*, 460, 1490  
 Zierau, O ..... 2250  
 Zimmer, B ..... 1378  
 Zitoun, P ..... 758  
 Zitzow, J ..... 492  
 Ziv-Gal, A ..... 2096\*  
 Zoeller, R ..... 1914, 1915  
 Zok, S ..... 271  
 Zollinger, T ..... 1443  
 Zong, Q ..... 925  
 Zorrilla, L ..... 102\*  
 Zucker, R ..... 1737  
 Zuehlke, U ..... 760  
 Zuppinger, C ..... 1476\*

A large rectangular area with horizontal ruling lines, intended for taking notes. The area is framed by a dark border at the top and bottom, and a decorative floral pattern on the sides.

# Abstract Keyword Index

The numerals following each keyword refer to the relevant abstract number(s).

- [18F]FDG microPET imaging and animal 3Rs ..... 992
- 1-bromopropane ..... 1389, 2231
- 1, 3 dinitrobenzene (DNB) ..... 2125
- 1, 3-butadiene ..... 2223
- 1, 3-Dichloropropene ..... 1108
- 1, 4-diamino-2-butanone ..... 2015
- 17-DMAG ..... 1284
- 17beta-estradiol ..... 314
- 1H MRS ..... 1866
- 2-AMINOANTHRACENE (2AA) ..... 683
- 2-Bromo-3'-chloropropiophenone ..... 1506
- 2-ethylhexanol ..... 303
- 2-Hydroxy-4-methoxybenzophenone ..... 514
- 2-methylfuran ..... 2348
- 2, 2'-Dithiobisbenzimidazole ..... 513
- 2, 3-Butanedione ..... 1268
- 2, 3-pentanedione ..... 209
- 2, 3, 7, 8-tetrachlorodibenzo-p-dioxin (TCDD) ..... 648, 666, 883, 1293, 2406
- 21st Century Toxicology ..... 2267
- 22RHC ..... 2246
- 28-Day Oral Study ..... 1545
- 3-cafeoyl, 4-dihydrocaffeoylquinic acid ..... 1785
- 3-D reconstructed tissues ..... 980
- 3-Indoxyl sulfate ..... 2194
- 3-MCPD fatty acid ester ..... 1952
- 3-Methylcholanthrene ..... 316
- 3-monochloropropane-1, 2-diol ..... 1952
- 3, 3' Diindolymethane ..... 657
- 3, 5-dichloroaniline ..... 2181
- 3D ..... 1072
- 3D cell culture ..... 2172
- 3D culture ..... 2247
- 3D human skin model ..... 707, 958
- 3D human skin models ..... 1694
- 3D liver mimic ..... 1461
- 3D-human dermal equivalents ..... 1700
- 3R ..... 516
- 3T3 neutral red uptake ..... 1479
- 4-hydroxynonenal ..... 165, 2030
- 4-t-OP ..... 1241
- 4'OH-DELTAMETHRIN ..... 592
- 4h human patch test ..... 1036
- 5-FU ..... 184
- 5-hydroxymethylcytosine ..... 546
- 6-formylindolo[3, 2-b]carbazole (FICZ) ..... 302, 325
- 6:2 fluorotelomer alcohol ..... 494
- 8-methoxypsoralen ..... 1041
- 8-oxodG ..... 437
- 96 well *in vitro* micronucleus ..... 1686
- a-Synuclein ..... 1862
- A549 ..... 442
- abandoned mine ..... 1162
- abatacept ..... 1807
- ABC transporters ..... 1930
- Abcb11 ..... 734
- ABCB6 ..... 663
- ABCC2 ..... 1066
- Abcg2 ..... 662
- Aberant Crypt Foci ..... 150
- absorption ..... 2371
- Abuse ..... 744
- Acacia sieberiana ..... 1308
- Accelerator mass spectrometry ..... 1232
- accommodation ..... 2510
- Acephate ..... 1414
- Acetaldehyde ..... 604
- acetaminophen ..... 233, 249, 627, 658, 660, 661, 664, 665, 1086, 1090, 1461, 1900, 2405
- Acetaminophen Hepatotoxicity ..... 628
- Acetaminophen overdose ..... 632
- Acetaminophen-induced liver injury ..... 630
- Acetylation ..... 1054, 1154
- acetylcholinesterase ..... 135, 340, 343, 2449
- Acetylcholinesterase reactivation ..... 342
- acetylcholinesterase reactivator ..... 576
- Acetylcholinesterase ..... 179
- Achatina ..... 635
- acidic formazan ..... 1037
- Acrolein ..... 65, 646, 2053, 2224, 2337
- Acrylamide ..... 140, 944, 2221, 2337
- Acrylonitrile ..... 813, 1949
- Activity Based Protein Profiling (ABPP) ..... 317
- Activity Related Cytoskeletal Associated Protein ..... 995
- acute behavioral neurotoxicity ..... 896
- Acute exposure ..... 1947
- acute inhalation exposure ..... 703, 704, 2224
- acute kidney injury ..... 283, 1882, 2187, 2200
- Acute liver failure ..... 657
- Acute lung injury ..... 741
- Acute pancreatitis ..... 196
- acute radiation syndrome ..... 740
- Acute toxicity ..... 1540, 1572, 1573, 1576, 2272
- acute toxicity test ..... 1444
- Adaptive Immune response ..... 733
- Adaptive immune system ..... 410
- Adducts ..... 1497, 1501
- adefovir ..... 1905
- Adhesion molecules ..... 390
- adipocyte differentiation ..... 2304
- adipogenesis ..... 586, 1273, 1744
- Adiponectin ..... 1128
- Adjuvant ..... 227
- ADME ..... 494, 500, 513, 514
- ADME/TK ..... 484
- ADMET ..... 41
- adnectin ..... 503, 1237
- Adolescents ..... 1420
- adipocytokines ..... 643
- Adriamycin ..... 1723
- adult stem cell ..... 2311
- adverse drug reactions ..... 824, 1652
- adverse outcome pathway ..... 143, 889, 1623
- Adverse Outcome Pathways ..... 854
- AEGL ..... 703, 704
- Aerosol ..... 574, 1541, 1542, 1543
- Aerosol toxicity ..... 1626
- aesthesia ..... 1031
- aflatoxin ..... 2325, 2327, 2436, 2437
- Aflatoxin B1 ..... 1106, 1690, 2316
- Aflatoxin B1-Lysine Adduct ..... 2318
- Aflatoxins ..... 1105, 2318
- African American ..... 190
- Ag Nanoparticles ..... 1327, 1337, 1352
- Age Susceptibility ..... 1123
- age-related macular degeneration ..... 2511
- age-related susceptibility ..... 2409
- agglomeration ..... 1344
- Agglomeration behavior ..... 1345
- Aggregate harvester exposures ..... 597
- Aggregation ..... 1766, 1862
- aging ..... 59, 700, 906, 1187
- aging individuals ..... 523
- AgNP ..... 1133, 1135
- Agranulocytosis ..... 408, 2031
- Agrochemical ..... 719
- Ah receptor ..... 302, 563, 1270, 1277, 1282
- AHR ..... 162, 387, 669, 693, 773, 811, 812, 873, 997, 1276, 1289, 1296, 1990, 1996, 2096, 2254
- AhR knockout mice ..... 1083
- AhR null Rat ..... 422
- AhR-deficient mice ..... 1292
- AhRR ..... 1289
- AIDS ..... 1706
- air monitoring ..... 2223, 2224
- air monitoring trends ..... 2238
- air pollution ..... 42, 43, 44, 45, 46, 60, 223, 561, 563, 948, 1385, 1500, 1604, 1606, 1607, 1945, 2099, 2101, 2105, 2478, 2481, 2482, 2500
- air pollution mixtures ..... 2502
- Air Quality ..... 768
- air-liquid interface ..... 240, 1341, 1464
- Air-liquid Interface Exposure ..... 1759
- air-liquid-interface (ALI) ..... 2361
- Airborne nanoparticles ..... 1762
- airborne particulate matter ..... 1195
- airway ..... 2298
- airway hyperresponsiveness ..... 254
- airway inflammation ..... 1313
- airway resistance ..... 433
- airway sensitization ..... 699
- Akt1 ..... 695
- albumin ..... 1168, 1478
- alcohol ..... 1302, 1589, 1598, 1600, 2057
- alcoholic liver disease ..... 650
- Aldehyde dehydrogenase ..... 312, 1399
- aldehydes ..... 671, 2023
- ALDH1B1 ..... 172
- Aldh2 knockout ..... 194
- aldrin ..... 2217
- Alkaline Phosphatase ..... 1152
- alkenylbenzenes ..... 2333
- All-Trans-Retinoic Acid ..... 2020
- allergen ..... 1438
- allergen-specific IgE ..... 254
- allergens ..... 403
- Allergic asthma ..... 396
- Allergic Contact Dermatitis ..... 252, 963, 1429, 2071
- Allergic Immunity ..... 1650
- allergy ..... 227, 241, 253, 448, 1439, 1443
- Allopregnanolone ..... 1831
- Allura Red AC ..... 1505
- Alpha-Synuclein ..... 1404, 1857
- alpha-T catenin ..... 189
- Alternative Animal Model ..... 964, 1447
- alternative animal models ..... 1445, 2255
- alternative eye irritation test ..... 977, 979, 982
- Alternative flame retardants ..... 903
- Alternative fuel ..... 580
- Alternative fuels ..... 562
- Alternative Method ..... 966
- Alternative Methods ..... 795, 956, 960, 1000, 1574, 2251
- alternative model ..... 961, 1446
- alternative models ..... 981
- alternative splicing ..... 170
- Alternative testing strategy ..... 965
- alternative to *in vivo* testing ..... 1479
- alternatives assessment ..... 1551, 1559, 2229
- alternatives to animals ..... 271
- Alternatives to Mammalian Models ..... 885, 886
- Aluminium ..... 2149
- Aluminum ..... 1183
- alveolar epithelial cells ..... 1762
- Alveolar macrophages ..... 224
- Alzet pumps ..... 488
- Alzheimer's ..... 779, 1873
- Alzheimer's Disease ..... 261, 1581, 1583, 1584, 1585, 1801
- ambient air ..... 2227
- Ambient Particulate Matter ..... 253, 1125
- Ames assay ..... 1692
- Ames II ..... 1686
- amines ..... 1263
- amino acids ..... 509
- aminoflavone ..... 1287
- aminoglutethimide ..... 406
- aminotransferases ..... 1355
- amidodrone ..... 234, 1720, 1726
- amorphous silica ..... 1754
- Amphibian metamorphosis ..... 96
- Amphotericin B ..... 919
- Amphotericin Monoester ..... 919
- AMPK ..... 1311, 1785
- AMPK activator ..... 1084
- Amyotrophic Lateral Sclerosis ..... 122
- anaerobic microbiota ..... 2278
- analgesic ..... 502, 1428
- Analytical ..... 595
- analytical method development ..... 1243
- Androgen Receptor (AR) ..... 108, 1932, 2250
- androgenic endocrine disruptor screening ..... 2250
- Anegen ..... 2176
- aneuploidy ..... 156, 1186, 1455, 1706
- aneurysm ..... 774
- angiogenesis ..... 130, 1457, 2001, 2390
- angiotensin ..... 1141
- angiotensin II ..... 773
- AngPTL4 ..... 1802
- Aniline ..... 2027
- animal ..... 1822
- Animal - human extrapolation ..... 345
- animal alternative ..... 623, 983
- animal care ..... 1477
- Animal distress ..... 705
- Animal model ..... 733, 801, 1236, 1431, 1815, 1872, 2058
- Animal Models ..... 724, 730, 1014
- animal models of human disease ..... 737
- animal testing ..... 1569, 1677
- Animal welfare ..... 730
- Anoikis ..... 161
- anorexia and emesis ..... 2320
- ANT ..... 655
- Anthrax ..... 345
- anti-drug antibody ..... 2059
- anti-EGFR and anti-IGFR ..... 1237
- antiandrogen ..... 1634, 1941
- antiandrogenic mixtures ..... 105
- Antibiotics ..... 2202
- antibody ..... 357
- antibody production ..... 420
- anticancer drugs ..... 1098, 2132
- antidiabetic agent ..... 1304
- antidotes ..... 2507
- antifungal ..... 309, 1321
- Antimalarial ..... 1319
- antimicrobial ..... 2455
- antimicrobial cleaning products ..... 979
- antinociception ..... 2058
- antiortho-phthalaldehyde ..... 254
- Antioxidant ..... 232, 1799
- Antioxidant enzymes ..... 1319
- Antioxidant property ..... 1783
- antioxidant response ..... 2025
- antioxidants ..... 233, 1853, 2007, 2452
- Antipsychotic drugs ..... 1124
- Antisense ..... 1817
- Antisense Oligonucleotides ..... 1816
- antiviral ..... 1809
- Antiviral drug ..... 344
- Antiviral drugs ..... 1204
- ANVISA ..... 1620
- Apoecorin ..... 2346
- apolipoprotein ..... 829
- apoptosis ..... 33, 80, 149, 154, 353, 380, 389, 399, 573, 904, 1088, 1140, 1155, 1159, 1714, 1716, 1718, 1719, 1722, 1726, 1728, 1729, 1730, 1731, 1732, 1733, 1798, 2083, 2378
- Apoptosis/cell survival ..... 228
- appetite suppressant ..... 1303
- appropriate solvent ..... 976
- aquaporin ..... 268
- aquatic animal ..... 1973
- ARfD ..... 1960
- aristolochic acid ..... 1484
- aryl hydrocarbon receptor (AhR) ..... 415, 2355
- ARNT ..... 167
- Aroclor 1254 ..... 1990
- aromatase ..... 524, 1929
- aromatic amines ..... 406

# Abstract Keyword Index (Continued)

The numerals following each keyword refer to the relevant abstract number(s).

ARPE-19 .....	1737	bacterial infection .....	2034	Bioindicator .....	1320, 1395	Body-residue based approach .....	1552
Arrhythmia .....	239	baicalin .....	286, 287	Bioinformatics .....	119, 578, 871, 886	body-weight loading .....	1829
Arsenic .....	168, 268, 385, 386, 473, 526, 541, 659, 1115, 1136, 1193, 1206, 1273, 1640, 1643, 1644, 1645, 1646, 1647, 1835, 2225, 2230, 2234, 2278, 2282, 2283, 2285, 2286, 2287, 2288, 2289, 2290, 2291, 2294, 2295, 2296, 2297, 2298, 2299, 2300, 2301, 2302, 2303, 2304, 2305, 2307, 2308, 2309, 2310, 2311, 2312, 2313, 2315, 2344	<i>Balanites aegyptiaca</i> .....	1305	Biointeractions .....	1761	bone .....	736, 1158, 1302, 1519, 1586, 1864
arsenic (+3 oxidation state) .....		BaP .....	688	biokinetic .....	1514	Bone endpoints .....	1220
methyltransferase .....	2299	Bariatric .....	1493	biokinetics .....	2374	bone marrow .....	1591
Arsenic (Organic arsenicals) .....	2292	Barnett Shale .....	768, 1568	biologic .....	1800	Bone marrow progenitor cells .....	250
arsenic exposure .....	472, 1249	Basic Red 51 .....	1040	Biologic Therapeutic .....	1003, 1803	Bone marrow toxicity .....	1819
Arsenic species .....	2306	Batracylin .....	1221	Biological limit values .....	622	Bone regulating hormones .....	1896
Arsenic toxicity .....	2279	BAX .....	1726	biological modeling .....	613, 624, 879, 885, 1914	bone resorption .....	1589
arsenical .....	2314	Bayesian .....	142	biological monitoring .....	1887	bone toxicity .....	1587
Arsenite .....	2284	Bayesian Network .....	134, 1627	biologically effective dose .....	805	Bone turnover .....	1896
Arsenobetaine .....	2306	BBDR-HPT axis .....	893	Biologicals .....	1815, 2059	BoNT/A .....	676
artificial skin .....	1040	Bcl-2 .....	1730	Bioluminescence .....	100	borate .....	2228
Artificial sweat .....	1496	BCOP .....	976, 977, 979, 981, 982	biomarker .....	25, 28, 29, 528, 800, 915, 925, 928, 929, 933, 934, 936, 937, 943, 953, 1058, 1089, 1265, 1603, 1613, 1614, 1808, 1864, 1875, 1879, 1880, 1883, 1888, 1889, 1892, 1898, 1899, 1901, 1902, 1903, 1910, 2119, 2120, 2122, 2124, 2126, 2191, 2197, 2401, 2402	Boric Acid .....	1021
aryl hydrocarbon receptor .....	171, 326, 323, 333, 392, 525, 612, 883, 1138, 1190, 1271, 1278, 1279, 1280, 1282, 1283, 1287, 1288, 1291, 1716, 2292, 2459	BCRP .....	524, 662	biomarkers ..	276, 591, 658, 801, 926, 935, 945, 1062, 1126, 1143, 1180, 1234, 1460, 1482, 1579, 1651, 1711, 1878, 1882, 1886, 1894, 1895, 1896, 2130, 2175, 2192, 2199, 2325, 2397, 2398	botanical drugs .....	2486
Aryl hydrocarbon receptor (AHR) .....	175, 666, 673, 811, 1281, 1392, 1929, 1994, 2460	BDE-100 .....	1993	biomarker qualification .....	1912	botanicals .....	957, 1796, 1959, 2336
Aryl hydrocarbon Receptor Repressor .....	1039	BDE-154 .....	1733	biomarker translation .....	26	Bovine Corneal Opacity and Permeability Assay .....	978
As3mt .....	2295	BDE-209 .....	559	Biomarkers ..	276, 591, 658, 801, 926, 935, 945, 1062, 1126, 1143, 1180, 1234, 1460, 1482, 1579, 1651, 1711, 1878, 1882, 1886, 1894, 1895, 1896, 2130, 2175, 2192, 2199, 2325, 2397, 2398	BPA .....	1570, 2096
asarone .....	2333	Beagle dog .....	2069, 2417	biomarkers for exposure .....	2437	BPA TBBPA .....	1930
asbestos .....	230, 231, 380, 381, 382, 383, 607, 1255, 1424, 1495, 1735, 2083	Beagle dogs .....	761	Biomarkers of early effects .....	942	BPA-glucuronide .....	485
<i>Aspergillus flavus</i> .....	2317	BEAS-2B .....	609, 687, 1773	Biomarkers of exposure .....	942	BPD .....	2408
assay development .....	99	BEAS-2B cell line .....	428	biomaterials .....	1326	Bradycardia .....	1148
assay kits .....	1269	behavior .....	57, 58, 322, 674, 835, 1023, 1389	biomonitoring .....	805, 1534, 1649, 1883	Brain .....	916, 1382, 1611, 1915, 2478, 2481
Assessment .....	722	behavioral model .....	1657	Biomonitoring Equivalent .....	804	Brain cancer .....	2372
Assessment factor .....	1947	behavioral toxicology .....	2451	Biomonitoring Equivalents .....	1248	Brain morphometry .....	1393
Assessment factors .....	1965	Behavioural Deficits .....	1022	biopersistence .....	819, 1749	brain stimulation reward .....	1658
Asthma .....	263, 416, 425, 438, 467, 475, 1947, 1974, 2384	behentrimonium chloride .....	972	Biosimilar .....	1800	branched DNA assay .....	2171
asthma models .....	219	benchmark dose .....	711, 718, 876, 1946, 1953, 2215, 2217	Biotechnology .....	1547	Brazil .....	1620
Astrocyte .....	918, 1373	benchmark dose analysis .....	705, 709	Biotherapeutics .....	849, 850, 851, 852, 853, 1620	Brcal .....	999
astrocytes .....	776, 1403	Benchmark Dose Model .....	1944	Biotransformation .....	288, 495, 1082, 1083, 1266	BrdU .....	1441
Ataxia .....	1695	Benchmark Dose Modeling .....	2429	Biotransformation/ Cytochrome P450 .....	311	Breast cancer .....	147, 169, 171, 479, 482, 544, 672, 695, 1176, 1296, 2274
Atherosclerosis .....	64, 83, 124, 770, 829, 2101, 2291	Benchmark Response .....	1955	birds .....	325	Bromate .....	615
ATM .....	685, 1695	Benefin .....	104	Birth Cohort Study .....	1249	bromide .....	2233
Atmospheric aging .....	2502	benzene .....	16, 481, 668, 1265, 1944, 2218, 2238, 2474	birth defects .....	477	Brominated Flame Retardant .....	484
atmospheric systems .....	1605	benzene metabolites .....	165	Bismuth .....	1761, 1769, 2385	brominated flame retardants .....	471, 491, 902, 903
atomic absorption spectroscopy .....	226	Benzidine-azo-dye .....	1496	Bismuth derivatives .....	1748	bronchiolitis obliterans .....	209
Atopic dermatitis .....	1314, 1315, 1789	Benzo(a)pyrene .....	306, 328, 331, 542, 618, 942, 1110, 2110	Bisphenol .....	1921	Brown Norway rat .....	728
atopy .....	402	benzo[a]pyrene (BaP) .....	313, 1966, 2189	Bisphenol A .....	1261, 18, 202, 203, 314, 396, 485, 486, 550, 989, 1551, 1830, 1925, 2093, 2106, 2112, 2115, 2117, 2329, 2330, 2331	BSEP .....	37, 1463, 1881
atrazine .....	324, 490, 583, 584, 682, 988, 1408, 1940, 2088	bile acid .....	1059, 1073, 1082, 1083, 1881	Bisphenol A (BPA) .....	329, 807, 2328	<i>Bufo bufo gargarizans Cantor</i> .....	1794
Aurora kinase .....	2176	Bile acid transport .....	881	Bisphenol AF .....	308, 904, 1934	BUN .....	2190
autism .....	745, 1250, 2482	Bile acid transporter .....	1087	Bivalves .....	2342	butyl paraben .....	1481
Autism Spectrum Disorder .....	1374	bile acids .....	1717	black mold .....	399	butyrylcholinesterase .....	368
autoantibodies .....	835	bile salt .....	1075	Bladder .....	2286, 2288	C x t .....	236
Autoimmune .....	379, 418, 536, 1807	biliary hyperplasia .....	631	Bladder cancer .....	188, 1186, 2234	c-Jun N-terminal kinase .....	628
Autoimmune disease .....	1424	biliary toxicity .....	946	bleomycin sulfate .....	743	<i>C. elegans</i> .....	1153, 1157, 1452, 1525, 1846, 1847, 2143, 2148, 2205
Autoimmunity .....	1425, 1426	Binary Mixtures .....	564	blood biomarker .....	1119	C14 labeled nanoparticles .....	2391
automation .....	1476, 1696	binding site .....	397	blood brain barrier .....	509, 1776	C6-glioma .....	1482
autonomic .....	1129	bioaccumulation .....	267, 276, 515, 746	blood cadmium .....	1162	Caco-2 .....	2169
autonomic function .....	1137	bioanalysis .....	518, 520, 521, 1178	blood concentrations .....	1514	Caco2 .....	1184
Autonomous bioluminescence .....	803	Bioanalytical .....	1707	blood lead .....	1509, 1901	cadmium .....	274, 384, 531, 652, 691, 1149, 1150, 1151, 1152, 1153, 1154, 1155, 1157, 1158, 1159, 1160, 1165, 1180, 1181, 1188, 1191, 1196, 1197, 1257, 1535, 1920, 1933, 2051, 2189, 2219, 2284
autophagy .....	170, 430, 685, 913, 1512, 1528, 1711, 1715, 1720, 1724, 1784, 1818, 2024, 2288, 2309	Bioassays .....	873	blood pressure .....	67, 73, 1137, 1511, 2168	cadmium chloride .....	1820
AVPV .....	998	Bioavailability .....	503, 955, 1968	blood vessel .....	769	cadmium resistance .....	1729
axonal degeneration .....	2447	bioavailable .....	2230	Blood-Cerebrospinal Fluid Barrier .....	1862	<i>Caenorhabditis elegans</i> .....	1366, 1444, 1450, 1451, 1456, 1494, 1845
Azathioprine .....	2352	Biochemistry .....	318, 762	Blood-CSF Barrier .....	1863	<i>Caesalpinia bonduc</i> .....	1783
AZT .....	2053	Biocide .....	269	Blood-retinal barrier .....	2174	Caffeic acid phenethyl ester .....	1932
B cell .....	2080	biocompatibility .....	200, 204, 205, 431	Blood-testis Barrier .....	511	calcitriol toxicity .....	2045
B lymphocytes .....	2086	biocompatibility testing .....	201	blueberry .....	533	calcium channel .....	1840
B(a)P .....	990	biodegraded hydrocarbons .....	565	BMAA .....	908	Calcium Sensing Receptor (CaSR) ..	2320
BAC .....	1217	Biodiesel .....	221, 241	Bmal1 mice .....	455	Calcium Signaling .....	918
BACE .....	2165	Biodiesel exhaust .....	214	BMD/BMDL .....	290, 601	California Proposition 65 .....	2244
background data .....	751, 1961	Biodiesel Inhalation Exposure .....	2360	body composition .....	753	Calu-3 cells .....	282
bacteria .....	197	Biodiesel/Alternative Fuels .....	1607			Cancer ... 153, 377, 700, 1116, 1182, 1191, 1192, 1193, 1225, 1493, 1550, 1771, 2231, 2280, 2284, 2309	
		Biodistribution .....	2362, 2386			Cancer mode of action ... 813, 1117, 1707	
		bioerodable .....	2512			cancer potency .....	2222
		Biofuel .....	580			Cancer Risk Assessment ... 837, 840, 841, 842, 1943, 1957, 1958, 1966, 2344	
		Biofuels .....	56			cancer slope factor .....	2221

candle .....	1554	Celastrol .....	145	Chlorine .....	236	committee recommendations .....	1972
canine .....	747, 1885, 1913, 2069	cell based .....	2262	chloroacetates .....	560	community health training .....	2434
canine telemetry .....	71	cell based assay .....	1437	chloroethanol .....	2212	community outreach .....	1242
cannabinoid .....	745	cell culture .....	2321	chloroethylaziridine .....	2089	Comparability .....	1808
Cannabinoids .....	158, 420, 421, 1423	cell culture media .....	77	Chlorpyrifos .....	508, 1248, 1379, 1416, 2448, 2450, 2451, 2452	Complement and cytokines .....	413
CAR .....	808, 880, 1294	cell cycle .....	293	Choline .....	629	Complementary and Alternative Medicine .....	1425
caract .....	755	Cell cycle arrest .....	447, 2018	cholinergic toxicity .....	1417	complex mixtures .....	563, 565, 2489
Caralluma fimbriata .....	1303	cell cycle regulation .....	382	cholesterol .....	1282, 1757	compound stability .....	2269
Carbamate pesticides .....	389	cell death .....	1067, 1727, 1745	Cholestasis .....	734, 1075, 1087, 1881, 2039	Computational .....	136, 880
Carbaryl .....	799	cell death/apoptosis .....	393	Cholesteryl ester .....	1282, 1757	Computational approaches .....	136, 824, 872, 1628
Carbofuran .....	602	cell microelectronic sensing .....	1480	Choline .....	629	computational biology .....	821, 823, 1297
carbon based nanomaterials .....	469	Cell proliferation .....	1473, 2286	Cholinesterase .....	348	Computational methods .....	2488
carbon black nanoparticles .....	444	cell signaling .....	79, 777	chronic toxicity .....	1829	computational model .....	605, 887, 1622
Carbon Capture .....	1608	cell uptake .....	1769	Chondrotoxicity .....	1829	computational modeling .....	34, 619, 625, 825, 892
carbon monoxide .....	2499	cell-nanomaterial cytotoxicity .....	1324	choroid plexus .....	1160, 1861	Computational Strategies .....	2421
Carbon Nanomaterials .....	426	Cells .....	1777	chromatin .....	529	Computational Toxicology .....	137, 126, 128, 130, 138, 578, 857, 862, 1000, 1674, 2253, 2349, 2486
carbon nanotube .....	429, 430, 446, 449, 1016	cellular .....	2277	Chromatin Structure .....	692	computational workflows .....	858
carbon nanotubes .....	19, 427, 428, 431, 439, 440, 443, 450, 451, 455, 464, 465	cellular immunity .....	2065	chromium .....	156, 688, 1107, 1165, 1166, 1169, 1170, 1171, 1172, 1186, 1950, 2235	conazole .....	1946
Carbon tetrachloride .....	633	Cellular microarray .....	2266	chromosome instability .....	1170	concentration addition .....	577
carbonaceous nanoparticles .....	461	Cellular oxidants .....	2038	chromosome number .....	432	concentration-response functions .....	802
carcinogen .....	1119, 1702	Cellular Response, Toxicity .....	186	chronic administration .....	1228	Concordance .....	1943
carcinogenesis .....	53, 145, 175, 316, 810, 1097, 1109, 1112, 1114, 1115, 1173, 1272, 1690, 1729, 1979, 2285, 2300, 2314	cellular transduction .....	1295	chronic exposure .....	2314	confined space .....	1240
Carcinogenesis screening .....	174	cellular uptake .....	1342	chronic kidney disease .....	2200	confocal microscopy .....	1323
Carcinogenic Dose Response .....	1565	Cellulase enzyme .....	2339	Chronic Oral Toxicity Study .....	1316	Confocal Raman Microscopy .....	1044
carcinogenicity .....	118, 752, 838, 1096, 1104, 1951	cellulose nanocrystal .....	1752	chronic organophosphate toxicity .....	2447	congenital malformations .....	1027
Carcinogenicity study .....	176, 178	Central Drugs Standard Control Organization .....	1618	chronic study .....	1330	connectivity mapping .....	549
Carcinoma .....	683	central nervous system .....	1360	chrysotile .....	231	consequence modeling .....	712
cardiac .....	1129, 2242	cerebellum .....	57, 1392	cigar smoke .....	1507	consistency .....	714
Cardiac adverse events .....	1124	ceria nanoparticle .....	819	Cigarette smoke .... 1138, 1727, 2355, 2369		Constitutive Androstane Receptor (CAR) .....	634, 642, 1284
cardiac function .....	1208	Cerium Dioxide .....	92, 818	cigarette smoke condensate .....	1486	consumer awareness .....	1678
Cardiac Injury .....	925, 1892	cerium oxide .....	2366	cinnamal .....	1542	consumer product .....	1577, 1974
Cardiac insulin resistance .....	1142	Cerium Oxide nanoparticles .....	814, 815, 817, 1751	Circadian .....	278	consumer products .....	1254
Cardiac Risk .....	72	CFU Assay .....	1204	Circadian Rhythm .....	1093, 1165, 1372, 1688	contact allergens .....	2072
cardiac safety .....	1556	Characterization .....	375	class switch recombination .....	384	contact hypersensitivity .....	1430
cardiolipin .....	1888, 2009	chemical additives .....	706	Clastogenicity .....	1503	contact lens .....	2509
cardiomyocyte .....	81, 1132, 1194, 1200	chemical adjuvancy .....	416	clathrin coated vesicles .....	1772	Containers .....	1264
cardiomyocytes .....	77, 82, 2475	chemical allergy .....	1756	clay-based enterosorbent .....	2437	contamination .....	1558
cardioprotection .....	1318	chemical carcinogenesis .....	1176	clearance .....	746, 1358	continuous data .....	711
Cardiopulmonary .....	212, 214	chemical exposure .....	2055	climate change .....	1605, 2500	contraception .....	2091
Cardiotoxicity .....	78, 81, 82, 85, 86, 90, 315, 373, 1126, 1826, 1880, 2098	chemical grouping .....	889	Clinical .....	2420	COPD .....	1627
cardiotoxicity mechanisms .....	1556	chemical hazard assessment .....	712, 1005, 1551, 1559, 2229	clinical signs and symptoms .....	364, 2055	Copper .....	206, 650, 1520
cardiovascular .....	3, 65, 70, 73, 74, 75, 76, 85, 213, 223, 754, 844, 1120, 1122, 1124, 1130, 1139, 1141, 1644, 2036, 2168	chemical injury .....	361	Clinical Toxicology .....	2210	Copper Transport .....	1863
Cardiovascular Disease .....	826	chemical mixture .....	1409	Cmax .....	38	cornea .....	1822, 2030
Cardiovascular diseases .....	2279	chemical mixture toxicity .....	105	CNS .....	238, 909, 1654, 1655, 1656	Corneal endothelium .....	1823
cardiovascular function .....	1125, 1144	chemical mixtures .....	558, 579, 1927	Co-carcinogenic effect .....	1105, 1106	Coronary .....	1134, 1135, 1147
cardiovascular health .....	831	chemical prioritization .....	127	Co-culture .....	224, 311, 2265	corticosterone .....	1940
cardiovascular response .....	23	Chemical properties .....	39	co-exposure .....	2501	Cosmetic .....	1694
Cardiovascular risk .....	848	Chemical Risk Assessment .....	1571, 1965	Coagulation .....	638	cosmetic ingredient review panel .....	1676
cardiovascular safety .....	85, 376	Chemical risk assessments .....	1653	coal ash .....	2211	cosmetic ingredients .....	869
Cardiovascular Toxicity .....	1131, 1145	Chemical structure .....	116, 129	cobalt .....	1168, 1514, 1515, 1555	cosmetic product .....	974
career .....	1630	Chemical warfare agent .....	338, 357, 367	Cobalt Chloride .....	1513	Cosmetics .....	113, 958, 1672, 1673, 1674, 1675, 1676, 1677, 1678
career planning .....	2043	chemical warfare agents .....	349, 364	Coffee beverage .....	2345	Cotinine .....	182
Carolina Breast Cancer Study .....	190	chemical warfare nerve agent .....	370	cognition .....	1865, 2479	CounterACT .....	338
CAS Registry Number 8002-05-9 .....	566	chemical-induced asthma .....	949	cognitive function .....	58	countermeasure .....	336
CASE Ultra .....	874	chemical-teratogenic interactions .....	123	collaboration study .....	973	countermeasures of radiation injury .....	2010
case-control study .....	1827	chemicals .....	1444, 1557	Collagen .....	251, 449, 2002	Courtroom .....	2041
castor oil .....	1308	cheminformatics .....	877, 1625	Collision nebulizer .....	1348	COX-2 .....	1780, 2082
Catecholamine .....	1841	chemistry .....	1876	colloidal silica nanoparticle .....	2370	CpG island methylation .....	543
category approach .....	2256	Chemopreventative .....	1797	Colon Cancer .... 158, 163, 306, 935, 1110, 1118		CPT-11 .....	320
category formation .....	889	chemoprevention .....	1306, 2317	chemotherapy .....	149	Cr(VI) .....	1173
Cathlecidin .....	2057	chemotherapeutic .....	2018, 2188	Chemotherapeutics .....	149	CRC detection .....	1876
Causal reasoning .....	1626	Chemotherapeutics .....	149	chemotherapies .....	75	Creatinine .....	1887, 2182
Causation .....	1579	Chemotherapy-induced peripheral neuropathy .....	1470	Chemotherapy-induced peripheral neuropathy .....	1470	critical path .....	1912
caveolin coated vesicles .....	1772	chemotypes .....	859	chemotypes .....	859	CRM1 .....	166
Caveolin-1 .....	1995	Chicken .....	2255	Chicken .....	2255	cross-presentation .....	409
CBA .....	2354	Chicken Litter .....	1537	chickens .....	2327	Crude Oil .....	566, 568
CD-1 Mouse .....	1961	child behavior problem .....	1394	children .....	475, 1835, 2412	crude oil pipeline .....	1976
CD36 .....	222	Children exposure .....	182	Children exposure .....	182	Crystalline silica .....	954
CD4+ T lymphocyte .....	415	children's health .....	1492, 780, 781, 782, 783, 785, 1836	children's health .....	1492, 780, 781, 782, 783, 785, 1836	CSF .....	2044
CD8+ T cells .....	383	China .....	1617	China .....	1617	CTLA4 .....	1807
CDDO-Im .....	905	Chiral .....	288, 590	Chiral .....	288, 590	Cucurbitacin B .....	677
CDKN2A .....	134	chiral PCBs .....	296	chiral PCBs .....	296	Cultivated ginseng .....	1314, 1789
Cedarwood oil .....	1300	Chk1 .....	681	Chk1 .....	681	Cumulative Risk .....	579, 878, 2498
				Chlorine .....	236	cumulative risk assessment .....	718

- Cumulative Toxicity ..... 2497  
 curcumin ..... 94  
 Cutaneous toxicology ..... 1050  
 CWA ..... 362  
 Cyanide intoxication ..... 2054  
 cyanobacteria ..... 247  
 cyclins ..... 2027  
 cyclooxygenase-2 ..... 586  
 cyclophosphamide ..... 2089  
 cynomolgus ..... 758, 1805  
 cynomolgus monkey ..... 760, 1236, 1237, 1803, 1804, 2044, 2066, 2100, 2107  
 Cynomolgus monkeys ..... 923, 2095  
 CYP ..... 1039  
 CYP gene expression ..... 282  
 CYP induction ..... 523  
 CYP1 ..... 325  
 CYP17 ..... 108  
 CYP1A1 ..... 811  
 CYP1A1/1A2 expression ..... 1992  
 CYP1A1/2 ..... 2338  
 CYP1A2 ..... 1391  
 CYP1B1 ..... 300  
 CYP26 ..... 1008  
 CYP2E1 ..... 2024  
 CYP2F1 ..... 297, 307  
 CYP2F2 ..... 307  
 CYP2S1 ..... 193, 686, 687  
 CYP3A4 ..... 332, 1209  
 CYP450 metabolism ..... 305  
 CYP4f ..... 2404  
 Cystatin C ..... 1156  
 cysteinyl leukotriene receptor 1 antagonist ..... 1713  
 cyto-/genotoxicity, human peripheral lymphocytes ..... 1491  
 cyto-/genotoxicity ..... 1489  
 cytochrome c ..... 2009  
 cytochrome P450 ..... 229, 244, 283, 284, 291, 302, 304, 313, 318, 319, 327, 571, 663, 1625, 1702, 2001, 2002, 2138, 2181, 2403, 2407  
 Cytochrome P450 1A1 ..... 315, 2292  
 cytochrome P45011a1 ..... 2093  
 Cytochrome P4501A ..... 316, 2408  
 cytokine ..... 1185  
 cytokine release ..... 385  
 cytokine signalling ..... 1477  
 cytokines ..... 652, 1438, 1440, 1843, 2354, 2407  
 cytokines and inflammatory gene expression ..... 1992  
 Cytoprotection ..... 2020  
 cytostatic ..... 1725  
 Cytotoxic T Lymphocyte (CTL) ..... 2065  
 Cytotoxic T Lymphocytes ..... 2067  
 cytotoxicity 88, 264, 585, 817, 1009, 1171, 1329, 1340, 1343, 1365, 1468, 1507, 1725, 1742, 1748, 1751, 1770, 1778, 1794, 1978, 2007, 2259, 2264  
 cytotoxicity profiling ..... 127  
 Cytotoxicity screening ..... 887  
 Cytotoxicity testing ..... 199  
 daidzein ..... 417  
 dampness ..... 399  
 dapagliflozin ..... 1219  
*Daphnia* ..... 1365, 1454, 2394  
*Daphnia magna* ..... 274  
 DART ..... 1020  
 Data Analysis ..... 1393  
 data exchange standard ..... 861  
 Data Integration ..... 855, 864, 871  
 data mining ..... 861  
 database ..... 856, 866, 867, 869, 890, 2256, 2375  
 database development ..... 2454  
 Database Uncertainty ..... 1980  
 dataset modelability ..... 144  
 DD generator ..... 1179  
 DDE ..... 479, 1924  
 DDI ..... 1047  
 DDT ..... 598  
 DecaBDE ..... 1559  
 Decabromodiphenyl Ether ..... 2129, 2140  
 decalin ..... 2215  
 decision tool ..... 723  
 Deepwater Horizon ..... 1539  
 Default Values ..... 594  
 DEHP ..... 710, 2104  
 DEL assay ..... 2440  
 Delayed neuropathy ..... 1414, 1415  
 Delphi ..... 2395  
 Delta-9-tetrahydrocannabinol ..... 419  
 Deltamethrin ..... 262, 301, 596  
 Demographic Differences ..... 305  
 Dendrimer Nanoparticles ..... 470  
 dendritic cells ..... 402, 2008  
 Dendritic Spines Morphology ..... 998  
 dental material ..... 2220  
 deoxynivalenol ..... 1889, 2079, 2320, 2326, 2350  
 depleted uranium ..... 123  
 Dermal ..... 513, 514, 1429  
 dermal absorption ..... 131, 594, 1044  
 dermal exposure ..... 407, 507, 1104  
 Dermal Safe Harbor Level ..... 2244  
 Dermal sensitization ..... 967  
 Dermal Toxicity ..... 1042, 1043, 1572, 1573, 1576  
 dermal toxicokinetics ..... 955  
 dermatotoxicity ..... 1436  
 detection ..... 1510  
 Detoxification function ..... 1068  
 developing brain ..... 993  
 development ..... 328, 331, 738, 997, 1017, 1024, 1382, 1449, 1634, 2202  
 development origins of health and disease ..... 991  
 developmental ..... 1030, 1632, 1635, 1636  
 developmental ..... 581, 1377, 1378  
 Developmental & Reproductive toxicity ..... 551, 1021, 1029, 2110, 2491, 2493  
 developmental abnormalities ..... 1027  
 Developmental and reproductive toxicity ..... 56, 1446  
 developmental and reproductive toxicology ..... 784, 1020  
 developmental basis of adult disease ..... 392  
 Developmental Exposure ..... 1007, 1570  
 Developmental Immunotoxicity ..... 415, 2076  
 developmental immunotoxicology ..... 392, 394  
 developmental neurotoxicity ..... 53, 330, 332, 1367, 1371, 1383, 1386, 1392, 1393, 1633, 1679, 1680, 1682, 1684  
 Developmental Neurotoxicity Testing ..... 784, 1445  
 Developmental Neurotoxicology ..... 1376, 1389, 2418  
 Developmental Origins of Adult Disease ..... 396, 398  
 developmental origins of disease ..... 1631  
 Developmental PAH toxicity ..... 334  
 developmental programming ..... 807  
 developmental toxicity ..... 324, 393, 490, 1001, 1013, 1387, 1453, 1833  
 developmental toxicity screen ..... 1025  
 Developmental Toxicology ..... 128, 781, 1014, 1472, 1925  
 developmental toxicology assay ..... 1026  
 Dexamethasone ..... 2451, 2512  
 Dexmedetomidine ..... 1370  
 DFP ..... 1418  
 Di(2-ethylhexyl)phthalate ..... 1005, 2244  
 Diabetes ..... 66, 725, 1096, 1159, 1523, 1782, 1916, 1933, 1987, 2017  
 diabetes mellitus ..... 1304  
 Diabetic ..... 2047  
 diabetic cardiomyopathy ..... 1731, 1824  
 diabetic vascular damage ..... 1825  
 diacetyl ..... 237, 1268  
 Diakyl metabolites ..... 1909  
 diarrhea ..... 1308  
 Dibenzofuran ..... 655  
 dibutyl phthalate ..... 1430  
 dichloroacetate ..... 151, 747  
 dichloromethane ..... 2049  
 dichlorvos ..... 588  
 Dicyclohexylamine ..... 1038  
 dieldrin ..... 1378, 2217  
 diesel ..... 240, 1116  
 diesel exhaust ..... 213, 214, 241, 260, 377, 1129, 1139, 1879, 2480  
 Diesel Exhaust Particle (Dep) ..... 2359  
 Diet ..... 235, 1234, 1251, 1643  
 diet-acclimation ..... 1006  
 diet-induced obesity ..... 1508  
 dietary ..... 1645  
 dietary exposure ..... 1647  
 Dietary Supplement ..... 1435, 1779  
 Dietary Supplements ..... 1555, 2484, 2487, 2490  
 diethylene glycol ..... 2186  
 Diethylnitrosamine ..... 642, 670  
 Diethylstilbestrol ..... 989  
 differential display ..... 164  
 Differentially Expressed Genes ..... 115, 680  
 Differentiated human neuroblastoma SH-SY5Y ..... 905  
 differentiation ..... 1206  
 Diffusion ..... 1046  
 Dihydroartemisinin ..... 1780  
 diindolylmethane ..... 1118  
 Diisocyanate ..... 425, 1432  
 diisocyanate asthma ..... 189  
 Diisocyanates ..... 1951  
 DILI ..... 678, 1063, 1089, 1214  
 DIM ..... 162  
 dimethylarsonic acid ..... 472  
 dimethylfumarate ..... 1433  
 dinitrotoluene ..... 143  
 dioxin ..... 892, 1917, 1986, 1999, 2092  
 Dioxin-like compounds ..... 1990  
 Dioxins ..... 1258, 2000  
 dioxins and furans ..... 1992, 2241  
 dipentyl phthalate ..... 2128, 2133  
 diphenyl diselenide ..... 1531  
 directed differentiation ..... 1202  
 Disease ..... 1638  
 diseases ..... 717  
 Dislodgeable foliar metabolites ..... 597  
 Dispersants ..... 575  
 disposition ..... 487, 2118  
 Disposition/Pharmacokinetics ..... 484, 1058  
 Disrupted-in-Schizophrenia 1 ..... 2153  
 Dissolution ..... 1361, 2388  
 Dissolution kinetics ..... 1336  
 dissolution of nanoparticles ..... 616  
 dithiocarbamate ..... 1405  
 Dithiocarbamates ..... 1404  
 Dityrosine ..... 1884  
 Diversity Outcross ..... 183  
 Division ..... 1910  
 DMSA ..... 1852  
 DMT1 ..... 1849  
 DNA adduct ..... 624, 1484, 1504  
 DNA adducts ..... 561  
 DNA damage ..... 365, 999, 1221, 1265, 1354, 1485, 1497, 1701, 1703, 1705, 1714, 2271, 2300, 2442  
 DNA damage response ..... 33, 569, 684, 690, 1328  
 DNA damage/repair ..... 2439  
 DNA demethylation ..... 546  
 DNA intercalation ..... 136  
 DNA lesions ..... 1498  
 DNA methylation ..... 147, 524, 527, 533, 538, 540, 544, 546, 1095, 1443, 1935, 2413, 2436  
 DNA methylation and gene expression ..... 2297  
 DNA Microarray ..... 1513  
 DNA repair ..... 30, 32, 33, 482, 614, 1022, 1169, 1170, 1516, 1690, 1704, 2394  
 DNA repair mechanisms ..... 1498  
 DNA-damage stress pathway ..... 34  
 DNA-PKcs ..... 1335  
 DNA-Protein-Crosslink ..... 953  
 DNEL ..... 1571, 1964  
 Docking ..... 119, 180  
 DOHaD ..... 986  
 dopamine ..... 778, 921, 1411, 1841, 1847, 1850, 1851, 2156, 2160  
 dopamine neuron ..... 1378  
 Dopamine Transporter ..... 1404, 2150  
 dopaminergic neuron ..... 2147  
 dopaminergic neurons .. 1202, 1521, 1549  
 Dorsal root ganglion ..... 1470  
 Dose ..... 1669  
 dose reconstruction ..... 800  
 Dose response characterization ..... 1926, 1977, 2240  
 dose response modeling ..... 2235  
 dose response relationships ..... 1596  
 dose-response ..... 882, 1594, 1629, 2334  
 dosimetry ..... 465, 604, 607, 789, 1488  
 Double Strand Breaks ..... 1169  
 Doxorubicin ..... 1880  
 Draize test ..... 1036, 1553  
 DRE ..... 2355  
 Dried Blood Spots (DBS) ..... 521  
 drinking water ..... 98, 1963, 2233, 2243  
 drinking water disinfection byproducts ..... 2259  
*drosophila* ..... 680, 1400, 1844  
*Drosophila melanogaster* ..... 583, 584  
*Drosophila* model ..... 330  
 drug abuse ..... 1654, 1655, 1657, 1659  
 drug allergy ..... 1436  
 drug delivery ..... 2508  
 Drug Development ..... 793, 1212  
 drug discovery ..... 824  
 Drug Discovery and Development ..... 1216  
 Drug disposition ..... 1066  
 Drug Hepatotoxicity ..... 2039  
 drug hypersensitivity ..... 728, 1431  
 Drug Impurities ..... 1506  
 Drug Induced toxicity ..... 1224  
 drug metabolism ..... 686, 1080, 1602, 2333, 2357  
 Drug metabolism and disposition ..... 649  
 Drug pair ..... 1062  
 drug safety ..... 2252, 2411  
 drug safety assessment ..... 86  
 drug screening ..... 90  
 drug toxicity ..... 623  
 Drug Toxicity/Screening ..... 1081, 2048  
 Drug-Drug Interactions ..... 499  
 Drug-Induced Kidney Injury ..... 1882  
 Drug-induced liver injury (DILI) ..... 636, 716, 881, 890, 1059, 1062, 1081, 22162, 399  
 drug-induced nephrotoxicity ..... 924  
 Drug-induced organ toxicity ..... 945  
 drug-induced vascular injury ..... 1875  
 drugs ..... 837, 838, 840, 841, 842, 1616  
 drugs of abuse ..... 295  
 DTH ..... 2065  
 Dual Oxidase ..... 255  
 dump ..... 266  
 Dyslipidemia ..... 1257  
 early biomarkers ..... 949  
 early life ..... 1454  
 Early life sensitivity ..... 895  
 Earthworms ..... 599  
 EBDC pesticides ..... 1184  
 ebselen ..... 336  
 ECG ..... 74  
 ECG analysis ..... 68  
 ECG intervals ..... 68

- Ecotoxicity Effects ..... 1346  
 Ecotoxicology ..... 1267, 1356  
 edaravone ..... 1403  
 EDSP ..... 102, 104, 602  
 Education ..... 1669, 1670, 1671, 2204, 2209  
 EEG ..... 69, 923, 1396  
 Effectopedia ..... 854  
 Effects of storage ..... 2345  
 effects screening levels ..... 1949  
 EGCG ..... 124, 313, 1098  
 EGFR ..... 1876  
 EGFR pathway ..... 1055  
 EGR-1 ..... 2085  
 Eicosanoids ..... 2404, 2406  
 elderly ..... 1921, 2414  
 electron spin  
   resonance (ESR) ..... 1747, 2013  
 electronic cigarettes ..... 141, 1753  
 Electrophile ..... 232, 1291  
 Electrophysiology ..... 89, 900, 901  
 Electroretinography ..... 749, 1231  
 Electrospray ..... 1348  
 Elemental Analysis ..... 1177  
 ELISA ..... 1884, 1885, 2328, 2354  
 Elsadek 123 ..... 797  
 embryo-fetal development ..... 1028, 1033, 1665  
 embryogenesis ..... 1030  
 Embryonic development ..... 999  
 Embryonic stem cell ..... 1194  
 Embryonic Stem Cell Test ..... 1025  
 embryonic stem cells ..... 1189, 1190, 1206, 1472  
 embryonic zebrafish ..... 137, 694  
 embryotoxicity ..... 1034  
 Emergency Responders ..... 476  
 emerging contaminants ..... 585  
 Emerging Issues ..... 1604  
 Emerging Markets ..... 1616  
 Emesis ..... 2324  
 EMG ..... 69  
 emissions ..... 1554  
 enantioselective oxidation ..... 296  
 endocannabinoid ..... 2450  
 Endocannabinoids ..... 395  
 endocrine ..... 104, 109, 547, 1594, 1922, 2108  
 endocrine active substance ..... 1928  
 endocrine active substances ..... 1596  
 Endocrine disruption ..... 96, 98, 101, 107, 112, 119, 298, 1382, 1592, 1937, 2138, 2253  
 endocrine disruptor ..... 110, 114, 273, 866, 1569, 1926, 1941, 2249  
 endocrine disruptor screening ..... 99  
 Endocrine Disruptor  
   Screening Program ..... 112  
 Endocrine Disruptors ..... 103, 106, 138, 1383  
 Endocrine Modulatory Effects ..... 1920  
 Endocrine Toxicology ..... 102, 625, 1109, 1934, 2132  
 endocrine-disrupting  
   chemicals (EDCs) ..... 1587, 1595, 2328  
 Endocrinology ..... 1919  
 endogenous ligand ..... 1270  
 endometrial cancer ..... 173  
 endothelial ..... 223  
 endothelial cell ..... 429, 430  
 Endothelial cells ..... 1092  
 endothelial dysfunction ..... 87, 2376  
 endothelial progenitor cells ..... 60  
 Endothelium ..... 2016  
 endothelium repair ..... 771  
 endotoxin ..... 245  
 endotoxin tolerance ..... 1259  
 energetics ..... 75  
 Engineered nanomaterials ..... 1358, 1741, 2464  
 engineered nanoparticles ..... 441  
 enniatin B ..... 1722  
 Enplasmic Reticulum  
   Stress Response ..... 356  
 ENU ..... 1688  
 Environmental Cardiology ..... 63  
 Environmental danger signals ..... 1652  
 Environmental disease ..... 867  
 environmental epigenetics ..... 530, 1007  
 environmental exposure ..... 1536, 2021, 2434  
 Environmental Genetics ..... 15  
 environmental pollutants ..... 717, 775  
 environmental pollution ..... 1662  
 Environmental safety assessment ..... 1552  
 environmental tobacco exposure ..... 1394  
 Environmental Toxicants ..... 157, 1642  
 environmental toxicology ..... 739, 871, 2206  
 Enzyme Ontogeny ..... 317  
 eosinophilia ..... 1515  
 Eosinophils ..... 636  
 EpiAirway ..... 1466  
 Epidemiology ..... 474, 698, 1646, 1924, 2496, 2505  
 EpiDerm ..... 959  
 Epididymis ..... 1048  
 Epididymis ..... 2136  
 Epigallocatechin Gallate ..... 183, 284  
 Epigenetic ..... 533, 1095, 2081  
 Epigenetic modification ..... 541  
 Epigenetic regulation ..... 543  
 epigenetic toxicology ..... 1196, 1197  
 Epigenetics ..... 18, 525, 527, 528, 529, 531, 532, 536, 537, 539, 545, 547, 548, 692, 731, 1079, 1443, 1449, 1584, 1637, 1638, 1641, 1642, 1710, 2076, 2188, 2414  
 epigenomics ..... 2409, 2410  
 epileptogenesis ..... 911  
 EpiOcular ..... 977  
 EpiSkin ..... 1037, 1580  
 epithelial barrier ..... 2335  
 epithelial to mesenchymal  
   transition ..... 1786  
 Epithelial-to-Mesenchymal  
   Transition ..... 171, 701  
 Epoxide Hydrolase ..... 540  
 epoxide/diol ..... 1897  
 ePPND ..... 1220  
 eQTL ..... 985  
 ER beta ..... 146  
 ER positive breast cancer ..... 2321  
 ER stress ..... 1528, 2170, 2351  
 ErbB2 Over-expression ..... 2036  
 Erionite ..... 379  
 ERK1/2 ..... 676  
 Erlotinib ..... 1715  
 ES-D and Caco-2 ..... 539  
 ESC ..... 1201  
 essential metals ..... 477  
 Essential Oil ..... 1310, 1321  
 essential oils ..... 1728  
 ESTERASES ..... 1413  
 estradiol ..... 197, 06, 109, 1004, 1010  
 Estragole ..... 1504  
 Estrogen ..... 100, 168, 1878  
 Estrogen Activity ..... 113  
 Estrogen carcinogenesis ..... 174  
 estrogen disruption ..... 739  
 estrogen receptor ..... 114, 116, 169, 866, 1004, 1287, 2115, 2248  
 Estrogen Receptor (ER) ..... 2249, 2250, 2253, 2336  
 Estrogen signaling ..... 110  
 Estrogen-related receptor- $\alpha$  ..... 1814  
 estrogenic activity ..... 111, 2332  
 estrogens ..... 1596  
 Ethanol ..... 506, 898, 1373, 2052  
 Ethanol Metabolism ..... 2040  
 ethyl tertiary-butyl ether ..... 194, 1091  
 Ethylene Oxide ..... 1708, 1709, 1969  
 Ethylhexylmethoxycinnamate ..... 303  
 Ethylmercury ..... 1528  
 Etoposide ..... 1718  
 European legislation ..... 1677  
 euthanasia ..... 1031  
 Evaluation ..... 1307  
 Evaporation rate ..... 133  
 Evidence ..... 2041  
 Evidence based toxicology ..... 2490  
 excess ..... 1127  
 Excipients ..... 2416  
 Excitotoxicity ..... 1874  
 Exenatide ..... 725  
 exercise ..... 216  
 Exfoliated Urothelial Cells ..... 2294  
 Exhaled Breath Condensate ..... 827  
 Exon skipping ..... 1499  
 exotoxicology ..... 271  
 Experimental design ..... 705, 800  
 Expert ..... 2041  
 expert system ..... 874  
 ExpoCast ..... 1244  
 Exponential ..... 2201  
 exposome ..... 1648  
 Exposure ..... 36, 37, 574, 591, 598, 765, 789, 878, 1245, 1247, 1255, 1266, 2220, 2239, 2318  
 Exposure assessment ..... 441, 798, 2232  
 exposure biomarkers ..... 349  
 exposure modeling ..... 1251, 1252, 1268  
 Exposure rate ..... 1239  
 Exposure Reconstruction ..... 799, 1907  
 Exposure Route ..... 92  
 Exposure Science ..... 855, 2463  
 exposure windows for TBTO ..... 993  
 Exposure-based waiving ..... 713  
 Exposure-Dose-Effect  
   Relationships ..... 1412  
 expression ..... 304  
 Extended restraint ..... 761  
 extraction ..... 1468  
 extracts ..... 200, 1768  
 extrapolation ..... 608, 891  
 eye ..... 2165  
 eye irritation ..... 974, 975, 980, 983  
 F344 rats ..... 1163  
 false positives ..... 1052, 2070  
 farm family exposure ..... 402  
 Farmworkers ..... 1909  
 fat ..... 1523  
 fatty acid oxidation ..... 1599, 2258  
 fatty acid synthase ..... 160  
 fatty liver ..... 1602  
 Fatty liver disease ..... 1598, 1599, 1601, 1603  
 FcRn ..... 1003  
 fear response ..... 1387  
 Fecal Biomarker ..... 1906, 1908  
 feed ..... 111, 2108  
 Feed formulation ..... 1934  
 Female minipigs ..... 748  
 Fenamiphos ..... 1414  
 fentanyl ..... 2214  
 fertility ..... 1033, 2112  
 fetal ..... 2131  
 Fetal alcohol spectrum disorder ..... 1299  
 fetal gene expression ..... 84  
 Fetal growth restriction ..... 1249  
 Fetal origins of adult health ..... 1408  
 Fetal/neonatal ..... 738  
 fetus ..... 1031  
 fever ..... 215  
 FFPE ..... 939, 951  
 FGF21 ..... 1140, 1996  
 Fiber ..... 727  
 Fibrinogen ..... 639, 2200, 2400  
 Fibrinolysis ..... 451  
 Fibroblast Cells ..... 575  
 Fibroblast-like synoviocytes ..... 1280  
 Fibrosis ..... 251, 446, 449, 743, 984, 1061, 1312, 2184  
 Fibrous particles ..... 445  
 FICZ ..... 693  
 FICZ, 6-formylindolo  
   [3, 2-b]carbazole ..... 669  
 filarial diseases ..... 1034  
 fine and nanoparticles ..... 1741  
 Firemaster 550 ..... 326  
 First in Human ..... 1213  
 First pass metabolism ..... 508  
 fish ..... 277, 281, 2334  
 Fish oil ..... 1309  
 fish testing ..... 271  
 flame retardant ..... 495, 581, 582, 1733  
 flame retardants ..... 1682, 2237  
 Flavin-Containing  
   Monooxygenase-3 ..... 664  
 flavonoids ..... 52  
 Flavonol ..... 1275  
 flavoring ..... 237  
 Flavorings ..... 478  
 Flow ..... 1459  
 Flow Cytometry ..... 1325, 1477, 2068  
 Fluoranthene ..... 306  
 fluorescent indicator for zinc ions ..... 1765  
 fluoride ..... 88, 736, 2190  
 Fluorinated compounds ..... 1388  
 Fluorochloridone ..... 601  
 fluorotelomer ..... 2113  
 fluorotelomers ..... 1544, 2227  
 Fluorotelomer alcohol ..... 493  
 Flutamide ..... 1928  
 folate ..... 192  
 Folate Deficiency ..... 1002  
 follicle ..... 2109  
 Folliculogenesis ..... 2094  
 Food ..... 1264, 1646  
 Food additive ..... 843, 848, 2335  
 Food Additives ..... 1564  
 Food Allergy ..... 1435  
 food safety ..... 47, 48, 49, 843, 846, 1547  
 Food-contact ..... 1564  
 foodborne illness ..... 2344  
 formaldehyde ..... 154, 589, 948, 953, 1254, 1568, 1902  
 Formulation Stability ..... 576  
*fosl1* ..... 1188  
 fracking ..... 706  
 Fracking, Natural Gas,  
   Nuclear Energy, Coal ..... 1608  
 Fractal Dimension ..... 1766  
 fracturing ..... 764  
 Fragrance Ingredient ..... 2103  
 framework ..... 1558  
 free concentration ..... 1478  
 free fatty acids ..... 2365  
 Free Radical ..... 818  
 free radicals ..... 1747, 1799  
 FRET-based fluorescent  
   Cd2+ indicator ..... 1161  
 Fuel Standards ..... 1607  
 Fullerene ..... 435, 447  
 Fullerenes ..... 1134, 2453  
 fumigant ..... 1240  
 fumonisin ..... 2319, 2325  
 Fumonisin B1 ..... 1106, 1886  
 Fumonisinins ..... 1105  
 Functional ..... 555  
 Functional Genomics ..... 679, 1448, 2410  
 functionalization ..... 22, 439  
*Fundulus heteroclitus* ..... 268, 323, 2110  
 Fungi ..... 1844  
 Fungicides ..... 278  
 furan ..... 545, 951  
 Fusarium Mycotoxins ..... 1446, 2324  
 fusarium toxin ..... 2322  
 Future of Air Pollution Research ..... 1609  
 G-protein coupled  
   receptor (GPCR) ..... 2308  
 GABA ..... 1854  
 GABA Receptor Antagonist ..... 1421  
 GABAA receptor ..... 621  
 Galantamine ..... 348  
 gamma secretase ..... 1033

# Abstract Keyword Index (Continued)

The numerals following each keyword refer to the relevant abstract number(s).

Gamma-ketoaldehydes .....	2005	Ginsenoside .....	1277	hazard communication .....	877	High Content Screening .....	2162
Gaseous .....	1503	GIS .....	2303	Hazard evaluation .....	813	High Content Screening Assay .....	2177
Gasoline .....	606, 1116	glia .....	350, 1868	Hazard ID .....	36	High Fat Diet .....	454, 989, 1802
gasoline emissions .....	377	glial cells .....	834	hazard identification .....	1578	High fructose diet .....	62
Gasoline Vapor .....	1386	Glial Fibrillary Acidic Protein .....	340	hazard screen .....	2237	High IgA (HIGA) mice .....	2190
gastric reduction .....	517	glioma .....	522	hazards .....	266	high-throughput analysis .....	1243
Gastrointestinal Biomarker ....	1906, 1908	global gene expression .....	682	HC-CT-AAS .....	2295	high-throughput exposure .....	1244
Gastrointestinal microflora .....	1357	Glomerular Filtration .....	2193	HCE-T .....	983	high-throughput screening .....	114, 116, 139, 174, 791, 803, 862, 891, 1338, 1452, 1653, 1674, 1735, 1855, 2195, 2251
gavage reflux .....	234	Glomerular Injury .....	2191	HCV-NS3 Inhibitor .....	2163	High-throughput screening (HTS) .....	1218
gecko .....	279	glucocorticoid .....	350	HDAC .....	2353	hip .....	1166
Gemcitabine .....	497	glucocorticoid receptor .....	2296	HDAC inhibitor .....	1838	hippocampal field potentials .....	992
gender .....	1085	glucose intolerance .....	59	hdo—blood pressure monitoring .....	760	hippocampal injury .....	833
gender comparison .....	753	Glucose Tolerance .....	727	head and neck cancer .....	1271	Hippocampus .....	1406, 1418, 1563
gender differences .....	1010	glucuronidation .....	320	Health .....	847	hiPS-derived cardiomyocytes .....	1208
gene expression .....	394	glucuronidation and sulfonation .....	308	health disparities .....	185	histamine .....	2334
gene array .....	213, 429	glutamate receptors .....	2145	health effects .....	141, 1604	histiotrophic nutrition .....	1018
gene expression .....	173, 209, 405, 540, 548, 552, 573, 648, 671, 674, 679, 683, 698, 936, 954, 1153, 1164, 1450, 1462, 1891, 1911, 2115, 2174, 2301	Glutamate transporter .....	1859	health hazard evaluation .....	565	histology .....	1017, 1611
Gene expression analysis .....	2357	glutathione .....	279, 627, 1160, 2029, 2033, 2283	Health Risk Assessment .....	570	Histone Modification .....	359
Gene Expression Profile .....	2070	glutathione S-transferase .....	2327	Heart .....	1123, 2242	Histone modifications .....	1640
gene expression, gene regulation .....	2076	Glutathione S-transferase M1 (GSTM1) .....	188	Heart disease .....	1984	histopathology .....	1238
gene interaction profiling .....	822	Glutathione-S-transferase (GST) .....	2201	Heart Rate .....	1137	HIV .....	87
Gene Ontology .....	822	glutathione .....	2026	heart rate variability .....	1526	HIV Drugs .....	511
Gene Polymorphisms .....	263	Glycidol .....	2340	Heat and chemical coexposure .....	1948	HIV gp120 .....	419
Gene regulation .....	142, 446, 686, 1079, 1097, 1292, 1858	Glycidol fatty acid ester .....	2340	heat shock .....	1730	HL-60 .....	681
gene regulation by AHR .....	2084	Glycidol Fatty Acid Esters .....	177	Heat Shock Protein .....	675	HLA-DRB1 .....	125
Gene regulation/Signal transduction .....	653, 1764	glycosylation .....	649	Heat shock protein-90(HSP90) .....	1284	HMDS .....	617
gene response .....	990	glyphosate .....	1411, 1937, 2242	Heated cigarette .....	217	HMGB1 .....	1870, 1900, 2034
Gene transfection .....	2266	Glyphosate herbicides .....	1410	heavy metal ion biosensing .....	1161	HNFs .....	1115
Gene-Environment Interaction .....	14, 15, 1241, 1685, 2153	GM-CSF .....	1804, 1805	heavy metals .....	274, 1532, 1536, 1795	HO-1 .....	1788
gene-gene interaction .....	121	Gold Nanoparticle .....	1359, 1360	Hematology .....	762, 1245	Honey Bee .....	278
general anesthesia .....	1369	gold nanoparticles .....	1331, 1345, 1353, 1366, 1776	Hematopoietic Stem Cells .....	1195	hormones .....	372
genetic .....	17	gonadotropin-releasing hormone ....	2092	Hematotoxicity .....	1204	HOTTIP .....	159
Genetic Toxicology .....	186, 796	gonads .....	9	Hematotoxicity, neutropenia prediction .....	1198	house dust mite .....	227
genetic and epigenetic mechanisms .....	2412	Göttingen minipigs .....	1029	hemodialyzer .....	202	household product .....	968
Genetic damage .....	432, 1832, 1836	gout .....	1279	hemoglobin .....	1902	Houston Ship Channel .....	2241
Genetic function approximation .....	610	GPED .....	1931, 1938	HepaRG .....	1465, 1478	HPG axis .....	1929
Genetic instability .....	434	gpt delta .....	751	HepaRG cells .....	1068	HPLC-ICP-MS .....	2293
genetic polymorphism .....	181, 185, 196	gpt delta mouse .....	1508	hepatic catabolism .....	1064	HSP90 .....	1811
genetic polymorphisms .....	2299	gpt delta rats .....	752	hepatic injury .....	1309	Human .....	1942, 2301
Genetic Susceptibility .....	15, 737, 783, 2474, 2475	Grain Processing .....	2339	hepatic progenitor cell .....	1203	human 3D airway model .....	1474
genetic toxicity .....	1536	grant writing .....	378	hepatic steatosis .....	437, 641	human B cells .....	2084
Genetic toxicology .....	792, 793, 794, 1694, 2442	grantsmanship .....	378	Hepatic transporters .....	1065	Human Blood Serum .....	1983
Genetic Variability .....	310, 2472, 2477	Granuloma .....	2136	Hepatitis B .....	2193	human cardiomyocytes .....	79
Genetically Modified .....	1957	Graphene .....	458	hepatitis B surface antigen .....	2064	human corneal model .....	973
Genetics .....	1364, 1642	GRAS .....	2347	Hepatoblastoma .....	1094	human epidermal keratinocytes .....	197, 1322, 1326
Genetics, Genomics, Epigenetics .....	14	green tea .....	124, 1086	Hepatocarcinogenesis .....	634, 1117	human ESC-derived cardiomyocytes .....	90
Genipin .....	2082	Green Tea Polyphenols .....	544, 1886	hepatocellular carcinoma .....	807, 943, 1094, 1111, 2050, 2435, 2436	Human exposure .....	505
genistein .....	1302, 2338	GreenScreen™ .....	1362	Hepatocyte .....	640, 654, 1080, 2172, 2264	human health benchmarks .....	1963
genistin .....	417	GRIK .....	122	hepatocytes .....	285, 588, 887, 1201, 1463, 1721	Human health risk assessment ..	26, 1980, 2049, 2211
Genome profiling .....	1702	groundwater .....	765, 2303	hepatotoxicity .....	248, 627, 629, 633, 635, 664, 732, 892, 929, 938, 946, 1056, 1057, 1063, 1076, 1088, 1089, 1305, 1355, 1601, 1710, 1894, 2172, 2173, 2175, 2265, 2352, 2405	human hematopoietic stem cell .....	1199
genome wide expression .....	583	growth .....	1889	hepatotoxicity .....	248, 627, 629, 633, 635, 664, 732, 892, 929, 938, 946, 1056, 1057, 1063, 1076, 1088, 1089, 1305, 1355, 1601, 1710, 1894, 2172, 2173, 2175, 2265, 2352, 2405	human hepatocytes .....	2039
genome-wide association study (GWAS) .....	121	growth factor targets of AhR .....	1271	hepatotumorigenicity .....	1091	Human induced pluripotent stem cells .....	901
genomic .....	17	GRP78 .....	667, 776	HepG2 .....	1993	Human iPSC .....	1200
Genomics .....	1146, 1297, 1979, 2409	GSH/GSSG .....	1381	HepG2 cells .....	2270	Human lung cells .....	1474
Genotoxic .....	35, 1539	GSTs .....	2025	heptotoxic compounds .....	937	human monocyte .....	1758
genotoxic impurities .....	837, 838, 839, 840, 841, 842, 2349	Guinea pig .....	1428, 2168	HER2 .....	677	human neural progenitor cells .....	1681
genotoxicity .....	31, 194, 453, 571, 575, 670, 1329, 1334, 1354, 1483, 1487, 1490, 1493, 1499, 1506, 1507, 1540, 1691, 1697, 1701, 1705, 1742, 1794, 1879, 1911, 1944, 2259, 2274, 2307, 2427, 2428, 2440, 2443	Gulf of Mexico Oil spill .....	1958	herbicides .....	1411	human placenta .....	1661
Genotoxicity—Mechanism of action .....	1502, 1689	Gut Satiety Hormones .....	2324	Herval extracts .....	1084	human Pregnane Xenobiotic Receptor .....	1274
Genotoxicity risk assessment .....	1489, 1699	gutkha .....	987	hES .....	1209	human prostate .....	994
Genotoxicology .....	2444	H19 .....	1011	HES1 .....	697	Human Relevance Framework .....	1101, 2460
Genotype .....	1916	H19 gene .....	535	heterotetramerization .....	312	human risk assessment .....	902
germ-free .....	287	H295R .....	2246	Hexabromocyclododecane .....	491	human skin penetration .....	1049
Gevokizumab .....	1020	H9c2 cells .....	84	hexahydro-1, 3, 5-trinitro-1, 3, 5-triazine, RDX .....	250	Humanized liver mouse .....	1693
GH .....	1913	HAART toxicity .....	2052, 2053	hexavalent chromium ....	517, 1167, 1575, 1967, 2236	Humidifier disinfectants .....	207, 1577
Ginkgo extract .....	1485	Haber's Rule .....	704	HG-CT-AAS .....	2293	humoral immune response .....	421
		HaCaT cells .....	1055	HIF .....	256, 1515	Humoral immunity .....	2095
		Hair dye .....	1040	High Content .....	38	Huntington .....	1860
		halotyrosine .....	2305	High Content Analysis .....	1470, 1189, 2396	hyaluronic acid .....	1203
		Hamster .....	2225	High Content Image Analysis .....	1450	hydraulic fracturing .....	706, 763, 765, 767, 1558
		Hanford miniswine .....	750	High Content Imaging .....	963, 1217	hydrodynamic particle size .....	1175
		haplotype .....	1691			Hydrogen Peroxide .....	255, 1270, 2345
		Hapten .....	1432			hydronephrosis .....	2203
		Harmful and Potentially Harmful Constituents .....	567				
		Harmonization .....	1954				
		Hazard .....	37				
		hazard assessment .....	710, 790				
		Hazard characterization .....	1974				

Hydroxyapatite .....	1778	<i>in vitro</i> - <i>in vivo</i> extrapolation .....	186, 746, 2275, 2457, 2458	inhalation exposure limits .....	2212	Iron .....	1177, 2161
hydroxylamine .....	1548	<i>in vitro</i> <i>in vivo</i> correlation .....	888, 2048	Inhalation Exposure System .....	374	Iron Deficiency .....	2158
hydroxylated PBDE .....	1988	<i>in vitro</i> alternative method .....	967	Inhalation kinetics .....	505	Iron Disturbance .....	1967
hydroxylated PCBs .....	1985	<i>in vitro</i> alternative .....	707, 1458, 2273	Inhalation nanotoxicology .....	814, 1749, 2374, 2380	iron metabolism .....	647
Hydroxylated polychlorinated biphenyl .....	138	<i>in vitro</i> Alternatives .....	504	inhalation safety assessment .....	225	iron nanoparticles .....	2365
Hyperoxia .....	2032, 2034	<i>in vitro</i> and Alternative Methods .....	978, 2245	Inhalation toxicity ....	459, 464, 1562, 2417	iron oxide .....	2160
Hyperoxic lung injury .....	2004, 2026, 2408	<i>in vitro</i> and clinical safety assessment .....	972	inhalation toxicology .....	1469	iron oxide nanoparticles .....	1745, 2391
hypersensitivity .....	423, 1440	<i>in vitro</i> assay .....	282, 969, 2461	Inhaled Dose Calculation .....	374	Iron Toxicity .....	1178
hypertension .....	773, 991, 1127, 2282	<i>in vitro</i> Comet .....	1697	Inhaled insulin .....	1228	Irradiation induced GI toxicity .....	1906
hypertrophy .....	84, 2183	<i>in vitro</i> cornea model .....	352	Inhaled Particles .....	826	irritants .....	1438
hypothalamic-pituitary-adrenal axis .....	1940	<i>in vitro</i> cytotoxicity .....	1331, 2476	Inhibin B .....	27, 1813, 1885, 2119, 2120, 2121, 2122, 2124, 2125, 2126	irritation .....	1469
Hypothalamic-pituitary-testicular axis .....	1918	<i>in vitro</i> exposure .....	221	Inhibition .....	348	ischaemia/ reperfusion injury .....	1318
hypothalamus .....	1549	<i>in vitro</i> Genotoxicity .....	1485, 2441	injection .....	1147, 1238	ischemia .....	1724
hypothermia .....	215	<i>in vitro</i> human tissues .....	1739	Injector .....	2060	Ischemic brain damage .....	913
hypothiocyanite .....	2019	<i>in vitro</i> inhalation toxicity .....	1464, 1471, 1474	injury .....	1121	ISO 10993 .....	201
hypothyroidism .....	54	<i>in vitro</i> liver model .....	1461	innate immune cells .....	1439	Isobornyl Acetate .....	2103
Hypoxia .....	65, 673	<i>in vitro</i> metabolism .....	269, 299	Innate Immunity .....	253, 258, 411, 412, 2019, 2298	isoeugenol .....	1543
I3C DIM .....	2353	<i>in vitro</i> Micronucleus Test .....	1489	Inorganic arsenic .....	2473	isoflavone .....	2321
IBD .....	2335	<i>in vitro</i> Micronucleus .....	1696, 1697	INrf2 (Keap1) .....	1100	Isolated Heart .....	93
ICGN .....	736	<i>in vitro</i> model system .....	1199	insecticides .....	1321	Isolated mitochondria .....	1081
ICH Guidelines .....	132	<i>in vitro</i> model .....	1661, 2137	Inspector Toxicology .....	1668	isoniazid .....	2031
ICP-AES .....	272	<i>in vitro</i> models .....	1502, 1689	Instrument development .....	609	isooctane .....	2243
ICP-MS .....	1178, 1323	<i>in vitro</i> neurotoxicity .....	899, 902	insulin .....	921	Isoprene .....	1565
ICP-QMS .....	1518	<i>in vitro</i> phototoxicity testing .....	971	insulin glargine .....	1096	Isoproterenol .....	1826
Idiosyncratic .....	656, 938, 1057	<i>in vitro</i> phototoxicity .....	1479	insulin resistance .....	60, 61, 62, 991, 2313	IVIVE .....	496, 613, 882, 898
Idiosyncratic drug reactions .....	732	<i>in vitro</i> screening .....	1074, 1210	insulin secretion .....	2012	IVNAA .....	1179
Idiosyncratic drug-induced liver injury .....	410, 1077, 1078	<i>in vitro</i> Skin Absorption .....	962, 1045	insulin sensitivity .....	1073	Jacketed External Telemetry .....	73
idiosyncratic liver damage .....	2399	<i>in vitro</i> skin irritation .....	968, 981	insulin signaling .....	659, 1157	Jatropha .....	1560
IFN beta-1b .....	1223	<i>in vitro</i> skin sensitization .....	965, 966, 1437	insulin signaling pathway .....	1187	Jet Fuel .....	562
IgE antibody .....	1434	<i>in vitro</i> systems .....	1473	Integrated Testing Strategies .....	1256, 2444	JET jacketed external telemetry .....	67
IGF-1 .....	1913	<i>in vitro</i> teratogenicity .....	1025	Integrated testing strategy .....	1707	Jewelry .....	2219
IGFR .....	160	<i>in vitro</i> tests .....	870	integration .....	2445	JNJ-35815208 .....	1814
IL-18 .....	967	<i>in vitro</i> to <i>in vivo</i> extrapolation .....	507, 510, 883, 895	integrative approach .....	551, 2272	JNK/ERK activation .....	1721
IL-1beta .....	1050	<i>in vitro</i> toxicity assays .....	899	integrative medicine .....	2485, 2490	JNK/ERK/GSK-3a/β .....	1718
IL-8 .....	1746	<i>in vitro</i> toxicity testing .....	86	Integrins .....	677	Jurkat T cells .....	1339, 2074, 2087
IL6 .....	2358	<i>in vitro</i> toxicology .....	1820	inter-laboratory reproducibility .....	975	juvenile .....	1834, 2098
Imaging .....	76, 1126	<i>in vitro</i> toxicology .....	1820	Inter-species Extrapolation .....	720	juvenile and pediatric safety .....	1045, 1831, 2415, 2416, 2417, 2418, 2420
imidazole-substituted oleic .....	2010	<i>in vivo</i> Comet assay .....	1487	inter-strain differences .....	647	Juvenile Idiopathic Arthritis .....	2420
immortalized cells .....	1462	<i>in vivo</i> genotoxicity assay .....	1699, 2255	Interactions .....	2497	juvenile toxicity .....	1833, 2411, 2415
Immortalized Z310 Cell Line .....	1861	<i>in vivo</i> imaging .....	803	Interference .....	1340	K-12 education .....	1666, 1668
immune .....	1332	<i>in vivo</i> liver Comet assay .....	1693	Interleukin 13 .....	218	K-12 outreach .....	1667, 1669, 1671
Immune enhancement .....	388	<i>in vivo</i> micronucleus assay .....	1693	Interleukin 17 .....	218, 387, 1439	Kahweol .....	1798
immune function .....	2067	<i>in vivo</i> Micronucleus .....	1698, 1740	interleukin 33 .....	462	Kainic Acid .....	1229, 1874
Immune response ....	436, 816, 1350, 1652	<i>in vivo</i> Studies .....	456	Internal exposure of environmental pollution .....	1239	KBrO3 .....	614
immune suppression .....	420	<i>in vivo</i> .....	2382	international cooperation .....	1574	Keap1, Nrf2 .....	341
immune system .....	1227	Inbred Mouse Strains .....	2392	interoperability .....	702	Keap1 .....	2014, 2358
Immune tolerance .....	732	IND .....	5	intestinal microflora .....	286	Keratinocyte .....	675
immune-modulating effect .....	409	India .....	1618	intestinal tissue model .....	623	Keratinocyte Differentiation .....	293
Immunoglobulin .....	1, 2086	indium .....	226	Intestine .....	319, 2178, 2368	Keratinocytes .....	1038
Immunohistochemistry .....	1092	indium tin oxide .....	424, 1175	intracellular Cd2+ monitoring .....	1161	KeratinoSens .....	1051
Immunology .....	395, 2319	indoor air .....	798	intracellular signaling .....	1367	Ketamine .....	1368
Immunophenotyping .....	422	indoors .....	1247	Intracellular trafficking .....	1765	key event .....	1099
Immunostimulation .....	411, 2063	induction/inhibition .....	2338	intradermal injection .....	1812	Key events .....	809
immunosuppression .....	612, 2078	Industrial .....	2465	Intranasal drug delivery .....	497	KFDA .....	1619
Immunotherapy .....	1806	industrial chelates .....	1893	intraocular drug .....	2511	kidney .....	492, 499, 527, 1155, 1156, 1180, 1181, 1890, 1903, 1905, 2167, 2188, 2197
immunotoxicity ...	386, 391, 393, 406, 414, 587, 1227, 1431, 1467, 1833, 2061, 2062, 2067, 2078, 2079, 2087, 2370, 2498	Infants .....	2419	intraocular lens .....	2510	kidney biomarker .....	1877
Immunotoxicity Testing .....	784	Infection .....	257, 2252, 2498	intrathecal .....	1236	kidney biomarkers .....	1904
Immunotoxicology ...	14, 401, 1050, 2059, 2062, 2077, 2080, 2444, 2466, 2469	Inflammasome .....	445	intratracheal instillation .....	207, 463, 1016	Kidney Injury .....	1820, 2196, 2199
impedance .....	1208, 1971	inflammation .....	32, 152, 196, 220, 242, 248, 256, 257, 259, 355, 373, 405, 413, 454, 637, 739, 742, 769, 770, 836, 1057, 1283, 1374, 1422, 1423, 1601, 2016, 2021, 2102, 2136, 2184, 2352, 2364, 2403, 2407, 2479	intrauterine growth restriction .....	1827	kidney toxicity .....	289, 2195, 2198, 2202
implantation .....	204	inflammatory .....	362	Intravenous dosing .....	756	kidney toxicity biomarker .....	952
IMX101 .....	1048	Inflammatory response .....	569, 2363	Intravenous infusion .....	1548	Kidney transporters .....	1065
<i>in silico</i> .....	129, 1632, 1692	Influenza A virus .....	436	Intravital microscopy .....	2372	KIM-1 .....	1890
<i>in silico</i> liver .....	553	informatics .....	787, 857, 872, 876	intravital .....	2511	Kinase .....	78, 525, 2277
<i>in silico</i> methods .....	839, 2486	infusion .....	1834	intrinsic clearance models .....	496	Kinase inhibitor .....	1819
<i>in silico</i> prediction .....	1628	inhalation .....	208, 211, 354, 414, 425, 493, 562, 580, 741, 761, 1349, 1809, 1950, 1970, 2216, 2218, 2232, 2385	iodide deficiency .....	1914	Kinases .....	180
<i>in silico</i> profilers .....	858	inhalation delivery .....	219, 225	iodine deficiency .....	1915	Kinetic Modeling .....	614
<i>in silico</i> toxicology .....	869	inhalation dose .....	216	Iodophorous compound .....	1245	kisspeptin .....	1898
<i>in situ</i> characterization .....	1755	inhalation dosimetry .....	230	Ion channels .....	72, 78, 2144	kiwifruit .....	1434
<i>in vitro</i> .....	40, 89, 240, 351, 640, 788, 820, 900, 957, 959, 974, 1026, 1203, 1310, 1367, 1440, 1459, 1465, 1488, 1679, 1682, 1738, 1839, 2178, 2247, 2265, 2274, 2276	inhalation exposure ....	20, 207, 225, 367, 453, 465, 815, 1163	Ionic strength .....	1336	KLH .....	2095
				ionising radiation .....	1390	knockout mice .....	283, 1286
				IPA .....	1626	knockout mouse .....	689
				iPS .....	1063	knockout rat .....	1278
				iPS Cardio .....	1465	Kolaviron .....	1318
				Irinotecan, Pharmacokinetics, Obesity .....	498	Korea .....	1619
				IRIS .....	1578	Korean adults .....	1511
						Korus FTA .....	1619
						Kow .....	515
						KRAS .....	1709

# Abstract Keyword Index (Continued)

The numerals following each keyword refer to the relevant abstract number(s).

Kupffer .....	637, 1072	lncRNA .....	545	Mango .....	152	metals .....	7, 281, 558, 776, 782,
Kupffer cell .....	1112	local lymph node assay .....	424, 963,	mannose receptor .....	1767	1182, 1185, 1192, 1347, 1409, 1500,	
Kupffer cells-hepatocytes .....	1333	1433, 1442		MAPKs signaling .....	1920	1510, 1533, 1534, 1537, 1538, 1539,	
L-BMAA .....	500	Long Evans rat .....	1041	Margin of Exposure .....	120, 718	1753, 1836, 2280, 2281, 2310, 2413	
L-carnitine .....	1368	Long Interspersed Nuclear		mass casualty incidents .....	2055	Metals and organics .....	276
LA-QPCR .....	1498	Element-1 (LINE-1 or L1) .....	701	mass spectrometry .....	360, 945,	metalworking fluids .....	1038
label-free .....	81, 82	long noncoding RNA .....	159	1235, 2166		metastasis .....	161, 1763, 2014
laboratory models		long-term cultures .....	1070	Mast Cell .....	2470	Metformin .....	1002
of human variability .....	2472	long-term risk assessment .....	2238	mast cells .....	587, 1337	Methemoglobin .....	1955
Lactation .....	1522	loss of heterozygosity .....	1486	maternal exposure .....	1250, 1379	methionine sulfoxide .....	1095
Langendorff .....	93	low dose .....	107, 1261, 1592,	Matrix Effect .....	519	method .....	1168
Large Therapeutic Peptides .....	518	1597, 1926, 1927, 1928		matrix metalloproteinase .....	534	Method development .....	516
LC-MS/MS .....	1922	low dose DNA damage .....	30, 31	maturity .....	2100	Method validation .....	1475
LC50 .....	40	low dose DNA damage response .....	34	Mauritian/asian origin .....	760	methods development .....	1972
LD50 .....	370	Low dose effects .....	105	MCF-7 .....	106	Methyl Bromide .....	599
leachable .....	202, 206	low-anxiety behavior .....	1114	MDMA .....	917	methyl parathion .....	1211
lead .....	18, 125, 532, 635,	Low-birth weight .....	2105	MDR1 .....	1791	methylation .....	526, 532, 535, 2290
934, 1007, 1251, 1252, 1509, 1511, 1512,		LP9/TERT-1 .....	460	mechanical damage .....	962	methylglyoxal .....	2017
1535, 1588, 1973, 2151, 2154, 2155,		LPS .....	1843	Mechanism .....	35, 1423	methylmercury .....	667, 1454, 1456,
2156, 2159, 2504		luciferase reporter .....	2273	Mechanism of Action .....	849, 850,	1521, 1523, 1524, 1525, 1526, 2143,	
Lead Exposure .....	2158, 2503, 2505, 2506	Luminiscent .....	1778	851, 852, 853, 2491		2144, 2145, 2146, 2147	
lead neurotoxicity .....	2152, 2157	lung .....	19, 21, 22, 24, 208, 229,	Mechanisms .....	954	Methyltriclosan .....	1936
Lead nitrate .....	315	458, 1350, 1750, 2305, 2393		mechanisms of disease .....	775, 1644	Mevalonate pathway .....	1723
Lead optimization .....	39	Lung cancer .....	457, 814, 1107,	mechanisms of toxicity .....	2504	MGMT expression .....	195
lead poisoning .....	2503, 2507	1575, 1641, 2236		Mechanistic .....	38	MGMT haplotypes .....	195
Learning .....	1385, 2155	lung cancer cells .....	151	Mechanistic evidence .....	1867	MGMT polymorphism .....	195
Learning and Memory .....	262	lung carcinogenesis .....	1709	Mechanistic model .....	1059	mice .....	762, 1183, 1430
left ventricular geometry .....	2282	lung carcinoma .....	461	Mechanistic Toxicogenomics .....	115	Michael Addition .....	1053
legislation .....	1678	Lung Cells .....	1759	mechanistic toxicology .....	553	microarray .....	97, 362, 875, 947,
Leishmania .....	388	lung deposition .....	802, 1358	mechlorethamine .....	351	1094, 1773, 2285	
leucine .....	509	lung development .....	985	Medaka .....	1299	microarray analysis .....	990, 1941
Leukemia .....	2315	lung disease .....	2003	medical device .....	198, 199, 200, 201,	Microarray gene expression .....	694
levels of concern .....	1956	Lung edema .....	1148	203, 206, 2508, 2509, 2510, 2513		microarrays .....	944, 1629
Levofloxacin .....	512	Lung Epithelium .....	134	Medicinal plant .....	1319, 1799	microbiome .....	1648, 1649, 1650
Lewisite and Sulfur Mustard .....	2213	lung fibrosis .....	210, 815, 2366	Medicine .....	1768	microbiota .....	1317
Leydig cell .....	682	Lung function .....	1835, 1945, 2369	Medium-term animal model .....	752	microcirculation .....	94, 95, 469, 2376
Leydig Cell Tumor .....	1101	Lung inflammation .....	1364, 2366	megakaryocyte .....	2179	microcystin .....	1451
LH surge .....	2088	lung injury .....	358, 452	Melatonin .....	592	microcystins .....	1480
Libby amphibole .....	230, 231	lung lining fluid .....	468	Memantine .....	1874	microdialysis .....	2449
Licorice .....	633	Lung tumors .....	1749	memory .....	1384, 2155	microelectrode .....	204, 205
Life-stage susceptibility .....	912	Lungs .....	433	Menadione .....	2037	microflora .....	1481
Lifecourse .....	781	lux .....	100	menopause .....	2336	microfluidic system .....	2245
Ligand .....	180	LXR .....	641	menstrual cycle .....	2100	microglia .....	247, 832, 833, 836,
Ligand binding .....	1277	LXR nuclear receptor .....	2291	Menthol .....	1727	1843, 1870, 2480	
linalool .....	1541	lymphocyte .....	2069	mentorship .....	1630	miconuclei .....	2443, 2446
LINE-1 Retrotransposon .....	542	lymphoma .....	167	mercaptopurine .....	2337	miconucleus .....	1492
lipid droplets .....	2008	lymphopoiesis .....	1586	Mercury .....	330, 332, 394, 418, 530,	miconucleus .....	1701, 2176
lipid mediators .....	2009	Lysosome .....	2164	1522, 1529, 1530, 2080, 2150, 2183		Micronucleus assay .....	1688, 2441
Lipid Membrane .....	435	lysyl oxidase .....	1150	Mesenchymal Stem Cells .....	1195	Micropillar/microwell chip .....	2266
Lipid Metabolism .....	1290, 2308	Macrophage .....	656, 1512, 1757, 2081	mesoporous silica nanoparticle .....	2370	microRNA .....	28, 152, 363, 423,
Lipid Rafts .....	400	macrophage inhibitory		Mesothelioma .....	383, 1495	924, 925, 926, 927, 928, 930, 931, 932,	
lipid regulation .....	2302	cytokine 1 .....	148, 2351	MeT-5A .....	434	933, 948, 950, 1119, 1600, 2198	
lipids .....	130, 1981, 1984	macrophage polarization .....	1767	Meta-analysis .....	479	microRNA microarray .....	1339
lipogenesis .....	1787	macrophages .....	220, 226, 248, 249, 346,	metabolic .....	2310	microRNAs .....	150, 657
Lipopolysaccharide .....	247, 1869, 2350	400, 438, 661, 1343, 1353, 1745		metabolic activation .....	292	microsomal epoxide hydrolase .....	181
Literature Mining .....	863, 865	MAEC .....	148	metabolic detoxification .....	292	Microtubule Associated	
Litigation .....	1579	magnetic resonance imaging .....	522	Metabolic Disease/Diabetes .....	1606	Protein 1 Light Chain 3 (LC) .....	1818
liver .....	249, 557, 630, 637, 638, 639,	Magnetic Resonance Spectroscopy .....	568	metabolic syndrome .....	61, 651, 1636	microvascular .....	3, 996
652, 653, 654, 661, 665, 806, 810, 880,		Male and female fertility .....	782	Metabolism .....	269, 285, 289, 291,	Miniature swine .....	74, 2047
885, 932, 947, 987, 1058, 1061, 1067,		male infertility .....	1241	317, 321, 553, 1649, 1942		minipig .....	1017, 1035
1071, 1072, 1074, 1079, 1082, 1097,		Male reproduction .....	584	Metabolism and disposition .....	308,	Minipigs .....	749
1112, 1183, 1294, 1459, 1518, 1724,		male reproductive development .....	2134	309, 495		miR-122 .....	1900
1911, 1919, 2258, 2316, 2331		Male reproductive toxicity .....	2142	Metabolite .....	1628	miR-208a .....	1826
liver bioreactor .....	496	Male reproductive		metabolite profiling .....	483	miR132 .....	1375
liver cancer .....	2432, 2433, 2438	toxicology .....	2135, 2137	metabolites .....	2323	Microvascular .....	92
Liver carcinogenesis .....	1108, 2297	mammalian target of rapamycin .....	1683	Metabolites in Safety Testing .....	1235	miRNA .....	534, 1069, 1102, 2197, 2304
Liver hypertrophy .....	808	mammary .....	97	Metabolome .....	1562	miRNA expression .....	541
liver injury .....	646, 733, 888	Mammary Carcinogenesis .....	177, 1923	Metabolomics .....	109, 275, 440, 550, 941,	miRNA microarray .....	329
Liver injury biomarker .....	2399	mammary gland .....	1635	1001, 1064, 1561, 1680, 2028, 2270		miRNA122 .....	929
Liver Metabolism .....	552	Mammary Glands .....	1015	Metal .....	473, 653, 1136, 1519, 1520	Mismatch repair .....	384
liver micronucleus .....	2445	Mammary Tumor .....	1093	Metal homeostasis .....	1989	MITC .....	414
liver regeneration .....	632	mancozeb .....	1403	metal mine .....	1162	mitochondria .....	80, 655, 913, 1174, 1218,
liver steatosis .....	647	Maneb .....	1184, 1406	metal oxide .....	1775	1784, 1982, 1993, 2164, 2262, 2264	
Liver toxicity .....	626, 631, 1060,	manganese .....	834, 1405, 1520, 1535,	metal oxide nanoparticles .....	2363, 2374,	Mitochondria Dysfunction .....	2151, 2173
1070, 1779, 1981		1750, 1848, 1849, 1850, 1851, 1852,		2389		mitochondria-targeted	
liver transporters .....	645, 884	1853, 1854, 1855, 1859, 1860, 1865,		Metal toxicity .....	1685, 2149	nano-complex .....	2010
Liver tumorigenesis .....	808	1866		metallic nanoparticles .....	2377	mitochondrial .....	2006, 2257, 2258
Liver tumors .....	809	Manganese (Mn) .....	1864	Metallothionein .....	1142, 1174,	Mitochondrial behavior .....	879
Liver X Receptor .....	1274	Manganese Exposure .....	1863, 2056	1181, 1182, 1187		Mitochondrial biogenesis .....	1856
liver-Cpr-null .....	319	Manganese neurotoxicity .....	729, 1856,			Mitochondrial dysfunction .....	626, 2024
LKB1 .....	1792	1857, 1858				Mitochondrial Function .....	2147
LLNA .....	964, 1441	Manganism .....	1850, 1851, 1852, 1853			Mitochondrial liabilities .....	2173

# Abstract Keyword Index (Continued)

The numerals following each keyword refer to the relevant abstract number(s).

- mitochondrial modulator ..... 1224  
Mitochondrial Toxicity ..... 1623,  
2022, 2171, 2261  
MitoPark mouse model ..... 729  
Mixture ..... 570, 581, 1566, 2111  
mixtures ..... 42, 43, 560, 574, 577,  
578, 582, 606, 721, 1383, 2134  
Mixtures, Metals ..... 698  
MMP ..... 1910  
Mn in human bone ..... 1179  
Mn-related differentially  
expressed proteins ..... 1861  
mode of action ..... 1969, 42,  
43, 44, 45, 46, 120, 549, 806, 809, 859,  
868, 1091, 1099, 1101, 1562, 1624, 1696,  
2222, 2236, 2270, 2460  
Mode-of-Action ..... 2492  
model ..... 133, 279, 621, 788, 1046  
model evaluation ..... 480  
modeling ..... 611, 708, 720, 1230  
modelling ..... 131  
models ..... 702  
moist snuff consumer ..... 941  
Molecular Docking ..... 321, 2180  
molecular dynamics ..... 2468  
molecular pharmacology ..... 1593  
Molecular Signature ..... 2424  
mollugin ..... 1790, 1791  
monitoring ..... 1568  
monkey ..... 757, 1130, 1223,  
1817, 1890, 1892  
Monoamine ..... 920  
Monoamine transporter ..... 1872  
monoclonal ..... 4  
monoclonal antibody ..... 1801,  
1802, 1803, 1804, 1805, 2107  
monocyte derived macrophage ..... 1751  
mononuclear phagocyte system ..... 819  
Monte Carlo simulation ..... 480  
*Morinda morindoides* ..... 1307  
mortality patterns ..... 717  
motor activity ..... 922  
motor function ..... 1391  
motor neurons ..... 2145  
mouse ..... 620, 1860, 2061, 2367  
Mouse Diversity Panel ..... 716  
mouse embryonic stem cells ..... 2152  
Mouse Epididymides ..... 2129  
mouse liver ..... 642  
mouse lung tumors ..... 457  
mouse lymphoma assay ..... 1486  
mouse model ..... 55, 1401, 1869, 1919  
mouse model of  
human population ..... 2474  
mouse populations ..... 2473  
mouse stem cells ..... 2475  
MPPD modeling ..... 1349  
MRI ..... 907, 993, 1613  
MRI biomarkers ..... 2056  
mRNA ..... 2139  
MRP ..... 1463  
Mrp2 deficiency ..... 2178  
Mrp4 ..... 660, 697  
MRS ..... 907, 908  
MTBE ..... 1457, 2222  
MTF-1 ..... 1188  
mu opioid receptor ..... 1222  
mucosal tissue ..... 2252  
multi-color flow cytometry ..... 2066  
multi-electrode array system ..... 1475  
multi-mycotoxins urinary  
exposure assessment ..... 1883  
multi-wall carbon nanotubes ..... 463  
Multi-walled carbon  
nanotube ..... 432, 457, 1147  
Multi-walled carbon  
nanotubes ..... 20, 441, 471, 817  
Multicase ..... 860, 874  
multigenerational toxicity ..... 950  
multiple myeloma ..... 481  
Multiple Reaction Monitoring ..... 1614  
Multiple Sclerosis ..... 125  
multiplex ..... 1725, 1877  
multipollutants ..... 2502  
Multiwall carbon nanotubes ..... 434  
Multiwalled Carbon  
Nanotubes ..... 433, 453, 462  
munitions ..... 515, 1295  
Murine local lymph node assay ..... 2071  
murine model ..... 398  
MUSST ..... 970  
mutagenesis ..... 1500, 1687  
Mutagenic activity ..... 1505  
mutagenicity ..... 1484, 1503, 1504,  
1508, 1708  
mutagenicity, genotoxicity ..... 839  
Mutation ..... 2446  
mutation assay ..... 1331  
MWCNT ..... 459  
mycotoxin ..... 2326  
mycotoxins ..... 391  
myeloid-derived suppressor cells ..... 461  
myelosuppression ..... 250, 568  
Myoc-estrogen ..... 1923  
Myocardial infarction ..... 1144  
Mytilus edulis ..... 264  
N-acetyl-B-D-  
glucosaminidase (NAG) ..... 2201  
N-Acetyltransferase 1 (NAT1) ..... 293  
N-acetyltransferases ..... 1054  
NAAQS ..... 1567, 1945  
NAC ..... 2263  
NADPH oxidase ..... 772, 1715  
NAFLD ..... 1064, 1065  
nail ..... 1901  
nano risk assessment ..... 444, 471  
nano titanium dioxide ..... 1737  
nanoaerosol ..... 1341  
Nanoarray ..... 2192  
Nanobody ..... 1809  
nanocarrier ..... 1767  
nanocomposites ..... 450  
nanodisk ..... 291  
nanoinformatics ..... 790  
nanomaterial ..... 407, 458, 996,  
1734, 1735, 1769, 2364  
Nanomaterials ..... 375, 789, 790,  
791, 1133, 1135, 1344, 1384, 1739, 1743,  
1768, 1774, 1970, 2097, 2371, 2421,  
2423, 2464, 2466, 2469  
Nanomedicine ..... 2469  
nanoparticle coatings ..... 1131  
nanoparticle ..... 816, 1673, 1741,  
1750, 1755, 1756, 1771, 2362, 2369,  
2386  
Nanoparticle toxicity ..... 411, 1324, 2396  
nanoparticles ..... 23, 91, 243, 438,  
439, 452, 454, 466, 467, 818, 1340,  
1342, 1346, 1351, 1361, 1363, 1738,  
1740, 1742, 1753, 1759, 1760, 1773,  
1777, 2367, 2375, 2384, 2387, 2422,  
2468, 2471  
nanoporous alumina ..... 1736  
nanosafety ..... 2395  
Nanoscale materials ..... 2425  
Nanosilica ..... 2382  
nanosilver ..... 1343, 1348, 1356, 1362  
nanostructured amorphous silica ..... 1754  
nanotechnology ..... 8, 448, 787,  
2467, 2470  
nanothermites ..... 1774  
nanotoxicity ..... 1332, 2373,  
2378, 2423, 2424  
nanotoxicology ..... 19, 21,  
22, 24, 179, 375, 440, 443, 455, 456, 464,  
468, 786, 788, 1325, 1333, 1338, 1350,  
1364, 1736, 1739, 1747, 1748, 1752,  
1758, 1761, 1764, 1766, 1775, 2379,  
2380, 2382, 2385, 2421, 2467, 2470  
Nanotubes ..... 460  
Naphthalene ..... 232, 297  
nasal ..... 234  
Nasal Toxicity ..... 235, 236, 1256  
NASH ..... 1066  
National Children's Study ..... 1828  
natriuretic peptide ..... 2401  
Natural Gas ..... 768  
natural killer cell ..... 381, 417  
natural products ..... 2484, 2485, 2487  
NBBS ..... 489  
NC-XRE ..... 666  
necrosis ..... 1088  
neonatal ..... 1388  
Neonatal dogs ..... 1831  
neonatal pharmacokinetics ..... 483  
Neonate ..... 1830  
Neonates ..... 2419  
neonicotinoid ..... 589  
Nephrotoxic ..... 1538  
nephrotoxicant ..... 1904  
Nephrotoxics ..... 2194  
Nephrotoxicity ..... 930,  
931, 1529, 1877, 1893, 1894, 1895, 2020,  
2181, 2182, 2185  
nerve agent ..... 135, 339, 343  
Nerve Agent Antidote ..... 576  
Nerve agents ..... 347  
Networks ..... 823  
Neural behavior ..... 1402  
Neural differentiation ..... 2152  
neural repair ..... 832  
neural stem cells ..... 1371  
neural tube defects ..... 1018  
Neurite Outgrowth ..... 676  
neuroapoptosis ..... 1370  
neurobehavioral ..... 1419  
neurodegeneration ..... 731, 777, 779,  
899, 1397, 1410, 1837, 1838, 1839, 1845,  
1846, 1847, 2148, 2447, 2483  
neurodegenerative diseases ..... 775  
Neurodevelopment ..... 715, 1410  
Neurodevelopmental ..... 1925  
Neurodevelopmental Toxicity ..... 2158  
neuroendocrine ..... 988  
neurogenesis ..... 54, 910  
Neuroinflammation ..... 243, 260, 261,  
262, 350, 832, 833, 834, 835, 1360, 1842,  
1868, 1870, 2404  
neurologic diseases ..... 2402  
Neurologic Symptoms ..... 1420  
neuromodulation ..... 1417  
Neuronal networks ..... 1475  
Neuropathology ..... 1610, 1611,  
1612, 1613, 1614  
Neuropathy ..... 12  
neuroprotection ..... 1369, 1781, 1872, 2418  
Neurotoxics ..... 905  
neurotoxicity ..... 52, 54, 56, 354, 418,  
487, 500, 778, 820, 907, 908, 915, 917,  
919, 923, 928, 1347, 1385, 1396, 1397,  
1398, 1447, 1451, 1581, 1582, 1612,  
1776, 1866, 2144, 2149, 2377, 2449  
neurotoxicity, pesticides ..... 1380  
Neurotoxicology ..... 6, 906, 1419, 1610, 1839  
neurotoxin ..... 918  
neurotransmitter release ..... 1417  
Neurotransmitters ..... 916  
neutrophil ..... 1090, 2364  
Neutrophils ..... 255, 636  
new methods ..... 1502, 1689  
Next Generation Sequencing ..... 115, 534  
NFkB ..... 167, 246, 412, 421, 678  
NGF ..... 2033  
NGS ..... 1069  
NHANES ..... 1244, 1253, 2505  
NHP ..... 2046  
nickel ..... 164, 272, 1164, 1640, 2384  
nickel compounds ..... 1163  
nickel occupational exposure ..... 1164  
Nickel oxide ..... 2378  
Nickel sulfate ..... 1145  
Nicotinamide  
Phosphoribosyltransferase ..... 2179  
Nicotine ..... 674, 1141, 1371, 1372,  
1379, 1546  
Nicotinic acetylcholine receptors ..... 903  
nicotinic receptor ..... 339  
Nitric Oxide ..... 685, 2037  
nitro-PAHs ..... 1714  
Nitroarenes ..... 1113  
nitrogen mustard ..... 336, 341, 352, 358, 359,  
365, 366, 369, 371  
Nitrosamines ..... 1494, 1566  
nitrosative stress ..... 911  
NK cells ..... 389  
NMDA receptor ..... 1368  
NNK ..... 166  
NOAEL ..... 1561, 2348  
Nociception ..... 1148  
noise ..... 828  
noise and artifact ..... 68  
non-animal testing ..... 982  
Non-genotoxic carcinogen ..... 1108  
Non-genotoxic carcinogens ..... 538, 1102  
Nonalcoholic fatty liver disease ..... 649  
Nonclinical predictivity ..... 376  
Nonclinical Safety Assessment ..... 1806,  
2415  
Nonclinical Toxicology ..... 872  
Nonclinical vehicles ..... 176  
nongenotoxic carcinogenesis ..... 2341  
Nonhuman primate (NHP) ..... 740, 743,  
2142, 2462  
Nonhuman primates ..... 1028, 1220, 1895  
nonmonotonic ..... 1593, 1594  
Nonmonotonic Dose Response ..... 1592,  
1595, 1597  
nonmutagenic carcinogens ..... 2440  
nonparametric Bayesian ..... 711  
norepinephrine ..... 910, 1841  
normal brain aging ..... 1681  
Normal human  
bronchial epithelial cells ..... 428  
normal propyl bromide ..... 910  
Normal ranges ..... 750  
Nose-only inhalation ..... 217  
Novel ..... 2060  
Novel biomarkers ..... 2038  
novel targets ..... 588  
Nrf2 ..... 153, 654, 678,  
726, 1085, 1100, 1149, 1290, 1406, 1681,  
1824, 1825, 2011, 2014, 2073, 2074,  
2075, 2358, 2359, 2393  
Nrf2 activation ..... 2072  
Nrf2-Keap1 ..... 1995  
NTP studies ..... 2487  
Nuclear Factor Kappa B ..... 1229  
nuclear hormone receptor ..... 2296  
nuclear receptor ..... 1117, 1118,  
1269, 1273, 1286  
Nuclear receptors ..... 663, 1295  
nucleoside analogs ..... 1706  
nucleoside reverse transcriptase  
inhibitor ..... 87  
nucleoside reverse transcriptase  
inhibitor safety ..... 2171  
Nucleotide Excision Repair ..... 1703  
Nursing Curriculum ..... 2210  
nutraceutical ..... 1167  
nutrition ..... 13  
'omics ..... 870  
'Omics Research ..... 1653  
OATP1B3 ..... 1480  
obesity ..... 726, 769, 770, 774, 1073,  
1317, 1606, 1636, 1792, 1987, 2435  
observed adverse effect levels ..... 2223  
Occupation in the coal,  
iron and steel industries ..... 188  
Occupational ..... 2506  
occupational asthma ..... 189  
Occupational epidemiology ..... 478  
occupational exposure ..... 530,  
1240, 2003, 2013  
occupational exposure level ..... 2216  
Occupational Exposure Limit ..... 1256, 1575,  
1954, 2228  
occupational exposure limits ..... 503  
occupational health ..... 50, 51, 622  
ochratoxin A ..... 2319

- Ocular ..... 360, 361, 1823, 2508, 2509, 2513
- Ocular Distribution ..... 501
- ocular drug delivery system ..... 2512
- ocular irritation ..... 978
- ocular irritation ..... 973, 980, 1553
- Ocular toxicity ..... 749, 1231, 1811
- ODD ..... 2281
- OECD 407 ..... 1545, 1561
- OECD 442B ..... 1441
- OECD Nanomaterials ..... 2383
- OECD Reference Nanomaterials ..... 1471
- OECD TG 414 ..... 2383
- OECD TG431 ..... 1580
- OEL ..... 2226
- Ofloxacin ..... 1491
- Okadaic acid ..... 539
- old age sensitivity ..... 896
- Oleanolic acid ..... 1087
- Oligonucleotide ..... 1817
- Oligonucleotides ..... 1499
- online workspace ..... 876
- Onset ..... 748
- Ontogeny ..... 692
- ontology ..... 868, 873
- oocyte ..... 2104, 2112
- opioid drugs ..... 1222
- ophthalmology ..... 755
- optimal experimental design ..... 572
- oral ..... 1891
- Oral Bioavailability ..... 1345
- Oral Cancer ..... 1967
- oral exposure limits ..... 2212
- oral tolerance ..... 2329
- oral toxicity ..... 2368
- Orellanine ..... 1837
- organ toxicity ..... 2177
- organelle-specific  
fluorescent proteins ..... 1765
- Organic Cation Transporter ..... 920
- Organochlorine ..... 1246, 1998
- Organochlorine Pesticides .. 83, 586, 1997
- organohalogen ..... 2237
- organophosphate ..... 135, 340, 1418, 2130, 2448, 2450, 2453
- organophosphate induced delayed  
neuropathy ..... 1413
- Organophosphate Nerve Agent ..... 363
- Organophosphate pesticides ..... 1909
- organophosphates ..... 322, 2452
- Organophosphorus Insecticides ..... 1684
- Organophosphorus  
pesticides ..... 587, 1420
- Organoselenium ..... 351
- organotypic models ..... 1476
- orofacial cleft ..... 121
- Oropharyngeal aspiration ..... 1352
- OSRI ..... 1569
- ossification ..... 1030
- osteoporosis ..... 1586, 1588, 1590
- OSW-1 ..... 1784
- ototoxic ..... 2499
- Outreach ..... 1670
- ovalbumin ..... 256
- Ovarian antral follicles ..... 2096
- Ovarian development ..... 2106
- Ovarian toxicity ..... 2090
- Ovarian toxicology ..... 2094
- ovary ..... 2089, 2109
- Oxidative injury ..... 912
- oxidative and nitrosative stress ..... 1426
- oxidative damage ..... 1722, 1832, 2161
- Oxidative Stress ..... 83, 153, 238, 260, 337, 405, 412, 437, 442, 560, 592, 619, 643, 772, 827, 830, 935, 1022, 1128, 1149, 1158, 1338, 1351, 1369, 1381, 1522, 1687, 1704, 1775, 1838, 1856, 1884, 1969, 2001, 2002, 2005, 2006, 2007, 2015, 2018, 2021, 2023, 2027, 2029, 2030, 2033, 2035, 2037, 2040, 2102, 2129, 2151, 2160, 2175, 2184, 2360, 2365, 2403, 2483
- oxidative stress and  
inflammation ..... 94, 95
- Oxidative stress genes regulation ..... 694
- Oxidative stress/ER-stress ..... 2381
- oxidatively modified lipids ..... 2008
- Oxidized Lipids ..... 2187
- oxime ..... 343
- oxLDL ..... 1136
- Oxycyte ..... 1226
- Oxylipins ..... 1897, 2406
- ozone ..... 59, 61, 62, 63, 215, 220, 222, 224, 235, 239, 258, 912, 1125, 2016, 2029, 2483
- ozone inhalation ..... 801
- ozone susceptibility ..... 216
- P-glycoprotein ..... 187, 510
- p16INK4a ..... 700
- p38MAPK ..... 1328
- P450 ..... 295, 1080, 1209, 1391
- p53 ..... 529, 1103, 1705, 2269
- packaging ..... 111
- Paclitaxel ..... 695
- PAH ..... 169, 335, 554, 721, 1942, 1968
- PAH metabolism ..... 181
- PAH mixtures ..... 569, 1966
- PAHs ..... 1956
- pain ..... 2046
- Paint ..... 2367
- palatogenesis ..... 1622
- Palmitate ..... 1140
- Palmitoylation ..... 1524, 2350
- Panax ginseng ..... 1299
- pancreas ..... 2035
- pancreatic cancer ..... 159, 192
- pancreatic ductal carcinoma ..... 172
- Pancreatitis ..... 725, 926, 1711
- Panel study ..... 212
- Papaverine ..... 497
- Papillary necrosis ..... 952
- Para-phenylenediamine ..... 1054
- paracetamol ..... 745
- Paralytic Shellfish Poisoning ..... 2342
- Paraoxon ..... 1732, 2453
- paraoxonase ..... 1010, 1527, 1916, 2279, 2448
- paraquat ..... 55, 600, 1381, 1398, 1401, 1402, 1721
- Parasite ..... 2330
- PFASs ..... 1837
- Parkinson's disease ..... 55, 187, 729, 731, 1399, 1400, 1401, 1685, 1840, 1842, 1845, 1855, 1867, 1869, 1888
- PARP-1 ..... 2287
- Particle exposure ..... 259
- particokinetics ..... 1734
- Particulate Material ..... 1285
- Particulate Matter ... 66, 80, 211, 238, 239, 261, 771, 772, 802, 828, 830, 1144, 1492, 1832
- Particulate Matter dust ..... 228
- Particulates ..... 452
- Partition Coefficients ..... 488
- Parvalbumin ..... 2154
- Passive smoke ..... 182
- Patch Test ..... 1429
- pathology ..... 1599
- Pathway Analysis ..... 679
- Pathways ..... 867, 891, 2398
- Pathways of Toxicity ..... 1217, 2247
- Pb ..... 1581, 1582, 1583, 1584, 1585
- Pb toxicity ..... 2153
- PBDE ..... 310, 1988
- PBDEs ..... 1828
- PBMC ..... 1816
- PBPK ..... 290, 490, 506, 507, 604, 616, 884, 896, 897
- PBPK and Biological modeling ..... 865
- PBPK Model ..... 606, 617, 618, 799, 898
- PBPK modeling ..... 474, 486, 622, 2362
- PBPK models ..... 2049
- PBPK, Biological modeling ..... 608
- PC3 prostate cancer cells ..... 146
- PCB ..... 155, 475, 778, 1023
- PCB 126 ..... 673, 1897
- PCB sulfate ..... 1266
- PCB153 ..... 1207
- PCBs ..... 1258, 1377, 1984, 1995
- PCLS ..... 1471
- PD-L1 ..... 1806
- pdr-1/parkin ..... 1849
- pedagogy ..... 1667, 2206
- pediatric ..... 2411
- PEG ..... 1810
- Penetration ..... 1048
- Penicillium mycotoxins ..... 2081
- Peptide ..... 1049, 2166
- Peptide reactivity ..... 960
- peptides ..... 245
- Peracetic acid ..... 2226
- perchlorate ..... 893, 1253, 1907, 2239
- perfluorinated compounds ..... 58
- Perfluoroalkanes ..... 1982
- Perfluoroalkyl acids ..... 564
- perfluorocarbon ..... 1226
- Perfluorochemicals ..... 504
- perfluorohexanoate ..... 280
- Perfluorooctanoic  
Acid ..... 1015, 1981, 2035
- Perfluoroundecanoic acid ..... 2116
- Perfluorooctanoic acid ..... 1009
- Performance Standards ..... 964
- Perinatal exposure ..... 2146, 2329, 2330
- peripheral neuropathy ..... 53
- Permethrin ..... 301
- Peroxydase ..... 294
- persistant organic pollutant ..... 1587
- Persistent and Bioaccumulating  
Toxic Pollutant ..... 1983
- Persistent organic pollutants ..... 390
- Persistent organic  
pollutants (POPs) ..... 491, 1376
- personal care products ..... 1111, 1552
- pesticide ..... 779, 1395, 1396, 1407
- Pesticide formulation ..... 594
- pesticide risk assessment ..... 265
- Pesticides ..... 108, 187, 347, 585, 590, 603, 783, 1044, 1247, 1258, 1397, 1399, 1400, 1409, 1419, 1960, 1963, 1998, 2434, 2455
- petroleum ..... 118, 566
- PFASs ..... 570
- PFOA ..... 404, 662, 806, 1004, 1635, 2456
- PFOS ..... 629, 1918, 1985
- PFSAs ..... 492
- Phagocytosis ..... 1467, 1738, 1764, 2068
- Phagotest ..... 1467
- Pharmaceutical ..... 1225, 2430, 2431
- Pharmaceutical agents ..... 1222, 1692
- Pharmaceutical Ecotoxicology ..... 265
- Pharmaceuticals ..... 1615
- Pharmacodynamic assay ..... 2063
- Pharmacodynamics ..... 2047, 2471
- Pharmacogenetics ..... 184, 716
- Pharmacogenomics ..... 184
- pharmacokinetic ..... 518, 519, 520, 615
- Pharmacokinetic modeling ..... 504
- pharmacokinetic/  
pharmacodynamic model ..... 1248
- pharmacokinetics ..... 286, 287, 344, 345, 486, 494, 512, 590, 595, 596, 608, 611, 708, 884, 1235, 1868, 2386, 2471
- Pharmacology ..... 70, 2272
- Pharmacophore ..... 321
- Phenobarbital ..... 670, 947, 1069
- phenotyping ..... 2066
- Phikud Navakot ..... 1316
- Phillyrin ..... 1792
- PhIP ..... 1103
- Phorbol ester ..... 1560
- Phosgene ..... 741, 1260
- Phosphatidylinositol-3 kinase ..... 2094
- Phospholipids ..... 519
- phosphoproteomic ..... 1931
- Phosphoproteomics ..... 2079
- phosphorylation ..... 2277
- photobeam ..... 922
- photocatalytic ROS production ..... 2388
- Photosafety evaluation ..... 971, 2260
- Photostability ..... 1215
- phototoxicity ..... 129, 1041, 1215, 1310, 1737, 2260, 2276
- Phthalate ..... 709, 897, 1012, 1019, 1024, 1830, 2109, 2131
- Phthalate esters ..... 2229
- phthalate mixtures ..... 2127
- phthalates ..... 798, 1005, 1018, 1935, 2134, 2461
- Phyllanthus amarus ..... 1304
- Physicochemical properties ..... 427, 1770, 2164, 2170
- Physicochemical characterization ..... 1175
- Physiological background ..... 750
- physiologically based  
kinetic modeling ..... 2458
- Physiologically Based  
Pharmacokinetic Model ..... 2495
- Physiologically Based  
Pharmacokinetic Models ..... 299, 894
- PI3K-regulated ER stress ..... 1719
- PI3K/Akt ..... 2143
- Pig-a ..... 1698, 1740, 2446
- PIGO mutation ..... 1704
- Pixuvri ..... 2098
- PKC epsilon ..... 1100
- PLA2 ..... 1717
- placenta ..... 1660, 1662, 1665
- placental form  
glutathione S-Transferase ..... 2316
- Placental Toxicology ..... 1664
- Placental Transfer ..... 1003, 1458, 1663
- placental transfer of  
monoclonal antibody ..... 1663
- planarian ..... 270
- Plasma Integrity ..... 520
- Plasma Protein Binding ..... 593
- plasminogen ..... 2017
- plastic ..... 2332
- Plasticizer ..... 309, 1019
- platelet ..... 2179
- Platelets ..... 630, 639, 734, 1301, 1819
- Platinum ..... 1427
- Platycodin D ..... 1787
- Platycodon grandiflorum* ..... 1311, 1312, 1313, 1786
- Pleural Fibrosis ..... 1424
- Pleurotus eryngii* ..... 1315
- plums ..... 1317
- pluripotency ..... 1190
- PM ..... 1567
- PM health effects ..... 1517
- PM2.5 ..... 63, 556, 1145
- Pol eta ..... 1687
- polyaromatic hydrocarbon (PAH) ..... 1975
- Polyaromatic Hydrocarbons ..... 299, 894
- polybrominated diphenyl  
ethers ..... 333, 610, 1827
- polybrominated diphenyl  
ethers (PBDEs) ..... 1250, 1828
- Polycarbonate ..... 203
- Polychlorinated biphenyl ..... 1375
- Polychlorinated Biphenyl Ether ..... 1374
- Polychlorinated biphenyls ..... 390, 1377, 1683, 1983, 1987, 1991, 1997
- Polychlorinated  
biphenyls (PCBs) ..... 474, 1989, 1994
- polycyclic aromatic  
hydrocarbons ..... 229, 323, 1113
- Polycyclic Aromatic  
Hydrocarbons, PAHs ..... 995
- Polyhexamethyleneguanidine  
phosphate ..... 210
- polymerase eta ..... 1172
- polymeric nanocapsules ..... 179, 2372
- polymers ..... 723
- Polymorphism ..... 1495, 2257, 2290
- polymorphisms ..... 191, 193
- Polypheols ..... 150

# Abstract Keyword Index (Continued)

The numerals following each keyword refer to the relevant abstract number(s).

PON1 .....	185, 191	protective effects .....	1167	Quinones .....	1782	reproduction .....	277, 1024, 2108, 2123
pooled analysis .....	709	protein .....	2346	(Regulatory) Developmental Toxicity .....	2383	Reproduction and Development .....	780, 2090, 2103, 2118, 2249
POP .....	1246	protein adduct .....	1878	R-spondin .....	2141	reproduction toxicity .....	2090
POPs .....	280	protein adduction .....	349	rabbit .....	1006	Reproduction-Developmental .....	327
population studies .....	2435	protein adducts .....	295, 1232, 1991	radiation .....	740	reproductive outcomes .....	603
population variability .....	2476	Protein Adsorption .....	431	Radiation mitigator .....	338	Reproductive System .....	1595
Porcine Model .....	2114	protein aggregation .....	1842, 1857	radiation sensitivity .....	151	reproductive toxicity .....	126, 2113
port catheter .....	2044	protein allergen .....	1434	radiofrequency .....	1490	Reproductive toxicology .....	537, 1455, 2127, 2128
portfolio analysis .....	986	Protein binding .....	658	Rainbow trout .....	1276	Reproductive/developmental toxicity .....	2116
post-marketing adverse event data .....	972	Protein Carbonylation .....	2023	raloxifene .....	146	Research .....	2208
postnatal .....	1384	protein corona .....	1322, 1327	rasH2 mouse .....	1104	research sample .....	877
potency ranking .....	1053	protein expression .....	79	Rat .....	27, 550, 631, 751, 755, 1526, 1548, 1657, 2128	Resistance .....	1723
Potential risk .....	1239	protein interaction .....	2425	rat developmental toxicity study .....	1008	resources .....	1671
Potential/Promotion .....	1413	protein kinase C .....	403	rat embryos .....	1034	respiratory .....	70, 754, 757, 1427, 1541, 1542, 1543, 1774
Poultry .....	2317	protein kinase C inhibitor .....	1821	rat hepatocyte sandwich culture .....	1070	respiratory allergy .....	699
Power Generation .....	1608	Protein Networks .....	822	rat hepatocytes .....	1713	Respiratory Disease .....	228
PPAR .....	557, 1102, 1290	Protein Nitration .....	2038	rat liver microsomes .....	284	respiratory effects .....	2216
PPAR-alpha .....	564	protein oxidation .....	1398	Rat Primary Hepatocytes .....	2162	Respiratory function .....	1233
PPAR-gamma .....	395	protein, lipid corona .....	1755	Rat whole embryo culture .....	1002, 1008	respiratory infection .....	984
PPARa .....	2405	Proteomics .....	558, 943, 1201, 1513, 2072	Rats .....	512, 1834, 1939	respiratory tract dosimetry .....	2363
PPARalpha .....	1272	Protocatechuic acid .....	1301	RccHan Wistar .....	944	Restraint device .....	759
PPARgamma .....	1590	Provisional Advisory Levels (PALs) .....	2214	REACH .....	10, 713, 1571, 1964, 2268	Restraint stress .....	759
Pre-Post natal toxicity .....	2107	proximal tubule .....	2183	reactive metabolites .....	1232	resveratrol .....	1110, 2185, 2347
pre/postnatal loss .....	1013	Pseudomonas aeruginosa .....	385	reactive oxygen .....	1589	retina .....	2165
preB lymphocyte .....	1591	PSOA .....	1545	Reactive oxygen species (ROS) .....	2003	Retinal photoreceptors .....	2159
Preclinical .....	1610, 1654, 1655, 1656	PSTC .....	1912	read-across .....	857	Retinal pigment epithelial cells .....	2174
preclinical biomarkers .....	1871	PTD .....	252	realistic exposure .....	1341	Retinal Toxicity .....	1231
preclinical safety .....	1228, 2193	puberty .....	1898	receptor crosstalk .....	1931	Retinoblastoma proteins .....	542
Preclinical safety evaluation .....	1814	PUFAs .....	1128	Receptor for Advanced Glycation Endproducts .....	66	retinoic acid .....	693
Preclinical study design .....	1213, 2142	Pulmonary .....	257, 258	recombinant .....	577, 1109, 2091	Retinoids .....	1269, 1298
precocious puberty .....	1923	pulmonary and Hepato-toxicity and Inflammation .....	2360	recombinant strain .....	2339	Retinopathy .....	2032
preconditioning .....	667	pulmonary arterial hypertension .....	218, 742	reconstructed human epidermis model .....	968	retrotransposition .....	312, 701
Prediction Model .....	965, 970	pulmonary effects .....	20	reconstructed human skin .....	959	reverse dosimetry .....	897, 1253
predictive .....	2195	pulmonary exposure .....	23	Redox .....	1205, 2161	Reverse Engineering .....	555
predictive ecotoxicology .....	265	pulmonary fibrosis .....	600	redox cyclers .....	2263	RfC .....	1964
Predictive <i>in vitro</i> model .....	1216	Pulmonary Function .....	462, 476, 478	Redox signaling .....	2036	Rheumatoid Arthritis .....	1280
predictive model .....	1205	Pulmonary Immunity .....	1650	reduction .....	2283	Rho GTPases .....	2180
Predictive Modeling .....	2425	Pulmonary inflammation .....	217	reference concentration .....	2215	Rho-kinase .....	1032
Predictive models .....	1632	Pulmonary Injury .....	359	reference values .....	1949	Rho-kinases .....	445
Predictive Myelotoxicity .....	1198	Pulmonary Instillation .....	1131	refinement .....	502, 1428	RIA .....	1922
predictive oral exposure model .....	728	Pulmonary Toxicity .....	456, 463, 2381	refuse .....	266	Ribosomal Insults .....	2085
Predictive Toxicology .....	128, 140, 605	Pulmonics .....	1648, 1651	Regeneration .....	1598	rice and grain consumption .....	472
pregnancy .....	473, 893, 996, 1006, 2051	Purified Diet .....	727	Regional Chapter .....	1666	risk .....	481, 722, 1566, 1643, 1743, 1950, 2218, 2220
pregnancy hormones .....	645	Purinergic receptor .....	628	regulation .....	1672	Risk and Safety assessment .....	1435, 1623, 2464
Pregnane X Receptor .....	1275	pyrethroid .....	487, 591, 593, 1380	Regulatory .....	792, 1573, 1576, 1612, 2042, 2043, 2465, 2513	Risk Assessment .....	2, 47, 48, 110, 177, 288, 450, 508, 517, 579, 607, 615, 619, 625, 702, 708, 714, 719, 723, 780, 794, 796, 804, 864, 875, 956, 1227, 1246, 1261, 1342, 1532, 1578, 1631, 1633, 1637, 1647, 1734, 1796, 1952, 1953, 1954, 1955, 1959, 1962, 1972, 1973, 1976, 1977, 1979, 2043, 2209, 2213, 2214, 2219, 2221, 2227, 2228, 2232, 2233, 2234, 2235, 2239, 2240, 2241, 2276, 2348, 2419, 2426, 2427, 2428, 2429, 2430, 2431, 2456, 2457, 2461, 2472, 2477, 2497
Pregnane X receptor (PXR) .....	1281	Pyrethroids .....	301, 488, 595, 596, 804, 1412, 1482	Regulatory Guidelines .....	794	risk characterization ratio .....	805
prematurity .....	984	Pyrethroids risk assessment .....	895	regulatory hazard classification .....	1572	Risk Communication .....	785, 1976, 2211
prenatal .....	987	pyrolysis .....	208	Regulatory Toxicology .....	1953	risk factors .....	482, 2438
prenatal exposure .....	2413	pyrrolidine dithiocarbamate .....	600	Regulatory Value .....	1565	risk factors for disease .....	2432
Preterm birth .....	2102, 2105	Qdot .....	2379	Reinstatement .....	744	Risk Management .....	785, 2209
Primary cardiomyocyte culture .....	1009	qHTS .....	127, 2269	relative potency factor (RPF) .....	1975	rituximab .....	1800
primary cell cultures .....	2048	QNAR .....	2422	relative risk .....	1899	RNA .....	2343
Primary hepatocyte .....	41	qRT-PCR .....	951	Renal .....	844	RNA sequencing .....	687
primary human hepatocytes .....	523, 645	QSAR .....	140, 624, 860, 890, 1982, 2267, 2268, 2423, 2424	renal biomarkers .....	2167	RNA-seq .....	335, 684, 688, 939, 1216, 1629
Primary neuronal cell culture .....	1684	QSAR modeling .....	1625, 2454	Renal Cell Carcinogenesis .....	2189	RNAi .....	2343
pro-inflammatory cytokines .....	244	QSAR models .....	1624	Renal damage .....	2194	RNAi screen .....	1848
probabilistic analysis .....	71	QSAR/QSTR modeling .....	144	Renal inflammation .....	2187	rodent .....	1023
Probiotics .....	1320	QT interval prolongation .....	71	renal toxicity .....	737, 1221, 2271	Rodents .....	1353
Product safety assessment .....	537, 2492, 2494	Quality assurance .....	1971	renin-angiotensin system .....	774	ROS .....	427, 548, 669, 735, 1173, 2012
progenitor cells .....	771	quality control .....	1971	repeated dose .....	648, 2445	ROS assay .....	2260
progesterone .....	2088	Quantitative Trait Locus Analysis .....	183	Repeated dose toxicity .....	870, 2116, 2256	rotenone .....	1846
progestins .....	277	Quantitative High-Throughput Screening .....	2476	Replace, Reduce, Refine .....	2458	route dependency .....	483
Programmed death-1 receptor .....	410	Quantitative Proteomics .....	952, 1214	replication stress .....	154	RTCATM high-throughput assay .....	1978
prohaptin .....	311, 1051	Quantitative Risk Assessment .....	2231			RTP801 .....	1405
prolactin .....	1917	Quantitative Structure Activity Relationship .....	610				
proliferation .....	172, 1790	Quantitative structure activity relationship (QSAR) .....	132, 703				
Prophylactic .....	259	Quantum dot nanoparticles .....	2392				
prophylactic vaccines .....	1812	quantum dots .....	2394				
Proposition 65 .....	1550	QuEChERS .....	1998				
Prostacyclins .....	221	Quercetin .....	1529				
Prostaglandin .....	242	Quinoid Metabolites .....	1991				
prostanoids .....	91	quinolone .....	1829				
Prostate cancer .....	149, 168, 170, 1098, 1103, 1717, 1797, 1932	Quinone Oxidoreductases .....	1782				
prostate diseases .....	994						
Prostate Inflammation .....	251						
proteasome inhibitor .....	1824, 1825						
Protection .....	1086						
protective .....	372						
Protective activity .....	1305						

# Abstract Keyword Index (Continued)

The numerals following each keyword refer to the relevant abstract number(s).

rutacarpine .....	285, 1788	SILAC .....	1214, 2031	sperm .....	29, 2139	Sustainability .....	2268
Ryanodine receptor .....	1375, 1683	silica .....	2097	sperm whale .....	1530	SWCNT .....	442
S-allyl cysteine .....	1793	silica nanoparticle .....	407, 409, 2381	spermatogenesis .....	605, 1712	synapse .....	1373
S-nitrosation .....	2287	silica nanoparticles .....	1746, 2371, 2376	Spermatogonial Stem Cells .....	2135	Synaptic mitochondria .....	2159
Safe Starting Dose .....	1230	silica-silver nanocomposite .....	1362	spheres .....	1262	Synaptophysin .....	2146
safety .....	754, 792, 1557, 1672, 1676, 2163, 2332, 2347	silver .....	1174, 1332, 1344, 1351, 1361	spina bifida .....	123	synthetic amorphous silica .....	1754
Safety assessment .....	40, 796, 1223, 1303, 1544, 1547, 1615, 1621, 1903, 2167, 2491	silver ions .....	197	spinal cord injury .....	836	system biology .....	552, 879
Safety Biomarker .....	930, 931	Silver nanomaterials .....	1356	splice variant .....	1840	systematic approach .....	710
Safety Evaluation .....	1617, 2462	silver nanoparticle .....	1349	Splicing factors .....	2140	systematic reviews .....	875
safety pharmacology .....	757, 1233	silver nanoparticles .....	616, 1322, 1323, 1324, 1325, 1326, 1328, 1329, 1333, 1334, 1335, 1336, 1347, 1354, 1355	spontaneous behaviour .....	1390	systemic REPs .....	2000
Saffron .....	1797	silver nanoparticles (AgNPs) .....	1339	spontaneous DNA damage .....	32	systems biology .....	16, 141, 551, 821, 823, 881, 938, 1000, 1631, 1633, 2196
Salicylamine .....	2005	Silver Nanotoxicology .....	1330, 1352	Sprague-Dawley Rat .....	176	Systems Biology and Toxicology .....	886
salmon .....	275	Silver nanowires .....	1365	Sprague-Dawley rats .....	756	Systems Genetics .....	1177, 2392
Salmonella mutagenicity .....	132	silymarin .....	1781	squalene .....	611	systems models .....	825
Salmonella/microsome assay .....	1496	Simulated Metabolism .....	93	SREBP-1 .....	641	Systems Toxicology .....	715, 786
Salmonella/microsome mutagenicity assay .....	860	simulation .....	1960	staining .....	1035	SYVN1 .....	2011
Salt .....	845, 847	simvastatin .....	2127	stakeholders .....	2395	T cell .....	380, 812, 2073
SAM .....	246	Single cell array .....	2439	standard assays .....	1334	T cell-dependent antibody response .....	2063
sandalwood .....	1728	single nucleotide polymorphism .....	190	STAT-3 .....	161	T cell responses .....	1760
Sandhoff disease .....	1871	Single walled carbon nanotube .....	436	Stat3 .....	1154, 2196	T cells .....	386, 419, 2075
SAR models .....	859	Singleminded-2s .....	672	statins .....	2022	T-2 toxin .....	2322
Sarin .....	342, 370	siRNA .....	2343	Statistical approaches .....	582	T-Box Transcription factors .....	142
Saxitoxin .....	2342	siRNA screening .....	361	Statistical Power .....	67	T47D-KBluc .....	2248
scaling .....	613	SIRT1 .....	1600	status epilepticus .....	621	tamoxifen .....	173, 1071, 1710
Scavenger Receptor A .....	1363	sister chromatid exchange, chromosome aberration .....	1491	STD10 .....	1230	tandem mass spectrometry .....	1501
Scavenger Receptors .....	1327, 1337	skeletal muscle toxicology .....	2311	STE .....	975	target organ toxicities .....	1213
Schedule Y .....	1618	skeleton .....	1035	steatohepatitis .....	643	targeted testing .....	2275
Schizophrenia .....	2154	SKH-1 mice .....	371	Steatosis .....	640, 1060, 1793, 2331	Tartrazine .....	1505
Science .....	1621	skin .....	133, 353, 355, 356, 366, 371, 1039, 1046, 1047, 1300, 1673, 1796	Stem Cell .....	363, 1200	tau .....	1390
Scientific Writing .....	2465	Skin Absorption .....	1049	stem cell biology .....	1207	tBHQ .....	2073, 2074, 2075
Screen .....	1455	skin allergy .....	1433	stem cell biology and toxicology .....	1211	TBX2 .....	1627
Screening .....	36, 89, 820, 900, 901, 1084, 2022	skin barrier .....	962, 1045	Stem cell differentiation .....	1744	TBX5 .....	696
screening-level risk assessment .....	1577	Skin cancer .....	157, 1306	stem cell models .....	950	TCDD .....	107, 162, 388, 612, 812, 997, 998, 1194, 1289, 1292, 1387, 1986, 1996, 2086, 2141, 2203
SDF-1beta .....	1731	Skin corrosion .....	707, 1580	Stem Cells .....	76, 932, 1001, 1191, 1192, 1193, 1196, 1197, 1202, 1205, 1462, 1679	TCDD Immunotoxicity .....	398, 1199, 2078, 2084
seafood .....	1956	Skin Dendritic Cells .....	2356	steroid .....	1821	TDAR .....	404, 2061, 2062
Seafood safety .....	1958	skin injury .....	346	Steroid Hormone .....	1593	TDAR cynomolgus monkey .....	2064
SEB .....	2353	Skin injury biomarkers .....	369	steroid sulfotase .....	651	TEF .....	1999
secondhand smoke .....	1259, 1394	Skin irritation .....	199, 958, 1036, 1037	Steroidogenesis .....	1012, 2093, 2245, 2246	TEF concept .....	2000
seizure .....	758, 1229, 1422	Skin metabolism .....	294	steroids .....	2091	telemetry .....	758, 1130, 1233
seizures .....	1421	Skin penetration .....	470, 955	stochastic gene expression .....	668	Telomere .....	155, 1172, 1703
selective AHR modulator .....	1279	Skin rash .....	1055	strain comparison .....	753	Telomeres .....	1994
Selective AHR modulators .....	175	Skin Sensitization .....	956, 960, 969, 970, 1051	strain comparisons .....	387	temperature regulation .....	2500
selenium .....	1530, 1531	skn-1 .....	1521	strain difference .....	1442, 2203	teratogenicity screen .....	1026
selenium tetrachloride .....	1531	Small Sample volume .....	2192	Strain Differences .....	668, 1986	Teratology .....	1028
selenoprotein P .....	659	small scale inhalation studies .....	219	stress .....	2156	terminology .....	1027
semantic web .....	868	Smallpox .....	344	Stress Response .....	1330	Terrorist .....	722
Semi-Volatile Organics .....	64	smartphone .....	1242	striated muscle .....	1460	tert-butyl-1, 4-benzoquinone .....	1291
SenCeeTox .....	1466	Smokeless Tobacco .....	916, 1532, 1546	Structural determinants .....	39	Tertiary oxime .....	342
SEND .....	2042	smoker .....	941	structure activity relationship (SAR) .....	21	Testes .....	27, 573, 2119
Senescence .....	447, 2312	SNP .....	192	styrene .....	307, 318, 1264	testes histopathology .....	2124
sensitization .....	424, 949, 957, 1052, 1466, 2070	SO2 .....	1567	subacute toxicity .....	459	testicular digenesis syndrome .....	126
Sensory Evoked Potentials .....	1386	Social Behavior .....	920	subcellular organization .....	825	Testicular toxicity .....	26, 601, 2125, 2126
sensory irritation .....	233	social housing .....	922, 1013	subchronic oral toxicity .....	1939, 2113	testing strategy .....	969
sepsis .....	245	Sodium .....	844, 845, 846, 847, 848	subchronic systemic toxicity .....	205	testis .....	25, 28, 304, 314, 531, 1012, 1634, 1712, 2120, 2121, 2122, 2130, 2132, 2139, 2501
sequencing .....	526	Soil .....	598	Subchronic toxicity .....	1540, 2340	testis histopathology .....	1813
Sequestosome 1 (p62) .....	1818	Soil Fumigants .....	599	subcutaneous .....	1238	testis in vitro .....	2137
serotonin .....	921, 1408, 1854	solid materials .....	976	Submicron particles .....	413	Testis steroidogenesis .....	1930
SERT .....	917	Solutions .....	1609	substrate oxidation .....	1060	Testisin .....	1935
Serum .....	1395	solvents .....	2499	sufficient similarity .....	572	Testosterone .....	298, 1924
sex difference .....	1123	Soman .....	347, 373	sulforaphane .....	341, 2012	tetanus toxoid .....	2064
sex differences .....	742, 1962	Soman vapor .....	354	Sulfur donor .....	2054	tetrachloroethylene .....	620
sex hormones .....	1921	sonication .....	443	sulfur mustard .....	337, 346, 355, 356, 360, 366, 367, 369	tetraculture .....	2361
Sex-specific .....	2004	sources .....	830	sulphur mustard .....	1501	Tetrahydrocannabinol .....	2077
Sexual maturity .....	748, 2462	Sp protein transcription factors .....	163	Sunscreens .....	303	tetramethylenedisulfotetramine .....	1421
SFDA .....	1617	Sp transcription factors .....	145	superoxide .....	2006	TETS .....	1422
SGLT2 .....	1219	Spatial Discrimination .....	995	Superparamagnetic .....	2391	Texas .....	2432, 2433, 2438
SGLT2 inhibitor .....	1219	Reversal Paradigm .....	995	superparamagnetic iron oxide nanoparticles .....	522	textile .....	1254
SH-SY5Y human cells .....	1415	Spatial learning and memory .....	1402	Surface Ligand Effect .....	1359	textile dyes .....	1700
shale gas .....	766	Spatial Memory .....	1376	surfactant corona .....	1762	TGF .....	1786
Shear Stress .....	1146	species .....	1166	surfactant proteins/function .....	468	TGHQ .....	681
shugoshin 1 .....	156	species comparison .....	1278	Surrogate endpoint .....	41	Th cell .....	381
Sick House Syndrome .....	1563	species differences .....	2025	surveillance .....	1534	thallium .....	272
Sidman electric shock avoidance test .....	914	species specificity .....	1297	Survival .....	1873	therapy .....	339, 368
signal transduction .....	403, 690, 1067	species-dependent .....	296	susceptibility .....	17, 24, 985, 1093, 2410, 2412, 2414, 2457, 2477	Thermal constraints .....	1948
signalling mechanisms .....	1185, 1746	Specificity protein transcription factors .....	158			thermal injury .....	95
		Specular microscopy .....	1823				

# Abstract Keyword Index (Continued)

The numerals following each keyword refer to the relevant abstract number(s).

thermal stress .....	680	toxicity mechanisms .....	2273	Triterpenoid .....	2359	Vitamin A .....	2032
Thermoregulation .....	1412	Toxicity pathway .....	555	Trivalent Arsenicals .....	2293, 2294	vitamin D .....	1127, 1538, 2057
thiamethoxam .....	589	Toxicity Pathways .....	1298, 2501	troponin .....	77, 2401	Vitamin D Receptor .....	1275
thickness .....	1822	toxicity prediction .....	858	trout hepatocytes .....	101	Vitamin E .....	1771, 2225
thioarsenicals .....	2278	Toxicity Study .....	2163	Trovaflaxacin .....	656, 1077, 1078	vitellogenesis .....	1938
thioredoxin .....	337, 2026	Toxicity testing .....	1962	TRP Channel .....	1285	vitellogenin .....	101
thioredoxin reductase .....	358, 2019	Toxicity testing in the		TRPV1 .....	252	vitrocell .....	2361
Thiostaurine .....	2040	21st century .....	1464	<i>Trypanosoma cruzi</i> .....	2015	VOCs .....	2118
Third trimester .....	2051	toxicity values .....	2454	TSPO .....	1871	volatile methyl siloxanes .....	617
Thirdhand smoke .....	1468	Toxicoeugenomics .....	1639	Tumor Pathology .....	1943	Volatile organic compounds .....	1844
Thorough QT study .....	376	toxicogenomics .....	16	Tumor Promotion .....	684, 1560	vomitoxin .....	2326
Thra1/Thra2 .....	2140	118, 426, 554, 691, 715, 791, 855, 939,		Tumor repressor .....	1858	vulnerable populations .....	878
Three dimensional model .....	1077	992, 1052, 1366, 1453, 1472, 1563, 1624,		Tumour profile .....	1961	VX .....	368, 372
three-dimensional .....	1891	2426, 2427, 2428, 2429, 2430, 2431, 2442		tumours .....	1549	Warburg Effect .....	672
Threshold .....	35, 2443, 2455	Toxicokinetics .....	516, 1043	Tungsten .....	1176, 1519, 1591	Water .....	281
threshold dose response .....	30, 31	toxicokinetic and		twins .....	191	water pollution .....	280
Threshold of Toxicological		pharmacokinetic .....	521, 747	two-generation reproduction .....	2097	weather .....	1605
Concern .....	713	toxicokinetics .....	489, 493, 506, 593, 719, 720	Type 1 Hypersensitivity .....	1427	Web Application .....	864
Threshold of Toxicological		toxicologic .....	2346	Type 2 diabetes .....	726	Weight of evidence .....	112, 1021,
Concern (TTC) .....	198	Toxicological .....	1307	Type IV hypersensitivity .....	2071	1951, 2456	
Thresholds .....	1553	Toxicology .....	460, 756, 821, 1570, 1637,	Tyrosine Kinase Inhibitors .....	1556	weighting .....	1999
thrombocytopenia .....	1226	1638, 2166, 2315		ubiquitination .....	237	welders .....	1107
Thrombosis .....	1301	toxicology education .....	1667, 2207	UCP2 .....	2028	welding .....	211, 2056
thymic atrophy .....	210	Toxicology Education Strategies .....	2207	UGT .....	157	Welding fumes .....	1132
Thymoma .....	178	Toxicology in <i>C. elegans</i> .....	1848	Ultrafine Particles .....	64, 561, 1122, 2479	well water .....	477
Thyroid disruption .....	1988	Toxicology outreach .....	1666	ultrasound .....	1143	whale cells .....	1171
thyroid disruptors .....	103, 572, 1985	ToxML .....	861	ultraviolet B .....	1716	Whole Blood .....	1555
thyroid hormone .....	1915	toys .....	1557	ultraviolet light .....	1283	Wild yam .....	147
thyroid hormones .....	1293, 1914	Traditional Chinese		Ultraviolet Radiation .....	2356	Wistar Han rat .....	178, 2121
thyroid tumor .....	1099	Medicine .....	2488, 2489	Uncertainty .....	1609	Wnt .....	1588
thyroperoxidase .....	99, 103	Traditional Medicine .....	1795	Uncertainty Factor .....	1980	Wnt signaling .....	632
TIAR .....	404	Traffic pollutants .....	212	Undergraduate .....	2205, 2208	Wood Smoke .....	1285
time-concentration-dependent		traffic-generated pollutants .....	829	undergraduate education .....	2206,	Workers .....	1948
response curve .....	1978	Traffic-Related Pollutants .....	827	2207, 2210		workers' exposure .....	828
TiO <sub>2</sub> .....	2393	TRAIL .....	1712	UPLC-MS/MS .....	1019	XBP1 .....	2011, 2170
tire .....	270	Training .....	2208	uranium .....	1516	xenobiotic metabolizing enzymes .....	1437
Tissue Distribution .....	501	transcriptomics .....	699	urban soil lead .....	1509	Xenobiotic .....	2114
tissue engineering .....	1476	transcript profile .....	549	Urethane .....	1698	xenoestrogens .....	1938
tissue factor .....	638, 1122	transcription .....	697, 1150	Urinary biomarker .....	1905, 1907	Xenograft .....	994, 1306, 2387
tissue fusion .....	1622	Transcription factor .....	543, 1114	urinary biomarkers .....	1893	Xenopus laevis .....	1293, 1936
tissue slices .....	1469	transcription factors .....	467	urinary C5b-9 .....	2191	XPC - NER .....	1691
titanate nanoparticle .....	1758	transcriptional activation .....	2111	Urinary microRNA .....	2199	XRF .....	1510
titanium and zinc thin coatings .....	1736	transcriptional dose response .....	1946	Urine .....	1234	yeast .....	1448, 1524
Titanium Dioxide .....	1744, 2390	transcriptomics .....	275, 557, 691, 816,	urine biomarker .....	927	zafirlukast .....	1713
Titanium dioxide nanoparticles .....	1763,	1211, 1294, 1651, 2087, 2375, 2459		Urine biomonitoring .....	597	Zea mays .....	1537
2380		transformation .....	164	urogenital sinus .....	2141	Zearalenone .....	2114, 2322, 2323
titanium nanoparticles .....	2368	Transforming Growth		Urothelium .....	1473	zebrafish .....	52, 273, 324,
TNF .....	246	Factor Beta .....	2356	US FDA .....	1675, 2042	326, 328, 331, 333, 335, 559, 735, 988,	
TNF- $\alpha$ .....	1078	transgenerational effects .....	547	Usnic acid .....	1779	1281, 1288, 1359, 1372, 1380, 1407,	
TNIP1 .....	675, 689	Transgenic .....	1873	usual intake .....	1645	1449, 1582, 1752, 2377, 2387	
Tobacco .....	567, 1533, 1899	transgenic mice .....	651, 1957	uterine artery .....	1032	zebrafish assay .....	1453
tobacco carcinogens .....	1494	transgenic mouse models .....	1801	Uterine Receptivity .....	2099	zebrafish development .....	322, 329
Tobacco documents .....	117	Transition metal oxides .....	1770	uterotrophic assay .....	2111	zebrafish embryo toxicity .....	1447, 2396
Tobacco Smoke .....	120, 671, 1259, 1488	transition metals .....	556	Vaccine .....	2060	zebrafish larvae .....	1445
tobacco-control policy .....	480	translation .....	25, 2398	Vaccine immunogenicity .....	401	ZFN .....	2169
Tokai High Avider rat .....	914	Translation Toxicology .....	1816	vaccine safety assessment .....	1812	zinc .....	270, 1517, 1518, 2307
Tolfenamic acid .....	163	Translational .....	777	vacuole .....	1810	zinc finger nucleases .....	1288
Toll-like receptor .....	397	translational biomarker .....	2402	Validation .....	795, 2251, 2267	zinc finger protein .....	1516
Toll-like Receptors .....	263	translational models .....	1659	variation .....	1887	zinc oxide .....	1757
Toluene .....	909	Translational toxicology .....	11,	vascular .....	1121, 1133, 1134	Ziram .....	1407
Topic modeling .....	117	933, 1212, 2484, 2485, 2488, 2489		vascular calcification .....	88, 2312	ZnO nanoparticles .....	2388
Topoisomerase I inhibitor .....	1225	translocation .....	2481	Vascular disease .....	1257	zoniperide .....	2261
topoisomerase II .....	165	Translocation and Clearance .....	2389	vascular function .....	831	zygote .....	2104, 2117
Torsade de Pointes .....	72	transparency .....	714	Vascular Injury .....	936, 1143,		
Total Allowable Concentration .....	2243	Transplacental .....	738	1146, 1875			
Total phenolic content .....	1783	transplacental exposure .....	554, 894,	vasoconstriction .....	1207		
Tox21 .....	786, 1298	1661, 1663		vasodilation .....	91		
Tox21-c .....	1680	transport .....	492, 511	Vav2-Rac1 .....	2180		
toxaphene .....	810	transporter .....	510, 1075, 1602, 2169, 2182	VEGF .....	1457, 2390		
Toxcast .....	137, 862, 888,	transporters .....	485, 499, 1525, 2148	vehicle .....	1442		
1452, 1686, 2275		transposon .....	528	ventilation .....	1252		
ToxCast hepatic outcomes .....	139	treatment .....	1695, 2507	ventricular remodeling .....	1138		
Toxic chemicals .....	364	Treg .....	382, 2083	vesicant injury .....	352, 353		
Toxic Equivalency Factors .....	2459	Trend .....	1550	vesicles shuttled along			
Toxic Island .....	2204	trends .....	2433	actin filaments .....	1772		
Toxic Load Model .....	374	Tribbles 3 .....	1142	veterinary toxicology .....	1436		
Toxicant Associated Steatohepatitis .....	644	Tributyltin .....	273, 914, 1590	Vinclozolin .....	298, 1927, 2138		
toxicity .....	29, 735, 846, 856, 1071, 1460,	trichlorfon .....	1415	Vinyl Chloride .....	644, 940		
1743, 1777, 2257, 2439		trichloroethene .....	1426	virtual liver .....	882		
toxicity assessment .....	1970	trichloroethylene .....	57, 289, 536,	Visual Cycle Modulator .....	501		
Toxicity Biomarkers .....	1212	620, 1061, 1497, 1867, 2271, 2473					
		triclosan .....	416, 1042, 1043, 1111, 1936				

A large rectangular area with horizontal ruling lines, intended for taking notes. The area is framed by a dark border at the top and bottom, and a decorative floral pattern on the sides.

# The Official Journal of the Society of Toxicology

## Toxicological Sciences



- *Premier, hypothesis-driven, original research articles in all areas of toxicology*
- *Advance Access—quick online publication, weeks ahead of print*
- *Optional open access for authors*

**VISIT OUR BOOTH AT TOXEXPO 2013**

OR VISIT US ONLINE AT

**[www.toxsci.oxfordjournals.org](http://www.toxsci.oxfordjournals.org)**

\* 2011 Journal Citation Reports (Thomson Reuters, 2012)

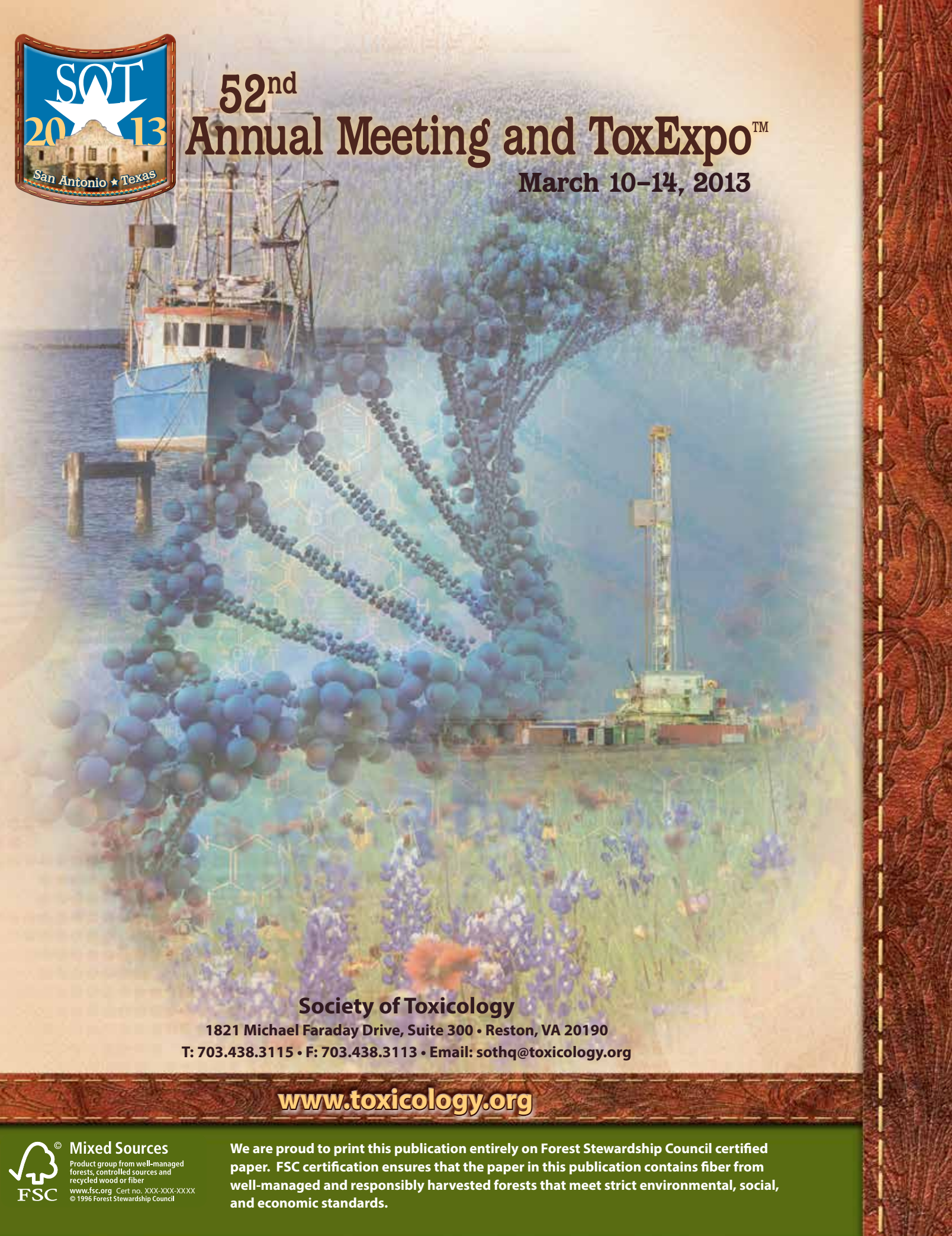
OXFORD  OPEN

**OXFORD**  
UNIVERSITY PRESS



# 52<sup>nd</sup> Annual Meeting and ToxExpo™

March 10–14, 2013



**Society of Toxicology**

1821 Michael Faraday Drive, Suite 300 • Reston, VA 20190

T: 703.438.3115 • F: 703.438.3113 • Email: [sothq@toxicology.org](mailto:sothq@toxicology.org)

**[www.toxicology.org](http://www.toxicology.org)**



**Mixed Sources**

Product group from well-managed  
forests, controlled sources and  
recycled wood or fiber  
[www.fsc.org](http://www.fsc.org) Cert no. XXX-XXX-XXXX  
© 1996 Forest Stewardship Council

We are proud to print this publication entirely on Forest Stewardship Council certified paper. FSC certification ensures that the paper in this publication contains fiber from well-managed and responsibly harvested forests that meet strict environmental, social, and economic standards.